REPORT
VOLUME V

COLUMBIA
ACCIDENT INVESTIGATION BOARD

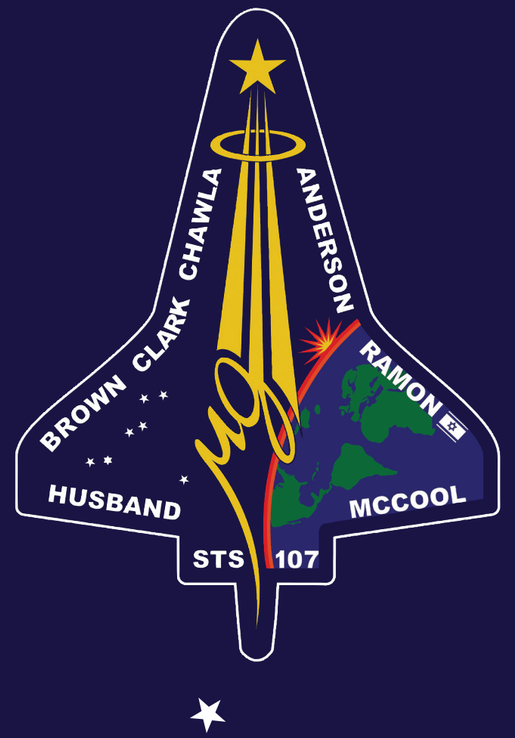

COLUMBIA ACCIDENT INVESTIGATION BOARD

OCTOBER
2003

REPORT VOLUME V
APPENDICES G.1 – G.9
OCTOBER 2003

COLUMBIA

ACCIDENT INVESTIGATION BOARD

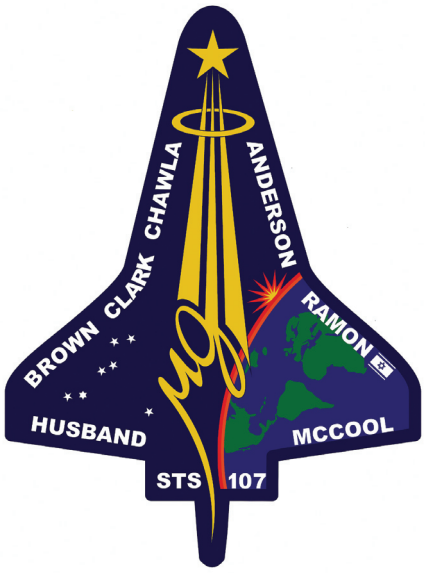

Note: Volumes II – VI contain a number of conclusions and recommendations, several of which were adopted by the Board in Volume I. The other conclusions and recommendations drawn in Volumes II – VI do not necessarily reflect the opinion of the Board, but are included for the record. When there is conflict, Volume I takes precedence.

REPORT VOLUME V

APPENDICES G.1 – G.9

OCTOBER 2003

On the Front Cover

This was the crew patch for STS-107. The central element of the patch was the microgravity symbol, μg, flowing into the rays of the Astronaut symbol. The orbital inclination was portrayed by the 39-degree angle of the Earth's horizon to the Astronaut symbol. The sunrise was representative of the numerous science experiments that were the dawn of a new era for continued microgravity research on the International Space Station and beyond. The breadth of science conducted on this mission had widespread benefits to life on Earth and the continued exploration of space, illustrated by the Earth and stars. The constellation Columba (the dove) was chosen to symbolize peace on Earth and the Space Shuttle Columbia. In addition, the seven stars represent the STS-107 crew members, as well as honoring the original Mercury 7 astronauts who paved the way to make research in space possible. The Israeli flag represented the first person from that country to fly on the Space Shuttle.

On the Back Cover

This emblem memorializes the three U.S. human space flight accidents – Apollo 1, Challenger, and Columbia. The words across the top translate to: "To The Stars, Despite Adversity – Always Explore"

The Board would like to acknowledge the hard work and effort of the following individuals in the production of Volumes II – VI.

Maj. Gen. John L. Barry	Executive Director to the Chairman
Dennis R. Jenkins	Investigator and Liaison to the Board
Lt. Col. Donald J. White	Technical Editor
Lt. Col. Patrick A. Goodman	Technical Editor
Joshua M. Limbaugh	Layout Artist
Joseph A. Reid	Graphic Designer
Christine F. Cole	Administrative Assistant
Jana T. Schultz	Administrative Assistant
Lester A. Reingold	Lead Editor
Christopher M. Kirchhoff	Editor
Ariel H. Simon	Assistant Editor
Jennifer L. Bukvics	Lead Project Manager
Donna J. Fudge	Senior Paralegal, Group II Coordinator
Susan M. Plott	Project Supervisor, Group III Coordinator
Ellen M. Tanner	Project Supervisor
Matthew J. Martin	Government Relations Consultant
Frances C. Fisher	ANSER Liaison

Limited First Printing, October 2003, by the
Columbia Accident Investigation Board

Subsequent Printing and Distribution by the
National Aeronautics and Space Administration
and the
Government Printing Office
Washington, D.C.

VOLUME I

PART ONE	THE ACCIDENT
Chapter 1	The Evolution of the Space Shuttle Program
Chapter 2	*Columbia*'s Final Flight
Chapter 3	Accident Analysis
Chapter 4	Other Factors Considered
PART TWO	WHY THE ACCIDENT OCCURRED
Chapter 5	From *Challenger* to *Columbia*
Chapter 6	Decision Making at NASA
Chapter 7	The Accident's Organizational Causes
Chapter 8	History as Cause: *Columbia* and *Challenger*
PART THREE	A LOOK AHEAD
Chapter 9	Implications for the Future of Human Space Flight
Chapter 10	Other Significant Observations
Chapter 11	Recommendations
PART FOUR	APPENDICES
Appendix A	The Investigation
Appendix B	Board Member Biographies
Appendix C	Board Staff

VOLUME II

CAIB TECHNICAL DOCUMENTS CITED IN THE REPORT

	Reader's Guide to Volume II
Appendix D.a	Supplement to the Report
Appendix D.b	Corrections to Volume I of the Report
Appendix D.1	STS-107 Training Investigation
Appendix D.2	Payload Operations Checklist 3
Appendix D.3	Fault Tree Closure Summary
Appendix D.4	Fault Tree Elements – Not Closed
Appendix D.5	Space Weather Conditions
Appendix D.6	Payload and Payload Integration
Appendix D.7	Working Scenario
Appendix D.8	Debris Transport Analysis
Appendix D.9	Data Review and Timeline Reconstruction Report
Appendix D.10	Debris Recovery
Appendix D.11	STS-107 Columbia Reconstruction Report
Appendix D.12	Impact Modeling
Appendix D.13	STS-107 In-Flight Options Assessment
Appendix D.14	Orbiter Major Modification (OMM) Review
Appendix D.15	Maintenance, Material, and Management Inputs
Appendix D.16	Public Safety Analysis
Appendix D.17	MER Manager's Tiger Team Checklist
Appendix D.18	Past Reports Review
Appendix D.19	Qualification and Interpretation of Sensor Data from STS-107
Appendix D.20	Bolt Catcher Debris Analysis

VOLUME III — OTHER TECHNICAL DOCUMENTS

Reader's Guide to Volume III

Appendix E.1 CoFR Endorsements

Appendix E.2 STS-107 Image Analysis Team Final Report

Appendix E.3 An Assessment of Potential Material Candidates for the "Flight Day 2" Radar Object Observed during the NASA Mission STS-107

Appendix E.4 *Columbia* Early Sighting Assessment Team Final Report

VOLUME IV — OTHER TECHNICAL DOCUMENTS

Reader's Guide to Volume IV

Appendix F.1 Water Absorption by Foam

Appendix F.2 Follow the TPS

Appendix F.3 MADS Sensor Data

Appendix F.4 ET Cryoinsulation

Appendix F.5 Space Shuttle STS-107 Columbia Accident Investigation, External Tank Working Group Final Report – Volume 1

VOLUME V — OTHER SIGNIFICANT DOCUMENTS

Reader's Guide to Volume V 5

Appendix G.1 Requirements and Procedures for Certification of Flight Readiness 7

Appendix G.2 Appendix R, Space Shuttle Program Contingency Action Plan 27

Appendix G.3 CAIB Charter, with Revisions 55

Appendix G.4 Group 1 Matrix Brief on Maintenance, Material, and Management 69

Appendix G.5 Vehicle Data Mapping (VDM) Team Final Report, Jun 13, 2003 281

Appendix G.6 SRB Working Group Presentation to CAIB 319

Appendix G.7 Starfire Team Final Report, Jun 3, 2003 351

Appendix G.8 Using the Data and Observations from Flight STS-107... Exec Summary 389

Appendix G.9 Contracts, Incentives, and Safety/Technical Excellence 453

Appendix G.10 Detailed Summaries: Rogers Commission Report, ASAP Report, SIAT Report

Appendix G.11 Foam Application and Production Chart

Appendix G.12 Crew Survivability Report

Appendix G.13 Aero/Aerothermal/Thermal/Structures Team Final Report, Aug 6, 2003

VOLUME VI — TRANSCRIPTS OF BOARD PUBLIC HEARINGS

Reader's Guide to Volume VI

Appendix H.1	March 6, 2003	Houston, Texas
Appendix H.2	March 17, 2003	Houston, Texas
Appendix H.3	March 18, 2003	Houston, Texas
Appendix H.4	March 25, 2003	Cape Canaveral, Florida
Appendix H.5	March 26, 2003	Cape Canaveral, Florida
Appendix H.6	April 7, 2003	Houston, Texas
Appendix H.7	April 8, 2003	Houston, Texas
Appendix H.8	April 23, 2003	Houston, Texas
Appendix H.9	May 6, 2003	Houston, Texas
Appendix H.10	June 12, 2003	Washington, DC

Reader's Guide to Volume V

Volume V of the Report contains appendices that were not cited in Volume I. These consist of documents produced by NASA and other organizations, which were provided to the Columbia Accident Investigation Board in support of its inquiry into the February 1, 2003 destruction of the Space Shuttle *Columbia*. The documents are compiled in this volume in the interest of establishing a complete record, but they do not necessarily represent the views of the Board. Volume I contains the Board's findings, analysis, and recommendations. The documents in Volume V are also contained in their original color format on the DVD disc in the back of Volume II.

THIS PAGE INTENTIONALLY LEFT BLANK

Volume V
Appendix G.1

Requirements and Procedures for Certification of Flight Readiness

This Appendix contains NASA NSTS 08117 Revision L, December 13, 1995 document Space Shuttle, Requirements and Procedures for Certification of Flight Readiness.

THIS PAGE INTENTIONALLY LEFT BLANK

National Aeronautics and
Space Administration

Lyndon B. Johnson Space Center
Houston, Texas 77058

NSTS 08117
REVISION L
DECEMBER 13, 1995

SPACE SHUTTLE

REQUIREMENTS AND PROCEDURES FOR CERTIFICATION OF FLIGHT READINESS

FOREWORD

Efficient management of the Space Shuttle Program (SSP) dictates that effective control of program activities be established. Requirements, directives, procedures, interface agreements, and system capabilities shall be documented, baselined, and subsequently controlled by SSP management.

Program requirements controlled by the Manager, Space Shuttle Program, are documented in, attached to, or referenced from Volumes I through XVIII of NSTS 07700. NSTS 08117, Requirements and Procedures for Certification of Flight Readiness Requirements, establishes a standard approach to be used jointly by contractors and NASA to incrementally review flight preparation of the Space Shuttle Vehicle (SSV). The requirements and procedures herein provide a means for assuring a uniform flight readiness assessment of all SSV elements.

All elements of the SSP must adhere to these baselined requirements. When it is considered by the Space Shuttle Program/Project Managers to be in the best interest of the SSP to change, waive, or deviate from these requirements, an SSP Change Request (CR) shall be submitted to the Program Requirements Control Board (PRCB) Secretary. The CR must include a complete description of the change, waiver, or deviation and the rationale to justify its consideration. All such requests will be processed in accordance with NSTS 07700, Volume IV, and dispositioned by the Manager, Space Shuttle Program, on a Space Shuttle PRCB Directive (PRCBD).

Loren J. Shriver
Manager, Launch Integration, KSC

CONTENTS

NSTS 08117

1.0	INTRODUCTION	1-1
1.1	PURPOSE	1-1
1.2	SCOPE	1-1
1.3	PROCESS DESCRIPTION	1-1
1.4	RESPONSIBILITIES	1-2
2.0	APPLICABLE DOCUMENTS	2-1
3.0	MILESTONE AND FRR REVIEW ACTIONS	3-1
4.0	DOCUMENTATION REQUIREMENTS	4-1
4.1	DEPOSITORY REQUIREMENTS	4-1
5.0	PROCEDURES	5-1
6.0	PROJECT MILESTONE REVIEWS	6-1
6.1	ELEMENT ACCEPTANCE REVIEW PROCESSES	6-1
6.1.1	Element Acceptance Reviews for Hardware Provided as Government Furnished Property	6-1
6.1.2	Element Acceptance Reviews for Hardware Provided as Contractor Furnished Property	6-2
6.2	PAYLOAD READINESS REVIEW (PRR)	6-3
6.2.1	Responsibilities	6-3
6.2.2	Review Requirements	6-4
6.3	SOFTWARE READINESS REVIEW (SRR)	6-5
6.3.1	Responsibilities	6-5
6.3.2	Review Requirements	6-6
7.0	PROGRAM MILESTONE REVIEWS	7-1
7.1	PRE-MATE MILESTONE REVIEWS	7-1
7.1.1	Responsibilities	7-1
7.1.2	ET/SRB Mate Milestone Review	7-1
7.1.3	Orbiter Rollout/ET Mate Milestone Review	7-3
7.2	FERRY FLIGHT READINESS MILESTONE REVIEW	7-5
7.2.1	Responsibilities	7-5
7.2.2	Organization	7-5

CONTENTS

NSTS 08117

	7.2.3	Review Requirements	7-6
8.0	**FLIGHT READINESS REVIEW (FRR)**		**8-1**
8.1	**POLICY**		**8-1**
8.2	**CERTIFICATION REQUIREMENTS**		**8-1**
	8.2.1	Flight Preparation Process Plans	8-1
8.3	**FLIGHT READINESS REVIEW PREPARATION**		**8-2**
8.4	**FLIGHT PREPARATION PROCESS EXCEPTIONS**		**8-3**
8.5	**RESPONSIBILITIES**		**8-3**
	8.5.1	Space Shuttle Vehicle Engineering	8-4
	8.5.2	EVA Project Office	8-7
	8.5.3	SSME	8-9
	8.5.4	External Tank	8-10
	8.5.5	Reusable Solid Rocket Motor	8-10
	8.5.6	Solid Rocket Booster	8-12
	8.5.7	Mission Operations Directorate (MOD)	8-12B
	8.5.8	Shuttle Processing	8-13
	8.5.9	(Deleted)	8-14
	8.5.10	ISS/Payloads Processing	8-14
	8.5.11	Flight Crew Operations	8-16
	8.5.12	Space Shuttle KSC Integration	8-16
	8.5.13	Space Shuttle Systems Integration	8-17
	8.5.14	Space Shuttle Customer and Flight Integration	8-19
	8.5.15	Space and Life Sciences	8-20
	8.5.16	Ferry Operations	8-21
	8.5.17	Space Shuttle SR&QA	8-22
	8.5.18	Space Flight Operations Contractor (SFOC)	8-22
	8.5.19	SSP Safety and Mission Assurance	8-28
8.6	**ORGANIZATION**		**8-28**
8.7	**REVIEW REQUIREMENTS**		**8-29**
9.0	**ACRONYMS AND ABBREVIATIONS**		**9-1**

APPENDICES

NSTS 08117

A	ORBITER FLIGHT PREPARATION PROCESS	A–i
B	EVA PROJECT FLIGHT PREPARATION PROCESS PLAN	B–i
C	SPACE SHUTTLE MAIN ENGINE (SSME) PROJECT FLIGHT PREPARATION PROCESS PLAN	C–i
D	EXTERNAL TANK PROJECT FLIGHT PREPARATION PROCESS PLAN	D–i
E	REUSABLE SOLID ROCKET MOTOR PROJECT FLIGHT PREPARATION PROCESS PLAN	E–i
F	SOLID ROCKET BOOSTER FLIGHT PREPARATION PROCESS PLAN	F–i
G	MISSION OPERATIONS FLIGHT PREPARATION PROCESS PLAN	G–i
H	SHUTTLE PROCESSING FLIGHT PREPARATION PROCESS PLAN	H–i
H	ATTACHMENT 1, SHUTTLE LOGISTICS FLIGHT PREPERATION PROCESS PLAN	H–11
I	(DELETED)	I–i
J	ISS/PAYLOADS PROCESSING FLIGHT PREPARATION PROCESS PLAN	J–i
J	ATTACHMENT 1, ISS/PAYLOADS LOGISTICS FLIGHT PREPERATION PROCESS PLAN	J–7
K	FLIGHT CREW OPERATIONS FLIGHT PREPARATION PROCESS PLAN	K–i
L	KSC INTEGRATION FLIGHT PREPARATION PROCESS PLAN	L–i
M	SPACE SHUTTLE SYSTEMS INTEGRATION OFFICE FLIGHT PREPARATION PROCESS PLAN	M–i
N	SPACE SHUTTLE CUSTOMER AND FLIGHT INTEGRATION AND THE PAYLOAD SAFETY REVIEW PANEL FLIGHT PREPARATION PROCESS	N–i
O	SPACE AND LIFE SCIENCES FLIGHT PREPARATION PROCESS PLAN	O–i
P	FERRY OPERATIONS FLIGHT PREPARATION PROCESS PLAN	P–i
Q	SPACE SHUTTLE SAFETY, RELIABILITY, AND QUALITY ASSURANCE FLIGHT PREPARATION PROCESS PLAN	Q–i
R	SPACE FLIGHT OPERATIONS CONTRACTOR FLIGHT PREPARATION PROCESS PLAN	R–i

1.0 INTRODUCTION

1.1 PURPOSE

The purpose of this document is to define the Space Shuttle Program (SSP) Flight Preparation Process (FPP). It defines the procedures for the Project Milestone Reviews, the Program Milestone Reviews and the Flight Readiness Review (FRR). It also defines the endorsement documentation required at the completion of the FRR which provides the Certification of Flight Readiness (CoFR) for a specific flight.

1.2 SCOPE

This document is applicable to JSC, KSC, MSFC, Stennis Space Center (SSC), and SSP NASA and contractor organizations and personnel involved in the conduct of Space Shuttle operations. The FPP consists of the required preparations for a Space Shuttle mission, from the baselining of the processing requirements to acceptance of the major hardware elements through processing, mating, launch, and ferry when required. The major elements of the FPP are the Project Milestone Reviews, three Program Milestone Reviews, and the FRR where the CoFR endorsement is signed. Reviews of the activities that support the FPP are considered part of the CoFR process.

This Revision L identifies the processes and requirements for all milestone reviews and the FRR for STS–78 and subsequent flights. Revision K applies to prior flights.

1.3 PROCESS DESCRIPTION

The FPP is structured to baseline a set of processing requirements through a series of requirements reviews and to incrementally review and status progress towards readiness for flight (reference Figure 1). It represents a commitment by each of the SSP element and project managers (NASA and contractor) certifying that their organizations have satisfactorily completed the requirements and their respective portions of the effort required to safely support each flight. The FPP is incrementally implemented through milestone reviews and an FRR which ensures the readiness of all organizations for the operational phase following each review. The FPP consists of Project Milestone Reviews, three Program Milestone Reviews and the FRR. The Project Milestone Reviews are the DD 250/1149–Element Acceptance Reviews, the Payload Readiness Review (PRR), the Software Readiness Review (SRR), and the organizational Pre–FRR Reviews. The three Program Milestone Reviews are the Pre–Mate Milestone Reviews, consisting of the External Tank (ET)/Solid Rocket Booster (SRB) Mate Milestone Review and the Orbiter Rollout/ET Mate Milestone Review, and a Ferry Flight Readiness Milestone Review which is conducted when a ferry is required. The CoFR endorsement is signed at the FRR. A Prelaunch Mission Management Team (PMMT) Review will be conducted on the Launch Minus Two (L–2) Day or Launch

Minus One (L–1) Day when the Mission Management Team (MMT) is activated to status the launch countdown and address any issues remaining from the FRR (reference Figure 2). (Reference NSTS 07700 Volume III, Flight Definition and Requirements Directive; NSTS 07700, Volume IV, Configuration Management Requirements; and NSTS 07700, Volume VIII, Operations, Appendix D.)

1.4 RESPONSIBILITIES

The Manager, Launch Integration shall manage the FPP. SSP organizations and their respective contractors are responsible for implementing the FPPs as outlined in the appendices of this document. The implementation will be done by certifying that the required work under their purview, as defined in the Flight Preparation Process Plans (FPPPs) for each certifying organization, has been satisfactorily completed and will safely support the specified flight.

The review secretariat function for Program Milestone Reviews and the FRR shall be the responsibility of the Space Flight Operations Contract (SFOC) Program Integration Office at KSC. The secretariat function for the Project Milestone Reviews, shall be the responsibility of the review Chair.

FIGURE 1

FLIGHT PREPARATION PROCESS

*NOTE: See Figure 2 for expansion.

NOTE: For specific timeline information, see JSC 25187, Flight Production Generic Template, Appendix A.

FIGURE 2

MILESTONE REVIEWS PROCESS

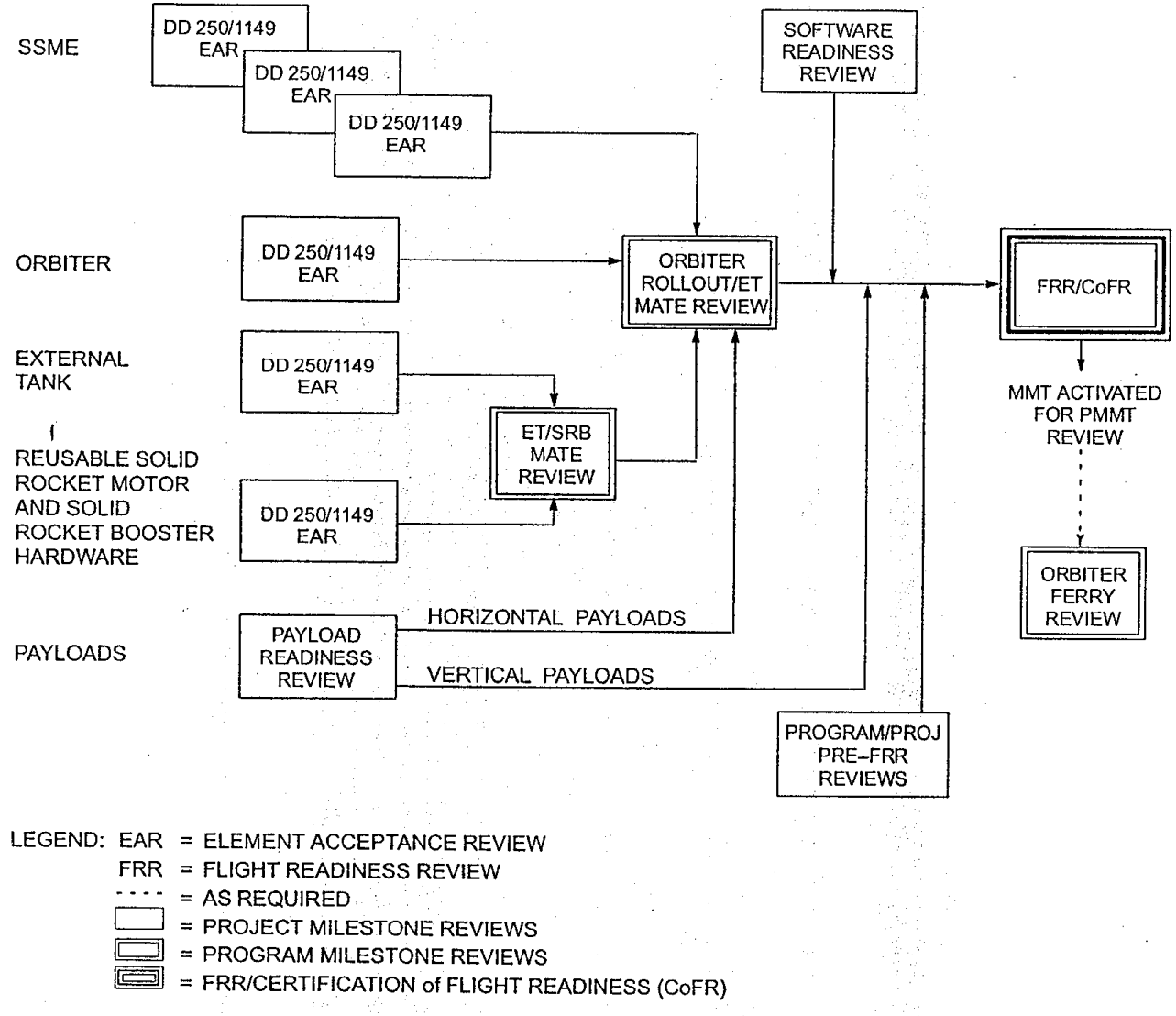

8.0 FLIGHT READINESS REVIEW (FRR)

Approximately two weeks prior to launch, a FRR will be conducted that will determine the readiness of the SSV, flight crew, and payloads. At the review, organizations identified in Paragraph 8.7b will certify the completion of all tasks and planned work required to prepare the flight/ground hardware/software, support facilities, and operations personnel to safely support a specific mission. Readiness for flight shall be determined through the review of necessary data to ensure satisfactory closeout of all FRR certification requirements, exceptions, and launch constraints, and be in sufficient detail to provide the Associate Administrator (AA), Office of Space Flight with the information needed to make a decision as to flight readiness.

8.1 POLICY

The FRR is an integrated senior management review chaired by the AA, Office of Space Flight who is supported by a review board. It is the policy of the AA, Office of Space Flight to make an assessment of mission readiness prior to each flight. This will be accomplished by a comprehensive review of all activities/elements necessary for the safe and successful conduct of all operations from prelaunch through post–landing and recovery operations. Government and contractor representatives will certify readiness in their areas of responsibility.

8.2 CERTIFICATION REQUIREMENTS

The CoFR endorsement certifies all organizations (NASA and contractor) have successfully completed their FPPs and products per their Flight Preparation Process Plans (FPPPs). During the transition period for the SFOC contract the transition plans and PDPs document the transfer of responsibilities from NASA to the contractor and should be referenced for complete CoFR accountability.

8.2.1 Flight Preparation Process Plans

Each organization's FPPP defines the processes and products the organization will complete for a each mission. The FPPP ensures the successful assembly, launch and completion of the flight. As applicable for each organization, the process plans shall encompass all major and critical operations, design, certification, analyses, testing, documentation, and requirements definition required for the each mission. The major processes involved are as follows:

a. Vehicle processing

b. Payload processing

c. Configuration management/requirements definition

d. Flight certification (including Launch Commit Criteria [LCC], flight rules, etc.)

e. Facility/equipment/GSE certification

f. Personnel certification

g. Special testing/analyses

h. Material review

i. Hazard analyses

j. Failure Modes and Effects Analysis/Critical Items List (FMEA/CIL)

k. Crew training/medical certification

l. Validation that external inputs are appropriate for this specific flight

In addition, the following products and processes which organizations participate in, but are not their unique responsibilities, shall be completed in support to external organizations:

a. Develop/validate/deliver products requested by external organizations

b. Delivery of hardware or software and support data

c. Operations and Maintenance Requirements and Specifications Document (OMRSD)/LCC requirements definition

d. Configuration drawings

e. Anomaly/discrepancy resolution

f. Flight rules requirements

g. Crew procedures requirements

h. Flight design definition

i. Flight constraints definition

j. Ferry requirements

k. Time, cycle, age life, interval inspection, and maintenance requirements

l. Flight Data File (FDF) requirements

8.3 FLIGHT READINESS REVIEW PREPARATION

Each organization shall be responsible for conducting a Pre–FRR in preparation for the SSP FRR which ensures their project FPPPs are satisfied. The program/projects shall

FIGURE 3
CoFR ENDORSEMENT

STS–____ CoFR ENDORSEMENT

ELEMENT	SERIAL NUMBER		PAYLOAD
ORBITER			
ET			
RSRM			
SSME			
SRB			

Projects having exceptions to this CoFR document are as follows (see Exception Log for details):

SSP Form 4042 (Rev Sep 02) Page 1 of 7

FIGURE 3
CoFR ENDORSEMENT – Continued

STS–____ CoFR ENDORSEMENT

The Flight Preparation Process Plans documented in NSTS 08117, Requirements and Procedures for Certification of Flight Readiness, have been satisfied. Required products and other responsibilities for each project (NSTS 08117, Section 8) have been or will be produced or completed.

a. Certified flight hardware elements have been delivered to the SFOC at the Kennedy Space Center.

b. Required hardware element processing specifications and requirements have been delivered to the SFOC.

c. All identified "out-of-family" events that occurred after delivery of hardware for launch processing/ assembly/testing have been resolved.

d. For "out-of-family" conditions detected during manufacturing, testing, or post-mission tear down and analysis, notification to the Space Shuttle Program has been made, and corrective action, if any, identified.

e. The as-built flight element configuration satisfies the released requirements and engineering, based on data compiled and reviewed by SFOC.

f. For the Space Shuttle Main Engine Project: Certified main engine controller software has been delivered for this mission.

CONTRACTOR			NASA	
SSME (8.5.3.1, 8.5.3.2, Apx. C)	PROGRAM MANAGER, ROCKETDYNE	DATE	MANAGER, SSME PROJECT, MSFC	DATE
ET (8.5.4.1, 8.5.4.2, Apx. D)	PROGRAM MANAGER, LMMSS	DATE	MANAGER, ET PROJECT, MSFC	DATE
RSRM (8.5.5.1, 8.5.5.2, Apx. E)	PROGRAM MANAGER, THIOKOL	DATE	MANAGER, RSRM PROJECT, MSFC	DATE
CONCURRENCE				
MSFC SHUTTLE PROJECTS	N/A		MANAGER, MSFC SHUTTLE PROJECTS	DATE

SSP Form 4042 (Rev Sep 02) Page 2 of 7

FIGURE 3
CoFR ENDORSEMENT – Continued

STS–____ CoFR ENDORSEMENT

The Flight Preparation Process Plans documented in NSTS 08117, Requirements and Procedures for Certification of Flight Readiness, have been satisfied. Required products and other responsibilities for each organization (NSTS 08117, Section 8) have been or will be produced or completed.

a. For Payload Processing: Flight and ground requirements, payload logistics, and configuration requirements provided by the flight projects, have been maintained, performed, or are planned to be performed per approved TOPs.

b. For EVA project: Audit, insight, and surveillance of SFOC activities have been completed or are planned for completion, and all discrepancies have been resolved. Oversight functions have been conducted in conjunction with Hamilton Sundstrand.

NASA

FLIGHT CREW OPERATIONS (8.5.11.1, 8.5.11.2, Apx. K)	DIRECTOR, FLIGHT CREW OPERATIONS	DATE
FERRY OPERATIONS (8.5.16.1, 8.5.16.2, Apx. P)	FERRY OPERATIONS MANAGER	DATE
SPACE AND LIFE SCIENCES (8.5.15.1, 8.5.15.2, Apx. O)	DIRECTOR, SPACE AND LIFE SCIENCES	DATE
SPACE SHUTTLE SR&QA (8.5.17.1, 8.5.17.2, Apx. Q)	MANAGER, SPACE SHUTTLE SR&QA	DATE

	CONTRACTOR		NASA	
PAYLOAD PROCESSING (8.5.10.1, 8.5.10.2, Apx. J)	PROGRAM MANAGER, CAPPS BOEING, KSC	DATE	DIRECTOR OF ISS/PAYLOAD PROCESSING	DATE
EVA (8.5.2.1, 8.5.2.2, Apx. B)	PROGRAM MANAGER, HAMILTON SUNDSTRAND	DATE	MANAGER, EVA PROJECT OFFICE	DATE

SSP Form 4042 (Rev Oct 02) Page 3 of 7

FIGURE 3
CoFR ENDORSEMENT – Continued

STS– ____ CoFR ENDORSEMENT

The Flight Preparation Process Plans documented in NSTS 08117, Requirements and Procedures for Certification of Flight Readiness, have been satisfied. Required products and other responsibilities (shared or independent) for each organization (NSTS 08117, Section 8) have been or will be produced or completed.

a. The following NASA organizations have completed or plan to complete audit, insight, and surveillance of contractor activities, and have resolved all discrepancies.

NASA

CUSTOMER AND FLIGHT INTEGRATION (8.5.14.1, 8.5.14.2, Apx. N)	MANAGER, SPACE SHUTTLE CUSTOMER AND FLIGHT INTEGRATION	DATE
KSC INTEGRATION (8.5.12.1, 8.5.12.2, Apx. L)	MANAGER, SPACE SHUTTLE KSC INTEGRATION	DATE
SHUTTLE PROCESSING (8.5.8.1, 8.5.8.2, Apx. H)	DIRECTOR OF SHUTTLE PROCESSING, KSC	DATE
MISSION OPERATIONS (8.5.7.1, 8.5.7.2, Apx. G)	DIRECTOR, MISSION OPERATIONS	DATE
SRB (8.5.6.1, 8.5.6.2, Apx. F)	MANAGER, SRB PROJECT, MSFC	DATE
SSP S&MA	MANAGER, SSP S&MA	DATE
SYSTEMS INTEGRATION (8.5.13.1, 8.5.13.2, Apx. M)	MANAGER, SPACE SHUTTLE SYSTEMS INTEGRATION	DATE
VEHICLE ENGINEERING (8.5.1.1, 8.5.1.2, Apx. A)	MANAGER, SPACE SHUTTLE VEHICLE ENGINEERING	DATE

SSP Form 4042 (Rev Sep 02) Page 4 of 7

FIGURE 3
CoFR ENDORSEMENT – Continued

STS–____ CoFR ENDORSEMENT

The Space Shuttle Flight Preparation Process Plans (shared or independent) documented in NSTS 08117, Requirements and Procedures for Certification of Flight Readiness, have been satisfied. Required products and other responsibilities (shared or independent) for the SFOC (NSTS 08117, Section 8) have been or will be produced or completed.

a. All out-of-family conditions have been identified and resolved with the NASA.

b. The SSV has been processed in accordance with requirements and policies baselined by the SSP.

UNITED SPACE ALLIANCE

SFOC SQ&MA CONCURRENCE	VICE PRESIDENT, SAFETY, QUALITY AND MISSION ASSURANCE, SFOC	DATE
SFOC (8.5.18.1, 8.5.18.2, Apx. R)	SSP, PROGRAM MANAGER, SFOC	DATE

Boeing endorses that the requirements for CoFR documented in SSP 50108 and the Boeing Flight CoFR Implementation Plan have been satisfied in accordance with the Boeing specific responsibilities for this flight. Any issues that have arisen since the Stage Operations Readiness Review (SORR) have been resolved or have been presented at the Flight Readiness Review. This certification is subject to clause H.43 of NAS 15-10000 (for ISS Missions).

BOEING

ISS PRIME CONCURRENCE	VICE PRESIDENT AND PROGRAM MANAGER, ISS, BOEING	DATE

SSP Form 4042 (Rev Oct 02) Page 5 of 7

NSTS 08117
Revision L

8–35

CHANGE NO. 71

FIGURE 3
CoFR ENDORSEMENT – Continued

STS– _____ CoFR ENDORSEMENT

NASA SSP READINESS

The preparation of all Space Shuttle Program and Project organizations for this mission has been reviewed. All required processes, products, and responsibilities are complete or will be completed prior to launch. Deviations, exceptions or waivers have been reviewed and will be dispositioned by the Prelaunch MMT Review for this mission. The Space Shuttle Program is ready to proceed with the conduct of this mission.

MANAGER, SPACE SHUTTLE PROGRAM INTEGRATION — DATE

MANAGER, LAUNCH INTEGRATION — DATE

MANAGER, SPACE SHUTTLE PROGRAM — DATE

NASA ISS PROGRAM READINESS

All necessary activities required to support the flight, stage and increment have been accomplished or are planned. All deviations, waivers, and exceptions have been reviewed and satisfactorily dispositioned. The International Space Station Program is ready to proceed with launch and on-orbit operations. Any issues that have arisen since the SORR have been resolved or have been presented at the Flight Readiness Review (for ISS Missions).

MANAGER, INTERNATIONAL SPACE STATION PROGRAM — DATE

CONCURRENCE

I concur that the Space Shuttle Program and the International Space Station Program (for ISS Missions) are ready to proceed with this mission.

DEPUTY ASSOCIATE ADMINISTRATOR FOR INTERNATIONAL SPACE STATION AND SPACE SHUTTLE PROGRAMS — DATE

SSP Form 4042 (Rev Oct 02) Page 6 of 7

FIGURE 3
CoFR ENDORSEMENT – Concluded

STS– ____ CoFR ENDORSEMENT

CONCURRENCE

As a member of the FRR Board, I concur that, pending completion of planned work, the Space Shuttle Program and International Space Station Program (for ISS Missions) are ready to execute this mission.

DIRECTOR, JOHNSON SPACE CENTER	DATE
DIRECTOR, KENNEDY SPACE CENTER	DATE
DIRECTOR, MARSHALL SPACE FLIGHT CENTER	DATE
DIRECTOR, STENNIS SPACE CENTER	DATE

As a member of the FRR Board, I concur that, pending completion of planned work, the Prime Mission is ready to execute this mission (for non-ISS missions).

ASSOCIATE ADMINISTRATOR FOR PRIME MISSION	DATE

NASA S&MA has reviewed the status of preparations for this mission and has performed an independent assessment of the readiness of the Space Shuttle Program for the conduct of this mission, and the readiness of the International Space Station for launch and on-orbit operations (for ISS missions). We are in concurrence with proceeding with this mission.

ASSOCIATE ADMINISTRATOR, SAFETY AND MISSION ASSURANCE	DATE

APPROVAL

The FRR Board has conducted a comprehensive assessment of the readiness of all flight and ground systems and supporting personnel. For ISS missions, the FRR Board has also conducted a comprehensive assessment of the readiness of the Launch Package/Cargo Element (LP/CE), ground hardware/software support facilities and personnel to support the flight, stage and increment including the readiness of the on-orbit stage to accept the LP/CE and return items. The Certificate of Flight Readiness has been endorsed by each program element. I have concluded, with the concurrence of the FRR Board, that pending completion of planned work, the Space Shuttle Program is ready to execute this mission and the International Space Station Program is ready for launch and on-orbit operations (for ISS missions).

ASSOCIATE ADMINISTRATOR, OFFICE OF SPACE FLIGHT (CHAIR, FRR BOARD)	DATE

SSP Form 4042 (Rev Oct 02) Page 7 of 7

NSTS 08117
Revision L

8–36A

CHANGE NO. 71

B2-000089

Volume V
Appendix G.2

Appendix R, Space Shuttle Program Contingency Action Plan

This Appendix contains NASA NSTS 07700, Volume VIII, Revision E, Appendix R; Space Shuttle Program Contingency Action Plan.

THIS PAGE INTENTIONALLY LEFT BLANK

APPENDIX R

SPACE SHUTTLE PROGRAM CONTINGENCY ACTION PLAN

THIS PAGE INTENTIONALLY LEFT BLANK

APPENDIX R

SPACE SHUTTLE PROGRAM CONTINGENCY ACTION PLAN

1.0 INTRODUCTION

1.1 PURPOSE

The purpose of this document is to serve as an integrated plan to predetermine the program response in the event of a Space Shuttle contingency. This plan will be implemented in concert with the OSF SFO Contingency Action Plan, and field center contingency plans. It has been written to augment each of these by providing the anticipated, integrated timelines of the formalized program response.

1.2 SCOPE

The Manager, Launch Integration, KSC has overall responsibility for contingency planning during flight preparation, launch ascent, and post-landing operations. During ascent, this responsibility continues until the Shuttle is established in a stable orbit or until landing, should a stable orbit not be achieved. The Manager, Launch Integration will hold a Mishap Response Teleconference (MRT) approximately one hour and 30 minutes after the contingency where specific actions will be levied by the MMT. Normal program elements will execute those actions along with this plan. The Manager, Space Shuttle Program will determine when the MMT no longer has operational oversight for this plan. The Manager, Launch Integration, KSC will retain responsibility for contingency operations until a formal investigation board is established, and/or until the Orbiter is returned to KSC.

1.3 DEFINITION

For the purpose of this plan, a program contingency is defined as any SSP-related failure, accident, or incident (involving SSP-controlled flight or test hardware, support equipment, or facilities) that significantly delays or jeopardizes the SSP or a flight, prevents accomplishment of a major objective, or terminates a flight prematurely.

NPD 8621.1G, NASA Policy Directive on NASA Mishap Reporting and Investigating Policy, defines six mishaps/contingencies in which the AA-OSF may become involved. They include Type A, B, and C Mishaps, mission failures, incidents, and close calls, all of which are defined in Table 1. The AA-OSF or delegated agent is the final authority in determining if an actual or suspected mission failure, accident, or incident constitutes a SSP contingency. All probable contingency situations will be reported to the AA-OSF or delegated agent for a final decision.

1.4 APPLICABILITY

This plan applies to any contingency situation during Space Shuttle operations where a multi-center response may be required. It applies to all SSP organizations and those agencies that support the SSP during a contingency operation. Use of this plan assumes the AA-OSF has declared, or will declare, an SSP contingency.

1.5 REFERENCED DOCUMENTS

This plan is intended to be consistent with the documents listed in Attachment 10 of this appendix.

1.6 NOTIFICATION

Those witnessing a potentially significant Shuttle Program incident will notify the appropriate element/project manager who in turn will notify the Manager, Space Shuttle Program. The Manager, Space Shuttle Program will be responsible for notifying the Deputy AA for International Space Station and Space Shuttle.

1.7 CONTINGENCY READINESS

Space Shuttle Program and Project personnel will participate in contingency response exercises that demonstrate the program's effective response. These will consist of exercises prescribed by NASA Headquarters' Office of Safety and Mission Assurance and as outlined in the OSF SFO Contingency Action Plan.

TABLE R.1

CONTINGENCY CRITERIA SUMMARY

Classes of Unexpected Events	Damage to Property, Facilities, or Equipment and/or Personnel Injury/Death		Investigation/Analysis
Type A Mishap	Greater than $1M	Death	AA-OSF appoints investigation board or Administrator chooses to appoint investigation board and board investigates mishap*
Type B Mishap	Equal to or greater than $250K but less than $1M	Permanent disability of 1 or more persons, or hospitalization of 3 or more persons.	AA-OSF or Deputy AA appoints investigation board and board investigates mishap*
Type C Mishap	Equal to or greater than $25K but less than $250K	Occupational injury or illness that results in a lost workday case.	Deputy AA appoints investigator or investigation team depending on significance of mishap*
Incident	Equal to or greater than $1K but less than $25K	Personal injury of less than Type C Mishap severity but more than first-aid severity.	Same as Type C mishap*
Mission Failure	A mishap of such severity that it prevents the achievement of primary NASA mission objectives as described in the Mission Operations Report or equivalent document.		An investigation board is required and Type A or B Mishap investigation procedures are followed*
Close Call**	No equipment/property damage equal to or greater than $1K	No injury or significant interruption of productive work	Investigated in accordance with its potential*

*If event involves more than one Center or has significant public interest, the AA-OSF, or delegated agent, may order an investigation board or recommend to the Administrator that the Space Shuttle Mishap Interagency Investigation Board be activated.

**Event which possesses high severity potential for any of the previous types of mishaps.

2.0 RESPONSIBILITIES

2.1 MANAGER, SPACE SHUTTLE PROGRAM

In accordance with the OSF SFO Contingency Action Plan, the Manager, Space Shuttle Program is responsible for ensuring that:

a. SSP contingency response actions are included in the OSF centers contingency plans.

b. The program is ready to manage appropriate actions to minimize losses, and preserve evidence, should a contingency occur.

c. The program is prepared to manage the contingency situation until a formal investigation board is established.

2.2 MANAGER, LAUNCH INTEGRATION, KSC

The Manager, Launch Integration, KSC is directly responsible for management of contingency activities after a suspected launch or EOM landing contingency has been reported. Immediately following a suspected contingency, the Manager, Launch Integration, KSC will implement this plan anticipating that the AA-OSF will declare the incident a program contingency.

The Manager, Launch Integration, KSC, will chair the MRT within one hour and 30 minutes after a contingency has been reported. The MMT will provide direct support to the Manager, Launch Integration, KSC.

The Manager, Launch Integration, KSC appoints the Chair of the Mishap Investigation Team (MIT), and activates the MIT, as necessary, with the approval of the AA-OSF.

2.3 MANAGER, SPACE SHUTTLE PROGRAM INTEGRATION

The Manager, Space Shuttle Program Integration is responsible for chairing the MMT during on-orbit activities. If a suspected mission contingency occurs, it is the responsibility of the Manager, Space Shuttle Program Integration, to coordinate and chair the MRT from JSC, and to inform the MMT.

Immediately following a suspected mission contingency, the Manager, Space Shuttle Program Integration, JSC will implement this plan anticipating that the AA-OSF will declare the incident a program contingency.

Responsibility for contingency operations will be transitioned back to the Manager, Launch Integration, KSC, after landing has occurred.

2.4 SPACE SHUTTLE PROGRAM ELEMENTS (MSFC PROJECTS/EVA/FCOD/PAYLOADS PROCESSING/SHUTTLE PROCESSING/SYSTEMS INTEGRATION/VEHICLE ENGINEERING)

In the event a failure, accident, or incident occurs involving SSP hardware or facilities, it is the responsibility of the respective element manager to take the following actions:

a. Assure that all possible action is taken to prevent injury to personnel, and damage or loss of equipment;

b. Notify, by the most expeditious means, the Manager, Space Shuttle Program; the respective Center Director; AA-OSF; and the Deputy AA-OSF;

c. Assure that the scene is secured against action that could impair investigation;

d. Protect records, logs, data books, film, etc.

e. Initiate preliminary on-site assessment to determine scope of potential contingency;

f. Initiate their respective center contingency action plans;

g. Support investigations of SSP contingencies under its own direction or under the direction of the lead center, a Headquarters Mishap Investigation Board (MIB), or any board established by the NASA Administrator or the President of the United States; and

h. Prevent sabotage and provide security.

2.5 MISSION OPERATIONS

When a potential contingency situation arises during mission operations, the Flight Director, as specified in JSC 12805, Flight Control Operations Handbook, will put contingency procedures into effect. All flight control and support personnel will be required to complete these procedures. Logs of each individual's equipment status prior to and at the time of the potential contingency will be completed. JSC Form 1441, Flight Director's Mission Log, will be used and completed as soon as possible after a mission contingency and prior to the release of the individual from the MCC or his/her support area. These logs will be collected by each area/specialty supervisor or lead flight controller, and forwarded to the Flight Director, who will provide the data to the MIB. A roster of all mission personnel will be provided in addition to the logs. At the time a contingency is suspected or declared, all personnel will immediately verify that their logs are up-to-date and will institute a "hands-off" policy with regard to switches, push-button indicators, knobs, recorders, etc., as is appropriate to continued flight safety. The MCC will remain active in support of the potential contingency until released by the AA-OSF

or the Manager, Space Shuttle Program. Upon release of the MCC, its functions in support of the contingency will be transferred to the Technical Action Center.

3.0 REQUIREMENTS

3.1 PERSONNEL NOTIFICATION

All Space Shuttle program elements shall provide predefined notification lists within their respective center contingency action plans to address any failure, accident, or incident involving program resources. These predefined notification lists will be executed within 60 minutes of the suspected incident. The notification shall include a description of the potential contingency; its cause, if known; associated information leading up to the potential contingency; any actions that have been initiated or are planned; and recommendations for a course of action.

The manning of action centers and communication networks also shall be predefined to ensure an organized and timely response. Attachment 2 describes the NASA Action Centers at NASA HQ, MSFC, KSC, JSC, and SSC.

3.1.1 Launch Notification Sequence

The Manager, Launch Integration, KSC will notify the members of the MMT who, in turn, will notify their respective organizations. The Flight Director shall notify the JSC MCC, and the LSO shall notify specific NASA and other government personnel.

3.1.2 Mission Notification Sequence

During SSP mission activities, officials will be notified through normal mission-monitoring activities. The SSP Manager will notify the Deputy AA for International Space Station and Space Shuttle or delegated agent of the potential contingency.

3.2 TEAM NOMINATIONS

The Manager, Launch Integration, KSC, or his designee shall be responsible for publishing a list of the qualified personnel two weeks prior to the FRR for each flight. This includes membership of the NASA MRT, MIT, RRT, and the Crew Recovery Team (CRT). MIT personnel will be on alert to depart for the contingency scene as soon as a contingency has been declared. A list of the positions to be filled for each team is included in Attachment 1.

The travel of all NASA personnel to an overseas landing site shall be approved by the AA-OSF, with responsibility delegated to the Manager, Launch Integration, KSC. All personnel deployments and manifests will be provided to the Office of External Rela-

tions at NASA HQs approximately two weeks prior to each mission to ensure timely visa requests.

3.2.1 Mishap Investigation Team

The MIT shall be responsible for immediately traveling to the contingency site to gather first-hand information, take witness statements, and preserve material, which could be valuable to the formal investigation board. The turnaround/ salvage teams shall not begin their operations until the Orbiter is released by the MIT. The MIT shall comply with NPD 8621.1G and the NASA Headquarters OSF SFO Contingency Action Plan. The MIT Chair is appointed by the Manager, Launch Integration, KSC and approved by the AA-OSF. Once deployed, all MIT members are considered on detail from their field centers and are responsible only to the Chair. If the Orbiter should land undamaged, a decision not to deploy the MIT may occur at the MRT. Reference Attachment 5 for the detailed MIT Operations Plan.

3.2.2 Rapid Response Team

KSC shall prepare a KSC Off-site Transportation Plan for TAL site deployment. The RRT will arrive at the contingency site within approximately 18 hours. These plans shall be modified realtime to reflect the actual condition of the Orbiter. The activation of the airlift shall begin when the LRD calls the DDMS Operations SOC to request airlift. The SOC shall then notify the Air Mobility Command (AMC) Tanker Airlift Control Center for actual aircraft deployment. KSC, in conjunction with the AMC Tanker Airlift Command Element (TALCE) (once in place), shall coordinate support for arriving aircraft at NASA and TAL facilities.

The RRT shall consist of personnel under the direction of the KSC GOM who will evaluate the condition of the Orbiter and determine any additional requirements to prepare the Orbiter for ferry. The RRT will modify existing contingency planning to accommodate the realities of the Orbiter configuration and landing site facilities. If Orbiter towing equipment is not available at the landing site, the RRT will transport towing equipment to the site, if possible. Most of the RRT shall be deployed from KSC. For a TAL, the aircraft will pick up personnel and equipment at the KSC SLF approximately six hours after the TAL declaration. Estimated deployment timelines are in Attachment 6 of this appendix.

a. Augmented Landing Site Rapid Response - Three landing sites in the European and African continents shall have personnel trained to participate in an Orbiter recovery. Personnel from the sites at which the Orbiter did not land will be utilized at the actual landing site. The aircraft used for transportation will be the SAR or MEDEVAC aircraft (C-130) stationed at the TAL sites. The KSC GOM shall identify the personnel, and the request for transportation will be coordinated with the DDMS and the DOD/SOC at PAFB.

b. Non-augmented Landing Site Rapid Response - Unscheduled Orbiter landings will likely occur at ALS where NASA and DOD personnel will be trained and equipped to take care of an Orbiter that has landed. However, the possibility remains that the landing of an Orbiter may occur at an airfield other than an ALS. If such a landing should occur, the capability may exist for equipment and personnel at the ALS to reach the Orbiter before any response aircraft from CONUS. The aircraft used will be the SAR or MEDEVAC aircraft stationed at Zaragoza Air Base (AB), Banjul, and/or Ben Guerir.

3.2.3 Crew Recovery Team

In the event of a non-CONUS landing, the JSC FCOD will send the KC-135 aircraft containing the CRT from JSC EFD to the location of the flight crew. The purpose of this aircraft is to return the flight crew to the U.S. Transportation of other JSC personnel on the KSC RRT will be provided to the KSC SLF. A DDMS provided aircraft will be used as a backup aircraft in the event that the NASA KC-135 is unavailable. The DOD, using available SAR/MEDEVAC aircraft, will provide evacuation for uninjured flight crew members to the nearest U.S. military base, if necessary. The estimated typical TAL timeline for the KC-135 deployment is in Attachment 6 of this appendix.

3.3 MISHAP RESPONSE TELECONFERENCE

A MRT will be established within one hour and 30 minutes after a suspected launch, on-orbit, or EOM landing contingency occurs.

a. Launch MRT - The KSC Launch Integration Staff Office will be responsible for coordination and set-up of the teleconference in Room 1R29 of the Launch Control Center. The teleconference will be effected by MCI communications. The Chair shall be the Manager, Launch Integration, KSC. The teleconference shall cover a review of pertinent facts, statements of contingency actions, and a review of deployment schedules of response teams. Access to the MRT will be predefined, and approved by the Manager, Launch Integration, KSC prior to the prelaunch MMT review.

b. Mission MRT - Upon notification of a suspected contingency, the Manager, Space Shuttle Program Integration will chair the MRT from JSC. The Space Shuttle Customer and Flight Integration Office, JSC will coordinate the teleconference.

A complete description of the MRT is included in this appendix in Attachment 3.

3.4 SEARCH AND RESCUE REQUIREMENTS

SAR capabilities will be provided through the DDMS on a per site basis. Given 24-hour advanced notice, Air MEDEVAC will be available at the primary CONUS EOM sites and the TAL sites. ELSs will have no prepositioned Shuttle support resources and the DOD SAR and MEDEVAC effort will be on a "best effort" basis.

3.4.1 Kennedy Space Center

KSC will have the following resources available for launch, RTLS, EOM, and near coastal bailout:

Required:

a. DOD HH-60 helicopters on standby at the SLF

b. One UH-1 NASA helicopter

c. One DOD HC-130 positioned 175 nm downrange (excluding EOM support)

d. One DOD HC-130 and KC-130 positioned at PAFB (excluding EOM support)

If available:

a. One E-2C positioned at PAFB (excluding EOM support)

b. One U.S. Navy ship with helicopter (excluding EOM support)

c. One Coast Guard cutter with helicopter

Each DOD helicopter will carry one medical doctor and two pararescuemen and have the capability to transport two astronauts in litters. Each HC-130 will have two 3-man pararescue teams with motorized inflatable rafts.

3.4.2 Edwards Air Force Base

When given 24-hour advanced notice, EAFB will have DOD UH-60 or UH-1 MEDEVAC helicopters available for EOM landings. Each UH-60 helicopter will carry one medical doctor, three Emergency Medical Technicians (EMTs), and up to three flight crew members. Each UH-1 helicopter will carry one medical doctor, one EMT, and two flight crew members.

3.4.3 White Sands Space Harbor

WSSH will have UH-1 MEDEVAC helicopters available for EOM landings, given 24-hour notice. Each helicopter will carry one medical doctor, one EMT, and two flight crew members.

3.4.4 TAL Sites

TAL sites will have available the following SAR/MEDEVAC resources to support a landing:

a. One DOD fixed-wing aircraft (C-130) at Banjul, The Gambia, for low inclination launches

b. One DOD fixed-wing aircraft (C-130) at Ben Guerir, Morocco

c. One DOD fixed-wing aircraft (C-130) at Zaragoza AB, Spain, for high inclination launches

The C-130 aircraft at Ben Guerir, Banjul, and Zaragoza will have two flight surgeons and nine pararescue specialists onboard. Each aircraft will be capable of transporting the entire flight crew. Fixed-wing assets along with equipment to support landing activities will be transported to Moron, Spain as needed.

3.5 EMERGENCY MEDICAL SERVICES

The Director, Space and Life Sciences Directorate, JSC has overall management responsibility for EMS operations. This will be implemented by the Medical Operations Branch through the FCR surgeon and through the respective site EMS coordinators. The on-scene physician is responsible for making realtime trauma treatment decisions until such times as the flight crew member is under the care of an Intermediate Medical Care Facility (IMCF) or Definitive Medical Care Facility (DMCF). Patient information will be relayed from the on-scene physician to the site EMS coordinator. EMS's are described more fully in Attachments 7 and 9 of this appendix.

3.6 COMMUNICATIONS

In the event of an unscheduled landing, all operational communications will remain in their landing support configuration until direction to do otherwise is obtained from the MMT or other appropriate site managers. Any other predefined communications in support of unscheduled landings will be activated after crew egress. It can be expected that the support role of some facilities will change to support this unscheduled event. For any unscheduled landings associated with the launch phase, the MMT will exercise its management role while still at the KSC LCC. Landings occurring after the MMT has arrived at JSC will be supported using the Action Center in the MCC. Landings at any non-CONUS bases with U.S. military presence will have telephone capability in place and active to either the tower or airport manager's facility. This phone line capability is provided by the DOD SOC. For landings at non-CONUS sites without U.S. military presence, the LSO in the MCC will utilize a hotline to the State Department. The State Department will contact the embassy in the country where the landing occurred. The

embassy will contact to the airport tower or airport manager's office. Within three days of a landing at a TAL site or non-CONUS ELS, DDMS will provide a 24-channel voice communications capability to handle non-secure communications with the DOD SOC and KSC.

3.6.1 MCC Communications

Handover of the Orbiter from the JSC FCT to the KSC turnaround team occurs at flight crew egress. At this time, the FCT and communication lines are nominally released. If a contingency landing should occur, continuing communications between the flight crew and the MCC Capsule Communicator (CAPCOM) and Flight Director will be required. This may occur via telephone or by leaving the flight communication channels active. It is to be expected that all communication channels will remain active until the MMT convenes. For an unscheduled landing, the voice control element and the LSO would remain on console in the MCC to provide support to those elements, which are involved in evaluating the situation.

3.6.2 TAL Sites

The primary TAL sites will have three International Maritime Satellite (INMARSAT) terminals available for use prior to launch. These circuits will provide primary communications to the MCC and LCC. The channels are:

a. Landing Field Prime 1

b. Weather Observer, which is time-shared between voice and data transmissions

The following circuit reallocations will occur after the landing:

c. The Landing Field Prime 1 circuit will be left to its normal functions and additional JSC/DDMS coordination, as necessary.

d. The Weather Observer circuit will be reconfigured to the Convoy Commander net, to be used for local UHF communications with units around the TAL site.

e. The Weather Aircraft circuit will be used for initial MCC communications including medical status, flight crew debrief, flight crew family conversations, and recording the flight crew's statement. Should a bailout occur, this circuit would be used by DDMS to communicate with the SAR aircraft.

In addition, each flight crew member will have a PRC-112 UHF handheld radio in his flight suit, capable of transmitting and receiving on 282.8 MHz and 243.0 MHz. Attachment 8 describes the communications available at each TAL site.

3.6.3 Daily Status Teleconference

A daily status teleconference will be established from the landing site to KSC to report the progress of turnaround operations. The time will be established after the MRT.

Participants will vary according to the condition of the Orbiter and the recovery and turn-around progress.

3.7 AVAILABLE LANDING SITES

There are a variety of landing sites loaded into the Orbiter software available for flight crew selection during flight by item execution on the horizontal situation display. High and low inclination launches have different sites defined in the software. In addition, landing sites are defined as either (1) augmented, with Shuttle-specific landing aids and NASA personnel available or, (2) emergency, with 8,500 feet of available runway and a TACAN. The sites available are listed in NSTS 07700, Volume X - Book 3. Personnel at DOD ALS's and overseas ELS's have received rescue training. Attachment 6 of this appendix lists the types of landings that could occur and a nominal contingency response timeline for each site. Annex 1 to Appendix R will be published as a separate document for each mission to specify the configuration and operations for each landing site. This document will assist KSC and DDMS in planning and staffing for required support.

3.7.1 Return to Launch Site

The RTLS scenario will return the Orbiter to the SLF within 25 minutes. The RTLS may be declared between approximately T+2:30 and T+4:05 minutes. A convoy will be located at the SLF with purge, towing, fire, and rescue capabilities. Attachment 6, Table R6.1, of this appendix details an estimated RTLS timeline.

3.7.2 Transoceanic Abort Landing

A TAL may result in the Orbiter landing at the prime TAL sites of Ben Guerir, Morocco; Moron AB, Spain; Zaragoza AB, Spain; or Banjul, The Gambia. The TAL may be declared between approximately T+2:30 minutes and MECO. The primary TAL site will be manned by approximately 40 predeployed people to provide landing aids and weather operations. Fire and rescue capabilities will be present. The DOD MEDEVAC aircraft will evacuate the flight crew to Naval Station Rota, Spain if uninjured, or to appropriate medical facilities if injured. The flight crew will remain together unless medical circumstances dictate otherwise. The USA Transportation Office has developed airlift schedules for RRT personnel and equipment. All TAL sites are downgraded after launch day, with most of the personnel support released. If a TAL occurs, the NASA GOM will have a prepared press statement for release to the local media thanking the local government and explaining the nature of the landing.

Attachment 6, Table R6.3, of this appendix details a typical TAL timeline.

3.7.2.1 Support Requirements Available at Each TAL Site

Different TAL sites are governed by different international agreements and may have site-unique support personnel and facilities available. A synopsis of the support

provided is included in Attachment 8 of this appendix on those sites that have a high probability of a TAL occurring.

3.7.3 Abort Once Around

The AOA will result in a landing at either EAFB, California; WSSH, New Mexico; or KSC, Florida. It may be declared from MECO to approximately T+30 minutes. There will be personnel at each location to support convoy operations. This convoy does not allow the vehicle to remain powered up, but has adequate equipment for purge (excluding WSSH) as well as fire and rescue operations if needed. KSC ground operations personnel will be immediately dispatched for ground turnaround activities. The vehicle will remain on the runway until KSC personnel arrive if it is damaged; otherwise, the Orbiter will be secured and towed to the deservice area. Warm air purge (excluding WSSH) and around the clock surveillance will be provided until the turnaround team arrives. Attachment 6, Table R6.4, of this appendix describes a typical AOA timeline.

3.7.4 Emergency Landing Sites

3.7.4.1 Primary Landing Site (PLS)

Daily PLS's are identified for each mission. These are the sites that provide the best opportunity for an emergency deorbit to a NASA-supported facility (EAFB, WSSH, KSC). It is also possible to have a Rev 3 Deorbit if the Orbiter is not cleared to continue to orbit. These landings will have minimal convoy support including purge, (excluding WSSH), fire, and rescue. The Orbiter will not remain powered up. The flight crew will return to JSC on the STA as soon as possible.

3.7.4.2 Non-NASA Supported Facility

For an emergency landing at a CONUS site, KSC personnel will be airlifted and equipment will be loaded and shipped by rail or truck from EAFB and KSC. It is estimated to take at least 72 hours to begin equipment deployment. The flight crew will be picked up by the JSC STA, as soon as possible, and returned to JSC. The response timeline will be similar for the AOA up through the teleconference and press conference.

3.7.4.3 Emergency Landing at Non-CONUS Site

For an emergency landing situation where the Orbiter lacks sufficient time or energy to reach a PLS, the software loads onboard the Orbiter provide guidance to a variety of landing sites. These sites will not have personnel predeployed, and if they are non-DOD airfields, they may not have received any Shuttle-unique rescue training. Some non-U.S. sites may not have been notified by NASA that they are in the software loads.

The profiles of the facilities available at each local U.S. Embassy are available through the U.S. State Department. The Embassies have been sent an Airgram giving pertinent details of an Orbiter landing, and actual notification of an impending Orbiter landing will be accomplished by the State Department via a flash message and telephone call. In these instances, the flight crew will retain responsibility for the Orbiter until either (1) they are evacuated out or, (2) a U.S. citizen with a secret clearance arrives at the landing site. The flight crew will carry onboard letters of explanation to the local officials giving simple precautionary instructions and telephone contacts. In the timeline, a C-130 is shown arriving at the site at L+5H. This assumes a landing has occurred at a site that could be reached by the SAR or MEDEVAC C-130 from an ALS within two hours. This time could vary significantly depending on how close to the ELS a U.S. presence is and on the suitability of the airfield. The RRT will arrive in a minimum of 25 hours, assuming the Landing Operation Team is already deployed to DFRF. Aircraft support from the AMC will be best effort. A typical timeline is described in Attachment 6, Table R6.5, of this appendix.

3.8 BAILOUT

Preparations for flight crew bailout will be initiated by starting cabin depressurization to equalize cabin pressure with the altitude. A nominal bailout will begin at 20,000 feet taking approximately two minutes to egress all flight crew members. A bailout may be declared at any time when it is known that there is insufficient energy to reach a runway. The Commander may declare a bailout without MCC knowledge if there is a loss of communications. DOD SAR forces are prepositioned at KSC and TAL sites to locate and/or retrieve the flight crew as soon as possible. Initial DOD SAR forces are under the control of the DOD SOC at PAFB, FL. The progress of the SAR effort shall be reported to the DOD LSO. The LSO will report efforts to the Flight Director and appropriate officials. A typical timeline is described in Attachment 6, Table R6.6, of this appendix.

3.9 CREW CHECKLISTS

The flight crew will carry onboard the Orbiter a series of checklists to aid in post-landing operations after a contingency landing at a non-EOM site. These will be located in the Flight Data File Maps and Charts book. The Initial Flight Crew Response is included in this appendix as Attachment 7.

3.10 ORBITER TURNAROUND

After the RRT begins initial safing and towing of the Orbiter, approximately 400 more personnel will be deployed for turnaround operations. These operations will be controlled by the TAL Orbiter Recovery Plan, which describes the responsibilities for the

management and conduct of the preparation and return of an Orbiter from a TAL site. The detailed plan for TAL Orbiter Recovery is included in this document as Appendix S.

3.11 SALVAGE OPERATIONS

In the event that the Orbiter/payload cannot be returned to KSC via normal ground turn-around and ferry procedures, SFOC-GO-0014, KSC NSTS Salvage Plan, will be implemented. This plan establishes the structure of the Shuttle salvage organization, the assignment of responsibilities, and management procedures to be used in conducting Orbiter/payload salvage operations.

Salvage operations requirements under the direction of KSC Shuttle Processing are as follows:

a. Develop, prepare, and implement the Space Transportation System (STS) Transportation and Salvage Plans.

b. Provide the organization and staffing of KSC/contractor personnel for recovery and salvage operations.

c. Coordinate with applicable government and commercial agencies for services, equipment, and personnel required to effect recovery and salvage operations.

d. Identify support hardware and equipment required for recovery and salvage operations.

e. Coordinate with and advise the Department of Defense (DOD) regarding the transportation of personnel and equipment and/or salvaged items of the Orbiter and its payload.

Salvage Operations will be conducted in support of and under the direction of the designated mishap investigation team or accident investigation board until the scene/hardware has been released from further investigation.

3.12 ACTING WORKING GROUPS

Activation - The MIB Chair will activate working groups appropriate to the contingency situation. The Manager, Space Shuttle Program, may also activate the working groups either prior to the appointment of a MIB Chair, or at the request of the AA-OSF or delegated agent or at the request of another Center Director. The appropriate center will provide personnel to support any working group established to evaluate the contingency including those specified in this plan.

As a basis for the selection of working groups for a specific contingency investigation, a description of various working groups is provided in the following paragraphs. Any or all

of the working groups may be activated. There is no limit to the number of specialized working groups that may be appointed.

The MIB Chair may rearrange the working group structures and define their roles as required. Maximum use should be made of government and contractor experts as consultants or advisors to the working groups and the MIB.

Responsibilities - Each activated working group is responsible to the MIB for performing the following functions within the scope of the group's assigned investigation activities:

a. Take all possible action to prevent injury to personnel and damage or loss of equipment, property or data.

b. Obtain and review contractor and NASA records pertaining to receipt, inspection, configuration control, assembly, reliability, quality control and checkout, as well as any other records pertinent to the investigation.

c. Obtain and review contractor and NASA procedures associated with the activity taking place at the time the contingency occurred.

d. Reconstruct the circumstances under which the contingency could have been initiated.

e. Perform interviews and obtain witness statements as soon as practical after the occurrence of the contingency.

f. Review all data, which may have a bearing on the contingency.

g. Report progress to the MIB on a periodic basis (daily, weekly, etc.) as required by the Board Chair.

h. Participate in MIB meetings when working groups of overlapping interest are reporting.

i. Perform other services as directed by the Chair of the Board of Investigation.

3.12.1 Impoundment/Classified Data Working Group

The Impoundment/Classified Data Working Group will review all data, information and findings to determine if security classification guidance is applicable, and where applicable, will ensure proper classification handling is implemented. This group will also have the overall responsibility for ensuring proper data impoundment procedures are followed and impoundment records are maintained.

3.12.2 Systems Integration Working Group

The Systems Integration Working Group is responsible for the analysis of the integrated Space Shuttle Launch Vehicle data which includes the environment, aerodynamics, flight dynamics, and total vehicle loads.

3.12.3 Vehicle Engineering Working Group

The Vehicle Engineering Working Group is responsible for all of the Orbiter systems-associated instrumentation, prelaunch and post-launch data applying to those systems, and associated support not covered by the Facilities and Ground Support Working Group.

3.12.4 Propulsion and Power Working Group

The Propulsion and Power Working Group examines Orbiter propulsion and power subsystems such as reaction control subsystem, auxiliary power unit, orbital maneuvering subsystem, and hydraulics, pyrotechnics, fuel cells and power reactant storage and distribution subsystems. This group will also assess the integrated main propulsion system for conditions that may have contributed to the contingency.

3.12.5 Navigation, Control, and Aeronautics Working Group

The Navigation, Control, and Aeronautics Working Group will analyze and document the performance of the integrated avionics system, define requirements and compare these data to preflight predictions and post-flight history, and reconstruct flight dynamics, as required.

3.12.6 Avionics and Software Working Group

The Avionics and Software Working Group will analyze and document the performance of the integrated avionics system (includes all essential onboard electronics and software). Coordinate the retrieval and interpretation of data from recovered avionics units. The group will interface with the Navigation, Control, and Aeronautics Working Group as appropriate.

3.12.7 Structures and Mechanics Working Group

The Structures and Mechanics Working Group will analyze the Orbiter structural integrity, loads, structural dynamics, materials, thermal protection system, thermal control system and the purge, vent, and drain system. Orbiter mechanical systems, including interfaces between the Orbiter and External Tank, and their performance will also be reviewed.

3.12.8 Crew and Thermal Systems Working Group

The Crew and Thermal Systems Working Group will examine Shuttle environmental control and life support systems and EVA equipment.

3.12.9 Mission Operations Working Group

The Mission Operations Working Group is responsible for the MCC, network control center, network stations, and the associated data which may have a bearing on

the contingency. Responsibilities may include a review of the flight plan, MCC, NCC, and network configurations and procedures, flight control, communications with the launch site and flight vehicle, and commands (including spurious signals) to the SSV or attached payload. This working group is also responsible for reviewing the adequacy of all operating procedures and actions. Adequacy pertains to the adherence to and compliance with the procedures, the effectiveness of the procedures, and the flight controller training and certification processes.

3.12.10 Flight Crew Operations Working Group

The Flight Crew Operations Working Group is responsible for analyzing any flight crew procedures, training, or other factors involving crew participation which may have a bearing on the contingency.

3.12.11 Payloads/Cargo Working Group

The Payloads/Cargo Working Group is responsible for all payloads, including payload support equipment and consumables. This responsibility also includes examining pre-launch and post-launch data, payload integration, engineering, hardware safety, checkout and payload status at the time of the contingency.

3.12.12 Photographic and TV Analysis Working Group

The Photographic and TV Analysis Working Group is responsible for analyzing all available photographic and video data which may have a bearing on the contingency. This working group will also be responsible for processing, screening, and analyzing optical products. The working group will define and manage all imagery enhancement required and will perform the intercenter coordination required for all photographic investigation products.

3.12.13 Records and Witnesses Working Group

The Records and Witnesses Working Group is responsible for obtaining and reviewing contractor and NASA records pertinent to the contingency, including records on receipt, inspection, configuration control, assembly, reliability, quality control, checkout, and modification. Records may be impounded, if required. This group will accumulate and review statements of witnesses as soon as possible after the contingency.

3.12.14 Timeline Working Group

The Timeline Working Group will analyze all data (telemetry, photographic, etc.) concerning the contingency and will correlate the chronological timeline which will be used by other working groups in their analyses.

3.12.15 Public Affairs Working Group

The Public Affairs Working Group is responsible for the coordination and release of information in accordance with the NASA management instructions and the operational procedures outlined in the Center support plans. The PAO representative will develop and coordinate all public releases with the MIB Chair and will also effect coordination through normal PAO channels.

3.12.16 Fire, Explosives, and Radiological Working Group

The Fire, Explosives, and Radiological Working Group is responsible for locating, identifying, and plotting the position of any fire, explosive, or radiological hazard patterns and the associated debris. This working group is also responsible for reconstructing the circumstances under which such hazards could have been initiated.

3.12.17 Medical and Toxicological Working Group

The Medical and Toxicological Working Group will analyze all medical factors which may have a bearing on the contingency and assess any actual or potential health hazards or stress associated with the mission. In the formation of this working group, reference should be made to the Medical Contingency Action Working Group, defined in Paragraph 3.12.18, established immediately following the contingency.

3.12.18 Medical Contingency Action Working Group

The Medical Contingency Action Working Group responsibilities are to identify the relevant circumstances under which an injury or death occurred, considering those factors which may have led to the injury or death; review all relevant medical documents including autopsy reports; and formulate recommendations concerning corrective action as appropriate.

3.13 OTHER WORKING GROUPS

In addition to the working groups listed above, the lead center for the investigation will support the following working groups.

3.13.1 Facilities and Ground Support Working Group

The Facilities and Ground Support Working Group will evaluate launch and landing facilities, test support systems, and ground support equipment that includes servicing and deservicing equipment at the primary, backup, secondary and contingency landing sites and at ground test sites.

3.13.2 Launch, Landing, and Retrieval Operations Working Group

The Launch, Landing, and Retrieval Operations Working Group is responsible for reviewing all flight, ferry, launch, landing, and ground service operations associated with

the contingency. This includes landing operations and deservicing at secondary and contingency landing sites, and at ground test sites.

3.13.3 Search, Recovery, and Reconstruction Working Group

The Search, Recovery, and Reconstruction Working Group is responsible for performing the search for and recovery of critical vehicle flight components for determination of the exact cause of the contingency. Upon recovery of the hardware, the working group will take precautions to maximize the use of the recovered components for failure analysis. These steps will include photographic documentation, preservation and sampling.

3.14 CONSULTANTS

The following consultants should be assigned by the MIB Chair and approved by the Center Director:

a. Counsel from the legal office will be available whenever witnesses are being questioned or when legal problems arise, or when legal advice is needed by the MIB.

b. The PAO will provide advice and assistance regarding news releases or public information.

c. A safety official; and

d. Others as required.

3.15 SPECIALISTS

As many specialists as necessary will be appointed by the Chair of the MIB. Specialists will participate in the MIB meetings and be available, at the request of the Chair, to assist the working groups. These specialists can be selected from outside NASA; however, non-government employees or non-full-time government employees will not be voting members of the MIB.

4.0 INVESTIGATION GUIDELINES

4.1 GENERAL

The investigation is conducted to determine the cause of the contingency and to recommend steps to prevent recurrence of such a contingency. If the MIT is activated following the MRT, all evidence and data collected will be turned over to the formal MIB, once established. The MIB and each working group involved in the investigation will

document their findings, determinations, conclusions, recommendations, and the procedural methods used during the investigation. Various guidelines for conducting an investigation are provided in the following paragraphs.

4.2 SUPPORT FACILITIES

The centers will support any investigation that may be required. Necessary resources to conduct the investigation - administrative, facilities, secretarial support, communications, data access and security systems - will be made available to the MIB. To the extent possible, the respective center will utilize existing facilities, organizations, and procedures for data handling and analysis.

4.3 SECURITY

Security, as it pertains to this plan, applies not only to classification of data, but also to restricting access to accident-sensitive areas to approved personnel only. NASA security regulations do not apply to the DOD supporting facilities, except for those specified instances where joint DOD/NASA agreements are available. Security coordination with contractor security services will be provided.

4.4 ACCIDENT SITE PRESERVATION

Those resources committed to support the SSP at the time of the contingency will be preserved in their operational state and configuration until released by the AA-OSF or MIT Chair. Space vehicle and launch or impact-site debris will be moved only as authorized by the AA-OSF or MIT Chair, except when mandatory for rescue personnel, firefighting, or removal of explosives. The DOD forces and equipment that are available for location and removal of salvageable components are responsible to the DOD for command and control. The AA-OSF or MIT Chair is responsible for requesting the DOD to utilize salvage equipment or move debris in the vicinity of KSC or adjacent shallow water areas, if required. The term vicinity applies to the Florida mainland and shallow waters of the Atlantic Ocean for which 45th Space Wing (45SW) agreements exist. The DOD Manager for Space Shuttle Support may be required to provide salvage/retrieval on a world-wide basis. Arrangements will be made to store damaged hardware, equipment, debris, etc., in controlled facilities, if necessary. Duties listed for the AA-OSF or MIT Chair in this paragraph will be assumed by the MIB Chair when investigation responsibility has been turned over to that board. Exceptions to this policy will be justified when equipment or actions are necessary to ensure personnel safety.

4.5 NETWORK INSTRUMENTATION

The Flight Director will make timely recommendations to the Manager, Space Shuttle Program, regarding equipment and network instrumentation to be released from further

flight or test support. The Manager, Space Shuttle Program, should reach early agreement with the DOD Manager on the appropriate status of configuration control for any pertinent DOD equipment. GSFC will be kept informed through the Network Director of all decisions involving the network and recorded data requirements.

4.6 DATA HANDLING

4.6.1 General

Data designated in the implementing message, such as realtime recordings of telemetry, plotboard charts, trajectory data, tape recordings, weather reports, digital command system and tone command tapes, acquisition aid data, signal-strength records, photographs, etc., will be reduced into legible format as soon as possible and distributed as required to support the investigation. The MIB Chair may specify any special data requirements for use by the investigating authority. All other mission data may be processed in a normal manner on a noninterference basis with data in support of the investigation.

4.6.2 Records

The Director of Mission Operations, the Manager, Space Shuttle Program, the Manager, Launch Integration, and the Manager, Space Shuttle Vehicle Engineering, may impound applicable/appropriate records and protect NASA records pertinent to the contingency. These may include records of receipt, inspections, modifications, reliability and quality control, assembly and checkout, configuration control, and resolutions of significant technical problems. A custodian within each working group will be designated for these records and will retain the records for use by the MIB.

4.6.3 Security of Data

Data associated with the contingency will not be reclassified. To ensure all data are available to the MIB, the distribution of these data will be restricted and accorded special handling procedures as specified in this plan. Except for direct support of continued flight operations, and to the extent permitted by law, no information or data will be released to any person without a need-to-know, as designated by the Manager, Space Shuttle Program until such time as the MIB Chair is appointed. To the extent provided by law, access to the processed and reduced data associated with the investigation will be limited to personnel involved with the failure investigation until the data are released by the MIB Chair.

4.6.4 Public Release

Any public release of information relating to a contingency is the responsibility of the PAO. The Manager, Space Shuttle Program, in consultation with the AA-OSF or

designated agent, will provide guidance to the Manager, Launch Integration and the Director of Public Affairs, Flight Director, DOD Representative, and other appropriate personnel until a duly appointed MIB assumes investigative responsibilities.

4.7 REPORTS

The Mishap Investigation Board Report shall consist of five volumes which are entitled:

a. Volume I: The Report

b. Volume II: Appendices

c. Volume III: Proposed Corrective Action Implementation Plan

d. Volume IV: Lessons Learned Summary

e. Volume V: Witness Statements/Recordings/Transcripts

The convening authority may also require the MIB to prepare intermediate reports. The MIB reports will be submitted to the convening authority and to other organizations as appropriate.

The working groups will report their progress periodically or at prearranged intervals as established by the MIB. Preliminary investigative reports will be reviewed at a time designated by the MIB Chair.

Time-lost reports will be filed for cases in which hospitalization for more than five days or death occurs.

The MIB will assemble lessons learned in the form of a summary of corrective actions.

4.7.1 Minority Reports

If a MIB member disagrees with the findings, conclusions, or recommendations of a majority of the MIB, a non-concurrence statement will be appended to the report and become a part of the report.

THIS PAGE INTENTIONALLY LEFT BLANK

Volume V
Appendix G.3
CAIB Charter with Revisions

This Appendix contains the Columbia Accident Investigation Board Charter.

THIS PAGE INTENTIONALLY LEFT BLANK

National Aeronautics and
Space Administration
Office of the Administrator
Washington, DC 20546-0001

February 2, 2003

Admiral Hal Gehman
3725 Lynnfield Drive
Williamsburg, VA

Dear Admiral Gehman:

This letter is to advise you that, pursuant to 42 U.S.C. §2473 (c)(1), Section 203 (c)(1) of the National Aeronautics and Space Act of 1958, as amended, and as a result of the loss of the Space Shuttle Columbia, I have formally activated the Columbia Accident Investigation Board. I am appointing you to be Chairman of this Board.

I am requesting your immediate and full cooperation with the investigation of the STS-107 Space Shuttle mishap of February 1, 2003. As Chairman of the Board, you are charged with all activities and responsibilities described in but not limited to the Columbia Accident Investigation Board Charter.

Among other things, the Board shall independently determine the facts, as well as the actual or probable causes of the Shuttle accident and recommend preventative or other appropriate actions to preclude recurrence of a similar nature. Our regulations stipulate that the Board issue a final report within 60 days from this date. However, if you feel that you need additional time to arrive at a responsible conclusion, do not hesitate to request such additional time as you deem fit. You are free to pursue whatever avenue you deem appropriate. A copy of the Charter is attached for your reference.

I have designated Mr. David Lengyel and Mr. Steven Schmidt from my staff to be your key points of contact. We will also make other staff available to directly support the Board's activities.

I am grateful for your dedication and service to our country in this time of great need. I trust that you will be diligent, thorough, and unrelenting in your work to determine the cause and prevent the recurrence of this tragedy.

Respectfully,

Sean O'Keefe
Administrator

C2-000031

Letter dtd 2 Feb 03 re Charter.pdf

CAB089-0072

Columbia Accident Investigation Board
Charter

1. GUIDELINES

In the case of a high-visibility, mission-related Shuttle mishap, the NASA Administrator may activate an International Space Station and Space Shuttle Mishap Interagency Investigation Board (the Board). Board activation is anticipated for events involving serious injury or loss of life, significant public interest, and other serious mishaps. The Board should consist of at least seven members, and be supported by the Office of Space Flight Headquarters and technical consultants as required.

2. ACTIVATION

The recommendation for the NASA Administrator to activate this Board will normally be made at either the Associate Administrator for the Office of Space Flight-directed Mishap Response Teleconference or as a decision at the Administrator's HCAT meeting and/or teleconference. For this case, the NASA Administrator has determined effective at 10:30 am February 1, 2003, to convene such a Board and to name it the Columbia Accident Investigation Board.

3. MEMBERSHIP

Chairman of the Board
Admiral Hal Gehman, USN

Board Members
Commander, Naval Safety Center, Rear Admiral Stephen Turcotte
Director, Plans and Programs, Headquarters Air Force Materiel Command,
Major General John Barry
Commander, HQ USAF Chief of Safety, Major General Kenneth W. Hess
Chief, Aviation Safety Division, Department of Transportation, Dr. James N. Hallock
Director of Accident Investigation, Federal Aviation Administration, Mr. Steven B. Wallace
Commander, 21st Space Wing, USAF, Brigadier General Duane Deal
Director, NASA Ames Research Center, Mr. Scott Hubbard

4. BOARD SUPPORT

Standing Board Support Personnel

Ex-Officio Member: Mr. Bryan O'Connor, Associate Administrator for Safety and Mission Assurance

Executive Secretary: Mr. Theron Bradley, Jr., NASA Chief Engineer

Additional Support Personnel. The Board may designate consultants, experts, or other government or non-government individuals to support the Board as necessary.

Task Force Team Support. Within 72 hours of activation of the Interagency Board, the AA/OSF, the AA/SMA, the NASA Field Center Director or NASA Program Associate Administrator (Non-

OSF or Non Mission Related), and the NASA Chief Engineer will meet to elect and recommend non Task Force Team members to the Mishap Board Chairman. Upon approval by the NASA Administrator, the Task Force Team members will convene and meet with the appropriate Working Group Team leads. The Task Force Team will support the Board and they will:

1. Be the formal interface between the Board and the activated Working Groups;
2. Monitor, collect, document, and file the reports of the Working Groups activated to support the mishap investigation;
3. Provide the Board members with requested information and reports from the Working Groups; and
4. Assist the Board in the preparation of interim and final reports as required.

5. BOARD RESPONSIBILITIES

The Board will:

1. Conduct activities in accordance with direction from the NASA Administrator and the provisions of applicable NASA management instructions.
2. Work with the NASA Administrator to schedule Board activities, interim Board reports, and submission of the final Board report.
3. Determine the facts, as well as the actual or probable causes of the Shuttle mishap in terms of primary cause(s), and potential cause(s) and recommend preventive and other appropriate actions to preclude recurrence of a similar mishap. The investigation will not be conducted or used to determine questions of culpability, legal liability, or disciplinary action.
4. Use the established NASA support structure of working groups, NASA Field Center support, and supporting facilities to conduct the investigations. This includes staff advisors as required for expertise in areas such as public affairs, legal, medical, safety, and security.
5. Activate the working groups appropriate to the mishap.
6. Obtain and analyze whatever facts, evidence, and opinions it considers relevant by relying upon reports of studies, findings, recommendations, and other actions by NASA officials and contractors or by conducting inquiries, hearings, tests, and other actions it deems appropriate. In so doing, it may take testimony and receive statements from witnesses. All elements of NASA will cooperate fully with the Board and provide any records, data, and other administrative or technical support and services that may be requested.
7. Impound property, equipment, and records to the extent that it considers necessary.
8. Document findings in terms of (a) the primary causes of the mishap; (b) contributing causes; (c) potential causes; and (d) pertinent observations.
9. Release mishap information and mishap investigation reports in accordance with applicable NASA policies.
10. Develop recommendations for preventative and other appropriate actions. A finding may warrant one or more recommendations or may stand alone.
11. Provide a final written report to the NASA Administrator not later than 60 days.

February 1, 2003

National Aeronautics and
Space Administration
Office of the Administrator
Washington, DC 20546-0001

February 6, 2003

Admiral Hal Gehman
3725 Lynnfield Drive
Williamsburg, VA 23081

Dear Admiral Gehman:

Please find, attached to this letter, a revised Charter for the Columbia Accident Investigation Board. I am pleased to make the changes you requested, which are incorporated in this new text. I thank you for your efforts, and those of the entire Board, as we all dedicate ourselves to determining the cause of the accident.

Respectfully,

Sean O 'Keefe
Administrator

Enclosure

C0-000010

CAB031-0250

Columbia Accident Investigation Board
Charter

1. GUIDELINES

In the case of a high-visibility, mission-related Shuttle mishap, the NASA Administrator may activate an International Space Station and Space Shuttle Mishap Interagency Investigation Board (the Board). Board activation is anticipated for events involving serious injury or loss of life, significant public interest, and other serious mishaps. The Board should consist of at least seven members, and be supported by the Office of Space Flight Headquarters and technical consultants as required.

2. ACTIVATION

The recommendation for the NASA Administrator to activate this Board will normally be made at either the Associate Administrator for the Office of Space Flight-directed Mishap Response Teleconference or as a decision at the Administrator's HCAT meeting and/or teleconference. For this case, the NASA Administrator has determined effective at 10:30 am February 1, 2003, to convene such a Board and to name it the Columbia Accident Investigation Board.

3. MEMBERSHIP

Chairman of the Board
Admiral Hal Gehman, USN

Board Members
Commander, Naval Safety Center, Rear Admiral Stephen Turcotte
Director, Plans and Programs, Headquarters Air Force Materiel Command,
Maj. General John Barry
Commander, HQ USAF Chief of Safety, Major General Kenneth W. Hess
Chief, Aviation Safety Division, Department of Transportation, Dr. James N. Hallock
Director of Accident Investigation, Federal Aviation Administration, Mr. Steven B. Wallace
Commander, 21st Space Wing, USAF, Brig. General Duane Deal
Director, NASA Ames Research Center, Mr. Scott Hubbard

4. BOARD SUPPORT

Standing Board Support Personnel

Ex-Officio Member: Mr. Bryan O'Connor, Associate Administrator for Safety and Mission Assurance

Executive Secretary: Mr. Theron Bradley, Jr., NASA Chief Engineer

Additional Support Personnel. The Board may designate consultants, experts, or other government or non-government individuals to support the Board as necessary.

Task Force Team Support. Within 72 hours of activation of the Interagency Board, the AA/OSF, the AA/SMA, the NASA Field Center Director or NASA Program Associate Administrator (Non-OSF or Non Mission Related), and the NASA Chief Engineer will meet to select and recommend

Task Force Team members to the Mishap Board Chairman. Upon approval by the NASA Administrator, the Task Force Team members will convene and meet with the appropriate Working Group Team leads. The Task Force Team will support the Board and they will:

1. Be the formal interface between the Board and the activated Working Groups;
2. Monitor, collect, document, and file the reports of the Working Groups activated to support the mishap investigation;
3. Provide the Board members with requested information and reports from the Working Groups; and
4. Assist the Board in the preparation of interim and final reports as required.

5. COLUMBIA ACCIDENT INVESTIGATION BOARD RESPONSIBILITIES

The Independent Board will:

1. Conduct activities in accordance with the provisions of applicable NASA policies and procedures.
2. Schedule Board activities, interim Board reports, and submission of the final Board report in coordination with the NASA Administrator.
3. Determine the facts, as well as the actual or probable causes of the Shuttle mishap in terms of dominant and contributing root causes and significant observations and, recommend preventive and other appropriate actions to preclude recurrence of a similar mishap. The investigation will not be conducted or used to determine questions of culpability, legal liability, or disciplinary action.
4. Use the established NASA support structure of working groups, NASA Field Center support, and supporting facilities to conduct the investigations. This includes staff advisors as required for expertise in areas such as public affairs, legal, medical, safety, and security.
5. Activate the working groups appropriate to the mishap.
6. Obtain and analyze whatever facts, evidence, and opinions it considers relevant by relying upon reports of studies, findings, recommendations, and other actions by NASA officials and contractors or by conducting inquiries, hearings, tests, and other actions it deems appropriate. In so doing, it may take testimony and receive statements from witnesses. All elements of NASA will cooperate fully with the Board and provide any records, data, and other administrative or technical support and services that may be requested.
7. Impound property, equipment, and records to the extent that it considers necessary.
8. Release mishap information and mishap investigation reports in accordance with applicable NASA policies.
9. Develop recommendations for preventative and other appropriate actions. A finding may warrant one or more recommendations or may stand alone.
10. Provide a final written report to the NASA Administrator not later than 60 days.

February 1, 2003
Revised: February 6, 2003

National Aeronautics and
Space Administration
Office of the Administrator
Washington, DC 20546-0001

February 18, 2003

Admiral Hal Gehman, USN (Ret)
Chairman
Columbia Accident Investigation Board
16850 Saturn Lane
Houston, Texas 77058

Dear Admiral Gehman,

Thank you for your comments on the charter changes proposed last week. Pursuant to your request, I have made further changes to the charter derived from our collective efforts to consult with Members of Congress. The enclosed charter reflects all revisions to this date.

The revised charter also reflects the appointments of Roger Tetrault and Sheila Widnall as members of the Board. You have advised that you are considering a recommendation to me for another appointment. In accord with our discussions, I am prepared to make such appointments you feel would contribute to the Board's work.

I am also in receipt of a copy of a letter addressed to you from NASA's Inspector General, Robert Cobb, on February 14, 2003, asking you to acknowledge your independence in certain respects. Please feel free to advise of any aspects of your charge you feel needs particular further emphasis. Of particular note relative to the Inspector General's views, you are charged in the charter to "obtain and analyze whatever facts, evidence, and opinions it (the Board) considers relevant" to "determine the facts, as well as the actual or probable causes of the Shuttle mishap… and recommend preventative and other actions to preclude recurrence of a similar mishap."

These charter provisions and others clearly demonstrate that your Board can and must act independently. Your Board is entitled to receive any information that NASA has. If there is any resistance, please let me know and we will assure cooperation. It is within your charter to determine causes, including whether NASA budget or management or any other factors created an environment which caused or contributed to the cause of this accident.

For these and other factors we have discussed several times over the past two weeks, I find the Inspector General's views and advice to be completely consistent with our mutual understanding of the Board's responsibility and conduct of operations for this important investigation.

Cordially,

Sean O'Keefe
Administrator

Columbia Accident Investigation Board
Charter

1. GUIDELINES

In the case of a high-visibility, mission-related Shuttle mishap, the NASA Administrator may activate an International Space Station and Space Shuttle Mishap Interagency Investigation Board (the Board). Board activation is anticipated for events involving serious injury or loss of life, significant public interest, and other serious mishaps. The Board should consist of at least seven members, and be supported by the Office of Space Flight Headquarters and technical consultants as the Board deems appropriate.

2. ACTIVATION

The recommendation for the NASA Administrator to activate this Board will normally be made at either the Associate Administrator for the Office of Space Flight-directed Mishap Response Teleconference or as a decision at the Administrator's HCAT meeting and/or teleconference. For this case, the NASA Administrator has determined effective at 10:30 am February 1, 2003, to convene such a Board and to name it the Columbia Accident Investigation Board.

3. MEMBERSHIP

Chairman of the Board
Admiral Hal Gehman, USN (Ret)

Board Members
Commander, Naval Safety Center, Rear Admiral Stephen Turcotte
Director, Plans and Programs, Headquarters Air Force Materiel Command,
Maj. General John Barry
Commander, HQ USAF Chief of Safety, Major General Kenneth W. Hess
Chief, Aviation Safety Division, Department of Transportation, Dr. James N. Hallock
Director of Accident Investigation, Federal Aviation Administration, Mr. Steven B. Wallace
Commander, 21st Space Wing, USAF, Brig. General Duane Deal
Director, NASA Ames Research Center, Mr. Scott Hubbard
Mr. Roger E. Tetrault
Dr. Sheila Widnall

4. BOARD SUPPORT

Standing Support Personnel Reporting to the Board

Ex-Officio Member: Mr. Bryan O'Connor, Associate Administrator for Safety and Mission Assurance

Executive Secretary: Mr. Theron Bradley, Jr., NASA Chief Engineer

Additional Support Personnel. The Board may designate consultants, experts, or other government or non-government individuals to support the Board as necessary. In addition, the Board may substitute non-NASA personnel as Executive Secretary at the discretion of the Chairman.

Task Force Team Support. Within 72 hours of activation of the Interagency Board, the AA/OSF, the AA/SMA, the NASA Field Center Director or NASA Program Associate Administrator (Non-OSF or Non Mission Related), and the NASA Chief Engineer will meet to select and recommend Task Force Team members to the Columbia Accident Investigation Board Chairman. Upon approval by the Board and appointment by the NASA Administrator, the Task Force Team members will convene and meet with the appropriate Working Group Team leads. The Task Force Team may to the extent that the Board deems appropriate:

1. Be the formal interface between the Board and the activated Working Groups;
2. Monitor, collect, document, and file the reports of the Working Groups activated to support the mishap investigation;
3. Provide the Board members with requested information and reports from the Working Groups; and
4. Assist the Board in the preparation of interim and final reports.

5. COLUMBIA ACCIDENT INVESTIGATION BOARD RESPONSIBILITIES

The Independent Board will:

1. Conduct activities in accordance with the policies and procedures adopted by the Board.
2. Schedule Board activities, interim Board reports, and submission of the final Board report as the Board deems appropriate.
3. Determine the facts, as well as the actual or probable causes of the Shuttle mishap in terms of dominant and contributing root causes and significant observations and, recommend preventive and other appropriate actions to preclude recurrence of a similar mishap. The investigation will not be conducted or used to determine questions of culpability, legal liability, or disciplinary action.
4. Use the established NASA support structure of working groups, NASA Field Center support, and supporting facilities to conduct the investigations, as the Board deems appropriate. The Board may use non NASA support as it deems appropriate.
5. Activate the working groups appropriate to the mishap.
6. Obtain and analyze whatever facts, evidence, and opinions it considers relevant by relying upon reports of studies, findings, recommendations, and other actions by NASA officials and contractors or by conducting inquiries, hearings, tests, and other actions it deems appropriate. In so doing, it may take testimony and receive statements from witnesses. All elements of NASA will cooperate fully with the

Board and provide any records, data, and other administrative or technical support and services that may be requested.

7. Impound property, equipment, and records to the extent that it considers necessary.
8. Release mishap information and mishap investigation reports, as the Board deems appropriate.
9. Develop recommendations for preventative and other appropriate actions. A finding may warrant one or more recommendations or may stand alone.
10. Provide a final written report at such time and in such manner as the Board deems appropriate which upon its completion will be immediately released to the public.

February 1, 2003
Revised: February 18, 2003

C2-000031

CAIB Charter dtd 18 Feb 03.pdf

CAB089-0060

News Release

National Aeronautics and
Space Administration

Washington, DC 20546
(202) 358-1600

Glenn Mahone/Bob Jacobs
Headquarters, Washington
(Phone: 202/358-1600)

Steve Nesbitt
Columbia Accident Investigation Board
(Phone: 713/301-9571)

For Release
Feb. 18, 2003

NOTE TO EDITORS: N03-019

SPACE SHUTTLE ACCIDENT INVESTIGATION BOARD CHARTER AMENDED

The NASA charter for the independent panel in charge of the Space Shuttle Columbia accident investigation has been amended. The changes allow the Space Shuttle Accident Investigation Board additional flexibility in acquiring support staff and expertise outside of NASA.

NASA Administrator Sean O'Keefe has indicated the charter will continue to be updated as necessary to ensure the panel, which is known as the Gehman Board, remains independent during the course of the investigation.

On Saturday, Admiral Harold W. Gehman, Jr., announced the addition of Dr. Shelia Widnall of the Massachusetts Institute of Technology, Cambridge, Mass., to the panel. Dr. Widnall, former Secretary of the Air Force from 1993 to 1997, is a world-renowned expert in aircraft turbulence and spiraling airflows. She will begin meeting with the other members of the Gehman Board Thursday, Feb. 20, in Houston.

An updated copy of the board's charter and letter from the NASA Administrator is on the Internet at **www.nasa.gov**.

-end-

C2-000031

News Release dtd 18 Feb 03.pdf

CAB089-0073

Volume V
Appendix G.4

Group 1 Matrix Brief on Maintenance, Material, and Management

This Appendix contains a working matrix of slides on maintenance, material, and management. These slides were used by Group I in tasking NASA to respond to requests for information or specific issues. Each matrix subject addresses an action/issue, background/facts, findings, recommendations and source documentation. By using this tool, Group I was able to engage NASA on potential final report inclusions.

THIS PAGE INTENTIONALLY LEFT BLANK

Group 1

INVESTIGATION MATRIX

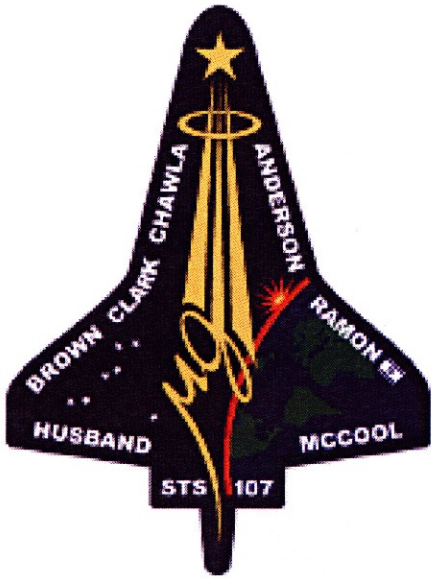

Print Presentation

Group 1 Investigation Matrix

	E/T Foam	RCC	Tile	Orbiter	Other	Organization	Contract
Design / Certification	1 (3)	5 (3)	10 (1)	13 (1)	18 (1)		28 (1)
Production	2 (4)	6 (1)			19 (4)	24 (3)	29 (4)
Mission Life		7 (1)					
Fleet Experience / Aging		8 (4)	11 (5)	14 (7)	20 (2)	25 (3)	
Maintenance	3 (2)	9 (4)	12 (1)	15 (5)	21 (1)	26 (3)	30 (3)
Launch / Ascent	4 (5)			16 (3)	22 (7)		
Orbit					23 (1)	27 (3)	
Entry				17 (3)			

Reset Matrix

ET – Foam
Design – Certification

1-1 ET Bipod Ramp Redesign

1-2 Geometry of LH2-IT Flange

1-3 Super Lightweight Tank Design Change

Matrix

Presenter	CAIB/Group 1	Date	FINAL	Slide	3 of 32

ET – Foam Design – Certification

- **Action / Issue:** Redesign of Bipod Fitting Enclosure
- **Background / Facts:**
  - Complex bipod attachment designed to be structurally optimal
    - TPS materials (incl. foam ramp) were incorporated into the design following structural optimization
  - Foam & SLA must be applied to a complex geometry
  - Combination of complex geometry and variable foam spraying techniques make current bipod foam ramp fabrication difficult
    - Only 6 spray operators are trained for foam application in this area
  - Bipod foam ramp has been redesigned twice in past
  - Foam from bipod ramp lost during ascent on at least 7 occasions:
    - STS-7 (ET-6), STS-32 (ET-32R), STS-50 (ET-50), STS-52 (ET-55), STS-62 (ET-62), STS-112 (ET-115), STS-107 (ET-93)

Presenter: M3/Material | Date: FINAL | Slide: 1 of 12 | Closed

ET – Foam Design – Certification

- **Findings:**
  - Bipod fitting enclosure redesign efforts are already underway
    - Effort was initiated after loss bipod ramp foam on STS-112
  - Lessons learned indicate use of SLA is not necessary
  - Five designs proposed
    - All eliminate SLA
    - Two minimize size of sprayed-on foam ramp with metal (Ti) fitting
    - One uses a bare metal (Ti) fitting
    - Two use an Inconel housing to protect the metal fitting
  - Leading candidate (2a) is a bare metal fitting with no foam
  - Preliminary Design Review scheduled for 17-19 Jun 03
  - Critical Design Review planned for ~15 July 03

Presenter: M3/Material | Date: FINAL | Slide: 2 of 12 | Closed

ET – Foam Design – Certification

- **Recommendations:**
  - NASA efforts to redesign the bipod fitting enclosure must continue.
    - Redesign efforts must include testing and analyses that account for the complex combination of aerodynamic loads, structural loads, aerodynamic heating, cryogenic backface temperatures, and changes in atmospheric pressure.
  - Tests and analyses must be sufficient to ensure that the loss of foam or hardware from this region will not happen in the future.
  - The redesign of the bipod fitting enclosure will be a Return-To-Flight requirement.
  - If foam is still required on bipod fitting:
    - Tighten acceptable temperature & humidity spray envelope
    - Standardize operator techniques
    - Consider use of robotics to fabricate bipod ramp
    - Develop and validate NDE techniques to check for defects

Presenter: M3/Material | Date: FINAL | Slide: 3 of 12 | Closed

ET – Foam Design – Certification

Bipod Configuration Overview

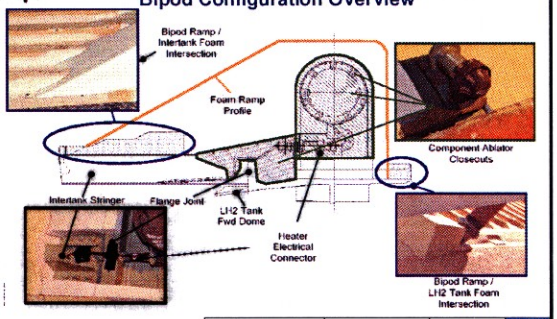

Presenter: M3/Material | Date: FINAL | Slide: 4 of 12 | Closed

ET – Foam Design – Certification

Historical Bipod Ramp Changes - 1

ET	STS	Launch Date
1	1	4/12/81
5	5	11/11/82
6	7	6/18/83
8	6	4/4/83
9	8	8/30/83
13	41D (14)	8/30/84
50	50	6/25/92

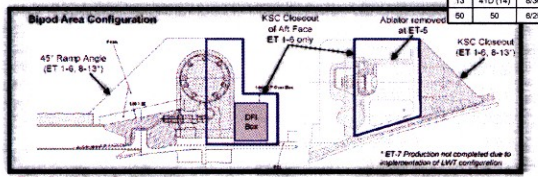

Early Bipod Area Configuration
- Forward face angle of 45 ± 5°
  - Edge straight into Intertank foam
- Development Flight Instrumentation (DFI) box and associated KSC closeout eliminated at ET-8
- SLA on bipod housing removed at ET-5
- Intertank foam configuration in area of bipod revised at ET-9
- Debris produced by -Y Bipod on ET-6 (STS-7)
  - Attributed to rework on forward ramp of closeout
    - Assessed repair criteria

Intertank Foam at Bipod

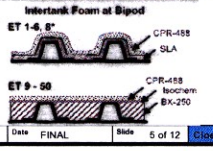

Presenter: M3/Material | Date: FINAL | Slide: 5 of 12 | Closed

ET – Foam Design – Certification

Historical Bipod Ramp Changes - 2

ET	STS	Launch Date
6	7	6/18/83
9	8	8/30/83
13	41D (14)	8/30/84
14	51C (20)	1/24/85
17	51B (24)	4/29/85
50	50	6/25/92
51	51	1/13/93
87	85	8/7/97

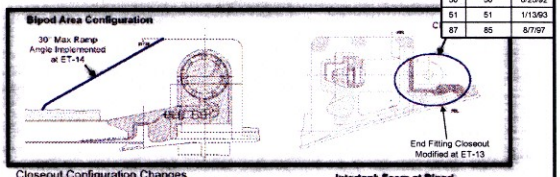

Closeout Configuration Changes
- PDL closeout under the clevis replaced the BX-250 closeout over the end fitting - KSC production flow enhancement
- Revised ramp impingement angle to 30° max with a 5.0 ± .1 inch radius at forward edge
  - Changed as a result of suspected foam debris on ET-6
  - ET 14-17 reworked at KSC
- Added restrictions to the allowable repair area
- Intertank foam configuration revised at ET-51 to eliminate the isochem / CPR-488 bond line
  - Foam loss during flight attributed to localized debonds

Intertank Foam at Bipod

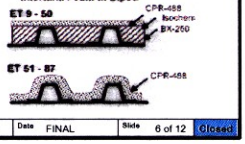

Presenter: M3/Material | Date: FINAL | Slide: 6 of 12 | Closed

1

ET – Foam Design – Certification

Historical Bipod Ramp Changes - 3

ET	STS	Launch Date
76	75	2/22/96
88	86	9/25/97
90	89	1/22/98
91	90	4/17/98
92	99	2/11/00
93	107	1/16/03
94	TBD	TBD
95	91	6/2/98

Bipod Area Configuration

Ramp intersection Changed at ET-76

Closeout Configuration Changes
- Forward ramp edge permitted to terminate straight into Intertank acreage foam
  - 0.25" step allowed for forward ramp termination
- Implemented NCFI 24-124 on intertank side wall at ET-88
- Intertank foam machined at ET 91, 93, 94, 95 & up

Intertank Foam at Bipod
ET 88 – 90, 92 — NCFI 24-124 Net Spray
ET 91, 93, 94, 95 & up — NCFI 24-124 Machined

Presenter M3/Material | Date FINAL | Slide 7 of 12 | Closed

ET – Foam Design – Certification

Considerations for All Bipod Fitting Enclosure Redesigns

- Multiple application closeout (eliminate/minimize voids)
- Minimize/Eliminate Foam Ramp Reshape ramp (More aerodynamic)
- Remove connector (eliminate closeout complexity) and splice in heater(s), bond wires to tank
- Eliminate Ablator (Cryopumping concern)
- Foam in fitting end cover/T stringer (cryopumping concern)

Presenter M3/Material | Date FINAL | Slide 8 of 12 | Closed

ET – Foam Design – Certification

REDESIGN OPTIONS & CHALLENGES

Option 1 – Manual spray with most foam of options, no validated NDE

Option 2 – Manual spray with minimum foam, no validated NDE

Option 2a – Non-LRU heater requires fitting removal for heater failure

Leading Candidate

Option 3 – Fairing attach plate under fitting adds complexity

Option 3a – Verification of multiple strip heaters under cover/fitting modifications.

Presenter M3/Material | Date FINAL | Slide 9 of 12 | Closed

ET – Foam Design – Certification

Heater Solution for Option 2a

- Main Drawback to Original Option 2a
  - No capability to replace heater strip (beneath fitting) on pad in case of strip failure
- Solution
  - Use redundant & replaceable rod heaters in copper plate beneath fitting

Heater slots in fitting (1.5" x 4.75" x .375")

Rod heater locations

Copper sheet between fitting and isolator

Copper Sheet with Integral Heater Pads

Presenter M3/Material | Date FINAL | Slide 10 of 12 | Closed

ET – Foam Design – Certification

Bipod Ramp Redesign Schedule

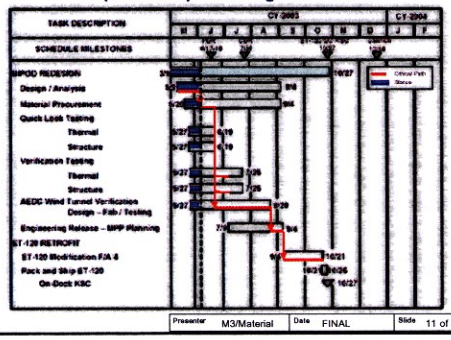

Presenter M3/Material | Date FINAL | Slide 11 of 12 | Closed

ET – Foam Design – Certification

- **Documentation:**
  - "Bipod Ramp Area Design & Analysis," provided to CAIB, 3 Mar 03
  - "Bipod Foam Redesign Update," PRCB Review, 26 Mar 03
  - "Construction of Bipod Attach Area and Bipod Ramp," Presented at the Michoud Assembly Facility, 13 Mar 03
  - S. Sparks and L. Foster, "ET Cryoinsulation," CAIB Public Hearing, 7 April 03
  - "ET Bipod Closeout Redesign System Design Review," @ MAF, 17 Apr 03
  - Personal Communication with S. Holmes & N. Otte, Marshall Space Flight Center, 1 April 03
  - "ET Bipod Aero Ramp Foam Verification/Certification," presented by M. Quiggle, Michoud Assembly Facility, 10 April 03
  - Discussion with M. Quiggle, J. Pilet, R. Steinbach, Michoud Assembly Facility, 15 May 03
  - "1.1.1 TPS Debris Fault Tree Closeout Briefing," S. Sparks at MSFC, 20 May 03
  - "External Tank Foam Loss," RFI B1-000039
  - Personal Correspondence with S. Holmes (MSFC), 5 may 03
  - "Bipod Foam Redesign Update," Presented to the Problem Resolution Control Board, 26 Mar 03
  - "Bipod Foam Redesign Update," Presented to the Problem Resolution Control Board, 9 May 03

Presenter M3/Material | Date FINAL | Slide 12 of 12 | Closed

ET – Foam Design – Certification

- **Action / Issue:** Geometry of the LH2-IT flange could contribute to foam loss
- **Background / Facts:**
  - LH2-IT geometry provides several paths where LN2 can possibly get into the flange area
  - Solid N2 to GN2 state transitions could possibly contribute to foam loss
  - A "Y" joint is formed where the LH2-IT connection is made provide a reservoir where LN2 can collect

Presenter M3/Material | Date FINAL | Slide 1 of 8 | Closed

ET – Foam Design – Certification

- **Findings:**
  - Bolt holes, shim gaps and stringer venting could provide a path for LN2 to get behind the foam in the flange closeout area
  - During ascent, stresses in flange area change between tension and compression
    - LN2 path back to the IT could possibly be sealed leading to foam being "popped" off
  - Foam loss from the LH2-IT flange region has been observed on ~70% of missions where imagery was available

Presenter M3/Material | Date FINAL | Slide 2 of 8 | Closed

ET – Foam Design – Certification

- **Recommendations:**
  - NASA must understand the relationship between the complex LH2-IT flange geometry and the high rate of foam loss from this region
    - Current testing efforts at MSFC and MAF should continue
  - NASA should use knowledge gained from testing and analysis of the current LH2-IT flange geometry to redesign this area
    - Redesign efforts should include, but not be limited to, considerations of:
      - minimizing the ability for nitrogen to come in contact with foam or SLA
      - replacing the existing intertank nitrogen purge with a helium purge
      - structural changes that eliminate or reduce all vent paths in the flange region

Presenter M3/Material | Date FINAL | Slide 3 of 8 | Closed

ET – Foam Design – Certification

LH2-IT Geometry

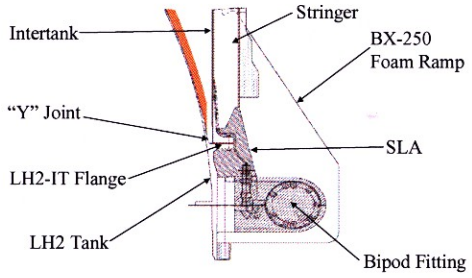

Presenter M3/Material | Date FINAL | Slide 4 of 8 | Closed

ET – Foam Design – Certification

LN2 Collection Areas

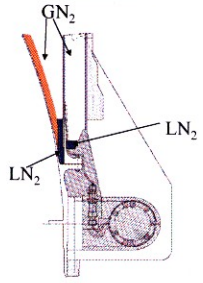

Presenter M3/Material | Date FINAL | Slide 5 of 8 | Closed

ET – Foam Design – Certification

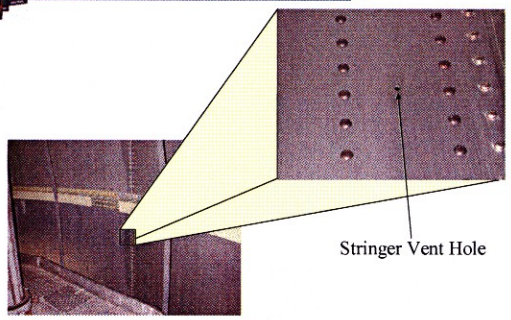

Presenter M3/Material | Date FINAL | Slide 6 of 8 | Closed

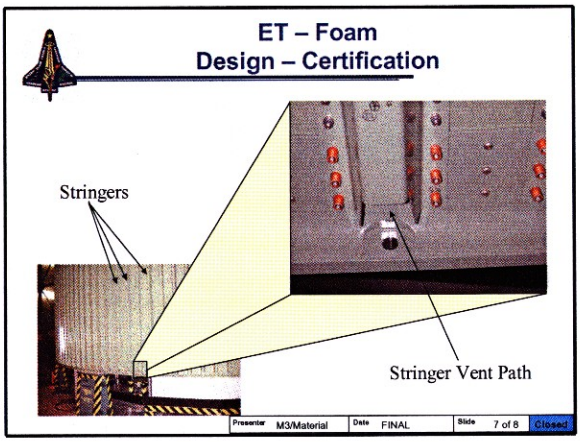
ET – Foam
Design – Certification
Stringers
Stringer Vent Path
Presenter M3/Material
Date FINAL
Slide 7 of 8
Closed

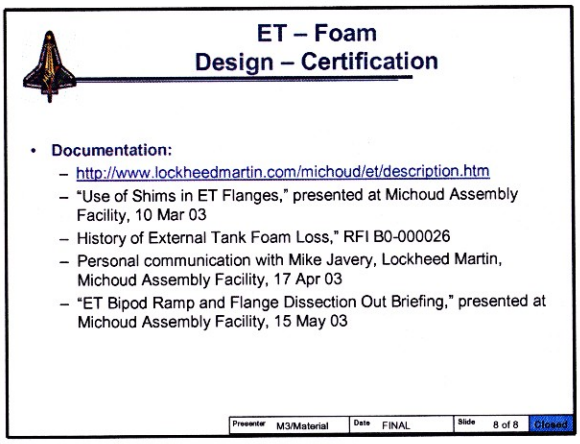
ET – Foam
Design – Certification
• Documentation:
– http://www.lockheedmartin.com/michoud/et/description.htm
– "Use of Shims in ET Flanges," presented at Michoud Assembly Facility, 10 Mar 03
– History of External Tank Foam Loss," RFI B0-000026
– Personal communication with Mike Javery, Lockheed Martin, Michoud Assembly Facility, 17 Apr 03
– "ET Bipod Ramp and Flange Dissection Out Briefing," presented at Michoud Assembly Facility, 15 May 03
Presenter M3/Material
Date FINAL
Slide 8 of 8
Closed

ET – Foam Design – Certification

- **Action / Issue:**
  - Stringer valley cracks have been documented as occurring on super lightweights more frequently than on other tanks
- **Background / Facts:**
  - Cracks in the valleys between stingers (external stiffening elements) on the intertank have been observed on several missions on all types of tanks
    - Standard weight [eg. ET-6]
    - Lightweight [eg. ET-29 & ET-35]
    - SLWT
  - However, the occurrence of these cracks have been identified more often beginning with the first SLWT, ET-96, launched with mission STS-91 in June 1998

Presenter M3/Material | Date FINAL | Slide 1 of 6 | Closed

ET – Foam Design – Certification

- **Findings:**
  - Subsequent to the change to super lightweight tanks, final inspection teams started seeing cracks in the intertank stringer valleys more frequently than on lightweight or standard tanks
    - It is believed these cracks form during tanking as a form of stress relief as the aluminum ET cools and contracts
      - Hypothesis: thinner, machined foam in these areas (part of the super lightweight design) is more susceptible to cracking
    - Ice/Debris Team inspection & documentation procedures have not changed with respect to stringer valley cracks
    - Cracks are more difficult to spot in machined foam
    - Thus, so the sudden increase in the numbers of cracks observed with the advent of the SLWT appears to be real.
  - A comprehensive review of historical records has not been performed
    - However a quick data search shows that these cracks were rarely recorded prior to the SLWT inception
  - These cracks, if underneath the bipod ramp, could provide a possible reservoir for LN2

Presenter M3/Material | Date FINAL | Slide 2 of 6 | Closed

ET – Foam Design – Certification

- **Recommendations:**
  - NASA should continue tests currently underway at MSFC and MAF to understand cryopumping and cryoingestion
    - The tests involving full-scale mock-ups of the LH2-IT should be monitored for the presence of stringer valley cracks
  - NASA should plan to continue additional analysis and testing on the SLWT configuration to understand the cause of these cracks, their effects, and ways to prevent them from occurring
    - If these cracks are found to be detrimental, NASA should take steps to prevent them

Presenter M3/Material | Date FINAL | Slide 3 of 6 | Closed

ET – Foam Design – Certification

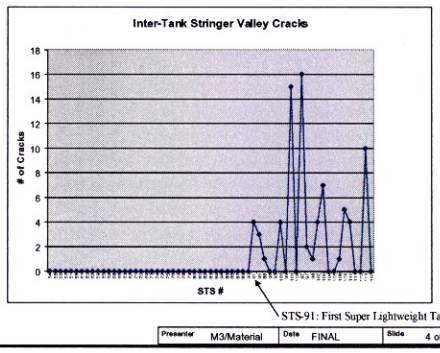

Presenter M3/Material | Date FINAL | Slide 4 of 6 | Closed

ET – Foam Design – Certification

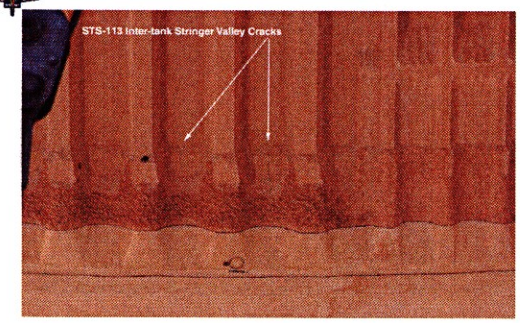

Presenter M3/Material | Date FINAL | Slide 5 of 6 | Closed

ET – Foam Design – Certification

- **Documentation:**
  - "Lessons Learned: From Space Shuttle External Tank Development – A Technical History of the External Tank", October 30, 2002
  - Final Inspection Intertank Cracks Request for Information, RFI #B1-000134
  - Discussions with Armando Oliu, 24 March 2003
  - Discussions at Michoud Assembly Facility, 02 April 2003
  - Personal Communication, J. Feeley, Michoud Assembly Facility, 12 Jun 03.
  - E-mail, M. Quiggle, Michoud Assembly Facility, 19-23 Jun 03.

Presenter M3/Material | Date FINAL | Slide 6 of 6 | Closed

1

ET – Foam Production

2-1 Blowing Agent Changes

2-2 Manual Spraying Operations

2-3 Processing Environment Controls for Foam Applications

2-4 NDE for ET During Production

Matrix

Presenter	CAIB/Group 1	Date	FINAL	Slide	4 of 32

ET – Foam Production

- **Action / Issue:**
  Concerns exist about changes to blowing agents used in ET foams and their influence on foam properties
- **Background / Facts:**
  - 1978: US bans CFCs in aerosol sprays
  - 1988: US Senate approves Montreal Protocol
  - 1988: Martin Marietta initiates activities to screen CFC alternates
  - 1990: Clean Air Act Amendment rules phase-out of CFCs by 2000
  - 1991: Martin Marietta selects best CFC alternative (HCFC 141b)
  - 1993: CFC 11 manufacture discontinued
    NASA chooses not to pursue "Essential Use Exemption" for production of CFC 11 after remaining stockpile exhausted
  - 1995: SS 1171 (HCFC 141b) chosen to replace BX 250 (CFC 11)
    CFC 11 stock secured by Martin Marietta to continue BX 250 production

Presenter M3/Material | Date FINAL | Slide 1 of 7 | Closed

ET – Foam Production

- **Background / Facts: (cont.)**
  - 1998: Problems with SS 1171 force continued use of BX 250
  - 2001: BX 265 (HCFC 141b) chosen to replace BX 250 (CFC 11)
  - 2002: BX 265 implemented on ET-117 (MAF) & ET-116 (KSC)
  - 2003: EPA phase-out of HCFC 141b production takes effect
    Waiver for continued HCFC 141b production approved for NASA
- **Findings:**
  - Thousands of tests conducted to develop & qualify each ET foam
  - Change in blowing agents for acreage foam (from CPR 488 to NCFI 24-124) caused "popcorning" earlier in ascent profile
    - Popcorning = small pieces lost from thrust panels
      - Popcorning earlier in ascent results in debris with higher energy
    - Early popcorning first observed on STS-84/ET-85
    - Resulted in extensive tile damage on STS-87/ET-89

Presenter M3/Material | Date FINAL | Slide 2 of 7 | Closed

ET – Foam Production

- **Findings: (cont.)**
  - First attempt to change blowing agents for closeout foam (from BX 250 to SF-1171) failed due to production issues
    - Second change attempt (from BX 250 to BX 265)successful; first flown on STS-113 with ET-116
- **Recommendations:**
  - NASA should transition to a new blowing agent only if performance improvements in the foam can be achieved (e.g., greater stability – less shedding)
  - Foam blowing agent requirements should be reviewed to verify they are sufficient and specify the correct properties & attributes
  - NASA should continue complete and thorough testing of foam blowing agents to understand flight implications and minimize risks

Presenter M3/Material | Date FINAL | Slide 3 of 7 | Closed

ET – Foam Production

New foams (w/HCFC 141b) meet all requirements

Foam / Property	(New) NCFI 24-124 (Old) CPR 488			(New) NCFI 24-57 (Old) NCFI 22-65			(New) PDL 1034 (Old) PDL 4034			(New) BX 265 (Old) BX 250		
(% of total foam)	(77%)			(7%)			(1%)			(14%)		
Application	LH2,LO2,RT sidewall			LH2 aft dome			Closeouts and repairs			LH2 forward dome, LO2 aft dome, closeouts		
Process	Spray			Spray			Pour/Mold			Spray		
Description	Isocyanurate			Isocyanurate			Urethane			Urethane		
Requirements	Spec Req.	Typ Prop	Flt Req.	Spec Req.	Typ Prop	Flt Req.	Spec Req.	Typ Prop	Flt Req.	Spec Req.	Typ Prop	Flt Req.
Density PCF	2.0-2.5 2.1-2.6	2.47 2.4	Lighter[4]	2.8-3.1 2.8-3.1	2.87 2.90	Heavier[4]	2.2-3.1 2.3-3.1	2.8 2.6	same[4]	1.9-2.6 1.8-2.6	2.4 2.4	same[4]
Tensile RT (psi)	30min 30min	66 64	19	60min 40min	88 71	19	60 60	113 104	19	30min 30min	82 76	19
Tensile -423°F (psi)	N/A[1]	34 41	19	N/A	48 47	19	N/A	49 49	19	N/A	82 83	19
Tensile +300°F (psi)	N/A	32 37	19	N/A	38 46	19	N/A	717 53	19	N/A	38[5] 47	19
Compression (psi)	30min 24min	33 49	26	30min 30min	49 51	39	30 30	61 42	26	30min 24min	36 46	39
Recession Rate @ 7 BTU/ft sq sec (in/sec)	N/A	0.0156 0.0188	lower[4]	N/A	0.0098[2] 0.0098[2]	same[4]	N/A	0.0343 0.0236	higher[4]	N/A	0.0177 0.024	lower[4]
Thermal Cond @ R/T BTU/hr ft °F	0.025	0.017 0.017	same[4]	0.0226 0.0188	0.0188 0.0186	higher[4]	0.015 0.016	0.015 0.012	higher[4]	0.015 0.015	0.013 0.011	higher[4]
Cryostrain (ue)	818-423	568-423 568-423	pass	568-423	568-423 568-423	pass	N/A	568-328 568-328	pass	N/A	568-423 568-423	pass

[1] N/A- Not Applicable
[2] @ + 200°F
[2] 200°F Values
[4] Means new vs. old
[3] @ 4 BTU/ft sq sec Radiant heating
[5] Max density 3.0 in dome area allowed. *7.4 – 2.8 PCF for thick/thin

Presenter M3/Material | Date FINAL | Slide 4 of 7 | Closed

ET – Foam Production

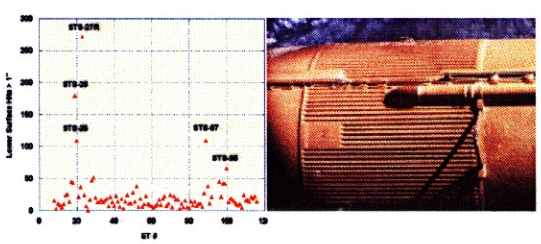

Presenter M3/Material | Date FINAL | Slide 5 of 7 | Closed

ET – Foam Production

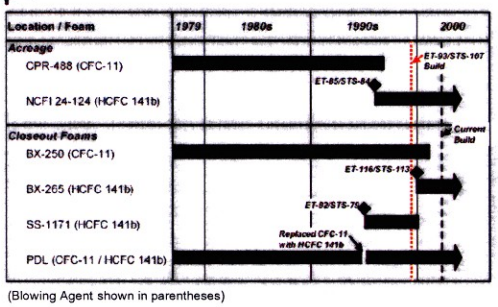

(Blowing Agent shown in parentheses)

Presenter M3/Material | Date FINAL | Slide 6 of 7 | Closed

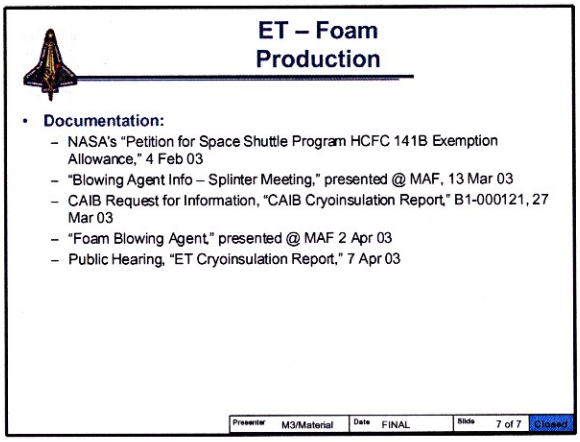
ET – Foam Production
• Documentation:
– NASA's "Petition for Space Shuttle Program HCFC 141B Exemption Allowance," 4 Feb 03
– "Blowing Agent Info – Splinter Meeting," presented @ MAF, 13 Mar 03
– CAIB Request for Information, "CAIB Cryoinsulation Report," B1-000121, 27 Mar 03
– "Foam Blowing Agent," presented @ MAF 2 Apr 03
– Public Hearing, "ET Cryoinsulation Report," 7 Apr 03
Presenter M3/Material
Date FINAL
Slide 7 of 7
Closed

ET – Foam Production

- **Action / Issue:**
  - Manual spraying operations of complex and closeout areas are not sufficiently controlled
- **Background / Facts:**
  - Operators must be qualified to hand spray foam
  - Each spraying operation is unique and is operator dependent
  - Control of spraying variables has been limited except in the flange closeout area
    - Special techniques with limited qualified operators are now used due to prior problems in the flange closeout area
  - Spraying operations can be either one or two people depending on the operator's preference
  - Complex shapes and access to the area being sprayed makes these operations even more difficult to control

Presenter M3/Material | Date FINAL | Slide 1 of 6 | Closed

ET – Foam Production

- **Findings:**
  - Dissection of various bipod and flange closeout areas has revealed that defects are introduced during the spraying operation
  - Defects tend to occur in complex geometry regions or where there is limited access for operators during the spray evolution
  - Defects are random and unpredictable
  - There have been limited attempts to control spraying variables except in the flange closeout area
  - Summary: complexity of areas to be sprayed + variability in operator techniques = a unique product with insufficient/unknown foam quality

Presenter M3/Material | Date FINAL | Slide 2 of 6 | Closed

ET – Foam Production

- **Recommendations:**
  - Efforts should be made to try and standardize (control) the hand spraying process as much as possible
    - If automated processes can be put in place to spray these areas, such as is currently done on the acreage foam, every effort should be made to make that transition
    - In areas where hand spraying must continue, operators should be qualified to spray all complex geometries
  - There should be no foam application processes requiring less than two people

Presenter M3/Material | Date FINAL | Slide 3 of 6 | Closed

ET – Foam Production

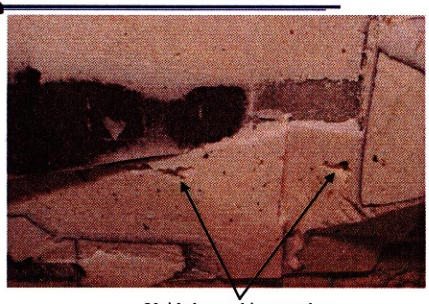

Voids located in complex geometry areas

Presenter M3/Material | Date FINAL | Slide 4 of 6 | Closed

ET – Foam Production

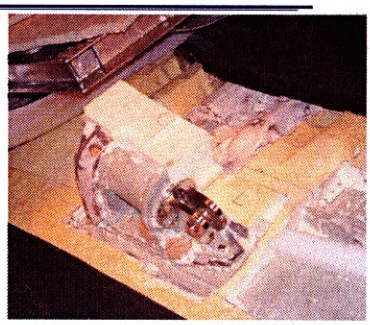

Complex spray areas around bipod fixture

Presenter M3/Material | Date FINAL | Slide 5 of 6 | Closed

ET – Foam Production

- **Documentation:**
  - Personal observations at Michoud Assembly Facility (MAF), February – May 2003
  - Discussions with Lockheed Martin personnel, MAF, February to May 2003
  - Discussion with Marshall Space Flight Center/MAF personnel, 02 April 2003
  - ET Shedding – Composite Request for Information, RFI #B0-000026
  - ET-120 Dissection Outbrief, 10 April 2003

Presenter M3/Material | Date FINAL | Slide 6 of 6 | Closed

ET – Foam Production

- **Action / Issue:**
  - Process controls (especially those for temperature and humidity) may be insufficient to permit consistently high quality foam application.
- **Background / Facts:**
  - Spraying operations must be within required environmental conditions
  - Boundaries of the environmental conditions are considered to be conservative to guarantee proper foam performance
  - Plug pulls are performed subsequent to spraying operations to verify proper material bonding and strength

Presenter M3/Material | Date FINAL | Slide 1 of 6 | Closed

ET – Foam Production

- **Findings:**
  - Most spraying operations occur at or near the outer acceptable boundaries of the processing envelope
  - Large variability in the response of the foam based on inherent randomness of foam cell structure
  - Plug pulls, as a single indicator, might not be sufficient to verify the foam's bonding and strength properties

Presenter M3/Material | Date FINAL | Slide 2 of 6 | Closed

ET – Foam Production

- **Recommendations:**
  - Foam loss history should be looked at for correlation to processing environments and plug pull values
  - The processing envelope should be revalidated and attempts should be made to try and perform spraying operations more towards the center of the defined envelopes vice at the outer edges
  - Plug pull requirements should also be revalidated and the actual usefulness of these tests to determine overall foam application worthiness should be questioned
    - Localized plug values might not be telling the story for the whole tank

Presenter M3/Material | Date FINAL | Slide 3 of 6 | Closed

ET – Foam Production

Recent TPS Processing Data

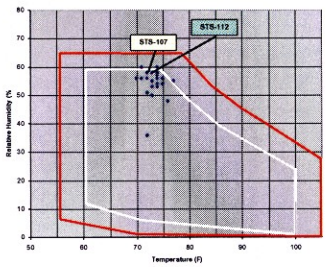

Absolute Limits in RED. Processing Envelope in WHITE.

Presenter M3/Material | Date FINAL | Slide 4 of 6 | Closed

ET – Foam Production

Recent TPS Processing Data

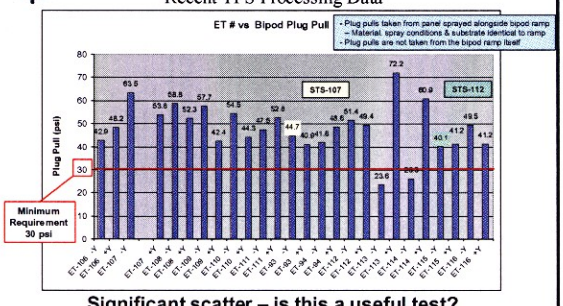

Significant scatter – is this a useful test?

Presenter M3/Material | Date FINAL | Slide 5 of 6 | Closed

ET – Foam Production

- **Documentation:**
  - CAIB Public Hearing – ET Cryoinsulation, Lee Foster and Scotty Sparks, 07 April 2003
  - Discussions with Michoud Assembly Facility personnel, February 2003

Presenter M3/Material | Date FINAL | Slide 6 of 6 | Closed

ET – Foam Production

- **Action / Issue:** No validated NDE techniques are available to identify subsurface damage within ET foam during or after production
- **Background / Facts:**
  - Extensive NDE is performed on welded aluminum sections of ET
  - No NDE performed on ET thermal protection system (TPS) except:
    - Visual checks during and after production
    - Eddy current checks for thickness
    - Preflight ice/debris inspections
    - Plug pulls & witness panels (*destructive* tests)
  - Previous efforts at MAF (1986-93) were unsuccessful in identifying NDE technologies that could be readily implemented
  - Boeing has had success using laser shearography on acreage foam of Delta-IV boosters, but
    - Geometry is much less complex than that of ET
    - Inspection requirement is for larger defects

Presenter M3/Material | Date FINAL | Slide 1 of 13 | Closed

ET – Foam Production

- **Findings:**
  - Previous tests of laser shearography on flat foam panels indicated the technique had promise as a potential NDE technique for foam
    - Some promise also seen on flat panels with intertank geometry
    - Additional work is required to develop technique for production
  - Production checks for foam quality are:
    - Visual -or-
    - Require destructive testing (plug pulls) -or-
    - Test representative foam sample rather than foam actually applied to tank ("witness panels")
  - Dissections of bipod foam ramps on ET-94, ET-120, and ET-124 revealed that production defects in foam are common
    - Laser Shearography and X-ray NDE indications provided minimal correlation with physical observations

Presenter M3/Material | Date FINAL | Slide 2 of 13 | Closed

ET – Foam Production

- **Findings:** (cont.)
  - MAF and MSFC are actively pursuing development of an NDE technique to use on hand-sprayed closeouts
    - Candidate techniques include: X-ray (radiography), backscatter X-ray, shearography, microwave, and terahertz
    - Experts in field among are in Working Group All post-build & KSC processing inspections of the ET are visual
    - No NDE is used to confirm or size regions needing repair
    - Visual examination relies on experienced personnel
      - Especially the Ice/Debris Team at KSC
  - LTI (John Newman) has estimated that 12-24 months is needed to develop shearography scanner hardware for the ET
    - Standards and procedures would also be required in addition to hardware

Presenter M3/Material | Date FINAL | Slide 3 of 13 | Closed

ET – Foam Production

- **Recommendations:**
  - Potential Return to Flight Recommendation: NASA should continue to pursue the development, validation, and implementation of NDE techniques that can be used to interrogate ET foam during production
  - NASA should continue to pursue the development, validation, and implementation of NDE techniques that can be used to interrogate ET foam following production (i.e. at KSC prior to launch)

Presenter M3/Material | Date FINAL | Slide 4 of 13 | Closed

ET – Foam Production

Laser shearography in use on Boeing Delta IV boosters

Presenter M3/Material | Date FINAL | Slide 5 of 13 | Closed

ET – Foam Production

NDE of 9" thick foam block revealed defects as small as 3" in diameter

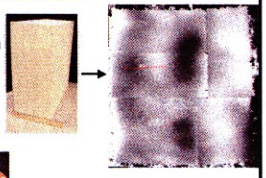

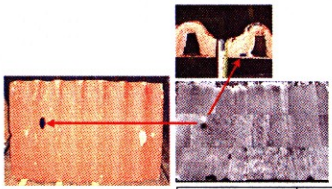

NDE of flat panels with intertank geometry yielded promising results

Presenter M3/Material | Date FINAL | Slide 6 of 13 | Closed

1

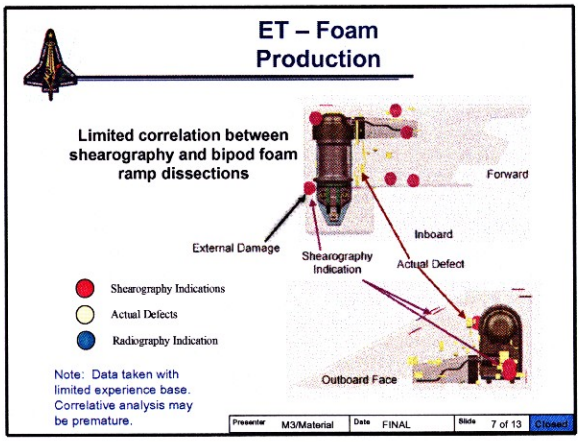
ET – Foam Production
Limited correlation between shearography and bipod foam ramp dissections
Forward
External Damage
Shearography Indication
Inboard
Actual Defect
Shearography Indications
Actual Defects
Radiography Indication
Outboard Face
Note: Data taken with limited experience base. Correlative analysis may be premature.
Presenter M3/Material
Date FINAL
Slide 7 of 13
Closed

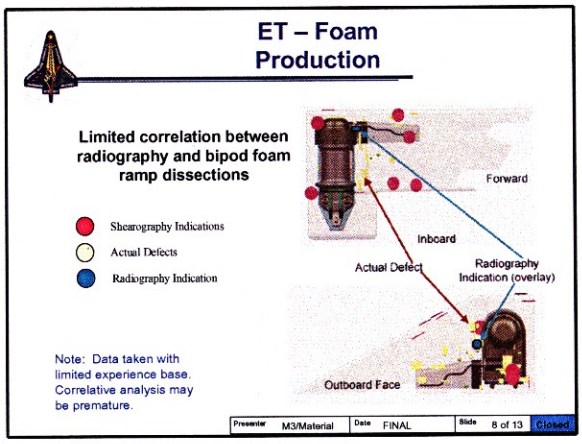
ET – Foam Production
Limited correlation between radiography and bipod foam ramp dissections
Forward
Shearography Indications
Actual Defects
Radiography Indication
Inboard
Actual Defect
Radiography Indication (overlay)
Outboard Face
Note: Data taken with limited experience base. Correlative analysis may be premature.
Presenter M3/Material
Date FINAL
Slide 8 of 13
Closed

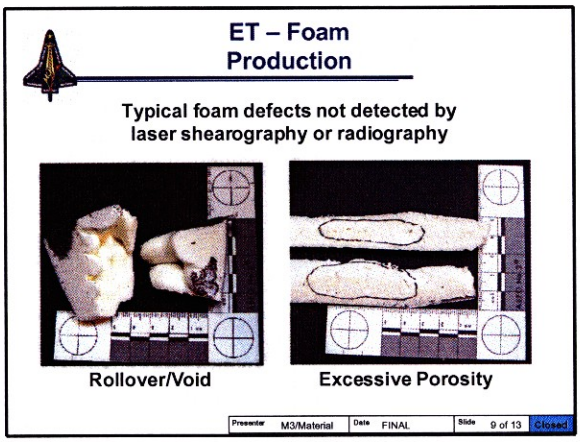
ET – Foam Production
Typical foam defects not detected by laser shearography or radiography
Rollover/Void
Excessive Porosity
Presenter M3/Material
Date FINAL
Slide 9 of 13
Closed

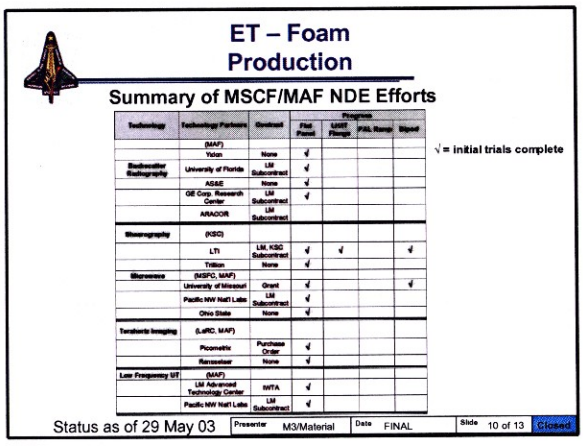
ET – Foam Production
Summary of MSCF/MAF NDE Efforts
√ = initial trials complete
Status as of 29 May 03
Presenter M3/Material
Date FINAL
Slide 10 of 13
Closed

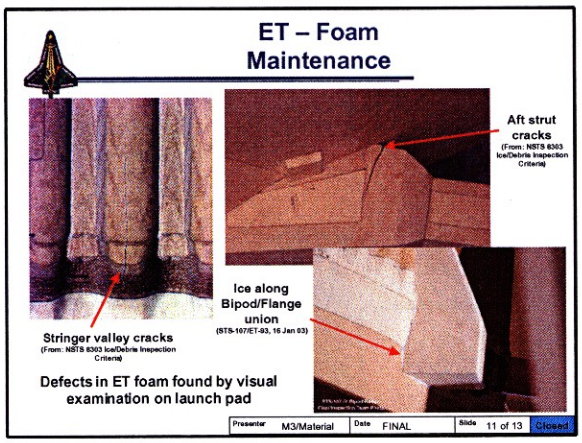
ET – Foam Maintenance
Aft strut cracks
(From: NSTS 8303 Ice/Debris Inspection Criteria)
Ice along Bipod/Flange union
(STS-107/ET-93, 16 Jan 03)
Stringer valley cracks
(From: NSTS 8303 Ice/Debris Inspection Criteria)
Defects in ET foam found by visual examination on launch pad
Presenter M3/Material
Date FINAL
Slide 11 of 13
Closed

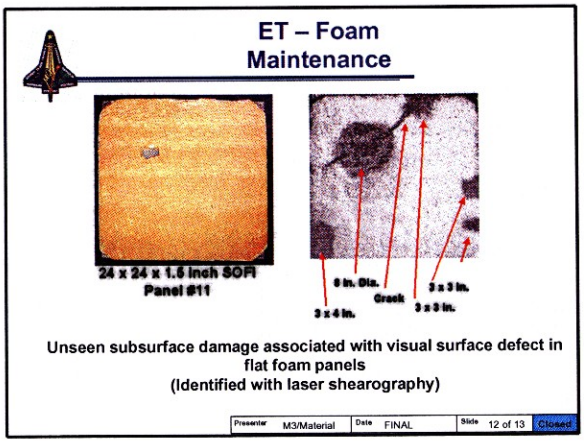
ET – Foam Maintenance
24 x 24 x 1.5 inch SOFI Panel #11
8 in. Dia.
Crack
3 x 4 in.
3 x 3 in.
3 x 3 in.
Unseen subsurface damage associated with visual surface defect in flat foam panels
(Identified with laser shearography)
Presenter M3/Material
Date FINAL
Slide 12 of 13
Closed

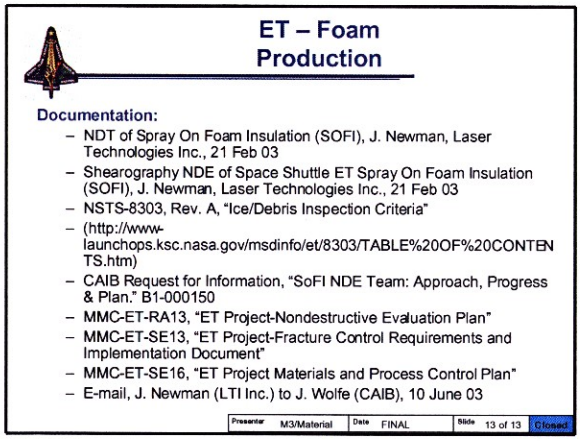
ET – Foam Production
Documentation:
– NDT of Spray On Foam Insulation (SOFI), J. Newman, Laser Technologies Inc., 21 Feb 03
– Shearography NDE of Space Shuttle ET Spray On Foam Insulation (SOFI), J. Newman, Laser Technologies Inc., 21 Feb 03
– NSTS-8303, Rev. A, "Ice/Debris Inspection Criteria"
– (http://www-launchops.ksc.nasa.gov/msdinfo/et/8303/TABLE%20OF%20CONTENTS.htm)
– CAIB Request for Information, "SoFI NDE Team: Approach, Progress & Plan." B1-000150
– MMC-ET-RA13, "ET Project-Nondestructive Evaluation Plan"
– MMC-ET-SE13, "ET Project-Fracture Control Requirements and Implementation Document"
– MMC-ET-SE16, "ET Project Materials and Process Control Plan"
– E-mail, J. Newman (LTI Inc.) to J. Wolfe (CAIB), 10 June 03
Presenter M3/Material
Date FINAL
Slide 13 of 13
Closed

3

ET – Foam Maintenance

3-2 ET Storage, Shipping, and Handling

3-4 Crushed Foam from Mate/De-Mate of ET-93

Matrix

Presenter	CAIB/Group 1	Date	FINAL	Slide	5 of 32

ET – Foam Maintenance

- **Action / Issue:** Foam crushed beneath the –Y (left side) bipod strut clevis during pre-launch mating & demating with the bipod strut may have contributed to the loss of the –Y bipod foam ramp from ET-93 during STS-107.
- **Background / Facts:**
  - ET-93 mated to SRBs on 8 May 02 in VAB; de-mated on 28 Aug 02
  - ET-93 mated to bipod on 24 Jun 02 in VAB; de-mated on 1 Aug 02
  - Operations carried out in accordance with standard procedures
  - Crushed foam seen after -Y strut removal (1.5" x 1.25" x 0.187")
    - Beneath –Y fitting-clevis joint after bipod struts removed
  - Thickness of foam in this area: 2.187"
  - Exposed crushed foam not permissible; Problem Report written
  - Testing was performed @ MAF and KSC (on ET-117) to determine:
    - If crushed foam on ET-93 could have caused loss of –Y bipod ramp
    - If limits specified in PR procedures were sufficient

Presenter M3/Material | Date FINAL | Slide 1 of 12 | Closed

ET – Foam Maintenance

ET-93 Processing Timeline at KSC

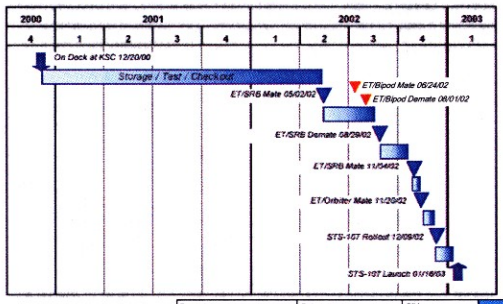

Presenter M3/Material | Date FINAL | Slide 2 of 12 | Closed

ET – Foam Maintenance

- **Findings:**
  - Crushed foam is always present at ET bipod attach points
    - Specifically designed to be an "interference fit"
  - KSC engineers decided to defer action on PR. Rationale:
    - Crushed foam was contained beneath bipod strut clevis after mating to a new set of bipod struts
    - Unexposed (i.e. contained) crushed foam is permissible
  - Inspection of region after installation of bipod struts showed that crushed foam did not extend further than 0.75" beyond bipod fitting-clevis joint
    - Within acceptable limits
  - STS-107 launched with crushed foam contained behind –Y bipod strut clevis

Presenter M3/Material | Date FINAL | Slide 3 of 12 | Closed

ET – Foam Maintenance

- **Findings: (cont.)**
  - Three other mate-de-mate instances occurred on shuttle program; unknown link between mating/de-mating & foam loss
    - ET-13 used on STS-14(41D)
      - No imagery to confirm/deny foam loss
    - ET-23 used on STS-27R
      - Handheld video imagery; bipod ramps not visible, no other loss noted
      - Mated & de-mated during checkout of Vandenberg AFB facilities
      - Extensive tile damage due to the loss of SRB ablator during launch
    - ET-80 used on STS-80
      - Lost 2 divots on flange under bipod
      - Lost one 10-inch diameter divot on intertank forward of –Y bipod ramp

Presenter M3/Material | Date FINAL | Slide 4 of 12 | Closed

ET – Foam Maintenance

- **Findings: (cont.)**
  - Crushed foam testing conducted at MAF & KSC (on ET-117)
    - Red dye indicated extent of damage to be limited to a maximum of 0.5" beyond region visibly crushed with aid of dye
      - Within acceptable limit
      - Receives little/no airflow with bipod strut installed
    - Undamaged foam thickness was over 2" on ET-117
      - No ice/frost potential
    - Localized damage would have no impact on performance of ramp
    - Results indicate no contribution from crushed foam to the loss of the bipod foam ramp on ET-93
- **Recommendations:**
  - None

Presenter M3/Material | Date FINAL | Slide 5 of 12 | Closed

ET – Foam Maintenance

Problem Report (PR ET-93-ST-003)

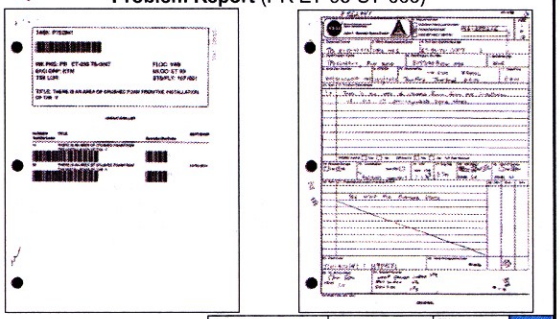

Presenter M3/Material | Date FINAL | Slide 6 of 12 | Closed

1

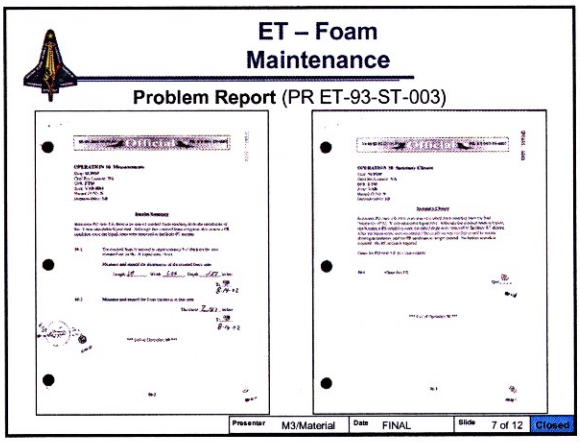
ET – Foam Maintenance
Problem Report (PR ET-93-ST-003)
Presenter M3/Material Date FINAL Slide 7 of 12 Closed

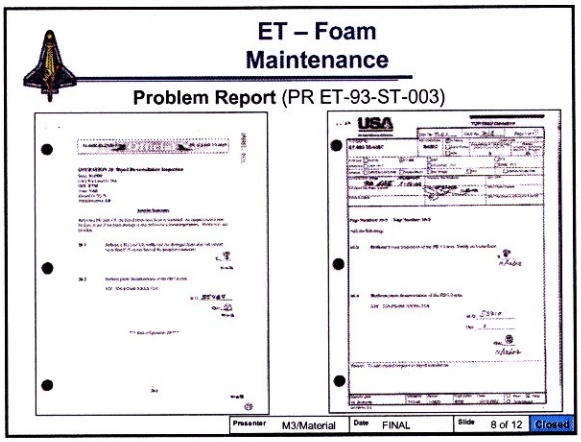
ET – Foam Maintenance
Problem Report (PR ET-93-ST-003)
Presenter M3/Material Date FINAL Slide 8 of 12 Closed

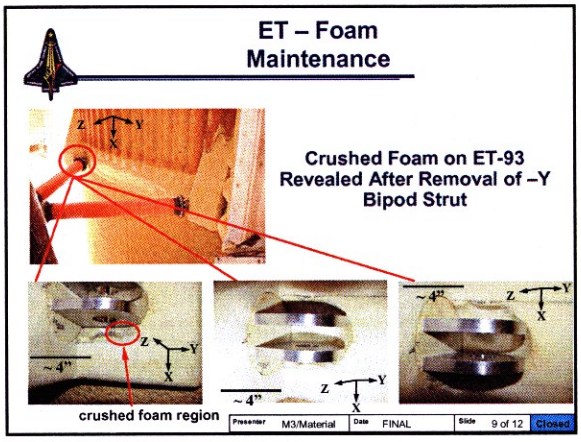
ET – Foam Maintenance
Crushed Foam on ET-93 Revealed After Removal of –Y Bipod Strut
~4"
crushed foam region
Presenter M3/Material Date FINAL Slide 9 of 12 Closed

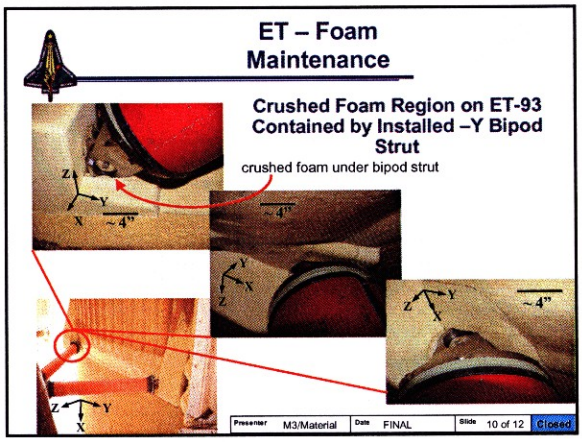
ET – Foam Maintenance
Crushed Foam Region on ET-93 Contained by Installed –Y Bipod Strut
crushed foam under bipod strut
~4"
Presenter M3/Material Date FINAL Slide 10 of 12 Closed

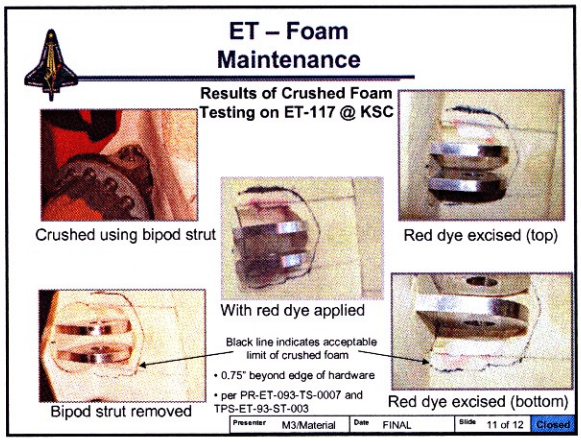
ET – Foam Maintenance
Results of Crushed Foam Testing on ET-117 @ KSC
Crushed using bipod strut
Red dye excised (top)
With red dye applied
Black line indicates acceptable limit of crushed foam
• 0.75" beyond edge of hardware
• per PR-ET-093-TS-0007 and TPS-ET-93-ST-003
Bipod strut removed
Red dye excised (bottom)
Presenter M3/Material Date FINAL Slide 11 of 12 Closed

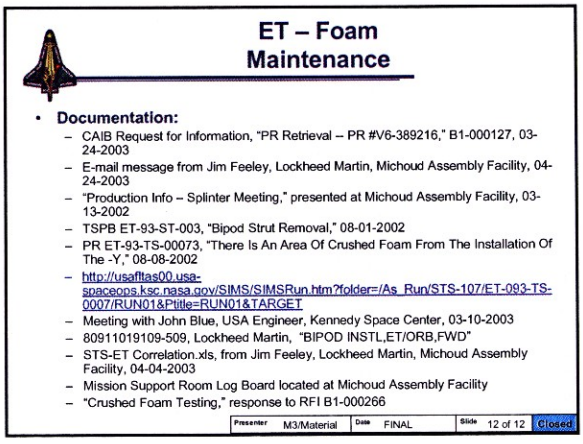
ET – Foam Maintenance
• Documentation:
– CAIB Request for Information, "PR Retrieval – PR #V6-389216," B1-000127, 03-24-2003
– E-mail message from Jim Feeley, Lockheed Martin, Michoud Assembly Facility, 04-24-2003
– "Production Info – Splinter Meeting," presented at Michoud Assembly Facility, 03-13-2002
– TSPB ET-93-ST-003, "Bipod Strut Removal," 08-01-2002
– PR ET-93-TS-00073, "There Is An Area Of Crushed Foam From The Installation Of The -Y," 08-08-2002
– http://usafltas00.usa-spaceops.ksc.nasa.gov/SIMS/SIMSRun.htm?folder=/As_Run/STS-107/ET-093-TS-0007/RUN01&Ptitle=RUN01&TARGET
– Meeting with John Blue, USA Engineer, Kennedy Space Center, 03-10-2003
– 80911019109-509, Lockheed Martin, "BIPOD INSTL,ET/ORB,FWD"
– STS-ET Correlation.xls, from Jim Feeley, Lockheed Martin, Michoud Assembly Facility, 04-04-2003
– Mission Support Room Log Board located at Michoud Assembly Facility
– "Crushed Foam Testing," response to RFI B1-000266
Presenter M3/Material Date FINAL Slide 12 of 12 Closed

ET – Foam Maintenance

- **Action / Issue:** A concern existed that improper storage and handling of the ET between its completion and launch may have damaged foam and contributed to foam loss during the ascent of STS-107.
- **Background / Facts:**
  - Post-build activities include storage at MAF, shipment to KSC, processing at KSC, and mating to SRBs and orbiter
- **Findings:**
  - Extensive documentation governs steps taken to care for ET
  - Storage takes place in locked, limited-access facilities
  - Tanks are pressured with nitrogen or helium to 6.0 +/- 0.5 psi
    - Pressure checked every 2 weeks at MAF, every week at KSC
  - Visual inspections performed every 90 days
  - ET is inspected 7 times between arrival at KSC and launch
    - This does not count daily inspections when stack exists

Presenter M3/Material | Date FINAL | Slide 1 of 9 | Closed

ET – Foam Maintenance

- **Findings (cont.):**
  - Protective covers are used for 14 areas with historically significant potential rates of damage due to collateral operations
  - Repairs performed by KSC with assistance from MAF if needed
    - Repaired areas inspected for "collateral" damage after repairs made
  - Post STS-107 paper review by KSC examined 56,000 pages of documentation
    - No contributing events identified
- **Recommendations:**
  - None
    - Processes appear to be in place and followed to ensure that shipping and handling is performed in a manner that minimizes damage to the ET

Presenter M3/Material | Date FINAL | Slide 2 of 9 | Closed

ET – Foam Maintenance

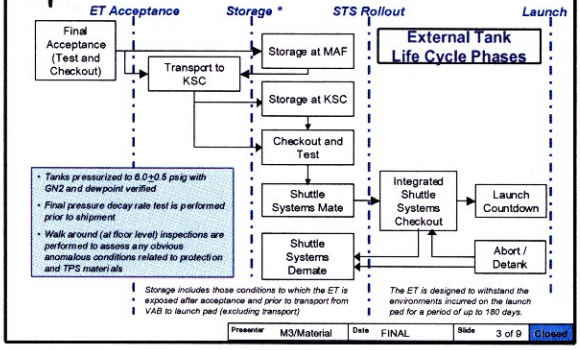

Presenter M3/Material | Date FINAL | Slide 3 of 9 | Closed

ET – Foam Maintenance

Maneuvering the ET at Michoud Assembly Facility

(~ 10 personnel act as spotters inside and outside the storage facility)

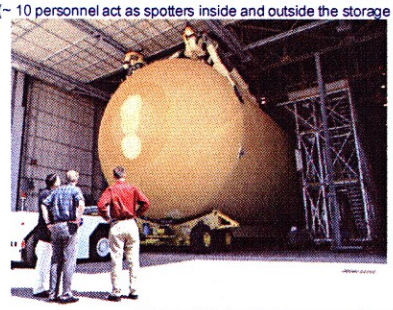

Presenter M3/Material | Date FINAL | Slide 4 of 9 | Closed

ET – Foam Maintenance

ET shipped from MAF to KSC via Barge

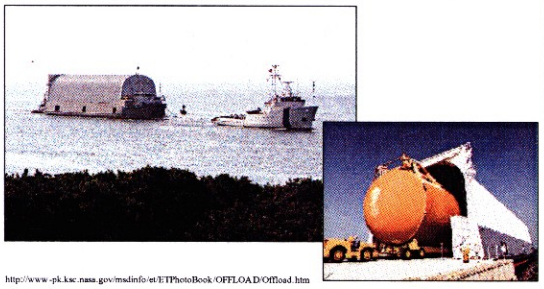

http://www-pk.ksc.nasa.gov/msdinfo/et/ETPhotoBook/OFFLOAD/Offload.htm

Presenter M3/Material | Date FINAL | Slide 5 of 9 | Closed

ET – Foam Maintenance

Raising the ET for Stacking in the Vehicle Assembly Building at KSC

Presenter M3/Material | Date FINAL | Slide 6 of 9 | Closed

1

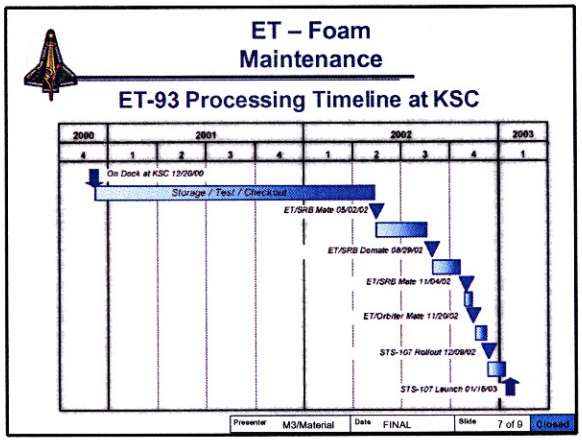
ET – Foam Maintenance
ET-93 Processing Timeline at KSC
2000
2001
2002
2003
On Dock at KSC 12/20/00
Storage / Test / Checkout
ET/SRB Mate 05/02/02
ET/SRB Demate 08/29/02
ET/SRB Mate 11/04/02
ET/Orbiter Mate 11/29/02
STS-107 Rollout 12/09/02
STS-107 Launch 01/16/03
Presenter M3/Material
Date FINAL
Slide 7 of 9
Closed

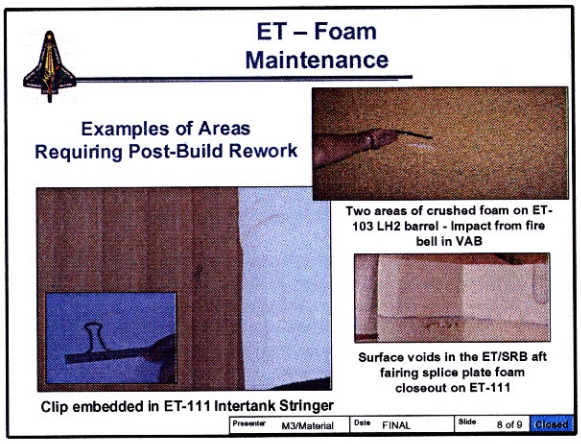
ET – Foam Maintenance
Examples of Areas Requiring Post-Build Rework
Two areas of crushed foam on ET-103 LH2 barrel - Impact from fire bell in VAB
Surface voids in the ET/SRB aft fairing splice plate foam closeout on ET-111
Clip embedded in ET-111 Intertank Stringer
Presenter M3/Material
Date FINAL
Slide 8 of 9
Closed

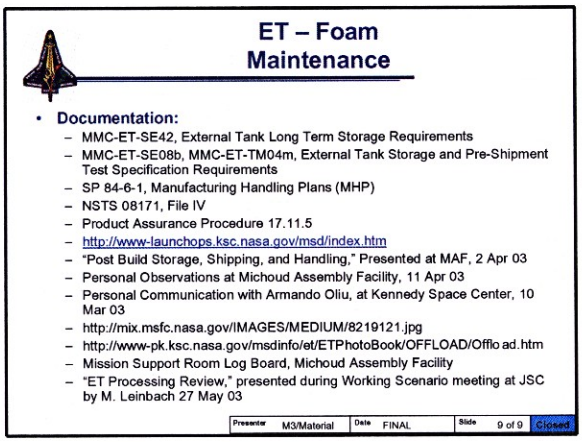
ET – Foam Maintenance
• Documentation:
– MMC-ET-SE42, External Tank Long Term Storage Requirements
– MMC-ET-SE08b, MMC-ET-TM04m, External Tank Storage and Pre-Shipment Test Specification Requirements
– SP 84-6-1, Manufacturing Handling Plans (MHP)
– NSTS 08171, File IV
– Product Assurance Procedure 17.11.5
– http://www-launchops.ksc.nasa.gov/msd/index.htm
– "Post Build Storage, Shipping, and Handling," Presented at MAF, 2 Apr 03
– Personal Observations at Michoud Assembly Facility, 11 Apr 03
– Personal Communication with Armando Oliu, at Kennedy Space Center, 10 Mar 03
– http://mix.msfc.nasa.gov/IMAGES/MEDIUM/8219121.jpg
– http://www-pk.ksc.nasa.gov/msdinfo/et/ETPhotoBook/OFFLOAD/Offlo ad.htm
– Mission Support Room Log Board, Michoud Assembly Facility
– "ET Processing Review," presented during Working Scenario meeting at JSC by M. Leinbach 27 May 03
Presenter M3/Material
Date FINAL
Slide 9 of 9
Closed

ET – Foam
Launch – Ascent

4-1 Cryopumping
4-2 ET Foam Loss History
4-3 Aerodynamic Loads on the Bipod Ramp
4-4 Foam Loss Related to Weather
4-5 Water Absorption by ET Foam

ET – Foam
Launch – Ascent

- **Action / Issue:** Cryopumping & Cryoingestion
- **Background / Facts:**
  - Cryoingestion: escape of N2 from intertank into SLA or foam
    - Gaseous N2 used to purge inner tank condenses to liquid on upper surface of LH2 tank
    - LN2 can leak through LH2-intertank flange shims, panel joints, and vent holes under stringers
    - LN2 can then enter voids in foam or can be absorbed by SLA
  - Cryopumping: entry of ambient air through cracks in foam
    - Type (2) Ambient air condenses on surface of LO2 or LH2 tanks
    - Air can come into contact with tank surface through cracks in foam
    - Air can then enter voids or debonds at foam/substrate interface
  - Theory:
    - Trapped liquid N2 or liquid air vaporizes during ascent as temp rises
    - Lacking an escape path, vaporization causes a pressure build-up
    - Pressure can force foam to shed off the ET

Presenter M3/Materials | Date FINAL | Slide 1 of 13 | Closed

ET – Foam
Launch – Ascent

- **Findings:**
  - Recent dissections of bipod ramps and LH2-intertank flanges (ET-94, ET-120, ET-124) revealed flaws (voids, disbonds, FOD) - potential cryoingestion/cryopumping sites
  - Cracks in intertank stringer valleys & other areas may contribute to cryopumping
  - No evidence exists of SLA having spalled off along with foam
  - Test #6 at MSFC (cryoingestion) revealed:
    - When conditions were correct for cryoingestion and subsequent vaporization, foam failure mode was characterized by cracking
    - Cracking relieved pressure permitting N2 to escape from beneath foam
    - No spalling of foam was observed
    - Test #6 conditions do not simulate the operational environment

Presenter M3/Materials | Date FINAL | Slide 2 of 13 | Closed

ET – Foam
Launch – Ascent

- **Findings: (cont.)**
  - Test #2 at MSFC (combined thermo/cryo/vacuum environment) revealed:
    - Conditions during tanking favor the formation of liquid and/or solid N2 in "Y" joint at intertank flange
    - Conditions are not correct for vaporization of liquid/solid N2 during ascent
  - MSFC will continue to change parameters on Test #2 to determine if N2 vaporization can be artificially induced
  - Bottom Line: Vaporization following ingestion of N2 from the intertank may be a contributing mechanism for foam loss but does not appear to be the sole driver

Presenter M3/Materials | Date FINAL | Slide 3 of 13 | Closed

ET – Foam
Launch – Ascent

- **Findings: (cont.)**
  - Test #6 at MSFC (cryoingestion) revealed:
    - When conditions were correct for cryoingestion and subsequent vaporization, foam failure mode was characterized by cracking
    - Cracking relieved pressure permitting N2 to escape from beneath foam
    - No spalling of foam was observed
    - Test #6 conditions do not simulate the operational environment
      - Rapid warm up of the backface is not representative of flight environment
        - » Even with rapid warming, it takes approximately 3-5 minutes to build up enough pressure to crack foam, time far outside STS-107 bipod foam loss
  - **Bottom Line: Test #2 and Test #6 together show that vaporization following ingestion of N2 from the intertank is probably not a contributor to bipod ramp foam loss during ascent**

Presenter M3/Materials | Date FINAL | Slide 4 of 13 | Closed

ET – Foam
Launch – Ascent

- **Recommendations:**
  - NASA (MSFC) should continue with the series of tests planned to investigate the loss of the bipod foam ramp from ET-93 during STS-107
    - These tests will focus on understanding the cryopumping/ingestion issue and its effect on and relationship to other environmental conditions that the ET experiences during launch and ascent.
  - NASA should perform independent (non-MSFC) testing to understand cryo-effects and other foam properties/behavior
  - Lessons learned from these tests must be used in the redesign of the bipod fitting enclosure and also in the redesign of the LH2-intertank flange area
  - Cryopumping and cryoingestion must be eliminated as potential initiating events for foam loss from the ET.

Presenter M3/Materials | Date FINAL | Slide 5 of 13 | Closed

ET – Foam
Launch – Ascent

Cryoingestion of LN2 from Intertank through Intertank-LH2 Flange in Bipod Region

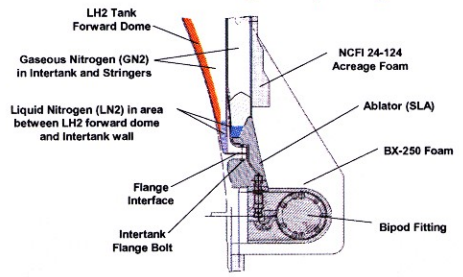

Presenter M3/Materials | Date FINAL | Slide 6 of 13 | Closed

ET – Foam Launch – Ascent

Theoretical Progression of LN2 Cryoingestion from Intertank

time →

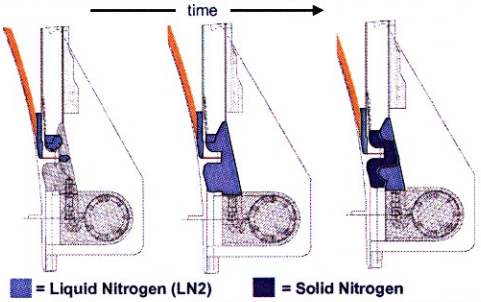

= Liquid Nitrogen (LN2) = Solid Nitrogen

Presenter M3/Materials | Date FINAL | Slide 7 of 13 | Closed

ET – Foam Launch – Ascent

Theoretical Progression of LN2 Cryoingestion from Intertank

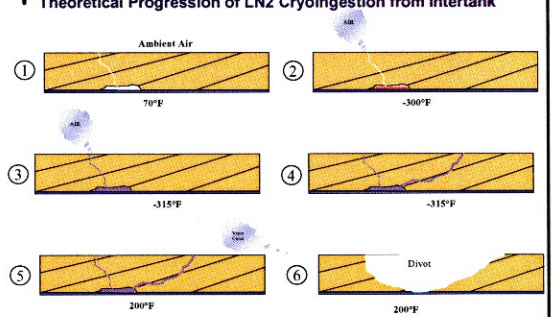

Presenter M3/Materials | Date FINAL | Slide 8 of 13 | Closed

ET – Foam Launch – Ascent

Typical Voids found during Dissection of ET-120 +Y Bipod Ramp

Potential Cryoingestion Paths

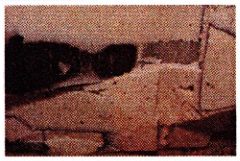

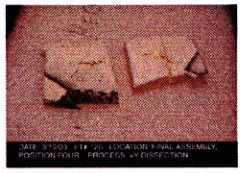

Presenter M3/Materials | Date FINAL | Slide 9 of 13 | Closed

ET – Foam Launch – Ascent

Stringer Valley Cracks on ET Intertank

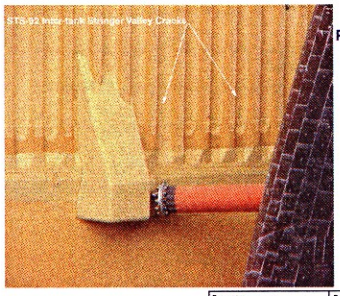

Potential Cryopumping Paths

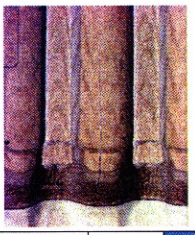

Presenter M3/Materials | Date FINAL | Slide 10 of 13 | Closed

ET – Foam Launch – Ascent

Bipod Thermal/Vacuum Cryogenic Test MSFC Test #2

Description

– Replicate the TPS configuration of the –Y bipod ramp and expose this area to simulated ground and flight environments in an attempt to replicate the probable scenario of foam loss similar to that experienced on STS-112

Objective

–Characterize TPS debris from bipod area resulting from the following ascent environments

- •Cryogenic back-face temperatures coupled with on-pad soak duration.
- •Back-face temperature ascent profile
- •Ascent pressure profile

–Characterize configuration of hardware and SLA-561 remaining after initial foam lossResults support fault tree blocks relating to foam loss and tile impact

Presenter M3/Materials | Date FINAL | Slide 11 of 13 | Closed

ET – Foam Launch – Ascent

Cryoingestion/Cryopumping Fundamental Data Test

MSFC Test #6

- **Description**
  - – Collect fundamental phenomenon investigation for the effects of cryo fluids on stacked structure and TPS configurations
- **Objective**
  - – Bridge testing results from small single material test articles to interaction effects of SLA with SOFI in controlled tests where specific fundamental characteristics may be observed and quantitatively evaluated for use in modeling the behavior of complex SLA and SOFI structures
    - Investigate SLA/foam debris liberation sensitivity to geometry
    - Characterize failure modes
    - Characterize cryopumping sensitivity to crack size
    - Investigate freezing effects of cryoingestion
    - Investigate rate effects of ingestion and venting
    - Investigate cryopumping behavior to configuration
    - Investigate pressure induced failure of SLA/foam
    - Investigate phenomena identified by the TEF

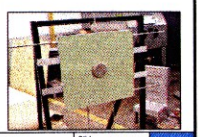

Presenter M3/Materials | Date FINAL | Slide 12 of 13 | Closed

2

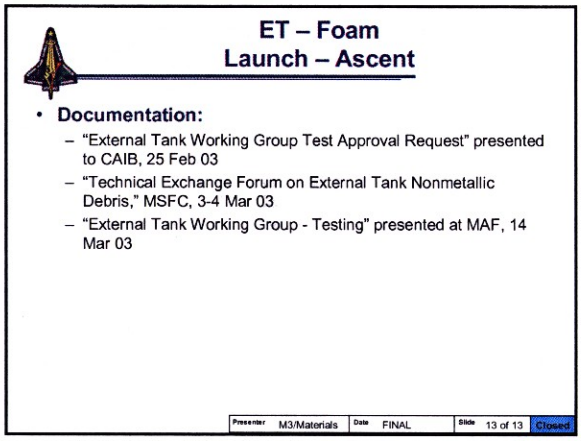
ET – Foam
Launch – Ascent
• Documentation:
– "External Tank Working Group Test Approval Request" presented to CAIB, 25 Feb 03
– "Technical Exchange Forum on External Tank Nonmetallic Debris," MSFC, 3-4 Mar 03
– "External Tank Working Group - Testing" presented at MAF, 14 Mar 03
Presenter M3/Materials
Date FINAL
Slide 13 of 13
Closed

ET – Foam
Launch – Ascent

- **Action / Issue:** The ET has shed foam since STS-01. Major events, such as the loss of portions of bipod foam ramps, have occurred periodically.
- **Background / Facts:**
  - Although tile damage is often used as the indicator of foam loss, no conclusive evidence exists linking tile damage with foam loss
    - Chemical sampling of tile damage sites for foam has been inconclusive
    - Debris sources are not limited to the ET
    - Use of imagery from launch, ascent, and ET separation is necessary to confirm foam loss
  - All 113 STS missions have been reviewed to determine availability of launch/ascent imagery data
  - No imagery coverage available on 34 missions
    - 16 Night Launches & 18 Day Launches with no camera coverage
  - Bottom line: Presence or absence of foam loss can be visually confirmed on 79 of 113 missions at this time

Presenter M3/Material | Date FINAL | Slide 1 of 12 | Closed

ET – Foam
Launch – Ascent

- **Findings:** *Recall, visual imagery available on 79 of 113 missions*
  - 65 missions experienced visually confirmed foam loss
    - Foam loss confirmed on **82%** of missions for which imagery was available
    - 55 experienced loss of foam from LH2-Intertank flange
    - 34 experienced loss of foam from Intertank acreage
    - At least 7 experienced loss of a portion of a bipod ramp (all –Y [left])
    - 12 experienced confirmed loss of foam from thrust panels ("popcorning")
    - 45 experienced loss of foam from other sites
    - Of the 57 without a bipod ramp loss, 39 experienced losses "near bipod"
  - Worst damage to orbiter tiles: STS-27R (OV-104)
    - Due to loss of SRB ablator material: **not** due to loss of ET foam
    - Hits to orbiter: 644 lower surface (272 >1") [707 total (298 > 1")]
  - Most damage to tiles from ET foam loss: STS-87 (OV-102)
    - Thrust panel popcorning
    - Hits to orbiter: 244 lower surface (109 >1") [308 total (132 > 1")]

Presenter M3/Material | Date FINAL | Slide 2 of 12 | Closed

ET – Foam
Launch – Ascent

- **Findings (con't):**
  - MSFC has taken actions on numerous occasions to eliminate or reduce foam loss from the ET
- **Recommendations:**
  - NASA must continue testing currently underway at MSFC and MAF to identify the root cause(s) for the generation of debris from the ET.
  - NASA must minimize the generation of debris from the ET.
  - NASA must establish programs to understand the possible damage resulting from debris impacts on other Space Shuttle elements.
  - NASA must institute a policy to provide (visual) imagery on 100% of launches to check for ET foam loss and other launch debris.

Presenter M3/Material | Date FINAL | Slide 3 of 12 | Closed

ET – Foam
Launch – Ascent

- **Recommendations (con't):**
  - NASA must harden each of the Space Shuttle elements (especially the orbiter) to maximize their impact damage tolerance.
  - NASA should take an integrated approach to address these recommendations
    - All future efforts that minimize the debris generated by each Space Shuttle element and maximize each element's impact damage tolerance must be mutually compatible.
  - NASA should consider eliminating a foam-covered ET from the Space Transportation System

Presenter M3/Material | Date FINAL | Slide 4 of 12 | Closed

ET – Foam
Launch – Ascent

Loss of –Y Bipod Ramp Foam, STS-7 (OV-99, ET-6)

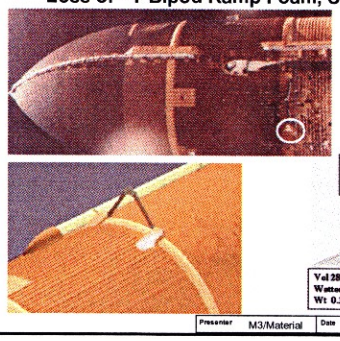

Presenter M3/Material | Date FINAL | Slide 5 of 12 | Closed

ET – Foam
Launch – Ascent

Loss of –Y Bipod Ramp Foam, STS-32R (OV-102, ET-32)

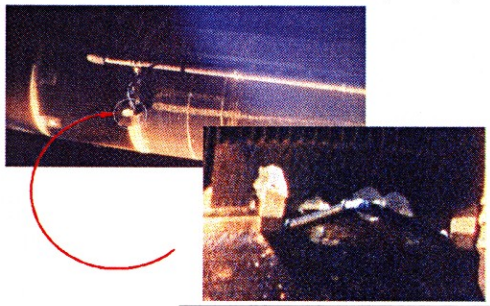

Presenter M3/Material | Date FINAL | Slide 6 of 12 | Closed

1

ET – Foam
Launch – Ascent

Loss of –Y Bipod Ramp Foam, STS-50 (OV-102, ET-43)

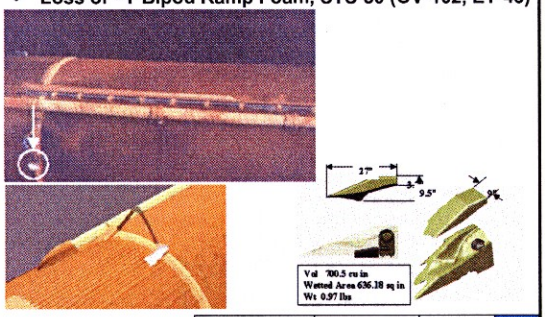

Presenter M3/Material | Date FINAL | Slide 7 of 12 | Closed

ET – Foam
Launch – Ascent

Loss of –Y Bipod Ramp Foam, STS-52 (OV-102, ET-55)

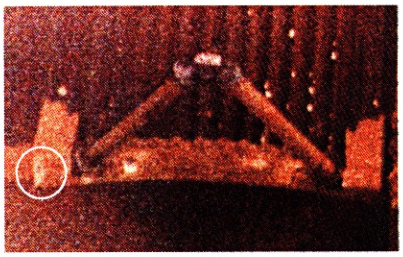

Presenter M3/Material | Date FINAL | Slide 8 of 12 | Closed

ET – Foam
Launch – Ascent

Loss of –Y Bipod Ramp Foam, STS-62 (OV-102, ET-62)

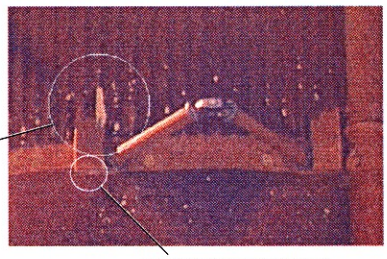

Presenter M3/Material | Date FINAL | Slide 9 of 12 | Closed

ET – Foam
Launch – Ascent

Loss of –Y Bipod Ramp Foam, STS-112 (OV-104, ET-115)

(Lost at ~ T+30 sec)

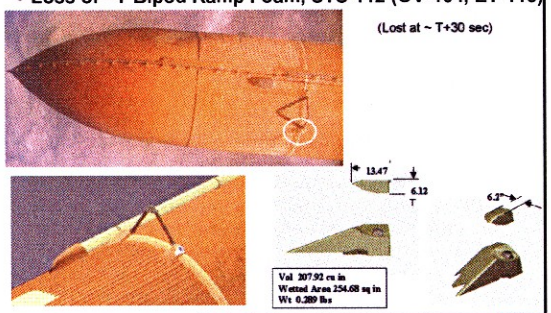

Presenter M3/Material | Date FINAL | Slide 10 of 12 | Closed

ET – Foam
Launch – Ascent

Summary of Some ET Project Office Efforts to Reduce Debris Shed by External Tank

STS	ET	Launch Date	Precipitating Event / Concern	Efforts to Reduce Debris
1	1	4/12/1981	Ice may form on instrumentation spirals and become debris	Removed instrumentation spirals on LO2 Tank to insure no ice debris
6	6 (LWT 1	4/1/83	Block change to Lightweight Tank enabled design changes	Redesign of Bipod Ramp angle from 45° to 30° on LWT-7
				Incorporated maximum feasible defect limits on Bipod ramp
				Incorporated improved fabrication procedures for LH2 tank cable tray ice frost ramps (two-step single-pour application versus one-step multi-pour process)
				Reduced SLA areas
				Created anti-gouger line
				Incorporated "ten-forty" foam configuration on areas of the intertank
27	21	8/14/1985	Large intertank divots observed on STS-26 & STS-26	Corrective action (drilled holes) applied in two-forty areas to preclude debris due to two/forty bond/gap issues
32R	32	1/9/1990	Intertank / Bipod divot observed on STS-32R	Added inspection to verify vent hole depth in two-forty areas
35	35	12/2/1990	Ten flange area divots observed on STS-35	Incorporated process improvements to reduce potential for void formation around the flange bolts
50	50	6/25/1992	Jack-pad area divot observed on STS-50	Changed jack-pad closeout method
48	48	7/31/1992	Intertank / Bipod divot observed on STS-50	Added more vent holes around bipod ramps in two-forty areas
54	51	1/13/1993	Previous problems with two-forty intertank foam	Incorporated two-gun spray foam application on intertank to replace two-forty foam
56	54	4/8/1993	Ten large, shallow divots on -Z Intertank Acreage	Enhancement of Process to reduce fall-over and crevicing
87	89	11/19/1997	Increased number of Orbiter tile hits	Reduced foam thickness
				Incorporated "vent" holes
112	115	10/7/2002	Bipod foam loss on STS-112	Proposed corrective action (to be presented 2/6/03): remove SLA from under the foam application

Presenter M3/Material | Date FINAL | Slide 11 of 12 | Closed

ET – Foam
Launch – Ascent

- **Documentation:**
  - CAIB Request for Information, "External Tank Foam Loss,"B1-00039
  - MAF Mission Support Room Log Board, Michoud Assembly Facility
  - http://www-pao.ksc.nasa.gov/kscpao/factoids/shfacts.htm (night launches)
  - STS-ET Correlation.xls, from Jim Feeley, MAF
  - CAIB Request for Information, "Debris Info STS-32 -35 -42 - 58 Summary.xls." B0-000026
  - CAIB Request for Information, "CAIB Cryoinsulation Report," B1-000121
  - CAIB Request for Information, "Discussions at MSFC…" (w/ Scotty Sparks & Steve Holmes), B1-000132
  - "Tile Chemical Analysis," Discussion & E-mail with Jorge Rivera @ MAF, 10 Apr 03
  - "ET Cryoinsulation," presented at the CAIB Public Hearing, L. Foster & S. Sparks, 7 Apr 03.

Presenter M3/Material | Date FINAL | Slide 12 of 12 | Closed

Ascent Debris Strike
Other (ET/Foam)

- **Action / Issue:** Complex aerodynamic loads on ET-93's bipod foam ramp may have caused it to fail during the ascent of STS-107
- **Background / Facts:**
  - Bipod foam ramp shed at 81 sec (Mach 2.46, $\alpha = 2.08^{o}$)
  - Ascent environment is very severe; flow field is complex
    - 3 intersecting shocks occur in bipod region
  - Airloads determined by numerous methods
    - Wind tunnel testing of 3% scale model
    - Computational Fluid Dynamics (CFD) analysis
    - Analytical (Hoerner) analysis

Presenter M3/Material | Date FINAL | Slide 1 of 15 | Closed

Ascent Debris Strike
Other (ET/Foam)

- **Findings:**
  - Early wind tunnel tests on flat-faced and 20° angle ramps confirmed a 1.1 safety factor against failure caused by aerodynamic loads
    - Additional analysis calculated a safety factor of 2.35
    - Wind tunnel testing was not performed on the current bipod ramp geometry (22°-30°) nor on flight configuration articles (SLA, underlying bipod fitting, etc.)
  - Wind tunnel testing was also performed on 3% scale model of Space Shuttle
    - Correlation between this testing and CFD/analytical models was good
    - MADS data from the OEX recorded recovered from STS-107 confirmed that CFD and analytical models were conservative
  - No flight instrumentation was used on early ETs to investigate airloads on bipod ramps
    - Instrumentation on early flights collected only bipod strut strains

Presenter M3/Material | Date FINAL | Slide 2 of 15 | Closed

Ascent Debris Strike
Other (ET/Foam)

- **Findings: (cont.)**
  - Aerodynamic loads predicted by CFD and analytical methods are significantly less than design requirements
    - Minimum safety factor is 1.4
  - Vibroacoustic analysis calculated a safety factor of 1.64 against the formation of divots
  - No finite element analysis was performed to determine the ability of the bipod foam ramps to withstand aerodynamic loads
    - Complexity of geometry and material makes such modeling difficult
    - Efforts are in place at MAF to develop a finite element modeling capability for foam protuberances
  - The complex combined aero/thermo/vibro/vacuum/acoustic is extremely difficult to simulate, thus, combined testing was never performed
    - "Worst case" conditions were solved and superimposed to determine the integrity of the bipod foam ramps under these conditions

Presenter M3/Material | Date FINAL | Slide 3 of 15 | Closed

Ascent Debris Strike
Other (ET/Foam)

- **Findings: (cont.)**
  - No studies of the behavior of partially failed (i.e. cracked, etc.) bipod foam ramps was ever performed
  - No evidence that aerodynamic loads, alone, caused bipod ramp to fail on ET-93 during STS-107
    - In fact, precited aero loads have a large radial load component (300 lb) forcing ramp to remain on ET
- **Recommendations:**
  - NASA must continue to improve its capabilities to perform analytical and numerical simulations of the complex combined environments to which the the ET is exposed.
    - These capabilities must be validated with test and/or flight data

Presenter M3/Material | Date FINAL | Slide 4 of 15 | Closed

Ascent Debris Strike
Other (ET/Foam)

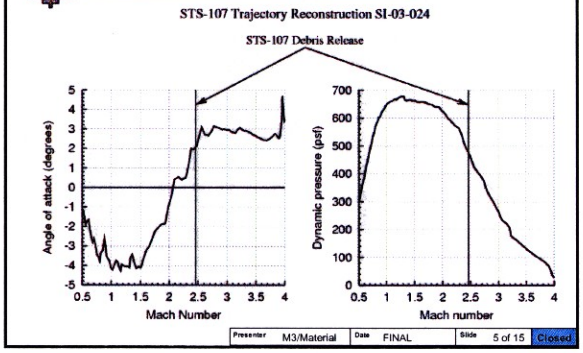

Presenter M3/Material | Date FINAL | Slide 5 of 15 | Closed

Ascent Debris Strike
Other (ET/Foam)

Flowfields

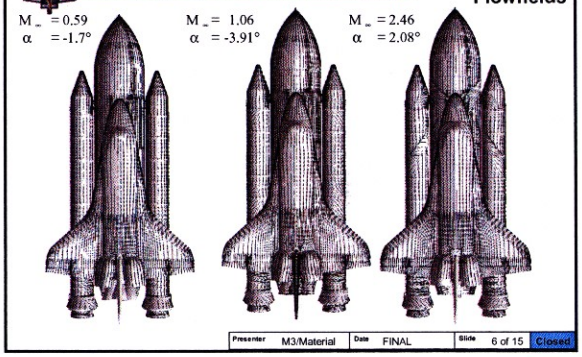

Presenter M3/Material | Date FINAL | Slide 6 of 15 | Closed

1

Ascent Debris Strike Other (ET/Foam)

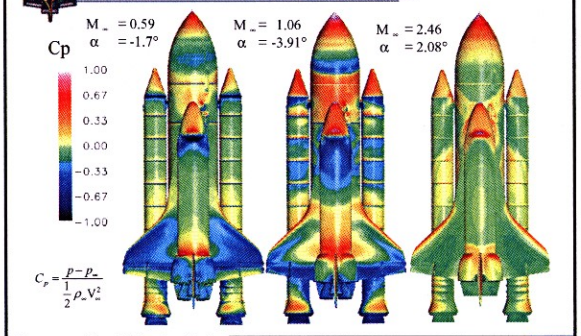

Pressure Coefficients (Cp)

Presenter M3/Material | Date FINAL | Slide 7 of 15 | Closed

Ascent Debris Strike Other (ET/Foam)

Flowfields in –Y Bipod Region

(Flowfields in +Y bipod region inaccurate due to simplifications in model)

JSC CFD
Mach no. = 2.46
Alpha = 2.08 °

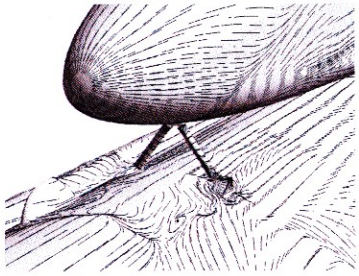

Presenter M3/Material | Date FINAL | Slide 8 of 15 | Closed

Ascent Debris Strike Other (ET/Foam)

Pressure Coefficients (Cp) in –Y Bipod Region

(Coefficients in +Y bipod region inaccurate due to simplifications in model)

- **Observations**
  - 3 intersecting shocks in bipod region
    - Complex flow features
      - Separated flow
      - Vortices ahead of bipod/bipod ramp
  - Significantly more complex local flow field than lower Mach numbers
  - Complex flow characteristics begin at approximately Mach = 1.4

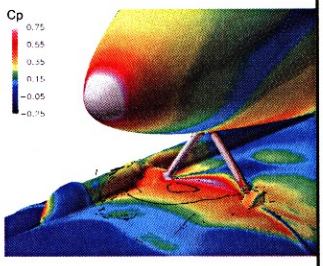

Presenter M3/Material | Date FINAL | Slide 9 of 15 | Closed

Ascent Debris Strike Other (ET/Foam)

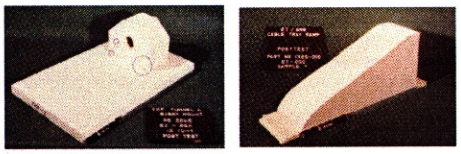

Original Bipod Ramp Wind Tunnel Test Components

Presenter M3/Material | Date FINAL | Slide 10 of 15 | Closed

Ascent Debris Strike Other (ET/Foam)

Comparison of Wind Tunnel Test Data With CFD Predictions for Pressure Coefficients Longitudinally Along the ET Surface

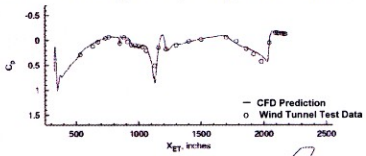

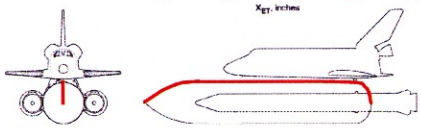

Path Along Which Data Was Taken and CFD Prediction Was Made

Presenter M3/Material | Date FINAL | Slide 11 of 15 | Closed

Ascent Debris Strike Other (ET/Foam)

Predicted Side (Y-direction) Force on ET-93's –Y Bipod Foam Ramp During STS-107

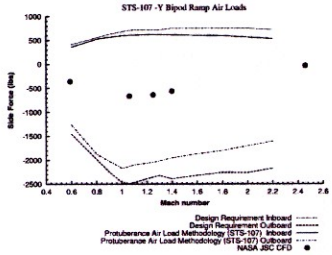

Presenter M3/Material | Date FINAL | Slide 12 of 15 | Closed

Ascent Debris Strike
Other (ET/Foam)

Predicted Bipod Foam Ramp Aerodynamic Loads

Axis	Design Requirements (lb) (Independent of Mach)	CFD predictions of Flight Loads		
		Mach 0.59	Mach 1.06	Mach 2.46
Max Axial Load (+aft)	899.4	254	637	48
Max Side Load (+/-) (+ inboard)	756.2/-2483.5	-359	-664	-24
Max Radial Load (+ inward)	1409.3	-332	-24	322

Includes Safety Factor of 1.4

Predictions Indicate Aerodynamic Loads Are Less Than Design Limits

Presenter: M3/Material | Date: FINAL | Slide: 13 of 15 | Closed

Ascent Debris Strike
Other (ET/Foam)

- **Documentation:**
  - "Bipod Airflow and Loads," presented by R. Gomez, RFI B1-000050, 23 Mar 03
  - "ET Bipod Aero Ramp Foam Verification / Certification," presented by M. Quiggle, at Michoud Assembly Facility, 10 Apr 03
  - "Ascent CFD Verification," RFI B1-000147, 22 Apr 03.
  - Personal Communication, M. Quiggle, at Michoud Assembly Facility, 15 May 03.
  - "1.1.1 TPS Debris Fault Tree Closeout Briefing," S. Sparks at MSFC, 20 May 03

Presenter: M3/Material | Date: FINAL | Slide: 14 of 15 | Closed

Absolute Angle for Flights at 39° Inclination

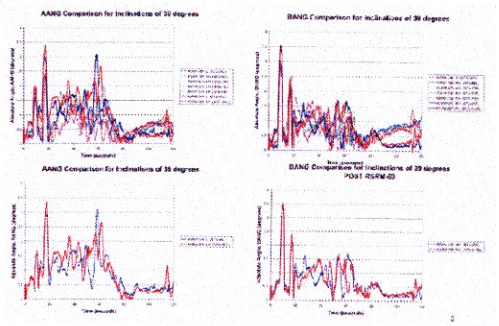

Presenter: M3/Material | Date: FINAL | Slide: 15 of 15 | Closed

3

ET – Foam
Launch – Ascent

- **Action / Issue:** Potential for Foam Loss to be Related to Weather
- **Background / Facts:**
  - Numerous suggestions (via PIAs and media) that foam loss is related to moisture absorption and/or ice formation
  - Weather office at KSC has provided the following historical info for the time during which the shuttle was outside for each mission: 1) daily rainfall, 2) min/max daily temps, 3) min/max daily rh, 4) min/max daily atm pressure, 5) max daily surface wind gusts & direction, 6) temp at start of tanking (fueling), 7) temp at launch
- **Findings:**
  - Average ET pre-launch exposure time for all missions is 38.5 days
    - ET-93 (used on STS-107) was on the pad for 39 days prior to launch
    - No apparent trend linking pre-launch exposure time to foam loss
  - No apparent trends linking foam loss with any weather variables analyzed

Presenter M3/Material | Date FINAL | Slide 1 of 3 | Closed

ET – Foam
Launch – Ascent

- **Recommendations:**
  - NASA should continue to investigate moisture absorption by foam and relate any results to pre-launch exposure of the ET to the atmosphere.
  - NASA should continue analyzing weather data in search of correlations between weather variables and foam loss. Particular attention should be given to identifying the importance of combinations of variables that might contribute to foam loss.
- **Documentation:**
  - RFI B1-00145 "Historical Weather Data," 27 Mar 03
  - John Madura, KSC Weather Office, 321-867-0814, john.t.madura@nasa.gov

Presenter M3/Material | Date FINAL | Slide 2 of 3 | Closed

ET – Foam
Launch – Ascent

Relationship Between Foam Loss and ET Pre-Launch Exposure

(Overlapping confidence intervals indicate no significant difference among categories of data)

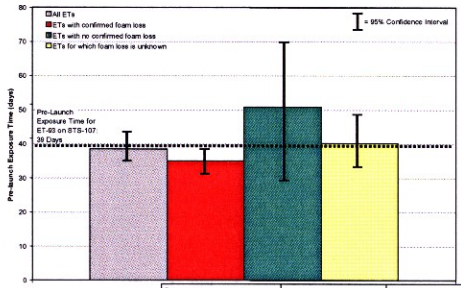

Presenter M3/Material | Date FINAL | Slide 3 of 3 | Closed

ET – Foam
Launch – Ascent

- **Action / Issue:** Moisture absorption by the External tank (ET) foam may have caused or exacerbated the foam loss event by increasing the mass of the piece shed from ET-93 during the ascent of STS-107
- **Background / Facts:**
  - PIA #644 cited a "review of publications" indicating closed-cell foam can absorb water and increase in mass by a factor of 10
  - B. Peterson (formerly of Texaco Chemical) cited experience with polyurethane foams that could absorb water at near-freezing temperatures if chemical constituents of foam were correct
  - Prof. L. Glicksman (M.I.T.) performed preliminary calculations
    - Showed water vapor could be absorbed into foam at 68°F and 100% rh
    - 6-hour tanking would result in absorption of 0.001 lb/ft² of water
  - Moisture absorption by foam is a concern in the building industry
    - PIA # 671 identified two commercially available codes designed to predict moisture absorption in foam
  - Incorrect analyses by media led to public misunderstandings

Presenter: M3/Material | Date: FINAL | Slide: 1 of 12 | Closed

ET – Foam
Launch – Ascent

- **Findings:**
  - ET foams do not have chemistry susceptible to moisture absorption
    - Peterson identified a specific EO/PO ratio (ethylene oxide / propylene oxide) that made foams absorptive near 32°F
    - EO is the hydrophyllic component (attractive to water)
    - EO/PO ratio of ET foams is zero
  - Regardless of chemistry, unlikely that closed-cell foam can absorb liquid water
    - Diffusional absorption of water vapor may be possible
  - Prof. Glicksman predicted ice and vaporization layers
    - Potential ice layer: thickness = 0.002 in, weight = 0.015 oz/ft²
    - Vaporization layer: thickness = 0.2 in, weight = 0.06 oz/ft²
  - Dr. Osheroff has performed simple experiments at Stanford
    - Immersion of foam in ice water suggests water permeates foam only to 0.004 in below surface
    - Consistent with depth of single layer of open cells at surface

Presenter: M3/Material | Date: FINAL | Slide: 2 of 12 | Closed

ET – Foam
Launch – Ascent

- **Findings: (cont.)**
  - MSFC previously performed water absorption tests under accelerated conditions (7 days at 125°F and 95% rh)
    - NCFI 24-124 acreage foam: 0.12% weight gain
    - BX 250 closeout foam: 0.16% weight gain
    - SS 1171 feedline foam: 0.42% weight gain
    - PDL 1034 poured foam: 0.83% weight gain
    - Both foams had machined surfaces (i.e. surface cells were open)
  - Recent additional tests conducted at MSFC (with Prof. Leon Glicksman of M.I.T. retained as a consultant)
    - Immersion of BX 250 & NCFI 24-124 in distilled, de-aired water at 125°F for over 60 hours
      - Water absorption equivalent to thickness of exposed surface layer of open cells
      - Consistent with Dr. Glicksman's calculations and Dr. Osheroff's experiments

Presenter: M3/Material | Date: FINAL | Slide: 3 of 12 | Closed

ET – Foam
Launch – Ascent

- **Findings: (cont.)**
  - Recent additional tests conducted at MSFC (cont.)
    - Vapor Phase Transmission through BX 250
      - Included thermal gradient of ~70°F to simulate tanking conditions
      - Level of transmission deemed insignificant (< 3 g/hr·m²)
      - Especially in light of low moisture absorption & limited tanking times
  - Bottom Line from recent tests at MSFC
    - "Absorbed" water limited to open cells on surface
    - Any water absorbed deeper into foam does so through vapor transmission at a very low rate
    - Water ingress through voids/cracks open to surface and subsequent vaporization & crack formation or growth is a possibility
  - Role of long voids, wormholes, knitlines may merit further testing
  - Future research should integrate test results into a mechanistic, quantitative failure mode model

Presenter: M3/Material | Date: FINAL | Slide: 4 of 12 | Closed

ET – Foam
Launch – Ascent

- **Group Recommendations:**
  - NASA should consider continued testing per Dr. Glicksman's suggestion
    - Investigating water ingress through unique features (long voids, etc.)
    - Developing failure mode model incorporating test results

Presenter: M3/Material | Date: FINAL | Slide: 5 of 12 | Closed

ET – Foam
Launch – Ascent

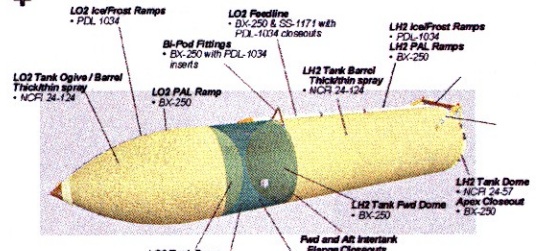

Types and Locations of ET Foams

Presenter: M3/Material | Date: FINAL | Slide: 6 of 12 | Closed

1

ET – Foam Launch – Ascent

Types of ET Foams

	NCFI 24-124	BX 250	NCFI 24-57	PDL 1034
% of Total Foam	(77%)	(14%)	(7%)	(1%)
Application Areas	LH2,L02,I/T sidewall	LH2 forward dome, L02 aft dome, closeouts	LH2 Aft Dome	Closeouts and repairs
Application Process	Automatic Spray	Manual Spray	Automatic Spray	Pour/Mold
Description	Isocyanurate	Urethane	Isocyanurate	Urethane

Presenter M3/Material | Date FINAL | Slide 7 of 12 | Closed

ET – Foam Launch – Ascent

Moisture Absorption by ET Foams

Exposure Conditions: 7 days @ 125°F and 95% rh

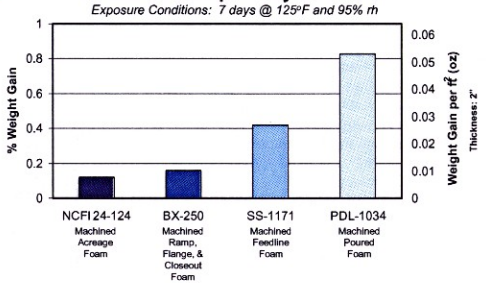

Presenter M3/Material | Date FINAL | Slide 8 of 12 | Closed

ET – Foam Launch – Ascent

ET Foam Moisture Absorption

Source: RFI B3-00060

- **NCFI 24-124**
  - Accelerated Exposure (7 days @ 125°F and 95% humidity)
    - 0.12% weight gain due to moisture absorption (machined foam)
  - Outdoor Exposure (28 day variable daily relative humidity)
    - 0.70% maximum weight gain due to moisture absorption (after 6 days)
    - 0.04% moisture loss after 28 days
- **Vented NCFI 24-124**
  - Concern: Holes in vented foam will wick moisture if ET is exposed to rain
  - Test performed: 5 repeated exposures of heavy rain and extreme freezing conditions caused no deterioration of the foam tensile properties

Presenter M3/Material | Date FINAL | Slide 9 of 12 | Closed

ET – Foam Launch – Ascent

ET Foam Moisture Absorption *(cont.)*

Source: RFI B3-00060

- **BX-250**
  - Accelerated Exposure (7 days @ 125°F and 95% humidity)
    - 0.16% weight gain due to moisture absorption (machined foam)
- **SS-1171**
  - Accelerated Exposure (7 days @ 125°F and 95% humidity)
    - 0.42% weight gain due to moisture absorption (machined foam)
- **PDL-1034**
  - Accelerated Exposure (7 days @ 125°F and 95% humidity)
    - 0.83% weight gain due to moisture absorption (machined foam)
- **Conclusion**
  - ET foam materials absorb insignificant amount of moisture under accelerated test conditions

Presenter M3/Material | Date FINAL | Slide 10 of 12 | Closed

ET – Foam Launch – Ascent

Closed-Cell Foam Morphology (BX-250 shown)

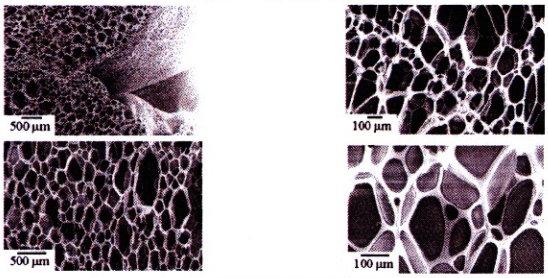

Presenter M3/Material | Date FINAL | Slide 11 of 12 | Closed

ET – Foam Launch – Ascent

- **Documentation:**
  - E-mail: Bruce Peterson to Johnny Wolfe, 27 Feb 03
  - E-mail: Leon Glicksman to MG Barry, 9 Mar 03
  - CAIB Request for Information, "External Tank Moisture Absorption," B3-00060
  - CAIB Request for Information, "ET Cryoinsulations," B1-000121
  - PIA 671 "Insulation & Moisture"
  - PIA 644 "Closed Cell Foam Can Absorb Water"
  - Discussion with Scotty Sparks (MSFC) at MAF, 16 Apr 03
  - Discussion with Dr. Osheroff (CAIB/Stanford) at MAF, 21 Apr 03
  - Response to RFI B1-000194 "ET Foam Moisture Absorption Testing," 1 Jun 03

Presenter M3/Material | Date FINAL | Slide 12 of 12 | Closed

RCC
Design – Certification

5-1 WLE Subsystem Design Requirements and Certification

5-2 RCC Impact Energy Requirements and Certification

Matrix

Presenter	CAIB/Group 1	Date	FINAL	Slide	7 of 32

Wing Leading Edge Design & Certification

- **Action / Issue:** Determine adequacy of the WLE subsystem requirements, design and certification
- **Background / Facts:**
  - RCC is a critical component of the TPS (safety-of-flight)
  - Performance and design requirements documented in specification MJ070-0001-1E, 7 Nov 02
    - TPS impact energy design requirement is 0.006 foot-lbs (paragraph 3.3.1.8.11)
    - Orbiter not designed to withstand launch debris or ice (paragraph 3.3.1.8.16)

Presenter M3/Material | Date FINAL | Slide 1 of 26 | Closed

Wing Leading Edge Design & Certification

- **Background / Facts :**
  - Procurement specification MC621-0007, Rev E requirement more stringent than design requirement
    - Impact/ground handling damage resistance limits defined in figure 3.1
    - Impact energy limit ranges from 1 to 2.25 foot-pounds based on part thickness
  - TPS mission life requirement of 100 missions with scheduled maintenance and refurbishment (paragraph 3.4.3)

Presenter M3/Material | Date FINAL | Slide 2 of 26 | Closed

Wing Leading Edge Design & Certification

- **Background / Facts:**
  - RCC system is mounted to the wing front spar using attach fittings bolted to the front spar
  - Wing front spar attach fittings redesigned from a 2-piece design using A-286 steel (OV-102) to a 1-piece design using Ti-6Al-4V titanium (subsequent orbiters)
  - The insulators used to protect the metallic components of the WLE have been redesigned to increase survivability against MMOD
  - Moment constraint fittings (spanner beams) were retrofitted on several OV-102 RCC panels as a result of an increase in the predicted loads
    - OV-102 spanner beams installed on panels 5 through 19

Presenter M3/Material | Date FINAL | Slide 3 of 26 | Closed

Wing Leading Edge Design & Certification

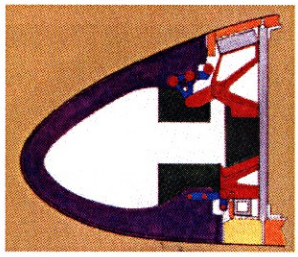

LI2200 | Inconel 718 | RCC | Inconel-
LI900 | A-286 steel | Aluminum | Dynaflex

Presenter M3/Material | Date FINAL | Slide 4 of 26 | Closed

Wing Leading Edge Design & Certification

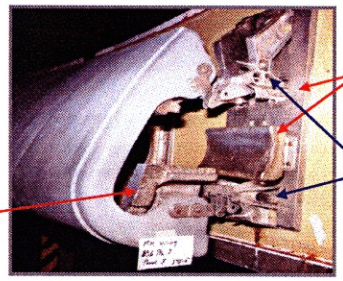

OV-102 RCC Panel 3 on Right Side

Presenter M3/Material | Date FINAL | Slide 5 of 26 | Closed

Wing Leading Edge Design & Certification

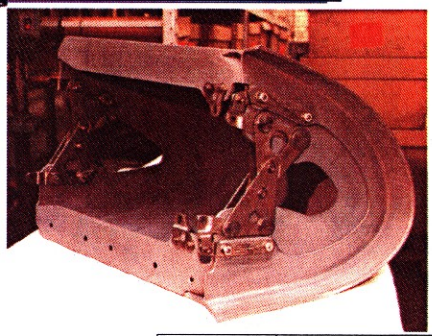

Presenter M3/Material | Date FINAL | Slide 6 of 26 | Closed

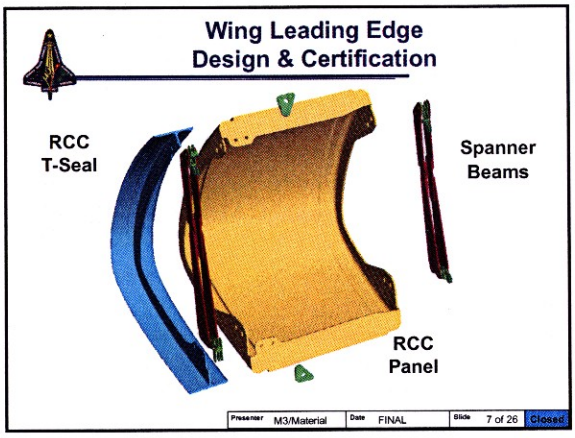
Wing Leading Edge
Design & Certification
RCC
T-Seal
Spanner
Beams
RCC
Panel
Presenter M3/Material
Date FINAL
Slide 7 of 26
Closed

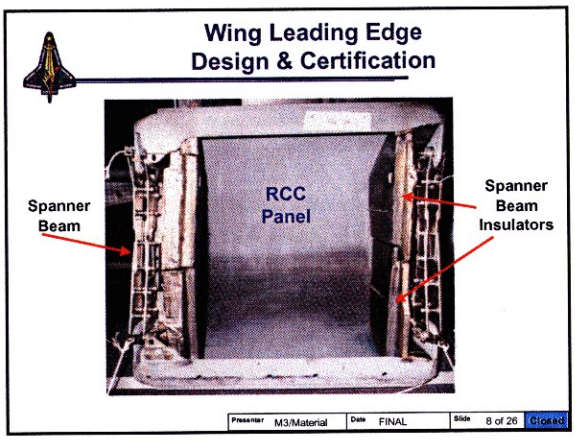
Wing Leading Edge
Design & Certification
Spanner
Beam
RCC
Panel
Spanner
Beam
Insulators
Presenter M3/Material
Date FINAL
Slide 8 of 26
Closed

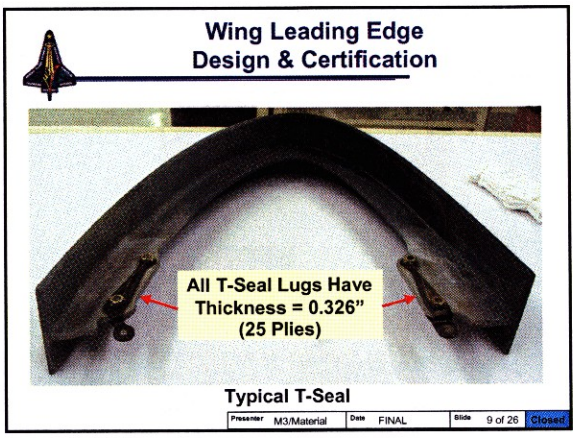
Wing Leading Edge
Design & Certification
All T-Seal Lugs Have
Thickness = 0.326"
(25 Plies)
Typical T-Seal
Presenter M3/Material
Date FINAL
Slide 9 of 26
Closed

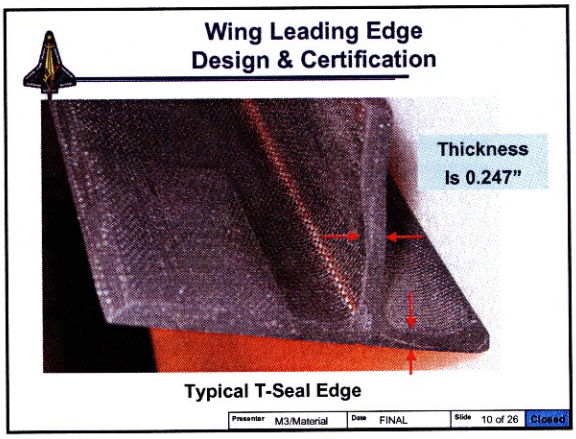
Wing Leading Edge
Design & Certification
Thickness
Is 0.247"
Typical T-Seal Edge
Presenter M3/Material
Date FINAL
Slide 10 of 26
Closed

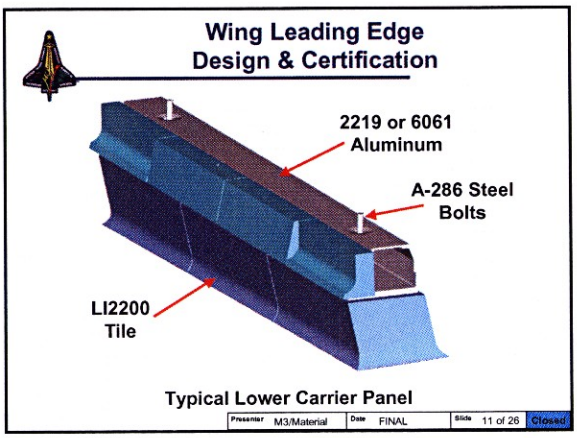
Wing Leading Edge
Design & Certification
2219 or 6061
Aluminum
A-286 Steel
Bolts
LI2200
Tile
Typical Lower Carrier Panel
Presenter M3/Material
Date FINAL
Slide 11 of 26
Closed

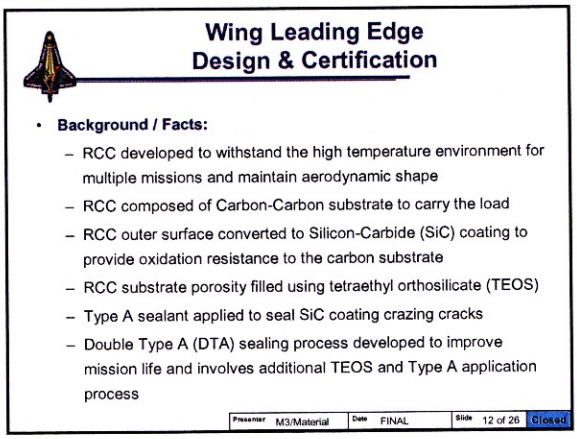
Wing Leading Edge
Design & Certification
• Background / Facts:
– RCC developed to withstand the high temperature environment for multiple missions and maintain aerodynamic shape
– RCC composed of Carbon-Carbon substrate to carry the load
– RCC outer surface converted to Silicon-Carbide (SiC) coating to provide oxidation resistance to the carbon substrate
– RCC substrate porosity filled using tetraethyl orthosilicate (TEOS)
– Type A sealant applied to seal SiC coating crazing cracks
– Double Type A (DTA) sealing process developed to improve mission life and involves additional TEOS and Type A application process
Presenter M3/Material
Date FINAL
Slide 12 of 26
Closed

Wing Leading Edge Design & Certification

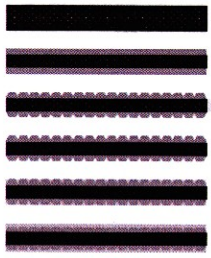

RCC Material System - Application Order is Top to Bottom

Presenter M3/Material | Date FINAL | Slide 13 of 26 | Closed

Wing Leading Edge Design & Certification

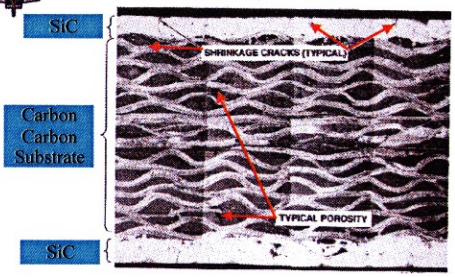

Representative Cross-Section of RCC Material

Presenter M3/Material | Date FINAL | Slide 14 of 26 | Closed

Wing Leading Edge Design & Certification

RCC Panel & T-Seal Weights

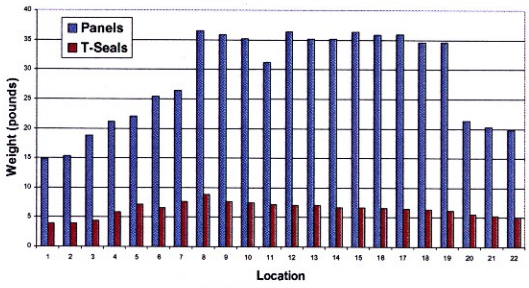

Presenter M3/Material | Date FINAL | Slide 15 of 26 | Closed

Wing Leading Edge Design & Certification

- **Background / Facts:**
  - Extensive analysis and testing was performed to certify the WLE subsystem to the performance requirements
  - Mechanical property (design allowables) documented in Vought Report 221RP00614, Rev A, 12 October 1994
    - Over 2,000 specimen tests were performed to characterize the RCC mechanical properties
  - Initial development tests did not reveal the susceptibility of RCC to subsurface oxidation

Presenter M3/Material | Date FINAL | Slide 16 of 26 | Closed

Wing Leading Edge Design & Certification

- **Background / Facts:**
  - Substrate mass loss significantly reduces flexure strength and impact energy resistance
  - Substrate mass loss has minimal affect on tension, compression and shear properties
  - Highest peak temperature occurs at Panel 9
  - Highest air loads occur at Panel 17

Presenter M3/Material | Date FINAL | Slide 17 of 26 | Closed

Wing Leading Edge Design & Certification

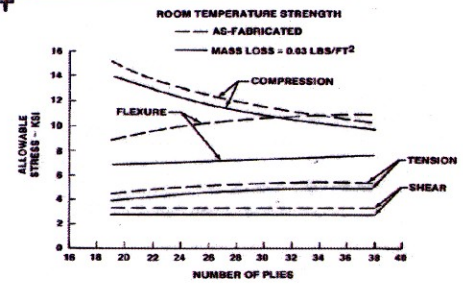

19 plies = 0.24" thick, 38 plies = 0.5" thick

Presenter M3/Material | Date FINAL | Slide 18 of 26 | Closed

Wing Leading Edge Design & Certification

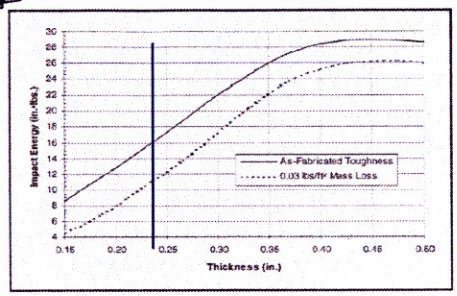

— Minimum WLE RCC Thickness

Presenter M3/Material | Date FINAL | Slide 19 of 26 | Closed

Wing Leading Edge Design & Certification

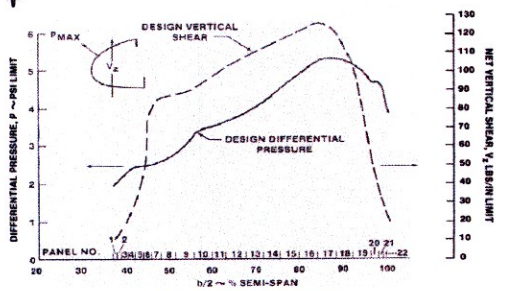

Figure 5 LESS Design Airloads

Presenter M3/Material | Date FINAL | Slide 20 of 26 | Closed

Wing Leading Edge Design & Certification

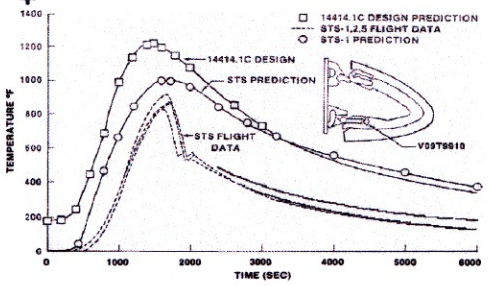

Figure 8 Wing LE Panel 9 Lower Attach Clevis Temperature

Presenter M3/Material | Date FINAL | Slide 21 of 26 | Closed

Wing Leading Edge Design & Certification

- **Findings (agreed to by Curry, Gordon, Grant):**
  - Impact of aging in terms of calendar time on corrosion, adhesive breakdown, etc. and impact to structural integrity must be determined
  - Safe-life design approach used for RCC mission life which is potentially an unsafe approach to ensure structural integrity
  - The residual strength of damaged RCC parts has not been demonstrated by testing with the exception of substrate oxidation, pinholes and craze cracks

Presenter M3/Material | Date FINAL | Slide 22 of 26 | Closed

Wing Leading Edge Design & Certification

- **Recommendations (agreed to by Curry, Gordon, Grant):**
  - Determine RCC component damage sources, frequency, and severity to include debris impact during ascent
  - Determine the damage tolerance capability for each damage type, location, and size ranges by calculating remaining service life and residual strength
  - Develop an NDE technique and capability to ensure damage limits have not been exceeded prior to each mission
  - Establish realistic service life duration expectation for remaining orbiters and revise operation and maintenance requirements accordingly

Presenter M3/Material | Date FINAL | Slide 23 of 26 | Closed

Wing Leading Edge Design & Certification

- **Documentation:**
  - Briefing by M. Gordon, "LESS/RCC Recovery and Reconstruction Data, OV-102 LESS/RCC Components Installed for STS-107", 1 March 2003
  - Boeing Specification MJ070-0001-1E, "Orbiter End Item Specification for the Space Shuttle Systems, Part 1, Performance and Design Requirements, 7 Nov 02
  - Briefing by D. Curry et al., "Orbiter RCC Design and Flight Experience", 28 July 1999

Presenter M3/Material | Date FINAL | Slide 24 of 26 | Closed

4

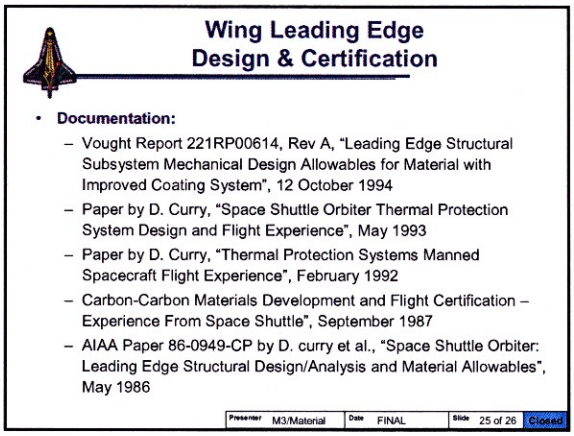
Wing Leading Edge
Design & Certification
• Documentation:
– Vought Report 221RP00614, Rev A, "Leading Edge Structural Subsystem Mechanical Design Allowables for Material with Improved Coating System", 12 October 1994
– Paper by D. Curry, "Space Shuttle Orbiter Thermal Protection System Design and Flight Experience", May 1993
– Paper by D. Curry, "Thermal Protection Systems Manned Spacecraft Flight Experience", February 1992
– Carbon-Carbon Materials Development and Flight Certification – Experience From Space Shuttle", September 1987
– AIAA Paper 86-0949-CP by D. curry et al., "Space Shuttle Orbiter: Leading Edge Structural Design/Analysis and Material Allowables", May 1986
Presenter M3/Material
Date FINAL
Slide 25 of 26
Closed

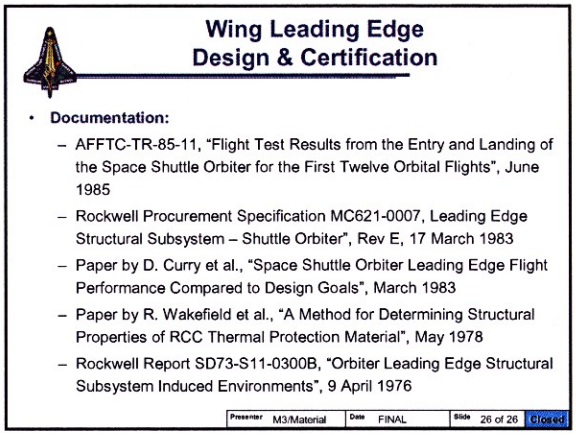
Wing Leading Edge
Design & Certification
• Documentation:
– AFFTC-TR-85-11, "Flight Test Results from the Entry and Landing of the Space Shuttle Orbiter for the First Twelve Orbital Flights", June 1985
– Rockwell Procurement Specification MC621-0007, Leading Edge Structural Subsystem – Shuttle Orbiter", Rev E, 17 March 1983
– Paper by D. Curry et al., "Space Shuttle Orbiter Leading Edge Flight Performance Compared to Design Goals", March 1983
– Paper by R. Wakefield et al., "A Method for Determining Structural Properties of RCC Thermal Protection Material", May 1978
– Rockwell Report SD73-S11-0300B, "Orbiter Leading Edge Structural Subsystem Induced Environments", 9 April 1976
Presenter M3/Material
Date FINAL
Slide 26 of 26
Closed

RCC Impact Energy Requirements

- **Action / Issue:** Determine adequacy of RCC impact requirements and certification
- **Background / Facts:**
  - Performance and design requirements documented in specification MJ070-0001-1E, 7 Nov 02
    - TPS impact energy design requirement is 0.006 foot-lbs (paragraph 3.3.1.8.11)
    - Orbiter not designed to withstand launch debris or ice (paragraph 3.3.1.8.16)
  - Procurement specification MC621-0007, Rev E requirement more stringent than design requirement
    - Impact energy limit ranges from 1 to 2.25 foot-pounds based on part thickness

Presenter M3/Material | Date FINAL | Slide 1 of 13 | Closed

Previous RCC Impact Testing

- **Background / Facts:**
  - Hypervelocity impact testing performed
    - Reference NASA-LARC Report TMX-74039, June 1977
    - Nylon projectile resulted in front face damage at 2.2 foot-pounds and both front and back face damage at 8.1 foot-pounds
    - Glass projectile resulted in front face damage at 0.2 foot-pounds
  - Hypervelocity impact testing performed in support of NRC MMOD study at JSC facility
    - 15 shots using 2017-T4 aluminum
    - Projectile energy ranged from 53 to 213 foot-pounds
    - Minimum damage: front face = 0.65" and back face = 0.87"

Presenter M3/Material | Date FINAL | Slide 2 of 13 | Closed

Previous RCC Impact Testing

- **Background / Facts :**
  - Low velocity ice impact testing performed
    - Reference Boeing report STS-82-0615
    - Specimen perforated at 132 foot-pounds normal to surface
  - Low velocity impact testing performed in an attempt to generate damage result seen on RCC panel 10R after STS-45 on OV-104-11
    - Aluminum projectile generated front face crater at 19.6 foot-pounds and front and rear face damage at 31.7 foot-pounds
    - Steel projectile generated front and rear face damage at 42.77 foot-pounds – best match of STS-45 damage
    - .22 short lead bullet did not damage specimen at 3.36 foot-pounds
    - Steel BB damaged front and rear face at 1.23 foot-pounds

Presenter M3/Material | Date FINAL | Slide 3 of 13 | Closed

WLE RCC Impact Fleet Experience Summary

Year	STS	OV	Flight #	Impact Location	Debris Type	Resulting Damage
1988	27R	104	3	T-Seal 7R	SRB Ablative	1 Dent, No SiC Loss
1992	45	104	11	Panel 10R	Man-Made Object	2 Dents with SiC Loss
1994	65	102	17	Panel 5L	MMOD	Small Crater
2003	107	102	28	Panel 5 to 10	ET Bi-Pod Foam	Under Evaluation

21 Flights Sampled, 43 Impacts Discovered due to Orbital Debris, Largest Damage = 0.2"

Presenter M3/Material | Date FINAL | Slide 4 of 13 | Closed

WLE RCC Impact Fleet Experience Foam/Ablative

- **Background / Facts:**
  - OV-104-03 impact damage to right wing discovered after STS-27R in 1988
    - Reference TPS post-flight report KL0-89-001
    - "Some of the RCC panels and tee seals had streaks on the OML"
    - "Rib station #7 had a dent near the upper trailing edge"
    - Most probable cause is the right SRB nose cap ablative insulating material
  - OV-102-28 ET bi-pod ramp foam impact to left wing during STS-107 in 2003

Presenter M3/Material | Date FINAL | Slide 5 of 13 | Closed

WLE RCC Impact Fleet Experience Man-Made Object

- **Background / Facts:**
  - OV-104-11 impact damage to panel 10R discovered after STS-45 in 1992
    - Reference S. Christensen briefing
    - Substrate was exposed and oxidized, panel scrapped
    - Failure analysis documented in LTR4088-2427
    - Impact was caused by a low velocity impact by a man-made object
    - Impact occurred before reentry heating
    - Ascent encounter determined to be possible
    - On-orbit encounter determined to be remote possibility

Presenter M3/Material | Date FINAL | Slide 6 of 13 | Closed

WLE RCC Impact Fleet Experience Man-Made Object

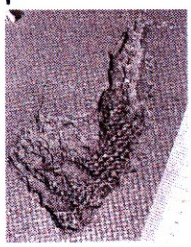

OML

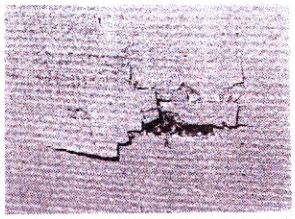

IML

OV-104-11, Panel 10R Impact Damage (1992)

Presenter M3/Material | Date FINAL | Slide 7 of 13 | Closed

WLE RCC Impact Fleet Experience MMOD

- **Background / Facts:**
  - OV-102-17 impact damage to panel 5L discovered after STS-65 in 1994
    - Most likely cause is a micro-meteorite (MMOD)
  - Hypervelocity impact to RCC components during flight is not unusual
    - 43 impacts occurred during the 21 flights sampled
    - Largest damage was 0.2"
    - No through-penetrations occurred

Presenter M3/Material | Date FINAL | Slide 8 of 13 | Closed

WLE RCC Impact Fleet Experience MMOD

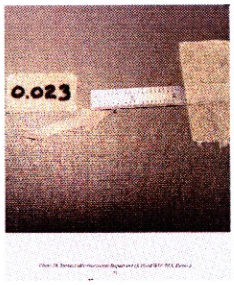

Crater Approximately 0.08" in Diameter

Depth Unknown but Reported not to be through-thickness

OV-102-17, Panel 5L Micro-meteorite (1994)

Presenter M3/Material | Date FINAL | Slide 9 of 13 | Closed

WLE RCC Impact Category: Potential Contributor

- **Findings (agreed to by Curry, Gordon and Grant):**
  - Impact energy design requirement is minimal
  - Impact energy capability exceeds original design requirements
- **Recommendations (agreed to by Curry, Gordon and Grant):**
  - Utilize foam impact test results to evaluate impact energy resistance and adequacy of current requirements
  - Establish realistic launch/ascent debris types (foam, SLA, etc.) and evaluate capability of WLE system to withstand the impacts via testing and analysis

Presenter M3/Material | Date FINAL | Slide 10 of 13 | Closed

WLE RCC Impact

- **Documentation:**
  - Boeing report KL0-03-001, Mission STS-112 OV-104 Flight 26 Thermal Protection System Post-Flight Assessment", May 2003
  - JSC report, "STS-112 Launch Film Screening Report", 12 October 2002
  - MSFC report, "STS-112 JSC Launch Video Screening Report", 8 October 2002

Presenter M3/Material | Date FINAL | Slide 11 of 13 | Closed

WLE RCC Impact

- **Documentation:**
  - Boeing Specification MJ070-0001-1E, "Orbiter End Item Specification for the Space Shuttle Systems, Part 1, Performance and Design Requirements, 7 Nov 02
  - Paper by D. Curry et.al., "Oxidation of Hypervelocity Impacted RCC", June 2000
  - NASA TP-2000-209760, "Oxidation of RCC Subjected to Hypervelocity Impact", March 2000
  - JSC Report 28768, "As-Flown Shuttle Orbiter Meteoroid/Orbital Debris Assessment", January 2000
  - JSC Report 28404, "STS-87 Orbiter Meteoroid/Orbital Debris Impact Damage Analysis", 7 August 1998
  - JSC Report 28398, "Hypervelocity Impact Testing of RCC", May 1998
  - Briefing by M. Hasselbeck, "Space Shuttle Orbiter On-Orbit Impact Critical Failure Criteria", 17 June 1997

Presenter M3/Material | Date FINAL | Slide 12 of 13 | Closed

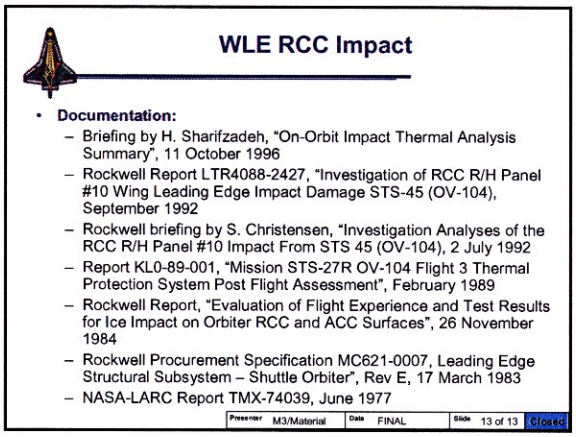
WLE RCC Impact
• Documentation:
– Briefing by H. Sharifzadeh, "On-Orbit Impact Thermal Analysis Summary", 11 October 1996
– Rockwell Report LTR4088-2427, "Investigation of RCC R/H Panel #10 Wing Leading Edge Impact Damage STS-45 (OV-104), September 1992
– Rockwell briefing by S. Christensen, "Investigation Analyses of the RCC R/H Panel #10 Impact From STS 45 (OV-104), 2 July 1992
– Report KL0-89-001, "Mission STS-27R OV-104 Flight 3 Thermal Protection System Post Flight Assessment", February 1989
– Rockwell Report, "Evaluation of Flight Experience and Test Results for Ice Impact on Orbiter RCC and ACC Surfaces", 26 November 1984
– Rockwell Procurement Specification MC621-0007, Leading Edge Structural Subsystem – Shuttle Orbiter", Rev E, 17 March 1983
– NASA-LARC Report TMX-74039, June 1977
Presenter M3/Material
Date FINAL
Slide 13 of 13
Closed

3

RCC Production

6-1 RCC Production Processes

Matrix

Presenter	CAIB/Group 1	Date	FINAL	Slide	8 of 32

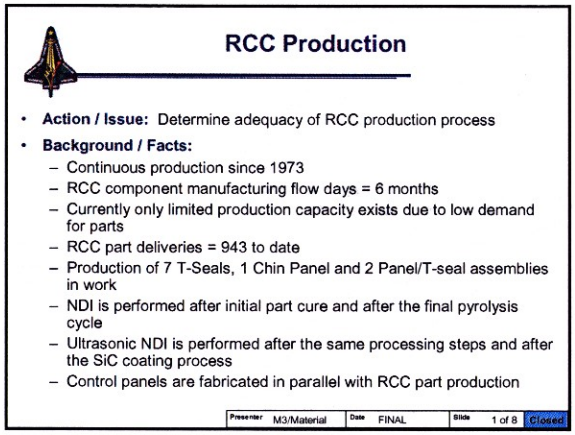
RCC Production
• Action / Issue: Determine adequacy of RCC production process
• Background / Facts:
– Continuous production since 1973
– RCC component manufacturing flow days = 6 months
– Currently only limited production capacity exists due to low demand for parts
– RCC part deliveries = 943 to date
– Production of 7 T-Seals, 1 Chin Panel and 2 Panel/T-seal assemblies in work
– NDI is performed after initial part cure and after the final pyrolysis cycle
– Ultrasonic NDI is performed after the same processing steps and after the SiC coating process
– Control panels are fabricated in parallel with RCC part production
Presenter M3/Material Date FINAL Slide 1 of 8 Closed

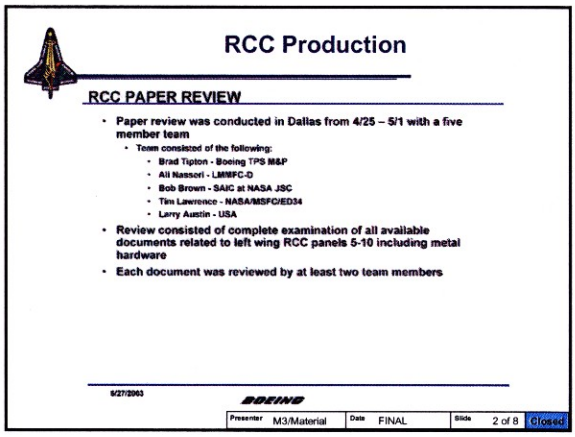
RCC Production
RCC PAPER REVIEW
• Paper review was conducted in Dallas from 4/25 – 5/1 with a five member team
• Team consisted of the following:
• Brad Tipton - Boeing TPS M&P
• Ali Nassori - LMMFC-D
• Bob Brown - SAIC at NASA JSC
• Tim Lawrence - NASA/MSFC/ED34
• Larry Austin - USA
• Review consisted of complete examination of all available documents related to left wing RCC panels 5-10 including metal hardware
• Each document was reviewed by at least two team members
5/27/2003
BOEING
Presenter M3/Material Date FINAL Slide 2 of 8 Closed

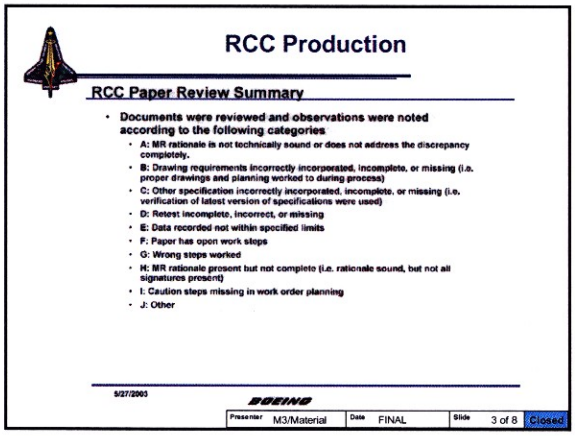
RCC Production
RCC Paper Review Summary
• Documents were reviewed and observations were noted according to the following categories
• A: MR rationale is not technically sound or does not address the discrepancy completely.
• B: Drawing requirements incorrectly incorporated, incomplete, or missing (i.e. proper drawings and planning worked to during process)
• C: Other specification incorrectly incorporated, incomplete, or missing (i.e. verification of latest version of specifications were used)
• D: Retest incomplete, incorrect, or missing
• E: Data recorded not within specified limits
• F: Paper has open work steps
• G: Wrong steps worked
• H: MR rationale present but not complete (i.e. rationale sound, but not all signatures present)
• I: Caution steps missing in work order planning
• J: Other
5/27/2003
BOEING
Presenter M3/Material Date FINAL Slide 3 of 8 Closed

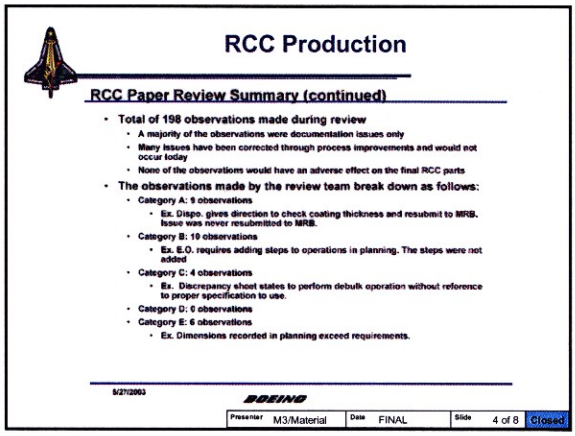
RCC Production
RCC Paper Review Summary (continued)
• Total of 198 observations made during review
• A majority of the observations were documentation issues only
• Many issues have been corrected through process improvements and would not occur today
• None of the observations would have an adverse effect on the final RCC parts
• The observations made by the review team break down as follows:
• Category A: 9 observations
• Ex. Disps. given direction to check coating thickness and resubmit to MRB. Issue was never resubmitted to MRB.
• Category B: 10 observations
• Ex. E.O. requires adding steps to operations in planning. The steps were not added
• Category C: 4 observations
• Ex. Discrepancy sheet states to perform debulk operation without reference to proper specification to use.
• Category D: 0 observations
• Category E: 6 observations
• Ex. Dimensions recorded in planning exceed requirements.
5/27/2003
BOEING
Presenter M3/Material Date FINAL Slide 4 of 8 Closed

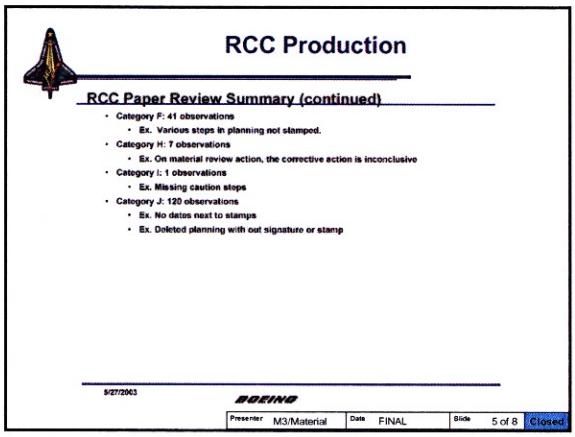
RCC Production
RCC Paper Review Summary (continued)
• Category F: 41 observations
• Ex. Various steps in planning not stamped.
• Category H: 7 observations
• Ex. On material review action, the corrective action is inconclusive
• Category I: 1 observations
• Ex. Missing caution steps
• Category J: 120 observations
• Ex. No dates next to stamps
• Ex. Deleted planning with out signature or stamp
5/27/2003
BOEING
Presenter M3/Material Date FINAL Slide 5 of 8 Closed

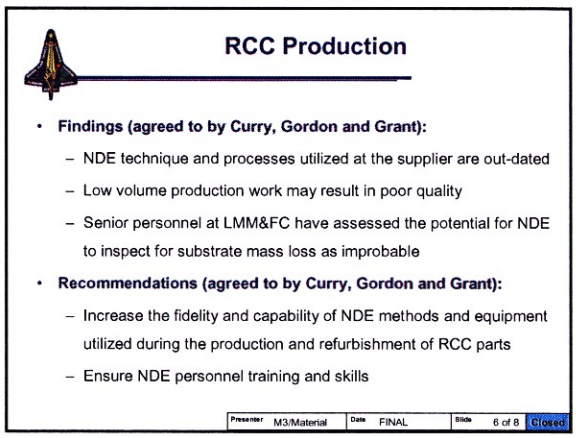
RCC Production
• Findings (agreed to by Curry, Gordon and Grant):
– NDE technique and processes utilized at the supplier are out-dated
– Low volume production work may result in poor quality
– Senior personnel at LMM&FC have assessed the potential for NDE to inspect for substrate mass loss as improbable
• Recommendations (agreed to by Curry, Gordon and Grant):
– Increase the fidelity and capability of NDE methods and equipment utilized during the production and refurbishment of RCC parts
– Ensure NDE personnel training and skills
Presenter M3/Material Date FINAL Slide 6 of 8 Closed

1

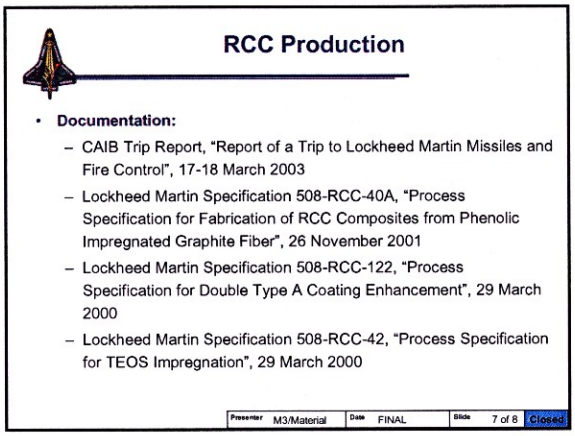
RCC Production
• Documentation:
– CAIB Trip Report, "Report of a Trip to Lockheed Martin Missiles and Fire Control", 17-18 March 2003
– Lockheed Martin Specification 508-RCC-40A, "Process Specification for Fabrication of RCC Composites from Phenolic Impregnated Graphite Fiber", 26 November 2001
– Lockheed Martin Specification 508-RCC-122, "Process Specification for Double Type A Coating Enhancement", 29 March 2000
– Lockheed Martin Specification 508-RCC-42, "Process Specification for TEOS Impregnation", 29 March 2000
Presenter M3/Material
Date FINAL
Slide 7 of 8
Closed

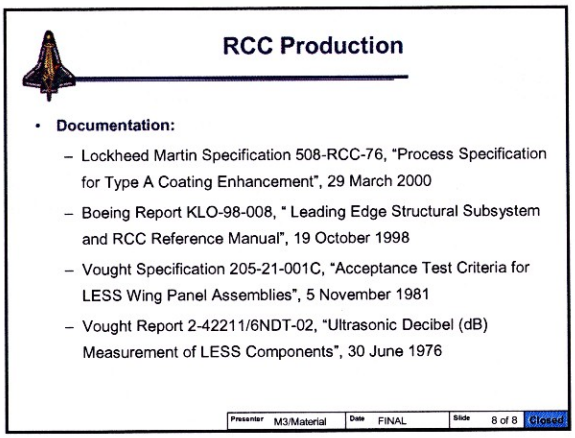
RCC Production
• Documentation:
– Lockheed Martin Specification 508-RCC-76, "Process Specification for Type A Coating Enhancement", 29 March 2000
– Boeing Report KLO-98-008, " Leading Edge Structural Subsystem and RCC Reference Manual", 19 October 1998
– Vought Specification 205-21-001C, "Acceptance Test Criteria for LESS Wing Panel Assemblies", 5 November 1981
– Vought Report 2-42211/6NDT-02, "Ultrasonic Decibel (dB) Measurement of LESS Components", 30 June 1976
Presenter M3/Material
Date FINAL
Slide 8 of 8
Closed

RCC
Mission Life

7-1 RCC Mission Life Capability

RCC Mission Life

- **Action / Issue:** Determine adequacy of RCC mission life analysis methodology
- **Background / Facts:**
  - Oxidation rate is the most important parameter to determine mission life
    - Function of temperature, pressure and heating time
    - Resulting mass loss reduces part strength
  - Repeated exposure to the flight environment degrades the oxidation protection system and increases amount of mass loss
  - Mass loss rate characterized by laboratory testing

Presenter M3/Material | Date FINAL | Slide 1 of 23 | Closed

RCC Mission Life

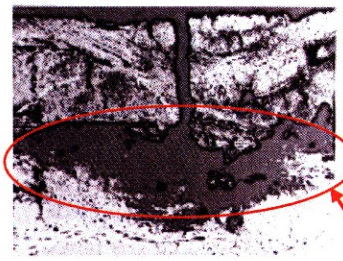

Presenter M3/Material | Date FINAL | Slide 2 of 23 | Closed

RCC Mission Life

- **Background / Facts:**
  - Arc jet test at Ames and JSC in 1973 first revealed mass loss with no apparent dimensional changes
  - Database generated for non-TEOS material
    - Arc jet and radiant exposure tests at JSC, ARC, LARC and Rockwell
    - Established strength reduction as a function of mass loss
    - Mass loss greater in plasma arc jet (convective) than radiant tests
    - Mass loss correlation (radiant/convective) developed from the test results (see charts 7 and 8 for convective heating results)
    - Established need for improved coating system

Presenter M3/Material | Date FINAL | Slide 3 of 23 | Closed

RCC Mission Life

Mass loss limit for internal surfaces is 0.10 psf

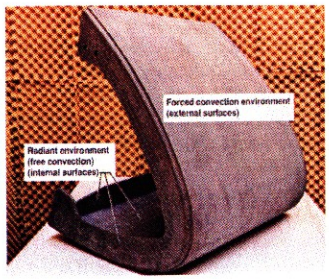

Mass loss limit for external surfaces is 0.03 psf

Presenter M3/Material | Date FINAL | Slide 4 of 23 | Closed

RCC Mission Life
Material System Evolution

- **Background / Facts:**
  - TEOS infiltration system baselined for OV-102 in March 1976
    - Mass loss correlation for radiant and convective heating developed in 1978
  - Surface porosity effects on mission life discovered in December 1978
  - Type A sealant developed in 1980 to seal surface porosity
    - Retrofitted onto OV-102 after 5th flight
    - Mass loss database developed in 1984
  - Double Type A (DTA) sealant developed to increase mission life
    - Baseline for OV-105 and all new parts
    - Mass loss database developed in 1994

Presenter M3/Material | Date FINAL | Slide 5 of 23 | Closed

RCC Mission Life
Convective Mass Loss Correlation

- **Background / Facts:**
  - RCC/SiC/TEOS/Type A material system plasma arc jet tests for convective mass loss conducted at JSC in 1984
    - 40 total specimens, 2 each at 20 combinations of temperature and pressure
    - Temperature ranged from 1000 to 3000 F
    - Pressure ranged from 0.01 to 0.05 atmospheres
  - Test results summary
    - SiC erosion occurred at temperatures at 2800 F and above
    - Specimens exposed to temperatures at 2700 F and below did not indicate a thickness change
    - Mass loss rates increase rapidly above 2500 F
    - See next 2 charts for actual results

Presenter M3/Material | Date FINAL | Slide 6 of 23 | Closed

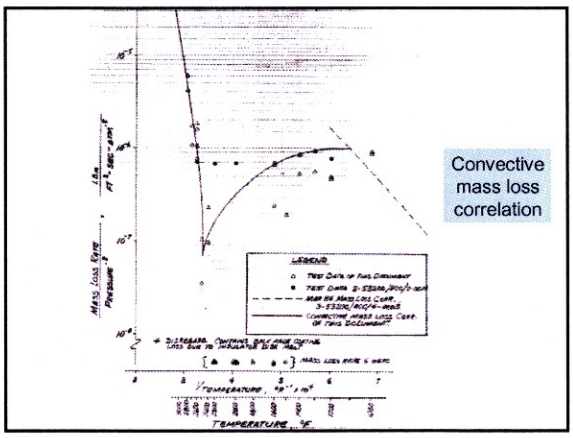

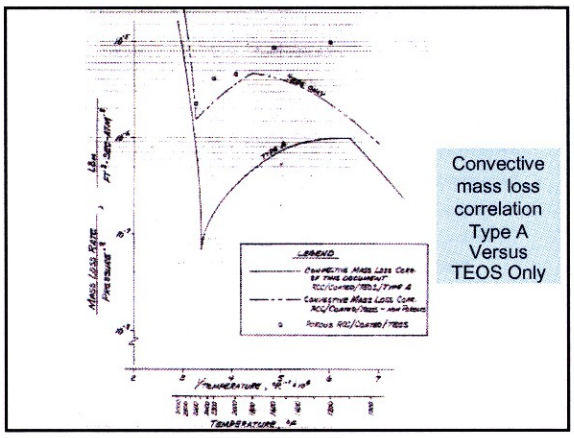

RCC Mission Life Determination

- **Background / Facts :**
  - Determination of mission lives due to operational aging includes both thermal and structural analysis results
    - Thermal analysis determines mass loss based on certification mission profiles (closest match to each actual mission)
    - Structural analysis determines strength based on air loads and thermal loads
  - Margin of safety is determined for longest possible mission life while preserving the required factor of safety = 1.4
  - Mission life limits are documented in NSTS 08171, Operations and Maintenance Requirements Specifications Document, File II, Volume 3

Presenter M3/Material | Date FINAL | Slide 9 of 23 | Closed

RCC Mission Life Margin of Safety Versus Factor of Safety

- **Background / Facts :**
  - MS = (Allowable Stress / Applied Stress * FS) - 1
  - MS = Margin of Safety
    - Required to be 0 or positive
  - FS = Factor of Safety
    - Shuttle program uses 1.4
    - USAF, USN, commercial aircraft use 1.5
  - Allowable stress based on mechanical design allowables database generated from over 2000 RCC specimens (A-basis, 99% of material expected to exceed the value)
    - Allowable stress for material generated for material at mass loss cut-off limits
  - When we hear that a location has a reduced "factor of safety" – it really means a negative margin of safety (reduction of FS is typically not an option)
  - SRB ETA ring is an example of a liberal allowance of a FS reduction – issue only known for 24 hours prior to ET tanking meeting

Presenter M3/Material | Date FINAL | Slide 10 of 23 | Closed

RCC Mission Life RCC Allowable Stress for Some Properties

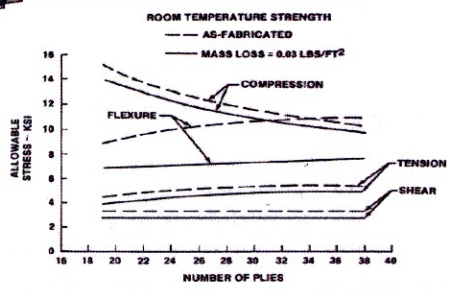

19 plies = 0.24" thick, 38 plies = 0.5" thick

Presenter M3/Material | Date FINAL | Slide 11 of 23 | Closed

RCC Mission Life

- **Background / Facts :**
  - OV-102 RCC components were not coated with Type A sealant for the first 5 missions – reduced mission lives from other orbiters
  - RCC Refurbishment intervals established to replenish Type A sealant to achieve desired mission life
  - Minor repair capability developed to allow for continued operation between scheduled OMM downtime
  - Minimum predicted life for WLE RCC component on OV-102 is 50 missions for panel/seal 9 assembly

Presenter M3/Material | Date FINAL | Slide 12 of 23 | Closed

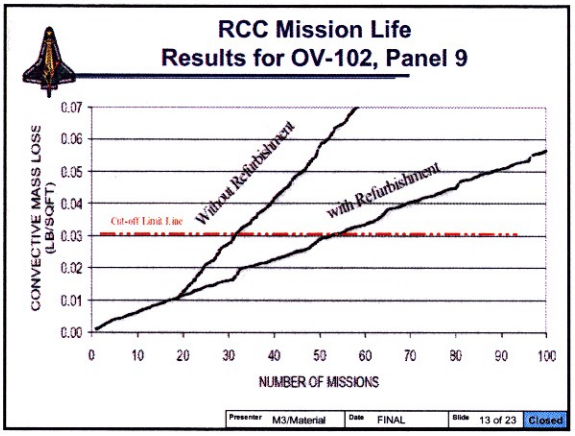
RCC Mission Life
Results for OV-102, Panel 9
CONVECTIVE MASS LOSS (LB/SQFT)
0.07
0.06
0.05
0.04
0.03
0.02
0.01
0.00
Without Refurbishment
with Refurbishment
Cut-off Limit Line
0
10
20
30
40
50
60
70
80
90
100
NUMBER OF MISSIONS
Presenter M3/Material
Date FINAL
Slide 13 of 23
Closed

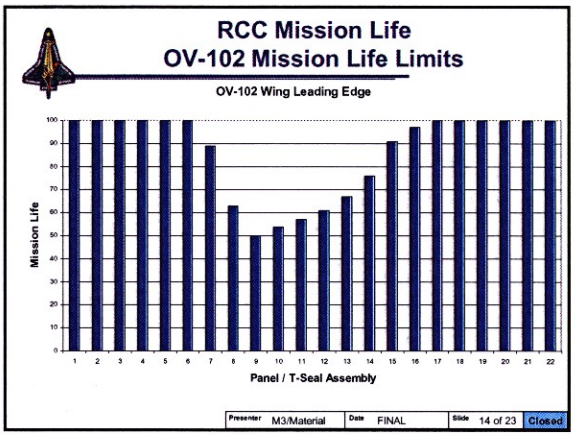
RCC Mission Life
OV-102 Mission Life Limits
OV-102 Wing Leading Edge
Mission Life
Panel / T-Seal Assembly
Presenter M3/Material
Date FINAL
Slide 14 of 23
Closed

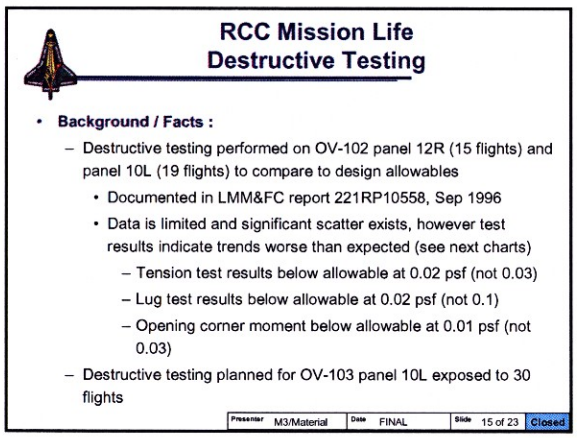
RCC Mission Life
Destructive Testing
• Background / Facts :
– Destructive testing performed on OV-102 panel 12R (15 flights) and panel 10L (19 flights) to compare to design allowables
• Documented in LMM&FC report 221RP10558, Sep 1996
• Data is limited and significant scatter exists, however test results indicate trends worse than expected (see next charts)
– Tension test results below allowable at 0.02 psf (not 0.03)
– Lug test results below allowable at 0.02 psf (not 0.1)
– Opening corner moment below allowable at 0.01 psf (not 0.03)
– Destructive testing planned for OV-103 panel 10L exposed to 30 flights
Presenter M3/Material
Date FINAL
Slide 15 of 23
Closed

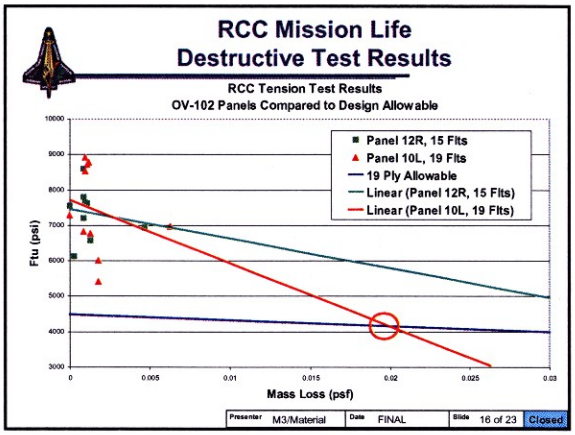
RCC Mission Life
Destructive Test Results
RCC Tension Test Results
OV-102 Panels Compared to Design Allowable
Panel 12R, 15 Flts
Panel 10L, 19 Flts
19 Ply Allowable
Linear (Panel 12R, 15 Flts)
Linear (Panel 10L, 19 Flts)
Ftu (psi)
Mass Loss (psf)
Presenter M3/Material
Date FINAL
Slide 16 of 23
Closed

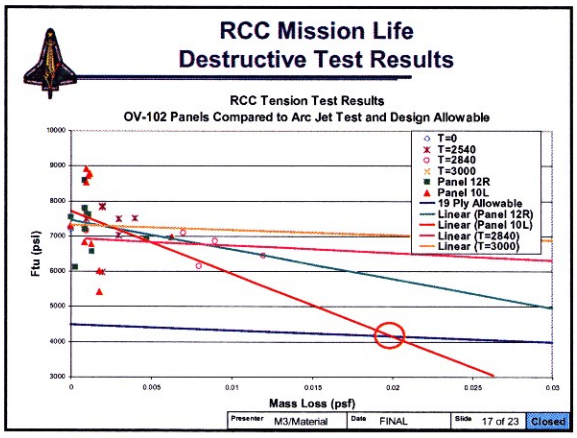
RCC Mission Life
Destructive Test Results
RCC Tension Test Results
OV-102 Panels Compared to Arc Jet Test and Design Allowable
T=0
T=2540
T=2840
T=3000
Panel 12R
Panel 10L
19 Ply Allowable
Linear (Panel 12R)
Linear (Panel 10L)
Linear (T=2840)
Linear (T=3000)
Ftu (psi)
Mass Loss (psf)
Presenter M3/Material
Date FINAL
Slide 17 of 23
Closed

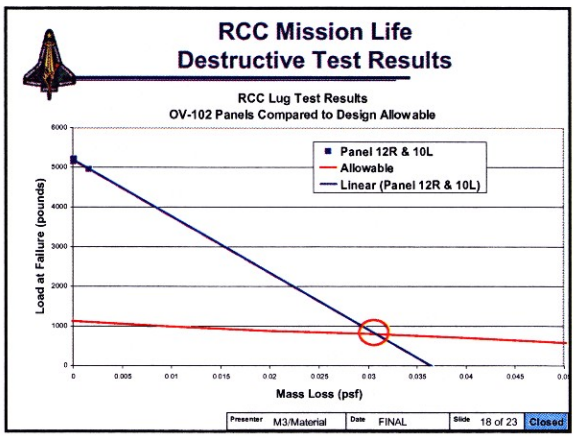
RCC Mission Life
Destructive Test Results
RCC Lug Test Results
OV-102 Panels Compared to Design Allowable
Panel 12R & 10L
Allowable
Linear (Panel 12R & 10L)
Load at Failure (pounds)
Mass Loss (psf)
Presenter M3/Material
Date FINAL
Slide 18 of 23
Closed

RCC Mission Life
Destructive Test Results

RCC Opening Corner Moment Test Results
OV-102 Panels Compared to Design Allowable

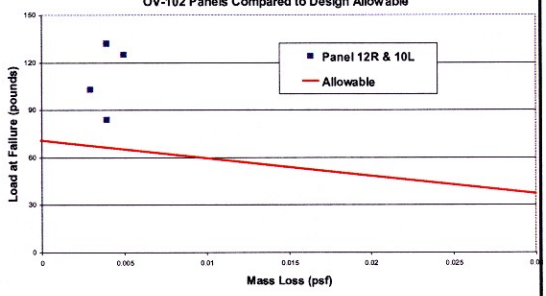

Presenter M3/Material | Date FINAL | Slide 19 of 23 | Closed

RCC Mission Life
Category: Potential Contributor

- **Findings:**
  - Insufficient data exists to compare predicted mass loss and strength to actual mass loss and strength on flown hardware due to repeated exposure
  - However, results to date indicate need to accelerate additional destructive testing of flown hardware
  - Only 2 tests were performed to determine oxidation associated with craze cracks used to develop tactile evaluation method for coating adherence reduction due to oxidation along interface
  - Recent NASA GRC examination of OV-102 panel 12R has revealed coating and substrate anomalies that warrant further investigation

Presenter M3/Material | Date FINAL | Slide 20 of 23 | Closed

RCC Mission Life
Category: Potential Contributor

- **Recommendations (Agreed to by Curry):**
  - Develop a plan to conduct destructive testing of flown RCC components that addresses:
    - Extensive NDE to select test specimen locations
    - Predicted mass loss rates and corresponding reduction in mechanical properties versus actual test results
    - Type A sealant loss on OML
    - Pinhole impact on coating adherence and mechanical property reductions
    - Oxidation associated with craze cracks
    - Substrate oxidation impact on mechanical properties
    - Impact energy resistance due to launch/ascent debris
  - Conduct testing of flown hardware ASAP per above plan

Presenter M3/Material | Date FINAL | Slide 21 of 23 | Closed

RCC Mission Life

- **Documentation:**
  - NASA GRC Briefing by A. Calomino, "Microstructural Characterization of RCC Materials", 16 May 2003
  - NSTS 08171, Operations and Maintenance Requirements and Specifications Document, File II, Volume 3, "Limited Life/Time/Cycle Items", 1 May 2003
  - Lockheed Martin Report 221RP10558, "RCC Pinhole/Sealant Loss Investigation", September 1996
  - Lockheed Martin Report 221RP10551, "OV-102 Panel / Seal Set 10L Mechanical Properties Tests", August 1996
  - Lockheed Martin Report 221RP10539, "RCC Pin-Hole / Sealant Loss Coating Adherence", May 1996

Presenter M3/Material | Date FINAL | Slide 22 of 23 | Closed

RCC Mission Life

- **Documentation:**
  - Paper by A. Eckel et.al, "Oxidation Kinetics of a Continuous Carbon Phase in a Nonreactive Matrix", 4 April 1995
  - NASA TM 106793, "Thermochemical Degradation Mechanisms for RCC Panels on the Space Shuttle, N. Jacobson, January 1995
  - NASA TM 104792, "Analysis of the Shuttle Orbiter RCC Oxidation Protection System", D. Curry et.al., June 1994
  - AIAA 94-2084, "Ablation Analysis of the Shuttle Orbiter Oxidation Protected RCC", June 1994
  - DIR NO. 3-53200/RCC/4-0006, "June 1984 Convective Mass Loss Correlation", 28 June 1984

Presenter M3/Material | Date FINAL | Slide 23 of 23 | Closed

RCC
Fleet Experience – Aging

8-1 RCC Maintenance Actions

8-2 Pinholes in RCC Components

8-3 Deterioration of Type A Sealant

8-4 NDE of RCC Components

Matrix

Presenter	CAIB/Group 1	Date	FINAL	Slide	10 of 32

WLE Maintenance Actions

- **Action / Issue:** WLE maintenance actions evaluated for negative trends or damage experience not already incorporated into new OMRSD requirements
- **Background:**
  - 3 RCC panel/seals have been replaced on OV-102
    - Replaced panel/seal 12R after 15 flights for destructive testing
    - Replaced panel/seal 10L after 19 flights for destructive testing
    - Replaced panel/seal 11L after 19 flights due to fit-up issues with the new panel/seal 10L
      - Removed panel/seal 11L (P/N 10211LA001) is currently in the spares pool

Presenter M3/Material | Date FINAL | Slide 1 of 20 | Closed

WLE Maintenance Actions

- **Background:**
  - 10 RCC panels and 8 seals have been repaired on OV-102
    - Repaired 7 panels and 6 seals on the left wing of OV-102
    - Repaired 3 panels and 2 seals on the right wing of OV-102
  - Refurbished 11 RCC panels and 12 seals on the left wing and 11 RCC panels and 11 seals on the right wing of OV-102

Presenter M3/Material | Date FINAL | Slide 2 of 20 | Closed

RCC Maintenance Actions

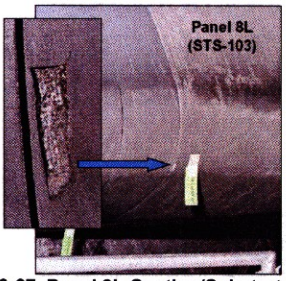

Suspected Oxidation At SiC and Substrate Interface

OV-103-27, Panel 8L Coating/Substrate Loss (Jan 00) Panel Scrapped

Presenter M3/Material | Date FINAL | Slide 3 of 20 | Closed

RCC Maintenance Actions

OV-102-26, T-Seal 11L Cavity (Dec 00)

Presenter M3/Material | Date FINAL | Slide 4 of 20 | Closed

RCC Maintenance Actions

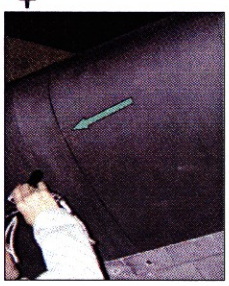

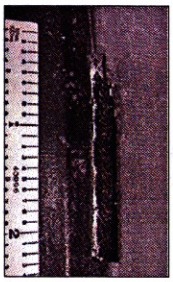

Suspected Oxidation At SiC and Substrate Interface

(2"L x 0.3"W x 0.18"D)

OV-103-29, Panel 10L Coating/Substrate Loss (Apr 01)

Presenter M3/Material | Date FINAL | Slide 5 of 20 | Closed

RCC Maintenance Actions

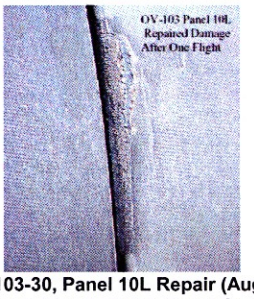

OV-103-30, Panel 10L Repair (Aug 01) Damaged After 1 Flight, Panel Scrapped

Presenter M3/Material | Date FINAL | Slide 6 of 20 | Closed

1

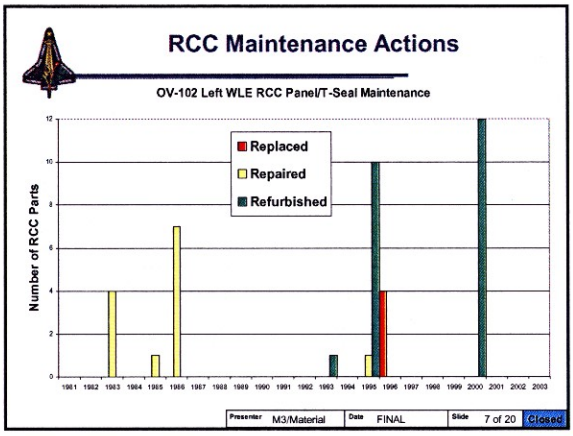
RCC Maintenance Actions
OV-102 Left WLE RCC Panel/T-Seal Maintenance
Number of RCC Parts
Replaced
Repaired
Refurbished
Presenter M3/Material
Date FINAL
Slide 7 of 20
Closed

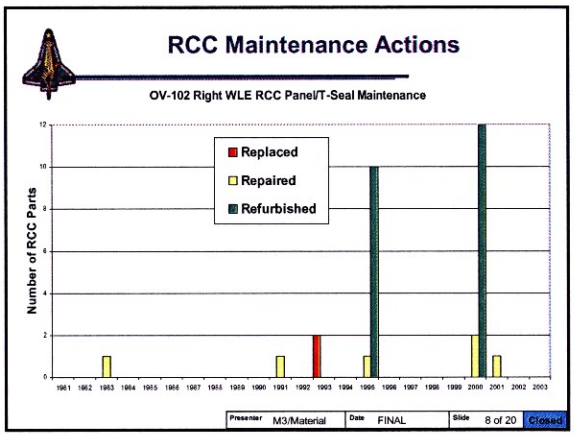
RCC Maintenance Actions
OV-102 Right WLE RCC Panel/T-Seal Maintenance
Number of RCC Parts
Replaced
Repaired
Refurbished
Presenter M3/Material
Date FINAL
Slide 8 of 20
Closed

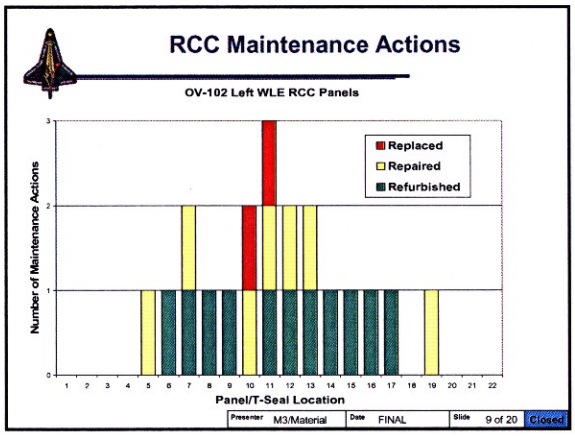
RCC Maintenance Actions
OV-102 Left WLE RCC Panels
Number of Maintenance Actions
Panel/T-Seal Location
Replaced
Repaired
Refurbished
Presenter M3/Material
Date FINAL
Slide 9 of 20
Closed

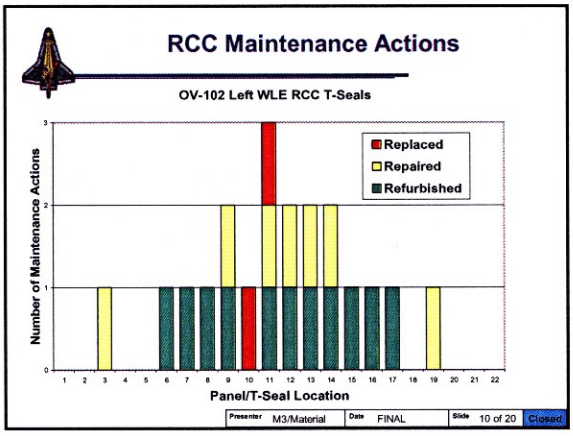
RCC Maintenance Actions
OV-102 Left WLE RCC T-Seals
Number of Maintenance Actions
Panel/T-Seal Location
Replaced
Repaired
Refurbished
Presenter M3/Material
Date FINAL
Slide 10 of 20
Closed

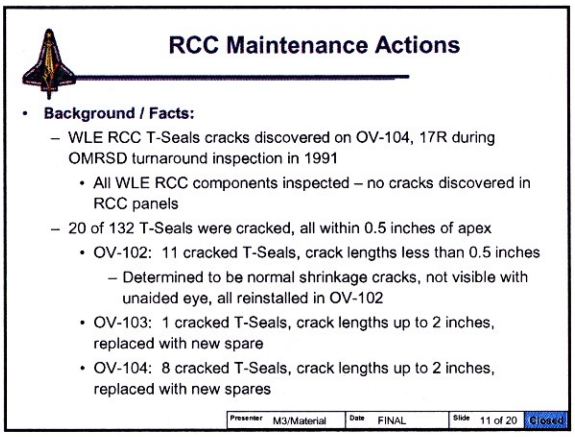
RCC Maintenance Actions
• Background / Facts:
– WLE RCC T-Seals cracks discovered on OV-104, 17R during OMRSD turnaround inspection in 1991
• All WLE RCC components inspected – no cracks discovered in RCC panels
– 20 of 132 T-Seals were cracked, all within 0.5 inches of apex
• OV-102: 11 cracked T-Seals, crack lengths less than 0.5 inches
– Determined to be normal shrinkage cracks, not visible with unaided eye, all reinstalled in OV-102
• OV-103: 1 cracked T-Seals, crack lengths up to 2 inches, replaced with new spare
• OV-104: 8 cracked T-Seals, crack lengths up to 2 inches, replaced with new spares
Presenter M3/Material
Date FINAL
Slide 11 of 20
Closed

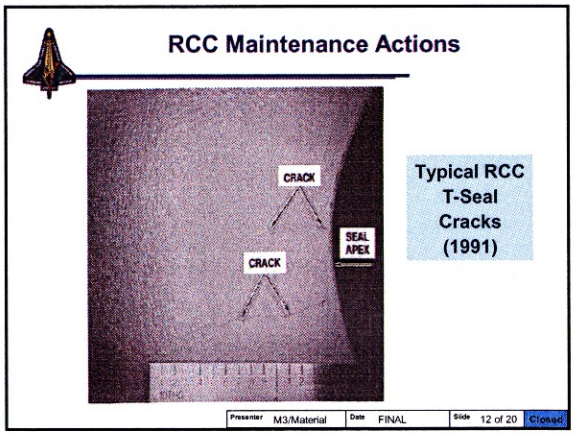
RCC Maintenance Actions
CRACK
CRACK
SEAL APEX
Typical RCC T-Seal Cracks (1991)
Presenter M3/Material
Date FINAL
Slide 12 of 20
Closed

RCC Maintenance Actions

- **Background / Facts:**
  - RCC T-Seal Cracking investigation documented in Rockwell Report LTR 4088-2401, November 1991
  - Sectioned OV-104, 17R (worst cracking) and 18R (3rd worst case) for failure analysis
    - No substrate cracks
    - Laminates significantly distorted
    - OV-104 panel 17R had oxidation damage
  - Removed coating from several other T-seals – no substrate cracks found
  - Conclusions from failure analysis (metallurgical, fractography, etc.)
    - Cracks only in SiC layer
    - Cracks due to variations in fabrication lay up process resulting in different laminate distortions

Presenter M3/Material | Date FINAL | Slide 13 of 20 | Closed

RCC Maintenance Actions

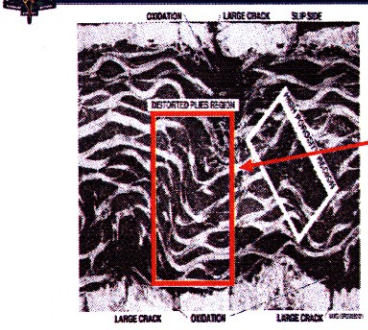

Distorted Plies Region

Presenter M3/Material | Date FINAL | Slide 14 of 20 | Closed

RCC Maintenance Actions

- **Background / Facts:**
  - Determined full length SiC layer crack does not affect static strength
  - Analyzed full-length substrate crack
    - Factor of safety > 1.4 for entry/landing
    - Factor of safety = 1.38 for ascent
  - Tested 2 T-seals for coating crack growth characteristics at a stress level of 80% of design limit in 1991
    - Tested OV-102 #9 left (between panels 9 and 10) for 400 cycles – determined via analysis and inspection negligible fatigue damage occurred and re-installed T-seal in OV-102
    - Tested OV-104 RH #18 for 100 cycles – no crack growth, part was scrapped for destructive testing

Presenter M3/Material | Date FINAL | Slide 15 of 20 | Closed

RCC Maintenance Actions

OV-104 RH 17 T-SEAL

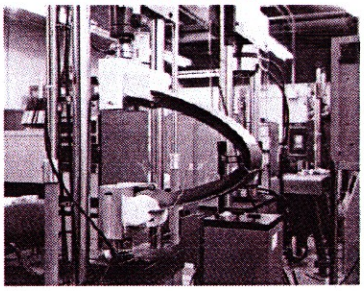

RCC T-Seal Fatigue Test Setup

Presenter M3/Material | Date FINAL | Slide 16 of 20 | Closed

WLE Maintenance Actions

- **Background / Facts:**
  - OV-102 wing leading edge spars have a history of degradation due to corrosion
    - Design corrosion protection system was a single coat of MB0125-055 primer (Koropon)
    - MB0130-119 Type II RTV adhesive applied as a galvanic barrier on forward most plane of corrugated spar
    - Design change incorporated at J2 OMDP to apply 2 coats of Koropon and cover with RTV topcoat as moisture and galvanic barrier
  - Inspection process updated
    - Full inspection performed every 4 and ½ years (V30KG0.060 and V30LG0.060) which requires removal of all RCC panels and associated support fittings and insulators
    - Sampling inspection performed every 3 years (V30KG0.065 and V30LG0.065) for 6 panels per side

Presenter M3/Material | Date FINAL | Slide 17 of 20 | Closed

WLE Maintenance Actions

- **Background / Facts:**
  - OV-102 inspections performed in conjunction with WLE refurbishment per MCR18457 during J2 resulted in significant corrosion findings
    - 41 doublers required on the right side
    - Multiple doublers required on the left side
  - Exploratory holes were drilled for core inspection and no corrosion was detected
  - Inspections during J3 did not detect evidence of corrosion on the WLE spars

Presenter M3/Material | Date FINAL | Slide 18 of 20 | Closed

3

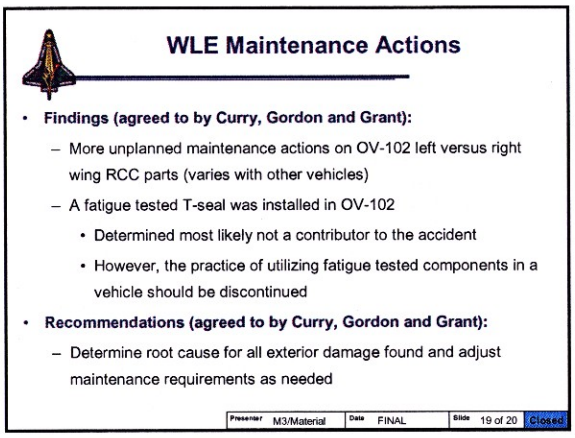
WLE Maintenance Actions
• Findings (agreed to by Curry, Gordon and Grant):
– More unplanned maintenance actions on OV-102 left versus right wing RCC parts (varies with other vehicles)
– A fatigue tested T-seal was installed in OV-102
• Determined most likely not a contributor to the accident
• However, the practice of utilizing fatigue tested components in a vehicle should be discontinued
• Recommendations (agreed to by Curry, Gordon and Grant):
– Determine root cause for all exterior damage found and adjust maintenance requirements as needed
Presenter M3/Material
Date FINAL
Slide 19 of 20
Closed

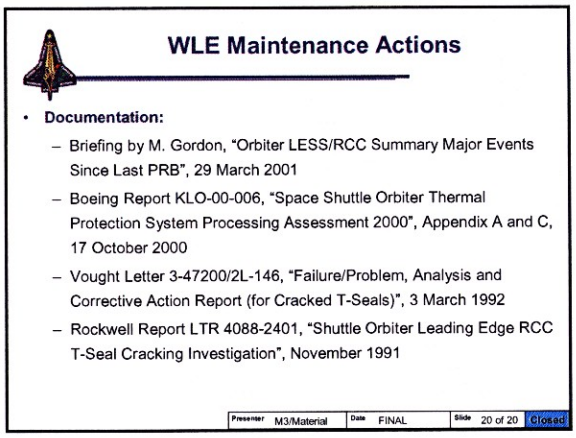
WLE Maintenance Actions
• Documentation:
– Briefing by M. Gordon, "Orbiter LESS/RCC Summary Major Events Since Last PRB", 29 March 2001
– Boeing Report KLO-00-006, "Space Shuttle Orbiter Thermal Protection System Processing Assessment 2000", Appendix A and C, 17 October 2000
– Vought Letter 3-47200/2L-146, "Failure/Problem, Analysis and Corrective Action Report (for Cracked T-Seals)", 3 March 1992
– Rockwell Report LTR 4088-2401, "Shuttle Orbiter Leading Edge RCC T-Seal Cracking Investigation", November 1991
Presenter M3/Material
Date FINAL
Slide 20 of 20
Closed

RCC Pinholes

- **Action / Issue:** Determine adequacy of pinhole corrective actions
- **Background / Facts:**
  - Pinholes first discovered on OV-102 after 12 flights in 1992
  - Pinholes subsequently found on all other orbiters
  - Pinhole size/quantity increased with flight exposure
  - Testing was performed to determine root cause of pinholes based on several theories
    - Zinc oxide contamination
    - Sea mist salt contamination
    - TEOS application

Presenter M3/Material | Date FINAL | Slide 1 of 16 | Closed

RCC Pinholes

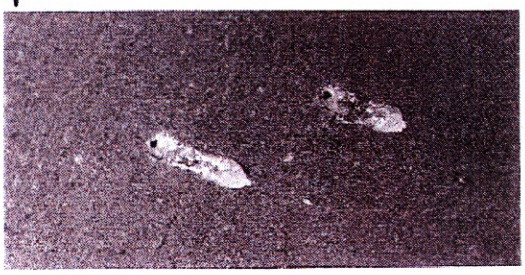

Typical Pinholes (1992) First Discovered on OV-102-12

Presenter M3/Material | Date FINAL | Slide 2 of 16 | Closed

RCC Pinholes

- **Background / Facts:**
  - OV-102 RCC panel 12R removed after 15th flight for detailed destructive evaluation in October 1993
    - Reference Rockwell Report LTR 6322-4039, Dec 1994
  - Optical and SEM evaluation performed on 15 pinholes
    - Majority of pin holes occur along craze cracks in SiC layer
    - Typically in thick regions of SiC layer – indicative of porous substrate
  - Pinhole glass chemistry determined
    - Silicon, oxygen, aluminum and zinc
  - Zinc not a part of the RCC material system – suggested contamination from external source
  - 6 samples collected from the RSS of pad 39A in July 1994 and zinc was identified via chemical analysis

Presenter M3/Material | Date FINAL | Slide 3 of 16 | Closed

RCC Pinholes

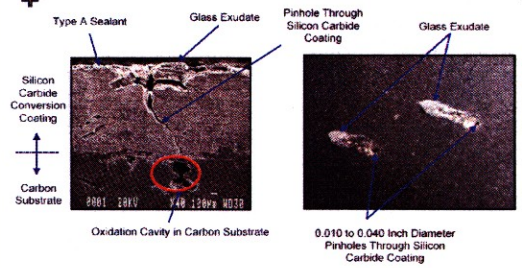

RCC Pinhole Cross-Section **RCC Pinhole Surface View**

OV-102 Panel 12R After 15th Flight

Presenter M3/Material | Date FINAL | Slide 4 of 16 | Closed

RCC Pinholes

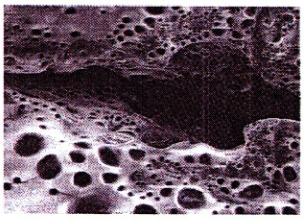

OV-102 Panel 12R After 15th Flight
Mouth of a Pinhole, Magnification Approximately 130X
Actual Pinhole Diameter = 0.01 Inches

Presenter M3/Material | Date FINAL | Slide 5 of 16 | Closed

RCC Pinholes

- **Background / Facts :**
  - Zinc oxide contamination determined to be root cause
    - Reference Boeing Report KL0-98-009, Launch Pad Zinc Fallout Determination, 22 December 1998
    - Launch pad service structure protected with a two-coat primer and topcoat system
    - Primer contains metallic zinc dust in a silica binder
    - Launch pad refurbishment process discontinued topcoat repairs
    - Weathering of exposed primer caused zinc oxide powdery residue
    - Rain washed the zinc oxide onto the orbiter
    - During reentry, zinc oxide reacts with the SiC layer resulting in pinholes and the zinc containing glass on the part surface

Presenter M3/Material | Date FINAL | Slide 6 of 16 | Closed

1

RCC Pinholes

- **Background / Facts:**
  - NASA review of old plasma arc jet test specimens indicated formation of small anomalies similar to pinholes but not typical of flight induced pinholes
  - Specimens with pinholes made from OV-102 panel 12R
    - Tested for 3.5 hours
    - Temperature ranged from 2400F to 3000F
    - Pressure ranged from 0.014 to 0.10 atmospheres
    - Testing did not significantly change pinhole dimensions nor substrate oxidation

Presenter M3/Material | Date FINAL | Slide 7 of 16 | Closed

RCC Pinholes

OV-102 Panel 12R Test Specimen Pinholes

Presenter M3/Material | Date FINAL | Slide 8 of 16 | Closed

RCC Pinholes

- **Background / Facts:**
  - Developed Type A sealant refurbishment process at Lockheed-Martin to repair pinholes
    - Process described in maintenance requirements portion of the briefing
    - Added step to fill pinholes with Type A sealant
    - Refurbishment does not prevent pinholes from reforming or restore carbon substrate integrity
  - Implemented refurbishment plan on all vehicles

Presenter M3/Material | Date FINAL | Slide 9 of 16 | Closed

RCC Pinholes

- **Background / Facts :**
  - Inspection accept/reject criteria established
    - Documented in ML0601-0002, RSI Acceptance Criteria for Operation Vehicles, 19 September 2002
    - All pinhole-related glass formations are acceptable regardless of the localized surface roughness associated with the formation (paragraph 4.12.9.1)
    - Pinholes are acceptable during routine processing flows (paragraph 4.12.9.2)
    - Pinholes greater than 0.04 inches are unacceptable during OMM (paragraph 4.12.9.3)

Presenter M3/Material | Date FINAL | Slide 10 of 16 | Closed

RCC Pinholes

- **Background / Facts :**
  - Launch pad sampling conducted in 1997 and 2003
  - Zinc fallout rate (mg/ft^2/day) comparisons:
    - Highest recorded value obtained in 2003 (8.69)
    - Other 9 locations in 2003 less than 1997 results
  - Zinc % content comparisons:
    - 2003 results consistently around 9% with one exception
    - 1997 results ranged from 10% to 25%
  - See next chart for results by locations

Presenter M3/Material | Date FINAL | Slide 11 of 16 | Closed

RCC Pinholes

Plate Location	Fallout Rate (mg/ft^2/day) 1997 Avg	2003	2003/ 1997	Zinc % Content 1997 Avg	2003	2003/ 1997
LH5/Plate 9	4.8	0.66	0.14	14.2	9.55	0.67
LH10/Plate 1	6.25	4.02	0.64	13.2	8.58	0.65
LH22/Plate 5	6.08	5.33	0.88	15.9	8.82	0.55
RH7/Plate 2	5.29	8.69	1.64	19	9.31	0.49
RH13/Plate 4	4.33	1.21	0.28	15.6	5.64	0.36
RH21/Plate 3	7.05	4.04	0.57	21.4	9.48	0.44
NC/Plate 6	1.97	0.56	0.28	10.4	8.91	0.86
AH/Plate 7	2.16	0.49	0.23	11.5	8.75	0.76
RSS/Plate 8	4.39	0.44	0.10	18.8	9.07	0.48
MLP/None	6.63	N/A	N/A	24.5	N/A	N/A

Highest values shown in red

Presenter M3/Material | Date FINAL | Slide 12 of 16 | Closed

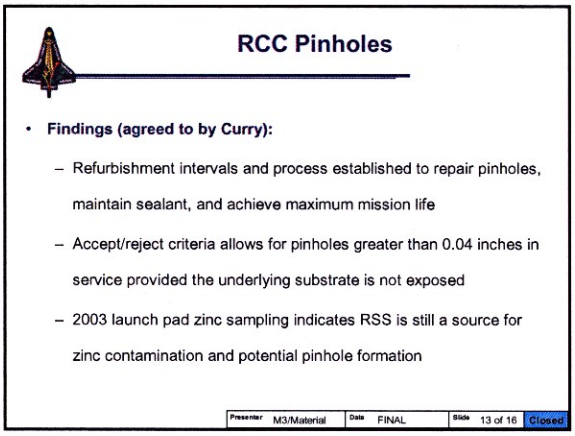
RCC Pinholes
• Findings (agreed to by Curry):
– Refurbishment intervals and process established to repair pinholes, maintain sealant, and achieve maximum mission life
– Accept/reject criteria allows for pinholes greater than 0.04 inches in service provided the underlying substrate is not exposed
– 2003 launch pad zinc sampling indicates RSS is still a source for zinc contamination and potential pinhole formation
Presenter M3/Material
Date FINAL
Slide 13 of 16
Closed

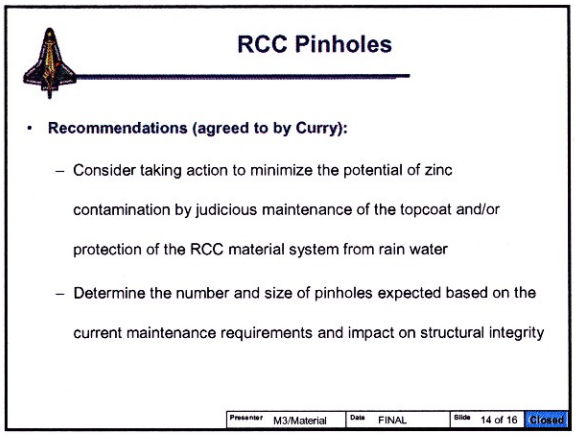
RCC Pinholes
• Recommendations (agreed to by Curry):
– Consider taking action to minimize the potential of zinc contamination by judicious maintenance of the topcoat and/or protection of the RCC material system from rain water
– Determine the number and size of pinholes expected based on the current maintenance requirements and impact on structural integrity
Presenter M3/Material
Date FINAL
Slide 14 of 16
Closed

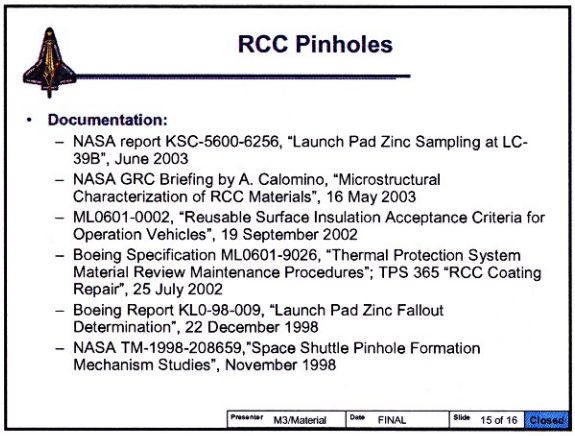
RCC Pinholes
• Documentation:
– NASA report KSC-5600-6256, "Launch Pad Zinc Sampling at LC-39B", June 2003
– NASA GRC Briefing by A. Calomino, "Microstructural Characterization of RCC Materials", 16 May 2003
– ML0601-0002, "Reusable Surface Insulation Acceptance Criteria for Operation Vehicles", 19 September 2002
– Boeing Specification ML0601-9026, "Thermal Protection System Material Review Maintenance Procedures"; TPS 365 "RCC Coating Repair", 25 July 2002
– Boeing Report KL0-98-009, "Launch Pad Zinc Fallout Determination", 22 December 1998
– NASA TM-1998-208659,"Space Shuttle Pinhole Formation Mechanism Studies", November 1998
Presenter M3/Material
Date FINAL
Slide 15 of 16
Closed

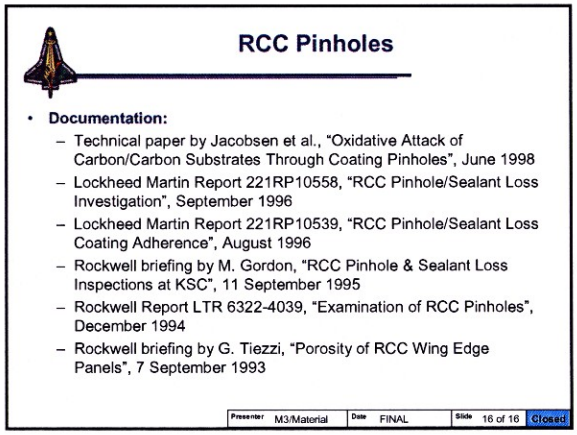
RCC Pinholes
• Documentation:
– Technical paper by Jacobsen et al., "Oxidative Attack of Carbon/Carbon Substrates Through Coating Pinholes", June 1998
– Lockheed Martin Report 221RP10558, "RCC Pinhole/Sealant Loss Investigation", September 1996
– Lockheed Martin Report 221RP10539, "RCC Pinhole/Sealant Loss Coating Adherence", August 1996
– Rockwell briefing by M. Gordon, "RCC Pinhole & Sealant Loss Inspections at KSC", 11 September 1995
– Rockwell Report LTR 6322-4039, "Examination of RCC Pinholes", December 1994
– Rockwell briefing by G. Tiezzi, "Porosity of RCC Wing Edge Panels", 7 September 1993
Presenter M3/Material
Date FINAL
Slide 16 of 16
Closed

RCC Type A Sealant

- **Action / Issue:** Deterioration of Type A sealant
- **Background / Facts:**
  - Discovered white residue on WLE RCC panels on OV-102, OV-104 and OV-105 in November 2001
  - Lab results determined deposits to be sodium carbonate
  - Root cause determined to be the Type A sealant converting to sodium carbonate when exposed to rain water

Presenter M3/Material | Date FINAL | Slide 1 of 5 | Closed

RCC Type A Sealant
Locations With White Residue

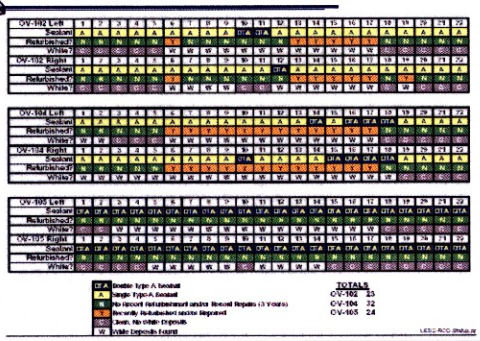

Presenter M3/Material | Date FINAL | Slide 2 of 5 | Closed

RCC Type A Sealant

- **Background / Facts:**
  - There are 3 possible outcomes for sodium carbonate deposits
    - Deposits are washed off and removed
      - Would decrease sealant effectiveness
    - Deposits remain on surface, melt on re-entry, and combine with glass
      - Favorable outcome, restores the composition of Type A sealant
    - Deposits remain on surface, melt on re-entry, and flow to other parts
      - Potentially damaging and needs to be monitored

Presenter M3/Material | Date FINAL | Slide 3 of 5 | Closed

RCC Type A Sealant

- **Findings (Agreed to by Curry):**
  - Root cause determined and found not to be detrimental to RCC
  - Deposits are potentially damaging to metallic hardware
- **Recommendations (Agreed to by Curry):**
  - Continue previous investigation of an improved sealant system
  - Continue monitoring for potential flow of deposits onto metallic hardware

Presenter M3/Material | Date FINAL | Slide 4 of 5 | Closed

RCC Type A Sealant

- **Action / Issue:** Deterioration of Type A sealant
- **Background / Facts:**
  - Discovered white residue on WLE RCC panels on OV-102, OV-104 and OV-105 in November 2001
  - Lab results determined deposits to be sodium carbonate
  - Root cause determined to be the Type A sealant converting to sodium carbonate when exposed to rain water

Presenter M3/Material | Date FINAL | Slide 1 of 5 | Closed

RCC Type A Sealant
Locations With White Residue

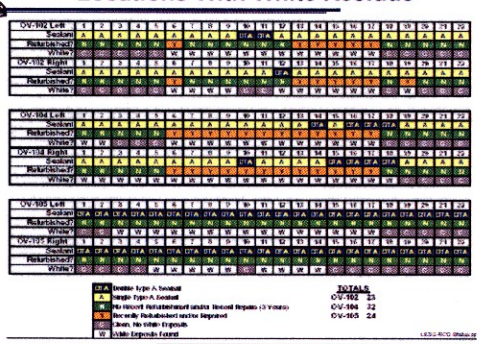

Presenter M3/Material | Date FINAL | Slide 2 of 5 | Closed

RCC Type A Sealant

- **Background / Facts:**
  - There are 3 possible outcomes for sodium carbonate deposits
    - Deposits are washed off and removed
      - Would decrease sealant effectiveness
    - Deposits remain on surface, melt on re-entry, and combine with glass
      - Favorable outcome, restores the composition of Type A sealant
    - Deposits remain on surface, melt on re-entry, and flow to other parts
      - Potentially damaging and needs to be monitored

Presenter M3/Material | Date FINAL | Slide 3 of 5 | Closed

RCC Type A Sealant

- **Findings (Agreed to by Curry):**
  - Root cause determined and found not to be detrimental to RCC
  - Deposits are potentially damaging to metallic hardware
- **Recommendations (Agreed to by Curry):**
  - Continue previous investigation of an improved sealant system
  - Continue monitoring for potential flow of deposits onto metallic hardware

Presenter M3/Material | Date FINAL | Slide 4 of 5 | Closed

RCC Type A Sealant

- **Documentation:**
  - NASA Labs at KSC letter KSC-MSL-0127-2001, "White Deposits Removed From OV-102, OV-104 and OV-105", 15 March 2001
  - Briefing by N. Jacobson et al., "Chemistry of Sodium Carbonate Deposits on the Orbiter Wing Leading Edge and Nose Cap"
  - Briefing by D. Curry et al., "Orbiter Reinforced Carbon/Carbon Advanced Sealant Systems Screening Tests", January 2000

Presenter M3/Material | Date FINAL | Slide 5 of 5 | Closed

1

RCC NDE

- **Action / Issue:** Determine NDE requirements for RCC components
- **Purposes of NDI:**
  1. Verify no carbon substrate defects exist of a quantify and size distribution that could result in structural failure
  2. Verify no SiC/substrate interface defects exist of a quantity and size distribution that could result in loss of the SiC layer and expose the carbon substrate
  3. Validate the mass loss analysis method/results and support determination of mission life capability for each RCC part

Presenter M3/Material | Date FINAL | Slide 1 of 25 | Closed

RCC NDE

- **Basis for Purpose 1 (Carbon Substrate):**
  - Visual and thermography NDE results of OV-104 panel 16R revealed surface and subsurface defect indications (see next chart)
  - X-Ray computed tomography NDI technique performed by Wyle Laboratories on same panel in Nov 02
    - Reference Wyle Laboratories Report, "CT Inspection of OV-104 RCC Panel", P. Engel, 22 November 2002
    - 75 CT slices were obtained
    - Subsurface defect indications were confirmed (see next 4 charts)

Presenter M3/Material | Date FINAL | Slide 2 of 25 | Closed

RCC NDE

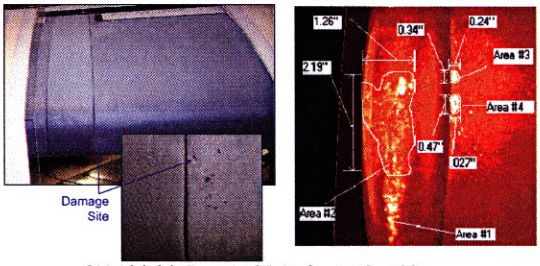

OV-104-24, Panel 16R Defects (Oct 02)
Visual and Thermography Results

Presenter M3/Material | Date FINAL | Slide 3 of 25 | Closed

RCC NDE

OV-104-24, Panel 16R CT by Wyle Labs (Nov 02)

Presenter M3/Material | Date FINAL | Slide 4 of 25 | Closed

RCC NDE

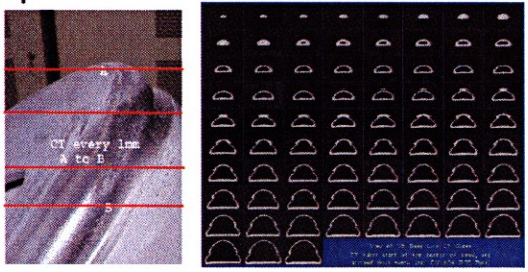

75 CT Slices Were Obtained on OV-104-24, Panel 16R

Presenter M3/Material | Date FINAL | Slide 5 of 25 | Closed

RCC NDE

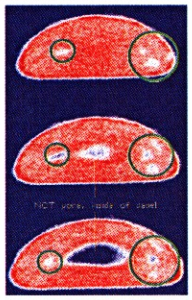

Subsurface Indications

OV-104-24, Panel 16R CT Results (Nov 02)

Presenter M3/Material | Date FINAL | Slide 6 of 25 | Closed

RCC NDE

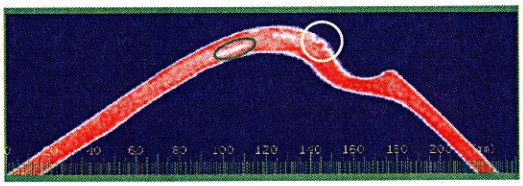

Subsurface Indications

Surface Defects

OV-104-24, Panel 16R CT Results (Nov 02)

Presenter M3/Material | Date FINAL | Slide 7 of 25 | Closed

RCC NDE

- **Basis for Purpose 1 (Carbon Substrate) Continued:**
  - A study was performed on OV-103 and OV-105 RCC panels using thermography
    - Reference briefing by KSC personnel
    - Concentrated on panels 7 through 12, left and right
    - All 24 panels appeared to be in good condition
  - As an additional test, OV-103 panel 16R was inspected using thermography
    - Subsurface defect indications observed (see next chart)

Presenter M3/Material | Date FINAL | Slide 8 of 25 | Closed

RCC NDE

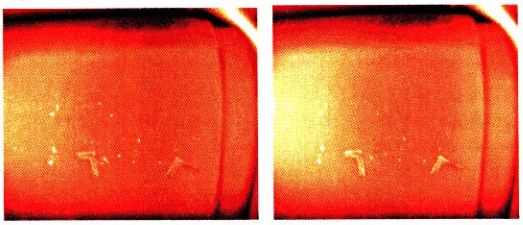

0.234-0.651 Seconds (Averaged) 0.334-0.851 Seconds (Averaged)

OV-103-30, Panel 16R Thermography Results (Nov 02)

Presenter M3/Material | Date FINAL | Slide 9 of 25 | Closed

RCC NDE

- **Basis for Purpose 2 (SiC Layer):**
  - 6 occurrences of SiC layer loss or damage have been identified
    - November 1997, OV-102-24 (STS-87), 3 damaged parts
      - Reference Boeing Report KLO-98-002, March 1998 (no photos included in report)
      - Panel 19R, 0.04" diameter, 0.035" deep exposing carbon substrate
      - Panel 17R, 0.1" x 0.2" x 0.025" deep exposing carbon substrate
      - Arrowhead, 0.2" x 0.15" x 0.026" deep exposing carbon substrate
    - January 2000, OV-103-27 (STS-103), Panel 8L, panel scrapped
    - December 2000, OV-102-26 (STS-93), T-Seal 11L
    - April 2001, OV-103-29 (STS-102), Panel 10L

Presenter M3/Material | Date FINAL | Slide 10 of 25 | Closed

RCC NDE

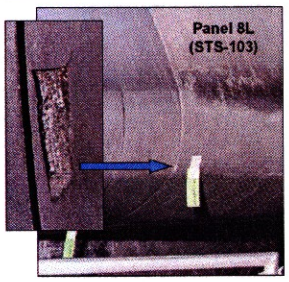

Suspected Oxidation At SiC and Substrate Interface

OV-103-27, Panel 8L SiC Loss (Jan 00), Panel Scrapped

Presenter M3/Material | Date FINAL | Slide 11 of 25 | Closed

RCC NDE

OV-102-26, T-Seal 11L SiC Damage (Dec 00)

Presenter M3/Material | Date FINAL | Slide 12 of 25 | Closed

2

RCC NDE

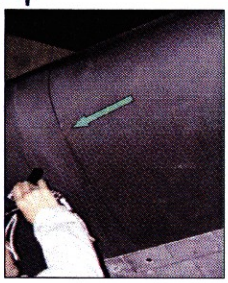

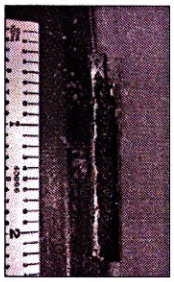

Suspected Oxidation At SiC and Substrate Interface

(2"L x 0.3"W x 0.018"D)

OV-103-29, Panel 10L SiC Loss (Apr 01)

Presenter M3/Material | Date FINAL | Slide 13 of 25 | Closed

RCC NDE

- **Basis for Purpose 2 (SiC Layer) Continued:**
  - Pinholes in SiC layer have potential to result in oxidation of the carbon substrate and/or SiC/substrate interface
    - Majority of pinholes occur along craze cracks in SiC layer
    - Typically in thick regions of SiC layer – indicative of porous substrate
  - Oxidation below the SiC layer has been discovered associated with pinhole locations (see next charts)

Presenter M3/Material | Date FINAL | Slide 14 of 25 | Closed

RCC NDE

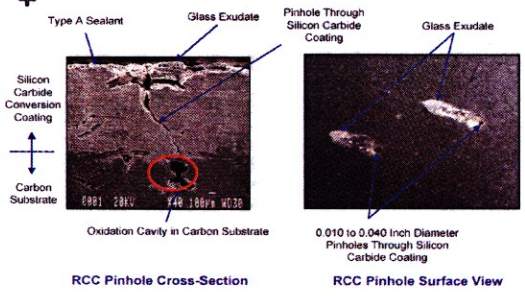

OV-102 Panel 12R After 15th Flight

Presenter M3/Material | Date FINAL | Slide 15 of 25 | Closed

RCC NDE

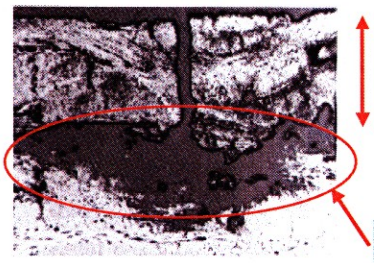

Silicon Carbide Layer (0.02" to 0.04")

Subsurface Oxidation

Presenter M3/Material | Date FINAL | Slide 16 of 25 | Closed

RCC NDE

- **Basis for Purpose 3 (Mission Life):**
  - Destructive testing performed on OV-102 panel 12R (15 flights) and panel 10L (19 flights) to compare to design allowables
    - Documented in LMM&FC report 221RP10558, Sep 1996
  - Data is limited and significant scatter exists, however test results indicate trends worse than expected (see next charts)
    - Tension test results below allowable at 0.02 psf (not 0.03)
    - Lug test results below allowable at 0.02 psf (not 0.1)
    - Opening corner moment below allowable at 0.01 psf (not 0.03)
  - Results indicate mass loss prediction method should be revalidated

Presenter M3/Material | Date FINAL | Slide 17 of 25 | Closed

RCC NDE

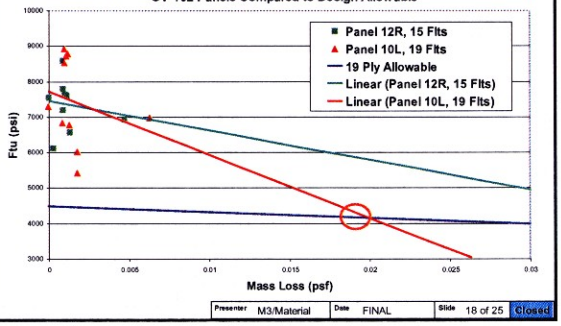

Presenter M3/Material | Date FINAL | Slide 18 of 25 | Closed

RCC NDE

RCC Lug Test Results
OV-102 Panels Compared to Design Allowable

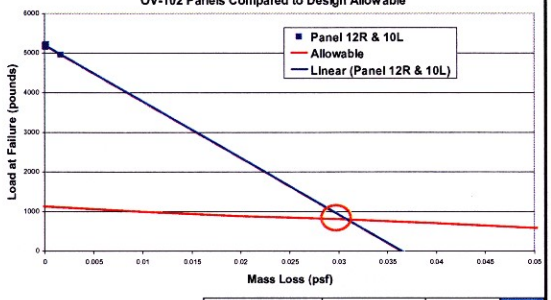

Presenter M3/Material | Date FINAL | Slide 19 of 25 | Closed

RCC NDE

RCC Opening Corner Moment Test Results
OV-102 Panels Compared to Design Allowable

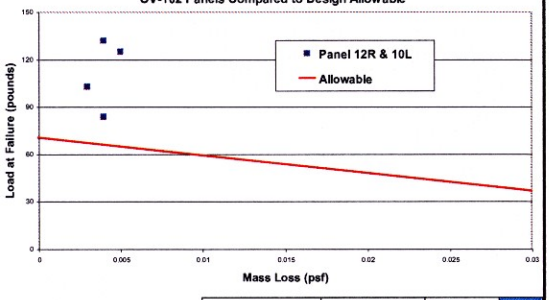

Presenter M3/Material | Date FINAL | Slide 20 of 25 | Closed

RCC NDE

- **Basis for Purpose 3 (Mission Life) Continued:**
  - X-ray Computed Tomography (CT) NDI technique demonstrated to be viable for determining variable RCC mass loss due to oxidation
    - Reference Rockwell Report MPR 6146-2000, "Evaluation of Carbon-Carbon Materials and Structures Using Computerized Tomography Techniques", March 1994
    - Rockwell Report LTR 5928-2442, "Prediction of RCC Flexural Strength Using CT Techniques", September 1992
    - Reference Rockwell Report MPR 5806-2020, "Determination of Mass Loss coated RCC Carbon-Carbon Orbiter Structures", May 1992

Presenter M3/Material | Date FINAL | Slide 21 of 25 | Closed

RCC NDE

- **Basis for Purpose 3 (Mission Life) Continued:**
  - MCR19643, "Develop a NDE Method for RCC Components", 11 March 2002 was presented to the ERB
  - Proposed a 3-year development program to develop a credible RCC NDE program
    - Fabricate and characterize NDE standards
    - Down-select NDE techniques
    - Fully characterize RCC flight hardware via destructive testing
    - Validate analysis predictions of mass loss and strength reduction using NDE results
  - Right approach!!! – schedule can be accelerated

Presenter M3/Material | Date FINAL | Slide 22 of 25 | Closed

RCC NDE

- **Findings (agreed to by Curry, Gordon and Grant):**
  - Damage and defects discovered on RCC components warrants development of NDI techniques to verify structural integrity
- **Recommendations (agreed to by Curry, Gordon and Grant):**
  - NDE all flown WLE RCC parts ASAP to support investigation
    - Determine defect quantity and size distribution
    - Use results to determine what parts should be included in the impact test program
  - Identify and implement NDE techniques for carbon substrate and SiC/substrate layer inspection as a **return to flight** criteria and for routine use
  - Develop and implement NDE techniques for carbon substrate mass loss to validate analysis methods and results (need date is TBD)

Presenter M3/Material | Date FINAL | Slide 23 of 25 | Closed

RCC NDE

- **Recommendations Continued (agreed to by Curry, Gordon and Grant):**
  - NDE technique development and application should address the following
    - NDE standards
    - Probability of detection
    - Inspector certification requirements
    - Basis for accept/reject criteria
    - Basis for inspection frequency
    - How NDE results will be used in the mission life analysis
    - If production NDE techniques and processes are used, demonstrate the adequacy to include detection capability, accept/reject criteria, and implications to structural integrity via mechanical testing as was performed originally

Presenter M3/Material | Date FINAL | Slide 24 of 25 | Closed

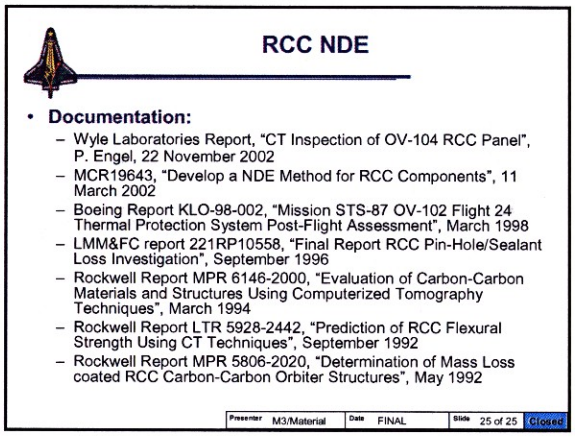
RCC NDE
• Documentation:
– Wyle Laboratories Report, "CT Inspection of OV-104 RCC Panel", P. Engel, 22 November 2002
– MCR19643, "Develop a NDE Method for RCC Components", 11 March 2002
– Boeing Report KLO-98-002, "Mission STS-87 OV-102 Flight 24 Thermal Protection System Post-Flight Assessment", March 1998
– LMM&FC report 221RP10558, "Final Report RCC Pin-Hole/Sealant Loss Investigation", September 1996
– Rockwell Report MPR 6146-2000, "Evaluation of Carbon-Carbon Materials and Structures Using Computerized Tomography Techniques", March 1994
– Rockwell Report LTR 5928-2442, "Prediction of RCC Flexural Strength Using CT Techniques", September 1992
– Rockwell Report MPR 5806-2020, "Determination of Mass Loss coated RCC Carbon-Carbon Orbiter Structures", May 1992
Presenter M3/Material
Date FINAL
Slide 25 of 25
Closed

RCC Maintenance

9-1 RCC Maintenance Requirements

9-2 RCC Maintenance Repair and Refurbishment Process

9-3 Left WLE Maintenance During OMM & Flows

9-4 LESS Hardware Use

Matrix

Presenter	CAIB/Group 1	Date	FINAL	Slide	11 of 32

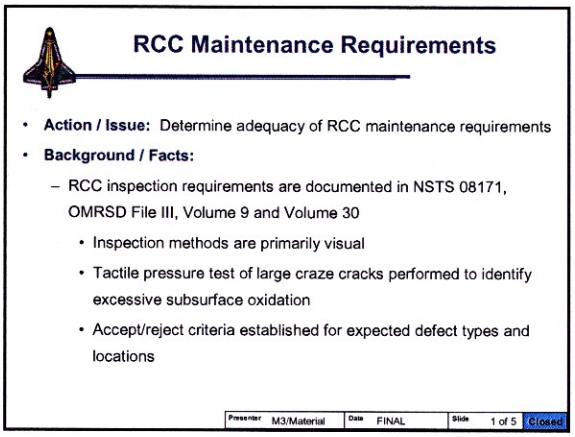
RCC Maintenance Requirements
• Action / Issue: Determine adequacy of RCC maintenance requirements
• Background / Facts:
– RCC inspection requirements are documented in NSTS 08171, OMRSD File III, Volume 9 and Volume 30
• Inspection methods are primarily visual
• Tactile pressure test of large craze cracks performed to identify excessive subsurface oxidation
• Accept/reject criteria established for expected defect types and locations
Presenter M3/Material
Date FINAL
Slide 1 of 5
Closed

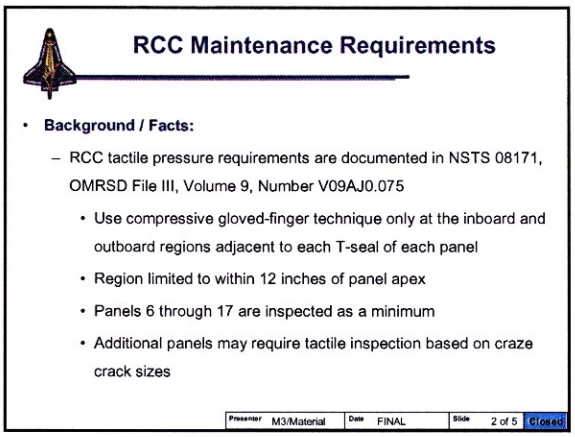
RCC Maintenance Requirements
• Background / Facts:
– RCC tactile pressure requirements are documented in NSTS 08171, OMRSD File III, Volume 9, Number V09AJ0.075
• Use compressive gloved-finger technique only at the inboard and outboard regions adjacent to each T-seal of each panel
• Region limited to within 12 inches of panel apex
• Panels 6 through 17 are inspected as a minimum
• Additional panels may require tactile inspection based on craze crack sizes
Presenter M3/Material
Date FINAL
Slide 2 of 5
Closed

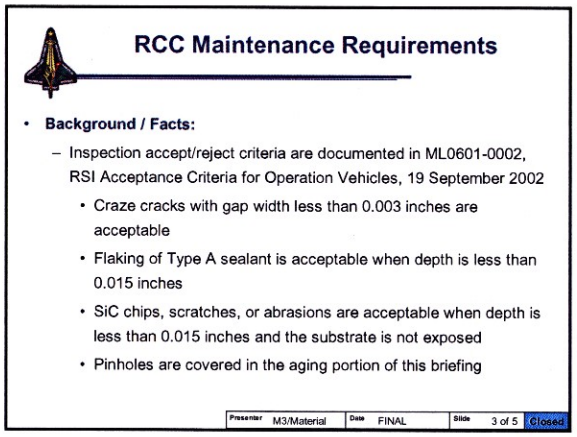
RCC Maintenance Requirements
• Background / Facts:
– Inspection accept/reject criteria are documented in ML0601-0002, RSI Acceptance Criteria for Operation Vehicles, 19 September 2002
• Craze cracks with gap width less than 0.003 inches are acceptable
• Flaking of Type A sealant is acceptable when depth is less than 0.015 inches
• SiC chips, scratches, or abrasions are acceptable when depth is less than 0.015 inches and the substrate is not exposed
• Pinholes are covered in the aging portion of this briefing
Presenter M3/Material
Date FINAL
Slide 3 of 5
Closed

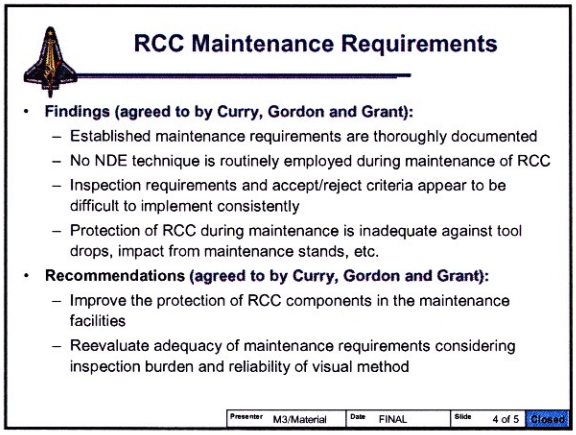
RCC Maintenance Requirements
• Findings (agreed to by Curry, Gordon and Grant):
– Established maintenance requirements are thoroughly documented
– No NDE technique is routinely employed during maintenance of RCC
– Inspection requirements and accept/reject criteria appear to be difficult to implement consistently
– Protection of RCC during maintenance is inadequate against tool drops, impact from maintenance stands, etc.
• Recommendations (agreed to by Curry, Gordon and Grant):
– Improve the protection of RCC components in the maintenance facilities
– Reevaluate adequacy of maintenance requirements considering inspection burden and reliability of visual method
Presenter M3/Material
Date FINAL
Slide 4 of 5
Closed

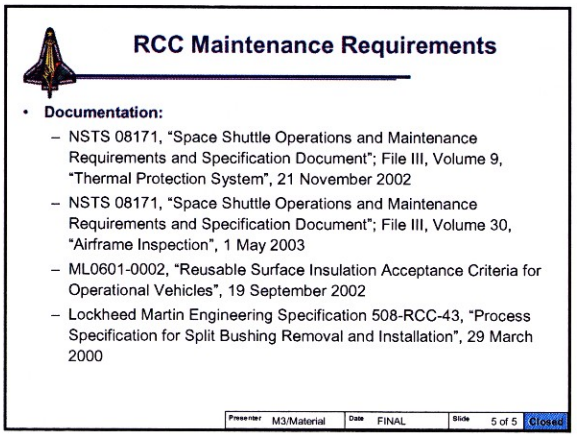
RCC Maintenance Requirements
• Documentation:
– NSTS 08171, "Space Shuttle Operations and Maintenance Requirements and Specification Document"; File III, Volume 9, "Thermal Protection System", 21 November 2002
– NSTS 08171, "Space Shuttle Operations and Maintenance Requirements and Specification Document"; File III, Volume 30, "Airframe Inspection", 1 May 2003
– ML0601-0002, "Reusable Surface Insulation Acceptance Criteria for Operational Vehicles", 19 September 2002
– Lockheed Martin Engineering Specification 508-RCC-43, "Process Specification for Split Bushing Removal and Installation", 29 March 2000
Presenter M3/Material
Date FINAL
Slide 5 of 5
Closed

RCC Repair & Refurbishment

- **Action / Issue:** Determine adequacy of RCC repair and refurbishment requirements
- **Repair Process:**
  - Repairs are performed using Boeing Specification ML0601-9026, Procedure TPS-365, RCC Coating Repair
  - Repairs to RCC parts limited to minor damage to Silicon-Carbide coating
    - Repairs are performed at KSC
    - Not authorized for pinholes and substrate damage
  - RCC repair involves the following process steps:
    - Part cleaning
    - Type A sealant application
    - Sanding of repaired region to meet flushness requirements

Presenter M3/Material | Date FINAL | Slide 1 of 9 | Closed

RCC Repair & Refurbishment

- **Refurbishment Process:**
  - Refurbishments are performed using Lockheed-Martin Specification 508-RCC-318, Refurbishment of Flown RCC Parts, 16 February 2000
  - Refurbishments to RCC parts performed to achieve the desired part mission life by replenishing the Type A sealant
  - Refurbishments performed by only Lockheed-Martin using the following process:
    - Type A sealant removed by sanding
    - Vacuum heat clean to bake-out contaminants
    - Pinholes repaired using Type A sealant forcefully wiped into the holes
    - TEOS impregnation and cure
    - Type A sealant application and cure
    - Reassembly of the metallic parts to the RCC panel

Presenter M3/Material | Date FINAL | Slide 2 of 9 | Closed

RCC Repair & Refurbishment

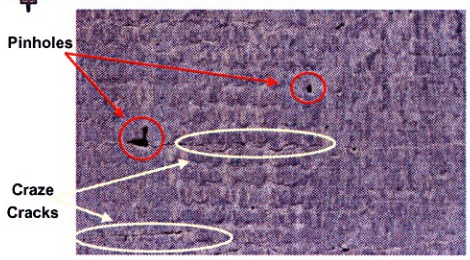

OV-102-17, T-Seal 9L After Sanding During Refurbishment, Magnification Approximately = 10X

Presenter M3/Material | Date FINAL | Slide 3 of 9 | Closed

RCC Repair & Refurbishment

- **Background / Facts:**
  - Refurbishment interval established based on destructive evaluation of OV-102 panel 12R after 15th flight
    - Reference Rockwell Report LTR 6322-4039, "Examination of RCC Pinholes", December 1994
    - Evaluation performed to characterize pinholes
    - Discovered that OML is losing the Type A sealant layer
  - Type A sealant thickness measured near 5 pinholes
    - Minimum ranged from 0.0001 to 0.0002 inches
    - Maximum ranged from 0.006 to 0.0014 inches

Presenter M3/Material | Date FINAL | Slide 4 of 9 | Closed

RCC Repair & Refurbishment

Type A Sealant Thickness Range 0.0002 to 0.0014 Inches

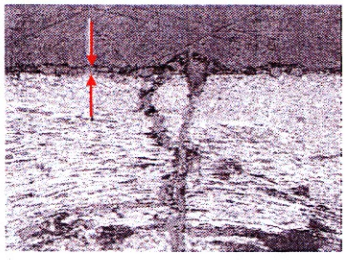

OV-102 Panel 12R After 15th Flight Pinhole Cross-Section, Magnification Approximately 200X

Presenter M3/Material | Date FINAL | Slide 5 of 9 | Closed

RCC Repair & Refurbishment

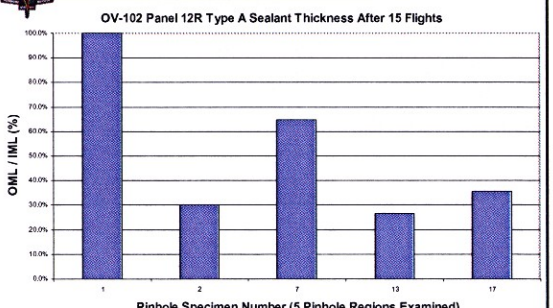

Presenter M3/Material | Date FINAL | Slide 6 of 9 | Closed

1

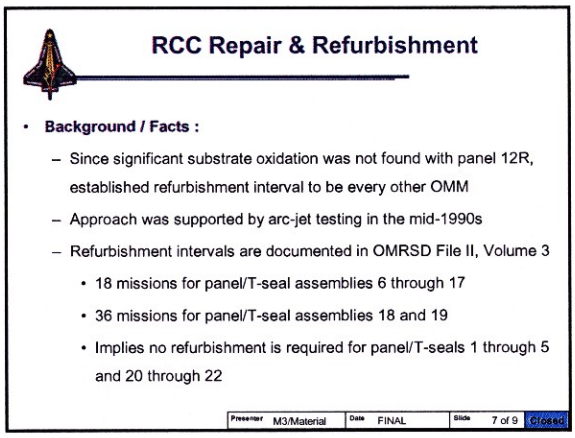
RCC Repair & Refurbishment
• Background / Facts :
– Since significant substrate oxidation was not found with panel 12R, established refurbishment interval to be every other OMM
– Approach was supported by arc-jet testing in the mid-1990s
– Refurbishment intervals are documented in OMRSD File II, Volume 3
• 18 missions for panel/T-seal assemblies 6 through 17
• 36 missions for panel/T-seal assemblies 18 and 19
• Implies no refurbishment is required for panel/T-seals 1 through 5 and 20 through 22
Presenter M3/Material
Date FINAL
Slide 7 of 9
Closed

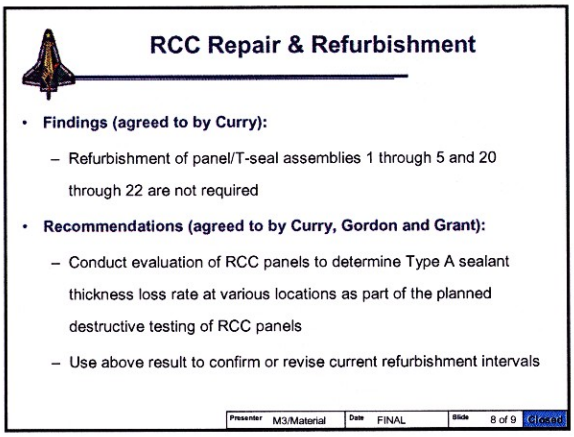
RCC Repair & Refurbishment
• Findings (agreed to by Curry):
– Refurbishment of panel/T-seal assemblies 1 through 5 and 20 through 22 are not required
• Recommendations (agreed to by Curry, Gordon and Grant):
– Conduct evaluation of RCC panels to determine Type A sealant thickness loss rate at various locations as part of the planned destructive testing of RCC panels
– Use above result to confirm or revise current refurbishment intervals
Presenter M3/Material
Date FINAL
Slide 8 of 9
Closed

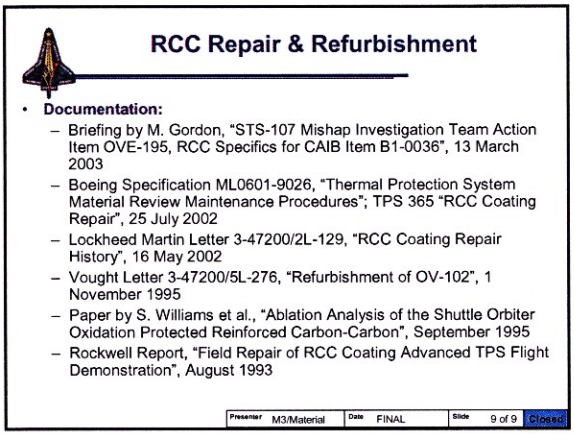
RCC Repair & Refurbishment
• Documentation:
– Briefing by M. Gordon, "STS-107 Mishap Investigation Team Action Item OVE-195, RCC Specifics for CAIB Item B1-0036", 13 March 2003
– Boeing Specification ML0601-9026, "Thermal Protection System Material Review Maintenance Procedures"; TPS 365 "RCC Coating Repair", 25 July 2002
– Lockheed Martin Letter 3-47200/2L-129, "RCC Coating Repair History", 16 May 2002
– Vought Letter 3-47200/5L-276, "Refurbishment of OV-102", 1 November 1995
– Paper by S. Williams et al., "Ablation Analysis of the Shuttle Orbiter Oxidation Protected Reinforced Carbon-Carbon", September 1995
– Rockwell Report, "Field Repair of RCC Coating Advanced TPS Flight Demonstration", August 1993
Presenter M3/Material
Date FINAL
Slide 9 of 9
Closed

RCC Maintenance OMM in 2000

- **Action / Issue:** Determine potential for left WLE maintenance actions to be a contributing cause of the accident
- **Background / Facts:**
  - OV-102 inducted into OMM after STS-93, 26th flight for OV-102
  - OMM conducted at Palmdale October 1999 through February 2001
  - All WLE RCC components were removed to accomplish required inspections
  - RCC panel/T-seals 6, and 13-17 were refurbished
  - RCC parts were inspected for pinholes, etc.
    - Pinholes in Panel 8 and 19 originally reported > 0.04 inches in diameter (TES-2-J3-0412, 0416)
    - Quality evaluated pinholes using optical comparator and determined them to be within acceptable limits

Presenter M3/Material | Date FINAL | Slide 1 of 13 | Closed

RCC Maintenance OMM in 2000

- **Background / Facts :**
  - After re-installation of the RCC components, step and gap measurements were found to be unacceptable (TES-2-J3-0495)
  - Complete removal of Left WLE subsystem was performed and the following issues were discovered
    - Spar fitting shims not per design (STR-2-J3-7033)
    - Lower access panel nutplate issues (STR-2-J3-6689)
    - Debonded nutplates, low running torque and damaged nuts (TES-2-J3-0439)
  - Evaluated 152 of the 176 fitting fasteners (24 were not evaluated since some fittings were already removed)
    - 104 of 152 (68%) were per drawing requirements
    - 48 of 152 (32%) had low torque values

Presenter M3/Material | Date FINAL | Slide 2 of 13 | Closed

RCC Maintenance OMM in 2000

OV-102 Fastener Detail

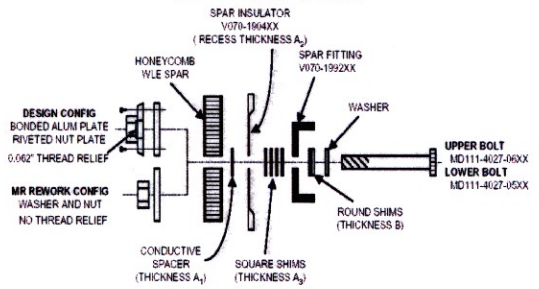

Presenter M3/Material | Date FINAL | Slide 3 of 13 | Closed

RCC Maintenance OMM in 2000

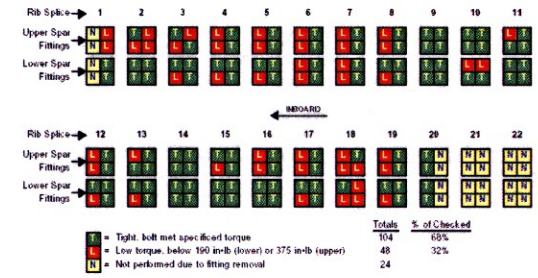

OV-102 Left Wing Torque Check Results

Presenter M3/Material | Date FINAL | Slide 4 of 13 | Closed

RCC Maintenance OMM in 2000

- **Background / Facts :**
  - Improper shims resulted in shank-out condition in some locations
    - Observed in MR nut and washer rework areas only
    - Shim stack returned to original build configuration
  - Bolt torque sequence standardized to reduce panel torsion and deformation
    - Sequence steps and torque increments defined
    - Torque checked after a minimum of 24 hours
  - Both OV-102 wings reworked to design configuration
  - Boeing Specification ML0301-0023 installation procedures revised

Presenter M3/Material | Date FINAL | Slide 5 of 13 | Closed

RCC Maintenance OMM in 2000

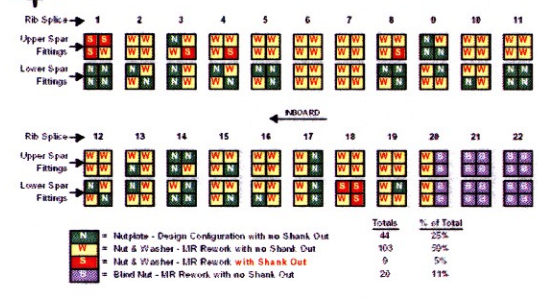

OV-102 Left Wing Fastener Shank-Out Check Results

Presenter M3/Material | Date FINAL | Slide 6 of 13 | Closed

1

RCC Maintenance

2. WLE Attach Fitting Bolt Torque

UA Closure Team

Related Fault Tree Block
- SFOML Wing 9-19 Loss of RCC Panel Due to Supporting Structure Failure

Finding
- Experience at the OV-102 OMM in Palmdale resulted in the program establishing a new baseline procedure for torquing the LESS attach fitting bolts to assure proper preload.
- Not all attachment fittings have been torqued per the new procedure.

OV-103: All RCC panels are currently off the vehicle and undergoing inspection per OMRSD. All fittings are off and will be torqued per the new procedure.

OV-104: Twelve panels (9-11 and 20-22) are now scheduled for removal and inspection this flow per existing OMRSD 3 year requirement. 8 fittings are scheduled for removal and torque per the new procedure.

OV-105: All fittings have been removed and will be torqued per the new procedure.

This material is PRELIMINARY information only. It is for limited distribution. DO NOT FORWARD. 18

Presenter M3/Material | Date FINAL | Slide 7 of 13 | Closed

RCC Maintenance After STS-109

- **Background / Facts:**
  - STS-109, 27th flight for OV-102 launched 1 March 2002
  - Post-flight processing performed May 2001 through Jan 2002
  - Upper wing discoloration discovered near panel 15 left
  - Upper and lower access panels removed for inspection
  - Baseball size hard object found
    - Most likely glass-backed white masking tape
    - Tape used for paint masking may have fallen into RCC cavity during OMM
  - Area cleaned and accepted with MR concurrence

Presenter M3/Material | Date FINAL | Slide 8 of 13 | Closed

RCC Maintenance After STS-109

Discoloration Near Panel 15L

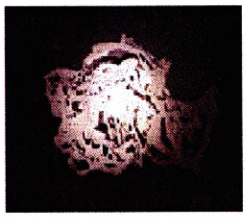

Ball of Masking Tape

OV-102-27, Post Flight Inspection

Presenter M3/Material | Date FINAL | Slide 9 of 13 | Closed

RCC Maintenance Before STS-107

- **Background / Facts:**
  - Pre-flight processing performed Mar 2002 through Aug 2002
  - STS-107, 28th flight for OV-102 launched 16 January 2003
  - OV-102 left wing horseshoe gap fillers were removed and replaced at panels 1, 19 and 20
    - Gap filler repaired during OMM J3 and found torn following STS-109

Presenter M3/Material | Date FINAL | Slide 10 of 13 | Closed

RCC Maintenance Before STS-107

- **Background / Facts :**
  - RCC angle seal 1L was removed to replace horseshoe gap filler
  - During bushing removal, the load applied was not calculated
    - Boeing specification MLO301-0023 states loads applied to RCC components should be kept below 30 pounds
    - PR disposition specified RCC loading should be kept below 20 pounds
  - Clevis fitting damaged during removal of the bushing
    - Replaced bolt and bushing
    - Damaged region was polished

Presenter M3/Material | Date FINAL | Slide 11 of 13 | Closed

RCC Maintenance OMM & Flows

- **Findings (agreed to by Curry, Gordon and Grant):**
  - Significant WLE maintenance performed during OMM J3
  - Few maintenance actions after OMM J3 and prior to STS-107
  - Not all the fittings on OV-104 are scheduled for bolt torque prior to next flight
- **Recommendations (agreed to by Curry, Gordon and Grant):**
  - Perform torque of OV-104 attach fitting bolts prior to next flight

Presenter M3/Material | Date FINAL | Slide 12 of 13 | Closed

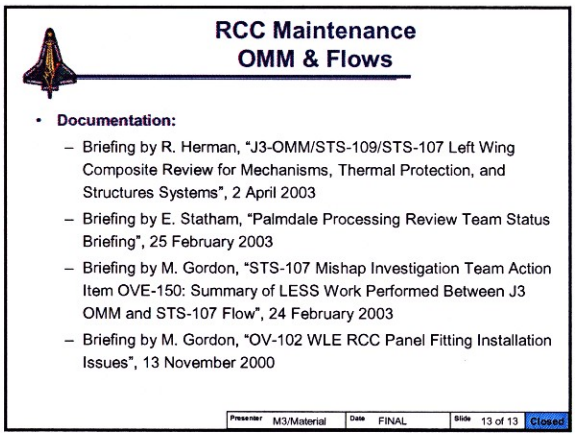
RCC Maintenance
OMM & Flows
• Documentation:
– Briefing by R. Herman, "J3-OMM/STS-109/STS-107 Left Wing Composite Review for Mechanisms, Thermal Protection, and Structures Systems", 2 April 2003
– Briefing by E. Statham, "Palmdale Processing Review Team Status Briefing", 25 February 2003
– Briefing by M. Gordon, "STS-107 Mishap Investigation Team Action Item OVE-150: Summary of LESS Work Performed Between J3 OMM and STS-107 Flow", 24 February 2003
– Briefing by M. Gordon, "OV-102 WLE RCC Panel Fitting Installation Issues", 13 November 2000
Presenter M3/Material
Date FINAL
Slide 13 of 13
Closed

3

RCC Maintenance

Maintenance Practices: LESS Hardware Use

- **Action / Issue:** Review/assess orbiter Leading Edge Structural Subsystem (LESS) maintenance practices regarding hardware use
- **Background:**
  - LESS consists of:
    - 22 Reinforced Carbon-Carbon (RCC) panels on each wing
    - 44 carrier panels: 22 upper, 22 lower on each wing
    - Numerous other components (spar insulators, clevis insulators, spanner beam insulators, attach fittings, brackets) and hardware (bolts, pins, sleeves, etc)
  - LESS subjected to thermal and aero stresses during reentry
    - Proper inspection/maintenance of components essential to system performing as designed/intended

Presenter: M3/Maintenance | Date: FINAL | Slide: 1 of 5 | Closed

RCC Maintenance

Maintenance Practices: LESS Hardware Use

- **Findings:**
  - Work Authorization Documents (WADs) very specific on most tasks
  - One exception: carrier panel (C/P) hardware (A286 bolt) reuse
    - 4 bolts per upper panel, 2 per lower panel
    - Engineers initially stated bolts are reused
    - Technicians stated hardware is discarded/replaced
    - Inspected multiple storage containers holding removed C/Ps
      - No bolts found
    - After further discussion, engineers restated bolts "can be reused" at technician's discretion, based on cleaning (using isopropyl alcohol) and visual inspection

Presenter: M3/Maintenance | Date: FINAL | Slide: 2 of 5 | Closed

RCC Maintenance

Maintenance Practices: LESS Hardware Use

- **Findings (cont'd):**
  - Unlike the predominance of WADs reviewed, the C/P WADs provide no clear guidance on hardware disposition
    - Both WADs (removal and installation of C/Ps) reviewed
    - No specific requirement to clean, inspect, or reuse (or replace)
  - By contrast, WADs covering removal of RCC panels clearly state "…identify, bag and retain hardware for future use" with respect to four separate component removals
    - Verified through physical inspection of removed components
  - Inconsistent/lacking guidance allows varying interpretations and creates the potential for process variation(s)

Presenter: M3/Maintenance | Date: FINAL | Slide: 3 of 5 | Closed

RCC Maintenance

Maintenance Practices: LESS Hardware Use

- **Findings (cont'd):**
  - Results of investigation by metallurgist
    - "There was no evidence of stress corrosion cracking at pre-launch conditions. There was no evidence of cumulative failures that started on previous missions."
- **Recommendations:**
  - Eliminate the potential for varying interpretations of carrier panel bolt reuse by making the WADs more specific

Presenter: M3/Maintenance | Date: FINAL | Slide: 4 of 5 | Closed

RCC Maintenance

Maintenance Practices: LESS Hardware Use

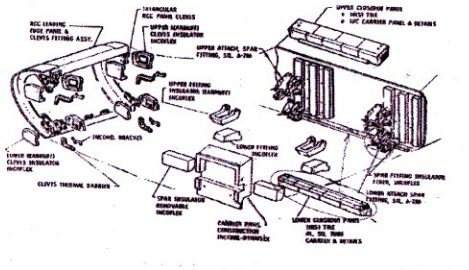

February 24, 2003

Presenter: M3/Maintenance | Date: FINAL | Slide: 5 of 5 | Closed

Tile
Design – Certification

10-1 Design for Impact Resistance

Matrix

Presenter	CAIB/Group 1	Date	FINAL	Slide	12 of 32

Tile Design – Certification

- **Action / Issue:**
  - Debris impact resistance of the tile TPS may be below safe levels.
- **Background / Facts:**
  - Current design requirements for impact damage as follows [17]:
    - The TPS shall not be designed to accommodate particle impact (such as from hail, rain, runway debris, meteoroids, etc.) whose kinetic energy levels exceed 0.006 ft-lb to the surface normal.
    - The Orbiter shall not be designed to withstand launch debris or ice.
  - Yet, tile damage occurs with every flight. In some cases localized structural heating due to the damage has been severe and could have caused loss of vehicle if located at another location [16]

STS-27

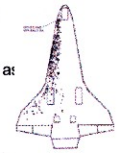

Presenter M3/Material | Date FINAL | Slide 1 of 11 | Closed

Tile Design – Certification

- **Background / Facts (cont'd):**
  - For the orbiter, TPS damage tolerance could be defined as the attribute that permits it to retain the required thermal protection for reentry after the structure has sustained described levels damage
  - Damage
    - Impact damage would include impact incurred during any phase of the mission
    - Other service induced damage could include undetected cracks along the densified layer in the tile
    - Maintenance induced damage would include undetected cracks incurred during maintenance (e.g. stepping on "piano key" tile)

STS-27R

Presenter M3/Material | Date FINAL | Slide 2 of 11 | Closed

STS-27R, OV-104, Flight 3

Robert "Hoot" Gibson

Presenter M3/Material | Date FINAL | Slide 3 of 11 | Closed

Composite of Post-Flight Damage

STS
1
35
50
51D
52
72
73
87
89
95
101
102
103
109
110
111

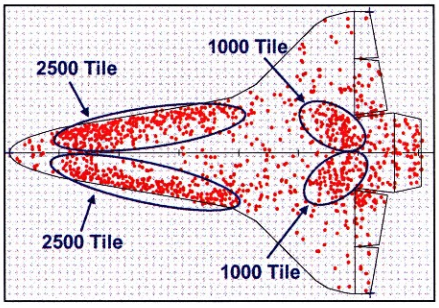

Presenter M3/Material | Date FINAL | Slide 4 of 11 | Closed

Tile Design – Certification

- **Background / Facts (cont'd):**
  - A 1998 Boeing effort did assess the TPS damage to OV-102 during STS-87 and the potential damage to OV-105 during the next flight (STS-89) [18]; *this type of analysis is the lead-in for impact damage resistant design; helps define requirement for tile impact resistance*
  - Criteria required to establish magnitude of survivable damage is being developed as part of the on-orbit repair development effort and could be used, in-part, to establish new tile impact resistance requirements

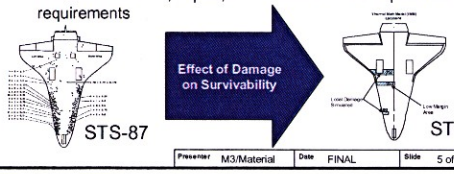

Presenter M3/Material | Date FINAL | Slide 5 of 11 | Closed

Tile Design – Certification

- **Background / Facts (cont'd):**
  - 1st generation tile (LI-900, LI-2200 and FRCI-12) have thin RCG coating that is not resistant to impact; cannot be coated with TUFI/RCG coating
  - 2nd generation tile (AETB-8) with TUFI/RCG coating has a factor of 6 increase in resistance to low-velocity impact damage [61] but can't be used over large areas on lower surface due to it higher thermal conductivity
  - 3rd generation tile (BRI-8) can be coated with TUFI/RCG and has conductivity similar to LI-900; design goal was also to have a strength similar to AETB-8
    - May be a one-for-one replacement for LI-900 lower surface acreage tile
    - Boeing IR&D funded BRI development prior to 2000
    - NASA upgrade program funded BRI development in 2000, 2001 and 2003
    - Additional development and testing required to fully ascertain its potential to replace lower surface LI-900 tile

Presenter M3/Material | Date FINAL | Slide 6 of 11 | Closed

Tile Design – Certification

- **Background / Facts (cont'd):**
  - Additional BRI development and testing required
    - Assess dimensional stability for complex shaped tile
    - Fully assess thermal characteristics (e.g. conductivity)
    - Material allowables
    - BRI at other densities
    - Evaluate impact resistance (various velocities and projectiles) based on damage tolerance requirements

LI-900

BRI-8

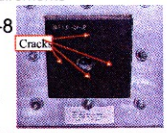

Hypervelocity Impact Testing

Presenter M3/Material | Date FINAL | Slide 7 of 11 | Closed

Tile Design – Certification

- **Findings:**
  - The loss of a single tile before entry interface on the lower surface of the orbiter forward of location $X_0$1357 could result in the loss of the orbiter. The loss of two tiles before entry interface on the lower surface of the orbiter forward of location $X_0$1357 would most likely result in the loss of the orbiter [67].
  - Some tile possess more risk than others: some tile have a greater probability of being struck by debris, some locations are subject to greater heat load, and some locations have are adjacent to critical non-structural components [72]
  - The orbiter has been subjected to debris strikes since its first flight. Yet the requirements to tolerate or resist debris impact are exceedingly weak for general impact resistance and nonexistent for debris impact during launch [17].

Presenter M3/Material | Date FINAL | Slide 8 of 11 | Closed

Tile Design – Certification

- **Findings (cont'd):**
  - Boeing has studied the consequence of impact damage resulting from debris impact under NASA sponsorship [74, 18]. The thermal and structural analysis performed as part of the study subsequent to the large debris impact damaged experienced during STS-87 [74, 18], demonstrated that plausible damage states could cause structural factors of safety to drop below 1.0 [46].
  - History has shown that the orbiters have suffered 10 tile loss events since Columbia first flew in April 1981. On average, that's one tile loss event every two years or 11 flights. One tile-loss event was directly attributable to debris impact from the SRB nose-cap.
  - A systematic approach to evaluate the effect of various tile damage scenarios on reentry survivability has not been performed.
  - As can be seen from the impact map, some areas of the orbiter are more likely to be damaged than others. Knowing the probability of where damage may occur is important, but the critical damage levels and consequences must also be ascertained.

Presenter M3/Material | Date FINAL | Slide 9 of 11 | Closed

Tile Design – Certification

- **Recommendations:**
  - Compute/analyze the distribution of known damage sizes and locations
  - Establish the critical damage size for each critical location
  - Identify the consequences of sustaining critical damage in a critical location
  - Compute the probability of sustaining critical damage in a critical location based upon a predictive model that accounts for impacts of debris emanating from various sources
  - Develop a tile designed to withstand the critical damage computed for various locations and install it at those critical locations

Presenter M3/Material | Date FINAL | Slide 10 of 11 | Closed

References

Number	Filename	Reference
16	STS-27_Post Flight.pdf	Mission STS-27 OV-104 (Atlantis) Flight 3 TPS Post Flight Assessment (Hoot Gibson)
17	Orbiter Vehicle End Item Specification for The Space Shuttle.pdf	Orbiter Vehicle End Item Specification for the Space Shuttle System, Part 1, Performance and Design Requirement, Contract NAS9-20000, 7 Nov 02
18	OV-102 STS-87 TPS Damage.ppt	Gatto, "OV-102 (STS-87) TPS Damage," Boeing Presentation -Space Shuttle Vehicle Engineering Office, 6 January 1998
60	MIL-HDBK-1530.pdf	"Military Handbook - Aircraft Structural Integrity Program, " MIL-HDBK-1530, 4 November 1996
61	TPS Imp Post-PRT Basic2.pdf	Boeing, "TPS Enhancement Study Options," UCN 23273 (presentation), 28 March 2003

Presenter M3/Material | Date FINAL | Slide 11 of 11 | Closed

Tile
Fleet Experience – Aging

11-1 Tile System Integrity

11-2 Lost Tiles

11-3 Lack of NDI/E

11-4 Potential for Corrosion

11-6 Tile Shrinkage

Matrix

Presenter	CAIB/Group 1	Date	FINAL	Slide	13 of 32

Tile System Integrity

- **Action / Issue:**
  - Tile system components may degrade as a function of thermal/mechanical loads, chemical environment, and calendar time

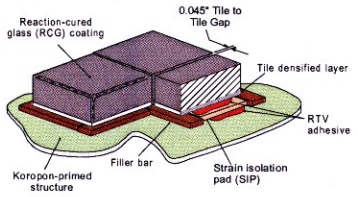

Tile System
RCG Coating
LI-900 LI-2200 FRCI-12 AETB-8
Densified Layer
RTV Adhesive
SIP
RTV Adhesive
Heatsink/Screed
Koropon Primer

Presenter M3/Material | Date FINAL | Slide 1 of 18 | Closed

What will be the Weak Link In the Future?

Evaluate each tile component for aging effects

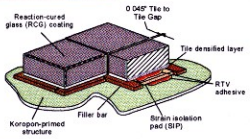

Material	Strength (psi) Material Allowable	Average
LI-900	13	23
LI-2200	35	60
FRCI-12	50	75
AETB-8	29	45
BRI-8*	20	33
0.090-in Class 1, Grade A SIP	45	
0.115-in Class 2, Grade A SIP	45	
0.160-in Class 3, Grade A SIP	25	
RTV 560/566	280	480
Koropon Primer	?	
RTV 577		

The question: Do these properties change as a function of thermal/mechanical loading, ground environment and/or time?

Presenter M3/Material | Date FINAL | Slide 2 of 18 | Closed

Coating/Tile/Densification Integrity

- **Background / Facts:**
  - Tile "poisoning" possible and inhibits efficacy of rewaterproofing; however, treatment of tile with multiple injection of DMES overcomes "poisoning"
  - Cooper test was used to evaluate mechanical strength under various loads
- **Findings:**
  - Evaluation of tile coating, substrate and densification to date indicates that tile should continue to be resistant to thermal/mechanical effects

Tile System
RCG Coating
LI-900 LI-2200 FRCI-12 AETB-8
Densified Layer
RTV Adhesive
SIP
RTV Adhesive
Heatsink/Screed
Koropon Primer

Presenter M3/Material | Date FINAL | Slide 3 of 18 | Closed

RTV Integrity

- **Background / Facts (cont'd):**
  - RTV Adhesive/Heatsink/Screed
    - Adhesive, heatsink and screed are all RTV silicone products supplied by General Electric
    - RTV known to degrade when exposed to certain environments
    - HMDS waterproofing used on OV-102 and OV-103; degrades RTV strength properties
    - A NASA/USA program is in place to sample and analyze RTV for degradation

Tile System
RCG Coating
LI-900 LI-2200 FRCI-12 AETB-8
Densified Layer
RTV Adhesive
SIP
RTV Adhesive
Heatsink/Screed
Koropon Primer

Presenter M3/Material | Date FINAL | Slide 4 of 18 | Closed

RTV Screed/Heatsink for OV-102

- **Background / Facts (cont'd)**
  - Red indicates original installation of OML screed/heatsink [63]
  - Tiles over screed/heatsink subjected to HMDS

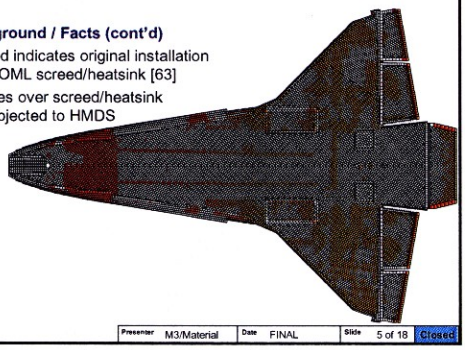

Presenter M3/Material | Date FINAL | Slide 5 of 18 | Closed

Major Factors For RTV Degradation Have Been Identified

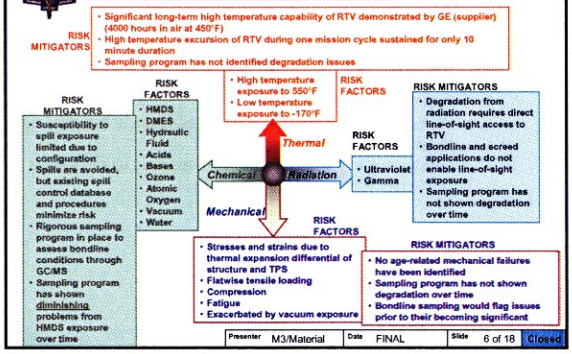

Presenter M3/Material | Date FINAL | Slide 6 of 18 | Closed

1

RTV Bondline Sampling Test Program (Since 1980s) [30]

Contractual Requirement Defines Key Locations
RTV Samples Removed During Ops & OMM
Assessment Made of RTV Bond During TPS Removal
RTV Specimens Tested and Analyzed at Boeing-HB
Analysis and Trends Presented to Customer Every 2 Years at TPS PRB

- **Samples are taken from key areas of Orbiter per OMRSD V09AW0**
  - Hydraulic Fluid Inspection - piano hinge/body flap
  - Screed/Heatsink Inspection - 7 locations (from 14 options)
  - Orbiter RTV Bondline Sampling - 10 locations
  - OMS RTV Bondline Sampling - 1 location per pod
- **Samples accompanied by Tile Removal PR**
  - Includes subjective evaluation of peel strength, tackiness
- **Samples sent to Boeing HB labs for analysis**
  - Derived Shore A Harness
  - Gas Chromatography/Mass Spectrometry (GC/MS)

Analysis Results Presented at TPS Process Review Boards Every 2 Years Do Not Show Degradation Trends

Presenter M3/Material | Date FINAL | Slide 7 of 18 | Closed

Thermal Effects on RTV

- **Background / Facts (cont'd):**
  - Maximum structural surface temperatures experienced by OV-102 [62]
  - At 250F, RTV/Koropon average strength drops to 220 psi; material allowable drops to 120 psi; at 350F, allowable drops to < 20 psi

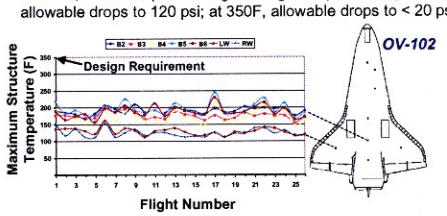

Presenter M3/Material | Date FINAL | Slide 8 of 18 | Closed

RTV Integrity

- **Background / Facts (cont'd):**
  - Sampling program in place since 1980s to identify age/environment related changes in material properties [29, 30]
  - To date, the sampling program has not found any negative trends [30]
  - The loss of two tiles before entry interface on the lower surface of the orbiter forward of X01357 would most likely result in the loss of the orbiter [67]
- **Findings:**
  - Sub-nominal bonds probably exist
- **Recommendations:**
  - Ensure continuation of sampling program; statistical analysis?; enough samples?
  - Relate results of sampling program to reduction in risk
  - Investigate effect of combined environment (thermal/mechanical/chemical) and age on degradation
  - Qualify subjective peel-strength evaluation process
  - Investigate methods to detect subnominal bonds (long-term)

Presenter M3/Material | Date FINAL | Slide 9 of 18 | Closed

Strain Isolation Pad (SIP) Integrity

Background / Facts (cont'd):

- Strain Isolation Pad (SIP)
  - SIP is a Nomex felt comprised of polyamide fibers formed into a pad
  - The felt is heat set at 500F for 30 minutes to provide dimensional stability and then coated with RTV (0.006"-0.010")
  - Multiple thicknesses are used:
    - 0.090-in for high modulus applications (e.g. next to thermal barriers around doors)
    - 0.160-in for most applications (acreage tile)
  - Due to buy-out of SIP in the 1980's SIP no longer manufactured
  - There is no shelf-life requirement for SIP

Tile System
RCG Coating
LI-900 LI-2200 FRCI-12 AETB-8
Densified Layer
RTV Adhesive
➡ SIP
RTV Adhesive
Heatsink/Screed
Koropon Primer

Presenter M3/Material | Date FINAL | Slide 10 of 18 | Closed

SIP Integrity

- **Background / Facts (cont'd):**
  - Material allowables development [H77]
    - Permanent extension of SIP (flatwise) occurs after exposure to cyclic mechanical loads [H77]
    - Testing to develop modulus included exposure of SIP (flatwise) to cyclic mechanical loads
    - Tensile strength (flatwise) specimens exposed up to 25 hrs at test temperature prior to test to failure

Presenter M3/Material | Date FINAL | Slide 11 of 18 | Closed

SIP Integrity

- **Background / Facts (cont'd):**
  - SIP properties are tested indirectly:
  - Indirect testing provides information about "threshold" strength, but cannot be used to model degradation effects
    - "Time-aged" SIP tested indirectly during recertification of tile:
      - Tile densification qualification using a new coloring agent
      - AETB tile certification for used on base heat shield
    - "Thermal/mechanical" aging indirectly tested for 26 missions during certification of of DMES rewaterproofing
    - "Thermal/mechanical" aging indirectly tested during certification of tile system for 100 Orbiter missions

Presenter M3/Material | Date FINAL | Slide 12 of 18 | Closed

SIP Integrity

- **Findings:**
  - SIP currently thought to be robust
- **Recommendations:**
  - Direct testing and evaluation of SIP to assess aging effects is not necessary
  - Establish periodic testing of SIP stock to monitor potential aging effects due to time and, currently unknown, degradation effects

Presenter M3/Material | Date FINAL | Slide 13 of 18 | Closed

Koropon Primer Integrity

- **Background / Facts (cont'd):**
  - Super Koropon used as a primer on aluminum surfaces of orbiter
  - Over-spray of Koropon results in reduction in cohesion properties
    - Over-spray occurred during orbiter assembly and has occurred during insulation installation
  - Strength of RTV applied over bare aluminum greater versus application over Koropon
  - At 120F the flatwise strength ("A" allowable) of RTV over Koropon and RTV over bare aluminum begins to diverge; the allowable for RTV over Koropon drops to 13 psi at 350F

Tile System

RCG Coating
LI-900 LI-2200 FRCI-12 AETB-8
Densified Layer
RTV Adhesive
SIP
RTV Adhesive
Heatsink/Screed
Koropon Primer

Presenter M3/Material | Date FINAL | Slide 14 of 18 | Closed

Koropon Primer Integrity

- **Background / Facts (cont'd):**
  - Koropon develops microcracks which enhances adhesion
  - Koropon softens when used under thick applications of RTV 577 and RTV 560
    - Screed thickness: 0.2 and 0.4 inches
    - Screed not applied over Koropon
  - The loss of two tiles before entry interface on the lower surface of the orbiter forward of X01357 would most likely result in the loss of the orbiter [67]

Tile System

RCG Coating
LI-900 LI-2200 FRCI-12 AETB-8
Densified Layer
RTV Adhesive
SIP
RTV Adhesive
Heatsink/Screed
Koropon Primer

Presenter M3/Material | Date FINAL | Slide 15 of 18 | Closed

Koropon Primer Integrity

- **Findings:**
  - No thermal/mechnical testing has been accomplished to evaluate the loss of cohesion due to Koropon over-spray
- **Recommendations**
  - Initiate a program to ascertain thermal/mechanical effects on over-spray adhesion
    - Identify areas of probable over-spray and sample

Presenter M3/Material | Date FINAL | Slide 16 of 18 | Closed

Overall Findings and Recommendations

- **Findings:**
  - Effect of age and operational exposure not completely understood
    - Subnominal tile component properties probably exist
      - Magnitude of degradation is unknown
  - The loss of two tiles before entry interface on the lower surface of the orbiter forward of X01357 would most likely result in the loss of the orbiter [67]
- **Recommendation:**
  - Implement a program to systematically characterize effect of aging on all tile system components relative to design conditions
    - Initial emphasis should be on Super Koropon and RTV

Presenter M3/Material | Date FINAL | Slide 17 of 18 | Closed

References

Number	Filename	Reference
29	RTV Scrap History and Age Life March 2001.ppt	Robert J. Perez, Tom Luce, Michael P. Gordon, "RTV Scrap History & Age Life," Material & Process Engineering, TPS PRB, March 2001
30	RTV aging.ppt	Mary Litwinski, "Integrity of RTV for TPS Applications," Boeing-HB M&P Engineering, 6 February 2003
62	ShuttleAeroheatingStatistics.xls	Gearld Kinder, Shuttle Aeroheating Statistics from Boeing, Huntington Beach Meeting 25 April 2003
63	OV-102 Screed_heatsink_recorded_prior_to_deliveryl.ppt	TIPs generated output depicting original installation of screed/heatsink

Presenter M3/Material | Date FINAL | Slide 18 of 18 | Closed

Tile Fleet Experience

- **Action / Issue:**
  - It is not possible to determine when the tile system has degraded to the point where there will be a loss of tile
- **Background / Facts:**
  - The loss of two tiles before entry interface on the lower surface of the orbiter forward of $X_0$1357 would most likely result in the loss of the orbiter [67]
  - Many tile losses resulted in a design modification or change in process
    - Did not know that something was wrong prior to flight
    - Development and certification testing/analysis did not predict failure
  - On average, tile is lost every 2 years (11 flights)
    - Last loss occurred 3 years ago (16 flights)

Presenter M3/Material | Date FINAL | Slide 1 of 9 | Closed

Lost Tiles – All Orbiters

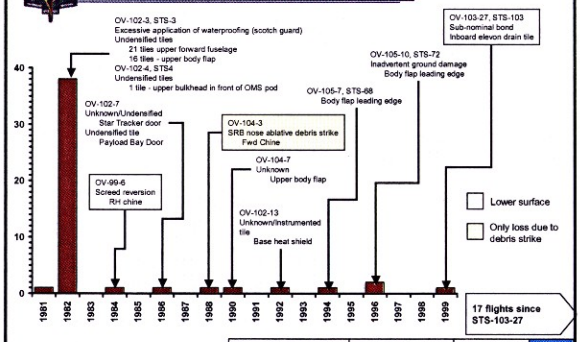

Presenter M3/Material | Date FINAL | Slide 2 of 9 | Closed

Right Wing Lost Tile

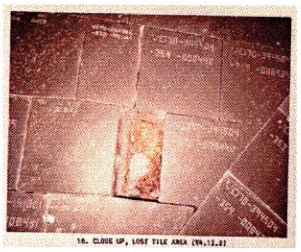

STS-41G
OV-99, Flight #6
5 October 1984

Screed remained in cavity; initiated "Soft Screed" hunt
Ultimately, 4011 tiles would be replaced

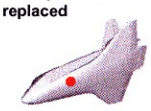

Cause: Sub-nominal bond due to RTV reversion after application of HMDS rewaterproofing

Presenter M3/Material | Date FINAL | Slide 3 of 9 | Closed

Left Elevon Burn Through

Not classified as a lost tile.

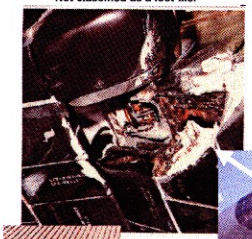

STS-51D
OV-103, Flight #4
12 April 1985

Severe TPS damage on left outboard elevon caused carrier panel burn-through and significant structural damage to the forward outboard corner of the elevon.

Tile found on ground after landing

Presenter M3/Material | Date FINAL | Slide 4 of 9 | Closed

Missing Chine Tile

STS-27R
OV-104, Flight #3
2 December 1988

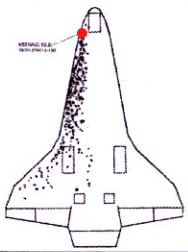

Cause: SRB Nose-cap Ablative Debris Strike

Presenter M3/Material | Date FINAL | Slide 5 of 9 | Closed

Lost Upper Body Flap Leading Edge Tile

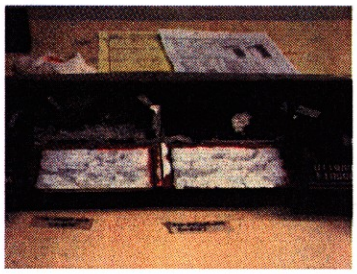

STS-72
OV-105, Flight #10
11 January 1996

Bonded SIP and tile densification layer remained in cavity.

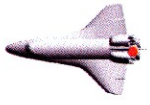

Cause: Inadvertent ground damage

Presenter M3/Material | Date FINAL | Slide 6 of 9 | Closed

Lost Inboard Elevon Drain Tile

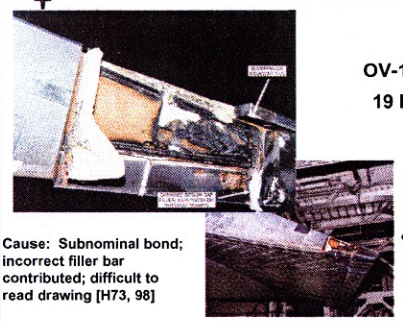

STS-103
OV-103, Flight #27
19 December 1999

Cause: Subnominal bond; incorrect filler bar contributed; difficult to read drawing [H73, 98]

Presenter M3/Material | Date FINAL | Slide 7 of 9 | Closed

Design / Mods / Manufacturing TPS Under Wing

- **Findings:**
  - Cannot predict tile failure
    - Failure due to design, maintenance process changes and inadvertent ground damage
  - Effect of aging difficult to predict and may be a risk contributor in the future
- **Recommendations:**
  - The fact that a dominant or common cause does not exist underscores the need to address tile system integrity on several fronts: design and process change certification, training for maintenance personnel, clear process instructions, design of processes to reduce sensitivity and variance and NDI/E or "health monitoring" system to aid in determining when tiles are damaged.
  - Continue RTV sampling program to help assure ability to to detect potential, and currently unknown, aging effects on tile system integrity

Presenter M3/Material | Date FINAL | Slide 8 of 9 | Closed

References

Number	Filename	Reference
47	OV104 Lost Tile PP Version 4.ppt	Karrie Hinkle, "STS-99 Flight Readiness Review, OV-103 Lost Elevon Tile, Boeing/USA " 18 January 2000
67	RE Criticality of Tile.htm	Email from Boeing
68	STS-4 Thermal Protection System Postflight Analysis Part II Tile, SIP, and Gap Filler Analysis.pdf	Laboratory analysis of lost tile and tile damage
69	STS-72_Book.pdf	Mission STS-72 OV-105 Flight 10 TPS Post-Flight Assessment, SE-1617T9, KLO-96-003, April 1996
70	Significant TPS Event History 29Mar03.XLS	TPS event history from SSM website; modified by Clare Paul to include analysis data contained in workbook
98	OV103ElevonDrainHole.pdf	Boeing Corrective Action Request - Elevon Drain Tile, Problem 103RF02-010

Presenter M3/Material | Date FINAL | Slide 9 of 9 | Closed

Tile Fleet Experience – Aging

- **Action / Issue:**
  - Bond-line integrity and/or strength is unknown
- **Background / Facts:**

  Bond-line Integrity
  - There are two techniques used to characterize bond-line integrity: a proof test (bond verification test) and the manual deflection test ("wiggle" test).
  - Bond verification (BV), for regular tile, is performed by attaching a specialized tensile test unit over the tile and utilizing a vacuum chuck tool. The maximum applied load is generally determined by using the known bond surface area multiplied by the stress levels given in table specification The load is held at the maximum value for at least one second. For a typical lower surface regular five-inch square SIP footprint, the test load required to achieve the required 10-psi would be 250-lbs.

Presenter M3/Material | Date FINAL | Slide 1 of 11 | Closed

Maintenance Turnaround Work TPS Under Wing

- **Background / Facts (cont'd):**
  - A partial bond could exist and the BV test would not detect it
  - There are specialized test load procedures for modified regular tile, irregular tile, structurally limited tile, tile bonded to filler bar, carrier panel tile, closeout tile and TUFI-coated and TUFI-RCG-coated tile.
  - Structurally limited tiles will be tested using reduced loads due to the structural limitations of the underlying substrate.
  - The tile bond is characterized as acceptable if the required tension load is sustained for one second without the tile pull-off.
  - Another method used to evaluate the tile to substrate bond is through the manual deflection test, also known as the "wiggle" test. This test requires an experienced technician to "wiggle" the tile and sense when the tile to substrate bond is unacceptable.

Presenter M3/Material | Date FINAL | Slide 2 of 11 | Closed

Current Method: Tile Bond Verification

Tile System Component Strength [H76]

Material	Strength (psi) Material Allowable	Average
LI-900	13	23
LI-2200	35	60
FRCI-12	50	75
AETB-8	29	45
BRI-8*	20	33
0.090-in Class 1, Grade A SIP	45	
0.115-in Class 2, Grade A SIP	45	
0.160-in Class 3, Grade A SIP	25	
RTV 560/566	280	480
Koropon Primer	7	
RTV 577		

Bond Verification

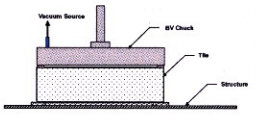

Type	Applied Stress (psi)
HRSI	10
LRSI	6-10
TUFI	10

Bond Verification Stress [H24]

Design Limit Stress (DLS)[65]

DLS (psi)	Number of Tile	Percent of Total
0-4	4862	33.00%
4-6	4792	32.52%
6-8	3320	22.53%
8-10	1065	7.23%
10-12	204	1.38%
12-14	269	1.83%
14-16	143	0.97%
16-20	44	0.30%
20-30	36	0.24%

Total of 14,735 Lower Surface Tiles

Presenter M3/Material | Date FINAL | Slide 3 of 11 | Closed

Tile BV Compared to DLS

- **Background / Facts (cont'd):**
  - BV occurs when tile replaced
  - 44% of tiles applied prior to first flight (1981) [H77]

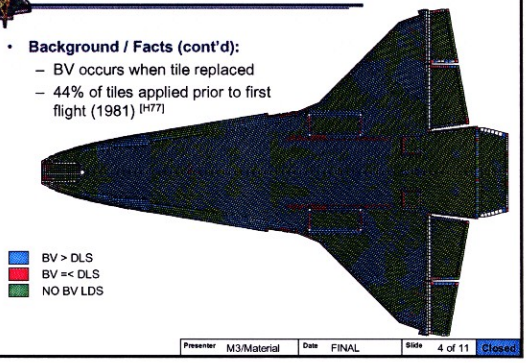

Presenter M3/Material | Date FINAL | Slide 4 of 11 | Closed

Heavy Reliance on Process Control and Sampling

- **Background / Facts (cont'd):**
  - There is a heavy reliance on process control to ensure tile system integrity
  - Sampling program removes tile and samples RTV [13]
    - Samples sent to Boeing HB labs for analysis
      - Derived Shore A Harness
      - Gas Chromatography/Mass Spectrometry (GC/MS)

Presenter M3/Material | Date FINAL | Slide 5 of 11 | Closed

Matrix of NDI/E Methods Evaluated Over the Years[10]

	Method	Year	Company	Used for	Flaw Size	Strength	Weakness	Tested on TPS
Off Orbiter	Film X-Ray	1980-2003	Lockheed & Boeing	Internal Voids	.025 inch x .025	Well established method	Requires standards	Yes Production Units
	CT	1996	EG&G	Internal Voids/ Density	No voids or inclusions Density shall be 8 +-1.0 pcf	Multi slices	Time consuming	Yes Production Units
	Acoustic Excitation	1986-1989	EG&G	Disbond	Target 10% disbond	Portable	No debonds were found	Yes
On Orbiter	Laser Vibrometry	1991	Navcon Engineering Network/Ometron	Disbond	Target 10% disbond	Portable	No debonds were found	Yes 1991 OV102 (43 Tiles)
	Shearography	1991 & 1997	Laser Technology	Disbond	Target 10% disbond	Portable	No debonds were found	Yes 1991 OV102 (43 Tiles) 1997 OV105 (470 Tiles)
	Reverse Geometry X-ray	1997	Digiray	Disbond	Target 10% disbond	Portable	No debonds were found	Yes OV105 (21 Tiles)

Presenter M3/Material | Date FINAL | Slide 6 of 11 | Closed

1

NDI/E Development and Evaluation

- **Background / Facts (cont'd)**
  - Boeing (Huntington Beach) is not in the business of developing tile bond-line NDI
    - Now allows NASA/vendors to test NDI/E on specially fabricated test panels [10]

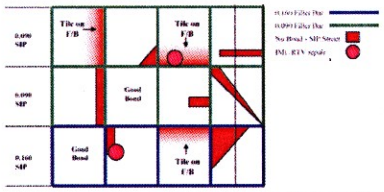

Presenter M3/Material | Date FINAL | Slide 7 of 11 | Closed

Boeing Proposed New NDI/E Methods for Tiles

- **Background / Facts (cont'd):**
  - The following new NDE Methods for detecting tile disbonds have been proposed[10]
    - Microwave Technology
      - Proposed by University of Missouri
      - Never funded or tested on TPS materials
    - Nonlinear Structural Dynamic Response
      - Proposed by Georgia Tech
      - Never funded or tested on TPS materials
    - Laser Vibration
      - Proposed by University of Central Florida
        - » Funded by NASA KSC
        - » Has been tested on Tiles

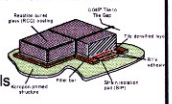

Presenter M3/Material | Date FINAL | Slide 8 of 11 | Closed

General Results of NDE/I Methods[10]

- **Background / Facts (cont'd):**
  - Changes in material properties, Tile (Silica & Air), SIP (Nomex), RTV thickness, Gap fillers (Fabric) and Aluminum structure limit accuracy / repeatability of NDE to detect disbonds
  - None of the methods or combination of them could accurately detect disbonds
    - Suspect NDE disbond tiles were removed and evaluated as a good bond
    - NDE method would show promise when used on disbonded test panel but fail when tested on the Orbiter
  - New Tile disbond panel has been made and sent to NASA Marshall Space Flight Center for evaluation

Presenter M3/Material | Date FINAL | Slide 9 of 11 | Closed

Lack of Tile NDI/E

- **Findings:**
  - There are no widely accepted NDI/E methods that are used to detect disbonds. General methods to detect a disbonds are in development, and the time when they will be available is unknown. A even more useful NDI/E method would be one that can measure the bond strength. This is an even more challenging problem and will not likely be resolved in the near future.
  - The loss of two tiles before entry interface on the lower surface of the orbiter forward of X01357 would most likely result in the loss of the orbiter [67]
  - NASA and Boeing seem to have a sense for the need to develop a method to better quantify the bond-line integrity and have tested various methods on test panels and the orbiters
- **Recommendations:**
  - It is recommended that efforts to develop and evaluate NDI/E methods to assess bond integrity be given increased emphasis

Presenter M3/Material | Date FINAL | Slide 10 of 11 | Closed

References

Number	Filename	Reference
10	Processes Used to Test Tile Bonds and Inspect RCC from SSM Website.ppt	
13	NSTS 08171 File 3 V09 Thermal Protection System.pdf	NSTS 08171- Space Shuttle Operations and Maintenance Requirements and Specifications document, File III , V09 - Thermal Protection System, 21 Nov 02
15	Tile NDE Boeing 28May97.pdf	A Boeing presentation that discusses the use of reverse geometry x-ray and shearography to NDI/E tile bond.
37	Tiles Replaced on OV-102.ppt	Tile Replaced on OV-102 from SSM Website
65	v102lower_paul.xls	TIPS generated Excel output from Jenny Tran, Boeing, Huntington Beach tabulating tile location, DLS, BV values and more
66	CAIBNDE TPS4-25-03.ppt	NDE Presentatin from Boeing, Huntington Beach 25 April 2003
67	RE Criticality of Tile.htm	Email from Boeing

Ref	Content
H23	Bond Verification and Design Limit Stresses
H24	ML0601-9024, Process 315 - Bond Verification of RSI Tiles
H76	Materials Properties Manual, Volume 3, Thermal Protection System Materials Data prepared by Laboratories and Test D/284, Rockwell International, August 1988
H77	Original Tile History for OV-102, RFI: B1-0090194

Presenter M3/Material | Date FINAL | Slide 11 of 11 | Closed

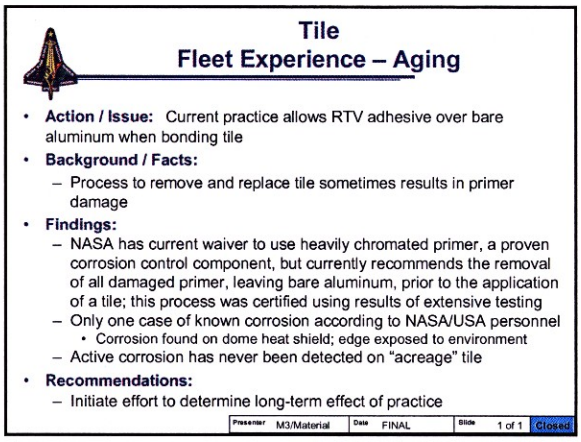
Tile
Fleet Experience – Aging
• Action / Issue: Current practice allows RTV adhesive over bare aluminum when bonding tile
• Background / Facts:
– Process to remove and replace tile sometimes results in primer damage
• Findings:
– NASA has current waiver to use heavily chromated primer, a proven corrosion control component, but currently recommends the removal of all damaged primer, leaving bare aluminum, prior to the application of a tile; this process was certified using results of extensive testing
– Only one case of known corrosion according to NASA/USA personnel
• Corrosion found on dome heat shield; edge exposed to environment
– Active corrosion has never been detected on "acreage" tile
• Recommendations:
– Initiate effort to determine long-term effect of practice
Presenter M3/Material
Date FINAL
Slide 1 of 1
Closed

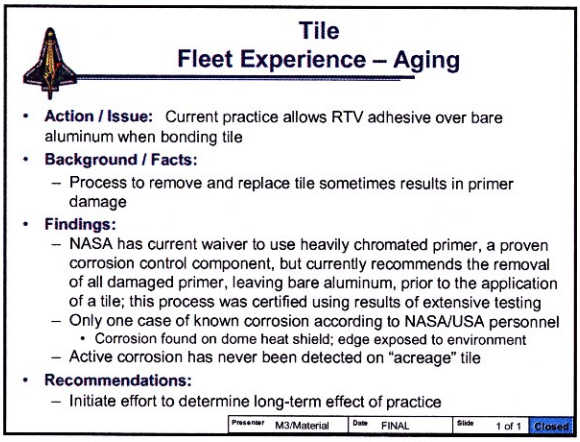

Tile
Fleet Experience – Aging

- **Action / Issue:** Current practice allows RTV adhesive over bare aluminum when bonding tile
- **Background / Facts:**
  - Process to remove and replace tile sometimes results in primer damage
- **Findings:**
  - NASA has current waiver to use heavily chromated primer, a proven corrosion control component, but currently recommends the removal of all damaged primer, leaving bare aluminum, prior to the application of a tile; this process was certified using results of extensive testing
  - Only one case of known corrosion according to NASA/USA personnel
    - Corrosion found on dome heat shield; edge exposed to environment
  - Active corrosion has never been detected on "acreage" tile
- **Recommendations:**
  - Initiate effort to determine long-term effect of practice

Presenter	M3/Material	Date	FINAL	Slide	1 of 1	Closed

1

Tile Shrinkage

- **Action / Issue:** Investigate orbiter fleet problems related to tile shrinkage
- **Background / Facts:**
  - Tile shrinkage does occur during manufacturing
  - Localized Heating Results in Tile Repair and Replacement
    - Localized High Heating in Flight Causes Tile Lips to Shrink Back, Corners to Round Off, Overhangs to Slump, and Tile to Tile Gaps to Widen
    - STS-91 Resulted in 8 Tile Replacements Due to Slumping on Reentry
      - ISS Missions Have More Severe Reentry Heating

Replacement of Complex Shaped Tiles Is Expensive

Presenter M3/Material | Date 5 June, 2003 | Slide 1 of 6 | Closed

Tile Shrinkage

- **Findings:**
  - Tile shrinkage generally not a safety-of-flight issue; it is a maintenance issue
  - Tile certification tests indicate total gap sizes from 0.075-0.093 inches after a 100 mission simulation.
    - Allowable gaps are on the order of 0.025-0.065 inches; filled gaps range from approximately 0.066-0.085 inches
  - Tile shrinkage of BRI-8 much less than LI-900
- **Recommendations:**
  - Revisit tile shrinkage as a function of temperature for acreage installations and assess long-term impact. If the ultimate solution to tile shrinkage is tile replacement at some time in the orbiters life, it may provide further impetus to migrate to a tougher tile system

Presenter M3/Material | Date 5 June, 2003 | Slide 2 of 6 | Closed

Areas That Typically Experience Slumping (Localized Shrinkage)

Complex Shaped Tiles

Tiles in Chin Area

Elevon Hinge Tiles

Nose Landing Gear Door Tile

Elevon Hinge Tiles

Presenter M3/Material | Date 5 June, 2003 | Slide 3 of 6 | Closed

Maximum Recorded OML Surface Temperatures

Temperatures Range from 1600F-2300F

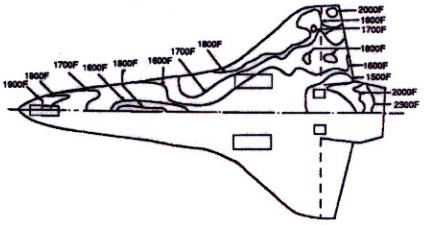

Presenter M3/Material | Date 5 June, 2003 | Slide 4 of 6 | Closed

Tile Shrinkage

- **Background / Facts (cont'd):**

Tile certification test results and temperature exposure profile

Block	Thermal Cycles	Cum. Cycles	Individual Wide Gaps: Tiles 16-24 (in)	Individual Wide Gaps: Tiles 38-46 (in)	Mission (after reboard)
6	6	16	0.085	0.060	Pre-Block 7
7	9	25	0.135	0.110	Post-Block 7
8	25	50	0.150	0.105	Post-Block 8
9	25	75	0.165	0.110	Post-Block 9
10	25	100	0.180	0.120	Post-Block 10
		Gap Increase	0.095	0.060	

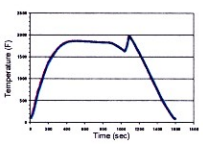

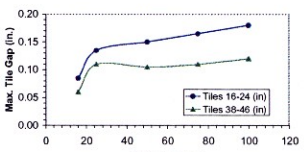

Presenter M3/Material | Date 5 June, 2003 | Slide 5 of 6 | Closed

Dimensional stability of BRI-8, LI-900, and AETB-8

- For these tests, entire tile exposed to high temperature
- Orbiter tile not exposed on all sides during mission
- These tests used to compare tile shrinkage of different tile materials

Before Test

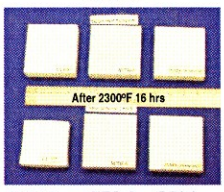

LI-900 AETB-8 BRI-8

IP: In-Plane
TTT: Through the Thickness

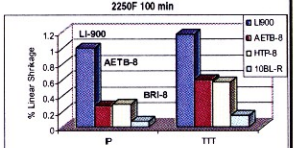

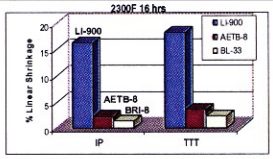

Presenter M3/Material | Date 5 June, 2003 | Slide 6 of 6 | Closed

1

Tile Maintenance

12-1 Tile Repair Discrepancies

Matrix

Presenter	CAIB/Group 1	Date	FINAL	Slide	14 of 32

Tile Maintenance

- **Action / Issue:**
  - Some repairs performed on tile were not consistent with standard procedures.
- **Background / Facts:**
  - USA and NASA personnel reviewed 137 lower surface TPS WADs to determine in search of discrepancies that could have contributed to OV-102 failure
- **Findings:**
  - Four of five tile repairs on the orbiter chine and lower surface were found to exceed TPS-211 repair criteria for maximum volume/depth.
  - One repair around the LMLG door was found to be outside repair criteria found TPS-211 due to the failure to remove an existing repair prior to rework.
  - USA/NASA reported the discrepancies did not present a safety-of-flight issue

Presenter M3/Material | Date FINAL | Slide 1 of 5 | Closed

STS-107 LH Wing TPS Process Review "Findings of Concern" [H22]

- **Findings:**

ID #	WAD	Wad Type	Area	Findings	Observations
105	MMID-2-28-6070	Finding	CHINE	Damage Volume exceeds TPS-211 Repair Criteria	Damage Volume exceeds TPS-211 Repair Criteria
102	MLWNG-2-28-7548	Finding	Gear	Damage was too deep for a TPS-211 Repair (Upper Surf Tile)	Damage Depth exceeds TPS-211 Repair Criteria (Investigation - Evaluation Indicated that TPS-311 is OK)
104	MLWNG-2-28-7576	Finding	Lower Wing Acreage	Damage was too deep for a TPS-211 Repair	Damage Depth exceeds TPS-211 Repair Criteria (Investigation - Evaluation Indicated that TPS-311 is OK)
107	MMID-2-28-6012	Finding	GEAR	Damage Volume exceeds TPS-211 Repair Criteria	Damage Volume exceeds TPS-211 Repair Criteria
106	MLWNG-2-28-7523	Finding	GEAR	Previous damage Not removed (Investigation - Evaluation Indicated that TPS-311 is ok)	Previous Damage Not removed (Investigation - Evaluation Indicated that TPS-311 is OK)

137 Total WADS reviewed for the LH Wing Lower Surface

71 Matrix DRs (Not TIPS Tracked) were reviewed but are not included on the maps (minor putty repairs TPS-211/311)

Presenter M3/Material | Date FINAL | Slide 2 of 5 | Closed

Example: Paper Study Find #105

Old Repair

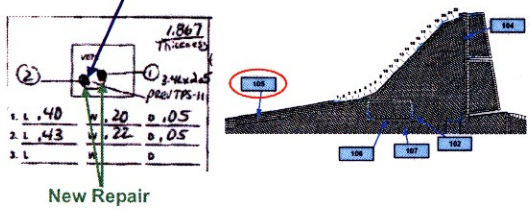

New Repair

Damage volume exceeds TPS-211 repair criteria. Volume exceeds limits. Previous repair should have been included in volume calculation [H22].

Presenter M3/Material | Date FINAL | Slide 3 of 5 | Closed

Tile Maintenance

- **Recommendations:**
  - Determine cause of process escapes
    - Training, process clarity, etc.
  - Establish and execute action plan to mitigate the cause of process escapes

See also: Orbiter Maintenance (14-3)

Presenter M3/Material | Date FINAL | Slide 4 of 5 | Closed

References

Ref	Tab Number	Content
H22	3	Kathy Laufenberg, USA, "OV-102 Flight 28-STS-107 Team A, TPS, CAIB Requests Repsponse," Tile Repair Procedures TPS-211 and -311, WADS for "high concern" TPS Damage; 7 March 2003

Number	Filename	Reference
64	WAD MMID-2-28-6070.tif	Paper Study Finding 105, Work Package MMID-2028-6070

Presenter M3/Material | Date FINAL | Slide 5 of 5 | Closed

Orbiter
Design / Certification

28-1 Orbiter Design Concerns

Matrix

Presenter	CAIB/Group 1	Date	FINAL	Slide	15 of 32

Orbiter Design Concerns

- **Action/Issue:**
  - Unexplained Anomaly (UA) team has uncovered additional orbiter design and maintenance concerns that should be addressed
- **Background:**
  - UA Team objective was to develop the effort required for safe Return to Flight utilizing UA logic and rationale should results of the investigation prove inconclusive
  - UA Team assessed possible causes from the Fault Tree and identified areas of concern that might warrant further action
  - UA Team also addressed the vulnerability of critical lower surface areas which, while not a contributor to the accident, had potential for a critical breach and warranted design review action before reflight
  - UA charts for issues not addressed in other locations of the Matrix follow

Presenter M3/Material | Date FINAL | Slide 1 of 14 | Closed

Orbiter Design Concerns

7. Door Seal Requirements

UA Closure Team

Related Fault Tree Block
- SFOML Wing 8-24

Findings

OVEI Specification states:

3.3.1.3.8 Access Doors – The primary structure shall be designed so that frequently-used doors including landing gear doors are not relied upon to carry primary body loads except local pressure loads. Sealing provisions shall be provided to preclude ingestion of adverse environments (i.e., hot gases, rain, dust, etc.)

- There is no specified requirement to assure environmental sealing of the NLG, MLG, and ET doors on a flight-by-flight basis
  - There are no seal compression verification requirements for MLG and NLG doors. A non-specified tactile check is performed after door closure which has initiated installation of gap fillers at the thermal barrier when purge leakage was considered excessive
  - Drawing requirement for ET door seal compression is 0.100 +/-0.050 inches with a recommended method for seal compression measurement after door re-rigging by ink imprint on tape. Not an every-flight activity

Presenter M3/Material | Date FINAL | Slide 2 of 14 | Closed

Orbiter Design Concerns

7. Door Seal Requirements (contd)

UA Closure Team

Findings (cont'd)
- Different materials are used for the door seals
  - ET = Teflon coated Silicon (very smooth surface)
  - NLG and MLG = Nomex coated Silicon (textured surface)
- The ET disconnect umbilical purge curtain ("baggie") which is destroyed during ascent consistently sandwiches unliberated remnants of the Kapton film baggie between door structure and environmental seal and/or thermal barrier. This potentially compromises seal integrity after door closure on orbit.

Concern
- Leakage bypassing the environmental seal on OV-104 (STS-51J and STS-61B) resulted in structural overtemp of the MLG wheel well frame edge and flow into the wheel well
- Leakage bypassing the environmental seal on OV-102 (STS-40) resulted in structural overtemp of ET door latch and flow into the aft fuselage compartment.

Presenter M3/Material | Date FINAL | Slide 3 of 14 | Closed

Orbiter Design Concerns

7. Door Seal Requirements (contd)

UA Closure Team

Recommendation
- Establish FMEAs for critical door seals and umbilical purge curtain
- Establish OMRSD requirement to verify sealing
- Review significance of seal coating differences
- Review ET door purge curtain design to eliminate compromising door sealing

Effectivity
- All vehicles – Return to Flight

Presenter M3/Material | Date FINAL | Slide 4 of 14 | Closed

Orbiter Design Concerns

Main Landing Gear Pressure Seal Configuration Shown

UA Closure Team

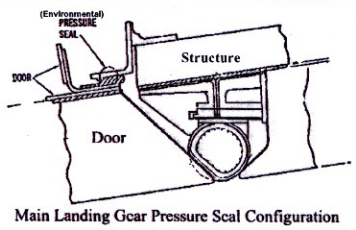

Main Landing Gear Pressure Seal Configuration

Presenter M3/Material | Date FINAL | Slide 5 of 14 | Closed

Orbiter Design Concerns

8. Carrier Panel Bonded Studs

UA Closure Team

Related Fault Tree Block:	SFOML-WING-8-12, 20, 17, 24 SFOML-WING-7-20
Finding:	Bonded Studs are used for TPS Tile Carrier Panel Attachment
Concern:	Flight and ground processing history indicates an unacceptable risk associated with the use of Bonded Studs for tile carrier panel attachment.
Recommendation:	The UA Closure Team recommends the elimination of bonded studs for future design. In addition, the team recommends an analysis of applications (including those existing as a result of prior Material Review action) to ensure positive margins if studs are completely debonded. In the event positive margins are not maintained, the team recommends redesign to an alternative fastener.
Effectivity:	Return to Flight

Presenter M3/Material | Date FINAL | Slide 6 of 14 | Closed

1

Orbiter Design Concerns

Bonded Stud Installation

UA Closure Team

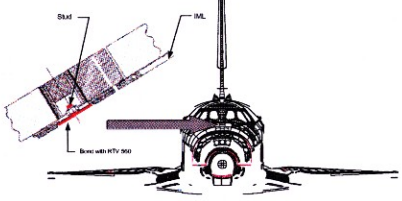

Presenter M3/Material | Date FINAL | Slide 7 of 14 | Closed

Orbiter Design Concerns

Lost Carrier Panel Caused by Debonded Stud

UA Closure Team

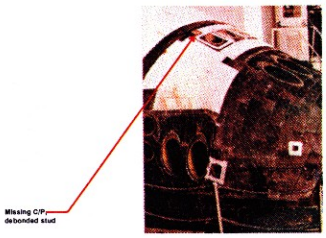

Presenter M3/Material | Date FINAL | Slide 8 of 14 | Closed

Orbiter Design Concerns

9. Elevon Cove Carrier Panel Fasteners

UA Closure Team

Related Fault Tree Block: SFOML-Wing-8-12, 20, 17, 24. SFOML-Wing-7-20

Finding: The elevon cove leading edge carrier panels are fastened to the seal panel with two #10 (0.186 in. dia.) fasteners engaging a self-locking thin wall insert. The carrier panels have been modified (per MCR 11656) since the original design, adding flow restrictors between the seal panel and carrier panel. The flow restrictors added preload to the fasteners, placing them in tension.

Concern: Failure of the insert or fastener would expose the primary seal panel to direct plasma flow during entry.

Recommendation: Perform a design study to re-evaluate the margins associated with the fastener/insert combination used in pre-loaded tension for this application.

Effectivity: Return to Flight

Presenter M3/Material | Date FINAL | Slide 9 of 14 | Closed

Orbiter Design Concerns

Cross Section Through Elevon Cove Shows Key Details

UA Closure Team

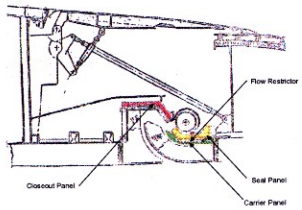

Presenter M3/Material | Date FINAL | Slide 10 of 14 | Closed

Orbiter Design Concerns

Elevon Cove Seal Carrier Panel Fastener Detail

UA Closure Team

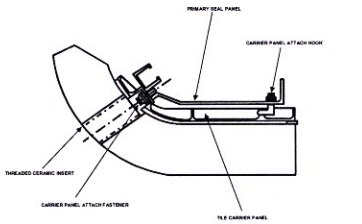

Presenter M3/Material | Date FINAL | Slide 11 of 14 | Closed

Orbiter Design Concerns

10. Elevon Cove Seals

UA Closure Team

Finding
The elevon cove seal has numerous critical TPS features. It is unique in that it is designed with known hot gas leak paths. The design has no FMEA. Leakage is allowed to levels up to 65 scfm and 110 scfm. Although there have been significant flight damage events in the early flights, the maintenance experience and processing have matured such that current thermal damage is minimal

Concern
Failure of any one of several structural features could result in significant risk to the elevon structure, wing structure and to the control surface effectiveness. In particular, loss of the "ski slope" tile, loss of the wiper seal carrier panel or loss of the honeycomb seal closeout panel would result in a significant hot gas breach.

Recommendation
Perform FMEA. Include potential effect of hot gas breach on control surface effectiveness as well as propagation of structural damage. Identify and quantify significant hazards.

Effectivity
Return to Flight

Presenter M3/Material | Date FINAL | Slide 12 of 14 | Closed

2

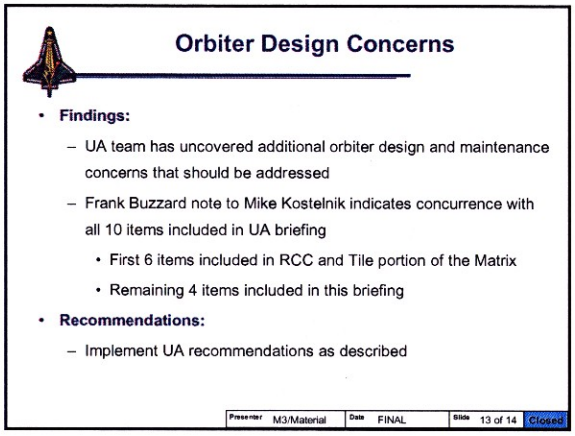
Orbiter Design Concerns
• Findings:
– UA team has uncovered additional orbiter design and maintenance concerns that should be addressed
– Frank Buzzard note to Mike Kostelnik indicates concurrence with all 10 items included in UA briefing
• First 6 items included in RCC and Tile portion of the Matrix
• Remaining 4 items included in this briefing
• Recommendations:
– Implement UA recommendations as described
Presenter M3/Material
Date FINAL
Slide 13 of 14
Closed

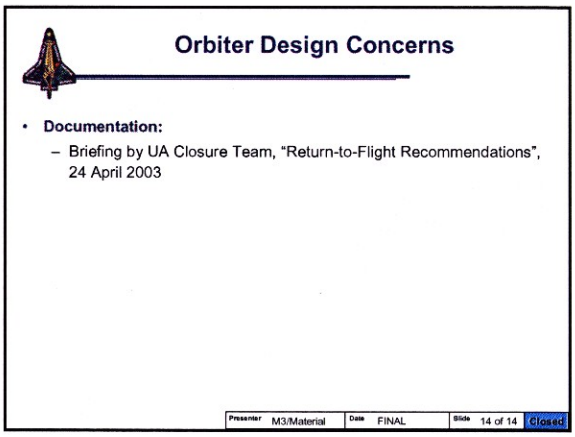
Orbiter Design Concerns
• Documentation:
– Briefing by UA Closure Team, "Return-to-Flight Recommendations", 24 April 2003
Presenter M3/Material
Date FINAL
Slide 14 of 14
Closed

Orbiter
Fleet Experience – Aging

13-1 Orbiter Service Life

13-2 Aging and Corrosion of OV-102

13-3 Corrosion found on and near forward fuselage (X0 582)

13-4 Environmentally Assisted Cracking of Carrier Panel Bolts

13-5 Challenges Associated with Wire Inspection

13-6 OV-102 Exposure to the Elements

13-7 Service Life of the Shuttle Fleet

Orbiter Service Life

- **Action / Issue:** Determine knowledge of OV-102 service life capability
- **Background / Facts:**
  - Comparison of key parameters used to determine orbiter structure service life to the most current fatigue loads spectra (PE Cycle 6.0) is documented in RSS99D0510D, "Space Shuttle Life Tracking", March 2003
  - Includes all missions from 1981 through February 2003 spanning STS-1 through STS-107
    - OV-102, Columbia, 28 flights
    - OV-103, Discovery, 30 flights
    - OV-104, Atlantis, 26 flights
    - OV-105, Endeavor, 19 flights

Presenter M3/Material | Date FINAL | Slide 1 of 18 | Closed

Orbiter Service Life

- **Background / Facts:**
  - Space shuttle has been analyzed for 4 different changes in usage
  - Most current fatigue loads spectra is designated Performance Enhancement
    - PE did not change descent or ferry flight regimes and includes DOLILU II

Number of Missions

	Starts with	All	OV-102	OV-103	OV-104	OV-105
First Flight			STS-1	STS-41D	STS-51J	STS-49
Date			4/12/1981	8/30/1984	10/3/1985	5/7/1992
All Flights	STS-1	113	28	30	26	19
DCR2 (RTF)	STS-26	88	21	24	24	19
DOLILU II	STS-70	44	11	10	12	11
PE	STS-88	21	3	5	6	7

Presenter M3/Material | Date FINAL | Slide 2 of 18 | Closed

Parameter Comparisons

	Number of Occurrences of Parameter in Life					
	All flts	OV-102	OV-103	OV-104	OV-105	Spectra
< 195,000						
195,000 - 205,000						
205,000 - 215,000						
215,000 - 225,000	1	1				4
225,000 - 235,000	2	1		1		7
235,000 - 245,000	12	2	5	1	1	12
245,000 - 255,000	32	4	9	7	7	38
255,000 - 265,000	51	17	13	12	8	21
265,000 - 275,000	8	2	1	1	3	18
275,000 - 285,000						
285,000 - 295,000						
Total	106	27	28	22	19	100

OV-102 orbiter liftoff weight is within fatigue spectra although rate of occurrences at 260K more than expected

Presenter M3/Material | Date FINAL | Slide 3 of 18 | Closed

Parameter Comparisons

	Number of Occurrences of Parameter in Life					
	All flts	OV-102	OV-103	OV-104	OV-105	Spectra
< 1094						
1094 - 1098	1				1	
1098 - 1102	4	3			1	2
1102 - 1106	16	10	4		2	10
1106 - 1110	19	5	3	5	5	10
1110 - 1114	30	2	7	13	6	6
1114 - 1118	16	1	8	3	3	13
1118 - 1122	10	3	4		1	23
1122 - 1126	7	2	1	1		15
1126 - 1130	2		1			21
1130 - 1134	1	1				
Total	106	27	28	22	19	100

OV-102 C.G. location is within fatigue spectra although a more forward shift from expected usage

Presenter M3/Material | Date FINAL | Slide 4 of 18 | Closed

Parameter Comparisons

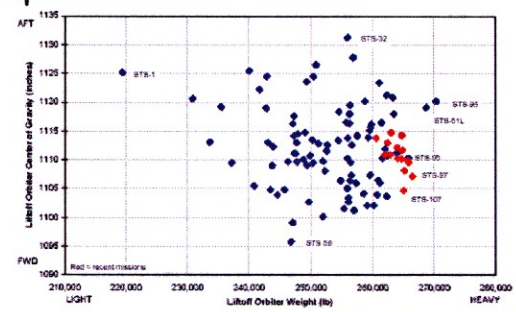

Presenter M3/Material | Date FINAL | Slide 5 of 18 | Closed

Parameter Comparisons

	Number of Occurrences of Parameter in Life					
	All flts	OV-102	OV-103	OV-104	OV-105	Spectra
< 600						
600 - 620	1	1				2
620 - 640	2	1				4
640 - 660	11	4	3	3	1	9
660 - 680	19	4	7	3	3	15
680 - 700	26	9	3	6	6	12
700 - 720	25	8	10	2	2	22
720 - 740	12	1	4	5	2	17
740 - 760	9		2	4	3	13
760 - 780	5			2	2	6
780 - 800						
Total	110	28	29	25	19	100

OV-102 max Q is well within the fatigue spectra

Presenter M3/Material | Date FINAL | Slide 6 of 18 | Closed

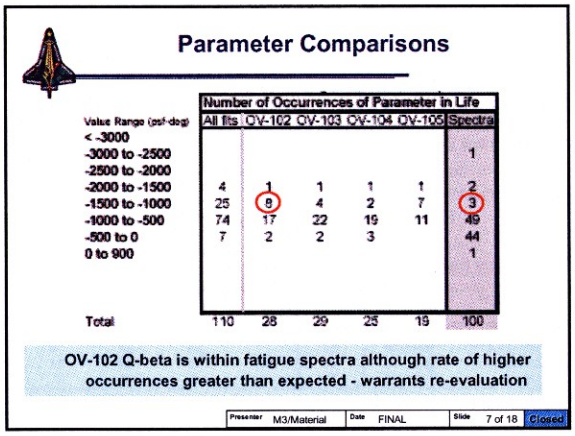
Parameter Comparisons
Number of Occurrences of Parameter in Life
Value Range (psf-deg)
All fits OV-102 OV-103 OV-104 OV-105 Spectra
< -3000 1
-3000 to -2500 2
-2500 to -2000 3
-2000 to -1500 4 1 1 1 1 2
-1500 to -1000 25 9 4 2 7 3
-1000 to -500 74 17 22 19 11 49
-500 to 0 7 2 2 3 44
0 to 900 1
Total 110 28 29 25 19 100
OV-102 Q-beta is within fatigue spectra although rate of higher occurrences greater than expected - warrants re-evaluation
Presenter M3/Material Date FINAL Slide 7 of 18 Closed

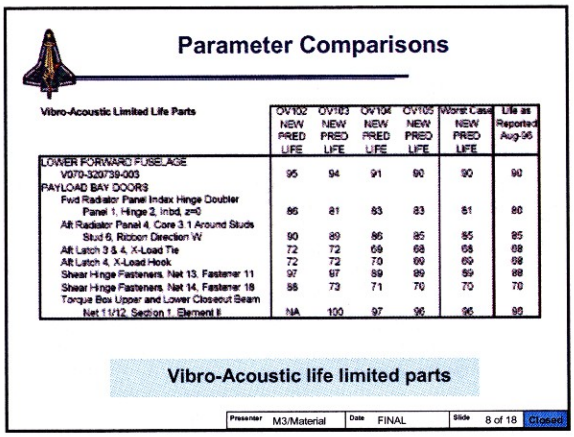
Parameter Comparisons
Vibro-Acoustic Limited Life Parts
OV102 NEW PRED LIFE
OV103 NEW PRED LIFE
OV104 NEW PRED LIFE
OV105 NEW PRED LIFE
Worst Case NEW PRED LIFE
Life as Reported Aug-96
LOWER FORWARD FUSELAGE
V070-320739-003 95 94 91 90 90 90
PAYLOAD BAY DOORS
Fwd Radiator Panel Index Hinge Doubler Panel 1, Hinge 2, Inbd, z=0 86 81 83 83 81 80
Aft Radiator Panel 4, Core 3.1 Around Studs Stud 6, Ribbon Direction W 90 89 86 85 85 85
Aft Latch 3 & 4, X-Load Tie 72 72 69 68 68 68
Aft Latch 4, X-Load Hook 72 72 70 69 69 68
Shear Hinge Fasteners, Net 13, Fastener 11 97 97 89 89 89 88
Shear Hinge Fasteners, Net 14, Fastener 18 86 73 71 70 70 70
Torque Box Upper and Lower Closeout Beam Net 11/12, Section 1, Element II NA 100 97 96 96 99
Vibro-Acoustic life limited parts
Presenter M3/Material Date FINAL Slide 8 of 18 Closed

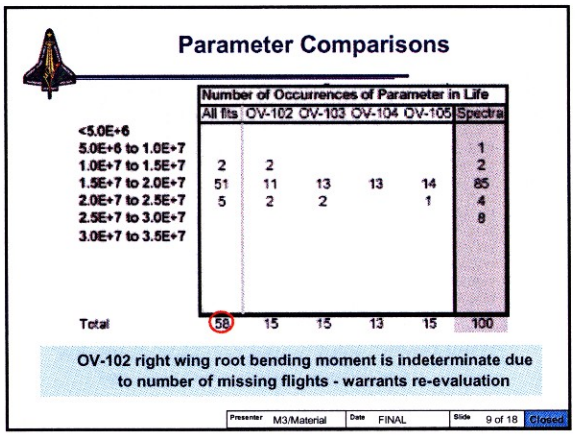
Parameter Comparisons
Number of Occurrences of Parameter in Life
All fits OV-102 OV-103 OV-104 OV-105 Spectra
<5.0E+6 1
5.0E+6 to 1.0E+7 2
1.0E+7 to 1.5E+7 2 2 85
1.5E+7 to 2.0E+7 51 11 13 13 14 4
2.0E+7 to 2.5E+7 5 2 2 1 8
2.5E+7 to 3.0E+7
3.0E+7 to 3.5E+7
Total 58 15 15 13 15 100
OV-102 right wing root bending moment is indeterminate due to number of missing flights - warrants re-evaluation
Presenter M3/Material Date FINAL Slide 9 of 18 Closed

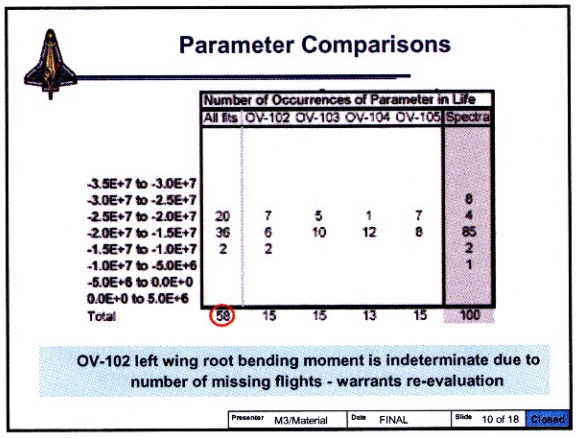
Parameter Comparisons
Number of Occurrences of Parameter in Life
All fits OV-102 OV-103 OV-104 OV-105 Spectra
-3.5E+7 to -3.0E+7 8
-3.0E+7 to -2.5E+7 4
-2.5E+7 to -2.0E+7 20 7 5 1 7 85
-2.0E+7 to -1.5E+7 36 6 10 12 8 2
-1.5E+7 to -1.0E+7 2 2 1
-1.0E+7 to -5.0E+6
-5.0E+6 to 0.0E+0
0.0E+0 to 5.0E+6
Total 58 15 15 13 15 100
OV-102 left wing root bending moment is indeterminate due to number of missing flights - warrants re-evaluation
Presenter M3/Material Date FINAL Slide 10 of 18 Closed

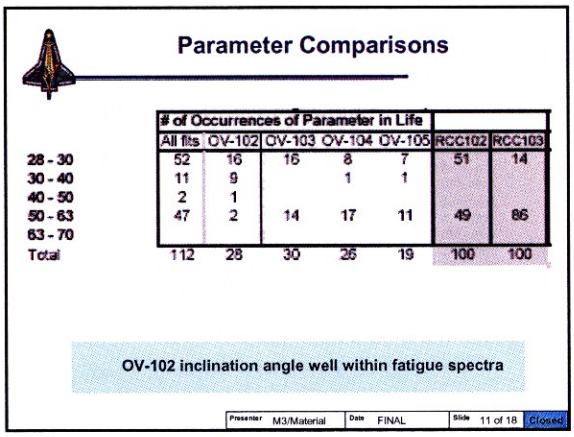
Parameter Comparisons
# of Occurrences of Parameter in Life
All fits OV-102 OV-103 OV-104 OV-105 RCC102 RCC103
28 - 30 52 16 16 8 7 51 14
30 - 40 11 9 1 1
40 - 50 2 1
50 - 63 47 2 14 17 11 49 86
63 - 70
Total 112 28 30 26 19 100 100
OV-102 inclination angle well within fatigue spectra
Presenter M3/Material Date FINAL Slide 11 of 18 Closed

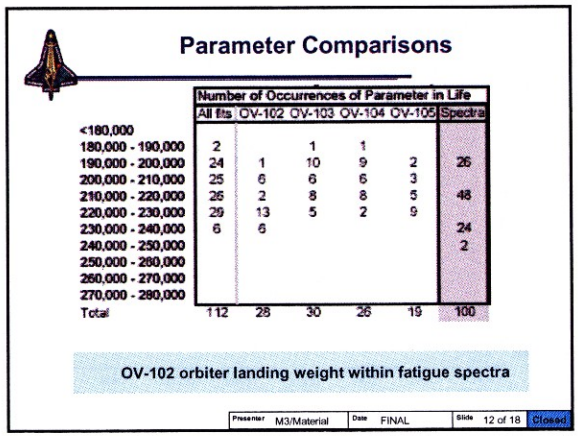
Parameter Comparisons
Number of Occurrences of Parameter in Life
All fits OV-102 OV-103 OV-104 OV-105 Spectra
<180,000
180,000 - 190,000 2 1 1
190,000 - 200,000 24 1 10 9 2 26
200,000 - 210,000 25 6 6 6 3
210,000 - 220,000 26 2 8 8 5 48
220,000 - 230,000 29 13 5 2 9
230,000 - 240,000 6 6 24
240,000 - 250,000 2
250,000 - 260,000
260,000 - 270,000
270,000 - 280,000
Total 112 28 30 26 19 100
OV-102 orbiter landing weight within fatigue spectra
Presenter M3/Material Date FINAL Slide 12 of 18 Closed

2

Parameter Comparisons

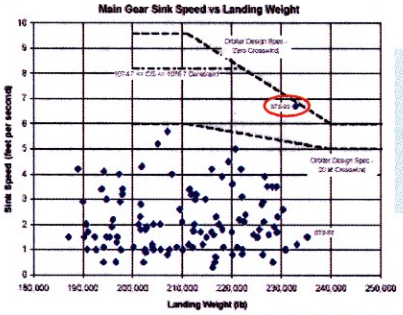

Hard landing data reviewed, well w/i structural limits

Presenter M3/Material | Date FINAL | Slide 13 of 18 | Closed

Wing Heating Load

- **Background / Facts:**
  - OV-102 had the highest predicted wing heating load for a location near the wing leading edge
    - Maximum heating load: OV-102 was 1.3 to 1.1 times higher than the other orbiters
    - Average heating load: OV-102 was 1.15 times higher than the other orbiters
  - OV-102 peak structural temperatures significantly less than certification peak temperatures
    - Wing bottom: 190 versus 326 F
    - Fuselage: 244 versus 326 F

Presenter M3/Material | Date FINAL | Slide 14 of 18 | Closed

Spectra Comparisons PE Versus 5.4

- **Background / Facts:**
  - At the request of the CAIB (reference RFI B1-120), 9 wing and vertical stabilizer control points crack growth life predictions were determined using the certification spectra (5.4) and compared to the current spectra (PE)
    - PE spectra 1.4 to 1.6 times more severe for wing bending moment
    - PE less severe for vertical stabilizer bending moment
  - Comprehensive analysis update performed for the airframe structure using the PE spectra (CAIB conducted spot check review)

Presenter M3/Material | Date FINAL | Slide 15 of 18 | Closed

Orbiter Actual Usage

- **Findings:**
  - Wing root bending moment results were not determined prior to STS-51
  - Parameters obtained and summarized in the Life Tracking report are not utilized to determine mission life capability (crack growth lives) for each orbiter based on actual usage
  - Fatigue testing of the wing structure has not been performed
  - Fatigue spectra appears to be adequate for near-term operations given the number of missions achieved (30 versus 100), however the spectra may need to be updated to safely achieve 100 missions

Presenter M3/Material | Date FINAL | Slide 16 of 18 | Closed

Orbiter Actual Usage

- **Recommendations:**
  - If possible, fill in the missing wing root bending moment data and re-evaluate adequacy of fatigue spectra
  - Carefully monitor the trends of the following parameters: liftoff weight, C.G. location, ascent Q-beta, ascent wing root bending moment
  - Develop the capability to determine mission life capability (crack growth lives) for each orbiter based on actual usage

Presenter M3/Material | Date FINAL | Slide 17 of 18 | Closed

Orbiter Actual Usage

- **Documentation:**
  - Responses to RFIs 120 and 195
  - Briefing by T. Kott, "Orbiter Life Cycle Analysis Process Overview", 3 April 2003
  - Boeing Report RSS99D0510D, "Space Shuttle Life Tracking", March 2003
  - Briefing by C. Modlin, "Orbiter Structural Life", 23 June 1992

Presenter M3/Material | Date FINAL | Slide 18 of 18 | Closed

Aging Structural Issues

- **Action / Issue:**
  - Aging and Corrosion
- **Background / Facts:**
  - Orbiter designed as maintenance-free for 10 years—all are now older than 10 years
  - Spar is aluminum honeycomb (known to be corrosion prone) in service for 24 years—concerns about galvanic couple between spar and IN718 or A-286 that could lead to degradation
  - Crevice corrosion known to occur on other shuttle locations with 2024-T81
  - 200 doublers reported on OV-102 in response to corrosion damage
  - Anecdotal evidence indicates that chromates leach out of primer after 6-12 years

Presenter M3/Material | Date FINAL | Slide 1 of 5 | Closed

Orbiter OMRS Corrosion Anomalies at KSC

Background/Facts (cont'd):

- Corrosion Problems Reports (PRs) are on the Increase

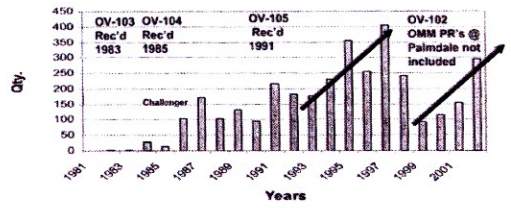

Presenter M3/Material | Date FINAL | Slide 2 of 5 | Closed

Orbiter Body Flap Cumulative Corrosion Occurrence versus Age

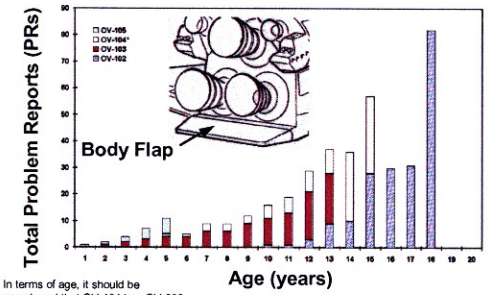

* In terms of age, it should be remembered that OV-104 has OV-099s body flap assy. Circa 1982.

Presenter M3/Material | Date FINAL | Slide 3 of 5 | Closed

Orbiter Corrosion

- **Findings:**
  - Corrosion is on the rise
- **Recommendations:**
  - Ascertain parameters that contribute to the aging of corrosion protection materials and processes
    - Chromate leach rates
    - Effect of chemical/thermal/mechanical environments and age
  - Quantify CPC efficacy and limitations
    - e.g. Reapplication frequency and outgassing
    - Expand use if appropriate
  - Continue to trend corrosion problems and address problems as early as possible

Presenter M3/Material | Date FINAL | Slide 4 of 5 | Closed

Orbiter Corrosion

- **Recommendations (cont'd):**
  - In order to better establish inspection requirements for corrosion based on environmental exposure, it's important to establish corrosion rates via test for environments, materials and structural configuration specific to the orbiter.
  - USAF and Navy aircraft structure very similar in construction to the orbiter. It may be beneficial to review their corrosion prevention and control practices.
  - Recent USAF and Navy R&D efforts aimed at providing practical modeling techniques for corrosion may also provide insight into the corrosion problem.
  - A USAF Air Mobility Command sponsored program developed an approach to ascertain the Economic Service Life for the KC-135. Their, and similar efforts by others, may be applicable to the obiter.

Presenter M3/Material | Date FINAL | Slide 5 of 5 | Closed

Corrosion Near Aft End of Crew Module

- **Action / Issue:**
  - Corrosion found on and near forward fuselage ($X_0$582) and was left unrepaired
- **Background / Facts:**
  - $X_0$582 is a frame near the aft end of the crew module
  - Corrosion found and repaired on forward side of X0 582
  - Corrosion "monitored" but not repaired near X0 576 (slightly forward of X0 582)
  - While corrosion was not removed, CPC was applied to forward fuselage floor
    - Use of CPC not straightforward; specialized application process required because outgassing may occur and interfere with Star Tracker

Presenter M3/Material | Date FINAL | Slide 1 of 7 | Closed

Corrosion Near Aft End of Crew Module

- **Background / Facts (cont'd):**
  - OV-102 had different construction to subsequent orbiters making it more susceptible
    - Goldized insulation blanket directly on aluminum stringers
    - Uncoated steel fasteners
  - However, construction used for other orbiters not "corrosion-proof"
    - Titanium fasteners (react with aluminum)
    - Aluminum not clad
    - No faying surface sealant
    - Susceptible materials

Presenter M3/Material | Date FINAL | Slide 2 of 7 | Closed

Location of $X_0$582 Corrosion

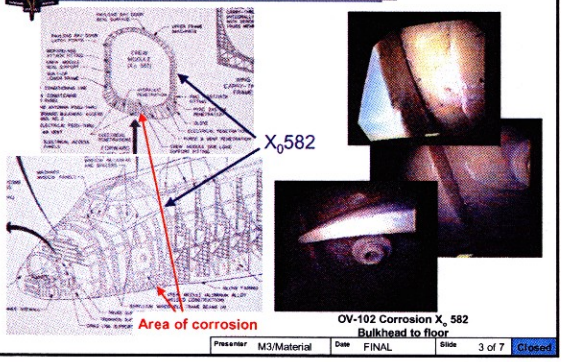

OV-102 Corrosion X_0 582 Bulkhead to floor

Presenter M3/Material | Date FINAL | Slide 3 of 7 | Closed

Location of $X_0$582 Corrosion

OV-102 Corrosion X_0 582 Bulkhead to floor

Borescope View of Typical "582" Corrosion

- **Using video borescope, corrosion found on lower forward fuselage skin panel and stringer areas. Extensive rework and corrosion protection of "582" bulkhead forward surface was accepted for unrestricted use.**
- **In addition to "582" frame, borescope inspection revealed suspect corrosion (X_0 576) on visible rivets and on the sides and feet of hat section stringers.**
- **This PR was deferred due to the inability to fully access the area in question to effect a repair. The condition is to be visually assessed on a recurrent basis.**

Source: OV-102 V30/31 Inspection Report September 1999 - February 2001

Presenter M3/Material | Date FINAL | Slide 4 of 7 | Closed

Corrosion Near Aft End of Crew Module

- **Findings:**
  - Access to area between crew module and outer hull difficult to access for inspection and repair
  - Concern that unmitigated corrosion could progress and degrade structure below minimum safe level
  - OV-102 lower fuselage construction in area forward of $X_0$582 was unique and caused it to be more susceptible to corrosion
  - Corrosion cannot be eliminated as a potential degradation mechanism on the other orbiters
- **Recommendations:**
  - To better understand potential impact, perform analysis of corrosion susceptibility, growth and damage consequences relative to factors influencing corrosion:
    - Material
      - Alloy, Temper, orientation, product form, anodized, clad/unclad

Presenter M3/Material | Date FINAL | Slide 5 of 7 | Closed

Corrosion Near Aft End of Crew Module

- **Recommendations (cont'd):**
  - Fasteners
    - Type, finish, AMS, wet/dry installed
  - Coating
    - Conversion coats, primer, CPC
  - Mechanical load orientation
  - Blanket insulation
    - Attachment material and method of attachment
    - Blanket material
  - Environment
    - Accidental fire suppression activation, OPF environment, rain exposure; pad exposure

Presenter M3/Material | Date FINAL | Slide 6 of 7 | Closed

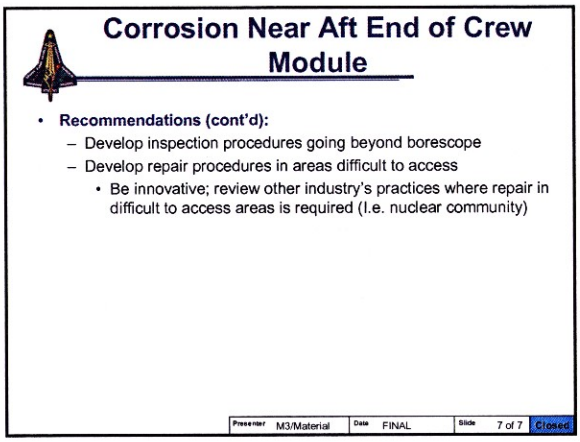
Corrosion Near Aft End of Crew Module
• Recommendations (cont'd):
– Develop inspection procedures going beyond borescope
– Develop repair procedures in areas difficult to access
• Be innovative; review other industry's practices where repair in difficult to access areas is required (I.e. nuclear community)
Presenter M3/Material
Date FINAL
Slide 7 of 7
Closed

Fastener Environmentally Assisted Cracking (EAC)

- **Action / Issue:**
  - Potential for environmentally assisted cracking of Inconel 718 and A-286.
- **Background / Facts:**
  - A-286 bolts are used as fasteners LESS components
  - Microbial or fungal corrosion can occur within an environment that contains carbon and a source of water such as condensate. A product of this corrosion process is acid that could degrade Inconel and A-286.
  - Other forms of environmentally assisted cracking are also possible.

Presenter M3/Material | Date FINAL | Slide 1 of 12 | Closed

Material of RCC Attachment Hardware

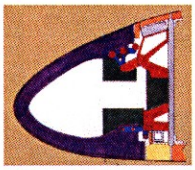

LI2200 LI900 | Inconel 718 A-286 steel | RCC Aluminum | Inconel-Dynaflex

V070-199362 (ship side clevis): A-286 CRES
V070-199751 (angle side clevis): 718 Inconel
V070-199689 (bushing): A-286 CRES
NAS6304U19H (bold): A-286 CRES

Presenter M3/Material | Date FINAL | Slide 2 of 12 | Closed

LESS Lower Carrier Panel

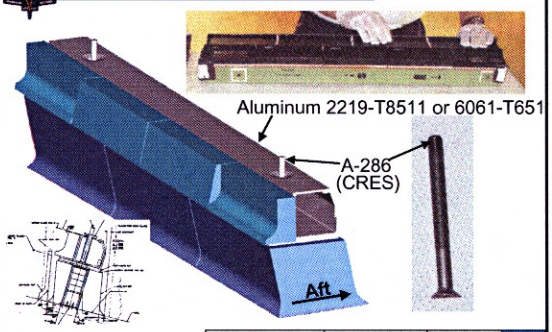

Presenter M3/Material | Date FINAL | Slide 3 of 12 | Closed

Material and Configuration

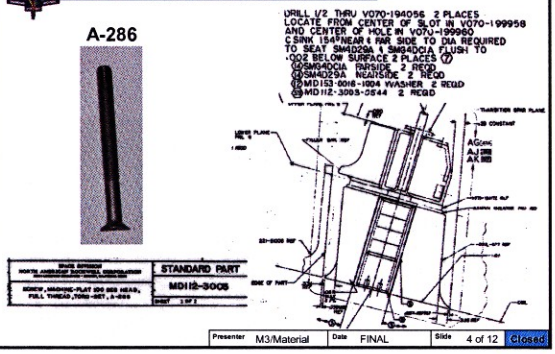

Presenter M3/Material | Date FINAL | Slide 4 of 12 | Closed

Recovered Spar Fitting

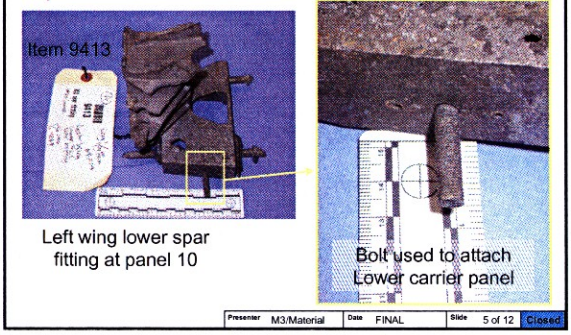

Presenter M3/Material | Date FINAL | Slide 5 of 12 | Closed

Carrier Panel A-286 Bolt

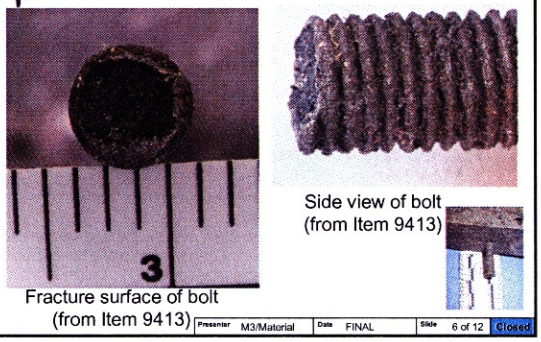

Presenter M3/Material | Date FINAL | Slide 6 of 12 | Closed

Carrier Panel A-286 Bolt

Higher magnification photos of fracture surface of bolt from Item 9413

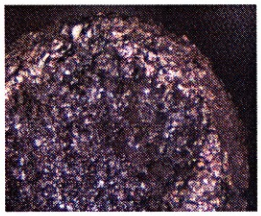

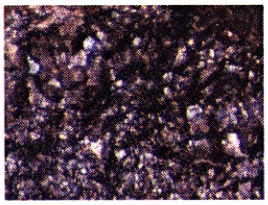

Presenter M3/Material | Date FINAL | Slide 7 of 12 | Closed

Fracture Surface

Similar features found on bolt from left wing lower spar fitting at panel 17

Fracture surface of bolt from Item 866

Side view of bolt

Presenter M3/Material | Date FINAL | Slide 8 of 12 | Closed

Higher magnification photos of fracture surface of bolt from Item 866

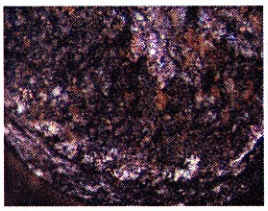

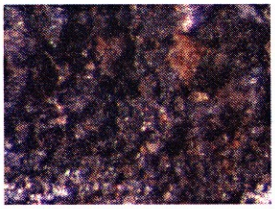

Presenter M3/Material | Date FINAL | Slide 9 of 12 | Closed

OV-102 Debris Sampled

Lower Spar Fittings Carrier Panel Bolts

Item	Inbrd/Outbd	Panel	Intact	Bent	Fractured	Bushing	Length at Fracture	Lat.	Long.
717	Outboard	2	X	X				31.61275	-94.72366
431	Inboard	3	X					31.61903	-94.74134
708	Outboard	3	X	X				31.62673	-94.73083
823	Inboard	5			Yes		5/8" beyond threads		
823	Outboard	5	X	X					
64805	Inboard	6		X	Yes		3/4" from edge of fitting	31.53335	-94.52234
64805	Outboard	6		X	Yes		1" beyond threads		
9413	Inboard	10		X	Yes		7/8" from edge of fitting	31.69806	-94.9649
	Outboard	10							
12203	Inboard	14	X			Yes		31.68358	-94.99158
12203	Outboard	14	X	X		Yes			
68	Inboard	15	X			Yes		31.68404	-95.0005
68	Outboard	15	X			Yes			
12239	Inboard	16	X	X		Yes		31.68989	-95.01096
12239	Outboard	16	X	X					
866	Inboard	17			Yes		11/16" from edge of fitting		
866	Outboard	17							
67060	Inboard	20		X	Yes		1/8" from edge of fitting	31.63379	-94.92818
67060	Outboard	20	X	X					
36	Inboard	21	X					31.68369	-95.01647
36	Outboard	21	X						

Presenter M3/Material | Date FINAL | Slide 10 of 12 | Closed

Fastener Environmentally Assisted Cracking (EAC)

Findings:

- Failure mode of recovered carrier panel bolts is consistent with high-temperature failure; failure is not due to EAC
- Current design and maintenance practices leave components at greater risk for corrosion

Recommendations:

- Obvious galvanic couples between aluminum and steel alloys should be avoided or clearly mitigated
- The use of TFE and MoS2 should be expressly forbidden in assembling components
- The use of primers and sealants such as RTV 560 and Korpon should be reviewed with respect to their possibly accelerating corrosion in real environments including in tight crevices.

Presenter M3/Material | Date FINAL | Slide 11 of 12 | Closed

Fastener Environmentally Assisted Cracking (EAC)

Recommendations (cont'd)

- The negligible and compressive stresses presently occurring in A286 bolts provide protection against failure; assuring the continued presence of such low to negative residual stresses should be part of acceptance and qualification procedures.
- The detailed general and impurity chemistry of all paints, adhesives, and sealants should be reviewed periodically at the ppb to ppm concentrations, and such results should be reviewed from a corrosion point of view.
- The procedures and criteria for qualifying materials and coatings from a corrosion point of view should be reviewed for their relevance and adequacy.
- A substantially higher level of understanding and appreciation of damaging effects of all relevant ambient and applied environments on critical materials should be incorporated into the design and maintenance of the orbiters

Presenter M3/Material | Date FINAL | Slide 12 of 12 | Closed

Maintenance Wiring Inspections

- **Action / Issue:** Kapton wiring, currently used in orbiters, poses inspection/maintenance challenges. Assess NASA actions to address these challenges.
- **Background:**
  - Each orbiter contains approximately 852,000 feet of wiring
    - Amounts vary depending on modifications/instrumentation
    - Most of the wiring is insulated with Kapton
- **Findings:**
  - Kapton (MIL-W-81381) refers to a type of insulation (technical name: aromatic polyimide) originally developed by DuPont in the 1960s

Presenter: M3/Maintenance | Date: FINAL | Slide: 1 of 10 | Open

Maintenance Wiring Inspections

- **Findings (cont'd):**
  - When the shuttle was built, Kapton was state-of-the-art, exhibiting many positive attributes
    - 50% less space, 25% less weight, tough, durable to a wide temperature range, will not melt/drip/propagate flame
    - Widely used in both military and civil aviation
    - Continues to be used today, though notable shortcomings have emerged over the years
  - Major concern is arc tracking
    - A phenomenon in which overheated wiring carbonizes
    - Overheating typically caused by broken insulation/arcing
    - Carbonized Kapton acts as a conductor; result: "soft shorts"
    - "Soft shorts" (as opposed to "hard shorts") continue to conduct below the tripping threshhold of circuit protection devices, thereby propagating further carbonization/damage

Presenter: M3/Maintenance | Date: FINAL | Slide: 2 of 10 | Open

Maintenance Wiring Inspections

- **Findings (cont'd):**
  - Major causes of insulation failure (splitting/cracking/flaking)
    - Improper installation during manufacture (unknown at the time), such as routing (tight bends), clamping (too tightly), or positioning wires against burred screw heads/rivet tails/sharp edges; causes insulation wear/failure due to vibration and/or maintenance
    - Wire stress during inspection/maintenance: repositioning by technicians for access and/or unintentional actions (stepping)
      - Determined to be the single largest cause on orbiters
    - Exposure to elements such as solvents/corrosives/moisture
    - Parallel, extensive AF study (1986) concludes most problems due to design, installation, and maintenance
  - OV-102/STS-93 (Jul 99) incident raised awareness: loss of power to two of six Main Engine Controller computers 5 sec after liftoff
    - Investigation identified root cause as damaged wire

Presenter: M3/Maintenance | Date: FINAL | Slide: 3 of 10 | Open

Maintenance Wiring Inspections

- **Findings (cont'd):**
  - NASA has taken numerous corrective actions since STS-93
    - Extensive inspections/corrective actions, starting with OV-102's J3 OMM (Sep 99); chit 1-month after roll-in complicated OMM
    - Other orbiters grounded for inspection (partial); full inspections to be completed during scheduled OMMs
    - Results of OV-102/J3 OMM used to refine inspection/ documentation methodologies (more comprehensive/specific tracking)
    - Improvements made in technician/inspector training and certification, maintenance procedures (e.g., calibrated crimpers)
    - Wiring inspection now required during any ground processing actions

Presenter: M3/Maintenance | Date: FINAL | Slide: 4 of 10 | Open

Maintenance Wiring Inspections

- **Findings (cont'd):**
  - OV-103 currently in OMM/undergoing remainder of wire inspection
    - Total discrepancies (stand down + OMM) nearing OV-102 proportions
  - Arc track testing using orbiter circuit protection/wiring displayed limited track lengths; worst case = 6.5 inches
    - Current mods include separating all critical wire paths from main bundles and individually protecting them
  - Numerous tests indicate Kapton is still the leading choice for orbiter environment despite development of hybrid insulators
  - Development of improved inspection equipment/techniques (to supplement visual) continues in the aviation community
  - Wholesale replacement, whether in military/commercial aviation, or the orbiter fleet, is costly
    - Hybrids used on new build B737/B757/F-15/F-22 (post-1995)

Presenter: M3/Maintenance | Date: FINAL | Slide: 5 of 10 | Open

Maintenance Wiring Inspections

- **Findings (cont'd):**
  - Modifications either complete, in progress, or scheduled show ongoing efforts to mitigate wiring problems
    - MCR 19448: Orbiter Wire Protection Enhancements addressed routing of redendant Crit 1 wires; 127 cases ID'd
    - MCR 19527: Orbiter Wire Redundancy Separation corrects all 127
    - MCR 19596: AC Bus Separation separates critical wires to C/B pnls
    - MCR 23167: Arc Track Protection continues efforts; Rev 1 for OV-102/Flt 29 (STS-107)
  - Approx 2,000 feet of orbiter wiring is inaccessible
    - Primarily below crew module
    - No plans to inspect over the life of the orbiter
    - No technician traffic/hands-on maintenance due to inaccessibility
    - NASA has confirmed, thru USA and Boeing, no Crit 1 wiring in inaccessible areas
    - Concern: installation-induced problems over 20+ yrs of service

Presenter: M3/Maintenance | Date: FINAL | Slide: 6 of 10 | Open

Maintenance
Wiring Inspections

- **Conclusions:**
  - NASA has taken extensive action to mitigate orbiter wiring-related problems
  - Kapton issues (especially age-related), are still not fully understood
- **Recommendations:**
  - Continue as expeditious as possible implementation of all wiring-related inspections/mods
  - Inspect/track/monitor wiring to determine aging effects
  - Develop plans to inspect inaccessible wiring as part of the Shuttle Service Life Extension Program
  - Assess the adequacy of Kapton wiring inspection/maintenance in non-orbiter areas, such as RSRM/ET and SRB/MLP separation bolts

Presenter: M3/Maintenance | Date: FINAL | Slide: 7 of 10 | Open

Maintenance
Added Wiring Insulation/Separation Examples

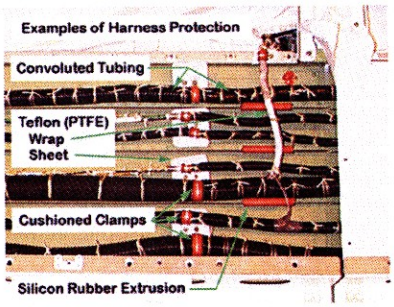

Presenter: M3/Maintenance | Date: FINAL | Slide: 8 of 10 | Open

103 J3 Wire Discrepancies Summary

919 OEL PRs as of 4/4/03

Total Discrepancies: 1793*

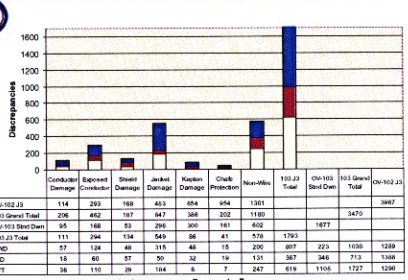

	Conductor Damage	Exposed Conductor	Shield Damage	Jacket Damage	Kapton Damage	Chafe Protection	Non-Wire	103 J3 Total	OV-103 Strd Dwn	103 Grand Total	OV-102 J3
OV-102 J3	114	293	169	463	654	954	1301				3967
103 Grand Total	206	462	187	847	386	202	1180			3470	
OV-103 Strd Dwn	95	168	53	295	300	181	602		1677		
103 J3 Total	111	294	134	549	86	41	576	1793			
FWD	57	134	46	315	48	15	200	817	223	1039	1289
MID	18	60	57	50	32	19	131	367	346	713	1388
AFT	36	110	29	184	6	7	247	619	1108	1727	1290

Damage by Type

*Multiple discrepancies may be documented on a single PR.
*Baseline assumption 2200 discrepancies.

Presenter: M3/Maintenance | Date: FINAL | Slide: 9 of 10 | Open

Maintenance – Wiring Inspections
Red Dashed Lines Indicate Inaccessible Wiring

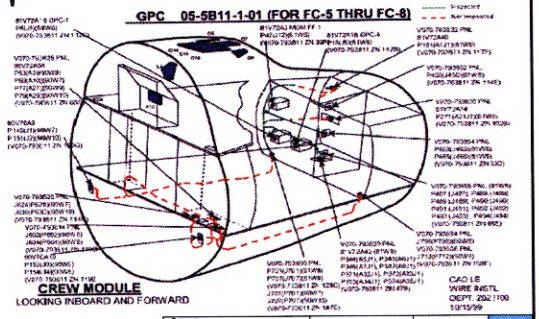

Presenter: M3/Maintenance | Date: FINAL | Slide: 10 of 10 | Open

Orbiter Environmental Exposure

- **Action / Issue:** Review/assess orbiter exposure to elements
- **Background / Facts**
  - OV-102 cumulative launch pad weather exposure - 3.3 years
    - Longest single exposure: STS-35/164 days (Apr-Dec 90)
  - Exposure to elements (rain, dew, salt air) has a negative impact
    - Corrosion to structure, oxidation/damage to RCC (suspected), wiring, etc.
- **Findings:**
  - Orbiter total exposure time (less –102) varies from 2.1 to 2.9 years
    - OV-102 leads fleet in total exposure time, but not in total launches
    - OV-102: 28 launches; OV-103: 30 launches
  - Rollovers/rollouts/rollbacks due to launch scrubs, follow-on maintenance, & ops checks contribute to prolonged exposure

Presenter M3/Maintenance | Date FINAL | Slide 1 of 15 | Closed

Orbiter Environmental Exposure

- **Findings (cont'd)**
  - STS-35's 164-day exposure driven by scrubbed launch attempts
    - Rollout to pad (22 Apr) for initial launch attempt (30 May)
      - Freon system repair - 14 add'l days
      - Launch scrubbed – 30 May (MPS LH2 leak)
      - Rollback – 12 Jun (following troubleshooting/maintenance preps)
    - Rollout to pad (9 Aug) for second launch attempt (1 Sep)
      - Stand down for payload telemetry repair – 6 add'l days
      - Launch scrubbed – 5 Sep (Orbiter H2 leak, maintenance at pad)
    - Third launch attempt (18 Sep)
      - Launch scrubbed – 18 Sep (MPS LH2 leak)
      - Rollback – 9 Oct (following troubleshooting, maintenance preps)
    - Rollout to pad (14 Oct) for fourth launch attempt
      - Special LH2 tanking tests performed – 2 add'l days
      - APU water valve problems; maintenance/servicing – add'l 16 days
      - Launched 2 Dec
    - STS-35 was an outlier compared with other missions (see chart)

Presenter M3/Maintenance | Date FINAL | Slide 2 of 15 | Closed

Orbiter Environmental Exposure

- **Findings (cont'd):**
  - Besides pad exposure, most notable vulnerability is during mate/demate/ferry ops; three incidents noted
  - Sep 99: OV-102 caught in rain at KSC during mating
    - 128 lbs/16 gals removed after arrival at Palmdale
  - Feb 01: OV-102 caught in rain at Palmdale after mating
    - 747/shuttle could only be partially hangared (see picture)
    - 112 lbs/14 gals removed after arrival at KSC
  - Feb 01: OV-104 caught in rain during mating at Edwards AFB
    - 1,600 lbs/200 gals removed after arrival at KSC
      - "Aft fuselage under bay 6 full of standing water"
      - "Five inches deep along back of 1307 bulkhead"
  - Mate/demate ops highly vulnerable to inclement weather
    - Lengthy operation; no shelter at any location
    - No positive pressure inside shuttle, as at pad

Presenter M3/Maintenance | Date FINAL | Slide 3 of 15 | Closed

Orbiter Environmental Exposure

- **Findings (cont'd):**
  - Exposure is a major contributor to corrosion on all orbiters; trending upward 10% annually
    - 140+ PRs written due to corrosion damage in the body flap cove area alone (low point in vertical position)
      - 84 on OV-102 (51 in last flow)
      - 19 on OV-103
      - 29 on OV-104
      - 6 on OV-105
    - Frequency/quantity of PRs citing corrosion increasing
      - 91% of occurrences since '92
    - Impact on logistics (reparability/availability of spare parts)
      - Components (e.g., body flap actuators) being replaced due to corrosion
      - Repair taking longer: some piece parts beyond repair, must be manufactured, lead times as long as 1 year away
      - No serviceable spare actuators & 2 "holes"; first available – Jun 03

Presenter M3/Maintenance | Date FINAL | Slide 4 of 15 | Closed

Orbiter Environmental Exposure

- **Findings (cont'd):**
  - Environmental (specifically weather) exposure constraints clearly outlined in RTOMI S0018.100, Adverse Environmental and Lightning Monitoring at LC39
    - Includes guidance on actions to be taken to minimize exposure to rain/hail/winds/freezing temps/tornadoes, etc.
- **Recommendations:**
  - Emphasize strict adherence to existing guidance
  - Take every opportunity to avoid/minimize/reduce exposure
    - Review/analyze launches where exposure was significantly over or under the mean (e.g., >1 standard deviation) for lessons learned
  - As some amount of exposure is unavoidable, an intensive corrosion program (inspection, treatment, prevention) is a must
    - See related "Action/Issue" slides on Corrosion and Service Life Extension Program (SLEP)

Presenter M3/Maintenance | Date FINAL | Slide 5 of 15 | Closed

Orbiter Environmental Exposure
Total Launch Pad Exposure by Orbiter

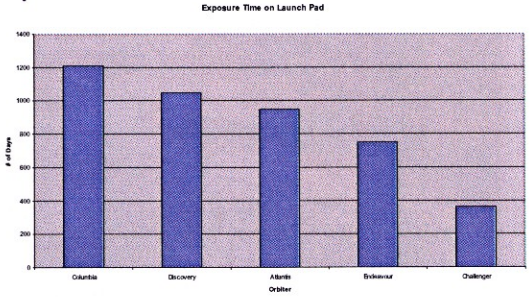

Presenter M3/Maintenance | Date FINAL | Slide 6 of 15 | Closed

Orbiter Environmental Exposure

Includes rollout/rollback/pad time

	Challenger	Endeavor	Atlantis	Discovery	Columbia	Total Fleet	Fleet minus Columbia
Total Days Exposed	361	749	948	1,050	1,208	4,316	3,108
# of Launches	10	19	26	30	28	113	85
Avg Days Per Launch	36.1	39.4	36.5	35.0	43.1	38.2	36.6

NOTE: STS-107 exposure time was 39 days
OV-102 exposed for as long as 164 days

Presenter M3/Maintenance Date FINAL Slide 7 of 15 Closed

Exposure Days By Mission

STS-35 (Far Right) An Outlier/STS-107 (Arrow) 1-Day Above Mean

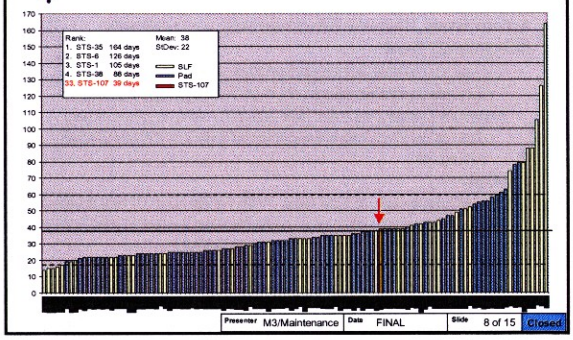

Presenter M3/Maintenance Date FINAL Slide 8 of 15 Closed

Exposure – Total Rain By Mission

STS-35 (far right): 20.6 in/STS-107 (arrow): 12.8 in/Fleet Avg: 5.5 in

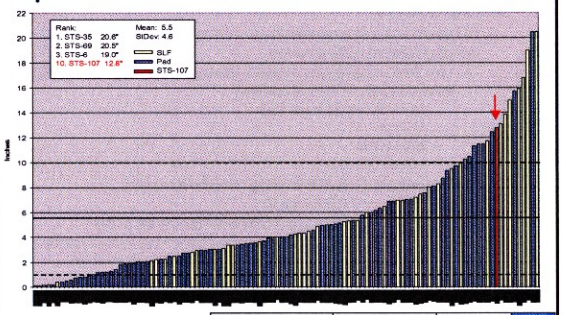

Presenter M3/Maintenance Date FINAL Slide 9 of 15 Closed

Environmental Exposure

Mate/Demate Ops Highly Vulnerable to Inclement Weather

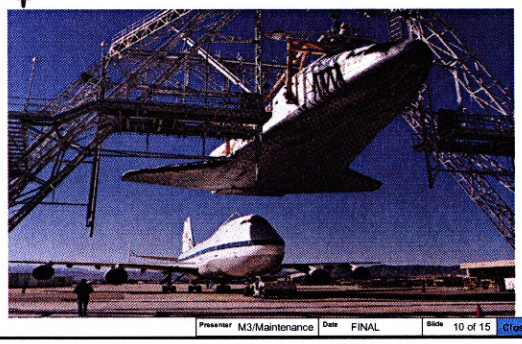

Presenter M3/Maintenance Date FINAL Slide 10 of 15 Closed

Orbiter Environmental Exposure

Partial Hangaring at Palmdale (Feb 01 Incident)

Presenter M3/Maintenance Date FINAL Slide 11 of 15 Closed

Orbiter Environmental Exposure

Increasing Corrosion Anomalies – PRs vs. Time

- Orbiter's Corrosion Problems are trending upward at 10% per year and some discrete locations > 10%.

Orbiter OMRS Corrosion Anomalies at KSC

Presenter M3/Maintenance Date FINAL Slide 12 of 15 Closed

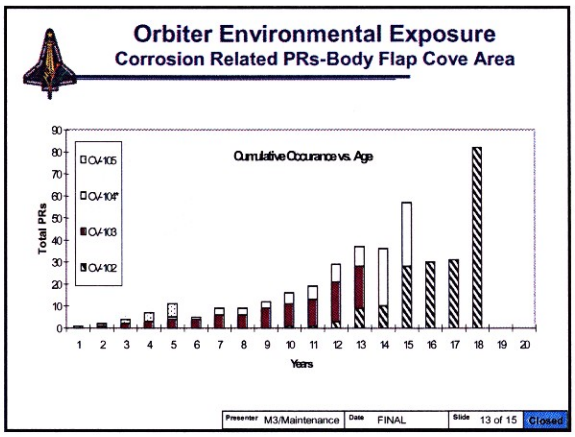
Orbiter Environmental Exposure
Corrosion Related PRs-Body Flap Cove Area
Cumulative Occurance vs. Age
OV-105
OV-104
OV-103
OV-102
Total PRs
Years
Presenter M3/Maintenance
Date FINAL
Slide 13 of 15
Closed

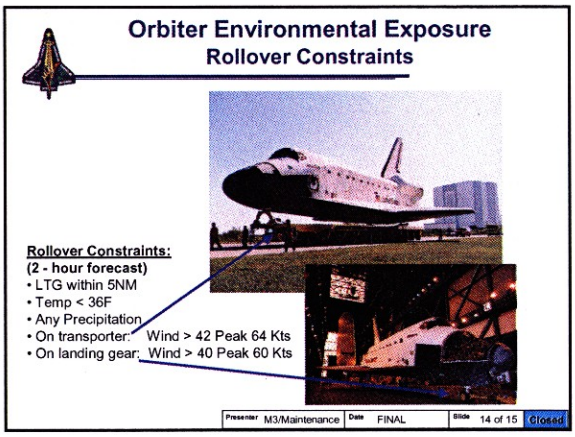
Orbiter Environmental Exposure
Rollover Constraints
Rollover Constraints:
(2 - hour forecast)
• LTG within 5NM
• Temp < 36F
• Any Precipitation
• On transporter: Wind > 42 Peak 64 Kts
• On landing gear: Wind > 40 Peak 60 Kts
Presenter M3/Maintenance
Date FINAL
Slide 14 of 15
Closed

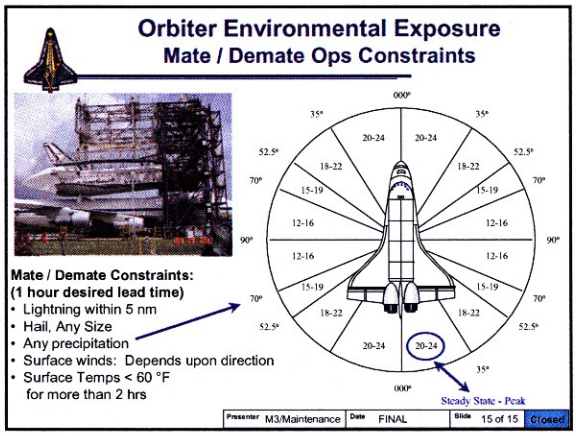
Orbiter Environmental Exposure
Mate / Demate Ops Constraints
Mate / Demate Constraints:
(1 hour desired lead time)
• Lightning within 5 nm
• Hail, Any Size
• Any precipitation
• Surface winds: Depends upon direction
• Surface Temps < 60 °F
for more than 2 hrs
000°
35°
52.5°
70°
90°
20-24
18-22
15-19
12-16
Steady State - Peak
Presenter M3/Maintenance
Date FINAL
Slide 15 of 15
Closed

Maintenance
Aging Vehicle/SLEP

- **Action / Issue:** Service Life Extension of Shuttle Fleet
- **Background / Facts:**
  - Shuttle fleet has been in service since 1980s
  - Originally programmed for replacement by early 21st century
  - Basic subsystem life requirement is 100 missions in 10 years
    - Performance and Design Requirement (PDRD FE093)
- **Findings:**
  - SLEP objective very general: Integrated Space Trans. Plan says "middle of next decade", DAA - ISS/SSP uses "2020 and beyond."
  - Original certification for 10 years, recertified in 1991 for 10 years
  - Limited structural data available: destructive testing of partial/ subscale structures at beginning, follow-on tests at subsystem level
  - SLEP initiated by HQ Code M Dec 2002, delegated to SSP Development Office is responsible for SLEP
  - First act…provide candidate projects list for SLEP independent panel review and final recommendation to Space Flight Leadership Council on May 7, 2003…over 100 collected

Presenter: M3/Maintenance | Date: FINAL | Slide: 1 of 8 | Closed

Maintenance
Aging Vehicle/SLEP

- **Findings:**
  - Used Analytical Hierarchy Process (AHP) tool to compare projects on impact to life extension, safety, urgency and cost.
  - 4 groups used to categorize the AHP priorities
    1. Must Do…imminent obsolescence or DMS concerns in 03; e.g. sustaining test equipment tasks for SSME and case hardware availability for RSRM.
    2. Current Commitments…e.g. CAU (glass cockpit), SSME Advanced Health Mgmt Sys (ph 1), Infrastructure (bldg, GSE), Industrial Engineering for Safety
    3. Foundational Activities…Aging vehicle studies, Mid-Life Certification, NDE upgrades, Project Feasibility Studies

    4a.b.c. Sustainability, Improvement, New Capabilities…e.g. obsolescence issues, vehicle health monitoring, Hydrazine Replacement, and crew survivability.
  - Used AHP to prioritize over 50 projects for first budget submission
  - Foundational Activities and Project Feasibility Studies may lead to increases in subsequent summit and budget cycles

Presenter: M3/Maintenance | Date: FINAL | Slide: 2 of 8 | Closed

Maintenance
Aging Vehicle/SLEP

- **Findings:**
  - Funding request in May for initial studies to identify tasks in most crucial sustainment programs…Mid-Life Recertification (MLR), Fleet Leader, Corrosion Control and Risk Management.
    - MLR will define tasks to be completed to recertify the STS for continued used through foreseeable life span
    - Results expected to identify necessary upgrades to structures and subsystems to assure safe operation as well as recommendations for additive maintenance and inspection programs
    - MLR funding undefined
    - Significant effort to prioritize previously identified candidate programs and add to budget request
  - Higher headquarters supportive but concerned over financial impact of CAIB recommendations

Presenter: M3/Maintenance | Date: FINAL | Slide: 3 of 8 | Closed

Maintenance
Aging Vehicle/SLEP

- **Recommendations:**
  - Sustainment program needs a clearly enunciated goal in terms consistently applied across NASA to focus efforts
  - Mid-Life Recertification is the foundation of SLEP. Accelerate funding to to ensure competitive consideration in budget request
  - NASA is charting new ground and seems to be accepting the financial reality that sustaining systems is a long-term commitment
    - Will require programmatic support (organizationally and financially) throughout the remainder of the system's operational life.
    - NASA should consider a sustainment-based reorganization and develop doctrine to guide them
  - Restrictively define the SLEP mission. Current construct establishes this program as the central repository for nearly any shuttle related project. This will leave SLEP vulnerable to budget cuts and dilution of NASA's ability to resolve sustainment issues.

Presenter: M3/Maintenance | Date: FINAL | Slide: 4 of 8 | Closed

Maintenance
Aging Vehicle/SLEP

Cost by SLEP Prioritization Categories

Real Year Dollars in Millions - Not in Full Cost

		FY03	FY04	FY05	FY06	FY07	FY08	FY09	Total FY04-FY08
FY04 President's Budget Request		299	364	367	297	301	304	--	1,633
Delta to Presidents Budget		18	-52	-59	-50	54	71		-35
Total POP 03 SLEP Recommendation		281	416	426	347	246	233	214	1,668
1	Should Start In Fiscal Year 2004	0	15	16	14	9	13	13	66
2	Commitments	261	274	234	156	136	126	124	926
3	Foundational Activities	3	23	31	23	12	24	12	113
4a	Sustainability	2	40	62	73	47	38	40	259
4b	Improvements	16	45	62	62	23	12	5	204
4c	New Capabilities	0	0	0	0	0	0	0	0
	Reserves	0	20	20	20	20	20	20	100

Presenter: M3/Maintenance | Date: FINAL | Slide: 5 of 8 | Closed

Maintenance
Aging Vehicle/SLEP

Real Year Dollars in Millions - Not in Full Cost

	FY03	FY04	FY05	FY06	FY07	FY08	FY09	Total FY04-FY08
Total POP 03 SLEP Recommendation	281	416	426	347	246	233	214	1,668
1 Should Start In Fiscal Year 2004	0	15	16	14	9	13	13	66
RSRM - Case Hardware Availability	0	5	5	5	5	5	5	25
Orbiter - Certify PRSD Tank Supplier & Procure Spares	0	4	8	8	4	8	8	31
SSME - Sustaining Test Equipment Tasks	0	6	3	1	0	0	0	10
2 Commitments	261	274	234	156	136	126	124	926
Vehicle Cockpit Avionics Upgrade (CAU)	89	91	77	14	0	0	0	182
Vehicle Main Landing Gear Tire & Wheel	3	3	0	0	0	0	0	3
SSME Advanced Health Management System (AHMS Phase 1)	8	4	3	2	1	0	0	10
Industrial Engineering for Safety	8	15	15	15	15	15	15	75
RSRM Obsolescence	12	18	19	20	20	21	21	98
Infrastructure	91	92	77	78	79	80	80	406
Others	50	51	43	27	21	10	8	152
3 Foundational Activities	3	23	31	23	12	24	12	113
Aging Vehicle Studies	2	10	14					24
Mid-Life Certification Assessment & Issue Mitigation								
Fleet Leader Program								
Corrosion Control								
STE Survey / Evaluation								
Non-Destructive Evaluation Upgrades								
Ground Test Program	0	4	10	20	9	21	9	64
Performance Trade Studies / Lift, Power	1	2	2					4
Improved Tools / Metrics	1	7	5	3	3	3	3	21
Probabilistic Risk Assessment								
Sustainability Health Metrics								
Analytical Hierarchy Tool System								

Presenter: M3/Maintenance | Date: FINAL | Slide: 6 of 8 | Closed

1

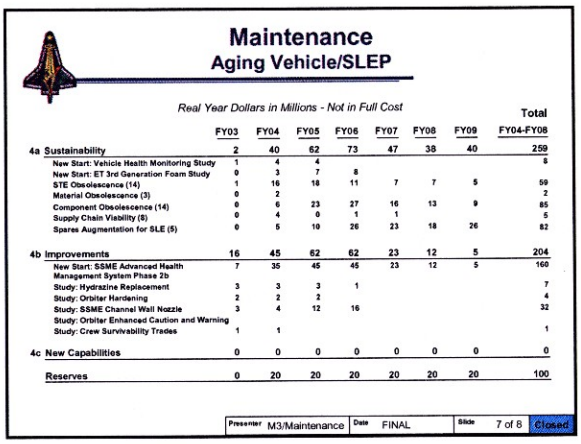

Maintenance
Aging Vehicle/SLEP

Real Year Dollars in Millions - Not in Full Cost

	FY03	FY04	FY05	FY06	FY07	FY08	FY09	Total FY04-FY08
4a Sustainability	2	40	62	73	47	38	40	259
New Start: Vehicle Health Monitoring Study	1	4	4					8
New Start: ET 3rd Generation Foam Study	0	3	7	8				
STE Obsolescence (14)	1	16	18	11	7	7	5	59
Material Obsolescence (3)	0	2						2
Component Obsolescence (14)	0	6	23	27	16	13	9	85
Supply Chain Viability (8)	0	4	0	1	1			5
Spares Augmentation for SLE (5)	0	5	10	26	23	18	26	82
4b Improvements	16	45	62	62	23	12	5	204
New Start: SSME Advanced Health Management System Phase 2b	7	35	45	45	23	12	5	160
Study: Hydrazine Replacement	3	3	3	1				7
Study: Orbiter Hardening	2	2	2					4
Study: SSME Channel Wall Nozzle	3	4	12	16				32
Study: Orbiter Enhanced Caution and Warning								
Study: Crew Survivability Trades	1	1						1
4c New Capabilities	0	0	0	0	0	0	0	0
Reserves	0	20	20	20	20	20	20	100

Presenter: M3/Maintenance | Date: FINAL | Slide: 7 of 8 | Closed

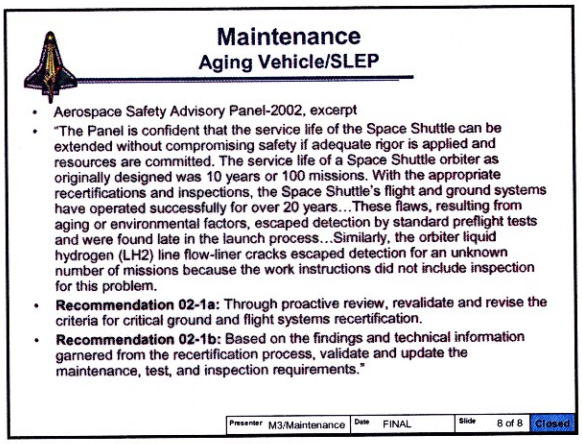

Maintenance
Aging Vehicle/SLEP

- Aerospace Safety Advisory Panel-2002, excerpt
- "The Panel is confident that the service life of the Space Shuttle can be extended without compromising safety if adequate rigor is applied and resources are committed. The service life of a Space Shuttle orbiter as originally designed was 10 years or 100 missions. With the appropriate recertifications and inspections, the Space Shuttle's flight and ground systems have operated successfully for over 20 years…These flaws, resulting from aging or environmental factors, escaped detection by standard preflight tests and were found late in the launch process…Similarly, the orbiter liquid hydrogen (LH2) line flow-liner cracks escaped detection for an unknown number of missions because the work instructions did not include inspection for this problem.
- **Recommendation 02-1a:** Through proactive review, revalidate and revise the criteria for critical ground and flight systems recertification.
- **Recommendation 02-1b:** Based on the findings and technical information garnered from the recertification process, validate and update the maintenance, test, and inspection requirements."

Presenter: M3/Maintenance | Date: FINAL | Slide: 8 of 8 | Closed

Orbiter Maintenance

14-1 Assessment of OV-102/STS-90 Hard Landing
14-2 Hypergolic Fuel Spill
14-3 WAD Accuracy
14-4 OV-102 Unique Wiring Configuration
14-5 OMDP – OMM

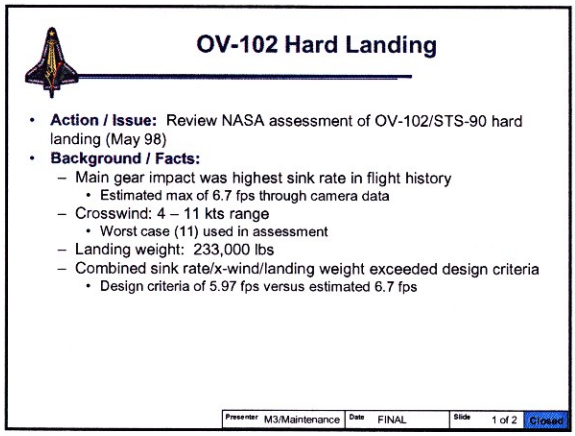

OV-102 Hard Landing

- **Action / Issue:** Review NASA assessment of OV-102/STS-90 hard landing (May 98)
- **Background / Facts:**
  - Main gear impact was highest sink rate in flight history
    - Estimated max of 6.7 fps through camera data
  - Crosswind: 4 – 11 kts range
    - Worst case (11) used in assessment
  - Landing weight: 233,000 lbs
  - Combined sink rate/x-wind/landing weight exceeded design criteria
    - Design criteria of 5.97 fps versus estimated 6.7 fps

Presenter	M3/Maintenance	Date	FINAL	Slide	1 of 2	Closed

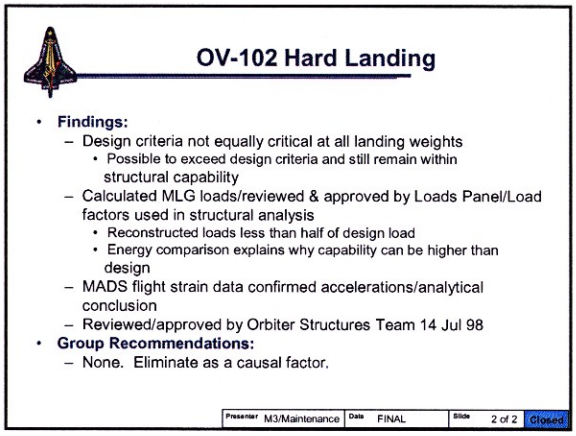

OV-102 Hard Landing

- **Findings:**
  - Design criteria not equally critical at all landing weights
    - Possible to exceed design criteria and still remain within structural capability
  - Calculated MLG loads/reviewed & approved by Loads Panel/Load factors used in structural analysis
    - Reconstructed loads less than half of design load
    - Energy comparison explains why capability can be higher than design
  - MADS flight strain data confirmed accelerations/analytical conclusion
  - Reviewed/approved by Orbiter Structures Team 14 Jul 98
- **Group Recommendations:**
  - None. Eliminate as a causal factor.

Presenter	M3/Maintenance	Date	FINAL	Slide	2 of 2	Closed

1

Maintenance
Structural Issues- Hypergolic Spill

- **Action / Issue:** Hypergolic Fuel Spill (McDonald-Gehman letter)
- **Background / Facts**
  - SIAT learned of hypergolic fuel spill 20 Aug 99 at KSC
  - Occurred during OV-102 prep for shipment to Palmdale
  - Issue briefed to Shuttle Operations Advisory Group 1 Nov 99
- **Findings**
  - 2.25 oz. dripped from GSE onto left wing inboard elevon trailing edge
  - Spill cleaned; 2 tiles removed for inspection; no damage found
  - USA employees at KSC received training; GSE improvements proposed to minimize risk of future spill
    - Quick disconnects now separated at vehicle/GSE interface only
  - Permanent panels now installed in each OPF, eliminates multiple QDs and flex lines on interface and test panel for each job
- **Group Recommendations**
  - None; spill was small/cleaned/assessed no effect on TPS or wiring

Presenter	Date	Slide	
M3/Maintenance	FINAL	1 of 2	Closed

Maintenance
Structural Issues- Hypergolic Spill

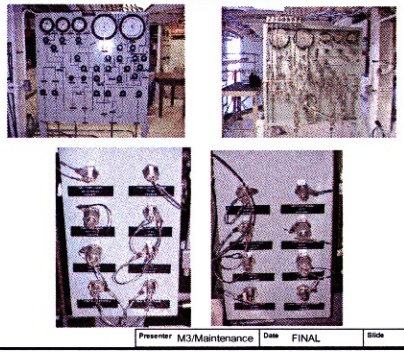

Presenter	Date	Slide	
M3/Maintenance	FINAL	2 of 2	Closed

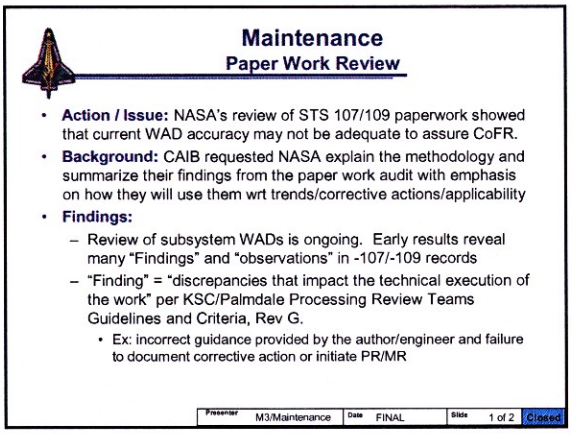
Maintenance
Paper Work Review
• Action / Issue: NASA's review of STS 107/109 paperwork showed that current WAD accuracy may not be adequate to assure CoFR.
• Background: CAIB requested NASA explain the methodology and summarize their findings from the paper work audit with emphasis on how they will use them wrt trends/corrective actions/applicability
• Findings:
– Review of subsystem WADs is ongoing. Early results reveal many "Findings" and "observations" in -107/-109 records
– "Finding" = "discrepancies that impact the technical execution of the work" per KSC/Palmdale Processing Review Teams Guidelines and Criteria, Rev G.
• Ex: incorrect guidance provided by the author/engineer and failure to document corrective action or initiate PR/MR
Presenter M3/Maintenance
Date FINAL
Slide 1 of 2
Closed

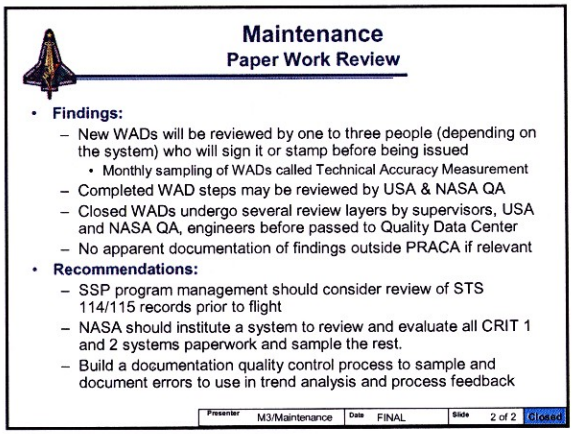
Maintenance
Paper Work Review
• Findings:
– New WADs will be reviewed by one to three people (depending on the system) who will sign it or stamp before being issued
• Monthly sampling of WADs called Technical Accuracy Measurement
– Completed WAD steps may be reviewed by USA & NASA QA
– Closed WADs undergo several review layers by supervisors, USA and NASA QA, engineers before passed to Quality Data Center
– No apparent documentation of findings outside PRACA if relevant
• Recommendations:
– SSP program management should consider review of STS 114/115 records prior to flight
– NASA should institute a system to review and evaluate all CRIT 1 and 2 systems paperwork and sample the rest.
– Build a documentation quality control process to sample and document errors to use in trend analysis and process feedback
Presenter M3/Maintenance
Date FINAL
Slide 2 of 2
Closed

Fire (Pyro /Wiring / etc.)
OV-102 Unique Wiring Configuration

- **Action / Issue:** Determine reason for OV-102's unique wiring configuration (left wing) and its role in data loss leading up to LOS
- **Background / Facts:**
  - OV-102 wiring outboard of MLG wheel well routed in 4 large bundles; other orbiters have 7 small bundles
- **Findings:**
  - As the first operational orbiter, OV-102 had additional instrumentation; nearly 90% of wires routed through this area associated with OEX data gathering and/or disconnected systems
  - Bundle securing method changed from clamps to tape straps in later orbiters; tape less able to secure large bundles – additional smaller diameter bundles (0.5 in or less) required
- **Group Recommendations:**
  - Not causal, but inclusion in OEX data analysis/sequence of events leading up to LOS will enhance investigation
  - Role in data loss sequence TBD; NASA wire heating tests ongoing

Presenter: M3/Maintenance | Date: FINAL | Slide: 1 of 2 | Closed

Fire (Pyro /Wiring / etc.)
Internal Hazard

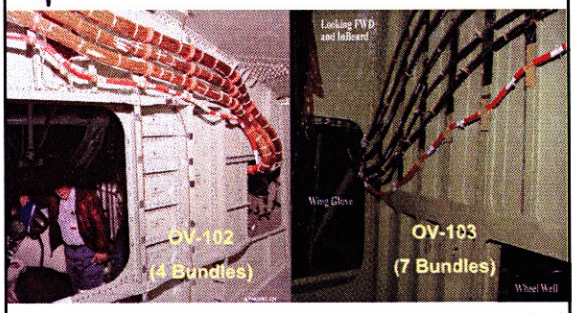

Presenter: M3/Maintenance | Date: FINAL | Slide: 2 of 2 | Closed

1

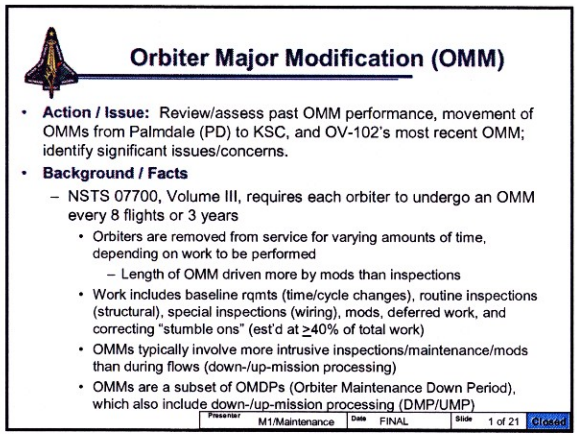
Orbiter Major Modification (OMM)
• Action / Issue: Review/assess past OMM performance, movement of OMMs from Palmdale (PD) to KSC, and OV-102's most recent OMM; identify significant issues/concerns.
• Background / Facts
– NSTS 07700, Volume III, requires each orbiter to undergo an OMM every 8 flights or 3 years
• Orbiters are removed from service for varying amounts of time, depending on work to be performed
– Length of OMM driven more by mods than inspections
• Work includes baseline rqmts (time/cycle changes), routine inspections (structural), special inspections (wiring), mods, deferred work, and correcting "stumble ons" (est'd at ≥40% of total work)
• OMMs typically involve more intrusive inspections/maintenance/mods than during flows (down-/up-mission processing)
• OMMs are a subset of OMDPs (Orbiter Maintenance Down Period), which also include down-/up-mission processing (DMP/UMP)
Presenter M1/Maintenance Date FINAL Slide 1 of 21 Closed

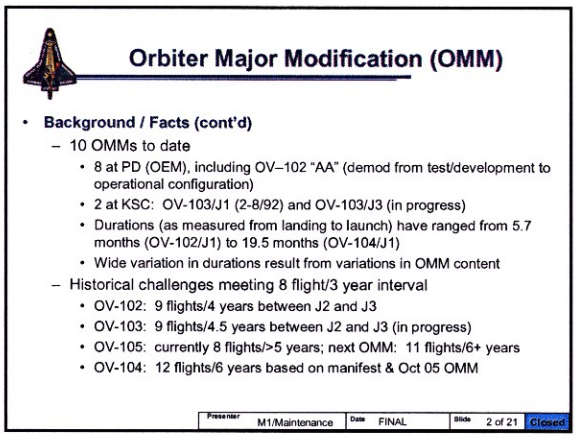
Orbiter Major Modification (OMM)
• Background / Facts (cont'd)
– 10 OMMs to date
• 8 at PD (OEM), including OV–102 "AA" (demod from test/development to operational configuration)
• 2 at KSC: OV-103/J1 (2-8/92) and OV-103/J3 (in progress)
• Durations (as measured from landing to launch) have ranged from 5.7 months (OV-102/J1) to 19.5 months (OV-104/J1)
• Wide variation in durations result from variations in OMM content
– Historical challenges meeting 8 flight/3 year interval
• OV-102: 9 flights/4 years between J2 and J3
• OV-103: 9 flights/4.5 years between J2 and J3 (in progress)
• OV-105: currently 8 flights/>5 years; next OMM: 11 flights/6+ years
• OV-104: 12 flights/6 years based on manifest & Oct 05 OMM
Presenter M1/Maintenance Date FINAL Slide 2 of 21 Closed

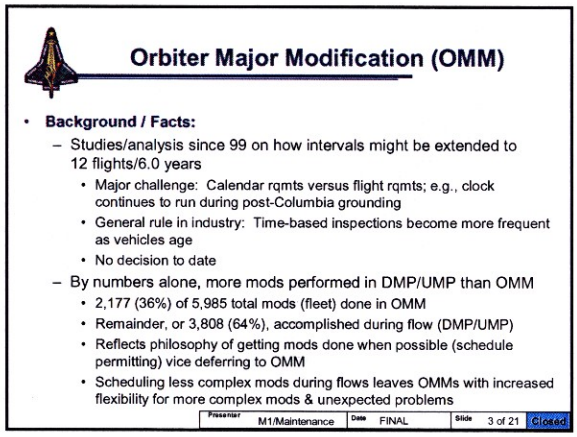
Orbiter Major Modification (OMM)
• Background / Facts:
– Studies/analysis since 99 on how intervals might be extended to 12 flights/6.0 years
• Major challenge: Calendar rqmts versus flight rqmts; e.g., clock continues to run during post-Columbia grounding
• General rule in industry: Time-based inspections become more frequent as vehicles age
• No decision to date
– By numbers alone, more mods performed in DMP/UMP than OMM
• 2,177 (36%) of 5,985 total mods (fleet) done in OMM
• Remainder, or 3,808 (64%), accomplished during flow (DMP/UMP)
• Reflects philosophy of getting mods done when possible (schedule permitting) vice deferring to OMM
• Scheduling less complex mods during flows leaves OMMs with increased flexibility for more complex mods & unexpected problems
Presenter M1/Maintenance Date FINAL Slide 3 of 21 Closed

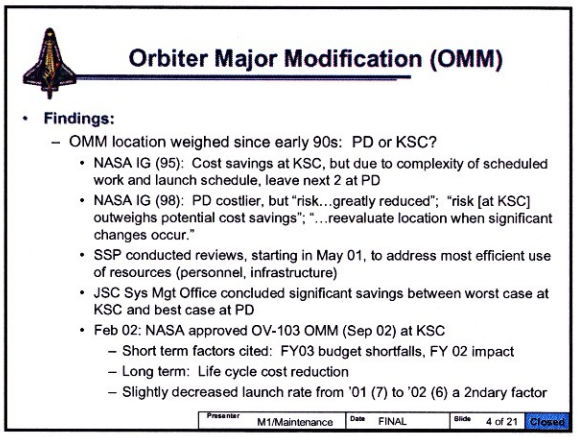
Orbiter Major Modification (OMM)
• Findings:
– OMM location weighed since early 90s: PD or KSC?
• NASA IG (95): Cost savings at KSC, but due to complexity of scheduled work and launch schedule, leave next 2 at PD
• NASA IG (98): PD costlier, but "risk…greatly reduced"; "risk [at KSC] outweighs potential cost savings"; "…reevaluate location when significant changes occur."
• SSP conducted reviews, starting in May 01, to address most efficient use of resources (personnel, infrastructure)
• JSC Sys Mgt Office concluded significant savings between worst case at KSC and best case at PD
• Feb 02: NASA approved OV-103 OMM (Sep 02) at KSC
– Short term factors cited: FY03 budget shortfalls, FY 02 impact
– Long term: Life cycle cost reduction
– Slightly decreased launch rate from '01 (7) to '02 (6) a 2ndary factor
Presenter M1/Maintenance Date FINAL Slide 4 of 21 Closed

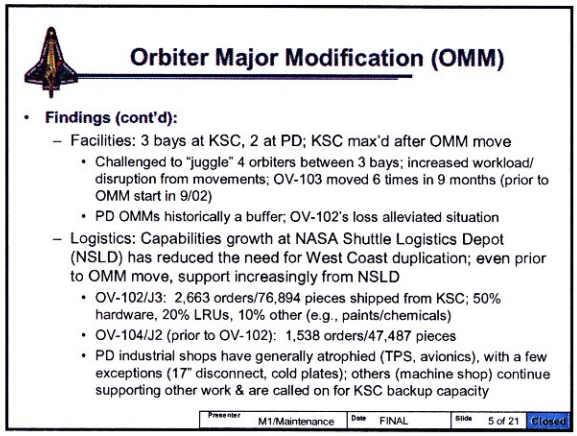
Orbiter Major Modification (OMM)
• Findings (cont'd):
– Facilities: 3 bays at KSC, 2 at PD; KSC max'd after OMM move
• Challenged to "juggle" 4 orbiters between 3 bays; increased workload/ disruption from movements; OV-103 moved 6 times in 9 months (prior to OMM start in 9/02)
• PD OMMs historically a buffer; OV-102's loss alleviated situation
– Logistics: Capabilities growth at NASA Shuttle Logistics Depot (NSLD) has reduced the need for West Coast duplication; even prior to OMM move, support increasingly from NSLD
• OV-102/J3: 2,663 orders/76,894 pieces shipped from KSC; 50% hardware, 20% LRUs, 10% other (e.g., paints/chemicals)
• OV-104/J2 (prior to OV-102): 1,538 orders/47,487 pieces
• PD industrial shops have generally atrophied (TPS, avionics), with a few exceptions (17" disconnect, cold plates); others (machine shop) continue supporting other work & are called on for KSC backup capacity
Presenter M1/Maintenance Date FINAL Slide 5 of 21 Closed

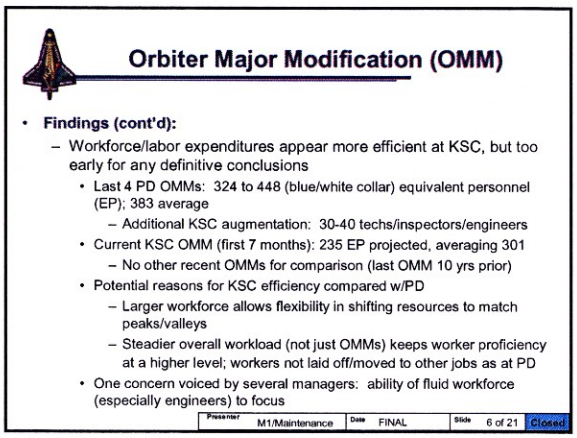
Orbiter Major Modification (OMM)
• Findings (cont'd):
– Workforce/labor expenditures appear more efficient at KSC, but too early for any definitive conclusions
• Last 4 PD OMMs: 324 to 448 (blue/white collar) equivalent personnel (EP); 383 average
– Additional KSC augmentation: 30-40 techs/inspectors/engineers
• Current KSC OMM (first 7 months): 235 EP projected, averaging 301
– No other recent OMMs for comparison (last OMM 10 yrs prior)
• Potential reasons for KSC efficiency compared w/PD
– Larger workforce allows flexibility in shifting resources to match peaks/valleys
– Steadier overall workload (not just OMMs) keeps worker proficiency at a higher level; workers not laid off/moved to other jobs as at PD
• One concern voiced by several managers: ability of fluid workforce (especially engineers) to focus
Presenter M1/Maintenance Date FINAL Slide 6 of 21 Closed

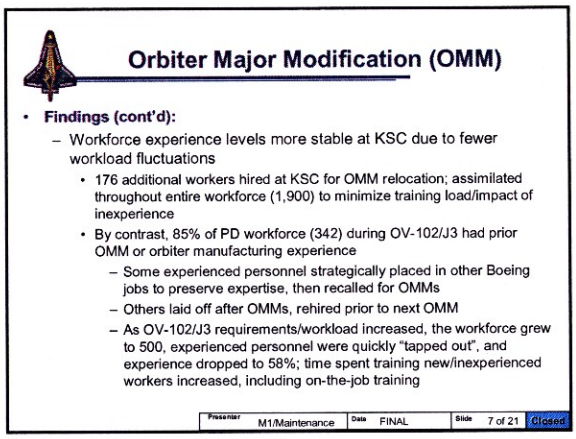
Orbiter Major Modification (OMM)
• Findings (cont'd):
– Workforce experience levels more stable at KSC due to fewer workload fluctuations
• 176 additional workers hired at KSC for OMM relocation; assimilated throughout entire workforce (1,900) to minimize training load/impact of inexperience
• By contrast, 85% of PD workforce (342) during OV-102/J3 had prior OMM or orbiter manufacturing experience
– Some experienced personnel strategically placed in other Boeing jobs to preserve expertise, then recalled for OMMs
– Others laid off after OMMs, rehired prior to next OMM
– As OV-102/J3 requirements/workload increased, the workforce grew to 500, experienced personnel were quickly "tapped out", and experience dropped to 58%; time spent training new/inexperienced workers increased, including on-the-job training
Presenter M1/Maintenance Date FINAL Slide 7 of 21 Closed

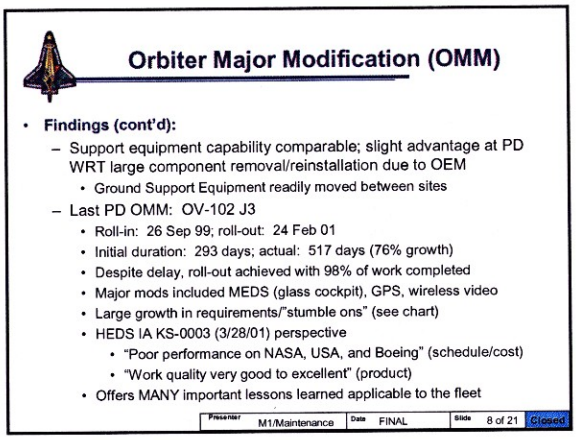
Orbiter Major Modification (OMM)
• Findings (cont'd):
– Support equipment capability comparable; slight advantage at PD WRT large component removal/reinstallation due to OEM
• Ground Support Equipment readily moved between sites
– Last PD OMM: OV-102 J3
• Roll-in: 26 Sep 99; roll-out: 24 Feb 01
• Initial duration: 293 days; actual: 517 days (76% growth)
• Despite delay, roll-out achieved with 98% of work completed
• Major mods included MEDS (glass cockpit), GPS, wireless video
• Large growth in requirements/"stumble ons" (see chart)
• HEDS IA KS-0003 (3/28/01) perspective
• "Poor performance on NASA, USA, and Boeing" (schedule/cost)
• "Work quality very good to excellent" (product)
• Offers MANY important lessons learned applicable to the fleet
Presenter M1/Maintenance Date FINAL Slide 8 of 21 Closed

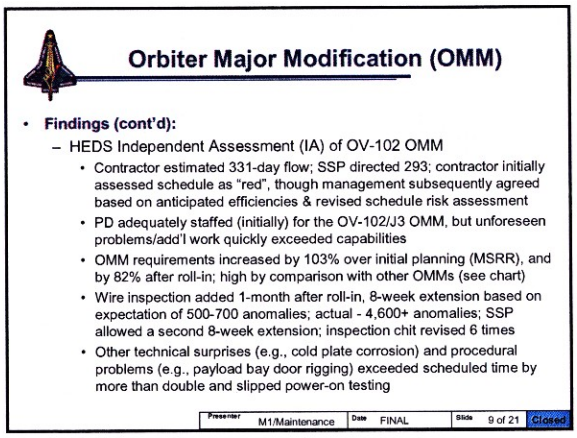
Orbiter Major Modification (OMM)
• Findings (cont'd):
– HEDS Independent Assessment (IA) of OV-102 OMM
• Contractor estimated 331-day flow; SSP directed 293; contractor initially assessed schedule as "red", though management subsequently agreed based on anticipated efficiencies & revised schedule risk assessment
• PD adequately staffed (initially) for the OV-102/J3 OMM, but unforeseen problems/add'l work quickly exceeded capabilities
• OMM requirements increased by 103% over initial planning (MSRR), and by 82% after roll-in; high by comparison with other OMMs (see chart)
• Wire inspection added 1-month after roll-in, 8-week extension based on expectation of 500-700 anomalies; actual - 4,600+ anomalies; SSP allowed a second 8-week extension; inspection chit revised 6 times
• Other technical surprises (e.g., cold plate corrosion) and procedural problems (e.g., payload bay door rigging) exceeded scheduled time by more than double and slipped power-on testing
Presenter M1/Maintenance Date FINAL Slide 9 of 21 Closed

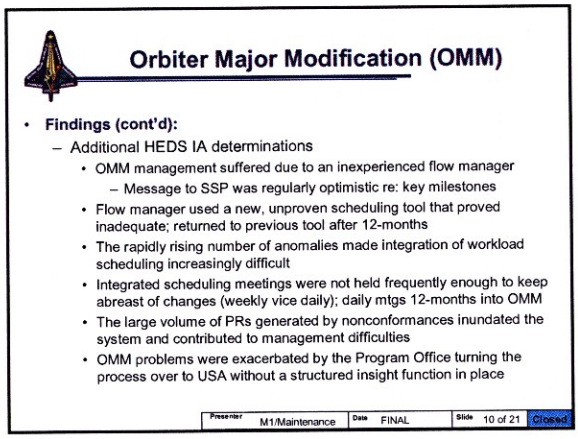
Orbiter Major Modification (OMM)
• Findings (cont'd):
– Additional HEDS IA determinations
• OMM management suffered due to an inexperienced flow manager
– Message to SSP was regularly optimistic re: key milestones
• Flow manager used a new, unproven scheduling tool that proved inadequate; returned to previous tool after 12-months
• The rapidly rising number of anomalies made integration of workload scheduling increasingly difficult
• Integrated scheduling meetings were not held frequently enough to keep abreast of changes (weekly vice daily); daily mtgs 12-months into OMM
• The large volume of PRs generated by nonconformances inundated the system and contributed to management difficulties
• OMM problems were exacerbated by the Program Office turning the process over to USA without a structured insight function in place
Presenter M1/Maintenance Date FINAL Slide 10 of 21 Closed

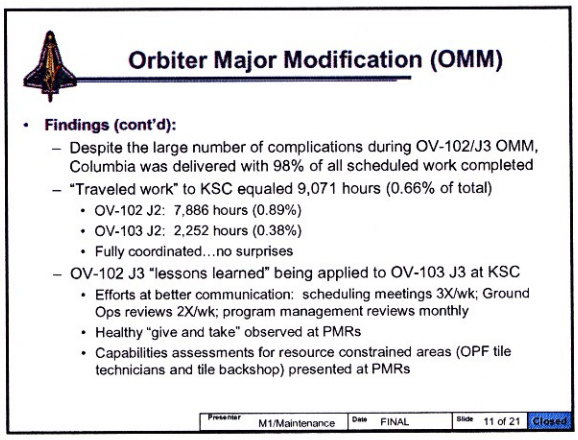
Orbiter Major Modification (OMM)
• Findings (cont'd):
– Despite the large number of complications during OV-102/J3 OMM, Columbia was delivered with 98% of all scheduled work completed
– "Traveled work" to KSC equaled 9,071 hours (0.66% of total)
• OV-102 J2: 7,886 hours (0.89%)
• OV-103 J2: 2,252 hours (0.38%)
• Fully coordinated…no surprises
– OV-102 J3 "lessons learned" being applied to OV-103 J3 at KSC
• Efforts at better communication: scheduling meetings 3X/wk; Ground Ops reviews 2X/wk; program management reviews monthly
• Healthy "give and take" observed at PMRs
• Capabilities assessments for resource constrained areas (OPF tile technicians and tile backshop) presented at PMRs
Presenter M1/Maintenance Date FINAL Slide 11 of 21 Closed

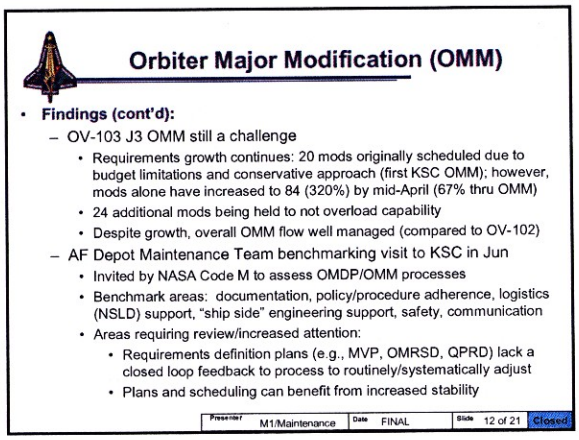
Orbiter Major Modification (OMM)
• Findings (cont'd):
– OV-103 J3 OMM still a challenge
• Requirements growth continues: 20 mods originally scheduled due to budget limitations and conservative approach (first KSC OMM); however, mods alone have increased to 84 (320%) by mid-April (67% thru OMM)
• 24 additional mods being held to not overload capability
• Despite growth, overall OMM flow well managed (compared to OV-102)
– AF Depot Maintenance Team benchmarking visit to KSC in Jun
• Invited by NASA Code M to assess OMDP/OMM processes
• Benchmark areas: documentation, policy/procedure adherence, logistics (NSLD) support, "ship side" engineering support, safety, communication
• Areas requiring review/increased attention:
• Requirements definition plans (e.g., MVP, OMRSD, QPRD) lack a closed loop feedback to process to routinely/systematically adjust
• Plans and scheduling can benefit from increased stability
Presenter M1/Maintenance Date FINAL Slide 12 of 21 Closed

Orbiter Major Modification (OMM)

- **Findings (cont'd):**
  - AF Depot Maintenance Team/OMM areas requiring review (cont'd)
    - Orbiter sustainment roadmap must be tied into OMM requirements
    - Gov't/contractor relationships require review to ensure the right OMM "behavior" is being incentivized
- **Conclusions:**
  - While there are specific baseline elements, no two OMMs are alike; variations occur as orbiters age (wiring inspection, cold plate corrosion), as mission rqmts change (reconfiguration for MIR) and, in some cases, due to lack of funding; improving schedule and funding stability can help reduce process variation and aid in better planning/scheduling and less turmoil
  - Increasing OMM intervals as orbiters age is counter to industry norms; for high performance systems, it raises even greater questions

Presenter: M1/Maintenance | Date: FINAL | Slide: 13 of 21 | Closed

Orbiter Major Modification (OMM)

- **Conclusions (cont'd):**
  - Relocation of OMMs to KSC provides many advantages over PD (e.g., a more stable, more fully/steadily employed workforce), but also creates new challenges
    - KSC advantages can still be overwhelmed if not carefully managed
    - Several NASA/USA/Boeing managers expressed concern over a fluid workforce's (especially engineers) ability to focus
  - The wire inspection chit and its timing (1-month after OV-102 roll-in) played a major role in OMM schedule slippage
    - A "must do", representative of technical surprises that will continue
  - OV-102 J3 OMM "lessons learned" have fleet implications because:
    - As orbiters age, workload will likely increase
    - The likelihood of technical surprises will also increase
    - A significant return-to-flight workload is highly probable
    - All of the above will generate new challenges, similar to those encountered during OV-102's OMM, for both managers/workforce

Presenter: M1/Maintenance | Date: FINAL | Slide: 14 of 21 | Closed

Orbiter Major Modification (OMM)

- **Recommendations:**
  - The Program Office MUST work to achieve greater stability in OMM-scheduled work, particularly the number of mods (biggest driver of schedule/workload variation); a continually changing schedule (rqmts growth) creates unnecessary turmoil/stress and increases the potential for quality escapes
  - Managers (NASA/USA) MUST understand workforce/facilities capabilities, schedule to those capabilities, and take necessary actions to avoid exceeding them (ref. Capabilities Assessment briefing)
  - The SSP Office MUST determine how it will effectively meet the challenges of inspecting/maintaining an aging orbiter fleet prior to increasing the OMM interval
  - NASA/USAF benchmarking efforts should be continued using the same personnel as much as possible for continuity

Presenter: M1/Maintenance | Date: FINAL | Slide: 15 of 21 | Closed

Orbiter Major Modification (OMM) Boeing/Palmdale

Presenter: M1/Maintenance | Date: FINAL | Slide: 16 of 21 | Closed

Orbiter Major Modification (OMM) History

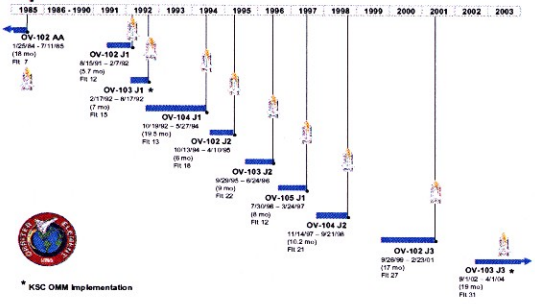

Presenter: M1/Maintenance | Date: FINAL | Slide: 17 of 21 | Closed

Orbiter Modifications OMM vs. Flow

ORBITER	MODS IN OMM	MODS IN FLOW	TOTAL MODS
OV-102	608	1,058	1,666
OV-103	675	936	1,611
OV-104	691	725	1,416
OV-105	203	1,089	1,292
TOTAL	2,177	3,808	5,985

Presenter: M1/Maintenance | Date: FINAL | Slide: 18 of 21 | Closed

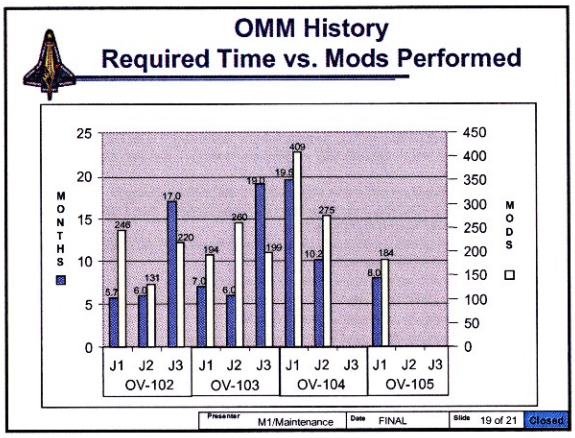

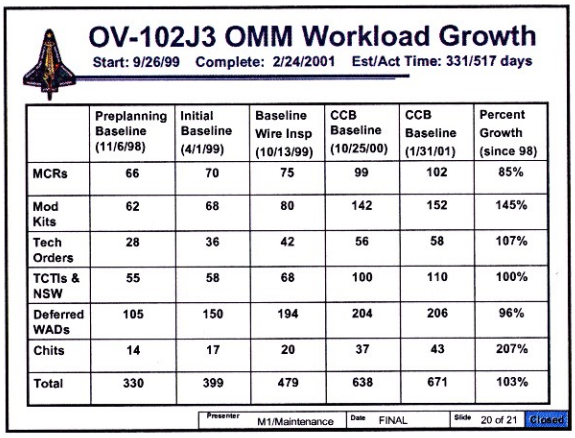

	Preplanning Baseline (11/6/98)	Initial Baseline (4/1/99)	Baseline Wire Insp (10/13/99)	CCB Baseline (10/25/00)	CCB Baseline (1/31/01)	Percent Growth (since 98)
MCRs	66	70	75	99	102	85%
Mod Kits	62	68	80	142	152	145%
Tech Orders	28	36	42	56	58	107%
TCTIs & NSW	55	58	68	100	110	100%
Deferred WADs	105	150	194	204	206	96%
Chits	14	17	20	37	43	207%
Total	330	399	479	638	671	103%

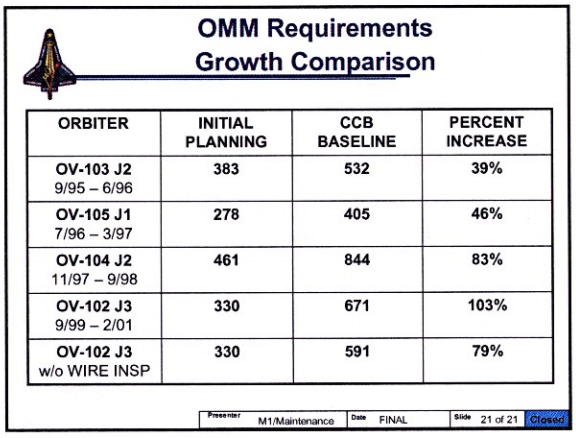

ORBITER	INITIAL PLANNING	CCB BASELINE	PERCENT INCREASE
OV-103 J2 9/95 – 6/96	383	532	39%
OV-105 J1 7/96 – 3/97	278	405	46%
OV-104 J2 11/97 – 9/98	461	844	83%
OV-102 J3 9/99 – 2/01	330	671	103%
OV-102 J3 w/o WIRE INSP	330	591	79%

Orbiter
Launch – Ascent

15-1 STS-107 Key Loads Parameters Versus Design and Experience

15-2 STS-107 Ascent Loads (DOLILU)

15-3 STS-107 OEX Ascent Data

Matrix

Presenter	CAIB/Group 1	Date	FINAL	Slide	18 of 32

STS-107 Vs Past Experience

- **Action / Issue:** Compare STS-107 key parameters to past experience and design limits
- **Background / Facts:**
  - STS-107 key parameters extracted from RSS99D0510D, "Space Shuttle Life Tracking", March 2003

Presenter M3/Material | Date FINAL | Slide 1 of 7 | Closed

STS-107 Vs Past Experience

STS-107 Versus Fleet Experience
Orbiter Weight at Liftoff and Landing

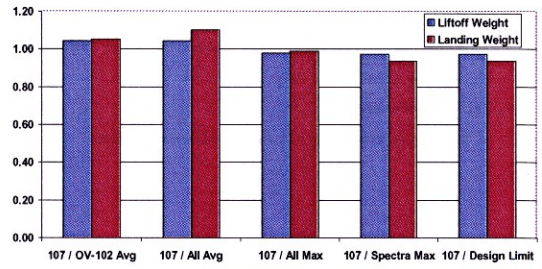

Presenter M3/Material | Date FINAL | Slide 2 of 7 | Closed

STS-107 Vs Past Experience

STS-107 Versus Fleet Experience
Ascent Max Q

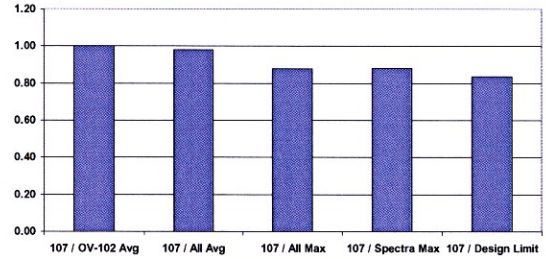

Presenter M3/Material | Date FINAL | Slide 3 of 7 | Closed

STS-107 Vs Past Experience

STS-107 Versus Fleet Experience
Ascent Q-Beta

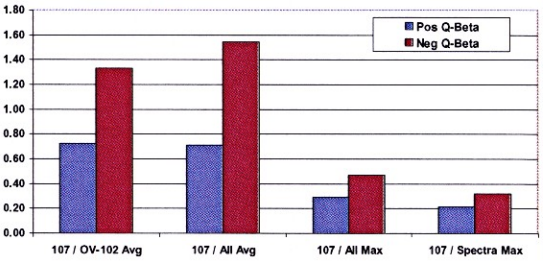

Presenter M3/Material | Date FINAL | Slide 4 of 7 | Closed

STS-107 Vs Past Experience

STS-107 Versus Fleet Experience
Wing Root Bending Moment During Ascent

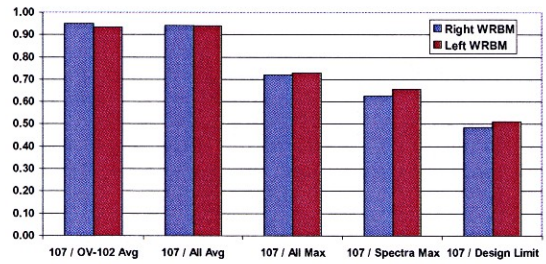

Presenter M3/Material | Date FINAL | Slide 5 of 7 | Closed

STS-107 Vs Past Experience

Parameter	Units	STS-107 Value	STS-109 Value	STS-93 Value	OV-102 Average	All Flights Average	All Flights Maximum	All Flights Minimum
Liftoff Orbiter Weight	lbs	265081	260965	270455	253760	254306	270455	219441
Liftoff Orbiter Center of Gravity	in	1164.7	1113.8	1120.2	1109.7	1112.2	1131.3	1095.8
Ascent Maximum Dynamic Pressure (Q)	psf	683.6	706.6	701.9	683.8	697.7	777.5	606.7
Ascent Q-Beta Positive Maximum	psf-deg	544.7	869.2	495.0	751.9	766.7	1606.2	
Ascent Q-Beta Negative Minimum	psf-deg	-1106.5	-878.5	-690.6	-881.4	-647.0		-1734.4
Ascent Beta Positive Maximum, M 0.9 to 1.0	deg	0.84	0.63	0.44	0.44	0.51	1.63	
Ascent Beta Negative Minimum, M 0.9 to 1.0	deg	-0.86	-0.39	-0.44	-0.66	-0.57		-1.80
Ascent Right Wing Root Bending Mx Positive	in-lb	1.714E+07	1.995E+07	1.806E+07	1.808E+07	1.822E+07	2.382E+07	
Ascent Left Wing Root Bending Mx Negative	in-lb	-1.801E+07	-1.851E+07	-1.866E+07	-1.828E+07	-1.823E+07		-2.471E+07
Landing Orbiter Weight	lbs	230648	222160	230721	220966	231117	235285	187200

Presenter M3/Material | Date FINAL | Slide 6 of 7 | Closed

1

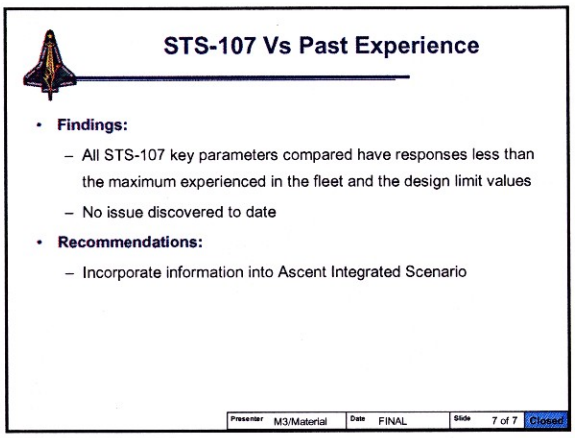
STS-107 Vs Past Experience
• Findings:
– All STS-107 key parameters compared have responses less than the maximum experienced in the fleet and the design limit values
– No issue discovered to date
• Recommendations:
– Incorporate information into Ascent Integrated Scenario
Presenter M3/Material
Date FINAL
Slide 7 of 7
Closed

STS-107 Launch/Ascent

- **Action / Issue:** Review STS-107 structural responses during ascent
- **Background / Facts:**
  - Structural response of Shuttle depends on a combination of:
    - Flight control commands
    - Shuttle responses (α and β changes, gimbal angles, LOX slosh, etc.)
    - Environment through which Shuttle ascends (winds, etc.)
  - Guidance commands in the Day of Launch I-Load Update (DOLILU) provide input to flight control software
    - Inputs to DOLILU: measured winds, atmospheric data, vehicle config.
    - What DOLILU targets: angle of attack (α), angle of sideslip (β), dynamic pressure (q) as function of Mach number
    - DOLILU Outputs: guidance commands to control
      - Vehicle pitch & yaw attitudes
      - SSME throttle
    - SSME & SRB gimbal angles controlled by flight control software
    - DOLILU is used to ensure vehicle is flown within an acceptable structural loads envelope

Presenter M3/Material | Date FINAL | Slide 1 of 34 | Closed

STS-107 Launch/Ascent

- **Background / Facts:** (cont.)
  - DOLILU inputs (winds)
    - Based on observation from Jimsphere balloon released at L-4:35
    - Verified using data from Jimspheres released at L-3:25, -2:15, & -1:10
    - STS-107 Data
      - L-4:35: Max wind shear of 41.0 fps at 34,300 feet = 74.0% of design limit
      - L-3:25: Max wind shear of 46.0 fps at 33,800 feet = 83.1% of design limit
      - L-2:15: Max wind shear of 43.6 fps at 33,400 feet = 78.6% of design limit
      - L-1:10: Max wind shear of 26.9 fps at 33,400 feet = 70.9% of design limit
      - No exceedances on any Jimsphere data
  - STS-107 Experience (wind shear) at MET = 57 sec and Mach 1.27
    - Not measured by vehicle – no capability to do so
  - Post-launch (L+15) Jimsphere confirmed wind shear was less than design limit
    - L+0:15: Max wind shear of 37.7 fps at 33,200 feet = 68.0% of design limit
    - Also ~40 ft/sec less than L-4:35 wind shear used for DOLILU
    - See next chart

Presenter M3/Material | Date FINAL | Slide 2 of 34 | Closed

STS-107 Launch/Ascent
L-04:30 and L+00:15 Jimsphere Data

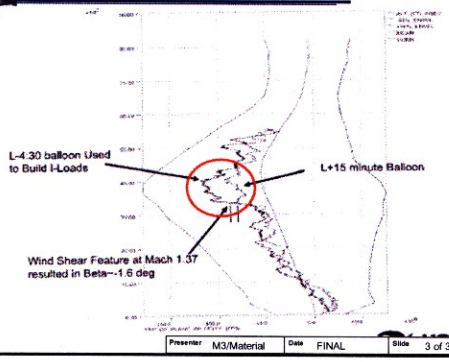

Presenter M3/Material | Date FINAL | Slide 3 of 34 | Closed

STS-107 Launch/Ascent

- **Background / Facts:** (cont.)
  - STS-107 Experience (wind shear) at MET = 57 sec (cont.)
    - Due to wind shear, the following Shuttle responses exceeded prior flight experience (See next 3 charts)
      - Orbiter β of 1.6 degrees
      - SRB gimbal angles
      - SSME #3 pitch gimbal angle

Presenter M3/Material | Date FINAL | Slide 4 of 34 | Closed

STS-107 Launch/Ascent
Angle of Sideslip (Beta)

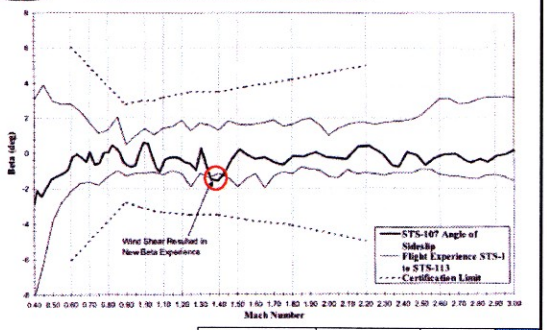

Presenter M3/Material | Date FINAL | Slide 5 of 34 | Closed

STS-107 Launch/Ascent
SRB Left Tilt & Rock Gimbal Position

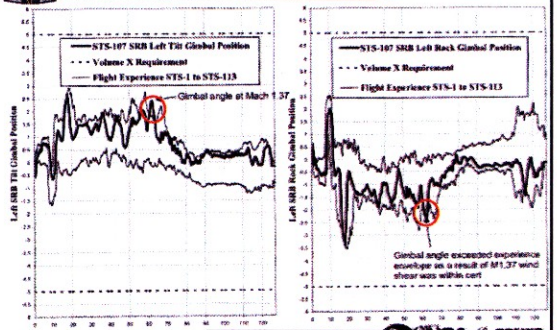

Presenter M3/Material | Date FINAL | Slide 6 of 34 | Closed

1

STS-107 Launch/Ascent
SSME-3 Pitch Gimbal Position

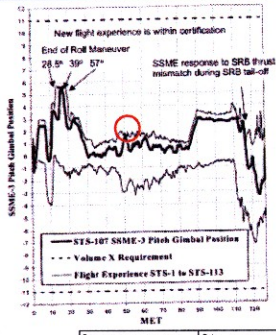

Presenter M3/Material | Date FINAL | Slide 7 of 34 | Closed

STS-107 Launch/Ascent

- **Background / Facts:** (cont.)
  - STS-107 Experience (winds shear) at MET = 57 sec (cont.)
    - Shuttle left & right wing responses were predicted ("reconstructed" using flex-body analysis), obtained via MADS data (OEX), and compared with previous missions and design limits (see next 11 charts)

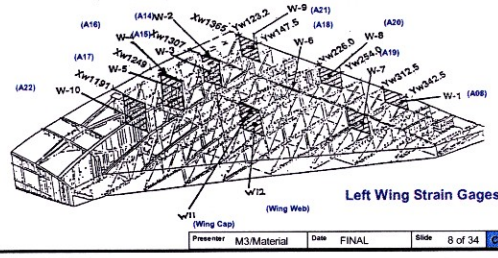

Presenter M3/Material | Date FINAL | Slide 8 of 34 | Closed

STS-107 Launch/Ascent
Gage # A08 Left

STS-107 (A08L) Flex Reconstructed Wing Load Indicator, MADS Data, And Maximum Rigid Reconstructed Peaks For Previous OV-102 Flights vs Redline Limit

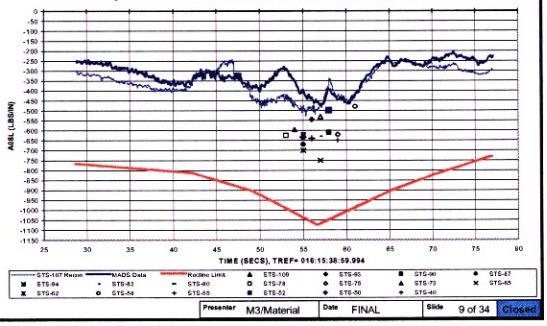

Presenter M3/Material | Date FINAL | Slide 9 of 34 | Closed

STS-107 Launch/Ascent
Gage #A08 Right

STS-107 (A08R) Flex Reconstructed Wing Load Indicator, MADS Data, And Maximum Rigid Reconstructed Peaks For Previous OV-102 Flights vs Redline Limit

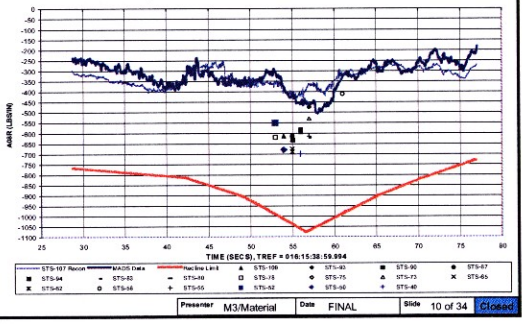

Presenter M3/Material | Date FINAL | Slide 10 of 34 | Closed

STS-107 Launch/Ascent
Gage # A14 Left and Right

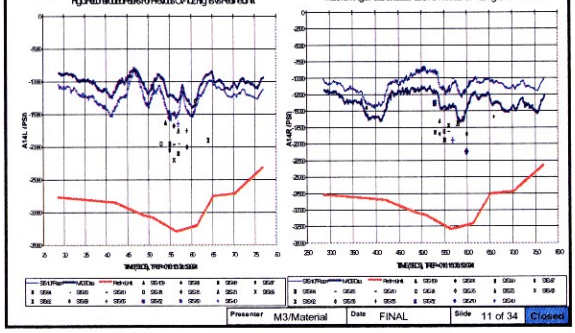

Presenter M3/Material | Date FINAL | Slide 11 of 34 | Closed

STS-107 Launch/Ascent
Gage # A15 Left and Right

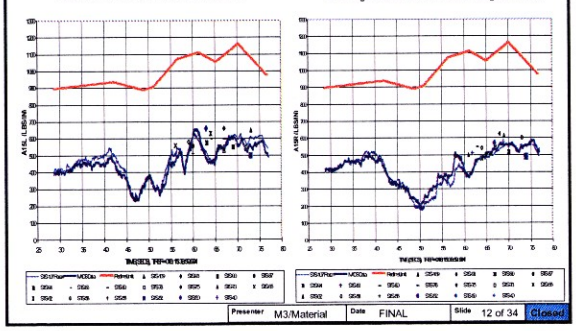

Presenter M3/Material | Date FINAL | Slide 12 of 34 | Closed

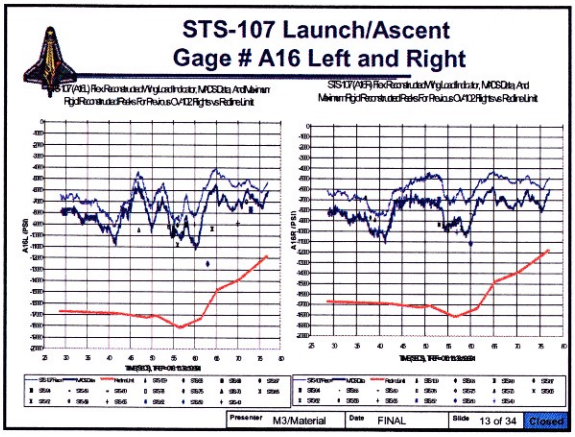
STS-107 Launch/Ascent
Gage # A16 Left and Right
M3/Material
FINAL
13 of 34
Closed

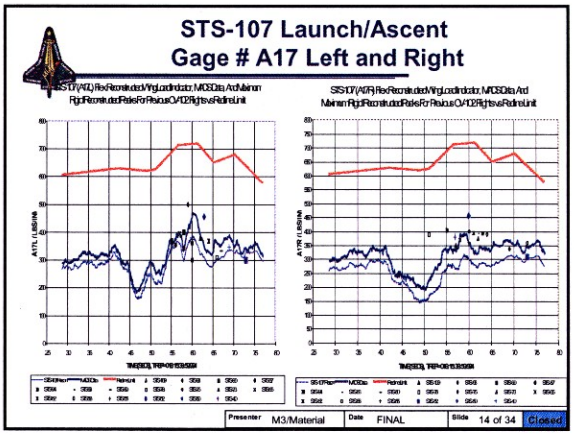
STS-107 Launch/Ascent
Gage # A17 Left and Right
M3/Material
FINAL
14 of 34
Closed

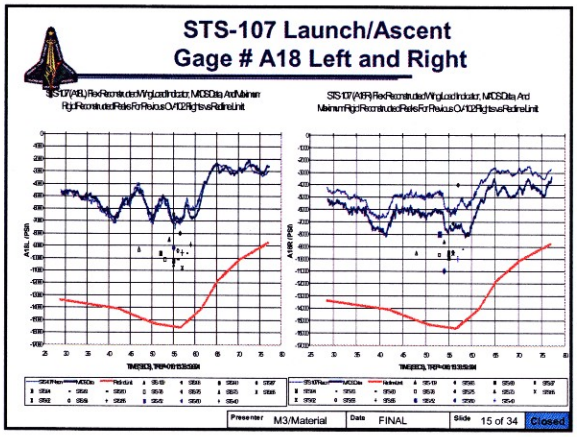
STS-107 Launch/Ascent
Gage # A18 Left and Right
M3/Material
FINAL
15 of 34
Closed

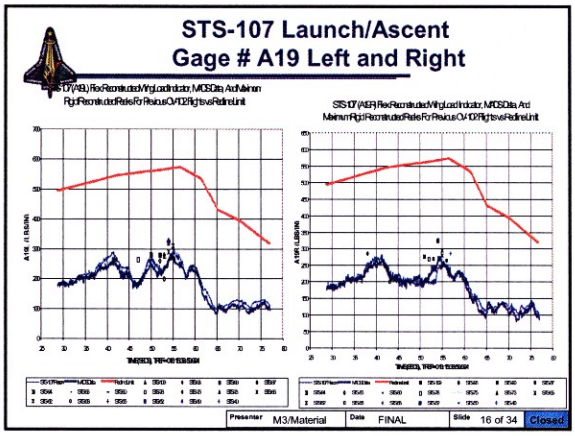
STS-107 Launch/Ascent
Gage # A19 Left and Right
M3/Material
FINAL
16 of 34
Closed

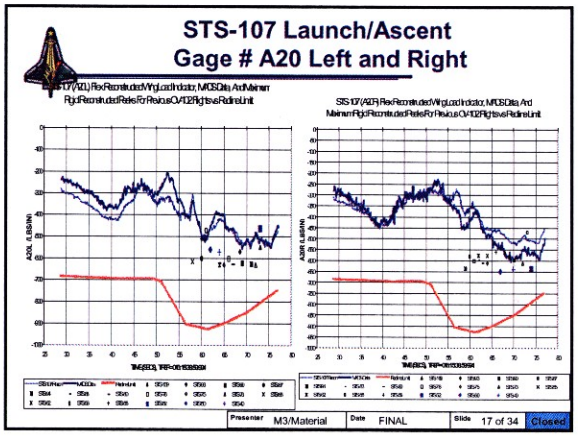
STS-107 Launch/Ascent
Gage # A20 Left and Right
M3/Material
FINAL
17 of 34
Closed

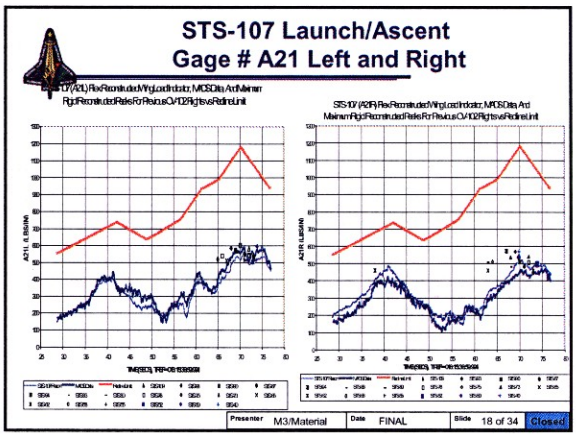
STS-107 Launch/Ascent
Gage # A21 Left and Right
M3/Material
FINAL
18 of 34
Closed

STS-107 Launch/Ascent
Gage # A22 Left and Right

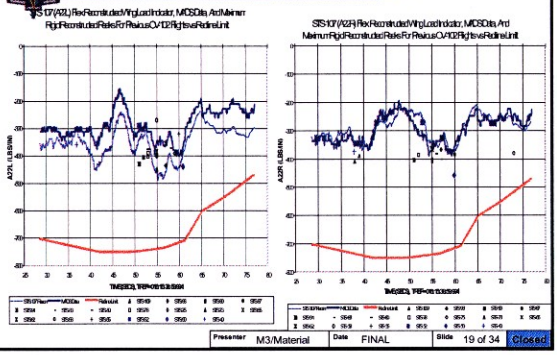

Presenter M3/Material | Date FINAL | Slide 19 of 34 | Closed

Reconstructed left wing root moment for previous flights

STS-107 Launch/Ascent

- **Background / Facts:** (cont.)
  - STS-107 Experience (winds shear) at MET = 57 sec (cont.)
    - Predicted ("reconstructed") wing root bending moment was compared to wing root bending moments from other missions

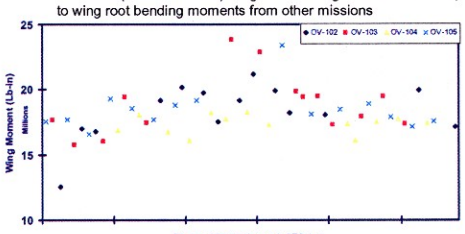

Presenter M3/Material | Date FINAL | Slide 20 of 34 | Closed

STS-107 Launch/Ascent

- **Background / Facts:** (cont.)
  - STS-107 Experience (ascent oads)
    - Max & min predicted ("reconstructed" using rigid body analysis) loads on ET-Orbiter attachments, struts, and orbiter body also measured and compared against design limit during ascent (see next 4 charts)
    - Highest % of limits indicated with red arrow ←

STS-107 Reconstructed Max/Min Attachment Loads

ET - Attachment Loads

Indicator Name	Upper Side % of Limit	Upper Side Mach	Upper Side Load (kips)	Upper Side Limit (kips)	Lower Side % of Limit	Lower Side Mach	Lower Side Load (kips)	Lower Side Limit (kips)
FT81	16.96	0.78	37.42	220.60	9.37	1.54	-14.19	-151.50
FT82	11.64	0.64	25.94	222.80	16.11	1.42	-23.67	-147.00
FT83	48.38	2.20	93.76	193.80	*	*	36.81	-80.40
FT84	*	*	-32.27	83.60	42.11	2.08	-84.77	-201.30
FT85	*	*	-1025.36	168.80	81.43	2.20	-1368.24	-1680.30
FT86	*	*	-1033.62	152.70	82.41	2.20	-1384.23	-1679.60
FT87	25.35	1.01	69.93	275.90	20.11	1.38	-39.21	-195.00
FT88	40.39	1.40	121.13	299.90	9.99	0.84	-20.45	-204.70
FT89	*	*	-21.21	269.90	39.43	1.40	-118.58	-300.70
FT80	30.26	1.50	92.84	306.80	*	*	3.19	-296.00
MT81	15.63	1.36	2731.63	17481.10	19.24	1.00	-4869.35	-25309.00
MT82	31.86	1.37	8078.14	25352.90	5.45	0.83	-991.29	-18189.30

Presenter M3/Material | Date FINAL | Slide 21 of 34 | Closed

STS-107 Launch/Ascent

STS-107 Reconstructed Max/Min Attachment Loads

Strut Loads

Indicator Name	Upper Side % of Limit	Upper Side Mach	Upper Side Load (kips)	Upper Side Limit (kips)	Lower Side % of Limit	Lower Side Mach	Lower Side Load (kips)	Lower Side Limit (kips)
P1	19.25	0.84	14.47	75.20	34.56	1.41	-33.00	-95.50
P2	15.27	0.90	11.67	76.40	27.27	1.53	-27.27	-100.00
P3	44.78	0.71	188.75	421.50	4.81	1.07	-11.62	-241.70
P4	55.02	1.36	251.93	457.90	*	*	20.29	-231.00
P5	*	*	-180.72	181.10	53.29	0.73	-436.74	-800.80
P6	*	*	-166.31	182.60	51.12	0.71	-412.50	-806.90
P7	15.02	0.99	18.80	125.10	22.32	1.26	-29.75	-133.30
P8	17.53	1.48	35.42	202.00	14.52	1.06	-27.16	-187.00
P9	39.06	1.37	103.50	265.00	*	*	6.83	-124.10
P10	9.99	0.84	21.35	213.70	40.39	1.40	-126.46	-313.10
P11	33.86	1.36	68.39	202.00	6.19	1.00	-11.58	-187.00
P12	27.01	1.48	71.57	265.00	0.08	0.88	-0.10	-127.20
P13	20.11	1.38	40.93	203.50	25.35	1.01	-73.00	-288.00

Presenter M3/Material | Date FINAL | Slide 22 of 34 | Closed

STS-107 Launch/Ascent

STS-107 Reconstructed Max/Min Attachment Loads

Orbiter - Attachment Loads

Indicator Name	Upper Side % of Limit	Upper Side Mach	Upper Side Load (kips)	Upper Side Limit (kips)	Lower Side % of Limit	Lower Side Mach	Lower Side Load (kips)	Lower Side Limit (kips)
FT01	15.49	0.87	14.20	91.70	31.46	1.54	-39.89	-126.80
FT02	26.80	1.39	18.07	67.40	20.10	0.82	-13.37	-66.50
FT03	19.61	1.36	62.66	319.50	20.83	1.00	-67.83	-325.70
FT04	13.47	0.83	37.14	275.70	36.90	1.38	-134.98	-365.80
FT05	19.50	1.36	20.72	105.70	20.83	1.00	-22.43	-107.70
FT06	29.67	1.42	29.23	98.50	6.43	0.87	-4.29	-66.60
FT07	*	*	-145.41	159.60	51.11	0.71	-360.47	-705.30
FT08	*	*	-157.97	158.20	53.30	0.73	-372.97	-699.80
FT09	24.50	1.54	2.67	10.90	11.59	0.87	-0.95	-8.20

Presenter M3/Material | Date FINAL | Slide 23 of 34 | Closed

STS-107 Launch/Ascent

Orbiter Unit Load Indicators - Left Side

Indicator Name	Upper Side % of Limit	Upper Side Mach	Upper Side Nominal Load	Upper Side Limit	Lower Side % of Limit	Lower Side Mach	Lower Side Nominal Load	Lower Side Limit
FWOL-F1	1.5	1.95	46.94	3103.00	62.5	0.86	-1938.01	-3103.00
FWOL-F2	*	*	*	0.00	39.1	1.30	-5562.40	-14225.00
FWOL-F4	*	*	-488.32	3448.00	65.6	0.92	-2260.92	-3448.00
FWOL-F5	59.6	1.00	404.41	679.00	*	*	*	0.00
FWOL-F6	73.6	0.86	348.74	474.00	*	*	*	0.00
MIDL-M1	*	*	*	0.00	32.2	1.10	-4761.89	-14806.00
MIDL-M2	50.4	1.10	7783.51	15444.00	*	*	*	0.00
MIDL-M3	*	*	*	0.00	40.9	1.36	-2695.55	-6584.00
MIDL-M4	*	*	*	0.00	27.1	1.38	-1851.70	-6835.00
MIDL-M5	*	*	*	0.00	46.6	1.10	-3535.50	-7586.00
MIDL-M6	*	*	*	0.00	34.0	1.55	-2423.70	-7130.00
MIDL-M7	69.4	1.55	17905.80	25806.00	*	*	*	0.00
MIDL-M8	70.0	1.25	14527.50	20766.00	*	*	*	0.00
MIDL-M10	*	*	*	0.00	56.2	1.14	-23742.60	-42228.00
MIDL-M18	*	*	*	0.00	39.5	1.09	-4738.97	-12000.00
MIDL-M19	*	*	*	0.00	40.5	1.08	-2729.22	-6731.00
MIDL-M21	*	*	*	0.00	71.6	1.55	-4347.18	-6074.00
MIDL-M22	64.6	1.55	14255.10	22050.00	*	*	*	0.00
PBOL-D1	*	*	-16.42	356.00	44.9	1.05	-159.89	-356.00
PBOL-D2	8.7	0.80	33.73	387.00	33.8	1.05	-130.83	-387.00
PBOL-D3	33.0	1.08	108.94	330.00	24.0	0.80	-79.07	-330.00
PBOL-D5	85.8	1.10	15694.90	18296.00	*	*	*	0.00
WNGL-W11	*	*	*	0.00	49.9	1.25	-6473.27	-12978.00
WNGL-W12	*	*	-146.32	591.00	54.3	1.25	-320.67	-591.00
AFTL-A1	*	*	*	0.00	25.2	1.37	-956.00	-3798.00
AFTL-A2	*	*	*	0.00	60.4	1.54	-4037.63	-6689.00
AFTL-A4	61.0	1.25	11455.50	18783.00	*	*	*	0.00
AFTL-A7	*	*	*	0.00	29.3	1.51	-7960.54	-27136.00
AFTL-A8	*	*	*	0.00	*	*	179.42	-22134.00
VTLL-T3	22.7	1.37	37808.90	166550.00	*	*	374.08	-166550.00
VTLL-T4	33.3	1.37	4199.12	12604.00	11.6	1.00	-1457.09	-12604.00
VTLL-T8	12.6	1.00	1865.12	14790.00	28.6	1.37	-4232.75	-14790.00

Presenter M3/Material | Date FINAL | Slide 24 of 34 | Closed

STS-107 Launch/Ascent

Orbiter Unit Load Indicators - Right Side

Indicator Name	Upper Side				Lower Side			
	% of Limit	Mach	Nominal Load	Limit	% of Limit	Mach	Nominal Load	Limit
FWDR-F1	4.3	1.93	134.68	3103.00	63.4	0.90	-1966.52	-3103.00
FWDR-F2	*	*	*	0.00	49.4	1.25	-7026.49	-14225.00
FWDR-F4	*	*	-442.48	3448.00	64.3	0.96	-2217.18	-3448.00
FWDR-F5	59.3	1.03	402.89	679.00	*	*	*	0.00
FWDR-F6	77.3	0.90	366.39	474.00	*	*	*	0.00
MIDR-M1	*	*	*	0.00	27.8	1.10	-4121.60	-14806.00
MIDR-M2	54.1	1.10	8048.37	15444.00	*	*	*	0.00
MIDR-M3	*	*	*	0.00	38.4	1.25	-2539.99	-6584.00
MIDR-M4	*	*	*	0.00	14.6	1.37	-999.14	-6835.00
MIDR-M5	*	*	*	0.00	46.8	1.10	-3548.93	-7586.00
MIDR-M6	*	*	*	0.00	32.3	1.54	-2299.55	-7130.00
MIDR-M7	67.3	1.55	17378.30	25806.00	*	*	*	0.00
MIDR-M8	58.4	1.58	12123.40	20766.00	*	*	*	0.00
MIDR-M10	*	*	*	0.00	61.0	1.15	-25745.00	-42228.00
MIDR-M18	*	*	*	0.00	41.5	1.10	-4984.86	-12000.00
MIDR-M19	*	*	*	0.00	41.7	1.09	-2804.78	-6731.00
MIDR-M21	*	*	*	0.00	68.1	1.54	-4134.30	-6074.00
MIDR-M22	63.4	1.54	13974.90	22050.00	*	*	*	0.00
PBDR-D1	5.4	0.80	19.12	356.00	48.1	1.06	-171.11	-356.00
PBDR-D2	15.8	0.80	61.29	387.00	42.7	1.08	-165.31	-387.00
PBDR-D3	18.9	1.11	62.42	330.00	11.2	0.90	-37.02	-330.00
PBDR-D5	85.8	1.10	15694.90	18296.00	*	*	*	0.00
WNGR-W11	*	*	*	0.00	46.9	0.86	-6086.19	-12978.00
WNGR-W12	*	*	-148.29	591.00	49.4	0.88	-291.98	-591.00
AFTR-A1	*	*	*	0.00	16.7	1.30	-634.12	-3798.00
AFTR-A2	*	*	*	0.00	39.9	1.53	-4008.70	-6689.00
AFTR-A4	49.0	1.31	9195.42	18783.00	*	*	*	0.00
AFTR-A7	*	*	*	0.00	30.9	1.41	-8378.90	-27136.00
AFTR-A8	*	*	*	0.00	1.2	1.41	-254.92	-22134.00
VTLR-T3	42.8	1.27	71219.80	166550.00	*	*	275.09	-166550.00
VTLR-T4	11.6	1.00	1456.76	12604.00	33.3	1.37	-4200.59	-12604.00
VTLR-T8	28.6	1.37	4230.32	14790.00	12.6	1.00	-1865.55	-14790.00

Presenter M3/Material | Date FINAL | Slide 25 of 34 | Closed

STS-107 Launch/Ascent
SRB Actuator Angular Deflections

- **Background / Facts:** (cont.)
  - STS-107 Experience (SRB gimbal oscillations)
    - STS-107 accelerometers & SRB actuators show 0.6 Hz oscillation
    - All missions experience a 0.6 Hz frequency content
      - 0.6 Hz frequency due to LOX slosh and winds
      - Missions 2, 51, 53, 84, 85, 90, 97, & 101 experienced similar oscillations
    - Left & right rock and tilt actuator positions were compared to program experience, Performance Enhancement (PE) mission experience, PE analysis database, and design limits (see next four charts)

Presenter M3/Material | Date FINAL | Slide 26 of 34 | Closed

STS-107 Launch/Ascent
SRB Actuator Angular Deflections
SRB Left Tilt Actuator Position

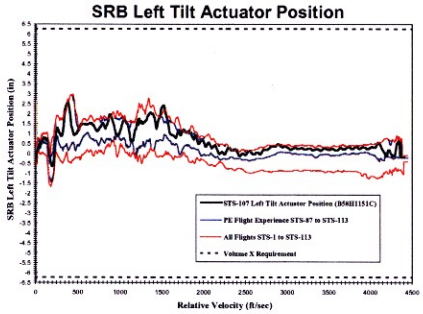

Presenter M3/Material | Date FINAL | Slide 27 of 34 | Closed

STS-107 Launch/Ascent
SRB Actuator Angular Deflections
SRB Left Rock Actuator Position

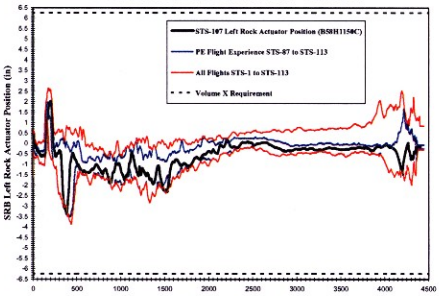

Presenter M3/Material | Date FINAL | Slide 28 of 34 | Closed

STS-107 Launch/Ascent
SRB Actuator Angular Deflections
SRB Right Tilt Actuator Position

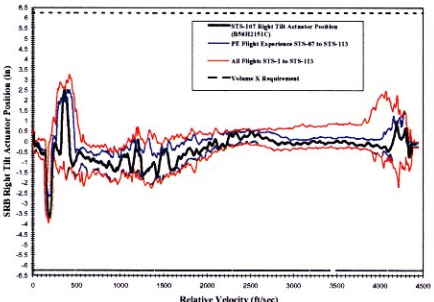

Presenter M3/Material | Date FINAL | Slide 29 of 34 | Closed

STS-107 Launch/Ascent
SRB Actuator Angular Deflections
SRB Right Rock Actuator Position

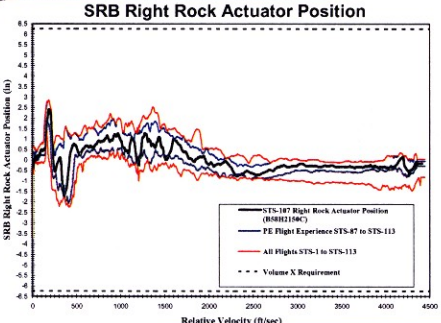

Presenter M3/Material | Date FINAL | Slide 30 of 34 | Closed

STS-107 Launch/Ascent

- **Findings:**
  - Out-of-experience events were within certification limits
  - Flight Control System operated as designed
  - During the wind shear event at MET = 57 sec, wind shears, sideslip (β) angle, SRB gimbal angles, SSME #3 gimbal angle, and observed & predicted left & right wing loads were all below design limits
    - All wing loads were ≤ 50% of design limits
  - Maximum attachment and orbiter body loads during entire ascent were below design limits
  - Wing instrumentation indicates more cycles on left vs. right wing
  - Left & right SRB rock and tilt actuator positions were within design limits
- **Recommendations:** None

Presenter M3/Material | Date FINAL | Slide 31 of 34 | Closed

STS-107 Launch/Ascent

- **Documentation:**
  - "STS-107 Natural Environments Data," Marshall Space Flight Center, Engineering Directorate, Environments Group, (ED44), 10 Feb 03
  - "DOLILU & Structural Loads," response to RFI B1-000123, 4 April 03
  - "STS-107 Integrated Ascent Timeline," 8 May 03
  - "STS-107 Flex Reconstructed Left Wing Unit Load Indicators, MADS Data, And Maximum Rigid Body Reconstructed Peaks For Previous OV-102 Flights Versus Variable Redline Limit," E Dougherty, 17 May 03
  - "STS-107 Flex Reconstructed Right Wing Unit Load Indicators, MADS Data, And Maximum Rigid Body Reconstructed Peaks For Previous OV-102 Flights Versus Variable Redline Limit," E Dougherty, 17 May 03
  - "RSRM Actuator responses During STS Missions," response to RFI B1-000170, file:
  - E-Mail from Rod Wallace, 3 June 03.

Presenter M3/Material | Date FINAL | Slide 32 of 34 | Closed

STS-107 Launch/Ascent
SSME-3 Pitch Gimbal Position @ SRB Tail-Off

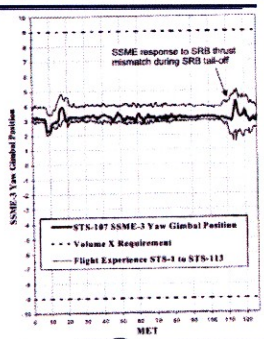

Presenter M3/Material | Date FINAL | Slide 33 of 34 | Closed

STS-107 Launch/Ascent
SRB Actuator Angular Deflections

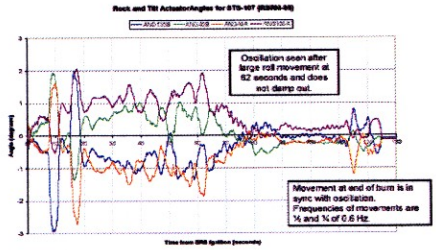

Presenter M3/Material | Date FINAL | Slide 34 of 34 | Closed

STS-107 OEX Ascent Data

- **Action / Issue:** Review STS-107 OEX ascent data for anomalies
- **Background / Facts:**
  - Ascent significant events included:
    - 60 seconds – wind shear occurred at Mach 1.37 at an altitude of approximately 32,000 Feet
    - 82 seconds – foam impacted orbiter wing at Mach 2.46 at an altitude of approximately 60,000 feet

Presenter M3/Material | Date FINAL | Slide 1 of 14 | Closed

STS-107 OEX Ascent Data

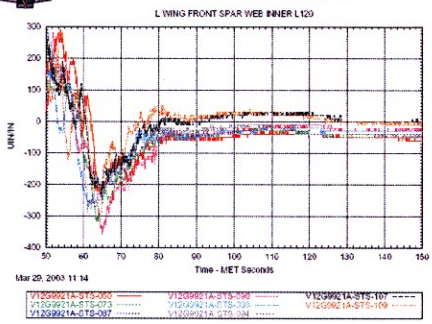

Strain gage on front spar behind RCC panel 9

Presenter M3/Material | Date FINAL | Slide 2 of 14 | Closed

STS-107 OEX Ascent Data

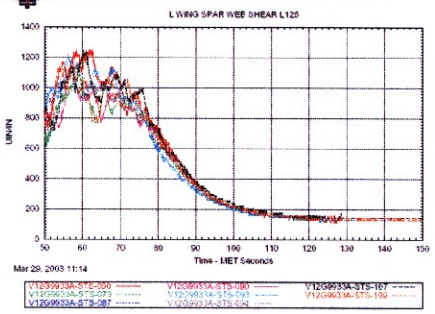

Strain gage on lower skin or spar at spar #3

Presenter M3/Material | Date FINAL | Slide 3 of 14 | Closed

STS-107 OEX Ascent Data

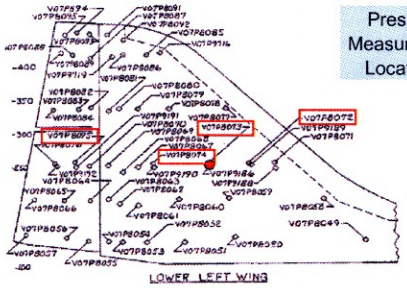

Pressure Measurement Locations

Presenter M3/Material | Date FINAL | Slide 4 of 14 | Closed

STS-107 OEX Ascent Data

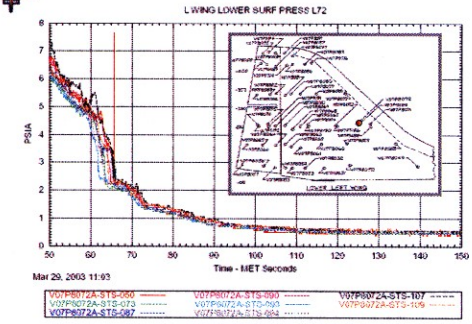

Presenter M3/Material | Date FINAL | Slide 5 of 14 | Closed

STS-107 OEX Ascent Data

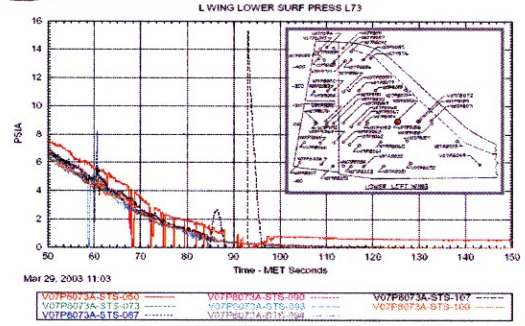

Presenter M3/Material | Date FINAL | Slide 6 of 14 | Closed

1

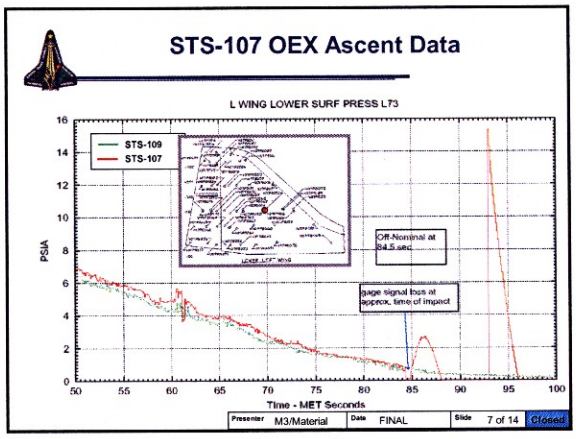
STS-107 OEX Ascent Data
L WING LOWER SURF PRESS L73
STS-109
STS-107
PSIA
Off-Nominal at 84.5 sec
Time - MET Seconds
Presenter M3/Material
Date FINAL
Slide 7 of 14
Closed

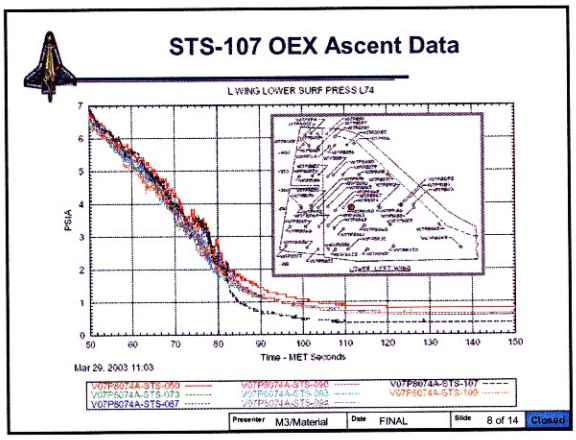
STS-107 OEX Ascent Data
L WING LOWER SURF PRESS L74
PSIA
Time - MET Seconds
Mar 29, 2003 11:03
Presenter M3/Material
Date FINAL
Slide 8 of 14
Closed

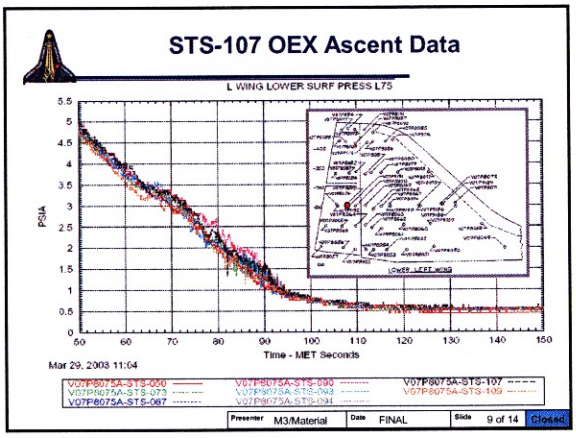
STS-107 OEX Ascent Data
L WING LOWER SURF PRESS L75
PSIA
Time - MET Seconds
Mar 29, 2003 11:04
Presenter M3/Material
Date FINAL
Slide 9 of 14
Closed

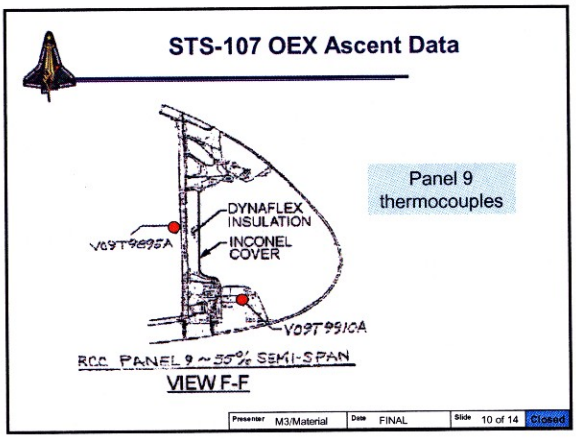
STS-107 OEX Ascent Data
DYNAFLEX INSULATION
INCONEL COVER
V09T9895A
V09T9910A
Panel 9 thermocouples
RCC PANEL 9 ~ 55% SEMI-SPAN
VIEW F-F
Presenter M3/Material
Date FINAL
Slide 10 of 14
Closed

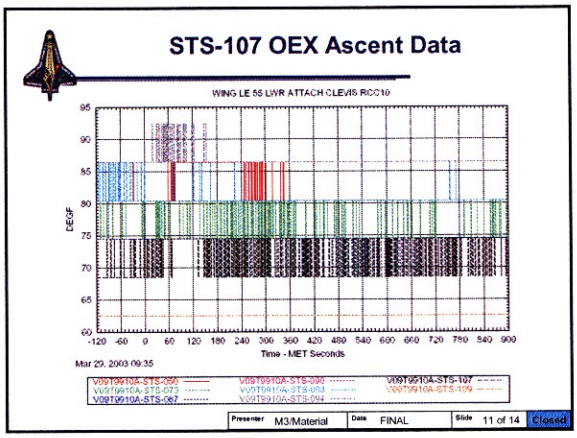
STS-107 OEX Ascent Data
WING LE 55 LWR ATTACH CLEVIS RCC10
DEGF
Time - MET Seconds
Mar 29, 2003 09:35
Presenter M3/Material
Date FINAL
Slide 11 of 14
Closed

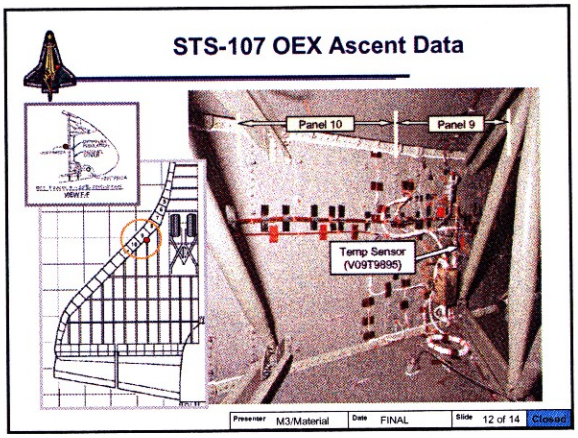
STS-107 OEX Ascent Data
Panel 10
Panel 9
Temp Sensor (V09T9895)
Presenter M3/Material
Date FINAL
Slide 12 of 14
Closed

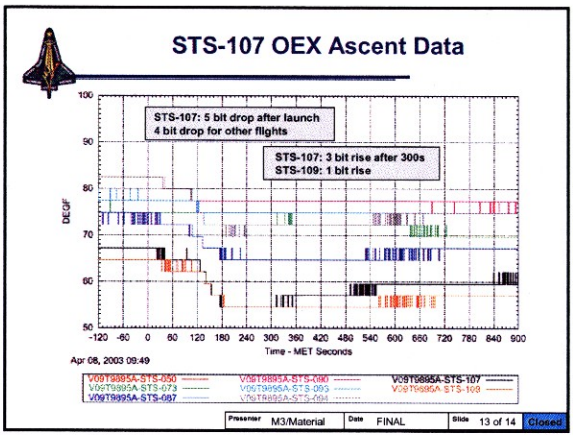
STS-107 OEX Ascent Data
STS-107: 5 bit drop after launch
4 bit drop for other flights
STS-107: 3 bit rise after 300s
STS-109: 1 bit rise
DEGF
100
90
80
70
60
50
-120 -60 0 60 120 180 240 300 360 420 480 540 600 660 720 780 840 900
Time - MET Seconds
Apr 08, 2003 09:49
V09T9895A-STS-050
V09T9895A-STS-073
V09T9895A-STS-087
V09T9895A-STS-090
V09T9895A-STS-095
V09T9895A-STS-107
V09T9895A-STS-109
Presenter M3/Material
Date FINAL
Slide 13 of 14
Closed

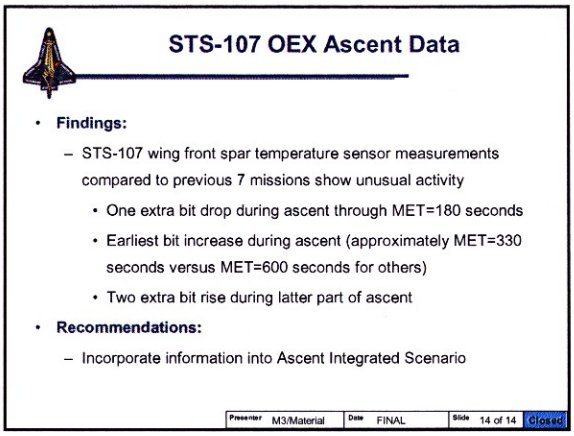
STS-107 OEX Ascent Data
• Findings:
– STS-107 wing front spar temperature sensor measurements compared to previous 7 missions show unusual activity
• One extra bit drop during ascent through MET=180 seconds
• Earliest bit increase during ascent (approximately MET=330 seconds versus MET=600 seconds for others)
• Two extra bit rise during latter part of ascent
• Recommendations:
– Incorporate information into Ascent Integrated Scenario
Presenter M3/Material
Date FINAL
Slide 14 of 14
Closed

Orbiter Entry

16-1 Effect of Roughness (Keq) on Orbiter Heat Load

16-2 Kapton Wiring

16-3 Premature Firing of Pyrotechnic Devices

Matrix

Presenter	CAIB/Group 1	Date	FINAL	Slide	19 of 32

Rough Wing Structural Issues

- **Action / Issue:**
  - Effect of Roughness (Keq) on Orbiter Heat Load
- **Background / Facts:**
  - Speculation that OV-102's wing was "rougher"—Keq nearly twice that of other orbiters
  - High Keq causes early transition to turbulent flow and greater heat load (hotter longer)
- **Findings:**
  - Found that OV-102 Keq similar to that of other orbiters
- **Recommendation:**
  - Continue to emphasize the importance of minimizing Keq

Presenter M3/Material | Date FINAL | Slide 1 of 7 | Closed

Boundary Layer Transition

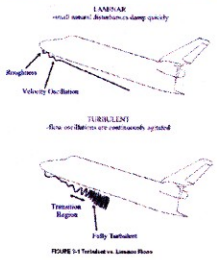

Presenter M3/Material | Date FINAL | Slide 2 of 7 | Closed

Step and Gap Measurement

- For an unfilled gap:
  s= step measured from low tile
  w= gap width

$Keq=((step)^2+(gap-0.045)^2)^{1/2}$

- For locations where the gap is 0.045" or less
  Keq=step

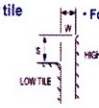

- For a gap filled with a gap filler or thermal barrier with a circular crown:
  s= step measured from low tile
  w= gap width
  d= recession from the low tile

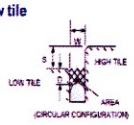

Presenter M3/Material | Date FINAL | Slide 3 of 7 | Closed

Measurement Locations

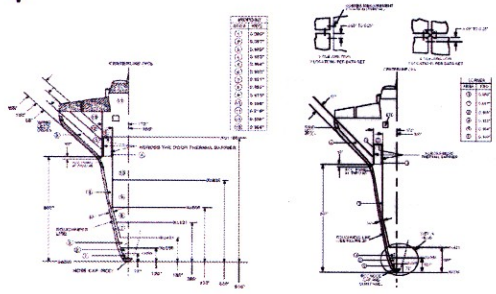

Presenter M3/Material | Date FINAL | Slide 4 of 7 | Closed

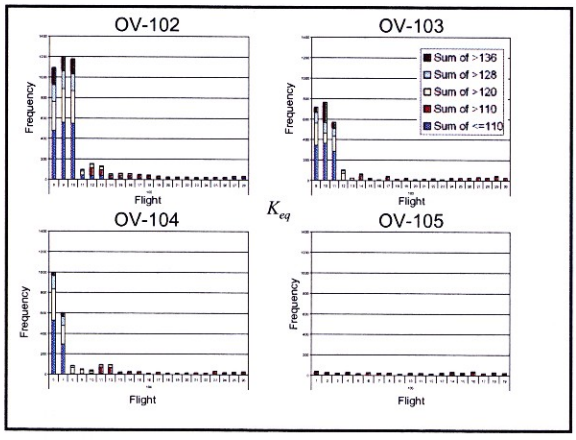

OV-102 Transition History

Flight	STS	X/l = 0.3	X/l = 0.6
8	28	1215	900
9	32	1210	1250
10	35	1225	1210
11	40	1200	1220
12	50	1300	1200
13	52	1230	1240
14	55	1068	1068
15	58	1260	1142
16	62	1214	1207
17	65		
18	73	1021	893
19	75	1260	1260
20	78		1261
21	80	1233	1233
22	83		
23	94	1040	1040
24	87	1281	1234
25	90	1186	1047
26	93	1328	1276
27	109		1199
28	107		
OV-102 Average		1204	1160
Fleet Average		1190	1173

Transition time from Entry Interface (sec.)

Presenter M3/Material | Date FINAL | Slide 6 of 7 | Closed

1

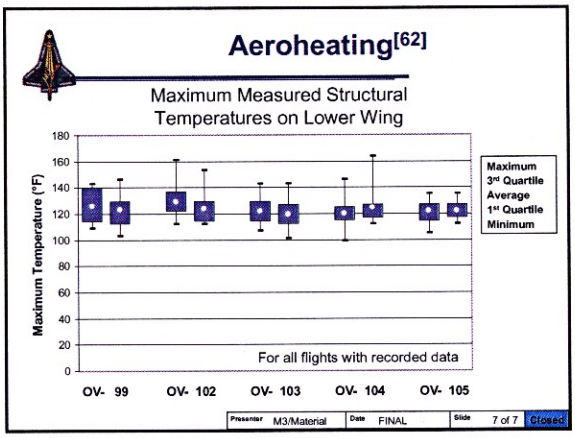
Aeroheating[62]
Maximum Measured Structural Temperatures on Lower Wing
Maximum Temperature (°F)
180
160
140
120
100
80
60
40
20
0
Maximum
3rd Quartile
Average
1st Quartile
Minimum
For all flights with recorded data
OV- 99
OV- 102
OV- 103
OV- 104
OV- 105
Presenter M3/Material
Date FINAL
Slide 7 of 7
Closed

Fire (Pyro /Wiring / etc.) Kapton Wiring as Causal

- **Action / Issue:** Assess Kapton wiring as a fire/explosion risk to OV-102/STS-107.
- **Background / Facts:**
  - Kapton insulation proven to degrade under certain conditions
  - Insulation degradation leads to risk of shorting between wires
    - "Arc tracking" along length of wire
    - Arcing can damage adjacent wires
- **Findings:**
  - In-depth inspection of OV-102 during J3 OMM (Sep 99 – Mar 01) identified/corrected numerous nonconformances (nearly 5,000)
    - Prompted by damaged insulation/shorted wire/loss of power to two of six main engine controller computers during STS-93 (Jul 99)
  - OV-102 inspection results formed a good baseline for subsequent studies/development of preventive measures
    - Most common cause: work-induced, either during inspection/maintenance
    - Other causes: improper installation (routing/securing) during manufacture; moisture intrusion, chemical spillage

Presenter M3/Maintenance | Date FINAL | Slide 1 of 4 | Closed

Fire (Pyro /Wiring / etc.) Internal Hazard

- **Findings (con't.):**
  - Despite numerous ongoing studies of alternate insulators, Kapton still viewed as a leading candidate
    - Various reasons: Kapton does not burn, but carbonizes at approx 650 degrees C; also lightweight, durable
  - Telemetry from OV-102's last minutes prior to breakup does not point to Kapton wiring as causal
    - Data from 14 left wing sensors analyzed: hydraulic line/wing skin/ wheel temperatures, tire pressure, & landing gear downlock position
    - Sensor failure signatures consistent with leading causal scenario of left wing thermal intrusion, NOT with Kapton-associated failure
  - Actual/extensive NASA testing immediately following Columbia tragedy verified failure signature analyses
    - Kapton wiring subjected to oven, blowtorch, and arc jet heating
  - Testing/analysis for years prior to STS-107 showed Kapton wiring w/low voltages & low currents associated with orbiter instrumentation (such as in the left wing) have a very low probability of arc tracking

Presenter M3/Maintenance | Date FINAL | Slide 2 of 4 | Closed

Fire (Pyro /Wiring / etc.) Internal Hazard

- **Conclusions:**
  - Based on extensive wiring inspections/maintenance/modifications to OV-102 prior to STS-107, analysis of sensor/wiring failure signatures, physical verification of those signatures, and prior Kapton wiring studies, Kapton's role as causal to Columbia's loss is highly unlikely
- **Recommendations:**
  - Inspection of remainder of fleet planned/being executed
    - Partial inspection completed on all orbiters during initial grounding
    - Complete inspection to occur during respective OMMs
      - -- OV-103 currently in progress with expected completion in Apr 04
      - -- OV-105 to be completed in 04 (input date accelerated to summer 03)
    - OV-104 must be fully inspected as soon as possible

Presenter M3/Maintenance | Date FINAL | Slide 3 of 4 | Closed

Fire (Pyro /Wiring / etc.) Internal Hazard

FLEET WIRE INSPECTION & REPAIR SUMMARY

Presenter: Doug White
Organization/Date: Orbiter/11-2-99

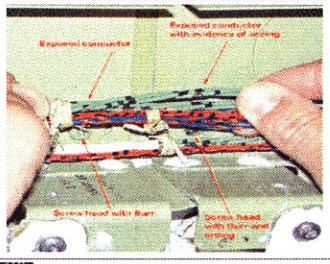

BOEING 3 USA

Presenter M3/Maintenance | Date FINAL | Slide 4 of 4 | Closed

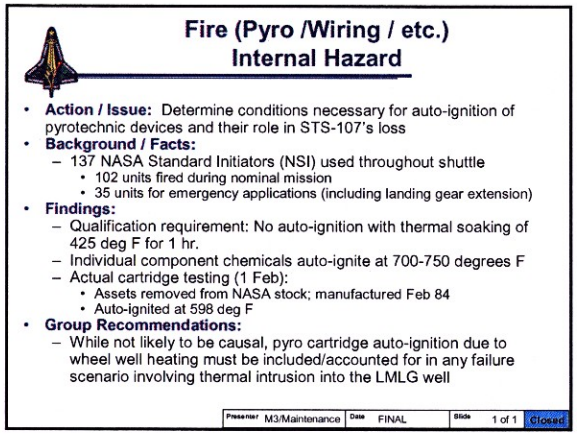

Fire (Pyro /Wiring / etc.) Internal Hazard

- **Action / Issue:** Determine conditions necessary for auto-ignition of pyrotechnic devices and their role in STS-107's loss
- **Background / Facts:**
  - 137 NASA Standard Initiators (NSI) used throughout shuttle
    - 102 units fired during nominal mission
    - 35 units for emergency applications (including landing gear extension)
- **Findings:**
  - Qualification requirement: No auto-ignition with thermal soaking of 425 deg F for 1 hr.
  - Individual component chemicals auto-ignite at 700-750 degrees F
  - Actual cartridge testing (1 Feb):
    - Assets removed from NASA stock; manufactured Feb 84
    - Auto-ignited at 598 deg F
- **Group Recommendations:**
  - While not likely to be causal, pyro cartridge auto-ignition due to wheel well heating must be included/accounted for in any failure scenario involving thermal intrusion into the LMLG well

Presenter: M3/Maintenance	Date: FINAL	Slide: 1 of 1	Closed

Other
Design – Certification

17-1 SRB ET Attach Ring Structure Factor of Safety

Matrix

Presenter	CAIB/Group 1	Date	FINAL	Slide	20 of 32

SRB ETA Ring

- **Action / Issue:** SRB ET attach (ETA) ring has reduced properties
- **Background / Facts:**
  - Recent material testing discovered strength values less than the design requirement
    - Minimum requirement is 180 ksi
    - Lowest value from 2 S/Ns is 144 and 150 ksi
  - Issue presented during ET tanking meeting on 16 Jan 03
  - SSP CR S091496 approved on 16 Jan 03
    - Waived the factor of safety requirement of 1.4, accepted 1.25
    - No full technical review prior to launch of STS-107
  - ETA design life is 40 missions (inspection interval is 13 missions), STS-107 ETA rings:
    - Left: S/N 19, 9 flights prior to launch
    - Right: S/N 6, 12 flights prior to launch

Presenter M3/Material | Date FINAL | Slide 1 of 12 | Closed

SRB ETA Ring

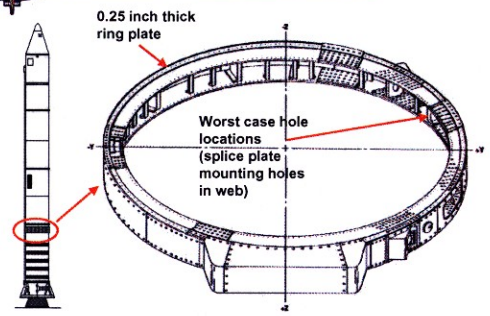

Presenter M3/Material | Date FINAL | Slide 2 of 12 | Closed

SRB ETA Ring

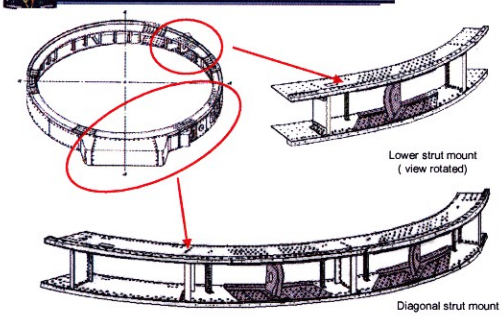

Presenter M3/Material | Date FINAL | Slide 3 of 12 | Closed

SRB ETA Ring

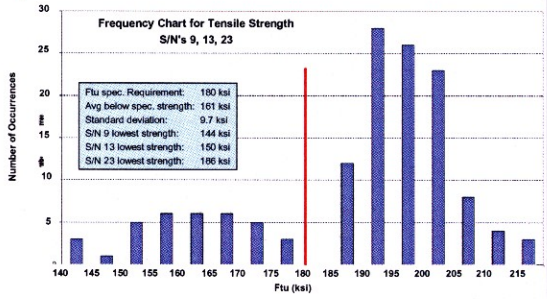

Presenter M3/Material | Date FINAL | Slide 4 of 12 | Closed

SRB ETA Ring

- **Background / Facts :**
  - STS-107 strength analysis performed using 147 ksi
    - Factor of safety reduced to 1.25 (ET tanking meeting value)
  - MSFC recommended using 136 ksi based on metallurgical assessment in March 2003
    - Factor of safety reduced to 1.16
  - Below design minimum thickness measured on 7 ETA rings in March 2003
  - Strength analysis being revised accounting for hardness test results correlated to strength and actual part thickness
    - Both the current analysis method (linear material properties) and non-linear analysis methods are being utilized

Presenter M3/Material | Date FINAL | Slide 5 of 12 | Closed

SRB ETA Ring

- **Background / Facts :**
  - Non-linear analysis method (takes advantage of entire material stress-strain response) to determine ultimate strength capability validated by test of specimen shown below
  - Good correlation between predicted and measured strains and failure load was obtained

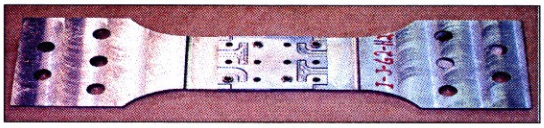

Presenter M3/Material | Date FINAL | Slide 6 of 12 | Closed

SRB ETA Ring

#	ETA Ring Area (same areas apply on fwd & aft web plates)	Ftu = 147 ksi (STS-107 Waiver) Linear analysis with Modulus of Rupture Factor of Safety	Ftu = 136 ksi Linear analysis with Modulus of Rupture Factor of Safety	Ftu = 136 ksi Non-linear analysis using Material Stress-Strain Curve Factor of Safety
1	W-131-W132	1.38	1.27	
2	W239-W240	1.36	1.26	
3	W248-W250	1.27	1.16	1.65
4	W200	> 1.40	1.35	
5	W208		1.31	
6	W260		1.29	
7	W41		1.30 (D-Holes)	

Summary of Original, Revised and Current Strength Analysis

Presenter M3/Material | Date FINAL | Slide 7 of 12 | Closed

SRB ETA Ring

- **Background / Facts :**
  - Total quantify of SRB ETA rings is 17
  - 9 rings were readily available for hardness and thickness measurements (the others require some level of disassembly) and have been completed
    - S/Ns: 5, 6, 9, 15, 16, 19, 22, 24, and 27
  - Strength analysis performed using linear analysis (more conservative) and actual hardness and thickness results
    - S/N 16 has a region with a factor of safety less than 1.4 and a region with low hardness results
    - The other 8 S/Ns have a minimum factor of safety > 1.4
    - S/N 15 has a couple of regions with marginal hardness results
  - All rings have factor of safety > 1.4 using non-linear analysis method
  - 9 rings have completed NDE in the critical regions
  - All rings will undergo a complete re-baselining NDE, S/Ns 9 and 24 are in-work to support first return to flight

Presenter M3/Material | Date FINAL | Slide 8 of 12 | Closed

SRB ETA Ring

No.	ETA Ring Serial No.		Critical Zone 1 FOS	Critical Zone 2 FOS	Critical Zone 3 FOS	Critical Zone 4 FOS	Critical Zone 5 FOS	Critical Zone 6 FOS	Critical Zone 7 FOS
1	S/N 09	Fwd	1.53	1.63	1.55	1.68	1.68	1.84	1.83
		Aft	1.45	1.64	1.62	1.60	1.56	1.66	N/A
2	S/N 24	Fwd	1.65	1.67	1.63	1.65	1.70	1.66	1.67
		Aft	1.63	1.53	1.48	1.58	1.72	1.71	N/A
3	S/N 05	Fwd	1.56	1.61	1.57	1.61	1.65	1.66	1.68
		Aft	1.59	1.57	1.59	1.65	1.76	1.65	N/A
4	S/N 22	Fwd	1.59	1.62	1.61	1.70	1.62	1.66	1.67
		Aft	1.75	1.63	1.64	1.65	1.87	1.72	N/A
5	S/N 16	Fwd	TBD						
		Aft							
6	S/N 27	Fwd	1.69	1.67	1.61	1.64	1.67	1.53	N/A
		Aft	1.65	1.59	1.57	1.62	1.65	1.69	N/A
7	S/N 15	Fwd	1.55	1.76	1.68	1.41	1.50	1.70	1.65
		Aft	1.41	1.72	1.69	1.42	1.65	1.68	N/A
8	S/N 6	Fwd	1.63	1.65	1.62	1.66	1.62	1.72	1.78
		Aft	1.65	1.59	1.65	1.61	1.71	1.73	N/A
9	S/N 19	Fwd	1.72	1.65	1.62	1.66	1.69	1.47	1.75
		Aft	1.71	1.68	1.66	1.77	1.70	1.70	N/A

Presenter M3/Material | Date FINAL | Slide 9 of 12 | Closed

SRB ETA Ring

- **Background / Facts :**
  - NASA's short-term plan:
    - Complete NDE on 9 uninstalled rings
    - Uninstall the remaining 8 rings and perform hardness and thickness measurements and NDE
  - NASA's long-term plan:
    - Replace ring web plates with new material or material that meets specification and proper thickness
    - Implementation plans have not been approved by the program

Presenter M3/Material | Date FINAL | Slide 10 of 12 | Closed

SRB ETA Ring
Category: Other Significant Finding

- **Findings:**
  - Short-term plan to include hardness and thickness measurements and NDE of the 8 remaining rings is adequate
  - 7 of the 9 rings measured to date appear to be adequate for limited use
  - Long-term plan is the best approach, funding and implementation schedule has not been authorized by the program
- **Recommendations:**
  - Don't use S/N 16 and 15 in their present condition
  - Accelerate implementation of long-term plan

Presenter M3/Material | Date FINAL | Slide 11 of 12 | Closed

SRB ETA Ring

- **Documentation:**
  - PCRB briefing, "SRB External Tank Attach Ring Status", June 5, 2003
  - MSFC/ED33 document, "Strength and Safe-Life Parameters for 4130 ET Attach Ring", 28 May 2003
  - Briefing by D. Martin, "SRB External Tank Attach Ring"; Action CAIB-NAIT-00154, B1-00153, 14 April 2003
  - Briefing by P. Gutierrez, "SRB External Tank Attach Ring Program Requirements Control Board", 26 March 2003
  - SRB ETA Ring Factor of Safety Change Request, 28 Jan 03
  - Briefing by R. Elliott, "STS-107 (BI116) ET Tanking Meeting Program – Solid Rocket Booster", 16 January 2003

Presenter M3/Material | Date FINAL | Slide 12 of 12 | Closed

Other Production

18-1 Maintaining Critical Technical Knowledge

18-2 S&MA Quality Assurance Organization

18-3 USA/NASA FOD Prevention Programs

18-5 Capabilities Analysis

Matrix

Presenter	CAIB/Group 1	Date	FINAL	Slide	21 of 32

Maintenance Turnaround Work Other

- **Action / Issue:** Active maintenance of critical technical institutional knowledge and know-how
- **Background / Facts:**
  - Aging workforce working on an aging fleet
- **Findings:**
  - USA has training program to grow workforce with expertise levels commensurate with training and experience
  - Available technical expertise for sustaining NASA QA technicians
    - Continuing education and training
  - Training challenges for existing workforce to adapt to new inspection and maintenance requirements
  - Impact of contractor culture, NASA culture
- **Group Recommendations:**
  - NASA should continue to monitor critical personnel issues

Presenter: M3/Maintenance | Date: FINAL | Slide: 1 of 7 | Closed

USA Proprietary Information Not for Release

USA Age Distribution

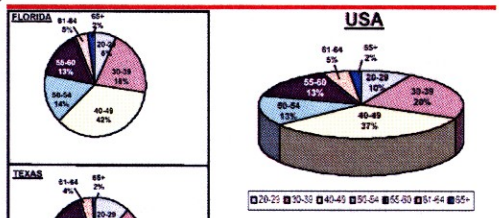

	USA	Texas	Florida
Headcount	10090	3539	6151
Average Age	45.3	43.3	46.6

1996 – 44.1 ⟶ 2002 – 45.3

Presenter: M3/Maintenance | Date: FINAL | Slide: 2 of 7 | Closed

USA Proprietary Information Not for Release

Workforce Aging

LENGTH OF SERVICE

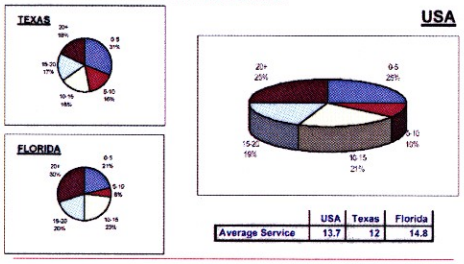

	USA	Texas	Florida
Average Service	13.7	12	14.8

Presenter: M3/Maintenance | Date: FINAL | Slide: 3 of 7 | Closed

USA Proprietary Information Not for Release

Engineer Aging

USA Engineer Process Age Trends

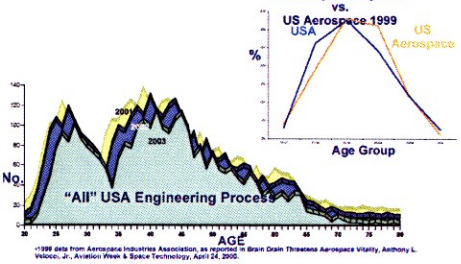

Presenter: M3/Maintenance | Date: FINAL | Slide: 4 of 7 | Closed

USA Proprietary Information Not for Release

Attrition in USA

USA Attrition Remains Below Industry

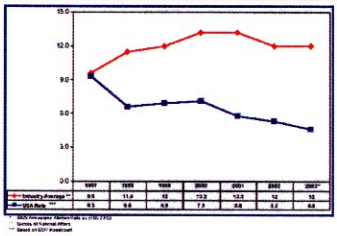

Presenter: M3/Maintenance | Date: FINAL | Slide: 5 of 7 | Closed

USA Proprietary Information Not for Release

USA Sources of Staffing

Hiring Sources

- Aerospace Companies - 50%
  - Lockheed
  - Raytheon
  - ITT
  - Northrop Grumman
  - Boeing
  - Honeywell
  - OSC
  - General Dynamics
- Non Aerospace Companies - 30%
  - Siemens
  - Harris Corporation
  - General Electrics
  - Booz Allen
  - Compaq
  - Petro Chemical Industry
- Recent Grads - 20%
  - Florida
  - Texas

15% Relocation

Presenter: M3/Maintenance | Date: FINAL | Slide: 6 of 7 | Closed

1

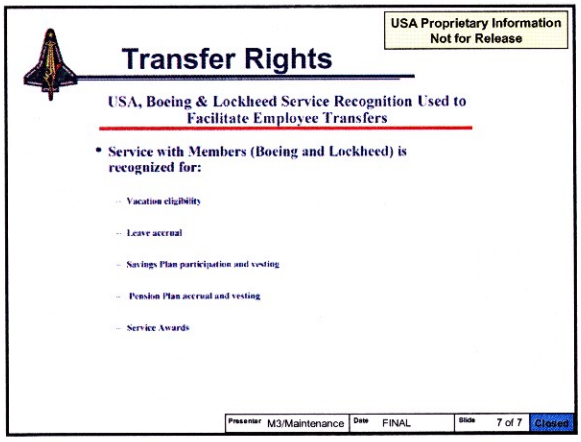
USA Proprietary Information
Not for Release
Transfer Rights
USA, Boeing & Lockheed Service Recognition Used to Facilitate Employee Transfers
• Service with Members (Boeing and Lockheed) is recognized for:
– Vacation eligibility
– Leave accrual
– Savings Plan participation and vesting
– Pension Plan accrual and vesting
– Service Awards
Presenter M3/Maintenance
Date FINAL
Slide 7 of 7
Closed

Maintenance
Safety & Mission Assurance

- **Action / Issue:** NASA/USA's Safety & Mission Assurance has had significant changes in workforce & inspection methodology
- **Background / Facts:**
  - Sufficiency of Government Mandated Inspection Points (GMIPs) was questionable by numerous testimonies
    - KSC GMIPs reduced from 44,000 in 89' to 22,500 in 96' to 8,500 now
- **Observations and interview information:**
  - Need thorough review of quality program requirements (doing non-value added looks but not some critical items – e.g., hydraulic pump installation, mating of SRBs)
  - Penny wise and pound foolish? (batteries, lights, inspection mirror tools)
  - Yielding to contractor (FOD definition, schedule, nonexistent unscheduled surveillance)
  - Unsupportive quality program management at KSC (instances of having to go to NASA HQ for resolution); dysfunctional organization of "camps"

Presenter: M3/Maintenance | Date: FINAL | Slide: 1 of 6 | Closed

Maintenance
Safety & Mission Assurance

- **Observations and interview information**
  - Abundance of "fly as is" dispositions
  - Government inspector hiring eval needed (DCMA and NASA PDs)
  - Disgruntled employees at MAF
  - Safety and security consistently rated strong
  - Potentially too few government inspectors
- **Findings:**
  - Quality assurance done by S&MA, SQ&MA and some engineering
  - QA's role in process improvement through interpretative trend analysis of PRACA and the Integrated Quality Support database is inconsistent and not integrated between the players
  - NASA inspectors inconsistently use the Hex or reject stamp for jobs closed out by SQ&MA (testimony given to CAIB staff)
    - Consequently, NASA S&MA has no means of tracking/trending for use as evaluation tool for personnel training and assessment

Presenter: M3/Maintenance | Date: FINAL | Slide: 2 of 6 | Closed

Maintenance
Safety & Mission Assurance

Government inspections ...

Spread thin (even for few GMIPs)	Reduced GMIPs
Flow delays waiting for inspectors	Reduced coverage (3 in OPFs?)
Contractor Pressure to inspect	Nothing other than GMIPs
Contract incentives to meet dates	Zero surveillance
Adversarial conditions	Reliance on "diving catches"

Underscored by SIAT and other recommendations

Presenter: M3/Maintenance | Date: FINAL | Slide: 3 of 6 | Closed

Maintenance
Safety & Mission Assurance

- **Findings:**
  - NASA involvement beyond GMIPs is very limited. Sampling of routine or non-critical tasks not formally done
  - GMIPs review process is ad hoc with no regular methodology for review of historic data to adjust QA emphasis
  - S&MA manning levels dropped due to retirements and moves to engineering posts without replacement
- **Interviews:**
  - KSC – with additional quality inspectors (several suggested by previous interviewees), and the head and deputy of the quality program
  - MAF -- with additional quality inspectors (several suggested by previous interviewees)

Presenter: M3/Maintenance | Date: FINAL | Slide: 4 of 6 | Closed

Maintenance
Safety & Mission Assurance

- **Reviews**
  - Contract regarding items such as FOD, engaging NASA inspectors during the flow
  - Facility upkeep and needs
  - Quality Planning Requirements Document
  - Quality inspector PDs
  - Past reports observations & recommendations (e.g., SIAT, Rogers, ASAP, GAO)
- **Recommendations:**
  - Independently-led bottom-up review of QPRD at KSC and MAF with intent to validate adequacy of oversight in terms of # of GMIPs, scope of authority outside the enumerated GMIPs and manpower
  - Add tasks to GMIPs that evaluate hardware and housekeeping
  - Build a regular review process to evaluate assurance program to provide trend analysis data, for training and inspection targeting

Presenter: M3/Maintenance | Date: FINAL | Slide: 5 of 6 | Closed

Maintenance
Safety & Mission Assurance

- **Recommendations:**
  - Broaden S&MA inspections to include statistically-driven sampling of all maintenance-related processes
    - Should go beyond GMIPs specific events to validate USA Quality inspection results and verify work quality before close out
    - Include a process to sample/validate documentation of maintenance for completion of the tasks and adequacy of the audit trail
  - Validate S&MA workforce is adequately sized and manned to accomplish it's mission to enforce quality and safety
  - Implement the NNBE "model for compliance verification"
  - Return to past closed loop discrepancy system
  - Return to true FOD definition, enforce "clean as you go" program
  - Ensure no closeout work can be done by a single person alone (e.g., foam spraying)
  - Allow employees to accomplish the duties in their PDs (!)
  - NASA Code Q examination of safety specialist manning and responsibilities at KSC (in relation to USA safety)

Presenter: M3/Maintenance | Date: FINAL | Slide: 6 of 6 | Closed

1

Maintenance
FOD Policy

- **Action / Issue:** USA / NASA Foreign Object Damage (FOD) Prevention Programs Require Evaluation
- **Background / Facts:**
  - USA program consists of daily debris walk-downs by management, workers "clean as you go," and statistically-based process sampling
  - 23 separate checks of launch pad complex from pre- to post-launch accomplished in varying levels of detail by various organizations
  - USA FOD prevention metrics differentiate "FOD" and "process debris"
    - "FOD" -- After job is stamped
    - "Processing Debris" -- Before job signoff or end of shift
      - No other NASA contractor uses this category
- **Findings:**
  - FOD prevention is highly emphasized in USA/NASA daily operations
  - Assessment of responsibility is delineated: S&MA (NASA) responsible for FOD and SQ&MA (USA) primarily responsible for Process Debris

Presenter: M3/Maintenance | Date: FINAL | Slide: 1 of 6 | Closed

Maintenance
FOD Policy

- NASA inspects and assesses FOD failures only after USA has closed a WAD
- "FOD" is an industry standard term – basis for prevention programs and immediately recognized as critical part of prevention
- Commonly expressed opinion: FOD was redefined to accommodate SFOC award fee determination
- FOD and Process Debris are "feeder" metrics that are rolled up into the TMR's scoring for inclusion in the SFOC award calculation.
  - First half FY 03 performance assessment: the "good" FOD rate canceled out the moderate Process Debris rate
  - Unique effect of splitting FOD into two metrics
  - Second half FY 02: 2nd straight poor performance in both categories, award fee impact minimal, received highest score ever in roll up
- FOD found on launch pad is a direct award fee impact

Presenter: M3/Maintenance | Date: FINAL | Slide: 2 of 6 | Closed

Maintenance
FOD Policy

- **Recommendations:**
  - Greater NASA involvement in FOD program beyond GMIPs or occasional process sampling may improve program emphasis
  - NASA's role regarding the FOD program should be evaluated for expansion of inspector involvement, and expansion of inspections
  - Add random "Process Surveillance" of all processes, including FOD prevention
  - Eliminate alternative definitions of FOD
    - Could be interpreted as diminishing significance
    - Eliminate lines that separate NASA and USA quality assurance by authority over FOD prevention
  - Realign Award fee algorithm to increase FOD impact

Presenter: M3/Maintenance | Date: FINAL | Slide: 3 of 6 | Closed

Maintenance
FOD Policy

Process Debris Statistics

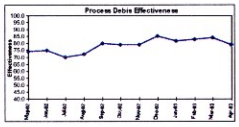

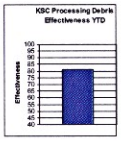

# of Reports	648	486	548	536	437	487	337	424	343	387	373
# Debris Free Reports	457	343	382	406	348	365	331	347	294	349	297
# of Debris Findings	171	113	166	130	87	102	99	77	73	73	76
Ineffectiveness	74	75	70	72	80	79	79	82	83	84	79
Process Debris Rate	25.9%	25.1%	30.0%	28.1%	20.4%	20.9%	21.1%	14.8%	18.2%	17.1%	16.1%	20.9%

Presenter: M3/Maintenance | Date: FINAL | Slide: 4 of 6 | Closed

Maintenance
FOD Policy

FOD Statistics

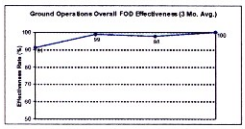

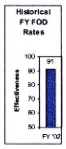

		FY '02						FY '03					
		APR - JUN			JLY - SEP			OCT - DEC			JAN - MAR		
# of Closeout Inspections		205			172			83			60		
# FOD Free Closeouts		187			170			81			60		
		APR	MAY	JUN	JLY	AUG	SEP	OCT	NOV	DEC	JAN	FEB	MAR
STS 107	# INSPECTIONS	21	45	48	1	1	0	3	8	9	6	0	
	# FOD FREE	18	36	42	1	1	0	3	8	9	6	0	
STS 114	# INSPECTIONS	0	1	4	0	0	0	0	1	10	38	1	
	# FOD FREE	0	1	4	0	0	0	0	1	10	38	1	
OTHER	# INSPECTIONS	34	23	29	52	42	76	28	21	3	2	13	
	# FOD FREE	34	23	29	52	41	75	27	20	3	2	13	

Presenter: M3/Maintenance | Date: FINAL | Slide: 5 of 6 | Closed

Maintenance
FOD Policy

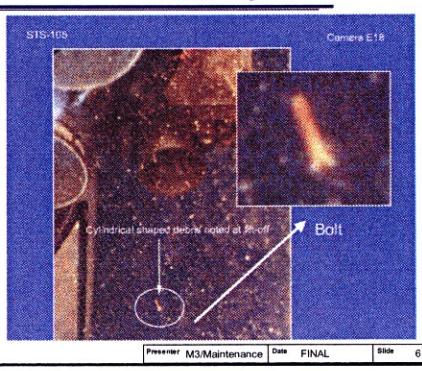

Presenter: M3/Maintenance | Date: FINAL | Slide: 6 of 6 | Closed

Maintenance Capabilities Analysis

- **Action / Issue:**
  - Do NASA/USA ground operations managers routinely assess their capability to support the launch schedule?
    - Do they have the tools to identify when they are approaching (or exceeding) the "ragged edge"?
    - At what point does a launch schedule become unsupportable from a ground processing viewpoint?
- **Background / Facts:**
  - Six launches originally planned for FY02/03; 4 more in FY04/1&2Q
    - Compare with 8 in FY 91/7 in FY 92
  - SSP combined workforce (NASA/USA) at KSC totals 4,400 today
    - Compare with 8,900 in FY 91/8,400 in FY 92
  - A professional, high-tech workforce (both white- and blue-collar) is typically not easily expanded to respond to fluctuating requirements

Presenter: M3/Maintenance | Date: FINAL | Slide: 1 of 13 | Closed

Maintenance Capabilities Analysis

- **Findings:**
  - Workload variations driven by numerous factors
    - Vehicle age, modifications, mission requirements, etc.
  - One example: OV-103, currently 8 months into J3 OMM
    - 28 percent growth over original tile replacement projections
    - 11.5 percent tile growth over original projected man hours
    - Potential additional tile growth ranges from 7 to 24 percent
      - From original 82,522 to 111,892 man hours
  - Second example: TPSF ("tile backshop")
    - Currently supporting OV-103 OMM, OV-104 flow
    - Test tile production (CAIB support) increasing rqmt by 473%
      - Mar – May 03: 128 originally projected, 606 now required

Presenter: M3/Maintenance | Date: FINAL | Slide: 2 of 13 | Closed

Maintenance Capabilities Analysis

- **Findings (cont'd):**
  - Both Orbiter Operations (OPF) and Integrated Logistics (TPSF) are assessing capabilities against requirements
    - Briefed at 1 May OV-103 OMDP Program Management Review
    - Presented various options to potential increases in requirements
      - Work employees longer, augment work force with additional manpower, slip delivery schedule
      - For TPSF, additional options included:
        - Reactivating Palmdale tile shop to produce test tiles
        - Augmenting KSC with Palmdale technicians
    - Both capability assessment efforts in a fledgling state
      - Represent efforts to communicate workforce constraints and mitigation options to higher management levels

Presenter: M3/Maintenance | Date: FINAL | Slide: 3 of 13 | Closed

Maintenance Capabilities Analysis

- **Findings (cont'd):**
  - Ground Operations managers also "plowing new ground" with capability assessments using "equivalent flow" (EF) model
    - Based on OPF standard flow of 315,000 man hours
    - Total (OPF/ET/Booster/Integration) of 525,000 man hours
    - OMM baseline being developed using OV-103
      - 700,000 man hours estimated
    - Adjustments made based on OMM/flow content
    - EF capabilities being applied against launch schedule (manifest) to determine shortfalls
      - Original FY 03/04 manifest exceeded EF capability by as much as 64%
      - Managers envision being able to level "peaks" and fill in "valleys"
      - Managers using EF capabilities to develop mitigation plans
      - Key question: How flexible can/will the launch schedule be?

Presenter: M3/Maintenance | Date: FINAL | Slide: 4 of 13 | Closed

Maintenance Capabilities Analysis

- **Findings (cont'd):**
  - What if the launch schedule is inflexible?
    - Work longer hours, increase workforce size, or adjust milestones internal to the processing flow
  - Longer hours bring well-recognized concerns
    - Potential for increased mistakes, injuries, higher costs
  - The workforce has been "leaned out" by 50 percent since 91
    - While more efficient than ever, surge capability is primarily thru overtime
    - Increasing the size of a professional, high-tech work force is not quick
    - Tile technician (OPF): approx 1 year necessary to work independently, longer until fully qualified
    - Tile technician (back shop): approx 3-months necessary to work independently, 3-5 years until fully qualified
  - Management must have the ability to routinely/accurately forecast capabilities, compare against requirements, and have sufficient lead time to take mitigating actions

Presenter: M3/Maintenance | Date: FINAL | Slide: 5 of 13 | Closed

Maintenance Capabilities Analysis

- **Recommendations:**
  - Ground Operations managers have been developing a complement of tools in recent years to do capability assessment modeling
    - They should expedite efforts to refine these models (e.g., the equivalent flow model) and use the results to take proper action(s) when requirements exceed capabilities
  - Managers need to develop sufficient confidence in capability assessments to use them in manifest and resource planning

Presenter: M3/Maintenance | Date: FINAL | Slide: 6 of 13 | Closed

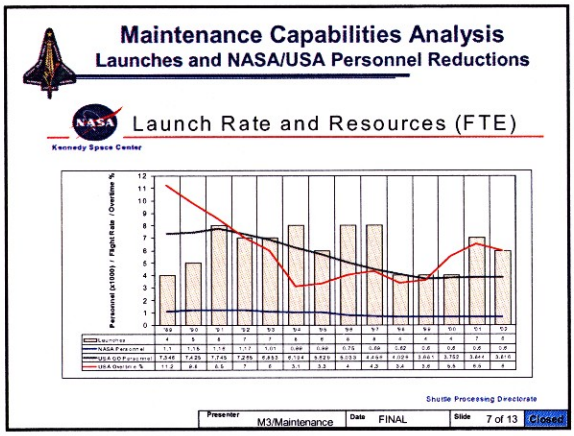
Maintenance Capabilities Analysis
Launches and NASA/USA Personnel Reductions
Launch Rate and Resources (FTE)
Kennedy Space Center
Shuttle Processing Directorate
Presenter M3/Maintenance
Date FINAL
Slide 7 of 13
Closed

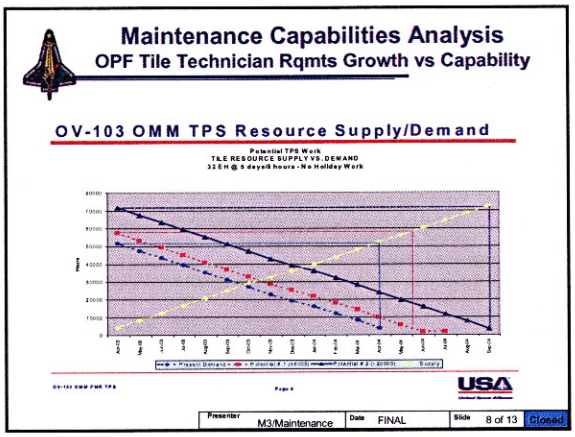
Maintenance Capabilities Analysis
OPF Tile Technician Rqmts Growth vs Capability
OV-103 OMM TPS Resource Supply/Demand
Presenter M3/Maintenance
Date FINAL
Slide 8 of 13
Closed

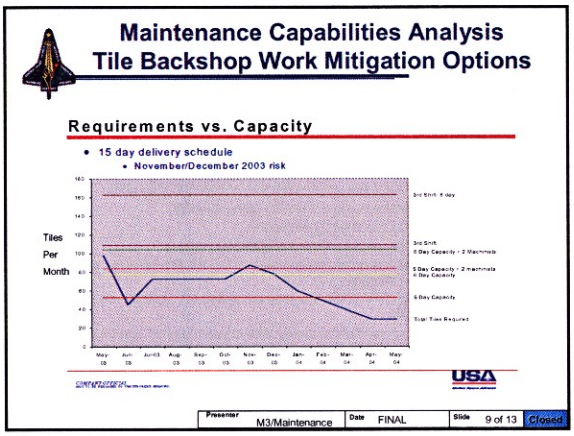
Maintenance Capabilities Analysis
Tile Backshop Work Mitigation Options
Requirements vs. Capacity
15 day delivery schedule
November/December 2003 risk
Tiles Per Month
Presenter M3/Maintenance
Date FINAL
Slide 9 of 13
Closed

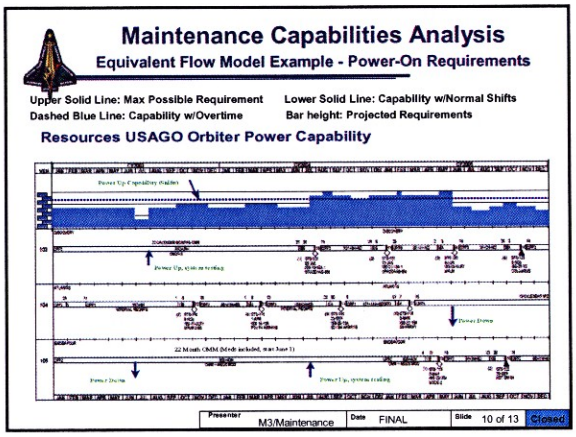
Maintenance Capabilities Analysis
Equivalent Flow Model Example - Power-On Requirements
Upper Solid Line: Max Possible Requirement
Lower Solid Line: Capability w/Normal Shifts
Dashed Blue Line: Capability w/Overtime
Bar height: Projected Requirements
Resources USAGO Orbiter Power Capability
Presenter M3/Maintenance
Date FINAL
Slide 10 of 13
Closed

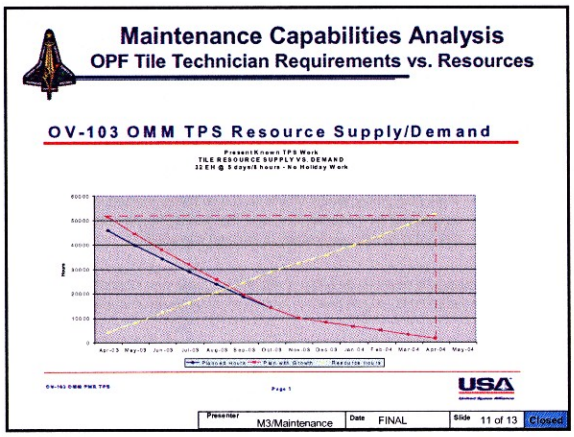
Maintenance Capabilities Analysis
OPF Tile Technician Requirements vs. Resources
OV-103 OMM TPS Resource Supply/Demand
Presenter M3/Maintenance
Date FINAL
Slide 11 of 13
Closed

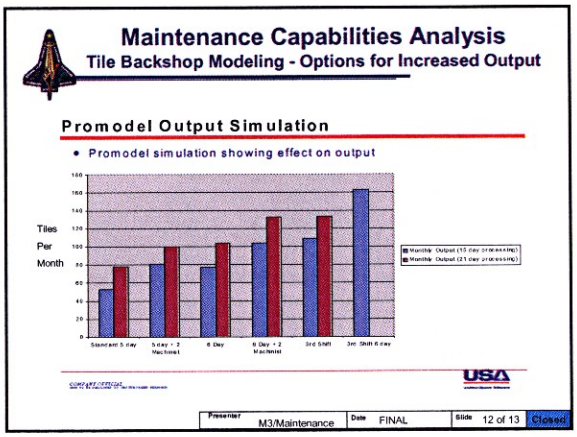
Maintenance Capabilities Analysis
Tile Backshop Modeling - Options for Increased Output
Promodel Output Simulation
Promodel simulation showing effect on output
Tiles Per Month
Presenter M3/Maintenance
Date FINAL
Slide 12 of 13
Closed

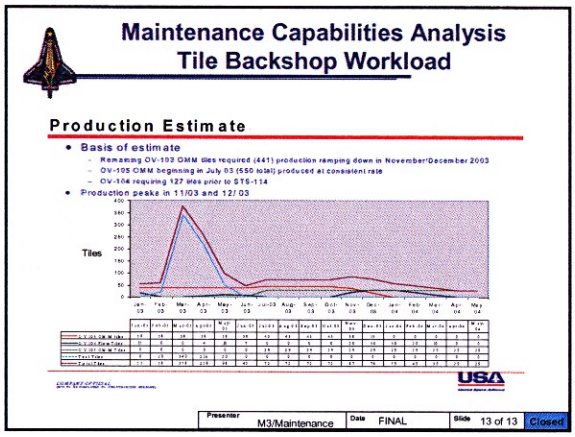
Maintenance Capabilities Analysis
Tile Backshop Workload
Production Estimate
Basis of estimate
Remaining OV-103 OMM tiles required (441) production ramping down in November/December 2003
OV-105 OMM beginning in July 03 (550 total) produced at consistent rate
OV-104 requiring 127 tiles prior to STS-114
Production peaks in 11/03 and 12/ 03
Tiles
USA
Presenter
M3/Maintenance
Date
FINAL
Slide
13 of 13
Closed

3

Other
Fleet Experience – Aging

19-1 Loose Carrier Panel Fasteners

19-2 Programming for Aging Infrastructure

Matrix

Presenter	CAIB/Group 1	Date	FINAL	Slide	22 of 32

Carrier Panels

- **Action / Issue:** Determine adequacy of maintenance requirements for carrier panel fasteners
- **Background / Facts:**
  - Upper and lower access/carrier panels closeout the WLE between the RCC panels and the wing front spar
  - OV-102 has 794 total carrier panels including the OMS pods
  - WLE lower carrier panel utilizes a gap filler referred to as a horsecollar
  - OV-102 left wing lower access panels had 27 horsecollars replaced, 9 HRSI tiles replaced, 9 fills in the gap filler material, 12 HRSI tile repairs and 7 MRs
  - OV-102 left wing upper access panels had 7 HRSI tiles replaced, 7 HRSI tile repairs and 7 MRs

Presenter M3/Material | Date FINAL | Slide 1 of 11 | Closed

Carrier Panels

- **Background / Facts:**
  - Post-flight inspection after STS-87 (OV-102-24, 1997) revealed a large step in the number 4R lower access panel
    - Reference Boeing Report KLO-98-002, "Mission STS-87 OV-102 Flight 24 Thermal Protection System Post-Flight Assessment", March 1998
    - A 0.4" gap under the head of the bolt was discovered during panel removal
    - No signs of overheating were noted
    - The remaining fasteners were inspected and low torque values were found but none were unseated (report doesn't provide quantity)
    - "Bolts were retorqued and the problem was resolved"

Presenter M3/Material | Date FINAL | Slide 2 of 11 | Closed

Carrier Panels

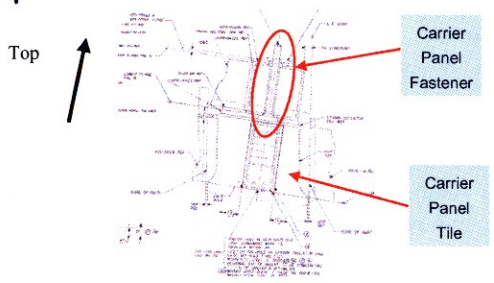

Presenter M3/Material | Date FINAL | Slide 3 of 11 | Closed

Carrier Panels

- **Background / Facts:**
  - During OV-103-25, STS-95, 1998 a carrier panel on the OMS pod Y-web door peeled back and structure under the panel was damaged during entry
  - Torque check of all the fasteners on OV-103's and OV-105's OMS pod Y-web doors were performed
    - OV-103 had 4 loose washers found spinning under the fastener heads, and 13 out of 44 fasteners with low torque
    - OV-105 had 7 fasteners found with low torque
  - Concluded "no concern for loose TPS carrier panel fasteners"
  - Recommended monitoring plan for fastener torque
    - 2 lower LESS carrier panels (1 LH and 1 RH)
    - 2 star tracker carrier panels
    - 2 OMS pod stringer carrier panels

Presenter M3/Material | Date FINAL | Slide 4 of 11 | Closed

Carrier Panels

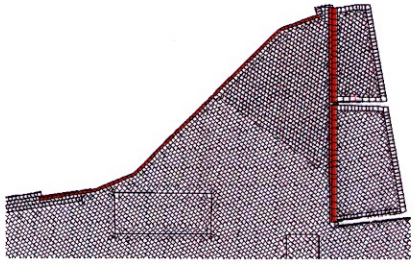

Wing Carrier Panel Locations Shown in Red

Presenter M3/Material | Date FINAL | Slide 5 of 11 | Closed

Carrier Panels

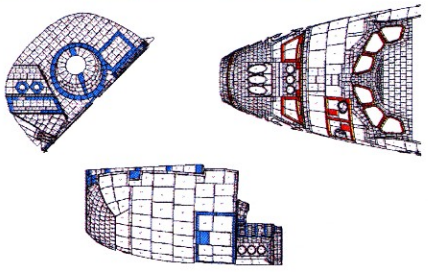

Other Carrier Panel Locations

Presenter M3/Material | Date FINAL | Slide 6 of 11 | Closed

1

Carrier Panels

L/H LESS PNL #7 DAMAGE TO TILE

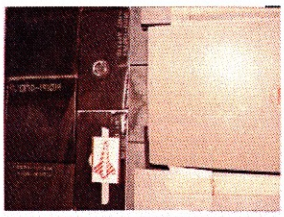

TILE SLUMPING ADJ TO RCC T-SEAL

OV-103-01, WLE Carrier Panel 7L Slumped Tile (1984)

Presenter M3/Material | Date FINAL | Slide 7 of 11 | Closed

Carrier Panels

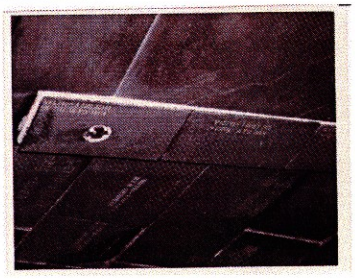

OV-103-04, WLE Loose Carrier Panel 16R (1985)

Presenter M3/Material | Date FINAL | Slide 8 of 11 | Closed

Carrier Panels

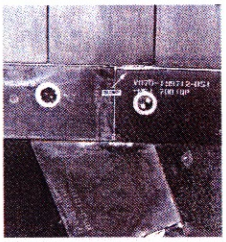

OV-104-21, WLE Carrier Panel 7L Slumped Tile (May 00)

Presenter M3/Material | Date FINAL | Slide 9 of 11 | Closed

Carrier Panels
Category: Other Significant Finding

- **Findings:**
  - Carrier panels have a history of having loose fasteners
  - Recommended monitoring plan appears to be inadequate (if it was even implemented)
- **Recommendations:**
  - Revisit carrier panel loose fastener issue and revised planned maintenance actions

Presenter M3/Material | Date FINAL | Slide 10 of 11 | Closed

Carrier Panels

- **Documentation:**
  - Briefing by A. Mirdamadi, "TPS Carrier Panel Fasteners Monitoring Plan", 30 March 1999
  - Meeting minutes by H. Ashkar, "8-27-98 Palmdale Visit Minutes", 27 August 1998
  - Briefing by S. Cavanaugh, "OV-102 Wing Leading Edge Carrier Panel", January 1998

Presenter M3/Material | Date FINAL | Slide 11 of 11 | Closed

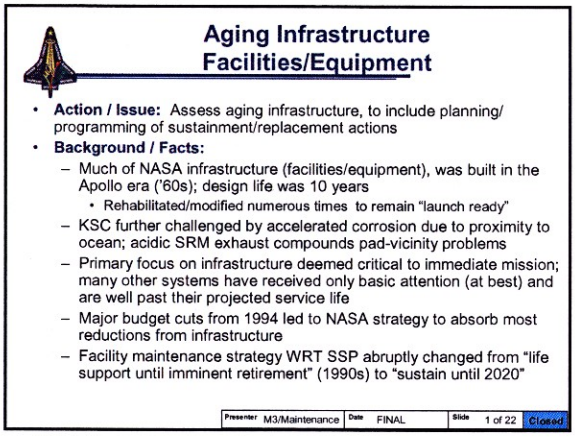
Aging Infrastructure
Facilities/Equipment
• Action / Issue: Assess aging infrastructure, to include planning/ programming of sustainment/replacement actions
• Background / Facts:
– Much of NASA infrastructure (facilities/equipment), was built in the Apollo era ('60s); design life was 10 years
• Rehabilitated/modified numerous times to remain "launch ready"
– KSC further challenged by accelerated corrosion due to proximity to ocean; acidic SRM exhaust compounds pad-vicinity problems
– Primary focus on infrastructure deemed critical to immediate mission; many other systems have received only basic attention (at best) and are well past their projected service life
– Major budget cuts from 1994 led to NASA strategy to absorb most reductions from infrastructure
– Facility maintenance strategy WRT SSP abruptly changed from "life support until imminent retirement" (1990s) to "sustain until 2020"
Presenter M3/Maintenance Date FINAL Slide 1 of 22 Closed

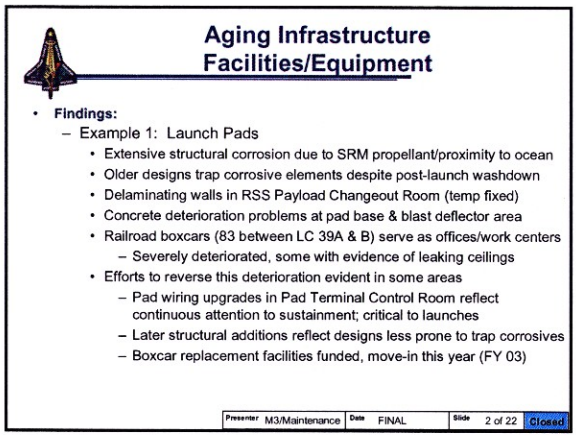
Aging Infrastructure
Facilities/Equipment
• Findings:
– Example 1: Launch Pads
• Extensive structural corrosion due to SRM propellant/proximity to ocean
• Older designs trap corrosive elements despite post-launch washdown
• Delaminating walls in RSS Payload Changeout Room (temp fixed)
• Concrete deterioration problems at pad base & blast deflector area
• Railroad boxcars (83 between LC 39A & B) serve as offices/work centers
– Severely deteriorated, some with evidence of leaking ceilings
• Efforts to reverse this deterioration evident in some areas
– Pad wiring upgrades in Pad Terminal Control Room reflect continuous attention to sustainment; critical to launches
– Later structural additions reflect designs less prone to trap corrosives
– Boxcar replacement facilities funded, move-in this year (FY 03)
Presenter M3/Maintenance Date FINAL Slide 2 of 22 Closed

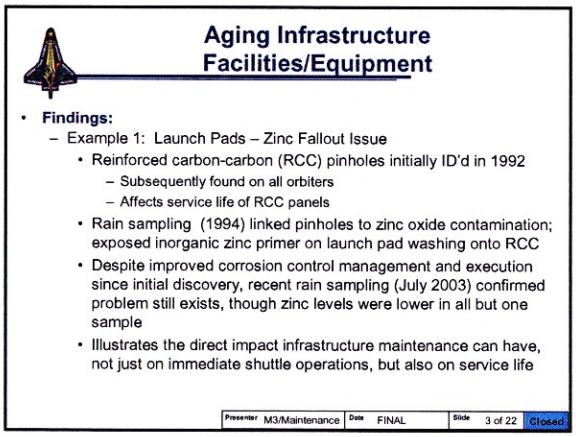
Aging Infrastructure
Facilities/Equipment
• Findings:
– Example 1: Launch Pads – Zinc Fallout Issue
• Reinforced carbon-carbon (RCC) pinholes initially ID'd in 1992
– Subsequently found on all orbiters
– Affects service life of RCC panels
• Rain sampling (1994) linked pinholes to zinc oxide contamination; exposed inorganic zinc primer on launch pad washing onto RCC
• Despite improved corrosion control management and execution since initial discovery, recent rain sampling (July 2003) confirmed problem still exists, though zinc levels were lower in all but one sample
• Illustrates the direct impact infrastructure maintenance can have, not just on immediate shuttle operations, but also on service life
Presenter M3/Maintenance Date FINAL Slide 3 of 22 Closed

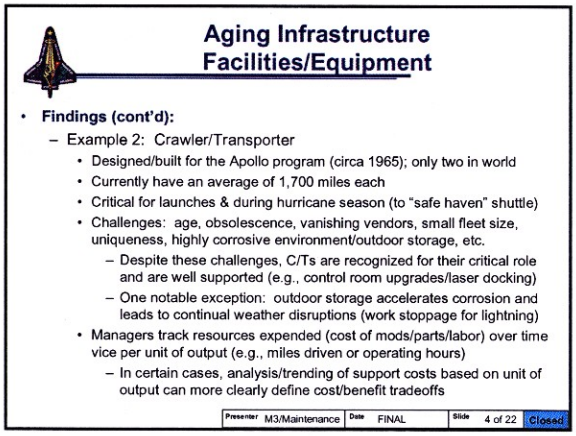
Aging Infrastructure
Facilities/Equipment
• Findings (cont'd):
– Example 2: Crawler/Transporter
• Designed/built for the Apollo program (circa 1965); only two in world
• Currently have an average of 1,700 miles each
• Critical for launches & during hurricane season (to "safe haven" shuttle)
• Challenges: age, obsolescence, vanishing vendors, small fleet size, uniqueness, highly corrosive environment/outdoor storage, etc.
– Despite these challenges, C/Ts are recognized for their critical role and are well supported (e.g., control room upgrades/laser docking)
– One notable exception: outdoor storage accelerates corrosion and leads to continual weather disruptions (work stoppage for lightning)
• Managers track resources expended (cost of mods/parts/labor) over time vice per unit of output (e.g., miles driven or operating hours)
– In certain cases, analysis/trending of support costs based on unit of output can more clearly define cost/benefit tradeoffs
Presenter M3/Maintenance Date FINAL Slide 4 of 22 Closed

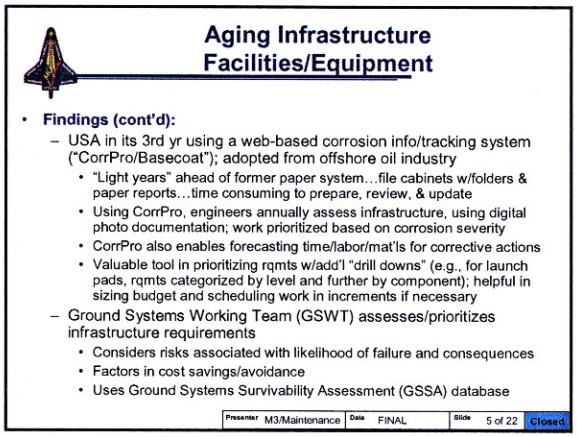
Aging Infrastructure
Facilities/Equipment
• Findings (cont'd):
– USA in its 3rd yr using a web-based corrosion info/tracking system ("CorrPro/Basecoat"); adopted from offshore oil industry
• "Light years" ahead of former paper system…file cabinets w/folders & paper reports…time consuming to prepare, review, & update
• Using CorrPro, engineers annually assess infrastructure, using digital photo documentation; work prioritized based on corrosion severity
• CorrPro also enables forecasting time/labor/mat'ls for corrective actions
• Valuable tool in prioritizing rqmts w/add'l "drill downs" (e.g., for launch pads, rqmts categorized by level and further by component); helpful in sizing budget and scheduling work in increments if necessary
– Ground Systems Working Team (GSWT) assesses/prioritizes infrastructure requirements
• Considers risks associated with likelihood of failure and consequences
• Factors in cost savings/avoidance
• Uses Ground Systems Survivability Assessment (GSSA) database
Presenter M3/Maintenance Date FINAL Slide 5 of 22 Closed

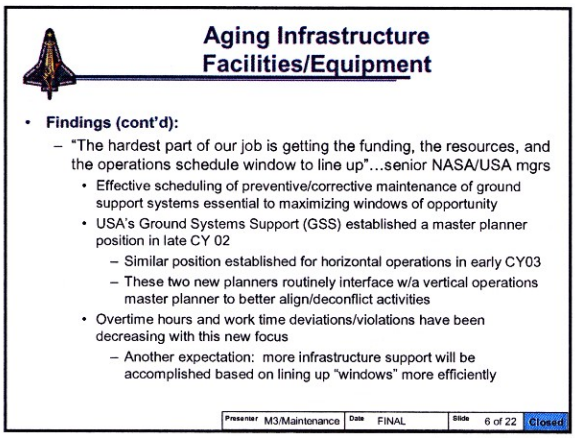
Aging Infrastructure
Facilities/Equipment
• Findings (cont'd):
– "The hardest part of our job is getting the funding, the resources, and the operations schedule window to line up"…senior NASA/USA mgrs
• Effective scheduling of preventive/corrective maintenance of ground support systems essential to maximizing windows of opportunity
• USA's Ground Systems Support (GSS) established a master planner position in late CY 02
– Similar position established for horizontal operations in early CY03
– These two new planners routinely interface w/a vertical operations master planner to better align/deconflict activities
• Overtime hours and work time deviations/violations have been decreasing with this new focus
– Another expectation: more infrastructure support will be accomplished based on lining up "windows" more efficiently
Presenter M3/Maintenance Date FINAL Slide 6 of 22 Closed

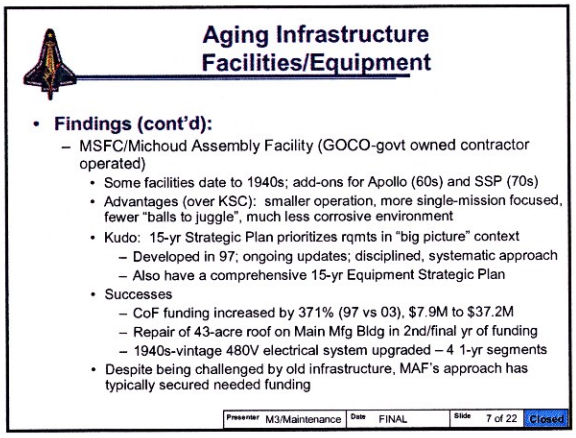
Aging Infrastructure
Facilities/Equipment
• Findings (cont'd):
– MSFC/Michoud Assembly Facility (GOCO-govt owned contractor operated)
• Some facilities date to 1940s; add-ons for Apollo (60s) and SSP (70s)
• Advantages (over KSC): smaller operation, more single-mission focused, fewer "balls to juggle", much less corrosive environment
• Kudo: 15-yr Strategic Plan prioritizes rqmts in "big picture" context
– Developed in 97; ongoing updates; disciplined, systematic approach
– Also have a comprehensive 15-yr Equipment Strategic Plan
• Successes
– CoF funding increased by 371% (97 vs 03), $7.9M to $37.2M
– Repair of 43-acre roof on Main Mfg Bldg in 2nd/final yr of funding
– 1940s-vintage 480V electrical system upgraded – 4 1-yr segments
• Despite being challenged by old infrastructure, MAF's approach has typically secured needed funding
Presenter M3/Maintenance
Date FINAL
Slide 7 of 22
Closed

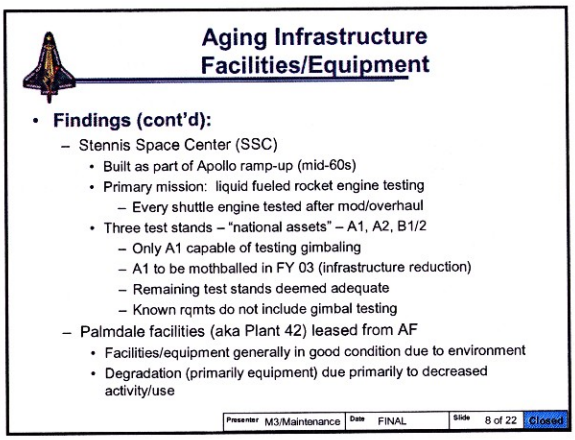
Aging Infrastructure
Facilities/Equipment
• Findings (cont'd):
– Stennis Space Center (SSC)
• Built as part of Apollo ramp-up (mid-60s)
• Primary mission: liquid fueled rocket engine testing
– Every shuttle engine tested after mod/overhaul
• Three test stands – "national assets" – A1, A2, B1/2
– Only A1 capable of testing gimbaling
– A1 to be mothballed in FY 03 (infrastructure reduction)
– Remaining test stands deemed adequate
– Known rqmts do not include gimbal testing
– Palmdale facilities (aka Plant 42) leased from AF
• Facilities/equipment generally in good condition due to environment
• Degradation (primarily equipment) due primarily to decreased activity/use
Presenter M3/Maintenance
Date FINAL
Slide 8 of 22
Closed

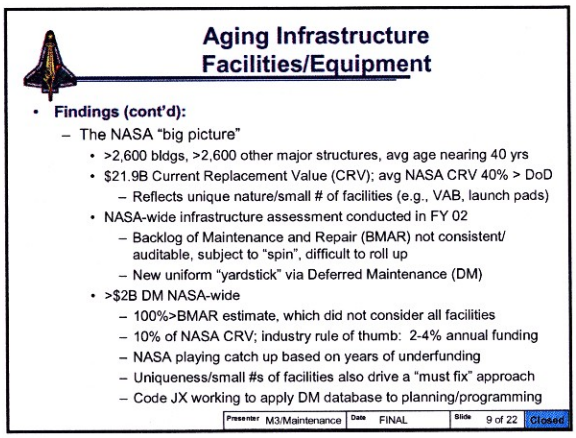
Aging Infrastructure
Facilities/Equipment
• Findings (cont'd):
– The NASA "big picture"
• >2,600 bldgs, >2,600 other major structures, avg age nearing 40 yrs
• $21.9B Current Replacement Value (CRV); avg NASA CRV 40% > DoD
– Reflects unique nature/small # of facilities (e.g., VAB, launch pads)
• NASA-wide infrastructure assessment conducted in FY 02
– Backlog of Maintenance and Repair (BMAR) not consistent/ auditable, subject to "spin", difficult to roll up
– New uniform "yardstick" via Deferred Maintenance (DM)
• >$2B DM NASA-wide
– 100%>BMAR estimate, which did not consider all facilities
– 10% of NASA CRV; industry rule of thumb: 2-4% annual funding
– NASA playing catch up based on years of underfunding
– Uniqueness/small #s of facilities also drive a "must fix" approach
– Code JX working to apply DM database to planning/programming
Presenter M3/Maintenance
Date FINAL
Slide 9 of 22
Closed

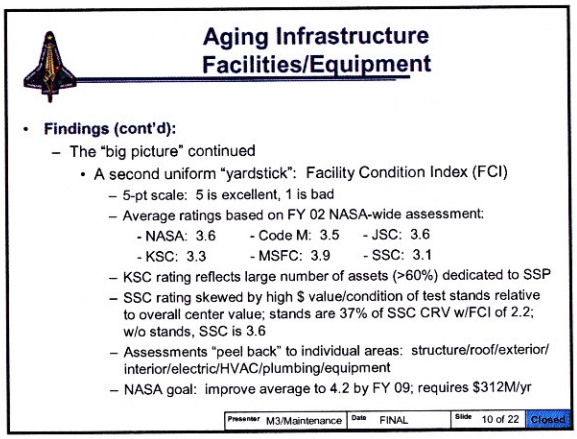
Aging Infrastructure
Facilities/Equipment
• Findings (cont'd):
– The "big picture" continued
• A second uniform "yardstick": Facility Condition Index (FCI)
– 5-pt scale: 5 is excellent, 1 is bad
– Average ratings based on FY 02 NASA-wide assessment:
- NASA: 3.6 - Code M: 3.5 - JSC: 3.6
- KSC: 3.3 - MSFC: 3.9 - SSC: 3.1
– KSC rating reflects large number of assets (>60%) dedicated to SSP
– SSC rating skewed by high $ value/condition of test stands relative to overall center value; stands are 37% of SSC CRV w/FCI of 2.2; w/o stands, SSC is 3.6
– Assessments "peel back" to individual areas: structure/roof/exterior/ interior/electric/HVAC/plumbing/equipment
– NASA goal: improve average to 4.2 by FY 09; requires $312M/yr
Presenter M3/Maintenance
Date FINAL
Slide 10 of 22
Closed

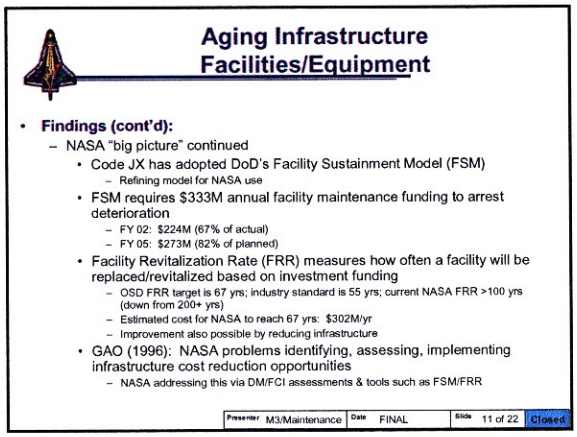
Aging Infrastructure
Facilities/Equipment
• Findings (cont'd):
– NASA "big picture" continued
• Code JX has adopted DoD's Facility Sustainment Model (FSM)
– Refining model for NASA use
• FSM requires $333M annual facility maintenance funding to arrest deterioration
– FY 02: $224M (67% of actual)
– FY 05: $273M (82% of planned)
• Facility Revitalization Rate (FRR) measures how often a facility will be replaced/revitalized based on investment funding
– OSD FRR target is 67 yrs; industry standard is 55 yrs; current NASA FRR >100 yrs (down from 200+ yrs)
– Estimated cost for NASA to reach 67 yrs: $302M/yr
– Improvement also possible by reducing infrastructure
• GAO (1996): NASA problems identifying, assessing, implementing infrastructure cost reduction opportunities
– NASA addressing this via DM/FCI assessments & tools such as FSM/FRR
Presenter M3/Maintenance
Date FINAL
Slide 11 of 22
Closed

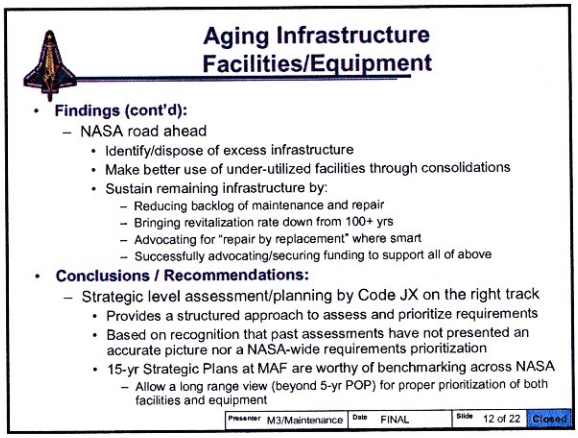
Aging Infrastructure
Facilities/Equipment
• Findings (cont'd):
– NASA road ahead
• Identify/dispose of excess infrastructure
• Make better use of under-utilized facilities through consolidations
• Sustain remaining infrastructure by:
– Reducing backlog of maintenance and repair
– Bringing revitalization rate down from 100+ yrs
– Advocating for "repair by replacement" where smart
– Successfully advocating/securing funding to support all of above
• Conclusions / Recommendations:
– Strategic level assessment/planning by Code JX on the right track
• Provides a structured approach to assess and prioritize requirements
• Based on recognition that past assessments have not presented an accurate picture nor a NASA-wide requirements prioritization
• 15-yr Strategic Plans at MAF are worthy of benchmarking across NASA
– Allow a long range view (beyond 5-yr POP) for proper prioritization of both facilities and equipment
Presenter M3/Maintenance
Date FINAL
Slide 12 of 22
Closed

Aging Infrastructure
Facilities/Equipment

- **Recommendations:**
  - KSC should continue its initiatives for improved scheduling integration; the recent add'n of master planners for horizontal ops & GSS to interface w/vertical ops is a great move in this direction
  - KSC GSS managers should consider tracking support costs relative to unit of output (vice over time) in selected areas; this can assist in tradeoff decisions on funding mods/upgrades vs replacement
    - Given the amount of aging infrastructure/equipment, this can be a valuable decision tool
  - KSC should continue efforts to improve management/prioritization of workload and costs thru systems such as CorrPro/BaseCoat
    - Explore application to non-corrosion related infrastructure
  - KSC should perform cost/benefit tradeoff analysis of constructing add'l shelters for equipment (not limited to CTs)
    - This will reduce weather deterioration/resulting maintenance and weather-induced work stoppages
  - KSC should examine current launch pad maintenance practices and make every effort to further reduce/eliminate zinc fallout
  - Other centers should benchmark MAF's 15-year infrastructure and equipment strategic plans; a "long view" of these critical issues is essential

Presenter M3/Maintenance | Date FINAL | Slide 13 of 22 | Closed

Aging Infrastructure
Managing Using CorrPro Software

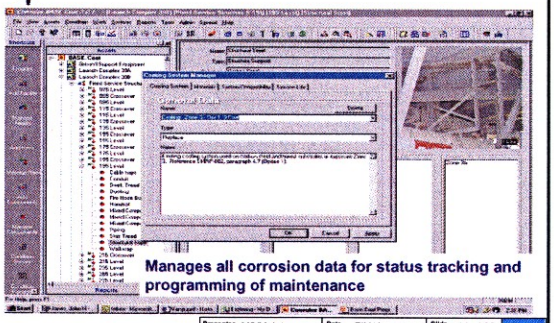

Manages all corrosion data for status tracking and programming of maintenance

Presenter M3/Maintenance | Date FINAL | Slide 14 of 22 | Closed

Aging Infrastructure
Severe Corrosion - Pad 39A

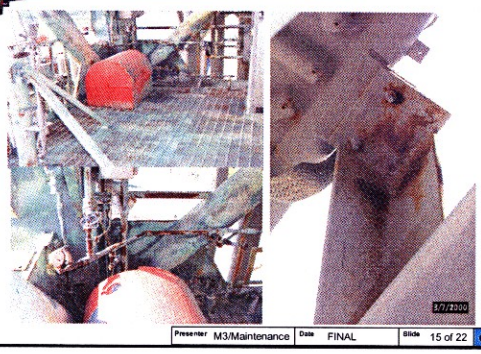

Presenter M3/Maintenance | Date FINAL | Slide 15 of 22 | Closed

Aging Infrastructure
Corrosion/Boxcars at Pad 39A

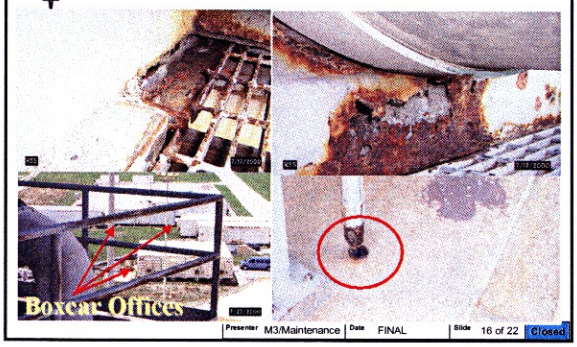

Presenter M3/Maintenance | Date FINAL | Slide 16 of 22 | Closed

Aging Infrastructure
VAB Deterioration

- Roof
- Siding
- Doors

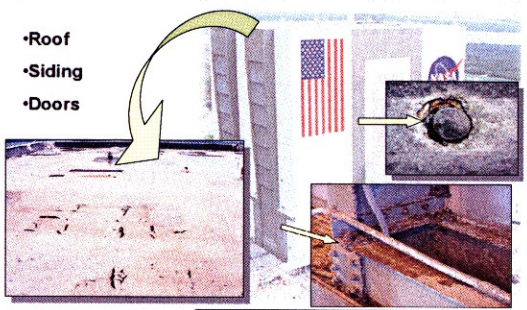

Presenter M3/Maintenance | Date FINAL | Slide 17 of 22 | Closed

Aging Equipment
C/T and MLP

Mobile Launch Platform

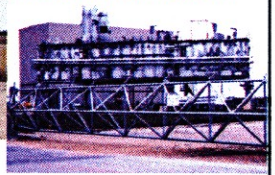

Presenter M3/Maintenance | Date FINAL | Slide 18 of 22 | Closed

3

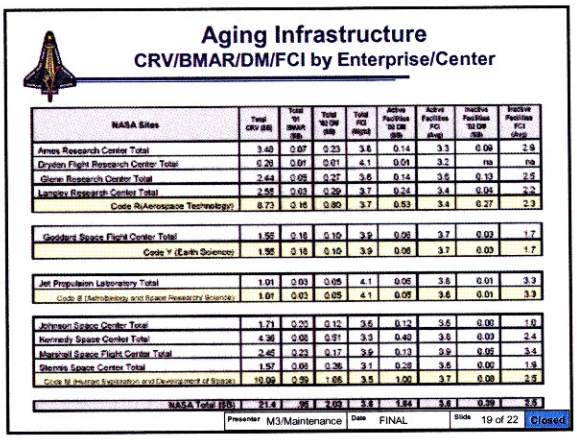

Aging Infrastructure
CRV/BMAR/DM/FCI by Enterprise/Center

NASA Sites	Total CRV ($B)	Total Yr BMAR ($B)	Total Yr DM ($B)	Total FCI (Avg)	Active Facilities Yr DM ($B)	Active Facilities FCI (Avg)	Inactive Facilities Yr DM ($B)	Inactive Facilities FCI (Avg)
Ames Research Center Total	3.40	0.07	0.23	3.6	0.14	3.3	0.09	2.9
Dryden Flight Research Center Total	0.29	0.01	0.01	4.1	0.01	3.2	na	na
Glenn Research Center Total	2.44	0.05	0.27	3.6	0.14	3.5	0.13	2.5
Langley Research Center Total	2.55	0.03	0.29	3.7	0.24	3.4	0.05	2.2
Code R(Aerospace Technology)	8.73	0.16	0.80	3.7	0.53	3.4	0.27	2.3
Goddard Space Flight Center Total	1.55	0.15	0.10	3.9	0.06	3.7	0.03	1.7
Code Y (Earth Science)	1.55	0.15	0.10	3.9	0.06	3.7	0.03	1.7
Jet Propulsion Laboratory Total	1.01	0.03	0.05	4.1	0.05	3.8	0.01	3.3
Code S (Astrobiology and Space Research/ Sciences)	1.01	0.03	0.05	4.1	0.05	3.8	0.01	3.3
Johnson Space Center Total	1.71	0.20	0.12	3.6	0.12	3.5	0.00	1.0
Kennedy Space Center Total	4.36	0.08	0.51	3.3	0.40	3.5	0.03	2.4
Marshall Space Flight Center Total	2.45	0.23	0.17	3.9	0.13	3.9	0.05	3.4
Stennis Space Center Total	1.57	0.08	0.26	3.1	0.20	3.5	0.00	1.9
Code M (Human Exploration and Development of Space)	10.09	0.59	1.05	3.5	1.00	3.7	0.08	2.5
NASA Total ($B)	21.4	.96	2.02	3.8	1.84	3.6	0.39	2.5

Presenter M3/Maintenance | Date FINAL | Slide 19 of 22 | Closed

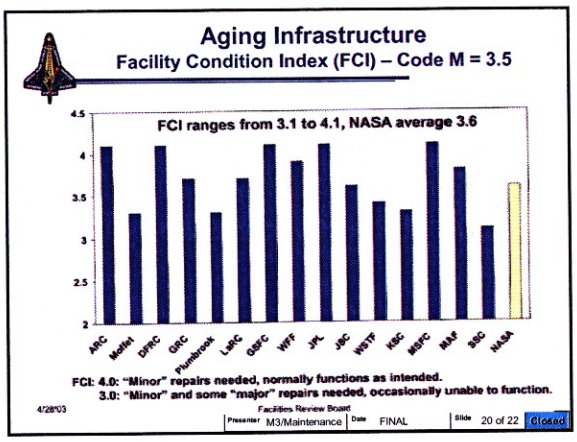

Aging Infrastructure
Facility Condition Index (FCI) – Code M = 3.5

FCI: 4.0: "Minor" repairs needed, normally functions as intended.
3.0: "Minor" and some "major" repairs needed, occasionally unable to function.

4/28/03 Facilities Review Board

Presenter M3/Maintenance | Date FINAL | Slide 20 of 22 | Closed

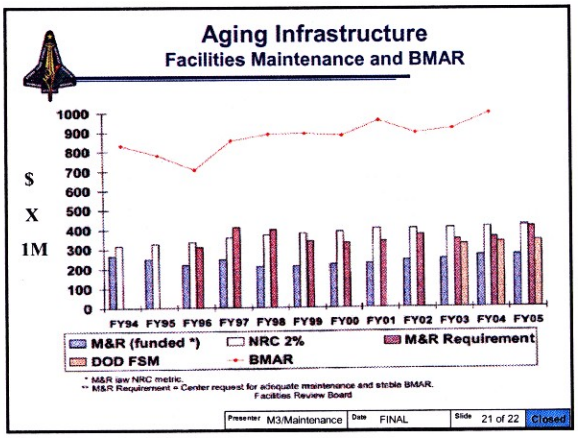

Aging Infrastructure
Facilities Maintenance and BMAR

* M&R iaw NRC metric.
** M&R Requirement = Center request for adequate maintenance and stable BMAR.
Facilities Review Board

Presenter M3/Maintenance | Date FINAL | Slide 21 of 22 | Closed

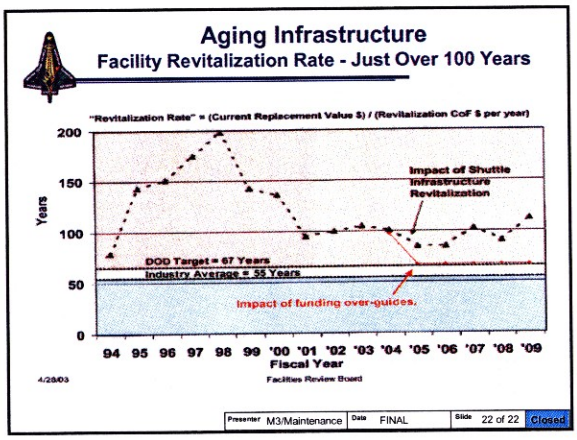

Aging Infrastructure
Facility Revitalization Rate - Just Over 100 Years

4/28/03 Facilities Review Board

Presenter M3/Maintenance | Date FINAL | Slide 22 of 22 | Closed

Other Maintenance

20-1 Engineering Orders

Matrix

Presenter	CAIB/Group 1	Date	FINAL	Slide	23 of 32

Maintenance
Engineering Orders

- **Action/Issue:** Backlog of unincorporated Engineering Orders (UEO) is significant and may impact the quality and timeliness of maintenance
- **Background:**
  - Last 5 ASAP reports document a large and growing number of UEOs (over 1600 with > 10 changes ea; now 1400 with removed from schedule)
  - NNBE referenced using Navy's zero level as a baseline
- **Facts:**
  - Observed examples of UEOs in shop and OPF
    - Observed the impact and difficulties of navigating EO with multiple unincorporated changes and potential for human error
    - NASA built a noteworthy plan to incorporate the most important changes to drawings for orbiter on basis of highest use and complexity (2002-2004)
- **Recommendations:**
  - Draft a plan to finish incorporating the >10 UEOs

Presenter: M3/Maintenance | Date: FINAL | Slide: 1 of 4 | Closed

Maintenance
Engineering Orders

Aerospace Safety Advisory Panel, 2002... report excerpt:

"Previously, the Panel has been concerned with the large number of orbiter drawings that are out of date. Many EO changes have not been incorporated into the drawings. Although they are noted on the drawings,engineers must refer to additional paperwork to understand the state of the hardware systems. Over 1,600 drawings have more than 10 unincorporated EOs. The orbiter program will update and incorporate all EOs on 59 of the most frequently used drawings by the end of 2003. Also during the year,an effort to address the 589 drawings referenced most frequently after those 59 will begin. The remaining drawings will be updated as opportunity permits. Orbiter program management has committed to maintaining the upgraded drawings at no more than 10 unincorporated EOs. The orbiter program is now reviewing the possibility of identifying the safety-critical drawings that should always be kept current.

Recommendation 02-8:

Identify drawings that are critical to flight safety, update them to include all EOs, and keep them current."

Presenter: M3/Maintenance | Date: FINAL | Slide: 2 of 4 | Closed

Maintenance
Engineering Orders

Drawings with unincorporated EOs past the 10 or 30 EO limits (Excluding OV 102)

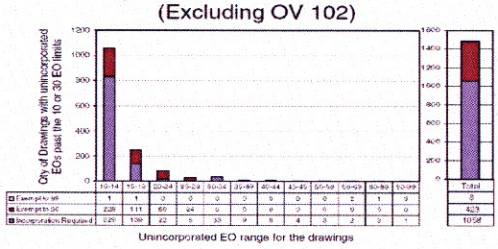

Presenter: M3/Maintenance | Date: FINAL | Slide: 3 of 4 | Closed

Maintenance
Engineering Orders

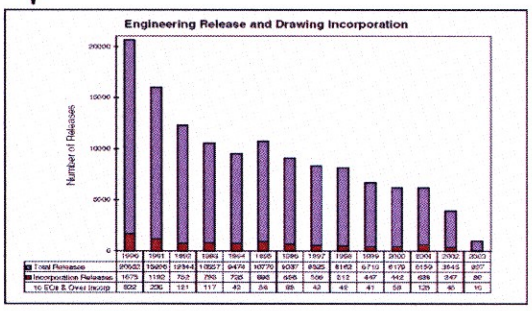

Presenter: M3/Maintenance | Date: FINAL | Slide: 4 of 4 | Closed

Other
Launch – Ascent

21-1 Day of Launch Assets, Hardware Security, and Scenarios
21-2 SRB Bolt Catchers
21-3 Separation Bolt Certification
21-4 RSRM Flex Boot Tear
21-5 STS-107 Impact Analysis
21-6 STS-107 Ascent Debris (Radar & Imaging)
21-7 Hold-Down Cable Anomaly

Willful Damage All Areas

- **Action/Issue:** Potential for willful damage
- **Background/Facts:**

Day-of-Launch Assets included:
- Fighters
- Helicopters
- Sea surveillance
- Ground security
- Sensors

"Tightest security ever … briefed to NSC"

Presenter M3 | Date FINAL | Slide 1 of 3 | Closed

Hardware Security

- **Background/Facts:**
  - Panel and door close-outs
    - Multiple technicians
    - Multiple contract quality inspectors
    - Multiple government inspectors

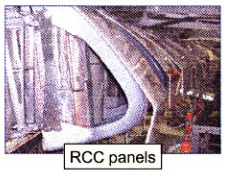

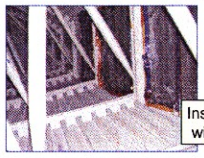

Presenter M3 | Date FINAL | Slide 2 of 3 | Closed

"Willful damage" scenarios

- **Background/Facts:**
  - Examining via testing (outside agencies involved)
  - HOWEVER … to be credible, each must still pass "tests"
    - Telemetry (digital, voice)
    - Imagery (still, video, telescopic)
    - Thermodynamics
    - Aerodynamics
    - Debris shedding, ground evidence
    - Documentation
    - And -- grounded in shuttle systems facts
- **Findings:**
  - Thus far, none meets the tests to be credible
  - FBI testing and chemical/metallurgical evidence do not support willful damage
- **Recommendations:**
  - Continue high level of diligence to prevent willful damage

Presenter M3 | Date FINAL | Slide 3 of 3 | Closed

Maintenance
Bolt Catcher

- **Action / Issue:** Did a malfunction of the SRB forward Bolt Catcher contribute to the accident chain of events?
- **Background / Facts:**
  - Function: Catch fired separation bolts attaching SRBs to ET
    - Upper catcher attached to ET, lower attached to SRB, different design
    - Good example of SIAT (99) documented concern with "fly what you test, test what you fly"
  - SUMMA and Harris manufacture, subKtr, USA serial #
    - Pulled from supply to install on ET, coated with (SLA) ablative which requires # removal-- MAF assigns new serial #
    - Serial # discrepancy between USA and MAF serial #s on STS --107

Presenter M3/Maintenance | Date FINAL | Slide 1 of 9 | Closed

Maintenance
Bolt Catcher

- **Background/Facts:**
  - Bolt Catcher never qualified as flown…79/80 tests
    - Attachment to ET qualified with through-bolts (vice inserts)
    - SLA 561 not applied on test articles
    - Reduced resistance aluminum honeycomb not tested
  - System changes certified by "analysis and similarity"
  - In-flight photograph of STS 107 Bolt Catcher black and unusable
  - Radar images at 126 seconds point originally considered normal
- **Findings:**
  - Tests run 27 May – 8 July of representative articles to evaluate/determine as-flown environment and safety margin
  - Test profiles designed to verify engineering profile of system performance as certified including as-flown configuration
    - 18 tests completed …4 bolts fired into instrumented catcher,seven stress tests of catcher to failure

Presenter M3/Maintenance | Date FINAL | Slide 2 of 9 | Closed

Maintenance
Bolt Catcher

Findings:

- Dynamic test #2 measured 46KIPs in Summa serial #50 dome
- Stress test #3 of catcher failed at weld at 44KIPs…engineering analysis expected bolt failure at 68,000lb
  - Same failure point as 1979 certification test
  - Implies 0.956 safety margin
  - Additional tests requested
- X-Ray film of #50 showed poor quality film and strong evidence of substandard welding…would not have been certified today
- STS-107, Summa catcher #1 installed on left SRB/ET
  - X-Ray film failed in quality as well as substandard weld

Presenter M3/Maintenance | Date FINAL | Slide 3 of 9 | Closed

Maintenance
Bolt Catcher

- **Findings**
- STS-107 launch radar data comparison with bolt catcher radar cross section (RCS) complete
  - Event #33 at 128 second similar in size to bolt catcher RCS
  - Lack of photographic evidence means event #33 cannot be ruled out as a possible bolt catcher or fragment.
- **Group Recommendations**
  - Certification by "analysis and similarity" flawed…how many other bolt catchers on SSP?
  - Remove all Bolt Catchers from service
  - Redesign system to assure 1.4 safety margin at a minimum

Presenter M3/Maintenance | Date FINAL | Slide 4 of 9 | Closed

Maintenance
Bolt Catcher

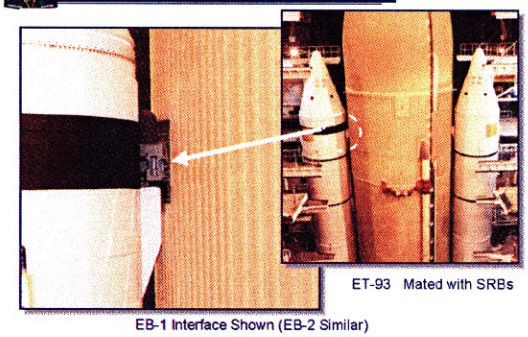

ET-93 Mated with SRBs

EB-1 Interface Shown (EB-2 Similar)

Presenter M3/Maintenance | Date FINAL | Slide 5 of 9 | Closed

Bolt Catcher

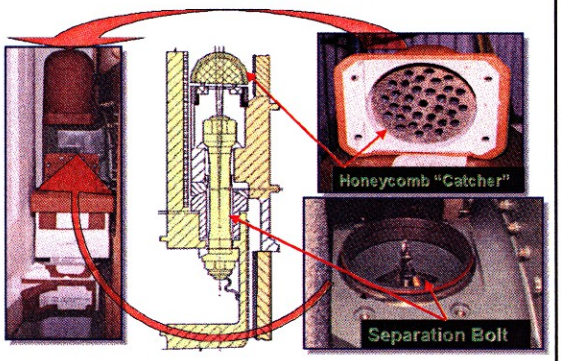

Presenter M3/Maintenance | Date FINAL | Slide 6 of 9 | Closed

1

Maintenance
Bolt Catcher (In-Flight Observations)

Mission	LH Vehicle	RH vehicle
STS-113	Not in FOV	Not in FOV
STS-112	Visible	Visible
STS-111	Visible	Visible
STS-110	Visible	Not in FOV
STS-109	Visible	Visible
STS-108	Dark Exposure	Dark Exposure
STS-106	Visible	Visible
STS-105	Visible	Visible
STS-104	Visible	Not in FOV
STS-103	Dark Exposure	Dark Exposure
STS-102	Not in FOV	Visible
STS-101	Visible	Visible
STS-100	Visible	Visible
STS-099	Visible	Visible
STS-098	No Film	No Film
STS-097	Poor Quality	Poor Quality
STS-096	Visible	Visible
STS-095	Visible	Visible
STS-093	Dark Exposure	Dark Exposure
STS-092	No Film	No Film
STS-091	Visible	Visible
STS-090	Visible	Visible
STS-088	Dark Exposure	Dark Exposure

FOV = Field of View "Visible" indicates that the bolt catcher was identifiable in its installed position in post-SRB separation photographs.

Presenter M3/Maintenance | Date FINAL | Slide 7 of 9 | Closed

Test Pic's

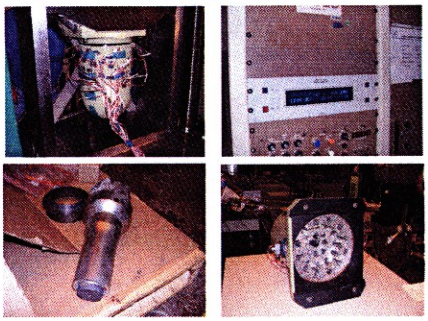

Presenter M3/Maintenance | Date FINAL | Slide 8 of 9 | Closed

Velocity Variation in X direction for Bolts+Bolt Catcher Debris

SRB's Separation Condition
BSM's at 100% Thrust
Bolt+Bolt-Catcher (Mass = 41.1 lbs)

Flowfield Conditions at SRB Separation:
Analysis / (STS-107 BET)
Altitude = 136,400 ft. / (155,000 ft)
Mach = 3.94 / (4)
Alpha = 0 degrees / (3.57 degrees)
Beta = 0 degrees / (-0.02 degrees)
Qbar = 52 psf / (25 psf)

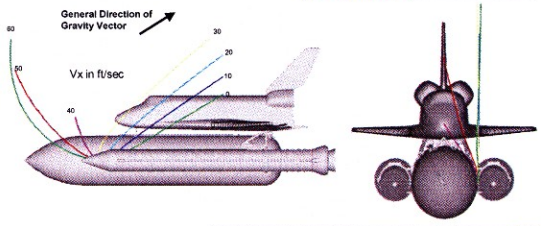

Presenter M3/Maintenance | Date FINAL | Slide 9 of 9 | Closed

Maintenance
Separation Bolt Certification

- **Action / Issue:** Separation bolts manufactured by Pacific-Scientific were not adequately NDI'd before flight on STS 107
- **Background / Facts:**
  - USA replaced Hi-Shear as the prime contractor for separation bolts in May 2000. Certification of new bolts may have been done without adequate NDI (magnetic particle) of the internal bore
- **Findings:**
  - P-S used Pacific Magnetic and Penetrant for NDI verification
  - PS/PMP used same NDI specifications as Hi-Shear
  - First lot (Lot AAN) used on STS 107 and installed on STS 114
    - All NDI results were approved and certified by PS, USA, and DCMA
  - 2nd lot (AAP) magnetic particle inspection eval'ed by DCMA NDI expert
    - Determined process inadequate WRT analysis of Magnetic Part. Insp.
    - ASTM E 1444-01, par. 5.7.3 stipulates use of a borescope

Presenter: M3/Maintenance | Date: FINAL | Slide: 1 of 4 | Closed

Maintenance
Separation Bolt Certification

- **Findings (con't):**
  - USA had verbally authorized PMP to deviate from the purchase order specification since borescope was not available
  - USA and DCMA NDI experts disagree over test sufficiency
  - USA built a Defect Standard Bolt with known flaws to evaluate process
    - "Initial assessment of PMP's inspection procedure by USA NDE confirms procedure meets engineering requirement imposed but could be improved"…USA briefing to CAIB
  - USA impounded existing supply of 1st lot: dedicated to test only
  - This situation is not a contributor to the STS-107 mishap
- **Recommendations:**
  - Use more stringent inspection criteria IAW ASTM E 1444, par. 5.7.3, Restricted Area Examination **with** borescope or new method that can adequately identify flaws in the ID

Presenter: M3/Maintenance | Date: FINAL | Slide: 2 of 4 | Closed

Maintenance
Separation Bolt Certification

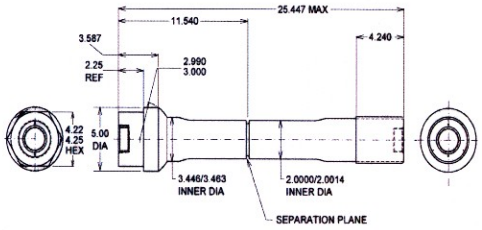

Presenter: M3/Maintenance | Date: FINAL | Slide: 3 of 4 | Closed

Maintenance
Separation Bolt Certification

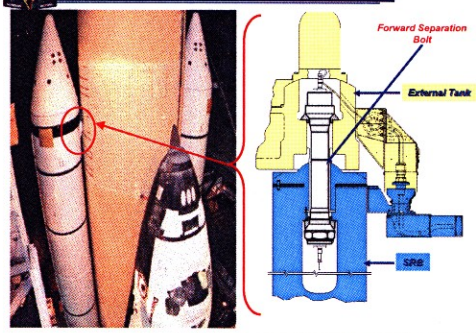

Presenter: M3/Maintenance | Date: FINAL | Slide: 4 of 4 | Closed

1

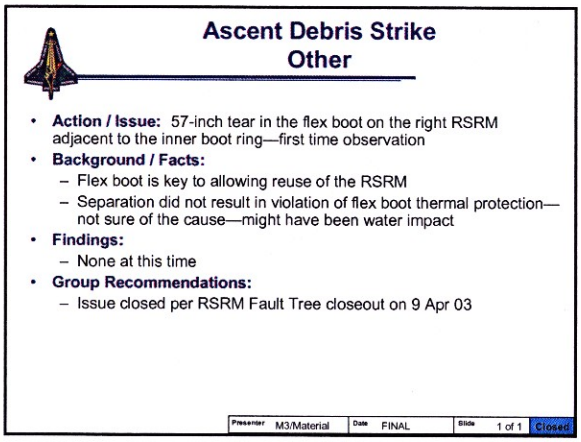
Ascent Debris Strike
Other
• Action / Issue: 57-inch tear in the flex boot on the right RSRM adjacent to the inner boot ring—first time observation
• Background / Facts:
– Flex boot is key to allowing reuse of the RSRM
– Separation did not result in violation of flex boot thermal protection—not sure of the cause—might have been water impact
• Findings:
– None at this time
• Group Recommendations:
– Issue closed per RSRM Fault Tree closeout on 9 Apr 03
Presenter M3/Material
Date FINAL
Slide 1 of 1
Closed

Ascent Impact Analysis
(includes Crater)

- **Action / Issue:**
  - The impact damage analysis process did not accurately predict the damage sustained by OV-102 during the ascent of STS-107
- **Background / Facts** (Impact Analysis Process):
  - Crater is a tool used in impact analysis
  - "Impact Analysis" includes Crater, thermal, & stress analyses
    - For STS-107, the impact analysis was performed using the image analysis team's assessment of debris size and location
    - Crater program predicted severe damage to several tiles
    - Thermal and stress analyses predicted localized heating but safe return of orbiter
  - Boeing's Debris Assessment Team recently experienced a transition from Huntington Beach to Houston

Presenter M3/Material | Date FINAL | Slide 1 of 17 | Closed

Ascent Impact Analysis
(includes Crater)

- **Background / Facts** (Crater):
  - Crater is a semi-empirical/semi-theoretical set of equations that results in a tile damage prediction for LI-900 tiles
    - Crater is only model used by NASA to predict impact damage to tiles
    - Crater is conservative and predicts worst case damage
  - Crater originally designed for "in family" (small < 3 in^3) hits
    - Crater is appropriately named; accounts for only for cratering (no other damage mechanisms considered)
    - Never intended to be used for large projectiles (STS-107 analysis)
      - Extrapolation to higher energy debris never validated through testing
    - Crater predicted severe damage to several tiles for STS-107
  - Crater's capabilities are limited by test data used to verify the model
  - Most probable cause of Columbia accident has been identified as impact damage to RCC panels
    - Revised photo analysis
    - Analysis of onboard instrumentation
    - Forensics

Presenter M3/Material | Date FINAL | Slide 2 of 17 | Closed

Ascent Impact Analysis
(includes Crater)

- **Findings** (Impact Analysis Process):
  - Basic types of analyses performed at Boeing-Huntington Beach (pre-transition) and Boeing-Houston (for STS-107) appear to have been the same
  - Boeing-HB and Boeing Houston differ in their assessment of the effectiveness of the training program
    - One key engineering analyst, as reported by HB had only several hours of training on Crater but not by the HB personnel
    - Boeing-Houston team believes training quality & quantity sufficient
      - Boeing Houston team states OJT occurred in Houston, independent of HB training to understand:
        - » Supporting documentation
        - » Crater equation development
        - » V* threshold development
      - Sensitivity studies reported to have been conducted prior to STS-107 final analysis release

Presenter M3/Material | Date FINAL | Slide 3 of 17 | Closed

Ascent Impact Analysis
(includes Crater)

- **Findings** (Impact Analysis Process):
  - Impact analysis uses an iterative, multidisciplinary (transport, impact, Crater, thermal, stress) team-based process
    - STS-107 analysis appears to have been done in the same manner however, without enough feedback between analysis components
      - Thermal analysis may have had minor errors due to communications issues with the Crater analysis hand-off

Presenter M3/Material | Date FINAL | Slide 4 of 17 | Closed

Ascent Impact Analysis
(includes Crater)

- **Findings** (Impact Analysis Process):
  - Photo analysis during the mission identified the most probable location of foam impact on wing acreage tile, not RCC
    - Also indicated no debris over top of wing – impact below WLE apex
  - The Orbiter RCC design requirements did not include debris impact tolerance
    - Some impact testing was performed, but was limited to small projectiles that resulted in localized "cratering" or penetration
      - Mostly ice tests, no foam tests
    - No impacts of the size and mass that occurred on STS-107 were previously predicted, analyzed, or tested.
  - The tools and models available to the analysis team during the flight did not account for the bending failure mode that is currently believed to be the failure cause on STS-107.
    - Data from preliminary detailed analyses and initial fiberglass impact test support this failure mode

Presenter M3/Material | Date FINAL | Slide 5 of 17 | Closed

Ascent Impact Analysis
(includes Crater)

- **Findings** (Crater):
  - Crater's use on STS-107 was far outside it's verified limits of applicability
  - Crater limitations:
    - Only for LI-900 tiles
    - Does not account for special geometry present on some tiles
    - Valid for ascent impact velocities only
      - Hypervelocity impacts not part of this methodology
    - Valid for a limited set of impactor materials
    - Impactor shapes limited to cylinder, rectangular block, or sphere
      - For rectangular block impactors, predicts damage for "edge" orientation only
    - Does not include effects of crossing tile boundaries in large impacts
    - Need to define more stringent limits to Crater's useage when tile depth reaches a defined % of total tile thickness

Presenter M3/Material | Date FINAL | Slide 6 of 17 | Closed

1

Ascent Impact Analysis
(includes Crater)

- **Findings** (Crater):
  - Crater works well within its established limits
    - In the experimental space in which Crater was developed (foam projectiles up to 3 in^3), it provides a reasonable solution
  - Extrapolating beyond the limits of Crater may be performed with:
    - Interpretation based on experience
    - An understanding that the accuracy of predictions will be reduced
  - Crater does not capture "non-cratering" effects on tile or substructural response
  - Crater is not a "turn-key" code
    - Effective use of Crater assumes users have knowledge of model's development and experience in interpreting results
  - Crater has been underutilized in developing acceptable debris/ice criteria for "In Family" hits

Presenter M3/Material | Date FINAL | Slide 7 of 17 | Closed

Ascent Impact Analysis
(includes Crater)

- **Findings** (Crater):
  - For STS-107, the Crater model predicted severe damage to several tiles
  - Crater results were interpreted using potentially un-conservative assumptions based upon inherent conservatism of model
    - Extent of tile damage assumed to stop at tile's densified layer

Presenter M3/Material | Date FINAL | Slide 8 of 17 | Closed

Ascent Impact Analysis
(includes Crater)

- **Recommendations** (Impact Analysis Process):
  - Boeing should not view the process for knowledge capture as "complete," despite the completion of the transition period
    - They should build on previous efforts to develop a systematic and comprehensive training process to ensure ongoing proficiency in critical tasks
    - Boeing/NASA should conduct an in-depth training curriculum for Boeing-Houston to assure proper understanding and interpretation of impact damage analysis models and procedures
    - Free & open communication between Boeing-Houston and Boeing-HB should be encouraged and financially supported until it is agreed that a full and proper transition is complete

Presenter M3/Material | Date FINAL | Slide 9 of 17 | Closed

Ascent Impact Analysis
(includes Crater)

- **Recommendations** (Impact Analysis Process):
  - Boeing, under NASA supervision, should review training matrices for transitioned personnel to verify individuals meet established requirements
    - Upon completing the review, action plans should be developed to remediate those not meeting set job criteria.
      - Boeing should risk manage the remediation process, not only on a group/technology area level, but also on an individual employee level.
        - » Particular attention should be given to new hires with low shuttle experience and areas with several inexperienced personnel.
      - Boeing should employ HB incumbents to remediate new/transitioned personnel failing to meet established job criteria
        - » Affected employee's time should be dedicated to the programmed remediation

Presenter M3/Material | Date FINAL | Slide 10 of 17 | Closed

Ascent Impact Analysis
(includes Crater)

- **Recommendations** (Impact Analysis Process):
  - Boeing should facilitate team building within their Houston-based Debris Assessment Team to achieve a greater degree of cohesion and more effective (i.e., "closed-loop") communication flows.
    - This could be accomplished through close monitoring by SSMs, holding regular staff meetings, group training sessions, and routine feedback sessions.
    - The desired outcomes of such efforts would be improved overall decision-making practices and calculation usage methodology. Upon completing the review, action plans should be developed to remediate those not meeting set job criteria.
  - When a decision is to be made by upper management, the engineering solutions given to management should include a quantifiable uncertainty analysis and risk analysis.

Presenter M3/Material | Date FINAL | Slide 11 of 17 | Closed

Ascent Impact Analysis
(includes Crater)

- **Recommendations** (Crater):
  - NASA/USA/Boeing should continue to develop a more robust, physics-based model to analyze impact damage to tile and RCC
    - Development should take advantage of expertise from all available resources
  - Boeing should work to develop a user's manual for thermal and stress analysis associated with impacts
  - Boeing should continue to encourage communication between Houston and Huntington Beach technical communities in the future

Presenter M3/Material | Date FINAL | Slide 12 of 17 | Closed

Ascent Impact Analysis
(includes Crater)

- **Documentation**
  - CAIB Request for Information, "ET Debris Impact Records," B1-000013
  - CAIB Request for Information, "Background Info on the CRATER Model." B1-000063
  - CAIB Request for Information, "CRATER Model Technical Discussions," B3-000186

Presenter M3/Material | Date FINAL | Slide 13 of 17 | Closed

Ascent Impact Analysis
(includes Crater)

Orbiter Impact Assessment Overview

Debris Source Identified
(Trajectory Analysis)
Impact Location/Speed/Angle Identified
(Crater Impact Damage Analysis)
Damage to TPS Tiles Identified
(Thermal Analysis)
Thermal Consequences of Damaged TPS Identified
(Stress Analysis)
Structural Consequences of Damaged TPS to Safe Return Identified

Presenter M3/Material | Date FINAL | Slide 14 of 17 | Closed

Ascent Impact Analysis
(includes Crater)

Damage Results From Crater Equations Show Significant Tile Damage

- **"Crater" indicates that multiple tiles would be taken down to densified layer**
  - **However, program was designed to be conservative due to large number of unknowns**
  - **Crater reports damage for test conditions that show no damage**

Crater predicts damage deeper than densified layer in 6 of 9 cases

Debris Size = 20" x 10" x 6"
(Density = 2.4 lb/ft³)

1/23/2003 | 5

Presenter M3/Material | Date FINAL | Slide 15 of 17 | Closed

Ascent Impact Analysis
(includes Crater)

Experimental Basis for Crater
- NASA, Boeing, and Texas A&M tests performed 1978-1982

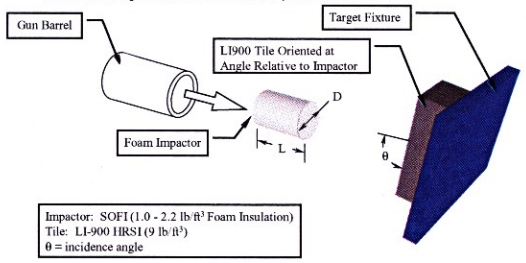

Impactor: SOFI (1.0 - 2.2 lb/ft³ Foam Insulation)
Tile: LI-900 HRSI (9 lb/ft³)
θ = incidence angle

Presenter M3/Material | Date FINAL | Slide 16 of 17 | Closed

Ascent Impact Analysis
(includes Crater)

Theoretical Basis for Crater
- Boeing penetration equation developed for Apollo program for meteoroid analysis was adapted to predict projectile penetration into TPS tiles

$$p = \frac{0.0195(L/d)^{0.45}(d)(\rho_p)^{0.27}(V - V^*)^{2/3}}{(S_T)^{1/4}(\rho_T)^{1/6}}$$

Where, for insulation debris
- p = penetration depth
- L = projectile length
- d = projectile diameter
- ρ_P = projectile density
- V = normal component of impact velocity = $V_0 \sin\theta$
- V^* = threshold normal velocity to penetrate tile coating
- S_T = tile compressive strength
- ρ_T = tile density
- 0.0195 = empirical constant

Presenter M3/Material | Date FINAL | Slide 17 of 17 | Closed

3

Ascent Debris

- **Action / Issue:** Review radar and optics results for evidence of debris during ascent
- **Background / Facts:**
  - STS-107 was tracked during ascent by Eastern Range land-based C-band radar and metric optics
  - Data was examined to identify any previously undetected debris
  - No radars detected debris prior to SRB separation
  - Only the Cocoa Beach Distant Object Attitude Measurement System (CB DOAMS) optical telescope observed debris around 81 seconds
    - 81.66 sec: single object between Orbiter nose cone and ET 1st detected, appeared white
    - 81.82 sec: struck under Orbiter's left wing, disintegrates into a cloud of orange-colored debris

Presenter M3/Material | Date FINAL | Slide 1 of 7 | Closed

Ascent Debris

- **Background / Facts:**
  - Debris detected by radar following SRB separation from T+150 to T+230 seconds
    - One radar (radar 0.14) detected 21 items
    - Another radar (radar 28.14) detected 6 items
    - Radar Cross-Section (RCS) ranged from –26 to –15 dBsm
    - Radar return signal was not of sufficient strength to determine approximate shape, size or rigidity of the debris
    - Radar analysis results are consistent with the debris analyses from previous STS missions

Presenter M3/Material | Date FINAL | Slide 2 of 7 | Closed

Ascent Debris
Radar 0.14 Results

CATALOG #	PIECE NUMBER	FIRST APPEARANCE	LAST APPEARANCE	MAX RCS (dBsm)	RANGE SEPARATION RATE (m/s)
①	**	80.4	87	5	14
②	1	152.5	156	*	*
3	2	152.5	162.5	-24	326
4	3	153	160	-23	229
5	4	156	170	-20	217
6	5	158.5	171	-21	309
7	6	164	170	-21	312
8	7	166.5	173	-21	357
9	8	167	184.5	-19	260
10	9	170	184.5	-19	265
11	10	174.5	180	-20	290
12	11	173	180	-21	206
13	12	174	175.1	-19	244
14	13	175.5	180	-18	180
15	14	178	180	-18	296
16	15	184	190	-20	236

Presenter M3/Material | Date FINAL | Slide 3 of 7 | Closed

Ascent Debris
Radar 0.14 Results (Continued)

CATALOG #	PIECE NUMBER	FIRST APPEARANCE	LAST APPEARANCE	MAX RCS (dBsm)	RANGE SEPARATION RATE (m/s)
17	16	187	192.5	-20	649
18	17	204.5	210	*	*
19	18	204.5	214	-26	326
20	19	204.5	212	-24	166
21	20	206	212	-24	225
22	21	211.5	228	-22	219

* The RCS and range separation rate of these pieces cannot be determined due to the low level of signal returns. RCS is estimated to be within 0 to 3 dB of the Minimum Detectable RCS.
** These events have been determined to be due to plume effects.

Presenter M3/Material | Date FINAL | Slide 4 of 7 | Closed

Ascent Debris
Radar 28.14 Results

CATALOG #	PIECE NUMBER	FIRST APPEARANCE	LAST APPEARANCE	MAX RCS (dBsm)	RANGE SEPARATION RATE (m/s)
23	2	152	158.5	*	*
24	4	154.5	162	-17	400
25	8 or 9	167	176.5	-20	221
26	14	179	187.5	-15	884
27	16	201	207	*	*
28	17 or 18	205	208.5	*	*

* The RCS and range separation rate of these pieces cannot be determined due to the low level of signal returns. RCS is estimated to be within 0 to 3 dB of the Minimum Detectable RCS.

Presenter M3/Material | Date FINAL | Slide 5 of 7 | Closed

Ascent Debris

- **Findings:**
  - Radar detected debris after T=150 seconds
    - Debris could not be identified
    - Radar returns similar to past STS missions
  - CB DOAMS observed debris between orbiter and ET at 81.66 seconds
- **Recommendations:**
  - Issue should be closed

Presenter M3/Material | Date FINAL | Slide 6 of 7 | Closed

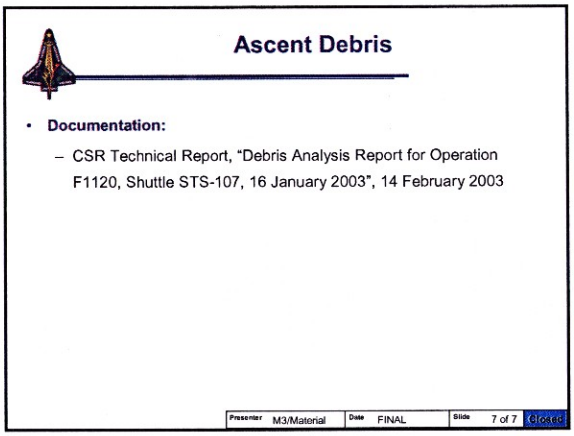
Ascent Debris
• Documentation:
– CSR Technical Report, "Debris Analysis Report for Operation F1120, Shuttle STS-107, 16 January 2003", 14 February 2003
Presenter M3/Material
Date FINAL
Slide 7 of 7

Maintenance
Hold Down Cable Anomaly

- **Action / Issue:** Could orbiter MECs/cabling failure to the hold down post (HDP) pyrotechnics and ET vent arm system (ETVAS) be catastrophic?
- **Background / Facts:**
  - PIA #3007 stated that STS 112 had a failure in the system that controls firing of the initiators in each SRB restraint nut
  - Redundancy in each Master Events Controller (MEC)
    - MEC#1 feeds A system, MEC#2 feeds B system
  - Each nut has two initiators, one on A system, one on B
  - Signal sent by MECs to nut to fire and ETVAS to retract
  - Either MEC will operate system in event of failure in the other
  - During STS-112 the Ground Launch Sequencer (GLS) issued "Cut Off" at T+ 3 Seconds
    - Post launch review indicated that system A HDP and ETVAS Pyrotechnic Initiator Controllers (PICs) did not discharge

Presenter: M3/Maintenance | Date: FINAL | Slide: 1 of 7 | Closed

Maintenance
Hold Down Cable Anomaly

- **Findings:**
  - Pyro systems A and B are independent and redundant
  - The HDP and ETVAS systems receive Fire commands at T-0
    - Fire 1 and Fire 2 commands are sent as a nearly simultaneous event
  - Each redundant pyro device is initiated by a dedicated PIC
    - 16 separate PICs for "A" and "B" HDP devices and four separate PICs for "A" and "B" ETVAS devices
  - The PIC design requires 3 separate commands to detonate its NASA Standard Initiator (NSI)
    - ARM—Activates the PIC's power supply and charges capacitor bank
    - Fire1—Activates a switching transistor controlling the PIC output return and enables the Fire2
    - Fire2—Activates a switching transistor controlling the PIC output
  - ETVAS pyro Fire commands are branched from the HDP Fire commands
  - HDP "A" PIC and ETVAS "A" PIC failed to discharge

Presenter: M3/Maintenance | Date: FINAL | Slide: 2 of 7 | Closed

Maintenance
Hold Down Cable Anomaly

- **Findings:**
  - Extensive analysis and study was initiated immediately
  - Approx. 25 different potential fault chains were considered as source of A system failure
  - Definite cause never determined, considered intermittent
  - Most probable cause: the fire 1 command wasn't transmitted properly from MEC 1 to PIC Rack 6743 in the MLP
  - Focus of command path anomaly is on T-0 electrical interface
    - Not cleared during investigation since normal function (T-0 separation) destroyed evidence
  - Inspection has detected wear and contamination at interface

Presenter: M3/Maintenance | Date: FINAL | Slide: 3 of 7 | Closed

Maintenance
Hold Down Cable Anomaly

- **Findings:**
  - STS-112 investigation recommendations implemented:
    - All T-0 Ground Cables have been replaced after every flight
    - T-0 interface to PIC rack cable in redesign, ETIC July 03
      - Old T-0 Ground cable and this Kapton
    - All Orbiter T-0 Connector Savers have been replaced
      - Pyro connectors prescreened with pin retention test
    - Connector saver mate will be verified using Videoscope
- **Recommendations:**
  - Inquiry released for failure potential on this CRIT IR system
  - Specifically, what is chance of a concurrent failure of a MEC/cable and one or more initiators? What would result? Can NASA redesign system to add cable from each system to every initiator so a signal system failure would not disable half of the initiators?

Presenter: M3/Maintenance | Date: FINAL | Slide: 4 of 7 | Closed

Maintenance
Hold Down Cable Anomaly

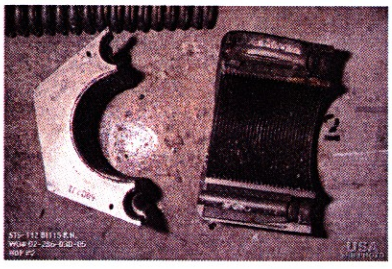

Presenter: M3/Maintenance | Date: FINAL | Slide: 5 of 7 | Closed

Maintenance
Hold Down Cable Anomaly

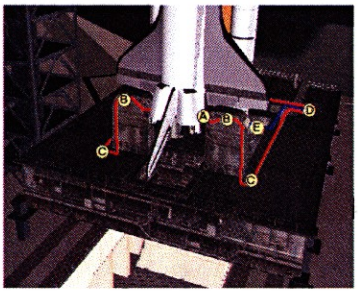

Presenter: M3/Maintenance | Date: FINAL | Slide: 6 of 7 | Closed

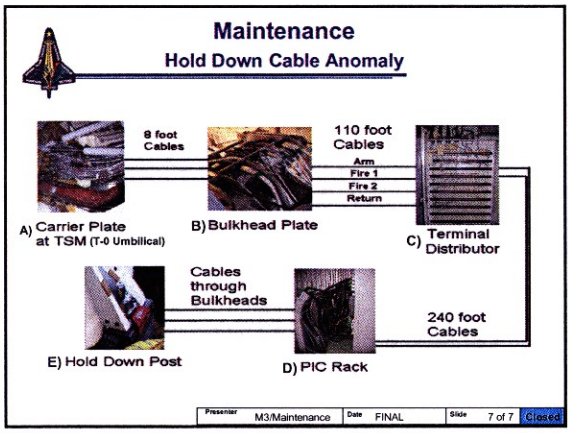
Maintenance
Hold Down Cable Anomaly
8 foot Cables
110 foot Cables
Arm
Fire 1
Fire 2
Return
A) Carrier Plate at TSM (T-0 Umbilical)
B) Bulkhead Plate
C) Terminal Distributor
Cables through Bulkheads
240 foot Cables
E) Hold Down Post
D) PIC Rack
Presenter M3/Maintenance
Date FINAL
Slide 7 of 7
Closed

Other Orbit

22-1 FD2 On-Orbit Object

Matrix

Presenter	CAIB/Group 1	Date	FINAL	Slide	25 of 32

FD2 – On-Orbit Object

- **Action / Issue:** Determine on-orbit object detected by ground radar during post-flight data review
- **Background / Facts:**
  - While on orbit, 3,180 separate radar or optical observations of Columbia were collected
  - Collection sites includes: Eglin AFB, Beale AFB, Navy Space Surveillance, Cape Cod, Maui, and Kirtland AFB
  - Each observation was individually examined **after** the accident
  - 1st Space Control Squadron and AFSPC Space Analysis Center personnel conducted detailed analysis
  - Post-flight processing discovered a small object in shuttle orbit
    - Object referred to by International Designator 2003-003B

Presenter M3/Material | Date FINAL | Slide 1 of 25 | Closed

FD2 – On-Orbit Object

- **Event Timeline:**
  - Jan 17, 1442Z: Shuttle reoriented
    - Moved from tail-first to right wing-first orientation
  - Jan 17, 1517Z: Shuttle reoriented
    - Returned to tail-first orientation
  - Jan 17, 1500-1615Z: Object 2003-003B separates
  - Jan 17, 1857Z: First confirmed sensor track
  - Jan 19, 2146Z: Last confirmed sensor track
  - Jan 20, 0145-0445Z: Object 2003-003B decays

Presenter M3/Material | Date FINAL | Slide 2 of 25 | Closed

FD2 – On-Orbit Object

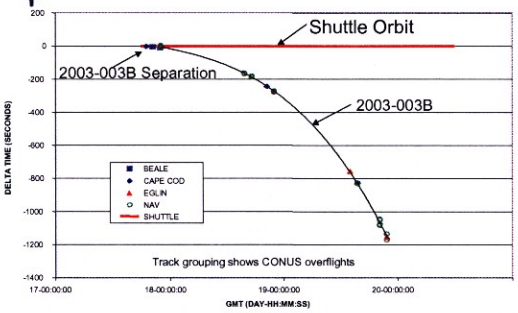

Presenter M3/Material | Date FINAL | Slide 3 of 25 | Closed

FD2 – On-Orbit Object

- **Background / Facts:**
  - On-orbit object 2003-003B detected by Cape Cod PAVE PAWS radar during passes on 3 days before de-orbiting
    - Day 1 Track: -18 to - 4 dBsm
    - Day 2 Track: -15 to - 2 dBsm
    - Day 3 Track: -13 to -1.75 dBsm
  - Object tumble rate increased with time
  - RCS varies from ~0.1 to ~0.7 m^2

Presenter M3/Material | Date FINAL | Slide 4 of 25 | Closed

FD2 – On-Orbit Object

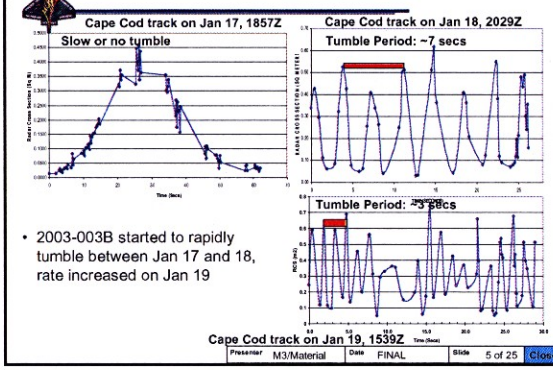

- 2003-003B started to rapidly tumble between Jan 17 and 18, rate increased on Jan 19

Presenter M3/Material | Date FINAL | Slide 5 of 25 | Closed

FD2 – On-Orbit Object

- **Background / Facts :**
  - Radar Cross-Section (RCS) combined with ballistics results used to determine potential FD2 object
    - Potential candidate orbiter parts must match both RCS and ballistics as a minimum
  - AFRL conducted RCS measurements of 26 orbiter parts to compare to on-orbit signature and 4 RCC pieces from STS-107 RH debris
  - US Space Command determined ballistics coefficient of on-orbit object and all parts measured for RCS signature
    - Ballistics coefficient = (Drag Coefficient * Area) / Mass
    - Area/Mass ratio for on-orbit object determined to be 0.1 meters^2 / kg

Presenter M3/Material | Date FINAL | Slide 6 of 25 | Closed

1

FD2 – On-Orbit Object

- **Background / Facts:**
  - Obtained RCS measurements for the following RH parts from OV-102 debris:
    - Part 51311, 8" x 13" RCC fragment with lip
    - Part 37736, curved RCC fragment with no lip
    - Part 2018, 8" x 11" RCC flat acreage
    - Part 51313, T-seal fragment at panel 8/9

Presenter M3/Material | Date FINAL | Slide 7 of 25 | Closed

FD2 – On-Orbit Object

- **Background / Facts:**
  - Parts that matched both RCS signature and ballistics:
    - RCC panel acreage piece if approximately 100 to 150 inch^2
  - Parts rejected due to RCS signature, ballistics or both include:
    - 14 blanket-type insulators or cloth-like material
    - 5 lower carrier panels with and without horsecollars
    - 4 RSI tiles
    - 1 RCC panel with all metallic hardware
    - 1 upper carrier panel

Presenter M3/Material | Date FINAL | Slide 8 of 25 | Closed

FD2 – On-Orbit Object

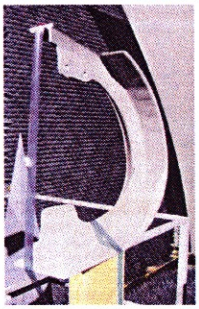

RCC T-Seal Measured for RCS Signature

Presenter M3/Material | Date FINAL | Slide 9 of 25 | Closed

FD2 – On-Orbit Object

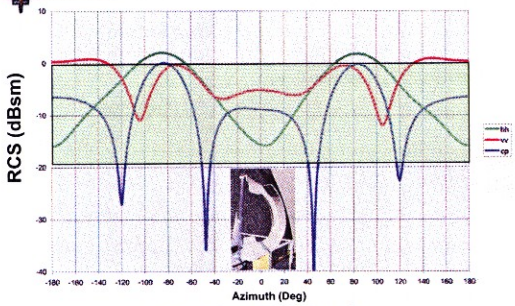

RCC T-Seal RCS Results

Presenter M3/Material | Date FINAL | Slide 10 of 25 | Closed

FD2 – On-Orbit Object

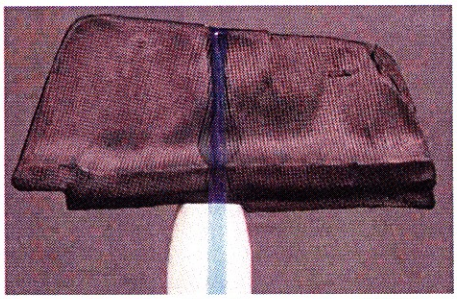

WLE Spanner Beam Insulator Measured for RCS Signature

Presenter M3/Material | Date FINAL | Slide 11 of 25 | Closed

FD2 – On-Orbit Object

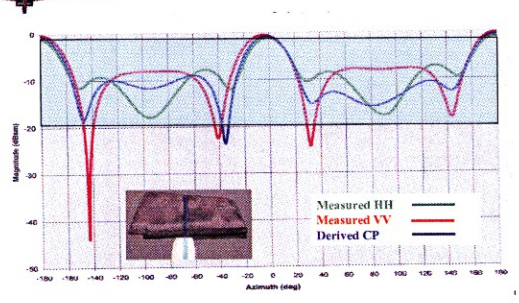

WLE Spanner Beam Insulator RCS Results

Presenter M3/Material | Date FINAL | Slide 12 of 25 | Closed

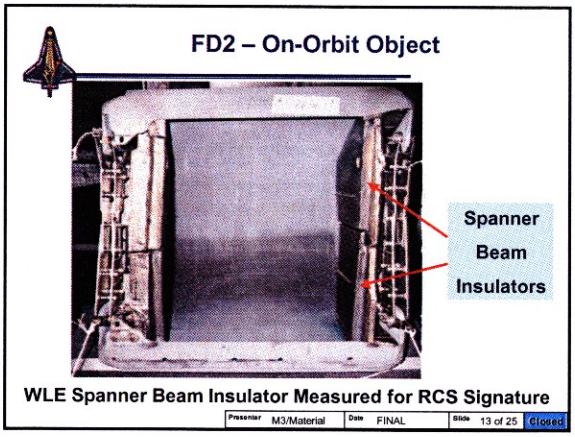
FD2 – On-Orbit Object
Spanner
Beam
Insulators
WLE Spanner Beam Insulator Measured for RCS Signature
Presenter M3/Material
Date FINAL
Slide 13 of 25
Closed

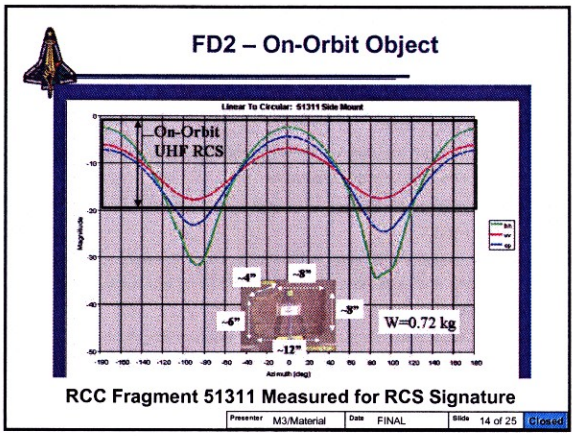
FD2 – On-Orbit Object
Linear To Circular: 51311 Side Mount
On-Orbit
UHF RCS
~4"
~8"
~6"
~8"
~12"
W=0.72 kg
RCC Fragment 51311 Measured for RCS Signature
Presenter M3/Material
Date FINAL
Slide 14 of 25
Closed

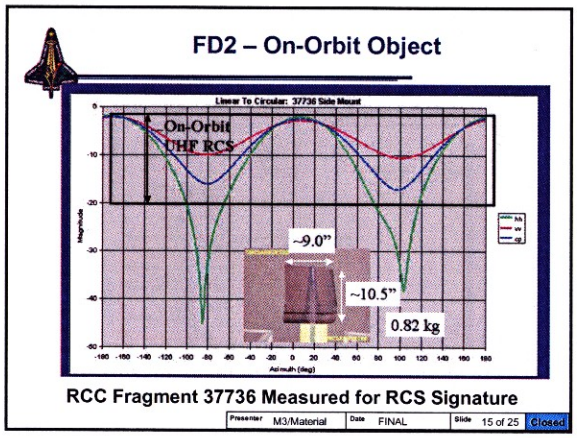
FD2 – On-Orbit Object
Linear To Circular: 37736 Side Mount
On-Orbit
UHF RCS
~9.0"
~10.5"
0.82 kg
RCC Fragment 37736 Measured for RCS Signature
Presenter M3/Material
Date FINAL
Slide 15 of 25
Closed

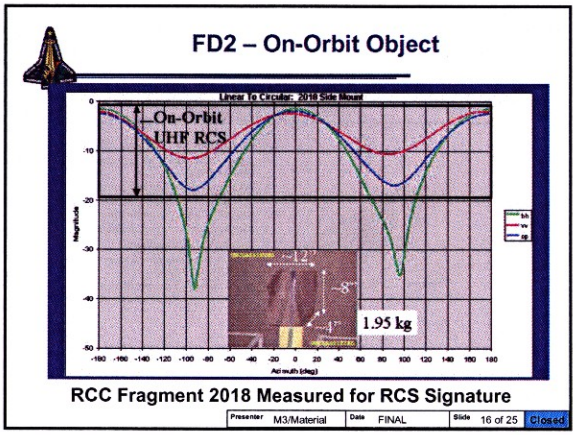
FD2 – On-Orbit Object
Linear To Circular: 2018 Side Mount
On-Orbit
UHF RCS
~8"
~4"
1.95 kg
RCC Fragment 2018 Measured for RCS Signature
Presenter M3/Material
Date FINAL
Slide 16 of 25
Closed

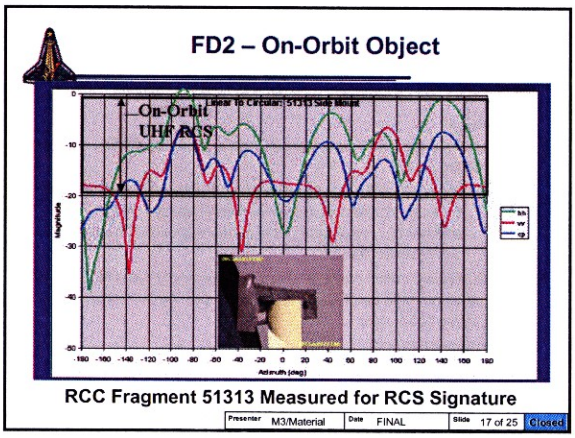
FD2 – On-Orbit Object
On-Orbit
UHF RCS
RCC Fragment 51313 Measured for RCS Signature
Presenter M3/Material
Date FINAL
Slide 17 of 25
Closed

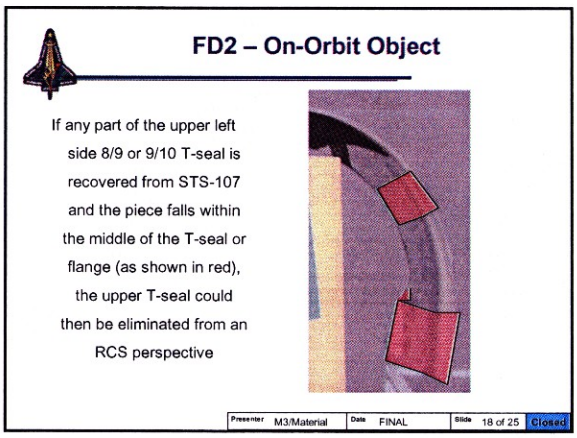
FD2 – On-Orbit Object
If any part of the upper left side 8/9 or 9/10 T-seal is recovered from STS-107 and the piece falls within the middle of the T-seal or flange (as shown in red), the upper T-seal could then be eliminated from an RCS perspective
Presenter M3/Material
Date FINAL
Slide 18 of 25
Closed

FD2 – On-Orbit Object
VHF RCS Data From Altair Radar

- **Background / Facts:**
  - A "Corrected" fragment of VHF RCS data was observed from FD2 object on-orbit from the Altair radar
    - Fidelity of this data set estimated by MIT Lincoln Laboratory to be +/- 3 dB.
  - AFRL tested VV/HH co-polarized RCS of 4 RCC debris components (T-seals and panel acreage) at VHF (158 MHz) with the following results:
    - Cannot eliminate the T-Seal, either whole or fragment
    - Cannot eliminate or exclude RCC panel acreage, especially if the piece has an edge or corner that produces a resonance effect

Presenter M3/Material | Date FINAL | Slide 19 of 25 | Closed

FD2 – On-Orbit Object
MIT Lincoln Lab Results

Summary

FOUO

- Paucity of RCS data eliminates possibility of directly measuring fragment size/shape
- Effort lead to extraction of considerable new RCS measurement data on fragment
  - ALTAIR UHF/VHF
  - Eglin UHF
  - NAVSPASUR Bi-static VHF
- New RCS data provides new insight into fragment
  - Motion dynamics
  - Bulk size
- Orbit analysis agrees with AFSPC estimate of fragment departure time
- Credible "flat-spin" motion model developed for fragment
  - Fits radar measured body motion across all 3 days
- Qualitative match made between time history of radar RCS measurements and RCS simulated for spinning ½ T-seal
  - Full T-seal match not nearly as good
  - Cross pole data does not show expected deep nulls

FOUO

MIT Lincoln Laboratory

Presenter M3/Material | Date FINAL | Slide 20 of 25 | Closed

FD2 – On-Orbit Object
MIT Lincoln Lab Results

Flat Spin Example
(Propeller Blade Concept)

FOUO

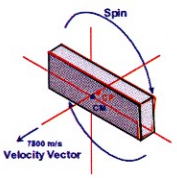

- Closure panel 15in x 5in x 2in
- 3/16in aluminum plate with 2in tiles on the back
- Free-molecular flow regime
- May be just enough restoring moment to keep face forward
- Twist provides rolling moment
- Exponential atmosphere
- Ballistic coefficient ~10 kg/m² (remains constant)
- Small twist +/-1deg produces ~2.6s spin period after 2 days

(Center of Pressure CP aft of Center of Mass CM)

FOUO

MIT Lincoln Laboratory

Presenter M3/Material | Date FINAL | Slide 21 of 25 | Closed

FD2 – On-Orbit Object
MIT Lincoln Lab Results

Spin Up Motion Model
Shuttle Fragment Frequency Points Computed From RCS Data

FOUO

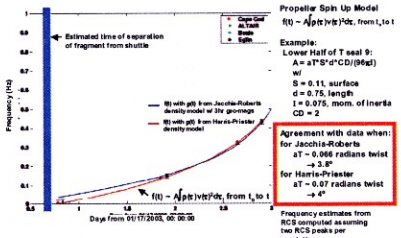

Consistent with T-Seal Design

FOUO

MIT Lincoln Laboratory

Presenter M3/Material | Date FINAL | Slide 22 of 25 | Closed

FD2 – On-Orbit Object
MIT Lincoln Lab Results for ½ T-Seal

Static Pattern: Half T-seal 9 HH
Data: Eglin Day 19 HH Polarization
Motion: 2.316 sec. Period

FOUO

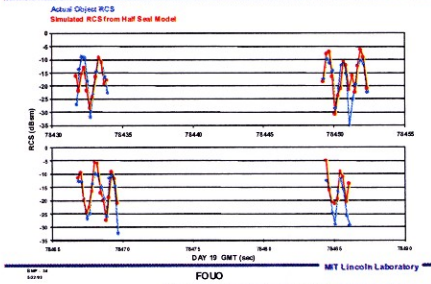

FOUO

MIT Lincoln Laboratory

Presenter M3/Material | Date FINAL | Slide 23 of 25 | Closed

FD2 – On-Orbit Object

- **Findings:**
  - 41 items screened for either ballistics and/or RCS testing by NASA, AFSPC, and AFRL
    - Only RCC T-Seal/T-Seal Fragment, RCC panel fragment in the 1/3 inch thick regions (lower portion of panel 8 and 9) or a spanner beam insulator could not be excluded based on RCS and ballistics results
  - Qualitative match made between time history of radar RCS measurements and RCS simulated for spinning ½ T-seal by MIT Lincoln Laboratory
- **Recommendations:**
  - Continuously evaluate potential on-orbit object as debris reconstruction efforts progress

Presenter M3/Material | Date FINAL | Slide 24 of 25 | Closed

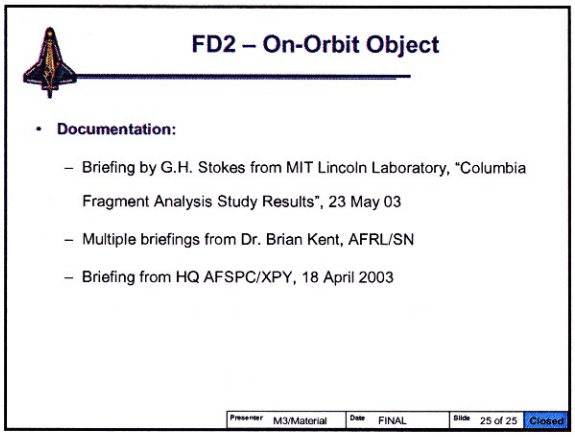
FD2 – On-Orbit Object
• Documentation:
– Briefing by G.H. Stokes from MIT Lincoln Laboratory, "Columbia Fragment Analysis Study Results", 23 May 03
– Multiple briefings from Dr. Brian Kent, AFRL/SN
– Briefing from HQ AFSPC/XPY, 18 April 2003
Presenter M3/Material
Date FINAL
Slide 25 of 25
Closed

5

Organization
Production

23-1 SSP Centralization/Decentralization

23-5 Contract Management Culture

23-6 CoFR Process Integrity

Matrix

Presenter	CAIB/Group 1	Date	FINAL	Slide	26 of 32

Production-Organization
Centralization/Decentralization in SSP

- **Action / Issue:** Organizational Characteristics, Policies, & Practices
- **Background / Facts:**
  - Centralized and formal communications, decision-making, and risk management to cope with "tight coupling" linked to the numerous events associated with "normal operations" to provide for immediate responses (e.g., FRR, COFR, etc.).
  - Decentralized and more informal communications, decision-making, and risk management to provide for deliberate analysis to handle unplanned "interactive complexity" of failures by those closest to subsystems (e.g., MMT, MER, etc.).
  - Scheduling demands, workload, staffing shortages/inexperience, performance incentives , etc. increase the opportunity for tighter coupling and additional interactive complexity for both normal and emergency operations.

Presenter: M3/Human Factors | Date: FINAL | Slide: 1 of 4 | Closed

Production-Organization
Centralization/Decentralization in SSP

- **Findings:** Demands associated with centralized and decentralized processes are incompatible, while the former presses for inputs to address scheduled events, the latter presses for time to thoroughly make assessments. Centralization leads to more prescribed meetings, documentation, etc., whereas decentralization tends to be more informal and have varied patterns of interactions, level of documentation, etc.
- **Recommendations:** SSP should be viewed as a flight test environment, therefore the post-launch management should be more formal and systematic, similar to that for the Pre-Launch COFR

Presenter: M3/Human Factors | Date: FINAL | Slide: 2 of 4 | Closed

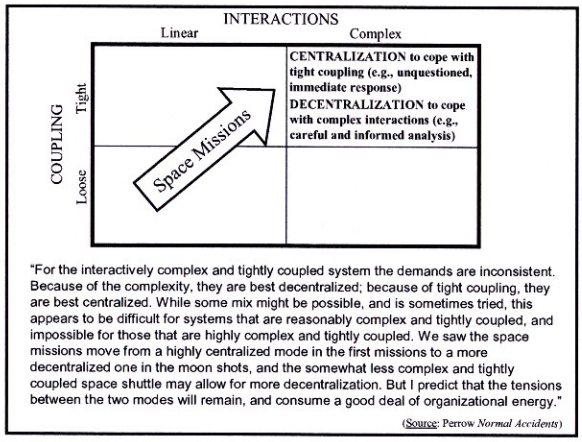

"For the interactively complex and tightly coupled system the demands are inconsistent. Because of the complexity, they are best decentralized; because of tight coupling, they are best centralized. While some mix might be possible, and is sometimes tried, this appears to be difficult for systems that are reasonably complex and tightly coupled, and impossible for those that are highly complex and tightly coupled. We saw the space missions move from a highly centralized mode in the first missions to a more decentralized one in the moon shots, and the somewhat less complex and tightly coupled space shuttle may allow for more decentralization. But I predict that the tensions between the two modes will remain, and consume a good deal of organizational energy."

(Source: Perrow *Normal Accidents*)

Centralization/Decentralization in SSP: Pre- vs. Post- Launch Comparison

- Pre-Launch:
  - Centralized Decision Making w/Defined CoC Roles/Actions
  - Formalized Mission Planning, Problem Resolution, & SOF Determination

  Theme:

  "*Prove There Is Not A SOF Problem*"
  - NASA Space Centers Visibly Interacting
  - Interactive Complexity Due To Geographic Dislocation & Component Integration Process
  - Tight Coupling Due to Mission Schedule & Stovepipe Operations; # CRIT 1 Hazards & Lack of Redundant Systems
- Post-Launch:
  - Centralized Decision Making w/Delegated Responsibilities
  - Less Formal Mission Monitoring, Anomaly Review, & SOF Determination

  Theme:

  "*Prove There Is A SOF Problem*"
  - JSC Primary w/Minimal Outside Center Input
  - Greater Interactive Complexity Due To Orbiter Technologies & Space Environment
  - Increased Tight Coupling Due to Real-time OPS & Little On-Orbit Flexibility; # CRIT 1 Hazards & Lack of Redundant Systems

Presenter: M3/Human Factors | Date: FINAL | Slide: 4 of 4 | Closed

1

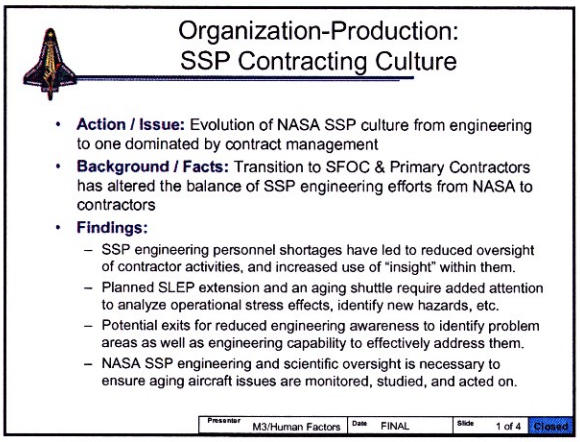
Organization-Production:
SSP Contracting Culture
• Action / Issue: Evolution of NASA SSP culture from engineering to one dominated by contract management
• Background / Facts: Transition to SFOC & Primary Contractors has altered the balance of SSP engineering efforts from NASA to contractors
• Findings:
– SSP engineering personnel shortages have led to reduced oversight of contractor activities, and increased use of "insight" within them.
– Planned SLEP extension and an aging shuttle require added attention to analyze operational stress effects, identify new hazards, etc.
– Potential exits for reduced engineering awareness to identify problem areas as well as engineering capability to effectively address them.
– NASA SSP engineering and scientific oversight is necessary to ensure aging aircraft issues are monitored, studied, and acted on.
Presenter M3/Human Factors Date FINAL Slide 1 of 4 Closed

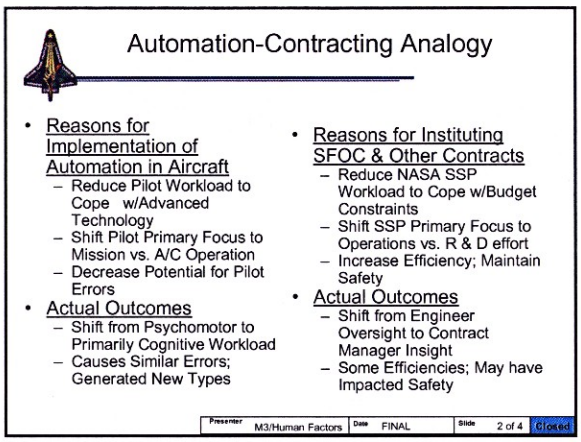
Automation-Contracting Analogy
• Reasons for Implementation of Automation in Aircraft
– Reduce Pilot Workload to Cope w/Advanced Technology
– Shift Pilot Primary Focus to Mission vs. A/C Operation
– Decrease Potential for Pilot Errors
• Actual Outcomes
– Shift from Psychomotor to Primarily Cognitive Workload
– Causes Similar Errors; Generated New Types
• Reasons for Instituting SFOC & Other Contracts
– Reduce NASA SSP Workload to Cope w/Budget Constraints
– Shift SSP Primary Focus to Operations vs. R & D effort
– Increase Efficiency; Maintain Safety
• Actual Outcomes
– Shift from Engineer Oversight to Contract Manager Insight
– Some Efficiencies; May have Impacted Safety
Presenter M3/Human Factors Date FINAL Slide 2 of 4 Closed

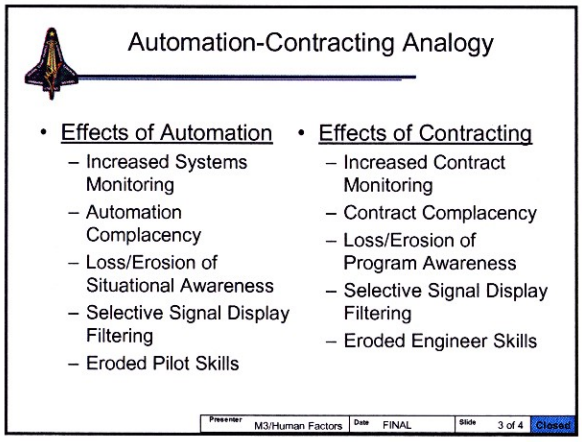
Automation-Contracting Analogy
• Effects of Automation
– Increased Systems Monitoring
– Automation Complacency
– Loss/Erosion of Situational Awareness
– Selective Signal Display Filtering
– Eroded Pilot Skills
• Effects of Contracting
– Increased Contract Monitoring
– Contract Complacency
– Loss/Erosion of Program Awareness
– Selective Signal Display Filtering
– Eroded Engineer Skills
Presenter M3/Human Factors Date FINAL Slide 3 of 4 Closed

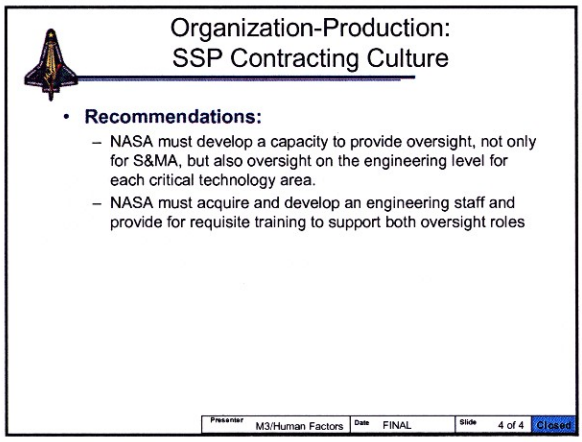
Organization-Production:
SSP Contracting Culture
• Recommendations:
– NASA must develop a capacity to provide oversight, not only for S&MA, but also oversight on the engineering level for each critical technology area.
– NASA must acquire and develop an engineering staff and provide for requisite training to support both oversight roles
Presenter M3/Human Factors Date FINAL Slide 4 of 4 Closed

Organization- Fleet Experience: Potential COFR Process Defense Breaches

- **Action/Issue:** Pre-Launch Factors May Impact COFR Process Effectiveness
- **Background/Facts:** Reason's "Swiss Cheese" Model is used to categorize/organize latent conditions of failed or absent defenses that "set the stage" for active failures which lead to incidents; it can also be used for examining those factors affecting decision-making
- **Findings:** SSP COFR is considered a rigorous, systematic process leading to accurate SOF launch decisions. It is perceived as being shielded from outside factors, yet if an organization, supervisor, or member is influenced by external factors, it can be contended the process can miss signals of absent/failed defenses, accept perceived minor deviations, or permit margin of safety reductions.

Presenter: M3/Human Factors | Date: FINAL | Slide: 1 of 5 | Closed

Potential COFR Process Defense Breaches: Applying Reason's "Swiss Cheese" Model

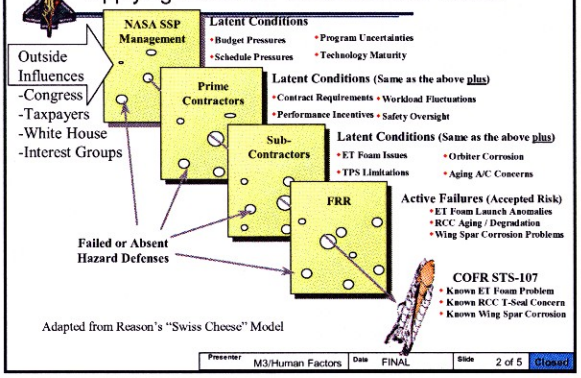

Adapted from Reason's "Swiss Cheese" Model

Presenter: M3/Human Factors | Date: FINAL | Slide: 2 of 5 | Closed

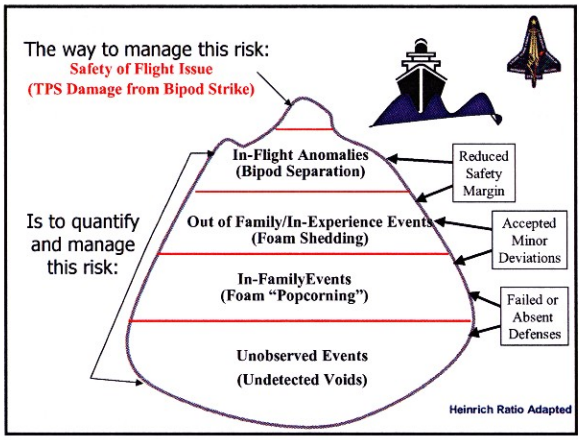

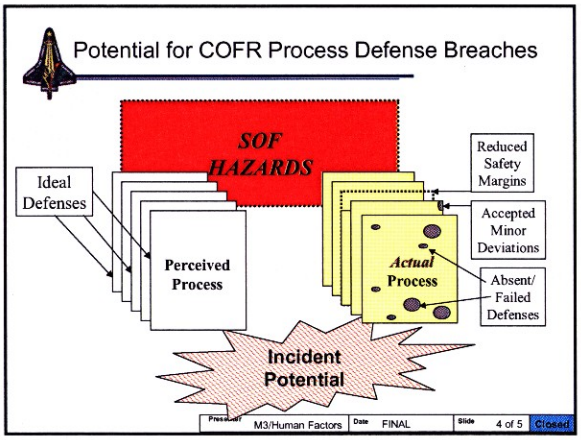

Organization-Fleet Experience: Potential COFR Process Defense Breaches

- **Recommendations:**
  - NASA should examine potential pre-launch factors that can influence FRRs and the subsequent COFR process to ensure external factors do not weigh-in on SOF decisions
  - NASA should ensure potential SOF information is actively sought and acted upon, not filtered and ignored due to pressure, complacency, or norms.

Presenter: M3/Human Factors | Date: FINAL | Slide: 5 of 5 | Closed

1

Organization
Fleet Experience – Aging

23-2 High Reliability Organizations

23-3 Risk Acceptance in the SSP

23-9 Role of Space Shuttle Systems Integration Office

Matrix

Presenter	CAIB/Group 1	Date	FINAL	Slide	27 of 32

Organization-Fleet Experience: SSP as a High Reliability Organization

- **Action / Issue:** The SSP needs to more closely align itself as an HRO
- **Background / Facts:** Organizations that have less than their "fair share" of failures (e.g., nuclear submarines, petrochemical plants, etc. despite:
  - managing complex & demanding technologies
  - meeting peak requirements & time pressures
  - routinely handling significant risks & hazards
  - executing dynamic/intensely interactive tasks

  are termed High Reliability Organizations (HROs). They exhibit "mindfulness", an ability to identify an maintain awareness of potentially hazardous situations and to act quickly to contain or mitigate them

Presenter M3/Human Factors | Date FINAL | Slide 1 of 6 | Closed

Organization-Fleet Experience: SSP as a High Reliability Organization

- **Background / Facts (con't):**
  - ✓ Preoccupation with failures- treating any performance lapses as a symptom of a system based problem
  - ✓ Reluctance to simplify interpretations- deliberately taking steps to create more complete/nuanced pictures
  - ✓ Sensitivity to operations- attending to front-line conditions for well-developed situational awareness
  - ✓ Commitment to resilience- develop capabilities to detect, contain, and recover from inevitable errors
  - ✓ Deference to expertise- encouragement of a fluid decision-making system using appropriate personnel

Presenter M3/Human Factors | Date FINAL | Slide 2 of 6 | Closed

Organization-Fleet Experience: SSP as a High Reliability Organization

- **Findings:** Pre-launch events as well as historical factors indicate the SSP is not fully aligned as an HRO. Some examples that the SSP does not fully exhibit the characteristics of a HRO, include :
  - ➢ *Preoccupation with Success:*
    - ET foam shedding accepted as in-family event
  - ➢ *Tendency to Simplify Interpretations:*
    - Shuttle is operational and its technology is mature
  - ➢ *Insensitivity to Operations:*
    - Effect of consolidation moves on experience and skill level
  - ➢ *Non-Commitment to Resilience:*
    - Predisposition for post-landing vs. on-orbit damage assessment
  - ➢ *Lack of Deference to Expertise:*
    - Limited post-launch JSC interactions w/centers (OPS vs. R&D)

Presenter M3/Human Factors | Date FINAL | Slide 3 of 6 | Closed

Table 1: Reasons for Spacecraft Failures

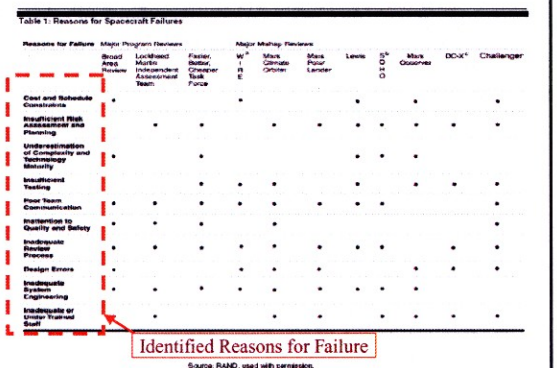

Source: RAND, used with permission.

Presenter M3/Human Factors | Date FINAL | Slide 4 of 6 | Closed

Reason for Failure (Taken from Rand report)	STS-107 Pre-Launch Issues
Cost & Schedule Constraints	OMM Overrun, #Mission Slips, & ISS Schedule
Insufficient Risk Assessment & Planning	Previous Foam, Tile, & RCC Events & Potential Interaction
Underestimation of Complexity & (Overestimation of) Technology Maturity	TPS- Tile/RCC & Foam (e.g., MFG, Install, Aging, & Repairs)
Insufficient Testing (e.g., Testing, Analysis, NDE, etc.)	TPS- Tile/RCC & Foam (e.g., MFG, Install, Aging, & Repairs)
Poor Team Communication	Stove-Piping of Component Operations & Horizontal Integration in Technology Areas
Inattention to Quality & Safety	SFOC Transition: NASA Insight vs. Oversight
Inadequate Review Process	TPS- Tile/RCC & Foam (e.g., MFG, Install, Aging, & Repairs)
Design Errors (e.g. Inadequate Specs, Criteria, etc.)	TPS- Tile/ RCC & Foam (e.g., Anomalies, Specifications, BiPOD, etc.)
Inadequate System Engineering	Component Integration Concerns (e.g., ET Foam Mating Damage)
Inadequate or Under Trained Staff	ENG: Staffing Levels, Size, & Experience* OMM: QA Insp., Aging Workers, & Workload*

*Not a factor in STS-107

Presenter M3/Human Factors | Date FINAL | Slide 5 of 6 | Closed

Organization-Fleet Experience: SSP as a High Reliability Organization

- **Recommendations:**
  - Re-examine treatment/resolution of past, present & future anomalies
  - Provide for greater hands-on presence & involvement of NASA personnel in all aspects of the SSP
  - Reform pre-/ post- launch reviews, add a pre-landing review, & retool on-orbit mission monitoring/support
  - Provide for improved post-launch & on-orbit vehicle assessment as well as on-orbit repair & escape
  - Establish a matrix of Subject Matter Experts to be enlisted for respective technology areas impacted by anomalies

Presenter M3/Human Factors | Date FINAL | Slide 6 of 6 | Closed

Organization-Fleet Experience:
Risk Acceptance in the SSP

- **Action / Issue:** **Risk Acceptance in the SSP**
- **Background / Facts:** Scholars studying NASA & SSP have raised the issue of **risk acceptance,** overlooking/failing to recognize the severity of possible problems (e.g.,Vaughan, Feynman, etc.)

"Experience Rationalization"

SPACE SHUTTLE PROGRAM
Space Shuttle Projects Office (MSFC)

STS-112/ET-115 Bipod Ramp Foam Loss

- Rationale for Flight
  - Current bipod ramp closeout has not been changed since STS-54 (ET-51)
  - Pre-Orbiter has not experienced "Safety of Flight" damage from loss of foam in 112 flights (including 3 known flights with bipod ramp foam loss)
  - There have been no design / process / equipment changes over the the last 60 ETs (flights)
  - All ramp closeout work (including ET-115 and ET-116) was performed by experienced practitioners (all over 20 years experience each)
  - Ramp foam application involves craftsmanship in the use of validated application processes
  - No change in inspection / Process control / Post application handling, etc.
  - Probability of loss of ramp TPS is no higher/no lower than previous flights
  - **The ET is safe to fly with no new concerns (and no added risk)**

Prior to Foam Closeout
After Final Foam Trim
Bipod Attach Fitting

Presenter M3/Human Factors | Date FINAL | Slide 1 of 8 | Closed

Organization-Fleet Experience:
Risk Acceptance in the SSP

How do We Know What to Fix?

There are things we know that we know,
There are things we do know that we don't know,
There are things we don't know that we don't know.

Honorable Donald Rumsfeld
U. S. Secretary of Defense
NATO HQ Press Conference, June '02

Presenter M3/Human Factors | Date FINAL | Slide 2 of 8 | Closed

Organization-Fleet Experience:
Risk Acceptance in the SSP

- **Findings:**
  - Risk acceptance may be a continuing phenomenon in the SSP.
    - Increase in waivers and "work arounds"
  - There seems to be repeated failure to identify and attend to weak signals occurring over time.
    - "foam loss never has been a SOF issue"
  - Bryan O'Connor (NASA HQ S&MA Officer) discusses 3 levels of the Risk Iceberg to describe Risk Acceptance in NASA:
    1. Known Knowns: Repeated or routine events and established facts.
    2. Known Unknowns: Known possible events, but unknown when or how they will happen. Also, recognizing the limits of one's knowledge.
    3. Unknown Unknowns: Rare (or have yet to occur) events. There is insufficient vigilance in the process to look for their possibility.
    4. *A possible fourth category:* Unknown Knowns: Situations where an abundance of data exists (known knowns), but it's too much information to filter through & select out the relevant data for a given situation in a timely manner. High signal to noise ratio (Thompson 2003). Especially relevant during crisis or unusual conditions, like mishaps.

Presenter M3/Human Factors | Date FINAL | Slide 3 of 8 | Closed

The Risk Iceberg

- Mishap recommendations
- Problem solutions
- IFA fixes

Known Knowns

- FMEA/Hazard controls
- Close call recommendations

Known Unknowns

- Ignored close calls?
- Old cert, new environment?
- Inadvertent excursions out of cert/family?
- Hardware talking…nobody listening?

Unknown Unknowns

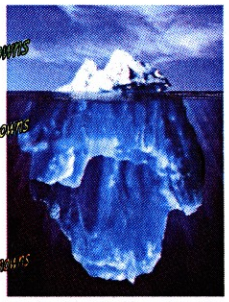

Taken from a briefing by Bryan O'Connor on 19 March 03

Presenter M3/Human Factors | Date FINAL | Slide 4 of 8 | Closed

Organization-Fleet Experience:
Risk Acceptance in the SSP

Collaborative Product Between NASA and CAIB

LEVELS OF RISK ICEBURG	SKILLS	ANALYTICAL TOOLS
• Known Known –Repeated / routine events –Established facts –Verifiable	• Classical surveillance techniques • Mentoring of engineering science • Structured analytical approaches	• Statistical Process Control • Test / checkout procedures • Trending analysis
• Known Unknowns –Known possible events –Unknown when or how –Limits of knowledge known	• Inquisitive surveillance • Predictive / imaginative hypothesis • Measurements of knowledge	• Predictive analyses / documentation • Controlled experimentation • Test – to – failure approaches • Fleet leader approaches
• Unknown Known –Data exist –Too much information to filter –"High signal to noise"	• Data management skills • Interpretation skills • "Art" form of surveillance	• Automated data search technology • Trending / Analytical techniques • Intelligent applications
• Unknown Unknown –Rare / yet to occur events –Unable to recognize possibility –Beyond limits of knowledge	• Out-of-box thinking / inquisitive • Exploratory surveillance • High experience / technical knowledge • Imaginative / Intuitive –Naïve Objectivity "fresh look" perspective	• Integrity programs • Fleet leader approaches • Test – analyze – fix approaches • Design for test

- All levels require skill development and maintenance (structured training, simulation, case studies, etc.)
- Great discipline and care must prevent one category from "sliding" into lower category
- Proper selection and execution of analytical tools will draw out and nurture (exercise) the desired skill

Presenter M3/Human Factors | Date FINAL | Slide 5 of 8 | Closed

Organization-Fleet Experience:
Risk Acceptance in the SSP

- **Recommendations:**
  SSP should increase its vigilance regarding Risk Acceptance by incorporating various preventative measures. For example:
  - A Personnel-focused Mentoring Program:
    - The SSP should establish ongoing relationships between experienced and less experienced personnel.
    - Senior personnel have knowledge stores, problem resolution experience, troubleshooting, and ability to detect nuances with complex systems.
    - Such attributes allow for practicing "art" vs. science of Shuttle engineering when confronted with situations where existing models and processes may not fit perfectly.
  - A Process-focused Program:
    - The SSP should consider incorporating a structured paradigm providing a disciplined approach to technical analyses & other critical processes.
      - The KNOT model (Known, Need to Know, Opinion, Thought to be Know) is used by some USAF analysts in cases of unexpected or unexplained failures. It can be used in combination with a "fishbone" model of fault-tree analysis.

Presenter M3/Human Factors | Date FINAL | Slide 6 of 8 | Closed

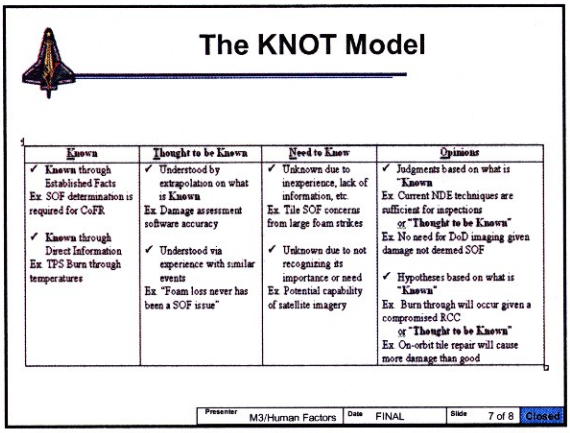

The KNOT Model

Known	Thought to be Known	Need to Know	Opinions
✓ **Known** through Established Facts Ex. SOF determination is required for CoFR ✓ **Known** through Direct Information Ex. TPS Burn through temperatures	✓ Understood by extrapolation on what is **Known** Ex. Damage assessment software accuracy ✓ Understood via experience with similar events Ex. "Foam loss never has been a SOF issue"	✓ Unknown due to inexperience, lack of information, etc. Ex. Tile SOF concerns from large foam strikes ✓ Unknown due to not recognizing its importance or need Ex. Potential capability of satellite imagery	✓ Judgments based on what is "**Known**" Ex. Current NDE techniques are sufficient for inspections or "**Thought to be Known**" Ex. No need for DoD imaging given damage not deemed SOF ✓ Hypotheses based on what is "**Known**" Ex. Burn through will occur given a compromised RCC or "**Thought to be Known**" Ex. On-orbit tile repair will cause more damage than good

Presenter: M3/Human Factors | Date: FINAL | Slide: 7 of 8 | Closed

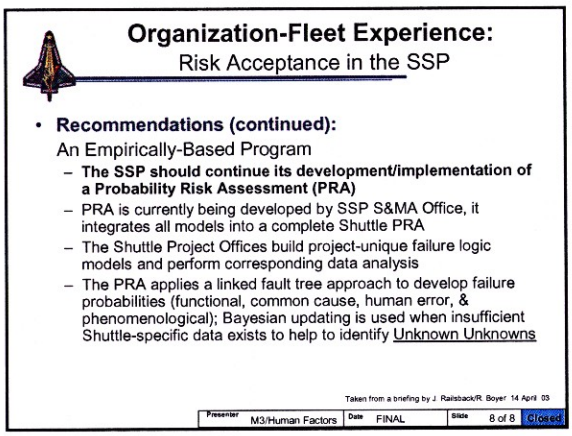

Organization-Fleet Experience:
Risk Acceptance in the SSP

- **Recommendations (continued):**
  An Empirically-Based Program
  - **The SSP should continue its development/implementation of a Probability Risk Assessment (PRA)**
  - PRA is currently being developed by SSP S&MA Office, it integrates all models into a complete Shuttle PRA
  - The Shuttle Project Offices build project-unique failure logic models and perform corresponding data analysis
  - The PRA applies a linked fault tree approach to develop failure probabilities (functional, common cause, human error, & phenomenological); Bayesian updating is used when insufficient Shuttle-specific data exists to help to identify Unknown Unknowns

Taken from a briefing by J. Railsback/R. Boyer 14 April 03

Presenter: M3/Human Factors | Date: FINAL | Slide: 8 of 8 | Closed

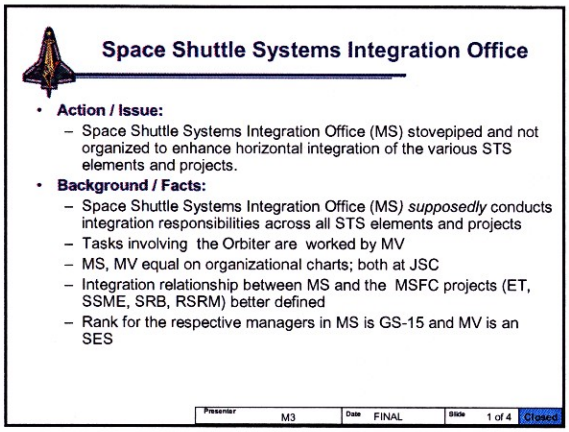
Space Shuttle Systems Integration Office
• Action / Issue:
– Space Shuttle Systems Integration Office (MS) stovepiped and not organized to enhance horizontal integration of the various STS elements and projects.
• Background / Facts:
– Space Shuttle Systems Integration Office (MS) supposedly conducts integration responsibilities across all STS elements and projects
– Tasks involving the Orbiter are worked by MV
– MS, MV equal on organizational charts; both at JSC
– Integration relationship between MS and the MSFC projects (ET, SSME, SRB, RSRM) better defined
– Rank for the respective managers in MS is GS-15 and MV is an SES
Presenter M3 Date FINAL Slide 1 of 4 Closed

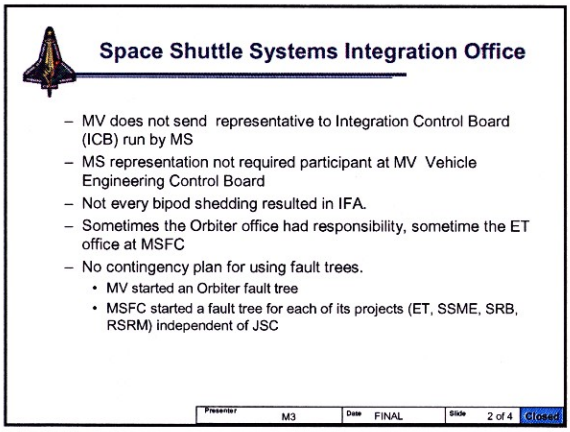
Space Shuttle Systems Integration Office
– MV does not send representative to Integration Control Board (ICB) run by MS
– MS representation not required participant at MV Vehicle Engineering Control Board
– Not every bipod shedding resulted in IFA.
– Sometimes the Orbiter office had responsibility, sometime the ET office at MSFC
– No contingency plan for using fault trees.
• MV started an Orbiter fault tree
• MSFC started a fault tree for each of its projects (ET, SSME, SRB, RSRM) independent of JSC
Presenter M3 Date FINAL Slide 2 of 4 Closed

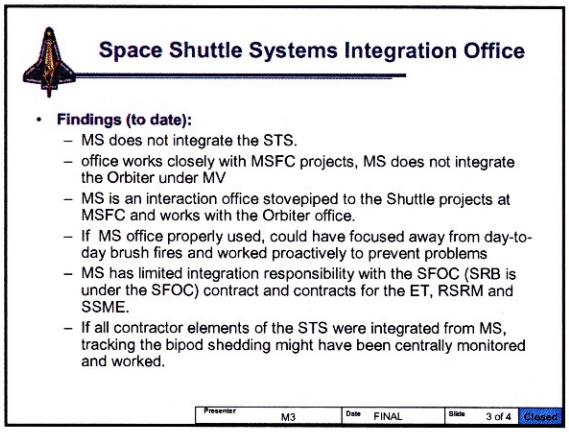
Space Shuttle Systems Integration Office
• Findings (to date):
– MS does not integrate the STS.
– office works closely with MSFC projects, MS does not integrate the Orbiter under MV
– MS is an interaction office stovepiped to the Shuttle projects at MSFC and works with the Orbiter office.
– If MS office properly used, could have focused away from day-to-day brush fires and worked proactively to prevent problems
– MS has limited integration responsibility with the SFOC (SRB is under the SFOC) contract and contracts for the ET, RSRM and SSME.
– If all contractor elements of the STS were integrated from MS, tracking the bipod shedding might have been centrally monitored and worked.
Presenter M3 Date FINAL Slide 3 of 4 Closed

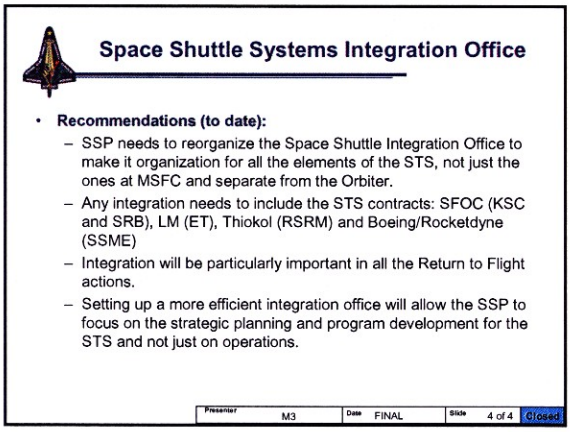
Space Shuttle Systems Integration Office
• Recommendations (to date):
– SSP needs to reorganize the Space Shuttle Integration Office to make it organization for all the elements of the STS, not just the ones at MSFC and separate from the Orbiter.
– Any integration needs to include the STS contracts: SFOC (KSC and SRB), LM (ET), Thiokol (RSRM) and Boeing/Rocketdyne (SSME)
– Integration will be particularly important in all the Return to Flight actions.
– Setting up a more efficient integration office will allow the SSP to focus on the strategic planning and program development for the STS and not just on operations.
Presenter M3 Date FINAL Slide 4 of 4 Closed

Organization Maintenance

24-2 Human Factors and Maintenance Operations

24-3 Human Factors in NDE, QA, and Inspection

24-4 Human Factors in FOD Prevention

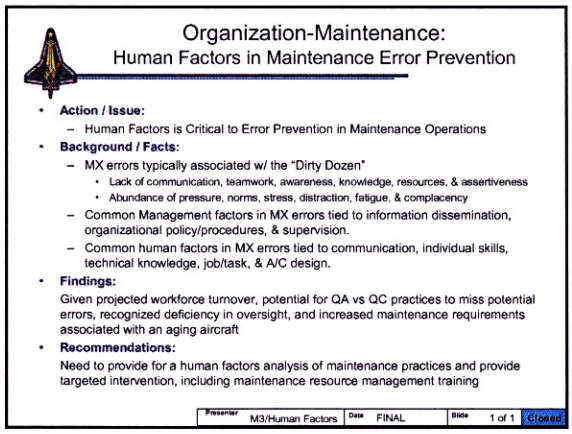

Organization-Maintenance:
Human Factors in Maintenance Error Prevention

- **Action / Issue:**
  - Human Factors is Critical to Error Prevention in Maintenance Operations
- **Background / Facts:**
  - MX errors typically associated w/ the "Dirty Dozen"
    - Lack of communication, teamwork, awareness, knowledge, resources, & assertiveness
    - Abundance of pressure, norms, stress, distraction, fatigue, & complacency
  - Common Management factors in MX errors tied to information dissemination, organizational policy/procedures, & supervision.
  - Common human factors in MX errors tied to communication, individual skills, technical knowledge, job/task, & A/C design.
- **Findings:**

  Given projected workforce turnover, potential for QA vs QC practices to miss potential errors, recognized deficiency in oversight, and increased maintenance requirements associated with an aging aircraft
- **Recommendations:**

  Need to provide for a human factors analysis of maintenance practices and provide targeted intervention, including maintenance resource management training

Presenter	M3/Human Factors	Date	FINAL	Slide	1 of 1	Closed

1

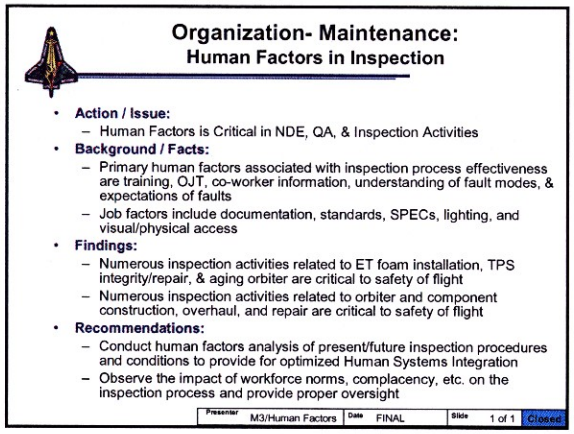

Organization- Maintenance:
Human Factors in Inspection

- **Action / Issue:**
  - Human Factors is Critical in NDE, QA, & Inspection Activities
- **Background / Facts:**
  - Primary human factors associated with inspection process effectiveness are training, OJT, co-worker information, understanding of fault modes, & expectations of faults
  - Job factors include documentation, standards, SPECs, lighting, and visual/physical access
- **Findings:**
  - Numerous inspection activities related to ET foam installation, TPS integrity/repair, & aging orbiter are critical to safety of flight
  - Numerous inspection activities related to orbiter and component construction, overhaul, and repair are critical to safety of flight
- **Recommendations:**
  - Conduct human factors analysis of present/future inspection procedures and conditions to provide for optimized Human Systems Integration
  - Observe the impact of workforce norms, complacency, etc. on the inspection process and provide proper oversight

Presenter	M3/Human Factors	Date	FINAL	Slide	1 of 1	Closed

1

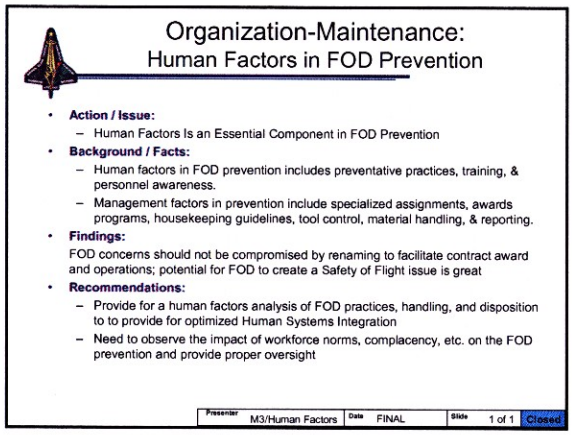
Organization-Maintenance:
Human Factors in FOD Prevention
Action / Issue:
Human Factors Is an Essential Component in FOD Prevention
Background / Facts:
Human factors in FOD prevention includes preventative practices, training, & personnel awareness.
Management factors in prevention include specialized assignments, awards programs, housekeeping guidelines, tool control, material handling, & reporting.
Findings:
FOD concerns should not be compromised by renaming to facilitate contract award and operations; potential for FOD to create a Safety of Flight issue is great
Recommendations:
Provide for a human factors analysis of FOD practices, handling, and disposition to to provide for optimized Human Systems Integration
Need to observe the impact of workforce norms, complacency, etc. on the FOD prevention and provide proper oversight
Presenter M3/Human Factors
Date FINAL
Slide 1 of 1
Closed

1

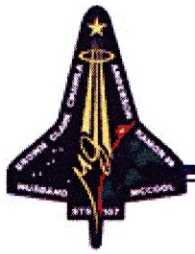

Organization
Orbit

23-4 Langley and JSC E-Mail Exchange

23-7 Engineer Simulation Training

23-8 Boeing Transition of Orbiter Support from CA to TX

Decentralization & Resilience in Handling Anomalies: LaRC-JSC Exchanges on MLG Concerns

- **Action / Issue:**
  - Decentralization is critical in detecting anomalies and providing for resilience
- **Background / Facts:**
  - Jan 27th JSC & LaRC engineers had phone/e-mail exchanges on the foam debris assessment (included charts indicating that the left MLG area could be involved).
  - JSC engineer stated there was concern the MLG door was "vulnerable", perhaps leading to a two flat tire landing (or compromising MLG). Discussed simulating landings to evaluate outcomes, but no formal request was pending; Explored doing "after hours" piggy-backing on astronaut training underway at NASA ARC.
  - LaRC engineer expressed concerns to JSC counterpart to be prepared in case a problem arose on landing; contacted management on JAN 28th an about concerns
  - Reviewed previous related data runs; JAN 30th provided scenarios tied to potential MLG problem (most had severe outcomes). Simulation results for a two flat tire landing provided on JAN 31st showed it was survivable/controllable condition.
  - Based on established working relationships, the negative scenario observations (with caveats) were passed to select JSC personnel for consideration, whereas favorable simulation results were given to a wider JSC audience for review.

Presenter: M3/Human Factors | Date: FINAL | Slide: 1 of 5 | Closed

Decentralization & Resilience in Handling Anomalies: LaRC-JSC Exchanges on MLG Concerns

- **Findings:**
  - Formal dissemination of foam debris assessment did not make it directly (or in a timely manner) to all potentially affected parties, especially those who may have the expertise for the proper diagnosis of associated problems and /or the development of mitigation/containment procedures.
  - Ineffective dissemination leads to informal channeling that can not be relied upon to get information expeditiously to affected system/technology experts and provide them an adequate chances to make inputs for decision-making.
  - E-mail/Powerpoint are tools for asynchronous communication (often to a select audience), however they can not be relied upon to ensure understanding, influence decision-making, or elicit action (especially from non-targeted recipients/respondents).
  - Note. The actions these working level engineers took to overcome limited horizontal integration between OPS and R&D (& NASA Centers) so as to network, marshal resources, and prepare for a potential contingency is an example of the resilient spirit that led to the successful return of Apollo 13.

Presenter: M3/Human Factors | Date: FINAL | Slide: 2 of 5 | Closed

Decentralization & Resilience in Handling Anomalies: LaRC-JSC Exchanges on MLG Concerns

- **Recommendations:**
  - Guidelines regarding communication of safety issues/concerns should be established to ensure early/full dissemination of information to recognized government and contractor system and technology experts who work OPS, R&D, etc. at all NASA Centers.
  - All channels of communication (e-mail, phone, etc.) should be open and encouraged to discuss/disseminate safety concerns, but assurance must be made that information is raised to appropriate management and safety oversight personnel.
  - Disseminate information prior to decision-making sessions (if possible) for preliminary review and potential comment to increase early feedback, participation from attendees, as well as comments from interested parties unable to attend.

Presenter: M3/Human Factors | Date: FINAL | Slide: 3 of 5 | Closed

Decentralization & Resilience in Handling Anomalies: LaRC-JSC Exchanges on MLG Concerns

- **References:**
  - E-mail exchanges on foam damage and LaRC and JSC interactions regarding the initial damage assessment. Complete set of email beginning on Jan. 23. (http://www.nasa.gov/pdf/2207main_COL_email_030226.pdf)
  - E-mail exchange on Jan. 28-31, 2003, on assessment of potential for a breach in the landing gear door or wheel well during re-entry into Earth's atmosphere (http://www.nasa.gov/pdf/2205main_COL_debris_email.pdf)
  - E-mail exchange within LaRC regarding main gear breach concerns on Jan. 31. (http://www.nasa.gov/pdf/2208main_COL_email_larc.pdf)
  - Daugherty, R. & Shuart, M. (10 MAR 03) NASA Langley Press Conference (http://www.spaceref.com/news/viewsr.html?pid=8270)
  - NASA HQ Records Management Bulletin 97.01 (http://www.hq.nasa.gov/office/codea/codeaq/recn9701.html)
  - NASA Information Systems Directorate e-mail Guidelines (http://isd.isc.nasa.gov/GA/computer/email/EmailDosDonts.html)
  - Palme, J. (23 MAY 99). Support for Decisions by E-mail. TERENA Conference (http://www.dsv.su.se/~jpalme/ietf/JPMADS.html)

Presenter: M3/Human Factors | Date: FINAL | Slide: 4 of 5 | Closed

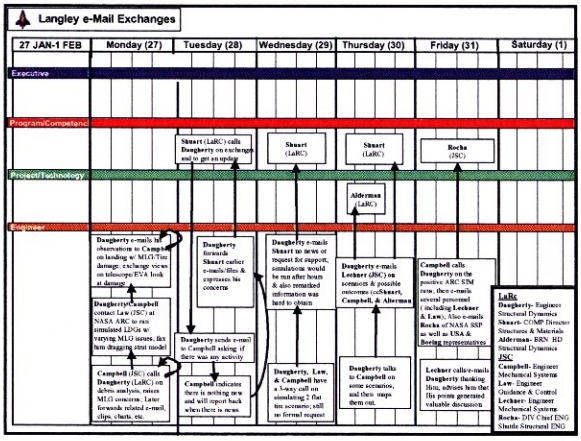

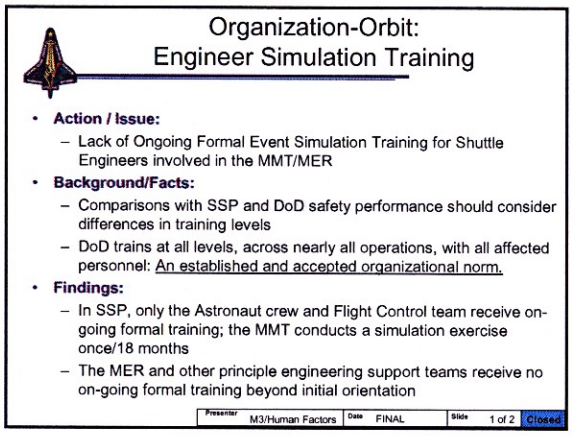
Organization-Orbit:
Engineer Simulation Training
• Action / Issue:
– Lack of Ongoing Formal Event Simulation Training for Shuttle Engineers involved in the MMT/MER
• Background/Facts:
– Comparisons with SSP and DoD safety performance should consider differences in training levels
– DoD trains at all levels, across nearly all operations, with all affected personnel: An established and accepted organizational norm.
• Findings:
– In SSP, only the Astronaut crew and Flight Control team receive on-going formal training; the MMT conducts a simulation exercise once/18 months
– The MER and other principle engineering support teams receive no on-going formal training beyond initial orientation
Presenter M3/Human Factors
Date FINAL
Slide 1 of 2
Closed

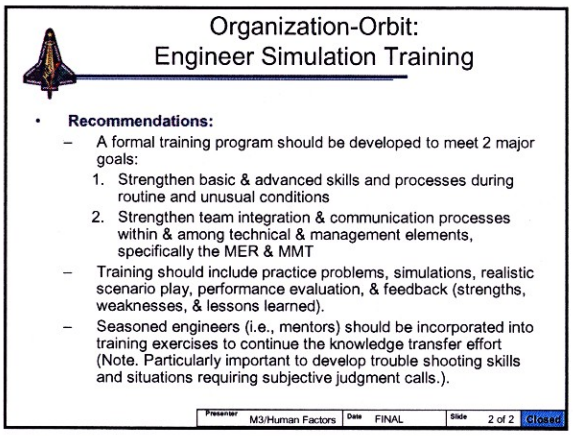
Organization-Orbit:
Engineer Simulation Training
• Recommendations:
– A formal training program should be developed to meet 2 major goals:
1. Strengthen basic & advanced skills and processes during routine and unusual conditions
2. Strengthen team integration & communication processes within & among technical & management elements, specifically the MER & MMT
– Training should include practice problems, simulations, realistic scenario play, performance evaluation, & feedback (strengths, weaknesses, & lessons learned).
– Seasoned engineers (i.e., mentors) should be incorporated into training exercises to continue the knowledge transfer effort (Note. Particularly important to develop trouble shooting skills and situations requiring subjective judgment calls.).
Presenter M3/Human Factors
Date FINAL
Slide 2 of 2
Closed

1

Organization-Orbit:
Boeing Transition of Orbiter Support from CA to TX

- **Action / Issue:**
  - Boeing transition (12/01-03/03) of Shuttle operations (OPS) support function from Huntington Beach, CA (HB) to Houston,TX (HOU) precipitated a large turnover in personnel with significant program experience and technical expertise.
  - To minimize effects from a potential loss of experience/expertise, Boeing planned a risk managed knowledge transition process, with an emphasis on key positions.
  - Process was not uniformly implemented, potentially impacting support capabilities.
- **Background:**
  - In Dittemore's March 6th testimony to the CAIB, he indicated the transition was a contractor-based initiative to get "engineering closer to the customer" and achieve ". . .efficiencies that would lower the overall cost".
  - Pre-transition Boeing had ~1,300 jobs: ~1,000 (76%) in HB & ~150 (12%) in HOU; Post-transition Boeing had ~500 jobs in HB (38%) & ~580 jobs (45%) in HOU.
  - Only 97 HB Boeing incumbents transferred to HOU, requiring over 330 jobs to be filled (This included both critical SSM and various engineering positions).

Presenter: M3/Human Factors | Date: FINAL | Slide: 1 of 14 | Closed

Organization-Orbit:
Boeing Transition of Orbiter Support from CA to TX

Boeing Proprietary Information Not for Release

- **Background (con't):**
  - By March 31, 2003 there were 531 total jobs that transferred from Huntington Beach to Houston and Florida
  - Of the 531 jobs that transferred, 140 people relocated from Huntington Beach. The remaining 391 positions were filled by replacements

Job Distribution by Category (March 31, 2003)

	Engineer	Management	Others	Totals
Total Jobs Transferred (est)	424	55	52	**531**
Relocations (est)	89	33	18	**140**
Replacements (est)	335	22	34	**391**

Presenter: M3/Human Factors | Date: FINAL | Slide: 2 of 14 | Closed

Organization-Orbit:
Boeing Transition of Orbiter Support from CA to TX

Overall, their plan appeared to be both systematic and comprehensive, encompassing:

- Knowledge capture process (KCP), to catalog incumbent KSAs through questionnaires, video interviews, and toolboxes
- Critical skill checklists, based on inputs from each incumbent performing a task comprising a given "job"
- HB competency managers and HOU Integrated Team Managers review of KCPs w/ corresponding checklists,
- Risk management of the task transition process, to effectively identify, assess, and address hazards; "Red-flagging" areas for additional oversight based risk
- 15-month transition timeline that covered two shuttle missions (STS 112 & 113), providing "real time" OJT
- Set 3-month period for individual job transition, to include face-to-face training
- Certification process for key positions (e.g.,Sub-System Manager) & Integrated Team Manager sign-off for others
- Established guidelines for identifying and selecting critical personnel and engineering replacement candidates
- Pairing a job candidate with respective incumbents for formal task training and mentoring whenever possible

Presenter: M3/Human Factors | Date: FINAL | Slide: 3 of 14 | Closed

Organization-Orbit:
Boeing Transition of Orbiter Support from CA to TX

- **Background (continued):**
  - Boeing transition review (11/02) accomplishments listed hired 95% of replacements, completed 85% of programmed training (70% completed all of the training), and replaced 98% of critical skills
  - Boeing HB site director indicated that a further endorsement of the transition's success was USA's consideration to use this KCP model in their organization.
  - Boeing performance and safety award fee scores were higher than pre-transition
- **Findings:**

  Witness Impressions of the Overall Transition Process
  - Despite the official reports' positive tone and the site director's comments, witnesses questioned the actual success of the transition process (including knowledge capture, individual training, and exit evaluation).
  - Witnesses characterized the process as compressed (and consequently rushed); lacking standardization, clear job-based criteria, and post transition group/ individual risk re-assessment.
  - Further, former analysts (aero, stress, thermo, & structures) had additional concerns that the transition could impact the on-orbit reported damage assessment process/findings.

Presenter: M3/Human Factors | Date: FINAL | Slide: 4 of 14 | Closed

Organization-Orbit:
Boeing Transition of Orbiter Support from CA to TX

- **Findings (continued):**

  Knowledge Capture Process (KCP)
  - Witnesses' General Observations:
    - The KCP was seen as "too little, too late."
    - Parts of the KCP were not as useful as others; whereas some felt the entire KCP was not useful at all.
    - The KCP was not as specific on analyses functions as it was in hardware areas; but lead analysts reported they did effectively document troubleshooting, problem-solving, lessons learned, etc.
    - Overall, there was a cumulative loss of experience across all technology areas. This concern was expressed to management in both formal and informal settings, including all-hands, staff, and hallway meetings.
    - HOU witnesses reported that while KCP was lacking, actual knowledge transfer process was sufficient
  - Questionnaires:
    - The job questionnaire documented inputs, processes, and products of a position.
    - Some witnesses indicated it was adequate, but it could not capture decades of experience.
    - It was perceived as too brief and inadequate, as it gathered only top-level, generic information about positions.

Presenter: M3/Human Factors | Date: FINAL | Slide: 5 of 14 | Closed

Organization-Orbit:
Boeing Transition of Orbiter Support from CA to TX

- **Findings (continued):**

  Knowledge Capture Process (KCP)
  - Video Interviews:
    - The video-taped interviews were intended as a "how-to" demonstration of procedures lending themselves to hands-on or hardware processes.
    - Many incumbents were not asked to participate in videotape interview.
    - Most felt they were useful for technical, hands-on tasks, but not useful for other activities, like procedures and analysis.
    - One analyst thought this was the only useful KCP component.
  - Toolboxes:
    - Incumbents were asked to make a complete listing of all files, references, locations of guiding documents, policies, analytical tools, software, etc. that would be relevant for a particular position.
    - While this compilation was not required of some lower-level engineers, most agreed that this was the most useful part of the KCP.
    - HOU engineers acknowledged there is continuing work being done on the toolboxes

Presenter: M3/Human Factors | Date: FINAL | Slide: 6 of 14 | Closed

Organization-Orbit:
Boeing Transition of Orbiter Support from CA to TX

- **Findings (continued):**

Knowledge Capture Process (KCP)

– Management Review:
  - Review of the KCP products after the incumbent compiled them was sporadic at best.
  - They generally indicated that their manager received it and in some cases reviewed it, and asked for clarification. In other cases they merely took it, with no revision or refinement.
  - The witnesses collectively stated there was no training on how to do the KCP, no standardization of the product produced, and it was not systematically/uniformly implemented.
  - The process was more difficult for senior personnel and for management types, e.g., to produce an effective video interview as stated above.
  - Overall, the KCP did not consistently follow the transition plan in many cases, especially for non-critical positions.

Presenter: M3/Human Factors | Date: FINAL | Slide: 7 of 14 | Closed

Organization-Orbit:
Boeing Transition of Orbiter Support from CA to TX

- **Findings (continued):**

Selection, Training, & Certification
– HOU mgmt. oversaw most new personnel hiring. Except for a few senior positions and transfers from HB, the HB supervisors were not involved in the selection process.
– KCP end products were collected from the incumbents and then provided to the Integrated Team Managers (ITMs) who oversaw the transition training for new hires and transfers. ITMs were either senior SSP people who transferred or experienced SSP people recruited from NASA or USA. There were some instances where the ITM themselves were new hires.
– Training utilized the HB incumbent when they were available. The incumbent conducted 2-3 weeks of training with the trainee at HB, while the ITMs oversaw the remainder of the training process at HOU.
– Training plans or checklists were to be covered over a 3-month period (approx.) for each job; all jobs were to be transitioned over an 18-month period. When incumbents and management were satisfied with trainee's performance, the incumbent was given a 60-day notice. Incumbent remained available to the trainee during this time period.
– New SSMs required a controlled, multi-step training and certification process. Certifications requirements and processes were approved by USA/NASA. Each SSM was evaluated by Boeing/Customer Boards foe final certification.

Presenter: M3/Human Factors | Date: FINAL | Slide: 8 of 14 | Closed

Organization-Orbit:
Boeing Transition of Orbiter Support from CA to TX

- **Findings (continued):**

Selection, Training, & Certification
– The transition's beginning phases appeared rushed. Thus some positions and any process perturbations (e.g., a candidate or incumbent leaving) compromised process integrity.
– Toward the transition's end, some witnesses stated there was pressure to finish training to complete the transition. Though incumbents were available for training candidates, they were not given 3 dedicated months to train: either the incumbent attended to other duties or the candidate was not on site.
– During the 3-month training period, the incumbent charged a special transition job order number, while the candidate charged to SSP.
  - There was some pressure not to exceed the allotted transition time, despite the trainee's proficiency status and/or checklist completion.
  - HOU management stated the training budget was under-run by $2M
– In contrast to HB incumbent experience, the replacement HOU based employees reported the training to be sufficient in quantity and quality.
– Most candidates were deemed proficient for normal tasks and conditions. However, incumbents indicated that training was conducted with an understanding that in unusual cases (out of family, etc.), the incumbent and trainee would work together.

Presenter: M3/Human Factors | Date: FINAL | Slide: 9 of 14 | Closed

Organization-Orbit:
Boeing Transition of Orbiter Support from CA to TX

- **Findings (continued):**

Selection, Training, & Certification
– Exit criteria for the training process was unclear to incumbents, other than completing the checklist/training plan. In some instances, the list was not completed or the candidate was not proficient to the task(s) by the time the transition ended. *Some witnesses expressed significant frustration and concern about this.*
– Most SSM training and certification processes were coordinated by managers. They indicated the process was rigorous and included USA/NASA participation. Most SSMs held significant seniority with the SSP. Although some portions of the certification process was not highly structured, most witnesses said this process went very well. Records indicated that the training and certification process for SSMs was well documented.
– The incumbent and candidate worked together for STS 112 & STS 113, two missions flown during the transition process. STS-107 was the first mission flown after transition completion, with HOU holding primary responsibility.
– After the transition was complete, incumbents provided further assistance ***only as requested by the new employee.***

Presenter: M3/Human Factors | Date: FINAL | Slide: 10 of 14 | Closed

Organization-Orbit:
Boeing Transition of Orbiter Support from CA to TX

- **Findings (continued):**
- Risk Management and Over-Site
  – Risk mitigation plans for each task/task group were incorporated into official Task Transition Plans. This process included assessment of probability,severity, and risk mitigation for each risk item. Tasks were identified and tasked on team schedules; monitoring of the knowledge capture, transition training, and certification/completion processes were employed. However, Witnesses observed the process as non-systematic in overall implementation.
  – Baseline risk assessments were not adjusted on an individual basis to consider experience level, "out of family" selection, etc.
  – A 02/02 NASA SSP S&MA risk mgmt. report indicated "yellow" (5- "high" likelihood & 2- "med-low" consequences) through FY 02 for supportability and safety due to the Boeing relocation; A 10/02 NASA SSP S&MA risk mgmt. report indicated "yellow" (4- high-med likelihood & 2- med-low consequences) for supportability and safety through FY 03 (est. Resolution 01/03) due to the Boeing relocation.
  – Listed as a "Top Issue", the impacts listed were "Low percentage of incumbent personnel willing to relocate" and "Could impact COFR process integrity." It also indicated various concerns: loss of existing skills and experience, challenges to replace personnel, incumbent retention to support contracted tasks and train replacements, and quality of NASA/USA available for out-of-family support.

Presenter: M3/Human Factors | Date: FINAL | Slide: 11 of 14 | Closed

Organization-Orbit:
Boeing Transition of Orbiter Support from CA to TX

- **Findings (continued):**

Risk Management and Over-Site
– STS-107 & STS-114 were listed as yellow due to some Orbiter replacement personnel generating flight products with approved work around plan and some System Integration personnel having no certified back-up. The action plan to mitigate risk was listed as "Transition plan has been developed and partnered with NASA" and "NASA and USA in oversight mode until transition completed".
– Once the transition process was complete, no re-assessment of individual risk was done.
– Boeing contracted Independent Risk Assessments (IRA) for the transition.
  - The goal was to complete staff training by the end of 12/02. "Victory Criteria" included: completing 90% of the hiring, 90% of the training, 90% of the critical skill replacement, 90% of the redeployment, and 100% SSMs trained and certified.
  - Their analysis indicated a 95% chance that criteria would **not** be met by the end DEC 02, a 50% chance by 02/02, and a chance it may extend until 03/03 (and until 05/04 without careful management).
  - Given the situation, they recommended a "supercharged" interview and pre-screening process; acceleration of making offers, hire decisions, reporting dates, and training start-up; carefully control/manage training time and work on scheduling (especially if incumbent is leaving).

Presenter: M3/Human Factors | Date: FINAL | Slide: 12 of 14 | Closed

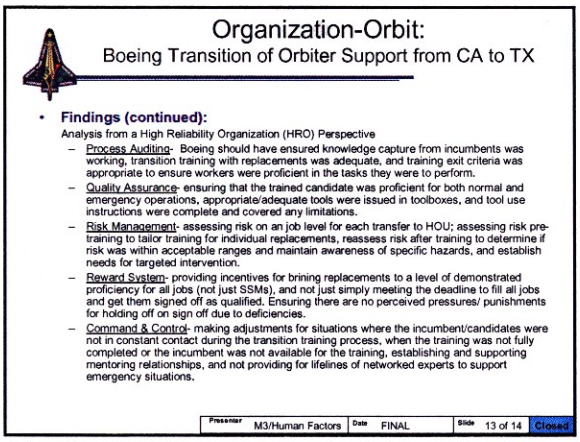
Organization-Orbit:
Boeing Transition of Orbiter Support from CA to TX
• Findings (continued):
Analysis from a High Reliability Organization (HRO) Perspective
– Process Auditing- Boeing should have ensured knowledge capture from incumbents was working, transition training with replacements was adequate, and training exit criteria was appropriate to ensure workers were proficient in the tasks they were to perform.
– Quality Assurance- ensuring that the trained candidate was proficient for both normal and emergency operations, appropriate/adequate tools were issued in toolboxes, and tool use instructions were complete and covered any limitations.
– Risk Management- assessing risk on an job level for each transfer to HOU; assessing risk pre-training to tailor training for individual replacements, reassess risk after training to determine if risk was within acceptable ranges and maintain awareness of specific hazards, and establish needs for targeted intervention.
– Reward System- providing incentives for brining replacements to a level of demonstrated proficiency for all jobs (not just SSMs), and not just simply meeting the deadline to fill all jobs and get them signed off as qualified. Ensuring there are no perceived pressures/ punishments for holding off on sign off due to deficiencies.
– Command & Control- making adjustments for situations where the incumbent/candidates were not in constant contact during the transition training process, when the training was not fully completed or the incumbent was not available for the training, establishing and supporting mentoring relationships, and not providing for lifelines of networked experts to support emergency situations.
Presenter M3/Human Factors
Date FINAL
Slide 13 of 14
Closed

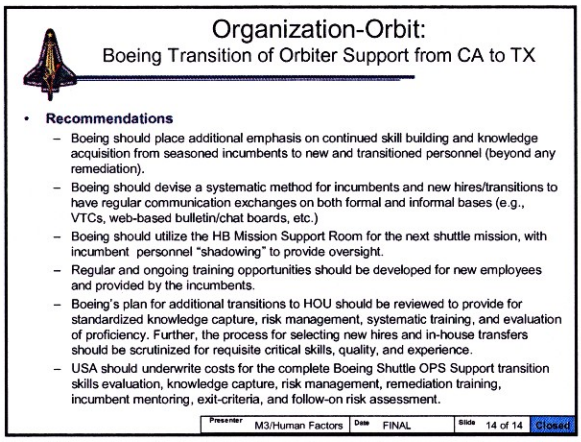
Organization-Orbit:
Boeing Transition of Orbiter Support from CA to TX
• Recommendations
– Boeing should place additional emphasis on continued skill building and knowledge acquisition from seasoned incumbents to new and transitioned personnel (beyond any remediation).
– Boeing should devise a systematic method for incumbents and new hires/transitions to have regular communication exchanges on both formal and informal bases (e.g., VTCs, web-based bulletin/chat boards, etc.)
– Boeing should utilize the HB Mission Support Room for the next shuttle mission, with incumbent personnel "shadowing" to provide oversight.
– Regular and ongoing training opportunities should be developed for new employees and provided by the incumbents.
– Boeing's plan for additional transitions to HOU should be reviewed to provide for standardized knowledge capture, risk management, systematic training, and evaluation of proficiency. Further, the process for selecting new hires and in-house transfers should be scrutinized for requisite critical skills, quality, and experience.
– USA should underwrite costs for the complete Boeing Shuttle OPS Support transition skills evaluation, knowledge capture, risk management, remediation training, incumbent mentoring, exit-criteria, and follow-on risk assessment.
Presenter M3/Human Factors
Date FINAL
Slide 14 of 14
Closed

Contract Design – Certification

25-1 Contracting & Financial Considerations

Matrix

Presenter	CAIB/Group 1	Date	FINAL	Slide	30 of 32

Budget and Finance Considerations

- **Action / Issue:** Budget and Finance Considerations Influence Shuttle Program Performance
- **Background / Facts:**
  - Cost pressure may adversely influence mission success at USA and sub-contractors as ISS cost overruns take greater share of NASA budget
  - Reduction at NASA funded level would be distributed to program based on NASA priorities. Cost growth in other priority programs could negatively affect funding on the SFOC and other SSP contracts.
- **Findings:**
  - Committee reports, new media, etc. indicate extensive cost growth on ISS

Presenter M3/Contracting | Date FINAL | Slide 1 of 6 | Closed

Budget and Finance Considerations

- **Group Recommendation:**
  - NASA should accelerate move to full cost accounting of the Space Shuttle Program in order to provide the adequate future funding in NASA and Centers' budget

Presenter M3/Contracting | Date FINAL | Slide 2 of 6 | Closed

SSP Budget

- Human Space Flight is approx 40% of NASA budget
- Space Shuttle is half of human space flight Budget
- No recent large congressional cuts
- FY2001 necessary to redirect advanced areas to address cost and program management needs of the ISS

Presenter M3/Contracting | Date FINAL | Slide 3 of 6 | Closed

Shuttle Budget History

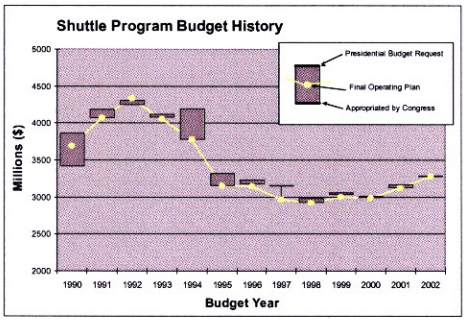

Presenter M3/Contracting | Date FINAL | Slide 4 of 6 | Closed

Shuttle Budget History

- 2002 reduced $50mil
- 2001 reduced $40mil for Mars initiative
- 2000 earmark of $40mil transfer to ISS
- 1999 reduced $31mil
- 1998 transferred $50mil to ISS
- 1997 transferred $190mil to ISS
- 1996 reduced $53mil; transferred $30mil to ISS
- 1995 general reduction $168 to Human Space Flight

Presenter M3/Contracting | Date FINAL | Slide 5 of 6 | Closed

SSP Budget

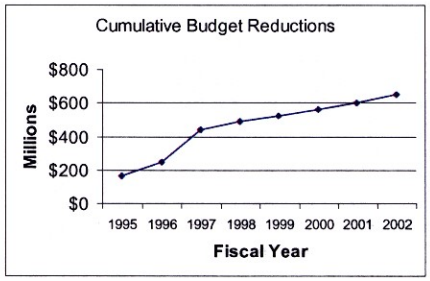

Presenter M3/Contracting | Date FINAL | Slide 6 of 6 | Closed

Contract Production

26-1 Non-SFOC Contracts
26-2 Foam Application Process not Specified as Contractual Requirement
26-3 ET Not Subject to Catastrophic Loss Penalty Clause
26-4 Pressure to Decrease Costs on SRB

Contracting Issues Non-SFOC Contracts

- **Action / Issue:** Non-SFOC Contracts "evolve" to shift emphasis away from cost savings
- **Background / Facts:**
  - MSFC has contract cognizance over Space Shuttle element contracts that are not part of the SFOC
- **Findings:**
  - MSFC evaluates whether contractor headcount had been reduced to minimum safe level and whether continued personnel reductions would have a negative rather than a positive effect
  - ATK Thiokol Propulsion has been Reusable Solid Rocket Booster (RSRM) supplier since 1974
  - Contracts from Buy 1 to Buy 4 included cost savings share line, allowing Thiokol to share in any savings below target cost
  - Current buy, while including a 1% incentive fee at target cost, contains no incentive for underrun

Presenter M3/Contracting | Date FINAL | Slide 1 of 18 | Closed

Contracting Issues Non-SFOC Contracts

- **Group Recommendation:**
  - NASA JSC should examine removing cost savings incentives from SFOC

Presenter M3/Contracting | Date FINAL | Slide 2 of 18 | Closed

Fee Structures of Non-SFOC

- Issue: SFOC was planned to include other "element" contracts as Phase 2
- Only SRB added (1998)
- Elements not included in SFOC
  - External Tank (ET)
  - Space Shuttle Main Engine (SSME)
  - Reusable Solid Rocket Motor (RSRM)

Presenter M3/Contracting | Date FINAL | Slide 3 of 18 | Closed

Non-SFOC:External Tank

- Michoud Assembly Facility (GOCO) operated by Lockheed Martin
- Estimated Cost (ET Production): $2.06 B
- Estimated Fees: $134.4 M (Incentive, Employee Motivation, Award)

Presenter M3/Contracting | Date FINAL | Slide 4 of 18 | Closed

ET

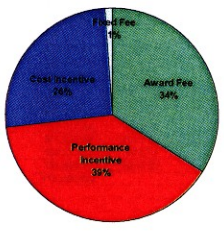

Presenter M3/Contracting | Date FINAL | Slide 5 of 18 | Closed

ET Production Award Fee

- Quality Performance 70%
  - Subcriteria: Quality of hardware; problem reporting/resolution; hardware performance; safety performance
- Management Performance 30%
  - Subcriteria: Project management; flight support; contract management

Presenter M3/Contracting | Date FINAL | Slide 6 of 18 | Closed

ET Award Fee

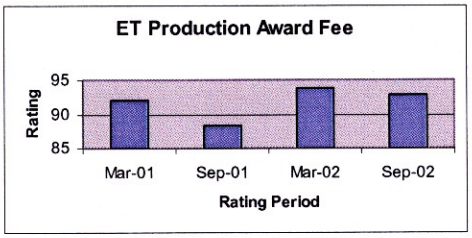

Presenter M3/Contracting | Date FINAL | Slide 7 of 18 | Closed

ET

Production Award Fee Pools

Period	Amount Available		Earned Amount	Earned Percent
October 1, 2000 - March 31, 2001	$1,499,664		$1,370,693	91.40%
April 1, 2001 - September 30, 2001	$2,493,361		$2,202,136	88.32%
October 1, 2001 - March 31, 2002	$3,273,186		$3,070,903	93.82%
April 1, 2002 - September 30, 2002	$2,498,684		$2,296,290	91.90%
Total	$9,764,895		$8,940,022	91.55%

MAF Operations & Maintenance Award Fee Pools

Period	Amount Available		Earned Amount	Earned Percent
October 1, 2000 - March 31, 2001	$345,327		$334,622	96.90%
April 1, 2001 - September 30, 2001	$485,448		$461,661	95.10%
October 1, 2001 - March 31, 2002	$658,718		$645,544	98.00%
April 1, 2002 - September 30, 2002	$761,736		$717,555	94.20%
Total	$2,251,229		$2,159,382	95.92%

B02063 – "Implementation of Friction Stir Welding" Award Fee Pools

Period	Amount Available		Earned Amount	Earned Percent
May 1, 2000 - March 31, 2001	$ 343,218-		$314,044	91.50%
April 1, 2001 - September 30, 2001	$297,000		$268,785	90.50%
October 1, 2001 - March 31, 2002	$128,000		$114,278	89.28%
April 1, 2002 - September 30, 2002	$84,687		$83,840	99.00%
Total	$852,905		$780,947	91.56%

Presenter M3/Contracting | Date FINAL | Slide 8 of 18 | Closed

Non-SFOC: Space Shuttle Main Engine

- Contractor: Boeing (formerly Rockwell/Rocketdyne)
- Current Contract Thru December 2003
- Estimated Total Cost: $1.04 B
- Estimated Fees: $123.6M (fixed, incentive,award)
  - 12% of cost

Presenter M3/Contracting | Date FINAL | Slide 9 of 18 | Closed

SSME

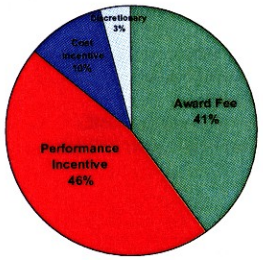

Presenter M3/Contracting | Date FINAL | Slide 10 of 18 | Closed

SSME Award Fee

- Management performance : 30%
- Flight support: 40%
- Safety, Reliability, QA: 30%
- Current Rating:
  - June 2002: 81.2
  - December 2002: 91.4

Presenter M3/Contracting | Date FINAL | Slide 11 of 18 | Closed

SSME Award Fee History

Evaluation Period	Start Date	End Date	Avail. Award Fee Dollars	Dollars Earned	Dollars Not Earned	Overall Score
1	1/1/02	6/30/02	$4,823,679	$3,916,827	$906,852	81.20%
2	7/1/02	12/31/02	$5,222,203	$4,773,094	$449,109	91.40%
3	1/1/03	6/30/03	$5,370,488			
4	7/1/03	12/31/03	$5,261,730			
5	1/1/04	6/30/04	$5,111,443			
6	7/1/04	12/31/04	$5,051,295			
7	1/1/05	6/30/05	$5,118,927			
8	7/1/05	12/31/05	$4,950,116			
9	1/1/06	6/30/06	$5,182,323			
10	7/1/06	12/31/06	$4,906,367			
			$50,998,571			

Presenter M3/Contracting | Date FINAL | Slide 12 of 18 | Closed

SSME Award Fee (prior)

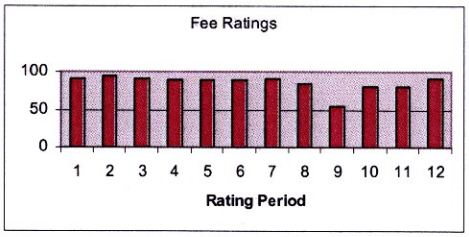

Presenter M3/Contracting | Date FINAL | Slide 13 of 18 | Closed

Reusable Solid Rocket Motor (RSRM)

- ATK THIOKOL PROPULSION HAS BEEN RSRM SUPPLIER SINCE 1974
- Current Contract value: $2.34 B
- Fee: 15%

Presenter M3/Contracting | Date FINAL | Slide 14 of 18 | Closed

RSRM

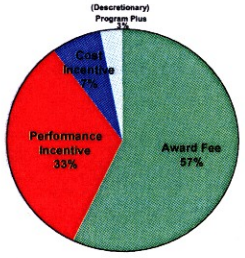

Presenter M3/Contracting | Date FINAL | Slide 15 of 18 | Closed

RSRM Award Fee

- Performance Management 50%
  - Subcriteria: Flight Support; Budget Management; Contract Management
- Safety, Reliability and QA 50%

Presenter M3/Contracting | Date FINAL | Slide 16 of 18 | Closed

RSRM Award Fee History

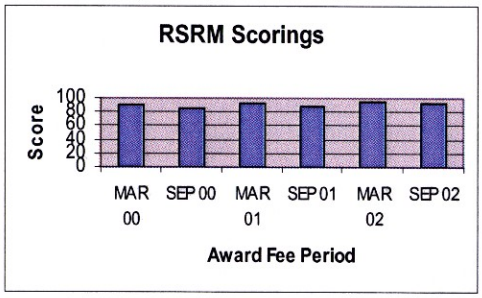

Presenter M3/Contracting | Date FINAL | Slide 17 of 18 | Closed

RSRM Award Fee History

Evaluation Period	Start Date	End Date	Avail. Award Fee Dollars	Dollars Earned	Dollars Not Earned	Overall Score
1	10/01/98	03/31/00	$21,013,756	$18,912,380	$2,101,376	90.0%
2	04/01/00	09/30/00	$9,711,956	$8,381,418	$1,330,538	86.3%
3	10/01/00	03/31/01	$15,142,213	$13,779,414	$1,362,799	91.0%
4	04/01/01	09/30/01	$16,690,226	$14,236,763	$2,453,463	85.3%
5	10/01/01	03/31/02	$14,234,638	$13,594,079	$640,559	95.5%
6	04/01/02	09/30/02	$14,032,556	$12,909,952	$1,122,604	92.0%
7	10/01/02	03/31/03	$16,905,169			
8	04/01/03	09/30/03	$17,204,304			
9	10/01/03	03/31/04	$13,381,973			
10	04/01/04	09/30/04	$11,838,699			
11	10/01/04	03/31/05	$10,169,653			
12	04/01/05	09/30/05	$6,914,057			
13	10/01/05	03/31/06	$2,237,675			
14	04/01/06	09/30/06	$1,001,715			
15	10/04/06	05/31/07	$750,576			

Presenter M3/Contracting | Date FINAL | Slide 18 of 18 | Closed

Contracting Issues External Tank

- **Action / Issue:** Foam Application Process not specified as contractual requirement
- **Background / Facts:**
  - External Tank Contract NAS8-00016 does not specify the application process to be used by Lockheed Martin Michoud Assembly Facility for the External Tank
- **Findings:**
  - ET Statement of Work (SOW) as included in the contract imposes the ET end Item Specification, CM02 and materials Process Control Plan as Type 1 documents.
  - Items below SE 16 level include engineering drawings, product processes and manufacturing plan (MPP)
  - NASA and DCMA are to review any changes the contractor that affect form, fit or function

Presenter M3/Contracting | Date FINAL | Slide 1 of 7 | Closed

Contracting Issues External Tank

- **Group Recommendation:**
  - NASA MSFC should consider specifying the ET Foam application process in the contract End Item Specification to maintain consistent control of the process

Presenter M3/Contracting | Date FINAL | Slide 2 of 7 | Closed

Contracting Issues External Tank

Contractual Flow Down for TPS Requirements 1 of 1

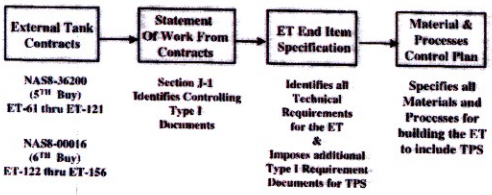

Presenter M3/Contracting | Date FINAL | Slide 3 of 7 | Closed

Contracting Issues External Tank

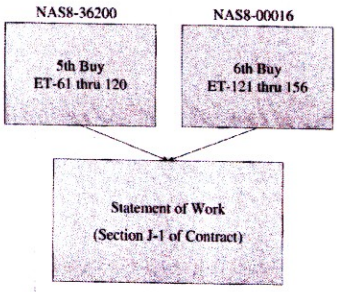

Presenter M3/Contracting | Date FINAL | Slide 4 of 7 | Closed

Contracting Issues External Tank

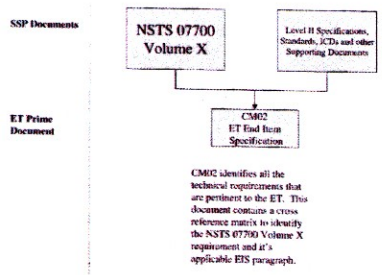

Presenter M3/Contracting | Date FINAL | Slide 5 of 7 | Closed

Contracting Issues External Tank

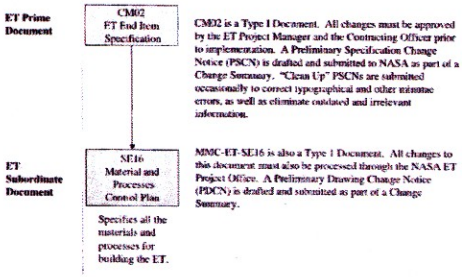

Presenter M3/Contracting | Date FINAL | Slide 6 of 7 | Closed

1

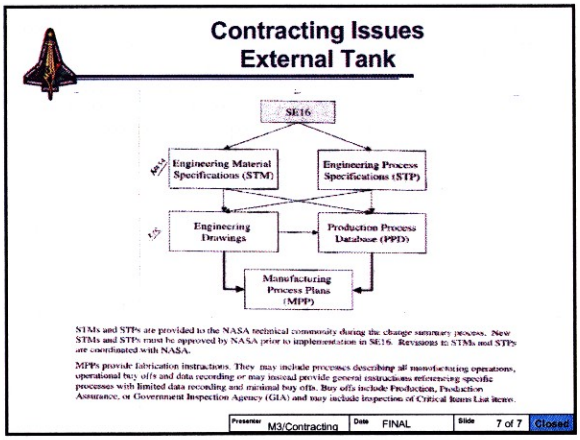
Contracting Issues
External Tank
SE16
Engineering Material Specifications (STM)
Engineering Process Specifications (STP)
Engineering Drawings
Production Process Database (PPD)
Manufacturing Process Plans (MPP)
STMs and STPs are provided to the NASA technical community during the change summary process. New STMs and STPs must be approved by NASA prior to implementation in SE16. Revisions to STMs and STPs are coordinated with NASA.
MPPs provide fabrication instructions. They may include processes describing all manufacturing operations, operational buy offs and data recording or may instead provide general instructions referencing specific processes with limited data recording and minimal buy offs. Buy offs include Production, Production Assurance, or Government Inspection Agency (GIA) and may include inspection of Critical Items List items.
Presenter M3/Contracting
Date FINAL
Slide 7 of 7
Closed

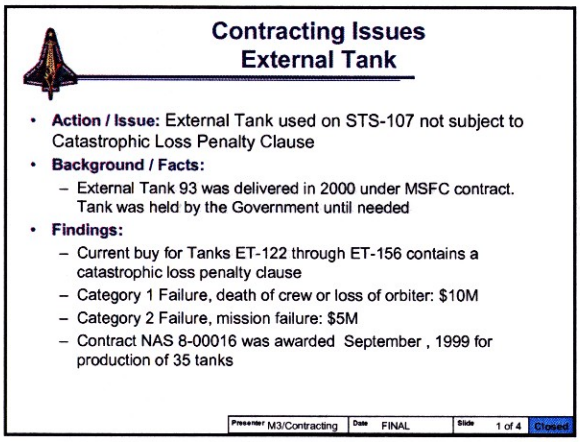
Contracting Issues
External Tank
• Action / Issue: External Tank used on STS-107 not subject to Catastrophic Loss Penalty Clause
• Background / Facts:
– External Tank 93 was delivered in 2000 under MSFC contract. Tank was held by the Government until needed
• Findings:
– Current buy for Tanks ET-122 through ET-156 contains a catastrophic loss penalty clause
– Category 1 Failure, death of crew or loss of orbiter: $10M
– Category 2 Failure, mission failure: $5M
– Contract NAS 8-00016 was awarded September , 1999 for production of 35 tanks
Presenter M3/Contracting
Date FINAL
Slide 1 of 4
Closed

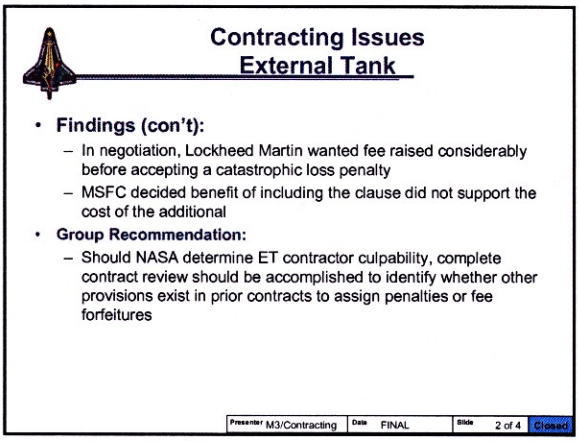
Contracting Issues
External Tank
• Findings (con't):
– In negotiation, Lockheed Martin wanted fee raised considerably before accepting a catastrophic loss penalty
– MSFC decided benefit of including the clause did not support the cost of the additional
• Group Recommendation:
– Should NASA determine ET contractor culpability, complete contract review should be accomplished to identify whether other provisions exist in prior contracts to assign penalties or fee forfeitures
Presenter M3/Contracting
Date FINAL
Slide 2 of 4
Closed

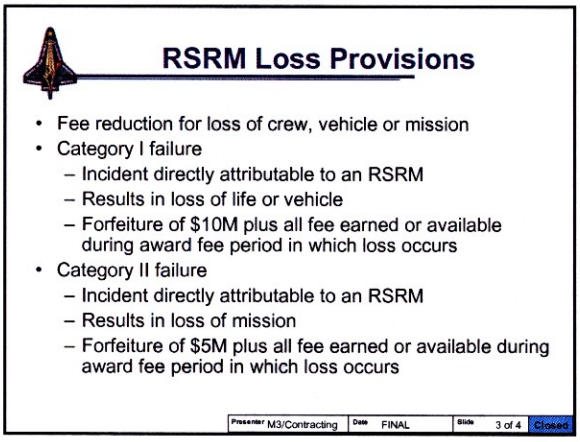
RSRM Loss Provisions
• Fee reduction for loss of crew, vehicle or mission
• Category I failure
– Incident directly attributable to an RSRM
– Results in loss of life or vehicle
– Forfeiture of $10M plus all fee earned or available during award fee period in which loss occurs
• Category II failure
– Incident directly attributable to an RSRM
– Results in loss of mission
– Forfeiture of $5M plus all fee earned or available during award fee period in which loss occurs
Presenter M3/Contracting
Date FINAL
Slide 3 of 4
Closed

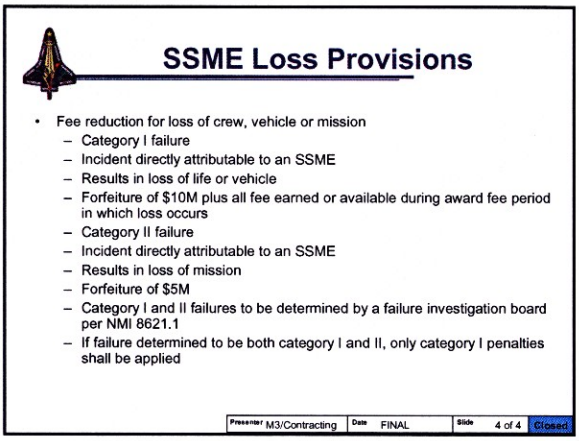
SSME Loss Provisions
• Fee reduction for loss of crew, vehicle or mission
– Category I failure
– Incident directly attributable to an SSME
– Results in loss of life or vehicle
– Forfeiture of $10M plus all fee earned or available during award fee period in which loss occurs
– Category II failure
– Incident directly attributable to an SSME
– Results in loss of mission
– Forfeiture of $5M
– Category I and II failures to be determined by a failure investigation board per NMI 8621.1
– If failure determined to be both category I and II, only category I penalties shall be applied
Presenter M3/Contracting
Date FINAL
Slide 4 of 4
Closed

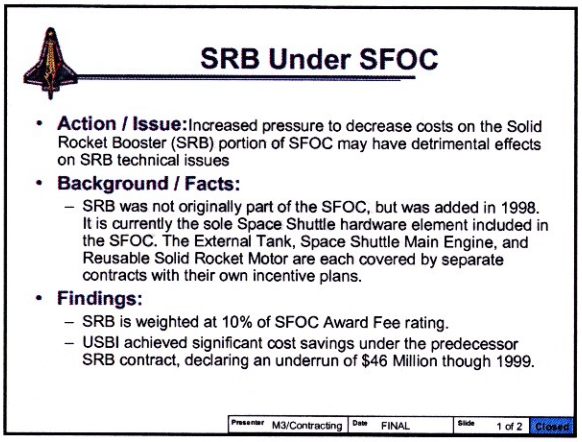
SRB Under SFOC
• Action / Issue: Increased pressure to decrease costs on the Solid Rocket Booster (SRB) portion of SFOC may have detrimental effects on SRB technical issues
• Background / Facts:
– SRB was not originally part of the SFOC, but was added in 1998. It is currently the sole Space Shuttle hardware element included in the SFOC. The External Tank, Space Shuttle Main Engine, and Reusable Solid Rocket Motor are each covered by separate contracts with their own incentive plans.
• Findings:
– SRB is weighted at 10% of SFOC Award Fee rating.
– USBI achieved significant cost savings under the predecessor SRB contract, declaring an underrun of $46 Million though 1999.
Presenter M3/Contracting
Date FINAL
Slide 1 of 2
Closed

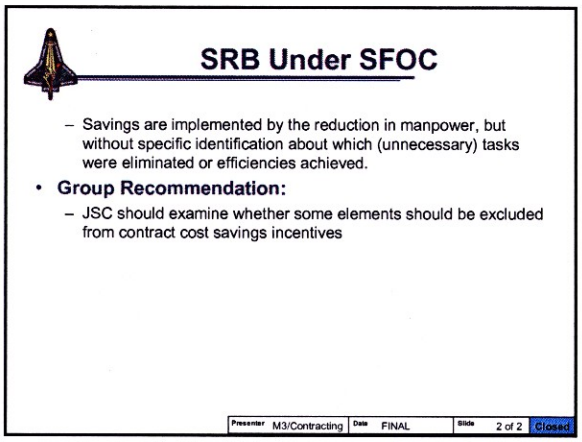
SRB Under SFOC
– Savings are implemented by the reduction in manpower, but without specific identification about which (unnecessary) tasks were eliminated or efficiencies achieved.
• Group Recommendation:
– JSC should examine whether some elements should be excluded from contract cost savings incentives
Presenter M3/Contracting
Date FINAL
Slide 2 of 2
Closed

Contract Maintenance

27-1 SFOC Fees and Cost Limitations

27-2 TMR Weights

27-3 USA Benefits

Matrix

Presenter	CAIB/Group 1	Date	FINAL	Slide	32 of 32

Space Shuttle Operations Contract

- **Action / Issue:** SFOC award fees, incentive fees, performance fees, and cost limitations may affect the profitability of the contract
- **Background / Facts:**
  - SFOC is susceptible to funding limitations
  - Reduction at NASA funded level would be distributed to program based on NASA priorities. Cost growth in other priority programs could negatively affect funding on the SFOC and other SSP contracts.
  - Using commercial business practices can reduce cost and provide increase profit incentives for cost reduction and performance
- **Findings:**
  - Fee Structure (see following slides)
- **Group Recommendation:**
  - NASA should review contract history to evaluate whether fee plan is rewarding cost savings at expense of performance

Presenter M3/Contracting | Date FINAL | Slide 1 of 14 | Closed

Space Shuttle Operations Contract Fee Structure

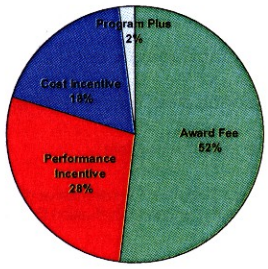

Presenter M3/Contracting | Date FINAL | Slide 2 of 14 | Closed

SFOC Performance Fee Plan

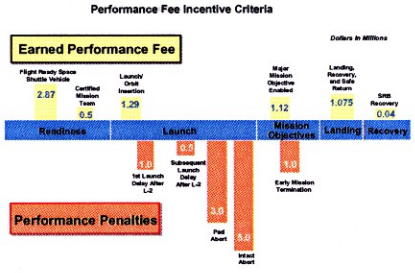

Presenter M3/Contracting | Date FINAL | Slide 3 of 14 | Closed

SFOC Performance Fees

- Available fee: $6Million (STS 80 – STS 91); $6.8Million (STS 95 STS 110)
- Total earned over 31 flights: $190 million
- Fees forfeited:
  - $1M STS 80 (OV-102), January 1997 (challenged by USA,resolved September 1997)
    - In Flight anomaly (IFA), inability to accomplish major mission objectives
  - $1M STS 92 (OV-103) September, 2000
    - 24-hour launch delay

Presenter M3/Contracting | Date FINAL | Slide 4 of 14 | Closed

SFOC Performance Fees

- Fee Not Earned (cont)
  - $2.87M STS 103 (OV-103): January 2000
    - Missed manifest launch date by more than 7 days - due to workmanship damage to wiring
  - $2,87M STS 99 (OV-105): March 2000
    - Workmanship damage to wiring
  - $2.879 STS 101 (OV-104): June 2000
    - Workmanship damage to wiring
  - $1.435M STS 109 (OV-102) May 2002
    - Missed manifest date, ready for launch criteria not met

Presenter M3/Contracting | Date FINAL | Slide 5 of 14 | Closed

Performance Fees Earned

SHUTTLE MISSION	AVAILABLE PERFORMANCE	DOLLARS EARNED	DOLLARS NOT EARNED
STS 80	$6,000,000	$5,000,000	$1,000,000
STS 81	$6,000,000	$6,000,000	$0
STS 82	$6,000,000	$6,000,000	$0
STS 83	$6,000,000	$6,000,000	$0
STS 84	$6,000,000	$6,000,000	$0
STS 85	$6,000,000	$6,000,000	$0
STS 94	$6,000,000	$6,000,000	$0
STS 86	$6,000,000	$6,000,000	$0
STS 87	$6,000,000	$6,000,000	$0
STS 89	$6,000,000	$6,000,000	$0
STS 90	$6,000,000	$6,000,000	$0
STS 91	$6,000,000	$6,000,000	$0
STS 95	$6,895,000	$6,895,000	$0
STS 88	$6,895,000	$6,895,000	$0
STS 96	$6,895,000	$6,895,000	$0
STS 93	$6,895,000	$6,895,000	$0
STS-103	$6,895,000	$4,025,000	$2,870,000
STS-99	$6,895,000	$4,025,000	$2,870,000
STS-101	$6,895,000	$4,025,000	$2,870,000
STS-106	$6,895,000	$6,895,000	$0
STS-92	$6,895,000	$5,895,000	$1,000,000
STS-97	$6,895,000	$6,895,000	$0
STS-98	$6,895,000	$6,895,000	$0
STS-102	$6,895,000	$6,895,000	$0
STS-100	$6,895,000	$6,895,000	$0
STS-104	$6,895,000	$6,895,000	$0
STS-105	$6,895,000	$6,895,000	$0
STS-108	$6,895,000	$6,895,000	$0
STS-109	$6,895,000	$5,460,000	$1,435,000
STS-110	$6,895,000	$6,895,000	$0
STS-111	$6,895,000	$6,895,000	$0
STS-112	$6,895,000	$6,895,000	$0

Presenter M3/Contracting | Date FINAL | Slide 6 of 14 | Closed

Award Fee

- Six-month periods
- Scores range from 0-100, reflect per cent of available fee
- Fee Determining Official (FDO) signs the performance determination
- Safety Score and Performance Score
- Contracting Officer's Technical Representative (COTR) recommends based on input from Performance Evaluation Board

Presenter M3/Contracting | Date FINAL | Slide 7 of 14 | Closed

Award Fee

- Performance Evaluation Team (PET) rates USA on 13 functional areas.
- Technical Management Representatives (TMR) provide numerical evaluations on areas of emphasis
- Identify Strengths and Weaknesses

Presenter M3/Contracting | Date FINAL | Slide 8 of 14 | Closed

SFOC Award Fee

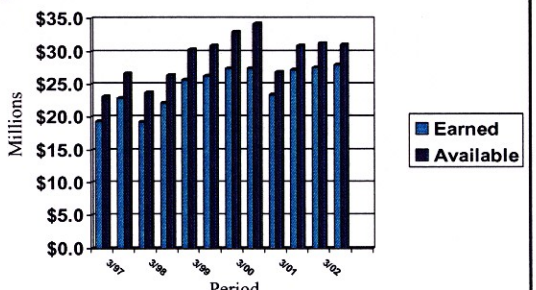

Presenter M3/Contracting | Date FINAL | Slide 9 of 14 | Closed

SFOC Award Fee History

EVALUATION PERIOD	START DATE	END DATE	AVAILABLE AWARD FEE	DOLLARS EARNED	DOLLARS NOT EARNED
1	10/1/1996	3/31/1997	$23,200,000	$19,488,000	$3,712,000
2	4/1/1997	9/30/1997	$26,661,483	$22,928,875	$3,732,608
3	10/1/1997	3/31/1998	$23,788,065	$19,268,333	$4,519,732
4	4/1/1998	9/30/1998	$26,425,761	$22,197,639	$4,228,122
5	10/1/1998	3/31/1999	$30,303,402	$25,757,894	$4,545,508
6	4/1/1999	9/30/1999	$30,971,263	$26,325,576	$4,645,687
7	10/1/1999	3/31/2000	$33,052,574	$27,433,636	$5,618,938
8	4/1/2000	9/30/2000	$34,327,255	$27,461,804	$6,865,451
9	10/1/2000	3/31/2001	$26,917,106	$23,415,781	$3,498,910
10	4/1/2001	9/30/2001	$30,915,116	$27,205,302	$3,709,814
11	10/1/2001	3/30/2002	$31,366,792	$27,602,777	$3,764,015
12	4/1/2002	9/30/2002	$31,073,024	$28,274,949	$2,796,423
13	10/1/2002	3/31/2003	**$41,218,518**		
14	4/1/2003	9/30/2003	**$41,906,566**		
15	10/1/2003	3/30/2004	**$42,102,291**		
16	4/1/2004	9/30/2004	**$49,178,918**		
17	10/1/2004	3/30/2005	**$484,163**		
18	4/1/2005	9/30/2005	**$436,857**		
19	10/1/2005	3/30/2006	**$387,583**		
20	4/1/2006	9/30/2006	**$368,279**		
21	10/1/2006	3/30/2007	**$348,238**		
22	4/1/2007	9/30/2007	**$343,043**		
23			**7,967**		
24					
25					
26					
27					
28					
TOTAL			**$525,784,264**	$297,360,566	$51,637,208

Presenter M3/Contracting | Date FINAL | Slide 10 of 14 | Closed

SFOC TMR Ratings

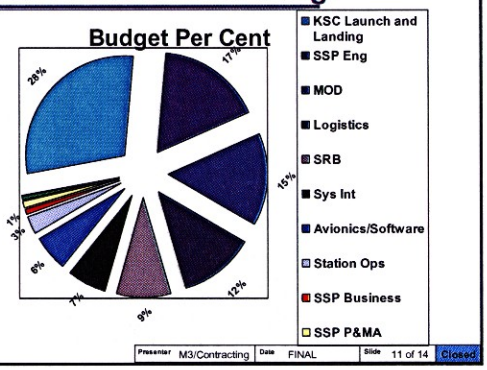

Presenter M3/Contracting | Date FINAL | Slide 11 of 14 | Closed

Boeing Subcontract to SFOC

- Boeing subcontract makes up largest share of SFOC
- Subcontract value is $2.3 B
  - Cost of $2.1B
  - Fees total $197.4M
- Award fee plan mirrors SFOC
- Award fees scores track to within 5% of SFOC score by agreement

Presenter M3/Contracting | Date FINAL | Slide 12 of 14 | Closed

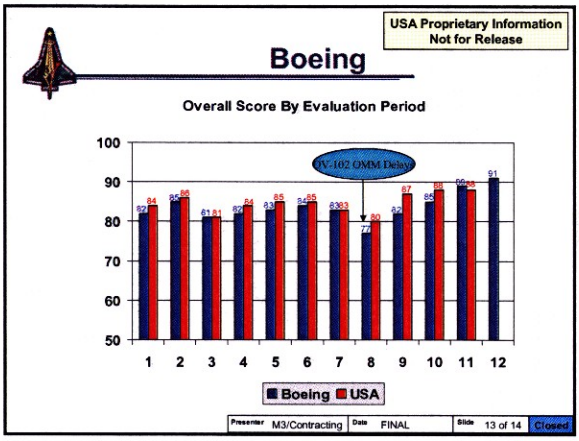
USA Proprietary Information
Not for Release
Boeing
Overall Score By Evaluation Period
OV-102 OMM Delay
100
90
80
70
60
50
1 2 3 4 5 6 7 8 9 10 11 12
Boeing USA
Presenter M3/Contracting
Date FINAL
Slide 13 of 14
Closed

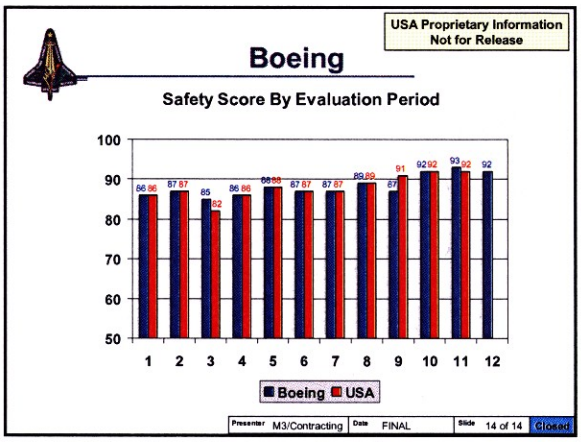
USA Proprietary Information
Not for Release
Boeing
Safety Score By Evaluation Period
100
90
80
70
60
50
1 2 3 4 5 6 7 8 9 10 11 12
Boeing USA
Presenter M3/Contracting
Date FINAL
Slide 14 of 14
Closed

Contracting Issues SFOC

- **Action / Issue:** Technical Management Representatives score weightings may hide substandard performance on contract requirements
- **Background / Facts:**
  - Each Technical Management Representative (TMR) assigns USA a performance grade in each of 6 areas. TMR Scores are weighted based on an individual share of the budget
  - Weighted scores are totaled to provide recommended score
- **Findings:**
  - 13 TMRs rate contractor performance every 6 months
  - Weighted scores become the recommendation to the PEB
  - Weights of TMRs on small share elements "disappear" when summary number produced

Presenter M3/Contracting | Date FINAL | Slide 1 of 5 | Closed

SFOC TMR Weighted Ratings

- **Group Recommendation:**
  - NASA should review low ratings regardless of budget weights; consider assigning award fee pools to each TMR to reward performance in each area rather than aggregate.

Presenter M3/Contracting | Date FINAL | Slide 2 of 5 | Closed

TMR Weighted scoring

KSC Launch and landing:	27.96%
SSP vehicle engineering:	17.67%
MOD:	14.47%
Integrated Logistics:	12.03%
Solid Rocket Booster:	9.26%
SSP SYS INT	6.99%
Avionics and Software	5.48%
Station Ops and Util	2.69%
SP Business	.89%
SSP S&MA	1.09%
Management Int	0.39%
FCOD	0.27%

Presenter M3/Contracting | Date FINAL | Slide 3 of 5 | Closed

SFOC TMR Weighted Ratings

- KSC Launch and Landing weighted at 30%
- Vehicle Engineering weighted at 17%
- System Integration weighted at 6.5%
- Safety and Mission Assurance weighted at 1.1%
- Reinforces commitment to meeting manifest

Presenter M3/Contracting | Date FINAL | Slide 4 of 5 | Closed

TMR Scores

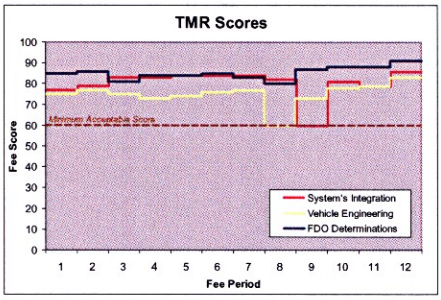

Presenter M3/Contracting | Date FINAL | Slide 5 of 5 | Closed

1

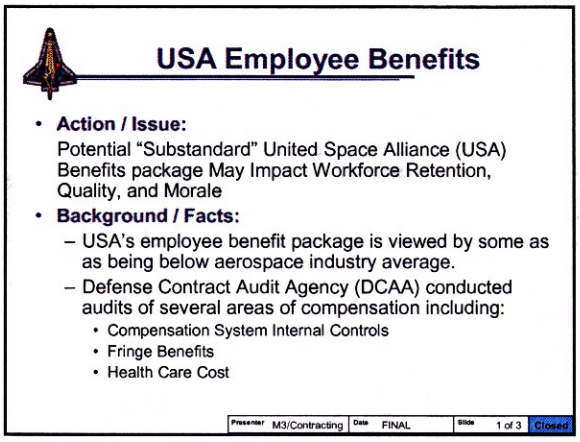
USA Employee Benefits
• Action / Issue:
Potential "Substandard" United Space Alliance (USA) Benefits package May Impact Workforce Retention, Quality, and Morale
• Background / Facts:
– USA's employee benefit package is viewed by some as as being below aerospace industry average.
– Defense Contract Audit Agency (DCAA) conducted audits of several areas of compensation including:
• Compensation System Internal Controls
• Fringe Benefits
• Health Care Cost
Presenter M3/Contracting
Date FINAL
Slide 1 of 3
Closed

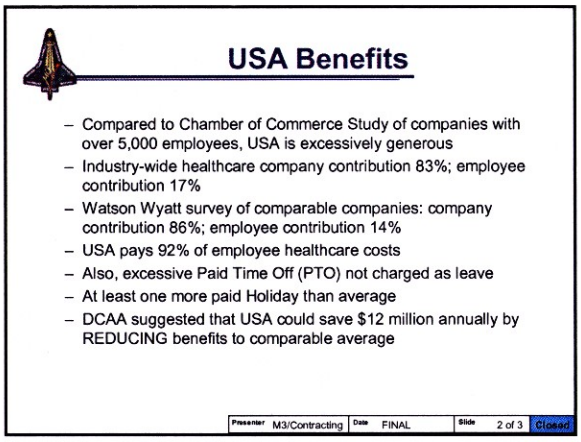
USA Benefits
– Compared to Chamber of Commerce Study of companies with over 5,000 employees, USA is excessively generous
– Industry-wide healthcare company contribution 83%; employee contribution 17%
– Watson Wyatt survey of comparable companies: company contribution 86%; employee contribution 14%
– USA pays 92% of employee healthcare costs
– Also, excessive Paid Time Off (PTO) not charged as leave
– At least one more paid Holiday than average
– DCAA suggested that USA could save $12 million annually by REDUCING benefits to comparable average
Presenter M3/Contracting
Date FINAL
Slide 2 of 3
Closed

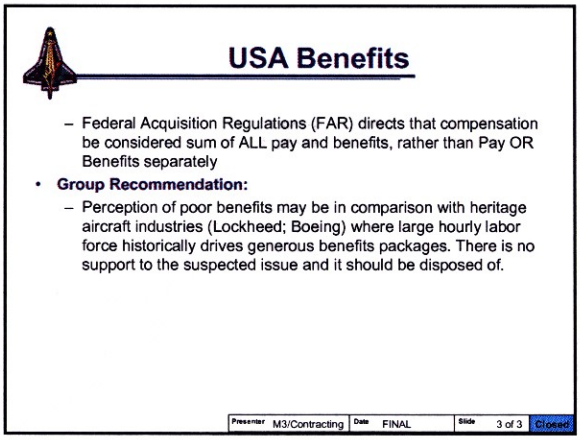
USA Benefits
– Federal Acquisition Regulations (FAR) directs that compensation be considered sum of ALL pay and benefits, rather than Pay OR Benefits separately
• Group Recommendation:
– Perception of poor benefits may be in comparison with heritage aircraft industries (Lockheed; Boeing) where large hourly labor force historically drives generous benefits packages. There is no support to the suspected issue and it should be disposed of.
Presenter M3/Contracting
Date FINAL
Slide 3 of 3
Closed

THIS PAGE INTENTIONALLY LEFT BLANK

Volume V
Appendix G.5

Vehicle Data Mapping (VDM) Team
Final report, Jun 13, 2003

This Appendix contains NSTS-37383 Vehicle Data Mapping Team Final Report in Support of the *Columbia* Accident Investigation, 13 June 2003.

THIS PAGE INTENTIONALLY LEFT BLANK

NSTS-37383

Vehicle Data Mapping (VDM) Team Final Report

in support of the *Columbia* Accident Investigation

June 13, 2003

Prepared by:

John D. Albright
NASA-JSC-EP4
VDM Team Data Manager

Approved and Submitted by:

Gene Grush
NASA-JSC-EP
VDM Team Lead

Table of Contents

Executive Summary **1**
1.0 INTRODUCTION **2**
2.0 PURPOSE AND SCOPE **3**
3.0 PRODUCTS AND SPECIAL ACTIVITIES **3**
3.1 VDM-P01: 3D Full Animation Event Sequence Playback 4
3.2 VDM-P02: Physical Mockup 7
3.3 VDM-P03: 3D Graphical Events Sequence 8
3.4 VDM-P04: 2D Static Storyboard 8
3.5 VDM-P05: 2D Graphical Events Sequence 10
3.6 VDM-P06: 3D CAD Modeling 11
3.7 VDM-P07: Wire Routing / Sensor Placement Reconstruction 13
3.8 VDM-P08: Events Timeline 14
3.9 VDM-P09: Instrumentation Listing and Sensor Location 15
3.10 VDM-P10: Sensor Signal Characterization For Failure Scenario 16
3.11 VDM-P11: Structure / Installation Drawings 17
3.12 VDM-P12: Wire Routing Details 17
3.13 VDM-P13: Closeout Photos 18
3.14 VDM Team ASA4 Anomaly Assessment 19
3.15 VDM Team Testing 20
3.16 VDM Team Leading Edge Wire Run Assessment 24
3.17 VDM Team Miscellaneous Tasks 25
4.0 CONCLUSIONS AND SIGNIFICANT FINDINGS **25**
APPENDIX A: VDM Team Product Flow Chart **28**
APPENDIX B: VDM Team Roster and Action List **29**
APPENDIX C: VDM Product Files for the Final Report **30**
APPENDIX D: Acronyms and Abbreviations **31**

Executive Summary

The Vehicle Data Mapping (VDM) Team was created to support the Orbiter Vehicle Engineering Working Group (OVEWG) investigation of the OV-102/*Columbia* accident that occurred during the STS-107 mission on February 1, 2003. The VDM team charter included the creation of unique and innovative data display products that aid in understanding the hardware configuration, sensor response data, and complex sequence of events during *Columbia's* entry.

In meeting this charter, approximately 125 personnel from NASA, Boeing, USA, and multiple support contractors from around the country produced seven major products and six supporting products in accordance with the VDM team product flowchart contained in Appendix A. Four special activities related to these products and encompassed by the VDM team charter were also pursued. All of these products and activities are discussed in detail in this report, along with related findings generated by the VDM team during this effort.

Due to the large volume of data produced by the VDM team, this report is best reviewed from the VDM team share drive or a compact disk (CD) containing all related product files, thus enabling embedded hyperlinks to work properly and maximizing data availability and organization. Accordingly, the planned method of distribution for this report is a CD. Note that a readme file is included to explain the general content and provide key usage instructions for the final report.

1.0 INTRODUCTION

The Vehicle Data Mapping (VDM) Team, headquartered at Johnson Space Center (JSC) and lead by NASA-JSC-EP/Gene Grush, was created to support the Orbiter Vehicle Engineering Working Group (OVEWG) investigation of the OV-102/*Columbia* accident that occurred during the STS-107 mission on February 1, 2003. The VDM team charter was as follows:

- To perform data collection, organization, and analysis for select vehicle parameters during entry.
- To research sensor installation details, wire routings, and power and signal conditioning configurations for associated instrumentation.
- To perform testing as required to anchor analytical models and define failure modes/signatures for associated instrumentation.
- To create unique and innovative data display products that aid in understanding the hardware configuration, sensor response data, and complex sequence of events during entry.

In general, the VDM team did not provide detailed interpretation of the flight data. Instead, the existing Problem Review Team (PRT) for each Orbiter subsystem performed this task with oversight from the Data Review and Timeline Reconstruction Team, who then used the results as an input to the master entry timeline. One exception, discussed later in this report, involved analyzing the timing and failure signatures of certain Orbiter sensors to identify trends and patterns in the data.

In meeting the VDM team charter, seven major products and six supporting data generation/gathering products were produced in accordance with the VDM team product flowchart contained in Appendix A. Four special activities related to these products and encompassed by the VDM team charter were also pursued. All of these products and activities are discussed in this report. To maximize efficiency and accountability, the VDM team structure and action tracking system were product oriented, including the assignment of a lead engineer for each product. To organize and control VDM team products and inputs, a VDM team headquarters (building 15, room 131) was established for meetings/telecons and display/storage of hardcopy data. A VDM team share drive was also established on a JSC server for display/storage of electronic files.

Over a 4-month period, approximately 125 personnel from NASA, Boeing, and United Space Alliance (USA) at JSC, Kennedy Space Center (KSC), Marshall Space Flight Center (MSFC), and Huntington Beach (HB), plus technical support personnel from Analytical Graphics, Inc., GHG Inc., IMC Incite, Lockheed Martin, Muniz Engineering, Inc. (MEI), Information Dynamics, Inc. (IDI), and SAIC, Inc., responded to action items and produced the products described in this report. A comprehensive list of VDM team members, action items (98 total), and action item response files is contained in Appendix B. During this process, the VDM team provided regular status briefings to the OVEWG, records of which are contained on the VDM team share drive. Similar or

supplemental information was also provided directly to the *Columbia* Accident Investigation Board (CAIB) in several instances upon request.

2.0 PURPOSE AND SCOPE

This report is intended to provide final documentation of the VDM team products and findings. Due to the large volume of data produced by the VDM team, this report is best reviewed from the VDM team share drive or a compact disk (CD) containing all related product files, thus enabling embedded hyperlinks to work properly and maximizing data availability and organization. Accordingly, the planned method of distribution for this report is a CD.

3.0 PRODUCTS AND SPECIAL ACTIVITIES

In accordance with the VDM team product flowchart contained in Appendix A, seven major products, six supporting data generation/gathering products, and four special activities were created and pursued to help document, visualize, and comprehend the data associated with *Columbia's* entry on STS-107. The major source of flight data used for this effort included telemetry data from the Operational Instrumentation (OI) sensors and Orbiter Experiment (OEX) recorder data from the Modular Auxiliary Data System (MADS) sensors. This data was obtained in hardcopy and/or electronic form directly from the Mission Evaluation Room (MER) via formal data requests. Also, as mentioned previously, a key input to many VDM team products and activities was the master entry timeline from the Data Review and Timeline Reconstruction Team, which was used for identification and annotation of key events.

Unless otherwise specified for individual products or activities, ending times for OI sensor data include loss of signal (LOS) at Greenwich Mean Time (GMT) 2003/032:13:59:32.136 (data set referred to as "107 data") and post-LOS at GMT 2003/032:14:00:31.102 (data set referred to as "107-edit data"). Similarly, the ending time for MADS sensor data is GMT 2003/032:14:00:14.290 (data set referred to as "OEX data"), with entry interface (EI) occurring at GMT 2003/032:13:44:09.000 (frequently used as a point of reference).

VDM team efforts initially focused on OI sensor data from the vehicle. The first OI indications of off-nominal performance involved a hydraulic line temperature on the inboard sidewall (Yo-105) of the left wheel well (V58T1703A, LMG Brake Line Temp D) at GMT 2003/032:13:52:17. Subsequently, other OI sensors began showing off-nominal trends. Of these, particular attention was given to the following 14 OI sensors (seven left wing, seven left wheel well) that went off-scale low (OSL) or unexpectedly changed state (starting at GMT 2003/032:13:52:56) prior to LOS:

Failure Order	MSID	Description	Sensor Location	Panel/ Connector	Mode
1	V09T1006A	LH Inbd Elev Lwr Skin Temp	Wing	Glove/P105	OSL
2	V58T0157A	Hyd 1 LH Inbd Elvn Actr Rtn Ln T	Wing	Glove/P105	OSL
3	V58T0394A	Hyd Sys 3 LOE Rtn Ln T	Wing	Glove/P105	OSL

4	V58T0257A	Hyd 2 LH Inbd Elvn Actr Rtn Ln T	Wing	Glove/P105	OSL
5	V58T0193A	Hyd Sys 1 LOE Rtn Ln T	Wing	Glove/P105	OSL
6	V09T1002A	LH Lwr Wing Skin Temp	Wing	Glove/P105	OSL
7	V09T1024A	LH Upr Wing Skin Temp	Wing	Glove/P105	OSL
8	V51P0570A	MLG LH Outbd Tire Press 1	W-well	W-well/P87	OSL
9	V51P0571A	MLG LH Inbd Tire Press 1	W-well	W-well/P87	OSL
10	V51T0574A	MLG LH Outbd Wheel Temp	W-well	W-well/P89	OSL
11	V51P0572A	MLG LH Outbd Tire Press 2	W-well	W-well/P89	OSL
12	V51T0575A	MLG LH Inbd Wheel Temp	W-well	W-well/P87	OSL
13	V51P0573A	MLG LH Inbd Tire Press 2	W-well	W-well/P89	OSL
14	V51X0125E	LH MLG Downlock Prox	W-well	W-well/P59	State

After the OEX recorder was recovered, attention was shifted to the MADS sensor data that provided 600+ additional pressure, temperature, and strain measurements of interest to the investigation, the first of which (V12G9921A, Left Wing Front Spar Strain) began showing signs of off-nominal performance at GMT 2003/032:13:48:39, approximately 3:38 sec before the first off-nominal OI sensor reading was detected.

The following sections in this report describe each VDM team product and special activity in detail. A complete list of these items is as follows:

- VDM-P01: 3D Full Animation Event Sequence Playback
- VDM-P02: Physical Mockup
- VDM-P03: 3D Graphical Events Sequence
- VDM-P04: 2D Static Storyboard
- VDM-P05: 2D Graphical Events Sequence
- VDM-P06: 3D CAD Modeling
- VDM-P07: Wire Routing / Sensor Placement Reconstruction
- VDM-P08: Events Timeline
- VDM-P09: Instrumentation Listing and Sensor Location
- VDM-P10: Sensor Signal Characterization for Failure Scenario
- VDM-P11: Structure / Installation Drawings
- VDM-P12: Wire Routing Details
- VDM-P13: Closeout Photos
- VDM Team ASA4 Anomaly Assessment
- VDM Team Testing
- VDM Team Leading Edge Wire Run Assessment
- Miscellaneous Tasks

3.1 VDM-P01: 3D Full Animation Event Sequence Playback

Product VDM-P01 is a digital video disk (DVD)-based movie/animation displaying telemetry data from select OI pressure and temperature sensors in the left wing, wheel well, and fuselage areas during entry. As of this writing, rev 2 is the latest version of the DVD, which conforms to rev 15 of the master entry timeline and rev 5 of product VDM-P05 (2D Graphical Events Sequence). As such, all animation sequences run from GMT 2003/032:13:51:00.000 to GMT 2003/032:14:00:31.000. In addition, a total of 39 OI

sensors are depicted in the CAD model used to create this product. A complete list of these sensors is contained in Appendix C. Note that this product does not attempt to visualize specific failure scenario sequences (e.g. hot gas plumes, structural deflections, debris shedding, etc.) due to the complex and speculative nature of these details, although similar computer graphics techniques could be employed for this purpose if desired.

The following key inputs were used to generate this product:

- Product VDM-P04: 2D Static Storyboard (including OI sensor data from the MER)
- Product VDM-P05: 2D Graphical Events Sequence
- Product VDM-P06: 3D Orbiter CAD models
- Product: VDM-P07: Wire Routing/Sensor Placement Reconstruction
- Product VDM-P12: Wire Routing Details
- Master entry timeline

The product contains the following main computer graphics sequences:

- A "flythrough" of the left wing and wheel well areas allowing user familiarization with the vehicle physical configuration and geometry. Wing structure, wire runs and sensors, and wheel-well contents are all depicted in detail. Due to their small size, the sensors called out in the master entry timeline are represented as "balloons." Minor license was taken in the X-Y-Z positioning of the sensor balloons to ensure that they would be visible with the camera angles selected. Callouts and highlighting are employed to identify relevant features.

- A wing plan-form sequence showing the left side of the vehicle, including the fuselage sidewall. When selected, this sequence progresses in real time from a point prior to the onset of anomalous sensor indications during the STS-107 entry. A digital clock supplemented by an analog timeline display indicates current time. Sensor temperature and pressure indications are represented by color changes of the balloons: green representing nominal indications, yellow-orange-red representing increasingly above-nominal indications, and light-medium-dark blue representing below-nominal indications. White and black are used to indicate off scale high (OSH) and OSL, respectively, while gray indicates a sync/data loss. A side view of the Orbiter in an inset window illustrates vehicle attitude and Reaction Control System (RCS) thruster and aerosurface activity (aerosurface positions are exaggerated for visibility), and a simplified ground track plot indicates geographic location. Captions are superimposed to call out significant events from the entry timeline.

- A wheel well close-up sequence providing an enlarged view of the left wheel well, including the landing gear structure, hydraulic lines, and wire runs. The same balloon color change conventions used in the wing plan form sequence are employed here.

- A trajectory/ground track sequence with four sub-windows: one for timeline and caption data, an Orbiter side view comparable to the plan form view, a "gun camera" (camera trailing behind the Orbiter) view to further enhance visualization of Orbiter attitude, and an augmented ground track in aeronautical map format.

A menu on the DVD allows the user to select between these various animation sequences. Standard DVD angle functions allow the user to switch between the wing plan form, wheel well, and trajectory sequences in real time.

The first three sequences described above were created in the Integrated Graphic Operations and Analysis Laboratory (IGOAL) at JSC using an in-house developed application called Enigma, with 3D solid models of the Orbiter created in Pro/Engineer under product VDM-P06 (3D CAD Modeling). The fourth sequence was also created at JSC (with significant technical support from Analytical Graphics, Inc.) using Satellite Tool Kit (STK) software. Special graphics features and unique data intervals related to the use of STK are as follows:

- Animations of the Orbiter's attitude and trajectory over the Earth surface, including RCS and aerosurface activity.
- Separate "gun camera" and "right wingtip" (camera looking towards the Orbiter right side) views.
- Ground track views ranging from simplified maps showing only the Pacific coastline and U.S. state borders to fully detailed aeronautical maps.
- Special captions denoting significant events from the master entry timeline.

Note that all STK features/views are terminated at LOS+5 sec (GMT 2003/032:13:59:37.396), with interpolation used to represent sensor data during the brief communication dropout periods included in the master entry timeline.

The Enigma and STK output files were originated in AVI format. The individual caption, aeronautical map ground track, and STK gun camera and wingtip windows were integrated into one "quad view" window using Discrete Logic Combustion software. Subsequent compression and reformatting to MPEG2 format was performed to support DVD authoring using Spruce Maestro software (with significant technical support from IMC Incite for nonlinear editing).

One of two known issues with the current rev 2 version of the VDM-P01 DVD is that captions were inadvertently omitted from the wing plan form sequence. These captions are present on all other sequences. The other issue is that the color-coding for the Environmental Control and Life Support System (ECLSS) nozzle temperature sensors on the forward fuselage was erroneously scaled. Rev 3 of the DVD is in now in work to correct these two issues, begin earlier in the entry profile (GMT 2003/032:13:48:00.000), and conform to rev 16 of the master entry timeline. However, it still will not contain any MADS sensor data.

An organized list of all electronic files on the VDM team share drive related to product VDM-P01 and applicable to this report is contained in Appendix C. Collectively, these files constitute the product itself, or they represent the product if not computer-based or not available in a compatible electronic format. They also contain supplemental information that describes or explains important product content, inputs/outputs, observations, and results/conclusions in much greater detail than this report. In the case of product VDM-P01, the product itself is a DVD and all files contained therein are duplicated on the VDM team share drive. As of this writing, the large number of intermediate source files used in creating the DVD are managed individually and do not reside in either location.

3.2 VDM-P02: Physical Mockup

Product VDM-P02 is 1/10 scale physical mockup of the Orbiter left wing that includes major structural components such as wing ribs and spars, wing leading edge (WLE) spars, partial fuselage bulkheads, wheel well and landing gear elements, and wire harnesses associated with select OI sensors. A total of 28 OI sensors are depicted in the mockup, including 8 pressures and 9 temperatures associated with the tires and hydraulic system lines/components in the wheel well; 2 skin temperatures in the wing; 1 bondline temperature on the mid-fuselage sidewall; and 8 hydraulic line/component temperatures in the elevon coves. A complete list of these sensors is contained in Appendix C.

Despite structural elements being present, the mockup does not attempt to present a highly accurate and detailed structural model of the wing. It also does not include wing skin, Thermal Protection System (TPS) components, aerosurface or landing gear actuators, fluid lines, or any MADS sensors and associated wire runs. Instead, the mockup was built early in the investigation when detailed drawings were first becoming available and OI sensor data was initially being analyzed. Therefore, the mockup represents a quick-response solution to providing a reasonably detailed physical model that could be used as an aid to the visualization of major components and key wire harnesses, along with the physical relationships between them.

Several key inputs were used to generate this product:

- Product VDM-P06: 3D CAD Modeling
- Product VDM-P12: Wire Routing Details
- Product VDM-P13: Closeout Photos

The mockup was constructed as follows:

- Prints of the major structural spars and cross sections at the ribs were plotted at 1/10 scale. These prints were applied to 3/16” foam-core single-sided adhesive board. This was cut to finished size using the prints as a guide for their outer shape. Slots were cut at each intersection to allow the ribs and spars to slip together. As updated versions of a spar or rib cross section became available,

the part was re-plotted and affixed to a new board. Then the new part would replace the older part. A functional landing gear assembly was also fabricated using plastic and foam to provide realistic structure for the attachment of select OI sensors.

- Wire runs for OI sensors shown were modeled with a variety of materials, including multicolored micro-gauge wires formed into bundles and 20 gauge insulated wires with color coding that matched the color scheme in use at the time of model construction. The OI sensors depicted on the mock-up include the mockup are referenced in Appendix C.

- For ease of transport, the wing model was built in two sections: from the 1365 spar at the elevon cove to the 1009 spar in the wing glove just forward of the wheel well, and from the 1009 spar to the 807 bulkhead at the wing chine interface.

The resulting mockup was used routinely during meetings, discussions, briefings, and throughout the VDM team investigation process to better visualize physical relationships and potential fluid flow paths through the left wing. The mockup was also provided to the CAIB upon request for temporary use while more detailed and accurate versions were being built to CAIB specifications. These improved mockups used similar construction techniques but slightly different materials, including clear polycarbonate backing for the wing rib sections to improve appearance, fidelity, and handling tolerance. They also included numerous TPS elements and many more sensors, had better internal vent path representations, and went further forward on the vehicle.

An organized list of all electronic files on the VDM team share drive related to product VDM-P02 and applicable to this report is contained in Appendix C. Collectively, these files constitute the product itself or they represent the product if not computer-based or not available in a compatible electronic format. They also contain supplemental information that describes or explains important product content, inputs/outputs, observations, and results/conclusions in much greater detail than this report.

3.3 VDM-P03: 3D Graphical Events Sequence

Product VDM-P03 no longer exists in the VDM team product flowchart. Its intent is captured by products VDM-P04 (2D Static Storyboard) and VDM-P05 (2D Graphical Events Sequence).

3.4 VDM-P04: 2D Static Storyboard

Product VDM-P04 refers to plots of relevant sensor data coupled with maps of vehicle hardware that emphasize the communication of overall vehicle status information during the last hour of the STS-107 mission. Above all, this product attempts to present the flight data in an unbiased and non-timeline format that is unrelated to any given failure scenario. The finished product consists of the following sub-elements:

- A five-sheet E-size (34 in x 44 in) poster displaying relevant sensors and associated data plots to illustrate performance trends. The first two sheets (S1, S2), created early in the investigation, contain OI pressure and temperature sensor locations, data plots, and a comparison between left and right sides of the vehicle on STS-107 through LOS. The last three sheets (S3, S4, S5), created later in the investigation after the OEX recorder was recovered, contain MADS pressure, temperature, and strain sensor locations, data plots, wire routings, and a comparison between STS-107 and three other *Columbia* missions (STS-073, -090, -109) through EI+1000 sec. All five sheets use a common color-coding scheme to represent sensor status (nominal, off-nominal, off-line). They also contain one or more applicable vehicle drawings/schematics to aid in visualizing sensor locations and wire runs as known at the time of product release.

- A 40-page booklet (a.k.a. quantitative report) containing similar OI and MADS sensor information to the poster but with more detail including closeout photos, sensor information spreadsheets, 3D CAD model pictures, cable burnthrough timing plots, and data plot grouping based on future analysis efforts.

- Presentation charts containing similar OI sensor information to the poster and booklet but in a concise presentation format. Two sets of charts exist, the first involving various OI sensors through LOS and the second involving the same OI sensors through the post-LOS time period.

Several key inputs were used to generate this product:

- Raw OI and MADS sensor data from the MER
- Product VDM-P06: 3D Orbiter CAD Modeling
- Product VDM-P07: Wire Routing/Sensor Placement Reconstruction
- Product VDM-P09: Instrumentation Listing and Sensor Location
- Product VDM-P12: Wire Routing Details
- Product VDM-P13: Closeout photos
- Master entry timeline

The raw OI and MADS sensor data used to create the P04 product was acquired in electronic form (CSV format) directly from the MER as soon as it became available. The data was then manipulated and plotted (i.e. reduced) by the P04 product team while concurrently identifying/verifying all active sensors on the vehicle. This process was repeated multiple times until confidence in the data sets reached a high level and the product reached its final state of maturity. To ensure accuracy, results were spot-checked by independent reviewers from other VDM product teams through comparison to hardcopy plots created in the MER. In addition to being used directly in the P04 product, the raw and reduced sensor data was also distributed to the following recipients/teams to save time, ensure consistency, and minimize data processing overhead in the MER:

- Product VDM-P01: 3D Full Animation Event Sequence Playback
- Product VDM-P05: 2D Graphical Events Sequence
- Data Review and Timeline Reconstruction Team
- Failure Scenario Team
- *Columbia* Accident Investigation Board (CAIB)

As of this writing, rev 6 is the latest version of the poster and booklet, and rev 5 is the latest version of the presentation charts, all of which correspond to rev 15 of the master entry timeline.

An organized list of all electronic files on the VDM team share drive related to product VDM-P04 and applicable to this report is contained in Appendix C. Collectively, these files constitute the product itself, or they represent the product if not computer-based or not available in a compatible electronic format. They also contain supplemental information that describes or explains important product content, inputs/outputs, observations, and results/conclusions in much greater detail than this report.

3.5 VDM-P05: 2D Graphical Events Sequence

Product VDM-P05 is a set of presentation charts depicting the overall sequence of events during *Columbia's* entry in a graphical step-by-step manner. The heart of the product is a top-level drawing of the Orbiter, with sensors of interest shown highlighted in their approximate X-Y-Z location and color-coded according to their readings relative to nominal values. Sensor color-coding is as follows, with nominal values defined by the individual subsystem PRT's (with oversight from the Data Review and Timeline Reconstruction Team):

- Green = good sensor with nominal readings
- Yellow = sensor off-nominal high (for temperature, $0°F<\Delta T<15°F$)
- Orange = temperature sensor is off-nominal high, $15°F<\Delta T<30°F$
- Shaded Red = temperature sensor is off-nominal high, $30°F<\Delta T<100°F$
- Solid Red = temperature sensor is off-nominal high, $\Delta T>100°F$
- Light Blue = temperature sensor is off-nominal low, $\Delta T<0°F$
- Shaded Blue = sensor has experienced wire damage, readings no longer represent reality
- Solid Blue = sensor has experienced wire damage, readings have gone off scale and no longer represent reality

To provide a more complete view of the Orbiter, the product is separated into two distinct parts. Each part can stand-alone or be combined for greater insight. Part 1 shows the vehicle from above ("plan view" looking at the X-Y plane), including all sensors and wire runs as viewed from that perspective for each event depicted. It also includes a ground track map to show the exact location of the Orbiter above the earth, corresponding altitude and Mach number information, and an indication of how many sensors went offline in each of the three main wire bundles routed through the left wing (i.e. those running down the outboard and forward walls of the wheel well, sometimes

referred to as bundles A, B, and C). Part 2 shows the vehicle from the port side (side view looking at the X-Z plane), including all sensors and some wire runs for each event depicted in part 1. It also includes an embedded plot of the highlighted sensor's output during a longer portion of the entry profile to give a broader view of trending at that sensor's location. Finally, a three dimensional perspective is shown from behind the vehicle to illustrate vehicle attitude.

Several key inputs were used to generate this product:

- Product VDM-P04: 2D Static Storyboard
- Product VDM-P09: Instrumentation List and Sensor Location
- Product VDM-P10: Sensor Signal Characterization (including the MADS sensor signature database)
- Product VDM-P13: Wire Routing Details
- Master entry timeline

This product went through many revisions, being continually updated as new information became available. Initial versions contained only a few sensors, all of which were OI measurements in the left wing and wheel well showing anomalous behavior during entry. As time passed and more information was obtained, additional sensors and other details were added, eventually expanding the scope of the product to include MADS and OI sensors, key wire runs, aerodynamic events, communication events, and debris events. As of this writing, rev 7 is the latest and intended final version of this product. It utilizes information from master entry timeline rev 17, MADS sensor signature database rev 4, and wire routing details through May 20, 2003.

In its final form, this product provides valuable insight into the sequence of events during entry by allowing a quick flip-through of the charts to visualize: (1) initial heating on the left wing leading edge, (2) heating/burnthrough of the sensor cables routed on the back side of the WLE spar, (3) heating/burnthrough of the sensor cables routed on the outboard and forward walls of the wheel well, (4) temperatures increasing inside the wheel well, and (5) heating/burnthrough of sensor cables routed inside the wheel well.

An organized list of all electronic files on the VDM team share drive related to product VDM-P05 and applicable to this report is contained in Appendix C. Collectively, these files constitute the product itself, or they represent the product if not computer-based or not available in a compatible electronic format. They also contain supplemental information that describes or explains important product content, inputs/outputs, observations, and results/conclusions in much greater detail than this report.

3.6 VDM-P06: 3D CAD Modeling

Product VDM-P06 is a complete solid model representation of *Columbia's* left wing, including wing structure, wheel well structure, main landing gear, hydraulic lines, select OI sensors and associated wire runs, and leading edge reinforced carbon-carbon (RCC) panels. Some areas and features of the mid fuselage are also included. Note that this

model represents the "as-designed" vehicle and does not attempt to recreate the "as-built" configuration, with the exception of certain OI sensor locations that were modified according to inputs from key KSC personnel with first-hand knowledge of the vehicle hardware configuration.

Several key inputs were used to generate this product:

- Product VDM-P07: Wire Routing/Sensor Placement Reconstruction
- Product VDM-P12: Wire Routing Details
- Engineering drawings from the Shuttle Drawing System (SDS)
- Hardcopy engineering drawings

NASA-JSC personnel coordinated the modeling effort. Additional inputs were provided from a variety of different NASA and Boeing organizations as follows:

Contributing Organization	Models Created/Provided
NASA-JSC Structural Engineering Division (ES), with assistance from Lockheed Martin support contractors	RCC Panels Spar Fittings Wing Spars Wing Ribs Main Landing Gear
NASA-KSC Shuttle Engineering Group	Wing Wiring Main Landing Gear
Boeing-Huntington Beach Structures Group	Mid Fuselage Structure Main Landing Gear Door Wing Glove Ribs Elevon Ribs and Actuators
Boeing-KSC Structures Group	Wheel Well Hydraulics Wing Tile Carrier Panels
Boeing-KSC Design Visualization Group	Main Landing Gear Uplock Mechanism
NASA-JSC Energy Systems Division (EP)	Mid Fuselage Tanks and Fluid Lines
NASA-MSFC	RCC Panel Fittings

The master model exists in Pro/Engineer format and resides in an Intralink database at JSC (Root Folder\Space Shuttle\Accident Investigation\Top Level\V070-000002_012_gen_assy.asm). Mirror sites exist at KSC, MSFC, and Boeing-HB. The overall assembly currently contains over 2000 individual components, models of which have different levels of fidelity. Early on, "envelope" models approximating basic component geometry were built. In some cases these models were sufficient. However, in most cases additional details were later added at the request of the model end-users. Models are named using their part numbers, and the assembly is structured to match the Orbiter drawing tree.

As part of the overall CAD modeling effort, detailed models were created for much of the fluid systems hardware located in the mid fuselage region of the Orbiter. This effort

was undertaken to develop a better representation of the vehicle in areas of potential interest, particularly those that may have been affected by off-nominal port fuselage sidewall temperatures. Models were developed for the Power Reactant Storage and Distribution (PRSD) tanks and select feedlines, in addition to the Main Propulsion System (MPS) gaseous helium (GHe) tanks and the ECLSS gaseous nitrogen (GN2) tanks located on the port side of the vehicle in mid-fuselage bays 7 though 11. These models were originally intended for integration into the overall vehicle assembly model. However, as it turns out, these components and areas were not of sufficient interest to warrant inclusion of these models.

Another aspect of the CAD modeling effort involved displaying the X-Y-Z locations of numerous OI and MADS sensors on the vehicle. Initial interest focused on OI sensors in the left wing, wheel well, and mid-fuselage areas. A total of 37 OI sensors were modeled as part of this activity, including the 14 sensors (seven left wing, seven left wheel well) that went OSL or unexpectedly changed state during entry prior to LOS. Later, additional OI temperature sensors from “area 40” on the vehicle were modeled after being identified as relatively sensitive external measurements that might provide additional insight into the local thermal environment. A total of 58 OI temperature sensors were modeled as part of this activity. Finally, after the recovery of the OEX recorder, a large number of MADS sensors were modeled based on relevance to the investigation. A total of 615 sensors were modeled as part of this activity, including pressure, temperature, and strain measurements throughout the vehicle. However, seven more sensors of interest were not modeled due to lack of location information.

For both OI and MADS sensors, X-Y-Z locations were obtained from a variety of sources, some of which were incomplete or in conflict with others. Best attempts were made to determine accurate locations when conflicts were present, and multiple checks were made to maximize accuracy of the final product. Although this was a CAD modeling task, the results of the effort relate directly to product VDM-P09 (Instrumentation Listing and Sensor Location) discussed in section 3.9. Accordingly, all files summarizing the sensors modeled and the associated X-Y-Z locations are kept with other VDM-P09 documents.

An organized list of all electronic files on the VDM team share drive related to product VDM-P06 and applicable to this report is contained in Appendix C. Collectively, these files constitute the product itself, or they represent the product if not computer-based or not available in a compatible electronic format. They also contain supplemental information that describes or explains important product content, inputs/outputs, observations, and results/conclusions in much greater detail than this report. In the case of product VDM-P06, all electronic files are in Pro/Engineer format and are maintained in a separate JSC Intralink database.

3.7 VDM-P07: Wire Routing / Sensor Placement Reconstruction

Product VDM-P07 consists of three sets of charts intended to organize and consolidate the large volume of design, installation, functionality, and performance information

related to the *Columbia* investigation that resides on the VDM team share drive. These files emphasize graphical display methods (3D CAD models, wire routing drawings, closeout photographs, etc.) to aid in visualizing hardware installation. Initially, key information was posted on the walls of the VDM team headquarters and incrementally provided to the OVEWG. Subsequently, this information was organized into a set of more detailed "hardware description" charts for distribution to the OVEWG and CAIB.

Several key inputs were used to generate this product:

- Product VDM-P06: 3D CAD Modeling
  - Pro-E integrated CAD model of OV-102 (pulled from JSC Intralink 3/11/03_8:00am)
- Product VDM-P12: Wire Routing Details
  - Boeing-HB plan view wire routing stick drawings (wing1_Rev4.ppt)
  - Boeing-HB wire routing blacklines (wing2part1_rev0.ppt, wing2part2_rev0.ppt, WIRE RUN SKETCH.ppt)
  - P105 Pinout Rev0_Galvez.ppt
  - Boeing-HB wheel well isometric (wheel well isometric-Rev4.ppt)
  - Boeing-HB wire routing blacklines (V070-796051 LMLG Dark Line Rev4 Pt 1 of 3.ppt)
  - Boeing-HB Wheel Well Plan View (Wing-wheelwell-Rev4.ppt)
- Product VDM-P13: Closeout Photos
  - OV-102 photographs from the Palmdale Orbiter Major Modification (OMM)
  - OV-102 KSC close-out photographs from SIMS
- Left wing and wheel well vent and leak path information provided by Boeing-Houston (Maingearwellvent_info3.xls)

An organized list of all electronic files on the VDM team share drive related to product VDM-P05 and applicable to this report is contained in Appendix C. Collectively, these files constitute the product itself, or they represent the product if not computer-based or not available in a compatible electronic format. They also contain supplemental information that describes or explains important product content, inputs/outputs, observations, and results/conclusions in much greater detail than this report. In the case of product VDM-P07, no further revisions of the hardware description charts are planned even though several key inputs, particularly those related to product VDM-P12 (Wire Routing Details), have already been appended or revised.

3.8 VDM-P08: Events Timeline

Due to the importance of the master entry timeline as an input to many of the VDM team products, this product consisted of assigning a VDM team member to be a liaison to the Data Review and Reconstruction Timeline Team. Although no electronic files were created, this product ensured a thorough understanding of the timeline team's products and conveyed VDM team needs, questions, and comments directly to the timeline team.

3.9 VDM-P09: Instrumentation Listing and Sensor Location

Product VDM-P09 consists of instrumentation system schematics and master measurement lists (MMLs) for all OI and MADS sensors on *Columbia* during STS-107. This information was used as a basic and critical input to many VDM team products, particularly those that involved data plotting, sensor signature characterization and trending analysis, and commonality assessment between measurements. Attributes of primary interest for each measurement included MSID, description, sensor type and X-Y-Z location, power supply and signal conditioner assignments, engineering units and range, sample frequency and most/least significant bit, etc. Since all of this information cannot be found in a single source for OI or MADS sensors, numerous files are used to capture the intent of this product.

Several key inputs were used to generate this product, some of which became part of the product itself due to complexity associated with file and database consolidation:

- For OI sensors:
  - Orbiter Instrumentation Program and Components List (ICPL), Orbiter 102, Flight 28, STS-107, dated 10/29/01
    - Volume one (Equipment List)
    - Volume two (Signal Conditioner and Telemetry Loading List)
    - Volume three (PCM MUX and downlink formats)
  - Electronic database version of the IPCL maintained at Boeing-HB
  - JSC 18366: Operational Instrumentation, Space Shuttle Orbiter, Temperature Measurement Locations, revised January 1992
  - Electronic MML Notebook on Boeing-KSC, NASA Systems website (http://p51.ksc.nasa.gov/aps/mml/)
- For MADS sensors:
  - JSC 23560 Modified for STS-107 (OV-102) Investigation: Modular Auxiliary Data System (MADS) / Orbiter Experiments (OEX) Measurement Locations, dated 4/16/03
- For all sensors:
  - Shuttle drawing system (SDS)

Inconsistencies exist between the items listed above, particularly with respect to sensor X-Y-Z location. Despite this conflict, an attempt was made to document the exact X-Y-Z locations used for sensor placement in product VDM-P06 (3D CAD Modeling) and correlate these placements to their respective sources. As of this writing, a supplemental action external to the VDM team exists to resolve any conflicts and consolidate all attributes mentioned above into a single source.

An organized list of all electronic files on the VDM team share drive related to product VDM-P09 and applicable to this report is contained in Appendix C. Collectively, these files constitute the product itself, or they represent the product if not computer-based or not available in a compatible electronic format. They also contain supplemental information that describes or explains important product content, inputs/outputs,

observations, and results/conclusions in much greater detail than this report. In the case of product VDM-P09, some of the files are just electronic versions of the documents mentioned above.

3.10 VDM-P10: Sensor Signal Characterization For Failure Scenario

Product VDM-P10 consists of a failure mode assessment for various OI and MADs sensors and associated signal conditioners on the vehicle. As such, the intent of this product was met through a combination of analysis and testing.

Analysis, described in this section, involved predicting sensor/signal conditioner outputs for a variety of fail-open and fail-short conditions based on a detailed knowledge of instrumentation system hardware configuration and functionality, along with past experience. In this case, efforts focused on a subset of the 14 OI sensors (seven left wing, seven left wheel well) that went OSL or unexpectedly changed state prior to LOS. This subset included five hydraulic system line/component temperatures in the wing and two tire pressures in the wheel well. For the temperatures, OSL readings were only predicted to be possible under certain fail-short conditions. For the tire pressures, OSL readings were predicted to be possible under both fail-short and fail-open conditions.

Testing, described in section 3.15, involved non-destructive open/short tests with actual sensors and flight-like signal conditioners to confirm analytical predictions. It also involved wire burnthrough tests with flight-representative cables, bundles, and harnesses in a variety of environments and configurations to recreate sensor output signatures observed during entry. As also mentioned in section 3.15, testing showed that breakdown in the Kapton insulation on the sensor wires at temperatures beginning at 750 °F produces a gradual decrease in resistance between adjacent conductors in a cable and adjacent cables in a bundle, eventually creating a hard-short condition that results in the predicted and observed OSL outputs.

An important extension of this product involved analyzing and interpreting/characterizing MADs sensor signatures to explain erratic behavior and address concerns about data validity. The primary objective was to establish a single point in time beyond which (or a range of time during which) the data for each relevant MADS sensor can be considered unreliable (a.k.a. “unphysical”). This was accomplished by first segregating the data according to measurement and sensor type. Examples include resistance temperature devices (RTDs) vs. thermocouples for temperature, Statham vs. Kulite transducers for pressure, and full-bridge gauges for strain. Then, failure modes and commonalities between the sensors were examined to explain the data observed. The result of this activity was a spreadsheet (referred to as the MADS sensor signature database) and set of charts to describe and categorize sensor signatures, define sensor commonalities, and identify the point (or range) in time where sensor data is considered invalid.

A further development of this effort involved using the MADS sensor signature database, instrumentation and sensor location data from product VDM-P09, and wire

routing information from product VDM-P12 to correlate MADS sensor failure timing with wire run locations, particularly along the WLE spar. This activity is described in detail in section 3.16.

An organized list of all electronic files on the VDM team share drive related to product VDM-P10 and applicable to this report is contained in Appendix C. Collectively, these files constitute the product itself, or they represent the product if not computer-based or not available in a compatible electronic format. They also contain supplemental information that describes or explains important product content, inputs/outputs, observations, and results/conclusions in much greater detail than this report. Note that all files related to testing are contained in section 3.15 and all files related to the WLE wire run assessment are contained in section 3.16.

3.11 VDM-P11: Structure / Installation Drawings

Product VDM-P11 no longer exists in the VDM team product flowchart. Its intent is effectively captured by products VDM-P06 (3D CAD Modeling) and VDM-P07 (Wire Routing / Sensor Placement Reconstruction (Drawings/Photos)).

3.12 VDM-P12: Wire Routing Details

Product VDM-P12 consists of simplified two-dimensional “stick” drawings and detailed three-dimensional “blackline” drawings to document sensor installation, wire routing, and connector pin-out details for all failed and non-failed OI and MADS sensors in the left wing and wheel well. Blackline drawings were created from engineering drawings and engineering orders (EOs) residing in the SDS. Closeout photos taken during *Columbia’s* third and most recent OMM (J2) at Boeing-Palmdale were also used to confirm sensor placements and wire routing details.

The task of gathering all the necessary information was broken down into areas and functions. Initial assessment involved the following items:

- Failed and non-failed OI sensors and wiring in the wing
- Failed and non-failed OI sensors and wiring in the wheel well
- Failed and non-failed end-effector power and control wires in the wing
- Failed and non-failed end-effector power and control wires in the wheel well

Significant findings of this initial effort included a determination that all seven OI measurements failing OSL in the wing were contained in a common wire bundle routed along the outboard and forward walls of the wheel well (one of three major bundles, sometimes referred to as A, B, and C). It was also determined that wires for these same sensors were routed through a common connector (P105) in the midbody interface connector panel located in the wing glove area (on the Yo-105 bulkhead between the Xo980 and Xo1009 spars). Other OI sensors not lost but located nearby did not share common wire routings with the failed OSL sensors. Additional indications were that six of the seven affected measurements in the wheel well shared common wire runs to the

wheel well interface connector panel. The seventh measurement shared portions of the same wire run but went to a different connector on the panel.

After the OEX recorder was recovered, the product scope was expanded to include stick drawings for all remaining sensors in the wing plus select blackline drawings of sensor installations and wire routings near the left WLE spar. This last task was necessary to support the Failure Scenario Team. The investigation of MADS sensors was by far the biggest effort of the wire routing team. Upon completion, it consisted of eleven batch files of strain gauge measurements (147 measurements total), seven batch files of wing pressure measurements (80 total), two batch files of wing and Orbital Maneuvering System (OMS) pod temperature measurements (23 total), and one acoustic sensor.

The total effort was divided among numerous engineering groups at KSC, JSC and Boeing-HB. Wire routing information was also used by KSC Orbiter Electrical (OEL) personnel for incorporation into their Pro/Engineer model that depicted key OI sensor wire runs, which was eventually incorporated into product VDM-P06 (3D CAD Modeling).

One interesting observation was that some of the blackline drawings conflict with the closeout photos taken during *Columbia's* last OMM. This is most likely due to flexibility in the way the wiring is installed in the vehicle, which pertains to the accessibility of the intended wire routing and the amount of wire the supporting fixtures (cable clamps, aluminum tape, etc.) can handle.

An organized list of all electronic files on the VDM team share drive related to product VDM-P12 and applicable to this report is contained in Appendix C. Collectively, these files constitute the product itself, or they represent the product if not computer-based or not available in a compatible electronic format. They also contain supplemental information that describes or explains important product content, inputs/outputs, observations, and results/conclusions in much greater detail than this report.

3.13 VDM-P13: Closeout Photos

Product VDM-P13 consists of an organized collection of photos, some available electronically and some not, to help define or confirm structural configurations, sensor locations and installation details, and wire runs applicable to other VDM team products. Where possible, OV-102 closeout photos taken just prior to the STS-107 mission or just after the last OMM (J2) were used as the preferred source of information for this purpose. However, OV-102 original build photos and other vehicle photos were also used as needed, with an acknowledged sense of uncertainty regarding the applicability to OV-102.

The overall photo collection created under product VDM-P13 includes some photos that are available in electronic form and some that are not. Sources of electronic photos include:

- The USA-KSC Still Image Management System (SIMS) website (http://kscgrndtsk1/SIMS/sims.htm)
- The NASA-KSC Investigation Links website (http://www-launchops.ksc.nasa.gov/etd/Investigation/Links.shtml)

Local copies of particularly relevant photos from these websites also reside on the VDM team share drive. Other photos are available electronically on CD or are available in hardcopy form only. An inventory of all photo items generated and tracked by the VDM team as part of product VDM-P13 is contained in Appendix C. As of this writing, all relevant photos have been retrieved and distributed so no additional work is planned on this product.

3.14 VDM Team ASA4 Anomaly Assessment

The aerosurface servoamplifier assembly #4 (ASA4) anomaly was discovered during review of the OI sensor pre-LOS data, which showed that the channel 4 position feedback signal on the speedbrake began to rise unexpectedly in the last three data samples before LOS, indicating speedbrake opening. However, the commanded and expected position of the speedbrake during entry is closed, as observed prior to this time. Post-LOS data showed the following additional anomalous events:

- Speedbrake position indication was bleeding off towards null.
- Right and left inboard and outboard elevon channel 4 isolation valves went to bypass
- A force fight occurred between channels 1-3 and channel 4 on the left outboard elevon for approximately 2 seconds
- Remote power converters (RPCs) that provide main power (bus A & C) and isolation valve power (bus B) to ASA4 both tripped

Upon discovering these events/conditions, a small group of VDM team members with expertise in flight control hardware, hydraulics, and electrical power distribution and control (EPDC) system hardware performed a root cause assessment for this anomaly. The first task was to gain a thorough understanding of the power/control circuits and functionality of the channel 4 flight control actuators. This was accomplished by mapping the wire routing for these signals and investigating the inner workings of the ASA4 box and associated actuator sensors/transducers. During this process, the following significant details were discovered:

- ASA4 receives DC power from three separate RPCs. Primary power is supplied by main buses A and C “OR’d” together through a diode logic circuit. Isolation valve power is supplied to ASA4 by main bus B.
- Excitation power (26 VAC) to the actuator position feedback and delta pressure transducers is derived internal to ASA4 from the main bus A and C feeds.

- Loss of DC power to ASA4 will cause the fail flags to be raised on all channel 4 actuators, thus causing the isolation valves to bypass (i.e. release channel 4 hydraulic pressure within the actuator power valve).
- Loss of excitation power to the actuator position feedback and delta pressure transducers will cause a transition in output to the null value
- Loss of DC power to the isolation valves will prevent valve bypass.
- Excitation wiring to the actuator position feedback and primary delta pressure transducers is separate from equivalent wiring to the secondary delta pressure transducer

After several detailed review meetings and discussions, the team concluded that the most likely events explaining the ASA4 anomaly were as follows:

- Two shorts occurred at approximately the same time due to burning wires between ASA4 and the left outboard elevon actuator
    - The first short involved the AC excitation power wires to the actuator position feedback sensor
    - The second short involved the DC power wires to the isolation valve
- The current-limiting feature of the RPCs feeding the shorts reduced the bus voltage to ASA4 with a corresponding degradation in ASA4 performance and eventual RPC trip
- The shorts combined with degraded performance of ASA4 and tripped RPCs resulted in a loss of AC power to the actuator position sensor and DC power to the isolation valve
    - Position feedback output transitions to null state starting a force fight
    - Isolation valve fails to bypass and end the force fight before RPC trip

In the end, these events were considered credible and consistent with the behavior of Kapton-insulated wires when exposed to a high heating environment. However, these events occurred very late in the entry timeline, had no negative effects on flight control performance at the time, and were a symptom of a larger problem involving hot plasma flow into the left wing.

An organized list of all electronic files on the VDM team share drive related to the ASA4 anomaly assessment and applicable to this report is contained in Appendix C. Collectively, these files constitute the product itself, or they represent the product if not computer-based or not available in a compatible electronic format. They also contain supplemental information that describes or explains important product content, inputs/outputs, observations, and results/conclusions in much greater detail than this report.

3.15 VDM Team Testing

The VDM team conducted nine separate test programs in support of the *Columbia* investigation. All nine test programs are summarized in this report, with additional test set-up details and test data available in separate reports and briefings contained on the

VDM team share drive and referenced in Appendix C. Important observations and/or conclusions resulting from each test program are also summarized below.

1. Main Landing Gear Uplock Release Cartridge Auto Ignition Test – ESTA

   This test was conducted at the Energy Systems Test Area (ESTA) at JSC. A class III main landing gear uplock release cartridge was placed in a thermal chamber and subjected to increasing temperature at 25 to 30 °F per minute until propellant ignition occurred. Results showed autoignition at 598 °F, far above any temperatures observed in the wheel well during entry.

2. Main Landing Gear (MLG) Proximity Sensor Failure Test – NSLD

   This test was conducted at the NASA Shuttle Logistics Depot (NSLD) at KSC. Proximity sensors in each wheel well detect uplock vs. downlock position of the main landing gear. Entry data from these sensors, included in the OI telemetry stream, showed an unexpected change of state from uplock to not-uplock on the left main gear uplock proximity sensor prior to LOS. To examine the failure modes of this sensor and its "proximity box" signal conditioner, a series of tests was run to characterize the output for simulated failures of the sensor cabling. Test conditions included various combinations of hard open circuits, hard short circuits, and soft short circuits for various combinations of conductors in the sensor cabling. Results showed which conditions provide a gear uplock vs. not - uplock output. Furthermore, it was determined that a soft short within a particular resistance range could cause a change in indicated output for a "target far" sensor like the one in question, but not for "target near" sensors like those that did not change state in flight. For this reason, it is presumed that the change of state in the left MLG downlock sensor is a false indication resulting from local heating/burning of the sensor wires.

3. Sensor / Signal Conditioner Failure Test – SAIL

   This test was conducted in the Shuttle Avionics Integration Laboratory (SAIL) at JSC. Entry data for numerous OI pressure and temperature sensors from before LOS showed unexpected output changes from nominal to OSL, some decaying quickly and others much more slowly. To examine the failure modes of these sensors (or equivalent electric circuits) and the associated signal conditioners, a series of tests was run to characterize the output for simulated failures of the sensor cabling. Test conditions included hard open circuits, hard short circuits, and soft short circuits for various combinations of conductors in the sensor cabling. Results showed those cable failures / combinations of failures that produce a normal, off scale high (OSH), or OSL output. More importantly, it was determined that multiple hard short and hard open combinations could produce an OSL output but always with a step-function signature. A smooth decay as seen in flight could only be produced under variable resistance conditions similar

to those generated in the wire burnthrough tests (to be described in the following sections).

4. Initial Cable Burnthrough Characterization Test (oxygen-acetylene torch) – ESTA

   This test was conducted at ESTA at JSC. Early in the STS-107 investigation, evidence from OI sensors indicated a left wing overtemperature condition. Accordingly, a quick test was performed to determine the behavior of Kapton-insulated cables when subjected to localized heating from a small oxygen-acetylene torch. Although this heat source was recognized to be very different than the flight plasma environment, the objective of the test was simply to provide generic data on the behavior of Kapton-insulated cables when rapidly heated. Individual twisted shielded cables and small harnesses consisting of multiple twisted shielded cables were all heated with the torch. Temperature and resistance between conductors within a single cable were measured and recorded. Results from single cable testing showed that a short gradually develops between conductors when heated, with some finite time required for the short to propagate. Based on available literature for Kapton insulation, this behavior is caused by breakdown of the insulation at high temperature as it transitions to being a conductor. Results from the harness testing showed that there can be a significant time delay in the onset of a short circuit for different cables depending on the location within a harness. These factors are presumed to explain the variability in signal decay profile (i.e. time from nominal to OSL) and times at which signal decay began for each sensor.

5. Hot Oven Cable Overtemperature Test (GN2 Environment) – ESTA

   This test was conducted at ESTA at JSC. To supplement the initial cable burnthrough test, a hot oven test was performed to characterize the behavior of a longer section of a Kapton-insulated twisted shielded cable when uniformly heated. Single cables were individually subjected to heating in a 12 in long tube oven. Temperature and resistance between the conductors in the cable were recorded. A nitrogen purge was implemented to minimize potential reaction between oxygen and the cable materials at elevated temperature. Heating of the test cables was performed at various rates by adjusting oven settings. Results showed that the short circuit between conductors in a cable initiates at 750 to 950 °F. Results also showed that the propagation time for the short (from essentially infinite resistance to some very low value) was a strong function of heating rate; higher heating rates produced a shorter propagation time. Although this result was qualitative in nature, since heating rates were not actually measured, the observed behavior did relate to the *Columbia* flight data where sensor failures showed varying times to decay from a nominal reading to OSL. The conductor-to-conductor resistance data from this test was subsequently applied to the sensor calibration curves and results of the SAIL testing to show the predicted vehicle signal conditioner output if the sensor cables were subjected to an overtemperature condition like that simulated in the oven. The

resulting plots of these simulated flight measurements showed a very similar profile to the flight data.

6. Hot Oven Cable Overtemperature Test (Vacuum Environment) – WSTF

   This test was conducted at the White Sands Test Facility (WSTF). Since the off-nominal sensor signatures were observed with the vehicle at such a high altitude, portions of the hot oven GN2 test were repeated at vacuum conditions to evaluate any effects of ambient pressure. Again, single Kapton-insulated twisted shielded cables were individually subjected to heating in a long vacuum oven with temperature and resistance between conductors measured and recorded. As expected, results showed the same resistance decay profile as seen during the hot oven tests in GN2, thus supporting previous conclusions.

7. Cable Burnthrough Thermal Model Calibration Test (small propane torch) – ESTA

   This test was conducted at ESTA at JSC. Early on in the investigation, the analysis team developed detailed thermal models of Orbiter cables, harnesses (multiple cables), and bundles (multiple harnesses) being impinged upon by hot gas flow. Cable and harness burnthrough testing was subsequently performed to provide engineering data to correlate/calibrate these thermal models. Various Kapton-insulated twisted shielded cables and 40-cable harnesses were heated with a small propane torch from various distances and incident angles to vary the local heat rates. Instrumented metal specimens, consisting of steel rods and tubes to simulate the size and shape of the flight cables and harnesses, were also heated with the torch and used as a calorimeter. Temperature and resistance between conductors within the cables and harnesses were recorded, as were numerous temperatures within the calorimeters. Results were used to support initial development and correlation of the thermal models. However, the small torch size was insufficient to allow testing of a large bundle similar in size to those carrying the sensor signal and excitation wires in the wing and wheel well areas. Therefore, complete thermal model calibration was not yet possible.

8. ESTA Cable and Bundle Burnthrough Test (large propane torch)

   To enable additional burnthrough testing on a large wire bundle representative of those being modeled/analyzed on the vehicle, a larger propane torch was used. Test bundles of 1.75 in diameter, consisting of 290 Kapton-insulated twisted shielded cables, were also built from flight spare inventory to simulate the wire bundles routed along the forward and outboard walls of the wheel well. Within each test bundle, temperature and resistance between conductors were measured and recorded on 33 individual cables. These bundles, along with instrumented metal calorimeters built to simulate the size and shape of large bundles, were then individually heated with the torch. Results were used to complete development and correlation of the thermal models.

9. Arc Jet Cable Bundle Failure Test

   This test was conducted in the Atmospheric and Reentry Materials Structural Evaluation Facility (ARMSEF) at JSC. During STS-107, many OI and MADS sensors showed anomalies in their output signals, likely related to localized cable heating. In this test, cable bundles simulating those carrying numerous OI and MADS sensor wires on the Orbiter were subjected to hot plasma impingement representative of the entry environment through various sized holes in an aluminum plate. The test bundles were approximately 1.75 in diameter and consisted of 290 separate 24 AWG, Kapton-insulated, twisted, shielded cables secured with flight-like aluminum cable clamps. Within each bundle, 33 separate cables were monitored for changes in conductor-to-conductor resistance as a function of temperature and time.

   The general purpose of the test was to gain an understanding of the convective heating environment and associated thermal failure mechanism for the cable bundles routed inside the left wing. The specific objective was to obtain the failure mechanism characteristics, failure initiation time, failure rate, and burn-through time for a cable bundle subjected to a representative plasma environment. Test results showed that arc jet plume heating could produce the same cable failure mechanism seen in previous torch tests (but much more quickly and dramatically) and the same sensor output signatures seen in flight. They also showed a very rapid erosion of the hole in the aluminum plate with a corresponding increase in cable failure rate. Finally, test-derived heating rate and cable failure rate data can be used to validate thermal models of the vehicle to support failure scenario development for the *Columbia* investigation.

3.16 VDM Team Leading Edge Wire Run Assessment

As an extension of product VDM-P10 (Sensor Signal Characterization for Failure Scenario), a detailed assessment was performed to examine the correlation between MADS sensor failure timing and sensor wire routing. The MADS sensor signature database from product VDM-P10 and wire routing information from product VDM-P12 were both used as inputs to this assessment.

Results of the assessment indicate that all 18 MADS sensors with wires contained in one of the five separate harnesses routed along the left WLE spar (sometimes referred to as A, B, C, D, and E) were lost. Furthermore, 17 out of 18 of these events occurred during a 10 sec time interval (EI+487 sec to EI+497 sec) preceding the loss of any other MADS sensors with different wire routings. The only exception involved four unrelated MADS sensors sharing a common power supply with the failed WLE-routed sensors. These four sensors are presumed to have been lost due to electrical commonality, not wire heating/burning away from the left WLE spar. Finally, wire routing geometry and sensor failure order (top to bottom, outboard to inboard) suggest specific boundaries for left WLE spar burnthrough behind RCC panel 8.

Based on engineering drawings and closeout photos, some uncertainty still exists regarding which sensor wires are contained in which of the five main WLE harnesses. The most notable example involves the WLE spar temperature sensor behind RCC panel 9, which was the last of the 18 WLE-routed sensors to fail and did so even after other MADS sensors in the three main wheel well wire bundles began to fail. Despite this uncertainty, confirmed information about the wire routing still provides strong evidence that a breach in the WLE spar occurred at RCC panel 8, allowing hot plasma to enter the wing.

The product resulting from this assessment is a set of presentation charts containing a tabular summary of all WLE-routed MADS sensors, a 3D CAD picture showing sensor locations and cable routings, closeout photos confirming these routings to the extent possible, and relevant plots of sensor data. This information is kept on the VDM team share drive and is also referenced in Appendix C.

3.17 VDM Team Miscellaneous Tasks

Several miscellaneous tasks were performed by select VDM team members based on expertise in Orbiter propulsion and power subsystems, including the Auxiliary Power Unit (APU); Electrical Power Distribution and Control (EPDC) System; Fuel Cells (FC); Hydraulics/Water Spray Boiler (Hyd/WSB); Main Propulsion System (MPS); Orbital Maneuvering System (OMS); Power Reactant Supply and Distribution (PRSD) System; Pyrotechnic Devices (Pyro); and Reaction Control System (RCS). In particular, hardware inventories and hazard assessments applicable to STS-107 were created to aid the debris recovery teams with hardware identification and handling safety. In addition, pre-flight data records that are not controlled (i.e. organized and stored) in any other configuration management system were identified and impounded, including Pyro acceptance data packages (ADPs) and Space Shuttle Engineering Integration (SSEI) flight readiness statements (FRSs).

An organized list of all electronic files on the VDM team share drive related to the miscellaneous tasks and applicable to this report is contained in Appendix C. Collectively, these files constitute the product itself, or they represent the product if not computer-based or not available in a compatible electronic format. They also contain supplemental information that describes or explains important product content, inputs/outputs, observations, and results/conclusions in much greater detail than this report.

4.0 CONCLUSIONS AND SIGNIFICANT FINDINGS

The VDM team charter included the creation of unique and innovative data display products that aid in understanding the hardware configuration, sensor response data, and complex sequence of events during *Columbia's* entry. Accordingly, the team focused on producing the products defined by the VDM team product flowchart in Appendix A and responding to all related action items listed in Appendix B. All VDM team products have been described in this report. Action items were not discussed but

relate directly to the VDM team products as indicated by the action tracking number and associated closeout files in Appendix B. Since the VDM team was not formally tasked with detailed interpretation of the flight data, significant findings are limited to those areas in which testing or analysis took place to create a product, pursue a special activity, or respond to an action. The resulting list of conclusions and findings is shown below. Most of these items have previously been discussed in this report.

- The VDM team produced seven major products and six supporting data generation/gathering products. Four special activities related to these products and encompassed by the VDM team charter were also pursued. Finally, the VDM team worked 98 formal action items. The content, revision status, and findings of each VDM team product and special activity were previously discussed in this report. As of this writing, only two action items remain open. The first involves plasma impingement testing of flight-representative cable bundles under VDM Team Testing (section 3.15). The second involves production of the latest and expected final revision of product VDM-P01 (3D Full Animation Event Sequence Playback, section 3.1).

- The first OI indications of off-nominal system performance involved a hydraulic line temperature on the inboard sidewall (Yo-105) of the left wheel well (V58T1703A, LMG Brake Line Temp D) at GMT 2003/032:13:52:17. Subsequently, other OI sensors began showing off-nominal trends. Of these, a total of 14 OI measurements went OSL or unexpectedly changed state (starting at GMT 2003/032:13:52:56) prior to LOS, as listed in section 3.0. Seven of these sensors were located in the left wing and seven were located in the left wheel well. All seven in the left wing shared a common wire bundle routed along the outboard and forward walls of the left wheel well. They also shared a common connector panel and connector in the wing glove area (midbody interface connector panel located on the Yo-105 bulkhead between the Xo980 and Xo1009 spars, connector P105). Six of the seven in the wheel well shared a common wire run along the aft wall (Xo1191 spar), ceiling, and forward wall (Xo1040 spar) of the wheel well, with the seventh signal sharing portions of this same run. All seven of these signals shared a common connector panel in the wheel well (wheel well interface connector panel located on the Y-105 bulkhead) but they did not all share a common wire bundle or connector.

- Recovery of the OEX recorder provided 600+ additional MADS pressure, temperature, and strain measurements of interest to the investigation, the first of which (V12G9921A, Left Wing Front Spar Strain) began showing signs of off-nominal performance at GMT 2003/032:13:48:39, approximately 3:38 sec before the first off-nominal OI sensor reading was detected.

- Based on analysis and testing performed by the VDM team, nearly all notable OI and MADS sensor signatures observed during entry (OI sensors lost OSL or unexpectedly changing state before LOS, MADS sensors showing erratic behavior then failing OSL or OSH, OI sensors indicating the ASA4 anomaly, etc.)

are consistent with plasma-induced heating/burnthrough and progressive shorting of the associated Kapton-insulated cables, rather than actual events occurring at the location of each sensor. Propagation of the short, as manifested in failure start time and signal decay time, is dependent on cable location within a harness/bundle and local heat flux, with arc-jet plasma impingement tests showing the greatest similarity to flight data.

- Product VDM-P05 (2D Graphical Events Sequence) provides an excellent overall view of the sequence of events that occurred during entry. The format and content of this product allow a quick flip-through of the charts to visualize: (1) initial heating on the left wing leading edge, (2) heating/burnthrough of the sensor cables routed on the back side of the WLE spar, (3) heating/burnthrough of the sensor cables routed on the outboard and forward walls of the wheel well, (4) temperatures increasing inside the wheel well, and (5) heating/burnthrough of sensor cables routed inside the wheel well. When combined with product VDM-P04 (2D Static Storyboard), a comprehensive view of all events and sensor data observed during entry is obtained.

- A comprehensive 3D solid model representation of the Orbiter's left wing was created in Pro/Engineer under product VDM-P06 (3D CAD Modeling). The top-level assembly file contains over 2000 individual components, including wing structure, wheel well structure, main landing gear, hydraulic lines, OI sensors and associated wire runs, and leading edge RCC panels. Additional modeling was performed to show fluid systems hardware located in the mid fuselage area adjacent to the left wheel well, in addition to 37 OI sensors in the left wing, wheel well, and mid-fuselage areas; 58 OI temperature sensors in area 40; and 615 MADS pressure, temperature, and strain sensors throughout the vehicle.

- An extension of product VDM-P10 (Sensor Signature Characterization for Failure Scenario, section 3.10) involved analyzing and interpreting/characterizing MADs sensor signatures to explain erratic behavior and address concerns about data validity. The result of this activity was a comprehensive sensor signature database representing MADS sensor failure signatures and timing. Related work on the leading edge wire run assessment (section 3.16) indicated that all 18 MADS sensors with wires contained in one of the five separate harnesses routed along the left WLE spar were lost. Furthermore, 17 out of 18 of these events occurred during a 10 sec time interval (EI+487 sec to EI+497 sec) preceding the loss of any other MADS sensors with different wire routings. The only exception involved four unrelated MADS sensors sharing a common power supply with the failed WLE-routed sensors. These four sensors are presumed to have been lost due to electrical commonality, not wire heating/burning away from the left WLE spar. Finally, wire routing geometry and sensor failure order (top to bottom, outboard to inboard) suggest specific boundaries for left WLE spar burnthrough behind RCC panel 8.

APPENDIX A: VDM Team Product Flow Chart

APPENDIX B: VDM Team Roster and Action List

NOTE:

Closeout files referenced in the VDM team action list are available in the final report folder on the VDM team share drive and on the final report CD. However, unlike the product document list in Appendix C, embedded hyperlinks to the action closeout files are not present. Instead, base filenames and file extensions are given without regard to revision or date. This was done to minimize action list upkeep as response files were continually being revised. For those files that are common to both lists, hyperlinks to the revision available at the time of this writing can be accessed from the product document list in Appendix C. For those that are not common (with the exception of 100+ MB raw data files associated with product VDM-P04), the base filenames and file extensions can be used to locate a particular document of interest in the final report folder on the VDM team share drive or on the final report CD (or better yet, the related product folder on the VDM team share drive where the latest revisions of all VDM files are kept).

APPENDIX C: VDM Product Files for the Final Report

Product/Activity	Files Applicable to VDM Final Report?
VDM-P01: 3D Full Animation Event Sequence Playback	YES
VDM-P02: Physical Mockup	YES
VDM-P03: 3D Graphical Events Sequence	NO
VDM-P04: 2D Static Storyboard	YES
VDM-P05: 2D Graphical Events Sequence	YES
VDM-P06: 3D CAD Modeling	YES
VDM-P07: Wire Routing / Sensor Placement Reconstruction (Drawings/Photos)	YES
VDM-P08: Events Timeline	NO
VDM-P09: Instrumentation Listing and Sensor Location	YES
VDM-P10: Sensor Signal Characterization For Failure Scenario	YES
VDM-P11: Structure / Installation Drawings	NO
VDM-P12: Wire Routing Details	YES
VDM-P13: Closeout Photos	YES
VDM Team ASA4 Anomaly Assessment	YES
VDM Team Testing	YES
VDM Team Leading Edge Wire Run Assessment	YES

APPENDIX D: Acronyms and Abbreviations

Acronym/Symbol	Definition
Δ	Delta
2D	2-Dimensional
3D	3-Dimensional
AC	Alternating Current
Actr	Actuator
ADP	Acceptance Data Pack
APU	Auxiliary Power Unit
ARMSEF	Atmospheric and Reentry Materials Structural Evaluation Facility at JSC
ASA	Aerosurface Servo Amplifier
AVI	Audio Video Interleave
AWG	American Wire Gauge
CAD	Computer
CAIB	*Columbia* Accident Investigation Board
CD	Compact Disk
CSV	Comma Separated Variable
DC	Direct Current
DVD	Digital Video Disk
ECLSS	Environmental Control and Life Support System
EI	Entry Interface
Elev	Elevon
EO	Engineering Order
EP	Energy Systems Division at JSC
EPDC	Electrical Power Distribution and Control
ES	Structures and Mechanics Division at JSC
ESTA	Energy Systems Test Area at JSC
FC	Fuel Cell
FDM	Frequency Division Multiplexer
FRS	Flight Readiness Statement
GHe	Gaseous Helium
GMT	Greenwich Mean Time
GN2	Gaseous Nitrogen
HB	Huntington Beach, CA
Hyd/WSB	Hydraulics / Water Spray Boiler
IDI	Information Dynamics, Inc.
IGOAL	Integrated Graphic Operations and Analysis Laboratory at JSC
Inbd	Inboard
IPCL	Instrumentation Program and Components List
JPEG	Joint Photographic Experts Group
JSC	Johnson Space Center
KSC	Kennedy Space Center

LH	Left Hand
LMLG	Left Main Landing Gear
LMG	Left Main Gear
Ln	Line
LOE	Left Outboard Elevon
LOS	Loss of Signal
Lwr	Lower
MADS	Modular Auxiliary Data System
MEI	Muniz Engineering, Inc.
MER	Mission Evaluation Room
MLG	Main Landing Gear
MML	Master Measurement List
MPEG	Moving Pictures Experts Group
MPS	Main Propulsion System
MSFC	Marshall Space Flight Center
MUX	Multiplexer
NASA	National Aeronautics and Space Administration
NSLD	NASA Shuttle Logistics Depot at KSC
OEL	Orbiter Electrical
OEX	Orbiter Experiments
OI	Orbiter Instrumentation
OMM	Orbiter Major Modification
OMS	Orbital Maneuvering System
OSH	Off-Scale High
OSL	Off-Scale Low
Outbd	Outboard
OVEWG	Orbiter Vehicle Engineering Working Group
PCM	Pulse Code Modulation
Press	Pressure
Prox	Proximity
PRSD	Power Reactant Storage and Distribution
PRT	Problem Review Team
Pyro	Pyrotechnic
RCC	Reinforced Carbon-Carbon
RCS	Reaction Control System
RPC	Remote Power Controller
RTD	Resistance Temperature Detector
Rtn	Return
SAIL	Shuttle Avionics Integration Laboratory
SDS	Shuttle Drawing System
SIMS	Still Image Management System
SSEI	Space Shuttle Engineering Integration
STK	Satellite Took Kit
T	Temperature
TPS	Thermal Protection System

Upr	Upper
USA	United Space Alliance
VAC	Volts AC
VDC	Volts DC
VDM	Vehicle Data Mapping
WLE	Wing Leading Edge
WSTF	White Sands Test Facility

THIS PAGE INTENTIONALLY LEFT BLANK

Volume V
Appendix G.6

SRB Working Group Presentation to CAIB

This Appendix contains the SRB Working Group Presentation to Columbia Accident Investigation Board, 28 May 2003.

THIS PAGE INTENTIONALLY LEFT BLANK

SRB Working Group Presentation to Columbia Accident Investigation Board CAIB

Solid Rocket Booster Working Group Agenda

SRB Working Group

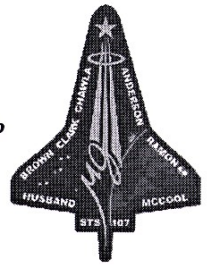

- **Executive Summary**
- List of Members, Advisors, Observers, and Others
- Method of Investigation
  - Special Circumstances
  - Investigation Process
- Fault Tree Closure Summary
- Summary

Preliminary - Investigation Sensitive

Executive Summary

SRB Working Group

Objective

- To Determine if the Solid Rocket Boosters (SRBs) were a contributor to the loss of the STS-107 crew and vehicle.

Approach

- Develop credible Fault Tree failure scenarios for events that could have contributed to the loss of STS-107. Follow structured and methodical approach for closure of all fault tree blocks.
- Perform in-depth hardware and documentation assessment using all available analysis, test, recovered hardware inspection, pedigree documentation, processes, and discrepancy data.

Fault Tree Summary

- **509 blocks (including Top Level block) rolled up into 88 closure blocks**

	Total Blocks	Closure Blocks	Multi-Element	Open Blocks
Load & Environments	70	18	1	0
Active Subsystems	14	2	3	0
Debris	424	68	35	4
Total	**508**	**88**	**39**	**4**

Preliminary - Investigation Sensitive

Executive Summary

SRB Working Group

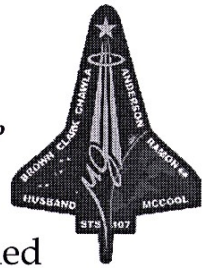

Fault Tree Closure Definitions

- **Closed** – Fault Tree Blocks in which the event or failure scenario has been deemed **Not Credible** by the SRBWG.
  - "**Not Credible**" is defined as "Extremely remote possibility that Failure Scenario caused the loss of STS-107. Either strong controls in place or hardware evidence shows event did not occur."
- **Open** – Fault Tree Blocks where SRBWG cannot obtain majority consensus on Failure Scenario being "**Not Credible**."

- Fault Tree Block B.1.3.2.4.2 (Debris Ejection from Motor (FWD BSM)) – **Closed (Minority Report)**
- Fault Tree Blocks B.1.3.4.4.3.1, B.1.3.4.4.3.2, B.1.3.4.4.3.3, B.1.3.4.4.3.4 (Bolt Catcher) – **Open** (Pending Test Results)
- Fault Tree Block number B.1.3.6.1.1 (Loss of Aft Separation Area ET Side TPS Causes Debris) is **closed** based on engineering judgment by the SRBWG. Final Debris Transport Analysis from Level II is pending but is related to return-to-flight rather than fault tree closure..

Preliminary - Investigation Sensitive

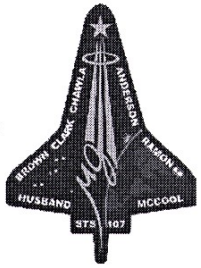

Acronym List

ACO	Assembly Check Out
AFT	Rear of the spacecraft
AMS	Aerospace Material Specification
AP	Ammonium Perchlorate
APRT	Ascent Performance and Reconstruction Team
APU	Auxilliary Power Unit
ATVC	Ascent Thrust Vector Control
BET	Best Estimate Trajectory
BI	Booster Identifier
BSM	Booster Separation Motor
BTA	Booster Trowelable Ablative
CDF	Confined Detonating Fuse
CDFA	Confined Detonating Fuse Assembly
CDFI	Confined Detonating Fuse Initiator
CDFM	Confined Detonating Fuse Manifold
CIL	Critical Items List
CSD	Chemical Systems Division now known as P&W Space Propulsion
CWSI	Critical Weld Stress Indicator
DAS	Data Acquisition System
DCMA	Defense Contract Management Agency
E&I	Electrical and Instrumentation
ECP	Engineering Change Proposal
ECR	Engineering Change Request
ED	Engineering Directorate
EMI	Electromagnetic Interference
ESD	Electrostatic Discharge
ET	External Tank
ETA	External Tank Aft
FEM	Finite Element Mode
FEM	Finite Element Model
FEP	Fluorinated Ethylene Propylene
FIV	Fuel Isolation Valve
FMEA/CIL	Failure Mode and Effects Analyses/Critical Items List
FOD	Foreign Object Debris
FOS	Factor of Safety
FSM	Fuel Supply Module
FT	Fault Tree
FWD	Forward
GNC	Guidance, Navigation and Control
GO	Ground Operations
HDI	High Density Indication
HDP	Holddown Post
ICD	Interface Control Document
IPR	In Process Review
JSC	Johnson Space Center
KSC	Kennedy Space Center
L&E	Loads and Environment
LCC	Launch Commit Criteria
LH	Left Hand
LOV	Loss of Vehicle
LSBR	Liquid Strand Burn Rate
LSC	Linear Shaped Charge
MAF	Michoud Assembly Facility
MCC-1	Marshall Convergence Coating - 1
MET	Mission Elapsed Time
MLP	Mobile Launch Platform
MLP	Mobile Launcher Platform
MPP	Manufacturing Process Plan
MSFC	Marshall Space Flight Center
NDE	Nondestructive Evaluation
NIS	Nonconformance Information System
NSD	NASA Standard Detonator
NSI	NASA Standard Initiator
NSI-PC	NASA Standard Initiator - Pressure Cartridge
OMI	Operations and Maintenance Instructions
OMRSD	Operations and Maintenance Requirement Specification Document
P&W	Pratt and Whitney
PDL	Polymer Development Labs
PIC	Pyrotechnic Initiator Controllers
PR	Problem Report
PRCBD	Program Requirements Change Board Directive
PSC	Primary Separation Cue

Executive Summary

SRB Working Group

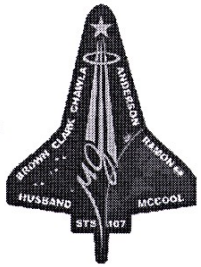

Acronym List

RCS	Reaction Control System
RH	Right Hand
ROD	Routing Operation Document
RSRM	Redesigned Solid Rocket Motor
RSS	Range Safety Systems
RTV	Room Temperature Vulcanizing
S&A	Safe and Arm
SIRB	Systems Integration Requirement Board
SLA	Super Light Ablator
SLET	Shelf Life Extension Test
SRB	Solid Rocket Booster
SRBTS	Solid Rocket Booster Tracking Subsystem
SRBWG	Solid Rocker Booster Working Group
SRM	Solid Rocket Motor
SSME	Space Shuttle Main Engine
SSP	Space Shuttle Program
TLI	Thrust Load Indicator
TPS	Thermal Protection System
TSM	Tail Service Mast
TVC	Thrust Vector Control
USA	United Space Alliance
USBI	United Space Booster, Incorporated
VAB	Vehicle Assembly Building
WADS	Work Authorization Documents

Solid Rocket Booster Working Group Agenda

SRB Working Group

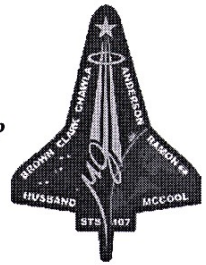

- Executive Summary
- **List of Members, Advisors, Observers, and Others**
- Method of Investigation
  - Special Circumstances
  - Investigation Process
- Fault Tree Closure Summary
- Summary

Note: The symbol ▣ indicates a link to back up information.

Preliminary - Investigation Sensitive

Solid Rocket Booster Working Group Team Members

SRB Working Group

SRB Working Group (NASA Team)

Darrell Davis	Thermal
Joe B. Davis	Pyrotechnics
Jeff Dilg	Structures
Don Ford	Systems Engineering
Joe Gentry	Structures
Rusty Jones	Loads/Environments
Joe Lusk	SRBWG Deputy Chair and Assistant Project Manager, SRB Project Office
Tina Malone	M&P
Malissa Meadows	E&I
Boris Pagan	TVC
Tom Reickhoff	Photo Analysis
Pete Rodriguez	SRBWG Chair and Deputy Manager, Structures, Mechanics and Thermal Department
George Story	BSM
Randall Tucker	S&MA
Renee Wilson	SRBWG Secretary

Preliminary - Investigation Sensitive

Other Key Players

SRB Working Group

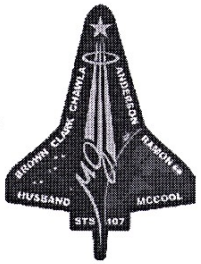

Review and Assessment

Peggy Frazier
Chantel Jacob
Mike Norris

Systems Fault Tree Review Team

Joe Brunty
Dan Mullane
Richard Sheppard
John Townsend

DCMA Key Players

Jim Anderson
Craig Bennett
Myles Campbell
Primo Correa
Carlos de Mattos
Joe Giedlinski
Robert Kaufmann
Robert Kauffman
Dave Kedell
Ron Koehn
Norm Powers
Tom Root
Mike Smutek
Terence Young

NASA S&MA MSFC and KSC

Foster Anthony
Shane Canerday
Neal Hooten
Art Morales
Robert Osterblum
Rick Sizemore

NASA MSFC SRB Resident Office at KSC

Homero Hidalgo
Tom Engler
Robin Ferebee
Sandy Norris

SRBWG Senior Advisory Group

Vince Caruso(retired), Former Manager, Systems Management and Integration Office, Space Shuttle Main Engine
Keith Coates(retired), Former Chief Engineer, Solid Rocket Motor Program
Erich Engler(retired), Former Chief, Structural Development Branch, Science and Engineering Directorate
Bob Henry(retired), Former Senior Technical Assistant to the Chief Engineer, Solid Rocket Booster Program
Bill Horton(retired), Former Chief Engineer, Solid Rocket Booster Program

Senior Independent Review

Moody Davis(retired), Former Manager, Testing and Operations Office, Chief Engineer's Office, Solid Rocket Motor Program
Jim Thomas(retired), Former Manager, Technical Operations Office, Solid Rocket Motor Program

Fault Tree Independent Review

Robert Schwinghamer(retired), former Assistant Center Director - Technical, MSFC

Preliminary - Investigation Sensitive

030-000063
SRB Working Group Presentation to Columbia Accident Investigation Board CAIB.pdf
CAB093-0009

Solid Rocket Booster Working Group Team Members

SRB Working Group

USA Investigation Team Leads/Key Players

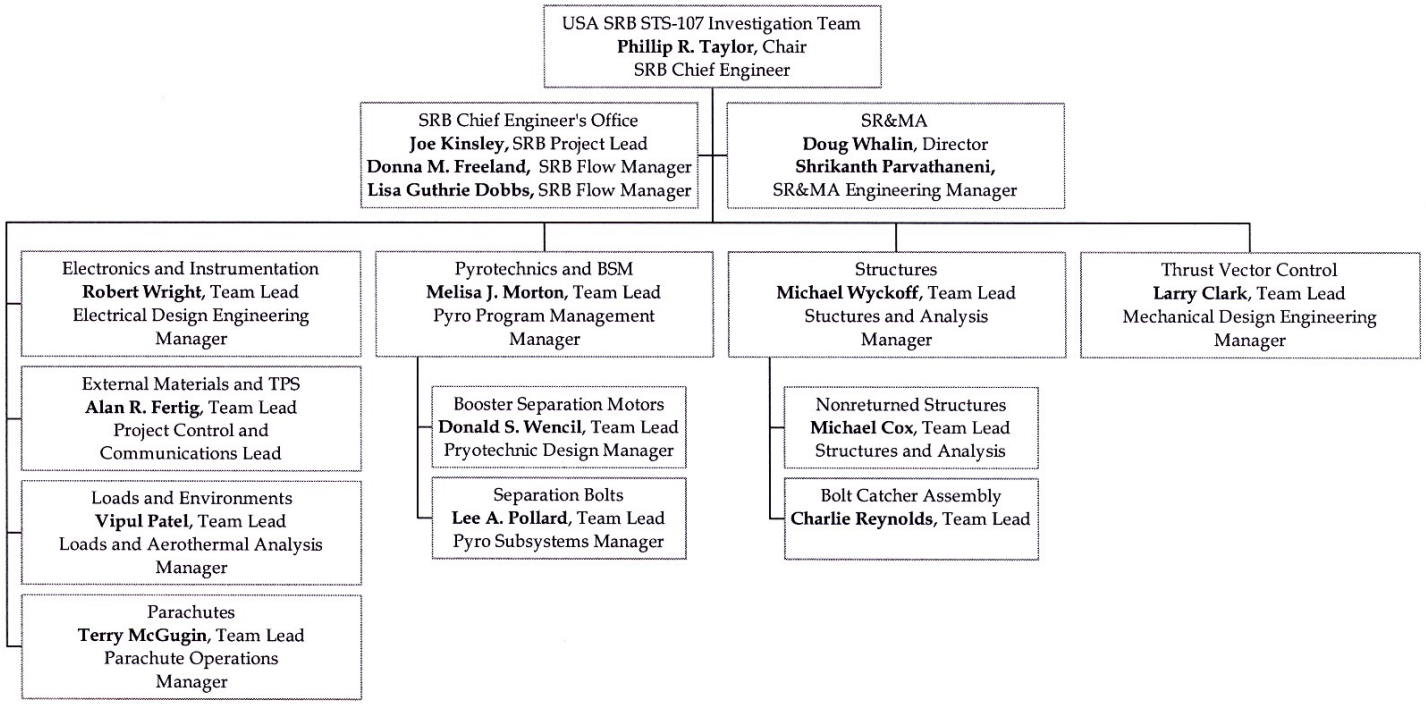

Preliminary - Investigation Sensitive

Solid Rocket Booster Working Group Agenda

SRB Working Group

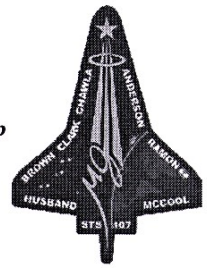

- Executive Summary
- List of Members, Advisors, Observers, and Others
- Method of Investigation
  - **Special Circumstances**
  - Investigation Process
- Fault Tree Closure Summary
- Summary

Preliminary - Investigation Sensitive

Special Circumstances

SRB Working Group

- **Hardware Status As of February 1, 2003:**
  - Open Assessment of STS-107 SRB/RSRM Hardware Completed on 1/20/03
  - The SRB/RSRM Disassembly Schedule Was Nearly Complete
  - Refurbishment Was in Work
  - USA Post Flight Assessment Team Performed Initial Thorough Assessment of Hardware
  - SRBWG Reviewed Post Flight Data and Photography plus Hardware as it was in the Disassembly and Refurbishment Process

Preliminary - Investigation Sensitive

Solid Rocket Booster Working Group Agenda

SRB Working Group

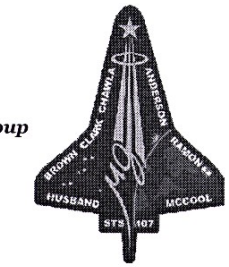

- Executive Summary
- List of Members, Advisors, Observers, and Others
- Method of Investigation
  - Special Circumstances
  - **Investigation Process**
- Fault Tree Closure Summary
- Summary

Preliminary - Investigation Sensitive

SRB Working Group Presentation to Columbia Accident Investigation Board CAIB.pdf
CAB093-0013

Investigation Process

SRB Working Group

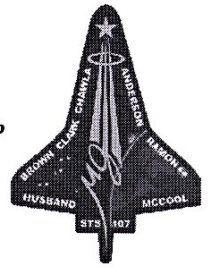

SRB Hardware classified into two categories

- **Retrieved Hardware**
  - Post-Flight Assessment
  - SRBWG Re-Assessment
  - Video and Photography
  - Flight Loads Analysis/Flight Data
  - 10MNL-0035 Requirements Document
- **Non-Retrieved Hardware**
  - Video and Photography
  - Comparison to Retrieved Hardware with Equal Processing
  - Flight Data (DAS, Telemetry)
  - Documentation Assessment Including:
    - As-designed vs. As-Built
    - Engineering Changes Affecting STS107
    - Problem Reports/Squawks/Non-Conformances
    - SRB Build-up and Consumables
    - Ground Operations Build-up Documents
    - NASA ALERTS
    - Hazard Analysis and CIL Correlation
    - SRB Waiver List Review

SRBWG Philosophy: "All Hardware is Guilty until Proven Innocent." John Key

Preliminary - Investigation Sensitive

Investigation Process

SRB Working Group

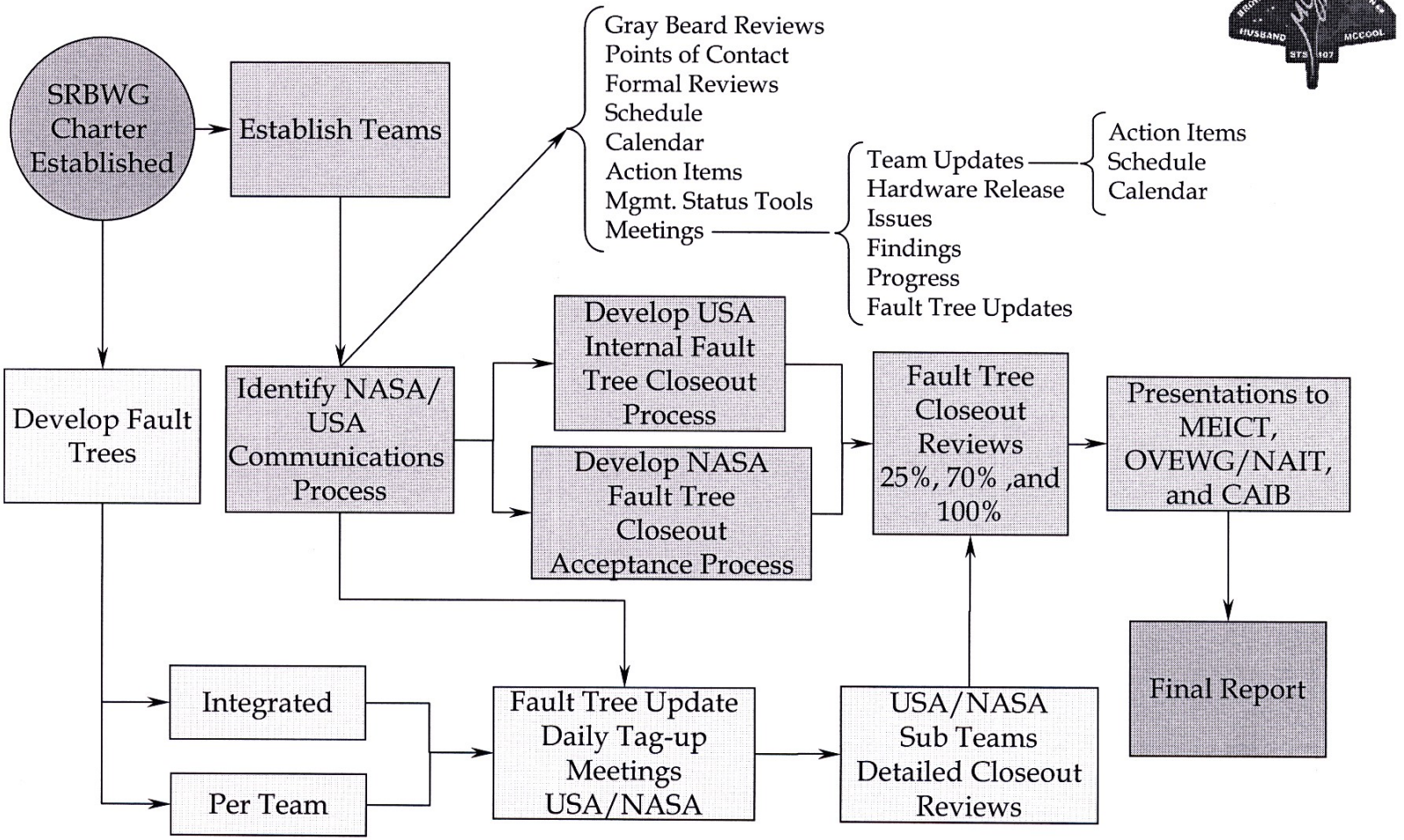

Page 15

Preliminary - Investigation Sensitive

C0-000063

Investigation Process

SRB Working Group

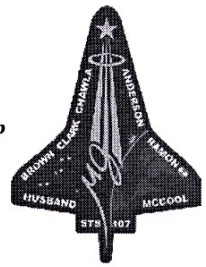

Operational Experience and Design Limits

- Knowledge of both existing data base and design limits (overall and second-by-second) needed to understand hardware performance
- Each Shuttle flight adds to our knowledge and experience base
- Deviations/Exceedances from the experience base result in executing planned activities to understand the "what", "how" and "why" of event.

Fault Tree Development

- Fault Tree developed and checked against Hazards Analysis and Critical Items List (CIL)

Independent Reviews

- Senior Advisory Group
  - 2 Reviews for Fault Tree Development
  - 3 Reviews for Closure Development
  - 2 Final Presentation Reviews
- MSFC Systems Team – 1 Fault Tree Development Review

SRBWG Fault Tree mapped to MEIC/Systems and CAIB Fault Tree

Preliminary - Investigation Sensitive

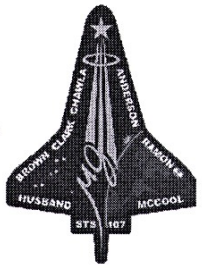

Fault Tree Closure Process

Closure Rationale Developed jointly by USA/SRBWG/DCMA

- USA Teams provided initial write-up
  - Including input from SRBWG members and DCMA
- USA SRB Chief Engineer Office Review
- SRBWG Chairman/MSFC S&MA performed individual **one-on-one** reviews with USA team lead and SRBWG discipline/hardware lead for each closure sheet
- Entire SRBWG and SRB Project Personnel performed final closeout review on each closure sheet. DCMA present at each closure discussions.

Preliminary - Investigation Sensitive

Solid Rocket Booster Working Group Agenda

SRB Working Group

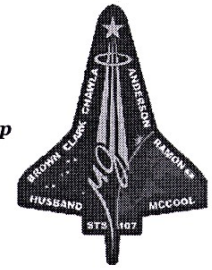

- Executive Summary
- List of Members, Advisors, Observers, and Others
- Method of Investigation
  - Special Circumstances
  - Investigation Process
- **Fault Tree Closure Summary**
- Summary

Preliminary - Investigation Sensitive

Solid Rocket Booster Working Group
Fault Tree Multi-Element Blocks

SRB Working Group

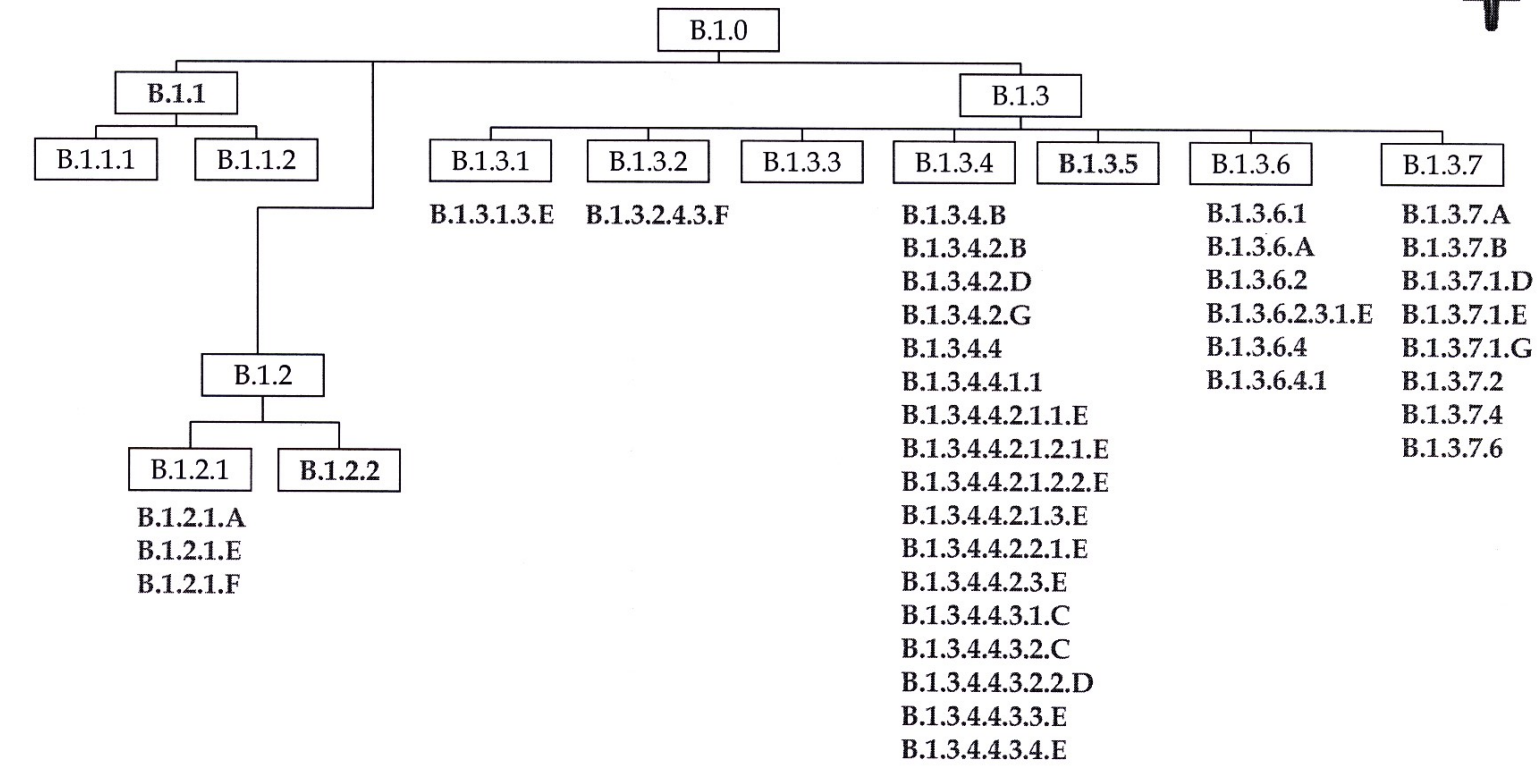

Preliminary - Investigation Sensitive

Solid Rocket Booster Working Group
SRBWG-to-MEICT Mapping

SRB Working Group

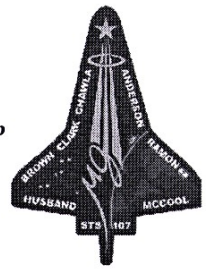

G525

B.1.3.1	B.1.3.4.4.1.A	B.1.3.6.4.1.B
B.1.3.1.1	B.1.3.4.4.1.B	B.1.3.6.4.1.1
B.1.3.2.A	B.1.3.4.4.1.1.A	B.1.3.6.4.1.2
B.1.3.2.B	B.1.3.4.4.1.1.B	B.1.3.6.5
B.1.3.2.1	B.1.3.4.4.1.1.1	B.1.3.7.A
B.1.3.2.2	B.1.3.4.4.1.1.2	B.1.3.7.B
B.1.3.2.4.A	B.1.3.4.4.2	B.1.3.7.1
B.1.3.2.4.1	B.1.3.5.A	B.1.3.7.1.1.A
B.1.3.2.4.2	B.1.3.5.B	B.1.3.7.1.1.B
B.1.3.2.4.3	B.1.3.5.C	B.1.3.7.2
B.1.3.2.4.4	B.1.3.5.1	B.1.3.7.2.B
B.1.3.2.5	B.1.3.5.2	B.1.3.7.2.M
B.1.3.3	B.1.3.6.A	B.1.3.7.2.S
B.1.3.4.A	B.1.3.6.B	B.1.3.7.3
B.1.3.4.B	B.1.3.6.1	B.1.3.7.4.1
B.1.3.4.1	B.1.3.6.1.1	B.1.3.7.4.2
B.1.3.4.1.1	B.1.3.6.2	B.1.3.7.5
B.1.3.4.2	B.1.3.6.3	B.1.3.7.6.A
B.1.3.4.2.C	B.1.3.6.3.G	B.1.3.7.6.B
B.1.3.4.2.M	B.1.3.6.4.A	B.1.3.7.6.C
B.1.3.4.2.N	B.1.3.6.4.B	
B.1.3.4.3	B.1.3.6.4.1.A	

G526

B.1.3.1
B.1.3.2.4.3
B.1.3.4.4.2
B.1.3.6.2

G649

B.1.3.6.1
B.1.3.6.1.1
B.1.3.7.1

G527

B.1.3.5.1	B.1.3.6.4.1.2
B.1.3.5.2	B.1.3.6.4.1.A
B.1.3.5.A-C	B.1.3.6.4.1.B
B.1.3.4.B	B.1.3.6.4.A
B.1.3.4.2	B.1.3.6.4.B
B.1.3.4.4.1.1.1	B.1.3.7.A
B.1.3.4.4.1.1.2	B.1.3.7.4.1
B.1.3.4.4.1.1.A	B.1.3.7.4.2
B.1.3.4.4.1.1.B	B.1.3.7.B
B.1.3.4.4.1.A	B.1.3.7.2
B.1.3.4.4.1.B	B.1.3.7.2.B
B.1.3.4.4.2	B.1.3.7.2.M
B.1.3.6.A	B.1.3.7.2.S
B.1.3.6.2	B.1.3.7.6.A-C
B.1.3.6.4.1.1	

G814

B.1.1.1.1	B.1.1.2.3.1.2.2
B.1.1.1.2.A-G	B.1.2.1, B.1.2.2
B.1.1.2.A	B.1.3.4.4.1.1.1
B.1.1.2.B	B.1.3.4.4.1.1.2
B.1.1.2.1	B.1.3.4.4.1.1.A
B.1.1.2.1.D	B.1.3.4.4.1.1.B
B.1.1.2.2	B.1.3.6.4.1.1
B.1.1.2.3	B.1.3.6.4.1.2
B.1.1.2.3.1.1.1	B.1.3.6.4.1.A
B.1.1.2.3.1.1.2	B.1.3.6.4.1.B
B.1.1.2.3.1.2.1	

Preliminary - Investigation Sensitive

Solid Rocket Booster Working Group
Fault Tree Multi-Element (1 of 5)

SRB Working Group

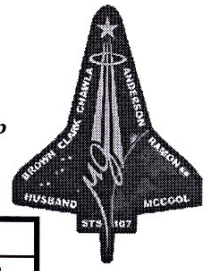

FT Cause ID#	Fault Tree (FT) Block Name	Level 2
B.1.1	Anomalous Loads and Environments on SRB Adversely Affect Mission, Vehicle & Crew	G499/G814
B.1.1.1 ®	Extreme Environments Adversely Affect SRB or SRB/ET Interface	
B.1.1.1.1	Extreme Natural Environments Adversely Affect SRB or SRB/ET Interface	
B.1.1.1.2.A	Adverse Effects From Conducted or Radiated Electro Magnetic Interface (EMI)	
B.1.1.1.2.B	Adverse Aerothermal Effects During Ascent	
B.1.1.1.2.C	Adverse Vibro-Acoustic Effects While on Pad or During Ascent	
B.1.1.1.2.D	Adverse Vehicle Dynamics Effects While on Pad or During Ascent	
B.1.1.1.2.E	Adverse Aerodynamic Effects During Ascent	
B.1.1.1.2.F	Improper Venting During Ascent	
B.1.1.1.2.G	Pryo Shock While on Pad or During Ascent	
B.1.1.2 ®	Anomalous Loads Adversely Affect SRB or SRB/ET Interfaces	
B.1.1.2.1	Anomalous Loads During Prelaunch Operations	
B.1.1.2.1.D	Adverse Loads Induced by SSME Thrust Build Up	
B.1.1.2.A	Anomalous Induced Loads Caused by Holddown Stud Hangup	
B.1.1.2.2	Anomalous Loads During Ascent	
B.1.1.2.B	Anomalous Loads During Liftoff	
B.1.1.2.3	Anomalous Loads During Booster Separation	
B.1.1.2.3.1.1.1	Premature Ignition (Aft BSM)	
B.1.1.2.3.1.1.2	Low/Inadequate Thrust Output for any Two BSMs (Aft BSM)	
B.1.1.2.3.1.2.1	Premature Ignition (Forward BSM)	
B.1.1.2.3.1.2.2	Low/Inadequate Thrust Output for any Two BSMs (Forward BSM)	

Preliminary - Investigation Sensitive

Solid Rocket Booster Working Group
Fault Tree Multi-Element (2 of 5)

SRB Working Group

FT Cause ID#	Fault Tree (FT) Block Name	Level 2
B.1.2.1	Anomalous Electrical & Instrumentation Subsystem Performance	
B.1.2.1.A	Anomalous SRB/ET Separation Performance	G499/G814
B.1.2.1.E	Anomalous SRB Guidance, Navigation & Control Performance (Rate-Gyro)	G499/G814
B.1.2.1.F	Anomalous SRB Electrical Power/Data Cable Performance	G499/G814
B.1.2.2	Anomalous Thrust Vector Control (TVC) Subsystem Performance	G499/G814
B.1.3.1	Nose Cap Assembly Damage/Malfunction Causes Debris	
B.1.3.1.3.E	Overload [Nose Cap Fastener]	G524/G526
B.1.3.2. ®	Frustum Assembly Damage/Malfunction Causes Debris	
B.1.3.2.4.3.F	Aerodynamic Loading Causes Debris	G524/G526

Preliminary - Investigation Sensitive

Solid Rocket Booster Working Group
Fault Tree Multi-Element (3 of 5)

SRB Working Group

FT Cause ID#	Fault Tree (FT) Block Name	Level 2
B.1.3.4 ®	Forward Skirt Assembly Damage/Malfunction Causes Debris	
B.1.3.4.B	Loss of Elec. Breakaway Cables & Connector Components (Sep. Plane) Causes Debris [Fwd Skirt]	G524/G526
B.1.3.4.2.B	Loss of Thrust Post Attach Components Causes Debris	G524/G527
B.1.3.4.2.D	Loss of Forward Skirt/RSRM Interface Hardware Causes Debris	G524/G527
B.1.3.4.2.G	Loss of SRB Fwd Crossover Components Causes Debris	G524/G527
B.1.3.4.4	Loss of Fwd. ET Attach Components Causes Debris	G524/G527
B.1.3.4.4.1.A	Debris Due to No Separation	
B.1.3.4.4.1.B	Debris Due to Premature Separation	
B.1.3.4.4.1.1	Debris Due to Improper Separation	G499/G814
B.1.3.4.4.1.1.A	Failure Outside of Fracture Plane Causes Debris	
B.1.3.4.4.1.1.B	Recontact Causes Debris	
B.1.3.4.4.1.1.1	Material Defects Causes Debris	
B.1.3.4.4.1.1.2	Manufacturing Defect Causes Debris	
B.1.3.4.4.2.1.1.E	Overload [RSS Crossover Fastener]	G524/G526
B.1.3.4.4.2.1.2.1.E	Overload [RSS Crossover Disconnect Housing]	G524/G526
B.1.3.4.4.2.1.2.2.E	Overload [RSS Crossover Subparts]	G524/G526
B.1.3.4.4.2.1.3.E	Overload [RSS Crossover Gimbal Cover]	G524/G526
B.1.3.4.4.2.2.1.E	Overload [RSS Crossover Fastener (ET side)]	G524/G526
B.1.3.4.4.2.3.E	Overload [RSS Crossover Gimbal Cover Fastener]	G524/G526
B.1.3.4.4.3.1.C	Overload [Bolt Catcher Attach Fastener]	G524/G526
B.1.3.4.4.3.2.C	Excessive Aerodynamic Loading	G524/G526
B.1.3.4.4.3.2.2.D	Excessive Force From Separation Bolts	G524/G526
B.1.3.4.4.3.3.E	Overload [Bolt Catcher ET Thrust Fitting or Inserts]	G524/G526
B.1.3.4.4.3.4.E	Excessive Separation Bolt Loading Causes Debris	G524/G526

Preliminary - Investigation Sensitive

Solid Rocket Booster Working Group
Fault Tree Multi-Element (4 of 5)

SRB Working Group

FT Cause ID#	Fault Tree (FT) Block Name	Level 2
B.1.3.5 ®	Tunnel Cover/Floor Plate Assembly Damage/Malfunction Causes Debris	G524/G527
B.1.3.5.1	Loss od Thermal Protection System (TPS) Causes Debris [Tunnel Cover/Floor Plate Assembly]	
B.1.3.5.A	Structural Damage to Tunnel Cover Assembly Caiuses Debris	
B.1.3.5.B	Loss of Electrical Cables and Connector Components causes Debris [Tunnel Cover/Floor {Plate Assy]	
B.1.3.5.2	Loss of Tunnel over/Floor Plate Components Causes Debris (SRB/RSRM)	
B.1.3.5.C	Improper Operation of Pyrotechnic Components Causes Debris [Tunnel Cover//Floor Plate Assembly]	
B.1.3.6 ®	ETA Ring/Aft Attach Strut Assembly Damage/Malfunction Causes Debris	
B.1.3.6.A	Loss of Elec. Breakaway Cables & Connector Components (Sep. Plane) [ETAR/Aft Attach Strut Assy]	G524/G527
B.1.3.6.1	Loss of Thermal Protection System (TPS) Causes Debris [ETAR/Aft Attach Strut Assy]	G524/G649
B.1.3.6.2	Aft Strut Component Failure (ET Strut Half)	G524/G527
B.1.3.6.2.3.1.E	Overload [Aft Strut ET Fastener]	G524/G526
B.1.3.6.4	Aft Separation Bolt Components Causes Debris	G524/G527
B.1.3.6.4.A	No Separation Causes Debris	
B.1.3.6.4.B	ETA Ring Structural Failure	
B.1.3.6.4.1	Improper Separation Causes Debris	G499/G814
B.1.3.6.4.1.A	Failure Outside of Fracture Plane Causes Debris	
B.1.3.6.4.1.B	Recontact Causes Debris (Strut Half)	
B.1.3.6.4.1.1	Material Defects Causes Debris	
B.1.3.6.4.1.2	Manufacturing Defect Causes Debris	

Preliminary - Investigation Sensitive

Solid Rocket Booster Working Group
Fault Tree Multi-Element (5 of 5)

SRB Working Group

FT Cause ID#	Fault Tree (FT) Block Name	Level 2
B.1.3.7 ®	Aft Skirt Assembly Damage/Malfunction Causes Debris	
B.1.3.7.A	Loss of Electrical Breakaway Cables & Connector Components (Separation Plane) [Aft Skirt]	G524/G527
B.1.3.7.B	Aft Skirt Assembly Structural Failure Causes Debris	G524/G527
B.1.3.7.1.D	Loss of RT455 without Hypalon From Aft Skirt Assembly Causes Debris	G524/G649
B.1.3.7.1.E	Loss of BTA without Hypalon From Aft Skirt Assembly Causes Debris	G524/G649
B.1.3.7.1.G	Loss of RTV133/RTV108 From Aft Skirt Assembly Causes Debris	G524/G649
B.1.3.7.2	Loss of Aft Skirt Components Causes Debris	G524/G527
B.1.3.7.4	Improper Operation of Pyrotechnic Components Causes Debris [Aft Skirt]	G524/G527
B.1.3.7.4.1	Improper Operation of SRB/MLP Holddown Release	
B.1.3.7.4.2	Improper Operation of Booster Separation Motor Ignition Components	
B.1.3.7.6	Loss of MLP Holddown Components Causes Debris	G524/G527
B.1.3.7.6.A	Loss of Aft Skirt Shoe Hardware Causes Debris (includes Shims and Ground Straps)	
B.1.3.7.6.B	Loss of GN2 Purge Line Assembly Causes Debris	
B.1.3.7.6.C	Loss of Holddown Hardware Causes Debris (includes Stud Washer, Nut & Breaklink Nut)	

Preliminary - Investigation Sensitive

Fault Tree Block Presentation Sequence

SRB Working Group

File #	Block ID.	Order of Presentation	Number of Closure Sheets	Title or related areas
File #1	B.1.1	6	18	Anomalous Loads and Environments on SRB Adversely Affect Mission, Vehicle and Crew
File #2	B.1.2	7	2	Anomalous Performance of Active Subsystems
File #3	B.1.3.1	5	2	Nose Cap Assembly Damage/Malfunction Causes Debris
File #4	B.1.3.2 B.1.3.3	2	11	Frustum Assembly Damage/Malfunction Causes Debris, Parachutes
File #5	B.1.3.4	1	20	Forward Skirt Assembly Damage/Malfunction Causes Debris
File #6	B.1.3.5 B.1.3.6	4	19	Tunnel Cover/Floor Plate, ET Attach Ring and Aft Attach Strut Cause Debris
File #7	B.1.3.7	3	16	Aft Skirt Assembly Damage/Malfunction Cause Debris
File #8				Executive Summary/Presentation
		Total	**88**	

Preliminary - Investigation Sensitive

Fault Tree Block Presentation Sequence

SRB Working Group

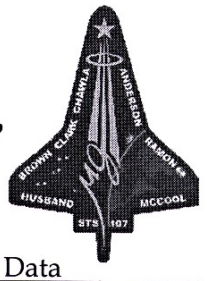

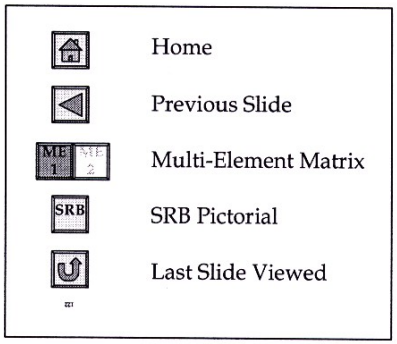

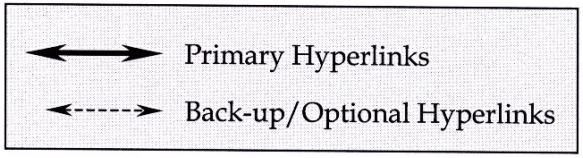

Photographic/Film Data

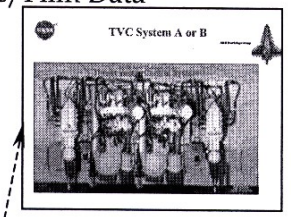

SRB Pictorial

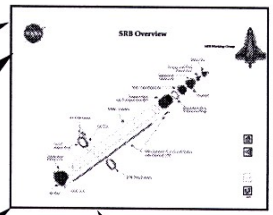

Fault Tree Block Closure Sheet

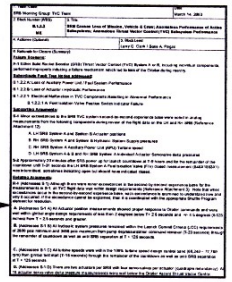

Fault Tree Branch Summary Sheet

Fault Tree Block Summary Sheet

Home

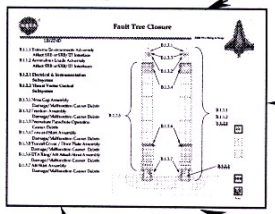

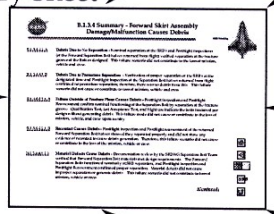

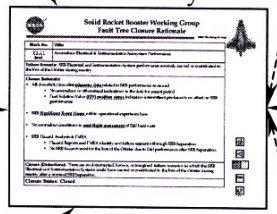

Engineering Data

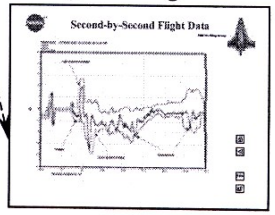

Fault Tree Branch

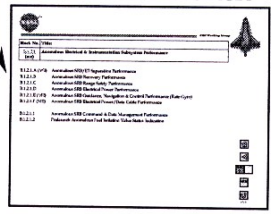

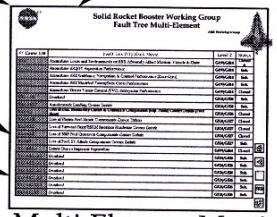

Multi-Element Matrix

Page 27

Preliminary - Investigation Sensitive

Solid Rocket Booster Working Group Agenda

SRB Working Group

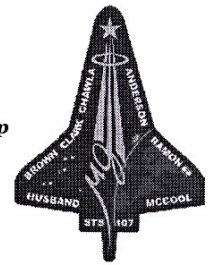

- List of Members, Advisors, Observers, and Others
- Method of Investigation
  - Working Group Organization
  - Special Circumstances
  - Investigation Process
- Fault Tree Closure Summary
- Summary

Preliminary - Investigation Sensitive

Summary

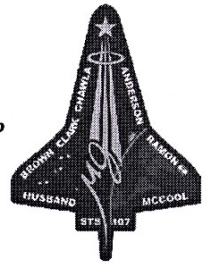

- All Multi-Element Fault Tree Blocks Have Been Addressed Individually or as a Sub-Block to a Higher Level Closure Sheet.
- All SRB Systems Performed Nominally within Specifications and with No Unexplainable Experience-Base Deviations.
- Solid Rocket Boosters are Known STS Debris Generators:
  - All Debris Generating Events Have Been Identified
    - Debris at Liftoff
    - Debris during Flight
    - Debris at Separation
    - Debris after Separation
- Four Bolt Catcher Fault Tree Blocks Remain Open until after Testing is Complete (Estimated Completion 6/9/03).
- Investigation Results Thus Far Indicate SRBs did not Cause Loss of STS-107.

SRB Launch through Recovery Environments

Preliminary - Investigation Sensitive

THIS PAGE INTENTIONALLY LEFT BLANK

Volume V
Appendix G.7

Starfire Team Final Report, Jun 3, 2003

This Appendix contains NSTS-37379 Starfire Team Final Report in Support of the Columbia Accident Investigation, 3 June 2003.

THIS PAGE INTENTIONALLY LEFT BLANK

NSTS-37379

Starfire Team Final Report

in support of the *Columbia* Accident Investigation

June 3, 2003

Submitted by:

/s/ Douglas White
Douglas White, USA
Team Leader

/s/ Kandy Jarvis
Kandy Jarvis, LMSO
Team Member

Dewey Houck, Boeing
Karen Watts, USA
Julian Christou, CFAO
Robert Fugate, SOR

Maj. Robert Johnson, USAF
Rick Cleis, SOR
Roger Petty, SOR
Rich Rast, SOR

This information is being distributed to aid in the investigation of the *Columbia* mishap and should only be distributed to personnel who are actively involved in this investigation.

Table of Contents

Executive Summary 3
1.0 INTRODUCTION 4
2.0 PURPOSE & SCOPE 4
3.0 DATA 5
4.0 DATA ANALYSIS 6
5.0 RESULTS 6
Table 1 – Anomalous Optical Signature (AOS) Results 7
Fig. 1: Turbulence near the nose/left wing/WLE. 7
Fig. 2: Asymmetric Gas Trail. 7
Fig. 3: WLE "Bulges" 8
Fig. 4: Asymmetric Bulge at Nose. 8
Fig. 5: Asymmetric Streaming of Gas from Aft of Orbiter. 8
Fig. 6: Flare 1 9
Fig. 6A: Flare 1. 10
6.0 CONCLUSIONS 10
7.0 RECOMMENDATIONS 10
APPENDIX A 12
ACRONYMS AND ABBREVIATIONS 12
APPENDIX B 13
TEAM MEMBER BIOGRAPHIES 13
APPENDIX C 15
CATEGORY CLASSIFICATION AND SUMMARY 15
APPENDIX D 18
Presentation 1 19
Presentation 2 21
APPENDIX E 36
DEFINITIONS 36

This information is being distributed to aid in the investigation of the *Columbia* mishap and should only be distributed to personnel who are actively involved in this investigation.

Executive Summary

The Starfire Team was created in support of the STS-107 Orbiter Vehicle Engineering (OVE) investigation effort. The team's charter was to review imagery, both still photography and video taken at the Starfire Optical Range (SOR) at Kirtland Air Force Base in New Mexico, in order to determine the state of the orbiter at that time in its re-entry.

As part of this investigation about 18,800 video frames and 3 digital stills were reviewed and a small portion of these were processed and analyzed. All were categorized as to potential return of information regarding the condition of the orbiter. A total of ten anomalous optical signatures (AOS) were identified and images associated with these signatures were processed to some degree. An AOS here is considered to be a visual appearance of the orbiter containing a characteristic that appears irregular; i.e., lack of symmetry, pulsation, scintillation. Difficulties arose due to motion blur related to the relative motion of the orbiter and camera, failure to track due to relative angular velocity, lack of comparative nominal condition images, saturation of images, and lack of resolution. In some cases these difficulties were prohibitive in determining a conclusion regarding the condition of the orbiter.

Of the ten AOS, two were concluded to be nominal (with the understanding an off-nominal condition contribution was indeterminate for one image), two were not classifiable as nominal or off nominal, and six were considered off nominal. See Table 1 for a summary. Of the six AOS identified as off nominal, the Wing Leading Edge (WLE) "bulge(s)" is the single AOS for which a nominal condition is least likely. Other AOS have a possibility of finding a nominal condition, albeit one not currently understood, as the source. The lack of comparative nominal condition data precludes any conclusion to the one hundred percent certainty level. If all ten AOS are compared, five provide for the possibility of an event occurring relating to the left wing.

Recommendations for the future, in the event such imagery is requested, would require that higher resolution video be obtained at high magnification, such as that taken through a telescope that is capable of tracking an object with a high angular velocity. The digital stills proved useful, but a greater number would be desired, with minimal saturation. Nominal condition re-entry imagery is deemed necessary for future studies of this type of orbiter condition analysis upon re-entry.

This information is being distributed to aid in the investigation of the *Columbia* mishap and should only be distributed to personnel who are actively involved in this investigation.

1.0 INTRODUCTION

The Starfire Team was formed in support of the Orbiter Vehicle Engineering Working Group (OVEWG) to aid the NASA community in the investigation of the STS-107 accident. The team was formed with members of various organizations, some associated with NASA, some not. A short biography of each member can be found in Appendix B of this report.

The Starfire Optical Range (SOR), a part of the Air Force Research Lab, acquired three still digital photographs and four videos of the Columbia as it passed over Albuquerque, New Mexico on re-entry. This was the first attempt by SOR to capture imagery of a shuttle on re-entry. SOR acquired color video through a handheld digital camera operated in movie mode, one video through a camera mounted on the elevation gimbal of the coelostat used to track the orbiter and two videos with different fields of view obtained with two telescopes looking through the 1.0-m clear aperture coelostat consisting of two flat mirrors that rotate to view different parts of the sky. Three still digital photographs were also acquired with a 3.5-inch telescope and CCD camera, also looking through the coelostat, though one of the stills imaged only a small fraction of the orbiter/plasma trail.

These images were obtained by engineers at SOR volunteering their time and using available equipment. The data collection was not an official tasking. Tracking of the orbiter had never before been attempted with this equipment. The degree of potential object brightness was unknown and that, coupled with a brightening sky due to imminent sunrise, made gain adjustments (to prevent saturation) on the instruments difficult. There was no opportunity to compensate for errors in the supplied vectors of the orbiter as the orbiter was obscured by cloud during the first 20 degrees of the pass; this compounded the difficulty of tracking a rapidly moving object in a small field of view (FOV).

The Starfire Team was formed to process and evaluate the resulting imagery for indications of the orbiter condition at that time in the re-entry path. The Starfire Team reviewed all images and identified those stills or frames of the videos that appeared most probable to achieve this goal. The team focused on the identified video frames and stills and performed various levels of image processing and analysis.

The Starfire Team provided regular status briefings to the OVEWG.

2.0 PURPOSE & SCOPE

This report defines and documents the Starfire Team investigation: determination of important stills and video frames, problems encountered, data analysis techniques, and data interpretation results.

The scope of the data interpretation included a limited number of the available video frames and two of the three stills. While other video frames were available, those of the orbiter with AOS were judged the most potentially revealing and only those were examined in detail.

Classification of priority resulted in four categories:

This information is being distributed to aid in the investigation of the *Columbia* mishap and should only be distributed to personnel who are actively involved in this investigation.

1) High potential of information return from analyses
2) Moderate potential of information return from analyses
3) Low potential of information return from analyses
4) No expected information return from analyses

After review of all available data, two of the three stills and one set of frames from the 5-millirad field-of-view (FOV) video were considered to be Category 1. A set of frames here is defined as a sequential subset of video frames extracted from the complete video, wherein the number of frames in a set varies according to the content. The remaining still, one set of frames from the 5-millirad FOV video, and one set of frames from the 700-microrad FOV video were classified to be Category 2. The remaining video frames that contained views of the orbiter, as well as the two remaining videos were considered to be Category 3. Any set of video frames that failed to capture the orbiter in its field of view was classified to be Category 4.

Several problems were encountered. The primary difficulty with analysis was the lack of nominal-condition comparative data. Other problems were unknown plate scales (i.e. size of objects), motion blurring, saturated images, unknown orientation (rotation), and resolution. Techniques for analyzing this type of imagery existed only in a limited fashion; this specific type of data did not previously exist.

Plate scales and orientation of a few images were determined by imaging starfields at the known elevation and azimuth of the image and calculating the scale and degree of rotation.

Data analysis techniques and interpretation required drawing on assorted personnel with backgrounds in image data reduction and analysis, astronomical data reduction and analysis, wire cad modeling, aerothermal modeling, and extrapolation of aerothermal conditions to visual results.

3.0 DATA

All video and stills were reviewed by the Starfire Team as well as independently reviewed by the STS-107 Image Analysis Team creating the timeline for the Columbia's re-entry. The review by the timeline team was used as a metric against category classification. The approximate Greenwich Mean Time (GMT) coverage encompassing all of the videos and stills wherein the orbiter is visible is 13:56:31 – 13:58:12.

The two videos that were not acquired through a telescope were considered of no value for the purpose of this team's work other than to confirm or deny possible changes in appearance of the orbiter's luminosity. These were videos EOC2-4-148-2 and EOC2-4-148-6. They were reviewed for possible changes in luminosity and no changes were seen that correlated with any AOS.

Video EOC2-4-148-4 is a 5 millirad FOV (~1/3 degree) digital video taken through a 14" Celestron telescope looking off two 1.5-m diameter flat mirrors positioned at 45 degrees to the line of sight that rotate about vertical and horizontal axes: a configuration known as a 1-m clear aperture coelostat. This arrangement causes images in the focal plane of a camera

This information is being distributed to aid in the investigation of the *Columbia* mishap and should only be distributed to personnel who are actively involved in this investigation.

to rotate as the mount tracks objects across the sky. Sets of frames ranged from Category 1 through Category 4. The orbiter was in the FOV intermittently.

Video EOC2-4-148-3 is a 700 microrad FOV video taken through a 7" Questar telescope also looking through the 1-m coelostat. Sets of frames ranged from Category 2 through Category 4. The orbiter was in the FOV infrequently.

Digital stills consist of JSC2003e03394 (GMT 13:57:14) and JSC2003e03395 (GMT 13:57:59). These were acquired with a 3.5-inch telescope and CCD camera, also looking through the coelostat. Both of these stills were classified Category 1. The third still (GMT 13:57:51) has been submitted for inclusion in the JSC Columbia Accident stills database, but as of yet has no JSC number. It was classified a Category 2. All three stills were taken with a CCD camera attached to a 3.5-inch Questar telescope looking through the 1.0-m coeleostat.

Appendix C identifies categorization of this data in both pre- and post- analysis status.

4.0 DATA ANALYSIS

After preliminary review and classification, those stills or sets of video frames in Categories 1 and 2 were examined. Sets of video frames were captured via two different programs ISEE & DPS Reality. Late in the analysis it was recognized that some small degree of signal was lost if video frames were taken from a second-generation copy rather than a digital clone or digital copy of the original. Video frames taken from a digital copy were examined and while slightly higher in quality, appeared to add no significance to the final results, thus the data were not reprocessed.

Adobe Photoshop was used to enhance contrasts, rotate images as required to correct to proper orientation due to the rotation of the mirror, and crop images. (Adobe resamples an image when it rotates an image; resampled images were not used in for final analysis.) Preliminary interpretation was performed. Stills and some single frames of video were processed with an iterative blind deconvolution method (Center for Adaptive Optics, Christou). Two of the stills were also processed using a regularized maximum likelihood method (Veridian, Thelen). Only the stills and frames processed by the blind deconvolution method were interpreted and then reviewed by the entire team.

After a detailed review, many images were reclassified. See Appendix C for details regarding classification/reclassification and a brief summary of results.

5.0 RESULTS

The Starfire Team reviewed about 18,800 frames of video and three digital stills. Ten possible AOS were identified and investigated. Due to the lack of comparative nominal condition imagery, in no case can an apparent AOS be confirmed to the one hundred percent level of certainty. One event not addressed here is Debris 16, a debris event noted

This information is being distributed to aid in the investigation of the *Columbia* mishap and should only be distributed to personnel who are actively involved in this investigation.

Anomaly	NASA # Video/Still	Conclusion
Turbulence near the nose/left wing, WLE	EOC2-4-0148-3	Unknown if off-nominal
Asymmetric gas trail	JSC2003e03394	Nominal
WLE "bulges"	JSC2003e03394	Off-nominal
Asymmetric bulge at nose	JSC2003e03394	Nominal
Asymmetric streaming of gas from aft of orbiter	EOC2-4-0148-4	Unknown if off-nominal
Flare 1	EOC2-4-0148-4	Off-nominal
Flare 2	EOC2-4-0148-4	Off-nominal
Flaring/Streaming	EOC2-4-0148-4	Off-nominal
Brightening of left wing	JSC2003e03395 EOC2-4-0148-4	Off-nominal
Nose or Tail brightening	JSC2003e03395 EOC2-4-0148-4	Off-nominal

Table 1 – Anomalous Optical Signature (AOS) Results

by the STS-107 Image Analysis Team constructing the timeline. The debris event is difficult to see and was not part of the scope of this task. Of all the AOS identified as off nominal, the Wing Leading Edge (WLE) "bulge(s)" is the AOS for which a nominal condition is least likely. Other AOS have a greater possibility of finding a nominal condition, albeit one not currently understood, as the source. See Table 1 for a list of the ten AOS, video/still the AOS is associated with, and conclusions. A brief discussion follows, identifying possible causes of the AOS identified and the conclusions drawn. Some additional information is contained in Appendix D.

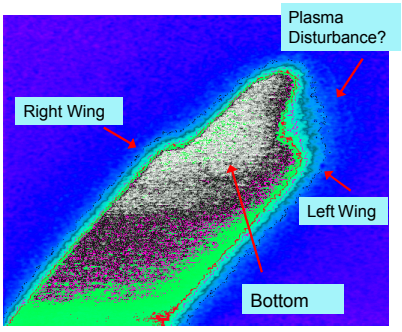

Fig. 1: Turbulence near the nose/left wing/WLE. NASA video EOC2-4-0148-3. It is unknown what a nominal optical signature of the flowfield at these specific conditions (speed, orientation, etc.) would look like. The signature is not overt nor does telemetry provide additional insight. No conclusion can be drawn regarding a nominal or off nominal condition.

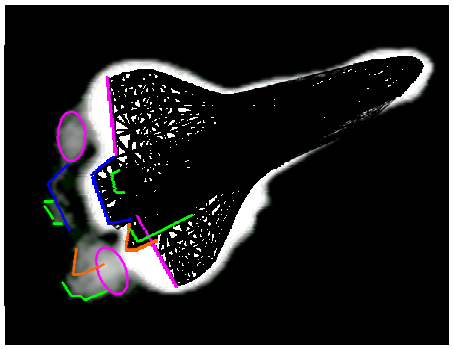

Fig. 2: Asymmetric Gas Trail. NASA Image JSC2003e03394. The processed image revealed structure in the gas trail. This structure could be correlated to specific source locations on the orbiter. Damage to the left wing could create additional enhancement of the gas trail that could not be distinguished from known sources. This optical signature is considered to represent a nominal condition with the caveat that an off-nominal condition could not be identified as such with this image.

This information is being distributed to aid in the investigation of the *Columbia* mishap and should only be distributed to personnel who are actively involved in this investigation.

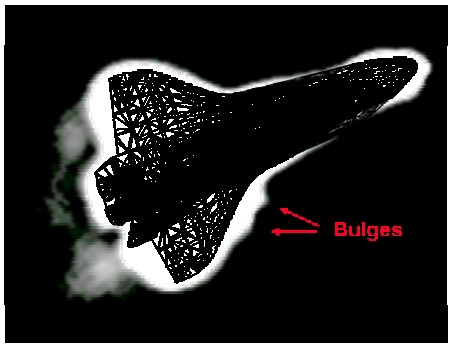

Fig. 3: WLE "Bulges". No currently understood nominal condition can support this optical signature. Possibilities for sources of this optical signature are: localized increase in temperatures (hot spots), local increase in reflectivity (unlikely), tile damage (unlikely), and damage to WLE. Viewing geometry and refraction could contribute. See Appendix D for some additional explanation. This is considered to represent an off-nominal condition.

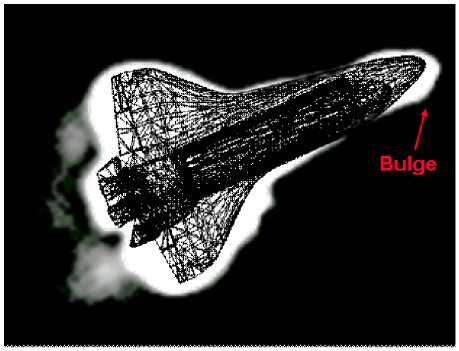

Fig. 4: Asymmetric Bulge at Nose. The nose is known to be the hottest spot and could produce an optical signature representative of a localized intensity increase. As the image displays the bottom of the orbiter (the wirecad model is "see-through" and somewhat misleading due to that), orientation and viewing angle is considered the most likely source of this optical signature. This is not inconsistent with Sandia's Plasma models. This is considered to represent a nominal condition.

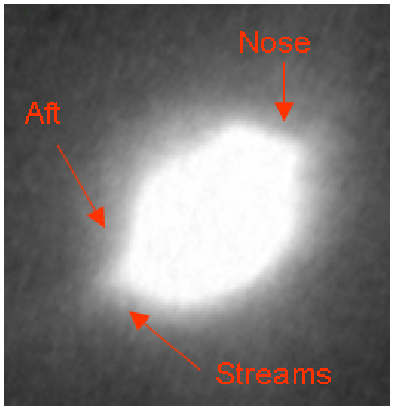

Fig. 5: Asymmetric Streaming of Gas from Aft of Orbiter. NASA video EOC2-4-0148-4. This is apparent in the video and not well represented by a still image. In the video, the image of the orbiter is highly saturated and is "lemon-shaped" in appearance. The image shown at the left has been rotated into its approximate correct orientation and would appear similar to the above digital still were it not so badly saturated. A "tail" of gas/plasma is evident at the aft of the orbiter (identified as "streams"). This tail appears to stream and pulse over time. One of the three digital stills is acquired during this period of time and shows an asymmetric gas trail (see Fig. 2). This streaming is likely related to the asymmetric gas trail seen in the still and the explanation for the asymmetric gas trail potentially applies to this streaming/pulsing tail. The asymmetric gas trail in the still is thought to be nominal (with consideration of the caveats mentioned in Fig. 2) and this suggests that this streaming effect may also represent a nominal case. Without nominal comparative data, no conclusion can be drawn regarding if this is a nominal or off nominal condition.

The last five AOS are to some degree interrelated. The five signatures are Flare 1, Flare 2, Flaring/Streaming, Brightening of Left Wing, and Nose or Tail Brightening. The Brightening of the Left Wing and Nose or Tail Brightening occurs simultaneously with Flare 1 and visually may help create the optical signature of Flare 1. Flare 1 shows brightening of the

This information is being distributed to aid in the investigation of the *Columbia* mishap and should only be distributed to personnel who are actively involved in this investigation.

left wing, the nose/tail, and a streaming signature (hot gas?) possibly located around the tail region. This does not imply tail damage, but rather one possibility presented is that normal tail interaction with the flowfield generates this optical signature. The general optical signature of Flare 1 persists (in time) and Flaring/Streaming is seen. The orbiter passes out of the FOV, then returns. As it leaves the FOV again, Flare 2 is seen. Flare 2 is merely a brightening with no significant change in the general optical signature associated with Flare 1, other than the increase in brightness. Only the imagery of Flare 1 is shown as all five optical signatures are essentially represented by the three images shown below.

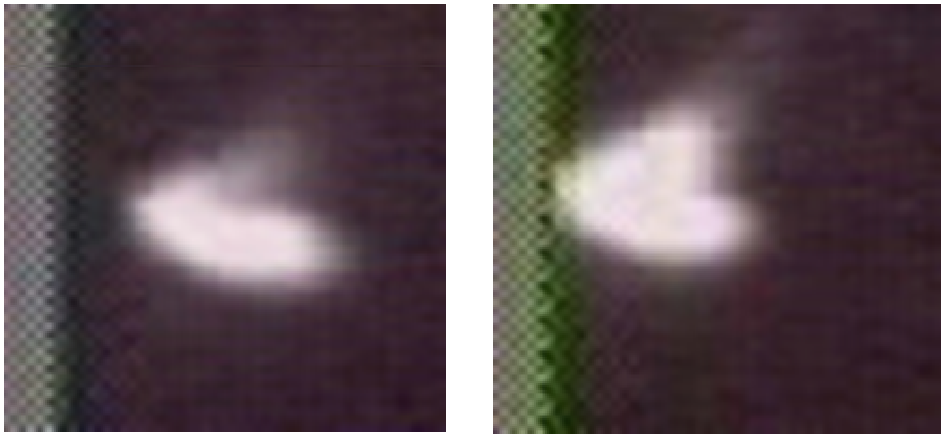

Fig. 6: Flare 1. NASA video EOC2-4-0148-4. Flare 1 is noted on the timeline for Columbia's re-entry and its AOS may in part be a brightening of the upper portion of the canopy and left wing of the orbiter. Images taken from the video are shown. To the left is the pre-flare appearance of the orbiter; to the right is Flare 1. The checkerboard pattern to the left of both images is the edge of the FOV. These images are approximately half a second apart in time. They have not been rotated to the proper orientation. Diffraction was considered as a possibility; diffraction is an effect of the optics seen as a brightening of an object as an object leaves the FOV of the telescope. This was tested for by SOR. Jupiter was used to represent the orbiter, as Jupiter was approximately the same visual size as the orbiter; the telescope was moved rapidly to simulate the orbiter's motion through the FOV. No similar brightening was noted. Although phase angle cannot be simulated (the orbiter was in daylight at the time), diffraction as the source of brightening is considered unlikely. The streaming of what is thought to be hot gas is not well represented by a still, but the aspect of the elongation of what may be hot gas can be seen in the digital still (Fig 6A), and contributes to the optical signature of Flare 1. Viewing angle may contribute to the signature seen in that the camera is viewing the aft of the orbiter. It is unknown to what degree the view is looking through a plasma trail, the opacity of the plasma trail, and if the plasma trail contributes to the "flare" signature. Additionally, shadowing due to phase angle of the sun may contribute to the signature.

This information is being distributed to aid in the investigation of the *Columbia* mishap and should only be distributed to personnel who are actively involved in this investigation.

Fig. 6A: Flare 1. NASA image JSC2003e03395. The second digital still analyzed was taken at about the same time as the right-hand image in Figure 6. The still is shown here after a blind deconvolution has been applied to the image and its contrast enhanced. It has been properly oriented and displays a wireframe overlay of the orbiter. The wireframe overlay has been approximately scaled. Exact placement relative to the image is unknown. See Appendix D for more details regarding these images and others. The flare image and the digital still are considered to represent an off-nominal condition, and all five AOS listed in the paragraph above Fig. 6 are considered off nominal.

6.0 CONCLUSIONS

Of the ten AOS identified in the Starfire datasets, two were classified as nominal, two were inconclusive and six were considered potentially off-nominal, with one of those six having no currently identifiable possibility of a nominal condition. If all ten AOS are compared, five provide for the possibility of an event occurring relating to the left wing. Based upon the AOS with no currently identifiable possibility of a nominal condition, the left wing WLE appears to be in an off-nominal state.

7.0 RECOMMENDATIONS

Recommendations for the future, in the event such imagery is requested, would require that higher resolution video is obtained at high magnification, such as that taken through a telescope that is capable of tracking an object with a high angular velocity. Resolution, saturation, and tracking were three keys issues that reduced the usefulness of the videos. An additional issue was that, due to the rotating coelostat, the orientation (rotation) of each frame of video was unknown and each processed frame's rotation had to be determined by acquiring starfield images at a later date. The digital stills proved useful, but a greater number would be desired, with minimal saturation.

Nominal condition re-entry imagery is deemed necessary if future comparative studies of this type of orbiter condition upon re-entry analysis is requested or planned.

This information is being distributed to aid in the investigation of the *Columbia* mishap and should only be distributed to personnel who are actively involved in this investigation.

APPENDICES

This information is being distributed to aid in the investigation of the *Columbia* mishap and should only be distributed to personnel who are actively involved in this investigation.

APPENDIX A
ACRONYMS AND ABBREVIATIONS

AOS	**Anomalous Optical Signature**
FOV	**Field of View (telescope)**
GMT	**Greenwich Mean Time**
OVE	**Orbiter Vehicle Engineering**
OVEWG	**Orbiter Vehicle Engineering Working Group**
SOR	**Starfire Optical Range**
WLE	**Wing Leading Edge**

This information is being distributed to aid in the investigation of the *Columbia* mishap and should only be distributed to personnel who are actively involved in this investigation.

APPENDIX B
TEAM MEMBER BIOGRAPHIES

Starfire Team Biographies

Julian Christou
Dr. Christou has over twenty years experience with image processing of both astronomical and artificial satellites. He obtained a Ph.D. in Astronomy from New Mexico State University and has worked at the National Optical Astronomy Observatories and Steward Observatory both in Tucson, Az., as well as the Starfire Optical Range. He is presently a research scientist with the Center for Adaptive Optics at the University of California, Santa Cruz.

Rick Cleis
Mr. Cleis works at the SOR. No Bio provided.

Robert Q. Fugate
Dr. Fugate is the Air Force Senior Scientist for Atmospheric Compensation and serves as the Technical Director, Starfire Optical Range, Directed Energy Directorate, Air Force Research Laboratory, Kirtland Air Force Base, N.M. The Range operates 1.5- and 3.5-meter telescopes, and a 1.0-meter beam director. Dr. Fugate conducts a research program on atmospheric propagation physics; atmospheric compensation using laser guide star adaptive optics; the acquisition, tracking and pointing of lasers to earth-orbiting satellites; and the development of sensors, instrumentation and mount control of large-aperture, ground-based telescopes. He has worked for the U.S. Air Force since 1970 in the fields of atmospheric propagation, electro-optical sensors and detection, space surveillance and adaptive optics.

Dewey Houck
Mr. Houck is currently a Senior Technical Fellow working in the Space and Intelligence Systems Division of IDS for Boeing/Autometric. He chairs Boeing/Autometric's Engineering Review Board that acts in an oversight capacity for Product Development and Program initiatives. He also chairs the Technology Steering Group responsible for commercial product investment decisions. Prior to the Boeing acquisition (of Autometric), he served as a member of the senior management team as Vice President for Technology development for Autometric. During that time, he administered all Research and Development activities including several geospatial, photogrammetric and visualization initiatives. Mr. Houck has Master's and Undergraduate degrees in Civil Engineering from Virginia Tech with specialization in Photogrammetry and Geodesy.

Kandy Jarvis
Ms. Jarvis has seven years experience at NASA, all with Lockheed Martin Space Operations. Her position is Senior Research Scientist as Lead for the Planetary Astronomy Group and Optical Lead for the Orbital Debris Program Office. In both positions she works with a variety of telescopic data, including the acquisition, data reduction, analysis, and interpretation of spectrophotometry and video and short exposure (5 – 20 seconds) images of starfields containing orbital debris.

This information is being distributed to aid in the investigation of the *Columbia* mishap and should only be distributed to personnel who are actively involved in this investigation.

Robert Johnson
Major Johnson is with the USAF and has a PhD. He works with cameras and optics. No Bio provided.

Roger Petty
Mr. Petty works at the SOR. He is an optical engineer. He performed as outdoor spotter and operated the handheld camera. No Bio provided.

Rich Rast
As an Air Force civilian, Mr. Rast served as chief orbital analyst at NORAD before coming to JSC in 1986. He left JSC after six years to become operations manager of SOR. He now works at AFRL's Satellite Assessment Center. He proposed that SOR image Columbia's re-entry to JSC-DM4's Gilman on December 9, 2002.

Karen Watts
Ms. Watts has six years of experience in the Space Shuttle Program, all with the United Space Alliance. Her current position is Pointing Operations Engineer in the Attitude and Pointing Office. The Pointing Office is responsible for manned spacecraft attitude determination and line-of-sight analysis.

R. Douglas White
Mr. White is currently the Director for Operations Requirements in the United Space Alliance Orbiter Element department. He began work on the space shuttle program in 1979 as an employee for Rockwell International in Downey, California. Mr. White has held increasingly responsible positions within the space shuttle program focusing on the areas of turnaround test requirements, engineering flight support, anomaly resolution, and Orbiter certification of flight readiness preparation. He joined United Space Alliance as a director in 1996. He holds a BS and MS in physics from UCLA.

Other Contributors:
Gil Carman: JSC NASA
Sina Farsiu: Engineering Department, Univ. of CA, Santa Cruz
Dr. Peyman Milanfar: Electrical Engineering Department, Univ. of CA, Santa Cruz
Scott Murray: JSC NASA
Dr. Brian J. Thelen: Veridian Systems Ann Arbor Research and Development Center

This information is being distributed to aid in the investigation of the *Columbia* mishap and should only be distributed to personnel who are actively involved in this investigation.

APPENDIX C
CATEGORY CLASSIFICATION AND SUMMARY

Type: Digital Still Photograph

NASA Number: JSC2003e03394
GMT Time: 13:57:14
Initial Classification: Category 1
Post Analysis: Category 1
Description: Saturated image of the underside of the orbiter.
Results: Image was analyzed, interpreted, and results presented. See Appendix D.

NASA Number: JSC2003e03395
GMT Time: 13:57:59
Initial Classification: Category 1
Post Analysis: Category 1
Description: Partially saturated image of the orbiter looking at the aft end.
Results: Image was analyzed, interpreted, and results presented. See Appendix D.

NASA Number: JSC2003exxxx (Still #3)
GMT Time: 13:57:51
Initial Classification: Category 2
Post Analysis: Category 3-4
Description: Plasma trail directly aft of orbiter.
Results: Image was analyzed and interpreted. Little to no information obtained.

Type: Video

NASA Number: EOC2-4-0148-2
Field of View: 5 degree
Frame Subset or Full Video?: Full Video
GMT Timespan: 13:56:47.22 – 13:58:11.29
Initial Classification: Category 3
Post Analysis: Category 3
Results: Video was reviewed. No significant anomalies seen other than those identified by the STS-107 Image Analysis Team. One piece of debris identified by the STS-107 Image Analysis Team: Debris 16. No further processing performed. Possibility of identifying additional debris with extensive processing of video.

NASA Number: EOC2-4-0148-6
Field of View: ~5 degree, RGB (color)
Frame Subset or Full Video?: Full Video
GMT Timespan: ~13:56:47 – 13:58:12
Initial Classification: Category 3
Post Analysis: Category 4

This information is being distributed to aid in the investigation of the *Columbia* mishap and should only be distributed to personnel who are actively involved in this investigation.

Results: Video was reviewed. No anomalies seen. No further processing performed.

Type: Video (cont.)

NASA Number: EOC2-4-0148-3
Field of View: 700 μrad
Frame Subset or Full Video?: Frame Subset
GMT Timespan: 13:57:23.0 – 13:57:23.3
Initial Classification: Category 2
Post Analysis: Category 2
Results: Video frame set = 7 fields (2 fields per frame, 29 frames per second). Video frames show motion-blurred orbiter. Effort was made to re-integrate images but relative velocity of orbiter and movement of camera prevented this effort. Field b, at GMT 13:57:23.1 was analyzed and interpreted. Results presented. See Appendix D.

NASA Number: EOC2-4-0148-3
Field of View: 700 μrad
Frame Subset or Full Video?: Full Video
GMT Timespan: 13:56:45.29 – 13:58:57.5 (excluding previously listed times)
Initial Classification: Category 3
Post Analysis: (Predominantly) Category 4
Results: Video was reviewed. In most frames, orbiter is not in the FOV. Occasional streaks of light suggest orbiter presence in or near the FOV. No further processing performed.

NASA Number: EOC2-4-0148-4
Field of View: 5 mrad
Frame Subset or Full Video?: Frame Subset
GMT Timespan: 13:57:11.14 – 13:57:18.3
Initial Classification: Category 2
Post Analysis: Category 3
Results: Video was reviewed. Includes time coverage of still JSC2003e03394. Orbiter is badly over-saturated; orbiter appears “lemon-shaped”. An undefined asymmetric streaming is seen at aft of orbiter; may relate to tail of orbiter; unknown if nominal or off nominal. Severe saturation prevents further analysis at this time. No further processing performed.

NASA Number: EOC2-4-0148-4
Field of View: 5 mrad
Frame Subset or Full Video?: Frame Subset
GMT Timespan: 13:57:49.23 – 13:58:01.11
Initial Classification: Category 1
Post Analysis: Category 2-3
Results: Video was reviewed. Includes time coverage of still JSC2003e03395. Orbiter is partially over-saturated; orbiter appears “horseshoe-shaped”. Aft of orbiter is toward camera. Two brightening events are seen to occur; these events are termed “Flare 1” and “Flare 2” in the timeline. Three hundred plus frames were extracted and processed with various methods by the CFAO. The orbiter is in and out of the FOV during this timespan. Two frames (13:57:54.14, 13:57:54.22) at the beginning of Flare 1 and peak of Flare 1 were analyzed and results presented; see Appendix D. No significant improvement was achieved

This information is being distributed to aid in the investigation of the *Columbia* mishap and should only be distributed to personnel who are actively involved in this investigation.

on most processed frames. Possibility of determining if the Flares are an optical effect related to the tail or nose with further study.

Type: Video (cont.)

NASA Number: EOC2-4-0148-4
Field of View: 5 mrad
Frame Subset or Full Video?: Full Video
GMT Timespan: 13:56:48.26 – 13:58:01.11 (excluding previously listed times)
Initial Classification: Category 2-4
Post Analysis: Category 3-4
Results: Video was reviewed. Orbiter is in the FOV intermittently. Excluding previously noted framesets, orbiter is motion blurred due to relative velocity of orbiter and motion of camera. No further processing performed.

This information is being distributed to aid in the investigation of the *Columbia* mishap and should only be distributed to personnel who are actively involved in this investigation.

APPENDIX D

Presentation 1: Select slides taken from first presentation to OVEWG
Presentation 2: Second presentation to OVEWG

This information is being distributed to aid in the investigation of the *Columbia* mishap and should only be distributed to personnel who are actively involved in this investigation.

Presentation 1

SPACE SHUTTLE PROGRAM
Space Shuttle Vehicle Engineering Office
NASA Johnson Space Center, Houston, Texas

USA United Space Alliance

BOEING LOCKHEED MARTIN

Starfire Optical Range Location

Presenter: Doug White
Date: Mar 3, 2003
Page 6

Preliminary

Location: Kirtland Airforce Base, NM

GMT coverage for the 5 deg fov: 13:56:47.22 – 13:58:11.29 (+/- 2 secs)

SPACE SHUTTLE PROGRAM
Space Shuttle Vehicle Engineering Office
NASA Johnson Space Center, Houston, Texas

USA United Space Alliance

BOEING LOCKHEED MARTIN

Still at 13:57:14

Presenter: Doug White
Date: Mar 3, 2003
Page 11

- Columbia observed from SOR, 1 Feb 2003, 13:57:14 UTC with Orbiter Attitude Overlay

Preliminary

Solid 3-D Model of Orbiter Attitude at 1 Feb 2003, 13:57:14 UTC (provided by E. Cross and A. Wheaton/SF5)

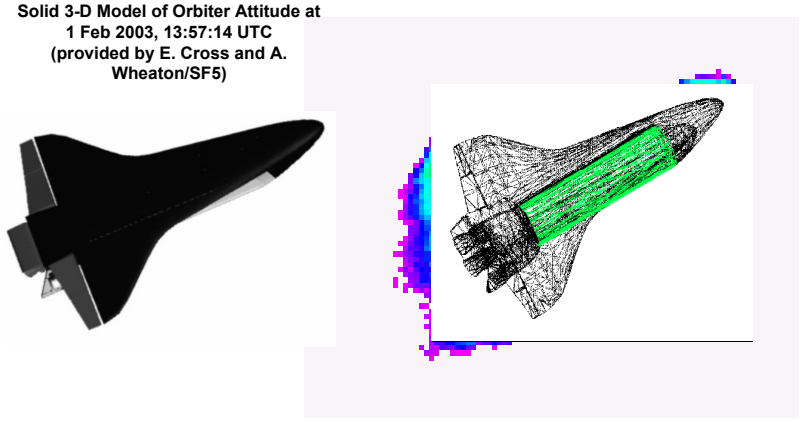

This information is being distributed to aid in the investigation of the *Columbia* mishap and should only be distributed to personnel who are actively involved in this investigation.

SPACE SHUTTLE PROGRAM
Space Shuttle Vehicle Engineering Office
NASA Johnson Space Center, Houston, Texas

Stills at 13:57:51 and 13:57:59

Presenter: Doug White
Date: Mar 3, 2003
Page: 13

Preliminary

13:57:51

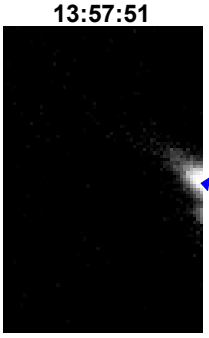

13:57:59

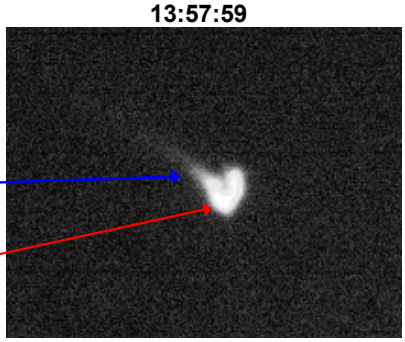

- Left Wing Is Visible in 13:57:59 Image
- Further Processing Is Underway
- Potential to Enhance Left Wing Chine and Left Wing Glove
- "Flare" Is Visible in Both
- Orientation Provided But Not Confirmed; these images are not yet corrected for orientation.

SPACE SHUTTLE PROGRAM
Space Shuttle Vehicle Engineering Office
NASA Johnson Space Center, Houston, Texas

Image Taken from 700 mRad Video, GMT 13:57:23

Presenter: Doug White
Date: Mar 3, 2003
Page: 21

Preliminary

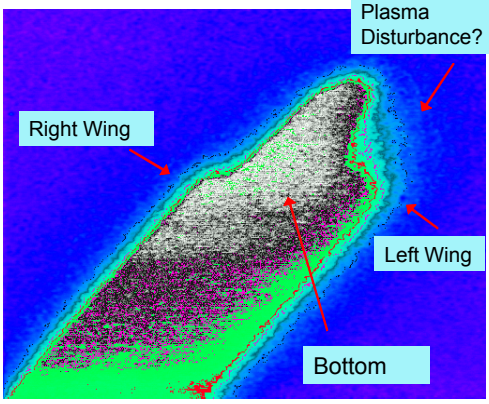

- Colors represent pixel values No processing was performed other than the intensity highlighting
- Left wing chine and glove are not visible at this viewing angle
- Apparent disturbance seen in leading plasma
- Indeterminate significance at this time
- No nominal shuttle re-entry images exist for comparison

Image has been cropped and pixel intensity modified to bring out detail

Orientation unknown

Viewing bottom of orbiter

This information is being distributed to aid in the investigation of the *Columbia* mishap and should only be distributed to personnel who are actively involved in this investigation.

Presentation 2

SPACE SHUTTLE PROGRAM
Space Shuttle Vehicle Engineering Office
NASA Johnson Space Center, Houston, Texas

STS-107 Investigation
Kirtland Photo Tiger Team
4/21/03

SPACE SHUTTLE PROGRAM
Space Shuttle Vehicle Engineering Office
NASA Johnson Space Center, Houston, Texas

Objective and Team Members

Presenter: Kandy Jarvis
Date: April 21, 2003
Page 2

- The Objective of This Tiger Team Was to Analyze the Still and Video Images Taken at the Starfire Optical Range (Kirtland AFB, NM) During the STS-107 Entry

- Tiger Team Members
  - Doug White, USA
  - Kandy Jarvis, Lockheed Martin
  - Dewey Houck, Boeing
  - Karen Watts, USA
  - John Neer, Lockheed Martin
  - Scott Murray, NASA

Preliminary

This information is being distributed to aid in the investigation of the *Columbia* mishap and should only be distributed to personnel who are actively involved in this investigation.

SPACE SHUTTLE PROGRAM
Space Shuttle Vehicle Engineering Office
NASA Johnson Space Center, Houston, Texas

Starfire Optical Range Team and Media

Presenter: Kandy Jarvis
Date: April 21, 2003 Page 3

Preliminary

- Starfire Optical Range Team
  - Major Robert Johnson, PhD, camera and optics
  - Mr. Rick Cleis, software and coelostat control
  - Mr. Roger Petty, optical engineer, outdoor spotter and handheld camera operator
  - Mr. Rich Rast, liaison with NASA to get vectors
  - Dr. Robert Q. Fugate, Senior Scientist and Technical Director, S OR (Unable to be there during the event)
- Media
  - 4 videos
  - 3 stills
  - A total of 5 cameras were used, some utilizing telescopes, some not

SPACE SHUTTLE PROGRAM
Space Shuttle Vehicle Engineering Office
NASA Johnson Space Center, Houston, Texas

Images Analyzed

Presenter: Kandy Jarvis
Date: April 21, 2003 Page 4

Preliminary

Revised Analyses of Starfire Optical Range Stills

13:57:14

13:57:59

Two Frames Taken from 5-mRad Video for Analyses

13:57:54.14

13:57:54.22

Stills and frames have been processed by Dr. J. Christou, Center for Adaptive Optics, UCSC using a blind deconvolution technique

This information is being distributed to aid in the investigation of the *Columbia* mishap and should only be distributed to personnel who are actively involved in this investigation.

SPACE SHUTTLE PROGRAM
Space Shuttle Vehicle Engineering Office
NASA Johnson Space Center, Houston, Texas

Starfire Optical Range Stills & Frames

Presenter: Kandy Jarvis
Date: April 21, 2003
Page 5

Preliminary

- Stills:
  - 3.5" telescope looking through a computer controlled 1.0 -m coelostat (rotating mirror)
  - The plate scale is known for these images
    - ~ Measurements of object can be done
    - Re-processing has altered plate scale
  - Orientation (rotation) is known
  - The stills have an ~5 mRad (~1/3 degree) field of view (fov)
- Video Frames:
  - 5 mRad fov: intensified CCD camera attached to a 14" telescope, looking through the 1.0-m coelostat
    - Orientation for every frame will change
    - Approximate Orientation known
  - Plate scales have been estimated
    - Re-processing has changed the plate scale

SPACE SHUTTLE PROGRAM
Space Shuttle Vehicle Engineering Office
NASA Johnson Space Center, Houston, Texas

Still at 13:57:14

Presenter: Kandy Jarvis
Date: April 21, 2003
Page 6

Preliminary

- Notes Regarding Attitude Comparison at Time: 1 Feb 2003, 13:57:1 4 UTC
  - Models account for 8 degree rotation (per 24 -Feb. SOR e-mail)
  - Elevons, body flap, and engines are modeled in neutral position
  - Groundsite observer viewing from slightly port, slightly forward of normal to orbiter belly
  - Model scales were done visually
    - Approximations were calculated based on wingtip to wingtip dista nce and nose to tail distance
    - Plate scale of original known; compared to deconvolved image and plate scale approximated
    - Model fit visually based upon approximated scale and compared ag ainst SOR's model

This information is being distributed to aid in the investigation of the *Columbia* mishap and should only be distributed to personnel who are actively involved in this investigation.

SPACE SHUTTLE PROGRAM
Space Shuttle Vehicle Engineering Office
NASA Johnson Space Center, Houston, Texas

Still at 13:57:14

Presenter Kandy Jarvis
Date April 21, 2003 Page 7

Preliminary

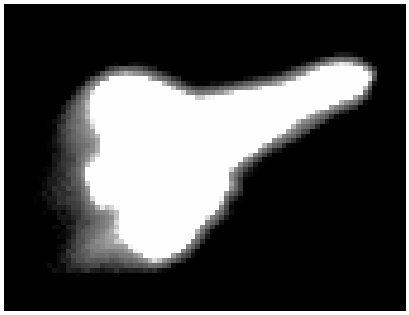

Raw Image

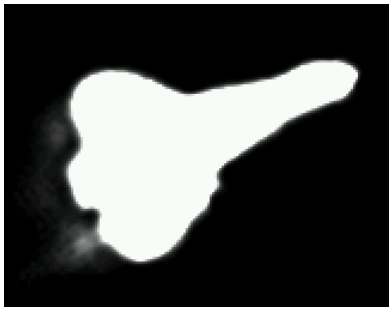

Re-Processed Image

SPACE SHUTTLE PROGRAM
Space Shuttle Vehicle Engineering Office
NASA Johnson Space Center, Houston, Texas

Still at 13:57:14

Presenter Kandy Jarvis
Date April 21, 2003 Page 8

Preliminary

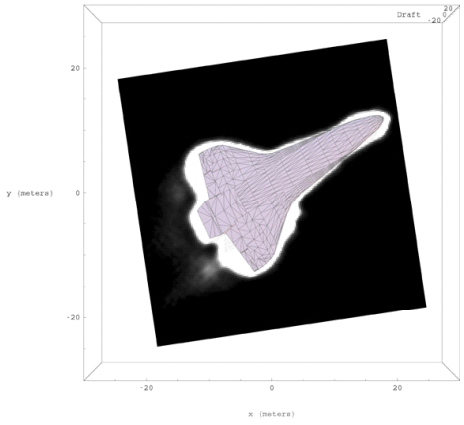

Starfire Optical Range Image (26 March 2003)
model overlay (R. Cleis, R. Fugate, R. Johnson)
image sharpened using deconvolution (J. Christou)
The model scaling and orientation are based on telemtery (latitude, longitude, and altitude from NASA) and observations (azimuth, elevation, and range from SOR). The image scaling and orientation were derived from measurements using star fields. The Columbia model was provided by NASA.

Mathematically scaled wireframe model overlain on re-processed image

- Model scaling based on telemetry
- Image scaling based on starfield measurements

The side of the orbiter and the tail were decreased in brightness in this overlay

This information is being distributed to aid in the investigation of the *Columbia* mishap and should only be distributed to personnel who are actively involved in this investigation.

SPACE SHUTTLE PROGRAM
Space Shuttle Vehicle Engineering Office
NASA Johnson Space Center, Houston, Texas

Still at 13:57:14

Presenter Kandy Jarvis
Date April 21, 2003 Page 9

Preliminary

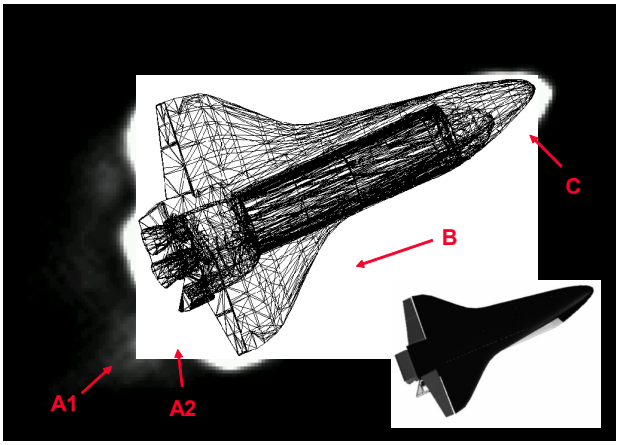

Wire frame 3-D Model of Orbiter Attitude at
1 Feb 2003, 13:57:14 UTC overlaid on still
Solid 3-D model provided as inset

3 Areas of Interest

- Asymmetric (A) Gas Flow Pattern
  - Left wing more elongated in vertical wake (A1)
  - Greater area brightened in aft wing area (A2)
- Asymmetry (B) of Wing (Left vs. Right)
  - Convex in region (Xo-1100, Yo-256), leading edge of left wing.
- Asymmetry (C) of Nose

SPACE SHUTTLE PROGRAM
Space Shuttle Vehicle Engineering Office
NASA Johnson Space Center, Houston, Texas

Still at 13:57:14

Presenter Kandy Jarvis
Date April 21, 2003 Page 10

Preliminary

Asymmetric Gas Flow (A1)

- When the re-processed image is adjusted to brighten the fainter pixels, details of the asymmetric gas are definable
  - Correlation between portions of the orbiter and the gas are possible
- The most probable correlations are presented
  - Other possibilities are not precluded and should be investigated by
    - •Modeling
    - •Wind tunnel testing
- Specifics of correlations follow

This information is being distributed to aid in the investigation of the *Columbia* mishap and should only be distributed to personnel who are actively involved in this investigation.

SPACE SHUTTLE PROGRAM
Space Shuttle Vehicle Engineering Office
NASA Johnson Space Center, Houston, Texas

Still at 13:57:14
Gas correlation

Presenter: Kandy Jarvis
Date: April 21, 2003 Page 11

Preliminary

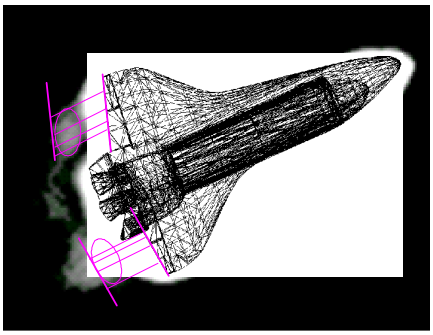

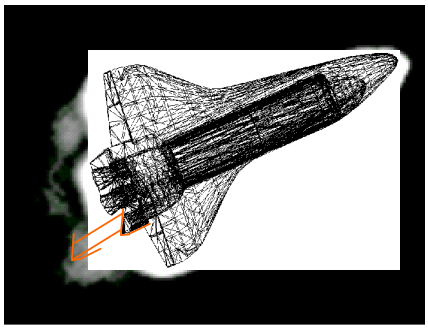

- Gas (elliptical circles) seen behind right wing
  - Assumed nominal
  - Assumed symmetric w/respect to left wing
- Gas flow from the tail identified

SPACE SHUTTLE PROGRAM
Space Shuttle Vehicle Engineering Office
NASA Johnson Space Center, Houston, Texas

Still at 13:57:14
Gas Correlation

Presenter: Kandy Jarvis
Date: April 21, 2003 Page 12

Preliminary

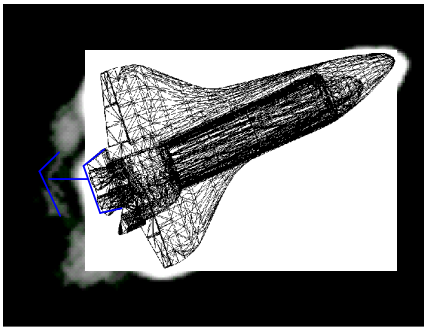

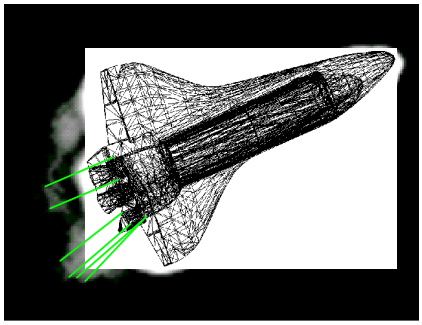

- Gas flow from the body flap identified
- Gas flow from the OMS pods suggested as explanation
- See next page for additional options

This information is being distributed to aid in the investigation of the *Columbia* mishap and should only be distributed to personnel who are actively involved in this investigation.

SPACE SHUTTLE PROGRAM
Space Shuttle Vehicle Engineering Office
NASA Johnson Space Center, Houston, Texas

Still at 13:57:14
Gas Correlation

Presenter: Kandy Jarvis
Date: April 21, 2003 Page: 13

Preliminary

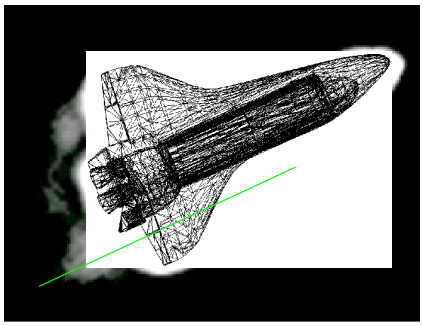

- **Flow from split between inboard and outboard elevons?**
  - Symmetry expected but not seen
  - Unlikely
- **Elevon position**
  - Right and left elevons are between 0.3 and 0.7 degrees different in position between 13:57:14.0 – 13:57:14.99
  - Unlikely but could contribute
- **"Bulges" in leading edge create turbulence and/or hot gas**
  - This possibility cannot be ruled out
  - Potential resultant gas flow should be modeled
- **Viewing geometry and refraction could contribute**

SPACE SHUTTLE PROGRAM
Space Shuttle Vehicle Engineering Office
NASA Johnson Space Center, Houston, Texas

Still at 13:57:14
Gas Correlation

Presenter: Kandy Jarvis
Date: April 21, 2003 Page: 14

Preliminary

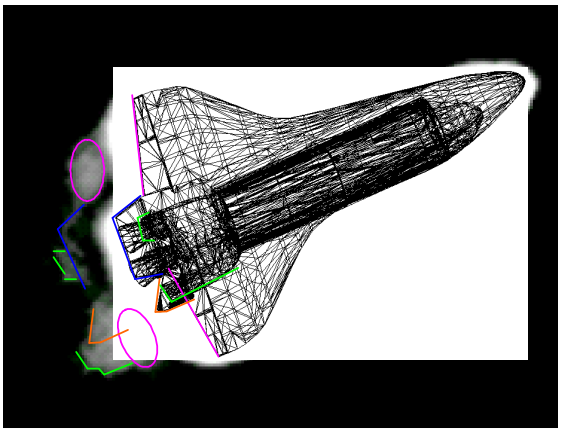

Correlation of Gas

This information is being distributed to aid in the investigation of the *Columbia* mishap and should only be distributed to personnel who are actively involved in this investigation.

SPACE SHUTTLE PROGRAM
Space Shuttle Vehicle Engineering Office
NASA Johnson Space Center, Houston, Texas

Still at 13:57:14

Presenter: Kandy Jarvis
Date: April 21, 2003 Page: 15

Preliminary

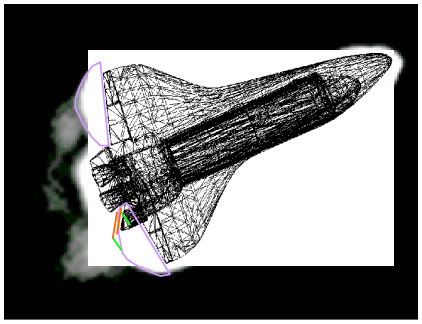

Greater area is brighter behind trailing edge of left wing (A2)

- Both wings show a gas flow pattern that is rounded; however, left wing has an additional bulge in area near elevon gap
- This brightened zone appears to correlate with the tail and left OMS pod/stinger
  - Some contribution could be from either the elevon, or from the "bulges" along the leading edge of the wing

SPACE SHUTTLE PROGRAM
Space Shuttle Vehicle Engineering Office
NASA Johnson Space Center, Houston, Texas

Still at 13:57:14

Presenter: Kandy Jarvis
Date: April 21, 2003 Page: 16

Preliminary

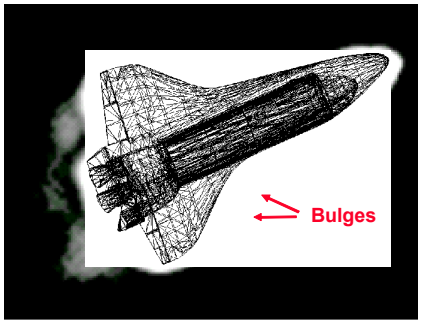

Two Bulges on Wing (B)

- Clearly outboard of wing-structure
- Shape is inconsistent with wing leading edge
- Inconsistent with flow pattern on right wing

Possible Causes

- Localized intensity increase
- Anomalous gas flow pattern

This information is being distributed to aid in the investigation of the *Columbia* mishap and should only be distributed to personnel who are actively involved in this investigation.

SPACE SHUTTLE PROGRAM
Space Shuttle Vehicle Engineering Office
NASA Johnson Space Center, Houston, Texas

Still at 13:57:14

Presenter Kandy Jarvis
Date April 21, 2003 Page 17

Preliminary

Localized intensity increase

- Local increase in temperature; hot spots
- Local increase in reflectivity (orbiter is in sunlight at this t ime)
  - Exposure of metal
  - This is considered unlikely, but is possible

Anomalous gas flow pattern in front of wing

- Tile damage?
  - Possible, but unlikely to change bow shock and wing shock shape (per aerothermo team)
- Damage to wing leading edge?
  - Could change local bow shock and wing shock shape (per aerothermo team)
- Viewing geometry and refraction could contribute

SPACE SHUTTLE PROGRAM
Space Shuttle Vehicle Engineering Office
NASA Johnson Space Center, Houston, Texas

Still at 13:57:14

Presenter Kandy Jarvis
Date April 21, 2003 Page 18

Preliminary

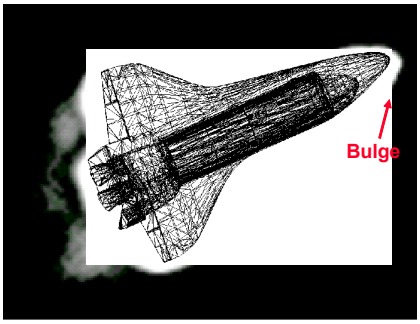

Asymmetry of Nose (C)

- Unknown if nominal
- Localized intensity increase
- Could be normal canopy shock seen from this angle
- Viewing geometry could hide symmetry

This information is being distributed to aid in the investigation of the *Columbia* mishap and should only be distributed to personnel who are actively involved in this investigation.

SPACE SHUTTLE PROGRAM
Space Shuttle Vehicle Engineering Office
NASA Johnson Space Center, Houston, Texas

Still at 13:57:14

Presenter: Kandy Jarvis
Date: April 21, 2003 Page: 19

Preliminary

Final Conclusions

- **Asymmetric gas behind left wing (A1)/brightened aft region(A2)**
  - Can be accounted for with structure of Orbiter
  - Contribution from leading edge "bulges" can not be ruled out
  - Contribution from elevon can not be ruled out
- **Bulges (B)**
  - Caused by either local increase in intensity or anomalous gas fl ow
    - Some possible causes of anomalous gas flow presented
      - » Modeling and wind tunnel testing investigations should aid in understanding and/or generate new theories
      - » Some measurements of angles of bulges in relation to orbiter may be possible if so requested by other teams
- **Nose asymmetry (C)**
  - Likely nominal condition
  - Flight data (OI and OEX) show no anomalous readings at the chin panel or vent nozzles at this time

Analyses of This Still is Considered Complete Unless Otherwise I nstructed

SPACE SHUTTLE PROGRAM
Space Shuttle Vehicle Engineering Office
NASA Johnson Space Center, Houston, Texas

Frames at 13:57:54.14 & 13:57:54.22

Presenter: Kandy Jarvis
Date: April 21, 2003 Page: 20

Preliminary

- Notes Regarding Attitude Comparison at Time: 1 Feb 2003, 13:57:5 4 UTC
  - Telemetry exists for 13:57:54.14 UTC; 13:57:54.22 was interpolat ed.
  - Elevons, body flap, and engines are modeled in neutral position
  - Ground observer viewing from vertical tail and slightly to port
  - Model scales were done visually
    - Approximations were calculated based on wingtip to wingtip dista nce
    - Plate scale of still (5 secs later) known; compared to deconvolved image and plate scale approximated
    - Model fit visually based upon approximated scale.
  - Orientation (rotation) of frames with overlays were estimated ba sed upon known orientation of wireframe.

This information is being distributed to aid in the investigation of the *Columbia* mishap and should only be distributed to personnel who are actively involved in this investigation.

SPACE SHUTTLE PROGRAM
Space Shuttle Vehicle Engineering Office
NASA Johnson Space Center, Houston, Texas

Frames at 13:57:54

Presenter: Kandy Jarvis
Date: April 21, 2003 Page 21

Preliminary

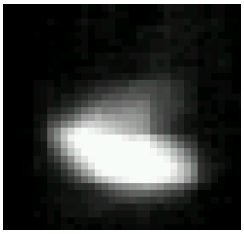

13:57:54.14

ß **Raw** **Re-Processed** à

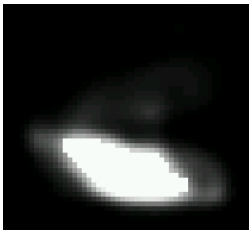

Note the "blocky" nature of the frames; this will generate some artifacts in the deconvolution process

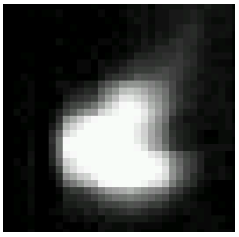

13:57:54.22

ß **Raw** **Re-Processed** à

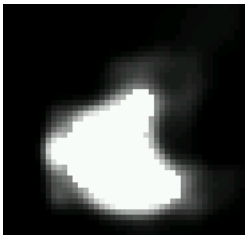

SPACE SHUTTLE PROGRAM
Space Shuttle Vehicle Engineering Office
NASA Johnson Space Center, Houston, Texas

Frame at 13:57:54.14

Presenter: Kandy Jarvis
Date: April 21, 2003 Page 22

Preliminary

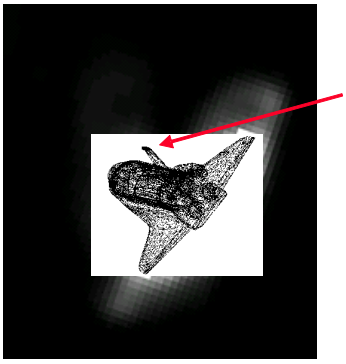

Re-processed, rotated

Tail

Artifacts?

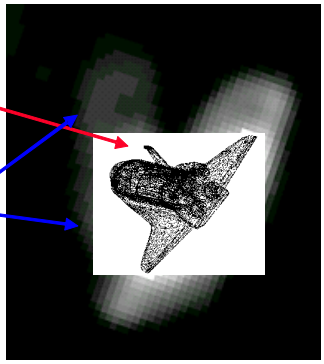

Faint pixels enhanced

•Only wings clearly visible
•Nose or SILTS pod/tail faintly visible

Currently unknown if the enhanced pixels represent artifacts or flow features, etc. Modeling, wind tunnel testing, and processing of video should help determi ne this

This information is being distributed to aid in the investigation of the *Columbia* mishap and should only be distributed to personnel who are actively involved in this investigation.

SPACE SHUTTLE PROGRAM
Space Shuttle Vehicle Engineering Office
NASA Johnson Space Center, Houston, Texas

Frame at 13:57:54.22 (Flare Event #1)

Presenter: Kandy Jarvis
Date: April 21, 2003 Page 23

Preliminary

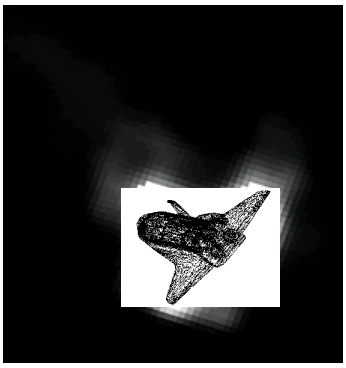

Re-processed, rotated

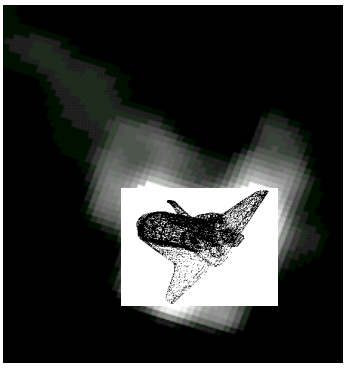

Faint pixels enhanced

•Increased intensity/visual blooming of nose or SILTS pod/tail
•Increased intensity/visual blooming of left wing

There are still multiple questions regarding the event seen here ; See discussion

SPACE SHUTTLE PROGRAM
Space Shuttle Vehicle Engineering Office
NASA Johnson Space Center, Houston, Texas

Frames at 13:57:54.14 & 13:57:54.22

Presenter: Kandy Jarvis
Date: April 21, 2003 Page 24

Preliminary

Current understanding of video images

- The left wing appears to brighten
- The nose/tail then appears to brighten
  - Possible causes
    - Changes in the flow field for the left wing and tail
    - An event in the left wing generates a flow field that, at this v isual aspect, appears to intersect with the tail
      - Flow field is generally too faint to see but when additive with nose/tail brightness, appears to cause an overall brightening of the nose/ tail region
      - The tail passes through the flow field as the orbiter moves forw ard and this enhances the brightening
      - An illumination of the wing illuminates area(s) previously in sh adow (nose or tail)
    - There are no overt indications in information from the orbiter t hat suggests the tail underwent any change at this moment in time. Newly acq uired MADS data has not yet been compared against these times.
    - Diffraction (see next page)

This information is being distributed to aid in the investigation of the *Columbia* mishap and should only be distributed to personnel who are actively involved in this investigation.

SPACE SHUTTLE PROGRAM
Space Shuttle Vehicle Engineering Office
NASA Johnson Space Center, Houston, Texas

Frames at 13:57:54.14 & 13:57:54.22

Presenter: Kandy Jarvis
Date: April 21, 2003 Page 25

Preliminary

Diffraction:

- As a bright object exits the field of view of a telescope, diffr action of the optics can create a brightening of that object
  - Both “flare events” in the time line occur at the edge of the fi eld of view
  - SOR has taken video of Jupiter at the same angular size as the o rbiter, and moved the telescope so Jupiter left the field of view at the sam e approximate location as the orbiter
    - No flash or flare was seen to occur
    - Can not re-create phase angle of the sun at that time (no stars in daylight)
  - There does appear to be a distinct visual change in the orbiter between pre-flare and post flare. Still at 13:57:59 shows brightened nose/t ail region
- This suggests diffraction is not a cause of the events seen

SPACE SHUTTLE PROGRAM
Space Shuttle Vehicle Engineering Office
NASA Johnson Space Center, Houston, Texas

Still at 13:57:59

Presenter: Kandy Jarvis
Date: April 21, 2003 Page 26

Preliminary

- Notes Regarding Attitude Comparison at Time: 1 Feb 2003, 13:57:5 9 UTC
  - Telemetry unavailable for 13:57:59 UTC; interpolated.
  - Orientation known (rotation)
  - Elevons, body flap, and engines are modeled in neutral position
  - Ground observer viewing from vertical tail and slightly to port
  - Model scales were done visually
    - Approximations were calculated based on wingtip to wingtip dista nce
    - Plate scale of original known; compared to deconvolved image and plate scale approximated
    - Model fit visually based upon approximated scale

This information is being distributed to aid in the investigation of the *Columbia* mishap and should only be distributed to personnel who are actively involved in this investigation.

SPACE SHUTTLE PROGRAM
Space Shuttle Vehicle Engineering Office
NASA Johnson Space Center, Houston, Texas

Still at 13:57:59

Presenter: Kandy Jarvis
Date: April 21, 2003 Page 27

Preliminary

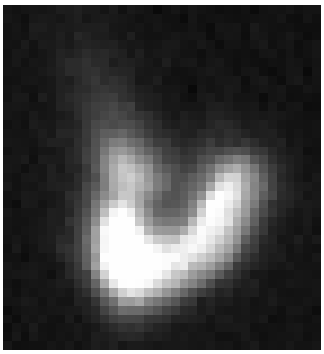

Raw Image in proper orientation

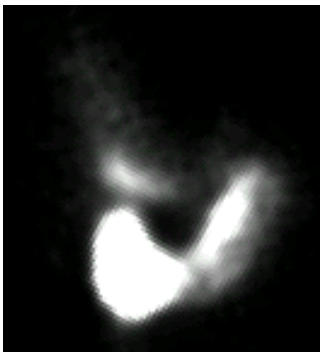

Re-Processed Image in proper orientation

SPACE SHUTTLE PROGRAM
Space Shuttle Vehicle Engineering Office
NASA Johnson Space Center, Houston, Texas

Still at 13:57:59

Presenter: Kandy Jarvis
Date: April 21, 2003 Page 28

Preliminary

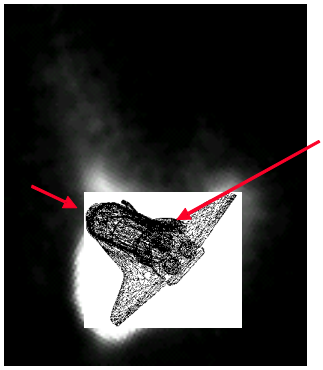

Re-processed

Shadowing due to relative location of sun

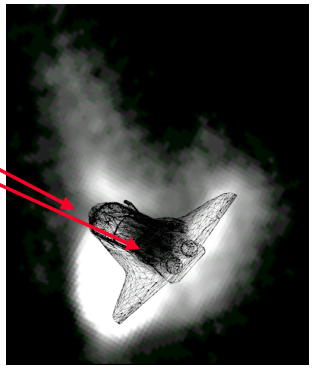

Faint pixels enhanced

The scale and exact placement of the wireframe overlay is still approximated

This information is being distributed to aid in the investigation of the *Columbia* mishap and should only be distributed to personnel who are actively involved in this investigation.

SPACE SHUTTLE PROGRAM
Space Shuttle Vehicle Engineering Office
NASA Johnson Space Center, Houston, Texas

Photo Still at 13:57:59

Presenter: Kandy Jarvis
Date: April 21, 2003
Page: 29

Preliminary

Current understanding of still

- The left wing has increased intensity
- The nose/tail has increased intensity
  - Improved resolution (vs. video frames) suggests
    - An event in the left wing generates a flow field that, at this v isual aspect, appears to intersect with the tail
      - Flow field is generally too faint to see but when additive with nose/tail brightness, appears to cause an overall brightening of the nose/ tail region
      - An illumination of the wing illuminates area(s) previously in sh adow (nose or tail)
    - There are no overt indications in information from the orbiter t hat suggests the tail underwent any change at this moment in time

SPACE SHUTTLE PROGRAM
Space Shuttle Vehicle Engineering Office
NASA Johnson Space Center, Houston, Texas

Next Steps

Presenter: Kandy Jarvis
Date: April 21, 2003
Page: 30

Preliminary

- SOR-AFRL Will
  - Provide video for plate scaling
  - Determine orientation of video frames of interest
- Acquiring Slightly Better Resolution Video Frames from Digital R ecording for Deconvolution
  - First set of frames have been acquired and will soon be processe d
- Continue Interpretation of Still 13:57:59 and Video Frames from 5 mRad Video
- Video Processing Will Search for Additional Signs of Debris
- Events Will Be Submitted for Entry Event Timeline as Confirmed

This information is being distributed to aid in the investigation of the *Columbia* mishap and should only be distributed to personnel who are actively involved in this investigation.

APPENDIX E
DEFINITIONS

Anomalous Optical Signature –A visual appearance of the orbiter containing a characteristic that appears irregular such as a lack of expected symmetry, pulsation of signal, or outline not matching the expected configuration.

Frames, Set of –A sequential subset of video frames extracted from the complete video, wherein the number of frames in a set varies according to the content.

Nominal –All conditions within normal expected parameters.

Off Nominal –A condition or conditions outside of normal expected parameters.

Orientation –The known compass direction of an image. This may be unknown due to the rotation of the imaging apparatus.

Pixel –A contraction of "picture elements"; a single energy flux detector.

Plate Scale –The ratio of a measurement on an image to the equivalent measurement of the imaged object.

Resample –An averaging of nearby values to generate a new value.

Resolution –The ability to separate closely spaced objects on an image.

Saturation –When the energy flux exceeds the sensitivity range of a detector or set of pixels. This overflow can also spread to adjoining pixels, altering their values.

Starfield –An image of a collection of identifiable stars at a known time that permits calculation of plate scale and compass orientation of an image.

This information is being distributed to aid in the investigation of the *Columbia* mishap and should only be distributed to personnel who are actively involved in this investigation.

Volume V
Appendix G.8

Using the Data and Observations from Flight STS-107... Exec Summary

This Appendix contains the report Using the Data and Observations From Flight STS-107 to Explain the Fatal Reentry of the Columbia Orbiter OV-102, Bertin, John J., Smiley, James W. This report develops possible scenarios that were considered by the Columbia Accident Investigation Board.

THIS PAGE INTENTIONALLY LEFT BLANK

USING THE DATA AND OBSERVATIONS FROM FLIGHT STS-107 TO EXPLAIN THE FATAL REENTRY OF THE COLUMBIA ORBITER OV-102

By
DR. JOHN J. BERTIN
DR. JAMES W. SMILEY
CONSULTANTS, CAIB SUPPORT GROUP

EXECUTIVE SUMMARY

In our role as Aerothermodynamic Consultants to the Columbia Accident Investigation Board (CAIB), we are documenting our interpretation of the key events, which led to the demise of OV-102 during Flight STS-107. In order to develop an understanding of aerothermodynamic environment and of the sequence of critical events that led to the demise of the Orbiter, meetings were held with NASA personnel and their contractors and with other consultants to Group 3 (Engineering and Technical Analysis) of the Columbia Accident Investigation Board (CAIB). During these meetings, we obtained film clips, timelines, basic data, interpretations of the data, and figures from power-point presentations. In these meetings, we exchanged ideas on what we thought were key events, about what was possible, what was likely, what was not possible, and what was not likely.

The authors would like to acknowledge the inputs (verbal and written) that we received from Rick Barton, Charles Campbell, Joe Caram, Ray Gomez, Dave Kanipe, Steve Labbe, Gerald J. Lebeau, Chris Madden, Fred Martin, Scott Murray, et al. [all of the Johnson Space Center (NASA)]; Stan Bouslog of Lockheed-Martin; and Jim Arnold, Howard Goldstein, Pat Goodman, Robert Hammond, Jim Mosquera, and Donald J. Rigali from the CAIB Technical Support Team. The authors have benefited from discussions with and from presentations made by the Group 3 members of the CAIB, Dr. James Hallock, G. Scott Hubbard, Dr. Doug Osherhoff, Roger Tetrault, and Dr. Sheila Widnall. The following text offers our interpretation of the significance of and the relationship between data and observations that are currently “known” about the fatal aerothermodynamic environment of flight STS-107 for the Columbia Orbiter, OV-102.

It is the intent of the authors to document a summary of key data and provide a realistic scenario that would explain the aerothermodynamic environment during the demise of Columbia OV-102. In this effort, we have attempted to match what we consider to be twelve critical events or observations that were determined from “data” gathered from the persons mentioned in the previous paragraph. The word “data” has been placed in quotes, since some “data” represent flight measurements whose time and magnitude are well known, other “data” represent debris whose origin and timing is somewhat subjective, and still other “data” are from computations and wind-tunnel tests and, thus, are dependent on the simulation models (numerical or experimental) used. Therefore, some of the observations based on our interpretation of the “data” may differ from the demise scenarios proposed by others using the same “data”. For instance, some of the information gleaned from the recovered debris may be in error, because the debris was misidentified or because the damage to the recovered debris may have occurred at a different time during the reentry. Furthermore, new information (in the form of additional recovered debris, analysis, etc.) may become available at some point in the future. For instance, data from the MADS recorder that was recovered after initial

investigations provided information over a longer time frame and from additional sensors. To allow for such uncertainties in the existing "data" and for the probability of new, additional data providing an improved understanding of the aerothermodynamic environment, most of the observations that the authors deem to be "critical" represent several pieces of information rather than a single datum point.

Furthermore, by matching the information from twelve "critical data/events", it is hoped that a reasonably accurate and coherent description of the evolving damage will be presented in this report. We will describe how the following sequence of events can be used to define a demise scenario, which is judged to be consistent with all of the "data".

1. The observation that foam particles from the external tanks impinged on the wing leading edge during the launch.

2. Radar signatures from the second day of the mission that showed a piece of debris drifting away from the Orbiter.

3. The strain-gage reading (beginning at EI + 270) and the temperature rise at two thermocouples located in the vicinity of RCC Panel 9 (beginning at EI + 290), as indicated by MADS data.

4. The perturbations to the heating and to the surface pressures due to the interaction between the bow shock wave and the wing-leading-edge shock wave are most severe in the region of RCC Panels 8 and 9.

5. Start of off nominal temperature histories at four sensors on left OMS Pod (beginning with lower than expected temperatures at EI + 340, followed by higher than expected temperatures at EI + 460).

6. The anomalous temperature increases that occurred at various locations in the main left-landing-gear wheel well (beginning at EI + 488).

7. The increase in temperatures at points located on the vertical side of the fuselage, as indicated both in thermocouples on the Orbiter itself and in the temperature sensitive coatings on the wind-tunnel models tested at the Langley Research Center (beginning at EI + 493).

8. Loss of all measurements from the wire bundle running along the backside of the wing spar (beginning at EI + 487) followed by the loss of measurements from the wire bundle running along the left main-landing gear wheel well, which included elevon measurements (beginning at EI + 527)

9. The observations regarding the damage to the wing leading edge, as determined from the recovered debris.

10. The modifications to the shock/shock interaction flow field that was described in "critical data/event" #4, as developed based on the developing damage scenario and correlated against the Kirtland photograph, i. e., observations by personnel from the Starfire Optical Range (at EI + 830.5/832.5).

11. Comparing selected histories showing that the actual flight was close to the planned flight up to EI + 900.

12. Using the rolling-moment-coefficient history to support findings for some of the previous eleven points.

It is recognized that there are other data (facts) and that some of these facts may become critical as an improved and more complete understanding of the demise is achieved. However, based on our understanding at this time, we believe that these twelve "critical data/events" are very important and that a demise scenario that incorporates all twelve has some credibility. The time-dependence of these twelve events will be based on the "Relation of Reentry Parameters" that are contained in the table presented in Table 1 and in Appendix A. Entry Interface (EI) occurred at GMT 13:44:09. Referring to Table 1, the reader can identify three, related early "events" that indicate anomalous behavior: the strain gage reading and the high temperatures for two thermocouples on the spar behind RCC Panel 9 (one on the clevis and one on the back face of the spar. These foreboding signs occurred by 13:49:00, with the Orbiter still approximately 1000 miles west of the California coast. The Orbiter was flying at altitudes in excess of 260,000 feet, where non-continuum effects are important in modeling the flow field and the peak convective heating has not been reached. Thus, it is believed that the initial damage that compromised the thermal protection system and that led to the demise of OV-102 was in place at the EI.

To readily access the figures and appendices of this report click on the hyperlinks located on the last page of this document.

GENERAL DISCUSSION

(1) The observation that foam particles from the external tanks impinged on the wing leading edge during launch.

A large piece of foam (debris) from the bipod area of the external tank (ET) is evident in the film of the STS-107 during launch. The trajectory of the debris, which is shown in Figure 1, indicates that the ET foam debris struck the wing leading edge 82 seconds after launch. Based on this trajectory, the likeliest area of impact was on RCC Panel 6, or slightly downstream. See Figure 2. As shown in Figure 3, RCC Panels 1 through 4 are located on the glove, which has a sweep angle of 81°. RCC Panels 5 through 7 are located on the intermediate spar, a. k. a., the transition spar. RCC Panels 8 through 19 are located on the wing spar, which is swept 45°,

Post-flight analysis of the MADS data indicated a small temperature rise in the measurement from a temperature sensor that was located behind the wing spar of RCC Panel 9. This is a possible additional piece of evidence that the damage occurred during the launch phase.

The authors believe that significant damage to the RCC panels in the vicinity RCC Panel 6 is consistent with the early thermal anomalies that were observed both in the sensors on and/or near the spar at the back of RCC Panel 9 and in some of the sensors in the left main-landing-gear wheel well. The anomalies that occurred in these two regions did not occur simultaneously, but were close in time. Thus, damage somewhere in the vicinity of RCC Panel 6 would be strategically placed to deliver hot gases that could both damage the wires on the back of the wing spar near these RCC panels and the wires on the main left-landing-gear wheel well. The hot gases from the breech in the wing leading edge would also flow down the chunnel (channel/tunnel) that exists between the RCC panels and the spar that follows the wing leading edge, producing the anomalous readings on the sensors at the spar at RCC Panel 9.

The wing-leading-edge subsystem (LESS) is shown in the sketch of Figure 4. The impact of the debris with a leading-edge RCC panel could have removed (all or part of) a T-seal or produced a hole or a crack in the RCC panel itself. In an attempt to further define the location and the extent of the debris-induced damage, NASA personnel and their contractors have been using computational fluid dynamic (CFD) codes. Additional work is needed to complete and to validate the analysis efforts, e. g., use the direct simulation Monte Carlo (DSMC) computational tools to provide an independent validation of the flow field at these low-density gas conditions. The modeling of the internal flow through the chunnel, starting with a breech of the leading-edge TPS (using the location and the nature of the breech to define the boundary conditions for a few likely initial conditions), and proceeding into the wing is a very complex task that should be completed. Of special interest is matching the computed results to the observed times for (1) the burn through of the MADS wires behind the spars, (2) the burn through of the bundle of wires that ran along the wall of the main left-landing-gear, and (3) the anomalous temperatures measured at various points inside the left main-landing-gear wheel well.

(2) Radar signatures from the second day of the mission that showed a piece of debris drifting away from the Orbiter.

Radar signatures from the second day of the STS-107 mission indicated that there was an object drifting away from the Orbiter, disappearing after a few orbits. The radar signature and the ballistic coefficient of the object were analyzed to determine what the object might be. Recent communications from personnel from the Lincoln Lab (as provided to Dr. Sheila Widnall) indicate that, in their judgment, the best match to the "data" would be a piece of a T-seal. However, the possibility exists that the impinging ET foam caused a piece of an RCC panel to be broken off. The exact configuration of the initial damage is not known.

(3) The strain-gage reading (beginning at EI + 270) and the temperature rise at two thermocouples located in the vicinity of RCC Panel 9 (beginning at EI + 290), as indicated by MADS data.

As shown in Figure 5, three sensors were located in the vicinity of RCC Panel 9: two thermocouples and a strain gage. AT GMT 13:48:39, the strain gage on the left wing spar at RCC Panel 9 starts an off-nominal increase, as indicated in Appendix A. This is only 270 seconds after EI. At this point in time, the Orbiter is located about 1000 miles west of the California coast, flying at 23,000 feet/second at an altitude in excess of 270,000 feet. Refer to Table 1. Referring to Table 1 and to Figure 6, the temperature sensed by the thermocouple on the Spar 9 Clevis starts to increase by (approximately) GMT 13:49:00, which is less than 300 seconds after EI. According to Table 1, the temperature sensed by the thermocouple on the back of Spar 9 starts to increase very rapidly with time beginning at GMT 13:51:09. Refer now to Figure 7. Signal is lost from the thermocouple on the clevis at (approximately) 55 deg F, 490 seconds after EI. At approximately 522 seconds after EI, signal is lost from the thermocouple on the back face of the spar at a temperature exceeding 240 deg F.

The authors believe that the increase in temperature of the two thermocouples that are located on or near Spar 9 was caused by hot gases entering through a breech in the thermal protection system (TPS), which occurred when the impingement of the ET foam debris damaged the leading-edge TPS. Based on the information currently available to the authors, the critical, it is their opinion that the initial damage probably occurred in the vicinity of RCC Panel 6. Hot gases from the shock layer entered through the breech in the TPS and flowed down the chunnel. Although the density of these gases is relatively low, their temperature is very high. If this is indeed the case, then these hot gases flowing through the chunnel also were destroying the intermediate spar, a. k. a., the transition spar, and parts of the wing spar. Assuming this model to be correct, the hot gases would flow through the gaps and around the edges of the insulative wrap that surrounds the sensors. Thus, convection would be added to conduction and radiation, as mechanisms contributing to the rate at which the measured temperature increases.

Based on the computed flow-field solutions by NASA and on the engineering experiences of the authors, the flow path of the ingested hot gases depends on the location and on the shape of the breech in the thermal protection system. If the initial damage were a hole in the RCC panel itself, there would be a strong component of flow outward along the chunnel and parallel to the wing leading edge, following the external streamlines. If the initial damage were a piece of T-seal, the ribs of the bounding RCC

panels would constrain the flow to the channel bounded by the ribs. This flow path is initially perpendicular to the wing leading edge. However, the high temperature gases flowing in this channel could quickly ablate the downstream rib, at which time the damage would function as a hole.

Some Observations at This Point (A)

The destruction of the spar is not the only problem caused by the hot gases flowing down the chunnel. Under normal circumstances, the locally high convective heating rates to the external surface of the RCC panels along the wing leading edge are balanced by radiation into the relatively cool cavity behind the curved RCC panels, i. e., into the chunnel volume. In addition, under normal circumstances, some energy is conducted away from the leading edge through the high temperature gradients in the reinforced carbon/carbon shell. But this is no longer possible. These hot gases flowing in the chunnel not only prevent the mechanisms for relief of the energy from the RCC panels, they create a situation where the panels are being heated from both sides. The hot gases in the chunnel prevent the energy relief from the high convective heating rates to the external surface of the RCC panels. This will strike first at the RCC panel where the convective heating from the flow in the shock layer is the greatest. As will be discussed, the shock/shock interaction pattern produced the highest convective heating rates in the vicinity of RCC Panel 9. This will be discussed in "critical data/event" #4.

The destruction of the intermediate (or transition) spar somewhere behind RCC Panels 6 through 8 provides a source for the problems soon to affect objects in the left main-landing-gear wheel well ("critical data/event" #6) and the early loss of the elevon signals, which is attributed to the wire burn through ("critical data/event" #8).

(4) The perturbations to the heating and to the surface pressures due to the interaction between the bow shock wave and the wing-leading-edge shock wave are most severe in the region of RCC Panels 8 and 9.

The bow shock wave intersects the wing-leading-edge shock wave, creating a shock/shock interaction, such as shown in Figure 8 [Ref. 1]. The interaction between the bow shock wave and the wing-leading-edge shock wave depends (among other parameters) on the gas chemistry, on the angle-of-attack, and on the sweep angle of the wing. The bow shock wave is relatively weak, so that flow in the shock layer near the wing root is supersonic and the pressure is relatively low. Far outboard, the wing-leading-edge shock wave depends on the sweep of the wing leading edge. If the leading edge is only slightly swept (as was the case for some of the early Orbiter concepts), the wing-leading-edge bow shock wave will be strong with high pressures in the downstream, subsonic flow. The low-pressure, supersonic flow inboard of the interaction adjusts to the high pressure, subsonic flow outboard of the interaction through a complex flow that contains regions of subsonic flow, of supersonic flow, impinging jets, and imbedded shock waves. See Figure 8(b). The surface of the wing leading edge that is subject to the impingement of this strong viscous/inviscid interaction may see heating rates more than an order-of-magnitude greater than the heating rates that would exist if there were no shock/shock interaction. However, in actuality, the wing-leading-edge sweep angle (for RCC Panels 8 through 18) is 45°. See Figure 3. Since the wing is highly swept, the wing-leading-edge shock wave will be relatively weak with low pressures in the downstream, supersonic flow. See Figure 8(c). Both the jet and the free-shear layer that are contained in the shock/shock interaction diffuse rapidly.

As a result, the shock/shock-induced perturbation to the heating in the region affected by impinging flow is relatively small for the current Orbiter configuration, i. e., approximately twice the heating that would exist if no shock/shock interaction were present.

Convective heating rates in the interaction region of the wing leading edge have been computed for the Shuttle Orbiter. The computed heat-transfer rates that are presented in Figure 9 indicate that the interaction between bow shock wave and the wing-leading-edge shock wave causes the heating to the surface in the interaction to be approximately twice the undisturbed value and that RCC Panel 9 experiences the highest heating. Because the Orbiter is operating at an angle-of-attack of 40-degrees, the stagnation line is on the windward surface just below the apex of the leading edge. Thus, the highest convective heating to the wing-leading-edge region affects RCC Panel 9, on the lower surface, just below the leading edge. As noted in the previous paragraphs, under normal circumstances, these incident heating rates would be accommodated by radiation from the back surface of the RCC panel into the cavity and by conduction through the reinforced carbon/carbon shell, away from the stagnation line. However, as shown in the sketch of Figure 10, the hot gases flowing up the chunnel not only eliminate the ability to transfer energy away from the wing leading edge, but they produce a situation where energy is added to the RCC panel from the inside as well as from the outside. It doesn't take long before the material near the stagnation line (on the lower surface) fails, leaving relatively sharp RCC plates, exposed to the flow. Thus, the authors believe that a second breech of the thermal protection system has occurred. The authors believe that this one is most likely to be on the lower surface of RCC Panel 9 $\pm$ one panel. The authors' belief that there are two breeches to the RCC panels along the wing-leading edge is based upon not only the sensor data, but upon the Kirtland photograph, which will be discussed as "critical data/event" #10. Gases quickly flow from the high pressure region in the shock layer near the stagnation line into the chunnel, causing the destruction of the lower surface of the panel. The authors believe that this is a significant change in the Orbiter Mold Line (OML). The changes in the OML of the wing leading edge modify the vortices that emanate from this region and that impinge on the leeward fuselage. Therefore, it is associated with the start of off-nominal temperature histories at the four sensors on the left OMS Pod, which are described in "critical data/event" #5.

(5) Start of off nominal temperature histories at four sensors on left OMS Pod (beginning with lower than expected temperatures at EI + 340, followed by higher than expected temperatures at EI + 460).

Refer to "The STS-107 Mishap Investigation – Combined Master Timeline, - Baseline Corrected" that is presented in Appendix A. It is noted that, at GMT 13:49:49, which is EI + 340, "Start of off-nominal temperature trends" for "4 Left OMS Pod Surface Temps". Initially, the rise rate is cooler, when compared to previous flights of the same inclination. That is followed by a warmer-than-expected temperature trend, beginning at EI + 460. It is noted in Appendix A that the "Sensor sees a sharp increase at EI + 910 and goes erratic at EI + 940."

Even for the baseline configuration, i. e., for the configuration without any damage to wing leading edge, free-vortex-layer types of separation are produced by the flow around the fuselage chine, around the highly swept glove (sweep angle of 81°) and around the transition section from the glove to the majority of the wing, which is swept 45°. The resultant viscous/inviscid interactions cause locally high heating rates and high

shear forces to act on the orbital maneuvering system (OMS) pod. However, as is evident in the data presented by Neumann [Ref. 2] and reproduced in Figure 11, the heating to the OMS Pod is a function of the angle-of-attack. The correlation between the local heating and the angle-of-attack is important, since the Space Shuttle Orbiter employs ramping during entry. That is, the angle-of-attack of the Orbiter during entry is initially high, i. e., approximately 40-deg. until Mach twelve is reached. Then, it is ramped down, reaching approximately 20-deg., when the flight Mach number is four. The reader should note that there are significant differences between the heat-transfer correlation based on the wind-tunnel data and that based on the flight data. These differences can be traced, at least in part, to real-gas effects, to Reynolds-number-related effects, and/or to low-density effects.

The first author had a similar experience involving a difference between viscous/inviscid correlations based on wind-tunnel data and those based on flight-test data from the Gemini program. During the design phase of the Gemini capsule, it was assumed that the reentry aerothermodynamic environment for Gemini capsule was similar to that for the Mercury capsule. Thus, the wind-tunnel test program that was conducted during the design phase of the Gemini was somewhat limited. However, the Mercury capsule flew at an angle-of-attack of zero degrees, while the Gemini capsule reentered at an angle-of-attack of approximately 20-deg. Because the Gemini capsule flew at non-zero angle-of-attack, a vortex-induced viscous/inviscid interaction produced locally high heating rates on the conical surface in the vicinity of the umbilical fairing. The locally high heating rates produced numerous, small holes in the surface of the conical frustum of the capsule that was made of Rene 41. Once the inspection of the recovered capsule revealed the damage, a post-flight wind-tunnel test was conducted with instrumentation specifically located to obtain information about the aerothermodynamic environment in the region of perturbed flow. The wind-tunnel data revealed that locally high heating rates due to the viscous/inviscid interaction caused by the presence of the flow over the umbilical fairing. Although the wind-tunnel tests revealed the presence of and the approximate strength of the perturbations, there were considerable differences between the severity and the locations of the flight-observed damage and those based on the wind-tunnel tests. The results were similar to those of Figure 11.

By EI + 290, anomalous readings have occurred at the three sensors near Spar 9, as discussed in section relating to “critical data/event” #3. By EI + 493, anomalous data will be evident in the data from sensors in the left main-landing-gear wheel well and on the vertical side of the Orbiter. There will be a loss of the measurements from wire bundles at various locations in the wing box, beginning at EI + 487. These anomalous data indicate there was a considerable mass flow of hot gases through a large fraction of the internal wing volume.

The off-nominal temperature trends that were discussed in the first paragraph of this section (first slightly below the expected values, then above the expected values) are attributed to changes in the free-vortex shear-layer pattern that dominates the leeward flow field. The changes in the vortex pattern are due to the changes in the Outer Mold Line and to hot gases that are flowing from the internal wing volume through the vents that are located on the upper surface of the wing. The specific location of the perturbations to the surface heat-transfer and surface pressure are sensitive to the angle-of-attack, to the Reynolds number, to the density ratio across the shock wave, etc.

Flow-field computations for an Orbiter with RCC Panel 6 removed that were presented by Labbe et al. [Ref. 3] are reproduced in Figure 12. The computations that were made with the FELISA code at the Langley Research Center (NASA) assume an inviscid flow with equilibrium air in a Mach 23.8 stream. Three principal observations are associated with the removal of RCC Panel 6:

"(1) Produces negative roll and yaw moments w/small magnitude
(2) Streamlines for the damaged vehicle track inboard of baseline
(3) Resultant shock raises pressures in proximity to temp measurements".

(6) The anomalous temperature increases that occurred at various locations in the main left-landing-gear wheel well (beginning at EI + 488).

The first sign that hot gases had reached the main left-landing-gear wheel well showed up in the brake-line temperature measurements. A "bit flip" in the "LMG Brake-Line Temp D" occurred at GMT 13:52:17 [Ref. 3]. This is temperature trace M in Figure 13. Thus, this event occurred 488 seconds after EI, which is approximately three minutes after the anomalous readings in the vicinity of Spar 9 ("critical data/event" #3). While a "bit flip" may well be within the experimental uncertainty and, therefore, will not be truly indicative of a problem, the LMG Brake-Line temp D was only one of many anomalous measurements that occurred in this time frame at sensors in the vicinity of the left main-landing-gear wheel well. Referring to Table 3, three "LMG Brake Line Temps" began unusual temperature increases in the time frame GMT 13:52:17 to GMT 13:52:41. Both the temperature measurement for LMG Brake-Line Temp C, which is trace I in Figure 13, and the temperature measurement for LMG Brake-Line Temp A, which is trace G in Figure 14, exhibit anomalous increases starting at GMT 13:52:41. These three gages cover X_0 coordinates from approximately 1100 through 1200. Thus, all three sensors are aft of the tires of the LMG. Because the rate of increase for the temperatures sensed in the wheel well was relatively slow, the hot gases didn't impinge directly on these sensors. Instead, the authors believe that the hot gases entered the cavity away from the sensors and gradually heated the volume of air that resided in the wheel well. Because of the severe damage on the tire and of the aluminum residue splattered on a door latch, the authors believe that the plume of hot gases could have entered that area through a breech near RCC Panel 6.

(7) The increase in temperatures at points located on the vertical side of the fuselage, as indicated both in thermocouples on the Orbiter itself and in the temperature sensitive coatings on the wind-tunnel models tested at the Langley Research Center (beginning at EI + 493).

It is noted in Appendix A that, by GMT 13:52:52, i. e., EI + 493, unusual temperature shifts were observed in five thermocouples on the fuselage and on the upper left wing. It is noted in Table 1 that "Mid fuse bond temp starts up" at GMT 13:54:22. The location of this sensor is noted in Table 3 as X_0 = 1410. Hasselback [Ref. 4] reports that, at GMT 13:53:29, "Fuselage side surface temp increase at X_0 1000.7". Because these anomalous fuselage side-wall temperatures were given a separate mention in the time line of Appendix A, it is given a separate data/event number in this report. However, the flow phenomena that cause these anomalous are essentially those associated with the anomalous heating to the left OMS Pod, i. e., "critical data/event" #5.

Wind-tunnel data from the 20-inch Mach 6 (Air Wind Tunnel) at the Langley Research Center (NASA) that are reproduced in Figure 15 show increased heating rates

on the side of the Orbiter fuselage both for only RCC Panel 6 removed and for only RCC Panel 9 removed.

(8) Loss of all measurements from the wire bundle running along the backside of the wing spar (beginning at EI + 487) followed by the loss of measurements from the wire bundle running along the left main-landing gear wheel well, which included elevon measurements (beginning at EI + 527).

Several of the wires carrying signals from the MADS sensors (including the two temperature measurements behind RCC Panel 9, one on the clevis and one behind the spar) run behind the RCC Panel 9 area wing spar along the back of the spar, forward to the front of the wheel well (about RCC Panel 5). See Figures 16 and 17. At EI + 487, the sensors whose wires run on the back of the left wing front spar begin going off-line, indicating a burn through of the spar. Over the next 10 seconds most of these signals go off line. The last one, the bottom-most wire, goes off-line at EI + 522. Since these wires are separated by about eighteen inches in most locations, the breech, at least its vertical dimension, had to be quite large. Beginning at approximately GMT 13:52:59, which is equivalent to EI + 530, the wires in the large bundles that run along the top of the wheel well (See Figure 17 and 18) begin to go off line. The first signal to go off line was the elevon lower skin temperature. Over the next minute or so most of the signals in these wire bundles go off line. See Figure 19. This would indicate a significant amount of heat was impinging on the wires and wheel well wall. NASA has performed a number of tests to investigate the burning of wire bundles. These test demonstrated that the rapid loss of the entire wire bundle requires very hot gases, with local heat rates of 80 to 90 Btu/ft^2-sec. It is likely that the wheel well wall had been penetrated at this time, since anomalies were showing up in the temperature measurements in the left main-landing-gear wheel well. Recall that the first observed “bit flip” in the wheel well was at EI + 488. While this single “bit flip” may or may not be significant by itself, within the next one to two minutes most of the temperature sensors on the landing gear in the wheel well began to increase. Refer to the discussion of “critical data/event” #6.

This sequence raises some dilemmas that need to be addressed. First, how do we get enough heat on the wheel well to burn the wires, but yet the sensors in the wheel well stay on line until the loss of the Orbiter and the temperatures only go up about 40^oF. Second, the hole through the spar has to be large enough (> 18 inches tall) to take out all the wires, creating a large path for the hot gases to go into the wing interior, yet much of the aluminum wing structure stays intact for another 8 minutes. One explanation could be that a T-seal (or portion of a T-seal) missing. With a T-seal the impinging jet would be narrow, but tall enough to cut all the MADS wires. It could take out the vertical array of wires without the massive heat a “circular hole” would deliver. Also, it would seem that the breech in the spar should be near where the wire bundles (MADS and OI) are close together so the required heat would be minimized. This would favor a breech through a lower number RCC panel. However two strain gages on the front of the wheel well did not go off-line (See Figure 18). This would tend to rule out RCC Panel 5, which is ahead of the front wheel well wall. If the initial damage were to a T-seal (or maybe created a hole just upstream of an RCC rib), the hole through the spar could be smaller and still burn a vertical array of wires. Interestingly enough, such a damage configuration would result in initial flow perpendicular to the spar and cut wires. After 2 to 3 minutes, the very hot gases impinging on the downstream edge of the slot would burn through the RCC rib. At this point the hot gases would tend to flow down the chunnel, damaging the downstream RCC panels and the spar.

(9) The observations regarding the damage to the wing leading edge, as determined from the recovered debris.

Many members of the Board and support staff have spent considerable time in Florida examining the recovered debris. Experts such as Jim Arnold, Howard Goldstein, Pat Goodman, Greg Kovacs, Mark Tanner, and Don Rigali have spent considerable time and effort analyzing the recovered debris. The present authors are not as knowledgeable as many others on the detailed interpretation of the reconstructed wing leading edge. Therefore, our conclusions rely on the photographs, reports, and oral feedback from these experts. Photographs of the reconstructed wing-leading-edge panels, RCC Panels 5 through 11, are presented in Figures 20(a), 20(b), and 20(c). Note that very little of the bottoms (windward surfaces) of RCC Panels 6 through 9 have been recovered. The authors interpret the damage pattern to RCC Panels 6 through 9, as supporting their belief that the foam-induced damage was centered on RCC Panel 6 and the subsequent damage caused by the blockage-of-relief/additional-heating from the chunnel gases led to the loss of most of RCC Panel 9. Because RCC Panel 9 is in the most severe region of the baseline shock/shock interaction region, it would be expected to suffer the most damage. Thus, we believe that the subsequent loss of RCC Panel 9 left two regions where substantial damage had occurred to the wing-leading-edge RCC panels relatively early. Of course, the absence of debris could mean simply that the debris has not been found. It appears that significant fractions of the upper section of RCC Panels 7 and 8 have been recovered. Thus, it appears that there was a surviving section of RCC panel(s) between the two gaps. This is consistent with the authors' belief that, by the time of the Kirtland photograph, there were two distinct notches in the wing leading edge, which were caused by the loss of a substantial amount of RCC Panel 6 (+/- one panel) and RCC Panel 9 (+/- one panel). Between these "missing" panels, a piece of the wing leading edge (what we believe to be the surviving pieces of RCC Panels 7 and 8) remains in place.

The experts report that there is a lot of unique damage in the vicinity of RCC Panels 8 and 9, noting that there is considerable slag deposited on the inner surfaces of the upper portions of the recovered panels. The relative metallic deposition on left wing materials is presented in Figure 21. Note that the metallic deposition is "heavy" to "very heavy" behind RCC Panels 7, 8, 9, and 10. Since the predominate flow stream will be up and out along the chunnel, this pattern would be consistent with an initial breech in the vicinity of RCC Panel 6 +/-1 panel with the hot gas plume impinging on the spar behind RCC Panels 7 and 8, causing splatter on the material in this area.

The authors believe the recovered portions of RCC Panels 6 through 10 are reasonably consistent with the demise history of the panels that will apply to "critical data/event" #10. Moving circumferentially around the wing leading edge in an x-y plane, the most severe convective heating occurred in the vicinity of the stagnation line in the shock/shock-interaction region, which is most severe for RCC Panel 9 $\pm$ one panel. See Figure 9. The burn through started at the stagnation line and proceeded to eat away the RCC shell in either direction. Thus, it is not surprising that the lower surface has not been found for any of these RCC panels. The hot gases flowing through the chunnel from the original ET foam-induced breech to the thermal protection system (TPS), which occurred in the vicinity of RCC Panel 6 +/-1 panel, ate away at numerous metal surfaces, depositing the residue as slag on the surviving inner surfaces of the leading edge TPS elements.

It would be reasonable to expect that, if any portion of an RCC panel were recovered, it would be upper portion of the panel. The lower portion (which is the windward portion and, therefore subjected to the greatest convective heating) of the panel may be destroyed during the expanding destruction of the reinforced carbon/carbon shell. Referring to Table 2 and Figure 20(c), the upper portions of RCC Panels 7 and 8 on the left wing have been recovered. Only the edges of the upper portion of RCC Panel 9 have been recovered. As of the date of this writing, the lower portions of these three RCC panels have not been found.

Some Observations at this Point (B)

Referring to the timeline record presented in Table 1 for the flight STS-107 of OV-102, the first debris was seen leaving the Orbiter at GMT 13:53:44. Hot gases have been entering through a breech, or breeches, that occurred in the vicinity of RCC Panels 6 though 10. Sensor measurements on the spar behind RCC Panel 9 indicate anomalies starting at approximately GMT 13:48:39, which is 270 seconds after EI. Temperatures sensed at various points in the LMG brake line exhibit anomalous behavior, starting at GMT 13:52:17 (or slightly later). Thus, the anomalous temperature measurements from the main left-landing-gear wheel well started approximately 488 seconds after EI.

Note that "critical data/events" # 3 and #5 through #9 take place over several minutes in time, affecting first sensors at the spar behind RCC Panel 9, which is relatively close to the wing leading edge, and then, approximately three minutes later, affecting brake line temperatures in the LMG wheel well. This pattern is consistent with a damage model that starts with a foam-impact-induced breech near RCC Panel 6 ± one panel. Hot gases flowing through the chunnel not only block the path for relieving the relatively high heating rates to the external surface of the RCC panels in the vicinity of the shock/shock interaction, but cause these critical panels to be heated from both sides. Because the shock/shock interaction to the baseline configuration produces relatively high heating rates centered in the vicinity of RCC Panel 9 (refer to Figure 9), the internal flow next creates catastrophic damage to the TPS in this region. Thus, the RCC panels in this region undergo growing damage, providing a second breech to the TPS. As noted earlier, at this point in time during reentry, there has been a significant change to the Orbiter Mold Line (OML).

Note that it is the authors' opinion that the limited data available to the authors at this time does not rule out the possibility that the initial foam-impact-induced breech might have affected an RCC panel downstream of RCC Panel 6. However, the Kirtland photograph, which will be discussed in the next section, indicates to us that there are two gaps in the wing leading edge. Regardless of where the initial breech of the wing leading edge occurred, the locally high pressures due to the shock/shock interaction that exist for the baseline Orbiter configuration are greatest on the surface of RCC Panel 9 +/- one panel. These pressures drive the hot gases into the wing volume, contributing to the heating to those gages on the spar behind RCC Panel 9. Then, within a few minutes, the gases break through the spar and the LMG wheel-well wall. Damage to the Orbiter is growing rapidly. The first five debris events (refer to Table 3) occurred in the time GMT 13:53:44 to 13:54:11. The demise of one or more RCC panels changes the Orbiter Mold Line (OML) geometry of the wing leading edge. Instead of encountering a rounded leading edge with gradually changing wing-leading-edge sweep angles, the

oncoming flow sees cavities or notches in the wing leading edge, flat faces of (what is left of) the spars, metal surfaces of high catalycity, etc. See Figure 22. Locally strong shock waves that are imbedded in the viscous/inviscid interaction change the nature of the interaction to one more like that of Figure 8(b). A significant increase occurs to the perturbations in heating to the erose leading edge formed by the damage to/loss of those RCC panels in the "transition zone", e. g., RCC Panels 6 through 9. All of this, occurs with the Orbiter flying at velocities in excess of 22,000 feet/second (Mach 22.5) and at an altitude of 227,000 feet where the flow is a continuum and the aerothermodynamic environment is severe.

The scenario now becomes one in which the damage accelerates dramatically.

(10) The modifications to the shock/shock interaction flow field of "critical data/event" #4, as developed based on the developing damage scenario and correlated against the Kirtland photograph, i. e., observations by personnel from the Starfire Optical Range (at EI + 830.5/832.5).

As noted in the previous paragraphs, debris events 1 through 5 take place from GMT 13:53:44 to GMT 54:11. See Tables 1 and 3. A number of tiles and/or pieces of individual RCC panels along the leading edge have been ablated, or lost. See Figures 20(a) through 20(c) and the "The Content of Left RCC Panels" in Table 2. Consistent with our premise, let us assume that there are at two gaps due to "missing" RCC panels from the wing leading edge. Missing is in quotes because parts of the panels are probably still in place. Furthermore, each notch may represent one or more RCC panels. Recall from the previous discussion that the initial, critical, foam-impingement-induced damage possibly affected RCC Panel 6 ± one panel. The early and rapid responses of the three sensors near the spar behind RCC Panel 9 led to the postulation that hot gases were flowing through the chunnel. The significant amount of metallic deposits on left-wing materials presented in Figure 21 further supports the contention that damage to RCC Panel 6 was the initial breech. Downstream, leading edge RCC panels were being heated from both sides, with disastrous effects. The most disastrous were to the RCC panels located where the shock/shock interaction heating was the greatest, RCC Panel 9. Thus, based on the previous discussion, we will assume that the two notches are centered on RCC Panel 6 and on RCC Panel 9. Refer to Figure 22.

As shown in the sketch of Figure 23, the loss of these segments along the wing leading edge present the oncoming flow with notches that contained flat faces, forward-facing corners, etc., instead of the gradually changing sweep angle and the rounded nose of the undamaged wing leading edge of the Orbiter. Locally strong shock waves, i. e., shock waves that are perpendicular to the oncoming flow, occur for each notch. A portion of each shock wave is normal to the oncoming flow, but only for a short distance. The notch-induced shock waves quickly curve away as the flow follows the RCC surface downstream of the corner. Thus, the shock shape has a "bubble-like" appearance in the plane of the paper.

The shock-layer structure postulated for each notch in the sketch of Figure 23 is similar to that obtained during the Mach 6 wind-tunnel tests that were conducted at the Langley Research Center. See Figure 24. Consider the curved shock wave associated with the notch created by the removal of RCC Panel 9 from the wind-tunnel model. The trace of the shock wave nearest the wing root, i. e., the trace that extends into the notch produced by the missing RCC Panel 9 is normal to the oncoming flow. Thus, the flow

immediately downstream of the normal shock wave is subsonic. As the shock wave curves, it becomes weaker and the flow immediately downstream of the shock wave is supersonic. Because the shock wave is curved, there is considerable vorticity in the shock layer flow approaching the wing leading edge. The curved shock wave associated with the notch of RCC Panel 6 would exhibit similar features. Furthermore, when these two curved shock waves intersect for this high angle-of-attack configuration, they create an extremely complex flow field.

Consider next the flow of the air in the shock layer just ahead of the wing leading edge. The density of the air in the shock layer will be greatest in the shock-layer flow downstream of the normal portions of the shock wave. The large density gradients that occur in the shock layer flow would cause light rays from a distant source on the far side of the vehicle to be bent as they pass through the shock layer. Light rays would bend due to the large second derivatives in the density of the air in the shock layer, producing dark areas in a photograph of the flow. This phenomenon is similar to the shadowgraph technique, which is used to visualize the shock-wave structure in a wind-tunnel flow. The stand-off distance from the shock wave to the vehicle surface is relatively small for these hypersonic flows. Thus, the shock layer flow in the shadowgraph may appear as a dark region in the plane of the photograph. The reader should note that this is a two-dimensional trace of a three-dimensional phenomenon.

A photograph of the Orbiter in flight was taken by personnel at the Starfire Optical Range is presented in Figure 25. This is called the Kirtland photograph. It was taken at EI + 830.5/832.5, which is just less than two minutes before the loss of signal. Note the similarity between the notch-induced shock-wave structure that the authors postulate for the flow near the wing root (refer to Figure 23) and the darkened area in the Kirtland photograph (refer to Figure 25), which contains two bubbles in the darkened area near the intersection of the wing with the fuselage. Many investigators have tried to define the place of the Orbiter within the darkened area. Two examples of these attempts are presented in Figures 26 and 27. Although the present authors do not necessarily agree with the phenomenological models proposed for these two figures, they do support our belief that damage to the wing-leading edge in the form of missing RCC panels produces a multiply-curved shock structure. The existence of two notches along the wing leading edge produces a shock-layer structure, which is consistent with the present authors' interpretation of the Kirtland photograph.

Assume that the breech of the wing leading edge through the loss of "two" RCC panels occurred near GMT 13:54:00, i. e., the time of debris events one through five. "Two" is in quotes, because the possibility exists that portions of adjacent RCC panels may also be missing during this time frame. Why does the darkened region in the Kirtland photograph, which was taken at GMT 13:57:59.5, which was approximately 240 seconds later, still correlate with the authors' model of the notch-induced perturbed flow? The authors believe that, while there is a considerable mass of hot gases flowing through the wing box, there is a considerable thermal mass available to absorb the energy in these hot gases. Thus, it takes awhile for the damage to the structures in the internal wing volume to reach the critical limit, where the left wing will break off. This occurs somewhere between the time of the Kirtland photograph (EI + 830.5/832.5) and the LOS (EI + 923).

(11) Comparing selected histories showing that the actual flight was close to the planned flight up to EI + 900.

Beginning at EI + 270 and continuing through EI + 923, which corresponded to LOS, the damage to OV-102 grows continuously. Breeches along the wing leading edge allow hot gases to flow through large portions of the internal wing volume, destroying structures in its path. Venting gases and the changes to the OML modify the vortical flow over the leeward surfaces of the Orbiter. Nevertheless, the "actual, or as flown trajectory" was very close to the "planned trajectory". Referring to Figure 28, the velocity history for the actual trajectory follows closely that for the planned trajectory through EI + 923. A similar comparison for the altitude history would produce the same degree of agreement.

It is noted in Appendix A that angle-of-attack modulation becomes active at EI + 562. "Entry Guidance enables limited delta angle of attack commands from the reference angle of attack to promote improved convergence to the reference drag profile". Referring to Figure 29, the reader can see that the "actual, or as-flown" angle-of-attack history follows "reasonably well" the "planned" angle-of-attack history until after EI + 900. The actual angle-of-attack was usually within one degree of the planned flight angle-of-attack.

Thus, despite the growing damage, many of the flight performance parameters remain close to nominal up to this time. At some time after (approximately) EI + 860, with the Orbiter over Texas, a substantial portion of the left wing probably broke away. From then on, there were a plethora of indicators of trouble.

(12) Using the rolling-moment-coefficient history to support findings for some of the previous eleven points.

The delta rolling moment history is presented in Figure 30. The strong oscillatory variations of the delta rolling moments that occur before GMT 13:50:00 were attributed to experimental uncertainty from the outset, as noted by Labbe et al. [Ref. 3]. From GMT 13:50:00 through GMT 13:53:00, the delta rolling moment was relatively constant and negative. The magnitude is within the experimental uncertainty. Furthermore, additional review of these data indicated that there had been flight-to-flight variations of similar magnitude from previous flights. Winds were offered as another factor that could have affected the data in this time frame. Because of these three factors, the authors have assumed that none of the delta rolling moment data for times before GMT 13:53:00 are definitive.

From GMT 13:53:00 to GMT 13:54:00, the delta rolling moments are negative (left-wing down) and becoming more negative with time. See Figure 30. In the same time frame are the first five debris events. Recall that, for the flow field that was computed for the Orbiter with RCC Panel 6 missing, there were negative rolling moments of small magnitude. See Figure 12.

Research activities have been conducted by personnel at the Langley Research Center (NASA) to determine the flow field of the Shuttle Orbiter at an angle-of-attack of 40°. Notches in the wing leading edge simulated missing RCC panels. The Mach 24.2 flow field was computed assuming that the Orbiter was missing RCC Panel 9 and that the air was in thermochemical equilibrium. Surface pressures for this computed flow

field are presented in the lower right-hand figure of Figure 31. Streamwise streaks of high pressure are associated with the vortices from the shock interactions and from the flow around the notches. The effect of the vortices are also exhibited in the streamwise streaks of high heating that bound the large area of lower left wing surface where the notch has perturbed the heating. See the lower left-hand figure of Figure 31.

High pressures act at the notch left by the loss of RCC Panel 9. The probable loss of a good portion of the spar behind that RCC panel provides a path for the hot gases to create devastation to the structures in large areas of the internal wing volume. Although temperature measurements in the LMG wheel well have been indicating problems for over two minutes, the damage to the wing front spar and internal struts is increasing. The timeline presented in Table 1 indicates that, during the same time frame that first five debris events occur. It is likely the upper interior wing honeycomb surface is being heated above the RTV (tile bonding adhesive) failure limit and the tiles are coming off. It is also possible a larger section of the honeycomb aluminum burns or comes lose which could correspond to the flash (burning of the vaporized aluminum) observed in this time period.

As the internal wing structure (spar and struts) melts, the dynamic pressure on the lower wing surface would likely cause some wing flexure, bending up or dimpling of the lower wing. Loss of the internal wing structure would put added loading on the remaining RCC panels causing them to break, consistent with observed panel tops cracked at the apex. A bent spanner beam was also found. These phenomena also contribute to the explanation of the increasingly positive rolling moment observed.

CONCLUDING REMARKS

This document develops a plausible scenario for the demise of the Shuttle Columbia based on what the authors judge to be 12 critical pieces of data. While there is lot still unknown and much we'll never know, the authors believe there is sufficient collaborating evidence to support the following conclusions:

1. At 82 seconds into the launch, the ET-foam debris strikes the wing, damaging the leading edge. For reasons discussed in the main body of the report, the authors believe the initial breech was in the vicinity of RCC Panel 6 ± one panel. This also would mean the breech was present at start of reentry.

2. Hot gases entering a breech near RCC Panel 6 have several negative effects. First, hot gases flow down the chunnel, causing the MADS sensors near spar 9 to have anomalous responses early in the entry. The slag and other melting metallic components are splattered onto the surfaces behind RCC Panels 7 through 10. See Figure 21. Second, the incoming plume impinges on the spar, eventually burning a hole. Third, the hot gases in the chunnel reduced the heat rejection capability of the RCC panels downstream (outboard) of RCC Panel 6. Since these RCC panels are in the region where the baseline shock/shock interaction pattern is most severe, a second breech in the TPS occurs near RCC Panel 9 ± one panel. Soon other RCC panels in the vicinity experience significant ablation. See Figure 20(c).

3. The hole through the spar has some defining characteristics. It has to burn all 4 MADS wire bundles on the back of the spar (making it about 18 inches high), yet focus enough heat on the OI (telemetry) wire bundles several feet away on the top of the wheel well to burn them quickly. A missing T-seal (or a portion thereof) near RCC Panel 6 ± one panel would allow a concentrated slit of hot gases to cut the wire bundles, without depositing heat to a large internal volume in the wheel well. Since the temperature sensors in the wheel well all increase together, but at a very slow rate (about 8 degrees per minute), the plume can't be impinging directly on these temperature sensors. Within a few minutes, the slit jet will change to a "circular" hole as the downstream rib burns through. The change in the geometry of the breech causes more of the hot gases to flow down the chunnel.

4. Damaged panels near RCC Panels 6 and 9 would explain the OMS-Pod heating transients because of the perturbation to the flow over the wing. This behavior is consistent with studies being conducted at the Langley Research Center (LaRC). Notches at two locations along the wing leading edge appear as a double hump in the leading edge flow field that is captured in the Kirtland photograph, which was taken when the Orbiter was visible to the Starfire Optical Range,

5. The debris damage shows a lot of unique damage in the region of RCC Panels 8 and 9. This is consistent with a secondary burn through in this max-heat area after hot gases get in the chunnel. The fact that much of the bottom panels in region 6 to 10 are missing would be consistent with burn through on the bottom high heat area. Probably first occurring at the shock-shock interaction centered on RCC Panel 9, but eventually affecting RCC Panels from 6 to 10. The tire in

the left wheel well shows unique burning, as does one of the main gear up-lock parts. This would be consistent with a jet originating behind RCC Panel 6 and burning through the wheel well near the tire. The tire would protect the temperature sensors in the wheel well from being directly hit and, as a good insulator, help diffuse the heat for a while giving in a more uniform heat up rate in the wheel well.

6. The small initial decrease in rolling moment is consistent with LaRC wind tunnel test with "missing" RCC panels. The hot gases will penetrate into the wing front spar region and the wing internal structure. As this wing support structure is destroyed the lower wing surface will begin to flex upward under the increasing dynamic pressure load as the atmospheric density increases. The changing shape could explain the continuing increase in roll moment up until the loss of signal at about EI + 923.

While there is much that will never be known about the demise the authors judge the scenario developed in this paper is reasonable and may best correlate with the available aero, thermal, debris, and timeline. At the time of this report, NASA has not yet completed an integrated Aerothermal-structural analysis starting with a breech in the vicinity of RCC Panel 6.

REFERENCES

[1] J. J. Bertin, Hypersonic Aerothermodynamics, AIAA Education Series, Washington, D. C., 1994.

[2] R. D. Neumann, "Defining the Aerothermodynamic Methodology", J. J. Bertin, R. Glowinski, and J. Periaux (eds.), Hypersonics, Volume I: Defining the Hypersonic Environment, Birkhaeuser Boston, Boston, 1989.

[3] S. Labbe, J. Caram, and C. Madden, "CAIB Public Hearing", Tuesday, 18 March 2003.

[4] M. Hasselbeck, "Preliminary Conclusions Based on MADS Data", April 2003.

To link to the figures and appendices please click on the following hyperlinks:

To see figures click on 2 Fatal Reentry of STS107 Data and Observations.ppt

To see appendix click on 3 Timeline-STS-107-REV17-BASELINE.xls

Figures for

Using the Data and Observations from Flight STS-107 to Explain the Fatal Reentry of the Columbia Orbiter OV-102

Relationship of reentry Parameters

Order of Magnitude Estimates Only!

Values from NASA briefs and text books
Prep. By Jim Smiley X7545

Rev 5
4/30/03

GMT	Time from EI min	Altitude Feet	Air Density slugs/ft3	Atmos Press #/sqft	Dynam Press #/sq ft	Equiv Sea L speed Mile/hr	Heat Rate analys Btu ft2sec	LE Temp analys deg-F	Mach	Vel ft/sec	Location	Key Entry Events Rev 14	Debris Events	Number Dens Mole/ft3 Later	Altitude Miles	Km	Mean free path Path lambda ft Inf gas reg	Lambda inches Free space	Mean free path lambda Layer Lmda fr/20 Later	no dens Free air	MAX KE 1/2pv*v*v per ft2 Btu/ft2sec	Air Flow lbm/ft2sec	Oxygen Flow rhoxvx.23 lbm/sqft-sec	Max Aluminum Burn rate if hot enou Mils per sqft-sec	Heat of Combustion if hot enough Btu per sqft-sec
13:44:00	0	400000	5.4E-11	~0	0	0	0	0	24.6	23000		13:44:09 Entry Interface			76	126	6	72		1.73E+16	0	4.0E-05	9.1E-06		0.00
13:44:15																									
13:44:30	:30						1	100														1.7E-04			
13:44:45																									
13:45:00	1:00						1	200														3.0E-04			
13:45:15																									
13:45:30	1:30						2	350														4.2E-04			
13:45:45																									
13:46:00	2:00	340000	7.5E-10		0	9	3	500		22920					64	107	0.700	8.405		2.42E+17		5.5E-04	1.3E-04	0.01	1.86
13:46:15																									
13:46:30	2:30	327000					7	800		22900					62	103						1.8E-03			
13:46:45																									
13:47:00	3:00	314000					10	1100		22890					59	99						3.0E-03			
13:47:15																									
13:47:30	3:30	301000					15	1300		22880					57	95						4.2E-03			
13:47:45																									
13:48:00	4:00	288000	7.4E-09	~0	2	28	22	1500	24.7	22850					55	91	0.071	0.853		2.38E+18	57	5.4E-03	1.3E-03	0.10	18.26
13:48:15																									
13:48:30	4:30	274000	1.4E-08	0.01	4	38	30	1750		23050					52	86	0.038	0.461		4.42E+18	108	1.0E-02	2.3E-03	0.19	34.10
13:48:45																									
13:49:00	5:00	260000	2.5E-08	0.021	7	52	36	2000	24.6	23100		RCC-9 Clevis heating			49	82	0.021	0.249		8.17E+18	202	1.9E-02	4.3E-03	0.35	63.27
13:49:15																									
13:49:30	5:30	256000	3.0E-08	0.030	8	56	42	2200		23050					48	81	0.017	0.209		9.75E+18	239	2.2E-02	5.2E-03	0.41	75.28
13:49:45																									
13:50:00	6:00	251500	3.7E-08	0.040	10	62	46	2400		23000					48	79	0.014	0.171		1.19E+19	290	2.7E-02	6.3E-03	0.50	91.57
13:50:15																									
13:50:30	6:30	247000	7.4E-08	0.051	20	88	52	2550		22950					47	78	0.007	0.085		2.38E+19	576	5.4E-02	1.3E-02	1.01	182.91
13:50:45												Start of peak heating													
13:51:00	7:00	243000	8.8E-08	0.058	23	95	55	2700	24.1	22900		RCC 9 Spar heating			46	77	0.006	0.072		2.82E+19	679	6.4E-02	1.5E-02	1.19	216.39
13:51:15																									
13:51:30	7:30	239000	1.0E-07	0.063	27	103	57	2750		22825					45	75	0.005	0.061		3.34E+19	797	7.6E-02	1.8E-02	1.41	255.73
13:51:45												51:46 Inertial Beta goes neg-stays neg													
13:52:00	8:00	236000	1.3E-07	0.080	33	113	58	2800	23.6	22750	300 w calif	52:05 first off nominal aero signal			45	74	0.004	0.050		4.04E+19	953	9.2E-02	2.1E-02	1.69	307.93
13:52:15												52:17 Brake line temp start to rise													
13:52:30	8:30	234800	1.3E-07	0.085	33	114	60	2800		22600		52:32 Supply H2O temp rise			44	74	0.004	0.049		4.18E+19	967	9.4E-02	2.2E-02	1.74	316.51
13:52:45												52:59 Elevon Lower skin Temp OSL													
13:53:00	9:00	233600	1.4E-07	0.089	36	119	62	2800	23.3	22500		53:01 First clear Off line roll moment			44	74	0.004	0.044		4.57E+19	1044	1.0E-01	2.4E-02	1.89	344.77
13:53:15												53:10 Hyd left OB/ Inbd elev OSL													
13:53:30	9:30	231000	1.5E-07	0.102	38	122	63	2850	23	22400	Calif coast	53:36 Inbd Elevon temp OSL			44	73	0.003	0.042		4.88E+19	1099	1.1E-01	2.5E-02	2.01	366.12
13:53:45												53:44 First debris leaves orbiter	# 1 to												
13:54:00	10:00	229000	1.7E-07	0.112	41	127	64	2900		22250		54:10 LG brake/strut temp up	#5		43	72	0.003	0.038		5.32E+19	1174	1.2E-01	2.7E-02	2.18	396.59
13:54:15												54:20 Slow aileron trim change													
13:54:30	10:30	227000	1.8E-07	0.121	44	132	64	2900	22.5	22100	CA/NV Bord	54:22 Mid fuse bond temp starts up	#6		43	72	0.003	0.035		5.79E+19	1253	1.3E-01	2.9E-02	2.36	428.95
13:54:45												54:33 Bright flash seen in video	Flash 1												
13:55:00	11:00	224800	1.9E-07	0.133	46	134	64	2900		21700			# 7 to		43	71	0.003	0.033		6.23E+19	1276	1.3E-01	3.1E-02	2.49	453.10
13:55:15													#10												
13:55:30	11:30	223500	2.1E-07	0.144	47	135	64	2900		21300	NV/UT Bord		# 11 to		42	71	0.003	0.031		6.61E+19	1281	1.4E-01	3.2E-02	2.59	471.86
13:55:45		222800	2.1E-07	0.150					21.6	21000		55:41 Mid Fus sill T start off N	#15		42	70	0.002	0.030		6.86E+19	1273	1.4E-01	3.3E-02	2.65	482.68
13:56:00	12:00	222000	2.3E-07	0.158	50	140	64	2900		20850		56:03 Wing temp trend down			42	70	0.002	0.027		7.41E+19	1346	1.5E-01	3.5E-02	2.84	517.47
13:56:15												56:16 temp in LMG all up													
13:56:30	12:30	220000	2.4E-07	0.171	51	142	64	2900		20780		56:30 Roll Reversal Initiated			42	69	0.002	0.027		7.60E+19	1367	1.6E-01	3.6E-02	2.91	529.13
13:56:45																									
13:57:00	13:00	218000	2.6E-07	0.186	56	148	64	2900	20.7	20700	AZ/NM bord	56:55 Roll reversal comp			41	69	0.002	0.024		8.36E+19	1486	1.7E-01	4.0E-02	3.19	579.80
13:57:15												57:19 Tire press small rise	#16												
13:57:30	13:30	215500	2.9E-07	0.190	61	155	64	2900		20350		57:28 Wing temp off line			41	68	0.002	0.022		9.42E+19	1592	1.9E-01	4.4E-02	3.53	642.54
13:57:45												57:54 Sys 2 LH Brake vlv temp inc	Flare 1			0									
13:58:00	14:00	213000	3.4E-07	0.233	69	164	63	2900	19.9	20000	NM	58:09 Sign chang e yaw and roll	Flare 2		40	67	0.002	0.018		1.10E+20	1767	2.2E-01	5.1E-02	4.06	738.44
13:58:15																0									
13:58:30	14:30	208000	3.9E-07	0.296	73	169	62	2850	19.3	19400	Littlefield	58:32Tire temp and press OSL			39	66	0.001	0.016		1.24E+20	1818	2.4E-01	5.5E-02	4.44	807.58
13:58:45																0									
13:59:00	15:00	204000	4.5E-07	0.341	81	178	60	2800	18.6	18900	Lubbock	59:06 LMG Down lock indication			39	64	0.001	0.014		1.45E+20	1960	2.7E-01	6.3E-02	5.04	917.09
13:59:15																0									
13:59:30	15:30	200700	4.8E-07	0.381	83	180	59	2800		18600		59:33 Two yaw jets firing			38	63	0.001	0.013		1.54E+20	1985	2.9E-01	6.6E-02	5.27	959.23
13:59:45											Dallas Tx	Growth in Bank attitude error				0									
14:00:00	16:00	200000	5.0E-07	0.400	84	181	58	2800		18300		Loss of all signals			38	63	0.001	0.013		1.60E+20	1969	2.9E-01	6.7E-02	5.40	983.08

CA-000112

2 Fatal Reentry of STS107 Data and Observations.ppt

CAB068-0201

Table 2

Content of Left RCC Panels

	Lower Closeout Panel	Lower RCC Panel	Upper RCC Panel	Upper Closeout Panel
1	X	X	X	X
2	X	X	X	
3	X		X	X
4	X		X	
5			X	X
6	X			X
7	X		X	
8	X Tiles Only		X	
9	X Tiles Only		X Edges Only	
10	X			
11	X			
12				
13		X		X
14		X	X	X
15	X	X	X	X
16	X	X	X	
17			X	
18		X		
19		X		
20				
21		X		
22	X	X		

CA-000112

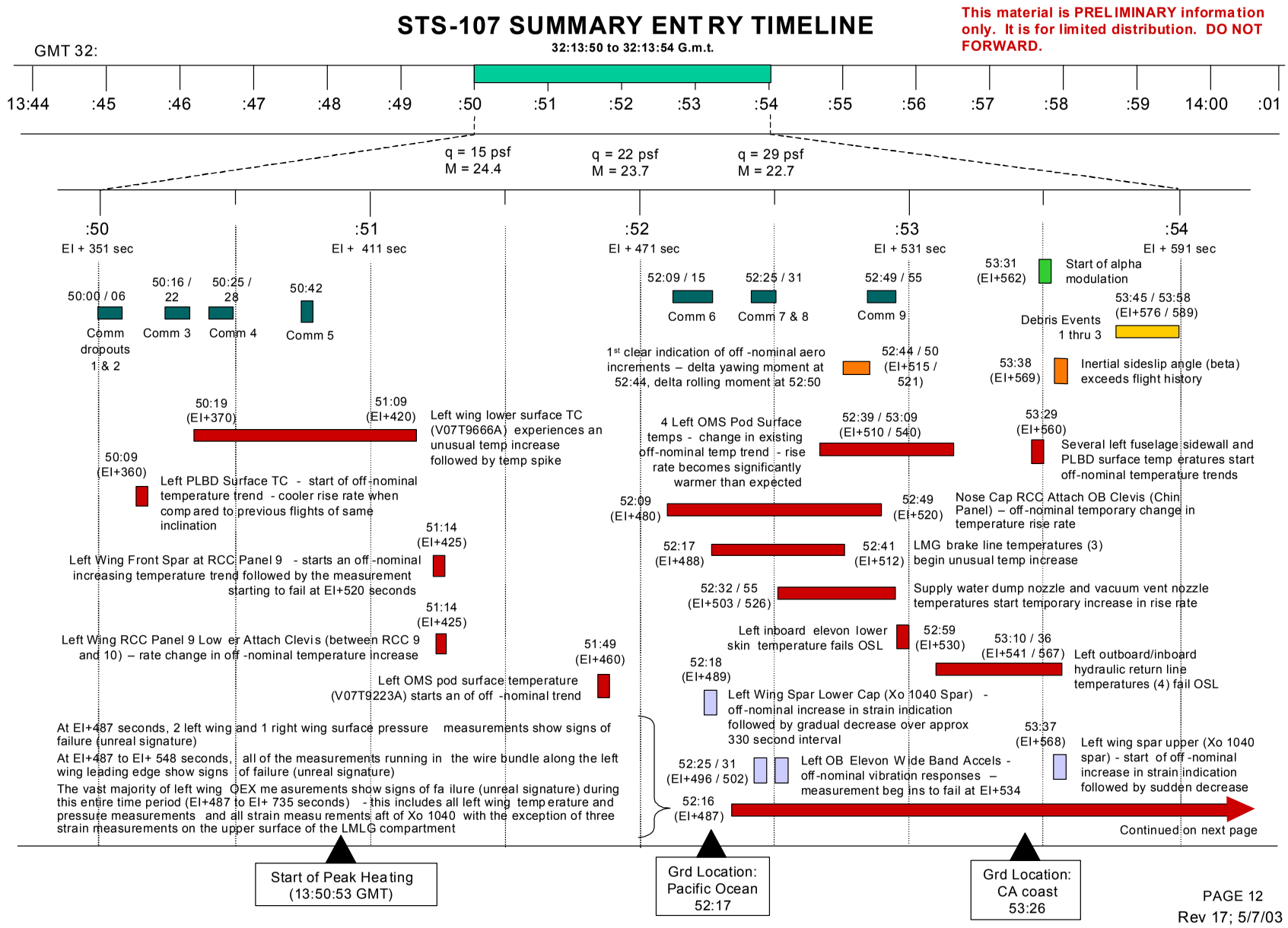

CA-000112

2 Fatal Reentry of STS107 Data and Observations.ppt

CAB068-0203

Figure 1

Ascent Debris Trajectory

- **Solid cylindrical protrusions were created through the debris locations in each view**

ET208 Camera Frame

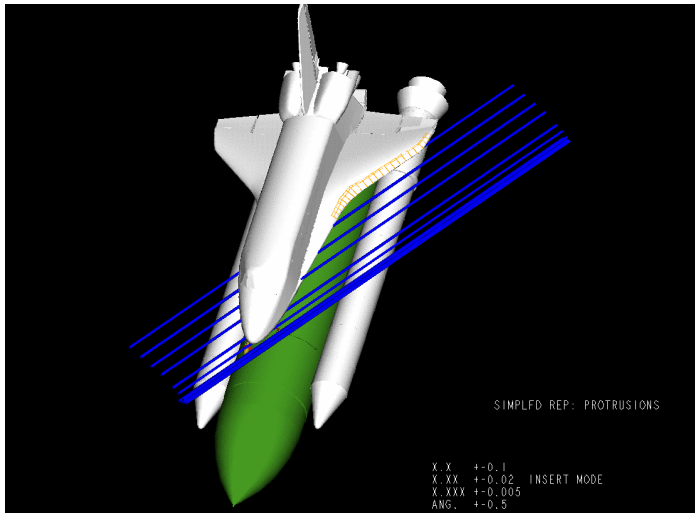

Trimetric View

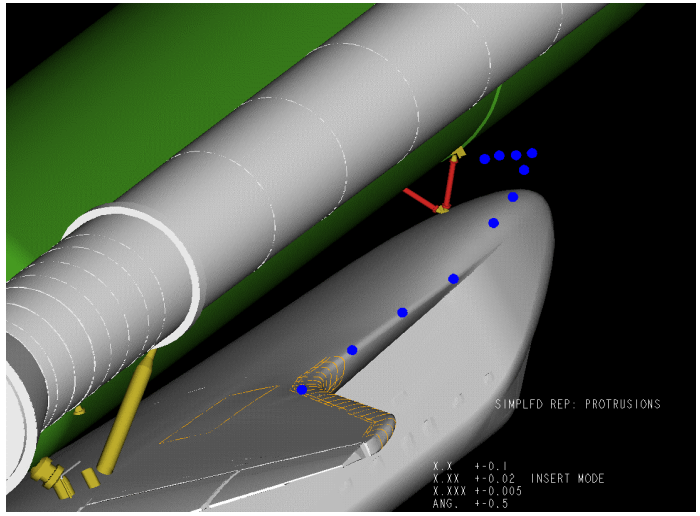

ET208 Camera View

Projection of Debris Trajectory onto Left Wing

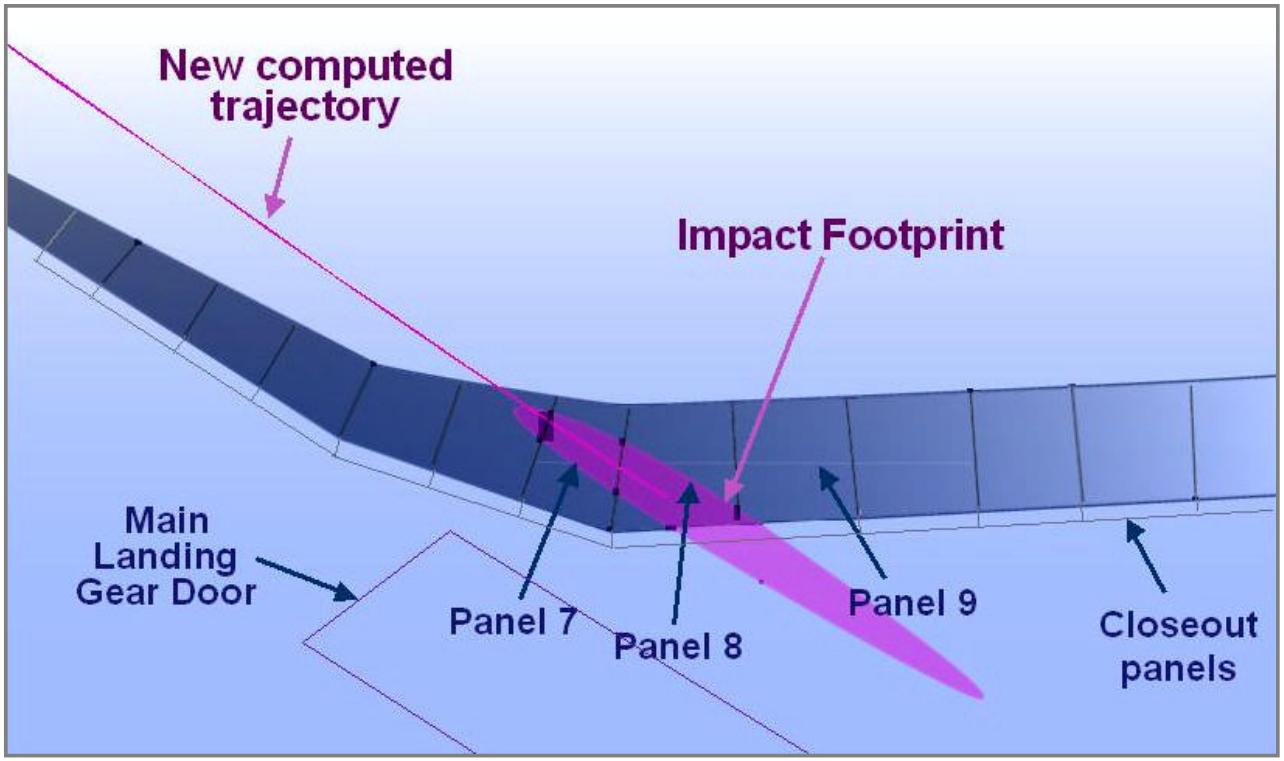

- Centerline of one-foot diameter trajectory "pipe" intersects the wing at approximately RCC panel 8, with the most likely foam impact predicted along panels 7 and 8

Figure 3

Left Wing Orientation

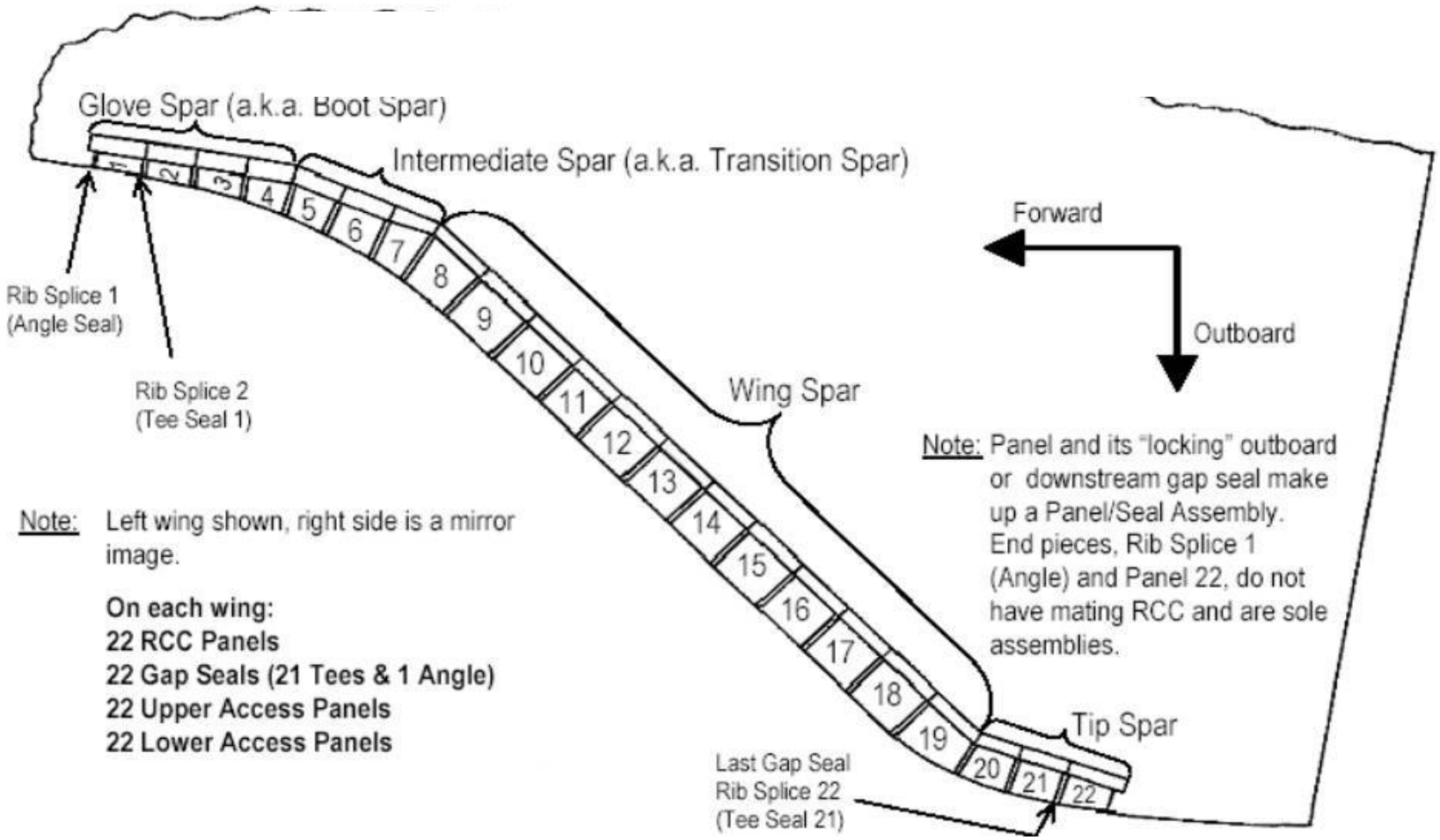

CA-000112

Left Wing Leading Edge

- Wing Leading Edge Subsystem (LESS) comprised of RCC panels, T-Seals, Upper and Lower Thermal Barriers, and associated mounting hardware

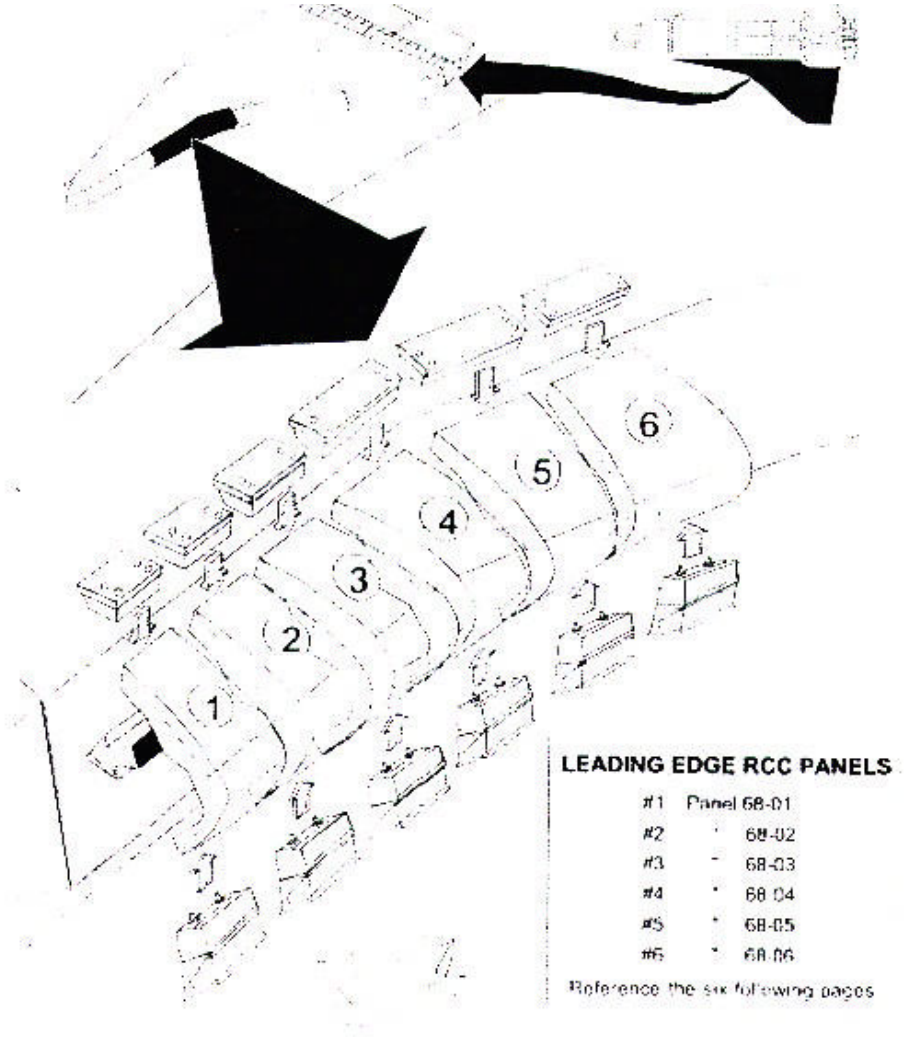

3/14/03

Figure 5

RCC Panel 9 Sensor Locations

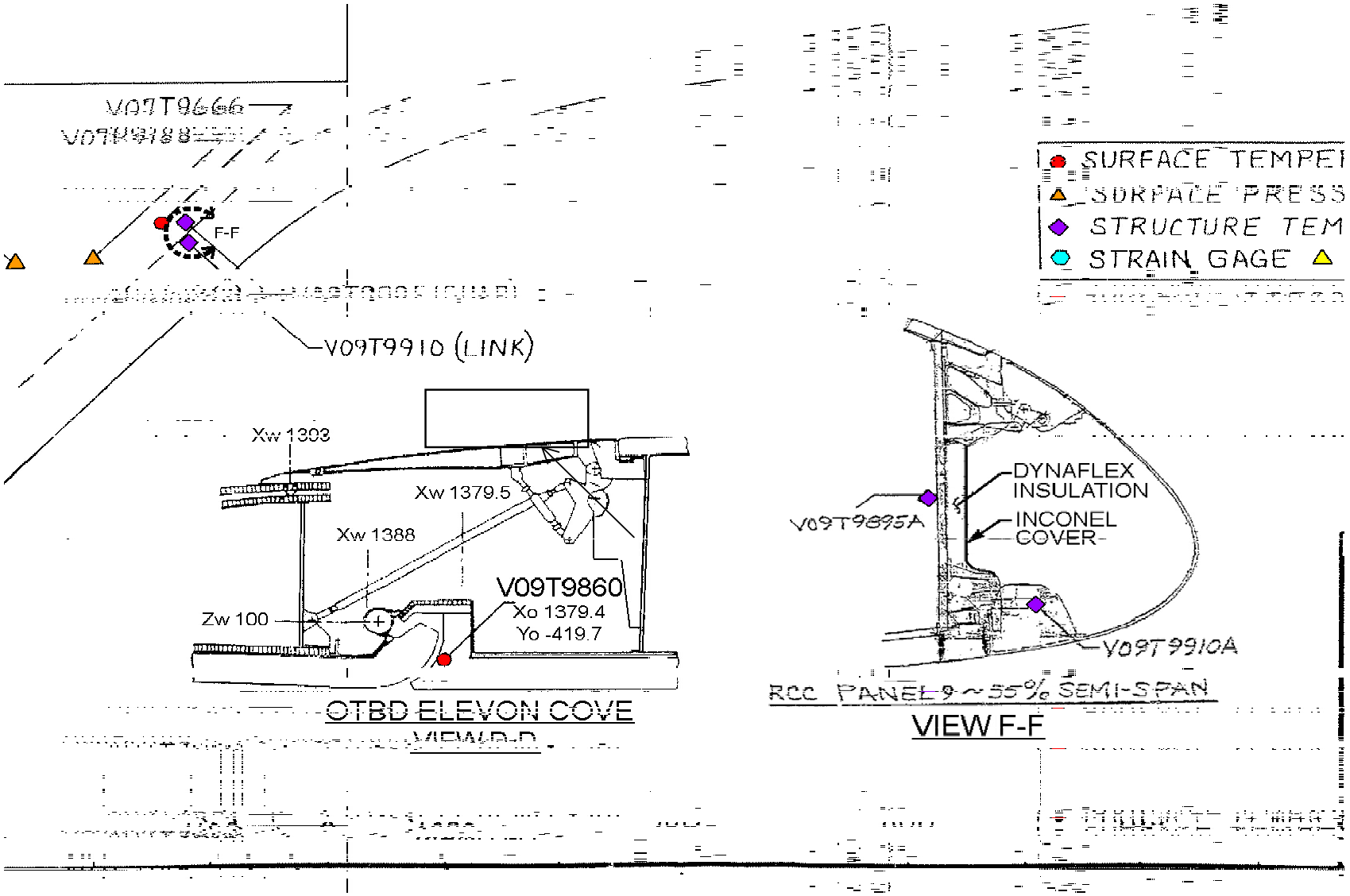

CA-000112

Figure 6

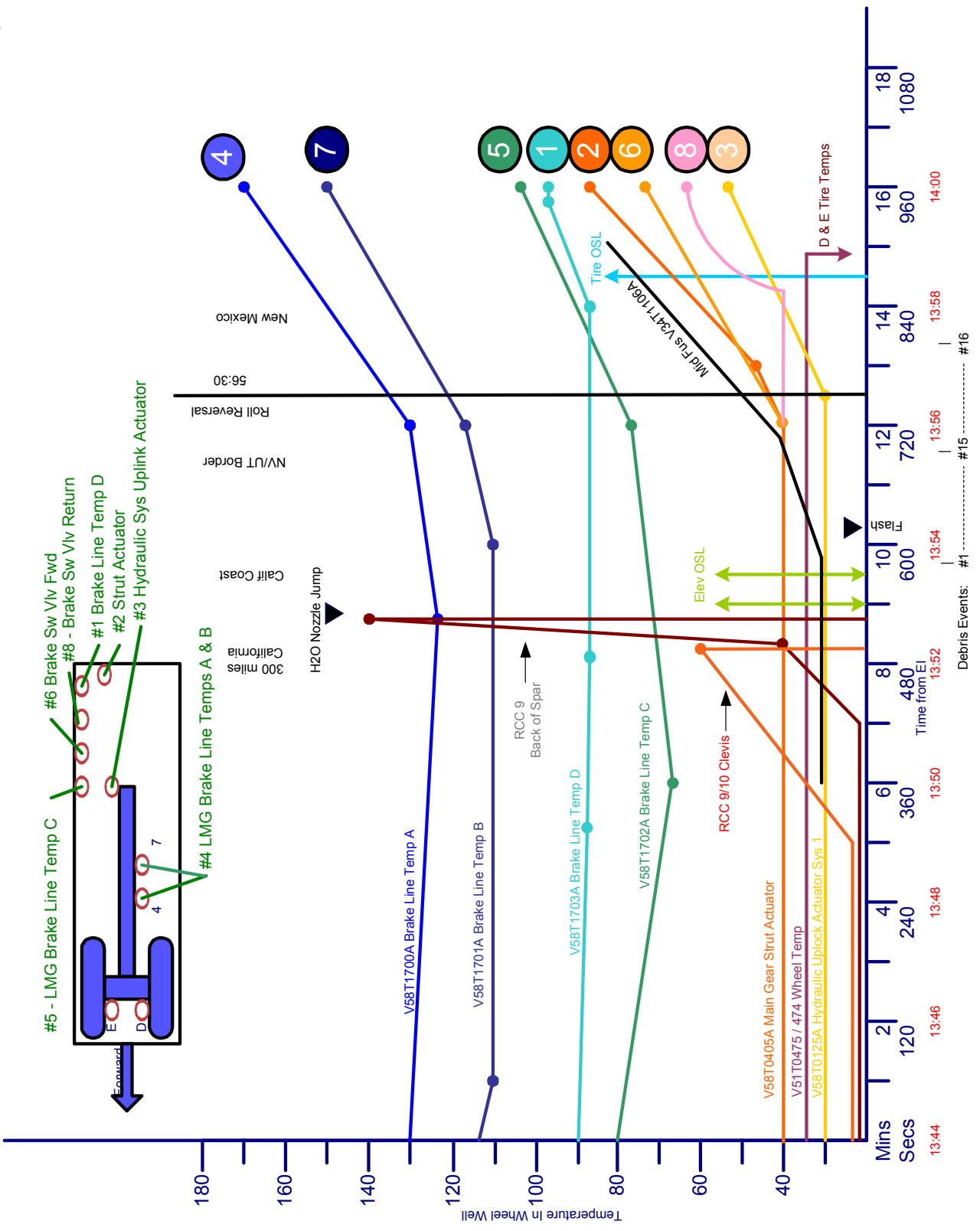

CA-000112

2 Fatal Reentry of STS107 Data and Observations.ppt

CAB068-0209

Figure 7

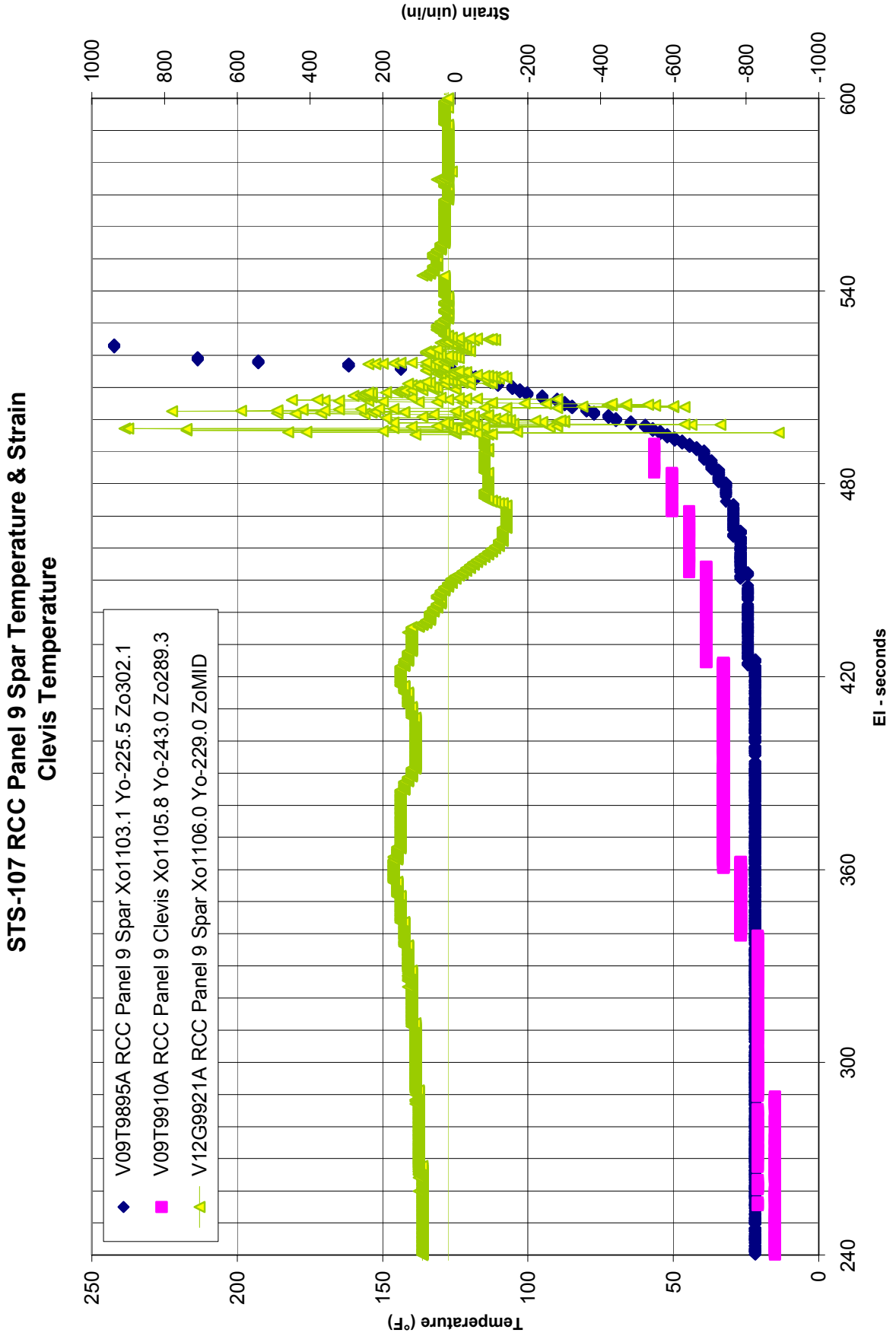

CAB068-0210

CA-000112

2 Fatal Reentry of STS107 Data and Observations.ppt

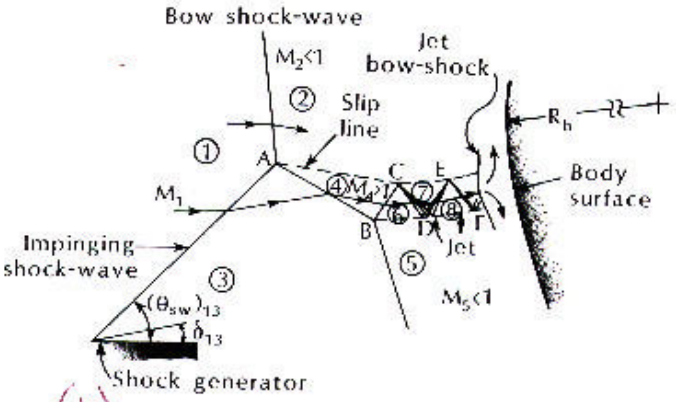

(b)

Fig. 9.14 Type IV shock/shock interaction pattern.

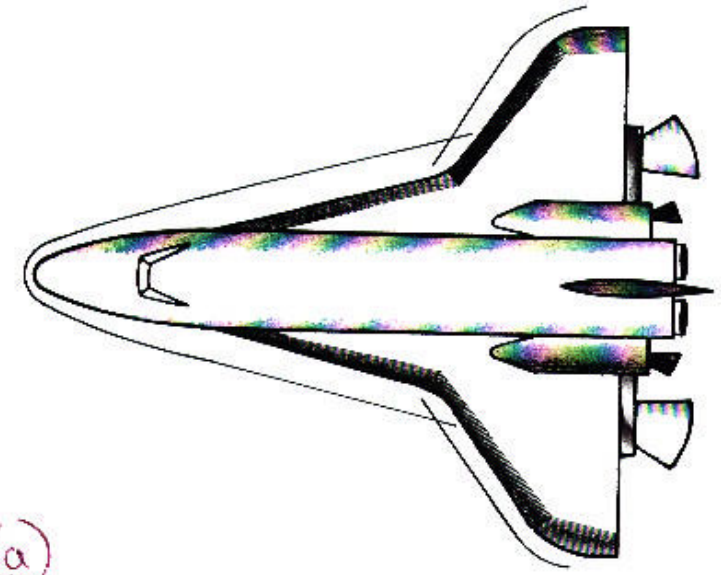

(a)

Fig. 9.3 Interactions between the bow shock wave and the

wing leading edge shock wave

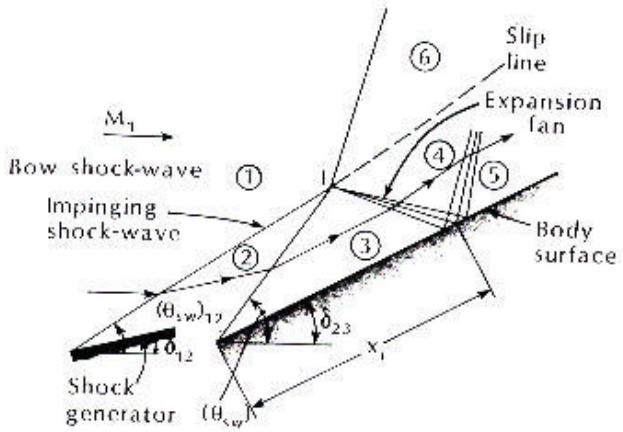

Fig. 9.19 Type VI shock/shock interaction pattern.

(c)

Surface Temperatures Radiation Equilibrium

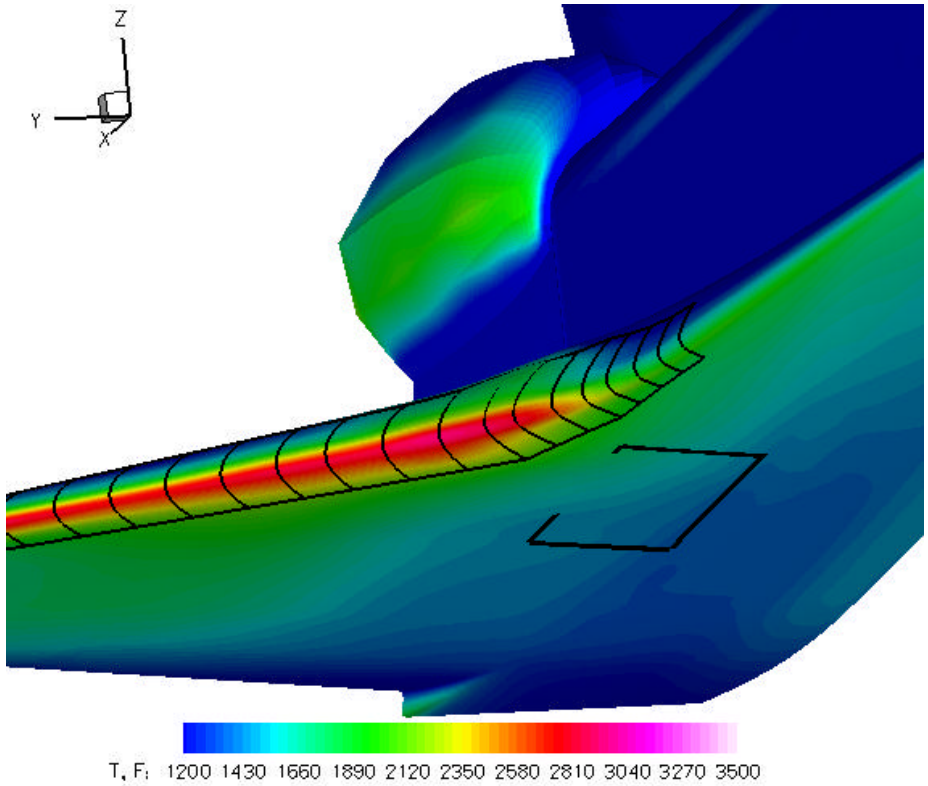

Temperatures, F

CFD Point #1

NASA LaRC LAURA CFD Solution

CFD Point #6

NASA ARC GASP CFD Solution

Temperatures, F

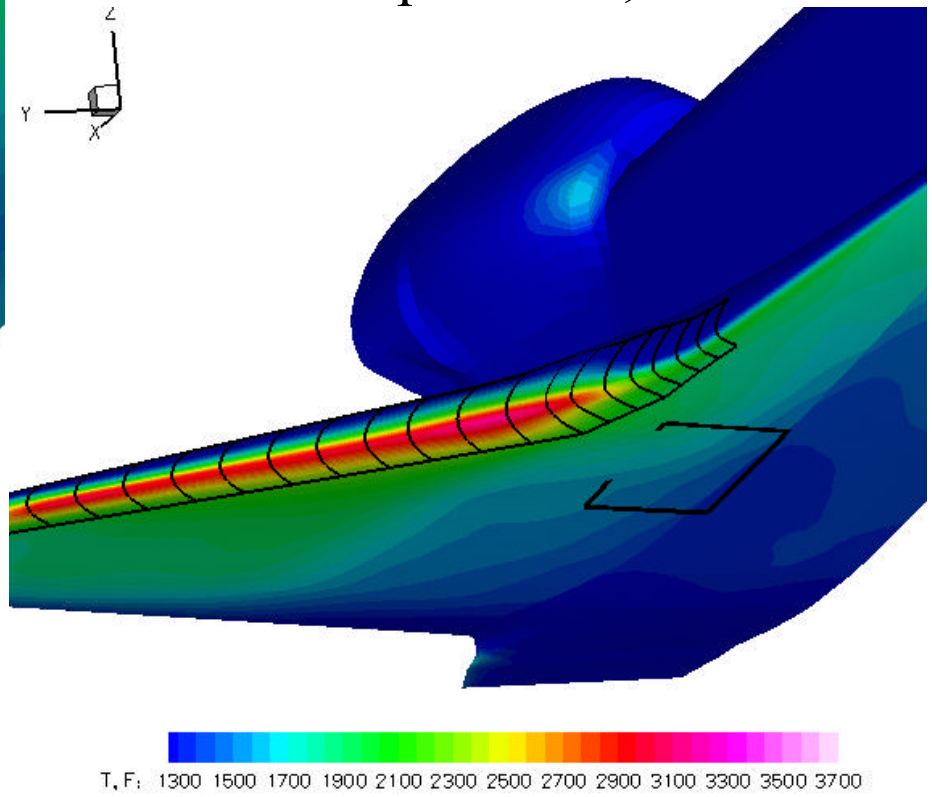

CA-000112

Hot gases enter the chunnel

- Flow behind RCC
- Outward through Chunnel

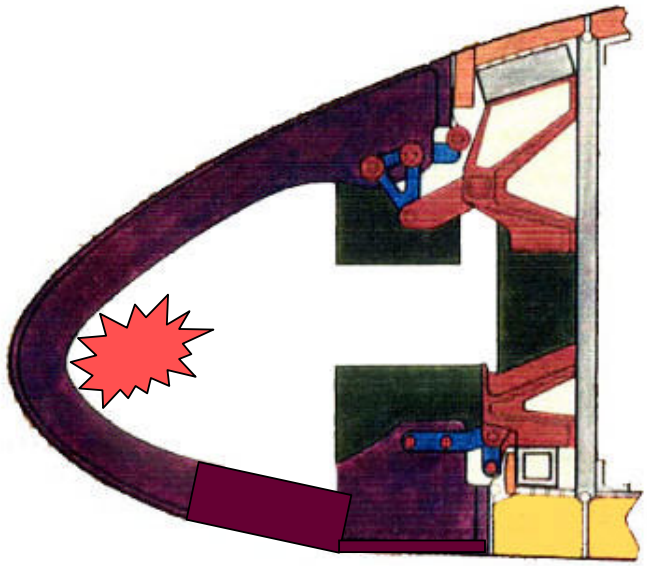

Jet of hot gases coming down the chunnel

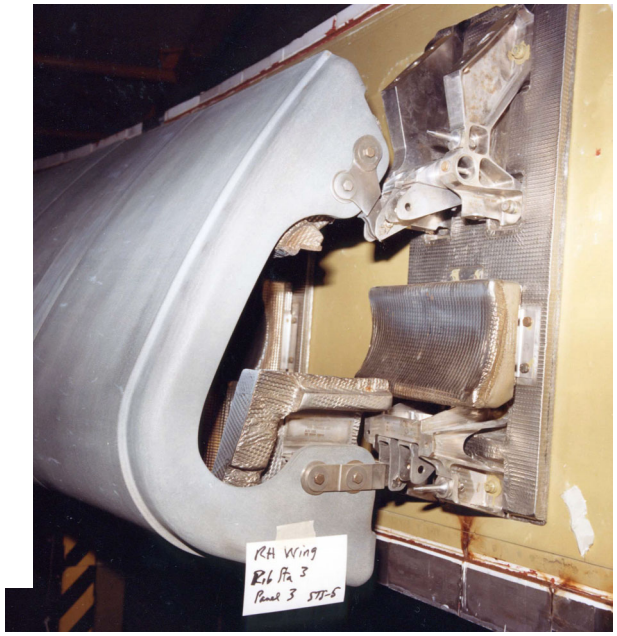

RCC
Aluminum
LI2200
LI900
Inconel-Dynaflex
Inconel 718
A-286 steel

Figure 11

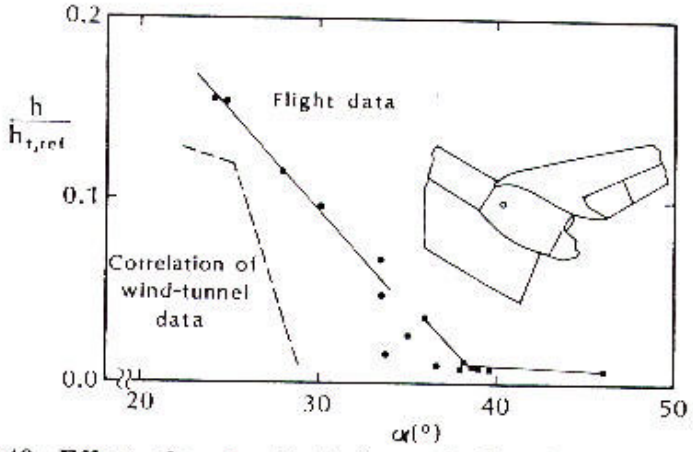

Fig. 9.40 Effect of angle-of-attack on the heating to the OMS pod, as taken from Ref. 38.

Orbiter OML Sensitivity CFD Analysis

Orbiter with RCC Panel 6 Removed – Mach 23.8

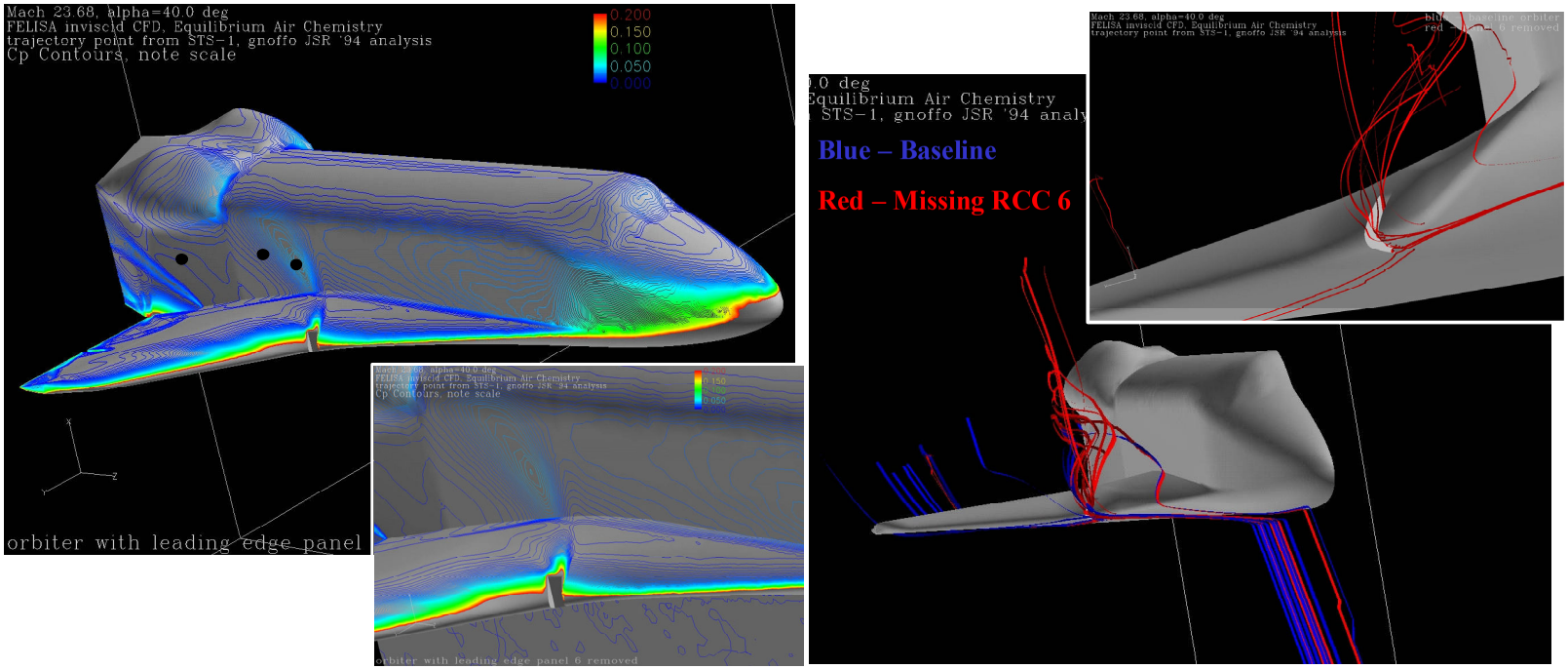

Results and Observations (CFD analysis)

- Produces negative roll and yaw moments w/small magnitude
- Streamlines for damaged vehicle track inboard of baseline
- Resultant shock raises pressure in proximity to temp measurements

17

Rev. 4 – Preliminary
Limited Distribution
DO NOT FORWARD

Limited Distribution
DO NOT FORWARD

Figure 13

VDM Team

Based on Master Time Line (MTL) 13

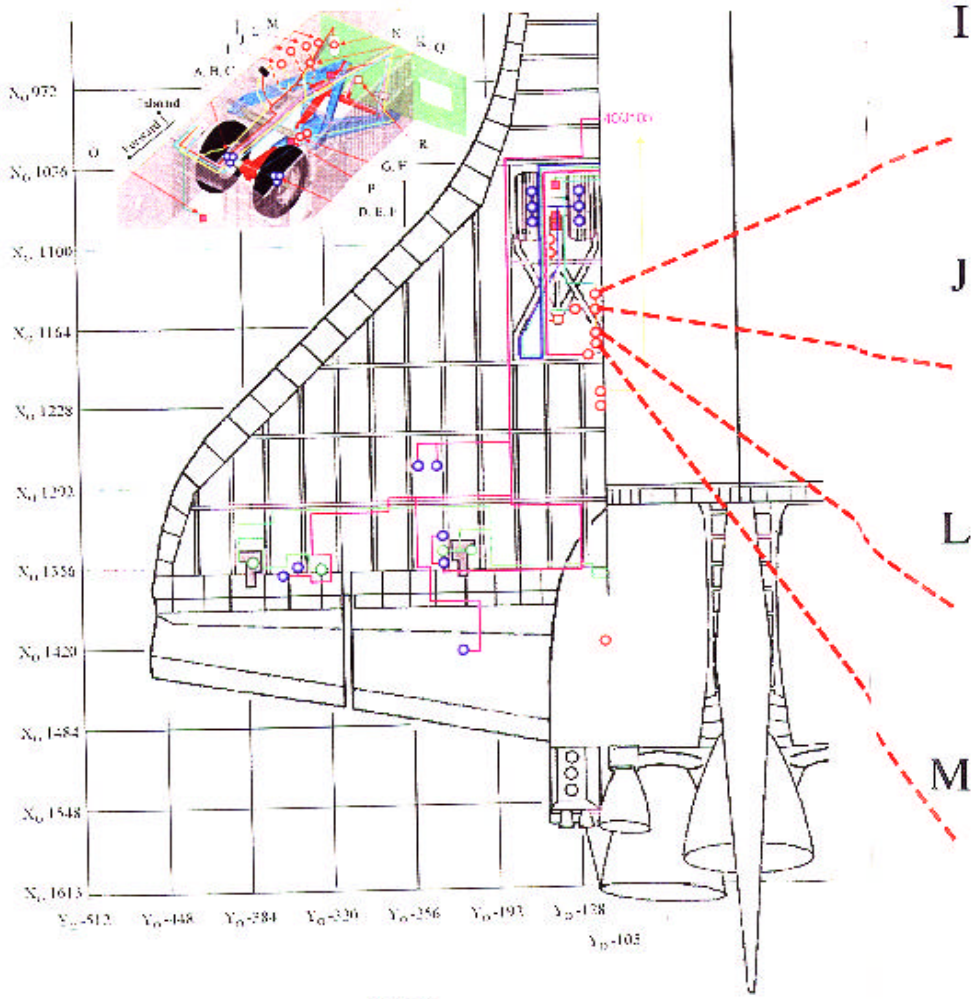

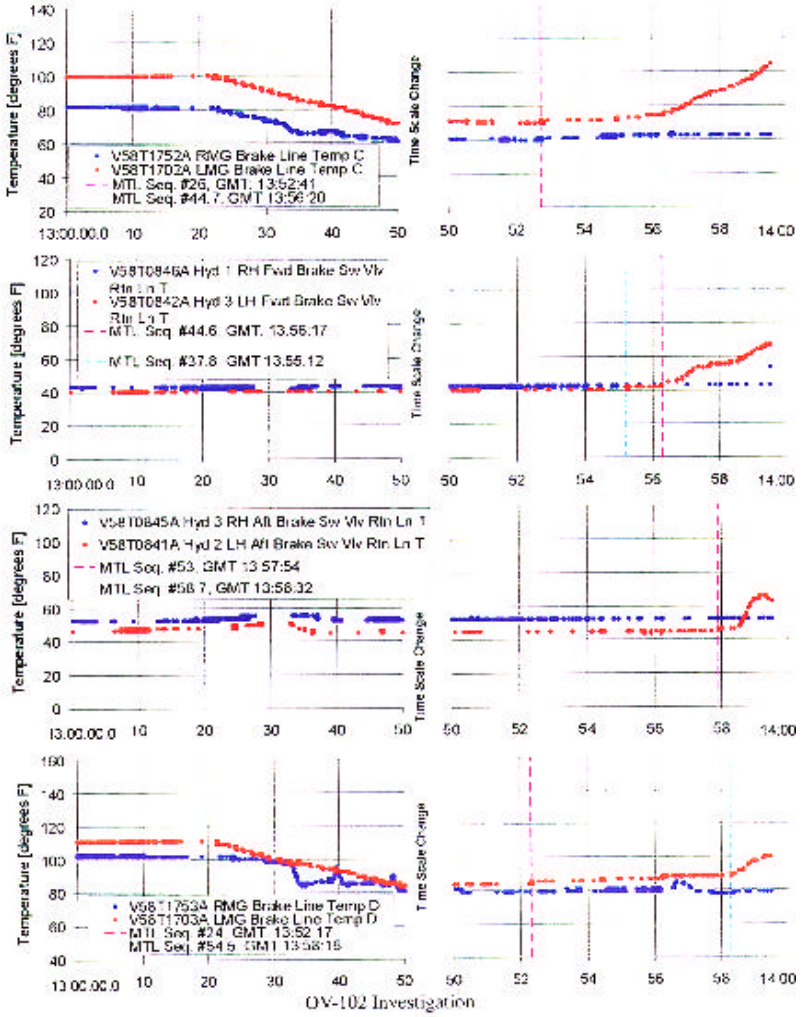

CA-000112

2 Fatal Reentry of STS107 Data and Observations.ppt

CAB068-0216

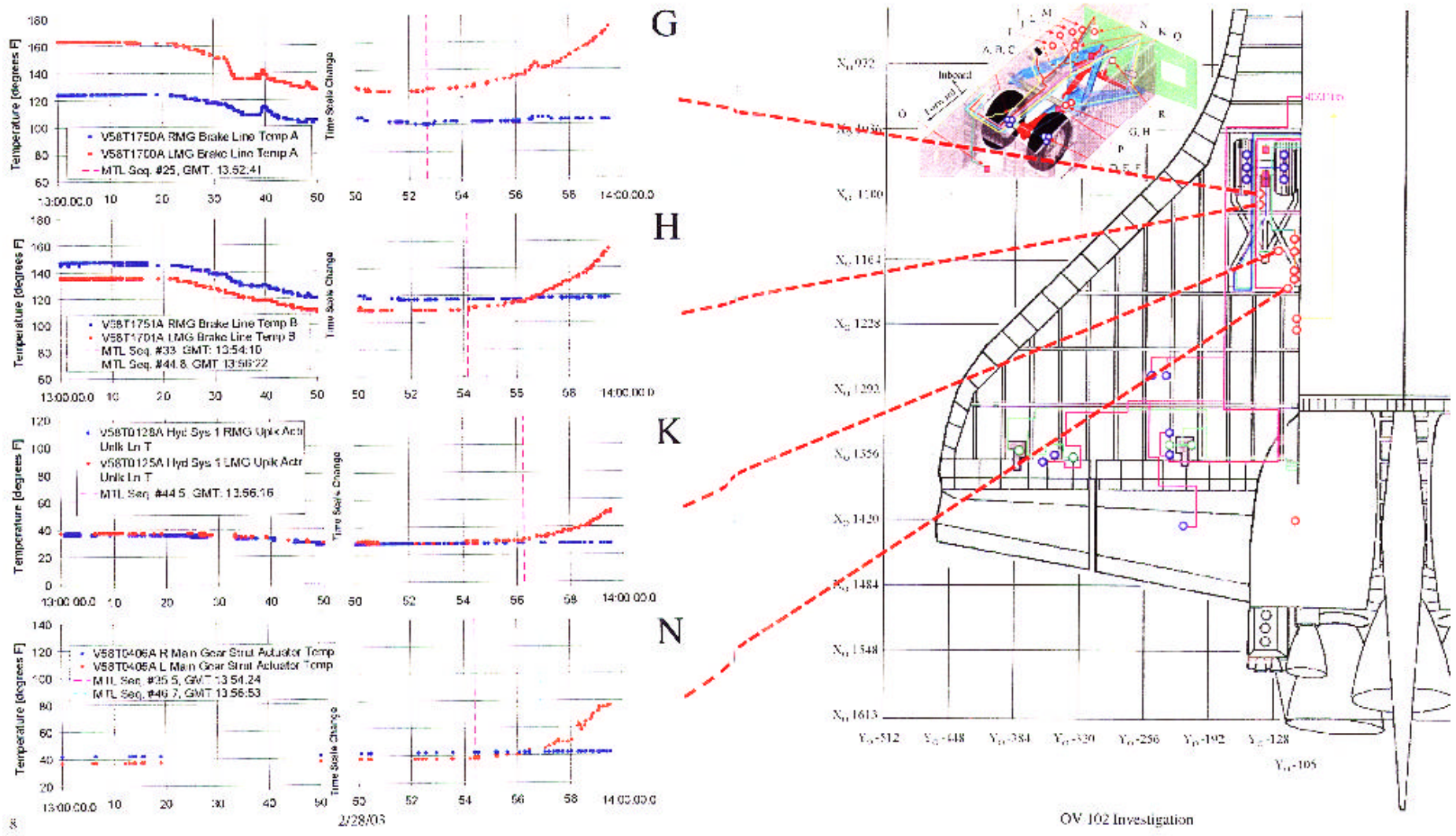
G
H
K
N
Temperature [degrees F]
Time Scale Change
V58T1750A RMG Brake Line Temp A
V58T1700A LMG Brake Line Temp A
MTL Seq. #25, GMT: 13:52:41
V58T1751A RMG Brake Line Temp B
V58T1701A LMG Brake Line Temp B
MTL Seq. #33, GMT: 13:54:10
MTL Seq. #44.8, GMT: 13:56:22
V58T0128A Hyd Sys 1 RMG Upik Actr Unlk Ln T
V58T0125A Hyd Sys 1 LMG Upik Actr Unlk Ln T
MTL Seq. #44.5, GMT: 13:56:16
V58T0406A R Main Gear Strut Actuator Temp
V58T0405A L Main Gear Strut Actuator Temp
MTL Seq. #35.5, GMT: 13:54:24
MTL Seq. #46.7, GMT: 13:56:53
2/28/03
OV-102 Investigation

Figure 15

Wind Tunnel Testing of Orbiter OML Deltas

Effect of RCC Panel Cutout Position on Orbiter Fuselage Nondimensional Heating, Panel 6 vs. Panel 9

Side fuselage heating 2 to 10 times nominal configuration heating.

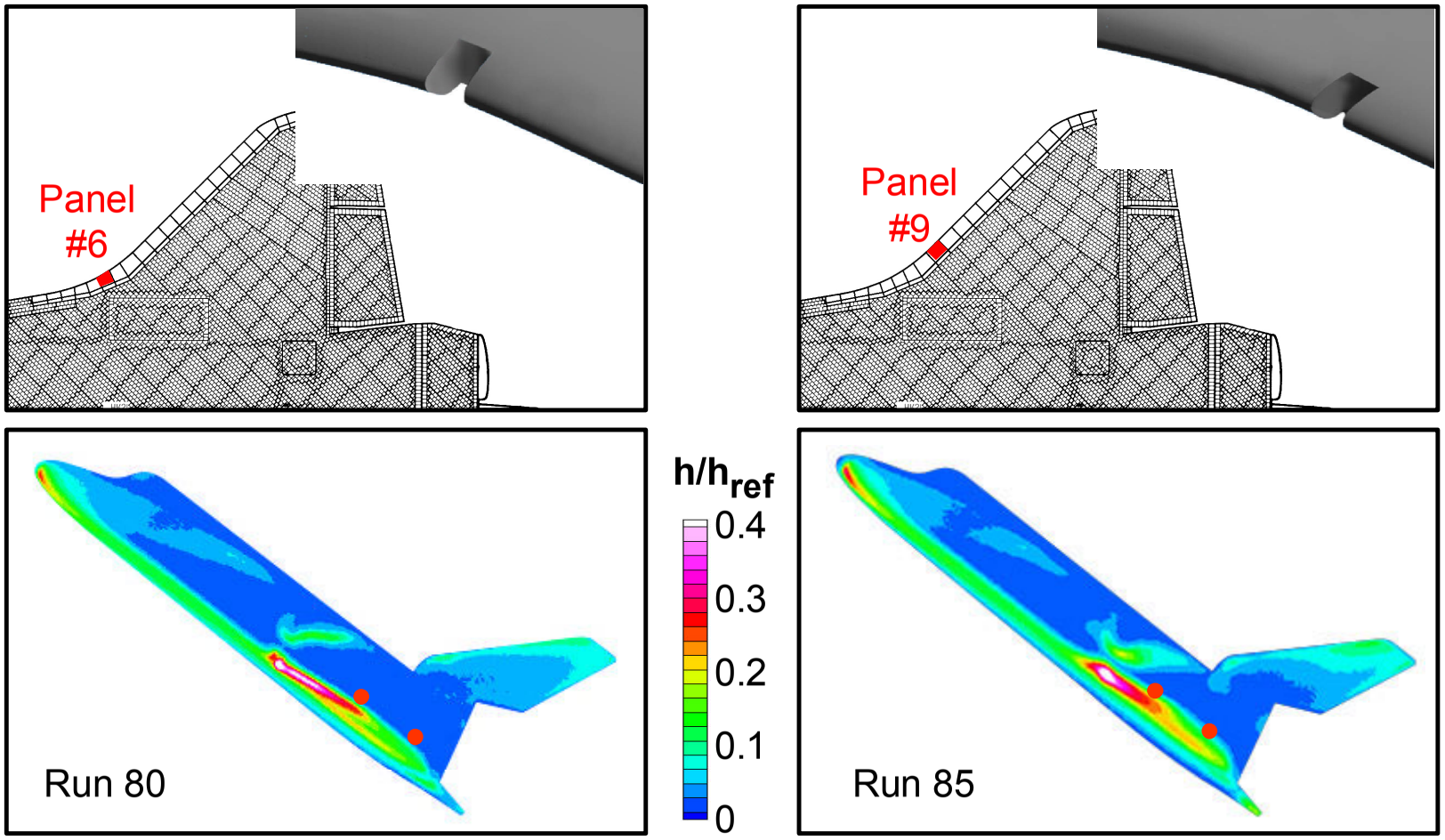

CA-000112

2 Fatal Reentry of STS107 Data and Observations.ppt

CAB068-0218

MADDS Wires on Back of Spar RCC 9 and 8

Figure 16

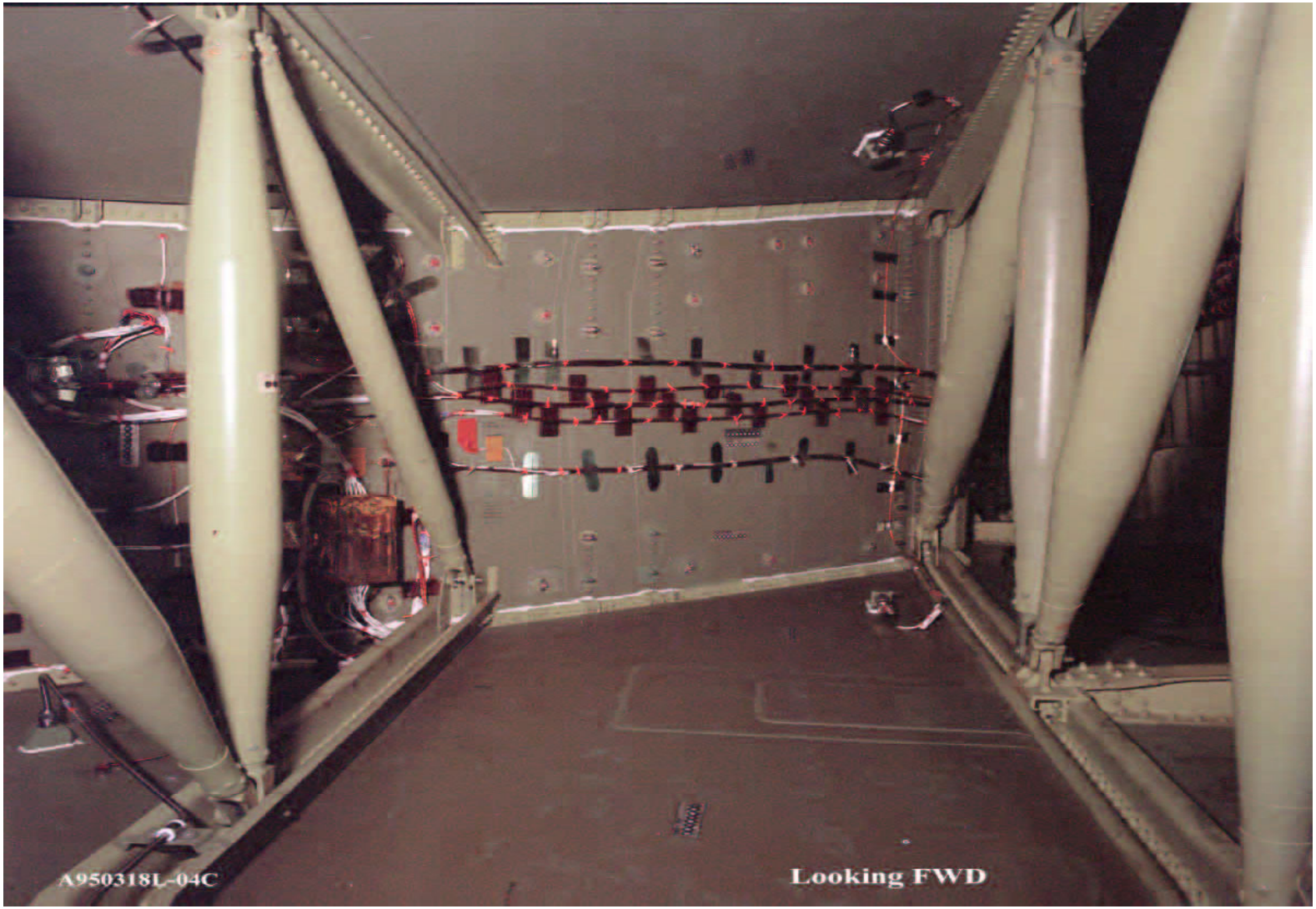

CA-000112

2 Fatal Reentry of STS107 Data and Observations.ppt

CAB068-0219

MADDS Wires on Back of Spar RCC 7 and 6 and IO Wires on Wheel Well

Figure 17

CA-000112

2 Fatal Reentry of STS107 Data and Observations.ppt

CAB068-0220

RCC Spar 5 on MADDS and OI Wires on Front of Wheel Well

CA-000112

2 Fatal Reentry of STS107 Data and Observations.ppt

CAB068-0221

Limited Distribution
DO NOT FORWARD

VDM Team

Figure 19

Based on Master Time Line (MTL) 13

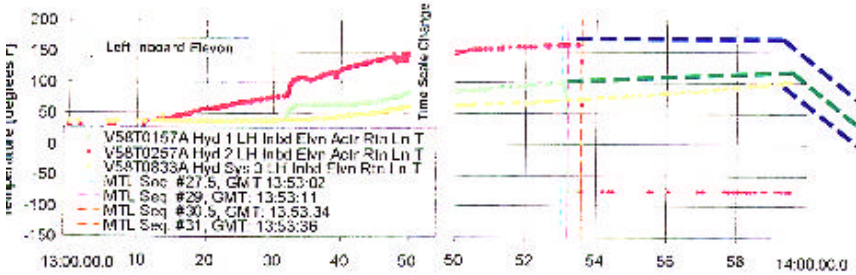

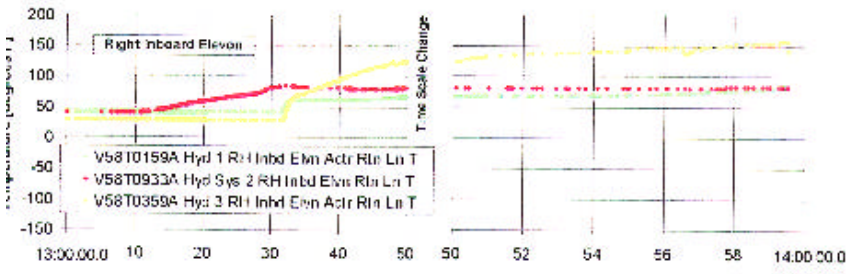

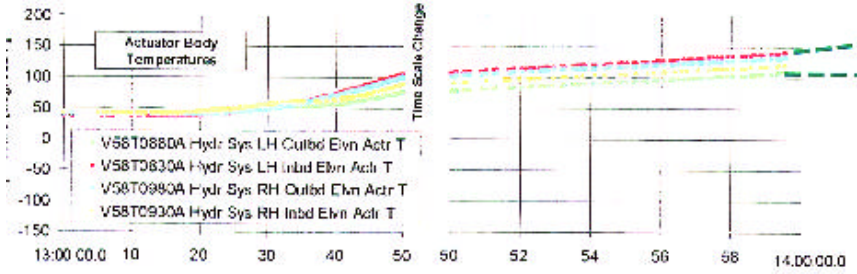

APU 2 Start, MTL Seq. #1, GMT 13:10:39

APU 1 Start, MTL Seq. #4, GMT 13:31:25
APU 3 Start, MTL Seq. #5, GMT 13:31:29

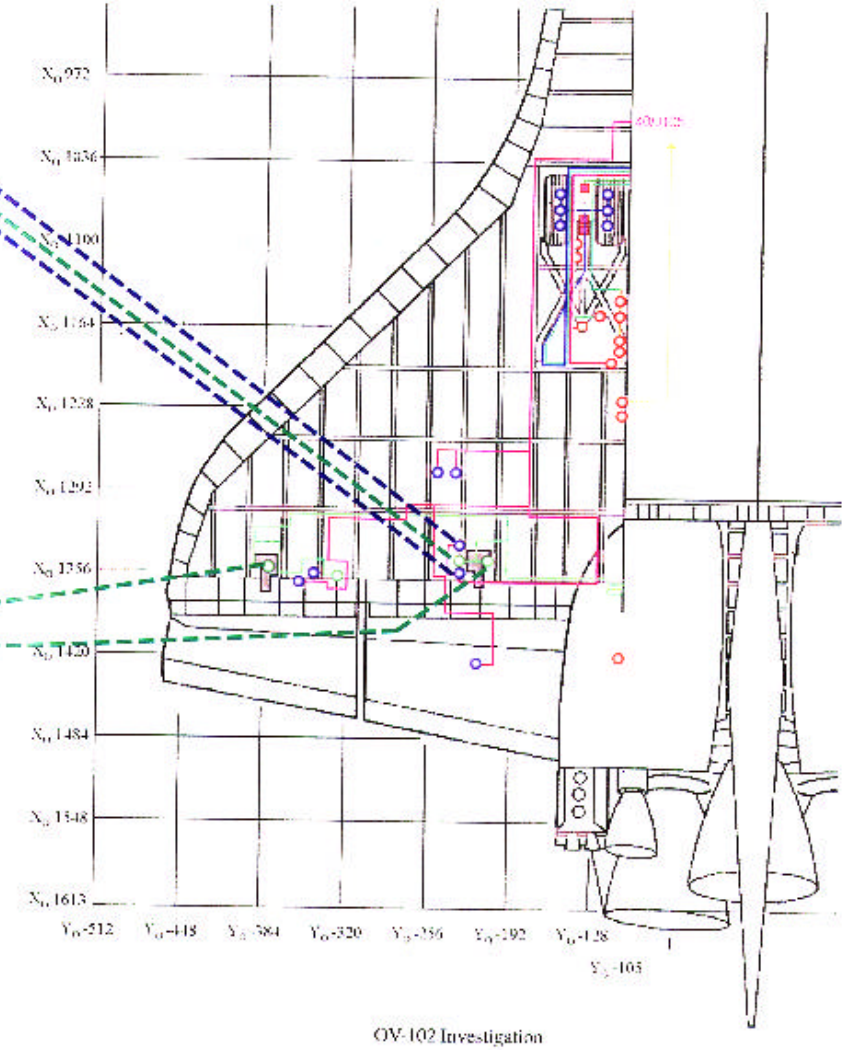

2/28/03

OV-102 Investigation

Left RCC Panels 5-8

- There is no RCC from panel 6
- Only upper RCC sections of 5, 7, and 8
- Interesting T Seal between 5 and 6

Panel 8 Panel 7 Panel 6 Panel 5

Predecisional Working Draft

CA-000112

Figure 20b

Left RCC Panels 7-11 Exhibit Unique Characteristics

Deposits and Erosion Indicate an Outboard Flow

Substantially Less RCC Material

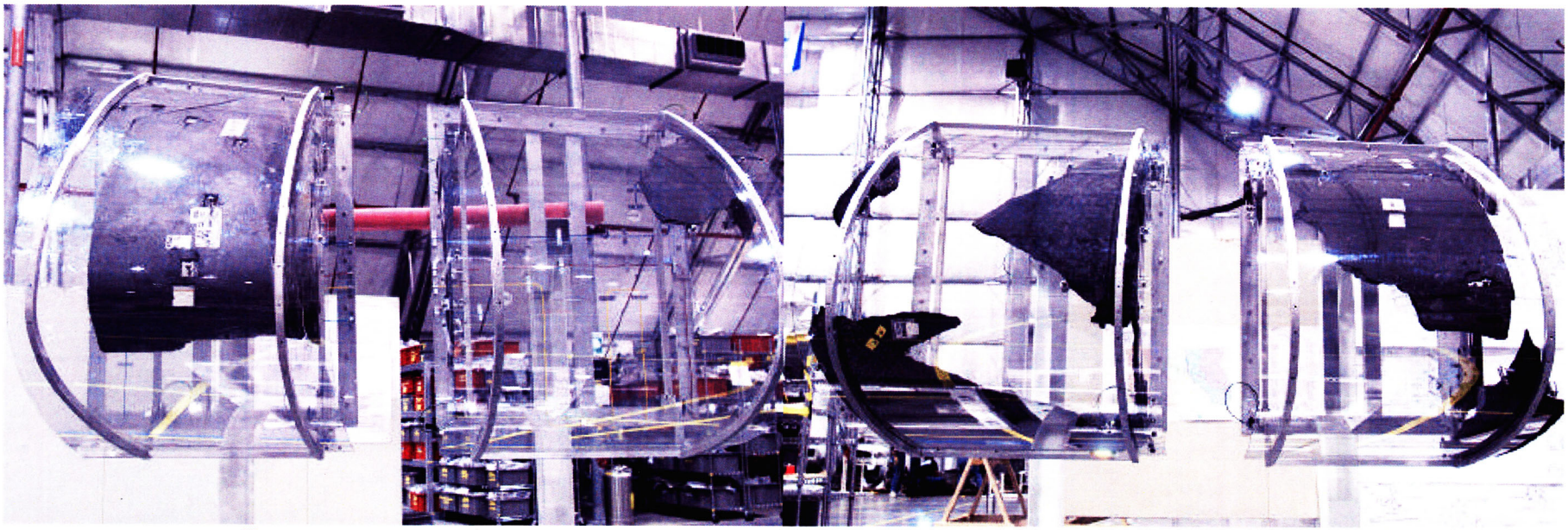

Panels 8 and 9

Panels 10 and 11

Virtual 3-D Reconstruction of Debris

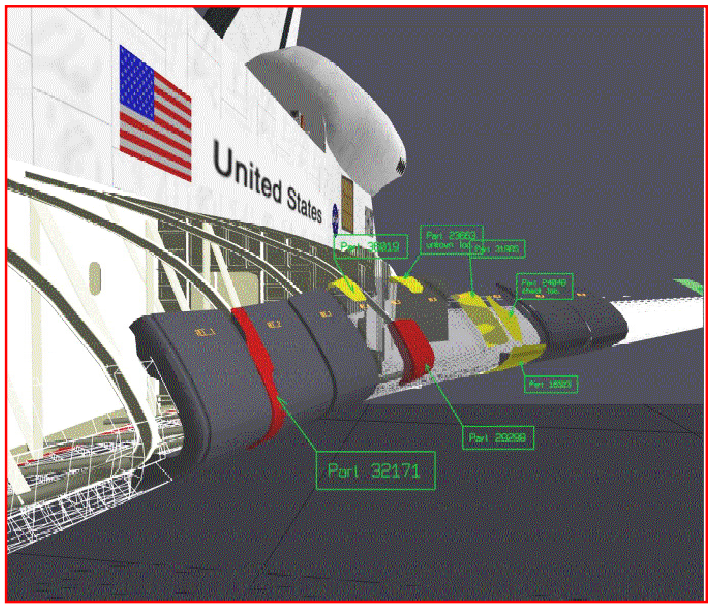

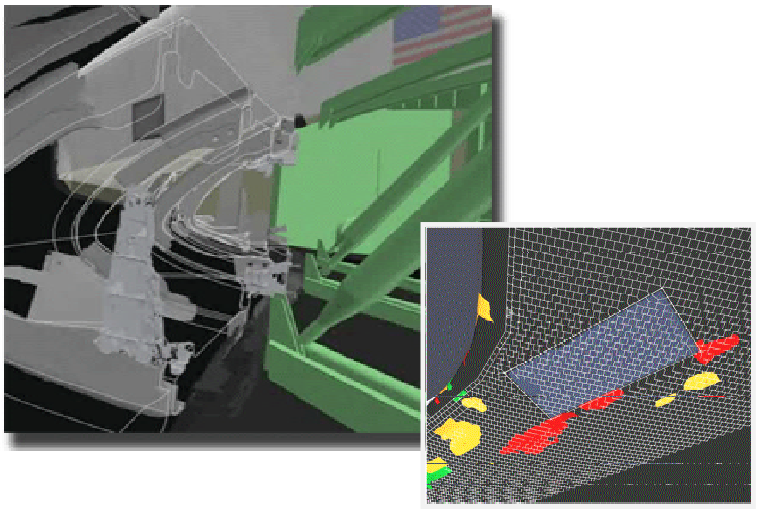

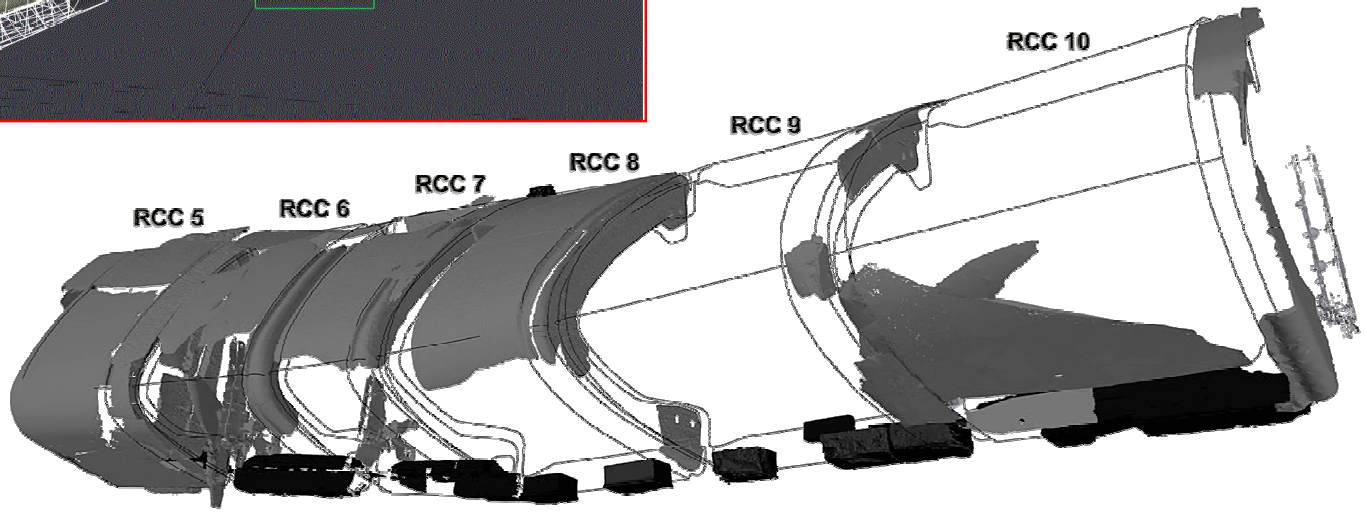

CA-000112

2 Fatal Reentry of STS107 Data and Observations.ppt

CAB068-0225

Figure 21

Relative Metallic Deposition on Left Wing Materials

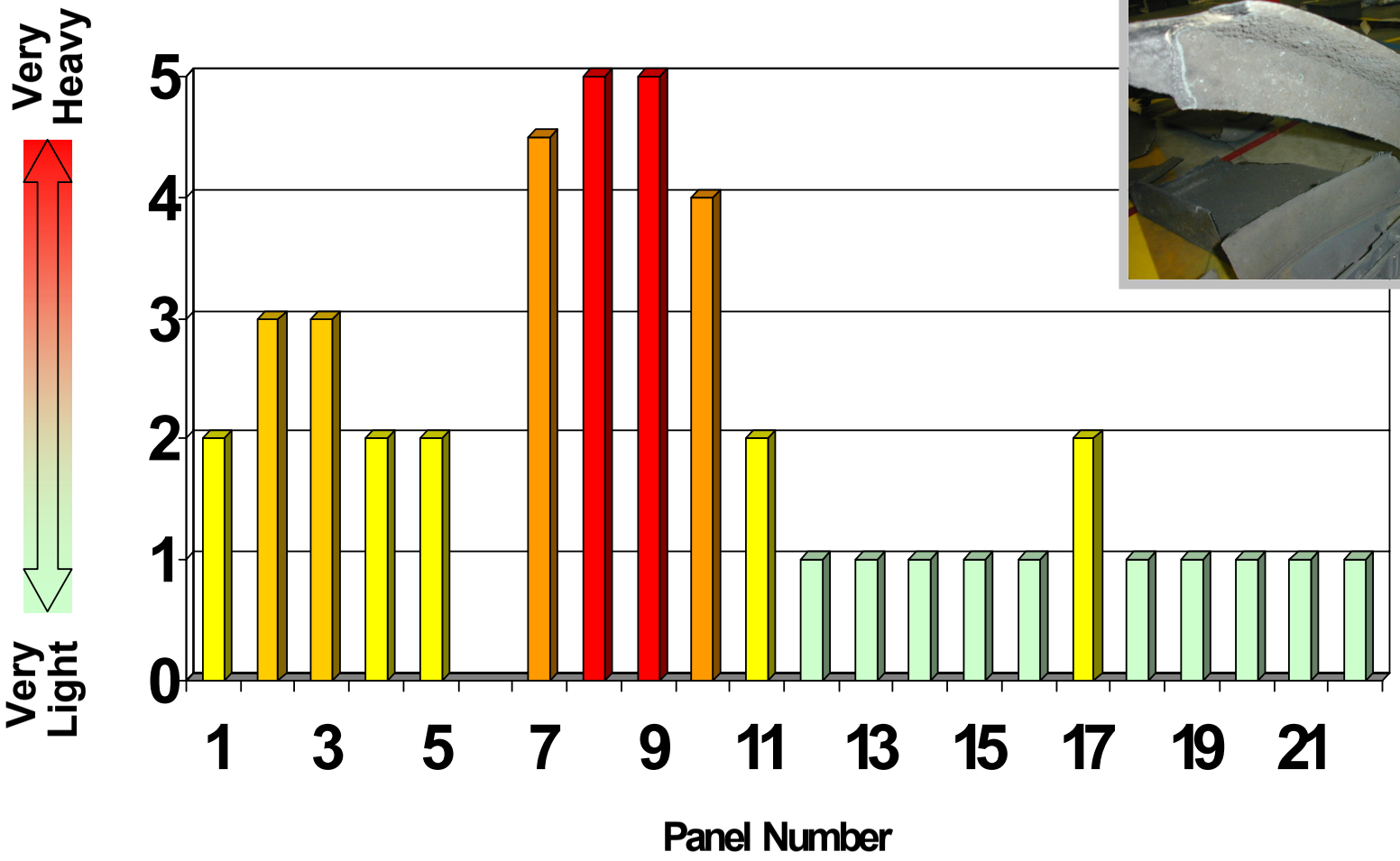

Distribution of metallic deposition volume was centered around panels 8 & 9

CA-000112

View From Bottom of Left-Wing (Similar to Kirtland Photography)

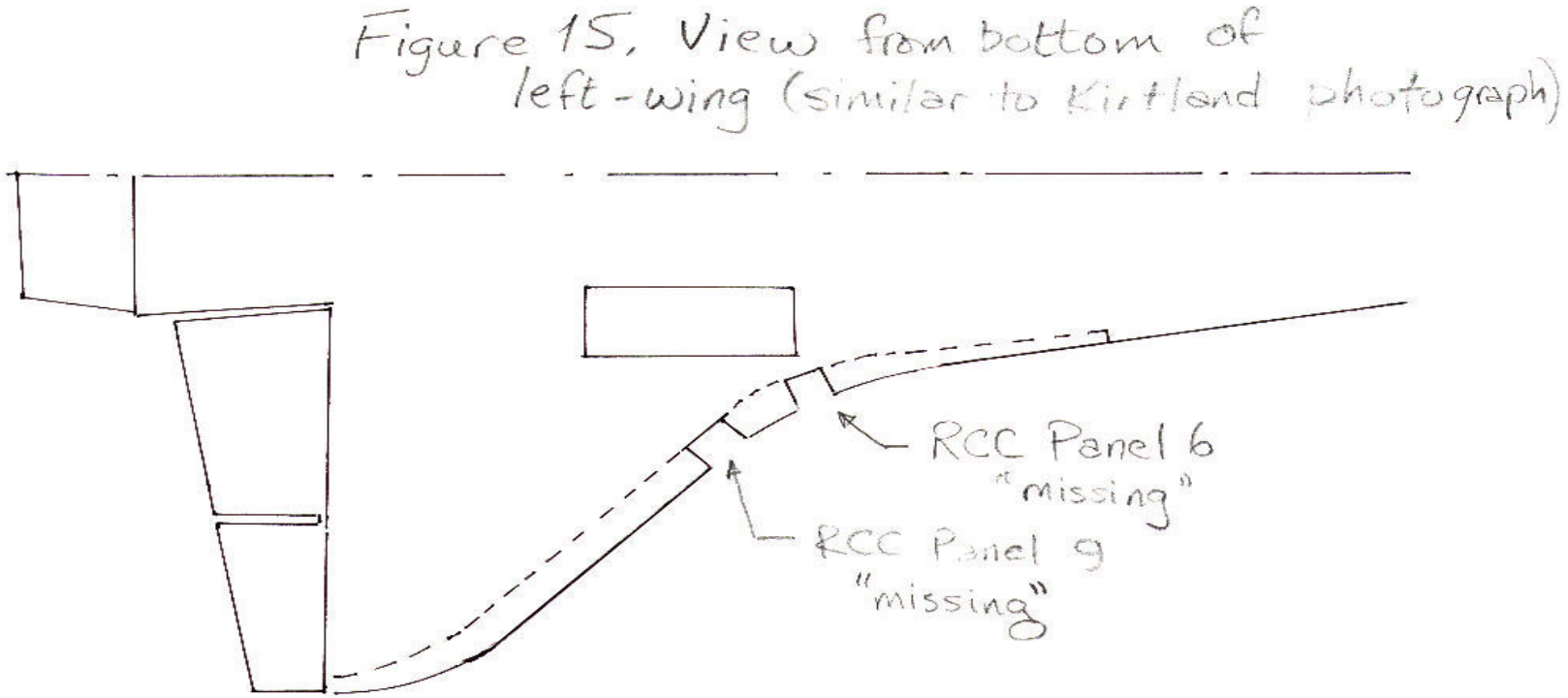

Figure 23

Shock-Shock Interaction for Left Wing, as Modified by Missing RCC Panels (RCC Panel 6 and RCC Panel 9)

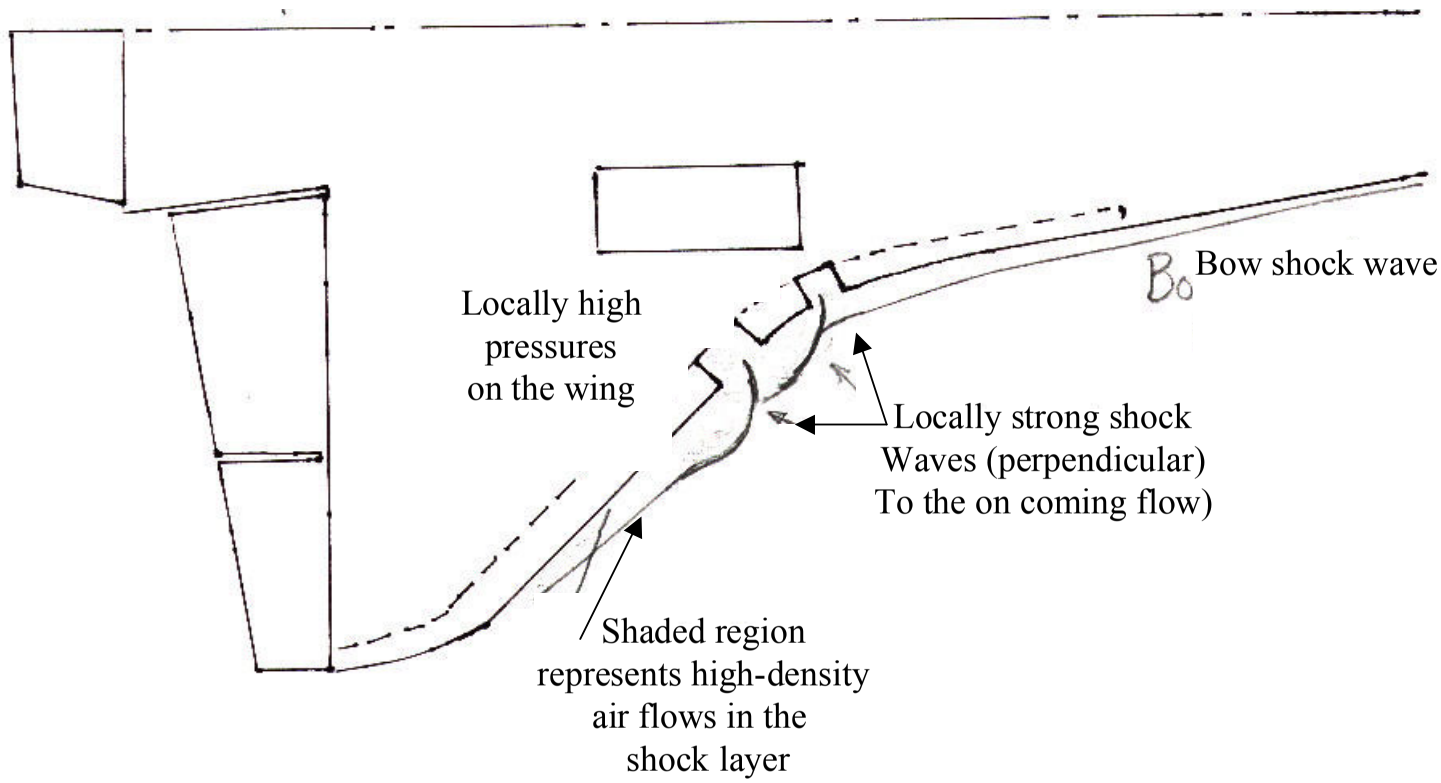

Orbiter Leeside Heating and Corresponding Shock Pattern

Mach 6 Air $\gamma_{eff} = 1.4$ $\alpha = 40$ deg $Re_{\infty, L} = 2.4 \times 10^6$ $\beta = 0$ deg

Note scale change

OMS pod heating increase

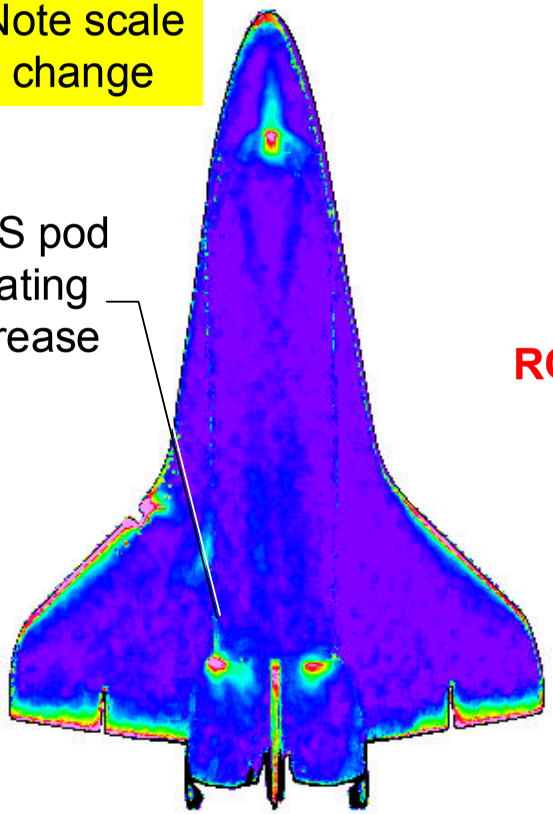

Missing RCC panel #9

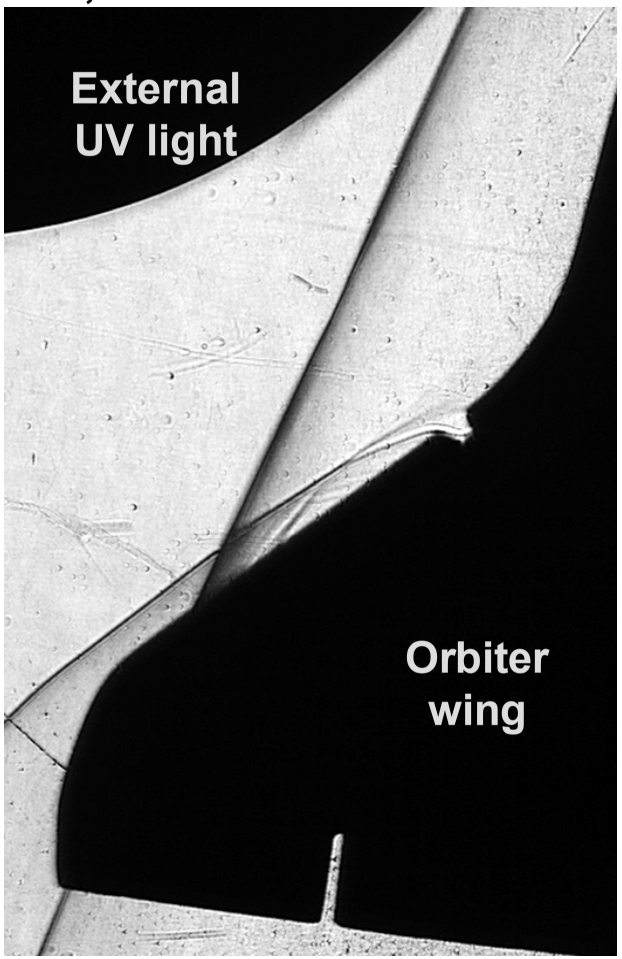

Leeside heating pattern

Shock patterns (path integrated)

CA-000112

2 Fatal Reentry of STS107 Data and Observations.ppt

CAB068-0229

Figure 25

Kirtland Image

Image straight overhead from Albuquerque
Approximately 13:57:24 GMT

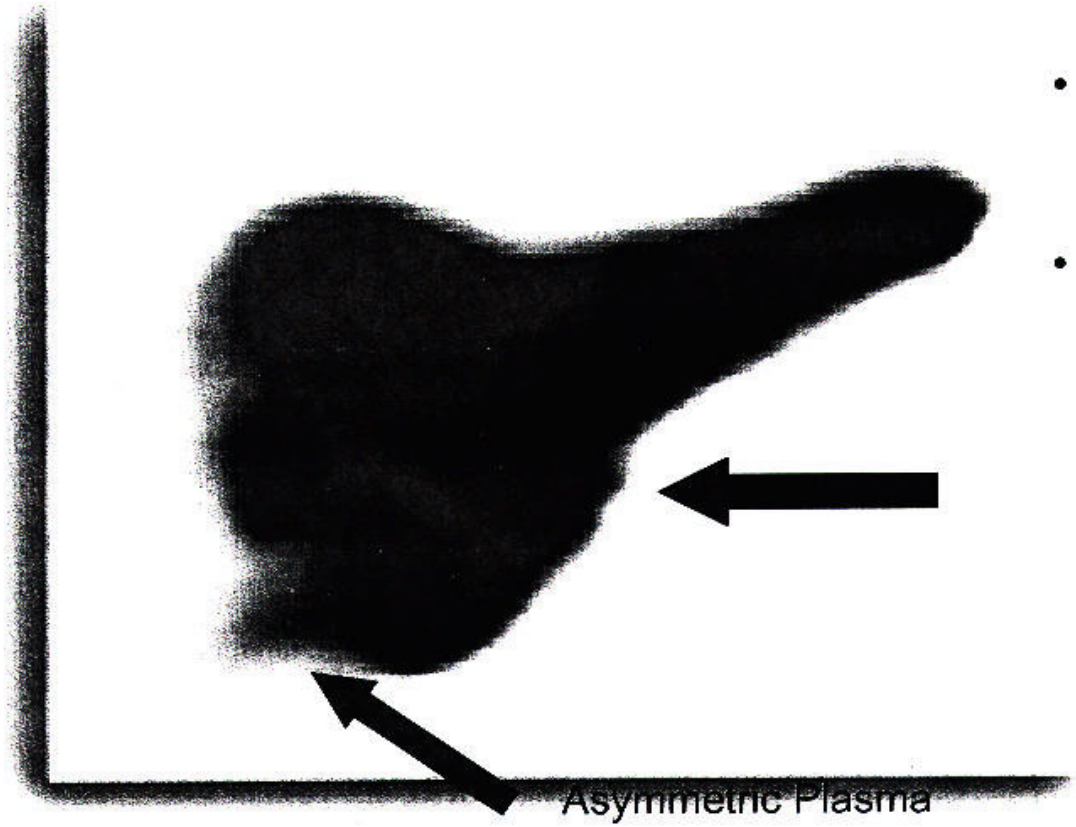

- Gregg Byrne's team thinks this apparent feature is real
- **Are RCC panels hinged up?**

Predecisional Working Draft

CA-000112

Kirtland Image

Image straight overhead from Albuquerque
Approximately 13:57:24 GMT

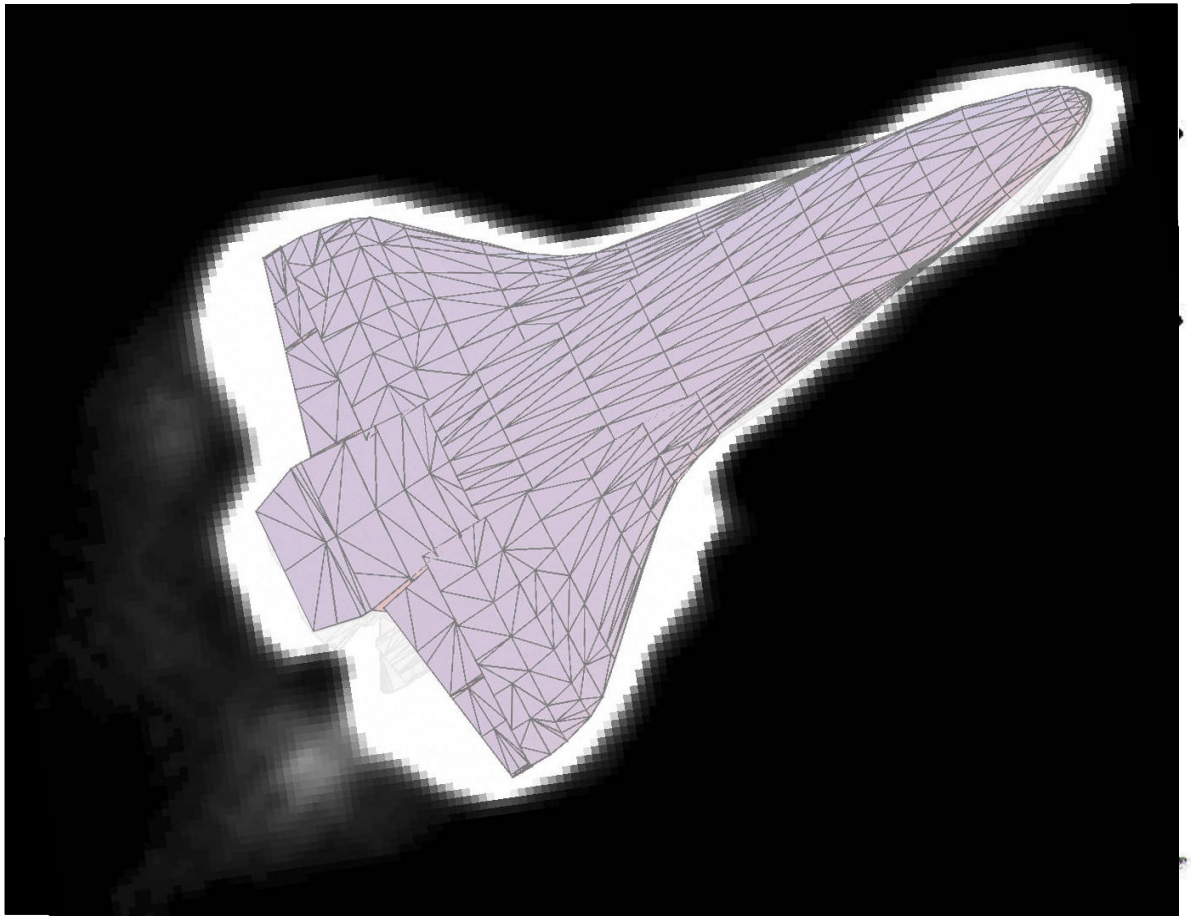

Gregg Byrne's team thinks this apparent feature is real

Are RCC panels hinged up?

CA-000112

2 Fatal Reentry of STS107 Data and Observations.ppt

CAB068-0231

Figure 27

Kirtland AFB Photo at 13:57:19

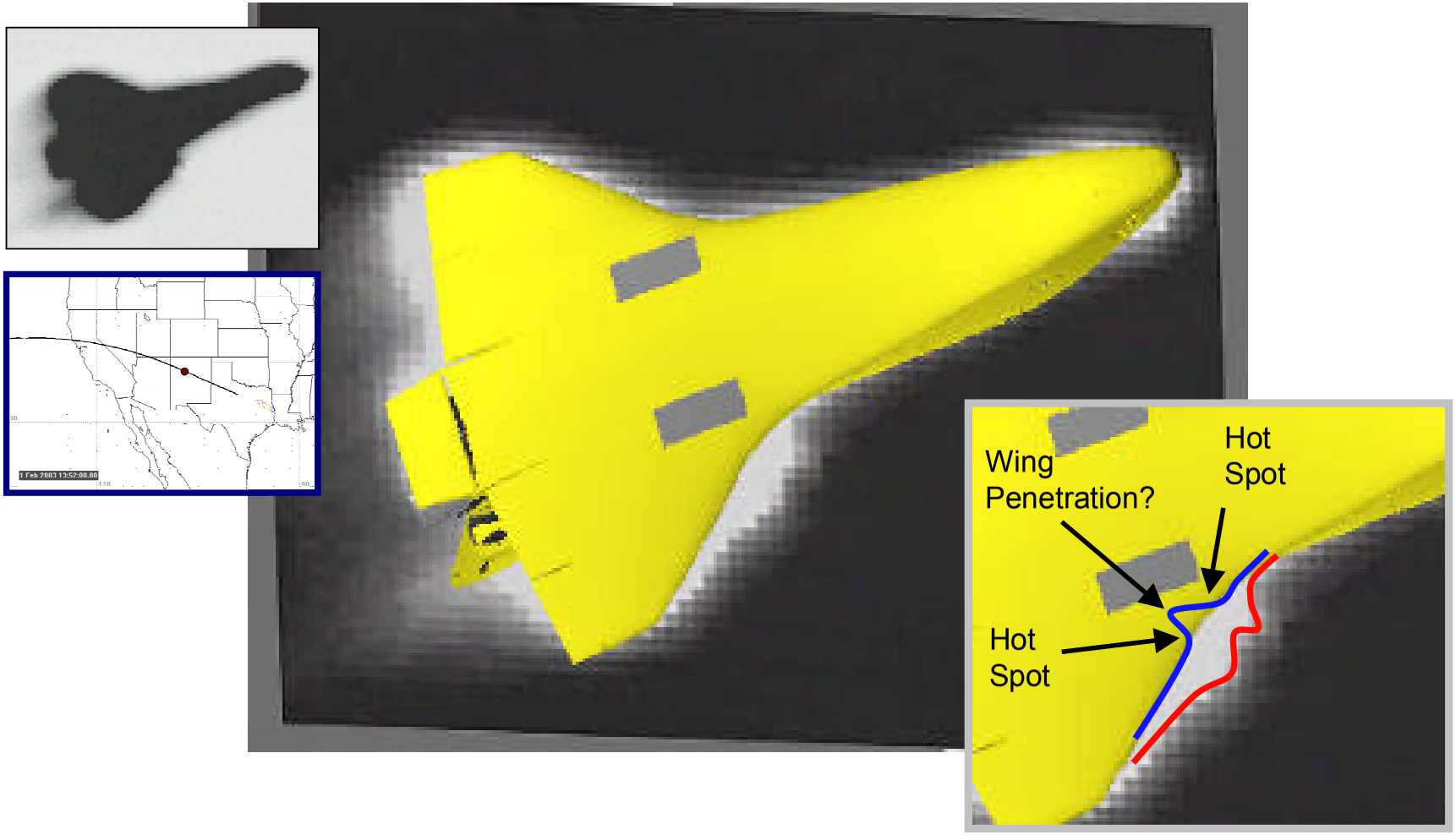

CA-000112

2 Fatal Reentry of STS107 Data and Observations.ppt

CAB068-0232

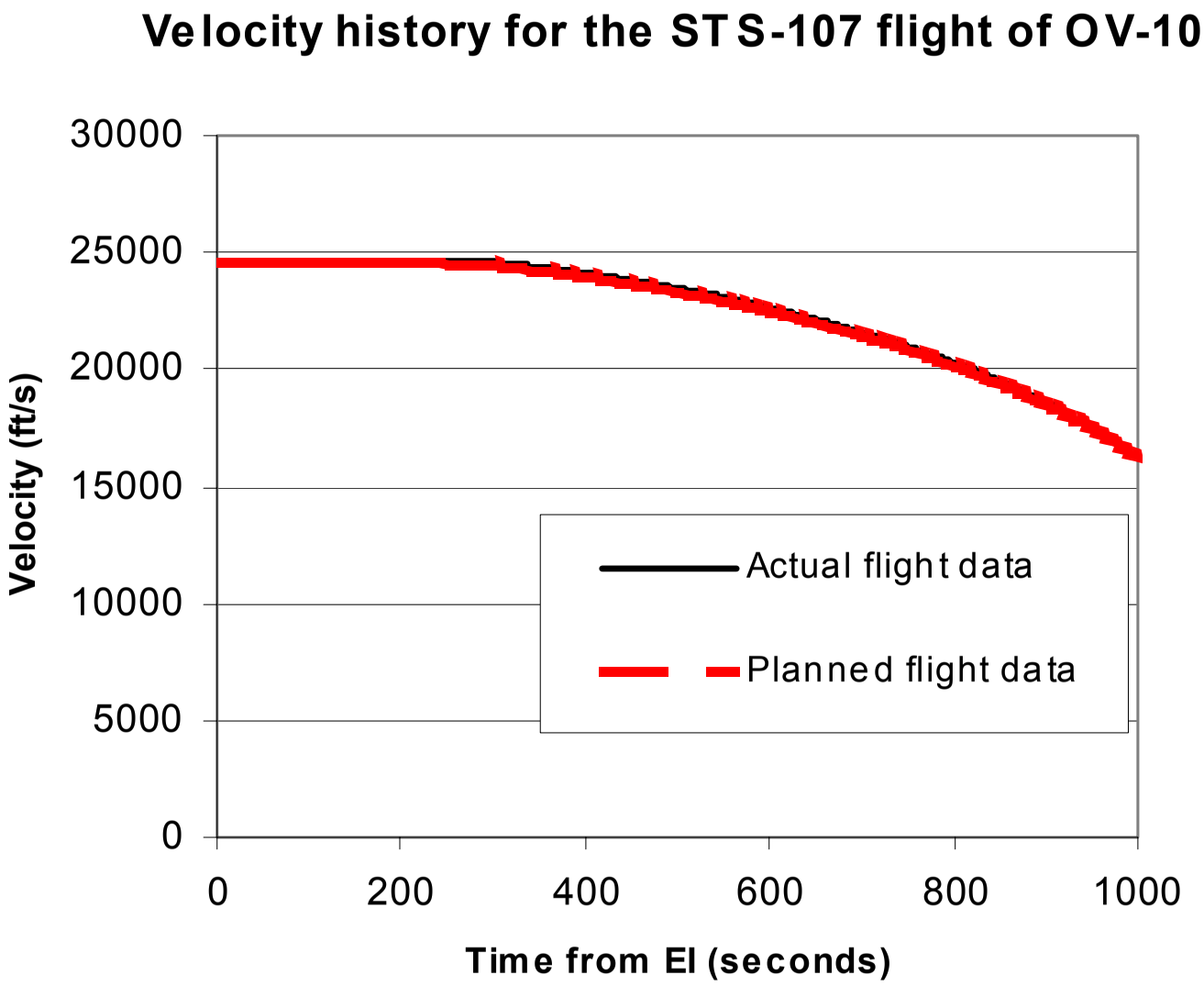
Velocity history for the STS-107 flight of OV-102
Velocity (ft/s)
30000
25000
20000
15000
10000
5000
0
0
200
400
600
800
1000
Time from EI (seconds)
Actual flight data
Planned flight data

Figure 29

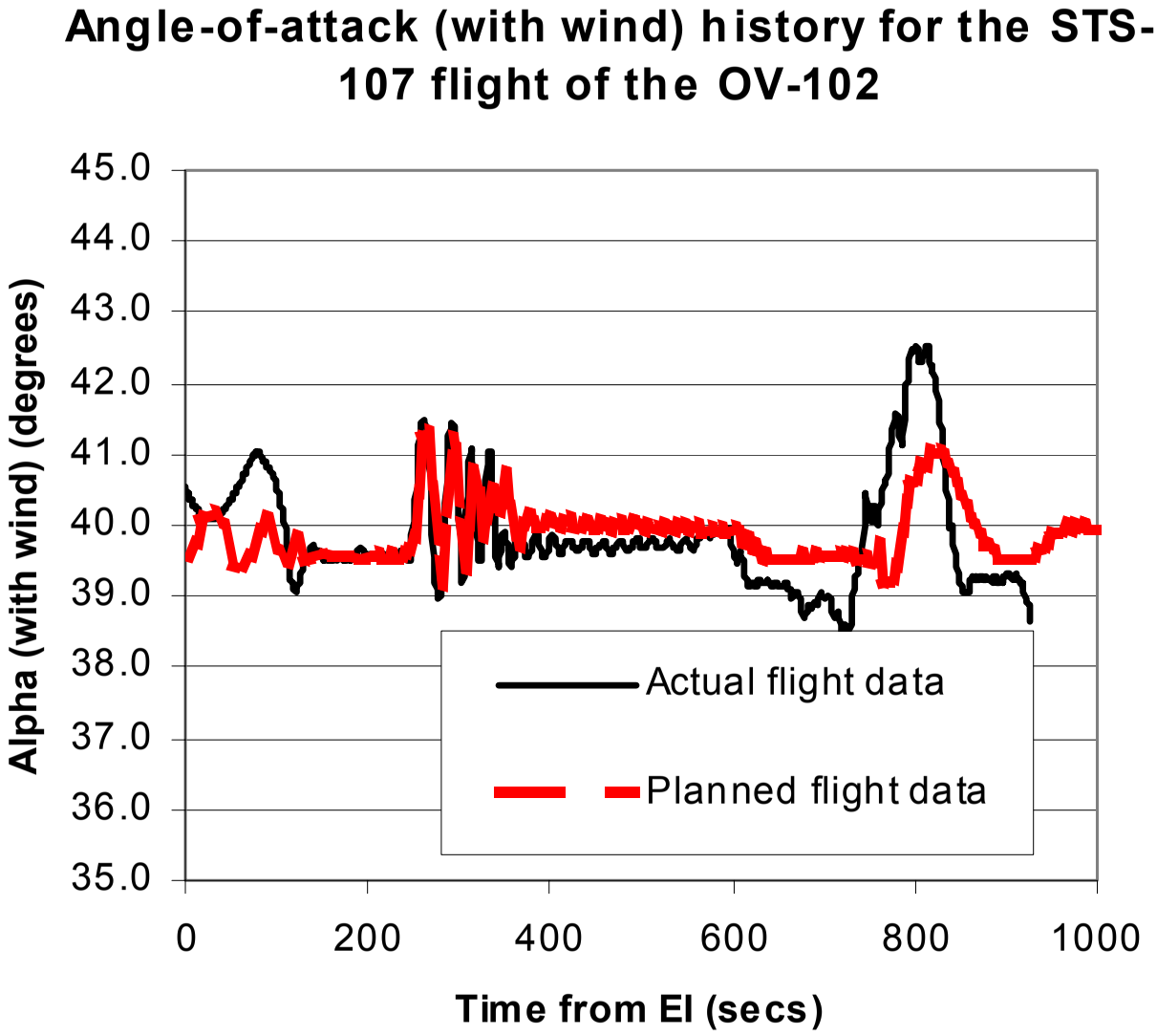

CA-000112

2 Fatal Reentry of STS107 Data and Observations.ppt

CAB068-0234

Sharp Change in Rolling Moment

Timeline Events vs. Δ Roll Aero Model Key Correlations

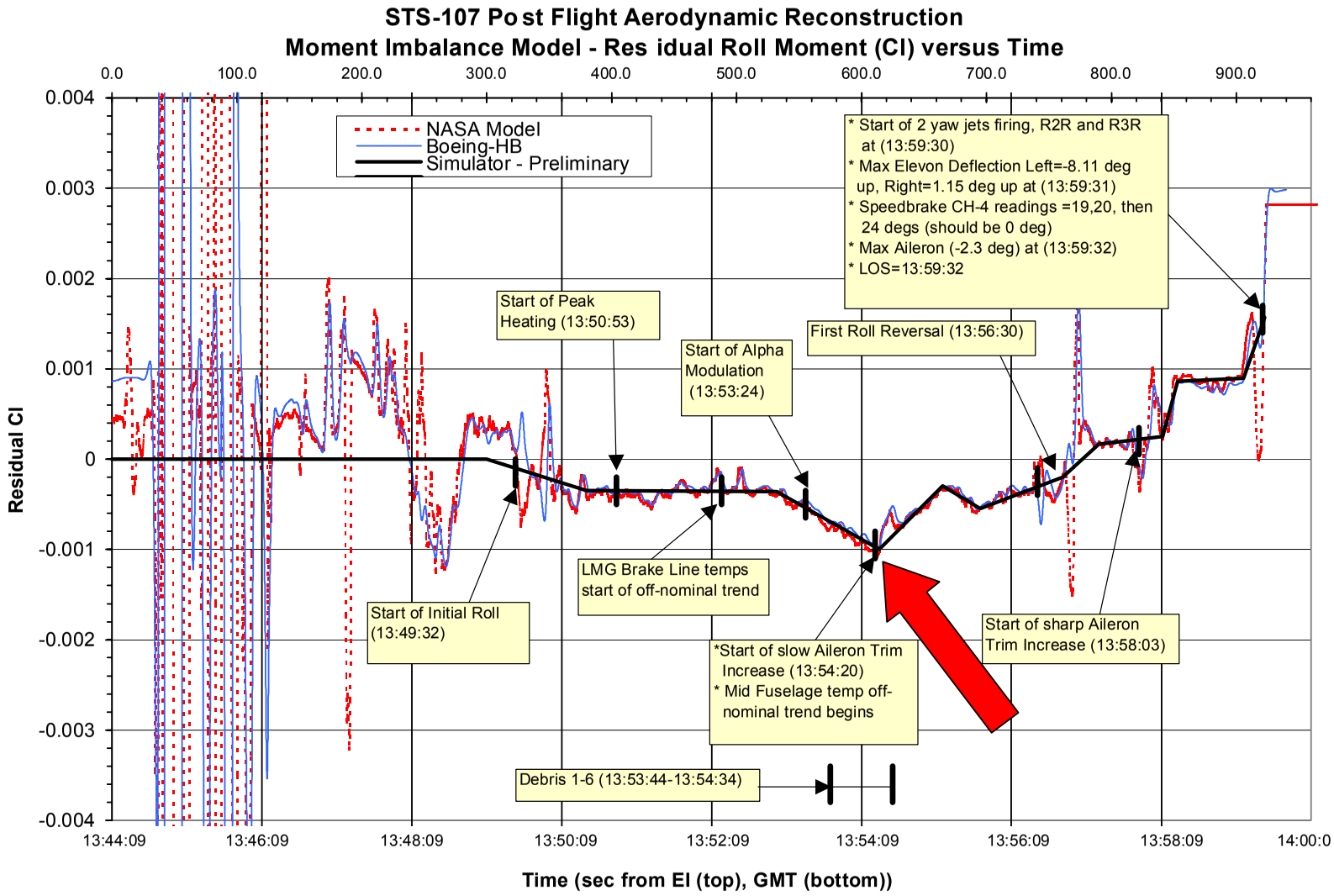

CA-000112

2 Fatal Reentry of STS107 Data and Observations.ppt

CAB068-0235

Figure 31

Missing RCC Panel 9 – Surface Flow Features

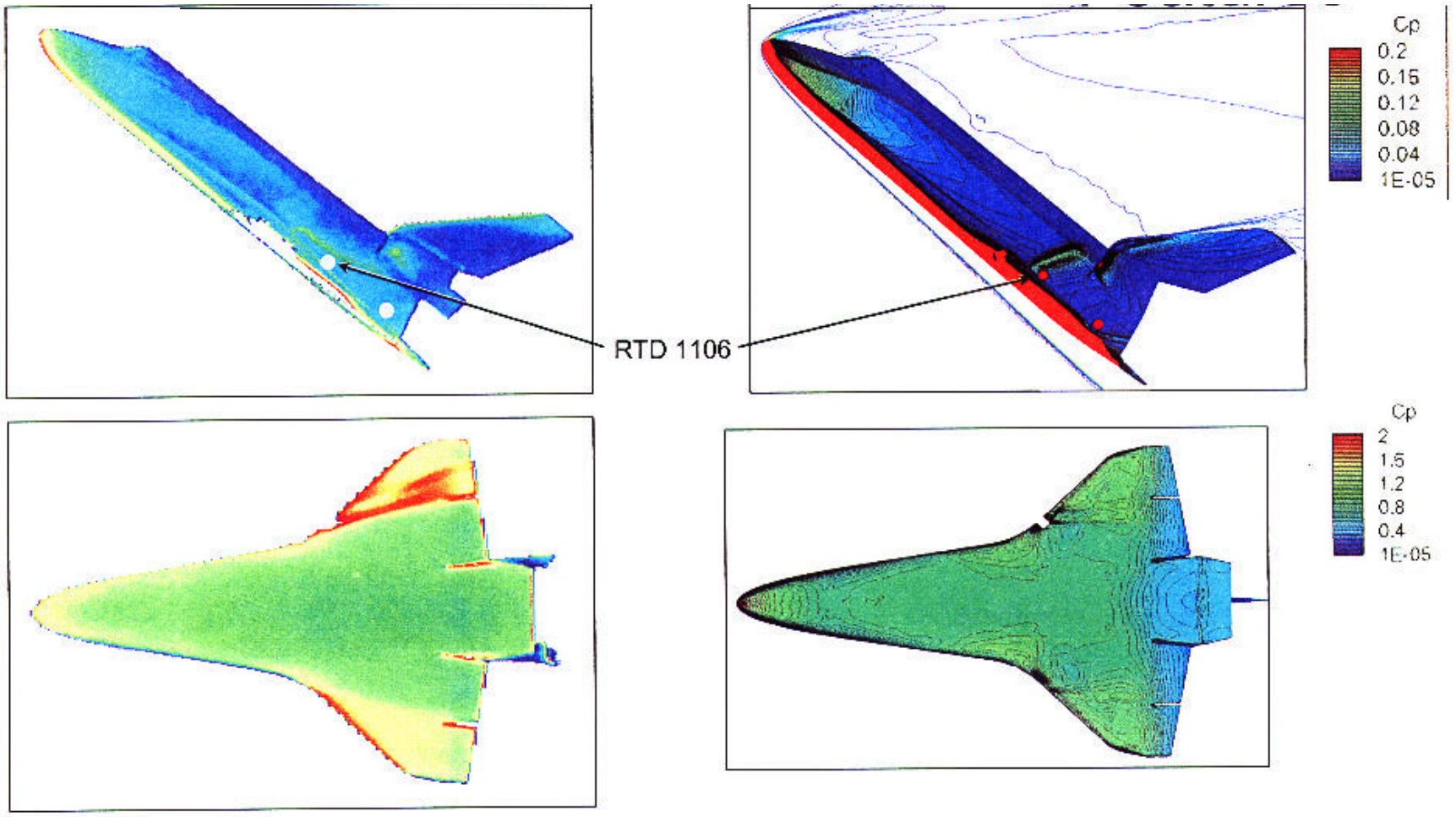

Experimental Aeroheating
20-inch CF4 tunnel, $\alpha = 40°$

FELISA Prediction of Surface Pressure
M = 24.2, Equilibrium air, $\alpha = 40°$

CA-000112

STS-107 Mishap Investigation - Combined Summary Time Line
-BASELINE-

Integ Time Line Team - REV 17 BASELINE **5/8/2003 11 AM**

Note: Rev 17 BASE integrates the OEX data timeline with the Baselined Rev 16 timeline plus IEE aero event changes (accounted for wind effects in aero increment derivation process).
Rev 17 was baselined by the OVE Working Group Team as of 5/7/03.

Sum No.	GMT GMT Day 32	EI sec	OEX data	Milestone	Entry Event	Remarks	MSID
1	13:10:39	EI+2010		TIG-5	APU 2 Start		
2	13:15:30	EI-1719		TIG	OMS TIG		
3	13:18:08	EI-1561			OMS End of Burn		
4	13:31:25	EI-764		EI-13	APU 1 Start		
5	13:31:29	EI-760			APU 3 Start		
5.5	13:39:28.559	EI-280.4	X		Start of OEX PCM Data Block		
6	13:44:09	EI+0		EI	Entry Interface (400,000 ft)	Mach 24.57	
6.1	13:45:39 / 48:59	EI+90 / EI+290	X		16 Temperature Sensors on the lower surface to the left of or at the centerline experience off-nominal early temperature trends (warmer temperature rise rate compared to previous flights of OV-102 at the same inclination)		V09T9849A V07T9784A V07T9666A V07T9786A V07T9468A V07T9787A V07T9470A V07T9788A V07T9711A V07T9478A V07T9713A V07T9480A **V07T9785A V09T9845A V09T9231A V07T9489A**
6.15	13:48:39	EI+270	X		Left Wing Front Spar at RCC Panel 9 - initiation of off-nominal trend in strain (small increase) followed by a more significant off-nominal signature to failure at EI+495 secs	The measurement began to fail at approximately EI+495 sec	V12G9921A X1106.0 Y-229.0 ZMID
6.2	13:48:59	EI+290	X		Left Wing RCC Panel 9 Lower Attach Clevis (between RCC 9 and 10) - initiation of an off-nominal temperature trend (early temperature increase compared to previous flights of same inclination)	The measurement began to fail at approximately EI+492 sec	V09T9910A X1112.0 Y-239.0 Z289.0
6.3	13:49:32	EI+323			Start of initial roll		
6.4	~13:49:39*	~EI+330*	X		Left Wing Front Spar Caps Strain Gage shows early off nominal downward trend	*Note: PCM3 entry data is in snapshot format (not continuous). Time indicated is at start of data segment where off-nominal signature is first observed, therefore event may have started earlier than noted.	V12G9169A X1107 Y232 Z?
6.45	13:49:49 / 49:59	EI+340 / EI+350	X		4 Left OMS Pod Surface temps - Start of off-nominal temperature trend - cooler rise rate when compared to previous flights of same inclination	Followed by the start of a warmer-than-expected temperature trend beginning in the EI+510 to EI+540 sec range	V07T9976A V07T9978A V07T9220A V07T9972A
QBAR = ~15 psf (~0.10 psi); Mach 24.4					**------ 32:13:50:00 ------**	EI + 351 sec; WLE Stagnation Temp: ~2520 F (STS-107 Nom EOM Design Pred)	
6.5	13:50:00 / 43	EI+351 / EI+394			Five events of unexpected return link comm drop-out (Comm events 1-5)	On upper left aft antenna (TDRS 171/W). Appears off-nominal based on previous flt data. Comm loss not continuous thru period indicated.	
6.7	13:50:09	EI+360	X		Left PLBD Surface TC BP3703T - Start of off-nominal temperature trend - cooler rise rate when compared to previous flights of same inclination	Followed by large increase in temperature at EI + 570 seconds	V07T9925A X1138.5 YLH Z441.4
6.9	13:50:19	EI+370	X		Left Wing Lower Surface Thermocouple BP2510T begins off-nominal temp increase from ~2000 deg F to ~2200 deg F over approx 50 seconds followed by a momentary 100 deg F temperature spike	The measurement subsequently fails at approximately EI+496 sec	V07T9666A X1121.1 Y-235.5 ZLWR
7	13:50:53	EI+404		Start of Peak Heating		Determined by analysis	
QBAR = ~19 psf (~0.13 psi); Mach 24.1					**------ 32:13:51:00 ------**	EI + 411 sec; WLE Stagnation Temp: ~2650 F	
7.2	13:51:14	EI+425	X		Left Wing Front Spar at RCC Panel 9 - start of off-nominal increasing temperature trend	Increasing trend continues until the measurement starts to fail at approximately EI+520 sec	V09T9895A X1102.2 Y-239.0 Z-239.0
7.25	13:51:14	EI+425	X		Left Wing RCC Panel 9 Lower Attach Clevis (between RCC 9 and 10) - start of a more rapid off-nominal increasing temperature trend	Increases until the measurement starts to fail at approximately at EI + 492 secs	V09T9910A X1112.0 Y-239.0 Z289.0
7.3	deleted					Rationale for deletion: Upon further evaluation of the data, it was determined that the remote sensor signatures had been seen in previous flights and/or could be explained by known events.	
7.35	deleted					Rationale for deletion: Moved to seq # 11.37 after further analysis.	
7.37	13:51:49	EI+460	X		OMS-L Pod HRS1 Surf T3-AFT - Start of off-nominal higher-than-expected temperature trend when compared to previous flights of same inclination	Sensor sees a sharp temp increase at EI+910 and goes erratic at EI+940	V07T9223A X1437.2 Y-126 Z422
QBAR = ~22 psf (~0.15 psi); Mach 23.7					**------ 32:13:52:00 ------**	EI + 471 sec; WLE Stagnation Temp: ~2700 F	
7.4	deleted					Rationale for deletion: Moved to seq # 8.75 after further analysis.	
7.45	13:52:09 / 52:55	EI+480 / EI+486			Four events of unexpected return link comm drop-out (Comm events 6-9)	On upper left aft antenna (TDRS 171/W). Appears off-nominal based on previous flt data. Comm loss not continuous thru period indicated.	

STS-107 Mishap Investigation - Combined Summary Time Line
-BASELINE-

Integ Time Line Team - REV 17 BASELINE

5/8/2003 11 AM

Note: Rev 17 BASE integrates the OEX data timeline with the Baselined Rev 16 timeline plus IEE aero event changes (accounted for wind effects in aero increment derivation process).
Rev 17 was baselined by the OVE Working Group Team as of 5/7/03.

Sum No.	GMT GMT Day 32	EI sec	OEX data	Milestone	Entry Event	Remarks	MSID	
7.46	13:52:09 / 52:49	EI+480 / EI+520	X		Nose Cap RCC Attach OutBoard Clevis (Chin Panel) - Temporary change in slope, then returns to "nominal" Note: Adjacent sensor V09T9888 (on centerline) does not show this signature		V09T9889A X262.0 Y-23.0 LWR	
7.47	13:52:16	EI+487	X		Two Left Wing and 1 Right Wing Surface Pressure measurements show signs of failure	First OEX data to show signs of failure	V07P8038A V07P8086A V07P8151A	
7.48	13:52:16 / 53:17	EI+487 / EI+522	X		All of the measurements running in the wire bundle along the left wing leading edge show signs of failure		15 of 15 measure-ments	
7.49	13:52:16 / 56:24	EI+487 / EI+735	X		The vast majority of left wing OEX measurements show signs of failure during this time period - this includes all left wing temperature and pressure measurements and all strain measurements aft of Xo 1040 with the exception of three strain measurements on the upper surface of the LMLG compartment Additionally, 30 right wing pressure measurements show signs of failure		Multiple measurements	
7.5	13:52:17	EI+488		Approx Vehicle Ground Location: 39.0 N / -129.2 W	Altitude 236,800 ft / Mach 23.6 - Over the Pacific Ocean, approx 300 miles West of California Coastline	Approx vehicle position when first off-nominal data was seen; Data source: STS-107 GPS Trajectory Data		
7.7	13:52:17	EI+488			LMG Brake Line Temps (D) - small increase in temperature ("bit flip up")	Initiation of temp rise ("bit flip up") - may be nominal based on rise rate comparison w/ flight experience	V58T1703A	
7.75	13:52:18	EI+489	X		Left Wing Spar Cap Lwr L103 (Xo 1040 Spar - Lower Cap) - off-nominal increase in strain indication followed by gradual decrease over approx 330 seconds interval until measurement failure at ~EI+935		V12G9048A	
7.77	13:52:24	EI+495	X		Left Wing Front Spar at RCC Panel 9 - strain gage goes erratic for approximatly 20 second - measurement appears to be failing	Subsequent data is suspect	V12G9921A X1106.0 Y-229.0 ZMID	
7.8	13:52:25	EI+496	X		Left Outboard Elevon Wide Band Accelerometers - off-nominal vibration response (approximately 2G peak-to-peak) V08D9729A - L OB Elevon Z-Vib (MUX1B Ch 2)		V08D9729A	
7.85	13:52:29	EI+500	X		OMS-L Pod HRSI Surf T1-AFT - Start of slightly off-nominal erratic trend when compared to previous flights of same inclination	Followed by drop in temperature at EI + 570 seconds and subsequent erratic temperature changes	V07T9219A X1507.1 Y-126.0 Z422.0	
7.9	13:52:31	EI+502	X		Left Outboard Elevon Wide Band Accelerometers - off-nominal vibration response (approximately 3G peak-to-peak) V08D9729A - L OB Elevon Z-Vib (MUX1B Ch 2)		V08D9729A	
8	deleted					Rationale for deletion: moved to seq #8.7		
8.5	13:52:32/55	EI+503			Supply H2O Dump Nozzle Temps (A, B) (2) and Vacuum Vent Temp (1) - transient (15 and 23 seconds, respectively) increase in typical rise rates.	GMT shown indicates initial rise duration. Supply H2O Dump Nozzle temps took additional 48 secs to return to nominal temp rise, vacuum vent temps took additional 40 secs to return to nominal rise.	V62T0440A V62T0551A	V62T0439A
8.6	13:52:34	EI+505	X		OMS-L Pod HRS1 Surf T2-AFT - Start of off-nominal lower-than-expected temperature trend (compared to previous flights of same inclination) until sensor sees a sharp temp increase at EI+910 and goes erratic at EI+940		V07T9222A X1486.9 Y-126 Z422.0	
8.65	13:52:39 / 53:09	EI+510 / EI+540	X		4 Left OMS Pod Surface temps - Change in existing off-nominal temperature trend (following a cooler rise rate than expected, the temperature trend that is significantly warmer when compared to previous flights of same inclination)		V07T9976A V07T9220A	V07T9978A V07T9972A
8.7	13:52:41	EI+512			LMG Brake Line Temps (A, C) (2) - start of off nominal trend	Unusual Temperature Increase	V58T1700A	V58T1702A
8.75	13:52:44 / 52:50	EI+515 / EI+521			First clear indication of off-nominal aero increments	Delta yawing and rolling moment coefficients indicate off-nominal trends. Derived by analysis.	n/a	
8.8	13:52:49.5 / 52:51.4	EI+520.5 / EI+522.4	X		2 Left Wing temperature sensors begin an off-nominal (typically erratic) response that appears to be an indication of the measurements (sensors/wiring) failing		V09T9895A V09T9849A	
9	deleted							
10	13:52:59	EI+530			Left INBD Elevon Lower Skin Temp (1) - OSL	Began trending down 3 secs earlier	V09T1006A	
QBAR = ~25.5 psf (~0.18 psi); Mach 23.2					------ 32:13:53:00 ------		EI + 531 sec; WLE Stagnation Temp: ~2800 F	
10.5	deleted					Rationale for deletion: Merged with seq # 8.75 after further analysis.		
10.6	13:53:03	EI+534	X		Left Outboard Elevon Wide Band Accelerometers - onset of signal saturation indicating likely measurement failure (approximately 10G peak-to-peak - off-scale)		V08D9729A	
11	13:53:10 / 36	EI+541 / EI+567			Hydraulic System Left Outbd / Inbd Elevon Return Line Temps (4) - OSL	OSL was preceded by Nominal Temp rise.	V58T0394A V58T0157A	V58T0193A V58T0257A

STS-107 Mishap Investigation - Combined Summary Time Line
-BASELINE-

Integ Time Line Team - REV 17 BASELINE

5/8/2003 11 AM

Note: Rev 17 BASE integrates the OEX data timeline with the Baselined Rev 16 timeline plus IEE aero event changes (accounted for wind effects in aero increment derivation process).
Rev 17 was baselined by the OVE Working Group Team as of 5/7/03.

Sum No.	GMT GMT Day 32	EI sec	OEX data	Milestone	Entry Event	Remarks	MSID
11.1	deleted					Rationale for deletion: alpha modulation time tag updated - moved to seq #11.25	
11.2	13:53:26	EI+557		Approx Veh Grd Location: 38.7 N / -123.5 W	Altitude 231600 ft / Mach 23.0 - Crossing the California Coastline	Data source: STS-107 GPS Trajectory Data	
11.21	13:53:29	EI+560	X		Left Fuselage Side Surface Temp BP3605T - start of off-nominal increasing temperature trend from ~180 deg F to 400 deg F	Trend followed by temperature drop and rise	V07T9253A X1000.7 Y-105 Z354.5
11.22	13:53:29	EI+560	X		Left PLBD Surface TC BP3603T - Start of slightly off-nominal erratic temperature trend when compared to previous flights of same inclination		V07T9913A X1003.8 YLH Z441.3
11.23	13:53:29	EI+560	X		Left PLBD Surface TC BP3703T - start of off-nominal temperature rise, peaking at EI+625, followed by temperature drop and subsequent off-nominal higher-than-expected temperature signature		V07T9925A X1138.5 YLH Z441.4
11.24	13:53:29	EI+560	X		Left Fuselage Side Surface TC BP3604T - Start of slightly off-nominal erratic temperature trend when compared to previous flights of same inclination		V07T9903A X1006 Y-105 Z398.4
11.25	13:53:31	EI+562		Alpha Modulation	Angle of attack (alpha) modulation active		V90H0803C
11.3	13:53:32 / 54:22	EI+563 / EI+565			Two events of unexpected return link comm drop-out (Comm events 10-11)	On upper left aft antenna (TDRS 171/W). Appears off-nominal based on previous flt data. Comm loss not continuous thru period indicated.	
11.35	13:53:37	EI+568	X		Xo 1040 Spar (MLG Forward Wall Spar) Strain Gage - Upper Cap - start of off-nominal increase in strain indication (over an approximate 115 second interval) followed by sudden decrease		V12G9049A X1040 Y-135 ZUPR
11.37	13:53:38	EI+569			Inertial sideslip angle (Beta) exceeds flight history.	The steady state navigation derived sideslip angle becomes out-of-family as compared to previous flight data at this point in the trajectory.	V90H2249C
11.4	13:53:44	EI+575	X		OMS-L Pod HRSI Surf T1-AFT - Start of off-nominal lower-than-expected temperature trend when compared to previous flights of same inclination	Sensor goes erratic at EI+940	V07T9219A X1507.1 Y-126.0 Z422.0
11.5	13:53:45 / 54:11	EI+576 / EI+602			1st reported debris (5) observed leaving the Orbiter just aft of Orbiter envelope (Debris # 1 thru 5)	EOC video # EOC2-4-0055, 0056, 0064, 00136 & 0201. No evidence of jet firings near events.	n/a
QBAR = ~29 psf (~0.20 psi); Mach 22.7					------ 32:13:54:00 ------		EI + 591 sec; WLE Stagnation Temp: ~2850 F
12	deleted						
13	13:54:10 / 55:12	EI+601 / EI+663			Left Main Gear Brake Line Temp B (1) / Strut Actuator Temp (1) / Sys 3 LMG Brake Sw Vlv Ret Line Temp (FWD) (1) - start of off nominal trend	Unusual Temperature Increase	V58T1701A V58T0842A V58T0405A
14	13:54:20	EI+611			Start of slow aileron trim change; Reversal in trend of derived rolling moment coefficient.	The aileron trim setting observed in flight first deviates from the predicted trim setting at this pt in trajectory (GMT is approximate (+/- 10 sec) for aileron). Also, observed roll moment changed from a negative to positive slope (derived by analysis).	V90H1500C (aileron trim) n/a (roll moment)
15	13:54:22	EI+613			Mid Fuselage LT BondLine Temp at x1215 (1) & LH Aft Fus Sidewall Temp at x1410 (1) - start of off nominal trend	Unusual increase in temperature rise rate	V34T1106A V09T1724A
15.2	13:54:29	EI+620	X		Left Fuselage Side Surface temp BP3605T peaks and starts downward trend		V07T9253A X1000.7 Y-105 Z354.5
15.3	13:54:33.3 / 54:37	EI+624.3 / EI+628			Flash #1 - Orbiter envelope suddenly brightened (duration 0.3 sec), leaving noticeably luminescent signature in plasma trail; plus Debris # 6 - report of very bright debris observed leaving the Orbiter just aft of the Orbiter envelope.	EOC video # EOC2-4-0026, 0034, & 0009B. R3R and R2R jet firings occurred near events. Debris events 6 & 14 are visually the biggest, brightest events & therefore may indicate the most significant changes to the Orbiter of the western debris events.	n/a
15.32	13:54:34	EI+625	X		Left Fuselage Side Surface temp BP3703T peaks and starts downward trend		V07T9925A X1138.5 YLH Z441.5
13.33	13:54:39	~EI+630	X		Strain Gages Centered on the Upper Surface of the Left MLG Wheel Wheel - Higher-than-expected strain indications observed in these gages	Note: PCM3 entry data is in snapshot format (not continuous), therefore event may have occurred earlier than noted	V12G9156A, V12G9157A, V12G9158A

STS-107 Mishap Investigation - Combined Summary Time Line
-BASELINE-

Integ Time Line Team - REV 17 BASELINE

5/8/2003 11 AM

Note: Rev 17 BASE integrates the OEX data timeline with the Baselined Rev 16 timeline plus IEE aero event changes (accounted for wind effects in aero increment derivation process).
Rev 17 was baselined by the OVE Working Group Team as of 5/7/03.

Sum No.	GMT GMT Day 32	EI sec	OEX data	Milestone	Entry Event	Remarks	MSID
13.34	13:54:39	~EI+630	X		Left Wing X1040 Spar Web - shows increase in strain	Note: Adjacent sensor V12G9165A did not show similar "off-nominal" signature at this time, also, PCM3 entry data is in snapshot format (not continuous), therefore event may have occurred earlier than noted	V12G9166A V12G9167A (V12G9165A-nominal)
QBAR = ~34.5 psf (~0.24 psi); Mach 22.1					------ 32:13:55:00 ------		EI + 651 sec; WLE Stagnation Temp: ~2900 F
15.35	13:55:04 / 55:29	EI+655 / EI+680			Debris # 7, 7A, & 8 thru 10 observed leaving the Orbiter just aft of Orbiter envelope. Debris 8, 9, & 10 were seen aft of the Orbiter envelope inside Debris Shower A (next event listed).	EOC video # EOC2-4-0005, 0017, 0021, 0028, 0030, 0098 & 0161. No evidence of jet firings near events except 7A where analysis still pending.	n/a
15.37	13:55:22 / 55:28	EI+673 / EI+679			Debris Shower A - Report of debris shower seen just aft of Orbiter envelope.	Seen just aft of Orbiter envelope. Over the course of these four seconds a luminsecent section of plasma trail is observed which appears to contain a shower of indefinite particles and multiple, larger discrete debris that includes Debris 8, 9, and 10.	Saw debris: EOC2-4-0098, 0161, 0005, 0030 Saw shower: EOC2-4-0017, 0021, 0028
15.4	deleted					Rationale for deletion: Upon further evaluation of the data, it was determined that the remote sensor signatures had been seen in previous flights and/or could be explained by known events.	
15.43	13:55:33 / 56:03	EI+684 / EI+714			Two events of return link comm drop-outs (Comm events 12 & 13)	On upper right aft antenna (TDRS 171/W). Uncertain if off-nominal based on previous flight data. Comm loss not continuous thru period indicated.	
15.44	13:55:34	EI+685	X		Xo 1040 Spar (MLG Forward Wall Spar) Strain Gage - Upper Cap - sudden drop in strain followed by gradual increase until erratic signature at approximately EI+930		V12G9049A X1040 Y-135 ZUPR
15.45	13:55:35 / 56:13	EI+686 / EI+724			Debris # 11, 11A, 11B, 11C & 12 thru 15 observed leaving the Orbiter just aft of Orbiter envelope. Debris #11B & #11C events were both seen at the head of a parallel plasma trail aft of the Orbiter envelope. Debris #12 event was preceded and followed by secondary plasma trails. Debris #13 event was followed by momentary brightening of plasma trail adjacent to debris. Debris #14 event consisted of very bright debris observed leaving the Orbiter.	EOC video # EOC2-4-0005, 0017, 0021, 0028, 0030, 0050, & 0098. No evidence of jet firings near events. (Nearest jet firings occur at 56:17.) Debris events 6 & 14 are visually the biggest, brightest events & therefore may indicate the most significant changes to the Orbiter of the western debris events.	n/a
15.5	13:55:41	EI+692			Mid Fuselage Port (Left) Sill Longeron Temp at X1215 - start of off nominal trend	Unusual Temperature Increase	V34T1118A
QBAR = ~40 psf (~0.28 psi); Mach 21.4					------ 32:13:56:00 ------		EI + 711 sec; WLE Stagnation Temp: ~2900 F
16	13:56:03 / 56:24	EI+714 / EI+735			Left Lower/Upper Wing Skin Temps - Trending down (2)	Indication of potential measurement failures	V09T1002A V09T1024A
16.5	13:56:16 / 56:53	EI+727 / EI+764			Hyd Sys 1 LMG Uplock Actuator Unlock Line Temp; Sys 3 LMG Brake Sw Vlv Ret Line Temp (FWD); LMG Brake Line Temp C; LMG Brake Line Temp B; Sys 3 Left Main Gear Strut Actuator Temp - all show a temp rise rate change.	Significant increase in temp rise rate on all four lines	V58T0125A V58T1701A V58T0842A V58T0405A V58T1702A
16.55	13:56:30 / 56:55	EI+741 / EI+766			First Roll Reversal initiation / completion		V90H1044C
16.6	deleted					Rationale for deletion: Comm dropout (event 14) is deleted since probably nominal due to completion of roll reversal resulting in elevation angle nearing 60 deg's (vertical tail interfence w/comm).	
QBAR = ~42 psf (~0.29 psi); Mach 20.7					------ 32:13:57:00 ------		EI + 771 sec; WLE Stagnation Temp: ~2900 F
16.65	13:57:09	EI+780	X		Fuselage Side Surf Thermocpl BP3976T - start of off-nominal trend (temp increase followed by temp drop / rise)		V07T9270A X1486.1 Y-124.8 Z307.1
16.67	13:57:09	EI+780	X		Fuselage Lower Surface BF Thermocpl BP220T - start of off-nominal trend (shallow temp drop)		V07T9508A X1560 Y-111.1 Z LWR
16.7	13:57:19 / 24	EI+790 / EI+795			MLG LH Outbd Tire Pressures 1 & 2 - start of small increase in pressures	Not seen in previous flights	V51P0570A V51P0572A

STS-107 Mishap Investigation - Combined Summary Time Line
-BASELINE-

Integ Time Line Team - REV 17 BASELINE **5/8/2003 11 AM**

Note: Rev 17 BASE integrates the OEX data timeline with the Baselined Rev 16 timeline plus IEE aero event changes (accounted for wind effects in aero increment derivation process).
Rev 17 was baselined by the OVE Working Group Team as of 5/7/03.

Sum No.	GMT GMT Day 32	EI sec	OEX data	Milestone	Entry Event	Remarks	MSID	
16.8	13:57:19 / 58:01.5	EI+790 / EI+832.5			Debris # 16 (very faint debris) observed leaving just aft of Orbiter followed by two events of assymmetrcial brightening of the Orbiter shape (Flares 1 and 2). (Occurred over eastern AZ and NM.)	Debris #16: EOC video # EOC2-4-00148-2. Flares #1 & 2: EOC2-4-00148-4. Observations by personnel from the Starfire Optical Range (Kirtland Air Force Base, NM).	n/a	
17	13:57:28 / 57:43	EI+799 / EI+814			Left Lower/Upper Wing Skin Temps (2) - OSL		V09T1002A	V09T1024A
18	deleted							
19	13:57:54				Sys 2 LH Brake Sw Vlv Return Temp (1)	Unusual Temperature Increase	V58T0841A	
QBAR = ~52.5 psf (~0.36 psi); Mach 19.8					------ 32:13:58:00 ------		EI + 831 sec; WLE Stagnation Temp: ~2880 F	
20	13:58:03				Start of sharp aileron trim Increase	GMT is approximate (+/- 10 sec)	V90H1500C	
20.3	13:58:04	EI+835	X		Left fuselage side surface temp BP3605T starts off-nominal temperature increase		V07T9253A X1000.7 Y-105 Z354.5	
20.5	13:58:04 / 58:19	EI+835 / EI+850			Increase in off-nominal aero increments.	Substantial increase in rate of change of rolling and yawing moment increments and initial indication of off-nominal pitching moment increment. Derived by analysis.	n/a	
21	deleted							
22	deleted							
22.5	13:58:16	EI+847			LMG Brake Line Temp D - Temp rise rate change	Significant increase in temp rise rate.	V58T1703A	
23	13:58:32 / 58:54	EI+863 / EI+885			MLG LH Inbd / Outbd Tire Pressures (4) - Decay to OSL		V51P0570A V51P0571A	V51P0573A V51P0572A
24	deleted							
25	13:58:39 / 58:48	EI+870 / EI+879			MLG LH Inbd/Outbd Wheel Temps (2) - OSL		V51T0574A	V51T0575A
25.5	13:58:40	EI+871			BFS Fault Msg (4) - Tire Pressures - 1st Message			
26	13:58:56	EI+887			BFS Fault Msg (4) - Tire Pressures - Last Message			
QBAR = ~63.5 psf (~0.44 psi); Mach 18.7					------ 32:13:59:00 ------		EI + 891 sec; WLE Stagnation Temp: ~2850 F	
27	13:59:06				Left Main Gear Downlocked Indication - Transferred ON		V51X0125E	
27.3	13:59:09 / 59:39	EI+900 / EI+930	X		Several left side temperature measurements show a rapid increase in temperature followed by erratic behavior and subsequent loss of the measurements at approximately EI+940		V07T9925A V07T9972A V07T9976A V07T9903A V07T9913A	V07T9976A V07T9978A V07T9222A V07T9223A
27.5	13:59:23	EI+914			Loss of MCC real-time data to the workstations in the FCR and MER			
27.7	13:59:26 / 59:28	EI+917 / EI+919			Abrupt increase in off-nominal aero increments.	Abrupt increase in rate of change of pitching, rolling, and yawing increments. Magnitude of aero increments starting to exceed ability of aileron to laterally trim the vehicle. Derived by analysis.	n/a	
28	13:59:30.66 / 59:30.68	EI+921.66 / EI+921.68			Start of two yaw jets firing (R2R and R3R)	Fired continuously until end of data at 13:59:37.4	V79X2634X	V79X2638X
29	13:59:31	EI+922			Observed elevons deflection at LOS	Left: -8.11 deg (up) Right: -1.15 deg (up)		
29.3	13:59:31.4 / 59:34.5	EI+922.4 / EI+925.5			Several events and PASS and BFS FSM messages during this time period all indicate the failure signature of ASA 4	ASAs responded appropriately. However, signature is indicative of failure of ASA 4.	V57H0253A (5 Hz)	
29.5	13:59:32	EI+923			Observed aileron trim at LOS	-2.3 degrees		
30	deleted							
31	deleted							
32	deleted							
32.5	13:59:32	EI+923		Approx Veh Grd Location: 32.9 N / -99.0 W	Altitude ~200700 ft / Mach ~18.1 - Near Dallas TX	Approximate Vehicle Ground Location at Loss of Signal based on GMT; Data source: STS-107 GPS Trajectory Data	n/a	
33	13:59:32.136	EI+923.136		LOS	Last valid downlink frame accepted by ODRC - OI / BFS / PASS. Start of reconstructed data.	Nominal loss of comm at this GMT (for ~15 sec max based on previous flt data)		
34	deleted							
35	13:59:35/36	EI+926 / EI+927			Sideslip on vehicle changes sign.	The event occurred between the two times listed. Aerodynamic forces due to sideslip are now reinforcing aerodynamic asymmetry.	n/a	
36	13:59:36	EI+927			Growth in Bank attitude error	Up until this time the flight control had been able to maintain the Bank error around 5 deg.		
37	13:59:36.8	EI+927.8			Aerojet DAP Requests Third Right Yaw RCS Jet (R4R)	This additional jet is required to counteract the increasing aerodynamic moments on the vehicle. Fired continuously until end of data at 13:59:37.4		
38	13:59:37.3	EI+928.3			Aerojet DAP Requests Third Right Yaw RCS Jet (R1R)	This additional jet is required to counteract the increasing aerodynamic moments on the vehicle. Fired continuously until end of data at 13:59:37.4		

STS-107 Mishap Investigation - Combined Summary Time Line
-BASELINE-

Integ Time Line Team - REV 17 BASELINE

5/8/2003 11 AM

Note: Rev 17 BASE integrates the OEX data timeline with the Baselined Rev 16 timeline plus IEE aero event changes (accounted for wind effects in aero increment derivation process).
Rev 17 was baselined by the OVE Working Group Team as of 5/7/03.

Sum No.	GMT GMT Day 32	El sec	OEX data	Milestone	Entry Event	Remarks	MSID
39	13:59:37.n	EI+928.n			Last aileron data	The aileron position is now approx -5.2 deg with approx -2.5 deg of aileron trim. The rate of change of aileron trim had reached the maximum allowed by the flight control system.	
40	13:59:37.396	EI+928.396		End of 5-second period of reconstructed data	End of first 5-seconds of the 32-second period of post-LOS data. Start of approximately 25 seconds of no data available	GMT derived by MER data personnel	n/a
40.5	13:59:39 / 14:00:19	EI+930 / EI+970	X		Beginning at EI+930 and continuing until the loss of sync on OEX data (EI+964.4 for PCM and EI+970.4 for FDM), essentially all of the OEX data for the entire vehicle becomes erratic and fails		
41	13:59:46.347 / 14:00:01.900*	EI+937.347 / EI+952.900			PASS Fault Message annunciation - ROLL REF PASS Fault Message annunciation - L RCS LEAK BFS Fault Message annunciations - L RCS LEAK (2)	*Time info corrupted on some of the events.	
QBAR = nn psf; Mach nn					------ 32:14:00:00 ------		EI + 951 sec; WLE Stagnation Temp: ~2800 F
42	14:00:02/06	EI+953 / EI+957			Debris A observed leaving the Orbiter - Large debris seen falling away from the Orbiter envelope.	EOC videos # EOC2-4-0024, EOC2-4-0018 & EOC2-4-0118	n/a
43	14:00:02.654	EI+953.654			PASS Fault Message annunciation - L RCS LJET		
44	14:00:02.660	EI+953.660		Beginning of 2-second period of reconstructed data	Start of last 2-seconds of the 32 second period of post-LOS data.		
					During this final 2 second period of reconstructed data, the data indicates the following systems were nominal: APUs were running and WSB cooling was evident. MPS integrity was still evident. Fuel cells were generating power and the PRSD tanks/lines were intact. Comm and navaids systems in the forward fuselage were performing nominally. RSB, Body Flap, main engine, and right wing temps appeared active. ECLSS performance was nominal. During this final 2 second period of reconstructed data, the data indicates the following systems were off-nominal: All three Hyd systems were lost. The left inbd/outbd elevon actuator temps were either OSL or no data exists. Majority of left OMS pod sensors were either OSH or OSL or no data exists. Elevated temps at bottom bondline centerline skin forward and aft of the wheel wells and at the port side structure over left wing were observed. EPDC shows general upward shift in Main Bus amps and downward shift in Main Bus volts. AC3 phase A inverter appeared disconnected from the AC Bus. GNC data suggests vehicle was in an uncommanded attitude and was exhibiting uncontrolled rates. Yaw rate was at the sensor maximum of 20 deg/sec. The flight control mode was in AUTO. (Note that all Nav-derived parameters (e.g., alpha) are suspect due to high rates corrupting the IMU state.)		
45	14:00:03.470 / 14:00:03.637*	EI+954.470 / EI+954.637			BFS Fault Message annunciation - L OMS TK P BFS Fault Message annunciation - Indeterminant BFS Fault Message annunciation - SM1 AC VOLTS PASS Fault Message annunciation - L RCS PVT	* Time info corrupted on some of the events.	
46	14:00:03.637	EI+954.637			PASS Fault Message annunciation - DAP DOWNMODE RHC	The s/w process which logs the PASS message runs every 1.92 seconds, so this event could have occurred as early as 14:00:01.717 GMT. However, during the 2 sec period, available vehicle data indicates RHC was in detent and DAP was in AUTO.	
47	14:00:04.826	EI+955.826		End of 2-second period of reconstructed data	Last identifiable OI Downlink frame		n/a
47.5	14:00:13.439	EI+964.439	X		OEX PCM loss of sync		
48	14:00:17 / 14:00:22	EI+968 / EI+973			Debris B and C observed leaving the Orbiter	EOC videos # EOC2-4-0024 & -0118 (for both B and C)	n/a
48.5	14:00:19.44	EI+970.44	X		FDM1 A end of data		
49	14:00:21 / 14:00:25	EI+972 / EI+976			Vehicle Main Body break-up	EOC videos # EOC2-4-0024, -0018 &-0118	n/a
50	14:00:53	EI+1004		End of Peak Heating		Determined by analysis	

= Nominal/Expected Event or Performance

Volume V
Appendix G.9

Contracts, Incentives, and Safety/Technical Excellence

This Appendix contains a Report to Columbia Accident Investigation Board: Contracts, Incentives, and Safety/Technical Excellence, Olson, Gary, Foster, Tim; 27 May 2003.

THIS PAGE INTENTIONALLY LEFT BLANK

Report to CAIB:

Contracts, Incentives, and Safety / Technical Excellence

Submitted by: Gary Olson and Tim Foster – 27 May2003

Contracts, Financial Incentives, and Safety / Technical Excellence

Summary

NASA efforts to enhance contractor performance have resulted in complex contracts with multiple incentives. The assumptions are:

- The opportunity to increase corporate profits motivates management and workers more than devotion to astronaut safety, to program success, and to their own livelihood;
- Contractors so motivated will act always in the government's interest with minimal oversight;
- These incentives enhance NASA leverage with sole source, non-competitive, cost-reimbursement contractors.

The extensive use of incentives, particularly award fees (the principal one) detracts from technical excellence and safety. For example, they:

- Make fee dollars, not technical excellence and safety, the primary focus for program oversight and review.
- Encourage complacency through high scores, emphasis on contractor strengths, and loophole-ridden "metrics" that often stipulate tolerance for errors and lateness.
- Devalue the contributions of many by assigning relative weights to work areas.

Because the outcome of incentive fee processes has become predictable – high fees (near or above the normal limit) –NASA probably will be unable to regain leverage and avoid contractor complacency absent competition. "Conventional wisdom" in NASA presumes that only aerospace firms can manage shuttle work.

The people and facilities at NASA sites, not corporate logos, are critical to program requirements. NASA's shuttle work is based on NASA-owned technology, done for the most part at NASA-owned facilities by a workforce trained by NASA and dedicated to the facility. Department of Energy, in similar situation, has had no shortage of reputable bidders for management and operating contact work.

The U.S. Naval Nuclear Propulsion Program is evidence that a technical program of comparable complexity and risk can be managed successfully without extensive reliance on contract financial incentives and without being beholden to incumbent contractors.

Recommendation: Rather than hoping to motivate contractors to manage the NASA shuttle program through cumbersome financial incentives, NASA should:

- Develop a strong, stable, self-sufficient Shuttle Program Office of experienced, expert technical personnel capable of effective program management and oversight.
- Establish leverage over contractors by opening to competition by aerospace and non-aerospace companies what are in effect management and operating contracts.

Contract Environment

The NASA Space Shuttle Program relies predominantly on Lockheed Martin and Boeing, either as direct component suppliers or, for operations, through their joint venture creation, United Space Alliance (USA). Lockheed Martin and Boeing formed USA as a

Contracts, Financial Incentives, and Safety / Technical Excellence

limited liability corporation in 1996 in response to NASA desires to consolidate work under the Space Flight Operations Contract (SFOC).[1]

For SFOC and for major shuttle component work, which NASA decided not to incorporate into SFOC as originally planned, NASA has relied on sole source, non-competitive, cost-reimbursement contracts since shuttle program inception in the early 1970s. These contracts indemnify the contractors against third party claims for injury, loss of life, and property damage arising from shuttle operations. Progress payments ensure these contractors substantial, positive cash flow.[2] In addition, the contractors are realizing fees for this work averaging about 10% of incurred cost, the limit prescribed by the Federal Acquisition Regulation for cost-reimbursement contracts.[3]

Without the discipline of competition or fixed priced contracting, NASA provides multiple contract financial incentives to motivate shuttle program contractors. The theory is that since contractors are in business to make money, the best way to promote excellence is to tie fee payments to performance.

The emphasis on contract financial incentives extends beyond NASA; it tends to be government-wide. When the budget process generates fewer dollar and manpower resources than program managers request, the differences are often attributed to "inefficiencies" and lead to calls for better forms of contracting. The goal is to so effectively structure contract incentives that contractors, looking to their own financial interests, will act in the Government's best interest with little need for oversight.

In evaluating the NASA financial incentives and possible impact on safety, the following sections discuss each contract financial incentive that NASA uses in major shuttle program contracts as they pertain to technical excellence and therefore safety.

Cost Incentive Fees

All major shuttle program contracts are, in part, cost-plus-incentive-fee contracts. From a negotiated target cost and target fee, contractors get more fee dollars if costs at completion underrun the negotiated target cost, but less fee if they overrun the negotiated target cost. The percentages of underrun and overrun sharing are defined in the contract.

Cost-plus-incentive contracts may or may not significantly motivate contractors to reduce cost, depending on the situation:

- In the case of the reusable solid rocket motor contract, NASA program managers became concerned that the contract provisions overly motivated contractor management to reduce personnel, potentially to the program's detriment. NASA officials, therefore, eliminated the contract underrun sharing provision.[4]
- Cost incentives, on the other hand, can equally motivate contractors to negotiate higher target costs and higher prices for contract changes, or to submit claims for contract price adjustments in the case of potential overruns.

[1] Boeing and Lockheed Martin each put up $1M to form USA. They appoint top USA management and share profits 50/50.

[2] Contractor billings, submitted every two weeks and paid within seven days, include incurred costs, accrued costs, and provisional fees.

[3] FAR 15.903

[4] NASA and the contractor agreed to redirect the equivalent fee potential to other areas.

- For repetitive, non-competitive contracts, a contractor might conclude that the long-term benefits of sustaining a high cost base for future contract negotiations outweigh the near-term advantages of driving down costs.

Determining whether these cost incentive contract provisions actually save money is difficult. However, to outsiders they seem to satisfy the feeling that contractors that spend less should get more fee.

On the plus side, cost-plus-incentive-fee provisions generate little, if any, additional effort or distraction for workforce or management. Beyond a possible tendency towards more aggressive contract price negotiations, these provisions should involve little, if any, additional administrative effort beyond that required for any other cost reimbursement contract; i.e., Government validation of costs incurred.

Conclusion – Cost Incentive Fees

Regardless of the extent to which they may or may not actually reduce costs, cost incentives as used in major shuttle program contracts do not seem likely to detract significantly from technical excellence and safety.

Performance Incentive Fees

Performance incentive arrangements pay fixed sums for meeting prescribed program milestones and impose penalties for failure to meet selected milestones. Performance-based contracting is not uniquely a NASA concept. Rather, the approach arose government-wide as a way to motivate contractors.

NASA policy ties performance incentive fees to objective milestones, either schedular or successful completion of specific tasks or events; e.g., delivery of a product, successful launch, or successful flight. Since successful completion often demonstrates safe operation, these performance standards also fall into the category of safety incentives.

These performance incentive fees are "all-or-nothing" payments. A contractor either earns the performance fee for that event or gets nothing – or may have to pay a penalty.

Whether tying fee payments to performance milestones provides any additional motivation to workers and management is not clear. These performance incentives did not preclude USA from missing milestones that resulted in fee forfeiture of from $1M to $3M each on five different occasions. Moreover, shuttle program managers note that contractor / customer relations become more contentious when a contractor might miss an incentivized milestone. In such situations, fee forfeiture can be avoided if the contractor can successfully blame the delay on others.

Whether or not these performance incentives provide added incentive, administration of performance-incentive-fee contract provisions does not seem to impose substantial additional workload on management and workers. The contract milestones tend to be ones that would be the focus of any effective program management system.

Conclusion—Performance Incentive Fees

There appears to be little evidence, one way or the other, that performance incentive fees enhance shuttle program contractor performance. However, they seem to pose little risk of burdening or distracting technical effort from primary functions beyond the possibility of inserting contractor financial and contract specialists more deeply into technical and production work.

Contracts, Financial Incentives, and Safety / Technical Excellence

Award fees

Background

In addition to having cost-plus-incentive-fee provisions, all major shuttle program contracts also have cost-plus-award-fee provisions. This means that every six months a performance evaluation board subjectively evaluates contractor performance, assigns a numeric performance grade, and recommends to a fee-determining official an award fee as a percentage of available fee assigned for that period.

Award Fee Process and Scoring

The purpose of the award fee is to make contractors more responsive to customer needs. Since contractors are in business to make money, the theory is people who actually manage and execute the work can best be motivated if they see a connection between their work and corporate profits. According to NASA policy, the award fee process is designed to promote "... more effective communications among Government and contractor personnel, at management levels where decisions can be made and results achieved."[5]

The award fee process seems inevitably to result in high scores and realized fee levels near or above the normal 10 percent maximum limit for cost reimbursement contracts.[6] The question is whether the high scores actually reflect exceptional performance across the board or are they largely a predictable outcome. Also, if the performance is as good as indicated, should the success be attributed primarily to the award fee process?

NASA policy specifies a contractor that satisfactorily meets contractual commitments will fall into the "good" range (score: 71-80). However, overall ratings for shuttle program contractors tend always to fall in the mid-80s to low-90s on a scale of 100. For the period preceding the Columbia accident, all major shuttle program contractors rated "excellent", which NASA policy defines as "exceptional performance".

The complexity of the performance evaluation process varies by contract. For SFOC, NASA contract monitors, called Technical Manufacturing Representatives, assess contractor strengths and weaknesses against nearly 400 elements grouped within thirteen functional areas. Some eighty of these elements are stated in the SFOC along with measures of performance, referred to as "metrics", for each one.

Each monitor assigns a numerical grade for his or her area of oversight. These scores, after weighting for relative importance and budget significance, determine the recommended overall contractor performance rating. Interestingly, the grades assigned by three of the twelve monitors determine 75 percent of the proposed SFOC award fee score.

For major shuttle program contracts other than SFOC, NASA managers also list strengths and weaknesses, and assign weights to perhaps a dozen areas of performance. However, the award-fee provisions are much simpler than the elaborate process followed in the SFOC. In essence, program managers for these contracts are not so constrained by metrics in arriving at their subjective evaluations of contractor performance.

[5] NASA *Award Fee Contracting Guide* section 3.7.1
[6] Under the Federal Acquisition Regulation, NASA may approve individual and class deviations from this limit.

Contracts, Financial Incentives, and Safety / Technical Excellence

The award fee process, occurring every six months with interim assessments at the midpoint, seems to have become the principal forum for reviewing work. But the process differs from more traditional reviews in that issues are translated into fee dollars.

To reduce performance evaluation to a score, the award fee process compares contractor strengths and weaknesses. This balancing of good with bad might be useful for rationalizing performance scores, but is of little value in accomplishing work. In the absence of these incentives, traditional reviews would emphasize problems, potential problems, actions needed on critical path items, and areas that need management attention.

Overall performance scores vary within a relatively small range from period to period.

There are reasons, aside from possible performance, why ratings tend to be much higher than "good".

- NASA policy encourages high awards, stating: "...an award fee contract should provide the contractor with a reasonable opportunity to earn the maximum award fee available".
- The NASA managers who have day-to-day responsibility for each area assign grades for contractor performance in that area. Poor contractor grades might reflect adversely on their own performance.
- Poor contractor performance scores could strengthen the hand of program critics and jeopardize program support for the budget arena.
- When contractors respond to a customer-identified area of emphasis, performance evaluators may feel obliged to increase the score, which over time can lead to rising grades.
- Higher grades are less subject to contractor rebuttal in front of the performance evaluation board.

Corporate Profit Maximization Is Not The Best Focus and Motivator for Those Who Actually Do the Work

The risk with award fees is that both customers and contractors begin focusing on the award fee process rather than on the work itself.

It is hard to imagine that, for all those involved in shuttle program work, the prospect of influencing in some small way corporate profits could surpass the incentives inherent in the work itself. They are contributing to a nationally recognized, prestigious program the fate of which (not to mention their own livelihood) depends upon public confidence and safety. The importance of their work to the safety of the astronauts they see working around them is certainly well recognized and to suggest the opportunity to earn the company a little extra fee would enhance their concern would be to do them a great disservice.

NASA policy requires grading based on evaluation factors weighted as to relative importance. This is not conducive to technical excellence. For example, does it promote technical excellence to assign, as NASA has in the SFOC, a 20 percent weight factor to "Operational Safety", which includes industrial safety? Or, does it inspire technical excellence to assign "Quality" the same 15 percent weighting as contractor performance in awarding contracts to small, minority, or disadvantaged business?

Contracts, Financial Incentives, and Safety / Technical Excellence

In a similar vein, the SFOC, as previously noted, defines more than 80 performance elements with associated "metrics", the apparent result of a procurement initiative to demonstrate commitment to performance-based contracting. From a practical standpoint, the metrics run counter to the pursuit of excellence.

Many of the contract metrics stipulate customer tolerance for errors or lateness. Others include loopholes that render them largely irrelevant. The following are examples of "expected" levels of performance. The contract also identifies for many items an even lower level of acceptable performance called maximum error rate.

- **Safety, Mission Assurance, and Product Assurance:**

  "Expectation: 85% of risk packages presented to the Government are accepted."

  "Expectation: 85% of items correctly assessed as no increased risk validated through use, Government audit, or Government surveillance."

  "Expectation: 15 mishaps per year." ("Mishaps" are injury to non-SFOC contractor personnel or damage to NASA property by accidents / incidents during processing.)

- **Quality Assurance:** "Expectation: 95% of all mandatory Government inspections are accepted.... Success rate of SFOC work volume greater than 90%."

- **Orbiter Logistics:** "Expectation: 96% of all reparable Orbiter hardware requirements satisfied by the negotiated need dates."

- **Backup Flight System (and Pass Flight Software):** "Slips or redelivery caused by BFS not meeting negotiated schedules or due to a redelivery to correct an error are allowed if no additional resource impact to outside organizations is incurred."

- **Launch Readiness:** "Expectation: 97% of all items on the initial launch countdown constraints list completed and closed prior to Launch Countdown Call-to-Stations."

- **Engineering, Maintenance, and Operations Support for Flight Operations System:** "Expectation: 5% late, but in no case impact safety, mission success, or major program schedule milestones."

Finally, the award fee process tends to result in making engineering and other technical personnel more accountable to financial and contracting people whose job is to try to win as large an award fee as possible. The rewards for portraying contractor performance in its best light are inconsistent with prompt and candid problem reporting and performance self-assessment, which is vital to successful management of complex technical programs.

Conclusions -- Award-fee contracts:

Continued reliance on award-fee provisions would significantly detract from emphasis on technical substance and problem resolution. An environment that, in effect, tries to make engineers and technical people their own corporate profit centers is not conducive to technical excellence.

Other Contract Financial Incentives

Major shuttle program contracts include other, less significant, financial incentives. These include:

- "Performance Plus" incentives. These are relatively small amounts program managers are able to use at their discretion to focus contractor attention on near-term actions.

Contracts, Financial Incentives, and Safety / Technical Excellence

- "Value Engineering" incentives. These are standard government contract provisions designed to encourage contractors to recommend cost-saving modifications to specification requirements. If accepted by the government, the contractor shares in the estimated savings.
- "Employee Incentives". USA, for example, makes a flat payment to all non-supervisory employees each year depending on USA success in earning award fee. NASA, however, is not involved in these incentive payments except that NASA, not USA, bears the full cost of this program.

Conclusion – Other Contract Financial Incentives.

Whether or not these incentives are effective, they seem to impose little or no additional effort or adverse impact on those who perform the work. The Program Plus incentive, however, further reinforces the notion that the customer, in effect, must "tip" the contractor to get its work done.

Fee Reduction for Catastrophic Loss.

The most prominent, safety-related contract financial incentive in all current major shuttle program contracts is a clause entitled "Fee Reduction for Catastrophic Loss".

As explained earlier, the government indemnifies shuttle program contractors from liability for such loss, whether loss of life, damage to government property, or other third party liability. The Catastrophic Loss clause, however, allows NASA to reduce contractor fee by a prescribed amount if NASA determines that the accident was due to that contractor's actions or failure to act. [7] The clause requires the NASA finding to be based on an accident board's finding.

Interestingly, only the most recent external tank contract contains the Catastrophic Loss clause. The contract under which Lockheed Martin delivered the external tank used on the last Columbia flight has no such clause. [8]

From a practical standpoint, the Catastrophic Loss clause – or any other clause of that sort, regardless of amount – is unlikely to enhance contractor management or workforce attention to safety. Even at $10M or more in forfeited fees, the damage to the corporate image due to loss of life and technical failure in such a highly visible program would be incomparably greater. Nor is there reason to believe the clause would stimulate managers and workers to apply higher standards than they would otherwise apply. Their connection to the program, to the astronauts, and to their own jobs is no doubt stronger than their devotion to corporate finance.

Conclusion – Catastrophic Accident Penalty.

The effect of the Catastrophic Accident clause on contract performance seems minimal – certainly not negative. However, having the provision is helpful to demonstrate a measure of recompense where a contractor is responsible. This provision, which

[7] The SFOC specifies no fee for the six-month period in which the accident occurred. The most recent external tank contract stipulates a $10M penalty. The Space Shuttle Main Engine and Reuseable Solid Rocket Motor contracts specify a $10M penalty and forfeiture of all fees for the six-month period in which the accident occurred.
[8] According to NASA officials, Lockheed Martin was unwilling to accept the clause without a corresponding increase in contract fee.

Contracts, Financial Incentives, and Safety / Technical Excellence

predetermines the forfeiture amount, is preferable to leaving the question open for possible litigation.

Overall Conclusion

NASA relies very extensively on contract financial incentives to motivate major shuttle program contractors. There is no evidence these contract provisions directly contributed to the Columbia accident. Nor is there evidence they actually motivate contractors and enhance excellence.

To the extent financial incentives might help focus additional attention on cost reduction and key milestones, they can be positive. If instead financial incentives encourage contractor personnel to try to game the system by initially inflating contract prices or by setting the stage constantly to be able to blame others for missed milestones, they can be counterproductive. Overall, however, the cost incentive and performance incentive processes demand little, if any, additional effort or distraction on the part of those actually doing the work. The cost incentive is based on incurred costs; the performance incentives on events or tasks most likely to be tracked in any event.

In contrast to the cost and performance incentives, the contract award fee provisions are cumbersome and counterproductive.

- The award fee process in practice results almost inevitably in high grades and near maximum fees for major shuttle program contractors. These high grades, together with an award fee process that emphasizes contractor strengths as well as weaknesses, can encourage complacency.
- The assignment of relative weights to elements of contract performance based on several factors, including budget share, although required for award fee purposes, can do more harm than good. It tends to diminish the importance of the contributions that all must make in contract execution.
- The award fee process now seems to be the primary forum for program oversight and review. That this forum must translate technical and production issues into fee dollars sends a message that money, not technical excellence, is the important objective.
- The “metrics”, which the NASA procurement community apparently required to be included in SFOC, tend to undermine excellence, not encourage it. The standards are filled with loopholes that make many of them useless. They concede customer tolerance for errors and late deliveries.

The Catastrophic Loss contract provision bears most directly on safety by prescribing that a contractor must forfeit $10M or more in cases where NASA determines that contractor is responsible for the accident. However, that management and the workforce would view this forfeiture of corporate fee as a more powerful incentive for safety than their inherent commitment to the safety of the astronauts, to the well being of the program, and their own livelihoods is unlikely.

Overall, the extensive use of contract financial incentives in the space shuttle program seems more a reaction to government-wide procurement policies than something NASA managers invented as an important program management tool. The award fee structure in the SFOC seems to have been primarily the work of procurement personnel, not technical program managers.

Contracts, Financial Incentives, and Safety / Technical Excellence

In a budget-constrained environment and under pressure to reduce its federal payrolls, NASA contracting efforts focus on trying to structure incentives so effective that the contractor, pursuing its own financial interests, will automatically work to the government's benefit – with limited NASA oversight. Consequently, management attention on both sides tends to focus on dollars vice technical excellence. Financial incentives are no substitute for oversight by experienced, expert technical customer representatives. To this end, NASA should ensure that the Space Shuttle Program Office becomes a strong, stable, and self-sufficient entity capable of performing that function.

Contract financial incentives, such as NASA uses for shuttle program work, are not the only path to technical excellence and safety. NASA's Administrator has characterized the highly successful Naval Nuclear Propulsion Program as perhaps the most similar to NASA's space shuttle program in terms of engineering challenge. Both must apply complex and demanding technologies in a hostile environment with the lives of crewmembers as well as National interests at stake. The Naval Nuclear Propulsion Program, however, goes about the task much differently insofar as contracting.

The Naval Nuclear Propulsion Program avoids financial incentives in contracts with its major prime contractors – opting instead for close oversight by relatively small, but technically competent, headquarters and field organizations. Naval Nuclear Propulsion Program prime contractors operate under low-fee, cost-plus-fixed-fee contracts that include no contract financial incentives.

The theory behind this approach is that the best way to sustain an environment conducive to technical excellence and objectivity is to free those doing the work from corporate pressures to maximize profits. Program decisions with respect to assigning work and whether to extend or re-compete management and operating contracts provide ample business leverage to ensure contractor responsiveness to program needs. NASA, in efforts to focus more clearly on technical substance, might be well advised to consider the Naval Nuclear Propulsion Program approach.

With nearly 30 years of cost-plus-award-fee contracting tradition for major shuttle program work, incumbent contractors have no doubt become accustomed to high profit, no-risk, no investment, and generous cash flow associated with these contracts. With this background, effecting any substantive change in contracting approach through sole source negotiations with incumbent contractors may be impossible.

Should NASA consider significant change, it should reevaluate "conventional NASA wisdom" that only aerospace firms are candidates to compete for what in most cases amounts to management and operating contracts similar to the contracts the Department of Energy uses for nuclear weapons and naval nuclear propulsion work. As with the Department of Energy, to a large extent, critical NASA resources are government-financed technology, government-owned facilities, and workforces largely acquired, trained, and supported for decades at government expense.

NASA has historically concluded that only aerospace firms can be considered for NASA shuttle program work – a conclusion most recently reinforced by the NASA Space Shuttle Competitive Sourcing Task Force study published last fall. In contrast, the Department of Energy solicits competitive bids for management and operating contracts with the result that nationally know construction firms, component manufacturers, non profit institutions, universities, and even aerospace firms regularly vie for the work at a fraction of the fee NASA pays for these services. If they can design nuclear weapons and

Contracts, Financial Incentives, and Safety / Technical Excellence

naval nuclear propulsion plants for the Department of Energy – why cannot NASA overcome its attachment to the aerospace industry to seek management and operating support from a broader base?

The transition of SFOC work to USA demonstrated that change of operating contractors at NASA -sites could be effected with minimum impact without adverse effect on personnel retention or on pensions. Under the circumstances, no valid reason seems to exist beyond tradition that NASA should remain principally beholden to two contractors, or to the aerospace industry, for work at NASA sites. Department of Energy experience suggests no shortage of firms willing to assume responsibility for managing and operating complex work at its government sites.

The challenge to NASA in effecting significant change may be less formidable once the agency realizes that the people and facilities at NASA sites, not corporate logos, are critical to program requirements.

REPORT
VOLUME V

COLUMBIA
ACCIDENT INVESTIGATION BOARD

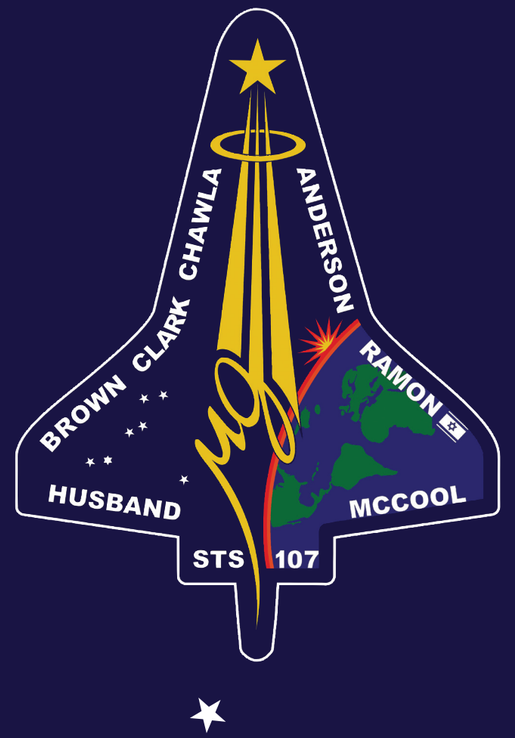

COLUMBIA ACCIDENT INVESTIGATION BOARD

OCTOBER
2003

REPORT VOLUME V
APPENDICES G.10 – G.12
OCTOBER 2003

COLUMBIA

ACCIDENT INVESTIGATION BOARD

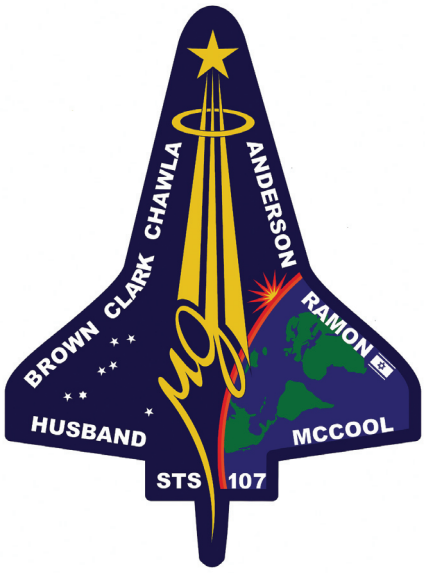

Note: Volumes II – VI contain a number of conclusions and recommendations, several of which were adopted by the Board in Volume I. The other conclusions and recommendations drawn in Volumes II – VI do not necessarily reflect the opinion of the Board, but are included for the record. When there is conflict, Volume I takes precedence.

REPORT VOLUME V

APPENDICES G.10 – G.12

OCTOBER 2003

On the Front Cover

This was the crew patch for STS-107. The central element of the patch was the microgravity symbol, μg, flowing into the rays of the Astronaut symbol. The orbital inclination was portrayed by the 39-degree angle of the Earth's horizon to the Astronaut symbol. The sunrise was representative of the numerous science experiments that were the dawn of a new era for continued microgravity research on the International Space Station and beyond. The breadth of science conducted on this mission had widespread benefits to life on Earth and the continued exploration of space, illustrated by the Earth and stars. The constellation Columba (the dove) was chosen to symbolize peace on Earth and the Space Shuttle Columbia. In addition, the seven stars represent the STS-107 crew members, as well as honoring the original Mercury 7 astronauts who paved the way to make research in space possible. The Israeli flag represented the first person from that country to fly on the Space Shuttle.

On the Back Cover

This emblem memorializes the three U.S. human space flight accidents – Apollo 1, Challenger, and Columbia. The words across the top translate to: "To The Stars, Despite Adversity – Always Explore"

The Board would like to acknowledge the hard work and effort of the following individuals in the production of Volumes II – VI.

Maj. Gen. John L. Barry	Executive Director to the Chairman
Dennis R. Jenkins	Investigator and Liaison to the Board
Lt. Col. Donald J. White	Technical Editor
Lt. Col. Patrick A. Goodman	Technical Editor
Joshua M. Limbaugh	Layout Artist
Joseph A. Reid	Graphic Designer
Christine F. Cole	Administrative Assistant
Jana T. Schultz	Administrative Assistant
Lester A. Reingold	Lead Editor
Christopher M. Kirchhoff	Editor
Ariel H. Simon	Assistant Editor
Jennifer L. Bukvics	Lead Project Manager
Donna J. Fudge	Senior Paralegal, Group II Coordinator
Susan M. Plott	Project Supervisor, Group III Coordinator
Ellen M. Tanner	Project Supervisor
Matthew J. Martin	Government Relations Consultant
Frances C. Fisher	ANSER Liaison

Limited First Printing, October 2003, by the
Columbia Accident Investigation Board

Subsequent Printing and Distribution by the
National Aeronautics and Space Administration
and the
Government Printing Office
Washington, D.C.

VOLUME I

PART ONE	THE ACCIDENT
Chapter 1	The Evolution of the Space Shuttle Program
Chapter 2	*Columbia*'s Final Flight
Chapter 3	Accident Analysis
Chapter 4	Other Factors Considered
PART TWO	WHY THE ACCIDENT OCCURRED
Chapter 5	From *Challenger* to *Columbia*
Chapter 6	Decision Making at NASA
Chapter 7	The Accident's Organizational Causes
Chapter 8	History as Cause: *Columbia* and *Challenger*
PART THREE	A LOOK AHEAD
Chapter 9	Implications for the Future of Human Space Flight
Chapter 10	Other Significant Observations
Chapter 11	Recommendations
PART FOUR	APPENDICES
Appendix A	The Investigation
Appendix B	Board Member Biographies
Appendix C	Board Staff

VOLUME II

CAIB TECHNICAL DOCUMENTS CITED IN THE REPORT

	Reader's Guide to Volume II
Appendix D.a	Supplement to the Report
Appendix D.b	Corrections to Volume I of the Report
Appendix D.1	STS-107 Training Investigation
Appendix D.2	Payload Operations Checklist 3
Appendix D.3	Fault Tree Closure Summary
Appendix D.4	Fault Tree Elements – Not Closed
Appendix D.5	Space Weather Conditions
Appendix D.6	Payload and Payload Integration
Appendix D.7	Working Scenario
Appendix D.8	Debris Transport Analysis
Appendix D.9	Data Review and Timeline Reconstruction Report
Appendix D.10	Debris Recovery
Appendix D.11	STS-107 Columbia Reconstruction Report
Appendix D.12	Impact Modeling
Appendix D.13	STS-107 In-Flight Options Assessment
Appendix D.14	Orbiter Major Modification (OMM) Review
Appendix D.15	Maintenance, Material, and Management Inputs
Appendix D.16	Public Safety Analysis
Appendix D.17	MER Manager's Tiger Team Checklist
Appendix D.18	Past Reports Review
Appendix D.19	Qualification and Interpretation of Sensor Data from STS-107
Appendix D.20	Bolt Catcher Debris Analysis

VOLUME III — OTHER TECHNICAL DOCUMENTS

Reader's Guide to Volume III

Appendix E.1 CoFR Endorsements
Appendix E.2 STS-107 Image Analysis Team Final Report
Appendix E.3 An Assessment of Potential Material Candidates for the "Flight Day 2" Radar Object Observed during the NASA Mission STS-107
Appendix E.4 *Columbia* Early Sighting Assessment Team Final Report

VOLUME IV — OTHER TECHNICAL DOCUMENTS

Reader's Guide to Volume IV

Appendix F.1 Water Absorption by Foam
Appendix F.2 Follow the TPS
Appendix F.3 MADS Sensor Data
Appendix F.4 ET Cryoinsulation
Appendix F.5 Space Shuttle STS-107 Columbia Accident Investigation, External Tank Working Group Final Report – Volume 1

VOLUME V — OTHER SIGNIFICANT DOCUMENTS

Reader's Guide to Volume V

Appendix G.1 Requirements and Procedures for Certification of Flight Readiness
Appendix G.2 Appendix R, Space Shuttle Program Contingency Action Plan
Appendix G.3 CAIB Charter, with Revisions
Appendix G.4 Group 1 Matrix Brief on Maintenance, Material, and Management
Appendix G.5 Vehicle Data Mapping (VDM) Team Final Report, Jun 13, 2003
Appendix G.6 SRB Working Group Presentation to CAIB
Appendix G.7 Starfire Team Final Report, Jun 3, 2003
Appendix G.8 Using the Data and Observations from Flight STS-107... Exec Summary
Appendix G.9 Contracts, Incentives, and Safety/Technical Excellence
Appendix G.10 Detailed Summaries: Rogers Commission Report, ASAP Report, SIAT Report 7
Appendix G.11 Foam Application and Production Chart 347
Appendix G.12 Crew Survivability Report 349
Appendix G.13 Aero/Aerothermal/Thermal/Structures Team Final Report, Aug 6, 2003

VOLUME VI — TRANSCRIPTS OF BOARD PUBLIC HEARINGS

Reader's Guide to Volume VI

Appendix H.1	March 6, 2003	Houston, Texas
Appendix H.2	March 17, 2003	Houston, Texas
Appendix H.3	March 18, 2003	Houston, Texas
Appendix H.4	March 25, 2003	Cape Canaveral, Florida
Appendix H.5	March 26, 2003	Cape Canaveral, Florida
Appendix H.6	April 7, 2003	Houston, Texas
Appendix H.7	April 8, 2003	Houston, Texas
Appendix H.8	April 23, 2003	Houston, Texas
Appendix H.9	May 6, 2003	Houston, Texas
Appendix H.10	June 12, 2003	Washington, DC

Reader's Guide to Volume V

Volume V of the Report contains appendices that were not cited in Volume I. These consist of documents produced by NASA and other organizations, which were provided to the Columbia Accident Investigation Board in support of its inquiry into the February 1, 2003 destruction of the Space Shuttle *Columbia*. The documents are compiled in this volume in the interest of establishing a complete record, but they do not necessarily represent the views of the Board. Volume I contains the Board's findings, analysis, and recommendations. The documents in Volume V are also contained in their original color format on the DVD disc in the back of Volume II.

THIS PAGE INTENTIONALLY LEFT BLANK

Volume V
Appendix G.10

Detailed Summaries

- Rogers Commission Report
- ASAP Report
- SIAT Report

THIS PAGE INTENTIONALLY LEFT BLANK

G.10 Past Reports Review

1.0 Past Reports Overview

The Columbia Accident Investigation Board was very interested in how other independent review boards had evaluated the Space Shuttle Program. A number of previously released reports were reviewed for relevance to the Columbia accident. At the highest level the Board looked at what general areas each of the reports had covered. These were broken up into nine categories, and most reports concentrated in a small subset of these areas. This evaluation provided the Board with insight into how NASA had previously responded to criticisms from independent evaluations, and also assisted the Board in determining how to frame new Findings and Recommendations for the strongest impact. The following table provides a general overview of the content of more than 45 previous reports.

Past Reports Review 1 of 3

	Infrastructure	Communication	Contracts	Risk Management	Quality Assurance	Safety Programs	Maintenance	Security	Workforce Issues
Rogers Report – 1986	●	●	●	●	●	●	●		
STS-29 Prelaunch Assessment – 1989				●					
"Augustine Report" – 1990		●	●	●			●		●
Paté-Cornell Report – 1990				●	●				●
"Aldridge Report" – 1992				●					
GAO: NASA Infrastructure – 1996	●								●
GAO: NASA Workforce Reductions – 1996	●								●
Super Light Weight Tank Independent Assessment – 1997				●	●				
Process Readiness Review – 1998				●			●		●
S&MA Ground Operations Report – 1998					●				
GAO: NASA Management Challenges – 1999		●	●	●					
Independent Assessment JS-9047 – 1999				●					
Independent Assessment JS-9059 – 1999				●					
Independent Assessment JS-9078 – 1999		●					●		
Independent Assessment JS-9083 – 1999					●				
S&MA Ground Operations Report – 1999					●	●			

Past Reports Review 2 of 3

	Infrastructure	Communication	Contracts	Risk Management	Quality Assurance	Safety Programs	Maintenance	Security	Workforce Issues
Space Shuttle Independent Assessment Team – 1999			●	●		●	●		●
Space Shuttle Ground Operations Report – 1999						●			
Space Shuttle Program (SSP) Annual Report – 1999						●			
GAO: Space Shuttle Human Capital & Safety – 2000						●			●
Independent Assessment JS-0032 – 2000					●				
Independent Assessment JS-0034 – 2000	●								
Independent Assessment JS-0045 – 2000					●				
IG Audit Report 00-039 – 2000			●						
NASA Independent Assessment Team – 2000		●		●	●	●			●
Space Shuttle Program Annual Report – 2000	●		●	●		●			
ASAP Report – 2001	●		●	●		●	●	●	●
GAO: NASA Critical Areas – 2001				●					
GAO: Space Shuttle Safety – 2001									●
Independent Assessment JS-1014 – 2001		●		●	●	●			
Independent Assessment JS-1024 – 2001		●			●				●

Past Reports Review 3 of 3

	Infrastructure	Communication	Contracts	Risk Management	Quality Assurance	Safety Programs	Maintenance	Security	Workforce Issues
Independent Assessment KS-0003 – 2001		●			●				●
Independent Assessment KS-1001 – 2001			●	●			●		
Workforce Survey-KSC– 2001				●	●				●
Space Shuttle Program Annual Report – 2001		●		●					
SSP Processing Independent Assessment – 2001				●	●	●			●
ASAP Report – 2002	●		●	●	●	●			●
GAO: Lessons Learned Process – 2002		●							
Independent Assessment KS-1002 – 2002					●				
Selected NASA Lessons Learned – 1992-2002		●		●	●	●	●		●
NASA Navy Benchmarking Exchange – 2002		●	●	●		●			●
Space Shuttle Program Annual Report – 2002	●			●		●			
ASAP Leading Indicators		●		●		●			
NASA Quality Management System – 2003					●				
QAS Tiger Team Report – 2003					●				
Shuttle Business Environment – 2003			●						

CAIB Review vs. Past Reviews

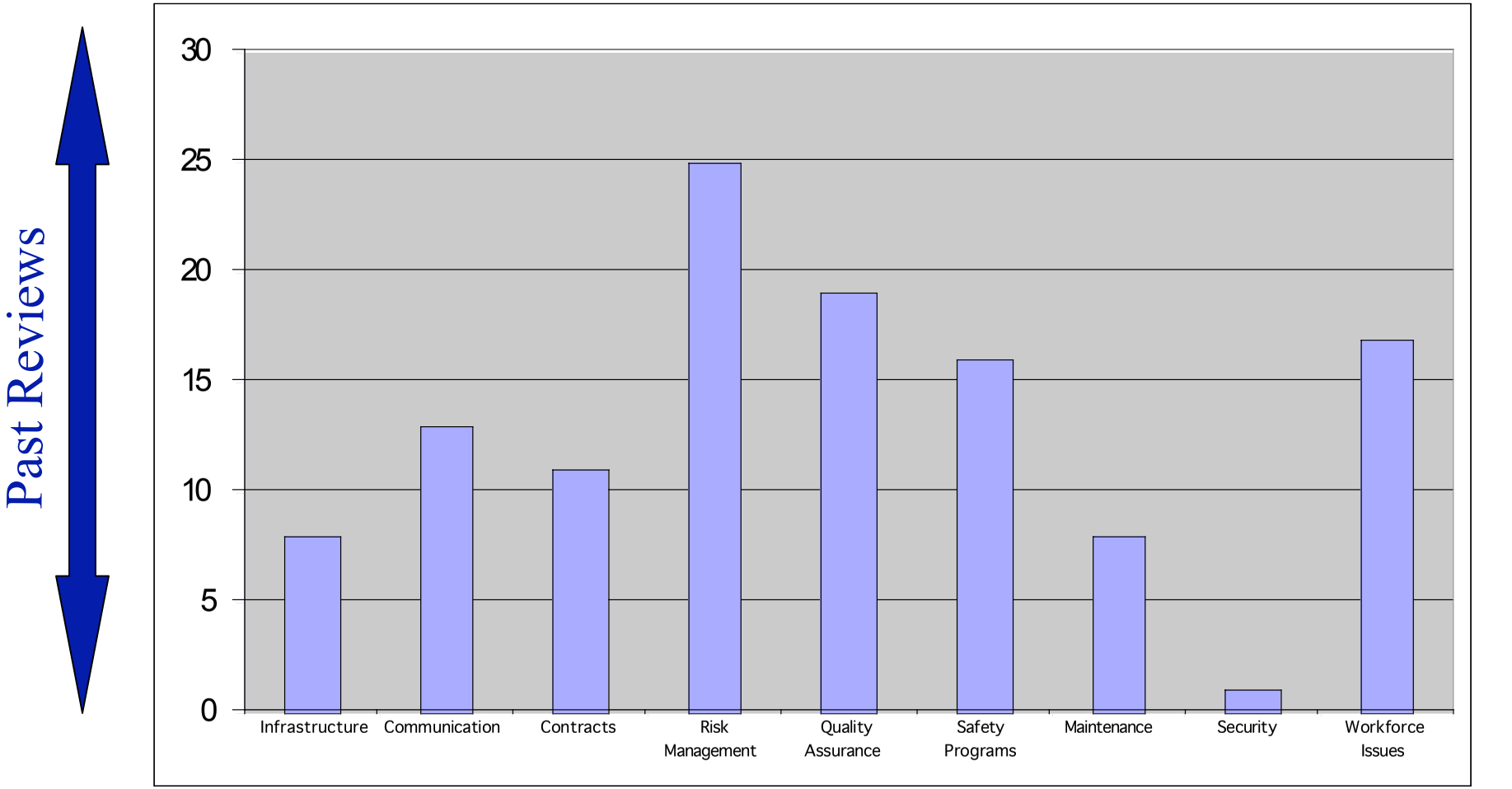

2.0 Detailed Report Summaries

In addition to the general overview, many previous reports – particularly from the annual Aerospace Safety Advisory Panel (ASAP) evaluation – were analyses in more detail to determine if there were consistent trends in how NASA dealt with external criticisms. The following table lists the Findings and Recommendations from a long list of advisory panels that have reviewed Space Shuttle operations. The last column details NASA's response to the Finding or Recommendation, if it was publicly released.

The table does not contain every Finding and Recommendation made in the reports that were analyzed, only those that seemed to have particular relevance to the NASA organization and culture as it affected STS-107. Many detailed technical recommendations that addressed specific hardware issues are not listed (and almost all were corrected by NASA in a timely manner), and recommendations that were not directed at the Space Shuttle Program are also not listed.

Independent Assessment Team *(Chartered by)*	Date of Report	Finding	Recommendation	NASA Response
Aerospace Safety Advisory Panel (*NASA Charter)*	March 2003	**Finding 02-1:** Many problems have not been discovered until late in the prelaunch sequence. In all of these cases, checkout, test, and inspection procedures were properly performed. The potentially hazardous discrepancies were not detected earlier because the test and inspection requirements did not dictate more specific or more stringent screening.	**Recommendation 02-1a:** Through proactive review, revalidate and revise the criteria for critical ground and flight systems recertification.	
			Recommendation 02-1b: Based on the findings and technical information garnered from the recertification process, validate and update the maintenance, test, and inspection requirements.	
Aerospace Safety Advisory Panel (*NASA Charter)*	March 2003	**Finding 02-2:** The growing Backlog of Maintenance and Repair (BMAR) and the change to Full Cost Accounting (FCA) may put infrastructure vital to safe operations at risk.	**Recommendation 02-2:** Reduce the BMAR on critical infrastructure as quickly as possible to ensure that this infrastructure remains safe and capable of supporting NASA's missions.	
Aerospace Safety Advisory Panel (*NASA Charter)*	March 2003	**Finding 02-3:** NASA has not established a guiding principle for locating safety organizations within its organizational structure. Unlike the DOD and industry, NASA's safety organizations are integrated into the assurance organization rather than into systems engineering.	**Recommendation 02-3:** Through appropriate management action, define an Agency-wide safety organizational structure—one that separates system safety engineering from system safety assurance.	
Aerospace Safety Advisory Panel (*NASA Charter)*	March 2003	**Finding 02-4:** NASA's safety policy direction is well formulated, but the Panel has observed that safety tends to be a comprehensive activity only late in the	**Recommendation 02-4a:** Consider integrating safety into systems engineering to support system development and sustaining engineering and supporting system safety assurance through an	

Independent Assessment Team *(Chartered by)*	Date of Report	Finding	Recommendation	NASA Response
		only late in the development cycle after design is complete, and occasionally only after an incident or mishap.	assurance through an independent reporting channel from the safety organization to the mission assurance organization.	
			Recommendation 02-4b: Establish independent funding mechanisms and appropriate authority, responsibility, and accountability for these new safety units.	
Aerospace Safety Advisory Panel (*NASA Charter)*	March 2003	**Finding 02-5:** NASA personnel do not view appointments to safety organizations as a positive career move.	**Recommendation 02-5:** Require that managers of major NASA programs and projects have experience in safety organizations.	
Aerospace Safety Advisory Panel (*NASA Charter)*	March 2003	**Finding 02-6:** NASA's application of root cause analysis appears to be inconsistent across the Agency and across programs.	**Recommendation 02-6a:** Continue the effort that has begun to assess the state of root cause analysis performed by NASA and its contractors. Provide the training and resources necessary to resolve any deficiencies.	
			Recommendation 02-6b: Explore the causes of cultural or contractual impediments, and devise ways to change the culture from a fixing orientation (identifying and eliminating deviations or symptoms of deeper problems) to a learning orientation in which both cultural and organizational factors are included in the search for the source of problems.	
			Recommendation 02-6c: Establish an oversight process for reviewing the root cause analyses and the resulting recommendations for all major failures or incidents.	

Independent Assessment Team *(Chartered by)*	Date of Report	Finding	Recommendation	NASA Response
Aerospace Safety Advisory Panel (*NASA Charter)*	March 2003	**Finding 02-7:** The shift to FCA in FY 2004 could negatively impact the ability to sustain safe and reliable operations.	**Recommendation 02-7:** Identify the impact of the implementation plans for FCA with respect to safe and reliable operations during and after the transition. Ensure that programs (including maintenance and modernization of hardware and software), personnel, infrastructure, and contractor services essential to safety are adequately funded.	
Aerospace Safety Advisory Panel (*NASA Charter)*	March 2003	**Finding 02-8:** The orbiter program is making progress in incorporating Engineering orders (EO) into engineering drawings.	**Recommendation 02-8:** Identify drawings that are critical to flight safety, update them to include all EOs, and keep them current.	
Aerospace Safety Advisory Panel (*NASA Charter)*	March 2003	**Finding 02-9:** Although progress is being made, there is no commitment to implementing crew escape capabilities for all regions of powered flight.	**Recommendation 02-9:** Complete the ongoing studies of crew escape design options. Either document the reasons for not implementing the NASA Program Guideline of Human Rating (currently in review) or expedite the deployment of such capabilities.	
Aerospace Safety Advisory Panel (*NASA Charter)*	March 2003	**Finding 02-10:** The Cockpit Avionics Upgrade (CAU) is making excellent progress toward meeting its objectives. The flight crews interviewed by the Panel were enthusiastic and unanimous in support of the effort. The Panel believes that Increment II must be completed in order to realize significant safety improvements in Shuttle operations.	**Recommendation 02-10:** Provide ongoing funding for the CAU through Increment II so that continuity between the two phases can be maintained.	
Aerospace Safety Advisory Panel (*NASA Charter)*	March 2003	**Finding 02-11:** The Cockpit Avionics Upgrade (CAU) project has not completed a credible hazard analysis. An orbiter hazard analysis including the CAU has not been planned.	**Recommendation 02-11:** Perform risk assessments and hazard analyses, both internal to the CAU and from the perspective of the entire orbiter, to confirm that there are no input error conditions that could result in flight crew actions	

Independent Assessment Team *(Chartered by)*	Date of Report	Finding	Recommendation	NASA Response
			detrimental to crew, mission, or vehicle safety.	
Aerospace Safety Advisory Panel (*NASA Charter)*	March 2003	**Finding 02-12:** Certain failure conditions may lead to conflicting data across display panels [of the CAU].	**Recommendation 02-12:** Through analysis, assess the probability of conflicting data among display screens. Confirm through simulated flight experiments that flight crew are able to identify information conflicts, that they are able to ascertain correct parameters, and that they can correct these errors without undue impact to flight safety or operations.	
Aerospace Safety Advisory Panel (*NASA Charter)*	March 2003	**Finding 01-18:** Funding cuts threaten to eliminate all effort on maintaining and updating surveillance and modeling of the orbital debris population as early as October 2002. [Actually in the ISS section, but directly applicable to SSP.]	**Recommendation 01-18:** Reexamine the decision to eliminate this important function and assure that the core MMOD effort is continued.	**NASA Response: Concur 01-18:** OSF is seeking to identify all users/stakeholders of the current Orbital Debris Program and identify appropriate program content and long-term Agency funding source(s) to ensure that NASA retains the capability for compliance with the Agency's Orbital Debris Policy for NASA missions. **Panel Assessment: Recommendation 01-18 is continuing.** The content of the Orbital Debris Program was adjusted in response to the budget reduction without increasing the risk to NASA missions. The program is currently funded by the two major users of the output - Space Shuttle and ISS. However, continued program funding is not resolved in the upcoming FY 2004 conversion to FCA.

Independent Assessment Team *(Chartered by)*	Date of Report	Finding	Recommendation	NASA Response
Aerospace Safety Advisory Panel (*NASA Charter)*	March 2003	**Finding 01-6:** The safety of NASA's human space flight programs will always be dependent on the ability of a skilled, experienced, and motivated workforce.	**Recommendation 01-6:** Accelerate efforts to ensure the availability of critical skills and to utilize and capture the experience of the current workforce.	**Panel Assessment: Recommendation 01-6 is continuing.** This issue will require aggressive action for the foreseeable future.
Aerospace Safety Advisory Panel (*NASA Charter)*	March 2002	**Finding 1:** The current and proposed budgets are not sufficient to improve or even maintain the safety risk level of operating the Space Shuttle and ISS. Needed restorations and improvements cannot be accomplished under current budgets and spending priorities.	**Recommendation 1:** Make a comprehensive appraisal of the budget and spending needs for the Space Shuttle and ISS based on, at a minimum, retaining the current level of safety risk. This analysis should include a realistic assessment of workforce, flight systems, logistics, and infrastructure to safely support the Space Shuttle for the full operational life of the ISS.	**Response (from 2002 ASAP Appendix)**: Concur: Both Shuttle and ISS Program Operating Plans (POP) identify the total resource requirements necessary to retain and improve safety risk. The development of these plans involves assessments from all organizations and receives the highest level of NASA management review. NASA management maintains a safety first decision process and will continue to be vigilant in developing as much operating margin as possible. The Office of Space Flight has recently initiated an assessment to address Space Shuttle fleet capability to fly safely until 2020. This assessment includes an analysis of workforce critical skills, flight systems upgrades, logistics and supportability, and any infrastructure upgrades requirements necessary to meet this goal. Any comprehensive assessment to support ISS beyond 2020 would occur in the future.
Aerospace Safety Advisory Panel (*NASA Charter)*	March 2002	**Finding 2:** Some upgrades not only reduce risk but also ensure that NASA's human space flight vehicles have sufficient assets for their entire service lives.	**Recommendation 2a:** Make every attempt to retain upgrades that improve safety and reliability, and provide sufficient assets to sustain human space flight programs.	**Response (from 2002 ASAP Appendix)**: Concur 2a: NASA and its contractors have continued to maintain and improve on the excellent safety practices and processes and as such, safety has not been compromised. Comprehensive analyses have identified potential upgrades projects that can further reduce risk if fully funded.

Independent Assessment Team *(Chartered by)*	Date of Report	Finding	Recommendation	NASA Response
				Examples of needed long-term supportability upgrades that are not currently funded include the Orbiter's communication and tracking system, components of the Orbiter's data handling system, and the SRB avionics subsystem. Every attempt is being made to apply available resources to the more promising areas of improvement.
			Recommendation 2b: If upgrades are deferred or eliminated, analyze logistics needs for the entire projected life of the Space Shuttle and ISS, and adopt a realistic program for acquiring and supporting sufficient numbers of suitable components.	**Response (from 2002 ASAP Appendix)**: Concur 2b: Long-term supportability analysis continues on a periodic basis between Orbiter, Logistics, and SMA. Most recent orbiter/logistics summit updated the supportability issues list in November 2001. SSP hardware element managers and SSP logistics managers have implemented a continuing supportability assessment analysis which is intended to maintain cognizance of potential supportability issues and to develop mitigation actions.
Aerospace Safety Advisory Panel (*NASA Charter)*	March 2002	**Finding 3:** Much of the Space Shuttle ground infrastructure has deteriorated and will not be capable of supporting the Space Shuttle for its realistic service life.	**Recommendation 3:** Revitalize safety-critical infrastructure as expeditiously as possible.	**Response (from 2002 ASAP Appendix)**: Concur 3: Human space flight is greatly dependent upon a capable ground infrastructure. The ISS and SSP management have worked closely with Center Directors in identifying the facilities, GSE, training, and test equipment necessary to continue and improve human space flight. As funding becomes available, it is applied to those areas having the greatest risk benefit.
Aerospace Safety Advisory Panel (*NASA*	March 2002	**Finding 4:** NASA is considering closing or deactivating some training and test facilities in an effort to economize.	**Recommendation 4:** Perform a detailed full life cycle safety and needs analysis including consideration of critical skills retention before making closure	**Response (from 2002 ASAP Appendix)**: Concur 4:Any consideration for training or test facility closure will be based upon an appropriate

Independent Assessment Team *(Chartered by)*	Date of Report	Finding	Recommendation	NASA Response
Charter)			decisions.	risk assessment that considers their significance to the readiness level of the crews or the vehicle.
Aerospace Safety Advisory Panel (*NASA Charter)*	March 2002	**Finding 5:** Space Shuttle privatization can have safety implications as well as affecting costs.	**Recommendation 5:** Include in all privatization plans an assessment by safety professionals of the ability of the approach to retain a reasonable level of NASA technical involvement and independent checks and balances.	**Response (from 2002 ASAP Appendix)**: Concur 5:All privatization discussions to date have included direct participation by the NASA Headquarters, Center, and SSP Safety organizations. A fundamental ground rule of any privatization option is that it must include the proper checks and balances as well as healthy tension between design and operations and include a value added independent assessment process. Current plans include numerous independent reviews of privatization concepts that will be structured to include safety professionals.
Aerospace Safety Advisory Panel (*NASA Charter)*	March 2002	**Finding 6:** The safety of NASA's human space flight programs will always be dependent on the availability of a skilled, experienced, and motivated workforce.	**Recommendation 6:** Accelerate efforts to ensure the availability of critical skills and to utilize and capture the experience of the current workforce.	**Response (from 2002 ASAP Appendix)**: Concur 6: Capturing the experience of the current workforce by continuing to hire and train young engineers is vital to the long-term safety of the Space Shuttle Program (SSP). NASA, USA, and the State of Florida have developed the Aerospace Technician Certification program, which provides a 2-year curriculum (4-year program in development) towards a space quality standard. Similar certification programs are in work for other aspects of SSP work. A Mentoring Program, focused on further development of technical and managerial skills, is also in place. The Prime Contractors have various hiring, training, and mentoring programs to facilitate skill development

Independent Assessment Team *(Chartered by)*	Date of Report	Finding	Recommendation	NASA Response
				and retention. The International Space Station (ISS) is early in the operational phase and has sufficient NASA civil service personnel to assist in the training and mentoring of new Boeing engineers. Further documentation is readily available on key subsystems and some hardware is still being procured. This will also allow an opportunity for new Boeing engineers to learn ISS systems in detail. In summary, this is an excellent time in the ISS program history to transfer and train new personnel and set in place a lower sustaining cost structure.
Aerospace Safety Advisory Panel (*NASA Charter)*	March 2002	**Finding 7:** Mishaps involving NASA assets are typically classified only by the actual dollar losses or injury severity caused by the event.	**Recommendation 7:** Consider implementing a system in which all mishaps, regardless of actual loss or injury, are assessed by a standing panel of independent accident investigation specialists. The panel would have the authority to elevate the classification level of any mishap based on its potential for harm.	**Response (from 2002 ASAP Appendix)**: Concur 7:NASA NPD 8621.1G defines a mishap as any unplanned occurrence or event resulting from any NASA operation or NASA equipment anomaly. Current human space flight problem reporting systems require reporting and analysis of all operational or equipment anomalies against criteria that includes addressing the potential for significant loss of life or assets. At this level, the investigative experts are the engineers, managers, and maintainers of the equipment. If an actual mishap were to occur, the Mishap Investigation Team (MIT) would be the first response. All members of this team have had accident investigation training and the Chairman has completed the NTSB accident investigation school and USC Aviation

Independent Assessment Team *(Chartered by)*	Date of Report	Finding	Recommendation	NASA Response
				Safety curriculums.
Aerospace Safety Advisory Panel (*NASA Charter)*	March 2002	**Finding 8:** There is no requirement for Mishap Investigation Boards (MIB) to include individuals specifically trained in accident investigation and human factors.	**Recommendation 8:** Adopt a requirement for the inclusion of accident investigation and human factors expertise on MIBs.	**Response (from 2002 ASAP Appendix)**: Concur 8: NPD 8621.1G states that it is NASA's policy to conduct NASA mishap investigations, using NASA MIBs, with properly trained personnel. At the Space Shuttle Program level, this has been implemented through the assignment of the Mishap Investigation Team. All members of this team have had accident investigation training and the Chairman has completed the NTSB accident investigation school and USC Aviation Safety curriculums.
Aerospace Safety Advisory Panel *(NASA Charter)*	March 2002	**Finding 9:** The first increment of the Cockpit Avionics Upgrade (CAU) has significant potential for long-term Space Shuttle risk reduction and provides a platform for still further improvements.	**Recommendation 9:** Maintain the previously planned funding to expeditiously implement the CAU.	**Response (from 2002 ASAP Appendix)**: Concur 9: CAU is currently adequately funded and authorized through PDR. Due to budget pressures NASA has reduced CAU funding to include only CAU Increment 1, which does provide key safety improvements. Increment 2 will be implemented on a deferred schedule using available sustaining engineering resources.
Aerospace Safety Advisory Panel *(NASA Charter)*	March 2002	**Finding 10:** Orbiter wiring inspections have shown instances where redundant wiring is carried in the same wire bundle.	**Recommendation 10:** Expedite efforts to route redundant wires in separate wire runs.	**Response (from 2002 ASAP Appendix)**: Concur 10: Orbiter project is currently expediting the separation of redundant wires. All that can be accomplished during a normal flow at KSC are being scheduled and those that cannot will be implemented during the vehicles next modification period.

Independent Assessment Team *(Chartered by)*	Date of Report	Finding	Recommendation	NASA Response
Aerospace Safety Advisory Panel *(NASA Charter)*	March 2002	**Finding 11:** Little definitive action has been taken to correct and preclude continuing the undesirable situation of excessive unincorporated EOs in the orbiter engineering drawings.	**Recommendation 11:** Expeditiously reduce the number of the drawing changes currently outstanding.	**Response (from 2002 ASAP Appendix)**: Concur 11: Orbiter project is currently working to reduce the number of outstanding drawing changes. The project is prioritizing the drawing updates based on criticality, complexity, and traffic. The highest priority tile drawings have been completed and other subsystems will follow.
Aerospace Safety Advisory Panel *(NASA Charter)*	March 2002	**Finding 12:** Space Shuttle logistics will face increasing challenges from vendor issues including closures, mergers, relocations, and changes in capability.	**Recommendation 12:** Continue to emphasize to all suppliers the importance of timely reporting of all significant business and organizational changes that could affect Space Shuttle logistics.	**Response (from 2002 ASAP Appendix)**: Concur 12:The Space Shuttle Process Control Working Group has been instrumental in communicating to the contractors and suppliers the importance of change control and notification. The Logistics departments continue to interact with the suppliers on a daily basis and have had good success with suppliers providing notification of changes. Several supplier conferences have been held at the Project level to reinforce this message. On January 23–24,2002,the SSP held its first Program-wide supplier conference in which this theme was communicated and reinforced by top management.
Aerospace Safety Advisory Panel *(NASA Charter)*	March 2002	**Finding 13:** Deferring the OMMs intensifies the risk that scheduled safety upgrades will never be completed, thereby further increasing the life cycle safety risk of operating the Space Shuttle.	**Recommendation 13:** Incorporate deferred safety-related modifications in the affected orbiters expeditiously. This should not be accomplished at the expense of other safety or operational upgrades, or the prudent maintenance of the Space Shuttle system and its infrastructure.	**Response (from 2002 ASAP Appendix)**: Concur 13: Orbiter project is currently incorporating a number of safety-related modifications and has placed priority on many proposed safety and risk reduction modifications.

Independent Assessment Team *(Chartered by)*	Date of Report	Finding	Recommendation	NASA Response
Aerospace Safety Advisory Panel *(NASA Charter)*	March 2002	**Finding 14:** It is reasonable to utilize the same engineering and technician workforce for routine Space Shuttle processing and OMDP work at KSC, since the work content is similar. Planning and management functions, however, differ significantly between line processing and heavy maintenance activities.	**Recommendation 14:** Designate separate, appropriately experienced management teams for the regular processing and OMDP work at KSC. These teams must be well coordinated, since they will be drawing on the same workforce.	**Response (from 2002 ASAP Appendix)**: Concur 14: The Orbiter Project has established an OMDP Management Plan, which designates a separate Orbiter management team for OMDP.
Aerospace Safety Advisory Panel *(NASA Charter)*	March 2002	**Finding 18 [Space Station, but applicable to SSP]:** Funding cuts threaten to eliminate all effort on maintaining and updating surveillance and modeling of the orbital debris population as early as October 2002.	**Recommendation 18:** Reexamine the decision to eliminate this important function and assure that the core MMOD effort is continued.	**Response (from 2002 ASAP Appendix)**: Concur 18: Office of Space Flight is seeking to identify all users/stakeholders of the current Orbital Debris Program and identify appropriate program content and long term Agency funding source(s) to assure NASA retains capability for compliance with Agency Orbital Debris Policy for NASA missions.
Aerospace Safety Advisory Panel *(NASA Charter)*	March 2002	**Finding 19:** The terrorist attacks on September 11 emphasized the need for increased security of all national assets, including NASA's computer systems. Since many of these systems safeguard the lives of astronauts and cosmonauts and the safety of valuable international assets, it is crucial that security vulnerabilities be fully understood and closely managed.	**Recommendation 19a:** Accelerate the schedule of penetration exercises to gain greater insights into computer security vulnerabilities; determine if further threat analysis should be conducted; review all vulnerabilities; and ensure that plans are adequately formulated to mitigate these vulnerabilities and that work is proceeding to prevent critical systems from being compromised.	**Response (from 2002 ASAP Appendix)**: Concur 19a: The Agency and Center IT security program is a risk-based management and acceptance process. The program continues to evolve to incorporate and facilitate tools and metrics for greater insight into security vulnerabilities. Currently the Centers perform quarterly vulnerability scans and metrics that are reported to the Agency. The vulnerabilities found are reviewed and worked through a defined process. Mission Critical systems external interfaces such as those of the JSC Mission Control Center with the JSC Institutional Network are included in these quarterly assessments. We

Independent Assessment Team *(Chartered by)*	Date of Report	Finding	Recommendation	NASA Response
				will continue to work to improve this process and capability as new technologies and tools become available.
			Recommendation 19b: Accelerate the schedule for the implementation of triple Data Encryption System (DES).	**Response (from 2002 ASAP Appendix)**: Concur 19b:The change to incorporate the triple DES has been negotiated with the contractor; a probabilistic risk assessment associated with losing S-band communications is being conducted prior to Program implementation.
NASA Office of Safety and Mission Assurance *(NASA Charter)*	31 October 2001	Under the sampling conditions (survey population, four orbiter in-flow, skill mix, staffing levels, experience level, etc.) and recognizing inherent sampling error and questionnaire limitations, the IAT finds that overall workplace induced stress does not appear to be a present safety concern. Based on the results of this assessment and the two previous assessments of USAGO workforce capability, the IAT reaffirms the previous finding that USAGO has established the capability to safely accomplish an evenly spaced flight rate of up to seven flights per year.	**Recommendation 1:** NASA KSC SSP management should commit to conducting independent workforce surveys on a periodic (e.g., semi-annual) basis. While the current survey represents only a snapshot in time it could serve as the starting point for periodic surveys that track workforce attitudes and perspectives regarding workplace satisfaction and safety. Future survey planning should consider sampling that includes all members of the workforce (including those individuals with zero WTD) as well as a wide range of questions addressing workplace factors that are recognized correlates to occupational safety and stress.	
NASA Office of Safety and Mission Assurance *(NASA Charter)*	31 October 2001	Skill-mix and training/certification imbalance imposes greater demands and stress on fully qualified (Level-1) workforce.	**Recommendation 5:** USAGO should continue to assess and manage skill mix/training issues to more effectively and safely meet workload demands. The IAT recommends that the NASA/USA refine and implement the Workforce Flexibility Model as a viable means to address skill mix,	

Independent Assessment Team *(Chartered by)*	Date of Report	Finding	Recommendation	NASA Response
			numbers, and training/certification imbalances.	
NASA Office of Safety and Mission Assurance *(NASA Charter)*	31 October 2001	Reported unsafe activities and/or conditions - a number of the individuals interviewed reported knowledge of unsafe activities or conditions in Space Shuttle ground operations.	**Recommendation 8:** NASA KSC SSP and USA management must redouble their efforts to improve workforce understanding and acceptance of Structured Surveillance as an important and necessary safety control process. The idea of structured surveillance as a means to maintain stable, capable, and controlled critical processes remains an excellent and essential concept for implementing checks and balances within the scope of a performance based contract.	
Aerospace Safety Advisory Panel *(NASA Charter)*	February 2001	**Finding 1:** The current planning horizon for the Space Shuttle does not afford opportunity for safety improvements that will be needed in the years beyond that horizon.	**Recommendation 1:** Extend the planning horizon to cover a Space Shuttle life that matches a realistic design, development, and flight qualification schedule for an alternative human-rated launch vehicle.	**NASA Response (Goldin, 24 May 2001):** Code M - Concur: It is prudent to assume that the Shuttle will continue to support human space flight well beyond the current planning date of 2012, probably at least until 2020. Industry and NASA studies indicate that there will not be a compelling case for funding, developing and certifying a Shuttle replacement system for human space flight until late in the next decade. Therefore, NASA is actively assessing further safety improvements, beyond the current suite of planned and funded upgrades, which may be implemented in the Shuttle within the next 5-7 years and which could significantly reduce the operational risk of the Shuttle for many years of continued operations.

Independent Assessment Team *(Chartered by)*	Date of Report	Finding	Recommendation	NASA Response
Aerospace Safety Advisory Panel *(NASA Charter)*	February 2001	**Finding 2:** There is no in-flight crew escape system for the Orbiter other than for abort below 20,000 feet during a controlled glide.	**Recommendation 2:** Complete the ongoing studies of crew escape design options and implement an improved system as soon as possible.	**NASA Response (Goldin, 24 May 2001):** Code M - Concur: The Space Shuttle Program (SSP) concurs with the recommendation and is investigating enhanced crew escape capability with the objective of making significant strides in reducing crew risk for vehicle failures, which result in the loss of the orbiter vehicle. A Crew Escape Study has been initiated to reexamine Space Shuttle crew escape options.
Aerospace Safety Advisory Panel *(NASA Charter)*	February 2001	**Finding 3:** Redundant hydraulic lines for the three orbiter hydraulic systems are not adequately separated to preclude loss of all hydraulic power in the event of a single catastrophic failure of adjacent hardware.	**Recommendation 3:** Provide the same degree of separation of redundant critical hydraulic lines as is given to redundant critical electrical wiring.	**NASA Response (Goldin, 24 May 2001):** Code M - Concur: Orbiter hydraulic systems utilize and will continue to implement the same considerations and degree of redundant system separation as is given redundant critical electrical wiring. Primary consideration is system placement such that a single catastrophic failure environment does not exist. Emphasis is placed on precluding events that may propagate from one function to another. Hazards associated with arc tracking can propagate to another wire in close proximity and therefore have influenced electrical wiring physical separation requirements. Hydraulic line hazards such as leakage or rupture cannot propagate to an adjacent hydraulic line. Extensive Failure Modes and Effects Analysis I Critical Items List (FMWCIL) and Hazard Analyses of the Orbiter systems and operational environment have not identified any credible single failure modes which would result in the loss of hydraulic power. Neither system is protected against

Independent Assessment Team *(Chartered by)*	Date of Report	Finding	Recommendation	NASA Response
				extreme externally induced events such as those that DOD separation requirements address.
Aerospace Safety Advisory Panel *(NASA Charter)*	February 2001	**Finding 4:** The ongoing effort to improve the work paper used at KSC by incorporating outstanding deviations and clarifying and simplifying the work instructions is proceeding well. Some lesser effort has been focused on improving the vehicle engineering drawings and reducing the engineering orders (EOs) they contain.	**Recommendation 4a:** Continue vigorous efforts to upgrade the work paper, even as the flight rate increases, in order to maintain the positive momentum that this worthwhile initiative has generated.	**NASA Response (Goldin, 24 May 2001):** Code M - Concur: Upgrading the paperwork continues to be a primary strategic initiative. The implementation of enhancements aimed at "work paper "Deviation" reduction continues to show positive results. The IPP (Intranet Provided Procedures) has enabled the technician to select and work paper that has been pre-approved by engineering, and other initiatives such as MAXIM0 are moving processing toward a more paperless work environment. All these initiatives combine to continue vigorous upgrade to the work paper quality while reducing the labor to achieve these gains.
			Recommendation 4b: Focus additional effort on updating vehicle engineering drawings with the objectives of incorporating as many EOs as possible and assuring the clarity of all information.	**NASA Response (Goldin, 24 May 2001):** Code M - Concur: Each SSP project has configuration control to minimize the number of EOs before engineering drawings are updated. Additional focus will be implemented on improving engineering drawings. For example, the tile drawings, which are complex high-use drawings, have been updated to incorporate their EOs and this process will be applied to other highly complex, high-use drawings on the vehicle. Additionally, the Space Shuttle Program is embarking upon a one-year pilot program to convert orbiter vehicle 2D drawings to 3D digital drawings which if

Independent Assessment Team *(Chartered by)*	Date of Report	Finding	Recommendation	NASA Response
				implemented would incorporate all of the outstanding EOs.
Aerospace Safety Advisory Panel *(NASA Charter)*	February 2001	**Finding 5:** The KSC facilities, ground support equipment, and test and checkout gear to support Space Shuttle processing and launch operations continue to age. The status of the potential readiness of these essential assets has been projected, but there is no detailed, funded plan to ensure that this aging infrastructure can safely support the Space Shuttle for its likely operational life.	**Recommendation 5:** Develop a detailed plan and budget to maintain and upgrade the KSC assets that are essential to the safe operation of the Space Shuttle for its reasonably expected flight life so that an appropriate infrastructure life extension program can be implemented.	**NASA Response (Goldin, 24 May 2001):** Code M - Concur: Infrastructure support and upgrades requirements for the KSC facilities, ground support equipment, and test and checkout equipment arc well defined and are updated yearly The SSP initiated an Infrastructure Revitalization Team to develop a detailed plan to upgrade the infrastructure at all element sites, in addition to KSC, for identified life through at least 2012. Infrastructure remains a top program initiative and significant investment is needed. Since there were no new initiatives funded from the FY 02 budget process, other programs within Human Space Flight are being considered to support infrastructure requirements.
Aerospace Safety Advisory Panel *(NASA Charter)*	February 2001	**Finding 11:** The critical skills challenge faced by NASA and its contractors in the Space Shuttle and ISS programs continues despite resumption of active recruiting of experienced and new employees.	**Recommendation 11:** Provide more effective incentives to retain employees with critical skills in such areas as Information Technology and Electrical/Electronic Engineering. Continue active recruiting of experienced and "fresh-out" employees, using appropriate incentives when necessary.	**NASA Response (Goldin, 24 May 2001):** Code M - Concur: Both NASA and its contractor management teams have recognized the challenges of competing for critical skills in today's work environment, and have begun focused development of organizational assessment programs with emphasis on skills maintenance. These programs are targeted to include multiple tools and approaches (such as pay incentives, cross training, mentoring, formal career development planning, etc) to maintain the appropriate balance of experienced skills as well as a continuous revitalization through the

Independent Assessment Team *(Chartered by)*	Date of Report	Finding	Recommendation	NASA Response
				steady introduction of recent graduates. NASA has established fresh out goals at OSF Centers, used recruitment or relocation (signing) bonuses when necessary to attract quality hires at all levels, and authorized the payment of more competitive salaries in critical skill areas.
Aerospace Safety Advisory Panel *(NASA Charter)*	February 2001	**Finding 12:** NASA's recent hiring of inexperienced personnel, along with continuing shortages of experienced, highly-skilled workers, has produced the challenge of training and integrating employees into organizations that are highly pressured by the expanded Space Shuttle flight rates associated with the ISS. There is no systematic effort to capture the knowledge of experienced personnel before they leave. Stress levels within the workforce are a continuing concern.	**Recommendation 12a:** Provide active mentoring and other career development incentives to bring new employees to full productivity as rapidly as can be accomplished with safety remaining paramount. Expand resources and delivery methods available to Agency level training programs to enable greater participation at Center and program levels.	**NASA Response (Goldin, 24 May 2001):** Code M - Concur: NASA and its contractors have made significant enhancements in the employee training and development arena. NASA civil servants now have individual career development plans tailored to meet their specific needs, including both hands on experience and appropriate training and education. Significant emphasis has also been placed on employee development with an Agency wide Leadership Development Initiative, a more systematized mentoring program, and increased usage of computer based training. The need to monitor stress levels and provide coping strategies has received considerable attention in all organizations, with significant progress made in this area. NASA has also recognized the importance of capturing the corporate knowledge in our aging workforce and transferring it to the next generation. Code F - General Response: NASA concurs with the recommendation(s). NASA and its contractors have made significant enhancements in the employee training and

Independent Assessment Team *(Chartered by)*	Date of Report	Finding	Recommendation	NASA Response
				development arena. Several NASA Centers have implemented individual career development plans for their workforce, or for specific segments and occupational categories. These workplans enable management and employees to plan and implement formal training initiatives, career development assignments, and job rotations which enhance current and future performance. Many Centers have also examined their need for leadership development, and have implemented new training initiatives designed to address these needs and requirements. More systematized mentoring programs and increased usage of computerized training have been implemented within the Agency. The need to monitor stress levels and provide coping strategies has also received increased attention across the Agency, with significant progress being made in this area. Code F - 12a: NASA concurs with the recommendation. As a result of beginning to hire new employees and fresh-outs, the NASA Centers have instituted, or have begun to revitalize, various orientation and other training programs designed to assimilate new employees into the workforce and provide mentoring and career development guidance. Many programs also include the requirement for specific types of training (e.g., technical or administrative), and include both on-the-job and developmental experiences over a period of time. Components in many

Independent Assessment Team *(Chartered by)*	Date of Report	Finding	Recommendation	NASA Response
				Centers' training programs also provide for guidance to supervisors in designing a training plan or individual development plan, providing mentoring and coaching, and evaluating work products and progress. The goals of these programs are to aid in the smooth and effective integration of new employees into the Center and Agency workforce by: providing a continuing and accelerated learning process: providing employees a way of identifying with the Center by understanding its mission and values; providing interaction with more senior staff and leaders; and providing opportunities to develop relationships with peers. At the Agency level, efforts are being initiated to establish a network of experienced practitioners who can provide mentoring and access to expertise in project management. At the Agency level, resources have been requested to enable NASA to expand the delivery methods being utilized to develop the workforce. Specific emphasis will be placed on the development of e-learning alternatives that can be accessed at all locations and levels, and increasing the ability to expand participation levels across the Agency. In addition, new capabilities are being developed to facilitate learning within intact teams, delivering tailored content directly to a project team at the point in time specific training is needed. In addition, some Centers have also increased their resources

Independent Assessment Team *(Chartered by)*	Date of Report	Finding	Recommendation	NASA Response
				available for training, and are instituting Center specific initiatives based upon Center needs. In addition, learning organization tools and methods being introduced in pilot projects within NASA are increasing organizational understanding, motivation, buy-in, and results. Examples of new initiatives include web-based course delivery and partnerships with universities for academic training.
			Recommendation 12b: Continue efforts, in partnership with NASA contractors, where appropriate, to provide hands-on experience.	**NASA Response (Goldin, 24 May 2001):** Code F - 12b: NASA concurs with the recommendation, and a primary emphasis in developing the workforce will continue to be reliance on valuable on-the-job experience. In addition, the NASA Academy of Program and Project Leadership is in the process or revising its career model to enable an expansion of the identification of experiential development. NASA's Professional Development Program also provides a combination of formal training, briefings, and developmental assignments within and outside the Agency.
			Recommendation 12c: Establish processes that capture the knowledge of experienced personnel before they leave or retire.	**NASA Response (Goldin, 24 May 2001):** Code F - 12c: NASA concurs with the recommendation. Several efforts are underway to more effectively capture the "lessons learned from experienced personnel nearing or at retirement. In addition, the NASA Academy of Program and Project Leadership has initiated a series of "Knowledge Sharing forums and has initiated an area on its website for

Independent Assessment Team *(Chartered by)*	Date of Report	Finding	Recommendation	NASA Response
				knowledge sharing and lessons learned. An emphasis is being placed on making maximum use and sharing of the experience of employees and managers both while they are still at NASA and after their retirement. Various avenues are being explored for access to this expertise both within NASA and gaining access to the knowledge base of those who leave the Agency. With regard to sharing knowledge within the Agency, NASA has also revised its Fellowship program to include a planned reentry requirement. The reentry plan requires individuals returning from longer-term University programs to identify with their management how their new learning will be shared within the Agency and how it will be applied strategically.
			Recommendation 12e: Implement an evaluation of the processes used to develop new hires into productive members of the workforce.	**NASA Response (Goldin, 24 May 2001):** Code F - 12e: NASA concurs with the recommendation. Centers will be evaluating systems and processes for developing their new hires, assimilating them into the workforce and sharing best practices.
Aerospace Safety Advisory Panel *(NASA Charter)*	February 2001	**Finding 13:** Recent downsizing and limitations on hiring have produced a workforce with aberrations in normal career development patterns and a potential future shortage of experienced leadership.	**Recommendation 13:** Develop and implement a long-term workforce plan, focused on retention, recruitment, training, succession, and career development needs, with at least a five-year time horizon that will ensure the availability of competent and experienced leaders. Also provide a strengthened capability in organizational development.	**NASA Response (Goldin, 24 May 2001):** Code F - Concur: NASA concurs with the recommendation. The recent experience with downsizing, coupled with Agency concerns about and aging workforce, demonstrate the importance of long-term human resources planning. In 1998, under the auspices of the Chief Engineer's Office, the Agency conducted a core capability assessment that focused on the physical and staffing needs of the

Independent Assessment Team *(Chartered by)*	Date of Report	Finding	Recommendation	NASA Response
				Enterprises and Centers of Excellence. This, and other similar activities, while very helpful, resulted in tactically-oriented decisions related to solving near-term human resource issues. The Agency is now embarking on a follow-on strategic resource planning activity, based on Centers' future vision and mission, taking into account workforce and facilities needed. This activity, led by the Associate Deputy Administrator, involves the active participation of the Enterprises and Centers and support from the Office of the Chief Financial Officer, the Office of Human Resources and Education, and the Office of the Chief Engineer. The result will provide a plan for each Center that links staffing, funding resources, mission and activities, and core competencies and will enable them to focus on recruitment, retention, training, succession and career development tailored to their individual circumstances. Once this activity has been completed, the Office of Human Resources and Education will continue to work with the Center Human Resources Directors to assess the impacts of demographic trends. Together the Human Resources community will develop plans that ensure that the Agency has the requisite staffing, training, career development, and recruiting and retention tools and programs necessary to support

Independent Assessment Team *(Chartered by)*	Date of Report	Finding	Recommendation	NASA Response
				the Agency mission. In addition, the Office of Human Resources and Education has been actively engaged, with input and support from the Enterprises and Centers, in a number of activities and initiatives to renew and revitalize the NASA workforce. These range from activities to recruit, retain, and continue development of a highly capable workforce today to endeavors to ensure a future source of highly qualified talent in the science, math, and technology disciplines needed to carry out the Agency mission over the long term. With respect to recruitment, the Agency is committed to marketing NASA as an "employer of choice." In order to be competitive with other employers, NASA recognizes that it must have a continuing presence on college and university campuses. The more than 140 on-cam pus recruitment trips scheduled for this coming fall and spring 2002 are typical of this presence. In addition, the Agency will continue to utilize the Presidential Management Intern Program and student employment programs as sources for entry-level hires. NASA will also continue to promote the Internet as a recruitment tool and to work collaboratively with professional organizations (i.e., National Association of Colleges and Employers and National Academy of Public Administration) in an effort to

Independent Assessment Team *(Chartered by)*	Date of Report	Finding	Recommendation	NASA Response
				remain competitive. Our NASA Centers utilize various hiring authorities that enable them to offer starting salaries above the minimum rate of a grade. The use of recruitment bonuses by the Centers to attract the "best and the brightest" has also increased significantly in the recent past. The number has increased more than 300% from FY 1999 to FY 2000 (from 20 in FY 1999 to 69 in FY 2000 and 14 in just the first quarter of FY 2001) - a trend that we fully expect to continue because of an increasingly competitive job market and high cost of living surrounding some of our Centers. In addition to these ongoing efforts, NASA will continue to be innovative in it recruitment efforts. We are implementing new automation tools, i.e., a position description management software package and two staffing software packages to improve the effectiveness and timeliness of the hiring process. We are enhancing the Agency's human resources websites to make them more responsive to applicant information needs. Further, we are developing new qualification requirements for cooperative education students in order to more effectively recruit. Additional non-permanent employment options are being pursued where they are practical and the Agency is working with the Office of Management and Budget (OMB) and the Office of Personnel

Independent Assessment Team *(Chartered by)*	Date of Report	Finding	Recommendation	NASA Response
				Management (OPM) to facilitate new employment options. The Agency has a new five-year plan for the employment of people with disabilities and will develop other outreach efforts designed to maintain a diverse workforce. A new National Recruitment Team, based at Headquarters, is currently being established to develop new Agency-wide recruitment strategies and tools to meet NASA's current and future hiring challenges in attracting and retaining a world-class, highly technical and diverse workforce. This team will facilitate and complement the Centers' recruitment efforts; collaborate with the Institutional Program Offices and Functional Offices; enhance relationships with universities; eliminate duplication of efforts; and facilitate targeted diversity and disability recruiting. The retention of a highly skilled workforce is equally vital. While the use of retention allowances has more than doubled from 5 in FY 1999 to 12 in FY 2000 (and 7 in the first quarter of FY 2001), this rate of usage has been impacted by downsizing and restructuring efforts in recent years and the continuing need to offer targeted buyouts to deal with our skills imbalances. NASA will continue to assess the skills of its workforce and restructure as necessary through buyout and early out retirement incentives to assure that NASA has the necessary

Independent Assessment Team *(Chartered by)*	Date of Report	Finding	Recommendation	NASA Response
				skills for present and future mission success. In addition, we continue to emphasize quality of work-life initiatives such as alternative work schedules, family friendly leave programs, part-time employment and job sharing, telecommuting, dependent day car and employee assistance programs. Promoting safety in the workplace, providing effective awards, recognition and stimulating work will enhance job satisfaction and foster retention. In the arena of developing competent and experienced leaders, in the last 18 months NASA conducted a leadership study and created a model to align development of our leaders to the NASA Strategic Plan and Strategic Management System. The study included benchmarking, working with universities, and the results of interviews of over 500 NASA/JPL employees performing in leadership roles from team lead to executive senior leader. This model provides a roadmap of skills and competencies for effective NASA leadership and is being used to respond to the training and developmental needs of the workforce. As part of NASA's strategy to prepare our next generation of leaders, there are several long-term developmental processes in place at both the Center and Agency level. These include the Senior Executive Service Candidate Development Program, the Professional Development Program, partnerships with

Independent Assessment Team *(Chartered by)*	Date of Report	Finding	Recommendation	NASA Response
				academia to provide fellowships in leadership and project management development, and Center-specific development programs. In addition, the curriculum for developing project management leaders is being reviewed to ensure that appropriate skills and competencies are developed. In the area of organization development, one of the features, which will be enabled by an increase in training resources, is the ability to provide intact team support. By providing developmental intervention to teams, NASA will be able to contribute to improved performance of teams, as well as better prepare individual team members for future opportunities. NASA is also engaged in a strategy to develop employees in the theories, methods and tools of learning organizations. Pilots are showing that these skills enhance motivation, communication, and understanding of complex systems. Several Centers have also increased their organizational development resources and capacity and are offering facilitation services to their organizations. The Agency is also looking at ways to help assure a future pipeline of talent from which the NASA and others can draw. FY 2001 marks the pilot year of the new NASA Undergraduate Student Research Program. This Agency-wide program was developed to extend and strengthen NASA's

Independent Assessment Team *(Chartered by)*	Date of Report	Finding	Recommendation	NASA Response
				commitment to educational excellence and university research, and to highlight the critical need to increase the Nation's undergraduate and graduate science, engineering, mathematics, and technology skill base. The Undergraduate Student Research Program will also build a national program bridge from existing NASA K12 Education Program activities **to** NASA Higher Education Program options that encourages and facilitates student interest in future professional opportunities with NASA and its partner organizations. Such opportunities might include NASA career employment: temporary assignment: undergraduate and graduate co-op appointment; or contractor positions.
Aerospace Safety Advisory Panel *(NASA Charter)*	February 2001	**Finding 14:** While NASA has made major changes to emphasize the need to utilize IV&V on safety critical projects, the technology is not well understood by program managers and other relevant NASA personnel.	**Recommendation 14:** Develop an appropriate user-centered course and require software assurance awareness training for all levels of management to help them become more cognizant of the IV&V processes and the value IV&V brings to a final product.	**NASA Response (Goldin, 24 May 2001):** Code AE - Concur: As the report points out, NASA has indeed made major changes to emphasize the need for IV&V on mission critical software. The software IV&V policy, criteria, and process for evaluation of projects is in place and being followed. The Office of the Chief Engineer has presented pertinent information to all Center Directors, emphasizing the importance of IV&V, and communicating the expectation that IV&V and the IV&V policy be incorporated in Center processes. The Goddard Space Flight Center has been making presentations about the policy, criteria, and process in greater detail to other levels of management including program and project managers whose projects meet the criteria for IV&V or

Independent Assessment Team *(Chartered by)*	Date of Report	Finding	Recommendation	NASA Response
				independent assessment by the IV&V facility. In addition, the Office of Human Resources and Development is planning the update of existing training in Verification and Validation, and Test and Evaluation to include IV&V and the appropriate application of the same.
Space Shuttle Independent Assessment Team *(NASA Charter)*	7 March 2000	**Issue 1:** NASA must support the SSP with the resources and staffing necessary to prevent the erosion of flight-safety critical processes.		**SSP Response (Abbey/Dittemore, 21 June 2000):** The Office of Space Flight (OSF) has recently conducted workforce reviews of staff workload and skill deficiencies at its Centers and programs, with particular emphasis on the SSP. Findings of these reviews, coupled with those of external groups such as the SIAT and the Aerospace Safety Advisory Panel (ASAP), led to the decision to terminate downsizing. All four OSF Centers, JSC, KSC, MSFC, and SSC, are in the midst of large-scale efforts to replace skill losses and increase the number of entry-level professionals. NASA has a plan in place to hire over 500 new employees in fiscal year 2000. Although only a portion of these new employees will be dedicated to the SSP, this action will help fill some of the most critical skill shortages, enable us to stabilize our flight safety skills resources, and build our cadre of future leaders. It is imperative that sufficient resources, including new hires, be dedicated in support of the SSP. Beginning in fiscal year 2001, the plan is to replace future losses on a one-for-one basis.

Independent Assessment Team *(Chartered by)*	Date of Report	Finding	Recommendation	NASA Response
				In addition, the recruiting strategy is to emphasize the identification of critical skill shortages and make those the top hiring priorities. The goal is to hire 50 to 70 percent of new personnel at the entry level in an effort to revitalize the workforce with high-caliber, recent graduates. To allow some of the best junior- and mid-level personnel the opportunity to broaden their functional experience, the SSP has created rotational opportunities at several Centers where they can gain experience at the program level. This early exposure to the significant operational and programmatic management challenges will enable them to enhance the flight safety critical process skills in the near term, and will better equip them to serve in leadership roles in the future.
Space Shuttle Independent Assessment Team *(NASA Charter)*	7 March 2000	**Issue 2:** The past success of the Space Shuttle program does not preclude the existence of problems in processes and procedures that could be significantly improved.		**SSP Response (Abbey/Dittemore, 21 June 2000):** The SIAT noted, "the SSP must rigorously guard against the tendency to accept risk solely because of prior success." The SSP wholeheartedly agrees. Regular senior management meetings are conducted that specifically address the issue of complacency and the inherent risk to the SSP relative to process and procedure change. A specific focus on process control has been established to increase the awareness throughout the SSP on changes that could increase the level of risk. A Process Control Implementation Plan, developed in cooperation with each of the major prime

Independent Assessment Team *(Chartered by)*	Date of Report	Finding	Recommendation	NASA Response
				contractors for the SSP, has been established that addresses the issue of process control at all levels of the NASA, contractor, vendor, and supplier product chain. A process control video has been developed for wide distribution throughout NASA and the contractor/vendor/supplier community to emphasize the importance of process control and to significantly increase the awareness of management and the workforce. Additionally, the SSP conducted a Program Manager's Review (PMR) in March 2000 where risk management was the sole topic. SSP senior management (NASA and contractors) participated and reviewed the risk management procedures that are utilized by each of the prime contractors. Emphasis was placed on the need for improvement and continued adherence to sound risk management principles. The SSP recognizes the critical importance of maintaining the rigor in planning, analyses, test, and execution that has been the strength of NASA and the space program. A continual emphasis on the SSP's primary goal, to fly safely, will be maintained to strengthen and increase the awareness of the management team and the workforce.
Space Shuttle Independent Assessment Team	7 March 2000	**Issue 3:** The SSP's risk management strategy and methods must be commensurate with the "one strike and you are out" environment of		**SSP Response (Abbey/Dittemore, 21 June 2000):** The foremost priority of the SSP is safety. This priority has extended to all aspects of the program with

Independent Assessment Team *(Chartered by)*	Date of Report	Finding	Recommendation	NASA Response
(NASA Charter)		Space Shuttle operations.		emphasis on public, crew, workforce, and asset protection. The program has accepted added cost and provided schedule relief in numerous situations in order to reduce safety risks. Emphasis on safety as the top priority has been implemented across all program elements, prime contractors, subcontractors, and suppliers. The SSP implements extensive risk management processes as documented in National Space Transportation System (NSTS) 07700. As a result of the SIAT, a section of NSTS 07700 will be dedicated to documenting the program's risk management plan (refer to response to SIAT recommendation #19). The SSP is a strong supporter of independent review processes such as the ASAP and considers knowledgeable review to be invaluable. The program has chartered several independent reviews utilizing technology expert representation. All findings and recommendations are reviewed and dispositioned by the SSP or appropriate organization. The SSP has taken many steps to ensure an appropriate risk management strategy, and will continue to strive for improving these processes (refer to response to SIAT recommendation #22). While the current risk management processes provide a focus for the program to succeed in safe and successful missions, the continuous recognition of and sensitivity to the unforgiving

Independent Assessment Team *(Chartered by)*	Date of Report	Finding	Recommendation	NASA Response
				environment of the Space Shuttle operational profile must always accompany even these disciplined processes.
Space Shuttle Independent Assessment Team *(NASA Charter)*	7 March 2000	**Issue 4:** SSP maintenance and operations must recognize that the Shuttle is not an "operational" vehicle in the usual meaning of the term.		**SSP Response (Abbey/Dittemore, 21 June 2000):** Safety is the number one priority of the SSP and is regularly reinforced throughout the workforce. Additionally, there is an emphasis on continual improvement of the Space Shuttle system; improvement in safety, improvement in efficiency, improvement in processes, etc. Ample evidence exists that demonstrate the SSP's commitment to safety as its highest priority goal (i.e., fleet standdown due to vehicle wiring issues, launch delays to allow time to understand and resolve technical issues, etc.). Safety "first" is a culture that exists throughout the SSP. The SSP agrees that the Space Shuttle is not a typical "operational" vehicle. As evident in the responses to the SIAT recommendations in this document, the SSP realizes the importance of maintaining rigor and conservatism in vehicle maintenance and operations. Refer to responses to SIAT Issue 2, Issue 5, and category 2 recommendations #3, 4, 5, 6, 10, 15, 26, 28, 32, 35, and 38 for additional detail on the conservatism and checks and balances in place for maintenance and operations procedures. These procedures are periodically reviewed. In addition, comprehensive

Independent Assessment Team *(Chartered by)*	Date of Report	Finding	Recommendation	NASA Response
				reexamination of maintenance procedures is in work as a result of the SIAT. Because of the nature of vehicle processing that does from flight to flight, it is reasonable to allow a certain level of standard repairs and "fair wear and tear" repair activities to exist. Standard repair, "fair wear and tear" specifications, and preapproved problem dispositions are used only for recurring conditions where the risks are well understood and acceptable. The "fair wear and tear" specification is a released engineering document that addresses cosmetic damage to hardware and allows the reflight of hardware with such damage under specified conditions, approved by engineering. Standard repairs are preapproved by the Program Material Review Board (PMRB) as delegated by the SSP Manager. The PMRB clearly defines the criteria that govern the use of such repair procedures. Adequate training on the use of these procedures and specifications is provided to the workforce.
Space Shuttle Independent Assessment Team *(NASA Charter)*	7 March 2000	**Issue 5:** The SSP should adhere to a "fly what you test/test what you fly" methodology.		**SSP Response (Abbey/Dittemore, 21 June 2000):** The SSP adopted a "fly what you test, test what you fly" verification methodology at the program's inception as the best approach for ensuring safe and successful operations. However, the extreme and complex environments coupled with their synergistic effects, which are experienced by a reusable spacecraft, did not allow for full-scale

Independent Assessment Team *(Chartered by)*	Date of Report	Finding	Recommendation	NASA Response
				vehicle or component testing to their operational limits. Therefore, the SSP baselined requirements for certification and verification by test and/or analysis, which are documented in the SSP Master Verification Plan (MVP), NSTS-07700-10-MVP01. The Space Shuttle used flight and ground test data to verify models and analytically predict performance at operational boundaries. For testing, either actual or representative flight hardware components were tested under the most realistic operational conditions achievable. Software was also thoroughly tested in avionics laboratories that contained equivalent or simulators of real flight computers and flight control hardware. Prior to first launch, a rigorous verification process was conducted by the program to assure that the flight vehicle, its components, and the associated or analytical were properly or analyzed simulation models tested to all the defined requirements. The program continues to use this same verification process for any significant redesign. The SSP originally implemented and continues to use a configuration control process that assures that flight hardware, software, and associated models remain consistent with this test-verified certification. Postflight data acquisition, data review, correlation with analytical simulations, and postflight inspections/systems testing of the hardware help to ensure that the systems maintain this test-verified

Independent Assessment Team *(Chartered by)*	Date of Report	Finding	Recommendation	NASA Response
				certification. The SSP used available ground and flight test data to characterize the Space Shuttle system performance and to certify the Space Shuttle for flight. Systems dispersions/uncertainties are used in designing the flight and the commit-to-flight processes to ensure safe margins during all flight phases. This preflight and postflight information is reviewed today prior to each Space Shuttle flight. It is natural that hardware and software changes have taken place in the 20 years since the original Space Shuttle certification. These can be classified as planned and unplanned changes. Planned changes are proposed, developed, and accomplished by the SSP to improve Space Shuttle safety, performance, or to account for obsolescence. Space Shuttle Main Engine (SSME) Block II, blanket thermal protection system (TPS), super-light-weight external tank (ET), and software operational increments (OI) upgrades are examples of planned Space Shuttle changes. Typically these types of changes go through the same rigorous testing, verification, and certification processes that the original Space Shuttle hardware went through during its development. Unplanned changes are primarily due to manufacturing defects of new or replaced parts or insufficient performance or failure of existing hardware.

Independent Assessment Team *(Chartered by)*	Date of Report	Finding	Recommendation	NASA Response
				These types of changes are typically very minor, and engineering judgments, supported by analyses, are made as to the extent of the required testing, reverification, and recertification requirements. All available information is used in this decision process for the safety of the Space Shuttle and its crew.
Space Shuttle Independent Assessment Team *(NASA Charter)*	7 March 2000	**Issue 6:** The SSP should systematically evaluate and eliminate all potential human single point failures,		**SSP Response (Abbey/Dittemore, 21 June 2000):** Operation of the Space Shuttle involves an extensive dependency on managers, engineers, technicians, operators, and crew personnel to perform their jobs in an efficient and accurate fashion. Various performance integrity techniques are employed to provide for assurance in executing these activities. The SSP utilizes a high degree of documented procedures and processes which are configuration controlled by the various program and project elements. These requirements flow down into specific maintenance and inspection criteria and are the basis for technician certification requirements and processes. Quality assurance techniques such as inspection, witness, surveys, and audits provide additional checks of performance accuracy. The SSP has had an extensive effort focused on increasing workforce awareness of process control, stamp warranty, and technician certification. In general, the focus has been to drive out the root cause of human error versus reliance on inspection programs. Forums such as the

Independent Assessment Team *(Chartered by)*	Date of Report	Finding	Recommendation	NASA Response
				Incident Error Review Board conduct analysis on maintenance issues and utilize various human factor analysis techniques to drive out contributing factors of human error. The establishment of the Process Control Forum, Chief Engineer Council, and the establishment of the SSP industrial engineering initiative have all been structured to provide for systematic evaluation and elimination of all barriers to error-free performance. Management review processes such as the Preventive/Corrective Action Review (PCAR) have been implemented to provide systematic review and evaluation of performance indicators in a proactive approach. A Government Mandatory Inspection Point (GMIP) represents a point in the flow process in which the work stops and a Government representative performs an observation or measurement. Often, a series of GMIPs were executed in a single flow process and ultimately led to a final checkout or inspection that verified system performance. In many cases, these intermediate inspections were redundant. This drove the program elements to reconsider the assignment of GMIPs and led to the formation of a specific analysis process to use in the evaluation of GMIPs. The SSP established criteria against which existing GMIPs would be reviewed and redundant GMIPs removed. The resultant reduction of GMIPs was based upon

Independent Assessment Team *(Chartered by)*	Date of Report	Finding	Recommendation	NASA Response
				technical justification utilizing established criteria. Extensive reviews of inspection requirements have been conducted over the years, and the SSP continues to utilize lessons learned to evaluate inspection requirements.
Space Shuttle Independent Assessment Team *(NASA Charter)*	7 March 2000	**Issue 7:** The SSP should work to minimize the turbulence in the work environment and its effect on the workforce.		**SSP Response (Abbey/Dittemore, 21 June 2000):** The workforce study conducted by SIAT members at KSC was confined to a small sample of workers. Although the survey raised legitimate concerns, the results of the study, particularly the magnitude of the concerns, may not necessarily be representative of the workforce in general. The issues raised by the study were known by NASA, United Space Alliance (USA), and the ASAP, who collectively believe that morale and focus have improved since the impact of the 1998 reduction in force. Nevertheless, NASA and USA took the SIAT concerns seriously, and USA initiated several actions to better understand the status of workforce morale and focus to correct open issues and improve morale and workforce focus. These actions included: • USA increased the number of face-to-face "skip level" meetings wherein senior managers meet with employees two or more levels below them in the chain of command to get direct input on issues of concern. These

Independent Assessment Team *(Chartered by)*	Date of Report	Finding	Recommendation	NASA Response
				meetings are held by the Space Flight Operations Contract (SFOC) Program Manager, the Associate and Deputy Associate Program Manager (APM) of Ground Operations (GO), and by the direct reports to the APM of GO. • USA commissioned Lord & Hogan, an independent consulting firm with experience in conducting workforce analysis, to administer an operational stress inventory and analysis. Lord & Hogan contacted the SIATto ensure the research instrument used would be endorsed by SIAT. The Lord & Hogan study included worker response to questionnaires, analysis of the responses, and follow-up focus group meetings to gain additional insight into concerns and issues. • USA established a management team to review the inputs from the "skip level" meetings and the Lord & Hogan survey. This team has recommended specific actions to resolve issues. USA management will follow through with a corrective action plan that implements the recommendations. • USA strengthened their communication

Independent Assessment Team *(Chartered by)*	Date of Report	Finding	Recommendation	NASA Response
				process with the establishment of a formal Leadership Council communication process. This council identifies information that should be communicated to the workforce, standardizes the messages, provides talking papers to managers, and flows the information through appropriate channels to ensure both "need to know" and "nice to know" information is provided to the workforce. The council has a feedback loop to measure the effectiveness of communication; thereby, continually improving the process. The issues raised by the SIAT study also were raised in the "skip level" meetings and in the Lord & Hogan survey. The results of the Lord & Hogan survey were very positive and showed that the USA employees in Florida were in the normal range compared to other companies in all categories of stress and coping behaviors. USA currently is conducting a similar study of its workforce in Texas and intends to conduct follow-on studies in both Florida and Texas in approximately 2 years as a comparison to the new baseline. The Space Shuttle launch schedule is expected to

Independent Assessment Team *(Chartered by)*	Date of Report	Finding	Recommendation	NASA Response
				increase to seven flights per year in 2001 and beyond. It is imperative that the SSP have the capability to safely meet that schedule. To assure that the program will continue to safely meet the manifest, USA is taking steps to improve the capability of the workforce in Florida. Actions include: • Hiring additional workers in GO and logistics to provide a workforce that is equivalent to the workforce that safely processed, launched, and recovered eight flights in 1997. This change from the continuous pressure to downsize since 1992 should have obvious positive morale effects. • Changing the Florida organization to align with processes in order to conduct work more efficiently and reduce the total workload. Initially, implementation of this "high performance organization" activity could induce stress, as does most change. The reorganization requires continuous communication and leadership from the initial stages throughout implementation of this reorganization to ensure the workforce remains focused on safely processing, launching, and recovering Space Shuttles. Although not specifically

Independent Assessment Team *(Chartered by)*	Date of Report	Finding	Recommendation	NASA Response
				mentioned as part of this issue, the morale and focus of Boeing's Palmdale workforce is an ongoing concern for NASA, USA, and Boeing. This concern comes mostly because the orbiter maintenance down (OMDP) periods are spaced with several months between the end of one and the beginning of another. The spacing leaves Boeing's Palmdale workforce with periods of very little Space Shuttle related work. This has caused and will continue to cause periodic reductions-in-force and rehiring. Boeing has taken several actions to mitigate the effects of this periodic work including: • Initiatives to increase Palmdale's non-SFOC work to provide additional opportunities for the workers. • Improvements in Boeing's Palmdale facilities to enhance work spaces, including better lighting, new equipment, refurbished work spaces, and adding a cafeteria. NASA and USA are extremely sensitive to workforce issues and are taking positive steps to ensure improvement. Continual monitoring of the workforce morale and focus is an SSP and USA priority.
Space Shuttle Independent Assessment Team *(NASA Charter)*	7 March 2000	**Issue 8:** The size and complexity of the shuttle system and the NASA/contractor relationships place extreme importance on understanding, communication, and		**SSP Response (Abbey/Dittemore, 21 June 2000):** The SIAT identified a number of recommendations relative to communication and information handling that are being addressed by the SSP as part of the SIAT response

Independent Assessment Team *(Chartered by)*	Date of Report	Finding	Recommendation	NASA Response
		information handling.		activity. The SSP continually emphasizes the importance of communication and has established processes, systems, and forums that facilitate information transfer and open discussion of issues and concerns. Weaknesses identified by the SIAT will be addressed.
Space Shuttle Independent Assessment Team *(NASA Charter)*	7 March 2000	**Issue 9:** Due to the limitations in time and resources, the SlAT could not investigate some Space Shuttle systems and / or processes in depth.		**SSP Response (Abbey/Dittemore, 21 June 2000):** The SSP considers the work associated **w**ith kno**w**ledgeable independent review processes to be invaluable to the continued success of the SSP. Relative to the SIAT, all SSP elements have thoroughly reviewed the SIAT report and have conducted internal reviews based upon the reported observations. A special PRCB was held to discuss implementation plans in response to the SIAT recommendations. The PRCB included all SSP elements to ensure maximum participation and dissemination of the information. Specific action items, as discussed in this report, were assigned to the SSP or SSP elements, as appropriate. In addition to the SLAT, USA has formed an independent team comprised of Lockheed, NASA, Boeing, and independent safety and human factors experts to review the maintenance practices related to orbiter processing. Additional reviews to examine other SSP elements will be considered. The SSP has been a strong promoter of independent review processes and has

Independent Assessment Team *(Chartered by)*	Date of Report	Finding	Recommendation	NASA Response
				financially supported and participated in numerous reviews. Numerous review processes, which are independent of the SSP, exist today. These include, but are not limited to, the ASAP, NASA Inspector General (IG), Government Accounting Office (GAO), National Research Council (NRC), Program Management Council (PMC), Center Systems Management Offices, and the (Headquarters/Code Q) Independent Assessment Office. In addition to these, NASA Headquarters, NASA Centers, and the SSP have chartered independent reviews on occasion to investigate specific topics or issues.
Space Shuttle Independent Assessment Team *(NASA Charter)*	7 March 2000		**Recommendation 1-1.** The reliability of the wire visual inspection process should be quantified (success rate in locating wiring defects maybe below 70% under ideal conditions).	**SSP Response (Abbey/Dittemore, 21 June 2000):** Initial qualitative assessments indicated approximately 70-80 percent of the wire defects are found during the first inspection. The remaining 30-20 percent of defects are found during the second inspection. Subsequent to the STS-103 pre-FRR, quantitative analysis at Palmdale indicates 86 percent of the defects are found during the first inspection with the remaining 14 percent found during the second inspection.
Space Shuttle Independent Assessment Team *(NASA Charter)*	7 March 2000		**Recommendation 1-2:** Wiring in OV-102 at Palmdale should be inspected for wiring damage in difficult-to-inspect regions. If any of the wires checked are determined to be especially vulnerable, they should be rerouted, protected, or replaced.	**SSP Response (Abbey/Dittemore, 21 June 2000):** Stringent inspection criteria were established to determine which vehicle areas must be inspected prior to flight of that vehicle. These criteria were approved at the STS-103 pre-FRR. In addition, an end-to-end wiring inspection of OV-102

Independent Assessment Team *(Chartered by)*	Date of Report	Finding	Recommendation	NASA Response
				at Palmdale is underway. These inspections include difficult-to-inspect regions. Wiring which is vulnerable to damage will be reported to the Space Shuttle Vehicle Engineering Office (SSVEO) to determine whether rerouting, additional protection, or replacement of the wiring is appropriate. To date, the OV-102 detailed wiring inspections have not identified any conditions which invalidate our basic inspection criteria for the other vehicles in the fleet.
Space Shuttle Independent Assessment Team *(NASA Charter)*	7 March 2000		**Recommendation 1-3:** The 76 CRIT 1 areas should be reviewed to determine the risk of failure and ability to separate systems when considering wiring, connectors, electrical panels, and other electrical nexus points. Each area that violates system redundancy should require a program waiver that outlines risk and an approach for eliminating the condition. The analysis should assume arc propagation can occur and compromise the integrity of all affected circuits. Another concern is that over 20% of this wiring can not be inspected due to limited access; these violation areas should as a minimum, be inspected during heavy maintenance and ideally be corrected.	**SSP Response (Abbey/Dittemore, 21 June 2000):** The same stringent inspection criteria were used to determine whether inspections of these 76 areas were appropriate prior to flight. Fifty-eight of the seventy-six areas were inspected on OV-103 prior to flight, based on these criteria. The 18 remaining areas were not inspected because the risk of damage during the inspection was greater than the benefit. The 18 remaining areas were inspected on OV-102 at Palmdale prior to the flight of OV-103. These inspections found no exposed conductor and no Kapton damage. In addition, all of the Palmdale inspections completed prior to STS-103 confirmed that the KSC inspection criteria were valid. The SSVEO presented a plan addressing the criticality 1 circuits located in the 76 criticality 1 areas to the PRCB on May 18, 2000. Preliminary estimates indicate approximately 80 percent of the waivered conditions can

Independent Assessment Team *(Chartered by)*	Date of Report	Finding	Recommendation	NASA Response
				be modified to separate system wiring. These modifications are planned to be implemented at the KSC during flow processing operations or during the vehicle orbiter major modifications, whichever is most appropriate. The remaining 20 percent can not be modified due to space limitations. These conditions will continue to be waived.
Space Shuttle Independent Assessment Team *(NASA Charter)*	7 March 2000		**Recommendation 1-4:** The Space Shuttle Program should review all waivers or deferred maintenance to verify that no compromise to safety or mission assurance has occurred.	**SSP Response (Abbey/Dittemore, 21 June 2000):** The SSP completed an extensive review of open waivers in January 2000. Waivers to SSP critical documents were reviewed to determine the quantity and quality of the waivers and the health of the waiver process. Currency of waiver rationale, technical validity, and potential for a requirement change were reviewed. The review concluded that although the waiver process is healthy, a periodic review of the waiver data base is appropriate.
Space Shuttle Independent Assessment Team *(NASA Charter)*	7 March 2000		**Recommendation 2-1:** NASA should expand existing data exchange and teaming efforts with other governmental agencies, especially concerning age effects.	**SSP Response (Abbey/Dittemore, 21 June 2000):** Several initiatives to expand data exchange and teaming efforts with the Federal Aviation Administration (FAA) and Department of Defense (DOD) are currently underway. The SSP has initiated conversations and planning with the Department of Navy and Wright-Patterson Air Force Base to take advantage of initiatives already in place and to coordinate a list of working groups and forums involving multiple Government aerospace agencies. The SSP

Independent Assessment Team *(Chartered by)*	Date of Report	Finding	Recommendation	NASA Response
				will participate in these forums and identify SSP points of contact. The SSP will document assignments and involvement in these forums and identify an appropriate SSP forum for reporting and dissemination of information obtained from the working interfaces. To address recommendation 31, the SSP will specifically identify wiring related working groups and establish the appropriate level of participation. The Manager, SSP Safety and Mission Assurance (SMA) has been appointed as the NASA representative to the Wire Safety Research Interagency Working Group chartered by the Office of Science and Technology Policy. In addition, the SSP established contact in mid-March with the chairman of the Aircraft Wiring and Inert Gas Generator (AWIGG) Working Group and established communications with the team. Membership rosters were exchanged and both the SSVEO and USA sent representatives to the May 15-19, 2000, meeting to further establish points of contact and exchange information. Formal membership and identification of specific SSP representatives will be documented.
Space Shuttle Independent Assessment Team *(NASA Charter)*	7 March 2000		**Recommendation 2-2:** A formal Aging and Surveillance Program should be instituted.	**SSP Response (Abbey/Dittemore, 21 June 2000):** The SSP currently has a strong System Integrity Assurance Program (SIAP), which includes consideration of all possible failure mechanisms including the

Independent Assessment Team *(Chartered by)*	Date of Report	Finding	Recommendation	NASA Response
				effects of aging, maintenance, or exposure. The SIAP requirements of NSTS 07700, Volume XI, were reviewed to ensure that current requirements are structured to incorporate effects of aging and handling on system integrity. The SIAP addresses requirements and responsibilities to ensure that the flight and critical ground systems retain their design performance, reliability, and safety. One key objective of the SIAP is to develop methods to maintain the quality, integrity, and discipline of the SIAP process over the life of the program. Specifically, SIAP paragraph 1.7.2.1 requires the projects and elements to monitor comprehensive maintenance, inspection, time/age/cycle, and refurbishment requirements to assure that their hardware retains design reliability, safety, and performance. Any effort associated with fair-wear specifications are required to comply with this. As a result of the SIAT, all program elements and projects are reviewing the SIAP requirements and specific implementation to meet these requirements. The SIAT makes reference to the "Aging Aircraft Program" in which NASA participates. It is not practical for the SSP to establish a similar program unique to the Space Shuttle, however, it is appropriate for the SSP to ensure results of recent investigations and

Independent Assessment Team *(Chartered by)*	Date of Report	Finding	Recommendation	NASA Response
				concerns associated with aerospace systems are incorporated within the SIAP process. The assignment of key points of contact (reference category 2 recommendation #1) will facilitate this dissemination of information from these conferences.
Space Shuttle Independent Assessment Team *(NASA Charter)*	7 March 2000		**Recommendation 2-3:** NASA and USA quality inspection and NASA engineers should review all CRIT 1 system repairs.	**SSP Response (Abbey/Dittemore, 21 June 2000):** KSC, JSC, and MSFC reviewed the process for review and signature of criticality 1 system repairs. Criticality 1 systems are defined as functional criticality 1 and 1R systems per the applicable failure mode and effects analysis/critical items list (FMEAJCIL) documentation. "Repairs" are material review (MR) items used to repair a design-released part. All MRs, regardless of criticality, are treated as "out-of-family." For orbiter systems, NASA system engineers (SE), USA GO; and Boeing Launch Support Services must sign all KSC GO MR dispositions regardless of criticality. Items that may be first time occurrences or out of the ordinary are thoroughly discussed within the appropriate Prevention/Resolution Team (PRT). The PRT consists of system experts at KSC, JSC, the design Center, and vendors. The PRT technically reviews the problem and agrees to the resolution. The NASA SE must be completely satisfied that all requirements are met and that the MR was properly processed prior to concurring to the repair. The

Independent Assessment Team *(Chartered by)*	Date of Report	Finding	Recommendation	NASA Response
				PMRB must review all orbiter MRs on hardware with failure mode criticality 1, 1R, 1S, 2 or 2R. The GO PMRB membership includes NASA and contractor engineering and quality representatives. All NASA Shuttle Logistics Depot (NSLD) component MR repairs, regardless of criticality, are reviewed and signed by USA quality, NASA quality, and Boeing NSLD engineers who are authorized MR board members. NASA engineering is involved in the repair of all orbiter flight hardware through the Problem Reporting and Corrective Action (PRACA) Corrective Action Request (CAR)/Sub-CAR) process and PRTs. Hardware at the NSLD is dispositioned for the NSLD PMRB approval per NSTS-07700, Volume IV, Section 4.3.2.9 and Appendix Z. PMRB membership includes NASA and contractor engineering and quality representatives. Requirements for Government quality inspections are documented in the Quality Planning Requirements Document (QPRD). Currently, Government quality inspections are required on final verification of configuration changes but not on MR repairs. As a result of the SIAT, a QPRD review is being performed by NASA quality personnel to ensure the proper level of inspection is documented. USA NSLD quality engineering worked closely with NASA quality

Independent Assessment Team *(Chartered by)*	Date of Report	Finding	Recommendation	NASA Response
				personnel to eliminate unnecessary NASA inspection points. Current NSLD metrics by NASA quality personnel shows no increase in findings since the reduction. The SSME Project, Solid Rocket Booster (SRB) Project, Reusable Solid Rocket Motor (RSRM) Project, ET Project, and JSC Space Shuttle Customer and Flight Integration Office also reviewed the MR repair process. The review concluded that the NASA and contractor engineering and quality personnel do review and process MR repairs. Based on the current process and past activities/data, NASA engineering does review all criticality 1 repairs and is compliant with the current NASA requirements. NASA will be required to approve changes to the QPRD, which specifies contractor and NASA inspection points. NASA KSC quality personnel are currently reviewing the QPRD to determine if any additional NASA quality inspection points are required.
Space Shuttle Independent Assessment Team *(NASA Charter)*	7 March 2000		**Recommendation 2-4:** The failure of all CRIT 1 units should be fully investigated and corrected without waivers.	**SSP Response (Abbey/Dittemore, 21 June 2000):** The SSP nonconformance process requires the investigation of safety critical systems failures and also considers the possibility of similar failure modes in other systems. It is the policy of the SSP to return all flight and ground hardware and-software to "print" per Section 1D506, Nonconforming Articles and Materials, of NSTS 5300.4

Independent Assessment Team *(Chartered by)*	Date of Report	Finding	Recommendation	NASA Response
				(1D-2). Furthermore, the investigative results of the failure and the proposed corrective actions are exposed to a wide scope of technical, project, and program reviews via the PRCB process. A waiver is used only after the design project and SSP management team review of corrective action options has resulted in concurrence that a "return to print" option is not mandatory and safety is not compromised. The nonconformances are recognized by the identification of variances from the SSP design and certification requirements (i.e., NSTS 077001Volume X, Flight and Ground Specification) or variances to form, fit, or function specifications in project level end item specifications. Finally, the SSP description of the integrated process for elevating and resolving problems is given in NSTS 07700, Volume XI, SLAP. Per Certification of Flight Readiness (CoFR) requirements, at each FRR all SSP elements are required to have verified that all applicable hardware and software meet all SSP baselined requirements for certification and redundancy. Any deviations, whether through disposition of replacement, repair, or "fly as is," must have had prior approval by the PRCB via the SSP waiver process. These items are also reviewed at the appropriate flight FRR. NSTS 07700, Volume IV, Section 4, directs all SSP elements to submit to the PRCB (for approval prior to

Independent Assessment Team *(Chartered by)*	Date of Report	Finding	Recommendation	NASA Response
				implementation) all proposed hardware or software dispositions which impact baselined program risk, redundancy, or certification requirements. Approval by the SSP Manager results in the development of a waiver to the applicable SSP requirements with the attendant documentation providing the technical rationale for flight acceptability and flight effectivity.
Space Shuttle Independent Assessment Team *(NASA Charter)*	7 March 2000		**Recommendation 2-5:** All testing of units must be minimized and documented as part of their total useful life. Similarly, maintenance operations must be fully documented.	**SSP Response (Abbey/Dittemore, 21 June 2000):** Testing of hardware life cycle, repair, and replacement items is controlled at KSC by established documentation and procedures. Efficient processing of the Space Shuttle components is a goal of the contractor and Government employees at KSC. Standard processing time is carefully monitored and appropriate justifications for performing nonstandard tasks on flight hardware, ground support equipment (GSE), and facility items alike must be provided. Currently, no testing of flight hardware is performed without authorization and documentation. Established Operations and Maintenance Requirements Specifications Document (OMRSD) requirements, PRACA, Test Preparation Sheet, or program level chits authorize testing of flight vehicle hardware and GSE. All of these documents currently have appropriate checks and balances that ensure only required work is performed. OMRSD

Independent Assessment Team *(Chartered by)*	Date of Report	Finding	Recommendation	NASA Response
				requirements conform to the MVP and test for failures modes defined by the FMEA/CIL. OMRSD reviews are periodically held with the goal of improving testing techniques. Per design Center recommendations, time and cycle requirements are levied on sensitive flight hardware items to protect their available lifetimes. OMRSD files also contain specific line replaceable unit (LRU) retest sections that guide the KSC engineer when determining the amount of systems retest required. GSE and facility items are tested only as directed by the appropriate group and must also have authorizing documentation.
Space Shuttle Independent Assessment Team *(NASA Charter)*	7 March 2000		**Recommendation 2-6:** The SIAT recommends comprehensive re-examination of maintenance and repair actions for adequate verification requirements (e.g., visual, proof test, or green run).	**SSP Response (Abbey/Dittemore, 21 June 2000):** The SSME Project, SSVEO, ET Project, RSRM Project, SRB Project, KSC GO and SSP Systems Integration have addressed this recommendation. All elements except SSVEO have completed their assessment and implementation-of any necessary corrective actions. SSVEO is scheduled to complete a review of NSTS 08151, Intermediate and Depot Maintenance Requirements Document (IDMRD) maintenance and Boeing Reusable Space System standard repairs by July 28, 2000. A schedule for implementation of any corrective action will be established as part of this review. All other elements have reviewed their repair/maintenance testing procedures and determined that processes and appropriate testing are in place to verify adequacy of any repairs. The

Independent Assessment Team *(Chartered by)*	Date of Report	Finding	Recommendation	NASA Response
				SSME Project determined, during the course of this review, that one type of nozzle tube repair had inadequate verification testing specified. The specification was revised to require acceptance test hotfire or proof testing prior to flight. All nozzles with this type repair have since been tested.
Space Shuttle Independent Assessment Team *(NASA Charter)*	7 March 2000		**Recommendation 2-7:** Human error management and development of safety metrics, e.g., Kennedy Space Center Shuttle Processing Human Factors team, should be supported aggressively and implemented program-wide.	**SSP Response (Abbey/Dittemore, 21 June 2000):** Human factors principles are being aggressively incorporated into ground processing at KSC. The Shuttle Processing Human Factors Team and the newly formed USA Industrial Engineering and Human Factors Department were staffed to implement human error and process management. Both entities are already working hand in hand to share data, resources, and expertise to develop human factors concepts. With the formation of the USA Industrial Engineering and Human Factors Department, the essential building blocks for this program are now in place. We will continue to improve by increasing the number of trained investigators, improving training, and enhancing data capture and trends analysis capability. As a supporting tool, the Tap Root analysis software is being investigated for use throughout USA to help implement a program wide root cause analysis process. The tool would not only be used by human factors team investigators but also by trained individuals throughout

Independent Assessment Team *(Chartered by)*	Date of Report	Finding	Recommendation	NASA Response
				the Space Shuttle management team (NASA & USA) to add more structure to root cause assessments and help implement better corrective actions. The joint USA and NASA KSC Shuttle Processing Human Factors Team is currently supporting several initiatives. These initiatives include the Work Instruction Task Team, which provides guidelines and training on effective procedure authoring and the Industrial and Work Space Design Team recently chartered to ensure human factors principles are incorporated into the concurrent engineering and ground system design processes. Both of these initiatives will have program wide effects in operations, maintenance, manufacturing, and design. A cross-functional team including human factors professionals has been established to review the Incident Prevention Board (IPB) process and make improvements to both the investigative process and identification and defining of effective corrective actions. The corrective action verification and effectiveness (CAVE) program is in place to verify corrective action effectiveness. This program will ensure that the recommendations of the industrial engineering and human factors team and the corrective action engineering group are implemented in a timely manner and that the actions taken were effective in

Independent Assessment Team *(Chartered by)*	Date of Report	Finding	Recommendation	NASA Response
				preventing or correcting occurrences. The SSP has established a quarterly PCAR where each program element presents their preventative and corrective actions and metrics. Some current activities of the Industrial Engineering and Human Factors Department are performance of on-site process analysis during critical tasks and continuation of development and deployment of human factors related training. USA has also begun to conduct training/outreach to the workforce in their monthly "tailgate meetings," and has reinstated the "Time Out" newsletter, which focuses on human factors issues. The SSP established a specific focus on industrial engineering (IE) and established an IE team that will include human factors in their activities. The focus of the IE team will be to identify specific improvements to the vehicle and/or GSE designs and processing procedures that will result in reduced risk to the workforce, increased maintainability, reduced risk of collateral damage, and an improvement in the overall processing of the hardware and vehicle systems.
Space Shuttle Independent Assessment Team *(NASA Charter)*	7 March 2000		**Recommendation 2-8:** Communications between the rank and file work force, supervisors, engineers and management should be improved.	**SSP Response (Abbey/Dittemore, 21 June 2000):** The USA contractor has taken aggressive actions to improve the communication between the workforce and senior management including biannual briefings from the Chief Executive Officer

Independent Assessment Team *(Chartered by)*	Date of Report	Finding	Recommendation	NASA Response
				(CEO), weekly Leadership Council Meetings at the management level, weekly SSP Manager Meetings, and weekly Employee Meetings conducted by directors and supervisors. Additionally, the USA Program Manager has reemphasized the "management by walking around" activity where management has significantly increased the amount of time spent out of the office visiting employees at their respective work sites. This has been especially emphasized at KSC for both the engineering and technician workforce. Meetings between senior management and 20-30 employees, without other management present, are routinely being conducted to get a better understanding of workforce issues and to receive feedback directly from the employees. Although the SIAt recommendation was more specifically targeted for the KSC workforce, the SSP has reemphasized the importance of communication between senior management and the workforce at all sites, both contractor and NASA. "All hands" meetings are routinely being conducted to communicate the SSP message on goals and objectives, to review "hot topics," to address current issues and concerns, and to obtain employee feedback on specific SSP activities.

Independent Assessment Team *(Chartered by)*	Date of Report	Finding	Recommendation	NASA Response
Space Shuttle Independent Assessment Team *(NASA Charter)*	7 March 2000		**Recommendation 2-9:** NASA should expand on the Human Factors research initially accomplished by the SIAT and the Air Force Safety Center. This work should be accomplished through a cooperative effort including both NASA and AFSC. The data should be controlled to protect the privacy of those taking the questionnaires and participating in interviews. Since major failures are infrequent occurrences, NASA needs to include escapes and diving catches (see Appendix 3) in their human factors assessments.	**SSP Response (Abbey/Dittemore, 21 June 2000):** As a continuation of the human factors research performed by the AFSC, USA hired an independent consultant, Lord and Hogan, to administer the occupational stress inventory and assess the results. A group of 700 USA GO employees were selected to participate in the survey and 589 were completed. Lord and Hogan also conducted face-to-face interviews of 95 participants in focus groups to validate the data and identify other issues. The survey results clearly indicated USA employees experience about the same amount of stress as employees in other industries. The focus groups indicated that USA employees believe that USA is focused on safety at all levels within the organization but USA needs to address workload, training, and other issues for the increased flight rate. These findings are consistent with the earlier ASAP findings. While the overall results are positive, USA is evaluating the detailed data to determine areas where it can improve and is addressing specific issues raised by the focus groups. A USA Workplace Action Team has been established to review the survey results and recommend proactive measures to help assure that USA can continue to effectively manage the pressures in the workplace as the flight rate increases. In response to program tasking, KSC NASA/USA GO have developed a system

Independent Assessment Team *(Chartered by)*	Date of Report	Finding	Recommendation	NASA Response
				to ensure both hardware and processing/safety "escapes" and "diving catches," as identified in the SIAT report, are identified and a risk assessment is performed to determine the appropriate level of reporting and corrective action. Human factors investigators are assigned to mishaps based upon a USA risk assessment score or at the discretion of USA management. All items are evaluated using the established USA risk assessment process and may be assigned as an IPB item. Additionally, the SSP Manager directed that process escapes be reported and tracked similar to in-flight anomalies. Process escapes are presented to the SSP Manager at the quarterly PCAR.
Space Shuttle Independent Assessment Team *(NASA Charter)*	7 March 2000		**Recommendation 2-10:** Maintenance practices should be reviewed to identify and correct those that may lead to collateral damage.	**SSP Response (Abbey/Dittemore, 21 June 2000):** In January 2000, a team was formed to assess hardware damage, provisions, current protection, and any associated issues with collateral damage in the orbiter aft fuselage. The team included Aft Shop (orbiter processing facility (OPF) and Pad), Palmdale, NASA, USA and Boeing subsystem engineering, Rocketdyne, GSE/tool engineering, and human factors personnel. The initial effort concentrated on the aft fuselage due to the hardware criticality and potential for damage. Standard processing, as well as contingency LRU removals, were examined. General safety and human factor concerns were

Independent Assessment Team *(Chartered by)*	Date of Report	Finding	Recommendation	NASA Response
				considered. Operational area and (OASIS) data were also reviewed. The team findings concentrated on the following areas: access concerns, areas at risk for collateral damage, potential for wire damage, GSE, LRU GSE, portable lighting, and training. To date, seven orbiter modifications are in work as a direct result of this team. A GSE/platform subteam addressed access andGSE concerns. The subteam has reviewed the maintenance procedures and platform installations and identified the areas of poor access for the horizontal and vertical platform sets. In addition to poor access areas, the team is reviewing the size and weight of the piece parts to help reduce the risk of collateral damage during installation and removal. The team has also documented access requirements for the change out of an SSME in the vertical, along with the fall protection concerns in this configuration. Engineering Support Requests (ESR) were approved for improvements to the horizontal and vertical platform sets (ESR K16789 and K16190) and implementation is in work. An auxiliary power unit (APU) access stand was created for general processing and LRU remove and replace (R&R). A Process Improvement Team (PIT) was also chartered to study maintenance procedures, onetime entry issues, additional training, lighting, and communication concerns. PIT findings have revealed the need for an integrated

Independent Assessment Team *(Chartered by)*	Date of Report	Finding	Recommendation	NASA Response
				approach to platform installation, hardware inspection, and protective cover installation. The team is also working with vendors to get improved fixed lighting to reduce the need for portable lighting. In addition, use of battery operated lights is under review. Wireless headsets are also being investigated. A main propulsion system (MPS) vacuum jacket line protection effort was kicked off to prevent line damage during processing. The lines are being protected with "elephant-hide" and a visual barrier ("No Step" ID) as immediate protection. In parallel, shop-aid thermo-foam plastic hardcovers are being designed and fabricated (Test Preparation Sheet SA19-1-629). This effort is in work and is being implemented to a prioritized list (by line damage history and high traffic areas). The methodology used to assess the aft compartment and maintenance procedures to mitigate risk to collateral damage will be employed for the orbiter payload bay and forward fuselage areas. Midbody and forward teams were kicked off and are working in parallel. The teams will continue to be chartered by management and will report back to the IPB for an integrated review and concurrence of recommended change. Based on increased emphasis on minimizing collateral damage, employee awareness was raised through communication and training in areas such as hardware handling and testing, foreign

Independent Assessment Team *(Chartered by)*	Date of Report	Finding	Recommendation	NASA Response
				object elimination, contamination protection, and equipment operation. The program will continue to apply these methodologies to other areas of the vehicle and maintain employee sensitivity.
Space Shuttle Independent Assessment Team *(NASA Charter)*	7 March 2000		**Recommendation 2-11:** Shuttle actuator soft goods should be adequately wetted to prevent downtime seepage.	**SSP Response (Abbey/Dittemore, 21 June 2000):** The current orbiter hydraulic system provides the best environment for seal operation to meet tight leakage requirements. The hydraulic system seals are maintained in a wetted environment at all times, including down time, and spare units are maintained on the shelf. The PRACA system data base shows there has not been any component replacement due to seal deterioration related to inadequate wetting. The orbiter currently meets the recommendation. SRB hydraulic LRUs incl;uding the actuators are refurbished after each flight. Following refurbishment, each unit is acceptance tested prior to being returned to stock. Preinstallation and postinstallation leakage tests are conducted on the entire hydraulic system for each SRB. Rigorous system level performance tests, including leakage tests, are done prior to each flight. System seal integrity is further verified at the vehicle level during the Space Shuttle Interface Test. No occurrences have been identified on the SRB program where post installation seal deterioration was related to inadequate wetting of the seal.

Independent Assessment Team *(Chartered by)*	Date of Report	Finding	Recommendation	NASA Response
Space Shuttle Independent Assessment Team *(NASA Charter)*	7 March 2000		**Recommendation 2-12:** Tank time and cycle data must be carefully logged to ensure safe life criteria are not exceeded.	**SSP Response (Abbey/Dittemore, 21 June 2000):** Time and life cycle life requirements for Space Shuttle flight tanks (ET, hydrogen, oxygen, orbiter maneuvering system (OMS) and reaction control system (RCS) propellant, N2, etc.) are found in OMRSD, File Two, Volume Ill. This file lists age sensitive items by part number. Information includes age and cycle life limits and required actions when life limits are reached. Items related to this file that have associated telemetry are tracked by a system called Time Age Cycle Control System (TACCS). TACCS is a data base that tracks the number of tank cycles by using software that accesses Launch Processing System (LPS) data for tank pressures whenever the vehicle is powered up. If the tank is at a vendor, cycles placed on the tank are recorded in the data pack. When the tank arrives back at KSC the data pack is reviewed and appropriate entries made into the TACCS data base. Any cycles not covered by telemetry and tank cycles at Palmdale are recorded into appropriate work authorization documents (WAD) or engineering logs. TACCS personnel review the WADs and entered data into the data base. Engineering is responsible for transferring tank cycle data from their logs to the TACCS data base. There have been limited instances when the cycle data was not accurately transferred to the TACCS data base. This disparity in cycle data is very small and does not constitute a problem since the number of

Independent Assessment Team *(Chartered by)*	Date of Report	Finding	Recommendation	NASA Response
				cycles accumulated to date on the tanks is only about 20 percent of the maximum allowed by the OMRSD. However, the SSP will correct the process to ensure accurate tank cycle data in the TACCS data base. When tanks reach 90 percent of their maximum life cycles per the OMRSD file, the appropriate system representative is notified for disposition. The SIATreport addressed exceeding the total number of hours that the tanks can be kept at flight operating pressure and the tracking of these data. The SSVEO has had a fleet leader program in place since 1978 for the Kevlar overwrap pressurant tanks. Data from this program indicate that tanks will not fail at ambient temperature for 100 years or more. Other orbiter tanks are not kept at flight pressures between flights, therefore, the total time spent at maximum pressure is small compared to their overall life. In addition, the design Center stress analysis group determined that there is no limit to the number of hours that the propellant tanks can remain at flight pressure.
Space Shuttle Independent Assessment Team *(NASA Charter)*	7 March 2000		**Recommendation 2-13:** Critical operations, especially those involving Self-Contained Atmospheric Protective Ensembles, must be staffed with technicians specifically experienced and properly trained with the operations.	**SSP Response (Abbey/Dittemore, 21 June 2000):** USA personnel are required to attend specific critical skills certification classes, based upon the requirements of their particular shop area. This is true for all certifications including self-contained atmospheric ensemble (SCAPE). Personnel must

Independent Assessment Team *(Chartered by)*	Date of Report	Finding	Recommendation	NASA Response
				attend and satisfactorily complete specific classes taught by certified instructors. Certifications are tracked and updated by the training department and the individual's specific directorate. On-the-job training (OJT) is often used to supplement certification training. Personnel, under the guidance of their management and an experienced certified senior technician, complete OJT packages. These packages are used in the actual work environment so training is hands on. Each area supervisor verifies that their personnel have the necessary skill and experience level to safely perform specific tasks and assigns them accordingly. Special efforts are made to team an experienced technician with a less experienced technician, until the supervisor feels confident in assigning the less experienced technician to a job without oversight. Cross training at various sites and with various systems is also strongly encouraged. USA and NASA at KSC are confident that only highly trained, certified, and experienced technicians are used in task execution. Standardization of this training for both horizontal and vertical operations is achieved via a "partnered" training plan.
Space Shuttle Independent Assessment Team *(NASA Charter)*	7 March 2000		**Recommendation 2-14:** Fleet Leader testing must be carefully scrutinized to ensure adequate simulation of operating conditions, applicability to multiple subsystems, and complete documentation of results.	**SSP Response (Abbey/Dittemore, 21 June 2000):** The Orbiter fleet leader program evaluation is in work and is expected to be complete in June 2000. Results and recommendations will be reviewed at the

Independent Assessment Team *(Chartered by)*	Date of Report	Finding	Recommendation	NASA Response
			results.	will be reviewed at the Vehicle Engineering Control Board (VECB). The current fleet lead testing and status was presented to the VECB in February 2000 along with the recommendation to evaluate additional potential fleet lead testing including fire extinguishers, landing deceleration systems, mechanical actuation hardware, hydraulics, and APUs. Test conditions were examined to ensure the correct test environments are applied to the fleet leader. Fleet leader testing of payload integration hardware has consisted of teardown inspections of two power harnesses and one data harness. The results were presented to the November 1999 PRCB. There was no indication of stress in the insulation as a result of bending, no degradation attributable to hi-pot testing, and no wiring damage hidden by the overbraid which was not attributable to the overbraid damage itself. All major SSME components achieved a fleet leader goal of demonstrating life requirements of 60 missions (7.5 hours operating time). After certification, hardware allowable life is based on 50 percent of the fleet leader operating time. The RSRM Project structured postfire inspection and refurbishment processes to ensure that flight hardware has met, and will continue to meet, all engineering

Independent Assessment Team *(Chartered by)*	Date of Report	Finding	Recommendation	NASA Response
				specification requirements. Conditions identified for further review by the postfire inspection activity are dispositioned in a closed loop system, which requires approval for closure by both NASA and contractor senior management. All observations noted during the inspections are entered into a data base for future reference and trending purposes. In addition, the "number of uses" is tracked for each component and compared to the design reuse requirements. This process ensures that requirements are met and identifies when replacement hardware should be procured. Furthermore, these data are presented as part of the CoFR process for review by both NASA and contractor senior management. Subsequent to these inspections, those components intended for reuse are subjected to a rigorous combination of nondestructive evaluation (NDE), proof-test, and inspection to satisfy the safe life requirements. As with the post'fire inspection process, the results of these activities are fully documented to provide a clear pedigree of the hardware intended for flight use. The SRB Project does not utilize a formal fleet leader program because the hardware is disassembled, thoroughly inspected, refurbished, and reassembled after each flight. LRU life is based on qualification of the design (structure LRUs = 40 missions, electronic LRUs = 20 missions, pyrotechnic LRUs = time, etc.).

Independent Assessment Team *(Chartered by)*	Date of Report	Finding	Recommendation	NASA Response
				Qualification is based on analysis, test, and/or similarity. LRUs are recertified for each flight by inspection and/or test. Critical functional parameters are trended. Pyrotechnic components are lot certified for a specific length of time by test, and their life is extended by test, if required. A teardown/analysis approach is utilized for evaluation of cables. A small sample of flight cables are withdrawn from inventory and subjected to more extensive testing, including destructive evaluation. The SRB Project continually monitors failures to determine their age/life implications and any associated impact on obsolescence and mission supportability. Fleet leader testing is not utilized in the verification of the ET since the tank is an expendable subsystem of the Space Shuttle. All SSP elements are exercising a fleet leader program, or a similar program, which meets the recommendation.
Space Shuttle Independent Assessment Team *(NASA Charter)*	7 March 2000		**Recommendation 2-15:** Vendor supplied training should be evaluated for all critical flight hardware.	**SSP Response (Abbey/Dittemore, 21 June 2000):** The vast majority of direct vendor training is provided to the NSLD. The NSLD was started in 1986 as a repair depot function to provide timely, cost effective local support to the SSP. The NSLD is currently certified to repair over 3,000 line items. The repair certification requirements are defined in JSC20423, Orbiter Repair Agency Design Activation and Operations Requirement

Independent Assessment Team *(Chartered by)*	Date of Report	Finding	Recommendation	NASA Response
				Document. Each time a new piece of hardware was transitioned from the original equipment manufacturer (OEM) to the NSLD, an extremely rigorous certification process was employed. This process included representatives from OEM engineering, NASA JSC systems engineering personnel, Rockwell (now Boeing) systems engineering personnel, NASA quality control personnel, NASA logistics personnel, and NSLD engineering/technicians. The process included transfer of knowledge on the theory of operation/design, detailed teardown/repair hands-on operations, and OEM design and specification documentation. Each piece of hardware, for which the NSLD is the certified repair agency, is considered unique. The requirements for how specific orbiter hardware was/is certified for repair at the NSLD is controlled by NSTS08151, Intermediate and Depot Maintenance Requirements Document (IDMRD), Vol. I, Maintenance Concepts Baseline. Both of these documents are subordinate documents to NSTS 07700. On complex items, training was done at both the OEM's plant as well as the NSLD. Actual certification and demonstration of hardware knowledge, troubleshooting, and repair capability was done at the NSLD. Each one of the individual certifications was video taped for documentation purposes as well as for review (if needed) for complex repairs. OJT

Independent Assessment Team *(Chartered by)*	Date of Report	Finding	Recommendation	NASA Response
				training packages were built. These packages mirrored the certification capability demonstration and conform to the requirements of the IDMRD for use in future training of engineers or technicians. KSC GO is limited to performing R&R of LRUs and is trained, certified, and procedure controlled to perform this task. There are rare exceptions where LRU replacements are allowed on the vehicle. For these cases, the design Center must concur with actions. Options include calling in certified vendor/depot support or certifying GO personnel to perform the repair. The former option presents an opportunity for GO personnel to work directly with vendor representatives, presenting a unique learning atmosphere for both parties. The latter option requires vendor and design Center (contractor and NASA) oversight and direct participation in initial training and procedure development for certification of GO personnel. Recertification curriculum is developed for administration by USA Integrated Logistics Technical Training & Development. Program control of this process is assured by documenting allowed repairs in the OMRSD LRU retest table. Changes to this document require PRCB approval.
Space Shuttle Independent Assessment Team	7 March 2000		**Recommendation 2-16:** The true mission impact of a second main engine pin failure (internal engine foreign object debris) during flight, similar to	**SSP Response (Abbey/Dittemore, 21 June 2000):** The need for such an analysis has been eliminated since there are no engines

Independent Assessment Team *(Chartered by)*	Date of Report	Finding	Recommendation	NASA Response
(NASA Charter)			that which took place last July, should be determined.	remaining in the flight fleet with deactivated main injector liquid oxygen (LOX) posts. Engine 2048 was the last such unit in the fleet. This unit was returned to the factory for a powerhead replacement. That work has since been completed and the engine returned to the active flight fleet at KSC. (Reference STS-93 In-Flight Anomaly Closure Report: STS-93-E-01). The need for LOX post deactivation was eliminated with design and manufacturing process improvements incorporated during the conversion to the Phase II + powerhead configuration. This non-pinned configuration is the only configuration now flying.
Space Shuttle Independent Assessment Team *(NASA Charter)*	7 March 2000		**Recommendation 2-17:** The SSP should consider more frequent lot sample hot fire testing of the Solid Rocket Booster motor segments at full-scale size to improve reliability and safety and verify continued grain quality.	**SSP Response (Abbey/Dittemore, 21 June 2000):** The SSP requires the RSRM Project to demonstrate all engineering/process changes on a full-scale static test motor prior to incorporation into the Space Shuttle flight program. This is accomplished through the use of a flight support motor (FSM) program conducted at the contractor facility in Utah. This program, presently conducted on approximate 12 month intervals, allows an engineering assessment/confirmation of the numerous analytical models used for nominal motor performance predictions and flight safety considerations of Senior Material Review Board conditions. However, these motors are only intended as substantiation that both the

Independent Assessment Team *(Chartered by)*	Date of Report	Finding	Recommendation	NASA Response
				individual and synergistic effects of the proposed changes have no adverse impacts resulting from their incorporation. Studies relative to "Corners-of-the-Box" and/or flaw test parameters have typically been limited to subscale test articles which contain inherent scale-up uncertainties leading to conservative boundary conditions when utilized for analytical calculations. Furthermore, the consideration of flaw testing to verify margins of safety on an FSM static test places some risk to the RSRM Project's qualification/verification resources. Within this context, the SSP concurred with the project's intention to define a full-scale engineering test motor (ETM) that would contain test objectives focused on flaw and margin assessments. The requirements for this test bed are currently being formalized targeting a presentation to the SSP requesting formal authority to proceed. The ETM firing is targeted for September of 2001.
Space Shuttle Independent Assessment Team *(NASA Charter)*	7 March 2000		**Recommendation 2-18:** An independent review process, utilizing NASA and external domain experts, should be institutionalized.	**SSP Response (Abbey/Dittemore, 21 June 2000):** The SSP currently utilizes numerous review processes, which are independent of the SSP. These reviews are performed repetitively, and essentially represent an institutionalized independent process. These include, but are not limited to, the ASAP, NASA IG, GAO, NRC, PMC, Center systems management Offices, and the (Headquarters/Code Q) Independent Assessment Office. In addition to these,

Independent Assessment Team *(Chartered by)*	Date of Report	Finding	Recommendation	NASA Response
				NASA Headquarters, NASA Centers, and the SSP have chartered independent reviews on occasion to investigate specific topics or issues. Many of these reviews were chartered prior to key program decisions being implemented. The SSP established a specific independent review process for the upgrades program including the Space Flight Advisory Committee, NASA Independent Program Assessment Office, and (Headquarters/Code Q) Independent Assessment Office. A sufficient number of independent formalizing a regular independent SSP review process. In addition, the Agency and the SSP periodically charter other specific independent assessments such as the SIAT to supplement the basic review processes utilized by the program. While there are numerous avenues for the workforce to voice their concerns, as a result of the SIAT, the program determined that value exists in the establishment of an independent process to draw out workforce issues. USA commissioned an independent consulting firm (Lord and Hogan) to conduct employee surveys on a periodic basis (approximately every 2 years) and has established a baseline as of February 2000. Additionally, an external group consisting of Lockheed, NASA, Boeing, and independent safety and human factors experts was established to conduct ongoing policy, procedure,

Independent Assessment Team *(Chartered by)*	Date of Report	Finding	Recommendation	NASA Response
				and best practice reviews.
Space Shuttle Independent Assessment Team *(NASA Charter)*	7 March 2000		**Recommendation 2-19:** NASA, USA, and the SSP element contractors should develop a Risk Management Plan and guidance for communicating risk as an integrated effort. This would flow SSP expectations for risk management down to working level engineers and technicians, and provide insight and references to activities conducted to manage risk.	**SSP Response (Abbey/Dittemore, 21 June 2000):** The SSP implements and utilizes extensive risk management processes. The requirements and processes are documented in NSTS 07700 and the various associated documents. This documentation serves as the risk management plan for the SSP and currently defines and integrates risk management activities across all SSP elements. A SSP PMR was held March 21-22, 2000, which focused on risk management implementation across all program elements. The PMR included participation from all NASA elements and Centers, prime contractors, Defense Contract Management Agency (DCMA), ASAP, and the SIAT risk management evaluators. Presentations included discussions of the various methods utilized by the contractors to involve their workforce and management in risk management processes. It was evident that e4xtensive risk management processes and analytical techniques are implemented across all SSP elements. In reviewing the complexity and diversity of the risk management processes, it was determined that a section of NSTS 07700, Volume I, would be dedicated to the documentation of the SSP risk

Independent Assessment Team *(Chartered by)*	Date of Report	Finding	Recommendation	NASA Response
				management processes and requirements. This documentation will include the program's risk management plan and a "roadmap" to existing documentation. The documentation will provide centralization of the various risk management elements incorporated throughout the program and establish a basis for the flow down of SSP expectations for risk management to the various program elements and contractors. It will provide insight and reference to activities conducted to manage risk. While this section is not intended to incorporate the specific requirements and procedures, it is intended to consolidate references to the various SSP risk management activities specified throughout NSTS 07700 and the associated SSP documents. The change to NSTS 07700 is target for implementation this summer.
Space Shuttle Independent Assessment Team *(NASA Charter)*	7 March 2000		**Recommendation 2-20:** Risk assessment matrix and Failure Modes and Effects Analysis should be updated based on flight failure experience, aging and maintenance history, and new information (e.g., wiring, hydraulics, etc.).	**SSP Response (Abbey/Dittemore, 21 June 2000):** Currently, the risk assessment matrix, FMEA/CILs, and hazards are updated based on flight failure experience, aging and maintenance history, and new information. For example, FMEA/CILs and hazards are updated when there is a new failure mode that was not considered previously. The new failure mode may cause a change in the risk matrix or cause a change in criticality. All increases in risk for FMEA/CILs or hazards are briefed at the applicable FRR. Prior to 1991, the SSP had a

Independent Assessment Team *(Chartered by)*	Date of Report	Finding	Recommendation	NASA Response
				requirement to include all failure history in the FMEA/CIL. The SSP approved deletion of that requirement on October 3, 1991, to eliminate duplicate information that can be obtained through other sources. This change also reduced the volume of CIL documentation updating and resulted in more efficient use of resources. Examples of information kept in other locations include: 1. Tests: Turnaround checkout testing is maintained in the OMRSD. 2. Failure History: Test failures, flight failures, unexplained anomalies, and other failures experienced during ground processing can be found in the PRACA data base. 3. Operational Use: Standard crew actions are maintained in flight rules and crew procedures. A web-based data warehouse with capability to cross reference CILs, hazards, and problem reports/failure history are under development. This capability should be available within 6 months.
Space Shuttle Independent Assessment Team	7 March 2000		**Recommendation 2-21:** The SSP should revise the risk matrix for probable and infrequent likelihood for CRIT 1R** and 1R* severity to require a greater level of	**SSP Response (Abbey/Dittemore, 21 June 2000):** In the 1995 timeframe, the SSP went through an extensive review of the Space Shuttle MVP with the specific

Independent Assessment Team *(Chartered by)*	Date of Report	Finding	Recommendation	NASA Response
(NASA Charter)			checkout and validation.	goal of identifying the appropriate level of checkout and verification while not overstressing the systems due to excessive testing. The team was challenged to find the proper balance between the risk of insufficient testing and the risk of overtesting. The team was a multifunctional SSP team and included safety, reliability and quality assurance (SR&QA) personnel. At one time, all criticality 1R1 and 1R2 systems were fully checked out on the ground. Excessive wear was resulting from this philosophy and on-orbit operations were not being considered in the validation approach. The team determined that on-orbit operating time or the time operating the systems in support of associated systems checkout should be considered in the checkout and validation of performance. This approach has reduced the wear and tear on many of the critical systems and has reduced the amount of system exposure to potentially induced damage. As noted in the wiring investigation, exposure to potential maintenance induced damage needs to be continuously balanced with the degree of ground maintenance and checkout required to verify system performance. To date, no in-flight failures are attributable to lack of ground checkout and validation. Continuous review of validation and checkout procedures is standard

Independent Assessment Team *(Chartered by)*	Date of Report	Finding	Recommendation	NASA Response
				practice and a current requirement associated with the MVP. For example, as a result of the OV-104 speedbrake power drive unit end cap found during ground testing at KSC prior to STS-101, an additional ground checkout procedure was added to each Vehicle flow to verify the end cap is properly seated and will not impede system operation.
Space Shuttle Independent Assessment Team *(NASA Charter)*	7 March 2000		**Recommendation 2-22:** NASA Safety and Mission Assurance surveillance should be restored to the Shuttle Program as soon as possible.	**SSP Response (Abbey/Dittemore, 21 June 2000):** NASA and the SSP have maintained an active SMA program and will continue to do so. The execution of these activities have contained two key elements: first, the safety, reliability, maintainability, and quality assurance (SRMQA) engineering; and second, analysis tasks performed in accordance with program requirements and the independent SMA oversight function provided in support of the Office of SMA (Headquarters/Cod.eQ)o NASA Center SRMQAorganizations have continued to be active participants in all aspects of the program. _1_ elements and supporting organizations have also been very active in executing SMA Program related surveillance. The SSP has taken several steps towards assuring a strong SMA program: • In 1996, an SSP position, Manager, SMA, was created

Independent Assessment Team *(Chartered by)*	Date of Report	Finding	Recommendation	NASA Response
				which provides a senior management authority associated with SSP SMA policy, requirements, and implementation. • All program elements have undergone training in DuPont Safety, fault tree analysis, root cause analysis, and obtained ISO quality system certification by third party registrar. • Resources for center SRMQA, which at one time were constantly threatened by Center priorities, are now provided directly under SSP funding. The SSP program operating plan (POP) reflects multiyear planning for SRMQA tasks throughout element and SRQA organizations and is fully supported by SSP management. • Supplier surveillance has been maintained through use of delegated tasks to the DCMA by the SSP Manager, SMA. This support has not decreased and has even recently been increased through the direct program funding of $4.5 million to support surveillance of contractor activities

Independent Assessment Team *(Chartered by)*	Date of Report	Finding	Recommendation	NASA Response
				associated with the SRB. • NASA implemented Government hiring of SMA personnel at all Centers. • In response to SSP requirements, the prime contractors implemented numerous safety and risk management initiatives. • Flight readiness processes include specific review and verification of SRMQA engineering products. • NASA and contract program elements have maintained an appropriate sustaining engineering function that is continuously involved in evaluation and analysis processes. These efforts are continuously reviewed at program forums such as the SSP Council, PMR, PCAR, and PMC. The Office of SMA (NASA Headquarters/Code Q) has also maintained a substantial SMA surveillance program. In 1996, the (Headquarters/Code Q) Independent Assurance Office located at JSC expanded its charter to include independent assessments associated with the SSP. In 1996, the Associate Administrator of SMA established the Human Exploration and Development of Space (HEDS) Assurance

Independent Assessment Team *(Chartered by)*	Date of Report	Finding	Recommendation	NASA Response
				Board-to provide senior NASA management with timely, objective, nonadvocate assessments of program health, status, and relative safety posture. This board meets on a monthly basis with NASA Administrator participation each 6 months and includes participation of the senior Center and program SMA managers. The Pre-Launch Assessment Review is chaired by the Associate Administrator of SMA and provides for independent assessment in support of CoFR. The Office of SMA also conducts process verification audits of the various SRMQA processes as an element of their surveillance activity and participates in numerous program reviews and problem resolution processes. SSP requirements address the various roles and responsibilities of both the SRMQA organizations and program elements in executing the SMA program. These requirements will be reviewed to ensure clarity between the SRMQA engineering activities which are conducted in direct support of the SSP and the independent assurance (IA) activities which are conducted in direct support of the Office of SMA. Organization charts and functional responsibilities will be revised to reflect clear and specific working relationships and responsibilities of these two functions. Specific assignment of individuals will be reviewed and revised to ensure clear and separate

Independent Assessment Team *(Chartered by)*	Date of Report	Finding	Recommendation	NASA Response
				reporting responsibilities. This review will be accomplished by August 1,2000.
Space Shuttle Independent Assessment Team *(NASA Charter)*	7 March 2000		**Recommendation 2-23:** The Safety & Mission Assurance role should include: mandatory participation on Prevention/Resolution Teams and in problem categorization, investigation of escapes and diving catches (see Appendix 3), and dissemination of lessons learned.	**SSP Response (Abbey/Dittemore, 21 June 2000):** As a result of this SIAT recommendation, verification that SSP requirements define SRMQA engineering's mandatory involvement and product expectations has been accomplished. Program requirements and processes including anomaly disposition, trending analysis, problem reporting, preventive/corrective action, and mishap investigations were reviewed and were confirmed to require mandatory participation by SRMQA engineering. These functions result in specific program products that are integral components of the problem resolution process. Verification of SMA dissemination of lessons learned was accomplished. Also, Headquarters/Code Q manages the NASA lessons learned data base and provides access to anyone within NASA and the contractor team. This system is active and supported. Products associated with determining safety and mission success involve a number of program elements and supporting disciplines. Safety reporting systems, IPBs, mishap and close call forums, and in/out of family anomaly reviews involve a diversity of program element

Independent Assessment Team *(Chartered by)*	Date of Report	Finding	Recommendation	NASA Response
				and contractor functions. As a result of the SIAT, the SSP Manager directed that escapes be treated similar to in-flight anomalies. Therefore, all escapes are briefed to SSP management at the quarterly PCAR. This requirement is applicable to all program elements including SRMQA organizations. The PCAR is conducted as a formal PRCB involving the mandatory participation of all elements including SRMQA organizations.
Space Shuttle Independent Assessment Team *(NASA Charter)*	7 March 2000		**Recommendation 2-24:** The SIAT believes that software systems (flight, ground, and test) deserve a thorough follow-on evaluation	**SSP Response (Abbey/Dittemore, 21 June 2000):** The SSP believes that the flight, ground, and test software systems are of world-class quality as evidenced by the metrics for product error rates. The SSP reviews these metrics on a regular basis and conducts reviews of the element processes and metrics. Flight software processes continue to be better than the industry standards for ISO 9001 and the Software Engineering Institute (SEI) Capability Maturity Model for Software (SW-CMM). Flight software personnel continues to exercise an independent verification and validation (IV&V) assessment throughout the general purpose computer (GPC) and SSME development processes. Software processes and performance have been assessed on numerous occasions (ASAP, GAO, NRC, arid Roger's Commission), with consistent findings of exemplary performance reported by these

Independent Assessment Team *(Chartered by)*	Date of Report	Finding	Recommendation	NASA Response
				reviews. While the SSP fully recognizes the complexity and criticality of software systems, the current control and review processes are considered to be rigorous, disciplined and sufficient. The SSP believes a follow-on SIAt evaluation is not warranted at this time.
Space Shuttle Independent Assessment Team *(NASA Charter)*	7 March 2000		**Recommendation 2-25:** Due to time constraints, the SIAT only examined Orbiter wiring; many other systems associated with the Shuttle also have critical wiring. The findings and recommendations in this report are applicable to all Shuttle systems, but unique conditions that may require additional actions.	**SSP Response (Abbey/Dittemore, 21 June 2000):** The SSP held an element wide wiring review at the September 16, 1999, PRCB. This review addressed extravehicular (EVA), cargo integration, Government-furnished equipment (GFE), GSE, RSRM, SRB, ET, and SSME wiring. Subsequent to that meeting,14 follow-up PRCB Actions pertaining to non-orbiter elements were issued, addressed, and closed. The scope of these actions includes wiring inspection status and protection, test plans and checkout procedures, fleet leader approach, engineering standards and requirements, as well as element unique activities such as bend radius life cycle analysis and teflon wiring utilization. The scope of SSP wiring attention has been and will continue to be inclusive of all program elements.
Space Shuttle Independent Assessment Team *(NASA Charter)*	7 March 2000		**Recommendation 2-25:** During the inspection of wiring, several connector issues were also apparent. Loose connector backshells and wire strain relief that can potentially chafe wiring were noted. Under certain conditions loose backshells can compromise electrical bonding between shielding and structure. Movement of the backshell can	**SSP Response (Abbey/Dittemore, 21 June 2000):** The orbiter OMRSD requires a visual inspection of electrical connectors every flow to verify proper mating and backshell attachment. The orbiter MLO303-0014 specification documents the requirements for backshell rework and connector manipulation. A recent

Independent Assessment Team *(Chartered by)*	Date of Report	Finding	Recommendation	NASA Response
			also cause chafing between the wiring and strain relief. In either case, these are unacceptable conditions and should be eliminated by periodic inspection and connector design.	investigation of chafing found between wiring and backsheil strain relief arms resulted in an update to this specification to provide additional strain relief. This specification is invoked on connectors with detected damage and connectors susceptible to damage due to configuration or frequent flexing. Backshell integrity is physically verified with every connector mate/demate operation and connector reworked. Payload integration wire harnesses are governed by the same ML0303-0014 specification as orbiter harnesses. A recent update to ML0303-0014, Paragraph 6.3.2.23, addresses added protection at the backshell strain relief tangs, where required, with the use of Mystic 7503 tape. A strain relief tang is used to secure the wires going into the connector to reduce strain on the contact locking mechanism. The wires entering a connector are spot tied to the tang so that any flexure of wire bundle stops tang. This configuration greatly reduces movement of the wires in the connector. The SSME design precludes wire looseness in backshell strain relief clamps. Silicone tape is used to fill gaps around wiring, and overmolds provide exterior protection. Inspection for loose backshells is included in periodic inspection requirements. There has been no comparable SSME failure history of wire damage due to

Independent Assessment Team *(Chartered by)*	Date of Report	Finding	Recommendation	NASA Response
				loose backshells. The RSRM Project conducted a review and evaluation of RSRM cabling and wiring. All RSRM cables utilizing backshell connectors are new for each flight. All cables undergo extensive electrical testing/checkout and visual inspection before and after installation. All RSRM cables utilizing backshell connectors are criticality 3. No postfight observations/trends were identified for RSRM cable backshell connectors in the history of the program. RSRMcables and connector designs are robust and reside in well protected, low traffic areas on the motor, therefore, greatly reducing the chance of contact damage. There are no postflight concerns/trends for any cable and connector issues. Current cable and connector inspections and tests are necessary and adequate; no additional inspection requirements/corrective actions have been identified. The SRB Project connector inspections (including backshell connections) are performed at the vendor prior to shipment, at SRB refurbishment operations for reusable cables, again at hardware issue, and then a final visual inspection is performed prior to hardware shipment to GO. SRB cable wiring is verified each flight by removal, refurbishment, inspection, and a series of tests. Cables are insulation resistance, dielectric withstanding voltage, and

Independent Assessment Team *(Chartered by)*	Date of Report	Finding	Recommendation	NASA Response
				continuity tested on the electrical bench. After installation, these tests are repeated. Prior to hardware shipment to GO, a visual inspection is performed. For the ancillary cables, these tests are performed by the SRB Project prior to shipment to GO. After installation by GO, these tests are repeated. Planned inspections of ET wiring design confirm correct assembly and installation. During assembly at Michoud, inspections verify the torque value of the connector backshells and the correct thread protrusion, spacing, and bend radius. Movement is controlled with tie-wraps, clamps, and Iockwire. A final inspection is performed for visual damage and proper configuration. ET harness assemblies are not exposed to high traffic areas due to enclosure in cable trays, tank interiors, and protective covers. The ET is not a reusable component of the Space Shuttle. Therefore, connectors are not routinely mated and demated which reduces the risk of improper installation.
Space Shuttle Independent Assessment Team *(NASA Charter)*	7 March 2000		**Recommendation 2-27:** Arc track susceptibility of aged wiring and circuit protection devices that are sensitive to arcing should be evaluated.	**SSP Response (Abbey/Dittemore, 21 June 2000):** The SSVEO has approved a comprehensive test plan to evaluate the arc track susceptibility of aged wiring and circuit protection devices. Arc tracking tests will be performed to obtain a baseline comparison between flown (OV-102) and new orbiter Kapton wire. These tests will be performed with orbiter circuit protection and source configurations using

Independent Assessment Team *(Chartered by)*	Date of Report	Finding	Recommendation	NASA Response
				various initiation methods and conditions to determine susceptibility to arc tracking under vehicle conditions. The testing is scheduled to take a year. Results will be presented to the SSP.
Space Shuttle Independent Assessment Team *(NASA Charter)*	7 March 2000		**Recommendation 2-28:** The need to examine wiring in areas that are protected or where damage may be induced by physical wiring inspection should be evaluated. Wiring should be continuously evaluated by conducting extensive electrical verifications on systems. When wiring damage is found in an area previously not examined, the remaining Orbiters should also be inspected	**SSP Response (Abbey/Dittemore, 21 June 2000):** OV-102 is undergoing an extensive wire inspection, which includes all accessible wire on the vehicle during OMDP. Any area where wiring is determined to be inaccessible is being photo documented. Wire inspections on OV-102 include all wire harnesses in the environment control and life support system (ECLSS) bay (high traffic area) and the aft compartment. The inspections include wires protected by convoluted tubing in order to develop an approach for inspecting protected wiring. The results of the OV-102 wire inspections will be used to update the OMRSD for future vehicle OMDP requirements. All safety and mission critical system functions are currently tested every flow per the requirements specified in the applicable OMRSD. OMRSD inspection requirements were updated and clarified to ensure adequate inspections are performed during normal vehicle processing. Standard problem resolution dictates that any findings on one vehicle will be assessed for its applicability to other vehicles, and corrective action will be implemented as required.

Independent Assessment Team *(Chartered by)*	Date of Report	Finding	Recommendation	NASA Response
Space Shuttle Independent Assessment Team *(NASA Charter)*	7 March 2000		**Recommendation 2-29:** Wire aging characteristics should be evaluated, including hydrolysis damage, loss of mechanical properties, insulation notch propagation, and electrical degradation. Testing should be performed by an independent laboratory.	**SSP Response (Abbey/Dittemore, 21 June 2000):** The SSVEO approved a comprehensive test plan to evaluate wire aging characteristics. The evaluation will be performed by two independent laboratories, Barcel and Lectromec, and by Boeing Huntington Beach. Old wire will be obtained from OV-102 and compared to new Kapton insulated wire. Testing will be performed on the flown wire to determine useful life remaining. Testing will be completed in August 2000.
Space Shuttle Independent Assessment Team *(NASA Charter)*	7 March 2000		**Recommendation 2-30:** A database that continually evaluates wiring system redundancy for the current design, modifications, repairs, and upgrades should be maintained. System safety should evaluate the overall risk created by wiring failures	**SSP Response (Abbey/Dittemore, 21 June 2000):** The SSP requirements for routing of redundant systems wiring are documented in NSTS 8080-1. This document specifies that electrical wiring of redundant systems, redundant subsystems, or redundant major elements of subsystems shall not be routed in the same wire bundle or through the same connector with wiring of the other redundant systems, subsystem, or subsystem element. A wire routing assessment was performed in 1994 addressing criticality 1 systems and wire routing violations. This assessment was documented in a report. An update to the report is in work with completion scheduled for October 2000. The report will become an official document baselined by the VECB chaired by the Manager, SSVEO. If a future vehicle modification will result in violation of the criticality 1 redundant wire routing requirements, the VECB will review the

Independent Assessment Team *(Chartered by)*	Date of Report	Finding	Recommendation	NASA Response
				proposed wiring and approve or disapprove associated violations.
Space Shuttle Independent Assessment Team *(NASA Charter)*	7 March 2000		**Recommendation 2-31:** NASA engineering should specifically participate in industry and government technology development groups related to wiring. The SAE AE-8 committees (specifically A and D) are excellent forums for identifying wiring issues.	**SSP Response (Abbey/Dittemore, 21 June 2000):** Several initiatives to expand data exchange and teaming efforts with the Federal Aviation Administration (FAA) and Department of Defense (DOD) are currently underway. The SSP has initiated conversations and planning with the Department of Navy and Wright-Patterson Air Force Base to take advantage of initiatives already in place and to coordinate a list of working groups and forums involving multiple Government aerospace agencies. The SSP will participate in these forums and identify SSP points of contact. The SSP will document assignments and involvement in these forums and identify an appropriate SSP forum for reporting and dissemination of information obtained from the working interfaces. To address recommendation 31, the SSP will specifically identify wiring related working groups and establish the appropriate level of participation. The Manager, SSP Safety and Mission Assurance (SMA) has been appointed as the NASA representative to the Wire Safety Research Interagency Working Group chartered by the Office of Science and Technology Policy. In addition, the SSP established contact in mid-

Independent Assessment Team *(Chartered by)*	Date of Report	Finding	Recommendation	NASA Response
				March with the chairman of the Aircraft Wiring and Inert Gas Generator (AWIGG) Working Group and established communications with the team. Membership rosters were exchanged and both the SSVEO and USA sent representatives to the May 15-19, 2000, meeting to further establish points of contact and exchange information. Formal membership and identification of specific SSP representatives will be documented.
Space Shuttle Independent Assessment Team *(NASA Charter)*	7 March 2000		**Recommendation 2-32:** Wiring subjected to hypergolic contamination should be replaced since high pH fluids are known to degrade polyimide type wire insulation.	**SSP Response (Abbey/Dittemore, 21 June 2000):** Orbiter wire is not exposed to hypergolics as part of planned operations. Current inspection procedures would detect this condition. The only credible scenario, which could result in wire exposure to hypergolics, would be in the case of a leak. If exposure occurs, the standard problem resolution process would dictate that the wiring be thoroughly inspected for discoloration and physical damage. If exposure and damage has occurred, the wire is removed and replaced.
Space Shuttle Independent Assessment Team *(NASA Charter)*	7 March 2000		**Recommendation 2-33:** The current quality assurance program should be augmented with additional experienced NASA personnel.	**SSP Response (Abbey/Dittemore, 21 June 2000):** The KSC SMA office is in the process of augmenting the existing workforce. Twenty-five quality specialists were hired to work in the SSP at KSC. Six existing, experienced NASA inspectors will augment the in-line processing effort by transferring from the Assembly and Refurbishment Facility.

Independent Assessment Team *(Chartered by)*	Date of Report	Finding	Recommendation	NASA Response
				In addition, three SMA engineering slots for the SSP (including one for checkout and launch control system (CLCS)) will be filled later this year. SMA will continue to evaluate resource requirements and work with Center management to prioritize their needs for future years.
Space Shuttle Independent Assessment Team *(NASA Charter)*	7 March 2000		**Recommendation 2-34:** Technician/inspector certification should be conducted by specially trained instructors, with the appropriate domain expertise.	**SSP Response (Abbey/Dittemore, 21 June 2000):** All required training, including recurring training, is tracked by USA and the qualification and certification sign-off system (QACSS). The training requirements are specific to the hardware, the processes, and the procedures used at KSC. The instructors, who train the hands-on personnel, represent the most knowledgeable individuals in their field of expertise. The selection process for instructors focuses on their education and training experience. A new instructor is assigned to an experienced, qualified instructor who is certified in the appropriate subject matter. The new instructor is mentored until signed-off by the experienced instructor and the manager. The instructor carries the certifications that he or she teaches. A senior instructor or their manager periodically observes instructors in their presentations. Students evaluate instructors at the end of each course and may evaluate at any time during the course. Course audits are conducted for courses tied to certifications at least every 3 years. However, course audits may be conducted at any time.

Independent Assessment Team *(Chartered by)*	Date of Report	Finding	Recommendation	NASA Response
Space Shuttle Independent Assessment Team *(NASA Charter)*	7 March 2000		**Recommendation 2-35:** The SIAT recommends an evaluation of depot repair documentation be performed to determine if the transition process attained a necessary and sufficient set of vendors for each Line Replaceable Unit, Shop. Replaceable Unit, and special test equipment.	**SSP Response (Abbey/Dittemore, 21 June 2000):** A project team was chartered to perform an evaluation of the certification process for identifying and obtaining documentation for transition of LRUs, shop replacement units (SRUs), and special test equipment (STE) to the NSLD. During certification, the NSLD works with the design Center and the OEM to establish a baseline of required repair documentation. The number of requests for vendor data and work stoppages due to lack of documentation was evaluated to determine whether sufficient vendor repair data are available. There is an average of 500 requests for documentation each week to the NSLD Technical Documentation Center. NLSD personnel and other SSP elements submit requests. Only a small percentage of these Evaluations of the NSLD work metrics indicate well requests are unable to be filled. Stoppage below 1 percent are due to lack of documentation. These factors indicate that sufficient documentation is available from the vendors. In those rare cases where NSLD repair documentation is not available, there is a process to obtain data by working with the design Center and USA procurement. Reasons for data not being available include increased repair capability after original certification (e.g., nonrepairable hardware must

Independent Assessment Team *(Chartered by)*	Date of Report	Finding	Recommendation	NASA Response
				be repaired due to obsolescence), lost or misplaced data, and limited documentation for STE. If the vendor still supports the program for documentation maintenance, USA procurement will contact the vendor and obtain the proper data. If the vendor or documentation is not available, the design Center will develop and release equivalent documentation through established authorization processes. For those cases where a vendor no longer supports the SSP, an alternate data maintenance agency is designated. All of the OEM's documentation is obtained, indexed, and maintained by the design Center that is designated as the "data maintenance" agency.
Space Shuttle Independent Assessment Team *(NASA Charter)*	7 March 2000		**Recommendation 2-36:** Teamwork and team support should be enhanced to mitigate some of the negative effects of downsizing and transition to Shuttle Flight Operations Contract. Most immediately needed is the provision of relief from deficits in core competencies, with appropriate attention to the need for experience along with skill certification. Further development of the use of cross-training and other innovative approaches to providing on-the-job training in a timely way should be investigated.	**SSP Response (Abbey/Dittemore, 21 June 2000):** Additional hiring is in progress by USA to meet the seven flights per year manifest with particular emphasis on critical skills and core competencies. Over the past 3 months, USA has hired approximately 164 people in the engineer, software, technician, and inspector categories at KSC. Over the same time period, approximately 64 were lost due to attrition. By the end of June 2000, USA expects to have an appropriate number of personnel to support the seven flights per year manifest. The experience level of the new hires is balanced. In addition, cross-training and certification levels are expanding in

Independent Assessment Team *(Chartered by)*	Date of Report	Finding	Recommendation	NASA Response
				Florida.
Space Shuttle Independent Assessment Team *(NASA Charter)*	7 March 2000		**Recommendation 2-37:** Work teams should be supported through improved employee awareness of stresses and their effect on health and work. Workload and "overtime" pressures should be mitigated by more realistic planning and scheduling; a serious effort to preserve "quality of life" conditions should be made.	**SSP Response (Abbey/Dittemore, 21 June 2000):** Following the initial concerns voiced by the SIAtabout the morale in Florida and possible effects on safety, USA commissioned an independent consultant, Lord and Hogan, to administer the occupational stress inventory. This inventory included an in-depth survey of the Florida workforce on the subject of stress and safety and face-to-face interviews of participants in focus groups. The results were remarkable for two reasons. First, the response rate to the survey was exceptionally high. Second, the responses showed USA to be well within expected norms compared to many other companies. USA is in the process of conducting the same survey for the Texas workforce. Both NASA and USA are sensitive to the "quality of life" environment of employees. Metrics and other management tools will continue to be used to emphasize this factor in management planning.
Space Shuttle Independent Assessment Team *(NASA Charter)*	7 March 2000		**Recommendation 2-38:** The inspection procedures of the Shuttle main engine high-pressure fuel lines and valves to find cracks should be reviewed. Currently, Columbia is at Palmdale and the vehicle is available for inspections of the main propulsion lines to verify whether this potentially serious problem exists.	**SSP Response (Abbey/Dittemore, 21 June 2000):** During the design of the orbiter's MPS hardware, materials were selected specifically for their resistance to hydrogen embrittlement. Hydrogen induced damage is not a concern in the low temperature/low pressure MPS. Nearly all high

Independent Assessment Team *(Chartered by)*	Date of Report	Finding	Recommendation	NASA Response
				pressure/high temperature components use "A" rated materials. Exceptions have been approved by the materials and process group based on their review of the specific stress environment for that item. To date, there have been no problems in the MPS hardware attributable to hydrogen embrittlement. In 1991 and 1996, the GH2 temperature probe and flow control valve, respectively, were inspected down to the individual piece part level and there was no evidence of hydrogen embrittlement. Since orbiter MPS materials were selected to preclude hydrogen embrittlement and it has been verified in limited inspections that no hydrogen embrittlement has occurred, a detailed, comprehensive, invasive inspection will not be performed (the configuration does not permit 100 percent inspection, even if desired). While hydrogen embrittlement is not a concern for MPS hardware, detailed inspections of all hardware removed for failure analysis will continue to look for signs of hydrogen embrittlement such as cracking and fatigue. These inspections will provide a periodic check for the onset of any potential failure mechanism, including hydrogen-related damage.
Space Shuttle Independent Assessment Team *(NASA Charter)*	7 March 2000		**Recommendation 3I-1:** Standard repairs on CRIT 1 components should be completely documented and entered in the Problem Resolution and Corrective Action system.	**SSP Response (Abbey/Dittemore, 21 June 2000):** All repairs (standard and nonstandard) are entered into either the Problem Reporting and Corrective Action (PRACA) system or lower level nonconformance systems per Space Shuttle Program (SSP) requirements; all require resolution,

Independent Assessment Team *(Chartered by)*	Date of Report	Finding	Recommendation	NASA Response
				corrective action, recurrence control, and accommodate trending, tracking, and risk mitigation. Additionally, a requirement is being added program wide to assure that all standard repair (SR) dispositions are uniquely coded in a consistent manner across the existing systems to provide easy access to the SR data base. The PRACA Evaluation Team (PET) will address this issue and recommend PRACA enhancements or structure changes as required. Additionally, the SSP will review program requirements pertaining to disposition and recording of SRs on criticality 1 components.
Space Shuttle Independent Assessment Team *(NASA Charter)*	7 March 2000		**Recommendation 3I-2:** The criteria for and the tracking of standard repairs, fair wear and tear issues, and their respective FMEA/CILs should be re-examined.	**SSP Response (Abbey/Dittemore, 21 June 2000):** The SSP criteria for SR's are contained in NSTS 5300.4(1D-2), Safety, Reliability, Maintainability, and Quality Provisions for the SSP, Section ID506. An SR is approved by a Material Review Board (MRB) to repair a nonconformance condition that shows a history of repetition and does not return material/hardware to drawing configuration. Space Shuttle MRBs and Program Material Review Board (PMRB) are authorized by NSTS 07700, Volume IV, Section 4.3.2.9, to disposition repairs per the process identified in NSTS 5300.4(1D-2), Section ID506. Any disposition, including SRs, by the MRB of a nonconformance affecting criticality 1 or 2 failure modes must be submitted to the

Independent Assessment Team *(Chartered by)*	Date of Report	Finding	Recommendation	NASA Response
				PMRB with an impact/no impact statement regarding the critical failure modes. If critical items list (ClL) waiver retention rationale for the hardware is affected, the disposition must be approved by the Program Requirements Control Board (PRCB). Fair wear and tear (FW&T) criteria for flight hardware are defined by the design Center and specified in the design drawings. FW&T items are parts or equipment exhibiting minor or cosmetic external defects generally attributed to handling or usage. All dispositions under SR or FW&T criteria are verified by the design project for compatibility with the certified operating environments applicable to the hardware item. All projects have data systems and procedures in place for documenting approved SR's and FW&T items. Criteria for tracking the occurrence of nonconformances, including those dispositioned as SR's, are defined in NSTS 08126, PRACA System Requirements. Currently no dedicated data field is assigned in PRACA for SR closures, and a text search must be made within the closure field to identify those nonconformances dispositioned as SRs. The SSP currently has an action in work to readdress the NSTS 08126, PRACA System Requirements, across the program per Shuttle Independent Assessment Team (SIAT) recommendation. In addition,

Independent Assessment Team *(Chartered by)*	Date of Report	Finding	Recommendation	NASA Response
				initiatives are in work that will enable electronic and query of SSP PRACA data (established per NSTS 07700, Vol. XI) by all SSP elements via the Shuttle Flight Operations Contract (SFOC) Advanced Data Acquisition and Management (ADAM) Data Warehouse. This action will be closed by verifying with each SSP element project that: (1) Documented procedures and instructions exist for defining SRs and FW&T items; (2) Procedures and data systems exist for tracking the occurrence of SR's and FW&T items within the project; (3) Procedures and criteria are in place for elevating to the PMRB dispositions involving hardware classified as criticality 1 or 2, and elevating to the PRCB dispositions affecting ClL retention rationale. This verification effort is expected to be completed by October 2000.
Space Shuttle Independent Assessment Team *(NASA Charter)*	7 March 2000		**Recommendation 3I-3:** The SIAT recommends comprehensive re-examination of maintenance and repair actions for adequate verification requirements (e.g., visual, proof test, or green run).	**SSP Response (Abbey/Dittemore, 21 June 2000):** The Space Shuttle Main Engine (SSME) Project, Space Shuttle Vehicle Engineering Office (SSVEO), External Tank (ET) Project, Reusable Solid Rocket Motor (RSRM) Project, Solid Rocket Booster (SRB) Project, KSC Ground Operations (GO), and Space Shuttle Systems Integration Office have addressed this recommendation. All elements except the SSVEO have completed their assessment and implementation of any

Independent Assessment Team *(Chartered by)*	Date of Report	Finding	Recommendation	NASA Response
				necessary corrective actions. The SSVEO is conducting a review of NSTS 08151, Intermediate and Depot Maintenance Requirements Document, maintenance and Boeing Reusable Space Systems (BRSS) SRs. Implementation of any corrective actions will be established as part of this review. All other elements have reviewed their repair/maintenance testing procedures and have determined that processes and appropriate testing are in place to verify adequacy of any repairs. The SSME Project determined, during the course of this review, that one type of nozzle tube repair had inadequate verification testing specified. The specification was revised to require acceptance test hotfire or proof testing prior to flight. All nozzles with this type repair have since been tested.
Space Shuttle Independent Assessment Team *(NASA Charter)*	7 March 2000		**Recommendation 3I-4:** The avionics repair facility should be brought up to industry standards.	**SSP Response (Abbey/Dittemore, 21 June 2000):** United Space Alliance (USA) is continuously evaluating initiatives in the area of safety, testing, repair, manufacturing, and facility improvements at the NASA Shuttle Logistics Depot (NSLD). The NSLD received the Occupational Safety and Health Administration's Standard of Excellence Star facility certification in 1997. Test equipment is being upgraded on a continual basis. Automated test stations and commercial off the shelf (COTS) test equipment are utilized where appropriate, and computer systems have been rehosted to newer

Independent Assessment Team *(Chartered by)*	Date of Report	Finding	Recommendation	NASA Response
				platforms. Examples of upgraded automated test equipment are for the heads up display electronics and orbiter cabling/crew compartment wiring special test equipment (STE). The STE is currently being evaluated at the NSLD for upgrade potential with priority placed on supportability improvements. Expert systems are a consideration in the equipment upgrade process. Tracking of equipment failures and causes are documented in logbooks and the data are a consideration in the upgrade process. Troubleshooting and failure analysis plans for in-flight hardware failures are documented on a Corrective Action Report (CAR)/sub-CAR and are thoroughly discussed within the appropriate Problem Resolution Team (PRT). The PRT is a combined effort between system experts at KSC, NSLD, the appropriate design Center (JSC/MSFC), and vendors that allows technically complete, coordinated resolution of problems, including failure trends and causes, at the "hands on" level. In the area of environmental controls, USA has instituted a strong campaign at the NSLD to help reduce potential electrostatic discharge (ESD) damage to flight and nonflight hardware (ESD safe floor wax, ESD safe binders, smocks, liners, etc), made electrical grounding improvements throughout the

Independent Assessment Team *(Chartered by)*	Date of Report	Finding	Recommendation	NASA Response
				facility, and upgraded the power drops and lighting in the Avionics Lab. Installation of an injected humidifier system in the avionics area has been approved, and implementation is currently in work. Other initiatives under consideration are power shut-off switches in the event of technician distress and use of insulated safety mats at workstations.
Space Shuttle Independent Assessment Team *(NASA Charter)*	7 March 2000		**Recommendation 3I-5:** Selected areas of staffing need to be increased (e.g., the Aerospace Safety Advisory Panel advised 15 critical functional areas are currently staffed one deep).	**SSP Response (Abbey/Dittemore, 21 June 2000):** The Office of Space Flight (OSF) has recently conducted workforce reviews of staff workload and skill deficiencies at its Centers and programs, with particular emphasis on the SSP. Findings of these reviews, coupled with those of external groups such as the SIAT and the Aerospace Safety Advisory Panel (ASAP), led to the decision to terminate downsizing. All four OSF Centers, JSC, KSC, MSFC, and SSC, are in the midst of large-scale efforts to replace skill losses and increase the number of entry-level professionals. NASA has a plan in place to hire over 500 new employees in fiscal year 2000. Although only a portion of these new employees will be dedicated to the SSP, this action will help fill some of the most critical skill shortages, enable us to stabilize our flight safety skills resources, and build our cadre of future leaders. It is imperative that sufficient resources, including new hires, be dedicated in support of the SSP. Beginning in fiscal year 2001,

Independent Assessment Team *(Chartered by)*	Date of Report	Finding	Recommendation	NASA Response
				the plan is to replace future losses on a one-for-one basis. In addition, the recruiting strategy is to emphasize the identification of critical skill shortages and make those the top hiring priorities. The goal is to hire 50 to 70 percent of new personnel at the entry level in an effort to revitalize the workforce with high-caliber, recent graduates. To allow some of the best junior- and mid-level personnel the opportunity to broaden their functional experience, the SSP has created rotational opportunities at several Centers where they can gain experience at the program level. This early exposure to the significant operational and programmatic management challenges will enable them to enhance the flight safety critical process skills in the near term, and will better equip them to serve in leadership roles in the future.
Space Shuttle Independent Assessment Team *(NASA Charter)*	7 March 2000		**Recommendation 3I-6:** The SIAT recommends that the SSP implement the Aerospace Safety Advisory Panel recommendations. Particular attention should be paid to recurring items.	**SSP Response (Abbey/Dittemore, 21 June 2000):** The SSP seriously considers all ASAP recommendations and responds in a timely fashion to those within program authority. The SSP provides to NASA Headquarters management, through an established review/assessment process involving Center review, a thorough and comprehensive input for use in the development of an overall NASA agency response to all ASAP recommendations. These SSP inputs provide the current status of activities implemented to address the specific issue and/or the needed implementation actions and plans to address

Independent Assessment Team *(Chartered by)*	Date of Report	Finding	Recommendation	NASA Response
				each ASAP recommendation. It should be noted that specific implementation of ASAP recommendations is not always possible by the SSP, as the issues often deal with Agency-wide issues (such as manpower levels) or integration complexities with external influences that are beyond the immediate control of the SSP. The SSP, while striving to implement appropriate recommendations, must deal with and address solution complexity, implementation time, and the availability of resources all within the framework of successfully carrying on the continued operational responsibilities and development commitments of the SSP. In all cases, the ASAP is well informed and briefed on the circumstances surrounding their recommendations. All recommendations are tracked, and the ASAP readdresses each year those issues/concerns that it considers open from the previous year, thereby, invoking an appropriate new/updated response through established processes.
Space Shuttle Independent Assessment Team *(NASA Charter)*	7 March 2000		**Recommendation 3I-7:** The SIAT believes that Aerospace Safety Advisory Panel membership should turnover more frequently to ensure an independent perspective.	**SSP Response (Abbey/Dittemore, 21 June 2000):** The following paragraph is the ASAP response to this recommendation. It is important to note that this text is taken directly from of the ASAP's "Plan for Assessment and Replenishment of the Membership of the Aerospace Safety Advisory Panel." "The ASAP is chartered to provide independent safety

Independent Assessment Team *(Chartered by)*	Date of Report	Finding	Recommendation	NASA Response
				oversight of NASA's programs and day-to-day activities, particularly those related to human flight. In order to cover adequately the range of activities in which NASA engages, the Panel needs a highly experienced and technically diverse corps of members and consultants. The historical effectiveness of the Panel has stemmed in part from the continuity of its membership. Even for experts in the aerospace industry, it takes a significant amount of time to become familiar with the NASA programs, their management and technical personnel and how the programs are managed and operated, The primary recruitment goal of the ASAP is therefore to identify the best possible members and consultants in each needed discipline who are likely to remain with the Panel for a significant period. The exception to this is for consultants recruited only for a specific, unusual task that is not expected to endure or recur."
Space Shuttle Independent Assessment Team *(NASA Charter)*	7 March 2000		**Recommendation 3I-8:** The root cause(s) for the decline in the number of problems being reported to the Problem Resolution and Corrective Action system should be determined, and corrective action should be taken if the decline is not legitimate.	**SSP Response (Abbey/Dittemore, 21 June 2000):** All the SSP elements reviewed their PRACA data to determine if their project experienced a decline in problem reports (PRs) and, if so, to determine the root cause. The SRB Project and the ET Project have not experienced declines but have seen steady or increased report activity tracing back through at least 7 years of PRACA history. The RSRM Project, SSME Project, and the SSVEO have experienced declines in PRACA reports

Independent Assessment Team *(Chartered by)*	Date of Report	Finding	Recommendation	NASA Response
				over at least the last 5 years. The RSRM Project, through increased technical understanding, design improvements, and tighter process controls, has experienced a continual decrease in reportable conditions. As the requirements for identifying reportable conditions has remained unchanged and the noted trend understood, no corrective action is under consideration at this time. The RSRM Project is extensively involved in postfire data evaluation and trending. The postfire anomaly data base and trending data bases extend the requirements for documentation to an additional level of detail. Although the problem reporting frequency to PRACA has decreased over time for the RSRM Project, the intensity and detail of the postfire evaluation and potential problem tracking has not diminished. The SSME Project has seen a decline since 1993and ascribes this in part to clarifications in 1993, 1998, and 1999 of their PRACA problem reporting criteria (the Unsatisfactory Condition Report (UCR)). The SSME Project attributes most of the downward trend to block engine improvements and effective response to issues and problems. The data on UCR's can be sorted by failure type and by component to a high degree of granularity, substantiating that their decline is attributed to effective implementation of

Independent Assessment Team *(Chartered by)*	Date of Report	Finding	Recommendation	NASA Response
				corrective actions. The SSVEO reviewed the decline in their PR's and attributes this to several legitimate factors. In 1994, KSC GO was authorized to use FW&T specifications, which allows acceptance of "cosmetic nonconformances" without remedial action and the attendant PR. There has also been a series of Memorandums of Understanding (MOUs) implemented for the SSVEO to reduce the number of problems reported to the design Center. These are utilized by the SSVEO technical community to document certain types of recurring hardware problems that are well understood by the design team and for which some type of corrective/remedial action has already been identified and approved. Both FW&T specifications and MOU implementation correlate with a corresponding decline in PR's. The SSVEO also cites that vehicle level testing has been reduced with each revision to the Operations and Maintenance Requirements and Specifications Document (OMRSD). As vehicle design, configuration, and processing techniques have matured, less modifications are being performed resulting in less overall problems. The SSVEO has initiated an internal study of the incoming PRs to determine if there is a significant reduction from any one of the reporting sites that would indicate where the reduction is primarily

Independent Assessment Team *(Chartered by)*	Date of Report	Finding	Recommendation	NASA Response
				originating. This study will be completed by September 2000. The PET is also investigating this issue across all the elements and will verify these initial assessments and recommend process changes if deemed necessary. It should be noted that with the observed decline in PRACA PRs, there has also been a corresponding reduction of inflight anomalies (IFA), which would indicate to the SSP an overall improvement of the Space Shuttle system.
Space Shuttle Independent Assessment Team *(NASA Charter)*	7 March 2000		**Recommendation 3I-9:** The root cause(s) for the missing problem reports from the Problem Resolution and Corrective Action system concerning Main Injector Liquid Oxygen Pin ejection, and for inconsistencies of the data contained within the existing problem reports should be determined. Appropriate corrective action necessary to prevent recurrence should be taken.	**SSP Response (Abbey/Dittemore, 21 June 2000):** A detailed search and review of the PRACA data base revealed 10 of the 12 engines that experienced ejection of liquid oxygen (LOX) post pins were documented in PRACA. The two omissions (engine 0006 in 1980 and 0110 in 1981) occurred before the baseline release of PRACA system requirements in 1982. The limited search capability in PRACA hindered the SIAT's ability to perform a comprehensive search. Criticality categorization differences assigned to SSME PRs (known as UCRs) and differences in interpretation of the event by the report generator contributed to the inconsistency observed in the finding. One interpretation assigned criticality based on the consequences associated with failure of the LOX post that was pinned (criticality 1 or 1R) and not the observed consequences of the LOX post pin ejection (benign or criticality 3). Rocketdyne has a handbook on UCR procedures and conducts

Independent Assessment Team *(Chartered by)*	Date of Report	Finding	Recommendation	NASA Response
				training and monthly audits of the system. The UCR form has evolved over time with additional fields created to standardize part identification and failure source. The UCR handbook and the training will be revised to ensure coding consistency and the form will be reviewed to consider if additional fields could further clarify and standardize the information recorded. The PET is also addressing advanced software improvements and data base management techniques that will aid consistent, complete data entry and enhance the search/trending capabilities of PRACA..
Space Shuttle Independent Assessment Team *(NASA Charter)*	7 March 2000		**Recommendation 3I-10:** A rigorous statistical analysis of the reliability of the problem reporting and tracking system should be performed**.**	**SSP Response (Abbey/Dittemore, 21 June 2000):** After discussions with the author of this recommendation, Dr. Tina Panontin, a plan was developed for a rigorous statistical sampling of the problem reporting and tracking system. A statistically significant sample of PRs (~900 total) spanning the last 5 years for the vehicle, Government furnished equipment, MSFC, and KSC PRACA systems will be analyzed by the JSC, MSFC, and USA quality organizations. A standardized statistical methodology will be developed to assure consistent analysis across the PRACA systems. The corrective actions applied to the sampled reports will be evaluated for effectiveness and any errors found in the review will be categorized and assessed for significance. The plan to accomplish this

Independent Assessment Team *(Chartered by)*	Date of Report	Finding	Recommendation	NASA Response
				will be presented to the PRCB in 2 months
Space Shuttle Independent Assessment Team *(NASA Charter)*	7 March 2000		**Recommendation 3I-11:** Reporting requirements and processing and reporting procedures should be reviewed for ambiguities, conflicts, and omissions, and the audit or review of system implementation should be increased.	**SSP Response (Abbey/Dittemore, 21 June 2000):** The SSP established a PET in February 2000. The team includes members from all SSP elements, projects, the SSP Office, and the Ames Research Center (ARC). The PET addressed this recommendation, as well as the findings from all PRACA audits completed over the past year. A review of program-level requirements has been completed. The revised requirements will be published in September 2000. All SSP project and element offices will follow up with a review of their PRACA requirements and processes to ensure compliance with the revised SSP requirements. The PET provides periodic status to the program at the PRCB. In addition to completing the PRACA requirements review, the PET will determine appropriate changes to improve the software systems for data entry, trending, and analysis. This PET will investigate utilizing state-of-the-art data base designs and techniques. To support this effort, the ARC established a pilot project investigating improved PRACA system automation and state-of-the-art data base design. Software upgrade review and implementation is schedule for completion in August 2001.

Independent Assessment Team *(Chartered by)*	Date of Report	Finding	Recommendation	NASA Response
Space Shuttle Independent Assessment Team *(NASA Charter)*	7 March 2000		**Recommendation 3I-12:** The SSP should revise the Problem Resolution and Corrective Action database to include integrated analysis capability and improved problem classification and coding. Also, improve system automation in data entry, trending, flagging of problem recurrence, and identifying similar problems across systems and sub-systems.	**SSP Response (Abbey/Dittemore, 21 June 2000):** The SSP established a PET in February 2000. The team includes members from all SSP elements, projects, the SSP Office, and the Ames Research Center (ARC). The PET addressed this recommendation, as well as the findings from all PRACA audits completed over the past year. A review of program-level requirements has been completed. The revised requirements will be published in September 2000. All SSP project and element offices will follow up with a review of their PRACA requirements and processes to ensure compliance with the revised SSP requirements. The PET provides periodic status to the program at the PRCB. In addition to completing the PRACA requirements review, the PET will determine appropriate changes to improve the software systems for data entry, trending, and analysis. This PET will investigate utilizing state-of-the-art data base designs and techniques. To support this effort, the ARC established a pilot project investigating improved PRACA system automation and state-of-the-art data base design. Software upgrade review and implementation is schedule for completion in August 2001.
Space Shuttle Independent Assessment Team *(NASA Charter)*	7 March 2000		**Recommendation 3I-13:** All critical data bases (e.g., waivers) need to be modernized, updated and made more user friendly.	**SSP Response (Abbey/Dittemore, 21 June 2000):** An activity to convert critical data bases from the mainframe environment to web based user interfaces was initiated in FY98. The SFOC ADAM Data Warehouse is

Independent Assessment Team *(Chartered by)*	Date of Report	Finding	Recommendation	NASA Response
				ADAM Data Warehouse is being utilized as the central repository using a web-based interface for searching and retrieving critical data. Currently, the SSP PRACAs, IFAs, critical hardware list, hazard reports, and time/age/cycle applications are completed and data are refreshed at least every 24 hours. The waivers, Space Shuttle integration accounting status system, launch commit criteria (LCC), and ClL will be incorporated into ADAM by December 2000. The completion of this activity will result in the data bases being updated and more user friendly.
Space Shuttle Independent Assessment Team *(NASA Charter)*	7 March 2000		**Recommendation 3I-14:** There are a number of cryogenic fluid mechanical joints and hot-gas mechanical joints that represent potential risks that should therefore be examined in detail.	**SSP Response (Abbey/Dittemore, 21 June 2000):** All cryogenic and hot gas joints currently receive extensive and continuing attention. This attention comes in the form of inspections, leak checks, problem trending, statistical process control (SPC) evaluation, and root cause problem resolution. The end result is that all hot gas and cryogenic joints are carefully monitored and controlled to ensure that the configuration flying is identical to that certified. Processes, inspections, and trending are in place to ensure proper installation and proper configuration. Furthermore, the projects have and are enhancing monitoring to identify trends in joint performance and manufacture before the trend becomes a problem. The Space Shuttle uses a variety of hot gas and

Independent Assessment Team *(Chartered by)*	Date of Report	Finding	Recommendation	NASA Response
				cryogenic joints. Many of these joints are not disturbed from flight to flight; a very small number are replaced with each launch. All joints were recertified during return to flight. A rigorous technical review, a review by the program manager, and a structured approval process assure modifications to the certified configuration receive proper engineering and management attention. Final approval for changes is received at the PRCB. There have been no significant changes to these systems from that certified for return to flight. The process for management review is documented in the NSTS 07700 documents. The SSP PRACA system is used to record and trend problems associated with Space Shuttle hardware including the hot gas and cryogenic joints. For all elements of the vehicle there has been no adverse or unusual problem activity associated with hot gas or cryogenic joints. All problems are reviewed in detail at the project level for trending and root cause solutions. For each flight, the entire vehicle, including the hot gas and cryogenic joints, undergoes comprehensive checkout and flight preparation as outlined in the OMRSD. The OMRSD and LCC are under program configuration control to assure appropriate and consistent testing of all equipment before launch. Testing and checkout of the

Independent Assessment Team *(Chartered by)*	Date of Report	Finding	Recommendation	NASA Response
				joints are different depending on the particular system but include inspections, pressure checks, hot fires, and leak tests as appropriate. The SSP, as well as the individual elements, employs a system of audits and inspections that ensure new hardware is manufactured in accordance with the requirements. While most of the cryogenic and hot gas joints are not changed on a routine basis, some very critical joints are new for each flight. It is very important that process drift or other inadvertent changes do not result in changes to the certified configuration of the joints. SPC, inspections, and process audits are routinely accomplished and reviewed to identify process changes or out of family occurrences and assure component compliance with engineering requirements. Each of the elements was asked to review their program for any unique criteria associated with their joints. The SSVEO has undertaken an effort to review all orbiter main propulsion system (MPS) and power reactant storage devices CILs. The intent is to ensure that failure modes are still accurate and that CIL retention rationale is still valid. All problems are documented in PRACA. The only significant PRACA entries concerning MPS leaks were associated with hydrogen leaks resulting in the scrub of STS-35 and STS-38 (1990). These problems resulted in an improvement to

Independent Assessment Team *(Chartered by)*	Date of Report	Finding	Recommendation	NASA Response
				the 17" disconnect components and have resulted in significantly reduced instances of "measurable hydrogen leakage. The SSME Project uses a fleet leader process so that flown configurations never exceed 50 percent of the fleet leader experience. Engines to be flown are first run in their final configuration. In addition, the engines undergo an extensive array of leak testing to ensure joint integrity. Routine inspections are accomplished to assure manufacturing compliance with engineering specifications. SPC is used in the manufacturing process to identify trends and out of family hardware. The RSRM Project performs extensive examination of the postflight performance of the joints within the motor. Reused components undergo extensive nondestructive evaluation (NDE), proof testing, and inspection to ensure that the components still satisfy engineering requirements. The entire refurbishment and build process undergoes an annual NASA Engineering Quality Audit (NEQA) to assure process integrity. SPC is one of the tools used to monitor and highlight changes in the build process. Independent review teams are used to review process and out of family occurrences. The SRB Project has only hot gas joints associated with the hydraulic power unit. These

Independent Assessment Team *(Chartered by)*	Date of Report	Finding	Recommendation	NASA Response
				joints undergo visual inspections and pressure decay tests to identify any leakage. Each new configuration is hot fired in its flight configuration to assure joint integrity. Routine management review of trends and problems is used to identify areas for special attention. The ET Project has a process that reports nonconformances and problems to the management level for review and action. SPC is currently in place at some areas within the assembly process but is being more fully implemented even at the subcontractor level.
Space Shuttle Independent Assessment Team *(NASA Charter)*	7 March 2000		**Recommendation 3I-15:** All internal Foreign Object Debris (e.g., pins) occurrences during the program should be listed, with pertinent data on date of occurrence, material, and mass. The internal Foreign Object Debris FMEA/CILs and history should be reviewed and the hazard categorized based on the worst possible consequence.	**SSP Response (Abbey/Dittemore, 21 June 2000):** To address this recommendation, Rocketdyne reviewed SSME design-generated foreign object debris (FOD). The design FOD analysis accounts for some degree of normal wear and tear, postulates internal sources such as breakage or loose pads, and analyzes the ensuing consequences. As stated by SLAT, Rocketdyne has an aggressive FOD-prevention program at their manufacturing and assembly plant that addresses other FOD sources. After reviewing all design-senerated FQD in the program history (169 analytical cases), all had the correct failure modes and effects analysis (FMEA)/ClL and hazard assessment. All engine components were reviewed and a data base was created that includes FOD source, failure date, material, mass, disposition, FMEA/ClL or hazard reference, correct

Independent Assessment Team *(Chartered by)*	Date of Report	Finding	Recommendation	NASA Response
				criticality assigned (yes/no), and a descriptive comment. All UCRs and material reports were reviewed for design-generated FOD and documented in this data base (over 1,000 entries). Every reported occurrence of FOD in the program requires the original analysis to be expanded and continually adds to the FOD knowledge base.
Space Shuttle Independent Assessment Team *(NASA Charter)*	7 March 2000		**Recommendation 3I-16:** Any type of engine repair that involves hardware modification - no matter how minor (such as liquid oxygen post pin deactivation) - should be briefed as a technical issue to the program management team at each Flight Readiness Review. The criticality of a standard repair should not be less than basic design criticality, based on worst-case consequences, and all failures of standard repairs should be documented and brought to the attention of the Material Review Board.	**SSP Response (Abbey/Dittemore, 21 June 2000):** The SSP requires all projects to control report, and review significant modifications, repairs, and process changes. The requirements are contained within the various volumes of NSTS 07700 and referenced documents, namely, Volumes IV and Xl; MVP 01; NSTS 08117; and NSTS 5300.4(1D-2) are the primary sources. These requirements can generally be categorized into information required at program reviews, configuration management (CM), and hardware nonconformance. To address program review requirements, NSTS 08117, Requirements and Procedures for Certification of Flight Readiness, requires that each participating project element identify changes since the last mission at each of the program milestone reviews. There is also a generic requirement for all elements to identify significant changes to the configuration baseline, including vehicle servicing and hardware manufacturing critical processes.

Independent Assessment Team *(Chartered by)*	Date of Report	Finding	Recommendation	NASA Response
				The program requirements for CM are defined in NSTS 07700, Volume IV, Book 1, Revision K, Configuration Management Requirements. This document defines the requirements, responsibilities, and procedures for all SSP elements/projects in the application of CM. The requirement for acceptance baseline configuration descriptions states that baseline configuration description shall describe and identify the as-designed configuration with exceptions that reflect the as-built and accepted configuration of an end item. Differences between the as-designed configuration and the as-built configuration must have NASA approved deviations or waivers or PMRB dispositions. Any changes to the acceptance baseline configuration must have the approval of the SSP or delegated program element/project. Configuration control of accepted flight hardware/software, including delegated authority, is defined in Volume IV. After a baseline is established, the process precludes any unauthorized configuration changes to that baseline. A procedure is defined to ensure that each proposed change to the baseline is completely described (including impacts); is thoroughly coordinated, reviewed, and evaluated; and is authorized and implemented in an approved manner. Additional requirements can be found in

Independent Assessment Team *(Chartered by)*	Date of Report	Finding	Recommendation	NASA Response
				NSTS 07700, Volume XI, System Integrity Assurance Plan. Generally, hardware repairs that are not returned to print are defined as a baseline nonconformance. Modifications can be defined as baseline configuration changes. The difference between the two is that a modification is a revision to the baseline and a nonconformance is a restricted/limited deviation from the baseline and, based on predetermined screening criteria, may require program approval. Hardware nonconformances are regulated by two program documents. NSTS 5300.4(1 D-2), Section 1D506, provides for repair or dispositio n of nonconforming hardware prior to Government acceptance. After acceptance by the Government, NSTS 07700, Volume IV, Book 1, Revision K, Configuration Management Requirements, Paragraph 4.3.2.9, Space Shuttle Material Review System, is the controlling document. Both documents require the establishment of a material review (MR) process. However, the NSTS 5300.4(ID-2) MR process does not require elevation of nonconformances to the program. It does require elevation to the NASA contracting officer based on specific criteria. For Government-accepted hardware, the Volume IV, Book 1, MR process includes criteria for MR dispositions of

Independent Assessment Team *(Chartered by)*	Date of Report	Finding	Recommendation	NASA Response
				nonconformances that must require program approval by the delegated configuration control board which is the PMRB. The SSP also delineates criteria for elevating a nonconformance beyond the PMRB to the PRCB.
Space Shuttle Independent Assessment Team *(NASA Charter)*	7 March 2000		**Recommendation 3I-17:** The design and the post Solid Rocket Booster recovery inspection and re-certification for flight should be looked at and analyzed in careful detail by follow-on independent reviews.	**SSP Response (Abbey/Dittemore, 21 June 2000):** The SRB Project has recently accomplished a NEQA. The RSRM Project conducts annual NEQAs at the prime contractor's facility and recently completed an audit in August 2000. These sessions cover a broad range of topics, including the design, recovery, and recertification process. In addition, the RSRM Project has pursued additional independent assessments on this same subject by teams comprised of senior level retired experts from industry and NASA with no significant issues identified. Finally, both projects are presently in the formulation process of establishing independent review teams to accomplish SIAT-type reviews on the individual projects. Team members will again be senior people having extensive knowledge and background experience relative to both Space Shuttle and SIAT-type reviews.
Space Shuttle Independent Assessment Team *(NASA Charter)*	7 March 2000		**Recommendation 3I-18:** The inspection and proof-test logic to screen for flaws or cracks in the Super-Light-Weight Tank should be reviewed in light of the reversal in fracture-stress-against-flaw-size between room and cryogenic temperatures.	**SSP Response (Abbey/Dittemore, 21 June 2000):** The super-lightweight tank (SLWT) parent material and welds are made of 2195 aluminum-lithium alloy. The proof test and nondestructive test (NDT) logic used to screen for flaws or cracks in aluminum 2195 was

Independent Assessment Team *(Chartered by)*	Date of Report	Finding	Recommendation	NASA Response
				extensively reviewed and accepted by a number of independent review teams. The logic was thoroughly reviewed and approved by the NASA MSFC Fracture Control Board with assistance from experts at other NASA Centers and industry. This topic was also a primary focus of the 1996 ASAP review of the ET Project. An independent verification team, a design certification review board, and the ASAP all concurred that the logic to certify and accept the SLWT was adequate, with full knowledge of the reversal phenomenon. The ET Project discussed the concerns cited in the SIAT report with SIAT member, Dr. James Newman of the NASA Langley Research Center. After this review, and based on the extensive previous reviews, all participants are confident in the NDT and proof test logic used to assure mission success on the SLWT.
Space Shuttle Independent Assessment Team *(NASA Charter)*	7 March 2000		**Recommendation 3I-19:** The SSP should explore the potential of adopting risk-based analyses and concepts for its critical manufacturing, assembly, and maintenance processes, and statistical and probabilistic analysis tools as part of the program plans and activities. Examples of these analyses and concepts are Process FMEA/CIL, Assembly Hazard Analysis, Reliability Centered Maintenance, and On Condition Maintenance.	**SSP Response (Abbey/Dittemore, 21 June 2000):** The SSP utilizes numerous analytical techniques and processes to determine and manage risk. Program requirements contained within NSTS 07700 specify the use of analytical methods in all aspects of program execution. SPC, process FMEA, hazard analysis, reliability centered analysis, and other techniques are implemented to various degrees across all program elements. The SSP has continued to explore the potential adaptation of various

Independent Assessment Team *(Chartered by)*	Date of Report	Finding	Recommendation	NASA Response
				quantitative risk analysis (QRA) processes. The System Safety Review Panel, with representatives from all program elements and safety, reliability, and quality assurance organizations, will review current probabilistic risk assessment/QRA techniques being utilized and determine an approach which maximizes value to risk management. The development of a QRA program standard and an implementation approach will be provided in the February 2001 timeframe. This will include methods of CM of integrated models, interface responsibilities, technical/managerial review processes, and processes for determining threshold decisions. With this information, a final evaluation of value-added will be conducted and the final recommendation presented to the SSP PRCB by April 2001.
Space Shuttle Independent Assessment Team *(NASA Charter)*	7 March 2000		**Recommendation 3I-20:** Failure analysis and incident investigation should identify root cause and not be artificially limited to a sub-set of possible causes.	**SSP Response (Abbey/Dittemore, 21 June 2000):** The SSP history demonstrates extensive experience and success in the conduction of failure analysis. These analyses are typically driven to the lowest practical level of potential cause for review. However, the SSP has taken steps to ensure that training syllabuses associated with failure analysis and root cause analysis have had increased emphasis placed on the importance of thorough root cause determination. Within the last year, SSP management level, team lead level, and analyst level personnel have attended root cause analysis training. The majority of contractor

Independent Assessment Team *(Chartered by)*	Date of Report	Finding	Recommendation	NASA Response
				employees have also received similar training as part of their ISO certification process. The SSP will verify that program elements have received root cause and failure analysis training by December 2000. Emphasis on accuracy of root cause analysis and clarification of the definition of cause at the lowest level responsible for the problem are being incorporated within the current revision to NSTS 08126 (SSP PRACA requirements) which is planned to be implemented by November 2000.
Space Shuttle Independent Assessment Team *(NASA Charter)*	7 March 2000		**Recommendation 3I-21:** Software requirements generated by Shuttle system upgrades must be addressed.	**SSP Response (Abbey/Dittemore, 21 June 2000):** The SSP believes it is meeting the intent of this recommendation. For each new Space Shuttle system upgrade, a review of existing software systems will continue to be accomplished to ensure the proper tradeoffs are performed to correctly integrate the new systems into the existing Space Shuttle architecture. All software modifications will utilize the mature, proven processes that have delivered safe, robust flight software in the past. Software changes identified will be scheduled for implementation, verification, and installation in a timeframe consistent with the installation date of the new Space Shuttle system upgrades. Workforce augmentation and training are planned to support upgrade driven software development, minimizing impact on the current operational software efforts. The SSP is assigning the responsibility for management of these internal software requirements to the appropriate upgrade project's

Independent Assessment Team *(Chartered by)*	Date of Report	Finding	Recommendation	NASA Response
				organization. The SSP is confident that this approach will address upgrade driven software modifications without adding undue risk to the program or crew.
Space Shuttle Independent Assessment Team *(NASA Charter)*	7 March 2000		**Recommendation 3I-22:** Enhanced software tools should be considered for potential improvements in reliability and maintainability as systems are upgraded.	**SSP Response (Abbey/Dittemore, 21 June 2000):** The SSP will continue to implement reliability and maintainability enhancements through the use of new/revised software tools and methods both to existing systems and in new platforms. The Space Shuttle flight operations contractor's standard software maintenance processes continually evaluate process improvements, including enhanced custom tools and COTS tools through formal methods. Recent improvements include conversion of data bases from hierarchical to relational, special risk analysis tools/methods, and reconfiguration data generation enhancements. As part of the cockpit avionics upgrade (CAU), the flight software contractor (USA) is examining current processes, procedures, and tools for potential improvements in productivity while maintaining or improving reliability and maintainability. Specifically, CAU is evaluating COTS real time operating systems, software development environments, and display generation tools for use in, and development of, the new command and display processor flight software. The SSP is confident that the use of these COTS products will improve reliability and maintainability without adding risk to the

Independent Assessment Team *(Chartered by)*	Date of Report	Finding	Recommendation	NASA Response
				program.
Space Shuttle Independent Assessment Team *(NASA Charter)*	7 March 2000		**Recommendation 3I-23:** An assessment of using lower fatigue-crack-growth thresholds and their impact on fracture critical parts or components needs to be reviewed to establish life and verify the inspection intervals. Retardation and acceleration model(s) should be used to assess the type of crack-growth history under the Orbiter spectra.	**SSP Response (Abbey/Dittemore, 21 June 2000):** NASGRO fracture mechanics analysis is the methodology and computerized tool used for all vehicle life predictions and inspection intervals. The crack growth threshold is a test derived quantity that is one of many terms in the NASGRQ crack growth equation. The NASGRO crack growth rate equation has a number of empirical coefficients, including the crack growth threshold, which is derived so that the equation matches test data. The current NASGRO equation obtains its threshold values according to the standard American Society for Testing and Materials methods. After incorporating the threshold value into the NASGRO equation, the other empirical parameters are derived to conservatively fit the material test data. If the crack growth threshold was lowered, then the other four parameters would be adjusted accordingly to still conservatively fit the material test data. Comparing the new version versus the current version of NASGRO, both would yield nearly identical results for the exact material test data. Retardation and acceleration were intentionally omitted from the NASGRO analysis to provide a more conservative prediction for

Independent Assessment Team *(Chartered by)*	Date of Report	Finding	Recommendation	NASA Response
				the vehicle application. The two occur together and are interrelated. Retardation (beneficial to life) is the dominant effect in aerospace applications and will be in effect on a larger number of the cycles than will acceleration. Aerospace industry experience has confirmed that ignoring retardation/acceleration is conservative. Aircraft users of NASGRO have stated that their designs could not tolerate the conservatism of the nonretardation version used on the vehicle. The SIAT concurred that for most aircraft spectra, omitting acceleration is conservative. Flight data have verified that the vehicle spectra is similar to other aircraft spectra and, therefore, does nothave any extreme ordering of cycles that would make it an exception. There has been more than 20 years of NASGRO experience in worldwide applications including the U. S. Navy, the U. S. Air Force, Boeing, Lockheed Martin, Grumman, Sikorsky, Raytheon, and United Technologies Corporation, all with no indication of under-conservative predictions. The SSVEO has high confidence in the current approach used to apply NASGR© analysis to vehicle structural life.
Space Shuttle Independent Assessment Team *(NASA Charter)*	7 March 2000		**Recommendation 3I-24:** Assessments of the impact of any new Orbiter flight loads on structural life should continue as responsibility for the Orbiter structure is transferred to the contractor.	**SSP Response (Abbey/Dittemore, 21 June 2000):** The JSC Engineering Directorate, Structures and Mechanics Division (SMD) will actively participate, in a leadership role, in any new design loads cycle for the

Independent Assessment Team *(Chartered by)*	Date of Report	Finding	Recommendation	NASA Response
				orbiter. An example of this type of activity would be the recently completed performance enhancement program, which significantly changed orbiter loads during ascent. These changes effected loads, stress, and structural life certification. In addition, SMD will routinely monitor and review the annual Structural Life Tracking Report produced by USA/Boeing to ensure that the orbiter continues to be operated within the certified boundaries for mission life certification. The Structural Life Tracking Report, Boeing document RSS99D0510A, tracks key structural parameters from mission to mission for each orbiter and is published for review every year.
Space Shuttle Independent Assessment Team *(NASA Charter)*	7 March 2000		**Recommendation 3I-25:** The Orbiter Corrosion Control Review Board should consider incorporating the framework suggested by the Federal Aviation Administration for Corrosion Prevention and Control Plans of commercial airplane operators into their corrosion database to provide focus to the more serious occurrences of corrosion.	**SSP Response (Abbey/Dittemore, 21 June 2000):** A review of typical corrosion prevention control plans (CPCPs) (DC-9/MD-80/747) revealed that the SSVEO covers the intent of this document by other methods. A CPCP defines corrosion levels as 1,2, or 3, with the requirement that all level 2 or 3 corrosion be reported to manufacturer: Level 1: Corrosion can be repaired within allowable limits SSVEO: Repaired by Standard Repair Procedure (SRP) Level 2: Corrosion is widespread or repair exceeds design limits SSVEO: Requires

Independent Assessment Team *(Chartered by)*	Date of Report	Finding	Recommendation	NASA Response
				MR activity; Reported to Corrosion Control Review Board (CCRB) Level 3: Corrosion is a potential airworthiness concern SSVEO: Elevated to Flight Readiness Review special topic A CPCP establishes areas to be inspected, inspection intervals, methods of inspection, methods of repair, and methods for reapplication of corrosion protection. Similarly, the SSVEQ relies on orbiter maintenance and requirements specifications, orbiter maintenance instructions, SRPs, and any resulting PR/MR documentation. The Federal Aviation Administration (FAA) requires that manufacturers and operators maintain a data base showing location of corrosion (level 2 or 3), the parts affected, and the cause of the corrosion. The SSVEO utilizes the PRACA data base that includes all PR/MR activity for corrosion found on the orbiter fleet. In 1996, KSC representatives of the CCRB built a data base by searching for and pulling the pertinent items from the PRACA data base that covered the time period of 1983 through 1996. The CCRB has initiated another PRACA search to update their data base, and this activity

Independent Assessment Team *(Chartered by)*	Date of Report	Finding	Recommendation	NASA Response
				should be completed by September 2000. The CCRB also maintains a corrosion data base on a NASA website that includes all significant issues reviewed by the CCRB. The SSVEO meets the recommendation with their existing mechanisms and procedures in place to satisfy the intent of a CPCP, which is to ensure that inspection and maintenance activities are sufficient to support flight safety.
Space Shuttle Independent Assessment Team *(NASA Charter)*	7 March 2000		**Recommendation 3I-26:** Hidden corrosion problems require a proactive inspection program with practical and reliable non-destructive evaluation techniques; at this point, this inspection is done on a randomized basis. An assessment of the impact of hidden (or inaccessible) corrosion and the repairs of identified corrosion on the integrity of the Orbiter structure should to be made.	**SSP Response (Abbey/Dittemore, 21 June 2000):** The SSVEO employs a rigorous, systematic, proactive inspection program. The OMRSD specifies areas to be inspected, inspection frequency, and inspection methods. The probability of hidden corrosion under the thermal protection system is considered to be extremely remote. Room temperature vulcanized material has been proven by test and experience to provide an excellent barrier against moisture. However, hidden corrosion in inaccessible areas continues to be a concern. The forward fuselage plenum is a prime example of this difficulty and recent discovery of significant corrosion on OV- 102 Xo 582 frame highlights this problem• An assessment of structural risk in the areas of corrosion found generally high tolerance for corrosion damage in the forward fuselage area. Various new (or improved) NDE techniques are constantly emerging. Promising NDE techniques include enhanced ultrasonic

Independent Assessment Team *(Chartered by)*	Date of Report	Finding	Recommendation	NASA Response
				and eddy current techniques, reverse geometry x-ray, and others. However, virtually all techniques require some direct access to the target area. To ensure that the SSVEO is utilizing the full capability of the available NDE technology to address the issue of hidden corrosion, Boeing is establishing a Structures/NDE Task Team to investigate possible methods for inspecting inaccessible areas. The task team will be chartered to identify structural areas currently considered inaccessible, determine which areas warrant further study (based on low margins), investigate possible NDE methods, and attempt to validate the technology at Palmdale during the next orbiter major modification. Where corrosion has been identified, the integrity of the repaired structure is verified via the PRIMR process. SRP or MR documentation defines procedures for removing corrosion using methods that will not damage the material for verifying the dimensions of the repaired area and for restoring the required corrosion protection. Stress analysis " verifies that the remaining material is sufficient or that further repairs (doublers) are required. If appropriate, design changes implemented as corrective action and corrosion prevention compounds are employed. The SSVEO meets the recommendation with existing processes to address general inspection and repair issues and by initiating a task team to address the inaccessible corrosion issue.

Independent Assessment Team *(Chartered by)*	Date of Report	Finding	Recommendation	NASA Response
Space Shuttle Independent Assessment Team *(NASA Charter)*	7 March 2000		**Recommendation 3I-27:** Current wire inspection and repair techniques should be evaluated to ensure that wire integrity is maintained over the life of the Shuttle vehicles. Several new inspection techniques are available that use optical, infrared, or electrical properties to locate insulation and conductor damage, and should be explored for use on the Shuttle.	**SSP Response (Abbey/Dittemore, 21 June 2000):** BRSS and the orbiter electrical wiring (OEW) PRT have reviewed orbiter wiring inspection and repair techniques. A new course was developed for all avionics personnel to address wiring inspection and repair methodologies. New repair techniques have been developed, and existing repair methodologies were reviewed and upgraded where necessary. BRSS proposed a plan to the SSVEO Vehicle Engineering Control Board to examine existing and emerging test methods and associated equipment for testing wire integrity. BRSS will work with vendors and developers to determine the effectiveness of test equipment in categorizing damage conditions and identifying degraded insulation properties due to aging wiring. Special consideration will be given to the ability of the test equipment to be used in the vehicle with a minimum of intrusiveness. Additionally, the ARC recently completed a Wire Integrity Research (WIRe) Pilot Study that addressed automated verification and validation of vehicle wiring configuration and automated condition assessment for maintenance. SSVEQ approval of the BRSS plan is pending the recommendations of the Ames WIRe Pilot Study that are expected at the end of August 2000. These two studies will contribute to the continued effort to ensure wire integrity across all the SSP elements.

Independent Assessment Team *(Chartered by)*	Date of Report	Finding	Recommendation	NASA Response
Space Shuttle Independent Assessment Team *(NASA Charter)*	7 March 2000		**Recommendation 3I-28:** All CRIT 2 circuits should be reviewed to determine to what extent redundancy has been compromised in wiring, connectors, electrical panels and other electrical nexus points. The primary concern is that single point failure sources may exist in the original design or have been created by system upgrades or modifications.	**SSP Response (Abbey/Dittemore, 21 June 2000):** The SSVEO has initiated several actions since the STS-93 wiring problem to address wiring redundancy issues. Design changes are being implemented to eliminate single wire criticality 1/1 functions. A risk ranking of electrical criticality 1R2 items for nominal flight and criticality 1/1 items for aborts is being performed to assess which should be targeted for correction first. Interim design solutions are being developed to protect criticality 1R wires and eliminate critical redundancy routing Violations in the fleet. The 1994 Wire Redundancy Separation Study is being updated to include design changes that have occurred since the initial study and assess routing violations for criticality 1/1 conditions. Since criticality 2 circuits do not cause loss of crew or vehicle by definition, they are lower in priority to the 1/1 and 1R2 circuits. The compared criticality criticality SSVEO believes the highest priority is to rectify the compromised redundant criticality 1/1 and criticality 1R2 circuits and will, therefore, continue to focus on the assessment and the implementation of those associated wiring modifications. In the future, when it becomes feasible, the SSVEO will perform an assessment of the criticality 2 and criticality 2R circuits, and based on the results of the assessment, appropriate design changes will be

Independent Assessment Team *(Chartered by)*	Date of Report	Finding	Recommendation	NASA Response
				implemented.
Space Shuttle Independent Assessment Team *(NASA Charter)*	7 March 2000		**Recommendation 3I-29:** The Shuttle program should form a standing wiring team that can monitor wire integrity and take program wide corrective actions. The team should include technicians, inspectors, and engineering with both contractor and government members. The chair of the team should have direct accountability for the integrity of the Shuttle wiring. One area that should be evaluated is the techniques conductor that has not yet developed into an electrical short.	**SSP Response (Abbey/Dittemore, 21 June 2000):** The OEW PRT has recently been expanded to include additional NASA and contractor representation from the orbiter community. The position of project manager for orbiter wiring has been established and is authorized to direct the PRT tasks. Status is given weekly to the SSVEO. KSC has been tasked by the SSP to expand the scope of the PRT to include all flight elements. A formal charter will be developed with program reporting requirements defined and membership expectations outlined. The OEW PRT is responsible to monitor all orbiter wire integrity issues and recommend corrective actions. The primary emphasis is on process controls, clarification of specifications, preventative wire protection (vehicle and ground support equipment), repair methodology, and wiring installation/modification concerns. This scope will be expanded to cover the entire SSP wiring community. To remain proactive, the SSP provides representation at the Aerospace Wiring and Inert Gas Generator Meetings that address issues with wire integrity across the aerospace industry. The orbiter wiring inspection process was

Independent Assessment Team *(Chartered by)*	Date of Report	Finding	Recommendation	NASA Response
				presented at the annual joint Department of Defense/FAA/NASA conference on aging aircraft. NASA ARC is conducting a wire study for the SSP, and BRSS is currently conducting tests to evaluate new inspection equipment that will assist in the detection of potential short circuits. The SSP is also planning updates to program wiring specification, inspection, maintenance, and repair documents to ensure recurrence is minimized.
Space Shuttle Independent Assessment Team *(NASA Charter)*	7 March 2000		**Recommendation 3I-30:** The long term use of primarily polyimide wiring should be minimized, and wire insulation constructions that have improved properties should be evaluated and compared to the current wire insulation used on the Shuttle program. Alternate wire constructions should be considered for modifications/repairs/upgrades. There are several aerospace wire insulation constructions that can provide more balanced properties.	**SSP Response (Abbey/Dittemore, 21 June 2000):** BRSS performed a study of new wire insulation for potential vehicle uses. Testing was performed over a wide range of criteria comparing vehicle Kapton (polyimide) wiring with six other aerospace wire constructions. After reviewing the test results, the engineering and safety community concluded these alternate wire constructions did not surpass the overall performance of the vehicle's current Kapton wiring. The SSP plans to continue using Kapton insulated wire for vehicle harnesses based on its superior test performance but will continue to evaluate new wiring constructions as they are introduced to the aerospace community.
Space Shuttle Independent Assessment Team *(NASA Charter)*	7 March 2000		**Recommendation 3L-1:** Where redundancy is used to mitigate risk, it should be fully and carefully implemented and verified. If it cannot be fully implemented due to design constraints, other methods of risk mitigation must be utilized.	**SSP Response (Abbey/Dittemore, 23 October 2000):** The Space Shuttle Program (SSP) reviewed all documentation pertaining to redundancy requirements for flight, payload, and ground support hardware and software. This

Independent Assessment Team *(Chartered by)*	Date of Report	Finding	Recommendation	NASA Response
				review verified that the requirements appropriately specify the method for identifying critical functions and hazards, the level of redundancy required to mitigate identified risks, the verification required of the redundancy approach, and the process to address risks that cannot be fully mitigated with redundant design. Every SSP element was involved in this review effort, confirming redundancy awareness and compliance across the program. These program level requirements and associated project level documents are kept current by a formal annual review and audit process. Once risks have been characterized and redundancy measures implemented into the design, a verification of their functionality is necessary. The process for ensuring proper implementation and certification is defined in the Space Shuttle Master Verification Plan. Redundant functional paths or subsystems are designed so that their operational status can be verified prior to each installation into the vehicle or during ground turn-around without removal of line-replaceable-units. Each element defines their system redundancy verification requirements in the Operations and Maintenance Requirements and Specifications Document, and subsequently verifiesthat the requirements have been correctly implemented into technical work instructions. Successful execution of these

Independent Assessment Team *(Chartered by)*	Date of Report	Finding	Recommendation	NASA Response
				work instructions for each Space Shuttle mission is verified at the Flight Readiness Review (FRR) via the Certificate of Flight Readiness (CoFR) process. For those situations where resources and design constraints do not permit the full implementation of redundancy requirements, other methods of risk mitigation are utilized per the hazard cause reduction precedence. The risk of hazard is either eliminated by appropriate design measures, prevented by use of safety devices, controlled by use of warning devices, or avoided by using special procedures. Furthermore, critical functions are required to be separated, protected from failure from similar causes, able to be isolated without disrupting redundant functions, and able to be fault-isolated without disconnections. To ensure compliance with all these requirements, the SSP formally directs every element to submit proposed hardware/software changesthat impact baselined program risk, redundancy, or certification requirements to the Program Requirements Control Board (PRCS) for disposition prior to implementation. Hardware or software configuration or performance that deviates from baselined requirements must be submitted by the design element on a waiver for program consideration. A waiver documents the technical rationale for flight

Independent Assessment Team *(Chartered by)*	Date of Report	Finding	Recommendation	NASA Response
				acceptability and effectivity, is dispositioned by the PRCB, and, if approved, is subsequently reviewed at the FRR per CoFR requirements.
Space Shuttle Independent Assessment Team *(NASA Charter)*	7 March 2000		**Recommendation 3L-2:** Serious consideration should be given to replacing the hydrazine power unit with a safer and easier to maintain advanced electric auxiliary power unit for the Thrust Vector Control hydraulic unit.	**SSP Response (Abbey/Dittemore, 23 October 2000):** NASA, United Space Alliance (USA), and Boeing-Reusable Space Systems (BRSS) are working to develop and implement an electric auxiliary power unit (EAPU) to replace the existing hydrazine auxiliary power unit. The overall objectives of the EAPU are to: • Reduce auxiliary power unit (APU) contribution to orbiter catastrophic risk from 30 percent to less than 5 percent. • Reduce APU criticality 1 items and hazards by more than 50 percent. • Increase APU system reliability by at least two orders of magnitude. • Reduce planned APU maintenance operations by more than 50 percent. The phase I feasibility study is complete and the phase II prototype development is in work. The development of phase III preliminary flight hardware is in the process of being authorized.
Space Shuttle Independent Assessment Team	7 March 2000		**Recommendation 3L-3:** Due to obsolescence, Shuttle Reaction Control System propellant valves and propellant flight-half couplings should be	**SSP Response (Abbey/Dittemore, 23 October 2000):** A BRSS study identified an improved reaction control system (RCS)

Independent Assessment Team *(Chartered by)*	Date of Report	Finding	Recommendation	NASA Response
(NASA Charter)			replaced with ones that are more tolerant of the oxidizer environment.	pilot operated valve (POV) and received approval from the NASA Space Shuttle Vehicle Engineering Office (SSVEO) to begin qualification testing. The improved POV is designed to be more tolerant of oxidizer-derived contamination by reducing the poppet cage contact area and increasing propellant flow through. The pilot poppet, pilot seat, and main seat materials were also changed to a more corrosion resistant stainless steel. The qualification program will be completed in early 2003, and implementation will be on an attrition basis. The qualification program for the redesigned 1Ainch and _ inch orbital maneuvering system and RCS air-half couplings is complete and certification approval was received from the SSVEO. The redesigned flight-half couplings were made more tolerant of oxidizer-derived contamination by reducing the sliding surface area and changing the poppet material from stainless steel to titanium. Oxidizer exposure tests verified the redesign measures. The redesigned parts will be installed on an attrition basis.
Space Shuttle Independent Assessment Team *(NASA Charter)*	7 March 2000		**Recommendation 3L-4:** The Problem Resolution and Corrective Action system should be revised using state-of-the-art database design and information management techniques.	**SSP Response (Abbey/Dittemore, 23 October 2000):** The SSP established a Problem Reporting and Corrective Action (PRACA) Evaluation Team (PET) in February 2000. The team includes members from all SSP elements, projects, the SSP Office, and the Ames Research Center (ARC). The

Independent Assessment Team *(Chartered by)*	Date of Report	Finding	Recommendation	NASA Response
				PET addressed this recommendation, as well as the findings from all PRACA audits completed over the past year. A review of program-level requirements has been completed. The revised requirements will be published in September 2000. All SSP project and element offices will follow up with a review of their PRACA requirements and processes to ensure compliance with the revised SSP requirements. The PET provides periodic status to the program at the PRCB. In addition to completing the PRACA requirements review, the PET will determine appropriate changes to improve the software systems for data entry, trending, and analysis. This PET will investigate utilizing state-of-the-art data base designs and techniques. To support this effort, the ARC established a pilot project investigating improved PRACA system automation and state-of-the-art data base design. Software upgrade review and implementation is schedule for completion in August 2001.
Space Shuttle Independent Assessment Team *(NASA Charter)*	7 March 2000		**Recommendation 3L-5:** Inspection technique(s) for locating corrosion under the tiles and in inaccessible areas should be developed. Inspection	**SSP Response (Abbey/Dittemore, 23 October 2000):** BRSS has established a structures/nondestructive evaluation (NDE) task team to investigate possible methods for inspecting inaccessible areas on the orbiter. The task team is chartered to ensure that the SSVEO is utilizing the full capability of the available NDE technology to address the issue of hidden corrosion. The team will identify structural areas

Independent Assessment Team *(Chartered by)*	Date of Report	Finding	Recommendation	NASA Response
				currently considered inaccessible, target the low margin areas for further study, investigate possible NDE methods, and attempt to validate the technology at Palmdale during the next orbiter major modification. Various new or improved NDE techniques are constantly emerging. Promising NDE techniques include enhanced ultrasonic and eddy current techniques, reverse geometry x-ray, and others. However, virtually all techniques require some direct access to the target area. The probability of hidden corrosion under the thermal protection system is considered to be extremely remote because room temperature vulcanized material has been proven by test and experience to provide an excellent barrier against moisture.
Space Shuttle Independent Assessment Team *(NASA Charter)*	7 March 2000		**Recommendation 3L-6:** Consideration should be given to modifying the Shuttle internal hydraulic line routing to the mold line to permit efficient facility hydraulic hose connections.	**SSP Response (Abbey/Dittemore, 23 October 2000):** The SSVEO authorized BRSS to design the relocation of the orbiter hydraulic ground servicing quick disconnects (QD) and landing gear extend/retract QDs to a new panel at the mold line. The modification eliminates the need to carry hydraulic ground servicing equipment into the aft compartment, thereby, reducing potential orbiter damage and improving vehicle turnaround time. The design has progressed through a preliminary design review and BRSS will come to the Vehicle Engineering Control Board (VECB) in October 2000 for implementation approval. Implementation will begin in November 2001, and

Independent Assessment Team *(Chartered by)*	Date of Report	Finding	Recommendation	NASA Response
				all vehicles will be modified by February 2002.
Space Shuttle Independent Assessment Team *(NASA Charter)*	7 March 2000		**Recommendation 3L-7:** Non-intrusive methods of reliably detecting wiring damage should be developed, including those areas no accessible to visual inspection.	**SSP Response (Abbey/Dittemore, 23 October 2000):** BRSS has proposed a plan to the VECB to examine existing and emerging test methods and associated equipment for testing wire integrity. BRSS will work with vendors and developers to determine the effectiveness of test equipment in categorizing damage conditions and identifying degraded insulation properties. Special consideration will be given to minimizing orbiter intrusion with these testing techniques. Additionally, ARC recently completed a wire integrity research pilot study that addressed automated verification and validation of orbiter wiring configuration and automated condition assessment for maintenance.
Space Shuttle Independent Assessment Team *(NASA Charter)*	7 March 2000		**Recommendation 3L-8:** Quantitative methods of risk assessment (likelihood of failure) should be developed.	**SSP Response (Abbey/Dittemore, 23 October 2000):** The SSP agrees with SIAT that quantitative risk assessment is essential to fly the Space Shuttle safely. The SSP currently utilizes many quantitative techniques to determine and manage risk. Program requirements contained within NSTS 07700 specify the use of analytical methods in all aspects of program execution. Statistical process control, process failure modes and effects analysis/critical items list, fault tree and event tree analysis, hazard analysis, reliability-centered analysis,

Independent Assessment Team *(Chartered by)*	Date of Report	Finding	Recommendation	NASA Response
				and other techniques are implemented to various degrees across alt program elements. These methods assess the probability and severity of failures through all mission phases. The SSP has generated a wealth of statistical and analytical data in the last 19 years of flight history and continues to explore the potential adaptation of various quantitative risk analysis (QRA) methods. The System Safety Review Panel (SSRP), with representatives from all program elements and safety, reliability, and quality assurance organizations, is reviewing current QRA techniques and will determine an approach to quantitative risk assessment for the program. To date, several meetings have been held by the SSRP involving the upgrades program, the safety community, NASA Headquarters, MSFC, and KSC to identify and agree on the requirements and priorities of quantitative software packages to support SSP operations and upgrade trade studies. Four software tools have been identified and three expert consultants have assisted the SSP to narrow the choices with the current favorite being a package called Sapphire. USA is working with the program to develop a probabilistic risk assessment (PRA)/QRA center of excellence to assist in the effort. The development of a PRA/QRA program standard and an implementation approach will be provided in the February 2001 timeframe. The SSRP will then determine if a

Independent Assessment Team *(Chartered by)*	Date of Report	Finding	Recommendation	NASA Response
				singular program-wide analytical methodology is the right solution, given the diversity and complexity of the SSP. A final evaluation will be conducted with the recommendation presented by the SSRP to the SSP PRCB in April 2001.
Space Shuttle Independent Assessment Team *(NASA Charter)*	7 March 2000		**Recommendation 3L-9:** Quantitative measures of safety (likelihood of error), including assessment surveying techniques should be developed, e.g., Occupational Stress Inventory and MEDA.	**SSP Response (Abbey/Dittemore, 23 October 2000):** The Incident Error Review Board at KSC is an example of one mechanism in place to assess maintenance process errors. Like the maintenance error decision aid (MEDA) used by the commercial airlines, this board analyzes all contributing elements to determine root cause and to formulate corrective actions. However, this approach is reactive and, much like MEDA, has limitations in that only significant events initiate board reviews. To be proactive, the SSP is aggressively incorporating human factor principles into the flight preparation process. The Space Shuttle Processing Human Factors Team and the USA Industrial Engineering and Human Factors Department were staffed to improve the SSP error management process. The two entities work cooperatively to share quantitative data, resources, and expertise to develop human factor concepts and perform on-site process analysis. Several initiatives underway include the Work Instruction Task Team that provides guidelines and training on effective procedure authoring and the Industrial and Work Space

Independent Assessment Team *(Chartered by)*	Date of Report	Finding	Recommendation	NASA Response
				Design Team recently chartered to ensure human factors are incorporated in the engineering and ground system design processes. Both programs will have widespread effects in operations, maintenance, manufacturing, and design. A statistical analysis of the PRACA system is also underway to assess problem report entry and classification errors, with corrective actions to be implemented by the PRACA Evaluation Team. USA commissioned Lord & Hogan, with the endorsement of the Shuttle Independent Assessment Team (SIAT),to administer an operational stress inventory and analysis. The results of the USA workforce surveys in Florida and Texas indicated positive results in the normal range compared to other companies in all categories of stress and coping behaviors. USA intends to conduct follow-on studies in approximately 2 years as a companion to the new baseline. NASA Centers are in the process of conducting various workforce surveys such as the Employee Stress Survey (ESS) and the Performance Evaluation Profile (PEP). These results are compiled and presented to the SSP as a series of measurements. The ESS specifically deals with occupational stress factors and the ability of the workforce to deal with stress issues. The PEP focuses on both industrial and flight safety and serves to evaluate the performance of the safety

Independent Assessment Team *(Chartered by)*	Date of Report	Finding	Recommendation	NASA Response
				program. The SSP will evaluate these results and, if necessary, take corrective actions. To further these efforts, the human factor teams will be chartered to develop quantitative measures of human performance and propose plans to address improvements within the industrial engineering for safety initiative currently chartered by SSP directive.
Space Shuttle Independent Assessment Team *(NASA Charter)*	7 March 2000		**Recommendation 3L-10:** Quantitative methods of risk assessment and safety (see above) need to be integrated to develop the ability to perform trade-off studies on the effect of new technology, aging, upgrades, process changes, etc., upon vehicle risk.	**SSP Response (Abbey/Dittemore, 23 October 2000):** The SSP agrees with SIAT that quantitative risk assessment is essential to fly the Space Shuttle safely. The SSP currently utilizes many quantitative techniques to determine and manage risk. Program requirements contained within NSTS 07700 specify the use of analytical methods in all aspects of program execution. Statistical process control, process failure modes and effects analysis/critical items list, fault tree and event tree analysis, hazard analysis, reliability-centered analysis, and other techniques are implemented to various degrees across alt program elements. These methods assess the probability and severity of failures through all mission phases. The SSP has generated a wealth of statistical and analytical data in the last 19 years of flight history and continues to explore the potential adaptation of various quantitative risk analysis (QRA) methods. The System Safety Review Panel (SSRP),

Independent Assessment Team *(Chartered by)*	Date of Report	Finding	Recommendation	NASA Response
				with representatives from all program elements and safety, reliability, and quality assurance organizations, is reviewing current QRA techniques and will determine an approach to quantitative risk assessment for the program. To date, several meetings have been held by the SSRP involving the upgrades program, the safety community, NASA Headquarters, MSFC, and KSC to identify and agree on the requirements and priorities of quantitative software packages to support SSP operations and upgrade trade studies. Four software tools have been identified and three expert consultants have assisted the SSP to narrow the choices with the current favorite being a package called Sapphire. USA is working with the program to develop a probabilistic risk assessment (PRA)/QRA center of excellence to assist in the effort. The development of a PRA/QRA program standard and an implementation approach will be provided in the February 2001 timeframe. The SSRP will then determine if a singular program-wide analytical methodology is the right solution, given the diversity and complexity of the SSP. A final evaluation will be conducted with the recommendation presented by the SSRP to the SSP PRCB in April 2001.
Aerospace Safety Advisory Panel *(NASA Charter)*	February 2000	**Finding 1:** The continuing downsizing at Office of Space Flight Field Centers, coupled with the effects of the prior hiring freeze and unplanned departures, has	**Recommendation 1:** NASA must continue to address workforce problems aggressively and establish program priorities that ensure a workforce capable of achieving long-term safe and effective	

Independent Assessment Team *(Chartered by)*	Date of Report	Finding	Recommendation	NASA Response
		produced critical skills deficits in some areas, growing workload pressure and stress levels, and a serious shortfall of younger S&Es.	operations. Emphasis should be placed on eliminating critical skills shortfalls and recruiting younger S&Es who can develop into experienced and skilled future leaders.	
Aerospace Safety Advisory Panel *(NASA Charter)*	February 2000	**Finding 2:** The combination of downsizing losses, hiring restrictions, and transition of responsibilities from NASA to contractors, such as USA, continues to limit the opportunities for junior and mid-level NASA managers to gain the operational knowledge and experience required for continued leadership in senior management positions.	**Recommendation 2:** Innovative arrangements between NASA and its contractors to provide entry-level and mid-level NASA S&Es with operational, "hands-on" experience should be strengthened and expanded. Project management training initiatives, such as the Academy of Program & Project Leadership (APPL), must strive to broaden their outreach to management teams and individuals at the Field Centers.	
Aerospace Safety Advisory Panel *(NASA Charter)*	February 2000	**Finding 3:** The Space Shuttle Program Office has instituted a set of Process Control Focus Groups whose goal is to implement "best practice" commonality in change control procedures across all supplier tiers.	**Recommendation 3:** Focus the active and dedicated support of senior management of the major contractors and all their subcontractors on implementing the process control "best practices" as soon as feasible. NASA must be fully apprised of all process changes even if they result in a product that meets requirements.	
Aerospace Safety Advisory Panel *(NASA Charter)*	February 2000	**Finding 4:** Although progress has been made to improve the quality, accuracy, and traceability of the work instructions ("paperwork" used in the processing of Space Shuttle Orbiters) much remains to be done to provide correct and unambiguous procedures. There are still too many unincorporated changes.	**Recommendation 4:** Efforts to improve the quality, accuracy, and traceability of the work paper as well as the timeliness of incorporation of changes to work instructions must be given higher priority by both NASA and USA in a coordinated, systematic effort.	
Aerospace Safety Advisory Panel	February 2000	**Finding 5:** There is no systematic plan to counter obsolescence and assure the availability of adequate facilities, GSE,	**Recommendation 5:** Develop and execute a plan to ensure that all needed support and test-and-checkout facilities and equipment are assured available	

Independent Assessment Team *(Chartered by)*	Date of Report	Finding	Recommendation	NASA Response
(NASA Charter)		and specialized test-and-checkout equipment throughout the expected lifetime of the Space Shuttle.	and protected from obsolescence for the maximum foreseeable life of the Space Shuttle.	
Aerospace Safety Advisory Panel *(NASA Charter)*	February 2000	**Finding 6:** Space Shuttle processing workload is sufficiently high that it is unrealistic to depend on the current staff to support higher flight rates and simultaneously develop productivity improvements to compensate for reduced head counts. NASA and USA cannot depend solely on improved productivity to meet increasing launch demands.	**Recommendation 6:** Hire additional personnel and support them with adequate training.	
Aerospace Safety Advisory Panel *(NASA Charter)*	February 2000	**Finding 7:** Due to attrition of experienced personnel, NASA and its contractors are assigning more newly trained personnel to Space Shuttle operations tasks. This has led to concerns in the workforce regarding the qualifications of some newly-assigned personnel.	**Recommendation 7:** NASA and its contractors must ensure that their training, certification, and task assignment processes are such that only suitably qualified engineering and technical personnel are performing Space Shuttle operations. Any training and licensing program to certify new personnel must include both testing of acquired skills and demonstrated proficiency on the assigned task.	
Aerospace Safety Advisory Panel *(NASA Charter)*	February 2000	**Finding 11:** The EVA Project Office has several planned initiatives to ensure the availability of adequate EVA resources to support the ISS and Space Shuttle. These initiatives cover acquisition of materiel, development of procedures, and improved training.	**Recommendation 11:** Expedite completion of the planned initiatives related to the safety of EVA so that maximum benefit can be realized during the upcoming intensive ISS assembly schedule.	

Independent Assessment Team *(Chartered by)*	Date of Report	Finding	Recommendation	NASA Response
Aerospace Safety Advisory Panel *(NASA Charter)*	February 2000	**Finding 12:** The funding of the EVA R&T program is not adequate to provide the maximum safety benefit in terms of new equipment and procedures that lower the risk of extravehicular activities.	**Recommendation 12:** Fund a robust EVA R&T program.	
Aerospace Safety Advisory Panel *(NASA Charter)*	February 2000	**Finding 14:** NASA has initiated an agency-wide program to deal with general computer security. Significant parts of NASA's initial plan depend upon the voluntary compliance of system users including contractors.	**Recommendation 14:** Expand the agency-wide security system development work to include less dependence on human compliance with the system. NASA should also require contractors to participate in its security efforts.	
Aerospace Safety Advisory Panel *(NASA Charter)*	February 2000	**Finding 16:** NASA has established an Avionics Upgrade Architecture Team (AUAT) charged with studying Space Shuttle avionics systems and recommending upgrades. The AUAT has conducted a thorough study and developed an excellent Block I upgrade plan that addresses the most serious needs, but as yet it is unfunded.	**Recommendation 16:** Proceed with full funding for the proposed Block I Space Shuttle avionics upgrades as rapidly as possible.	
Aerospace Safety Advisory Panel *(NASA Charter)*	February 2000	**Finding 17:** Part of the AUAT's initial approach is to install three mission computers to augment the existing General Purpose Computers (GPCs). The specific functions to be offloaded from the GPCs to the mission computers have yet to be determined. Eventually, the AUAT plans to consider moving some "Crit 1" functions to the mission computers.	**Recommendation 17:** Do not move any "Crit 1" functions to the mission computers unless memory requirements in the GPC demand it and then only after an appropriate risk analysis is performed.	

Independent Assessment Team *(Chartered by)*	Date of Report	Finding	Recommendation	NASA Response
NASA Office of Safety and Mission Assurance *(NASA Charter)*	16 April 1999	The review team evaluated the assumptions, supporting data, and maturity of selected strategic initiatives (fifteen of the twenty-one Phase 2 initiatives) and arrived at an estimated savings of 224 as opposed to the USA/GO projection of 287. This 78 percent-yield (see Chapter 14, Table 14-1) suggests that USA/GO will achieve roughly three-quarters of their goal to increase flight rate capability from 5 flights-per-year to 8 flight-per-year.		
NASA Office of Safety and Mission Assurance *(NASA Charter)*	16 April 1999	The review team estimates that effective implementation of the USA/GO Strategic Initiatives will establish the capability to safely accomplish a steady-state flight rate of up to seven per year. Ultimate verification of processing capability can only be determined after analysis of actual steady-state flow performance.		
NASA Office of Safety and Mission Assurance *(NASA Charter)*	16 April 1999	The team noted that effective implementation has not yet been achieved in the safety-related Structured Surveillance Phase II initiative, where human-factors issues (communication, inspection dynamic, worker acceptance) exist. Increased USA management attention is warranted in this area. The inspection "work review process" must be acknowledged and accepted by the entire USA workforce as a		

Independent Assessment Team *(Chartered by)*	Date of Report	Finding	Recommendation	NASA Response
		critical element in assuring flight safety.		
Aerospace Safety Advisory Panel *(NASA Charter)*	February 1999	**Finding 1:** Budget and personnel ceiling constraints on the hiring of engineers, scientists, and technical workers are moving NASA toward a crisis of losing the core competencies needed to conduct the Nation's space flight and aerospace programs in a safe and effective manner.	**Recommendation 1:** Provide NASA's human space flight Field Centers, particularly KSC, JSC, and MSFC, with the budgetary resources and administrative flexibility needed to strengthen their human resource capabilities.	**NASA Response (in 1999 ASAP appendix):** NASA concurs with the recommendation; and, we fully recognize the near heroic efforts at each of our installations that have brought us within striking distance of our downsizing targets. At the beginning of fiscal year 1993, the NASA employment level was 24,900 FTE. As a result of the March 1993 Executive Order to reduce Federal Civilian FTE by 100,000, the NPR recommendations and additional OMB directed cuts in 1994,NASA received an out-year target of 20,906. Additional budget reductions occurred that required us to initiate the Zero Base Review, which was completed in 1995.The ZBR recommended an FY 2000 FTE level of 17,488. Since that time we have carefully managed an FTE reduction to a planned 18,545 FTE for FY 99 and 17,970 for FY 00. Our final "go to" target is now 17,574 FTE for FY 04. Currently 7 of our 10 Centers are at or below our lowest "go to" numbers. To NASA's credit, our accomplishments were achieved without resort to the ravages of a reduction-in-force. Voluntary losses to date include in excess of 4,500 buyouts, 1,300 early outs, and more than 800 intercenter transfers. As a result of the downsizing challenges, we provided relief to the OSF Centers in the FY

Independent Assessment Team *(Chartered by)*	Date of Report	Finding	Recommendation	NASA Response
				00 budget process as follows: FY 99-153 FTE; FY 00-110 FTE; FY 01-103 FTE; FY 02-59 FTE; and, FY 03-68 FTE. This relief has enabled the innovative use of temporary and extended term appointments, as well as increasing the number of permanent hires available to fill critical skill positions. In addition, we are currently reviewing their request for additional relief, as identified in the recent Core Capability Assessment (CCA). OSF management has proposed several augmentation and/or hiring models that address both short and long term needs regarding replacement and enhancement of critical workforce competencies. One objective of the current CCA review is to help chart a strategy that will provide the OSF Centers with the requisite flexibility to attract and retain the core competency talent pool necessary to ensure safe mission and program success.
Aerospace Safety Advisory Panel *(NASA Charter)*	February 1999	**Finding 2:** Shortfalls in workforce training within both NASA and USA, caused by downsizing and the related difficulty of hiring new people to fill skill shortages, can jeopardize otherwise safe operations.	**Recommendation 2:** NASA and USA should review critical skills training and certification requirements and institute programs to ensure the full proficiency of the workforce and the safety of the products being released.	**NASA Response (in 1999 ASAP appendix):** NASA concurs in the recommendation and, in cooperation with USA, has already reviewed certification requirements for flight controllers, training instructors, and other key operating positions. Training plans and certification requirements for critical positions have been documented and maintained. For example, the management role in launch countdown and landing is supported by a well–defined training and certification plan. NASA and its contractors are continually reviewing critical skills

Independent Assessment Team *(Chartered by)*	Date of Report	Finding	Recommendation	NASA Response
				training and certification requirements to ensure controls are in place to validate and ensure employee proficiency. Quality initiatives are being developed to provide improved processes for cross training, automated training tools, inline automated certification validation, and enhancements in the closed loop verification of operators and system operational performance. Meanwhile, training capacity for new employees, both NASA and contractor, has been increased through intensive simulator training at a new USA "training academy." A saturation-type training environment has been designed to improve training at the beginning of the regular certification process and produce employees better qualified for critical process work. In training and orientation programs, NASA emphasizes the priority of safety and the responsibility of employees to voice their concerns about inadequate assurances of safe products.
Aerospace Safety Advisory Panel *(NASA Charter)*	February 1999	**Finding 3:** The combined effect of workforce downsizing, the recent hiring freeze, and the SFOC transition, especially at KSC, has raised the possibility that NASA senior managers in the future will lack the necessary hands-on technical knowledge and inline experience to provide effective insight of operations.	**Recommendation 3:** NASA should develop and promulgate training and career paths, with a special focus on providing hands-on technical knowledge and experience, so that NASA's future senior managers will possess the range of skills and experience required for effective insight of the SFOC.	**NASA Response (in 1999 ASAP appendix):** NASA concurs in the recommendation and is intensifying and refocusing its efforts in training and in support of career development at all levels. At the operating level, NASA managers are instructed to plan and to take advantage of all opportunities to obtain operational experience through audit, surveillance, and other interfaces to provide hands-on experience to NASA personnel.

Independent Assessment Team *(Chartered by)*	Date of Report	Finding	Recommendation	NASA Response
				(list with lots of detail omitted) Additionally, employees are provided cross training and specialized training as needed and strongly encouraged to take advantage of program related training. The key to developing future generations of senior managers is to provide hands-on experience, with progressively more responsible assignments through one's career. Both NASA and the contractors continually seek improvements in the succession planning and preparations for the next generation of supervisors and managers. Special consideration is given to assuring that broad training and hands-on operational/technical job assignments and opportunities are consciously addressed for promising candidates for future senior management positions. NASA's training philosophy also emphasizes on-the-job work experiences supplemented by classroom instruction, participation in outside academic programs and industry through assignments in such private sector organizations as Boeing, Newport News Shipbuilding, and USA. At the agency planning level, the training budget has provided for an increase of 20% for the Office of Space Flight from FY1997 through

Independent Assessment Team *(Chartered by)*	Date of Report	Finding	Recommendation	NASA Response
				FY2000.Current agency Program Operating Plan (POP) guidelines call for funding training at 2-3.25% of salary levels, an extremely generous ratio for government and rivaling progressive private sector organizations. The NASA Academy of Program and Project Leadership (APPL) is building on ten years of educational and developmental activities and is striving to facilitate the flow of current knowledge and techniques to the full engineering and science workforce. APPL is making available information and automated tools on-line and seeking to develop expert systems. APPL is also working directly to support intact teams with information and techniques and attempting to better organize case studies and archives into a more effective knowledge base. The APPL program is also adding an Accelerated Leadership Option to the Project Management Development Process (PMDP) which will enable NASA engineers to obtain a Master's of Science in Engineering and Management degree from MIT.APPL is continuing and expanding a multifaceted program of classroom work, developmental work assignments, and dissemination of information and guidance. Finally, NASA is well along in an update of its Leadership Development Model;

Independent Assessment Team *(Chartered by)*	Date of Report	Finding	Recommendation	NASA Response
				documenting the technical, managerial, and executive competencies required to direct the work of the agency through the foreseeable future. This model will guide the scope and emphasis of training and development programs, including a new approach to succession planning, to ensure that NASA's leaders at all levels have the knowledge and skills to meet their responsibilities.
Aerospace Safety Advisory Panel *(NASA Charter)*	February 1999	**Finding 4:** It is often difficult to find meaningful metrics that directly show safety risks or unsafe conditions. Safety risks for a mature vehicle, such as the Space Shuttle, are identifiable primarily in specific deviations from established procedures and processes, and they are meaningful only on a case-by-case basis. NASA and USA have a procedure for finding and reporting mishaps and "close calls" that should produce far more significant insight into safety risks than would mere metrics.	**Recommendation 4:** In addition to standard metrics, NASA should be intimately aware of the mishaps and close calls that are discovered, follow up in a timely manner, and concur on the recommended corrective actions.	**NASA Response (in 1999 ASAP appendix):** NASA agrees with the recommendation. In addition to standard metrics, NASA is intimately aware of the mishaps and close calls and is directly involved in the investigations and approval of corrective actions. Current requirements contained in various NASA Center and contractor safety plans include procedures for reporting of mishaps and close calls. These reports are investigated and resolved under the leadership of NASA representatives with associated information being recorded and reported to NASA management. NASA is intimately aware of and participates in the causal analysis and designation of corrective action for each mishap. Additionally, NASA performs trend analysis of metrics as part of the required insight activities. Definitions relating to "close call" have been expanded to include any observation or employee comment related to safety improvement. Close call reporting has been emphasized in contractor and

Independent Assessment Team *(Chartered by)*	Date of Report	Finding	Recommendation	NASA Response
				NASA civil servant performance criteria and a robust management information system is being incorporated to monitor and analyze conditions and behavior having the potential to result in a mishap. Various joint NASA/contractor forums exist to review, evaluate, and assign actions associated with reported close calls. As an example, the KSC NASA Human Factors Integration Office leads the NASA/Contractor Human Factors Integrated Product Team (IPT) in the collection, integration, analysis, and dissemination of root cause and contributing cause data across all KSC organizations. The KSC Human Factors IPT is also enhancing the current close call process which includes tracking of mishaps with damage below $1000 and injuries with no lost workdays. The SSP has revised it's Preventive/Corrective Action Work Instruction to include mandatory quarterly review of close call reports. Several initiatives are in place to increase awareness of the importance of close call reporting and preventive/corrective action across the SSP and the supporting NASA Centers and contractors. Under this new approach to close call reporting, a metric indicating an increase in close call reporting and preventive action is considered highly desirable as it indicates an increased involvement by the workforce in identifying and resolving potential hazards. Care is taken in over

Independent Assessment Team *(Chartered by)*	Date of Report	Finding	Recommendation	NASA Response
				emphasizing the number of close calls reported as a performance metric to prevent reluctance in reporting. NASA is working hard to shift the paradigm from the negative aspects of reporting close calls under the previous definition to being a positive aspect of employee identification of close calls under the new definition.
Aerospace Safety Advisory Panel *(NASA Charter)*	February 1999	**Finding 5:** A principal cause of Space Shuttle processing errors is incorrect documentation ("paperwork").	**Recommendation 5:** NASA and USA must place increased priority on determining error sources, causes, and corrective actions for inadequacies in the documentation on which Space Shuttle processing is based and develop a management system that drastically reduces the time that it takes to incorporate paperwork changes.	**NASA Response (in 1999 ASAP appendix):** NASA concurs with the recommendation. NASA and USA have established metrics to identify the types of errors and error sources in the processing documentation. During daily interface, NASA and USA discuss these metrics and perform causal analysis to identify the need for corrective action. For critical procedures, USA has implemented a check and balance in the work instruction generation process to increase the procedure quality before it is worked. Additionally, NASA and USA have an initiative to reduce the complexity of work procedures, increase the procedure standardization, and reduce the time for paperwork generation for work not requiring engineering disposition. More importantly, USA is developing, as a high priority, a paperless system. Specifically, the Ground Operations organization at KSC is implementing an integrated on-line system that ensures total process rigor and mitigates the potential for human error in accomplishing space flight work. This

Independent Assessment Team *(Chartered by)*	Date of Report	Finding	Recommendation	NASA Response
				system incorporates recognized "best practices" for authoring work documents including on-line review and approval, and the ability for authors to automatically update and incorporate work document deviations. Required checks and balances are inherent in the system to maintain the integrity, safety and quality of both flight and ground work performed. Work documents will clarify user understanding by incorporating enhanced explanations with in-line graphics, sound and video where required. The goal of this activity is to ensure that a properly certified person, utilizing the right work instructions, has safely accomplished all required work.
Aerospace Safety Advisory Panel *(NASA Charter)*	February 1999	**Finding 6:** While spares support of the Space Shuttle fleet has been generally satisfactory, repair turnaround times (RTAT) have shown indications of rising. Increased flight rates will exacerbate this problem.	**Recommendation 6:** Refocus on adequate acquisition of spares and logistic system staffing levels to preclude high RTATs, which contribute to poor reliability and could lead to a mishap.	**NASA Response (in 1999 ASAP appendix):** NASA concurs with the recommendation. During calendar year 1998,RTAT's for both the NASA Shuttle Logistics Depot and the original equipment manufacturer fluctuated, but at year's end, the overall trend was downward through concerted NASA and vendor efforts. These efforts are aimed at providing better support at the current flight rate and for higher flight rates in the future. Logistics is working to find innovative ways to extend the lives of aging line replaceable units (LRUs) and their support/test equipment. Logistics has initiated the Space Council (an industry group with 11 other company executives addressing such topics as verification reduction, ISO compliance, and upgrades) to

Independent Assessment Team *(Chartered by)*	Date of Report	Finding	Recommendation	NASA Response
				assure the supplier base continues its outstanding support to the SSP. Examples of LRUs being evaluated and enhanced include: Star Trackers, auxiliary power units, inertial measurement units, multifunction electronic display system (MEDS),Ku-band, orbiter tires, and manned maneuvering units. NASA/KSC Logistics and USA Integrated Logistics have made progress on a long-term supportability tool. The tool will provide information, including historical repair trend data for major LRUs, RTATs, and "what if" scenarios based on manipulation of factors (e.g., flight rate, turnaround times, loss of assets, etc.) to determine their effect on the probability of sufficiency. This will be a tool, not a substitute, for human analytical decision making.
Aerospace Safety Advisory Panel *(NASA Charter)*	February 1999	**Finding 7:** NASA aircraft used for both Space Shuttle operations and astronaut training are increasingly out of date and, in several respects, may be approaching the unsafe. This is noticeably so in the case of the Shuttle Training Aircraft (STA) and the T-38 aircraft.	**Recommendation 7:** Continue to execute and accelerate as much as possible the current plans for the modernization and safety assessment of astronaut training aircraft.	**NASA Response (in 1999 ASAP appendix):** NASA believes that the current aircraft used as astronaut training aircraft are maintained in a safe condition. NASA remains committed to safe operation of all the training aircraft. Measures to ensure that the NASA T-38s and STAs used for astronaut training are maintained in a safe configuration and in good material and structural condition are in place. (lots more T-38 detail omitted) NASA will continue to evaluate new programs and seek new initiatives to meet the requirements as they

Independent Assessment Team *(Chartered by)*	Date of Report	Finding	Recommendation	NASA Response
				evolve, such as adding avionics for compatibility with the future free flight concept in the air traffic control system. STA: NASA has four STAs and one spare Gulfstream II (GII) that will be modified into an STA when it is either required by the Shuttle flight rate or in the event that one of the four STAs becomes unusable.
Aerospace Safety Advisory Panel *(NASA Charter)*	February 1999	**Finding 8:** The use of simulated Space Shuttle launch and flight operations for training and rehearsal has proven to be an effective technique for enhancing safety and efficiency and is especially valuable in the case of special or rarely performed procedures or after a long hiatus of effort.	**Recommendation 8:** Simulation-based training should be included in difficult or infrequent Space Shuttle operations whenever feasible. This type of training is especially needed after there has been a significant hiatus in performing an operation.	**NASA Response (in 1999 ASAP appendix):** NASA concurs with the recommendation. NASA and USA have beneficially increased simulation-based training at KSC. The pursuit of a separate simulation training room and simulation team will allow NASA and USA to further increase the number of simulations that can be performed each flow. Additionally, KSC will use the new collaborative engineering environment to enhance simulation capabilities.
Aerospace Safety Advisory Panel *(NASA Charter)*	February 1999	**Finding 18:** The EVA project lacks sufficient operational assets to meet unplanned contingencies. There are no spare Extravehicular Mobility Units (EMU). Only five U.S. Simplified Aid for EVA Rescue (SAFER) flight units will be available to meet a requirement to maintain three units on orbit. In addition, only four Russian SAFER units are planned.	**Recommendation 18:** To meet contingencies that are almost certain to arise, additional EMU's and SAFER units or their critical long lead components should be procured as soon as possible.	**NASA Response (in 1999 ASAP appendix):** NASA concurs with the ASAP recommendation. With respect to the EMU, the inventory of life support system (LSS) hardware will be 14 (13 Class I and 1 Class II) by October 1999.Exceedences to our supply begin in 2000. In order to achieve a 90 percent probability of sufficiency, NASA must increase its inventory by two LSSs. NASA plans on addressing this issue within the Program Operating Plan (POP) 99.We plan to upgrade the current

Independent Assessment Team *(Chartered by)*	Date of Report	Finding	Recommendation	NASA Response
				Class II LSS to Class I and upgrade the certification unit to Class II. This will increase our inventory to 15. NASA also plans to go forward with the recommendation to procure an additional LSS to achieve 16 LSSs. (lots more LSS detail omitted) With respect to the USA SAFER, NASA concurs with the ASAP recommendation on obtaining critical long lead components. In fact, the majority of the long lead components have already been procured. These components are expected to support the USA SAFER flight units for their 7-year life. NASA can normally support the requirement to maintain three USA SAFER flight units on orbit with five flight units in service. The current rotation plan utilizes two of the flight units to accommodate rotation of back-to-back missions where the turnaround time is approximately 1 month. With one flight unit out of service, four USA SAFER flight units can be rotated to maintain three units on orbit for 92 percent of the flights per the International Space Station (ISS) assembly sequence dated February 22, 1999.The remaining 8 percent of the flights can also be supported with contingent coordination ahead of time to reduce the turnaround time from approximately 1.5 months to approximately 1 month. (lots more SAFER detail omitted)

Independent Assessment Team *(Chartered by)*	Date of Report	Finding	Recommendation	NASA Response
Aerospace Safety Advisory Panel *(NASA Charter)*	February 1999	**Finding 25:** The NASA Standard Initiator (NSI) on a SAFER unit tested on STS-86 on October 1, 1997, did not activate because of a marginal design of the activating power supply. As a result, the unit could not function. The certification testing for the firing circuit did not identify the power supply inadequacy. Also, an inadequate NSI emulator was used for most of the original SAFER certification (qualification) and acceptance tests.	**Recommendation 25a:** The design and implementation of flight systems critical to safety and mission success should, at least, provide redundancy for system startup.	**NASA Response (in 1999 ASAP appendix):** NASA concurs with the ASAP finding that the NSI drive circuit of the USA SAFER was marginal in its design to the point where the drive circuit failed to activate the NSI during a demonstration on STS-86.The failure was due to lack of margin within the subsystem to drive the NSI and not due to lack of redundancy (a backup subsystem) to the subsystem. Adding redundancy (a backup subsystem) to drive the NSI would not resolve the lack of margin as both the primary and backup subsystems would still fail to drive the NSI without sufficient margin. This condition was addressed by addition of a new NSI circuit with increased margin to fire the NSI on demand. In addition the new NSI contains redundant components where possible. The USA SAFER is categorized as emergency hardware and is designed for use only after the EVA crewmember had inadvertently separated from structure due to a tether failure or a tether disconnection. The combination of the tether and USA SAFER provide a functional redundancy to each other and a fail-operational system, which can sustain one failure in the tether (functional after one failure) and still retains the capability to continue with the EVA. A subsequent failure of the tether (two failures) and a functional USA SAFER provide a fail-safe system,

Independent Assessment Team *(Chartered by)*	Date of Report	Finding	Recommendation	NASA Response
				which still retains the capability to successfully terminate the mission by using the USA SAFER to bring the inadvertently-separated EVA crewmember back to safety. Once the USA SAFER is needed to perform self-rescue in its role as the fail-safe device, its failure to perform due to any reason would result in loss of the EVA crewmember. Because the USA SAFER is to provide the fail-safe capability, as the functional redundancy to the tether, it was designed as a single-string system. As such, redundancy was not required for all subsystems and components. Adding redundancy to the activation subsystem alone would not increase the probability of saving an inadvertently separated crewmember since other critical subsystems (propulsion and mechanism) are still single-string. NASA will evaluate redesigning the next generation be fully redundant in critical functions.
			Recommendation 25b: All NASA Centers should review the design requirements for reliable activation of the NSI and assure they are adequate to be communicated to their suppliers, especially those who are responsible for the design of firing circuits. All designs currently using NSI's should be reviewed to assure that the firing circuits are adequate and have been appropriately tested.	**NASA Response (in 1999 ASAP appendix):** NASA agrees with the ASAP recommendation. The new USA SAFER NSI circuit employs the capacitive discharge approach which has been well proven by the SSP. Peer reviews were held to evaluate the new circuit design, and a series of tests were performed with the complete flight circuit. Also, the Engineering Directorate's Pyrotechnic Subsystem Manager performed a comprehensive review of all known uses of the NSI to ensure an acceptable design existed and that appropriate

Independent Assessment Team *(Chartered by)*	Date of Report	Finding	Recommendation	NASA Response
				certification/ acceptance tests had been accomplished. Lastly, a User's Guide (JSC-28596) for the NSI was developed to assist developers in selecting the appropriate NSI, designing the appropriate NSI drive circuit, and testing the complete NSI subsystem.
			Recommendation 25c: Qualification tests of safety-critical equipment must use flight-quality hardware. Any exceptions must require high-level program approval.	**NASA Response (in 1999 ASAP appendix):** NASA concurs with ASAP recommendation to use flight-quality hardware to support qualification testing. The new USA SAFER circuit certification was completed with the successful firing of 15 flight NSIs consecutively.
Aerospace Safety Advisory Panel *(NASA Charter)*	February 1999	**Finding 29:** The Space Shuttle General Purpose Computers (GPC) are outmoded and limit the ability to incorporate necessary software changes and hardware upgrades.	**Recommendation 29:** NASA should begin the process of replacing the Space Shuttle GPC's. As part of this effort, NASA should also modularize the flight software.	**NASA Response (in 1999 ASAP appendix):** The Space Shuttle Program is addressing the finding and recommendation identified by the ASAP. A review of the GPC and its flight software was performed in April 1998. Based on current estimates on GPC mean time between failures, the flight hardware and spares are expected to be available through at least 2016 (and likely significantly later). The flight software estimate on memory availability and usage has projected that memory capacity would be expected to reach its limit in the 2005-2006 timeframe. A software architecture strategy as part of the overall SSP avionics upgrade effort is being developed which will mitigate the memory capacity concern. This strategy will partition the critical software such as flight control and guidance from software that

Independent Assessment Team *(Chartered by)*	Date of Report	Finding	Recommendation	NASA Response
				requires periodic change. The result of this partition would allow those stable software functions like flight control to remain within the current GPC's while allowing those functions that frequently change to be migrated to a newer computer technology. The offloading of the software functions such as display processing and systems management from the current GPCs should permit current GPC memory capacity to remain acceptable through at least 2020. Additionally the software subject to frequent change would be located within a system, which will be designed to be more easily reconfigurable than the existing system. In summary, a supportability concern does not exist for the current GPCs. Continued use of the existing GPCs and their established processes will maintain high levels of safety. Software partitioning involving the offloading of software functions to a more flexible system will provide sufficient memory availability for future GPC software changes. This approach will provide an evolutionary and a migration path to full GPC upgrade if it is later required.
Aerospace Safety Advisory Panel *(NASA Charter)*	February 1999	**Finding 30:** There is no formal requirement that dependent Space Shuttle I-loads be recalculated or checked when an I-load patch is to be uplinked.	**Recommendation 30:** NASA should create a dependency matrix of all I-loads. Furthermore, it should assess its Space Shuttle and ISS procedures and ensure that they are all fully documented.	**NASA Response (in 1999 ASAP appendix):** NASA believes that we already meet the intent of the recommendation. Flight Operations processes and documentation ensures proper I-load change implementation for all flight design I-loads, including uplinkable I-loads. These procedures include positive verification that the selected or uplinked values do not violate subsystem,

Independent Assessment Team *(Chartered by)*	Date of Report	Finding	Recommendation	NASA Response
				element, or integrated vehicle certification and that the update meets mission requirements. I-load dependencies are verified as part of the certification assessment. Procedures for verifying I-loads to be uplinked vary. In some instances uplinked Iloads change vehicle response in a way that impacts several of the remaining I-loads; i.e., Day-of-Launch I-load Update (DOLILU). Those verification assessments include an analysis which uses a high fidelity computer model to simulate integrated vehicle response to the new I-loads. These simulations include models of the onboard flight software of sufficient detail to verify that all applicable I-load interactions are assessed. In other cases, specific I-load dependencies are evaluated. A number of flight design uplinks involve an uplink of values that are generated and verified days or sometimes months before launch. These I-loads include vehicle navigation, targeting, and abort parameters. Verification procedures for these I-loads are identical to that used during the normal flight design template. For all cases, procedures clearly specifying verification requirements including specific I-load dependency evaluations, as applicable, are in place and under configuration control.
Aerospace Safety Advisory Panel *(NASA*	February 1999	**Finding 31:** Present plans depend on human procedures to achieve lockout to prevent inadvertent or	**Recommendation 31:** NASA should use a computerized authorization to achieve lockout of commands to actual hardware from anyone not	**NASA Response (in 1999 ASAP appendix):** NASA concurs with the ASAP recommendation. The CLCS Project will undertake a study

Independent Assessment Team *(Chartered by)*	Date of Report	Finding	Recommendation	NASA Response
Charter)		unauthorized access to actual hardware when using the new Checkout and Launch Control System (CLCS).	authorized to issue such a command in CLCS.	with the Shuttle engineering community to determine how these lockouts could be implemented. The results will include a preliminary set of requirements for CLCS and other systems, such as the Shuttle Data Center and Simulation Systems, an operational risk assessment for implementing these changes, and a rough order of magnitude cost assessment for implementing these changes. The study will be completed in a timely manner so that implementation can be accomplished in time to avoid extensive revalidation of CLCS application software. Progress reports will be presented to the ASAP during their CLCS review meetings.
Aerospace Safety Advisory Panel *(NASA Charter)*	February 1999	**Finding 32:** NASA does not have a plan in place to deal with the problem of maintaining the many commercial off-the-shelf (COTS) software development tools used in its programs.	**Recommendation 32:** NASA should develop a general strategy and provide program wide guidelines for addressing the maintenance of COTS tools.	**NASA Response (in 1999 ASAP appendix):** NASA concurs with the finding that no program-wide plan exists addressing the maintenance of COTS software development tools. A programmatic action has been assigned to develop the usage requirements for COTS/modified off-the-shelf software including the associated development tools. These guidelines will document maintenance and selection guidelines to be used by all of the applicable program elements.
NASA Office of Safety and Mission Assurance *(NASA Charter)*	27 October 1998	The review team could not determine whether or not USA-proposed process improvements will achieve efficiencies necessary, in the time required, to support increased manifest demands in mid-to-late 1999.		

Independent Assessment Team *(Chartered by)*	Date of Report	Finding	Recommendation	NASA Response
NASA Office of Safety and Mission Assurance *(NASA Charter)*	27 October 1998	The team noted that opportunities exist to achieve efficiencies in administrative and management processes, which support the core work control/review and change control infrastructure. The strength of USA management leadership and commitment will determine the outcome.		
NASA Office of Safety and Mission Assurance *(NASA Charter)*	27 October 1998	In any event, NASA management must closely monitor implementation of proposed USA process initiatives to assure that a stable infrastructure, capable of handling sustained higher flight rates, is developed. Flight safety will be assured as long as key ground operations processes remain in place. When the ground operations system becomes saturated it will be important to understand how "people in the process" (human factors) respond.		
NASA Office of Safety and Mission Assurance *(NASA Charter)*	27 October 1998	Although no objective evidence was found to indicate that the work requirements would have any adverse impact on safety or quality, the KSC/SMA planning process is not sufficiently mature to provide evidence that the increased flight rate can be supported within current workforce ceilings.	It is recommended that the KSC/SMA organization notify the Office of Safety and Mission Assurance when it has completed the critical process definition effort and the workforce analysis planning. At that time a delta assessment will be performed to assess the completeness of the activity.	
Aerospace Safety Advisory Panel *(NASA*	February 1998	**Finding 1:** Operations and processing in accordance with the Space Flight Operations Contract	**Recommendation 1a:** Both NASA and the SFOC contractor, USA, should reaffirm at frequent intervals the dedication to safety before	**NASA Response (in 1998 ASAP appendix):** The Space Shuttle Program concurs with the ASAP affirmation that safety is our first priority. The

Independent Assessment Team *(Chartered by)*	Date of Report	Finding	Recommendation	NASA Response
Charter)		(SFOC) have been satisfactory. Nevertheless, lingering concerns include: the danger of not keeping foremost the overarching goal of safety before schedule before cost; the tendency in a success-oriented environment to overlook the need for continued fostering of frank and open discussion; the press of budget inhibiting the maintenance of a well-trained NASA presence on the work floor; and the difficulty of a continued cooperative search for the most meaningful measures of operations and processing effectiveness.	schedule before cost.	potential for safety impacts as a result of restructuring and downsizing are recognized by NASA at every level. From the Administrator down there is the communication of and the commitment to the policy that safety is the most important factor to be considered in our execution of the program and that restructuring and downsizing efforts are to recognize this policy and solicit and support a zero tolerance position for safety impacts. The restructuring efforts across the Program in pursuit of efficiencies which might allow downsizing of the workforce consistently stress that such efficiencies must be enabled by identification and implementation of better ways to accomplish the necessary work, or the unanimous agreement that the work is no longer necessary, but that in either case that the safety of the operations are preserved. In the case of the restructuring and downsizing enabled by the SFOC transition of some responsibility and tasks to the contractor, the transition plans for these processes and tasks specifically address the safety implications of the transition. Additionally, the Program has required the NASA Safety and Mission Assurance (S&MA) organizations to review and concur on the transition plans as an added assurance. Other Program downsizing efforts have similar emphasis embedded in the definition and implementation of their restructuring, and the S&MA organizations are similarly committed as a normal

Independent Assessment Team *(Chartered by)*	Date of Report	Finding	Recommendation	NASA Response
				function of their institutional and programmatic oversight to assure this focus is not compromised. Additionally, the Program priorities of 1) fly safely, 2) meet the manifest, 3) improve mission supportability, and 4) reduce cost are incorporated into almost every facet of planning and communication within both the NASA and contractor execution of the Program. Besides the continuous presentation of these priorities in employee awareness media, the Program highlights their relative order in the formal consideration of design and/or process changes being considered by the various Program control boards. Additionally, these priorities are the focus point for most of the Program management forums such as the Program Management Reviews and SFOC Contract Management Reviews (CMRs). They are specified as the basis for the Program Strategic Plan, as well as the SFOC goals and objectives used by the contractor and NASA to manage and monitor the success of the SFOC. Finally, these priorities are embedded in the SFOC award fee process (which provides for four formal reviews each year). Specifically, the award fee criteria provide for both safety and overall performance gates which, if not met by the contractor, would result in loss of any potential cost reduction share by the contractor. In summary, NASA and all of the contractors supporting the

Independent Assessment Team *(Chartered by)*	Date of Report	Finding	Recommendation	NASA Response
				Space Shuttle Program have always been and remain committed to assuring that safety is of the highest priority in every facet of the Program operation. While downsizing does increase the challenge of management to execute a successful Program, process changes, design modifications, employee skills maintenance, and reorganizations are all part of the management challenges to be faced and resolved, and maintenance of the high level of attention to safety in resolving these challenges is recognized by NASA and the contractors alike as not being subject to compromise.
			Recommendation #1b NASA should develop and promulgate training and career paths leading to qualification for senior NASA Space Shuttle management positions.	**NASA Response (in 1998 ASAP appendix):** While it is true that the roles for NASA management and technical personnel are being reduced in number and reshaped to focus on the critical areas of anomalies and changes, these roles and the ongoing role of assessing the contractor's performance against the contract and Program requirements should provide a continued source of trained and capable future NASA senior managers. NASA has an active commitment to development of the skills for senior managers for all functional areas of the Agency, and Space Shuttle Program senior managers are generally products of both their in-line experiences as well as these career development programs. It is anticipated at this time that the roles for NASA personnel and the career development programs which have served NASA well to this point will be sufficient to assure a

Independent Assessment Team *(Chartered by)*	Date of Report	Finding	Recommendation	NASA Response
				continuation of highly qualified and capable senior managers in the future. Given the nature of the still evolving definition of the NASA and prime contractor roles and responsibilities for the SFOC operational model, it is reasonable to provide special attention to this concern, and the Program will ensure that specific consideration is given to this concern in the transition plans being developed and implemented by the functional and institutional organizations across the Program.
			Recommendation 1c: NASA should continue to ensure that a trained and qualified Government personnel presence is maintained on the work floor.	**NASA Response (in 1998 ASAP appendix):** NASA/KSC has maintained a physical presence on the work floor since the beginning of the Shuttle Processing Contract and will continue this presence for SFOC, Payload Ground Operations Contract, and Base Operations Contract. NASA engineering, operations, safety, and quality personnel maintain a surveillance and audit presence of overall operations for insight purposes and are formally involved for selected tasks being performed. Presence on the floor monitoring hazardous or safety critical operations has been maintained through the transition to performance based contracting and will be maintained in the future. The frequency and depth of the insight and presence may be adjusted as justified by the results of the contractor's performance, but the value of these checks and balances has long been recognized by NASA and will be maintained. To a lesser degree, this same floor

Independent Assessment Team *(Chartered by)*	Date of Report	Finding	Recommendation	NASA Response
				presence is executed at production sites through Resident Office presence and periodic audit and surveillance activities by NASA Center personnel. While there is a focused initiative to minimize Government mandatory inspection points (GMIPs) across the Program, it is mutually recognized by NASA and USA that the criticality of some checks and balances in critical processes demands that some small percentage (10–15 percent) will be maintained on the production and processing floors. This presence also supports the desired training and qualification needs for NASA to remain a smart customer. Finally, there are functional roles anticipated for continued NASA participation, such as flight controllers, astronauts, and launch directors which will also provide a significant avenue for NASA skills maintenance in the long-term management model.
			Recommendation 1d: NASA and USA should continue to search for, develop, test, and establish the most meaningful measures of operations and processing effectiveness possible.	**NASA Response (in 1998 ASAP appendix):** Both NASA and USA recognize the value of meaningful measures of the operational and processing effectiveness for the Program and continually strive to evolve and improve on the measures currently in place. The SFOC Performance Measurement System (PMS) has been a significant development project since the beginning of the contract, continues to take shape as the primary repository for the performance metrics which

Independent Assessment Team *(Chartered by)*	Date of Report	Finding	Recommendation	NASA Response
				provide management insight into the cost, and technical performance across the complete contract. Once the system is complete and populated with viable metrics, NASA will validate the system. The goal is to complete the validation by the fall of 1998. Key metrics are reviewed quarterly at the SFOC CMR, and individual functional areas such as flight operations and ground processing use these on a continual basis for their management execution and insight. Additional measures are continually developed at the Program level and within individual functional areas to enhance the understanding of performance trends, and when proven to be effective management tools, these metrics roll into the PMS and/or other forums and products used to manage the Program.
Aerospace Safety Advisory Panel *(NASA Charter)*	February 1998	**Finding 2:** The Kennedy Space Center (KSC) has been successfully phasing in the structured surveillance process for safety and quality for some time. The development of metrics using structured surveillance information has lagged data collection.	**Recommendation 2:** KSC should continue to expand the use of structured surveillance and to focus effort on the development of valid and reliable metrics to assess program performance from structured surveillance results.	**NASA Response (in 1998 ASAP appendix):** We concur. The development of reliable metrics with which to measure performance of the SFOC in all areas including safety and quality is progressing at KSC. There are several examples of this. At KSC, NASA Safety has developed a data base for the Space Shuttle Program, revised its surveillance approach, and developed a method by which proper measurements can be evaluated and analyzed in determining safety program management effectiveness and contractual statement of work compliance. These new metrics will enable NASA

Independent Assessment Team *(Chartered by)*	Date of Report	Finding	Recommendation	NASA Response
				Safety to more effectively measure contractor performance. The Quality Surveillance Record data base is currently being modified to clarify the method by which deficiencies and observations are counted and to better define failure codes and other data collected. These changes will increase the reliability of the data used to assess program performance and will be implemented in early July. In the interim, the existing data base has been modified and focuses on surveillance data collection for tasks which GMIPs were deleted through the GMIP reduction efforts. KSC has developed an expanded surveillance system that will provide extensive insight into the contractor's overall operation by process analysis. The process analysis program was initiated in October 1997, and there are presently 11 Quality Process Analysts working the pilot program at KSC. This system will provide added insight into the contractor's processes, procedures, and policies.
Aerospace Safety Advisory Panel *(NASA Charter)*	February 1998	**Finding 3:** NASA Safety and Mission Assurance (S&MA) auditors at KSC overseeing operations requiring Self-Contained Atmospheric Protective Ensemble (SCAPE) are not certified for SCAPE.	**Recommendation #3:** In order to be in a position to conduct valid safety and quality audits of SCAPE operations, NASA should ensure that personnel involved are certified so that, when necessary, they can observe the tasks while they are performed.	**NASA Response (in 1998 ASAP appendix):** The Space Shuttle Program concurs that safety and quality audits of SCAPE operations be performed. However, KSC's position is that NASA's safety and quality personnel monitoring SCAPE tasks will not be exposed to the additional risk of SCAPE operations as personnel can accomplish monitoring tasks by observing and communicating through the

Independent Assessment Team *(Chartered by)*	Date of Report	Finding	Recommendation	NASA Response
				audio and video capabilities of the Operational Intercommunication System and operational television (OTV). All SCAPE tasks are conducted on recorded communications channels that are monitored in the control room, and the majority of tasks are observable on the OTV system. NASA quality and safety personnel have performed those audits for several years without being SCAPE certified.
Aerospace Safety Advisory Panel *(NASA Charter)*	February 1998	**Finding 4:** To compensate for skills deficiencies related to staff departures from KSC, both NASA and USA are making extensive use of cross training of personnel, both technicians and engineers. Individuals who have been cross-trained also should have recent "hands-on" experience before they undertake a cross-trained task.	**Recommendation 4:** NASA and USA should develop and use valid and reliable measures of the readiness of personnel to take on tasks for which they have been trained but on which they have only limited or episodic experience. The cross-training program could include a regularly scheduled rotation of duties so that the multiply trained individual has the opportunity to employ all of the acquired skills and knowledge at appropriate intervals.	**NASA Response (in 1998 ASAP appendix):** NASA is in full agreement with the Panel's position that individuals who have been cross-trained also should have recent hands-on experience before performing tasks. The combined NASA/USA training and certification plan identifies those skills that require hands-on training as part of the certification process. Personnel selected for cross-training are required to be certified to perform other jobs in the same family of skills (i.e., mechanical systems, avionics systems, electrical distribution systems). With this knowledge base, those identified for cross-training will be required to meet the same training and performance requirements established for the given task. Performance is measured to verify that the individual has obtained the stated objectives of the instructional tool being used. In the case of hands-on training, the employee is required to demonstrate 100% command of the task being performed. The certification process is controlled by the

Independent Assessment Team *(Chartered by)*	Date of Report	Finding	Recommendation	NASA Response
				KSC Certification Board, which operates under approved certification procedures. The Certification Board, chaired by the USA S&MA Director at KSC, approves and implements certification/recertification requirements.
Aerospace Safety Advisory Panel *(NASA Charter)*	February 1998	**Finding 5:** The reduction of Government Mandatory Inspection Points (GMIP) at KSC has significantly lagged the downsizing of NASA quality personnel responsible for processing these GMIPs. This has resulted in an expanded workload among remaining NASA quality inspectors and made it more difficult to conduct analyses needed to identify further GMIP reductions. There has been a similar reduction of NASA safety inspectors and engineers at KSC without a commensurate reduction in oversight requirements while, at the same time, the addition of new safety audit or insight responsibilities has taken place.	**Recommendation 5:** Any downsizing of personnel by both NASA and USA should be preceded by the reduction of commensurate workload associated with Space Shuttle processing, such as reduction of GMIPs and NASA safety inspections.	**NASA Response (in 1998 ASAP appendix):** NASA concurs with the recommended approach of reducing the workload in Space Shuttle processing before proceeding with downsizing NASA and USA personnel; however, we have not been as successful in this area as desired. In the downsizing effort implemented in February 1998, USA experienced an unexpectedly high level of voluntary attrition in certain critical functions - an outcome that was predicted by ASAP members and others. Although USA experienced shortages of critical skills and staffing to minimum levels for short periods of time in selected areas, USA and NASA worked together to overcome these deficits and assure that the scheduled missions through STS-91 were safely executed. This was done by a combination of launch schedule relief, back-filling USA shortages with NASA expertise, and re-hiring technical expertise to train and certify USA staff, thus eliminating shortages in critical skills. Evaluation of GMIPs for potential elimination by process engineering and quality engineering staff continues. It is estimated that approximately 6,000 of the original 22,000 GMIPs will

Independent Assessment Team *(Chartered by)*	Date of Report	Finding	Recommendation	NASA Response
				remain in place at the end of this effort. This is a level assessed as commensurate with the current NASA quality inspection workforce. NASA Headquarters Office of Safety and Mission Assurance (OSMA) continues to evaluate the situation at KSC regarding NASA and USA workforce reductions by assessing process efficiencies and workload indicators. Indicators of process effectiveness include overtime rates and first-time quality rates. Although the efforts are not yet complete, OSMA anticipates that as GMIPs are reduced overtime rates for NASA quality inspections will drop. Additionally, if the development of process efficiency initiatives by USA are effective, then, when implemented, OSMA anticipates that USA engineering and technician overtime rates will drop and first-time quality rates, based on NASA surveillance sampling, will increase.
Aerospace Safety Advisory Panel *(NASA Charter)*	February 1998	**Finding 6:** The Super Light Weight Tank (SLWT) has completed its design certification review, and proof tests on the first tank have been satisfactorily passed. The only remaining test to complete certification of the SLWT is the cryogenic loading test that will be run on the first production tank on the launch pad. The diligent attention that has been given to quality control, particularly to material inspection and weld integrity, has made this program successful.	**Recommendation 6:** NASA should ensure that the current manufacturing and quality control procedures continue to be rigidly adhered to and conscientiously followed in production.	**NASA Response (in 1998 ASAP appendix):** NASA concurs with this recommendation. MSFC and Lockheed Martin Michoud Space Systems (LMMSS), the External Tank prime contractor, periodically perform a NASA Engineering and Quality Audit (NEQA) which focuses on both the processes and the flight hardware. The audit is conducted by experienced MSFC and LMMSS technical and management personnel and the operators and inspectors that actually utilize those processes. LMMSS also performs internal and supplier audits throughout the year. In

Independent Assessment Team *(Chartered by)*	Date of Report	Finding	Recommendation	NASA Response
				addition, on-site MSFC Science and Engineering, Safety and Mission Assurance, and DCMC personnel provide continuous insight and guidance through surveillance and limited oversight activities. Finally, adherence to manufacturing and quality control procedures is one of the primary focuses of the on-site government personnel.
Aerospace Safety Advisory Panel *(NASA Charter)*	February 1998	**Finding 9:** Support of the Space Shuttle fleet with operational spares has been maintained by the effective efforts of the logistics function. While spares support has been adequate for the current flight rate, any increase in flight rate might not be supportable.	**Recommendation 9:** Although NASA has established programs for dealing with suppliers and bringing additional component overhaul "in house," efforts in these areas need to be continuously reexamined to speed up the restoration and upgrading of line-replaceable units. Such efforts are especially needed to eliminate "dead" time while units are awaiting restoration.	**NASA Response (in 1998 ASAP appendix):** The Space Shuttle Program concurs with the ASAP concerns for the availability of line replaceable units (LRUs). Logistics monitors LRU spares posture through the probability of sufficiency calculations within the LRU data system. This system can be programmed to determine spares requirements for various flight rates. At this time, an appreciable increase in flight rate would be required to jeopardize supporting the Space Shuttle Program with most of the current LRUs. (Lots of detail omitted) Additionally, through the use of industrial engineering principles and work teams, Logistics has taken action to reduce the NASA Shuttle Logistics Depot (NSLD) backlog and increase output for fiscal year 1998. To date, backlog has decreased 8 percent since October 1 by increasing output. These efforts are aimed at providing better support at the current flight rate but are also the type of efforts that will allow higher flight rates in the

Independent Assessment Team *(Chartered by)*	Date of Report	Finding	Recommendation	NASA Response
				future.
Aerospace Safety Advisory Panel *(NASA Charter)*	February 1998	**Finding 10:** Transition and development of the logistics tasks for the orbiter and its ground operations under the SFOC are proceeding efficiently and according to plan.	**Recommendation 10:** NASA and USA should continue the task of management integration of the formerly separate logistics contracts and retain and expand the roles of the experienced logistics specialists therein.	**NASA Response (in 1998 ASAP appendix):** The Space Shuttle Program concurs with the ASAP philosophy of logistics integration. Integrated Logistics has been successful in integrating Ground Logistics and more recently, Flight Operations Logistics with Orbiter Logistics insight. As new elements are integrated within USA, the sharing of new techniques and best in class practices is occurring. Logistics is recognized as a key member of both the NASA and contractor teams; their input is actively sought on key decisions, and they are members of key decision-making boards and panels.
Aerospace Safety Advisory Panel *(NASA Charter)*	February 1998	**Finding 11:** As reported last year, long-term projections are still suggesting increasing cannibalization rates, increasing component repair turnaround times, and loss of repair capability for the Space Shuttle logistics programs. If the present trend is not arrested, support difficulties may arise in the next 3 or 4 years.	**Recommendation 11:** NASA and USA should reexamine and take action to reverse the more worrying trends highlighted by the statistical trend data.	**NASA Response (in 1998 ASAP appendix):** The Space Shuttle Program has recognized the concerns for long-term supportability and is proactively pursuing improvements. Cannibalizations continue to be closely monitored and are well within limits. There have been several concerns during this past year (seals and cryo heater controllers) that are requiring the adjustment of sparing levels. The Logistics organization is aggressively pursuing a solution to specific problems as well as pursuing innovations to keep the rate below the standard. As mentioned in the response to Finding #9, the NSLD backlog is now decreasing as

Independent Assessment Team *(Chartered by)*	Date of Report	Finding	Recommendation	NASA Response
				a result of USA action. This should ultimately reduce the repair turn around time for hardware although short term increases can be expected. Other initiatives such as the replacement of unserviceable test equipment at vendors are also in progress. Logistics and Engineering are developing common tools to integrate upgrade actions, resolve supportability issues, and mitigate the loss of repair capability. The Problem Resolution Teams have increased the interfaces with Logistics, Engineering, and management to ensure a proactive and integrated effort in identifying problem areas and identifying solutions. Numerous initiatives are under way. Finally, NASA has funded through Space Shuttle upgrades the prototyping of a new expert logistics system which shows promise in ranking issues according to severity. This data might then be used to assure that limited funding available is used as economically and wisely as possible in order to minimize risk in the most vulnerable areas.
Aerospace Safety Advisory Panel *(NASA Charter)*	February 1998	**Finding 19:** The Checkout and Launch Control System (CLCS) program at KSC has not been provided with funding for Independent Verification and Validation (IV&V) that is safety critical for a software effort of this size.	**Recommendation 19:** The CLCS should be provided with adequate funding for software IV&V.	**NASA Response (in 1998 ASAP appendix):** KSC concurs with the ASAP recommendation relative to IV&V funding for the CLCS Project. A Memorandum of Agreement (MOA) was signed on May 5, 1998, between the Software IV&V Facility and KSC, for the performance application of IV&V techniques and methods to the CLCS software. The scope of this

Independent Assessment Team *(Chartered by)*	Date of Report	Finding	Recommendation	NASA Response
				memorandum will include performing IV&V on selected catastrophic/critical/high risk CLCS software components. The selected software components will consist of CLCS system software. The specific areas to be analyzed will be system redundancy, command support, data distribution and processing, constraint management, and the safing system related software. The software related to safing includes the Emergency Safing System and those control logic modules associated with safing (some of which may reside within application software). The analysis will consist of requirements, design, code, and test analysis, as applicable for the life cycle of the software being analyzed. The application interfaces with the system software will also be analyzed. In addition, the IV&V Facility will perform system level analysis of the system test plan and system tests performed along with software engineering and integration analysis of the CLCS system as a whole. This MOA is effective from May 1, 1998, until September 30, 2000. The work identified in this MOA will require a staffing level of about 16 full time equivalents (FTEs). This staffing level will be comprised of 15 FTEs from the IV&V contractor located at the IV&V Facility and at KSC. The remaining one FTE will be a civil service personnel. Staffing at KSC

Independent Assessment Team *(Chartered by)*	Date of Report	Finding	Recommendation	NASA Response
				will be comprised of eight contractor FTEs with the remainder residing at the Fairmont Facility. The Space Shuttle Program has agreed to fund this effort at $4.5M over the life of the MOA.
Aerospace Safety Advisory Panel *(NASA Charter)*	February 1997	**Finding 1:** One consequence of the implementation of the Space Flight Operations Contract (SFOC) is a reduction in opportunities for NASA personnel to maintain detailed, day-to-day work floor interfaces with their contractor counterparts both at space flight centers and major contractor facilities. This could compromise NASA's ability to carry out its assessment function.	**Recommendation 1:** In order to carry out its assessment role, NASA must maintain some physical presence on the work floor at the space flight centers and major contractor facilities. NASA must ensure that the people staffing these surveillance positions are and continue to be appropriately skilled, thoroughly knowledgeable about the Space Shuttle, and sufficiently experienced with both the subsystem they oversee and the total Space Shuttle system.	**NASA Response (in 1997 ASAP appendix):** NASA concurs with the finding and is sensitive to the need to maintain a skilled and capable workforce in both the management and technical functions necessary for Space Shuttle program (SSP) success, and the Agency will work with the contractor in establishing the eventual organizational roles and responsibilities to assure that success. The transition process will be managed at a pace to ensure that necessary skills are maintained within the Government/contractor workforce. The assessment function that NASA will perform in the future Shuttle operations architecture will require the maintenance of a solid skill base within the Agency. NASA will retain the capability to review all anomalies in operations and system performance, as well as all changes to operations and to systems. NASA's role in requirements control will also provide continuous exposure to designs and operations within the program. The participation of NASA engineering and management in the development of Shuttle upgrades will provide further opportunity for the maintenance of an inherent skill base. Finally, there will

Independent Assessment Team *(Chartered by)*	Date of Report	Finding	Recommendation	NASA Response
				be functional roles for NASA personnel, such as astronauts, flight controllers, and mission directors, that will provide an avenue for skills development and maintenance.
Aerospace Safety Advisory Panel *(NASA Charter)*	February 1997	**Finding 2:** It is not clear how NASA Space Shuttle supervisory personnel will be trained and acquire the experience levels necessary to function effectively in senior management positions when the SFOC is fully implemented and the traditional learning ladder positions are staffed by the contractor.	**Recommendation #2:** NASA should develop and promulgate training and career paths leading to preparation and qualification as potential senior NASA Space Shuttle management.	**NASA Response (in 1997 ASAP appendix):** NASA has an active commitment to the development of the skills of senior managers for all functional areas of the Agency. Space Shuttle program senior managers are generally products of both their in-line experiences as well as the NASA career development programs. It is anticipated at this time that the roles for NASA personnel and the career development programs that have served NASA well to this point will be sufficient to assure a continuation of highly qualified and capable senior managers in the future. Given the evolving nature of the NASA and prime contractor roles and responsibilities for the SFOC operational model, it is reasonable to focus special attention on this issue; the program will ensure that specific consideration is given to management development in the transition plans being developed and implemented across the program.
Aerospace Safety Advisory Panel *(NASA Charter)*	February 1997	**Finding 3:** No objective measure has yet been developed, or is likely possible, that can shed significant light on the impact of downsizing on the safety of Space Shuttle operations.	**Recommendation 3:** In the absence of a valid predictive safety metric, NASA should ensure that all functions affected by downsizing and necessary for safe operations are assigned to people who have the knowledge, skills, and time to carry them out.	**NASA Response (in 1997 ASAP appendix):** NASA concurs; all of the contractors supporting the Space Shuttle program remain committed to assuring that safety is the highest priority in every facet of the program. The program recognizes the concerns that downsizing may raise, and it will assure that knowledgeable and skilled individuals are assigned to all

Independent Assessment Team *(Chartered by)*	Date of Report	Finding	Recommendation	NASA Response
				critical Shuttle functions, including those being downsized. The plans for the transition of processes and tasks under the SFOC specifically address the safety implications of the transition. As an added assurance, the Shuttle program has required that the NASA Safety and Mission Assurance (SMA) organizations review and concur on the transition plans. Other program downsizing efforts have a similar emphasis on safety embedded in them, and both program management and the SMA management are committed to assure that this focus is not compromised.
Aerospace Safety Advisory Panel *(NASA Charter)*	February 1997	**Finding 4:** Post-flight discovery of a wrench and an equipment nameplate in the forward skirt of one STS-79 Solid Rocket Booster (SRB) has heightened concern for the overall integrity of Space Shuttle processing quality assurance procedures.	**Recommendation 4:** NASA, in concert with the several Space Shuttle contractors, should conduct an in-depth review of Space Shuttle processing quality assurance procedures focused on creating a more formal, documented approach to accounting for tools and other material introduced to and removed from flight hardware work areas.	**NASA Response (in 1997 ASAP appendix):** The Space Shuttle program element contractors presented their tool control programs to the Space Shuttle System Safety Review Panel (SSRP) meeting in December 1996. The SSRP reviewed the tool control programs of all the contractors and determined that each of the tool programs was effective for the type of work performed. The SSRP recommended that tool accounting audits be maintained or increased, and that metrics be maintained to assure that each tool control program remains effective. In a letter dated March 20, 1997, the Space Shuttle Systems Integration Office confirmed that NSTS 07700, "Space Shuttle Program Definition and Requirements," requires tool control for only the launch and landing project, and recommended that Volume XI of NSTS 0770 be expanded to include tool control at the manufacturing

Independent Assessment Team *(Chartered by)*	Date of Report	Finding	Recommendation	NASA Response
				facilities. A change request to NSTS 07700, Volume XI, adding the program requirement to include tool control at the element manufacturing facilities, was approved by the Program Requirements Control Board (PRCB) on July 10, 1997.
Aerospace Safety Advisory Panel *(NASA Charter)*	February 1997	**Finding 5:** NASA plans to operate the Space Shuttle until at least 2012. This will require safety and operational upgrades to hardware, software, and logistics support.	**Recommendation 5:** NASA should complete Space Shuttle upgrades as soon as possible to take advantage of opportunities for earliest risk reduction and operational improvement.	**NASA Response (in 1997 ASAP appendix):** The SSP upgrade strategy is founded on the premise that safety, reliability, and supportability improvements must be made to support human space transportation until a suitable replacement is available. To manage and focus these efforts more effectively, the SSP established the Office of SSP Development on January 16, 1997. The Space Shuttle upgrades program is being implemented from a systems perspective. Upgrades will be integrated and prioritized across all flight and ground systems, ensuring that individual upgrades are compatible and that their impact is assessed across the entire program. A phased approach to the SSP upgrades is already under way. Phase I, to be completed by the year 2000, emphasizes safety and performance enhancements for the International Space Station (ISS) assembly and utilization. Ongoing efforts within all SSP elements are also under way to identify Phase II candidate and Phase III/IV studies. Primary emphasis remains on safety and risk reduction by improving reliability and maintainability, eliminating obsolescent components, and

Independent Assessment Team *(Chartered by)*	Date of Report	Finding	Recommendation	NASA Response
				improving vehicle performance. As those upgrade candidates are identified by the program elements, the SSP is committed to expediting implementation to maximize safety and reduce overall program risk.
Aerospace Safety Advisory Panel *(NASA Charter)*	February 1997	**Finding 6:** The orbiter Reaction Control System (RCS) thruster valves continue to leak in flight. NASA h as aggressively attacked this problem with some success. Procedural changes have improved thruster reliability, and the incidence of leakage has been reduced but not eliminated.	**Recommendation 6:** Continued attention must be focused on the elimination of the root causes of RCS valve leakage/failures.	**NASA Response (in 1997 ASAP appendix):** Several remedial actions have been and are being implemented as a result of a 1995 tiger team investigation into the causes of RCS valve leakage/failure. This has resulted in many procedural changes and several potential hardware improvement concepts. The procedural changes are reducing the number of in-flight thruster valve failures. Many of the hardware improvements are entering a development testing phase. Examples of procedure and hardware changes include: (examples omitted)
Aerospace Safety Advisory Panel *(NASA Charter)*	February 1997	**Finding 7:** A new gas generator valve module for the Improved Auxiliary Power Unit (IAPU) is currently entering the process of certification. When fully certified, the IAPU with this new valve is planned to be qualified for 75 hours of operation between scheduled teardowns and overhauls (in excess of 10 years at projected use rates).	**Recommendation 7:** Once certification is achieved for 75 hours of IAPU operation, NASA should establish a periodic inspection and test program to assure that IAPUs continue to perform in accordance with requirements throughout their service life.	**NASA Response (in 1997 ASAP appendix):** An IAPU maintenance plan is being developed by the NASA and contractor technical community. Current activity is focused on developing a maintenance specification, evaluating long-term life of elastomeric components, and organizing a parts tracking/usage database. At the conclusion of this effort in late FY 1997, a longterm maintenance plan will be baselined for implementation. Supplementing this to provide long-term service life information is a fleet leader test program at WSTF. The WSTF program is currently

Independent Assessment Team *(Chartered by)*	Date of Report	Finding	Recommendation	NASA Response
				scheduled to conclude in FY 1999 and is to demonstrate 75-hour run time and evaluate 10+ year teardown and overhaul time.
Aerospace Safety Advisory Panel *(NASA Charter)*	February 1997	**Finding 8:** The Space Shuttle is about to receive two major avionics upgrades - a triple redundant Global Positioning System (GPS) installation and the Multi-Function Electronic Display System (MEDS)- both of which require significant changes to the Primary Flight Software (PFS) and Backup Flight Software (BFS) systems.	**Recommendation #8:** The Space Shuttle program should ensure that both the GPS and MEDS software changes are thoroughly tested in the Shuttle Avionics Integration Laboratory (SAIL) using the normal and enhanced test protocols that have proved to be robust when testing major modifications.	**NASA Response (in 1997 ASAP appendix):** The SSP concurs that all software and hardware changes need thorough testing, and it recognizes the extremely important role that SAIL testing fulfills in the complement of testing for software certification. All Shuttle software or hardware upgrades are assessed to determine integrated verification test requirements. The SSP and its contractors cooperate to produce integrated hardware and software test implementation plans, test requirements documents, and integrated test schedules to assure that the required resources, including SAIL, are available. All these plans are reviewed and approved by the program. Thorough testing of each new capability is then performed and analyzed. This same rigorous process that is used for flight software Operational Increment (OI) updates will be applied to the MEDS, GPS, other Shuttle upgrades, and future software updates.
Aerospace Safety Advisory Panel *(NASA Charter)*	February 1997	**Finding 9:**The Multi-Function Electronic Display System (MEDS) in the orbiter is being implemented with display functions and formats that mimic the present electro-mechanical and cathode ray tube presentations. There are significant potential safety and operational benefits from	**Recommendation 9:** The Space Shuttle program should commit to a significantly enhanced MEDS display as soon as possible. The MEDS advanced display working group or a similar multidisciplinary team should be tasked with identifying specific modifications and an associated timetable so that the opportunities inherent in MEDS	**NASA Response (in 1997 ASAP appendix):** The SSP has established an enhanced MEDS program that includes hardware and software enhancements to take full advantage of MEDS capabilities. This includes hardware expansion as well as utilization of inherent MEDS capabilities to provide better displays and improve crew

Independent Assessment Team *(Chartered by)*	Date of Report	Finding	Recommendation	NASA Response
		enhancing the amount, type, and format of information shown on the MEDS displays.	can be realized.	situational awareness. Additionally, an SSP Cockpit Upgrade Team is being formed to develop advanced display and application concepts for future implementation into MEDS/enhanced MEDS/future avionics upgrades capability. The Cockpit Upgrade Team will also participate in avionics upgrades discussions in order to anticipate future hardware and software changes and develop advanced cockpit applications to further improve crew awareness and reduce crew training requirements. Initial testing of new applications for enhanced MEDS will begin in June 1997.
Aerospace Safety Advisory Panel *(NASA Charter)*	February 1997	**Finding 10:** The Block II SSME development program has proceeded well, except for the Alternate Turbopump Program High Pressure Fuel Turbopump (ATP HPFTP). The HPFTP has suffered significant failures in testing, which were traced to shortcomings in hardware design details. Corrective actions have been implemented on the HPFTP. Block II engine testing has resumed for this major safety improvement.	**Recommendation 10:** Continue the development and certification test programs as originally planned. Accumulate the specified test operating times for the modified ATP HPFTP, and employ the number of test pumps as per the original test plan.	**NASA Response (in 1997 ASAP appendix):** The SSME project is committed to meet the original development and certification plan requirements. The schedule for certification has been adjusted to accommodate comprehensive resolution of the development problems. Scheduled completion of certification testing is now February 1998. As originally planned, the total "hot-fire time" for development and certification will exceed 60,000 seconds, utilizing eight HPFTP units. Certification will be based on two units with 22 tests each, and "hotfire time" of 11,000 seconds per pump or 22,000 seconds total certification time.
Aerospace Safety Advisory Panel *(NASA*	February 1997	**Finding 11:** The schedule for the first flight of the Block II engine has slipped, from September 1997 to December 1997.	**Recommendation 11:** Maintain the full scope of the planned test programs. Assure the availability of test stand A-2 at SSC for as long as it is	**NASA Response (in 1997 ASAP appendix):** The development and certification test programs will be maintained as originally

Independent Assessment Team *(Chartered by)*	Date of Report	Finding	Recommendation	NASA Response
Charter)		This schedule is optimistic and contains no slack for future development problems. The schedule also requires continued availability of three test stands at the Stennis Space Center (SSC).	needed for the Block II engine test programs so that three test stands continue to be available.	planned. Test stand availability has been coordinated with other program test requirements to support completion of Block II HPFTP certification testing in February 1998. Three test stands are required only until July 1997 to support this schedule. A mid-May milestone to initiate construction authorization for the July reconfiguration of Test Stand A-1 for X-33 testing will be reassessed based on fuel pump development status at that time. The other two test stands will remain dedicated to SSME testing. After test stand modification, conversion back to SSME test configuration would take approximately 1 month. The first flight of the Block II configuration has been reassigned to STS-91, currently scheduled for May 1998. Due to the development problems with the ATP HPFTP and the associated schedule slips, the SSP has elected to certify an interim Block II configuration, designated Block IIA. Block IIA will consist of Rocketdyne's current HPFTP in conjunction with the other Block II components and will provide the safety and reliability benefits of the large throat main combustion chamber at the earliest opportunity. This configuration will be certified to fly nominal missions at 104% to 104.5% rated power level (RPL) and will maintain the current 109% RPL contingency abort capability.

Independent Assessment Team *(Chartered by)*	Date of Report	Finding	Recommendation	NASA Response
Aerospace Safety Advisory Panel *(NASA Charter)*	February 1997	**Finding 12:** The Block II engine will be certified for operation at 109% power level only for abort situations. Accordingly, the test program provides only limited cumulative test time at this thrust level.	**Recommendation 12:** After completion of the current planned Block II certification test program, conduct a certification extension test program that will demonstrate the highest thrust level for safe continuous operation achievable by the Block II configuration. This program should attempt to achieve at least the 109% power level.	**NASA Response (in 1997 ASAP appendix):** The Block II program was developed to "improve the safety, reliability, and robustness of the SSME" by providing lower operating temperatures, pressures, shaft speeds, and other critical parameters. An increase in operating power level from 104% to 104.5% will offset some of the weight gain of Block II. The Block II SSME was never intended to increase Space Shuttle ascent performance or increase payload capability to orbit. However, additional performance has been accepted for a few specific missions at the cost of some of the improved safety margin. There is a commitment that the ISS flights will provide 106% engine power level certification to achieve mandatory critical payloads to orbit. The Block II certification will also provide a 109% intact abort capability, which will allow the vehicle system to better optimize abort scenarios. Implementation recommendations for use of 109% throttle for intact aborts will be made by the Shuttle operations element once certification is complete.
Aerospace Safety Advisory Panel *(NASA Charter)*	February 1997	**Finding 13:** Changes in the Pressure Sensitive Adhesive (PSA) and the cleaning agent for the J-flap of the RSRM were driven by environmental regulations. The certification testing for these changes included a Flight Support Motor (FSM) firing without the application of side loads,	**Recommendation 13:** Employ the application of side loads in all future RSRM FSM firings.	**NASA Response (in 1997 ASAP appendix):** The SSP and RSRM project agree with this recommendation when aft field joint test objectives warrant inclusion on an FSM test motor. During Space Shuttle return-toflight RSRM redesign, the assessment of strut loading on the solid rocket motors concluded that the only influence was at the

Independent Assessment Team *(Chartered by)*	Date of Report	Finding	Recommendation	NASA Response
		a significant condition for RSRM field joints for which the J-flap plays a role.		aft field joint. The influence on the aft field joint gap openings was predicted to be less than 0.001 inch, roughly an order of magnitude less than the contribution of the internal motor pressures. Side loads were included on two RSRM static test motors (QM-7 and -8) in a comprehensive effort to include every element of flight loading influencing the aft field joint gap openings. Joint gap openings were not measured directly, but the sealing systems performed as expected. Gap openings were measured on the RSRM structural test article-3, where testing showed side loads influence to be less than 0.0005 inch out of a total of 0.0084 inch for aft field joints only. The consideration to include side loads on all future tests would not come without technical penalty. To accommodate the side load forces, the aft test stand must be locked out, and as such, no thrust measurements are obtained. Also, no thrust vector control (TVC) duty cycling is performed during the side load events, which requires modification to the baseline static test duty cycle; for certain test objectives, this is an important requirement consideration. This baseline TVC duty cycle is utilized to allow direct performance comparisons between static tests, primarily associated with nozzle and aft dome materials or components. Therefore, a generic inclusion of side loads on all future FSM tests would require elimination of other test

Independent Assessment Team *(Chartered by)*	Date of Report	Finding	Recommendation	NASA Response
				considerations, which, depending on specific test objectives, might be a qualification necessity. In conclusion, the RSRM static test policy includes side loads on full-scale static test motors where there are test objectives associated with the aft field joints, which could be influenced by side loads.
Aerospace Safety Advisory Panel *(NASA Charter)*	February 1997	**Finding 14:** There are many material and process changes in work for the RSRM in response to both environmental regulations and obsolescence issues. A vital part of the certification program for these changes is the demonstration of the acceptability of the changes during an FSM firing. At present, FSM firings are scheduled at 2-year intervals instead of the 1-year or 18-month intervals previously used.	**Recommendation 14:** Considering the large number of changes in RSRM materials and processes and the importance of proper simulation of operating conditions in any certification test program, NASA should re-evaluate its decision to have 2 years between FSM firings.	**NASA Response (in 1997 ASAP appendix):** The RSRM project presented an assessment of static test motor frequency to the PRCB on February 27, 1997, and recommended static tests at 1-year intervals. The recommendation was accepted by the PRCB. An initiative is under way to ensure that the maximum possible benefit is obtained from each test.
Aerospace Safety Advisory Panel *(NASA Charter)*	February 1997	**Finding 15:** A substantial program effort is under way to eliminate the asbestos used in RSRM manufacture and replace it with more environmentally acceptable (i.e., "asbestos- free") materials. Although some of the materials tested to date meet specifications, they do not provide as high structural and thermal margins as the asbestos-containing materials.	**Recommendation 15:** To maintain flight safety, NASA should not eliminate the use of asbestos in RSRM manufacture. An environmental waiver should be obtained to continue its use in RSRM insulation, liners, inhibitors, and other motor parts in the event of future regulatory threat to the asbestos supplier.	**NASA Response (in 1997 ASAP appendix):** NASA currently has no plan to introduce nonasbestos-based replacements for asbestos-based components in RSRM production. The RSRM production and flight history are baselined with asbestos-based materials, primarily NBR rubber. Asbestos is also a constituent of liner and adhesives. The production, handling, and disposal processes for these materials are performed in compliance with strict state, Federal, and local controls and regulations regarding asbestos material. There are no currently identified regulations to ban

Independent Assessment Team *(Chartered by)*	Date of Report	Finding	Recommendation	NASA Response
				production or use of asbestos materials in the RSRM supply chain. Because there is no existing or pending regulation, pursuit of waivers or exemptions is not applicable at this time. NASA considers it prudent to continue low-level development of possible alternative nonasbestos materials. This reflects NASA's sensitivity to the environment, worker safety and health issues, and the fact that the shelf life of these materials precludes the option to stockpile. This development effort is being carried out to provide limited contingency development at a routine pace. The recommendations by both the ASAP and the RSRM initiatives to find alternative materials are consistent with program policy documented in SSP letter MS 96-071, dated September 16, 1996. The policy seeks to balance flight safety and environmental protection goals.
Aerospace Safety Advisory Panel *(NASA Charter)*	February 1997	**Finding 16:** The 2195 aluminum-lithium alloy used in the tank walls and domes of the new Super Light Weight Tank (SLWT) has a lower fracture toughness at cryogenic temperatures than was anticipated in the design. To compensate for this potentially critical short-coming, NASA has limited the pressure used in the full tank proof test and has recognized that acceptance of each SLWT for flight is highly	**Recommendation 16a:** Assure that the acceptance tests of the 2195 material and the quality control procedures used in the manufacture of each SLWT continue to be sufficiently stringent, clearly specified, conscientiously adhered to, and their use unambiguously documented.	**NASA Response (in 1997 ASAP appendix):** The SSP and Marshall Space Flight Center (MSFC) will continue to ensure that material acceptance testing and the quality control procedures used in the manufacturing of SLWTs are of a sufficient quality to validate that each tank is fully in compliance with all program requirements and is safe to fly.

Independent Assessment Team *(Chartered by)*	Date of Report	Finding	Recommendation	NASA Response
		dependent on far more stringent quality control of the materials and processes used to manufacture the SLWT than is required for the current external tanks.		
			Recommendation 16b: The criticality of these quality control operations makes it mandatory for NASA to retain buyoff of the results of those fabrication operations and tests that are essential in determining SLWT safety.	**NASA Response (in 1997 ASAP appendix):** The SSP and MSFC will retain NASA approval of the quality control program and changes to that baseline.
			Recommendation 16c: As quality control data on the size of flaws detected in 2195 aluminum-lithium material are collected, they should be used in an updated analysis of the SLWT structure, because it may permit the verifiable spread between flight limit stress and proof stress to be raised above that presently reported.	**NASA Response (in 1997 ASAP appendix):** The simulated service database has been developed from data collected on fracture specimens with flaws that are 0.175 inch long. The data verify a 2.9% positive spread between the flight and proof-test conditions. Using the demonstrated flaw detectability level for our nondestructive evaluation dye penetrant process (0.086 inch long) would increase the spread to approximately 14%. Because of uncertainties, it is NASA's standard policy to use a factor of two on our flaw detectability limit. This methodology provides the proper risk allocation between the nondestructive evaluation capability and proof-test levels. The use of a flaw size of 0.175 inch for the simulated service tests is conservative for the SLWT.
Aerospace Safety Advisory Panel *(NASA Charter)*	February 1997	**Finding 17:** Transition of logistics functions under Phase 1 of the Space Flight Operations Contract (SFOC) appears to be taking place smoothly. Key personnel are maintaining	**Recommendation 17:** Continue adherence to established systems, and make maximum use of the inherent capability of the incumbent personnel in the logistics systems.	**NASA Response (in 1997 ASAP appendix):** NASA concurs. The established NASA Logistics Operations continues to monitor the established logistics systems and enhance others in order to maintain insight into the

Independent Assessment Team *(Chartered by)*	Date of Report	Finding	Recommendation	NASA Response
		continuity in management techniques and processes.		logistics activity. Both the SFOC contractor and NASA Logistics Organization have retained incumbent key personnel with critical logistics skills to minimize the transitional risks and continue to support the SSP. Currently, the SFOC contractor is studying the horizontal consolidation of like functions and processes. NASA Logistics Operations will monitor the contractor's progress to assure that the logistics systems resulting from this consolidation will be capable, effective, efficient, and, above all, not adversely impacting the safety of operations.
Aerospace Safety Advisory Panel *(NASA Charter)*	February 1997	**Finding 18:** Long-term projections suggest increasing cannibalization rates, component repair turnaround times, and loss of repair capability for the Space Shuttle logistics and support programs.	**Recommendation 18:** Take early remedial action to control this potential situation, such as maintaining sufficient spares and extending repair and overhaul capability.	**NASA Response (in 1997 ASAP appendix):** NASA is closely monitoring logistics trends. The areas of emphasis stress long-term logistics support indicators, specifically backlog and repair turnaround. While an increase in repair turnaround time has been noted, vehicle support remains at the same high level. Budget reductions in past years have meant that fewer spares have been produced and less repairs were performed, but NASA and the contractor will continue to manage the process to maintain acceptable levels of support. Presently, logistics performance measurement data do not indicate any adverse trends in cannibalization rates. NASA has directed SFOC management to maintain an emphasis on logistics supportability during the transition of all contract responsibilities. The SFOC

Independent Assessment Team *(Chartered by)*	Date of Report	Finding	Recommendation	NASA Response
				contractor has been directed to maintain key personnel with critical logistics skills to minimize transitional risks and provide continuity to Shuttle logistics support. In addition, SFOC is required to develop and submit original equipment manufacturer (OEM) contingency plans for responding to known and potential support issues at effected OEMs. All known supportability threats are tracked and evaluated to determine the associated risk and required actions for resolution. The SFOC has the appropriate processes in place to both monitor and respond to loss of subcontractor capability. The NASA Shuttle Logistics Depot (NSLD) has been certified to make some repairs where there has been a loss of critical supplier capability. The SFOC is also considering consolidating similar work at one vendor so that the NSLD is not the only repair agent.
		Finding 19: Obsolescence of components and systems on the Space Shuttle is an increasing problem threatening critical spares availability.	**Recommendation 19:** Alternative components must be developed and certified, and, where necessary, systems must be redesigned to use available or adaptable units.	**NASA Response (in 1997 ASAP appendix):** NASA continues to identify and coordinate obsolescence issues concerning hardware, special test equipment, vendor capability, and environmental restrictions with the appropriate design center. Each issue is evaluated for logistics impacts, and this information is communicated to or within the design center so that appropriate action can be taken to initiate any required redesigns, modifications, or enhancements. A Kennedy Space Center (KSC) logistics priority list is

Independent Assessment Team *(Chartered by)*	Date of Report	Finding	Recommendation	NASA Response
				maintained to communicate logistics' top concerns to design center management. While obsolescence will continue, a team approach to problem identification, prioritization, and resolution appears to be providing effective problem resolution. Additionally, the Shuttle upgrade program is designed to assure that potential problem areas are addressed so as to preclude disruption in meeting manifest requirements.
Aerospace Safety Advisory Panel *(NASA Charter)*	February 1997	**Finding 27:** NASA's Agency-wide software safety policy allows projects latitude to tailor their software safety plan for safety-critical software. It does not, however, require projects to obtain center Safety and Mission Assurance (S&MA) approval of the tailored software safety plans nor does it require Verification and Validation (V&V) per se. mile the software assurance standard does mention V&V, it does not require any independence of V&V for safety-critical software.	**Recommendation 27a:** NASA should require approval of a project's tailored software safety plan by both the center S&MA organization and by one administrative level higher than that making the request.	**NASA Response (in 1997 ASAP appendix):** NASA agrees with the intent of this recommendation but believes the requirements for formal system safety program plans and software management plans exist and, with proper and firm enforcement, fulfill the objective of this recommendation. To be sure that these requirements are perfectly understood, the Office of Safety and Mission Assurance (OSMA) will update NSS 1740.13, "NASA Software Safety Standard," to explicitly state that the program/project manager for programs/projects perform an assessment to determine, based on the level of criticality and risk, the scope and level of Independent Verification and Validation (IV&V) to be planned. The results of the assessment will be formally reviewed by Center Safety and Mission Assurance (SMA). The program/project manager, in consultation with SMA, will tailor an approach to ensure that the appropriate V&V requirements are established

Independent Assessment Team *(Chartered by)*	Date of Report	Finding	Recommendation	NASA Response
				and implemented. The OSMA will place more emphasis on the implementation and enforcement of these existing requirements. Process verification, recently established in the OSMA, will be used to evaluate and enforce these existing policy and requirements more aggressively. NASA is committed to assuring that required program management plans and any subordinate plans such as software or safety management plans cover the essential requirements for programs where warranted by cost, size, complexity, lifespan, risk, and consequence of failure. Additional changes are being incorporated into NPG 7120.5, "NASA Program/Project Management Guide" (currently under development), to ensure that necessary and sufficient requirements will be fulfilled for programs having software vulnerabilities. SMA organizations at each level are to be a party to these decisions and are to intervene where necessary to assure that proper and clearly documented decisions are made by the appropriate level of management. The Program Management Councils could play a role in adjudicating any issues with the content of program management plans.
Aerospace Safety Advisory Panel *(NASA Charter)*	February 1997	**Finding 28:** NASA has put considerable effort into the reorganization of its software activities and has made significant progress. It does not yet, however, have a	**Recommendation 28:** NASA should ensure that there is a clear, universally well-understood, widely promulgated, and enforced NASA Policy Directive on the roles and responsibilities of its	**NASA Response (in 1997 ASAP appendix):** NASA agrees with the recommendation. The July 1996 (draft) program plan for the Fairmont (IV&V) Facility is the contract between Code

Independent Assessment Team *(Chartered by)*	Date of Report	Finding	Recommendation	NASA Response
		comprehensive, clear set of roles and responsibilities for various groups within the Agency with respect to software development, safety, V&V, and software process development.	various organizations vis-a-vis software development and safety. Moreover, that Policy Directive should specify organizational roles and responsibilities solely on the basis of technical and administrative capability.	Q and the Facility and will be updated for future funding and delegation of the software assurance program. NASA concurs that the draft plan now contains ambiguities but will be clarified in the next update. The IV&V Facility's reporting structure will be finalized in the upcoming proposed Ames Research Center reorganization. It is anticipated that the IV&V Facility will be moved from under the direction of Code I at Ames and installed as the equivalent of a Directorate in the new ARC organization. The IV&V Facility Business Plan currently defines the roles and responsibilities of the IV&V Facility. NASA Headquarters will establish and document at the policy level the roles in the Agency for all software, including embedded and flight system software. The policies document will explain how the roles and responsibilities of the Agency-wide software efforts mentioned in the finding (e.g., CIO, COE-IT, IV&V Facility) fit together in a synergistic manner within the Agency. The new NPD 2820 will define Agency policy for program/project utilization of the IV&V Facility. The Chief Information Officer, the Chief Engineer's Office, the Office of Safety and Mission Assurance, and the Software Working Group will be responsible for increasing Agency awareness of all the software-related resources, policies, and existing standards. The newly

Independent Assessment Team *(Chartered by)*	Date of Report	Finding	Recommendation	NASA Response
				implemented Code Q process verification activity will validate Agency project managers' awareness of software assurance policy and procedures for compliance in software development efforts.
Aerospace Safety Advisory Panel *(NASA Charter)*	February 1996	**Finding 1:** Cutbacks in government and contractor personnel and other resources at the Kennedy Space Center (KSC) and the planned transition of tasks from government to contractor workers will create a new mode of Space Shuttle operations. Those involved in day-to-day Shuttle operations and management are in the best position to determine how to maintain the stated program priorities - fly safely, meet the manifest and reduce costs, in that order.	**Recommendation 1:** Additional reductions in staff and operations functions should be accomplished cautiously and with appropriate inputs from the KSC NASA/contractor team itself.	**NASA Response (in 1996 ASAP appendix):** KSC operations continue to focus on the program goals of flying safely, meeting the manifest, and reducing costs, with flying safely being paramount. Teamwork between NASA and its contractors has enabled us to meet program challenges in the past, and we will rely on that same teamwork to meet the challenges of the Space Flight Operations Contract (SFOC) transition. Reductions in personnel will be proportional to requirement reductions as opposed to budget reductions. Requirements reductions which will reduce work content should come from the program as well as efficiencies which are originated at KSC. KSC plans to use a phased methodology to control change and risk. In a partnering relationship, NASA and United Space Alliance (USA) will jointly plan change, implement change, then stabilize and assess the results before making further changes. "Partnering" provides NASA visibility and management insight into the transition process and ensures desired levels of safety and quality are maintained. By implementing a disciplined transfer of mature systems, proven procedures, and experienced personnel into SFOC, we feel that we can

Independent Assessment Team *(Chartered by)*	Date of Report	Finding	Recommendation	NASA Response
				accomplish a seamless transition without disturbing the infrastructure that has made this program such a success.
Aerospace Safety Advisory Panel *(NASA Charter)*	February 1996	**Finding 2:** Obsolescence of Space Shuttle components is a serious operational problem with the potential to impact safety. Many original equipment manufacturers are discontinuing support of their components. NASA is, therefore, faced with increasing logistics and supply problems.	**Recommendation 2:** NASA should support augmenting the current comprehensive logistics and supply system so that it is capable of meeting Space Shuttle Program needs in spite of increasing obsolescence.	**NASA Response (in 1996 ASAP appendix):** NASA concurs with the finding that current tracking and control systems are providing timely information to deal with logistics problems. With regards to the specific need for better visibility into the subject of obsolescence, it was with that concern in mind that the Safety and Obsolescence (S&O) activity was established as a process for identifying and responding to trends indicative of aging and to identify areas where replacement parts may no longer be available. The S&O process baselined in NSTS 08198 provides a rigorous prioritization approach which factors in the criticality of the systems and nonsafety related risks involved with Shuttle flight and ground processing hardware. This process identifies the most serious problems and generates data used to support requests to program management for correction of the identified concerns.
Aerospace Safety Advisory Panel *(NASA Charter)*	February 1996	**Finding 3:** The Return to Launch Site (RTLS) abort maneuver is one of the highest risk off-nominal Space Shuttle flight procedures. A Space Shuttle Main Engine (SSME) shutdown leading to an intact abort is more likely than a catastrophic engine	**Recommendation 3:** NASA should pursue with vigor efforts to minimize Space Shuttle exposure to the RTLS maneuver through all available means.	**NASA Response (in 1996 ASAP appendix):** NASA has and will continue to increase the reliability of the hardware to decrease the probability of any abort and to make operational trades to balance the risks between the available abort modes. The RTLS abort mode is fully certified and has been a

Independent Assessment Team *(Chartered by)*	Date of Report	Finding	Recommendation	NASA Response
		failure. Exposure of an ascending Space Shuttle to the risk of performing the demanding RTLS maneuver might be significantly minimized by operating the Block II SSME at higher thrust levels at appropriate times. Certification of alternative Space Shuttle landing approaches for use during contingency aborts and installation of Global Positioning System (GPS) could also contribute to the minimization of RTLS risk (see Finding #5).		requirement throughout the design and certification of the vehicle. Options to improve abort capability, such as increased SSME throttling or utilization of GPS to increase operating flexibility, are continually evaluated. A decision for certifying the Block II SSME intact throttle to 109 percent is scheduled for late 1996. Routinely operating at higher thrust settings may add additional risk, which needs to be evaluated versus RTLS exposure. A review of the GPS implementation schedule is under way. Single-string GPS is in development for three vehicles to gather flight test experience. Software development for three-string GPS is also currently in work. As development and flight testing continues, the GPS contribution to minimizing RTLS risk will be assessed. While the RTLS intact abort mode is certified and is considered to be acceptable, however, improvements to decrease the risks of RTLS will continue to be evaluated. Each flight is designed to meet RTLS constraints, and operational considerations are continually reviewed to ensure that the proper trades are being made to balance risks. While many alternatives have been considered, none can eliminate the requirement for RTLS capability, and, to date, all are predicted to have risk greater than that associated with the current certified abort modes.

Independent Assessment Team *(Chartered by)*	Date of Report	Finding	Recommendation	NASA Response
Aerospace Safety Advisory Panel *(NASA Charter)*	February 1996	**Finding 4:** The Range Safety System (RSS) destruct charges have been removed from the liquid hydrogen tank of the External Tank (ET). The risk studies, which supported this removal, also suggested that the RSS charges had to be retained on the Liquid Oxygen (LOX) tank of the ET. It is preferable to omit as much ordnance as possible from flight vehicles to reduce the possibility of inadvertent activation.	**Recommendation 4:** Studies supporting the need for the RSS destruct system on the LOX tank should be updated in light of the current state of knowledge, operating experience and the introduction of the new Super Lightweight Tank (SLWT) to determine if it is now acceptable to remove the ordnance.	**NASA Response (in 1996 ASAP appendix):** Studies have been completed, and the Space Shuttle program has formally eliminated the requirement for an ET RSS and approved removal of ET RSS hardware. Deactivation of the system is planned with a phased implementation of hardware removal on tanks that culminates in a total removal by ET-96. RSS hardware removal may begin as early as ET-87. The first SLWT (ET-96) will not have any RSS hardware installed, thus increasing the Shuttle safety by removing the possibility of inadvertent activation of the tank destruct system.
Aerospace Safety Advisory Panel *(NASA Charter)*	February 1996	**Finding 5:** The Orbiter and its landing sites continue to be configured with obsolescent terminal navigation systems. The existing Tactical Air Control and Navigation (TACAN) and Microwave Scanning Beam Landing System (MSBLS) systems are increasingly difficult to maintain, vulnerable and expensive. Continued reliance upon them limits landing options in the event of a contingency abort. Replacement of TACAN and MSBLS with now available precise positioning GPS in a triple redundant configuration would ameliorate and most likely solve these problems.	**Recommendation 5:** Accelerate the installation of a triple redundant precise positioning service GPS in all Orbiters.	**NASA Response (in 1996 ASAP appendix):** The Space Shuttle orbiter project is accelerating the first installation of three-string GPS to the orbiter maintenance down period (OMDP) scheduled for OV-104 in 1998. This improves the date for the last TACAN flight by 2 years, from 2002 to 2000. The FY 1998 OMDP is the earliest date that can be accommodated by hardware design, certification, and flight software development. Software development and hardware installation during the OMDP are the pacing items in bringing the three-string system on line. The requirements to install the wiring, antenna, and control panel modifications for the three-string system have been estimated to be approximately 5,000 man-hours of work on each vehicle. Implementing any change of this size during

Independent Assessment Team *(Chartered by)*	Date of Report	Finding	Recommendation	NASA Response
				a vehicle flow in the KSC Orbiter Processing Facility would create prohibitive launch flow impacts, thus relegating the change to OMDP. The single-string system now being implemented for OV-103, -104, and -105 is essential to verifying GPS performance. Plans to thoroughly evaluate and certify the GPS as the primary Shuttle navigational system are being prepared. The additions to GPS flight software necessary to support just the single-string system require the single largest software change since the initial development of the Space Shuttle program. The additional changes to go from single-string to the operational three-string system will be approximately the same size. Production of this software is being given the highest priority. The backup flight software system (BFS) will support the single string-system on STS-79. Primary flight software for the Shuttle is developed in operational increments. GPS software was originally considered for 01-26 in 1994; however, it was necessary to give priority to software associated with payload performance enhancements that enable construction of the International Space Station. A special OI-26B was created to add single-string GPS capability to the primary flight software. 01-27 will be devoted to the three-string system. Meanwhile, NASA is considering utilizing single-string GPS data for additional

Independent Assessment Team *(Chartered by)*	Date of Report	Finding	Recommendation	NASA Response
				risk reduction for contingency aborts and emergency de-orbits. Software and hardware improvements and supporting certification will allow for first flight of the three-string GPS in January 1999 on STS-96. The Space Shuttle program continues to investigate upgrades that will minimize the risks of contingency abort modes.
Aerospace Safety Advisory Panel *(NASA Charter)*	February 1996	**Finding 6:** Orbiter Reaction Control System (RCS) oxidizer thruster valve leaks are occurring with increasing frequency. More recently, RCS fuel thruster valve leaks have also been observed. Because isolation of leaking thrusters can be implemented by manifold shut off and thruster redundancy is provided, leaking thrusters have not been considered a serious safety hazard. RCS leaks in the vicinity of rendezvous targets such as Mir and the International Space Station (ISS) could, indeed be a serious safety hazard.	**Recommendation 6:** Do what is necessary to eliminate the RCS thruster valve leaks now and in the future.	**NASA Response (in 1996 ASAP appendix):** A comprehensive program to improve thruster reliability and eliminate RCS thruster leaks has been put in place. The majority of oxidizer valve leaks are attributed to the long-term accumulation of nitrates that form in the presence of moisture. The changes fall into three categories: operations improvements, improved maintenance of valves, and design changes. Changes in the way turnaround operations are performed consist of emphasizing the maintenance of the RCS propellant system in a hard-filled/wetted state, improved thermal conditioning to keep the thrusters always above the minimum temperature, and reduction of moisture intrusion into the system. These principles have been incorporated into written procedures at KSC and are currently in use. In addition, a molecular sieve is being implemented at the launch pad to reduce the residual iron and water in the RCS oxidizer. Periodic flushing of thruster and valve passages to remove accumulations of nitrates has been implemented. The thruster flushing essentially returns

Independent Assessment Team *(Chartered by)*	Date of Report	Finding	Recommendation	NASA Response
				the thruster to an as- new condition in terms of nitrate accumulation. Thruster flushing has been performed at each OMDP beginning with OV-103 in July 1995. Subsequent intervals for flushing are planned at every other orbiter maintenance down period (OMDP), subject to change based on evolving failure rates from nitrate accumulation. Two design approaches to achieve a more reliable valve have been evaluated, and one has been chosen for implementation. The first design solution proposed was to abandon the current pilot operated valve (POV) in favor of a direct acting valve (DAV). In addition to technical problems involving reliability of required bellows, it was determined that removing and replacing all the oxidizer valves in the fleet was cost prohibitive. It was determined that the cost-effective approach could be achieved by replacing certain internal parts of the existing valve with redesigned parts on an attrition basis. The redesigned parts modify the areas of the current valve that have been shown to be sensitive to nitrate contamination. Examples of design changes are reduction of seal surface contact area, adoption of a conical seal geometry, and a stronger spring with more valve closing capability. In summary, a comprehensive, cost-effective program to improve thruster reliability and minimize leaks

Independent Assessment Team *(Chartered by)*	Date of Report	Finding	Recommendation	NASA Response
				has been defined and is in various stages of implementation. The effectivity of various elements of the program will be carefully monitored and the program adjusted according to results.
Aerospace Safety Advisory Panel *(NASA Charter)*	February 1996	**Finding 7:** The use of Alumina Enhanced-Thermal Barrier (AETB) tiles with Toughened Uniplace Fibrous Insulation (TUFI) coating on the Orbiter has the potential to enhance safety and reduce life cycle cost.	**Recommendation 7:** NASA should make a thorough study of the potential use of the AETB/TUFI tiles in order to determine if it is cost effective to qualify the tiles for flight.	**NASA Response (in 1996 ASAP appendix):** The use of AETB tiles with the TUFI h as been considered extensively in the last year for use on the Shuttle. AETB/TUFI tiles have been flown as technology demonstrations in support of the X-33 program. These tiles were installed on the lower body flap and base heat shield of the orbiter. Tiles with density of 12 pounds/cubic foot were attached to the body flap. Those attached to the base heat shield had a density of 8 pounds/cubic foot. The use of TUFI coating with the FRCI-12 substrate has been identified as a practical option for certain damage prone areas of the orbiter. Certification of this combination for multiple flights will be relatively inexpensive because of similarity between the current coating and TUFI. However, the weight of FRCI-12 with the TUFI coating excludes its use for large area applications. Weight is a critical parameter as the Space Shuttle program strives for performance improvements in support of Space Station assembly flights. The AETB-12 tile substrate, which is the most mature AETB material, offers few benefits over the current certified FRCI- 12. The

Independent Assessment Team *(Chartered by)*	Date of Report	Finding	Recommendation	NASA Response
				AETB-8 shows some promise as it would be weight competitive with the LI-900 configuration. Development of AETB-8 technology continues, but it is not in production. Studies will be performed to determine whether it is cost effective to certify and implement this tile configuration. These studies will determine whether the lower maintenance costs would provide an adequate payback.
Aerospace Safety Advisory Panel *(NASA Charter)*	February 1996	**Finding 8:** The SSME has performed well in flight during this year. While some launches were delayed because of problems or anomalies discovered during pre-launch inspections and checkout or development engine test firings at the Stennis Space Center (SSC), such issues were thoroughly and rapidly investigated and resolved.	**Recommendation 8:** Continue the practice of thorough and disciplined adherence to inspection and checkout of engines prior to commitment to flight as well as prompt and thorough resolution of any anomalies discovered.	**NASA Response (in 1996 ASAP appendix):** A disciplined adherence to procedures and a commitment to complete resolution of all anomalies will be maintained.
Aerospace Safety Advisory Panel *(NASA Charter)*	February 1996	**Finding 9:** The Block II engine, in near-final configuration, re-entered development testing in mid October 1995. Testing of what had been expected to be the final configuration was begun later that month. The High Pressure Fuel Turbopump (HPFTP) was a principal cause of the late restart of testing primarily because of slips in obtaining some redesigned turbopump components. The remaining time to achieve the scheduled first flight of the Block II configuration is very tight and allows for little, if any, problem correction	**Recommendation 9:** Do not let schedule pressure curtail the planned development and certification program.	**NASA Response (in 1996 ASAP appendix):** The Space Shuttle program and the SSME project are committed to completing the development and certification program of the Block II engine. Current planning supports the utilization of the Block II SSME for ISS missions, but the Shuttle has adequate performance with Block I engines for the initial Space Station flights.

Independent Assessment Team *(Chartered by)*	Date of Report	Finding	Recommendation	NASA Response
		during development and certification testing. The improved ruggedness and reliability of this version of the SSME is critical to the assembly and operation of the ISS.		
Aerospace Safety Advisory Panel *(NASA Charter)*	February 1996	**Finding 10:** Post flight inspection of recovered RSRMs from STS-71 and STS-70 identified gas paths leading to primary O-ring heat erosion in joint #3 of the RSRM nozzles. Heat erosion in this joint could compromise Space Shuttle mission safety. NASA stopped all launches until the anomaly was resolved and corrective repairs made.	**Recommendation 10:** NASA should continue to investigate and resolve all potential Space Shuttle flight safety problems in this same forthright manner.	**NASA Response (in 1996 ASAP appendix):** NASA concurs. Anomalies that could compromise Space Shuttle mission safety will be resolved before subsequent Shuttle launches.
Aerospace Safety Advisory Panel *(NASA Charter)*	February 1996	**Finding 11:** The schedule for firings of Flight Support Motors (FSM) for evaluating changes made to the RSRM has been stretched out. Now, accelerating obsolescence and new environmental regulations have increased the need for the data supplied by FSM firings.	**Recommendation 11:** Do not further stretch out FSM firings.	**NASA Response (in 1996 ASAP appendix):** NASA concurs with the finding and, based on current funding profiles, plans to abide by the schedule associated with FSM firings.
Aerospace Safety Advisory Panel *(NASA Charter)*	February 1996	**Finding 12:** The development of the Super Lightweight Tank (SLWT) using Aluminum Lithium (Al-Li) material entails several unresolved technical issues. These include a low fracture toughness ratio and problems in large scale joint welding. There are also critical structural integrity tests, which are behind schedule. Resolution of these issues could impact the delivery	**Recommendation 12:** Satisfactory resolution of these issues must be achieved prior to SLWT flight.	**NASA Response (in 1996 ASAP appendix):** NASA recognizes the concerns expressed in the findings and recommendations for this item. Appropriate efforts and planning have been implemented within the SLWT project to focus the needed resources on development of resolutions to the issues noted and support delivery of ET-96 to meet the International Space Station first element launch in December 1997.

Independent Assessment Team *(Chartered by)*	Date of Report	Finding	Recommendation	NASA Response
		of the SLWT.		Progress/changes that address these issues since the last Aerospace Safety Advisory Panel review follow. (lots of details omitted)
Aerospace Safety Advisory Panel *(NASA Charter)*	February 1996	**Finding 29:** The Dryden Flight Research Center's Basic Operations Manual (BOM) describes a pro-active attitude toward safety, which is exemplary and worthy of emulation throughout NASA.	**Recommendation 29:** Other Centers and NASA contractors could profit from the use of the Dryden BOM as a model.	**NASA Response (in 1996 ASAP appendix):** NASA agrees that the Dryden Flight Research Center's Basic Operations Manual (BOM) describes a proactive attitude toward safety that is exemplary and worthy of emulation throughout NASA. The Dryden BOM was installed on the Internet 2 years ago and can be accessed from the Dryden home page. This will ensure its availability to other NASA centers and contractors for use as a model in developing or improving their own operations documentation.
Aerospace Safety Advisory Panel *(NASA Charter)*	February 1996	**Finding 31:** The Senior Managers' Safety Course conceived and conducted by JSC is an outstanding overview of philosophies, techniques and attitudes essential to a successful safety program.	**Recommendation 31:** A safety course for senior managers similar to the one conducted at JSC should be established at other NASA centers and Headquarters. Consideration should also be given to exporting the course to major NASA contractors and including its elements in managerial training programs.	**NASA Response (in 1996 ASAP appendix):** The Senior Managers Safety Course conducted at JSC has become the benchmark at NASA for establishing enhanced safety awareness at the Center Director level. The Associate Administrator for Safety and Mission Assurance coordinated and promoted the awareness course during presentations on April 9-l 1, 1996, in Houston, Texas, to NASA Center Directors, senior managers, and senior safety, reliability, maintainability, and quality assurance personnel. Attendees highly praised the course and recommended enhancing senior participation by request of the NASA Deputy Administrator. The Deputy

Independent Assessment Team *(Chartered by)*	Date of Report	Finding	Recommendation	NASA Response
				Administrator will invite all Center Directors to a second presentation at JSC in the fall of 1996. The goal will be to transport this course using the "train the trainer" concept to each participating NASA center, with the objective of keeping safety and mission success foremost in every NASA operation.
Aerospace Safety Advisory Panel *(NASA Charter)*	February 1996	**Finding 32:** NASA's ongoing reorganization and the intention to pass responsibility for Space Shuttle operations to a single Space Flight Operations Contractor (SFOC) have potential safety implications. To this point, other than an effect on morale at the KSC due to uncertainty, no significant problems have surfaced.	**Recommendation #32:** NASA leadership and top management should continue active and detailed involvement in the safety aspects of planning for and over- sight of the NASA reorganization in general and Space Shuttle operations in particular.	**NASA Response (in 1996 ASAP appendix):** NASA's top priority throughout the restructuring process and implementation of the SFOC has been, and will continue to be, maintenance of safety. Safety considerations are currently embedded in the program management processes and will remain so. To help assure this, the Associate Administrator for Safety and Mission Assurance (S&MA) at NASA Headquarters has formed a Human Exploration and Development of Space (HEDS) Assurance Board, which includes in its membership the S&MA Directors of JSC, MSFC, KSC, and SSC and the Shuttle S&MA Technical Manager's Representative (TMR) from the Program Office. The HEDS Assurance Board charter is to monitor program safety implementation and provide guidance through transition to the SFOC. The Lead Center Director (LCD) at JSC has established the position of Associate Director (Technical) with responsibility for overseeing program safety and providing recommendations to the Center Director. (Astronaut John Young currently occupies this position.) The LCD receives weekly SFOC

Independent Assessment Team *(Chartered by)*	Date of Report	Finding	Recommendation	NASA Response
				implementation status from the Program Manager as well as monthly program issues reports, which are shared with the Associate Administrator for Space Flight. Additionally, the Program Manager provides status briefings to the OSF Management Council (the Associate Administrator for Safety and Mission Assurance is a member) quarterly or as requested. The implementation of Space Shuttle program streamlining and the SFOC is, therefore, receiving top-level management visibility and guidance on a routine basis. Even so, NASA is being extremely careful in implementing the SFOC. For example, particular attention is being paid to safety considerations at KSC, where the flight hardware will be processed by the SFOC. There, NASA will be instituting an extensive audit, surveillance, and independent assessment of SFOC processing activities that are required to be compliant with existing NASA-approved processes. The KSC management team will be retained as an integral part of the program management structure and will maintain insight into SFOC launch, landing, logistics, and S&MA activities. This team will continue to play a major role in Flight Readiness Review (FRR) activities with full membership on the FRR Board. Finally, we believe execution with the incumbent operations support contractors for the SFOC provides maximum assurance of

Independent Assessment Team *(Chartered by)*	Date of Report	Finding	Recommendation	NASA Response
				continuation of safe operations.
Aerospace Safety Advisory Panel *(NASA Charter)*	February 1996	**Finding 33:** The plan for Space Shuttle restructuring and downsizing provides that NASA personnel will be involved in the resolution of any off-nominal events which are beyond the operating experience base or "out-of-family." This places extreme importance on the development and implementation of the definition of an out-of-family situation.	**Recommendation 33:** NASA personnel with direct Space Shuttle operations experience should be involved not only in the derivation of the definition of out-of-family but also in the day-to-day decisions on what constitutes an out-of-family event.	**NASA Response (in 1996 ASAP appendix):** The Space Shuttle program management plans to maintain full capability for identifying, evaluating, and resolving all anomalous performance of Space Shuttle systems. To support this objective, the program has developed general definitions of "In-Family" and "Out-of-Family" characteristics for all Shuttle systems and processes, which will serve as performance classification criteria. NASA will use its most experienced and skilled personnel to develop detailed definitions and data bases. With the implementation of the Space Flight Operations Contract (SFOC), the program is transferring responsibility for routine operations activities to the contractor, which will be accountable for classifying performance as either "In-Family" or "Out-of-Family" per the definitions and consistent with well-defined systems and processes performance data bases. The SFOC contractor will be required to report and interface with NASA on a daily basis to ensure that appropriate data are exchanged to identify "Out-of-Family" issues. Additionally, NASA will perform audit and surveillance of the operation using ADVISORY PANEL NASA technical and operations experts. Metrics will be developed that will support the identification of

Independent Assessment Team *(Chartered by)*	Date of Report	Finding	Recommendation	NASA Response
				"Out-of Family" issues as well as the health of the processes. For evaluating those issues reported as "Out-of-Family," the program will retain a core team of NASA experts in each area (e.g., KSC ground operations, JSC flight operations, orbiter, flight software, etc.) that will be capable of performing independent assessment of issues and making recommendations to the Program Manager. In this approach, the Program Manager requires these NASA experts to concur in "Out-of-Family" resolutions.
Aerospace Safety Advisory Panel *(NASA Charter)*	February 1996	**Finding 35:** While hardware typically gets adequate coverage from the Safety and Mission Assurance organizations at the NASA Centers, there is evidence that software does not.	**Recommendation 35:** The Headquarters Office of Safety and Mission Assurance should examine the depth of the software assurance process at each of the Centers and promulgate NASA-wide standards for adequate coverage.	**NASA Response (in 1996 ASAP appendix):** NASA agrees with the importance of this recommendation. The NASA Software Assurance Standard (NASA-STD-2201-93) promulgates commonality and provides direction on what activities are to be performed for software assurance across the Agency. The NASA Software Safety Standard (NSS 1740.13) was added to the Safety Standards series in 1996. The addition of the software safety standard and guidebook will assist projects to plan and budget for software safety as software increases in criticality and importance in NASA systems. (lots of detail on ISS omitted) One such process to be verified is the software assurance process as it is applied at the center with respect to NASA-STD-2201-

Independent Assessment Team *(Chartered by)*	Date of Report	Finding	Recommendation	NASA Response
				93. Process Verification will provide the Agency the confidence that proper skills and personnel exist to adequately perform software assurance for each center. Software assurance has a high priority to be verified within the first year of the PV initiative.
Aerospace Safety Advisory Panel *(NASA Charter)*	March 1995	**Finding 7:** The Russian Androgynous Peripheral Docking System (APDS) for docking the Space Shuttle with the Mir uses 12 active hooks on the Space Shuttle side which mate with an equal number of passive hooks on the Mir. The design currently provides no positive means of determining whether any or all of the hooks are secured. NASA has decided it is an acceptable risk to fly the first docking mission, STS-71, without an indicator. Having to rely on the pyros as presently supplied by the Russian Space Agency poses risk because of lack of knowledge relating to the pyros' pedigree and certification. A second contingency demate procedure is available involving the Extravehicular Activity (EVA) removal of 96 bolts at a different interface. Implementing either backup method to separate Shuttle from Mir may leave the Mir port unusable for future dockings.	**Recommendation 7:** NASA should develop an indicator system.	**NASA Response (in 1995 ASAP appendix):** The second APDS unit, which is being procured from RSC-Energia for the second and subsequent Mir missions, also does not have individual structural hook position indicators. The addition of indicators was discussed with RSC-Energia, however, the APDS manufacturing and delivery schedule precluded installation. Johnson Space Center (JSC) and Rockwell engineers have shown, through test and analysis, that there is no threat to crew and vehicle safety for the remote failure case of two adjacent hooks failing to close properly. Combinations of failures that would result in crew injury or vehicle damage are considered to be of remote probability, the risk therefore being acceptable for the Phase I program. The Shuttle program has reviewed the test and analysis results and approved the APDS baseline without position indicators for the Mir missions.

Independent Assessment Team *(Chartered by)*	Date of Report	Finding	Recommendation	NASA Response
Aerospace Safety Advisory Panel *(NASA Charter)*	March 1995	**Finding 8:** If the primary system fails, the first backup separation system for the APDS is a set of pyro bolts which disengage the 12 active hooks.	**Recommendation 8:** NASA should emphasize increasing the reliability of the primary mating/demating mechanisms in order to reduce the likelihood of having to use either of the backups. NASA should also obtain an acceptable certification of the supplied pyro bolts. Failing that, NASA should procure fully certified substitute bolts.	**NASA Response (in 1995 ASAP appendix):** The APDS mechanism hardware has been demonstrated by test to fully meet its design environments. Additional detail regarding critical mechanical components was jointly developed by RSC-Energia, JSC, and Rockwell engineering, and analysis of those components has been completed. The analysis supports test results which demonstrate design margin for the life of the Mir program. Additionally, the results for this analysis will be used as a guideline in developing maintenance requirements for future Mir and Station missions, The pyrotechnics, installed in the APDS, have completed a confidence test that was developed by Rockwell and NASA engineering in conjunction with RSC-Energia and with the concurrence of NASA S&MA. NASA is pursuing design improvements of the RSC-Energia bolts for Station missions and is also working on the development of an American-built pyrotechnic bolt. RSC-Energia has not been receptive to the idea of installing American bolts in the APDS; however, assembly schedules do not require a decision until late 1995, and discussions with RSC-Energia are continuing.
Aerospace Safety Advisory Panel *(NASA Charter)*	March 1995	**Finding 9:** Significant additional payload mass capability is required to meet the demands of the ISS assembly and supply plans. Much of the needed increase in capacity will be achieved	**Recommendation 9:** Emphasis should be placed on the adequate integration of all of the changes into the total system.	**NASA Response (in 1995 ASAP appendix):** Integration of major changes into the existing Space Shuttle vehicle is receiving emphasis by the Space Shuttle program. The Space Shuttle program has had a system in place for

Independent Assessment Team *(Chartered by)*	Date of Report	Finding	Recommendation	NASA Response
		through weight reduction programs on a number of Space Shuttle elements and subsystems. The large number of simultaneous changes creates potential tracking and communication problems among system managers.		many years to integrate all of the changes into the total system. This system has proven effective. The system consists of technical panels, integrated product teams, and control boards. A technical panel exists for each major functional area (e.g., Loads and Dynamics, Thermal). These technical panels integrate and review the technical aspects of the analysis and testing. The functional areas are integrated by the integrated product teams (e.g., Propulsion System Integration Group) and at joint panel meetings. The control boards, at the project and program level, provide a final technical review and integration, and management direction for cost and schedule control. The NASA Element Project Offices and prime contractors are represented on the technical panels, integrated product teams, and control boards, allowing cross communication and input at all levels of the process. There is a System Integration Plan for each of the major performance enhancements that defines the responsibilities of the affected elements, identifies deliverable products and hardware, and defines the system schedule for that enhancement to support the first element launch.
Aerospace Safety Advisory Panel	March 1995	**Finding 10:** The New Gas Generator Valve Module (NGGVM): when certified and retrofitted to the fleet, should mitigate	**Recommendation 10:** NASA should attempt to introduce the NGGVM into the fleet as soon as possible as a safety and logistics improvement.	**NASA Response (in 1995 ASAP appendix):** NASA intends to introduce the NGGVM into the fleet on an opportunity basis. The ground

Independent Assessment Team *(Chartered by)*	Date of Report	Finding	Recommendation	NASA Response
(NASA Charter)		many of the problems with the current Improved Gas Generator Valve Module in the Improved Auxiliary Power Unit (IAPU). The NGGVM development program is proceeding well.	logistics improvement.	rule for this plan is to maintain a minimum Kennedy Space Center (KSC) stock level of five spare IAPUs to support any unplanned line replaceable unit removals. Any other IAPUs not required to support this stock level will be shipped to Sundstrand to undergo the NGGVM modification. By leaving this number of spare IAPUs on the shelf at KSC and modifying any units available beyond that, the NGGVM implementation into the fleet can be completed in late 1998 or early 1999. Upgrade and modification of three Auxiliary Power Units currently not used for flight as an expedient to the NGGVM fleet retrofit is not cost effective.
Aerospace Safety Advisory Panel *(NASA Charter)*	March 1995	**Finding 11:** The decision has been made to install the entire Multi-Function Electronic Display System (MEDS) in each Orbiter during a single Orbiter Maintenance and Down Period (OMDP). An Advanced Orbiter Displays/System Working Group has been formed to plan for the next generation of MEDS formats and display enhancements.	**Recommendation 11:** NASA should support the Advanced Orbiter Displays/System Working Group and set a timetable for the introduction of enhanced display formats which will improve both safety and operability. It should also maintain its commitment to completing the MEDS installations during a single OMDP.	**NASA Response (in 1995 ASAP appendix):** NASA established the Advanced Orbiter Displays/System Working Group to define next-generation cockpit displays that will take advantage of MEDS data processing capabilities to improve safety and operability. The Government/industry working group is currently defining requirements for enhanced displays as well as a timetable for both evaluation of candidate displays in MEDS testbeds and introduction of new displays into orbiters. NASA identified several advantages to installing MEDS hardware in orbiters during a single OMDP. Current OMDP planning as well as the schedule for first flight of MEDS on each orbiter reflects the single OMDP installation plan.

Independent Assessment Team *(Chartered by)*	Date of Report	Finding	Recommendation	NASA Response
Aerospace Safety Advisory Panel *(NASA Charter)*	March 1995	**Finding 12:** The Tactical Air Control and Navigation (TACAN) and Microwave Scanning Beam Landing System (MSBLS) on-board receivers are obsolescent and increasingly difficult to maintain. The MSBLS receivers also have known design problems which can lead to erroneous guidance information if the Orbiter is operating with only two of the three receiver complement. A Global Positioning System (GPS) test is underway on one of the Orbiters using the backup flight software and computer. The use of GPS could replace both the TACAN and MSBLS systems as well as assisting ascent and on-orbit operations.	**Recommendation 12:** Given the potential of GPS to improve safety and reliability, reduce weight and avoid obsolescence and the many existing and potential problems with the use of TACAN and MSBLS, a full GPS implementation on the Orbiter should be accomplished as soon as possible.	**NASA Response (in 1995 ASAP appendix):** The Space Shuttle program is currently reviewing a plan to fully implement the GPS capabilities. The GPS hardware/software implementation plan calls for completing the installation of a redundant GPS hardware capability as early as the year 2000. The software implementation will be completed with delivery of the 0I-27 operational increment by December 1997 with a first flight effectivity in the summer of 1998. The redundant GPS hardware installation will be accomplished during the OMDP for each orbiter.
Aerospace Safety Advisory Panel *(NASA Charter)*	March 1995	**Finding 13:** Growth in the requirements for on-board data processing will continue as the Space Shuttle is used in support of Shuttle/Mir, ISS and other future missions. The length of time over which the General Purpose Computer and its software will be able to meet these growing needs effectively is likely inadequate.	**Recommendation 13:** NASA should expedite a long-range strategic hardware and software planning effort to identify ways to supply future computational needs of the Space Shuttle throughout its life-time. Postponing this activity invites a critical situation in the future.	**NASA Response (in 1995 ASAP appendix):** We concur that continued reliance on the Space Shuttle beyond 2005 will demand some major revisions to the core General Purpose Computer (GPC) hardware and software, if for no other reason than the inability to maintain hardware based on early 1980 technology. Such a revision, given the tightly coupled interdependencies of the present core architecture, would logically be accomplished as a major "block" update rather than gradually evolving to a new architecture. The block update approach can also serve to reduce future operations costs by stabilizing avionics hardware and

Independent Assessment Team *(Chartered by)*	Date of Report	Finding	Recommendation	NASA Response
				software during the Station assembly era. In accord with that concept, the Space Shuttle program is considering an approach that would freeze the GPC software at roughly the turn of the century, following the incorporation of Station-driven enhancements. That freeze would allow for diversion of engineering resources, heretofore devoted to routinely evolving enhancements, to pursue a true significant block update sufficient to sustain the Space Shuttle past 2020. As the foundation for such a possible architecture, the JSC Engineering Directorate has developed a Reduced Instruction Set Computer (RISC) for high-fidelity emulation of the present GPC. That emulation is capable of real-time bit-level execution of actual object code produced by the HAL/S compiler. It will soon be made available to allow flight software developers a target machine for early development testing. At the present time, such early testing is a premium because of the limited availability of real GPCs. The extension of the emulator concept, as a candidate to replace the actual flight GPCs, is the next logical step. It would preserve critical flight code, thereby minimizing the reverification costs, while still providing a modern platform for growth. In summary, NASA does have the essential formative elements for a long-range strategic hardware and

Independent Assessment Team *(Chartered by)*	Date of Report	Finding	Recommendation	NASA Response
				software upgrade effort in work. Existing limited resources and ongoing program activities obviously preclude any definitive strategic planning until completion of the current program-wide restructuring activities. Once those activities are complete, a more definitive plan and schedule, predicated on critical examination of limited available resources, can be developed.
Aerospace Safety Advisory Panel *(NASA Charter)*	March 1995	**Finding 14:** The STS-64 mission involved a higher than usual level of windshield hazing which could have led to a situation in which the astronauts' view of the landing runway was obscured. MSBLS and TACAN are obsolescent. There is also the possibility that false indications by MSBLS under certain scenarios could result in an unacceptable risk of a landing mishap. Thus, there is a clear need for early upgrade of Orbiter and support facility autoland equipment and crew flight rules and training improvement.	**Recommendation 14:** NASA should improve the autoland equipment on the Orbiter; for example, replacing MSBLS and TACAN with GPS. In the interim, NASA should ensure that operations and failure modes of MSBLS are fully examined and understood. NASA should also reexamine the training of crews for executing automatic landings, including autoland system familiarization. Astronaut commanders and pilots should discuss circumstances which might warrant autoland use prior to each mission and be prepared for all reasonable contingencies in its operation.	**NASA Response (in 1995 ASAP appendix):** Incorporation of GPS is being pursued as aggressively as funding and technical constraints will allow. The program has approved plans and funding to provide a single-string GPS capability that can be flown in the summer of 1997 as a first step toward TACANIMSBLS replacement. Plans for a full three-string operational system have been approved for 01-27, and detailed costs and schedules are being assessed by the program. The failure modes of the MSBLS have been analyzed and are documented in the program's Critical Item List. The finding made by the ASAP regarding the STS-64 mission, involving a higher than usual level of windshield hazing that could have led to a situation in which the astronaut's view of the landing runway was obscured, is incorrect. The STS-64 orbiter Quick Look Reports states: "Orbiter Windows 3 and 4 exhibited light hazing and streaks were seen on 4." Additionally, the Commander

Independent Assessment Team *(Chartered by)*	Date of Report	Finding	Recommendation	NASA Response
				(Richard N. Richards, 4th flight) reports that the window hazing was not unusual at all, typical of what is usually seen, and an excellent view of the runway was obtained at all times during the approach, landing, and rollout phases of the flight. The STS-64 vehicle touchdown parameters were excellent, confirming that the Commander had an excellent view of all visual aids throughout the approach and landing. (These touchdown parameters include touchdown airspeed of 198 knots versus 195 planned, touchdown distance of 2386 feet versus predicted 2505, sink rate at touchdown of 1.0 feet per second, and a threshold crossing height of 20 feet. All parameters are excellent.) Extensive analysis of the orbiter autoland system has been performed by various organizations in NASA, including exhaustive reviews by NASA Safety and Mission Assurance personnel. Those results have been briefed to all levels of NASA management. The Space Shuttle program has not identified/defined any hardware or software change that is necessary to improve the autoland capability. The operational use of the autoland capability remains at the discretion of the mission commander. To educate pilots and commanders on the use of this emergency system, Mission Operations Directorate (MOD) provides a briefing that covers the capabilities and limitations of

Independent Assessment Team *(Chartered by)*	Date of Report	Finding	Recommendation	NASA Response
				the autoland system, as well as the contingency cases for which it is a viable alternative (i.e.? both pilots incapacitated, or a highly inaccurate weather forecast for landing). In addition, each crew has a session in the Shuttle Mission Simulator, as well as the Shuttle Training Aircraft where the autoland system is demonstrated and discussed.
Aerospace Safety Advisory Panel *(NASA Charter)*	March 1995	**Finding 15:** It has become necessary to execute a partial disassembly of both the engines and turbopumps after each flight because of the accumulation of special inspection requirements and service life limits on components of the current (Phase II) SSMEs. These inspections are performed with rigor and appropriate attention to detail. included in the parameters used in the algorithms that determine engine health.	**Recommendation 15:** In order to control risk, NASA must maintain the present level of strict discipline and attention to detail in carrying out inspection and assembly processes to ensure the reliability and safety of the SSMEs even after the Block I and Block II upgrades are introduced.	**NASA Response (in 1995 ASAP appendix):** NASA agrees with this recommendation and will continue to perform the detailed inspections of the Phase II Space Shuttle Main Engines (SSME) that are currently defined. The postflight inspections of both the Block I and Block II SSMEs will be significantly less in frequency than those for today's Phase II SSME due to the major design changes, especially in the turbopumps. However, the program plans to use the same level of strict discipline and attention to detail in carrying out the new inspection program as it has in the past.
Aerospace Safety Advisory Panel *(NASA Charter)*	March 1995	**Finding 16:** The re-start of the Advanced Turbopump Program (ATP) High Pressure Fuel Turbopump (HPFTP) and the start of the Large Throat Main Combustion Chamber (LTMCC) developments were authorized in the spring of 1994. Combined with the ongoing component developments of the Block I engine, this will produce a Block II engine which will contain all of the major component	**Recommendation 16:** Continue the development of the Block II modifications for introduction at the earliest possible time.	**NASA Response (in 1995 ASAP appendix):** NASA agrees with this recommendation. The first flight of the Block I SSME was on STS-70, which was launched on July 13, 1995. The Block II SSME will be available for flight in September 1997.

Independent Assessment Team *(Chartered by)*	Date of Report	Finding	Recommendation	NASA Response
		improvements that have been recommended over the past decade to enhance the safety and reliability of the SSME. Both the Block I and Block II programs have made excellent progress during the current year and are meeting their technical objectives.		
Aerospace Safety Advisory Panel *(NASA Charter)*	March 1995	**Finding 17:** In order to provide an engine health monitoring system that can significantly enhance the safety of the SSME, improvements must be made in the reliability of the engine sensors and the computational capacity of the controller. It is also essential to eliminate the difficulties with the cables and connectors of the Flight Accelerometer Safety Cut-Off System (FASCOS) so that vibration data can be included in the parameters used in the algorithms that determine engine health.	**Recommendation 17:** Expand and emphasize the program to improve engine health monitoring. Continue the program of sensor improvements.	**NASA Response (in 1995 ASAP appendix):** The Space Shuttle program is implementing Discharge Temperature Thermocouples as a replacement for the current temperature sensors on the SSMEs. No other health monitoring improvements are funded at this time because the design was not mature enough to make this a cost-effective project.
Aerospace Safety Advisory Panel *(NASA Charter)*	March 1995	**Finding 18:** The Block II SSME can improve safety if an abort is required because it can be operated more confidently at a higher thrust level. This will permit greater flexibility in the selection among abort modes.	**Recommendation 18:** NASA should reexamine the relative risks of the various abort types given the projected operating characteristics of the Block II SSMEs. Particular emphasis should be placed on the possibility of eliminating or significantly reducing exposure to a Return to Launch Site abort.	**NASA Response (in 1995 ASAP appendix):** Operating the Block II SSMEs at a higher power level requires completion of two certification activities-the Block II SSME hardware certification and the integrated vehicle intact abort certification (loads, thermal, guidance, navigation and control). Because the internal environments and stresses are significantly reduced for Block II SSMEs, the Space Shuttle program approved certification testing to include log-percent power level for intact abort operations. This allows for the future

Independent Assessment Team *(Chartered by)*	Date of Report	Finding	Recommendation	NASA Response
				consideration of increasing the power level for intact aborts to 109 percent pending the results of certification testing. If the increase in power level for intact aborts proves feasible, it would reduce, but not eliminate, exposure to the Return-to-Launch Site abort mode. Performance enhancements vehicle ascent certification environments are currently being developed using 106-percent power level for intact abort operations to improve abort performance and to minimize the risk of design impacts to the Space Shuttle vehicle. A delta certification plan to incorporate log-percent power level for intact abort operations is currently being developed. Implementation of the plan is contingent on a successful Block II SSME test program, the results of vehicle thermal and structural loads trade studies, and the delta certification cost and schedule. Further, even if certification is successful, the decision to utilize log-percent power level for intact aborts will depend on actual flight experience with the Block II SSMEs.
Aerospace Safety Advisory Panel *(NASA Charter)*	March 1995	**Finding 19:** The liquid oxygen tank aft dome gore panel thickness of the Super Lightweight Tank (SLWT) has been reduced significantly on the basis of analyses. To stiffen the dome, a rib was added. The current plan to verify the strength of the aft dome involves a proof test only to limit	**Recommendation 19:** The SLWT aft dome should either be tested to ultimate loads or its strength should be increased to account for the uncertainties in extrapolation.	**NASA Response (in 1995 ASAP appendix):** NASA agrees with this recommendation. At the joint NASA and Martin Marietta Aluminum Lithium Test Article (ALTA) Design Review on August 19, 1994, an aft LO2 dome test was added to the ALTA test program. Adding this stability test will permit the aft dome

Independent Assessment Team *(Chartered by)*	Date of Report	Finding	Recommendation	NASA Response
		load. Buckling phenomena cannot be extrapolated with confidence between limit and ultimate loads.		to be verified to the ultimate load condition. The as-planned test satisfies the buckling concerns of Finding #19.
Aerospace Safety Advisory Panel *(NASA Charter)*	March 1995	**Finding 20:** The structural tests of a segment of an SRB aft skirt in the baseline configuration did not duplicate the strains and stresses previously measured in the tests of the full-scale aft skirt Structural Test Article (STA-3). This suggests that segment testing of the proposed bracket modification to improve the aft skirt's factor of safety may not be valid.	**Recommendation 20:** NASA should reassess the use of the segment test method and reconsider the use of a full scale test article for qualifying the proposed bracket reinforcement.	**NASA Response (in 1995 ASAP appendix):** At the time of the NASA response to the March 1994 ASAP Annual Report, two initial test condition baselining test articles (TA) had been tested to 100- and 70-percent load levels. The TA-1 and TA-3 test loads were analytically derived and validated using empirical data from these tests and STA-3. The TA-3 baseline testing showed excellent correlation with strain response curves measured during the STA-3 test. In addition, a second test article was tested to failure. Strain data obtained from these two specimens was compared to the STA-3 strain data (up to 12%percent loads which was the maximum load level achieved prior to failure initiation during the STA-3 test program). Data from second baseline test, the bracket test, and STA-3 are depicted in the figure below. The strain measurements for the critical weld region for the full-load applications (0 to 12%percent loads) exhibit an average correlation within 8.6 percent and, at 128-percent load levels, the average correlation is within 9.6 percent. (lots of details omitted) In summary, component test results indicate that the external bracket significantly enhances critical weld factors of safety. In addition to

Independent Assessment Team *(Chartered by)*	Date of Report	Finding	Recommendation	NASA Response
				providing substantive quantitative verification of existing analytical techniques, the completed evaluation of the test program results has provided no challenge to or indictment of current flight rationale. The resultant potential benefits from introduction of the bracket are limited. The design change has minimal potential for increasing the Shuttle lift-off wind allowables (and associated probability of launch), as other elements are similarly constraining. The elimination of the Advanced Solid Rocket Motor effort precludes near-term concerns for substantially increased skirt loading. The significant component, subscale and full-scale analysis and test, along with individualized measurements of each aft skirt, provide a level of understanding such that no further concerns exist for a demonstrated 1.28 factor of safety in the critical weld area. Therefore, implementation of the bracket is not planned at this time, and the program plans to change the appropriate specification requirement to reflect this factor of safety to avoid repetitive flight by-flight waivers.
Aerospace Safety Advisory Panel *(NASA Charter)*	March 1995	**Finding 21:** The effort by the NASA logistics organization and its principal contractors has resulted in satisfactory performance. There remain a few problems, such as a tendency towards increased cannibalization, which still require attention.	**Recommendation 21:** Every effort should be made to avoid cannibalizations, particularly on critical components such as the SSME and the IAPU.	**NASA Response (in 1995 ASAP appendix):** While there were some increases in cannibalizations in mid-1994, continued management attention has maintained an overall decreasing trend in cannibalizations. Close attention to related indicators will continue. There are currently four spare IAPUs on the shelf at KSC. No IAPU cannibalizations have

Independent Assessment Team *(Chartered by)*	Date of Report	Finding	Recommendation	NASA Response
				occurred since 1993.
Aerospace Safety Advisory Panel *(NASA Charter)*	March 1995	**Finding 23:** There is a plan to consolidate all logistics elements at KSC except Spacelab over the next three or four years. This should unify the entire logistics and supply organization. The realignments are intended to eliminate duplication of effort, gain efficiency in support and materially reduce the cost of operation.	**Recommendation 23:** Proceed as outlined in the NASA plan.	**NASA Response (in 1995 ASAP appendix):** A single organization consolidating all KSC logistics elements was officially established on April 17, 1995. This new organization integrates logistics functions from the Payload Management and Operations Directorate, the Installation Management and Operations Directorate, the Engineering Development Directorate, and the Shuttle Management and Operations Directorate. This new organization, known as the Logistics Operations Directorate, is now proceeding with internal realignments to eliminate duplication, increase efficiency, and reduce costs while improving customer service.
Aerospace Safety Advisory Panel *(NASA Charter)*	March 1995	**Finding 29:** The Simplified Aid for EVA Rescue (SAFER) was successfully flight tested on the STS-64 mission. Although designed as a rescue device for an astronaut who becomes untethered, SAFER has demonstrated its potential to assist in other safety-critical situations such as contingency EVAs. Five SAFER flight units have been ordered. Plans are to deploy them on Mir and Space Station as well as to carry them on the Space Shuttle only when an EVA is planned.	**Recommendation 29:** Once the flight units are available, NASA should consider routinely flying SAFER units on all Space Shuttle missions which do not have severe weight limitations, This will permit them to be used for those contingency EVAs in which safety can be improved by giving crew members the capability to translate to the location of a problem to make an inspection or effect a repair.	**NASA Response (in 1995 ASAP appendix):** NASA has considered routinely flying SAFER units on all Space Shuttle missions which do not have severe weight limitations and has decided that it is not required. SAFER was specifically designed to be used to rescue an EVA crewmember who had become inadvertently detached from a structure under the circumstances where the Shuttle could not credibly effect a rescue (for example, during Space Station operations when the Shuttle is either not at the Station or is docked to it). As such, it is

Independent Assessment Team *(Chartered by)*	Date of Report	Finding	Recommendation	NASA Response
				classified as an "emergency" device and only needs to be single-string (i.e., zero-fault tolerant). SAFER is not required for other (operational) EVAs. All known, credible, contingency EVAs can be safely accomplished without it. There currently exists an EVA method to get to the External Tank (ET) umbilical doors located on the Orbiter without SAFER, for which each EVA crewmember is briefed prior to flight. Furthermore, the cost of making SAFER operational on all Shuttle flights would be high. To be used as other than an emergency device, significant redesign would be required to make it at least single-fault tolerant. SAFER cannot be stowed on the Primary Life Support Subsystem in the airlock; therefore, special stowage would be required on each flight. Flying two SAFER units on each flight would require stowage for about 8 cubic feet and 200 pounds. Additional EVA training would also be required each time SAFER is flown, regardless of whether or not it is planned to be used. Given the above reasons including the fact that all known, credible, contingency EVAs can be safely accomplished without SAFER, NASA believes that implementing this recommendation is not appropriate at this time.

Independent Assessment Team *(Chartered by)*	Date of Report	Finding	Recommendation	NASA Response
Aerospace Safety Advisory Panel *(NASA Charter)*	March 1994	**Finding 5:** The organization and management of Space Shuttle launch operations at Kennedy Space Center (KSC) continue to benefit from a "continuous improvement process" managed by the Shuttle Processing Contractor (SPC). Greater employee involvement, better communications, strengthened employee training and the use of task teams, process improvement teams, and a management steering committee have been major factors in this improvement.	**Recommendation 5:** A strong commitment to achieving "continuous improvement," despite budget cutbacks, should be maintained, at the same time recognizing the paramount priority of safety.	**NASA Response (in 1994 ASAP appendix):** The SPC continues its deep commitment to Continuous Improvement (CI) with over 550 active process improvement teams and 86 percent of their 6,600-person workforce trained in the principles and precepts of CI. The underlying theme of all SPC initiatives is their pledge for the highest level of performance at the lowest possible cost with absolute dedication to safety and quality.
Aerospace Safety Advisory Panel *(NASA Charter)*	March 1994	**Finding 6:** More than 1,200 positions have been eliminated by the SPC since September 1991 with only about 22 percent being achieved through involuntary separations. Present reductions have been achieved without an apparent adverse effect on the safety of launch processing. A comparable further reduction has been called for by the end of FY 1995. These additional reductions cannot likely be made without a higher probability of impacting safety.	**Recommendation 6:** KSC and SPC management must be vigilant and vocal in avoiding any unacceptable impacts on safety as a result of cost reductions planned for FY 1995 and beyond.	**NASA Response (in 1994 ASAP appendix):** KSC and SPC management are firmly committed to the precept that safety will not be compromised as a result of cost reductions. Procedures for processing a safe space vehicle have been established and are strictly followed. These procedures are revised only after a thorough review by technical and safety personnel to ensure that safety will not be compromised. Schedule times are flexible; safety requirements are not. As the cost reductions continue, KSC is committed to processing only the number of vehicles that can be completed safely within available resources.
Aerospace Safety Advisory Panel *(NASA Charter)*	March 1994	**Finding 7:** Several problems at KSC have been attributed to human factors issues. KSC has recently formed a human factors task force to address these problems.	**Recommendation 7:** KSC should ensure that the human factors task force includes individuals with training and experience in the field. Specific assistance should be sought from appropriate research centers and technology groups	**NASA Response (in 1994 ASAP appendix):** The Management Steering Committee, chaired by the KSC Launch Director, established a CI team to support the Incident Error Review Board (IERB) in

Independent Assessment Team *(Chartered by)*	Date of Report	Finding	Recommendation	NASA Response
			within NASA.	assessing human-error factors. This team reviewed the human-factors aspects of the Freon Coolant Loop Number 1 Pump Package incident on OV-105/STS-61 and made nine specific recommendations concerning the incident. A tenth recommendation addressed the need for the team to obtain training in human factors principles. The CI Human Factors Team has since received training on human factors from the Battelle Memorial Institute in a seminar conducted at KSC. Some team members attended a class on incident investigation taught by The Central Florida Chapter of the National Safety Council. The team has subsequently added a new member with extensive experience in human factors from Analex Space Systems, Inc. The team will continue to pursue additional human factors training.
Aerospace Safety Advisory Panel *(NASA Charter)*	March 1994	**Finding 8:** KSC has developed a Structured Surveillance Program with the objectives of decreasing overall process flow time, increasing "first-time quality," and reducing cost. The program approach involves reducing the reliance on inspections for assuring quality. Structured Surveillance also is proving valuable as a tool for the effective deployment of quality assurance resources.	**Recommendation 8:** The Structured Surveillance program should be continued and cautiously expanded.	**NASA Response (in 1994 ASAP appendix):** KSC has improved structured surveillance data elements, data collection methods, and metrics for the entire program at KSC (both Government and contractor) and has discussed these improvements with the Panel. To ensure effective implementation of the Government application of the structured surveillance program, the leadership of this effort has been moved up to the directors of the two implementing organizations. These directors co-chair a newly formed control board that manages the generation and modification of the

Independent Assessment Team *(Chartered by)*	Date of Report	Finding	Recommendation	NASA Response
				policies, procedures, and training necessary for full implementation of structured surveillance.
Aerospace Safety Advisory Panel *(NASA Charter)*	March 1994	**Finding 9:** Thermal damage was noted on the STS-56 (OV-103) elevon tiles. The slumping of the tiles indicated that the tile surface reached a temperature of approximately 1,000 degF. A temperature of this magnitude suggests that the temper and strength of the underlying aluminum structure could have been affected.	**Recommendation 9:** NASA should initiate an analysis to determine the temperature profile of the underlying aluminum structure of the elevens and its possible consequences on the strength of the Orbiter structure.	**NASA Response (in 1994 ASAP appendix):** On STS-56 (OV-103), an alternate forward elevon schedule (part of Center of Gravity Expansion Activities, Detailed Test Objective (DTO) 251) was flown. This was the maximum-up schedule (12 degrees up) ever flown. There was some tile slumping (caused by temperatures exceeding 1500 degrees F) at the center hinge location, but detailed postflight vehicle inspection confirmed that the aluminum structure was neither damaged nor subjected to unacceptable temperatures. Positive Margins-of-Safety have been verified subsequently through thermal design analysis. A redesign has been certified and is currently being installed on all four vehicles. This new design will allow a full-up (16 degrees) elevon without overheating of the underlying structure. Prior to incorporation of this modification, the elevon schedule had been constrained to 7 degrees up.
Aerospace Safety Advisory Panel *(NASA Charter)*	March 1994	**Finding 10:** The Shuttle tiles have provided effective heat protection. However, the surface of the tiles is easily damaged and their shrinkage and distortion properties are not as low as desired. A new tile formulation with superior characteristics and possibly lower density is being explored.	**Recommendation 10:** NASA is encouraged to support the development of thermal protection tiles with improved mechanical properties and lower density than the current Shuttle tiles. Autoland in a contingency mode, but do not plan to demonstrate Autoland until a firm requirement mandates a demonstration."	**NASA Response (in 1994 ASAP appendix):** NASA is considering several improvements to the Tile Protective System (TPS). On SIX-51 (OV-105), a tougher tile coating on Fiber Reinforced Composite Insulation (FRCI-12) tiles was flown as a DTO on a few door tiles on the base heatshield. There were no hits on these tiles. However, the DTO will

Independent Assessment Team *(Chartered by)*	Date of Report	Finding	Recommendation	NASA Response
				be flown a number of times to obtain a good evaluation of the improvement expected from this coating. This tougher coating will enhance turnaround activities by minimizing tile replacement due to coating damage.
Aerospace Safety Advisory Panel *(NASA Charter)*	March 1994	**Finding 11:** NASA has made excellent progress on the engineering of the Multipurpose Electronic Display System (MEDS) for retrofitting Orbiter displays. However, there is no formal program to identify and include the safety advantages possible from a fully exploited MEDS.	**Recommendation 11:** A thorough review of the performance and safety improvements possible from a completely developed MEDS should be conducted based on crew inputs to system designers and researchers. A definitive plan should be developed to determine the schedule/cost implications of such improvements, and, if warranted, implementation should be scheduled as soon as possible.	**NASA Response (in 1994 ASAP appendix):** The MEDS, when operational, will provide a foundation for potential upgrades and enhancements to the current crew displays that will improve safety. The initial MEDS program must be on line in a timely manner to replace aging electro-mechanical devices. The flight crew, mission operations, engineering, training, and safety, reliability, and quality assurance program personnel have all agreed that the "transparency" achieved by designing enhanced displays similar in function and appearance to the current displays is the optimum solution initially. By designing similar but enhanced displays, the impacts for a mixed fleet while MEDS is being installed are minimized in the areas of training and flight software. There is only one single-motion-base simulator, therefore, crews training for MEDS or non-MEDS equipped vehicles will be able to train on displays that are similar to those they will use in flight. Similar display formats do not require any changes to the existing flight software. Once trainers and laboratories are equipped with MEDS, the test beds will be in place to evaluate display

Independent Assessment Team *(Chartered by)*	Date of Report	Finding	Recommendation	NASA Response
				upgrades. The next phase of the total orbiter displays-and-controls update activities will be to achieve a world-class state-of-the-art system by expanding the total complement to digital electronics replacing current wiring and switches as practical. Planning for this phase is beginning, but the exact implementation schedule will be dependent on funding availability as well as future human-tended spacecraft planning.
Aerospace Safety Advisory Panel *(NASA Charter)*	March 1994	**Finding 12:** The Improved Auxiliary Power Unit (IAPU) has experienced problems that have impacted Space Shuttle processing and logistics.	**Recommendation 12:** A new focus on increasing the reliability of the total IAPU system should be initiated and supported until the identified problems are solved.	**NASA Response (in 1994 ASAP appendix):** To improve Auxiliary Power Unit (APU) reliability, a continuous improvement program has been underway since the STS 51-L accident. Results from this program include the completion of an IAPU "upgrade" project (which eliminated injector tube corrosion, exhaust housing cracking, and some Criticality 1 concerns), a new design for the turbine wheel, an improved APU controller and fuel isolation valve, and the more reliable "Path a" Gas Generator Valve Module (GGVM). These changes have resulted in a greatly reduced rate of APU in-flight anomalies and fewer delays to the Shuttle processing and logistics support activities. Elements of the continuous improvement program not yet complete, but now underway include development of an entirely new GGVM, certification of a new material for the fuel pump thermal isolator, and development of more vibration-resistant thermostats. As the new

Independent Assessment Team *(Chartered by)*	Date of Report	Finding	Recommendation	NASA Response
				GGVM is incorporated in the fleet, the APU should be totally certified for its planned 75-hour life capability.
Aerospace Safety Advisory Panel *(NASA Charter)*	March 1994	**Finding 13:** In its response to the Panel's last Annual Report, NASA indicated that "The program is reviewing the operational flight rules pertaining to Autoland, we have budgeted upgrades in software and hardware to improve the Autoland functionality, the life sciences organization is collecting physiological data and developing countermeasures to ensure adequate crew performance as the mission duration increases. We are confident with using Autoland in a contingency mode, but do not plan to demonstrate Autoland until a firm requirement mandates a demonstration."	**Recommendation #13:** The focus of Autoland should not be exclusively on long-duration missions. NASA should formulate a complete set of operational procedures needed for emergency use of Autoland, taking into account a full range of operational scenarios and equipment modifications that might be beneficial. These include upgrades to the Microwave Scanning Beam Landing System (MSBLS) receiver group, and installation and certification of Global Positioning System (GPS) capability.	**NASA Response (in 1994 ASAP appendix):** It is agreed that the Autoland system should not be focused just on long-duration missions. Currently, mission planning requirements do not include missions longer than approximately 18 days, including the Space Station program. The entry systems requirements including piloting techniques are continuously assessed for improvements. Autoland backup capabilities as well as heading alignment cone piloting enhancements are being developed and will be incorporated as we continue to implement the flight program. MSBLS/GPS type systems are being considered and will be brought on line as improvements are practical No specific training or procedures are required for the emergency use of Autoland, as the only manual tasks required of the crew in an Autoland scenario (e.g., deploying landing gear, postlanding braking, air data probe deployment, and navigation sensor data incorporation) are identical to those performed in a manual landing. Present flight rules define orbiter and landing-site equipment that must be functioning to perform an Autoland landing. The decision to engage Autoland in a contingency is left to the commander's discretion to protect the safety of the crew.

Independent Assessment Team *(Chartered by)*	Date of Report	Finding	Recommendation	NASA Response
				Exact flight rules to define all Autoland engagement criteria exceed the number of failure cases addressed by the current flight rules. A program to expand these criteria would require large resource commitments to develop and is not currently in the planning.
Aerospace Safety Advisory Panel *(NASA Charter)*	March 1994	**Finding 14:** The SSME has performed well in flight but has been the cause of launch delays and on-pad launch aborts that were primarily attributable to manufacturing control problems.	**Recommendation 14:** Continue to implement the corrective actions developed by the NASA and Rocketdyne manufacturing process review teams and devise techniques for detecting and/or precluding recurrence of the types of problems identified.	**NASA Response (in 1994 ASAP appendix):** The process audit teams and the NASA and Rocketdyne incident investigation teams have both identified process improvements which either have been or will be incorporated into all areas of the engine program. These process improvements will improve detection and preclude the recurrence of manufacturing control problems in any of our new or recycled hardware and substantially reduce the likelihood of associated problems leading to launch delays or launch pad aborts.
Aerospace Safety Advisory Panel *(NASA Charter)*	March 1994	**Finding 15:** "Sheetmetal" cracks in the Phase II (current) High Pressure Fuel Turbopump (HPFTP) have become more frequent and are larger than previously experienced. This has led to the imposition of a 4,250-second operating time limit and a reduction of allowable crack size by a factor of four. Congress has delayed the funding for restarting the development of the alternate HPFTP. This new turbopump design should eliminate the cracking problem.	**Recommendation 15:** Restart the development and certification of the alternate HPFTP immediately.	**NASA Response (in 1994 ASAP appendix):** NASA fully agrees with the recommendation to restart the alternate HPFTP immediately. Congressional authority to restart the program was received on April 14, 1994. The Space Shuttle program (SSP) is proceeding with the restart. The alternate HPFFP will be incorporated into the Block II SSME configuration with first flight scheduled for September 1997.

Independent Assessment Team *(Chartered by)*	Date of Report	Finding	Recommendation	NASA Response
Aerospace Safety Advisory Panel *(NASA Charter)*	March 1994	**Finding 16:** The approved parts of the engine component improvement programs, now organized into block changes, are progressing well. The Block I grouping will enter formal certification testing by mid-1994. Progress in the Block II effort is, however, hampered by the delay in restarting the alternate HPPTP development effort.	**Recommendation 16:** Continue efforts to complete all of the Block II development as soon as possible.	**NASA Response (in 1994 ASAP appendix):** NASA fully agrees with this recommendation and is firmly committed to developing and implementing all of the SSME safety improvements, including the Alternate HPFTP and the Large Throat Main Combustion Chamber. Upon completion of these modifications, a significant reduction in Shuttle operational risk will be realized. Initiation of full-scale development testing is currently planned for mid-1995, with first- flight capability scheduled for September 1997.
Aerospace Safety Advisory Panel *(NASA Charter)*	March 1994	**Finding l7:** Engine sensor failures have become more frequent and are a source of increased risk of launch delays, on-pad aborts, or potential unwarranted engine shutdown in flight.	**Recommendation 17:** Undertake a program to secure or develop and certify improved, more reliable engine condition sensors.	**NASA Response (in 1994 ASAP appendix):** Improved hot gas temperature-sensing instrumentation is undergoing development testing and is planned for the first flight in FY 1995. A two-step improvement process for pressure and flow measuring instrumentation is also under way. As a first step, a new screening selection process has been developed for immediate implementation to improve sensor quality control. The second step, redesigning and improving sensors, is being implemented as these improvements become available.
Aerospace Safety Advisory Panel *(NASA Charter)*	March 1994	**Finding 18:** The SSME health monitoring system comprising the engine controller and its algorithms, software, and sensors is old technology. The controller's limited computational capacity precludes incorporation of more state-of-the-art algorithms and decision rules. As a result, the	**Recommendation 18:** The SSME program should undertake a comprehensive effort to improve the capability and reliability of the SSME health monitoring system. Such a program should include not only improved sensors but also a more capable controller and advanced algorithms.	**NASA Response (in 1994 ASAP appendix):** NASA agrees that the development and implementation of an advanced health monitoring system for the SSME is potentially worth pursuing. A system currently being considered would incorporate more processing capability in an upgraded controller and allow the utilization of

Independent Assessment Team *(Chartered by)*	Date of Report	Finding	Recommendation	NASA Response
		probabilities of either shutting down a healthy engine or failing to detect an engine anomaly are higher than necessary.		advanced health monitoring software algorithms. With an improved system of this nature, the probability of shutting down a healthy engine would be reduced while the probability of preventing a catastrophic failure would be increased. NASA is reviewing proposals that would certify and implement this new capability into the Block II SSME configuration.
Aerospace Safety Advisory Panel *(NASA Charter)*	March 1994	**Finding 19:** A segment of an aft skirt will be used to test the effectiveness of an external bracket modification in reducing the overall bending stress of the skirt. The validity of using an 11-inch-wide test specimen to determine the effectiveness of the bracket is yet to be demonstrated.	**Recommendation 19:** NASA should evaluate the first specimen test results to see if the strains in the weld area duplicate the strains found when a full aft skirt was tested in the Static Test Article-3 (STA-3) test. If not, another test approach should be pursued.	**NASA Response (in 1994 ASAP appendix):** Tests on three of the four aft skirt test specimens have been completed. The baseline test article (TA-l), which represents the current aft skirt configuration, has been subjected to 100 percent of the developed load case. Based on a thorough evaluation of the TA-1 test data and correlation of the data with STA-3 test results, it is clear that the weld area strain field developed in the TA-1 test article correlates well with the strain field in this same area on the STA-3 aft skirt. This correlation confirms the validity of the test approach being used. The second test article (TA-4) was also in the baseline configuration and was subjected to a maximum load of 70 percent of the developed load case. This article utilized the photoelastic method for determining the strain field as opposed to using the typical strain gage method used on all other articles in this test program. This test verified that the STA-3 strain field could be duplicated on two-separate articles within acceptable limits and that no high strain areas were

Independent Assessment Team *(Chartered by)*	Date of Report	Finding	Recommendation	NASA Response
				overlooked during the analytical study of the test article response. The third test article (TA-2), which has an external bracket for the reduction of strain in critical weld region, was subjected to 205 percent of the developed load case with no structural anomalies occurring. Comparisons of the baseline configuration article (TA-1) and the bracketed configuration article (TA-2) were made at 100 percent loads. This comparison demonstrated that there was approximately a 50 percent reduction in the average weld strain in the critical weld region. The baseline configuration article (TA-1) was tested to failure during June 1994. This test defined the weld failure strain for the TA-1 article. Test data obtained from this test is being compared to the results of the 205 percent TA-2 test and the STA-3 test to develop a comparative assessment of the benefit gained by the addition of the external bracket modification If this assessment does not reveal adequate stress reduction, additional testing may be indicated.
Aerospace Safety Advisory Panel *(NASA Charter)*	March 1994	**Finding 20:** A small crack was found in the inner wall of a forward Redesigned Solid Rocket Motor (RSRM) casing used for STS-54. Although slightly above the specified minimum detectable size, it was well within the acceptable limits for safe flight. This was the first time that a crack had been found in a	**Recommendation 20:** The X-ray and magnetic particle inspection program criteria should be re-evaluated to assess their ability to detect cracks of the size found.	**NASA Response (in 1994 ASAP appendix):** A single crack was detected during standard refurbishment of the forward segment flown on STS-54. The subsequent investigation determined that an inclusion introduced into the metal during the manufacturing process caused the crack to form during heat treatment of the cylinder. The segment had been flown four

Independent Assessment Team *(Chartered by)*	Date of Report	Finding	Recommendation	NASA Response
		forward segment, although cracks have previously been detected in other segments. The crack occurred during the manufacturing heat treatment process because of an inclusion in the parent material.		times prior to detection of the crack. Prior to each of these flights, the cylinder was proof tested, which demonstrated safe life (4 mission cycles) in the membrane region where this crack was found. All areas of the RSRM metal hardware (case, nozzle, igniter) have been reevaluated with respect to critical flaw size and whether proof test, magnetic particle inspection or other nondestructive evaluation methods are required to demonstrate compliance to safe life requirements. As a part of this reevaluation, an RSRM hardware configuration specific magnetic particle inspection probability of detection (POD) study was completed. Prior to this study, crack detection threshold limits were based on industry standards. This RSRM magnetic particle inspection POD study incorporated RSRM specific geometries, physical access, gauss levels, surface finishes, potential flaw types, inspection times, and multiple operators. The results demonstrated that, in the areas of the RSRM hardware upon which magnetic particle inspection is solely relies, the detectable flaw size is smaller than the critical flaw size. Proof test is the method of choice used to demonstrate safe life in the case membrane region, not magnetic particle inspection. X-ray inspection is not used for crack detection in RSRM metal hardware. Magnetic particle inspection capability

Independent Assessment Team *(Chartered by)*	Date of Report	Finding	Recommendation	NASA Response
				has been reevaluated and, as a result of an RSRM hardware configuration specific POD study, detection capability versus location is well characterized. In those areas that rely solely on magnetic particle inspection, the detectable flaw size is smaller than the critical flaw size.
Aerospace Safety Advisory Panel *(NASA Charter)*	March 1994	**Finding 21:** The Advanced Solid Rocket Motor (ASRM) project has been canceled. Some elements from the ASRM development have possible reliability and/or performance benefits if they were applied to the RSRM.	**Recommendation 21:** Examine the potential applicability and cost-effectiveness of including selected ASRM design features in the RSRM.	**NASA Response (in 1994 ASAP appendix):** The RSRM project has continued to consider ASRM design attributes, as motivated by RSRM flight results, performance goals, obsolescence issues, and cost enhancements. Examples of these are the RSRM project's ongoing initiative to replace metal parts vapor degrease cleaning with an aqueous process and the ongoing initiative to remove asbestos from the primary RSRM insulation material. Both of these obsolescence replacement activities have drawn from previous ASRM activity. There are numerous ASRM design attributes for potential consideration for future adoption in the RSRM. These include, in part, propellant formulation (hydroxyl-terminated polybutadiene), sealing system designs, pressure vessel design and materials, some attributes of the nozzle design and some manufacturing process automation, such as insulation strip winding and Real Time Radiography (RTR) for nozzle and case inspections. At present, the RSRM project is considering incorporation of the previous ASRM RTR system into the RSRM

Independent Assessment Team *(Chartered by)*	Date of Report	Finding	Recommendation	NASA Response
				hardware verification process and the use of ASRM manufacturing equipment for nozzle fabrication. Based on collective consideration of the implementation cost impacts and RSRM flight demonstrated hardware performance, no requirements have been established to pursue the ASRM sealing system pressure vessel, or nozzle design attributes. However, future justifications in these areas are possible based on continuing RSRM flight evaluation or increased Shuttle program performance requirements.
Aerospace Safety Advisory Panel *(NASA Charter)*	March 1994	**Finding 22:** A chamber pressure excursion of 13 psi (equivalent to a thrust perturbation of 54,000 pounds) occurred in one of the RSRMs of STS-54 at 67 seconds of motor operation. A thorough investigation of the phenomenon was initiated and found that the most probable cause was the expulsion of a "slug" of liquid slag (aluminum oxide) generated during normal propellant combustion. Analyses showed that, even under statistical worst-case conditions, the safety of the Shuttle system is not compromised by such perturbations. Some testing and analyses are still scheduled to complete the investigation.	**Recommendation 22:** Complete and document the investigation, and continue the established practice of monitoring chamber pressures and examining possible remedial actions.	**NASA Response (in 1994 ASAP appendix):** The RSRM project has concluded its investigation and has determined that the generic cause of chamber pressure excursions is the periodic expulsion of liquid slag (aluminum oxide). Slag is produced during normal propellant combustion and is temporarily accumulated in the aft end of the nozzle prior to being "dumped" through the nozzle. The RSRM project has implemented the recommendations set forth by the Panel and has established a program to continue to evaluate multiple parameters that could affect the pressure perturbations. The results and findings of these studies are being reviewed and changes to the processes or specification will be made if it is concluded that they will be beneficial to the program. A very detailed study of many process and material parameters that influence slag formation has been conducted

Independent Assessment Team *(Chartered by)*	Date of Report	Finding	Recommendation	NASA Response
				to determine if a statistical correlation exists between these parameters and the pressure perturbations. Examples of these parameters include humidity, time in process, ammonium perchlorate (AP) moisture content, mix times, cast times, viscosity, mechanical properties, and many others. No special causes or process deviations related to pressure perturbations have been identified. Analyses have shown that, under the worst case conditions, the safety of the Shuttle system is not compromised by the pressure phenomenon. The results of this extensive study are currently being documented by Thiokol. Chamber pressures are being analyzed or monitored by Statistical Process Control charts. Eighteen acceptance tests are conducted for each lot of AP. The flight and static test pressure perturbation history is reviewed before every launch. Additionally, several other studies are being conducted to improve the predictability of pressure excursions. Quench bomb tests recorded with high-speed film have been used to identify burn-rate differences in the various propellant mixes. Five-inch diameter spin motor tests are being conducted to evaluate the amount of slag that is generated in a motor. This testing employs a design of experiments to evaluate the effects of ground AP, unground AP, differences in AP vendors, aluminum-particle sizes and vendor differences, particle- size

Independent Assessment Team *(Chartered by)*	Date of Report	Finding	Recommendation	NASA Response
				distributions, iron oxide surface area, and several other parameters.
Aerospace Safety Advisory Panel *(NASA Charter)*	March 1994	**Finding 23:** A Super Light Weight External Tank (SLWT) has been proposed as a means of increasing the payload performance of the Space Shuttle. The tank would employ structural changes and be made from an Aluminum-Lithium (Al-Li) alloy. The SLWT appears to involve no safety decrement and low technical risk.	**Recommendation 23:** The impact of the SLWT on the total system should be carefully examined.	**NASA Response (in 1994 ASAP appendix):** The External Tank Project and Shuttle program are thoroughly committed to an integrated system approach to the design and development of the SLWT. A systems integration plan to ensure the timely assessment of SLWT effects on the Shuttle system, and to ensure program-wide-managed implementation is currently in development.
Aerospace Safety Advisory Panel *(NASA Charter)*	March 1994	**Finding 24:** The Integrated Logistics Panel (ILP), which meets at 6-month intervals to report and coordinate the activities of the NASA Centers and their contractors, is performing a vital service in helping to control the entire Space Shuttle logistics program.	**Recommendation 24:** The ILP should continue to be supported as an effective means of maintaining control and coordination of the entire logistics program.	**NASA Response (in 1994 ASAP appendix):** NASA Centers and contractors continue to support the ILP and related integration activities. All project elements benefit from the exchange of technical data presented at ILP meetings. NSTS 07700, Volume XII, "Integrated Logistics Requirements", the program's requirements for integrated logistics was recently updated, and the ILP provided a focus for this effort. The ILP will continue to serve as the forum for problem solving, technical information exchange, and the appropriate level of control, coordination, and integration of Shuttle logistics support.
Aerospace Safety Advisory Panel *(NASA Charter)*	March 1994	**Finding 25:** The Vision 2000 cost-reduction program promulgated in May 1993 includes some major changes in the logistics and support areas.	**Recommendation 25:** All changes that might impair logistics and support functions in the name of cost-cutting should be most carefully reviewed before implementation.	**NASA Response (in 1994 ASAP appendix):** As the program continues to plan for the future, the Vision 2000 approach to the program will remain relevant. The Vision 2000 approach is based on the following two principles: operate within SSP experience and locate

Independent Assessment Team *(Chartered by)*	Date of Report	Finding	Recommendation	NASA Response
				decision making near operations. Notwithstanding the advantages these principles offer to the current Shuttle logistics community, the SSP office will remain vigilant and exercise caution when making cost-cutting decisions and changes necessitated by funding reductions.
Aerospace Safety Advisory Panel *(NASA Charter)*	March 1994	**Finding 26:** Introduction of the Just-In-Time (JIT) manufacturing and shelf-stocking concept by NASA logistics at KSC is a potentially effective method of cost control.	**Recommendation 26:** JIT should be used with caution and with a thorough understanding of how it may impact the availability of Space Shuttle spares and hardware supplies.	**NASA Response (in 1994 ASAP appendix):** All projects have cautiously considered the JIT method of spares provisioning and are in different stages of planning and implementation. Launch and Landing Project (L&L) has applied the JIT method to manufacturing activity. In addition, L&L is further studying alternative methods of prioritizing repair work which may be applied to JTT repairs at a later date. Operational availability will be uppermost in any JIT implementation decision strategy affecting spares and hardware supplies.
Aerospace Safety Advisory Panel *(NASA Charter)*	March 1994	**Finding 31:** NASA's past approach to software development has been to incorporate it within the individual programs, allowing them to determine their own requirements and development, verification, and validation procedures. In the future, as the complexity of NASA's computer systems and the need for interoperability grow, this mode of operation will be increasingly less satisfactory. While NASA has some good software practices, it does not have the overall management	**Recommendation 31:** NASA should proceed to develop and implement an Agency-wide policy and process for software development, verification, validation, and safety as quickly as possible.	**NASA Response (in 1994 ASAP appendix):** A software process action team, sanctioned by the Acting Deputy Administrator and the Information Resource Management Council, is working on Agency software issues including roles, responsibilities, standards, and procedures. The Office of Safety and Mission Assurance is leading the Agency in strategic planning for the Agency-wide software program with a NASA working group consisting of members from Centers, industry, and academia.

Independent Assessment Team *(Chartered by)*	Date of Report	Finding	Recommendation	NASA Response
		policies, procedures, or organizational structure to deal with these complex software issues.		A Software Safety Standard has been completed. Our present plan is to establish this as an interim standard for 1 year at which time it will become a mandatory requirement for newly developed software. The Software Independent Verification and Validation Facility will focus on the Agency software processes for development, verification, and validation in accordance with the Software Strategic plan currently being developed.
Aerospace Safety Advisory Panel *(NASA Charter)*	March 1994	**Finding 32:** NASA has consolidated Life and Microgravity Sciences and Applications, including human factors in NASA Headquarters Code U. A space Human Factors & Engineering Program Plan is being prepared to guide future research activities. There remains, however, a clear need for more operational human factors input in both the Space Shuttle and Space Station programs.	**Recommendation 32:** The Program Plan should be expanded to include support of the operating space flight programs to ensure that sufficient human factors expertise is included.	**NASA Response (in 1994 ASAP appendix):** The Life and Biomedical Sciences and Applications Division is committed to developing a new, dynamic Space Human Factors Engineering Program that will integrate human factors knowledge and methodologies into the Shuttle and Space Station programs. Leadership of this program resides within the Environmental Systems and Technology Branch of Code U, which is responsible for directing an integrated Space Human Factors Engineering research and development program. New processes and procedures will be developed to enhance crew training, augment the design of complex automated systems, and use extreme and isolated environments to conduct analog studies. Research programs will continue; however, the primary focus of the program will shift from knowledge acquisition to knowledge application. This shift will extend human factors support to operational areas and emphasize the improvement of processes and

Independent Assessment Team *(Chartered by)*	Date of Report	Finding	Recommendation	NASA Response
				products. The Space Human Factors Engineering Program Plan developed in 1993, is being revised to reflect this shift of emphasis, and an implementation plan will be developed to establish and maintain this new focus. Emphasis will be placed on identifying specific, adequate funding for meaningful results, and promoting the added value of human factors through concurrent engineering throughout the Agency. A Space Human Factors Engineering Customer Team, currently being established at Headquarters with representatives from Codes U, M, R, and Q, is being received in -a spirit of cooperation and collaboration. These changes should create a safer and more productive operational environment for all flight and ground activities planned for current and future programs.
Aerospace Safety Advisory Panel *(NASA Charter)*	March 1993	**Finding 9:** The Space Shuttle automatic landing system needs only minimal additional analysis and a few system design changes to extend its performance limits and to support a complete definition of flight rules for its use. Cancellation of the detailed test objective for an automatic landing on the flight of STS-53 has further delayed the specification of these capabilities and the appropriate operational role of the automatic landing system.	**Recommendation 9:** Define the requirements and demonstrate the capability for an automatic landing system as soon as possible.	**NASA Response (in 1993 ASAP appendix):** The orbiter currently has a capability for automatic landings, to be used as a contingency when the commander and the pilot are incapacitated or incapable of landing the orbiter using nominal Control Stick Steering (CSS). Certification of contingency Autoland has involved partial flight demonstration; on STS-2, -3, and –4 Autoland (automatic landing) was engaged from 10,000 ft. to as low as 125 ft. Further certification testing of contingency Autoland has not been identified as a requirement. Postflight data from each mission have been

Independent Assessment Team *(Chartered by)*	Date of Report	Finding	Recommendation	NASA Response
				reviewed and indicate no instances of unexpected divergence by the nonactive contingency Autoland from the reference trajectory. The requirements for demonstrating an automatic landing on the Shuttle have been developed as part of a DTO. However, this DTO is not currently scheduled. Reasonable mission rules, placards, microwave landing system calibration, and crew training requirements have been identified. Software changes desirable to enhance redundancy management of navigation sensors have been developed, though not yet implemented. Options for automation of landing gear deployment, air data probe deployment, braking, and nosewheel switching have been developed for incorporation in a long-duration orbiter program. We currently have no plan to demonstrate the Autoland System. This policy is the same as not demonstrating a Return to Launch Site or Transatlantic Abort (RTLS or TAL). The policy is not to take any additional risk for demonstration purposes without a firm requirement. As you know, the Office of Space Flight (OSF) is reviewing a crew exchange to preclude pilots from landing on long-duration flights to Space Station which extend beyond the crew's certified capability to land. Additionally, the OSF has developed an on-orbit simulator for practicing landings prior to entry. This

Independent Assessment Team *(Chartered by)*	Date of Report	Finding	Recommendation	NASA Response
				will enhance crew performance during landing. In summary, the program is reviewing the operational flight rules pertaining to Autoland, we have budgeted upgrades in software and hardware to improve the Autoland functionality, the life sciences organization is collecting physiological data and developing countermeasures to ensure adequate crew performance as the mission duration increases. We are confident with using Autoland in a contingency mode, but do not plan to demonstrate Autoland until a firm requirement mandates a demonstration.
Aerospace Safety Advisory Panel *(NASA Charter)*	March 1993	**Finding 10:** NASA has funded the development and installation of a Multi-Purpose Electronic Display System (MEDS) for retrofit into the Orbiter. This system will replace the conventional electro- mechanical instruments with flat panel displays.	**Recommendation 10:** The inherent operational and potential safety benefits of Multi-Purpose Electronic Display System.	**NASA Response (in 1993 ASAP appendix):** The magnitude of the modifications to the orbiter vehicles to incorporate the MEDS is quite large. This is known to involve removal and installation of flight deck panels, installation of avionic Line Replaceable Unit (LRU) cooling ducts, and installation of new LRU wiring and the LRUs themselves. The nature of these modifications coupled with the subsystem development schedule, testing schedule, and delivery dates of MEDS hardware, warrant installation of the MEDS during orbiter maintenance/interval inspection down periods. First flight is scheduled in the fourth quarter of FY 1996.

Independent Assessment Team *(Chartered by)*	Date of Report	Finding	Recommendation	NASA Response
Aerospace Safety Advisory Panel *(NASA Charter)*	March 1993	**Finding 11:** The inventory of Auxiliary Power Units is currently being upgraded to an Improved Auxiliary Power Unit configuration to improve reliability and service life. The upgrade program, however, projects a condition of zero spares in the future due to time limits on some parts.	**Recommendation 11:** NASA should take the steps necessary to preclude a situation of zero Improved Auxiliary Power Unit spares.	**NASA Response (in 1993 ASAP appendix):** The entire orbiter fleet will be upgraded to fly only IAPUs with the completion of the OV-104 Orbiter Maintenance Down Period (OMDP) 1. The spares posture is improving, but cannibalization will continue to be a possibility until all older APUs are upgraded to IAPUs and are available for installation in the field.
Aerospace Safety Advisory Panel *(NASA Charter)*	March 1993	**Finding 13:** The results of flight tests on the Orbiter Columbia (OV-102) using pressure and strain gage measurements on the wing showed that the calculated ascent loads on the wing are conservative. Additional flight tests to be conducted will measure the pressure distribution and strains on the wing and tail of OV-102. These data are required to substantiate that the predicted applied and internal loads on the wing and tail are conservative.	**Recommendation 13:** Conduct the planned tests as expeditiously as possible. Particular emphasis should be placed on the loads on the tail.	**NASA Response (in 1993 ASAP appendix):** The Space Shuttle program has conducted a series of structural DTOs flights to collect the pressure and strain gage data on wing loads. Additional DTOs are planned for STS-55 and STS-58. The collected flight data will be used to verify the orbiter aerodynamic data base which has been used in loads analyses. Vehicle loads analyses are expected to be completed by October 1994.
Aerospace Safety Advisory Panel *(NASA Charter)*	March 1993	**Finding 14:** The Space Shuttle Main Engine program is doing well and has sufficient spares. However, the engines still require meticulous attention to detail in inspections and tests.	**Recommendation 14:** Continue the vigilant implementation of the inspection and test procedures while design solutions for known weaknesses are being addressed.	**NASA Response (in 1993 ASAP appendix):** The SSME program will continue vigilant implementation of improved inspection techniques and acceptance test procedures. Design solutions, recurrence controls, limitations, and product improvements are addressed routinely to assure and increase operating margins and safety margins.
Aerospace Safety Advisory Panel *(NASA Charter)*	March 1993	**Finding 15:** The individual major component improvement programs are making progress. However, a total engine upgrade is being	**Recommendation 15:** The identified Space Shuttle Main Engine design improvements are vital to the reduction of Space Shuttle operational risk. Therefore, NASA should	**NASA Response (in 1993 ASAP appendix):** The identified SSME design improvements are vital to the reduction of Space Shuttle operational risk. Therefore,

Independent Assessment Team *(Chartered by)*	Date of Report	Finding	Recommendation	NASA Response
Charter)		delayed because the High Pressure Fuel Turbopump (HPFTP) part of the Advanced Turbopump Program (ATP) is on hold. The highly effective Large Throat Main Combustion Chamber (LTMCC) has finally been made a formal part of the Space Shuttle Main Engine program by NASA but has been denied appropriations by Congress. Schedule disparities among the various component improvements lead to interim certifications of components in engine configurations that will never fly and to unnecessary duplication of certification tests.	reinstate the Advanced Turbopump Program High Pressure Fuel Turbopump development; continue to press for approval of the Large Throat Main Combustion Chamber; and examine carefully the benefits of integrating all the individual modifications into a block change program.	NASA should reinstate the ATP HPFTP development as well as continue to press for approval of the LTMCC, and examine carefully the benefits of integrating all the individual modifications into a block change program.
Aerospace Safety Advisory Panel *(NASA Charter)*	March 1993	**Finding 16:** Three Flight Support Motors have been used to date to verify quality and qualify design improvements, reproducibility, and replacement materials for the Redesigned Solid Rocket Motor (RSRM). In the near future, new materials will be needed in the RSRM to replace those eliminated for environmental or safety concerns. It will also be necessary to qualify new vendors to replace those who have left the industry or are no longer willing to supply components for the RSRM.	**Recommendation 16:** To maintain safety and performance, NASA should continue the use of Flight Support Motors for quality control, validation of design improvements, and qualification and verification of new materials, processes, facilities, and equipment.	**NASA Response (in 1993 ASAP appendix):** It is NASA's intention to continue to qualify new materials or process changes incorporated into the RSRM via the FSM program. The next FSM is FSM-4, scheduled for November 1993. The timing of these changes and the subsequent qualification efforts are subject to budgetary constraints.
Aerospace Safety Advisory Panel *(NASA Charter)*	March 1993	**Finding 21:** The Kennedy Space Center has begun a pilot Structured Surveillance Program with the objective of increasing the efficiency of the	**Recommendation 21:** Before Structured Surveillance can be fully implemented, it must be carefully evaluated to assure that it is fully supportive of safe flight operations.	**NASA Response (in 1993 ASAP appendix):** The Structured Surveillance program is in the early stages of development with emphasis on maintaining safe flight operations. Operations

Independent Assessment Team *(Chartered by)*	Date of Report	Finding	Recommendation	NASA Response
		quality control function in order to enhance launch turnaround processing. This program appears to have great potential.		and Maintenance Requirements Specifications (OMRSs) derived from Critical Items Lists (CILs) or Hazard Report acceptance rationale will continue to have the previous level of quality assurance inspections. Acceptance and installation of Criticality 1 hardware will also continue to have both contractor and NASA inspections. Evaluation of the results of the pilot program indicates increased efficiency of the processing effort and continued effectiveness of the quality assurance activities. We are moving slowly into this program with close management attention to assure safe flight operations.
Aerospace Safety Advisory Panel *(NASA Charter)*	March 1993	Finding 23: A new high bay Orbiter Processing Facility (OPF-3) has been opened at the Kennedy Space Center. In addition to advanced support equipment, OPF-3 has vastly improved lighting, which should decrease accident risk and increase productivity.	**Recommendation 23:** NASA should upgrade the lighting in the other Orbiter Processing Facilities as soon as possible to avoid differences across the high bays and maximize safety and productivity.	**NASA Response (in 1993 ASAP appendix):** KSC acknowledges the findings and agrees with the recommendation. Actions are in process to improve the lighting disparities. Because the most significant differences are in platform configurations and light-reflective surfaces, all surfaces that can reflect light on High Bay 1 and 2 platforms are being painted white. The floors in High Bay 1 are also being painted white and those in High Bay 2 are scheduled to be painted white in August 1993.
Aerospace Safety Advisory Panel *(NASA Charter)*	March 1993	**Finding 24:** The NASA Shuttle Logistics Depot has great potential for improving repair turnaround times and enhancing the logistics program. At present, however, repair turnaround tunes are still significantly longer than desired due largely to	**Recommendation 24:** The Space Shuttle Program needs to establish a more effective method of moving units through the repair cycle in order to achieve the full potential of the NASA Shuttle Logistics Depot.	**NASA Response (in 1993 ASAP appendix):** The protracted failure analysis times, especially those involving original equipment manufacturers (OEMs), are the most prominent contributors to the long repair turnaround times. Such turnaround times involving OEMs have averaged about

Independent Assessment Team *(Chartered by)*	Date of Report	Finding	Recommendation	NASA Response
		protracted failure analysis times.		four times those at the NSLD. The failure analysis capability at the NSLD has been enhanced during the past year. Initiatives are also underway with the Johnson Space Center (JSC) Orbiter and GFE project to improve the overall failure analysis process relative to identification of requirements as well as location where the analysis is performed. The increasing utilization of the KSC NSLD capability for both failure analysis and repair will significantly improve the average repair turnaround time and the overall logistics program in general.
Aerospace Safety Advisory Panel *(NASA Charter)*	March 1993	**Finding 29:** At the request of the NASA Administrator, the Panel examined the organizational structure of the Office of Safety and Mission Quality and the counterpart organizations at NASA Centers. The study concluded that the current organizational arrangement provides an appropriate and effective relationship between NASA Headquarters and the Centers.	**Recommendation 29:** Maintain the current organizational structure, but clarify the functions and duties of the Headquarters Office of Safety and Mission Quality and those of Center Directors and, if necessary, issue revised NASA Management Instructions.	**NASA Response (in 1993 ASAP appendix):** The role and responsibilities of the Headquarters Office of Safety and Mission Quality (Code Q) have been realigned as the result of the recent internal NASA Headquarters red team/blue team reviews. Based on the teams' findings, the name of Code Q has been changed to the "Office of Safety and Mission Assurance" to more accurately reflect its function. Other changes have been instituted to streamline the overall activity and realign resources to better support the evolving needs of NASA programs and missions. A NM1 incorporating these changes was signed on April 9, 1993. Although the mandate of the OSMA will continue to emphasize its role as the Agency's "safety conscience," the changes ensure an appropriate and harmonious balance between

Independent Assessment Team *(Chartered by)*	Date of Report	Finding	Recommendation	NASA Response
				Code Q's independent program oversight and support functions. The Office will provide an upfront contribution to programs (prevent problems by building in safety, reliability, and quality assurance at the earliest possible stage), focus efforts to manage the quality process for NASA payloads, and increase system engineering/concurrent engineering capabilities, while expanding risk-management capabilities to support program managers in meeting schedule and budget constraints during critical decision making processes. The strategic thrust of the Office over the next 2 years will be to: (1) Integrate SRM&QA requirements at the appropriate stage of a program; (2) Advocate SRM&QA oversight and assessment functions across the Agency; (3) Develop and promote NASA-wide risk-management practices; (4) Maintain a strong contributing SRM&QA presence in NASA programs and operations; and (5) Develop and advance engineering standards and practices.
Aerospace Safety Advisory Panel *(NASA Charter)*	March 1993	**Finding 34:** NASA research and test facilities are a national asset, key to the United States' continuing leadership in space and aeronautics. Regrettably, some of the infrastructure is not being adequately maintained, and the development of new, state-of-the-art facilities has been lagging.	**Recommendation 34:** NASA should develop an integrated long-range infra-structure plan that assures the maintenance of existing assets and develops new facilities to continue American leadership in space and aeronautics research and development.	**NASA Response (in 1993 ASAP appendix):** NASA has embarked on a comprehensive study to develop a coordinated national plan for world-class aeronautical and space facilities that meets the current and projected need for commercial and Government-sponsored research and development, and for Government space operations. The plan will be coordinated with the Department of

Independent Assessment Team *(Chartered by)*	Date of Report	Finding	Recommendation	NASA Response
				Defense, Department of Energy, Department of Commerce, Department of Transportation, and the National Science Foundation. Industry representatives have been contacted to ensure that private-sector interests are considered. The plan will address shortfalls in existing capability, new facility requirements, and consolidation and phaseout of existing facilities. The development of the Facility Plan will be accomplished by three task groups: Aeronautics R&D Facilities, Space R&D Facilities, and Space Operations Facilities; all three of which are of interest to constituencies in the private sector. The results of the study will be an essential component of our internal planning to improve and continue to maintain our facility infrastructure.
Aerospace Safety Advisory Panel *(NASA Charter)*	March 1993	**Finding 36:** NASA has embraced the concept of Total Quality Management (TQM). However, TQM implementation across NASA centers and contractors appears to vary from highly visible and apparently productive efforts to activities that seem to have more form than substance.	**Recommendation 36:** NASA should review its internal Total Quality Management program to assure that it is properly structured as a support function and includes not only motivation, but also appropriate leadership and training for both TQM instructors and hands-on employees.	**NASA Response (in 1993 ASAP appendix):** NASA's Continual Improvement Office (Code T) is currently completing efforts to provide planning for a structured implementation of TQM. Coordination with points-of-contact at each NASA facility and outside industry experts has been conducted, and a NASA-wide Implementation Plan has been written. The plan provides for a phased program to examine established initiatives and approaches at all NASA Centers, benchmark successful activity, coordinate a consensus commitment across NASA, and achieve partnership working arrangement with outside organizations. Contractor/NASA metrics,

Independent Assessment Team *(Chartered by)*	Date of Report	Finding	Recommendation	NASA Response
				and an internal/external Supplier Ratings System (SRS) have been developed using the guidelines and selected provisions of the Baldridge Award, President Award, NASA Low Trophy, and other similar criteria. These measures will be used to gauge the performance of NASA's Continual Improvement activities. Overall, this effort will result in a network of leadership, support, and training that meets the strategic goals and directions of the Agency.
Aerospace Safety Advisory Panel *(NASA Charter)*	March 1992	**Finding 6:** The results of flight tests indicate that the turbulent flow over the body flap creates a spectrum of hinge moments greater than that used in the original structural fatigue analysis. It also has been determined that an additional load path exists from the flap to the supporting structure. Further, the flap actuators were found to be more flexible than originally assumed. Additional tests are to be conducted to evaluate hinge moments and actuator flexibility.	**Recommendation 6:** NASA should evaluate, as rapidly as possible, the results of the new tests and loads analyses to reestablish the allowable number of flights for the body flap.	**NASA Response (in 1992 ASAP appendix):** Concur. The Space Shuttle Program has baselined a set of loads to account for the increased buffet environment. Additionally, the Space Shuttle Program has implemented a plan to measure loads during missions. Assessments have shown adequate mission life of the body flap for current missions and overall life still is being evaluated. Additionally, the Shuttle Modal Inspection System (SMIS) is being used to track potential damage of the body flap.
Aerospace Safety Advisory Panel *(NASA Charter)*	March 1992	**Finding 7:** NASA has developed a Shuttle Modal Inspection System (SMIS) for detecting changes in stiffness in structural/mechanical systems due to factors such as wear or cracking. The SMIS has shown good results when used on the Orbiter body flap and elevon systems (including actuators and supporting structures). However, it is not a	**Recommendation 7:** The SMIS procedure should be used only to augment more conventional NDI methods.	**NASA Response (in 1992 ASAP appendix):** Concur. Successful tests have indicated that the SMIS is a reliable method to detect changes in stiffness and dynamic behavior of the Orbiter body flap, elevon, and rotor speed brake (control surfaces). The SMIS is not intended to replace current inspection procedures but is to supplement standard inspection procedures to help detect early damage in areas

Independent Assessment Team *(Chartered by)*	Date of Report	Finding	Recommendation	NASA Response
		complete replacement for more conventional nondestructive inspection (NDI) methods. These conventional methods are capable of detecting cracks in primary structures with a "critical crack length" too small to cause a detectable change in stiffness and hence be measurable by SMIS.		that cannot be inspected. NASA has not deleted any structural inspection requirements documented in the Operational Maintenance Requirements and Specifications Document (OMRSD).
Aerospace Safety Advisory Panel *(NASA Charter)*	March 1992	**Finding 8:** Thermal protection system tiles are inspected for damage after every flight by specially trained and highly experienced inspectors using tactile techniques. These inspectors determine if the tiles are loose and help to identify problems in step and gap. The current procedure is largely qualitative and highly dependent on the skill of the individual inspectors.	**Recommendation 8:** A program to select and train new inspectors should be instituted to ensure the availability of an adequate cadre of qualified inspectors throughout the life of the Orbiters. In addition, further effort should be applied to the development of a quantitative inspection technique.	**NASA Response (in 1992 ASAP appendix):** Concur. NASA has a program in place to train and qualify inspectors to inspect TPS tiles. In addition, quantitative techniques are being investigated to reduce the technique-sensitive characteristics of the current, operator-dependent, inspection techniques. Currently, all new tile inspections require bond verification testing. Any postflight tile suspect bond conditions also are verified along with conducting engineering "deflection" tests. A dozen certified bond inspectors presently are being used to qualitatively evaluate suspect tile bonds. The individuals have been trained on-the-job and consist of contractor and government engineers. The number of trained personnel will remain the same unless unforeseen increases in bond anomalies occur. The Kennedy Space Center (KSC) is actively pursuing the development and implementation of an alternative nondestructive evaluation (NDE) method for performing tile bond

Independent Assessment Team *(Chartered by)*	Date of Report	Finding	Recommendation	NASA Response
				verification. Presently, a math model of the tile system is being formulated that will be used to evaluate the abilities of NDE systems being developed by two independent contractors. These NDE systems use vibration imaging patterns correlated to bond discrepancies to identify bond anomalies.
Aerospace Safety Advisory Panel *(NASA Charter)*	March 1992	**Finding 9:** The Space Shuttle Program requires both turnaround and periodic major Orbiter overhaul functions.	**Recommendation 9:** Overhaul and major modification efforts should be organizationally and functionally separated from routine turnaround operations because of the different types of planning and management skills and experience required.	**NASA Response (in 1992 ASAP appendix):** The Space Shuttle Program has dedicated Orbiter Maintenance Down Periods (OMDP) at 3-year intervals for the performance of major modifications, structural inspections and other interval inspections. The decision to retain the same organizational structure at the Kennedy Space Center (KSC) for planning and management of both OMDPs as well as turnaround processing is based on the following: (list omitted)
Aerospace Safety Advisory Panel *(NASA Charter)*	March 1992	**Finding 10:** The Space Shuttle design presently includes an automatic approach guidance system that requires crew participation and does not control all landing functions through touchdown and rollout to wheel stop. The present system never has been flight tested to touchdown, but a detailed test objective for such a test is in preparation. The availability of a certified automatic landing system would provide risk reduction benefits in situations such as weather problems after de-orbit	**Recommendation 10:** Future mission plans suggest the potential for significant risk reduction if the present Space Shuttle automatic landing capabilities are fully developed and certified for operational use. System development should include consideration of hardware, software, and human factors issues.	**NASA Response (in 1992 ASAP appendix):** The current autoland system capability is functionally adequate and verified as a backup entry system with some crew participation required. Beginning with STS-53, a two-flight detailed test objective will evaluate autolanding performance through wheel stop. Further, a program study is under way to define the necessary hardware, software, human factors, and system analyses required to support an upgraded autoland system for extended duration Space Shuttle flights where this autoland system could be the

Independent Assessment Team *(Chartered by)*	Date of Report	Finding	Recommendation	NASA Response
		and Orbiter windshield damage.		prime mode for entry operations.
Aerospace Safety Advisory Panel *(NASA Charter)*	March 1992	**Finding 11:** NASA continued its software independent verification and validation (IV&V) activities during the year. This independent review has demonstrated its value by finding failure modes that previously were unknown. The Safety and Mission Quality organization has taken on greater responsibilities for software safety.	**Recommendation 11:** NASA should continue to support a software IV&V oversight activity. The present process should be reviewed to ascertain whether it can be streamlined. The IV&V oversight activity should include the development of detailed procedures for test generation. NASA should not attempt to duplicate, through IV&V or otherwise, the actual performance of all verification and validation tests.	**NASA Response (in 1992 ASAP appendix):** Concur. The Space Shuttle Program has formally baselined the embedded V&V process and established the requirements in NSTS 08271, Flight Software Verification and Validation Requirements; formally established a V&V policy requiring program elements to adhere to this process; and assigned the SR&QA organization as the independent overseer assuring adherence to this process. The Space Shuttle V&V process includes maintenance of detailed test procedures on many levels for the existing test facilities available to the program. Although the program feels very strongly. that the embedded V&V process is excellent, the NRC has been requested to evaluate the Space‘ Shuttle’s embedded V&V process relative to the need for IV&V. NRC’s evaluation is in process with planned completion targeted for September 1992. Additionally, NASA plans construction of an IV&V facility in Fairmont, WV in 1992. Methods of improving and streamlining the IV&V process will be studied at this facility. Based on criticality and category of the software to be independently validated and verified, the NASA IV&V activity will permit tailoring to specific software project needs.

Independent Assessment Team *(Chartered by)*	Date of Report	Finding	Recommendation	NASA Response
				It is not the intent of these independent activities to duplicate all verification and validation (V&V) tests, but to provide support and consistency to enhance the V&V process.
Aerospace Safety Advisory Panel *(NASA Charter)*	March 1992	**Finding 12:** The new Space Shuttle general purpose computer (GPC) apparently has performed well. The Single Event Upsets (SEUs) were no more numerous than expected. Based upon NASA's model of SEUs, the accuracy of the predictions is excellent, and supports NASA's estimate that the probability of an SEU-induced failure is negligibly small. Nevertheless, there still is concern about the eventual saturation of usable memory on the GPC.	**Recommendation 12:** NASA should initiate a small study on alternatives for future GPC upgrades and/or replacements. This should involve other NASA organizations that have been studying computer evolution.	**NASA Response (in 1992 ASAP appendix):** The GPC Error Detection and Correction circuitry cyclically accesses each word in the 256K memory every 1.7 seconds. Because any SEU error is corrected at that rate, there is minimal chance of the memory being "saturated," regardless of the duration of exposure, The same circuitry also generates a count whenever it encounters and corrects such an error, thereby providing corroborating data to compare with the environmental analyses performed to predict SEU rates. The same EDAC architecture is used in the Space Station onboard 386 processors. That processor family also has been selected for the new Space Shuttle Multifunction Electronic Display System (MEDS). It is anticipated that the MEDS will allow future mission-related software growth without directly impacting the flight-critical code in the GPCs. Available usable memory in the GPC appears to be adequate well into the next decade. It is probable that hardware obsolescence will arrive well before practical memory limits are reached. Considerations for GPC upgrades should be initiated in the next 3 to 4 years through the Assured Shuttle Availability (ASA) process.

Independent Assessment Team *(Chartered by)*	Date of Report	Finding	Recommendation	NASA Response
Aerospace Safety Advisory Panel *(NASA Charter)*	March 1992	**Finding 13:** The replacement of some requested software upgrades with crew procedures is a matter of serious concern particularly when the functions addressed could be handled with greater reliability and safety by software. The crew already has to cope with a very large number of procedures.	**Recommendation 13:** NASA should conduct a thorough review of all crew procedures that might be performed by the computer system to determine whether they are better done manually by the crew or by the software. Human factors specialists and astronauts should participate.	**NASA Response (in 1992 ASAP appendix):** Concur. As part of the software upgrade process, reviews are held to determine which activities are best shifted from the crew procedures. Astronauts have actively participate in these processes and reviews. Human factors specialists also contribute to this process. The Space Shuttle Program has and will continue to implement flight software automation of crew procedures that are deemed a significant threat to flight safety or mission success due to the level of difficulty. Tasks for which manual procedures are adequate are judged based on the trade-off of value added/implementation risk against other flight software priorities. During the requirements baselining of the last three Operational Increments (i.e., 01-21, -22, -23), a significant number of software change requests were approved that automated existing crew procedures. Examples include (1) single engine auto contingency abort, which defined the automation of vehicle maneuvers following the failure of two Space Shuttle Main Engines; (2) abort sequencing redesign, which automated some of the crew procedure for aborts; (3) Transatlantic Abort Landing (TAL) droop control, which automated crew procedures to keep the vehicle above a minimum target altitude; and (4) Universal Pointing Future Maneuver-Digital Autopilot

Independent Assessment Team *(Chartered by)*	Date of Report	Finding	Recommendation	NASA Response
				(DAP) that significantly reduces the crew procedures for selecting the most appropriate DAP configuration to enter from 14 separate entries to a single entry.
Aerospace Safety Advisory Panel *(NASA Charter)*	March 1992	**Finding 14:** There are currently a sufficient number of flightworthy engines to provide each Orbiter with a flight set as well as provide an adequate number of spares.	**Recommendation 14:** Maintain this position. level tests have begun for both	**NASA Response (in 1992 ASAP appendix):** Thank you. We intend to maintain a good posture on spare engines.
Aerospace Safety Advisory Panel *(NASA Charter)*	March 1992	**Finding 25:** In spite of significant advances over the past year, there is still a need to improve the effectiveness of launch processing at KSC. It is rare when a vehicle is taken to the pad and launched without delays. Subsystem problems sometimes either require rolling the vehicle back to the Vehicle Assembly Building (VAB) or they cause delays at the pad.	**Recommendation 25:** Continue efforts to improve the effectiveness of launch processing operations. Each occurrence of a problem at the pad should be reviewed to determine why it was not caught in the VAB or Orbiter Processing Facility.	**NASA Response (in 1992 ASAP appendix):** Concur. NASA is committed to a series of new initiatives designed to enhance the hands-on accountability of individuals at the task level and improve processing flow. The Space Shuttle Program has requested all Space Shuttle projects to continue striving for efficiencies in the checkout requirements and the implementing procedures at KSC. The Space Shuttle Program recently completed a project-by-project review of the OMRSD requirements. The goal was to eliminate or reduce "vehicle" checkout requirements that were considered redundant testing or over-testing of a system. This is now beginning to appear in the OMIs as efficiencies to operations. A policy that has been put in place by the Space Shuttle Program defers testing of a function until reaching the pad if (1) that function is required to be checked out in an integrated test and (2) the system/component can be reasonably repaired or removed/replaced at the pad. Process reviews and process

Independent Assessment Team *(Chartered by)*	Date of Report	Finding	Recommendation	NASA Response
				analyses by the task teams still are being promoted as another technique to improve processing operations.
Aerospace Safety Advisory Panel *(NASA Charter)*	March 1992	**Finding 26:** Morale among launch processing personnel at KSC improved over the past year. This most likely is the result of a heightened sense of individual responsibility, improved systems training, and a better supervisory/management approach.	**Recommendation 26:** Continue and expand the approaches that have been successful over the past year.	**NASA Response (in 1992 ASAP appendix):** Concur.
Aerospace Safety Advisory Panel *(NASA Charter)*	March 1992	**Finding 29:** Procedures for tracking, analyzing, and providing corrective action for hardware problems arising at KSC are complex and lengthy involving numerous entities. There is no overall coordination effort to ensure that appropriate corrective action is taken.	**Recommendation 29:** The Space Shuttle Program should establish a coordinating function that is responsible for ensuring that proper and timely action is taken by responsible organizations in correcting problems that occur during launch preparation.	**NASA Response (in 1992 ASAP appendix):** Concur. A joint KSC/JSC problem process improvement team chartered by the Space Shuttle Program (SSP) has been formed to analyze the Orbiter discrepant hardware/logistic processing flow. The sequence of events presently required to process discrepant hardware is undergoing assessment to determine how best to streamline and make the system more responsive. Recommended changes are scheduled for presentation to the SSP in mid-1992. In addition, the Space Shuttle Critical Process Improvement Team has completed a review of the current NASA management/ contractor interface relationships for logistics for all Space Shuttle elements. A report identifying issues and corrective actions has been submitted to the Space Shuttle Program.

Independent Assessment Team *(Chartered by)*	Date of Report	Finding	Recommendation	NASA Response
Aerospace Safety Advisory Panel *(NASA Charter)*	March 1992	**Finding 42:** Despite acknowledged examples of contributions to aviation safety analyses through human factors research, NASA has not marshalled its resources in this field to study similar problems in spaceflight orbital and ground operations. Efforts in this arena have been stymied by a lack of appreciation of its potential value and the absence of clear guidelines regarding programmatic responsibilities.	**Recommendation 42:** In view of the anticipated increase in manned spaceflight activity during the present decade involving joint Space Shuttle and Space Station activities, NASA human factors resources should be marshaled and coordinated effectively to address the problems of risk assessment and accident avoidance.	**NASA Response (in 1992 ASAP appendix):** Concur. NASA currently sponsors a pilot project at the Kennedy Space Center to determine the value to the safety program of incorporating human factors principles. This project focuses primarily on facility design and acquisition. The Space Station Processing Facility has been selected to serve as a demonstration vehicle. Draft guidelines have been developed and are being tested in the pilot project prior to publication and NASA-wide implementation.
Aerospace Safety Advisory Panel *(NASA Charter)*	March 1991	**Finding 1:** NASA has planned to implement the wing/fuselage modifications indicated by the results of the 6.0 load analysis. Modification work has been scheduled for OV-102, and plans are being developed for the remainder of the fleet.	**Recommendation 1:** The implementation of these modifications should be accomplished as soon as possible so that the restricted flight envelope (green squatcheloid) parameters can be safely upgraded.	**NASA Response (in 1991 ASAP appendix):** Concur. Modifications are scheduled for each vehicle's Orbiter Maintenance Down Period (OMDP). The OMDP has been incorporated into the Space Shuttle Program to provide dedicated times for performing detailed vehicle structural inspections, subsystem inspections and internal functional checks as well as modifications. All vehicle modifications will be complete by mid-1993.
Aerospace Safety Advisory Panel *(NASA Charter)*	March 1991	**Finding 2:** The uncertainties surrounding crew performance after extended stays in space suggest a need for an alternative to manual landings.	**Recommendation 2:** The Space Shuttle Program should complete the development of a reliable autoland system for the Orbiter as a backup.	**NASA Response (in 1991 ASAP appendix):** Concur. The existing Shuttle autoland system is certified and is a reliable backup for 16-day Extended Duration Orbiter missions. A significant program to collect crew performance data is being undertaken by the Office of Space Science and Applications during flights involving incremental increases of on-orbit duration. Current plans involve flying four lo-day flights and three 13-day flights prior to the first

Independent Assessment Team *(Chartered by)*	Date of Report	Finding	Recommendation	NASA Response
				16-day flight. Crew performance data will be evaluated and must be judged acceptable prior to commitment to the next increment of extended duration.
Aerospace Safety Advisory Panel *(NASA Charter)*	March 1991	**Finding 3:** With plans to extend Orbiter use well into the next century, it will be necessary to upgrade the Orbiter computer systems several times. The present, rather ad hoc, approach of treating each upgrade as an independent action will be unsatisfactory for the long term.	**Recommendation 3:** NASA should accept the need for an upgrade involving a complete software reverification approximately every 10 years. A study should be undertaken to plan a path of evolution for all future changes in avionics computer hardware and software for the life of the Space Shuttle Program. The study should involve independent assessment to ensure the broadest possible perspective.	**NASA Response (in 1991 ASAP appendix):** Concur. NASA has just completed integrating the Improved General Purpose Computer (IGPC) into the fleet. This upgrading of the orbiter computers included an extensive reverification of the flight software. Integrated testing of the flight hardware and software was one of the milestones in the certification of the IGPC hardware and flight software. In addition, the Shuttle software is incrementally upgraded and released for flight approximately every eight months. These upgrades are validated, verified, and certified through an extensive and thorough process. Future computing capability beyond recent incorporation of the IGPC is under development in the Assured Shuttle Availability (ASA) Program in the Multifunction Electronics Display Subsystem (MEDS). The plan for the subsequent lo-15 years involves maintaining the existing system. Issues involving obsolescence and enhanced performance will continue to be reviewed.
Aerospace Safety Advisory Panel *(NASA Charter)*	March 1991	**Finding 4:** The Space Shuttle flight software generation process is very complex. It includes numerous carefully designed safeguards intended to ensure that no faulty software is ever	**Recommendation 4:** NASA should conduct an independent review of its entire software generation, verification, validation, object build, and machine loading process for the Space Shuttle. The goals should be to ascertain whether the	**NASA Response (in 1991 ASAP appendix):** Concur. An independent review has been completed of NASA's entire software generation, verification, validation, object code build, and machine loading process. As part of the

Independent Assessment Team *(Chartered by)*	Date of Report	Finding	Recommendation	NASA Response
		loaded. When errors have occurred, or when concerns have been raised about steps in the procedure, new safeguards have been added. The whole process is long, complicated, and involves a plethora of organizations and computers.	process can be made less complex and more efficient.	post-511 activity, NASA contracted with Intermetrics Inc., as the independent verification and validation (IV&V) contractor. NASA is developing a policy to define the scope of our independent oversight activity. To assist in this task, NASA has requested the National Research Council to perform an independent review of the IV&V process to include software generation, object code build, and machine loading.
Aerospace Safety Advisory Panel *(NASA Charter)*	March 1991	**Finding 14:** The external tank project is moving along very well.	**Recommendation 14:** Keep up the good work.	**NASA Response (in 1991 ASAP appendix):** Thank you.
Aerospace Safety Advisory Panel *(NASA Charter)*	March 1991	**Finding 15:** This past year, NASA management has postponed Space Shuttle launches when technical uncertainties existed, declared a hiatus during the Christmas season and interrupted launch operations until the cause of hydrogen leaks could be determined and resolved. This is clear evidence of NASA management's commitment to the principle of "safety first, schedule second."	**Recommendation 15:** NASA management should maintain this policy even as Shuttle launches become more frequent.	**NASA Response (in 1991 ASAP appendix):** Strongly concur.
Aerospace Safety Advisory Panel *(NASA Charter)*	March 1991	**Finding 16:** Reports indicate that launch processing operations at the Kennedy Space Center (KSC) are being carried out with a declining rate of incidents. This is a trend in the right direction since the extreme sensitivity of Shuttle launch processing requires reducing errors	**Recommendation 16:** KSC, the Shuttle Processing Contractor, and associate contractors should continue to make all possible efforts to reduce incidents. However, care must be exercised to ensure that any observed decrease in incident reports is not merely an artifact of the reporting system. In particular, if management's response to	**NASA Response (in 1991 ASAP appendix):** Concur. KSC and the Shuttle Processing Contractor (SPC) are continuing to try to reduce incidents, even beyond the success we have had to date. We are accomplishing this through a network of preplanning, communication, and coordination that encourages everyone to work

Independent Assessment Team *(Chartered by)*	Date of Report	Finding	Recommendation	NASA Response
		to the lowest possible levels.	incident reporting is perceived as punitive in nature, the net result may be a suppression of reporting with a resultant reduction in the information available to management on which to identify problems and design remedial actions. Total Quality Management (TQM) techniques can be of great assistance. Likewise, the inclusion of human factors professionals on incident investigation teams can be very beneficial. Therefore, KSC should consider both an enhanced TQM program and a broader use of human factors.	together and understand that they are an essential part of the task at hand. Management takes no punitive action against any worker for incidents unless it is clearly shown that the worker had a preconceived negative intent or makes the mistake repetitively (more than twice). For repetitive errors, the worker is simply reassigned to other tasks and/or retrained. Any repetitive error is automatically evaluated from the human factors viewpoint. It should be noted that human factors concepts have been used throughout the creation and verification of all Orbiter Maintenance Instructions (OMIs) and the initial performances of all tasks involved in vehicle processing. With quality control checks at all levels from planning, engineering, OMI creation, and progressive steps of task team work, we are practicing TQM and reducing incidents. We will continue to use enhanced TQM and a broader use of human factors, as appropriate.
Aerospace Safety Advisory Panel *(NASA Charter)*	March 1991	**Finding 17:** There is a perception among some workers at KSC that disciplinary actions for errors are overly severe.	**Recommendation 17:** NASA and its contractors should make every effort to communicate the facts and rationale for disciplinary actions to the work force and involve workers in incident reviews. TQM techniques can be of great assistance. There is simply no substitute for sincere communication between management and labor in dispelling negative perceptions.	**NASA Response (in 1991 ASAP appendix):** Concur. NASA is very concerned about the potential that such a perception may exist. KSC and SPC have instituted a program of vertical and lateral communications that extends from the highest KSC management levels (both civil service and SPC) down through middle management, engineering, and the task team technical floor workers. Practices include weekly meetings at top management levels, daily reviews at middle management and throughout engineering, and per shift (or

Independent Assessment Team *(Chartered by)*	Date of Report	Finding	Recommendation	NASA Response
				more) coordination sessions at the task team level. There are also horizontal channels for coordination from hands-on-workers, logistics/supply elements, and support operations. It is continually stressed throughout these channels that disciplinary action for errors will not be severe or punitive unless the errors or incidents result from clearly proven negative intent. All employees are advised of their obligation to come to work fit and able, and to perform the tasks carefully and successfully. Any error is discussed with the responsible employee and efforts made to help him or her understand how to avoid a repetition.
Aerospace Safety Advisory Panel *(NASA Charter)*	March 1991	**Finding 18:** There are cases in which recurring waivers are sought and issued for the same subsystem or component on successive Space Shuttle flights. For example, waivers have had to be issued to fly with the tumble valve disabled on the external tank.	**Recommendation 18:** Continuing waivers for the same condition should not be permitted. If it is deemed acceptable to fly repeatedly with a configuration that varies from specifications, the specifications should be altered rather than risk diluting the significance of waivers by making them routine. For example, the underlying specification for the tumble valve could be changed to require its inclusion only on high inclination launches.	**NASA Response (in 1991 ASAP appendix):** Concur in principle. The ASAP is correct in suggesting that there are continuing waivers where the specification can be changed; a good example is the tumble valve. Based on Flight Data for tanks with an active tumble system, the tumble systems were disabled on selected flights based on analysis of External Tank (ET) Rupture Altitude and the corresponding debris footprint. Flight and tracking data were used to determine the correlation between non-tumble system tank trajectories, ET motion, ET Rupture Altitude and the ET Debris Model. Based on these analyses and flight tests, the applicable specification was changed to preclude the necessity for continuing ET Tumble System Waivers. However, it should be pointed out that waiver disposition is never "routine." As outlined above, a request for waivers

Independent Assessment Team *(Chartered by)*	Date of Report	Finding	Recommendation	NASA Response
				or to change a specification requires rigorous supporting data (many times flight data) presented through a series of at least three change control boards. Specifications have been, and will continue to be, changed where it is proved that the limits should be revised for all flights.
Aerospace Safety Advisory Panel *(NASA Charter)*	March 1991	**Finding 19:** The Mission Control computer support system is quite old, relatively slow, and has monochrome displays primarily of tabular data. The advantages of applying current technology to Mission Control are being explored with the Real-Time Data System at the Johnson Space Center (JSC).	**Recommendation 19:** NASA should embark upon a systematic process to replace the old Mission Control system with one based upon up-to-date computer and human interface system technology.	**NASA Response (in 1991 ASAP appendix):** Concur. Since 1986, NASA has been in a phased process of upgrading the operational elements of the Mission Control Center (MCC) to incorporate advanced technology. This includes the replacement and upgrade of mainframe computers, and the placement over the last 2 years of current generation workstations in the MCC that are capable of using advanced techniques for analyzing and displaying data. These enhancements are part of a comprehensive multi-year plan developed to introduce new technology into the operating environment.
Aerospace Safety Advisory Panel *(NASA Charter)*	March 1991	**Finding 24:** Out-of-production, aging, and obsolescent parts are a growing problem.	**Recommendation 24:** Increased emphasis should be given to ensuring the availability of sufficient quantity of up-to-date hardware.	**NASA Response (in 1991 ASAP appendix):** Concur. NASA recognizes the potential problem posed by obsolete parts. KSC has instituted a three-part program to minimize the impact that obsolescence could have on orbiter logistics supportability. The program includes identification of potentially obsolete parts; evaluation of available prevention options; and tracking of obsolescence data, including actions taken. These actions are taken in conjunction with the Assured Shuttle Availability Program. The increased emphasis on

Independent Assessment Team *(Chartered by)*	Date of Report	Finding	Recommendation	NASA Response
				parts obsolescence should ensure the ability of KSC to provide up-to-date hardware for orbiter launch processing.
Aerospace Safety Advisory Panel *(NASA Charter)*	March 1991	**Finding 25:** There does not appear to be a comprehensive and realistic plan for scheduling and accomplishing major overhaul of the Orbiter fleet.	**Recommendation 25:** To help ensure structural integrity of each vehicle, much greater effort must be devoted to these tasks. A comprehensive program should be developed for the orderly overhaul of Orbiters that are expected to operate into the 21st century.	**NASA Response (in 1991 ASAP appendix):** Concur. The Space Shuttle Program has developed and instituted a plan by which the orbiter vehicles are inspected and modified every 3 years. This plan involves the use of specific orbiter flow periods commonly referred to as Orbiter Maintenance Down Period (OMDP) to perform vehicle structural inspections and modifications. The orbiter structural inspection will verify the integrity of primary structural elements of the vertical tail, flight control surfaces, aft fuselage, mid-fuselage, landing gear, crew module and forward fuselage. Critical elements will be inspected for corrosion, fatigue, deformation and cracks, which would result in reduced structural integrity. Flow periods of 188 days have been allocated for an OMDP. OV-102 is the first vehicle to be scheduled for an OMDP and will begin in FY 91. OV-103 and OV-104 are currently scheduled to begin their modification/inspections periods in FY 92. The Space Shuttle Program will continue to use OMDPs to inspect and modify each orbiter throughout a vehicles operational lifetime to ensure each orbiter's structural integrity and upgrade the systems as required to ensure operations through 2020.

Independent Assessment Team *(Chartered by)*	Date of Report	Finding	Recommendation	NASA Response
Aerospace Safety Advisory Panel *(NASA Charter)*	March 1991	**Finding 29:** The use of Fault Tree Analysis and Failure Modes and Effects Analysis techniques proved to be valuable in solving the hydrogen leak problems on STS-35 and STS-38. Their use led to the identification of probable sources of the hydrogen leaks, the probable causes of these leaks, and the nature of the corrective actions needed.	**Recommendation 29:** Use of these techniques for problem resolution should be encouraged throughout NASA. Suitable training programs should be established to ensure proper implementation.	**NASA Response (in 1991 ASAP appendix):** Concur. Fault-tree analysis (FTA) and Failure Modes and Effects Analysis (FMEA) are techniques fundamental to the NASA systems engineering disciplines. They are used throughout system development to enable early identification of problems, and assign hardware and software criticality. Critical Item Lists (CILs) are tabulated by criticality level and require review, resolution, or waiver before flight is approved. FTA is used by the safety organizations to provide top-down analyses of safety-critical problems, while the FMEA is a bottom-up approach that begins at the parts level. Both formal and informal on-the-job training in these techniques is provided.
Aerospace Safety Advisory Panel *(NASA Charter)*	March 1991	**Finding 30:** NASA has a TQM program intended to improve quality and productivity within NASA and its contractors. The implementation of the TQM (or its equivalent) concept, however, has been quite variable across the NASA Centers and contractors.	**Recommendation 30:** The principles of TQM have merit when implemented by a dedicated and concerned management. NASA should implement a consistent TQM methodology that ensures adherence to those principles and participation of all levels of the work force.	**NASA Response (in 1991 ASAP appendix):** Concur. NASA's ongoing emphasis on quality and productivity improvement (QPI) began in 1982, with an internal and external focus. In 1986, a special emphasis was placed on the external efforts in recognition that the majority of the NASA budget is allocated to contractors. In fact, Martin-Marietta/Michoud (which was referenced in the ASAP report) was evaluated under the NASA Excellence Award Program and won in 1987 for their quality achievements. In 1989-90, a renewed emphasis was placed on internal QPI programs, while still maintaining our external efforts. In February 1990,

Independent Assessment Team *(Chartered by)*	Date of Report	Finding	Recommendation	NASA Response
				NASA formally launched an internal TQM initiative, and recently conducted a NASAwide TQM assessment. We are now planning an internal TQM evaluation initiative patterned after the George M. Low Trophy (NASA's Quality and Excellence Award program) using TQM criteria contained in the President's Award for Quality and Productivity Improvement. NASA top-level management is committed to successfully implementing the TQM program and will be directly involved in formulating strategies for achieving NASA TQM program goals. The TQM Steering Committee, consisting of NASA senior management, will report on the status and progress of TQM implementation at their Fall 1991 meeting.
Aerospace Safety Advisory Panel *(NASA Charter)*	March 1991	**Finding 31:** NASA has a management instruction (NM1 8621.1E) that addresses "Mishap Reporting and Investigation." This NM1 includes a specification of board composition. It does not, however, realistically address the need for human factors input in such investigations. It notes that if human factors are thought to be substantially involved, then human factor input is to be sought from a "NASA or resident NASA contractor physician" rather than a trained human factors expert. Also, this NM1 does not require investigation of "close	**Recommendation 31:** Inclusion of a member on the incident/accident investigation board with specific human factors expertise should be given much greater consideration. "Close-call" investigations should be more formalized.	**NASA Response (in 1991 ASAP appendix):** Concur. NASA is investigating the human element in all NASA mishaps. Efforts are currently underway to refine and update NM1 8621.1E. Part of this effort will be the transition of NASA Mishap Investigation Board Membership requirements to the Basic Safety Manual, NHB 1700.1. Consideration will be given to incorporating a requirement to have a Human Factors Engineering professional assigned to a NASA Mishap Investigation Board during this transition. The NASA Headquarters Safety Division is sponsoring a Human Error Avoidance Project at KSC that includes funding for a full-time Human Factors Engineering professional.

Independent Assessment Team *(Chartered by)*	Date of Report	Finding	Recommendation	NASA Response
		calls."		This individual will be available to participate in future mishap investigations at KSC. Formalization of the NASA close-call investigation process is also a NASA concern. The update to NM1 862LlE will stipulate investigation of Type A, B, and C mishap-related close-calls as a requirement in the Basic Policy for NASA Mishap Reporting and Investigation. Under the current policy, all close-calls must be reported; close-call reports are evaluated at NASA Headquarters and, when necessary, an investigation board is established.
Aerospace Safety Advisory Panel *(NASA Charter)*	March 1990	**Finding 1:** Until November 1989, the two principal manned space flight programs - the Space Shuttle and Space Station Freedom - were managed independently, each under the cognizance of a separate Associate Administrator. Since the Challenger accident, Space Shuttle management has exhibited a noteworthy degree of effectiveness and stability. In contrast, Space Station Freedom management has suffered from a lack of continuity in its top-level personnel. Also, the independent status of both programs created some confusion concerning future operational responsibilities. The recent reorganization of the Office of Space Flight places both programs under one Associate Administrator. This change in NASA	**Recommendation 1:** NASA, the Administration, and the Congress should support the recent reorganization of the Office of Space Flight and allow that office time to accomplish its objective of achieving a unified and cohesive manned space flight program.	**NASA Response (in 1990 ASAP appendix):** NASA concurs with the finding regarding the recent reorganization and establishment of the Office of Space Flight under a single Associate Administrator. All necessary actions have been taken within Space Station Freedom Program (SSFP) elements to ensure the smooth transition of the organization involved so that the goal of a "unified and cohesive manned space flight program" can be achieved.

Independent Assessment Team *(Chartered by)*	Date of Report	Finding	Recommendation	NASA Response
		management is a positive step in seeking stability and cohesiveness in manned space flight activity, especially in flight operations and budgetary planning.		
Aerospace Safety Advisory Panel *(NASA Charter)*	March 1990	**Finding 3:** The return-to-flight of the Space Shuttle has been characterized by extensive preflight reviews. The majority of these, including the roll-out, solid rocket booster/external tank mating, and flight readiness reviews have been conducted face-to-face at the Kennedy Space Center. With the increasing flight rate, the travel and scheduling involved in the multiplicity of meetings are becoming a financial and physical burden. Some of the reviews are being shifted to video or telephone conferences. These techniques conserve travel time and budget, but could reduce the effectiveness of the management review process.	**Recommendation 3:** The flight readiness, Launch-2 day, and Launch-1 day reviews should continue to be conducted as face-to-face meetings at the Kennedy Space Center. The balance of the prelaunch reviews for each flow may be conducted as either actual meetings or by remote conferencing techniques. This would depend upon interflight schedules and the number/importance of unique problems or issues associated with a particular flight.	**NASA Response (in 1990 ASAP appendix):** NASA concurs with the recommendation. The Flight Readiness Review, and the Launch-2 Day and Launch-l Day reviews will continue to be conducted as face-to-face reviews at the Kennedy Space Center. For the L-2/L-1 reviews, some JSC support elements (flight directors, weather, etc.) must remain at JSC to support, the terminal count. Therefore, some JSC elements have been supporting, and will continue to support the L-2 and L-1 reviews by telephone. The Level III project reviews, ET/SRB MATE Review, Orbiter OPF Rollout Review, and Launch Site Flow Reviews can be conducted by telephone with proper representation, Detail requirements, formats, and designated face-to-face meetings are contained within the NSTS 7000, Level I, Program Requirements Document, Appendix 8 (NSTS Operations).
Aerospace Safety Advisory Panel *(NASA Charter)*	March 1990	**Finding 5:** Interruptions in Space Shuttle operations for any reason can have serious consequence to the Space Station Freedom assembly. The Panel, thus far, has seen little evidence of contingency planning by NASA for such eventualities. Contingency planning	**Recommendation 5:** NASA should develop a contingency plan that addresses the issues arising from possible interruptions of Space Shuttle operations during the assembly of Space Station Freedom.	**NASA Response (in 1990 ASAP appendix):** NASA concurs and has actions presently underway. All of the Space Station Freedom stages prior to permanently manned capability (PMC) have an orbital lifetime of at least 1 year and generally closer to 2 years in the normal operating altitude. In the case of a Space Shuttle standdown, NASA

Independent Assessment Team *(Chartered by)*	Date of Report	Finding	Recommendation	NASA Response
		should extend through all phases of operation. The Panel believes this to be an important area for NASA to emphasize in operational planning.		could boost any of these stages to higher orbits with orbital lifetime of approximately 2 to 4 years, depending on solar cycle. After PMC, an Assured Crew Return Vehicle (ACRV) will be present; and in the event of a shuttle standdown, the crew could be returned via the ACRV and the station boosted to a higher orbit. These results will be reviewed during the Space Station Program preliminary design review in December.
Aerospace Safety Advisory Panel *(NASA Charter)*	March 1990	**Finding 12:** Review of the data from postflight inspections of orbiter windows indicates that frequency of damage to the windows is greater than previously believed.	**Recommendation 12:** NASA should consider incorporating thicker or improved glass to enhance the safety margin of the windows as well as implementation of operational techniques such as pre-selecting on-orbit attitudes and entry angle of attack to minimize exposure to debris or thermal effects.	**NASA Response (in 1990 ASAP appendix):** Review of postflight inspections of orbiter window shows that frequency of damage to windows is well within values predicted by Rockwell at the beginning of the program. Thicker windows have been considered in the past as an improvement that would reduce turnaround time for the orbiter. Though improved glass will undoubtedly improve the thermal pane's ability to withstand impacts by reducing the stress on the pane's surface, there always will be a hypervelocity particle that can penetrate the pane. A redundant thermal pane window design may be feasible to incorporate within the vehicle to provide another layer of protection against the risk associated with a failed thermal pane. Vehicle on-orbit operational attitudes that could minimize exposure to debris have been reviewed, though more work needs to be done. Uncertainties in the analysis data presented to date are greater than the risk reduction a different attitude would give.

Independent Assessment Team *(Chartered by)*	Date of Report	Finding	Recommendation	NASA Response
				The probability of a particle large enough to penetrate the thermal pane is very small, about 10 to the minus 4 for a 7-day mission. Thus, the risk is small for continuing to operate without attitude restrictions. The effect on the vehicle during entry for the crack and/or loss of a thermal pane is being studied. Entry profiles that could be flown to minimize thermal stresses on a cracked window and surrounding structure will be evaluated once the damaged window study has been completed. Current mission rules require an orbiter entry at a cabin pressure of 10.2 psi for the loss of a thermal pane, thereby minimizing stresses on the remaining panes and window structure.
Aerospace Safety Advisory Panel *(NASA Charter)*	March 1990	**Finding 14:** NASA faces a significant problem with respect to its Space Shuttle computers that has not been addressed: a third generation of computers to replace the new computers to be installed in 1991. While it may seem premature to consider a third generation computer before the second generation has been installed, the rate at which computer technology is advancing compels such a consideration.	**Recommendation 14:** NASA should begin planning now for a process of regular upgrades to the Space Shuttle and the Space Station Freedom computers including, perhaps, a transition to the use of a common underlying computer architecture for the two systems.	**NASA Response (in 1990 ASAP appendix):** NASA concurs with this recommendation for the long term but disagrees that this is a near-term issue. NASA believes that efforts currently underway are sufficient to identify and provide any necessary upgrades to the Space Shuttle and Space Station Freedom computing systems. The new Space Shuttle General Purpose Computer (GPC) is scheduled for its first flight on STS-41 in October 1990. Design work for the new GPC began in January 1984, and the first new computers will be flown in late 1990 or early 1991. The calendar time required to design, test, and certify such a man-rated system practically assures that system to be

Independent Assessment Team *(Chartered by)*	Date of Report	Finding	Recommendation	NASA Response
				technologically obsolete for most of its operational life. The expected life of the new GPCs is 15 years. Subsequent major changes to the computer system architecture would require revision of the complete avionics package. NASA believes that any consideration of possible further improvements to the GPCs or to the computer system should be an integral part of the Assured Shuttle Availability (ASA) Program. The Space Station Freedom Program (SSFP) is planning for the upgrading of computers and/or software as improved technology permits. This planning, documented in its highest level program document, the Program Requirements Document (PRD), and in its second level requirements document, the Program Definition and Requirements Document (PDRD), is in two areas. First, the SSFP is planning for mainframe computer hardware and support software replacement every 7 years and workstation replacement every 5 years during the program's operational phase. Second, the program is establishing evolutionary requirements allowing the flexibility to upgrade to advance technology as it becomes available. As a result, requirements for the operational Space Station Information System require a design that isolates applications software (both flight and ground) from the underlying computing system, This promotes the migration of ground hardware and

Independent Assessment Team *(Chartered by)*	Date of Report	Finding	Recommendation	NASA Response
				software to the flight systems or from facility to facility, and maximizes flexibility for replacement of flight hardware during the life of the program. Transition to the use of a common computer architecture in both the Space Shuttle and Space Station is not considered feasible due to the differences in the underlying design philosophy of the two systems. The Space Shuttle, although relying on five computers (four primary and one backup), is essentially a centralized system fully integrated with the avionics package. Migrating the Space Shuttle computer architecture to some other design, such as that employed by the Space Station, would require the complete redesign of the avionics system. The Space Station, on the other hand, employs a decentralized system utilizing microcomputing technology as its driving force. Additionally, these systems employ radically different operating systems, programming languages, and are subject to different weight and volume constraints.
Aerospace Safety Advisory Panel *(NASA Charter)*	March 1990	**Finding 20:** The desire to eliminate the tumble valve has resulted in carrying a waiver for each flight since STS-27. The tumble valve has been disengaged for a number of flights and this has not resulted in External Tank debris footprints outside acceptable limits.	**Recommendation 20:** The program should either remove the tumble valves in their entirety and eliminate the specification requirement or conduct a process by which waivers are no longer needed for each flight.	**NASA Response (in 1990 ASAP appendix):** In all flights where the tumble valve has been activated, the reentry footprint has remained typical of a tumbling tank and outside the geographical limits of 25 nautical miles from United States landmass and 200 nautical miles from foreign land masses. Mission specific analyses are performed to assure that predicted ET

Independent Assessment Team *(Chartered by)*	Date of Report	Finding	Recommendation	NASA Response
				reentry footprints are satisfactory and to establish any risk associated with contingency aborts. The tumble valve will be disabled for missions where the footprint is such that the tumble valve is not required. NASA and DOD Range Safety agree the footprint uncertainties pose no risk to adjacent landmarks. When generic certification of ET entries without an active tumble valve is complete, the tumble valve system will be removed. This generic certification is planned to be completed by the end of FY91 and would enable NASA to eliminate this critical flight hardware from the External Tank.
Aerospace Safety Advisory Panel *(NASA Charter)*	March 1990	**Finding 21:** There is clear evidence that many of the problems that hampered launch processing prior to the Challenger accident are being addressed such as excessive overtime, lack of clarity in work instructions, shortage of spare parts, and heavy paperwork burden. However, these pre-Challenger problems have not been totally eliminated.	**Recommendation 21:** NASA and the Shuttle Processing Contractor must work diligently to eliminate deviations and errors that still occur frequently in the processing activities. Communications between the Shuttle Processing Contractor middle management and hands-on technicians must be continually improved.	**NASA Response (in 1990 ASAP appendix):** NASA and the Shuttle Processing Contractor (SPC) realize that to safely process vehicles in support of the planned flight rate, occurrences of worker error must be further reduced. To decrease the likelihood of worker fatigue contributing to processing mistakes, the KSC continues to strictly adhere to the overtime policy outlined in Kennedy Management Instruction (KMI) 1700.2. Over the past year, less than 1 percent overtime exceeded the 60 hour/week criteria outlined in the KMI. In May 1989, NASA/SPC formed a joint Processing Enhancement Team (PET) to reevaluate overall processing procedures. Efforts have focused on three major areas. First, the PET is working to assure that the work task preparation is complete, i.e.,

Independent Assessment Team *(Chartered by)*	Date of Report	Finding	Recommendation	NASA Response
				all documentation, people, and parts are available when required. Second, the team is working to guarantee that the right people and equipment are available to resolve processing problems as they occur. And third, the PET has found that to enhance processing, standardization is required of planning and scheduling procedures. These representative steps are aimed at clarifying instructions that each worker must abide by in safely completing his task. Availability of spare parts has improved markedly since return-to-flight. The Line Replacement Unit (LRU) fill rate is roughly 89 percent compared to an average of 80 percent prior to STS-51L. The transition of logistics management responsibility to KSC has greatly improved the support posture. Steps also have been taken in this area by placing commonly used items in the OPF to assure availability to workers. Reduction in the amount of, technician downtime has resulted. The Shuttle Processing and Data Management System II (SPDMS II) is the descriptive title for a computer hardware, software, documentation, and processing system that will provide technical and management information support to shuttle ground processing activities. The project will significantly improve the work control system at KSC by providing faster, more accurate work scheduling, tracking, and approval to support the projected flight rate. Initial phases of this project are now

Independent Assessment Team *(Chartered by)*	Date of Report	Finding	Recommendation	NASA Response
				being implemented, with continued incorporation planned over the next 2 years. NASA/SPC believes the steps summarized above will mitigate the potential for processing errors. A system has been set up by the PET whereby workers can communicate their concerns and ideas about the specific processing tasks to appropriate directorate representatives. Managers continue to emphasize that safety will not be compromised to meet launch schedules. NASA/SPC remains committed to continue improving workmanship and strengthening communication channels between managers and hands-on technicians.
Aerospace Safety Advisory Panel *(NASA Charter)*	March 1990	**Finding 40:** There is a need to monitor the aging and reliability of components as a function of time in service. Typically, monitoring is accomplished with fleet leader statistics. Unfortunately, as presently employed, fleet leader numbers can be relatively uninformative or even misleading. For example, these data do not permit managers to assess whether the fleet leader is representative of the entire system or simply an outlier.	**Recommendation 40:** Statistics on single fleet leaders should be augmented by simple data that identify the distribution of the entire fleet. For items that have been procured in relatively large numbers, this might be expressed as percentages. For relatively unique items, information on the three or four of the oldest and youngest items might be provided.	**NASA Response (in 1990 ASAP appendix):** NASA agrees. Historically, fleet leader statistics were used almost exclusively; however, this is not the case today. The SSME is the only item using a modified fleet leader concept in that it uses multiple fleet leaders to obtain a more representative sample of the fleet distribution. This minimizes the likelihood of a single fleet leader being an outlier. Use of a single fleet leader is atypical rather than typical. Fleet leader information is supplemented by such techniques and data sources as stress analysis, fracture analysis, qualification test results, life limit tests, and additional inspections of critical hardware. The process is no longer restricted solely to the fleet leader statistics.

Independent Assessment Team *(Chartered by)*	Date of Report	Finding	Recommendation	NASA Response
				Initially, the fleet leader is the prime source of data defining the anticipated fleet distribution. However, as additional devices are built, tested and put into operation additional data becomes available to "temper" the initial judgment of the initial fleet distribution. Information is retained at the contractors on each device and these statistics are compared using in-house studies to guide judgment on retention of items and the flight worthiness of them. These data are reviewed prior to each flight and bear heavily on the decisions to retain/reuse items and on the ultimate launch decision.
Aerospace Safety Advisory Panel *(NASA Charter)*	March 1989	**Finding 1-A:** Strengthening the role of NASA Headquarters (Level I) and STS program management (Level II), coupled with tighter management and budgetary controls over NASA's R&D Centers (Level III), has clarified responsibilities within the total STS program and strengthened authority and accountability at all levels. Of special importance is the position of Deputy Director (NSTS) for Operations as the focal point of the highly complex shuttle processing and launch activities at the Kennedy Space Center.	**Recommendation A:** It is essential that this more disciplined management structure - characterized by clear lines of authority, responsibility and accountability - continue in place once the launch rate accelerates in order to support NASA's commitment to the operating principle of "Safety first; schedule second."	**NASA Response (in 1989 ASAP appendix):** NASA agrees. The Space Transportation System (STS) management system is reviewed on a continuing basis to ensure that established clear lines of authority, responsibility, and accountability are effectively entrenched to accommodate planned accelerated launch rates. The Management Councils involving the NASA Manned Space Flight Center Directors and the monthly General Management Status Reviews serve to enhance NASA visibility within the STS program and provide assurance of management strengthened authority and accountability at all levels. Primary emphasis continues to be placed on preventing communication breakdown and ensuring that vital information pertinent to the decision-making process is provided to appropriate levels of management in near real-

Independent Assessment Team *(Chartered by)*	Date of Report	Finding	Recommendation	NASA Response
				time, In addition, the Deputy Associate Administrator for Systems Assurance, Code QA, is developing an audit/survey process that will be used to assess the acceptability and responsiveness of the SRM&QA efforts in each NASA program, including the National Space Transportation System (NSTS) program. One of the major purposes of this audit/survey process will be to further ensure that clear, effective, efficient lines of authority, responsibility, and accountability are established and remain in place. Efforts to date have concentrated on: analyzing existing policy documents and their flow throughout NASA; and developing a generic, model survey plan that will be the blueprint for conducting a survey of NSTS Level 2 and Level 3 during the first quarter of FY 1990. NASA has no intention of letting the strengthened Level I, II, and III roles degrade. The operating principle of "Safety First, Schedule Second" will continue as NASA policy.
Aerospace Safety Advisory Panel *(NASA Charter)*	March 1989	**Finding 1-B:** The Safety, Reliability, Maintainability and Quality Assurance (SRM&QA) function is now stronger, more visible, better staffed and better funded since establishment of the position of the Office of Associate Administrator for SRM&QA which reports directly to the Administrator. The Panel notes that the incumbent,	**Recommendation B:** Across-the-board budget cuts that jeopardize the recently strengthened SRM&QA function must be denied. Funding to maintain essential safety-related documentation of STS systems must be provided.	**NASA Response (in 1989 ASAP appendix):** NASA agrees that problems such as funding cuts that jeopardize the continuing strengthening of the SRM&QA function must be resolved. Across-the-board budget cuts not only have a debasing effect on Safety, but on all areas of NASA. Management realizes that it is necessary to look at the overall NASA program to evaluate the best and most efficient way to administer

Independent Assessment Team *(Chartered by)*	Date of Report	Finding	Recommendation	NASA Response
		George Rodney, is a part of the key decision loops and has established the beginnings of an essentially independent "certification" process within NASA. However, there is recent evidence that budgetary pressures within the Shuttle program are causing project directors to propose budget cuts in various SRM&QA activities (e.g., safety documentation associated with the Space Shuttle Main Engine, such as FMEA/CILs and Hazard Analyses, and oversight of major STS projects).		resources. In several areas, prior major efforts have reduced the outstanding work load so that available resources can be channeled elsewhere for best overall results relating to Safety. For example, in the area of Failure Modes and Effects Analysis/Critical Items Lists (FMEA/CILs) and hazard analyses, a major rebaselining of all hazards was undertaken during the hiatus after STS-51L. The rebaselining effort has been completed; hazard and FMEA/CIL evaluations are now needed only when new hazards are discovered or when configuration changes and new development designs are initiated. This is a considerably smaller effort than during the rebaselining effort, where all existing hazards were revisited and reevaluated. While the hazard FMEA/CIL process is and will continue to be proactive, the quantity of analyses will vary based on design changes to the systems, the elements being deployed, and those hazards that are discovered during operation/evaluation periods. Resolution and documentation of problems associated with hazard analyses and FMEA/CIL findings will continue. However, the backlog of problems and, therefore, the effort is decreasing as problems are resolved. To help identify common funding problems within the Safety community, Headquarters Safety Division, Code QS, convenes a

Independent Assessment Team *(Chartered by)*	Date of Report	Finding	Recommendation	NASA Response
				Quarterly Center Safety Directors Meeting. This meeting allows the Safety Community to air safety issues that require additional funding and/or personnel. In addition, the Associate Administrator for SRM&QA periodically meets with the SR&QA Directors from the nine NASA Centers. The agenda at these sessions permits open discussion of problems and issues, such as problems created by funding cuts and reallocation of resources. With the insight acquired through this forum, the problems can be addressed at the Headquarters level, and appropriate action can be initiated with cognizant program managers. This facilitates the resolution of impacts created by funding problems and maintains the vitality of a healthy NASA-wide Safety program.
Aerospace Safety Advisory Panel *(NASA Charter)*	March 1989	**Finding 1-C:** Management communications, a necessary component in achieving a successful STS program, have improved, both horizontally and vertically within NASA. In particular, the reinstatement of the Management Council, an entity that fosters direct and regular communication among all top STS managers and center directors, has brought a higher level of awareness of common problems and coordinated action to resolve them. This, in turn, has resulted in better informed and effective design certification reviews	**Recommendation C:** As the flight rate increases, greater attention to maintaining these improved communication channels will be required.	**NASA Response (in 1989 ASAP appendix):** NASA agrees with the need to maintain the improved and strengthened management communications channels. NASA fully intends to maintain the higher level of awareness that now exists in the Space Transportation System (STS) program management structure. NASA also plans to continue the Management Council to foster direct and regular communication, and to ensure better informed and effective assessment of STS program concerns and actions as the flight rate increases.

Independent Assessment Team *(Chartered by)*	Date of Report	Finding	Recommendation	NASA Response
		(DCRs) and flight readiness reviews (FRRs).		
Aerospace Safety Advisory Panel *(NASA Charter)*	March 1989	**Finding 1-D:** NASA, along with many other Federal agencies, has suffered through more than a decade of hostility directed toward Federal employees and a related failure to maintain salary comparability at the higher management levels. NASA urgently needs greater flexibility and resources in competing for and retaining the skilled personnel who are required to carry forward the Nation's space and aeronautical programs.	**Recommendation D:** Although the salary comparability question will be settled by the Administration and Congress, NASA should speak out clearly about the increasing costs of the present situation and the specific steps that are needed to once again make NASA careers among the most desirable and respected.	**NASA Response (in 1989 ASAP appendix):** NASA agrees that specific steps are needed to make NASA careers among the most desirable and respected. This has been a priority issue within NASA, and various approaches have been implemented to raise and maintain the professional stature of NASA personnel. However, the monetary reward and/or pay structure are legislated external to the Agency. Competing with industry for top talent, especially in high cost of living areas, is a serious problem. Within the Agency, various career development programs that permit career growth have been implemented. Also, job flexibility programs permit personnel to change positions and jobs horizontally within the Agency, as well as vertically, to gain varied background and experiences. This approach provides new and interesting personal challenges and, at the same time, promotes interest and growth. Training and recruitment programs at both professional and nonprofessional levels also continue as a top priority at NASA Headquarters and the Centers. The NASA Quality and Productivity Improvement Programs Office has as a primary responsibility, the function of finding better

Independent Assessment Team *(Chartered by)*	Date of Report	Finding	Recommendation	NASA Response
				ways to stimulate productivity and providing methods and programs for rewarding professional achievement. Recognition for performance is an important factor in retaining the skilled work force. In summary, there is a problem in attracting and keeping professional personnel. The salary base commensurate with responsibility, which is legislated external to the Agency, as well as the uncertainty of funding for existing and new space programs have made attracting and keeping top-level managers and engineers a serious problem. This is an Administration and Congressional issue.
Aerospace Safety Advisory Panel *(NASA Charter)*	March 1989	**Finding 3:** NASA's decision to procure the Advanced Solid Rocket Motor (ASRM) is based on the premise that the new motor will benefit from advanced solid rocket motor technology and new manufacturing methods and thus would evolve into a safer and more reliable motor than the current redesigned solid rocket motor (RSRM). On the basis of safety and reliability alone it is questionable whether the ASRM would be superior to the RSRM which has undergone extensive design changes until the ASRM has a similar background of testing and flight experience. This may take as long as 10 years from go-ahead. In the interim, the current design is	**Recommendation 3:** The ASAP recommends that NASA review its decision to procure the Advanced Solid Rocket Motor and postpone any action until other alternatives, including consideration of long range objectives for future launch requirements have been thoroughly evaluated.	**NASA Response (in 1989 ASAP appendix):** The NASA decision to procure the ASRM was made after thorough review of the major factors involved, including an assessment of potential alternative courses of action. Several of the more significant considerations that lead to the NASA decision to proceed with the ASRM Program are discussed below. There have been major improvements in the National Space Transportation System (NSTS) as a whole, and in the RSRM in particular, since the STS-51L accident. RSRM joint integrity is much improved, and the degree of field joint and nozzle-to-case joint rotation during motor ignition has been reduced significantly. However, O-ring expansion is still required

Independent Assessment Team *(Chartered by)*	Date of Report	Finding	Recommendation	NASA Response
		the current design is expected to have had over 160 additional firings prior to the introduction of the ASRM. Furthermore, it is not evident why the new manufacturing processes planned for the ASRM cannot be applied to the manufacture and assembly of the RSRM. Consequently, it is not clear to the ASAP why NASA is proceeding with its plan to develop a new and expensive solid rocket motor, especially as there are still many elements of the STS system which, if modified or replaced, would add significantly to the safety of the operation. Furthermore, NASA has not thoroughly evaluated other alternative choices to the ASRM such as liquid rocket boosters.		to preclude hot gas leakage. [The ASAP report (page 4) notes the need to develop a resilient O-ring material for primary and secondary seals to eliminate the required (RSRM) field joint heaters.] The RSRM factory joints do not meet the redundant, verifiable seal design criterion, due to joint rotation. Every feasible precaution, short of complete redesign, has been taken to ensure that all RSRM joints will function as intended, and NASA has high confidence in RSRM joint integrity. However, the RSRM joint designs are not the best concepts now available, and are not optimally tolerant of off-nominal conditions or unanticipated combinations of events. RSRM joint integrity thus remains a concern for the long term. The Advanced Solid Rocket Motor (ASRM) provides a positive solution to joint integrity by incorporation of welded factory joints and mechanical field joints that close upon motor pressurization. The mechanical joint closure criterion applies to & joints (igniter to case, segment to segment, and nozzle to case). The redesign of joints to use face seals rather than bore seals minimizes assembly damage potential and permits visual seal inspection until the final mating. Joint heaters, and their attendant failure modes, are eliminated. Furthermore, it is anticipated that insulation design improvements will further reduce potential debonds

Independent Assessment Team *(Chartered by)*	Date of Report	Finding	Recommendation	NASA Response
				and/or leakage paths. Another ASRM design criterion leads to obviation of the Space Shuttle Main Engine (SSME) "throttle bucket" during the maximum dynamic pressure regime with the attendant elimination or reduction of about 175 Criticality l/lR failure modes for the STS. Information gained from actual flight experience has been show-n that the safety factors for water impact loads, internal insulation, and nozzle erosion on the current motors are lower than the original design criteria; these deficiencies are to be rectified in the ASRM. Due to ASRM design innovations, it is anticipated that, relative to the RSRM, Criticality 1 failure modes will be reduced by approximately 30 percent, failure causes will be reduced by approximately 25 percent, and failure points will be reduced by approximately 30 percent. Flight reliability is as dependent upon the method of manufacturing as it is upon design. The current motor manufacturing is highly labor intensive, and historical contractor data indicate that 40 to 50 percent of the encountered defects are workmanship faults. Furthermore, workmanship faults are prevalent in the entire family of solid rocket motor (SRM) failures. These findings led to the conclusion that ASRM should be designed for the prudent automation of manufacturing

Independent Assessment Team *(Chartered by)*	Date of Report	Finding	Recommendation	NASA Response
				processes to minimize defects and maximize reproducibility. Short of a major redesign, which would be tantamount to a noncompetitive ASRM procurement, the RSRM will never achieve the aforementioned flight safety and reliability enhancements. Moreover, the ASRM significantly enhances industrial, environmental, and public safety. The ASRM will eliminate all asbestos-bearing insulation and other material applications in favor of equally effective materials that are noncarcinogenic. The manufacturing automation will minimize the exposure of the work force to hazardous operations; and the new production and test facilities will incorporate features for environmental protection in anticipation of ever increasing stringency in environmental constraints. (lots more omitted)
Aerospace Safety Advisory Panel *(NASA Charter)*	March 1989	**Finding 5-E:** As the flight schedule picks up in FY 1989, there remains the clear and present danger of slipping back into the operating environment at KSC that helped to contribute to the Challenger accident. At the same time, the need to achieve greater efficiency and cost-effectiveness in turnaround procedures is clear. In this situation, NASA's commitment to the operating principle of "Safety first; schedule second" must be retained. If experience of the past is a guide to the future,	**Recommendation 5-E:** NASA must resist the schedule pressures that can compromise safety during launch operations. This requires strong enforcement by NASA of the directives governing STS operations.	**NASA Response (in 1989 ASAP appendix):** NASA and our contractors recognize the complex problem of increasing launch site efficiency while resisting schedule pressures that may compromise safety. Some of the specific actions that Kennedy Space Center has taken include: review of problems caused by human-induced error to ascertain whether additional training, job reassignment, or procedure change is required; and constant review of areas of high overtime/stress for schedule change and reassignment of personnel. In

Independent Assessment Team *(Chartered by)*	Date of Report	Finding	Recommendation	NASA Response
		the pressures to maintain or increase flight rate will be intense.		addition, NASA has established formalized training programs designed to reduce the potential for human error. The schedule and scheduling process are constantly reviewed and updated, as necessary, to ensure that all formal protocols are completed regardless of the affect on ability to launch on a specific date. NASA management from the top level through the first-line supervisor exercises constant vigilance to ensure that satisfactory working schedules and environments are maintained at all times in accordance with the operating principle, "Safety First, Schedule Second." NASA continues to closely monitor workload imposed by the baselined STS flight rate. Manpower levels currently budgeted to support the STS flight schedule have been sized to assure that the processing workload can continue to be accomplished in a safe manner. Both staffing and overtime data continue to be reviewed by top management on a weekly basis to assure rigorous adherence to the overtime policy in Kennedy Management Instruction (KMI) 1700.2.
Aerospace Safety Advisory Panel *(NASA Charter)*	March 1989	**Finding D-1:** In 1988 NASA issued several NMIs and NHBs that provide policies and direction designed to improve the identification, evaluation	**Recommendation D-1:** The risk management policies and initial implementing methodologies which have been issued in 1988 need to be evolved further. Practical quantitative risk assessment and	**NASA Response (in 1989 ASAP appendix):** The risk management function is evolving. NASA is vigorously refining the NASA Management Instructions (NMIs) and NASA

Independent Assessment Team *(Chartered by)*	Date of Report	Finding	Recommendation	NASA Response
		and disposition of safety risks. In particular, NM1 8070.4 titled "Risk Management policy for Manned Flight Programs" calls for a risk management process that includes categorization and prioritization of "risks" using qualitative techniques for ratings of the frequency expectation and severity of the potential mishaps. The documents also provide for use of quantitative risk analysis to provide a more definitive ordering of risks for purposes of risk management.	other relative risk-level rating techniques should be actually developed. They should then be applied to help define the risk levels of flight and ground systems. enhancing changes, and, if so, define these changes.	Handbooks (NHBs) to reflect the latest risk management policy developments. Independent risk assessments are being performed on Galileo and Ulysses payloads utilizing updated risk management methodology. This risk methodology includes the development of credible accident scenarios derived from initiating events that could cause potential mishaps. It incorporates both qualitative and quantitative system response analyses of initiating events induced by hardware or software anomalies malfunction(s), human error, environmental influences, or probable combinations of these factors. Also, the risk assessment methods are being restructured as further development and state-of-the-art knowledge are gained from ongoing risk assessment activities arena. Practical quantitative risk methods and risk-level techniques are being matured by NASA in structured workshop sessions and supporting policies with a view toward incorporation into the risk management efforts in the National Space Transportation System (NSTS), space station, and payload areas.
Aerospace Safety Advisory Panel *(NASA Charter)*	March 1989	**Finding D-2:** The Panel has found strong commitment by each of the Center Director Offices to the rebuilding of the System Safety Functions in NASA. They have provided valuable guidance, encouragement and some level of financial support to the difficult restructuring, staffing and new policy	**Recommendation D-2:** In addition to continuing their good work we believe that additional vigorous assistance is required on the part of each Center Director's Office to assure the allocation of resources that are necessary so that the promising progress toward a truly effective Systems Safety capability does not falter and wither away after a few successful STS flights.	**NASA Response (in 1989 ASAP appendix):** NASA strongly agrees that a key element to the successful implementation of a NASA-wide Safety Program is the committed support of the Center Directors who must continue to be the champions of safety engineering. To ensure that progress made at the Centers is maintained, the Office of the Associate

Independent Assessment Team *(Chartered by)*	Date of Report	Finding	Recommendation	NASA Response
		implementation activities at their respective Centers. We are concerned that program resource cuts may be beginning to erode the progress which has been made.	The Center Directors must be seen as major champions of safety engineering within NASA.	Administrator for SRM&QA, Code Q, has initiated the following efforts: (list omitted)
Aerospace Safety Advisory Panel *(NASA Charter)*	March 1989	**Finding D-3:** At JSC there is a clear commitment from the Director's level down to implementing the general policies and requirements of NM1 8070.4, and to improving techniques for risk assessment and risk mitigation. We observed that the SRM&QA organization is still not completely staffed. The organization has assembled hazard information that is used in the decisions of whether or not to fly. Whether this same information can be used to identify safety enhancing changes has yet to be examined.	**Recommendation D-3:** Examine the collected data to see if it can be used to identify safety enhancing changes, and, if so, define these changes.	**NASA Response (in 1989 ASAP appendix):** The review process for National Safety Transportation System (NSTS) safety issues and associated hazard reports, conducted by the System Safety Review Panel (SSRP) and the Levels I and II Program Requirements Control Board (PRCB), results in thorough review of the safety problems involved. As part of this process, recommended changes required for hazard mitigation and/or control are actions levied on the responsible NSTS element(s). Detailed responses and presentations are made to the review boards up to the Level I PRCB, which is chaired by the NSTS Program Director. Therefore, identifying and recommending safety-enhancing changes in response to identified hazards are integral parts of the hazard review process at levels up to and including NASA Headquarters. These changes include: revisions/changes/additions (to Flight Rules and Launch Commit Criteria); improvements in manufacturing, inspection, test, and quality control procedures; and design changes to mitigate or reduce the risk involved (subject to budgetary review and approval by the NSTS

Independent Assessment Team *(Chartered by)*	Date of Report	Finding	Recommendation	NASA Response
				Program Director).
Aerospace Safety Advisory Panel *(NASA Charter)*	March 1989	**Finding D-4:** At JSC the ASAP was presented a new approach to hazard rebaselining and rating, and a new format for the Mission Safety Assessment report &ISA). The new report is basically a set of evaluated fault trees which identify the potential system mishaps which might result from various hardware or human faults. For STS-26, 25 "significant risk" mishaps were "selected" for evaluation. All items selected had worst-case severity levels of "loss of crew and/or vehicle." All items were also rated as "unlikely," which was the lowest probability rating used in the hazard rating matrix. Thus, the MSA did not address even the relative risk-levels of the selected potential mishaps. However, the system safety organization did color-code various faults - red, which designates that Improvement is Highly Desirable (IHD). Because all of the items elected for inclusion in the MSA are rated as unlikely to occur and therefore "safe to fly," there remain a large number of undifferentiated items designated MD.	**Recommendation D-4:** The ambiguity regarding risk levels implied by the red color-coded MSA needs to be removed. NASA needs to provide a much more objective (quantitative) and data- based risk assessment methodology that will differentiate the "unlikely" events for purposes of assessing the principal contributors to risk on STS and Space Station type programs.	**NASA Response (in 1989 ASAP appendix):** The Mission Safety Assessment (MSA) focuses in more detail on risks considered issues for the current and subsequent launches. Since the ASAP visit, the MSA has been reevaluated and is now considered a program baseline safety assessment to be updated periodically, not mission specific. It is derived from the approved Hazard Report (HR) set, which forms the program baseline safety risk. Renaming of the document is under consideration and the safety community is developing a replacement document that will be mission-specific and unique, the final title of which is not yet determined. It will provide visibility to top management of significant changes or potential significant changes to the baseline safety risk. It will indicate launch constraints and resolved safety risk factors. Basic requirements for the mission-unique safety risk assessment report need to be changed, and changes to the requirements are being pursued. The requirement for the MSA to be published 30 days prior to a launch is unrealistic as some safety risk data probably will not be achieved in time for consideration in the report as happened on STS-26. It is expected that the new requirement for safety risk assessments will be keyed to milestones such as the Flight

Independent Assessment Team *(Chartered by)*	Date of Report	Finding	Recommendation	NASA Response
				Readiness Review (FRR) and the L-2 Day Review, and it will have a format that will permit rapid, last-minute updates. All risks in the STS-26 were considered "unlikely," but were also more significant than others that had been received at the time of publication. Several HRs were subsequently submitted with a probability of occurrence of "likely," and they have been incorporated in subsequent MSA editions. All the events had the potential of being catastrophic events. The fault-tree approach presents these basic and conditional events. From this analysis, the MSA evaluated the hazard controls in the design and procedural area (i.e., redundancy, safety factors, launch commit criteria) for possible improvement to further mitigate the risk. The MSA used a qualitative approach to assessing the relative levels of risk. The NSTS safety community is considering changes to the three-level probability of occurrence to provide greater differentiation. Also, future editions 'of the MSA will use the results of probabilistic risk assessments, when available, to help define the relative level of risk for prioritization. NASA's effort to identify and quantify risk contributors has proceeded with several different approaches: probabilistic risk assessment (PRAs), individual statistical analyses, and prioritization of Failure Modes and Effects

Independent Assessment Team *(Chartered by)*	Date of Report	Finding	Recommendation	NASA Response
				Analysis/Critical Items List (FMFA/CIL) items (system/component coupled with a Criticality 1 failure mode). Relative to the PRA effort, a risk assessment for the Galileo mission [which uses a radioisotope thermoelectric generator (RTG) power source] was conducted. The assessment focused on events leading to breech of the RTG case. Shuttle element risks and individual risk contributors were developed using fault trees, random failure distribution approximations, and Bayesian techniques. However, none of the above efforts obviate the need for detailed, accurate, and easily accessible data bases containing test and flight failure data. The current Program Compliance Assessment Status System (PCASS) data base contains problem reports on component failures. For analysis purposes, data fields containing the specific FMEA failure mode need to be included to facilitate initial analyses; such an effort is now under consideration. A space station requirement document for a failure history data base is being developed. Apart from individual assessments and development of data bases, a more quantitative approach for identifying and assessing principal risk contributors has been explored using the current hazard analyses as a foundation. In this approach, detailed causes and scenario paths leading to damage states are developed. Likelihoods ascribed to the scenario nodes

Independent Assessment Team *(Chartered by)*	Date of Report	Finding	Recommendation	NASA Response
				and, in turn, probabilities are approximated for each potential path and damage state. Examples using auxiliary power unit hazards have been developed. This approach is being evaluated as a quantitative enhancement for hazard assessment.
Aerospace Safety Advisory Panel *(NASA Charter)*	March 1989	**Finding D-5:** Functional areas such as system-safety engineering at the Centers appear not to have received the resource support necessary to fulfill their responsibilities. The SRM&QA organizations at the centers appear to be relatively loosely coupled to Headquarters.	**Recommendation D-5:** The various systems safety organizations throughout NASA should get stronger assistance from Headquarters especially regarding financial support.	**NASA Response (in 1989 ASAP appendix):** NASA agrees that Center SRM&QA organizations should continue to receive strong support from Headquarters. During fiscal year (FY) 1989, 50 percent of the Headquarters SRM&QA budget is being transferred directly to the Centers. In FY 1990, we plan to increase this to 70 percent. Since January 1986, we have been able to increase the number of civil service and Jet Propulsion Laboratory personnel directly assigned to SRM&QA functions by approximately 39 percent. During that same period, the number of support contractor personnel performing SRM&QA functions has increased by nearly 95 percent. These statistics verify that the Centers have a strong and eloquent voice in Headquarters. As a consequence, NASA feels that within the context of existing Federal Budget constraints, the Center SRM&QA organizations have been well supported. Center SRM&QA organizations report and are directly responsible to the Center Directors. The Office of SRM&QA functions in a senior staff capacity at Headquarters providing a

Independent Assessment Team *(Chartered by)*	Date of Report	Finding	Recommendation	NASA Response
				focal point for NASA-wide SRM&QA activities, programmatic direction, policy formulation, and resources support. The link between Headquarters and field SRMLQA operations is sufficiently strong to provide proactive and vigorous SRM&QA program management.
Aerospace Safety Advisory Panel *(NASA Charter)*	March 1989	**Finding D-6:** At MSFC the ASAP found an excellent SRM&QA organizational structure and good progress in staffing it with experienced engineering personnel. As other centers have done, they have engaged the services of two contractors to aid in developing the analysis techniques for practical, more quantitative risk assessment.	**Recommendation D-6:** MSFC is to be commended for their progress in evolving its SR&QA function and these efforts should receive continuing high-level support.	**NASA Response (in 1989 ASAP appendix):** The achievements of the Safety, Reliability, Maintainability, and Quality Assurance (SRM&QA) organization at Marshall Space Flight Center (MSFC) are recognized and applauded. Also noteworthy is MSFC taking the lead in establishing the management and engineering requirements for Maintainability, which is a relatively new key discipline within the Agency. MSFC and the other Center SRM&QA organizations will continue to receive the high-level support required to ensure their continued viability as effective spokespersons for System Safety, Reliability, Maintainability, and Quality Assurance.
Aerospace Safety Advisory Panel *(NASA Charter)*	March 1988	**Finding A-1-a:** NASA has responded positively to ASAP's recommendations and those of the Presidential Commission dealing with reorganization of NASA and the National Space Transportation System, including the reestablishment of an independent safety, reliability, maintainability, and quality assurance function.	**Recommendation A-1-a:** NASA's top management should continue to support vigorously the new agency and programmatic organizational structure. The Office of SRM&QA should continue to be provided with the management support and resources it needs to carry out its essential oversight and review function in a fully independent and comprehensive manner.	**NASA Response (in 1988 ASAP appendix):** The Associate Administrator (AA) for Safety, Reliability, Maintainability, and Quality Assurance (SRM&QA) is on an equal organizational basis with the top program officials within the Agency. The AA also has access, both on an as required and on a regularly scheduled basis, with the other top management officials within the Agency. Additionally, requests for resources, both budgetary and

Independent Assessment Team *(Chartered by)*	Date of Report	Finding	Recommendation	NASA Response
				personnel, are given careful and deliberate consideration. NASA is committed to providing a vigorous and independent oversight and review function through the Office of Safety, Reliability, Maintainability and Quality Assurance. This capability has been developed and is in place. NASA's long-range plans include the maintenance of this established capability and the continual strengthening of the SRM&QA functions within the Agency.
Aerospace Safety Advisory Panel *(NASA Charter)*	March 1988	**Finding A-1-b:** In the investigation of the Challenger accident, it was revealed that a breakdown developed in the Shuttle management structure over the course of time. Explanations for this abound. Nevertheless, the view persists that if the management breakdown could have been averted, vital information pertinent to the decision-making process could have reached responsible management in a more timely manner.	**Recommendation A-1-b:** Once a management system for a program has been adopted, especially for long-term projects, it would seem prudent for the NASA Administrator to be apprised periodically of its functioning to ensure that changes in personnel and program direction have not resulted in deterioration of the management structure.	**NASA Response (in 1988 ASAP appendix):** NASA agrees. How well the management system functions is a key element in the assessment of NASA programs. The management system, much like technical or budgetary elements, is being reviewed periodically, with the results provided to the NASA Administrator. Among the management mechanisms in NASA that enable this to occur are the various Management Councils that involve the appropriate NASA Center Directors, and the monthly General Management Status Reviews (GMSR) where the various NASA Associate Administrators report directly to the Administrator. The direction and discipline applied for these reviews ensures that the intent and content of these reviews cover all aspects of technical as well as programmatic problems facing the Agency, the Centers, and programs. All changes in key personnel, management structure and organizations and the status relative to performance,

Independent Assessment Team *(Chartered by)*	Date of Report	Finding	Recommendation	NASA Response
				problems, and concerns are continually reviewed as part of the agendas for these reviews. In addition, the SRM&QA organization, Code Q, is strengthening the Agency's audit system capability, which includes the periodic survey and assessment of the Centers' technical and management and reporting systems.
Aerospace Safety Advisory Panel *(NASA Charter)*	March 1988	**Finding A-1-c:** The STS is a complex system with many R&D-like characteristics. To employ the system so that there is an acceptable level of risk requires much effort and vigilant attention to detail.	**Recommendation A-1-c:** NASA should adopt the goal of using the STS only in those circumstances where human presence in space is needed for mission success. Otherwise, access to space should be gained by using unmanned expendable rockets. Given the expected long-term requirements of the Space Station and other space projects of national importance, the need to begin development of an unmanned heavy lift vehicle is clear. These initiatives should be part of a long-term comprehensive national space policy that sets clear objectives, determines the best way to accomplish these objectives, and then commits the United States to a realistic schedule and budget.	**NASA Response (in 1988 ASAP appendix):** NASA agrees and is working toward this goal. However, the Space Shuttle must be utilized to reduce the current payload backlog. The President's national space policy, which sets forth a long-term balanced and clear cut set of goals, principles, and guidelines, states that the Space Transportation System (STS) will be used to maintain the Nation's capability in manned space flight and to support critical programs requiring manned presence and other unique STS capabilities. The policy also states that the United States' national space transportation capability will be based on a mix of vehicles, consisting of the STS, unmanned launch vehicles and in space transportation systems. NASA strongly supports this policy and is intent upon meeting its objectives. As stated in the response to the 1986 ASAP report, the mixed fleet analysis study has been completed. The resulting plan is currently being implemented for a mixed fleet of launch vehicles. The March 1988 Mixed Fleet Manifest

Independent Assessment Team *(Chartered by)*	Date of Report	Finding	Recommendation	NASA Response
				for flights through September 1993 shows 16 NASA and National Oceanic and Atmospheric Administration (NOAA) spacecraft previously planned for the shuttle being reassigned for launching on expendable launch vehicles (ELVs). In addition, some 20 DOD payloads have been off-loaded from the shuttle to ELVIS. NASA also agrees with the need for development of an unmanned heavy-lift vehicle. The Agency is a partner with the Air Force in the definition of an Advanced Launch System (ALS) and is also conducting initial studies of an unmanned, cargo version of the Space Shuttle, Shuttle C.
Aerospace Safety Advisory Panel *(NASA Charter)*	March 1988	**Finding A-1-d:** The reevaluation and recertification of all hardware and software systems on the STS, has produced an extremely heavy work load related to launch processing including more paperwork, many modifications to existing systems, and a greatly expanded test program.	**Recommendation A-1-d:** NASA, the Shuttle Processing Contractor (SPC), and supporting contractors must exercise the most intensive and unrelenting scrutiny to prevent human error from occurring. In particular, the natural tendency to sign off routinely on complex documents approved at lower levels, shortcut test procedures, or otherwise work around nagging problems must be avoided at all costs.	**NASA Response (in 1988 ASAP appendix):** Both NASA and contractor management are sensitive to the need to prevent human error from occurring. Increased discipline has been manifested by additions to manpower in the areas of engineering support to the on-line workforce and additional quality control personnel, with clear direction for increased emphasis on planning and control of work. In the SRM&QA area, the ratio of quality control inspector-to- technicians has been increased in all areas from pre-STS 51-L levels. Certification and recertification training also continues to be provided for the work-force. NASA, the Shuttle Processing Contractor (SPC), and element contractor management periodically review these programs to

Independent Assessment Team *(Chartered by)*	Date of Report	Finding	Recommendation	NASA Response
				assure that each critical discipline area is properly supported. Additionally, the currently budgeted Shuttle Processing Data Management System (SPDMS) is being implemented to lessen the paperwork burden. This automated system will improve the work control system by providing for faster, more accurate problem disposition with appropriate management visibility. In addition to the above, the NASA Headquarters SRM&QA Office, Code Q, has revised the System Safety Handbook whereby a chapter is devoted to Human Factors considerations and requirements. Code Q will also validate the effectivity of organizational functions, systems and staffing through selected staff assistance surveys. Such overview actions will permit insight for determination relative to existence and application of adequate discipline within the system.
Aerospace Safety Advisory Panel *(NASA Charter)*	March 1988	**Finding A-2:** NASA and the STS contractors have been redoing the FMEAs, CILs and hazard analyses for all elements of the Shuttle system. We found that, although there were great differences in the specific techniques and data management employed by different organizations, the work was thorough and of high quality. Only a limited number of new failure modes were uncovered in the original designs. There were, of course, new modes identified for designs that had changes	**Recommendation A-2:** (1) NASA should take steps to establish uniform methodology for conducting FMEA/CIL/Hazard Analyses for the agency as a whole. (2) In addition to the above, NASA should develop and implement a consistent method of prioritization of items in the CIL so that appropriate attention can be given to the greater risks. (3) Data developed from the FMEA/CIL/Hazard Analysis process should be organized in such a fashion that it provides the deciding authority with information permitting him or her to assess the risk and make	**NASA Response (in 1988 ASAP appendix):** (1) As part of the revalidation process for the STS "Return to Flight", the National Space Transportation System (NSTS) Program issued NSTS 22206, "Instructions for Preparation of Failure Modes and Effects Analysis (FMEA) and Critical Items List (CIL)" and NSTS 22254, "Methodology for Conduct of NSTS Hazards Analyses (HA)." The purpose of these documents is to provide consistent methods for the

Independent Assessment Team *(Chartered by)*	Date of Report	Finding	Recommendation	NASA Response
		designs that had changes incorporated or planned. One result of the rework is that the number of Criticality 1I and 2 items increased dramatically. This occurred primarily because of new ground rules as to levels at which components would be addressed. NASA is considering various techniques for prioritizing the CIL so that the "highest risk" items can receive the highest levels of attention. The ASAP strongly supports this concept. A more definitive prioritization for such risk management purposes would require a more quantitative methodology to establish safety-risk levels.	her to assess the risk and make informed decisions.	preparation, maintenance, and publication of the FMEA/CIL/HAs. These documents are being used by the SRM&QA Office to develop NASA handbooks that will provide the Agency-wide guidelines. Drafts of these handbooks have already been prepared, and it is anticipated that the final documents will be issued prior to the end of FY 88. (2) A procedure (NSTS 22491, "Instructions for Preparation of Critical Items Risk Assessment") was developed and issued by the NSTS Program to implement a method of categorizing NSTS failure modes by severity of effect and likeliness of occurrence and prioritizing them from most severe effect to least severe effect. In addition, a method (Memorandum NA2/87-L046, "Implementation of Hazard Prioritization Technique", September 29, 1987) for categorizing Hazards by likelihood of occurrence and severity was also implemented in order to determine a risk index for each hazard. These methodologies are being incorporated into an overall Agency Risk Management Program being developed by the SRM&QA Office. (3) The NSTS Program has developed a new closed-loop accounting system known as the System Integrity Assurance Program (SIAP). A key feature of SIAP is its Program Compliance Assurance and Status System (PCASS). This is a computer-based information system which functions as a database that integrates a number of

Independent Assessment Team *(Chartered by)*	Date of Report	Finding	Recommendation	NASA Response
				information systems. FMEA/CIL and Hazards Analyses data are a part of this data base. PCASS has the potential to provide, in near real-time, an integrated view of a number of risk assessment parameters to NSTS Program decision-makers.
Aerospace Safety Advisory Panel *(NASA Charter)*	March 1988	**Finding A-3-c:** Prior to the STS 51-L accident, there was no cross-reference listing between the operational maintenance requirements specifications document (OMRSD) and the critical items list (CIL). Since the accident, an OMRSDIFMEAICIL matrix has been generated to help ensure that a focus is kept on all critical items in every step of the processing procedure. One of the short comings in the procedures prior to the 51-L accident was the lack of traceability of OMRSD requirements to the operations and maintenance instructions (OMI). An operations and maintenance plan (OMP) is now in use to provide this traceability. A closed-loop requirements accounting system is expected to be in place for STS-26R. This will be a partially manual system for STS-26R but is expected to be fully automated by February 1989.	**Recommendation A-3-c:** NASA should continue its efforts to establish clear-cut and uniform policies for the Shuttle Processing Procedures and for the flow of all evaluations top-down as well as bottom-up in a consistent and rational manner.	**NASA Response (in 1988 ASAP appendix):** NASA is continuing its efforts to have clear and uniform policies for shuttle processing procedures and evaluations. NASA and its contractors are expending major efforts to properly identify, document, and cross reference all shuttle critical items in the CIL, OMRSD, OMIs and OMP. These documents have all been thoroughly reviewed, revised, and reformatted for that specific purpose, and matrices allow tracing a CIL item throughout the series. Closed-loop OMP - OMI - OMRSD Accounting has been initiated and is in place supporting STS-26R KSC processing. The complete automation of this system is in process and on schedule to be partially available for STS-26 and completed by February 1989. This system will provide for uniform implementation of policy and create a greater awareness of the critical portions of shuttle processing and facilitate problem identification, resolution, and anomaly evaluations. The PCASS system will also be used to track and provide the status of Criticality 1 & 1R hardware problems.

Independent Assessment Team *(Chartered by)*	Date of Report	Finding	Recommendation	NASA Response
Aerospace Safety Advisory Panel *(NASA Charter)*	March 1988	**Finding A-3-d:** The content and format of the launch commit criteria document are being improved significantly. The format change will make it easier to use. In addition to these changes, the command chain during the countdown has been modified to include a "Mission Management Team" to whom the Launch Director will report. There is a concern that no clear distinction is being made between a "redline" and other criteria whose values are, advisedly, subject to interpretation or evaluation.	**Recommendation A-3-d:** Clear, unambiguous distinctions should be made in the Launch Commit Criteria between "redlines" and other parameters monitored during launch operations.	**NASA Response (in 1988 ASAP appendix):** The Launch Commit Criteria have been thoroughly reviewed by all concerned elements of the shuttle program to remove all ambiguous and unnecessary guidelines and leave only clear and concise criteria. Except for some introductory material about the document and general information on crew restrictions, only true "redlines" remain. These true "redlines? have no built-in margins and are intended for countdown holds, shutdowns, or recycles, depending on the phase of the count. All of the "redlines" that can be automated are being automated. The automation stops the countdown (clock) when any "redline" (limit) is reached prior to T-31 seconds, to allow a considered decision by the appropriate experts and program management on whether to proceed with or terminate the countdown, or take an alternate course. Encountering a "redline" after T-31 seconds leads to a shutdown and/or recycle of the launch countdown.
Aerospace Safety Advisory Panel *(NASA Charter)*	March 1988	**Finding B-1-a:** The restructured SRM&QA organization and operational mode appears to meet the recommendations made by the Presidential Commission, the Congress and the Aerospace Safety Advisory Panel and the internal NASA working groups. The policies and plans promulgated by the Associate Administrator/SRM&QA are being implemented by	**Recommendation B-1-a:** Official direction, through an appropriate document(s), should be provided to all programs/projects on the decision process for risk decisions. Without such direction for each specific program/project, risk decisions will not be made with a commonly understood and agreed-upon definition of the factors pertinent to the decision. The AA/SRM&QA should ensure that implementation of directed SRM&QA activities are conducted in an orderly,	**NASA Response (in 1988 ASAP appendix):** The risk management NMIs and NHBs, as discussed in Section B.1.c on the next page, provide direction on the risk disposition decision process, which is the central function of risk management. These directives and handbooks will be applicable to all programs. As appropriate, they provide for qualitative analyses with likelihood and severity treated categorically, and uncertainty reflected in the potential variability of the

Independent Assessment Team *(Chartered by)*	Date of Report	Finding	Recommendation	NASA Response
		the NASA centers. There is a new team spirit evolving throughout the SRM&QA world within NASA and its contractors that bodes well for the future.	thorough and timely manner to support the various milestones set by program/project offices.	categorizations. They also provide for quantitative analyses with likelihood and severity combined in numerical risk estimates, and uncertainty expressed as numerical distributions of the possible variations in the estimates. The development of the Risk Management Program Plan for each program is a program management responsibility. Guidance is provided in the NMIs and the NHBS, and the Safety Division (QS) Risk Management Program Manager provides additional assistance in the development of the plan and its implementation, as required. The Risk Management Program Manager in Code QS also supports or participates in program risk management assurance activities designed to provide oversight of the program's risk management process. Code Q will, through its audit, oversight, and independent assessment charter, provide personnel and resources to ensure that the programs properly implement the risk management program plans.
Aerospace Safety Advisory Panel *(NASA Charter)*	March 1988	**Finding B-1-b:** NASA has successfully instituted a variety of new procedures and reports to ensure and monitor safety. These are being given much attention in the efforts to resume STS flights. As regular Shuttle flights resume and become more routine, there is a danger of complacency setting in.	**Recommendation B-1b:** Because there is danger of complacency setting in, it is recommended that NASA review and audit the safety assessment process implementation on a periodic basis. Particular emphasis should be placed on the quality of the information reaching decision-makers. A regular review of the process will help managers discriminate between meaningful changes in system safety and unanticipated	**NASA Response (in 1988 ASAP appendix):** The Office of SRM&QA is well aware of the dangers of complacency and its impact on the safety of the various programs. One of the principal functions of the Deputy Associate Administrator for System Assurance is to establish and implement an audit/oversight function that will determine the SRM&QA acceptability and posture of each program. Program trade-offs and

Independent Assessment Team *(Chartered by)*	Date of Report	Finding	Recommendation	NASA Response
			alterations in the reporting process.	engineering decisions, vis-a-vis their effects on safety, are key elements to be reviewed, as well as the safety data that was generated to support these decisions. The expanded audit process and methodology, with plans and schedules, are being developed with the support of the NASA Headquarters Code Q support contractor. Audits will take place on a regular and/or as needed basis. Audit teams will consist of SRM&QA personnel from Headquarters, the Centers, support contractors, and outside experts in selected disciplines. The reporting systems and decision-making processes will be incorporated into the audit checklists to ensure that alterations to management systems and changes to reporting procedures are recognized with changes being properly assessed. Additionally, the Safety Division, QS, will continue to monitor the degree of implementation of the Agency safety policies by means of its own assistance visits and assessment/reviews. A training course is also being developed for personnel who will participate in audits, reviews, and surveys to assure effectiveness of the audit system. Maintaining the safety awareness and motivation of the workers at the floor level is also critical to the prevention of complacency and maintaining the safety assessment process. In support of this, the Safety Division is developing an Agency level Safety Awards Program that will provide top level recognition to project

Independent Assessment Team *(Chartered by)*	Date of Report	Finding	Recommendation	NASA Response
				groups, facility groups, or individuals who have demonstrated superior safety performance.
Aerospace Safety Advisory Panel *(NASA Charter)*	March 1988	**Finding B-1-c:** New NASA Management Instructions and Notices related to risk assessment and risk management policies are being developed. These instructions provide important new thinking and enabling policies that could lead to a more comprehensive and objective safety-risk management methodology for NASA. As yet, there is no organizational or functional structure for systems safety engineering that could implement effectively such a comprehensive program.	**Recommendation B-1c:** The ASAP recommends that (I) NASA complete NASA Management Instructions and Notices and their implementing handbooks and promulgate them as soon as possible. (2) NASA develop as rapidly as possible a more integrated systems safety engineering functional structure (possibly within the Headquarters SRM&QA organization with similar organizations at the centers).	**NASA Response (in 1988 ASAP appendix):** (1) NM1 8070.4, "Risk Management Policy for Manned Flight Programs," was promulgated on February 3, 1988. NMIs are also in draft and under review on risk management for unmanned programs and for research and technical facilities. These NMIs will identify, in general terms, the roles of qualitative and quantitative risk assessment in support of risk disposition decision-making. The NMIs also reflect recognition of the need to tailor these roles to specific applications, in accordance with appropriateness criteria that are related to the significance of the risks of concern, the information available for risk assessment, and the resources required for assessment and integration of results. NHB s are also being developed to aid in the implementation of the processes defined in the NMIs. A draft NHB on risk management program tools and techniques is currently under review. An NHB on risk management program roles and responsibilities has been developed, and a draft is currently available. The first NHB is a compendium of advanced qualitative and quantitative risk assessment and risk decision-making methods. The second NHB delineated the functions and interfaces of program and

Independent Assessment Team *(Chartered by)*	Date of Report	Finding	Recommendation	NASA Response
				facility management, engineering, system safety, and other Code Q elements. It further delineates the roles and responsibilities in risk management assurance. The primary role of program and facility management is recognized, as is the role of system safety in risk management support. The key role of oversight and special technical assistance in risk management assurance is particularly noted. In addition, a two-volume Safety Risk Management Program Plan has been published. It serves as a basic information source on risk management program objectives, rationale, and basic methodology.
Aerospace Safety Advisory Panel *(NASA Charter)*	March 1988	**Finding B-1-d:** The majority of NASA's safety efforts have focused on hardware reliability and the training and preparation of astronauts and pilots. There are potential safety problems that can arise from human errors at any level of the system because of its inherent complexity.	**Recommendations B-1-d:** More emphasis should be placed on the study of potential design-induced human errors.	**NASA Response (in 1988 ASAP appendix):** NASA Code QS is already providing additional emphasis on identifying and, when possible, preventing by design the potential safety problem areas arising from human errors. One chapter of the revised System Safety Handbook is devoted to Human Factors, Considerations, and Requirements. Continued emphasis will be applied towards incorporating these concerns into contract statements of work or as overall applicable contract requirements. Review of appropriate progress will be conducted during design and safety reviews to ensure that design takes into consideration human factors requirements. Additionally, Code QS intends to validate the effectiveness of the

Independent Assessment Team *(Chartered by)*	Date of Report	Finding	Recommendation	NASA Response
				multiplicity of discipline products and interfaces generated within the highly-matrixed SRM&QA organizational functions through selected staff assistance surveys.
Aerospace Safety Advisory Panel *(NASA Charter)*	March 1988	**Finding 5-a:** Work Environment at KSC. The work environment at KSC associated with launch processing can induce human error. NASA, the Shuttle Processing Contractor (SPC), and support contractors have generally recognized this fact through such actions as tightened discipline and accountability, improved worker safety programs, strict guidelines to control overtime, better training programs, and the better availability of spare parts and related equipment. However, there are still occasional reports of schedule pressure and the associated potential for error or acceptance of excessive risk.	**Recommendation 5-a:** Top management at NASA and the SPC should exercise continuing vigilance to ensure that a satisfactory working environment is achieved and maintained at KSC. The ASAP's dictum of "Safety first; schedule second" must be observed by each and every person involved in the STS program.	**NASA Response (in 1988 ASAP appendix):** NASA and its contractors have recognized that the complexity of STS launch processing can induce human error, and that there are risks associated with schedule pressure. The actions cited are intended to mitigate the possibility of such errors. As an example, SRM&QA management has taken a major step to this end by forming a Personnel Initiatives Panel (PIP). The purposes of the PIP are as follows: (1) identify organization problems, recommend corrective action, and provide a means of communication up to all levels of management; (2) establish the SR&QA function as an aggressive contributor for the overall team; (3) promote a workforce that is manned with quality people who are dedicated to superior performance and the pursuit of excellence; and (4) develop a comprehensive program to attract, develop, motivate, and retain the best professional talent available. By adhering to these tenets, NASA feels that the "safety first" belief can best be instilled in every worker. KSC policy is in place to assure that overtime is Carefully monitored and controlled, and that worker

Independent Assessment Team *(Chartered by)*	Date of Report	Finding	Recommendation	NASA Response
				fatigue due to excessive overtime does not contribute to errors during processing. Additionally, recently approved manpower increases, along with initiatives to increase operational efficiency, are serving to improve the working environment.
Aerospace Safety Advisory Panel *(NASA Charter)*	February 1987	**Finding General-1:** The Panel finds the recent reorganization of Space Shuttle management to be a positive step in recapturing or rebuilding a spirit of mutual respect and trust at all levels. The Panel recommends that: a priority objective of the new management team must be to enforce NASA's management instructions and to define clearly the responsibilities and authority of the NASA centers; a willingness of all NASA centers to pull together, to subordinate parochial interests, and to help each other is absolutely crucial if the Space Shuttle program is to succeed.		**NASA Response (in 1987 ASAP appendix):** We agree. In the Phillips' study, the Crippen report, and in the reorganization of the shuttle management, we have addressed the roles and responsibilities of all levels of management to specify the relationship between the various program offices and centers. NASA Management Instructions (NMIs), Program Approval Documents (PADS) and supporting policies are being reviewed to clearly define the responsibilities and authority of the centers. The elevation of direct control of the program to Headquarters establishes a programmatic chain that is independent of the NASA center organizations. However, the center directors are responsible and accountable for the technical excellence and performance of each of the National Space Transportation System (NSTS) project elements at their respective centers. Further, the center directors will ensure that their institution provides the required support to the NSTS program. In addition, the center directors, along with the Associate Administrator,

Independent Assessment Team *(Chartered by)*	Date of Report	Finding	Recommendation	NASA Response
				Office of Space Flight (CSF) are working together as members of the OSF Management Council which meets on a scheduled basis to oversee all CSF responsibilities and provide an independent review and assessment of the NSTS program.
Aerospace Safety Advisory Panel *(NASA Charter)*	February 1987	**Finding General-2:** The Panel finds that NASA and the Congress need to appreciate that the Space Shuttle is a system which remains primarily developmental with some operational characteristics. It is recommended that NASA needs to emphasize the developmental characteristic or it is likely to miss key elements of the Space Transportation System management challenge.		**NASA Response (in 1987 ASAP appendix):** In the detailed program assessment conducted after the 51-L accident, it has become evident to the top management within NASA that much of NSTS is still in the developmental stage and significant areas of the system will probably remain essentially developmental throughout the life of the program. We agree with the Panel that there is a need to emphasize the development characteristics in order to provide required management oversight and operational awareness. Also, it will be the duty of NASA to work closely with the Congress to come to a mutual understanding of the developmental stage of the system. This will be a critical task to get budget approval in areas of continued development. We seek assistance from ASAP to emphasize in their interface with the members of Congress and their staff the developmental nature of the shuttle system. NASA has already taken steps to strengthen its development effort on the shuttle program. In the critical main engine program, the single engine test rate has been substantially increased. The new plan calls for an average of 12 tests per

Independent Assessment Team *(Chartered by)*	Date of Report	Finding	Recommendation	NASA Response
				month through February 1988, and 10 tests per month through the mid-1990's. This is an increase over the previous plan of eight tests per month through mid-1990 and six tests per month through the mid-1990s. In the Solid Rocket Motor (SRM) program, it is planned to continue full scale firings of production motors at the rate of one to two per year following final qualification firings. These firings will be used to verify maintenance of critical processes, establish life of reusable components, and qualify any design changes. Another example is in the flight software area where a Level II Software Change Control Board has been set up. This board, made up of high level experts, reviews each proposed software change, determines impact, and approves or disapproves the change.
Aerospace Safety Advisory Panel *(NASA Charter)*	February 1987	**Finding General-8:** The Panel recommends that NASA top management should address the growing problem of recruiting and retaining talented engineers and managers due to inadequate Federal salaries. This is not just a Space Shuttle problem.		**NASA Response (in 1987 ASAP appendix):** We agree with this recommendation. NASA has traditionally relied on its highly visible mission, work environment, and career advancement opportunities to attract high-caliber scientists and engineers. However, in the past several years, 70 percent of all graduating entry-level engineers have declined NASA engineering job offers. The reason most often given for not accepting these job offers is inadequate salaries and/or benefits. Entry level technical salaries continue to be significantly less in the Federal sector than in private industry. NASA's most recent experiences show

Independent Assessment Team *(Chartered by)*	Date of Report	Finding	Recommendation	NASA Response
				that quality scientists and engineers with bachelor's degrees are accepting entry offers in private industry of $26,000 - $29,000; and some exceptional graduates with master's degrees, offers of $30,000 - $34,000. Under the Federal system, NASA can only offer $23,866 and $28,347, respectively. The Personnel Programs Division, Code NP, has been and will continue to document all data reflecting national recruitment trends and situations, Such data, including specific NASA recruitment and turnover data was recently presented to CMB. NASA management will continue to take every opportunity to give testimony to Congress, CMB, and OPM and to support needed changes to the Federal personnel system. Additionally, Code NP in conjunction with field installation personnel offices has initiated and developed a new personnel concept. This concept, centering around a new pay and compensation package, has the NASA Administrator's support. This new personnel system is needed to strengthen NASA's recruitment and retention posture with private industry, as well as to improve the overall quality of the NASA working environment. In expressing its concern regarding the salary structure for technical persons within NASA, the ASAP Report stated that: "It appears that in order to progress in terms of salary, people must move into

Independent Assessment Team *(Chartered by)*	Date of Report	Finding	Recommendation	NASA Response
				management ranks, making it difficult to keep experienced, highly qualified people in the technical ranks (p.58-91." We do not agree with this statement. In fact, the opposite is true. NASA employs approximately 6,500 E-13, 14, and 15 level non-managerial technologists compared to 3,000 management officials at the same grade levels.) It is at these grade levels where the preponderance of technical expertise is found within NASA and where Federal salaries are generally comparable to those in the private sector.
Aerospace Safety Advisory Panel *(NASA Charter)*	February 1987	**Finding General-9:** The Panel, in an independent review, concurs with the National Research Council (NRC) Panel conclusions on Space Shuttle Flight Rates and Utilization, that is, an upper limit of 8-10 flights per year with a three Orbiter fleet and 11-13 with a four Orbiter fleet. Further, the Panel recommends that the Space Shuttle be used only where manned missions are deemed mandatory, and expendable launch vehicles should be used for all other missions.		**NASA Response (in 1987 ASAP appendix):** In general, the flight rates projected by NASA are consistent with the conclusions of the NRC Panel. Their four orbiter flight rate of about 12 flights per year was characterized as a reasonable expected sustainable level. The rationale was that four flights per year can be achieved by each orbiter, but that only three of the four orbiters can be relied upon to be available on a continuing basis, due to unexpected problems and related maintenance and inspection requirements. The NRC also concluded that the space shuttle should have the capacity to surge above this sustainable level for short periods of time. NASA's current planning is based on a gradual buildup to 11 flights per year in the first four years after operations resume, with a later increase to 13 or 14 when the replacement orbiter joins the fleet. The actual flight rates will be adjusted on the basis of operational

Independent Assessment Team *(Chartered by)*	Date of Report	Finding	Recommendation	NASA Response
				experience, with appropriate contingency allowances in the shuttle processing schedules to minimize the buildup of launch pressure. For greater assurance of access to space and to reduce the demands on the shuttle for payloads that do not require its unique capabilities, Dr. Fletcher directed Admiral Truly, Associate Administrator for Space Flight, to conduct a NASA-wide study of a mixed fleet strategy, using expendable launch vehicles to augment the shuttle. The study recommended that Delta, Atlas, and Titan class vehicles be utilized for those payloads that could be launched on ELVs (about 25 percent of the NASA payloads). It also recommended that for the period beyond 1992, NASA, with the DOD, should develop a heavy lift launch vehicle capability to meet the needs of this Nation. Implementation plans for both recommendations are being developed as part of the ongoing NASA planning and budgeting process.
Aerospace Safety Advisory Panel *(NASA Charter)*	February 1987	**Finding Safety-1:** The Panel finds that three fundamental weaknesses appear evident. First, there has been a lack of in-line responsibility and authority in the Headquarters organization for establishing policy for the safety engineering function throughout NASA. Second, the elements of the safety functions that have been accomplished at various locations did not include responsibility for defining	**Recommendation Safety-1:** Within the newly established Safety, Reliability, Maintainability and Quality Assurance (SRM&QA) organization, NASA should develop the operating policy for all NASA SRM&QA and have the authority to ensure implementation. At each Center there should be a NASA Safety Engineering function reporting to the Center Director. This function should be matrixed into the various programs/projects and should be responsible for implementation of safety	**NASA Response (in 1987 ASAP appendix):** NASA has significantly strengthened the SRM&QA function both at headquarters and at the field centers. The Associate Administrator for SRM&QA reports directly to the Administrator and is responsible for developing operating policy for the NASA SRM&QA functions throughout NASA. He has the authority to ensure implementation of these policies. Each of the flight centers has a SRM&QA Director who reports directly

Independent Assessment Team *(Chartered by)*	Date of Report	Finding	Recommendation	NASA Response
		and controlling the validation and certification programs. Third, there is a conscious lack of quantitative approaches to determine failure-mode probabilities for the purposes of defining acceptable margins, and the relative likelihood of resulting system interactive hazards.	policies established by the Headquarters organization. NASA should continue to independently review all payload components with regard to their individual inherent safety, and should analyze the safety implications of the potential interactions of payloads in the event of a malfunction of any individual one.	to the center director. There is a safety engineering function within the center SRM&QA Director's organization. It is our intent to matrix SRM&QA personnel to their line organization for overview and oversight purposes. SRM&QA responsibilities within the programs will reside with the line organizations and they will have their own personnel to accomplish the safety engineering functions within the program/project. Additional personnel may be matrixed between program projects for this purpose to assure full compliance with SRM&QA objectives.
Rogers Commission *(Presidential Charter)*	6 June 1986		**Recommendation I – Design**: The faulty Solid Rocket Motor joint and seal must be changed. This could be a new design eliminating the joint or a redesign of the current joint and seal. No design options should be prematurely precluded because of schedule, cost or reliance on existing hardware.	**Original Response (Fletcher, 14 July 1986):** On March 24, 1986, the Marshall Space Flight Center (MSFC) was directed to form a Solid Rocket Motor (SRM) joint redesign team to include participation from MSFC and other NASA centers as well as individuals from outside NASA. The team includes personnel from Johnson Space Center, Kennedy Space Center, Langley Research Center, industry, and the Astronaut Office. To assist the redesign team, an expert advisory panel was appointed which includes 12 people with six coming from outside NASA. **Ultimate Result:** The result was the Redesigned Solid Rocket Motor (RSRM), later renamed the Reusable Solid Rocket Motor.

Independent Assessment Team *(Chartered by)*	Date of Report	Finding	Recommendation	NASA Response
Rogers Commission *(Presidential Charter)*	6 June 1986		**Recommendation I – Independent Oversight**: The Administrator of NASA should request the National Research Council to form an independent Solid Rocket Motor design oversight committee to implement the Commission's design recommendations and oversee the design effort.	**Original Response (Fletcher, 14 July 1986):** In accordance with the Commission's recommendation, the National Research Council (NRC) has established an Independent Oversight Group chaired by Dr. H. Guyford Stever and reporting to the NASA Administrator. The NRC Oversight Group has been briefed on Shuttle system requirements, implementation, and control; Solid Rocket Motor background; and candidate modifications. The group has established a near-term plan that includes briefings and visits to review in- flight loads; assembly processing; redesign status; and other solid rocket motor designs, including the Titan. Longer term plans are being formulated by the group including participation in the Solid Rocket Motor preliminary design review in September 1986.
Rogers Commission *(Presidential Charter)*	6 June 1986		**Recommendation II – Shuttle Management Structure**: The Shuttle Program Structure should be reviewed. The project managers for the various elements of the Shuttle program felt more accountable to their center management than to the Shuttle program organization. Shuttle element funding, work package definition, and vital program information frequently bypass the National STS (Shuttle) Program Manager. A redefinition of the Program Manager's responsibility is essential. This redefinition should give the Program Manager the requisite authority for all ongoing STS operations. Program funding and all Shuttle	**Original Response (Fletcher, 14 July 1986):** The Administrator has appointed General Sam Phillips, who served as Apollo Program Director, to study every aspect of how NASA manages its programs, including relationships between various field centers and NASA Headquarters. General Phillips has broad authority from the Administrator to explore every aspect of NASA organization, management and procedures. His activities will include a review of the Space Shuttle Office of Safety, Reliability, and Quality Assurance, and to the

Independent Assessment Team *(Chartered by)*	Date of Report	Finding	Recommendation	NASA Response
			Program work at the centers should be placed clearly under the Program Manager's authority.	existing Aerospace Safety Advisory Panel. On June 25, 1986, Astronaut Robert Crippen was directed to form a fact-finding group to assess the Space Shuttle management structure. The group will report recommendations to the Associate Administrator for Space Flight by August 15, 1986. Specifically, this group will address the roles and responsibilities of the Space Shuttle Program Manager to assure that the position has the authority commensurate with its responsibilities. In addition, roles and responsibilities at all levels of program management will be reviewed to specify the relationship between the program organization and the field center organizations. The results of this study will be reviewed with General Phillips and the Administrator with a decision on implementation of the recommendations by October 1, 1986.
Rogers Commission *(Presidential Charter)*	6 June 1986		**Recommendation II – Astronauts in Management**: The Commission observes that there appears to be a departure from the philosophy of the 1960s and 1970s relating to the use of astronauts in management positions. These individuals brought to their positions flight experience and a keen appreciation of operations and flight safety.	**Original Response (Fletcher, 14 July 1986):** Rear Admiral Richard Truly, a former astronaut, has been appointed as Associate Administrator for the Office of Space Flight. Several active astronauts are currently serving in management positions in the agency. The Crippen group will address means to stimulate the transition of astronauts into other management positions. It will also determine the appropriate position for the Flight Crew Operations Directorate within the NASA organizational structure.

Independent Assessment Team *(Chartered by)*	Date of Report	Finding	Recommendation	NASA Response
Rogers Commission *(Presidential Charter)*	6 June 1986		**Recommendation II – Shuttle Safety Panel:** NASA should establish an STS Safety Advisory Panel reporting to the STS Program Manager. The Charter of this panel should include Shuttle operational issues, launch commit criteria, flight rules, flight readiness and risk management. The panel should include representation from the safety organization, mission operations, and the astronaut office.	**Original Response (Fletcher, 14 July 1986):** A Shuttle Safety Panel will be established by the Associate Administrator for Space Flight not later than September 1, 1986, with direct access to the Space Shuttle Program Manager. This date allows time to determine the structure and function of this panel, including an assessment of its relationship to the newly formed Office of Safety, Reliability, and Quality Assurance, and to the existing Aerospace Safety Advisory Panel.
Rogers Commission *(Presidential Charter)*	6 June 1986		**Recommendation III – Criticality Review and Hazard Analysis**: NASA and the primary Shuttle contractors should review all Criticality 1, 1R, 2, and 2R items and hazard analyses. This review should identify those items that must be improved prior to flight to ensure mission safety. An Audit Panel, appointed by the National Research Council, should verify the adequacy of the effort and report directly to the Administrator of NASA.	**Original Response (Fletcher, 14 July 1986):** On March 13, 1986, NASA initiated a complete review of a1 Space Shuttle program failure modes and effects analyses (FMEAs) and associated critical item lists (CILs). Each Space Shuttle project element and associated prime contractor is conducting separate comprehensive reviews which will culminate in a program-wide review with the Space Shuttle Program Manager at Johnson Space Center later this year. Technical specialists from outside the Space Shuttle program have been assigned as formal members of each of these review teams. AI1 Criticality 1 and 1R critical item waivers have been cancelled. The teams are required to reassess and resubmit waivers in categories recommended for continued program applicability. Items which cannot be revalidated will be redesigned, qualified, and certified for flight. All Criticality 2 and 3 CILs are

Independent Assessment Team *(Chartered by)*	Date of Report	Finding	Recommendation	NASA Response
				being reviewed for proper categorization. This activity will culminate in a comprehensive final review with NASA Headquarters beginning in March 1987. As recommended by the Commission, the National Research Council has agreed to form an Independent Audit Panel, reporting to the NASA Administrator, to verify the adequacy of this effort.
Rogers Commission *(Presidential Charter)*	6 June 1986		**Recommendation IV – Safety Organization**: NASA should establish an Office of Safety, Reliability and Quality Assurance to be headed by an Associate administrator, reporting directly to the NASA Administrator. It would have direct authority for safety, reliability, and quality assurance throughout the agency. The office should be assigned the work force to ensure adequate oversight of its functions and should be independent of other NASA functional and program responsibilities.	**Original Response (Fletcher, 14 July 1986):** The NASA Administrator announced the appointment of Mr. George A. Rodney to the position of Associate Administrator for Safety, Reliability, and Quality Assurance on July 8, 1986. The responsibilities of this office will include the oversight of safety, reliability, and quality assurance functions related to all NASA activities and programs and the implementation of a system for anomaly documentation and resolution to include a trend analysis program. One of the first activities to be undertaken by the new Associate Administrator will be an assessment of the resources including workforce required to ensure ad- equate execution of the safety organization functions. In addition, the new Associate Administrator will assure appropriate interfaces between the functions of the new safety organization and the Shuttle Safety Panel which will be established.

Independent Assessment Team *(Chartered by)*	Date of Report	Finding	Recommendation	NASA Response
Rogers Commission *(Presidential Charter)*	6 June 1986		**Recommendation V – Improved Communications**: The Commission found that Marshall Space Flight Center project managers, because of a tendency at Marshall to management isolation, failed to provide full and timely information bearing on the safety of flight 51-L to other vital elements of Shuttle program management.	**Original Response (Fletcher, 14 July 1986):** On June 25, 1986, Astronaut Robert Crippen was directed to form a team to develop plans and recommended policies for the following: 1. Implementation of effective management communications at all levels. 2. Standardization of the imposition and removal of STS launch constraints and other operational constraints. 3. Conduct of Flight Readiness Review and Mission Management Team meetings, including requirements for documentation and flight crew participation. Since this recommendation is closely linked with the recommendation on Shuttle management structure, the study team will incorporate the plan for improved communications with that for management restructure. This review of effective communications will consider the activities and information flow at NASA Headquarters and the field centers which support the Shuttle program. The study team will present findings and recommendations to the Associate Administrator for Space Flight by August 15,

Independent Assessment Team *(Chartered by)*	Date of Report	Finding	Recommendation	NASA Response
				1986.
Rogers Commission *(Presidential Charter)*	6 June 1986		**Recommendation VI – Landing Safety:** NASA must take actions to improve landing safety.	**Original Response (Fletcher, 14 July 1986):** A Landing Safety Team has been established to review and implement the Commission's findings and recommendations on landing safety. All Shuttle hardware and systems are undergoing design reviews to insure compliance with the specifications and safety concerns. The tires, brakes, and nose wheel steering system are included in this activity, and funding for a new carbon brakes system has been approved. Runway surface tests and landing aid requirement reviews had been under way for some time prior to the accident and are continuing. Landing aid implementation will be complete by July 1987. The interim brake system will be delivered by August 1987. Improved methods of local weather forecasting and weather-related support are being developed. Until the Shuttle program has demonstrated satisfactory safety margins through high fidelity testing and during actual landings at Edwards Air Force Base, the Kennedy Space Center landing site will not be used for nominal end-of-mission landings. Dual Orbiter ferry capability has been an issue for some time and will be thoroughly considered during the upcoming months.

Independent Assessment Team *(Chartered by)*	Date of Report	Finding	Recommendation	NASA Response
Rogers Commission *(Presidential Charter)*	6 June 1986		**Recommendation VII – Launch Abort and Crew Escape:** The Shuttle program management considered first-stage abort options and crew escape options several times during the history of the program, but because of limited utility, technical infeasibility, or program cost and schedule, no systems were implemented.	**Original Response (Fletcher, 14 July 1986):** On April 7, 1986, NASA initiated a Shuttle Crew Egress and Escape review. The scope of this analysis includes egress and escape capabilities from launch through landing and will provide analyses, concepts, feasibility assessments, cost, and schedules for pad abort, bailout, ejection systems, water landings, and powered flight separation. This review will specifically assess options for crew escape during controlled gliding flight and options for extending the intact abort flight envelope to include failure of 2 or 3 main engines during the early ascent phase. In conjunction with this activity, a Launch Abort Reassessment Team was established to review all launch and launch abort rules to ensure that launch commit criteria, flight rules, range safety systems and procedures, landing aids, runway configurations and lengths, performance versus abort expo- sure, abort and end-of-mission landing weights, runway surfaces, and other landing-related capabilities provide the proper margin of safety to the vehicle and crew. Crew escape and launch abort studies will be complete on October 1, 1986, with an implementation decision in December 1986.
Rogers Commission *(Presidential Charter)*	6 June 1986		**Recommendation VIII – Flight Rate:** The nation's reliance on the Shuttle as its principal space launch capability created a relentless pressure on NASA to increase the flight rate. Such reliance on	**Original Response (Fletcher, 14 July 1986):** In March 1986 NASA established a Flight Rate Capability Working Group. Two flight rate capability studies are under way: (1) a

Independent Assessment Team *(Chartered by)*	Date of Report	Finding	Recommendation	NASA Response
			a single launch capability should be avoided in the future. NASA must establish a flight rate that is consistent with its resources. A firm payload assignment policy should be established. The policy should include rigorous controls on cargo manifest changes to limit the pressures such changes exert on schedules and crew training.	study of capabilities and constraints which govern the Shuttle processing flows at the Kennedy Space Center and (2) a study by the Johnson Space Center to assess the impact of flight specific crew training and software delivery/ certification on flight rates. The working group will present flight rate recommendations to the Office of Space Flight by August 15, 1986. Other collateral studies are still in progress which address Presidential Commission recommendations related to spares provisioning, maintenance, and structural inspection. This effort will also consider the National Research Council independent review of flight rate which is under way as a result of a Congressional Subcommittee request. NASA strongly supports a mixed fleet to satisfy launch requirements and actions to revitalize the United States expendable launch vehicle capabilities. Additionally, a new cargo manifest policy is being formulated by NASA Headquarters which will establish manifest ground rules and impose constraints to late changes. Manifest control policy recommendations will be completed in November 1986.
Rogers Commission *(Presidential Charter)*	6 June 1986		**Recommendation IX – Maintenance Safeguards:** Installation, test, and maintenance procedures must be especially rigorous for Space Shuttle items designated Criticality 1. NASA should	**Original Response (Fletcher, 14 July 1986):** A Maintenance Safeguards Team has been established to develop a comprehensive plan for defining and implementing actions to

Independent Assessment Team *(Chartered by)*	Date of Report	Finding	Recommendation	NASA Response
			establish a system of analyzing and reporting performance trends of such items. Maintenance procedures for such items should be specified in the Critical Items List, especially for those such as the liquid-fueled main engines, which require unstinting maintenance and overhaul.	comply with the Commission recommendations concerning maintenance activities. A Maintenance Plan is being prepared to ensure that uniform maintenance requirements are imposed on all elements of the Space Shuttle program. This plan will define the structure that will be used to document (1) hardware inspections and schedules, (2) planned maintenance activities, (3) maintenance procedures configuration control, and (4) maintenance logistics. The plan will also define organizational responsibilities, reporting, and control requirements for Space Shuttle maintenance activities. The maintenance plan will be completed by September 30, 1986. A number of other activities are underway which will contribute to a return to safe flight and strengthening the NASA organization. A Space Shuttle Design Requirements Review Team headed by the Space Shuttle Systems Integration Office at Johnson Space Center has been assigned to review all Shuttle design requirements and associated technical verification. The team will focus on each Shuttle project element and on total Space Shuttle system design requirements. This activity will culminate in a Space Shuttle Incremental Design Certification Review approximately 3 months prior to the next Space Shuttle launch. In consideration of the

Independent Assessment Team *(Chartered by)*	Date of Report	Finding	Recommendation	NASA Response
				number, complexity, and interrelationships between the many activities leading to the next flight, the Space Shuttle Program Manager at Johnson Space Center has initiated a series of formal Program Management Reviews for the Space Shuttle program- These reviews are structured to be regular face-to-face discussions involving the managers of all major Space Shuttle program activities. Specific subjects to be discussed at each meeting will focus on progress, schedules, and actions associated with each of the major program review activities and will be tailored directly to current program activity for the time period involved. The first of these meetings was held at Marshall Space Flight Center on May 5-6, 1986, with the second at Kennedy Space Center on June 25, 1986. Follow-on reviews will be held approximately every 6 weeks. Results of these reviews will be reported to the Associate Administrator for Space Flight and to the NASA Administrator.

Only **Findings** and **Recommendations** relevant to the Space Shuttle Program have been extracted from each report.

The Organizations making the reports – and their charters - are as follows:

Aerospace Safety Advisory Panel (ASAP): "The Panel shall review safety studies and operations plans referred to it and shall make reports thereon, shall advise the Administrator with respect to the hazards of proposed operations and with respect to the adequacy of proposed or existing safety standards, and shall perform such other duties as the Administrator may request." NASA Authorization Act of 1968 | Public Law 90-67, 42 U.S.C. 2477

Space Shuttle Independent Assessment Team (SIAT): The Space Shuttle Independent Assessment Team was chartered in September 1999 by the NASA Administrator to provide an independent review of the Space Shuttle subsystems and maintenance practices.

Volume V
Appendix G.11

Foam Application and Production Chart

This Appendix contains the Foam Application and Production spreadsheet developed by Group I in support of their investigation in the area of ET Foam. The spreadsheet is too large to reproduce in hardcopy and is included on the DVD only.

THIS PAGE INTENTIONALLY LEFT BLANK

MISSION DATA

#	STS	STS aka	OV	OV flt #	ET	ET wt.	Date	Pad	MLP	Day or Night	Landing Location	ET Age @ Launch (days)	ET Exposure (days)	Tanking Time (hrs)	Mission Time (hrs)	LS >1	LS Tot	OV>1	OV Tot	Camera	-Y bipod visible?	+Y bipod visible	FOAM LOSS NOTED?	Bipod	NEAR Bipod?	Flange	Intertank	Thrust Panel	Other	Cause	Corrective Action	SRB Mate/Demate from ET	Orbiter Mate/Demate from ET	Rollout/Rollback	Dry OV (incl. SSMEs) (lbs.)	Cargo & Crew (lbs.)	OV Consumables (lbs.)
1	1		102	1	1	H	04/12/81	A	1	D	E	653	105	3.50	54				247	16	Y	Y	Y	N		N	N	N	Y			11/03/80	11/24/80	12/29/80			
2	2		102	2	2	H	11/12/81	A	1	D	E	258	74	2.50	54				109	Y	Y	Y	N	N		N	N	N	N			06/30/81	08/10/81	08/31/81			
3	3		102	3	3	H	03/22/82	A	1	D	W	175	35	3.00	192				113	Y	Y	Y	Y	N		Y	Y	N	Y			01/04/82	02/03/82	02/16/82			
4	4		102	4	4	H	06/27/82	A	1	D	E	161	33	3.00	169				122	Y	Y	Y	Y	N		Y	Y	N	Y			04/17/82	05/19/82	05/26/82			
5	5		102	5	5	H	11/11/82	A	1	D	E	169	52	3.00	122				161	Y	Y	Y	Y	N	Y	Y	Y	N	Y			08/19/82	09/10/82	09/21/82	172566	35902	37957
6	6		99	1	8	L	04/04/83	A	2	D	E	208	126	4.00	120	21	89	36	120	35	Y	Y	Y	N		Y	N	N	Y			10/21/82	11/23/82	11/30/82	168736	51032	37219
7	7		99	2	6	H	06/18/83	A	1	D	E	327	24	3.00	146	41	153	48	253	35	Y	Y	Y	-Y		Y	Y	N	Y			03/02/83	05/24/83	05/26/83	169044	41134	39448
8	8		99	3	9	L	08/30/83	A	2	N	E	230	29	3.00	145	3	29	7	56		N	N	?	?		?	?	?	?			06/23/83	07/26/83	08/02/83	168832	34008	39953
9	9		102	6	11	L	11/28/83	A	1	D	E	206	43	7.00	248	9	49	14	58		N	N	?	?		?	?	?	?			???	???	11/08/83	176231	36402	35180
10	11	41B	99	4	10	L	02/03/84	A	2	D	K	339	23	5.00	191	11	19	34	63	35	Y	Y	Y	N	Y	Y	Y	N	Y			01/03/84	01/08/84	01/12/84	169166	37743	43496
11	13	41C	99	5	12	L	04/06/84	A	1	D	E	259	19	5.00	168	5	27	8	36		N	N	?	?		?	?	?	?			02/28/84	03/15/84	03/19/84	169433	42040	42931
12	14	41D	103	1	13	L	08/30/84	A	2	D	E	352	79	3.00	145	10	44	31	111		N	N	?	?		?	?	?	?			04/09/84	08/04/84	08/09/84	169944	51483	42194
13	17	41G	99	6	15	L	10/05/84	A	1	D	K	295	23	3.00	197	25	69	36	154	35	Y	Y	Y	N		N	Y	N	Y			06/19/84	09/10/84	09/13/84	170667	27994	43882
14	19	51A	103	2	16	L	11/08/84	A	2	D	K	286	17	3.00	192	14	66	20	87		N	N	?	?		?	?	?	?			10/02/84	10/19/84	10/23/84	169711	49661	43980
15	20	51C	103	3	14	L	01/24/85	A	1	D	K	448	20	3.00	74	24	67	28	81		N	N	?	?		?	?	?	?			10/30/84	12/23/84	01/05/85			
16	23	51D	103	4	18	L	04/12/85	A	1	D	K	353	16	3.00	168	43	111	46	152		N	N	?	?		?	?	?	?			02/14/85	03/23/85	03/28/85	169481	40610	40318
17	24	51B	99	7	17	L	04/29/85	A	2	D	E	409	33	3.00	168	45	110	62	140	35	Y	N	Y	?		N	Y	N	Y			01/09/85	04/11/85	04/15/85	170953	35422	40879
18	25	51G	103	5	20	L	06/17/85	A	1	D	E	347	14	3.00	170	109	231	144	315		N	N	?	?		?	?	?	?			05/02/85	05/29/85	06/04/85	169802	49042	37532
19	26	51F	99	8	19	L	07/29/85	A	2	D	E	431	31	3.00	191	179	482	226	553	35	Y	Y	Y	N		Y	Y	N	Y			05/31/85	06/26/85	06/29/85	170948	38742	43043
20	27	51I	103	6	21	L	08/27/85	A	1	D	E	398	22	3.00	170	21	96	33	141		N	N	?	?		?	?	?	?			07/02/85	07/30/85	08/06/85	169919	48781	43354
21	28	51J	104	1	25	L	10/03/85	A	2	D	E	287	35	3.00	98	7	66	17	111		N	N	?	?		?	?	?	?			08/09/85	08/13/85	08/30/85			
22	30	61A	99	9	24	L	10/30/85	A	1	D	E	348	15	3.00	169	24	129	34	183	35	Y	Y	Y	N	Y	N	N	Y			09/30/85	10/12/85	10/16/85	171084	36388	36279
23	31	61B	104	2	22	L	11/26/85	A	2	N	E	459	15	3.00	165	37	177	55	257		N	N	?	?		?	?	?	?			10/22/85	11/08/85	11/12/85	170127	53027	38290
24	32	61C	102	7	30	L	01/12/86	A	1	D	E	208	42	3.00	146	20	134	39	193	16	Y	Y	Y	N		N	Y	N	Y			11/14/85	11/22/85	12/02/85	176549	37894	40480
25	33	51L	99	10	26	L	01/28/86	B	2	D		319	38	3.00	0						N	N	?	?		?	?	?	?			12/10/85	12/17/85	12/22/85	172162	57545	38929
26	26R		103	7	28	L	09/28/88	B	2	D	E	1261	87	3.00	97	47	342	55	411	H	Y	Y	N	N		N	N	N	N			06/10/88	06/24/88	07/04/88	171978	51180	31459
27	27R		104	3	23	L	12/02/88	B	1	D	E	1530	31	3.00	105	272	644	298	707		N	N	?	?		?	?	?	?			09/21/88	10/24/88	11/02/88			
28	29R		103	8	36	L	03/13/89	B	2	D	E	1189	39	3.00	120	18	100	23	132	H	Y	Y	Y	N	Y	Y	N	Y	Y			12/15/88	01/25/89	02/03/89	172149	52640	31446
29	30R		104	4	29	L	05/04/89	B	1	D	E	1450	44	3.00	97	53	134	56	151		N	N	?	?		?	?	?	?			03/02/89	03/11/89	03/22/89	172098	52878	36380
30	28R		102	8	31	L	08/08/89	B	2	D	E	1484	25	3.00	121	13	60	20	74	16,35,H	Y	Y	Y	N	Y	Y	Y	N	Y		Y	05/22/89	07/04/89	07/15/89			
31	34		104	5	27	L	10/18/89	B	1	D	E	1723	51	3.00	120	17	51	18	53		Y	N	?	?		?	?	?	?			07/29/89	08/21/89	08/29/89	172329	53721	31565
32	33R		103	9	38	L	11/22/89	B	2	N	E	1317	27	3.00	120	21	107	21	118		N	N	?	?		?	?	?	?			09/02/89	10/05/89	10/27/89			
33	32R		102	9	32	L	01/09/90	A	3	D	E	1609	43	3.00	261	13	111	15	120	16,35	Y	Y	Y	-Y	Y	Y	N	Y	Y	Y		11/01/89	11/21/89	11/28/89	179735	31735	44593
34	36		104	6	33	L	02/28/90	A	1	N	E	1597	35	3.00	106	17	62	19	81		N	N	?	?		?	?	?	?			12/22/89	01/19/90	01/25/90			
35	31R		103	10	34	L	04/24/90	B	2	D	E	1674	40	3.00	121	11	33	12	48		N	N	?	?		?	?	?	?			02/23/90	03/06/90	03/16/90	172036	34236	42892
36	41		103	11	39	L	10/06/90	B	2	D	E	1635	32	3.00	98	13	64	16	76	H	N	N	?	?		N	N	N	N			08/01/90	08/27/90	09/05/90	172562	55036	31903
37	38		104	7	40	L	11/15/90	A	1	N	K	1609	88	3.00	118	7	70	8	81		N	N	?	?		?	?	?	?			09/12/90	10/03/90	10/12/90			
38	35		102	10	35	L	12/02/90	B	3	N	E	1850	164	3.00	215	15	132	17	147	H	Y	Y	Y	N		Y	N	N	Y	Y	Y	03/22/90	08/02/90	10/14/90	178847	38800	38864
39	37		104	8	37	L	04/05/91	B	1	D	E	1906	22	3.00	144	7	91	11	115	H	N	N	Y	?		Y	N	N	N			02/04/91	03/08/91	03/15/91	172272	46082	37404
40	39		103	12	46	L	04/28/91	A	2	D	K	1327	49	3.00	199	14	217	16	237	H	N	N	?	?		N	N	N	N			12/18/90	03/25/91	04/01/91	172883	33052	41401
41	40		102	11	41	L	06/05/91	B	3	D	E	1776	35	3.00	218	23	153	25	197	H,16?	Y	Y	Y	N		Y	N	N	N			04/17/91	04/25/91	05/02/91	180375	39117	32429
42	43		104	9	47	L	08/02/91	A	1	D	K	1323	39	3.00	213	24	122	25	131	H	Y	N	?	?		?	?	?	?	Y		06/03/91	06/19/91	06/25/91	172179	54799	32369
43	48		103	13	42	L	09/12/91	A	3	D	E	1829	32	3.00	128	14	100	25	182		N	N	?	?		?	?	?	?			07/24/91	08/01/91	08/12/91	172770	26978	40306
44	44		104	10	53	L	11/24/91	A	1	N	E	846	33	3.00	167	6	74	9	101		N	N	?	?		?	?	?	?			09/26/91	10/18/91	10/23/91	172322	52859	34670
45	42		103	14	52	L	01/22/92	A	3	D	E	994	35	3.00	193	38	159	44	209	H	Y	N	Y	?	Y	N	Y	N	N	N	N	11/04/91	12/13/91	12/19/91	172707	37890	32859
46	45		104	11	44	L	03/24/92	A	1	D	K	1840	34	3.50	214	18	122	22	172	H	Y	N	Y	?	Y	Y	N	N	N			01/22/92	02/13/92	02/20/92	172140	25963	35547
47	49		105	1	43	L	05/07/92	B	2	D	E	2005	56	3.00	213	6	55	11	114		N	N	?	?		?	?	?	?			02/17/92	03/07/92	03/13/92	172749	44886	38698
48	50		102	12	50	L	06/25/92	A	3	D	K	1333	23	3.00	332	28	141	45	184	16,35,H	Y	Y	Y	-Y		Y	N	N	Y	Y	Y	04/09/92	05/29/92	06/03/92	180784	38315	38596
49	46		104	12	48	L	07/31/92	B	1	D	K	1561	51	3.00	191	11	186	22	236	H	Y	Y	N	N		N	N	N	N			05/15/92	06/05/92	06/11/92	171994	40185	43852
50	47		105	2	45	L	09/12/92	B	2	D	K	1923	19	3.00	191	3	48	11	108	16,35,H	Y	Y	Y	N	Y	Y	Y	N	Y	Y	N	07/13/92	08/20/92	08/25/92	172859	38812	32897
51	52		102	13	55	L	10/22/92	B	3	D	K	994	27	2.50	237	6	152	16	290	16,35,H	Y	Y	Y	-Y		Y	Y	N	Y			09/09/92	09/20/92	09/26/92	181201	32341	36828
52	53		103	15	49	L	12/02/92	A	1	D	E	1577	25	3.00	175	11	145	23	240	H	Y	Y	Y	N	Y	Y	N	N			10/13/92	11/03/92	11/08/92	173438	33943	36516
53	54		105	3	51	L	01/13/93	B	2	D	K	1440	42	3.00	144	14	80	14	131	16,35,H	Y	Y	Y	N	Y	Y	Y	N	Y			11/05/92	11/23/92	12/03/92	173073	54495	31844
54	56		103	16	54	L	04/08/93	B	1	N	K	1256	25	3.00	222	18	94	36	156	H	Y	Y	Y	N		N	Y	N	N	N	Y	02/10/93	03/02/93	03/15/93	173563	27278	36412
55	55		102	14	56	L	04/26/93	A	3	D	E	1082	79	3.00	240	10	128	13	143	H,16?	Y	Y	Y	N	Y	Y	N	N	Y			01/12/93	02/02/93	02/07/93	180891	39484	35093
56	57		105	4	58	L	06/21/93	B	2	D	K	979	55	3.00	240	10	75	12	106	16,35,H	Y	Y	Y	N	Y	Y	Y	Y	Y			03/08/93	03/25/93	04/28/93	173363	35196	44144
57	51		103	17	59	L	09/12/93	B	3	D	K	900	80	3.00	236	8	100	18	154	H	Y	Y	Y	N	Y	Y	N	N	Y			06/02/93	06/18/93	06/25/93	173664	52473	35341
58	58		102	15	57	L	10/18/93	B	1	D	E	1180	33	3.00	336	23	78	26	155	16,35,H	Y	Y	Y	N	Y	Y	Y	N	Y	N		07/21/93	08/12/93	09/16/93	181268	38442	36393
59	61		105	5	60	L	12/02/93	B	2	N	K	889	36	3.00	260	7	59	13	120	H	N	N	?	?		?	?	?	?			10/06/93	10/21/93	10/28/93	173685	32016	44577
60	60		103	18	61	L	02/03/94	A	3	D	K	842	25	3.00	199	4	48	15	106	H	Y	Y	N	N		N	N	N	N			11/29/93	01/05/94	01/10/94	173781	35012	37143
61	62		102	16	62	L	03/04/94	B	1	D	K	773	23	3.00	335	7	36	16	97	16,35,H	Y	Y	Y	-Y	Y	Y	Y	N	Y			01/20/94	02/03/94	02/10/94	181475	36350	38754
62	59		105	6	63	L	04/09/94	A	2	D	E	737	22	3.00	270	10	47	19	77	16,35,H	Y	Y	Y	N	Y	Y	Y	N	Y			02/23/94	03/14/94	03/19/94	173853	40423	32573
63	65		102	17	64	L	07/08/94	A	3	D	K	718	24	3.00	354	17	123	21	151	16,35,H	Y	Y	Y	N	Y	Y	Y	N	Y			05/03/94	06/09/94	06/15/94	181576	39732	37991
64	64		103	19	66	L	09/09/94	B	2	D	E	591	23	3.00	236	18	116	19	150		N	N	?	?		?	?	?	?			07/27/94	08/11/94	08/18/94	173579	32194	35661
65	68		105	7	65	L	09/30/94	A	1	D	E	697	47	3.00	270	9	59	15	110	16,35,H	Y	Y	Y	N	Y	Y	Y	N	Y			06/16/94	07/21/94	09/13/94	173891	40911	32601
66	66		104	13	67	L	11/03/94	B	3	D	E	535	25	3.00	263	22	111	28	148	16,35,H	Y	Y	Y	N	Y	Y	Y	N	Y			09/14/94	10/04/94	10/10/94	173051	30635	40552
67	63		103	20	68	L	02/03/95	B	2	N	K	546	25	3.00	198	7	84	14	125		N	N	?	?		?	?	?	?			11/08/94	01/05/95	01/10/95	173605	31156	42864
68	67		105	8	69	L	03/02/95	A	1	N	E	484	23	3.00	399	11	47	13	76	H	Y	Y	N	N		N	N	N	N			12/13/94	02/03/95	02/08/95	174223	34923	47349
69	71		104	14	70	L	06/27/95	A	3	D	K	495	63	3.00	235	24	149	25	164	16	Y	Y	Y	N	Y	Y	Y	N	Y			03/15/95	04/20/95	04/26/95	173189	33963	41936
70	70		103	21	71	L	07/13/95	B	2	D	K	435	58	3.00	214	5	81	9	127	H	Y	Y	N	N		N	N	N	N			04/13/95	05/03/95	06/14/95	173728	52140	32716
71	69		105	9	72	L	09/07/95	A	1	D	K	433	59	3.00	260	22	175	27	198	16	Y	Y	Y	N		N	N	N	Y			05/31/95	06/28/95	08/08/95	173869	37782	44733
72	73		102	18	73	L	10/20/95	B	3	D	K	381	54	3.00	382	17	102	26	147	16,35,H	Y	Y	Y	N		N	N	N	Y			08/05/95	08/21/95	08/28/95	182071	39838	35418
73	74		104	15	74	L	11/12/95	A	2	D	K	360	33	3.00	197	17	78	21	116	16,35	Y	Y	Y	N		Y	N	N	N			09/11/95	10/03/95	10/11/95	173255	30086	44925
74	72		105	10	75	L	01/11/96	B	1	N	K	342	37	2.92	214	3	23	7	55	H,16	N	N	?	?		N	N	N	N			11/09/95	12/01/95	12/06/95	174465	27771	44775
75	75		102	19	76	L	02/22/96	B	3	D	K	330	25	2.92	338	11	55	17	96	H,16,35	Y	Y	Y	N		Y	N	N	Y			01/08/96	01/24/96	01/29/96	181514	38894	41083
76	76		104	16	77	L	03/22/96	B	2	N	E	303	24	3.17	221	5	32	15	69		N	N	?	?		?	?	?	?			02/05/96	02/20/96	02/28/96	173405	31342	41473
77	77		105	11	78	L	05/19/96	B	1	D	K	307	34	3.17	241	15	48	17	81	16,35,H	Y	Y	Y	N	Y	Y	Y	N	Y			03/21/96	04/08/96	04/16/96	174484	40955	39314
78	78		102	20	79	L	06/20/96	B	3	D	K	281	23	3.17	406	5	35	12	85	16,35,H	Y	Y	Y	N	Y	Y	N	N	N			05/03/96	05/21/96	05/29/96	182433	37873	36189
79	79		104	17	82	L	09/16/96	A	1	N	K	188	38	3.00	243	8	61	11	103	H	Y	Y	N	N		N	N	N	N			08/05/96	08/13/96	09/05/96	173550	34533	41357
80	80		102	21	80	L	11/19/96	B	3	D	K	368	35	3.00	424	4	34	8	93	16,35,H	Y	Y	Y	N	Y	Y	Y	N	Y			09/26/96	10/10/96	10/16/96	181558	37388	42871
81	81		104	18	83	L	01/12/97	B	2	N	K	262	34	3.00	244	14	48	15	100	H	N	N	?	?		Y	N	N	N			11/14/96	12/04/96	12/10/96	174043	34669	41455
82	82		103	22	81	L	02/11/97	A	1	N	K	390	26	3.17	240	14	53	18	103	H	Y	Y	N	N		N	N	N	N			12/09/96	01/11/97	01/17/97	175820	31998	44168
83	83		102	22	84	L	04/04/97	A	3	D	K	291	25	3.50	95	7	38	13	81	16,H	Y	Y	Y	N	Y	Y	N	N	Y			01/30/97	03/05/97	03/11/97	181532	40462	37973
84	84		104	19	85	L	05/15/97	A	2	N	K	281	22	3.17	221	10	67	13	103	H	Y	Y	Y	N	Y	Y	Y	N	N			03/24/97	04/20/97	04/24/97	173265	34927	41432
85	94		102	23	86	L	07/01/97	A	1	D	K	266	21	3.00	371	11	34	12	90	16,35,H	Y	Y	Y	N	Y	Y	Y	N	Y			05/12/97	06/04/97	06/11/97	181842	40448	37989
86	85		103	23	87	L	08/07/97	A	3	D	K	246	25	3.50	284	6	37	13	102	H	Y	N	?	?		N	N	N	N			06/20/97	07/07/97	07/14/97	175865	37478	36758
87	86		104	20	88	L	09/25/97	A	2	N	K	251	39	3.00	259	27	100	131	129		N	N	?	?		?	?	?	?			07/24/97	08/11/97	08/18/97	173505	36730	41560
88	87		102	24	89	L	11/19/97	B	1	D	K	146	22	3.00	377	109	244	132	308	16,35,H	Y	Y	Y	N		Y	N	Y	N	Y	Y	09/25/97	10/24/97	10/29/97	182091	40630	38973
89	89		105	12	90	L	01/22/98	A	3	N	K	167	35	3.00	212	38	95	40	138		N	N	?	?		?	?	?	?			11/11/97	12/12/97	12/19/97	175377	34880	40326
90	90		102	25	91	L	04/17/98	B	2	D	K	154	26	3.00	382	11	76	20	131	16,35,H	Y	Y	Y	N		Y	N	Y	N			02/26/98	03/16/98	03/23/98	181658	41983	38629
91	91		103	24	96	S	06/02/98	B	1	D	K	141	32	3.00	236	45	145	50	198	16,35,H	Y	Y	Y	N	Y	Y	Y	Y	N			03/26/98	04/27/98	05/02/98	175951	42272	41750
92	95		103	25	98	S	10/29/98	B	2	D	K	147	39	3.00	213	42	139	45	187	16,35,H	Y	Y	Y	N	Y	Y	Y	Y	Y			08/25/98	09/14/98	09/21/98	176161	45134	44560
93	88		105	13	97	S	12/04/98	A	3	D	K	249	47	3.00	283	21	80	25	116	H	Y	Y	Y	N		Y	N	Y	Y			09/22/98	10/12/98	10/19/98	175329	44497	44200
94	96		103	26	100	S	05/27/99	B	2	D	K	183	24	3.00	235	66	160	72	199	H	Y	Y	Y	N		Y	Y	Y	N			03/16/99	04/15/99	05/20/99	176287	40748	44777
95	93		102	26	99	S	07/23/99	B	1	N	K	360	47	2.92	119	42	161	49	208		N	N	Y	?		?	?	Y	?			12/01/99	06/02/99	06/07/99	180714	57441	32232
96	103		103	27	101	S	12/19/99	B	2	N	K	24	37	3.00	191	13	84	24	153		N	N	Y	?		?	?	Y	?	Y	N	08/26/99	11/02/99	11/13/99	176346	27159	44654
97	99		105	14	92	L	02/11/00	A	3	D	K	298	61	3.00	270	21	75	25	87	16,35,H	Y	Y	Y	N	Y	Y	N	Y				06/29/99	12/02/99	12/13/99	175882	41818	39039
98	101		104	21	102	S	05/19/00	A	1	D	K	473	56	3.00	236	19	70	27	113	16,35,H	Y	Y	Y	N	Y	Y	N	Y				02/03/00	03/13/00	03/25/00	176456	42344	43728
99	106		104	22	103	S	09/08/00	B	2	D	K	444	26	3.00	283	17	73	17	105	16,35,H	Y	Y	Y	N	Y	Y	Y	N	Y			04/04/00	08/07/00	08/14/00	176466	41981	43606
100	92		103	28	104	S	10/11/00	A	3	N	E	498	31	3.00	310	14	86	27	113		N	N	?	?		?	?	?	?			07/06/00	08/30/00	09/11/00	176407	42236	44445
101	97		105	15	105	S	11/30/00	B	1	N	K	503	31	3.00	250	10	78	10	84		N	N	?	?		?	?	?	?			09/27/00	10/25/00	10/31/00	175852	48974	41744
102	98		104	23	106	S	02/07/01	A	2	N	E	418	30	3.00	209	8	73	13	102		N	N	?	?		?	?	?	?			11/13/00	12/04/00	01/26/01	176461	45336	42330
103	102		103	29	107	S	03/08/01	B	3	D	K	455	25	2.92	210	10	44	14	100	35,H	N	N	?	?		N	N	N	N			01/10/01	02/02/01	02/12/01	176415	43794	44588
104	100		105	16	108	S	04/19/01	A	1	D	E	434	29	3.00	286	4	42	13	92	16,35,H	Y	Y	Y	N	Y	Y	N	N	Y			02/26/01	03/17/01	03/22/01	175924	45379	43965
105	104		104	24	109	S	07/12/01	B	2	D	K	435	22	3.00	307	24	108	26	126	H, 16?	Y	Y	Y	N	Y	Y	N	N	N			04/16/01	05/29/01	06/21/01	176559	41468	44925
106	105		103	30	110	S	08/10/01	A	3	D	K	380	40	3.00	285	15	108	25	144	16,35,H	Y	Y	Y	N	Y	Y	N	N	Y			05/24/01	06/13/01	07/02/01	176545	43423	42509
107	108		105	17	111	S	12/05/01	B	1	N	K	258	36	3.00	284	17	81	22	95		N	N	?	?		?	?	?	?			09/26/01	10/24/01	10/31/01	176072	44241	44605
108	109		102	27	112	S	03/01/02	A	2	D	K	358	38	3.00	286	14	63	18	98	16,35,H	Y	Y	Y	N	Y	Y	Y?	N	N			11/27/01	01/16/02	01/23/02	181579	34459	44627
109	110		104	25	114	S	04/08/02	B	3	D	K	294	28	3.00	250	18	70	22	110	16,35,H	Y	Y	Y	N	Y	Y	N	N			01/21/02	03/06/02	03/

GHT, CENTER OF GRAVITY, & PAYLOAD

WE

s.)		CENTER OF GRAVITY [CG] (in.)						PAYLOAD	RAINFALL					TEMPERATURE (F)							DEWPOINT (F)						RELATIVE HUMDITY (%rh)						SPE
OV Gross @ Liftoff (lbs.)	Integrated Vehicle Gross @ Liftoff (lbs.)	OV Xcg (in.)	OV Ycg (in.)	OV Zcg (in.)	Shuttle Xcg (in.)	Shuttle Ycg (in.)	Shuttle Zcg (in.)	PAYLOAD (S=secret)	TOTAL on Pad	1-Day MAX	AVG Daily	Launch Day	TOTAL 5 Day Pre-Launch	AVG on Pad	MAX on Pad	MIN on Pad	AVG Launch Day	MAX Launch Day	MIN Launch Day	At Tanking Start	At Launch	AVG on Pad	MAX on Pad	MIN on Pad	AVG Launch Day	MAX Launch Day	MIN Launch Day	AVG on Pad	MAX on Pad	MIN on Pad	AVG Launch Day	MAX Launch Day	MIN Launch Day	AVG on Pad
								DFI	6.00	2.22	0.06	0.00	0.00	60	87	23	67	79	55	65	58	49	75	9	60	68	52	69	100	13	73	93	93	12
								OSTA/DFI	13.11	2.11	0.18	0.00	0.61	76	93	49	68	75	61	63	75	68	78	48	59	62	55	77	100	36	76	93	93	12
								OSS/DFI	2.96	1.45	0.08	0.00	0.00	68	89	41	76	87	65	68	81	59	71	35	68	71	64	74	100	22	77	100	100	12
								DOD/DFI	8.02	2.39	0.24	0.02	1.27	80	91	69	80	88	72	72	85	73	78	64	75	78	71	80	100	45	82	100	100	12
246425	4488857	1116.7	0.2	379.6	1416.7	0.3	418.3	SBS/TELE	4.02	1.12	0.08	0.02	0.02	74	88	51	73	79	66	66	71	67	77	43	65	67	63	78	100	41	79	96	96	12
256987	4490778	1127.6	0.4	382.8	1416.6	0.3	419.1	TDRS A	19.00	1.89	0.15	0.00	0.78	63	84	35	65	78	52	53	76	56	73	23	56	63	49	78	100	25	72	96	96	14
249626	4486449	1122.0	-0.8	381.1	1416.8	0.0	418.6	MULT P/L	6.97	1.78	0.29	0.00	0.00	77	89	63	76	83	69	73	71	70	77	47	69	71	66	79	100	26	77	90	90	12
242793	4495896	1124.7	0.2	382.0	1412.6	0.3	418.0	MULT P/L	4.85	1.53	0.17	0.42	0.88	82	96	71	81	89	73	89	74	75	81	71	75	79	71	80	100	52	84	100	67	10
247813	4506789	1109.7	-0.1	378.9	1411.8	0.2	418.2	S/L 1	5.37	1.03	0.12	0.00	0.05	66	84	41	77	83	71	73	78	57	74	33	68	69	67	75	100	34	78	93	93	11
250405	4505048	1124.4	0.2	381.4	1412.3	0.3	418.5	MULT P/L	2.11	0.53	0.09	0.00	0.53	61	83	38	66	75	57	61	57	53	69	32	58	63	53	77	100	27	78	96	96	13
254404	4509231	1113.5	0.2	383.4	1412.4	0.2	418.9	LDEF/SMM	3.65	2.15	0.19	0.00	2.80	67	86	48	61	71	51	63	57	56	71	34	45	49	41	70	100	25	60	86	86	14
263621	4519789	1118.5	-0.2	382.8	1411.2	0.4	419.5	MULT P/L	15.94	2.76	0.20	0.31	0.31	78	97	53	78	85	71	74	75	70	78	49	73	76	69	77	100	32	82	96	96	10
242543	4497865	1119.1	-0.1	381.6	1417.1	0.2	418.0	MULT P/L	3.37	1.96	0.15	0.00	0.00	76	92	58	74	83	64	67	68	68	76	55	62	65	58	76	100	44	67	84	84	12
263352	4524849	1120.9	0.0	382.6	1413.3	0.2	419.4	MULT P/L	4.25	2.46	0.25	0.00	1.04	75	89	52	63	72	54	56	66	67	77	41	54	59	49	77	100	39	71	93	93	12
								DOD (S)	0.09	0.07	0.00	0.00	0.01	53	80	21	51	67	34	32	64	42	64	8	42	52	32	69	100	26	72	96	96	12
250409	4506364	1126.0	-0.2	381.7	1412.2	0.2	418.6	MULT P/L	0.40	0.32	0.03	0.04	0.04	67	86	45	70	73	66	67	69	56	69	34	57	63	51	69	100	28	69	81	81	14
247254	4501978	1114.5	-0.2	381.4	1411.3	0.3	418.3	S/L 3	0.12	0.09	0.00	0.00	0.00	68	91	33	77	85	68	69	85	59	72	29	64	72	55	73	100	29	68	96	96	11
256376	4514774	1109.8	0.2	379.6	1412.5	0.3	418.8	MULT P/L	3.03	1.03	0.22	0.00	1.91	80	96	68	80	90	69	73	70	72	78	62	73	76	69	77	100	32	75	100	100	12
252733	4514313	1111.5	-0.5	381.8	1412.2	0.2	418.7	(ATO) S/L 2	5.24	1.10	0.17	0.00	0.01	80	94	67	81	88	73	73	86	73	78	66	75	77	72	78	100	44	81	100	100	11
262054	4519949	1120.6	0.2	382.4	1413.3	0.3	419.4	MULT P/L	7.47	1.18	0.34	1.18	2.33	81	91	72	79	85	73	78	73	75	79	70	75	77	72	81	100	50	86	100	100	10
								DOD (S)	9.93	2.13	0.28	1.09	2.23	79	92	68	82	88	75	76	82	73	79	62	76	77	74	82	100	51	83	100	100	12
243751	4505113	1108.4	-0.3	380.1	1410.0	0.2	418.0	S/L DI	3.12	1.47	0.21	0.46	2.63	78	88	67	76	85	67	71	84	72	77	66	70	73	67	80	100	58	79	100	100	10
261444	4515538	1110.3	0.0	379.3	1412.6	0.2	419.2	MULTI P/L	0.19	0.11	0.01	0.00	0.00	75	85	62	73	82	63	77	71	69	76	62	66	70	62	82	100	58	80	100	100	11
254923	4511561	1111.2	0.9	380.6	1411.0	0.3	418.8	MULTI P/L	9.53	4.14	0.23	0.00	5.23	61	83	26	61	70	51	60	51	53	72	17	54	58	49	76	100	26	79	96	96	11
268636	4529681	1119.0	-0.3	384.0	1413.0	0.2	419.9	(FAILED)	7.18	4.14	0.19	0.00	0.18	59	82	25	36	46	25	31	37	50	69	4	13	21	4	74	100	18	36	53	53	11
254617	4522407	1118.1	0.3	380.6	1412.5	0.2	418.7	TDRS C	14.98	2.89	0.17	0.06	0.11	81	94	69	79	87	71	71	86	73	85	62	70	74	65							10
								DOD (S)	4.31	3.28	0.18	0.00	0.03	70	85	51	58	65	51	54	57	61	74	32	40	47	32							11
256235	4522277	1116.3	0.6	380.8	1412.5	0.3	418.8	TRDS D	3.38	1.12	0.09	0.00	0.40	65	85	32	70	81	58	63	62	54	71	11	54	58	49							13
261356	4527426	1123.4	0.5	382.6	1413.4	0.3	419.3	MAGELLAN	2.78	0.79	0.06	0.00	0.52	72	91	51	74	83	65	65	82	62	76	37	64	66	61							12
								DOD (S)	4.33	1.61	0.17	0.28	0.28	83	96	71	84	94	73	84	79	72	78	66	73	77	68							10
257615	4523573	1114.1	0.4	380.7	1412.5	0.2	418.9	GALILEO	13.89	5.47	0.27	1.17	1.17	81	93	66	81	88	73	74	85	72	78	61	71	73	69							10
								DOD (S)	2.22	1.02	0.08	0.59	0.59	70	85	48	65	69	61	62	68	61	71	27	60	67	53							12
256063	4519487	1131.3	-0.8	381.3	1413.2	0.2	418.9	LDEF	5.29	1.38	0.12	0.00	0.00	60	84	24	61	69	52	65	54	51	72	16	55	58	51					96	96	11
								DOD (S)	4.49	1.61	0.13	0.01	0.01	69	85	46	69	75	63	69	63	59	72	31	54	59	49	71	100	30	65	80	80	14
249164	4514688	1114.8	-0.5	384.2	1411.8	0.2	418.6	HST	2.48	0.97	0.06	0.00	0.04	70	86	49	70	80	60	71	67	59	73	34	59	63	54	67	100	29	64	83	83	13
259501	4527138	1115.2	-0.1	381.4	1412.9	0.2	419.0	ULYSSES	2.26	0.84	0.07	0.00	0.59	80	95	65	80	86	74	76	74	71	78	58	69	73	65	76	100	43	73	90	90	10
								DOD (S)	16.84	4.35	0.19	0.00	0.00	78	97	48	72	77	67	76	69	70	79	40	59	62	55	76	100	30	64	76	76	11
256511	4521514	1106.5	-0.5	378.1	1412.1	0.2	418.7	ASTRO	20.52	4.35	0.13	0.00	0.76	74	93	48	72	78	65	71	69	66	83	40	60	63	56	74	100	30	65	81	81	11
255758	4519945	1116.7	-0.3	381.7	1412.4	0.2	418.8	GRO	8.28	3.74	0.38	0.85	0.85	69	87	50	74	79	68	71	74	60	71	44	66	68	64	74	100	38	81	96	96	14
247336	4513048	1111.1	0.0	382.5	1411.2	0.3	418.3	DOD AFP 675	6.98	1.53	0.14	0.00	1.29	69	89	33	82	88	75	78	76	60	76	3	73	75	71	74	100	19	79	96	96	13
251921	4519792	1100.2	-0.1	376.4	1411.4	0.2	418.3	SLS 1	6.48	2.10	0.19	0.13	0.46	78	91	63	79	86	71	78	74	70	77	62	71	74	67	77	100	45	73	90	90	11
259347	4523118	1113.9	-0.2	380.4	1412.6	0.2	419.0	TDRS E	11.73	1.33	0.30	0.00	2.72	81	93	71	83	92	74	74	86	73	78	67	75	78	71	78	100	48	77	96	96	11
240054	4502671	1125.5	-0.9	381.9	1411.2	0.2	417.8	UARS	4.05	2.01	0.13	0.00	1.80	81	94	70	80	88	71	85	81	73	79	66	71	74	67	79	100	42	77	100	100	10
259851	4522576	1116.2	0.0	381.0	1412.7	0.3	419.1	DOD DSP	0.75	0.37	0.02	0.00	0.06	69	83	44	64	73	54	66	54	61	73	37	56	71	41	75	100	31	70	96	96	11
243456	4507474	1104.8	-0.1	378.3	1410.6	0.2	417.8	IML-01	2.97	2.60	0.12	0.00	0.19	60	79	32	55	73	37		66	53	69	26	48	60	35							11
233650	4496035	1113.1	-0.3	377.6	1409.8	0.2	417.2	ATLAS	2.75	1.24	0.08	0.00	0.11	66	86	43	67	71	62	64	67	56	70	34	56	60	51							12
256333	4519154	1119.6	-0.3	383.9	1412.4	0.2	419.0	INTELSTAT	4.57	1.60	0.08	0.01	0.01	67	87	43	70	78	61	66	61	56	72	27	58	65	51							12
257695	4520103	1105.5	-0.5	378.7	1412.0	0.2	418.8	USML-1 EDO	6.14	2.65	0.27	0.02	2.19	80	93	68	80	87	72	72	85	72	78	67	74	77	70							14
256031	4516789	1113.7	-0.4	382.4	1411.9	0.2	418.9	TSS/EUR	11.45	2.92	0.22	0.00	0.00	81	96	68	81	87	75	75	84	73	79	63	74	76	72							12
244568	4506804	1104.1	-0.4	379.2	1410.5	0.3	417.9	S/L J	1.42	0.70	0.07	0.00	0.60	80	92	70	79	86	72	75	84	73	77	67	73	74	71							10
250370	4514565	1109.5	-0.3	377.5	1411.4	0.1	418.2	LAGEOS-2	6.35	2.95	0.24	0.00	0.00	75	88	59	74	78	69	71	77	66	78	51	58	62	54							12
243897	4506587	1112.4	0.1	380.7	1410.7	0.2	418.0	DOD	4.06	2.18	0.16	0.00	0.00	69	86	41	55	68	42	49	55	61	74	34	49	57	40							13
259412	4522840	1116.2	0.3	381.3	1412.6	0.2	419.0	TDRS F	3.05	1.12	0.07	0.00	0.43	67	83	38	74	79	68	70	72	60	71	31	68	70	66				78	96	60	11
237253	4501920	1109.5	-0.3	379.3	1410.1	0.2	417.5	ATLAS 2	2.02	0.70	0.08	0.00	0.27	75	85	35	68	75	61	70	72	57	72	14	54	59	48	70	96	29	61	83	38	28
255468	4519000	1101.5	-0.7	377.5	1411.5	0.3	418.6	S/L D2	8.09	2.51	0.10	0.06	0.06	73	85	10	72	83	61	66	76	51	72	-4	64	68	60	66	100	13	70	93	46	25
252703	4518566	1112.7	-0.1	383.0	1412.0	0.2	418.7	S'HAB 1/EUR	1.21	0.50	0.02	0.04	0.04	83	94	64	82	87	77	66	76	65	77	47	72	74	69	68	96	31	72	87	57	25
261478	4523125	1116.5	-0.6	381.6	1412.8	0.2	419.2	ACTS/ORF	12.44	2.50	0.16	0.00	1.14	83	97	69	79	87	70	73	72	74	80	64	73	76	69	73	100	37	75	93	57	11
256103	4517138	1103.4	-0.4	378.1	1411.5	0.2	418.6	SLS 2 EDO	3.98	1.25	0.12	0.00	1.27	78	92	64	75	82	67	67	79	70	79	53	69	72	66	71	100	29	77	90	64	11
250278	4511794	1113.5	-0.1	381.7	1411.4	0.2	418.5	HST SERV	1.00	0.40	0.03	0.00	0.00	70	87	39	69	77	61	70	65	62	75	29	57	60	54	72	93	42	61	73	49	12
245936	4509010	1104.4	-0.8	380.1	1410.7	0.2	418.1	S'HAB 2	3.72	1.40	0.15	0.00	1.62	61	81	40	50	60	40	46	41	54	71	30	34	38	30	74	96	37	68	82	54	13
256579	4519801	1107.4	-0.6	379.2	1412.0	0.2	418.7	USMP 2/EDO	9.70	6.35	0.40	0.00	0.88	68	83	45	58	70	45	49	54	60	72	30	37	43	30	72	100	21	49	76	21	14
246849	4511411	1098.8	-0.5	378.7	1410.7	0.2	418.1	SRL1	2.04	1.65	0.09	0.00	0.06	71	88	52	75	78	71	49	71	62	77	37	63	65	60	69	96	32	63	71	55	12
259299	4523441	1104.8	-0.4	378.8	1412.2	0.2	418.9	IML 2/EDO	3.92	3.07	0.16	0.00	0.11	82	94	72	83	88	77	77	88	74	78	67	75	78	71	73	93	44	73	87	59	14
241434	4503921	1105.6	-0.6	379.5	1410.4	0.2	417.8	LAINCH - LITE 1	3.38	1.34	0.15	0.00	0.71	81	93	71	80	89	71	74	83	73	79	66	74	77	70	73	96	30	55	79	30	10
247403	4510613	1099.3	-0.5	378.5	1410.7	0.2	418.1	SRL 2	10.47	3.00	0.22	0.00	0.19	79	91	66	78	86	70	75	71	73	82	65	70	74	66	77	100	51	65	79	51	10
244238	4508715	1112.0	-0.1	379.4	1411.1	0.2	417.9	ATLAS 3	4.96	1.50	0.19	0.00	1.97	76	87	60	73	81	64	65	81	68	77	56	62	64	60	72	100	44	58	66	50	11
247625	4511630	1111.6	-0.3	382.4	1411.4	0.2	418.3	S'HAB 3	3.03	2.25	0.12	0.00	0.51	59	77	38	65	76	53	69	54	49	69	22	52	58	45	68	99	25	68	99	37	12
256495	4520187	1117.1	-0.1	381.5	1412.4	0.2	418.9	ASTRO 2/EDO	1.86	1.35	0.08	0.00	0.67	64	82	31	66	73	58		63	54	71	13	59	64	54	76	100	16	87	100	74	13
249088	4511586	1110.0	-0.1	380.1	1411.3	0.2	418.3	S/LM S/MM-1	11.33	3.20	0.18	0.00	4.90	79	95	60	83	92	73	73	90	70	79	56	74	77	71	79	100	36	81	100	61	12
258584	4521772	1120.6	0.0	380.9	1412.9	0.2	419.0	TDRS-G	11.46	5.60	0.20	0.00	1.99	80	95	69	80	87	72		84	73	80	62	74	77	70	82	100	42	85	99	71	12
256384	4519114	1112.9	-0.1	383.3	1412.3	0.2	419.0	WSF 2	20.47	5.65	0.35	0.05	1.09	82	95	71	81	88	73	75	84	76	82	67	75	77	72	85	100	42				12
257327	4521581	1101.6	-0.5	377.1	1411.8	0.2	418.7	USML-2 EDO	15.75	2.75	0.29	0.00	1.38	81	94	70	78	83	73	77	78	74	81	59	72	76	68	85	100	58	87	100	73	11
248266	4512395	1112.5	-0.5	381.6	1411.5	0.2	418.3	S/MM 2	5.36	2.60	0.17	0.00	0.89	75	87	48	63	77	48		48	66	78	37	56	70	41	78	100	41	80	96	64	12
247011	4514647	1117.7	-0.1	381.7	1411.9	0.2	418.2	SFU - RETR	7.04	3.80	0.19	0.00	0.06	59	82	30	54	69	39	51	40	50	73	18	41	47	34	78	100	25	64	91	36	12
261491	4526493	1106.2	-0.4	379.9	1412.7	0.2	419.1	TSS, USMP/EDO	1.87	1.75	0.07	0.00	0.00	61	81	32	71	81	61	62	76	48	68	16	63	65	60	73	100	24	85	100	69	12
246220	4509631	1110.1	-0.1	379.9	1411.2	0.2	418.1	S/MM -3, S'HAB	8.74	4.00	0.36	0.00	2.03	63	86	37	56	66	46	60	46	51	71	23	36	43	29	74	100	31	62	92	31	15
254753	4519162	1106.5	-0.2	380.5	1411.8	0.1	418.7	S'HAB TEAMS	1.27	1.24	0.04	0.00	0.00	74	88	51	77	87	66	75	66	65	74	45	66	71	60	78	100	45	76	96	55	11
256495	4517477	1102.6	-0.4	377.3	1411.4	0.2	418.6	LMS/EDO	5.77	2.40	0.26	3.37	5.53	78	92	64	80	88	72	73	83	70	77	58	73	76	70	81	100	49	86	100	71	12
249440	4510469	1109.6	0.0	379.8	1411.3	0.3	418.3	S/MM-4, S'HAB	9.37	3.35	0.25	0.24	0.24	81	93	68	82	88	75	82	79	73	81	64	76	79	72	79	100	45	82	94	69	11
261817	4524735	1106.1	-0.5	381.1	1412.4	0.2	419.2	ORFEUS-SPAS 2	0.91	0.36	0.03	0.00	0.35	72	88	46	68	79	57	59	79	62	75	34	59	63	55	74	100	30	74	100	48	11
250167	4511011	1110.5	0.1	379.7	1411.6	0.2	418.4	S/MM-5, S'HAB	0.41	0.30	0.01	0.00	0.21	64	82	36	59	68	50	59	52	58	72	25	53	55	50	81	100	36	82	97	67	9
251986	4513855	1112.1	0.1	381.5	1411.8	0.2	418.6	HST, SM-2	0.20	0.18	0.01	0.00	0.05	61	82	32	56	63	48	57	52	54	72	10	49	55	43	78	100	23	82	99	64	11
259967	4521509	1101.6	-0.2	378.0	1411.9	0.1	418.9	MSL 01, EDO	2.47	0.97	0.10	0.00	0.00	71	88	52	66	79	52	52	77	62	73	30	57	61	52	73	100	30	58	72	43	13
249624	4509832	1109.0	0.0	379.7	1411.2	0.2	418.4	S/MM-6, S'HAB	2.98	1.23	0.14	0.00	1.61	73	91	55	73	82	63	79	64	66	79	46	67	70	63	74	100	40	74	91	56	12
260279	4519333	1102.1	-0.3	378.2	1411.6	0.2	419.0	MSL 01, EDO	5.00	1.25	0.24	0.68	1.28	82	93	72	83	90	75	75	90	75	81	66	77	81	72	78	98	52	81	96	66	12
250101	4512125	1104.4	-0.1	379.8	1411.0	0.3	418.4	CHRISTA/SPAS	3.52	1.40	0.14	0.11	2.41	83	95	72	82	88	75	77	84	76	81	68	76	79	73	78	99	53	85	98	71	13
251795	4512024	1109.7	0.1	379.7	1411.5	0.3	418.5	S/MM-7, S'HAB	7.02	1.40	0.18	0.49	1.45	81	93	66	85	90	79	90	81	74	82	61	78	81	75	78	100	19	85	96	74	12
261694	4521900	1104.1	-0.3	378.5	1412.1	0.2	419.1	USMP4, SPTN	3.50	1.50	0.16	0.00	0.00	69	88	48	69	75	63	64	72	59	75	39	58	64	52	76	100	40	78	99	57	11
250583	4511879	1112.7	-0.2	380.3	1411.6	0.2	418.5	S/MM-8, S'HAB	3.55	1.57	0.10	0.30	0.31	66	82	45	70	72	68	73	70	58	73	28	67	70	64	81	100	26	90	100	80	12
262270	4523683	1103.9	-0.3	378.0	1412.4	0.2	419.1	NEUROLAB	0.15	0.11	0.01	0.00	0.00	70	86	46	75	82	68	70	82	60	73	39	67	70	63	76	100	30	72	89	54	15
259973	4514649	1109.0	-0.9	381.3	1412.1	0.1	419.2	S/MM-9, S'HAB	0.52	0.25	0.02	0.00	0.05	78	99	55	89	99	79	84	95	67	79	48	74	77	70	72	100	24	73	99	47	12
265855	4520191	1110.3	-0.5	382.2	1412.9	0.2	419.6	S'HAB, HOST	2.74	0.52	0.07	0.00	0.00	80	91	61	73	84	61	61	82	71	84	46	60	68	52	76	100	42	70	97	42	12
264026	4518489	1111.2	-1.1	383.3	1412.8	0.2	419.6	ISS 2A, NODE, PMA 1,2	5.01	2.37	0.11	0.00	0.12	73	88	54	72	82	61	72	70	64	75	46	65	70	59	74	98	37	78	90	66	10
261812	4514231	1112.3	-0.7	381.3	1412.2	0.2	419.3	ISS 2A, 1, S'HAB

EATHER DATA

WIND ED (kts)		WIND DIR. (deg)		TOTAL WIND SPEED (fps)						IN-PLANE WIND SPEED (fps)						OUT-OF-PLANE WIND SPEED (fps)						PRESSURE (mb)						ET PRODUCTION					-Y Bipod Ramp (Ha	
MAX on Pad	MAX Launch Day	AVG on Pad	Launch Day	@ 0 ft.Altitude	@ 10K ft.Altitude	@ 20K ft. Altitude	@ 30Kft.Altitude	@ 40K ft.Altitude	@ 50K ft.Altitude	@ 0 ft.Altitude	@ 10K ft.Altitude	@ 20K ft. Altitude	@ 30Kft.Altitude	@ 40K ft.Altitude	@ 50K ft.Altitude	@ 0 ft.Altitude	@ 10K ft.Altitude	@ 20K ft. Altitude	@ 30Kft.Altitude	@ 40K ft.Altitude	@ 50K ft.Altitude	AVG on Pad	MAX on Pad	MIN on Pad	AVG Launch Day	MAX Launch Day	MIN Launch Day	Start Date	Completion Date	ET DD-250	Ship Date	Days in Storage Before Shipment	Substrate Temp (°F)	Cell Temp (°F)	Cell Humidity (%rh)	Complete Date	Complete Day
26	12	234	130	6	32	11	40	56	82	3	32	-11	-40	-53	-72	5	4	0	-1	-18	-40	1019	1033	999	1024	1027	1024			06/29/79							
22	17	141	340	25	33	45	110	129	113	-4	10	-20	-68	-100	-106	-25	-31	-40	-87	-81	-39	1017	1025	1010	1016	1022	1016			02/27/81							
26	11	193	90	5	31	66	76	106	93	5	-29	-66	-73	-102	-89	-1	-12	0	-20	-27	-26	1018	1031	1006	1015	1020	1017			09/28/81							
28	11	152	130	10	15	28	10	11	27	5	-14	-27	-10	-7	-27	9	6	8	1	-9	-5	1015	1021	1006	1019	1018	1015			01/17/82							
18	13	160	90	16	8	30	58	142	78	16	-1	-6	-16	-58	-22	0	-8	-29	-56	-130	-75	1017	1024	1007	1023	1021	1019			05/26/82							
28	12	222	110	13	15	50	93	107	112	11	-15	-49	-92	-107	-111	-7	3	12	-16	4	12	1016	1028	991	1016	1017	1009			09/08/82							
22	12	128	40	1	12	17	39	63	32	1	5	-17	-39	-43	-32	-1	-11	-1	5	-46	-3	1014	1018	1006	1015	1016	1014			07/26/82							
16	9	151	220	6	8	5	14	28	12	-6	-5	-2	2	22	8	-1	-6	5	-14	-17	9	1018	1022	1011	1013	1021	1018			01/12/83							
15	11	222	160	19	45	55	77	71	77	-16	-45	-55	-70	-50	-64	11	-4	-4	-33	-50	-43	1016	1024	1009	1015	1017	1012			05/06/83							
19	9	283	160	0	19	55	104	111	72	0	-13	-54	-97	-106	-72	0	14	-10	-37	-34	-1	1020	1030	1011	1018	1021	1016			03/01/83							
27	12	202	270	15	59	62	142	170	106	-12	-56	-62	-136	-163	-105	-9	-18	-5	-39	-50	-11	1013	1023	995	1013	1023	1019			07/22/83							
18	8	139	90	1	15	12	31	42	20	1	-15	-12	-30	-42	-6	0	-2	-3	-9	4	19	1017	1023	1010	1018	1022	1019			09/13/83							
25	11	126	90	3	9	13	21	75	27	2	2	-5	-12	-4	14	2	9	-12	-17	-75	-23	1016	1023	1007	1022	1019	1015			12/15/83							
16	12	105	40	10	44	45	118	90	76	3	-3	-41	-116	-81	-74	-9	-44	-19	-20	-39	-17	1018	1025	1010	1024	1012	1010			01/27/84							
17	10	265	210	15	79	111	154	162	151	-11	-79	-111	-153	-154	-150	10	-6	-10	21	50	13	1020	1029	1011	1020	1016	1011			11/03/83							
20	12	163	60	17	25	37	62	128	83	13	10	-37	-51	-101	-56	11	23	-2	-35	-79	-62	1020	1027	1013	1026	1023	1019			04/24/84							
14	12	145	300	13	41	38	44	62	61	10	6	-7	5	-17	17	-9	-41	-37	-44	-60	-59	1020	1030	1012	1014	1016	1014			03/16/84							
20	11	147	170	5	20	20	29	51	48	-5	-16	-7	-23	-11	-42	2	12	-19	-18	-50	-24	1017	1022	1012	1020	1018	1014			07/05/84							
21	8	148	60	10	16	13	17	42	38	10	3	7	12	8	28	2	-16	-11	-12	-41	-25	1017	1023	1007	1018	1021	1016			05/24/84							
15	12	159	120	15	35	26	17	24	24	15	31	22	10	20	20	0	16	13	14	14	14	1017	1024	1013	1022	1019	1016			07/25/84							
25	11	95	150	17	6	7	7	11	19	-9	-3	-2	7	-7	6	15	5	7	2	-8	-18	1017	1022	1007	1017	1022	1019			12/20/84							
14	10	115	190	17	43	70	55	63	56	7	-32	-30	-25	-43	-34	15	29	63	49	46	45	1016	1025	1004	1006	1014	1011			11/16/84							
16	8	112	170	3	5	20	11	45	61	2	-4	-14	-9	-45	-60	2	3	-14	-6	-2	-11	1021	1025	1014	1020	1020	1015			08/24/84							
19	14	213	360	10	9	58	172	221	129	-6	4	-55	-171	-219	-127	-8	-8	18	21	27	20	1021	1032	1008	1021	1027	1020			06/18/85							
27	18	246	300	17	72	97	110	153	136	-14	-65	-88	-103	-153	-134	-10	-30	-41	-39	0	-21	1020	1032	1007	1021	1023	1020			03/15/85							
18	12	132	68	10	22	12	24	25	35	9	21	12	24	-14	-30	-5	6	2	-1	-21	-18	1017	1024	1009	1018	1018	1015			04/16/85							
21	13	188	338	22	46	69	146	174	142	4	32	-25	-108	-151	-97	-22	-33	-64	-98	-87	-104	1018	1028	1002	1026	1020	1015			09/24/84							
22	11	224	248	16	10	56	57	81	81	-14	-3	-44	-40	-69	-80	8	-9	-35	-41	-43	-13	1021	1032	1011	1017	1020	1017			12/10/85							
18	9	187	90	11	2	45	61	138	123	8	-1	-45	-61	-134	-116	7	-1	6	1	31	40	1018	1026	1010	1020	1018	1016			05/15/85							
15	12	132	113	10	21	25	16	9	16	-6	-17	-17	-10	-9	7	-8	12	-18	-12	-1	-14	1018	1024	1010	1012	1017	1015			07/16/85							
18	11	123	158	13	19	29	50	41	48	-7	-18	-25	-50	-39	-44	11	6	14	2	-11	-19	1015	1020	1005	1014	1019	1016			01/29/85							
55	13	198	360	16	24	64	78	108	103	-8	-18	-54	-65	-91	-100	14	16	34	44	59	25	1017	1027	1010	1014	1027	1025			04/15/86							
19	7	257	300	4	57	97	118	140	137	-3	-48	-83	-105	-137	-121	-3	31	50	54	27	64	1020	1028	1007	1020	1023	1019			08/14/85							
22	10	166	40	11	17	28	67	166	75	5	13	-20	-9	-70	-28	10	11	-19	-66	-150	-70	1021	1035	1009	1028	1026	1014			10/15/85							
20	11	136	90	11	15	10	78	77	69	11	15	1	-62	-70	-57	0	-3	-10	-47	-31	-39	1019	1029	1006	1020	1029	1026			09/23/85							
15	12	107	100	23	27	14	41	82	63	23	24	-10	-30	-72	-59	0	-11	-10	-27	-38	-22	1017	1022	1011	1018	1020	1017			04/15/86							
19	12	138	80	28	4	14	52	130	75	28	-1	-14	-49	-127	-73	-3	4	-3	-19	-27	-16	1017	1029	1007	1027	1024	1014			06/20/86							
20	12	132	110	21	10	20	93	139	80	21	-8	-20	-89	-138	-77	-1	6	-3	-27	-19	-22	1018	1029	1006	1024	1024	1021			11/08/85							
24	11	130	90	18	8	42	84	127	113	17	-4	-42	-84	-124	-112	-5	7	1	-9	-26	16	1019	1027	1006	1024	1026	1021			01/15/86							
29	11	166	170	12	11	45	61	97	85	-2	-10	-40	-61	-96	-85	12	5	-20	-3	-12	-3	1017	1030	999	1015	1016	1010			09/09/87							
15	8	137	40	6	31	26	3	10	32	-6	-22	-17	1	9	-13	1	-22	-19	-3	-5	-29	1017	1024	1008	1009	1015	1011			07/25/86							
22	12	174	170	16	26	19	56	63	30	3	-16	6	53	60	29	16	20	18	-18	-18	-9	1018	1023	1013	1018	1018	1015			12/18/87							
16	8	123	30	12	18	27	49	78	49	10	17	27	48	72	44	7	-5	2	8	29	21	1017	1021	1013	1017	1020	1018			09/09/86							
16	13	183	320	8	51	61	109	122	79	-7	-49	-58	-99	-117	-69	-4	12	18	46	34	38	1019	1025	1013	1019	1024	1021			07/31/89							
18	9	210	110	10	27	47	81	97	75	10	-27	-41	-74	-50	-35	0	5	-22	-33	-83	-66	1019	1036	1007	1021	1024	1018			05/03/89							
20	14	193	60	23	35	86	157	176	154	18	-10	-51	-81	-93	-93	-15	-34	-70	-135	-149	-123	1018	1026	1008	1015	1014	1011			03/11/87							
19	16	196	350	13	69	147	143	131	87	-8	-58	-127	-119	-107	-58	-10	38	74	80	75	65	1017	1026	1008	1012	1023	1014			11/10/86							
25	19	177	160	22	31	25	67	106	60	11	-18	-23	-65	-87	-60	19	25	11	17	61	-7	1014	1020	1008	1013	1013	1009			10/31/88							
25	10	191	80	10	8	12	31	67	28	-8	-8	9	-27	20	21	-6	2	8	15	64	18	1017	1024	1008	1019	1020	1017			04/22/88							
19	10	124	40	16	17	6	4	7	19	16	17	-3	-4	5	-3	1	-2	-5	0	5	-19	1019	1022	1015	1019	1021	1017			06/08/87							
19	13	123	60	27	31	24	82	139	69	20	14	16	-65	-122	-55	-18	-28	-18	-49	-67	-42	1016	1029	1008	1027	1016	1013			02/01/90							
18	10	173	200	10	80	91	109	107	77	-10	-23	-63	-35	-73	-35	1	-77	-65	-103	-78	-69	1019	1026	1012	1018	1018	1016			08/08/88							
27	11	164	200	9	8	57	78	87	69	0	-8	-45	-68	-81	-60	9	0	35	38	33	33	1021	1027	1009	1020	1016	1010			02/03/89							
58	54	177	113	16	9	22	33	91	119	14	-2	0	10	13	-72	7	-9	-22	-31	-90	-95	1017	1034	1006	1016	1020	1014			10/30/89							
58	18	216	148	16	20	36	65	73	87	-14	-20	-36	-64	-68	-79	8	-4	-3	-14	-27	-37	1017	1034	993	1018	1017	1013			05/10/90							
113	19	128	138	10	8	24	64	110	52	10	7	20	47	52	49	0	4	-14	-44	-97	-16	1016	1024	1006						10/16/90							
22	7	176	80	6	23	12	28	55	48	-5	-20	-9	-27	-44	-48	-2	10	-7	9	32	-3	1017	1024	1013	1020	1017	1013			03/27/91							
22	7	132	30	10	2	7	23	22	28	-3	0	-2	-18	-19	-28	-10	2	7	-14	-11	3	1017	1021	1009	1015	1021	1017			07/26/90							
23	12	188	60	11	19	38	47	90	69	10	-5	-34	-35	-61	-63	-4	-18	-18	-31	-66	-28	1019	1028	1005	1025	1020	1012			06/27/91							
18	12	173	10	15	46	114	131	161	141	2	-25	-86	-62	-83	-71	-15	-39	-75	-116	-138	-122	1023	1033	1007	1027	1017	1013	01/09/89	10/15/91	10/15/91	07/23/93	647				06/27/91	Thu
24	14	158	270	16	47	82	127	139	120	-12	-32	-57	-85	-108	-93	-11	-34	-59	-94	-87	-76	1019	1027	1003	1015	1025	1022	04/28/89	01/16/92	01/21/92	10/01/93	624				09/17/91	Tue
23	12	177	100	32	21	37	84	133	116	16	21	-18	-53	-99	-73	28	3	-32	-65	-89	-90	1017	1026	1011	1024	1018	1015	06/24/89	04/19/92	04/02/92	11/11/93	571				11/17/91	Sun
39	11	180	130	15	29	31	34	44	28	15	25	25	30	40	28	3	15	18	15	18	-3	1018	1023	1014	1021	1022	1019	09/25/89	07/13/92	07/20/92	01/08/94	544				04/07/92	Tue
14	9	101	60	12	3	5	34	64	38	4	-2	-5	-32	-57	-32	11	2	1	-13	-30	-21	1018	1022	1013	1018	1020	1018	01/28/90	01/20/93	01/26/93	05/12/94	477				09/17/92	Thu
13	12	166	80	3	9	23	57	94	120	3	7	21	-20	-71	-86	2	6	9	-53	-62	-83	1016	1021	1011	1016	1014	1011	11/25/89	10/21/92	11/02/92	02/24/94	491				06/30/92	Tue
22	10	116	50	16	5	8	6	13	49	14	5	-8	5	12	5	7	0	-2	2	5	-49	1016	1023	1011	1022	1019	1014	04/15/90	04/16/93	05/17/93	06/08/94	418				01/06/93	Wed
22	9	221	210	10	51	98	174	184	110	-10	-14	-34	-127	-137	-89	-3	-49	-92	-119	-123	-65	1018	1029	1007	1018	1016	1012	06/25/90	07/27/93	08/06/93	07/21/94	359				04/23/93	Fri
24	17	249	340	8	51	56	99	136	87	-7	-44	-53	-83	-131	-85	-4	26	19	54	37	17	1020	1030	1009	1016	1027	1023	08/25/90	10/26/93	11/03/93	09/15/94	324				06/25/93	Fri
21	9	141	280	13	38	11	30	81	65	9	-14	-4	-8	-13	-23	9	-35	-10	-29	-80	-61	1015	1022	1006	1017	1017	1012	01/20/91	01/21/94	02/17/94	11/10/94	293				09/25/93	Sat
30	8	142	60	5	2	16	26	25	14	4	-2	6	8	2	13	-3	1	15	25	25	-5	1016	1022	1012	1016	1016	1012	04/25/91	04/11/94	05/04/94	12/09/94	242	72	72	50	01/06/94	Thu
30	13	135	140	11	37	43	64	68	26	-6	-11	-11	-9	-35	-14	10	35	42	63	58	22	1014	1022	1006	1012	1016	1011	09/28/91	06/02/94	07/01/94	03/09/95	280	71	71	60	03/01/94	Tue
22	11	135	340	9	17	15	73	86	41	0	-10	-14	-59	-64	-31	-9	-14	4	-43	-58	-27	1014	1021	1005	1012	1017	1013	01/04/92	08/12/94	10/04/94	04/06/95	237	75	75	54	04/22/94	Fri
30	14	165	330	19	54	72	82	110	76	2	-39	-37	-61	-91	-30	-19	-38	-62	-55	-62	-70	1017	1025	1006	1018	1017	1013	05/17/92	10/14/94	11/17/94	06/01/95	230	76	76	56	06/24/94	Fri
22	8	233	200	5	32	59	95	124	98	-4	-31	-58	-92	-120	-97	-3	-7	12	-23	-30	-12	1019	1030	1005	1019	1017	1007	07/10/92	01/13/95	02/03/95	07/13/95	181	76	76	51	08/31/64	Mon
23	6	198	40	9	23	51	97	143	56	8	-23	-31	-64	-30	-36	-4	0	-40	-73	-140	-43	1019	1036	1008	1015	1018	1015	09/10/92	02/10/95	03/29/95	08/10/95	181	75	75	47	10/21/94	Fri
24	15	264	260	11	65	98	119	177	149	-1	-33	-56	-88	-155	-125	-11	-56	-80	-80	-86	-81	1017	1031	1004	1016	1011	1004	11/05/92	04/04/95	05/24/95	10/19/95	198	71	71	54	12/08/94	Thu
16	8	121	100	5	14	6	76	119	44	-5	7	-5	-75	-119	-43	1	12	2	-15	0	-9	1020	1026	1013	1018	1024	1021	04/05/93	05/25/95	07/17/95	12/07/95	196	71	71	53	02/17/95	Fri
22	15	142	270	6	24	25	19	29	16	2	-22	-15	-17	-27	-9	-6	-11	-20	-8	-10	-13	1017	1022	1011	1015	1018	1015	06/09/93	07/17/95	09/13/95	01/11/96	178	70	70	58	04/22/95	Sat
24	12	170	160	15	17	23	30	42	34	-5	-17	4	1	5	9	14	-2	-23	-30	-42	-33	1015	1022	1006	1015	1012	1009	12/20/93	12/13/95	03/12/96	04/25/96	134	76	76	54	09/19/95	Tue
20	8	148	210	13	43	67	96	129	128	-13	-39	-63	-59	-72	-121	-2	-17	-22	-76	-107	-42	1019	1031	1007	1015	1025	1022	08/18/93	09/05/95	11/17/95	03/21/96	198	73	73	58	06/10/95	Sat
22	12	181	10	13	57	95	136	175	149	4	-46	-81	-126	-156	-129	-12	-34	-49	-51	-79	-75	1020	1030	1007	1022	1019	1015	02/12/94	02/19/96	04/25/96	09/18/96	212	72	72	57	11/10/95	Fri
18	11	192	320	6	62	115	139	159	122	-4	-62	-114	-135	-155	-116	-5	1	-14	34	36	38	1022	1029	1014	1022	1021	1018	10/20/93	10/23/95	01/18/96	04/11/96	171	72	72	56	07/25/95	Tue
30	10	184	110	11	6	48	68	80	76	10	-5	-44	-33	-56	-69	6	-4	-20	-59	-58	-32	1018	1027	1005	1022	1016	1012	03/25/94	04/22/96	06/17/96	11/07/96	199	71	71	56	01/18/96	Thu
32	9	190	100	5	25	65	100	186	137	1	-19	-53	-80	-138	-100	-5	-16	-37	-60	-124	-93	1016	1025	1002	1016	1020	1017	05/08/94	06/20/96	08/07/96	10/03/96	105	72	72	57	03/15/96	Fri
26	17	156	100	15	20	21	14	25	23	5	-13	-20	-10	8	-2	-14	-16	-8	-10	-24	-23	1016	1021	1010	1015	1020	1018	06/07/94	08/22/96	10/08/96	01/09/97	140	71	71	49	05/17/96	Fri
22	9	184	60	8	20	19	17	1	22	3	-17	-15	12	-1	-22	-7	-10	-12	-12	0	2	1018	1020	1013	1017	1020	1018	07/21/94	11/04/96	12/04/96	03/27/97	143	76	76	55	07/23/96	Tue
30	19	113	180	3	34	46	43	30	38	-3	-34	-42	-38	-12	0	-1	1	-18	-20	-28	-38	1015	1021	1009	1010	1020	1017	08/25/94	01/09/97	01/17/97	04/24/97	105	71	71	52	10/23/96	Wed
17	10	230	360	21	66	88	97	166	160	4	-66	-87	-97	-154	-156	-21	8	-15	-3	62	36	1016	1027	1005	1022	1019	1011	10/04/94	06/24/97	06/26/97	07/10/97	16	73	73	54	04/11/97	Fri
20	13	173	140	16	20	49	49	105	118	-4	-19	-49	-40	-83	-98	15	-5	-2	-28	-65	-66	1018	1033	1003	1014	1018	1012	11/29/94	08/05/97	08/08/97	08/21/97	16	74	74	50	06/07/97	Sat
21	18	177	180	16	19	32	105	170	116	1	-14	-23	-56	-109	-78	16	-13	-22	-89	-130	-86	1018	1032	1005	1018	1025	1022	06/20/95	11/14/97	11/14/97	12/04/97	20	77	77	55	09/17/97	Wed
32	11	163	270	10	10	39	75	96	92	-4	6	-8	10	12	31	-9	-8	-38	-74	-95	-86	1014	1021	1005	1011	1018	1015	06/28/95	01/09/98	01/12/98	01/29/98	20	72	72	56	11/29/97	Sat
18	8	111	40	11	9	35	35	78	89	4	-9	-29	-33	-78	-86	-10	-2	-19	-13	1	-22	1017	1025	1010	1017	1024	1021	02/16/96	05/27/98	06/04/98	06/12/98	16	73	73	56	04/18/98	Sat
22	9	145	100	5	16	27	37	43	35	3	-10	13	35	28	15	4	12	24	-13	-32	-32	1019	1026	1001	1022	1024	1021	12/12/95	03/27/98	03/30/98	04/02/98	6	72	72	46	02/18/98	Wed
30	13	161	210	3	39	42	83	103	66	-2	-29	-32	-66	-80	-46	-2	-27	-28	-50	-65	-47	1015	1021	1008	1016	1020	1016	09/20/96	10/16/98	11/25/98	12/13/98	58	74	74	58	08/06/98	Thu
22	9	123	130	5	16	24	43	73	39	-5	15	23	34	66	32	-1	-6	-8	-26	-32	-22	1018	1024	1014	1016	1023	1020	05/02/96	07/28/98	07/28/98	08/07/98	10	74	74	59	06/10/98	Wed
16	8	187	320	5	27	48	114	140	117	-3	-27	-43	-112	-117	-105	-4	5	21	24	76	51	1020	1031	1008	1019	1024	1020	01/06/97	11/30/98	11/25/99	01/15/99	46	71	71	60	10/07/98	Wed
25	8	229	230	11	36	81	97	148	100	-6	-30	-51	-51	-43	-56	9	-20	-63	-82	-142	-83	1021	1037	1001	1020	1029	1024	04/28/97	04/19/99	04/19/99	04/23/99	4	74	74	52	02/26/99	Fri
24	10	162	120	5	49	27	55	88	94	3	43	27	3	-27	24	4	24	1	-55	-84	-91	1017	1027	1003	1022	1017	1014	03/26/97	01/29/99	02/01/99	04/02/99	63	75	75	58	12/01/98	Tue
22	9	123	30	8	12	12	18	51	31	7	12	12	13	49	31	-5	1	-3	-12	-13	-2	1016	1022	1009	1015	1013	1010	06/10/97	06/22/99	06/22/99	09/22/99	92	74	74	54	05/10/99	Mon
19	12	150	60	20	8	43	101	109	97	20	5	-13	-65	-80	-36	2	6	-41	-77	-74	-90	1015	1024	1009	1023	1018	1015	09/15/97	05/29/99	06/01/99	06/10/99	12	73	73	52	04/02/99	Fri
18	9	238

PRODUCTION & FOAM APPLICATION DATA FOR EXTERNAL TANK

PRODUCTION & F

DUCTION DATA AVAILABLE FOR ET-1 THROUGH ET-60

NO PRODUCTI

DUCTION DATA AVAILABLE FOR ET-1 THROUGH ET-60

NO PRODUCTI

DUCTION DATA AVAILABLE FOR ET-1 THROUGH ET-60

NO PRODUCTI

nd Spray)			-Y Bipod Spindle Face (Hand Spray)								-Y Bipod Beneath S.F. (Hand Spray)								+Y Bipod Ramp (Hand Spray)								+Y Bipod Spindle Face (Hand Spray)								+Y Bip		
Complete Time	Personnel	Personnel	Substrate Temp (°F)	Cell Temp (°F)	Cell Humidity (%rh)	Complete Date	Complete Day	Complete Time	Personnel	Personnel	Substrate Temp (°F)	Cell Temp (°F)	Cell Humidity (%rh)	Complete Date	Complete Day	Complete Time	Personnel	Personnel	Substrate Temp (°F)	Cell Temp (°F)	Cell Humidity (%rh)	Complete Date	Complete Day	Complete Time	Personnel	Personnel	Substrate Temp (°F)	Cell Temp (°F)	Cell Humidity (%rh)	Complete Date	Complete Day	Complete Time	Personnel	Personnel	Substrate Temp (°F)	Cell Temp (°F)	Cell Humidity (%rh)
1520	BN		76	76	55	06/05/91	Wed	1445	BR		75	75	58	06/14/91	Fri	1030	BN					07/16/91	Tue	1150	BR		76	76	55	06/05/91	Wed	1440	BR		74	74	61
2300	AP		75	75	50	09/03/91	Tue	2330	AR		75	75	58	09/07/91	Sat	130	AP					09/25/91	Wed	2150	AP		78	78	52	08/29/91	Thu	2300	AR		75	75	50
1125	BR		71	71	46	11/27/01	Tue	1240	BR		77	77	50	12/11/91	Wed	1035	BR					01/15/92	Wed	1500	BR		75	75	36	12/05/91	Thu	1330	BN		76	76	51
2125	AT		75	75	58	03/18/92	Wed	2100	BJ		78	78	48	03/26/92	Thu	1845	BJ					04/14/92	Tue	845	BR		75	75	58	03/18/92	Wed	2100	BJ		78	78	46
2045	AP		75	75	58	09/03/92	Thu	1815	AR		76	76	56	09/09/92	Wed	2230	AR					09/30/92	Wed	2040	AP		76	76	52	08/17/92	Mon	2300	AR		75	75	54
640	BR		2	72	57	06/11/02	Tue	1445	BR		74	74	57	06/23/92	Tue	1100	BN					07/02/92	Thu	700	BR		72	72	57	06/11/92	Thu	1435	BR		75	75	54
1110	BR		74	74	56	12/10/92	Thu	1345	BR		74	74	58	12/23/92	Wed	1442	BR					01/21/93	Thu	1510	BR		74	74	56	12/10/92	Thu	1330	BR		74	74	58
1350	AP		75	75	58	03/02/93	Tue	1230	AR		73	73	52	03/10/93	Wed	1445	AR					04/15/93	Thu	1330	AP		74	74	51	03/01/93	Mon	1445	AR		74	74	50
1315	BU		74	74	56	06/03/93	Thu	1240	BR		74	74	60	06/14/93	Mon	1500	BR					07/15/93	Thu	1110	BU		74	74	56	06/03/93	Thu	1233	BR		73	73	54
2150	BE		75	75	56	09/13/93	Mon	2255	BD		76	76	56	09/16/93	Thu	2330	BD					10/14/93	Thu	1330	AL		74	74	57	09/20/93	Mon	1300	BD		75	75	57
2130	AT		73	73	48	12/04/93	Sat	2230	BJ		74	74	38	12/17/93	Fri	100	AT		75	75	36	01/20/94	Thu	115	AT		73	73	60	12/03/93	Fri	2200	BJ		74	74	44
1350	BR		74	74	54	02/10/64	Mon	1100	BN		70	70	56	02/18/94	Fri	1500	BN		72	72	48	03/17/94	Thu	1345	BR		70	70	50	02/11/94	Fri	1030	BN		72	72	55
2115	AT		74	74	58	04/05/94	Tue	300	CY		74	74	64	04/15/94	Fri	100	BJ		76	76	58	05/17/94	Tue	2205	AT		74	74	58	04/05/94	Tue	119	CY		74	74	64
1050	BN		74	74	60	06/15/94	Wed	1000	BE		73	73	60	06/17/94	Fri	950	BD		73	73	57	07/19/94	Tue	1100	BR		73	73	60	06/14/94	Tue	1320	BD		73	73	60
1000	AP		77	77	56	08/15/94	Mon	1340	AR		78	78	52	08/17/94	Wed	1710	AR		76	76	50	09/21/94	Wed	940	AP		77	77	62	08/15/94	Mon	2250	AR		77	77	56
100	AT		72	72	54	10/06/94	Thu	150	BJ		72	72	64	10/08/94	Sat	2250	BJ		75	75	50	11/09/94	Wed	1050	BR		72	72	54	10/06/94	Thu	210	BJ		72	72	64
1440			70	70	54	11/29/94	Tue	640	BR		74	74	40	12/02/94	Fri	610	BR		71	71	59	01/09/95	Mon	1500			70	70	54	11/28/94	Mon	635	RBR		74	74	40
1250	AP		75	75	36	01/31/95	Tue	1030	AP		70	70	29	02/08/95	Wed	530	AP		73	73	54	03/14/95	Tue	1000	AP		73	73	36	02/01/95	Wed	820	AP		71	71	31
1305	BR		73	73	48	03/03/95	Fri	2120	H		73	73	48	04/14/95	Fri	1700	H		70	70	58	04/22/95	Sat	1330	BR		74	74	52	03/27/95	Mon	2250	H		74	74	52
1445	CZ		71	71	60	08/31/95	Thu	1405	CZ		76	76	60	09/06/95	Wed	1330	CZ		74	74	58	09/26/95	Tue	1000	CZ		73	73	54	09/11/95	Mon	1300	AP		71	71	60
1050	BU		75	75	53	05/18/95	Thu	115	H		74	74	56	05/30/95	Tue	2100	H		74	74	54	06/16/95	Fri	300	CI		76	76	46	05/19/95	Fri	2240	BY		73	73	59
2210	BW		73	73	50	10/09/95	Mon	2100	H		74	73	50	10/25/95	Wed	1800	H		73	73	52	11/17/95	Fri	2120	AT		73	73	50	10/06/95	Fri	2230	H		73	73	49
2250	AT		78	78	59	07/11/95	Tue	2240	CR		75	75	59	07/15/95	Sat	1850	CR		75	75	56	07/29/95	Sat	2250	CI		75	75	54	06/28/95	Wed	2320	CR		78	78	54
1110	BN		73	73	42	12/19/96	Thu	1300	BN		68	68	38	01/03/96	Wed	1325	BN		73	73	42	02/02/96	Fri	1400	R	BR	73	73	42	12/19/95	Tue	1300	R2BR		73	73	33
2130	DF		75	75	50	03/06/96	Wed	2145	DF		72	72	44	03/08/96	Fri	2150	DF		73	73	42	04/03/96	Wed	2125	CY		73	73	44	02/29/96	Thu	2030	CY		73	73	46
800	AX		72	71	48	04/30/96	Tue	1400	AX		72	72	49	05/07/96	Tue	1300	DE		71	72	41	05/30/96	Thu	1350	AX		72	71	48	04/30/96	Tue	1400	AX		72	72	49
1855	CY		74	74	64	07/08/96	Mon	2130	CY		76	76	54	07/12/96	Fri	1915	CY		75	75	51	08/23/96	Fri	1415	R	AX	75	75	69	07/09/96	Tue	1100	BD		72	72	48
1440	BD		71	71	60	09/18/96	Wed	1000	AR		72	72	52	10/16/96	Wed	1030	AR		71	71	52	10/23/96	Wed	1440	AR		70	70	57	09/25/96	Wed	1235	AR		71	71	56
1410	BR		74	74	54	03/28/97	Fri	1310	BR		74	74	56	04/02/97	Wed	1500	BR		75	75	49	05/01/97	Thu	1415	BR		73	73	52	03/25/97	Tue	1330	BR		74	74	56
1230	CG		73	73	57	05/29/97	Thu	1055	CI		73	73	58	06/03/97	Tue	1830	CI		75	75	58	06/17/97	Tue	1330	CI		72	72	54	05/29/97	Thu	1730	CI		73	73	56
230	AB		76	76	56	09/03/97	Wed	255	BD	HD	75	75	52	09/08/97	Mon	420	BD	HD	73	73	42	10/07/97	Tue	230	AB		76	76	56	09/03/97	Wed	250	BD		76	76	54
1120	BN	BR	72	72	50	11/19/97	Wed	1455	BR		74	74	56	11/22/97	Sat	1500	BN		72	72	48	12/08/97	Mon	1410	BR		72	72	46	11/18/97	Tue	1445	BR		71	71	57
1345	BD		73	73	61	04/02/98	Thu	2030	DF		74	74	44	04/05/98	Sun	2245	DF		74	74	50	04/25/98	Sat	1100	BD		73	73	60	03/31/98	Tue	2030	DF		73	73	53
1330	AO		73	73	42	02/07/98	Sat	200	BE		73	73	48	02/09/98	Mon	1325	AO		72	72	52	02/28/98	Sat	1350	BR		73	73	42	02/06/98	Fri	1355	AO		73	73	39
1200			75	75	58	07/17/98	Fri	1340	BN		75	75	60	07/22/98	Wed	1515	BN		74	84	27	08/11/98	Tue	1320	BD		75	75	58	07/17/98	Fri	1340	BR		75	75	60
245	BD		74	74	56	05/24/98	Sun	1705	AR		73	73	60	05/28/98	Thu	855	AR		75	75	58	06/19/98	Fri	245	BD		74	74	56	05/24/98	Sun	1700	AR		73	73	60
235	CI		74	74	57	09/18/98	Fri	200	M		74	74	54	09/24/98	Thu	200	M		73	73	53	10/10/98	Sat	1430	BD		72	72	60	10/01/98	Thu	1430	BD		72	72	56
1120	BD	HD	72	72	46	02/18/99	Thu	1030	BD	HD	74	74	48	02/21/99	Sun	1050	BD	HD	72	72	51	03/05/99	Fri	950	BD		72	72	46	02/18/99	Thu	1030	R		74	74	48
2200	AT		77	77	56	11/20/98	Fri	1710	J		74	74	52	11/23/98	Mon	2310	J		75	75	59	12/20/98	Sun	2210	BW		77	77	56	11/20/98	Fri	1715	DF		72	72	52
235	BU		74	74	56	04/27/99	Tue	2145	S		75	75	46	04/30/99	Fri	2305	J		74	74	54	05/10/99	Mon	245	BL		74	74	56	04/27/99	Tue	2145	J		75	75	50
720	BD		73	73	53	03/28/99	Sun	20	M		74	74	54	03/31/99	Wed	852	R		73	73	52	04/20/99	Tue	740	AR		72	72	52	03/26/99	Fri	450	M		73	73	53
115	BU		70	70	60	05/26/99	Wed	1230	CG		71	71	61	05/31/99	Mon	40	T		75	75	58	06/16/99	Wed	1330	BD		70	70	60	05/26/99	Wed	1230	CG		71	71	60
1405	BN		73	73	56	09/28/99	Tue	1450	BR		71	71	54	10/01/99	Fri	1500	BN		72	72	58	10/14/99	Thu	1030	BR		73	73	56	09/28/99	Tue	1450	BR		72	72	55
2315	BW		76	76	56	08/21/99	Sat	2105	O		78	78	56	08/27/99	Fri	2200	O		74	74	57	09/09/99	Thu	2340	BW		78	78	56	08/19/99	Thu	1845	L		77	77	58
2230	BW		71	71	56	11/30/99	Tue	45	T		71	71	56	12/07/99	Tue	500	T		75	75	54	12/17/99	Fri	2310	BW		71	71	56	11/30/99	Tue	45	T		71	71	56
2245	L		74	74	56	02/16/00	Wed	1040	DF		72	72	45	02/21/00	Mon	1330	DF		76	76	48	03/21/00	Tue	2200	AT	BW	76	76	54	02/17/00	Thu	950	DF		75	75	50
2140	F	BD	72	72	55	04/25/00	Tue	1945	A	BD	73	73	56	05/01/00	Mon	2130	D	Q	77	77	55	05/23/00	Tue	2145	F	BD	73	73	57	04/24/00	Mon	1830	A	L	73	73	56
530	M		73	73	52	06/27/00	Tue	500	M		76	76	58	07/11/00	Tue	720	H		74	74	60	08/01/00	Tue	2230	L		75	75	57	06/28/00	Wed	600	H		76	76	58
1100	B	BN	74	74	42	01/12/01	Fri	1450	BN		76	76	58	01/15/01	Mon	1050	BN		71	71	56	01/30/01	Tue	1040	BR	BN	74	74	42	01/12/01	Fri	1445	BR	A	76	76	58
830	BR	BN	74	74	56	05/01/01	Tue	1250	BN		74	74	54	05/03/01	Thu	1320	AY		74	74	53	05/13/01	Sun	1030	BN		74	74	56	05/01/01	Tue	1250	BR		74	74	54
2130	BW		74	74	54	02/20/01	Tue	2050	L		75	75	46	02/23/01	Fri	1410	L		75	75	46	03/18/01	Sun	1350	BD	HD	74	74	54	02/20/01	Tue	1820	J		73	73	56
2200	AB		76	76	55	06/15/01	Fri	430	H	C	76	76	55	06/21/01	Thu	530	H	E	74	74	53	07/26/01	Thu	945	BR		76	76	55	06/15/01	Fri	430	H	C	76	76	55
1425	BR		72	72	56	09/18/01	Tue	1435	BR		72	72	61	09/21/01	Fri	1315	BR		71	71	60	10/10/01	Wed	1425	BR		72	72	56	09/18/01	Tue	1435	BR		72	72	61
1045	BN	BR	73	73	58	08/21/00	Mon	1510	BN		72	72	60	08/25/00	Fri	1015	BN		74	74	58	09/14/00	Thu	1310	BR	BN	73	73	58	08/21/00	Mon	1510	BR		72	72	60

FOAM APPLICATION DATA FOR EXTERNAL TANK

PRODUCTION & FOAM APPLICATION DA

ON DATA AVAILABLE FOR ET-1 THROUGH ET-60

NO PRODUCTION DATA

ON DATA AVAILABLE FOR ET-1 THROUGH ET-60

NO PRODUCTION DATA

ON DATA AVAILABLE FOR ET-1 THROUGH ET-60

NO PRODUCTION DATA

od Beneath S.F. (Hand Spray)					Aft Half of LH/IT Flange Closeout (Hand Spray)									Fwd Half of LH/IT Flange Closeout (Hand Spray)									Intertank Acreage (Machine Spray)																							
Complete Date	Complete Day	Complete Time	Personnel	Personnel	Substrate Temp (°F)	Cell Temp (°F)	Cell Humidity (%rh)	Complete Date	Complete Day	Complete Time	Personnel	Personnel	Personnel	Personnel	Substrate Temp (°F)	Cell Temp (°F)	Cell Humidity (%rh)	Complete Date	Complete Day	Complete Time	Personnel	Personnel	Personnel	Substrate Temp at Upper Flange -1 (°F)	Substrate Temp at Upper Flange -2 (°F)	Substrate Temp at Upper Flange -3 (°F)	Substrate Temp at Upper Flange -4 (°F)	Substrate Temp at Lower Flange -1 (°F)	Substrate Temp at Lower Flange -2 (°F)	Substrate Temp at Lower Flange -3 (°F)	Substrate Temp at Lower Flange -4 (°F)	Cell Temp (°F)	Cell Humidity (%rh)	Complete Date	Complete Day	Complete Time	Personnel	Personnel	Personnel
07/09/91	Tue	1115	BN					10/24/90	Wed	2135	CE							11/06/90	Tue	2040	CE			130								102	15	03/16/90	Fri	1821	AE	HW	IU
09/03/91	Tue	2310	AP					01/04/91	Fri	1300	BB							01/15/91	Tue	1200	AH			126							128	100	14	06/04/90	Mon	1418	DG		
12/12/91	Thu	1030	BR					05/15/91	Wed	1530	AN							05/31/91	Fri	1250	BX			128								98	16	08/17/90	Fri	1921	AS		
03/27/92	Fri	2045	AT		82	76	54	08/01/91	Thu	1700	AN				74	74	46	08/16/91	Fri	2300	AW			132								102	14	10/31/90	Wed	1056	CA		
08/20/92	Thu	2035	AP		73	72	56	05/20/92	Wed	1315	BB				77	73	56	06/16/92	Tue	1053	BB			129								98	15	06/13/91	Thu	1426	Z	IJ	HC
06/30/92	Tue	1045	BA		74	74	46	12/12/91	Thu	1630	AQ				74	74	34	01/10/92	Fri	1230	BB			125								102	10	12/07/90	Fri	1739		HJ	GC
12/23/92	Wed	1438	BR		77	75	58	08/19/92	Wed	1445	BX				76	75	56	09/01/92	Tue	1130	BB			126								109	22	09/06/91	Fri	1916		EW	GS
03/12/93	Fri	1500	AR		85	85	23	11/06/92	Fri	1930	BZ				72	72	50	11/17/92	Tue	1210	AH			130			145				131	104	10	12/18/91	Wed	1305	BK		
06/17/93	Thu	1440	BR		71	71	40	02/12/93	Fri	1450	AH				75	75	46	02/26/93	Fri	1115	BX			127								104	12	02/14/92	Fri	1416	AI	IJ	GC
09/22/93	Wed	1225	BD		75	77	51	05/25/93	Tue	1100	AN				78	74	54	06/04/93	Fri	1355	AN			130								102	20	07/09/92	Thu	1143		HX	IT
12/18/93	Sat	2045	AT		79	74	54	08/13/93	Fri	1215	BB				77	75	48	08/24/93	Tue	1340	BX			126								97	10	12/02/92	Wed	1405	DK		
03/02/94	Wed	1330	BN		75	73	57	10/13/93	Wed	1025	BO				77	76	40	10/28/93	Thu	1130	BO			126								102	10	03/11/93	Thu	2313	AU	HW	JB
04/15/94	Fri	110	BJ		73	77	36	01/11/94	Tue	730	BX				73	74	30	01/21/94	Fri	1350	BO			132								104	10	04/05/93	Mon	1915		HI	IT
06/17/94	Fri	940	BD		72	72	38	03/03/94	Thu	1415	BX				72	76	42	03/15/94	Tue	1400	CF			126								98	20	06/16/93	Wed	1149	DJ	GV	II
08/24/94	Wed	1300	AR		75	68	56	04/20/94	Wed	1410	BO				73	73	46	04/29/94	Fri	1415	BB			126								97	21	10/21/93	Thu	1957	AA		
10/08/94	Sat	2300	BJ		76	77	56	07/12/95	Wed	1100	BO				74	74	52	07/19/94	Tue	1345	BO			130								100	9	02/02/94	Wed	1340	CM	JB	II
12/02/94	Fri	600	BR		74	74	46	09/09/94	Fri	1430	CK				74	74	54	09/15/94	Thu	1400	BO			132								100	18	03/26/94	Sat	1322	V		
02/09/95	Thu	1300	AP		74	75	42	11/01/94	Tue	1550	AE				76	57	52	11/09/94	Wed	1415	BX			125								101	18	05/05/94	Thu	1555	BS	JB	HW
04/14/95	Fri	1700	H		72	77	32	01/03/95	Tue	1435	BX				74	74	52	01/16/95	Mon	2115	CK			125								96	19	06/17/94	Fri	1331		HL	HI
09/14/95	Thu	1300	CZ		75	75	54	05/31/95	Wed	1055	BX				74	74	54	06/08/95	Thu	1345	BX			131				127				99	19	12/15/94	Thu	2223	AM	GJ	IM
05/26/95	Fri	2315	BY		74	76	34	02/22/95	Wed	1105	BX				73	76	36	03/03/95	Fri	1640	BX			125				125				100	20	09/10/94	Sat	621	CC	FZ	HI
10/17/95	Tue	2300	H		77	74	54	07/14/95	Fri	1430	BO				73	72	58	07/21/95	Fri	1345	BO			130				139				100	20	01/31/95	Tue	1420	BV	JC	HW
07/07/95	Fri	1800	CR		75	75	50	04/08/95	Sat	1145	BX				75	75	54	04/20/95	Thu	710	BX			127				125				97	21	11/05/94	Sat	857		HW	GD
01/09/96	Tue	1335	BR		74	74	52	09/18/95	Mon	1500	BX				73	73	52	09/26/95	Tue	1440	BX			126				131				98	24	04/22/95	Sat	0632	DM	GJ	HI
03/04/96	Mon	2245	CY		73	73	46	11/14/95	Tue	1345	BX				75	75	52	11/28/95	Tue	1340	BX			127				139				100	18	06/10/95	Sat	730		JB	HI
05/07/96	Tue	1300	DE		73	74F	46	01/31/96	Wed	1800	CF				76	78	48	02/08/96	Thu	1345	BX			125				134				99	19	06/23/95	Fri	932		HI	FW
07/11/96	Thu	1455	BD		74	75	35	04/10/96	Wed	1410	BX				74	75	46	04/18/96	Thu	1930	BX			128				135				100	20	08/22/95	Tue	1325	CH		
10/10/96	Thu	830	AR		75	75	54	06/17/96	Mon	1505	BX				82	79	52	06/27/96	Thu	1430	BX			130				126				105	19	12/05/95	Tue	1416		FZ	DD
04/02/97	Wed	1500	BR		75	75	56	01/05/97	Sun	1500	BX				95	95	22	01/09/97	Thu	1440	BX			131				129				105	10	12/21/95	Thu	1510		FN	DD
06/04/97	Wed	1500	CI		78	77	53	03/17/97	Mon	1430	DA				76	76	50	03/21/97	Fri	1410				136				128				96	19	03/14/96	Thu	1407	CH		
09/09/97	Tue	230	BD		76	78	56	07/26/97	Sat	1230	DA				76	76	54	07/30/97	Wed	1615	BX			126				137				102	16	05/23/96	Thu	1338	BS	HI	FF
12/01/97	Mon	1350	BR		74	74	42	10/22/97	Wed	1450	AH	BX			78	72	59	10/26/97	Sun	820	AH			138				127				92	20	10/02/96	Wed	2219	CA		
04/07/98	Tue	2150	DF		74	73	58	03/05/98	Thu	2230	CK				74	74	36	03/09/98	Mon	810	BX			134				125				102	16	01/22/97	Wed	1638		FZ	HI
02/08/98	Sun	1430	AO		74	77	35	01/11/98	Sun	1225	CD				76	76	46	01/15/98	Thu	1350	BX			135				130				103	8	12/07/96	Sat	1305	CH		
07/22/98	Wed	1515	BR		74	74	46	06/04/98	Thu	1800	DA				80	80	40	06/11/98	Thu	805	CD			125				129				102	20	10/07/97	Tue	1457		GJ	IM
05/28/98	Thu	850	AR		78	78	52	04/16/98	Thu	1410	BO	BX			76	76	46	04/20/98	Mon	1630	BX			126				127				101	22	08/19/97	Tue	655		IH	DD
10/04/98	Sun	1225	BD		75	75	56	08/02/98	Sun	2045	BX				75	75	54	08/07/98	Fri	2045	BX			125				128				102	18	10/31/97	Fri	1521	DM	HI	GD
02/21/99	Sun	1100	R		78	79	42	01/16/99	Sat	1125	BX				78	78	52	01/20/99	Wed	1935	DA			125				125				100	21	09/15/98	Tue	1227		HT	GH
11/22/98	Sun	2030	DF		76	80	46	10/26/98	Mon	1520	DA				80	80	50	10/31/98	Sat	1450	BX			126				126				103	17	12/22/97	Mon	1956		GJ	IM
04/30/99	Fri	100	S		78	78	48	02/06/99	Sat	1900	BX				78	79	52	02/09/99	Tue	2200	BX			125				127				105	18	04/14/98	Tue	127		GJ	IM
04/06/99	Tue	1450	R		74	76	30	02/23/99	Tue	540	BX				71	73	39	03/03/99	Wed	1350	BO			123				125				197	23	06/08/98	Mon	142			
06/01/99	Tue	630	T		75	72	53	05/02/99	Sun	2315	CX				76	76	54	05/06/99	Thu	1400	AS			125							130	100	23	08/23/98	Sun	1523	BC		
10/04/99	Mon	1300	BR		75	75	58	08/19/99	Thu	2348	CL	CX			76	76	56	08/23/99	Mon	600	DA	BX		128				125				105	15	11/22/98	Sun	1544		IF	HF
08/24/99	Tue	1900	L		78	78	52	07/30/99	Fri	1410	BX				77	77	54	08/02/99	Mon	1445	BX			126				127				103	12	12/23/98	Wed	504	AK	GJ	IF
12/07/99	Tue	500	T		77	79	47	10/31/99	Sun	1410	AS				76	76	48	11/05/99	Fri	635	BX			125				125				104	19	03/14/99	Sun	1247	AV	IF	FQ
02/23/00	Wed	850	DF		75	75	49	01/05/00	Wed	1415	GF	GF			74	75	48	01/09/00	Sun	830	DA	GF		126				125				105	15	04/21/99	Wed	1441		HM	IF
05/01/00	Mon	2130	D	Q	74	74	52	02/26/00	Sat	940	BX				73	75	50	03/03/00	Fri	1205	DA			125				125				101	18	06/07/99	Mon	1948		FZ	EZ
07/11/00	Tue	715	H		76	76	44	04/26/00	Wed	1050	BX				74	74	56	05/05/00	Fri	545	BX			126				125				105	17	07/07/99	Wed	2105	CT	FN	IF
01/15/01	Mon	1400	BR		76	78	49	12/14/00	Thu	700	DA				80	80	40	12/17/00	Sun	1650	BX			126				127				103	20	12/16/99	Thu	1213		FG	IF
05/04/01	Fri	810	BR		78	78	50	04/11/01	Wed	1400	CK	GF			78	78	52	04/17/01	Tue	550	DA	GF		127				125				105	17	05/15/00	Mon	1527		GJ	IM
02/22/01	Thu	2300	J		73	73	32	01/22/01	Mon	1130	AS	AH	GZ	CK	78	79	44	01/28/01	Sun	630	DA	GF		128				126				102	5	04/04/00	Tue	1606		GJ	IF
06/21/01	Thu	525	H	E	75	75	48	05/15/01	Tue	1400	DA				74	76	46	05/19/01	Sat	845	DA			127	127	128	130	126	126	126	127	101	20	06/29/00	Thu	319		GM	IM
09/21/01	Fri	1315	BR		75	76	52	07/13/01	Fri	1400	DA	GF	IC	BX	75	76	53	07/24/01	Tue	1355	BX	DA	IC	127				133				98	22	01/24/00	Mon	1722		EN	FL
08/25/00	Fri	1015	BR		74	74	54	06/15/00	Thu	1150	BX				76	76	54	06/25/00	Sun	1440	BX			130				129				105	19	08/16/99	Mon	2001	CT	GJ	DD

TA FOR EXTERNAL TANK

			LO2 Tank Acreage (Machine Spray)													LH2 Barrel Acreage (Machine Spray)													
Personnel	Personnel	Personnel	St380 Substrate Temp (°F)	St800 Substrate Temp (°F)	St840 Substrate Temp (°F)	Cell Temp (°F)	Cell Humidity (%rh)	Complete Date	Complete Day	Complete Time	Personnel	Personnel	Personnel	Personnel	Personnel	St2088 Substrate Temp (°F)	St1129 Substrate Temp (°F)	Cell Temp (°F)	Cell Humidity (%rh)	Complete Date	Complete Day	Complete Time	Personnel	Personnel	Personnel	Personnel	Personnel	PRCB # (PCBD ...) & Date
AVAILABLE FOR ET-1 THROUGH ET-60																													
AVAILABLE FOR ET-1 THROUGH ET-60																													S044812A, 2/6/90
AVAILABLE FOR ET-1 THROUGH ET-60																													S044824C, 6/14/91
																													S044848H, 9/1/92
																													S044876C, 8/6/92
																													S044880A, 11/30/92
																													S044897L, 5/23/94
HJ			149	127	126	100	12	07/09/90	Mon	2127	V					125	127	99	21	08/16/90	Thu	142		HG	HF	FA			
			144	127	129	104	8	09/26/90	Wed	1552	BM					126	154	100	15	09/26/90	Wed	1408	CO						
			154	132	130	99	10	03/08/91	Fri	1058	CJ	HX	IT	JA		126	142	99	19	12/14/90	Fri	1557	AJ	HB	FE	GH	JA		
			141	127	125	94	18	05/09/91	Thu	1549	AE					127	152	99	15	05/07/91	Tue	1430	CB						
JC	JA		155	127	128	101	17	10/03/91	Thu	1515	X	IJ	GC	HA	GS	127	129	103	7	01/17/92	Fri	1549	V	FE	GD	HW			
HX			137			99	15	08/27/91	Tue	1729		HX	IT	GI		100	106	100	22	08/06/91	Tue	1655		HB	GD	FE			
DX	EC		145	127	133	100	15	05/15/92	Fri	1655		DD	HY	EC	GT	125	132	103	11	04/29/92	Wed	2217	GS	HW	HB	FE	GL		
			147	127	127	103	16	08/18/92	Tue	1420	BS					128	148	103	20	08/06/92	Thu	2250	V						
EC	GS		159	128	130	97	18	11/18/92	Wed	1415	AZ	DD	GC	IX	EC	127	145	103	17	10/09/92	Fri	1516	DH	IL	HE	IX	FE		
JB	GS		137	130	126	130	10	03/24/93	Wed	1138		HW	GD	IX	JB	126	131	99	23	12/15/92	Tue	2134		HB	FE	GX	IX		
			128	131	128	98	24	05/07/93	Fri	2258	DM					125	135	103	14	04/23/93	Fri	1606	DJ						
FF			157	127	135	98	18	07/30/93	Fri	1958	AZ	HW	GD			132	150	105	17	07/13/93	Tue	1345	BX	HX	FE	IE	GT		
JB	HO		157	127	128	102	15	10/05/93	Tue	1559		II	HL	HY	GS	125	153	103	19	09/23/93	Thu	1435		HX	DX	FE	GS		
IT	EC		139	125	130	101	13	01/10/94	Mon	1522	GS	JB	II	HW	FQ	126	151	98	20	11/19/93	Fri	1520	DK	HX	FE	HY			
			135	125	131	98	10	02/11/94	Fri	1630	BP					125	142	101	14	01/14/94	Fri	1053	CB						
FF	HO		154	126	126	104	17	05/13/94	Fri	1508	BS	II	GD	HO	HW	125	134	102	11	03/12/94	Sat	1520							
				140		93	21	07/09/94	Sat	1601	CT					125	140	103	22	05/28/94	Sat	1910	AW						
FQ	HO		146	137	131	92	18	08/06/94	Sat	1721	CT	IM	FF	HO	GK	125	139	101	24	08/05/94	Fri	1603	DO						
FQ	GS		139	126	129	100	14	09/28/94	Wed	1226		IM	FQ	GT		126	139	102	20	09/16/94	Fri	1515		HQ	FE	ET			
FQ	ET		149	126	134	104	15	03/31/95	Fri	1325	BS	HI	FW			123	140	102	19	03/30/95	Thu	830	DJ	GP	II	HV	GS		
FQ	GT		147	125	126	97	12	12/02/94	Fri	1323	V	HW	GD	HO		128	135	105	19	11/03/94	Thu	1827	AG	FE	GB	DX	ET		
FQ	HO		146	125	127	105	18	05/09/95	Tue	1537	AB	HI	GD	HO		132	141	105	19	05/19/95	Fri	726	AW	DZ	II	HY	HO		
HO			145	125	126	104	14	02/14/95	Tue	1610	V	JC	FQ	HO		129	140	102	13	01/19/95	Thu	1348		EE	II	FS	HO		
GD			153	127	133	100	18	07/21/95	Fri	1915	CT	DD	FW	FZ		126	127	101	22	07/07/95	Fri	1457	DB	DZ	II	HY			
FW	GV		145	126	130	100	23	09/12/95	Tue	0410 .		FZ	DD	GD	HO	125	131	88	25	09/23/95	Sat	1703		DZ	II	GE	HO		
ET			137	126	130	104	16	11/14/95	Tue	1148		HW	GD	HO		127	133	99	19	11/17/95	Fri	2250		DZ	HB	GE	HO		
			141	126	127	105	11	01/13/96	Sat	1819	BV	FZ	HW	GD	HO	129	155	97	25	01/26/96	Fri	2058	Y	DZ	IF	FD	HO		
FW	EI		152	126	128	105	10	03/22/96	Fri	2121		FZ	HW	GD	HO	126	134	100	22	04/28/96	Sun	0913		DZ	IF	FW	HO		
FO	ET		134			95	22	06/10/96	Mon	1553	V	FZ	DD	GD	IX	125	127	94	14	11/13/96	Wed	600		DZ	GR	FS	HO	S062127, 1/13/00	
			149	128	127	101	10	09/29/96	Sun	1158	CH					127	134	95	10	12/21/96	Sat	1034	AF						
HO			150	125	127	105	8	02/07/97	Fri	1148	CN	FC	HI	GH	BS	129	141	95	24	06/03/97	Tue	2232	GB	EE	II	HZ	HP		
			142	130	132	102	19	08/18/97	Mon	1202	DI					130	146	100F	21	09/19/97	Fri	1724		FE	HX	FD	HT		
FO	IX		140	126	126	104	18	02/04/98	Wed	638		FB	HX	GH	GW	126	131	99	20	01/29/98	Thu	1210		DZ	HX	FQ	EI		
			154	127	128	102	19	12/04/97	Thu	1511	DM					128	147	99	22	12/04/97	Thu	2125		DZ	IF	IK	GW		
GD	HP		126	130	149	100	20	04/26/98	Sun	657		GJ	DD	JD	EI	126	148	94	23	05/01/98	Fri	1315		DZ	FL	HY	EI		
DX	HK		158	131	132	103	9	03/13/98	Fri	1317		HR	IM	FW	EI	125	150	102	12	03/03/98	Tue	1932		DZ	HH	FW	GW		
FF			156	125	132	103	19	06/28/98	Sun	1313	BC	GJ	IF	GH	GW	127	153	99	23	06/22/98	Mon	1459	AF	EE	DD	HY	GW		
GY			157	128	142	99	20	12/02/98	Wed	359		GJ	FZ	JD	HF	126	134	98	21	12/03/98	Thu	1226		DZ	II	HY	EY		
FQ	EI		143	125	125	103	18	09/17/98	Thu	145	CA	HN	IF	JD	EI	127	131	101	21	09/19/03	Fri	1353	DJ	DZ	II	HY	GW		
FW	EI		141	125	128	104	17	10/14/98	Wed	1345		GJ	IM	GD	HQ	126	145	102	19	11/24/98	Tue	1830		DZ	II	HY	EY		
			160	128	131	105	17	01/20/99	Wed	124		GM	DD	GD	FF	126	140	100	22	01/19/99	Tue	1415		DZ	II	HY	FF		
		G	156	126	136	105	12	03/10/99	Wed	1529	AN					126	143	103	19	04/04/99	Sun	2146		EE	HB	GE	EI		
			159	125	131	100	72	07/21/99	Wed	1418		GJ	FZ	EZ	EY	126	140	196	22	05/13/99	Thu	0		DZ	HI	GE	EI		
JD			130	126	126	105	19	06/30/99	Wed	2036	P	GJ	FL	FI		143	127	103	19	07/01/99	Thu	2200	CP	DZ	II	HY	DT		
EI	BT		144	125	127	100	17	09/12/99	Sun	630	CN	GJ	EU	EZ	EY	142	125	105	18	10/07/99	Thu	1708	CS	DZ	DD	HY	EY		
EZ	EI		150	128	128	101	21	10/03/99	Sun	811		FY	HX	HM	EY	126	143	106	16	12/02/99	Thu	536		DZ	HH	GW			
EY	EN		152	130	125	104	20	12/04/99	Sat	314	N	GJ	IF	GD	GW	126	143	104	19	01/22/00	Sat	1201		EV	HH	DX	EI		
EZ	FF		148	125	128	105	15	01/16/00	Sun	702	N	GJ	EU	GW		126	144	105	19	03/15/00	Wed	1518	DB	EE	DD	GU	EI		
GD	EI		154	128	125	105	19	08/11/00	Fri	520		HR	FL	HM	IY	128	143	90	23	11/24/00	Fri	2228		EE	II	HY	EI		
EZ			151	125	129	105	16	10/30/00	Mon	1451		HR	DD	JD	EI	143	126	94	20	03/14/01	Wed	1126		IB	II	GD	FF		
GD	EI		146	125	127	105	15	09/07/00	Thu	1624		GJ	IG	EZ	EI	129	143	100	18	12/13/00	Wed	2252		IB	DD	HY	EI		
GE	EI		156	130	135	101	15	12/22/00	Fri	1457		IF	FW	EI		129	156	89	22	04/20/01	Fri	1538		FR	DD	HY	EI	S06215, 12/19/02	
EZ	EI		154	127	135F	99	11	03/26/01	Mon	156	CQ	IV	HM	EI	AK	133	160	102	17	06/01/01	Fri	1441		DZ	II	DX	HF		
GA	EY		150	125	127	92	26	03/04/00	Sat	729	DN	IF	IM	EZ	EI	127	141	99	17	04/26/00	Wed	1851	CW	DZ	DD	HY	EI		

| | | |

OV Gross @ Liftoff (lbs.)	Integrated Vehicle Gross @ Liftoff (lbs.)	OV Xcg (in.)	OV Ycg (in.)	OV Zcg (in.)	Shuttle Xcg (in.)	Shuttle Ycg (in.)	Shuttle Zcg (in.)		TOTAL on Pad	1-Day MAX	AVG Daily	Launch Day	TOTAL 5 Day Pre-Launch	AVG on Pad	MAX on Pad	MIN on Pad	AVG Launch Day	MAX Launch Day	MIN Launch Day	At Tanking Start	At Launch	AVG on Pad	MAX on Pad	MIN on Pad	AVG Launch Day	MAX Launch Day	MIN Launch Day	AVG on Pad	MAX on Pad	MIN on Pad	AVG Launch Day	MAX Launch Day	MIN Launch Day	AVG on Pad	
255224	4515290	1111.9	-0.2	380.8	1412.2	0.2	418.8		5.45	1.92	0.14	0.11	0.73	72	89	51	71	80	63	68	71	64	75	42	62	67	57	76	99	35	73	91	69	12	
7668	8524	6.5	0.3	1.8	1.2	0.1	0.6		4.57	1.39	0.09	0.39	1.10	8	5	15	10	8	11	11	12	8	4	19	12	10	13	4	2	11	10	10	21	3	
1414	1572	1.2	0.1	0.3	0.2	0.0	0.1		0.84	0.26	0.02	0.07	0.20	1	1	3	2	2	2	2	2	2	1	3	2	2	2	1	0	2	2	2	4	0	
255305	4514796	1110.2	-0.3	380.3	1412.3	0.2	418.8		5.36	1.95	0.14	0.11	0.74	73	89	52	73	81	64	68	74	64	76	44	64	68	59	75	99	35	73	91	66	13	
7801	9231	6.7	0.4	1.8	1.5	0.1	0.6		4.59	1.39	0.09	0.44	1.26	7	4	15	8	7	10	10	10	8	4	18	9	8	11	4	2	11	9	9	21	3	
1896	2244	1.6	0.1	0.4	0.4	0.0	0.1		1.11	0.34	0.02	0.11	0.31	2	1	4	2	2	2	2	3	2	1	4	2	2	3	1	0	3	2	2	5	1	
257318	4515393	1112.9	-0.5	379.9	1413.0	0.2	418.9		6.83	3.04	0.24	0.01	0.46	71	87	51	69	77	60	64	70	63	75	43	59	64	54	76	99	32	71	91	66	12	
6352	13198	10.0	0.2	1.9	1.8	0.1	0.5		3.79	2.27	0.13	0.02	0.83	9	5	17	10	8	12	12	13	10	3	20	14	12	16	3	2	12	15	9	30	1	
4706	9777	7.4	0.2	1.4	1.3	0.1	0.4		2.81	1.68	0.10	0.01	0.61	7	4	13	7	6	9	9	9	7	3	15	10	9	12	2	1	9	11	7	22	1	
253298	4516356	1113.7	-0.1	381.0	1411.9	0.2	418.6		8.27	2.48	0.16	0.04	0.66	73	90	53	70	78	63	66	71	65	77	44	62	66	58	78	99	33	80	95	71	12	
4438	5411	5.5	0.4	0.9	0.8	0.0	0.3		5.57	1.64	0.08	0.08	0.75	10	7	17	12	11	13	13	17	10	5	23	15	14	15	3	2	11	7	7	13	1	
3075	3750	3.8	0.3	0.6	0.5	0.0	0.2		3.86	1.13	0.05	0.06	0.52	7	5	12	9	8	9	9	12	7	4	16	10	10	11	2	1	8	5	5	9	1	
255475	4515958	1114.4	-0.1	381.7	1412.2	0.2	418.9		5.04	1.77	0.14	0.14	0.74	72	88	50	69	78	61	68	67	63	75	40	59	64	54	76	##	35	72	90	74	12	
8056	7809	5.6	0.3	1.5	0.8	0.1	0.6		4.24	1.34	0.10	0.32	0.88	8	5	14	11	10	13	13	13	9	4	19	14	13	16	4	1	11	11	11	23	1	
2497	2420	1.7	0.1	0.5	0.2	0.0	0.2		1.31	0.42	0.03	0.10	0.27	2	2	4	3	3	4	4	4	3	1	6	4	4	5	1	0	3	3	3	7	0	
s.)		CENTER OF GRAVITY [CG] (in.)							RAINFALL					TEMPERATURE (F)								DEWPOINT (F)						RELATIVE HUMDITY (%rh)						SPE	
GHT, CENTER OF GRAVITY, & PAYLOAD																																			WE
								DFI	6.00	2.22	0.06	0.00	0.00	60	87	23	67	79	55	65	58	49	75	9	60	68	52	69	100	13	73	93	93	12	
								OSS/DFI	2.96	1.45	0.08	0.00	0.00	68	89	41	76	87	65	68	81	59	71	35	68	71	64	74	100	22	77	100	100	12	
								DOD/DFI	8.02	2.39	0.24	0.02	1.27	80	91	69	80	88	72	72	85	73	78	64	75	78	71	80	100	45	82	100	100	12	
246425	4488857	1116.7	0.2	379.6	1416.7	0.3	418.3	SBS/TELE	4.02	1.12	0.08	0.02	0.02	74	88	51	73	79	66	66	71	67	77	43	65	67	63	78	100	41	79	96	96	12	
256987	4490778	1127.6	0.4	382.8	1416.6	0.3	419.1	TDRS A	19.00	1.89	0.15	0.00	0.78	63	84	35	65	78	52	53	76	56	73	23	56	63	49	78	100	25	72	96	96	14	
249626	4486449	1122.0	-0.8	381.1	1416.8	0.0	418.6	MULT P/L	6.97	1.78	0.29	0.00	0.00	77	89	63	76	83	69	73	71	70	77	47	69	71	66	79	100	26	77	90	90	12	
250405	4505048	1124.4	0.2	381.4	1412.3	0.3	418.5	MULT P/L	2.11	0.53	0.09	0.00	0.53	61	83	38	66	75	57	61	57	53	69	32	58	63	53	77	100	27	78	96	96	13	
242543	4497865	1119.1	-0.1	381.6	1417.1	0.2	418.0	MULT P/L	3.37	1.96	0.15	0.00	0.00	76	92	58	74	83	64	67	68	68	76	55	62	65	58	76	100	44	67	84	84	12	
247254	4501978	1114.5	-0.2	381.4	1411.3	0.3	418.3	S/L 3	0.12	0.09	0.00	0.00	0.00	68	91	33	77	85	68	69	85	59	72	29	64	72	55	73	100	29	68	96	96	11	
252733	4514313	1111.5	-0.5	381.8	1412.2	0.2	418.7	(ATO) S/L 2	5.24	1.10	0.17	0.00	0.01	80	94	67	81	88	73	73	86	73	78	66	75	77	72	78	100	44	81	100	100	11	
243751	4505113	1108.4	-0.3	380.1	1410.0	0.2	418.0	S/L DI	3.12	1.47	0.21	0.46	2.63	78	88	67	76	85	67	71	84	72	77	66	70	73	67	80	100	58	79	100	100	10	
254923	4511561	1111.2	0.9	380.6	1411.0	0.3	418.8	MULTI P/L	9.53	4.14	0.23	0.00	5.23	61	83	26	61	70	51	60	51	53	72	17	54	58	49	76	100	26	79	96	96	11	
256235	4522277	1116.3	0.6	380.8	1412.5	0.3	418.8	TRDS D	3.38	1.12	0.09	0.00	0.40	65	85	32	70	81	58	63	62	54	71	11	54	58	49							13	
								DOD (S)	4.33	1.61	0.17	0.28	0.28	83	96	71	84	94	73	84	79	72	78	66	73	77	68							10	
256063	4519487	1131.3	-0.8	381.3	1413.2	0.2	418.9	LDEF	5.29	1.38	0.12	0.00	0.00	60	84	24	61	69	52	65	54	51	72	16	55	58	51					96	96	11	
256511	4521514	1106.5	-0.5	378.1	1412.1	0.2	418.7	ASTRO	20.52	4.35	0.13	0.00	0.76	74	93	48	72	78	65	71	69	66	83	40	60	63	56	74	100	30	65	81	81	11	
255758	4519945	1116.7	-0.3	381.7	1412.4	0.2	418.8	GRO	8.28	3.74	0.38	0.85	0.85	69	87	50	74	79	68	71	74	60	71	44	66	68	64	74	100	38	81	96	96	14	
251921	4519792	1100.2	-0.1	376.4	1411.4	0.2	418.3	SLS 1	6.48	2.10	0.19	0.13	0.46	78	91	63	79	86	71	78	74	70	77	62	71	74	67	77	100	45	73	90	90	11	
243456	4507474	1104.8	-0.1	378.3	1410.6	0.2	417.8	IML-01	2.97	2.60	0.12	0.00	0.19	60	79	32	55	73	37		66	53	69	26	48	60	35							11	
233650	4496035	1113.1	-0.3	377.6	1409.8	0.2	417.2	ATLAS	2.75	1.24	0.08	0.00	0.11	66	86	43	67	71	62	64	67	56	70	34	56	60	51							12	
257695	4520103	1105.5	-0.5	378.7	1412.0	0.2	418.8	USML-1 EDO	6.14	2.65	0.27	0.02	2.19	80	93	68	80	87	72	72	85	72	78	67	74	77	70							14	
244568	4506804	1104.1	-0.4	379.2	1410.5	0.3	417.9	S/L J	1.42	0.70	0.07	0.00	0.60	80	92	70	79	86	72	75	84	73	77	67	73	74	71							10	
250370	4514565	1109.5	-0.3	377.5	1411.4	0.1	418.2	LAGEOS-2	6.35	2.95	0.24	0.00	0.00	75	88	59	74	78	69	71	77	66	78	51	58	62	54							12	
243897	4506587	1112.4	0.1	380.7	1410.7	0.2	418.0	DOD	4.06	2.18	0.16	0.00	0.00	69	86	41	55	68	42	49	55	61	74	34	49	57	40							13	
259412	4522840	1116.2	0.3	381.3	1412.6	0.2	419.0	TDRS F	3.05	1.12	0.07	0.00	0.43	67	83	38	74	79	68	70	72	60	71	31	68	70	66				78	96	60	11	
237253	4501920	1109.5	-0.3	379.3	1410.1	0.2	417.5	ATLAS 2	2.02	0.70	0.08	0.00	0.27	75	85	35	68	75	61	70	72	57	72	14	54	59	48	70	96	29	61	83	38	28	
255468	4519000	1101.5	-0.7	377.5	1411.5	0.3	418.6	S/L D2	8.09	2.51	0.10	0.06	0.06	73	85	10	72	83	61	66	76	51	72	-4	64	68	60	66	100	13	70	93	46	25	
252703	4518566	1112.7	-0.1	383.0	1412.0	0.2	418.7	S'HAB 1/EUR	1.21	0.50	0.02	0.04	0.04	83	94	64	82	87	77	66	76	65	77	47	72	74	69	68	96	31	72	87	57	25	
261478	4523125	1116.5	-0.6	381.6	1412.8	0.2	419.2	ACTS/ORF	12.44	2.50	0.16	0.00	1.14	83	97	69	79	87	70	73	72	74	80	64	73	76	69	73	100	37	75	93	57	11	
256103	4517138	1103.4	-0.4	378.1	1411.5	0.2	418.6	SLS 2 EDO	3.98	1.25	0.12	0.00	1.27	78	92	64	75	82	67	67	79	70	79	53	69	72	66	71	100	29	77	90	64	11	
256579	4519801	1107.4	-0.6	379.2	1412.0	0.2	418.7	USMP 2/EDO	9.70	6.35	0.40	0.00	0.88	68	83	45	58	70	45	49	54	60	72	30	37	43	30	72	100	21	49	76	21	14	
246849	4511411	1098.8	-0.5	378.7	1410.7	0.2	418.1	SRL1	2.04	1.65	0.09	0.00	0.06	71	88	52	75	78	71	49	71	62	77	37	63	65	60	69	96	32	63	71	55	12	
259299	4523441	1104.8	-0.4	378.8	1412.2	0.2	418.9	IML 2/EDO	3.92	3.07	0.16	0.00	0.11	82	94	72	83	88	77	77	88	74	78	67	75	78	71	73	93	44	73	87	59	14	
247403	4510613	1099.3	-0.5	378.5	1410.7	0.2	418.1	SRL 2	10.47	3.00	0.22	0.00	0.19	79	91	66	78	86	70	75	71	73	82	65	70	74	66	77	100	51	65	79	51	10	
244238	4508715	1112.0	-0.1	379.4	1411.1	0.2	417.9	ATLAS 3	4.96	1.50	0.19	0.00	1.97	76	87	60	73	81	64	65	81	68	77	56	62	64	60	72	100	44	58	66	50	11	
249088	4511586	1110.0	-0.1	380.1	1411.3	0.2	418.3	S/LM S/MM-1	11.33	3.20	0.18	0.00	4.90	79	95	60	83	92	73	73	90	70	79	56	74	77	71	79	100	36	81	100	61	12	
256384	4519114	1112.9	-0.1	383.3	1412.3	0.2	419.0	WSF 2	20.47	5.65	0.35	0.05	1.09	82	95	71	81	88	73	75	84	76	82	67	75	77	72	85	100	42				12	
257327	4521581	1101.6	-0.5	377.1	1411.8	0.2	418.7	USML-2 EDO	15.75	2.75	0.29	0.00	1.38	81	94	70	78	83	73	77	78	74	81	59	72	76	68	85	100	58	87	100	73	11	
248266	4512395	1112.5	-0.5	381.6	1411.5	0.2	418.3	S/MM 2	5.36	2.60	0.17	0.00	0.89	75	87	48	63	77	48		48	66	78	37	56	70	41	78	100	41	80	96	64	12	
261491	4526493	1106.2	-0.4	379.9	1412.7	0.2	419.1	TSS, USMP/EDO	1.87	1.75	0.07	0.00	0.00	61	81	32	71	81	61	62	76	48	68	16	63	65	60	73	100	24	85	100	69	12	
254753	4519162	1106.5	-0.2	380.5	1411.8	0.1	418.7	S'HAB TEAMS	1.27	1.24	0.04	0.00	0.00	74	88	51	77	87	66	75	66	65	74	45	66	71	60	78	100	45	76	96	55	11	
256495	4517477	1102.6	-0.4	377.3	1411.4	0.2	418.6	LMS/EDO	5.77	2.40	0.26	3.37	5.53	78	92	64	80	88	72	73	83	70	77	58	73	76	70	81	100	49	86	100	71	12	
261817	4524735	1106.1	-0.5	381.1	1412.4	0.2	419.2	ORFEUS-SPAS 2	0.91	0.36	0.03	0.00	0.35	72	88	46	68	79	57	59	79	62	75	34	59	63	55	74	100	30	74	100	48	11	
259967	4521509	1101.6	-0.2	378.0	1411.9	0.1	418.9	MSL 01, EDO	2.47	0.97	0.10	0.00	0.00	71	88	52	66	79	52	52	77	62	73	30	57	61	52	73	100	30	58	72	43	13	
249624	4509832	1109.0	0.0	379.7	1411.2	0.2	418.4	S/MM-6, S'HAB	2.98	1.23	0.14	0.00	1.61	73	91	55	73	82	63	79	64	66	79	46	67	70	63	74	100	40	74	91	56	12	
260279	4519333	1102.1	-0.3	378.2	1411.6	0.2	419.0	MSL 01, EDO	5.00	1.25	0.24	0.68	1.28	82	93	72	83	90	75	75	90	75	81	66	77	81	72	78	98	52	81	96	66	12	
261694	4521900	1104.1	-0.3	378.5	1412.1	0.2	419.1	USMP4, SPTN	3.50	1.50	0.16	0.00	0.00	69	88	48	69	75	63	64	72	59	75	39	58	64	52	76	100	40	78	99	57	11	
262270	4523683	1103.9	-0.3	378.0	1412.4	0.2	419.1	NEUROLAB	0.15	0.11	0.01	0.00	0.00	70	86	46	75	82	68	70	82	60	73	39	67	70	63	76	100	30	72	89	54	15	
259973	4514649	1109.0	-0.9	381.3	1412.1	0.1	419.2	S/MM-9, S'HAB	0.52	0.25	0.02	0.00	0.05	78	99	55	89	99	79	84	95	67	79	48	74	77	70	72	100	24	73	99	47	12	
265855	4520191	1110.3	-0.5	382.2	1412.9	0.2	419.6	S'HAB, HOST	2.74	0.52	0.07	0.00	0.00	80	91	61	73	84	61	61	82	71	84	46	60	68	52	76	100	42	70	97	42	12	
264026	4518489	1111.2	-1.1	383.3	1412.8	0.2	419.6	ISS 2A, NODE, PMA 1,2	5.01	2.37	0.11	0.00	0.12	73	88	54	72	82	61	72	70	64	75	46	65	70	59	74	98	37	78	90	66	10	
261812	4514231	1112.3	-0.7	381.3	1412.2	0.2	419.3	ISS 2A, 1, S'HAB	2.06	0.91	0.09	0.21	0.24	75	91	55	80	88	72	75	72	66	77	45	73	75	70	74	100	33	75	98	51	14	
270387	4524972	1120.6	0.0	380.8	1413.9	0.2	419.8	CHANDRA (AXAF)	6.90	3.06	0.15	0.00	0.00	80	93	68	83	91	75	91	75	73	82	61	74	77	70	75	100	22	63	81	45	11	
248159	4506419	1114.3	-0.1	381.3	1411.7	0.2	418.4	HST REPAIR 3A	5.13	1.72	0.14	0.00	2.39	66	81	43	61	70	52	68	61	59	70	34	56	59	52	79	100	36	83	98	68	11	
256739	4520450	1104.7	0.2	381.4	1412.1	0.3	418.9	SRTM	6.00	1.76	0.10	0.00	0.00	60	81	34	60	75	45	46	72	51	70	21	48	54	41	74	100	27	68	90	45	12	
262528	4519455	1110.8	-0.2	380.6	1412.6	0.2	419.3	ISS 2A.2a, S'HAB	2.23	0.71	0.04	0.00	0.05	72	90	43	73	82	63	73	63	60	73	30	64	66	61	70	100	29	67	81	53	13	
262053	4519178	1110.9	0.0	380.6	1412.6	0.2	419.3	ISS 2a.2B, S'HAB	6.88	5.58	0.25	0.01	3.81	81	93	66	82	88	75	77	82	73	79	64	77	79	75	77	98	50	84	97	71	12	
265268	4522246	1108.2	-0.5	381.9	1412.7	0.2	419.5	ISS 6A, MPLM, SSRMS	1.92	1.71	0.07	0.00	0.00	68	88	45	59	72	45	45	70	59	73	37	46	54	37	71	97	27	54	78	30	13	
262952	4520159	1110.9	0.1	381.8	1412.8	0.3	419.4	ISS 7A, AIRLOCK	2.52	0.60	0.11	0.65	1.38	78	88	66	81	88	73	81	75	72	77	63	75	77	72	77	97	52	76	92	59	13	
262477	4518170	1113.0	-0.6	382.3	1412.8	0.2	419.4	ISS 7A.1, MPLM	5.06	1.40	0.13	0.00	0.00	79	90	70	81	90	72	72	84	73	79	66	75	77	72	78	95	52	76	93	58	13	
260665	4515646	1113.8	-0.8	381.0	1412.6	0.2	419.2	HST SM-03B	4.21	2.04	0.13	0.00	0.00	64	86	37	56	66	45	46	55	55	72	19	44	54	34	75	99	21	58	72	44	12	
264763	4520964	1110.2	-0.8	381.8	1413.0	0.2	419.5	ISS 8A, ITS, SO, MT	1.19	1.08	0.04	0.00	0.03	70	88	54	70	75	64	66	75	61	73	45	55	57	52	73	100	32	61	69	52	12	
264047	4518077	1112.2	-0.5	383.0	1412.9	0.2	419.5	ISS-UF2	1.85	0.63	0.05	0.00	0.00	77	93	61	78	84	72	72	82	66	75	54	71	73	68	77	100	24	80	86	74	12	
265812	4521314	1109.8	-0.2	383.0	1412.8	0.3	419.7	ISS-9A	0.55	0.31	0.02	0.05	0.05	79	90	66	77	84	70	72	82	72	77	66	73	75	70	78	96	48	82	95	69	11	
265081	4526034	1104.7	-0.5	378.5	1412.6	0.2	419.3	FREESTAR	12.78	5.88	0.33	0.00	0.07	57	79	34	58	70	45	46	64	50	70	27	49	59	39	75	100	31	77	99	55	12	

| | | |

| | | |

| | | |

| | | |

MISSION DATA

	STS		OV		ET		LAUNCH& LAND					TIMES				TILE Damage				IMAGERY			FOAM LOSS												RAINFALL			
#	STS	STS aka	OV	OV flt #	ET	ET wt.	Date	Pad	MLP	Day or Night	Landing Location	ET Age @ Launch (days)	ET Exposure (days)	Tanking Time (hrs)	Mission Time (hrs)	LS >1	LS Tot	OV>1	OV Tot	Camera	-Y bipod visible?	+Y bipod visible	FOAM LOSS NOTED?	Bipod	NEAR Bipod?	Flange	Intertank	Thrust Panel	Other	Cause	Corrective Action	SRB Mate/Demate	Orbiter Mate/Demate	Rollout/Rollback	TOTAL on Pad	1-Day MAX	AVG Daily	Launch Day
7	7		99	2	6	H	06/18/83	A	1	D	E	327	24	3.00	146	41	153	48	253	35	Y	Y	Y	-Y		Y	Y	N	Y			03/02/83	05/24/83	05/26/83	6.97	1.78	0.29	0.00
33	32R		102	9	32	L	01/09/90	A	3	D	E	1609	43	3.00	261	13	111	15	120	16,35	Y	Y	Y	-Y	Y	Y	Y	N	Y	Y	Y	11/01/89	11/21/89	11/28/89	5.29	1.38	0.12	0.00
48	50		102	12	50	L	06/25/92	A	3	D	K	1333	23	3.00	332	28	141	45	184	16,35,H	Y	Y	Y	-Y		Y	N	N	Y	Y	Y	04/09/92	05/29/92	06/03/92	6.14	2.65	0.27	0.02
51	52		102	13	55	L	10/22/92	B	3	D	K	994	27	2.50	237	6	152	16	290	16,35,H	Y	Y	Y	-Y		Y	Y	N	Y			09/09/92	09/20/92	09/26/92	6.35	2.95	0.24	0.00
61	62		102	16	62	L	03/04/94	B	1	D	K	773	23	3.00	335	7	36	16	97	16,35,H	Y	Y	Y	-Y	Y	Y	Y	N	Y			01/20/94	02/03/94	02/10/94	9.70	6.35	0.40	0.00
111	112		104	26	115	S	10/07/02	B	3	D	K	376	28	3.00	250	22	81	25	106	16,35	Y	Y	Y	-Y	Y	Y	N	Y	Y	Y			06/25/02	09/04/02	09/10/02	0.55	0.31	0.02	0.05
113	107		102	28	93	L	01/16/03	A	1	D		805	39	3.00	382					H	N	N	Y	-Y		?	?	?	?			11/04/02	11/20/02	12/09/02	12.78	5.88	0.33	0.00
						Average of all ETs						688	38	3	217	23	101	31	143													Average of all ETs			5.45	1.92	0.14	0.11
						Std Dev of all ETs						543	22	0	84	34	83	40	91													Std Dev of all ETs			4.57	1.39	0.09	0.39
						+/- 95% C.I. for all ETs						100	4	0	16	6	15	7	17													+/- 95% C.I. for all ETs			0.84	0.26	0.02	0.07
						Average of all ETs w/Bipod Foam Loss						888	30	3	278	20	112	28	175													Average of all ETs w/Bipod Foam Loss			6.83	3.04	0.24	0.01
						Std Dev of all ETs w/Bipod Foam Loss						470	8	0	79	14	47	15	82													Std Dev of all ETs w/Bipod Foam Loss			3.79	2.27	0.13	0.02
						+/- 95% C.I. for all ETs w/Bipod Foam Loss						348	6	0	58	10	35	11	60													+/- 95% C.I. for all ETs w/Bipod Foam Loss			2.81	1.68	0.10	0.01

WEATHER DATA

	TEMPERATURE (F)								DEWPOINT (F)						RELATIVE HUMDITY (%rh)						WIND SPEED (kts)			WIND DIR.		PRESSURE (mb)						ET PRODUCTION							
TOTAL 5 Day Pre-Launch	AVG on Pad	MAX on Pad	MIN on Pad	AVG Launch Day	MAX Launch Day	MIN Launch Day	At Tanking Start	At Launch	AVG on Pad	MAX on Pad	MIN on Pad	AVG Launch Day	MAX Launch Day	MIN Launch Day	AVG on Pad	MAX on Pad	MIN on Pad	AVG Launch Day	MAX Launch Day	MIN Launch Day	AVG on Pad	MAX on Pad	MAX Launch Day	AVG on Pad	Launch Day	AVG on Pad	MAX on Pad	MIN on Pad	AVG Launch Day	MAX Launch Day	MIN Launch Day	Start Date	Completion Date	ET DD-250	Ship Date	Days in Storage Before Shipment	Substrate Temp (°F)	Cell Temp (°F)
0.00	77	89	63	76	83	69	73	71	70	77	47	69	71	66	79	100	26	77	90	90	12	22	12	128	40	###	1018	1006	1015	1016	1014			07/26/82				
0.00	60	84	24	61	69	52	65	54	51	72	16	55	58	51					96	96	11	19	7	257	300	###	1028	1007	1020	1023	1019			08/14/85				
2.19	80	93	68	80	87	72	72	85	72	78	67	74	77	70							14	25	19	177	160	###	1020	1008	1013	1013	1009			10/31/88				
0.00	75	88	59	74	78	69	71	77	66	78	51	58	62	54							12	19	13	123	60	###	1029	1008	1027	1016	1013			02/01/90				
0.88	68	83	45	58	70	45	49	54	60	72	30	37	43	30	72	100	21	49	76	21	14	24	14	158	270	###	1027	1003	1015	1025	1022	####	01/16/92	01/21/92	10/01/93	624		
0.05	79	90	66	77	84	70	72	82	72	77	66	73	75	70	78	96	48	82	95	69	11	20	10	105	10	###	1021	1009	1016	1018	1015	####	09/24/01	09/26/01	12/14/01	81	74	74
0.07	57	79	34	58	70	45	46	64	50	70	27	49	59	39	75	100	31	77	99	55	12	19	9	271	140	###	1029	1007	1023	1026	1021	####	11/01/00	11/02/00	12/14/00	43	73	73
0.73	72	89	51	71	80	63	68	71	64	75	42	62	67	57	76	99	35	73	91	69	12	23	12	169	156	###	1026	1008	1019	1020	1016			**Avg. ET-61 thru 115**		179	73	73
1.10	8	5	15	10	8	11	11	12	8	4	19	12	10	13	4	2	11	10	10	21	3	11	5	42	100	2	4	4	4	4	4			**Std Dev ET-61 thru 115**		168	2	2
0.20	1	1	3	2	2	2	2	2	2	1	3	2	2	2	1	0	2	2	2	4	0	2	1	8	18	0	1	1	1	1	1			**+/- 95% C.I. ET-61 thru 115**		45	0	0
0.46	71	87	51	69	77	60	64	70	63	75	43	59	64	54	76	99	32	71	91	66	12	21	12	174	140	###	1025	1007	1018	1020	1016			**Avg. ET-61 thru 115**		249	74	74
0.83	9	5	17	10	8	12	12	13	10	3	20	14	12	16	3	2	12	15	9	30	1	3	4	66	113	3	5	2	5	5	5			**Std Dev ET-61 thru 115**		325	1	1
0.61	7	4	13	7	6	9	9	9	7	3	15	10	9	12	2	1	9	11	7	22	1	2	3	49	83	2	4	1	4	4	3			**+/- 95% C.I. ET-61 thru 115**		368	1	1

NO PRODUCTIO

-Y Bipod Ramp (Hand Spray)						-Y Bipod Spindle Face (Hand Spray)								-Y Bipod Beneath S.F. (Hand Spray)					
Cell Humidity (%rh)	Complete Date	Complete Day	Complete Time	Personnel	Personnel	Substrate Temp (°F)	Cell Temp (°F)	Cell Humidity (%rh)	Complete Date	Complete Day	Complete Time	Personnel	Personnel	Substrate Temp (°F)	Cell Temp (°F)	Cell Humidity (%rh)	Complete Date	Complete Day	Complete Time
) PRODUCTION DATA AVAILABLE FOR ET-1 THROUGH ET-60																			**NO PR(**
	09/17/91	Tue	2300	AP		75	75	50	09/03/91	Tue	2330	AR		75	75	58	09/07/91	Sat	130
58	07/13/01	Fri	2200	AB		76	76	55	06/15/01	Fri	430	H	C	76	76	55	06/21/01	Thu	530
58	09/01/00	Fri	1045	BN	BR	73	73	58	08/21/00	Mon	1510	BN		72	72	60	08/25/00	Fri	1015
54						72	74	54						74	74	53			
4						10	2	5						2	2	7			
1						3	0	1						1	1	2			
58						75	75	54						74	74	58			
0						2	2	4						2	2	3			
#NUM!						2	2	5						2	2	3			

PRODUCTION & FOAM APPLICATION DATA FOR EXTERNAL

		+Y Bipod Ramp (Hand Spray)								+Y Bipod Spindle Face (Hand Spray)									
Personnel	Personnel	Substrate Temp (°F)	Cell Temp (°F)	Cell Humidity (%rh)	Complete Date	Complete Day	Complete Time	Personnel	Personnel	Substrate Temp (°F)	Cell Temp (°F)	Cell Humidity (%rh)	Complete Date	Complete Day	Complete Time	Personnel	Personnel	Substrate Temp (°F)	Cell Temp (°F)
ODUCTION DATA AVAILABLE FOR ET-1 THROUGH ET-60																	**NO PRODUCT**		
AP					09/25/91	Wed	2150	AP		78	78	52	08/29/91	Thu	2300	AR		75	75
H	E	74	74	53	07/26/01	Thu	945	BR		76	76	55	06/15/01	Fri	430	H	C	76	76
BN		74	74	58	09/14/00	Thu	1310	BR	BN	73	73	58	08/21/00	Mon	1510	BR		72	72
		74	74	52						74	74	54						74	74
		2	2	7						2	2	6						2	2
		0	1	2						1	1	2						0	0
		74	74	56						76	76	55						74	74
		0	0	4						3	3	3						2	2
		#NUM!	#NUM!	4						3	3	3						2	2

TANK — PRODUCTION & FOAM APPLICATION DATA FOR EXTERNAL TANK

+Y Bipod Beneath S.F. (Hand Spray)						Aft Half of LH/IT Flange Closeout (Hand Spray)										Fwd Half of LH/IT			
Cell Humidity (%rh)	Complete Date	Complete Day	Complete Time	Personnel	Personnel	Substrate Temp (°F)	Cell Temp (°F)	Cell Humidity (%rh)	Complete Date	Complete Day	Complete Time	Personnel	Personnel	Personnel	Personnel	Substrate Temp (°F)	Cell Temp (°F)	Cell Humidity (%rh)	Complete Date
ION DATA AVAILABLE FOR ET-1 THROUGH ET-60																**NO PRODUCTION DATA AVA**			
50	09/03/91	Tue	2310	AP					01/04/91	Fri	1300	BB							01/15/91
55	06/21/01	Thu	525	H	E	75	75	48	05/15/01	Tue	1400	DA				74	76	46	05/19/01
60	08/25/00	Fri	1015	BR		74	74	54	06/15/00	Thu	1150	BX				76	76	54	06/25/00
53						75	75	48								76	76	48	
7						2	3	8								4	4	8	
2						1	1	2								1	1	2	
55						75	75	51								75	76	50	
5						1	1	4								1	0	6	
6						1	1	5								2	#NUM!	6	

PRODUCTION & FOAM APPLICATION DATA FOR EXTERNAL TANK

Flange Closeout (Hand Spray) | Intertank Acreage (Machine Spray)

Complete Day	Complete Time	Personnel	Personnel	Personnel	Substrate Temp at Upper Flange -1 (°F)	Substrate Temp at Upper Flange -2 (°F)	Substrate Temp at Upper Flange -3 (°F)	Substrate Temp at Upper Flange -4 (°F)	Substrate Temp at Lower Flange -1 (°F)	Substrate Temp at Lower Flange -2 (°F)	Substrate Temp at Lower Flange -3 (°F)	Substrate Temp at Lower Flange -4 (°F)	Cell Temp (°F)	Cell Humidity (%rh)	Complete Date	Complete Day	Complete Time	Personnel	Personnel
ILABLE FOR ET-1 THROUGH ET-60																	**NO PRODUCTION DATA AVAILAE**		
Tue	1200	AH			126							128	100	14	06/04/90	Mon	1418	DG	
Sat	845	DA			127	127	128	130	126	126	126	127	101	20	06/29/00	Thu	319		GM
Sun	1440	BX			130				129				105	19	08/16/99	Mon	2001	CT	GJ
					128	127	128	138	128	126	126	129	103	17					
					3	#DIV/0!	#DIV/0!	11	4	#DIV/0!	#DIV/0!	2	13	4					
					1	#DIV/0!	#DIV/0!	3	1	#DIV/0!	#DIV/0!	0	4	1					
					128	127	128	130	128	126	126	128	102	18					
					2	#DIV/0!	#DIV/0!	#DIV/0!	2	#DIV/0!	#DIV/0!	1	3	3					
					2	#DIV/0!	#DIV/0!	#DIV/0!	2	#DIV/0!	#DIV/0!	1	3	4					

				LO2 Tank Acreage (Machine Spray)															
Personnel	Personnel	Personnel	Personnel	St380 Substrate Temp (°F)	St600 Substrate Temp (°F)	St840 Substrate Temp (°F)	Cell Temp (°F)	Cell Humidity (%rh)	Complete Date	Complete Day	Complete Time	Personnel	Personnel	Personnel	Personnel	Personnel	St2058 Substrate Temp (°F)	St1129 Substrate Temp (°F)	Cell Temp (°F)
BLE FOR ET-1 THROUGH ET-60																**NO PRODUCTION DATA AVAILABLE FO**			
				144	127	129	104	8	09/26/90	Wed	1552	BM					126	154	100
IM	GE	EI		156	130	135	101	15	12/22/00	Fri	1457		IF	FW	EI		129	156	89
DD	GA	EY		150	125	127	92	26	03/04/00	Sat	729	DN	IF	IM	EZ	EI	127	141	98.5
				147	127	129	102	17									127	140	102
				8	3	4	5	9									6	10	14
				2	1	1	1	2									1	3	4
				150	127	130	99	16									127	150	96
				6	3	4	6	9									2	8	6
				7	3	5	7	10									2	9	7

LH2 Barrel Acreage (Machine Spray)

Cell Humidity (%rh)	Complete Date	Complete Day	Complete Time	Personnel	Personnel	Personnel	Personnel	Personnel	PAYLOAD (S=secret)	PRCB # (PCBD ...) & Date
R ET-1 THROUGH ET-60									MULT P/L	
									LDEF	S044812A, 2/6/90
									USML-1 EDO	S044876C, 8/6/92
									LAGEOS-2	
15	09/26/90	Wed	1408	CO					USMP 2/EDO	
22	04/20/01	Fri	1538		FR	DD	HY	EI	ISS-9A	S06215, 12/19/02
17	04/26/00	Wed	1851	CW	DZ	DD	HY	EI	FREESTAR	
19										
4										
1										
18										
4										
4										

MISSION DATA

	STS		OV		ET		IMAGERY			FOAM LOSS									
#	STS	STS aka	OV	OV flt #	ET	ET wt.	Camera	-Y bipod visible?	+Y bipod visible	FOAM LOSS NOTED?	Bipod	NEAR Bipod?	Flange	Intertank	Thrust Panel	Other	Cause	Corrective Action
6	6		99	1	8	L	35	Y	Y	Y	N		Y	N	N	Y		
7	7		99	2	6	H	35	Y	Y	Y	-Y		Y	Y	N	Y		
8	8		99	3	9	L		N	N	?	?		?	?	?	?		
10	11	41B	99	4	10	L	35	Y	Y	Y	N	Y	Y	Y	N	Y		
11	13	41C	99	5	12	L		N	N	?	?		?	?	?	?		
13	17	41G	99	6	15	L	35	Y	Y	Y	N		N	Y	N	Y		
17	24	51B	99	7	17	L	35	Y	N	Y	?		N	Y	N	Y		
19	26	51F	99	8	19	L	35	Y	Y	Y	N		Y	Y	N	Y		
22	30	61A	99	9	24	L	35	Y	Y	Y	N	Y	Y	N	N	Y		
25	33	51L	99	10	26	L		N	N	?	?		?	?	?	?		
1	1		102	1	1	H	16	Y	Y	Y	N		N	N	N	Y		
2	2		102	2	2	H	Y	Y	Y	N	N		N	N	N	N		
3	3		102	3	3	H	Y	Y	Y	Y	N		Y	Y	N	Y		
4	4		102	4	4	H	Y	Y	Y	Y	N		Y	Y	N	Y		
5	5		102	5	5	H	Y	Y	Y	Y	N	Y	Y	Y	N	Y		
9	9		102	6	11	L		N	N	?	?		?	?	?	?		
24	32	61C	102	7	30	L	16	Y	Y	Y	N		N	Y	N	Y		
30	28R		102	8	31	L	16,35,H	Y	Y	Y	N	Y	Y	Y	N	Y		Y
33	32R		102	9	32	L	16,35	Y	Y	Y	-Y	Y	Y	Y	N	Y	Y	Y
38	35		102	10	35	L	H	Y	Y	Y	N		Y	N	N	Y	Y	Y
41	40		102	11	41	L	H,16?	Y	Y	Y	N		Y	N	N	N		
48	50		102	12	50	L	16,35,H	Y	Y	Y	-Y		Y	N	N	Y	Y	Y
51	52		102	13	55	L	16,35,H	Y	Y	Y	-Y		Y	Y	N	Y		
55	55		102	14	56	L	H,16?	Y	Y	Y	N	Y	Y	N	N	Y		
58	58		102	15	57	L	16,35,H	Y	Y	Y	N	Y	Y	Y	N	Y	N	
61	62		102	16	62	L	16,35,H	Y	Y	Y	-Y	Y	Y	Y	N	Y		
63	65		102	17	64	L	16,35,H	Y	Y	Y	N	Y	Y	Y	N	Y		
72	73		102	18	73	L	16,35,H	Y	Y	Y	N		N	N	N	Y		
75	75		102	19	76	L	H,16,35	Y	Y	Y	N		Y	N	N	Y		
78	78		102	20	79	L	16,35,H	Y	Y	Y	N	Y	Y	N	N	N		
80	80		102	21	80	L	16,35,H	Y	Y	Y	N	Y	Y	Y	N	Y		
83	83		102	22	84	L	16,H	Y	Y	Y	N	Y	Y	N	N	Y		
85	94		102	23	86	L	16,35,H	Y	Y	Y	N	Y	Y	Y	N	Y		
88	87		102	24	89	L	16,35,H	Y	Y	Y	N		Y	N	Y	N	Y	Y
90	90		102	25	91	L	16,35,H	Y	Y	Y	N		Y	N	Y	N		
95	93		102	26	99	S		N	N	Y	?		?	?	Y	?		
108	109		102	27	112	S	16,35,H	Y	Y	Y	N	Y	Y	Y?	N	N		
113	107		102	28	93	L	H	N	N	Y	-Y		?	?	?	?		
12	14	41D	103	1	13	L		N	N	?	?		?	?	?	?		
14	19	51A	103	2	16	L		N	N	?	?		?	?	?	?		
15	20	51C	103	3	14	L		N	N	?	?		?	?	?	?		
16	23	51D	103	4	18	L		N	N	?	?		?	?	?	?		
18	25	51G	103	5	20	L		N	N	?	?		?	?	?	?		
20	27	51I	103	6	21	L		N	N	?	?		?	?	?	?		
26	26R		103	7	28	L	H	Y	Y	N	N		N	N	N	N		
28	29R		103	8	36	L	H	Y	Y	Y	N	Y	Y	N	Y	Y		
32	33R		103	9	38	L		N	N	?	?		?	?	?	?		
35	31R		103	10	34	L		N	N	?	?		?	?	?	?		
36	41		103	11	39	L	H	N	N	?	?		N	N	N	N		
40	39		103	12	46	L	H	N	N	?	?		N	N	N	N		
43	48		103	13	42	L		N	N	?	?		?	?	?	?		
45	42		103	14	52	L	H	Y	N	Y	?	Y	N	Y	N	N	N	N
52	53		103	15	49	L	H	Y	Y	Y	N	Y	Y	N	N	N		
54	56		103	16	54	L	H	Y	Y	Y	N		N	Y	N	N	N	Y
57	51		103	17	59	L	H	Y	Y	Y	N	Y	Y	N	N	Y		
60	60		103	18	61	L	H	Y	Y	N	N		N	N	N	N		
64	64		103	19	66	L		N	N	?	?		?	?	?	?		
67	63		103	20	68	L		N	N	?	?		?	?	?	?		
70	70		103	21	71	L	H	Y	Y	N	N		N	N	N	N		
82	82		103	22	81	L	H	Y	Y	N	N		N	N	N	N		
86	85		103	23	87	L	H	Y	N	?	?		N	N	N	N		
91	91		103	24	96	S	16,35,H	Y	Y	Y	N	Y	Y	Y	Y	N		
92	95		103	25	98	S	16,35,H	Y	Y	Y	N	Y	Y	Y	Y	Y		
94	96		103	26	100	S	H	Y	Y	Y	N		Y	Y	Y	N		
96	103		103	27	101	S		N	N	Y	?		?	?	Y	?	Y	N
100	92		103	28	104	S		N	N	?	?		?	?	?	?		
103	102		103	29	107	S	35,H	N	N	?	?		N	N	N	N		
106	105		103	30	110	S	16,35,H	Y	Y	Y	N	Y	Y	N	N	Y		
21	28	51J	104	1	25	L		N	N	?	?		?	?	?	?		
23	31	61B	104	2	22	L		N	N	?	?		?	?	?	?		
27	27R		104	3	23	L		N	N	?	?		?	?	?	?		
29	30R		104	4	29	L		N	N	?	?		?	?	?	?		
31	34		104	5	27	L		Y	N	?	?		?	?	?	?		
34	36		104	6	33	L		N	N	?	?		?	?	?	?		
37	38		104	7	40	L		N	N	?	?		?	?	?	?		
39	37		104	8	37	L	H	N	N	Y	?		Y	N	N	N		
42	43		104	9	47	L	H	Y	N	?	?		?	?	?	?	Y	
44	44		104	10	53	L		N	N	?	?		?	?	?	?		
46	45		104	11	44	L	H	Y	N	Y	?	Y	Y	N	N	N		
49	46		104	12	48	L	H	Y	Y	N	N		N	N	N	N		
66	66		104	13	67	L	16,35,H	Y	Y	Y	N	Y	Y	Y	N	Y		
69	71		104	14	70	L	16	Y	Y	Y	N	Y	Y	Y	N	Y		
73	74		104	15	74	L	16,35	Y	Y	Y	N		Y	N	N	N		
76	76		104	16	77	L		N	N	?	?		?	?	?	?		
79	79		104	17	82	L	H	Y	Y	N	N		N	N	N	N		
81	81		104	18	83	L	H	N	N	?	?		Y	N	N	N		
84	84		104	19	85	L	H	Y	Y	Y	N	Y	Y	Y	N	N		
87	86		104	20	88	L		N	N	?	?		?	?	?	?		
98	101		104	21	102	S	16,35,H	Y	Y	Y	N	Y	Y	N	Y	Y		
99	106		104	22	103	S	16,35,H	Y	Y	Y	N	Y	Y	Y	N	Y		
102	98		104	23	106	S		N	N	?	?		?	?	?	?		
105	104		104	24	109	S	H, 16?	Y	Y	Y	N	Y	Y	N	N	N		
109	110		104	25	114	S	16,35,H	Y	Y	Y	N	Y	Y	N	N	N		
111	112		104	26	115	S	16,35	Y	Y	Y	-Y	Y	Y	N	Y	Y	Y	
47	49		105	1	43	L		N	N	?	?		?	?	?	?		
50	47		105	2	45	L	16,35,H	Y	Y	Y	N	Y	Y	Y	N	Y	Y	N
53	54		105	3	51	L	16,35,H	Y	Y	Y	N	Y	Y	Y	N	Y		
56	57		105	4	58	L	16,35,H	Y	Y	Y	N	Y	Y	Y	Y	Y		
59	61		105	5	60	L	H	N	N	?	?		?	?	?	?		
62	59		105	6	63	L	16,35,H	Y	Y	Y	N	Y	Y	Y	N	Y		
65	68		105	7	65	L	16,35,H	Y	Y	Y	N	Y	Y	Y	N	Y		
68	67		105	8	69	L	H	Y	Y	N	N		N	N	N	N		
71	69		105	9	72	L	16	Y	Y	Y	N		N	N	N	Y		
74	72		105	10	75	L	H,16	N	N	?	?		N	N	N	N		
77	77		105	11	78	L	16,35,H	Y	Y	Y	N	Y	Y	Y	N	Y		
89	89		105	12	90	L		N	N	?	?		?	?	?	?		
93	88		105	13	97	S	H	Y	Y	Y	N		Y	N	Y	Y		
97	99		105	14	92	L	16,35,H	Y	Y	Y	N	Y	Y	Y	N	Y		
101	97		105	15	105	S		N	N	?	?		?	?	?	?		
104	100		105	16	108	S	16,35,H	Y	Y	Y	N	Y	Y	N	N	Y		
107	108		105	17	111	S		N	N	?	?		?	?	?	?		
110	111		105	18	113	S	16,35,H	Y	Y	Y	N	Y	Y	Y	N	N		
112	113		105	19	116	S		N	N	?	?		?	?	?	?		
							79	72	66	65	7	39	55	34	12	45		
										Y	Y		Y	Y	Y	Y	=	Y
										8	60		21	41	66	31		
										N	N		N	N	N	N	=	N
										40	46		37	37	35	37		
										?	?		?	?	?	?	=	?

ET & Foam Data Trend

ET & Foam Data Trending.xls

Camera							
-Y bipod visible?							
+Y bipod visible							
FOAM LOSS NOTED?							
Bipod							
NEAR Bipod?							
Flange							
Intertank							
Thrust Panel							
Other							

-Y Bipod Foam Loss by Orbiter

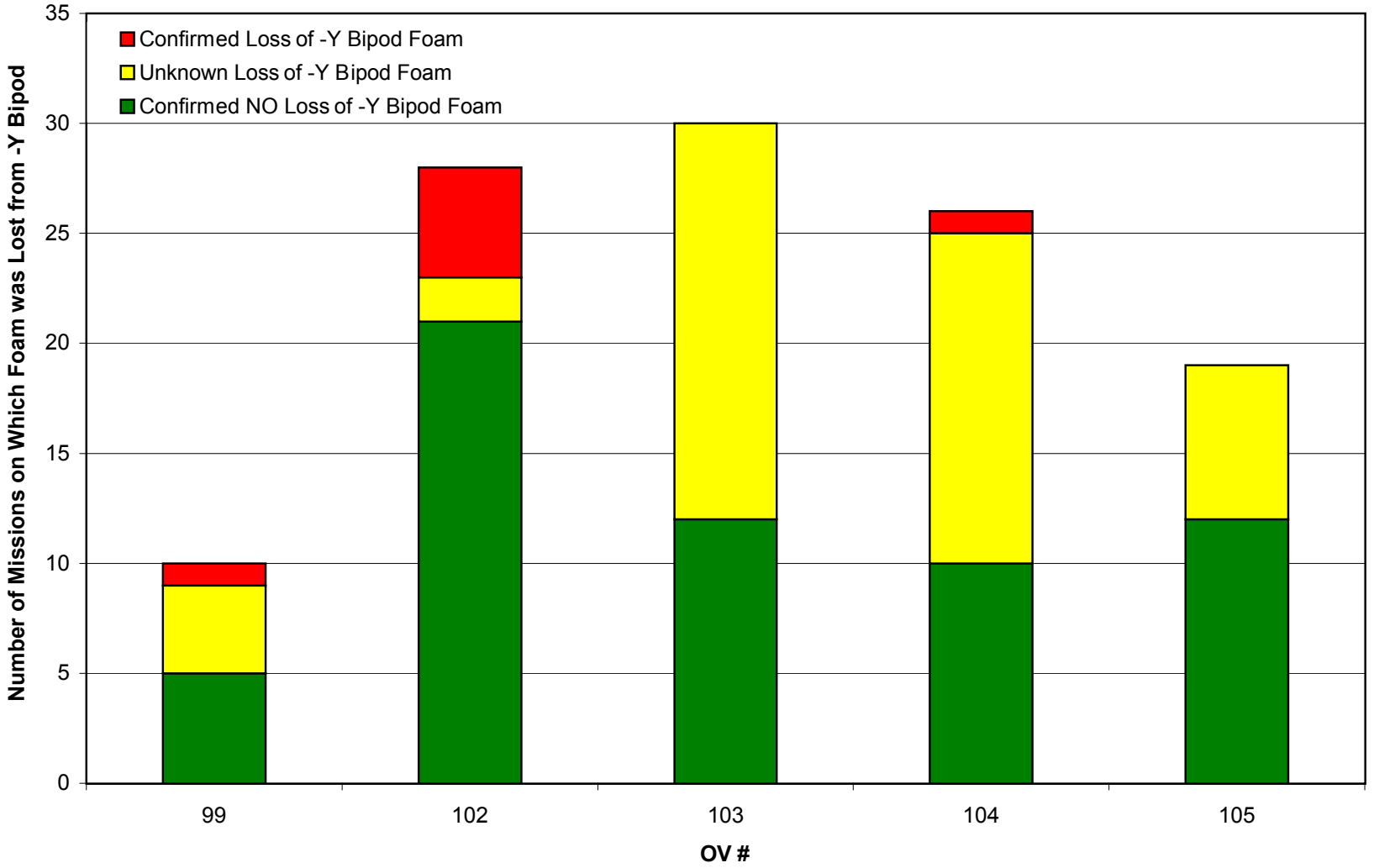

ET & Foam Data Trend

ET & Foam Data Trending.xls

CAB099-0023

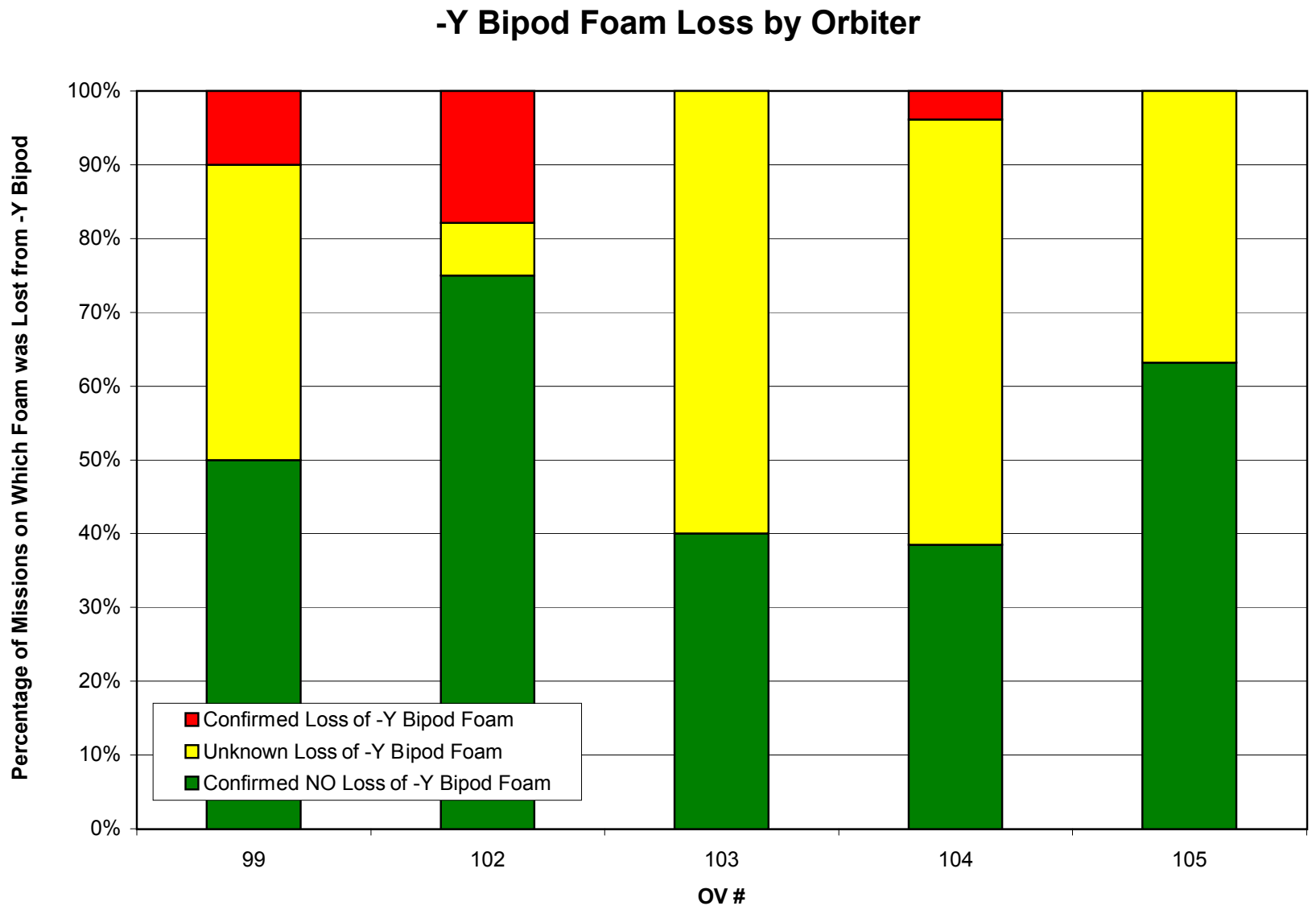
-Y Bipod Foam Loss by Orbiter
Percentage of Missions on Which Foam was Lost from -Y Bipod
100%
90%
80%
70%
60%
50%
40%
30%
20%
10%
0%
Confirmed Loss of -Y Bipod Foam
Unknown Loss of -Y Bipod Foam
Confirmed NO Loss of -Y Bipod Foam
99
102
103
104
105
OV #

Total (Upper & Lower Surface) Tile Hits

From Post-Mission Examinations of Orbiter

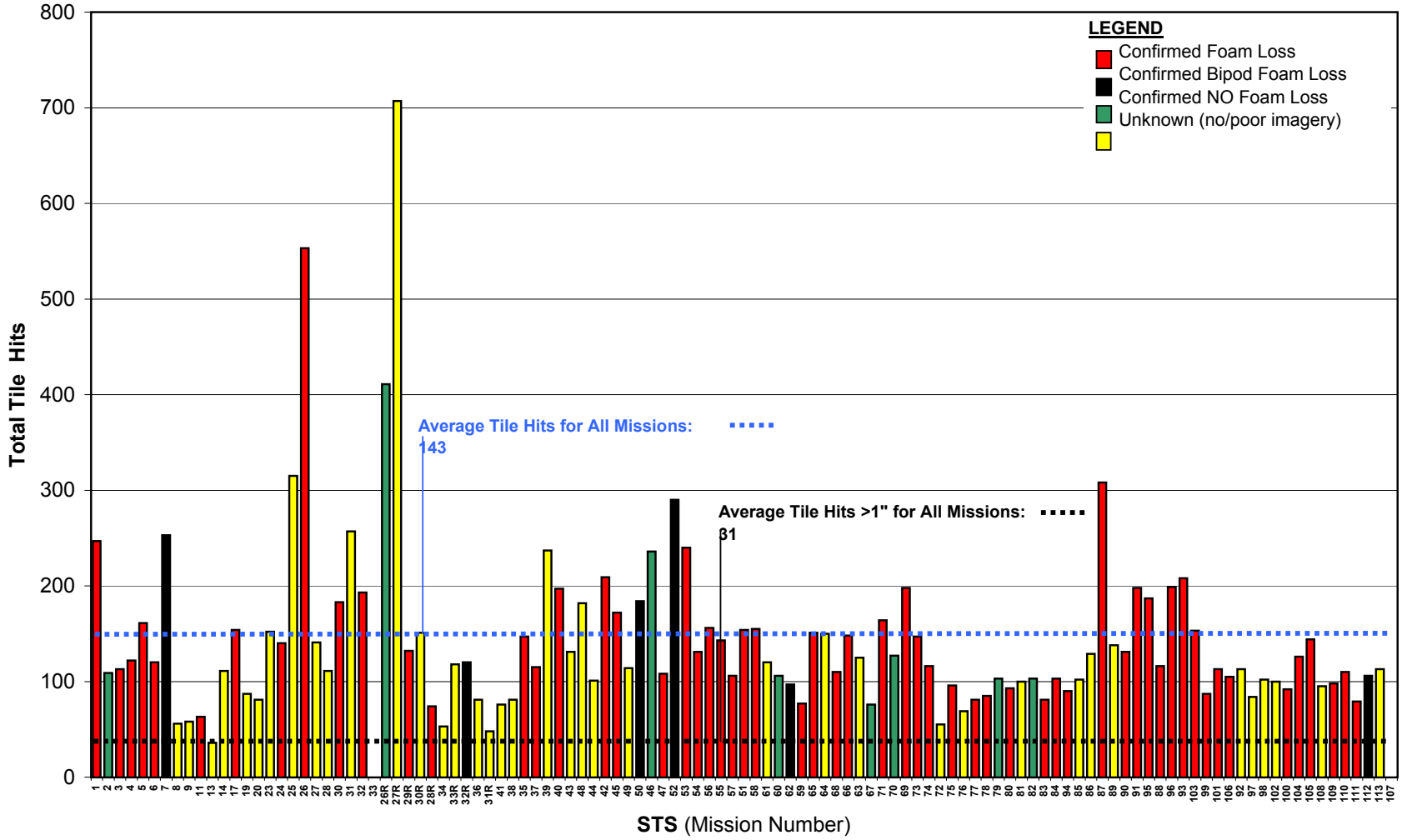

ET & Foam Data Trend

ET & Foam Data Trending.xls

CAB099-0025

Lower Surface Tile Hits

From Post-Mission Examinations of Orbiter

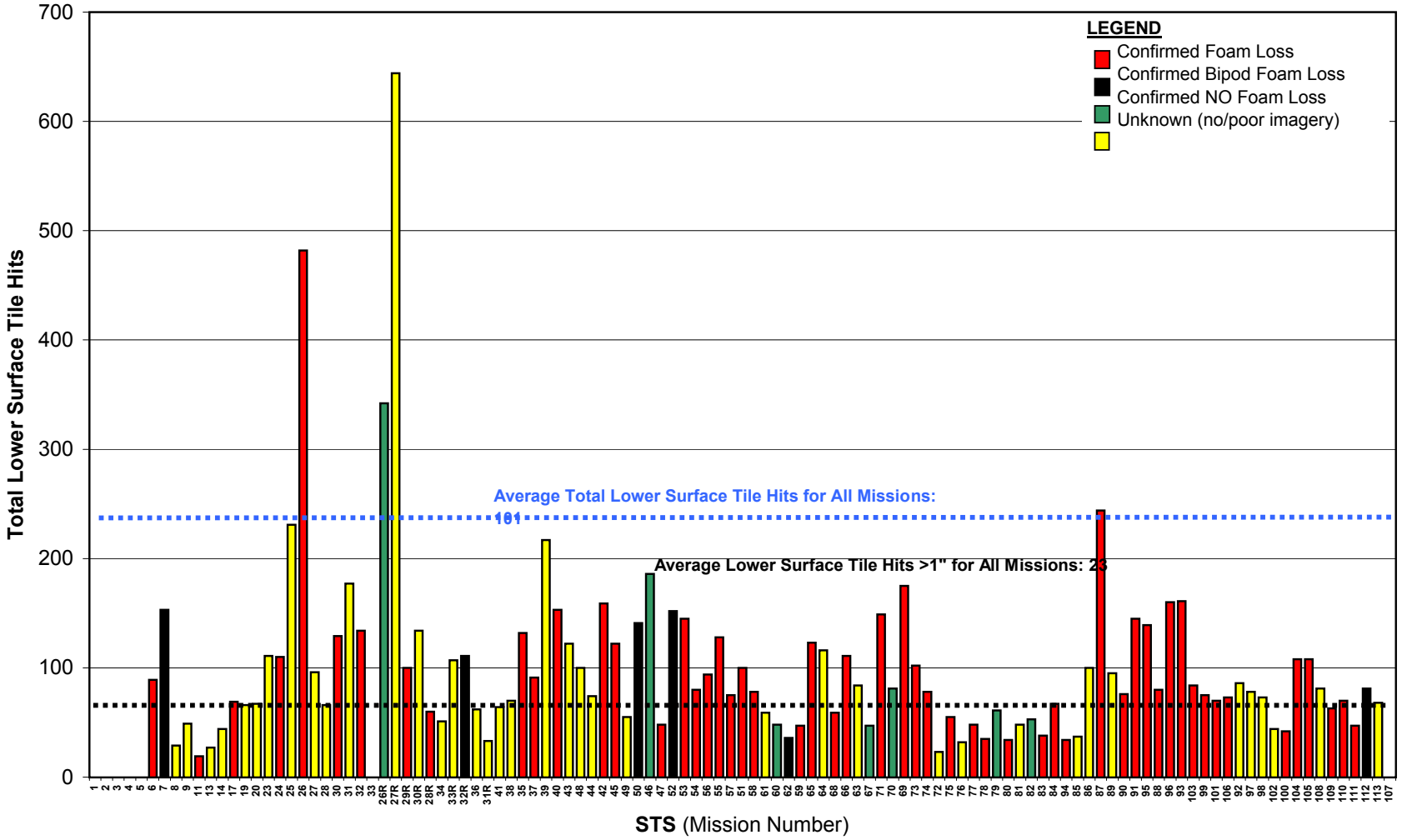

External Tank Age

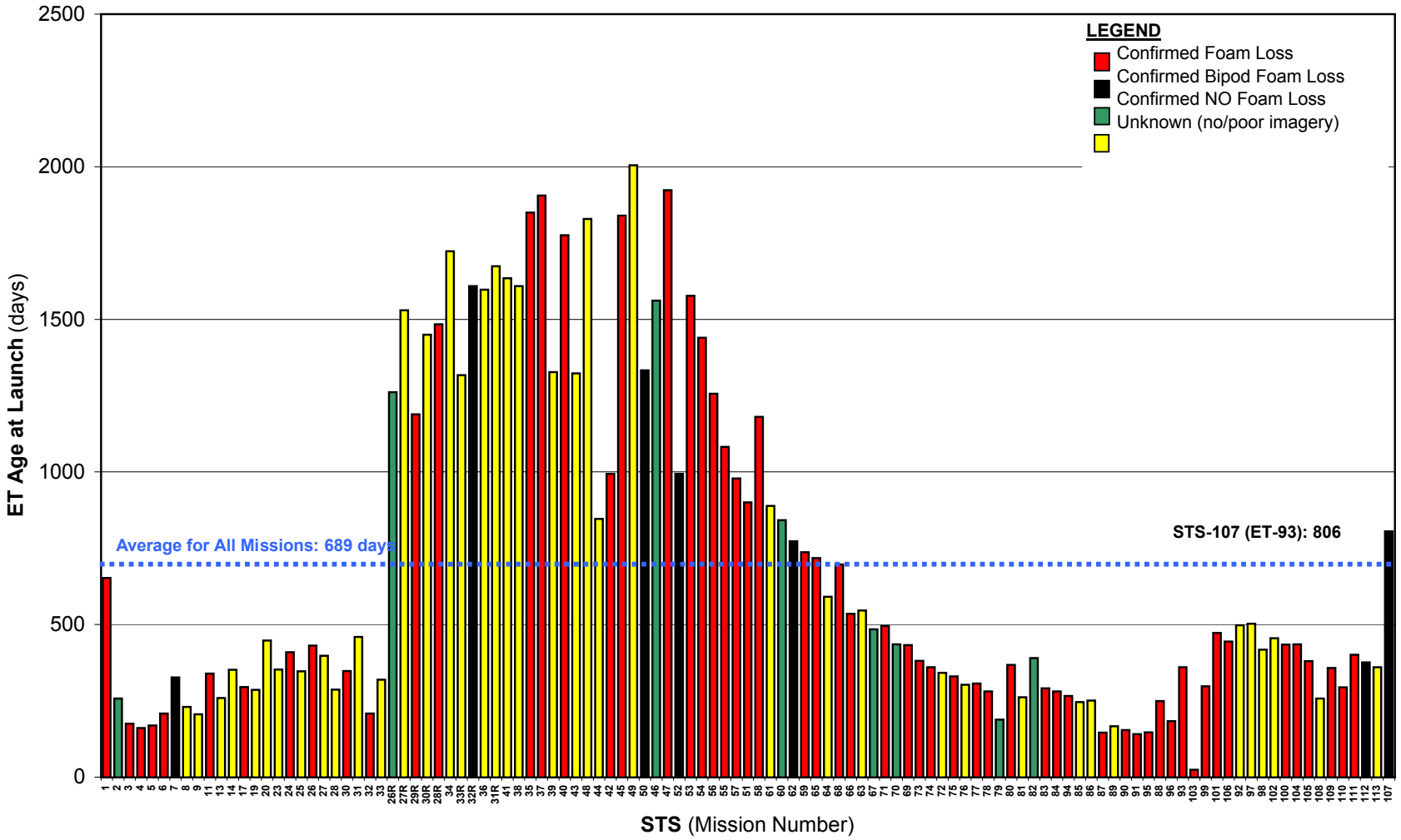

ET & Foam Data Trend

ET & Foam Data Trending.xls

External Tank Age

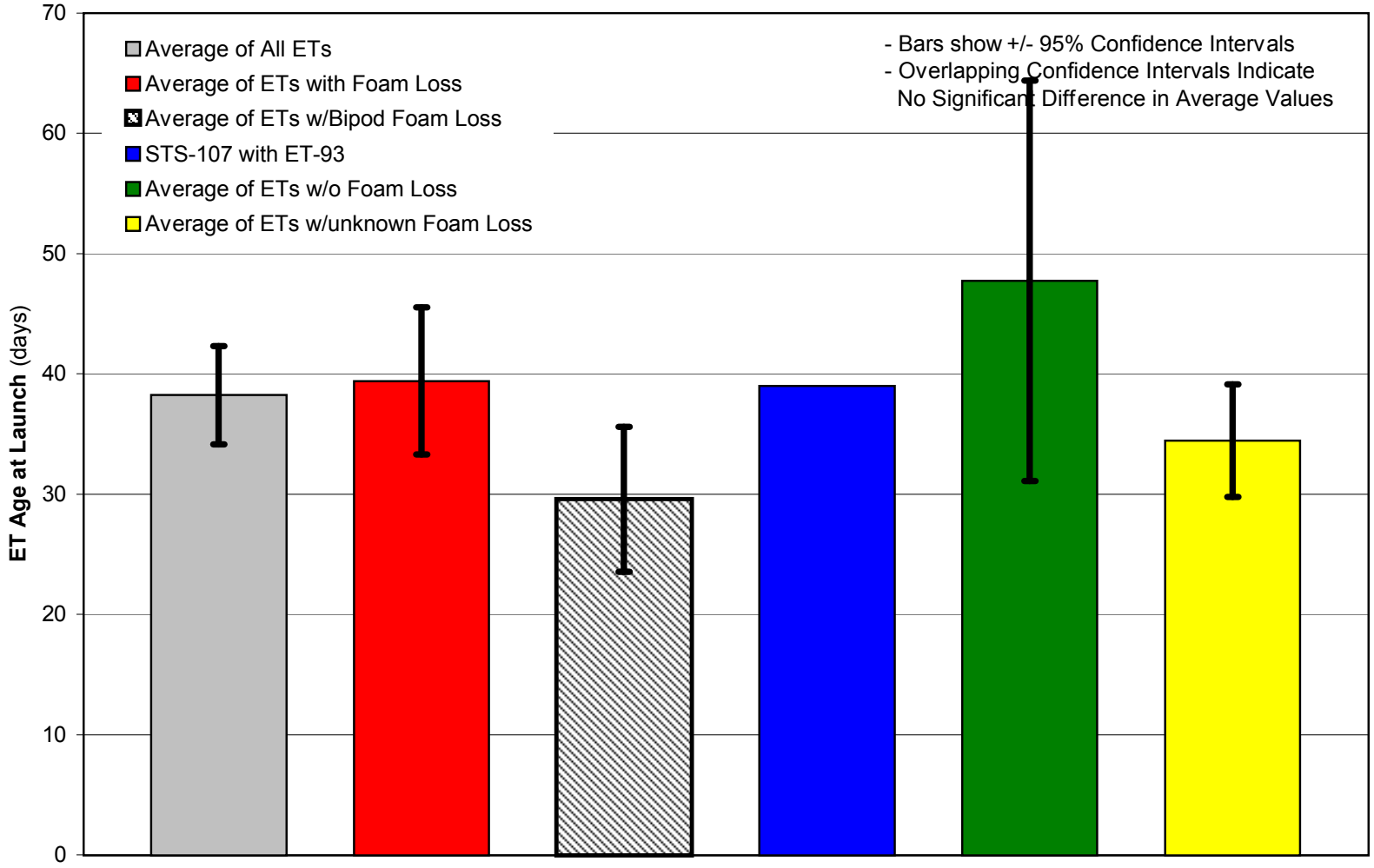

ET & Foam Data Trend

ET & Foam Data Trending.xls

CAB099-0028

External Tank Pre-Launch Exposure Time

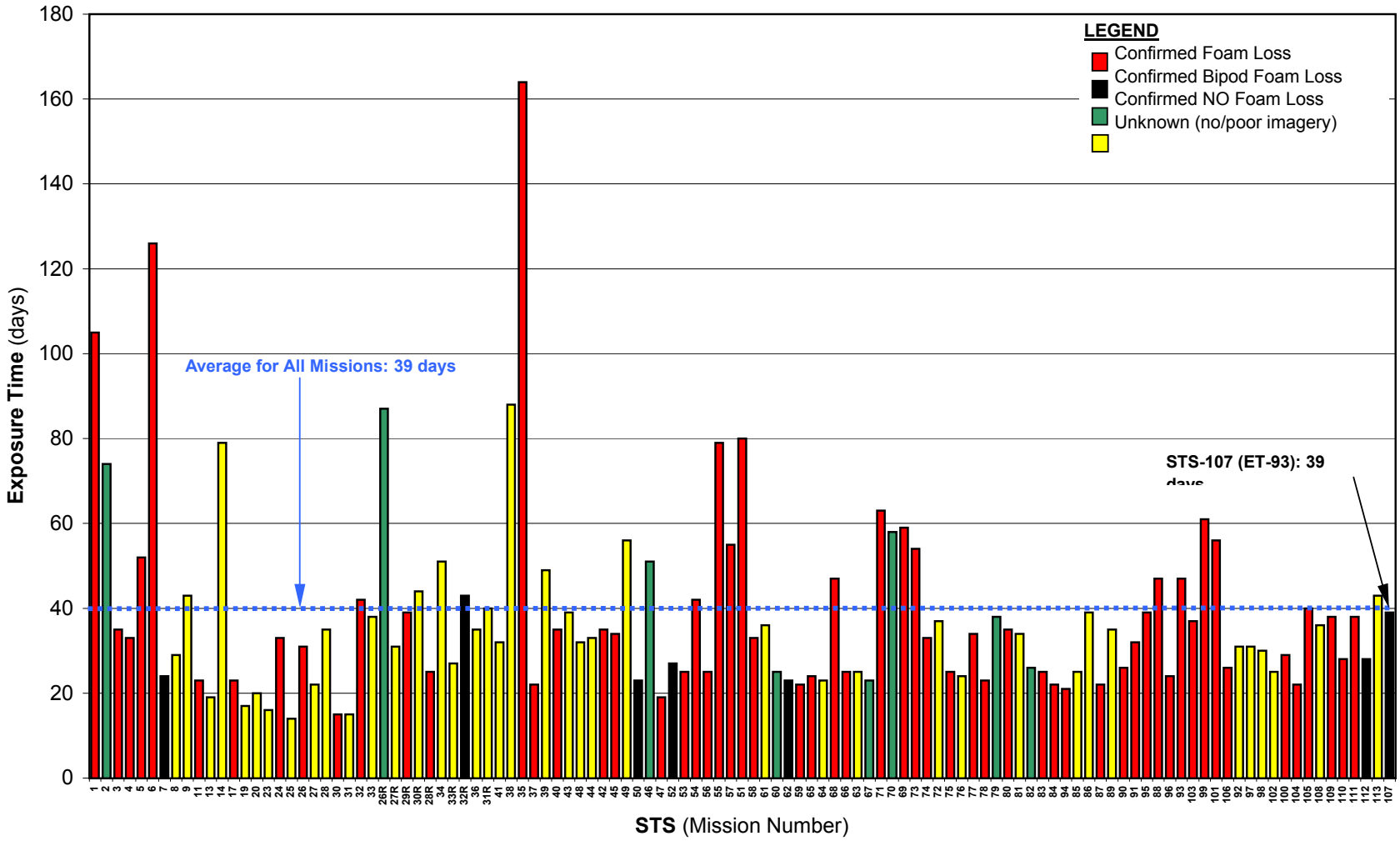

External Tank Pre-Launch Exposure Time

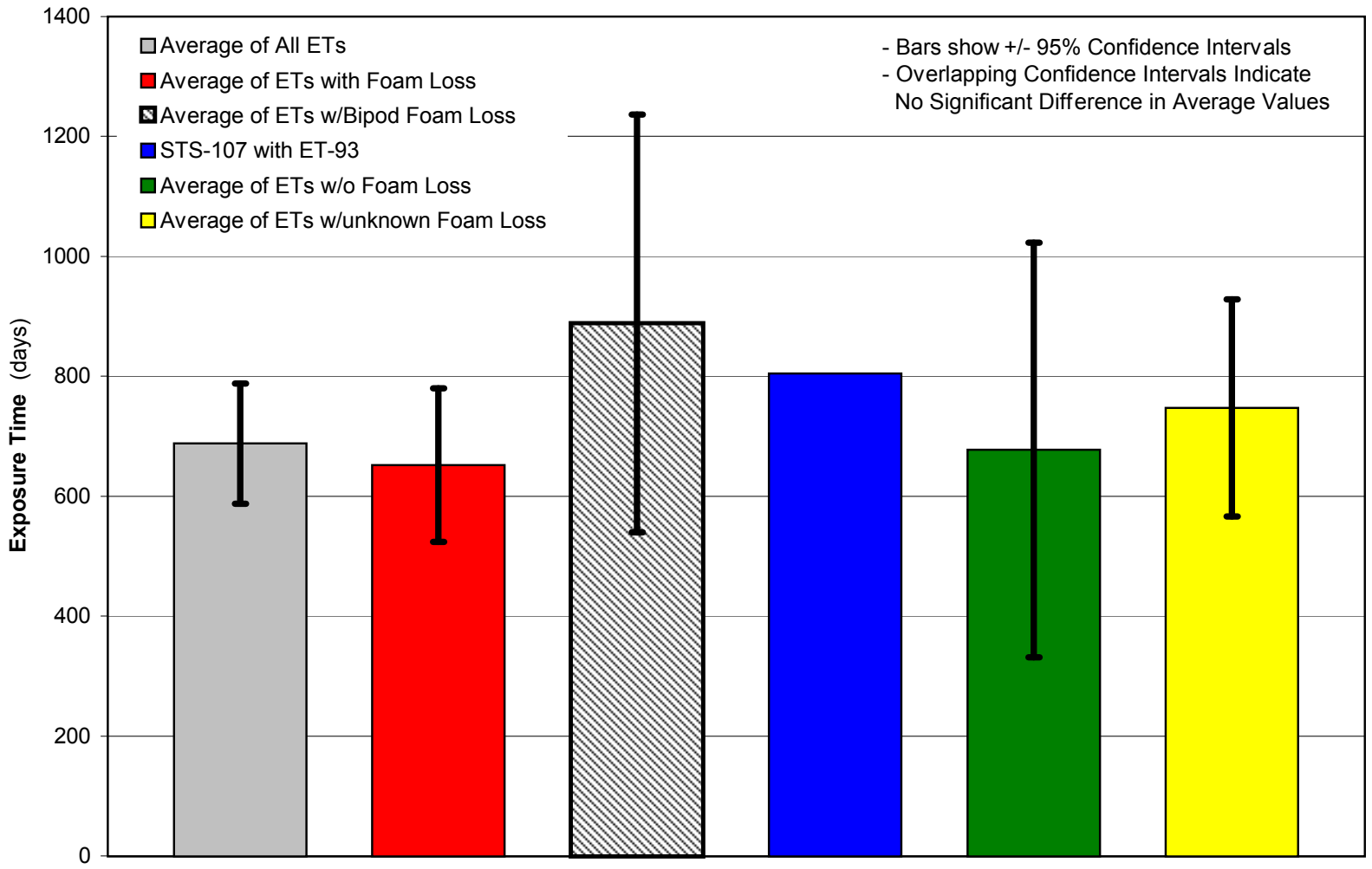

Total Pre-Launch Rainfall

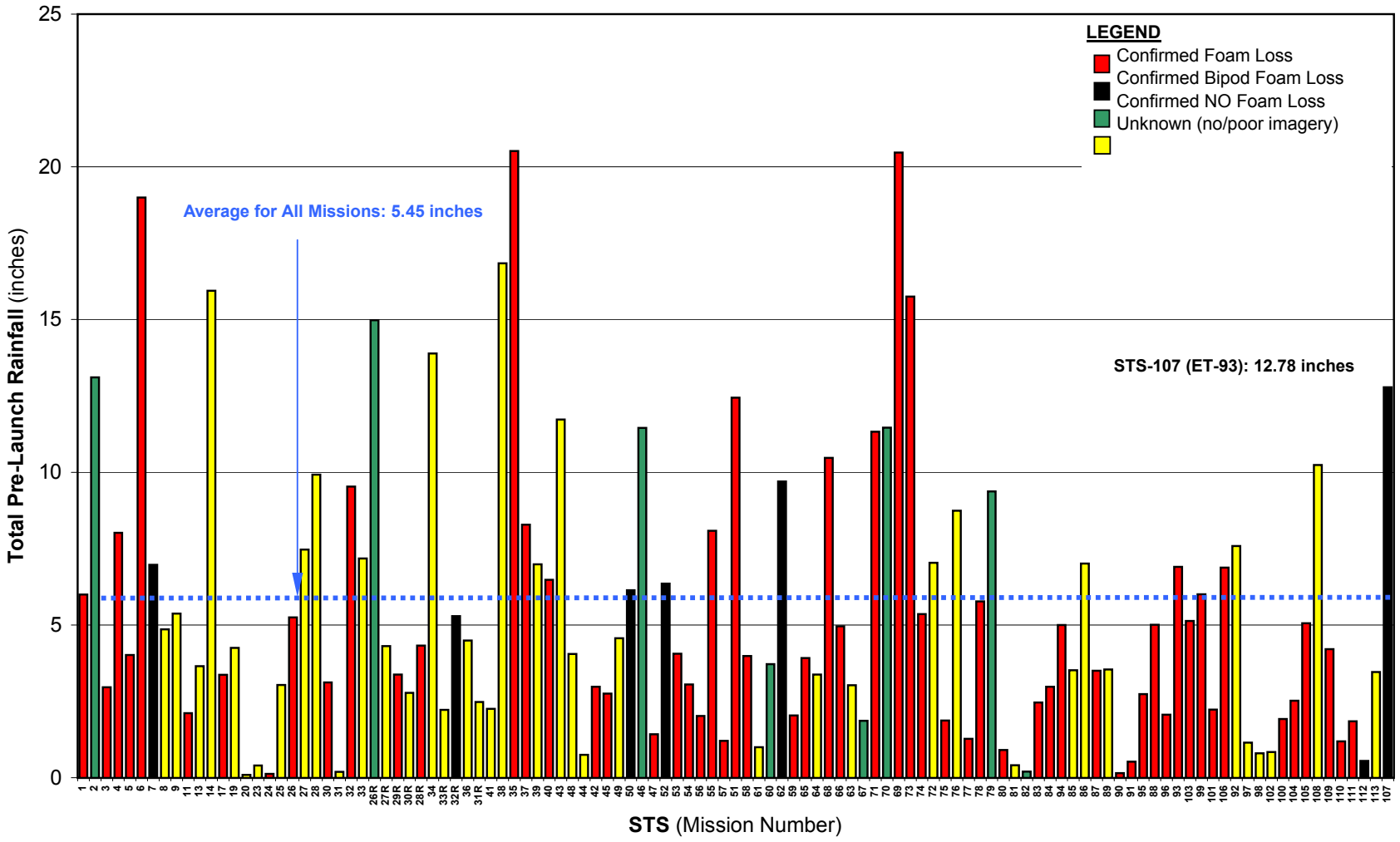

ET & Foam Data Trend

ET & Foam Data Trending.xls

CAB099-0031

Total Pre-Launch Rainfall

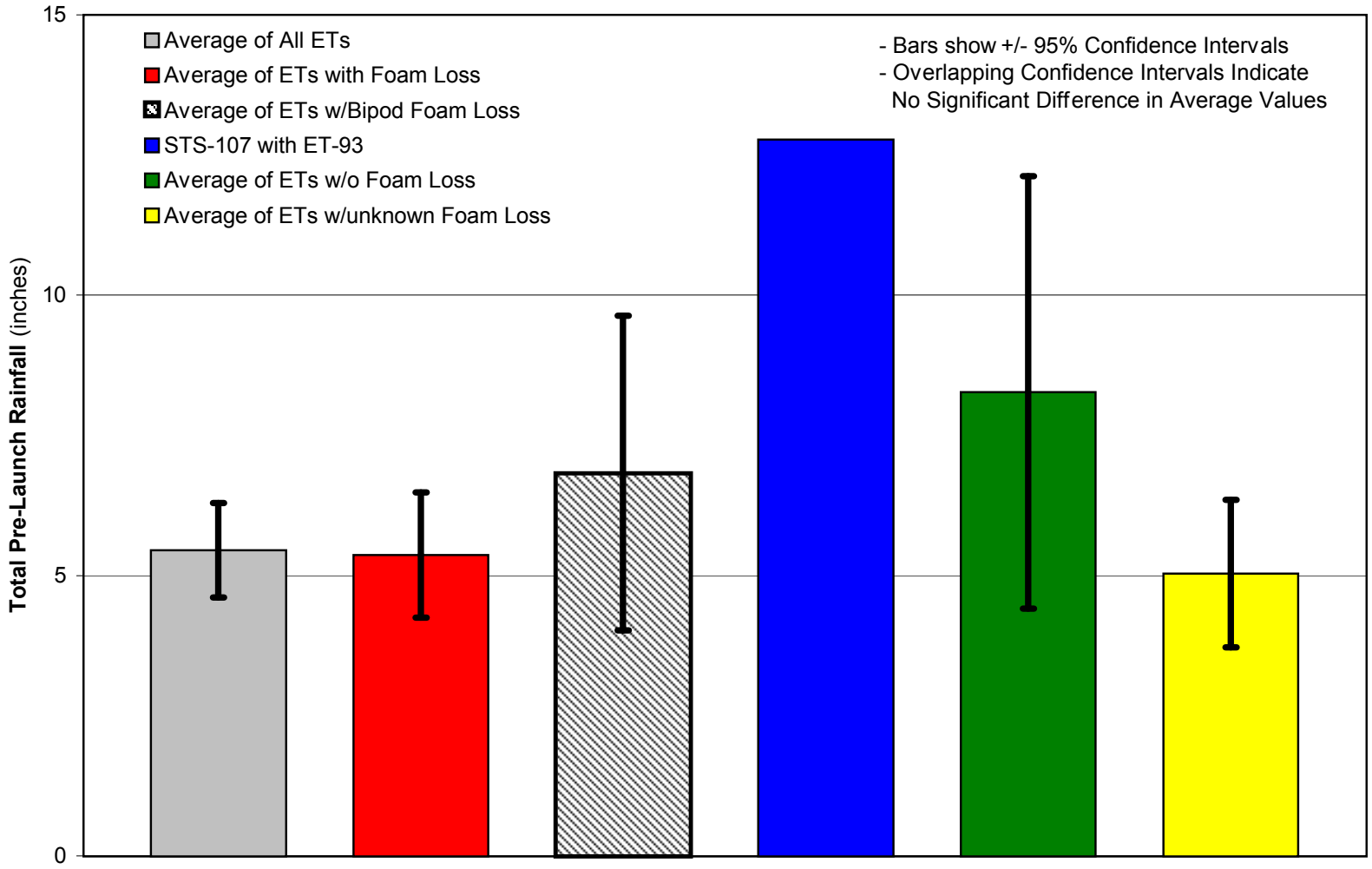

Single-Day Maximum Rainfall During Pre-Launch Period

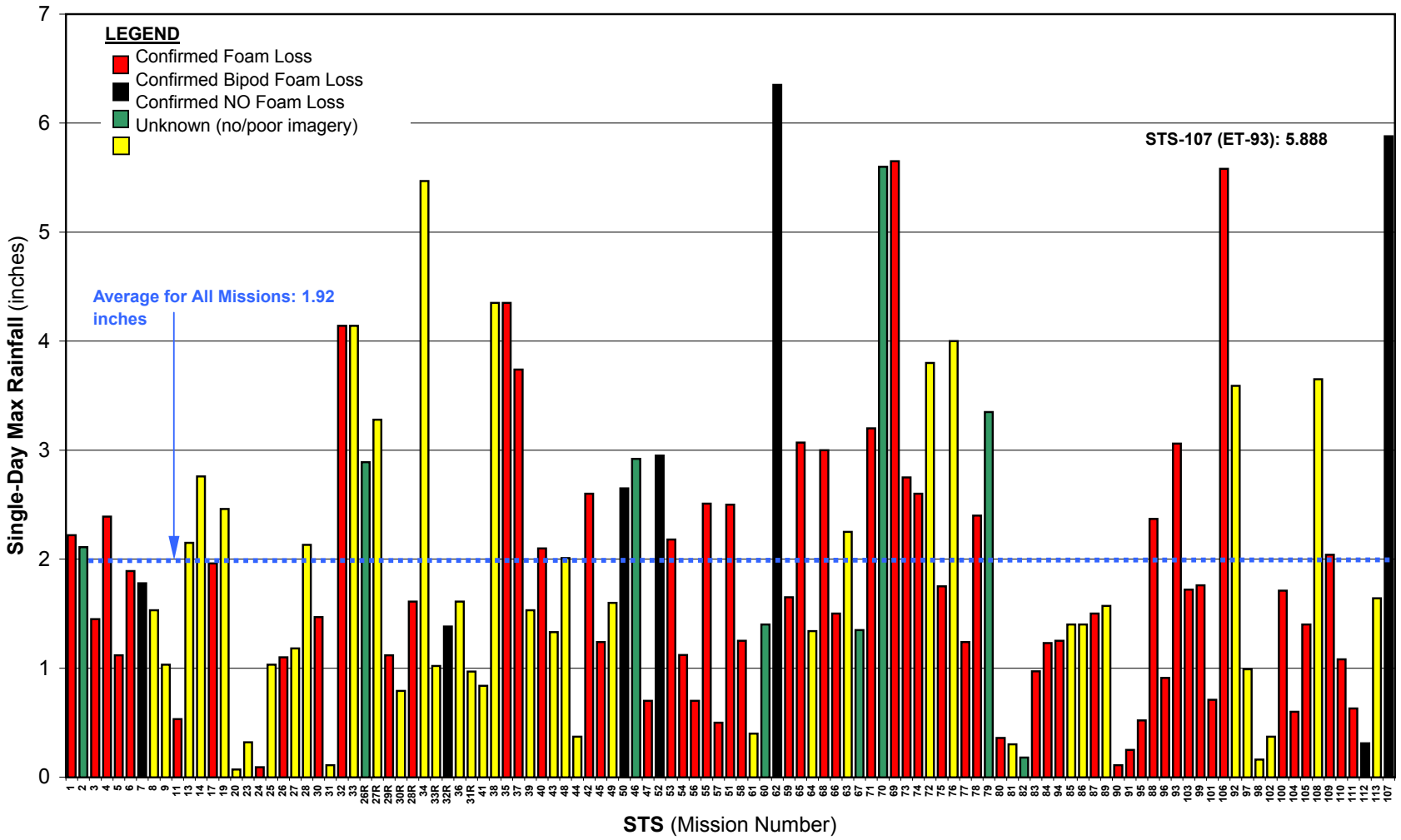

Single-Day Maximum Rainfall During Pre-Launch Period

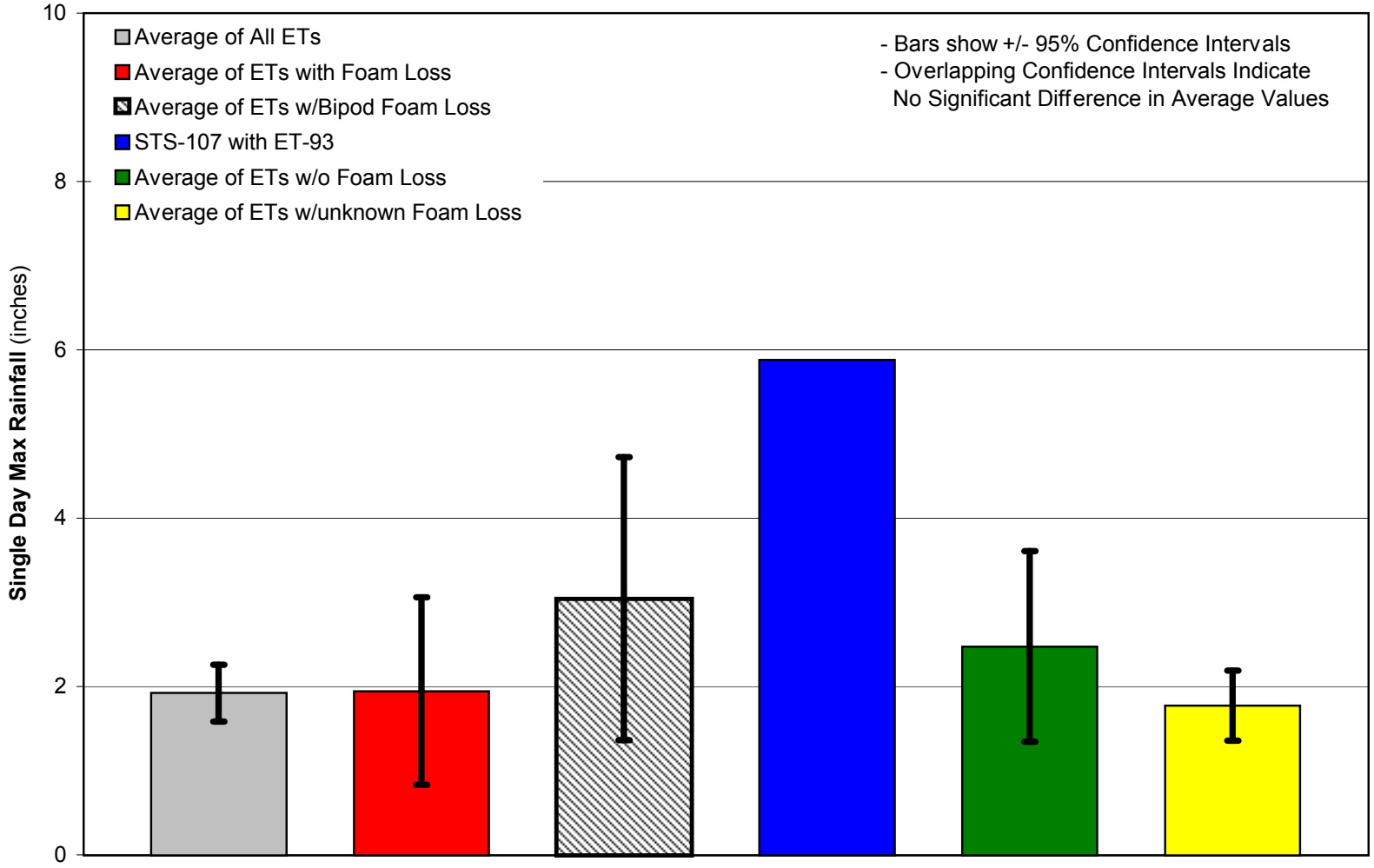

Average Daily Rainfall During Pre-Launch Period

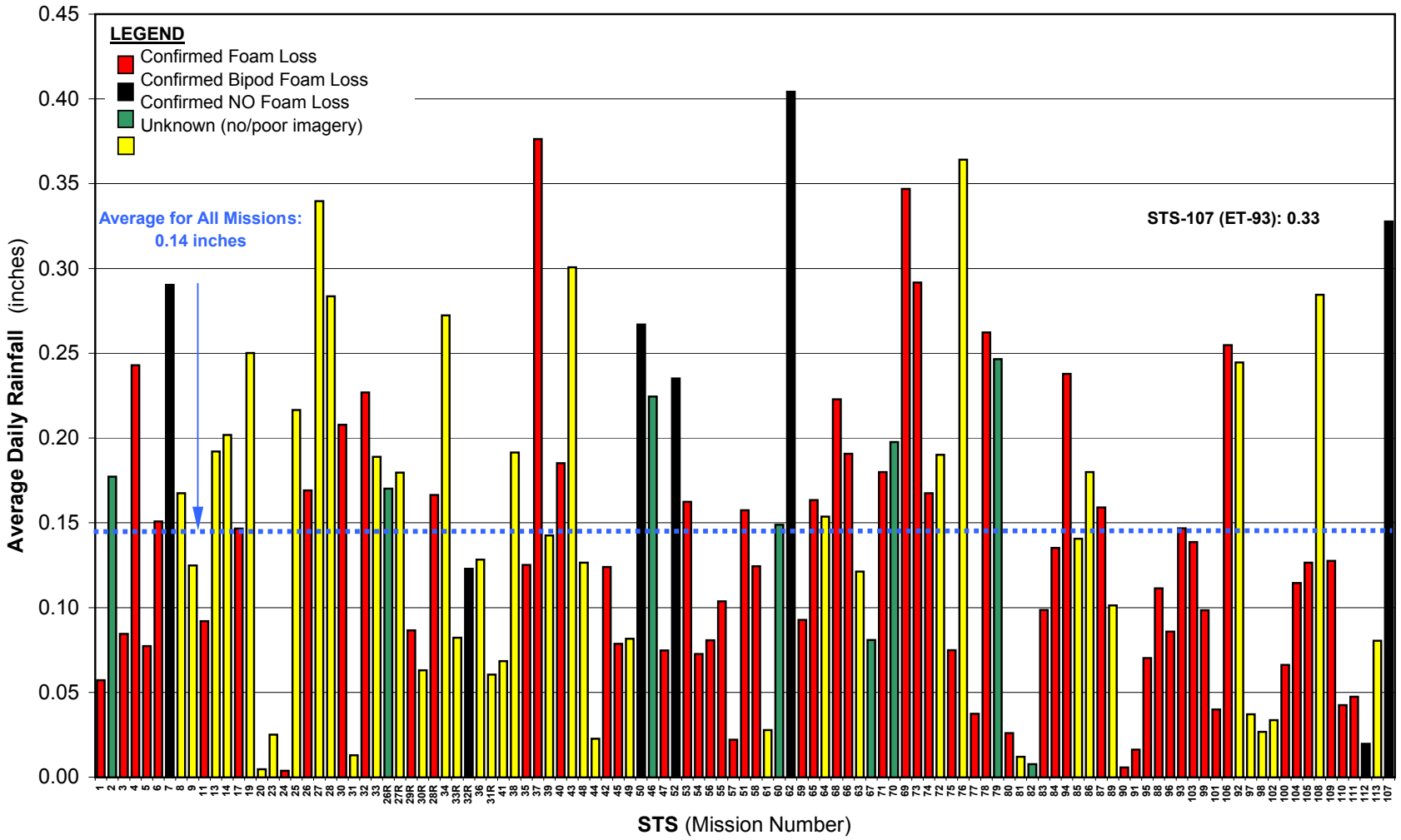

Average Daily Rainfall During Pre-Launch Period

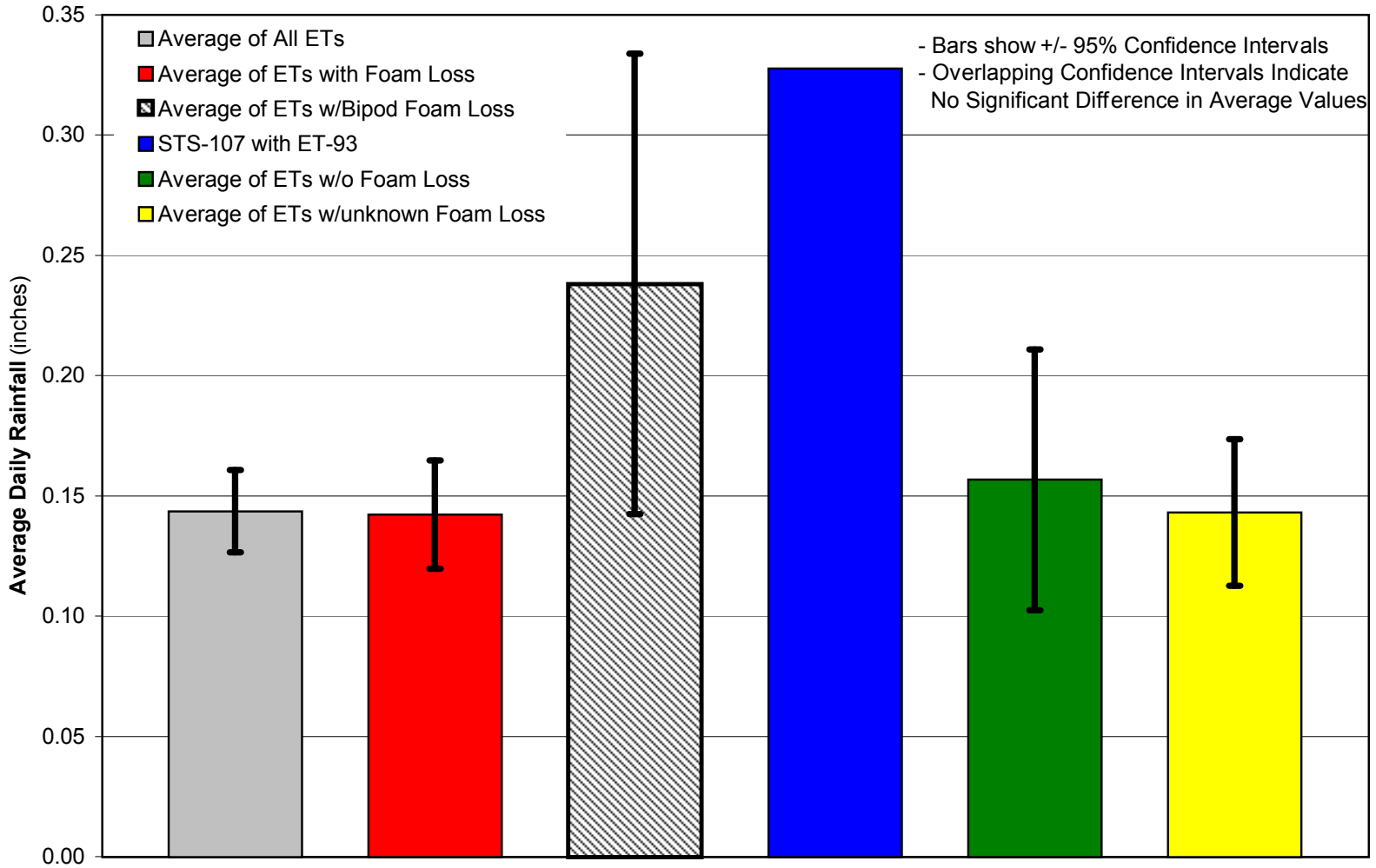

Total Rainfall During 5 Days Before Launch

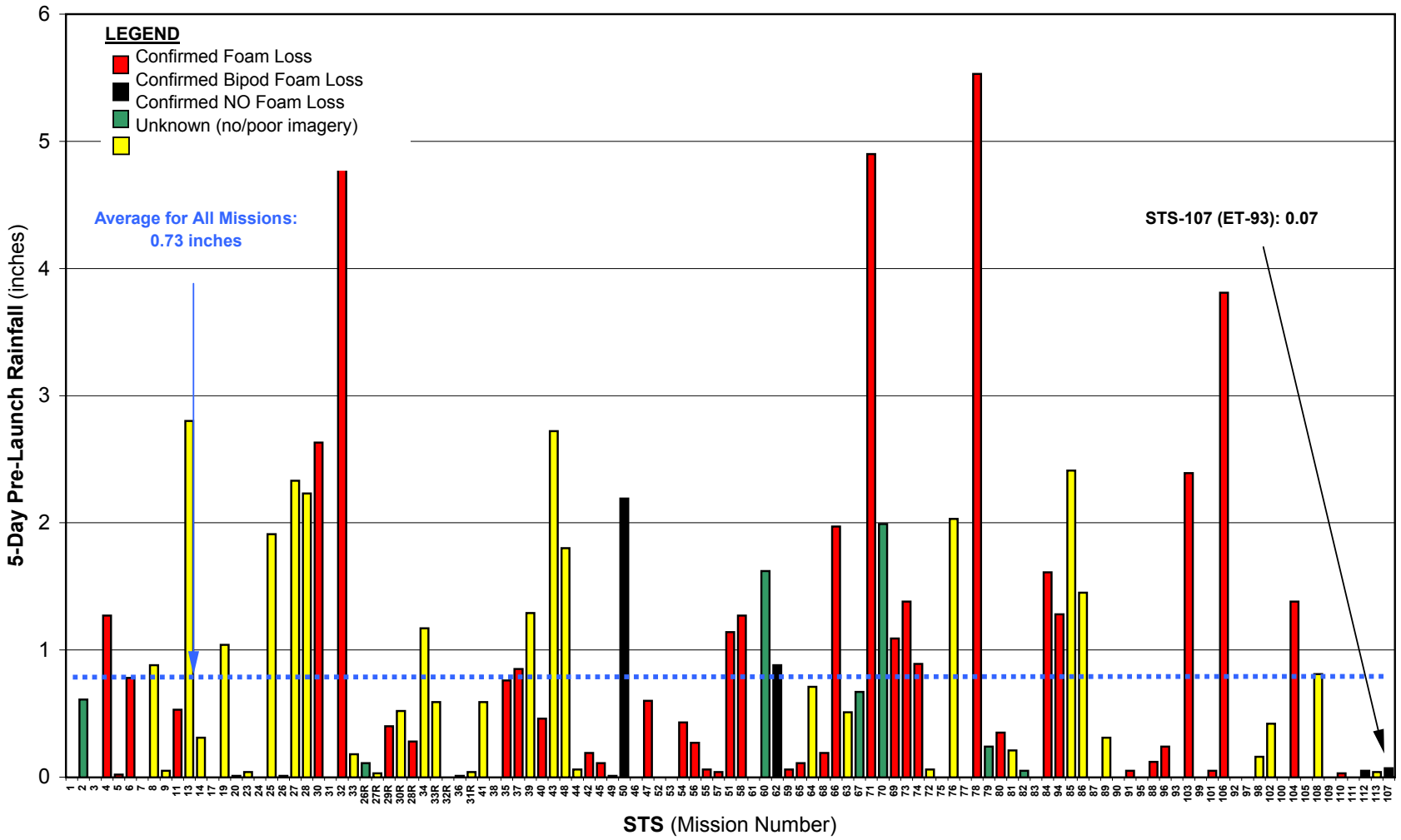

Total Rainfall During 5 Days Before Launch

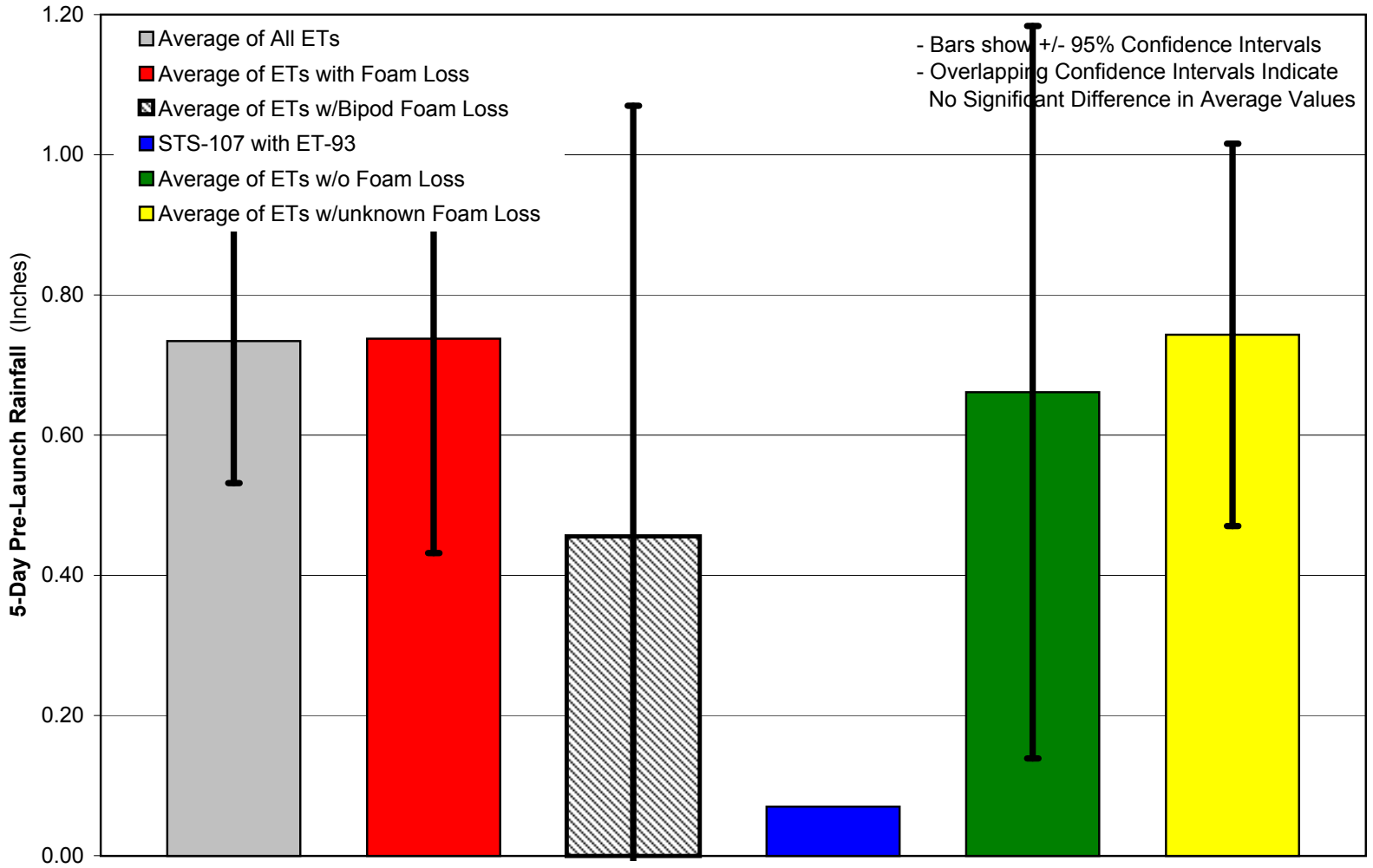

Rainfall On Launch Day

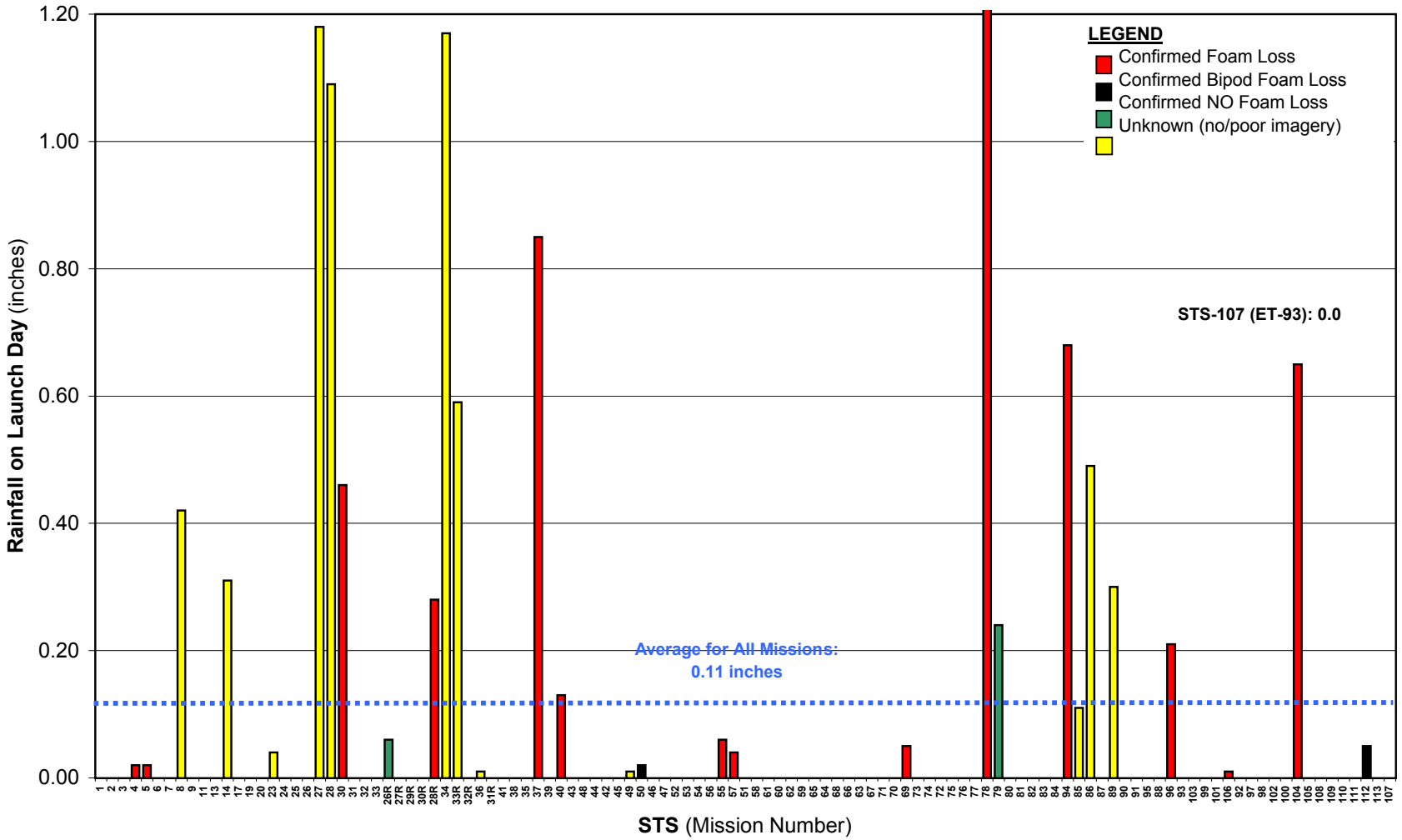

Rainfall on Launch Day

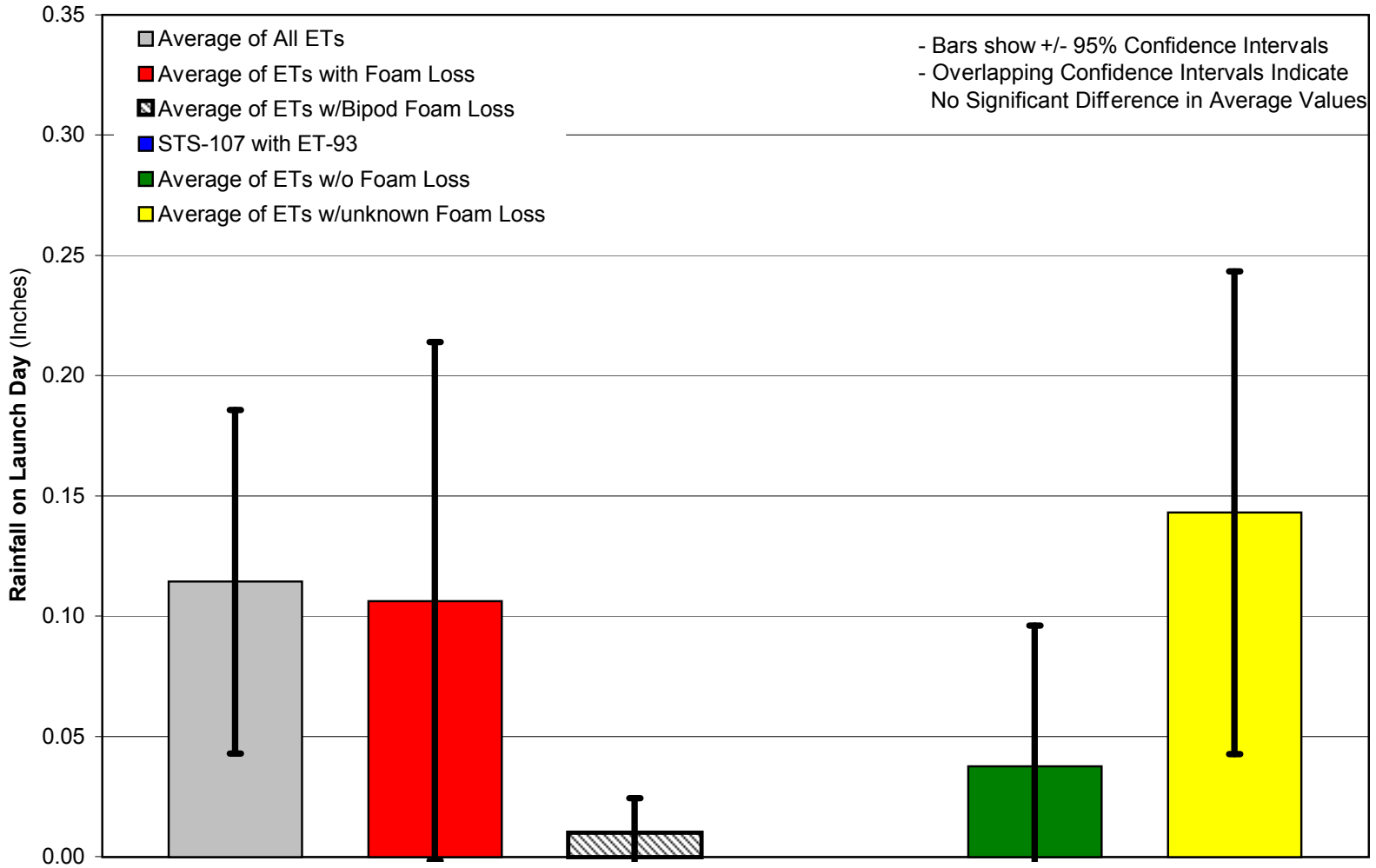

Average Temperature During Pre-Launch Period

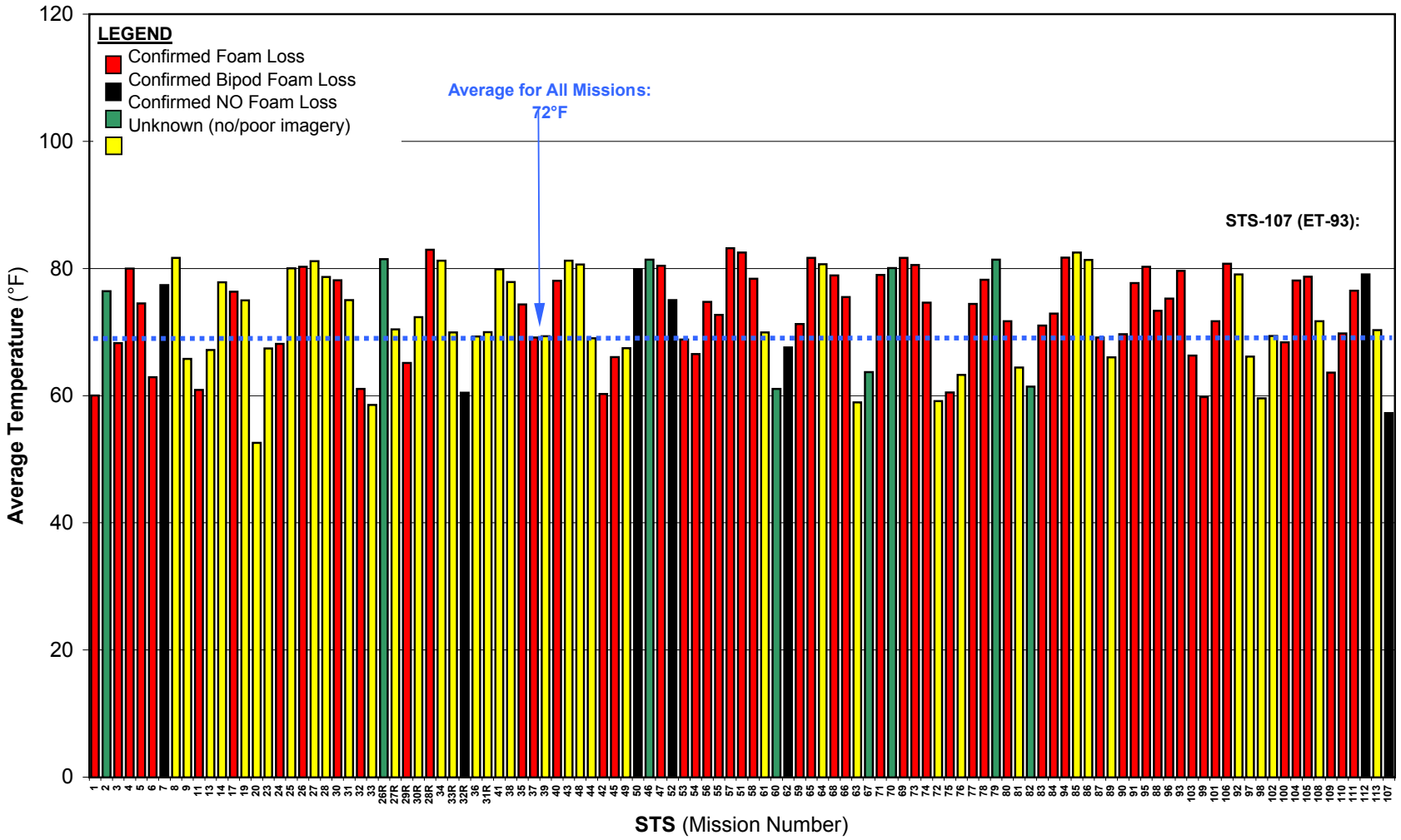

ET & Foam Data Trend

ET & Foam Data Trending.xls

CAB099-0041

Average Temperature During Pre-Launch Period

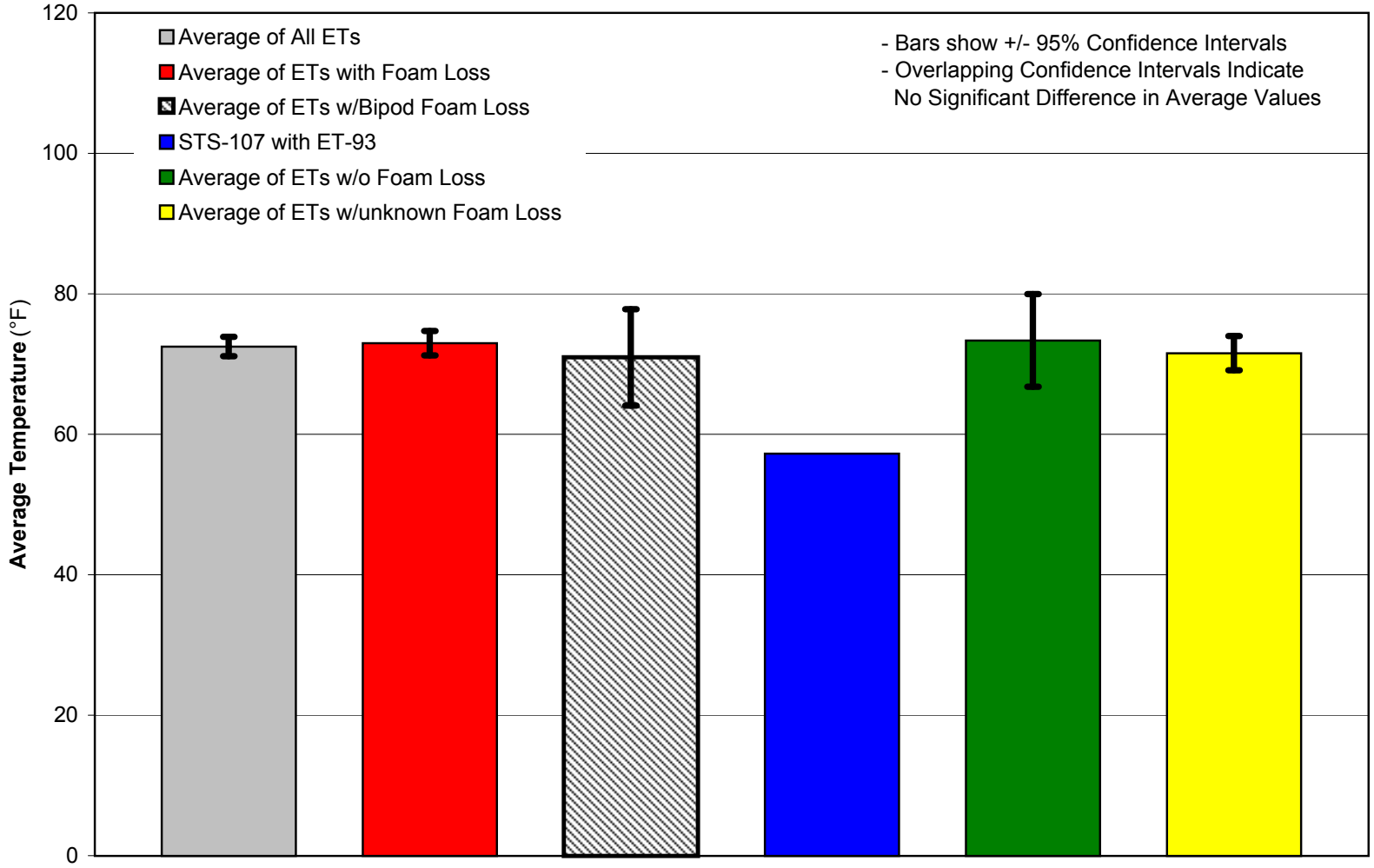

Maximum Temperature During Pre-Launch Period

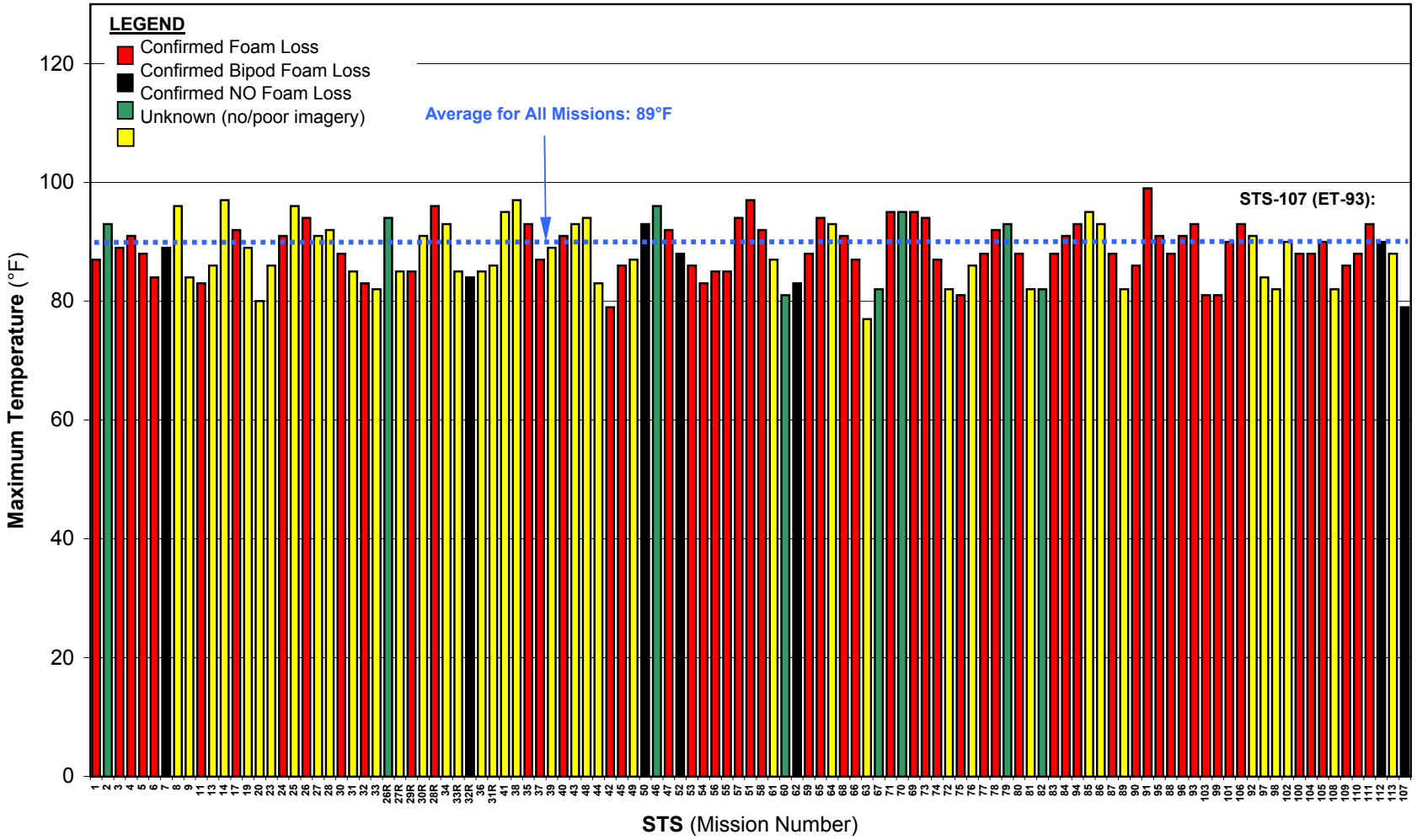

Maximum Temperature During Pre-Launch Period

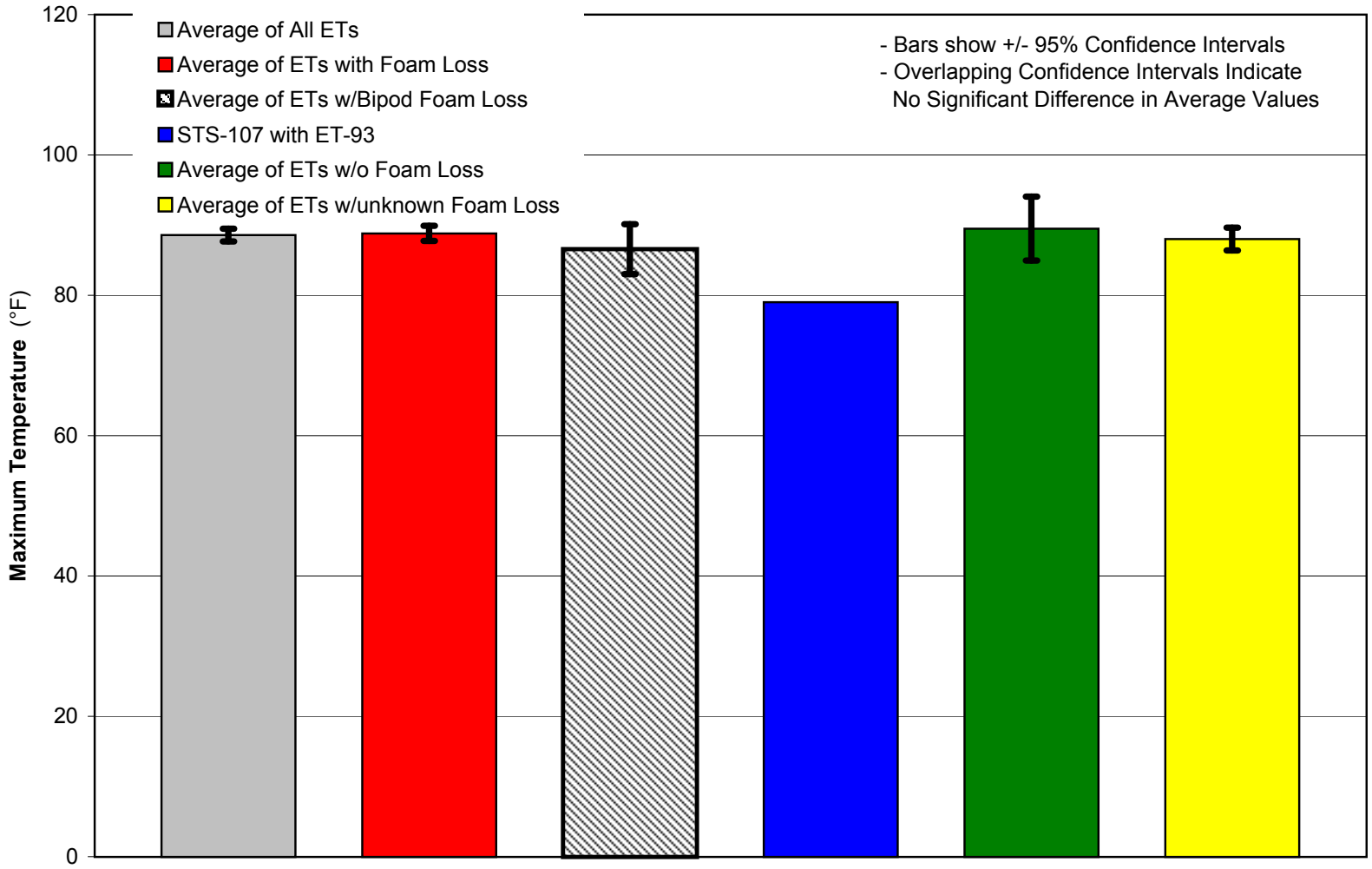

Minimum Temperature During Pre-Launch Period

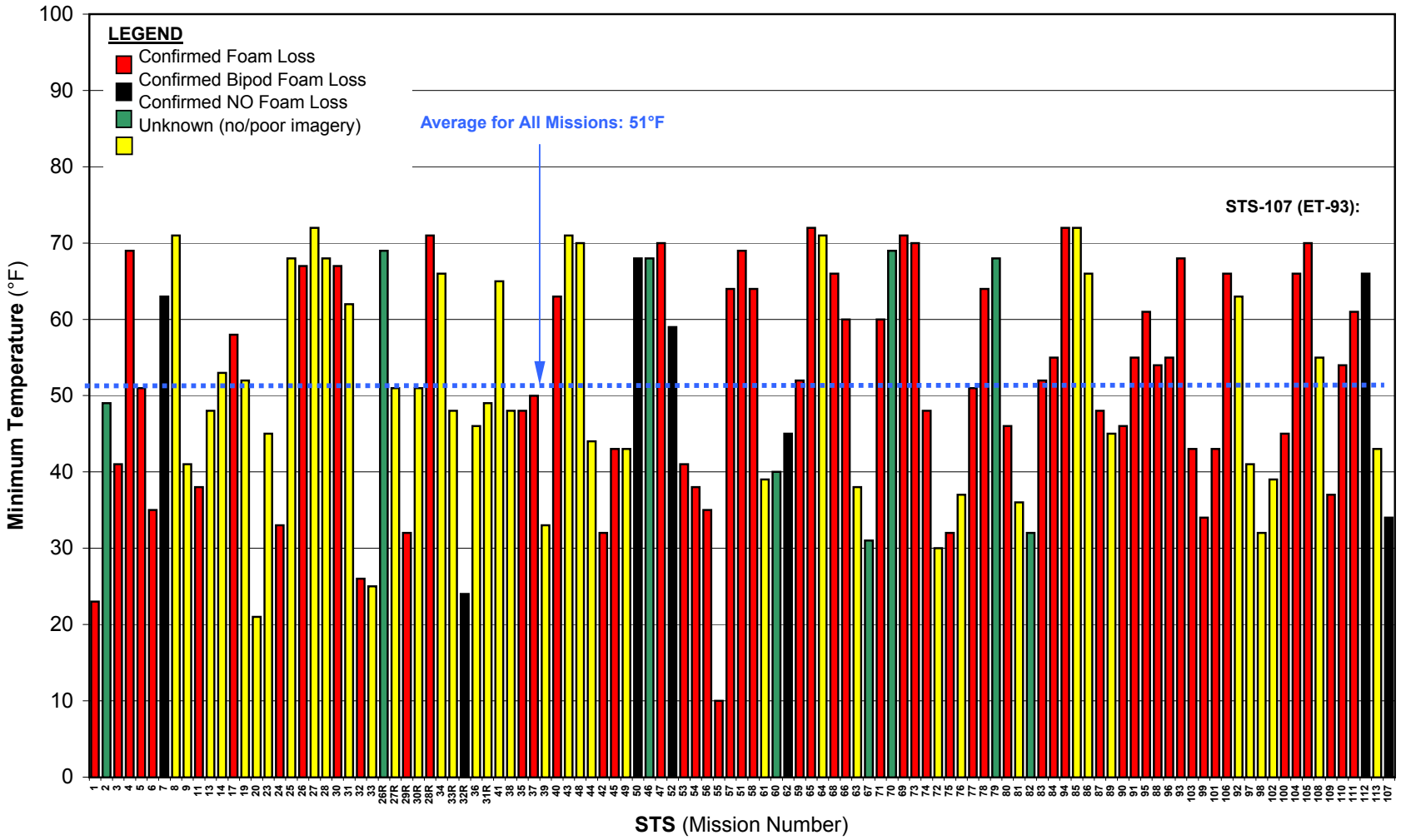

Minimum Temperature During Pre-Launch Period

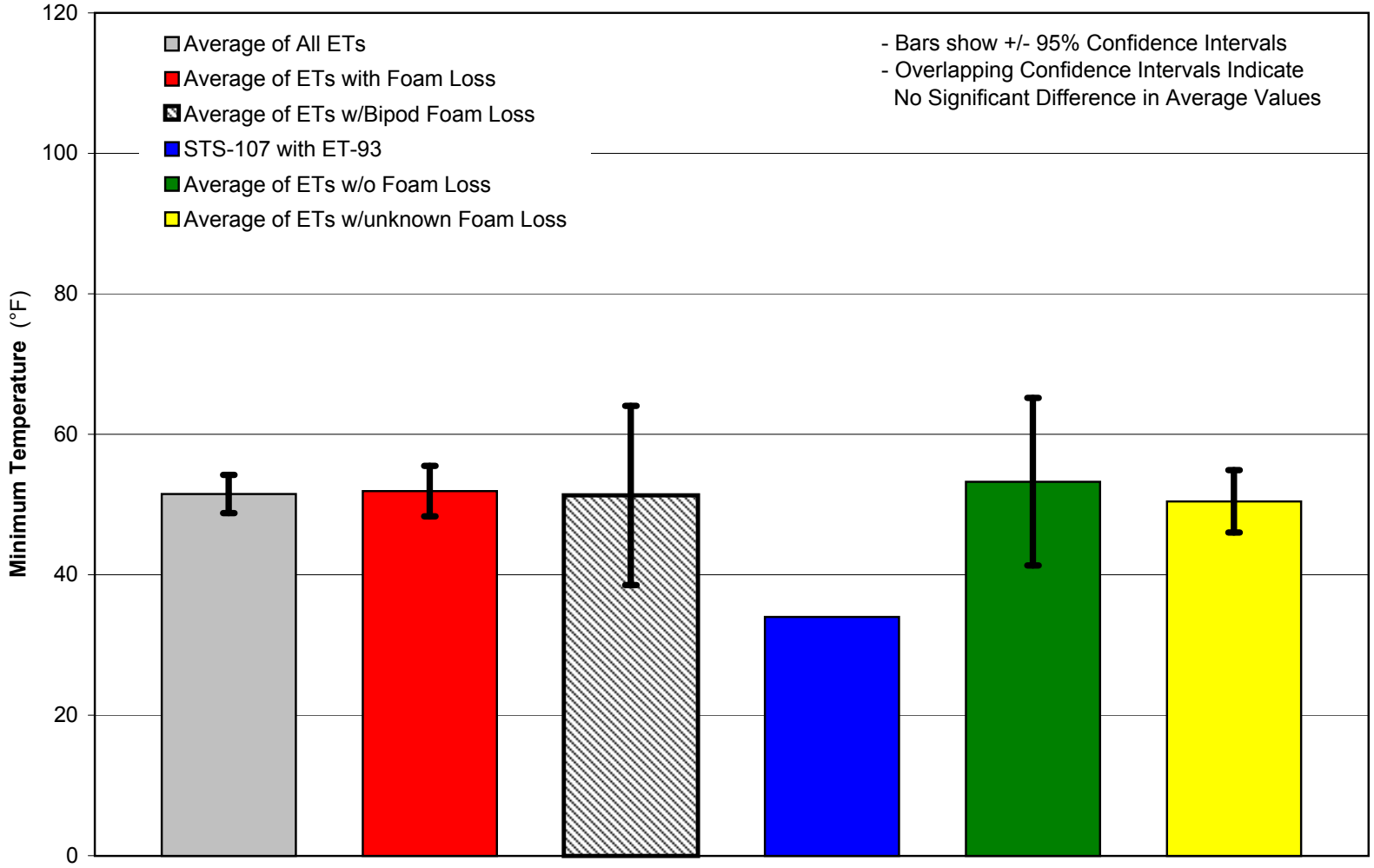

Average Temperature on Launch Day

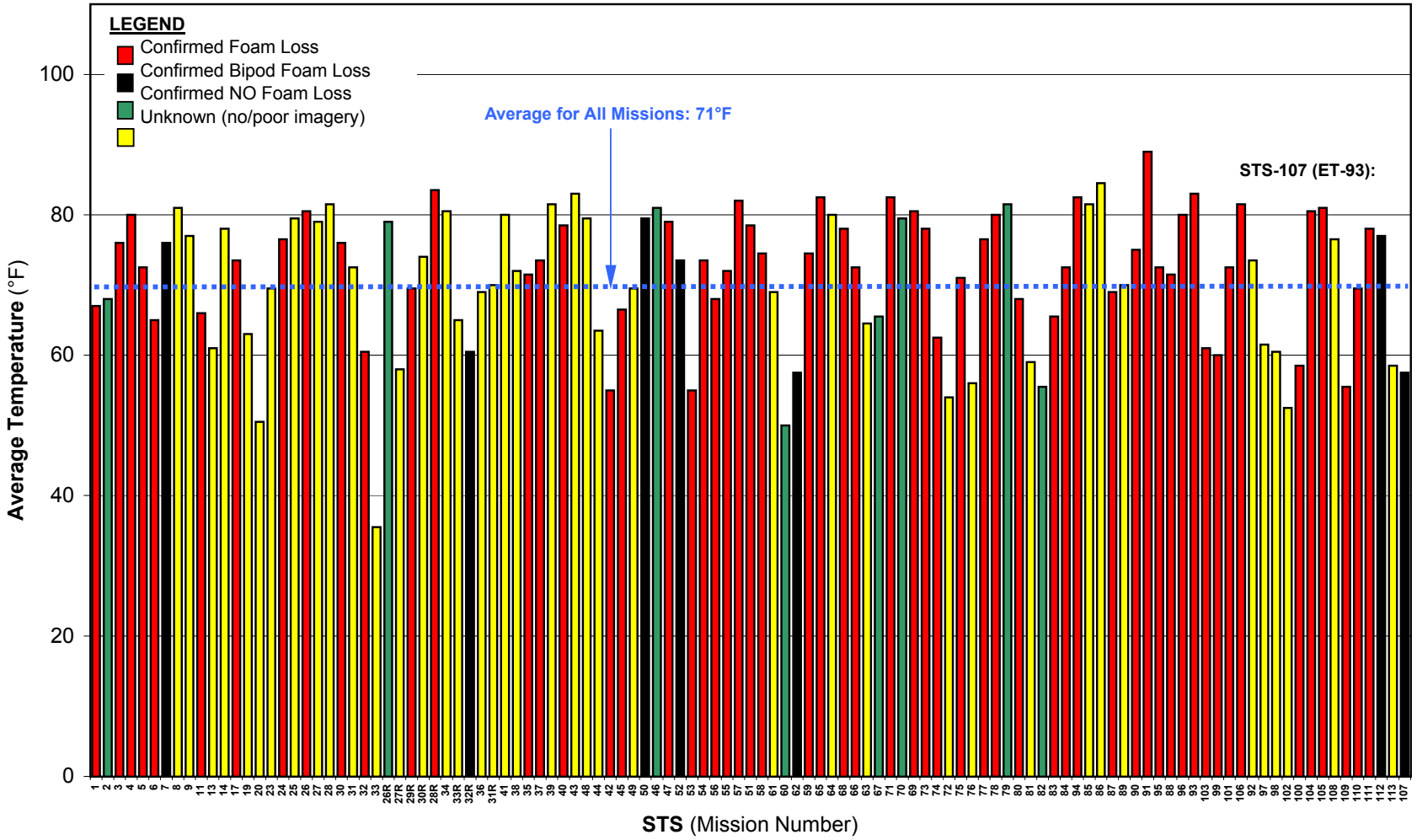

ET & Foam Data Trend

ET & Foam Data Trending.xls

CAB099-0047

Average Temperature on Launch Day

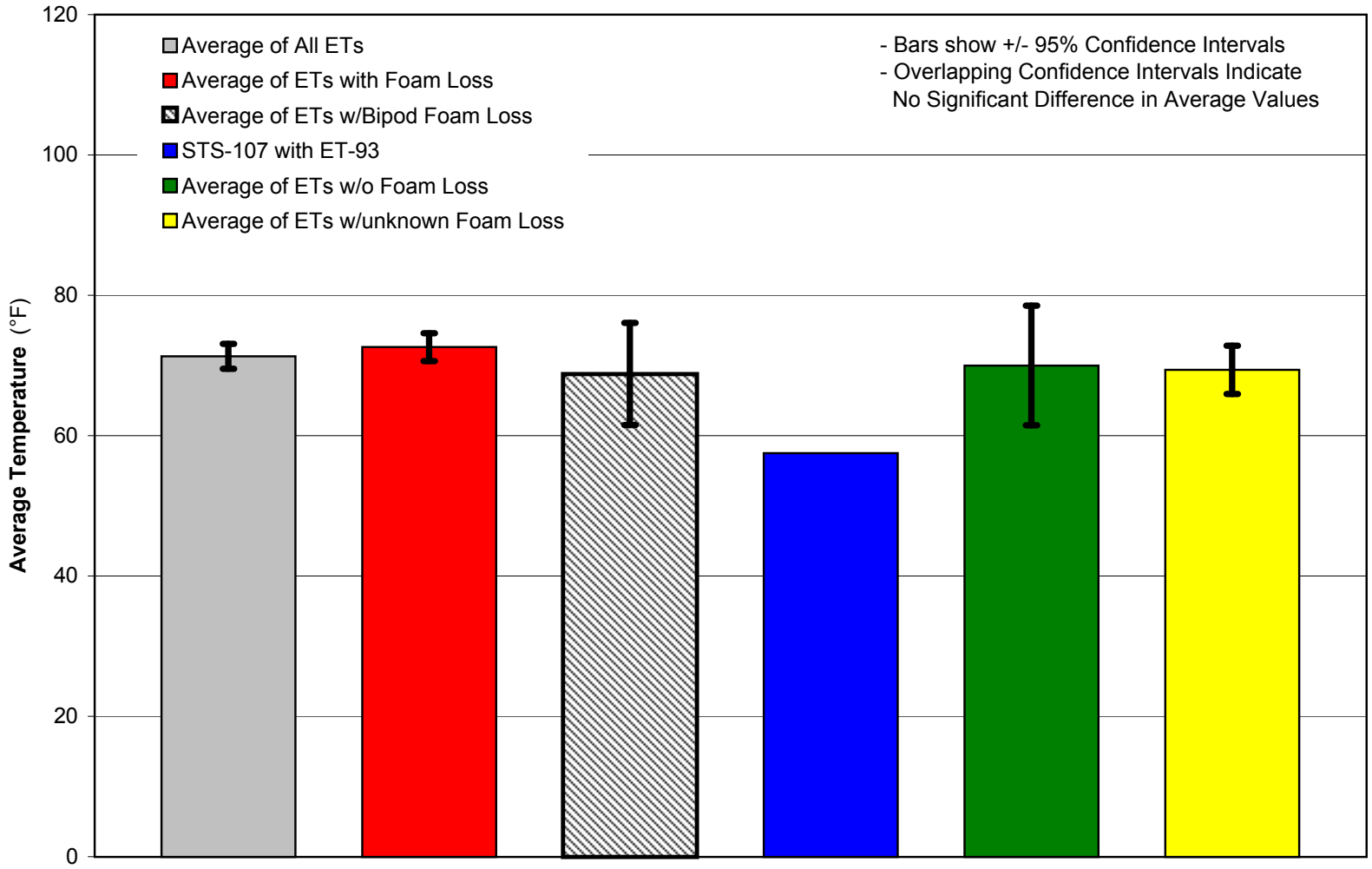

Maximum Temperature on Launch Day

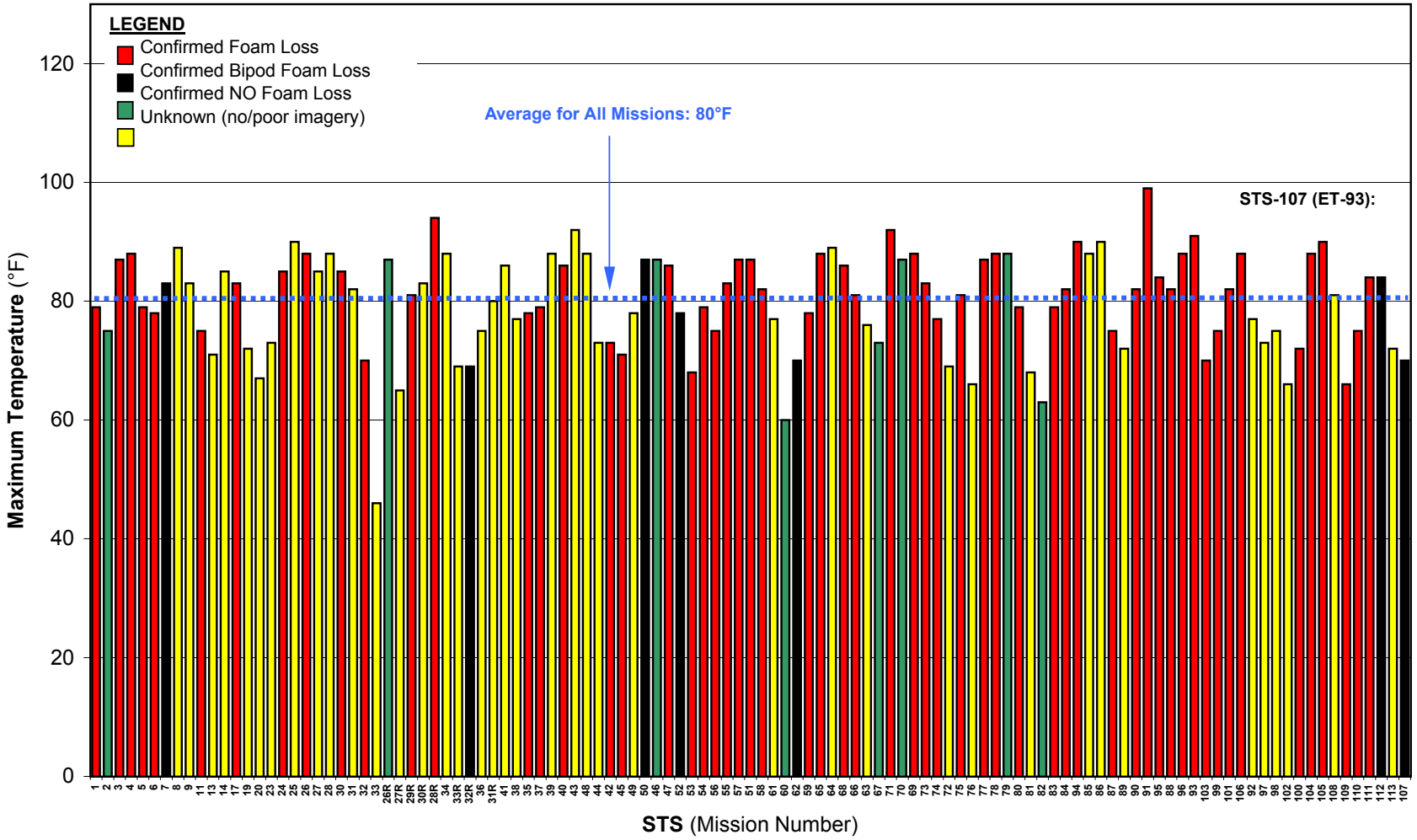

Maximum Temperature on Launch Day

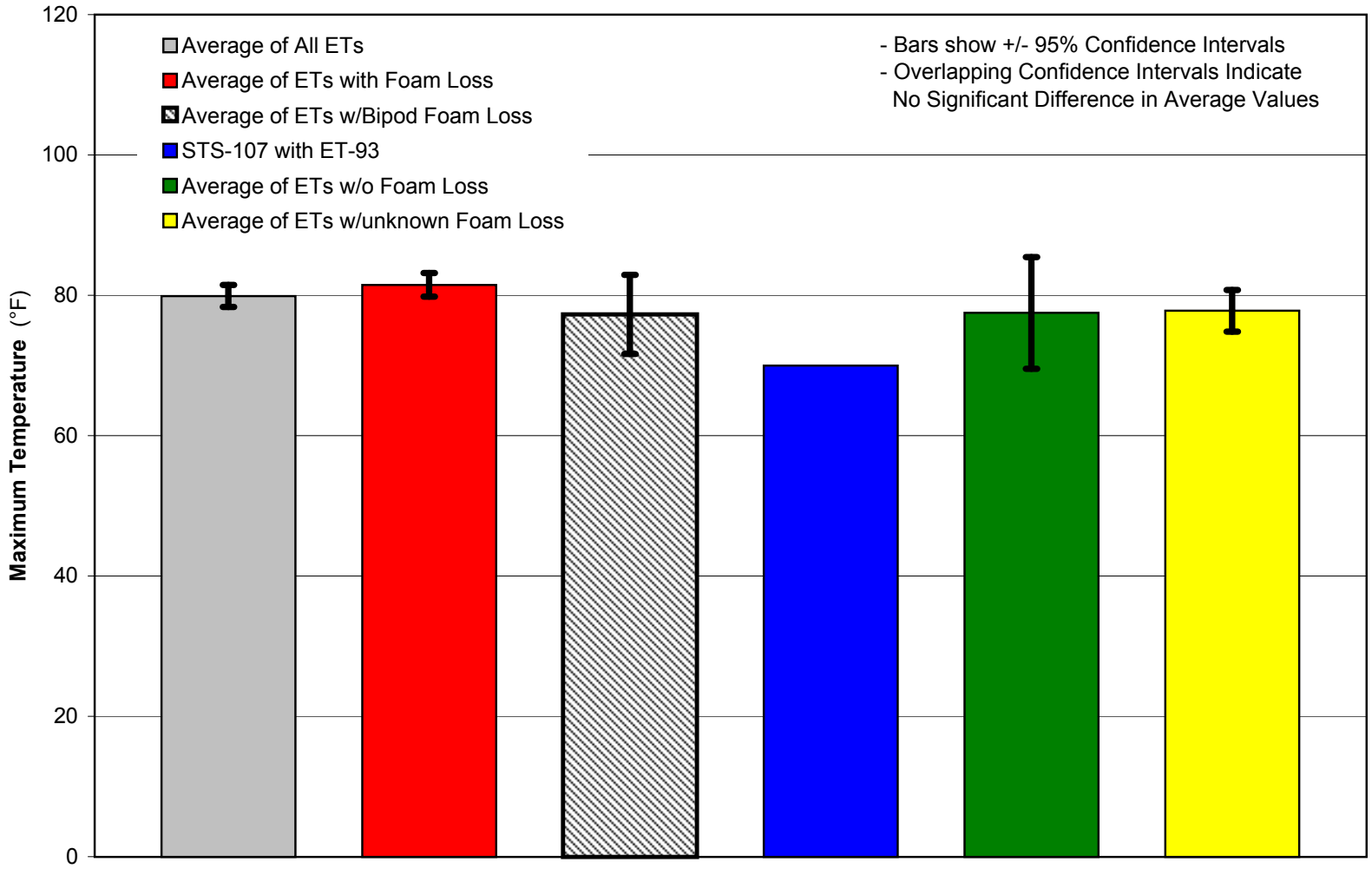

Minumum Temperature on Launch Day

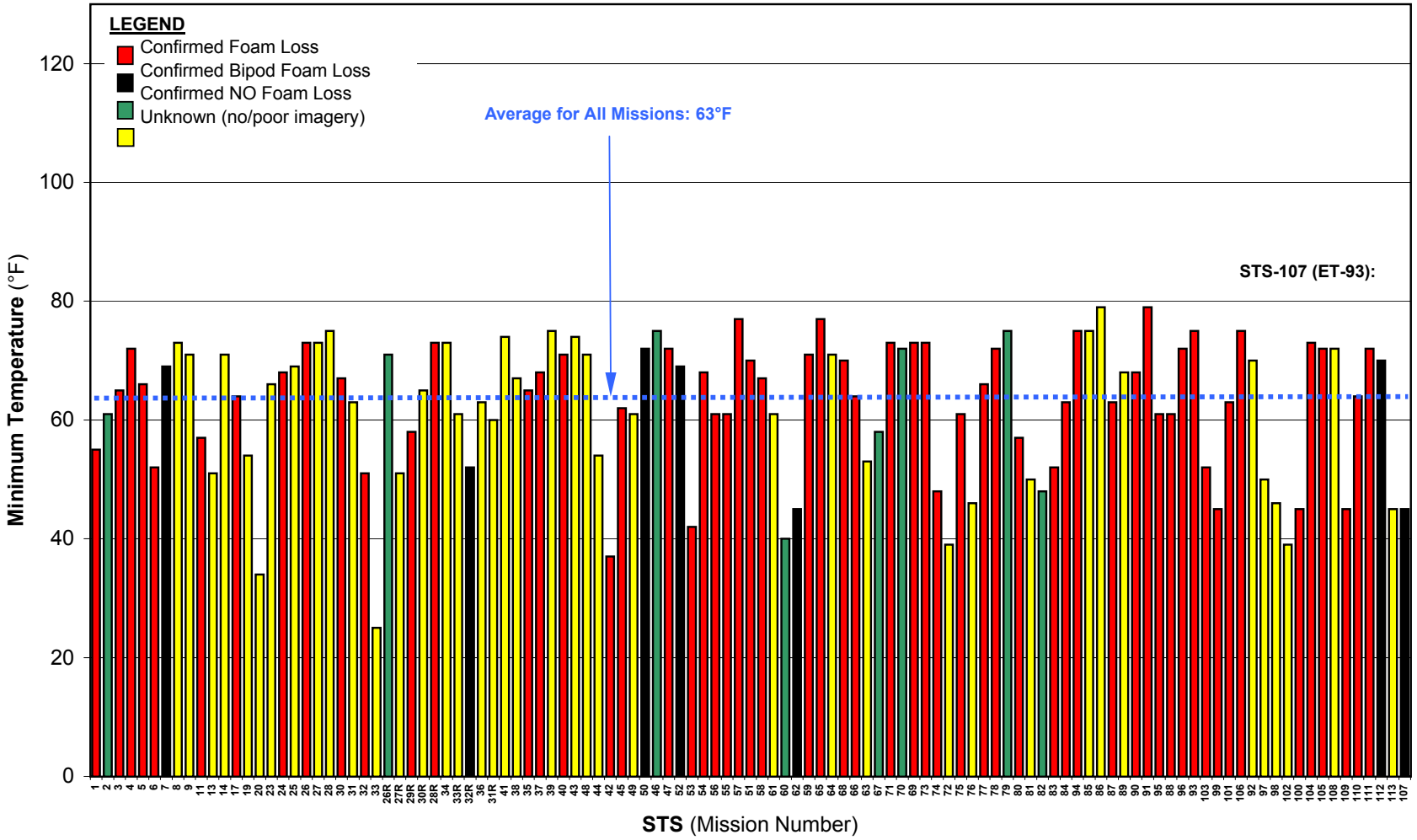

Minimum Temperature on Launch Day

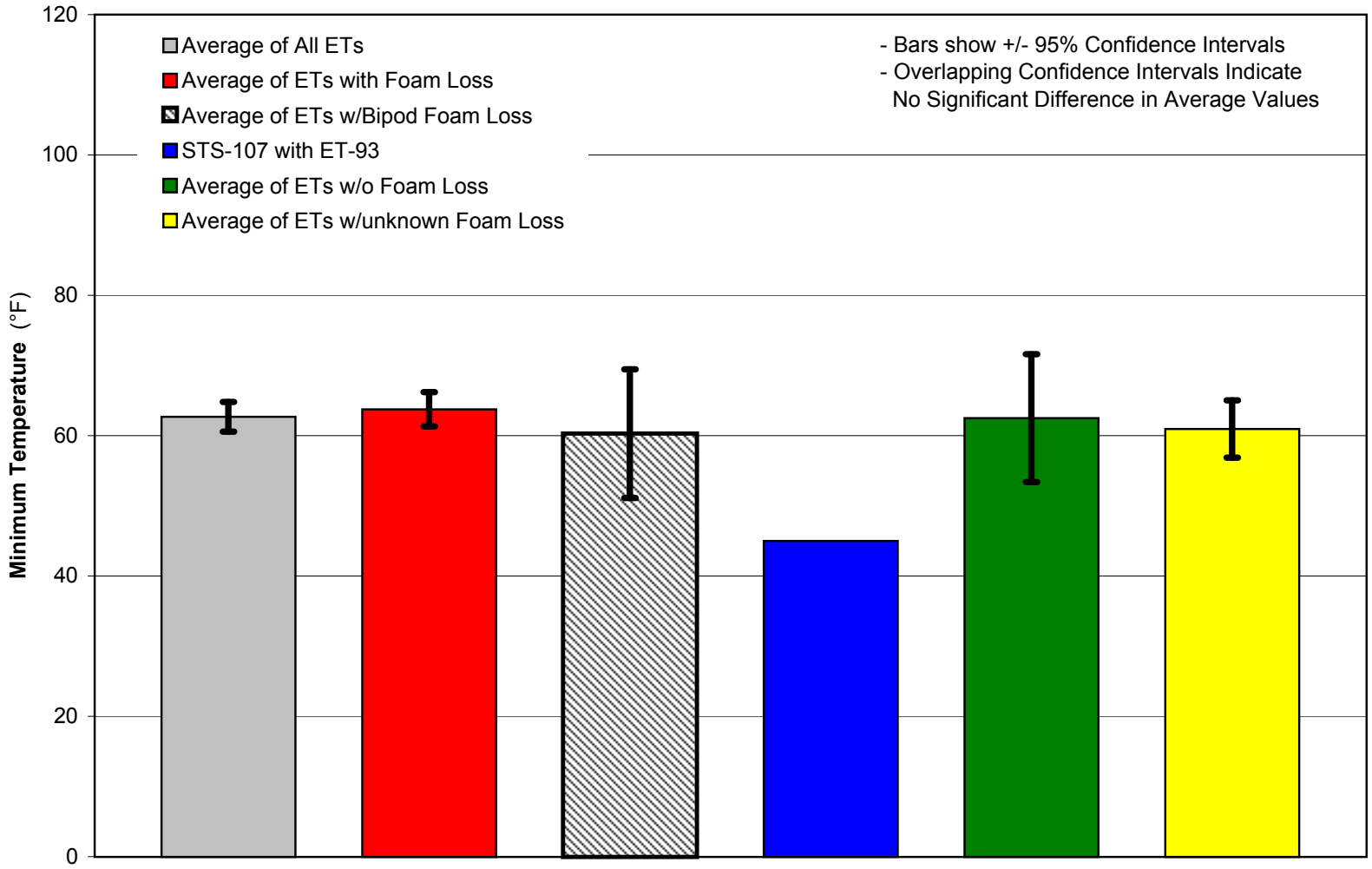

Temperature At Start of Tanking on Launch Day

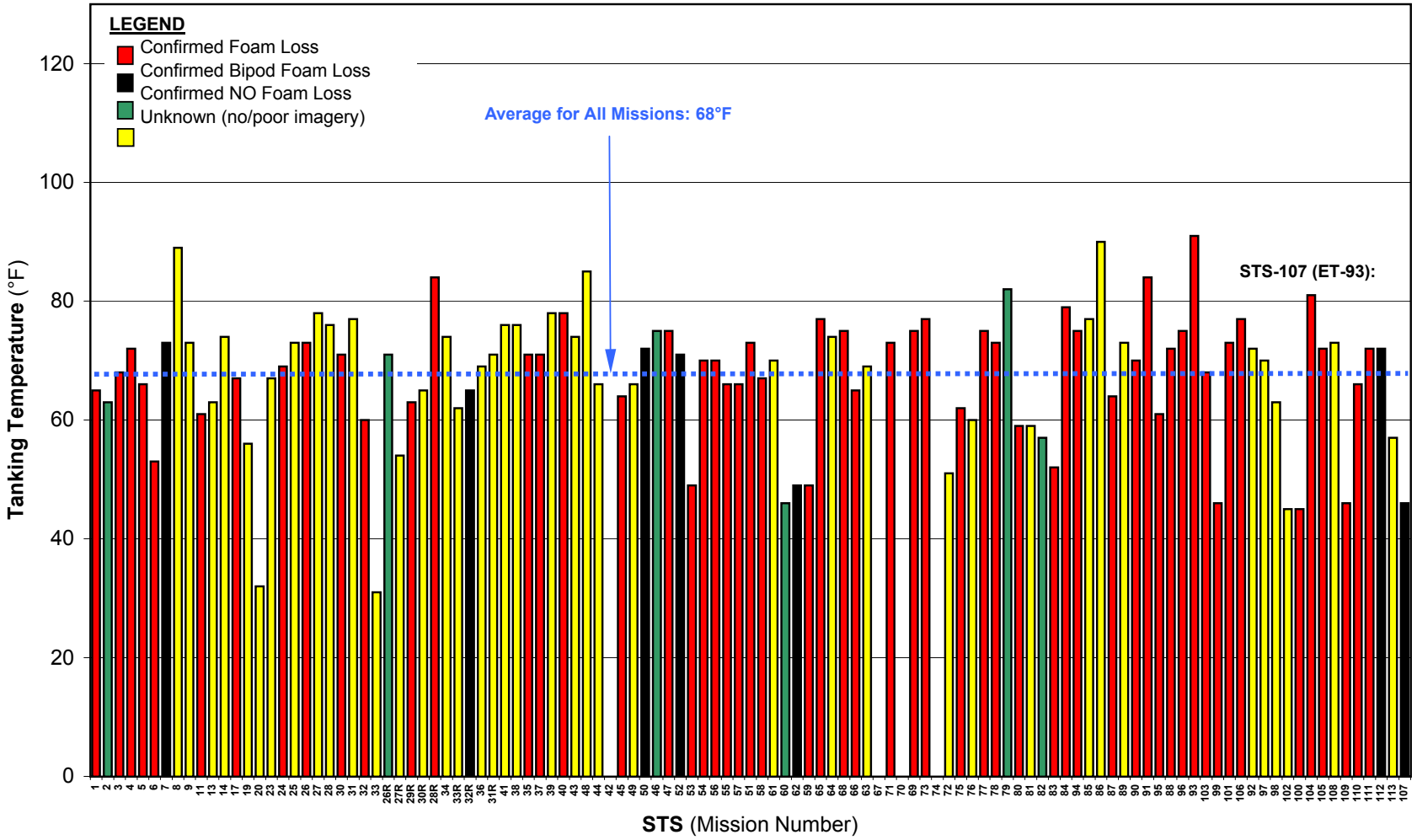

Temperature At Start of Tanking on Launch Day

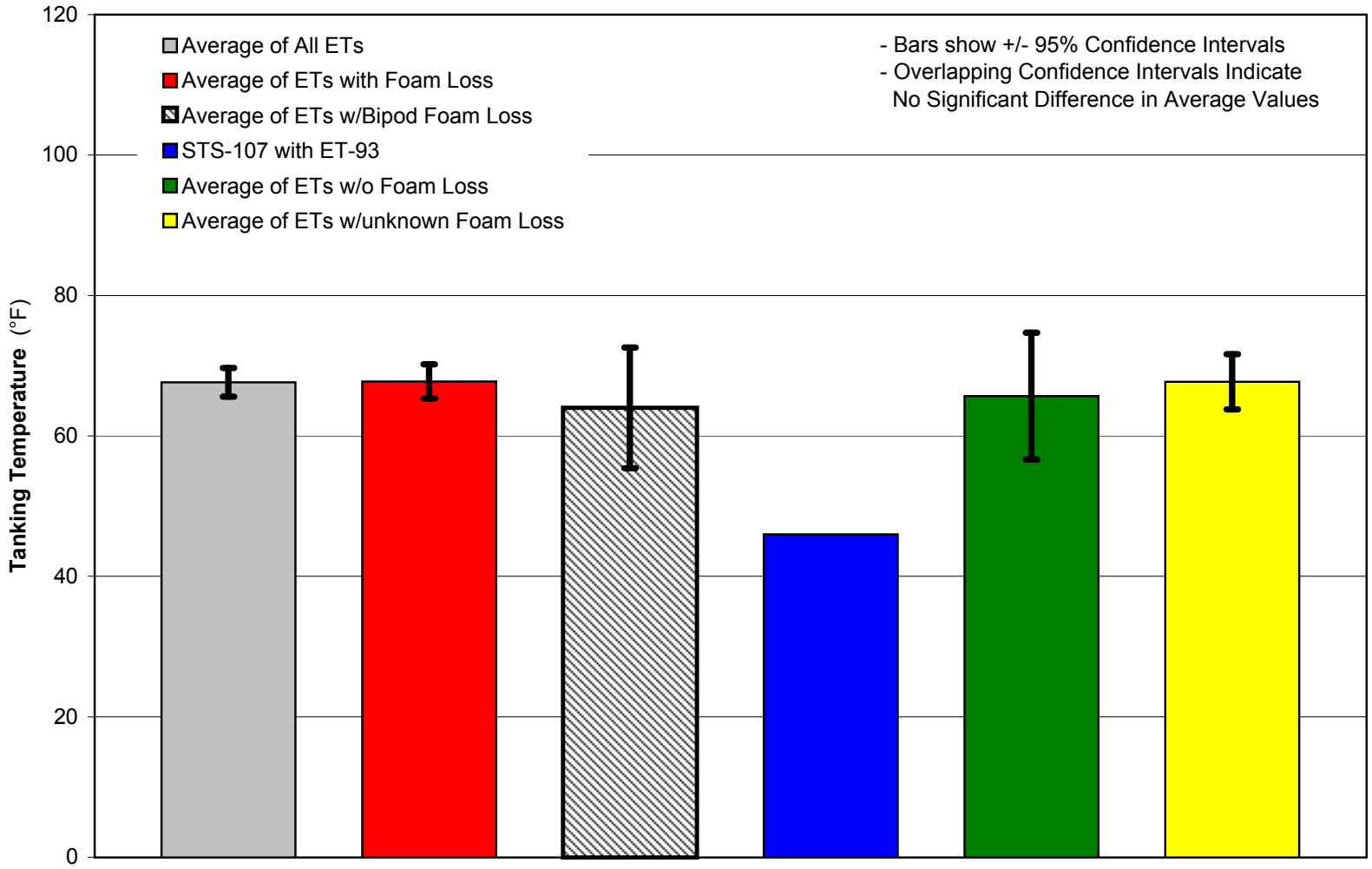

Temperature At Launch

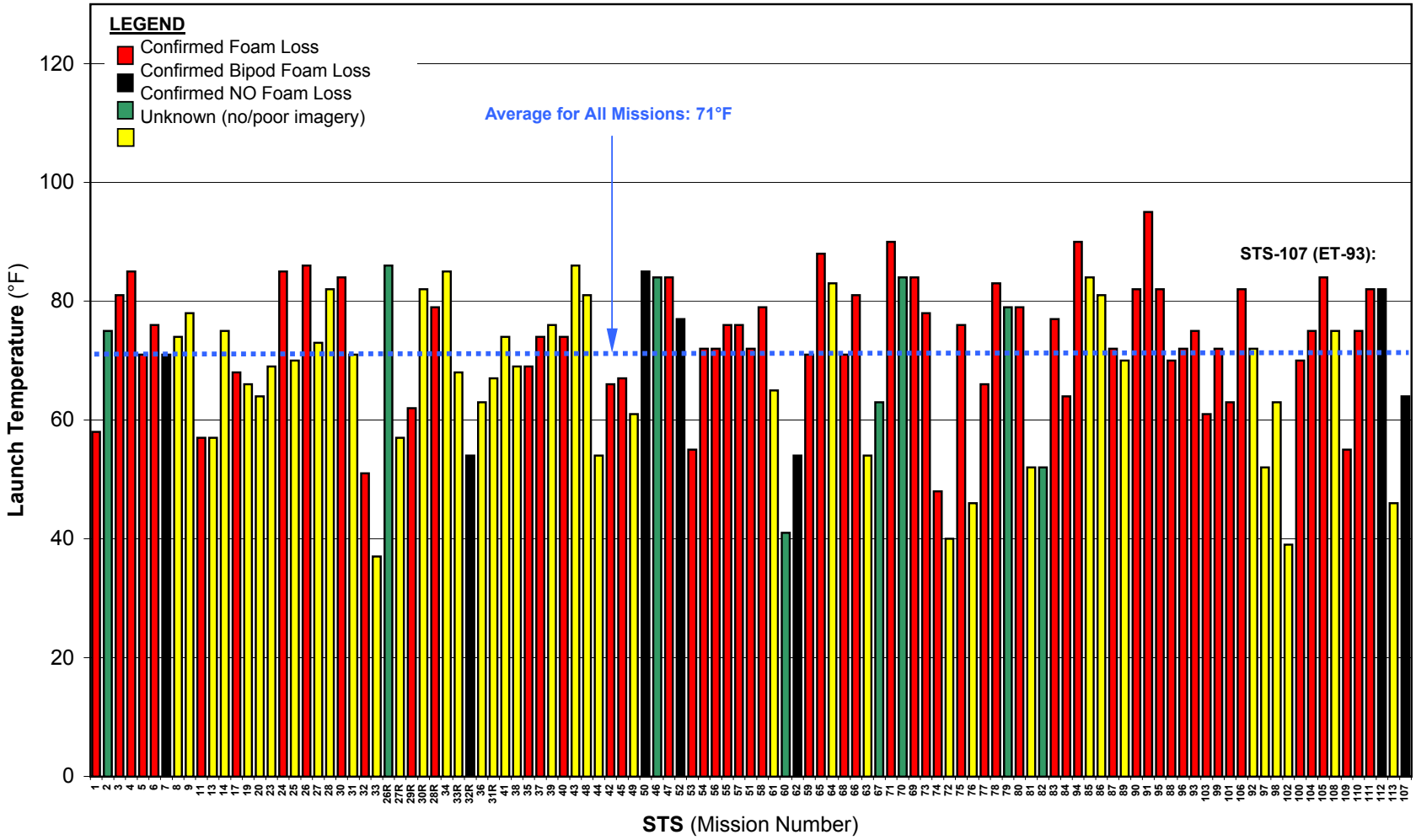

Temperature At Launch

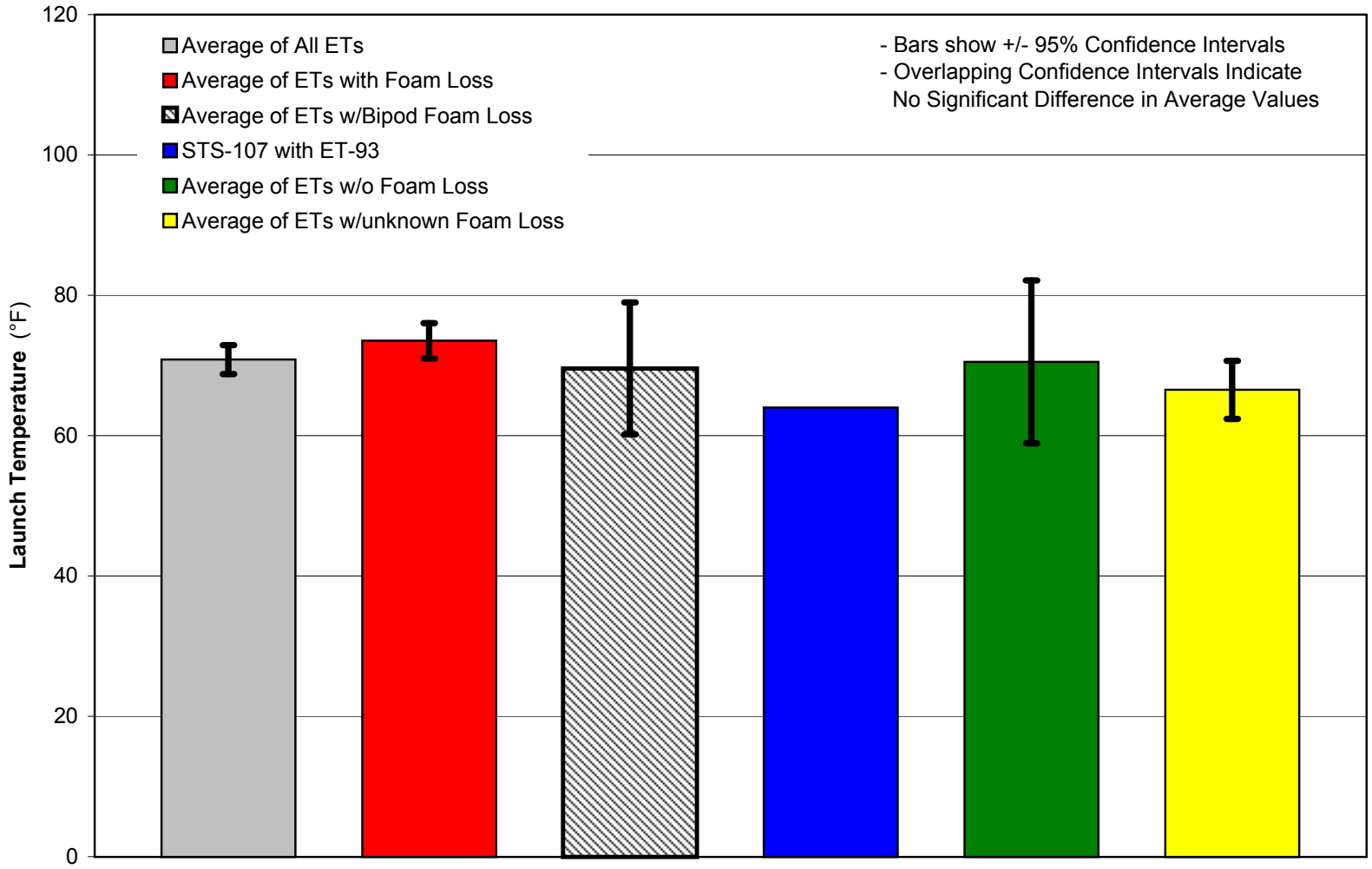

Average Dewpoint Temperature During Pre-Launch Period

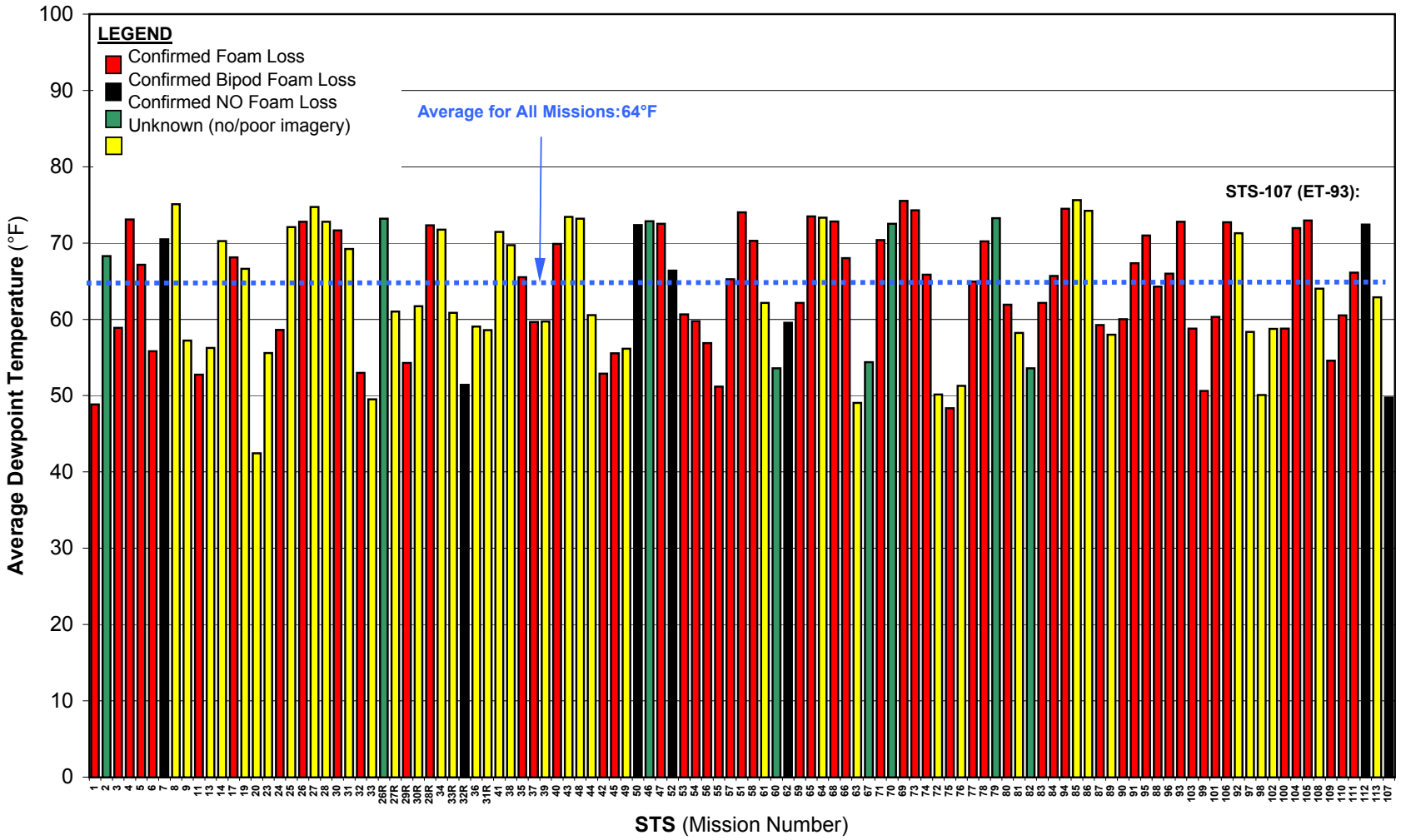

Maximum Dewpoint Temperature During Pre-Launch Period

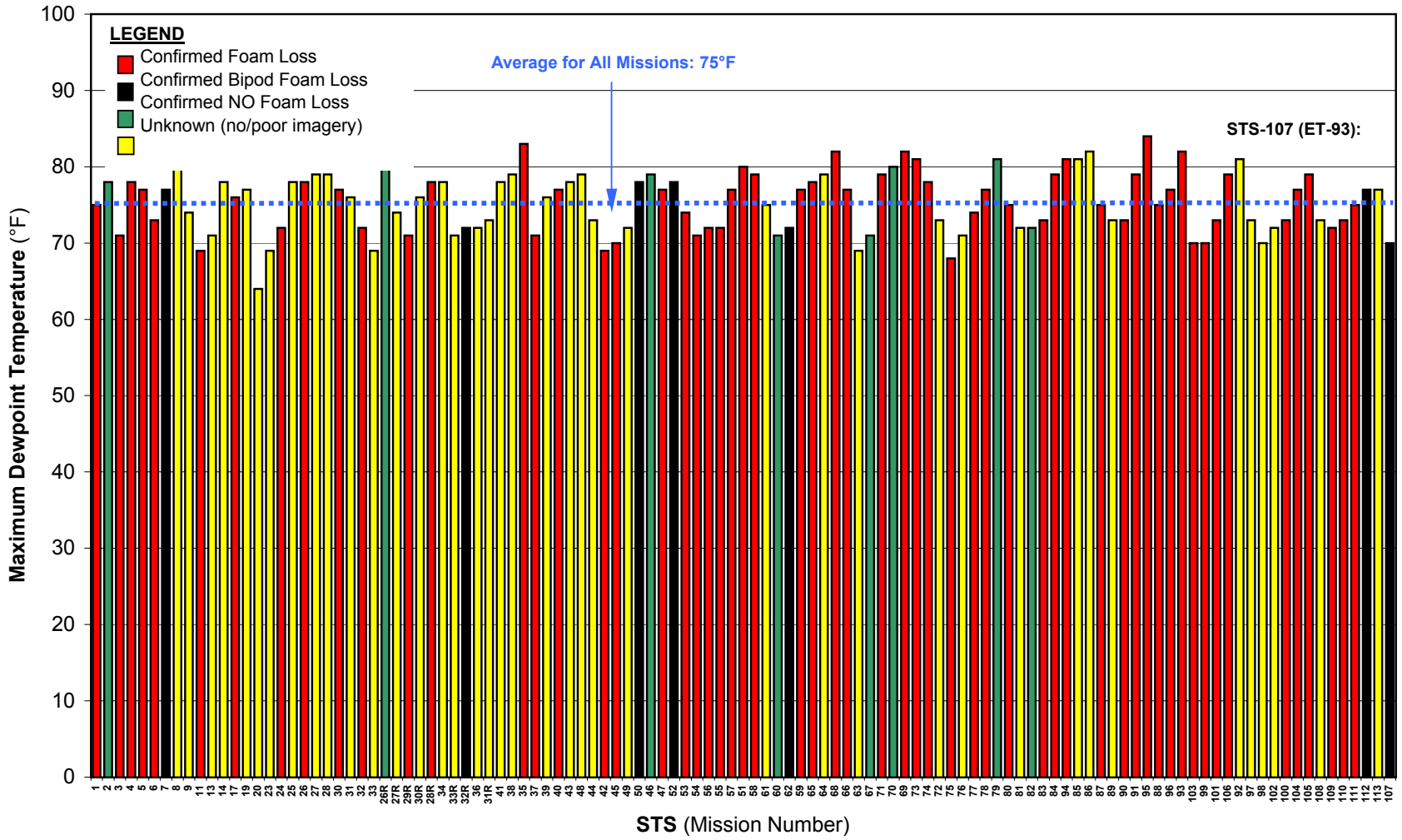

Minimum Dewpoint Temperature During Pre-Launch Period

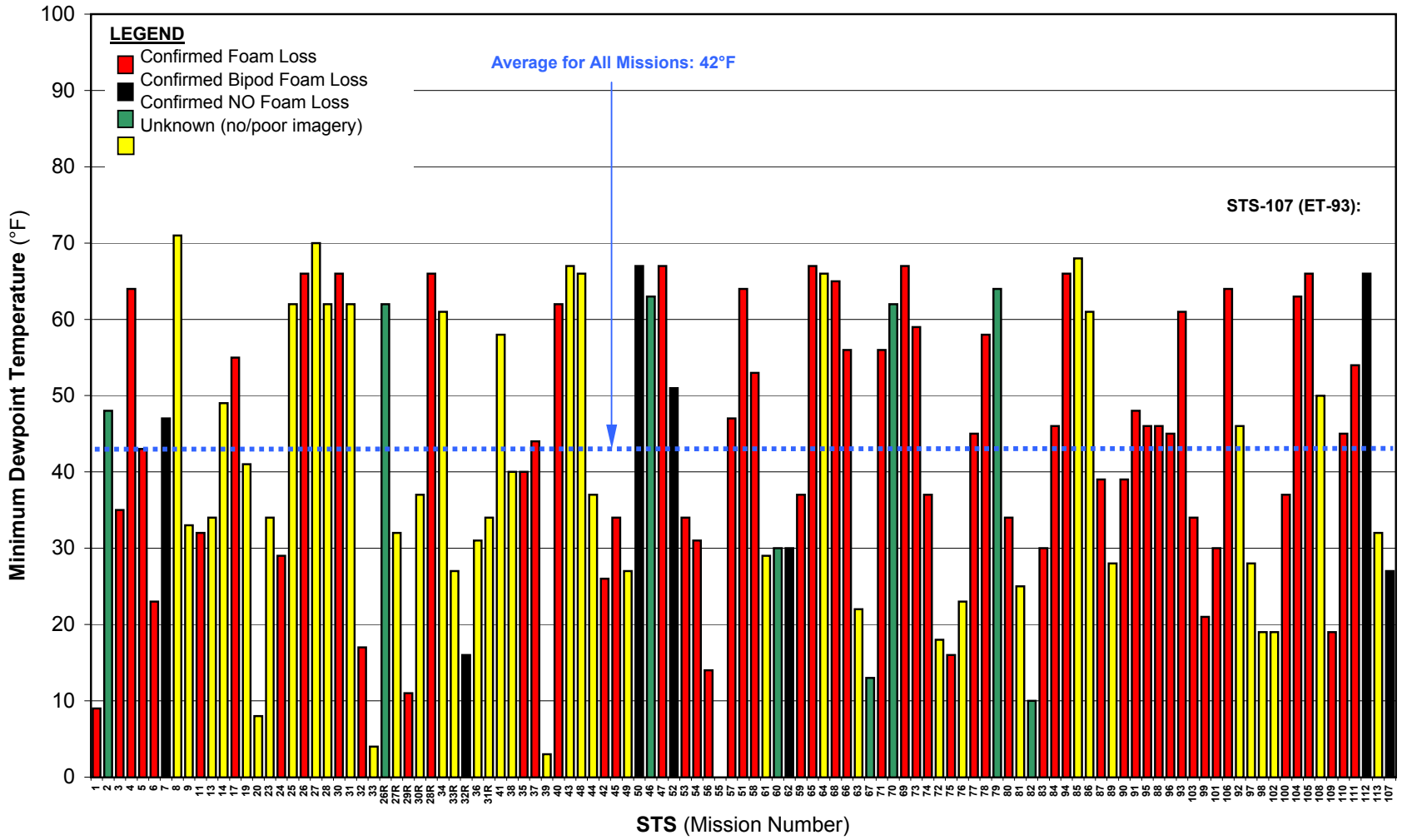

Average Dewpoint Temperature on Launch Day

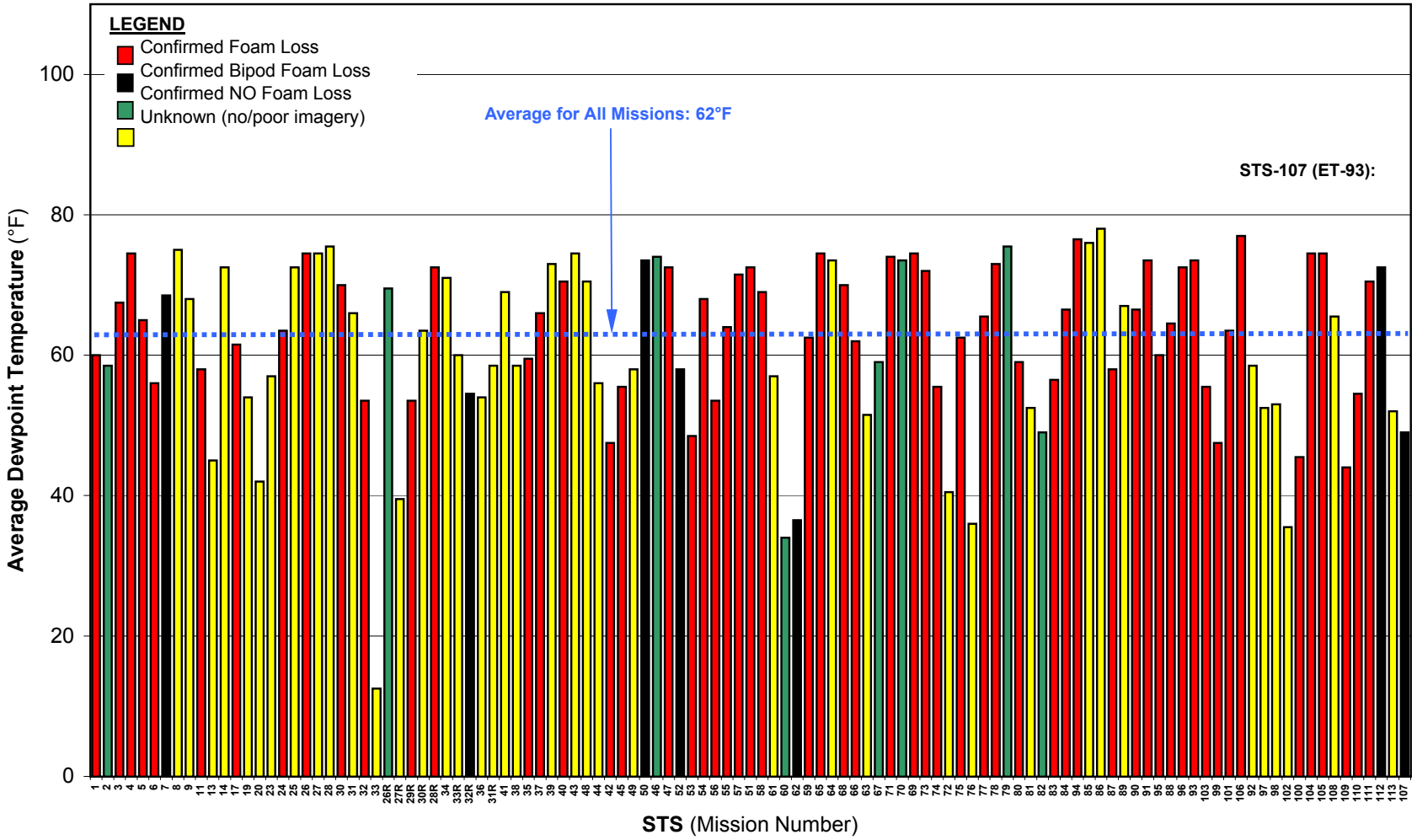

Maximum Dewpoint Temperature on Launch Day

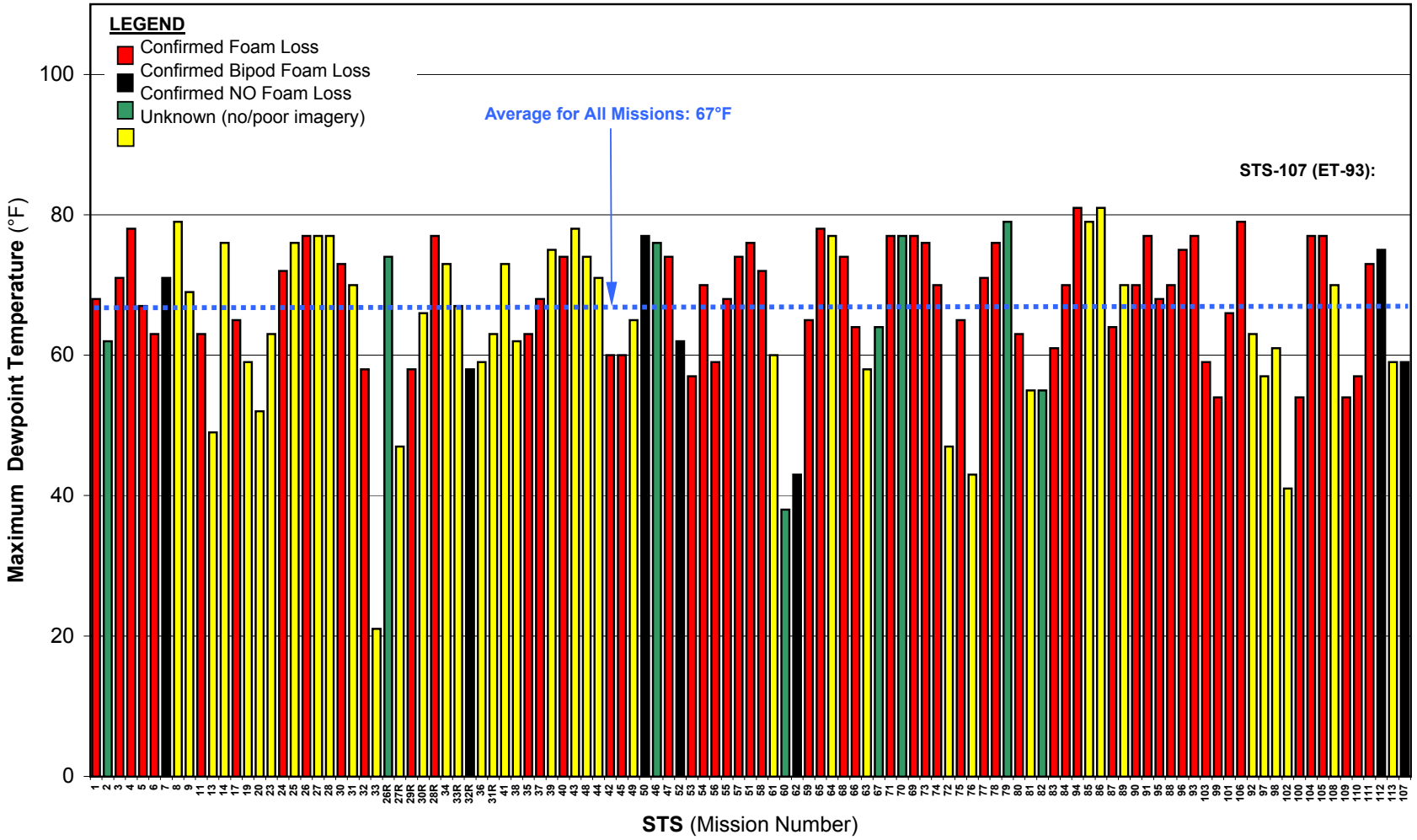

Minimum Dewpoint Temperature on Launch Day

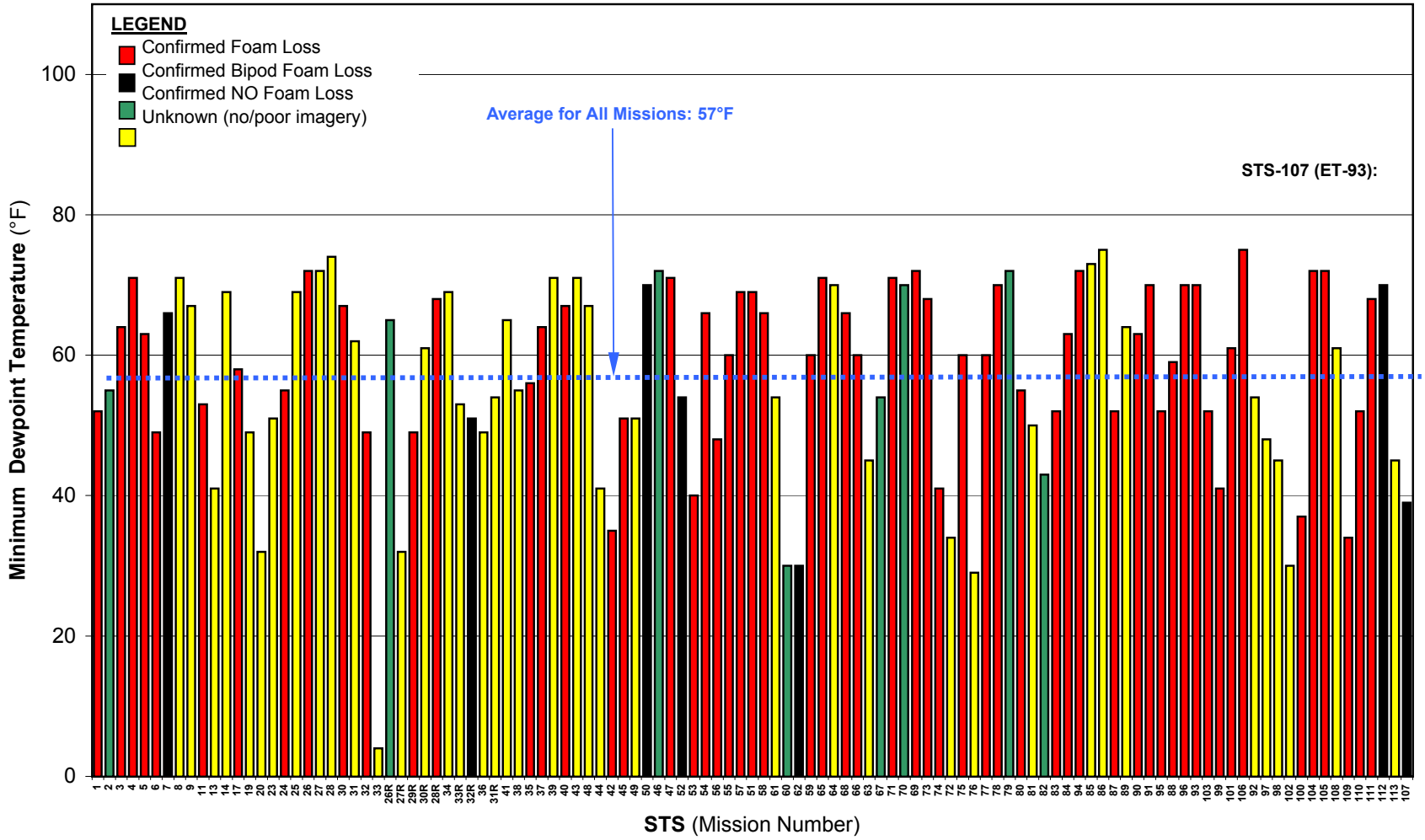

Average Humidity During Pre-Launch Period

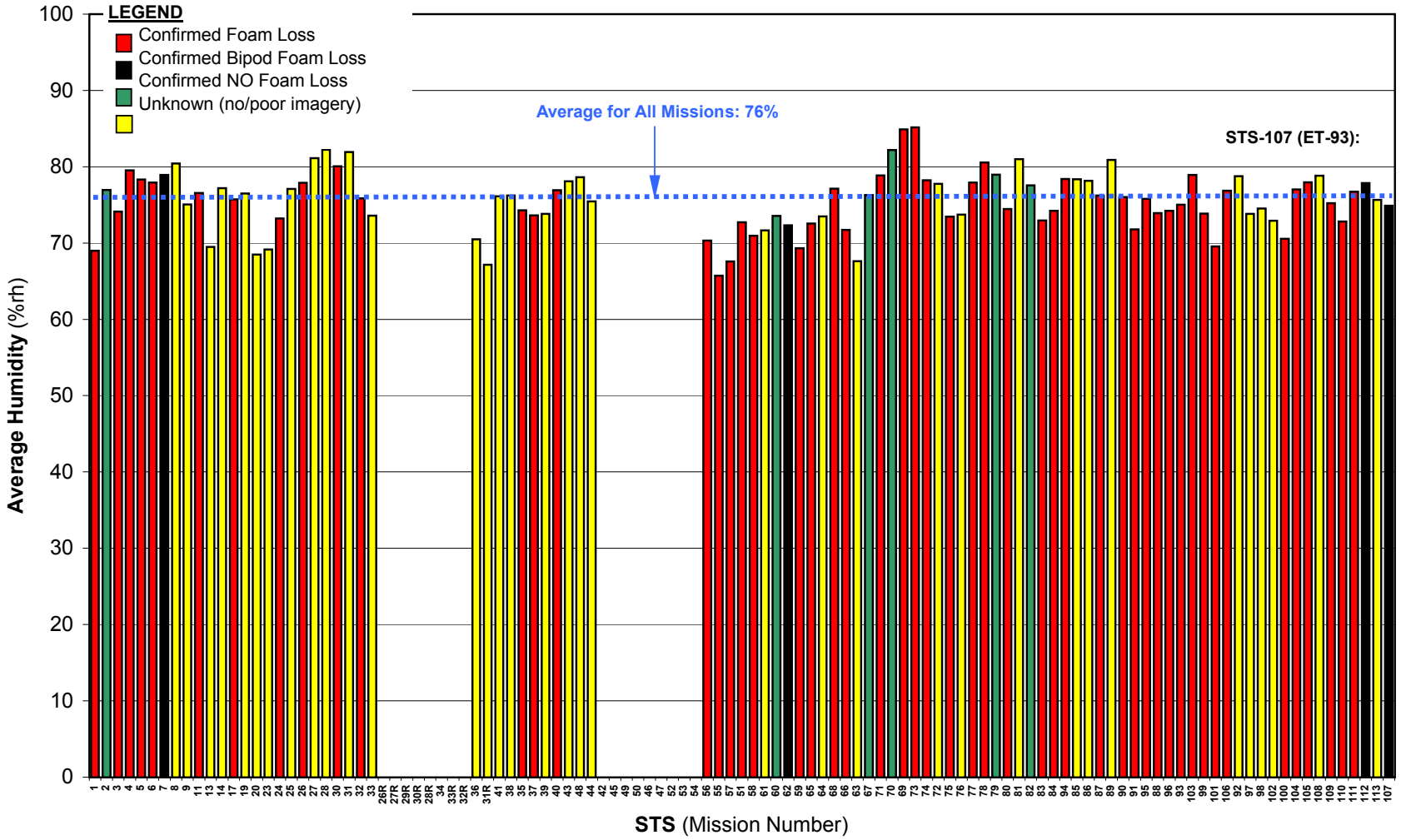

Maximum Humidity During Pre-Launch Period

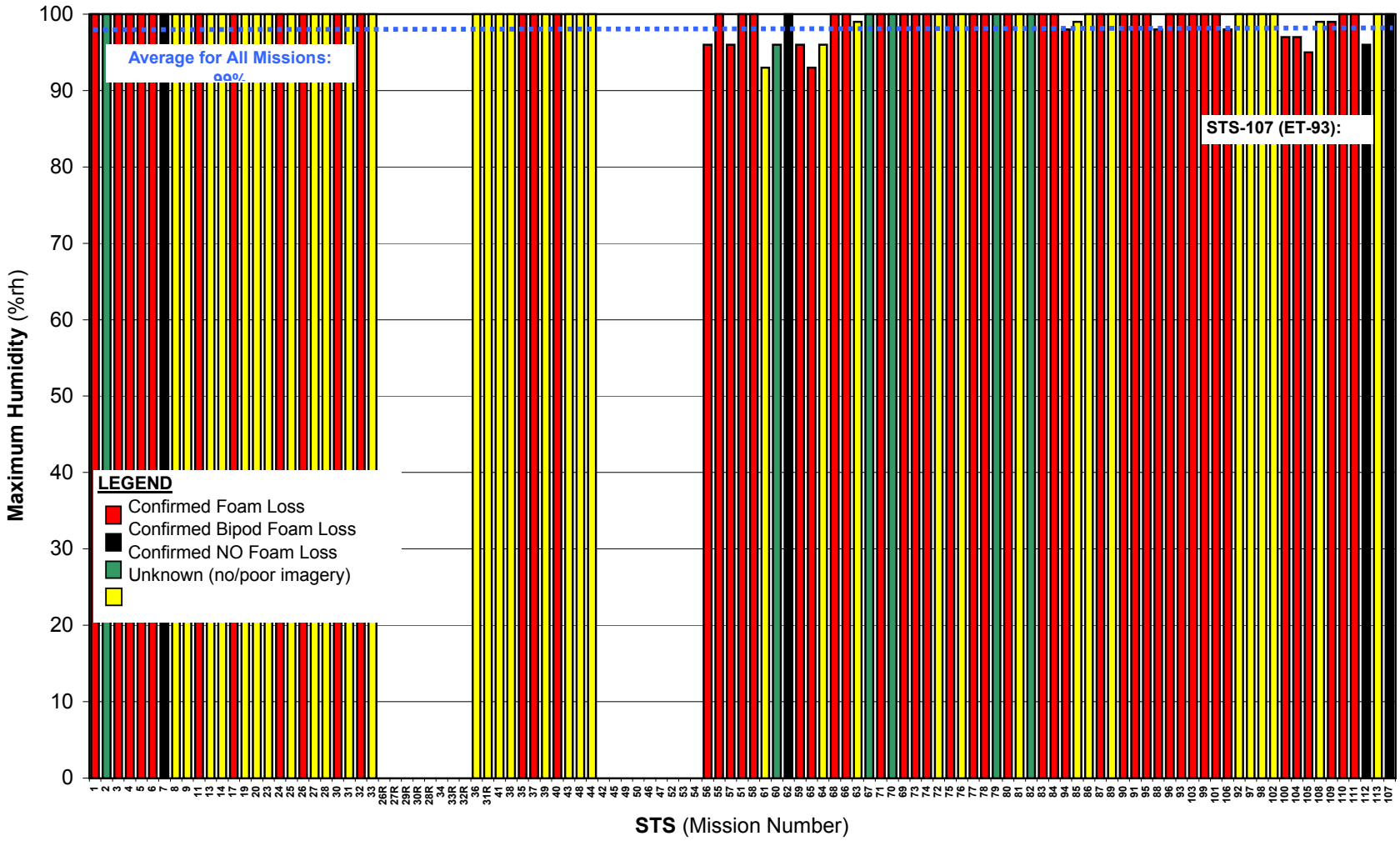

Minimum Humidity During Pre-Launch Period

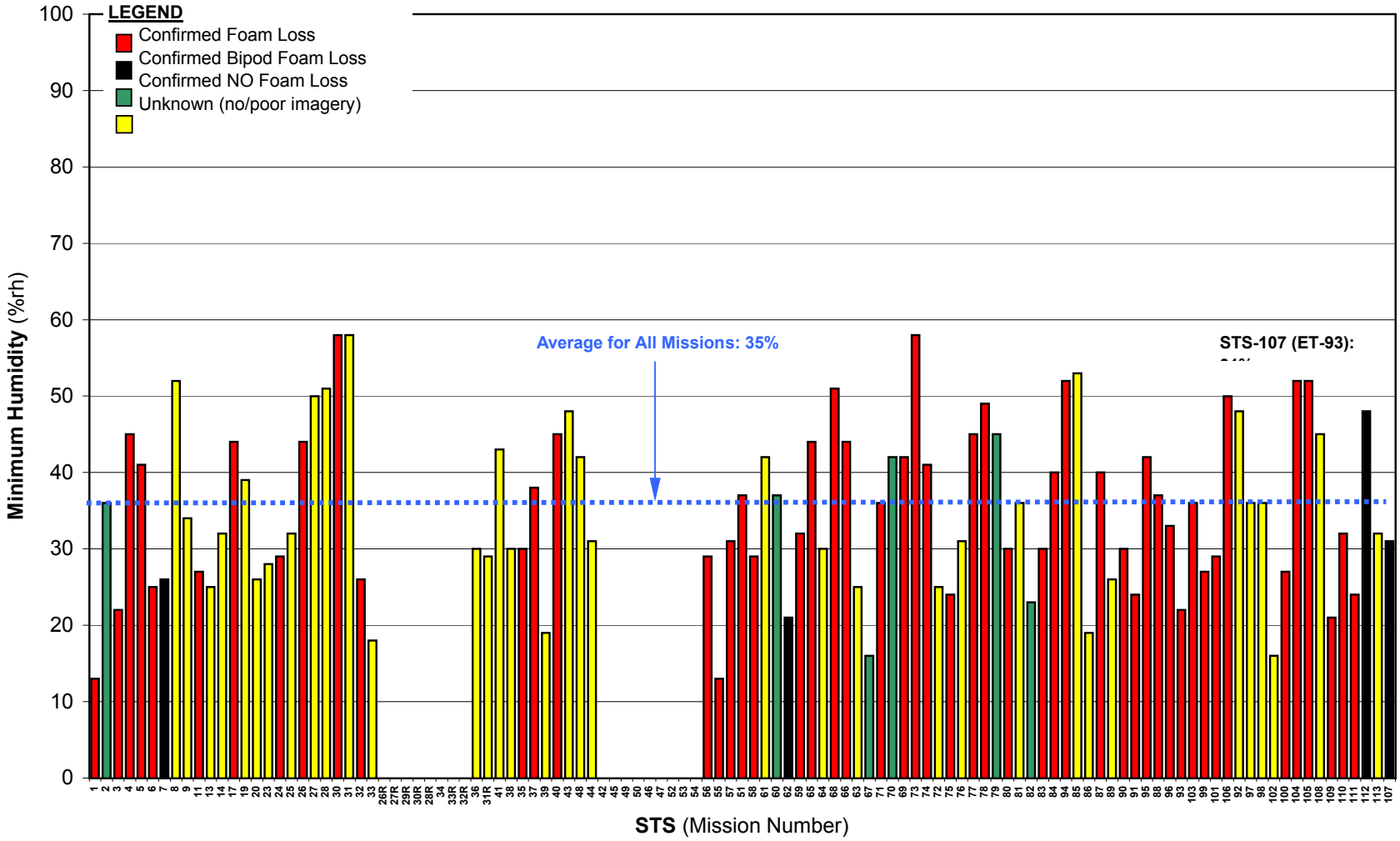

Average Humidity on Launch Day

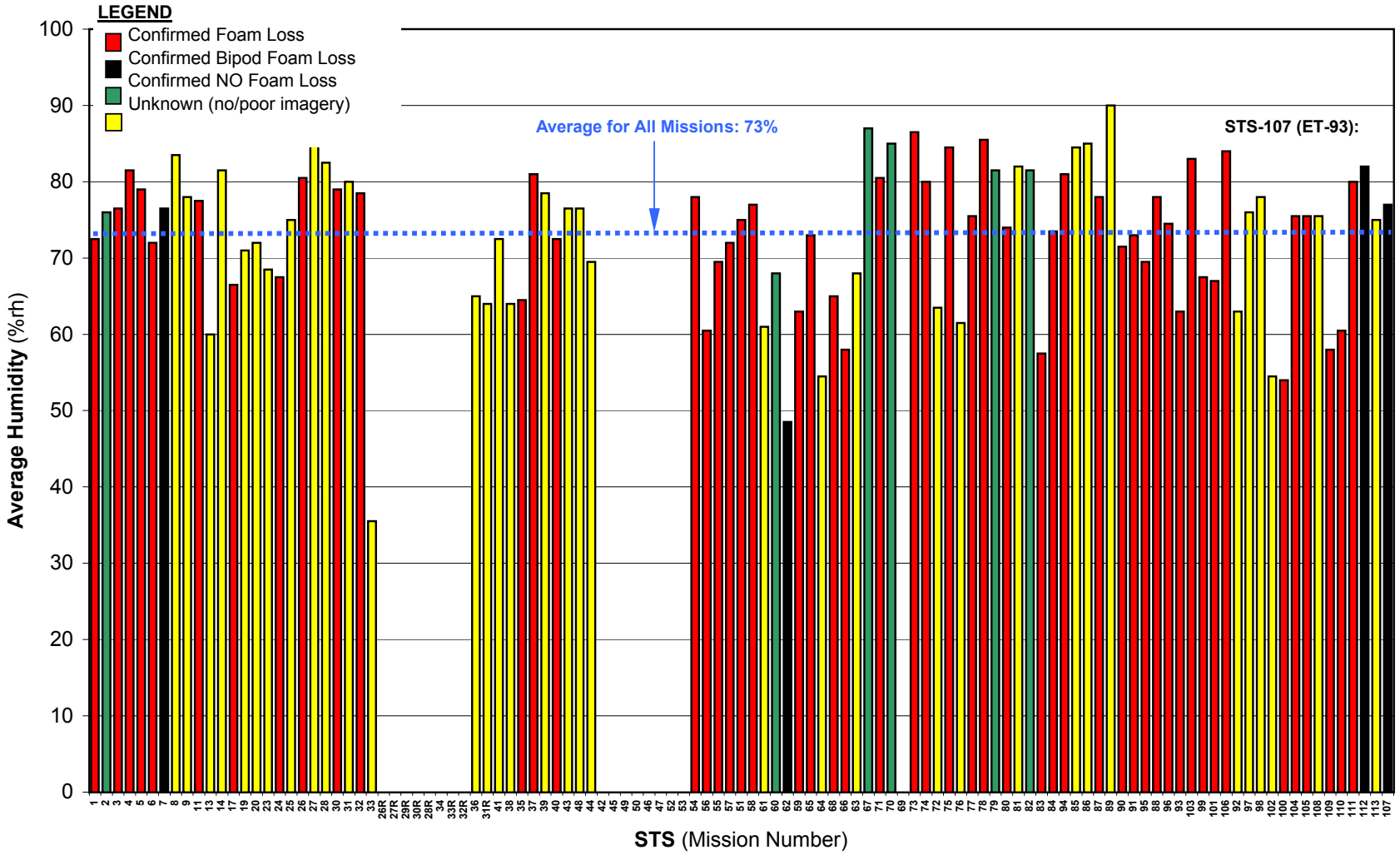

Maximum Humidity on Launch Day

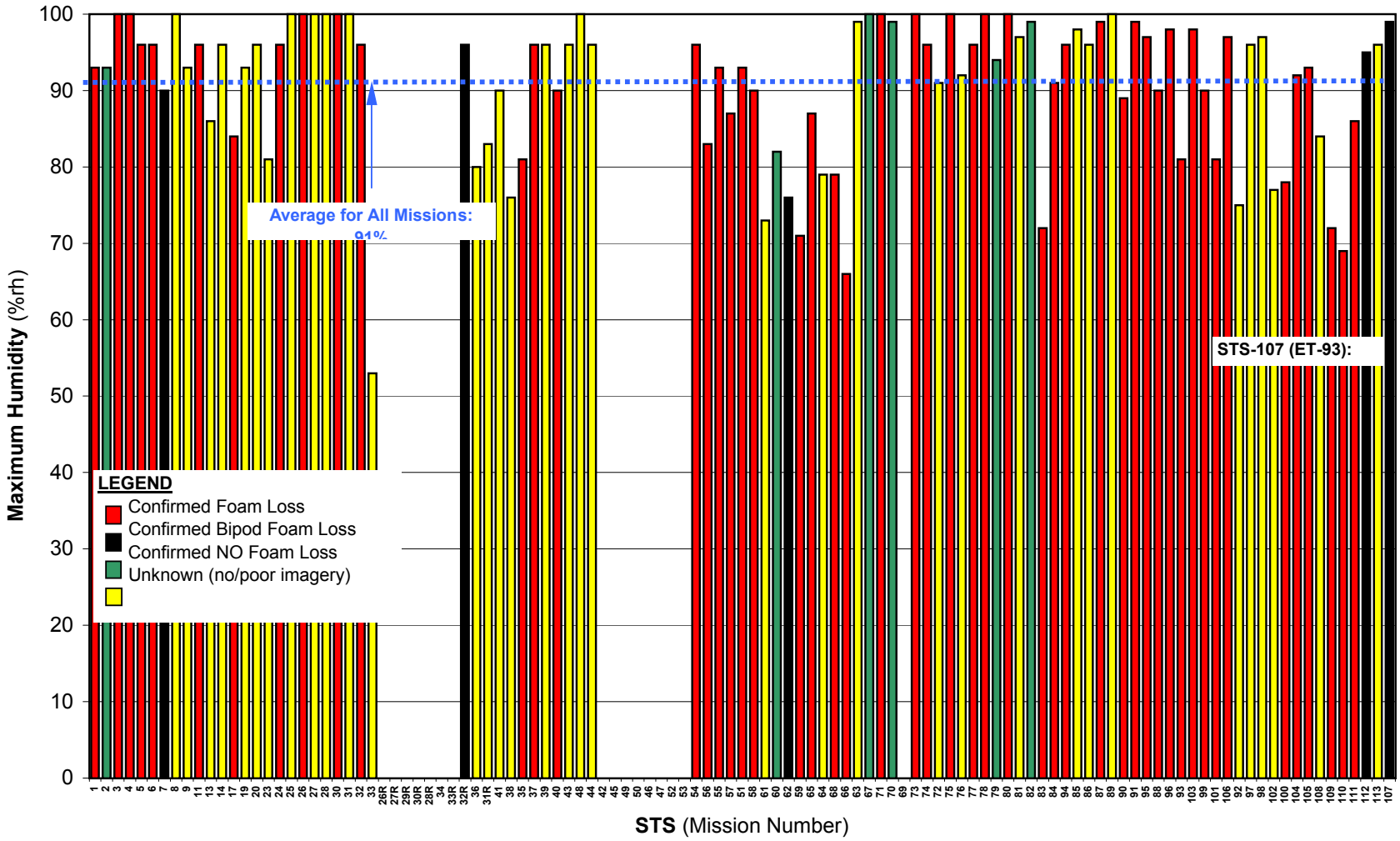

Minimum Humidity on Launch Day

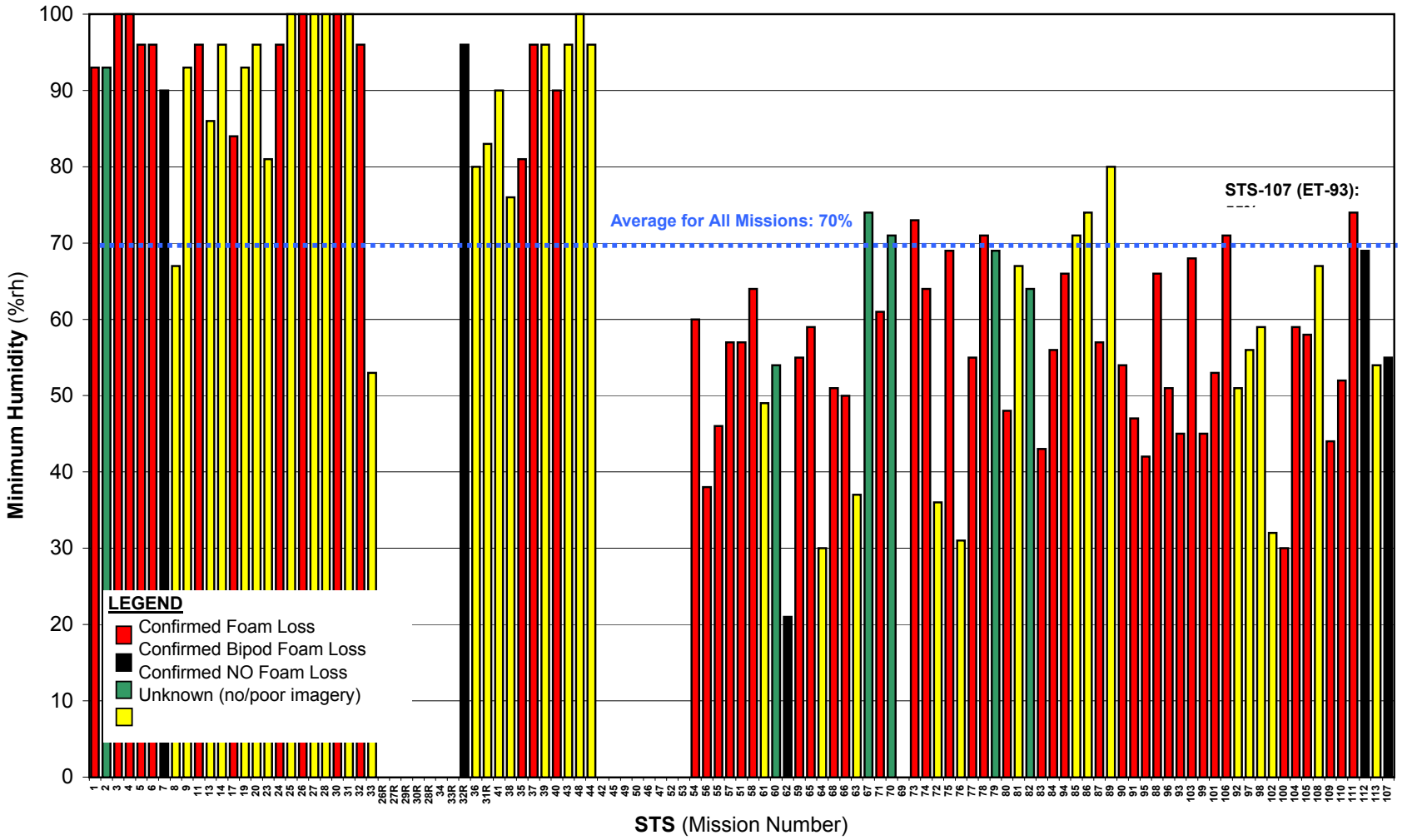

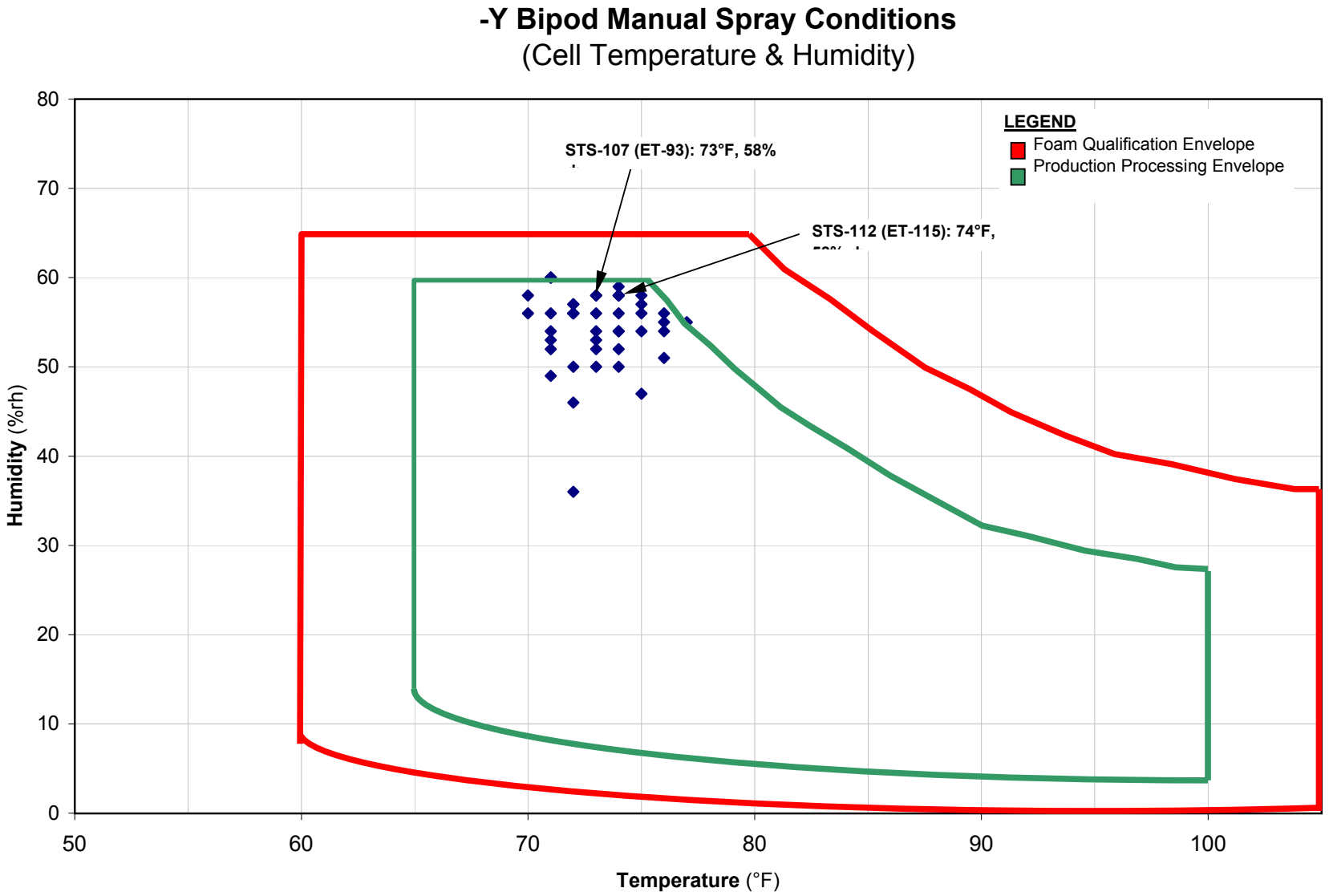
-Y Bipod Manual Spray Conditions
(Cell Temperature & Humidity)
LEGEND
Foam Qualification Envelope
Production Processing Envelope
STS-107 (ET-93): 73°F, 58%
STS-112 (ET-115): 74°F,
Humidity (%rh)
Temperature (°F)
0
10
20
30
40
50
60
70
80
50
60
70
80
90
100

-Y Bipod Manual Spray Conditions
(Cell Temperature & Humidity)

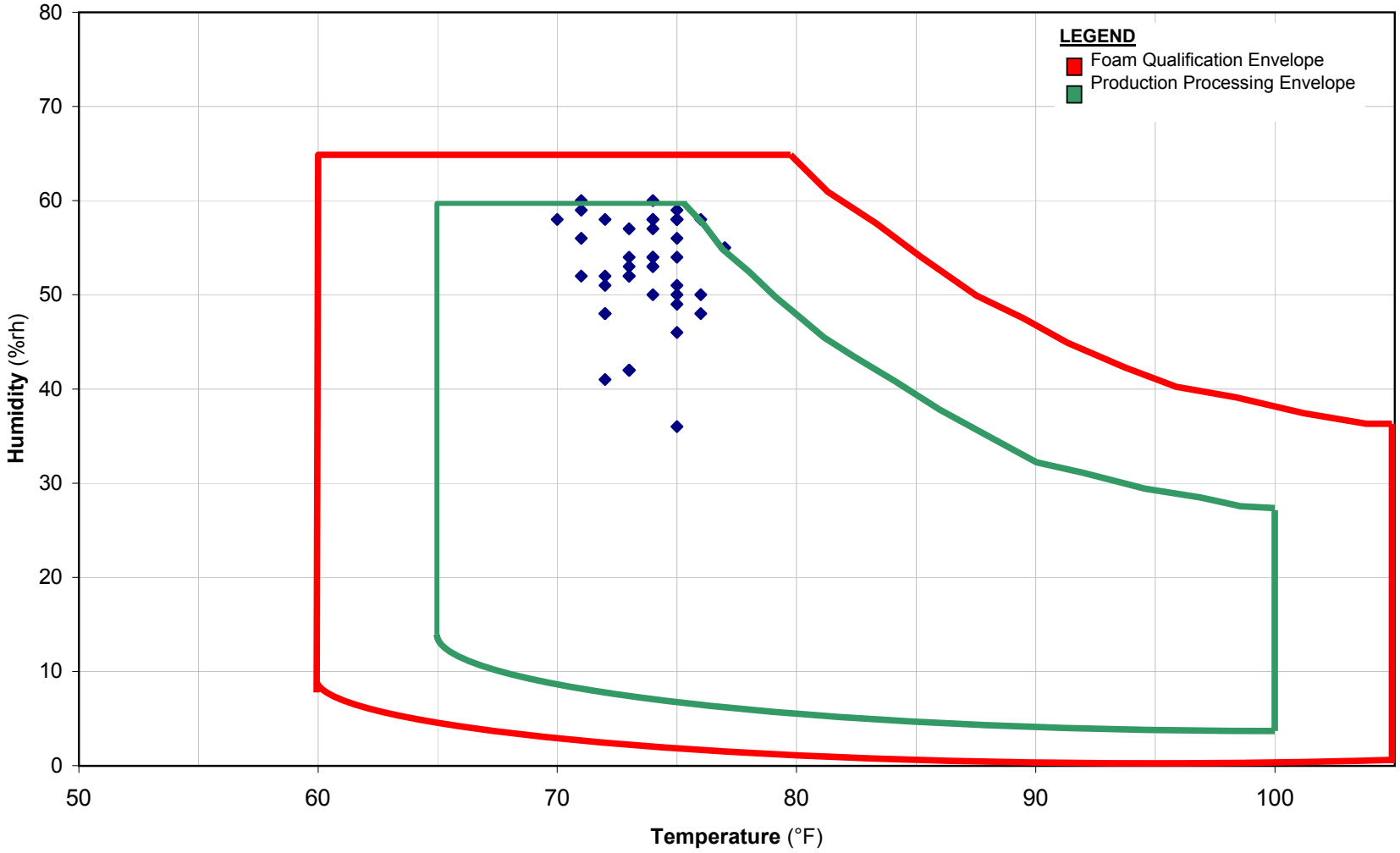

STS-Mission ET Bipod Ramp Imagery and Damage Summary	B1-00173				
History of Foam Damage	OrlandoSentinel		15-Apr-02		
External Tank Foam Loss	B1-00039				
MAF Mission Support Room Log Board	at MAF				
Night Launches:	http://www-pao.ksc.nasa.gov/kscpao/factoids/shfacts.htm				
STS-ET Correlation.xls	Jim Feeley, MAF				
Debris Info STS-32 -35 -42 - 58 Summary.xls	B0-000026				
CAIB Cryoinsulation Report	B1-000121				
Discussions at MSFC (Scotty Sparks & Steve Holmes)	B1-000132				
tanking.xls	B1-000145				
Exposure Data for OVs.xls	B1-000145				
History of External Tank Foam Loss	B0-000026				
Pad_SLF_Mission_Summaries_1981-2003.xls (Rain)	B1-000145				
STS-XXX_L.xls (Climate)	B1-000145				
Production Data	B1-000131				
E-mail from P Munafo 10 July w/loads data, etc.	3 Jul 03 Telecon				

		tanking.xls (from B1-000167)								
STS	Launch	Tanking	Tanking							
		Start Date	Start	Stop	Duration	All Times Eastern				
107	1/16/2003	1/16/2003	219	519	3.00					
113	1/16/2003	1/16/2003	1120	1420	3.00					
112	10/7/2002	10/7/2002	650	950	3.00					
111	6/5/2002	6/5/2002	757	1057	3.00					
110	4/8/2002	4/8/2002	714	1014	3.00					
109	3/1/2002	2/28/2002	2101	1	3.00					
108	12/5/2001	12/5/2001	754	1054	3.00					
105	8/10/2001	8/10/2001	750	1050	3.00					
104	7/12/2001	7/11/2001	2008	2308	3.00					
100	4/19/2001	4/19/2001	545	845	3.00					
102	3/8/2001	3/7/2001	2117	7	2.92					
98	2/7/2001	2/7/2001	916	1216	3.00					
97	11/30/2000	11/30/2000	1310	1610	3.00					
92	10/11/2000	10/11/2000	952	1252	3.00					
106	9/8/2000	9/7/2000	2350	250	3.00					
101	5/19/2000	5/18/2000	2117	17	3.00					
99	2/11/2000	2/11/2000	410	710	3.00					
103	12/19/1999	12/19/1999	1030	1330	3.00					
93	7/23/1999	7/22/1999	1454	1754	3.00					
96	5/27/1999	5/26/1999	2154	54	3.00					
88	12/4/1998	12/3/1998	1810	2110	3.00					
95	10/29/1998	10/29/1998	540	840	3.00					
91	6/2/1998	6/2/1998	914	1214	3.00					
90	4/17/1998	4/17/1998	529	829	3.00					
???	1/22/1998	1/22/1998	1252	1552	3.00					
87	11/19/1997	11/19/1997	626	926	3.00					
86	9/25/1997	9/25/1997	1339	1639	3.00					
85	8/7/1997	8/7/1997	151	521	3.50					
94	7/1/1997	7/1/1997	530	830	3.00					
84	5/15/1997	5/14/1997	1847	2157	3.17					
83	4/4/1997	4/4/1997	540	840	3.00					
82	2/11/1997	2/10/1997	1904	2204	3.00					
81	1/12/1997	1/12/1997	1937	2237	3.00					
80	11/19/1996	11/19/1996	603	903	3.00					
79	9/16/1996	9/15/1996	1933	2243	3.17					
78	6/20/1996	6/20/1996	159	509	3.17					
77	5/19/1996	5/18/1996	2140	50	3.17					
76	3/22/1996	3/21/1996	1752	2102	3.17					
75	2/22/1996	2/22/1996	658	953	2.92					
72	1/11/1996	1/10/1996	1958	2253	2.92					
74	11/13/1995	11/12/1995	2248	48	3.00					
73	10/20/1995	10/20/1995	130	430	3.00					
69	9/7/1995	9/7/1995	249	549	3.00					
70	7/13/1995	7/13/1995	121	421	3.00					
71	6/27/1995	6/27/1995	612	912	3.00					
67	3/2/1995	3/1/1995	1717	2017	3.00					
63	2/3/1995	2/2/1995	1531	1831	3.00					
66	11/3/1994	11/3/1994	336	636	3.00					
68	9/30/1994	9/29/1994	2256	156	3.00					
64	9/9/1994	9/9/1994	810	1110	3.00					
65	7/8/1994	7/8/1994	423	723	3.00					
59	4/9/1994	4/9/1994	2245	145	3.00					
62	3/4/1994	3/4/1994	33	333	3.00					
60	2/3/1994	2/2/1994	2250	150	3.00					
61	12/2/1993	12/1/1993	2007	2307	3.00					
58	10/18/1993	10/18/1993	233	533	3.00					
51	9/12/1993	9/11/1993	2325	225	3.00					
57	6/21/1993	6/21/1993	47	347	3.00					
55	4/26/1993	4/26/1993	230	530	3.00					
56	4/8/1993	4/7/1993	1610	1910	3.00	ESTIMATED				
54	1/13/1993	1/13/1993	32	332	3.00					
53	12/2/1992	12/1/1992	2239	139	3.00					
52	10/22/1992	10/22/1992	256	526	2.50					
47	9/12/1992	9/12/1992	203	503	3.00					
46	7/31/1992	7/31/1992	136	436	3.00					
50	6/25/1992	6/25/1992	347	647	3.00					
49	5/7/1992	5/7/1992	1016	1316	3.00					
45	3/24/1992	3/24/1992	2310	240	3.50					
42	1/22/1992	1/22/1992	33	333	3.00					
44	11/24/1991	11/24/1991	1011	1311	3.00					
48	9/12/1991	9/12/1991	1037	1337	3.00					
43	8/2/1991	8/2/1991	241	541	3.00					

40	6/5/1991	6/4/1991	2340	240	3.00						
39	4/28/1991	4/27/1991	2241	141	3.00						
37	4/5/1991	4/5/1991	58	358	3.00						
35	12/2/1990	12/1/1990	1708	2008	3.00						
38	11/15/1990	11/15/1990	1010	1310	3.00						
41	10/6/1990	10/5/1990	2315	215	3.00						
31	4/24/1990	4/24/1990	11	311	3.00						
36	2/28/1990	2/27/1990	1840	2140	3.00	ESTIMATED FROM A PREVIOUS ATTEMPT					
32	1/9/1990	1/8/1990	2150	50	3.00	ESTIMATED					
33	11/22/1989	11/22/1989	1010	1310	3.00						
34	10/18/1989	10/18/1989	407	707	3.00	ESTIMATED FROM PREVIOUS DAY ATTEMPT					
28	8/8/1989	8/7/1989	2310	210	3.00	ESTIMATED FROM PREVIOUS DAY ATTEMPT					
30	5/4/1989	5/4/1989	528	828	3.00						
29	3/13/1989	3/12/1989	2350	250	3.00	ESTIMATED FROM PREVIOUS DAY ATTEMPT					
27	12/2/1988	12/1/1988	2220	120	3.00	ESTIMATED FROM PREVIOUS DAY ATTEMPT					
26	9/29/1988	9/29/1988	139	439	3.00						
51L	1/28/1986	1/28/1986	418	718	3.00						
61C	1/12/1986	1/11/1986	2235	1035	12.00	ESTIMATED FROM LAUNCH TIME (L-8)					
61B	11/26/1985	11/26/1985	1109	1409	3.00						
61A	10/30/1985	10/30/1985	340	640	3.00						
51J	10/3/1985	10/3/1985	200	500	3.00						
51I	8/27/1985	8/26/1985	2300	200	3.00	ESTIMATED FROM LAUNCH TIME (L-8)					
51F	7/29/1985	7/29/1985	628	928	3.00						
51G	6/17/1985	6/16/1985	2313	213	3.00						
51B	4/29/1985	4/29/1985	340	640	3.00						
51D	4/12/1985	4/12/1985	100	400	3.00	ESTIMATED FROM LAUNCH TIME (L-8)					
51C	1/23/1985	1/23/1985	455	755	3.00						
51A	11/7/1984	11/6/1984	2358	258	3.00						
41G	10/5/1984	10/4/1984	2243	143	3.00						
41D	8/30/1984	8/30/1984	15	315	3.00	ESTIMATED FROM PREVIOUS DAY ATTEMPT					
41C	4/6/1984	4/5/1984	2038	338	5.00						
41B	2/3/1984	2/2/1984	2345	245	5.00						
9	11/28/1983	11/27/1983	2240	540	7.00						
8	8/30/1983	8/29/1983	1800	2100	3.00	ESTIMATED					
7	6/18/1983	6/18/1983	13	313	3.00						
6	4/4/1983	4/4/1983	530	930	4.00	ESTIMATED					
5	11/11/1982	11/10/1982	2330	230	3.00	ESTIMATED					
4	6/27/1982	6/27/1982	300	600	3.00	ESTIMATED					
3	3/22/1982	3/22/1982	200	500	3.00	ESTIMATED					
2	11/12/1981	11/12/1981	200	530	2.50	ESTIMATED FROM LAUNCH TIME (L-8)					
1	4/12/1981	4/11/1981	2330	300	3.50	ESTIMATED					

No imagery of the +Z axis +/-90 degrees available

No loss of TPS noted

								View				
STS	**ET**	**Vehicle**	**Launch Date**	**Useable ET Crew Photos**	**Useable ET Umbilical Well Photos**	**Day/ Night**	**Notes**	**-Y**	**+Y**	**Bipod Ramp**	**Flange**	**LO2 Tank**
107	093	102	01/16/03	Yes	No	Day	***Columbia Accident*** Crew downlink video views -Y/-Z side of ET - No visual observations	N	N	Ground base films note most likely loss of -Y bipod ramp at 81 seconds MET	No loss of TPS noted	No loss of TPS noted
113	116	105	11/24/02	No	No	Night	Due to dark conditions no useable ET imagery was obtained	N	N	No data obtained	No data obtained	No data obtained
112	115	104	10/07/02	No	Yes	Day	N/A	Y	Y	Portion (approximately 12"x7") of the -Y Bipod Ramp TPS is missing exposing the bipod spindle	1 divot (3" dia) in LH2 tank flange near the -Y jack-pad closeout with exposed primed substrate 1 divots (2.5"x1.5") in LH2 tank flange just forward of the +Y jack pad closeout	No loss of TPS noted
111	113	105	06/05/02	Yes	Yes	Day	N/A	Y	Y	No loss of TPS noted	3 divots (1.5" dia) in LH2 tank flange near the +Y jack-pad closeout 1 divot (1.5" dia) at the +Y bipod ramp-to-LH2 tank interface	No loss of TPS noted
110	114	104	04/08/02	Yes	Yes	Day	ET intertank, LO2 tank, and the ET nose cone were not imaged Shadows from the late afternoon limited the 35mm umbilical camera views in the +Y direction of the ET LO2 feedline. The +Y ET Thrust Panel was not imaged 16mm umbilical camera film with the 10 mm lens (FL-101) was out of focus	Y	Y	No loss of TPS noted	2 divots (approximately 5" x 5") between the bipod. One of the divots encompasses a significant portion of the +Y Jack Pad closeout	No loss of TPS noted
109	112	102	03/01/02	Yes	Yes	Day	N/A	Y	Y	No loss of TPS noted	3 divots between bipod ramps (one small and two 6" dia) 2 smal divots (3" dia) +Y of LH2 PAL Ramp near thrust panel	No loss of TPS noted
108	111	105	12/05/01	No	No	Night	No data obtained	N	N	No data obtained	No data obtained	No data obtained
105	110	103	08/10/01	Yes	Yes	Day	N/A	Y	Y	No loss of TPS noted	Small divots observed between the bipod struts	No loss of TPS noted
104	109	104	07/12/01	Yes	Yes	Day	Large areas of the +Z not visible	Y	Y	No loss of TPS noted	1 small divot in the LH2 tank flange at +Y 1 small divot between bipod struts	No loss of TPS noted
100	108	105	04/19/01	Yes	Yes	Day	All images were in clear focus, field of view and the lighting was excellent	Y	Y	No loss of TPS noted	2 divots (4" dia and 10" dia) between the bipod struts near centerline 1 divot (4"-6" dia) in the LH2 tank flange closeout -Y/+Z quadrant	No loss of TPS noted
102	107	103	03/08/01	Yes	Yes	Day	Lighting was excellent for areas to the +Y side of the LO2 feedline, the -Y side of the ET was in deep shadow 16 mm umbilical cameras not flown on this mission	N	N	No apparent loss of TPS noted - Area in deep shadow	No loss of TPS noted	No loss of TPS noted
098	106	104	02/07/01	No	No	Night	Due to dark conditions no useable ET imagery was obtained	N	N	No data obtained	No data obtained	No data obtained
097	105	105	11/30/00	No	No	Night	Crew photos too distant to determine ET foam loss 35mm imagery too dark and 16mm umbilical cameras disabled	N	N	No data obtained	No data obtained	No data obtained
092	104	103	10/11/00	No	No	Night	Due to dark conditions no useable ET imagery was obtained	N	N	No data obtained	No data obtained	No data obtained
106	103	104	09/08/00	Yes	Yes	Day	N/A	Y	Y	No loss of TPS noted	Numerous divots occurred in the LH2 tank flange closeout 3 divots (4"-6" dia) in LH2 tank flange closeout between the LO2 feedline and +Y thrust panel with exposed primed substrate in two of the divots 3 divots (4"-6" dia) in LH2 tank flange closeout between the bipod struts Possible divot in LH2 tank flange closeout under pressline	No loss of TPS noted
101	102	104	05/19/00	Yes	Yes	Day	SRB Mounted Cameras installed to observe NCFI popcorning phenomenon - 228 popcorn-type (small shallow) divots in Intertank thrust panel foam First ET will fully implemented thrust panel foam venting - Venting thrust panel foam reduced the size of the foam divots	Y	Y	No loss of TPS noted	Possible divot in the LH2 tank flange closeout on centerline (seen in crew photos only)	No loss of TPS noted
099	092	105	02/11/00	No	Yes	Day/Night	Good frontal lighting on the ET after the Orbiter shadow moved away Implemented partial venting of thrust panel foam	Y	Y	No loss of TPS noted	1 divot (18"X6") +Y side of the LH2 tank cable tray. The divot extended from the LH2 tank-to-intertank flange closeout into the intertank net spray foam 1 divot (7"x5") in the LH2 tank flange closeout on centerline between the bipod struts with exposed primed substrate 2 divots (6"-7"dia) divots in the LH2 tank flange closeout in the -Y/+Z quadrant outboard of the -Y bipod ramp	No loss of TPS noted
103	101	103	12/20/99	No	No	Night	SRB Mounted Cameras installed to observe NCFI popcorning phenomenon - 78 popcorn-type (small shallow) divots in Intertank thrust panel foam Implemented partial venting of thrust panel foam	N	N	No data obtained	No data obtained	No data obtained
093	099	102	07/23/99	No	No	Night/Day	Crew photos too distant to determine ET foam loss SRB Mounted Cameras installed to observe NCFI popcorning phenomenon - 210 popcorn-type (small shallow) divots in Intertank thrust panel foam	N	N	No data obtained	No data obtained	No data obtained
096	100	103	05/27/99	Yes	No	Day	SRB Mounted Cameras installed to observe NCFI popcorning phenomenon - 449 popcorn-type (small shallow) divots in Intertank thrust panel foam	Y	Y	No loss of TPS noted	Two small light spots (possible divots) were detected in the LH2 tank flange closeout between the bipod struts	Small divots (2 or 3) in the foward ogive (pencil sharpener area) that exceed the typically observed normal ablation. "Popcorn" type divots close to the +Z axis in an area from the nose cone aft to approximately XT-480.

Acreage				
Intertank	**LH2 Tank**	**Components**	**Substrate Exposed**	**# of Tankings**
No loss of TPS noted	No loss of TPS noted	No loss of TPS noted	No	1
No data obtained	No data obtained	No data obtained	N/A	3
One shallow TPS divot was observed on the LH2 tank near the ice/frost ramp at station Sta-1857. The area is shallow and approximately 5-inches long by 3-inches wide.	No loss of TPS noted	No loss of TPS noted	Flange closeout	1
1 divot (6"x2") near the GO2 pressline ramp at Sta 897 with exposedprimed substrate. This area is not sanded or vented	No loss of TPS noted	No loss of TPS noted	Flange closeout	2
No loss of TPS noted	No loss of TPS noted	No loss of TPS noted	No	2
No loss of TPS noted	No loss of TPS noted	1 small divot (3" dia) with foam still partially attached on the +Y thrust strut near the aft /inboard side 1 divot (8" dia) with foam still partially attached on the +Y thrust strut near the forward flange	No	1
No data obtained	No data obtained	No data obtained	N/A	2
No loss of TPS noted	1 divot near the base of the LO2 feedline support bracket closeout at station Sta 1377 1 divot (2"x6") observed near the Sta 1270 location	No loss of TPS noted	No	2
No loss of TPS noted	No loss of TPS noted	No loss of TPS noted	No	1
No loss of TPS noted	1 divot(4" dia) was noted just aft of the +Y bipod spindle housing closeout	1 divot (6"x 4") was seen on the +Y longeron TPS closeout, near the thrust strut joint to the longeron	No	1
No loss of TPS noted	No loss of TPS noted	No loss of TPS noted	No	1
No data obtained	No data obtained	No data obtained	N/A	1
No data obtained	No data obtained	No data obtained	N/A	1
No data obtained	No data obtained	No data obtained	N/A	2
4 shallow divots were located on stringer head 1 divot (8"Lx2"W) just forward of the flange closeout and almost on centerline with the bipod 2 small divots on stringer head TPS forward of the +Y bipod housing closeout in the intertank acreage	2 shallow divots (2" dia) approximately 12 inches aft of the flange closeout/bipod	1 small divot on the +Y thrust strut knuckle (appeared to be the result of a debris impact) 1 divot in the leading edge of the Sta 1787 ice/frost ramp (may have taken some acreage NCFI as well	Flange closeout	2
Intertank thrust panel popcorning (See notes)	No loss of TPS noted	Possible divot in +Y longeron closeout 1 divot (4"x2") in the forward surface outboard edge of the +Y vertical strut cable tray closeout 7 divots, possibly caused by ice debris impacts, in the +Y thrust strut TPS near the flange/knuckle	No	4
1 divot (approximately 18"L) at the +Y thrust panel to stringer interface just forward of the LH2 tank-to-intertank flange	No loss of TPS noted	3 divots on the pressline ice/frost ramp upper closeout at Sta 1722	Flange closeout	2
Intertank thrust panel popcorning (See notes)	No data obtained	No data obtained	N/A	2
Intertank thrust panel popcorning (See notes)	No data obtained	No data obtained	N/A	3
Intertank thrust panel popcorning (See notes) Light spots, possible small divots, were visible in the intertank +Z stringers forward of the bipod	No loss of TPS noted	No loss of TPS noted	No	1

No imagery of the +Z axis +/-90 degrees available

No loss of TPS noted

								View					
STS	**ET**	**Vehicle**	**Launch Date**	**Useable ET Crew Photos**	**Useable ET Umbilical Well Photos**	**Day/ Night**	**Notes**	**-Y**	**+Y**	**Bipod Ramp**	**Flange**	**LO2 Tank**
088	097	105	12/04/98	Yes	No	Night/Day	No usable umbilical imagery ere available due to the dark conditions Crew phots provided views of the aft dome, aft hardpoint, LH2 tank acreage, LO2 tank acreage, portions of the intertank and the nose cone.	Y	Y	No loss of TPS noted	10" divot in LH2 tank flange closeout extending into -Y thrust panel acreage	No loss of TPS noted
095	098	103	10/29/98	Yes	Yes	Day	SRB Mounted Cameras installed to observe NCFI popcorning phenomenon - 152 popcorn-type (small shallow) divots in Intertank thrust panel foam	Y	Y	No loss of TPS noted	2 divots (7" dia) between bipod 1 divot near +Y bipod flange	No loss of TPS noted
091	096	103	06/02/98	Yes	Yes	Day	First flight of umbilical well cameras on OV103	Y	Y	No loss of TPS noted	6" divot between bipod struts in LH2 tank flange closeout Two divots (4 to 6 diameter) in -Y/+Z quadrant of LH2 tank flange closeout 10" divot in LH2 tank flange closeout near -Y thrust panel	No loss of TPS noted
090	091	102	04/17/98	Yes	Yes	Day	N/A	Y	Y	No loss of TPS noted	One 6" dia divot in LH2 tank flange closeout at centerline Three divots in -Y/+Z quadrant (2 divots approximately 4 - 6" dia and one divot 10" dia, with exposed primed substrate) of LH2 tank flange closeout One divot (3" dia) in +Y/+Z quadrant of LH2 tank flange closeout	No loss of TPS noted
089	090	105	01/22/98	No	No	Night	No data obtained	N	N	No data obtained	No data obtained	No data obtained
087	089	102	11/19/97	Yes	Yes	Day	IFA-87-T001, Intertank thrust panel foam popcorning phenomenon associated with NCFI	Y	Y	No loss of TPS noted	8" divot outboard of LO2 feedline in LH2 tank flange closeout	No loss of TPS noted
086	088	105	09/25/97	No	No	Night	No data obtained	N	N	No data obtained	No data obtained	No data obtained
085	087	105	08/07/97	Yes	No	Day	No loss of TPS noted (+Z / -Y side visible)	Y	N	No loss of TPS noted	No loss of TPS noted	No loss of TPS noted
094	086	102	07/01/97	Yes	Yes	Day	N/A	Y	Y	No loss of TPS noted	No loss of TPS noted	No loss of TPS noted
084	085	104	05/15/97	Yes	No	Night	No umbilical cameras installed on OV104 ET separation not visible due to darkness until later when the ET crossed the terminator line	Y	Y	No loss of TPS noted	1 divot (6" dia) in LH2 tank flange closeout between bipod struts	No loss of TPS noted
083	084	102	04/04/97	Yes	Yes	Day	35 mm film jammed Good data from 16mm Handhelds back lighting by sun	Y	Y	No loss of TPS noted	5 divots (approximately 9 to 11" dia) in LH2 tank flange closeout at -Y/+Z quadrant outboard of -Y bipod 3 divots (6 to 7" dia) in LH2 tank flange closeout between bipod struts	No loss of TPS noted
082	081	103	02/11/97	Yes	No	Night	No umbilical cameras instaled on OV103 Good image of +Y axis No loss of TPS noted	Y	Y	No apparent loss of TPS noted	No loss of TPS noted	No loss of TPS noted
081	083	104	01/12/97	Yes	No	Night	Good images of -Z / +Y axis	N	N	No apparent loss of TPS noted	Six divots in LH2 tank flange closeout +Y axis (aft of thrust panel)	No loss of TPS noted
080	080	102	11/19/96	Yes	Yes	Day	N/A	Y	Y	No loss of TPS noted	No loss of TPS noted	No loss of TPS noted
079	082	104	09/16/96	Yes	No	Night	Crew photos taken after ET cross terminator line (long range views) No loss of TPS noted	Y	Y	No loss of TPS noted - Cannot verify fwd ramp due to angle	No loss of TPS noted	No loss of TPS noted
078	079	102	06/20/96	Yes	Yes	Day	N/A	Y	Y	No loss of TPS noted	4 divots in LH2 tank flange closeout - 1 in +Y/+Z quadrant - 2 in -Y/+Z quadrant - 1 adjacent to -Y jack pad closeout	No loss of TPS noted
077	078	105	05/19/96	Yes	Yes	Day	N/A	Y	Y	No loss of TPS noted	No loss of TPS noted	No loss of TPS noted
076	077	104	03/22/96	No	No	Night	No ET sep imagery - SRB sep only	N	N	No data obtained	No data obtained	No data obtained
075	076	102	02/22/96	Yes	Yes	Day	N/A	Y	Y	No loss of TPS noted	4 divots in LH2 tank flange closeout ranging from 6 to 12" dia (1 at -Y/+Z and 3 at +Y/+Z)	5" dia divot just below flange closeout +Y side
072	075	105	01/11/96	Yes	Yes	Night	Data obtained from 16mm umbilical or 35mm crew photos	N	N	No apparent loss of TPS noted - Bipods in shadow	No loss of TPS noted	No loss of TPS noted

Acreage				
Intertank	**LH2 Tank**	**Components**	**Substrate Exposed**	**# of Tankings**
Several divots (2"-3") could be discerned in thrust panel TPS to the -Z side of the EB fitting and forward of the fitting	No loss of TPS noted	No loss of TPS noted	No	2
Intertank thrust panel popcorning (See notes) 1 divot (7" long) near +Z aero vent 10 small divots on stringers forward of the bipod 11 divots (3"-7" dia) on +Y thrust panel forward of EB	1 divot (6" dia) between LO2 feedline and cable tray near Sta 1860 2 divots (3" dia) just forward of the crossbeam	No loss of TPS noted	No	1
Several (20 -25) small shallow divots were detected in the -Y thrust panel acreage	Small divot just aft of -Y bipod ramp in LH2 acreage	No loss of TPS noted	No	2
No loss of TPS noted	No loss of TPS noted	Small divots in -Y and +Y thrust struts	10" dia divot in flange	1
No data obtained	No data obtained	No data obtained	N/A	1
Numerous divots forward and aft of EB fitting on +Y and -Y thrust panel	No loss of TPS noted	No loss of TPS noted	No	1
No data obtained	No data obtained	No data obtained	N/A	1
No loss of TPS noted	No loss of TPS noted	No loss of TPS noted	No	1
7 small shallow divots on Intertank stringer heads forward of the forward of the bipod	22 divots (2"-3" dia) concentrated forward of aft crossbeam 1 divot (16"x10") between pressline and LO2 feedline at Sta 1528 1 divot (14"x2") outboard of Sta 1593 ice/frost ramp 1 divot (5" dia) adjacent to Sta 1623 LO2 feedline bracket with possible primer showing 1 divot (6"x4") between the pressline and LO2 feedline at Sta 1722	1 divot (6"x6") in -Y bipod jack pad closeout with substrate exposed 1 divot (4"x2") in leading edge of ice/frost ramp at Sta 1657	Jack pad closeout	1
3 shallow divots in stringer heads near LO2 PAL ramp 10 shallow divots forward of bipod 8 shallow divots around -Y bipod	No loss of TPS noted	Jack pads - Two shallow divots extending to upper barrel acreage	No	1
No loss of TPS noted	No loss of TPS noted	2 divots (approximately 3" dia) on -Y thrust strut - One on flange closeout and one just aft of flange	No	1
No loss of TPS noted	No loss of TPS noted	No loss of TPS noted	No	1
No loss of TPS noted	No loss of TPS noted	No loss of TPS noted	No	1
1 divot forward of -Y bipod ramp approximately 10" long and possibly showing substrate 2 divots (approximately 4" long) between bipod struts just forward of the flange closeout. One of the divotswith exposed primed substrate 1 divot (15" long) forward of the LO2 feedline fairing near Sta 930 with exposed primed substrate	1 divot (6" dia) in -Y/+Z quadrant	4 shallow divots (approximately 2"-3") on +Y vertical strut outboard surface 1 divot (5" dia) on -Y vertical strut	Intertank acreage	1
No loss of TPS noted	No loss of TPS noted	No loss of TPS noted	No	1
No loss of TPS noted	No loss of TPS noted	No loss of TPS noted	No	1
30 small shallow divots in stringer valleys around -Y bipod 10 small shallow divots around +Y bipod ramp	4 shallow divots in LH2 acreage just below -Y bipod	Missing portion of ice/frost ramp at Sta 760 Part of +Y jack pad (4" x '4") with primed substrate exposed 1 divot (4"x2") in forward, inboard corner of ice/frost ramp at Sta 1464 1 divot (12"x4"x1") on -Y thrust strut flange	Jack pad closeout	1
No data obtained	No data obtained	No data obtained	N/A	1
No loss of TPS noted	No loss of TPS noted	No loss of TPS noted	No	1
No loss of TPS noted	No loss of TPS noted	No loss of TPS noted	No	1

No imagery of the +Z axis +/-90 degrees available

No loss of TPS noted

								View				
STS	**ET**	**Vehicle**	**Launch Date**	**Useable ET Crew Photos**	**Useable ET Umbilical Well Photos**	**Day/ Night**	**Notes**	**-Y**	**+Y**	**Bipod Ramp**	**Flange**	**LO2 Tank**
074	074	104	11/12/95	No	Yes	Day	16mm/10 lens did not run	Y	Y	No loss of TPS noted	3" dia divot in LH2 tank flange closeout in +Y/+Z quadrant adjacent to PAL ramp	No loss of TPS noted
073	073	102	10/20/95	Yes	Yes	Day	N/A	Y	Y	No loss of TPS noted	No loss of TPS noted	No loss of TPS noted
069	072	105	09/07/95	No	Yes	Day	N/A	Y	Y	No loss of TPS noted	No loss of TPS noted	No loss of TPS noted
070	071	103	07/13/95	Yes	No	Day	Good images of +Z and -Z	Y	Y	No loss of TPS noted	No loss of TPS noted	No loss of TPS noted
071	070	104	06/27/95	No	Yes	Day	No handheld photography	Y	Y	No loss of TPS noted	1 shallow divot aft of -Y bipod closeout	No loss of TPS noted
067	069	105	03/03/95	Yes	No	Night	View of +Z with handhelds No apparent loss of TPS noted	Y	Y	No loss of TPS noted	No loss of TPS noted	No loss of TPS noted
063	068	103	02/03/95	No	No	Night	No umbilical cameras installed on OV103 No data obtained	N	N	No data obtained	No data obtained	No data obtained
066	067	104	11/03/94	Yes	Yes	Day	First flight of umbilical well cameras on OV104	Y	Y	No loss of TPS noted	1 divot (5" dia) in -Y/+Z quadrant of LH2 tank flange 1 divot (7" dia) adjacent to -Y bipod in the LH2 tank flange 1 divot (5") +Y of the PAL ramp in the LH2 tank flange	1 divot (4") near LO2 presline at Sta 514 1 divot (9") near LO2 pressline at Sta 676
068	065	105	09/30/94	Yes	Yes	Day	N/A	Y	Y	No loss of TPS noted	1 divot (6" dia) on +Y side of LO2 feedline in the LH2 tank flange	No loss of TPS noted
064	066	103	09/09/94	No	No	Sunset	No umbilical cameras installed OV103 No view of +Z side from crew photos	N	N	No data obtained	No data obtained	No data obtained
065	064	102	07/08/94	Yes	Yes	Day	N/A	Y	Y	No loss of TPS noted	2 divots (6" - 8" dia) in the LH2 tank flange outboard of PAL ramp with exposed primed substrate	No loss of TPS noted
059	063	105	04/09/94	Yes	Yes	Day	N/A	Y	Y	No loss of TPS noted	6 divots (ranging from 6" - 10" dia) in the LH2 tank flange - 2 divots outboard of LO2 feedline - 3 divots between -Y bipod and -Y thrust panel - 1 divot at the -Y bipod spindle outboard bondline	No loss of TPS noted
062	062	102	03/04/94	Yes	Yes	Day	N/A	Y	Y	1 small shallow divot (3"x1") near the aft face of the box section of the ramp	No loss of TPS noted	No loss of TPS noted
060	061	103	02/03/94	Yes	No	Day	No umbilical cameras installed OV103	Y	Y	No loss of TPS noted	No loss of TPS noted	No loss of TPS noted
061	060	105	12/02/93	Yes	No	Night	18 handheld images 36 min after sep	N	N	No apparent loss of TPS noted	No loss of TPS noted	No loss of TPS noted
058	057	102	10/18/93	Yes	Yes	Day	N/A	Y	Y	No loss of TPS noted	1 divot (19" dia) outboard of -Y bipod in the LH2 tank flange	No loss of TPS noted
051	059	103	09/12/93	Yes	No	Day	No umbilical cameras installed OV103 Orbiter damaged during payload deployment	Y	Y	No loss of TPS noted	1 divot (8" dia) outboard of -Y bipod closeout in the LH2 tank flange	No loss of TPS noted
057	058	105	06/21/93	Yes	Yes	Day	N/A	Y	Y	No loss of TPS noted	7 small divots between bipod (size not reported) 1 divot near LO2 feedline (size not reported) 2 divots at +Y, aft of EB fitting (size not reported) 1 divot (approximately 10" dia) at -Y, aft of EB fitting (size not reported)	No loss of TPS noted
055	056	102	04/26/93	Yes	Yes	Day	N/A	Y	Y	No loss of TPS noted	1 divot at -Y thrust panel (size not reported) in LH2 tank flange	No loss of TPS noted
056	054	103	04/08/93	Yes	No	Dawn	No umbilical cameras installed OV103	Y	Y	No loss of TPS noted	1 divot (16"-24") at +Y thrust panel in LH2 tank flange	No loss of TPS noted
054	051	105	01/03/93	Yes	Yes	Day	N/A	Y	Y	No loss of TPS noted	3 divots on -Y/+Z quadrant (size not reported) in LH2 tank flange	No loss of TPS noted
053	049	103	12/02/92	Yes	No	Day	No umbilical cameras installed OV103	Y	Y	No loss of TPS noted	3 divots in +Y/+Z quadrant (size not reported) in LH2 tank flange 1 divot in -Y/+Z quadrant (size not reported) in LH2 tank flange	No loss of TPS noted
052	055	102	10/22/92	Yes	Yes	Day	N/A	Y	Y	Lower outboard corner (8" X 4") of -Y bipod ramp missing	No loss of TPS noted	No loss of TPS noted
047	045	105	09/12/92	Yes	Yes	Day	N/A	Y	Y	No loss of TPS noted	4 divots (6"-8" dia) at +Z corner of +Y thrust panel in LH2 tank flange 2 divots (8" dia) at +Z corner of -Y thrust panel in LH2 tank flange 1 divot (10"-12" dia) in -Y/+Z quadrant in LH2 tank flange 1 divot (6"-8" dia) just forward of -Y jack pad closeout in LH2 tank flange	No loss of TPS noted
046	048	104	07/31/92	Yes	No	Day	No umbilical cameras installed OV104 Crew photos showed limited views at ET sep + 12 min - No loss of TPS noted	Y	Y	No loss of TPS noted	No loss of TPS noted	No loss of TPS noted
050	050	102	06/25/92	Yes	Yes	Day	N/A	Y	Y	Large portion (26" x 10") of -Y bipod ramp missing	No loss of TPS noted	No loss of TPS noted
049	043	105	05/07/92	No	No	Day	No data obtained	N	N	No data obtained	No data obtained	No data obtained

Acreage				
Intertank	**LH2 Tank**	**Components**	**Substrate Exposed**	**# of Tankings**
No loss of TPS noted	No loss of TPS noted	No loss of TPS noted	No	2
No loss of TPS noted	No loss of TPS noted	8" x 6" divot on -Y longeron to vertical strut / cable tray attach point came off shortly after ET sep	No	5
No loss of TPS noted	Numerous shallow "popcorn" type divots forward of crossbeam on LH2 tank	No loss of TPS noted	No	1
No loss of TPS noted	No loss of TPS noted	No loss of TPS noted	No	1
8 stringer head divots 2 forward of bipod at Sta 1080 1 forward of bipod on centerline at Sta 960 1 forward of LO2 feedline at Sta 860 1 forward/outboard of -Y bipod at Sta 1080 3 between LO2 feedline and EB-2 at Sta 1080	5" dia divot just inboard of LO2 feedline at Sta 1377 5" dia divot between LO2 feedline and presline at Sta 1377 (substrate exposed)	No loss of TPS noted	Divot between feedline and pressline	2
No loss of TPS noted	No loss of TPS noted	No loss of TPS noted	No	1
No data obtained	No data obtained	No data obtained	N/A	1
3 divots on Intertank stringer heads 1 divot (14" dia) forward of the -Y bipod 1 divot (17"x3.5") at centerline with exposed primed substrate 1 divot (24" x 3.5") with exposed primed substrate	1 shallow divot aft of bipod	No loss of TPS noted	Divots on stringer heads	1
1 divot (12"x4") on stringer head at Sta 1050, -Y of centerline with exposed primed substrate	1 divot (5" dia) aft of flange closeout between -Y thrust panel and -Y bipod	No loss of TPS noted	Intertank acreage	2
No data obtained	No data obtained	No data obtained	N/A	1
3 shallow divots in stringer valleys just forward of +Y bipod	1 divot (6" dia) aft of flange between +Y bipod and LO2 feedline	Small divot in pressline ramp at Sta 1152 Small divot in pressline ramp at Sta 1787	Flange closeout	1
No loss of TPS noted	1 divot (8" dia) aft of -Y bipod with substrate exposed 1 divot (6" dia) on -Y axis just below flange Numerous (greater than usual) small divots just forward of the ET/Orb crossbeam	No loss of TPS noted	8" divot in LH2 acreage	2
1 divot (14" x 4") on stringer head forward of -Y bipod ramp Numerous (approximately 35) small divots in vicinity of bipod	1 divot (5.5" dia) between +Y bipod and LO2 feedline	No loss of TPS noted	No	1
No loss of TPS noted	No loss of TPS noted	No loss of TPS noted	No	1
No loss of TPS noted	No loss of TPS noted	No loss of TPS noted	No	2
1 divot (28" x 4.6") on Intertank centerline with exposed primed substrate 4 small divots forward of +Y bipod	No loss of TPS noted	Portions of both jack pad closeouts were missing with exposed primed substrate	Intertank acreage Jack pad closeouts	3
No loss of TPS noted	1 divot (8" dia) just aft of flange between bipod	1 divot (10"-12") in -Y longeron closeout Missing foam on +Y thrust strut flange closeout	No	4
Numerous (approximately 70) small divots on stringer heads forward of bipod 1 divot (6" dia) on -Y thrust panel 9 divots (6" - 8" dia) +Z of -Y thrust panel	No loss of TPS noted	1 divot (6"-8" dia) on -Y longeron 1 divot on +Y thrust strut flange with exposed primed substrate	+Y thrust strut flange	2
No loss of TPS noted	4 divots just aft of flange closeout (smallest divot = 4.7")	No loss of TPS noted	No	2
No loss of TPS noted	No loss of TPS noted	No loss of TPS noted	No	2
2 divots (8" x 4") between bipod just forward of flange 1 divot (8" x 3") on stringer head in -Y/+Z quadrant	3 divots (4"-6" dia) just aft of flange - 1 divot below +Y bipod spindle - 1 divot below -Y bipod ramp - 1 divot below -Y thrust panel	+Y jack pad closeout missing	No	1
No loss of TPS noted	No loss of TPS noted	No loss of TPS noted	No	1
Several (20) small divots on stringer heads forward of bipod	1 divot (5" dia) between ET centerline and LO2 feedline at Sta 1399 with exposed primed substrate	-Y jack pad closeout partially missing	LH2 tank divot	1
1 divot (8") just above flange at -Y 1 divot (14"-16") just forward of bipod	1 divot (4" x 6") aft of LH2 PAL ramp adjacent to cable tray 1 divot (4"-6") just aft of -Y bipod spindle	No loss of TPS noted	No	1
No loss of TPS noted	No loss of TPS noted	No loss of TPS noted	No	1
No loss of TPS noted	1 divot (7" dia) near inboard base of Sta 1377 feedline bracket	+Y jack pad closeout (6" dia) and portion of adjacent material missing	No	1
No data obtained	No data obtained	No data obtained	N/A	2

No imagery of the +Z axis +/-90 degrees available

No loss of TPS noted

								View					
STS	**ET**	**Vehicle**	**Launch Date**	**Useable ET Crew Photos**	**Useable ET Umbilical Well Photos**	**Day/ Night**	**Notes**	**-Y**	**+Y**	**Bipod Ramp**	**Flange**	**LO2 Tank**
045	044	104	03/24/92	Yes	No	Day	No umbilical cameras installed OV104	Y	N	No loss of TPS noted	4 divots on -Y side 6 divots on +Y side	No loss of TPS noted
042	052	103	01/22/92	Yes	No	Day	No umbilical cameras installed OV103	Y	N	No loss of TPS noted	2 divots (8"-12") in the -Y/+Z quadrant just forward of the flange	No loss of TPS noted
044	053	104	11/24/91	No	No	Night	No data obtained	N	N	No data obtained	No data obtained	No data obtained
048	042	103	09/12/91	No	No	Day	No umbilical cameras installed OV103	N	N	No data obtained	No data obtained	No data obtained
043	047	104	08/02/91	Yes	No	Day	No umbilical cameras installed OV104 Poor quality photo of -Y only - No apparent loss of TPS	Y	N	No loss of TPS noted	No apparent loss of TPS noted	No apparent loss of TPS noted
040	041	102	06/05/91	Yes	Yes	Day	Umbilical photos of +Z and handheld photos of -Y	Y	Y	No loss of TPS noted	1 divot (6"-8" dia) in LH2 tank flange below +Y ET/SRB fitting	No loss of TPS noted
039	046	103	04/28/91	Yes	No	Day	No umbilical cameras installed OV103	N	N	No apparent loss of TPS noted	No loss of TPS noted	No loss of TPS noted
037	037	104	04/05/91	Yes	No	Day	No umbilical cameras installed OV104 No view of +Z	N	N	No apparent loss of TPS noted	2 divots (12"-14" dia) at -Y	No loss of TPS noted
035	035	102	12/02/90	Yes	No	Night	Umbilical cameras failed to operate	Y	N	No loss of TPS noted	12 divots on +Z, 6 of the divots had major dimension of 8"-10"	No loss of TPS noted
038	040	104	11/19/90	No	No	Night	No umbilical cameras installed OV104 No data obtained	N	N	No data obtained	No data obtained	No data obtained
041	039	103	10/06/90	Yes	No	Day	No umbilical cameras installed OV103 No loss of TPS noted	N	N	No apparent loss of TPS noted - Too distant to discern details	No loss of TPS noted	No loss of TPS noted
31R	034	103	04/24/90	No	No	Day	No umbilical cameras installed OV103 No data obtained	N	N	No data obtained	No data obtained	No data obtained
036	033	104	02/28/90	No	No	Night	No umbilical cameras installed OV103 No data obtained	N	N	No data obtained	No data obtained	No data obtained
032R	032	102	01/09/90	No	Yes	Day	N/A	Y	Y	No loss of TPS noted	No loss of TPS noted	No loss of TPS noted
33R	038	103	11/22/89	No	No	Night	No data obtained No umbilical cameras installed OV103	N	N	No data obtained	No data obtained	No data obtained
034	027	104	10/18/89	No	No	Day	No umbilical cameras installed OV104 Poor quality photo of -Y only	Y	N	No data obtained	No data obtained	No data obtained
028R	031	102	08/08/89	Yes	Yes	Day	N/A	Y	Y	No loss of TPS noted	1 divot (4"x8") in LH2 tank flange closeout outboard of PAL ramp	No loss of TPS noted
030R	029	104	05/04/89	No	No	Day	No umbilical cameras installed OV104 No data obtained	N	N	No data obtained	No data obtained	No data obtained
029R	036	103	03/13/89	Yes	No	Day	No umbilical cameras installed OV103	Y	Y	No loss of TPS noted	Divots (12"-20" dia) at +Y/+Z Numerous smaller divots in LO2 and LH2 flanges	No loss of TPS noted
027R	023	104	12/02/88	No	No	Day	No umbilical cameras installed OV104 No data obtained	N	N	No data obtained	No data obtained	No data obtained
026R	028	103	09/29/88	Yes	No	Day	No umbilical cameras installed OV103 Crew photos are poor quality	Y	Y	No loss of TPS noted	No loss of TPS noted	No loss of TPS noted
033 51L	026	99	01/28/86	No	No	Day	***Challenger Accident*** No data obtained	N	N	No data obtained	No data obtained	No data obtained
032 61C	030	102	01/12/86	No	Yes	Day	16mm umbilical cameras only No crew photos located at KSC	Y	Y	No loss of TPS noted	No loss of TPS noted	No loss of TPS noted
031 61B	022	104	11/26/85	No	No	Night	No umbilical cameras installed OV104 No data obtained	N	N	No data obtained	No data obtained	No data obtained
030 61A	024	99	10/30/85	No	Yes	Day	35mm umbilical cameras only No crew photos located at KSC	Y	Y	No loss of TPS noted	Divot approximately 2 inches in dia. located in the flange closeout between the bipod ramps. Divot approximately 2 inches in dia. Located in the flange closeout +Y of the feedline.	No loss of TPS noted
028 51J	025	104	10/03/85	Yes	No	Day	No umbilical cameras installed OV104 Crew photos showed only -Y side, +Y side too distant to detect foam loss	N	N	No data obtained	No data obtained	No data obtained
027 51I	021	103	08/27/85	No	No	Day	No umbilical cameras installed OV103 Unable to locate crew photos at KSC No imagery available (per J. Disler/ JSC)	N	N	No data obtained	No data obtained	No data obtained

Acreage				
Intertank	**LH2 Tank**	**Components**	**Substrate Exposed**	**# of Tankings**
No loss of TPS noted	No loss of TPS noted	No loss of TPS noted	No	2
No loss of TPS noted	No loss of TPS noted	No loss of TPS noted	No	1
No data obtained	No data obtained	No data obtained	N/A	1
No data obtained	No data obtained	No data obtained	N/A	1
No apparent loss of TPS noted	No apparent loss of TPS noted	No apparent loss of TPS noted	No	3
No foam loss noted	No foam loss noted	No foam loss noted	No	2
No loss of TPS noted	No loss of TPS noted	No loss of TPS noted	No	1
No loss of TPS noted	No loss of TPS noted	No loss of TPS noted	No	4
No loss of TPS noted	1 divot just aft of -Y bipod	No loss of TPS noted	No	6
No data obtained	No data obtained	No data obtained	N/A	1
No loss of TPS noted	No loss of TPS noted	No loss of TPS noted	No	1
No data obtained	No data obtained	No data obtained	N/A	2
No data obtained	No data obtained	No data obtained	N/A	3
5 divots just forward of the flange closeout - 2 divots (12"-14" dia) - 1 divot (14" dia) on centerline extending to flange - 1 divot (6" dia) just aft of flange outboard of -Y bipod ramp 1 divot (28" dia) surrounding part of the forward part of the -Y bipod ramp	2 divots near centerline at Sta 1250 and 1320	1 divot in +Y jack pad closeout with exposed primed substrate	Jack pad closeout	2
No data obtained	No data obtained	No data obtained	N/A	1
No data obtained	No data obtained	No data obtained	N/A	2
1 divot (23" x 15") in the two-tone area just forward of the +Y bipod ramp	No loss of TPS noted	5 small divots noted on +Y thrust strut flange closeout 1 divot in ice/frost ramp at Sta 1270	No	1
No data obtained	No data obtained	No data obtained	N/A	2
4 divots (6"-12" dia) at -Y thrust panel	1 divot (6" dia) on +Y longeron	No loss of TPS noted	No	1
No data obtained	No data obtained	No data obtained	N/A	2
No loss of TPS noted	No loss of TPS noted	No loss of TPS noted	No	5
No data obtained	No data obtained	No data obtained	N/A	2
1 divot (15"x20") in two-tone foam just forward of the -Y bipod ramp 1 divot (30"x12") in two-tone foam between bipod struts	No loss of TPS noted	1 divot (7"x3") in LH2 cable-tray clamshell closeout	No	5
No data obtained	No data obtained	No data obtained	N/A	1
No loss of TPS noted	No loss of TPS noted	1 divot (4" dia) in +Z surface of Sta 1115 feedline flange closeout	No	1
No data obtained	No data obtained	No data obtained	N/A	2
No data obtained	No data obtained	No data obtained	N/A	3

No imagery of the +Z axis +/-90 degrees available

No loss of TPS noted

								View				
STS	**ET**	**Vehicle**	**Launch Date**	**Useable ET Crew Photos**	**Useable ET Umbilical Well Photos**	**Day/ Night**	**Notes**	**-Y**	**+Y**	**Bipod Ramp**	**Flange**	**LO2 Tank**
026 51F	019	99	07/29/85	No	Yes	Day	35mm umbilical cameras only Unable to locate crew photos at KSC	Y	Y	No loss of TPS noted	The -Y jack pad closeout is missing. This area is approximately 5 inches by 5 inches with substrate exposed. This area is located within the flange closeout between the bipod ramps.	No loss of TPS noted
025 51G	020	103	06/17/85	No	No	Day	No umbilical cameras installed on OV103 Unable to locate crew photos at KSC No imagery available (per J. Disler/ JSC)	N	N	No data obtained	No data obtained	No data obtained
024 51B	017	99	04/29/85	No	Yes	Day	35mm umbilical cameras only - Sun angle washed out view of ET making it hard to detect foam loss Unable to locate crew photos at KSC	Y	N	No loss of TPS noted	No loss of TPS noted	No loss of TPS noted
023 51D	018	103	04/12/85	No	No	Day	No umbilical cameras installed on OV103 Unable to locate crew photos at KSC No imagery available (per J. Disler/ JSC)	N	N	No data obtained	No data obtained	No data obtained
020 51C	014	103	01/24/85	No	No	Day	No umbilical cameras installed on OV103 Unable to locate crew photos at KSC No imagery available (per J. Disler/ JSC)	N	N	No data obtained	No data obtained	No data obtained
019 51A	016	103	11/08/84	No	No	Day	No umbilical cameras installed on OV103 Unable to locate crew photos at KSC No imagery available (per J. Disler/ JSC)	N	N	No data obtained	No data obtained	No data obtained
017 41G	015	99	10/05/84	No	Yes	Day	35mm umbilical cameras only Unable to locate crew photos at KSC	Y	Y	No loss of TPS noted	No data obtained	No data obtained
014 41D	013	103	08/30/84	No	No	Day	No umbilical cameras installed on OV103 Unable to locate crew photos at KSC No imagery available (per J. Disler/ JSC)	N	N	No data obtained	No data obtained	No data obtained
013 41C	012	99	04/06/84	No	No	Day	Unable to locate crew or umbilical photos at KSC No imagery available (per J. Disler/ JSC)	N	N	No data obtained	No data obtained	No data obtained
011 41B	010	99	02/03/84	No	Yes	Day	35mm umbilical cameras only Unable to locate crew photos at KSC	Y	Y	No loss of TPS noted	No loss of TPS noted	No loss of TPS noted
009 041A	011	102	11/28/83	No	No	Day	Unable to locate crew or umbilical photos at KSC No imagery available (per J. Disler/ JSC)	N	N	No data obtained	No data obtained	No data obtained
008	009	99	08/30/83	No	No	Night	Unable to locate crew or umbilical photos at KSC No imagery available (per J. Disler/ JSC)	N	N	No data obtained	No data obtained	No data obtained
007	006	99	06/18/83	No	Yes	Day	35mm umbilical cameras only Unable to locate crew photos at KSC	Y	Y	Portion (approximately 18"x12") of the -Y Bipod Ramp TPS is missing. Spindle is not exposed	1 divot (4"dia) outboard of the cable tray in the flange closeout	No loss of TPS noted
006	008	99	04/04/83	No	Yes	Day	35mm umbilical cameras only Unable to locate crew photos at KSC	Y	Y	No loss of TPS noted	1 divot (10" x 4") located +Y of the LO2 feedline extending into the Intertank acreage TPS 1 divot (3" dia) in the flange closeout between the bipod ramps.	No loss of TPS noted
005	005	102	11/11/82	No	Yes	Day	GH2 pressline on -Y side	Y	Y	No loss of TPS noted	4 divots (2" to 6" dia) outboard of LH2 PAL ramp 1 divot (approximately 7" dia) between bipod	No loss of TPS noted
004	004	102	06/27/82	No	Yes	Day	GH2 pressline on -Y side Sun angle (backlighting) washed out view of ET above Sta 1623	Y	Y	No loss of TPS noted	3 divots (approximately 6" dia) just outboard of PAL ramp 1 divot (approximately 4" dia) between LO2 feedline and pressline	No loss of TPS noted
003	003	102	03/22/82	No	Yes	Day	GH2 pressline on -Y side	Y	Y	No loss of TPS noted	4 divots (ranging 4" to 8") at +Z 1 divot (approximately 6" x 12") outboard of +Y cable tray - Included portion of LH2 L7tank acreage foam 3 small divots (approximately 3" dia) on +Y/+Z quadrant	No loss of TPS noted

Acreage				
Intertank	**LH2 Tank**	**Components**	**Substrate Exposed**	**# of Tankings**
13 divots (7"-30" dia) in two-tone foam forward of the bipod struts 1 divot (3" dia) located in the intertank acreage TPS +Y axis just forward of the flange closeout 1 divot (16" dia) located just forward of the +Y bipod ramp 3 divots (10" dia) located in the intertank thrust panel 2-tone foam near the +Y EB fitting	No loss of TPS noted	Small divots (< 1 inch dia.) on LO2 feedline flange closeouts +Z surface 1 divot (8"x5") on the +Z surface of Sta 1856 feedline flange closeout with exposed primed substrate 1 divot (6" dia) located on the +Z surface of Sta 1609 feedline flange closeout	Sta 1856 feedline flange	2
No data obtained	No data obtained	No data obtained	N/A	1
9 divots (10" dia) located in the intertank two-tone foam just forward of the bipod struts	2 divots (3"-4" dia) located in the LH2 +Z axis acreage TPS just aft of the flange closeout	No loss of TPS noted	No	1
No data obtained	No data obtained	No data obtained	N/A	1
No data obtained	No data obtained	No data obtained	N/A	1
No data obtained	No data obtained	No data obtained	N/A	2
1 divot (5" dia) located in the intertank two-tone foam forward and between the bipod struts 1 divot (18"-20" dia) located in the 2-tone foam forward of the +Y bipod ramp	1 divot (3" dia) in the LH2 acreage +Z axis at Sta 1623 - Appears to be in plug-pull repair area	1 divot (6" dia) on the LO2 feedline flange at Sta 1870 with exposed primed substrate	Sta 1870 feedline flange	1
No data obtained	No data obtained	No data obtained	N/A	4
No data obtained	No data obtained	No data obtained	N/A	1
1 divot (10" dia) located in the intertank two-tone foam area just forward and inboard of the +Y bipod ramp	1 divot (2" dia) located in the LH2 acreage TPS 12 inches below the +Y bipod ramp	-Y jack pad closeout is missing Area is approximately 5" x 5" with substrate exposed	Jack pad closeout	1
No data obtained	No data obtained	No data obtained	N/A	2
No data obtained	No data obtained	No data obtained	N/A	1
Numerous (approximately 25) shallow divots (less than 4" dia) located in the intertank acreage TPS +Z axis just forward of the bipod struts	Numerous (approximately 40) divots (less than 2" dia) located in the upper LH2 acreage TPS +Z axis between Sta 1129 and Sta 1200	Divots in ice/frost ramps ranging from 4" dia up to most of the upper ramp closeouts missing at Stations 1916, 1851, 1787, 1722, 1657, 1528, and 1464. Most of these areas of missing foam exposed cable tray SLA sidewall substrate	Ice/frost ramps	1
No loss of TPS noted	1 divot (3"dia) located outboard of LO2 feedline in acreage TPS at Sta 1610	1 divot (5" dia) in LO2 feedline flange closeout at Sta 1958 with exposed substrate 1 divot (3" dia) in LO2 feedline flange closeout at Sta 1856 1 divot(2" dia) in LO2 feedline flange closeout at Sta 1609	Sta 1958 LO2 feedline flange	3
3 divots (1" to 2") just forward of +Y bipod ramp 3 divots (1" dia) forward of bipod	1 divot (2" dia) between pressline and feedline near Sta 1800 Numerous (30) divots (ranging 2"W x 2 to 10"L) just aft of +Z flange Numerous divots along entire length of GH2 pressline	Missing upper portion of GH2 pressline ice/frost ramp at Sta 1430	No	2
3 divots (2" to 3" dia) forward of bipod	1 divot (3" dia) just forward of longeron Numerous small divots (approximately 40) between pressline and feedling along entire length of LH2 tank Several (7 -9) divots (2" -3" dia) in acreage just aft of +Z flange	4 divots (3" to 4" dia) in LH2 PAL ramp along the entire length 1 divot (15"L x 8"W) on LH2 PAL ramp with 1 divot (20"L x 8"W) on forward end of LH2 PAL ramp with exposed SLA and exposed primed substrate	LH2 PAL ramp	2
3 divots (2" to 3" dia) forward of bipod	Numerous (35) divots (ranging 2" to 6" dia) between flange and Sta 1377	No loss of TPS noted	No	2

No imagery of the +Z axis +/-90 degrees available

No loss of TPS noted

								View				
STS	**ET**	**Vehicle**	**Launch Date**	**Useable ET Crew Photos**	**Useable ET Umbilical Well Photos**	**Day/ Night**	**Notes**	**-Y**	**+Y**	**Bipod Ramp**	**Flange**	**LO2 Tank**
002	002	102	11/12/81	No	Yes	Day	GH2 pressline on -Y side Foam loss divots are difficult to detect due to white paint No loss of TPS ntoed	Y	Y	No loss of TPS noted	No loss of TPS noted	No loss of TPS noted
001	001	102	04/12/81	No	Yes	Day	GH2 pressline on -Y side Foam loss divots are difficult to detect due to white paint	Y	Y	No loss of TPS noted	No loss of TPS noted	No loss of TPS noted

Acreage				
Intertank	**LH2 Tank**	**Components**	**Substrate Exposed**	**# of Tankings**
No loss of TPS noted	No loss of TPS noted	No loss of TPS noted	No	2
No loss of TPS noted	1 divot (16"x12") in LH2 acreage near Sta 1851adjacent to GH2 pressline 1 divot (15"x10") located in LH2 acreage near Sta 1721adjacent to GH2 pressline 1 divot (5" dia) with what appears to be exposed primed substrate located at approximately Sta 2068, aft of the GH2 Pressline run.	No loss of TPS noted	LH2 acreage	6

No imagery of the +Z axis +/-90 degrees available

No loss of TPS noted

								View					
STS	**ET**	**Vehicle**	**Launch Date**	**Useable ET Crew Photos**	**Useable ET Umbilical Well Photos**	**Day/ Night**	**Notes**	**-Y**	**+Y**	**Bipod Ramp**	**Flange**	**LO2 Tank**
			Total Flight History									
							External Tank			**Bipod Ramp**	**Flange**	**LO2 Tank**
			# of flights with usable imagery				79	72		79	79	79
			# of flights with no loss of TPS noted				14			74	30	76
			# of flights with known loss				65			6	49	3
							82%			8%	62%	4%

Acreage				
Intertank	**LH2 Tank**	**Components**	**Substrate Exposed**	**# of Tankings**
Note: Thrust panel popcorning not considered				
Intertank	**LH2 Tank**	**Components**	**Substrate Exposed**	
79	79	79	79	
44	45	49	55	
35	34	30	24	
44%	43%	38%	30%	

LWT	ET	STS	MLP/PAD	ORBITER	DD250	SRB MATE	ORB MATE	ROLLOUT	TANK/FRF**	LAUNCH	MISSION	Contingency SIM	# of Launches
1 (SWT)	1	1	1/A	Columbia	6/29/1979	11/3/1980	11/24/1980	12/29/1980	1/22/81 Tanking	4/12/1981	1		113
									02/20/81 FRF				
2 (SWT)	2	2	1/A	Columbia	2/27/1981	6/30/1981	8/10/1981	8/31/1981	09/14/81 Tanking	11/12/1981	2		112
3 (SWT)	3	3	1/A	Columbia	9/28/1981	1/4/1982	2/3/1982	2/16/1982	02/26/82 Tanking	3/22/1982	3		111
4 (SWT)	4	4	1/A	Columbia	1/17/1982	4/17/1982	5/19/1982	5/26/1982	06/02/82 Tanking	6/27/1982	4		110
5 (SWT)	5	5	1/A	Columbia	5/26/1982	8/19/1982	9/10/1982	9/21/1982	09/28/82 Tanking	11/11/1982	5		109
1	8	6	2/A	Challenger	9/8/1982	10/21/1982	11/23/1982	11/30/1982	12/18/82 FRF	4/4/1983	6		108
									01/25/83 FRF				
6 (SWT)	6	7	1/A	Challenger	7/26/1982	3/2/1983	5/24/1983	5/26/1983	None	6/18/1983	7		107
2	9	8	2/A	Challenger	1/12/1983	6/23/1983	7/26/1983	8/2/1983	None	8/30/1983	8		106
4	11	9	1/A	Columbia	5/6/1983	8/24/1983	9/24/1983	1) 09/28/83	10/11/83 Tanking	11/28/1983	9		105
							ROLLBACK?	2) 11/08/83					
-----	-----	10	-----	-----	-----	-----	-----	-----	-----	Cancelled			
3	10	11/41B	2/A	Challenger	3/1/1983	1/3/1984	1/8/1984	1/12/1984	None	2/3/1984	10		104
-----	-----	12	-----	-----	-----	-----	-----	-----	-----	Cancelled			
5	12	13/41C	1/A	Challenger	7/22/1983	2/28/1984	3/15/1984	3/19/1984	None	4/6/1984	11		103
6	13	14/41D	2/A	Discovery	9/13/1983	4/9/1984	1) 05/14/84	1) 05/19/84	06/02/84 FRF	8/30/1984	12		102
						ROLLBACK?	2) 08/04/84	2) 08/09/84					
-----	-----	15	-----	-----	-----	-----	-----	-----	-----	Cancelled			
8	15	17/41G	1/A	Challenger	12/15/1983	6/19/1984	9/10/1984	9/13/1984	None	10/5/1984	13		101
		18	-----	-----	-----	-----	-----	-----	-----	Cancelled			
9	16	19/51A	2/A	Discovery	1/27/1984	10/2/1984	10/19/1984	10/23/1984	None	11/8/1984	14		100
7	14	20/51C	1/A	Discovery	11/3/1983	10/30/1984	12/23/1984	1/5/1985	None	1/24/1985	15		99
-----	-----	21	-----	-----	-----	-----	-----	-----	-----	Cancelled			
10	17	22/51E	2/A	Challenger	3/16/1984	1/9/1985	2/12/1985	2/15/1985	None	Cancelled			
16	23	OV	---	Enterprise	9/24/1984	2/1/1985		Stack-On-Pad	(Inert) 01/23-24/85	(Destack) 03/08/85			
11	18	23/51D	1/A	Discovery	4/24/1984	2/14/1985	3/23/1985	3/28/1985	None	4/12/1985	16		98
10	17	24/51B	2/A	Challenger	3/16/1984	1/9/1985	4/11/1985	4/15/1985	None	4/29/1985	17		97
13	20	25/51G	1/A	Discovery	7/5/1984	5/2/1985	5/29/1985	6/4/1985	None	6/17/1985	18		96
12	19	26/51F	2/A	Challenger	5/24/1984	5/31/1985	6/26/1985	6/29/1985	None	7/29/1985	19		95
14	21	27/51I	1/A	Discovery	7/25/1984	7/2/1985	7/30/1985	8/6/1985	None	8/27/1985	20		94
18	25	28/51J	2/A	Atlantis	12/20/1984	8/9/1985	8/13/1985	8/30/1985	09/12/85 FRF	10/3/1985	21		93
17	24	30/61A	1/A	Challenger	11/16/1984	9/30/1985	10/12/1985	10/16/1985	None	10/30/1985	22		92
15	22	31/61B	2/A	Atlantis	8/24/1984	10/22/1985	11/8/1985	11/12/1985	None	11/26/1985	23		91
23	30	32/61C	1/A	Columbia	6/18/1985	11/14/1985	11/22/1985	12/2/1985	None	1/12/1986	24		90
19	26	33/51L	2/B	Challenger	3/15/1985	12/10/1985	12/17/1985	12/22/1985	None	1/28/1986	25		89
										(In-Flight Failure)			
21	28	26R	2/B	Discovery	4/16/1985	6/10/1988	6/24/1988	7/4/1988	08/01/88 Tanking	09/29/88	26		88
									08/10/88 FRF				
16	23	27R	1/B	Atlantis	9/24/1984	9/21/1988	10/24/1988	11/2/1988	None	12/2/1988	27		87
29	36	29R	1/B	Discovery	12/10/1985	12/15/1988	1/25/1989	2/3/1989	None	3/13/1989	28		86
22	29	30R	1/B	Atlantis	5/15/1985	3/2/1989	3/11/1989	3/22/1989	None	5/4/1989	29		85
24	31	28R	2/B	Columbia	7/16/1985	5/22/1989	7/4/1989	7/15/1989	None	8/8/1989	30		84
20	27	34	1/B	Atlantis	1/29/1985	7/29/1989	8/21/1989	8/29/1989	None	10/18/1989	31		83
31	38	33R	2/B	Discovery	4/15/1986	9/2/1989	10/5/1989	10/27/1989	None	11/22/1989	32		82
25	32	32R	3/A	Columbia	8/14/1985	11/1/1989	11/21/1989	11/28/1989	None	1/9/1990	33		81
26	33	36	1/A	Atlantis	10/15/1985	12/22/1989	1/19/1990	1/25/1990	None	2/28/1990	34		80
27	34	31R	2/B	Discovery	9/23/1985	2/23/1990	3/6/1990	3/16/1990	None	4/24/1990	35		79
32	39	41	2/B	Discovery	4/15/1986	8/1/1990	8/27/1990	9/5/1990	None	10/6/1990	36		78
33	40	38	1/A	Atlantis	6/20/1986	9/12/1990	10/3/1990	10/12/1990	10/24/1990	11/15/1990	37		77
28	35	35	3/B	Columbia	11/8/1985	3/22/1990	8/2/1990	10/13/1990	10/30/1990	12/2/1990	38		76
30	37	37	1/B	Atlantis	1/15/1986	2/4/1991	3/8/1991	3/15/1991	None	4/5/1991	39		75
39	46	39	2/A	Discovery	9/9/1987	12/18/1990	3/25/1991	4/4/1991	None	4/28/1991	40		74
34	41	40	3/B	Columbia	7/25/1986	4/17/1991	4/25/1991	5/2/1991	None	6/5/1991	41		73
40	47	43	1/A	Atlantis	12/18/1987	6/3/1991	6/19/1991	6/25/1991	None	8/2/1991	42		72
35	42	48	3/A	Discovery	9/9/1986	7/24/1991	8/1/1991	8/12/1991	None	9/12/1991	43		71
46	53	44	1/A	Atlantis	7/31/1989	9/26/1991	10/18/1991	10/23/1991	None	11/24/1991	44		70
45	52	42	3/A	Discovery	5/3/1989	11/4/1991	12/13/1991	12/19/1991	None	1/22/1992	45		69
37	44	45	1/A	Atlantis	3/11/1987	1/22/1992	2/13/1992	2/20/1992	None	3/24/1992	46		68
36	43	49	2/B	Endeavour	11/10/1986	2/17/1992	3/7/1992	3/13/1992	4/6/1992	5/7/1992	47		67
43	50	50	3/A	Columbia	10/31/1988	4/9/1992	5/29/1992	6/3/1992	None	6/25/1992	48		66
41	48	46	1/B	Atlantis	4/22/1988	5/15/1992	6/5/1992	6/11/1992	None	7/31/1992	49		65
38	45	47	2/B	Endeavour	6/8/1987	7/13/1992	8/20/1992	8/25/1992	None	9/12/1992	50		64
48	55	52	3/B	Columbia	2/1/1990	9/9/1992	9/20/1992	9/26/1992	None	10/22/1992	51		63
42	49	53	1/A	Discovery	8/8/1988	10/13/1992	11/3/1992	11/8/1992	None	12/2/1992	52		62
44	51	54	2/B	Endeavour	2/3/1989	11/5/1992	11/23/1992	12/3/1992	None	1/13/1993	53		61
47	54	56	1/B	Discovery	10/30/1989	2/10/1993	3/2/1993	3/15/1993	None	4/8/1993	54		60
49	56	55	/A	Columbia	5/10/1990	1/12/1993	2/2/1993	2/7/1993	None	4/26/1993	55		59
51	58	57	2/B	Endeavour	10/16/1990	3/8/1993	3/25/1993	4/28/1993	None	6/21/1993	56		58
52	59	51	/B	Discovery	3/27/1991	6/2/1993	6/18/1993	6/25/1993	None	9/12/1993	57		57
50	57	58	/B	Columbia	7/26/1990	7/21/1993	8/12/1993	9/16/1993	None	10/18/1993	58		56
53	60	61	/B	Endeavour	6/27/1991	10/6/1993	10/21/1993	10/28/1993	None	12/2/1993	59		55
54	61	60	/B	Discovery	10/15/1991	11/29/1993	1/5/1994	1/10/1994	None	2/3/1994	60		54
55	62	62	1/B	Columbia	1/21/1992	1/20/1994	2/3/1994	2/10/1994	None	3/4/1994	61		53
56	63	59	2/A	Endeavour	4/2/1992	2/23/1994	3/14/1994	3/19/1994	None	4/9/1994	62		52
57	64	65	3/A	Columbia	7/20/1992	5/3/1994	6/9/1994	6/15/1994	None	7/8/1994	63		51
59	66	64	2/B	Discovery	1/26/1993	7/27/1994	8/11/1994	8/18/1994	None	9/9/1994	64		50
58	65	68	1/A	Endeavour	11/2/1992	6/16/1994	7/21/1994	7/27/1994	None				49
							ROLLBACK?	9/13/1994		9/30/1994	65		
60	67	66	3/B	Atlantis	5/17/1993	9/14/1994	10/4/1994	10/10/1994	None	11/3/1994	66		48
61	68	63	2/B	Discovery	8/6/1993	11/8/1994	1/5/1995	1/10/1995	None	2/3/1995	67		47
62	69	67	1/A	Endeavour	11/3/1993	12/13/1994	2/3/1995	2/8/1995	None	3/2/1995	68		46
63	70	71	B	Atlantis	2/17/1994	3/15/1995	4/20/1995	4/26/1995	None	6/26/1995	69		45
64	71	70	B	Discovery	5/4/1994	4/13/1995	5/3/1995	5/11/1995	(Rollback)	----------			
								6/14/1995		7/13/1995	70		44
65	72	69	1/A	Endeavour	7/1/1994	5/31/1995	6/28/1995	7/6/1995	(Rollback)	----------			
								8/7/1995		9/7/1995	71		43
66	73	73	B	Columbia	10/4/1994	8/5/1995	8/21/1995	8/28/1995	None	10/20/1995	72		42
67	74	74	2/A	Atlantis	11/17/1994	9/11/1995	10/3/1995	10/11/1995	None	11/12/1995	73		41
68	75	72	1/B	Endeavour	2/3/1995	11/9/1995	12/1/1995	12/6/1995	None	1/11/1995	74		40
69	76	75	3/B	Columbia	3/29/1995	1/8/1996	1/24/1996	1/29/1996	None	2/22/1996	75		39
70	77	76	2/B	Atlantis	5/24/1995	2/5/1996	2/20/1996	2/28/1996	None	3/22/1996	76		38
71	78	77	1/B	Endeavour	7/17/1995	3/21/1996	4/8/1996	4/16/1996	None	5/19/1996	77		37
72	79	78	3/B	Columbia	9/13/1995	5/3/1996	5/21/1996	5/29/1996	None	6/20/1996	78		36
73	80	79	2/A	Atlantis	11/17/1995	6/6/1996	6/24/1996	7/1/1996	None	Demate			
75	82	79	/A	Atlantis	3/12/1996	8/5/1996	8/13/1996	8/20/1996	None	9/16/1996	79		35
73	80	80	/A	Columbia	11/17/1995	9/26/1996	10/10/1996	10/16/1996	None	11/19/1996	80		34
76	83	81	/A	Atlantis	4/25/1996	11/14/1996	12/4/1996	12/10/1996	None	1/12/1997	81		33
74	81	82	1/A	Discovery	1/18/1996	12/9/1996	1/11/1997	1/17/1997	None	2/11/1997	82		32
77	84	83	3/A	Columbia	6/17/1996	1/30/1997	3/5/1997	3/11/1997	None	4/4/1997	83		31
78	85	84	2/A	Atlantis	8/7/1996	3/24/1997	4/20/1997	4/24/1997	None	5/15/1997	84		30
79	86	94	1/A	Columbia	10/8/1996	5/12/1997	6/4/1997	6/11/1997	None	7/1/1997	85		29
80	87	85	3/A	Discovery	12/4/1996	6/20/1997	7/7/1997	7/14/1997	None	8/7/1997	86		28
81	88	86	2/A	Atlantis	1/17/1997	7/24/1997	8/11/1997	8/18/1997	None	9/25/1997	87		27
82	89	87	1B	Columbia	6/26/1997	9/25/1997	10/24/1997	10/29/1997	None	11/19/1997	88		26
83	90	89	3A	Endeavour	8/8/1997	11/11/1997	12/12/1997	12/19/1997	None	1/22/1998	89		25
84	91	90		Columbia	11/14/1997	2/26/1998	3/16/1998	3/23/1998	None	4/17/1998	90		24
89	96	91		Discovery	1/12/1998	3/26/1998	4/27/1998	5/2/1998	5/18/1998	6/2/1998	91		23
91	98	95		Discovery	6/4/1998	8/25/1998	9/14/1998	9/21/1998	None	10/29/1998	92		22
90	97	88		Endeavour	3/30/1998	9/22/1998	10/12/1998	10/19/1998	None	12/4/1998	93		21
93	100	96	2B	Discovery	11/25/1998	3/16/1999	4/15/1999	4/21/1999	(Rollback)	----------			
"	"	"	"	"	"	"	"	5/20/1999	None	5/27/1999	94		20
92	99	93		Columbia	7/28/1999	12/1/1999	6/2/1999	6/7/1999	None	7/23/1999	95		19
94	101	103	B	Discovery	11/25/1999	8/26/1999	11/2/1999	11/13/1999	None	12/19/1999	96		18
85	92	99	A	Endeavour	4/19/1999	6/29/1999	12/2/1999	12/13/1999	None	2/11/2000	97		17
95	102	101	A	Atlantis	2/1/1999	2/3/2000	3/13/2000	3/25/2000	None	5/19/2000	98		16
96	103	106	B	Atlantis	6/22/1999	4/4/2000	8/7/2000	8/14/2000	None	9/8/2000	99		15
97	104	92	A	Discovery	6/1/1999	7/6/2000	8/30/2000	9/11/2000	None	10/9/2000	100		14
98	105	97	B	Endeavour	7/16/1999	9/27/2000	10/25/2000	10/31/2000	None	11/30/2000	101		13
99	106	98	A	Atlantis	12/17/1999	11/13/2000	12/4/2000	1/3/2001	(Rollback)	----------			
"	"	"	"	"	"	"	"		None	2/7/2001	102		12
100	107	102	B	Discovery	12/9/1999	1/10/2001	2/2/2001	2/12/2001	None	3/8/2001	103		11
101	108	100	A	Endeavour	2/10/2000	2/26/2001	3/17/2001	3/22/2001	None	4/19/2001	104		10
102	109	104	B	Atlantis	5/3/2000	4/16/2001	5/29/2001	6/21/2001	None	7/12/2001	105		9
103	110	105	A	Discovery	7/26/2000	5/24/2001	6/13/2001	7/2/2001	None	8/10/2001	106		8
104	111	108	B	Endeavour	3/22/2001	9/26/2001	10/24/2001	10/31/2001	None	12/5/2001	107		7
105	112	109	A	Columbia	3/8/2001	11/27/2001	1/16/2002	1/23/2002	None	3/1/2002	108		6
107	114	110		Atlantis	6/18/2001	1/21/2002	3/6/2002	3/12/2002	None	4/8/2002	109		5
106	113	111		Endeavour	4/30/2001	2/28/2002	4/22/2002	4/29/2002	None	6/5/2002	110		4
108	115	112	B	Atlantis	9/26/2001	6/25/2002	9/4/2002	9/10/2002	None	10/7/2002	111		3
109	116	113		Endeavour	11/28/2001	9/11/2002	9/30/2002	10/12/2002	MMT SIM 11/1/02	11/23/2002	112		2
86	93	107	A	Columbia	11/2/2000	5/8/2002	6/24/2002	*	*	*	*		

LWT	ET	STS	MLP/PAD	ORBITER	DD250	SRB MATE	ORB MATE	ROLLOUT	TANK/FRF**	LAUNCH	MISSION	Contingency SIM	# of Launches
					Demate	8/28/2002	*	*	*	*			
						11/4/2002	11/20/2002	12/9/2002	None	1/16/2003	113		1
										(Re-entry Failure)			
Upcoming Flights													
110	117	114	B	Atlantis	2/6/2002	1/7/2003	1/29/2003						
						Demate	*3/11/2003*	*TBD*	*None*	*TBD*	*114*		
111	118	115	B	Endeavour		*TBD*	*TBD*	*TBD*	*None*	*TBD*	*115*		
112	119	116	B	Atlantis		*TBD*	*TBD*	*TBD*		*TBD*			

** Reflects 1) tanking tests to fill ET to various levels in support of some test objective, 2) Flight Readiness Firings in support of similar objectives, & 3) some info relative to rollback etc that have nothing to do with either tanking or firing

DATES IN RED ARE SUBJECT TO CHANGE

Mission	Bipod Ramp Visible		Damage to Ramp Visible		Other Damage Near ET Bipod	Camera Views of ET Bipod Ramps			Comments
	Left (-Y)	Right (+Y)	Left (-Y)	Right (+Y)		16 mm Umbilical	35 mm Umbilical	Handheld	
STS-26	No	No	No	No		No	No	Yes	
STS-27	No	No	No	No		No	No	Yes	
STS-28	Yes	Yes	No	No	Divot	Yes	Yes	Yes	Large divot immediately forward of +Y bipod ramp
STS-29	Yes	Yes	No	No	Divots	No	No	No	Divots on LH2 tank/intertank closeout flange
STS-30	No	No	No	No		No	No	No	
STS-31	No	No	No	No		No	No	No	
STS-32	Yes	Yes	No	No	Divot	Yes	Yes	No	Divot on intertank forward of -Y bipod ramp
STS-33	No	No	No	No		No	No	No	
STS-34	Yes	No	No	No		No	No	Yes	
STS-35	No	No	No	No		No	No	No	
STS-36	No	No	No	No		No	No	No	
STS-37	No	No	No	No		No	No	No	
STS-38	No	No	No	No		No	No	No	
STS-39	No	No	No	No		No	No	No	
STS-40	Yes	Yes	No	No		Yes	No	No	
STS-41	No	No	No	No		No	No	Yes	
STS-42	Yes	No	No	No	Two divots	No	No	Yes	Divots on intertank near -Y bipod ramp
STS-43	Yes	No	No	No		No	No	Yes	
STS-44	No	No	No	No		No	No	No	
STS-45	No	No	No	No	Divots	No	No	Yes	Divots on LH2/intertank closeout flange in -Y direction from -Y bipod ramp
STS-46	No	No	No	No		No	No	No	
STS-47	Yes	Yes	No	No	Divots	Yes	Yes	Yes	Divots on LH2/intertank closeout flange underneath bipod
STS-48	No	No	No	No		No	No	No	
STS-49	No	No	No	No		No	No	No	
STS-50	Yes	Yes	**Yes**	No		Yes	Yes	Yes	26x10 inch divot on -Y bipod ramp
STS-51	Yes	Yes	No	No	Divots	No	No	Yes	Divot on LH2/Intertank closeout flange adjacent to -Y bipod ramp
STS-52	Yes	Yes	**Yes**	No		Yes	Yes	Yes	Foam missing on left corner of -Y bipod ramp. -Y jack pad closeout missing
STS-53	Yes	Yes	No	No	Divots	No	No	Yes	Two divots on LH2/Intertank closeout flange near -Y bipod ramp
STS-54	Yes	Yes	No	No	Divots	Yes	Yes	Yes	Divots on closeout under bipod. Right bipod jack pad closeout missing.
STS-55	Yes	Yes	No	No	Divots	No	No	Yes	TPS divots near bipod. +Y bipod jack pad closeout missing
STS-56	No	No	No	No		No	No	Yes	IFA for divots on -Z side of ET
STS-57	Yes	Yes	No	No	Divots	Yes	Yes	Yes	Small Intertank TPS divots forward of bipod
STS-58	Yes	Yes	No	No	Divots	Yes	Yes	Yes	TPS divots near bipod. Both bipod jack pad closeouts missing
STS-59	Yes	Yes	No	No	Divots	Yes	Yes	Yes	28 inch intertank stringer head divot forward of bipod
STS-60	Yes	Yes	No	No		No	No	Yes	
STS-61	Yes	No	No	No		No	No	No	
STS-62	Yes	Yes	No	No	Intertank Divot	Yes	Yes	Yes	14 inch intertank stringer head divot forward of -Y bipod ramp. TPS divots
STS-63	No	No	No	No		No	No	No	
STS-64	No	No	No	No		No	No	No	
STS-65	Yes	Yes	No	No	Divots	Yes	Yes	Yes	6 inch divot near +Y bipod ramp
STS-66	Yes	Yes	No	No	Divots	Yes	Yes	Yes	14 inch intertank stringer head divot forward of -Y bipod ramp
STS-67	Yes	Yes	No	No		No	No	Yes	
STS-68	Yes	Yes	No	No	Divot	Yes	Yes	Yes	10 inch divot on intertank stringer head forward of bipod
STS-69	Yes	Yes	No	No		Yes	No	No	
STS-70	Yes	Yes	No	No		No	No	Yes	
STS-71	Yes	Yes	No	No	Divots	Yes	No	Yes	24 inch intertank stringer head divot forward of bipod
STS-72	Yes	Yes	No	No		Yes	No	No	
STS-73	Yes	Yes	No	No		Yes	Yes	Yes	
STS-74	Yes	Yes	No	No		Yes	Yes	No	
STS-75	Yes	Yes	No	No		Yes	Yes	No	
STS-76	No	No	No	No		No	No	No	
STS-77	Yes	Yes	No	No		Yes	Yes	Yes	Portion of +Y jack pad closeout missing. Multiple, small TPS divots
STS-78	Yes	Yes	No	No	Divots	Yes	Yes	Yes	Divot on intertank closeout flange between bipod legs
STS-79	No	No	No	No		No	No	No	
STS-80	Yes	Yes	No	No	Divots	Yes	Yes	Yes	10 inch divot on stringer head forward of bipod. Two divots under bipod
STS-81	No	No	No	No		No	No	No	
STS-82	No	No	No	No		No	No	No	
STS-83	Yes	Yes	No	No	Divots	Yes	No	Yes	3 divots between bipod legs. 5 divots on flange in -Y direction from bipod
STS-84	Yes	Yes	No	No	Divots	Yes	Yes	Yes	3 divots between bipod legs (largest 9 inches). Few divots forward of bipod
STS-85	No	No	No	No		No	No	Yes	
STS-86	No	No	No	No		No	No	No	
STS-87	Yes	Yes	No	No		Yes	Yes	Yes	
STS-88	No	No	No	No		No	No	Yes	
STS-89	No	No	No	No		No	No	No	
STS-90	Yes	Yes	No	No		Yes	Yes	Yes	
STS-91	Yes	Yes	No	No	Divots	Yes	Yes	Yes	Small divot on LH2 tank TPS aft of -Y bipod. 1 divot under bipod
STS-92	No	No	No	No		No	No	No	
STS-93	No	No	No	No		No	No	Yes	
STS-94	Yes	Yes	No	No	Divot	Yes	Yes	Yes	6 inch piece of foam missing from -Y jack pad closeout
STS-95	Yes	Yes	No	No	Divots	Yes	Yes	Yes	Divots on closeout flange under bipod.
STS-96	Yes	Yes	No	No		Yes	Yes	Yes	
STS-97	Yes	No	No	No		No	No	Yes	
STS-98	No	No	No	No		No	No	No	
STS-99	Yes	Yes	No	No	Divot	Yes	Yes	Yes	Divot on closeout flange under bipod
STS-100	Yes	Yes	No	No	Divot	Yes	Yes	Yes	Divot on closeout flange under bipod
STS-101	Yes	Yes	No	No	Divot	Yes	Yes	Yes	Divot on closeout flange under bipod
STS-102	Yes	Yes	No	No		No	Yes	Yes	
STS-103	No	No	No	No		No	No	No	
STS-104	Yes	Yes	No	No	Divot	No	No	Yes	Divot on closeout flange under bipod
STS-105	Yes	Yes	No	No	Divots	Yes	Yes	Yes	Divot on closeout flange under bipod
STS-106	Yes	Yes	No	No	Divots	Yes	Yes	Yes	Divot on closeout flange under bipod
STS-107	No	No	No	No		No	No	Yes	Downlink video only
STS-108	No	No	No	No		No	No	No	
STS-109	Yes	Yes	No	No	Divots	Yes	Yes	Yes	5 divots in bipod area
STS-110	Yes	Yes	No	No	Divots	Yes	Yes	Yes	Divots on closeout between bipod legs
STS-111	Yes	Yes	No	No	Divots	Yes	Yes	Yes	Divots on closeout between bipod legs
STS-112	Yes	Yes	**Yes**	No	Divots	Yes	Yes	Yes	Left bipod ramp partially missing
STS-113	No	No	No	No		No	No	No	

PRELIMINARY

ET TPS Foam Loss

STS	ET	Vehicle	Launch Date	Useable ET Crew Photos	Useable ET Umbilical Well Photos	Day/ Night	Notes	Photo Catalogued	Bipod Ramp	Flange	Acreage: LO2 Tank	Acreage: Intertank	Acreage: LH2 Tank
033 51L	026	99	01/28/86	No	No	Day	Challenger accident		No data obtained	No data obtained	No data obtained	No data obtained	No data obtained
032 61C	030	102	01/12/86	No crew photos found	16mm only	Day			No loss of TPS noted	No loss of TPS noted	No loss of TPS noted	Divot in I/T 2-tone foam just forward of the -Y bipod ramp. The divot measured approximately 15 inches by 20 inches. Divot in intertank 2-tone foam between bipods. The divot measures 30 inches by 12 inches.	No loss of TPS noted
031 61B	022	104	11/26/85	No	No	Night	No data obtained		No data obtained	No data obtained	No data obtained	No data obtained	No data obtained
030 61A	024	99	10/30/85	No crew photos found	35mm only	Day			No loss of TPS noted	Divot approximately 2 inches in dia. located in the flange closeout between the bipod ramps. Divot approximately 2 inches in dia. Located in the flange closeout +Y of the feedline.	No loss of TPS noted	No loss of TPS noted	No loss of TPS noted
028 51J	025	104	10/03/85	Yes	No umbilical photos found	Day	-Y visible +Y side too distant to detect foam loss		No loss of TPS noted	No data obtained	No data obtained	No data obtained	No data obtained
027 51I	021	103	08/27/85	No crew photos found	No umbilical photos found	Day	No crew or umbilical photos located at KSC.		No data obtained	No data obtained	No data obtained	No data obtained	No data obtained
026 51F	019	99	07/29/85	No crew photos found	35mm only	Day			No loss of TPS noted	The -Y jack pad closeout is missing. This area is approximately 5 inches by 5 inches with substrate exposed. This area is located within the flange closeout between the bipod ramps.	No loss of TPS noted	Thirteen large divots in intertank 2-tone foam ranging form 7 inches to 30 inches in dia. located forward of the bipods. Divot approximately 3 inches in dia. located in the intertank acreage TPS +Y axis just forward of the flange closeout. Divot appro	No loss of TPS noted
025 51G	020	103	06/17/85	No crew photos found	No umbilical photos found	Day	No crew or umbilical photos located at KSC.		No data obtained	No data obtained	No data obtained	No data obtained	No data obtained
024 51B	017	99	04/29/85	No crew photos found	35mm only	Day	Sun angle washed out view of ET making it hard to detect foam loss.	√	No loss of TPS noted	No loss of TPS noted	No loss of TPS noted	Nine large divots (10 inches in dia.) located in the intertank 2-tone foam just forward of the bipods.	Two divots approximately 3-4 inches in dia. Located in the LH2 +Z axis acreage TPS just aft of the flange closeout.
023 51D	018	103	04/12/85	No crew photos found	No umbilical photos found	Day	No crew or umbilical photos located at KSC.		No data obtained	No data obtained	No data obtained	No data obtained	No data obtained
020 51C	014	103	01/24/85	No crew photos found	No umbilical photos found	Day	No crew or umbilical photos located at KSC.		No data obtained	No data obtained	No data obtained	No data obtained	No data obtained
019 51A	016	103	11/08/84	No crew photos found	No umbilical photos found	Day	No crew or umbilical photos located at KSC.		No data obtained	No data obtained	No data obtained	No data obtained	No data obtained
017 41G	015	99	10/05/84	No crew photos found	35mm only	Day	No crew or umbilical photos located at KSC.		No data obtained	No data obtained	No data obtained	Divot approximately 5 inches in dia. located in the intertank 2-tone foam forward and between the bipods. Divot approximately 18-20 inches in dia. located in the 2-tone foam forward of the +Y bipod ramp.	Divot in the LH2 acreage +Z axis at Sta 1623. The divot appears to be loss of 3 inch dia. plug pull repair area.
014 41D	013	103	08/30/84	No crew photos found	No umbilical photos found	Day	No crew or umbilical photos located at KSC.		No data obtained	No data obtained	No data obtained	No data obtained	No data obtained
013 41C	012	99	04/06/84	No crew photos found	No umbilical photos found	Day	No crew or umbilical photos located at KSC.		No data obtained	No data obtained	No data obtained	No data obtained	No data obtained
011 41B	010	99	02/03/84	No crew photos found	35mm only	Day			No loss of TPS noted	The -Y jack pad closeout is missing. This area is approximately 5 inches by 5 inches with substrate exposed. This area is located within the flange closeout between the bipod ramps.	No loss of TPS noted	Divot approximately 10 inches in dia. located in the intertank 2-tone foam area just forward and inboard of the +Y bipod ramp.	Divot approximately 2 inches in dia. located in the LH2 acreage TPS 12 inches below the +Y bipod ramp.
009 041A	011	102	11/28/83	No crew photos found	No umbilical photos found	Day	No crew or umbilical photos located at KSC.		No data obtained	No data obtained	No data obtained	No data obtained	No data obtained
008	009	99	08/30/83	No crew photos found	No umbilical photos found	Day	No crew or umbilical photos located at KSC.		No data obtained	No data obtained	No data obtained	No data obtained	No data obtained
007	006	99	06/18/83	No crew photos found	35 mm only	Day		√	A portion of the -Y Bipod Ramp TPS is missing. The area is approximatel y 18" x 12". The bipod spindle is not exposed.	One small divot approximately 4 inches in dia. Located outboard of the cable tray in the flange closeout.	No loss of TPS noted	Approximately 25 shallow divots all less than 4 inches in dia. located in the intertank acreage TPS +Z axis just forward of the bipods	Approximately 40 divots all less than 2 inches in dia. located in the upper LH2 acreage TPS +Z axis between Sta 1129 and Sta 1200.
006	008	99	04/04/83	No crew photos found	35mm only	Day			No loss of TPS noted	Divot (10" x 4") located in flange closeout and extending into the Intertank acreage TPS. The divot is located +Y of the LO2 feedline. Small shallow 3 inch dia. Divot located in the flange closeout between the bipod ramps.	No loss of TPS noted	No loss of TPS noted	Small divot approximately 3 inches in dia. Located outboard of LO2 feedline in acreage TPS at Sta 1610
005	005	102	11/11/82	No crew photos found	Yes	Day	GH2 pressline on -Y side		No loss of TPS noted	4 divots (2" to 6" dia) outboard of LH2 PAL ramp 1 divot (approximately 7" dia) between bipod	No loss of TPS noted	3 divots (1" to 2") just forward of +Y bipod ramp 3 divots (1" dia) forward of bipod	1 divot (2" dia) between pressline and feedline near Sta 1800 Numerous (30) divots (ranging 2"W x 2 to 10"L) just aft of +Z flange Numerous divots along entire length of GH2 pressline
004	004	102	06/27/82	No crew photos found	Yes	Day	GH2 pressline on -Y side Sun angle (backlighting) washed out view of ET above Sta 1623		No loss of TPS noted	3 divots (approximately 6" dia) just outboard of PAL ramp 1 divot (approximately 4" dia) between LO2 feedline and pressline	No loss of TPS noted	3 divots (2" to 3" dia) forward of bipod	1 divot (3" dia) just forward of longeron Numerous small divots (approximately 40) between pressline and feedling along entire length of LH2 tank Several (7 -9) divots (2" -3" dia) in acreage just aft of +Z flange

Components	Substrate Exposed
No data obtained	N/A
Divot 7 inch by 3 inch in LH2 cable-tray clamshell closeout.	No
No data obtained	
Divot approximately 4 inches in dia. In +Z surface of Sta 115 feedline flange closeout.	No
No data obtained	N/A
No data obtained	N/A
Small divots (< 1 inch dia.) on LO2 feedline flange closeouts +Z surface. Divot 8 inches long by 5 inches wide with substrate exposed located on the +Z surface of Sta 1856 feedline flange closeout. Divot approximately 6 inches in dia. located on the +Z	Yes
No data obtained	N/A
No loss of TPS noted	No
No data obtained	N/A
No data obtained	N/A
No data obtained	N/A
Divot approximately 6 inches in dia. with substrate exposed located in LO2 feedline at Sta 1870.	Yes
No data obtained	N/A
No data obtained	N/A
No loss of TPS noted	Yes
No data obtained	N/A
No data obtained	N/A
Divots in ice/frost ramps ranging from 4 inches in dia. To most of the upper ramp closeouts missing at Sta 1916, Sta 1851, Sta 1787, Sta 1722, Sta 1657, Sta 1528, Sta 1464. Most of these areas of missing foam exposed cable tray SLA sidewall substrate.	Yes
Divot in LO2 feedline flange closeout at Sta 1958 with exposed substrate. Divot is approximately 5 inches in dia. Divot in LO2 feedline flange closeout at Sta 1856. Divot is approximately 3 inches in dia. Divot in LO2 feedline flange closeout at Sta 1	Yes
Missing upper portion of GH2 pressline ice/frost ramp at Sta 1430	No
4 divots (3" to 4" dia) in LH2 PAL ramp along the entire length 1 divot (15"L x 8"W) on LH2 PAL ramp 1 divot (20"L x 8"W) on forward end of LH2 PAL ramp	No

003	003	102	03/22/82	No crew photos found	Yes	Day	GH2 pressline on -Y side		No loss of TPS noted	4 divots (ranging 4" to 8") at +Z 1 divot (approximately 6" x 12") outboard of +Y cable tray - Included portion of LH2 L7tank acreage foam 3 small divots (approximately 3" dia) on +Y/+Z quadrant	No loss of TPS noted	3 divots (2" to 3" dia) forward of bipod	Numerous (35) divots (ranging 2" to 6" dia) between flange and Sta 1377
002	002	102	11/12/81	No crew photos found	Yes	Day	GH2 pressline on -Y side Foam loss divots are difficult to detect due to white paint.		No loss of TPS noted	No loss of TPS noted	No loss of TPS noted	No loss of TPS noted	No loss of TPS noted
001	001	102	04/12/81	No crew photos found	Yes 16mm only	Day	GH2 pressline on -Y side Foam loss divots are difficult to detect due to white paint		No loss of TPS noted	No loss of TPS noted	No loss of TPS noted	No loss of TPS noted	Divot approximately 16 inch by 12 inch (occurred after ET Sep.) in LH2 acreage near Sta 1851adjacent to Pressline. Divot approximately 15 inch by 10 inch located in LH2 acreage near Sta 1721adjacent to Pressline. 5 inch dia. Divot with what appears

No loss of TPS noted	N/A
No loss of TPS noted	No
No loss of TPS noted	Yes

Launch Year	Mission	Rollover	Rollout	Rollback	TCDT	Launch	Land	Ferry Complete	Vehicle	OV	Pad	Dates of Exposure		Days on Pad	OV Exposure Dates		OV Exposure Days	
												Start	End					
2003																		
	STS-107	20-Nov-02	9-Dec-02			16-Jan-03	1-Feb-03		Columbia	OV-102	39A	9-Dec-02	16-Jan-03	39	1-Feb-03			
2002																		
	STS-113	30-Sep-02	12-Oct-02			23-Nov-02	7-Dec-02		Endeavour	OV-105	39A	12-Oct-02	23-Nov-02	43				
	STS-112	4-Sep-02	10-Sep-02			7-Oct-02	18-Oct-02		Atlantis	OV-104	39B	10-Sep-02	7-Oct-02	28				
	STS-111	22-Apr-02	28-Apr-02		17-May-02	5-Jun-02	19-Jun-02	29-Jun-02	Endeavour	OV-105	39A	28-Apr-02	5-Jun-02	39	19-Jun-02	29-Jun-02		
	STS-110	6-Mar-02	12-Mar-02		19-Mar-02	8-Apr-02	19-Apr-02		Atlantis	OV-104	39B	12-Mar-02	8-Apr-02	28				
	STS-109	16-Jan-02	28-Jan-02		9-Feb-01	1-Mar-02	12-Mar-02		Columbia	OV-102	39A	28-Jan-02	1-Mar-02	33				
2001																		
	STS-108	24-Oct-01	31-Oct-01		9-Nov-01	5-Dec-01	17-Dec-01		Endeavour	OV-105	39B	31-Oct-01	5-Dec-01	36				
	STS-105	13-Jun-01	2-Jul-01		23-Jul-01	10-Aug-01	22-Aug-01		Discovery	OV-103	39A	2-Jul-01	10-Aug-01	40				
	STS-104	29-May-01	21-Jun-01		29-Jun-01	12-Jul-01	24-Jul-01		Atlantis	OV-104	39B	21-Jun-01	12-Jul-01	22				
	STS-100	17-Mar-01	22-Mar-01		30-Mar-01	19-Apr-01	1-May-01		Endeavour	OV-105	39A	22-Mar-01	19-Apr-01	29				
	STS-102	1-Feb-01	12-Feb-01		14-Feb-01	8-Mar-01	21-Mar-01		Discovery	OV-103	39B	12-Feb-01	8-Mar-01	25				
	STS-98	4-Dec-00	3-Jan-01	19-Jan-01	6-Jan-01	7-Feb-01	20-Feb-01	? Yes	Atlantis	OV-104	39A	3-Jan-01	19-Jan-01	17	20-Feb-01	? Yes		
	STS-98		26-Jan-01			7-Feb-01	20-Feb-01		Atlantis	OV-104	39A	26-Jan-01	7-Feb-01	13				
2000																		
	STS-97	25-Oct-00	31-Oct-00		7-Nov-00	30-Nov-00	11-Dec-00		Endeavour	OV-105	39B	31-Oct-00	30-Nov-00	31				
	STS-92	24-Aug-00	11-Sep-00			11-Oct-00	24-Oct-00		Discovery	OV-103	39A	11-Sep-00	11-Oct-00	31				
	STS-106	7-Aug-00	13-Aug-00		18-Aug-00	8-Sep-00	20-Sep-00		Atlantis	OV-104	39B	13-Aug-00	8-Sep-00	27				
	STS-101	17-Mar-00	25-Mar-00		7-Apr-00	19-May-00	29-May-00		Atlantis	OV-104	39A	25-Mar-00	19-May-00	56				
	STS-99	2-Dec-99	13-Dec-99		14-Dec-99	11-Feb-00	22-Feb-00		Endeavour	OV-105	39A	13-Dec-99	11-Feb-00	61				
1999																		
	STS-103	4-Nov-99	13-Nov-99		17-Nov-99	19-Dec-99	28-Dec-99		Discovery	OV-103	39B	13-Nov-99	19-Dec-99	37				
	STS-93	2-Jun-99	7-Jun-99		24-Jun-99	23-Jul-99	27-Jul-99		Columbia	OV-102	39B	7-Jun-99	23-Jul-99	47				
	STS-96	12-Apr-99	23-Apr-99	8-May-99		27-May-99			Discovery	OV-103	39B	23-Apr-99	8-May-99	16				
	STS-96		20-May-99			27-May-99	6-Jun-99		Discovery	OV-103	39B	20-May-99	27-May-99	8				
1998																		
	STS-91	27-Apr-98	2-May-98		7-May-98	2-Jun-98	12-Jun-98		Discovery	OV-103	39A	2-May-98	2-Jun-98	32				
	STS-90	17-Mar-98	23-Mar-98		31-Mar-98	17-Apr-98	10-May-98		Columbia	OV-102	39B	23-Mar-98	17-Apr-98	26				
	STS-89	12-Dec-97	19-Dec-97		10-Jan-98	22-Jan-98	31-Jan-98		Endeavour	OV-105	39A	19-Dec-97	22-Jan-98	35				
	STS-95	14-Sep-98	21-Sep-98			29-Oct-98	7-Nov-98		Discovery	OV-103	39B	21-Sep-98	29-Oct-98	39				
	STS-88	15-Oct-98	21-Oct-98			4-Dec-98	15-Dec-98		Endeavour	OV-105	39A	21-Oct-98	4-Dec-98	45				
1997																		
	STS-87	24-Oct-97	29-Oct-97			19-Nov-97	5-Dec-97		Columbia	OV-102	39B	29-Oct-97	19-Nov-97	22				
	STS-86	11-Aug-97	18-Aug-97			25-Sep-97	6-Oct-97		Atlantis	OV-104	39A	18-Aug-97	25-Sep-97	39				
	STS-85	7-Jul-97	14-Jul-97		22-Jul-97	7-Aug-97	19-Aug-97		Discovery	OV-103	39A	14-Jul-97	7-Aug-97	25				
	STS-94	4-Jun-97	11-Jun-97			1-Jul-97	17-Jul-97		Columbia	OV-102	39A	11-Jun-97	1-Jul-97	21				
	STS-84	19-Apr-97	24-Apr-97		28-Apr-97	15-May-97	24-May-97		Atlantis	OV-104	39A	24-Apr-97	15-May-97	22				
	STS-83	5-Mar-97	11-Mar-97		13-Mar-97	4-Apr-97	8-Apr-97		Columbia	OV-102	39A	11-Mar-97	4-Apr-97	25				
	STS-82	11-Jan-97	17-Jan-97		22-Jan-97	11-Feb-97	21-Feb-97		Discovery	OV-103	39A	17-Jan-97	11-Feb-97	26				
	STS-81	5-Dec-96	10-Dec-96		17-Dec-96	12-Jan-97	22-Jan-97		Atlantis	OV-104	39B	10-Dec-96	12-Jan-97	34				
1996																		
	STS-80	9-Oct-96	16-Oct-96		22-Oct-96	19-Nov-96	7-Dec-96		Columbia	OV-102	39B	16-Oct-96	19-Nov-96	35				
	STS-79	24-Jun-96	1-Jul-96	10-Jul-96	27-Aug-96	16-Sep-96	26-Sep-96		Atlantis	OV-104	39A	1-Jul-96	10-Jul-96	10				
	STS-79	13-Aug-96	20-Aug-96	4-Sep-96		16-Sep-96			Atlantis	OV-104		20-Aug-96	4-Sep-96	16				
	STS-79		5-Sep-96			16-Sep-96			Atlantis	OV-104		5-Sep-96	16-Sep-96	12				
	STS-78	20-May-96	30-May-96		4-Jun-96	20-Jun-96	7-Jul-96		Columbia	OV-102	39B	30-May-96	20-Jun-96	22				
	STS-77	9-Apr-96	16-Apr-96		23-Apr-96	19-May-96	29-May-96		Endeavour	OV-105	39B	16-Apr-96	19-May-96	34				
	STS-76	19-Feb-96	28-Feb-96		5-Mar-96	22-Mar-96	31-Mar-96	12-Apr-96	Atlantis	OV-104	39B	28-Feb-96	22-Mar-96	24	31-Mar-96	12-Apr-96		
	STS-75	23-Jan-96	29-Jan-96			22-Feb-96	9-Mar-96		Columbia	OV-102	39B	29-Jan-96	22-Feb-96	25				
	STS-72	30-Nov-95	6-Dec-95			11-Jan-96	20-Jan-96		Endeavour	OV-105	39B	6-Dec-95	11-Jan-96	37				
1995																		
	STS-74	3-Oct-95	12-Oct-95		17-Oct-95	12-Nov-95	20-Nov-95		Atlantis	OV-104	39A	12-Oct-95	12-Nov-95	32				
	STS-73	21-Aug-95	28-Aug-95		11-Sep-95	20-Oct-95	5-Nov-95		Columbia	OV-102	39B	28-Aug-95	20-Oct-95	54	5-Nov-95			
	STS-69	28-Jun-95	5-Jul-95	1-Aug-95		7-Sep-95			Endeavour	OV-105	39A	5-Jul-95	1-Aug-95	28				
	STS-69		8-Aug-95			7-Sep-95	18-Sep-95		Endeavour	OV-105	39A	8-Aug-95	7-Sep-95	31				
	STS-70	3-May-95	11-May-95	8-Jun-95		13-Jul-95			Discovery	OV-103	39B	11-May-95	8-Jun-95	29				
	STS-70		15-Jun-95			13-Jul-95	22-Jul-95		Discovery	OV-103	39B	15-Jun-95	13-Jul-95	29				
	STS-71	20-Apr-95	26-Apr-95			27-Jun-95	7-Jul-95		Atlantis	OV-104	39A	26-Apr-95	27-Jun-95	63				
	STS-67	3-Feb-95	8-Feb-95		14-Feb-95	2-Mar-95	18-Mar-95		Endeavour	OV-105	39A	8-Feb-95	2-Mar-95	23				
	STS-63	5-Jan-95	10-Jan-95		17-Jan-95	3-Feb-95	11-Feb-95		Discovery	OV-103	39B	10-Jan-95	3-Feb-95	25				
1994																		
	STS-66	3-Oct-94	9-Oct-94			3-Nov-94	14-Nov-94	? Yes	Atlantis	OV-104	39B	9-Oct-94	3-Nov-94	26	14-Nov-94	? Yes		
	STS-68	21-Jul-94	27-Jul-94	24-Aug-94	13-Sep-94	30-Sep-94	11-Oct-94		Endeavour	OV-105	39A	27-Jul-94	24-Aug-94	29				
	STS-68		13-Sep-94			30-Sep-94			Endeavour	OV-105	39A	13-Sep-94	30-Sep-94	18				
	STS-64	11-Aug-94	19-Aug-94			9-Sep-94	20 Spe 94		Discovery	OV-103	39B	19-Aug-94	9-Sep-94	22				
	STS-65	8-Jun-94	15-Jun-94			8-Jul-94	23-Jul-94		Columbia	OV-102	39A	15-Jun-94	8-Jul-94	24				
	STS-59	14-Mar-94	19-Mar-94			9-Apr-94	20-Apr-94	2-May-94	Endeavour	OV-105	39A	19-Mar-94	9-Apr-94	22	20-Apr-94	2-May-94		
	STS-62	3-Feb-94	10-Feb-94			4-Mar-94	18-Mar-94		Columbia	OV-102	39B	10-Feb-94	4-Mar-94	23				
	STS-60	4-Jan-94	10-Jan-94			3-Feb-94	11-Feb-94		Discovery	OV-103	39A	10-Jan-94	3-Feb-94	25				
1993																		
	STS-56	2-Mar-93	15-Mar-93			8-Apr-93	17-Apr-93		Discovery	OV-103	39B	15-Mar-93	8-Apr-93	25				
	STS-61	21-Oct-93	28-Oct-93			2-Dec-93	13-Dec-93		Endeavour	OV-105	39B	28-Oct-93	2-Dec-93	36				
	STS-58	11-Aug-93	17-Sep-93			18-Oct-93	1-Nov-93	9-Nov-93	Columbia	OV-102	39B	17-Sep-93	18-Oct-93	32	1-Nov-93	9-Nov-93		
	STS-51	18-Jun-93	26-Jun-93			12-Sep-93	22-Sep-93		Discovery	OV-103	39B	26-Jun-93	12-Sep-93	79				
	STS-57	24-Mar-93	28-Apr-93			21-Jun-93	1-Jul-93		Endeavour	OV-105	39B	28-Apr-93	21-Jun-93	55				
	STS-55	2-Feb-93	8-Feb-93			26-Apr-93	6-May-93	14-May-93	Columbia	OV-102	39A	8-Feb-93	26-Apr-93	78	6-May-93	14-May-93		
	STS-54	23-Nov-92	3-Dec-92			13-Jan-93	19-Jan-93		Endeavour	OV-105	39B	3-Dec-92	13-Jan-93	42				
1992																		
	STS-53	3-Nov-92	8-Nov-92			2-Dec-92	9-Dec-92	18-Dec-92	Discovery	OV-103	39A	8-Nov-92	2-Dec-92	25	9-Dec-92	18-Dec-92		
	STS-52	20-Sep-92	26-Sep-92			22-Oct-92	1-Nov-92		Columbia	OV-102	39B	26-Sep-92	22-Oct-92	27				
	STS-47	17-Aug-92	25-Aug-92			12-Sep-92	20-Sep-92		Endeavour	OV-105	39B	25-Aug-92	12-Sep-92	19				
	STS-46	4-Jun-92	11-Jun-92			31-Jul-92	8-Aug-92		Atlantis	OV-104	39B	11-Jun-92	31-Jul-92	51				
	STS-50	29-May-92	3-Jun-92			25-Jun-92	9-Jul-92		Columbia	OV-102	39A	3-Jun-92	25-Jun-92	23				
	STS-49	7-Mar-92	13-Mar-92			7-May-92	16-May-92	30-May-92	Endeavour	OV-105	39B	13-Mar-92	7-May-92	56	16-May-92	30-May-92		
	STS-45	13-Feb-92	19-Feb-92			24-Mar-92	2-Apr-92		Atlantis	OV-104	39A	19-Feb-92	24-Mar-92	35				
	STS-42	12-Dec-91	19-Dec-91			22-Jan-92	30-Jan-92	16-Feb-92	Discovery	OV-103	39A	19-Dec-91	22-Jan-92	35	30-Jan-92	16-Feb-92	1.23	4.4
1991																		
	STS-44	18-Oct-91	23-Oct-91			24-Nov-91	1-Dec-91	8-Dec-91	Atlantis	OV-104	39A	23-Oct-91	24-Nov-91	33	1-Dec-91	8-Dec-91		
	STS-48	25-Jul-91	12-Aug-91			12-Sep-91	18-Sep-91	26-Sep-91	Discovery	OV-103	39A	12-Aug-91	12-Sep-91	32	18-Sep-91	26-Sep-91		
	STS-43	19-Jun-91	25-Jun-91			2-Aug-91	11-Aug-91		Atlantis	OV-104	39A	25-Jun-91	2-Aug-91	39				
	STS-40	26-Apr-91	2-May-91			5-Jun-91	14-Jun-91	21-Jun-91	Columbia	OV-102	39B	2-May-91	5-Jun-91	35	14-Jun-91	21-Jun-91		
	STS-39	9-Feb-91	15-Feb-91	7-Mar-91		28-Apr-91	6-May-91		Discovery	OV-103	39A	15-Feb-91	7-Mar-91	21				
	STS-39	25-Mar-91	1-Apr-91			28-Apr-91			Discovery	OV-103	39A	1-Apr-91	28-Apr-91	28				
	STS-37	8-Mar-91	15-Mar-91			5-Apr-91	11-Apr-91	18-Apr-91	Atlantis	OV-104	39B	15-Mar-91	5-Apr-91	22	11-Apr-91	18-Apr-91		
1990																		
	STS-35	16-Apr-90	22-Apr-90	12-Jun-90		2-Dec-90	10-Dec-90		Columbia	OV-102	39B	22-Apr-90	12-Jun-90	52				
	STS-35	2-Aug-90	9-Aug-90	9-Oct-90		2-Dec-90			Columbia	OV-102	39B	9-Aug-90	9-Oct-90	62				
	STS-35		14-Oct-90			2-Dec-90			Columbia	OV-102	39B	14-Oct-90	2-Dec-90	50				
	STS-38	8-Jun-90	18-Jun-90	9-Aug-90		15-Nov-90	20-Nov-90		Atlantis	OV-104	39A	18-Jun-90	9-Aug-90	53				
	STS-38	2-Oct-90	12-Oct-90			15-Nov-90			Atlantis	OV-104	39A	12-Oct-90	15-Nov-90	35				
	STS-41	27-Aug-90	4-Sep-90			6-Oct-90	10-Oct-90	16-Oct-90	Discovery	OV-103	39B	4-Sep-90	6-Oct-90	33	10-Oct-90	16-Oct-90		
	STS-31	5-Mar-90	15-Mar-90			24-Apr-90	29-Apr-90	7-May-90	Discovery	OV-103	39B	15-Mar-90	24-Apr-90	41	29-Apr-90	7-May-90		
	STS-36	19-Jan-90	25-Jan-90			28-Feb-90	4-Mar-90	13-Mar-90	Atlantis	OV-104	39A	25-Jan-90	28-Feb-90	35	4-Mar-90	13-Mar-90		
	STS-32	16-Oct-89	28-Nov-89			9-Jan-90	20-Jan-90	26-Jan-90	Columbia	OV-102	39A	28-Nov-89	9-Jan-90	43	20-Jan-90	26-Jan-90		
1989																		
	STS-33	5-Oct-89	27-Oct-89			22-Nov-89	27-Nov-89	4-Dec-89	Discovery	OV-103	39B	27-Oct-89	22-Nov-89	27	27-Nov-89	4-Dec-89		
	STS-34	21-Aug-89	29-Aug-89			18-Oct-89	23-Oct-89	29-Oct-89	Atlantis	OV-104	39B	29-Aug-89	18-Oct-89	51	23-Oct-89	29-Oct-89		
	STS-28	3-Jul-89	14-Jul-89			8-Aug-89	13-Aug-89	21-Aug-89	Columbia	OV-102	39B	14-Jul-89	8-Aug-89	26	13-Aug-89	21-Aug-89		
	STS-29	23-Jan-89	3-Feb-89			13-Mar-89	18-Mar-89	24-Mar-89	Discovery	OV-103	39B	3-Feb-89	13-Mar-89	39	18-Mar-89	24-Mar-89		
	STS-30	11-Mar-89	22-Mar-89			4-May-89	8-May-89	15-May-89	Atlantis	OV-104	39B	22-Mar-89	4-May-89	44	8-May-89	15-May-89		
1988																		
	STS-27	22-Oct-88	2-Nov-88			2-Dec-88	6-Dec-88	13-Dec-88	Atlantis	OV-104	39B	2-Nov-88	2-Dec-88	31	6-Dec-88	13-Dec-88		
	STS-26	21-Jun-88	4-Jul-88			29-Sep-88	30-Oct-88	8-Oct-88	Discovery	OV-103	39B	4-Jul-88	29-Sep-88	88	30-Oct-88	8-Oct-88		
1987																		
	No Shuttle Flights																	
1986																		
	51-L	16-Dec-85	22-Dec-85			28-Jan-86			Challenger	OV-099	39B	22-Dec-85	28-Jan-86	38				
	61-C	22-Nov-85	2-Dec-85			12-Jan-86	18-Jan-86	23-Jan-86	Columbia	OV-102	39A	2-Dec-85	12-Jan-86	42	18-Jan-86	23-Jan-86		
1985																		
	61-B	7-Nov-85	12-Nov-85			26-Nov-85	5-Dec-85	7-Dec-85	Atlantis	OV-104	39A	12-Nov-85	26-Nov-85	15	5-Dec-85	7-Dec-85		
	61-A	12-Oct-85	16-Oct-85			30-Oct-85	6-Nov-85	11-Nov-85	Challenger	OV-099	39A	16-Oct-85	30-Oct-85	15	6-Nov-85	11-Nov-85	1.16	
	51-J	12-Aug-85	30-Aug-85			3-Oct-85	7-Oct-85	11-Oct-85	Atlantis	OV-104	39A	30-Aug-85	3-Oct-85	35	7-Oct-85	11-Oct-85		
	51-I	30-Jul-85	6-Aug-85			27-Aug-85	3-Sep-85	8-Sep-85	Discovery	OV-103	39A	6-Aug-85	27-Aug-85	22	3-Sep-85	8-Sep-85		
	51-F	24-Jun-85	29-Jun-85			29-Jul-85	6-Aug-85	11-Aug-85	Challenger	OV-099	39A	29-Jun-85	29-Jul-85	31	6-Aug-85	11-Aug-85		

	51-G	29-May-85	4-Jun-85			17-Jun-85	24-Jun-85	28-Jun-85	Discovery	OV-103	39A	4-Jun-85	17-Jun-85	14	24-Jun-85	28-Jun-85		
	51-B	10-Feb-85	15-Feb-85	4-Mar-85		29-Apr-85	6-May-85	11-May-85	Challenger	OV-099	39A	15-Feb-85	4-Mar-85	18	6-May-85	11-May-85		
	51-B	10-Apr-85	15-Apr-85			29-Apr-85			Challenger	OV-099	39A	15-Apr-85	29-Apr-85	15				
	51-D	23-Mar-85	28-Mar-85			12-Apr-85	19-Apr-85		Discovery	OV-103	39A	28-Mar-85	12-Apr-85	16				
	51-C	21-Dec-84	5-Jan-85			24-Jan-85	27-Jan-85		Discovery	OV-103	39A	5-Jan-85	24-Jan-85	20				
1984																		
	51-A	18-Oct-84	23-Oct-84			8-Nov-84	16-Nov-84	?Yes	Discovery	OV-103	39A	23-Oct-84	8-Nov-84	17	16-Nov-84	?Yes	4.42	
	41-G	8-Sep-84	13-Sep-84			5-Oct-84	13-Oct-84	? Yes	Challenger	OV-099	39A	13-Sep-84	5-Oct-84	23	13-Oct-84	? Yes		
	41-D	12-May-84	19-May-84	14-Jul-84		30-Aug-84	5-Sep-84	10-Sep-84	Discovery	OV-103	39A	19-May-84	14-Jul-84	57	5-Sep-84	10-Sep-84		
	41-D	1-Aug-84	9-Aug-84			30-Aug-84			Discovery	OV-103	39A	9-Aug-84	30-Aug-84	22				
	41-C	14-Mar-84	19-Mar-84			6-Apr-84	13-Apr-84	18-Apr-84	Challenger	OV-099	39A	19-Mar-84	6-Apr-84	19	13-Apr-84	18-Apr-84		
	41-B	6-Jan-84	12-Jan-84			3-Feb-84	11-Feb-84		Challenger	OV-099	39A	12-Jan-84	3-Feb-84	23				
1983																		
	STS-9	24-Sep-83	28-Sep-83	19-Oct-83		28-Nov-83	8-Dec-83	15-Dec-83	Columbia	OV-102	39A	28-Sep-83	19-Oct-83	22	8-Dec-83	15-Dec-83		
	STS-9	3-Nov-83	8-Nov-83			28-Nov-83			Columbia	OV-102	39A	8-Nov-83	28-Nov-83	21				
	STS-8	26-Jul-83	2-Aug-83			30-Aug-83	5-Sep-83	9-Sep-83	Challenger	OV-099	39A	2-Aug-83	30-Aug-83	29	5-Sep-83	9-Sep-83		
	STS-7	21-May-83	26-May-83			18-Jun-83	24-Jun-83	29-Jun-83	Challenger	OV-099	39A	26-May-83	18-Jun-83	24	24-Jun-83	29-Jun-83		
	STS-6	23-Nov-82	30-Nov-82			4-Apr-83	9-Apr-83		Challenger	OV-099	39A	30-Nov-82	4-Apr-83	126				
1982																		
	STS-5	9-Sep-82	21-Sep-82			11-Nov-82	16-Nov-82	22-Nov-82	Columbia	OV-102	39A	21-Sep-82	11-Nov-82	52	16-Nov-82	22-Nov-82		
	STS-4	19-May-82	26-May-82			27-Jun-82	4-Jul-82	15-Jul-82	Columbia	OV-102	39A	26-May-82	27-Jun-82	33	4-Jul-82	15-Jul-82		
	STS-3	3-Feb-82	16-Feb-82			22-Mar-82	30-Mar-82	6-Apr-82	Columbia	OV-102	39A	16-Feb-82	22-Mar-82	35	30-Mar-82	6-Apr-82		
1981																		
	STS-2	10-Aug-81	31-Aug-81			12-Nov-81	14-Nov-81	25-Nov-81	Columbia	OV-102	39A	31-Aug-81	12-Nov-81	74	14-Nov-81	25-Nov-81		
	STS-1	24-Nov-80	29-Dec-80			12-Apr-81	14-Apr-81	28-Apr-81	Columbia	OV-102	39A	29-Dec-80	12-Apr-81	105	14-Apr-81	28-Apr-81		
														4316				
														Days	**Days**			
													Columbia	1208	1208			
													Discovery	1050	1050			
													Atlantis	948	948			
													Endeavour	749	749			
													Challenger	361	361			
													Total Days	4316	4316			

Mission	Vehicle	Reference	Comments
STS-32	OV-103 Discovery	Debris Damage Assessment	The majority of debris damage was located on the lower surface, which was attributed to ice debris released from the umbilical area during ET separation. This umbilical ice debris was seen in the ET separation films and phots taken by cameras mounted in the OV-102 umbilical wells. These films also showed a loss of TPS from the ET intertank near the bipod. The largest piece of material lost was approximately 24" x 18". Loss of TPS from this area was the source of considerable debris damage for earlier flights and probably was a contributor to the lower surface damage for STS-32. "Jagged" steel particles of this type (from the frangible nuts) represent a potentially catostrophic source of damage to the vehicle, although the transport mechanism and risk are very uncertain due to the liftoff environment.
STS-35	OV-102 Columbia	Debris Damage Assessment	one of the damage sites, on the lower surface of the bodyflap, exhibited significant thermal erosion (app.. 3/4 inch in depth and melting adjacent tiles coating material. The largest lower surface damage site was located on the right hand wing chine, affected four tiles, but had a maximum depth of only 1/4 inch. This damage may be a result of impact from ET TPS debris. Photos of the separated ET, taken by the flight crew, indicate a loss of foam TPS at the juncture of the intertank and LH2 tank. This item was documented as an in-flight anomaly and is under investigation.
STS-35	OV-102 Columbia		ET TPS debris classified as IFA (35-T-001)
STS-35	OV-102 Columbia	Debris Damage Assessment	one of the damage sites, on the lower surface of the bodyflap, exhibited significant thermal erosion (app.. 3/4 inch in depth and melting adjacent tiles coating material. The largest lower surface damage site was located on the right hand wing chine, affected four tiles, but had a maximum depth of only 1/4 inch. This damage may be a result of impact from ET TPS debris. Photos of the separated ET, taken by the flight crew, indicate a loss of foam TPS at the juncture of the intertank and LH2 tank. This item was documented as an in-flight anomaly and is under investigation.
STS-42	OV-103 Discovery	Debris Damage Assessment	The majority of the hits occurred on the Orbiter lower surface which had a total of 159 hits. 38 of the lower surface hits had a major dimension of one inch or greater and 14 of the lower surface hits had a major dimension of 3 inches or greater. The large shallow hits on the wing glove lower surfaces were not typical. Analysis concluded that loss of ET intertank foam is the probable source of increased debris damage. An IFA was documented. STS-42 and STS-44 were the first two flights using the two gun spray process on the intertank. It is also the second flight (behind STS-44_ without intertank vent holes.
STS-58	OV-102 Columbia	Debris Damage Assessment	Photos of the separated ET taken using the cameras located in the Orbiter umbilical well showed a significant loss of TPS from the ET intertank. The jack pad closeout material was missing as was a strip of foam material from an intertank stringer. The loss of jack pad closeout material has occurred previously but the amount of material missing from the stringer (down to the primer) is unusual. Both of these conditions were documented as an inflight anomaly (IFA STS-58-T-1).

Mission	Pad	Days.Exposed	Total	DailyMax	DailyAvg
STS-100	39A	29	1.920	1.710	0.066
STS-101	39A	56	2.231	0.710	0.040
STS-102	39B	25	0.840	0.370	0.034
STS-103	39B	37	5.130	1.720	0.139
STS-104	39B	22	2.520	0.600	0.115
STS-105	39A	40	5.060	1.400	0.127
STS-106	39B	27	6.880	5.580	0.255
STS-107	39A	39	12.780	5.880	0.328
STS-108	39B	36	10.240	3.650	0.284
STS-109	39A	33	4.210	2.040	0.128
STS-110	39B	28	1.190	1.080	0.043
STS-111	39A	39	1.850	0.630	0.047
STS-112	39B	28	0.550	0.310	0.020
STS-113	39A	43	3.460	1.640	0.080
STS-42	39A	24	2.974	2.600	0.124
STS-44	39A	33	0.750	0.370	0.023
STS-45	39A	35	2.750	1.240	0.079
STS-46	39B	51	11.450	2.920	0.225
STS-47	39B	19	1.420	0.700	0.075
STS-48	39A	32	4.050	2.010	0.127
STS-49	39B	56	4.570	1.600	0.082
STS-50	39A	23	6.140	2.650	0.267
STS-51	39B	79	12.440	2.500	0.157
STS-52	39B	27	6.350	2.950	0.235
STS-53	39A	25	4.060	2.180	0.162
STS-54	39B	42	3.050	1.120	0.073
STS-55	39A	78	8.085	2.510	0.104
STS-56	39B	25	2.020	0.700	0.081
STS-57	39B	55	1.210	0.500	0.022
STS-58	39B	32	3.980	1.250	0.124
STS-59	39A	22	2.040	1.650	0.093
STS-60	39A	25	3.720	1.400	0.149
STS-61	39A/B	36	1.000	0.400	0.028
STS-62	39B	24	9.700	6.350	0.404
STS-63	39B	25	3.030	2.250	0.121
STS-64	39B	22	3.380	1.340	0.154
STS-65	39A	24	3.920	3.070	0.163
STS-66	39B	26	4.960	1.500	0.191
STS-67	39A	23	1.860	1.350	0.081
STS-68	39A	47	10.470	3.000	0.223
STS-69	39A	59	20.470	5.650	0.347
STS-70	39B	58	11.460	5.600	0.198
STS-71	39A	63	11.330	3.200	0.180
STS-72	39B	37	7.035	3.800	0.190
STS-73	39B	54	15.750	2.750	0.292
STS-74	39A	32	5.360	2.600	0.168
STS-75	39B	25	1.870	1.750	0.075
STS-76	39B	24	8.740	4.000	0.364
STS-77	39B	34	1.270	1.240	0.037
STS-78	39B	22	5.770	2.400	0.262
STS-79	39A	38	9.370	3.350	0.247
STS-80	39B	35	0.910	0.360	0.026
STS-81	39B	34	0.410	0.300	0.012
STS-82	39A	26	0.200	0.180	0.008
STS-83	39A	25	2.465	0.970	0.099
STS-84	39A	22	2.975	1.230	0.135
STS-85	39A	25	3.515	1.400	0.141
STS-86	39A	39	7.015	1.400	0.180
STS-87	39B	22	3.500	1.500	0.159
STS-88	39A	45	5.010	2.370	0.111
STS-89	39A	35	3.545	1.570	0.101
STS-90	39B	26	0.150	0.110	0.006
STS-91	39A	32	0.520	0.250	0.016
STS-92	39A	31	7.582	3.590	0.245
STS-93	39B	47	6.900	3.060	0.147
STS-94	39A	21	4.995	1.250	0.238
STS-95	39B	39	2.740	0.520	0.070
STS-96	39B	24	2.060	0.910	0.086
STS-97	39B	31	1.150	0.990	0.037
STS-98	39A	30	0.800	0.160	0.027
STS-99	39A	61	6.003	1.760	0.098
STS-1	39A	105	5.9961	2.220472	0.057105362
STS-2	39A	74	13.11	2.110236	0.177165354
STS-3	39A	35	2.9567	1.448819	0.08447694
STS-4	39A	33	8.0157	2.389764	0.242901456
STS-5	39A	52	4.0197	1.11811	0.077301635
STS-6	39A	126	18.996	1.889764	0.150762405
STS-7	39A	24	6.9685	1.779528	0.290354331
STS-8	39A	29	4.8543	1.531496	0.167390714
STS-9	39A	43	5.3701	1.031496	0.124885552
STS-41-B	39A	23	2.1142	0.531496	0.091920575
STS-41-C	39A	19	3.6496	2.149606	0.192084542
STS-41-D	39A	79	15.945	2.759843	0.201833948
STS-41-G	39A	23	3.3701	1.96063	0.146525163
STS-51-A	39A	17	4.252	2.46063	0.250115794
STS-51-C	39A	20	0.0945	0.070866	0.004724409
STS-51-D	39A	16	0.4016	0.318898	0.025098425
STS-51-B	39A	33	0.122	0.090551	0.003698401
STS-51-G	39A	14	3.0315	1.031496	0.216535433
STS-51-F	39A	31	5.2441	1.098425	0.169164338
STS-51-I	39A	22	7.4724	1.181102	0.339656407
STS-51-J	39A	35	9.9252	2.129921	0.283577053
STS-61-A	39A	15	3.1181	1.468504	0.207874016
STS-61-B	39A	15	0.1929	0.110236	0.012860892
STS-61-C	39A	42	9.5315	4.141732	0.226940382
STS-51-L	39B	38	7.1811	4.141732	0.188976378
STS-26	39B	88	14.98	2.889764	0.170230852
STS-27	39B	24	4.311	3.279528	0.179625984
STS-28	39B	26	4.3268	1.610236	0.166414294
STS-29	39B	39	3.378	1.11811	0.086614173
STS-30	39B	44	2.7756	0.791339	0.063081603
STS-31	39B	41	2.4803	0.968504	0.060495487
STS-32	39A	43	5.2874	1.38189	0.122962827
STS-33	39B	27	2.2205	1.019685	0.08223972
STS-34	39B	51	13.886	5.468504	0.272271113
STS-35	39A/B	164	20.516	4.350394	0.125096025
STS-36	39A	35	4.4921	1.610236	0.128346457
STS-37	39B	22	8.2795	3.740157	0.376342162
STS-38	39A	88	16.843	4.350394	0.191392269
STS-39	39A	49	6.9843	1.531496	0.142535754
STS-40	39B	35	6.4803	2.098425	0.185151856
STS-41	39B	33	2.2559	0.838583	0.068360773
STS-43	39A	39	11.728	1.330709	0.300726832

	Production				-Y Bipod Ramp (Hand Spray)								-Y Bipod Spindle Face (Hand Spray)								-Y Bipod Beneath S.F. (Hand Spray)								+Y Bipod Ramp (Hand Spray)								+Y B	
ET	Start Date	Completion Date	Ship Date	Days in Storage Before Shipment	Substrate Temp (°F)	Cell Temp (°F)	Cell Humidity (%rh)	Complete Date	Complete Day	Complete Time	Personnel	Personnel	Substrate Temp (°F)	Cell Temp (°F)	Cell Humidity (%rh)	Complete Date	Complete Day	Complete Time	Personnel	Personnel	Substrate Temp (°F)	Cell Temp (°F)	Cell Humidity (%rh)	Complete Date	Complete Day	Complete Time	Personnel	Personnel	Substrate Temp (°F)	Cell Temp (°F)	Cell Humidity (%rh)	Complete Date	Complete Day	Complete Time	Personnel	Personnel	Substrate Temp (°F)	Cell Temp (°F)
61	01/09/89	10/15/91	07/23/93	647				06/27/91	Thu	1520	BN		76	76	55	06/05/91	Wed	1445	BR		75	75	58	06/14/91	Fri	1030	BN					07/16/91	Tue	1150	BR		76	76
61	**Additional Data As Noted By Partial Respray**																																					
62	04/28/89	01/16/92	10/01/93	624				09/17/91	Tue	2300	AP		75	75	50	09/03/91	Tue	2330	AR		75	75	58	09/07/91	Sat	130	AP					09/25/91	Wed	2150	AP		78	78
63	06/24/89	04/19/92	11/11/93	571				11/17/91	Sun	1125	BR		71	71	46	11/27/01	Tue	1240	BR		77	77	50	12/11/91	Wed	1035	BR					01/15/92	Wed	1500	BR		75	75
64	09/25/89	07/13/92	01/08/94	544				04/07/92	Tue	2125	AT		75	75	58	03/18/92	Wed	2100	BJ		78	78	48	03/26/92	Thu	1845	BJ					04/14/92	Tue	845	BR		75	75
65	11/25/89	10/21/92	02/24/94	491				06/30/92	Tue	640	BR		2	72	57	06/11/02	Tue	1445	BR		74	74	57	06/23/92	Tue	1100	BN					07/02/92	Thu	700	BR		72	72
65	**Additional Data As Noted By Partial Respray**																																					
66	01/28/90	01/20/93	05/12/94	477				09/17/92	Thu	2045	AP		75	75	58	09/03/92	Thu	1815	AR		76	76	56	09/09/92	Wed	2230	AR					09/30/92	Wed	2040	AP		76	76
67	04/15/90	04/16/93	06/08/94	418				01/06/93	Wed	1110	BR		74	74	56	12/10/92	Thu	1345	BR		74	74	58	12/23/92	Wed	1442	BR					01/21/93	Thu	1510	BR		74	74
68	06/25/90	07/27/93	07/21/94	359				04/23/93	Fri	1350	AP		75	75	58	03/02/93	Tue	1230	AR		73	73	52	03/10/93	Wed	1445	AR					04/15/93	Thu	1330	AP		74	74
69	08/25/90	10/26/93	09/15/94	324				06/25/93	Fri	1315	BU		74	74	56	06/03/93	Thu	1240	BR		74	74	60	06/14/93	Mon	1500	BR					07/15/93	Thu	1110	BU		74	74
70	01/20/91	01/21/94	11/10/94	293				09/25/93	Sat	2150	BE		75	75	56	09/13/93	Mon	2255	BD		76	76	56	09/16/93	Thu	2330	BD					10/14/93	Thu	1330	AL		74	74
71	04/25/91	04/11/94	12/09/94	242	72	72	50	01/06/94	Thu	2130	AT		73	73	48	12/04/93	Sat	2230	BJ		74	74	38	12/17/93	Fri	100	AT		75	75	36	01/20/94	Thu	115	AT		73	73
72	09/28/91	06/02/94	03/09/95	280	71	71	60	03/01/94	Tue	1350	BR		74	74	54	02/10/64	Mon	1100	BN		70	70	56	02/18/94	Fri	1500	BN		72	72	48	03/17/94	Thu	1345	BR		70	70
73	01/04/92	08/12/94	04/06/95	237	75	75	54	04/22/94	Fri	2115	AT		74	74	58	04/05/94	Tue	300	CY		74	74	64	04/15/94	Fri	100	BJ		76	76	58	05/17/94	Tue	2205	AT		74	74
74	05/17/92	10/14/94	06/01/95	230	76	76	56	06/24/94	Fri	1050	BN		74	74	60	06/15/94	Wed	1000	BE		73	73	60	06/17/94	Fri	950	BD		73	73	57	07/19/94	Tue	1100	BR		73	73
75	07/10/92	01/13/95	07/13/95	181	76	76	51	08/31/64	Mon	1000	AP		77	77	56	08/15/94	Mon	1340	AR		78	78	52	08/17/94	Wed	1710	AR		76	76	50	09/21/94	Wed	940	AP		77	77
76	09/10/92	02/10/95	08/10/95	181	75	75	47	10/21/94	Fri	100	AT		72	72	54	10/06/94	Thu	150	BJ		72	72	64	10/08/94	Sat	2250	BJ		75	75	50	11/09/94	Wed	1050	BR		72	72
77	11/05/92	04/04/95	10/19/95	198	71	71	54	12/08/94	Thu	1440			70	70	54	11/29/94	Tue	640	BR		74	74	40	12/02/94	Fri	610	BR		71	71	59	01/09/95	Mon	1500			70	70
77	**Additional Data As Noted By Partial Respray**																																					
78	04/05/93	05/25/95	12/07/95	196	71	71	53	02/17/95	Fri	1250	AP		75	75	36	01/31/95	Tue	1030	AP		70	70	29	02/08/95	Wed	530	AP		73	73	54	03/14/95	Tue	1000	AP		73	73
78	**Additional Data As Noted By Partial Respray**																																					
79	06/09/93	07/17/95	01/11/96	178	70	70	58	04/22/95	Sat	1305	BR		73	73	48	03/03/95	Fri	2120	H		73	73	48	04/14/95	Fri	1700	H		70	70	58	04/22/95	Sat	1330	BR		74	74
80	08/18/93	09/05/95	03/21/96	198	73	73	58	06/10/95	Sat	1050	BU		75	75	53	05/18/95	Thu	115	H		74	74	56	05/30/95	Tue	2100	H		74	74	54	06/16/95	Fri	300	CI		76	76
81	10/20/93	10/23/95	04/11/96	171	72	72	56	07/25/95	Tue	2250	AT		78	78	59	07/11/95	Tue	2240	CR		75	75	59	07/15/95	Sat	1850	CR		75	75	56	07/29/95	Sat	2250	CI		75	75
82	12/20/93	12/13/95	04/25/96	134	76	76	54	09/19/95	Tue	1445	CZ		71	71	60	08/31/95	Thu	1405	CZ		76	76	60	09/06/95	Wed	1330	CZ		74	74	58	09/26/95	Tue	1000	CZ		73	73
83	02/12/94	02/19/96	09/18/96	212	72	72	57	11/10/95	Fri	2210	BW		73	73	50	10/09/95	Mon	2100	H		74	73	50	10/25/95	Wed	1800	H		73	73	52	11/17/95	Fri	2120	AT		73	73
84	03/25/94	04/22/96	11/07/96	199	71	71	56	01/18/96	Thu	1110	BN		73	73	42	12/19/96	Thu	1300	BN		68	68	38	01/03/96	Wed	1325	BN		73	73	42	02/02/96	Fri	1400	R	BR	73	73
85	05/08/94	06/20/96	10/03/96	105	72	72	57	03/15/96	Fri	2130			75	75	50	03/06/96	Wed	2145	DF		72	72	44	03/08/96	Fri	2150	DF		73	73	42	04/03/96	Wed	2125	CY		73	73
85	**Additional Data As Noted By Partial Respray**																																					
86	06/07/94	08/22/96	01/09/97	140	71	71	49	05/17/96	Fri	800	AX		72	71	48	04/30/96	Tue	1400	AX		72	72	49	05/07/96	Tue	1300	DE		71	72	41	05/30/96	Thu	1350	AX		72	71
87	07/21/94	11/04/96	03/27/97	143	76	76	55	07/23/96	Tue	1855	CY		74	74	64	07/08/96	Mon	2130	CY		76	76	54	07/12/96	Fri	1915	CY		75	75	51	08/23/96	Fri	1415	R	AX	75	75
88	08/25/94	01/09/97	04/24/97	105	71	71	52	10/23/96	Wed	1440	BD		71	71	60	09/18/96	Wed	1000	AR		72	72	52	10/16/96	Wed	1030	AR		71	71	52	10/23/96	Wed	1440	AR		70	70
89	10/04/94	06/24/97	07/10/97	16	73	73	54	04/11/97	Fri	1410	BR		74	74	54	03/28/97	Fri	1310	BR		74	74	56	04/02/97	Wed	1500	BR		75	75	49	05/01/97	Thu	1415	BR		73	73
89	**Additional Data As Noted By NCD**																																					
90	11/29/94	08/05/97	08/21/97	16	74	74	50	06/07/97	Sat	1230	CG		73	73	57	05/29/97	Thu	1055	CI		73	73	58	06/03/97	Tue	1830	CI		75	75	58	06/17/97	Tue	1330	CI		72	72
91	06/20/95	11/14/97	12/04/97	20	77	77	55	09/17/97	Wed	230	AB		76	76	56	09/03/97	Wed	255	BD	HD	75	75	52	09/08/97	Mon	420	BD	HD	73	73	42	10/07/97	Tue	230	AB		76	76
92	04/28/97	04/19/99	04/23/99	4	74	74	52	02/26/99	Fri	1120	BD	HD	72	72	46	02/18/99	Thu	1030	BD	HD	74	74	48	02/21/99	Sun	1050	BD	HD	72	72	51	03/05/99	Fri	950	BD		72	72
93	06/11/99	11/01/00	12/14/00	43	73	73	58	09/01/00	Fri	1045	BN	BR	73	73	58	08/21/00	Mon	1510	BN		72	72	60	08/25/00	Fri	1015	BN		74	74	58	09/14/00	Thu	1310	BR	BN	73	73
94	08/28/99	01/10/01	Still at MAF		74	74	56	10/26/00	Thu	1000	BD	HD	73	73	50	10/09/00	Mon	1305	BD	HD	74	74	54	10/17/00	Tue	1110	BD	HD	72	72	51	11/10/00	Fri	1730	BD	HD	73	73
95	**NOT BUILT**																																					
96	06/28/95	01/09/98	01/29/98	20	72	72	56	11/29/97	Sat	1120	BN	BR	72	72	50	11/19/97	Wed	1455	BR		74	74	56	11/22/977	/22/9	1500	BN		72	72	48	12/08/97	Mon	1410	BR		72	72
97	12/12/95	03/27/98	04/02/98	6	72	72	46	02/18/98	Wed	1330	AO		73	73	42	02/07/98	Sat	200	BE		73	73	48	02/09/98	Mon	1325	AO		72	72	52	02/28/98	Sat	1350	BR		73	73
98	02/16/96	05/27/98	06/12/98	16	73	73	56	04/18/98	Sat	1345	BD		73	73	61	04/02/98	Thu	2030	DF		74	74	44	04/05/98	Sun	2245	DF		74	74	50	04/25/98	Sat	1100	BD		73	73
99	05/02/96	07/28/98	08/07/98	10	74	74	59	06/10/98	Wed	245	BD		74	74	56	05/24/98	Sun	1705	AR		73	73	60	05/28/98	Thu	855	AR		75	75	58	06/19/98	Fri	245	BD		74	74
100	09/20/96	10/16/98	12/13/98	58	74	74	58	08/06/98	Thu	1200			75	75	58	07/17/98	Fri	1340	BN		75	75	60	07/22/98	Wed	1515	BN		74	84	56	08/11/98	Tue	1320	BD		75	75
101	01/06/97	11/30/98	01/15/99	46	71	71	60	10/07/98	Wed	235	CI		74	74	57	09/18/98	Fri	200	M		74	74	54	09/24/98	Thu	200	M		73	73	53	10/10/98	Sat	1430	BD		72	72
102	03/26/97	01/29/99	04/02/99	63	75	75	58	12/01/98	Tue	2200	AT		77	77	56	11/20/98	Fri	1710	J		74	74	52	11/23/98	Mon	2310	J		75	75	59	12/20/98	Sun	2210	BW		77	77
102	**Additional Data As Noted By Partial Respray 1**																																					
102	**Additional Data As Noted By Partial Respray 2**																																					
103	06/10/97	06/22/99	09/22/99	92	74	74	54	05/10/99	Mon	235	BU		74	74	56	04/27/99	Tue	2145	S		75	75	46	04/30/99	Fri	2305	J		74	74	54	05/10/99	Mon	245	BL		74	74
104	09/15/97	05/29/99	06/10/99	12	73	73	52	04/02/99	Fri	720	BD		73	73	53	03/28/99	Sun	20	M		74	74	54	03/31/99	Wed	852	R		73	73	52	04/20/99	Tue	740	AR		72	72
105	10/28/97	07/16/99	08/05/99	20	75	75	57	06/08/99	Tue	115	BU		70	70	60	05/26/99	Wed	1230	CG		71	71	61	05/31/99	Mon	40	T		75	75	58	06/16/99	Wed	1330	BD		70	70
106	02/15/98	12/14/99	02/24/00	72	72	72	56	10/08/99	Fri	1405	BN		73	73	56	09/28/99	Tue	1450	BR		71	71	54	10/01/99	Fri	1500	BN		72	72	58	10/14/99	Thu	1030	BR		73	73
107	03/08/98	10/10/99	03/16/00	158	75	75	56	09/07/99	Tue	2315	BW		76	76	56	08/21/99	Sat	2105	O		78	78	56	08/27/99	Fri	2200	O		74	74	57	09/09/99	Thu	2340	BW		78	78
108	05/29/98	02/07/00	07/13/00	157	73	73	50	12/14/99	Tue	2230	BW		71	71	56	11/30/99	Tue	45	T		71	71	56	12/07/99	Tue	500	T		75	75	54	12/17/99	Fri	2310	BW		71	71
109	07/22/98	05/02/00	10/20/00	171	74	74	54	03/02/00	Thu	2245	L		74	74	56	02/16/00	Wed	1040	DF		72	72	45	02/21/00	Mon	1330	DF		76	76	48	03/21/00	Tue	2200	AT	BW	76	76
110	08/25/98	07/14/00	11/02/00	111	74	74	56	05/05/00	Fri	2140	F	BD	72	72	55	04/25/00	Tue	1945	A	BD	73	73	56	05/01/00	Mon	2130	D	Q	77	77	55	05/23/00	Tue	2145	F	BD	73	73
111	12/06/98	09/22/00	03/22/01	181	74	74	58	07/20/00	Thu	530	M		73	73	52	06/27/00	Tue	500	M		76	76	58	07/11/00	Tue	720	H		74	74	60	08/01/00	Tue	2230	L		75	75
112	04/26/99	03/06/01	05/03/01	58	72	72	36	01/20/01	Sat	1100	B	BN	74	74	42	01/12/01	Fri	1450	BN		76	76	58	01/15/01	Mon	1050	BN		71	71	56	01/30/01	Tue	1040	BR	BN	74	74
113	10/05/99	04/27/01	05/17/01	20	70	70	56	03/12/01	Mon	2130	BW		74	74	54	02/20/01	Tue	2050	L		75	75	46	02/23/01	Fri	1410	L		75	75	46	03/18/01	Sun	1350	BD	HD	74	74
114	11/03/99	06/15/01	08/30/01	76	73	73	53	05/07/01	Mon	830	BR	BN	74	74	56	05/01/01	Tue	1250	BN		74	74	54	05/03/01	Thu	1320	AY		74	74	53	05/13/01	Sun	1030	BN		74	74
115	01/24/00	09/24/01	12/14/01	81	74	74	58	07/13/01	Fri	2200	AB		76	76	55	06/15/01	Fri	430	H	C	76	76	55	06/21/01	Thu	530	H	E	74	74	53	07/26/01	Thu	945	BR		76	76
116	02/27/00	11/26/01	01/13/02	48	71	71	60	10/10/01	Wed	1425	BR		72	72	56	09/18/01	Tue	1435	BR		72	72	61	09/21/01	Fri	1315	BR		71	71	60	10/10/01	Wed	1425	BR		72	72
117	03/22/00	01/31/02	04/18/02	77	74	74	46	11/16/01	Fri	1020	BN		74	74	48	11/05/01	Mon	2130	BD		74	74	49	11/09/01	Fri	30	BW		73	73	52	12/05/01	Wed	1030	BQ	BN	74	74
118	04/19/00	04/05/02	06/27/02	83	74	74	54	01/25/02	Fri	2200	M		72	72	54	01/17/02	Thu	1840	M		74	74	58	01/20/02	Sun	1700	M		73	73	50	03/19/02	Tue	635	BU		72	72
119	05/30/00	05/21/02	10/24/02	156	73	73	58	03/20/02	Wed	200	AB		71	71	44	03/06/02	Wed	440	H		72	72	58	03/12/02	Tue	515	H		71	71	52	03/22/02	Fri	230	AB		71	71
120	06/26/00	07/16/02			74	74	58	05/08/02	Wed	1130	AX		72	72	60	04/22/02	Mon	1430	BE		74	74	58	04/29/02	Mon	1235	BE		75	75	58	05/27/02	Mon	1030	BE		72	72
121	07/26/00	09/04/02			75	75	58	06/20/02	Thu	1445	BU		75	75	64	06/09/02	Sun	1700	BR		73	73	54	06/15/02	Sat	1500	BR		73	73	50	07/13/02	Sat	1110	BR	BN	75	75

ipod Spindle Face (Hand Spray)						+Y Bipod Beneath S.F. (Hand Spray)							Aft Half of LH/IT Flange Closeout (Hand Spray)									FwdHalf of LH/IT Flange Closeout (Hand Spray)									Intertank Acrea										
Cell Humidity (%rh)	Complete Date	Complete Day	Complete Time	Personnel	Personnel	Substrate Temp (°F)	Cell Temp (°F)	Cell Humidity (%rh)	Complete Date	Complete Day	Complete Time	Personnel	Personnel	Substrate Temp (°F)	Cell Temp (°F)	Cell Humidity (%rh)	Complete Date	Complete Day	Complete Time	Personnel	Personnel	Personnel	Personnel	Substrate Temp (°F)	Cell Temp (°F)	Cell Humidity (%rh)	Complete Date	Complete Day	Complete Time	Personnel	Personnel	Personnel	Substrate Temp at Upper Flange 1 (°F)	Substrate Temp at Upper Flange 2 (°F)	Substrate Temp at Upper Flange 3 (°F)	Substrate Temp at Upper Flange 4 (°F)	Substrate Temp at Lower Flange 1 (°F)	Substrate Temp at Lower Flange 2 (°F)	Substrate Temp at Lower Flange 3 (°F)	Substrate Temp at Lower Flange 4 (°F)	Cell Temp (°F)	Cell Humidity (%rh)
55	06/05/91	Wed	1440	BR		74	74	61	07/09/91	Tue	1115	BN					10/24/90	Wed	2135	CE							11/06/90	Tue	2040	CE			130								102	15
52	08/29/91	Thu	2300	AR		75	75	50	09/03/91	Tue	2310	AP					01/04/91	Fri	1300	BB							01/15/91	Tue	1200	AH			126							128	100	14
36	12/05/91	Thu	1330	BN		76	76	51	12/12/91	Thu	1030	BR					05/15/91	Wed	1530	AN							05/31/91	Fri	1250	BX			128								98	16
58	03/18/92	Wed	2100	BJ		78	78	46	03/27/92	Fri	2045	AT		82	76	54	08/01/91	Thu	1700	AN				74	74	46	08/16/91	Fri	2300	AW			132								102	14
57	06/11/92	Thu	1435	BR		75	75	54	06/30/92	Tue	1045	BA		74	74	46	12/12/91	Thu	1630	AQ				74	74	34	01/10/92	Fri	1230	BB			125								102	10
52	08/17/92	Mon	2300	AR		75	75	54	08/20/92	Thu	2035	AP		73	72	56	05/20/92	Wed	1315	BB				77	73	56	06/16/92	Tue	1053	BB			129								98	15
56	12/10/92	Thu	1330	BR		74	74	58	12/23/92	Wed	1438	BR		77	75	58	08/19/92	Wed	1445	BX				76	75	56	09/01/92	Tue	1130	BB			126								109	22
51	03/01/93	Mon	1445	AR		74	74	50	03/12/93	Fri	1500	AR		85	85	23	11/06/92	Fri	1930	BZ				72	72	50	11/17/92	Tue	1210	AH			130			145				131	104	10
56	06/03/93	Thu	1233	BR		73	73	54	06/17/93	Thu	1440	BR		71	71	40	02/12/93	Fri	1450	AH				75	75	46	02/26/93	Fri	1115	BX			127								104	12
57	09/20/93	Mon	1300	BD		75	75	57	09/22/93	Wed	1225	BD		75	77	51	05/25/93	Tue	1100	AN				78	74	54	06/04/93	Fri	1355	AN			130								102	20
60	12/03/93	Fri	2200	BJ		74	74	44	12/18/93	Sat	2045	AT		79	74	54	08/13/93	Fri	1215	BB				77	75	48	08/24/93	Tue	1340	BX			126								97	10
50	02/11/94	Fri	1030	BN		72	72	55	03/02/94	Wed	1330	BN		75	73	57	10/13/93	Wed	1025	BO				77	76	40	10/28/93	Thu	1130	BO			126								102	10
58	04/05/94	Tue	119	CY		74	74	64	04/15/94	Fri	110	BJ		73	77	36	01/11/94	Tue	730	BX				73	74	30	01/21/94	Fri	1350	BO			132								104	10
60	06/14/94	Tue	1320	BD		73	73	60	06/17/94	Fri	940	BD		72	72	38	03/03/94	Thu	1415	BX				72	76	42	03/15/94	Tue	1400	CF			126								98	20
62	08/15/94	Mon	2250	AR		77	77	56	08/24/94	Wed	1300	AR		75	68	56	04/20/94	Wed	1410	BO				73	73	46	04/29/94	Fri	1415	BB			126								97	21
54	10/06/94	Thu	210	BJ		72	72	64	10/08/94	Sat	2300	BJ		76	77	56	07/12/95	Wed	1100	BO				74	74	52	07/19/94	Tue	1345	BO			130								100	9
54	11/28/94	Mon	635	RBR		74	74	40	12/02/94	Fri	600	BR		74	74	46	09/09/94	Fri	1430	CK				74	74	54	09/15/94	Thu	1400	BO			132								100	18
36	02/01/95	Wed	820	AP		71	71	31	02/09/95	Thu	1300	AP		74	75	42	11/01/94	Tue	1550	AE				76	57	52	11/09/94	Wed	1415	BX			125								101	18
52	03/27/95	Mon	2250	H		74	74	52	04/14/95	Fri	1700	H		72	77	32	01/03/95	Tue	1435	BX				74	74	52	01/16/95	Mon	2115	CK			125								96	19
46	05/19/95	Fri	2240	BY		73	73	59	05/26/95	Fri	2315	BY		74	76	34	02/22/95	Wed	1105	BX				73	76	36	03/03/95	Fri	1640	BX			125					125			100	20
54	06/28/95	Wed	2320	CR		78	78	54	07/07/95	Fri	1800	CR		75	75	50	04/08/95	Sat	1145	BX				75	75	54	04/20/95	Thu	710	BX			127					125			97	21
54	09/11/95	Mon	1300	AP		71	71	60	09/14/95	Thu	1300	CZ		75	75	54	05/31/95	Wed	1055	BX				74	74	54	06/08/95	Thu	1345	BX			131					127			99	19
50	10/06/95	Fri	2230	H		73	73	49	10/17/95	Tue	2300	H		77	74	54	07/14/95	Fri	1430	BO				73	72	58	07/21/95	Fri	1345	BO			130					139			100	20
42	12/19/95	Tue	1300	R2BR		73	73	33	01/09/96	Tue	1335	BR		74	74	52	09/18/95	Mon	1500	BX				73	73	52	09/26/95	Tue	1440	BX			126					131			98	24
44	02/29/96	Thu	2030	CY		73	73	46	03/04/96	Mon	2245	CY		73	73	46	11/14/95	Tue	1345	BX				75	75	52	11/28/95	Tue	1340	BX			127					139			100	18
48	04/30/96	Tue	1400	AX		72	72	49	05/07/96	Tue	1300	DE		73	74F	46	01/31/96	Wed	1800	CF				76	78	48	02/08/96	Thu	1345	BX			125					134			99	19
69	07/09/96	Tue	1100	BD		72	72	48	07/11/96	Thu	1455	BD		74	75	35	04/10/96	Wed	1410	BX				74	75	46	04/18/96	Thu	1930	BX			128					135			100	20
57	09/25/96	Wed	1235	AR		71	71	56	10/10/96	Thu	830	AR		75	75	54	06/17/96	Mon	1505	BX				82	79	52	06/27/96	Thu	1430	BX			130					126			105	19
52	03/25/97	Tue	1330	BR		74	74	56	04/02/97	Wed	1500	BR		75	75	56	01/05/97	Sun	1500	BX				95	95	22	01/09/97	Thu	1440	BX			131					129			105	10
54	05/29/97	Thu	1730	CI		73	73	56	06/04/97	Wed	1500	CI		78	77	53	03/17/97	Mon	1430	DA				76	76	50	03/21/97	Fri	1410				136					128			96	19
56	09/03/97	Wed	250	BD		76	76	54	09/09/97	Tue	230	BD		76	78	56	07/26/97	Sat	1230	DA				76	76	54	07/30/97	Wed	1615	BX			126					137			102	16
46	02/18/99	Thu	1030	R		74	74	48	02/21/99	Sun	1100	R		78	79	42	01/16/99	Sat	1125	BX				78	78	52	01/20/99	Wed	1935	DA			125					125			100	21
58	08/21/00	Mon	1510	BR		72	72	60	08/25/00	Fri	1015	BR		74	74	54	06/15/00	Thu	1150	BX				76	76	54	06/25/00	Sun	1440	BX			130					129			105	19
48	10/09/00	Mon	1030	BD	HD	74	74	52	10/18/00	Wed	1030	BD	HD	77	77	51	07/31/00	Mon	1530	IC	IC			74	73	50	08/09/00	Wed	1500	IX	IC		127					131			98	21
46	11/18/97	Tue	1445	BR		71	71	57	12/01/97	Mon	1350	BR		74	74	42	10/22/97	Wed	1450	AH	BX			78	72	59	10/26/97	Sun	820	AH			138					127			92	20
42	02/06/98	Fri	1355	AO		73	73	39	02/08/98	Sun	1430	AO		74	77	35	01/11/98	Sun	1225	CD				76	76	46	01/15/98	Thu	1350	BX			135					130			103	8
60	03/31/98	Tue	2030	DF		73	73	53	04/07/98	Tue	2150	DF		74	73	58	03/05/98	Thu	2230	CK				74	74	36	03/09/98	Mon	810	BX			134					125			102	16
56	05/24/98	Sun	1700	AR		73	73	60	05/28/98	Thu	850	AR		78	78	52	04/16/98	Thu	1410	BO	BX			76	76	46	04/20/98	Mon	1630	BX			126					127			101	22
58	07/17/98	Fri	1340	BR		75	75	60	07/22/98	Wed	1515	BR		74	74	46	06/04/98	Thu	1800	DA				80	80	40	06/11/98	Thu	805	CD			125					129			102	20
60	10/01/98	Thu	1430	BD		72	72	56	10/04/98	Sun	1225	BD		75	75	56	08/02/98	Sun	2045	BX				75	75	54	08/07/98	Fri	2045	BX			125					128			102	18
56	11/20/98	Fri	1715	DF		72	72	52	11/22/98	Sun	2030	DF		76	80	46	10/26/98	Mon	1520	DA				80	80	50	10/31/98	Sat	1450	BX			126					126			103	17
56	04/27/99	Tue	2145	J		75	75	50	04/30/99	Fri	100	S		78	78	48	02/06/99	Sat	1900	BX				78	79	52	02/09/99	Tue	2200	BX			125					127			105	18
52	03/26/99	Fri	450	M		73	73	53	04/06/99	Tue	1450	R		74	76	30	02/23/99	Tue	540	BX				71	73	39	03/03/99	Wed	1350	BO			123					125			197	23
60	05/26/99	Wed	1230	CG		71	71	60	06/01/99	Tue	630	T		75	72	53	05/02/99	Sun	2315	CX				76	76	54	05/06/99	Thu	1400	AS			125							130	100	23
56	09/28/99	Tue	1450	BR		72	72	55	10/04/99	Mon	1300	BR		75	75	58	08/19/99	Thu	2348	CL	CX			76	76	56	08/23/99	Mon	600	DA	BX		128					125			105	15
56	08/19/99	Thu	1845	L		77	77	58	08/24/99	Tue	1900	L		78	78	52	07/30/99	Fri	1410	BX				77	77	54	08/02/99	Mon	1445	BX			126					127			103	12
56	11/30/99	Tue	45	T		71	71	56	12/07/99	Tue	500	T		77	79	47	10/31/99	Sun	1410	AS				76	76	48	11/05/99	Fri	635	BX			125					125			104	19
54	02/17/00	Thu	950	DF		75	75	50	02/23/00	Wed	850	DF		75	75	49	01/05/00	Wed	1415	GF	GF			74	75	48	01/09/00	Sun	830	DA	GF		126					125			105	15
57	04/24/00	Mon	1830	A	L	73	73	56	05/01/00	Mon	2130	D	Q	74	74	52	02/26/00	Sat	940	BX				73	75	50	03/03/00	Fri	1205	DA			125					125			101	18
57	06/28/00	Wed	600	H		76	76	58	07/11/00	Tue	715	H		76	76	44	04/26/00	Wed	1050	BX				74	74	56	05/05/00	Fri	545	BX			126					125			105	17
42	01/12/01	Fri	1445	BR	A	76	76	58	01/15/01	Mon	1400	BR		76	78	49	12/14/00	Thu	700	DA				80	80	40	12/17/00	Sun	1650	BX			126					127			103	20
54	02/20/01	Tue	1820	J		73	73	56	02/22/01	Thu	2300	J		73	73	32	01/22/01	Mon	1130	AS	AH	GZ	CK	78	79	44	01/28/01	Sun	630	DA	GF		128					126			102	5
56	05/01/01	Tue	1250	BR		74	74	54	05/04/01	Fri	810	BR		78	78	50	04/11/01	Wed	1400	CK	GF			78	78	52	04/17/01	Tue	550	DA	GF		127					125			105	17
55	06/15/01	Fri	430	H	C	76	76	55	06/21/01	Thu	525	H	E	75	75	48	05/15/01	Tue	1400	DA				74	76	46	05/19/01	Sat	845	DA			127	127	128	130	126	126	126	127	101	20
56	09/18/01	Tue	1435	BR		72	72	61	09/21/01	Fri	1315	BR		75	76	52	07/13/01	Fri	1400	DA	GF	IC	BX	75	76	53	07/24/01	Tue	1355	BX	DA	IC	127				133				98	22
48	11/05/01	Mon	2130	BD		74	74	49	11/09/01	Fri	30	BW		72	72	56	10/02/01	Tue	700	DA				76	76	55	10/06/01	Sat	1230	DA	AQ		131	129	127	134	125	128	127	127	98	22
54	01/17/02	Thu	1840	M		74	74	58	01/20/02	Sun	1700	M		76	76	48	12/22/01	Sat	1100	BX				78	78	38	12/27/01	Thu	1745	BX			131	128	126	126	125	125	126	126	94	24
44	03/06/02	Wed	440	H		72	72	58	03/12/02	Tue	510	H		76	78	45	09/22/02	Sun	1510	DA				75	75	40	01/26/02	Sat	2320	CX			132	132	128	128	125	126	125	126	104	13
60	04/22/02	Mon	1020	AX		75	75	58	04/30/02	Tue	1300	AX		74	74	54	03/09/02	Sat	1115	BX				70	74	48	03/16/02	Sat	235	AS			128	130	125	129	127	126	127	127	105	10
64	06/09/02	Sun	1700	BR		74	74	58		Sat		BR		74	71	55	04/18/02	Thu	1450	BX				73	75	48	04/26/02	Fri	1410	DA			127	129	128	129	125	125	125	125	103	18

ge (Machine Spray)									LO2 Tank Acreage (Machine Spray)										LH2 Barrel Acreage (Machine Spray)															
Complete Date	Complete Day	Complete Time	Personnel	Personnel	Personnel	Personnel	Personnel	Personnel	St380 Substrate Temp (°F)	St800 Substrate Temp (°F)	St840 Substrate Temp (°F)	Cell Temp (°F)	Cell Humidity (%rh)	Complete Date	Complete Day	Complete Time	Personnel	Personnel	Personnel	Personnel	Personnel	St2058 Substrate Temp (°F)	St1129 Substrate Temp (°F)	Cell Temp (°F)	Cell Humidity (%rh)	Complete Date	Complete Day	Complete Time	Personnel	Personnel	Personnel	Personnel	Personnel	Sprayer Codes Used for "Personnel" Column
03/16/90	Fri	1821	AE	HW	IU	HJ			149	127	126	100	12	07/09/90	Mon	2127	V					130	146	101	20	07/05/90	Thu	1603		HB	GH	HL		A
																						125	127	99	21	08/16/90	Thu	142		HG	HF	FA		B
06/04/90	Mon	1418	DG						144	127	129	104	8	09/26/90	Wed	1552	BM					126	154	100	15	09/26/90	Wed	1408	CO					C
08/17/90	Fri	1921	AS						154	132	130	99	10	03/08/91	Fri	1058	CJ	HX	IT	JA		126	142	99	19	12/14/90	Fri	1557	AJ	HB	FE	GH	JA	D
10/31/90	Wed	1056	CA						141	127	125	94	18	05/09/91	Thu	1549	AE					127	152	99	15	05/07/91	Tue	1430	CB					E
12/07/90	Fri	1739		HJ	GC	HX			155	127	128	97	11	07/25/91	Thu	1722		HX	IT	GI		100	106	100	22	08/06/91	Tue	1655		HB	GD	FE		F
									137			99	15	08/27/91	Tue	1729		HX	IT	GI														G
06/13/91	Thu	1426	Z	IJ	HC	JC	JA		155	127	128	101	17	10/03/91	Thu	1515	X	IJ	GC	HA	GS	127	129	103	7	01/17/92	Fri	1549	V	FE	GD	HW		H
09/06/91	Fri	1916		EW	GS	DX	EC		145	127	133	100	15	05/15/92	Fri	1655		DD	HY	EC	GT	125	132	103	11	04/29/92	Wed	2217	GS	HW	HB	FE	GL	I
12/18/91	Wed	1305	BK						147	127	127	103	16	08/18/92	Tue	1420	BS					128	148	103	20	08/06/92	Thu	2250	V					J
02/14/92	Fri	1416	AI	IJ	GC	EC	GS		159	128	130	97	18	11/18/92	Wed	1415	AZ	DD	GC	IX	EC	127	145	103	17	10/09/92	Fri	1516	DH	IL	HE	IX	FE	K
07/09/92	Thu	1143		HX	IT	JB	GS		137	130	126	130	10	03/24/93	Wed	1138		HW	GD	IX	JB	126	131	99	23	12/15/92	Tue	2134		HB	FE	GX	IX	L
12/02/92	Wed	1405	DK						128	131	128	98	24	05/07/93	Fri	2258	DM					125	135	103	14	04/23/93	Fri	1606	DJ					M
03/11/93	Thu	2313	AU	HW	JB	FF			157	127	135	98	18	07/30/93	Fri	1958	AZ	HW	GD			132	150	105	17	07/13/93	Tue	1345	BX	HX	FE	IE	GT	N
04/05/93	Mon	1915		HI	IT	JB	HO		157	127	128	102	15	10/05/93	Tue	1559		II	HL	HY	GS	125	153	103	19	09/23/93	Thu	1435		HX	DX	FE	GS	O
06/16/93	Wed	1149	DJ	GV	II	IT	EC		139	125	130	101	13	01/10/94	Mon	1522	GS	JB	II	HW	FQ	126	151	98	20	11/19/93	Fri	1520	DK	HX	FE	HY		P
10/21/93	Thu	1957	AA						135	125	131	98	10	02/11/94	Fri	1630	BP					125	142	101	14	01/14/94	Fri	1053	CB					R
02/02/94	Wed	1340	CM	JB	II	FF	HO		154	126	126	104	17	05/13/94	Fri	1508	BS	II	GD	HO	HW	125	134	102	11	03/12/94	Sat	1520						S
03/26/94	Sat	1322	V						153	126	125	102	20	06/24/94	Fri	1853	BS					125	140	103	22	05/28/94	Sat	1910	AW					T
										140		93	21	07/09/94	Sat	1601	CT																	V
05/05/94	Thu	1555	BS	JB	HW	FQ	HO		155	128	130	93	11	07/29/94	Fri	1435	CM	IM	FF	HO	GK	127	149	104	16	07/19/94	Tue	1307	CB	HX	HQ	FE	GT	X
									146	137	131	92	18	08/06/94	Sat	1721	CT	IM	FF	HO	GK	125	139	101	24	08/05/94	Fri	1603	DO					Y
06/17/94	Fri	1331		HL	HI	FQ	GS		139	126	129	100	14	09/28/94	Wed	1226		IM	FQ	GT		126	139	102	20	09/16/94	Fri	1515		HQ	FE	ET		Z
09/10/94	Sat	621	CC	FZ	HI	FQ	GT		147	125	126	97	12	12/02/94	Fri	1323	V	HW	GD	HO		128	135	105	19	11/03/94	Thu	1827	AG	FE	GB	DX	ET	AA
11/05/94	Sat	857		HW	GD	HO			145	125	126	104	14	02/14/95	Tue	1610	V	JC	FQ	HO		129	140	102	13	01/19/95	Thu	1348		EE	II	FS	HO	AB
12/15/94	Thu	2223	AM	GJ	IM	FQ	ET		149	126	134	104	15	03/31/95	Fri	1325	BS	HI	FW			123	140	102	19	03/30/95	Thu	830	DJ	GP	II	HV	GS	AD
01/31/95	Tue	1420	BV	JC	HW	FQ	HO		146	125	127	105	18	05/09/95	Tue	1537	AB	HI	GD	HO		132	141	105	19	05/19/95	Fri	726	AW	DZ	II	HY	HO	AE
04/22/95	Sat	0632	DM	GJ	HI	GD			153	127	133	100	18	07/21/95	Fri	1915	CT	DD	FW	FZ		126	127	101	22	07/07/95	Fri	1457	DB	DZ	II	HY		AF
06/10/95	Sat	730		JB	HI	FW	GV		145	126	130	100	23	09/12/95	Tue	0410	.		FZ	DD	GD	HO	125	131	88	25	09/23/95	Sat	1703		DZ	II	GE	HO	AG
											133	99	21	**Partial Respray**					FZ	DD	GD	HO												AH
06/23/95	Fri	932		HI	FW	ET			137	126	130	104	16	11/14/95	Tue	1148			HW	GD	HO		127	133	99	19	11/17/95	Fri	2250		DZ	HB	GE	HO	AI
08/22/95	Tue	1325	CH						141	126	127	105	11	01/13/96	Sat	1819	BV	FZ	HW	GD	HO	129	155	97	25	01/26/96	Fri	2058	Y	DZ	IF	FD	HO	AJ
12/05/95	Tue	1416		FZ	DD	FW	EI		152	126	128	105	10	03/22/96	Fri	2121		FZ	HW	GD	HO	126	134	100	22	04/28/96	Sun	0913		DZ	IF	FW	HO	AK
12/21/95	Thu	1510		FN	DD	FO	ET		147	130	127	102	20	05/21/96	Tue	2322	AD	FZ	DD	GD	IX	127	136	96	25	11/13/96	Wed	600		EE	II	HU	IX	AL
									134			95	22	06/10/96	Mon	1553	V	FZ	DD	GD	IX	125	127	94	14	11/13/96	Wed	600		DZ	GR	FS	HO	AM
03/14/96	Thu	1407	CH						149	128	127	101	10	09/29/96	Sun	1158	CH					127	134	95	10	12/21/96	Sat	1034	AF					AN
05/23/96	Thu	1338	BS	HI	FF	HO			150	125	127	105	8	02/07/97	Fri	1148	CN	FC	HI	GH	BS	129	141	95	24	06/03/97	Tue	2232	GB	EE	II	HZ	HP	AO
09/15/98	Tue	1227		HT	GH	GY			157	128	142	99	20	12/02/98	Wed	359		GJ	FZ	JD	HF	126	134	98	21	12/03/98	Thu	1226		DZ	II	HY	EY	AP
08/16/99	Mon	2001	CT	GJ	DD	GA	EY		150	125	127	92	26	03/04/00	Sat	729	DN	IF	IM	EZ	EI	127	141	99	17	04/26/00	Wed	1851	CW	DZ	DD	HY	EI	AQ
11/10/99	Wed	1215		GN	EU	EZ	EY		155	126	125	103	18	05/07/00	Sun	318		EX	IM	EZ	EI	130	154	96	17	06/07/00	Wed	2123		DZ	HI	HZ	EI	AR
																																		AS
10/02/96	Wed	2219	CA						142	130	132	102	19	08/18/97	Mon	1202	DI					130	146	100F	21	09/19/97	Fri	1724		FE	HX	FD	HT	AT
12/07/96	Sat	1305	CH						154	127	128	102	19	12/04/97	Thu	1511	DM					128	147	99	22	12/04/97	Thu	2125		DZ	IF	IK	GW	AU
01/22/97	Wed	1638		FZ	HI	FO	IX		140	126	126	104	18	02/04/98	Wed	638		FB	HX	GH	GW	126	131	99	20	01/29/98	Thu	1210		DZ	HX	FQ	EI	AW
08/19/97	Tue	655		IH	DD	DX	HK		158	131	132	103	9	03/13/98	Fri	1317		HR	IM	FW	EI	125	150	102	12	03/03/98	Tue	1932		DZ	HH	FW	GW	AX
10/07/97	Tue	1457		GJ	IM	GD	HP		126	130	149	100	20	04/26/98	Sun	657		GJ	DD	JD	EI	126	148	94	23	05/01/98	Fri	1315		DZ	FL	HY	EI	AY
10/31/97	Fri	1521	DM	HI	GD	FF			156	125	132	103	19	06/28/98	Sun	1313	BC	GJ	IF	GH	GW	127	153	99	23	06/22/98	Mon	1459	AF	EE	DD	HY	GW	AZ
12/22/97	Mon	1956		GJ	IM	FQ	EI		143	125	125	103	18	09/17/98	Thu	145	CA	HN	IF	JD	EI	127	142	98	23	09/13/98	Sun	1410		EU	II	HY	GW	BA
																						133	137	99	23	09/14/98	Mon	1137	DJ	DZ	II	HY	GW	BB
																						127	131	101	21	09/19/03	Fri	1353	DJ	DZ	II	HY	GW	BC
04/14/98	Tue	127		GJ	IM	FW	EI		141	125	128	104	17	10/14/98	Wed	1345		GJ	IM	GD	HQ	126	145	102	19	11/24/98	Tue	1830		DZ	II	HY	EY	BF
06/08/98	Mon	142	**ABORT Spray 1: Pressure**						160	128	131	105	17	01/20/99	Wed	124		GM	DD	GD	FF	126	140	100	22	01/19/99	Tue	1415		DZ	II	HY	FF	BJ
08/23/98	Sun	1523	BC	**I/T Moved:Cell H**			G		156	126	136	105	12	03/10/99	Wed	1529	AN					126	143	103	19	04/04/99	Sun	2146		EE	HB	GE	EI	BK
11/22/98	Sun	1544		IF	HF				159	125	131	100	72	07/21/99	Wed	1418		GJ	FZ	EZ	EY	126	140	196	22	05/13/99	Thu	0		DZ	HI	GE	EI	BL
12/23/98	Wed	504	AK	GJ	IF	JD			130	126	126	105	19	06/30/99	Wed	2036	P	GJ	FL	FI		143	127	103	19	07/01/99	Thu	2200	CP	DZ	II	HY	DT	BM
03/14/99	Sun	1247	AV	IF	FQ	EI	BT		144	125	127	100	17	09/12/99	Sun	630	CN	GJ	EU	EZ	EY	142	125	105	18	10/07/99	Thu	1708	CS	DZ	DD	HY	EY	BN
04/21/99	Wed	1441		HM	IF	EZ	EI		150	128	128	101	21	10/03/99	Sun	811		FY	HX	HM	EY	126	143	106	16	12/02/99	Thu	536		DZ	HH	GW		BO
06/07/99	Mon	1948		FZ	EZ	EY	EN		152	130	125	104	20	12/04/99	Sat	314	N	GJ	IF	GD	GW	126	143	104	19	01/22/00	Sat	1201		EV	HH	DX	EI	BP
07/07/99	Wed	2105	CT	FN	IF	EZ	FF		148	125	128	105	15	01/16/00	Sun	702	N	GJ	EU	GW		126	144	105	19	03/15/00	Wed	1518	DB	EE	DD	GU	EI	BQ
12/16/99	Thu	1213		FG	IF	GD	EI		154	128	125	105	19	08/11/00	Fri	520		HR	FL	HM	IY	128	143	90	23	11/24/00	Fri	2228		EE	II	HY	EI	BR
04/04/00	Tue	1606		GJ	IF	GD	EI		146	125	127	105	15	09/07/00	Thu	1624		GJ	IG	EZ	EI	129	143	100	18	12/13/00	Wed	2252		IB	DD	HY	EI	BS
05/15/00	Mon	1527		GJ	IM	EZ			151	125	129	105	16	10/30/00	Mon	1451		HR	DD	JD	EI	143	126	94	20	03/14/01	Wed	1126		IB	II	GD	FF	BT
06/29/00	Thu	319		GM	IM	GE	EI		156	130	135	101	15	12/22/00	Fri	1457		IF	FW	EI		129	156	89	22	04/20/01	Fri	1538		FR	DD	HY	EI	BU
01/24/00	Mon	1722		EN	FL	EZ	EI		154	127	135F	99	11	03/26/01	Mon	156	CQ	IV	HM	EI	AK	133	160	102	17	06/01/01	Fri	1441		DZ	II	DX	HF	BV
08/09/00	Wed	1606	AV	AW	EN	IF	EZ	CH	160	128	131	95	18	05/20/01	Sun	1354	GJ	DD	GL	EI		129	149	97	20	11/29/01	Thu	1136	CS	EE	II	DX	DJ	BW
10/18/00	Wed	1555			EC	FL	GD	EI	150	125	127	104	16	07/27/01	Fri	422	EN	IF	FW	EI		127	150	89	18	11/26/01	Mon	356		DZ	II	GA	EI	BX
12/09/00	Sat	1542	BT		EC	IM	GH		158	125	135	103	17	10/12/01	Fri	126	GJ	FZ	FD	EI		132	147	95	22	12/16/01	Sun	1228	CU	EE	DD	DX		BY
03/16/01	Fri	2229			HR	DD	GH		155	125	128	97	23	12/07/01	Fri	2229	GJ	IF	GH	EI		130	153	99	13	02/01/02	Fri	2244		DZ	DD	GA		BZ
04/23/01	Mon	1448	BT		EC	IF	ID		157	130	135	100	11	02/24/02	Sun	345	AV	GJ	EU	ID		128	153	98	19	03/13/02	Wed	438	AK	EV	DD	DV	EI	CA
																																		CB
																																		CD
																																		CE
																																		CF
																																		CH
																																		CI
																																		CJ
																																		CK
																																		CL
																																		CM
																																		CN
																																		CO
																																		CP
																																		CQ
																																		CR
																																		CS
																																		CT
																																		CU
																																		CW
																																		CX
																																		CY
																																		CZ
																																		DA
																																		DB
																																		DC
																																		DT
																																		DE
																																		DF
																																		DG
																																		DH
																																		DI
																																		DJ
																																		DK
																																		DL
																																		DN
																																		DO
																																		ET
																																		EU
																																		EV
																																		EW
																																		EX
																																		EY
																																		EZ
																																		FA
																																		FG
																																		FB
																																		FC
																																		FD
																																		FE
																																		FF
																																		EC
																																		FI
																																		FJ
																																		FL

ET & Foam Data Trend

ET & Foam Data Trend

	FM
	FR
	FN
	FO
	FS
	GD
	DX
	FV
	FW
	FY
	FZ
	GA
	GB
	GC
	GE
	DT
	GF
	EI
	GH
	GI
	GK
	GL
	GJ
	GM
	DZ
	GS
	GP
	GQ
	GR
	GU
	GV
	HO
	GW
	GX
	GY
	GZ
	HA
	DV
	HB
	HC
	HD
	HE
	HF
	HG
	HH
	HI
	HJ
	HK
	HP
	HL
	HQ
	HM
	HN
	HR
	HS
	HT
	HU
	HV
	HY
	HW
	HX
	HZ
	EN
	IB
	IC
	ID
	IE
	IF
	IG
	IH
	II
	IJ
	IK
	IL
	IM
	IT
	IU
	IV
	IW
	IX
	IY
	IX
	JA
	JB
	JC
	JD

Summary of Mass Properties for Flights That Lost ET Bi-Pod TPS

						Orbiter Liftoff Mass Properties				Integrated Vehicle Liftoff Mass Properties			
	Flight	Orbiter Vehicle	Dry Orbiter & SSMEs	Cargo & Crew	Orbiter Consumables	Orbiter Gross Liftoff Weight	Orbiter Xcg*	Orbiter Ycg*	Orbiter Zcg*	Integrated Veh Gross Liftoff Weight	Shuttle Xcg	Shuttle Ycg	Shuttle Zcg
	FLIGHTS WITH KNOWN FOAM LOSS												
7	STS-7	OV-099	169044	41134	39448	249626	1122.0	-0.8	381.1	4486449	1416.8	0.0	418.6
32	STS-32	OV-102	179735	31735	44593	256063	1131.3	-0.8	381.3	4519487	1413.2	0.2	418.9
50	STS-50	OV-102	180784	38315	38596	257695	1105.5	-0.5	378.7	4520103	1412.0	0.2	418.8
52	STS-52	OV-102	181201	32341	36828	250370	1109.5	-0.3	377.5	4514565	1411.4	0.1	418.2
62	STS-62	OV-102	181475	36350	38754	256579	1107.4	-0.6	379.2	4519801	1412.0	0.2	418.7
112	STS-112	OV-104	177322	44073	44417	265812	1109.8	-0.2	383.0	4521314	1412.8	0.3	419.7
107	STS-107	OV-102	182487	42493	40101	265081	1104.7	-0.5	378.5	4526034	1412.6	0.2	419.3
	OTHER FLIGHTS												
100	STS-100	OV-105	175924	45379	43965	265268	1108.2	-0.5	381.9	4522246	1412.7	0.2	419.5
101	STS-101	OV-104	176456	42344	43728	262528	1110.8	-0.2	380.6	4519455	1412.6	0.2	419.3
102	STS-102	OV-103	176415	43794	44588	264797	1114.3	-0.2	382.4	4521809	1413.1	0.2	419.5
103	STS-103	OV-103	176346	27159	44654	248159	1114.3	-0.1	381.3	4506419	1411.7	0.2	418.4
104	STS-104	OV-104	176559	41468	44925	262952	1110.9	0.1	381.8	4520159	1412.8	0.3	419.4
105	STS-105	OV-103	176545	43423	42509	262477	1113.0	-0.6	382.3	4518170	1412.8	0.2	419.4
106	STS-106	OV-104	176466	41981	43606	262053	1110.9	0.0	380.6	4519178	1412.6	0.2	419.3
108	STS-108	OV-105	176072	44241	44605	264918	1111.7	-0.3	382.8	4519872	1412.9	0.2	419.6
109	STS-109	OV-102	181579	34459	44627	260665	1113.8	-0.8	381.0	4515646	1412.6	0.2	419.2
110	STS-110	OV-104	177273	42766	44724	264763	1110.2	-0.8	381.8	4520964	1413.0	0.2	419.5
111	STS-111	OV-105	176970	42362	44715	264047	1112.2	-0.5	383.0	4518077	1412.9	0.2	419.5
113	STS-113	OV-105	177030	44430	44514	265974	1109.6	-0.2	383.2	4521249	1412.9	0.2	419.7
26	STS-26	OV-103	171978	51180	31459	254617	1118.1	0.3	380.6	4522407	1412.5	0.2	418.7
29	STS-29	OV-103	172149	52640	31446	256235	1116.3	0.6	380.8	4522277	1412.5	0.3	418.8
30	STS-30	OV-104	172098	52878	36380	261356	1123.4	0.5	382.6	4527426	1413.4	0.3	419.3
31	STS-31	OV-103	172036	34236	42892	249164	1114.8	-0.5	384.2	4514688	1411.8	0.2	418.6
34	STS-34	OV-104	172329	53721	31565	257615	1114.1	0.4	380.7	4523573	1412.5	0.2	418.9
35	STS-35	OV-102	178847	38800	38864	256511	1106.5	-0.5	378.1	4521514	1412.1	0.2	418.7
37	STS-37	OV-104	172272	46082	37404	255758	1116.7	-0.3	381.7	4519945	1412.4	0.2	418.8
39	STS-39	OV-103	172883	33052	41401	247336	1111.1	0.0	382.5	4513048	1411.2	0.3	418.3
40	STS-40	OV-102	180375	39117	32429	251921	1100.2	-0.1	376.4	4519792	1411.4	0.2	418.3
39	STS-41	OV-103	172562	55036	31903	259501	1115.2	-0.1	381.4	4527138	1412.9	0.2	419.0
41	STS-41B	OV-099	169166	37743	43496	250405	1124.4	0.2	381.4	4505048	1412.3	0.3	418.5
41	STS-41C	OV-099	169433	42040	42931	254404	1113.5	0.2	383.4	4509231	1412.4	0.2	418.9
41	STS-41D	OV-103	169944	51483	42194	263621	1118.5	-0.2	382.8	4519789	1411.2	0.4	419.5
41	STS-41G	OV-099	170667	27994	43882	242543	1119.1	-0.1	381.6	4497865	1417.1	0.2	418.0
42	STS-42	OV-103	172707	37890	32859	243456	1104.8	-0.1	378.3	4507474	1410.6	0.2	417.8
41	STS-43	OV-104	172179	54799	32369	259347	1113.9	-0.2	380.4	4523118	1412.6	0.2	419.0
40	STS-44	OV-104	172322	52859	34670	259851	1116.2	0.0	381.0	4522576	1412.7	0.3	419.1
39	STS-45	OV-104	172140	25963	35547	233650	1113.1	-0.3	377.6	4496035	1409.8	0.2	417.2
46	STS-46	OV-104	171994	40185	43852	256031	1113.7	-0.4	382.4	4516789	1411.9	0.2	418.9
47	STS-47	OV-105	172859	38812	32897	244568	1104.1	-0.4	379.2	4506804	1410.5	0.3	417.9
48	STS-48	OV-103	172770	26978	40306	240054	1125.5	-0.9	381.9	4502671	1411.2	0.2	417.8
49	STS-49	OV-105	172749	44886	38698	256333	1119.6	-0.3	383.9	4519154	1412.4	0.2	419.0
5	STS-5	OV-102	172566	35902	37957	246425	1116.7	0.2	379.6	4488857	1416.7	0.3	418.3
51	STS-51	OV-103	173664	52473	35341	261478	1116.5	-0.6	381.6	4523125	1412.8	0.2	419.2
51	STS-51A	OV-103	169711	49661	43980	263352	1120.9	0.0	382.6	4524849	1413.3	0.2	419.4
51	STS-51B	OV-099	170953	35422	40879	247254	1114.5	-0.2	381.4	4501978	1411.3	0.3	418.3
51	STS-51D	OV-103	169481	40610	40318	250409	1126.0	-0.2	381.7	4506364	1412.2	0.2	418.6
51	STS-51F	OV-099	170948	38742	43043	252733	1111.5	-0.5	381.8	4514313	1412.2	0.2	418.7
51	STS-51G	OV-103	169802	49042	37532	256376	1109.8	0.2	379.6	4514774	1412.5	0.3	418.8
51	STS-51I	OV-103	169919	48781	43354	262054	1120.6	0.2	382.4	4519949	1413.3	0.3	419.4
51	STS-51L	OV-099	172162	57545	38929	268636	1119.0	-0.3	384.0	4529681	1413.0	0.2	419.9
53	STS-53	OV-103	173438	33943	36516	243897	1112.4	0.1	380.7	4506587	1410.7	0.2	418.0
54	STS-54	OV-105	173073	54495	31844	259412	1116.2	0.3	381.3	4522840	1412.6	0.2	419.0
55	STS-55	OV-102	180891	39484	35093	255468	1101.5	-0.7	377.5	4519000	1411.5	0.3	418.6
56	STS-56	OV-103	173563	27278	36412	237253	1109.5	-0.3	379.3	4501920	1410.1	0.2	417.5
57	STS-57	OV-105	173363	35196	44144	252703	1112.7	-0.1	383.0	4518566	1412.0	0.2	418.7
58	STS-58	OV-102	181268	38442	36393	256103	1103.4	-0.4	378.1	4517138	1411.5	0.2	418.6
59	STS-59	OV-105	173853	40423	32573	246849	1098.8	-0.5	378.7	4511411	1410.7	0.2	418.1
6	STS-6	OV-099	168736	51032	37219	256987	1127.6	0.4	382.8	4490778	1416.6	0.3	419.1
60	STS-60	OV-103	173781	35012	37143	245936	1104.4	-0.8	380.1	4509010	1410.7	0.2	418.1
61	STS-61	OV-105	173685	32016	44577	250278	1113.5	-0.1	381.7	4511794	1411.4	0.2	418.5
61	STS-61A	OV-099	171084	36388	36279	243751	1108.4	-0.3	380.1	4505113	1410.0	0.2	418.0
61	STS-61B	OV-104	170127	53027	38290	261444	1110.3	0.0	379.3	4515538	1412.6	0.2	419.2
61	STS-61C	OV-102	176549	37894	40480	254923	1111.2	0.9	380.6	4511561	1411.0	0.3	418.8
60	STS-63	OV-103	173605	31156	42864	247625	1111.6	-0.3	382.4	4511630	1411.4	0.2	418.3
64	STS-64	OV-103	173579	32194	35661	241434	1105.6	-0.6	379.5	4503921	1410.4	0.2	417.8
65	STS-65	OV-102	181576	39732	37991	259299	1104.8	-0.4	378.8	4523441	1412.2	0.2	418.9
66	STS-66	OV-104	173051	30635	40552	244238	1112.0	-0.1	379.4	4508715	1411.1	0.2	417.9
65	STS-67	OV-105	174223	34923	47349	256495	1117.1	-0.1	381.5	4520187	1412.4	0.2	418.9
64	STS-68	OV-105	173891	40911	32601	247403	1099.3	-0.5	378.5	4510613	1410.7	0.2	418.1
69	STS-69	OV-105	173869	37782	44733	256384	1112.9	-0.1	383.3	4519114	1412.3	0.2	419.0
70	STS-70	OV-103	173728	52140	32716	258584	1120.6	0.0	380.9	4521772	1412.9	0.2	419.0
71	STS-71	OV-104	173189	33963	41936	249088	1110.0	-0.1	380.1	4511586	1411.3	0.2	418.3
72	STS-72	OV-105	174465	27771	44775	247011	1117.7	-0.1	381.7	4514647	1411.9	0.2	418.2
73	STS-73	OV-102	182071	39838	35418	257327	1101.6	-0.5	377.1	4521581	1411.8	0.2	418.7
74	STS-74	OV-104	173255	30086	44925	248266	1112.5	-0.5	381.6	4512395	1411.5	0.2	418.3
75	STS-75	OV-102	181514	38894	41083	261491	1106.2	-0.4	379.9	4526493	1412.7	0.2	419.1
76	STS-76	OV-104	173405	31342	41473	246220	1110.1	-0.1	379.9	4509631	1411.2	0.2	418.1
77	STS-77	OV-105	174484	40955	39314	254753	1106.5	-0.2	380.5	4519162	1411.8	0.1	418.7
78	STS-78	OV-102	182433	37873	36189	256495	1102.6	-0.4	377.3	4517477	1411.4	0.2	418.6
79	STS-79	OV-104	173550	34533	41357	249440	1109.6	0.0	379.8	4510469	1411.3	0.3	418.3
8	STS-8	OV-099	168832	34008	39953	242793	1124.7	0.2	382.0	4495896	1412.6	0.3	418.0
80	STS-80	OV-102	181558	37388	42871	261817	1106.1	-0.5	381.1	4524735	1412.4	0.2	419.2
81	STS-81	OV-104	174043	34669	41455	250167	1110.5	0.1	379.7	4511011	1411.6	0.2	418.4
82	STS-82	OV-103	175820	31998	44168	251986	1112.1	0.1	381.5	4513855	1411.8	0.2	418.6
83	STS-83	OV-102	181532	40462	37973	259967	1101.6	-0.2	378.0	4521509	1411.9	0.1	418.9
84	STS-84	OV-104	173265	34927	41432	249624	1109.0	0.0	379.7	4509832	1411.2	0.2	418.4
85	STS-85	OV-103	175865	37478	36758	250101	1104.4	-0.1	379.8	4512125	1411.0	0.3	418.4
86	STS-86	OV-104	173505	36730	41560	251795	1109.7	0.1	379.7	4512024	1411.5	0.3	418.5
87	STS-87	OV-102	182091	40630	38973	261694	1104.1	-0.3	378.5	4521900	1412.1	0.2	419.1
86	STS-88	OV-105	175329	44497	44200	264026	1111.2	-1.1	383.3	4518489	1412.8	0.2	419.6
89	STS-89	OV-105	175377	34880	40326	250583	1112.7	-0.2	380.3	4511879	1411.6	0.2	418.5
9	STS-9	OV-102	176231	36402	35180	247813	1109.7	-0.1	378.9	4506789	1411.8	0.2	418.2
90	STS-90	OV-102	181658	41983	38629	262270	1103.9	-0.3	378.0	4523683	1412.4	0.2	419.1
89	STS-91	OV-103	175951	42272	41750	259973	1109.0	-0.9	381.3	4514649	1412.1	0.1	419.2
92	STS-92	OV-103	176407	42236	44445	263088	1114.8	-0.3	382.3	4520549	1413.0	0.2	419.4
91	STS-93	OV-102	180714	57441	32232	270387	1120.6	0.0	380.8	4524972	1413.9	0.2	419.8
94	STS-94	OV-102	181842	40448	37989	260279	1102.1	-0.3	378.2	4519333	1411.6	0.2	419.0
93	STS-95	OV-103	176161	45134	44560	265855	1110.3	-0.5	382.2	4520191	1412.9	0.2	419.6
96	STS-96	OV-103	176287	40748	44777	261812	1112.3	-0.7	381.3	4514231	1412.2	0.2	419.3
97	STS-97	OV-105	175852	48974	41744	266570	1107.2	-0.5	383.4	4524795	1412.9	0.2	419.7

98	STS-98	OV-104	176461	45336	42330	264127	1110.3	-0.5	382.6	4519380	1412.7	0.2	419.5
99	STS-99	OV-105	175882	41818	39039	256739	1104.7	0.2	381.4	4520450	1412.1	0.3	418.9
27	STS-27	DOD											
28	STS-28	DOD											
33	STS-33	DOD											
36	STS-36	DOD											
38	STS-38	DOD											
51	STS-51C	DOD											
51	STS-51J	DOD											
			Note: * Conversion from Orbiter to Shuttle coordinate system:										
				Shuttle Xcg = Orbiter Xcg + 741 inches									

STS	Total Wind Speed, fps (per altitude, ft)						IP Wind Speed, fps (per altitude, ft)						OP Wind Speed, fps (per altitude, ft)					
	0	10k	20k	30k	40k	50k	0	10k	20k	30k	40k	50k	0	10k	20k	30k	40k	50k
1	6	32	11	40	56	82	3.000	31.761	-10.998	-39.976	-52.949	-71.719	5.196	3.900	0.192	-1.396	-18.232	-39.754
2	25	33	45	110	129	113	-4.341	10.198	-20.430	-67.723	-100.252	-106.185	-24.620	-31.385	-40.095	-86.681	-81.182	-38.648
3	5	31	66	76	106	93	4.830	-28.536	-66.000	-73.410	-102.388	-89.397	-1.294	-12.113	0.000	-19.670	-27.435	-25.634
4	10	15	28	10	11	27	5.000	-13.908	-26.915	-9.925	-6.923	-26.590	8.660	5.619	7.718	1.219	-8.549	-4.689
5	16	8	30	58	142	78	16.000	-0.697	-6.237	-15.987	-57.757	-21.500	0.000	-7.970	-29.344	-55.753	-129.723	-74.978
6	13	15	50	93	107	112	11.258	-14.672	-48.515	-91.587	-106.935	-111.386	-6.500	3.119	12.096	-16.149	3.734	11.707
7	1	12	17	39	63	32	0.500	4.689	-16.959	-38.620	-42.966	-31.878	-0.866	-11.046	-1.186	5.428	-46.075	-2.789
8	6	8	5	14	28	12	-5.890	-4.702	-1.710	1.706	22.362	8.336	-1.145	-6.472	4.698	-13.896	-16.851	8.632
9	19	45	55	77	71	77	-15.564	-44.829	-54.866	-69.786	-50.205	-63.836	10.898	-3.922	-3.837	-32.542	-50.205	-43.058
41b	0	19	55	104	111	72	0.000	-12.958	-53.989	-97.092	-105.567	-71.989	0.000	13.896	-10.494	-37.270	-34.301	-1.257
41c	15	59	62	142	170	106	-11.657	-56.112	-61.764	-136.499	-162.572	-105.419	-9.440	-18.232	-5.404	-39.140	-49.703	-11.080
41d	1	15	12	31	42	20	0.946	-14.918	-11.535	-29.799	-41.770	-5.513	0.326	-1.568	-3.308	-8.545	4.390	19.225
41g	3	9	13	21	75	27	1.888	2.025	-4.659	-12.343	-3.925	13.906	2.331	8.769	-12.137	-16.989	-74.897	-23.144
51a	10	44	45	118	90	76	3.256	-3.069	-40.784	-116.207	-80.891	-74.052	-9.455	-43.893	-19.018	-20.490	-39.453	-17.096
51c	15	79	111	154	162	151	-11.147	-78.808	-110.578	-152.501	-154.071	-150.425	10.037	-5.511	-9.674	21.433	50.061	13.161
51d	17	25	37	62	128	83	12.830	9.768	-36.949	-51.400	-100.865	-55.538	11.153	23.013	-1.936	-34.670	-78.805	-61.681
51b	13	41	38	44	62	61	9.508	5.706	-7.251	4.599	-17.090	16.814	-8.866	-40.601	-37.302	-43.759	-59.598	-58.637
51g	5	20	20	29	51	48	-4.728	-16.180	-6.511	-22.537	-11.473	-41.569	1.628	11.756	-18.910	-18.250	-49.693	-24.000
51f	10	16	13	17	42	38	9.877	3.327	7.456	12.229	8.014	28.240	1.564	-15.650	-10.649	-11.809	-41.228	-25.427
51i	15	35	26	17	24	24	15.000	30.903	22.286	10.231	19.660	19.660	0.000	16.432	13.391	13.577	13.766	13.766
51j	17	6	7	7	11	19	-8.756	-3.090	-1.693	6.619	-7.360	5.555	14.572	5.143	6.792	2.279	-8.175	-18.170
61a	17	43	70	55	63	56	7.185	-31.955	-29.583	-24.969	-42.966	-33.702	15.407	28.773	63.442	49.005	46.075	44.724
61b	3	5	20	11	45	61	2.121	-3.597	-14.387	-9.011	-44.938	-60.073	2.121	3.473	-13.893	-6.309	-2.355	-10.593
61c	10	9	58	172	221	129	-6.428	3.945	-55.161	-170.718	-219.353	-127.412	-7.660	-8.089	17.923	20.962	26.933	20.180
51L	17	72	97	110	153	136	-13.926	-65.254	-87.912	-102.694	-153.000	-134.326	-9.751	-30.429	-40.994	-39.420	0.000	-21.275
26	10	22	12	24	25	35	8.660	21.148	11.780	23.967	-13.980	-30.001	-5.000	6.064	2.290	-1.256	-20.726	-18.026
27	22	46	69	146	174	142	4.198	31.954	-24.727	-108.499	-150.688	-96.844	-21.596	-33.090	-64.417	-97.693	-87.000	-103.852
29	16	10	56	57	81	81	-14.127	-3.420	-43.520	-39.596	-68.692	-80.003	7.512	-9.397	-35.242	-41.002	-42.923	-12.671
30	11	2	45	61	138	123	8.175	-1.486	-44.562	-60.991	-134.463	-116.299	7.360	-1.338	6.263	1.065	31.043	40.045
28	10	21	25	16	9	16	-6.293	-16.989	-17.366	-10.285	-8.912	7.014	-7.771	12.343	-17.983	-12.257	-1.253	-14.381
34	13	19	29	50	41	48	-7.456	-18.070	-25.364	-49.970	-39.412	-44.184	10.649	5.871	14.059	1.745	-11.301	-18.755
33	16	24	64	78	108	103	-7.512	-18.113	-54.275	-64.665	-90.576	-99.940	14.127	15.745	33.915	43.617	58.821	24.918
32	4	57	97	118	140	137	-2.571	-47.804	-83.145	-105.139	-137.428	-120.964	-3.064	31.044	49.959	53.571	26.713	64.318
36	11	17	28	67	166	75	5.333	12.633	-20.478	-9.325	-70.155	-28.096	9.621	11.375	-19.096	-66.348	-150.447	-69.539
31	11	15	10	78	77	69	11.000	14.616	1.392	-62.294	-70.343	-57.204	0.000	-3.374	-9.903	-46.942	-31.319	-38.584
41	23	27	14	41	82	63	23.000	24.470	-9.548	-30.469	-72.402	-59.201	0.000	-11.411	-10.239	-27.434	-38.497	-21.547
38	28	4	14	52	130	75	27.847	-1.236	-13.641	-48.546	-127.159	-73.361	-2.927	3.804	-3.149	-18.635	-27.029	-15.593
35	21	10	20	93	139	80	20.987	-8.192	-19.805	-88.936	-137.647	-76.901	-0.733	5.736	-2.783	-27.191	-19.345	-22.051
37	18	8	42	84	127	113	17.303	-4.000	-41.994	-83.540	-124.225	-111.900	-4.961	6.928	0.733	-8.780	-26.405	15.727
39	12	11	45	61	97	85	-2.290	-9.621	-40.446	-60.916	-96.277	-84.948	11.780	5.333	-19.727	-3.192	-11.821	-2.966
40	6	31	26	3	10	32	-5.942	-22.300	-17.397	0.726	8.660	-13.016	0.835	-21.534	-19.322	-2.911	-5.000	-29.233
43	16	26	19	56	63	30	2.778	-16.007	5.555	52.949	60.247	28.532	15.757	20.488	18.170	-18.232	-18.419	-9.271
48	12	18	27	49	78	49	9.830	17.303	26.934	48.397	72.320	44.041	6.883	-4.961	1.883	7.665	29.219	21.480
44	8	51	61	109	122	79	-6.857	-49.485	-58.335	-98.788	-117.274	-69.095	-4.120	12.338	17.835	46.065	33.628	38.300
42	10	27	47	81	97	75	9.998	-26.590	-41.499	-73.997	-49.959	-35.210	-0.175	4.689	-22.065	-32.946	-83.145	-66.221
45	23	35	86	157	176	154	17.619	-9.647	-50.550	-80.861	-93.266	-92.680	-14.784	-33.644	-69.575	-134.575	-149.256	-122.990
49	13	69	147	143	131	87	-8.004	-57.868	-127.306	-118.552	-107.309	-58.214	-10.244	37.580	73.500	79.965	75.139	64.654
50	22	31	25	67	106	60	10.666	-18.221	-22.658	-64.717	-86.830	-59.553	19.242	25.080	10.565	17.341	60.799	-7.312
46	10	8	12	31	67	28	-7.660	-7.608	8.776	-27.371	19.589	21.132	-6.428	2.472	8.184	14.554	64.072	18.370
47	16	17	6	4	7	19	15.939	16.873	-3.355	-3.999	4.684	-3.299	1.394	-2.072	-4.974	0.070	5.202	-18.711
52	27	31	24	82	139	69	20.065	14.074	16.368	-65.488	-121.572	-55.106	-18.067	-27.621	-17.552	-49.349	-67.389	-41.525
53	10	80	91	109	107	77	-9.976	-23.390	-63.214	-35.487	-72.974	-34.957	0.698	-76.504	-65.460	-103.062	-78.255	-68.607
54	9	8	57	78	87	69	0.000	-7.995	-44.917	-68.220	-80.665	-60.349	9.000	-0.279	35.093	37.815	32.591	33.452
56	16	9	22	33	91	119	14.381	-2.177	0.000	10.198	12.665	-71.616	7.014	-8.733	-22.000	-31.385	-90.114	-95.038
55	16	20	36	65	73	87	-13.856	-19.563	-35.912	-63.580	-67.684	-78.849	8.000	-4.158	-2.511	-13.514	-27.346	-36.768
57	10	8	24	64	110	52	9.998	7.064	19.660	46.807	51.642	49.455	0.175	3.756	-13.766	-43.648	-97.124	-16.069
51	6	23	12	28	55	48	-5.481	-20.493	-9.456	-26.630	-44.496	-47.934	-2.440	10.442	-7.388	8.652	32.328	-2.512
58	10	2	7	23	22	28	-2.756	0.450	-1.812	-17.874	-18.858	-27.847	-9.613	1.949	6.761	-14.474	-11.331	2.927
61	11	19	38	47	90	69	10.337	-4.597	-33.552	-34.928	-61.380	-63.035	-3.762	-18.436	-17.840	-31.449	-65.822	-28.065
60	15	46	114	131	161	141	2.347	-25.053	-86.037	-61.501	-82.921	-70.500	-14.815	-38.579	-74.791	-115.666	-138.004	-122.110
62	16	47	82	127	139	120	-11.702	-32.054	-56.962	-84.980	-108.023	-93.258	-10.912	-34.374	-58.986	-94.379	-87.476	-75.518
59	32	21	37	84	133	116	15.514	20.796	-17.938	-52.863	-98.838	-73.001	27.988	2.923	-32.361	-65.280	-88.994	-90.149
65	15	29	31	34	44	28	14.772	24.858	25.080	30.294	40.196	27.847	2.605	14.936	18.221	15.436	17.896	-2.927
64	12	3	5	34	64	38	3.708	-2.158	-4.938	-31.524	-56.509	-31.503	11.413	2.084	0.782	-12.737	-30.046	-21.249
68	3	9	23	57	94	120	2.544	6.792	21.325	-20.427	-70.943	-86.321	1.590	5.905	8.616	-53.214	-61.670	-83.359
66	16	5	8	6	13	49	14.381	4.988	-7.795	5.481	12.053	5.122	7.014	-0.349	-1.800	2.440	4.870	-48.732
63	10	51	98	174	184	110	-9.613	-14.057	-33.518	-127.256	-136.739	-88.992	-2.756	-49.024	-92.090	-118.668	-123.120	-64.656
67	8	51	56	99	136	87	-6.928	-44.167	-52.623	-83.028	-130.732	-85.402	-4.000	25.500	19.153	53.919	37.487	16.600
71	13	38	11	30	81	65	9.192	-13.618	-3.581	-8.269	-12.671	-23.294	9.192	-35.476	-10.401	-28.838	-80.003	-60.683
70	5	2	16	26	25	14	3.886	-1.854	5.734	8.465	1.744	12.887	-3.147	0.749	14.937	24.583	24.939	-5.470
69	11	37	43	64	68	26	-5.500	-11.434	-11.129	-8.907	-35.023	-13.778	9.526	35.189	41.535	63.377	58.287	22.049
73	9	17	15	73	86	41	-0.314	-9.751	-14.419	-59.058	-63.910	-30.943	-8.995	-13.926	4.135	-42.908	-57.545	-26.898
74	19	54	72	82	110	76	2.316	-38.844	-37.083	-60.938	-91.194	-29.696	-18.858	-37.512	-61.716	-54.869	-61.511	-69.958
72	5	32	59	95	124	98	-4.330	-31.180	-57.711	-92.178	-120.317	-97.270	-2.500	-7.198	12.267	-22.983	-29.998	-11.943
75	9	23	51	97	143	56	7.872	-22.996	-31.399	-63.638	-29.731	-35.996	-4.363	-0.401	-40.189	-73.207	-139.875	-42.898
76	11	65	98	119	177	149	-0.767	-33.477	-56.210	-88.434	-154.808	-124.962	-10.973	-55.716	-80.277	-79.627	-85.811	-81.151
77	5	14	6	76	119	44	-4.891	7.000	-5.481	-74.604	-119.000	-43.038	1.040	12.124	2.440	-14.501	0.000	-9.148
78	6	24	25	19	29	16	1.854	-21.571	-14.695	-17.077	-27.251	-8.947	-5.706	-10.521	-20.225	-8.329	-9.919	-13.265
79	15	17	23	30	42	34	-5.376	-16.907	3.994	0.524	5.119	8.800	14.004	-1.777	-22.651	-29.995	-41.687	-32.841
80	13	43	67	96	129	128	-12.803	-39.282	-63.350	-59.104	-72.136	-121.026	-2.257	-17.490	-21.813	-75.649	-106.946	-41.673
81	13	57	95	136	175	149	3.583	-46.114	-81.431	-126.097	-155.926	-129.038	-12.496	-33.504	-48.929	-50.947	-79.448	-74.500
82	6	62	115	139	159	122	-3.857	-61.991	-114.143	-134.871	-154.925	-116.029	-4.596	1.082	-14.015	33.627	35.767	37.700
83	11	6	48	68	80	76	9.526	-4.528	-43.503	-32.967	-55.573	-68.879	5.500	-3.936	-20.286	-59.474	-57.547	-32.119
84	5	25	65	100	186	137	0.523	-19.429	-53.245	-79.864	-138.225	-100.195	-4.973	-15.733	-37.282	-60.182	-124.458	-93.434
94	15	20	21	14	25	23	5.130	-12.586	-19.605	-10.071	8.139	-1.604	-14.095	-15.543	-7.526	-9.725	-23.638	-22.944
85	8	20	19	17	1	22	2.867	-17.143	-14.555	12.433	-0.982	-21.879	-7.469	-10.301	-12.213	-11.594	0.191	2.300
86	3	34	46	43	30	38	-2.719	-33.979	-42.343	-37.967	-11.722	0.000	-1.268	1.187	-17.974	-20.187	-27.615	-38.000
87	21	66	88	97	166	160	3.647	-65.508	-86.663	-96.941	-153.913	-155.899	-20.681	8.043	-15.281	-3.385	62.185	35.992
89	16	20	49	49	105	118	-4.141	-19.406	-48.970	-40.138	-82.741	-97.826	15.455	-4.838	-1.710	-28.105	-64.644	-65.985
90	16	19	32	105	170	116	0.558	-13.667	-23.019	-55.642	-109.274	-77.619	15.990	-13.199	-22.229	-89.045	-130.228	-86.205
91	10	10	39	75	96	92	-4.226	5.878	-8.109	10.438	11.699	31.466	-9.063	-8.090	-38.148	-74.270	-95.284	-86.452
95	11	9	35	35	78	89	3.762	-8.835	-29.353	-32.675	-77.988	-86.356	-10.337	-1.717	-19.062	-12.543	1.361	-21.531
88	5	16	27	37	43	35	2.868	-10.069	12.676	34.542	28.211	14.792	4.096	12.434	23.840	-13.260	-32.453	-31.721
96	3	39	42	83	103	66	-2.121	-28.523	-31.698	-66.287	-80.046	-45.847	-2.121	-26.598	-27.554	-49.951	-64.820	-47.476
93	5	16	24	43	73	39	-4.924	14.937	22.553	33.884	65.612	31.947	-0.868	-5.734	-8.208	-26.473	-32.001	-22.369
103	5	27	48	114	140	117	-3.214	-26.504	-43.142	-111.509	-117.414	-105.159	-3.830	5.152	21.042	23.702	76.249	51.289
99	11	36	81	97	148	100	-5.665	-30.192	-50.975	-51.402	-43.271	-55.919	9.429	-19.607	-62.949	-82.261	-141.533	-82.904
101	5	49	27	55	88	94	2.868	42.856	26.984	2.878	-27.194	24.329	4.096	23.756	0.942	-54.925	-83.693	-90.797
106	8	12	12	18	51	31	6.553	11.984	11.644	13.377	49.262	30.924	-4.589	0.628	-2.903	-12.044	-13.200	-2.162
92	20	8	43	101	109	97	19.924	4.815	-12.572	-64.922	-79.718	-36.337	1.743	6.389	-41.121	-77.370	-74.338	-89.937
97	5	23	27	75	141	73	0.436	-3.994	2.822	-65.596	-131.635	-52.512	-4.981	-22.651	-26.852	-36.361	-50.530	-50.710
98	1	12	23	43	71	76	0.966	1.046	-13.192	-29.326	-42.729	-51.832	-0.259	-11.954	-18.840	-31.448	-56.703	-55.583
102	6	45	94	137	182	133	-0.523	-6.263	-41.207	-70.560	-112.050	-87.256	-5.977	-44.562	-84.487	-117.432	-143.418	-100.376
100	15	25	39	70	64	65	12.287	-12.120	-1.361	-8.531	1.117	-26.438	8.604	-21.865	-38.976	-69.478	-63.990	-59.380
104	8	31	17	9	31	19	-7.970	-29.944	-14.572	4.769	30.205	18.070	-0.697	-8.023	-8.756	-7.632	-6.973	-5.871
105	11	4	6	11	38	7	7.778	0.763	-0.314	-9.011	-37.907	6.578	7.778	-3.927	-5.992	-6.309	-2.651	-2.394
108	16	32	33	51	8	23	14.501	22.627	4.593	5.331	4.474	15.390	6.762	22.627	32.679	50.721	-6.632	-17.092
109	21	16	65	113	186	129	20.681	4.141	-64.753	-111.283	-169.919	-124.604	-3.647	15.455	5.665	19.622	75.653	33.388
110	23	32	20	29	58	105	-2.005	-10.418	-14.863	-20.145	-23.591	-70.259	22.912	30.257	13.383	-20.861	-52.986	-78.030
111	8	23	0	13	25	33	2.071	13.192	0.000	-10.777	-19.151	19.860	7.727	18.840	0.000	-7.270	-16.070	-26.355
112	13	18	23	50	46	21	9.192	8.450	15.390	19.537	5.606	-4.007	-9.192	-15.893	-17.092	-46.025	-45.657	-20.614
113	3	14	25	110	129	99	-0.776	-6.356	-18.868	-100.490	-122.686	-88.210	-2.898	-12.474	-16.401	-44.741	-39.863	-44.945
107	6	38	94	122	179	161	5.298	-36.705	-89.893	-112.302	-158.048	-148.201	2.817	-9.835	-27.483	-47.669	-84.035	-62.908

Volume V
Appendix G.12
Crew Survivability

While not the root cause of the mishap, understanding the cause of the loss of the crew will provide information that can be utilized in the design and planning of future space missions and vehicles to increase the probability of survival in the event of mishap.

THIS PAGE INTENTIONALLY LEFT BLANK

Crew Survivability Report

Submitted by Group II
James P. Bagian, MD, Medical Consultant and Chief Flight Surgeon
Donald J. White, Lt. Col., USAF, Life Sciences Investigator

PREFACE

Within two weeks of the STS-107 accident, NASA formed a Crew Survivability Working Group (CSWG) at the request of the Columbia Accident Investigation Board. The summary, which follows, was derived from investigation and analysis by the CAIB as well as the CSWG. The CSWG work dated 30 June 03 has been de-identified by crewmember and is attached as part of this appendix. The information presented in Volume 1 page 77 of the CAIB report, was drawn from this summary.

PURPOSE

While not the root cause of the mishap, understanding the cause of the loss of the crew will provide information that can be utilized in the design and planning of future space missions and vehicles to increase the probability of survival in the event of mishap.

VEHICLE INTEGRITY

In an effort to identify the integrity of *Columbia*'s pressurized cabin (the crew module – CM) prior to or during the catastrophic breakup of the vehicle, a detailed review of the environmental control and life support systems parameters that were down linked was performed. All cabin environmental parameters measured were nominal.

Although an additional 32 seconds of *Columbia*'s down linked data was recorded post LOS, there were no changes identified for the environmental control systems parameters over these 32 seconds. Additionally, the OEX accelerometer data during this period, and 17 seconds beyond, was not physiologically challenging and did not exceed any physiologic tolerance limits.

NO EVIDENCE OF AN EXPLOSION

Forensic evaluation of all recovered crew module / forward fuselage (CM/FF) components does not provide evidence for an over-pressurization and/or explosion event. This conclusion is supported by both the lack of forensic evidence and by lack of a credible source. Water tanks from below the mid-deck floor, along with both Forward Reaction Control System (FRCS) tanks were shown not to have undergone explosive failure.

An analysis was performed to establish the maximum delta pressure that could be generated assuming a sufficient heat rate was provided to cause all five tanks to burst simultaneously. The analysis concluded, given the tank sizes, initial temperature and pressure conditions, and water volumes, that the maximum delta pressure that could be created within the volume where the water tanks are located is only 50 psia. Based on this, the water tank rupture as a contributing factor towards seat failures, was dismissed.

Additionally, explosives experts from the FBI reviewed the crew cabin hardware at KSC and came to the conclusion that an explosive force was not a factor in the failure of this hardware.

STRUCTURAL FAILURE

Separation of the CM/FF assembly from the rest of the vehicle likely occurred at the interface between the Xo576 and Xo582 bulkheads. Subsequent break up of the assembly occurred as a consequence of ballistic heating and dynamic loading events. Materials evaluation of fractures on both primary and secondary structure elements suggests that structural failures occurred at stress and strain rates that, absent high temperature, would not have resulted in failure.[1]

MEDICAL AND LIFE SCIENCES

An extensive medical, crew health, STS-107 medical open items and in-flight anomaly review was completed. Space and Life Sciences Directorate Flight Readiness Review data were investigated. The Armed Forces Institute of Pathology

and Federal Bureau of Investigation conducted forensic analyses after recovery from the debris field. Death occurred after 14:00:19 (GMT) and was due to the physical environment associated with Crew Module catastrophic failure; death was due to blunt trauma and hypoxia with no evidence of lethal injury from thermal effects.

Data from Orbiter and Other Sources

Cabin Atmosphere

In an effort to identify the integrity of *Columbia*'s pressurized cabin prior to or during the catastrophic breakup of the vehicle, a detailed review of the environmental control and life support systems down linked parameters was performed. The cabin environmental data was nominal shirtsleeve environment. An additional 32 seconds plus two follow-on seconds of *Columbia*'s down linked and GPC data, respectively, were recorded post LOS (Table 1), there were no changes identified for the environmental control systems parameters.

• Cabin Pressure	14.64 psia
• Cabin Temperature	71.6 deg F
• Humidity	37.9%
• ppO2 Levels (3 Sensors)	3.14 psia (Sensor A), 3.14 psia (Sensor B), 3.16 psia (Sensor C)
• DP/dt	0.004 psi/min
• ppCO2	1.96 mmHg
• Cabin Temp Setting	0 or full cool/full HX flow
• N2 Supply Pressures	1011 psia (Sys 1), 1067 psia (Sys 2) – Nominal
• O2 Supply Pressures	822 psia (Sys 1), 809 psia (Sys 2) – Nominal

Table 1.

Flight Dynamics

Trajectory Reconstruction Process

The fundamental objectives of this effort were twofold: to identify, as accurately as possible, 1) the point in the trajectory of the *Columbia* when the crew module separated from the rest of the vehicle and 2) when the crew module itself began to disintegrate. Therefore, for the most part, all efforts were concentrated on the forward part of the vehicle and the crew module. The procedure used in this process is very straightforward. A piece of debris-of-interest is identified and its weight, size, and aerodynamic characteristics are determined. Using this information, its ballistic number is calculated. Knowing the location on the ground where a piece of debris was found, a trajectory program is executed in an iterative fashion to determine at what point in *Columbia*'s trajectory did that piece of debris have to have been released in order to land at that particular point on the ground. In other words, where do the trajectories of the piece of debris and the CM/FF intersect? It is at this point that the debris separated from the CM/FF.

Obviously, there are several assumptions made in the course

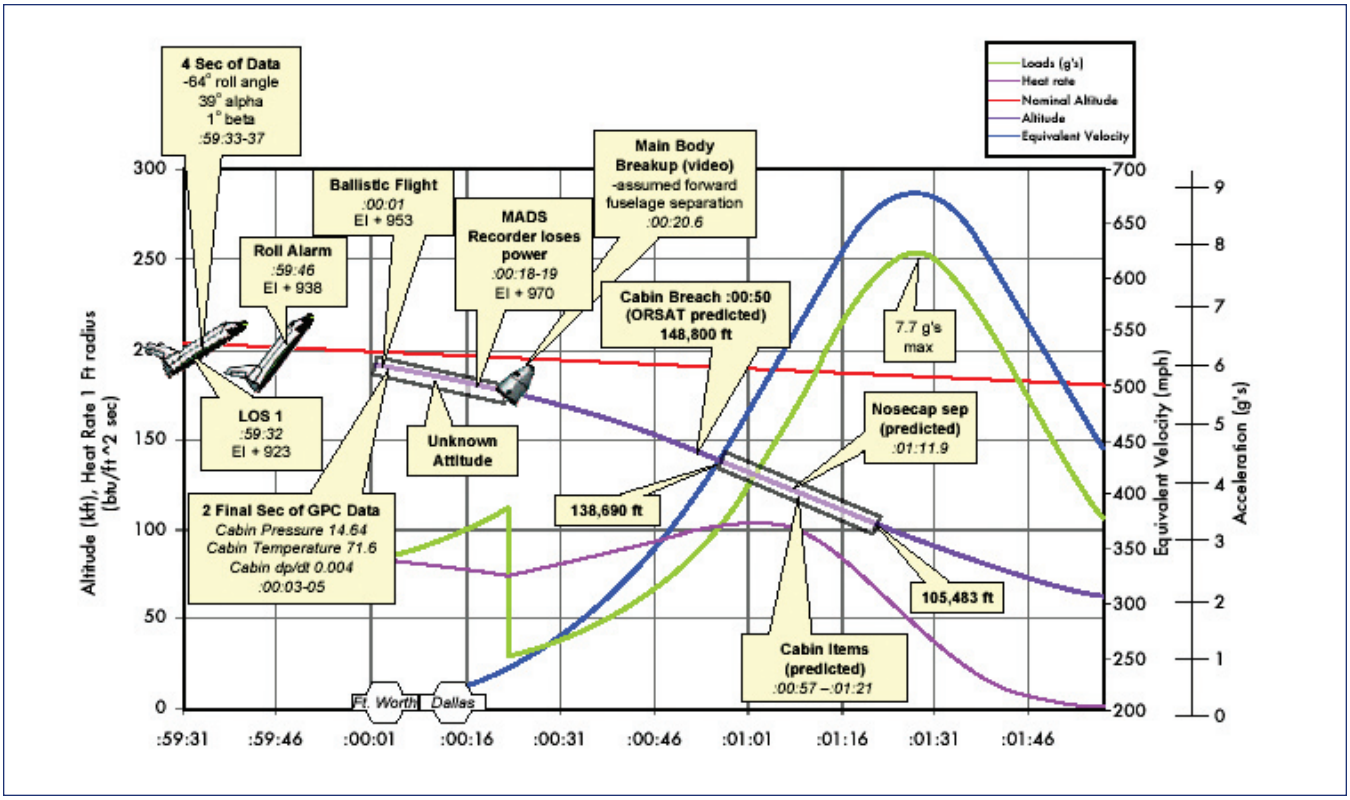

Figure 1.

of this process. The weight and area of the object as it was found may not be the same as when it became separated. Due to heating, structural loads, etc., the configuration of a given object may change. Similarly, defining the aerodynamic characteristics contains a certain amount of uncertainty since it is done computationally (although, at these altitudes, simple Newtonian assumptions are quite good). From that point of view, the most reliable objects would be spherical since the aerodynamic characteristics of a sphere are well known.

Data Sources

The first source of information was the official Rev 15 timeline and was continually refined as more data became available. All of the results derived from this process necessarily had to fit the official timeline or provide a strong rationale for revising it. Most of the information from the timeline are known quantities that were used a facts for this investigation.

Much information was gathered regarding debris and materials that originated from the crew module. This included crew equipment (helmets, radios, etc), objects definitely located in the crew module (toilet, racks, instrumentation, etc), and structural debris. These pieces were characterized as to weight, size, and aerodynamics and subjected to the iterative trajectory process mentioned above. The results were then plotted to determine their origin with respect to the orbiter's trajectory.

Flight Dynamics

Trajectory Reconstruction

An overall summary of the disintegration scenario can be seen in Figure 1. In addition to the timeline markers are some predicted events as well as load and heat rate calculations for the crew module on its trajectory. The band superimposed on the trajectory (starting about 14:00:58) indicates the window within which all of the debris analyzed originates. This would indicate that the destruction of the crew module took place over approximately 24 seconds. It is significant to note that the heat rate peaks near the beginning of this period while the load environment is increasing throughout the period. Thus, it is postulated that the cabin was exposed to significant heat load together with an increasing load environment. This resulted in the complete destruction of the vehicle and is also consistent with the structural analysis of the CM debris.

In spite of the diversity of items analyzed, and the uncertainty in the circumstances of their release, the analysis demonstrates that they cluster about an area along the trajectory that is about 24 seconds long which began at an altitude of approximately 140,000 feet and ended at 105,00 feet. A thermal entry model, ORSAT, was used to predict when entry heating would cause structural failure of CM. ORSAT predicted approximately 140,000 feet, which is consistent with the independent aerodynamic model. Another corroborating piece of evidence of ORSAT's ability to accurately predict heat-induced damage is its prediction of the thermal damage to helmet visors. ORSAT forecasted that the laminate helmet visor would experience melting of one laminate and not the other. Subsequently, when the helmets were located in the debris field, the damage observed was what ORSAT predicted. This leads to the conclusion that the crew module was breached early in that window and was in the process of continual disintegration throughout the 24 seconds.

Ground Based Analysis

In addition to the trajectory analyses, the debris footprint on the ground was analyzed to see if there were any patterns that could be used to infer the sequence of events. This analysis was limited strictly to the crewmembers and the equipment they were closely associated with at the time of the event. The most western piece of crew equipment found was a helmet from the mid-deck. The breakdown as to location of the remaining crew equipment showed that the mid-deck crew equipment was the farthest west and the flight deck crew equipment was at the eastern end of the debris field. Therefore, it seems reasonable to conclude that the crew equipment on the mid-deck separated from the CM before the flight deck crew equipment.

It is also interesting to note the order in which debris was found on the ground. With one exception, and taking into account missing items, the debris pattern is repeatable between crew positions.

Forensic Hardware Investigation

Crew Worn Equipment

Based on recovery of the wrist rings from the ACES suits that were worn by the crew during entry it could be determined that 3 crewmembers were not wearing their gloves at the time of the mishap. Based on the recovery of the helmets, it was determined that one of the crewmembers was not wearing their helmet at the time of the mishap.

Structure

Recovered Debris

Approximately 45% of the original crew module mass was recovered. Some major structural elements recovered, included portions of the forward and aft crew module bulkheads, window frames, mid-deck floor components, airlock and hatches. About 70% of the flight deck panels, and 80% of the mid-deck floor were recovered. Less than 20% of locker metal structure and fragments of the plastic and composite material of the locker trays were recovered. The Mid-deck Access Rack (MAR) was found nearly intact. Although some foam, fabric and paper were recovered, the bulk of the items recovered consisted of metal, plastic and composite materials. It is estimated that less than 30% of items stowed in the lockers were recovered. The EVA tool and suit debris (stowed mostly in the airlock for entry) were weighed, with 40% of the original mass recovered. The condition of the recovered debris items varied widely; from highly melted, twisted and torn, to near pristine (Figure 2). Overall, the damage distribution of crew module debris is consistent with surrounding debris from the forward fuselage structure.

Figure 2.

Figure 3.

Debris recovered from the crew module experienced noticeably less aerodynamic heating than other portions of the vehicle. Primary and secondary structure elements failures occurred at high temperatures evidenced by broomstraw[2] fractures. Five major attach points that suspend the crew module inside the forward fuselage were recovered, the port and starboard side fittings were recovered with evidence of high heating.[3]

Structural Failures

Separation of the CM/FF assembly from the rest of the vehicle likely occurred at the interface between the Xo576 and Xo582 bulkheads. Each fitting exhibited failures at both its crew module interface and Xo582 frame interface. The crew module interface failed at the longeron tab on both the port and starboard sides. On the Xo582 frame interface, the starboard side experienced a lug tensile failure while the port side fittings pulled through the Xo582 frame. Both the port and starboard side struts of the Y-linkage failed in tension at the clevis end fittings. The port side failed in proximity to the Xo582 ring frame, the starboard side in proximity to the Xo576 bulkhead. The Z-link failed at the attach point to the Xcm200 bulkhead. The joint failed by a combination of both fastener tensile failure and fastener insert pullout. This is similar to what happened in the *Challenger* mishap. Subsequent break up of the assembly occurred as a consequence of ballistic heating and dynamic loading events.[4]

Mid Deck Floor Structure

Approximately 80% of the mid-deck floor was recovered. Generally, mid deck floor panel and structure components experienced heating, but not of sufficient magnitude to cause melting of metallic components (with the exception of the LiOH door (Figure 3) and a few very localized areas on two recovered structure items). Heating was however sufficient to cause significant damage to the Aeroglaze topcoat (paint) and in some cases the Koropon primer.

Flight Deck Floor Structure

Unlike the mid deck floor, it is estimated that less than 10% of the flight deck floor was recovered. This is attributed to the substantial amount of heating experienced in this area.

Generally, only small portions of flight deck floor panels, structure, and seat components were recovered. In all cases, debris components are highly melted and/or deposited with splattered aluminum on all surfaces. None of the coating materials (topcoat or primer) survived.

The magnitude and distribution of heating experienced by flight deck components suggests a prolonged attachment to the larger crew module structure during re-entry (i.e. high ballistic number). Heating patterns on all debris components appears to be defined by the attachment to surrounding structure. This suggests these items were released from the crew module later in the break-up sequence as compared to items from the mid-deck locations. Ground plots of fallen debris also support this conclusion.

Crew Module Pressure Shell

Relatively speaking, some debris recovered from the crew module experienced noticeably less aerodynamic heating than other portions of the vehicle. No substantial portions of the CM shell were recovered. Those portions which were recovered such as pieces of the airlock, mid-deck LiOH door, and related structures showed failure and melting of thin sections where the contiguous ribbed sections were essentially undamaged indicating that the heating rate, duration of heating, and total energy input was not of such a magnitude to overcome the limited thermal capacity of the contiguous ribbed regions. Relatively speaking, more of the pressure shell was recovered from the lower crew module area than anywhere else

Heating was sufficient to burn away nearly all exposed thin sections of the exterior pressure shell (including bulkhead areas), and exposed thin section areas of internal components. Although some recovered debris has significant thermal damage, evaluation of heat patterns do not suggest any evidence that an internal cabin fire occurred before vehicle break-up.[5]

Seat Structure

A rather large collection of seat debris items was recovered. Since the majority of the lightweight seat design is common to all seven seat locations, positive seat assignment on most of the recovered seat debris was not possible. Major differences in the magnitude of thermal exposure were identified on flight deck vs. mid deck seat locations. As with the flight deck structure, flight deck seat components were highly melted and/or deposited with splattered aluminum on all surfaces. In contrast, mid-deck seat structural components did not experience any melting at all. The mid-deck seat 6 and 7 locations (Figure 3) did however collect significant deposits of melted aluminum from the LiOH door that these two seats were attached to. This melting appears to have occurred due to the LiOH floor panel having the seats and crew still attached at the time of separation from the CM.

Hardware Forensics Evaluation

Separation of the CM/FF assembly from the rest of the vehicle occurred as a consequence of heating and structural loading experienced outside of the vehicle design envelope. Although significant loading events initiated this separation, failure of the crew module structure was not instantaneous. Failure modes assessed on crew module structural components suggest that fractures occurred subsequent to and as a result of elevated temperature exposure (corresponding to a significant reduction of material properties). Thus, subsequent break-up of both the crew module and forward fuselage structure occurred as a consequence of the combined environments provided by ballistic heating and aerodynamic loading.

CONCLUSIONS

Acceleration levels seen by the crew module prior to its catastrophic failure were not lethal. LOS occurred at 8:59:32. The death of the crewmembers was due to blunt trauma and hypoxia. The exact time of death – sometime after 9:00:19 a.m. Eastern Standard Time – cannot be determined because of the lack of direct physical or recorded evidence.
Failure of crew module was precipitated by thermal degradation of structural properties that resulted in a catastrophic sequential structural failure that happened very rapidly as opposed to a catastrophic instantaneous 'explosive' failure. Crew module separation from the forward fuselage is not an anomalous condition in the case of a vehicle loss of control as has been the case in both 51-L (*Challenger*) and STS-107 (*Columbia*).

SUMMARY

It is irrefutable, as conclusively demonstrated by items that were recovered in pristine condition whose locations were within close proximity to some crewmembers, that it was possible to attenuate the potentially hostile environment that was present during CM break-up to the point where physically and thermally induced harmful effects were virtually eliminated. This physical evidence makes a compelling argument that crew survival under environmental circumstances seen in this mishap could be possible given the appropriate level of physiological and environmental protection.

1. Determine the cause of the loss of the crew – the loss of the crew occurred from blunt force and hypoxia. The exact time of death is indeterminate due to the lack of evidence of initiation and rate of cabin decompression.

2. Thermally induced degradation of structural properties of the CM resulted in its catastrophic structural failure. This failure subjected the crew to lethal environmental factors that included windblast, low atmospheric pressure and entry heating.

RECOMMENDATIONS:

NASA should investigate techniques that will prevent the structural failure of the CM due to thermal degradation of structural properties and determine their feasibility for application.

Future crewed vehicles should incorporate the knowledge gained from the 51-L and STS-107 mishaps in assessing the feasibility of designing vehicles that will provide for crew survival even in the face of a mishap that results in the loss of the vehicle.

Crew procedures and techniques for use of CWE should be standardized and complied with by all crewmembers.

Footnotes

[1] NSTS-60501, STS-107 *Columbia* Reconstruction Report, Debris Assessment, Conclusion, pg. 117, June 30, 2003

[2] NSTS-60501, STS-107 *Columbia* Reconstruction Report, Appendix A, pg. 147, June 30, 2003

[3] NSTS-60501, STS-107 *Columbia* Reconstruction Report, Debris Assessment Sub-Systems, Crew Module, pg. 103, June 30, 2003

[4] NSTS-60501, STS-107 *Columbia* Reconstruction Report, Debris Assessment Sub-Systems, Crew Module, pg. 103, June 30, 2003

[5] NSTS-60501, STS-107 *Columbia* Reconstruction Report, Debris Assessment Sub-Systems, Crew Module, pg. 103, June 30, 2003

Note: This appendix contains draft recommendations that were reviewed by the Board. The conclusions drawn in this report do not necessarily reflect the conclusions of the Board; when there is conflict, the statements in Volume I of the Columbia Accident Investigation Board Report take precedence.

The information contained in the following pages was compiled by the CAIB/NASA JSC Crew Survival Working Group.

Assumptions/Findings

Data from Orbiter and Other Sources

Cabin Atmosphere

In an effort to identify the integrity of *Columbia*'s pressurized cabin prior to or during the catastrophic breakup of the vehicle, a detailed review of the environmental control and life support systems downlinked parameters was performed. The following measurements (all nominal) were recorded at mission control at the time of loss of signal (LOS) from *Columbia*:

- Cabin Pressure — 14.64 psia
- Cabin Temperature — 71.6 deg F
- Humidity — 37.9%
- ppO2 Levels (3 Sensors) — 3.14 psia (Sensor A), 3.14 psia (Sensor B), 3.16 psia (Sensor C)
- DP/dt — 0.004 psi/min (this is the zero point due to the sensor bias)
- ppCO2 — 1.96 mmHg
- Cabin Temp Setting flow — 0 or full cool/full HX
- N2 Supply Pressures — 1011 psia (Sys 1), 1067 psia (Sys 2) – Nominal
- O2 Supply Pressures — 822 psia (Sys 1), 809 psia (Sys 2) – Nominal

An additional 32 seconds, plus two (2) follow-on seconds, of *Columbia*'s downlinked and GPC, respectively, data were recorded post LOS, there were no changes identified for the environmental control systems parameters.

As far as the Modular Auxiliary Data System Recorder, which was recovered from the *Columbia* debris, there are no environmental control systems parameters recorded on this system.

Water Tank Analysis

When members of the CSWG initially reviewed the crew cabin debris at the Kennedy Space Center (KSC), some of the debris suggested there may have been an explosive force from below the middeck up toward the top of the vehicle. In particular, middeck seats failed in the middle of the leg posts, as opposed to the connection points on the middeck floor, which are the weakest point structurally.

Based in particular on the seat failure, an assessment was done to identify the hardware located below the crew cabin capable of generating an increased pressure (or force) due to high delta temperatures or pressures. The only hardware identified was the four (4)potable water tanks and one (1) wastewater tank located immediately below the pressurized cabin.

An analysis was performed to establish the maximum delta pressure that could be generated assuming a sufficient heat rate was provided to cause all five (5) tanks to burst simultaneously. The analysis concluded, given the tank sizes, initial temperature and pressure conditions, and water volumes, that the maximum delta pressure that could be created within the volume where the water tanks are located is only 50 psia. Based on this, the water tank rupture as a contributing factor towards seat failures, were dismissed.

Additionally, explosives experts from the FBI reviewed the crew cabin hardware at KSC and came to the conclusion that an explosive force was not a factor in the failure of this hardware.

Cabin Depressurization

An analysis was performed to determine the time required for the cabin to depress to the altitude pressure at 200,000 feet (0.0028 psia) from a nominal 14.7 psia cabin pressure. Five (5) cases were analyzed, (a) bulkhead (BH) penetrations of 2.54 in2, (b) BH penetrations + 2" diameter hole (equivalent to eject the Waste Collector Subsystem (WCS) Commode Control Handle (CCH) ball), (c) 36" diameter hole (equivalent to the Airlock "A" hatch), (d) 36" diameter hole + BH penetrations + 2" WMC penetration, and (e) 72" diameter hole + BH penetrations + 2" diameter WMC penetration.

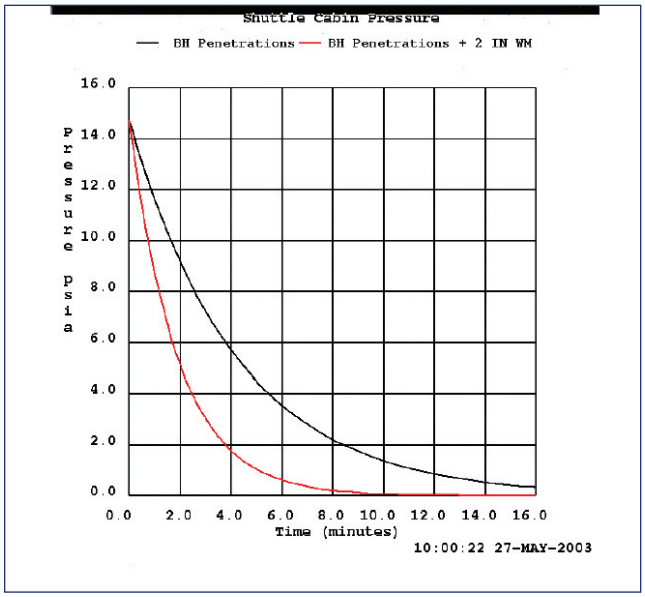

Figure XYZ Cabin Depressurization Cases (a) and (b).

Each case was selected to understand the range of possible depressurization rates, as a function of possible CM breakup scenario. Case (b) was selected as the WCS CCH ball was one of the furthest west CM item found. Case (c) was selected to simulated loss of the Airlock "A" hatch.

The analysis results are reflected in the graph below. Clearly, depress rate significantly varies, from minutes to seconds of useful cabin atmosphere. The CSWG is still analyzing data and hardware in an attempt to, at a minimum bound the depress rate. Depending on the scenario chosen, one can conclude whether or not the crew had or did not have time to execute various malfunction/contingency procedures.

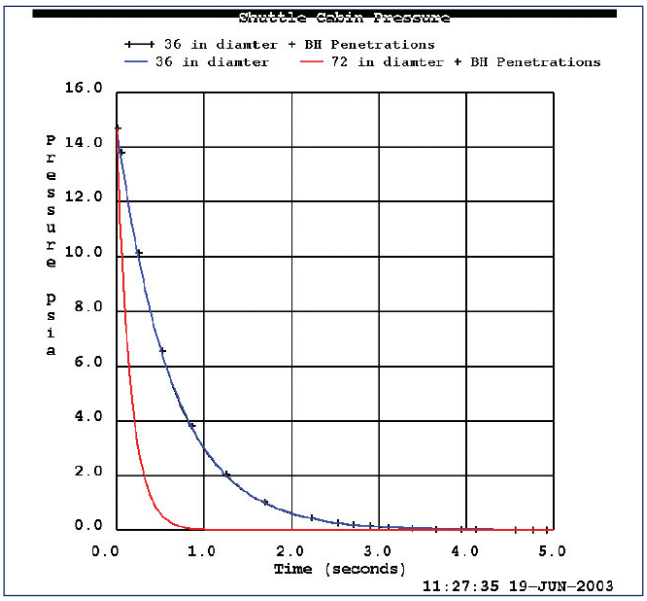

Figure XYZ Cabin Depressurization Cases (c), (d), and (e). Blue (or upper) curve contains both (c) and (d) cases.

Forensic Hardware Investigation

Shuttle Crew Escape Equipment (CEE)

Helmets and Suit-Disconnects

General Condition

Seven out of seven helmets along with six out of seven suit-side disconnects were recovered. Five of the seven helmets were recovered with the suit-side disconnect ring still attached. Thus, failure occurred predominantly between the suit-disconnect and suit fabric interface. Detailed inspection of all helmets and helmet to suit-disconnect interfaces suggests all but one crew member had their helmet on and properly installed at the time of crew module failure.

In general, the condition of each helmet shows effects from both mechanical and thermal loading. Effects from thermal loading were generally consistent across all helmets, except for the helmet that was not worn at the time of the mishap (much better condition). The effects from mechanical loading were generally consistent across all seven helmets. The magnitude and distribution of mechanical damage was not severe (except for that caused by ground impact).

Thermal Condition

Thermal effects were apparent throughout all helmet surfaces. Significant variations in general thermal condition were noted from helmet to helmet (both interior and exterior helmet surfaces). Reflective tape was missing from all outer helmet surfaces. Various amounts and depths of fiberglass delaminations were observed. Some white paint survived, outside of areas removed via fiberglass delamination. Residual paint on exterior helmet surfaces shows signs of damage consistent with impact from a large number of small debris items ("crater-like" pitting).

Both shallow and deep delaminations on helmet exterior surfaces appear associated with thermal effects. Significant variations in both location and magnitude of "hot spots" (i.e. stagnation points) were observed on exterior helmet surfaces:

Relatively small amounts of residual melted suit material were discovered, all of which was confined to the helmet / suit disconnect ring area. On all helmets except the one that was not worn, melted suit material was observed on both sides of the helmet / suit-side disconnect interface. Melted materials appear consistent with suit bladder materials (Nylon and Teflon), but not with Nomex. In all cases, the relative absence of Nomex material anywhere on internal or external helmet surfaces was noted. Close inspection of the suit / bladder clamp interface on the suit-side disconnect ring yielded only Nylon and Teflon materials (absent Nomex). As a result, it is suggested that the Nomex material failed mechanically before the chemical break-down temperature was reached (500°C). Thus, temperature may have degraded suit/helmet interface, yet the two were not melted apart. Deposition of melted suit material onto the helmet and suit-side disconnect areas appears to have occurred after mechanical separation of the helmet (small fragments of suit material were still clamped into suit-side disconnect upon mechanical separation).

On three of the seven helmets, the upper visor reinforcement bar survived with some Lexan / Plexiglass visor material still attached (large amount on helmet not worn). Upper and lower visor bars along with visor materials on each of the other four helmets did not survive. The visor is constructed of a two materials laminate: Polycarbonate and Polymethylmethacrylate. In all cases, the Polymethylmethacrylate flowed and the Polycarbonate did not. Subsequent laboratory analysis of visor materials suggests that helmet visor materials achieved temperatures between the range of 300 – 400 °C (572 - 752 F).

Mechanical Condition

In all cases, the helmet structure remained intact and the helmet profile was preserved in original form. Generically speaking, the helmets experienced a wide range of localized mechanical damage (fractures), but did not experience massive structural damage from external surface impacts (prior to ground impact). External helmet impacts were insignificant in size and random in distribution. Internal impacts were observed on all helmets.

Hold-down cables on each helmet (except the unworn helmet) were severed at the attach points to the cable guide

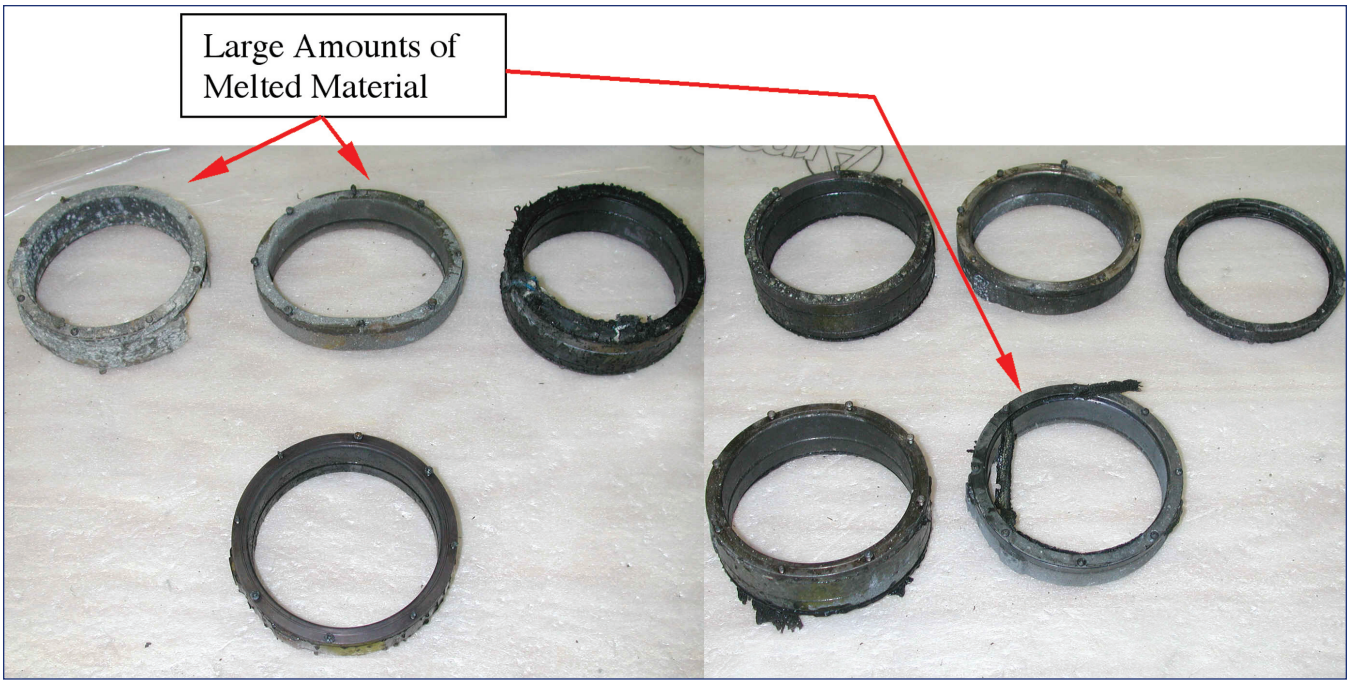

Recovered Glove Disconnects.

tubes (mechanical overload). All cable guide tubes (except the unworn helmet) experienced significant plastic deformation. Guide tubes display evidence of external contaminants (i.e. melted suit material) and thermal effects on top of fractures / localized deformation. This implies that mechanical loading was followed by exposure to thermal environment. Relative rotation of the helmet to suit-disconnect ring was observed all helmets (except the unworn helmet) anywhere from 90 to 180 degrees from forward nominal. Major cable guide tube deformation and helmet rotation supports evidence for a significant loading event, i.e. helmets were removed via mechanical (not thermal) mechanism.

Only one of the seven helmets (the unworn helmet) was recovered with the bailer bar still attached. All others were mechanically removed, yet the bailer bar cam mechanism remained in place (yet damaged) on both the starboard and port side helmet interfaces. The bailer bar latch mechanism on five out of seven helmets survived in good condition. This would not be expected if the crewmembers had achieved a "visor down" position (mechanical separation of bailer bar would also fracture latch assembly). The other two helmets experienced latch mechanism separation (fractured fasteners) before subsequent deposition of melted suit materials. This suggests sequence of events, i.e. latch separation followed by suit melting. Neither of these two helmets show evidence of indentation / deformation which could be associated with forces expected if the bailer-bar "ripped" the latch from the helmet-side disconnect ring. Thus, it is unlikely that any of the crewmembers achieved a helmet "visor down" position.

Glove Disconnects

A total of ten glove disconnect debris items were recovered corresponding to six out of seven crewmembers. Exposure to entry heating environments is apparent throughout. However, the level of heating varied substantially from item to item. Items from some crewmembers experienced significantly greater heating than comparable items on other crewmembers. Also, significant differences in heating were noted from the left to right sides on some crewmembers equipment. Detailed inspection of recovered debris items suggests that three of the seven crewmembers did not have gloves properly installed during re-entry.

Melted aluminum material was deposited onto exposed glove disconnect rings in 5 of 7 cases. The source of this material appears to be external to the glove disconnect rings (i.e. surrounding structure).

Melted suit material was discovered on all recovered glove disconnect items. Close inspection of the suit / bladder clamp interface on the suit-side disconnect ring yielded mainly nylon and Teflon materials (absent Nomex). In all cases, minimal amounts of Nomex remained clamped at the interface. Overall, the amount of residual melted suit material appears to correlate with the general magnitude of heating (i.e. higher magnitude heating resulted in the pyrolysis of residual suit material). As with the helmets, deposition of melted suit material onto the glove disconnects areas appears to have occurred after mechanical separation (small fragments of suit material were still clamped into suit-side disconnect upon mechanical separation). Thus, failure modes at the suit-side disconnect ring (between the suit-side ring and suit material interface) were similar to those observed at the suit-side helmet disconnect location (see Helmet section above).

Emergency Oxygen System (EOS)

Two EOS bottle/reducer subassemblies are flown per crewmember and are located within the harness assembly. Ten total individual EOS bottle/reducers have been found to-date, each with no oxygen remaining. All 10 individual EOS bottle/reducers present similar appearances. Material of construction consists of an outer stainless steel, cryogenically formed, bottle and a metallic regulator assembly.

No Nylon material, from the harness that contains the EOS, was visibly found adherent to the bottle/regulator assembly. Minor evidence of elevated temperatures is visibly identifiable, however, directional burn marks and discrete externally induced impacts are visible. As with most *Columbia* hardware, ground-induced corrosion is also evident. X-ray revealed all regulators have been activated, however, this could have occurred with separation of the bottles from the harness. Final determination if any crewmember in-fact activated an EOS is still under analysis.

Overall appearance suggests each EOS bottle/reducer assembly experienced similar thermal and mechanical environments. Each EOS assembly was mechanically extracted from the harness as temperatures were rising, then for a short duration and nearly simultaneously, experienced ballistic heating and some metal pellet-like impacts

SEAWARS

Two SEAWARS are flown per crewmember (left/right) and are part of the Personal Parachute Assembly (PPA) risers, which interface to the harness. Six total SEAWARS have been found to-date, none auto-ignited, and those inspected with both male/female buckle sections still attached. All six SEAWARS present similar appearances, consisting of the SEAWARS assembly still attached to approximately 12" of Nylon harness strap remnant. Material of construction consists of an outer aluminum casing, plastic external components, various internal electronic components, and an interfacing Nylon harness strap.

Only two of six SEAWARS have been inspected to-date (remaining to-be inspected by end of JUL 2003). Each SEAWARS has evidence of directional melting, burning, and mechanical loading. Each SEAWARS was found with only the lower Nylon strap, a surviving length consistent with failure at the waist. While the terminating ends show evidence of melting, they do not suggest significant melting. Localized heating on the metallic SEAWARS Frost fitting (i.e., buckle) suggests intense heat exposure, perhaps ballistically induced, for a short duration. Final determination if any crewmember was wearing these during genesis of these melt features is still under analysis.

Overall appearance suggests each inspected SEAWARS experienced similar thermal and mechanical environments. Each SEAWARS was mechanically extracted from the harness webbing as temperatures were rising, then for a short duration and nearly simultaneously, experienced ballistic heating, followed by nearly no hot metal shower event

TSUB-A SARSAT

One TSUB-A SARSAT beacon is flown per crewmember and is located within the Personal Parachute Assembly (PPA). Six total TSUB-A SARSATs have been found to-date, none successfully auto-activated. All six TSUB-A SARSATs present similar appearances. Material of construction consists of an outer aluminum casing, plastic external switches, and various internal electronic components.

No PPA Nylon material was visibly found adherent to the outer aluminum casing. Various amounts of paint survived and displayed evidence of impact with multiple small hot metallic pellets, plus ground-induced corrosion. All external plastic has been melted, with some directional features possibly attributed to final component ballistic heating. Internal inspection revealed minor solder re-flow, with majority of components mechanically and electrically intact. Two units were externally powered and properly functioned.

Overall appearance suggests each TSUB-A SARSAT experienced similar thermal and mechanical environments. Each TSUB-A was mechanically extracted from the PPA as temperatures were rising, then for a short duration and nearly simultaneously, experienced high ballistic heating and a hot metal pellet-like shower.

AN/PRC-112

One AN/PRC-112 radio/beacon is flown per crewmember and is located within right side, ACES outer pocket. Four total AN/PRC-112s have been found to-date. All four AN/PRC-112s present similar appearances. Material of construction consists of an outer aluminum casing, plastic external switches, plastic external battery pack, and various internal electronic components.

No ACES Nomex material was visibly found adhered to the outer aluminum casing. Various amounts of paint survived and displayed evidence of impact with multiple small hot metallic pellets, plus ground-induced corrosion. All external plastic has been melted or missing, with some directional features possibly attributed to final component ballistic heating. Internal inspection revealed evidence of moderate burning, with center-most components only experiencing minor solder re-flow. Each AN/PRC-112's "control module" (which contains unique crew ID) was successfully extracted and externally powered to determine crew ID.

Overall appearance suggests each AN/PRC-112 experienced similar thermal and mechanical environments. Each AN/PRC-112 was mechanically extracted from the ACES external pocket as temperatures were rising, then for a short duration and nearly simultaneously, experienced high ballistic heating and a hot metal pellet-like shower.

Structure

Recovered Debris

Overall, approximately 40-50% of the original crew module mass was recovered. Some major structural elements were recovered, including major portions of:

- forward and aft crew module bulkheads
- window frames
- mid-deck floor components
- airlock and hatches

About 70% of the flight-deck panels and about 80% of the mid-deck floor were recovered. Less than 20% of locker metal structure was found, only plastic and composite material fragments of the locker trays. The Mid-deck Access Rack (MAR) was found nearly intact.

Although some foam, fabric and paper were recovered, the bulk of the items recovered consisted of metal, plastic and composite materials. It is estimated that less than 30 percent of items stowed in the lockers were recovered. The EVA tool and suit debris (stowed mostly in the airlock for entry) was weighed, and 40% of the original mass was recovered.

Generally, the condition of the recovered debris items varied widely; from highly melted, twisted and torn, to near pristine. Overall, the damage distribution of crew module debris is consistent with surrounding debris from the forward fuselage structure.

Heating

Relatively speaking, some debris recovered from the crew module experienced noticeably less aerodynamic heating than other portions of the vehicle. Heating was however sufficient enough to burn away nearly all exposed thin sections of the exterior pressure shell (including bulkhead areas), and exposed thin section areas of internal components. Although recovered debris components do show significant effects from heating, evaluation of heat patterns do not suggest any evidence that an internal cabin fire occurred before vehicle break-up.

No Evidence Supporting An Explosion Event

Forensic evaluation of all recovered crew module / forward fuselage components does not provide evidence for an overpressurization and/or explosion event. This conclusion is supported by both the lack of forensic evidence and by lack of a credible source. (Water tanks from below the mid-deck floor, along with both Forward Reaction Control System (FRCS) tanks were recovered in good condition.)

Structural Failures

Separation of the crew module / forward fuselage assembly from the rest of the vehicle likely occurred at the interface between the Xo576 and Xo582 bulkheads. Subsequent break up of the assembly occurred as a consequence of ballistic heating and dynamic loading events. Materials evaluation of fractures on both primary and secondary structure elements suggests that structural failures occurred at high temperatures that reduced the material properties of the elements. Therefore, structural failure occurred at reduced levels of stress and strain rates than otherwise would have resulted in structural failure.

Crew Module Attach Fittings

Four major attach points that suspend the crew module inside the forward fuselage were recovered:

- Both the port & starboard XYZ-fittings (V070-332032) attaching the crew module longeron tab to the Xo582 frame
- The double strut Y-link attaching the lower center Xo576 bulkhead to the Xo582 frame
- The single Z-link attaching the Xo378 bulkhead to the Xcm200 bulkhead

Both the port and starboard side XYZ fittings were recovered intact with evidence of high heating. Both titanium fittings experienced significant thermal exposure / melting, predominantly on the upper surfaces. In comparison, the starboard side fitting experienced significantly greater heating than the port side.

Each fitting exhibited failures at both its crew module interface and Xo582 frame interface. The crew module interface failed at the longeron tab on both the port and starboard sides. Fasteners along the joint remained intact. On the Xo582 frame interface, the port side experienced a lug tensile failure while the starboard side fittings pulled through the Xo582 frame.

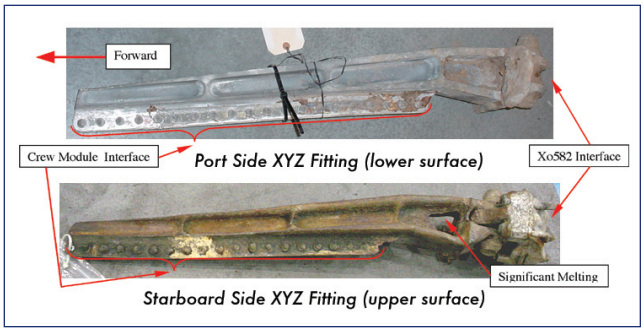

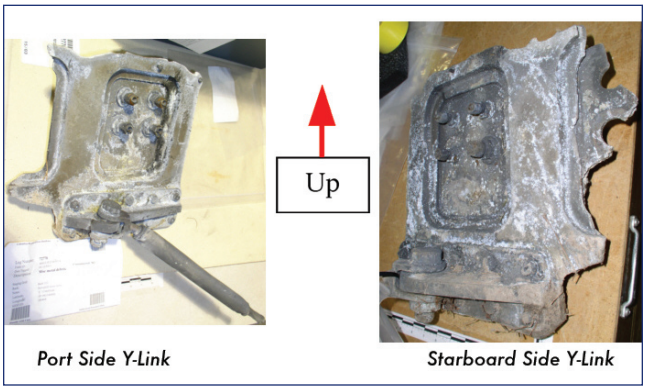

Both the port and starboard side Xo576 interfaces of the double strut Y-link assembly were recovered (the Xo582 side interface was not recovered). Both the port and starboard side struts of the Y-linkage failed in tension at the clevis end fittings. The port side failed in proximity to the Xo582 ring frame, the starboard side in proximity to the Xo576 bulkhead.

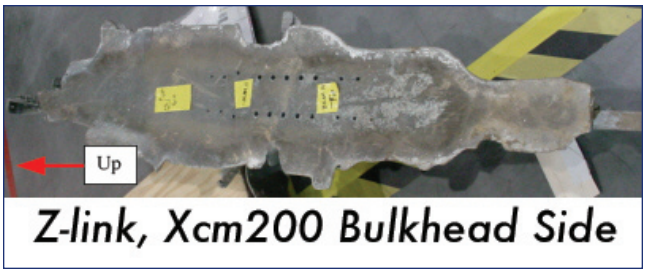

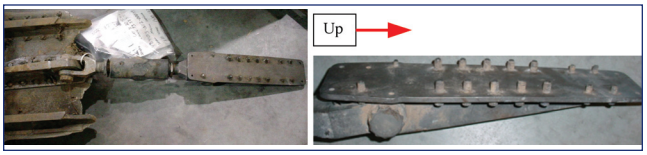

The Z-link failed at the attach point to the Xcm200 bulkhead. The joint failed by a combination of both fastener tensile failure and fastener insert pullout

Detailed inspection of each linkage failure suggests the failure mode was affected by a reduction in material properties associated with elevated temperatures.

Mid Deck Floor Structure

A substantial portion of the mid-deck floor was recovered (approximately 80%). In comparison with other crew module structure, more of the mid-deck floor was recovered than anything else. Generally, mid deck floor panel and structure components experienced heating, but not of sufficient magnitude to cause melting of metallic components (exceptions include the LiOH door and a few very localized areas on two recovered structure items). Heating was however sufficient to cause significant damage to the Aeroglaze topcoat (paint) and in some cases the Koropon primer.

The magnitude and distribution of heating experienced by mid deck components suggests that these items were either:

1. Released from the crew module early in the break-up sequence
2. Shielded by surrounding structure until final separation

Assessment of debris field ground plots supports the former, not the latter scenario.

Heating patterns on all debris components appears to be independent of attachment to surrounding structure. This implies that the recovered debris items not only were released early, but that they separated quickly from the surrounding structure. Deceleration occurred quickly due to low mass/area ratios (ballistic numbers).

The only recovered mid deck floor item which experienced significant re-entry heating was the LiOH door floor panel, with the corresponding seat 6 and 7 attachments. The panel itself was highly melted, with thin sections completely missing. Detailed inspection of heat patterns suggest that directional heating occurred along a flow vector directed "bottom-up." The mid deck seat 6 and 7 locations collected

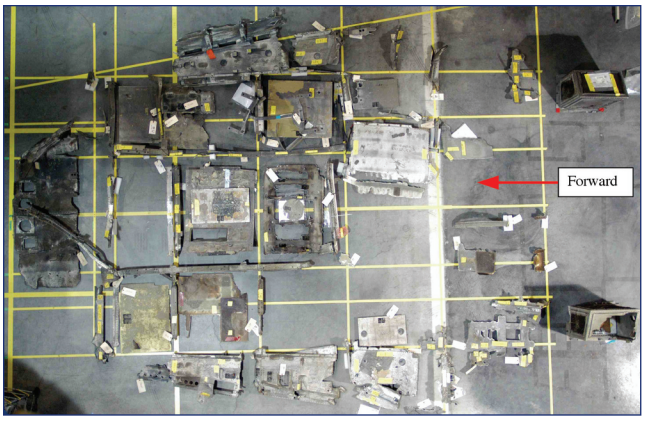

Mid Deck Floor Debris (looking down).

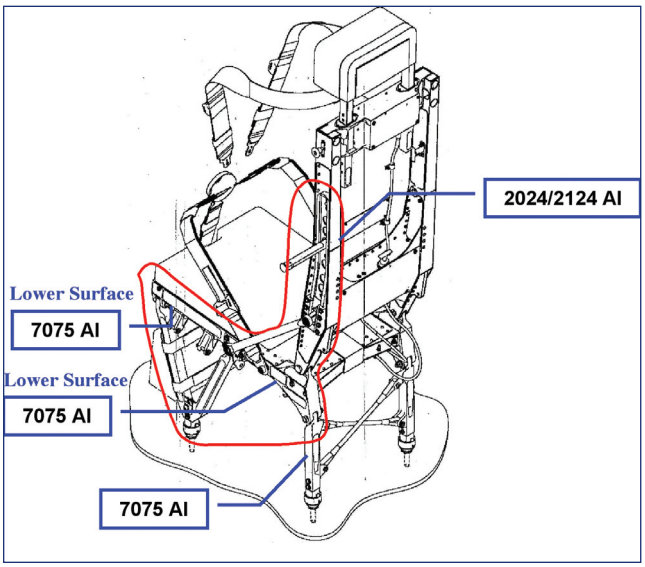

Mid Deck: Materials Sampling Analysis on Recovered Seat Debris Items.

LiOH Door Floor Panel With Seat 6 & 7 Attach Points.

deposits of melted aluminum consistent with the mid-deck floor panel they were attached to (verified by materials analysis and consistent with the flow direction). Materials

consistent with the surrounding pressure shell and/or structure were not found.

Thus, seats 6 and 7 remained attached to the LiOH door floor panel during thermal exposure, and experienced this environment completely separate from the surrounding structure. The magnitude of ballistic heating experienced on this debris item can be rationalized by the fact that this is by far the heaviest piece of recovered mid deck floor structure and thus possessed a high ballistic number when released from the crew module. The heating effects seen suggest that a ballistic number was higher than would be attributable to just the mass of the LiOH door and seats 6 & 7 alone.

Flight Deck Floor Structure

Unlike the mid deck floor, it is estimated that less than 10% of the flight deck floor was recovered. This is attributed to the substantial amount of heating experienced in this area.

Generally, only small portions of flight deck floor panels, structure, and seat components were recovered. In all cases, debris components are highly melted and/or deposited with splattered aluminum on all surfaces. None of the coating materials (topcoat or primer) survived.

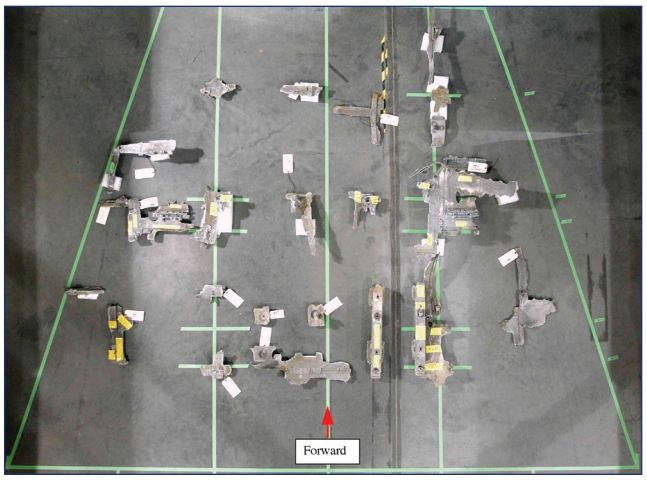

Flight Deck Floor Debris (looking down).

The flight deck seat locations collected substantial deposits of melted aluminum from locations throughout the cabin area (verified by materials analysis). Materials consistent with the bulkheads and outer pressure shell (2219 aluminum), the surrounding primary and secondary structure (2219, 2024, 2124, and 7075 aluminum), and the seat itself (2024 and 7075 aluminum) were discovered on both upper and lower surfaces of recovered seat debris. See below for a description of findings:

Thus, the flight deck seats remained attached to both flight deck floor panels and surrounding structure during thermal exposure.

The magnitude and distribution of heating experienced by flight deck components suggests a prolonged attachment to

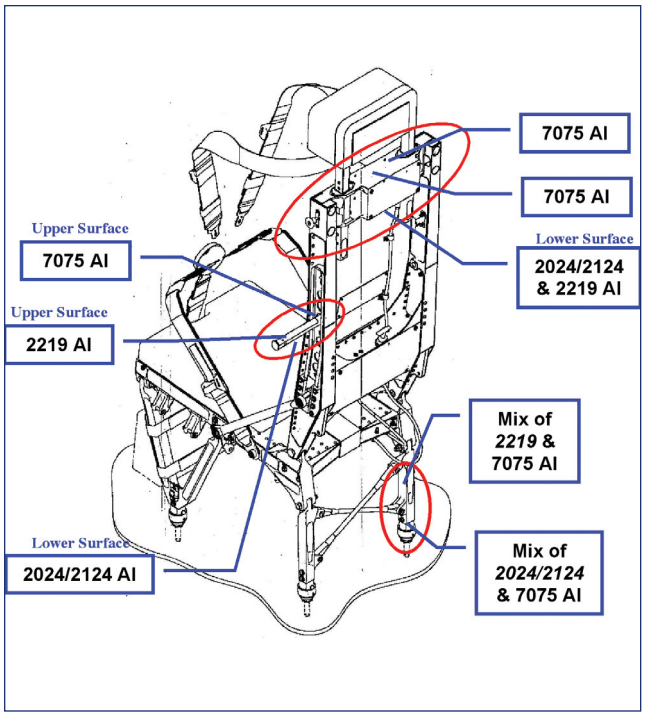

Flight Deck: Materials Sampling Analysis on Recovered Seat Debris Items.

the larger crew module structure during re-entry (i.e. high ballistic number). Heating patterns on all debris components appears to be defined by the attachment to surrounding structure. This suggests these items were released from the crew module later in the break-up sequence than comparable items from mid deck locations. Ground plots of fallen debris also support this conclusion.

Forward Bulkhead Structure

The failure mode of the forward bulkhead structure has not been determined. Debris items recovered from the forward bulkhead show heating patterns initiating from multiple directions. All of the recovered stiffeners appear to have sheared along their attach points, consistent with a bulkhead bending failure. Some failure modes appear to have been affected by elevated temperatures.

Further Analysis of the forward bulkhead structural failure is still in work.

Aft Bulkhead Structure

The failure mode of the aft bulkhead structure has not been determined. Debris items recovered from the aft bulkhead show heating patterns initiating from multiple directions. All of the recovered stiffeners appear to have sheared along their attach points, consistent with a bulkhead bending failure. Some failure modes appear to have been affected by elevated temperatures.

Further Analysis of the forward bulkhead structural failure is still in work.

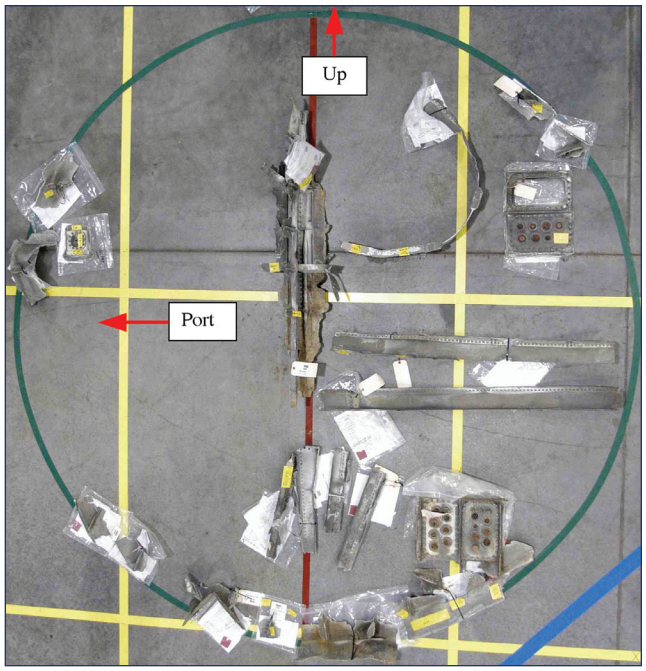

Forward Bulkhead Debris (looking forward).

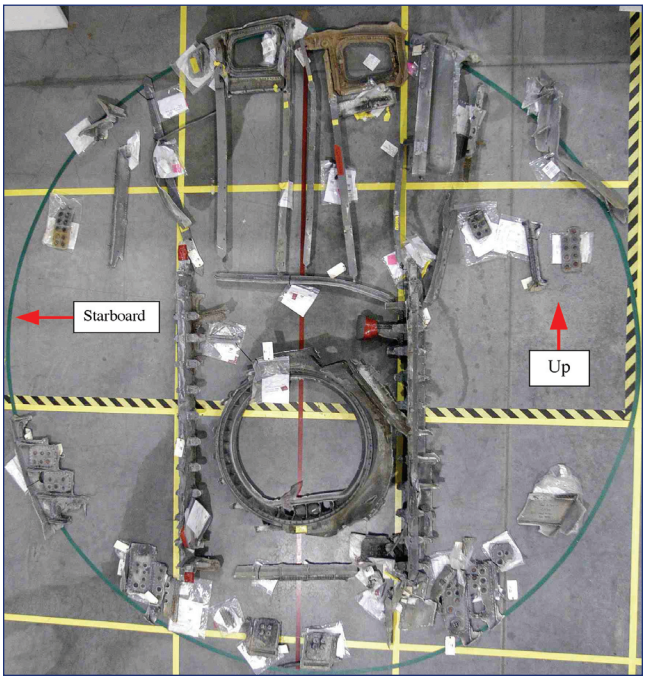

Aft Bulkhead Debris (looking aft).

Pressure Shell

Barely ANY of the exterior pressure shell was recovered. Apparently, re-entry heating was sufficient to burn / melt away nearly all exposed thin sections (including bulkhead areas). In general, the only pieces of the pressure shell remaining were found attached to corresponding structure. Relatively speaking, more of the pressure shell was recovered from the lower crew module area than anywhere else .

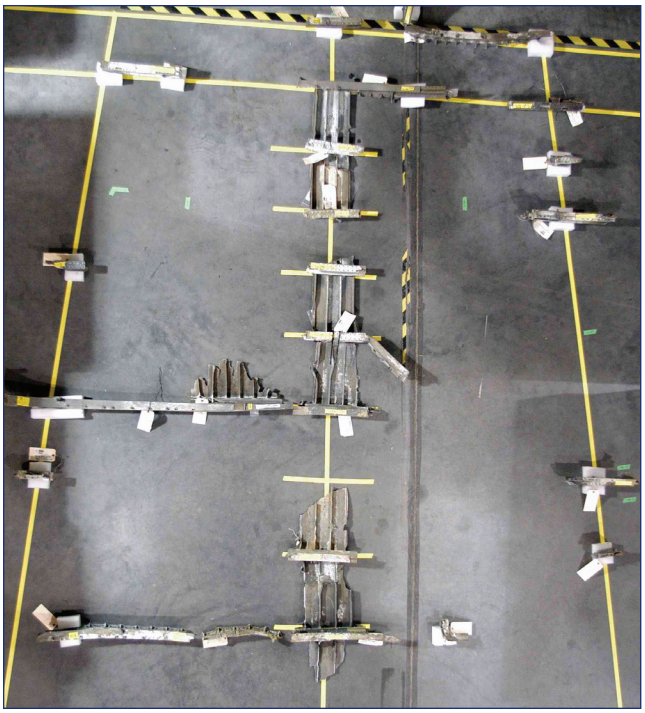

Lower Crew Module Pressure Shell Debris.

Seat Structure

A rather large collection of seat debris items was recovered. Since the majority of the lightweight seat design is common to all seven seat locations, positive seat assignment on most of the recovered seat debris was not possible. However, several key components were identified to seat locations on four flight deck (seats 1,2,3, & 4) and two mid deck (seats 6 & 7) locations. The only consistent piece of seat debris that was positively identified to each of the six seat locations was a failed portion of the upper seat back (see below for a detailed discussion).

Generically, major differences in the magnitude of thermal exposure were identified on flight deck vs. mid deck seat locations. As with the flight deck structure, flight deck seat components were highly melted and/or deposited with splattered aluminum on all surfaces. In contrast, and consistent with most mid deck structure, mid deck seat structural components did not experience any melting at all. The mid deck seat 6 and 7 locations did however collect significant deposits of melted aluminum from the LiOH door that these two seats were attached to (see Mid Deck Floor section).

In nearly all cases, seat components generally fractured into relatively small pieces. It is noted that nearly all seat component fractures occurred at minimum thermal cross-sectional areas (minimum thermal mass), away from any large heat sink locations. It is also noted that nearly all thin-sheet aluminum materials (close-out panels on seat pan and seat back) are completely missing (i.e. overloaded / melted away). Common seat component fracture locations are shown below:

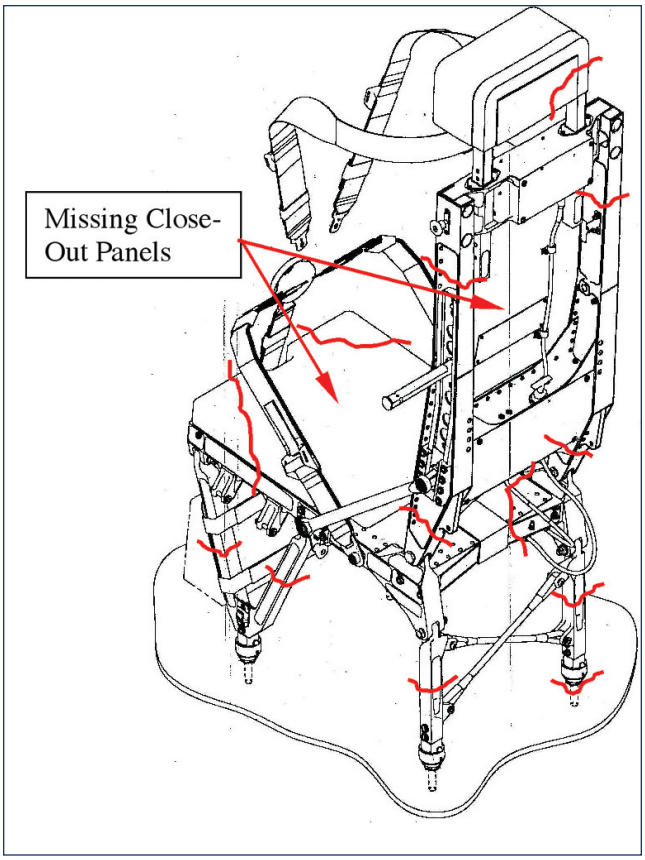

Common Seat Failure Locations (shown in red)
(NOTE: Mission Specialist seat shown; Components below seat pan on Commander/Pilot seat are different in design).

Upon inspection of fracture surfaces, a very unique "delamination" type fracture pattern was identified that is consistent throughout the seat component debris items. Several fractures almost appear as if the 7075 aluminum material is constructed of a laminate material (see below) when in actual fact the material is solid aluminum plate not a laminate structure. This phenomenon was termed as "broom-straw" fractures (see Example below).

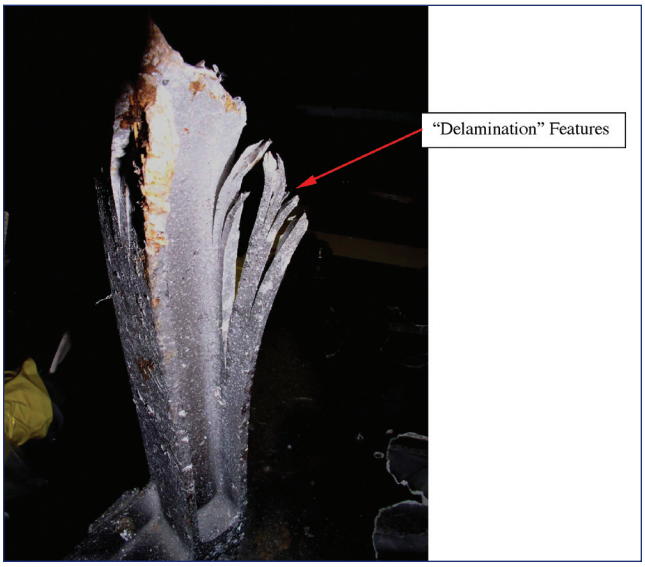

Example of "Broom-Straw" Fracture.

This fracture mode is consistent with elevated temperatures and relatively high strain rates. Metallurgical evaluation in proximity to, and away from crack surfaces discovered heavy grain boundary precipitation. Equiaxed grains were discovered along crack surfaces. These features are consistent with failures at high temperatures. Significant LACK of ductility surrounding fracture areas suggests failures occurred at relatively high strain rates for the thermal environment that was experienced. Thus, it is concluded that seat failure occurred as a result of thermal exposure (material property degradation) prior to mechanical overload.

Upper Seat Backs / Seat Restraint Recoil Mechanisms

Six out of seven "Upper Seat Back" debris items were recovered (all but Seat 5). Each item was positively identified to a seat position. Each recovered upper seat back debris item contains the upper seat strap recoil mechanism and some amount of strap material, which had recoiled back into the mechanism subsequent to strap failure. A description of the debris location and an example of one recovered upper seat back debris item follows:

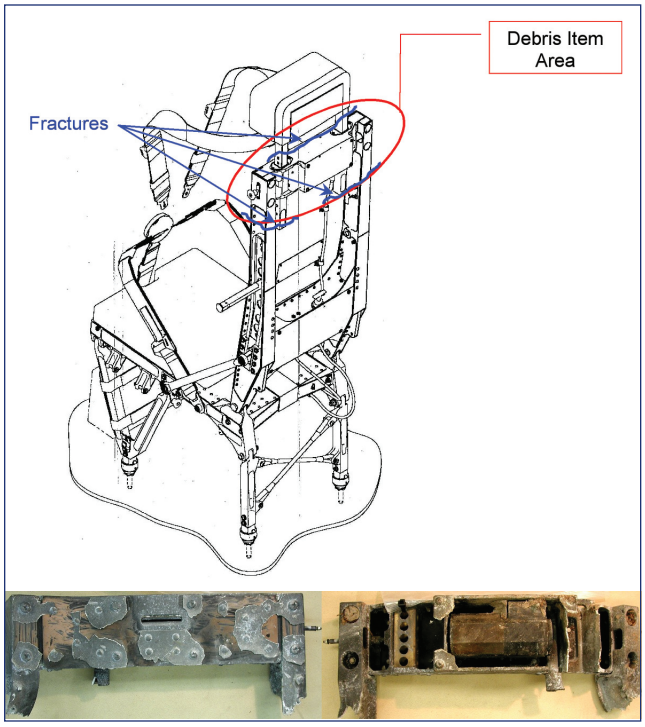

Schematic of "Upper Seat Back" Debris Location, and Example of Representative Debris Item (front and back shown).

In all cases, fractures at the upper seat back location occurred at the minimum thermal cross section, away from heat sinks on either side. These fractures are consistent with the general seat failure mechanism (thermal heating followed by mechanical overload).

In all cases, a significant amount of melted / splattered strap material was discovered internal to the upper back seat cavity. Melting appears associated with air flow entering the upper seat back strap entry point. Melt patterns suggest melting occurred AFTER the seat straps had been recoiled into the housing (i.e. post-failure). Thus, it can be concluded that crewmembers were removed prior to completion of thermal heating event.

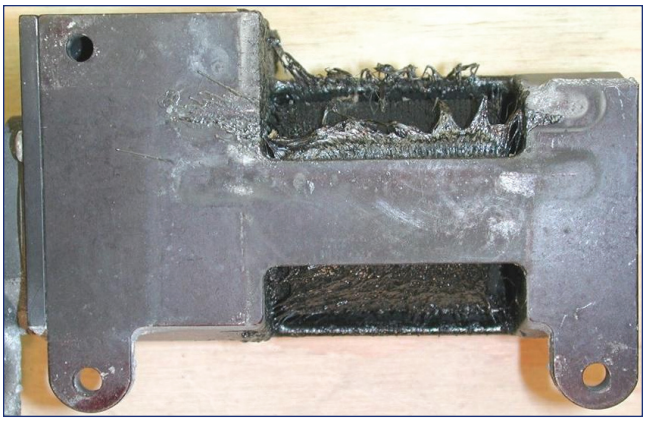

Example of Strap Melt Patterns Surrounding Recoil Mechanism.

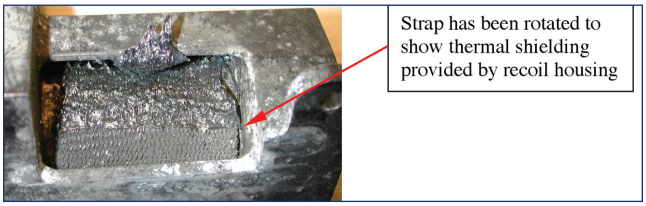

Close-Up of Strap Melt Patterns.

As the condition of the residual strap material contains evidence of thermal / loading history, each recoil mechanism was removed and disassembled to expose the straps for inspection. Upon inspection, strap failures occurred at varying positions along the strap length. Seat 1 & 2 experienced strap failures at or near the end of the strap, at the recoil mechanism (fully extended position). The seat 7 strap failed at approximately 50% of full extension. Seat 3 shows evidence that the strap experienced a significant dynamic loading event at the fully extended position ("bird-caging" near the recoil mechanism observed). All others straps failed at locations ranging from 50 - 90% of strap length (away from recoil attach point).

Comparing the ends of the recovered straps, 5 of 6 strap ends terminate along a "straight line" (all but seat 2). Away from the melted areas (in close proximity), the residual strap material remains flexible / resilient. This appears consistent with melting that occurred AFTER the strap had recoiled back into the housing (straight lines correspond to edges of the exposed strap pass-through areas). Had failure occurred by thermal means only, a thermal exposure gradient over some finite length would be expected. This was not present in any of the six recovered straps. It is thus concluded that all straps failed via mechanical overload of thermally compromised material.

Once the straps were fully extended for inspection, the presence of metallic debris material was discovered on both upper and lower strap surfaces. Overall, melted metallic material was deposited onto exposed seat harness strap material on 4 of 6 recovered upper seat back recoil mechanisms. Material deposition occurred BEFORE separation from seats, yet AFTER the crew module pressure shell had been breached.

Evidence from upper seat strap materials suggests that 4 of 6 straps were "extended" (50-100%) at the time of failure. 5 of 6 were fully extended at some point in time before catastrophic failure. Also, the presence of melted metallic material on extended straps suggests that the crew remained in their seats during exposure to the thermal re-entry environment.

5-Point Seat Belt Buckle

Only one of seven 5-point seat belt buckles was recovered. Positive identification was not possible. The one recovered buckle experienced significant re-entry heating. This resulted in substantial melting of the outer plastic housing. The structure however remained intact, with all five clasps still in place.

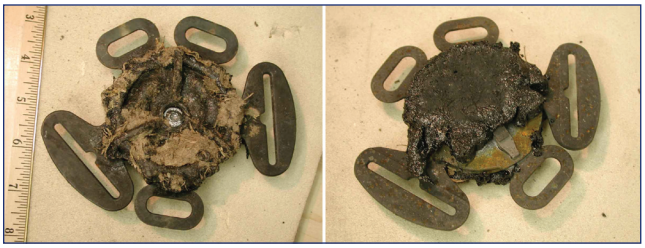

Recovered 5-Point Seat Belt Buckle (front and back shown).

Surprisingly, the two upper strap attach clasps were bent *outward* (away from the crewmember). All other clasps appeared nominal. The buckle assembly was disassembled in an attempt to locate "witness marks" which may have been caused by mechanical loading. Nothing was found.

Break-Up Sequence

Overall, crew module debris items experienced a significant variation in both the magnitude and direction of heating experienced during re-entry. The distribution of directional heating / splatter patterns observed throughout the recovered crew module debris items is essentially RANDOM. Minus the mid deck floor components, the magnitude and orientation of significant heating appears to be defined by the attachment to surrounding structure. In general, most failure modes are consistent with fracture at high temperature.

It can be concluded that the break-up of crew module structure was not instantaneous, but rather a sequential failure / separation of major structural components.

Hardware Forensics Evaluation: General Conclusions

Separation of the crew module / forward fuselage assembly from the rest of the vehicle occurred as a consequence of heating and structural loading experienced outside of the vehicle design envelope. Although significant loading events initiated this separation, failure of the crew module structure was not instantaneous. Failure modes assessed on crew module structural components suggest that fractures occurred subsequent to elevated temperature exposure (corresponding to a significant reduction of material properties). Thus, subsequent break-up of both the crew module and forward fuselage structure occurred as a consequence of the combined environments provided by ballistic heating and aerodynamic loading.

Failure modes assessed on crew module and/or forward fuselage components cannot be linked to the root cause of the STS-107 *Columbia* crash.

The information contained in this work was compiled by the CAIB/NASA JSC Crew Survival Working Group. The conclusions drawn in this work do not necessarily reflect the conclusions of the Board; when there is conflict, the statements in Volume I of the Columbia Accident Investigation Board Report take precedence.

COLUMBIA
ACCIDENT INVESTIGATION BOARD

REPORT
VOLUME V

COLUMBIA ACCIDENT INVESTIGATION BOARD

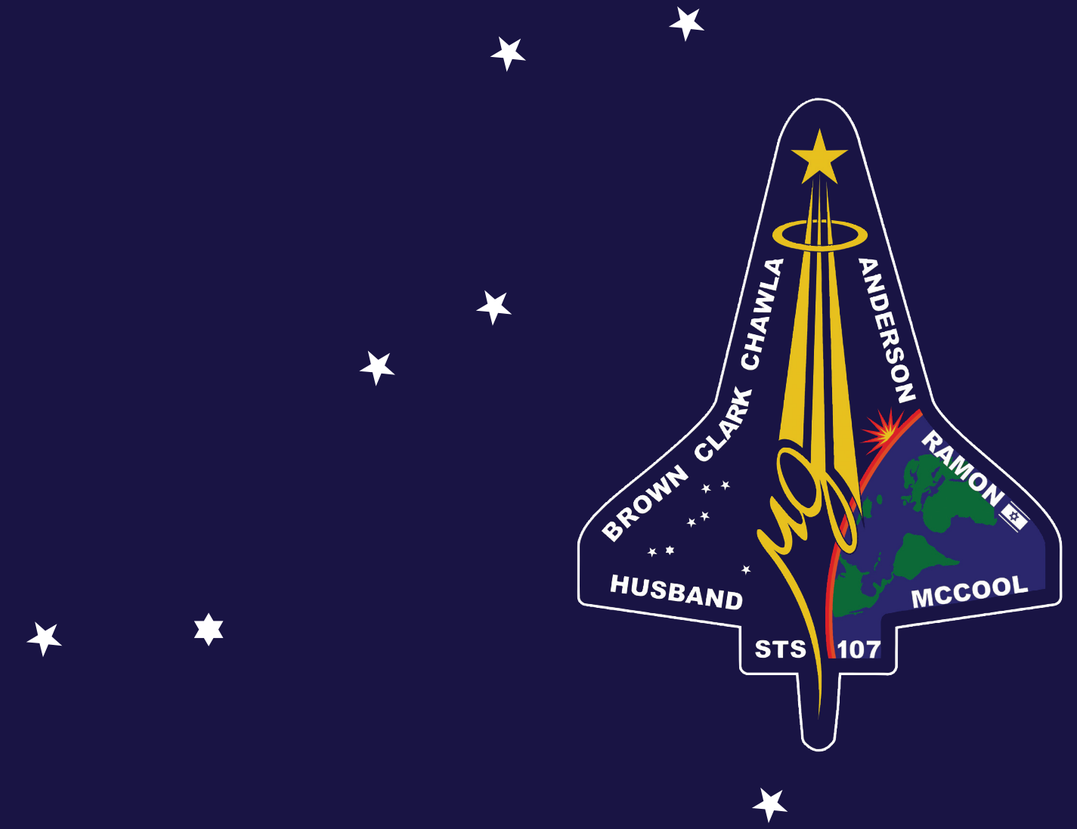

OCTOBER
2003

REPORT VOLUME V
APPENDIX G.13
OCTOBER 2003

COLUMBIA

ACCIDENT INVESTIGATION BOARD

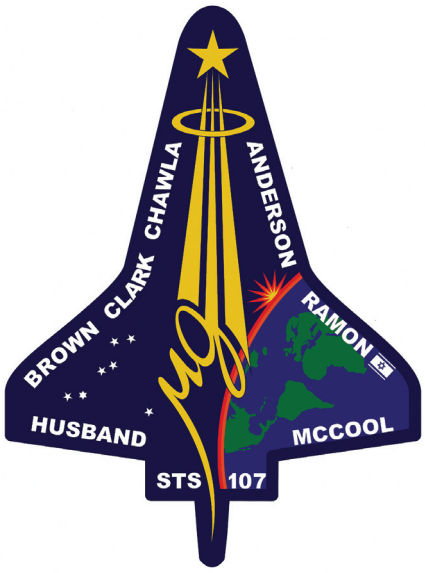

Note: Volumes II – VI contain a number of conclusions and recommendations, several of which were adopted by the Board in Volume I. The other conclusions and recommendations drawn in Volumes II – VI do not necessarily reflect the opinion of the Board, but are included for the record. When there is conflict, Volume I takes precedence.

REPORT VOLUME V
APPENDIX G.13
OCTOBER 2003

On the Front Cover

This was the crew patch for STS-107. The central element of the patch was the microgravity symbol, μg, flowing into the rays of the Astronaut symbol. The orbital inclination was portrayed by the 39-degree angle of the Earth's horizon to the Astronaut symbol. The sunrise was representative of the numerous science experiments that were the dawn of a new era for continued microgravity research on the International Space Station and beyond. The breadth of science conducted on this mission had widespread benefits to life on Earth and the continued exploration of space, illustrated by the Earth and stars. The constellation Columba (the dove) was chosen to symbolize peace on Earth and the Space Shuttle Columbia. In addition, the seven stars represent the STS-107 crew members, as well as honoring the original Mercury 7 astronauts who paved the way to make research in space possible. The Israeli flag represented the first person from that country to fly on the Space Shuttle.

On the Back Cover

This emblem memorializes the three U.S. human space flight accidents – Apollo 1, Challenger, and Columbia. The words across the top translate to: "To The Stars, Despite Adversity – Always Explore"

The Board would like to acknowledge the hard work and effort of the following individuals in the production of Volumes II – VI.

Maj. Gen. John L. Barry	Executive Director to the Chairman
Dennis R. Jenkins	Investigator and Liaison to the Board
Lt. Col. Donald J. White	Technical Editor
Lt. Col. Patrick A. Goodman	Technical Editor
Joshua M. Limbaugh	Layout Artist
Joseph A. Reid	Graphic Designer
Christine F. Cole	Administrative Assistant
Jana T. Schultz	Administrative Assistant
Lester A. Reingold	Lead Editor
Christopher M. Kirchhoff	Editor
Ariel H. Simon	Assistant Editor
Jennifer L. Bukvics	Lead Project Manager
Donna J. Fudge	Senior Paralegal, Group II Coordinator
Susan M. Plott	Project Supervisor, Group III Coordinator
Ellen M. Tanner	Project Supervisor
Matthew J. Martin	Government Relations Consultant
Frances C. Fisher	ANSER Liaison

Limited First Printing, October 2003, by the
Columbia Accident Investigation Board

Subsequent Printing and Distribution by the
National Aeronautics and Space Administration
and the
Government Printing Office
Washington, D.C.

VOLUME I

PART ONE	THE ACCIDENT
Chapter 1	The Evolution of the Space Shuttle Program
Chapter 2	*Columbia*'s Final Flight
Chapter 3	Accident Analysis
Chapter 4	Other Factors Considered
PART TWO	WHY THE ACCIDENT OCCURRED
Chapter 5	From *Challenger* to *Columbia*
Chapter 6	Decision Making at NASA
Chapter 7	The Accident's Organizational Causes
Chapter 8	History as Cause: *Columbia* and *Challenger*
PART THREE	A LOOK AHEAD
Chapter 9	Implications for the Future of Human Space Flight
Chapter 10	Other Significant Observations
Chapter 11	Recommendations
PART FOUR	APPENDICES
Appendix A	The Investigation
Appendix B	Board Member Biographies
Appendix C	Board Staff

VOLUME II

CAIB TECHNICAL DOCUMENTS CITED IN THE REPORT

	Reader's Guide to Volume II
Appendix D.a	Supplement to the Report
Appendix D.b	Corrections to Volume I of the Report
Appendix D.1	STS-107 Training Investigation
Appendix D.2	Payload Operations Checklist 3
Appendix D.3	Fault Tree Closure Summary
Appendix D.4	Fault Tree Elements – Not Closed
Appendix D.5	Space Weather Conditions
Appendix D.6	Payload and Payload Integration
Appendix D.7	Working Scenario
Appendix D.8	Debris Transport Analysis
Appendix D.9	Data Review and Timeline Reconstruction Report
Appendix D.10	Debris Recovery
Appendix D.11	STS-107 Columbia Reconstruction Report
Appendix D.12	Impact Modeling
Appendix D.13	STS-107 In-Flight Options Assessment
Appendix D.14	Orbiter Major Modification (OMM) Review
Appendix D.15	Maintenance, Material, and Management Inputs
Appendix D.16	Public Safety Analysis
Appendix D.17	MER Manager's Tiger Team Checklist
Appendix D.18	Past Reports Review
Appendix D.19	Qualification and Interpretation of Sensor Data from STS-107
Appendix D.20	Bolt Catcher Debris Analysis

VOLUME III — OTHER TECHNICAL DOCUMENTS

Reader's Guide to Volume III

Appendix E.1	CoFR Endorsements
Appendix E.2	STS-107 Image Analysis Team Final Report
Appendix E.3	An Assessment of Potential Material Candidates for the "Flight Day 2" Radar Object Observed during the NASA Mission STS-107
Appendix E.4	*Columbia* Early Sighting Assessment Team Final Report

VOLUME IV — OTHER TECHNICAL DOCUMENTS

Reader's Guide to Volume IV

Appendix F.1	Water Absorption by Foam
Appendix F.2	Follow the TPS
Appendix F.3	MADS Sensor Data
Appendix F.4	ET Cryoinsulation
Appendix F.5	Space Shuttle STS-107 Columbia Accident Investigation, External Tank Working Group Final Report – Volume 1

VOLUME V — OTHER SIGNIFICANT DOCUMENTS

Reader's Guide to Volume V

Appendix G.1	Requirements and Procedures for Certification of Flight Readiness
Appendix G.2	Appendix R, Space Shuttle Program Contingency Action Plan
Appendix G.3	CAIB Charter, with Revisions
Appendix G.4	Group 1 Matrix Brief on Maintenance, Material, and Management
Appendix G.5	Vehicle Data Mapping (VDM) Team Final Report, Jun 13, 2003
Appendix G.6	SRB Working Group Presentation to CAIB
Appendix G.7	Starfire Team Final Report, Jun 3, 2003
Appendix G.8	Using the Data and Observations from Flight STS-107... Exec Summary
Appendix G.9	Contracts, Incentives, and Safety/Technical Excellence
Appendix G.10	Detailed Summaries: Rogers Commission Report, ASAP Report, SIAT Report
Appendix G.11	Foam Application and Production Chart
Appendix G.12	Crew Survivability Report
Appendix G.13	Aero/Aerothermal/Thermal/Structures Team Final Report, Aug 6, 2003

VOLUME VI — TRANSCRIPTS OF BOARD PUBLIC HEARINGS

Reader's Guide to Volume VI

Appendix H.1	March 6, 2003	Houston, Texas
Appendix H.2	March 17, 2003	Houston, Texas
Appendix H.3	March 18, 2003	Houston, Texas
Appendix H.4	March 25, 2003	Cape Canaveral, Florida
Appendix H.5	March 26, 2003	Cape Canaveral, Florida
Appendix H.6	April 7, 2003	Houston, Texas
Appendix H.7	April 8, 2003	Houston, Texas
Appendix H.8	April 23, 2003	Houston, Texas
Appendix H.9	May 6, 2003	Houston, Texas
Appendix H.10	June 12, 2003	Washington, DC

Reader's Guide to Volume V

Volume V of the Report contains appendices that were not cited in Volume I. These consist of documents produced by NASA and other organizations, which were provided to the Columbia Accident Investigation Board in support of its inquiry into the February 1, 2003 destruction of the Space Shuttle *Columbia*. The documents are compiled in this volume in the interest of establishing a complete record, but they do not necessarily represent the views of the Board. Volume I contains the Board's findings, analysis, and recommendations. The documents in Volume V are also contained in their original color format on the DVD disc in the back of Volume II.

THIS PAGE INTENTIONALLY LEFT BLANK

Volume V
Appendix G.13

Aero/Aerothermal/Thermal/Structures Team Final Report, Aug 6, 2003

This Appendix contains NSTS-37398 Aero/Aerothermal/Thermal/Structures Team Final Report in Support of the *Columbia* Accident Investigation, 6 August 2003.

THIS PAGE INTENTIONALLY LEFT BLANK

NSTS-37398

Aero/Aerothermal/Thermal/Structures Team Final Report

in support of the *Columbia* Accident Investigation

August 6, 2003

Submitted by

Original signature obtained
Pam Madera, USA
Team Lead

Original signature obtained
Steve Labbe, NASA JSC
Aerodynamics

Original signature obtained
Joe Caram, NASA JSC
Aerothermodynamics

Original signature obtained
Chris Madden, NASA JSC
Thermal

Original signature obtained
Mike Dunham, Boeing
Stress, Loads and Dynamics

Contributing Authors - Aerodynamics

Karen Bibb, NASA Langley Research Center
Greg Brauckmann, NASA Langley Research Center
Olman Carvajal, Boeing-Houston
Kevin Dries, NASA Johnson Space Center
Randy Lillard, NASA Johnson Space Center
Ramadas K. Prabhu, LESC-Hampton
Karuna Rajagopal, Boeing-Huntington Beach
James Reuther, NASA Ames Research Center
William I. Scallion, NASA Langley Research Center
Jeff Stone, Boeing-Huntington Beach

Contributing Authors – Aerothermodynamics

Steve Alter, NASA Langley Research Center
Steve Barson, Boeing Rocketdyne Propulsion and Power
Maria Bobskill, Ph. D. , NASA Langley Research Center
Stan Bouslog, Lockheed Martin
Katie Boyles, NASA Johnson Space Center
Kevin Bowcut, Ph. D., Boeing Huntington Beach
Charles Campbell, NASA Johnson Space Center
Steve Fitzgerald, NASA Johnson Space Center
Michail Gallis, Ph. D., Sandia National Laboratories
Peter Gnoffo, Ph. D. , NASA Langley Research Center
Scott Halloran, Boeing Rocketdyne Propulsion and Power
Tom Horvath, NASA Langley Research Center
Randy Lillard, NASA Johnson Space Center
Joe Olejniczak Ph. D., NASA Ames Research Center

Tom Paul, Lockheed Martin
Jeff Payne, Sandia National Laboratories
Don Picetti, Boeing Huntington Beach
Karuna Rajagopal, Ph. D., Boeing Huntington Beach
James Reuther, Ph. D, NASA Ames Research Center
Joe Ruf, NASA Marshall Space Flight Center
Greg Schunk, NASA Marshall Space Flight Center
John Sharp, NASA Marshall Space Flight Center
Joel Stolzfus, NASA Johnson Space Center White Sands Test Facility
Ricky Thompson, NASA Langley Research Center
K. C. Wang, Boeing Houston
Vince Zoby, NASA Langley Research Center

Contributing Authors - Thermal

Donald Curry, NASA Johnson Space Center
Steven Del Papa, NASA Johnson Space Center
Ronald Lewis, NASA Johnson Space Center
Dan Newswander, NASA Johnson Space Center
Don Picetti, Boeing Huntington Beach
Alvaro Rodriguez, NASA Johnson Space Center

Contributing Authors – Stress

Jason Adair, BNA-Houston
Charles Park, BNA- Huntington Beach
Paul Parker, BNA-Houston
Shawn Sorenson, BNA-Houston

Table of Contents

Executive Summary 1
1 INTRODUCTION 2
2 PURPOSE & SCOPE 2
3 METHODOLOGY 3
4 AERODYNAMICS 5
4.1 Introduction 5
4.1.1 Team Objectives 5
4.1.2 Nominal Orbiter Aerodynamic Entry Flight Overview 5
4.1.3 Chronology of Investigation – Test & Analysis 5
4.1.4 Approach / Processes – Methodology to Achieve Objectives 6
4.2 Aerodynamic Extraction 11
4.2.1 Atmospheric Model 11
4.2.2 GSFC/DAO Upper Atmospheric Wind Model 12
4.2.3 Aerodynamic Increment Extraction Results 12
4.2.4 Correlation to Working Scenario 13
4.3 Damage Assessment Aero 23
4.3.1 Wind Tunnel Testing 23
4.3.2 Damage Assessment Using Computational Fluid Dynamics 42
4.4 Application of Data to the Working Scenario 85
4.4.1 Correlation of CFD & WTT – Results by Timeline Section 85
4.4.2 Damage Progression Theory and Supporting Aero 92
4.5 Summary – conclusions & observations 110
4.6 References – Aerodynamics 111
4.7 Appendices – Aerodynamics 112
4.7.1 Aerodynamic Definitions, Coordinate Systems and References 112
4.7.2 Surface Pressure Entry Data Evaluation 116
4.7.3 Wind Tunnel Test Matrix – Comprehensive Listing 119
4.7.4 FELISA Inviscid CFD - Comments and Additional Analysis 122
4.7.5 OVERFLOW CFD Analysis of Leeside Flow field Interactions 127
4.7.6 Aerodynamic Investigation using CART3D CFD Analysis 134
4.7.7 Aerodynamic Investigation using USA CFD Analysis 142
4.7.8 CFD Tools: 142
5 AEROTHERMODYNAMICS 146
5.1 Introduction 146
5.1.1 Team Objective 146
5.1.2 Aerothermodynamics Overview –Orbiter Perspective 146
5.1.3 Approach to Determining Required Environments 147
5.2 Orbiter External Aerothermodynamic Environments (Nominal & Damaged Configurations) 148
5.2.1 Orbiter OML/Skin Flight Data Observations 148
5.2.2 Orbiter Certified Body Point Heating Methodology 160
5.2.3 Wind Tunnel Testing 171
5.2.4 Computational Fluid Dynamics (CFD) and Direct Simulation Monte Carlo (DSMC) 195
5.2.5 Application of External Environments Data to the Working Scenario 271

5.3 Damaged Orbiter Internal Aerothermodynamic Environments 282
5.3.1 Process of Determining Internal Aerothermodynamic Environments 282
5.3.2 External/Internal Environments – Engineering Analysis 287
5.3.3 Plume Model Development 297
5.3.4 Effects of Burning Aluminum 325
5.3.5 Coupled Venting and Thermal Model of Wing 330
5.3.6 3D CFD & DSMC of Wing Leading Edge Cavity 363
5.3.7 Application of Data to the Working Scenario 466
5.4 Aerothermodynamic Environments Summary 482
5.5 References 485
5.6 Appendix for Aerothermodynamics 493
5.6.1 Engineering Tools 493
5.6.2 Wind Tunnel Facilities & Measurement Techniques 493
5.6.3 CFD/DSMC Tools 495
5.6.4 Hypersonic Boundary Layer Transition Effective Trip Height Calculation 501
5.6.5 STS-107 End of Mission (EOM) 3 Pre-Entry Trajectory 503
6 THERMAL 510
6.1 Panel 8/9 Spar & Clevis Thermal Analysis 510
6.1.1 Damaged Tee-seal 511
6.2 Spar Burn Through Analysis 512
6.3 Wheel Well Thermal Analysis 512
6.4 Wire Bundle Burn-Through Tests 514
6.5 Wire Bundle Burn-Through Thermal Analysis 517
6.5.1 Tee-seal scenario 519
6.6 Orbiter Sidewall Bondline Thermal Analysis 519
6.7 Damaged Wing Leading Edge Coupled Aero-Thermal-Structural Analysis 520
6.8 Chin Panel Temperature Anomaly 522
6.9 Truss Tube Thermal Analysis 522
6.10 RCC Knife Edge Tests 523
6.11 Leading Edge Reinforced Carbon-Carbon (RCC) Hole Growth Thermal Analysis 525
7 STRESS 577
7.1 Panel 9 Spar Strain Gauge Evaluation 577
7.1.1 Analysis Objective 577
7.1.2 Analytical Approach 578
7.1.3 Model Description 578
7.1.4 Thermal Profiles 579
7.1.5 Results 582
7.1.6 Conclusions 584
7.2 1040 Spar Strain Gauge Evaluation 587
7.2.1 Analysis Objective 587
7.2.2 Analysis Inputs, Models, Assumptions, and Approach 587
7.2.3 Results 590
7.2.4 Conclusions 592
7.3 Overall Wing MADS Evaluation 593
7.3.1 Analysis Objective 593
7.3.2 Analysis Inputs, Models, Assumptions, and Approach 593
7.3.3 Results 594
7.3.4 Conclusions 597
7.4 Accelerometer Evaluation 597
7.4.1 Ascent 597
7.4.2 Descent 611
7.4.3 Summary 618
7.5 Feasible Wing Deformation Prior to Loss of Signature 619
7.5.1 Analysis Objective 619
7.5.2 OV-102 Wing Finite Element Model 619
7.5.3 Load Cases 620

7.5.4 Analytical Procedure 621
7.5.5 Analysis Results 625
7.5.6 Conclusions 637
7.6 Stress Appendix 638
7.7 Reference – MADS PCM Installation Drawings 652
8 CONCLUSIONS 653
9 CREDITS 655
10 Acknowledgements 656
References 656
Appendix A - Acronyms and Abbreviations 658
Appendix B - Team Member List & Biographies 661

Executive Summary

The Aerodynamic/Aerothermodynamic/Thermal/Structures (AATS) Team was formed by the Orbiter Vehicle Engineering Working Group (OVEWG) to assist in the STS-107 Columbia Accident Investigation. The primary objective of this team was to provide an analytical basis for a most probable damage scenario for the STS-107 entry. This team was not chartered with the task of defining how the initial damage was incurred.

The approach used by the AATS Team was to postulate the approximate location and extent of damage experienced by Columbia during entry. The team would then formulate analyses or tests that would emulate the vehicle aerodynamic, thermal, or structural responses to the postulated hardware damage. The results of the analyses or tests were compared to anomalous MADS and OI measured data or off-nominal aerodynamic increments associated with the STS-107 entry to determine if the postulated damage condition was feasible. Results were then integrated to ensure that the postulated damage condition could be supported across the technical disciplines. Where appropriate to ensure consistency, corresponding analysis of damage conditions were completed for the ascent phase of flight. Finally, postulated damage conditions were evaluated to ensure that they would not conflict with the condition of recovered hardware or other flight data.

The AATS Team efforts were primarily focused on postulated damage conditions starting at entry interface (EI) and extending to approximately 615 seconds from EI. Evaluations of off-nominal indications during this time frame were expected to provide the best insight into identifying the initial damage condition. An evaluation of damage conditions consistent with aerodynamic increments just prior to loss of signal (LOS) was conducted for completeness.

The culmination of multiple analyses substantiates a most probable entry damage scenario that begins with damage to the wing leading edge reinforced carbon-carbon (RCC) prior to EI. Analyses indicate that the initial damage was consistent with a breach in the lower portion of RCC panel 8. The breach can be described as an aperture with an area equivalent to that of a six to ten inch diameter hole. From the beginning of the entry profile, hot gas was ingested into the wing leading edge cavity behind the RCC panels. The flow of hot gas into the cavity was disturbed by complex internal geometry increasing both the local pressure in the cavity and the heating of local surfaces. The increase in RCC cavity pressure and internal flow patterns increased flow out of the vents located at the top of the cavity. By approximately EI+340 seconds from EI, the vent paths were increased slightly due to thermal degradation. Flow out of the upper vents resulted in a disturbance of flow on the leeside of the vehicle, thereby displacing the strake and canopy vortices and temporarily reducing heating to the left sidewall and left Orbital Maneuver System (OMS) pod. Heating of local surfaces inside the RCC cavity eventually resulted in burn through of the wing leading edge spar by approximately EI plus 487 seconds. The transverse momentum of the flow of hot gas entering the RCC cavity was redirected as the flow impinges on RCC ribs and spanner beam hardware and insulation. As a result, the plume entering the intermediate wing was directed normal from the spar toward the main landing gear compartment wall. The impingement of the plume in this region resulted in burning of the four OI/MADS wire bundles, burn through of the main landing gear compartment wall, and burn through of the upper wing skin. Burn through of the main landing gear compartment wall resulted in an abnormal temperature rise of main landing gear components in the wheel well due to convective heating. Increased outer mold line heating of the left sidewall and OMS pod can be explained by redirection of the wing leading edge windward flow to the leeside through either a severely damaged and/or missing upper RCC carrier panel(s), severely damaged or missing full RCC panel (e.g. panel 9), or damaged upper wing just aft of the wing leading edge. These damage conditions are also consistent with anomalous aerodynamic increments between EI+500 to EI+600 seconds. Damage in the left wing cavity continued to progress until loss of signal. This damage resulted in a significant depression being formed on the lower surface of the left wing due to burn though of intermediate wing truss tubes and compromised structural strength associated with heating internal to the wing. The depression in the lower wing resulted in external flow patterns that effectively increased the lift and drag on the left wing resulting in the positive rolling moment and negative yawing moment just prior to loss of signal. This report details the tests and analyses results that lend credence to this damage progression as a plausible explanation of Columbia's final moments of flight.

1 INTRODUCTION

The AATS Team was formed by the Orbiter Vehicle Engineering Working Group (OVEWG) to aid the NASA community in the investigation of the STS-107 accident. The team was formed with members from various organizations and technical disciplines throughout the NASA and contractor communities. The team was organized with sub-team leads for each significant technical area as shown in Figure 1.1. A short biography of team leads and a list of team members can be found in Appendix B of this report.

This report summarizes the analyses performed by the AATS Team to support scenario development and to address actions levied and/or requests made by the Columbia Accident Investigation Board, OVEWG, and other teams supporting the investigation.

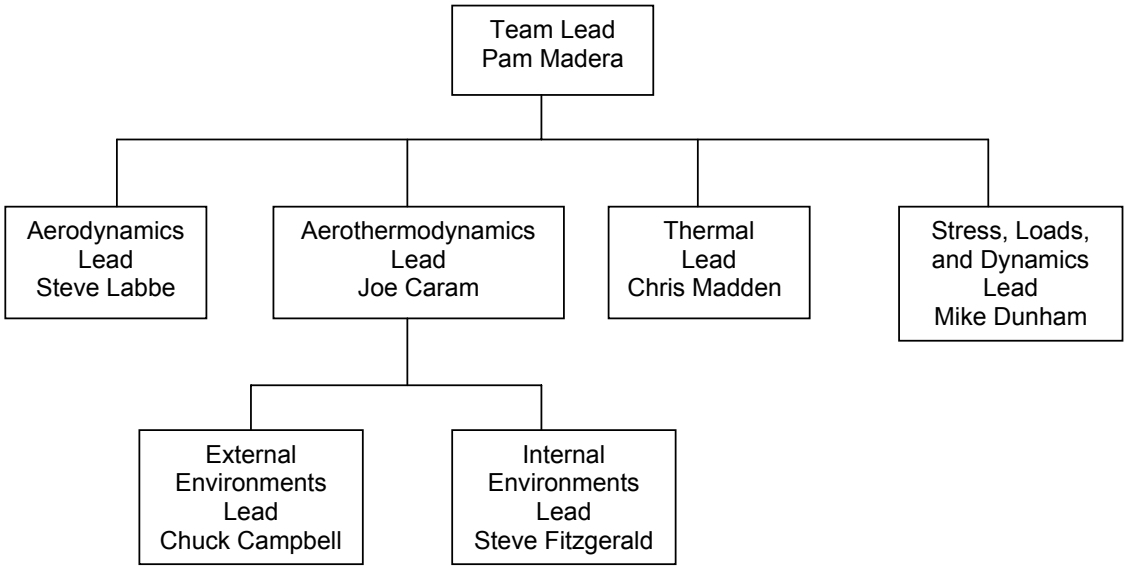

Figure 1-1 Team Organization

2 PURPOSE & SCOPE

This report documents the analyses performed by the AATS Team that provided substantiation for a most probable damage scenario for the Columbia accident. Damage conditions were analyzed to a level of fidelity that would provide the NASA OVEWG, NAIT, and CAIB sufficient insight to ensure that the appropriate corrective action steps would be taken prior to return to flight. In some cases, engineering level analysis was sufficient to understand the off-nominal conditions. This team was not chartered with the task of defining how the initial damage was incurred.

The AATS Team efforts were primarily focused on postulated damage conditions starting at entry interface (EI) and extending to approximately 615 seconds from EI. Evaluations of off-nominal indications during this time frame were expected to provide the best insight to identify the initial damage condition.

An evaluation of damage conditions consistent with aerodynamic increments just prior to loss of signal (LOS) was conducted for completeness.
It should be noted that analyses and tests conducted for the investigation were performed on representative geometries. The fact that these geometries were chosen for investigation purposes should not be misconstrued as exactly reproducing the damaged configuration encountered in flight. These

representative damage configurations, however, do provide insight into the nature and level of damage necessary to result in the loss of Columbia and her STS-107 crew.

3 METHODOLOGY

The completion of the scope of this team's charter required a significant amount of analyses to be completed in a short amount of time. To accomplish the largest amount of work in the shortest amount of time, many analysis efforts were performed parametrically in parallel with comparisons and integration completed at various points throughout the investigation. Some tasks were performed in sequence out of necessity. For example, most of the final thermal analyses could not be completed until internal aerothermodyanmic environments were developed. Wherever possible, independent and/or redundant processes and tools were used to help ensure the validity of the analysis results and subsequent conclusions.

Overall, the approach used by the AATS Team was to postulate the approximate location and extent of damage experienced by Columbia during entry. The team would then formulate analyses or tests that would emulate the aerodynamic, thermal, and structural responses of the postulated hardware damage. The results of the analysis or test were compared to anomalous MADS and OI measured data and off-nominal aerodynamic increments associated with the STS-107 entry to determine if the postulated damage condition was feasible. Results were then integrated to ensure that the postulated damage condition could be supported by each technical discipline. Progression of damage was reviewed to make sure it made logical sense. Where appropriate, corresponding analysis of damage conditions were completed for the ascent phase of flight. Finally, postulated damage conditions were evaluated to ensure that they would not conflict with the condition of recovered hardware or other flight data.

Completion of these steps required the identification of key off nominal data that required the postulation of damage conditions. Figure 3-1provides a high level summary of key data measurements and events that were identified to be evaluated.

GMT Time mm:ss	Time after EI sec	Key Data Measurements and Events
48:39	270	RCC panel 9 spar strain gauge shows off nominal response
48:59	290	Clevis fitting 9/10 sees first indication of temperature increase
49:49	340	OMS pod temperature experiences reduced heating
51:14	425	Panel 9 spar temperature starts off-nominal rise
52:16	487	First MADS measurement begins to fail behind wing spar
52:17	488	First temperature rise in wheel well (LMG brake line bit flip)
52:17	488	Xo 1040 spar strain gauge shows off-nominal response
52:19	490	Unusual response in chin panel outboard clevis temperature
52:30	501	Unusual water dump and vacuum vent nozzle temperature response
52:44	515	Start of delta yaw
52:50	521	Start of delta roll
54:09	600	Debris 5 (Flash "0")
54:10	601	Start of significant temperature rise in wheel well (LMG brake line b)
54:11	602	Reversal of delta roll trend
54:20	611	Start of Slow Aileron Trim Change
54:22	613	Mid Fuse and sidewall temperature rise
54:33	624	Flash 1

Figure 3-1 Key Data Measurements and Events

Several of the events occurred in nearly coincident time frames as shown in Figure 3-2. These corresponding events were reviewed to identify areas of commonality and to ensure consistency in damage progression.

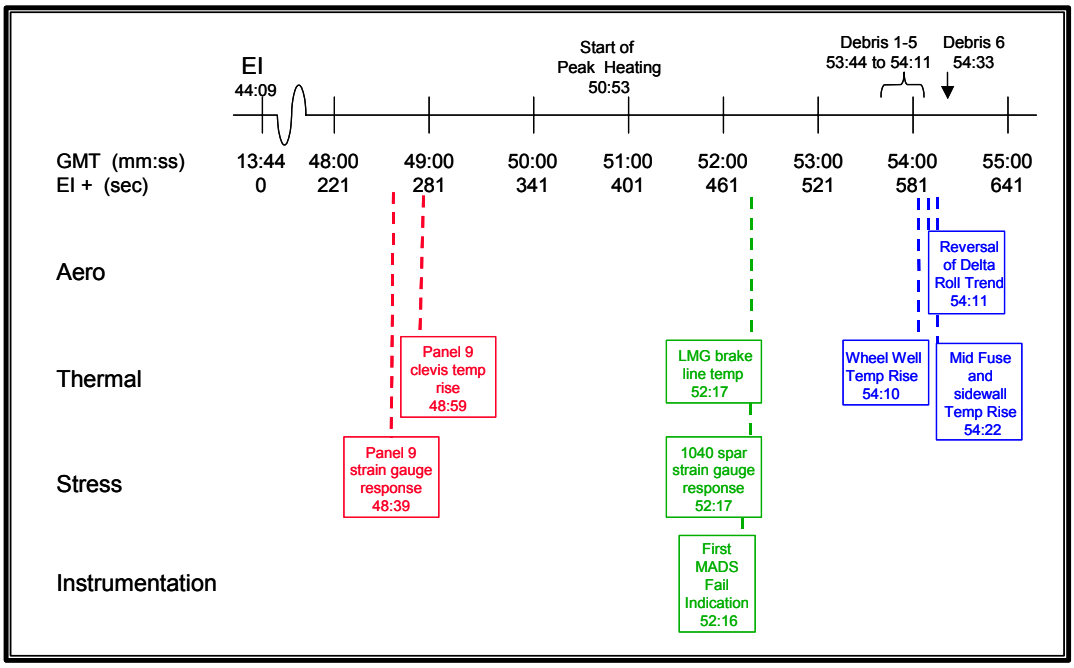

Figure 3-2 Corresponding Events

The AATS Team worked closely with the Scenario team. Analyses were used to formulate a most probable scenario of initial damage and damage progression within the scope of the team's charter. Coordination with the Scenario Team and the Technical Integration Team helped ensure that AATS analysis activities did not conflict with other investigation data/findings.

4 AERODYNAMICS

4.1 Introduction

4.1.1 Team Objectives

The STS-107 entry flight aerodynamic reconstruction effort had two primary objectives. The first was to define the aerodynamic forces and moments experienced by Columbia during atmospheric flight from entry interface (EI) up to the point of loss of signal (LOS) + 5 sec (the last reliable data set point). These extracted forces and moments were then compared to predictions obtained from the orbiter operational aerodynamic data base (OADB) with the resulting differences attributed to the effects of vehicle damage. This served as the basis for the second objective which focused on reproducing the observed off nominal force and moment aerodynamics through wind tunnel (WT) test and/or computational fluid dynamics (CFD) analysis of postulated damaged orbiter configurations. Developing a match between the extracted off nominal aerodynamics and the damage assessment test and analysis results was then used as one basis to substantiate or refute plausible damage scenarios. The ultimate goal was to correlate these results with a vehicle damage scenario that progressed from an initial stage at EI to a considerably more aerodynamically significant damaged configuration just prior to LOS, while maintaining consistency with results from the aerodynamic heating and other analyses. In the end, this leads to a damaged configuration that produced the overwhelming off nominal asymmetric aerodynamic moments resulting in Columbia's loss of control and vehicle breakup.

4.1.2 Nominal Orbiter Aerodynamic Entry Flight Overview

The Orbiter entry is initiated by the firing of the Orbiter Maneuvering System (OMS) jets, slowing the Orbiter and allowing the vehicle to descend to the atmospheric EI, nominally at an altitude of 400,000 feet. During the initial entry phase, which extends to a dynamic pressure of 20 psf. (approx. 250,000 ft), vehicle lateral/directional control and trim is provided by a combination of RCS jet firings, aileron deflections, and sideslip angle. This hypersonic entry flight phase, continuing down through a Mach number of less than five, is accomplished at a high angle of attack during which the blanketing effect of the wing and fuselage essentially precludes any use of the rudder for yaw control. With the rudder not activated until Mach 5, prior to this point in the entry the lateral axis is trimmed solely by aileron deflection with a resulting sideslip angle to balance the roll and yaw moments, augmented by occasional RCS yaw ret firings. Range control is achieved through a series of banking maneuvers while following a predetermined angle of attack schedule. STS-107 trajectory parameters from EI to LOS (approximately Mach 18 near 200,000 ft) are included in Figure 4.1-1 to Figure 4.1-3. Note that for the extent of the STS-107 entry, Columbia was in a high Mach Number, low dynamic pressure flight condition near the 40 deg nominal entry angle-of-attack.

Typically, a terminal phase would then begin as angle of attack is reduced below 18 degrees. As the vehicle continues its descent, air data probes are then extended (at approximately Mach 5) to provide air data relative to the Orbiter. Subsonic flight is attained at an altitude of approximately 40,000 ft. Range control during subsonic flight is obtained by angle of attack modulation with velocity control maintained by the rudder speed-brake. The approach and landing interface occurs at 10,000 ft and a pre-flare is initiated at the appropriate altitude, followed by a deceleration float and touchdown.

Aerodynamic coordinate systems, reference lengths and areas, etc. are included in Aerodynamic Appendices, Section 4.7.1

4.1.3 Chronology of Investigation – Test & Analysis

The STS-107 aerodynamic investigation began with a focus on the orbiter lower wing, primarily in the region of the main landing gear (MLG) door. This was based on the preliminary ascent foam debris impact assessment and operational instrumentation (OI) indications of off-nominal temperature and pressure sensor data in the left wing, particularly in the MLG wheel well. Testing was initiated in the Langley Research Center (LaRC) 20-Inch Mach 6 Air Tunnel, concentrating on lower surface tile damage scenarios, boundary layer transition effects and potential MLG door and/or wheel well cavity exposure.

Further analysis of the ascent debris trajectory suggested that foam may have impacted the WLE. Additionally, preliminary forensics of recovered Columbia hardware suggested WLE damage as an increasingly likely scenario. An LaRC inviscid (FELISA) CFD analysis of a damaged WLE reinforced carbon-carbon (RCC) panel, corroborated by preliminary LaRC WT test results, indicated side fuselage heating augmentation consistent with the OI data. Thus, the aerodynamic investigation priority was shifted to a WLE damage assessment with a concentrated effort to understand the aerodynamic and aerothermodynamic effects of damaged or missing WLE RCC panels. This combined aerodynamic/aerothermal approach was a fundamental part of the investigation process. The evaluations included WT testing in the LaRC Mach 6 air and carbon tetra-fluoride (CF4) hypersonic facilities complemented with CFD analysis by various groups from across the agency. These results were focused even further by the recovery of the Orbiter Experiments (OEX) recorder and associated pressure, temperature and strain data as well as continuing forensic analysis of Columbia's recovered WLE components.

Subsequently the Technical Integration Team conducted a failure analysis technical interchange meeting (TIM) where, based on all the latest investigation information a decision was approved by the Orbiter Vehicle Engineering Working Group (OVEWG) board to concentrate on WLE RCC Panel 5-9 damage as the primary working scenario. Test and analysis of missing partial WLE RCC panels was initiated based on the recovery of portions of each of Columbia's left hand side WLE panels. These results extended the data set for missing full RCC panels to a range of WLE damage configurations. Additionally, leeside flow field effects became a focus of the investigation based on off-nominal readings from the mid fuselage and OMS pod surface thermocouples as well as the unique damage patterns on the left hand side OMS pod and vertical tail. The source of these leeside flow disturbances was evaluated by addressing increased venting as well as the development of various holes through the wing.

As a final investigation thrust, the potential for orbiter lower surface wing deformation was evaluated. This ultimately provided the best match as the source of the changing trends in the aerodynamic moments. Finally, the results of the test and analysis were combined into a potential damage progression path that can reproduce the extracted off-nominal aerodynamics from EI to just prior to LOS.

4.1.4 Approach / Processes – Methodology to Achieve Objectives

The STS-107 Aerodynamic Reconstruction process is illustrated by the flow chart depicted in Figure 4.1-4. The process consisted of two primary phases: Step 1) an Aerodynamic Extraction which then served as the basis for Step 2) Aerodynamic Damage Assessment.

4.1.4.1 Aerodynamic Extraction

Aerodynamic (aero) increments were extracted from flight data to establish the off-nominal aero moments due to damage using an iterative approach. Evaluation tools were developed to extract the un-modeled yawing, rolling and pitching moment increments as well as the normal, axial and side force increments using a three-step process. First, flight parameters including Mach number, angle–of-attack and sideslip, and control surface settings, were used to extract a predicted set of nominal forces and moments using the Orbiter OADB. Second, flight measured acceleration and rate data, estimated orbiter mass properties and estimated atmospheric data were used to extract flight aerodynamic forces and moments based on the standard aircraft equations of motion. Then, the difference between the two sets of data (flight extracted minus nominal Orbiter OADB) produced the un-modeled (off-nominal) delta aerodynamic forces and moments experienced in flight. Figure 4.1-5 provides an outline of this process.

These force and moment increments were then provided to the GN&C flight trajectory simulation for evaluation. Simulations of the STS-107 entry trajectory were performed with and without the off-nominal delta aerodynamic increments and provided trajectory data and flight control system responses. A comparison of the STS-107 flight sensor data against the simulated trajectory predictions with the off-nominal aero increments was used to assess the adequacy of the increments. While the technique employed essentially forces a match between flight and simulation, the distribution of the off-nominal flight response between aerodynamics, atmospheric conditions, model uncertainty, etc. was critical to establishing the final aero increment magnitudes to be attributed solely to damage. After multiple iterations of this process, a good match was produced by taking into account all of these aspects of the flight

reconstruction. The resulting aero increments were considered defined and ready to serve as a measure for the damage assessment evaluation.

4.1.4.2 Damage Assessment

Assessing the change in aerodynamics due to damage required a definition of modified configurations such as those shown in Figure 4.1-6 & Figure 4.1-7, for test and analysis, consistent with a postulated damage scenario. As previously mentioned in the chronology of the investigation, the range and specifics of the postulated damage varied as the investigation matured. For example, WLE damage was initially modeled by removal of entire RCC panels. As new data and findings emerged, the postulated damage configurations were modified (e.g. the follow on test of missing partial WLE RCC panels) to be more consistent with the latest available information and the rapid pace of the investigation. It should be noted that evaluation of the damaged configurations was approached as an integrated aerodynamic and aerothermodynamic effort. This combined aerodynamic/aerothermal approach was a fundamental part of the process throughout the investigation. The test and analysis results were balanced against both of these aspects in judging their merits in supporting any particular damage scenario. The aerothermal results are detailed in Section 5.2.

Also essential to the assessment were reliable hypersonic test facilities and analysis capabilities. All of the wind tunnel tests conducted in support of this investigation were completed in either of two LaRC hypersonic wind tunnel test facilities, the 20-Inch Mach 6 Air Tunnel or the 20-Inch Mach 6 CF4 Tunnel. The vast majority of the testing was ultimately conducted in the CF4 facility because of the established capability of this facility to reproduce high Mach number (13-18) orbiter aerodynamic characteristics by accurately simulating the relevant flow field gas dynamics (see Sections 4.3.1 and 5.2.3.1 for more details). Complementing the WT testing was the application of various CFD analysis codes. These ranged from basic Newtonian estimation routines (SNEWT-JSC & CBAERO-ARC) to inviscid Euler calculations (CART3D-JSC & FELISA-LaRC) as well as several high-fidelity viscous Navier-Stokes simulations (Overflow-JSC, LAURA-LaRC, GASP-ARC & USA-Boeing). CFD analyses results were provided for both wind tunnel and flight conditions (including high temperature gas chemistry effects). The CFD analysis tools were employed in various ways to support damage assessment and evaluation. First, Newtonian and inviscid methods were used as a rapid screening tool for postulated damage scenarios. The CFD flow fields generated for the various damaged configurations were reviewed to gain a more complete understanding of the resulting aerodynamic deltas. Additionally, the CFD analysis was used to evaluate Mach number and angle-of-attack sensitivities as well as WT-to-flight extrapolation. Finally, CFD analysis was employed heavily to interrogate the contribution of leeside flow interactions and any resulting contribution to the delta aerodynamic patterns. These test and analysis capabilities and results are covered in detail in Section 4.3.

For each damage scenario, wind tunnel test models and CFD analysis grids were modified to represent a damaged configuration. The method to establish the change in aerodynamics utilized a baseline run for comparison. First, the nominal or clean configuration aerodynamic baseline was established for each wind tunnel run or CFD analysis. Then the model/grid geometry was modified to represent the damaged configuration under consideration. The test or analysis was repeated with this modified model and the delta aerodynamic force (normal, axial & side) and moments (roll, pitch & yaw) were determined as the difference (Delta = damaged – baseline). These assessment results were collected for the varied set of damaged configurations being considered, including lower surface wing gouges, raised MLG door forward edge, MLG door removed / open wheel well cavity, MLG and door deployed, missing WLE RCC panels (2-12 individually and in combination), partial RCC panels missing (lower half to apex), T-Seal slot, holes through wing with upper and/or lower carrier panel missing, wing deformation including lower surface depressions, as well as vertical tail and leeside interaction – see WT Test matrix (Aerodynamic Appendices, Section 4.7.3) and CFD Analysis case matrix (Table 4.3-6).

All the test and analysis results were then used in developing a match between the extracted off nominal aerodynamics and the damage assessment delta aerodynamics as well as the external aerodynamic heating patterns. The ultimate goal was to correlate these results with vehicle damage consistent with the final working scenario that progressed from an initial damage stage at EI to a considerably more aerodynamically significant damaged configuration just prior to LOS.

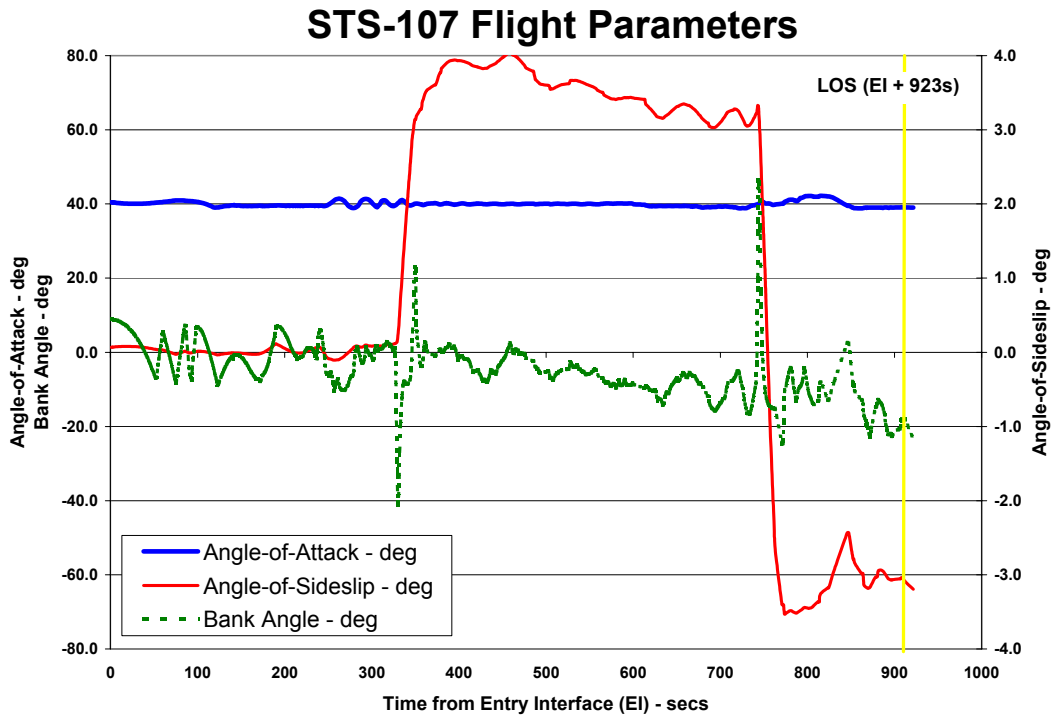

Figure 4.1-1 STS-107 Angle-of-Attack, Sideslip & Bank

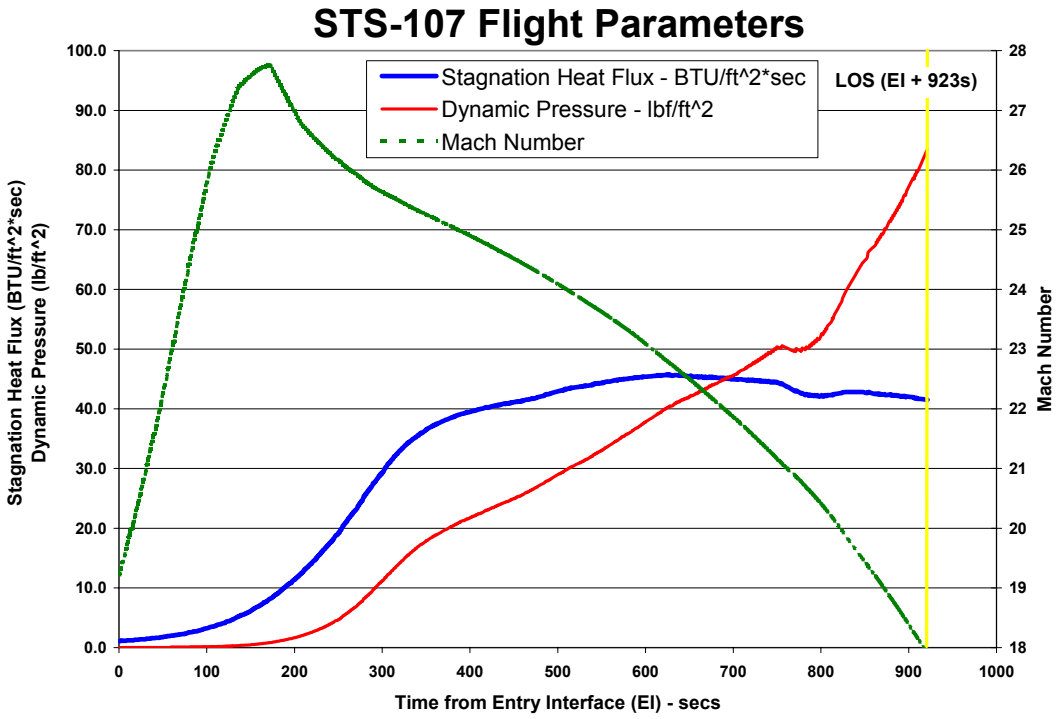

Figure 4.1-2 Mach No., Dynamic Pressure & Stagnation Heat Flux

8

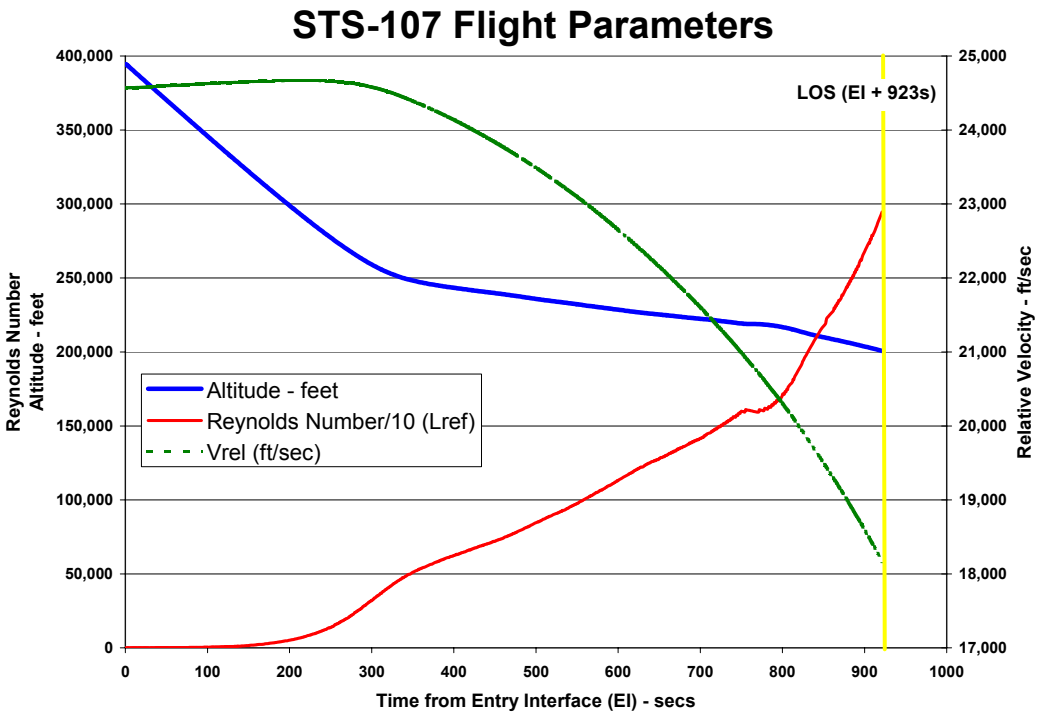

Figure 4.1-3 Altitude, Velocity & Reynolds No.

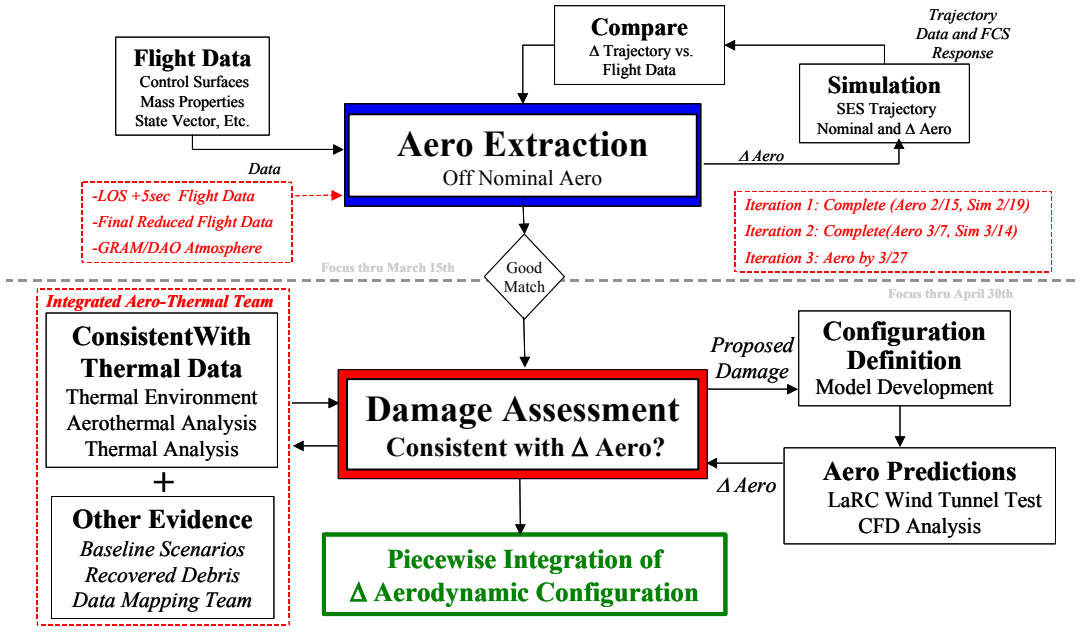

Figure 4.1-4 Aerodynamic Reconstruction Process

1) Orbiter aerodynamic database defines nominal aerodynamics

Input Flight Data:
Control Surfaces (δa, δe, δr, δbf) & RCS Jets
Air Data (Mach, Alpha, Beta, Qbar, Vinf)
Angular Rates (P,Q,R)
Mass Properties

Orbiter Aero Data Book Table Lookup

Nominal Aerodynamic F&M Coefficients:
C_N – Normal C_Y – Side
C_A – Axial C_l – Roll
C_m – Pitch C_n – Yaw

2) Aerodynamic coefficients extracted from flight data

Input Flight Data:
Accelerations (Ax, Ay, Az)
Angular Rates (P,Q,R)
Atmosphere (winds, Qbar)
Mass Properties

Aircraft Equations of Motion

Flight Aerodynamic F&M Coefficients:
C_N – Normal C_Y – Side
C_A – Axial C_l – Roll
C_m – Pitch C_n – Yaw

3) Flight extracted - Nominal Database = Unmodeled (delta aero) F&Ms

$$\Delta Cn_{Reconstructed} = Cn_{Flight\ Extracted} - Cn_{Aero\ Database}$$

Figure 4.1-5 Aerodynamic Extraction Methodology

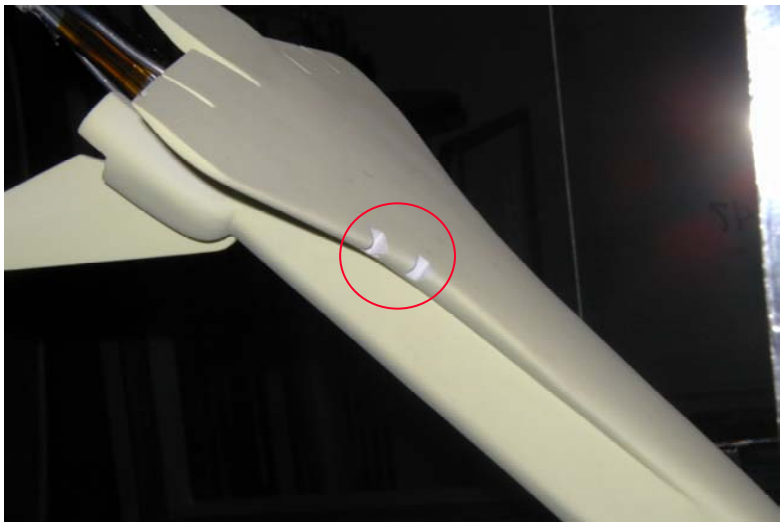

Figure 4.1-6 WT Model with WLE RCC panels (6 & 9) removed

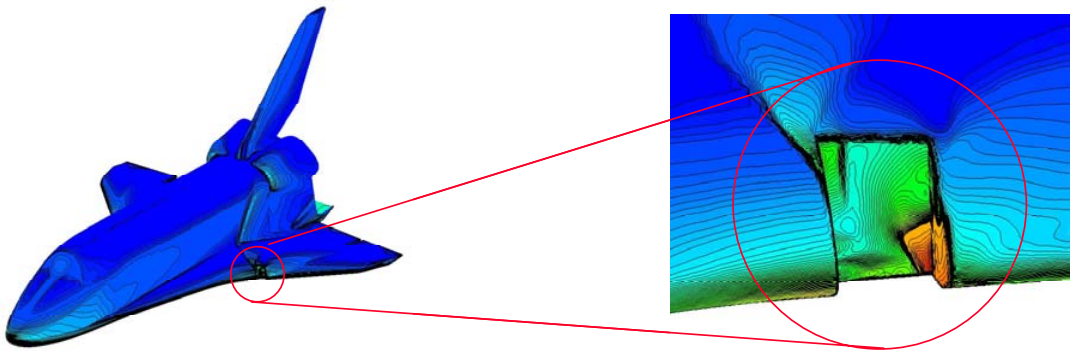

Figure 4.1-7 FELISA Grid with WLE RCC panel 9 removed

4.2 Aerodynamic Extraction

Aerodynamic (aero) increments were extracted from flight data to establish the off-nominal aero moments due to damage using an iterative approach. This section addresses the details of the atmospheric model, high altitude winds and the aerodynamic extraction process and results.

4.2.1 Atmospheric Model

An accurate simulation of the STS-107 entry depended in part on a reliable model of the environment through which the vehicle flew. By using the flight data from EI-5 to LOS and the wind information provided by experts from the Data Assimilation Office (DAO) and the Marshall Space Flight Center (MSFC), atmospheric parameters such as density, temperature, and pressure at a set of altitude reference points were derived with a process slightly modified from that used previously for post-flight analysis. Results compared favorably with the independent assessment of corresponding parameters from DAO/MSFC and contributed greatly to the fidelity of the resulting match between the integrated simulation output and the down listed flight data.

The original atmospheric reconstruction process used as its inputs a pre-defined set of 22 down listed measurements from the Orbiter Data Reduction Complex (ODRC), including such information as vehicle position and orientation, rates and accelerations, and control surface deflections, over the time period for which the atmospheric data was to be derived. This information along with data from the Orbiter OADB was used in an iterative process to generate an estimate of the atmospheric density, pressure, and temperature of the environment. This technique was then revised to make use of higher fidelity data compiled as a part of this investigation, as well as data that was not available when the code was originally developed.

Wind data from DAO/MSFC, for example, was incorporated into the determination of the values for angle of attack, sideslip, and true airspeed. As shown in Figure 4.2-1, the angle of attack (α) and sideslip (β), are defined by the angles the body-fixed frame must be rotated around the - Y_b and Z_b axes, respectively, to align the X_b axis along the velocity vector. At high altitudes where there is no sensed air data available, a navigation-based angle of attack and sideslip are determined on-board relative to the Earth-fixed velocity provided by the inertial measurement unit (IMU). However, when the vehicle is flying through an atmosphere that is moving relative to the ground, the velocity of the vehicle relative to the Earth differs from that relative to the air. Thus, the true air speed (TAS) is comprised by the difference in the Earth-fixed velocity and the wind velocity, and it is this vector into which the body axis must be rotated to determine the environment angle of attack and sideslip.

Since the process resulted in rather noisy output at very high altitudes and there was no flight data available below 200,000 ft, the Global Reference Atmosphere Model (GRAM) data was used in those regions for the final data file delivery. In the lower altitude region, the GRAM data was used up to 190,000 ft, and a spline fit was used to smoothly connect the GRAM and reconstructed data in the intervening

10,000 ft region. At very high altitudes, the extremely low densities were not reliably reconstructed by the process, and the resulting temperature and pressure profiles were quite noisy. The GRAM data was identified as a reasonable approximation to this noisy data, and was substituted for reconstructed atmospheric data above 320,000 ft. Thus a smooth and continuous set of data representing the entire atmosphere was created for use in subsequent simulations. The final set of density, pressure, and temperature profiles appear as illustrated in Figure 4.2-2.

4.2.2 GSFC/DAO Upper Atmospheric Wind Model

In the course of the investigation, it became apparent that a more complete understanding of the atmosphere and in particular a more precise estimation of the high altitude winds and density encountered during entry was critical to the reconstruction of the flight and the associated aerodynamic increments. Since a direct and independent measurement of the density and winds is not available from the onboard data system an effort was initiated to use meteorological resources to generate an atmosphere along the orbiter trajectory for the time of entry.

Generation of a meteorologically derived atmosphere had not been done since very early in the space shuttle program and therefore there was a development effort involving many resources in the meteorological community. The DAO at the Goddard Space Flight Center (GSFC) was the principal organization tasked to provide the atmosphere. The DAO uses space and ground based resources on a regular basis to assimilate measured data for atmospheric research. In order to better support the requirement for high altitude (> 200,000 ft) meteorological data, the DAO additionally assimilated data from the Sounding of the Atmosphere using Broadband Emission Radiometry (SABER) instrument on the Thermosphere Ionosphere Mesosphere Energetics and Dynamics (TIMED) satellite. Through the assimilation process and several iterations, the DAO was eventually able to generate atmosphere data up to an altitude of approximately 250,000 ft., Figure 4.2-3to Figure 4.2-5.

The DAO atmosphere was then faired with the GRAM February atmosphere by the MSFC. Details of the DAO assimilation and fairing methodology can be found in the STS-107 Natural Environments Document (Aerodynamic Reference 4.6 2).

4.2.3 Aerodynamic Increment Extraction Results

Three aerodynamic predictor tools were modified or developed to extract the STS-107 aerodynamic increments. These tools provided a source for rapid comparison between Orbiter OADB aero and flight predicted aero derived from the observed motion of the vehicle. Two existing tools had been developed as part of the experimental X-38 and X-40 flight test programs. Application of these tools to STS-107 was validated by processing flight data and simulator results from two previous Columbia flights (STS-109 & STS-73). A third tool was developed for the analysis using existing Orbiter OADB look-up routines to provide further substantiation. Also, hand calculations completed the analysis and served as a verification of results. Finally, an independent evaluation focused on the time frame from EI to EI+ 600 sec also confirmed these results.

As input flight data was analyzed and refined by the Integrated Entry Environment (IEE) team and as new atmospheric data became available, the aerodynamic increment model went through four revisions to improve accuracy by accounting for all relevant aspects of the flight reconstruction. Wind correction adjustments made to angle-of-attack and sideslip using the final DAO atmosphere greatly influenced the aerodynamic increment results in the fourth and final revision (Figure 4.2-6 thru Figure 4.2-10) (reducing the magnitude of the rolling and yawing moments by approximately 50%). Various uncertainties were also assessed to characterize the relative magnitude of the off-nominal aero forces and moments against other potential asymmetric aerodynamic contributions. These design level asymmetries are also depicted in the figures (note labels). The aerodynamic increment model reference table (Figure 4.2-14) was provided to the GN&C community for inclusion in flight simulations.

Evaluation of the resulting increments indicates that off-nominal aerodynamics were not apparent during the early portion of the STS-107 flight. The first clear indication of off-nominal yawing and rolling moments does not occur until EI + 515 and EI + 521 seconds, respectively. A corresponding small deviation in side

force can also be correlated to this time. The delta pitching moment is first observed in an off-nominal trend much later in the flight, around EI + 836 sec. Further review of data shows that substantial deviation in all three moments does not begin until around EI + 850 sec, which then continues through LOS. For clarity, an expanded section showing the substantial deviation in all three moments late in flight are provided in Figure 4.2-11 through Figure 4.2-13.

As discussed in the derived atmosphere model section, at high altitudes where there is no sensed air data available, the extraction technique must utilize the orbiter on board (normal) acceleration as an input to estimate the atmospheric density profile. As applied, this produces a normal force increment of zero. While necessary to accurately define the density, the zero normal force increment result is not considered accurate. Accounting for limitations presented by the data available, extracting accurate side and axial force increments were considered higher priority and the normal force extraction was thus sacrificed in the process.

Furthermore, it should be noted that the extracted force increments due to damage are a very small percentage (1-2%) of the expected total forces. This is consistent with the small off-nominal moments seen for the majority of the entry flight time. Considering the accuracy of the data available to extract these force increments, it was determined that the forces would not be considered a good measures of the damage induced aerodynamics. Therefore, the damage assessment did not attempt to match the aerodynamic force increments.

On the other hand, the extracted moments provide direct indication of off-nominal asymmetric aerodynamics. In flight the orbiter flight control system is continuously maintaining a trimmed (or zero moment) condition. Any small (non-zero) offset from this trimmed flight condition will manifest itself in the derived off-nominal moment increments. These delta aerodynamic moment increments are thus clear indicators of off-nominal aero and were the primary focus of the damage assessment efforts.

4.2.4 Correlation to Working Scenario

A thorough review of the final increments indicates that initially the damage to Columbia's left wing was too small to produce significant aero effects. The extracted moments early in entry (prior to EI + 500 sec) tend to correlate well with past OV-102 flight results from STS-109 and STS-73 (Figure 4.2-15 to Figure 4.2-17). Combined with the level of uncertainties accounted for in this flight regime, the near zero increments are consistent with no significant damage. As the flight progresses, a clear break in the previous flight trends becomes obvious in the rolling and yawing moment increments at a point after EI + 500 sec. The pitching moment increment, however trends well with previous flights (particularly STS-73) until even later in entry and can only be considered truly off-nominal sometime after EI + 800 sec.

To aid in the reconstruction effort and present correlation between vehicle reaction, debris sightings and onboard measurements, the increments were presented with these events labeled (Figure 4.4-20 to Figure 4.4-23). The correlation with this other available data provides the basis for defining the initial indication of off-nominal aerodynamics around EI+515 sec. While relatively small, the initial rolling and yawing moment increments are both negative. In this flight regime the only possible source of aerodynamic asymmetries are either due to a Yc.g. offset (i.e. other than on the centerline), a very small bent airframe term or the high altitude winds. Asymmetric boundary layer transition (ABLT) has been seen on a number of orbiter entry flights, but never this early in the entry profile, (in fact never prior to the end of STS-107 flight near Mach 18). Additionally, this (-roll/-yaw) pattern is inconsistent with previous asymmetric boundary layer transition observations which have always produced a +roll and -yaw for a left side ABLT. Since winds and c.g. offset have been accounted for and ABLT ruled out, the damage to Columbia's left wing is the only remaining source of the off-nominal aerodynamics.

A distinct change in the aerodynamic increment trend occurs at EI + 602 sec corresponding precisely with Debris Event No. 5 as well as the onset of the slow but steady aileron trim change response by Columbia's flight control system. At this point in flight, the rolling moment increment trend changes from increasing negative to increasing positive. It is postulated that this corresponds to an abrupt configuration change as the left wing damage progressed (this will be elaborated on in Section 4.5). After this point, both rolling (+) and yawing moment (-) trends increase in what is essentially a linear fashion until EI + 836 sec. It should be noted that up to this point in flight the aerodynamic increments are still relatively small (less that than

the worst case asymmetric aerodynamic design levels). The orbiter flight control system has continued to easily account for this slight change in the vehicles aerodynamics and trimmed flight is maintained. At EI + 766 sec, the Orbiter completes the initial roll reversal with no apparent impact from the damaged left wing. However, around EI + 836 sec the aileron trim begins a sharp increase and the rate of rolling and yawing moment increment growth abruptly increases. These extracted moments eventually exceed asymmetric aerodynamic design levels as defined by the Orbiter OADB ABLT after EI + 877 sec.

Between EI + 920 and 928 sec (LOS + 5 sec) the off-nominal rolling and yawing moments dramatically increase in magnitude to levels exceeding 6 times the asymmetric aerodynamic design levels. Flight control responds by maximizing the aileron trim rate and eventually fires all 4 RCS yaw jets continuously to maintain trimmed flight. This rapid increase in the off nominal moments near the end of flight effectively saturates Columbia's flight control system trim capability and eventually led to loss of control and vehicle breakup. For further explanation of the vehicle response to the off nominal aerodynamics encountered see the STS-107 Integrated Entry Environment Team Final Report, Aerodynamic Reference 3.

Based on these observations, the final aero increments indicate that initial damage did not produce significant changes in the nominal aerodynamic properties of the vehicle early in flight (prior to EI + 515 sec). Therefore, the aerodynamic extraction cannot be used to conclude damage to Columbia's wing existed at EI. These increments should primarily be used for flight reconstruction and as a screening mechanism for wind tunnel and CFD damage progression assessments in correlation with the aerothermodynamic evaluations and the other available data.

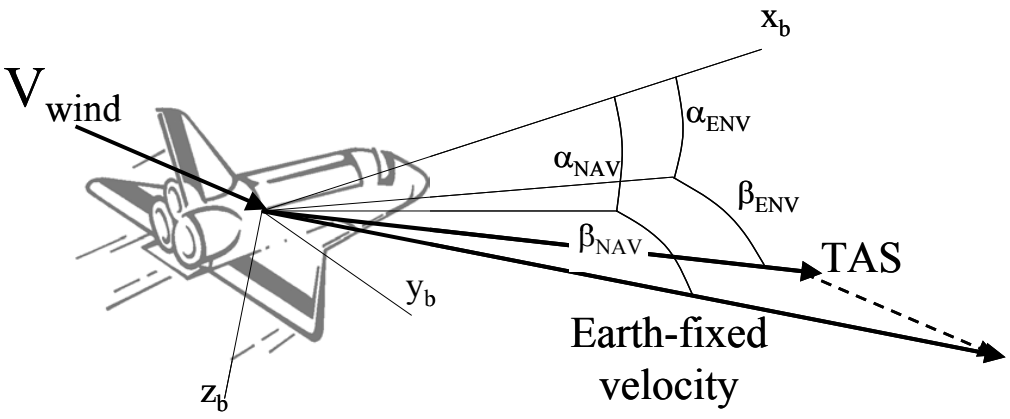

Figure 4.2-1 Determination of Angle-of-Attack & Sideslip

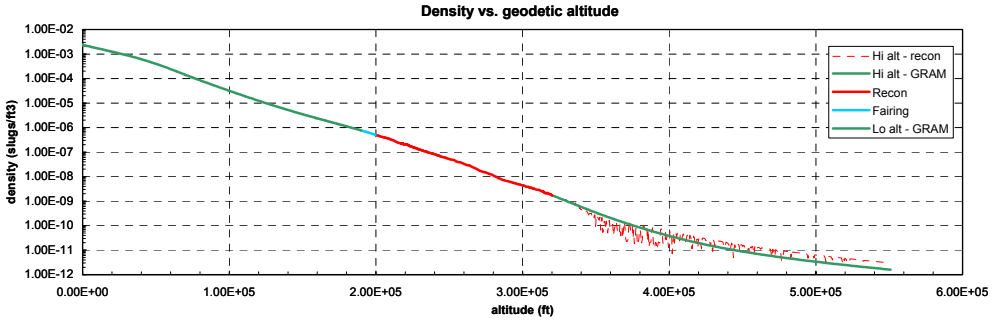

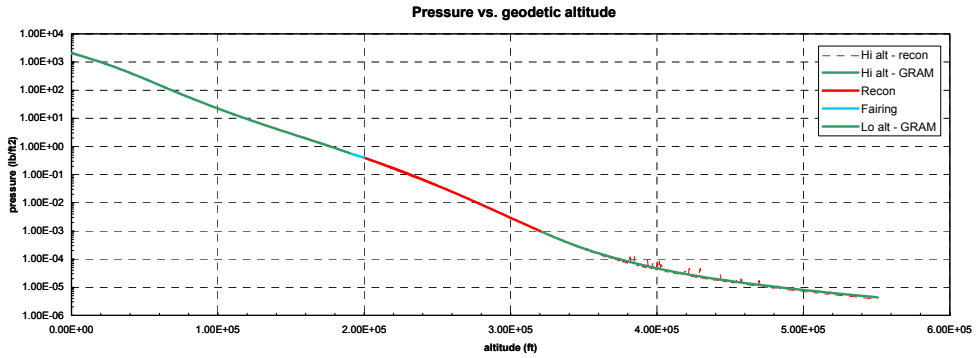

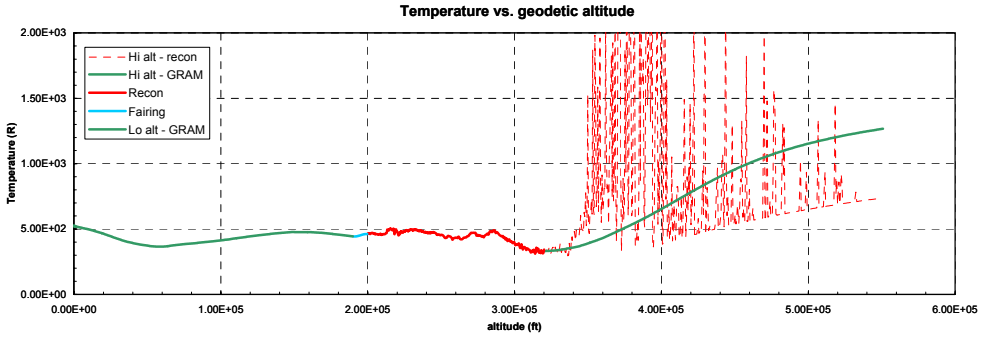

Figure 4.2-2 Reconstructed Atmospheric Density, Pressure & Temperature

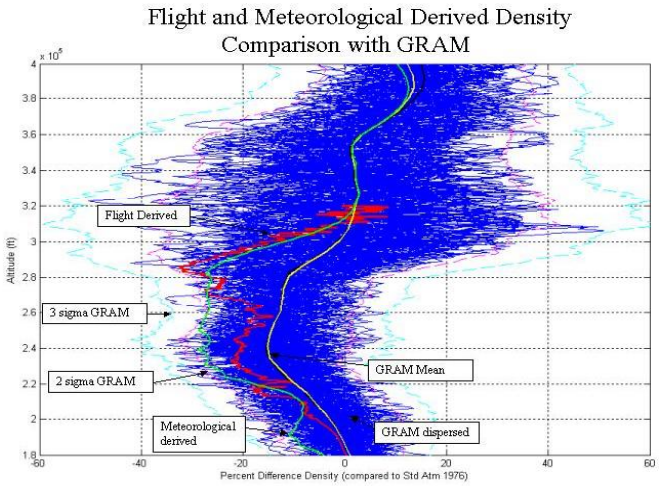

Figure 4.2-3 Flight & Meteorological Derived Density

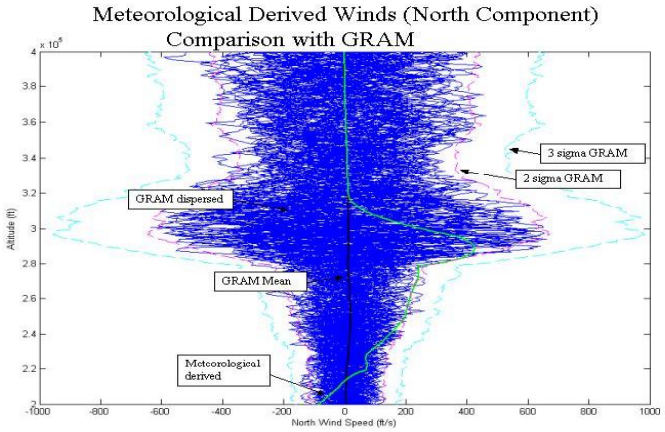

Figure 4.2-4 Meteorological Derived Winds (North Component)

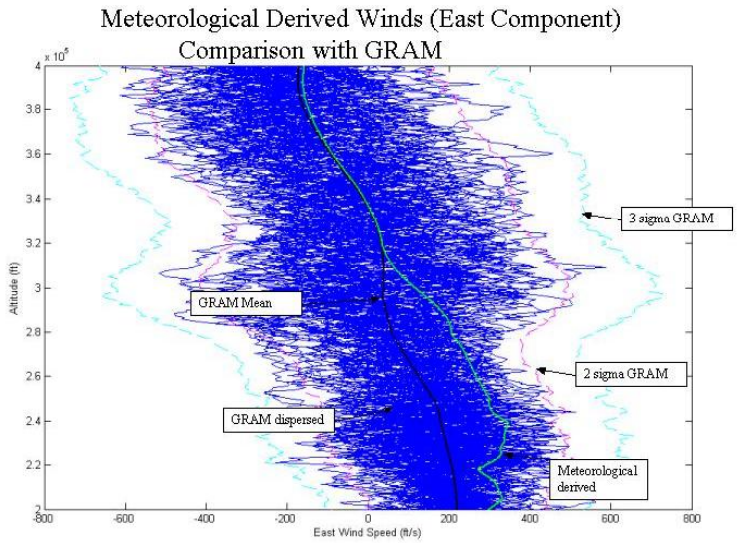

Figure 4.2-5 Meteorological Derived Winds (East Comp.)

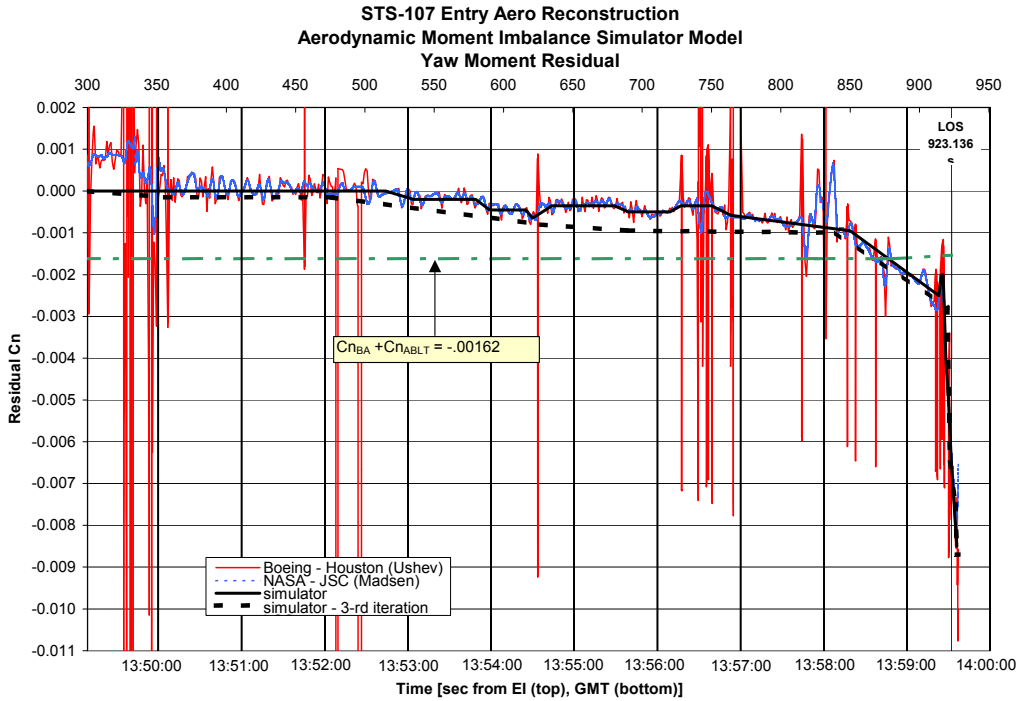

Figure 4.2-6 Delta Yawing Moment Coefficient

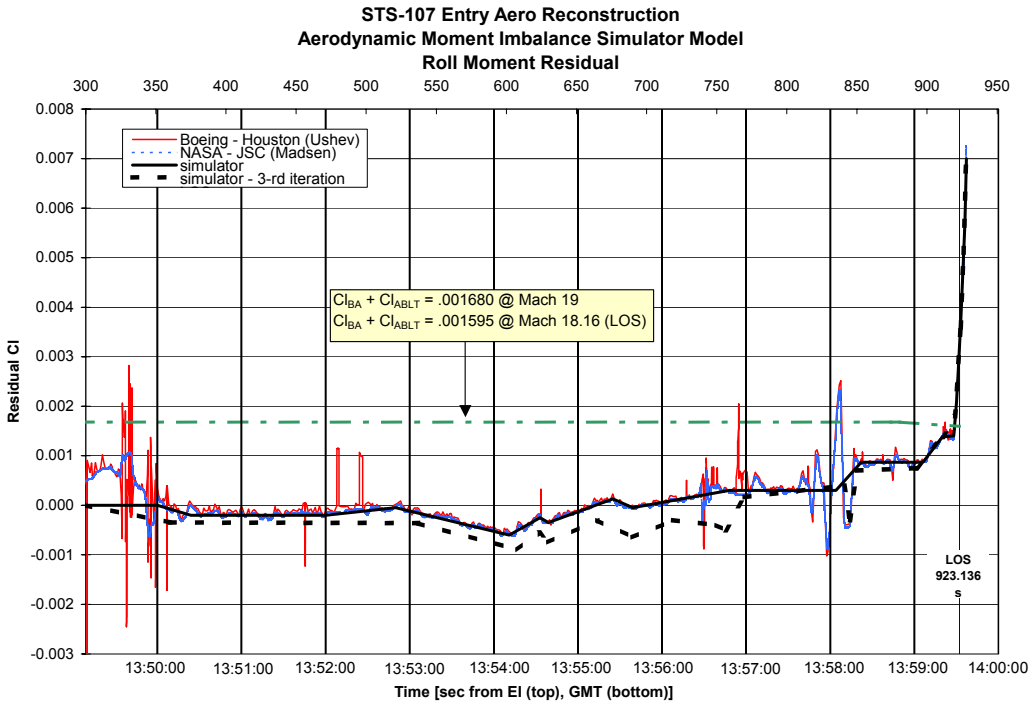

Figure 4.2-7 Delta Rolling Moment Coefficient

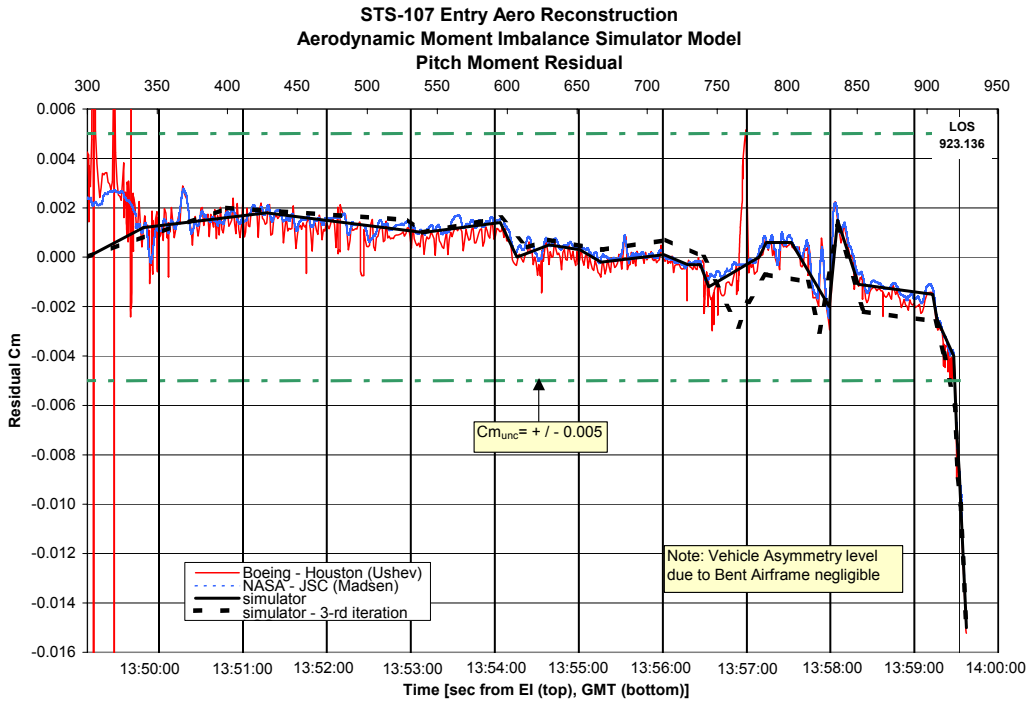

Figure 4.2-8 Delta Pitching Moment Coefficient

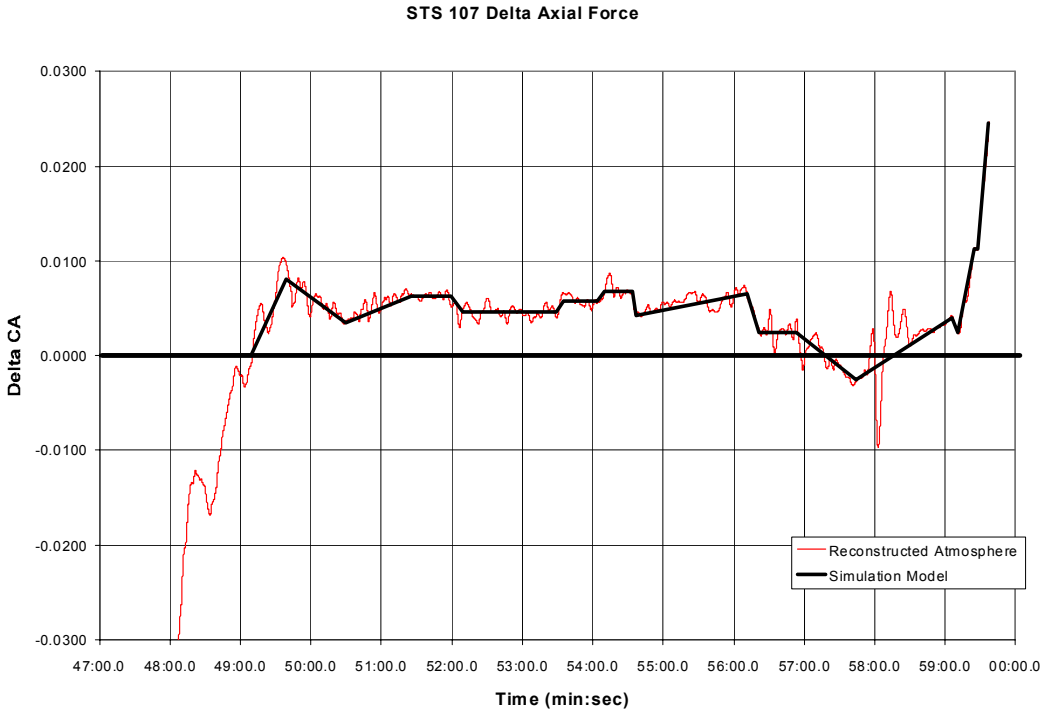

Figure 4.2-9 Delta Axial Force Coefficient

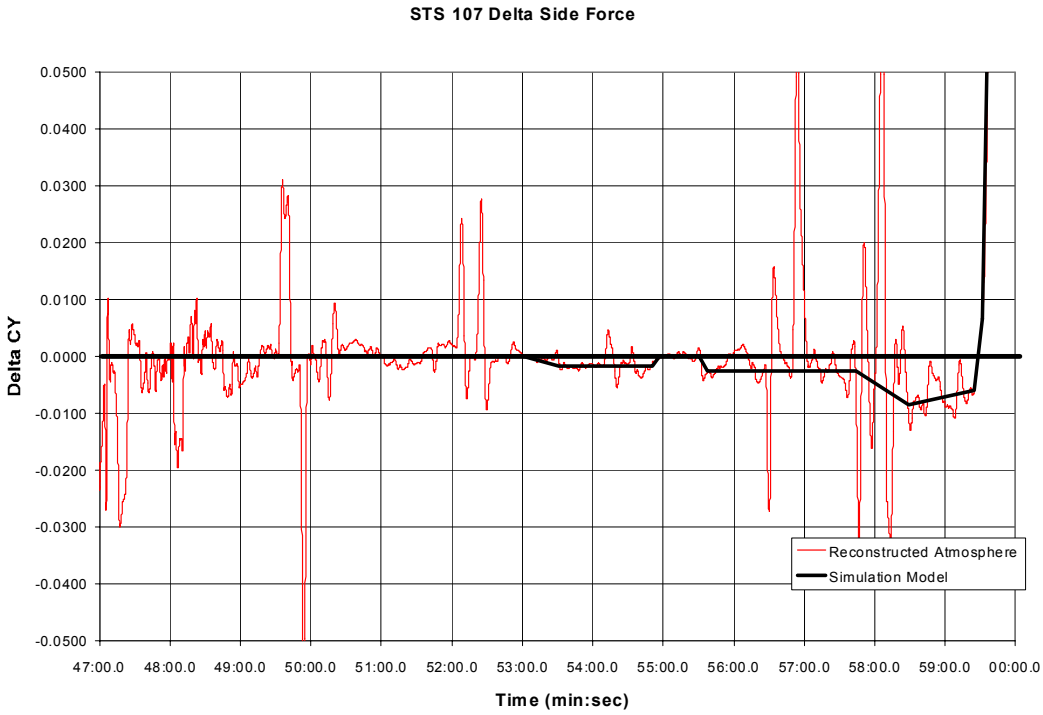

Figure 4.2-10 Delta Side Force Coefficient

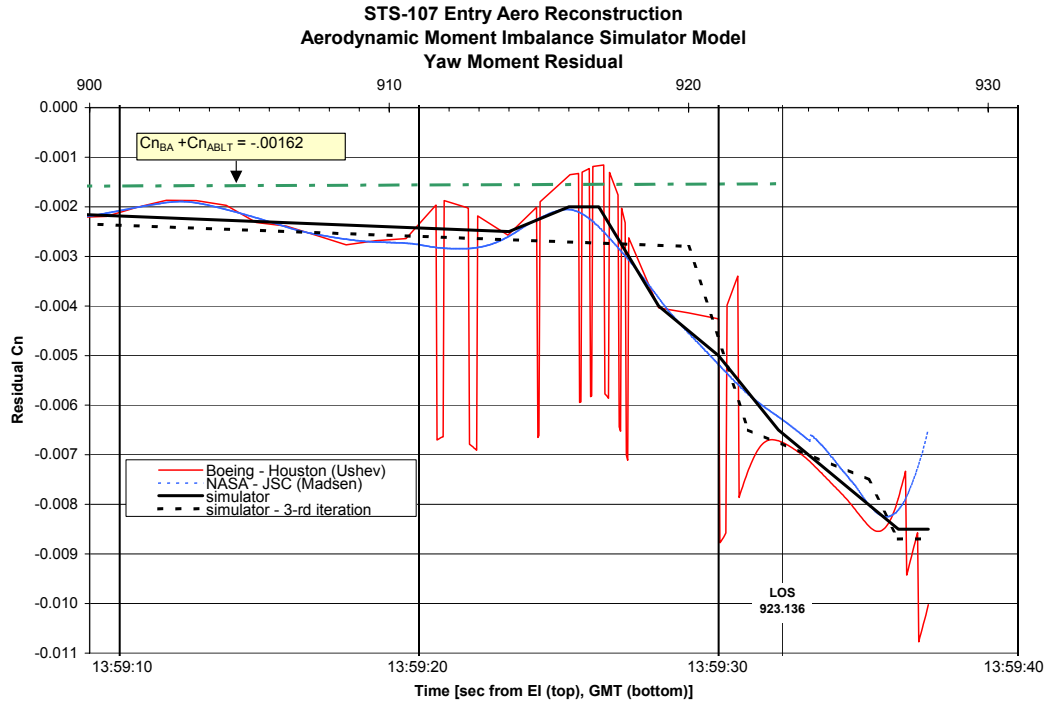

Figure 4.2-11 Delta Yawing Moment Coefficient (just prior to LOS)

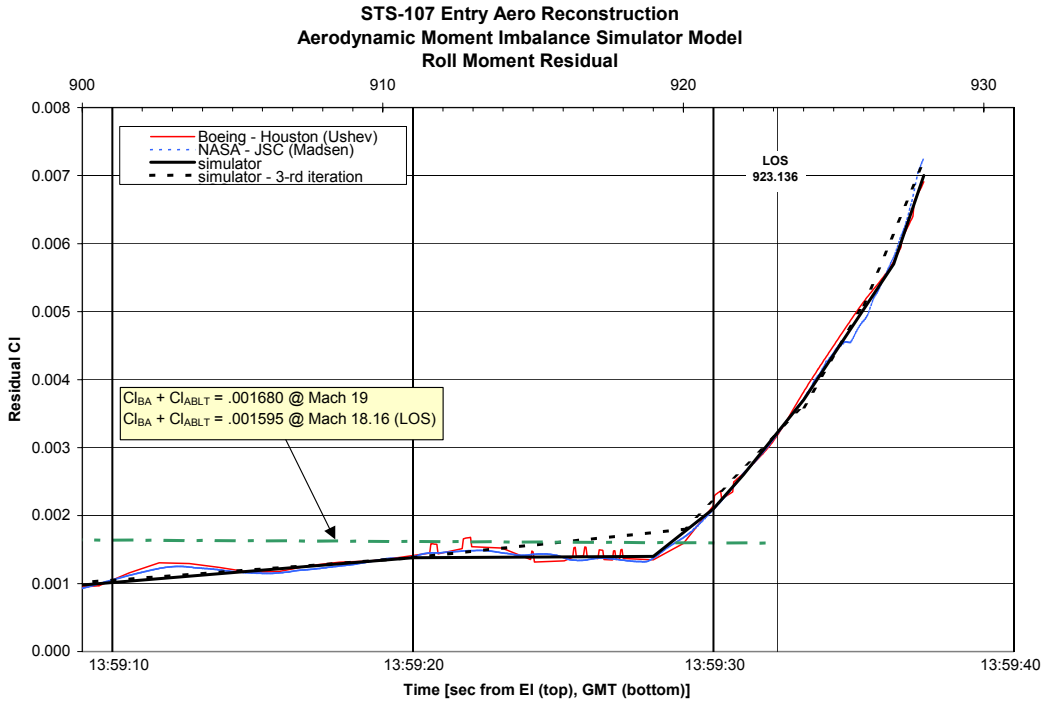

Figure 4.2-12 Delta Rolling Moment Coefficient (just prior to LOS)

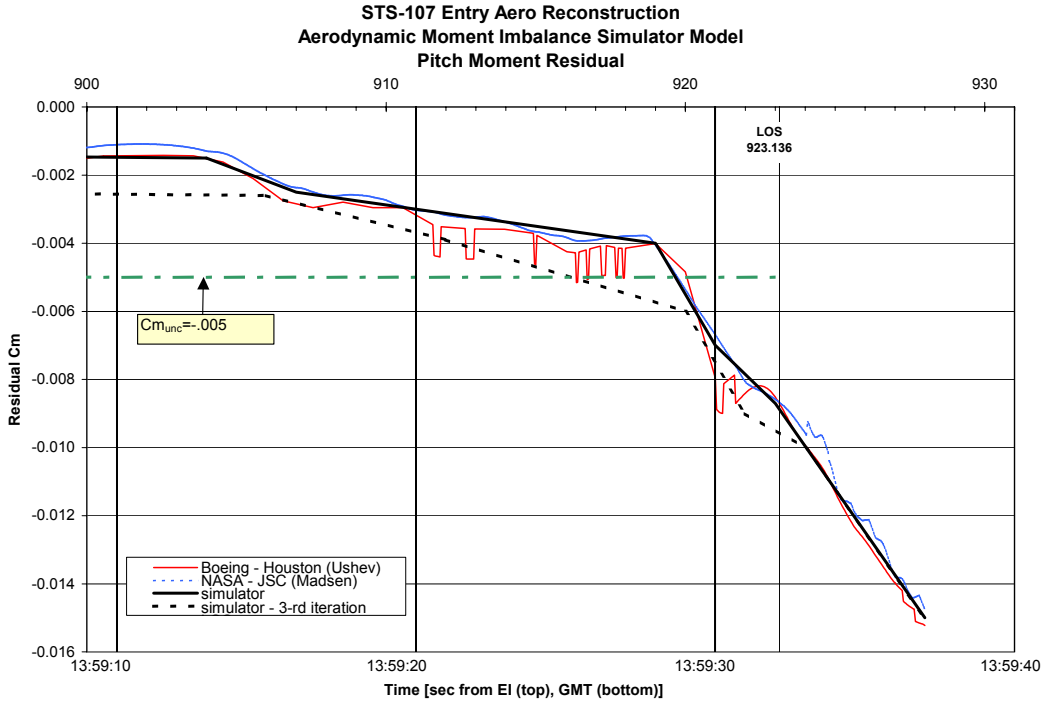

Figure 4.2-13 Delta Pitching Moment Coefficient (just prior to LOS)

STS-107 Simulator Moment Imbalance Model – Reference Table

(time is seconds from EI)

Pitch Moment (Cm) Imbalance

Time	Cm
0	0.00000
300	0.00000
340	0.00120
428	0.00180
540	0.00100
595	0.00140
607	0.00000
630	0.00050
652	0.00030
667	-0.00020
712	0.00010
729	-0.00030
738	-0.00030
744	-0.00120
780	0.00000
785	0.00060
803	0.00060
830	-0.00200
836	0.00150
851	-0.00110
904	-0.00150
907	-0.00250
919	-0.00400
921	-0.00700
923	-0.00870
928	-0.01500

Yaw Moment (Cn) Imbalance

Time	Cn
0	0.00000
300	0.00000
356	0.00000
515	0.00000
535	-0.00020
580	-0.00020
590	-0.00045
616	-0.00045
621	-0.00065
635	-0.00035
680	-0.00035
690	-0.00050
720	-0.00050
728	-0.00035
750	-0.00035
764	-0.00058
850	-0.00095
914	-0.00250
916	-0.00200
917	-0.00200
919	-0.00400
921	-0.00500
923	-0.00650
927	-0.00850
928	-0.00850

Roll Moment (Cl) Imbalance

Time	Cl
0	0.00000
351	0.00000
375	-0.00020
471	-0.00020
521	-0.00005
602	-0.00060
624	-0.00025
630	-0.00035
676	0.00013
690	-0.00005
759	0.00030
835	0.00030
853	0.00087
897	0.00087
911	0.00138
919	0.00140
921	0.00210
922	0.00260
924	0.00370
927	0.00570
928	0.00700

Axial Force (CA) Imbalance

Time	CA
0	0.00000
360	0.00000
368	0.00100
440	0.00100
445	0.00050
495	0.00050
510	0.00120
597	0.00300
606	0.00490
632	0.00200
742	0.00200
764	0.00400
769	0.00250
892	0.00480
897	0.00580
902	0.00450
916	0.01250
919	0.01250
928	0.02450

Side Force (CY) Imbalance

Time	CY
0	0.00000
349	0.00000
354	-0.00070
695	-0.00160
719	-0.00190
730	-0.00050
740	-0.00050
745	-0.00120
860	-0.00120
862	0.00000
875	0.00000
880	-0.00200
895	0.00000
924	-0.00400
928	-0.02222

Figure 4.2-14 STS-107 Delta Aero Increment Model

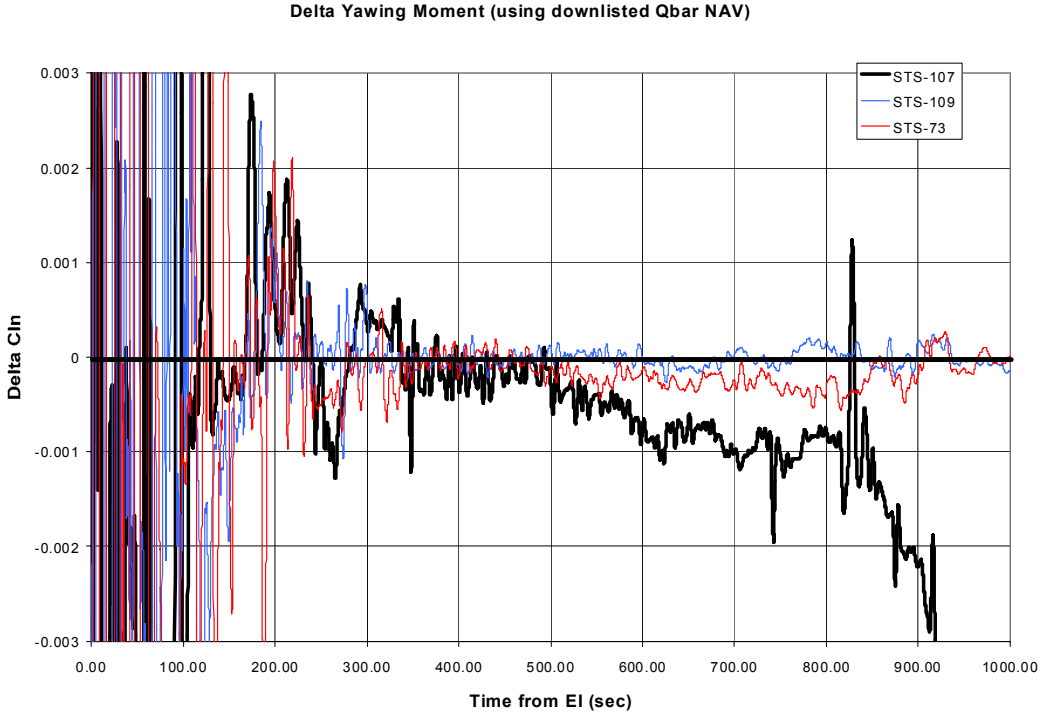

Figure 4.2-15 Delta Yawing Moment (STS-107, 109 & 73)

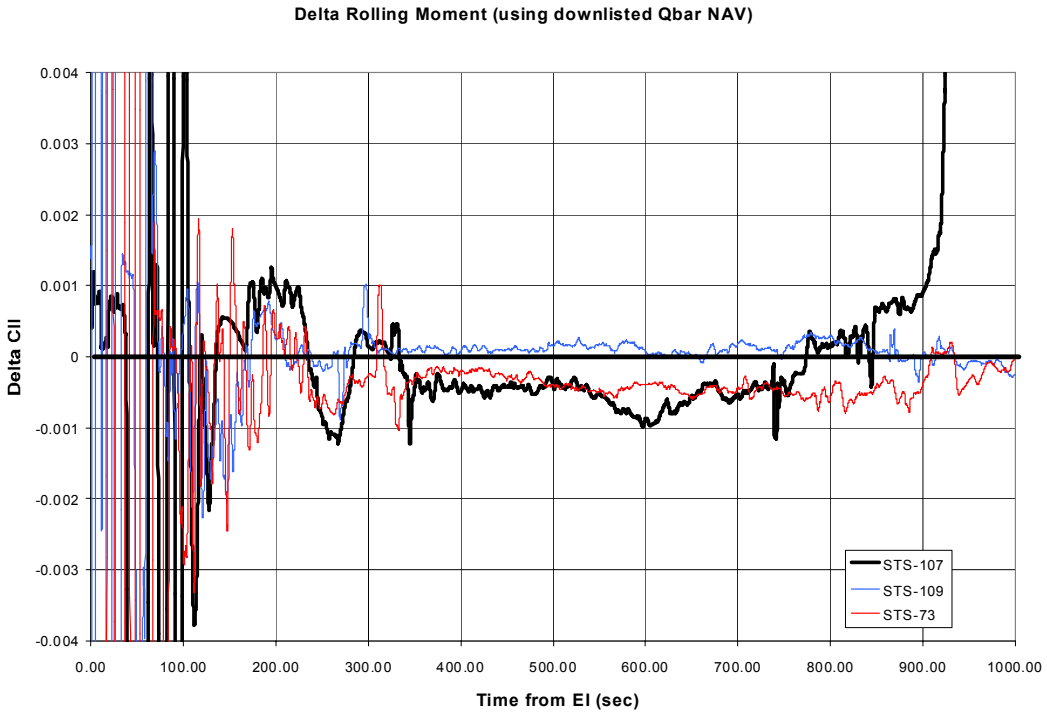

Figure 4.2-16 Delta Rolling Moment (STS-107, 109 & 73)

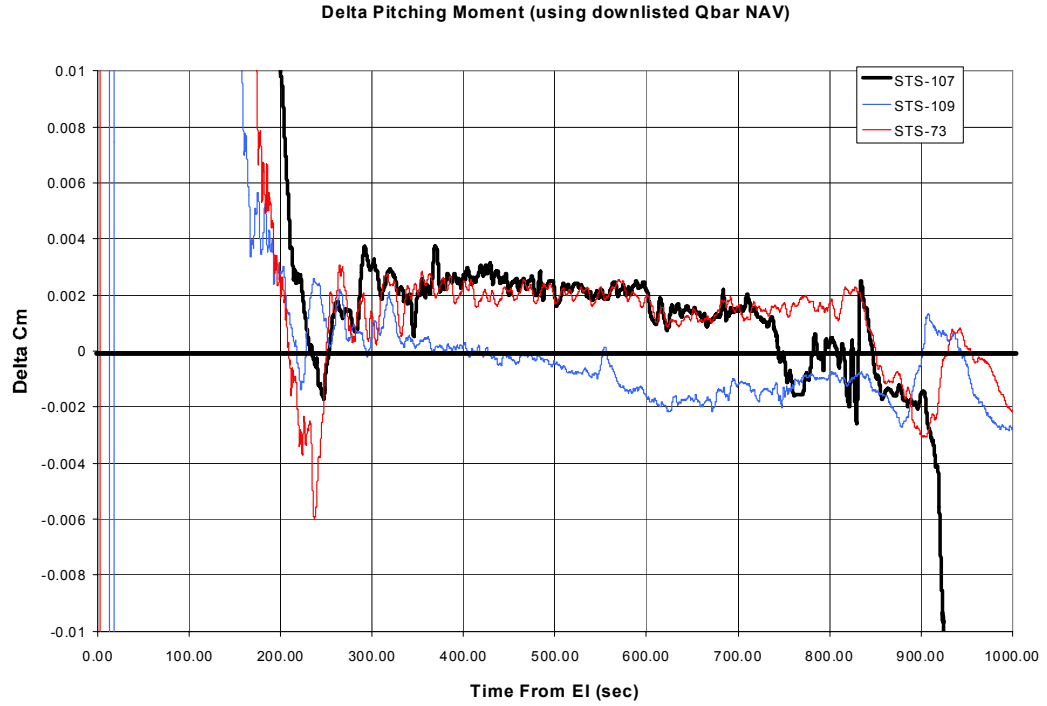

Figure 4.2-17 Delta Pitching Moment (STS-107, 109 & 73)

4.3 Damage Assessment Aero

4.3.1 Wind Tunnel Testing

Aerodynamic tests in support of the Columbia accident investigation were conducted in two hypersonic wind tunnels at the NASA Langley Research Center. The primary purpose of these tests was to measure the forces and moments generated by a variety of outer mold line alterations (damage scenarios). Simultaneously acquired global heat transfer mappings were obtained for a majority of the configurations tested. Schlieren photography visualizing the shock structures in the flow was utilized when possible. The damage scenarios evaluated included asymmetric boundary layer transition, gouges in the windward surface acreage thermal protection system tiles, wing leading edge damage (partially and fully missing RCC panels), holes through the wing from the windward surface to the leeside, deformation of the wing windward surface, and main landing gear door and/or gear deployment. The aerodynamic data were compared to the magnitudes and directions observed in flight, and the heating images were evaluated in terms of the location of the generated disturbances and how these disturbance might relate to the response of discreet gages on the Columbia Orbiter vehicle during entry.

4.3.1.1 Wind Tunnel Facilities

The two facilities used in this investigation were the 20-Inch Mach 6 Air Tunnel and the 20-Inch Mach 6 CF4 Tunnel. These facilities are conventional (as compared to impulse), low-enthalpy, blow-down type hypersonic tunnels. The Mach 6 air tunnel uses heated, dried, and filtered air as the test gas. Typical operating conditions for the tunnel are: stagnation pressures from 30 to 500 psia; stagnation temperatures from 760 to 1000 °R, free stream Mach number from 5.8 to 6.1; free stream unit Reynolds numbers from 0.5 to 8 million per foot; a free stream and post-normal shock ratio of specific heats (gamma) of 1.4; and a normal shock density ratio of 5.3. The facility has a two-dimensional contoured nozzle leading to a closed, solid-wall test section with dimensions of 20.5 by 20 inches. The test core varies from 12 to 14 inches depending on the operating condition. Nominal run time is approximately 60 to 120 seconds, although longer runs times are possible.

The CF4 Tunnel uses heated, dried, and filtered carbon tetrafluoride (Freon 14; molecular weight of 88 which is three times heavier than air) as the test gas. Typical operating conditions for the tunnel are: stagnation pressures from 85 to 2000 psia; stagnation temperatures up to 1300 °R, free stream Mach number from 5.9 to 6.0; free stream unit Reynolds numbers from 0.02 to 0.55 million per foot; a free stream gamma of 1.21 and a post-normal shock gamma of 1.10; and a normal shock density ratio of 11.7. The facility has a contoured axisymmetric nozzle with a nozzle exit diameter of 20 inches, leading to an open-jet test section. The test core varies from 12 to 14 inches depending on the operating condition. Nominal run time is approximately 20 seconds.

The test conditions in the two facilities for the tests performed for this investigation are summarized below. The majority of the runs in the Mach 6 air tunnel were made at a length Reynolds number of 2.4 million (based on a reference body length of 1290.3 inches full scale), which corresponds roughly to flight at Mach 19 and 207,00 feet, near loss of signal. The majority of the runs in the CF4 tunnel were made at a length Reynolds number of 0.36 million (based on a reference body length of 1290.3 inches full scale), which corresponds roughly to flight at Mach 25 and 256,00 feet.

Nominal Flow Conditions in NASA LaRC Aerothermodynamics Laboratory

Facility	M_∞	q_∞ (psi)	$P_{t,1}$ (psi)	$T_{t,1}$ (°R)	ρ_2/ρ_∞	Re_∞/ft ($x10^6$)
20-Inch Mach 6 Air	5.90	1.04	60	890	5.2	1.0
	5.94	2.10	125	910	5.3	2.1
	5.96	3.05	180	910	5.3	3.0
20-Inch Mach 6 CF4	5.94	0.65	750	1180	11.7	0.27
	5.94	1.27	1330	1210	11.7	0.45

4.3.1.2 Applicability of Wind Tunnels to STS-107 Flight Conditions

The loss of STS-107 occurred during entry at high Mach number and enthalpy levels, and relatively low Reynolds numbers. At these flight conditions high-temperature effects (i.e. flow chemistry) are significant due to the dissociation-recombination and ionization of the gas as it passes through the vehicle bow and wing shocks. These high-temperature effects increase the shock density ratio and lower the specific heat ratio (gamma) of the gas within the shock layer, causing shocks to lie closer to the vehicle surface and altering their interaction locations; these high-temperature effects cause the gas to expand to lower pressures than would occur for a non-reacting gas. The CF4 tunnel provides a simulation of these high-temperature effects via its low value of gamma, which is near the value in the Orbiter windward flow field at hypervelocity flight conditions. For example, lower pressure levels than expected on the rear windward portion of the Shuttle were identified as the root cause of the so-called Orbiter pitch-up anomaly that occurred during the first flight of Columbia, STS-1, wherein the Orbiter experienced a nose-up pitch increment relative to pre-flight predictions. The CF4 tunnel has been used to successfully demonstrate the magnitude and direction of this pitch-up increment. While the ability of the CF4 tunnel to accurately simulate the leeside flow has not been validated to the extent of the windward flow, the damage scenarios investigated have their initiation on the wing leading edge and the windward surface, and thus the CF4 tunnel is expected to provide credible simulation of their effects.

The Mach 6 air tunnel uses a perfect gas, but all the flow physics phenomena such as flow separation-reattachment, boundary layer transition, and shock-shock interactions, will be present. The high-temperature effects may alter the level and location of these phenomena, but should not add or delete from them. Thus the Mach 6 air tunnel may be used as a preliminary or screening facility, with the CF4 tunnel used to refine the results. A more detailed discussion of the use of these facilities and their relation to the flight environment can be found in section 5.2.3.1.

4.3.1.3 Wind Tunnel Models

Two types of force-and-moment models were used in this investigation, one made from stainless steel and several from cast silica ceramic. The steel model was an existing 0.0075-scale model that was modified to allow testing of gear and door deployment. A wheel well with a maximum depth of 0.35 inches was machined into the wing, a door was fabricated with a tab to allow installation on the model, and a simplified gear was constructed consisting of a single rod ending in a wheel assembly. The ceramic models were built from a mold that used the steel model as a pattern. Individual models were slip cast, and then a steel sleeve was bonded to the inside to accept the strain-gage force balance. The ceramic models then had the locations of the RCC and carrier panels marked using a coordinate measurement system by the LaRC surface verification laboratory. Individual missing panels were removed using the location marks as a guide. Several photographs of the models with the different damage scenarios are shown in Figure 4.3-1. All models had 0° control surface deflections of the elevons and body flap. The gap between the inboard and outboard elevons was present for the ceramic models, but was filled in for the steel model.

4.3.1.4 Test Techniques

Force and moment measurements were obtained using a six-component water-cooled balance. The balance was selected to maximize accuracy of the lateral-directional data. One balance was used for the steel model and another for the lighter-weight ceramic models. Usual corrections for balance interactions, weight tares, and sting bending were made. A baseline (no damage, 0° control surface deflections) set of aerodynamic coefficients was established for each model over an angle-of-attack range from 38° to 42°. This baseline was then subtracted from subsequent runs of the different damage scenarios to provide the residual aerodynamic increments.

The global heat-transfer mappings obtained in the Mach 6 air tunnel were obtained using an infrared (IR) imaging system with an un-cooled micro-bolometer-based focal plane array detector. The measured infrared radiation was converted to surface temperatures using the emittance of the target, which for the phosphor-coated fused silica model was determined to be 0.906. The global heat-transfer mappings obtained in the CF4 tunnel were generated with the two-color relative-intensity phosphor thermography

technique. IR techniques are not applicable to the CF4 tunnel as the freon gas absorbs the infrared radiation. The ceramic models were coated with phosphors that fluoresce in two regions of the visible spectrum when illuminated with ultraviolet light. The fluorescence intensity is dependent upon the amount of incident ultraviolet light and the local surface temperature of the phosphors. A temperature calibration of the system conducted prior to the study provides tables used to convert the ratio of green and red intensity images to global temperature mappings. For both the infrared and phosphor techniques, the global heat-transfer images are computed assuming one-dimensional semi-infinite heat conduction. The advantage of these techniques is their non-intrusive and global resolution of the quantitative heat-transfer data. These thermography techniques were used to identify the heating footprints associated with complex, three-dimensional flow phenomena such as boundary layer transition locations, flow separation and reattachment locations, etc. that would be extremely difficult to resolve using discrete measurement techniques.

4.3.1.5 Results from 20-Inch Mach 6 Air Tunnel

4.3.1.5.1 Raised boundary layer trips and gouge

At the beginning of the investigation the primary area of interest was early asymmetric boundary layer transition (ABLT), and in damage to the acreage tiles on the windward surface. Damage scenarios tested in the Mach 6 tunnel therefore included a single boundary layer trip at RCC panel 6 (0.6 inch high full scale), a gouge in the center of the main landing gear door (approximately 7 by 32 by 4 (WxLxD) inches, full scale), a raised main landing gear door (raised 0.9 inch full scale), and 7 trips (0.6 inch high full scale) arrayed span-wise across the leading edge of the door (to further simulate a raised door panel). In addition a “full” asymmetric transition configuration was tested which had 10 trips along the wing leading edge as well as 2 trips well forward near where surface protuberances were observed to cause early transition during flight of STS-28 (x/l =0.26). The extent of the turbulent flow generated by these disturbances is shown in Figure 4.3-2. The turbulent wedge from the single trip at RCC panel 6 is swept outboard and affects only the outermost portion of the left wing, as compared to the trips along the forward edge of the main landing gear door, which affect the flow more inboard. These individual trips were more effective than the raised door (not shown) as the door acted more like a two-dimensional trip or step, which is not as effective in promoting turbulent flow. The gouge did not produce turbulent flow, although a small increase in heating was generated. The “full” asymmetric transition case is seen to provide turbulent flow over the aft 2/3 of the left side of the model windward surface. The aerodynamic increments generated by these OML changes are shown in Figure 4.3-3(rolling moment) and Figure 4.3-4 (yawing moment). The gouge in the door and the raised door had minimal effect on the model aerodynamics. The single trip at RCC panel 6 and the 7 trips at the door leading edge had similar effects to each other, causing a positive rolling moment (right wing down) and a small negative yawing moment (nose left). All increments were less than the “full” ABLT condition.

4.3.1.5.2 Main Landing Gear/Door Deployment

Possible deployment of the main landing gear was examined by testing various combinations of the gear, door, and an open wheel well. In general the results were similar to those determined in the CF4 tunnel and will be discussed in the next section.

4.3.1.6 Results from 20-Inch CF4 Tunnel

4.3.1.6.1 Main Landing Gear/Door Deployment

Deployment of the main landing gear and door was tested in the CF4 tunnel, as well as the Mach 6 air tunnel. Although not a leading initial damage scenario, this scenario was examined due to the large aerodynamic moments observed towards the end of flight, which to this point had not been observed in any of the tunnel tests. An open wheel well (no door), door alone, gear alone, and door and gear deployed were tested. Filler plates were used to create three different depths of the open wheel well in order to simulate the presence of the gear (it was thought that the presence of the gear would tend to fill in the cavity, making the wheel well effectively shallower). A sketch of these configurations is shown in Figure 4.3-5. The aerodynamic results in terms of delta rolling, yawing, and pitching moments for these configurations are shown in Figure 4.3-6. Large rolling and yawing moments were generated for the door

and/or gear combinations (lines D and E) consistent with flight, but pitching moments were in the opposite direction than those inferred from flight measurements. However, for the open wheel well configurations (lines A and B), as the cavity was made shallower, all three moments increased, and in the same direction as flight. This trend is consistent with “open” and “closed” type cavity flows. For the deeper cavity, some flow re-circulates within the cavity, but the main flow essentially passes over the cavity; as the depth is decreased, the flow impinges on and attaches to the cavity floor, a shock is formed as the flow reaches the aft wall, and the pressure on the cavity floor is significantly increased. This increased pressure generates the rolling, yawing, and pitching moments observed.

4.3.1.6.2 Missing Full RCC Panels

As the investigation progressed it was known that two temperature instruments on the left side of the fuselage (V34T1106A, V09T1724A) had experienced large increases in heating rates. Investigators at Langley had modified the wing leading edge with a “notch”, both experimentally and computationally, and side fuselage disturbances near these gages were produced by both techniques. Given this knowledge, an extensive survey of wing leading edge damage in terms of missing RCC panels was undertaken. Five ceramic models were fabricated with one or more missing RCC panels. The missing panel area was filled and a baseline data set was again generated. The filled area was then removed and incremental aerodynamic data obtained. Simultaneous heat transfer images were obtained, but their discussion is left to section 5.2.3.4, where results from dedicated heat transfer models are presented. The aerodynamic results for single missing panels as a function of panel location are shown in Figure 4.3-7 through Figure 4.3-9. The solid line represents a least-square linear fit to all the single-panel-missing data. The results show a nearly constant negative value of delta roll for a given missing panel location (Figure 4.3-7). This left-wing-down roll is believed to be due to loss of lift on the left wing due to the loss of area. Delta yawing moment (Figure 4.3-8) exhibited a relatively strong dependence on missing panel location, with a more nose-left yawing moment generated for the more outboard locations. The solid forward facing rear wall and side walls of the notch generate a shock system causing a local high-pressure area, and combined with the larger moment arm for more outboard locations, leads to the observed trend. Delta pitching moment (Figure 4.3-9) showed a dependence on missing panel location also, as nose-down pitch increased for more outboard panel locations. Multiple missing RCC panels were also tested; for instance, one series of tests started with panel 6 out, then 5 and 6, then 5 through 7. A sample of these results is given in Figure 4.3-10 through Figure 4.3-12, where delta roll, yaw, and pitch are plotted as a constant against time from entry interface. The dominant trend is that the delta roll, delta yaw, and delta pitch increments all become progressively more negative (left wing down, nose left, nose down) as the number of missing panels is increased. Superposition of single missing RCC panels was somewhat successful in predicting two-panel out increments, but less so for three or more panels missing.

A brief series of tests examined Reynolds number effects. Missing RCC panel 9, and missing RCC panels 6 and 9 together, were tested at two Reynolds numbers, 0.27 and 0.46 per foot. No significant Reynolds number effect was observed for this factor of two variation in Reynolds number.

4.3.1.6.3 Missing Partial RCC Panels

As more of the debris was recovered and analyzed, a scenario emerged that a partially damaged RCC panel or panels may more appropriately model the actual damage, as opposed to a full panel missing. Thus a series of tests was undertaken to look at the effect of missing lower RCC panels. The wing leading edge was modified by removing the lower portion of the panel from the wing apex to the start of the lower carrier panel. The aerodynamic results for individually removed lower panels 4 through 9 are shown in Figure 4.3-13 through Figure 4.3-15. The solid line again represents a least-square linear fit to the data. For comparison, the linear fit to the full panel out data presented in the previous section is shown by the dashed line. Overall, the magnitudes of the rolling, yawing, and pitching moment increments for missing partial panels were smaller than those for a full missing panel. The rolling moment increment was slightly more positive (right wing down) for a more outboard missing panel location. This trend is believed due to the locally increased pressure acting on the underside of the RCC panel cutout, and thus as the moment arm increases with increasing outboard location, the roll becomes more positive. The yawing moment was nearly constant for any particular missing panel location, which was different than for the full panel out data where a strong dependence on panel location was observed. The pitching moment was again more nose-down for more outboard panel locations.

A recurring question was what wing leading edge or windward surface damage scenario would provide aerodynamic characteristics observed in flight and simultaneously generate leeside disturbances (side fuselage heating) also observed in flight. This had been shown to be possible for a full missing panel. Phosphor thermography images taken for the series of missing lower RCC panels (Figure 4.3-16) show that for panel 4, and to a lesser extent panel 5, a disturbance is generated that moves to the leeside of the model. This disturbance is not observed for missing partial panels 6 or 9. The relative location of the partially missing panel to the local attachment line largely determines if the disturbance is swept to the leeside.

4.3.1.6.4 Holes and Slots through the Wing

Another mechanism examined for flow reaching the leeside was through holes or slots in the upper surface. For one series of tests, small holes (0.030-inch diameter model scale, 4 inch diameter full scale) were drilled through the wing, from windward surface to the leeside, at the carrier panel locations behind RCC panels 6, 9, and 12 (separate runs). No effect of these holes through the wing was seen in either the aerodynamic increments or the side fuselage images. For another series of tests, a 0.030-inch hole was drilled from the windward surface (center, aft end of the partially missing panel 8) to the leeside side through upper carrier panel 8. Afterwards this hole was widened to a 0.030-inch slot, in effect removing most of the upper carrier panel. Phosphor thermography images of the fuselage side are shown in Figure 4.3-17. A slight effect on heating to the OMS pod can be seen for the single hole. The slot creates a larger disturbance in the leeside flow field, resulting in increased heating on the side of the fuselage and the OMS pod, similar to that observed for a full missing panel, though the heating rate is lower. The aerodynamic increments in rolling and pitching moments associated with the hole and slot are very small, but there is a measurable increase in the nose-left yawing moment increment when the hole is widened to a slot, as shown in Figure 4.3-18.

4.3.1.6.5 Effect of Vertical Tail

Another aspect that was investigated was whether flow to the leeside was impinging on or in some way affecting the flow on the vertical tail. A piece of the vertical tail had been found that showed damage to the left side, but not the right. In addition, the tail was seen as a possible contributor to the large roll and yaw increments seen late in flight, and especially for the change in rolling moment behavior after EI + 600 sec. A model was tested with the tail on and off, with and without panel 9 missing. As observed from the table in Figure 4.3-19 for missing RCC panel 9, the increments with and without the vertical tail are very close in value, leading to the conclusion that the tail was not affected nor a contributor to the moments in question.

4.3.1.6.6 Windward Surface Depression

A final series of aerodynamic tests were performed to determine if a damage scenario related to deformation of the left wing would cause the change in direction of the rolling moment seen to occur 602 seconds after entry interface. Influenced by the results from the open wheel well, a shallow depression was created in the left wing windward surface to simulate what might occur as the wing internal structure was degraded and the lower skin was pressed inward by the greater external surface pressure. A single groove was milled into the lower surface of the model, starting just behind RCC panel 8. The length of this groove was varied in three increments with the longest groove extending slightly past the aft end of the wheel well. This groove was then widened to simulate progressive damage. Measured aerodynamic moments show (Figure 4.3-20 through Figure 4.3-22) that a minimum length of the groove is needed to provide a measurable increase in rolling moment, similar to the critical depth of the open wheel well. The required aspect ratio (L/h) of the groove is greater than for the open wheel well; this effect may be related to the angle of the local streamlines, in that they will cross the groove as opposed to running parallel to it, thus in effect shortening the groove and reducing the aspect ratio. However, the depression does indeed cause a positive (right wing down) rolling moment as observed in flight, and the magnitude of the rolling moment increases as the width of the depression is increased. Furthermore, the yawing moment and pitching moment generated by the depression are similar in magnitude and in the same direction as observed for flight.

4.3.1.7 Observations:

4.3.1.7.1 Asymmetric Boundary Layer Transition

The preliminary work done in the Mach 6 air tunnel focused primarily on ABLT. For the damage scenarios examined, the rolling and yawing moments generated were consistent in terms of direction with the Shuttle ABLT model, which is a positive rolling moment (right wing down) combined with a negative (nose left) yawing moment. These results are inconsistent with the extracted STS-107 flight data for the early portion of the flight, which have a left-wing down rolling moment combined with a nose-left yawing moment, indicating that asymmetric transition was not an initiating cause of the accident. Boundary layer transition may have been a contributor later in the flight, when the rolling moment trend became positive.

4.3.1.7.2 Progressive Damage Scenario

As a final summation to the aerodynamic work, a progressive build-up of individual damage scenarios was developed and compared to the flight moment increments. The results are shown in figures Figure 4.3-23 through Figure 4.3-25. The time from entry interface is subjective, as are the damage scenarios themselves. Nonetheless, a plausible scenario can be developed, which has the same trends as the flight data, although an exact correlation of flight magnitudes and time is not achieved. The initial damage is loss of the lower portion of RCC panel 8. The magnitudes of the moment increments are small, as they were for the first 500 seconds of flight. This initial damage is followed by the addition of the slot through the upper portion of carrier panel 8, and then the complete removal of panel 9 at 615 seconds from entry interface (EI). It was at this time (615 seconds) that significant heating to the side fuselage was seen, and both the slot in carrier panel 8 and the complete removal of panel 9 allow flow to impinge on the leeside of the vehicle. The reversal in direction of the rolling moment is attributed to the windward surface depression, with the magnitude increasing as the size of the depression is increased (as more of the internal wing structure is degraded). The yawing and pitching moments continue their increasing negative trend as the depression is enlarged.

Figure 4.3-1 Wind Tunnel Test Model Configurations

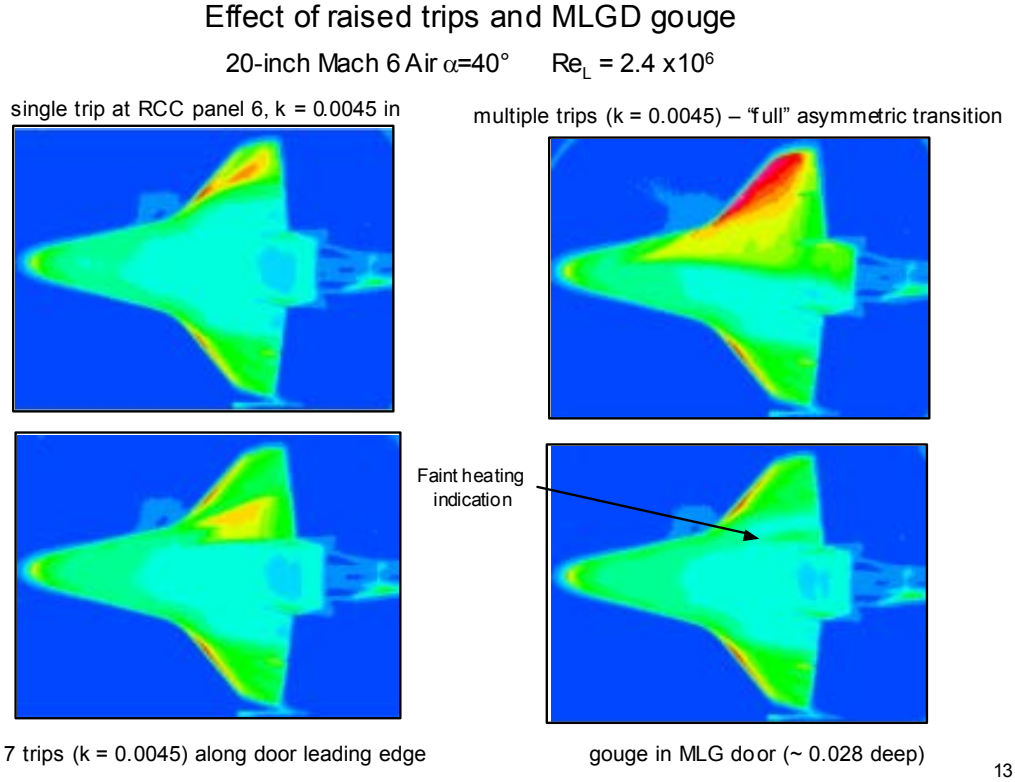

Figure 4.3-2 Infra-red Thermography Images Showing Extent of BL Transition

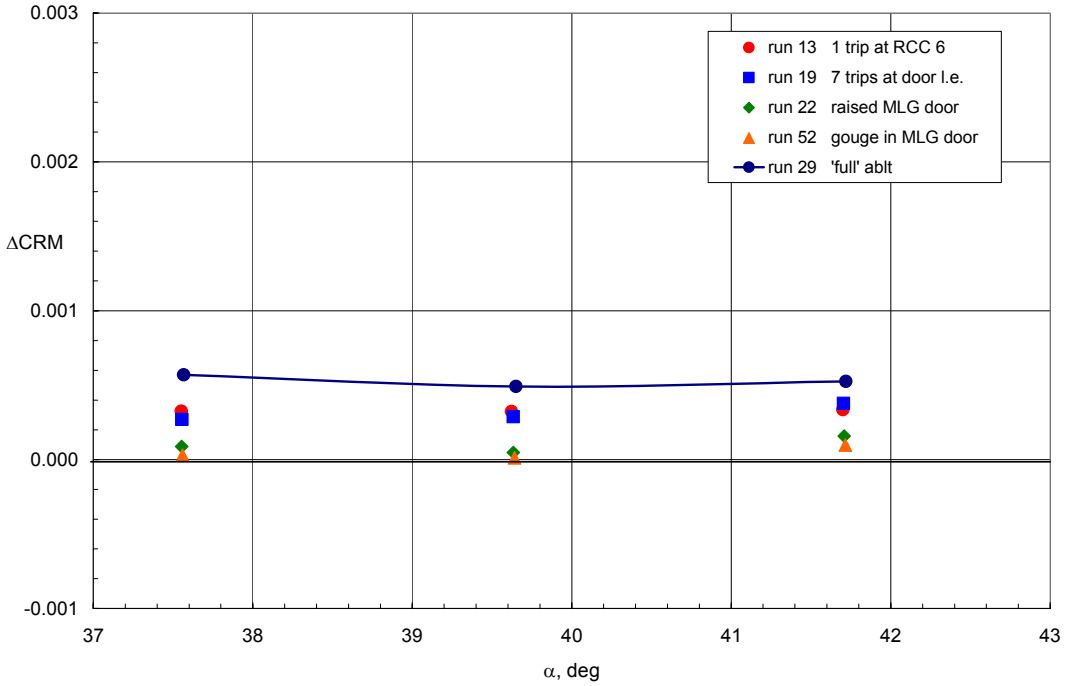

Figure 4.3-3 Boundary Layer Transition Aerodynamic Increments (Delta Roll)

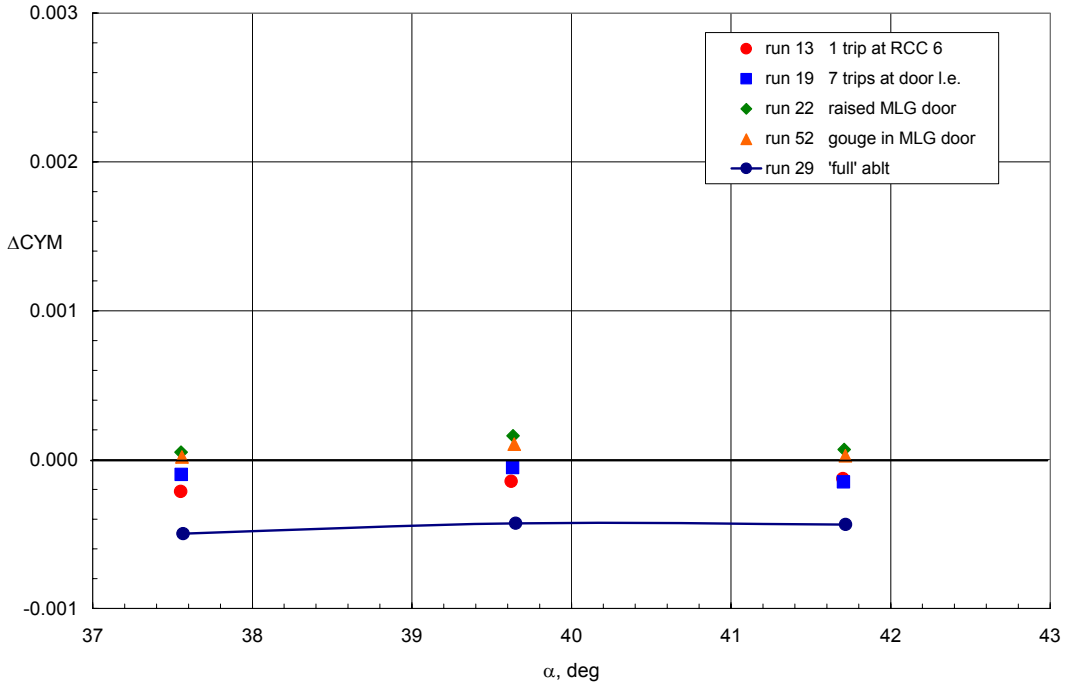

Figure 4.3-4 Boundary Layer Transition Aerodynamic Increments (Delta Yaw)

Test Configurations – Steel Model

Large OML Changes

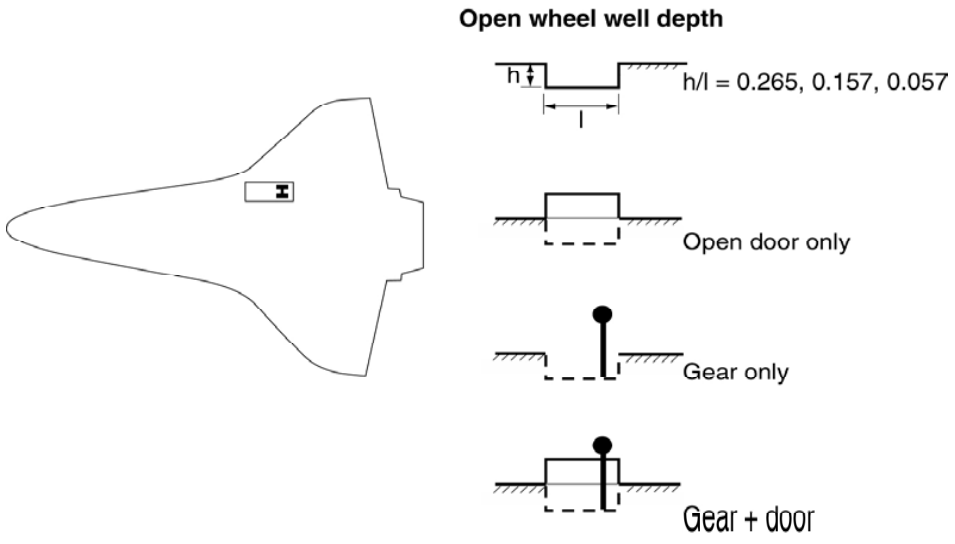

Figure 4.3-5 Stainless Steel Model Configurations Tested

MLG Door / Gear Scenarios in 20-Inch CF4 Tunnel

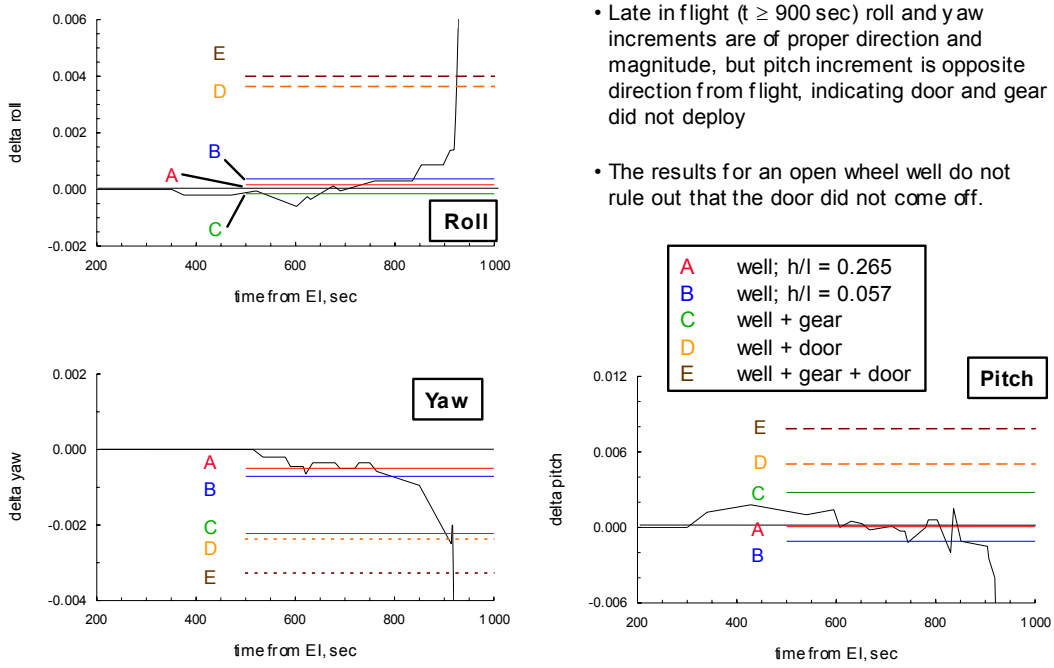

- Late in flight (t ≥ 900 sec) roll and yaw increments are of proper direction and magnitude, but pitch increment is opposite direction from flight, indicating door and gear did not deploy
- The results for an open wheel well do not rule out that the door did not come off.

Figure 4.3-6 Aerodynamic Increments (Roll, Pitch, Yaw) for MLG Door Scenarios

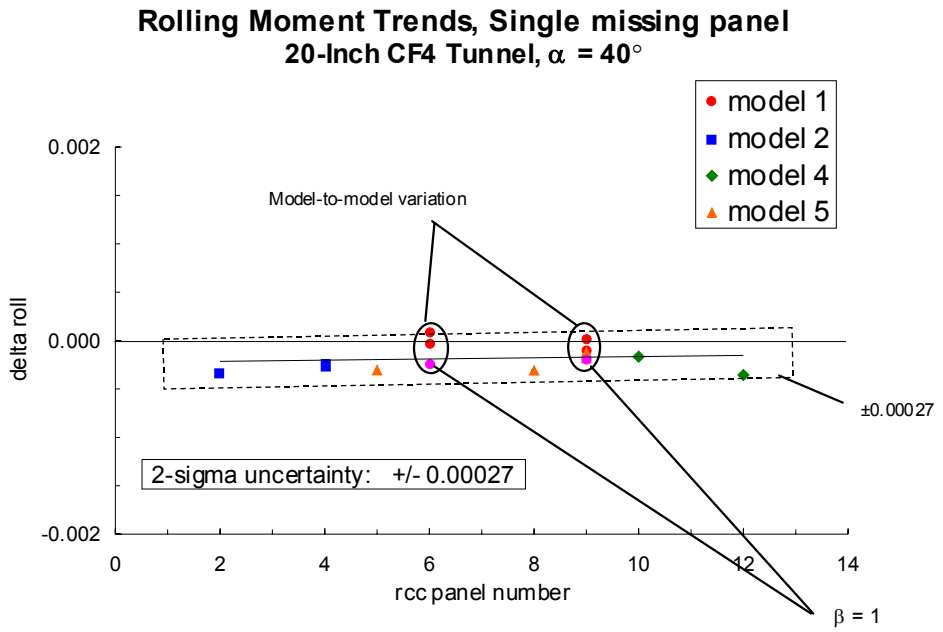

• Roll increment is relatively constant for a given missing panel

Figure 4.3-7 Aerodynamic Increment (delta Roll) – Missing Full RCC Panel by Location

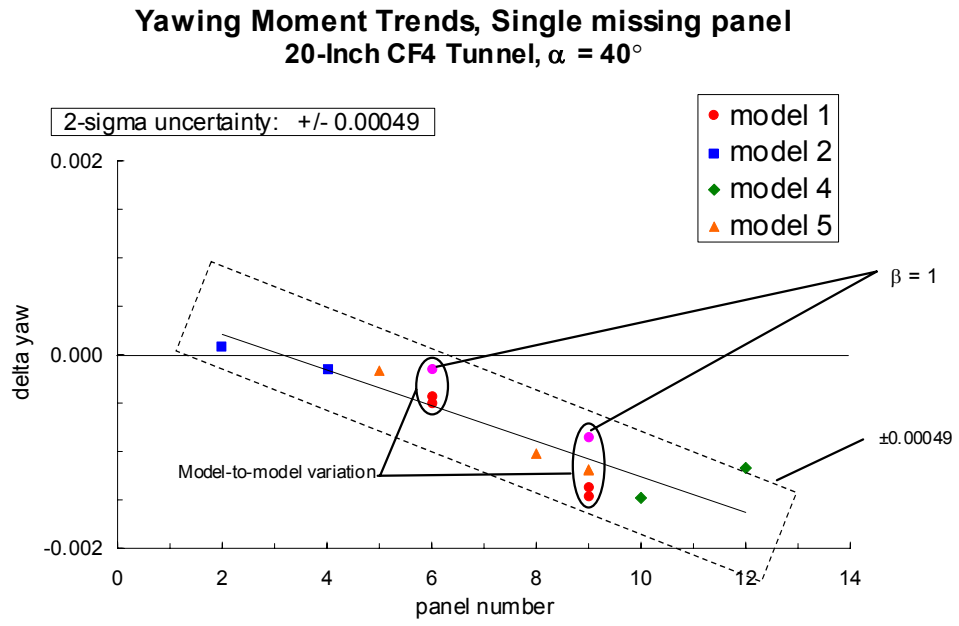

• Yaw increment is highly dependent on panel outboard location

Figure 4.3-8 Aerodynamic Increment (delta Yaw) – Missing Full RCC Panel by Location

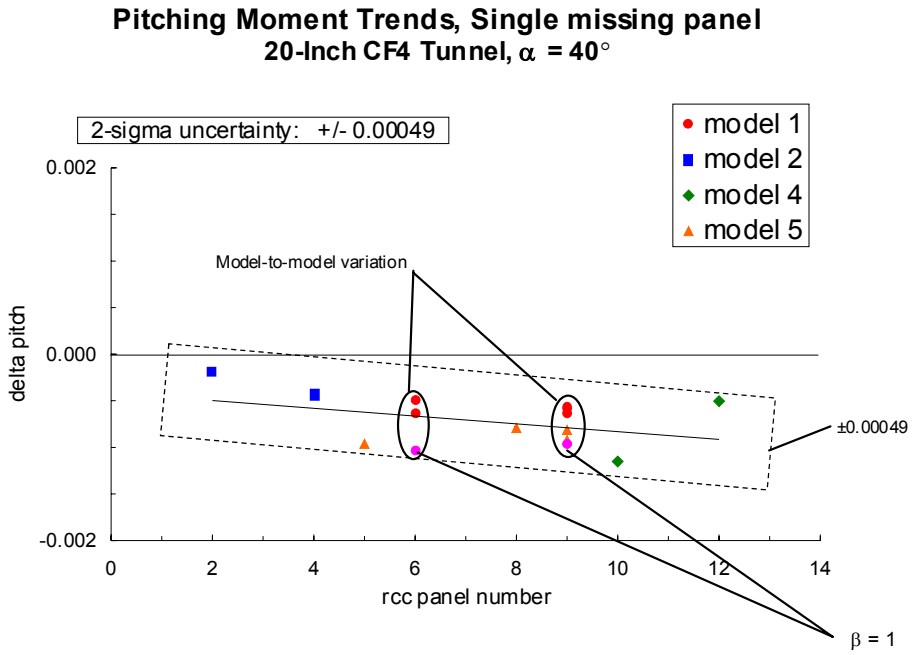

• Pitch increment is moderately dependent on panel location

Figure 4.3-9 Aerodynamic Increment (delta Pitch) – Missing Full RCC Panel by Location

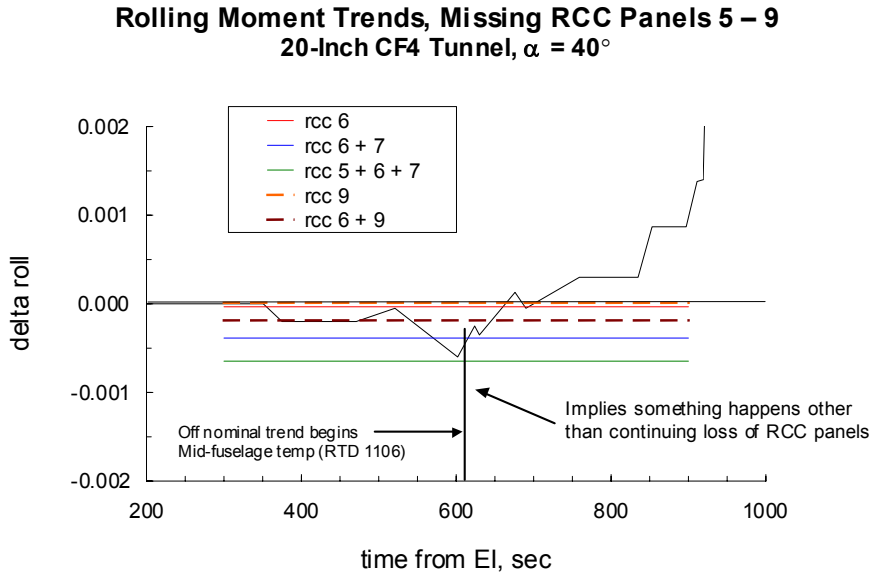

• Roll increment increases w ith increasing number of panels missing
• Tw o adjacent panels have larger increment than two separated panels
• Roll trend reverses at 615 sec; opposite effect from losing more leading edge panels

Figure 4.3-10 Rolling Moment Increment Trends - Missing RCC Panels 5-9

Yawing Moment Trends, Missing RCC Panels 5 – 9
20-Inch CF4 Tunnel, α = 40°

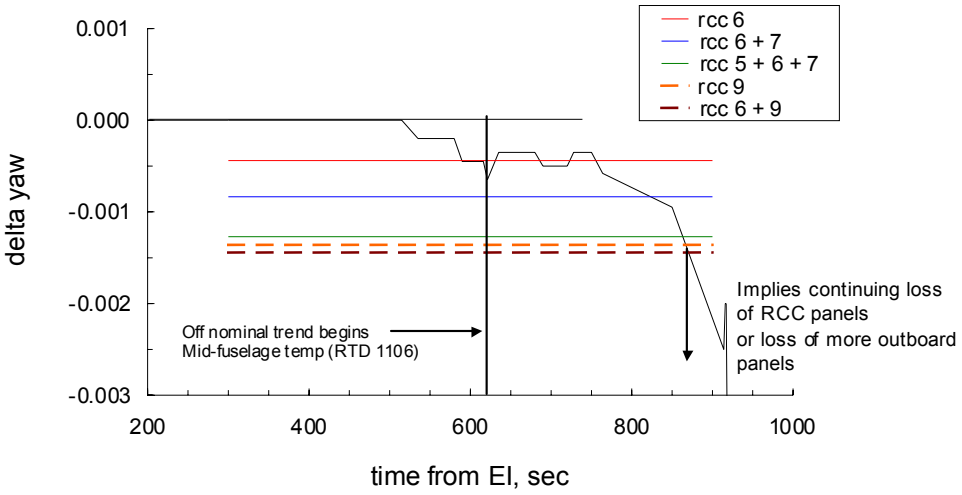

- Yaw increment increases for more outboard panels
- Yaw increment increases with increasing number of panels missing

Figure 4.3-11 Yawing Moment Increment Trends - Missing RCC Panels 5-9

Pitching Moment Trends, Missing RCC Panels 5 – 9
20-Inch CF4 Tunnel, α = 40°

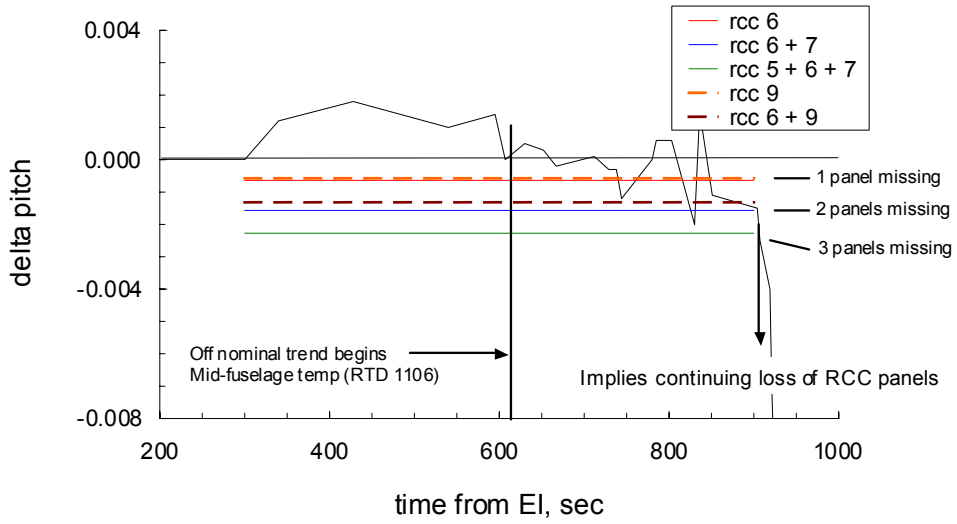

- Pitch increment nearly independent of panel outboard position
- Pitch increment increases nose-down with increasing number of panels missing

Figure 4.3-12 Pitching Moment Increment Trends - Missing RCC Panels 5-9

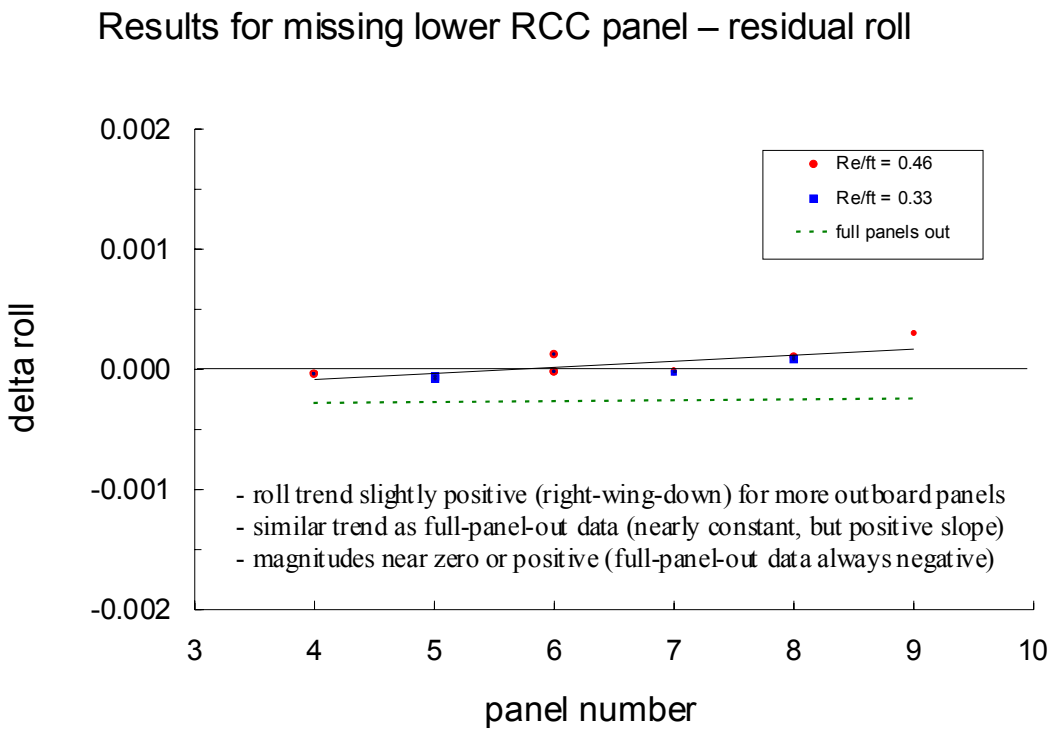

Figure 4.3-13 Aerodynamic Increment (delta Roll) – Missing Partial RCC Panel by Location

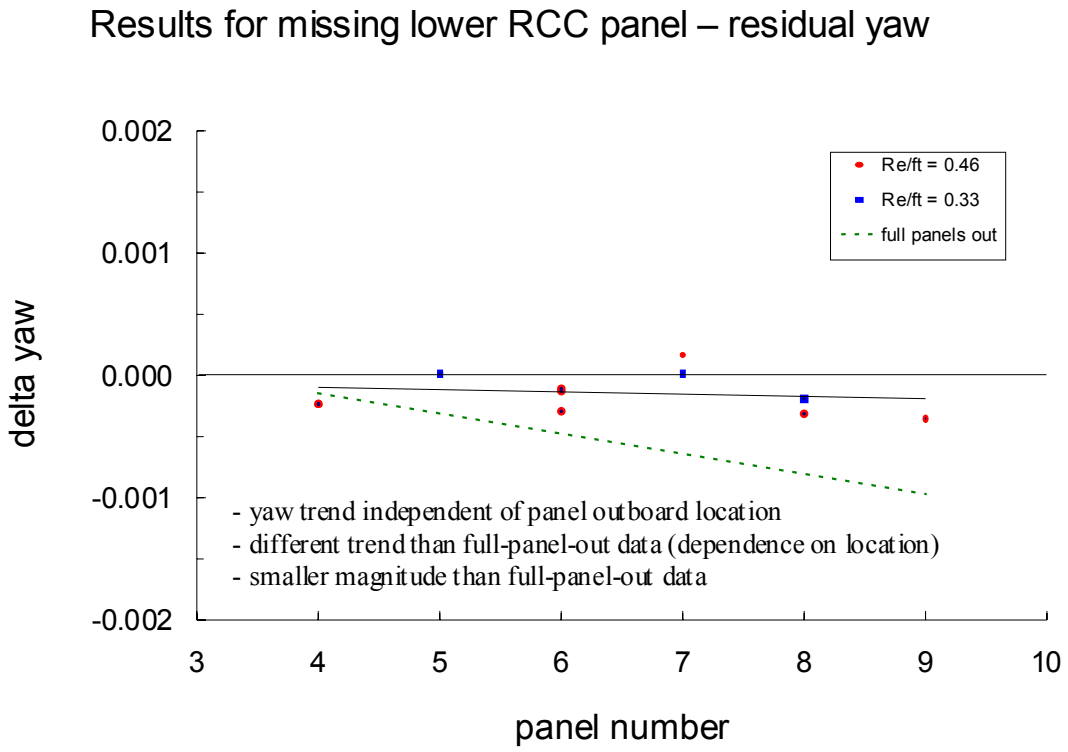

Figure 4.3-14 Aerodynamic Increment (delta Yaw) – Missing Partial RCC Panel by Location

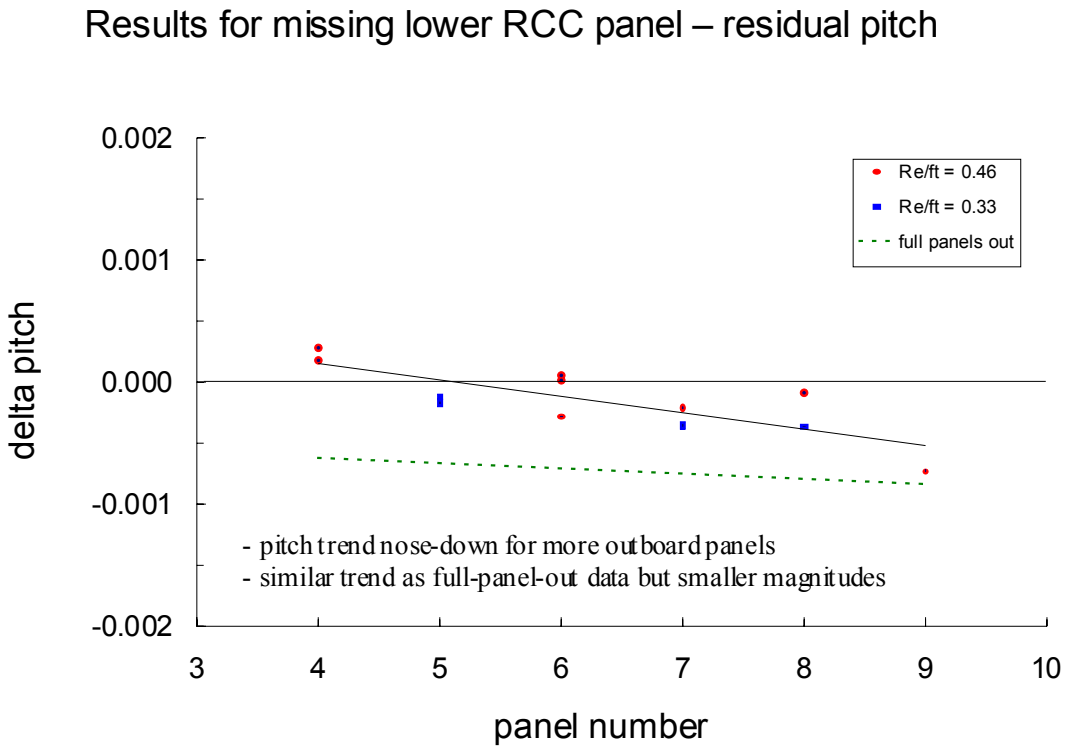

Figure 4.3-15 Aerodynamic Increment (delta Pitch) – Missing Partial RCC Panel by Location

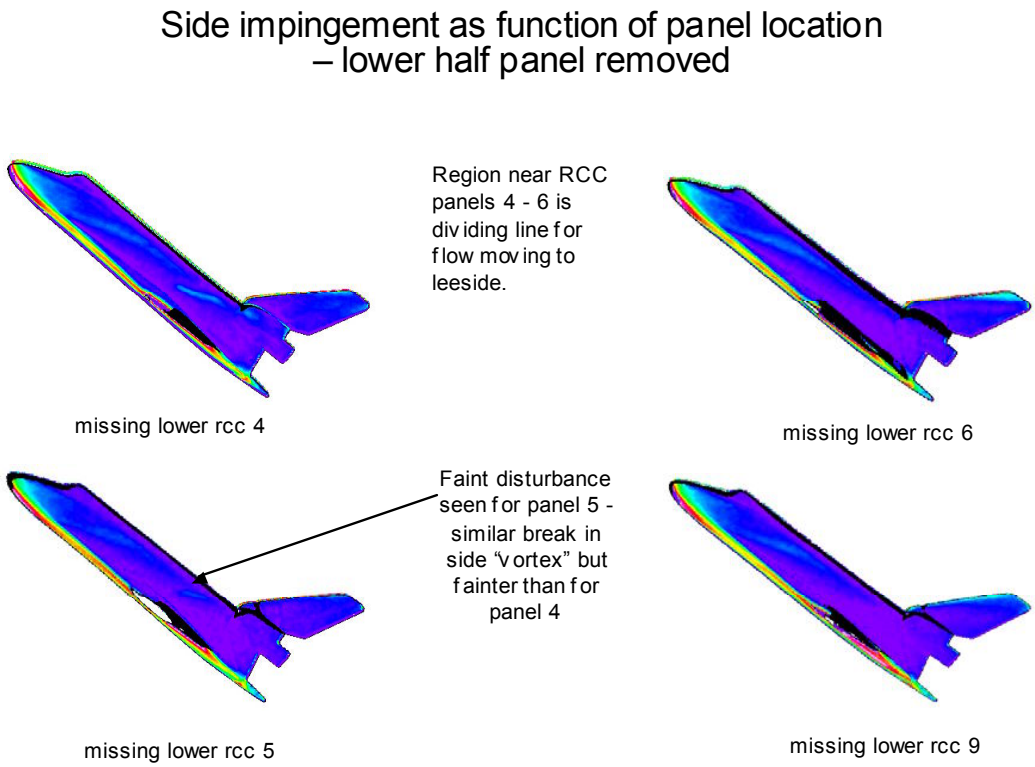

Figure 4.3-16 Side Fuselage Heating Augmentation – Missing Partial RCC Panel

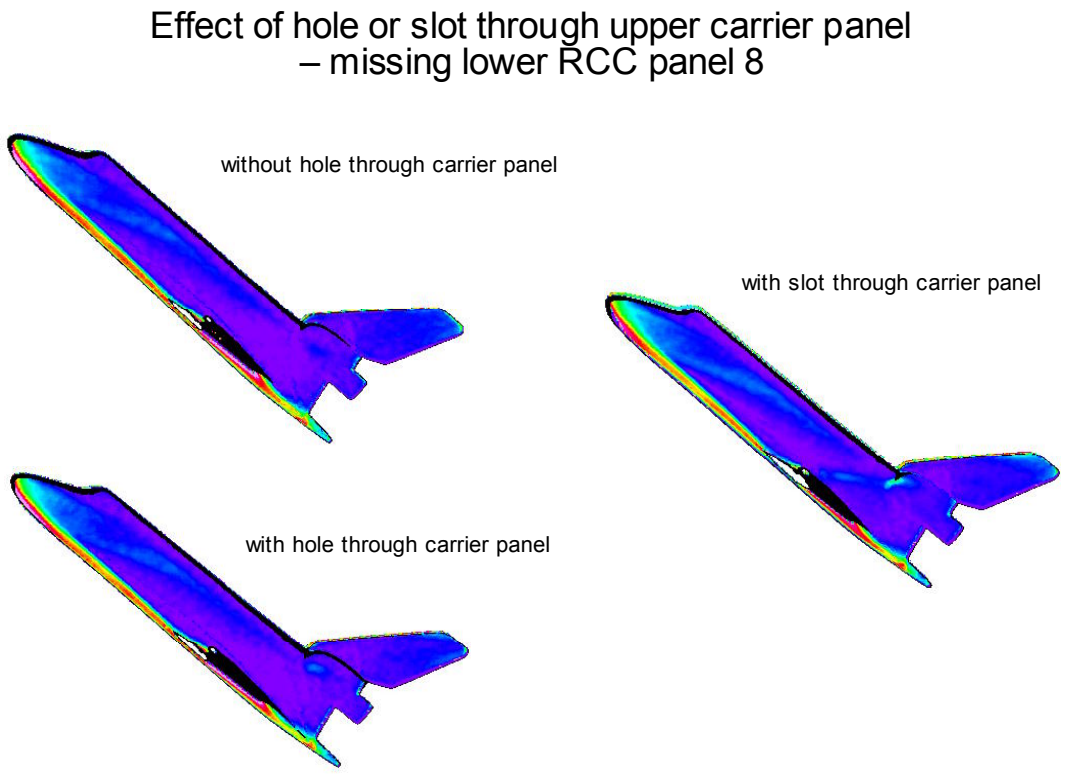

Figure 4.3-17 Side Fuselage Heating Augmentation – Missing Partial RCC Panel + Hole/Slot

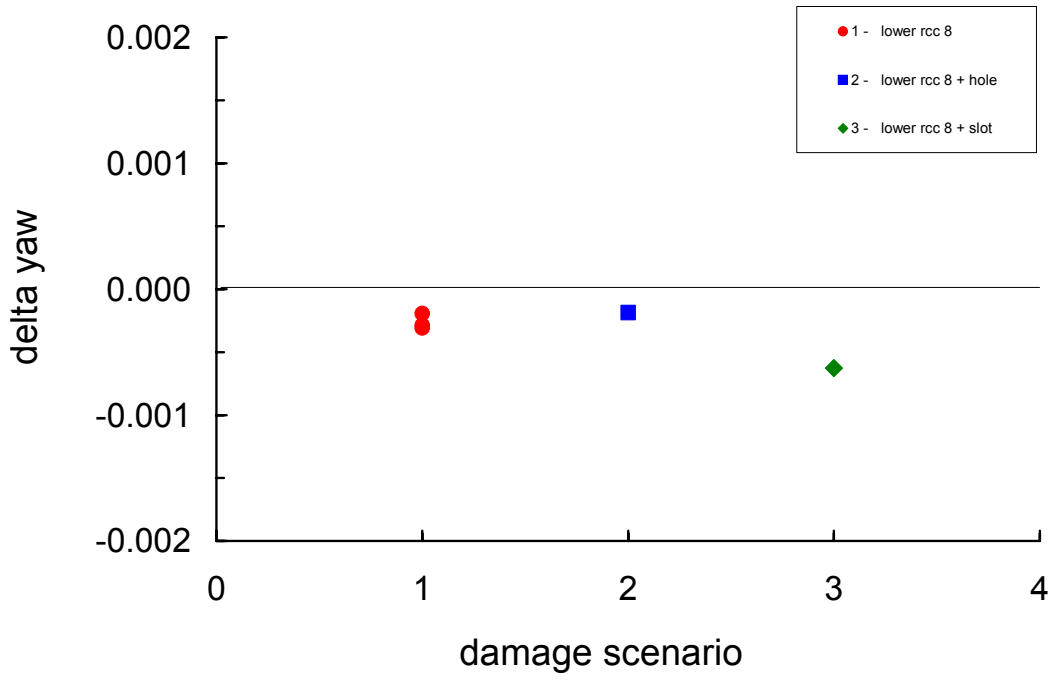

Figure 4.3-18 Aerodynamic Increment (delta Yaw) – Missing Partial RCC Panel + Hole/Slot

37

Vertical Tail on / off, missing Panel 9

Run	Tail	Alpha	Re/ft	ΔCrm	ΔCym	ΔCm	ΔCY	Model
30	on	40.2	0.45	-0.00006	-0.00115	-0.00105	0.00013	A
44	on	40.5	0.46	0.00007	-0.00131	-0.00128	-0.00037	5
45	on	40.5	0.45	0.00008	-0.00132	-0.00128	0.00022	5
63	off	40.5	0.46	-0.00007	-0.00122	-0.00125	-0.00006	5
64	off	40.5	0.44	-0.00013	-0.00122	-0.00117	0.00006	5
Avg	on	40.4	0.45	0.00003	-0.00126	-0.00120	-0.00001	
Avg	off	40.5	0.45	-0.00010	-0.00122	-0.00121	0.00000	
Delta		-0.1	0.00	0.00013	-0.00004	0.00001	-0.00001	

Effect of vertical tail is negligible, for missing RCC panel 9

Figure 4.3-19 Aerodynamic Increments -- Missing Full RCC Panel 9 with & w/o Vertical Tail

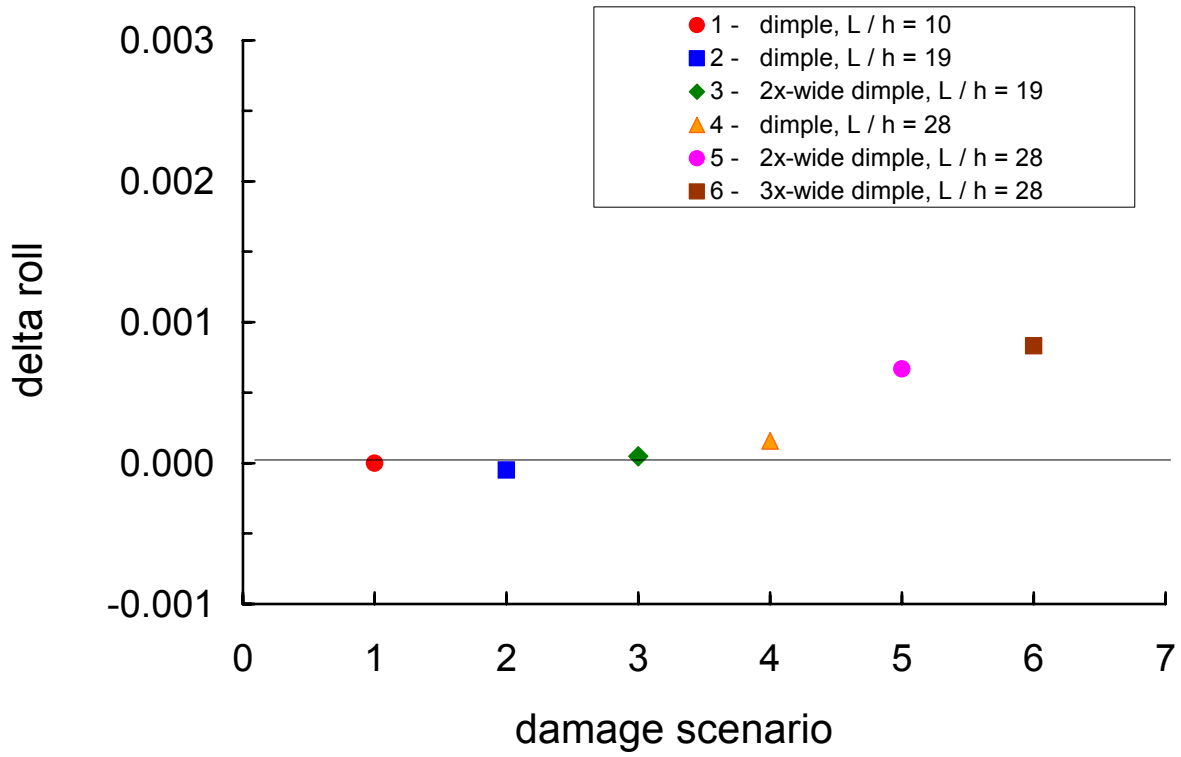

Figure 4.3-20 Aerodynamic Increment (delta Roll) – Lower Wing Surface Deformation / Dimple

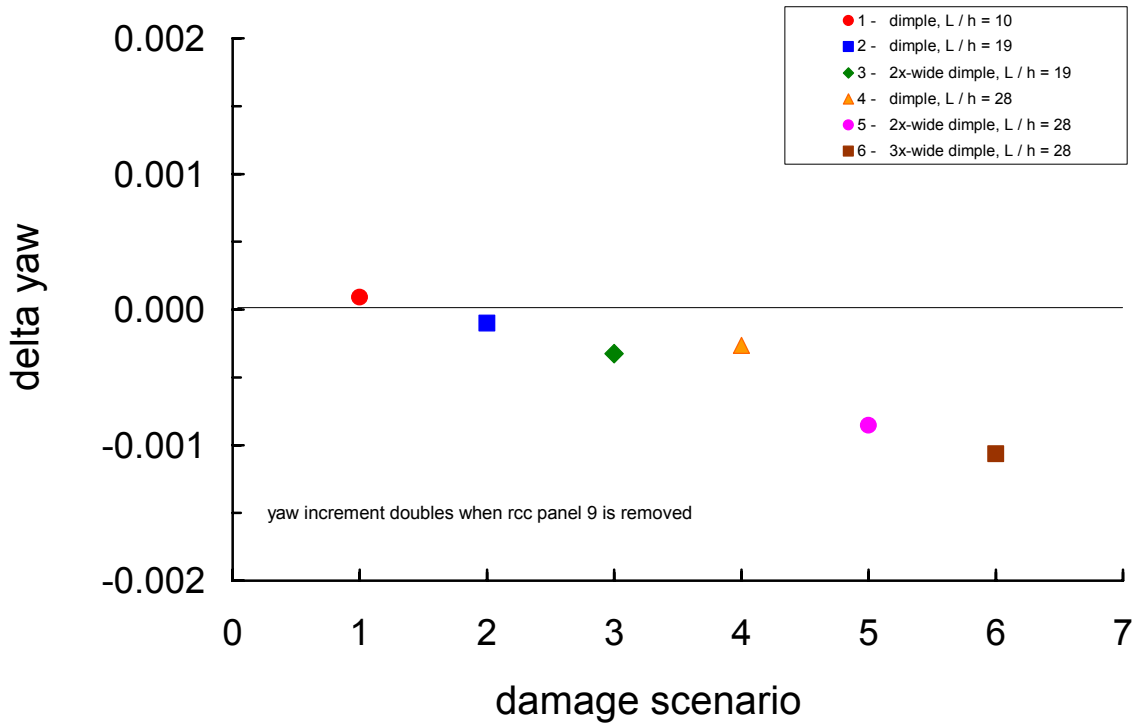

Figure 4.3-21 Aerodynamic Increment (delta Yaw) – Lower Wing Surface Deformation / Dimple

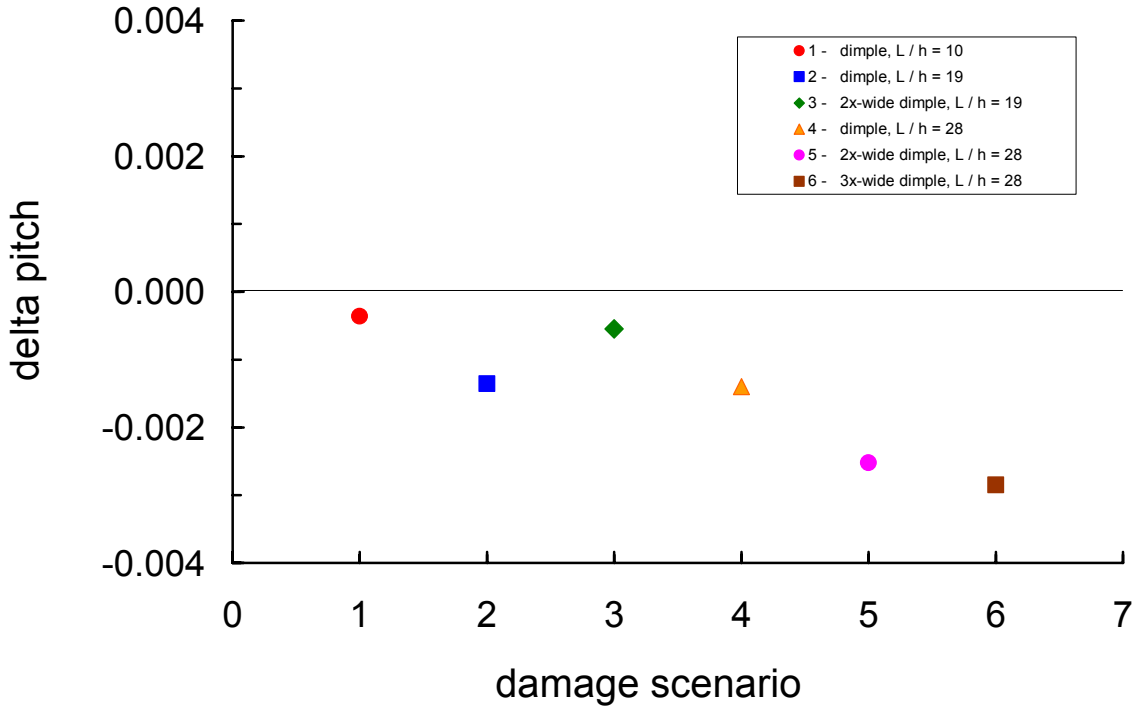

Figure 4.3-22 Aerodynamic Increment (delta Pitch) – Lower Wing Surface Deformation / Dimple

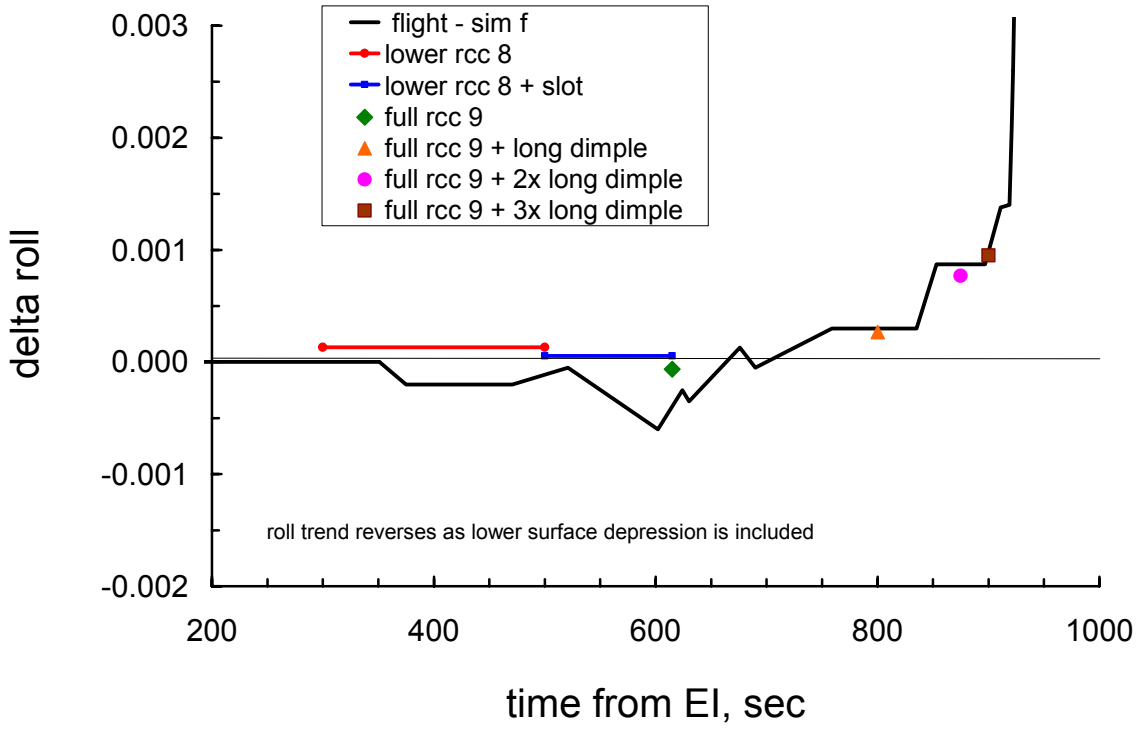

Figure 4.3-23 Aerodynamic Increment (delta Roll) – Damage Progression

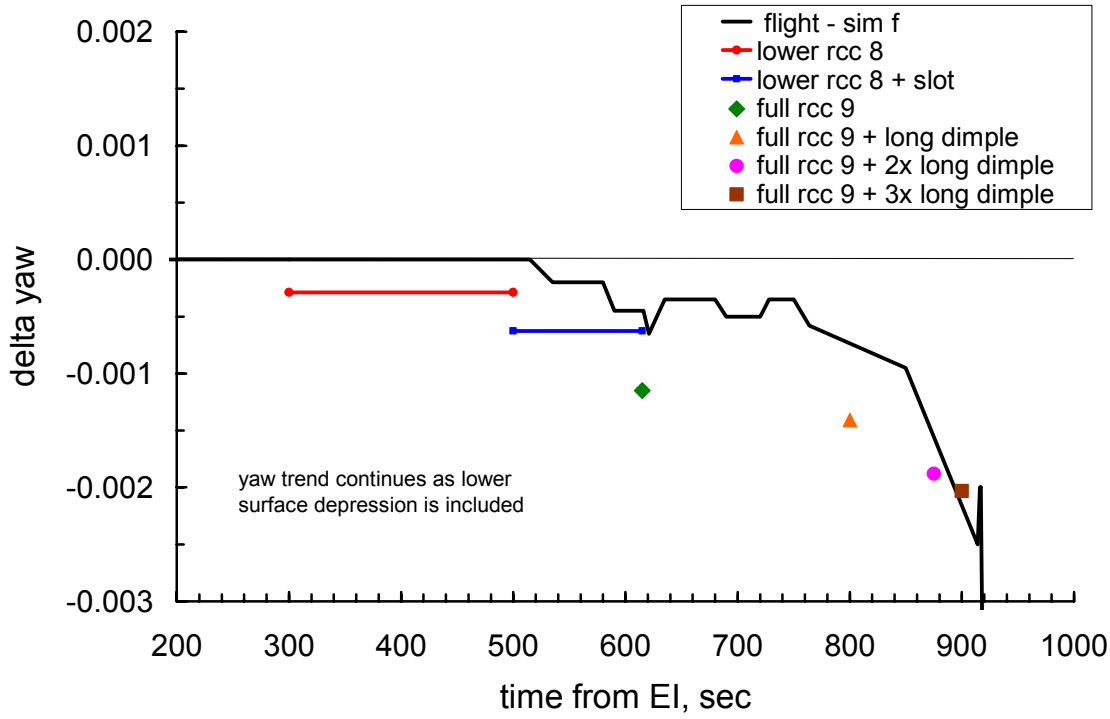

Figure 4.3-24 Aerodynamic Increment (delta Yaw) – Damage Progression

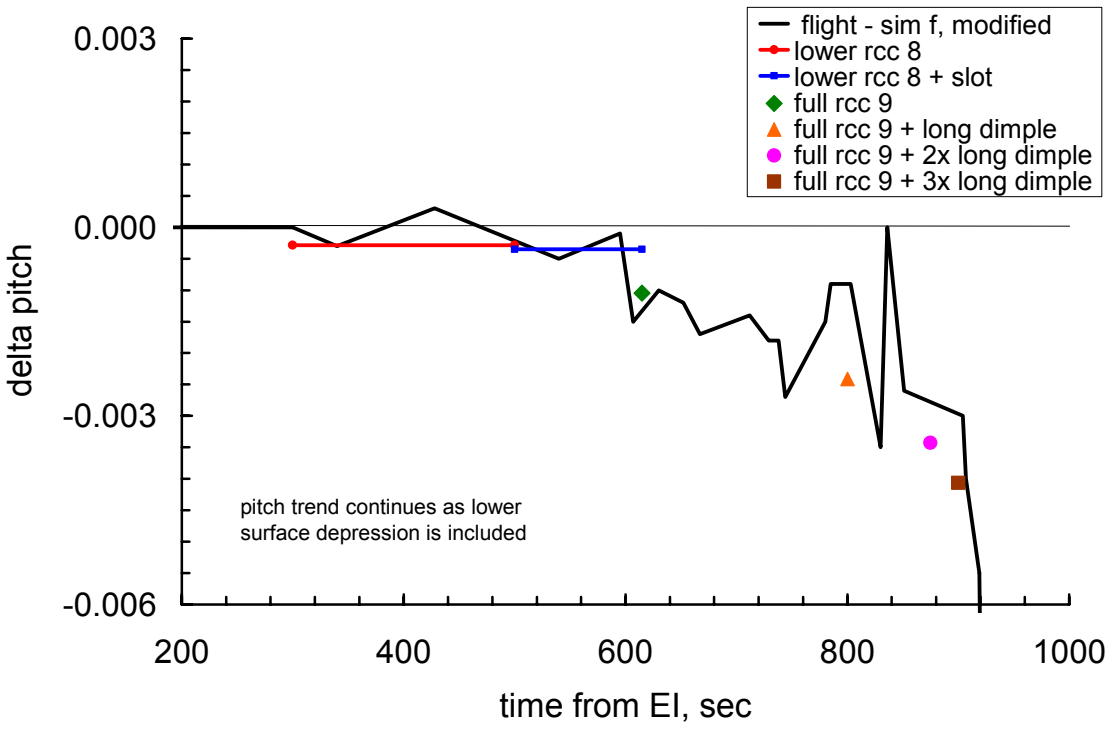

Figure 4.3-25 Aerodynamic Increment (delta Pitch) – Damage Progression

4.3.2 Damage Assessment Using Computational Fluid Dynamics

Computational tools were used to complement the wind tunnel testing of Columbia damage scenarios. The ability to simulate flight and wind tunnel conditions provided a bridge between the extensive wind tunnel test program and the STS-107 flight. The flow solutions provided a detailed view of the flow field characteristics and the contribution of orbiter components (vertical tail, wing, etc.) to aerodynamic forces and moments. In some cases, rapid, inviscid, unstructured CFD methods were able to guide the wind tunnel efforts. The inviscid methods are limited by the inability to accurately simulate viscous dominated flows such as occur in the highly separated flow region on the leeward side of the orbiter, but still proved very useful in a screening capacity. The structured mesh viscous methods are limited by the time it takes to develop a mesh for a complex geometry and in solution time. Having a limited number of the more accurate viscous solutions available provided a valuable check on the lower fidelity inviscid methods and served as an additional bridge between wind tunnel and flight conditions.

The sections below present the background for and data from computations that contributed to the understanding of the final damage scenario. Additional work performed by the analysts to verify assumptions of the computations, and on early analysis that led to the final working scenario is presented in the Aerodynamic Section Appendices.

4.3.2.1 CFD Analysis Introduction / Application Description

Several computational tools of varying levels of fidelity were used to predict aerodynamic forces and moments in support of the investigation. The inviscid methods provided a rapid meshing capability and a highly parallelized solution algorithm that allowed them to be used to screen a large number of damage scenarios over the course of the investigation. Development of the computational meshes for the viscous solver took much longer (weeks instead of a day), and the flow solutions were more computationally intensive (days/weeks instead of hours); thus the viscous solvers were used primarily as a check on the more abundant (from an aerodynamic perspective) inviscid work. The application of the various flow solvers utilized is briefly described and summarized in Table 4.3-1. Each is described in more detail in Aerodynamic Appendices Section 4.7.8.

The inviscid, unstructured mesh tool FELISA was the computational 'workhorse' of the aerodynamic investigation. It provides the capability to turn around complex geometries (mesh + solution) in under 2 days. Additionally its unique (among inviscid solvers) capability to model the flight environment with equilibrium air chemistry as well as the perfect gas environment of the Mach 6 air facility and the environment of the CF_4 tunnel provided ground test to flight condition trending. The inviscid, Cartesian mesh code CART3D was used to provide a set of rapid solutions at the Mach 6 air wind tunnel conditions. The viscous overset mesh solver OVERFLOW provided several Mach 6 laminar air solutions and was used to specifically address leeside flow interactions including the effects of the SILTS pod on the vertical tail. The viscous solvers GASP, USA and LAURA provided a set of solutions for the undamaged orbiter at hypervelocity flight conditions with full non-equilibrium chemistry, matched against a several solutions corresponding to wing leading edge damage scenarios, and a few coupled external/internal solutions.

4.3.2.2 STS-107 CFD Analysis Case Definition

Several sets of flow conditions were used in the analysis process. In the initial phase of the investigation, flow conditions and corresponding solutions for the STS-2 trajectory that have been widely reported in the open literature, and are listed in Table 4.3-2, were used as investigators geared up to support the investigation. Once the flight data from STS-107 became available, a joint effort undertaken by the aerodynamic and the aerothermodynamic teams, established a common set of flight conditions for use in all computational analyses. Table 4.3-4 lists the CFD points that were chosen along the STS-107 trajectory. Together, the 10 points span the range of STS-107 atmospheric flight conditions from entry interface (EI) to loss of signal (LOS). Points labeled condition AA and condition A were chosen for DSMC analysis at rarefied gas dynamic conditions, while the points, B and 1 - 6 were chosen for continuum flow (Navier-Stokes and Euler) methods. The conditions labeled 1-6 were chosen along the trajectory to correspond to key events that were noted in the initial evaluation of the OI data, and are described in Table 4.3-4. The CFD points were established well before the OEX data recorder was recovered and the MADS data became available. A final point, condition VN, was added near the end of the investigation to capture

the point at which the vacuum vent and water supply nozzle thermocouples indicate a brief off-nominal increase in temperature rise rate.

The challenge associated with the selection of the points was the lack of detailed atmospheric information during STS-107 entry flight combined with the need to quickly establish common CFD conditions to support the rapid pace of the investigation. In order to establish the complete set of conditions for these data points, several sources of information were combined. The most crucial data came from the GPS tracking that accompanied the OI telemetry data set. The GPS data provided the most accurate information on position (altitude, longitude, latitude) and relative velocity (speed, flight path angle, azimuth angle). The aerodynamic/ aerothermodynamic teams next assessed the OI data, which provided inertial navigation data information. While these data sets were less accurate in providing velocity and position compared to the GPS data, they did provide reasonably accurate information on vehicle attitude (alpha, beta and bank) as well as the actual control surface deflections (body flap, inboard and outboard elevons). To complete the needed data set, the February GRAM atmosphere model was utilized. An important note regarding the GPS velocity and OI derived vehicle attitude information is that neither accounts for the presence of any winds. When the CFD points were defined, the DAO/MSFC atmospheric reconstruction had not yet been developed. Furthermore, no attempt was made to re-compute the atmospherically derived parameters or account for the effect of wind on vehicle velocity and attitude parameters. By the time the DAO/MSFC atmospheric model became available, the computationally expensive CFD calculations were well under way. It is important to note that the delta aerodynamic analyses show little sensitivity to Mach number and angle of attack. Table 4.3-3 gives an accounting of how all the parameters were calculated. Figure 4.3-26 through Figure 4.3-29 depict various key trajectory parameters and labels the chosen CFD analysis conditions.

Additionally, CFD cases were run at wind tunnel conditions for both the Langley Mach 6 air and CF_4 facilities. The wind tunnel flow conditions used for the various flow solvers are shown in Table 4.3-5.

4.3.2.3 Configuration Summary and Analysis

All of the baseline and damaged configurations that were analyzed and the flow solver(s) and conditions used for analysis are summarized in Table 4.3-6. The scenarios are grouped by type/progression of damage, with baseline geometries listed first. The damaged configurations are grouped into three categories. The first group is for single and multiple missing RCC panels (full or partial), and includes the initial panel 6 damage simulation. The second grouping is a series of cases for progressive damage, increasing in severity, in the region of RCC panel 9. The third group of computations was for windward surface deformations, including an open wheel well and windward surface depressions/dimples (these simulate possible structural deformation of the wing skin due to the internal heating damage to the intermediate wing structure). The following subsections discuss the geometries, flow conditions, and analysis tools and present flow field images as well as the delta aerodynamic moment increments. The delta aerodynamic forces are not discussed here, as the extraction of these quantities from the flight data was considered unreliable.

4.3.2.3.1 Baseline Geometry and Analysis

While it would have been ideal for every computational and wind tunnel model to be generated from the same solid CAD model, time constraints and the availability of existing models already tailored to each particular application led to the decision to ‘go with what we have’ and to assess the impact of this decision when a common geometry became available. An 1997 CAD geometry was the basis for all of the computational meshes that existed prior to the Columbia accident. The 2003 CAD geometry was made available to all of the investigators shortly after the accident, and served as the geometry for the common baseline mesh (detailed in Aerothermodynamics Section 5.2.4.2) used for all of the structured mesh viscous computations. Table 4.3-7 lists the geometries that various computational meshes were generated from, and their relationship to the two ‘official’ CAD definitions. An effort was made to ensure that all investigators were modeling the damage consistently. The common geometries that were used to model the damaged orbiter are listed in Table 4.3-8.

An important assumption was made in all of the analysis, both wind tunnel and computational. Even if the model did not exactly capture the absolute aerodynamics of the orbiter at flight conditions, the delta

aerodynamic coefficients (calculated as *delta* = *damaged* – *baseline*) yield a reasonable approximation (when the damaged and baseline models are as close as possible with the exception of the damage area). For the computations great care was taken to have comparable mesh spacing in areas not affected by the damage. This eliminated any potential for deltas due to mesh differences corrupting the results.

Several geometric modeling simplifications were made for the various computations on an individual code and scenario basis. Early in the investigation, many computations were made excluding the vertical tail. The vertical tail is typically not important for hypersonic aerodynamics at high angle of attack conditions, and it's presence in a simulation adds a significant number of mesh points while hindering solution convergence. As it became apparent via Columbia's recovered debris forensics that there was significant off-nominal flow to the OMS pod and vertical tail, the tail was added into most computational models. Additionally, except for one set of OVERFLOW calculations, none of the computational models included the SILTS pod located on the tip of Columbia's vertical tail. For most cases, only half-body (i.e., 180°) simulations were computed, assuming no flow across the centerline of the vehicle. This modeling decision is the norm for CFD simulations as it facilitates more rapid simulations. While the assumption of no flow across the centerline was not strictly valid for the simulations where the leeside flow of the vehicle was interacting with flow through WLE damage, both FELISA and OVERFLOW results indicated that this assumption had little effect on predicted aerodynamic forces and moments (See Aerodynamic Appendices, section 4.7.5 for details of the OVERFLOW evaluation.) Also, the base of the orbiter was not modeled, another typical simplification for hypersonic simulations when the primary interest is heating or aerodynamic screening. The complex separated base flow typically requires a large mesh, and further slows convergence. It was apparent early in the investigation that damage was centered near the WLE or the wheel well, and that any effect to the base flow was likely insignificant. For many of the viscous simulations, the body flap was not included and neither were the gaps between the inboard and outboard elevons and the fuselage. Since the investigation was primarily concerned with the delta aerodynamics, no attempt was made to model the body flap and elevons at STS-107 flight deflections; all control surfaces were set at the zero degrees or trail position. Unless otherwise noted, all computations presented here assume a half-body, and do not compute the base flow. Additionally, a notation is made when the tail or body flap is not present in the computation.

Flow solutions on the baseline (undamaged) geometry were used by the Aerodynamics Team to compute the differences in aerodynamic forces and moments between the baseline and the damaged configurations, and for flow field comparisons. The External Aerothermodynamics Team also made extensive use of the baseline solutions to determine environments for engineering heating methods. To understand how well the inviscid and viscous computational methodologies reproduced the Orbiter OADB, a comparison was made between the OADB data and CFD results. Solutions computed on the baseline geometry as well as a missing panel 6 geometry with FELISA, and on the baseline geometry (without the body flap) with LAURA were utilized for this evaluation

The total normal and axial forces, and pitching moments for the solutions at CFD conditions 1 through 6 are plotted against time from EI of the STS-107 trajectory in Figure 4.3-30 (Note: side force, rolling and yawing moments are all zero for the symmetric baseline). The force and moments for the FELISA solutions are computed with and without the body flap, to serve as a bridge between the Orbiter OADB data and the LAURA computations. For pitching moment, the FELISA data is in better agreement with both the Orbiter OADB data and LAURA computations later in the flight, suggesting that the inviscid equilibrium chemistry model is not as appropriate for the higher Mach number range (M > 21). The trend in the LAURA predictions against FELISA without the body flap is similar to the trend of the Orbiter OADB data against the full FELISA solution, suggesting that the LAURA data is in good agreement with the flight database. The FELISA missing panel 6 result is also included in Figure 4.3-30 to illustrate how relatively small the delta aerodynamics due to damage are with respect to the absolute aerodynamics. A detailed discussion of this topic is included in the Aerodynamic Appendices Section 4.7.4.2.

4.3.2.3.2 Full RCC Panel missing

A damage scenario considered early in the investigation was that an entire RCC panel or perhaps several panels had been lost. This scenario was reinforced by an early FELISA computation (and subsequent wind tunnel testing) that showed windward flow passing through a notch in the WLE created by a simulated missing RCC panel. The notch was modeled with solid side surfaces and the open channel

behind the RCC panels was not represented. The flow was compressed as it passed through the notch, sending a jet over the leeward surface of the wing where it impinged on the side of the fuselage. This was this first evidence of a source for the augmented heating recorded by Columbia's fuselage and OMS pod surface temperature measurements. Consequently, a large portion of the computational effort in the investigation was spent looking at missing RCC panel configurations to gain an understanding of the effect of location and size of WLE damage on the aerodynamics and aerodynamic heating characteristics of the vehicle. The bulk of the computations were performed utilizing FELISA at both CF4 tunnel and flight conditions to establish a link between the wind tunnel results and the STS-107 flight data. A limited number of CART3D and OVERFLOW solutions were exercised at Mach 6 air and at flight Mach numbers with perfect gas (see Aerodynamic Appendices sections 4.7.5 (OVERFLOW) and 4.7.6 (CART3D) for more details), to provide additional insight into the trends shown with the wind tunnel and with FELISA. Additionally fully reacting Navier-Stokes calculations, primarily in support of the aerothermodynamic evaluation, were completed using LAURA, GASP and USA codes for several specific WLE damage cases. (see Aerodynamic Appendices Section 4.7.7 (USA) and Aerothermodynamics Section 5.2.4.5 (LAURA & GASP) for more details). Even though the debris recovery and subsequent analysis led to a more complex picture of the damage progression, the insight into the delta aerodynamics and the corresponding flow field characteristics gained by systematically looking at missing RCC damage proved invaluable to the investigation.

Numerous codes and both wind tunnels were utilized to study the effect of missing panel 6. While this damage was later ruled out for the STS-107 flight by recovered debris and while it had a very small impact on the aerodynamics, it offers an opportunity to explore the flow physics that are associated with wing leading edge damage. The initial panel 6 missing configuration was defined in the days after the accident without the benefit of a CAD definition, and, as shown in Figure 4.3-31, does not encompass the full RCC panel. This geometry roughly corresponds to the panel 6 'notch' geometry that was also evaluated in the wind tunnel.

Streamlines for both the baseline (blue) and missing RCC panel 6 (red) configurations are shown in Figure 4.3-32, for a FELISA computation at an STS-2, Mach 24 condition. With the orbiter at a 40° angle-of-attack, there is a strong expansion around the WLE, and the leeside flow field pressure and density are very low. When a section of material (such as an RCC panel) is removed from the orbiter WLE, the resulting gap has the effect of channeling the higher energy flow from the windward to the leeside, forming a jet-like flow structure. This 'jet' of high enthalpy flow carries substantially higher momentum than the surrounding leeside flow, and therefore is not significantly influenced by it. Pressure contours shown in Figure 4.3-33 (STS-107 Mach 24.2 condition) show the footprint of a shock on the leeside surface, and flow impingement on the side fuselage. This impingement would have the effect of increasing the heating rate on the side fuselage, a trend that was identified by the OI flight data early in the investigation. The effect of the missing panel on the windward surface is localized. The windward view of streamlines in Figure 4.3-32 show that the flow pattern is not affected just inboard of the missing panel, and the Cp (pressure coefficient) contours in Figure 4.3-33 indicate that the pressure distribution on the windward acreage of the damaged wing is essentially unchanged by the damage.

The full list of missing RCC panel cases analyzed computationally is given in Table 4.3-10, with the configuration details (tail/no tail, etc) and the flow conditions for each computation. Figure 4.3-34(a-e) shows the missing panel configurations as run with FELISA, except for the cases with all panels 1-7 removed. The surface pressure (C_p) contours on the side fuselage are shown in Figure 4.3-35 for each configuration at the STS-107 CFD condition 2 (Mach 24.2, α=40°). The disturbance on the fuselage moved further down the body and produced a higher C_p as the location of the missing RCC panel moved outboard (Figure 4.3-35a). For multiple missing panels, the trends are not as clear. There is a significant increase (> 2x) in the peak pressure on the side fuselage for missing panels 6+7 as compared to 6 only (Figure 4.3-35b). Removing more panels (5+6+7 or 1-7) spreads the region of influence, and the peak pressure drops. Figure 4.3-36 shows the leeside view for missing panels 6, 6+7, and 9. The influence of the size and orientation of the missing panel(s) is evident in the footprint of the expansion out of the channel and the shock due to the resulting 'jet' directed towards the fuselage. The missing panel 9 and missing panels 6+7 results show significantly stronger interaction on the wing leeside than the panel 6 removed case. For missing panels 6+7, the disturbance actually expands upstream of the damage area, indicating the strength of the jet relative to the leeside flow.

All computational methodologies consistently produced negative delta yawing (ΔCn) and pitching moments (ΔCm), and near zero to negative delta rolling moments (ΔCl) for a full missing RCC panel. Magnitudes of the predicted aerodynamic moments varied with the geometry, and to a lesser degree with flow condition (Mach 6 air, CF4, flight). The trends observed are very similar to those measured in the wind tunnel.

The delta aerodynamic moments computed with FELISA for several panel out configurations at flight (CFD condition 2, Mach 24.2) and CF4 are compared to the CF4 wind tunnel results in Figure 4.3-37. The x-axis of the plot is simply the configuration (labeled individually). The lines connecting the points for each configuration are included only to illustrate the trends; there is no expectation that interim damages can be predicted. Overall, the trend agreement between the computations and the wind tunnel is excellent. As additional RCC panels are removed, the moment increments become more negative. Delta pitching and rolling moments are relatively constant as the missing panel location moves outboard, while the yawing moment increment shows a more negative trend as the missing panel moves outboard. A single FELISA solution at flight (CFD condition 2, Mach 24.2) was computed for the full missing RCC panel 6 (RCC + carrier panel) to compare to the initial, or notched panel 6 results. Removing more material at the same location has a noticeable impact on the pitch and roll increments, but little effect on the yawing moment increment.

While the trends shown by the FELISA computations are consistent with the CF4 wind tunnel results, there is definite variation in magnitudes. Comparing the computed CF4 data to the WT measured values, FELISA over-predicts the roll, under-predicts the pitch increment, with close agreement for the yawing increment. When comparing flight condition to CF4 predictions, the flight computations produce consistently lower (larger value, more negative) pitch and yaw increments, while predicting higher (smaller value, more positive) rolling moment increments. While these differences appear large on the scales plotted in Figure 4.3-37, the magnitude of all of the delta moments for the missing panel configurations are represent very small aerodynamic values. The level of correlation between the flight and CF4 computations and the wind tunnel data shown in Figure 4.3-37 strongly suggest that the trends shown in the wind tunnel results are valid for STS-107 flight conditions.

The delta aerodynamic moments from missing panel computations using OVERFLOW, CART3D, LAURA, GASP, are shown in Figure 4.3-38, with the data in Figure 4.3-37 repeated. There is some variation in the geometries for the missing panel 6 and missing panel 9 cases, making exact comparisons impracticable. The CART3D computations did not include a vertical tail, the viscous GASP and LAURA computations terminated the grid systems at the body flap, and both GASP and OVERFLOW results were completed with and without the vertical tail (OVERFLOW with the SILTS pod – Aerodynamic Appendices section 4.7.5). Despite this range of geometry, the agreement for missing panel 6 is reasonable, with near zero increments. There is more of a spread for the missing panel 9 computations with larger increments indicated. Only CART3D and FELISA were used for the multiple missing panels. The CART3D Mach 6 computations indicate the same trends as FELISA and the wind tunnel, but with less variation for the multiple missing panels. For wing leading edge damage the results from all the various tools all indicate relatively small, negative moment increments with similar trends as the damage varies. While the variation suggest the exact magnitudes are uncertain, the body of data suggests the trends are legitimate and can be used to understand how this type of damage of relates to the STS-107 reconstruction.

With computational simulations, the contributions to the vehicle aerodynamics of each vehicle component (vertical tail, wing, etc.) can be isolated. Figure 4.3-39 shows the definition of the vertical tail, wing, OMS pod, and fuselage regions of the orbiter for which component contributions of the delta aerodynamics were calculated. Figure 4.3-40 shows the contributions of each of these regions to the total delta aerodynamic moments for missing panel configurations at flight conditions (CFD condition 2, Mach 24.2). Also shown are the total aerodynamic moments for the CF4 tunnel results. As in Figure 4.3-37, the missing panel configuration is plotted along the x-axis,. Each component is color coded according to the colors in Figure 4.3-39, and labeled on the plot, with the solid symbols representing flight computations. Figure 4.3-41 repeats the format of Figure 4.3-40, with hollow symbols for predictions at CF4 WT conditions.

Figure 4.3-40(a) and Figure 4.3-41(a) clearly show that the pressure loads to the wing dominate the delta pitching moment for both flight and CF4 conditions. For the multiple missing panel cases (6+7, 5+6+7) at flight conditions, Figure 4.3-40(b) and (c) show that the delta rolling and yawing moments are also dominated by the wing. For the single missing panels, however, the influences of the vertical tail and wing

balance each other in roll, essentially yielding a zero total increment. The vertical tail, the fuselage and the wing all produce negative increments for yawing moment, thereby providing a relatively large, negative delta yawing moment. The vertical tail contributions are more pronounced in flight for missing panel 9 than for missing panel 6. The CF4 (Figure 4.3-40) conditions show more influence of the vertical tail on the delta rolling and yawing moments for all configurations, with only missing panel 9 giving a positive contribution to the total delta rolling moment. Overall the component breakdown results indicate that there is not a large enough delta rolling moment contribution from the vertical tail to cause a substantial positive (right wing down) total delta rolling moment as seen late in flight.

Several of the missing panel configurations were run at multiple flight conditions to establish trends in the delta aerodynamics due to variations in the flight conditions. Figure 4.3-42 shows the computed delta aerodynamic moments and the extracted flight increments plotted against time from EI. The angle of attack varies between 38° and 42° (See Table 4.3-4for the flow conditions at each point). The CF4 computational and wind tunnel results are also shown to the right of the trajectory data. The delta pitching moment shows little variation, for each missing panel configuration, over the trajectory. The delta rolling moment shows somewhat of a negative trend toward the end of the trajectory, but the variation is small. Only the delta yawing moment shows a definite (more positive, smaller value) trend across the trajectory. A more systematic study where angle of attack and flow condition were varied independently confirmed that only the delta yawing moment was strongly influenced by the Mach number; these results are contained in Aerodynamic Appendices Section 4.7.4.4..

Overall, the computational results (both for flight and CF4 conditions) for missing panel damage scenarios were consistent with the wind tunnel results. The flow field analysis from these computations clearly indicates that when the windward flow is diverted by WLE damage, the flow field on the leeside of the vehicle is disturbed in a way that is consistent with the increased heating patterns observed during the STS-107 flight. The aerodynamic test and analysis results demonstrate that as more material is removed from the WLE all of the delta moments trend to more negative values. This is counter to the trend toward a more positive rolling moment seen later (after EI + 600 sec) in the STS-107 flight. These two observations taken together suggest the initial STS-107 aerodynamic increments are consistent with WLE damage. However, an additional damage progression scenario, other than simply continuing loss of RCC panel(s), is required to explain the aerodynamic trends later in flight.

4.3.2.3.3 Progressive Damage in Region of RCC Panel 9

As the investigation progressed, the primary damage location was focused towards RCC panels 8-9. The recovered WLE hardware also suggested that, at least initially, the damage was not as extensive as a full missing RCC panel. The second grouping of damaged configurations is a series of damaged configurations, increasing in severity, in the region of RCC panel 9. The damage scenarios and complete set of flow conditions for FELISA cases are shown in Table 4.3-11. Representative cross-sections of the wing in the region of panel 9 are shown for each damage scenario in Figure 4.3-43. For ease of discussion, these damages will be referred to as (a) – (g), as ordered in Figure 4.3-43. Damages (a) – (d) are partial damages to RCC panel 9, and (e) – (g) correspond toe full RCC panel 9 missing configurations. Damage (a) is the lower half of RCC panel 9 missing, with solid walls, and is the same configuration as tested in the CF4 wind tunnel. Damage (b) is a 1.0 inch slot from windward to leeside, at the front edge of the upper and lower carrier panels. Damage (c) is the lower half panel 9 with an internal cavity 'carved' out, and the upper carrier panel removed to create a flow path from windward to leeside. This geometry is repeated in damage (d), with an additional 810 in^2 of leeside material removed aft and inboard of the upper carrier panel, for a total leeside exit area of ~1000 in^2. The full panel missing geometries include an RCC panel 9 missing, damage (e) and the full RCC and both (upper and lower) carrier panels missing damage (f), (this data is repeated from the section on missing full RCC panels). Damage (g) has the same damage as in (d), but with the full RCC panel removed. Both damages (d) and (g) were created in an effort to direct as much mass flow as possible towards the OMS pod and vertical tail, to establish if it was possible to generate the positive delta rolling moment observed in flight by directing flow from the windward to leeside through a hole in the upper wing surface aft of the leading edge. Additional evaluation of progressive wing damage using CART3D is discussed in Aerodynamic Appendices Section 4.7.6.

The leeside flow fields for several of these damages at flight conditions (CFD condition 4, M=20.2) are shown in Figure 4.3-44. The flow patterns on the leeside wing and the side fuselage appear very similar,

despite the fact that the flow is coming through very different size damage geometries. The strength of the impingement (maximum Cp) on the side fuselage increases as the size of the hole increases beyond the upper carrier panel area, but is relatively constant for cases (d) – (g). The similarities in the flow patterns and pressure levels suggest that it is very difficult to isolate the damage size and location from correlations with the side fuselage MADS data. A wide range of damage scenarios, that enable windward to leeward flow, appear equally valid.

The delta aerodynamic moments for FELISA cases with progressive damage in the RCC panel 9 region, at flight (CFD condition 4, M=20.2) and CF4 conditions, are shown in Figure 4.3-45. The half panel 9 geometry (a) gives a very small increment in rolling (positive) and yawing (negative) moments, as no windward flow is diverted to the leeside. The delta aerodynamics for the one inch wide slot at RCC panel 9 are essentially zero. Establishing a larger flow path by removing the whole upper carrier panel 9 (c) continues the small positive increment to the rolling moment, and significantly shifts the yawing moment to a more negative value. When the size of the hole on the leeside is increased (d) from 188 in^2 (size of the upper carrier panel) to 998 in^2, there is little change in the delta rolling moment, and a small increase in the delta yawing moment. For the full panel out cases, the delta rolling moment becomes more negative as more WLE material is removed, from (e) to (f), while the delta yaw stays constant. When the additional leeside material is removed in (g), the delta yawing moment becomes less negative, and the delta rolling moment remains unchanged.

The component breakdown of the contributions to the delta aerodynamic moments is shown in Figure 4.3-46 and Figure 4.3-47 (See Figure 4.3-39 for the component definition). For delta rolling moment, the vertical tail gives a consistently positive contribution, which is offset to some degree by the wing. The half panel cases ((c) and (d), primarily) result in a small contribution from the wing, and thus a positive rolling moment. The full panel cases ((e) – (g)) have more contribution from the wing, resulting in a slightly negative rolling moment. The delta yawing moment is consistently negative, with fuselage and tail contributing more for the flight cases than the CF4. This analysis of component contributions to the total delta aerodynamics further underscores the observation that a large positive roll does not come from the flow over the vertical tail.

The leeside flow fields suggest that any of the damage progression configurations enabling flow to the leeside ((c) – (g)) can produce a significant disturbance on the side fuselage and OMS pod. The aerodynamic data, however, indicate that the damage that produces the more positive delta rolling moment (albeit near zero) is one with only partial damage to the RCC panel with flow to the leeside through an area behind the RCC, rather than a complete RCC panel missing. This set of damage scenarios did not produce a large positive rolling moment increment as observed late flight (EI + 800 sec). Indeed, it is clear that progressively damaging a particular RCC panel does not produce the steadily increasing trend in rolling moment increment seen in flight. This suggests that there must be another type of damage in addition to the WLE damage scenarios examined.

4.3.2.3.4 Windward Surface Deformation (Depressions and WLE Deformation)

One of the clearest trends in the reconstructed flight data was a change in the trend of the delta rolling moment that occurred around 600 seconds after EI. This change in rolling moment trend, and particularly the relatively large positive rolling moment late in flight (> EI + 800 sec), was not explained by any of the full or partial RCC panel damage configurations. Early wind tunnel tests with shallow wheel well cavities exposed had indicated that windward surface cavities could produce the positive roll and negative yaw observed late in flight.
A third group of computations conducted to investigate windward surface depressions/dimples in an attempt to model the structural deformation of the wing due to the heating damage to the intermediate wing internal structure. The depressions are assumed to result from the wing skin “dimpling” due to failure of the ribs and delamination of the wing honeycomb skin panels. Figure 4.3-48(a) shows an intermediate length (L=98”) depression that extends to the end of the wheel well, and has a depth that is approximately half (d=2.8”) of the depth modeled in the wind tunnel. Figure 4.3-48(b) shows the damage configuration that corresponds to full length, “single wide” (1w) depression with RCC panel 9 removed that was also tested in the CF4 tunnel. The depression created in the ceramic wind tunnel model was milled such that the interior corners were rounded, as opposed to sharp edges in the FELISA model. Aerodynamic

increments for the intermediate length dimple at 2 depths and a full length depression with and without RCC panel 9 removed were computed with FELISA for flight and CF4 conditions. The structural analysis group at JSC performed a FEM simulation of the global deformation of the wing, assuming failure and degraded strength of the structure in the intermediate wing box area. Additional engineering calculations were made on the damaged structure to simulate the localize deformation of the wing skin. Figure 4.3-48(c) shows the resulting geometry, as modeled with FELISA. The structural analysis efforts to understand the wing deformation late in flight are covered in Section 7.5. An additional geometry, which was an attempt to deform the WLE by rotating several of the RCC panels, around RCC panel 9, is included in this group. Figure 4.3-49 shows the deformed geometry overlay on the original. In the region of RCC panel 9, the WLE is rotated up. The amount of rotation tapers off away from RCC panel 9. Table 4.3-12 summarizes the damaged geometries and flow conditions that were run with FELISA for the windward surface deformation cases.

Windward surface pressure contours and surface streamlines are shown in Figure 4.3-50 for CF4 conditions and in Figure 4.3-51 for flight (CFD Condition 4, M=20.2) conditions, for several of the windward surface damage configurations. The depression configurations that simulate the 'single wide' wind tunnel geometries show a very strong compression along the aft face of the damaged area. The shorter length depression shows the same flow pattern in the expansion area at the front of the depression as the longer length. Thus, the longer depression has more area that is at a higher pressure than the baseline. Additionally, the shallower depression shows a smaller and weaker compression at the aft face of the depression. The character of the flow patterns for the damage resulting from the structural analysis is quite different than for the 'single wide' geometries. Since there are no sharp slope changes, a gentle expansion then recompression of the flow occurs within the dimpled area, and therefore a smoother and smaller variation in the surface pressure. This results in smaller delta aerodynamic moments than for the wind tunnel cases configurations.

The delta aerodynamics for the windward damage cases and corresponding CF4 tunnel data are shown in Figure 4.3-52. The WLE deformation case showed zero delta rolling and pitching moments, and a relatively small increment in yawing moment. The zero increment in rolling moment is due to canceling contributions of an increase in normal force (giving positive rolling moment) and a positive side force (which gives a negative rolling moment). It is possible that a WLE deformation that rotates more RCC panels at a smaller angle so less side force is produced would show a positive delta rolling moment. The agreement between the computations and wind tunnel for the single wide depressions is comparable for the delta yawing and pitching moments, but is not as good quantitatively for rolling moment as has been shown for other damaged configurations evaluated (See Figure 4.3-37 and Figure 4.3-45). The computations show the largest positive rolling moment for any of the damage configurations assessed, and is positive for all of the depressions considered. The wind tunnel only showed positive delta rolling moment for the longer depressions. This discrepancy is likely due to a combination of geometry differences (particularly the contoured back wall of the depression for the wind tunnel model) and a strong viscous component to this cavity-like flow. The damage from the structural analysis dimple configuration shows a smaller, though still positive rolling moment increment, and very small pitch and yawing moment increments. This is expected, in part because the strong compression at the back of the single width depression will produce larger delta moments when compared to the more gentle sloping of the structural analysis depression.

In addition to showing computed and measured delta aerodynamics, Figure 4.3-52 also shows an estimate, using simple superposition, of the delta aerodynamics for the cases where the windward surface damage was combined with a missing RCC panel. The superposition values compare well with the computed values for the longer, single width depression combined with missing RCC panel 9, and indicate that the postulated structural damage would produce the positive roll and negative yaw that was seen in flight.

Overall, the delta aerodynamics computed with FELISA for windward surface damage configurations corroborate the trends produced in the wind tunnel. The data trends support the hypothesis of progressive internal structural damage occurring late in the flight that produces a gradual windward surface deformation. This gradual deformation produces the steady increase in rolling moment and yawing moment increments seen late in flight.

Tables

Computational Tools Used in STS-107 Investigation - Aerodynamic Analysis					
Code / Tool	**Physics Model**	**Mesh type**	**Available Gas Models**	**Mach number range**	**Analysts**
FELISA	Inviscid	unstructured	perfect gas air, CF4 gas, equilibrium air	restricted by continuum flow boundaries	LaRC (Bibb, Prabhu)
CART3D	Inviscid	cartesian unstructured	perfect gas air	<10 (applied @ Mach 6)	JSC (Dries, Greathouse)
OVERFLOW	Viscous	structured, overset	perfect gas air	<18 (applied @ Mach 6)	JSC (Lillard)
LAURA	Viscous	structured	perfect gas, equilibrium, non-equilibrium, CF4	restricted by continuum flow boundaries	LaRC (Gnoffo, Bobskill, Thompson)
GASP	Viscous	structured	perfect gas, equilibrium, non-equilibrium	restricted by continuum flow boundaries	ARC (Reuther, Jones)
USA	Viscous	structured	perfect gas, equilibrium, non-equilibrium	restricted by continuum flow boundaries	Boeing-HB (Rajagopal)

Table 4.3-1 CFD Flow Solvers used in Aerodynamic Analysis for STS-107 Investigation

OEX / STS-2 Conditions							
Case	Mach	Angle-of-Attack (Alpha) deg	Angle-of-Sideslip (Beta) deg	Velocity ft/sec	Density slug/ft^3	Temperature °R	Reynolds Number / ft
STS-2a	18.07	40˚	0º	18429.4	3.1673E-07	433.1	9070
STS-2b	24.3	40˚	0º	22704.5	1.1200E-07	363.6	17950

Table 4.3-2 STS-2 Conditions Utilized in Initial Phase of Investigation

Parameter	Derivation	Comment
altitude	GPS data	
longitude	GPS data	
latitude	GPS data	
Velocity	GPS data	should be wind corrected to get true airspeed
flight path angle	GPS data	should be wind corrected
azmithul angle	GPS data	should be wind corrected
density	GPS altitude + GRAM February model	should be updated with DOA/MSFC atmosphere
temperature	GPS altitude + GRAM February model	should be updated with DOA/MSFC atmosphere
dynamic pressure	GPS velocity + density	should be updated with DOA/MSFC atmosphere
viscosity	Sutherland Law + Temperature	should be updated with DOA/MSFC atmosphere
Mach number	GPS velocity + Temperature	should be updated with DOA/MSFC atmosphere
Reynolds number	GPS velocity + Temperature	should be updated with DOA/MSFC atmosphere
Stagnation radiative equilibrium Heat Flux	Fey-Ridell + GPS data + GRAM data	should be updated with DOA/MSFC atmosphere
Stagnation radiative equilibrium Temperature	Fey-Ridell + GPS data + GRAM data	should be updated with DOA/MSFC atmosphere
Alpha	OI inertial navigation data	should be wind corrected
Beta	OI inertial navigation data	should be wind corrected
Bank	OI inertial navigation data	should be wind corrected
Body Flap	OI data	
Left Inboard Elevon	OI data	
Left Outboard Elevon	OI data	
Right Inboard Elevon	OI data	
Right Outboard Elevon	OI data	

Table 4.3-3 Parameter Calculation Method for STS-107 Investigation Conditions

Point Name	Comments	GMT (mm:ss.ss)	Time past e.i. (sec)	Altitude (ft)	VREL (ft/sec)	Mach Num.	Reynolds # per foot (Re/ft)	Alpha (deg)	Beta (deg)
Condition AA	350,000 ft DSMC point	45:40.0	91.04	350,274	24,622	25.10	26	40.78	-0.29
Condition A	300,000 ft DSMC vs NS comparison point	47:26.6	197.60	300,004	24,666	27.04	456	39.55	0.30
Condition B	Early Entry Navier-Stokes solution point	49:00.7	291.68	261,730	24,603	25.70	2,679	41.35	-0.07
Condition 1	Start Peak Heat	50:53.0	404.00	243,048	24,116	24.87	5,872	40.17	-0.06
Condition 2	First Off Nominal Event	52:20.4	491.36	236,527	23,554	24.17	7,644	39.99	-0.25
Condition VN	Off nominal vent nozzle temp. rise rate	52:45.3	516.32	234,623	23,368	23.94	8,274	40.04	-0.50
Condition 3	Mid Fuselage Bond Line Temperatures @ x=1215 and 1410 start off nominal trend	54:24.2	615.20	227,423	22,505	22.91	10,997	39.59	-0.47
Condition 4	Start of elevon roll trim corrections	57:35.2	806.24	216,064	20,210	20.30	16,244	42.01	-0.69
Condition 5	Near start of sharp aileron trim	58:23.2	854.24	209,368	19,428	19.35	20,729	38.87	-0.52
Condition 6	Last Good GPS point	59:30.4	921.44	200,767	18,164	17.88	27,409	39.02	-1.16

Point Name	Comments	GMT (mm:ss.ss)	Time past e.i. (sec)	Density (slugs/ft^3)	Temp (deg R)	Dynamic Pressure (lbf/ft^2)	Viscosity (slugs/(ft*sec))	Stag. heat flux (BTU/ft^2*sec)	Stag. rad. eq. Temp. (deg R)
Condition AA	350,000 ft DSMC point	45:40.0	91.04	3.345E-10	400.4	0.1014	3.169E-07	2.820	1,627
Condition A	300,000 ft DSMC vs NS comparison point	47:26.6	197.60	5.181E-09	346.2	1.5762	2.802E-07	11.102	2,289
Condition B	Early Entry Navier-Stokes solution point	49:00.7	291.68	3.314E-08	381.5	10.0292	3.043E-07	27.844	2,881
Condition 1	Start Peak Heat	50:53.0	404.00	7.568E-08	391.2	22.0077	3.108E-07	39.651	3,147
Condition 2	First Off Nominal Event	52:20.4	491.36	1.017E-07	395.2	28.2189	3.135E-07	42.559	3,203
Condition VN	Off nominal vent nozzle temp. rise rate	52:45.3	516.32	1.113E-07	396.4	30.3782	3.142E-07	43.528	3,221
Condition 3	Mid Fuselage Bond Line Temperatures @ x=1215 and 1410 start off nominal trend	54:24.2	615.20	1.552E-07	401.4	39.2967	3.176E-07	45.643	3,258
Condition 4	Start of elevon roll trim corrections	57:35.2	806.24	2.610E-07	412.5	53.3117	3.248E-07	42.119	3,195
Condition 5	Near start of sharp aileron trim	58:23.2	854.24	3.515E-07	419.6	66.3299	3.294E-07	42.824	3,208
Condition 6	Last Good GPS point	59:30.4	921.44	5.064E-07	429.3	83.5424	3.356E-07	41.502	3,182

Point Name	Comments	GMT (mm:ss.ss)	Time past e.i. (sec)	Bank (deg)	Body Flap (deg)	Lf. Inbd. El. (deg)	Lf. Outbrd. Elv. (deg)	Rt. Inbrd. Elv. (deg)	Rt. Outbrd. Elv. (deg)
Condition AA	350,000 ft DSMC point	45:40.0	91.04	-0.19	-4.32	1.97	1.88	1.97	1.96
Condition A	300,000 ft DSMC vs NS comparison point	47:26.6	197.60	1.36	-4.28	1.97	1.91	1.97	1.96
Condition B	Early Entry Navier-Stokes solution point	49:00.7	291.68	1.79	-4.46	-1.03	-1.06	-1.27	-1.25
Condition 1	Start Peak Heat	50:53.0	404.00	78.55	1.18	-2.30	-2.32	-3.54	-3.55
Condition 2	First Off Nominal Event	52:20.4	491.36	72.77	1.19	-2.71	-2.67	-3.53	-3.51
Condition VN	Off nominal vent nozzle temp. rise rate	52:45.3	516.32	72.05	1.19	-2.74	-2.74	-3.50	-3.45
Condition 3	Mid Fuselage Bond Line Temperatures @ x=1215 and 1410 start off nominal trend	54:24.2	615.20	66.75	1.23	-2.17	-2.21	-3.18	-3.19
Condition 4	Start of elevon roll trim corrections	57:35.2	806.24	-68.57	-1.81	-4.58	-4.58	-3.51	-3.50
Condition 5	Near start of sharp aileron trim	58:23.2	854.24	-56.75	-0.26	-3.27	-3.14	-1.37	-1.38
Condition 6	Last Good GPS point	59:30.4	921.44	-63.85	0.09	-6.07	-6.03	-1.63	-1.64

Table 4.3-4 STS-107 Investigation CFD Case Flight Conditions

Mach 6 Air Conditions (LaRC Tunnel)							
Case	Mach	alpha,	beta,de	velocity, ft/sec	density, slug/ft^	T, °R	Reynolds Number / ft
LAURA Wind Tunnel	5.94	40°	0º	3092.9	6.3517E-05	113.0	2.08 Million/ft
OVERFLOW Wind Tunnel	5.96	40°	0º	3096.0	2.5556E-05	112.3	2.98 Million/ft
Perfect Gas, FELISA,CART3D	6	40°	0º	---	---	---	---

Mach 6 CF4 Conditions (LaRC Tunnel)							
Case	Mach	alpha,	beta,de	velocity, ft/sec	density, slug/ft^	T, °R	Reynolds Number / ft
LAURA, low Re	5.894	40°	0º	2917.5	1.4805E-05	357.7	0.17 Million/ft
LAURA, high Re	5.902	40°	0º	2934.1	4.7026E-05	361.2	0.55 Million/ft
LAURA, final	5.913	40°	0º	2910.9	3.8915E-05	353.0	0.46 Million/ft
FELISA	5.85	40°	0º	2994.0	2.9393E-05	387.4	---

Table 4.3-5: Wind Tunnel Conditions Utilized in STS-107 Investigation

Scenario		Flow Solver	Mach 6	CF4	Flight
WLE Damage - Full / Partial Missing RCC					
Panel 6 removed	includes LaRC initial panel 6, RCC 6, and RCC+carrier panel 6	**FELISA**	X	X	X
		CART3D	X		
		OVERFLOW	X		
		LAURA			X
		GASP			X
		USA			X
Panels 6-7 removed	includes RCC 6+7, and RCC+carrier panel 6+7	**FELISA**		X	X
		CART3D	X		
Panels 5-7 removed	includes RCC 5+6+7, and RCC+carrier panel 5+6+7	**FELISA**		X	X
		CART3D	X		
Panel 9 removed	includes RCC 9, and RCC+carrier panel 9, LAURA/GASP also with open RCC channel	**FELISA**		X	X
		CART3D	X		
		OVERFLOW	X		
		GASP			X
		LAURA			X
Panels 1-7 removed		**FELISA**		X	X
		CART3D	X		
Half Panels Removed	CART3D (7, 8, 9), FELISA (9), GASP (6, 9)	**FELISA**		X	
		GASP			X
		CART3D	X		
Missing T-Seal 9		**CART3D**	X		
Progressive Damage near RCC Panel 9					
Half Panel 9	solid walls	**FELISA**		X	
		CART3D	X		
		GASP			X
Half Panel 9 with RCC cavity, upper carrier panel missing	GASP has vented walls, no upper cavity	**FELISA**		X	X
		GASP			X
Half Panel 9 with cavity, upper carrier panel missing, additional leeside material removed		**FELISA**		X	X
RCC Panel 9 removed		**FELISA**		X	X
RCC + carrier panels at 9 removed		**FELISA**		X	X
RCC 9, upper carrier 9, and additional leeside material removed		**FELISA**		X	X
Lower Carrier Panel 8 w/large upper wing hole		**CART3D**	X		
Half 8 (w/Full Panel 9 removed or small upper wing hole or large upper wing hole)		**CART3D**	X		
Windward Surface Damage					
WLE deformation	GEOLAB modification	**FELISA**		X	
B. Scallion dimple (depression created between the 163 and 192 ribs)	2 lengths, 2 depths, with and without RCC 9 removed	**FELISA**		X	X
Depression from structural analysis	Depth = 5.09"	**FELISA**		X	X

Table 4.3-6 Master Configuration Matrix for STS-107 Aerodynamic Analysis

Geometry Model / Mesh	Original Geometry Source	Comments
LaRC legacy structured mesh	1997 CAD defiinition	
gridTool model		All FELISA meshes were built from a gridTool watertight surface model, which was built from the LaRC legacy structured mesh.
FELISA unstructured surface mesh		CART3D meshes were built using the FELISA baseline mesh for the surface geometry
ARC legacy structured mesh		
Boeing legacy structured mesh		
Common Baseline Grid	2003 CAD definition	.igs and .stp exported geometry (R. Gomez-JSC)

Table 4.3-7 Geometry Pedigree for Baseline Geometries

Auxilliary Geometry for Damage Analysis	Short Name	Source	Comments
SILTS Pod	SILTS Pod	JSC Engineering	Simplified representation estimatedfrom SILTS Pod drawings
LaRC initial panel 6	LaRC initial panel 6	OEX Aerothermodynamics Symposium, NASA CP 3248, Part2, page 759	Estimated RCC panel 6 location from drawing in report -- *referred to as initial panel 6 definition or panel 6 "notch"*
Initial RCC Panel Definition	Greathouse RCC	Orbiter Drawings	RCC panel corner points were digitized from orbiter drawings. Leading edge was cut into individual pieces to approximate RCC panels 1-22
Dries/GEOLAB RCC and Carrier Panel Definition	Dries/GEOLAB	Drawing 221-50000 Rev. A, General Arrangement; Drawing MD-V70-10-002, Wing Reference System Diagram; LESS/RCC Recovery and Reconstruction Data	Panel locations provided by JSC/K. Dries and integrated into CAD definition by LaRC/GEOLAB

Table 4.3-8 Damage Geometry Pedigree

Scenario	Configuration Details	geometry pedigree	Flow Solver	STS-2	STS-107						CF4 Air Tunnel	Mach 6 Air Tunnel
					1	2	3	4	5	6		
Baseline, half body	with vertical tail, bodyflap	1997	FELISA	a, b	X	X	X	X	X	X	X	X
		1997	CART3D									X
	full body with vertical tail, bodyflap	1997	USA									
		1997	FELISA								β=-1°, +1°	
	vertical tail with SILTS pod	2003	OVERFLOW									X
	without bodyflap	1997	LAURA	a, b	X	X	X			X		
		2003	LAURA	a, b	X	X	X			X	X	X
		2003	GASP	a, b	X	X	X			X	X	X
	without vertical tail	1997	FELISA			X						
		1997	CART3D									X
		2003	OVERFLOW									X
	without vertical tail, bodyflap	1997	GASP									

Table 4.3-9 Baseline Orbiter Cases

Scenario	Configuration Details	geometry pedigree	Flow Solver	STS-2	STS-107						CF4 Air Tunnel	Mach 6 Air Tunnel
					1	2	3	4	5	6		
Full missing RCC panels												
Panel 6 removed	LaRC panel 6, vertical tail, bodyflap	1997	**FELISA**	**a, b**	**X**	**X**	**X**	**X**	**X**	**X**	**X**	**X**
	LaRC panel 6, no vertical tail	1997	**CART3D**									**X**
	LaRC panel 6, no vertical tail	2003	**OVERFLOW**									**X**
	LaRC panel 6. without bodyflap	1997	**LAURA**		**X**							
	RCC only, without bodyflap	2003	**GASP**		**X**							
	RCC + carrier panel 6, vertical tail, bodyflap	1997	**FELISA**			**X**						
	??	1997	**USA**						**X???**			
panels 6-7 removed	RCC + carrier panel, vertical tail, bodyflap	1997	**FELISA**		**X**	**X**	**X**	**α = 38°, 40°, 42°**	**X**	**X**	**X, α = 40°**	
	RCC only, no vertical tail	1997	**CART3D**									**X**
panels 5-7 removed	RCC + carrier panel, vertical tail, bodyflap	1997	**FELISA**			**X**					**X**	
	RCC only, no vertical tail	1997	**CART3D**									**X**
panel 9 removed	RCC + carrier panel, vertical tail, bodyflap	1997	**FELISA**		**X**	**X**	**X**	**X**			**X**	
	RCC only, no vertical tail	1997	**CART3D**									**X**
	RCC only, vertical tail, bodyflap	1997	**FELISA**		**X**	**X**		**X**			**X**	
	RCC + carrier panel, vertical tail, bodyflap, full (360°)	1997	**FELISA**								**β=-1°, 0°, +1°**	
	RCC only, with vertical tail and SILTS pod, full (360°)	2003	**OVERFLOW**									**X**
	RCC only, without vertical tail	2003	**OVERFLOW**									**X**
	RCC only, without tail, without bodyflap	2003	**GASP**		**X**							
	RCC only, without tail, without bodyflap. **Vented RCC channel**	2003	**GASP**		**X**							
	RCC only, vented RCC channel	2003	**LAURA**		**X**							
panels 1-7 removed	RCC only, no vertical tail	1997	**FELISA**			**X**					**X**	
			CART3D									**X**

Table 4.3-10 Missing RCC cases, FELISA

Scenario	Configuration Details	geometry pedigree	Flow Solver	STS-2	STS-107						CF4 Air Tunnel	Mach 6 Air Tunnel
					1	2	3	4	5	6		
Progressive Damage near RCC Panel 9												
half panel 9	solid walls, with vertical tail, bodyflap	1997	FELISA								X	
		1997	CART3D									X
	solid walls, without vertical tail, no bodyflap	2003	GASP		X							
	vented RCC channel, without vertical tail, no bodyflap	2003	GASP		X							
slot behind RCC panel 9	width ~ .5"	1997	FELISA								X	
	width ~ 1"	1997	FELISA								X	
half panel 9 with RCC cavity, upper carrier panel missing		1997	FELISA					X			X	
	vented RCC channel, without vertical tail, no bodyflap	2003	GASP		X							
half panel 9 with cavity, upper carrier panel missing, additional leeside material removed		1997	FELISA					X			X	
RCC 9 removed	RCC 9 only	1997	FELISA		X	X		X			X	
RCC + carrier panels at 9 removed		1997	FELISA			X	X	X			X	
RCC 9, upper carrier 9, and additional leeside material removed		1997	FELISA			X		X			X	

Table 4.3-11 Progressive Damage at RCC Panel 9, FELISA Cases

Scenario	Configuration Details	geometry pedigree	Flow Solver	STS-2	STS-107						CF4 Air Tunnel	Mach 6 Air Tunnel
					1	2	3	4	5	6		
Windward Surface Damage												
wheel well cavity open	d = 6", 15", 30"		FELISA								X	
WLE deformation	GEOLAB modification		FELISA								X	
scallion dimple (depression created between the 163 and 192 ribs)	L=98", d=2.8"	1997	FELISA								X	
	L=98", d=5.4"	1997	FELISA								X	
	L=150", d=5.3"	1997	FELISA			X	X	X			X	
	L=150", d=5.3", RCC 9 removed	1997	FELISA			X	X	X			X	
depression from structural analysis	d = 5.09"	1997	FELISA			X	X	X			X	

Table 4.3-12 Windward Surface Damage, FELISA Cases

Figures

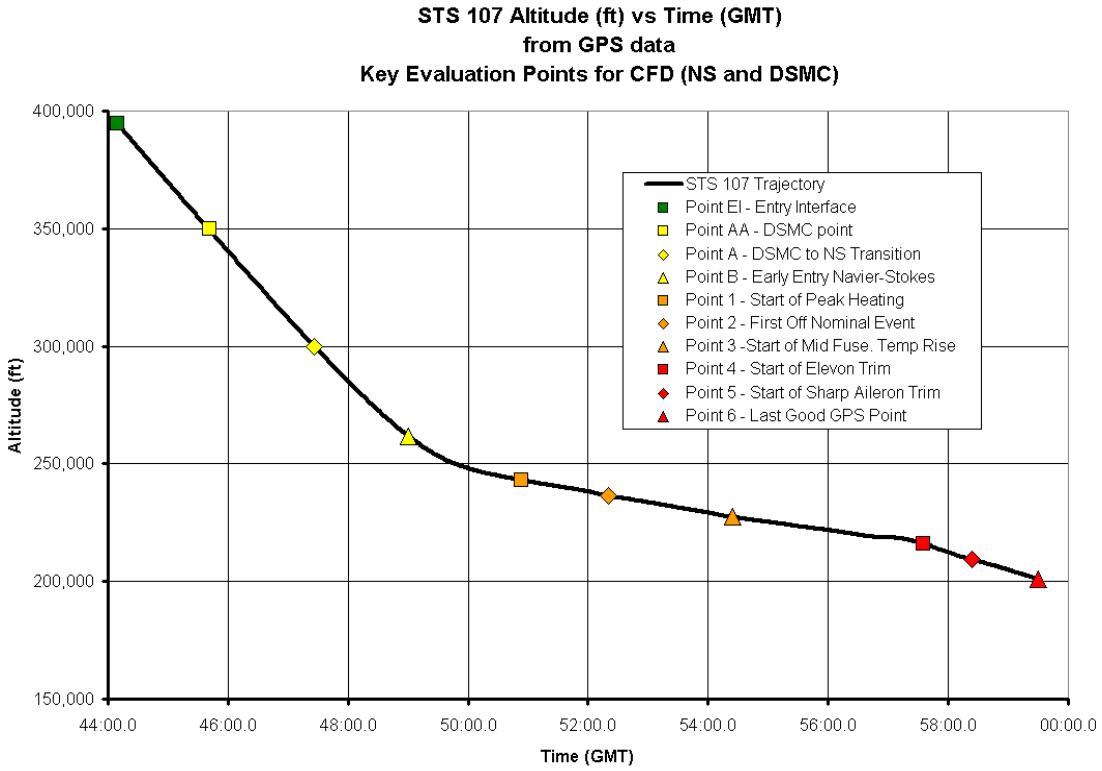

Figure 4.3-26 STS-107 Trajectory (Altitude vs. Time)

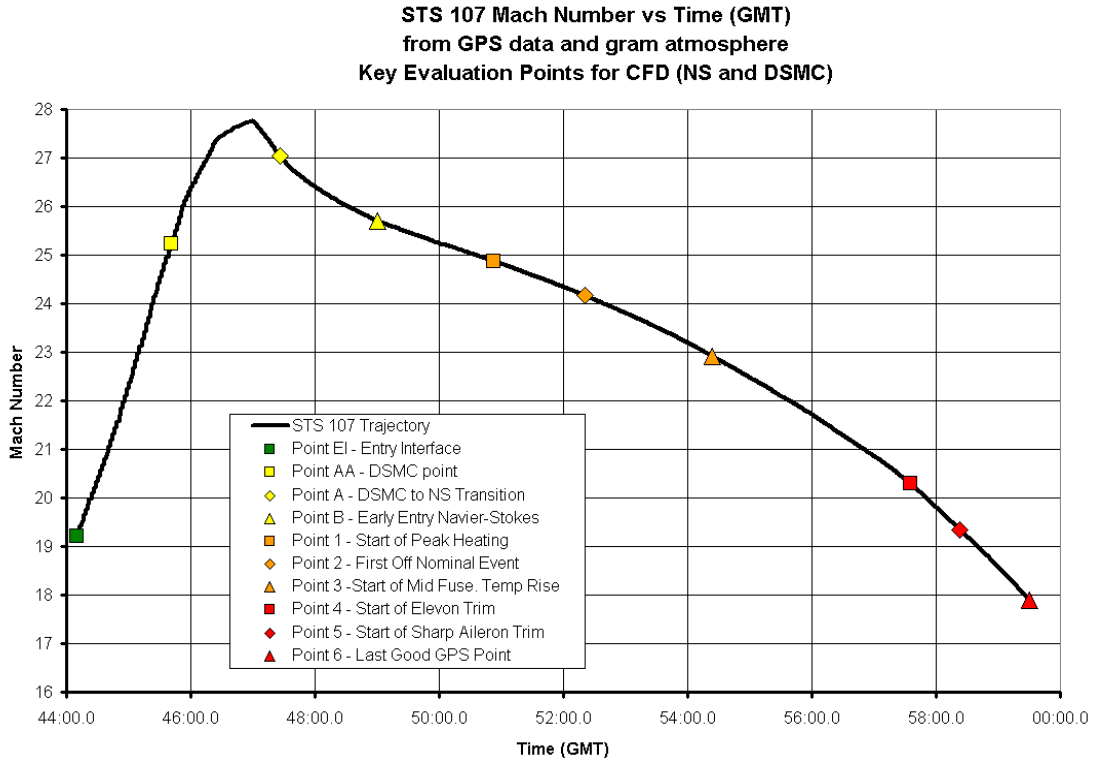

Figure 4.3-27 STS-107 Trajectory (Mach No. vs. Time)

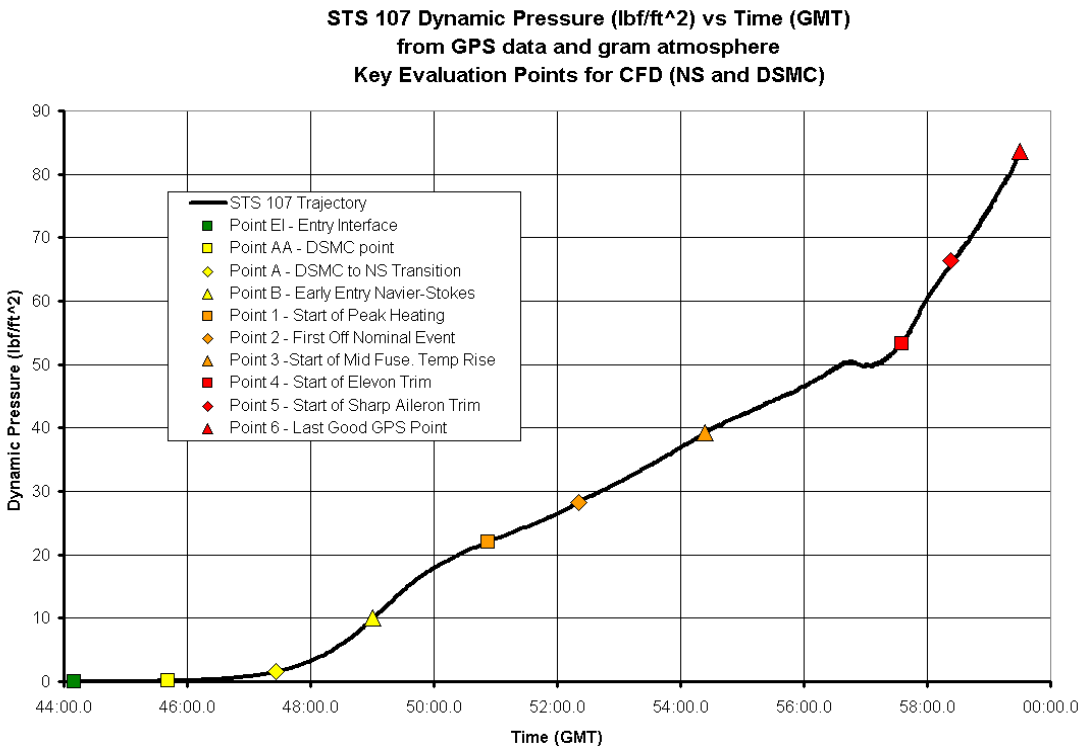

Figure 4.3-28 STS-107 Trajectory (Dynamic Pressure vs. Time)

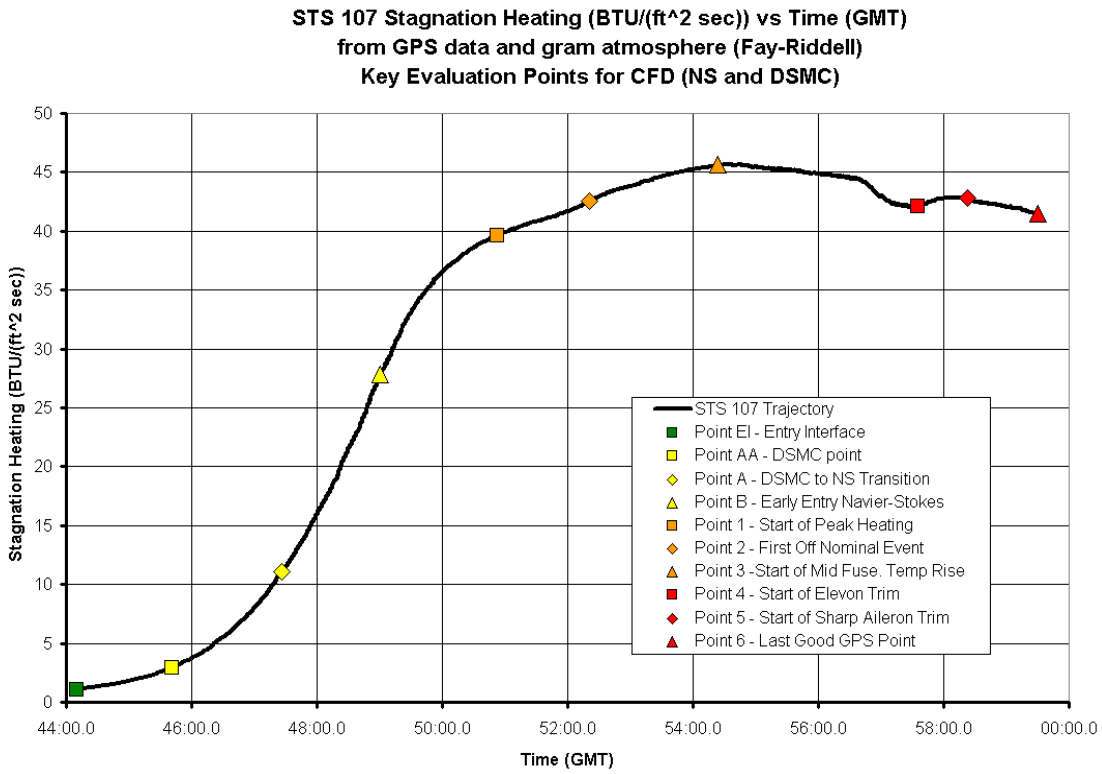

Figure 4.3-29: STS-107 Trajectory (Stagnation Point Heating vs. Time)

Comparison of Inviscid FELISA to Viscous LAURA Solutions and Flight Database

- Aerodynamic Coefficients vs. Time from Entry Interface
  - FELISA - Equilibrium Air
  - LAURA – Finite Rate Chemistry, Thermal Equilibrium
  - Angle of attack varies over flight
- LAURA geometry doesn't include bodyflap, FELISA loads reduced with and without bodyflap.
- FELISA has elevon gaps, LAURA does not.

FELISA vs. LAURA
(no bodyflap)

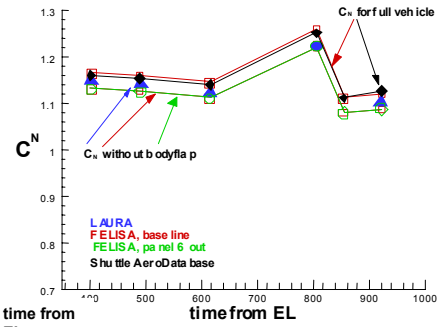

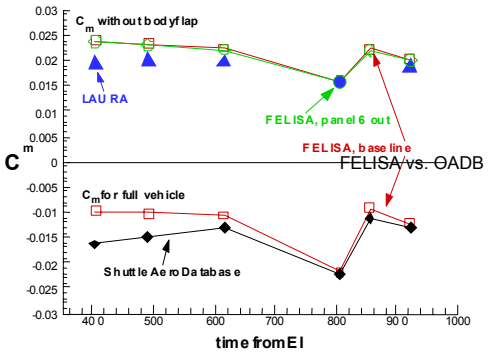

FELISA vs. OADB

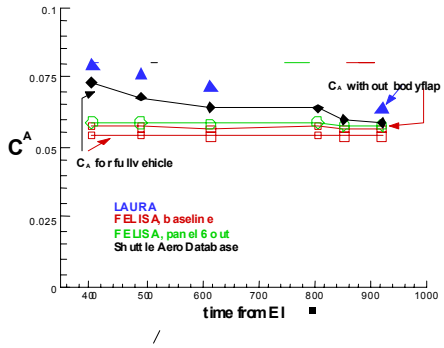

Figure 4.3-30 Baseline Aerodynamic Comparisons (Orbiter OADB vs. CFD Prediction)

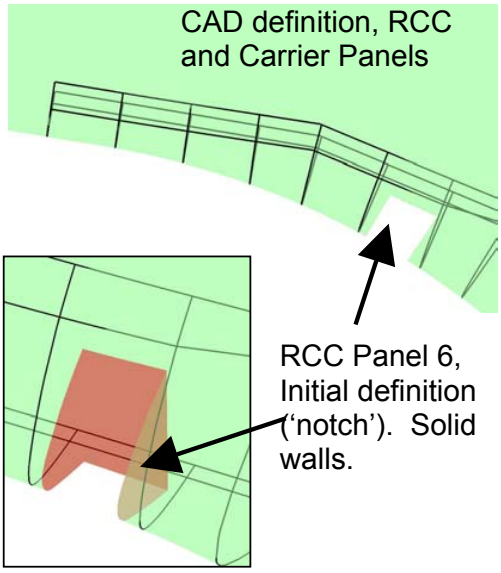

Figure 4.3-31 RCC Panel 6, Initial Definition

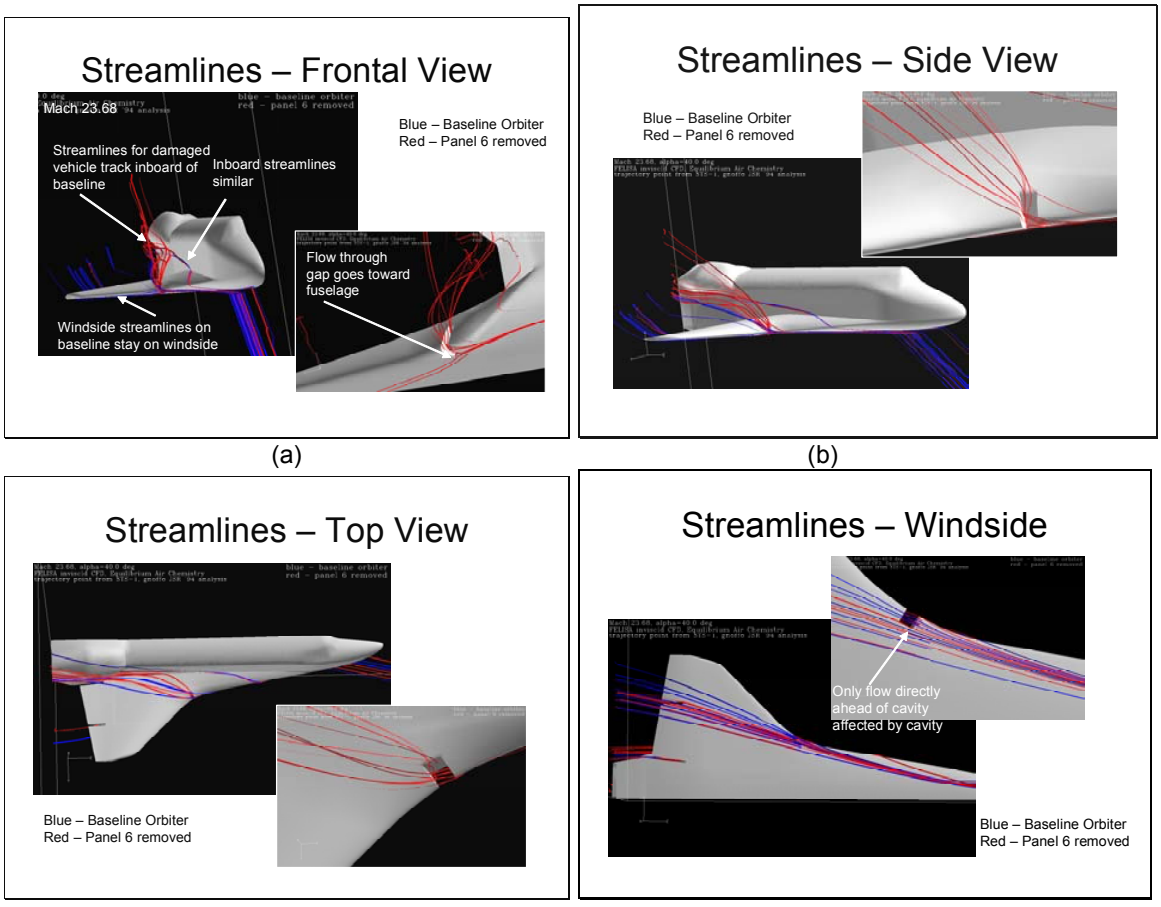

Figure 4.3-32 Nominal & Missing RCC Panel 6, Streamlines

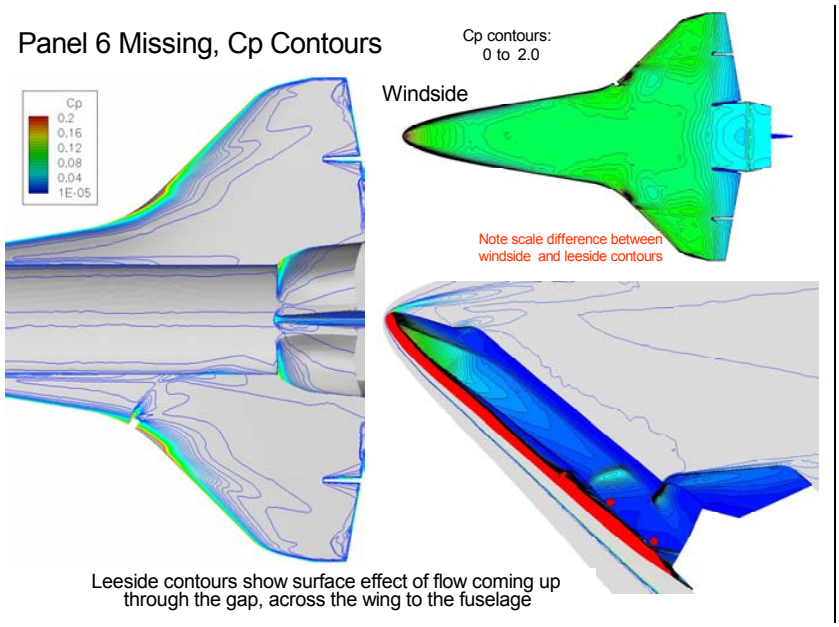

Figure 4.3-33 Panel 6 Missing – Surface Pressure Distribution

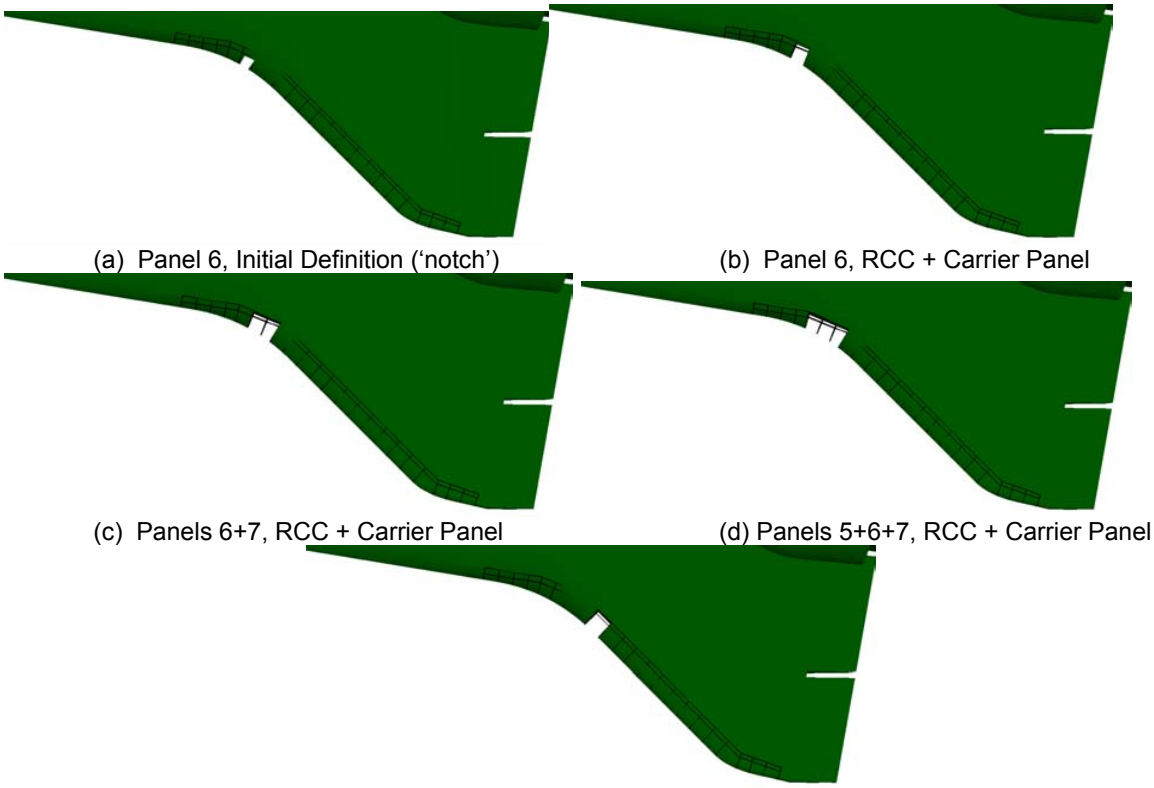

(a) Panel 6, Initial Definition ('notch')

(b) Panel 6, RCC + Carrier Panel

(c) Panels 6+7, RCC + Carrier Panel

(d) Panels 5+6+7, RCC + Carrier Panel

(e) Panel 9, RCC + Carrier Panel

Figure 4.3-34 Missing RCC Panel Geometries, FELISA

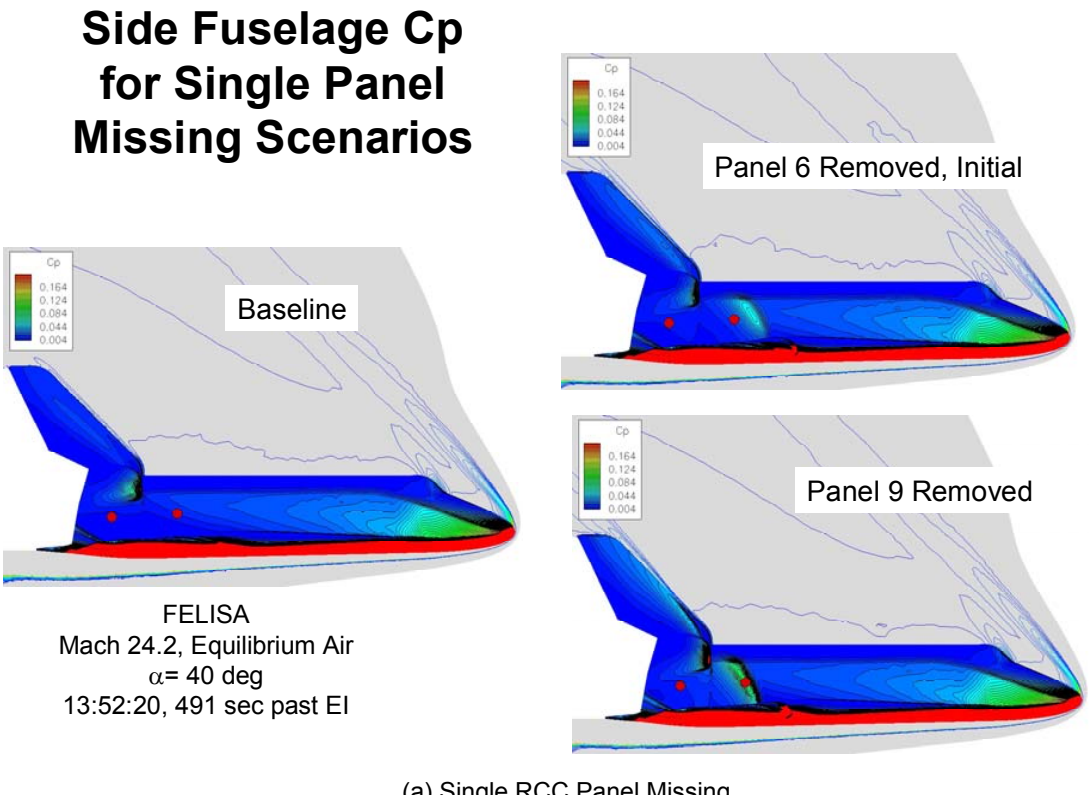

(a) Single RCC Panel Missing

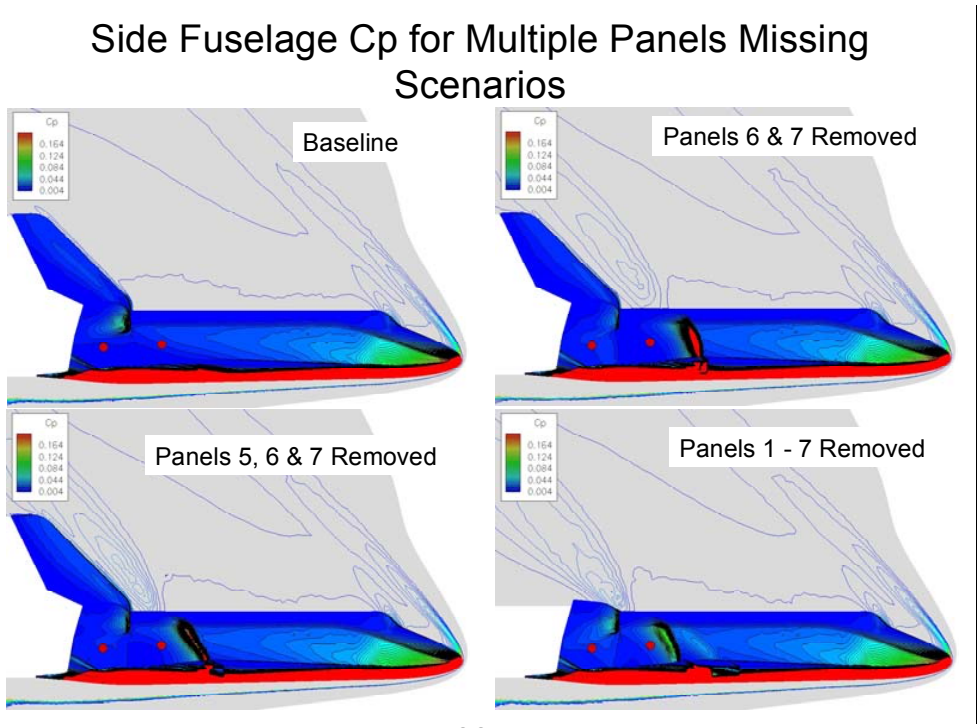

(b) Multiple RCC Panels Missing

Figure 4.3-35 Missing Panels, FELISA Cp Contours, side view

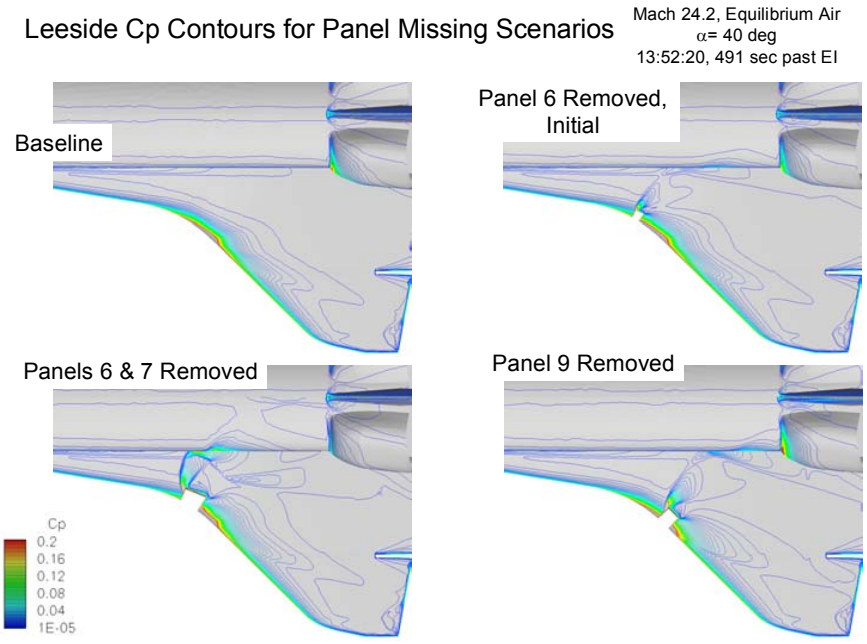

Figure 4.3-36 Missing Panels, FELISA Cp Contours, Leeside View

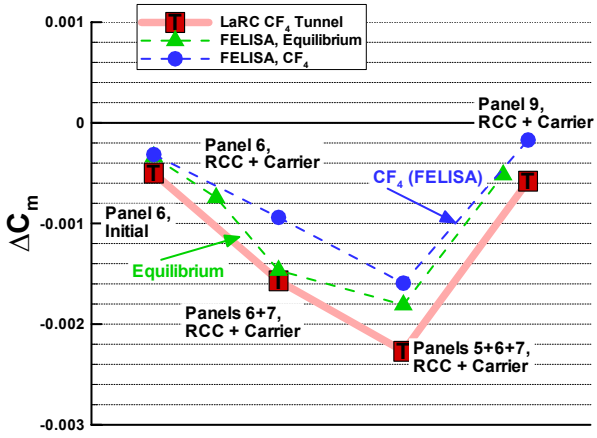

(a) Delta Pitching Moment

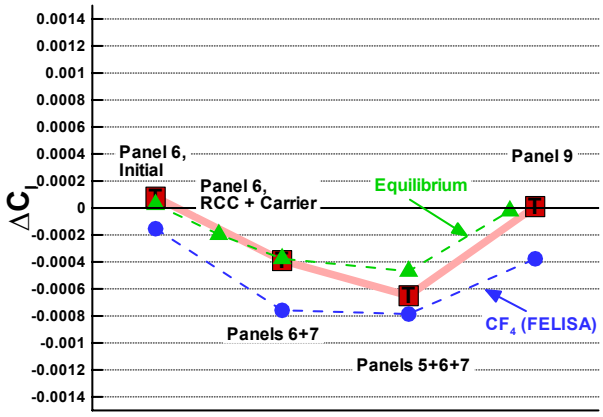

(b) Delta Rolling Moment

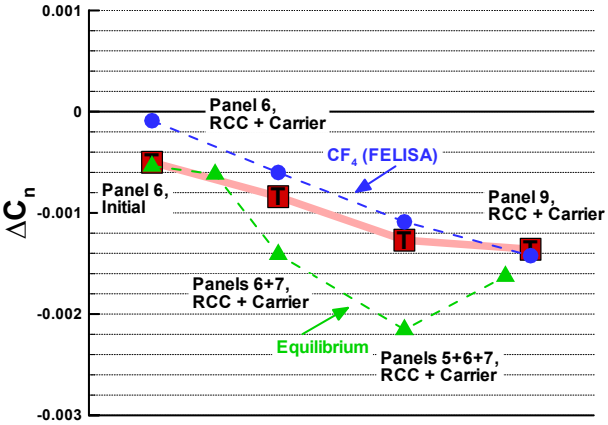

(c) Delta Yawing Moment

Figure 4.3-37 Missing Panel Delta Aero, FELISA and CF4 Tunnel

64

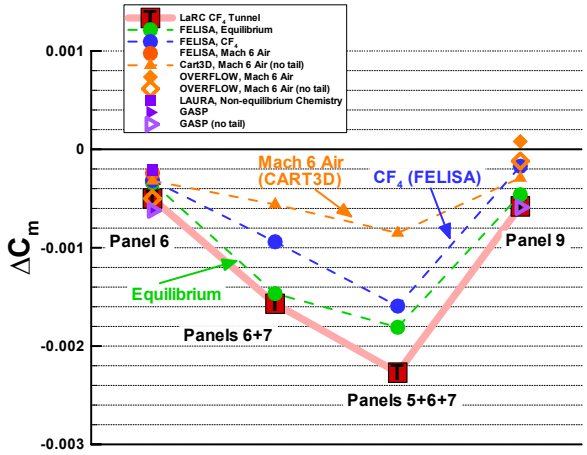

(a) Delta Pitching Moment

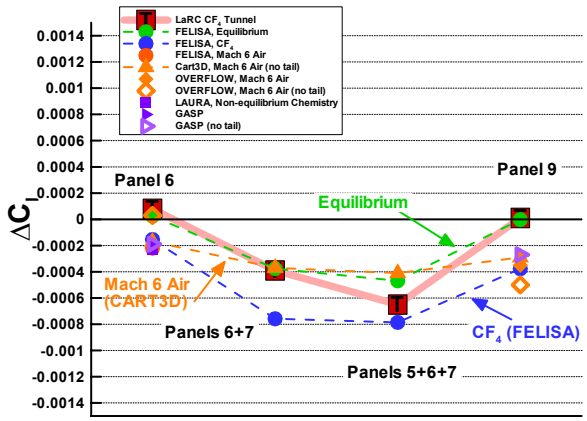

(b) Delta Rolling Moment

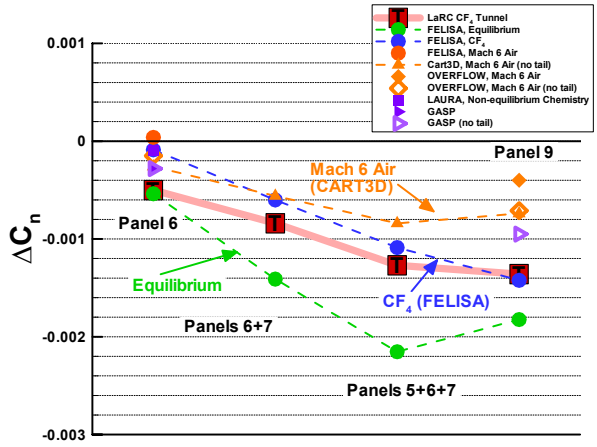

(c) Delta Yawing Moment

Figure 4.3-38 Missing Panel Delta Aero, All Computations and CF4 Tunnel

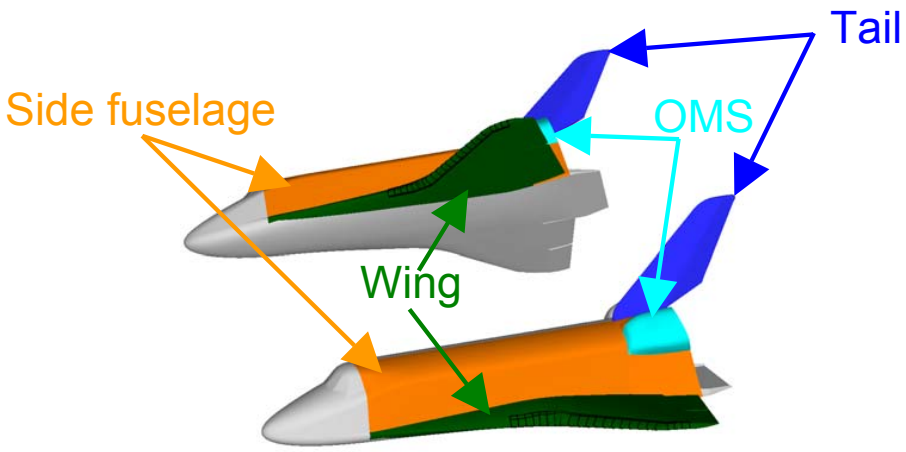

Figure 4.3-39 Orbiter Delta Aerodynamic Component Definition

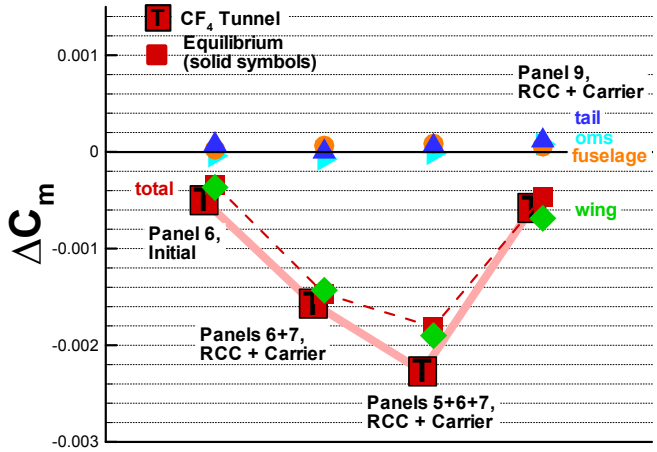

(a) Delta Pitching Moment

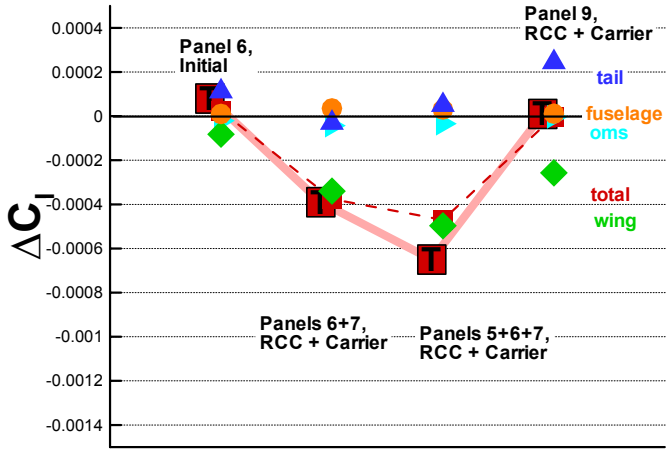

(b) Delta Rolling Moment

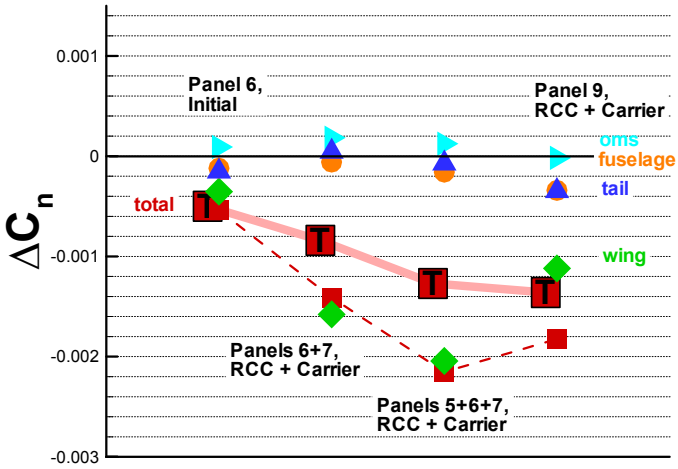

(c) Delta Yawing Moment

Figure 4.3-40 Missing Panel Delta Aero Component Breakdown(Flight Condition 2)

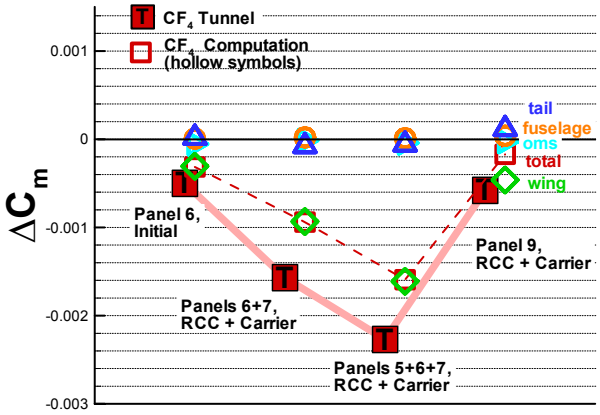

(a) Delta Pitching Moment

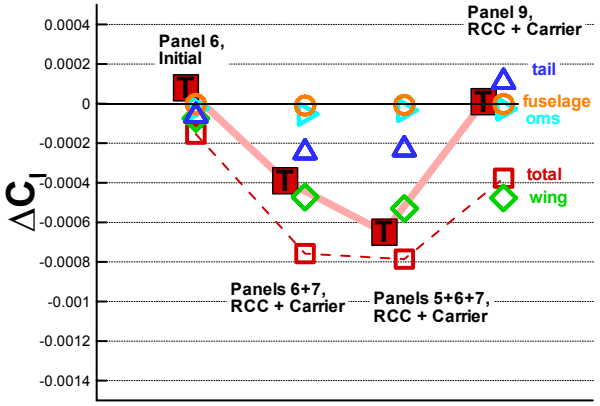

(b) Delta Rolling Moment

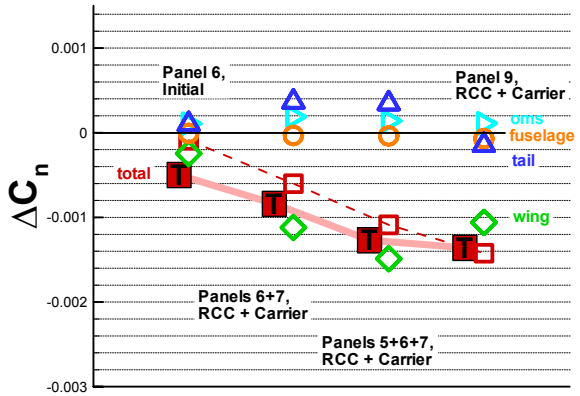

(c) Delta Yawing Moment

Figure 4.3-41 Missing Panel Delta Aero Component Breakdown (CF4 WT Condition)

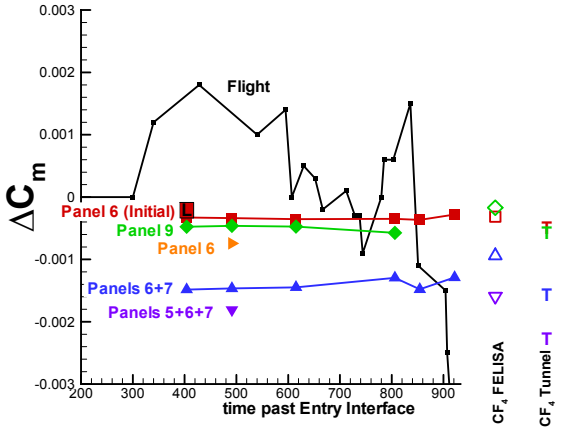

(a) Delta Pitching Moment

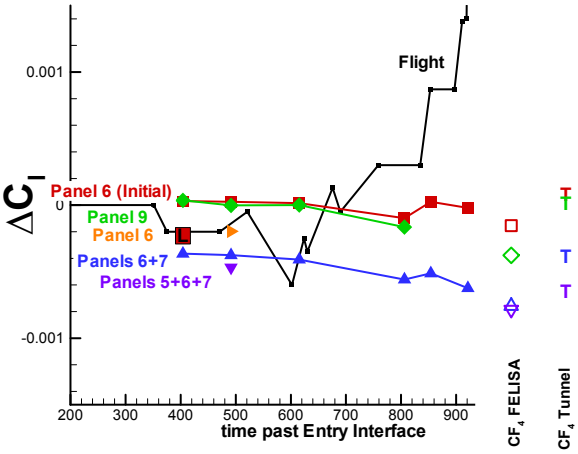

(b) Delta Rolling Moment

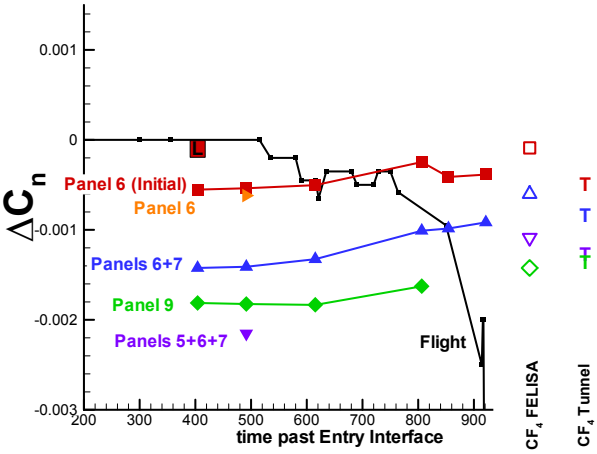

(c) Delta Yawing Moment

Figure 4.3-42 Missing Panel Delta Aero, Across Trajectory

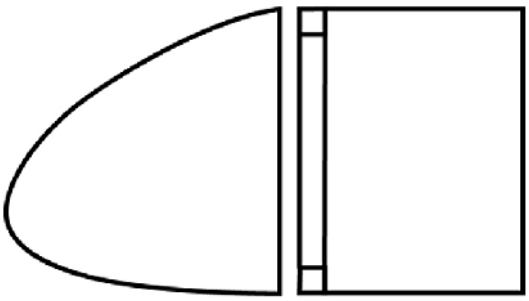

(a) Partial Panel 9 Damage, Slot

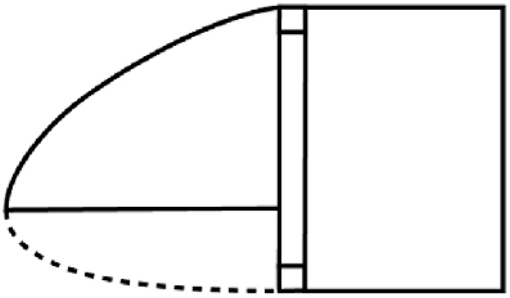

(b) Partial Panel 9 Damage, Half-Panel 9

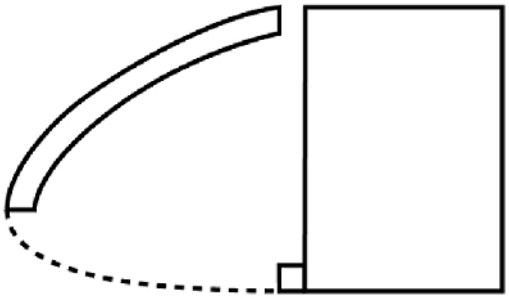

(c) Half Panel 9 with Cavity and Upper Carrier Panel 9 Removed

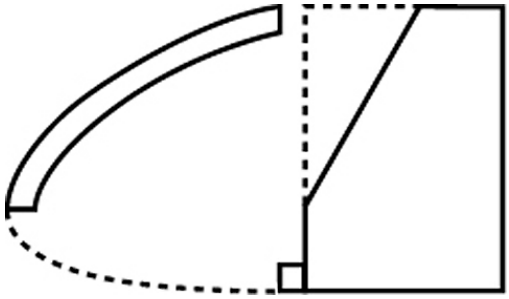

(d) Half Panel 9 with Cavity, Upper Carrier Panel 9, and Leeside Material removed

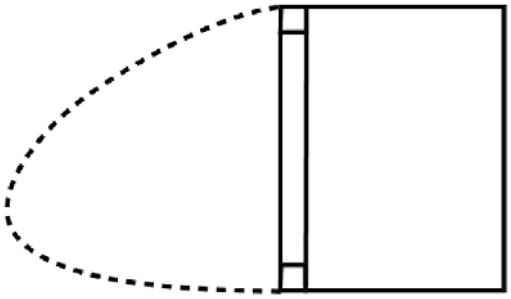

(e) RCC 9 Removed

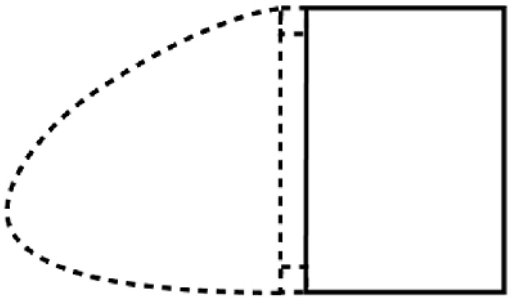

(f) Panel 9 Removed, RCC + Carrier Panel

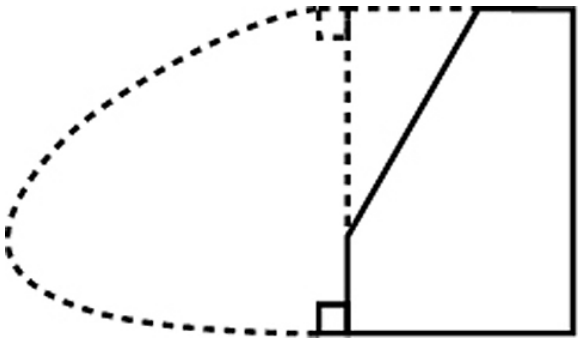

(g) RCC Panel 9, Upper Carrier Panel 9, and Leeside Material Removed

Figure 4.3-43 RCC Panel 9 Progressive Damage Configurations

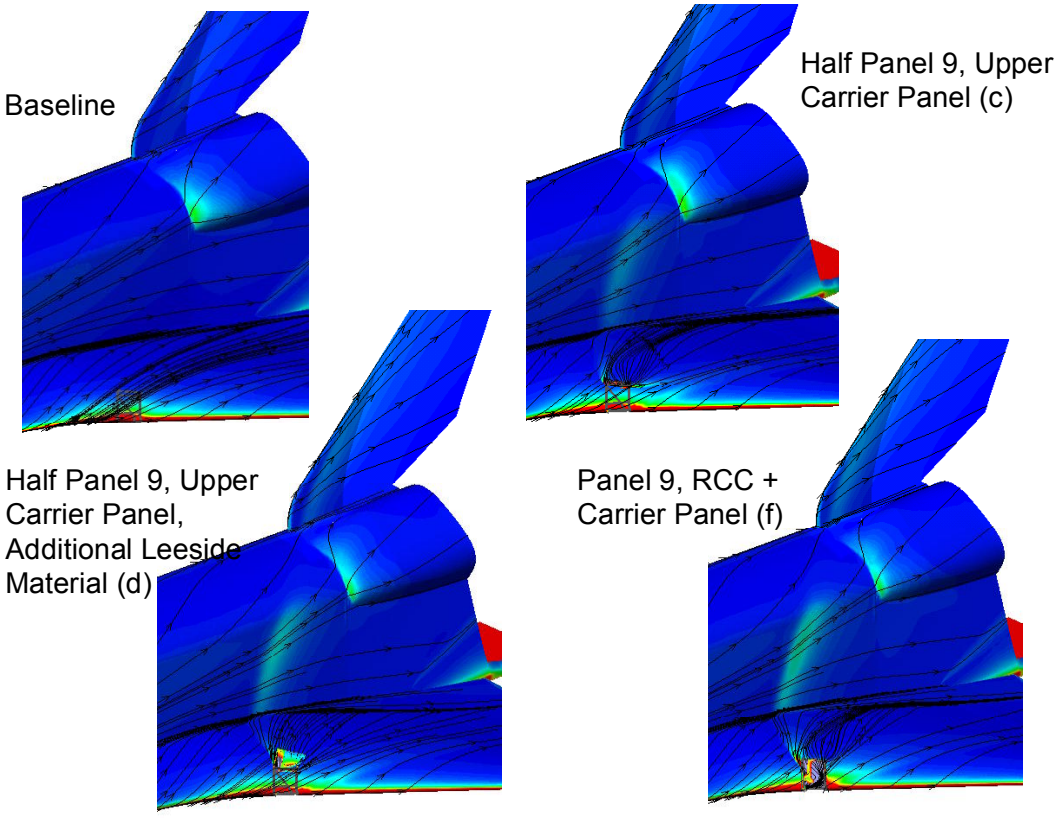

Figure 4.3-44: Leeside Flow field for Selected Panel 9 Progressive Damage Configurations

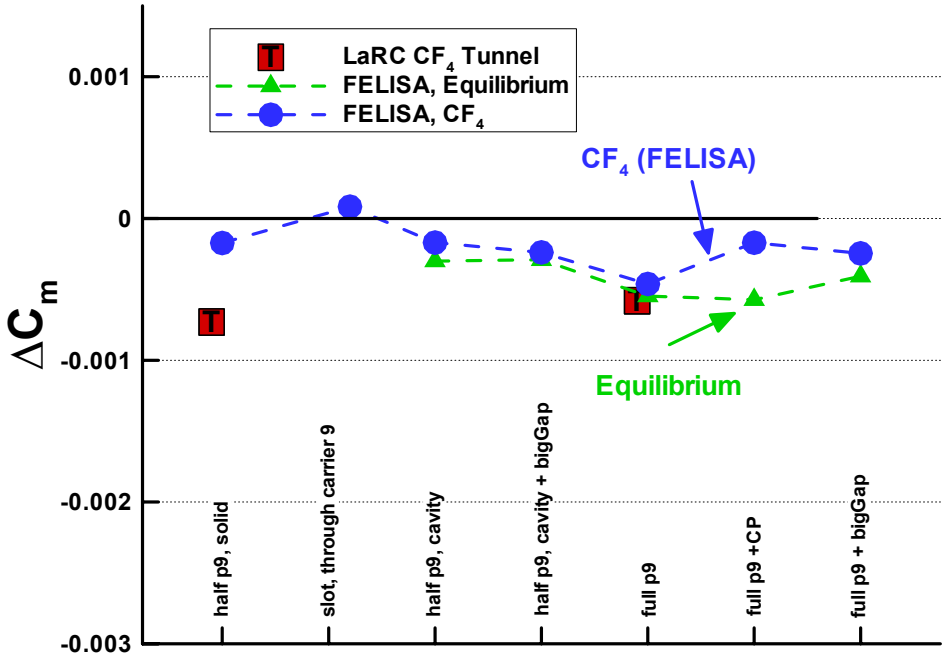

(a) Delta Pitching Moment

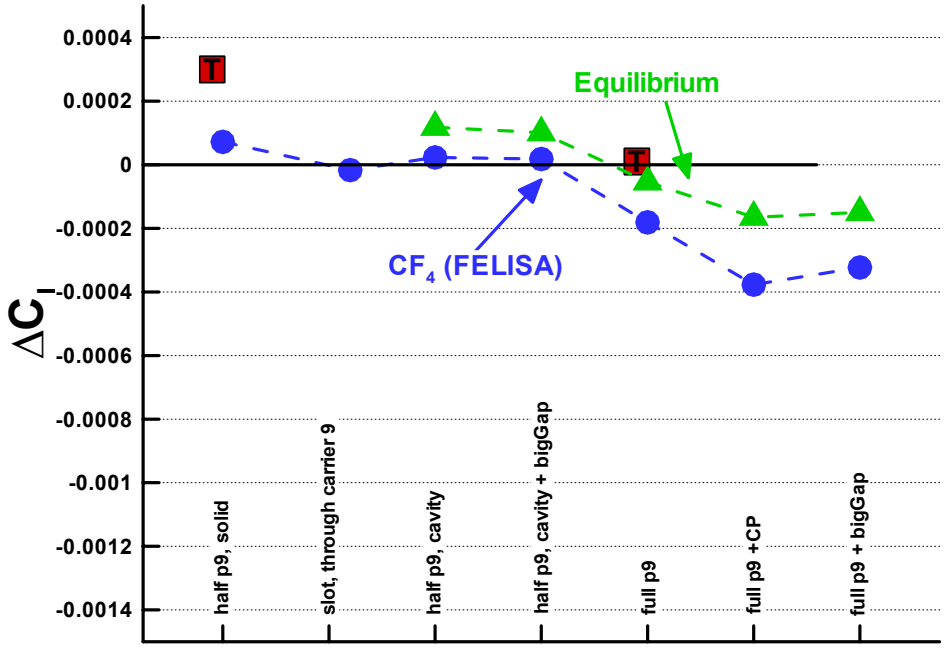

(b) Delta Rolling Moment

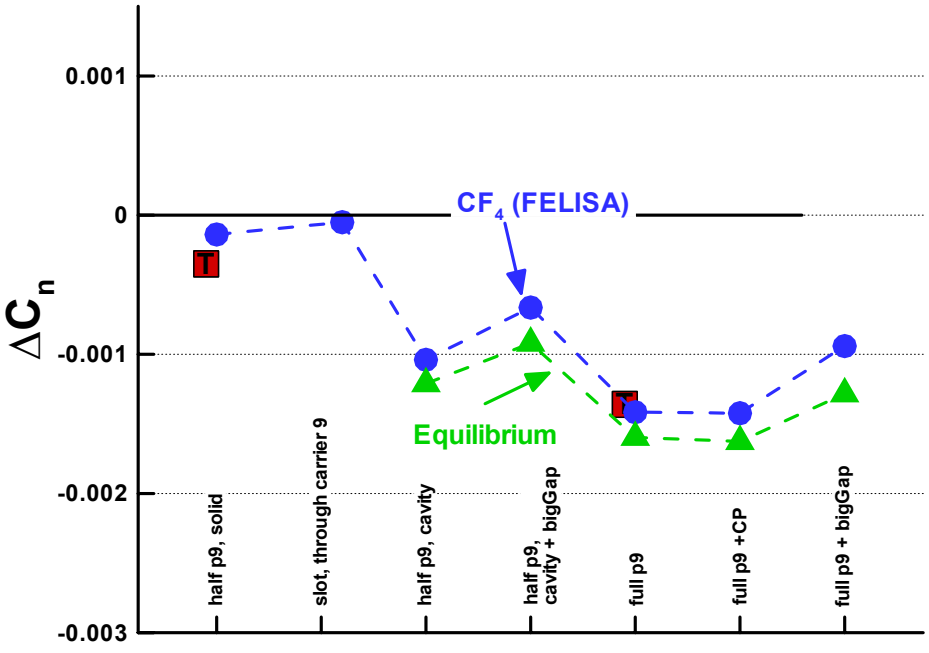

(c) Delta Yawing Moment

Figure 4.3-45 Partial Panel 9 Damage Progression, Delta Aero

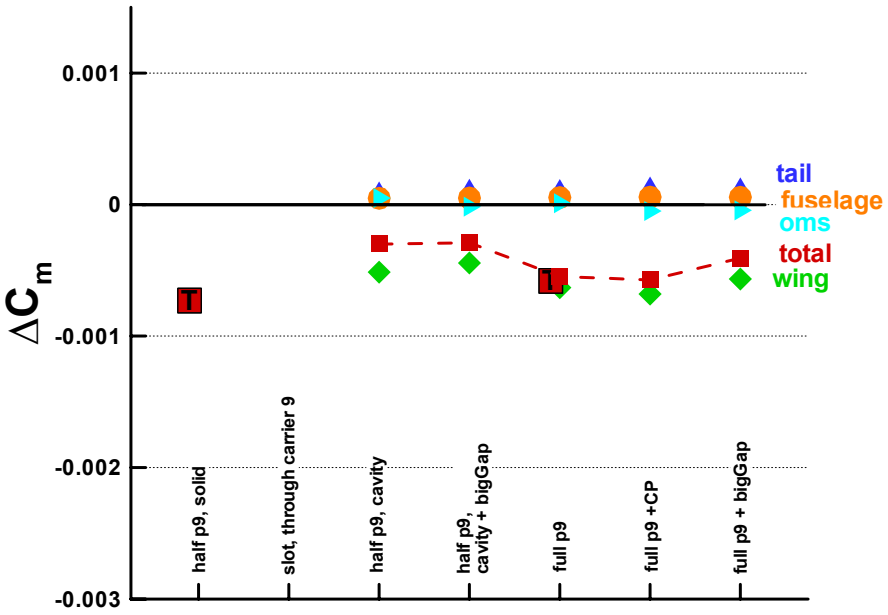

(a) Delta Pitching Moment

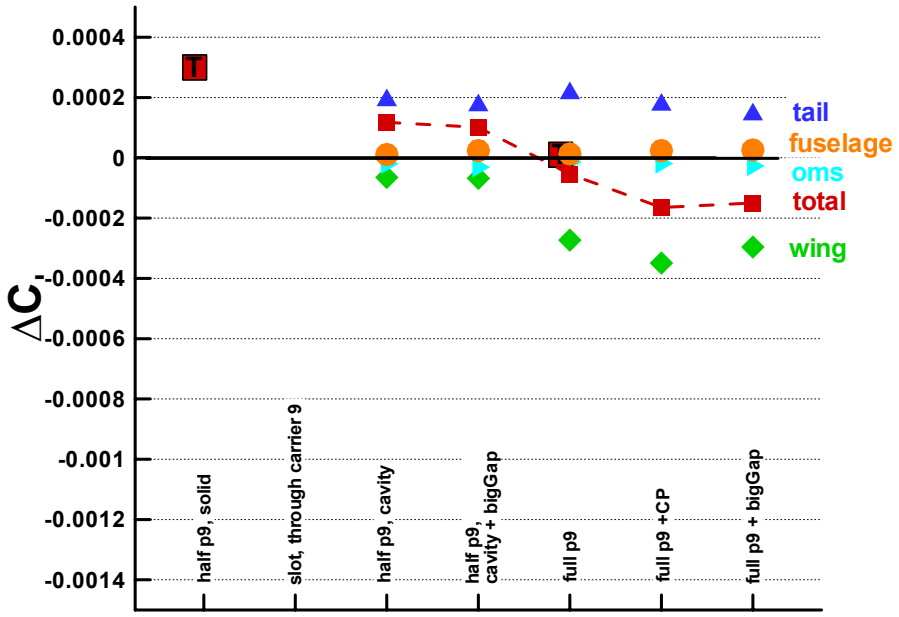

(b) Delta Rolling Moment

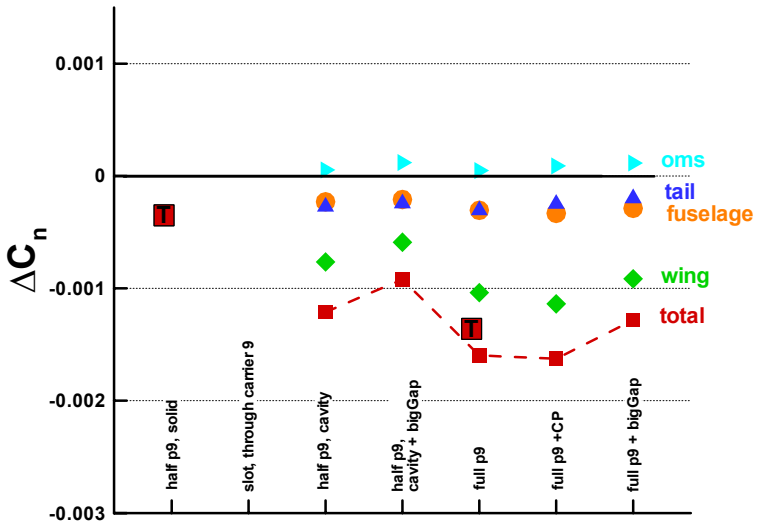

(c) Delta Yawing Moment

Figure 4.3-46 Partial Missing Panel 9 Delta Aero Component Breakdown(Flight Condition 2)

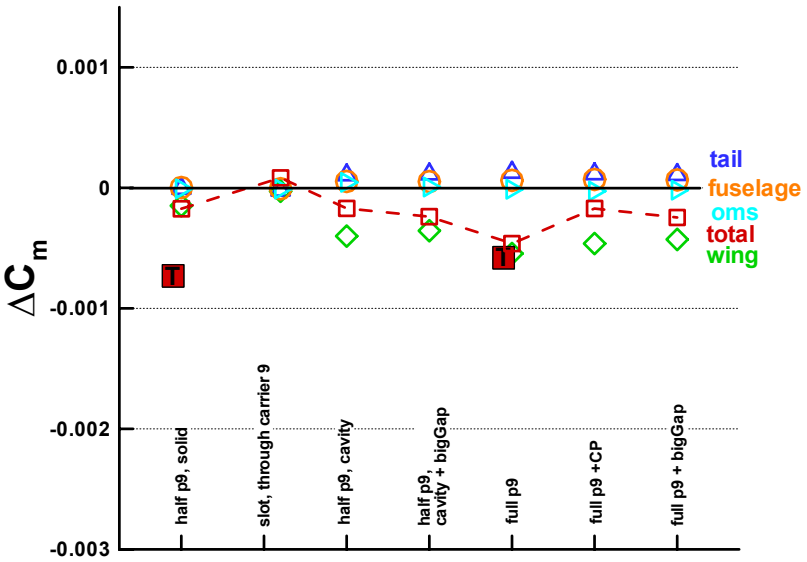

(a) Delta Pitching Moment

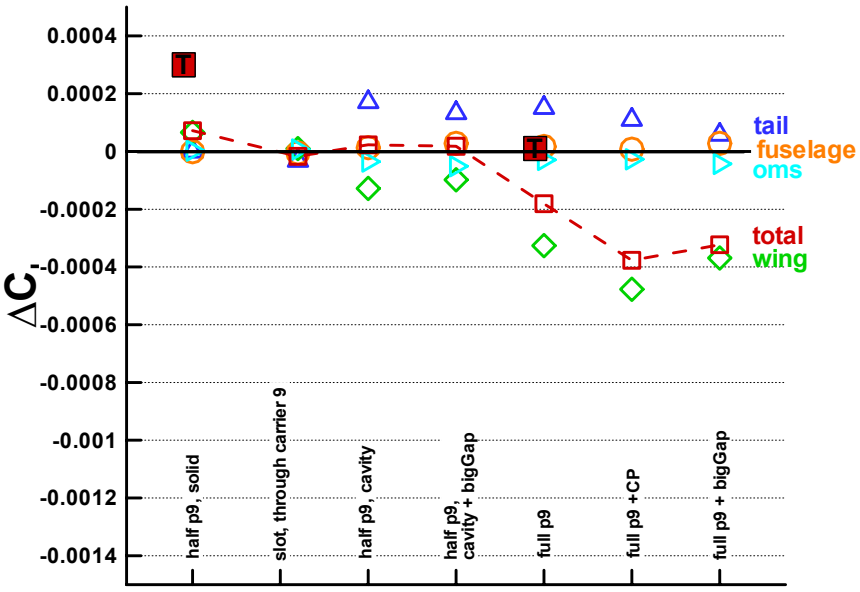

(b) Delta Rolling Moment

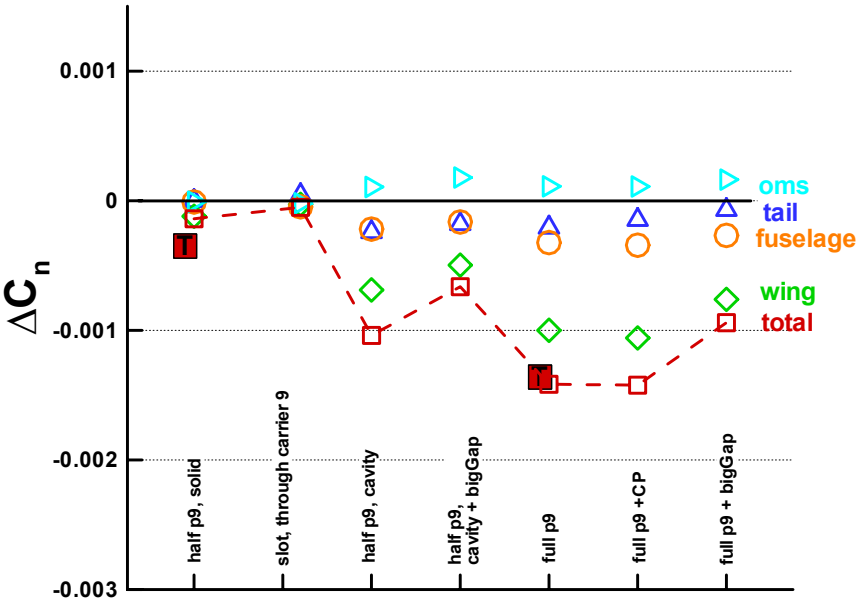

(c) Delta Yawing Moment

Figure 4.3-47 Partial Missing Panel 9 Delta Aero Component Breakdown(CF4 WT Condition)

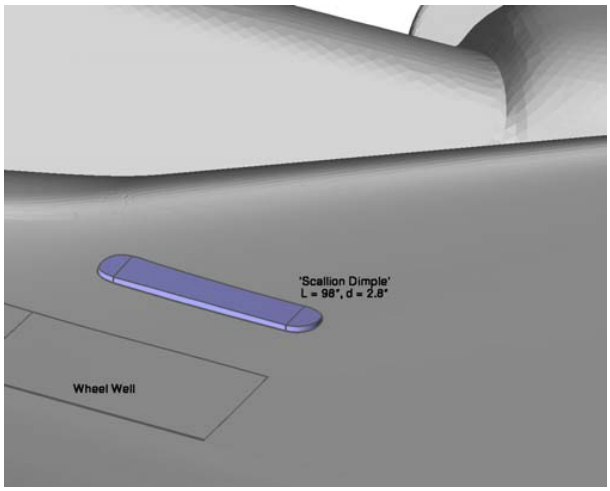

(a) Intermediate Length Windward Surface Depression

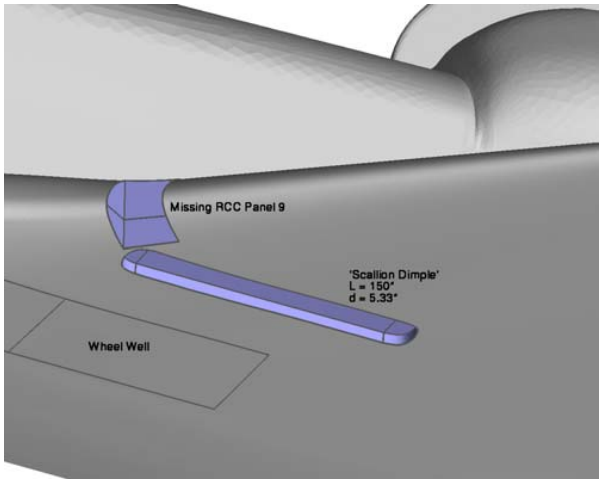

(b) Long Windward Surface Depression with RCC Panel 9 Removed

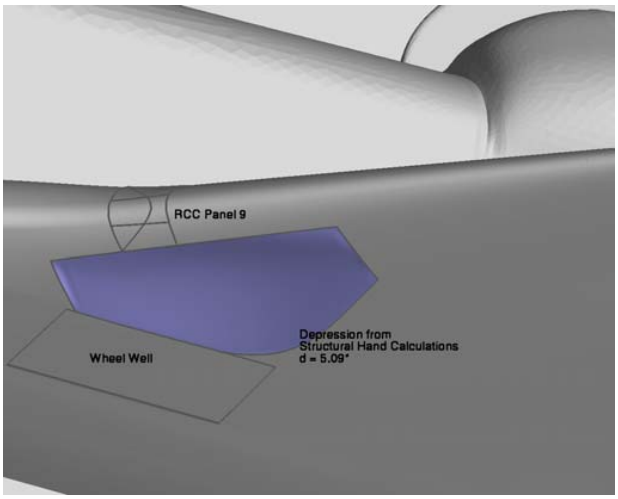

(c) Depression from Structural Calculations, d = 5.03”

Figure 4.3-48: Windward Surface Damage Configurations

Wing Leading Edge Deformation

- Geometry Assumptions:
  - spar compromised at panel 8-9
  - RCC will twist upwards and toward back
  - Deformation allowed in red and black regions
- Aero Effect:
  - Increased angle of attack in panel 7-10 region

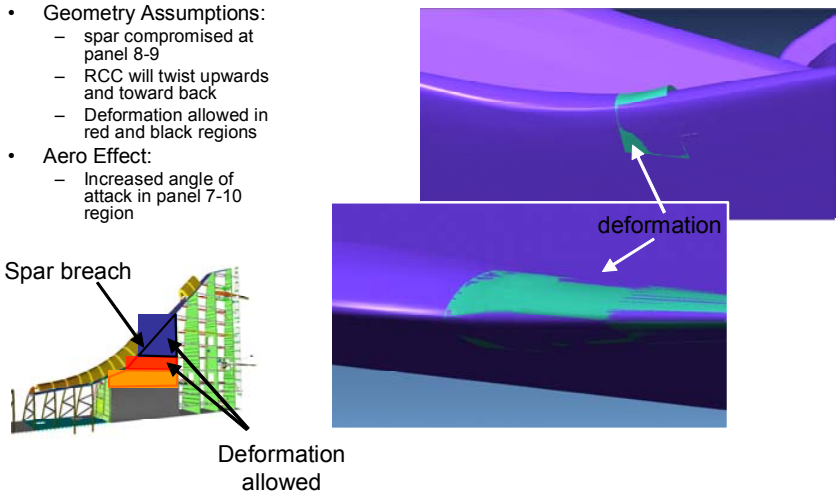

Figure 4.3-49 Geometry for Wing Leading Edge Deformation

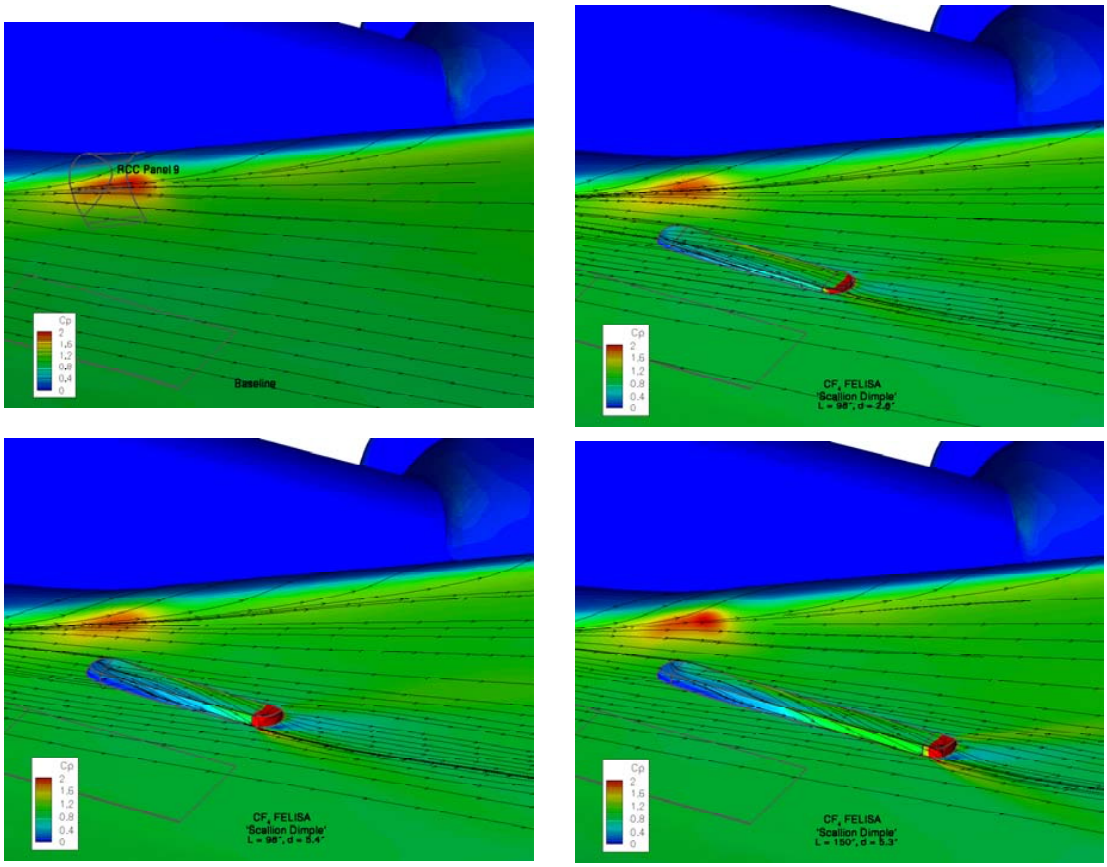

Figure 4.3-50: Pressure Contours and Streamlines - Windward Surface Depressions (CF4 WT Condition)

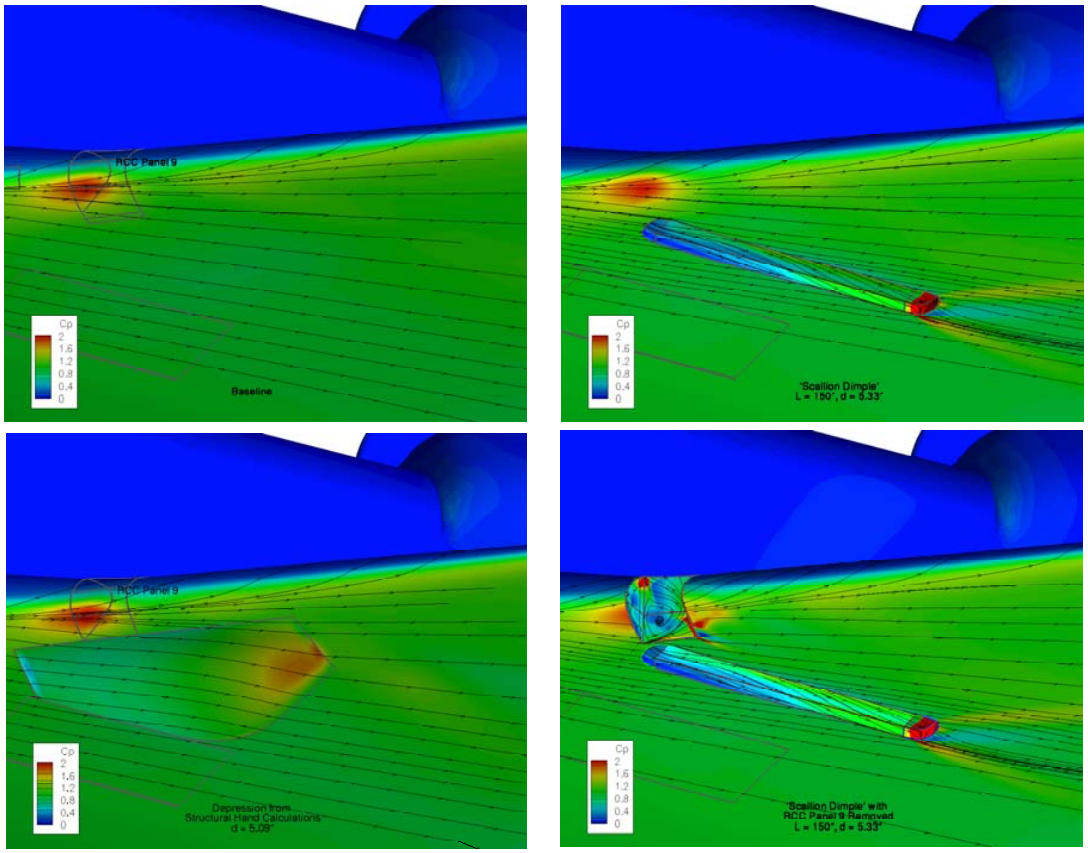

Figure 4.3-51: Pressure Contours and Streamlines - Windward Damage Configurations (Flight CFD Condition 4)

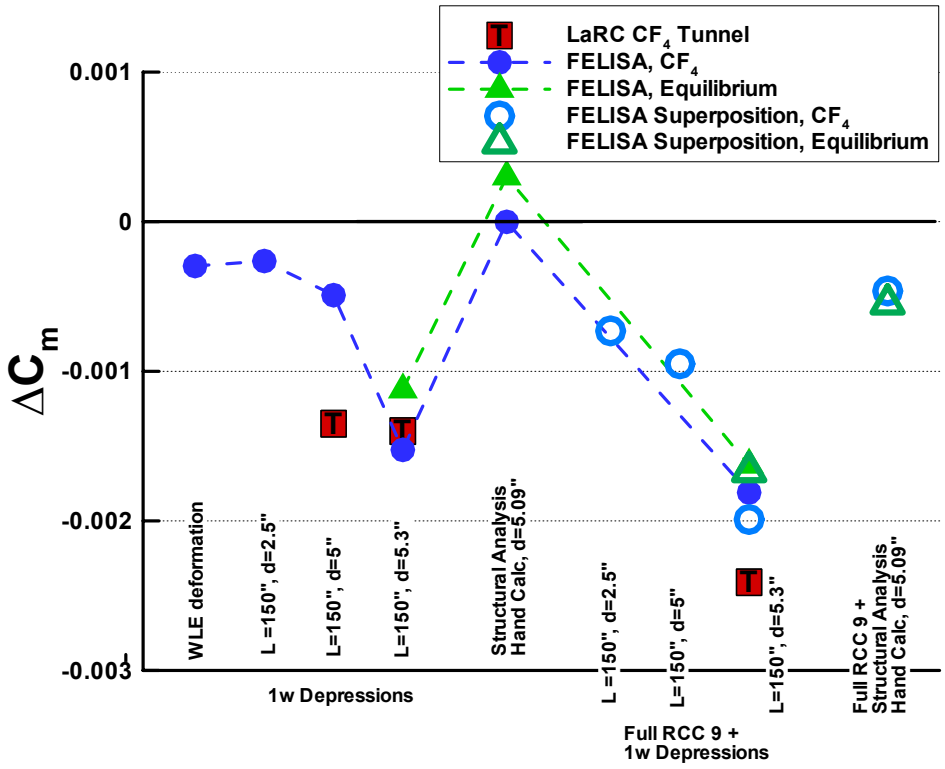

(a) Delta Pitching Moment

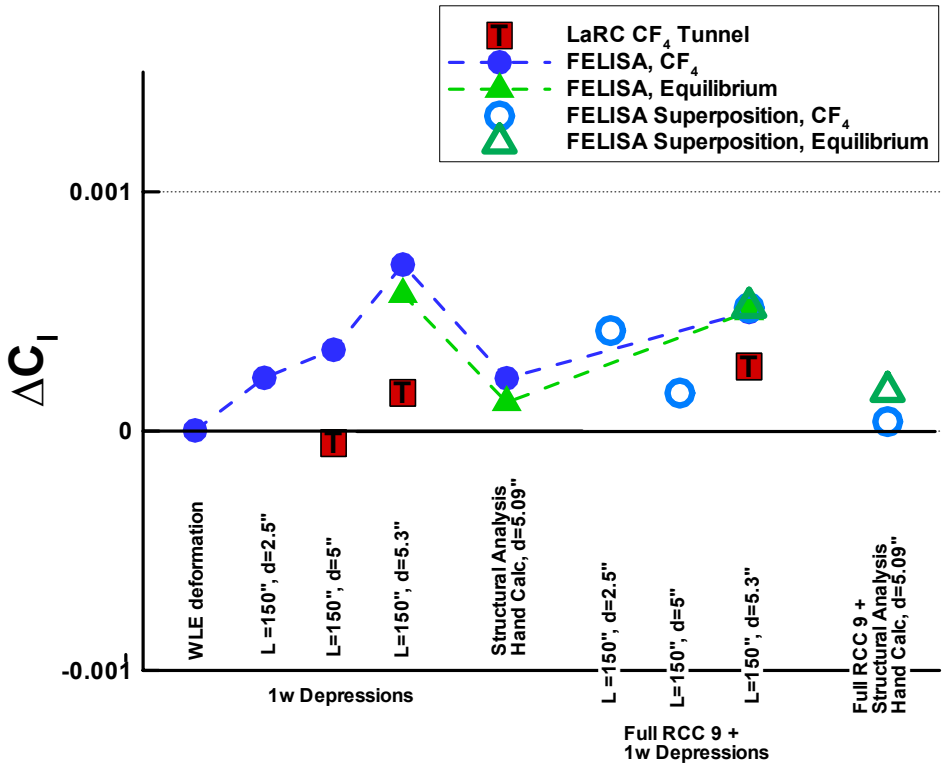

(b) Delta Rolling Moment

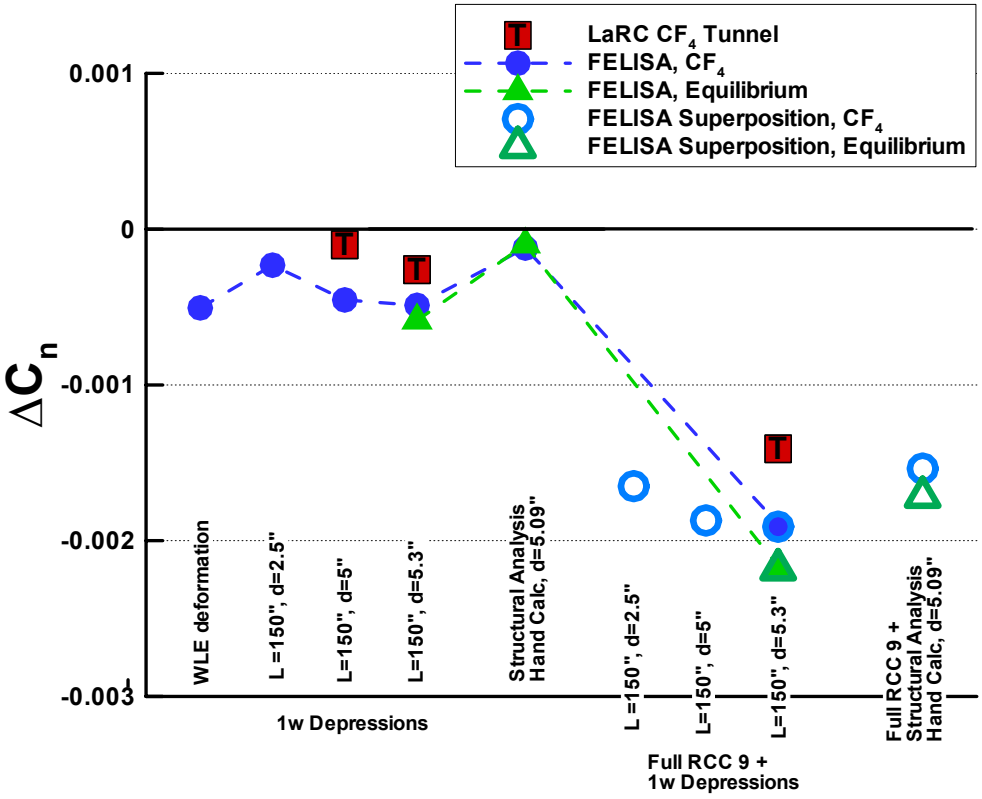

(c) Delta Yawing Moment

Figure 4.3-52 Windward Structural Damage, Delta Aerodynamic Moments

4.4 Application of Data to the Working Scenario

4.4.1 Correlation of CFD & WTT – Results by Timeline Section

The ultimate goal of the STS-107 aerodynamic reconstruction was to correlate the CFD analysis and WT test damage assessment results to the extracted flight delta aerodynamics from an initial damage stage at EI through a damage propagation that is consistent with the final working scenario. To develop a postulated damage progression the timeline was divided into four periods. Each timeline period represents a particular damaged configuration stage along the progression. The test and analysis results of a representative damaged configuration are then compared with the extracted aero increments for each timeline period. When providing a match, these comparisons lead to a postulated damage progression. Consistency with the working scenario is achieved by correlating to other available sources of data, timeline events, aerothermal, thermal, stress test and analysis results, OEX data signatures, recovered hardware forensics, etc. The resulting damage progression and data correlations are explained in this section.

4.4.1.1 Initial Timeline Section – No Observable Aerodynamic Increments

As stated in Section 4.3, off-nominal aerodynamics were not apparent during the initial portion of Columbia's STS-107 entry flight profile. This initial timeline period starts at EI (GMT 13:44:09) and extends to EI + 515 sec (GMT 13:52:44) corresponding to flight conditions which range from Mach 28 down to 24.4, with dynamic pressure increasing from 0 to 25 psf while descending through altitudes from 400,000 to 235,000 ft. The official timeline (and working scenario) identifies several major events during this period of flight (see Figure 4.4-20).

The initial portion of this time frame EI to EI + 330 sec / GMT 13:44:09 -13:49:39 suggests a breach or hole in a WLE RCC panel (5-9) existing at EI. This conclusion is supported by instrumentation near RCC Panel 9 responding to an apparent WLE internal flow thermal event. No identifiable aerodynamic increments are observed during this time frame. This is followed by a period from EI + 330 to 460 sec / GMT 13:49:39 -13:51:49 in which the initial indication of a leeside flow disturbance becomes apparent. This leeside disturbance is identified via left hand side OMS pod and fuselage surface temperature measurements indicating substantially reduced heating levels (below those seen on previous Columbia flights). Again no identifiable aerodynamic increments are observed in this time frame. Based on analysis and internal wing measurements the wing leading edge spar is breached sometime in the period covering EI + 460 to 515 sec / GMT 13:51:49 -13:52:44. This corresponds to the timeframe where all measurements along WLE Spar along with numerous others within left wing fail. Still, no identifiable aerodynamic increment is observed.

It is apparent from the data that during this initial (515 sec) atmospheric flight period the orbiters left wing is damaged to the extent that internal and external thermal events are occurring, without any clear indication of off-nominal aerodynamics. Several results from the investigation's test and analysis of probable initial damage support this observation.

An analysis, to define internal heating to the WLE spar, was completed for a circular hole in RCC panel 6 using the LaRC Navier-Stokes LAURA code. Hole sizes of 2, 4 and 6 inch diameter were analyzed at STS-107 flight condition 1 (Mach 24.7, AOA =40.2, h=243,000 ft). As shown in Figure 4.4-1, there is little if any change (even locally) to the computed external surface temperature distribution. As expected the aerodynamic normal and axial force increments extracted for this case are negligible (less than 0.3% of the total). In the wind tunnel this level of damage and its potential disruption of the flow field was evaluated by placing boundary layer trips along the wing leading edge. In Figure 4.4-2, the measured surface heating distribution shows that a relatively small area of the lower wing surface is affected for a single trip located at RCC panel 6. It should be noted that on STS-107 starting around EI + 370 sec, an external surface thermocouple, (V07T9666A) downstream of RCC panel 9 indicates a small increase in heating, similar to what this type of lower

surface heating augmentation could produce (see Aerothermodynamics Section 5.2.1.2). However, the associated aerodynamic moment increments measured for this test run are very small (essentially zero) and are listed in Table 4.4-1.

The reduced levels of heating on the fuselage and OMS Pod require some interaction of the higher energy windward flow with the relatively low energy leeside flow. While this interaction produces the change in heating during this time period, there is no associated change in aerodynamics. The source of the reduced heating has been attributed to flow exiting the WLE cavity through design vent locations along the wing upper surface at the RCC / carrier panel interface (see Aerothermodynamics Section 5.2.3.5). Several wind tunnel runs with either a single or multiple holes through (windward to leeward) the wing at these venting locations were conducted early in the investigation to identify any potential aerodynamic effects. In Figure 4.4-3, the measured surface heating distribution shows a fairly widespread disturbance over the lower wing surface due to the presence of these holes. However, the associated aerodynamic moment increments measured in these runs are also very small (essentially zero) and are listed in Table 4.4-1. (Note subsequent testing to better characterize the venting as the source of the reduced heating has been successful – however these dedicated aerothermal tests did not include simultaneous aerodynamic force and moment measurements – see Aerothermodynamics Section 5.2.3.4.). Given the suspected initial breach in the lower surface of an RCC panel, progression to a missing partial panel damaged configuration is plausible. Wind tunnel testing (section 4.3.1.6.3) and CFD analysis (section 4.3.2.3.3) results indicate little or no aerodynamic increments for this type of damage. Additionally the observed orbiter data (loss of measurements) suggests the onset of internal wing damage occurring during this time period. This is consistent with growing upper surface damage and increased venting or flow through an upper carrier panel, via the WLE breach yielding the observed aerothermodynamic response but still producing little or no aerodynamic change.

4.4.1.2 Timeline Section Two – Initial Onset of Aerodynamic Increments

The first clear indication of off-nominal aerodynamics has been identified at EI + 515 sec (GMT 13:52:44). This second timeline period extends from that point to EI + 602 sec (GMT 13:54:11) and corresponds to flight conditions ranging from Mach 24.4 down to 23.2, with dynamic pressure continuing to increase from 25 to 37 psf as Columbia descended from an altitude of 235,000 to 229,000 ft. The official timeline identifies several major events during this period of flight (see Figure 4.4-21) including a significant change in the leeside flow disturbance. The fuselage and OMS Pod measurements that were indicating reduced heating levels begin registering increased heating levels (above those seen on previous Columbia flights). Nearly all (99%) of the left wing instrumentation in the 4 major wire bundles which run along the MLG wheel well have failed by the end of this period. Additionally, the first four instances (captured by ground observers) of debris leaving the orbiter are recorded. During this time period the delta yawing and rolling moment increments show a slow steady negative growth trend. By EI + 602 sec, the off nominal delta yawing moment has increased to -0.00045 with delta rolling moment increasing to -0.0006.

Based on the WT test and CFD analysis results, WLE RCC panel damage provides the best match to the aerodynamic and aerothermodynamic events observed during this time period. Extensive test and analysis of missing full WLE RCC panels was conducted to provide a comprehensive evaluation of this particular damage scenario. As mentioned, a follow on partial missing WLE RCC panel test and analysis was conducted in order to maintain consistency with the latest recovered hardware forensics, which included significant portions of every left wing RCC panel except for panel 9. (The details are covered in Section 4.3.1.6 – WT test and Section 4.3.2.3 – CFD analysis).

In testing and analysis the clearest way to affect the leeside flow field was to provide a path for the higher energy windward flow to pass through the wing. A missing RCC panel produces this flow path. Additionally, depending on panel location, it produced augmented heating to the side of the fuselage and OMS pod, consistent with the onboard measurements. In
Figure 4.4-4 WT test aerodynamic heating measurements and

Figure 4.4-5 CFD analysis surface pressures the side fuselage effects due to the flow field interaction are clearly indicated. The aerodynamics for missing RCC panels are summarized in Figure 4.4-6 and presented along with the flight extracted aerodynamic increments for rolling and yawing moment. The shaded area represents the range of CF4 wind tunnel test data for all of the single panel testing. Several specific WT test and CFD analysis points are also included. The data shows that a missing RCC panel will produce the negative roll and yaw increments consistent with this time period (Yawing moment test data being slightly larger in magnitude than the flight data, rolling moment slightly lower). At the EI + 602 sec time point the data for a missing RCC Panel 9 is possibly the best match to the aerodynamic increments (as well as the side fuselage/OMS Pod heating augmentation pattern, see Aerothermodynamics Figure 5.2.3-16).

The recovered debris is more consistent with a partial WLE damage scenario. As mentioned previously, the WT test and CFD analysis of these configurations produced little if any rolling moment increment (actually positive for partial panels 8 & 9, see Figure 4.3-13) and a reduced (relative to a full panel) yawing moment increment (see Figure 4.3-14). Given that WLE damage most likely started as a breach in the lower half of the RCC, an expected progression would be growth to a partial panel type damage configuration. However, the side fuselage impingement is not evident from WT test results of missing partial RCC panels 6 through 9, see Figure 4.3-16. All test and analysis results show that to produce the augmented heating on the fuselage, flow through the wing (or WLE) is required. Combining a missing half panel 9 with a missing upper carrier panel did produce OMS Pod and possibly side fuselage heating augmentation without any significant aerodynamic increments. Based on these results, a partial panel damage configuration is more consistent with the initial timeline period (EI to EI + 515 sec where no clear indication of aerodynamic increments is consistent with the partial panel missing data) than with this second time period.

Another suggested damage progression involved multiple missing RCC panels. Test and analysis were conducted for this damage scenario in an attempt to match the flight extracted aerodynamics time history. Results, shown for yawing moment in Figure 4.4-7 and rolling moment in Figure 4.4-8, cover single then multiple missing panel combinations ranging over RCC panels 5 through 9. For rolling moment the continuing loss of WLE panels produces the maximum negative rolling moment observed at EI + 602 sec, while the yawing moment grows well beyond the levels observed during this time period. While this yawing moment trend is consistent with the time history beyond EI + 602 sec, the rolling moment trend is not. This implies that the damage progression must have involved something other than a continuing loss of RCC panels.

4.4.1.3 Timeline Section Three – Rolling Moment Increment Trend Reversal

At EI + 602 sec (GMT 13:54:11) the delta rolling moment trend abruptly reverses sign from increasing negative to a gradual increasing positive trend which continues for nearly all of the remainder of flight. The third timeline period focuses on this distinct event and extends to EI + 710 sec (GMT13:55:59). Flight conditions range from Mach 23.2 to 21.7, dynamic pressure from 37 to 47 psf over altitudes from 229,000 to 222,000 ft. The official timeline identifies continuing major events during this period of flight (see Figure 4.4-21). Several of these occur within approximately 10 seconds of the abrupt rolling moment trend reversal. These include observed Debris event 5 (@ EI + 602 sec), as well as the start of the slow aileron trim change, mid-fuselage bondline off-nominal temperature trends indicating increased sidewall heating levels and off scale low temperatures in the left hand elevon hydraulic system (all @ EI + 611 sec). These are followed by several observed flash events, Debris event 6 considered particularly large as well as Debris events 7 through 13 through the end of this period. During this timeline period while the delta rolling moment is gradually increasing in a positive trend, the delta yawing moment remains relatively constant. At the EI + 710 sec point, the delta rolling moment has become positive at +0.0001 and the delta yawing moment is essentially unchanged at -0.005.

The combination of a negative yawing and rolling moment increment prior to EI + 602 sec has been attributed to the increased drag and decreased lift on the left wing produced by wing leading edge

damage. The abrupt change in rolling moment trend requires an increasing wing lift condition and/or a side force increment developing on the leeside (above the c.g.). Numerous potential contributing sources were evaluated in order to develop the most probable explanation for this significant event.

The onset of ABLT was first considered as a possible explanation for the observed trend. While no orbiter entry has previously experienced boundary layer transition prior to Mach 19, given the suggested extent of damage to the wing leading edge, the possibility of an early ABLT seemed plausible. While the change in rolling moment trend is consistent with a left wing ABLT, the fact that the delta yawing moment remains constant is not. To illustrate this, Figure 4.4-9, shows the flight extracted delta rolling and yawing moment with wind tunnel predicted ABLT increments applied at EI + 602 sec. The increments were established from a wind tunnel run forcing full ABLT over the left hand side of the orbiter (full ABLT as shown in Figure 4.3-2 through Figure 4.3-4). These results clearly illustrates that early ABLT is not consistent with the yawing moment and therefore cannot be the source of the delta rolling moment trend reversal.

Another plausible explanation considered involved the potential for disturbed flow over the inboard elevon surface thereby altering the control surface effectiveness yielding the change in the rolling moment increment trend. This theory was bolstered by the recovered left hand inboard (LHIB) elevon actuator (debris item 7327) which incurred significant damage including a casing burn through suggesting the possibility of high energy flow through the wing and onto the actuator. However, the wing box primary vent is through the mid-fuselage and there is no design vent through the aft spar, (however there is some leakage). Also, the flipper door vents are intended to vent the elevon cove area only and not the wing. Therefore, no clear design flow path exists. Also the inboard elevon hinge moment data, Figure 4.4-10, shows no indication of off-nominal behavior during this time period and particularly nothing is evident at EI + 602 sec. Additionally, LHIB Elevon temperature sensors remained operational with nominal data throughout the time period. Based on the data available and these observations, there is no indication of flow exiting from aft spar and disturbing elevon flow field during this time period so as to contribute to the change in the rolling moment increment trend

From the point of wing leading edge spar breach (approx. EI + 460 sec) the internal wing cavity was ingesting the high energy air and being pressurized. In this time period, based on the MLG measurements, it is suspected that the outboard wall of the wheel well cavity is breached and allowing this cavity to pressurize. Recovered left hand MLG door and adjacent structure and TPS indicate patterns suggesting potential outflow from the wheel well at some point during the flight. It was postulated that this jet flow exiting the MLG door area could interact with the external flow field and produce the observed rolling moment increment trends.

A baseline solution for CFD Point 1 (Table 4.3-4 - Mach 24.7, AOA =40.2, h=243,000 ft) in the STS-107 accident investigation was modified to include effects of a scarfed, conical nozzle directed toward the centerline of the vehicle from the forward, inboard corner of the landing gear door. The intent of the simulation was to approximately model effects of a relatively large internal wing pressure, fueled by combusting aluminum, which deforms the corner of the landing gear door and directs a jet across the windward surface. This simulation did not include details of aluminum combustion but does consider extremes of internal conditions ($p_{internal}$ = **2** $\rho_\infty V_\infty^2$ and $T_{internal}$ = 4000 K) that are expected to provide an upper limit on this potential effect. *(An associated analysis of flow through a breach in the leading edge of Panel 6 into a vented cavity indicates internal pressures of* ***(1/8)*** $\rho_\infty V_\infty^2$ *fed by an external pressure of (1/2)* $\rho_\infty V_\infty^2$*).* The analysis includes interaction of the shock layer flow with the jet. The scarfed nozzle has a 3-inch diameter throat and a 1.3 ft^2 elliptical footprint on the windward surface. Perturbations to baseline aerodynamic coefficients are expected to scale with throat area for the specified internal conditions because the interaction disturbs only a small region (roughly double the exit area) in the vicinity of the exit plane. Aerodynamic coefficient perturbations are of order 10^{-3} to 10^{-5} of right-half-body values. These values account for both interaction and any potential thrust generated by the exiting jet. The exiting jet is substantially entrained in the windward boundary layer with relatively weak perturbations to the external flow as

shown in Figure 4.4-11. These results indicate that external flow interaction with an exiting jet is an unlikely source for the delta rolling moment trend reversal.

The recovered hardware included a portion of the left hand OMS pod and several portions of the vertical tail (VT). All showed a consistent pattern of heavy damage with Aluminum deposits on the left hand side, while the right hand side remained relatively clean. This forensic evidence combined with the increased heating indications on the left hand fuselage sidewall plus the relatively large moment arm available via the VT suggest disturbed flow on the left hand side of the vehicle as an explanation for the rolling moment increment trends. Flow through wing leading edge damage and/or a hole through the upper wing surface with a resulting leeside (Fuselage, OMS, VT) flow interaction could produce the relatively small delta pressure on the VT required to reproduce delta rolling and yawing moment trends seen during this time period.

It has already been noted that flow through the WLE via a missing RCC panel produces an interaction with the leeside flow field and that this interaction increases the heating rate on both the fuselage side and the OMS pod. As part of the investigation into this leeside interaction being correlated to the aerodynamic increment pattern, other flow paths through the wing were investigated. Debris event 5 is better characterized to be more like a flash event and is closely followed by Flash event 1 and then immediately followed by Debris event 6 (see Figure 4.4-21) which is considered by evaluation as the largest debris shed by the orbiter. Together, these have been hypothesized to be the onset of an upper wing surface breach (flashes representing venting of ingested gas/burned internal wing components) and then Debris event 6 is the release of a large section of the upper wing skin. Therefore the additional flow paths through the wing investigated included flow in through lower WLE damage and out via missing upper carrier panels or missing upper surface acreage as well as holes directly through the wing from windward to leeward side.

An extensive evaluation to characterize the leeside interaction effects was undertaken through WT test, CFD analysis and hand calculations to determine the plausibility of this contribution and evaluate the various potential sources for windward surface flow to interact with the leeward side flow. It should be noted that the leeside flow field with strake vortex along with OMS pod and VT interaction is extremely complicated, even without the added complexity of interaction due to wing damage. This complexity is illustrated in Figure 4.4-12, showing the details of the flow patterns and the local interactions over this region of the orbiter at hypersonic flight conditions.

As stated, some of Columbia's recovered hardware came from the VT. Figure 4.4-13 shows recovered Columbia hardware, VT Spar, debris item No. 52092. The difference in damage to the left and right sides is evident. Additionally the left hand side pattern suggests an aft-to-fore / base-to-tip flow direction. CFD analysis was conducted to investigate the possibility of this flow pattern and the changes to this interaction as a function of wing damage. In Figure 4.4-14 the flow patterns from inviscid calculations are shown for both a baseline and a missing RCC panel 9 case. These are compared against the direction inferred from the damage pattern. The missing panel has a small effect on the flow pattern over the VT. The patterns seen on the recovered hardware are not consistent with the CFD results. These inviscid calculations and analysis for various Panel 9 damage scenarios (including holes through the wing) are detailed in section 4.3.2.3.3. This includes a breakdown of the contributions from different orbiter components (Wing, Fuselage, Tail, OMS). In Figure 4.3-39 through Figure 4.3-41 this breakdown is detailed. These results suggest that while the VT can contribute partially to the positive delta roll trend, change to the wing flow field remains the principle contributor to the aerodynamic moment increments.

Because of the complexity and concerns that an inviscid solver may not adequately capture these leeside interactions, Navier-Stokes CFD analysis was also completed for a RCC Panel 9 missing case to further assess these interactions. In Figure 4.4-15 the change in pressure on the vertical tail is shown along with the delta aerodynamic increments. This analysis of the tail flow field and the delta pressures clearly demonstrate differences in the flow field for the Panel 9 missing case. However, the delta pressure change is very small, likewise the delta aero increment from the vertical tail is very small. For this case an order of magnitude less than the increments from the wing (see

Table 4.7-6). The details of this analysis are reported in the Aerodynamics Appendices, Section 4.7.4.

As a final check to ensure that the nature of this highly separated flow field was not being misinterpreted, several wind tunnel test runs were made with and without the VT. The details of these test runs are covered in 4.3.1.6.5 with the actual test data listed in Figure 4.3-19. The aerodynamic increments with and without the vertical tail are very close in value, supporting the conclusion that the vertical tail was not the major contributor to the delta aerodynamic increments for a missing panel 9 configuration.

One other point to put forth concerns consistency with the flight data extraction. If interaction with the vertical tail was the primary contributor to the change in delta rolling moment trends via increased pressure on the left hand side of the vertical tail, this would manifest itself in a positive (being out the right wing) side force increment. Flight data extraction of the side force increment shows a small but negative (out the left wing) side force increment (Figure 4.2-10) during this time period. This inconsistency between extracted force and moments implies the primary contributor must be a change in lift, likely produced by the wing, to yield the rolling moment increment trend.

While clear evidence of leeside flow field interaction exists for the fuselage and VT (i.e. recovered debris, temperature measurements, etc.), the reproduction of required delta pressure pattern has not materialized in either test or analysis. Leeside interaction is not the primary contributing source to the delta rolling moment trend reversal in this time period.

Lower surface damage configurations were initially centered around the MLG/wheel well area and were assessed via WT testing of the stainless steel model in the LaRC Mach 6 air facility. Various damaged configurations were evaluated including MLG and door deployed as well as three open wheel well cavities of various depths. The results of the testing produced several important observations.

The MLG and door deployed configuration produced both large positive rolling moment and large negative yawing moment increments similar to extracted aerodynamic trends seen just prior to LOS. However the configuration also produced a large positive pitching moment increment (see lines D & E in Figure 4.3-6). This wind tunnel measured pitching moment increment is not consistent with the large negative pitching moment extracted from flight just prior to LOS. Based on these results it is clear that the MLG did not deploy prematurely.

Another extension of these results was to utilize the MLG (only) down, with no door, test configuration as representative of lower wing surface damage that results in a forward facing step. Test results for this configuration produce both large -yawing and -rolling increments as shown in (Figure 4.4-16) This is not consistent with the (-yaw/+roll) flight extracted trends seen late in flight and suggest that whatever damage Columbia's left wing was enduring did not result in a lower surface forward facing step.

An open wheel well of various depths was investigated as part of this series of testing. These results provided the first indication that an open cavity on lower wing produces (+) rolling and (-) yawing moment increments, consistent with changing trend for roll moment and constant yaw moment seen after EI + 602 sec. (see
Figure 4.4-16). As can be seen in the data the shallower cavity yields larger increments (both yaw and roll).

The lower surface cavity wind tunnel results combined with forensic evidence, the extracted aerodynamic flight data patterns and wing structural design/loading suggest a lower surface deformation as the damaged configuration that best reproduces the observed change in rolling and yawing moments. The gradual aerodynamic moment increment growth is consistent with leeward debris and not loss of windward surface material. A lower surface deformation or recession could yield the necessary gradual change to windward surface by slowly growing in area and/or depth. To

assess this scenario in more detail a combined aerodynamic, internal heating and structural analysis was completed.

The orbiter intermediate wing structure was not designed to carry large loads and essentially supports the lower and upper skin and the associated distributed loads. The WLE spar, the outboard wheel well wall and the 1191 spar provide the primary strength and serve to outline the intermediate wing area (Figure 4.4-17). Structural analysis was used to define possible wing deformation considering the aerodynamic loads and potential internal wing damage. Finite element model analysis provided global wing deformation. Associated stress calculations were then used to provide localized skin deformation. The hot gas entering the intermediate wing does so as a high energy plume, therefore damage to much of the internal structure is likely to have occurred. The predicted wing deformation (global and local) was heavily influenced by the hypothesized damage which included reduced structural modulus to represent missing or severe damage to the WLE spar behind one RCC panel, reduced strength of the spar caps, missing wing truss tubes, and loss of wing skin inner face sheet. For structural analysis details see Section 7.5.

Structural and surface deflections from the analysis were provided to the aerodynamics group for assessment. The global structural deformation is relatively small. Even considering the damage, the overall delta between an undamaged wing and a damaged wing yielded a deflection change of less than 0.8 inches. The wing deflection (z-component) is shown in Figure 4.4-18. Newtonian aerodynamic analysis of this deformation produced a small -yawing and +rolling moment increments.

Similarly the local surface skin deflections as generated through stress analysis were also evaluated. These provided relatively large (maximum of 5+ inches) surface deflections Figure 4.4-19. Newtonian as well as inviscid (FELISA - Section 4.3.2.3.4 and CART3D) calculations were completed on this localized damaged configuration. These calculations also produced small -yawing and +rolling moment increments. Note that the global and local wing deformations were not combined and these cases were independently assessed. While the CFD analysis yields the correct signs (-yaw/+roll) the values are relatively low.

Wind tunnel testing of lower surface recession was completed in the LaRC CF4 tunnel. Test configurations considered a range of width and length for a 5 inch deep recession behind RCC panels 8 and 9. Three lengths were considered ranging from Xo=1146 to 1243. Single, double and triple wide recessions were tested (single being 23 inches wide). Testing was done with and without RCC panel 9 missing. These results are summarized in Section 4.3.1.6.6 and the configurations and results are shown in Figure 4.3-20 through Figure 4.3-22. These lower surface depressions do result in a positive (right wing down) rolling moment as observed in flight, and the magnitude of the rolling moment increases as the width of the depression is increased. Furthermore, the yawing moment and pitching moment generated by the depression are similar in magnitude and in the same direction as observed for flight.

The test and analysis concentrated on this timeline period in an attempt to identify the cause of the distinct pattern in the flight extracted aerodynamics. Several possible contributors to the change in rolling moment trend were identified and include leeside flow field effects, potential (very) early ABLT and flow through the wing. However, none of these serve as the primary contributor. Of all of the plausible explanations evaluated, only a lower wing surface deformation appears consistent with the data and therefore the rolling moment delta trend change is attributed to wing deformation.

4.4.1.4 Timeline Section Four – Progressive Damage Aerodynamics

The fourth timeline period covers what is essentially the remainder of flight from EI + 710 sec through EI + 918 sec (GMT13:55:59 – 13:59:27), just prior to LOS. Flight conditions range from Mach 21.7 to 17.8, dynamic pressure from 47 to 83 psf over altitudes from 222,000 down to 200,000 ft. The official timeline identifies continuing major events during this period of flight (see Figure 4.4-22 and Figure 4.4-23). These include debris events 14-17, loss of instrumentation within the

wheel well cavity, the sharp increase aileron trim rate, loss of upper and lower wing skin (OI) temperature measurements each suggesting a continuing degradation of the left wing. However Columbia does complete a planned roll reversal around EI + 765 sec with nominal performance indicating major vehicle and wing integrity still exists.

While the exact state of Columbia's damaged left hand wing is unknown, despite the extensive internal wing damage, the hypersonic aerodynamic asymmetries remain manageable, with the orbiter windward surface still basically intact. Based on the continuing observations of debris loss, the expected continual damage to the wing internal structure, the gradual increase in +rolling moment increment and - yawing moment increment as well as the onset of a -pitching moment increment, that the lower surface wing deformation remains the most plausible explanation for the aerodynamics observed during this time period.

The results for progressive growth in the lower wing surface deformation are summarized in section 4.3.1.6.6 (wind tunnel testing) and section 4.3.2.3.4 (CFD analysis). The wind tunnel test configurations and results are shown in Figure 4.3-20 through Figure 4.3-22. The data indicates that as the lower surface depression width increases from a single to triple wide configuration, the rolling moment (+), yawing moment (-) and pitching moment (-) increments each gradually increase in magnitude as observed in flight during this time period.

CFD analysis of the single wide lower surface depressions provided similar trends as the wind tunnel for rolling, yawing and pitching moment Figure 4.3-52. When combined (by superposition) with RCC panel 9 missing the resulting rolling moment (+), yawing moment (-) and pitching moment (-) increments each reach magnitudes consistent with those observed in flight during this period. Also included in these plots are the data for the localized lower wing skin deformation as predicted by stress analysis for a substantially damaged intermediate wing structure. While the CFD analysis yields the correct signs (-yaw/+roll) the values are relatively low for this case.

Overall, the delta aerodynamics computed and measured for windward surface damage configurations correlate well with the increments observed late in flight. The data trends support the hypothesis of progressive internal structural damage that produces a gradual windward surface deformation. This gradual deformation produces the steady increase in rolling moment and yawing moment as well as the pitching moment increments seen during this late period in flight.

4.4.2 Damage Progression Theory and Supporting Aero

Based on the damage assessment and timeline period correlations covered in Section 4.4.1, the following is a postulated damage progression theory based on the results of the aerodynamic investigation. This damage progression, approached from an aerodynamic perspective, is consistent with the working scenario and attempts to maintain consistency with other data from the investigation. References are made to figures which include a combination of aerodynamic extraction results and the major timeline events noted.

An initial WLE breach (small hole or slot) in an RCC panel exists at entry interface. By EI + 300 sec thermal events are occurring internal to the WLE cavity, however no identifiable aerodynamic increments are observed. The breach continues to grow into a larger hole and between EI + 300 to 450 sec has resulted in the loss of most of a lower RCC (7,8 or 9?) panel. The partial missing RCC panel configuration produces little if any delta aerodynamic effect, nothing observable (see Figure 4.4-20). Breach of the WLE spar follows somewhere between EI + 450 to 500 sec and internal wing pressurization and heating damage begin. Still no external aerodynamic effect is observed. As the WLE damage progresses it results in the onset of high energy windward flow passing through the WLE and interacting with the leeside flow field between EI + 500 to 600 sec (see Figure 4.4-21). The OMS pod and side fuselage surface temperature measurements indicate increased heating as a result of this interaction. This is most likely the result of loss of a considerable portion of RCC Panel 9 and/or an upper carrier panel (9,10 or 11?) and produces the first clear indication of off nominal aerodynamic increments (-yaw & -roll). Both continue to slowly increase with negative growth trends

for approximately 90 seconds. By EI + 600 sec internal wing damage has become significant. The four major OI/MADS wire bundles have burned through and the MLG wheel well wall is likely breached, much of the intermediate wing structure has been significantly damaged. Soon after, breaches through the left hand wing upper surface begin to develop as marked by a series of flash events, Debris 5 (or Flash "0") at EI +602 sec and Flash 1 (EI +624 sec) indicating a forced external venting of the gas and damaged material built up in the intermediate wing. At EI + 627 sec, Debris 6 (the largest observed debris event) most likely represents a large portion of the upper wing surface departing the orbiter. This release of the internal pressure buildup relieves the offset to the external lower surface pressure and combined with the extensive internal wing damage results in the onset of a lower wing surface deformation or dimple. Initiated at the EI + 602 sec mark, this corresponds to the Debris 5 flash event, the onset of the slow aileron trim change and the change in the delta rolling moment increment trend, which abruptly changes sign and begins positive growth. Beyond EI + 630 sec (see Figure 4.4-22), the WLE damage becomes extensive, perhaps to the point of loss of lower RCC Panel 8 and most or all of RCC Panel 9. The combination of WLE damage and lower surface wing deformation produces the slow growth in the delta rolling (+) and yawing (-) moment increments. The continuing observed debris events are postulated as primarily upper surface structure and TPS, so despite the extensive wing damage, the hypersonic aerodynamic asymmetries remain manageable, with the orbiter windward surface still basically intact. As the lower surface deformation continues to grow, between EI + 700 to 850 sec, it produces gradually larger delta rolling (+) and delta yawing (-) moment increments. Even with the developing damage to the left wing, Columbia completes a planned roll reversal with nominal performance at approximately EI + 765 sec. Shortly after this maneuver, at EI + 835 sec (see Figure 4.4-23) the aileron trim rate increases sharply in response to a corresponding sharp increase in the growth of both the rolling and yawing moment increments. The initial delta pitching (-) moment increment is now also observed. As large scale wing deformation continues to grow beyond EI + 870 sec the asymmetric aerodynamics exceed design levels. Columbia manages trimmed flight for approximately another 60 sec, eventually requiring the use of all 4 RCS aft yaw jets and maximum rate of aileron to maintain trim. However, the asymmetric yaw and roll moment growth increases drastically exceeding 6 times the design levels just prior to LOS + 5 sec. Under this extreme asymmetric condition, the flight control system can no longer maintain trimmed flight. Columbia soon departs from controlled flight leading to the loss of vehicle and crew.

The damage assessment results summarized in section 4.4.1 can be mapped to this progressive damage scenario. Since the exact damaged configuration can never truly be known, a subjective placement of the measured aerodynamic increments along the timeline of the extracted increments is reasonable. In Figure 4.4-24 through Figure 4.4-26 the rolling, yawing and pitching moment increments from the LaRC CF4 wind tunnel test results of configurations in line with the damage progression outlined above are presented. The time history trends of the yawing, rolling and pitching moment increments can be matched remarkably well. Although an exact correlation of flight magnitudes and time is not achieved, since the exact damaged configuration is unknown, a plausible damage progression scenario has been developed which has the same aerodynamic trends as the extracted flight data.

As a final comment on the damaged configuration test and analysis results, it must be pointed out again that the nature of this analysis and the conclusions to be drawn from them should be limited to a proper engineering perspective. The test and analysis conducted for the aerodynamic (and aerothermodynamic) portion of the investigation were performed on representative geometries. The representative geometries that have been assessed were chosen in a very dynamic investigation environment as engineers interpreted the latest results from wind tunnel testing, CFD analysis, flight measurement evaluation, recovered hardware forensics, etc. The fact that these geometries were chosen for investigation purposes should not be misconstrued as exactly reproducing the damaged configuration encountered in flight. These representative damaged configurations, however, do provide an insight into the nature and level of damage necessary to result in the loss of Columbia and her STS-107 crew.

TABLES

CASE	Damage Location	ΔCm	ΔCn	ΔCl
Boundary Layer Trip	RCC Panel 6	-0.00062	-0.00015	0.00032
Boundary Layer Trip	RCC Panel 6 (fwd)	-0.00019	-0.00004	0.00019
Holes Through Wing	4 holes (Mach 6)	0.00012	-0.00008	0.00017
Hole Through Wing	Carrier Panel 6 (CF4)	0.00040	0.00006	-0.00005
Hole Through Wing	Carrier Panel 9 (CF4)	0.00010	-0.00004	0.00000
Hole Through Wing	Carrier Panel 12 (CF4)	0.00014	-0.00003	-0.00004
Flight Extracted	**EI to EI + 515 sec**	**0.0000**	**0.0000**	**0.0000**

Table 4.4-1 Aerodynamic Increments – WT Results for BL Trips & Hole(s) Through Wing

	Full-vehicle baseline	Δ interaction (new-baseline)	Δ thrust	Δ net
axial	.0781751	$1.23\ 10^{-7}$	$3.07\ 10^{-7}$	$4.30\ 10^{-7}$
side	0	$3.66\ 10^{-5}$	$-8.12\ 10^{-5}$	$-4.46\ 10^{-5}$
normal	1.1322635	$-3.03\ 10^{-5}$	$4.08\ 10^{-5}$	$1.05\ 10^{-5}$
roll	0	$-2.79\ 10^{-5}$	$2.76\ 10^{-5}$	$-0.03\ 10^{-5}$
pitch	.0279899	$3.98\ 10^{-5}$	$2.67\ 10^{-6}$	$4.25\ 10^{-5}$
yaw	0	$8.50\ 10^{-6}$	$-5.53\ 10^{-6}$	$2.97\ 10^{-6}$

Table 4.4-2 Aerodynamic Increments – LAURA CFD – Jet exiting MLG door w/External Flow Interaction

FIGURES

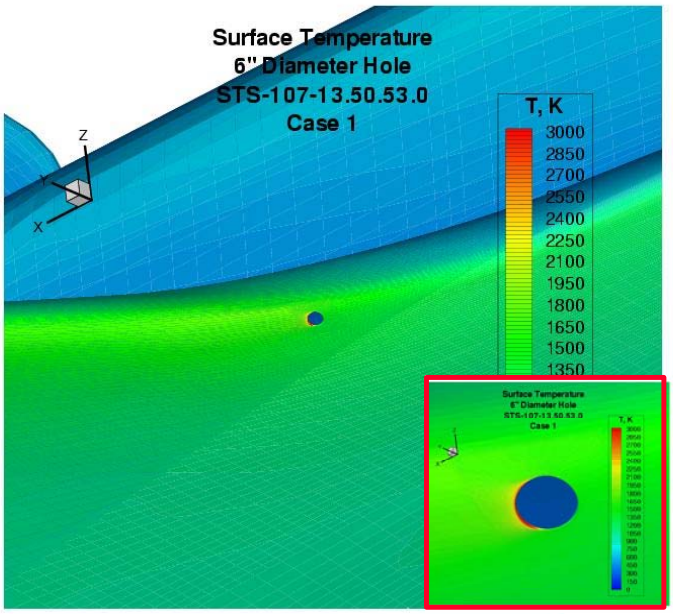

Figure 4.4-1 Surface Temperature - LAURA CFD Analysis – 6" Hole in WLE RCC Panel 6

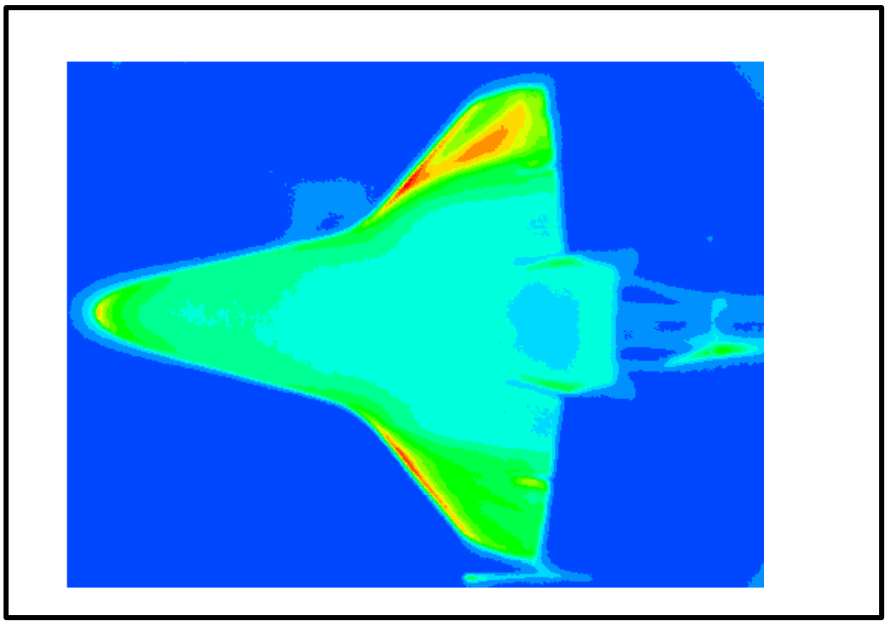

Figure 4.4-2 Infra-red Thermography Surface Heating Distribution – BL Trip at RCC Panel 6

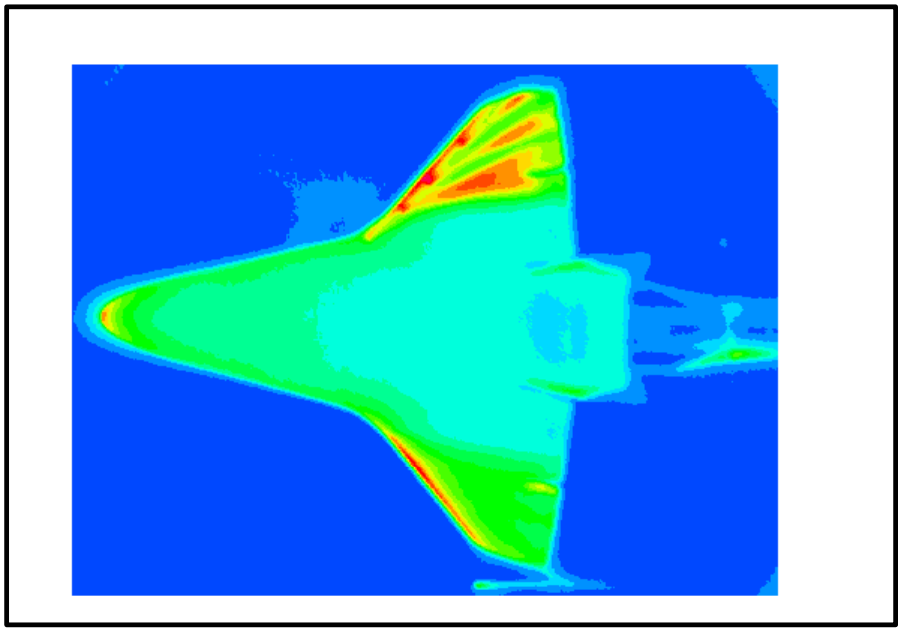

Figure 4.4-3 Infra-red Thermography Surface Heating Distribution – Holes (4) at RCC Vent Locations

Experimental Aeroheating -- 20-inch CF4 tunnel, $\alpha = 40°$

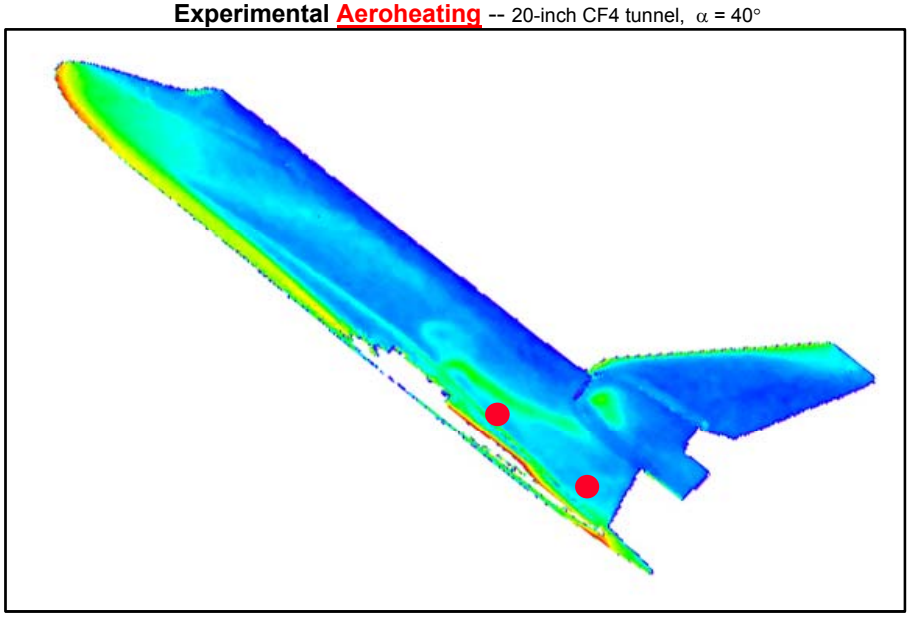

Figure 4.4-4 Phosphor Thermography WT Test Surface Heating Distribution – RCC Panel 9 Missing

FELISA Prediction of Surface Pressure

M = 24.2, Equilibrium air, $\alpha = 40°$

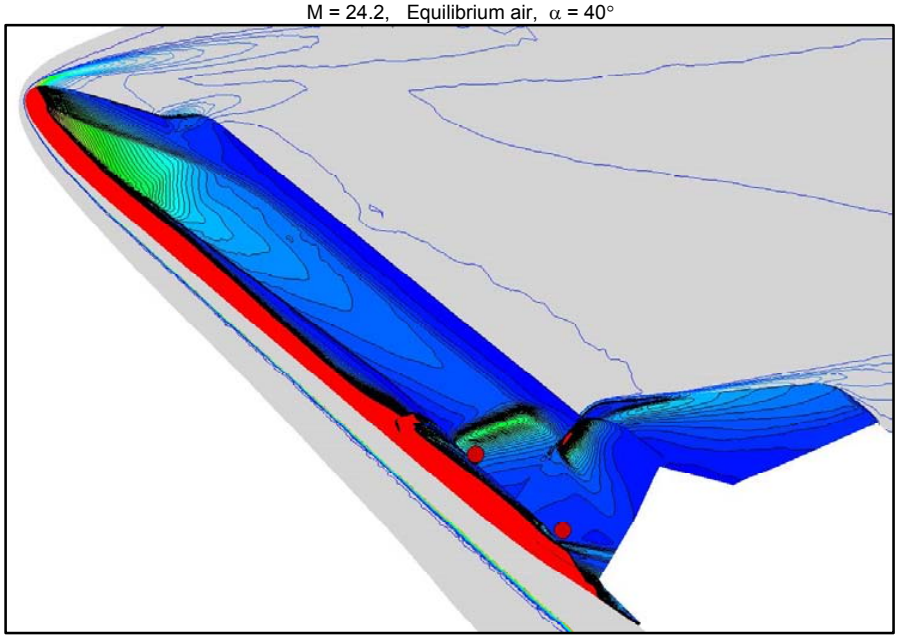

Figure 4.4-5 Surface Pressure Distribution – CFD Analysis - RCC Panel 9 Missing

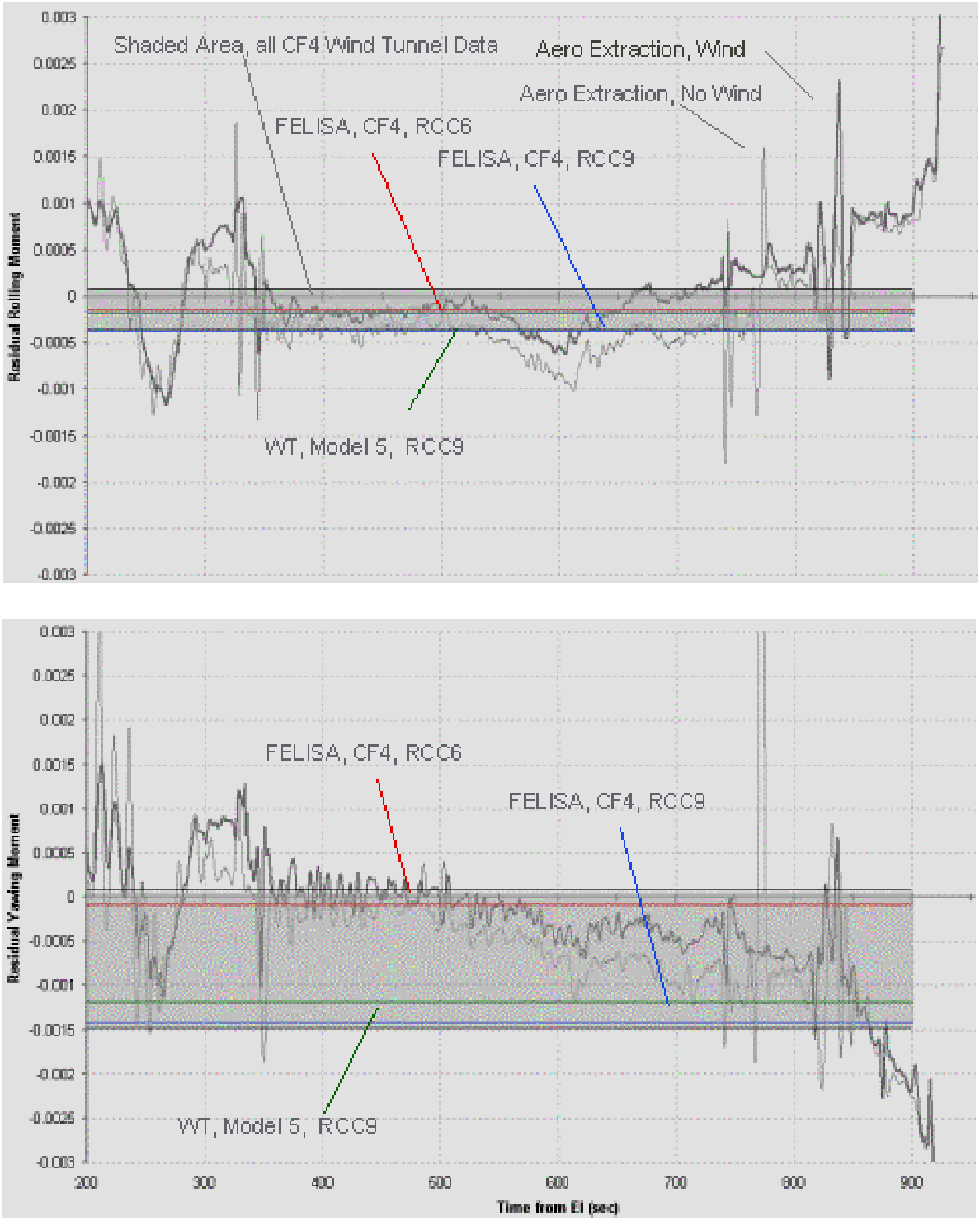

Figure 4.4-6 LaRC CF4 WT Test & FELISA (Inviscid) CFD Results – Single Panel Damage Predicted Delta Aerodynamics vs. Flight Extracted Increments

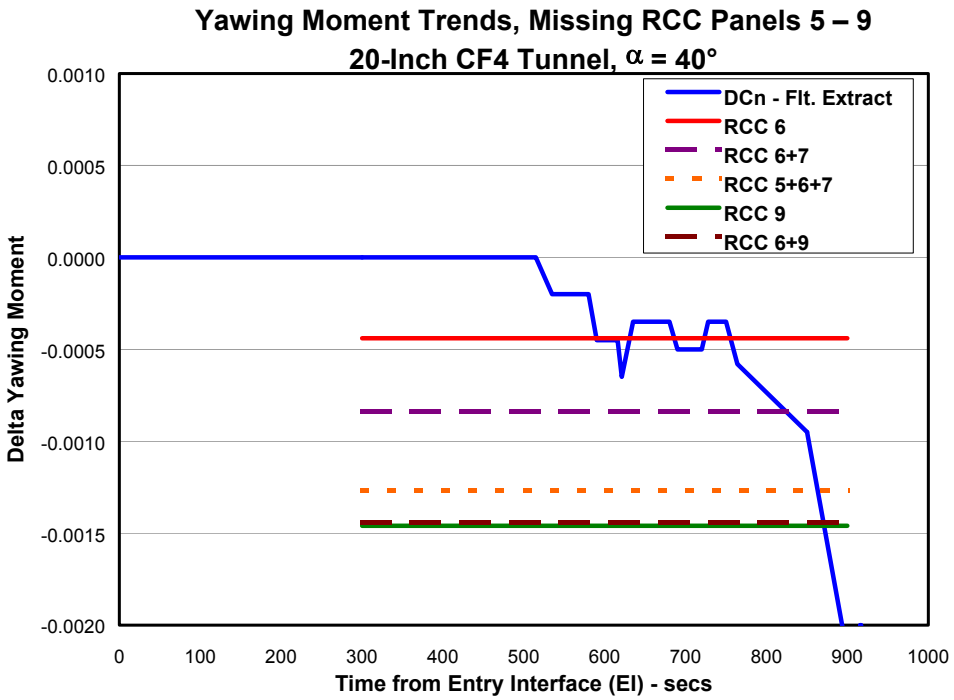

Figure 4.4-7 Aerodynamic Increment (delta Yaw) - Multiple RCC Panels Missing

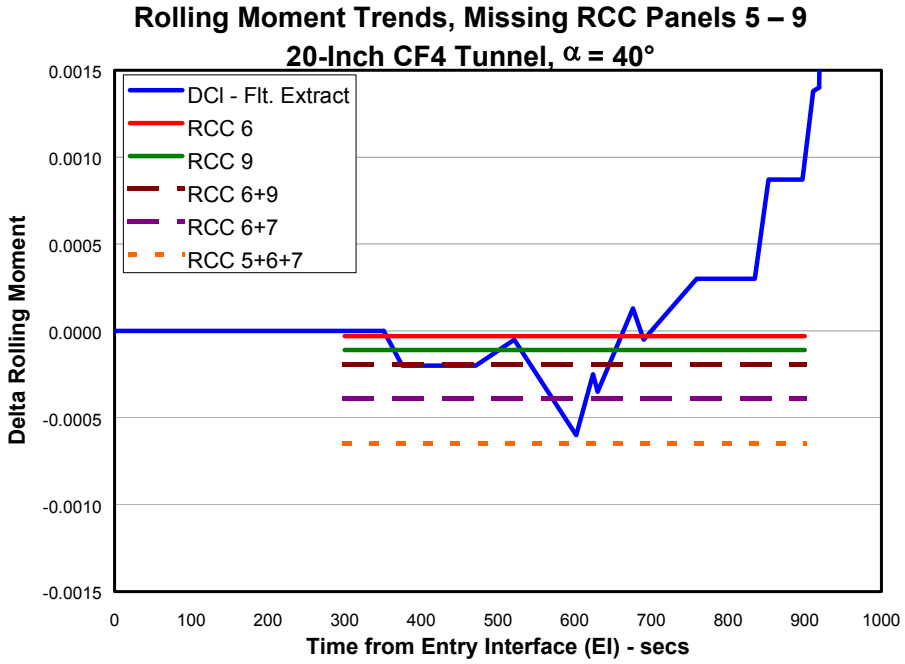

Figure 4.4-8 Aerodynamic Increment (delta Roll) - Multiple RCC Panels Missing

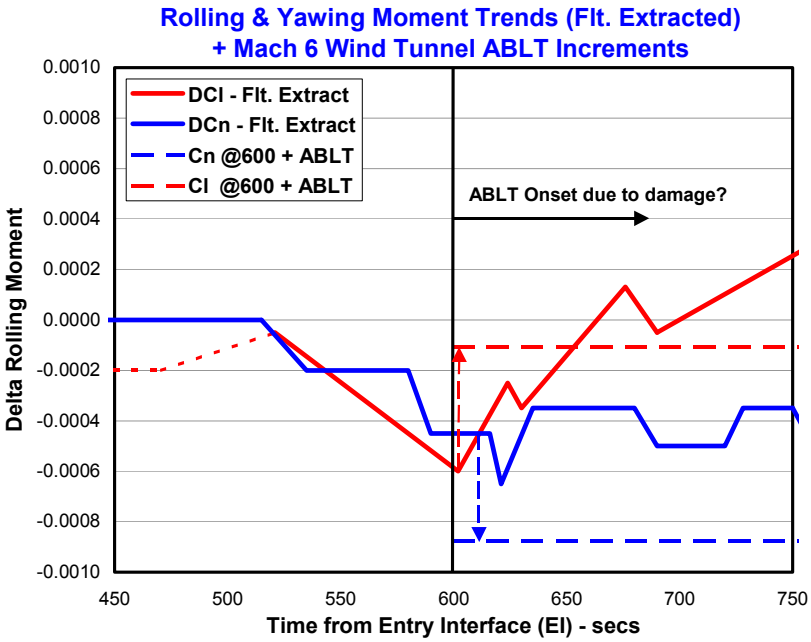

Figure 4.4-9 Delta Rolling Moment Trend Change - Early ABLT Onset?

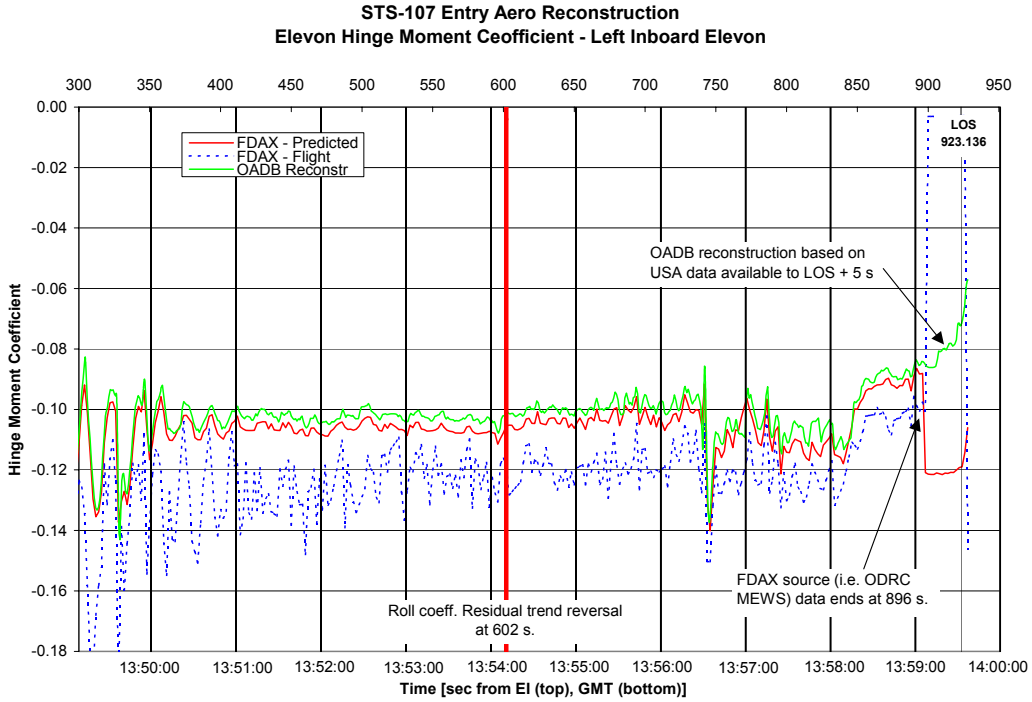

Figure 4.4-10 Delta Rolling Moment Trend Change – Disturbed flow over LHIB Elevon?

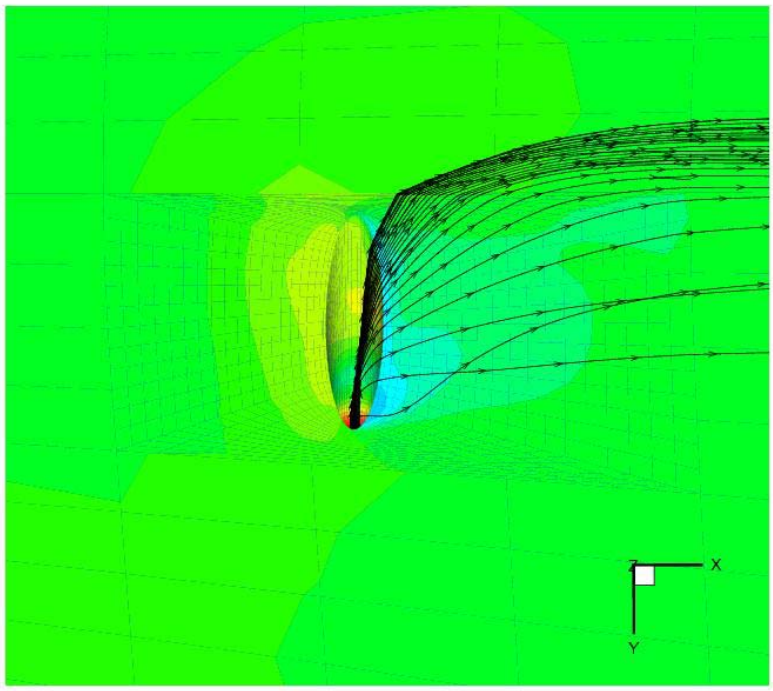

Figure 4.4-11 Delta Rolling Moment Trend Change – Flow Interaction w/Exiting Jet?

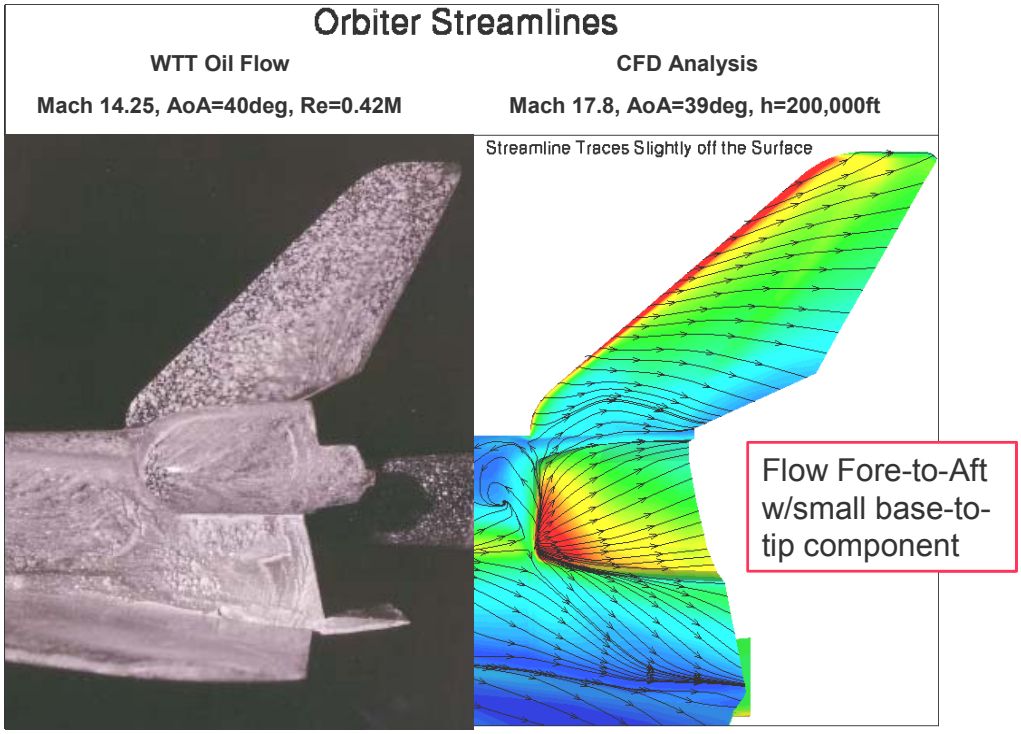

Figure 4.4-12 Orbiter Leeside (Fuselage, VT, OMS) Flow Field Visualization

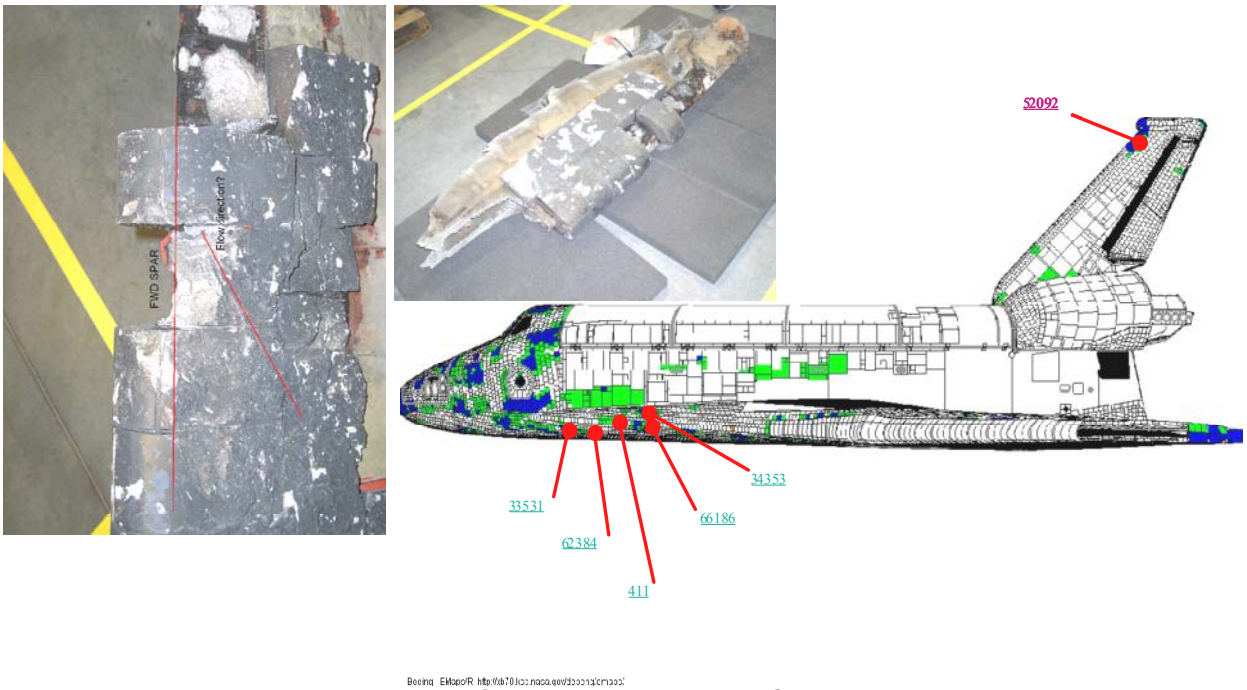

Figure 4.4-13 Recovered Columbia Hardware - VT Spar Debris Item 52092

FELISA --Inviscid Solver
Mach 24.2, Equilibrium Air, q = 28.2 psf, α= 40 deg (13:52:20, EI+491 sec)

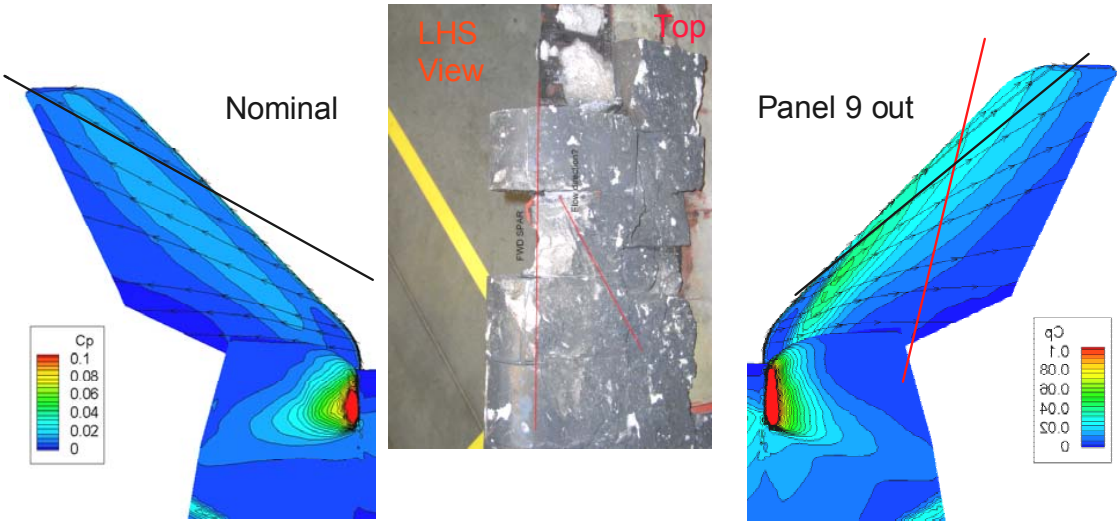

Figure 4.4-14 VT Flow Patterns - FELISA CFD Results - Baseline & w/Panel 9 Missing

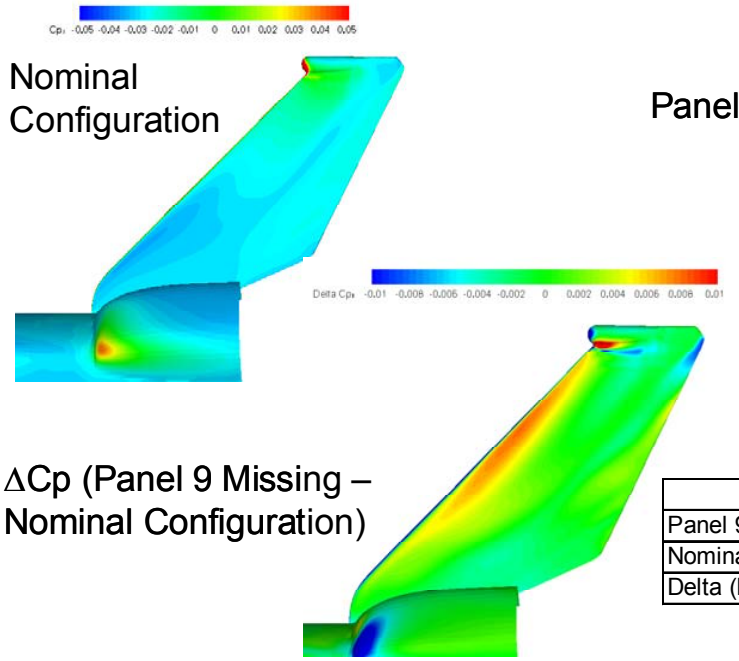

	Cl	Cm	Cn
Panel 9 (P9)	-0.00026	-0.00614	-0.00063
Nominal (clean)	0.00001	-0.00623	-0.00002
Delta (P9 - clean)	-0.00027	0.00009	-0.00061

Figure 4.4-15 Leeside Flow Interaction - Overflow CFD analysis - Delta CP on Vertical Tail

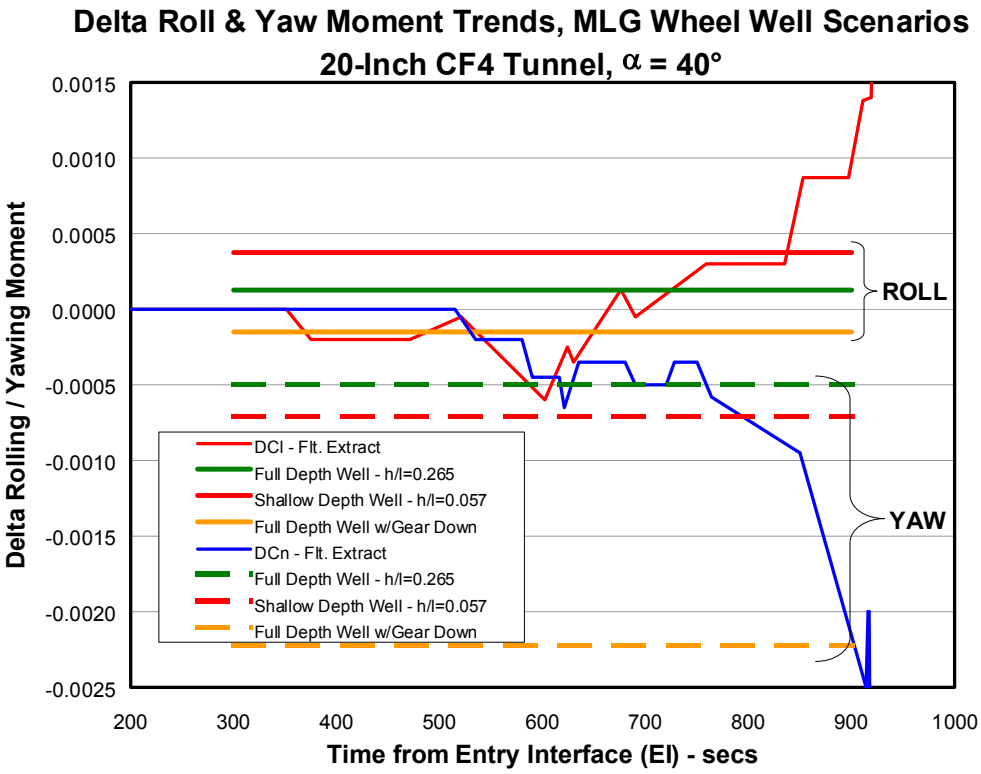

Figure 4.4-16 Delta Aero Increments - Roll & Yaw (MLG Wheel Well Scenarios)

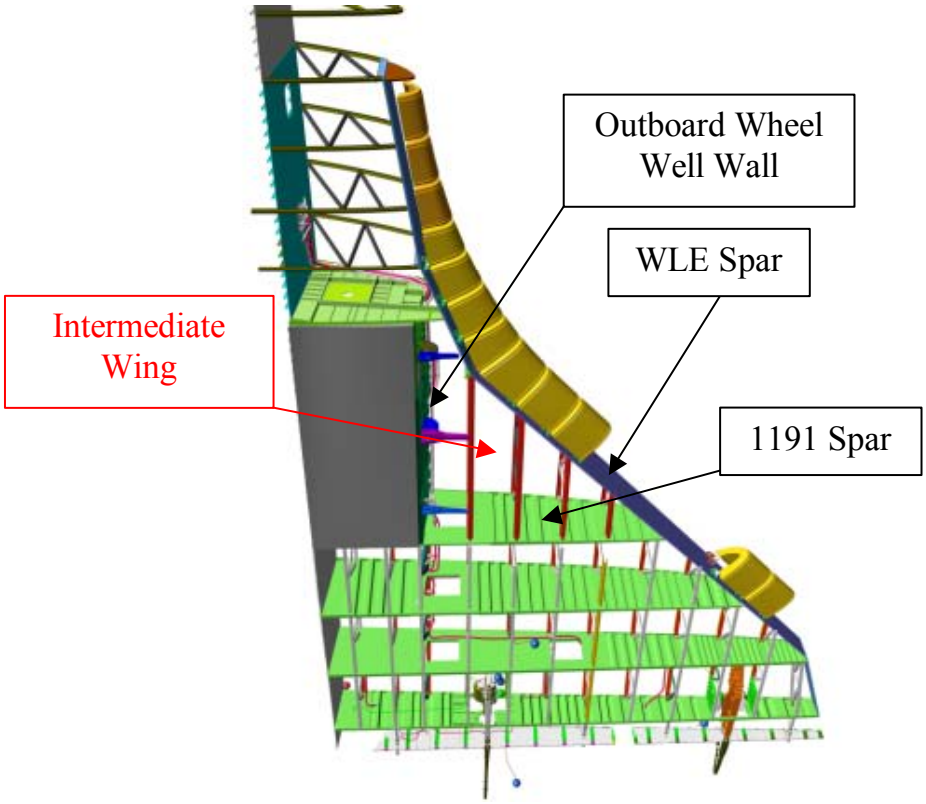

Figure 4.4-17 Orbiter Wing Structure Layout - Intermediate Wing Area

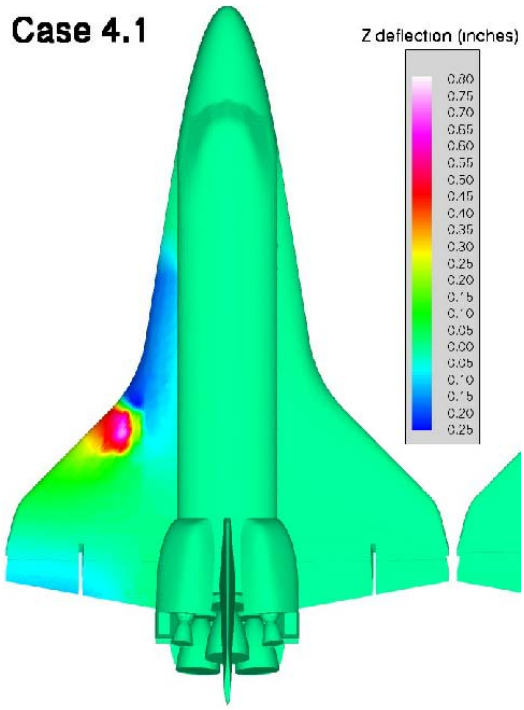

Figure 4.4-18 Orbiter Wing Structure Delta Deflection – Surface (z) Change With Damage

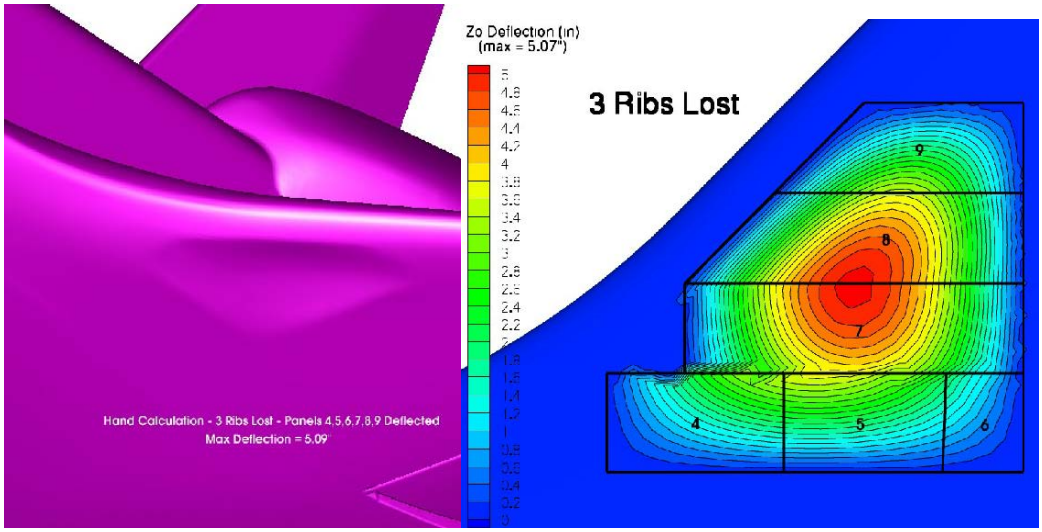

Figure 4.4-19 Orbiter Wing Surface (Skin) Deflection (z) – With Damage – 3 Ribs lost

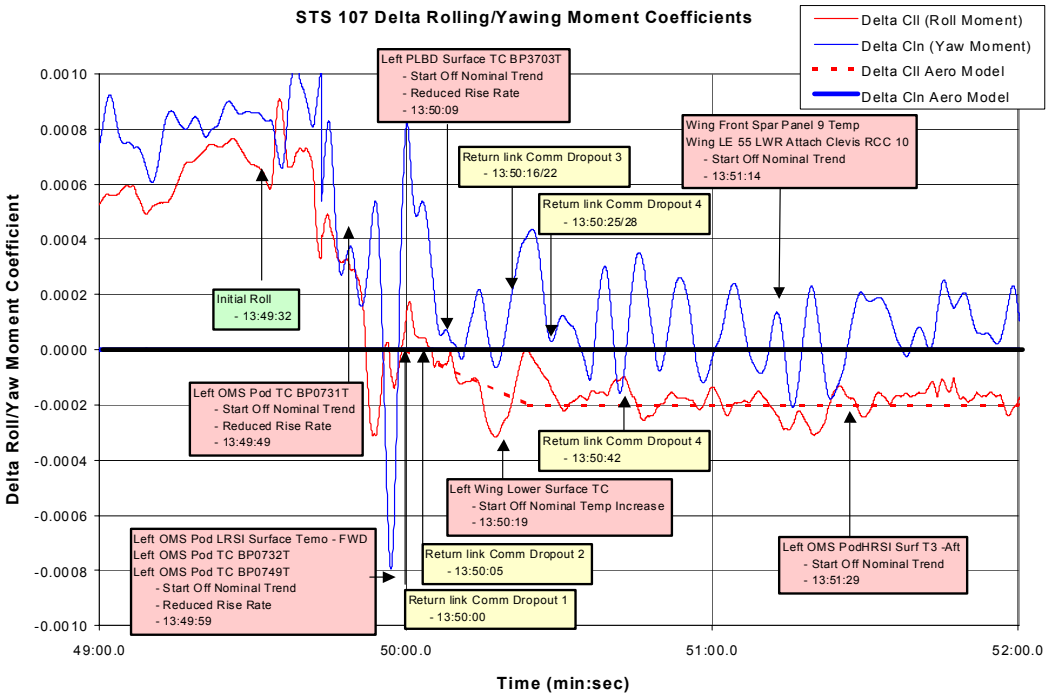

Figure 4.4-20 Aero Increments GMT 13:49:00 to 13:52:00

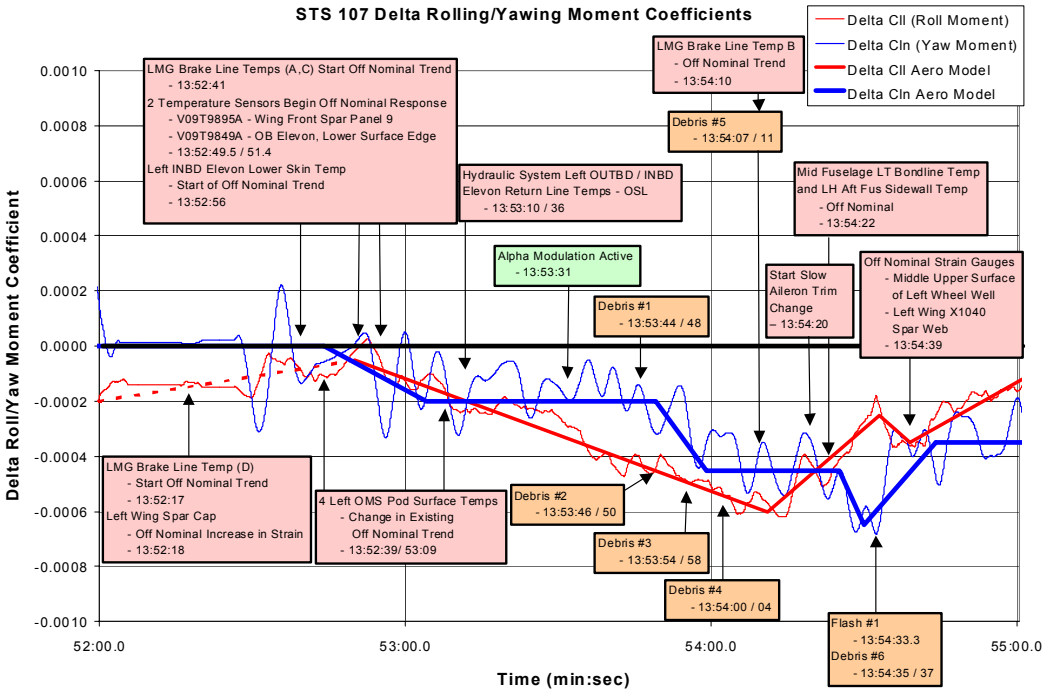

Figure 4.4-21 Aero Increments GMT 13:52:00 to 13:55:00

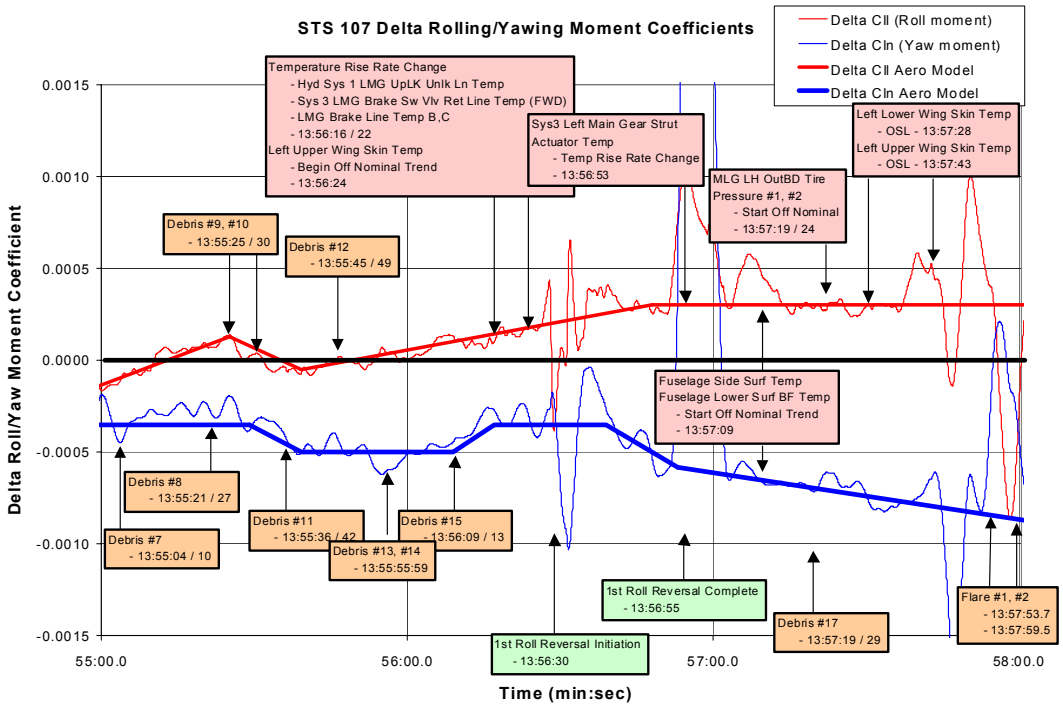

Figure 4.4-22 Aero Increments GMT 13:55:00 to 13:58:00

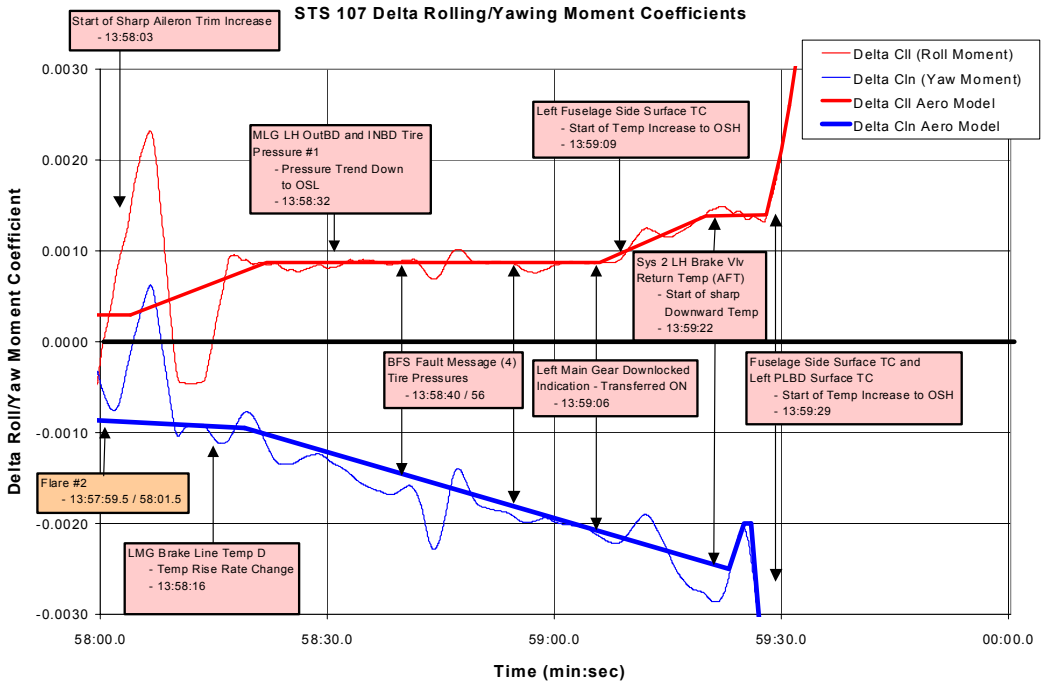

Figure 4.4-23 Aero Increments GMT 13:58:00 to 13:59:30

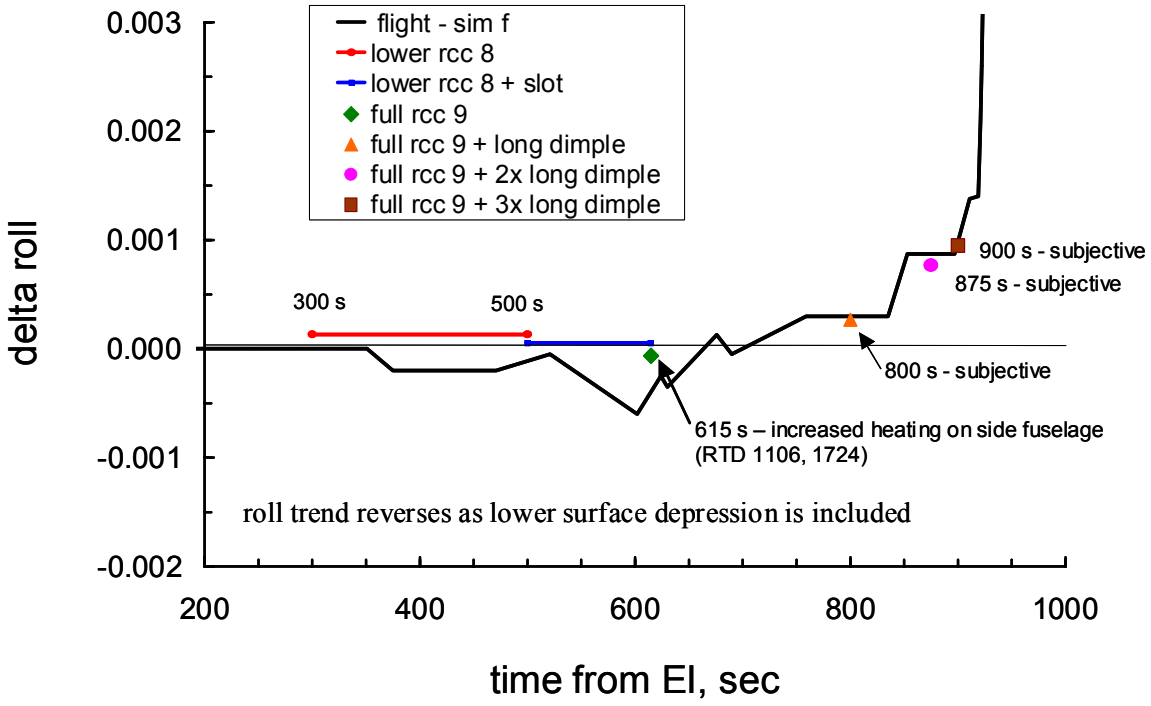

Figure 4.4-24 Aerodynamic Damage Progression Scenario – Delta Rolling Moment

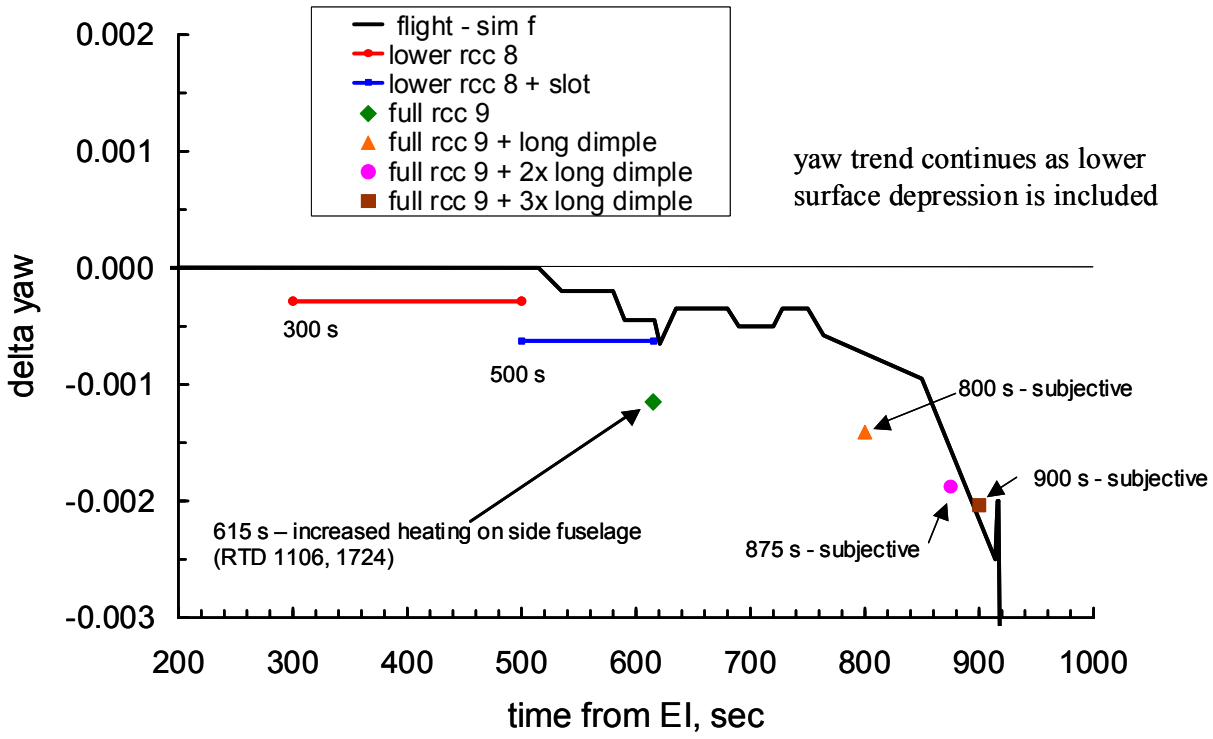

Figure 4.4-25 Aerodynamic Damage Progression Scenario – Delta Yawing Moment

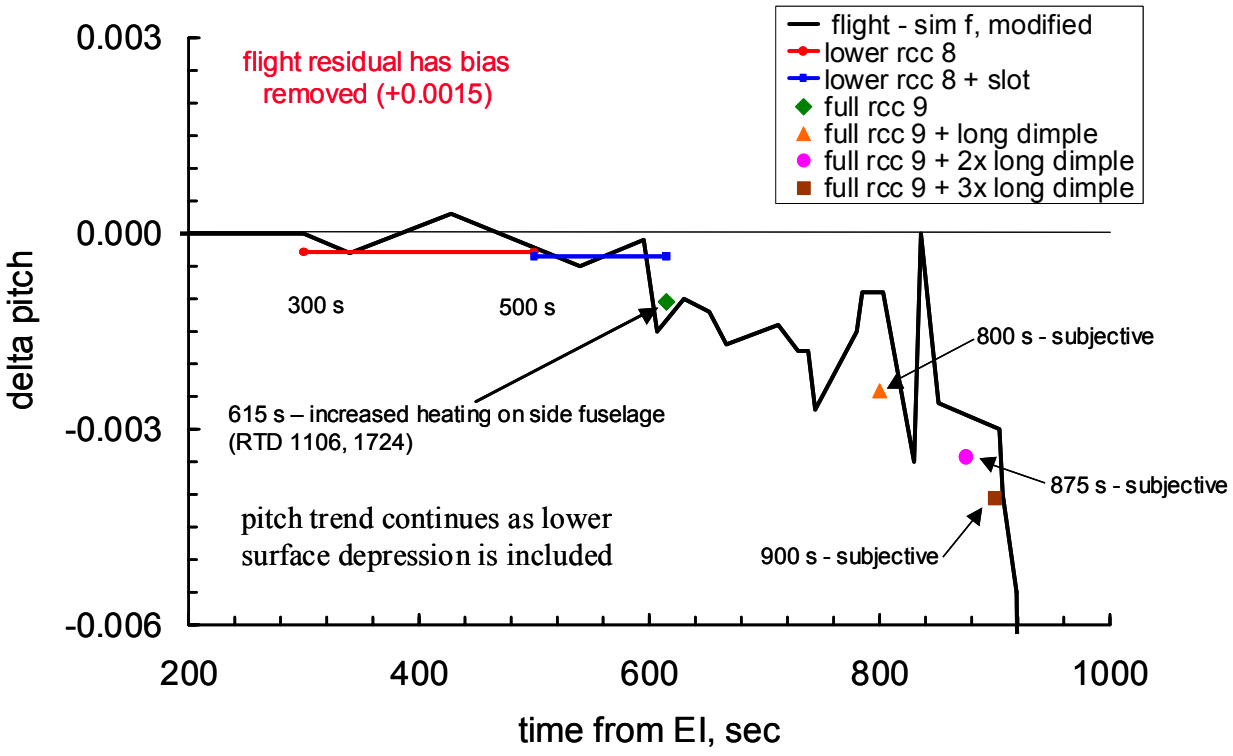

Figure 4.4-26 Aerodynamic Damage Progression Scenario – Delta Pitching Moment

4.5 Summary – conclusions & observations

1) Flight measured Orbiter rates, accelerations, trajectory parameters, control surface deflections, etc. can be used to define the off-nominal aerodynamics experienced by Columbia during STS-107 entry flight. The off-nominal aero is characterized by delta aerodynamic force and moment increments (Delta defined as Actual - Nominal).
2) High altitude winds have a pronounced effect on the magnitude of the off-nominal delta aerodynamic forces and moments, as much as 50%, but do not effect the trends vs. time.
3) Off nominal aerodynamic increments are not clearly evident until after EI + 515 sec.
4) At EI + 602 sec, the rolling moment increment trend abruptly reverses from increasing negative to increasing positive, corresponding to several other timeline events. These include the first evidence of flight control system compensation for asymmetric aero due to damage as well as debris event No. 5 (or Flash event "0").
5) The extracted moments do not exceed asymmetric aerodynamic design levels as defined by the Asymmetric Boundary Layer Transition (ABLT) model until very late in the flight timeline (after the EI + 877 sec point).
6) The flight control system manages the growing asymmetry as designed throughout the flight up to Loss of Signal (LOS).
7) The off nominal aerodynamics increase rapidly in the last 60 sec of flight producing overwhelming asymmetric moments (after EI + 920 sec) resulting in Columbia's loss of control leading to vehicle breakup.
8) Wind tunnel test and CFD analysis of proposed damaged configurations has been successful in producing aerodynamic increments consistent with a progressive damage scenario.
9) Initial delta aerodynamic yawing (-) and rolling (-) increments are not consistent with early ABLT which has always produced opposite signs for these moments.
10) Wing leading edge (RCC panel) damage produces the (-) roll and (-) yaw increments early in flight (plus the augmented heating observed on the side fuselage and OMS pod).
11) The primary source of the rolling moment trend change (@EI + 602 sec) cannot be attributed to leeside (VT, OMS, fuselage) interaction
12) Lower wing surface deformation (i.e. cavity or depression) produces the (-) yawing and (+) rolling moment increment trends seen later in the flight. These deformations are consistent with anticipated internal wing damage due to ingestion of hot gas through a Wing Leading Edge breach.
13) Increments measured for Main Landing Gear / Door deployment while matching the roll and yaw increments later in flight do not match the pitching moment. Based on this data the Main Landing Gear did not prematurely deploy.
14) Based on WT test and CFD analysis results a progressive damage scenario can be matched to the extracted aerodynamic increments that is consistent with other observed data trends, analysis and recovered hardware forensics.
15) The test and analysis conducted for the aerodynamic (and aerothermodynamic) portion of the investigation were performed on representative geometries. The fact that these geometries were chosen for investigation purposes should not be misconstrued as exactly reproducing the damaged configuration encountered in flight. These representative damaged configurations, however, do provide an insight into the nature and level of damage necessary to result in the loss of Columbia and her STS-107 crew.

4.6 References – Aerodynamics

1) Operational Aerodynamic Design Data Book, STS85-0118-1 CHG 8, August, 1996
2) STS-107 Natural Environments Report, MSFC ED44 (03-012), May 16, 2003
3) STS-107 Integrated Entry Environment (IEE) Team Final Report, NSTS-37382, May 30, 2003
4) OV-102 Investigation Vehicle Data Mapping (VDM) Team Quantitative Report, Preliminary - Rev. 6, May 02, 2003.

4.7 Appendices – Aerodynamics

4.7.1 Aerodynamic Definitions, Coordinate Systems and References

The following figures (pages from the Orbiter OADB) summarize the Orbiter aerodynamic coordinate system, aerodynamic definitions, moment reference center and the reference areas and lengths.

The aerodynamic force and moment sign convention is illustrated in Figure 3.1.5-4 which also includes the longitudinal equations for conversion from stability to body axis system.

STABILITY AXIS

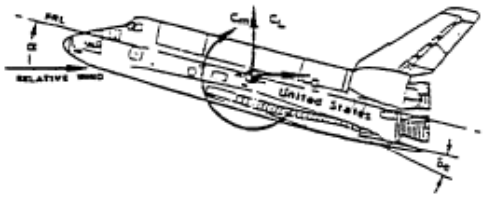

Conversion to body axis system:

$C_N = C_L \cos \alpha + C_D \sin \alpha$

$C_A = C_D \cos \alpha - C_L \sin \alpha$

BODY AXIS

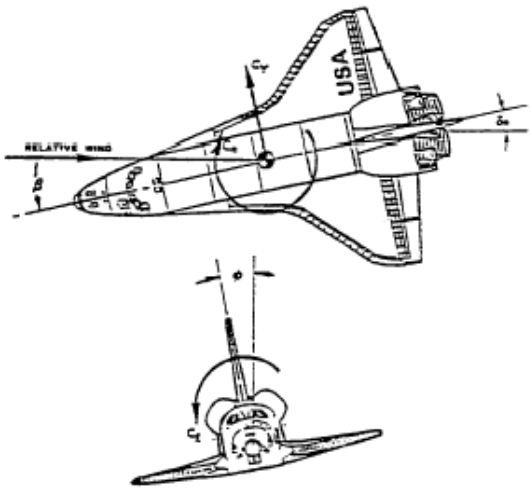

Figure 3.1.5-4
ORBITER SIGN CONVENTION

4.2.1.1 LONGITUDINAL AERODYNAMICS. The basic aerodynamic characteristics for the longitudinal degrees-of-freedom are presented as full-scale, rigid and elastic, forces and moment in both the stability and body axis systems (cf.Section 3.1.5). These forces and moments are defined for three phases or categories:

1.) ON-ORBIT (PAYLOAD BAY DOORS OPEN)

2.) ON-ORBIT (PAYLOAD BAY DOORS CLOSED)

3.) ENTRY

The total longitudinal forces and moment for the Orbiter Vehicle are defined as:

LIFT FORCE, $L_{TOTAL} = \bar{q}\, S_w C_{L_{TOTAL}} + L_{RCS}$ (lb)

NORMAL FORCE, $N_{TOTAL} = \bar{q}\, S_w C_{N_{TOTAL}} + N_{RCS}$ (lb)

DRAG FORCE, $D_{TOTAL} = \bar{q}\, S_w C_{D_{TOTAL}} + D_{RCS}$ (lb)

AXIAL FORCE, $A_{TOTAL} = \bar{q}\, S_w C_{A_{TOTAL}} + A_{RCS}$ (lb)

PITCHING MOMENT, $M_{TOTAL} = \bar{q}\, S_w \bar{c}_w C_{m_{TOTAL}} + M_{RCS}$ (ft-lb)

where, $\bar{q}$ = dynamic pressure (lb/ft^2)

S_w = Wing Reference Area (2690.00 ft^2)

$\bar{c}_w$ = Wing Mean Aerodynamic Chord (39.56 feet) (see Figure 3.1.5-2b)

RCS flow field interactions are defined as contributions to the total forces or moment rather than coefficients since the terms due to jet thrust and impingement are independent of dynamic pressure and cannot, therefore, be normalized in the conventional manner.

4.2.1.2 LATERAL-DIRECTIONAL AERODYNAMICS. The basic aerodynamic characteristics for the lateral-directional degrees-of-freedom are presented as full-scale, rigid and elastic, force and moments in the body-axis system (cf. Section 3.1.5). The lateral-directional characteristics are defined under the same three categories listed in Section 4.2.1.1.

The total lateral-directional force and moments for the Orbiter Vehicle are defined as:

SIDE FORCE, $Y_{TOTAL} = \bar{q}\, S_w C_{Y_{TOTAL}} + Y_{RCS}$ (lb)

YAWING MOMENT, $\mathcal{N}_{TOTAL} = \bar{q}\, S_w b_w C_{n_{TOTAL}} + \mathcal{N}_{RCS}$ (ft-lb)

ROLLING MOMENT, $\mathcal{L}_{TOTAL} = \bar{q}\, S_w b_w C_{\ell_{TOTAL}} + \mathcal{L}_{RCS}$ (ft-lb)

where, $\bar{q}$ = dynamic pressure (lb/ft^2)

S_w = Wing Reference Area (2690.00 ft^2)

b_w = Wing Span (78.057 ft)
(see Figure 3.1.5-2b)

RCS flow field interactions are defined as contributions to the total force or moments rather than coefficients since the terms due to jet thrust and impingement are independent of dynamic pressure and cannot, therefore, be normalized in the conventional manner.

3.1.5 ORBITER VEHICLE. The aerodynamic design of the Orbiter Vehicle configuration is the result of a selection which would achieve high cross-range aerodynamically and which would be capable of trimmed flight over a wide range of angles of attack. The double-delta wing planform, combined with a moderately low fineness ratio (approximately 5) body, minimizes interference heating effects, provides the required L/D ratio to meet cross-range requirements, and possesses an acceptable trim range over the flight Mach regime. Figure 3.1.5-1 presents a general arrangement drawing of the Orbiter Vehicle.

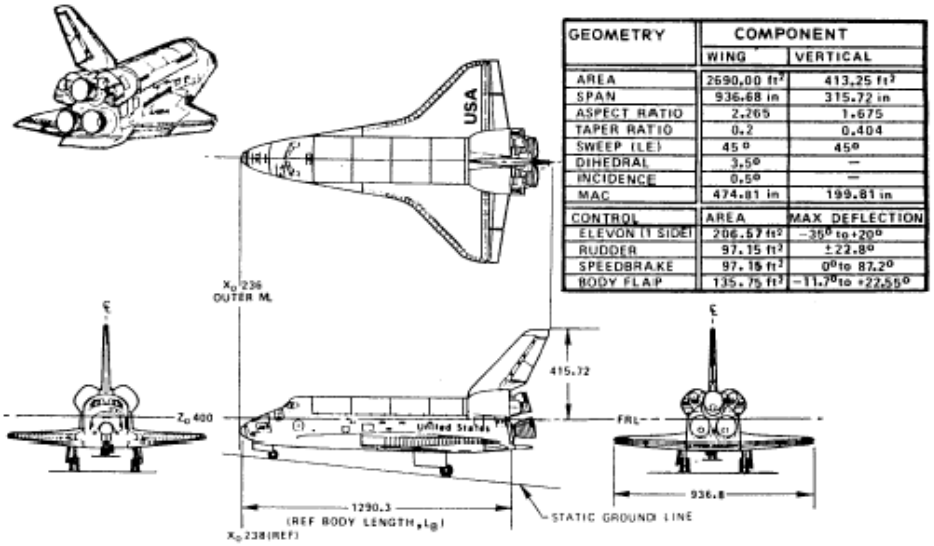

GEOMETRY	COMPONENT	
	WING	VERTICAL
AREA	2690.00 ft²	413.25 ft²
SPAN	936.68 in	315.72 in
ASPECT RATIO	2.765	1.675
TAPER RATIO	0.2	0.404
SWEEP (LE)	45°	45°
DIHEDRAL	3.5°	—
INCIDENCE	0.5°	—
MAC	474.81 in	199.81 in
CONTROL	AREA	MAX DEFLECTION
ELEVON (1 SIDE)	206.57 ft²	−35° to +20°
RUDDER	97.15 ft²	±22.8°
SPEEDBRAKE	97.15 ft²	0° to 87.2°
BODY FLAP	135.75 ft²	−11.7° to +22.55°

Figure 3.1.5-1
ORBITER GEOMETRY

Orbiter Vehicle design geometry is presented in Figure(s) 3.1.5-2 (a through f). The Orbiter Vehicle axis system for design drawing and mass properties statements is illustrated in the sketch. This axis system is defined in the Space Shuttle Master Dimensions Specification (Reference 3-7) and on Figure 3.1.5-2. All vehicle and design drawing axes systems are in accordance with NASA Phase B Technical Directives 2519 and 2519A.

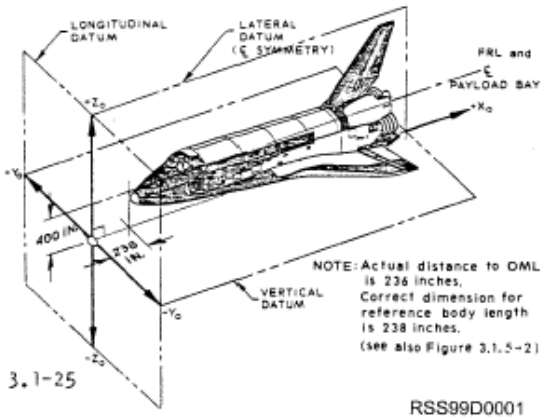

4.7.2 Surface Pressure Entry Data Evaluation

Orbiter Experiments (OEX) pressure data was installed on Columbia in support of the Ascent Wing Loads Verification Program. The pressure transducers were therefore sized (typically 0 to 16 psia) for ascent load environments and analysis of these flight results were incorporated into the Performance Enhancement Design Airloads database. These specific requirements limited the use of data for the entry phase. Entry data review was typically performed for the Mach 3.5 to 0.6 region which covers the Operational Entry Airloads Database. Since culmination of the Airloads Verification Program, the typical extent of the entry review was for instrument functionality and signature comparisons with past flights.

Analysis of the OEX recorder pressure data for STS-107 was made possible with the finding, identification and processing of the OEX data recorder. This data included 181 wing pressure measurement gages on two of the three Pulse Code Modulation (PCM) units of the recorder. PCM1 had 91 gages while PCM2 had 90 gages with no measurements recorded on PCM3. A previous instrument survey performed for STS-109 (Columbia's previous flight) had identified that only 116 gages were producing useable data. These 116 gages break down as 68 for left wing (41 upper, 27 lower) and 48 for the right wing (34 lower and 14 upper). The only active pressure gages on Columbia during STS-107 were those on the wings.

Analysis of the STS-107 OEX entry pressure data was of very limited use for aerodynamic evaluation. Even though data was recorded to EI + 970 seconds, the useful recorded pressures typically do not start until around 1420 seconds after EI near Mach 3.5, Figure 4.7-1. Since the extent of STS-107 entry was above this condition and at such high altitude, low density conditions, no useful aerodynamic data was recorded. Most pressure gages exhibited pressure "spikes" in the EI + 480-660 sec and 930-970 sec regions, with these trends identified on both wings Figure 4.7-2. OEX pressure data utilization was limited to identification of these off-nominal signatures. The first gages to exhibit this behavior and the failure patterns were provided to the Time Line Group for inclusion of OEX pressure data into the master time line in support of the working scenario.

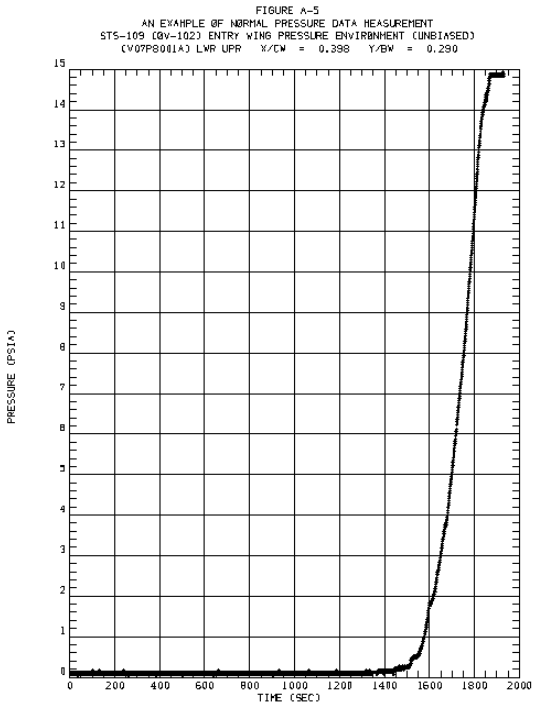

Figure 4.7-1 Typical OEX Entry Pressure Gage Signature (STS-109)

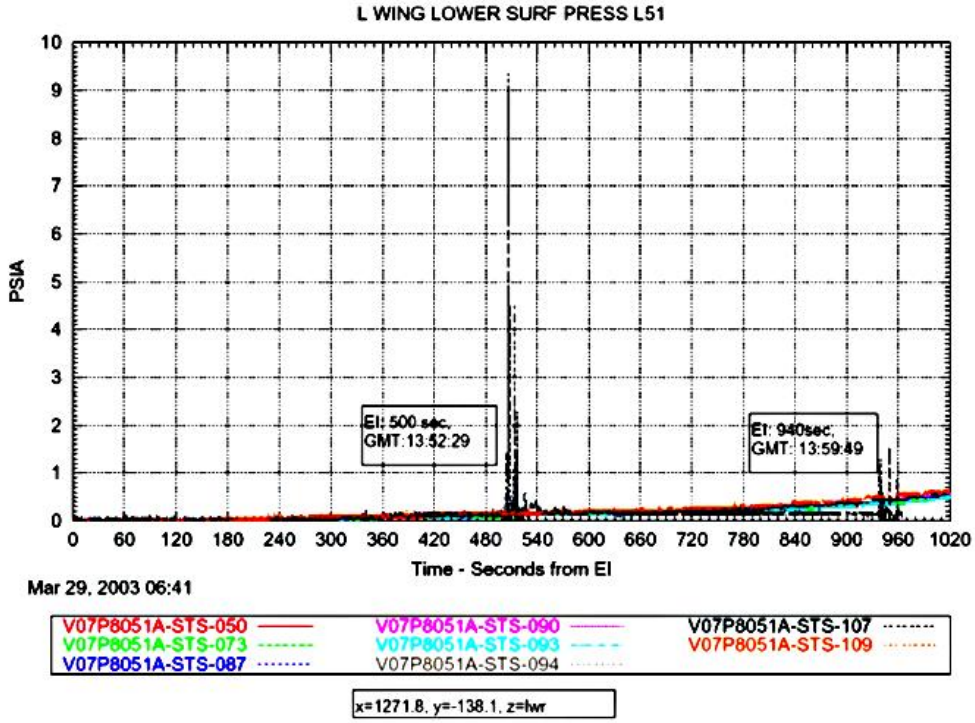

Figure 4.7-2 Typical OEX Entry Pressure Gage Signature (STS-107)

4.7.3 Wind Tunnel Test Matrix – Comprehensive Listing

Test	Run	Re/ft	Alpha	Beta	Mach	Gamma	Model	Configuration
6853	9	3.0	37.5	0.0	6.00	1.40	ceramic 1	baseline - ceramic 1; Re/ft = 3.0e6
6853	10	2.9	37.6	0.0	6.00	1.40	ceramic 1	baseline - ceramic 1, repeat; Re/ft = 3.0e6
6853	11	2.9	37.5	0.0	6.00	1.40	ceramic 1	baseline - ceramic 1, repeat; Re/ft = 3.0e6
6853	12	3.0	37.6	0.0	6.00	1.40	ceramic 1	trip at rcc panel 6 (1 trip, 0.0035 in)
6853	13	2.9	37.6	0.0	6.00	1.40	ceramic 1	trip at rcc panel 6 (1 trip, 0.0045 in)
6853	14	2.9	37.6	0.0	6.00	1.40	ceramic 1	trip at rcc panel 9 (1 trip, 0.0045 in)
6853	15	3.0	37.6	0.0	6.00	1.40	ceramic 1	trip at rcc panel 9 (1 trip, 0.0045 in)
6853	16	3.0	37.6	0.0	6.00	1.40	ceramic 1	trip at rcc panel 6 (1 trip, 0.0050 in)
6853	17	3.0	37.5	0.0	5.99	1.40	ceramic 1	trip at rcc panel 6 (1 trip, 0.0045 in)
6853	18	3.0	37.6	0.0	5.99	1.40	ceramic 1	trip at MLG door le,outboard corner (1 trip, 0.0045 in)
6853	19	3.0	37.6	0.0	5.99	1.40	ceramic 1	trips along MLG door le (7 trips, 0.0045 in)
6853	20	3.0	37.6	0.0	5.99	1.40	ceramic 1	trips along MLG door le (7 trips, 0.0045 in)
6853	21	3.0	37.6	0.0	5.99	1.40	ceramic 1	trips along MLG door le,down side (12 trips, 0.0045 in)
6853	22	3.0	37.6	0.0	5.99	1.40	ceramic 1	raised MLG door (1 "trip", 0.0065 in)
6853	23	3.0	37.5	0.0	5.98	1.40	ceramic 1	raised MLG door w/ slash (1 "trip", 0.0065 in)
6853	24	3.0	37.6	0.0	5.98	1.40	ceramic 1	trip at rcc panel 6; match test 6852 (1 trip, 0.0035 in)
6853	25	3.0	37.6	0.0	5.98	1.40	ceramic 1	trip at rcc panel 6, biased windward (1 trip, 0.0035 in)
6853	26	3.0	37.6	0.0	5.98	1.40	ceramic 1	trip at rcc panel 6, biased leeward (1 trip, 0.0035 in)
6853	27	2.9	37.5	0.0	5.98	1.40	ceramic 1	trip at rcc panel 6, biased windward (1 trip, 0.0065 in)
6853	28	3.0	37.6	0.0	5.98	1.40	ceramic 1	"full" ablt (10 trips along wing le)
6853	29	3.0	37.6	0.0	5.98	1.40	ceramic 1	"full" ablt (10 trips along wing le, 2 fwd)
6853	31	3.0	37.6	0.0	5.98	1.40	ceramic 1	baseline - ceramic 1, repeat; Re/ft = 3.0e6
6853	33	2.1	37.5	0.0	5.96	1.40	steel 1	baseline - steel 1; Re/ft = 2.0e6
6853	34	3.0	37.8	0.0	5.98	1.40	steel 1	baseline - steel 1; Re/ft = 3.0e6
6853	36	2.0	37.5	0.0	5.96	1.40	steel 1	open wheel well, L/H = 3.8, Re/ft = 2.0e6
6853	37	3.0	37.8	0.0	5.98	1.40	steel 1	open wheel well, L/H = 3.8, Re/ft = 3.0e6
6853	39	3.0	37.8	0.0	5.98	1.40	steel 1	open wheel well, L/H = 6.4, Re/ft = 3.0e6
6853	41	3.0	37.8	0.0	5.98	1.40	steel 1	open wheel well, L/H = 17.5, Re/ft = 3.0e6
6853	42	2.1	37.5	0.0	5.97	1.40	steel 1	open wheel well, L/H = 17.5, Re/ft = 2.0e6
6853	44	3.0	37.8	0.1	5.98	1.40	steel 1	open wheel well w/ door; L/H = 3.8
6853	46	3.0	37.9	0.1	5.98	1.40	steel 1	open wheel well w/ door and gear; L/H = 3.8
6853	48	3.0	37.8	0.0	5.98	1.40	steel 1	open wheel well w/ gear; L/H = 3.8
6853	49	3.0	37.8	0.0	5.98	1.40	steel 1	baseline - steel 1, repeat; Re/ft = 3.0e6
6853	51	3.0	37.6	0.0	5.98	1.40	ceramic 1	missing rcc panel 6
6853	52	3.0	37.6	0.0	5.98	1.40	ceramic 1	gouge in MLG door
6853	53	3.0	37.6	0.0	5.98	1.40	ceramic 1	holes through carrier panels 6, 9, 12, 16
6853	54	3.0	37.6	0.0	5.98	1.40	ceramic 1	baseline - ceramic 1, repeat; Re/ft = 3.0e6
6853	55	0.0	37.8	0.7	5.97	1.40	steel 1	baseline - steel 1; Re/ft = 3.0e6; beta = 0.7
6853	57	3.0	37.8	0.7	5.97	1.40	steel 1	open wheel well, L/H = 3.8; beta = 0.7
6853	58	3.0	37.8	0.7	5.98	1.40	steel 1	open wheel well w/ gear; L/H = 3.8; beta = 0.7
6853	59	3.0	37.9	0.8	5.98	1.40	steel 1	open wheel well w/ door + gear; L/H = 3.8; beta = 0.7
6853	60	3.0	37.8	0.7	5.98	1.40	steel 1	open wheel well w/ door; L/H = 3.8; beta = 0.7
6853	61	3.0	37.9	-0.8	5.98	1.40	steel 1	open wheel well w/ door + gear; L/H = 3.8; beta = -0.8
6853	62	3.0	37.8	-0.8	5.98	1.40	steel 1	open wheel well w/ door; L/H = 3.8; beta = -0.8
6853	63	3.0	37.8	-0.9	5.98	1.40	steel 1	baseline - steel 1; beta = -0.8

Table 4.7-1 Test LaRC 6853-Mach 6 Air Hypersonic Wind Tunnel Facility - STS-107 Investigation

Test	Run	Re/ft	Alpha	Beta	Mach	Gamma	Model	Configuration
144	10	0.46	38.1	0.0	5.93	1.22	steel 1	baseline - steel 1
144	11	0.46	40.2	0.0	5.90	1.21	steel 1	baseline - steel 1, repeat
144	12	0.45	42.2	0.0	5.89	1.21	steel 1	baseline - steel 1, repeat
144	13	0.44	38.2	0.0	5.95	1.22	steel 1	baseline - steel 1, repeat
144	14	0.45	40.2	0.0	5.93	1.22	steel 1	open wheel well, L/H = 3.8
144	16	0.45	42.2	0.0	5.91	1.21	steel 1	open wheel well, L/H = 17.5
144	17	0.45	38.2	0.0	5.90	1.21	steel 1	open wheel well w/ door and gear; L/H = 3.8
144	18	0.44	40.2	0.0	5.89	1.21	steel 1	open wheel well w/ door; L/H = 3.8
144	19	0.46	42.2	0.0	5.94	1.22	steel 1	open wheel well w/ gear; L/H = 3.8
144	20	0.45	38.2	0.0	5.93	1.22	steel 1	open wheel well, L/H = 6.4
144	28	0.15	40.0	0.0	6.00	1.23	steel 1	baseline - steel 1; Re/ft = 0.15
144	29	0.41	40.2	0.0	5.88	1.21	steel 1	baseline - steel 1, repeat
144	43	0.47	37.2	0.0	5.96	1.22	ceramic 1	baseline - ceramic 1
144	44	0.45	40.1	0.0	5.94	1.22	ceramic 1	baseline - ceramic 1, repeat
144	45	0.47	42.2	0.0	5.94	1.22	ceramic 1	baseline - ceramic 1, repeat
144	47	0.47	40.1	0.0	5.92	1.22	ceramic 1	missing rcc panel 9
144	48	0.45	40.1	0.0	5.90	1.21	ceramic 1	missing rcc panels 6 and 9
144	49	0.46	40.2	0.0	5.90	1.21	ceramic 1	missing rcc panel 6
144	50	0.44	40.1	0.0	5.89	1.21	ceramic 1	baseline - ceramic 1, repeat
144	51	0.47	38.0	0.0	5.94	1.22	ceramic 1	missing rcc panel 6, repeat
144	52	0.47	40.1	0.0	5.93	1.22	ceramic 1	missing rcc panels 6 and 7
144	54	0.44	37.7	0.0	5.91	1.21	ceramic 2	baseline - ceramic 2
144	55	0.47	39.8	0.0	5.95	1.22	ceramic 2	baseline - ceramic 2, repeat
144	56	0.46	41.8	0.0	5.93	1.21	ceramic 2	baseline - ceramic 2, repeat
144	58	0.48	40.0	0.0	5.96	1.22	ceramic 2	missing rcc panel 4
144	59	0.48	40.0	0.0	5.95	1.22	ceramic 2	missing rcc panels 2 and 4
144	60	0.45	40.0	0.0	5.92	1.22	ceramic 2	missing rcc panel 2
144	61	0.46	40.3	0.0	5.90	1.21	ceramic 1	missing rcc panels 5, 6, and 7
144	62	0.45	40.0	0.0	5.89	1.21	ceramic 4	baseline - ceramic 4
144	64	0.45	37.9	0.0	5.89	1.21	ceramic 4	baseline - ceramic 4, repeat
144	65	0.47	42.0	0.0	5.94	1.22	ceramic 4	baseline - ceramic 4, repeat
144	66	0.47	40.2	0.0	5.93	1.22	ceramic 4	missing rcc panel 10
144	67	0.46	40.2	0.0	5.91	1.21	ceramic 4	missing rcc panels 10 and 12
144	68	0.46	40.2	0.0	5.90	1.21	ceramic 4	missing rcc panel 12
144	69	0.46	40.3	0.0	5.90	1.21	ceramic 1	missing rcc panels 5, 6, 7, and 8
144	70	0.45	40.4	0.0	5.89	1.21	ceramic 1	baseline - ceramic 1, repeat
144	71	0.47	40.3	0.0	5.94	1.22	ceramic 1	missing rcc panel 9, repeat
144	72	0.46	40.3	0.1	5.93	1.22	ceramic 1	missing rcc panels 5, 6, 7, 8, and 9
144	73	0.46	40.2	0.0	5.91	1.21	ceramic 4	missing rcc panels 9 and 10
144	74	0.46	40.2	0.0	5.90	1.21	ceramic 4	missing rcc panels 9 and 10, repeat
144	75	0.45	40.2	0.0	5.88	1.21	ceramic 4	missing rcc panels 9, 10 and 12
144	76	0.46	39.8	0.0	5.89	1.21	ceramic 2	baseline - ceramic 2, repeat
144	77	0.47	39.8	0.0	5.94	1.22	ceramic 2	hole through carrier panel 6
144	78	0.46	40.0	0.0	5.93	1.22	ceramic 2	hole through carrier panel 9
144	79	0.46	40.0	0.0	5.91	1.21	ceramic 2	hole through carrier panel 12
144	80	0.45	37.7	0.0	5.90	1.21	ceramic 2	baseline - ceramic 2, repeat
144	81	0.45	41.9	0.0	5.89	1.21	ceramic 2	baseline - ceramic 2, repeat
144	82	0.45	38.0	0.0	5.88	1.21	ceramic 1	baseline - ceramic 1, repeat
144	83	0.47	40.1	0.0	5.94	1.22	ceramic 1	baseline - ceramic 1, repeat
144	84	0.46	40.0	0.0	5.92	1.22	ceramic 2	missing rcc panel 4, repeat
144	85	0.46	40.0	0.1	5.91	1.21	ceramic 2	missing rcc panels 2 and 4, repeat
144	86	0.45	40.2	0.1	5.90	1.21	ceramic 4	missing rcc panels 9, 10, 11 and 12
144	88	0.27	37.3	0.0	5.92	1.22	ceramic 5	baseline - ceramic model 5; Re/ft = 0.26e6
144	89	0.44	37.8	0.0	5.87	1.21	ceramic 5	baseline - ceramic model 5; Re/ft = 0.46e6
144	90	0.30	39.3	0.0	6.00	1.23	ceramic 5	baseline - ceramic model 5, repeat; Re/ft = 0.26e6
144	91	0.46	39.9	0.0	5.93	1.22	ceramic 5	baseline - ceramic model 5, repeat; Re/ft = 0.46e6
144	92	0.28	39.3	0.0	5.96	1.22	ceramic 5	baseline - ceramic model 5, repeat; Re/ft = 0.26e6
144	93	0.45	39.9	0.0	5.90	1.21	ceramic 5	baseline - ceramic model 5, repeat; Re/ft = 0.46e6
144	94	0.27	41.4	0.0	5.92	1.22	ceramic 5	baseline - ceramic model 5, repeat; Re/ft = 0.26e6
144	95	0.44	42.0	0.0	5.87	1.21	ceramic 5	baseline - ceramic model 5, repeat; Re/ft = 0.46e6
144	96	0.27	41.3	0.0	5.98	1.23	ceramic 5	baseline - ceramic model 5, repeat; Re/ft = 0.26e6
144	97	0.45	41.9	0.0	5.92	1.22	ceramic 5	baseline - ceramic model 5, repeat; Re/ft = 0.46e6
144	98	0.27	39.5	0.0	5.94	1.22	ceramic 5	missing rcc panel 9; Re/ft = 0.26e6
144	99	0.45	40.1	0.1	5.89	1.21	ceramic 5	missing rcc panel 9; Re/ft = 0.46e6
144	100	0.28	39.5	0.0	5.94	1.22	ceramic 5	missing rcc panels 6 and 9; Re/ft = 0.26e6
144	101	0.45	40.1	0.1	5.87	1.21	ceramic 5	missing rcc panels 6 and 9; Re/ft = 0.46e6
144	102	0.46	39.9	0.0	5.89	1.21	ceramic 5	baseline - ceramic model 5, repeat; Re/ft = 0.46e6
144	103	0.47	40.0	0.0	5.94	1.22	ceramic 5	missing rcc panel 8, right wing
144	104	0.46	39.9	0.0	5.92	1.22	ceramic 5	baseline - ceramic model 5, repeat; Re/ft = 0.46e6
144	105	0.46	40.1	0.0	5.90	1.21	ceramic 5	missing rcc panel 5, right wing
144	106	0.46	39.9	1.1	5.90	1.21	ceramic 5	baseline - ceramic model 5; Re/ft = 0.46e6; beta = 1

Table 4.7-2 Test LaRC 144 - CF4 Hypersonic Wind Tunnel Facility - STS-107 Investigation

Test	Run	Re/ft	Alpha	Beta	Mach	Gamma	Model	Configuration
148	13	0.45	38.2	0.0	5.91	1.21	ceramic A	baseline - ceramic A, repeat
148	14	0.47	38.1	0.0	5.95	1.22	ceramic A	single windward groove, L/H = 10.0
148	15	0.47	38.1	0.0	5.92	1.22	ceramic A	single windward groove, L/H = 18.9
148	16	0.46	38.1	0.0	5.91	1.21	ceramic A	single windward groove, L/H = 27.8
148	17	0.45	38.4	0.0	5.90	1.21	ceramic C	baseline - ceramic C
148	19	0.46	38.4	0.0	5.90	1.21	ceramic C	baseline - ceramic C
148	20	0.43	38.4	0.0	5.88	1.21	ceramic C	missing lower rcc 9
148	21	0.47	38.4	0.0	5.93	1.22	ceramic C	missing lower rcc 7
148	22	0.46	38.4	0.0	5.92	1.22	ceramic C	baseline - ceramic C, repeat
148	23	0.46	38.1	0.0	5.92	1.22	ceramic A	double windward groove, L/H = 27.8; missing rcc 9
148	24	0.46	38.1	0.0	5.91	1.21	ceramic A	double windward groove, L/H = 27.8
148	25	0.46	38.2	0.0	5.90	1.21	ceramic A	double windward groove, L/H = 18.9
148	26	0.47	38.1	0.0	5.95	1.22	ceramic A	double windward groove, L/H = 18.9, repeat
148	27	0.45	38.1	0.0	5.92	1.22	ceramic A	double windward groove, L/H = 27.8; missing rcc 9, repeat
148	28	0.47	38.2	0.0	5.92	1.22	ceramic A	double windward groove, L/H = 27.8, repeat
148	29	0.45	38.1	0.0	5.89	1.21	ceramic A	baseline - ceramic A, repeat
148	30	0.46	38.2	0.0	5.89	1.21	ceramic A	missing rcc panel 9
148	31	0.45	38.0	0.0	5.95	1.22	ceramic A	baseline - ceramic A, repeat
148	32	0.46	38.1	0.0	5.93	1.22	ceramic A	single windward groove, L/H = 27.8; missing rcc 9
148	34	0.45	38.3	0.0	5.91	1.21	ceramic B	baseline - ceramic B
148	35	0.45	38.3	0.0	5.90	1.21	ceramic B	baseline - ceramic B, repeat
148	36	0.44	38.4	0.0	5.89	1.21	ceramic B	missing lower rcc panel 4
148	37	0.47	38.3	0.0	5.95	1.22	ceramic B	missing lower rcc panel 4, repeat
148	38	0.43	38.2	0.0	5.92	1.22	ceramic B	missing lower rcc panel 6
148	39	0.44	38.2	0.0	5.90	1.21	ceramic B	missing lower rcc panel 6, repeat
148	40	0.43	38.3	0.0	5.89	1.21	ceramic B	missing lower rcc panel 8
148	41	0.44	38.3	0.0	5.89	1.21	ceramic B	missing lower rcc panel 8, repeat
148	43	0.42	38.4	0.0	5.89	1.21	ceramic 5	baseline - ceramic 5
148	44	0.46	38.4	0.0	5.94	1.22	ceramic 5	missing rcc panel 9
148	45	0.45	38.4	0.0	5.92	1.22	ceramic 5	missing rcc panel 9, repeat
148	46	0.44	38.4	0.0	5.92	1.22	ceramic 5	baseline - ceramic 5
148	47	0.34	38.0	0.0	5.94	1.22	ceramic B	missing lower rcc panel 8; Re/ft = 0.35e6
148	48	0.33	37.9	0.0	5.92	1.22	ceramic B	missing lower rcc panel 8, with through hole; Re/ft = 0.35e6
148	49	0.32	37.9	0.0	5.90	1.21	ceramic B	baseline - ceramic B; Re/ft = 0.35e6
148	50	0.20	37.5	0.0	5.97	1.23	ceramic C	baseline - ceramic C; Re/ft = 0.20e6
148	51	0.33	38.0	0.0	5.91	1.21	ceramic C	baseline - ceramic C; Re/ft = 0.35e6
148	52	0.33	38.1	0.0	5.90	1.21	ceramic C	missing lower rcc panel 5
148	53	0.32	38.1	0.0	5.88	1.21	ceramic C	missing lower rcc panel 5, repeat
148	54	0.32	38.1	0.0	5.88	1.21	ceramic C	baseline - ceramic C, repeat; Re/ft = 0.35e6
148	55	0.31	38.1	0.0	5.87	1.21	ceramic C	missing lower rcc panel 7
148	57	0.21	37.8	0.0	5.99	1.23	ceramic 2	simulated leeside venting (fence); Re/ft = 0.20
148	61	0.45	38.5	0.0	5.90	1.21	ceramic 5	baseline - ceramic 5, tail removed
148	62	0.46	38.5	0.0	5.90	1.21	ceramic 5	baseline - ceramic 5, tail removed
148	63	0.47	38.5	0.0	5.95	1.22	ceramic 5	missing rcc panel 9, tail removed
148	64	0.45	38.5	0.0	5.92	1.22	ceramic 5	missing rcc panel 9, tail removed, repeat
148	65	0.44	38.1	0.0	5.90	1.21	ceramic A	triple windward groove, L/H = 27.8
148	67	0.45	38.2	0.0	5.89	1.21	ceramic A	triple windward groove, L/H = 22.5; faired aft edge
148	68	0.47	38.0	0.0	5.95	1.22	ceramic A	triple windward groove, L/H = 27.8, missing rcc 9
148	69	0.46	38.1	0.0	5.93	1.22	ceramic A	triple windward groove, L/H = 27.8, missing rcc 9, repeat
148	70	0.45	38.2	0.0	5.91	1.21	ceramic B	missing lower rcc panel 8, with through slot
148	75	0.20	37.8	0.0	5.98	1.23	ceramic 2	simulated leeside venting (fence); Re/ft = 0.20
148	76	0.46	37.8	0.1	5.92	1.22	ceramic 2	simulated leeside venting (fence); Re/ft = 0.46
148	81	0.20	40.0	0.0	6.01	1.24	ceramic 2	simulated leeside venting (fence), missing rcc 9; Re/ft = 0.20
148	82	0.43	40.0	0.0	5.89	1.21	ceramic 2	simulated leeside venting (fence), missing rcc 9; Re/ft = 0.46
148	86	0.50	40.2	0.0	5.98	1.23	sla D	leeside vent
148	87	0.48	40.2	0.0	5.95	1.22	sla D	leeside vent w/ windward cavity
148	88	0.46	40.2	0.0	5.93	1.22	sla D	leeside vent w/ missing T-seal (8/9)
148	89	0.17	40.2	0.0	5.90	1.21	sla D	leeside vent w/ missing T-seal (8/9); Re/ft = 0.17
148	90	0.44	40.3	0.0	5.88	1.21	sla D	leeside vent (sealed) w/ windward cavity
148	91	0.47	40.3	0.0	5.95	1.22	sla D	leeside vent (sealed) w/ windward cavity, repeat
148	92	0.47	40.3	0.0	5.94	1.22	sla D	leeside vent w/ windward cavity

Table 4.7-3 Test LaRC 148 - CF4 Hypersonic Wind Tunnel Facility - STS-107 Investigation

4.7.4 FELISA Inviscid CFD - Comments and Additional Analysis

The work presented in Section 4.3.2, Damage Assessment Using Computational Fluid Dynamics, summarized the delta aerodynamics produced by numerous damage scenarios. This sections contains supporting computations that verified some of the assumptions used in the analysis and a discussion of how convergence is assessed.

4.7.4.1 Flow Solver Convergence

Two criteria are used in assessing convergence of a FELISA solution. The methodology in FELISA preserves total enthalpy, and thus the maximum and minimum total enthalpies are tracked. Since the primary utilization of FELISA is to compute aerodynamic loads, their convergence is also evaluate. Figure 4.7-3 shows the typical set of plots that are evaluated to assess convergence. Even though the residual is still dropping, the aerodynamic loads and the enthalpies have converged to a steady state. For many of the damage scenarios evaluated, the solver did not converge to a steady state solution. This is not unexpected given the types of damage (particularly the WLE damage) being evaluated. The convergence history of the loads for the baseline and the damaged configuration were co-plotted, to determine if the oscillation of the aerodynamic loads was larger than the delta aerodynamics. Figure 4.7-4 shows the aerodynamic loads convergence for a damaged (windward surface depression) and a baseline solution, where the damaged solution has reached a steady state. Figure 4.7-5 shows the same plot for a damaged solution (half panel 9 with upper carrier panel removed) that shows definite oscillations in the loads. The oscillations, however are small compared to the difference between the damaged and the baseline. The practical implication of the unsteady nature of many of the computations is that there is an bound on the delta aerodynamics, and that the idea that it is the trend of many computations that is important in the analysis of these damage scenarios.

4.7.4.2 Comparison of Absolute Aerodynamics for Flight, CF4, and Mach 6 Air

All of the delta aerodynamic analysis described in Section 4.3.2 was based on the assumption that even if the total aerodynamics did not compare exactly with the 'true' aerodynamics, the delta aerodynamics for the damaged configurations would compare well with the 'true' delta aerodynamics due to damage. Indeed, when the delta aerodynamics for wind tunnel, inviscid flight, viscous flight, and even Mach 6 perfect gas air simulations were compared, the trends gave a consistent picture. Figure 4.7-6 shows the total aerodynamics plotted against time from EI for the baseline and missing RCC panel 6+7 at flight conditions, and the baseline and missing RCC panel 6 for CF4 and Mach 6 air conditions. This figure shows that the difference between the flight, CF4, and Mach 6 air aerodynamics is much larger than the deltas between the baseline and the damaged aerodynamics for a given configuration.

4.7.4.3 Aerodynamics for Full (360°) Configurations, Baseline and Damaged

In order to assess the impact of using half body configurations for the delta aerodynamics, a set of computations was made with a full configuration, with an undamaged right side, and a missing RCC panel 9 on the left. The asymmetric aerodynamics (side force, rolling and yawing moments) are shown in Figure 4.7-7(a), and the symmetric loads (axial and normal force, and pitching moment) in Figure 4.7-7(b), plotted against sideslip. The half body aerodynamics (at β=0°) are shown, and indicate that there is little difference between the full and half-body aerodynamics.

4.7.4.4 Systematic Angle of Attack and Mach number Effect in Delta Aerodynamics

The delta aerodynamics presented in Figure 4.3-42 show the missing RCC panel aerodynamics for a range of flight conditions, which have varying Mach and angle of attack. Several computations were run to isolate the Mach number and the angle of attack effect in the delta aerodynamics, for the missing RCC panels 6+7 configuration. Figure 4.7-8 shows the delta aerodynamics plotted against Mach number (which is opposite in trend from time from EI) for an angle of attack of 40° Only the delta yawing moment showed a strong trend, decreasing with increasing Mach number. The delta

rolling and pitching moments showed a very shallow trend toward positive with increasing Mach number. Figure 4.7-9 shows the aerodynamics and delta aerodynamics plotted against angle of attack, for a constant Mach number of 20.2 (CFD condition 4). While the typical trends with angle of attack are observed in the symmetric aerodynamics (normal force in particular), the delta aerodynamics show are not affected by angle of attack,

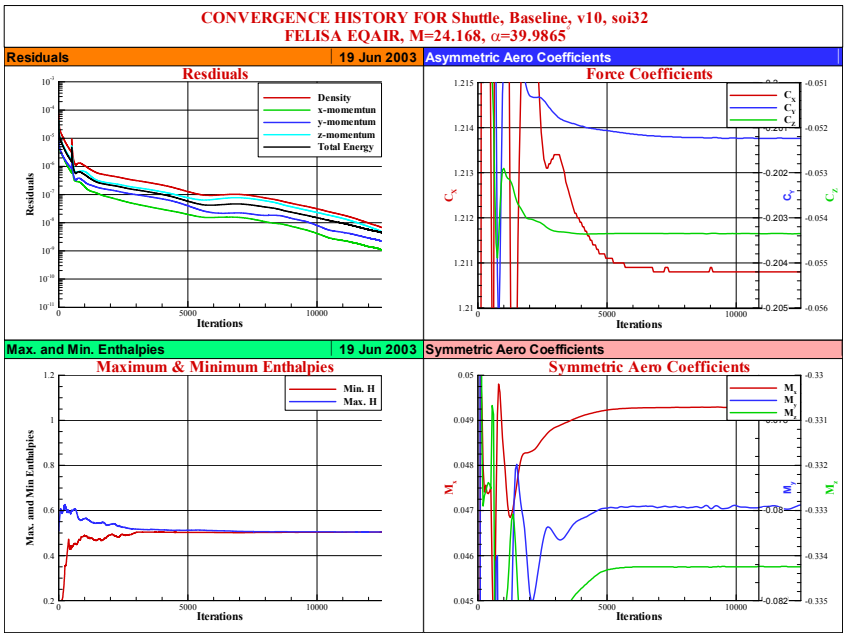

Figure 4.7-3 Typical Convergence History Plots from FELISA

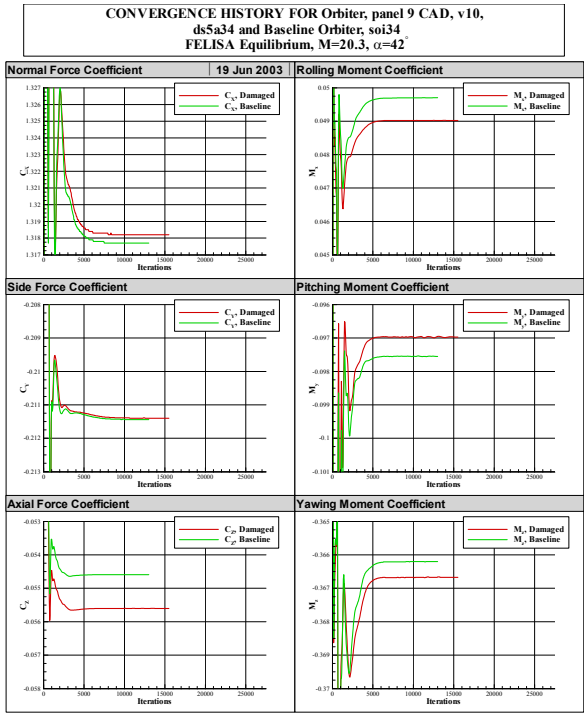

Figure 4.7-4 Aerodynamic Force and Moment Convergence for Steady Solution

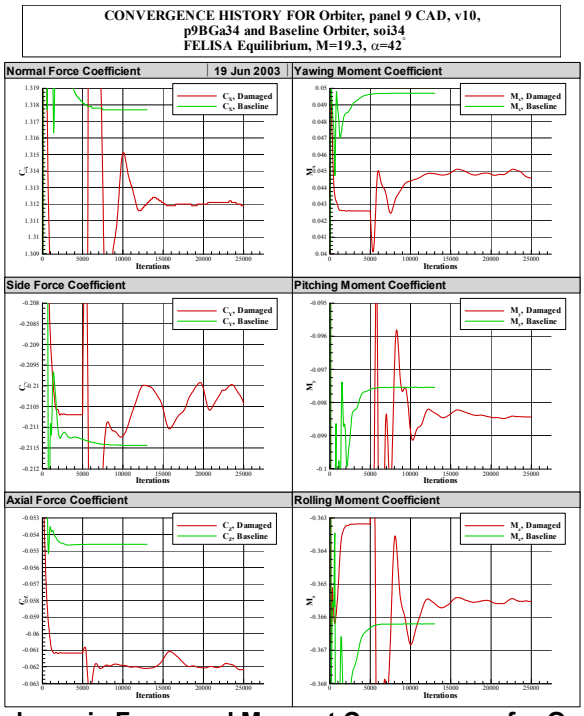

Figure 4.7-5 Aerodynamic Force and Moment Convergence for Oscillating Solution

FELISA Prediction of Aerodynamic Coefficients for Flight and Wind Tunnel Conditions, a = 40°

- At this scale, effect of missing panel small except in axial direction at
- Flight cases are for panels removed, CF_4 and Mach 6 are for panel 6 only.
- CF_4 doesn't match flight, but is closer than Mach

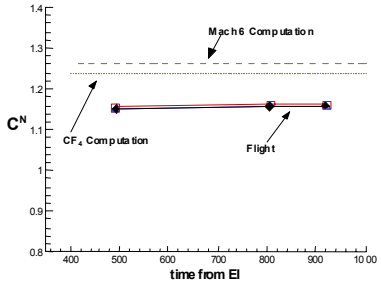

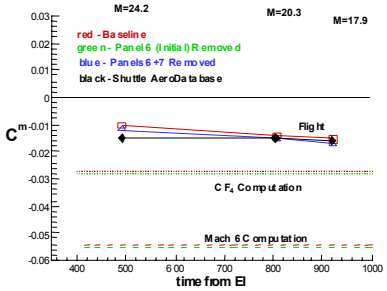

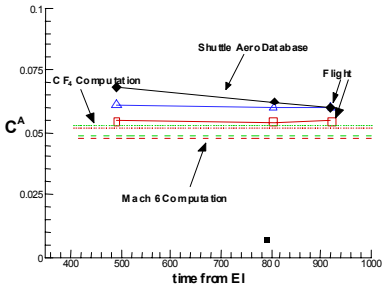

Figure 4.7-6 Comparison of Total Aerodynamics for Flight, CF4, & Mach 6 WT Conditions

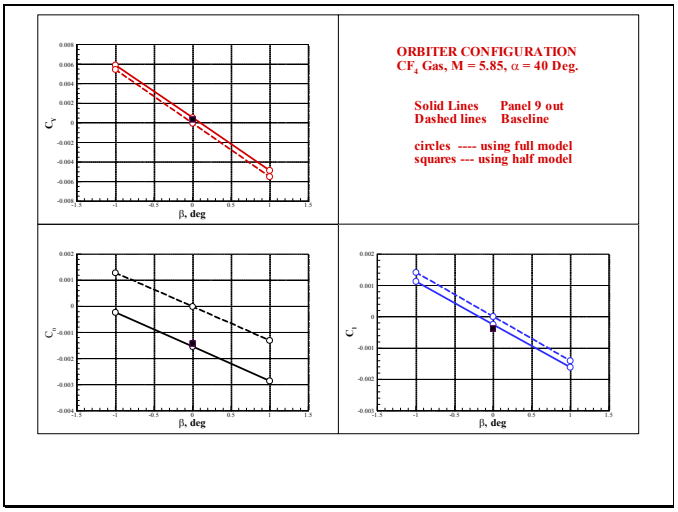

(a) Asymmetric Forces and Moments

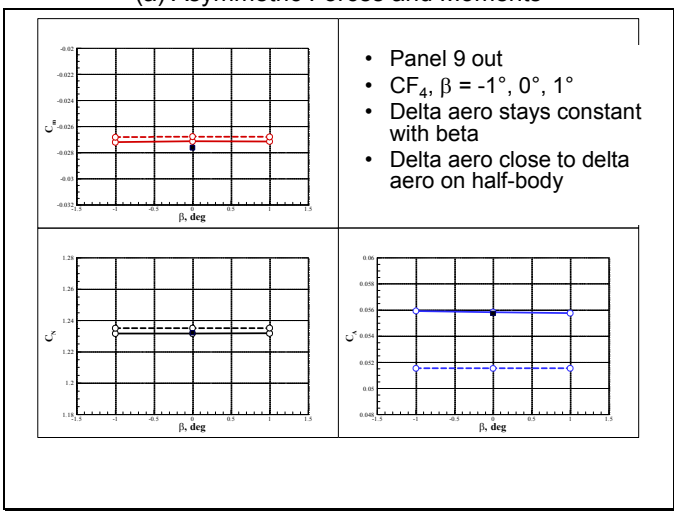

(b) Symmetric Forces and Moments

Figure 4.7-7 Forces and Moments for Baseline and Missing RCC Panel 9 for Range of Sideslip Angles

Effect of Mach Number, Hence Flow Chemistry, on Aerodynamic Coefficients and Deltas , a = 40°

- Pitch shows an increase with Mach, normal force a slight decrease
- Delta pitch flat, delta rolls shows slight increase, yaw shows significant decrease. Helps explain discrepancies between CF4 and flight computations.

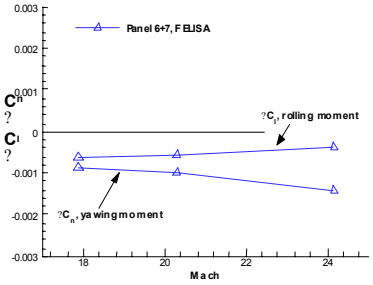

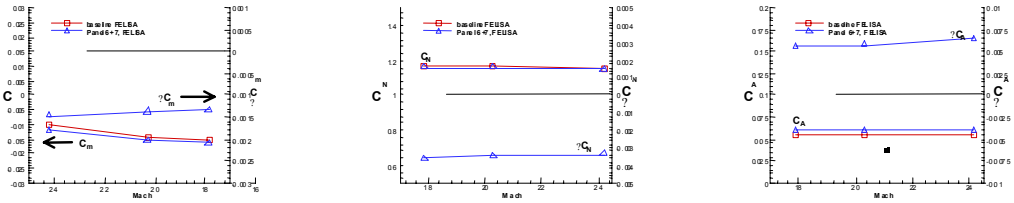

Figure 4.7-8 Effect of Mach Number on Delta Aerodynamics

Effect of Angle of Attack on Aerodynamic Coefficients and Deltas
FELISA, M = 20.3

- Forces and moments show typical trends with alpha
- Deltas have no significant trends for symmetric or asymmetric loads

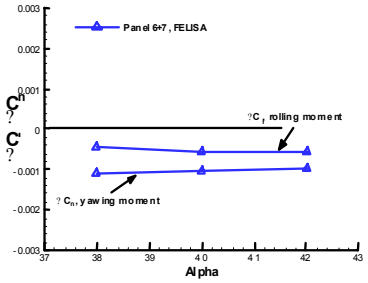

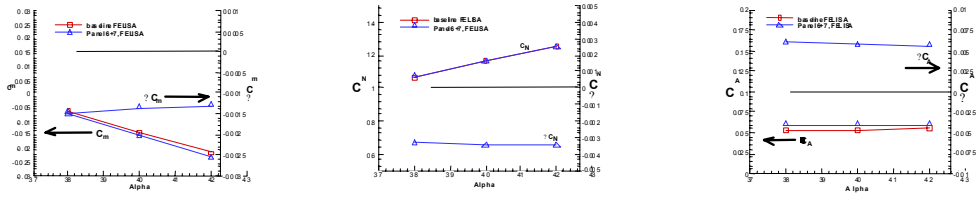

Figure 4.7-9 Effect of Angle of Attack on Delta Aerodynamics

4.7.5 OVERFLOW CFD Analysis of Leeside Flow field Interactions

4.7.5.1 Brief CFD Intro / Application Description

Missing RCC panel Navier Stokes solutions were done with the OVERFLOW code. Delta aero increments were extracted and the flow fields were analyzed for differences between missing panel solutions and the nominal configuration. Delta aero increments were obtained, including component aero from the wing, fuselage, and tail. The simulations were done to compare with the LaRC Mach 6 air tunnel. The wind tunnel model scale was 0.0075 of the full-scale orbiter corresponding to a vehicle length of approximately 9.678". The free stream conditions for the test and analysis were Mach = 5.96 at a Re / ft = 2.976 Million and Tinf = 112.27 R.

4.7.5.2 Configurations Analyzed

Three configurations were analyzed: baseline (no damage), panel 6 missing (original Karen Bibb geometry), and panel 9 missing. The grids were obtained from the External Aerothermal group's common grid for the nominal configuration (Aerothermodynamics Section 5.2.4.2). The common grid was modified to have overset boundaries in place of block zonal. The panel 6 and panel 9 grids were then created to match the resolution of the common grid in the missing panel region. The only difference between the grid systems was the addition of the missing panel grids. Figure 4.7-10 shows the surface grid for panel 9. The original grids were run for half the vehicle (without a VT). After evaluating the solutions, the flow field around the tail was desired so the symmetric grids were copied into both halves of the vehicle and combined to create the full geometry. The vertical tail, including the SILTS pod was added to the overset grid system. The missing panel grids didn't change, although only the RCC panel 9 missing configuration was computed on the vertical tail grid system.

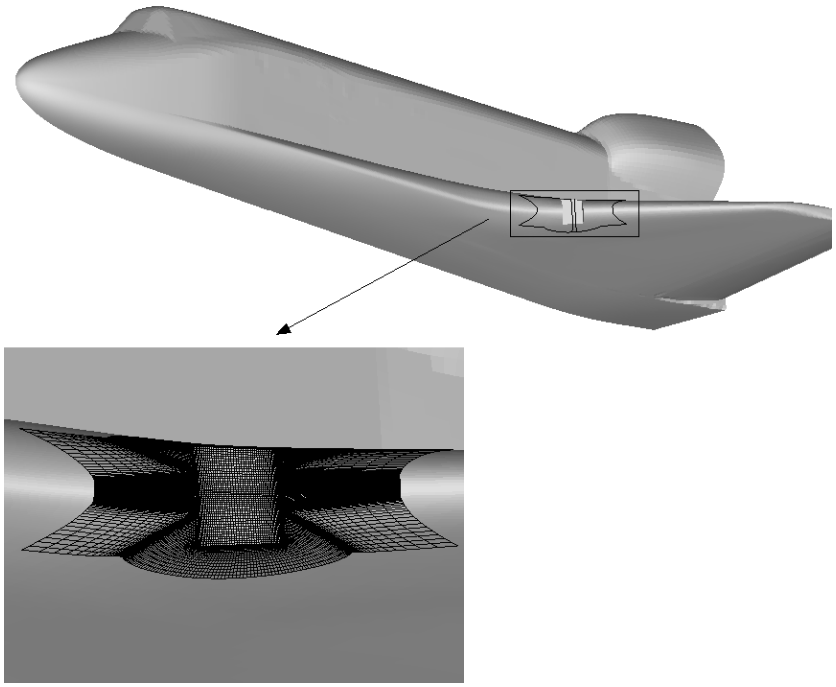

Figure 4.7-10 Surface Grid of a Missing RCC panel 9

4.7.5.3 Delta Aerodynamic Results

Table 4.7-4 shows the results for the original grid system (no VT). The delta aero increments in roll and yaw were very small for panel 6 removed.

	Cl	Cm	Cn
p6	0.09209	-0.00918	0.01287
p9	0.09156	-0.00881	0.01230
clean	0.09205	-0.00869	0.01302
Delta (p6 - clean)	0.00003	-0.00050	-0.00015
Delta (p9 - clean)	-0.00050	-0.00012	-0.00071

Table 4.7-4 Delta Aero Increments - Original grid system (no vertical tail)

The solutions done for the full grid system (baseline and the missing panel 9) with the vertical tail included gave similar delta aero as the original grid system without the tail. Table 4.7-5 shows these results.

	Cl	Cm	Cn
p9	-0.00034	-0.00615	-0.00043
clean	0.00001	-0.00623	-0.00002
Delta (p9 - clean)	-0.00035	0.00008	-0.00040

Table 4.7-5 Delta Aero Increments - Full grid system (w/vertical tail)

To better understand the source of the delta aero, the aero results were broken into the fuselage, wing, and vertical tail components. Table 4.7-6 shows these aero components. The fuselage and tail increments are very small in comparison to the wing increments. This points to the wing having the largest affect on the delta aero increments.

(p9 - clean)	ΔCl	ΔCm	ΔCn
FUSELAGE	0.000016	-0.000046	-0.000022
WING	-0.000355	0.000159	-0.000418
TAIL	-0.000010	-0.000041	0.000039
TOTAL	-0.000348	0.000084	-0.000403

Table 4.7-6 Delta Aero Increments (component breakdown) - Full grid system

4.7.5.4 Observations – Missing RCC Panels (Original Grid System)

Figure 4.7-11 shows the surface Cp for the baseline configuration. Figure 4.7-12 and Figure 4.7-13 show the surface Cp for the panels 6 and 9 removed, respectively. The black dots on the figures represent several of the flight temperature measurement gage locations.

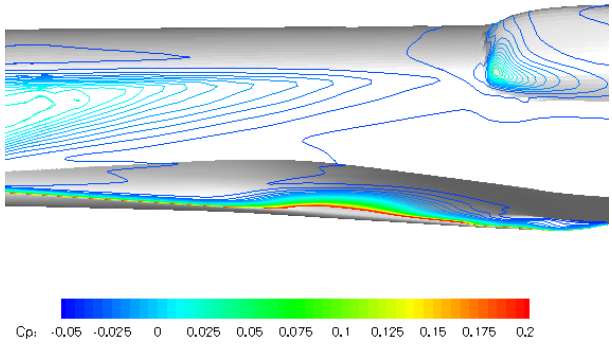

Figure 4.7-11 Surface Pressure (Cp) Baseline (no damage) Configuration.

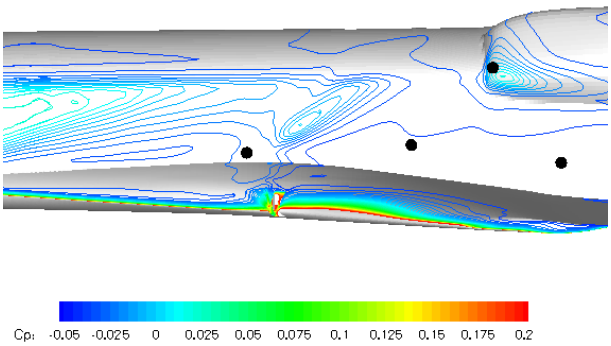

Figure 4.7-12 Surface Pressure (Cp) – Missing RCC Panel 6

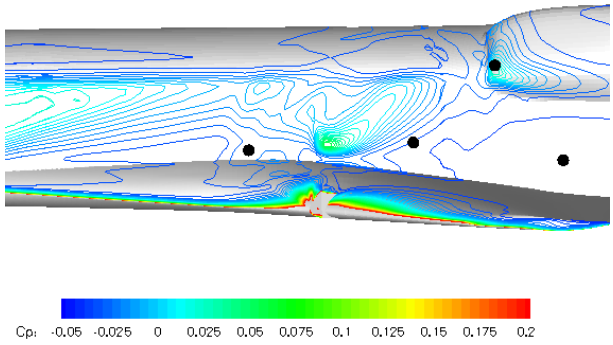

Figure 4.7-13 Surface Pressure (Cp) – Missing RCC panel 9

The interaction between the flow coming through the panel and the fuselage is very apparent for the panel 9 missing case. This impingement is much stronger with panel 9 missing than with panel 6 missing.

4.7.5.5 Observations – Missing RCC Panels (Full Grid System)

To further investigate the leeside interaction, the surface pressures on the vertical tail were analyzed to provide more information on tail pressure increments. Figure 4.7-14 shows the delta pressure coefficient (Cp panel 9 missing – nominal configuration) on the tail. It is evident from this figure the flow field on the tail is disturbed, but the maximum delta Cp values are on the order of 0.01, representing a very small change.

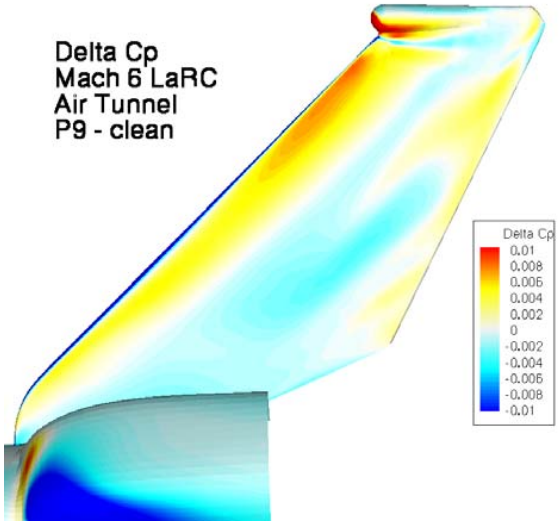

Figure 4.7-14 Delta Pressure (Cp) – Vertical Tail Surface (P9 – Baseline)

Figure 4.7-15 shows surface streamlines (k = 3 surface) for both the baseline configuration and the panel 9 missing. The largest difference between the 2 configurations is the flow on the lower part of the tail. The direction of the flow in this region changed directions.

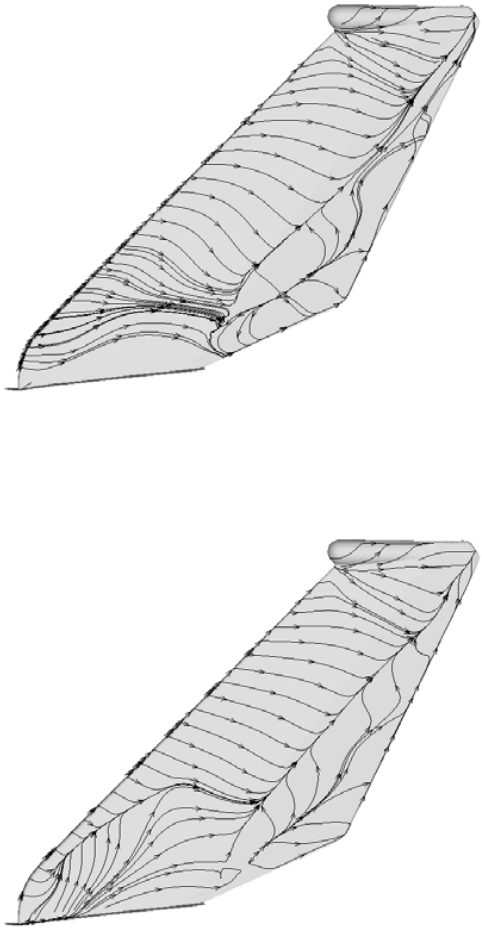

Figure 4.7-15 Surface Streamlines – Baseline and Panel 9 Configurations

The flow field on the leeside of the vehicle is directly affected by the vortex that emanates from the intersection of the wing and the fuselage (strake). Figure 4.7-16 represents this vortex by using volume ribbons. The vortex starting from the left strake never crosses the centerline of the vehicle for the baseline configuration. This is not the case for the missing panel 9 configuration. The vortex is disturbed towards the leading edge of the wing and is then pushed across the pitch plane in front of the tail. This dramatically affects the flow field on the leeside.

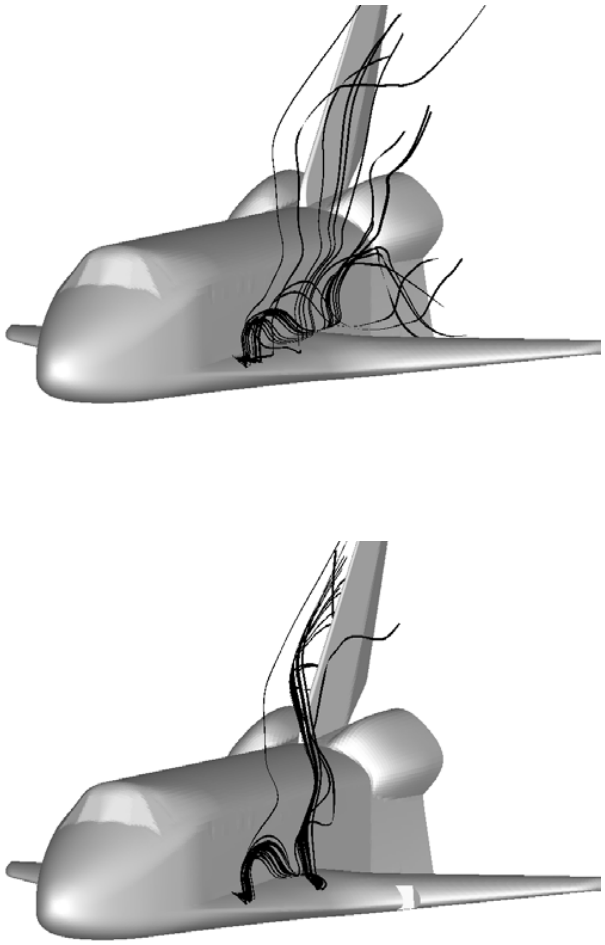

Figure 4.7-16 Volume Ribbons Emanating From the Strake - Baseline & RCC Panel 9 Missing

Based on the volume ribbon patterns, a delta pressure (Cp) plot (similar to Figure 4.7-14) was made showing the leeside of the vehicle, including the tail. Figure 4.7-17 shows this delta Cp plot. The figure shows that the flow on the port and starboard side of the tail is disturbed.

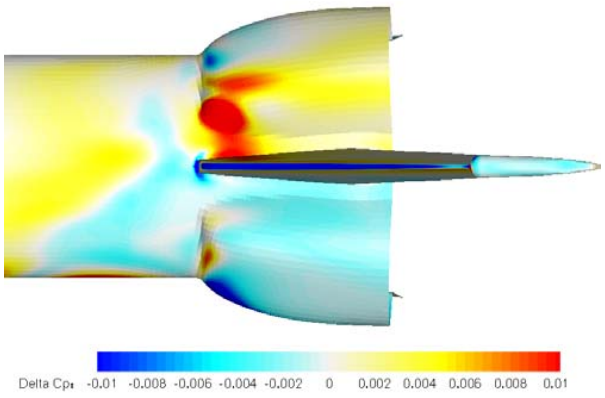

Figure 4.7-17 Delta Pressure (Cp) On the Vertical Tail Surface (P9 – Baseline).

4.7.5.6 Conclusions

The delta aerodynamic increments predicted by the OVERFLOW analysis at Mach 6 tunnel conditions are consistent with test measurements and other sources for Panel 6 or Panel 9 missing. Although the analysis of the tail flow field and the delta pressure coefficient demonstrate differences in the flow field, the delta aero increment from the tail was very small (an order of magnitude less than the increments from the wing).

4.7.6 Aerodynamic Investigation using CART3D CFD Analysis

4.7.6.1 Introduction

CART3D is a high fidelity, inviscid analysis package that uses adaptively refined Cartesian grids to discretize the volume around a defined surface geometry. It is used for conceptual and preliminary aerodynamic design and enables rapid CFD analysis on complex geometries.

4.7.6.2 STS-107 CART3D Case Definition

All the cases were completed at wind tunnel conditions of Mach 6 and 40-degrees angle of attack (corresponding to the LaRC Mach 6 air wind tunnel, Table 4.3-5).

4.7.6.3 Configurations Analyzed

In support of the STS-107 Investigation, different damage scenarios have been analyzed to try and reproduce the aerodynamics observed during Columbia's final flight. These damage scenarios were produced using two different geometries, one without a vertical tail and one including the tail. Karen Bibb, LaRC supplied the grids used to represent the baseline surface geometries. The LaRC GEOLAB defined the WLE RCC panel cutouts used to produce the different damaged configurations analyzed. Figure 4.7-18a shows the clean geometry without the vertical tail, and Figure 4.7-18b shows the clean geometry with the tail. The surface grid for the initial geometry without the vertical tail had a low resolution grid on the leeside, especially in the OMS pod region. Nominally, the resolution is appropriate because at hypersonic conditions, there are not significant aerodynamic interactions and flow features on the leeside of the vehicle. Since the initial analysis focused on WLE damage, this grid was sufficient to resolve the wing surface pressures. Once the analysis shifted to focus on the effects on the OMS pod and tail, the more refined surface grid with the vertical tail was required to ensure the leeside surface pressures were adequately resolved.

There were fourteen damage configurations analyzed using CART3D (listed in Table 4.7-7). Initial analysis focused on WLE damage. The first five configurations analyzed were for entire WLE RCC panels missing on the geometry without a vertical tail. The five configurations analyzed were: RCC 6 missing, RCC 9 missing, RCC 6 and 7 missing, RCC 5-7 missing, and RCC 1-7 missing. Figure 4.7-19 shows RCC 9 missing and an outline of RCC panels 1-7. Note that to model a missing RCC panel in this analysis, solid sidewalls in the cavity were included as a simplification over the actual geometry with an open channel between the RCC and the WLE spar. Additionally, the missing geometry accounts for removal of only the RCC panel and not the carrier panel geometry. Therefore, the back wall surface is approximately 4 to 6 inches forward of the WLE spar.

Based on debris forensics that suggested WLE damage could not include entire panels missing, partial RCC panel damage configurations were addressed. The next four cases analyzed were the lower (or windward half) of the RCC panel missing as well as a missing T-Seal. Three half-panel damage cases were computed: half of RCC 7 missing, half of RCC 8 missing, and half of RCC 9 missing. The T-Seal case was for T-Seal 9 removed, resulting in an open slot or gap between RCC panels 8 and 9. All four damaged configurations were analyzed using the geometry without the vertical tail.

Damage progression cases were analyzed next in an attempt to understand the sensitivity of the delta aerodynamics to increased levels of damage and further investigate leeside interaction effects. The final five cases were computed on the more refined (increased resolution) surface grid for the geometry with the vertical tail. The five cases were: half of RCC 7 missing, half of RCC 8 and all of RCC 9 missing, half of RCC 8 and hole #1 through the wing, lower (windward surface) carrier panel 8 and hole #2 through the wing, and half of RCC 8 and hole #2 through the wing. Hole #1 is the width of RCC 8, 20-inches long and is oriented directly behind RCC 8 funning inboard and aft. Hole #2 is 46-inches long, 28-inches wide and oriented behind RCC 9 and 10, running inboard and aft. Figure 4.7-20 thru Figure 4.7-25 show the holes and missing parts of the RCC and carrier panel.

4.7.6.4 Delta Aerodynamic Results

Table 4.7-7 lists the values of the aerodynamic coefficients for the clean configurations (with & without vertical tail) and the resulting delta values for the damaged configurations analyzed.

	Axial force (+ Aft)	Side force (+ Right)	Normal force (+ Up)	Rolling Moment (+ Right Wing down)	Pitching Moment (+ Nose Up)	Yawing Moment (+ Nose to the Right)
	Delta CA	**Delta CY**	**Delta CN**	**Delta Cl**	**Delta Cm**	**Delta Cn**
Without Vertical Tail						
Clean	**0.05100**	**0.14983**	**1.26233**	**0.18748**	**-0.06117**	**0.02718**
Panel 6	0.00115	0.00096	-0.00126	-0.00017	-0.00032	-0.00026
Panel 9	0.00202	0.00036	-0.00193	-0.00030	-0.00028	-0.00074
Panels 6-7	0.00255	0.00116	-0.00259	-0.00037	-0.00056	-0.00056
Panels 5-7	0.00336	0.00127	-0.00306	-0.00041	-0.00085	-0.00084
Panels 1-7	0.00358	0.00096	-0.00501	-0.00069	-0.00150	-0.00099
Half 7	-0.00023	0.00039	-0.00374	-0.00007	-0.00283	-0.00008
half 8	-0.00019	0.00046	-0.00394	-0.00013	-0.00263	-0.00011
Half 9	-0.00006	0.00032	-0.00371	-0.00005	-0.00281	-0.00012
T-Seal 9	-0.00024	0.00051	-0.00423	-0.00017	-0.00242	-0.00001
With Vertical Tail						
Clean	**0.05125**	**0.14347**	**1.25942**	**0.18578**	**-0.06233**	**0.03068**
Half 7	0.00021	0.00023	-0.00013	-0.00001	0.00003	-0.00010
Half 8 Full 9	0.00421	0.00159	-0.00454	-0.00067	-0.00028	-0.00156
Half 8 & Hole #1	0.00026	-0.00095	-0.00023	-0.00017	-0.00019	0.00025
Carrier Panel 8 & Hole #2	-0.00002	0.00004	-0.00036	0.00003	-0.00014	-0.00002
Half 8 & Hole #2	0.00061	0.00056	-0.00145	-0.00023	0.00037	-0.00024

Table 4.7-7 CART3D CFD Analysis - Results by Configuration - Delta Aero Coefficients

During latter portion (after EI + 700 sec) of the STS-107 entry flight, Columbia demonstrated a negative delta yaw and a positive delta roll when compared to a nominal entry trajectory. Most of the damage configurations analyzed by CART3D show a negative delta yaw and a negative delta roll, which corresponds to the earlier portion (before EI + 600 sec) of STS-107 entry. The windward half of RCC 8 missing with hole #1 in the wing configuration shows a negative delta roll and a positive delta yaw, a pattern not seen in flight. The windward carrier panel 8 missing with hole #2 in the wing configuration shows a positive delta roll and a negative delta yaw, but the deltas are relatively small.

Figure 4.7-27a shows the surface pressure in terms of pressure coefficient (Cp) on the leeward side of the shuttle for the clean configuration. Figure 4.7-27b through Figure 4.7-29 show the Cp on the leeward side for the complete RCC panel removed damaged configurations. Notice the increase in pressure on the side of fuselage near the region of augmented heating recorded by onboard instrumentation. For these Mach 6 computations on this lower grid resolution system, none of the whole RCC panel out cases affects the pressure on the OMS pod or the area around the base of the tail.

The results from the half RCC missing configurations however do show an increase in the pressure on the OMS Pod. Figure 4.7-29 shows the surface pressure distribution on the OMS Pod for the clean configuration. Figure 4.7-31 and Figure 4.7-32a show the surface pressure distribution on the OMS Pod for the half-panel missing cases, and Figure 4.7-32b is for the missing T-Seal. For half of RCC 7 and half of RCC 8, the pressure on the forward section of the OMS Pod increases. The pressure also increases for the missing T-Seal case, and there is a slight change for the half of RCC 9 missing case. Although there were no OMS pod surface pressure measurements, recovered OMS pod debris indicates significant impact damage most likely attributed from flow through the WLE damage. These cases would support the observation that the initial damage was inboard of RCC 9 as the pressure change on the OMS pod decreases as the damage moves outboard.

The five configurations with the tail were run to evaluate the pressure impact on the tail and the OMS Pod as a possible source for the change in extracted rolling moment after EI + 600 sec. Figure 4.7-33 shows the surface pressure distribution on the tail and OMS Pod for the clean configuration. Figure 4.7-33 through Figure 4.7-36 show the surface pressure distribution on the tail and OMS Pod for the five damage configurations. The half of RCC 8 and all of RCC 9 case had the largest overall impact on the Cp distribution. There was an increase on the tail, OMS Pod and the side of the fuselage. Both Hole #2 cases showed significant impact on the tail and the OMS Pod. Half of RCC 8 and hole #1 increased the pressure on the side of the fuselage. However, it decreased the pressure on the OMS pod and tail because of the orientation of the hole with respect to RCC panel 8. The results indicate only a small amount of interaction with relatively low changes in pressure over a limited area of the vertical tail and OMS pod. Based on these and other results it was concluded that the leeside flow interaction with the vertical tail and OMS pod was not the primary source for the trend change in extracted rolling moment.

4.7.6.5 Observations

The complete loss of an RCC panel matches the early off-nominal flight trends, but does not match the trends later in flight. Additionally complete RCC panel loss increases the pressure only on the side of the fuselage, consistent with other side fuselage observations, but does not impact the vertical tail region (at the computed Mach 6 condition). However, the loss of the windward half of RCC panels 7 and 8 redirects the flow onto the OMS pod and tail area, which increases the pressure in those areas. These increases are not large enough to produce the delta roll and delta yaw trends seen in flight, but are consistent with debris forensics and elevated heating rates observed on the OMS pod

One of the most influential damage configurations is a hole through the wing. The effect on the OMS pod and tail area is driven by the orientation of the hole with respect to the flow field and alignment of the fuselage. The delta aerodynamics for these cases is more consistent with early flight trends.

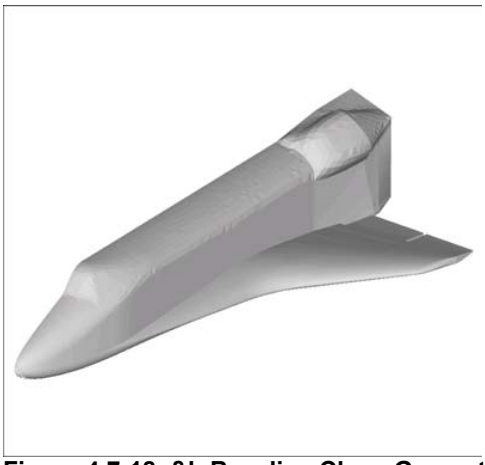

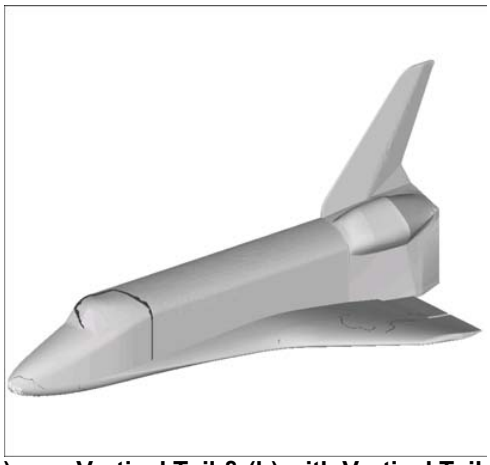

Figure 4.7-18a&b Baseline Clean Geometry (a) – no Vertical Tail & (b) with Vertical Tail

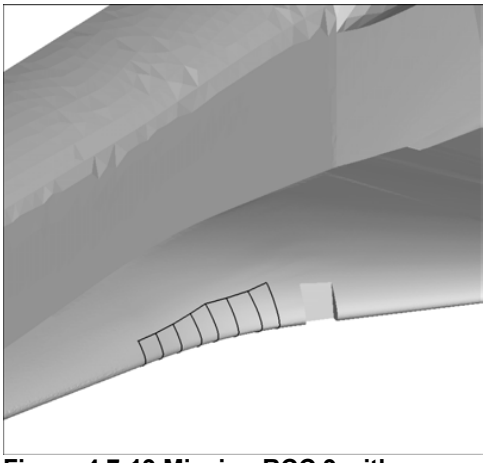

Figure 4.7-19 Missing RCC 9 with Outline of RCC 1 thru 7

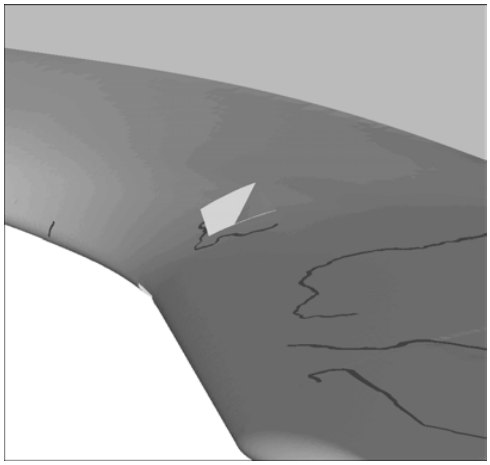

Figure 4.7-20 Windward View – Missing Lower Half of RCC 8 w/Hole #1 thru Wing

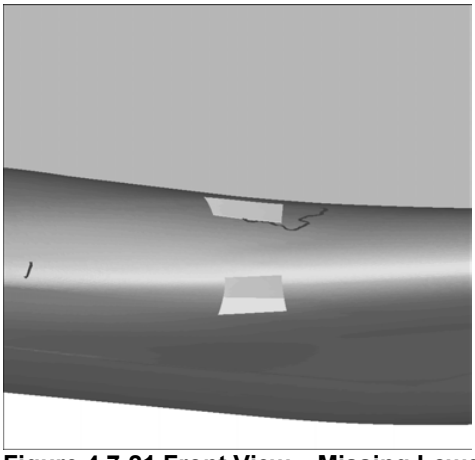

Figure 4.7-21 Front View – Missing Lower Half of RCC 8 w/Hole # 1 thru Wing

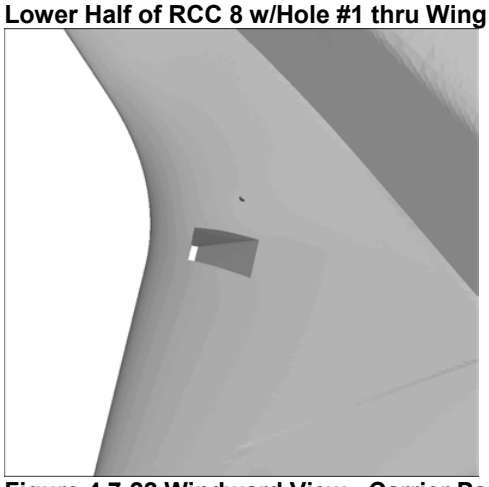

Figure 4.7-22 Windward View - Carrier Panel 8 Missing and Hole # 2 in Wing

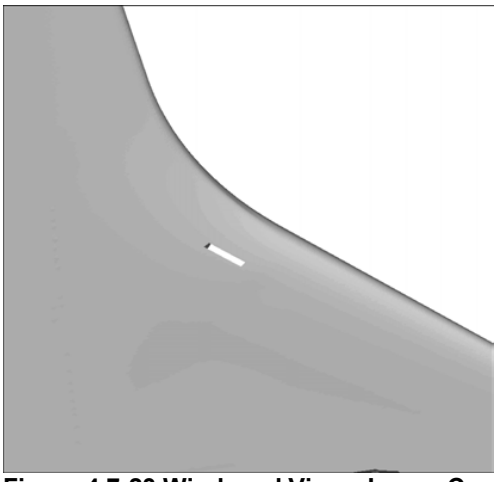

Figure 4.7-23 Windward View - Lower Carrier Panel 8 Missing and Hole #2 through Wing

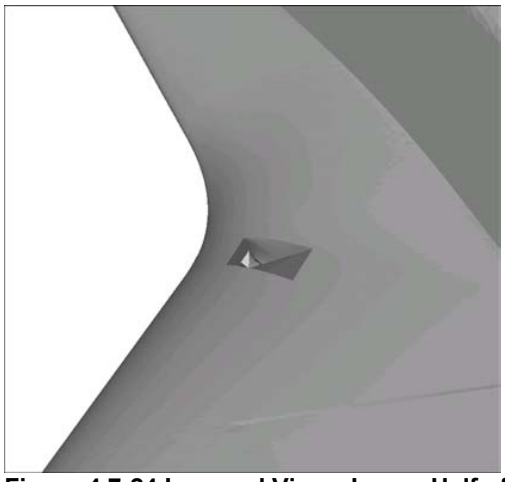

Figure 4.7-24 Leeward View - Lower Half of RCC 8 Missing and Hole # 2 through Wing

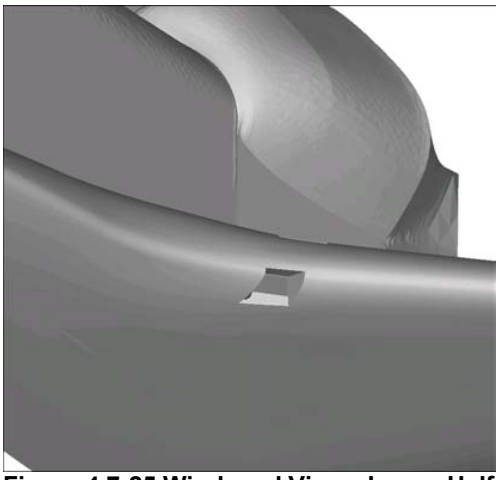

Figure 4.7-25 Windward View - Lower Half of RCC 8 Missing and Hole # 2 Through Wing

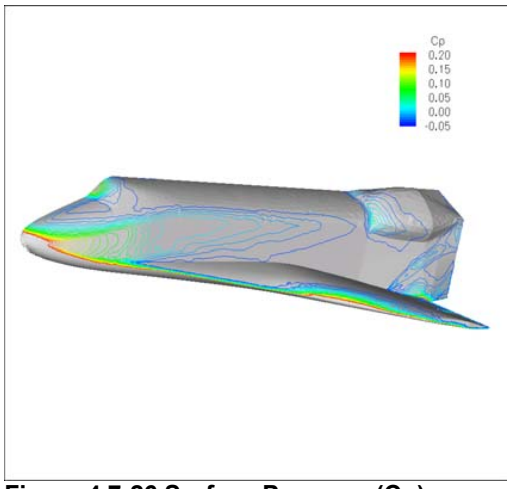

Figure 4.7-26 Surface Pressure (Cp) – Baseline Configuration

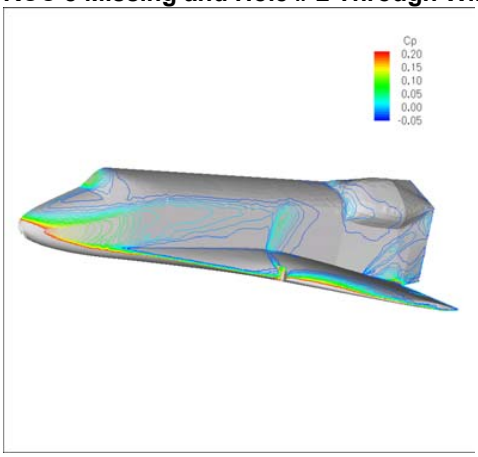

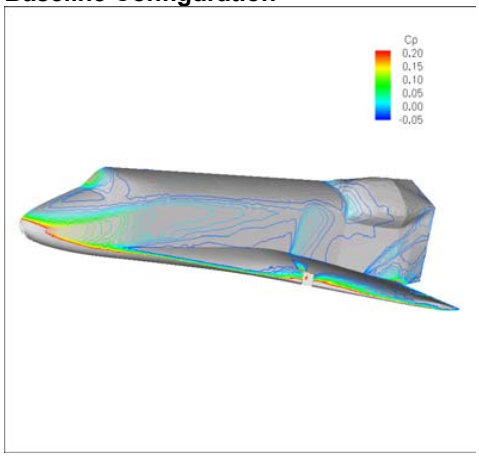

Figure 4.7-27a&b - Surface Pressure (Cp) – (a) Missing Panel 6 & (b) Missing Panel 9

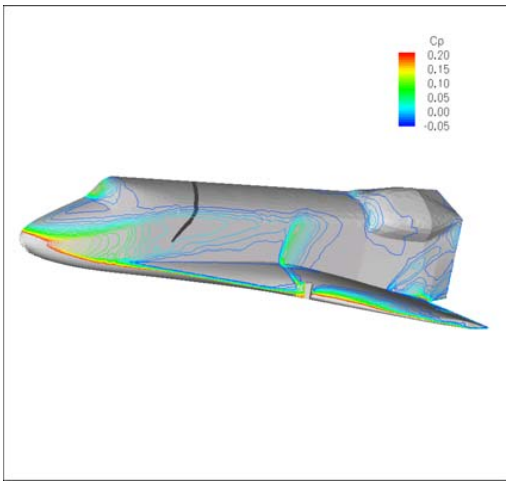

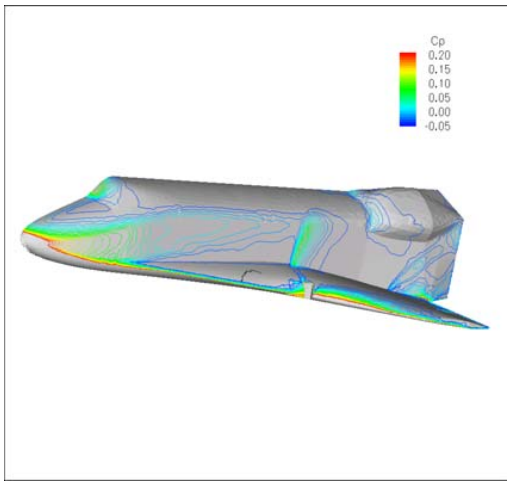

Figure 4.7-28a&b - Surface Pressure (Cp) - (a) Missing RCC Panels 6&7 & (b) Missing 5-7

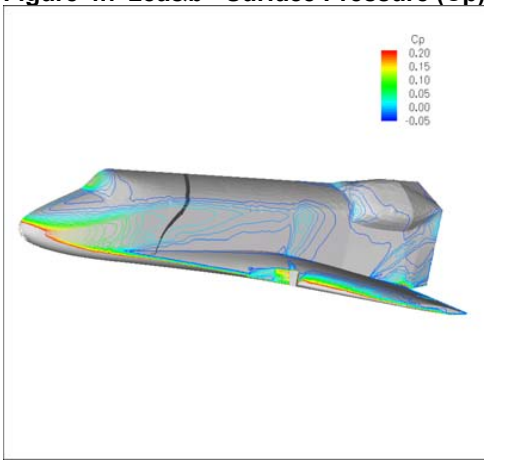

Figure 4.7-29 Surface Pressure (Cp) - Missing RCC Panels 1 through 7

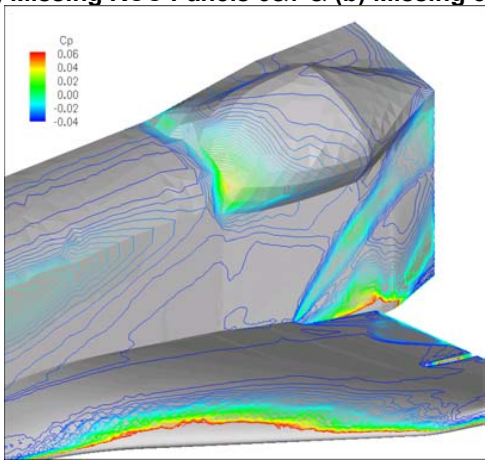

Figure 4.7-30 Surface Pressure (Cp) – Baseline Configuration (OMS Pod)

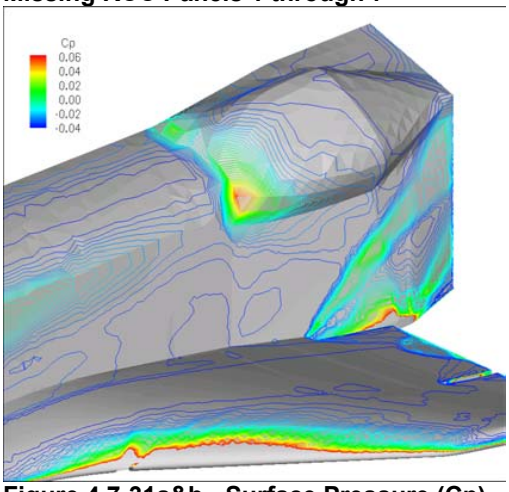

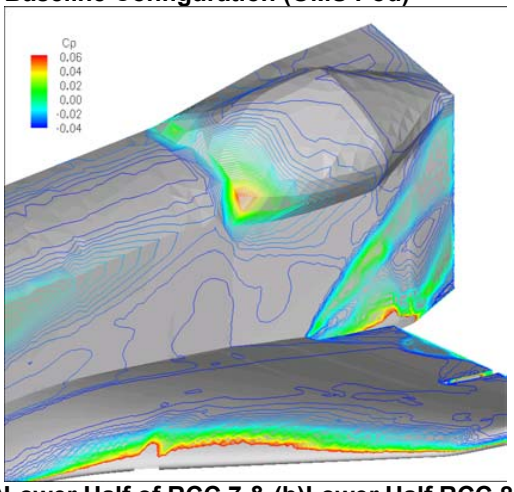

Figure 4.7-31a&b - Surface Pressure (Cp) - (a)Lower Half of RCC 7 & (b)Lower Half RCC 8

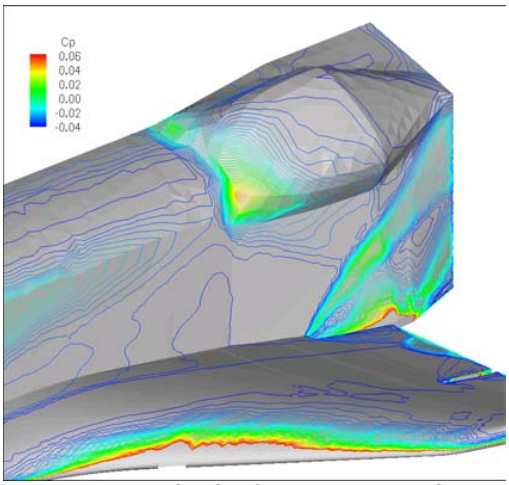

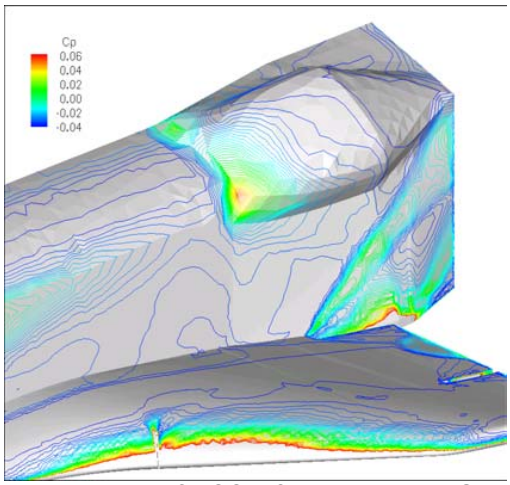

Figure 4.7-32a&b Surface Pressure (Cp) - Missing Lower Half RCC 9 & (b) Missing T-Seal 9

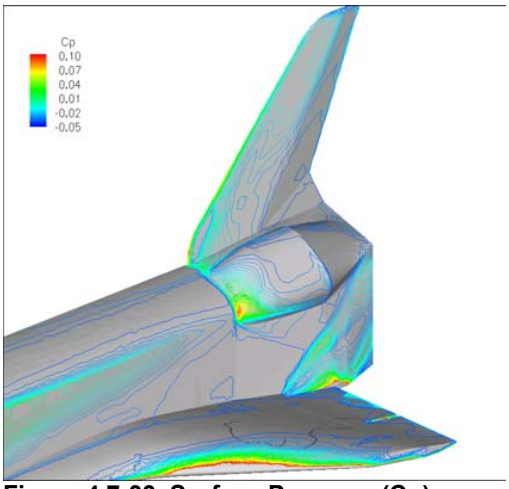

Figure 4.7-33 Surface Pressure (Cp) - Baseline Configuration (OMS & VT)

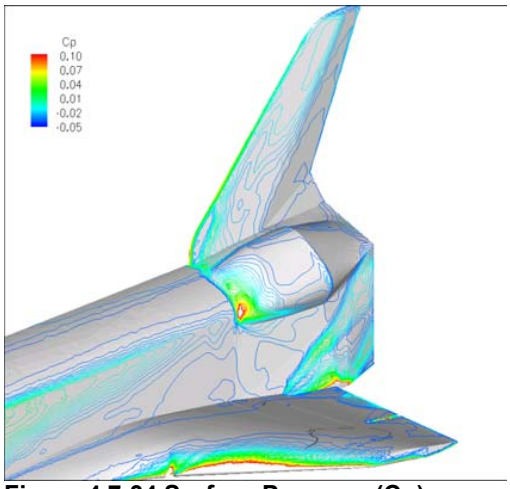

Figure 4.7-34 Surface Pressure (Cp) - Lower Half of RCC 7 Missing

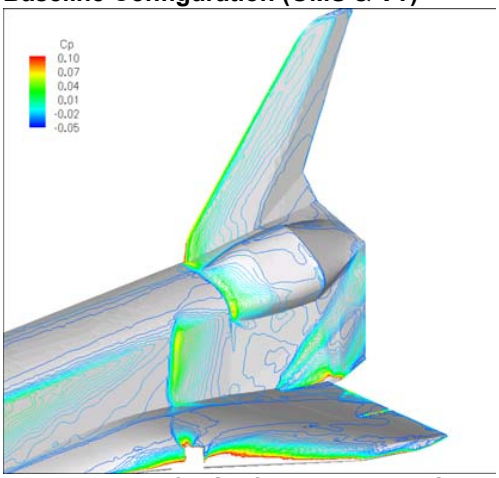

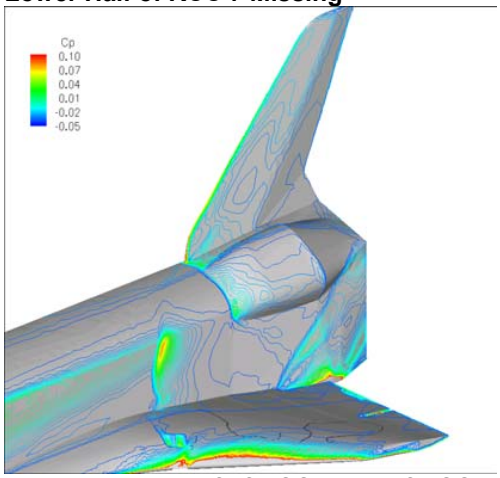

Figure 4.7-35a&b Surface Pressure (Cp) - (a) Missing Lower Half of RCC 8+ all of RCC 9 (b) Missing Lower Half of RCC 8 + Hole No. 1 through Wing

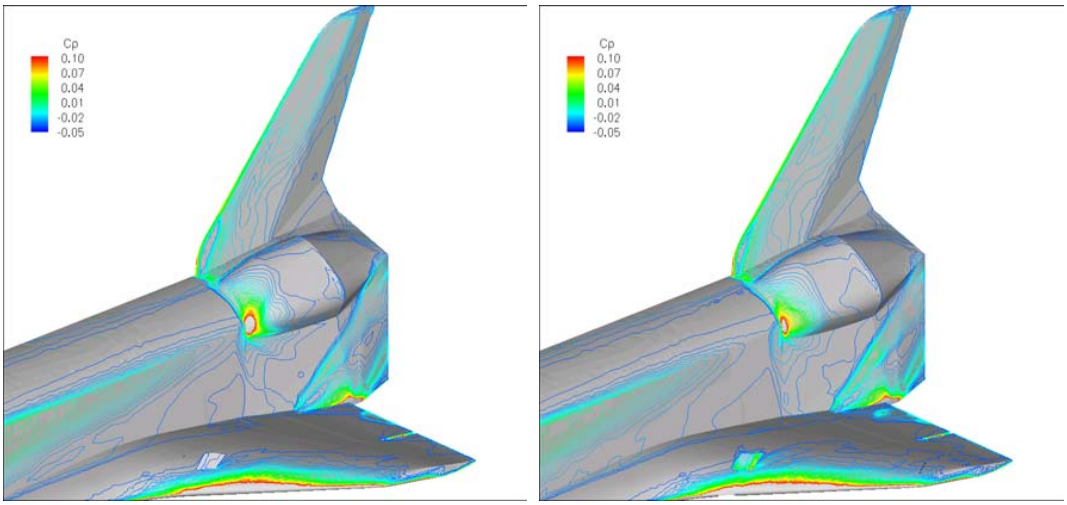

Figure 4.7-36a&b Surface Pressure (Cp) - (a) Lower Carrier Panel 8 Missing + Hole No. 2 Through Wing & (b) Lower Half of RCC 8 Missing + Hole No. 2 Through Wing

4.7.7 Aerodynamic Investigation using USA CFD Analysis

Boeing-Huntington Beach completed a CFD analysis of a damaged orbiter configuration (missing RCC Panel 6) using their USA Navier-Stokes solver at flight conditions.

4.7.7.1 USA Description

The unified solution algorithm (USA) code is a very versatile flow solver that can be used to compute numerical solutions to a large class of aerodynamic and aerothermodynamic problems by solving the Euler or Reynolds averaged Navier-Stokes (RANS) equations. The discretization is of TVD formulation using finite volume framework. Various Riemann solvers can be used with the preferred one being the modified Lax-Freidrichs scheme. A multi-zonal structural grid bookkeeping method facilitates the treatment of complex geometric topologies. A real gas approach based on a finite rate chemistry formulation can be coupled or uncoupled with the fluid dynamics to treat reacting and non-reacting gaseous species. In this work, the approximate factorization scheme using the implicit time marching option was used. The simulations were speeded up using grid-sequencing. The convergence of flow simulations were confirmed by monitoring the time history of surface results.

4.7.7.2 STS 107 CFD case definition

This analysis was done to quantify the effect on the force and moment coefficients due to the removal of the leading edge panel number 6. The cavity was modeled without any representation of the actual exposed interior components of the wing leading edge. The geometry represents the initial panel 6 definition. As detailed in Section 4.3.2.3.2 this is somewhat less than the full panel 6 geometry.

Configurations analyzed

There were two real gas CFD cases considered under this effort. The first one consisted of analysis of the intact vehicle and the second was for vehicle with RCC panel 6 missing. Flight conditions consisted of free stream Mach 18 and angle of attack of 40 degrees. Equilibrium air assumptions were utilized to handle this Mach number. A third case with perfect gas assumption was also conducted for the baseline geometry.

4.7.7.3 Delta Aerodynamic results

CASE	Geometry	Chemistry	CA	CN	CLM	CLL	CLN
OADB	OADB	-	0.06284	1.1598	-0.01667	0	0
1	Baseline	Real Gas/Equilbrium	0.06861	1.1158	-0.01297	0	0
2	"	Perfect gas	0.06439	1.201	-0.04693	0	0
3	RCC#6 Off	Real Gas/Equilbrium	0.069	1.1587	-0.0248	-0.0004	-0.0015

4.7.7.4 Observations/Conclusions

The analysis were carried out using an orbiter half model. The rolling moment and yawing moments were estimated from two half model solutions with the assumption of flow being essentially axial along the symmetry plane. The magnitude of these numbers were of the same order as the error band for the solution convergence and hence not highly reliable.

4.7.8 CFD Tools:

4.7.8.1 FELISA Inviscid Mesh Generation and Flow Solver

Computations of the present study were performed using the FELISA unstructured grid software. This software package consists of a set of computer codes for unstructured grid generation, and the simulation of three-dimensional steady inviscid flows using unstructured tetrahedral grids.

The mesh generation process starts with the definition of a geometry. The computational domain must be a watertight solid. The solid can be developed within a solid modeling CAD package (i.e., Unigraphics or Pro-Engineer), a geometry preprocessor such as GridTool, or by hand. For all of the FELISA work on the Columbia Accident Investigation, the baseline and damaged geometry models were developed within GridTool, with the starting baseline geometry as the structured grid developed at LaRC several years ago using a 1997 Orbiter CAD model. (A solid model based on the 2003 Orbiter CAD model was developed for use with FELISA, but it came available in the middle of the investigation, and the decision was made to continue using the original model.) The second step in the mesh generation process is to graphically define the spacing functions, which determine local mesh size, within either GridTool or GridEx. (GridEx is a mesh generation package under development at LaRC, and has the option of using the FELISA mesh generator). The mesh generation takes place in 2 steps. The surface is triangulated with either the FELISA-SURFACE code, or within the GridEx tool. Generation of the tetrahedral volume mesh is performed using the FELISA-3D_mesh code. Both surface and volume grids are essentially isotropic with little or no stretching. Once the baseline geometry and the mesh spacing were defined for the flight and CF4 conditions, producing a mesh for a new damage scenario only took a couple of hours of preparation work, and 4-8 hours of computer time. Mesh sizes for the damage scenario cases ranged from 2.5 to 5.5 million nodes, up to 30 million tetrahedral elements.

Two flow solvers are available with FELISA--one applicable for transonic flows, and the other for hypersonic flows. The hypersonic flow solver has options for perfect gas, equilibrium air, CF4, CO2, and several other gases (including Mars, Neptune, and Titan atmosphere) in equilibrium. This solver also has the capability of solving chemical non-equilibrium flow, and real gas (chemical and thermal non-equilibrium) flow. This software package has been used extensively for inviscid computations for X-34, X-33, X-37, Mars landers, and also for the Space Shuttle Orbiter at high angles of attack (see Ref. 1). The hypersonic flow solver with the equilibrium air and with the CF4 options was used for the present computations. The solvers are parallelized using MPI for rapid computations. For this investigation, the code was run both a local cluster of PC's with up to 24 processors, and on the NAS Origin 3000 system, 'chapman', with up to 64 processors. Wall clock time for obtaining a converged solution ranged from 8 – 24 hours, and depended on mesh size and the complexity of the damage scenario.

Post-processors such as the aerodynamic analysis routine are part of the software package. More information on FELISA software may be found in Ref. 2. A description of the hypersonic flow solver may be found in Ref. 3.

1. R. K. Prabhu: "Inviscid Flow Computations of the Shuttle Orbiter for Mach 10 and 15 and Angles of Attack 40 to 60 Degrees," NASA/CR-2001-211267, December 2001.

2. J. Peiro, J. Peraire, and K. Morgan: "FELISA System Reference Manual and User's Guide," University College Swansea Report, 1993.

3. K. L. Bibb, J. Peraire, and C. J. Riley: "Hypersonic Flow Computations on Unstructured Meshes," AIAA Paper 97-0625, January 1997.

4.7.8.2 Overflow

OVERFLOW is a structured (overset) grid, Navier-Stokes flow solver. It uses a finite-difference formulation, with flow quantities stored at the grid nodes. OVERFLOW has central- and Roe upwind-difference options, and uses a diagonalized, implicit approximate factorization scheme for the time advance. Local time stepping, multigrid and grid sequencing are used to accelerate convergence to a steady state. In this study, 2nd-order central differencing with Jameson-type 2nd/4th-order scalar dissipation is used. Thin-layer viscous terms are computed in wall-normal directions by default.

References:

D.C. Jespersen, T.H. Pulliam, and P.G. Buning, "Recent Enhancements to OVERFLOW," AIAA-97-0644, AIAA 35th Aerospace Sciences Meeting, Reno, NV, Jan. 1997.
http://science.nas.nasa.gov/~jesperse/papers/aiaa97-0644.ps.Z

P.G. Buning, D.C. Jespersen, T.H. Pulliam, G.H. Klopfer, W.M. Chan, J.P. Slotnick, S.E. Krist, and K.J. Renze, "OVERFLOW User's Manual, Version 1.8s," NASA Langley Research Center, Nov. 2000.

4.7.8.3 CART3D

CART3D is a high fidelity inviscid analysis package developed at NASA Ames Research Center. The geometry required is represented as a closed, watertight, triangulated surface. From this triangulated surface, CART3D produces the volume mesh. The volume mesh is a topologically unstructured, adaptively refined, Cartesian mesh produced around the geometry. The user can control the initial mesh division, the number of refinement levels, and specify certain regions for more cell refinement to develop a useable volume mesh. Using the volume mesh, CART3D uses a domain-decomposition, scalable, multi-level solver to solve the inviscid flow Euler equations.

For more information, visit the CART3D home page at
http://people.nas.nasa.gov/~aftosmis/cart3d/cart3Dhome.html

4.7.8.4 GASP

The GASP Real-Gas Navier-Stokes code was the primary code for solutions accomplished at Ames Research Center. This code originated as a commercially available code developed at AeroSoft, Inc (ref ARC1), but has been modified at ARC to enhance both capability and robustness specifically for hypersonic reentry applications (ref ARC2, ARC3, ARC4).

The GASP Reynolds Averaged Navier-Stokes code is a three-dimensional (3D) finite-volume code. Upwind flux options exist for this code, but for the present solutions the van Leer (ref ARC5) inviscid flux formulation was applied in all three directions. A formally 3rd order upwind-biased MUSCL scheme combined with min-mod limiter is selected to provide higher order accuracy. Experience at ARC with this code has indicated that wall normal spacing is sufficient to obtain accurate heat transfer with the Van Leer flux formulation and 3rd order accuracy provided the wall node Cell Reynolds number is kept below a value of 5. For most of the calculations provided in the present work the wall node Cell Reynolds number is approximately 1, which yields the best results in convergence and accuracy. Time advancement to steady state is accomplished with either a 2D Approximate Factorization, AF2, in the nominal cross-flow plane with planar relaxation in the streamwise direction, or, alternatively, with a point-Jacobi algorithm with inner iterations. Experience at ARC has shown that these two time-advancement schemes as implemented in GASP are nearly identical in convergence, robustness and speed.

The 5-species finite reaction rate model for dissociating air of Park (ref ARC6) was used in these calculations using GASP. In this chemistry model, air is composed primarily of molecular nitrogen, N2, and molecular oxygen, O2, with the possibility of dissociation at high temperature into atomic nitrogen, N, and atomic oxygen, O, followed by formation of NO. For the high Mach number, high altitude portion of a low Earth orbit reentry trajectory as considered herein, the molecular oxygen, O2, present in the atmosphere will almost entirely dissociate into atomic oxygen, O, upon encountering the bow shock. However, N2 will undergo but slight dissociation with lesser amounts of N and NO formed. The reaction rates are typically slow enough that little recombination occurs for hypersonic flows prior to the exit boundary except for that due to the catalytic effect of certain thermal protection surface materials.

The real-gas air chemistry has an important effect on the hypersonic flow about the orbiter by altering the shock location since energy is required to dissociate the molecular oxygen through the shock, the temperature and density rise through the shock are not as great as would otherwise occur for a perfect gas thereby reducing the effective gamma for the real gas in the shock relations. A further real-gas effect is that chemical energy is released at the shuttle surface due to recombination of O to O2 as a consequence of the catalytic behavior of the RCG shuttle tile material. This catalytic wall effect yields a higher heating rate to the wall than for non-catalytic materials.

Species transport properties are calculated using Blottner relations with mixture properties calculated using Eucken relations. See ref ARC1 for further details.

Stewart (ref ARC7) characterized the surface catalytic recombination of air due to various thermal protection system insulation materials including RCG as used on the windward side of the shuttle orbiter. RCG and other

catalytic materials act to enhance the rate of recombination of atomic oxygen into molecular oxygen and of atomic nitrogen into molecular nitrogen. Molecular NO is assumed to experience no catalytic effect. In the process, additional thermal energy is released to the wall due to the chemical reaction occurring at the surface.

The primary wall boundary condition used for these shuttle calculations is that of radiative equilibrium combined with the above RCG catalytic behavior. In this viscous wall boundary condition, there is an assumption that the radiative heat transfer from the wall exactly balances the thermal energy transfer to the wall due to convective heat transfer combined with energy release to the wall due to the surface catalytic chemical reaction. The radiative equilibrium boundary condition requires the simultaneous solution of 4 species equations (molecular NO is not considered catalytic) combined with an equation for the energy balance, all of which are written at the wall node. To then solve this wall boundary condition for each Navier-Stokes solver iteration, a Newton-Raphson method achieves quadratic convergence.

Additional boundary conditions used include conventional point-to-point zonal boundaries, adiabatic viscous wall, free-stream, and a specified back-pressure outflow boundary condition. Point-wise boundary conditions can be specified optionally for any of the 6 faces of each grid block and were used for the vented cavity panel 9 solutions.

Most of the solutions delivered were laminar throughout the solution domain. However, some eddy-viscosity turbulence models calculations were conducted to establish approximate turbulence heating enhancements and for validation purposes. Turbulence models implemented into this code include the Baldwin-Lomax algebraic model of Baldwin-Lomax (Ref ARC7) and the 2-eq SST/K-Omega turbulence model of Menter(Ref ARC8). These models have compressibility corrections suitable for hypersonic flows and have been validated for heat transfer in hypersonic strong interactions as implemented in the ARC version of the GASP code(see Ref ARC3). A means for specification of turbulence transition is implemented in the code, but is not used for the present work.

The GASP code was run initially on a serial processor computer (Intel 2 GHz XEON processor running RedHat Linux v 7.3). These early runs were for fully catalytic solid surface rather than RCG on grids of approximately 3/4 million grid points and took 96 hours. To improve throughput, subsequent work was moved to the NAS parallel-processing cluster, chapman, which is based on up to 1024 SGI Origin O3K cpus. For the parallel processor runs, the grids were decomposed into as many as 48 grid blocks each of which was then run on a separate SGI processor in the NAS chapman cluster. With grids of 1.9 million grid points, the chapman parallel processor runs took approximately 48 hours.

Convergence criterion was based on examination of residual history, temperature and pressure history for selected surface points during the entire iteration sequence, and when convergence was nearly complete examination of delta T and delta P surface plots separated by 50 to 200 iterations. Typically the L2 residual would drop by 5 orders of magnitude and the selected surface temperatures and pressures would become constant. The delta T and delta P surface plots were facilitated by the gasptools package written by D. Prabhu and M. Wright of Ames and which is based on perl scripts making use of the GASP print utility and the Tecplot plotting package. Typically the delta T surface plots were examined for constant temperature within 5 degrees over the entire shuttle surface. Some of the damage cases exhibited some oscillation of approximately a 10 degree K magnitude which was deemed acceptable inasmuch as there existed a physical basis.

4.7.8.5 USA

The unified solution algorithm (USA) code is a very versatile flow solver that can be used to compute numerical solutions to a large class of aerodynamic and aerothermodynamic problems by solving the Euler or Reynolds averaged Navier-Stokes (RANS) equations. The discretization is of TVD formulation using finite volume framework. Various Riemann solvers can be used with the preferred one being the modified Lax-Freidrichs scheme. A multi-zonal structural grid bookkeeping method facilitates the treatment of complex geometric topologies. A real gas approach based on a finite rate chemistry formulation can be coupled or uncoupled with the fluid dynamics to treat reacting and non-reacting gaseous species. In this work, the approximate factorization scheme using the implicit time marching option was used. The simulations were speeded up using grid-sequencing. The convergence of flow simulations were confirmed by monitoring the time history of surface results.

5 AEROTHERMODYNAMICS

5.1 Introduction

5.1.1 Team Objective

The objective of the aerothermodynamics team was to define local and acreage predicted heating environments of the Orbiter for nominal and damaged configurations in support of the Columbia accident investigation. These environments were used to explain the anomalies in the flight data and were provided to the thermal structures team in support of various thermal analyses, Figure 5.1.3-1.

5.1.2 Aerothermodynamics Overview –Orbiter Perspective

The discipline of aerothermodynamics as applied to the Orbiter principally refers to the aerodynamically induced heating of the vehicle during high speed flight. Significant aerodynamic heating occurs at Mach numbers of 2 and above. For the Orbiter, the highest heating is observed during re-entry from orbit as it descends into the earth's atmosphere traveling at Mach numbers greater than 25.

The heating is a result of the conversion of Orbiter kinetic energy into thermal energy. As the Orbiter passes through the atmosphere at high Mach numbers a shock wave is formed in front of the vehicle, called the bow shock. The bow shock processes convert the kinetic energy into thermal energy by reducing the air speed while tremendously increasing its temperature. Just behind the shock wave, the air can reach temperatures as high as 10,000° F. At these temperatures, the majority of the molecules that make up air, N_2 and O_2, dissociate into their respective atomic constituents. Such dissociated gases are termed high temperature gases. After passing through the bow shock, the heated dissociated gas flows around the vehicle, and thus the energy of the gas will be convectively transferred to heat the surface. Because this heating is extreme during re-entry, a thermal protection system (TPS) is required.

In order to determine the rate at which the heat is transferred to the surface of a vehicle, the flow physics that the vehicle will encounter must be understood, i.e., bow shocks, wing shocks, shock interactions, surface boundary layers and boundary layer state (laminar, transitional, or turbulent), shock-boundary layer interactions, and boundary layer separation and reattachment zones. The heat transfer rate will be a function of the vehicle geometry, its orientation to the flow, the surface temperature of the vehicle, the trajectory being flown through the atmosphere, and the TPS properties. Lastly, at Mach numbers greater than about 5, in a regime called hypersonic, chemical reactions in the air due to the energy exchange are significant. These reactions not only affect the heating of the vehicle but also its aerodynamics.

Flow chemistry affects the shock waves, pressure distributions, and heating distribution around the vehicle. As mentioned previously, at the speeds of Orbiter atmospheric re-entry, all of the molecular oxygen and most of the molecular nitrogen dissociate into their atomic forms via an endothermic reaction. This dissociation occurs due to the heating caused by the initial bow shock. The flow chemistry within this dissociated region may be considered in either a chemical equilibrium or non-equilibrium state, which also has an effect on the heat transfer rate. Determining the state depends upon the speed of the chemical reactions compared with the speed of the vehicle. It is during the phase of re-entry in which the dissociated region of the flow is also in a chemically non-equilibrium state that interaction of the dissociated gas with the TPS surface material properties can have a significant impact on the amount of heat being transferred to the vehicle. Surfaces that are non-catalytic inhibit the recombination of atomic nitrogen and oxygen and thus minimize the amount of heat transfer, whereas fully catalytic surfaces maximize the heat being transferred from the gas to the surface. In the case of the Orbiter TPS, both the tiles and leading edge materials are considered partially catalytic and are closer to non-catalytic than fully catalytic. This low partial catalytic property was designed into the TPS system to reduce the amount of chemical recombination energy transferred to the surface.

All of these issues must be considered when providing heating environments to be used in follow-on analyses. For a more thorough discussion on aerothermodynamics and high temperature gas dynamics, please refer to the works of Bertin and Anderson.

5.1.3 Approach to Determining Required Environments

As mentioned, there are many factors that need to be understood in order to determine Orbiter heating environments. Most of the previous work on determining these environments focused on a nominal Orbiter configuration during the TPS design and certification. Determining the environments for a damaged Orbiter is a more difficult problem. First, the size, shape, and location of the original and progressing damage are unknown. Second, because the damage exposes internal structure and permits external gases to enter internal cavities, the problem becomes a mixed internal-external flow problem. Finally, the problem is further complicated by the fact that as the damage to the Orbiter progressed, both the external and internal geometry changed, and the free stream conditions were also continuously changing.

During the design and operation of the Orbiter, and the design of more advanced vehicles since, numerous tools and testing techniques have been developed, and they were applied in support of this investigation. These tools include engineering methods using simplified geometries (e.g., spheres for nose caps, cylinders for wing leading edges), computational fluid dynamics (CFD), direct simulation Monte Carlo techniques (DSMC), and wind tunnel testing along with the associated instrumentation. The certified Orbiter heating model was also used as the benchmark for the Orbiter external heating environment as well as existing computational and testing data. This certified heating model is described in Section 5.2.2. The tools and techniques utilized for the certified Orbiter heating model were applied to nominal configurations with as-designed outer mold line (OML) geometry lines. There have been very limited pre-accident studies involving heating of the internal structure as a result of a penetration in the TPS. Those particular studies dealt with micrometeoroid penetrations and not the larger scale damage being considered as the root cause of the Columbia accident. The consideration of large scale damage to the Orbiter represented a new area of engineering analysis, especially for the determination of the internal heating environments.

In order to provide the external and internal heating environments needed for the investigation, a team of engineers and scientists from government, industry, and academia was formed. Two sub-teams were then formed - one focusing on external heating environments and the other on internal heating environments. The team decided that the damage configurations to be assessed were to be treated as static or at most quasi-static, in order to reduce the complexity of the analyses being performed. Also, it was recognized that since there was no time for a formal verification process of the environments being provided, the use of engineering best practices, multiple solution sources, and team review of the data would be sufficient. The idea was that the data were to be used in support of determining the plausibility of a given scenario and not to define the exact environments, because the exact configuration of the damage would never be known.

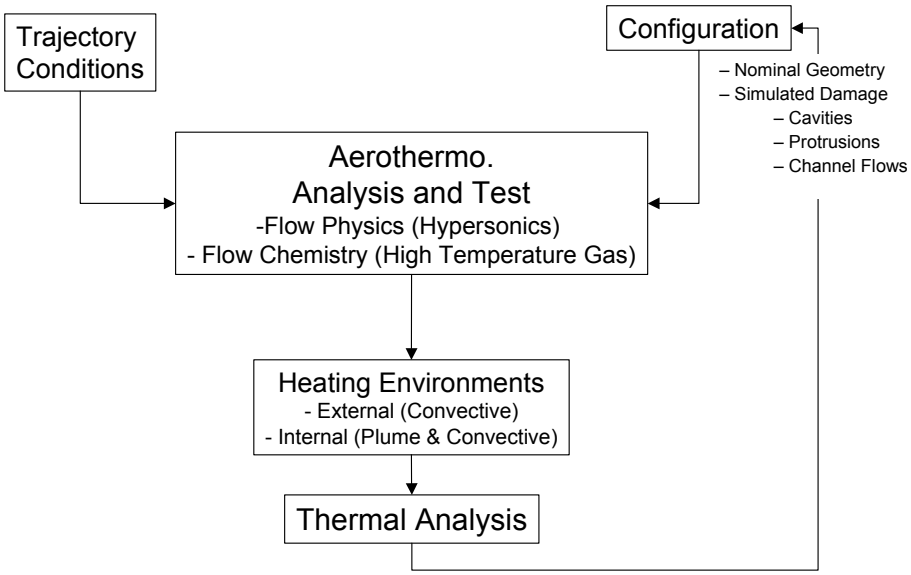

Figure 5.1.3-1 Aerothermodynamics Analysis Process

5.2 Orbiter External Aerothermodynamic Environments (Nominal & Damaged Configurations)

External aerothermodynamic environments for both nominal and damaged Orbiter configurations were needed for several aspects of the investigation. These include assessing the flight data using the aerothermodynamic results directly, qualitatively and/or quantitatively, or as input to the internal environments and thermal analysis teams. This section will review the relevant STS-107 flight data pertaining to the external environment and the working scenario, provide background on the certified Orbiter entry heating methodology, present the results from wind tunnel testing and computational analyses, and, finally, apply those data to the working scenario issues described in this section.

5.2.1 Orbiter OML/Skin Flight Data Observations

During the STS-107 re-entry, several off-nominal sensor readings on the Orbiter OML were recorded on the recovered Modular Auxiliary Data System (MADS) recorder. Also, several Orbiter Instrumentation (OI) sensors on the inner structure showed off nominal readings. Although there were a significant number of other off-nominal sensor readings in the MADS and OI data, those discussed in this section are pertinent relative to the external flow field and how they relate to the working scenario. The specific sensors to be discussed in this section include the surface thermocouples (T/Cs) on the left side fuselage and left OMS pod, the temperature sensors on the chin panel expansion seal, vacuum vent nozzle, water dump nozzle, and a surface T/C just behind the RCC Panel 9 and Panel 10 interface. Although not Orbiter flight data, the Kirtland photo image will be discussed in this section as it potentially shows a damaged Orbiter configuration.

5.2.1.1 Side Fuselage and OMS Pod

From the data available via the OI system, three measurements on the side fuselage indicated off nominal increased heating responses compared with previous flight data. The most significant of these increased heating responses was from V34T1106A, the location of which is shown in Figure 5.2.1-1. On the MADS there were 11 out of 14 surface T/Cs that indicated off-nominal response during the STS-107 re-entry prior to LOS. Those sensors showed both increased and reduced heating effects on the left side fuselage and OMS pod (locations depicted in Figure 5.2.1-1), as compared with previous flight data. Figure 5.2.1-2a – f show examples of these comparisons. The reduced heating was noted on the forward portion of the OMS pod and two sensors on the side fuselage-payload bay door area and began as early as 49:49 GMT (EI+340 sec). It is noteworthy that during this early part of the STS-107 flight, between 49:49 GMT (EI+340 sec) and about 52:09 GMT (EI+480 sec), only off-nominal low heating rates were

observed in any of the available side fuselage or OMS pod sensor data. Between 52:39 (EI+510 sec) and 53:09 GMT (EI+540 sec) the heating began to increase above the nominal range at various gauge locations compared with previous flights. This heating increase began with two measurements on the forward part of the OMS pod, V07T9978 and V07T9976. The different onset times for off nominal increased heating at the various gauge locations are a significant indicator of damage progression occurring on the Orbiter, Figure 5.2.1-1 and Figure 5.2.1-3.

An analysis was performed to back out the relative decrease or increase in heating that was observed. Since these were surface T/C's, an radiation equilibrium wall condition assumption can be made such that

$$\frac{\dot{q}_{STS-}}{\dot{q}_{Nominal}} \cong \frac{T^4_{STS-}}{T^4} .$$

In this relation, $\dot{q}$ is the heat transfer rate and T is the surface temperature in degrees Rankine. Using an average over previous flight data as a nominal value, a ratio of the disturbed to nominal heating was obtained. For all the sensors that experienced reduced heating during the early portion of the flight, before 52:09 GMT (EI+480 sec), the ratio of heating ranged from 0.6 to 0.8. The sensors on the OMS pod that showed reduced heating experienced heating ratios of 0.6 to 0.7 compared with previous flights. During the segment of the flight where off-nominal higher heating rates were observed, after 52:09 GMT (EI+480 sec), the heating ratios across several sensors on the side fuselage and OMS pod varied from 1.7 to 5.2.

A close examination of the temperature response of V07T9220 indicates at least two significant events during the period between 52:39 GMT (EI+510 sec) and 57:19 GMT (EI+850 sec), Figure 5.2.1-4. Observed debris events were co-plotted on the side fuselage and OMS pod data to investigate any correlation to the observed temperature increases, Figure 5.2.1-5, Figure 5.2.1-6, and Figure 5.2.1-7. The data for these gauges indicate that significant external changes were occurring on the Orbiter even before the first debris event was observed. Other flight data indicate that the wing spar had already been breached by the time the increased heating on the OMS pod was experienced. However, debris events 5 and 6 (with the flash) stand out as correlating well with changes in the slope of the temperature response. These data indicate a progression of damage on the wing that resulted from initial damage in the panel 5 through 9 region.

Finally, a check on the surface emittance of tiles recovered from the OMS pod region was performed to assess whether or not surface contamination could be the cause of the observed temperature response. If the heating environment were nominal, then the emittance of the TPS would have had to decrease to 0.3 from the nominal 0.85 value in order to match the temperature response, Figure 5.2.1-8. The emittance of these post-accident tiles was measured at NASA KSC and was shown to be nearly the same as a pristine tile. Therefore, the side fuselage and OMS pod measurements are believed to be accurate indicators of the reduced and increased heating.

5.2.1.2 Wing Surface T/C V07T9666A

V07T9666A is a surface T/C located on the lower wing immediately aft of the panel 9 / 10 interface, Figure 5.2.1-9. The data, Figure 5.2.1-10, indicate that this sensor begins to show an off-nominal behavior at 50:19 GMT (EI+370 sec). This start of off-nominal time is 30 seconds after the start of decreased heating recorded on the side fuselage and OMS pod. As can be seen in the figure, there were other flights in which an off-nominal temperature behavior can be observed for this T/C. However, the earlier off-nominal responses for the T/C are not of similar signature to the data seen for STS-107. No proven explanation can be provided for the previous off-nominal flight data but one theory is that the T/C temperature is demonstrating a sensitivity to the shock interaction. Shock interaction regions are areas within the flow field where two or more strong shock structures intersect. For the Orbiter, a very strong shock interaction occurs between the bow shock and wing shock, resulting in locally higher heating and pressure. In fact, the very high heating experienced on the Orbiter wing leading edge, in the region where the wing transitions from the strake section to the main wing section, results directly from the bow-

shock/wing-shock interaction. The heating produced by such an interaction can be very localized, implying very large surface heating gradients in the immediate vicinity of the interaction. The precise location of this interaction is a function of many variables related to high-speed aeroheating environments, and even small changes in these variables can cause significant changes in the actual position of the shock-shock interaction and hence the underlying heating experienced at the surface. No further discussion will be provided in this report on the off-nominal low data, but this information was noted here for completeness. The off-nominal high readings for STS-107 continue until the V07T9666A T/C fails at approximately 52:25 GMT (EI+496 sec).

The off-nominal trend for the V07T966A instrument occurs prior to any of the debris events that were observed, so no correlation can be made to observed debris. However, as was noted previously, instrumentation inside of the WLE and along the wing spar, i.e. V09T9910A, V12G9921A, V12G9169A, indicated that heating was already occurring in the WLE cavity when the off-nominal temperature at V07T9666A was noted. Thus, the temperature response of this gauge potentially indicates a worsening condition either inside the WLE cavity or at the original damage site itself.

5.2.1.3 Chin Panel and Vacuum Vent / Water Supply Dump Nozzles

Four additional temperature measurements indicated off-nominal behavior on the vehicle. However, these were located more forward on the fuselage than the sensors previously discussed. Additionally, these instruments are not surface thermocouples, but are instead Resistance Temperature Devices (RTDs) which were typically attached to structural elements of the Orbiter. The first of these was one of two RTDs located on the Nose Cap/Chin Panel expansion seal, Figure 5.2.1-11. The other three were located on the left side of the Orbiter; one associated with the vacuum vent nozzle and the other two with the water supply dump nozzle located just above the waste water dump nozzle, Figure 5.2.1-12.

The chin panel sensor, V09T9889A, was the first of these sensors to indicate off-nominal trends at 52:09 GMT (EI+480 sec) but it recovers to the “nominal” slope by 52:49 GMT (EI+520 sec), Figure 5.2.1-13. Note that V09T9880A, only 23 inches away on the centerline, did not show this off-nominal signature. Also in Figure 5.2.1-13, the vacuum vent, V62T0551A, and water supply dump nozzles temperature sensors, V62T0440A & 0439A (not shown), indicate similar behavior albeit at a slightly different start time of 52:32 GMT (EI+503 sec). However, the vacuum vent RTD recovered to the previous slope at 52:47 GMT (EI+518 sec), prior to the water supply nozzle RTD at 52.55 GMT (EI+526 sec). The slope of the temperature curves seen by these sensors essentially doubles between times 52:32 GMT (EI+503 sec) and 52.52 GMT (EI+523 sec). These vent nozzle temperature rise rate increases equate to an additional heat transfer rate of approximately 0.038 BTU/sec (40 Watts). Note that the nozzle temperatures were recorded via downlink on the OI system, and that off-nominal measurements were bounded by communication dropouts. The data dropouts were two of several unexplained communication blackouts (as noted by the gaps in the downlink data) that occurred prior to LOS.

As has been mentioned, the responses from these forward fuselage sensors are unusual in that their readings return to their nominal trends after a short period of off-nominal response. However, it is noted that the RTD response of the waste water dump nozzle, V62T0519A, located seven inches below the supply nozzle, V62T0520A, showed no indication of off-nominal response during the entire entry. Lastly, there was a surface T/C, V07T9522A, located just aft of and above the vent nozzle group that showed nominal behavior for the entire entry except for a sharp decrease in the data over one cycle. These data along with the observed debris data have been co-plotted in Figure 5.2.1-14. As can be seen, no clear relationship can be observed between the debris events and response of the sensors that performed nominally. Although not shown, the response of the chin panel gauge does coincide with the estimated time of the wing spar breach (see Section 6 for further details).

5.2.1.4 Kirtland Photo

As the Orbiter was passing over the Albuquerque, New Mexico area, images of the Orbiter were obtained from the Kirtland AFB Starfire Optical Range. Figure 5.2.1-15 shows the principle image of the set. Although a thorough analysis of the images was made (see Image Analysis Team Report), no direct evidence of damage to the Orbiter could be discerned. However, damage to the Orbiter, especially the WLE, could be inferred from the anomalous bulges noted on the left wing. The principle source of light

from an Orbiter re-entering the Earth's atmosphere is high temperature gas immediately behind the shock layer. It was hypothesized that the bulges in the light emission could be a result of a deformed wing shock or additional embedded shocks due to a damaged wing configuration, or additional illumination due to particulates in the flow field emanating from the damage site. Based upon the results of the analyses and testing presented below, this potential explanation will be discussed further in the external environments applications section.

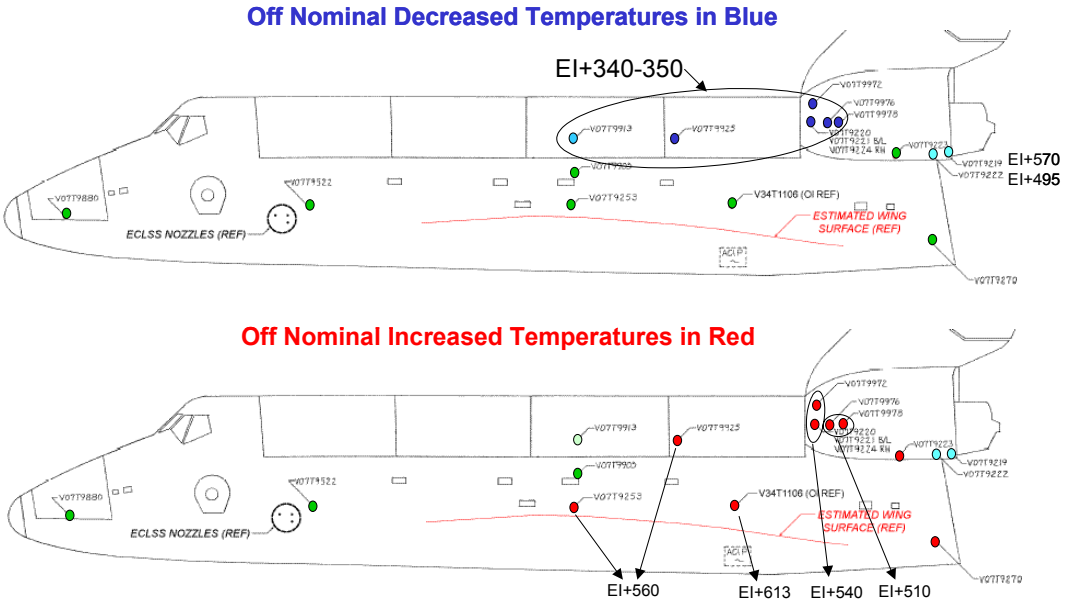

Figure 5.2.1-1 Left Side Fuselage and OMS Pod T/C locations. Times indicate when off nominal condition first observed.

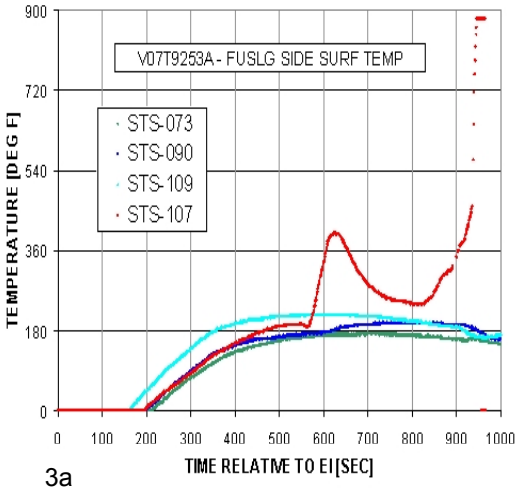

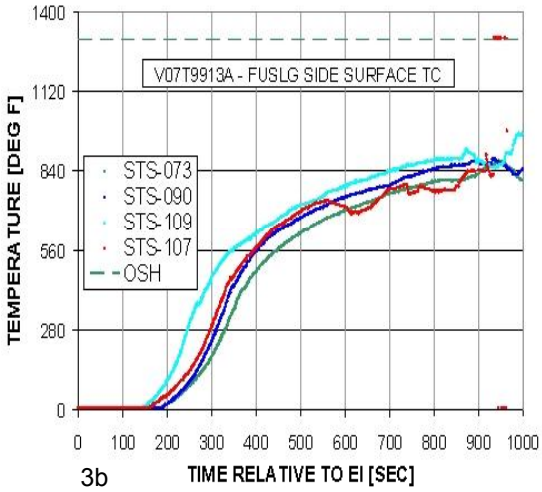

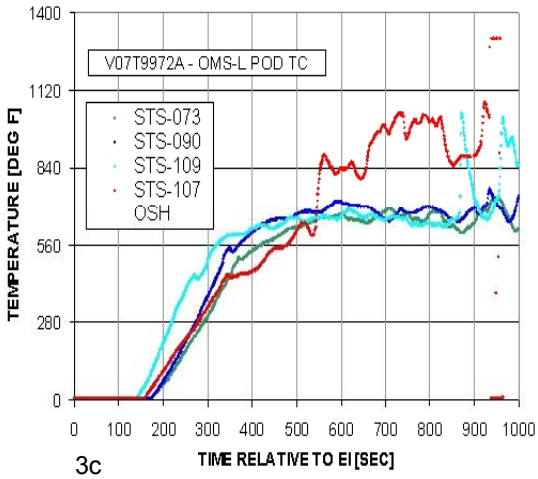

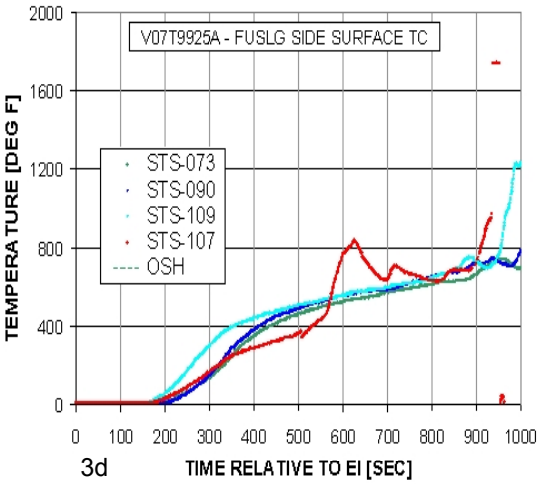

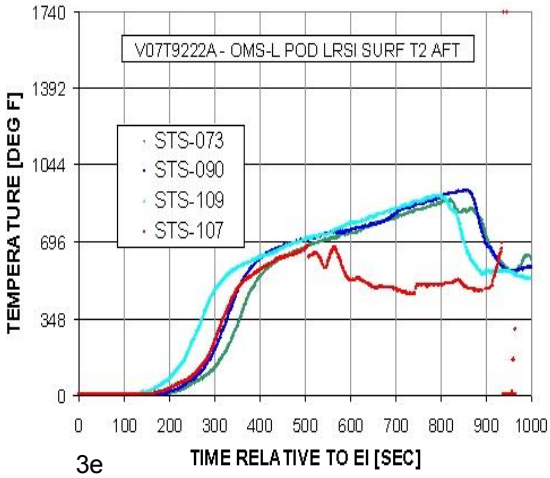

Figure 5.2.1-2a – 3e STS-107 Orbiter Side Fuselage and OMS Pod temperature comparisons with previous flights of Columbia.

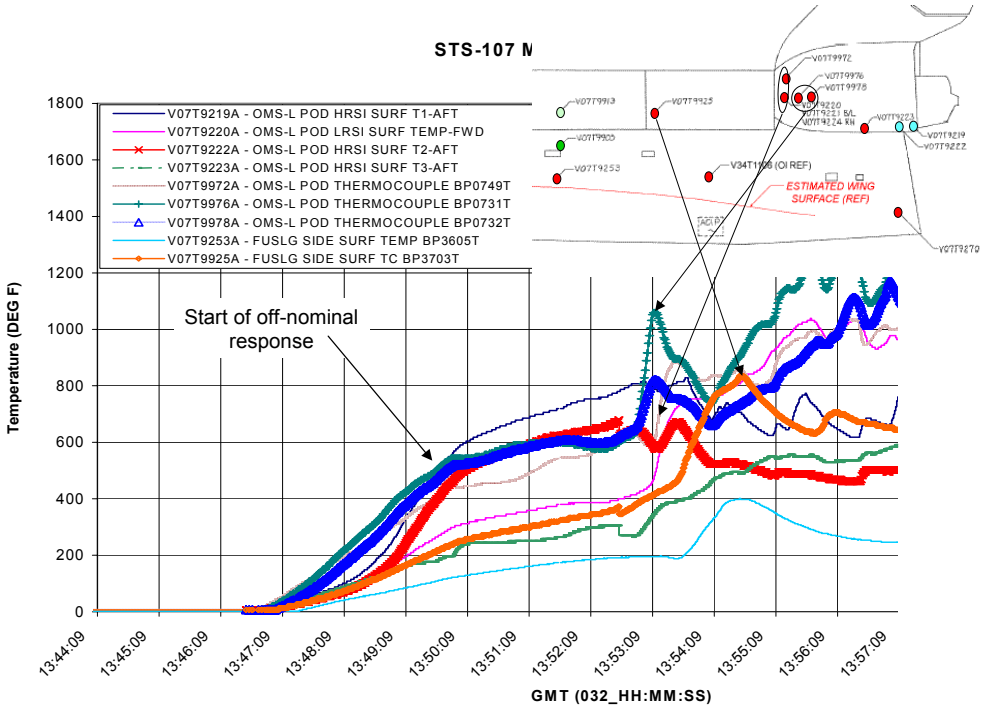

Figure 5.2.1-3 Left Side Fuselage and OMS Pod Off-Nominal Responses Indicate Aft to Forward Progression of Increased Heating

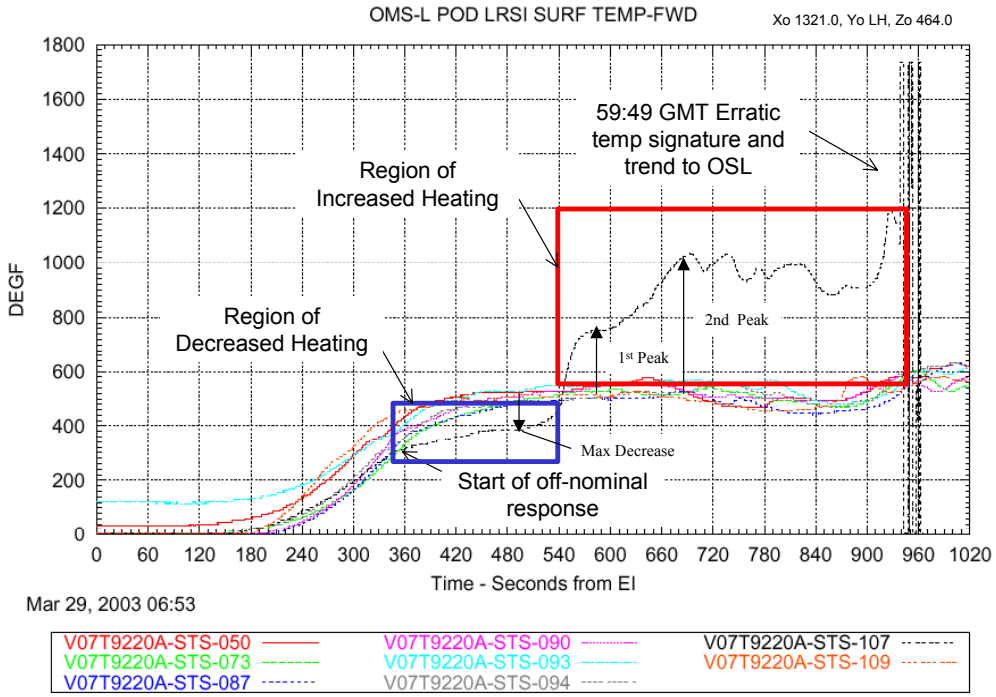

Figure 5.2.1-4 An example of Left OMS Pod temperature response that indicates at least two significant events during the period of increased heating

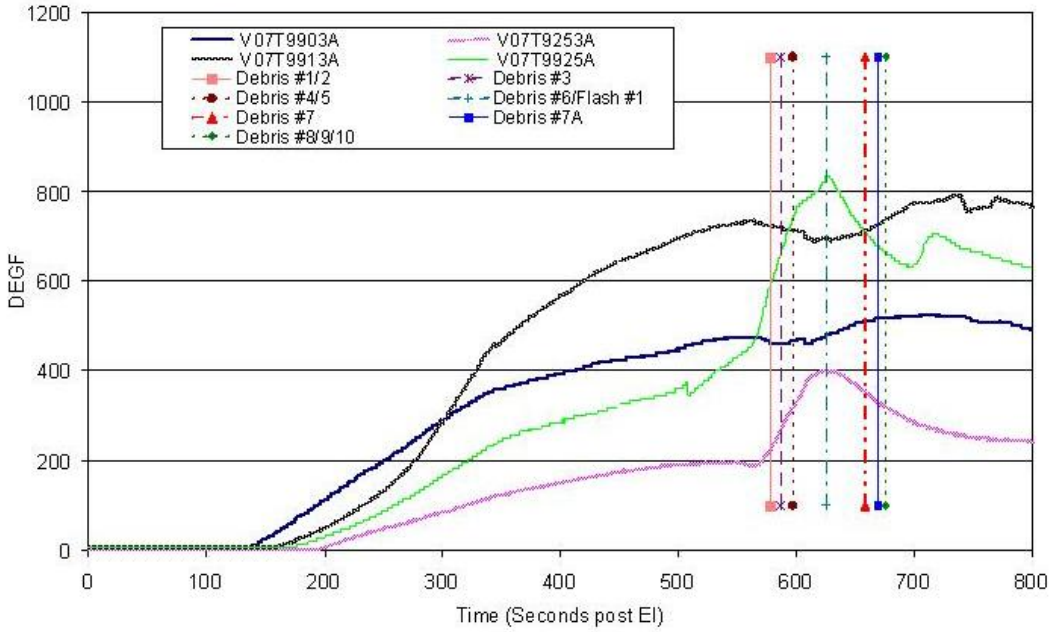

Figure 5.2.1-5 Mid Fuselage and Aft-Left Side Payload Bay Surface T/Cs response along with Debris Events 1 through 10

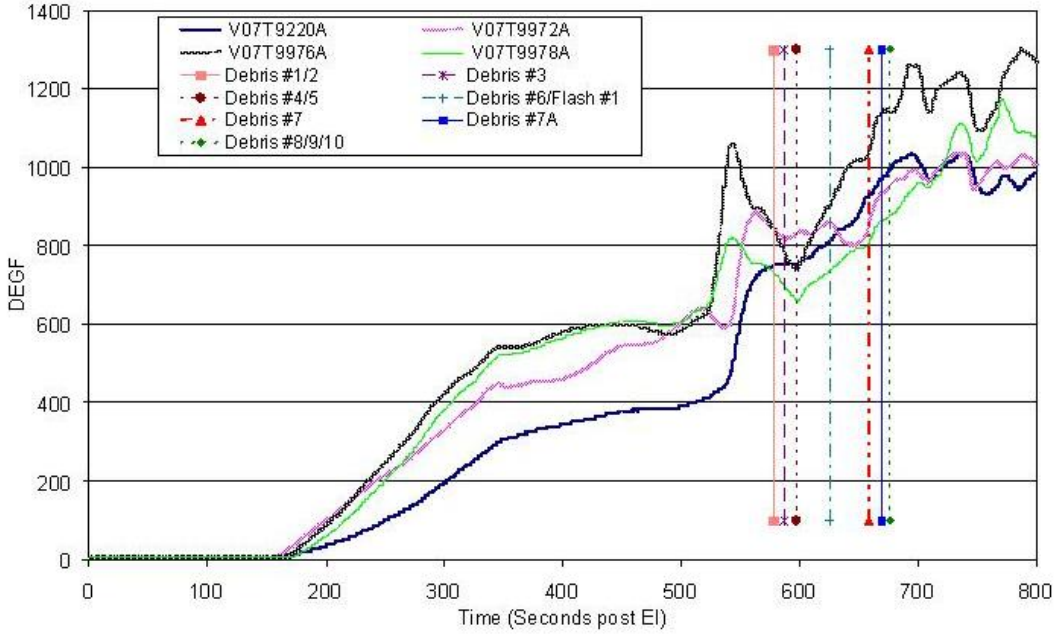

Figure 5.2.1-6 Forward Left OMS Pod Surface T/C responses along with Debris Events 1 through 10

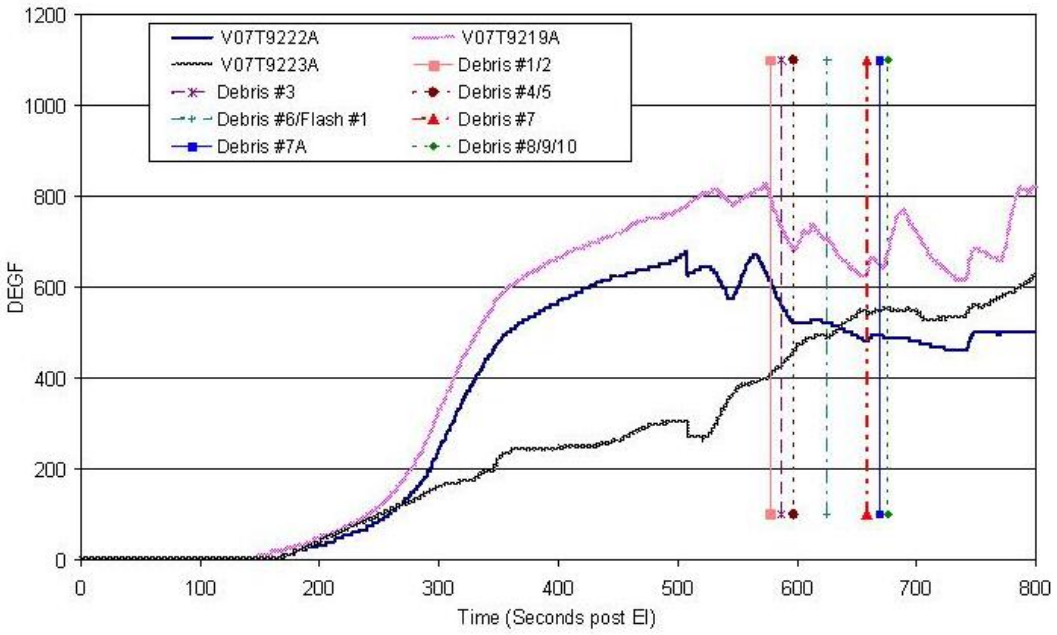

Figure 5.2.1-7 Mid and Aft Left OMS Pod Surface T/C responses along with Debris Events 1 through 10

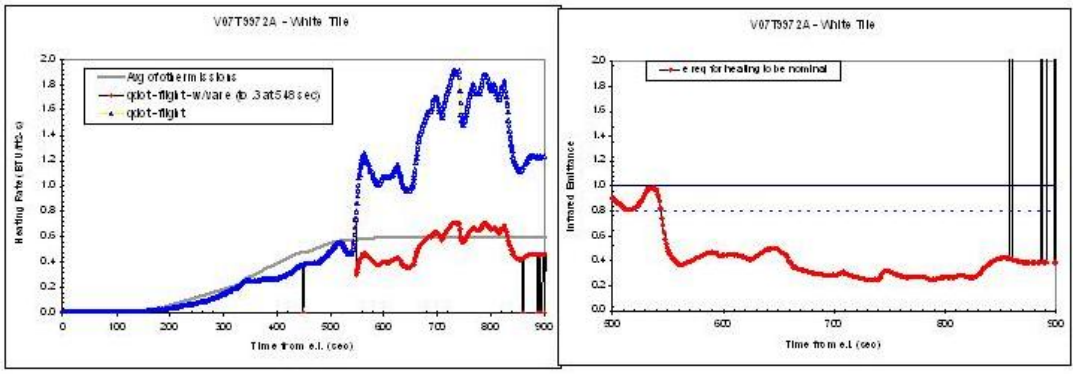

Figure 5.2.1-8 Emittance change needed to return inferred heating rates to previous flight average

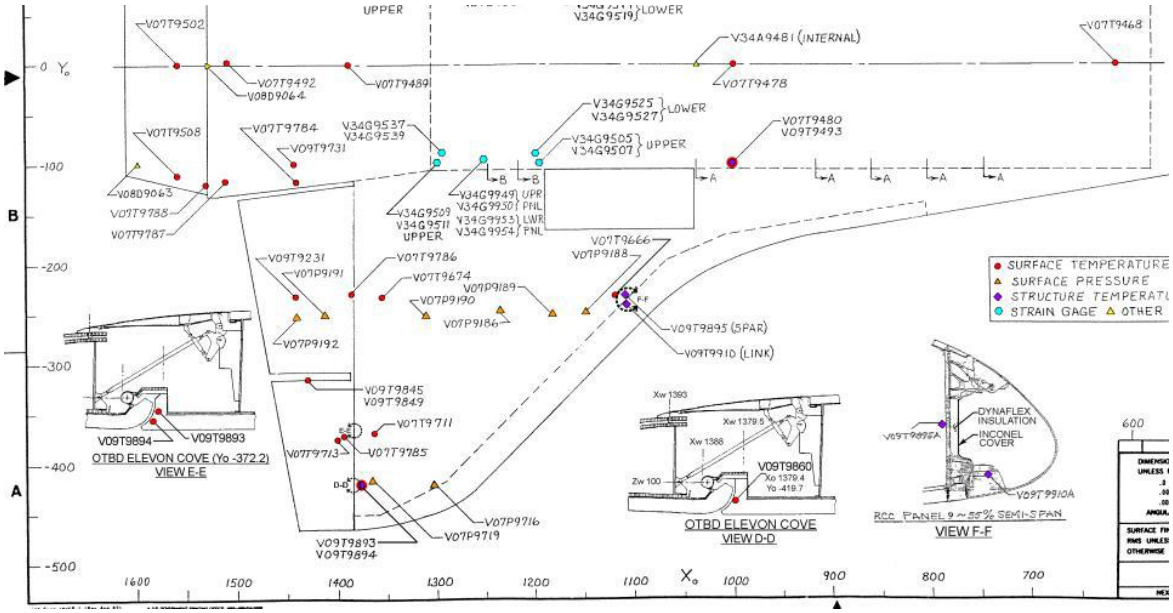

Figure 5.2.1-9 Lower Left Wing MADS instrumentation locations

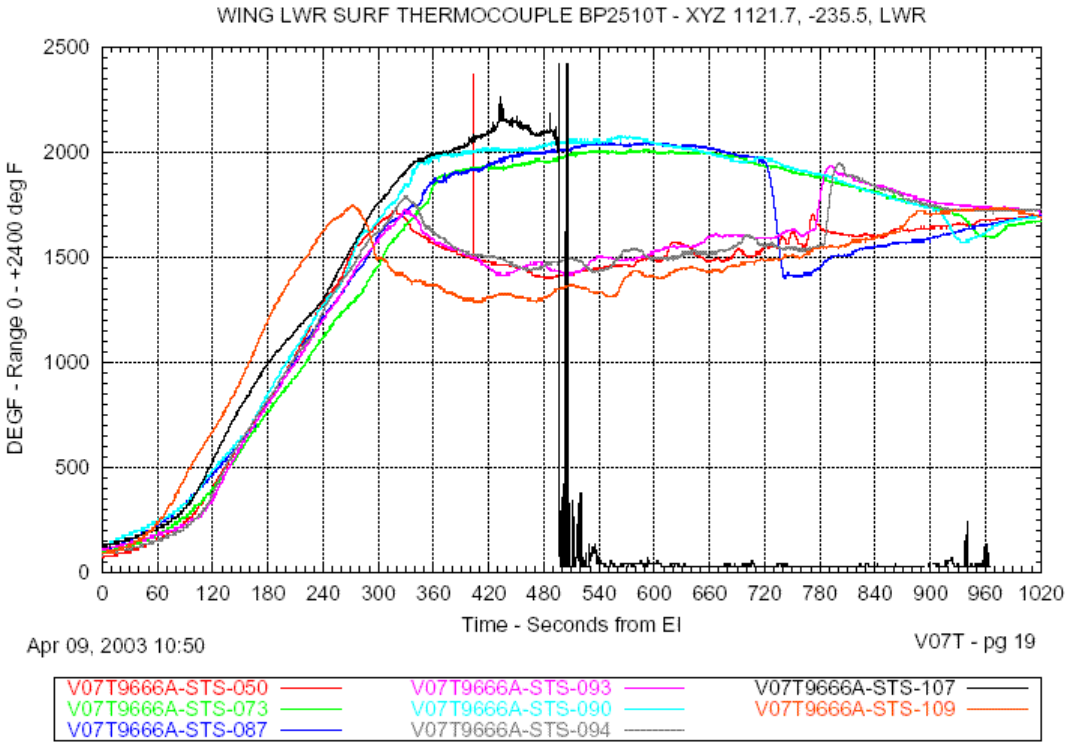

Figure 5.2.1-10 Temperature response of V07T9666A compared with previous flights of Columbia

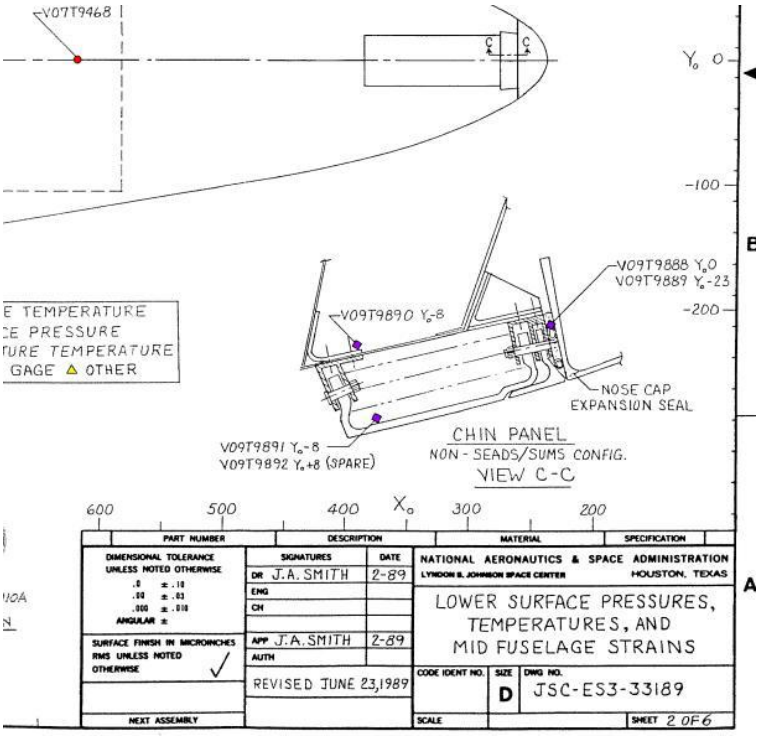

Figure 5.2.1-11 Nose Cap / Chin Panel Expansion Seal Instrument Locations

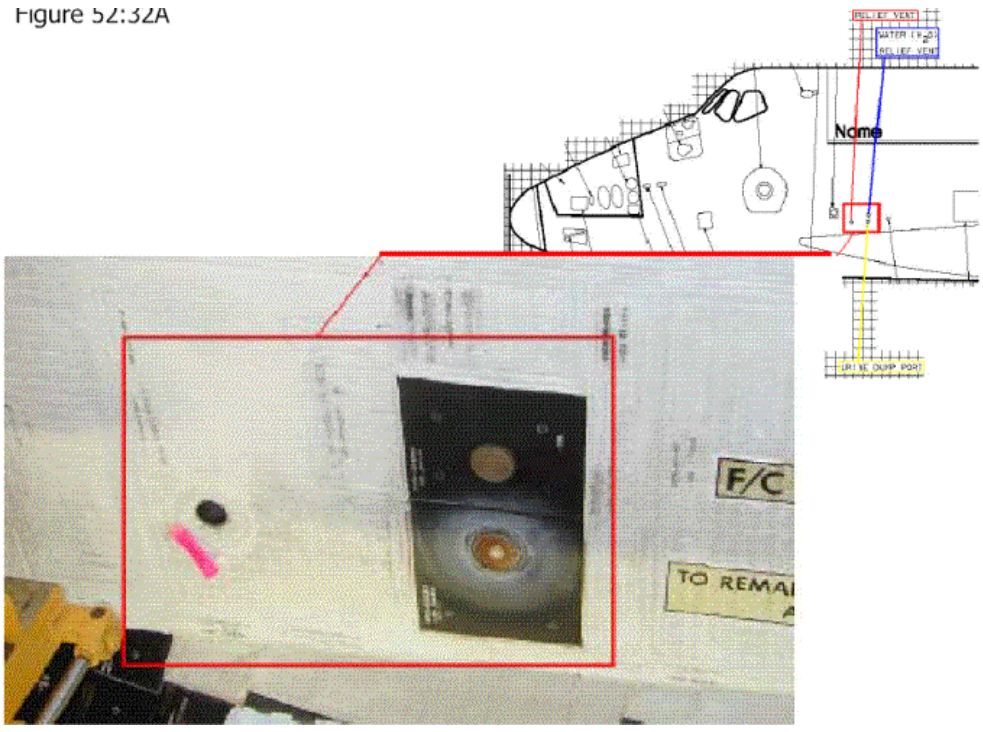

Figure 5.2.1-12 Vacuum Vent and Water Dump Nozzle Locations

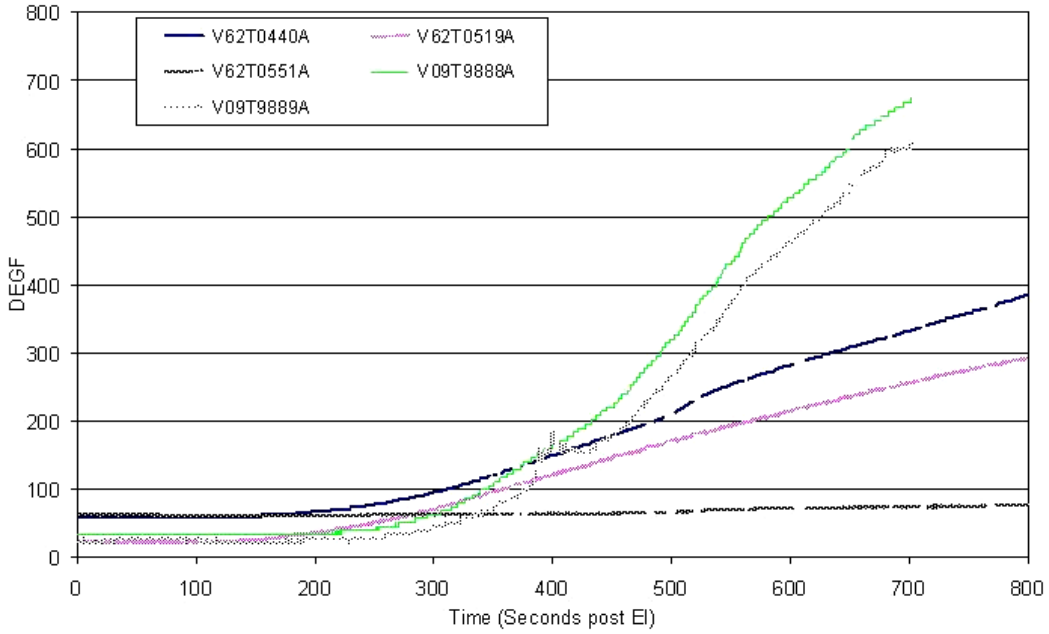

Figure 5.2.1-13 Chin Panel (V09T9880A and V09T9889A), Vacuum Vent (V62T0551A), Water Supply Dump Nozzle (V62T0440A), and Water Waste Dump Nozzle (V62T0519A)

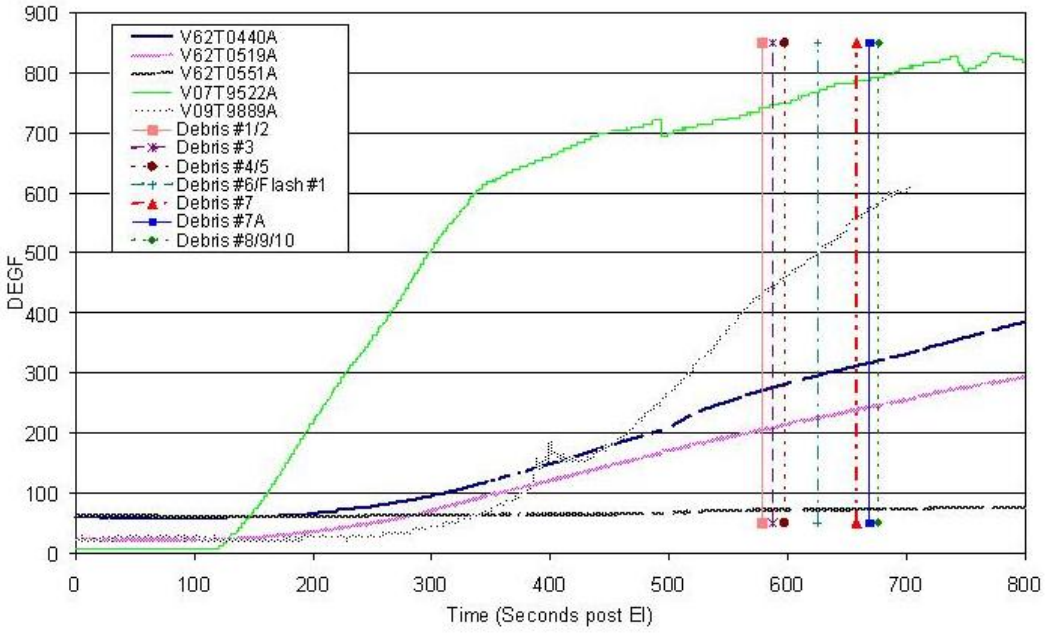

Figure 5.2.1-14 Chin Panel, Vent Nozzles, and local Surface T/C data plotted along with Debris Events 1 through 10.

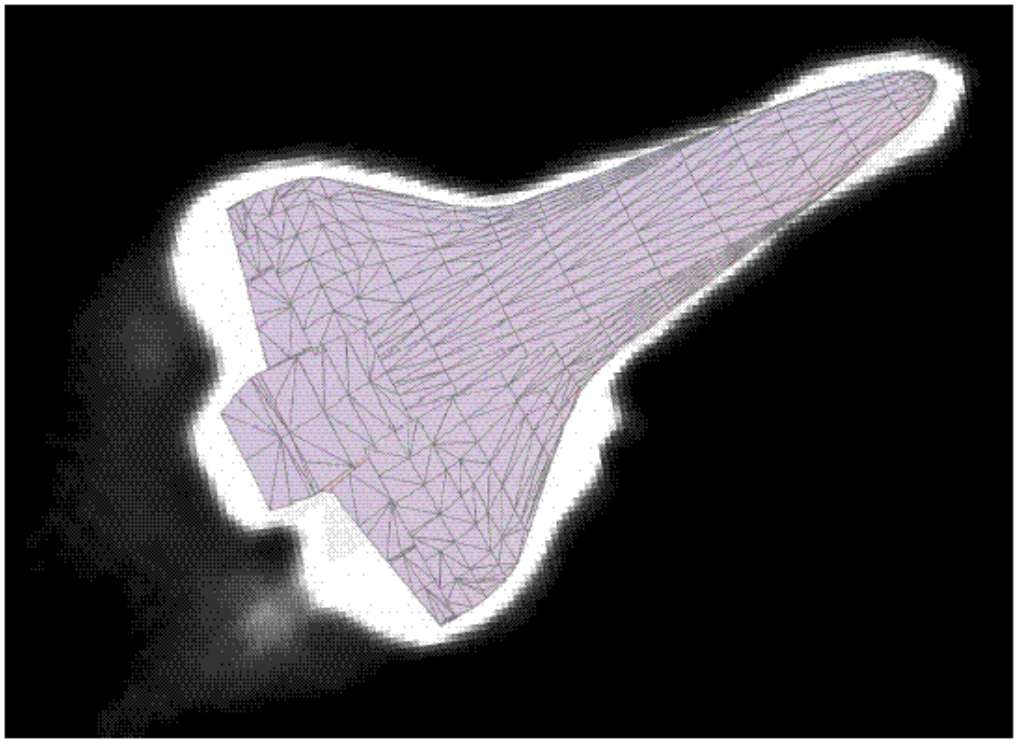

Figure 5.2.1-15 Kirtland AFB image taken at 13:57:14 GMT. Image has been enhanced and an Orbiter wire frame overlaid. View is of windward side of the Orbiter. Orbiter was in a left wing down roll attitude when this image was obtained.

5.2.2 Orbiter Certified Body Point Heating Methodology

5.2.2.1 Background on Body Point Heating Model Development

Entry aerodynamic heating of the Shuttle Orbiter is a result of the flow of air at high speed over the Orbiter. Friction between the air filaments as they stream over the orbiter surface, and compression near the stagnation regions of the nose and leading edges, convert kinetic energy of motion into heat. This heated gas environment envelops the Orbiter during its critical re-entry phase of flight.

Aerodynamic heating rates are influenced by all properties of the flow field as well as conditions at the body surface. In the external flow, the density, velocity, pressure, streamline pattern, and chemical composition must all be determined before heating calculations can be performed accurately.

The approach used for the development of Shuttle aerodynamic heating prediction methodology was to draw upon a vast knowledge available in the literature and combine it with Shuttle Orbiter wind tunnel data and Orbiter flight test data.

Use of wind tunnel data was strongly emphasized in the development of a heating prediction methodology. Where wind tunnel data were not available, analytical methods were used. It was the design philosophy (Figure 5.2.2-1) that, by proper use of wind tunnel data and analytical methods and by identifying and accounting for uncertainties in a logical manner, a minimum risk approach to the aerothermodynamic design of the Orbiter, without unnecessary conservatism, would be achieved. A nominal fairing/interpretation of wind tunnel data was used to develop the methodology. Verification of these methods was based on flow field solutions and data from developmental flight tests (OFT). A detailed description of the Orbiter entry heating prediction methods and database can be found in Rockwell International Document STS 83-0948 (1988).

5.2.2.2 Body Point Heating for Nose Cap, Wing Leading, Main Landing Gear Door

The basic approach for the Orbiter acreage is to break down the Orbiter into simple geometric shapes: sphere, cylinder, cones and wedges (Figure 5.2.2-2). These Simple Geometric Shapes (SGS) are correlated with wind tunnel data and adjusted to a nominal fit of the data. The SGS are then extrapolated to flight, while the adjustment factor is held constant. The adjustment factor accounts for Orbiter location, angle of attack, and Reynolds number variation. This approach works well for the Orbiter lower surfaces.

5.2.2.2.1 Fuselage Lower Surface (Nose Cap, Main Landing Gear Door)

The fuselage lower surface was divided into regions of both blunt body and slender body flows (Figure 5.2.2-3). The region of slender body flows was designated to be where the change in slope of the local velocity went to zero.

The bluntness of the Orbiter nose affects the downstream heating rate by altering the surface pressure distribution and by increasing the entropy of the flow at the boundary layer edge. For a cone, this bluntness causes the pressure to increase for a distance of one or two nose radii to a value greater than that for a sharp cone.

In the blunt body flow region, heat transfer film coefficients from wind tunnel data ratioed to reference sphere heat transfer values were applied to flight conditions adjusted by a slender body transfer factor. The reference sphere heating values were computed by the Fay & Riddell (1958) stagnation heating formulation with a variable Lewis number term. The heating distribution around the orbiter stagnation point at a 40° angle of attack is shown in Figure 5.2.2-4.

At the stagnation point in the sonic flow zone, the slender body adjustment factors have a value of 1.0 and increase to the slender body value of 1.6 at X/L = 0.208 for alpha equal to 30°. For angle of attack greater than 30°, the slender body interaction zone is held constant at X/L = 0.20, although the adjustment factor is allowed to vary (Figure 5.2.2-5).

The slender body adjustment factors were determined by ratioing laminar flat plate theory values at flight to those at wind tunnel conditions. This resulted in the blunt to slender body transfer distribution of Figure 5.2.2-6.

The blunt body flow region is characterized by high pressure gradients, which, in the axial direction can be approximated by a Newtonian-Prandtl Meyer expansion (Figure 5.2.2-7), while the heat transfer can be approximated for wind tunnel conditions with a Cohen and Beckwith (1961) similar solution (Figure 5.2.2-8).

In the slender body region, a system was developed to modify Eckert's flat plate theory for streamline divergence by a series of factors as shown in Figure 5.2.2-9. Streamline patterns were obtained from oil flow data. To do this, wind tunnel data were compared with SGS using a nominal fit of the data, and laminar factors (LAMFACs) were developed. These laminar factors were allowed to vary with angle of attack. The LAMFACs were correlated with two angles of attack (α_{REF}) selected as reference conditions (1,2). Slopes of the LAMFAC (designated: Q_{SLOPE}) were developed about these two alphas, and reference laminar factors were established. This resulted in an angle of attack variation in equation form:

$$ALFAC = 1 + \frac{(\alpha - \alpha_{REF}) * Q_{SLOPE}}{LAMFAC_{REF}}$$

The SGS was adjusted by the product of ALFAC *$LAMFAC_{REF}$ to account for divergence. The assumption was made that both ALFAC and LAMFAC developed in the wind tunnel at $\gamma = 1.4$ and basically Mach 8 had the same variations and magnitude under flight conditions. An example of the variation in LAMFAC with angle of attack can be found in Figure 5.2.2-10 through Figure 5.2.2-12 for the lower surface body point 1600. Figure 5.2.2-11 shows the variation of wind tunnel test data and flat plate theory with angle of attack. When this information was converted to LAMFAC, the distribution in Figure 5.2.2-12 was obtained.

The origin of the flow used in the flat plate calculation was assumed to be at X/L = 0. When applied to points aft of X/L = 0.2, the small variation in angle of attack on stagnation point movement would be negligible in the wetted flow length. Forward of X/L = 0.2 (blunt body) the flow length did not fit directly into heating methodologies (heating ratios), although it is still of importance to boundary layer transition calculations.

Spalding and Chi (1964) turbulent flat plate values were adjusted using turbulent factors which were developed along similar patterns to the laminar factors. Turbulent factors also vary with angle of attack and body location and correlate similarly to the laminar factor equation.

Laminar factors were generally based on wind tunnel data from test OH39, OH49B and OH50B having model scales of 0.0175 and 0.04.

The existence of chemical non-equilibrium in the shock layer during much of the Orbiter's entry trajectory, coupled with the relatively non-catalytic behavior of the TPS materials, necessitate an additional correction to laminar equilibrium heating values on the nose cap and lower surface. This adjustment is in the form of a catalytic heating parameter (η) inferred from flight data:

$$(q_{wall})_{catalytic} = h_{eq}(i_r - i_w - \eta i_d)$$

where h_{eq} is the equilibrium heat transfer coefficient, i_r is recovery enthalpy, i_w is the wall enthalpy and i_d is dissociation enthalpy. Here, $\eta = 0$ implies equilibrium heating and $\eta = 1$ is equivalent to non-catalytic wall heating.

The catalytic resistance coefficient, η, is developed from a recombination rate constant dependent on surface recombination efficiency and gas properties at the surface. Thermocouple data from STS-2, STS-3 and STS-5 were used to determine the numerical form of the temperature dependent recombination

efficiency. Detailed discussion of the non-catalytic heating approach and correlation technique is presented in Miller (1984).

5.2.2.2.2 Wing Leading Edge Heating Methodology

In the philosophy of simple geometric theories, the wing leading edge would be thought of as a swept cylinder. However, there are several features that move this approach to only a starting solution for the problem. First, an airfoil attached to the leading edge affects the shock shape and thereby affects the effective radius of the cylinder. Second, the intersection of the bow shock with the leading edge shock (Figure 5.2.2-13) produces several features as discussed in various sources. The shuttle wing leading edge shock region was interpreted to experience a type V interference pattern (Figure 5.2.2-14). This type of shock interaction results in a new shock that strikes the leading edge at about 55% semi-span (dependent on angle of attack) and disturbs the wing lower surface. Also formed is a jet shear layer that strikes the outboard section of the wing, scrubbing both the upper and lower surfaces.

Based on wind tunnel data from wind tunnel test OH66, the effective radius variation with angle of attack was developed (Figure 5.2.2-15). By using this curve along with the modified swept cylinder equation, the effect of shock impingement can be determined (Figure 5.2.2-16). This figure represents the effect of shock impingement at 55% semi-span. Therefore, as the shock position moves with angle of attack, the maximum heating footprint moves leading to a maximum heating at the 55% semi-span between 35 and 40 degrees angle of attack. At the other angles of attack, maximum heating would occur at a different span-wise location.

Wind tunnel data applied directly to flight were used. Data were applied in terms of film coefficients (local to reference sphere ratio) as a function of angle of attack and leading edge location. For span locations where no data existed, the modified swept cylinder was used.

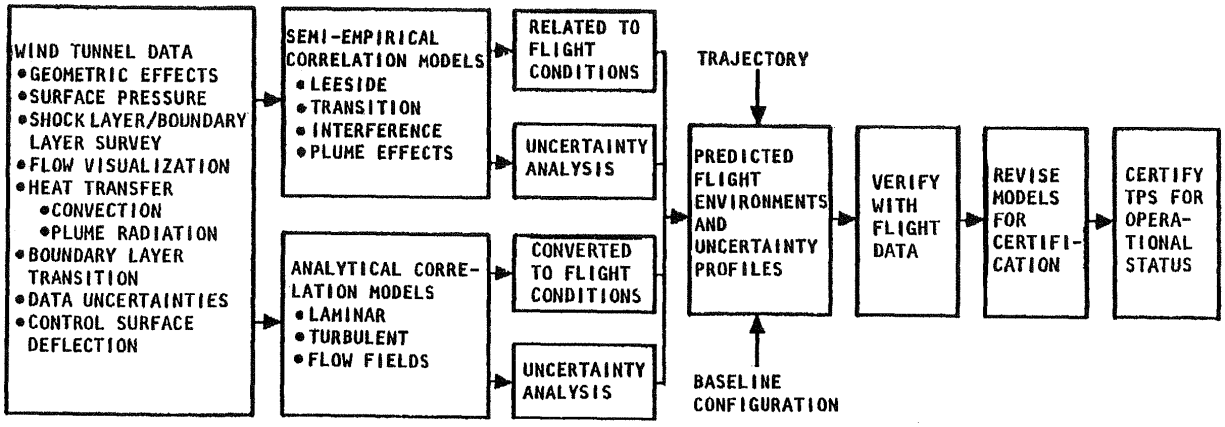

Figure 5.2.2-1 Orbiter Entry Heating Design and Certification Logic

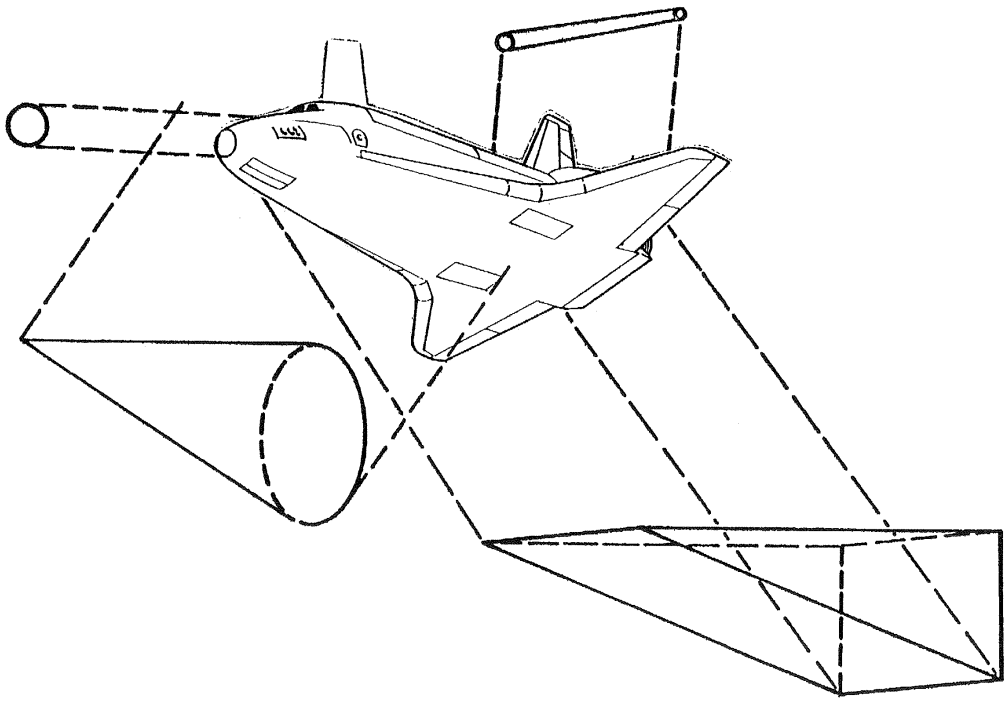

Figure 5.2.2-2 Simple Geometric Modeling (SGS)

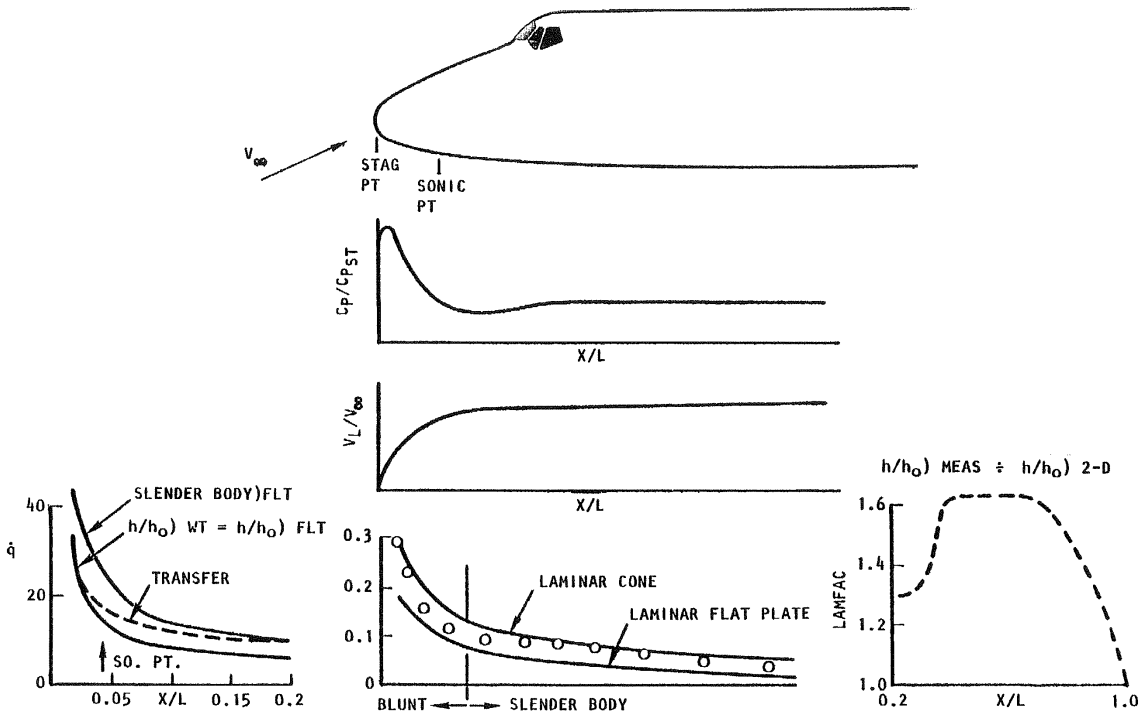

Figure 5.2.2-3 Fuselage Lower Surface Heating Extrapolation to Flight

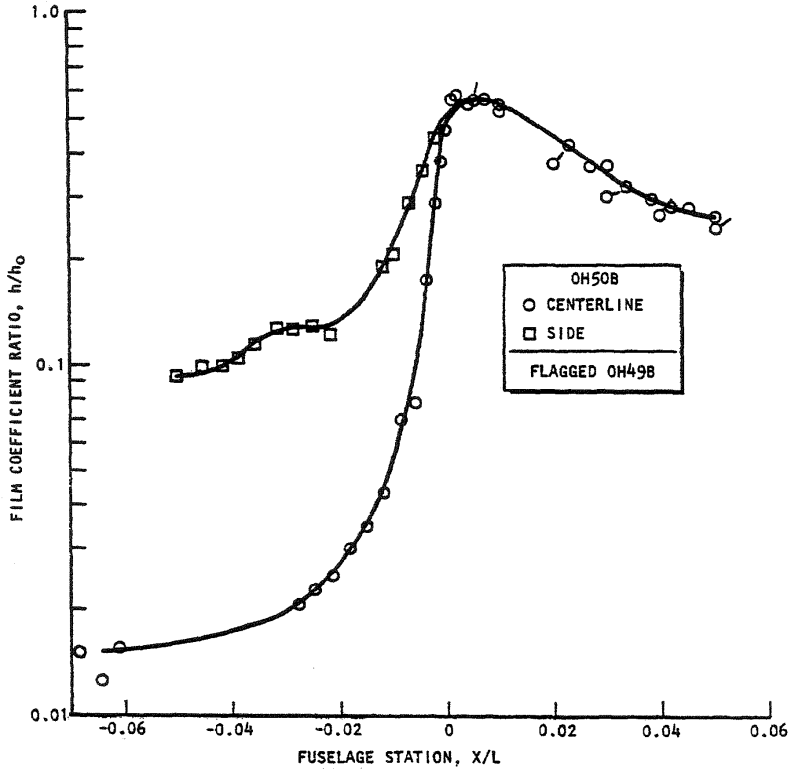

Figure 5.2.2-4 Heating Distribution Around the Orbiter Stagnation Point at Alpha = 40°

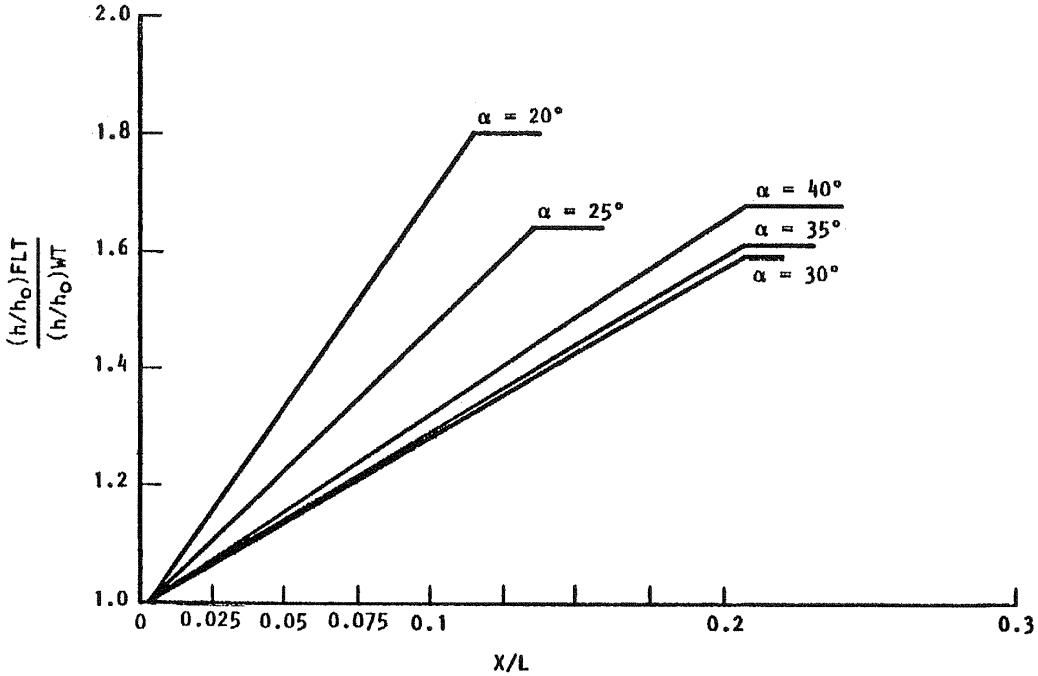

Figure 5.2.2-5 Wind Tunnel to Flight Scaling

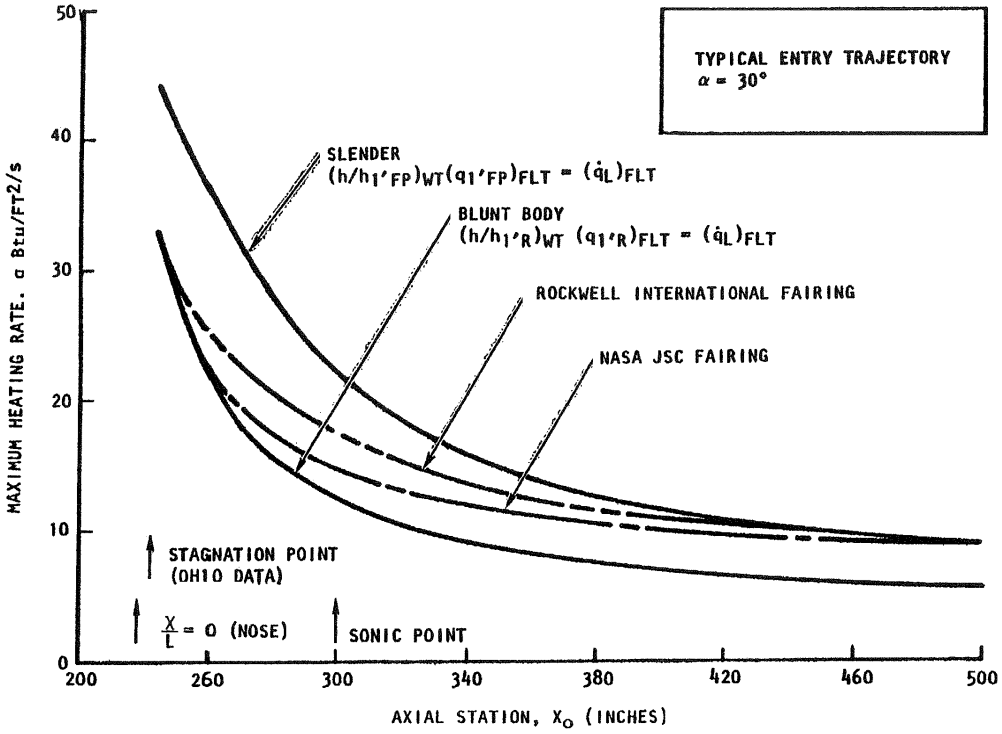

Figure 5.2.2-6 Blunt-Body-to-Slender Body Transfer Determination

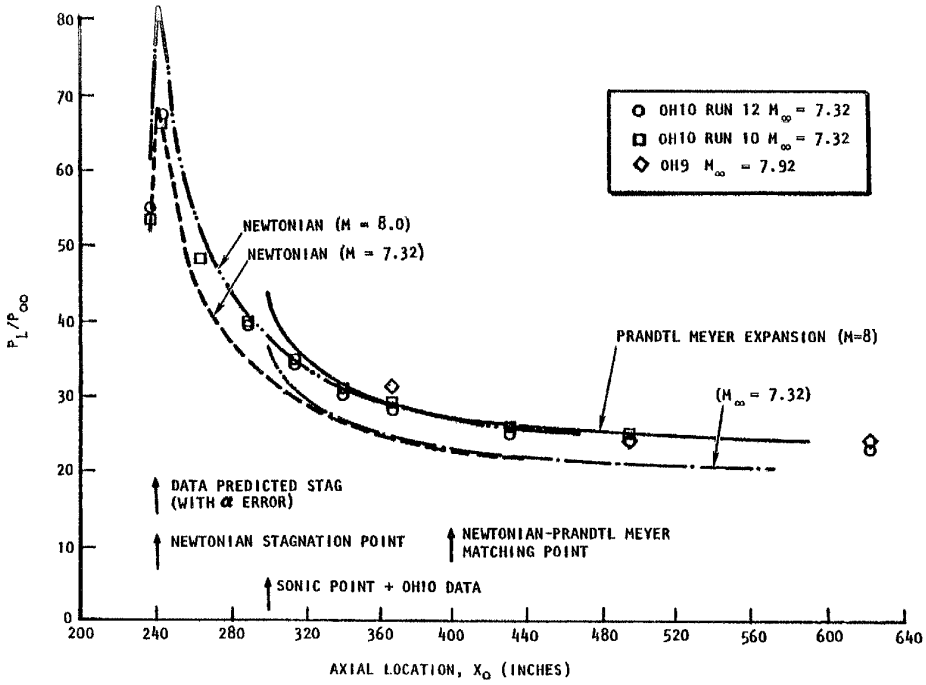

Figure 5.2.2-7 Forebody Pressure Modeling Under Wind Tunnel Conditions (Alpha = 30°)

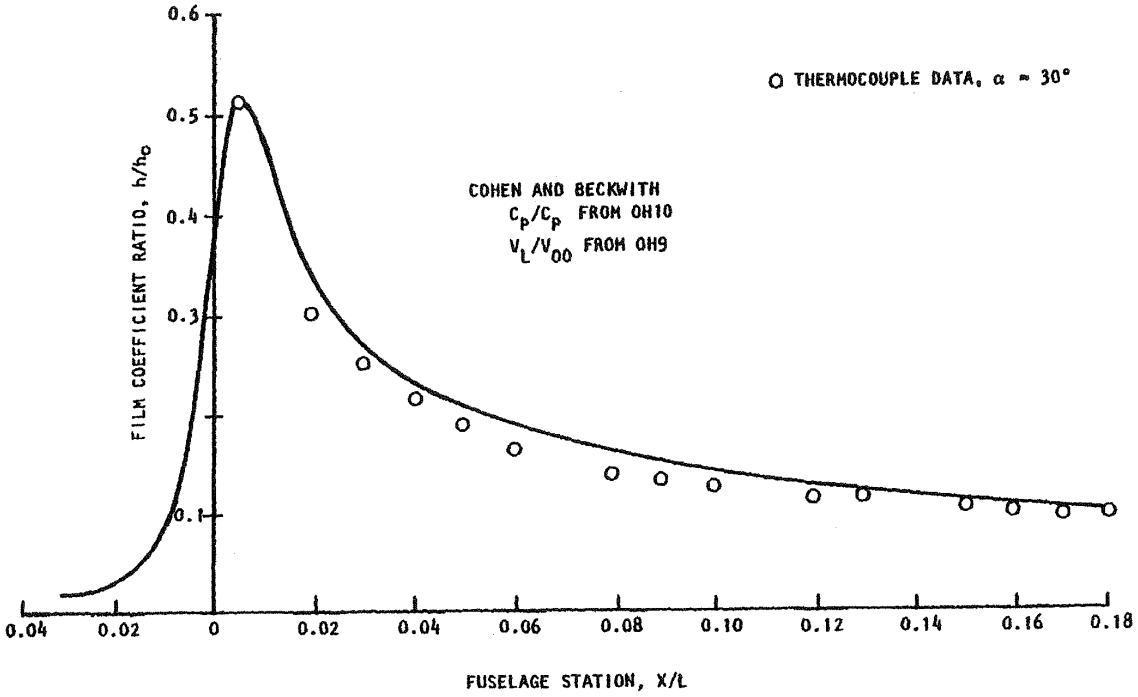

Figure 5.2.2-8 Cohen and Beckwith Modeling of Fuselage Forebody

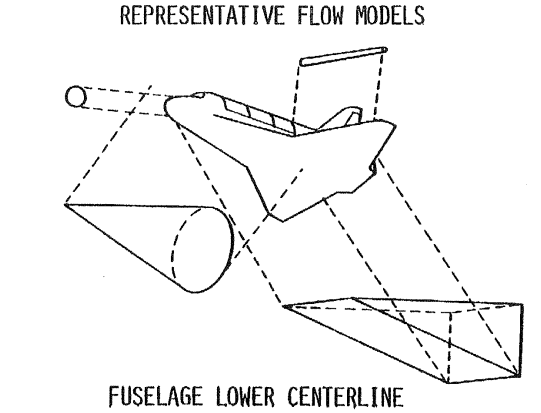

LAMINAR FLAT PLATE – ECKERT H*

$$h^*_{FP)} = \frac{0.332\,(\rho^*\mu^*)^{\frac{1}{2}}(V_L)^{\frac{1}{2}}(32.16)}{(X)^{\frac{1}{2}}(P_R)^{\frac{2}{3}}}$$

$h_{FP)}$ WIND TUNNEL : INPUT PERFECT GAS PROPERTIES

$h_{FP)}$ FLIGHT : INPUT FLIGHT PROPERTIES

$\therefore h)_{FLT} = h_{FP)_{FLT}} \cdot$ (LAMINAR FACTOR)

$\frac{X}{L}$	LAMINAR FACTOR α = 40 DEG
0.2	1.71
0.3	1.86
0.4	1.95
0.5	1.88
0.6	1.82
0.7	1.81
0.8	1.93
0.9	1.83
1.0	1.31

Figure 5.2.2-9 Orbiter Lower Surface Methodology, Slender Body Approach

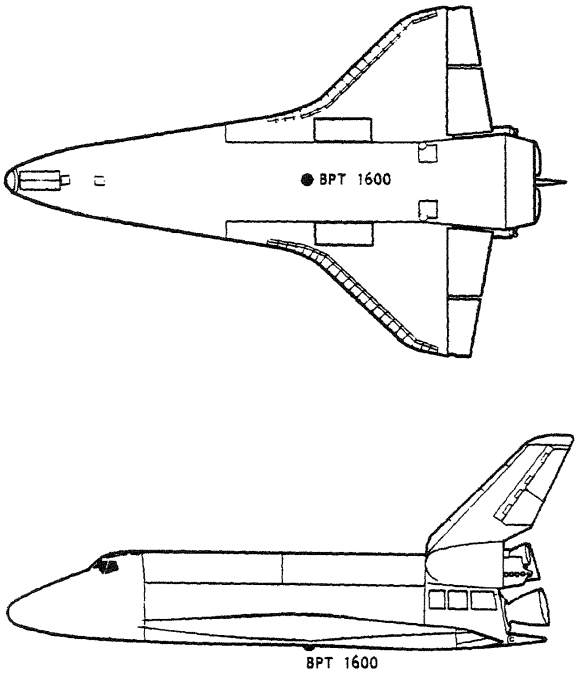

Figure 5.2.2-10 Typical Lower Surface Location

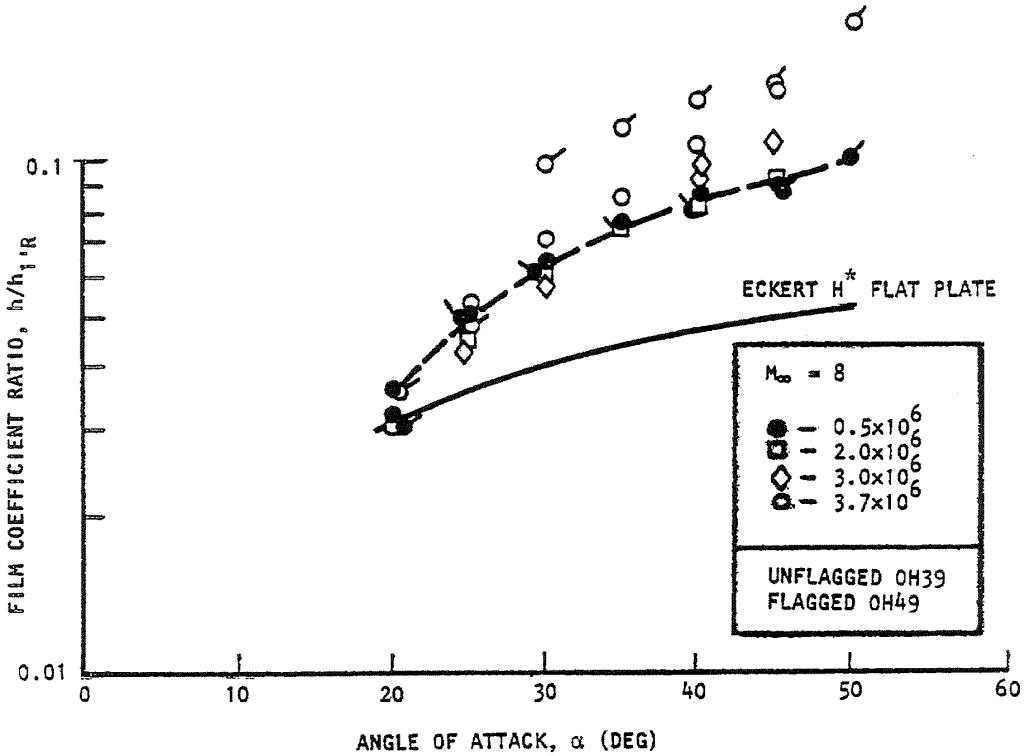

Figure 5.2.2-11 Local Heating Variation With Angle of Attack on Fuselage Lower Surface Centerline at X/L = 0.6

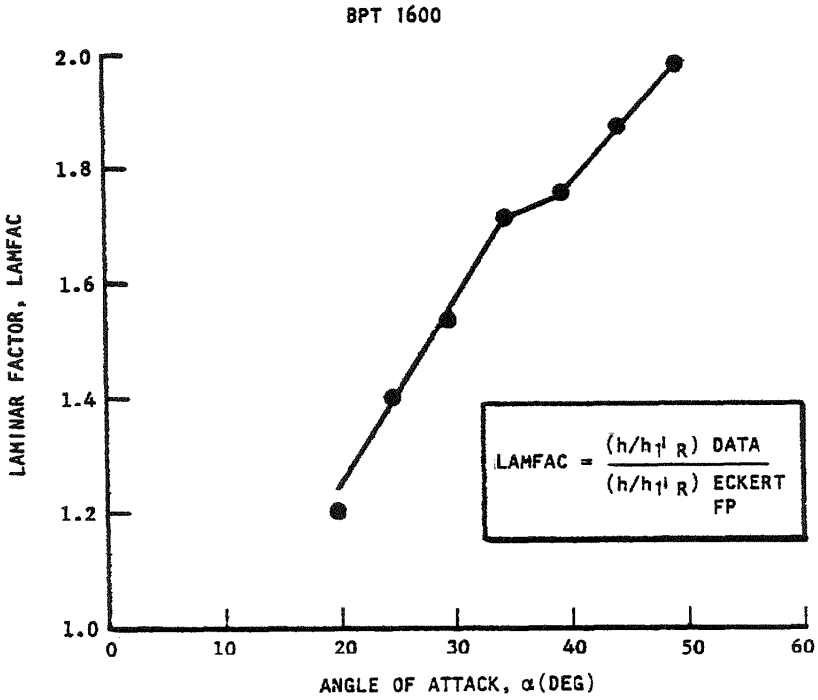

Figure 5.2.2-12 Fuselage Lower Surface Centerline Laminar Factor Laminar Variation With Angle of Attack

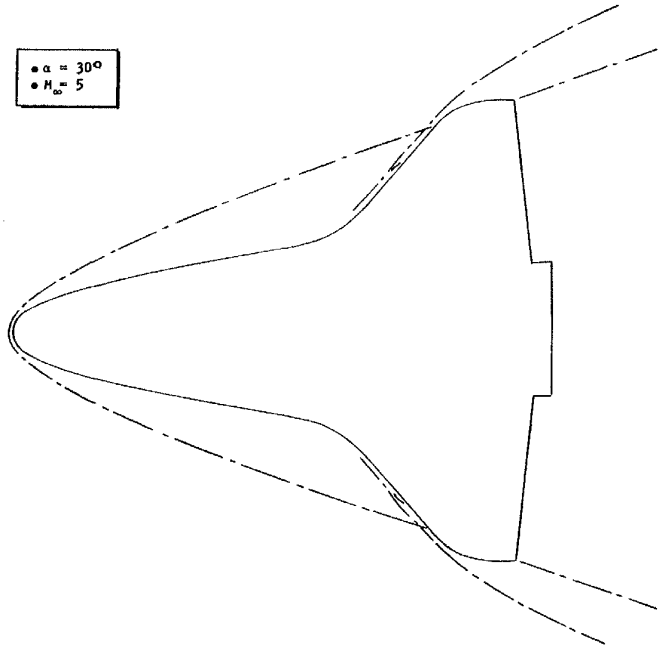

Figure 5.2.2-13 Shock Patterns Based on Wind Tunnel Shadowgraph

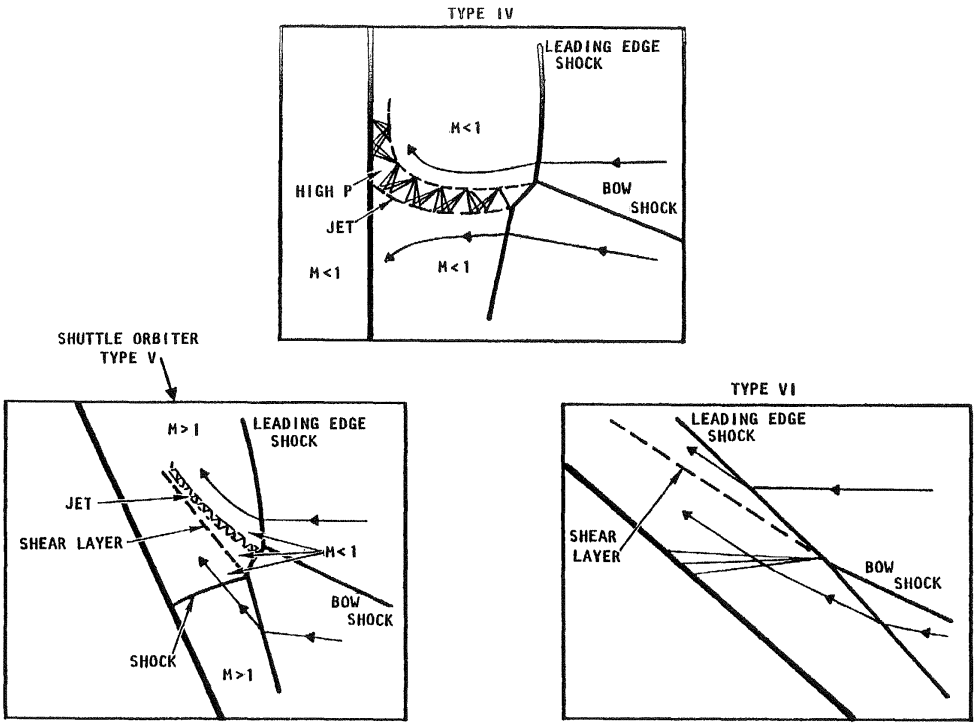

Figure 5.2.2-14 Variation in Shock Impingement Patterns

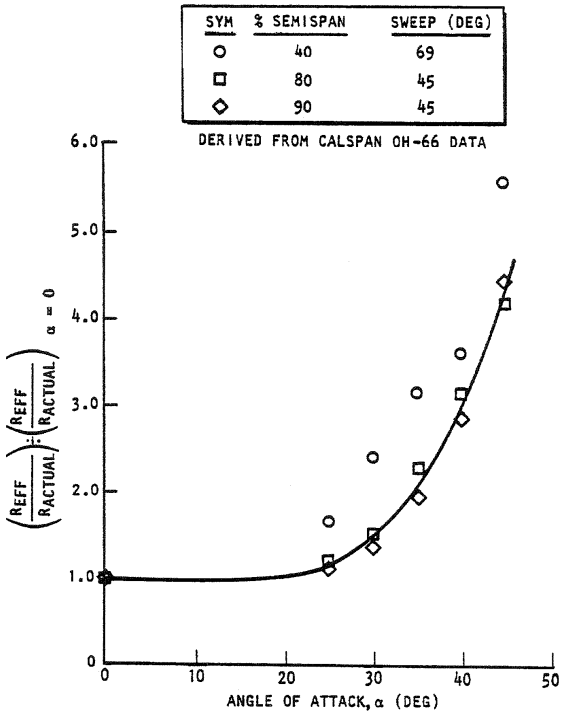

Figure 5.2.2-15 Angle of Attack Effect on Leading Edge Effective Radius

$$\text{SHOCK EFFECT} = \left(\frac{R_{EFF}}{R_{ACTUAL}}\right)_{\text{FIGURE 1-107}} \div \left(\frac{R_{EFF}}{R_{ACTUAL}}\right)_{\text{55\% SEMISPAN}}$$

DERIVED FROM CALSPAN OH-66 DATA

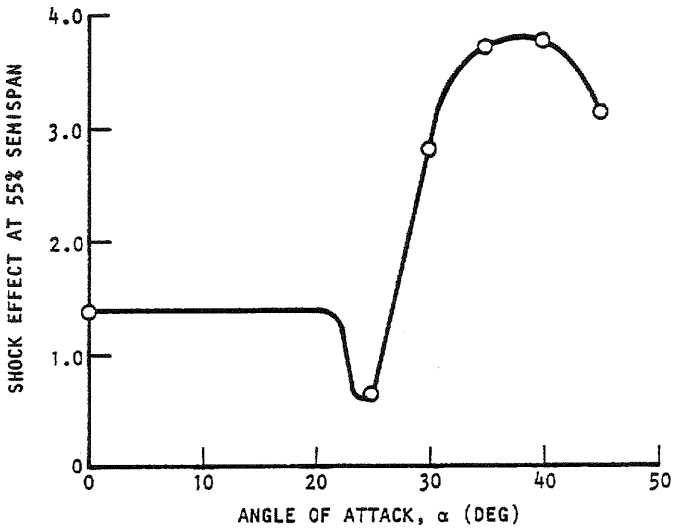

Figure 5.2.2-16 Angle of Attack Effect on Shock Impingement Effects

5.2.3 Wind Tunnel Testing

The purpose of this section is to describe the hypersonic aerothermodynamic wind-tunnel program conducted at the NASA Langley Research Center in support of the STS-107 accident investigation. The primary objective of the testing was to provide information regarding surface heating characteristics on scaled Orbiter models with surface perturbations to simulate various forms of localized damage to the thermal protection system (TPS). With very limited flight information available during the first weeks after the loss of STS 107, initial experimental testing covered a broad spectrum of TPS damage. As the investigation developed, increasing emphasis was placed on obtaining test data consistent with the subsequent body of recovered debris and extracted Orbiter OEX flight recorder data. Presentation of all heating test data associated with TPS damage, particularly that associated with early scenarios, has not been attempted in this section; emphasis has instead been placed on the data relevant to the working scenario involving damage to RCC panels 5-9.

Presently, the NASA has three active hypersonic wind tunnels (collectively referred to as the Langley Aerothermodynamics Laboratory) in the NASA LaRC inventory of ground-based facilities for hypersonic aerodynamic and aero-heating testing. Two facilities, the NASA LaRC 20–Inch Mach 6 Air and the 20–Inch Mach 6 CF_4 Tunnels, were utilized to characterize both heating and aerodynamic effects associated with damage scenarios. The high run productivity of the Mach 6 air tunnel was essential for assessments of damage scenarios involving large numbers of geometric parametrics. This initial screening capability was ideal for establishing test priorities and optimizing use of the more appropriate Mach 6 CF_4 tunnel. In addition, the wind tunnel results helped to focus application of higher fidelity CFD tools for damage simulations at flight conditions. Testing was not pursued in other facilities because appropriate testing techniques to perform rapid simultaneous aerodynamic and global aero-heating measurements on the Orbiter configuration were not available. Other NASA high enthalpy facilities or shock tunnels outside of NASA, while capable of generating high velocity/enthalpy conditions, were not amenable to the quick, parametric screening necessary for an investigation of this scope. The characterization of leeward flow fields in shock tunnels would also present challenges due to extremely short run times.

Documentation of global surface heat transfer, complimentary surface streamline patterns, and shock shapes are provided in this section for various simulated damage scenarios. Test parametrics include angles of attack from 38 to 42 deg, sideslip angles of $\pm$1 deg, unit Reynolds numbers from 0.05×10^6 to 6.5×10^6/ft, and normal shock density ratios of 5 (Mach 6 air) and 12 (Mach 6 CF_4). The model scale utilized in these studies was 0.0075 (approximately 10 inches).

5.2.3.1 Mach 6 Air and Mach 6 CF_4 Applicability Flight

Aeroheating events leading to the loss of Columbia occurred during hypervelocity entry at low Reynolds numbers and high Mach number (25 to 18) and enthalpy levels. This complex flight environment is characterized by the excitation of energy modes in the gas as it passes through the bow shock wave of the Orbiter. At high enthalpy conditions, high temperature effects result in dissociation, recombination, and ionization of the air, and these in turn dictate changes in the shock layer flow. An effect with large impacts on the flow field is the reduction of the ratio of specific heats (herein referred to as γ) relative to a non-reacting perfect gas. In hypervelocity flight, decreases in γ within the windward and leeward Orbiter flow field result in increases in the density ratio across shock waves. The change in density ratio produces differences in shock layer structure including shock inclination and standoff distances and hence, shock interaction locations. Larger degrees of flow compression and expansion can exist relative to a non-reacting gas and these changes have been shown to directly influence Orbiter aerodynamics. While it is recognized that a nominal Orbiter entry environment cannot be duplicated in any one ground-based facility, aeroheating effects due to localized damage are first and foremost the result of flow physics or fluid dynamic phenomena (e.g., boundary layer/shear layer transition, shock-shock and shock-boundary layer interaction, flow separation-reattachment) associated with a given vehicle geometry, attitude, and flight condition. High temperature chemistry effects at high flow enthalpy levels "alter" the aerodynamic or aeroheating characteristics due to flow physics, but do not add new flow physics phenomena or delete any.

Testing in the perfect gas environment of a Mach 6 air tunnel captures all pertinent flow physics phenomena but does not provide information as to how the results may be influenced by flow chemistry. To address the effects of flow chemistry, the experimental test program was designed to take advantage of the simulation capability of the 20–Inch Mach 6 CF_4 Tunnel. Orbiter damage scenarios were first screened in the Mach 6 air tunnel for aerodynamic and aerothermodynamic consistency; the most promising were then tested in the CF_4 tunnel. This conventional-type (as opposed to impulse-type) low enthalpy hypersonic tunnel has relatively long run times and avoids complex chemistry typically associated with high enthalpy facilities. Modeling of the effects of flow chemistry that occur at the actual flight conditions is accomplished by using a heavier-than-air test gas that exhibits a low ratio of specific heats and a correspondingly high normal shock density ratio characteristic of air at reacting hypersonic conditions. In conjunction with the Mach 6 air tunnel, this CF_4 tunnel provides the capability to test at the same free-stream Mach and Reynolds numbers, but at two values of density ratio (approximately 5 in air and 12 in CF_4). The Mach 6 CF_4 density ratio of 12 is relatively close to the values of 15-18 encountered near Orbiter re-entry peak. Thus, generating large density ratio values simulates many of the aerodynamic and aeroheating effects associated with a high temperature gas. Synergistic tests of the Orbiter in these facilities led Miller (1982) to conclude that the effects of density ratio on the non-dimensional windward surface heating at hypersonic entry angles of attack were small.

Prior to the application of CFD with complex reacting chemistry air, perfect-gas engineering codes were used quite successfully to predict aerodynamic/aero-heating characteristics at hypervelocity conditions where the effects of flow chemistry were significant. This was accomplished via modifications to the perfect gas equations by the introduction of an effective gamma to "account" for high temperature effects. The effective gamma (herein referred as γ_{eff}) was based on the normal-shock density ratio value and the free-stream Mach number (for Mach numbers > 10) at re-entry conditions. Thus, one method to bridge between perfect air and heavy gas hypersonic wind tunnels and flight is through the use of an effective gamma. Brauckmann (1995) used gamma defined as local enthalpy divided by internal energy to successfully characterize the STS-1 pitch-up anomaly by relating Orbiter aerodynamic measurements made in the CF_4 tunnel to flight predictions. For the Orbiter at flight Mach numbers above 18, γ_{eff} is approximately 1.11. In the Mach 6 CF_4 and air tunnels, the value is 1.13 and 1.40, respectively. A close agreement between flight prediction and measured windward bow shock inclination and standoff distance is shown in Figure 5.2.3-1. In addition, there is general agreement between the flight and Mach 6 CF_4 tunnel conditions for predicted pressure coefficients and non-dimensional heating distributions (and wing bow shock interaction locations) on the Orbiter windward surface (Figure 5.2.3-2). These two observations imply very good ground-based simulation capability of the Orbiter windward flow field.

Compressibility (Mach number) effects were not addressed explicitly via testing in the two facilities. However, during hypervelocity/hypersonic entry the Orbiter is at relatively high angles of attack and thus the local Mach number over a majority of the windward surface is supersonic (typically between 2 and 3). For blunt to moderately blunt configurations such as the Orbiter at entry angles-of-attack, aerodynamic characteristics are essentially independent of Mach number. In terms of viscous simulation in the continuum (Reynolds number) regime, the flight free stream Reynolds number based on vehicle length was below 0.5×10^6 up to the point of the first measured off-nominal heating event on the side fuselage and OMS pod regions. The free stream Reynolds number for STS-107 had increased to approximately 2.4×10^6 at loss of signal near M=18. In the Mach 6 air testing, Reynolds number based on model length was varied between 0.3×10^6 and 6.5×10^6, and the majority of testing occurred at 2.4×10^6. The length Reynolds number in the Mach 6 CF_4 tunnel was varied between 0.05×10^6 and 0.55×10^6 with most of the testing at 0.4×10^6. These Mach 6 CF_4 conditions are more representative of the flight conditions prior to loss of signal (higher altitude and Mach number). In the design of wind tunnel experiments, local conditions are often more appropriate when, for example, boundary layer correlations are sought. For the Orbiter at M=18 in flight, the edge Mach number at X/L=0.6 is approximately 3 with a post normal shock Reynolds number of 0.4×10^6 (Bouslog, 1995). The corresponding conditions for the Mach 6 air tunnel (at X/L=0.6) are 2.3 and 0.42×10^6, respectively. During a nominal Orbiter entry at Mach numbers greater than 18, the windward (Bouslog, 1995) and leeward (Throckmorton, 1995) flows are laminar. Wall-to-total temperature ratio was 0.60 and 0.45 for the air and CF_4 tunnels, respectively. Flight wall-to-total temperature ratio for the Orbiter near Mach 18 at flight conditions is generally within the range of 0.2 to 0.3.

In terms of facility limitations, it is recognized that acoustic disturbances are inherent for any hypersonic ground-based facility having a turbulent boundary layer on the nozzle wall. This fact may promote transition in an attached or separated wall boundary layer earlier than may occur in flight. Surface roughness related transition data provided to the investigation for correlation purposes were based upon a fully effective roughness criterion, whereby turbulence is initiated immediately downstream of the roughness element site. When vehicle surface roughness is present (a typical boundary layer transition bypass), it is generally accepted within the transition community that facility noise from conventional tunnels has little effect on transition as long as roughness heights are large enough to be considered effective.

One of the largest unknowns associated with the ground-based testing performed as part of the STS-107 investigation is the extrapolation to flight of wind tunnel based leeside flow field characteristics. Data derived from conventional air facilities regarding leeward flow separation, reattachment, transition of separated or attached leeward flow, and leeward vortex interactions all present significant scaling issues as discussed by Haney (1995). Historically, the CF_4 tunnel has not been heavily utilized for characterization of separated, leeward (or wake) flows. Rather, it has been used for aerodynamic studies associated with blunt planetary entry configurations where the inviscid forebody flow is primarily governed by the normal shock density ratio (Jones, 1969). If, in hypervelocity flight, the Orbiter leeside flow is non-reacting or frozen due to the rapid flow expansion around the leading edge, it is quite possible that the CF_4 simulation (with a free-stream $\gamma = 1.22$) will provide a rather good representation of coupled leeside flow physics and flow chemistry. It will be equally important in the future to determine how well CFD can accurately capture the "challenging" leeside flow physics (e.g., flow separation/reattachment, vortical flow) at wind tunnel conditions before the complexity of flow chemistry at flight conditions is introduced. In Mach 6 CF_4 results for the Orbiter, it has been observed that the spatial location of maximum OMS pod heating is closer to the location observed in flight (i.e., the high temperature black tile on the flight vehicle) relative to that inferred from test results in Mach 6 air. It is suggested by these observations that perturbations to the nominal leeward flow field from certain damage scenarios may also be better represented by the Mach 6 CF_4 tests (as opposed to Mach 6 air) as the disturbances generally originate from the windward surface.

5.2.3.2 Orbiter Configurations Tested

Baseline Orbiter Models

More than 70 cast ceramic models of the Orbiter configuration were manufactured as part of the investigation and they all share a common construction technique. Initially, during the first weeks of the investigation, existing ceramic 0.0075 scale models of the Orbiter from a prior NASA JSC/LaRC collaboration (Berry, 2002) were utilized. The expansive scope of aeroheating testing needed for the investigation, however, required additional models to be fabricated. To accomplish this quickly, a pre-existing epoxy based mold constructed from the 0.0075 scale metallic force & moment model (used during the early phases of the aerodynamic testing-see Section 4.3.1) was used to slip cast each new ceramic model. A magnesia ceramic was used to backfill the ceramic shells, thus providing strength and support to the base mounted sting support structure. Ceramic models used during simultaneous aerodynamic and aeroheating tests were constructed in a similar fashion, but were modified to accept a six-component balance. An overview of model fabrication used exclusively for thermal testing is shown in Figure 5.2.3-3. In order to obtain accurate heat-transfer data with the phosphor or IR technique, the ceramic models are cast with a material having low thermal diffusivity and well-defined, uniform, isotropic thermal properties. The phosphor coatings typically do not require refurbishment between runs in the wind tunnel and have been measured to be approximately 0.001 inch thick. Details concerning the model fabrication technique and phosphor coating can be found in Buck (1993, 2000). Fiducial marks were placed on the model side fuselage surface at the locations for RTDs V34T1106A and V09T1724A (Orbiter coordinates provided by NASA JSC) and axial stations X/L= 0.25, 0.50, 0.75, and 0.90. These fiducial marks were used to assist in more accurately determining spatial locations of surface heating features.

Modified Orbiter Models

Damage to the Orbiter was simulated on the ceramic models in several ways and was driven by the leading scenario(s) at the time of testing. Initial modifications to the model surface involved placing discrete protuberances at strategic locations on the windward surface (e.g., left main landing gear door) and along the left wing leading edge (along individual RCC or adjacent carrier panels). Subsequent

modeling of damage scenarios was more intrusive and involved machining cavities or holes through the wing. Damage in the form of a completely missing isolated RCC panel 6 was initially attempted with hand tools and later with milling operations. The approximate locations of RCC panels, carrier panels, and TPS damage for these early tests were taken from technical drawings of the TPS layout (Joels, 1982) and transferred to the model surface via transparency. A higher fidelity, more systematic approach to characterizing wing leading edge damage was undertaken and involved construction of 13 models (see Figure 5.2.3-3) each with an individual missing RCC panel (1-13). RCC panel and adjacent upper and lower carrier panel locations were provided in the form of a CAD file. These locations were transferred to the model as discrete points via the surface verification laboratory at NASA LaRC. Additional models were constructed to characterize thermal effects associated with multiple missing RCC panels, partially missing panels (with and without vent paths down the RCC channel or to the leeside) on the wing upper surface, and missing T-seals. The leading edge channel formed by the Orbiter RCC panels was not captured with the ceramic models. Thus, removal of an RCC panel or T-seal yielded solid walls and hence no lateral pressure relief.

Simulation of leading edge damage with a leading edge channel (lateral pressure relief) similar to the flight vehicle required a unique approach to model construction. A solid model CAD file (1997 definition-see sec 5.2.3.2) was modified to approximate the volume of the RCC channel (Figure 5.2.3-4). A rapid prototyping technique was used to "grow" a resin stereolithography (SLA) model. Thermal protection of the resin model was provided for by application of a ceramic coating to the resin model. Qualitative thermal imaging was accomplished via the phosphor thermography technique. To characterize the thermal effects associated with RCC channel venting to the leeside, a similar approach was taken. A resin model was internally modified (see Figure 5.2.3-5) to blow CF_4 or nitrogen gas through a continuous 0.01-inch vent gap along the upper wing near the RCC/carrier panel interface.

5.2.3.3 Results for Mach 6 Air

Wing Leading Edge Discontinuities

The sensitivity of global aeroheating distributions on the windward and side fuselage surfaces to several forms of simulated RCC panel 6 damage is summarized in Figure 5.2.3-6 and Figure 5.2.3-7, respectively. These results, obtained using IR thermography, all correspond to the same model residence time in the flow and indicate local areas of increased surface temperature relative to the nominal configuration. The typical surface protuberances placed along the wing leading edge would correspond to a 13-inch x 13-inch full scale surface raised 0.5-inch above the nominal outer mold line. While shown to be effective at promoting boundary layer transition on the windward surface, the raised disturbances along the leading edge did not produce temperature augmentations on the side fuselage at these Mach 6 air conditions. The temperature image corresponding to run 47 in Figure 5.2.3-7 was the first direct experimental evidence that simulated RCC panel damage in the form of a "notch" could produce a localized heating anomaly on the Orbiter side fuselage.

Missing Wing RCC Panel Survey

The sensitivity of Orbiter side fuselage surface heating to simulated RCC panel damage for completely missing individual panels is summarized in Figure 5.2.3-8. At the time of testing, the body of recovered debris did not refute the possibility of entire RCC panels missing and it was felt that this form of damage would be easier to model computationally. Higher fidelity, parametric removal of individual leading edge RCC panels 1-13 was undertaken to characterize the location and magnitude of the heating disturbance on the side fuselage. The results were obtained using phosphor thermography and indicate local areas of increased surface heating relative to the nominal wing leading edge. Global heating distributions are presented in terms of the ratio of enthalpy-based heat-transfer coefficients h/h_{REF}, where h_{REF} corresponds to the Fay and Riddell (1958) predicted sphere stagnation-point heating with a 1-ft radius at flight scale (i.e., radius equal to 0.09-inches at wind tunnel scale). Unless noted otherwise, a constant maximum color value of 0.25 was selected for data presentation to maintain consistency when viewing or comparing images. On the contour scale, the colors tending towards red indicate areas of higher heating (temperatures) while the colors towards blue represent areas of lower heating.

A localized heating disturbance on the side fuselage (Figure 5.2.3-8) was evident for all panel locations RCC (1-13). Although the heating magnitudes associated with the disturbance were generally insensitive to the location of the missing panel, the inclination of the heating pattern on the side fuselage was

dependent on the span-wise location of the RCC damage. The nearly vertical side fuselage heating footprint associated with missing RCC panel 1 approached a nearly horizontal orientation (parallel to the Orbiter reference waterline) as the systematic removal of individual RCC panels progressed outboard to missing RCC panel 12. A missing RCC panel at the location of the Mach 6 air wing/bow shock interaction (RCC panel 12) did not result in abrupt changes to the side fuselage heating footprint in terms of location or magnitude. In addition, no large location or magnitude changes to the surface heating associated with missing RCC panel 12 were observed for small changes in angle-of-attack (Figure 5.2.3-9), sideslip (Figure 5.2.3-10), or a factor of 4 increase in Reynolds number (Figure 5.2.3-11). Heating images taken from above the model (Figure 5.2.3-12) indicated that disturbances created from wing leading edge damage could produce leeward flow field perturbations strong enough to reduce the OMS pod heating for missing RCC inboard of panel 9. In contrast, local heating augmentations to the forward face of the OMS pod were measured for missing $9 \leq$ RCC panel ≤ 11. Comparison of Schlieren images revealed the local shock structure complexity associated with missing RCC panel 8 (Figure 5.2.3-13) relative to a baseline undamaged wing leading edge (Figure 5.2.3-14).

Holes Through Wing

Limited parametric studies of simulated damage in the form of a wing breach from the windward surface to the leeward surface were attempted in this facility and were primarily associated with aerodynamic testing (see Section 4.3.1). Initially, circular holes dimensionally consistent with the width of a carrier panel (approximately 4 inches full scale) were placed at the interfaces for carrier panels 5, 9, 12, and 16. The holes were found to force boundary layer transition on the windward surface to the damage site. The model and IR setup for the aerodynamic tests at this point in time precluded imaging the side fuselage. Since the model also incorporated damage in the form of missing RCC panel 6, it is believed that effects (if any) from the carrier panel holes would have been dominated by the disturbance from the missing RCC panel.

TPS damage in the form of a much larger breach through the wing was attempted, but the side fuselage heating measurements were considered qualitative due to compromised phosphor coatings on the models that were used. The holes were orientated normal to the wing chord and were located near the left main landing gear door. One hole location was approximately located at the center of the forward bulkhead (X=1040-inches in Orbiter coordinates) and the second location was near the center of the outboard bulkhead (Y=167-inches in Orbiter coordinates). At each location, the wing hole diameter was systematically changed from 0.0625 to 0.125 and 0.25-inch at wind tunnel scale (8.3, 16.7, and 33.3-inch full scale). While the compromised phosphor coating considerably degraded the image quality, it was evident that no change in side surface heating was apparent for any tested combination of location or diameter.

Aerothermodynamics Associated with Asymmetric Boundary Layer Transition

Boundary layer transition on the Orbiter during re-entry is known to introduce small changes in the aerodynamics of the vehicle. Thus, in order to assess the sensitivity of Orbiter aerodynamics to several forms of simulated damage, damage resulting in boundary layer transition was evaluated. The surface heating results complementing the companion aerodynamic tests (see Section 4.3.1) were obtained using IR thermography. The results indicated several surface protuberances (corresponding to a 6-inch x 6-inch full scale surface raised 0.5 to 1-inch above the nominal outer mold line) placed along the wing leading edge would effectively promote Asymmetric Boundary Layer Transition (ABLT) on the windward surface. As mentioned in Section 4.0, the corresponding aerodynamic data provided the first direct evidence that while ABLT could produce measurable aerodynamic increments consistent with the Orbiter ABLT model for flight, the trends were inconsistent with STS-107 flight data.

5.2.3.4 Results for Mach 6 CF_4

Windward Surface Protuberances

A limited data set was obtained in the Mach 6 CF_4 tunnel to determine (1) if the Orbiter windward surface boundary layer could be forced turbulent with discrete isolated roughness, and (2) if the results were positive, could they be mapped onto a previously developed Orbiter boundary layer transition correlation developed in the Mach 6 air tunnel (Berry, 2002). The forced boundary layer transition results are summarized in Figure 5.2.3-15. Surface protuberances were placed on the windward centerline near X/L of 0.26. This location corresponds to the location of a protuberance observed on flight STS-73 which

resulted in an "early" high Mach number (approximately 19) boundary layer transition event. The protuberances correspond to a 6 x 6-inch full scale surface raised approximately 0.5, 0.9, and 1.5-inch above the nominal outer mold line. Boundary layer edge conditions were computed with a method consistent with the Mach 6 air correlation and yielded protuberance height-to-boundary layer thickness ratio (k/δ) values of 0.2 to 1.75. The discrete data points in Figure 5.2.3-15 correspond to laminar, incipient and effective roughness and these Mach 6 CF_4 data are compared with previously correlated Mach 6 air perfect gas results (solid curves). This limited data set represents the first discrete roughness boundary layer transition data on the Orbiter acquired in the Mach 6 CF_4 facility. Because complicated effects interact to produce boundary layer transition, and a comprehensive study could not be carried out (due to time constraints) of how the current limited Mach 6 CF_4 data set relates to the previously developed correlation of Berry (2002) for Mach 6 air, assessments of boundary layer transition for STS-107 utilized the previously developed correlation.

Missing Wing RCC Panel Survey

The sensitivity of side fuselage heating distributions to RCC panel damage in the Mach 6 CF_4 facility for completely missing panels is summarized in Figure 5.2.3-16. At the time of this testing, the body of recovered wing debris suggested that loss of an entire RCC panel was not likely, except for RCC panel 9. Higher fidelity, parametric removal of individual leading edge RCC panels (1-13) was pursued to characterize the location and magnitude of the heating disturbance on the side fuselage and to compare with the Mach 6 air results. Similar to the previously obtained Mach 6 air data, the CF_4 results were obtained using phosphor thermography and indicate local areas of increased surface heating relative to the nominal configuration. As discussed previously, global heating distributions are presented in terms of the ratio of enthalpy-based heat-transfer coefficients h/h_{REF}, and unless noted otherwise, a constant color bar maximum value of 0.25 was selected with colors tending towards red indicative of areas of higher heating (temperatures).

A localized heating disturbance on the side fuselage (Figure 5.2.3-16) was evident for all RCC panel locations (1-13). The relationship of the heating pattern inclination on the side fuselage to missing panel span-wise location was different from that observed for Mach 6 air. The local disturbance in the Mach 6 CF_4 facility was "directed" at the OMS pod, resulting in heating augmentations to the forward face of the OMS pod for missing panel $1 \leq RCC \leq 10$ (in contrast to heating reductions in Mach 6 air). Similar to the Mach 6 air trends, however, heating magnitudes associated with the disturbance on the side fuselage were generally insensitive to the location of the missing panel. A missing RCC panel at the location of the wing/bow shock interaction for Mach 6 CF_4 (RCC panel 9) did not result in abrupt location or magnitude changes to the side fuselage heating footprint. Similar to the observation in Mach 6 air results, the side fuselage heating footprint approached a nearly horizontal orientation (parallel to the Orbiter reference waterline) as the systematic removal of individual RCC panels progressed outboard. No significant Reynolds number effects were observed for TPS damage in the form of missing RCC panels. Based upon the Mach 6 air results, no Mach 6 CF_4 heating sensitivity studies were attempted for angle-of-attack and sideslip.

The leading edge channel formed by the wing spar and RCC panels on the flight vehicle was not captured with the solid ceramic models. Removal of an individual RCC panel by a milling machine yielded solid walls and hence, no lateral pressure relief. Limited tests on ceramic-coated resin models with a leading edge channel were conducted to investigate this. Characterization of any differences in the leeside flow field associated with a missing RCC panel and lateral pressure relief along the wing leading edge was felt necessary. Although qualitative in terms of heating magnitudes, the comparison of side fuselage heating patterns associated with an open and closed leading edge channel (Figure 5.2.3-17) suggests that the local heating disturbance propagates further forward (i.e., further upstream) when the damaged cavity is allowed to vent down the RCC channel.

Partial RCC Panel Damage

As the debris recovery effort drew to a close, the body of evidence indicated that partially damaged RCC panels (as opposed to entirely missing panels) was likely. Sensitivity of the Orbiter side fuselage heating associated with several forms of RCC panel 9 damage are shown in Figure 5.2.3-18. At this wing leading edge location only a missing T-seal or a completely missing RCC panel lead to off-nominal heating disturbances on the side fuselage or OMS pod. The missing T-seal was located at the RCC 8/9 interface and was sized to simulate a gap taken from the leading edge back to the wing spar. The gap width was

approximately 1.3-inch full scale, which corresponds roughly to the correct width for a removed T-seal. In contrast to the completely missing RCC panel, the missing T-seal disturbance did not indicate any off nominal side fuselage heating and affected only the lower side surface of the OMS pod.

The various forms of lower RCC panel 9 damage did not result in side fuselage/OMS pod off nominal heating (Figure 5.2.3-18). However, this was not the case for all wing leading edge locations, as shown in Figure 5.2.3-19. The test results indicated that the extent of RCC panel damage in relation to the wing leading edge attachment line largely determines if the disturbance is "swept" to the leeside. Qualitative heating images associated with the companion force and moment tests indicated the threshold for disturbances propagated to the leeside from half RCC panel damage was between RCC 5 and 6 (see Section 4.3.1, Figure 4.3.16). In other words, half RCC panel damage at panels 1 to 4 produced fuselage side heating disturbances in the Mach 6 CF_4 facility, whereas half RCC panel damage outboard of panel 5 did not.

Holes Through Wing

Limited parametric studies for simulated damage in the form of a breach from the wing windward surface to the leeward surface were attempted in the Mach 6 CF_4 facility for dedicated aero-heating tests. Wing hole parametrics were primarily associated with the simultaneous aerodynamic/aero-heating testing (see sec 4.3.1). Similar to the Mach 6 air results discussed previously, holes through the wing (located at the center of carrier panels 6, 9, 12) were found to increase heating on the windward surface, a characteristic of boundary layer transition. With regard to the dedicated aeroheating tests, an early qualitative result with a single circular hole placed at the RCC/carrier panel 5/6 interface did not result in off-nominal heating to the side fuselage/OMS pod (Figure 5.2.3-20). Heating associated with missing RCC panel 6 is shown for comparison. The hole was orientated normal to the wing chord with the diameter dimensionally consistent with the width of a carrier panel.

Venting from Discrete Locations along Wing Upper Surface with RCC Panel Damage

Qualitative heating images associated with the companion force and moment tests indicated that disturbance propagation to the side fuselage with partial RCC panel damage (the lower surface missing) for panels outboard of RCC 5 was possible. In order to investigate a partial panel damage case that might lead to leeside heating effects, the stagnated flow in the damaged panel region was allowed to vent via a carrier panel slot (see Sec 4.3.1). This experimental evidence coupled with a developing understanding of recovered Columbia debris prompted an effort to qualitatively characterize the possible influence of mass addition on the leeside flow field. The ceramic-coated resin models that possessed a wing leading edge channel were further modified to include venting paths to the leeward surface. The total estimated venting area was first computed per unit panel; a series of circular holes with the per panel vent area were drilled into the leading edge channel near each RCC/carrier panel interface. The channel was allowed to pressurize via damage in the form of a completely missing RCC panel 9. No attempt was made to measure local pressure or mass flow rate along the wing leading edge. The qualitative data presented in Figure 5.2.3-21 reveals little effect of this venting via circular holes on side fuselage heating patterns. Since the model also incorporated damage in the form of missing RCC panel 9, it is believed that effects (if any) from the discrete carrier panel venting holes were dominated by the disturbance from the missing RCC panel.

Venting from Continuous Gap Along Upper Wing Surface with/without RCC Panel Damage

To isolate possible venting effects from major RCC damage that dominates the leeward flow field, qualitative tests were first conducted on a ceramic-coated resin model with an undamaged leading edge. In contrast to the previous resin model with discrete holes, new resin models with a continuous 0.01-inch wide vent gap running along the upper wing RCC/carrier panel interface were fabricated (see Figure 5.2.3-5). The gap width on the model was a limitation of the manufacturing process and is approximately a factor of 10 larger than the actual vent gap width at model scale. Gaseous CF_4 was fed to the gap internally via a free-stream flow field pitot tube and allowed to vent to the leeside through the gap. A pressure measurement inside the wing provided a pressure measurement for the flow being fed into the RCC channel. The internal gap pressure measurement divided by the computed surface pressure exceeded a factor of 2, indicating the flow was sonic at the gap (surface pressure predictions at wind tunnel conditions provided by methods detailed in Section 5.2.4). The qualitative data presented in Figure 5.2.3-22 suggests that mass addition (venting) to the leeside via this continuous vent gap behind RCC 1 to 22 forces wing flow separation and leeside flow field perturbations, resulting in off-nominal low

heating on both the side fuselage and the OMS pod. The maximum contour ratio of enthalpy-based heat-transfer coefficients h/h_{REF}, was changed to 0.10 for the leeward planform image to provide more detail associated with the heating patterns (h/h_{REF} = 0.25 for the side fuselage images).

Having demonstrated leeside flow field perturbations from venting, attempts at controlling mass flow rates using gaseous nitrogen were made. As with the previous CF_4 venting study, the qualitative heating tests were conducted on a ceramic-coated resin model with an undamaged leading edge. The objective of these tests was to correlate the off nominal low side fuselage/OMS pod heating using a local jet momentum to free-stream momentum ratio. The form of the momentum ratio was based on previous work by Stone and Cary (1972), and Zukoski and Spaid (1964). The experimental results shown in Figure 5.2.3-23 at two free-stream Reynolds numbers reveal off-nominal low side fuselage heating for momentum ratios > 0.35, and OMS pod heating reductions for momentum ratios > 0.80. These momentum ratios were determined by assuming sonic orifice conditions. The maximum contour ratio of enthalpy-based heat-transfer coefficients h/h_{REF}, was changed to 0.10 for these side fuselage images to provide more detail associated with the heating patterns. These results provide experimental data suggesting that a threshold scaling parameter ratio of about 0.3 or greater is required to cause side fuselage effects, and a threshold value of 0.5 or greater is required for OMS pod effects.

To conclude the wing venting characterization study, a cavity near the lower surface carrier panel of RCC panel 8 was machined into the previously tested resin model (Figure 5.2.3-24) permitting the wing leading edge channel to pressurize and vent to the wing leeward surface along the gap. The initial wing hole–to-vent gap area ratio was approximately 0.5. It has been previously shown that lower half panel RCC damage at this location (RCC panel 8) does not affect leeside heating, whereas the lower RCC panel damage shown in Figure 5.2.3-24 produces leeside heating effects. Similar to the previous venting scenarios, regions of off-nominal low heating were evident on the side fuselage/OMS pod as shown in Figure 5.2.3-24. In this image, the maximum contour ratio of enthalpy-based heat-transfer coefficients h/h_{REF}, was changed to 0.10 for the leeward planform image to provide more detail associated with the heating patterns (h/h_{REF} = 0.25 for the side fuselage images). Increasing the wing hole-to-vent gap area ratio to approximately 1 produced similar effects (not shown) on the off nominal heating.

5.2.3.5 General Experimental Observations

Description of Leeside Flow

The purpose of this section is to provide a brief overview of the Orbiter leeside flow field and to provide insight into how some of the RCC damage scenarios may have affected the side fuselage/OMS pod heating. An interpretation of the Orbiter leeside flow, Figure 5.2.3-25, taken from Baranowski (1983), captures the complexity of the three-dimensional flow structures that affect the Orbiter's leeward surfaces Figure 5.2.3-25 (a). The leeside is dominated by regions of strong flow expansions, flow separation/reattachment (which may be laminar, transitional, or turbulent), shock interactions, and vortical flow. For these reasons, the leeward flow field is highly sensitive to compressibility and viscous effects, and may be chemically frozen.

Flow features in the upper payload bay area with angles-of-attack less than 35 deg, are thought to be dominated by a vortex pair that interact along the centerline, Figure 5.2.3-25 (b, c, and d-1). At angles-of-attack between 35 and 45 deg, this vortex pair moves off the surface as depicted in Figure 5.2.3-25 (1d-2). Below this primary vortex pair a "quasi" boundary layer forms within which secondary or tertiary embedded vortices can develop. The so-called "vortex" scrubbing often used to describe the heating along the Orbiter side fuselage is, in actuality, reattachment of flow that has separated from the upper wing surface. It is this complex system of separated /re-circulating flow that is potentially perturbed by disturbances emanating from wing leading edge damage. Baranowski (1983), writes "…properties in the upper fuselage vortices are likely to be influenced by flow originating along the strake [wing] leading edge and impinging on the side fuselage." It is reasonable to assume that wing damage which alters the leading edge flow separation characteristics could have first-order effects on side fuselage/OMS pod heating.

Leeside Flow with Wing Leading Edge Damage

The effects of a missing RCC panel on Orbiter leeside flow as inferred from surface heating and corresponding streamline patterns are shown in Figure 5.2.3-26. Flow separation from the wing upper

surface and subsequent reattachment on the side fuselage as described by Baranowski (1983) is apparent from the surface oil flow streamline patterns. Locally displaced flow separations/reattachments (inferred from streamline patterns) are shown in Figure 5.2.3-26. Displacement of the embedded wing shock(s) as depicted in Figure 5.2.3-25 (1d-2) is also probable. It is believed that a jet-like plume originating from the wing leading edge damage is responsible for the observed heating augmentations. Until computational predictions demonstrate the ability to accurately capture the complex surface phenomenon (i.e., leeside wing separation, reattachment for both damaged and undamaged leading edges) as shown in Figure 5.2.3-26, the nature of the perturbed off-surface leeside flow remains speculative.

Off-Nominal Leeside Heating Trends

Side fuselage/OMS pod heating augmentations and reductions resulting from various damage scenarios have been identified from the ground-based tests. However, the off-nominal heating disturbances inferred from the experimental data were highly localized. In addition, the exact damage to Columbia is unknown and time dependent. These two factors are strong indicators that comparisons of wind tunnel derived augmentation/reduction factors to flight thermocouple and RTD magnitudes be performed with prudence.

The heating data presented in Figure 5.2.3-22 through Figure 5.2.3-24 suggest that in the absence of major leading edge damage (that tends to dominate the leeward flow field and results in *both* off-nominal high and low heating), mass addition via a degraded upper surface vent slot along the RCC 1-22/carrier panel interface can produce off-nominal low heating on both the side fuselage and OMS pod. As the heating data measurements were made on resin models, they are considered qualitative. However, it was determined that the side fuselage areas indicated in Figure 5.2.3-22 showed heating reductions of approximately 65% to 75% of the nominal surface heating. In terms of momentum ratio, a threshold for leeside venting effects was experimentally determined and should be correlated against flow field predictions involving both leading edge damage and leeside venting. However, the experimental data do suggest that a momentum ratio of at least approximately 0.3 is required to provide changes in leeside heating on the Orbiter.

Side fuselage heating augmentations associated with missing RCC panels were found to range from 2 to 12. In Mach 6 air, no changes to the surface heating associated with missing RCC panel 12 were observed for small changes in angle-of-attack (Figure 5.2.3-9), sideslip (Figure 5.2.3-10), or a factor of 4 increase in Reynolds number (Figure 5.2.3-11). Similar to the Mach 6 air trends, side fuselage heating peak magnitudes associated with missing RCC panels in Mach 6 CF_4 were generally insensitive to the location of the missing panel as shown Figure 5.2.3-16.

The test results in both facilities indicate that missing RCC panel damage outboard of RCC panel 10 leads to the heating footprint becomes nearly horizontal to the Orbiter reference waterline. In this orientation, the disturbance would act much like a “fluid fence” and would effectively prevent flow from flowing up through the elevon/fuselage gap to impinge on the lower aft corner of the OMS pod such as occurs with a nominal configuration (Haney, 1995).

Effect of Normal Shock Density Ratio on Heating Patterns

Side fuselage localized heating disturbances for normal shock density ratios of approximately 5 (γ_{eff} = 1.4) and 12 (γ_{eff} = 1.13) are contrasted in Figure 5.2.3-27 for individual missing RCC panels (1, 5, and 9). It has been noted earlier that for a missing RCC panel inboard of panel 10, the local heating disturbance on the side fuselage was more inclined from vertical in Mach 6 CF_4 than in Mach 6 air. That effect results in heating augmentations to the forward face of the OMS pod (see also Figure 5.2.3-16). For CF_4, it is speculated that local differences in γ on the leeside contribute to leading edge separation differences on the upper surface of the wing. It is not unreasonable to assume that differences in the wing embedded shock structure associated with air and CF_4 for a missing RCC panel would affect the flow to the leeside in a contrasting manner. Stronger flow expansions characteristic of a lower γ would imply larger flow turning angles as the separated flow off the wing is swept aft. If in flight, the Orbiter leeside flow is non-reacting or frozen due to the rapid flow expansion around the leading edge, it is quite possible that the Mach 6 CF_4 simulation (with a value of freestream γ limited to 1.22) provides a better representation than Mach 6 air (γ = 1.4) of coupled leeside flow physics and chemistry associated with hypervelocity flight.

Detailed computational and experimental studies of this topic would be required to address this question more comprehensively. However, at this time, the maturity of CFD to contribute significantly to a better characterization of the leeside flow field and γ effects is an open topic of discussion.

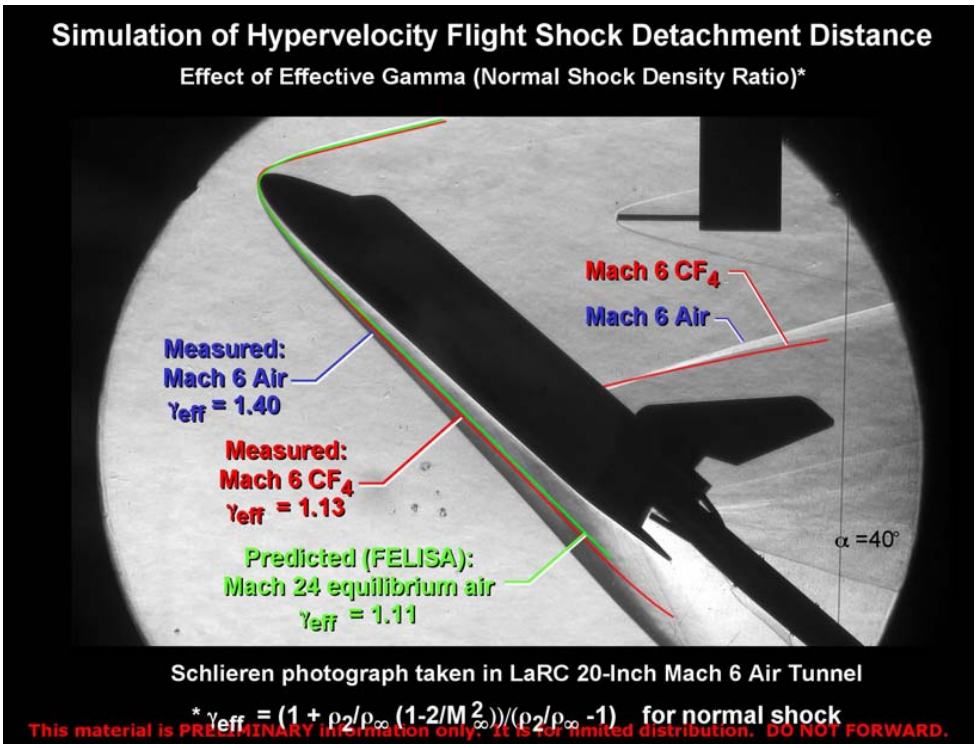

Figure 5.2.3-1 Simulation of Hypervelocity Flight Shock Detachment Distance

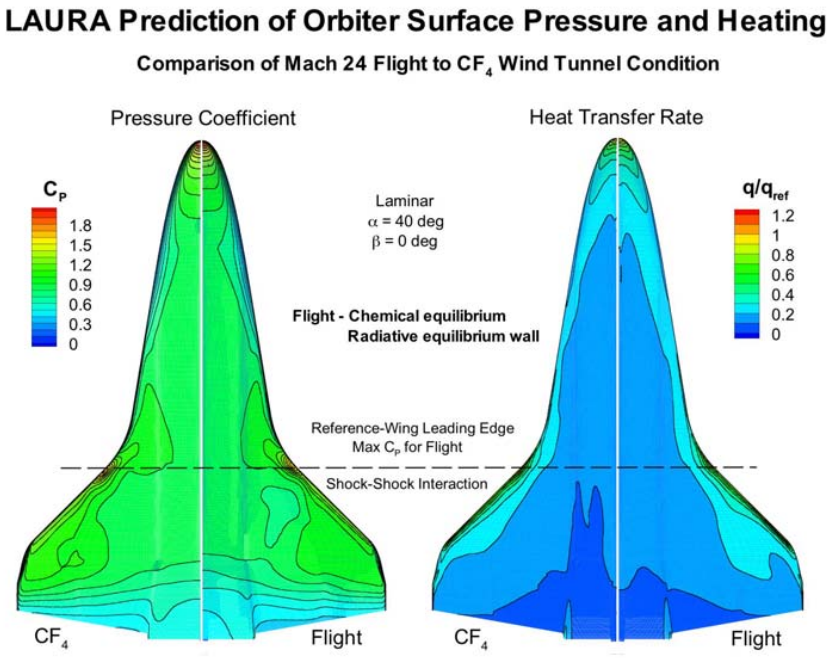

Figure 5.2.3-2 LaRC LAURA solutions of Orbiter windward surface pressure and heat flux

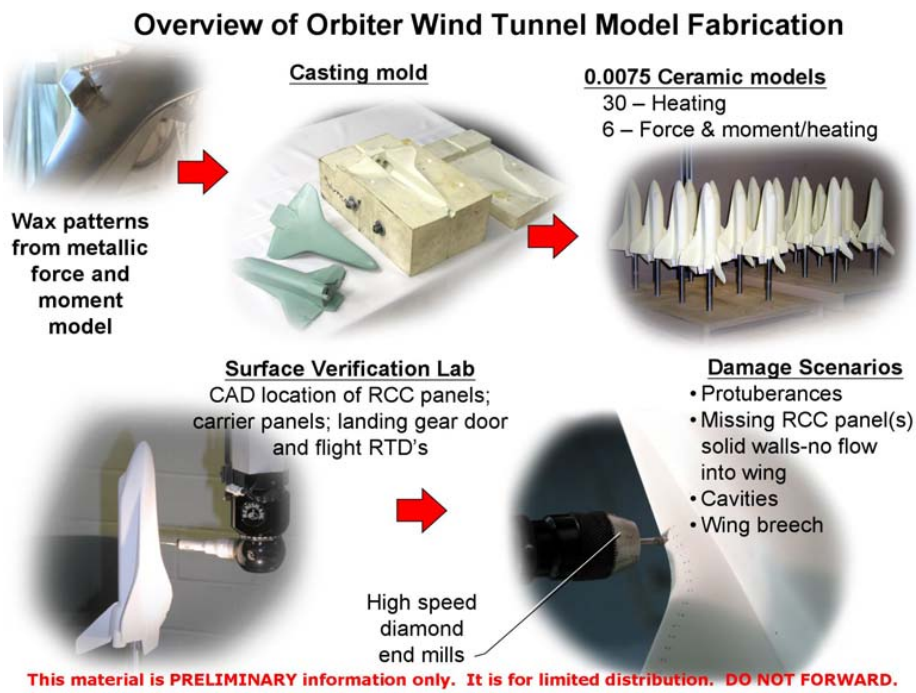

Figure 5.2.3-3 Ceramic model fabrication process

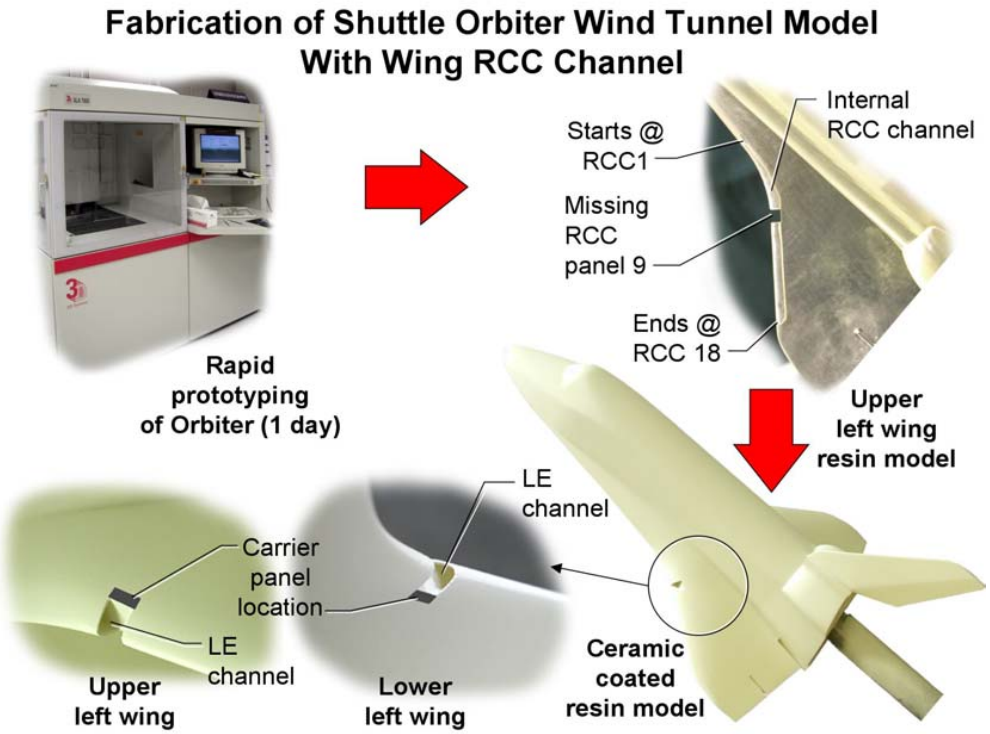

Figure 5.2.3-4 SLA model fabrication process of Orbiter with WLE cavity

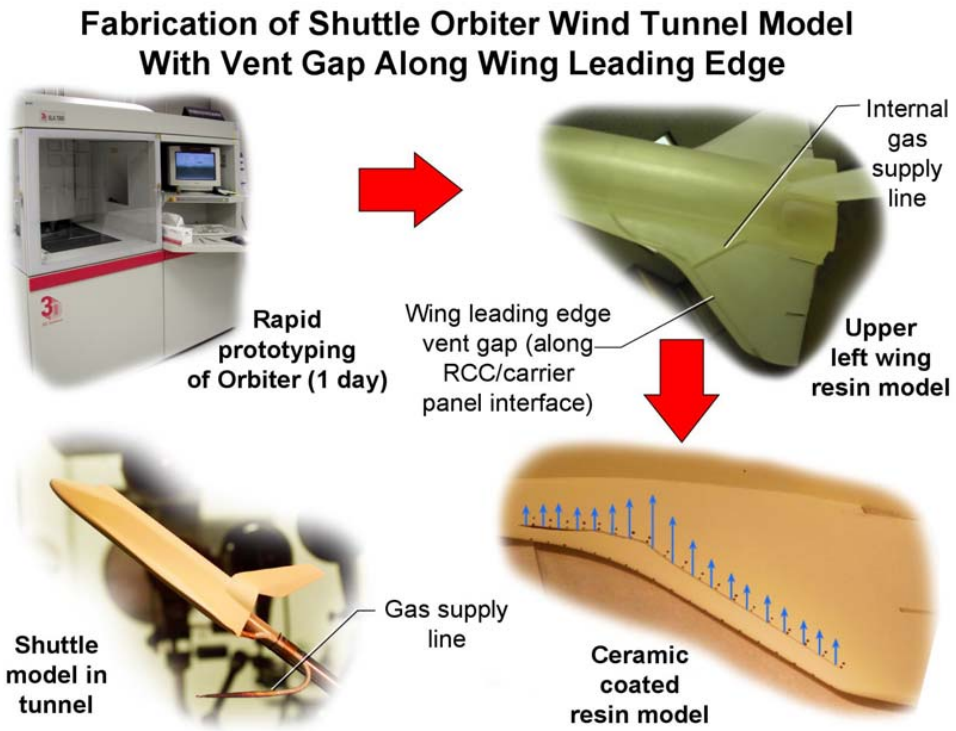

Figure 5.2.3-5 SLA fabrication process of Orbiter with WLE vented cavity and gas supply line

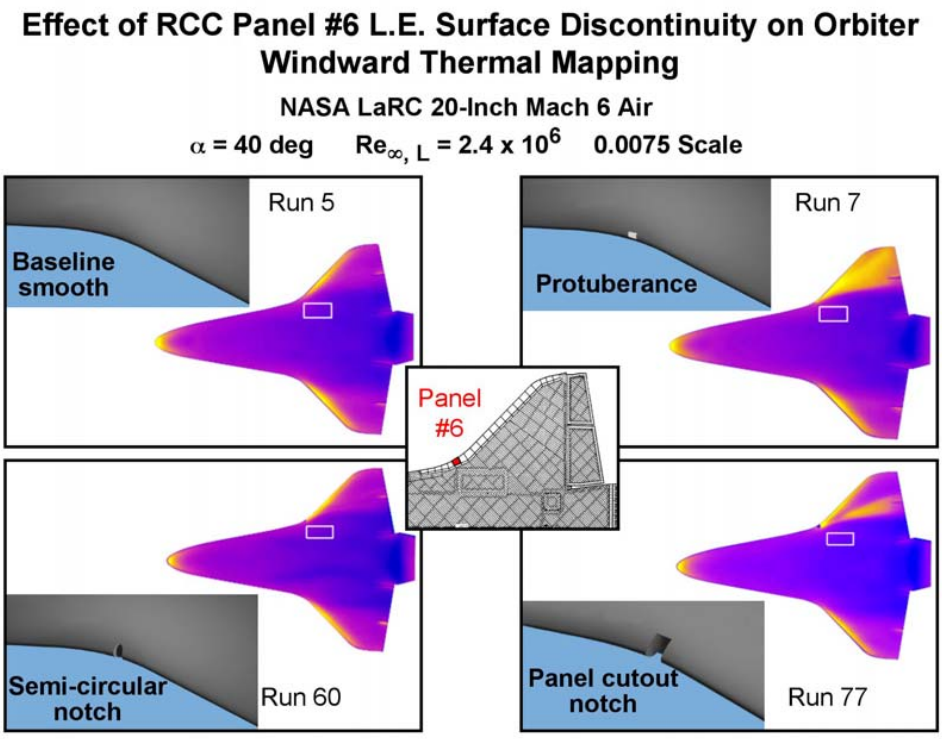

Figure 5.2.3-6 Effect of RCC Panel 6 surface discontinuity, windward view

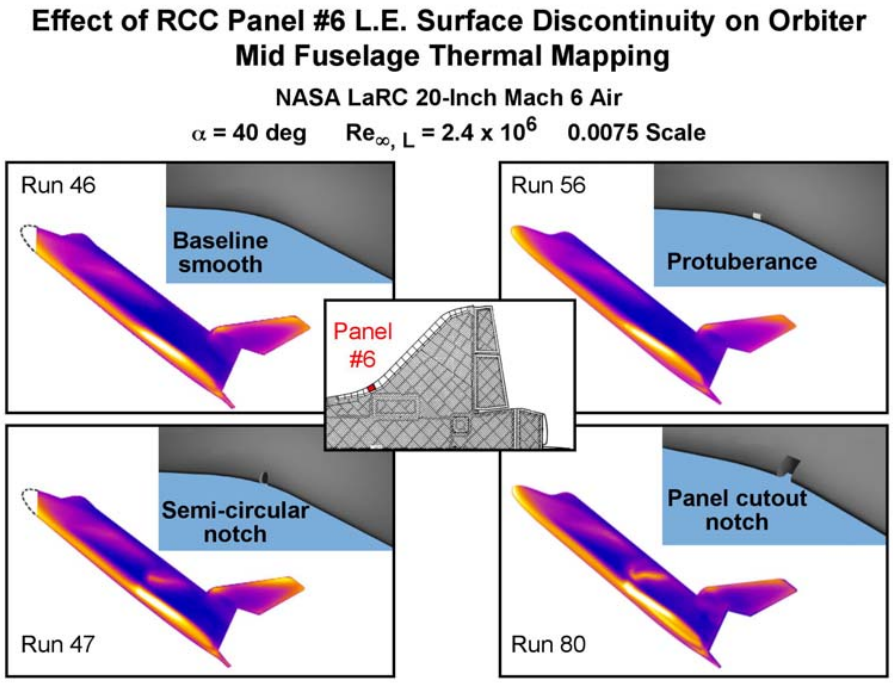

Figure 5.2.3-7 Effect of RCC Panel 6 surface discontinuity, side fuselage view

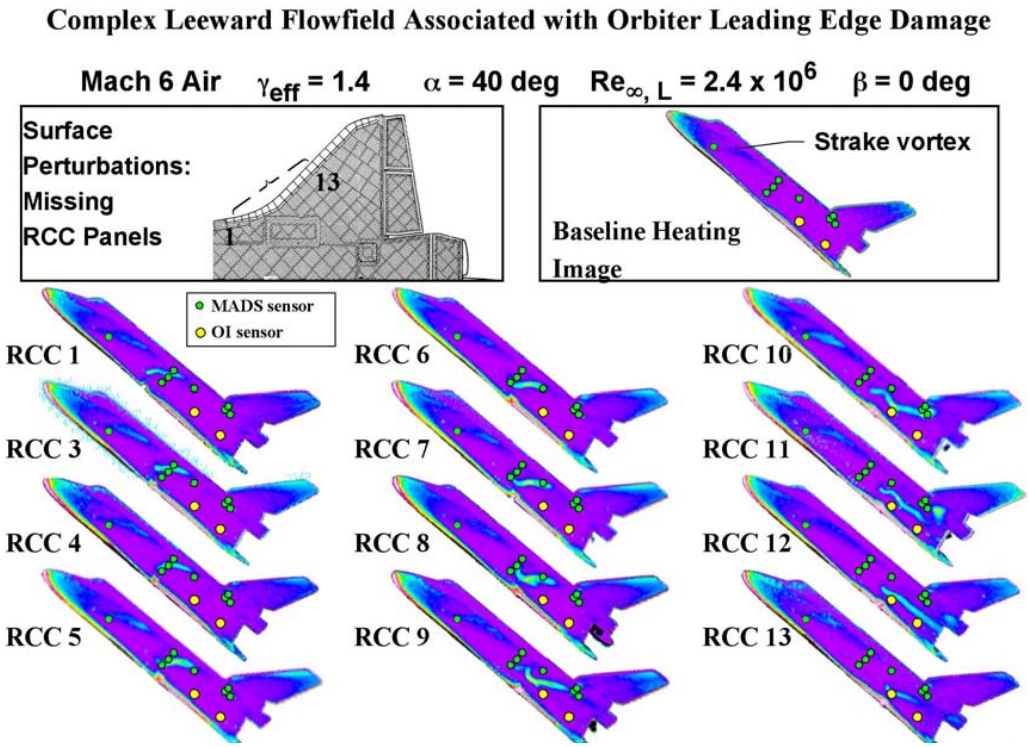

Figure 5.2.3-8 Mach 6 Air results of full RCC panel removed

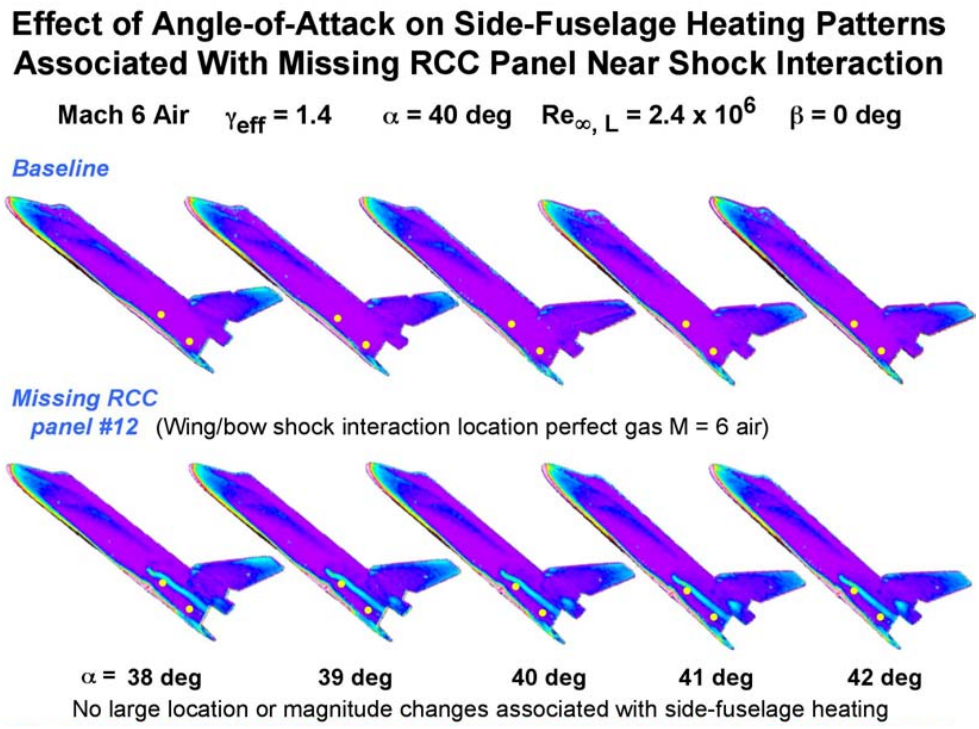

Figure 5.2.3-9 Assessment of the effect of angle of attack on side fuselage heating

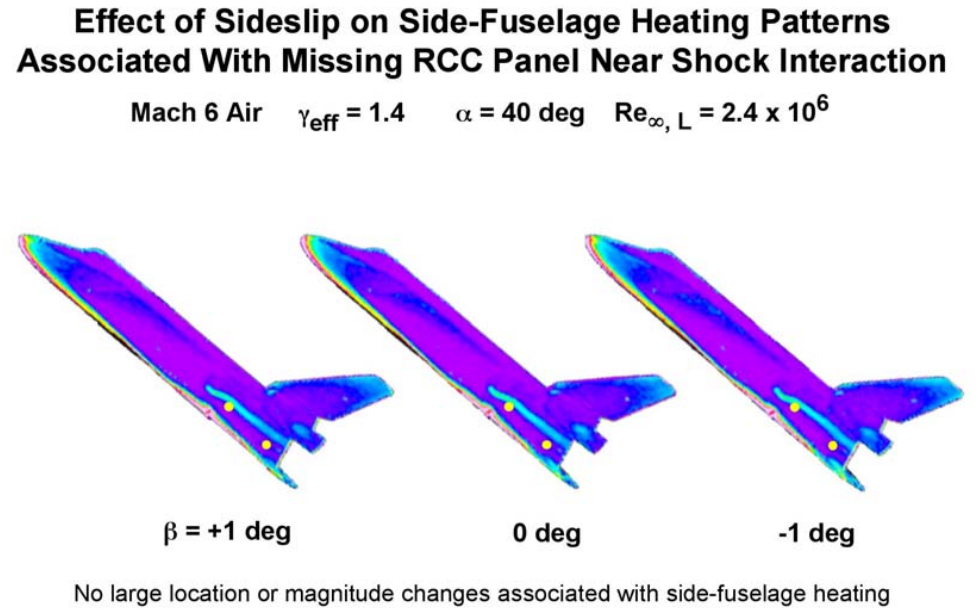

Figure 5.2.3-10 Assessment of the effect of angle of sideslip on side fuselage heating

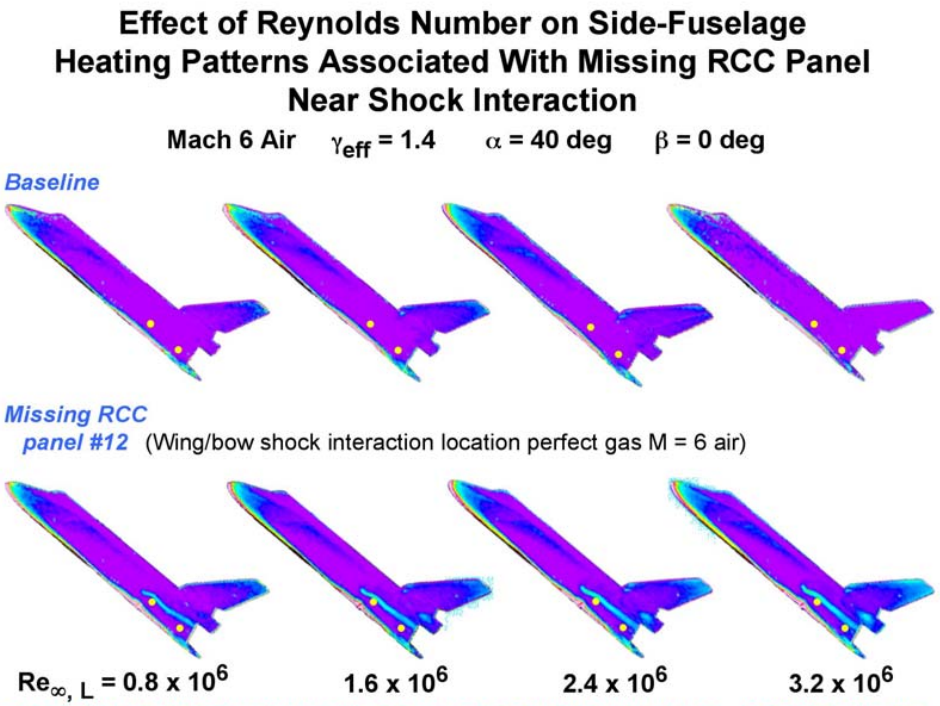

Figure 5.2.3-11 Assessment of the effect of Reynolds Number on side fuselage heating

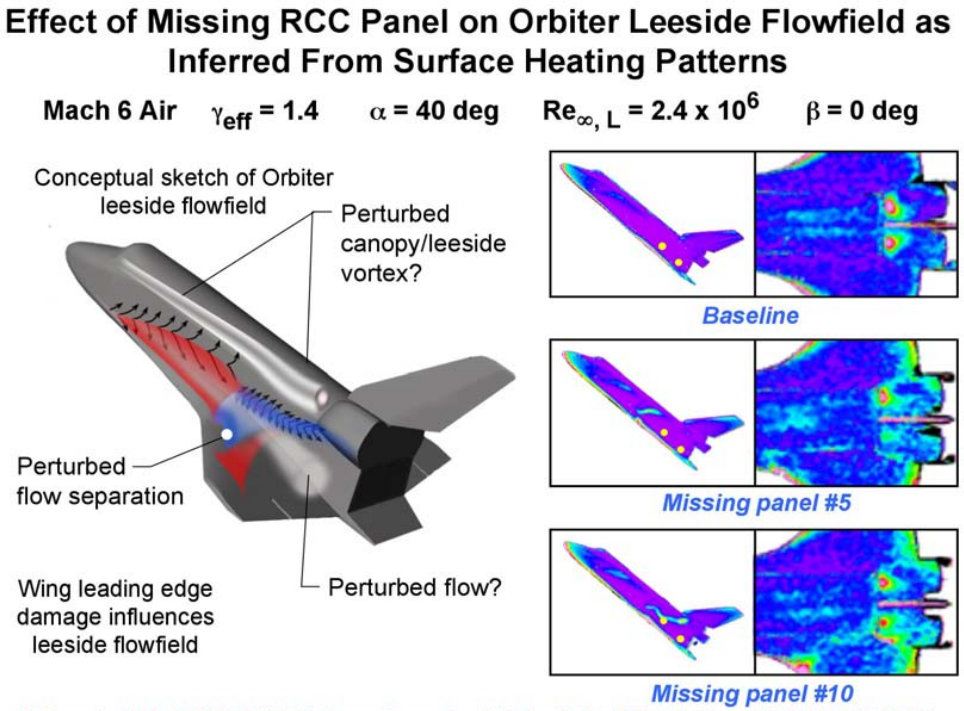

Figure 5.2.3-12 Orbiter leeside flow field changes as a result of WLE damage

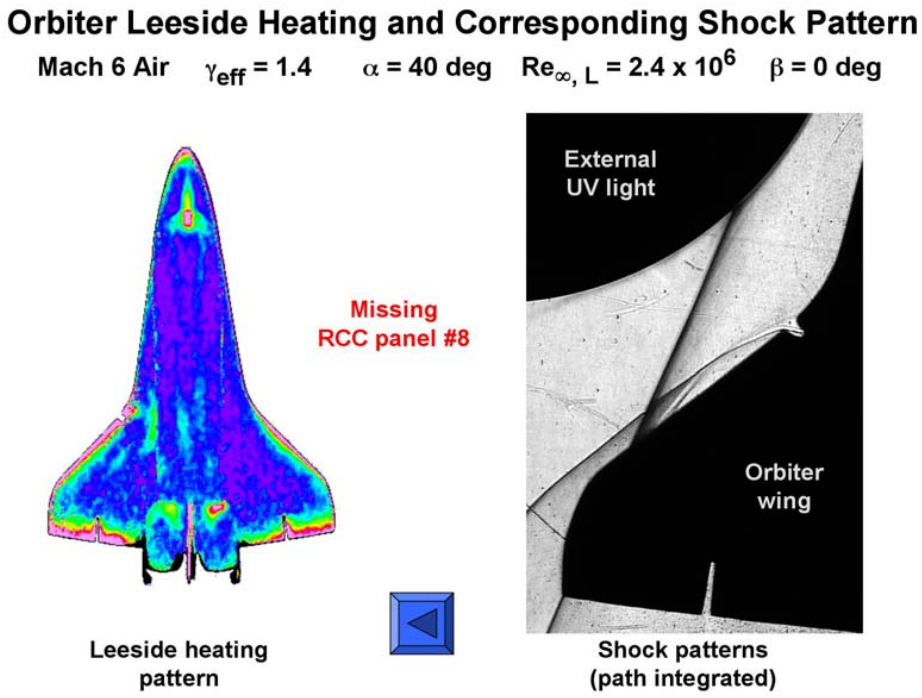

Figure 5.2.3-13 RCC Panel 8 Removed leeside heating and shock pattern

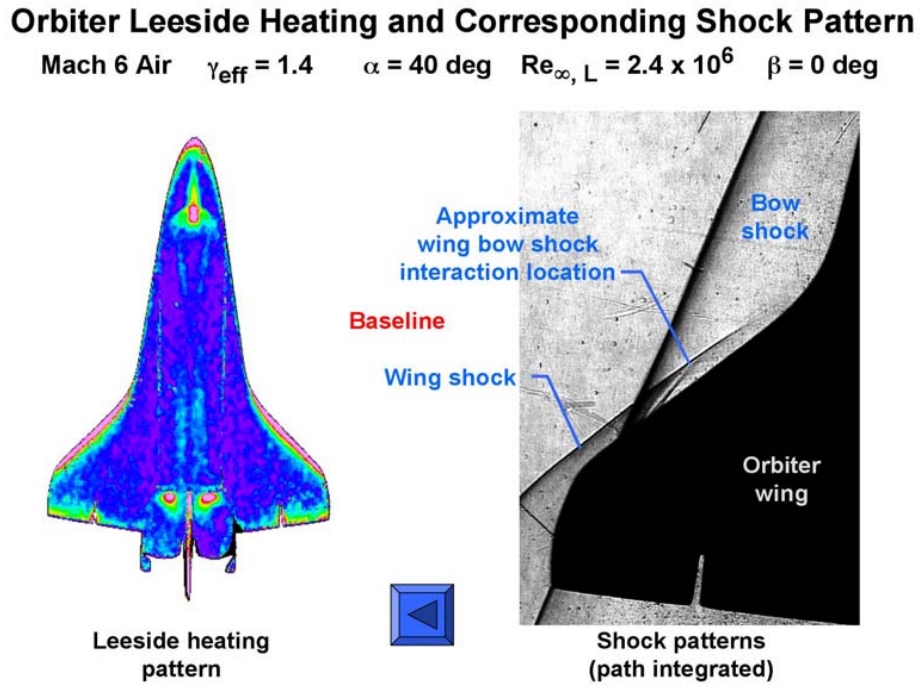

Figure 5.2.3-14 Baseline leeside heating and shock pattern

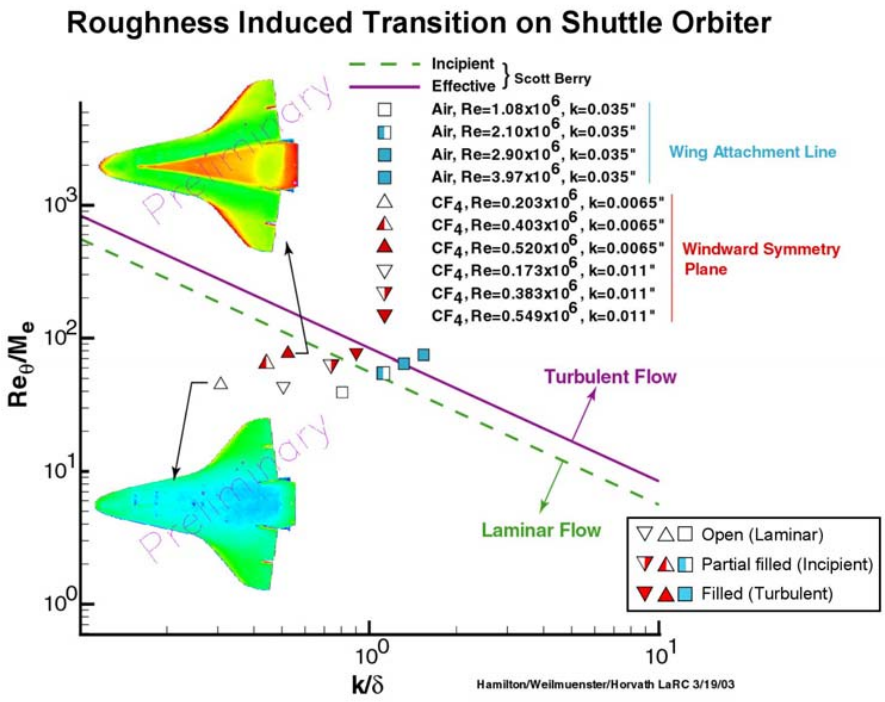

Figure 5.2.3-15 Roughness induced transition on the Orbiter. Berry correlation as compared to wind tunnel test results in both Mach 6 Air and Mach 6 CF_4

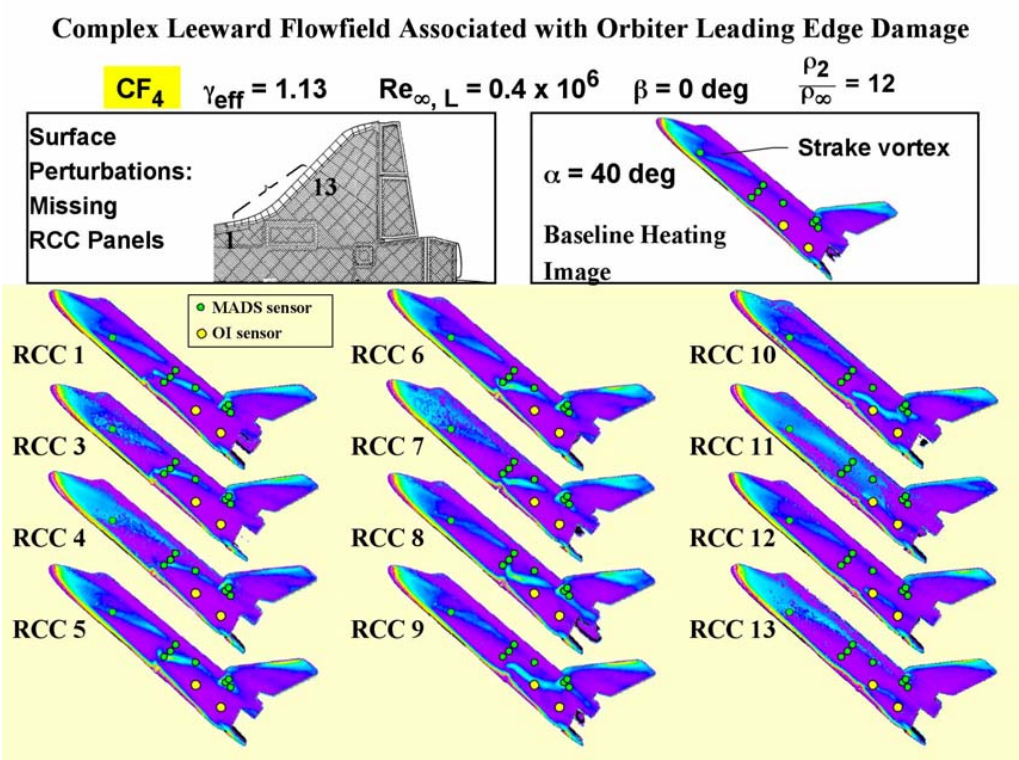

Figure 5.2.3-16 Mach 6 CF4 results for full RCC panels removed

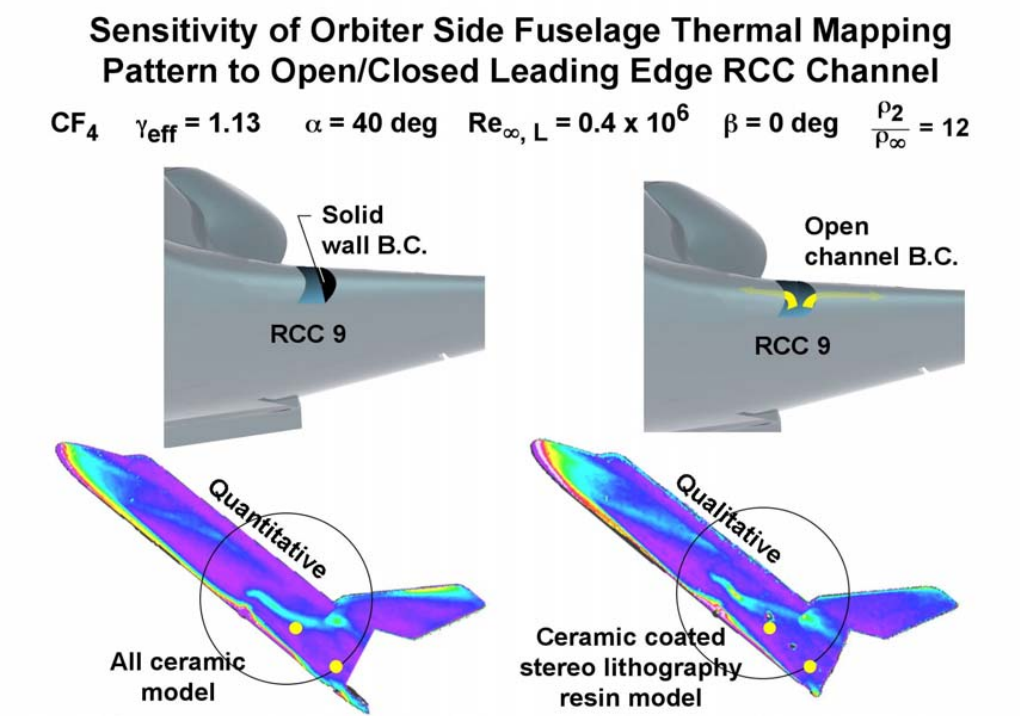

Figure 5.2.3-17 Effect of closed versus opened WLE cavity on side fuselage heating footprint

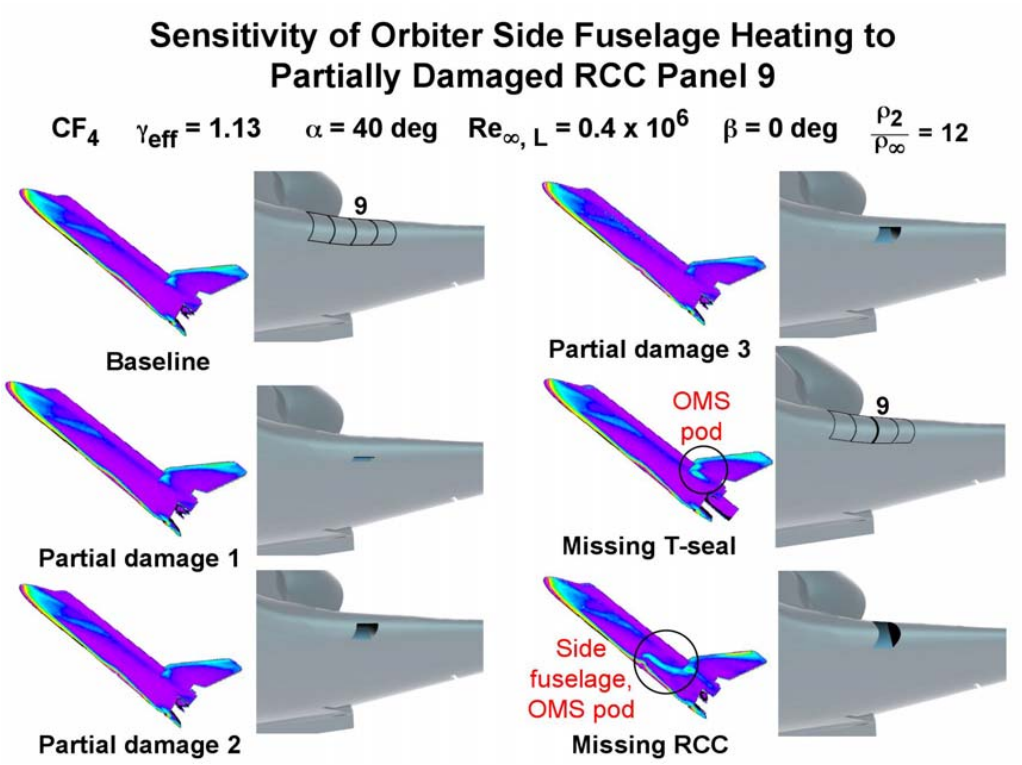

Figure 5.2.3-18 Effect of various types of panel 9 damage on side fuselage heating

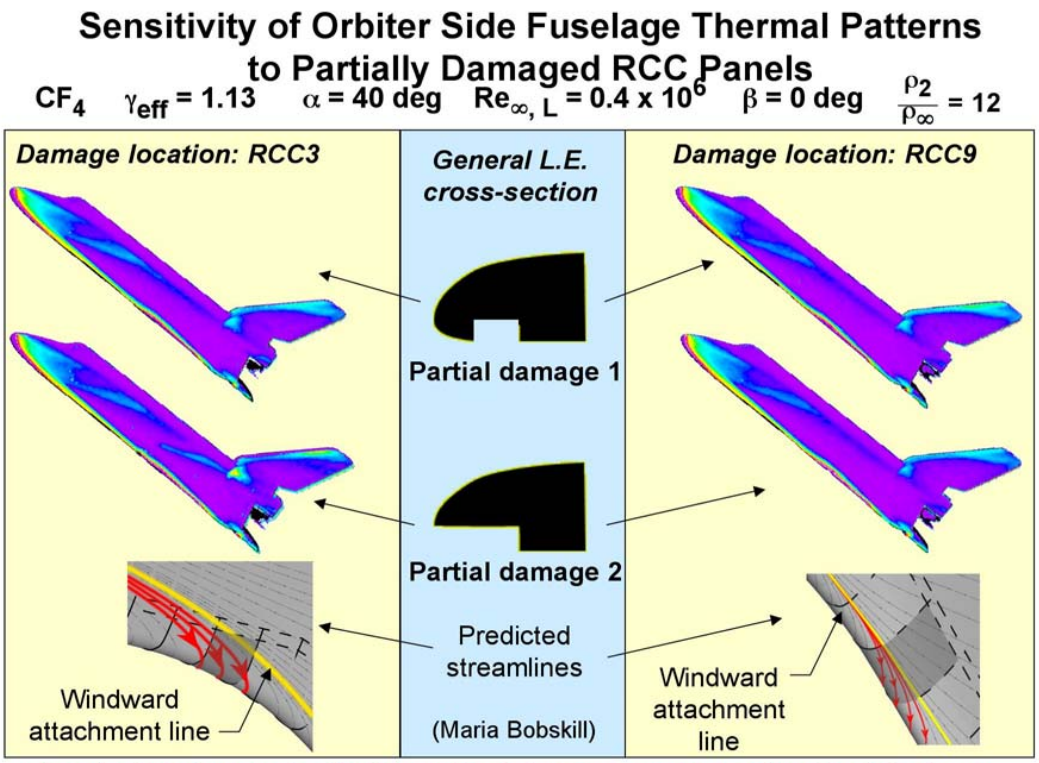

Figure 5.2.3-19 Partial panel damage assessment

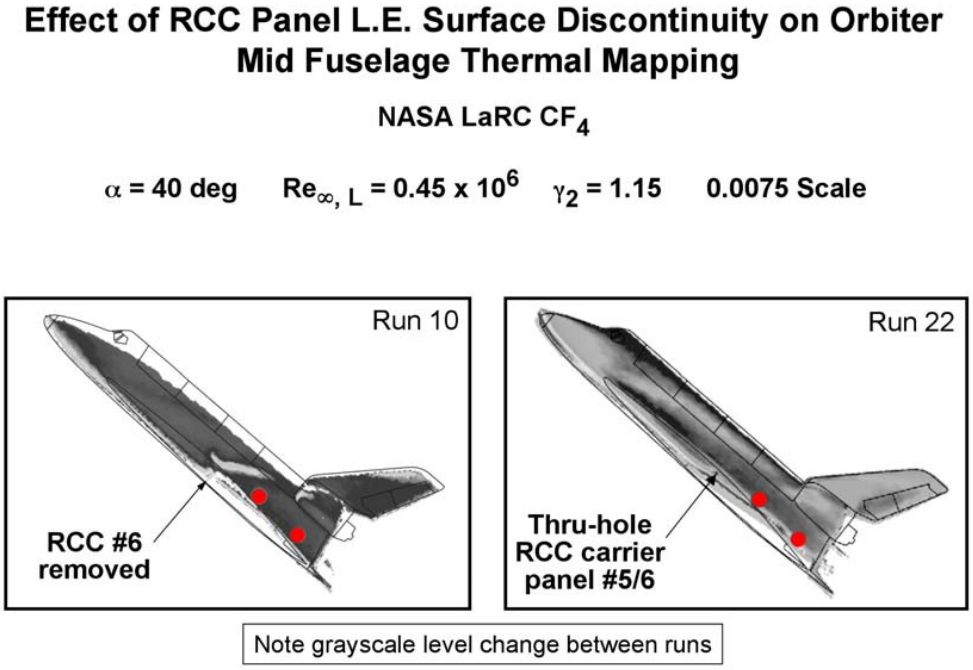

Figure 5.2.3-20 Hole through the wing assessment

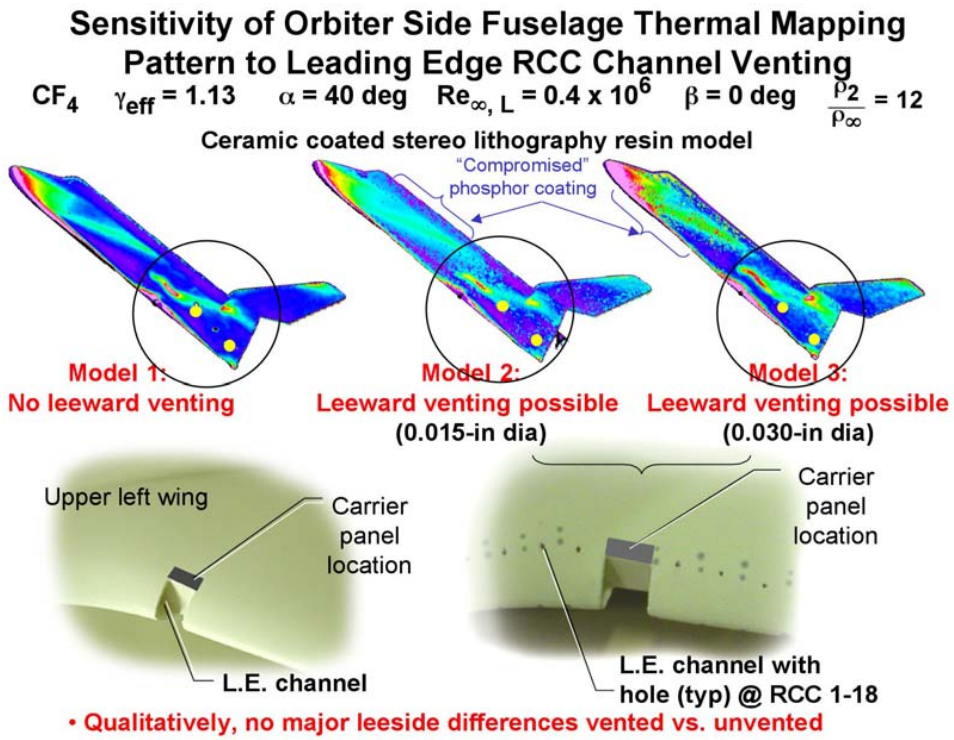

Figure 5.2.3-21 Initial assessment of venting with panel 9 missing and WLE cavity

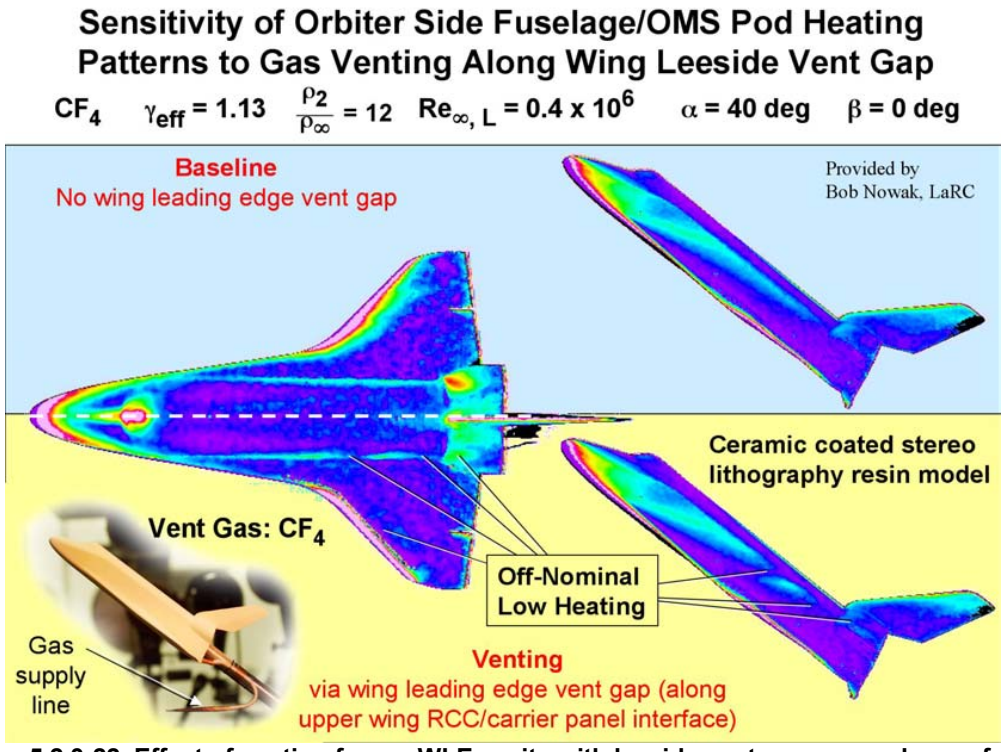

Figure 5.2.3-22 Effect of venting from a WLE cavity with leeside vents; gas supply was from a pitot probe in the flow field

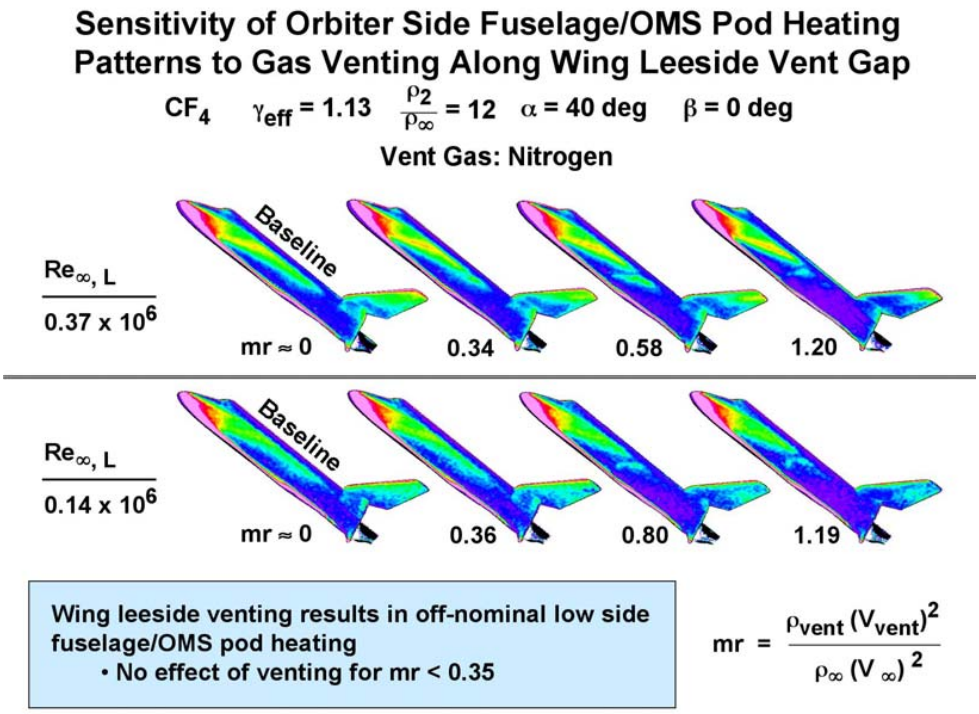

Figure 5.2.3-23 Reynolds Number and Momentum Ratio variation effects on side fuselage heating; gas supply from regulated GN2

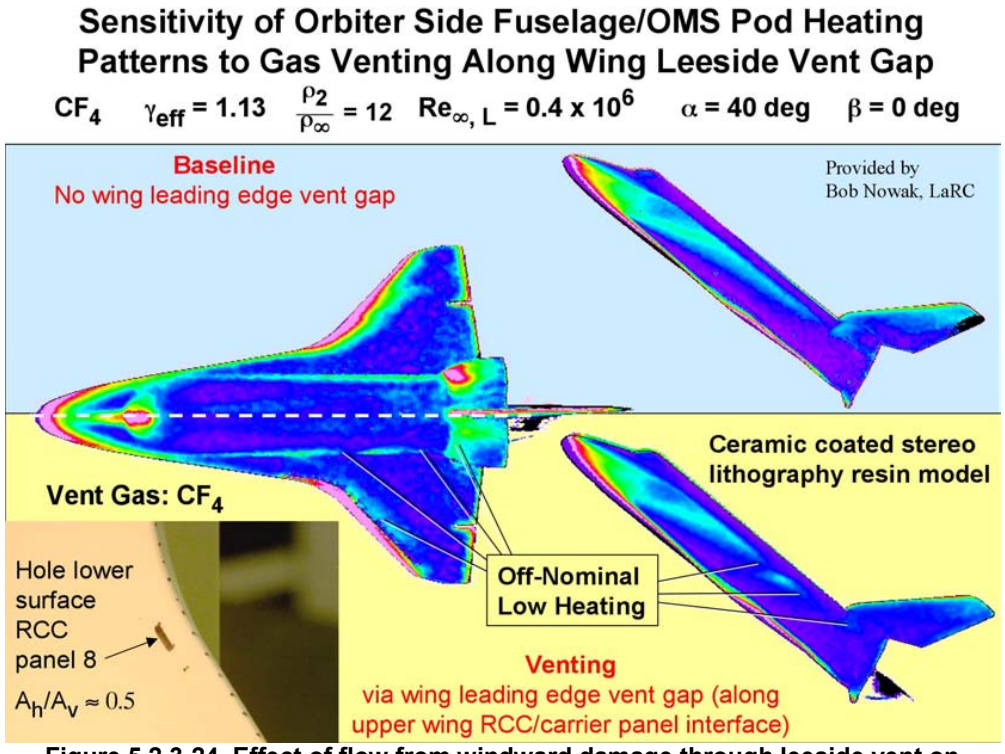

Figure 5.2.3-24 Effect of flow from windward damage through leeside vent on side fuselage heating

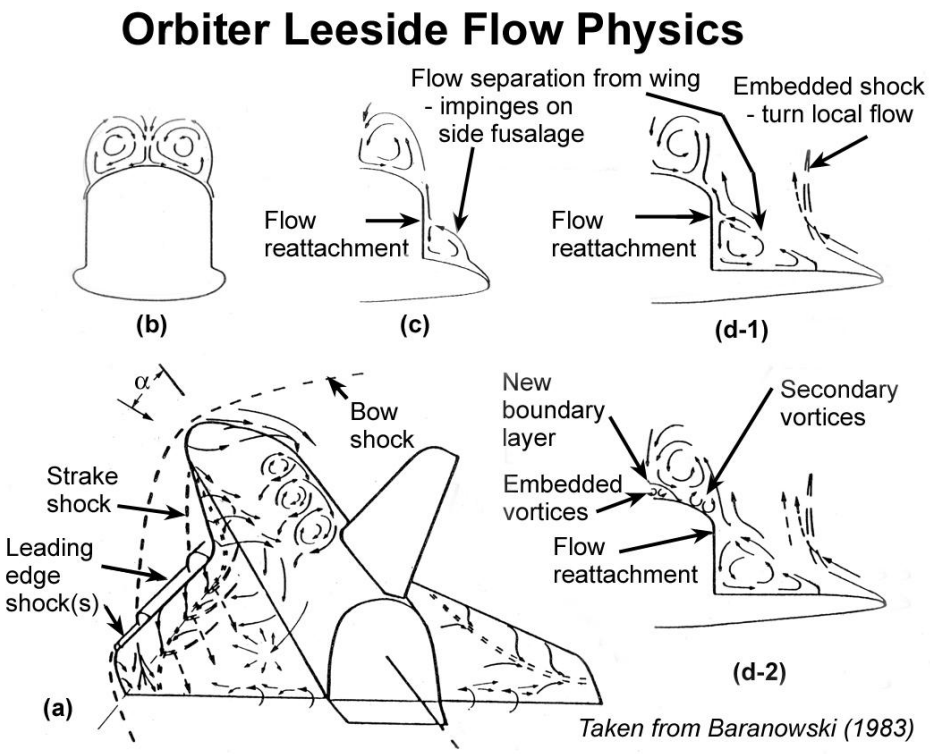

Figure 5.2.3-25 Orbiter Leeside Flow Physics

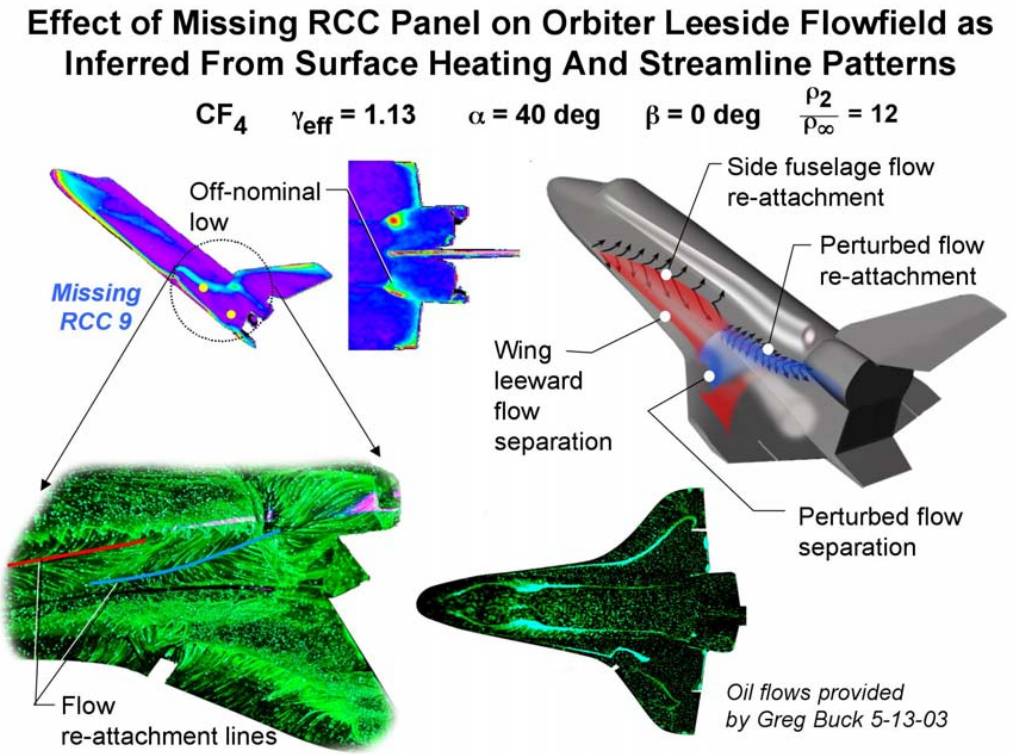

Figure 5.2.3-26 Phosphor Oil Flow showing leeside surface flow separation

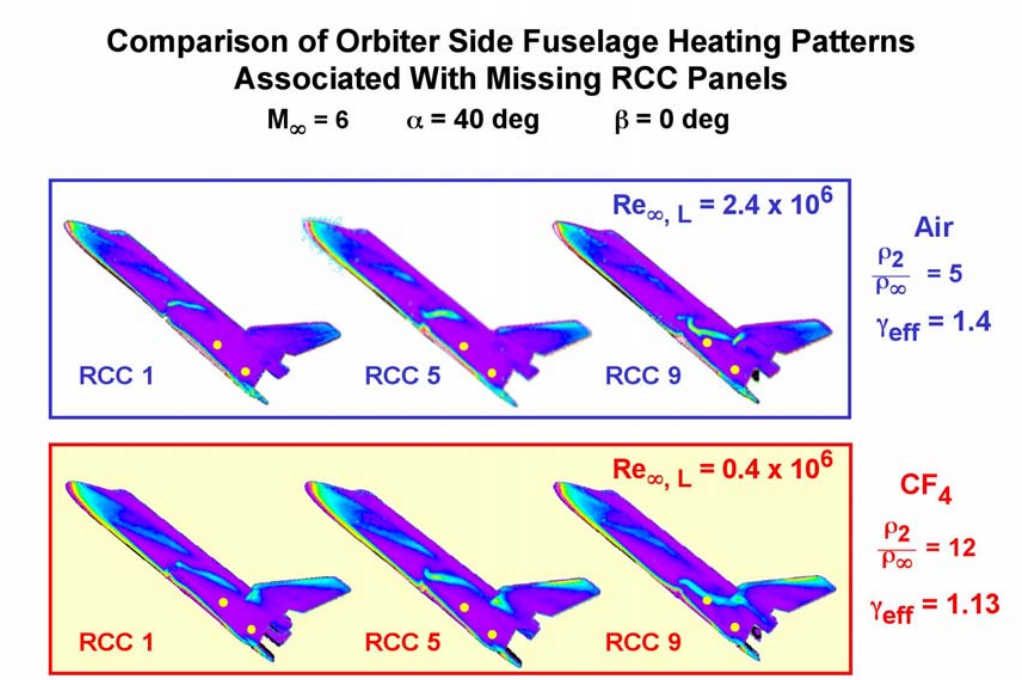

Figure 5.2.3-27 Comparison of Orbiter Side Fuselage Heating Patterns Associated with Missing RCC Panels

5.2.4 Computational Fluid Dynamics (CFD) and Direct Simulation Monte Carlo (DSMC)

5.2.4.1 Introduction for CFD and DSMC

Investigations of the Orbiter's external flow field encompassed several aspects of numerical analyses, from the high altitude rarefied regime to the lower altitude continuum regime. Since no ground-based facility can reproduce the Orbiter environments during hypervelocity re-entry conditions, the use of numerical simulations to understand the flow field at flight conditions was critical during the investigation. The analyses goals were primarily focused on two topics, providing nominal external flow field information supporting localized engineering analyses, and damaged configuration solutions to investigate changes in the aerodynamic and aerothermodynamic characteristics of the Orbiter. Because the magnitude of these analyses is daunting, a parallel effort across several organizations was required. The Navier-Stokes tools employed in the continuum regime analyses included GASP, LAURA, OVERFLOW, SACCARA and USA. The Direct Simulation Monte Carlo (DSMC) tools utilized in the rarefied regime included DAC and ICARUS. More details on each of the tools can be found in the Appendices.

Several concerns affected how the effort was approached, and effective utilization of the array of organizations and tools required the team to follow a staged route in the generation of the External Environments. Concerns with how the effort was approached center around aspects of validation and calibration of the numerical results. Information provided from STS-107 OI data highlighted the idea that significant efforts would be required to assess Orbiter leeside heating environments, yet no extensive leeside calibration effort has ever been performed with Orbiter flight data. In addition, concerns also exist about the validity of numerical simulations for damaged leading edge geometries. In light of these concerns, many leeside environment aspects and the damaged leading edge environment aspects from the numerical solutions must be viewed with an appropriate perspective. The perspective to take is that the solutions relied on established best practices at the time of the investigation. However, they are in essence uncalibrated for the leeside flow field and/or damaged leading edge configurations. Some effort was undertaken to assess the accuracy of the solutions by performing a comparison with STS-2 flight-derived surface temperatures and heat flux. Further information from that study is included in Section 5.2.4.3 (CFD/DSMC Validation). In addition, a study was initiated to characterize our ability to model the hypersonic leeside Orbiter flow field at wind tunnel conditions. Further information from that study is also included in Section 5.2.4.3 (CFD/DSMC Validation). Despite the concerns above about perspective and calibration, it is important to point out that the simulations can still provide much insight into the flow field characteristics and physical mechanisms at work on the Orbiter leeside. Also, an approach of using the results more in an engineering sense than in an absolute quantitative or scientific sense is what will drive interpretations of the CFD and DSMC numerical results to be presented in later sections.

As mentioned above, effectively utilizing the External Environment team's assets (tools, people and computers) to develop relevant CFD solutions required the use of a staged route. The first step in this staged route involved relying on established best practices to generate a suite of initial solutions on the undamaged Orbiter configuration with grid systems that were already available. However, the existing CFD grid systems from the various contributing organizations were markedly different in their intended purpose, resolution and even their Orbiter geometry representation. Thus, while these initial solutions were being generated for STS-107-specific re-entry conditions, an effort was undertaken to standardize the team on a single Orbiter CAD definition and generate a Common Baseline grid system that could be used to generate an extended set of solutions for both nominal and damage scenario configurations. Further information on this common grid generation effort can be found in Section 5.4.2 (Grid Development). Because of the difference in resolution requirements between DSMC and Navier-Stokes solutions, the Common Baseline grid developed for the Navier-Stokes studies was inappropriate for the DSMC analyses. For this reason, the decision was made to use a heritage DSMC Orbiter surface grid that has been shown to agree well with Orbiter aerodynamic flight data in previous studies. Later, as our understanding of the available flight data grew and was affected by a rapid and dynamic environment of investigation, the External Environments team simulations took on three distinct aspects. These aspects are nominal solution environments, to be covered in Section 5.2.4.4, providing damaged leading edge simulations, covered in Section 5.2.4.5, and providing simulations on other damage configurations that supported the effort to focus down to the Working Scenario. Those additional efforts will not be covered in any detail in this report, however.

5.2.4.2 Grid Development

Many aspects of numerical analyses are driven as much by process requirements as the particular physical modeling assumptions. In the simulation of hypersonic or hypervelocity flow fields, local changes in surface definition or grid density can affect the flow field results. These localized changes can be difficult to attribute specifically to either the surface definition or differences in results obtained by different tools and/or users. In order to move beyond discrepancies generated by differences in surface definition or grid resolution among the various numerical tools, an effort was undertaken to standardize the Aerodynamics and Aerothermodynamics teams on a common surface definition. In addition, the External Environments team standardized their Navier-Stokes simulations on a Common Baseline grid system. However, the DSMC simulations did not utilize the Common Baseline grid system. The Common Baseline grid developed for the External Environments Navier-Stokes studies was inappropriate for the DSMC analysis because of the resolution of the surface geometry. Over-discretization of the surface reduces the sampling count used to convert the microscopic events simulated by DSMC into macroscopic properties, thus increasing the statistical noise. Therefore, for the DSMC calculations, the decision was made to use a heritage DSMC Orbiter surface grid that has been shown to agree well with actual Orbiter flight data in previous studies. Efforts to standardize the Aerodynamics and Aerothermodynamics teams on a specific CAD definition are described in this section. In addition, details on the CAD definition developed as a standard for the Aerodynamics and Aerothermodynamics teams are provided. Also included is an overview of the Common Baseline grid system utilized by the External Environments team.

A majority of the viscous flow simulations performed for the Space Shuttle Orbiter Columbia accident investigation utilized structured volume grids. Structured grids are comprised of a logical or computational domain, characterized by three mutually orthogonal curvilinear coordinate directions. The orthogonal coordinates, in combination with a mapping that dictates how the points are placed on the surface of the vehicle, describe a vehicle to be analyzed. The mapping is referred to as a topology. It links the physical domain where the vehicle is typically described with Cartesian coordinates such as (x,y,z), to the computational domain where the coordinates are typically (i,j,k) and form a cube. In a structured grid, the most important issues to be addressed are the integrity of the outer mold lines that define the surface of the vehicle, the topology, and the quality of the grid with respect to the viscous flow solver to be used. Each of these issues will be discussed within the context of presenting our overall grid generation approach.

Initial computations performed by NASA (ARC, LaRC, and JSC), Boeing, and SNL made use of existing surface and volume grids for viscous flow simulations. The geometry description in use by most organizations prior to the STS-107 investigation was a version of the Shuttle Orbiter developed by Mississippi State University, under contract to NASA-JSC in 1997. This geometry, referred to as the ’97 definition, had several problematic regions on the vehicle, including an abnormally thick leading edge in the region of wing crank, and improperly modeled geometry at the wing tip/aileron junction. At the time of the accident, however, Navier-Stokes grids from the various organizations based on the ’97 definition were the most accurate available. Thus, these initial meshes were used to commence computational fluid dynamic (CFD) simulations.

Despite inaccuracies in the ’97 definition, NASA –LaRC developed a damaged RCC panel 6 geometry on that database. The volume grid was a modified version of an existing single-block volume grid, originally consisting of more than 9 million points. The damaged panel 6 geometry was estimated from existing Space Shuttle Orbiter Experimentation (OEX) documents. The surface and volumes of the previously existing grid system were modified to accommodate a damaged panel utilizing the “embedded” O-grid technique, and a new volume grid of 18 blocks and more than 18 million points was developed. This definition of panel 6 damage, referred to as the panel 6 “notch” grid, was used in many different computations performed at LaRC, Boeing, SNL, and JSC. It was so-named because the length of the missing RCC panel 6 was one half of the actual panel; hence it was a mere notch in the wing leading edge. Owing to its early availability, the panel 6 “notch” definition was used for many of the initial damaged RCC computations In addition, the generation of a volume grid on this early geometry definition provided extremely valuable insights towards developing structured volume grids for all subsequent leading edge damage scenarios.

In parallel with the CFD calculations that began on the pre-existing meshes, a new effort was initiated by the External Environments team to develop a common baseline grid. Following several discussions with representatives from all groups, an embedded O-grid topology was chosen. The embedded O-grid topology provides flexibility, enabling accurate computation of various damage scenarios with significantly reduced volume grid regeneration. As shown in Figure 5.2.4-1, there are three possible structured grid topologies. Each topology is so-named because of its structure; the O-grid looks like an O, and similarly for the C- and H-grids.

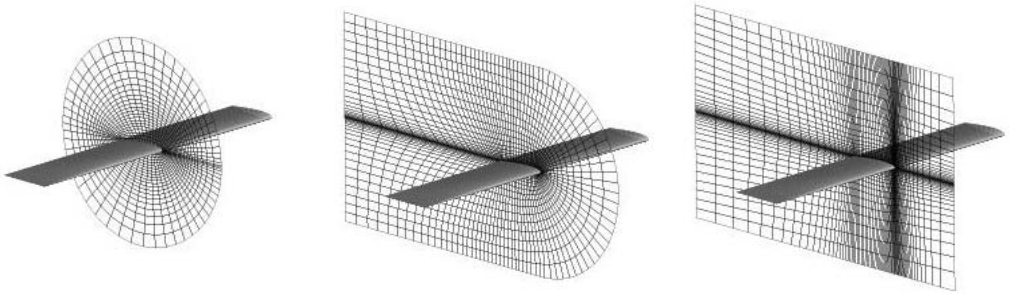

Figure 5.2.4-1 O-, C-, and H-grid topologies

For the common baseline grid, an O-grid wrapping around the entire vehicle from the top to the bottom was used as a starting point. The wings were then isolated topologically with C-grids so that grid resolution along the span of the wings would be completely independent of the main O-grid that wraps around the vehicle, as shown in Figure 5.2.4-3. This topology was chosen specifically because it permits blocks on the wing within the

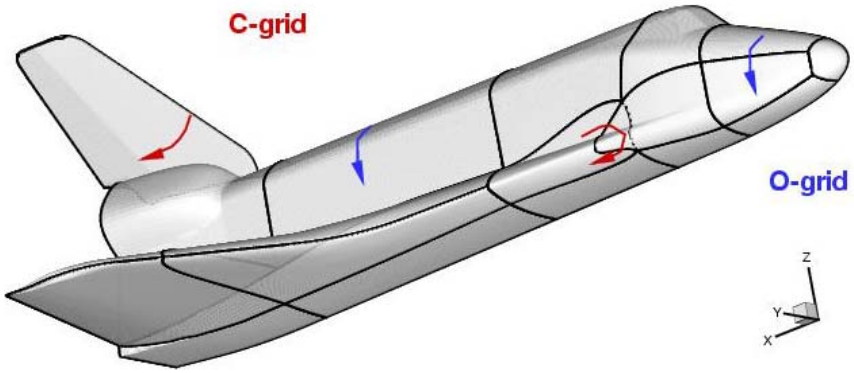

Figure 5.2.4-2
Figure 5.2.4-3 Common grid baseline topology

C-grid to be removed and replaced with an “embedded” O-grid, thus focusing grid points to a damaged leading edge area by altering the spacing and clustering.

Common baseline grid development began with the creation of a smooth outer mold line (OML) version that could be used to benchmark all the flow solvers from the various organizations. As noted previously, initial computations used the ’97 OML definition for the grid systems. The ’97 geometry definition had several accuracy issues, mentioned above, that needed to be addressed. These issues led to the development of a new, more accurate geometry description from computer-aided design (CAD) data provided by NASA -JSC to NASA-LaRC and ARC. The geometric description provided by NASA-JSC was not a complete geometry, as it had several regions where surfaces describing the wing and fuselage were not sealed. This produced holes where a grid could not be generated. Thus, the CAD representation was slightly modified to ensure that a solid model could be mathematically described with the data provided by NASA-JSC. To ensure a good solid model, the CAD representation was modified by filling in the “holes” and smoothing over gaps between the control surfaces and the respective hinge lines. In addition, the control surfaces were positioned based on initial STS-107 flight data. The resulting

surface definition became the '03-definition of the Space Shuttle Orbiter and it was utilized for the common baseline grid generation.

The process used in the common baseline grid generation, as well as many of the subsequent surface and volume grids used for viscous flow simulations is shown in Figure 5.2.4-4.

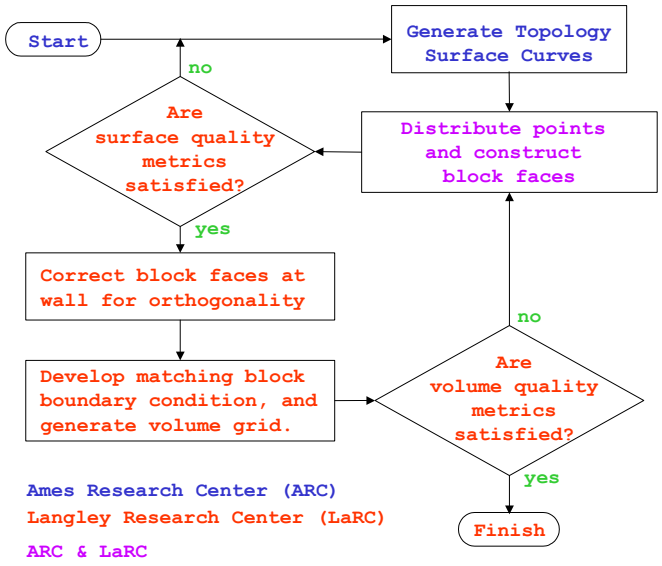

Figure 5.2.4-4 Grid generation process with ARC and LaRC

The first step in generating the common baseline grid system was the development of the basic grid topology. After the topology was developed, the next step involved the detailed generation of the surface meshes over the entire OML of the Orbiter. Next, initial block faces for all of the non-surface faces that defined the volume grid boundaries were created to produce a complete first sketch of the entire mesh. After these initial surfaces were constructed, the surface grids and initial block faces were evaluated for overall grid quality. Modifications were then made to ensure orthogonality of the grid lines emanating from the wall and to ensure that the grid metrics could be satisfied for grid stretching. Once an acceptable quality was reached for the OML surface and block interfaces, an initial volume grid was generated. Newly developed technologies were developed by LaRC to ensure slope continuity across matching block boundaries, producing superior grids that could meet grid quality metrics requirements established by the team. These requirements will be discussed in more detail later in this sub-section.

The primary grid generation software used at NASA-ARC was the GridGen software from Pointwise Inc., while NASA-LaRC utilized a combination of GridGen, the Volume Grid Manipulator (VGM), and the Three-Dimensional Grids about Anything using Poisson's Equations with upgrades from Ames and Langley (3DGRAPE/AL) for grid generation. NASA-LaRC also used the CFD Analyzer software from AMTEC Engineering Inc. for grid quality evaluations. The GridGen software was used to develop the initial surface grids by constructing grid lines on the baseline IGES-format database. GridGen was also used to construct the volume grids. However, due to limitations in GridGen, the interfaces of all blocks with edges coinciding with the OML were modified with VGM. This was done to ensure that the block interfaces were locally orthogonal to the vehicle OML. After block interface modification, the VGM software was used to develop a C-II continuous boundary condition across matching block volume grids. The volume grids were then elliptically smoothed in GridGen. In some rare instances where GridGen was unable to produce a volume grid with all positive cell volumes, the 3DGRAPE/AL software was used to generate the volume grid. After GridGen smoothing, all volume grids were modified and improved with VGM to reduce grid stretching. Finally, individual organizations re-positioned the outer boundary location of the baseline common grid to closely match the bow shock location for a given flight condition. The

repositioning of the outer boundary also allowed re-stretching in the normal direction to optimize the grid distribution in the shock layer.

The development of all surface and volume grids for the damage scenarios investigated by the External Environments team used the baseline common grid as a starting point. Several complete volume grids were generated to model various damage conditions of the Shuttle Orbiter, including Missing Main Landing Gear door tiles (MLG), a forward dump valve investigation, and Missing Reinforced Carbon-Carbon (RCC) panel 6 and Missing RCC panel 9 configurations. In addition, the Aerodynamics team used this grid system for portions of their Navier-Stokes analyses. In a general sense, therefore, each grid was generated with the same process identified in Figure 5.2.4-4. Also, as the damage scenarios varied, only the wing region was modified to accommodate a given damage scenario. This is illustrated in Figure 5.2.4-5, where the wing blocks and the attached fuselage blocks (shaded yellow) are modified to accommodate a damage scenario. This figure also shows the "embedded" O-grid, which encompasses the damage site. Using this topology, the center square on the wing leading edge representing a missing RCC panel was resolved with many more grid points than in the nominal geometry grid. However, this additional grid density did not affect any other portion of the vehicle. This approach made generation of new damage scenario volume grids easier and more efficient because only the wing leading edge region blocks needed to be re-constructed. All subsequent damage scenarios were generated with this type of topology, enabling the development of several different volume grids for the Shuttle Orbiter within a two-month period. It is estimated that this procedure saved 50% of the grid generation time compared with rebuilding a new volume grid each time a different damage scenario was considered.

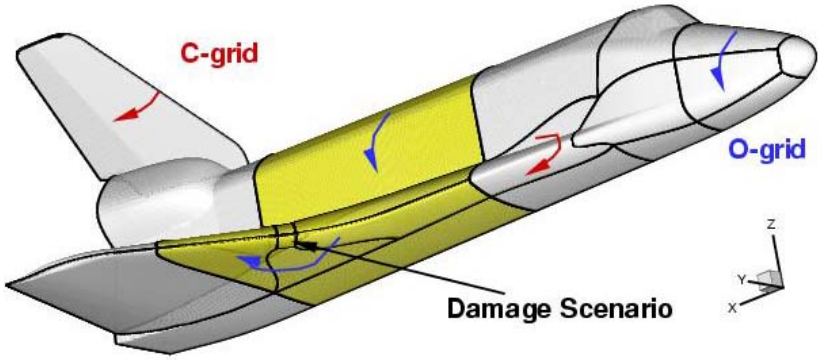

Figure 5.2.4-5 Damage scenario topology

Grid quality metrics used to assess the common baseline grid were defined based on extensive experience at NASA-LaRC in grid generation. The grid metrics used to determine the quality of the grid with respect to CFD include cell-to-cell stretching, interior and near-wall orthogonality, and cell volume. Based on previous work in structured grid generation, grid stretching should be less than a factor of 1.5 from one point to the next. Grid line orthogonality at the wall should be within 10 degrees of orthogonal, and cell volumes should be positive. These metrics are used to assess the grid quality by evaluating the maximum stretching, and minimum orthogonality, as well as the root mean square (RMS) and three-sigma values of the metrics, assuming a normal distribution. Based on anecdotal evidence obtained with the grids used for this effort, failure to adhere to reasonable limits for these metrics can result in inaccurate flow simulations. This evidence also suggests that grids with large values for these metrics will suffer from slower convergence of flow field residuals. Tabulated in Table 5.2.4-1 are the grid metrics for the common baseline grid, generated with the previously identified software and process. Note that the ξ-direction is streamwise from nose to tail, the η-direction is from top of the vehicle to the bottom, and the ζ-direction is from the wall to the outer bow-shock within the flow field. These directions represent the three mutually orthogonal computational coordinates that are used in the mapping of the grid to the geometry, using the topologies described. The common baseline grid contains nearly 3.5 million points and 20 blocks, and was suitable for computations by all viscous-flow CFD software used by the team.

Table 5.2.4-1 Baseline common grid quality metrics

	Minimum	Average ± 3σ	Maximum
I-Stretching (ξ)	1.000	1.048 ± 0.132	2.775
J-Stretching (η)	1.000	1.015 ± 0.132	2.775
K-Stretching (ζ)	1.000	1.013 ± 0.075	1.763
J-K Orthogonality (ξ)	0.018	0.671 ± 0.708	1.000
I-K Orthogonality (η)	0.042	0.729 ± 0.621	1.000
I-J Orthogonality (ζ)	0.023	0.836 ± 0.528	1.000

Additional Comments on Damage Scenario Meshes

Using the embedded-O mesh topology, the exterior grid resolution is focused toward the damage location. As previously noted, separate external meshes were created for the RCC panel 6 and panel 9 cases. The missing panel meshes allow the flexibility to assess a wide range of damage at a specific panel location. The inner perimeter of the focused embedded-O follows the OML at the RCC panel of interest. The External Environments team utilized two different topologies to investigate the damaged RCC panel parametrics. One group utilized a simple H-mesh interior for the missing RCC cavity. This topology required that Navier-Stokes spacing was achieved, tangential to the OML surface in the radial direction, as the external embedded-O mesh approached the perimeter of the damage location. The cavity itself is modeled with a simple H-topology that has Navier-Stokes spacing against each block face. The internal topology is broken out into a series of H blocks to permit various or progressive damage scenarios to be considered. For example the interior of an RCC panel removed cavity had separate H-grids for the carrier panels the RCC panel and the RCC channel interior. Each internal block maintained Navier-Stokes spacing against each of its six faces such that once the mesh was constructed any combination of upper/lower carrier panel and/or RCC panel could be computed without any re-gridding or re-stretching.

The second mesh topology used for damage scenarios employed a double-O mesh topology interior for the missing RCC cavity. While this topology required the creation of seven internal cavity blocks to ensure that Navier-Stokes clustering was obtained against all interior faces of the cavity, it did not require the Navier-Stokes clustering of the exterior grid except in the traditional normal direction. The inside of the cavity for the second option is constructed with a central H-mesh that is enclosed on six sides by unique blocks. Each of the surrounding six blocks has Navier-Stokes spacing against a single outward facing block face. This topology completely isolates the Navier-Stokes spacing, used against each of the interior walls, from propagating outside of the cavity region. However, the topology also requires interior cavity meshes (not the external mesh) to be constructed independently for the upper and lower panel out cases. Figure 5.2.4-6 shows a cut through the double-O interior mesh topology for the full panel 6 removed case. Similar interior mesh configurations were constructed for the full panel 9 out geometry and the two half panel out geometries.

For each damage grid option, the exterior mesh is built in two halves corresponding to upper and lower halves of the Orbiter, and is split at the wing leading edge water line. This split construction permits a missing upper half panel, a missing lower half panel, or a complete panel missing to be simulated from a single grid system. Furthermore, for each option the exterior meshes were clustered against all OML surfaces with Navier-Stokes spacing to meet a cell Reynolds number of approximately 1. Even the H-block that extends from the OML surface of the damage location to the outer boundary (present for both damage scenario topologies) has the same Navier-Stokes spacing. This exterior mesh construction, for either option, allows the various damage configurations such as smooth OML, half panel out and full panel out to be computed with changes only to the interior cavity mesh boundary conditions.

Both options allowed the region of the damaged RCC panel that vents into the leading edge channel to be modeled with an outflow boundary condition. The first option, with a simple H mesh interior to the cavity, was chosen for the LAURA simulations. It allowed the flexibility to easily re-distribute the grid to

satisfy a surface grid spacing criterion. However, this capability also resulted in a larger grid system due to the competing requirements of Navier-Stokes spacing in the radial/tangential direction along the perimeter of the damage location and the less than 1.5 point-to-point stretching ratio. The only way to meet both demands was to increase the number of points within the external common grid topology. The second option allowed the flexibility to model various damage scenarios using a single external grid system that could have considerably fewer points since there were no demands on Navier-Stokes spacing in the tangential/radial direction, but this flexibility was obtained at the expense of a topologically more complex internal cavity grid system and the need to have independent internal cavity meshes for either half- or full panel out scenarios. The two topologies are depicted in Figure 5.2.4-6 and Figure 5.2.4-7. Both topologies were utilized for the damaged RCC panel parametrics considered, and the various simulations performed with GASP and LAURA will be described in more detail in the damage scenario description of the CFD results.

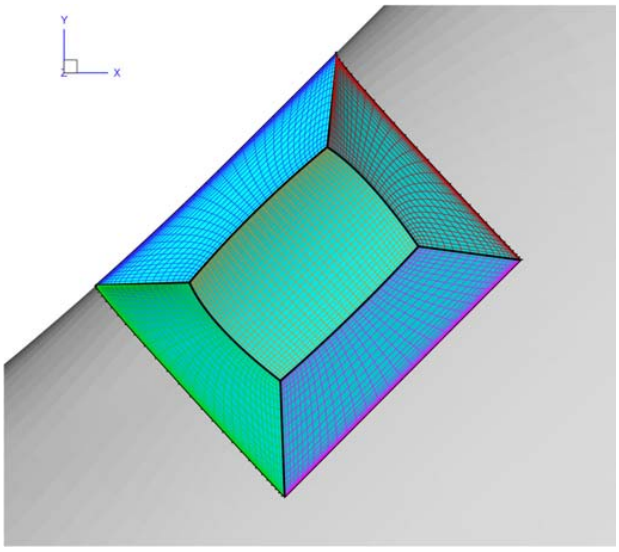

Figure 5.2.4-6 Cut through full panel out interior cavity mesh for GASP simulations

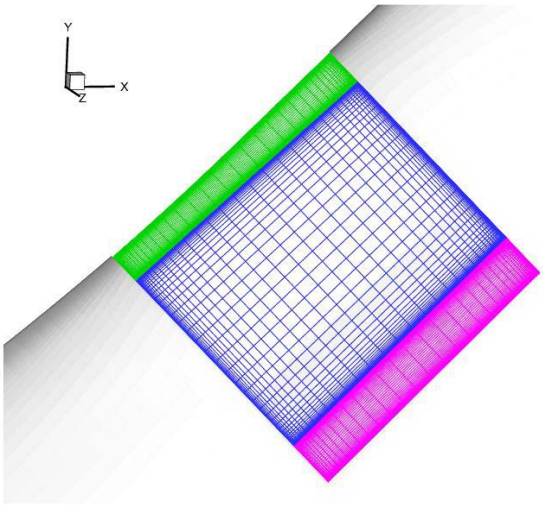

Figure 5.2.4-7 Cut through full panel out cavity mesh for LAURA Panel 9 simulation

5.2.4.3 CFD/DSMC Verification for the Orbiter Configuration

In order to determine laminar and turbulent heating rates and surface temperature uncertainty bands for the primary Navier-Stokes solvers used in the investigtion, researchers from Boeing Huntington Beach, NASA-ARC, and NASA-LaRC computed Navier-Stokes CFD solutions to compare against STS-2 flight data at three trajectory points, two laminar and one turbulent. Results from this study are provided in the following section. The CFD codes USA, LAURA, and GASP were used for the simulations by the Boeing-Huntington Beach, NASA-LaRC, and NASA-ARC groups, respectively, and are described in Section 5.6. Since this work was done prior to the completion of the common CFD grid, the grids available to each group at the time of STS-107 were used. They did not include body flap or elevon deflections and had been constructed primarily to capture windward side heating.

In order to make a comparison with flight data, three STS-2 trajectory points were simulated using the free-stream conditions shown in Table 5.2.4-2. The Mach 24 point was selected to approximate the conditions at the start of the peak heating region on the STS-107 trajectory. The Mach 18 point was selected to approximate the point on the STS-107 trajectory for which good GPS data were available. The Mach 7 point was selected to provide a turbulent comparison case.

Table 5.2.4-2 Freestream conditions for STS-2 computations

Case	M	V	ρ	T	alt.	Re/L
		(m/s)	(kg/m^3)	(K)	(km)	(1/m)
t = 75260 s	24.3	6920.0	5.7500E-05	202.00	72.400	28439
t = 75950 s	18.1	5617.0	1.6260E-04	240.60	64.400	56430
t = 76310 s	7.7	2486.0	1.9130E-03	256.90	45.070	278700
Case	**M**	**V**	**ρ**	**T**	**alt.**	**Re/L**
		(ft/s)	($slug/ft^3$)	(R)	(ft)	(1/ft)
t = 75260 s	24.3	22714.0	1.1152E-07	363.29	237670	8822
t = 75950 s	18.1	18430.0	3.1558E-07	433.07	211440	17958
t = 76310 s	7.7	8156.0	3.7094E-06	462.56	147870	88576

Comparisons between the computed and flight derived surface heat transfer rate data provide an additional measure of confidence in the numerical simulations at flight conditions. The results of these comparisons using the experimental data derived by Throckmorton and Hartung are discussed in the following paragraphs. Additionally, code-to-code comparisons are presented for predicted surface pressures. All calculations were made with a 5 species nonequilibrium chemistry model assuming thermal equilibrium. A radiative equilibrium wall boundary condition with the emissivity set to 0.90 was used. The RCG catalysis model from Stewart was used for the entire vehicle for each of the solvers. In the case of the Mach 7 condition,. NASA-LaRC used the Cebecci-Smith turbulence model, while NASA-ARC used the Baldwin-Lomax turbulence model.

Mach 24 Results

Figure 5.2.4-8 shows STS-2 flight data for surface heat flux plotted over the computed results for the windward side of the orbiter. The two tiles covered with a catalytic coating are indicated in the figure. The GASP and LAURA results are in general agreement, and the comparison with the data is good. The solutions are not expected to match the data in the body flap region since neither Ames nor Langley modeled the actual body flap deflection in their solutions.

Figure 5.2.4-9 gives a more quantitative comparison of the results along the windward centerline. The comparison between both predictions and the flight data is excellent for the non-catalytic locations

upstream of the body flap. A fully-catalytic GASP solution is also shown in Figure 5.2.4-9. The prediction matches the data at the downstream catalytic tile, but under-predicts the heating at the upstream catalytic tile. This under-prediction is not surprising since the computation is not modeling the physical situation of a catalytic tile surrounded by non-catalytic tiles. The heating on the isolated catalytic tile downstream of non-catalytic tiles should be higher than the heating at the same location downstream of catalytic tiles. The higher heating can be attributed to higher atomic species mass fractions in the boundary layer. The atomic species exist in higher quantities for the non-catalytic upstream tiles case because a lower-catalycity surface suppresses recombination of the atomic constituents. Thus, for an isolated catalytic tile in the vicinity of non-catalytic tiles, more atomic species exist in the approaching boundary layer, providing more potential for catalytic heat transfer.

The heating rate uncertainty, defined as the difference of the computed and flight derived heating rates divided by the flight derived heating rate, is shown in Figure 5.2.4-10 at every measurement location. The same data are also presented in Figure 5.2.4-11 as a function of axial co-ordinate down the Orbiter.

Figure 5.2.4-12 shows the computed heat transfer rates from GASP and LAURA on a slice through the Orbiter at a location of X = 1215 in Orbiter coordinates, which passes just downstream of the main landing gear (MLG) door. The agreement between the two codes on the wind side and around the wing leading edge is quite good. On the leeside, the results differ by as much as 100%, although this is not surprising since neither grid was optimized to capture leeside heating. In fact, the grid used for the GASP calculations is particularly coarse. The Z-location of RTD V34T1106 is indicated in the figure.

The heating results for a slice at Y = 167 in are shown in Figure 5.2.4-13. This slice is along the outboard edge of the MLG. On the wind side, the predictions of the two codes are within 10% of each other, and the heating rates on the WLE are within 2%. Figure 5.2.4-14 shows the predicted heating rates along the WLE. The codes are in good agreement except in the downstream region where the LAURA heating rates are about 30% higher than the GASP heating rates. Given the difference in grid resolution between the two solutions, a difference of 30% is not unreasonable. In addition, the shock-shock interaction region is a particularly difficult feature to resolve numerically. Because of this and the fact that a comprehensive calibration study using Orbiter wing leading edge heating flight data has not been performed, questions remain about what is required to obtain an accurate flight prediction.
The comparison of windward centerline pressure predicted by GASP and LAURA is shown in Figure 5.2.4-15. The two codes give similar answers, except for the wiggles in the GASP solution between $0.3 < X/L < 0.5$. These wiggles are caused by waves in the surface geometry used to create the GASP grid. Later comparisons for STS-107 cases computed on the common grid showed good agreement between the GASP and LAURA results.

Mach 18 Results

The results for Mach 18 are similar to the results for Mach 24. Figure 5.2.4-16 shows the computed and flight derived surface heat transfer rates on the windward side of the Orbiter. Figure 5.2.4-17 shows a comparison between the CFD predictions and the flight data on the windward centerline. Figure 5.2.4-18 and Figure 5.2.4-19 show the uncertainties in the computed data. The off-centerline results show the same trends as in the Mach 24 case. GASP and LAURA agree within about 10% of each other on the wind side, but differ on the lee side due to the differences in the grids.

Mach 7 Results

Figure 5.2.4-20 shows the computed and measured heat transfer rates for the Mach 7 turbulent trajectory point. In GASP the Baldwin-Lomax model was turned on at X/L = 0.4. In LAURA, the Cebecci-Smith turbulence model was turned on at X/L = 0.3. The flight data indicates transition in the region $0.3 < X/L < 0.5$. The GASP computation predicts higher heating than the LAURA computation. The higher heating in GASP can be seen clearly in Figure 5.2.4-21 where results on the windward centerline are presented. Figure 5.2.4-22 and Figure 5.2.4-23 show the uncertainties in the computed data.

Summary of STS-2 Surface Heating Comparisons

The agreement among the CFD codes utilized in this comparison to STS-2 flight derived heat flux data is generally very good considering that different codes and different meshes were used. There are some windward oscillations in the GASP solutions due to waviness in the surface grid. In addition, differences between the results from LAURA and GASP are apparent on the lee side. However, as mentioned previously, the grids were not tailored to capture leeside heating, and it is likely that lack of grid resolution is the reason for the differences among the codes. Only a comprehensive calibration study of leeside flow heating environments on the Orbiter can establish whether differences in leeside heating between the two solvers are due to grid resolution.

Table 5.2.4-3 shows the standard deviation of the computed heat transfer rates from the flight data for the windward surface gauges upstream of the body flap and elevons, forward of X = 1433.2 in. The laminar results are within about 15% of the data, while the turbulent results are within 30% of the data. The poorer than expected comparison with the turbulent results could be due to the fact that the radiative equilibrium assumption at the wall may not be valid. The flight data do show differences of up to 20% between the inferred radiative equilibrium heat fluxes and convective heat fluxes, suggesting that the surface is not in radiative equilibrium.

Table 5.2.4-3 Standard deviation of heating results

	LAURA	GASP	USA
M=24 Laminar	12.50%	12.60%	N/A
M=18 Laminar	11.20%	15.30%	N/A
M=7 Turbulent	27.70%	27.20%	N/A

Comparisons of Computed and Measured Surface Streamlines at Wind Tunnel Conditions

The simulation of leeside flows with computational fluid dynamics is a challenging endeavor, and the inclusion of leading edge damage parametrics into the activity makes the effort even more difficult. Most activities for the simulation of hypersonic flow fields have focused on the windward regions where surface heating drives the selection of thermal protection systems. In the case of the Space Shuttle Orbiter, no comprehensive leeside flow field calibration study has ever been performed. Because of this lack of historical base, the leeside results included in this report need to be looked at from an engineering perspective, as mentioned in Section 5.2.4.1. In order to provide some information on the quality of the leeside flow field results from the CFD simulations, LAURA computations were performed to simulate a wind tunnel experiment in the LaRC Mach 6 CF_4 wind tunnel. The computation was performed using the thin layer formulation of the Navier-Stokes equations assuming laminar flow and vibrational equilibrium. The grid used for these computations had 2 million cells, most of which were devoted to the vehicle windward side, and was derived from the '97 geometry definitions. The grid covered the leeward side and windward side of the vehicle but did not extend into the wake. The model scale for the computations was 0.75%. The angle of attack was 40 degrees and the sideslip angle was 0 degrees. A constant wall temperature boundary condition of 300 K was assumed, and the Mach 6 CF_4 CFD computation was run with the following free-stream conditions:

Mach = 5.902
Velocity = 889.84 m/s
Density = 1.9417e-2 kg/m3
Temperature = 198.38 K
Reynolds Number= 0.44 million/ft

The CF_4 wind tunnel experiment, run at 40 degrees angle of attack, had the following free-stream conditions:

Mach = 5.94
Velocity = 880 m/s
Density = 1.97e-2 kg/m3
Temperature = 190 K
Reynolds Number = 0.47 million/ft

The two sets of conditions are very similar, but are not an exact match because the CFD conditions were chosen before the wind tunnel experiment was performed. However, these free stream conditions are considered similar enough to provide a valid comparison. Computed and measured streamlines on the lee side of the vehicle are shown in Figure 5.2.4-24. The experimental streamlines, shown in the top of the figure, were obtained from post-run images using an oil flow technique. The lower images are computed surface streamlines from the LAURA simulation at the wind tunnel conditions listed above. While differences, possibly due to grid resolution, are observed in the computed and measured locations of the strake vortex separation line on the aft portion of the wing leeside, the code predicted the separation and reattachment line locations of the strake and canopy vortices. In general, good agreement was observed in this first comparison of leeside surface streamlines between the viscous solver LAURA and CF_4 wind tunnel measurements. The level of agreement in the streamline patterns between the experimental and numerical results demonstrates the confidence level that can be expected for the leeside flow simulation. Certain aspects of the flow field show quite reasonable agreement, e.g., the separation and reattachment locations on the fuselage and inboard wing regions, while others show less agreement, e.g., the outboard region of the wing leeside. The LAURA simulation was obtained using best practices available at the time of the accident, which do not include an a priori knowledge of what is necessary and sufficient to model the lee side of the Orbiter flow field. This statement is true for both wind tunnel and flight conditions. These results reinforce the statement made in Section 5.2.4.1 and reiterated here. Critical insight can be gained into the flow field characteristics and physical mechanisms at work on the Orbiter leeside. But, an approach towards interpreting the results more in an engineering sense than a scientific sense must be used for any of the leeside numerical results in this report because an established practice for obtaining accurate Orbiter leeside simulations is not known at this time.

Comments on DSMC Verification

A comparison of DSMC heating results with STS-2 flight data was also considered. After reviewing the available STS-2 data from Throckmorton and Hartung, it was decided that a comparison could not be made with the DSMC methodology. This was because the surface thermocouple data available showed little or no temperature response at the higher altitudes where it is reasonable to employ the DSMC method. Therefore, it was determined that an aerodynamic comparison previously made between STS-62 flight data and DSMC results would serve as verification that the surface geometry selected was acceptable to use for the DSMC analysis work done to support this investigation. More information on that study can be found in Boyles (2003). The Orbiter surface geometry used in the study by Boyles was also used for the 350,000 ft altitude DSMC solution performed for the STS-107 investigation, and the 300,000 ft altitude DSMC solution utilized a slightly finer resolution Orbiter definition. In addition to the conclusion to rely on the aerodynamic study as sufficient calibration for the STS-107 investigation, the judgment was made to accept the heating results obtained using the best practices available at the time of the accident. Therefore, to date, no comprehensive comparison has been made of DSMC heating results for the Orbiter at rarefied re-entry conditions.

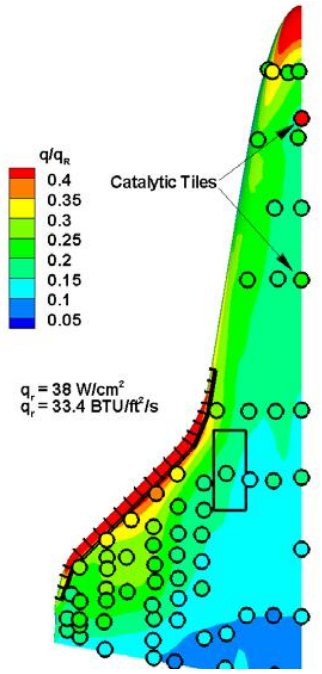

a) GASP

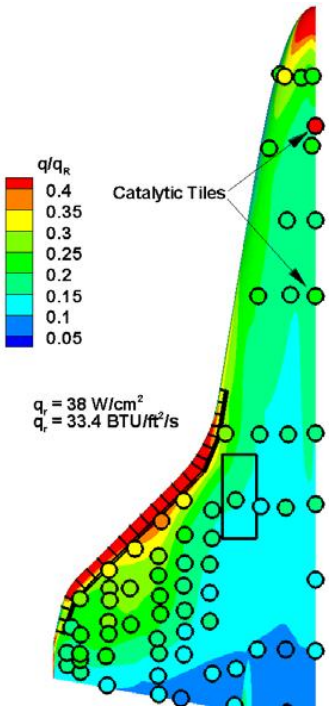

b) LAURA

Figure 5.2.4-8 Windward surface temperature predictions from GASP and LAURA compared with flight data at Mach 24. Experimental data are plotted inside the circular symbols. The symbol size is made larger than the measurement extent to aide visualization of the data.

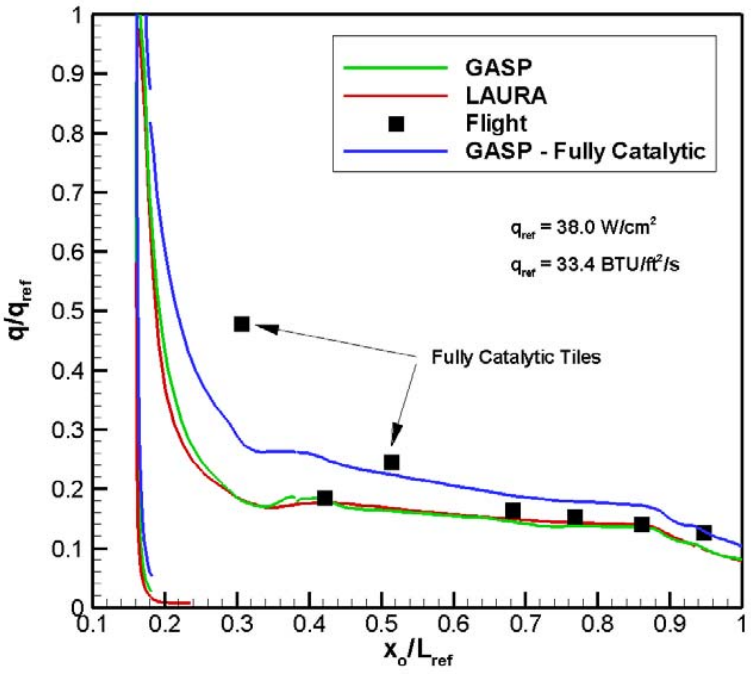

Figure 5.2.4-9 Windward centerline heat transfer rate for Mach 24. L_{ref} = 37.24 m = 1466 in

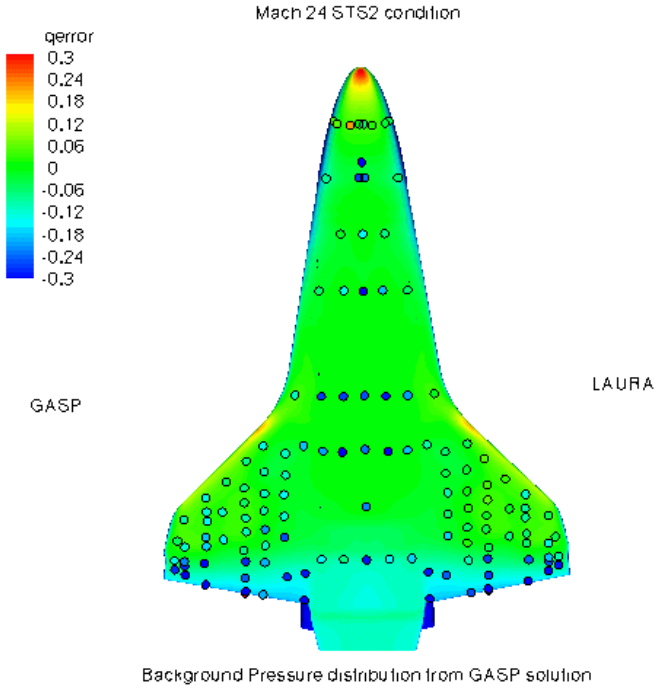

Figure 5.2.4-10 Windward heating rate uncertainty at Mach 24 plotted over pressure contours $q_{error} = (q_{cfd} - q_{flight})/q_{flight}$.

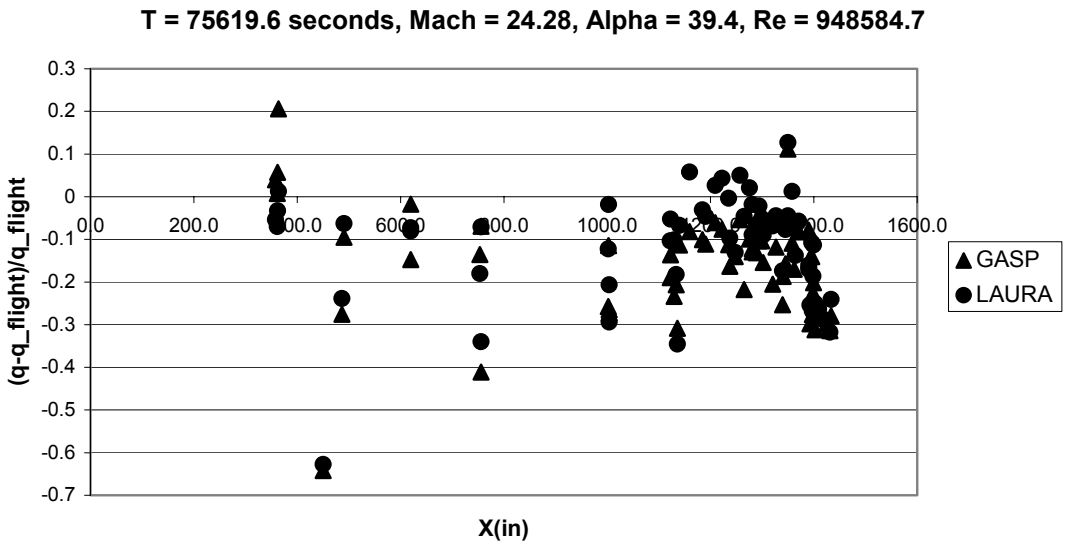

Figure 5.2.4-11 Heating rate uncertainty at Mach 24 as a function axial distance along the orbiter

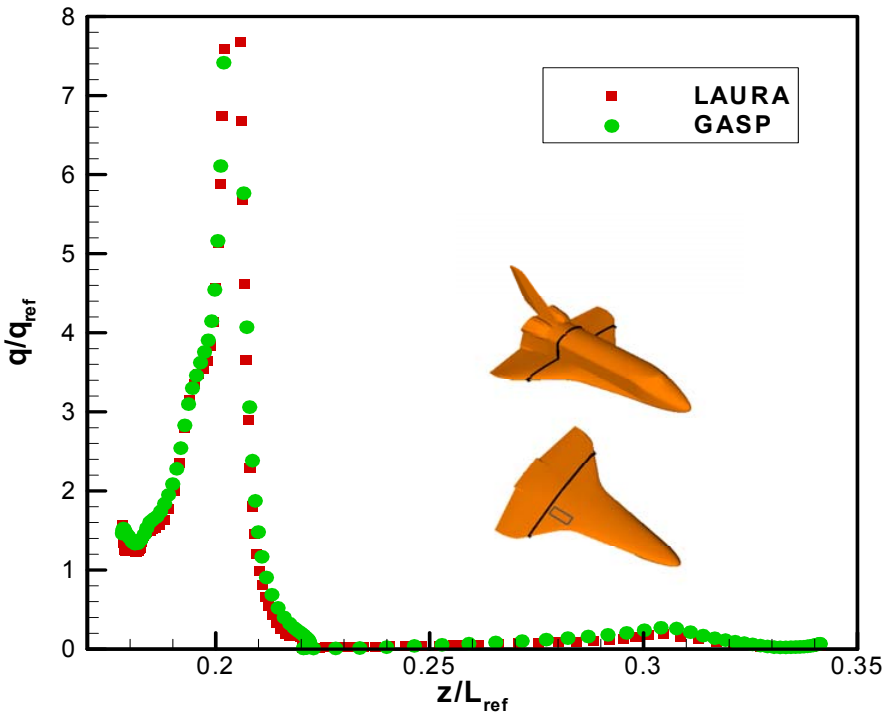

a) Wind side and lee side.

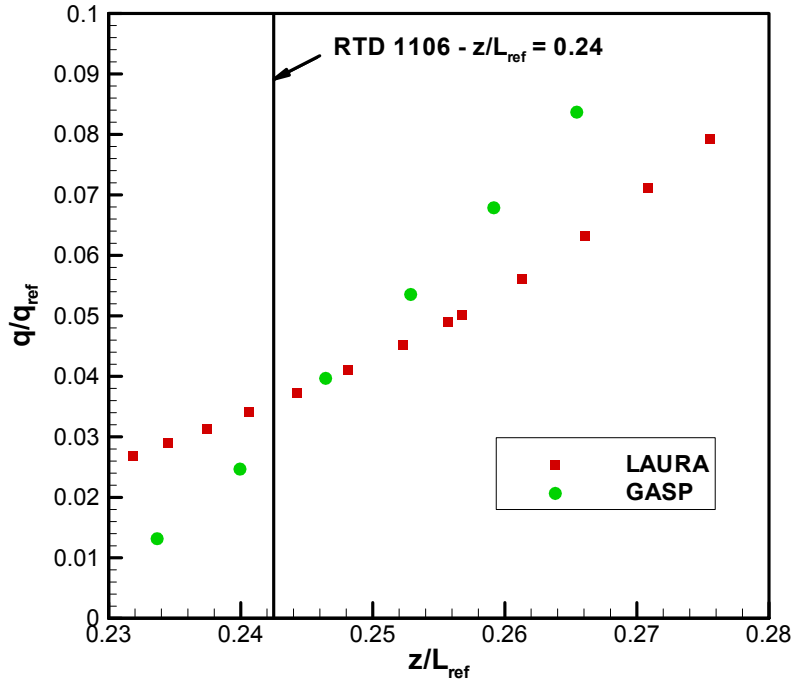

b) Zoom of leeside region.

Figure 5.2.4-12 Comparison of GASP and LAURA heat transfer rates along a cut at X = 1215 in. The location of the MLG is shown in the inset. q_{ref} = 3.55 W/cm^2 = 3.13 BTU/ft^2/s. L_{ref} = 37.24 m = 1466 in.

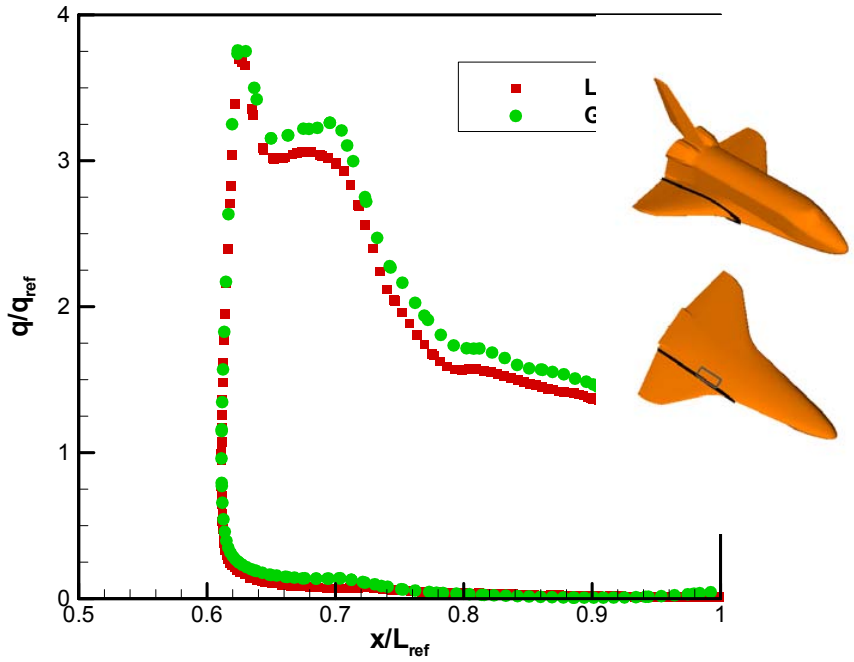

Figure 5.2.4-13 Comparison of GASP and LAURA heat transfer rates along a cut at Y = 167 in. The MLG location MLG is shown in the inset. q_{ref} = 3.55 W/cm^2 = 3.13 BTU/ft^2/s. L_{ref} = 37.24 m = 1466 in.

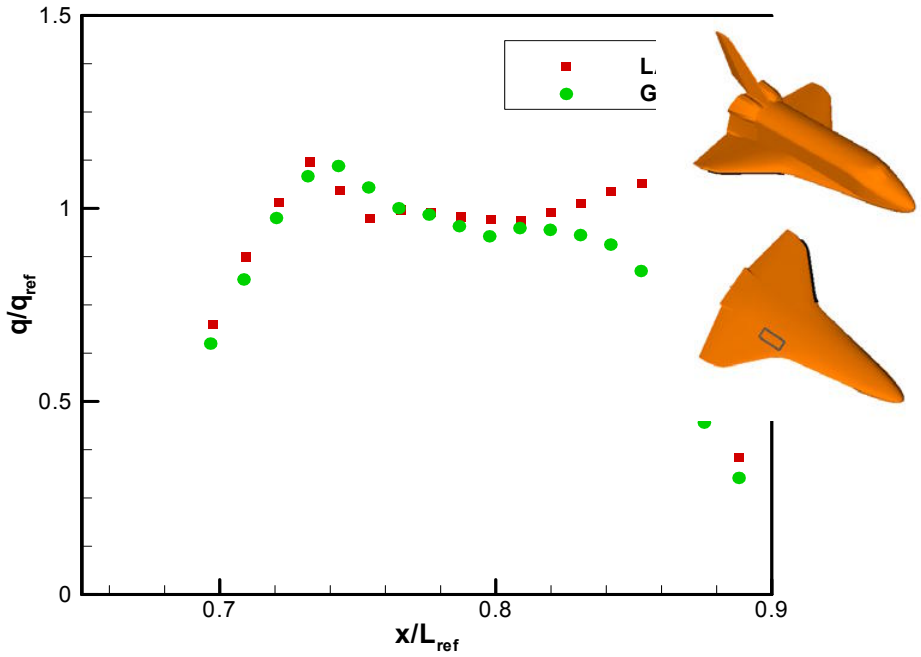

Figure 5.2.4-14 Comparison of GASP and LAURA heat transfer rates along the wing leading edge. q_{ref} = 37.8 W/cm^2 = 33.2 BTU/ft^2/s. L_{ref} = 37.24 m = 1466 in.

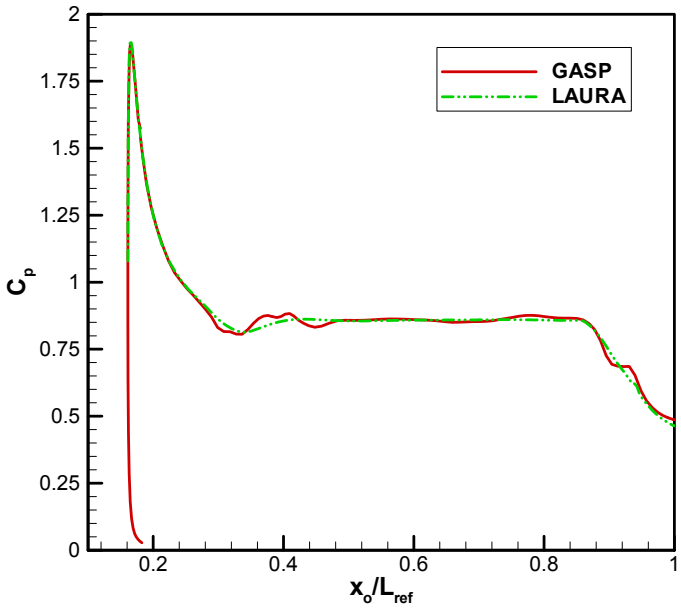

Figure 5.2.4-15 Computed windward centerline pressure distributions from GASP and LAURA. L_{ref} = 37.24 m = 1466 in.

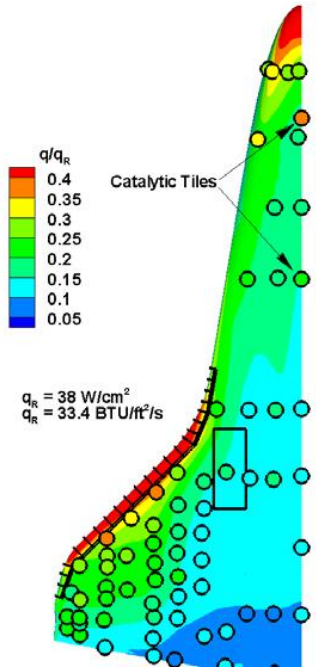

a) GASP

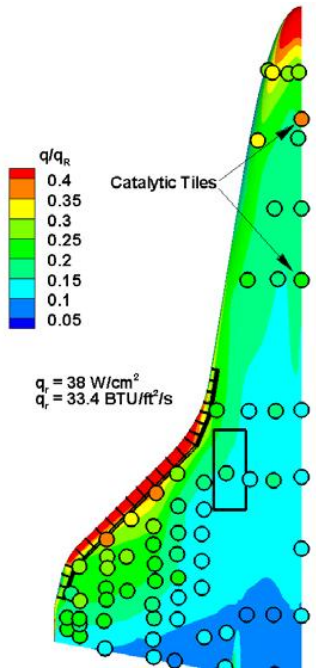

b) LAURA

Figure 5.2.4-16 Windward surface temperature predictions from GASP and LAURA compared with flight data at Mach 18. Experimental data are plotted inside the circular symbols. The symbol size is made larger than the measurement extent to aide visualization of the data.

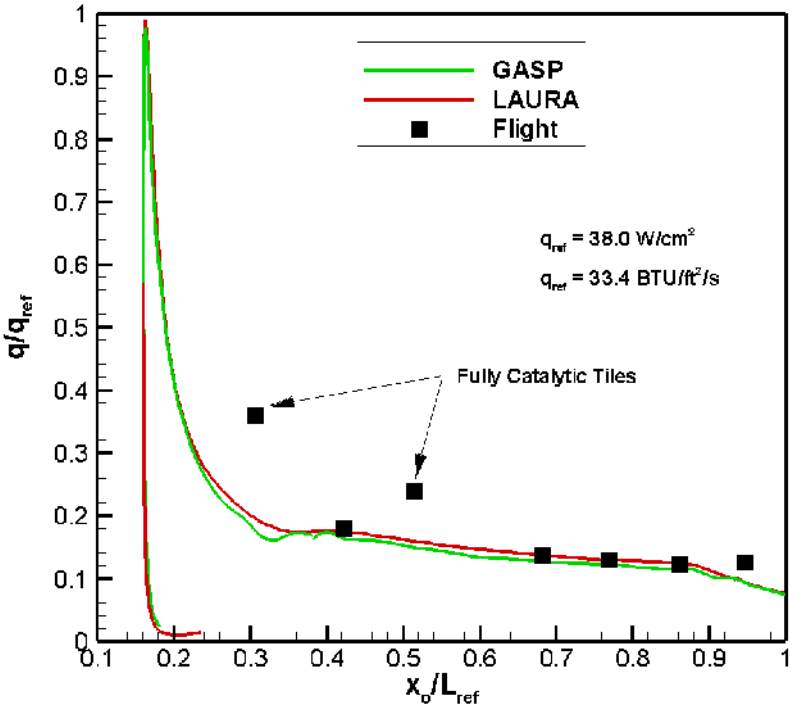

Figure 5.2.4-17 Windward centerline heat transfer rate for Mach 18. L_{ref} = 37.24 m = 1466 in.

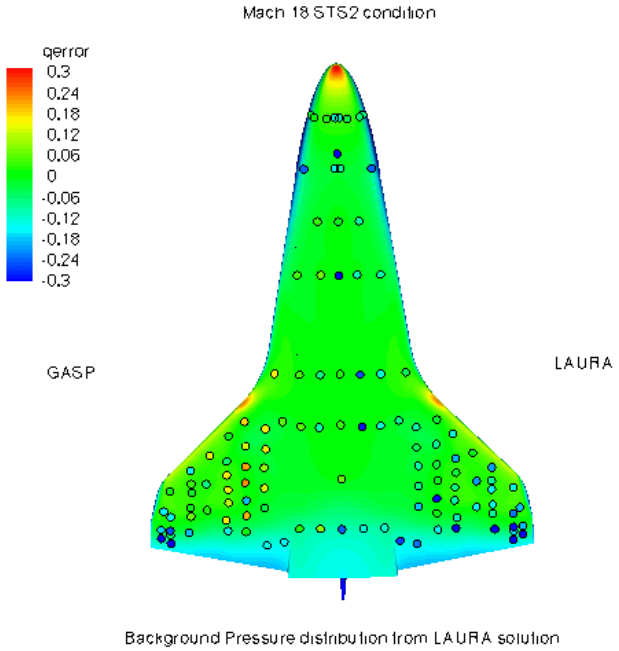

Figure 5.2.4-18 Windward heating rate uncertainty at Mach 18 plotted over pressure contours $q_{error} = (q_{cfd} - q_{flight})/q_{flight}$.

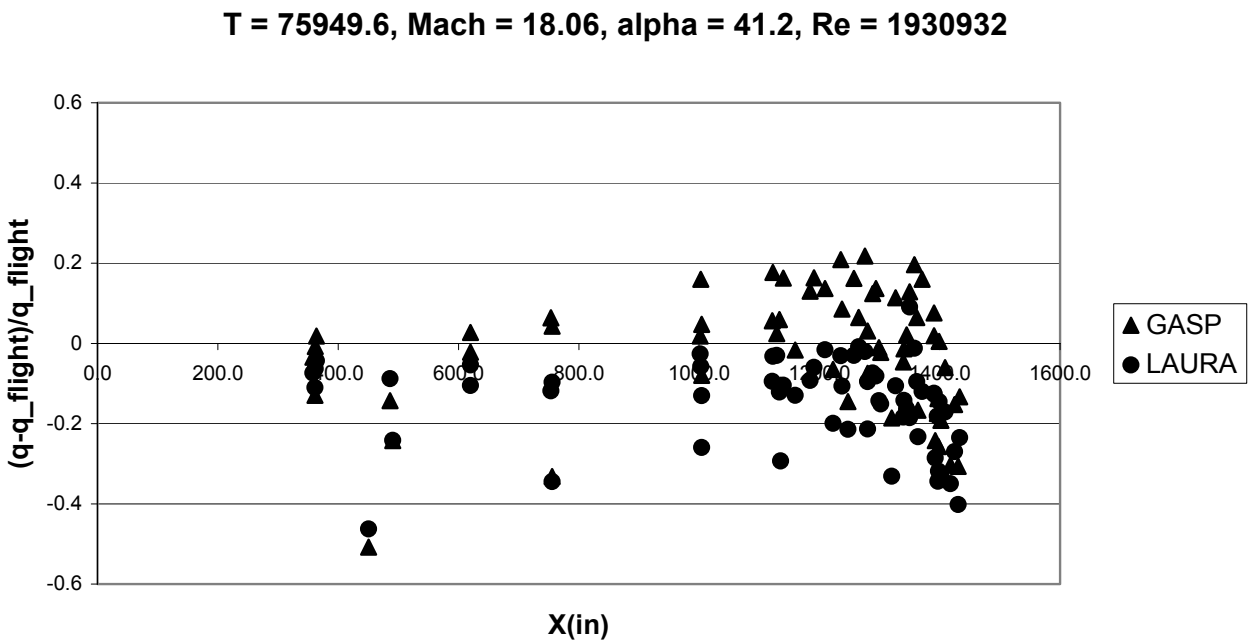

Figure 5.2.4-19 Heating rate uncertainty at Mach 18 as a function axial distance along the orbiter

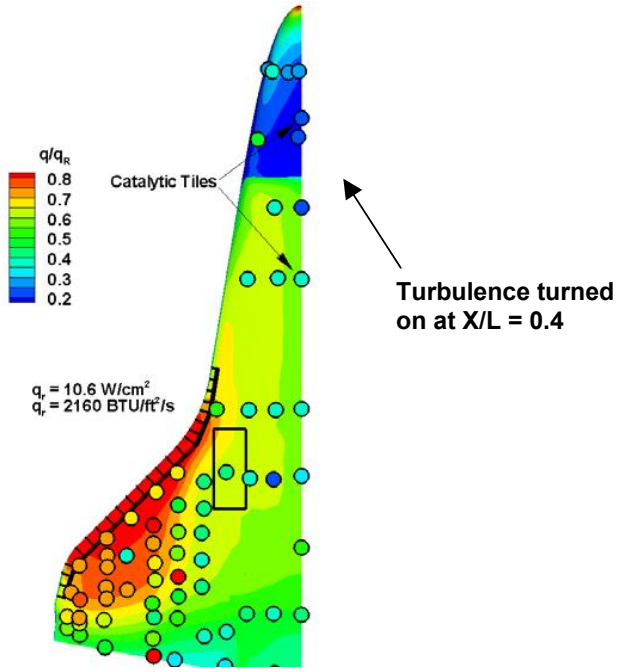

a) GASP

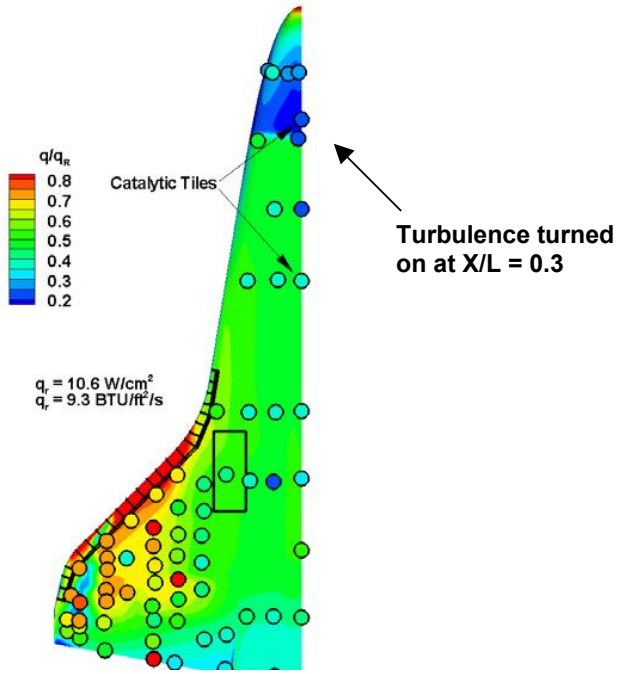

b) LAURA

Figure 5.2.4-20 Windward surface temperature predictions from GASP and LAURA compared with flight data at Mach 7. Experimental data are plotted inside the circular symbols. The symbol size is made larger than the measurement extent to aide visualization of the data.

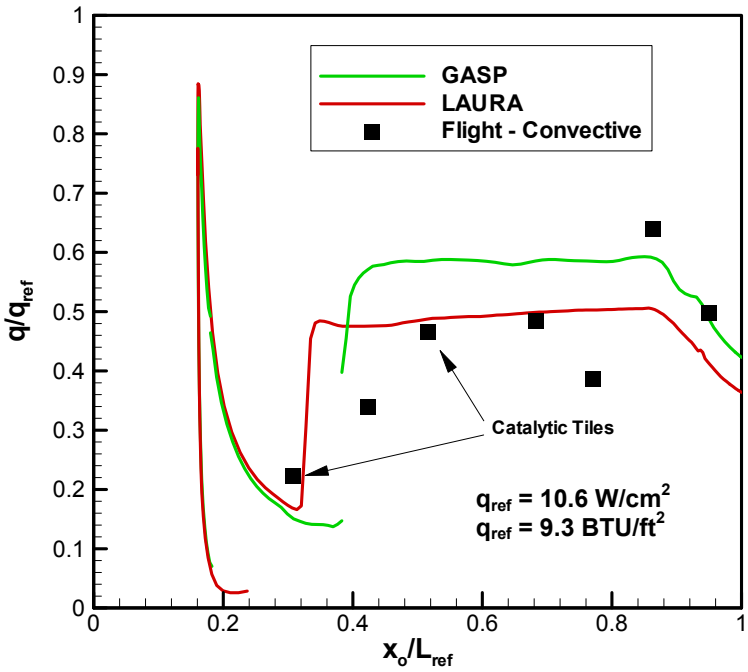

Figure 5.2.4-21 Windward centerline heat transfer rate for Mach 7. L_{ref} = 37.24 m = 1466 in.

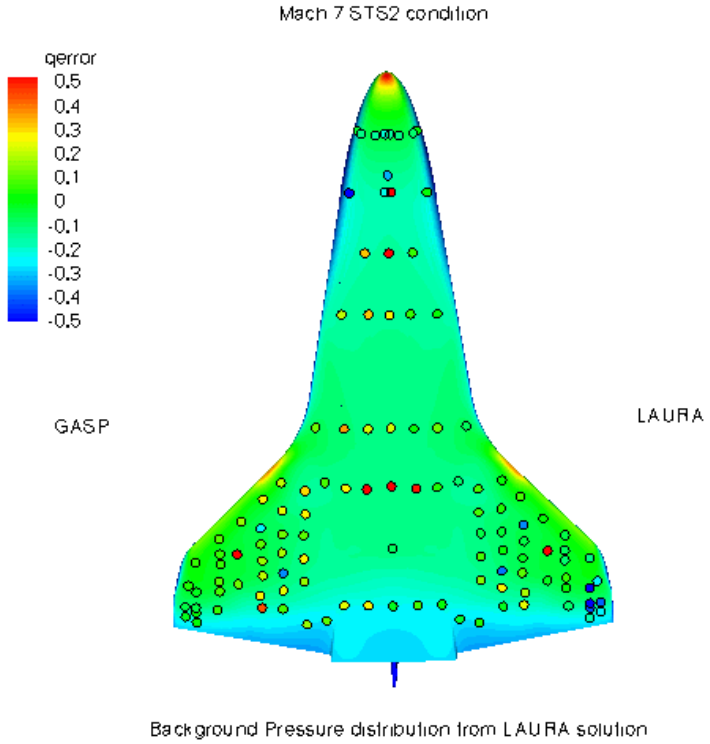

Figure 5.2.4-22 Windward heating rate uncertainty at Mach 7 plotted over pressure contours q_{error} = $(q_{cfd} - q_{flight})/q_{flight}$.

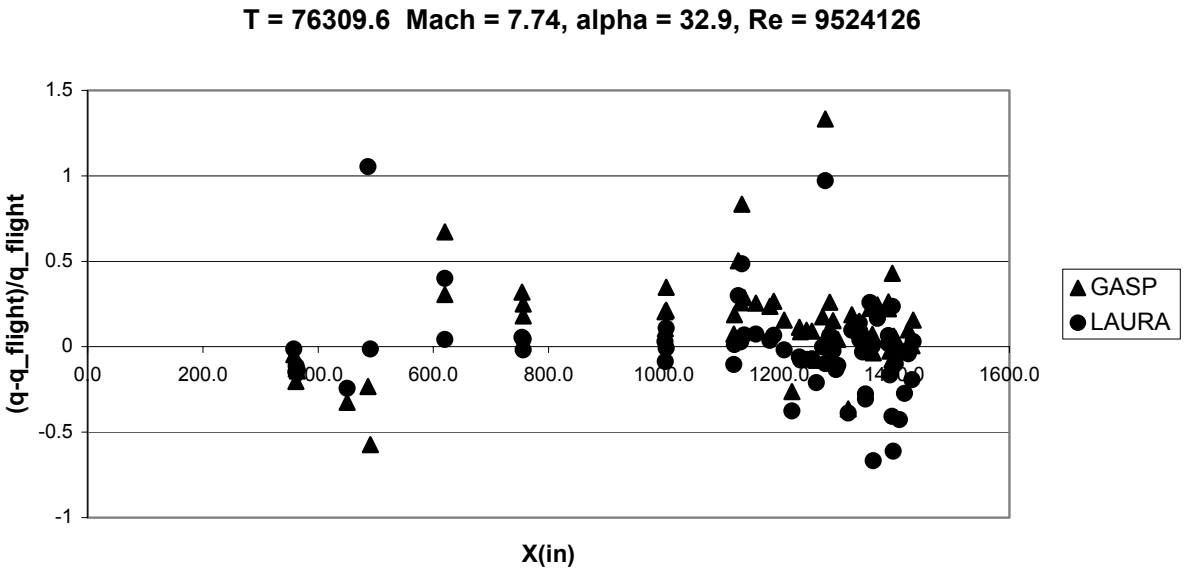

Figure 5.2.4-23 Heating rate uncertainty at Mach 7 as a function of axial distance along the orbiter

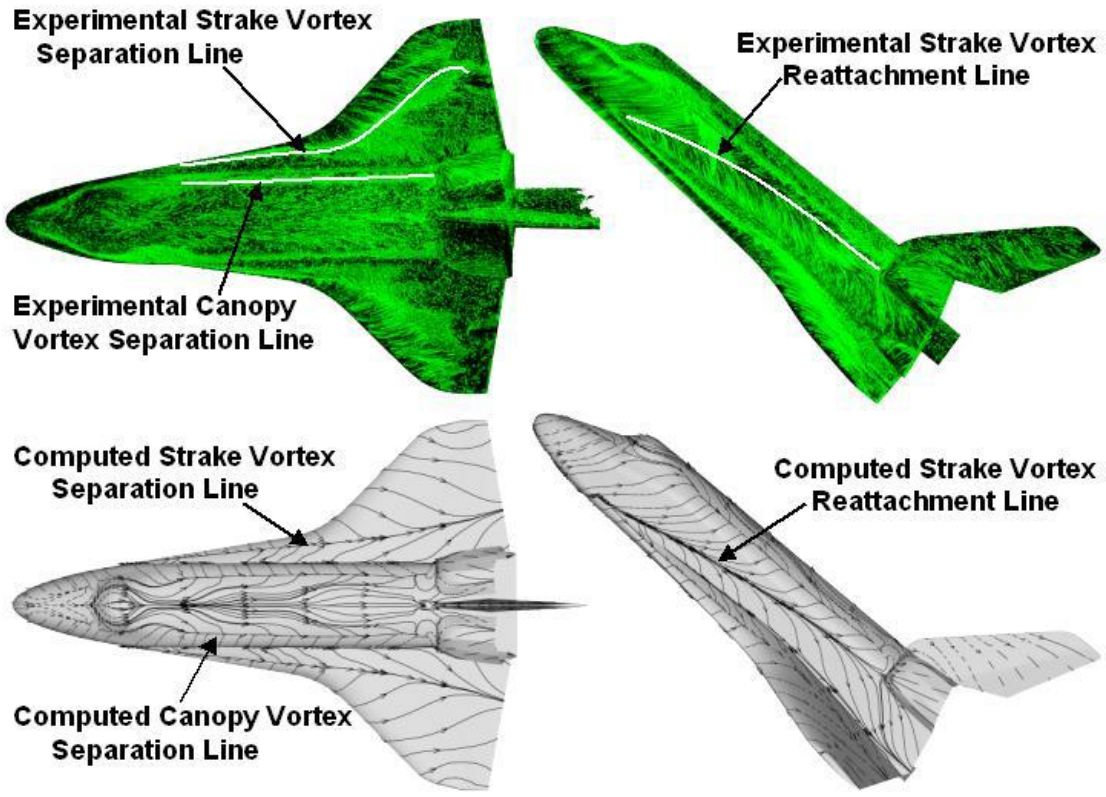

Figure 5.2.4-24 Comparison of Computed and Experimental Surface Streamlines on the Lee Side of the Baseline Orbiter in the CF_4 Wind Tunnel

5.2.4.4 Nominal Orbiter Configuration – Flight Environments

5.2.4.4.1 Introduction

The Orbiter re-entry environment exposes the vehicle to extreme high temperature gases, thus demanding as robust a thermal protection system as possible. The detailed physical features in the very complex Orbiter flow field during re-entry can be appreciated by examining high-fidelity CFD simulations calculated at the actual flight conditions. Thus, a need for understanding the details of local flow field features for the nominal Orbiter geometry led to the calculation of a suite of numerical solutions at STS-107-specific flight conditions. Details about the trajectory conditions identified to perform the simulations can be found in the Aerodynamics Section. The trajectory conditions cover the entire duration of the STS-107 entry trajectory, and as a whole provide a valuable database for the aero/aerothermal team. Because the Orbiter experiences conditions on re-entry that range from a very rarefied environment down to a fully continuum environment, the suite of nominal geometry solutions includes simulations appropriate to both regimes.

The external environment simulations along the STS-107 trajectory were performed by Boeing-Huntington Beach, NASA-ARC, NASA-JSC, NASA-LaRC and Sandia National Laboratories. The software tools used to perform these simulations included Navier-Stokes solvers (GASP, LAURA, SACCARA, USA) appropriate to the continuum regime, and DSMC software (DAC) appropriate to the rarefied regime. The database of solutions generated is provided in Table 5.2.4-4 , where the solutions obtained are listed by trajectory condition, grid basis, and software tool. The abbreviations for the entries correspond to 5-species chemical non-equilibrium using Reaction Cured Glass surface properties (Noneq), fully catalytic surface properties with 5-species non-equilibrium chemistry (FC), and equilibrium chemistry (Eq). The DAC solutions utilized a 6-species, non-equilibrium chemistry gas model, and a fully diffuse, non-catalytic surface with radiation equilibrium surface temperature boundary condition and an emissivity of 0.9. The Navier-Stokes simulations (GASP, LAURA, SACCARA and USA) all used laminar flow assumptions with a radiation equilibrium temperature boundary condition, and an emissivity of 0.9. Further details on the software tools can be found in the Appendices. As noted in the Grid Generation section, the initial nominal geometry grids mentioned in Table 5.2.4-4 were used to generate initial Navier-Stokes solutions immediately after the loss of Columbia. The common baseline grid was subsequently developed and was used to generate the additional solutions listed. The modified common baseline grid utilized for the SACCARA simulation used a grid system which had a resolution doubled in the streamwise and circumferential directions, and it encompassed only the front half of the Orbiter The DAC simulations utilized a surface definition already available at the time of the accident..

5.2.4.4.2 Description of the Nominal Orbiter Configuration Flow Field

Four of the flow field solutions shown in Table 5.2.4-4 were selected to present predicted surface pressure and thermal loads experienced by Columbia and to present the properties of the gas in close proximity to the Orbiter surface. The four solutions correspond to trajectory points with the following conditions:

CFD Point 1: EI+404 sec.; Mach = 24.9; Altitude = 243,000 ft; Alpha = 40°; Dyn. press. = 22.0 psf.
CFD Point 6: EI+921 sec.; Mach = 17.9; Altitude = 200,767 ft; Alpha = 40°; Dyn. press. = 83.5 psf.
DSMC Point A EI+197 sec.; Mach = 27.0; Altitude = 300,003 ft; Alpha = 40°; Dyn. press. = 1.6 psf.
DSMC Point AA EI+ 91 sec.; Mach = 25.1; Altitude = 350,274 ft; Alpha = 41°; Dyn. press. = 0.1 psf

Figure 5.2.4-25 presents the flow field Mach number distribution around the Orbiter as predicted by the LAURA code. Two views are shown – a pitch plane cut and a constant span cut through Panel 9. The first view shows that the bow shock is relatively close to the windward surface of the vehicle for the nominal 40-degree angle-of-attack re-entry. The second view shows that the distance between the Panel 9 wing leading edge surface and the shock is approximately 7 inches for a flight condition near Mach 25. Figure 5.2.4-26 and Figure 5.2.4-27 present the flow field number density distribution around the Orbiter for DSMC Points AA and A as predicted by the DAC code. The view shown is of the x-z plane down the centerline of the vehicle. Since the conditions of DSMC Points AA and A are more rarefied than the CFD points, the boundary layers shown in Figure 5.2.4-26 and Figure 5.2.4-27 merge with the shock layer,

creating a large compression region. This effect is more pronounced in Figure 5.2.4-26, with DSMC Point AA being the most rarefied.

Table 5.2.4-4 Nominal Geometry Hypersonic Orbiter Simulations at Flight Conditions

Trajectory Point		Common Baseline Grid			Modified Common Baseline Grid	Initial Grids	
	DAC	GASP	LAURA	USA	SACCARA	GASP	LAURA
AA	X	N/A	N/A	N/A		N/A	N/A
A	X	Noneq				Noneq & FC	Noneq
B		Noneq	Noneq	Eq		Noneq & FC	Noneq
1		Noneq	Noneq	Noneq & Eq		Noneq & FC	Noneq
2		Noneq				Noneq & FC	Noneq
3		Noneq	Noneq	Noneq & Eq		Noneq & FC	Noneq
4		Noneq				Noneq & FC	Noneq
5		Noneq				Noneq & FC	Noneq
6		Noneq				Noneq & FC	Noneq
VN					Eq		

Surface streamlines are presented in Figure 5.2.4-28 for the wing leading edge region at CFD point 1. An attachment line exists along the leading edge, which separates the flow that remains on the windward side from the flow that is swept over onto the leeward side of the vehicle. Note that the flow moves outboard along the attachment line. These streamlines provide an indication of where local disturbances on the surface will propagate downstream on the vehicle. Figure 5.2.4-29 through Figure 5.2.4-34 present the surface pressure distributions in the wing leading edge region for CFD Points 1 and 6 and DSMC Points AA and A, respectively. Absolute pressures in pounds per square foot (psf) are presented along with pressure coefficients. The pressure coefficient is defined as,

$$C_p = \frac{P_{local} - P_\infty}{\frac{1}{2}\rho_\infty V_\infty^2}$$

where P_{local} = local surface pressure, P_∞ = free stream atmospheric pressure, ρ_∞ = free stream atmospheric density, and V_∞ = relative velocity of vehicle. The pressure distributions for the CFD and DSMC flight conditions are very similar as depicted by the pressure coefficients. However, the wing leading edge peak pressure magnitudes change from ~0.001 psf at Mach 25.1 and 350,000 ft, ~0.01 psf at Mach 27.0 and 300,000 ft, ~35 psf at Mach 24.9 and 243,000 ft, and finally to ~140 psf at Mach 17.9 and 200,000 ft.

Figure 5.2.4-35 through Figure 5.2.4-40 present both the heat flux and Stanton number distributions on the wing leading edge region. The Stanton number is defined as,

$$St = \frac{q}{\rho_\infty V_\infty H_{total}}$$

where q = local heat flux, and H_{total} = total free stream enthalpy. The quantity $\rho_\infty V_\infty H_{total}$ is a measure of the total energy in the flow field and therefore the Stanton number provides an indication of how much of the total energy contained within the flow is transferred to the surface of the vehicle. Thus, a value of 1.0 for the Stanton number corresponds to complete energy accommodation to the surface. The results shown in Figure 5.2.4-35 Figure 5.2.4-36 , Figure 5.2.4-37 , and Figure 5.2.4-38 illustrate that the heating

distributions are very similar over the Mach 24.9 to 17.9 range, with the peak heat flux occurring along the attachment line of leading edge in the vicinity of RCC panels 8 and 9. Because the Orbiter GN&C attempts to guide the vehicle along a constant heat flux boundary between these Mach numbers, it should be expected that the peak heat flux remains fairly consistent in these illustrations. One additional observation is worthwhile. The Navier-Stokes results included here predict the magnitude of the peak heat flux in the region of leading edge panel 8 to be in the 38 to 40 Btu/ft^2-sec range. However, DeVenezia, et al. have shown that flight data typically indicate values of approximately 50 Btu/ft^2-sec for the same region. Clearly, the CFD results tend to under-predict the heating to this leading edge region of the vehicle. To date, no comprehensive Navier-Stokes calibration effort has ever been undertaken using the available Orbiter re-entry leading edge heating data.

However, an engineering code, XF0002, developed by Boeing and calibrated with Orbiter flight data can be used to predict peak heat fluxes to leading edge panel 9. The RCC panel 9 flight certified indicator in XF0002 is known as BP (Body Point) 5505. The XF0002 predicted heat flux and surface temperature histories are provided in Figure 5.2.4-41.

While the DSMC heating distributions at Mach 25.1 and Mach 27.0 are somewhat similar to those of the two CFD points, the area where the peak heat flux occurs along the attachment line of leading edge panels 8 and 9 is not as well defined, especially for DSMC Point AA. This lack of definition is due to the more diffuse nature of the flow under rarefied conditions. In addition, the significantly lower density at DSMC Points AA and A results in a peak wing leading edge heating rate of only about 2 Btu/ft^2-sec and 10 Btu/ft^2-sec, respectively. Note from Figure 5.2.4-35 and Figure 5.2.4-36 that the peak Stanton number for the continuum conditions is only 2 to 5%, while in Figure 5.2.4-38 and Figure 5.2.4-40 the peak Stanton number is approximately 25 to 50%. This is because at the rarefied high altitude conditions corresponding to DSMC Points AA and A, the flow is non-continuum. As a vehicle approaches completely rarefied conditions, where individual molecules do not interact, the Stanton number for a fully accommodated surface approaches 1 at the stagnation point. This rarefied flow effect is thus evident at the peak heating location on the wing leading edge, as illustrated in the DSMC heating figures.

Figure 5.2.4-42 presents radiation equilibrium surface temperature distributions for the wing leading edge region for CFD Points 1 and 6. The peak temperatures are along the leading edge attachment line and highest on Panels 8 and 9. As discussed previously, the peak temperatures predicted by the CFD codes are low and flight-calibrated values are presented in Figure 5.2.4-41. Figure 5.2.4-43 and Figure 5.2.4-44 show the radiation equilibrium surface temperature distribution for the wing leading edge region at DSMC Points AA and A. Note that no further discussion of the nominal geometry DSMC results will be included here, since the discussion to follow was important to the STS-107 investigation only for the continuum regime.

Another critical aspect of the flow environment experienced by the Orbiter during re-entry is the extreme gradients in flow field properties between the vehicle surface and the free stream. In order to illustrate these gradients, three locations in the leading edge (LE) region were selected to provide estimates of the local boundary-layer thickness, total enthalpy profiles, and static temperature profiles near the surface. Figure 5.2.4-45 provides a sketch describing the location of these three points – LE Panel 6, LE Panel 9 and Main Landing Gear Door forward outboard corner.

Figure 5.2.4-46 through Figure 5.2.4-51 provide predictions of the total enthalpy and static temperature variation of the gas near the surface of the Orbiter. These profiles for the CFD Point 1 flight condition, Mach 24.9 at an altitude of 243,000 feet, are provided in Figure 5.2.4-46 - Figure 5.2.4-48 for the locations shown in Figure 5.2.4-45 . On each of these plots the estimated boundary-layer thickness is noted. This estimate was obtained by locating the distance from the surface that the total enthalpy attains a value approximately 99% of the total free-stream value of 11,730 Btu/lb$_m$. For the 243,000 ft flight condition, the gas static temperatures are approximately 10,000 degrees Rankine at the boundary-layer edge. The thinnest boundary layer occurs at Panel 9. Figure 5.2.4-49 - Figure 5.2.4-51 provide the same information at the CFD Point 6 flight condition, Mach 17.9 and an altitude of 201,000 feet. For this flight condition, the boundary layer is considerably thinner at Panel 9 with a thickness of ~0.3 inches and the edge gas temperatures have decreased to about 7,000 degrees Rankine. This decrease in total enthalpy or total temperature corresponds to a decrease in kinetic energy of the Orbiter by approximately

40% between the conditions at CFD Point 1 and 6. Thus, roughly one-half the energy of the vehicle had been dissipated by the time Columbia reached LOS at about Mach 18.

Species concentration comparisons in the shock layer ahead of LE Panel 9 and the Orbiter nose stagnation point are provided in Figure 5.2.4-52 and Figure 5.2.4-53, respectively. These predictions were obtained from the LAURA solution at CFD Point 1. At the nose, the shock is approximately 2.5 inches from the surface and at Panel 9 it is about 7 inches from the surface. For both locations the oxygen is completely dissociated, thus only atomic oxygen is present in the shock layer. However, very near the surface some recombination occurs as the atomic oxygen mass fractions drop slightly. If the surface had been modeled as a fully catalytic surface instead of with the catalysis properties for the Reaction Cured Glass tile coating, full recombination of oxygen would have been predicted. For the nose shock layer, a significant amount of the nitrogen is dissociated with a peak atomic nitrogen mass fraction of about 0.38. This is in contrast to the Panel 9 shock layer, where the atomic nitrogen mass fraction is less than 0.1.

5.2.4.4.3 Orbiter Forebody CFD–Chin Panel / Vent Nozzle Cases

A focused set of simulations was conducted to investigate the anomalous chin panel and vent/dump nozzle instrumentation responses. See Section 5.2.1 for more information on the anomalous flight data characteristics. One theory to explain the increase in the temperature rise at the vent/dump nozzles is that an increase in sideslip angle moved the vortex at the wing body junction closer to the Orbiter fuselage, producing the increased heating. Thus, an effort to determine if the small changes in the angle of sideslip at those flight conditions could produce increased heating at the relevant vehicle OML locations was investigated. . In order to evaluate these anomalies, the common baseline grid of the nominal Orbiter was truncated at 50% of its length and additional grid, equivalent to what was removed by deleting the aft, was applied to the forebody. The resulting grid system had twice the resolution in the streamwise and circumferential directions compared with the baseline common mesh. The highly refined forebody grid were developed in order to provide the most accurate solution possible. In addition to flight simulations using the forward one-half of the Orbiter, a calibration was performed at wind tunnel conditions before attempting the flight simulations.

OH109 Orbiter Wind Tunnel Test Overview

Test OH109 was designed to investigate the effect of sideslip on heat transfer rate. The test was performed at Mach 8 for a range of Reynolds numbers and sideslip angles. A 0.04 scale thin-walled model of the shuttle was used in the experiment. The model was instrumented with thermocouples, and included thermocouples near the vent nozzles. These wind tunnel data provided a direct measurement of temperature rise rate near the vent nozzles and heat transfer data to benchmark the simulation tools.

The wind tunnel test measured the temperature rise rate on the surface of the model. The wind tunnel conditions were a Mach number of 8, side slip angle of –2.02°, -1.01°, -0.5°, 0.0°, angle of attack of 40.0, and a Reynolds number of $5x10^5$/ft. The flight vehicle was nominally at a Mach number of 24, angle of attack of 40°, a wind-corrected sideslip angle of 0.2°, and Reynolds number of $8x10^3$/ft when the instrumented vent nozzles recorded a doubling of the temperature rise rate. If the nominal temperature rise rate is measured at 0° sideslip, doubling the 0° sideslip temperature rise rate measured in the wind tunnel should produce a curve analogous to the off-nominal temperature rise rate observed in flight. In Figure 5.2.4-54 the white line near the wing-body junction is the vortex core location. Figure 5.2.4-55 shows the Orbiter forebody on the right and wind tunnel data comparisons on the left. The representative off-nominal curve shown in Figure 5.2.4-55 is the value the temperature rise rate would need to reach in order to match the increase observed in flight. The representative off-nominal curve is the dark line with no symbols. The arrow points to a line of thermocouples that are used for comparison in the image on the left. The red circles on the shuttle forebody are the location of the water dump, waste dump and vacuum nozzles. The plot on the left shows the temperature rise rate for sideslip angles from–2° to 0°. The wind tunnel data show only a moderate increase in temperature rise at a sideslip angle of –2°. The increase is approximately 20%, substantially less than the factor of two increase required to resemble the flight data. While the wind tunnel test did not match flight conditions and did not capture all the physical

phenomena that occurs in flight, the general data trend should be captured. Thus, the theory that the underlying cause of increased temperature rise rate is a sideslip effect is not supported by the available wind tunnel data. Even at an order of magnitude larger sideslip angle than the slip angle observed in flight, the increase in temperature rise rate from the wind tunnel data is only 20% of the flight observed increase.

Wind Tunnel Test OH109 Comparisons with Simulations

The experimental data taken in test OH109 provided an opportunity to benchmark the SACCARA prediction of heat transfer rates. A simulation was run on the truncated common baseline grid. The conditions computed matched the OH109 test: Mach number of 7.83, angle of attack of 40.04°, sideslip angle of -1.01°, Reynolds number of 4.938×10^5 and wall temperature of 505 °R. Figure 5.2.4-56 shows pressure contours along the centerline and the outflow boundary. Streamlines were placed near the wing-body junction vortex. Also, comparisons with the experimental data were made with a normalized heat transfer coefficient using the following definitions:

TT = tunnel total temperature, °R
QDOT = heat transfer rate, BTU/ft^2-sec
TW = wall temperature, °R
H(TT) = QDOT/(TT-TW), BTU/ ft^2-sec-°R
H(REF) = heat transfer coefficient derived from a Fay and Riddell based equilibrium stagnation point heating

Figure 5.2.4-57 shows the computed normalized heat transfer coefficient on both the in-wind side and the out-of-wind side, where the simulation results are co-plotted with the experimentally measured in-wind heat transfer coefficient. The Y- data were extracted from the simulation in-wind side and the Y+ data were extracted from the out-of-wind side. The comparisons are shown along the line of thermocouples indicated by the arrow shown in the right hand image. The diamonds depicted on the Orbiter fuselage represent the experimental data locations shown in the figure.

As illustrated in Figure 5.2.4-57, the in-wind and out-of-wind results have the same trends with a maximum change of approximately 20% in heat transfer coefficient. The simulation predicts a higher heat transfer coefficient that the experimental data. However, in comparison with the wind tunnel data, the predictions provide a conservative estimate of the heating rate. The in-wind and out-of-wind results show only modest differences in the heat transfer coefficient for the sideslip angle considered. An on-going study is under way to quantify the grid independence of the simulations. In addition, the experimental uncertainty in the OH109 data needs to be quantified before any conclusions can be drawn.

Simulation at flight conditions

One possible explanation for the flight observed temperature rise rate increase on the vent nozzles is that a gap or step located at the chin panel could have introduced a localized region of turbulent intermittency. The approach taken to examine this possible explanation was to run a simulation of the flight condition where the rise rate was observed, and to use the predicted surface quantities to determine where a disturbance would have to originate to affect the vent nozzles. Flight conditions for the simulation were selected based on the timesat which the vent nozzles were showing an increased rise rate, as in Section 5.1.2. The free stream conditions for this case use the VN (vent nozzle) identifier and are provided in the Aerodynamics section. Roughly, the conditions for the vent nozzle case are a Mach number of 24, altitude of 235,000 ft, with an angle of attack of approximately 40° and sideslip angle of -0.5°. The simulation was run on the same truncated common baseline grid used in the wind tunnel calibration study discussed above. Of particular interest in the flight simulation results is the behavior of the surface streamlines integrated from the surface shear stress vector. These streamlines should provide insight into the path a disturbance would follow. In Figure 5.2.4-58 , the water dump nozzle location and the vacuum vent location are indicated by the red circles, while the waste dump nozzle and thermocouple V07T9522A are shown in black. Figure 5.2.4-58 shows a number of streamlines on the Orbiter surface, along with colored contours of shear stress magnitude. The results show that the flight measurements are all located along the reattachment line. In relation to the attachment line, the vacuum nozzle is

located near its center, the waste dump nozzle is located below it, and the water dump nozzle and thermocouple are located above it. Figure 5.2.4-59 shows surface streamlines passing through the measurement locations for the vent/waste dump nozzle temperature instruments. The streamlines are tightly packed together until they reach the vacuum vent nozzle, where they begin diverging from one another. On the left of Figure 5.2.4-60 is an image of the front view, and on the right side is a close up of the nozzle. The front view shows that a disturbance in the chin panel region could propagate back to the nozzle locations. The close up of the nozzle locations shows that a disturbance could affect each nozzle differently, but with three streamlines passing the measurement locations, a clear case cannot be made. The simulation results do support the theory that a chin panel disturbance could have been the cause of the temperature rise rate. However, these results do not provide enough evidence to draw any conclusions. Since the temperature rise-rate returned to its nominal behavior after about 15 seconds of abnormality, it is very difficult to make any firm conclusions without additional data.

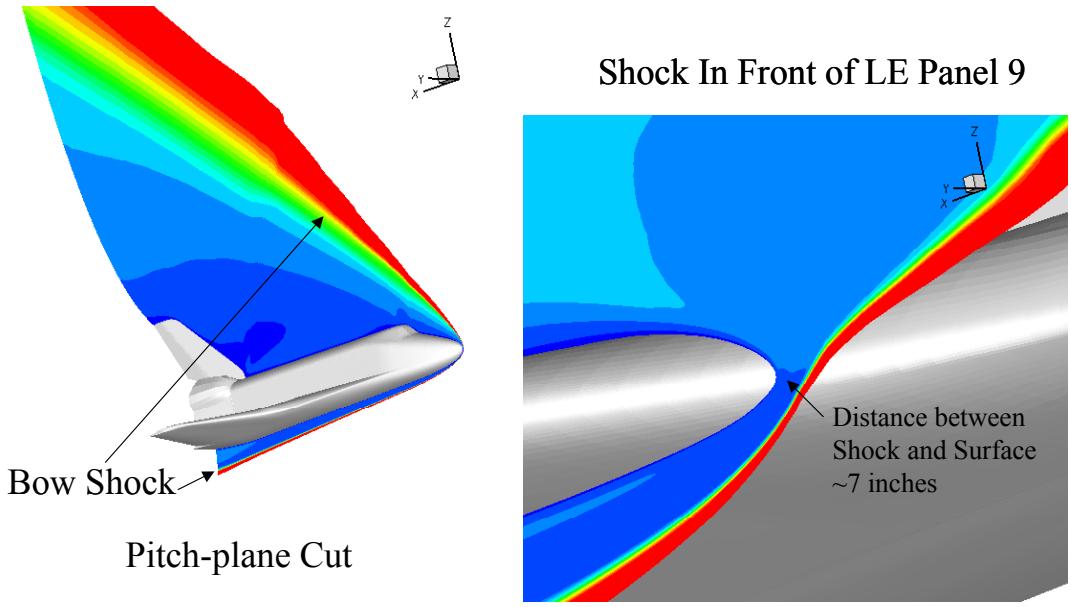

Figure 5.2.4-25 Shock Wave Structure around the undamaged Orbiter at CFD Point 1

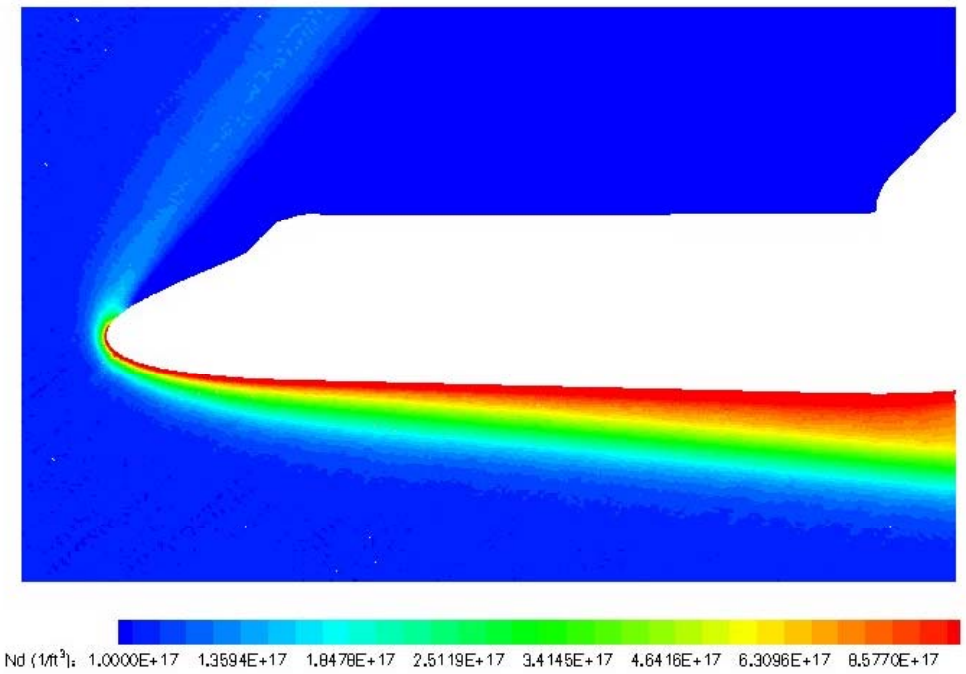

Figure 5.2.4-26 Number Density Distribution around Orbiter for DSMC Point AA

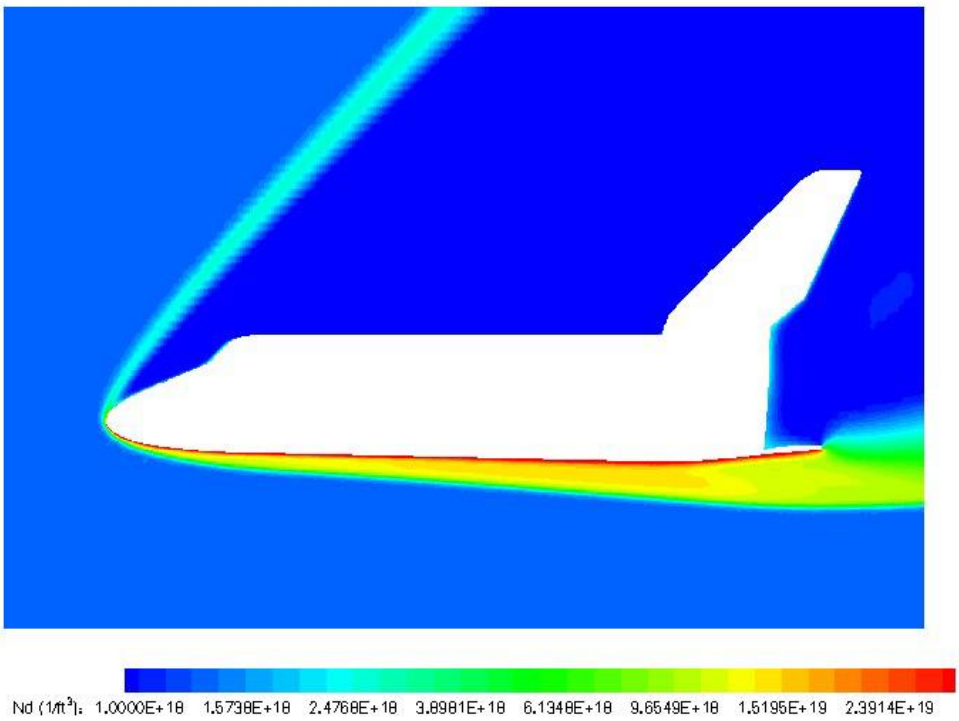

Figure 5.2.4-27 Number Density Distribution around Orbiter for DSMC Point A

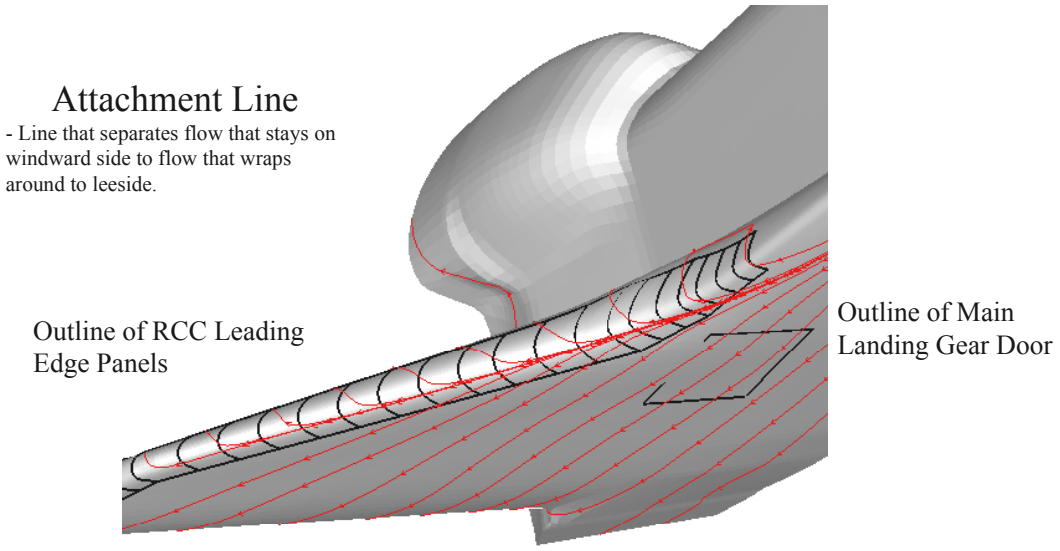

Figure 5.2.4-28 Surface Streamlines in the Wing Leading Edge Region

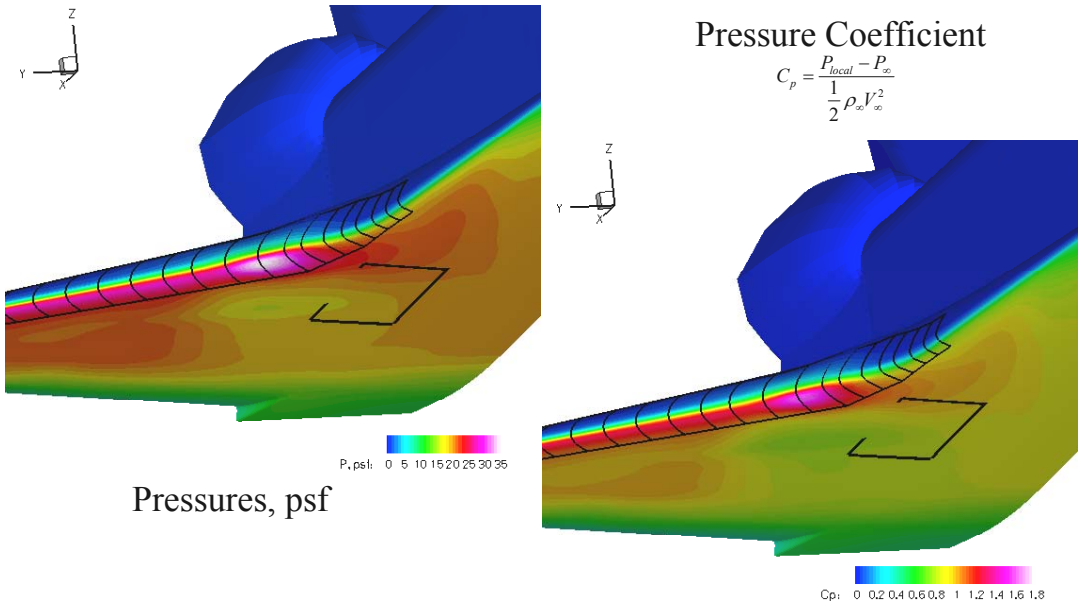

Figure 5.2.4-29 Surface Pressures for CFD Point 1, Mach 24.9

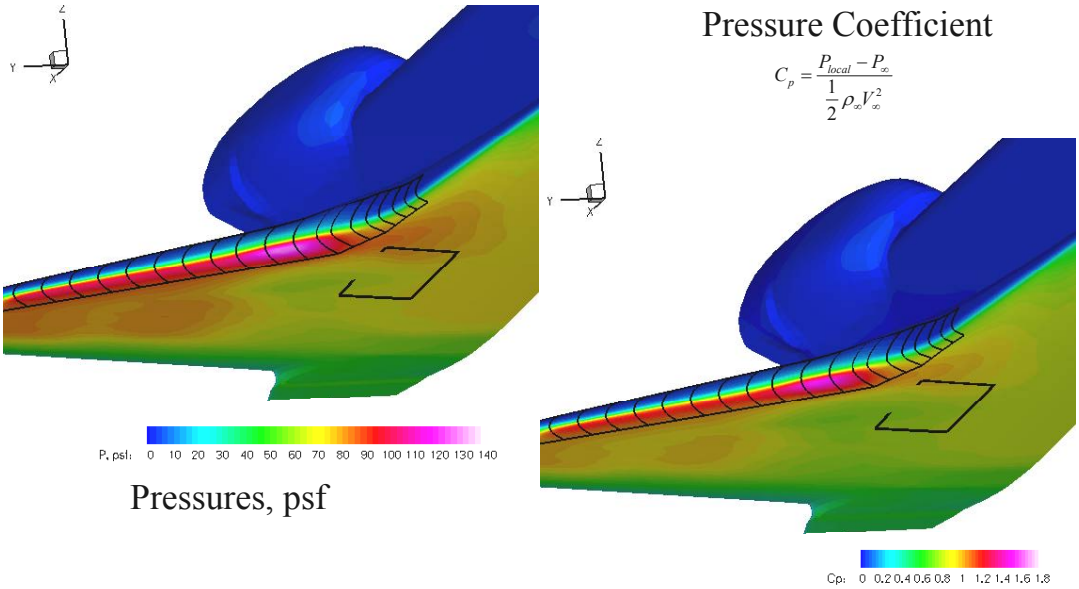

Figure 5.2.4-30 Surface Pressures for CFD Point 6, Mach 17.9

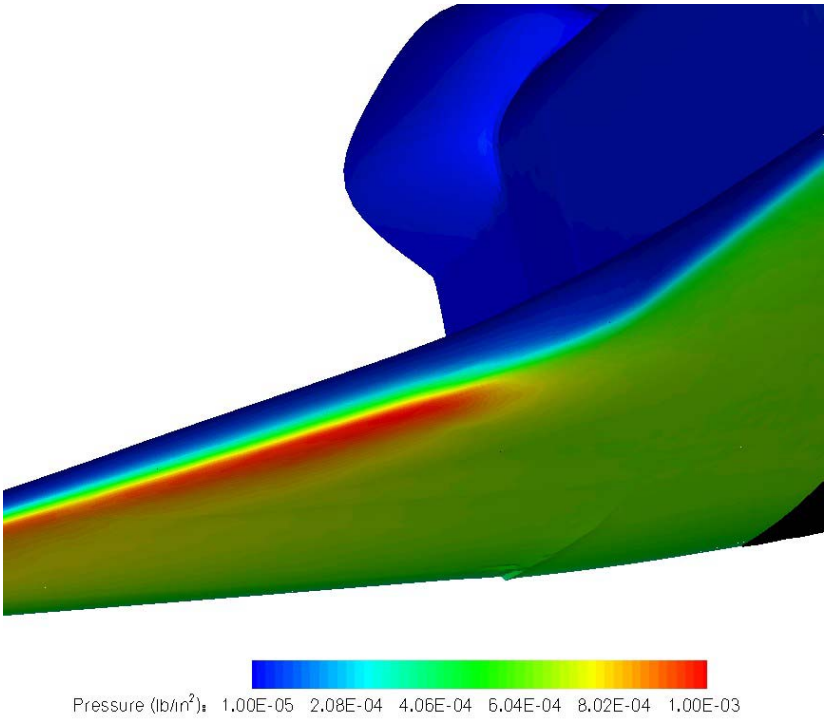

Figure 5.2.4-31 Surface Pressure for DSMC Point AA, Mach 25.1

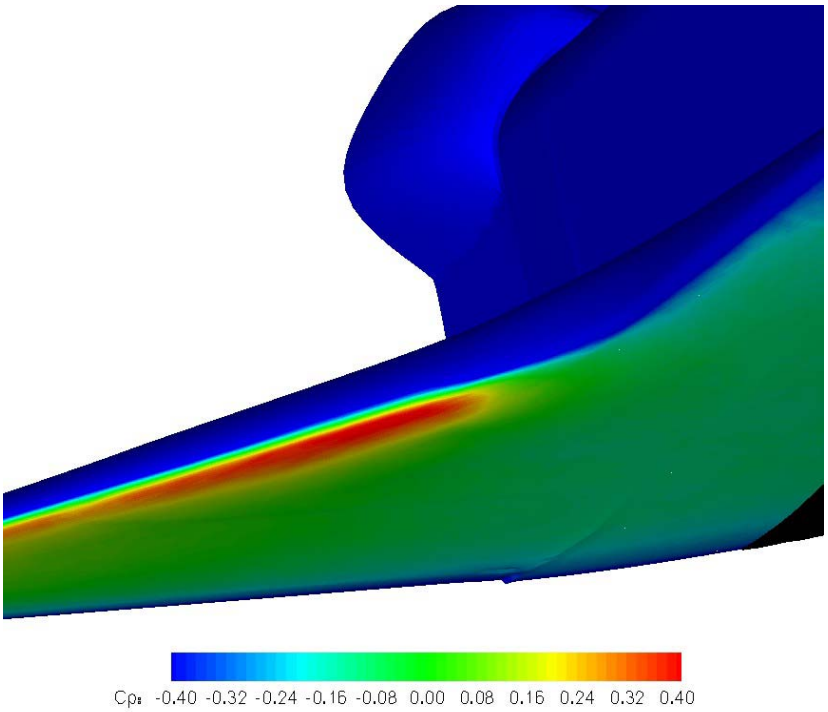

Figure 5.2.4-32 Surface Pressure Coefficient for DSMC Point AA, Mach 25.1

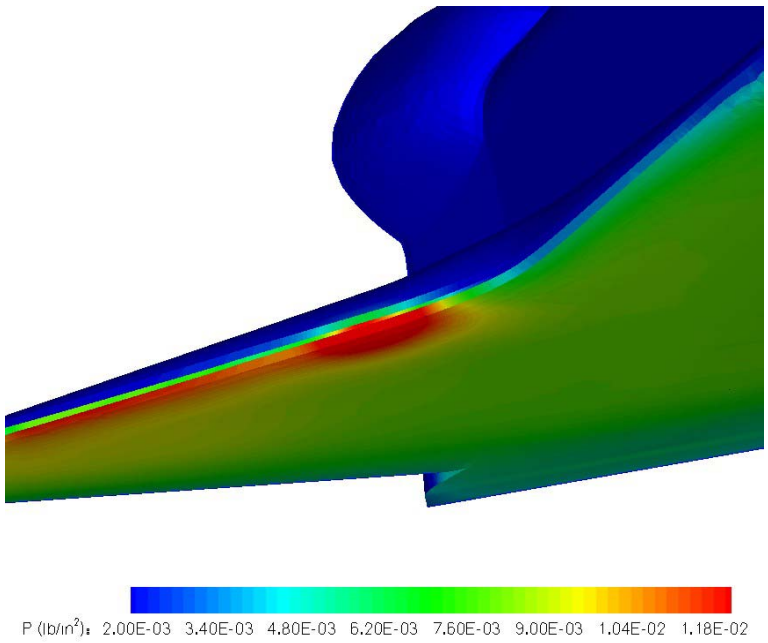

Figure 5.2.4-33 Surface Pressure for DSMC Point A, Mach 27.0

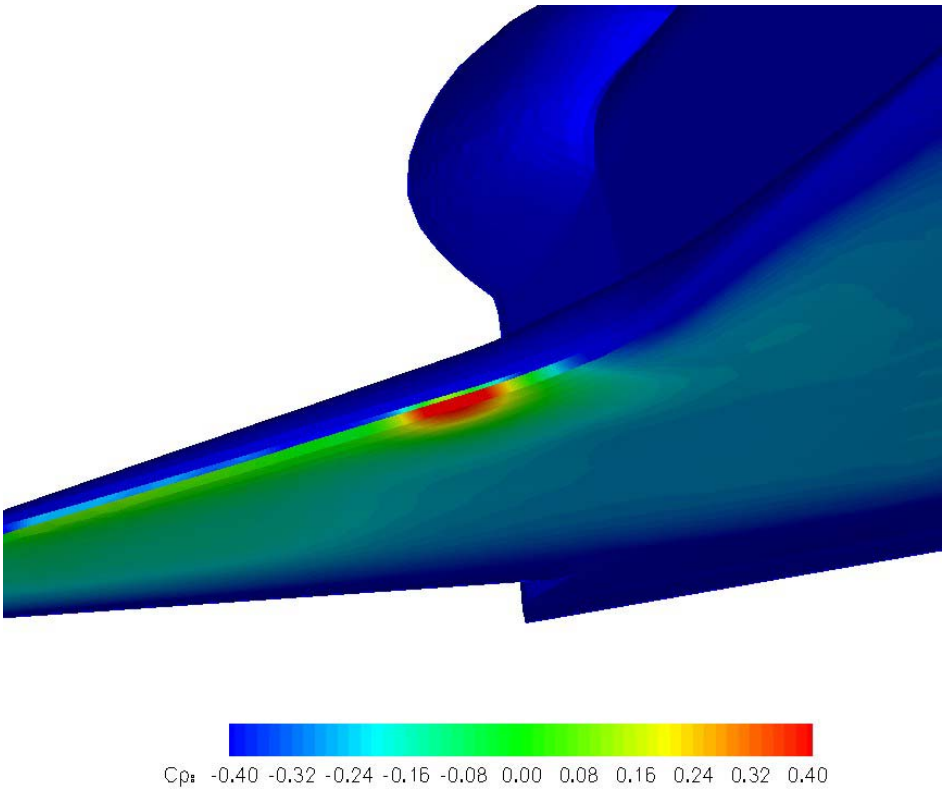

Figure 5.2.4-34 Surface Pressure Coefficient for DSMC Point A, Mach 27.0

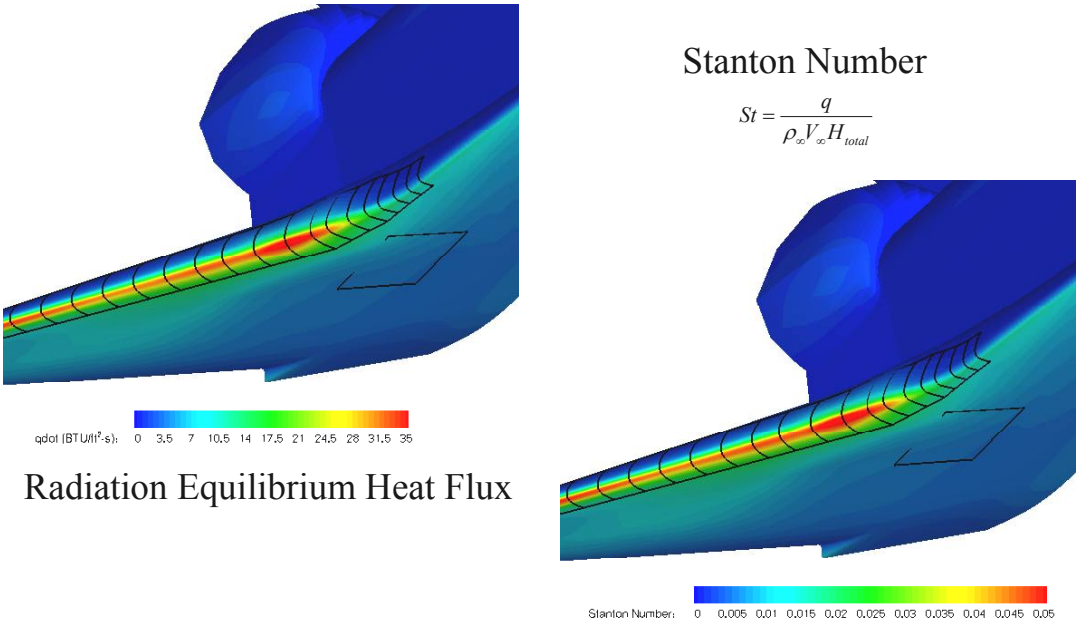

Figure 5.2.4-35 Surface Heat Flux Distributions for CFD Point 1, Mach 24.9

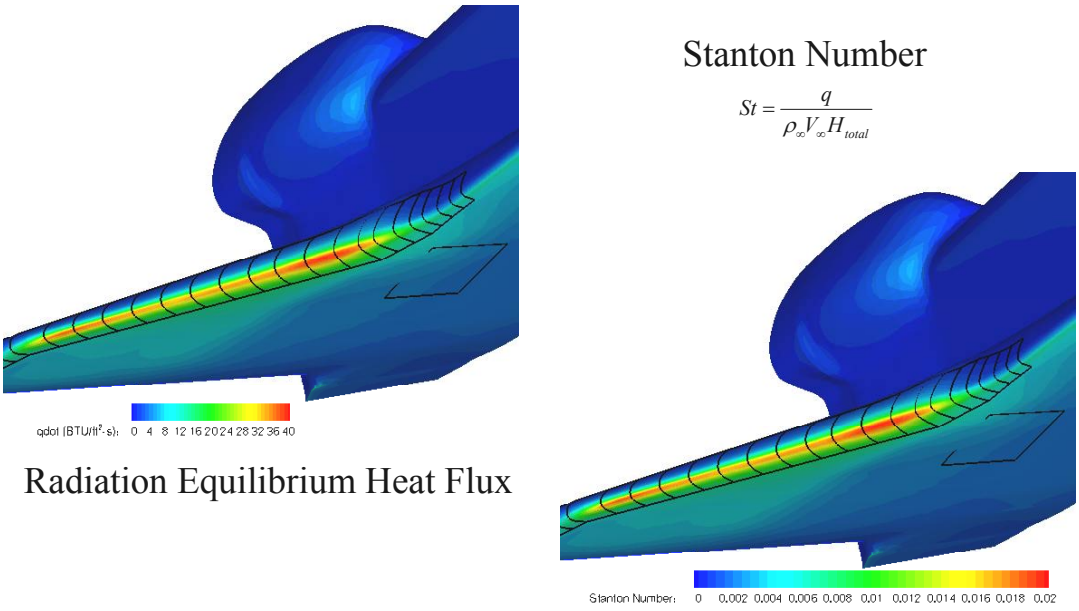

Figure 5.2.4-36 Surface Heat Flux Distributions for CFD Point 6, Mach 17.9

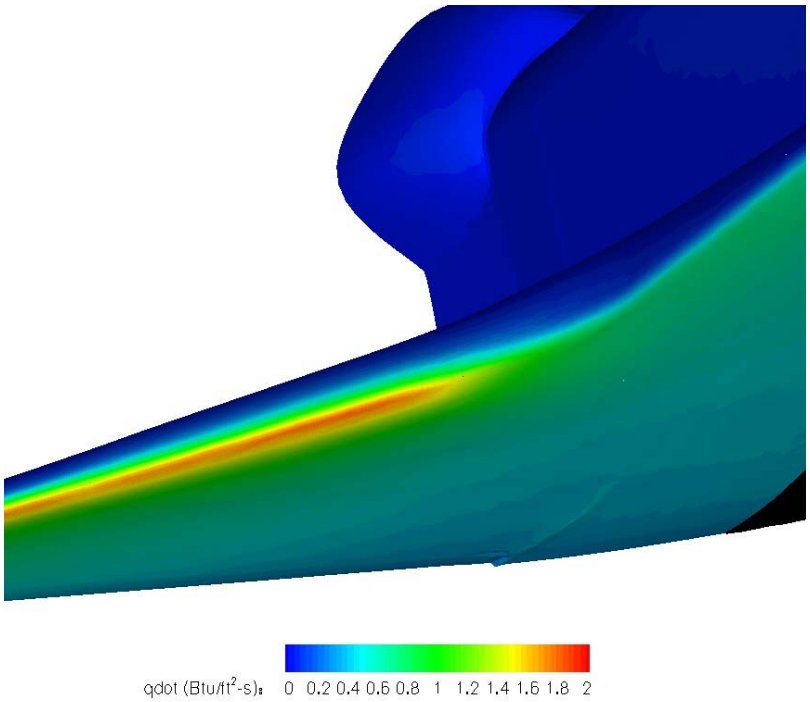

Figure 5.2.4-37 Surface Heat Flux Distribution for DSMC Point AA, Mach 25.1

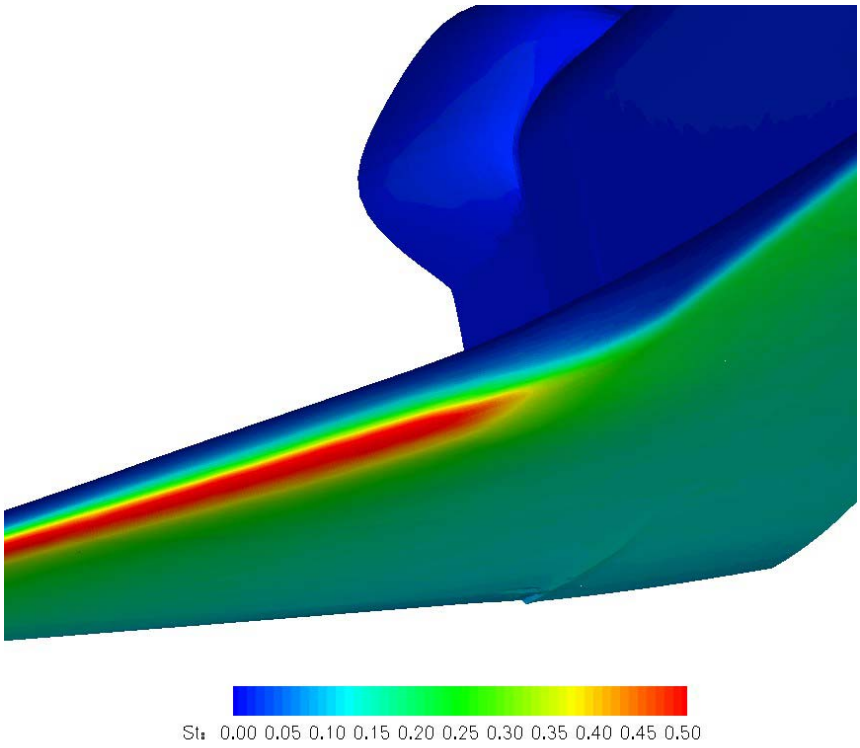

Figure 5.2.4-38 Stanton Number Distribution for DSMC Point AA, Mach 25.1

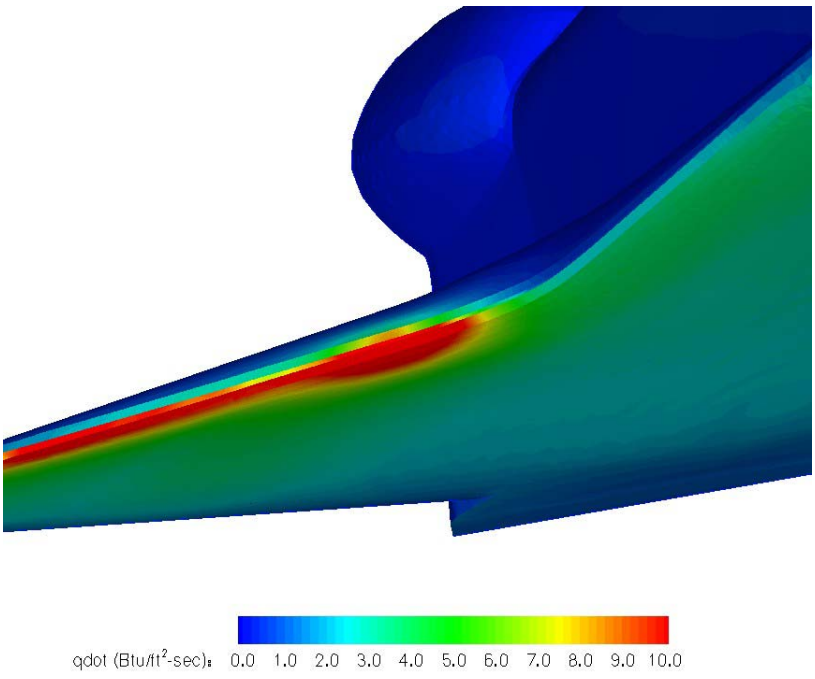

Figure 5.2.4-39 Surface Heat Flux Distribution for DSMC Point A, Mach 27.0

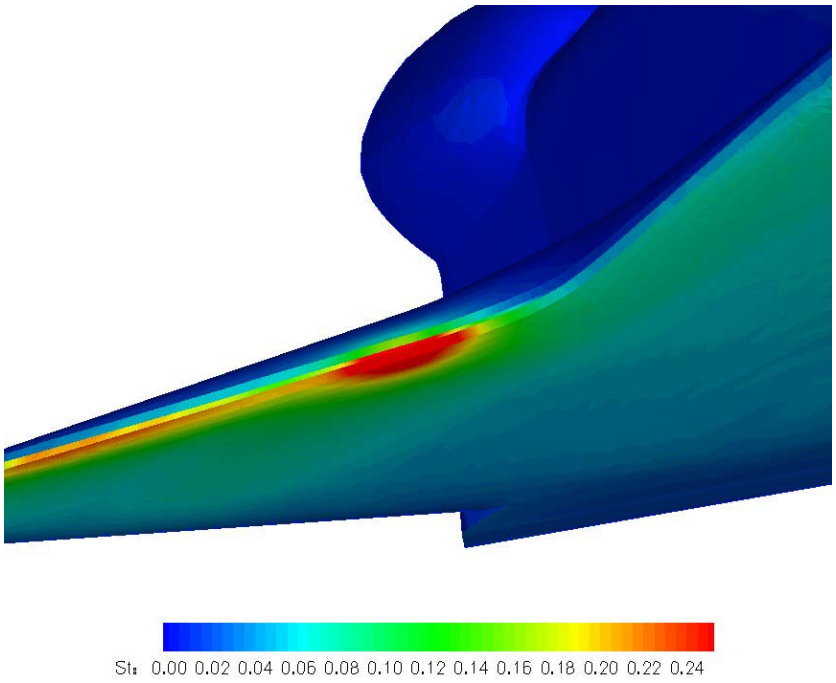

Figure 5.2.4-40 Stanton Number Distribution for DSMC Point A, Mach 27.0

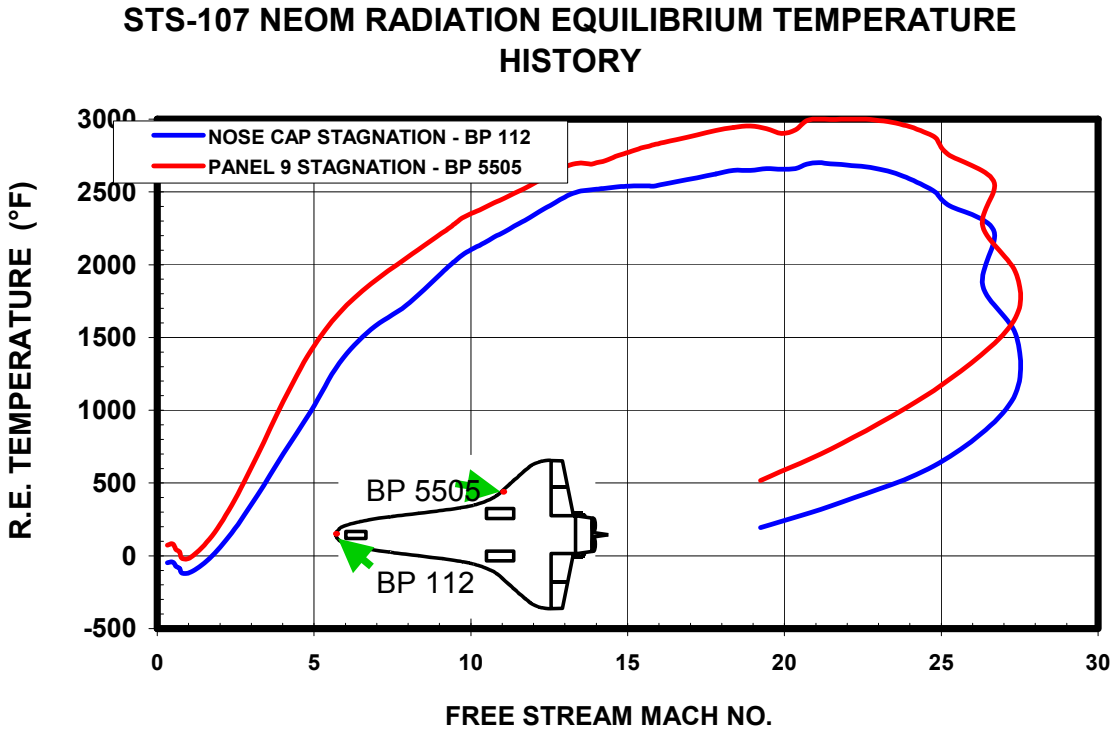

Figure 5.2.4-41 Flight Calibrated Estimate of Peak Heat Flux History on Panel 9

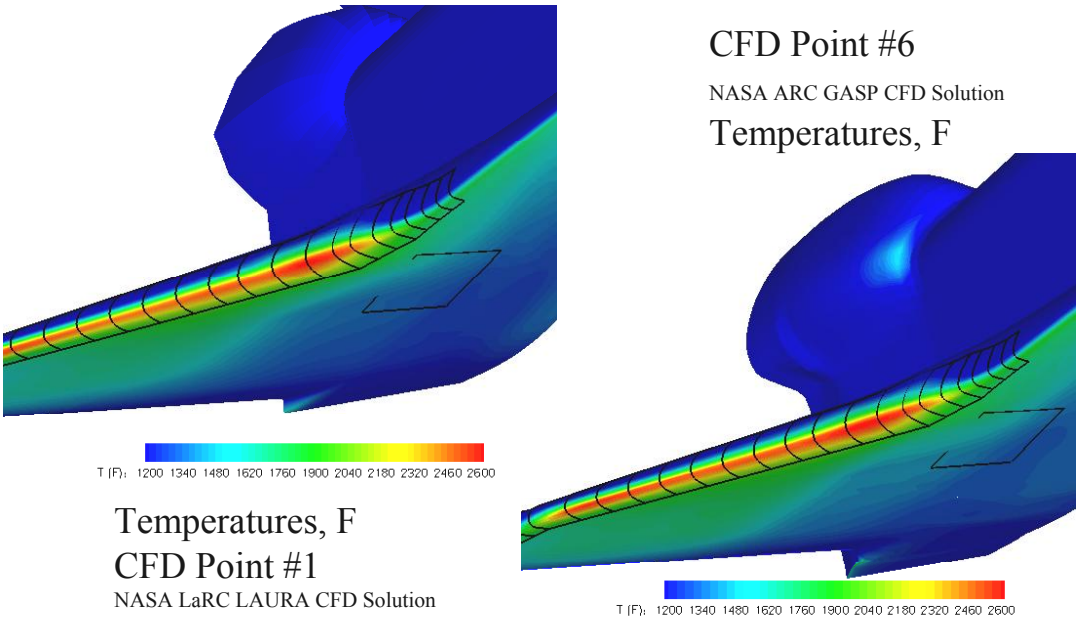

Figure 5.2.4-42 Radiation Equilibrium Surface Temperatures In the Wing Leading Edge Region

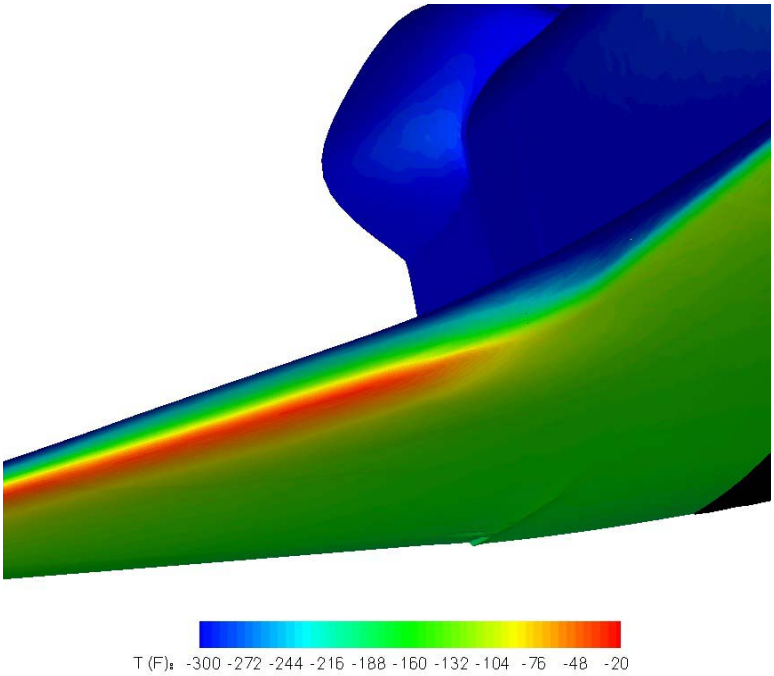

Figure 5.2.4-43 Radiation Equilibrium Surface Temperatures In the Wing Leading Edge Region for DSMC Point AA

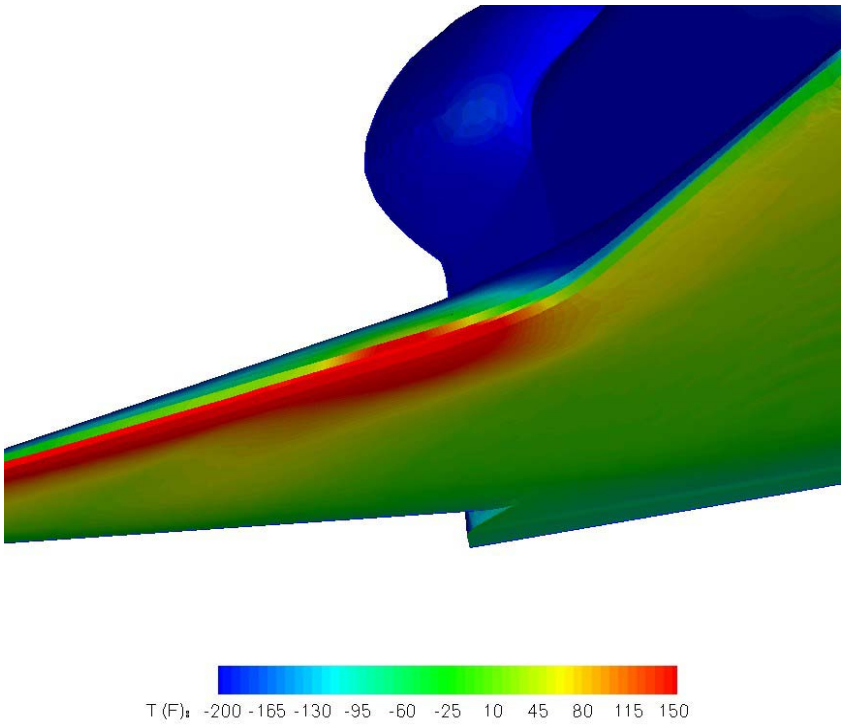

Figure 5.2.4-44 Radiation Equilibrium Surface Temperatures In the Wing Leading Edge Region for DSMC Point A

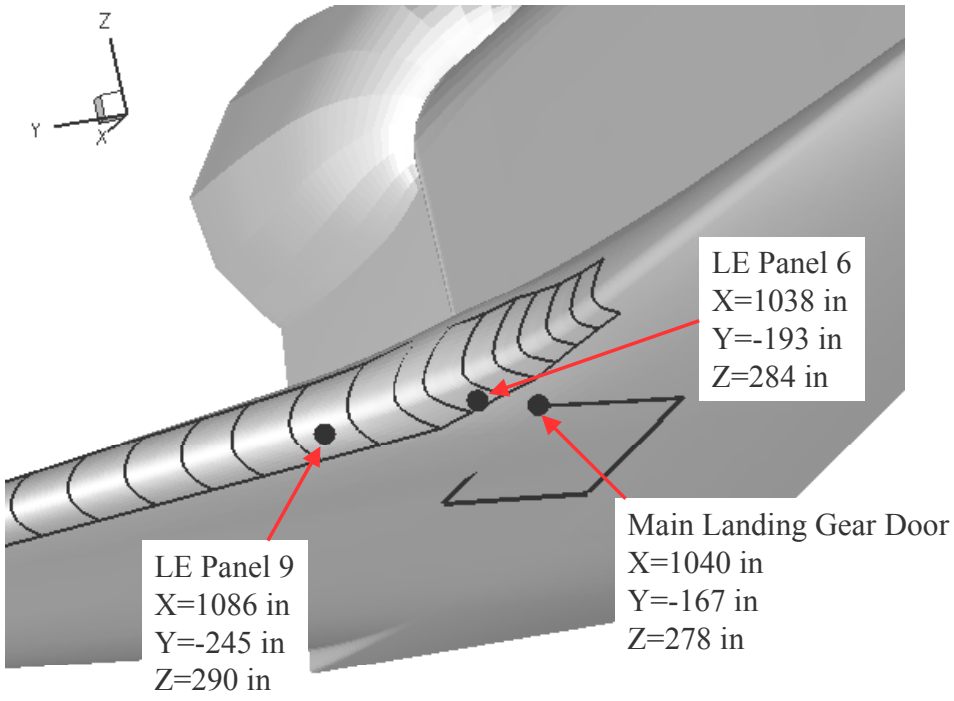

Figure 5.2.4-45 Boundary-layer Temperature and Enthalpy Profile Locations on Orbiter

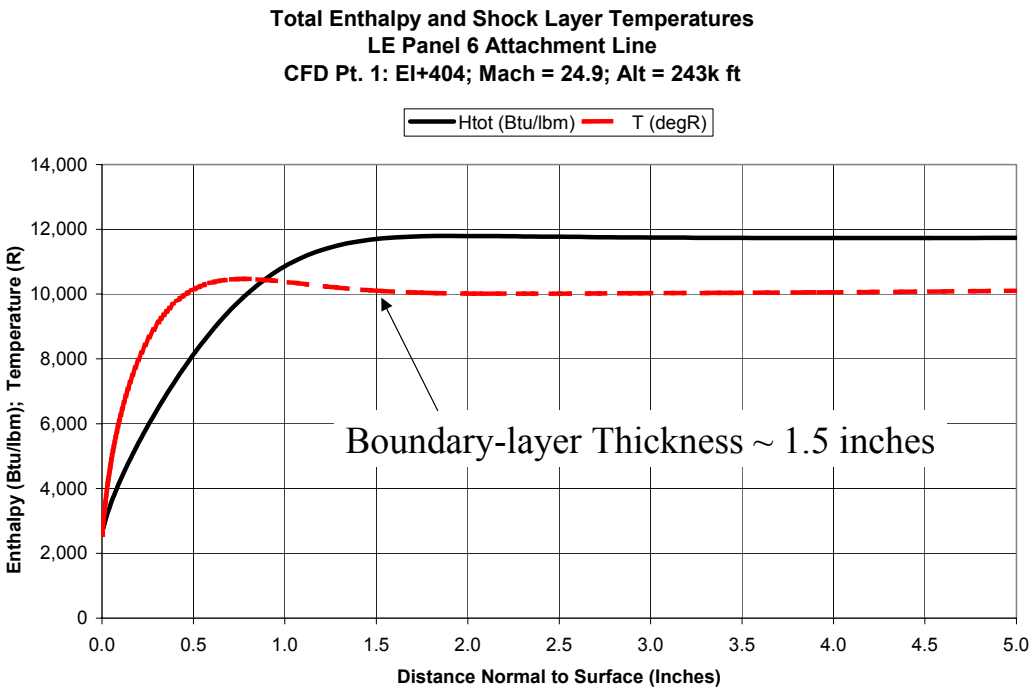

Figure 5.2.4-46 Total Enthalpy and Static Temperature Variation from LE Panel 6 Surface into Flow Field: CFD Point 1, Mach 24.9

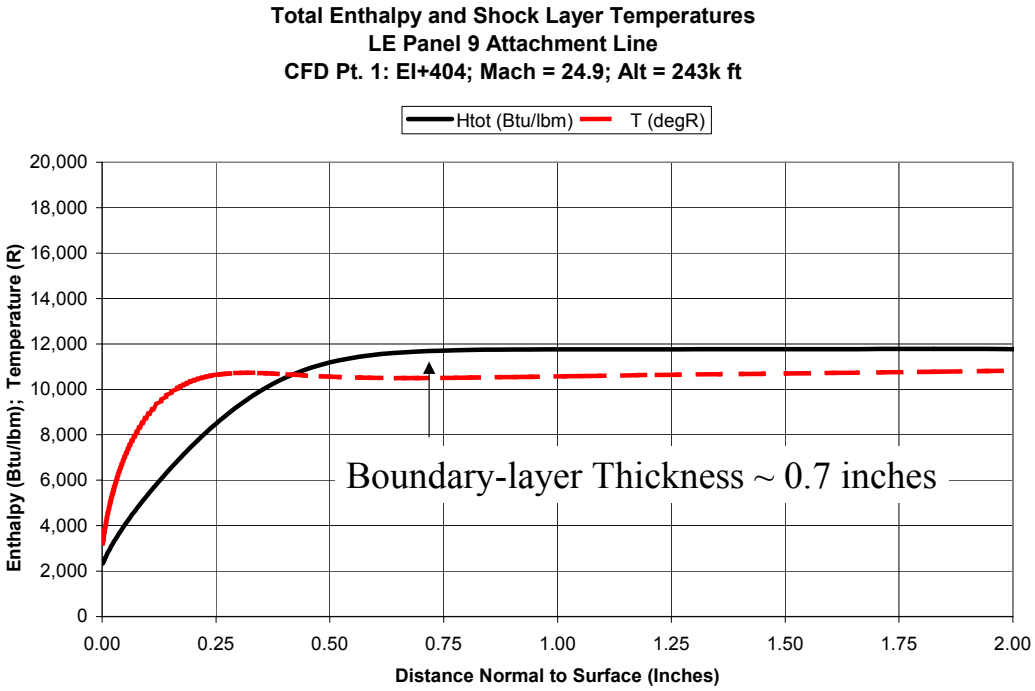

Figure 5.2.4-47 Total Enthalpy and Static Temperature Variation from LE Panel 9 Surface into Flow Field: CFD Point 1, Mach 24.9

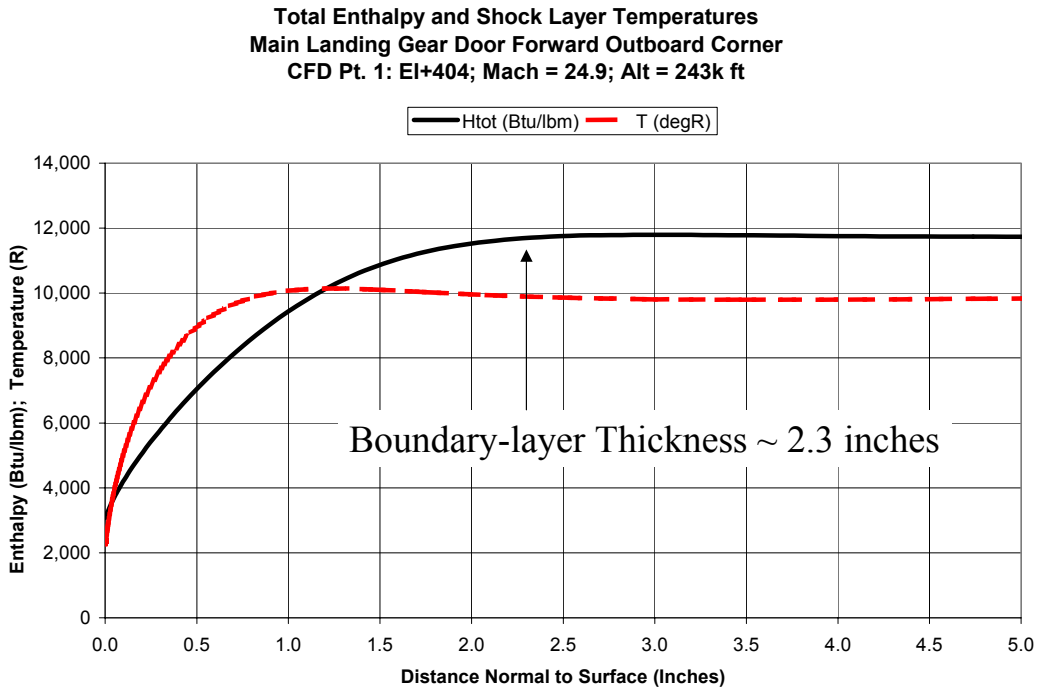

Figure 5.2.4-48 Total Enthalpy and Static Temperature Variation from Main LG Door Surface into Flow Field: CFD Point 1, Mach 24.9

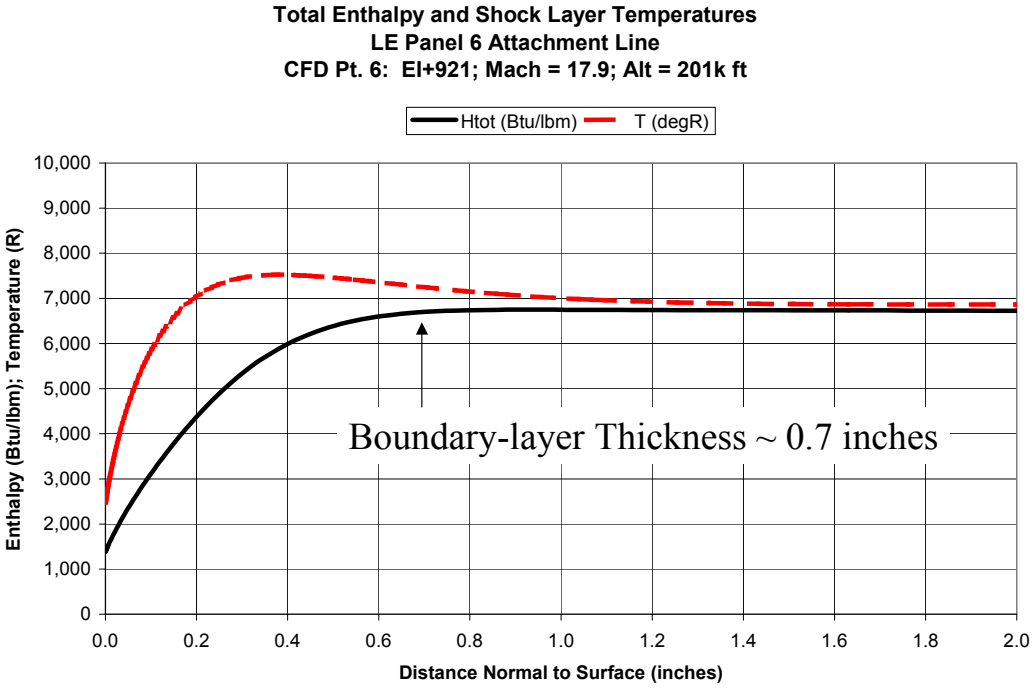

Figure 5.2.4-49 Total Enthalpy and Static Temperature Variation from LE Panel 6 Surface into Flow Field: CFD Point 6, Mach 17.9

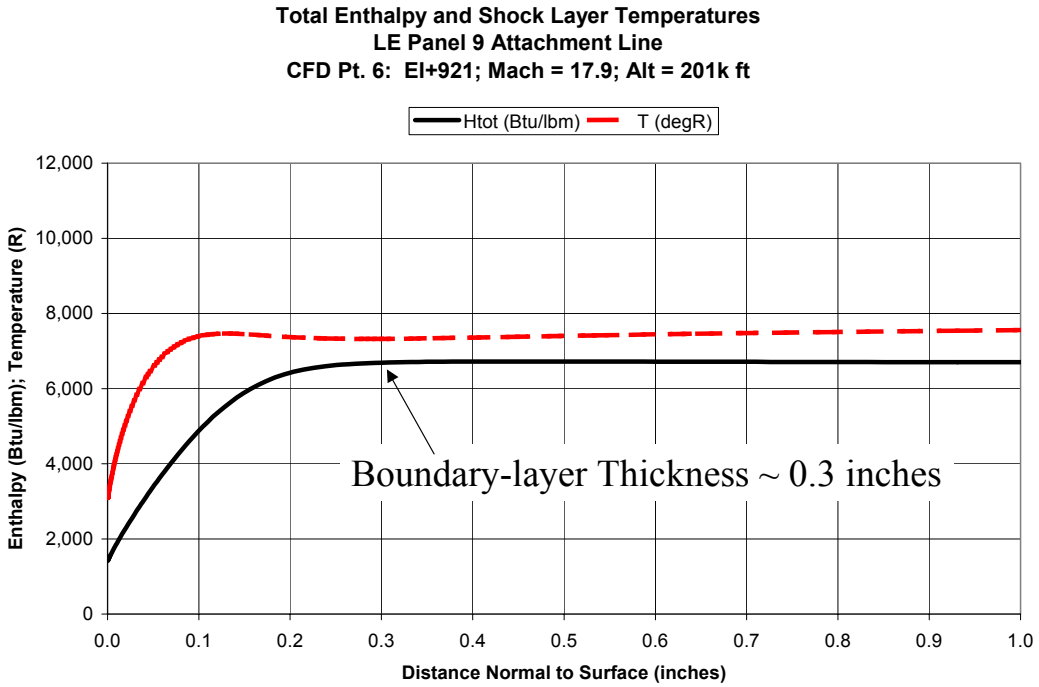

Figure 5.2.4-50 Total Enthalpy and Static Temperature Variation from LE Panel 9 Surface into Flow Field: CFD Point 6, Mach 17.9

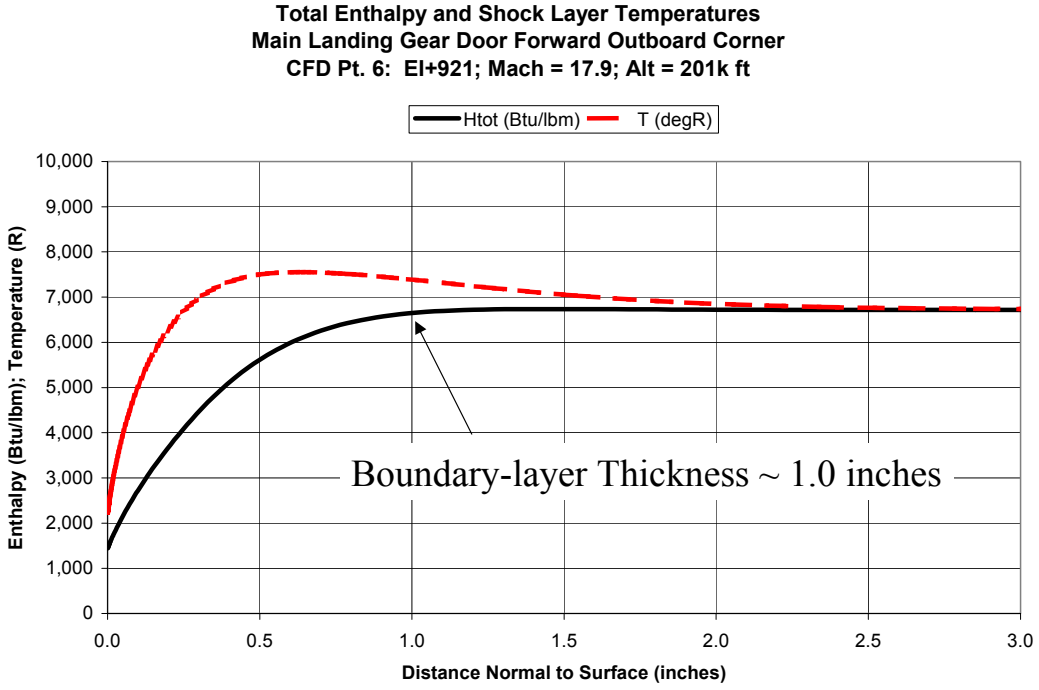

Figure 5.2.4-51 Total Enthalpy and Static Temperature Variation from Main LG Door Surface into Flow Field: CFD Point 6, Mach 17.9

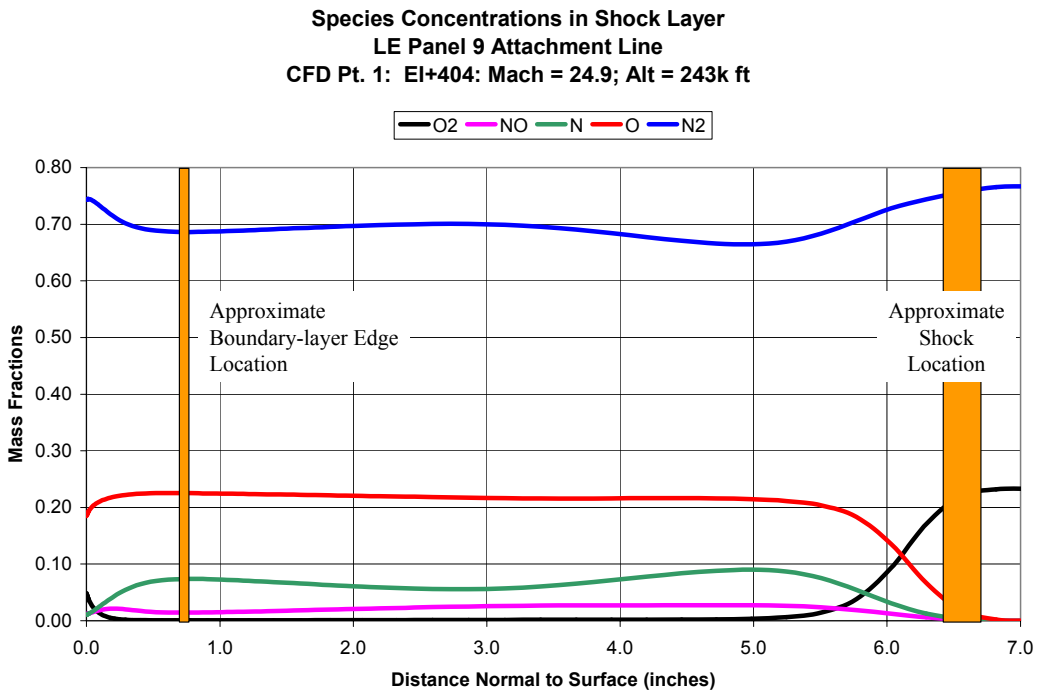

Figure 5.2.4-52 Predicted Species Mass Fractions in the LE Panel 9 Shock Layer: CFD Point 1, Mach 24.9

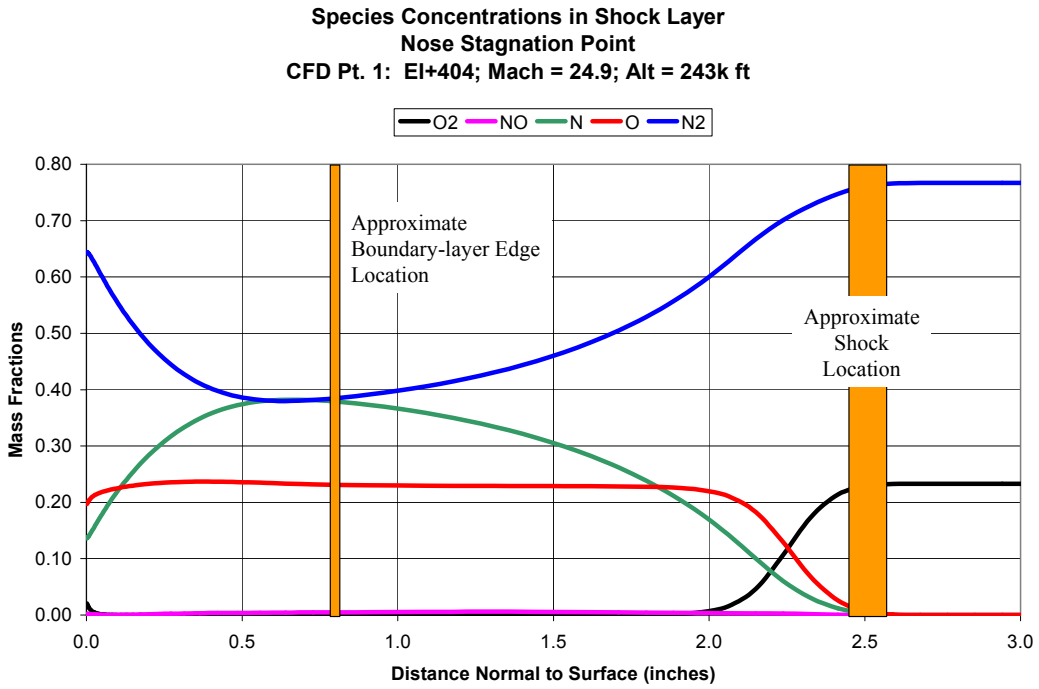

Figure 5.2.4-53 Predicted Species Mass Fractions in the Orbiter Nose Shock Layer: CFD Point 1, Mach 24.9

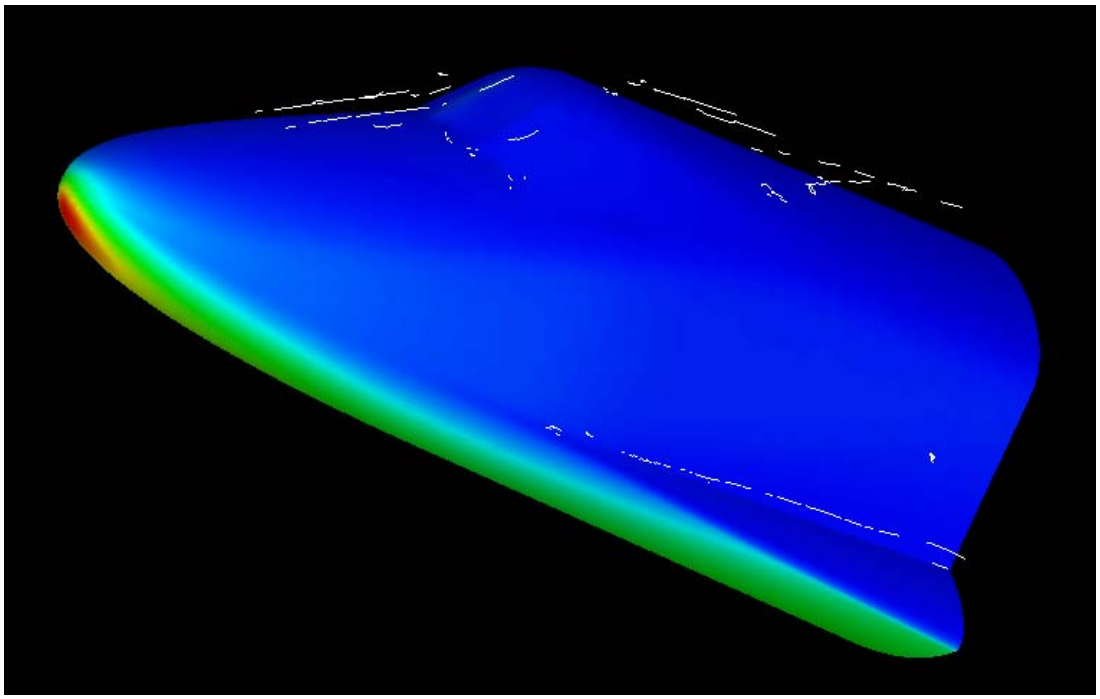

Figure 5.2.4-54 Pressure Contours and Vortex Location for wind tunnel conditions

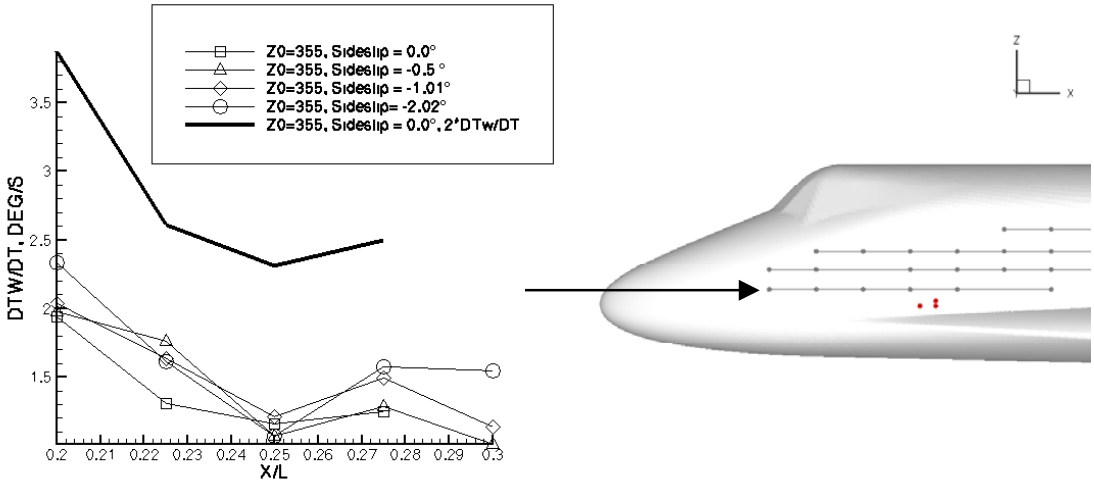

Figure 5.2.4-55 Wind Tunnel Measured Temperature Rise Rate

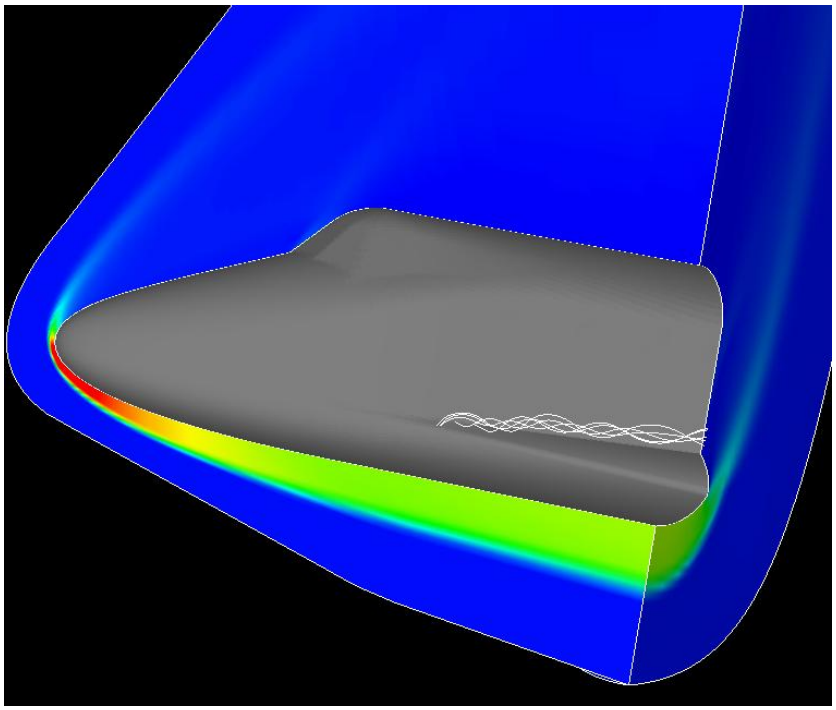

Figure 5.2.4-56 Pressure contour and vortex core location for wind tunnel conditions

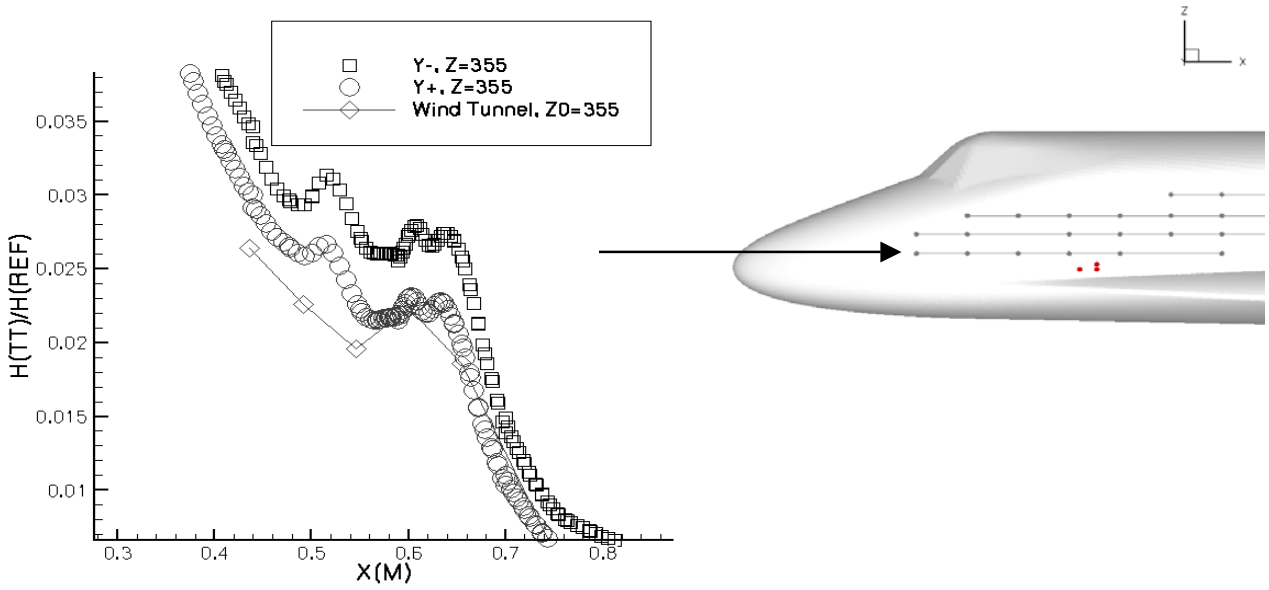

Figure 5.2.4-57 Comparisons with wind tunnel data

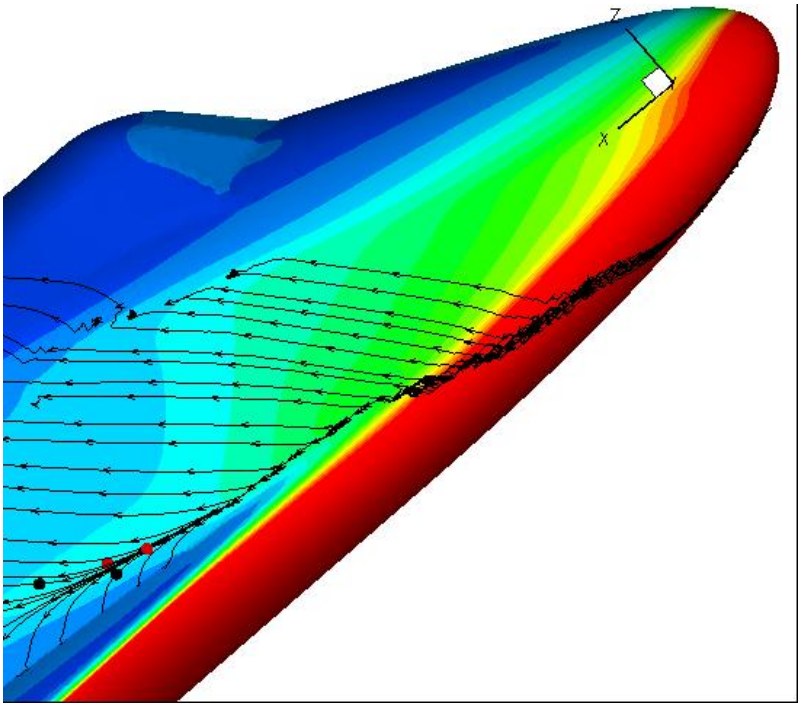

Figure 5.2.4-58 Shear stress contours and surface streamlines at flight conditions

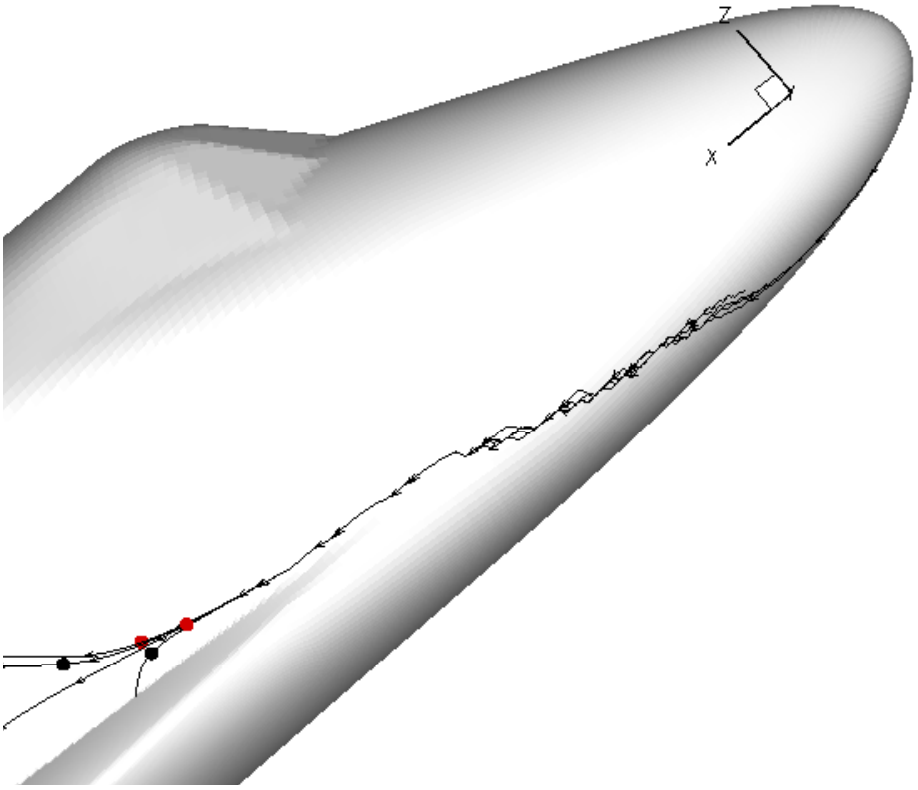

Figure 5.2.4-59 Nozzles and thermocouple streamlines at flight conditions

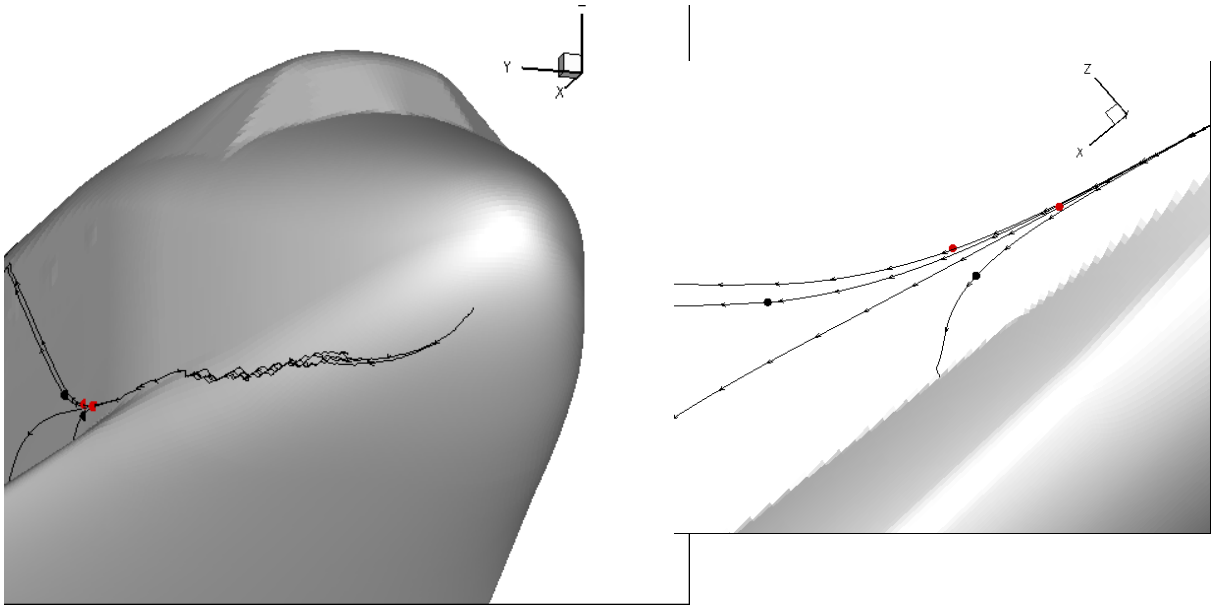

Figure 5.2.4-60 Front view and close-up of nozzles at flight conditions

5.2.4.5 *Damaged Orbiter Configurations Solutions*

5.2.4.5.1 Introduction

Computational aerothermodynamics was used to investigate the effects of damage to the Orbiter leading edge during Earth re-entry. The primary motivation in performing these RCC panel damage scenario CFD calculations was to gain a greater understanding of the detailed effects that various leading edge damage types and locations would have on overall vehicle dynamics and surface heating. Of particular interest in these CFD solutions was how the damage location and type would affect surface heating at the sensor locations on the side fuselage and OMS pod, where Columbia data were available. Another high priority aspect to be examined via the CFD solutions was the detailed off-body flow characteristics resulting from OML damage. Also, in order to aid the in the investigation of the delta aerodynamics (Section 4), these CFD solutions presented in this section were used to evaluate the damage effects on surface pressure and hence, on the integrated aerodynamic forces and moments. Obtaining a detailed understanding of RCC wing panel damage on the actual temperatures and heating for the wing spar, internal RCC channel insulation and other internal wing leading edge hardware was considered to be of secondary importance for these CFD computations. It is well understood that very small changes in damage topology or location will have very substantial effects on the actual heating values in the vicinity of the damage. The unknown nature of the actual STS-107 damage, combined with its likely rapid progression, makes quantitative internal cavity temperature and heating predictions virtually impossible. Furthermore, to attain even an engineering level of credibility on internal cavity heating, the cavity geometries would have to be more realistic and represent the actual internal wing leading edge hardware. Also, physically representative wall boundary conditions for the internal wing materials (emissivity and catalycity) and proper treatment of the internal radiative conditions would be necessary. Not only would these new kinds of boundary condition have to be implemented in our CFD codes, but they would have to be validated as well. Section 5.3 of this report focuses more on the interior heating details; thus this

section will not examine the physics or flow features within the cavities generated by removing RCC panels.

The studies described in this section were conducted at the start of peak heating where the external flow is characterized by high angle of attack, hypervelocity conditions: CFD case 1 condition (404 seconds from EI, free-stream Mach number = 24.83, angle of attack = 40.2 degrees, and altitude = 243,000 ft). Members of NASA-ARC Reacting Flow Environments (ASA) Branch and NASA-LaRC Aerothermodynamics Branch performed these computations using GASP (Appendix 5.6) and LAURA (Appendix 5.6), respectively. The entire flow field for these damage cases was assumed to be laminar and in a state of chemical nonequilibrium (5 reacting species), and in a state of thermal equilibrium. The boundary condition at all solid surfaces (both the OML and the internal cavity surfaces) used RCG catalysis assumptions developed by Stewart, radiative equilibrium, and an emissivity of 0.89. Complete details of the computational strategy and convergence acceptance and quality checking for both GASP and LAURA are provided in Appendix 5.6.

The damaged geometries considered in this work included an approximation of a complete missing panel 6 (herein referred to as the panel 6 “notch”), a fully removed and lower half removed panel 6, a lower half removed panel 9 with and without flow into the RCC channel, a complete missing panel 9 with and without flow into the RCC channel, and a lower half removed panel 9 with flow into the RCC channel and the upper carrier panel missing. These cases as well as the results observed from the computations are described more fully in the following sub-sections. A main point in considering the solutions below is that not all possible types of damage were explored nor were any thermal analyses performed to define in a precise way the actual damage experienced by STS-107. Rather the boundaries of a matrix of possible damage scenarios to the leading edge were explored. This matrix of damage solutions was used to establish the locations, extent and magnitude of associated temperature and heat flux anomalies that might credibly occur on the exterior surface of the Orbiter. Since special focus will later be placed on the effect that leading edge damage has on leeside heating of the fuselage side and the OMS pod, it is important to note the key parameters that appear to drive these effects: (1) the topology, size and location of any wind side wing leading edge damage, (2) the magnitude of venting into the interior wing, (3) the extent of venting to the lee side by hot gases within the RCC channel, and (4) the extent and nature of any breech that allows hot windside gases to pass directly to the leeward side of the vehicle. Thus, as mentioned in section 5.2.1.1, an engineering perspective is taken in the interpretation of these numerical results.

RCC Panel 6, Baseline Smooth OML Solution with Embedded-O Mesh (ARC)

The first in the series of GASP CFD computations for damaged RCC panel scenarios was that of the smooth OML panel 6 case. The computational mesh leaves both the upper and lower RCC half panels in place and therefore is simply another smooth OML solution. The main difference between this calculation at CFD condition 1 and the comparable GASP solution discussed in section 5.2.4.4.2 is the grid. The same forebody and aft body grids are used in the two GASP calculations, but the mid-body external grid for the current calculation uses an imbedded-O topology that focuses on the outer perimeter of RCC panel 6. Since this panel is left in place, the body surface face of the exterior H-grid that sits in the “eye” of the imbedded-O topology simply covers theRCC panel 6 OML. The calculation can be thought of as another comparison/validation case for the common baseline mesh solutions at CFD condition 1. Because of the use of the imbedded-O grid used in the earlier nominal GASP calculation (1.86 million for the current calculation, 1.06 million for the earlier nominal GASP calculation) its primary purpose here is to isolate possible solution problems related to the modified exterior grid or the complicated internal cavity grid. Also, when differences between the temperatures or heat fluxes of damaged and undamaged configurations are examined, the use of identical exterior meshes for both solutions greatly simplifies the differencing process.

Figure 5.2.4-68 and Figure 5.2.4-69 show side and top planform views of the normalized heating rates seen on the configuration for this nominal configuration case. These views shall be used repeatedly for all ARC-computed damage scenario CFD solutions presented later in this section. These images provide a viewpoint to understand changes in surface heating over regions of the vehicle where flight data were obtained during the STS-107 re-entry. The results of this computation are in very close agreement in

terms of temperature and heat flux compared with the corresponding solution obtained from the baseline common mesh discussed in section 5.2.4.4.2.

RCC Panel 6, Full "Notch" Out Solution with Solid Side Walls (LaRC)

For expediency in assessing the effects of leading edge damage, a grid approximating a missing RCC panel 6 was generated early in the investigation for the first damage scenario CFD case at flight conditions. Coordinates defining RCC panel 6 were estimated from existing literature since this work occurred prior to acceptance and distribution of a common CAD geometry within the investigation team. Subsequent comparison of the estimated panel 6 coordinates with the actual size and location revealed that the approximated missing panel was centered about the correct location but was roughly only 2/3 of the full panel. Figure 5.2.4-61 shows a planform view of the missing panel modeled in this work compared with the size and location of the actual RCC panels. The exterior grid for this "notched" panel 6 out case was developed at LaRC very early in the investigation before the common grid development had taken place. Details of the grid are presented in section 5.2.4.2. The grid uses an O-H topology to define the interiorof the missing RCC panel 6 cavity. This topology allows grid cells to be clustered against the solid side and back surfaces to capture viscous boundary-layer behavior. This current cavity grid can be thought of as a hybrid between two cavity grid alternatives described in section 5.2.4.2. The grid has an H topology in the spanwise direction and an O topology in the streamwise direction. The interior cavity grid was composed of 5 matching blocks, one in the center and four surrounding it with their outward faces forming the backplane and the matching faces to the RCC panel 6 OML. Each of the two spanwise faces of thesefive cavity blocks meets the side walls of the cavity. To construct the missing panel geometry, solid vertical surfaces were used to slice the nominal Orbiter geometry along the sidewalls and backplane, thereby forming the leading edge cavity. In reality, the sidewalls of a cavity formed by a missing RCC panel are hollow. This would allow flow into the channel on either side, but such venting was not modeled in the present computation. The backplane of the cavity is a rough approximation of the main wing spar in this simulation; however, no other internal geometry components (e.g., spanner bars, carrier panels, earmuffs) were modeled. The solution was obtained with LAURA using thin-layer Navier-Stokes equations on a grid that had been coarsened to one-half the available grid density in directions parallel to the surface, with full resolution normal to the Orbiter surface. This coarsened grid totaled approximately 8.5 million points, 2.5 million of them located within the missing RCC panel cavity.

Figure 5.2.4-62 shows one aspect of the resulting flow solution where a slice that crosses the RCC cavity has been extracted in the planform plane. The flooded contours on this figure show the flow field density levels for the case where the RCC panel is missing. It can be seen in the figure that shock waves are anchored at both the inboard and outboard leading-edge corners of the missing RCC panel. These embedded shocks are formed around the recirculating flow within the cavity at the inboard corner and from impingement of flow on the outboard corner. Both shocks form weak interactions with the wing bow-shock downstream of the cavity. Solid contour lines are overlaid on the figure to depict the density contours in this area for the case of a baseline geometry with no missing RCC panels. By comparison the presence of the cavity appears to have a very small effect on the outer bow shock and downstream flow in this plane. The only differences noted are the additional features described for the missing panel case. This observation regarding the downstream flow also held true for other planes around the leading edge.

While the missing RCC panel 6 "notch" effect was minimal along the wing leading edge, its impact was very evident in the wing leeside flow. Figure 5.2.4-63 through Figure 5.2.4-65 show temperature contours plotted in vertical planes that have been extracted from the flow field at three axial stations (at the missing RCC panel 6 "notch", midway between RCC panel 6 and the OMS pods, and at the front face of the OMS pods). These figures compare the flow fields of the nominal (i.e., undamaged) Orbiter geometry with the flow field predicted on the leeside with the RCC panel 6 "notch". The sequence of figures shows a jet flowing out of the cavity toward the side fuselage and then the subsequent flow development along the fuselage. In probing the computed flow field it can be ascertained that the jet flow leaves the cavity and travels across the wingspan toward the symmetry plane. Then, it impacts the fuselage at a nearly perpendicular angle. At the fuselage, the jet is turned abruptly downstream. The accompanying temperature increase in the flow field is due to both the hot gas flowing from the wind side and the impact of this jet on the fuselage.

The irregular flow effect on the Orbiter lee side is most evident in the surface pressure and heating experienced on the side fuselage. Figure 5.2.4-66 and Figure 5.2.4-67 illustrate these effects by showing contours of the increase in predicted surface pressure and heating rate over the nominal case. The pressure effect is computed as a difference in pressure coefficient and the effect on heat transfer is shown as a ratio of off-nominal to nominal heating. The area of pressure and heating increases are located almost directly transverse to the missing RCC panel 6. Both areas show an angled orientation sloping upward and aft. This result is in general agreement with wind-tunnel measurements of heating with missing RCC panel 6 geometry in terms of both location and orientation (Section 5.2.3). The maximum heating augmentation from the current prediction is ~5 times the nominal rate.

RCC Panel 6, Lower Half Panel Out Solution with Solid Side Walls (ARC)

The first damage scenario at flight conditions with an accurate definition of the RCC panels considered removing the lower half of RCC panel 6. A cavity was constructed into the wing leading edge by generating surfaces defining the spar, the inboard and outboard sides of RCC panel 6, and a constant waterline to define the vertical extent of panel loss. For the wing spar surface, a cutting plane was created that extends upward from the wing lower surface and parallel to the wing spar. The location of the vertical damage extent utilized a cutting plane that extends aft from the leading edge apex at a constant Z or waterline. Cutting planes between the edges that define the inboard and outboard RCC panel 6 side boundaries defined the width of the damage cavity. A pictorial representation of this geometry for a similar damage configuration at RCC Panel 9 is depicted in Figure 5.2.4-78. Solid wall RCG radiative equilibrium boundary conditions are applied along all of these interior cavity cut planes to fully define the boundary conditions.

The exterior mesh used for this calculation is the same as that used for the smooth OML RCC panel 6 case discussed above. It contained 1.86 million mesh points and 40 blocks, while the 7-block interior cavity mesh topology, which was described in detail in section 5.2.4.2 as the second alternative, contained 164 thousand points. Due to the short time frame allowed to complete this case and the long run times needed to converge a solution with leading edge damage, only a single CFD case was run. The conditions used for the GASP CFD code corresponded to point 1 in table 4.3-4 from section 4.3.2.2.

The cavity geometry is somewhat fictitious in that the inboard and outboard side walls should actually have vents into the RCC channel. Furthermore, the solid wall applied at the constant waterline cut plane actually has no physical basis. Finally, none of the internal RCC channel components such as the earmuffs, hardware insulation, or RCC panel attachment hardware were modeled. Instead, the interior of the RCC cavity was modeled with smooth straight walls. Nevertheless, to understand how significant windward RCC damage affects the leeside flow, this RCC half panel out cavity calculation was a helpful bounding case. In addition, an RCC half panel damage scenario solution at flight conditions helped to provide insight into differences between wind tunnel data and these flight simulations.

Figure 5.2.4-70 and Figure 5.2.4-71 show the analogous side and planform views of the damaged configuration with MADS (circles) and OI (boxes) sensors noted on the images. What is directly observable by comparing these images with the smooth OML images seen in Figure 5.2.4-68 and Figure 5.2.4-69, is that there is virtually no difference between the surface heating on the lee side, except for the region closest to the damage site. The conclusion from this solution is that having a lower half panel missing at the RCC panel 6 location has very little effect on the side fuselage or OMS pod heating. This result is consistent with the wind tunnel trends presented in Section 5.2.2. As a final note, the half RCC panel 6 out case calculation shows that there is some effect on the windward heating downstream of the damage region, although the images of this effect are not included in this report.

RCC Panel 6, Full Panel Out Solution with Solid Side Walls (ARC)

A follow-on to the RCC panel 6 half out case, simulated the loss of an entire RCC panel 6. Again cutting planes were constructed along the spar definition and at the RCC panel side boundaries. All of the new cavity-defining surfaces were specified as solid boundaries with RCG catalysis and radiative equilibrium. This cavity definition, as for the previous RCC half panel out case, was also somewhat flawed. No venting down the RCC channel was included, and hardware such as the insulating earmuffs and RCC panel retaining hardware was entirely missing. Both the backwall and the two side walls were modeled

as smooth featureless surfaces. Nevertheless, since our focus was on heating effects that occur away from the damage location, it provided a reasonable approximation of the loss of an entire RCC panel.

The mesh used for the exterior of the Orbiter was identical to that used for the two previous ARC RCC panel 6-related calculations. Inside the cavity, the 7-block interior mesh topology with 252 thousand points was used. CFD point 1 was used to define the conditions for GASP and only this single case was run.

Figure 5.2.4-72 and Figure 5.2.4-73 show the now familiar side and planform views of Orbiter leeside heating. Immediately evident from these images is that removal of the complete RCC panel 6 results in a rather significant heating change on the side fuselage and OMS pod. Figure 5.2.4-74 illustrates heat flux ratios on the side fuselage between the current complete-panel-removed solution and the smooth OML equivalent solution. Dramatic heat rate differences are indeed present. Very striking in the figure is the fact that locations of both significantly greater heating and moderate cooling relative to the undamaged OML solution are present on the vehicle. In particular, the OMS pod heating is dramatically reduced while a section on the side of the fuselage near the wing root and *ahead* of the actual damage location experiences heating levels that are dramatically higher than normal. Notice that the side fuselage region experiencing increased heating is quite large and that it is preceded upstream by a section of *reduced heating*. The increased heating of the side fuselage is due to impingement of the jet originating from the RCC cavity. The decreased heating on the OMS pod region may be due to changes in the position of the leeside wing-strake vortices, that normally run along paths that cause significant vortex scrubbing and hence heating effects on the OMS pod.

To illustrate the structure of the jet coming from the RCC cavity, Figure 5.2.4-75 through Figure 5.2.4-77 show temperature contours for cuts through the flow-field solution at three constant X locations. Side-by-side comparisons for both half RCC panel out and full RCC panel out with the smooth OML solutions are depicted. It is noted again that virtually no differences are seen in the leeside region for the half RCC panel out case. However, for the full panel out case, dramatic flow-field structures, not present in the smooth OML solution, are revealed. The very hot regions of these flow structures, which are especially evident at the X = 27 m and X = 30 m cuts, may be considered secondary shocks that are standing off the side of the fuselage. The shocks appear to be caused by an impinging jet hitting almost perpendicular to the side fuselage which emanates from the upper half of the RCC panel 6 removed cavity. The fact that the jet structure traverses the flow-field in the cross-stream direction while the free-stream flow is at Mach 25 emphasizes the strength of the jet. The removal of the panel can be thought of as creating a scoop down into the windside flow. The scoop turns the flow inward toward the body, and since on the leeside conditions are very nearly at a vacuum there is no resistance to this jet heading directly toward the side fuselage. Furthermore, once on the lee side, the jet must be traveling with considerable speed since it creates a secondary bow shock that stands off the side of fuselage. The temperature experienced by the flow as it traverses this secondary side-fuselage shock reaches levels that are near those present in the primary bow shock on the wind side of the vehicle. The cooler than normal region ahead of the jet impingement on the side of fuselage is a result of the jet flow moving aside the leeside flow that would normally be slowly accelerating along the side of body.

RCC Panel 9, Baseline Smooth OML Solution with Embedded-O Mesh (ARC)

In addition to the RCC panel 6 studies discussed above, studies at flight conditions focused on RCC panel number 9 were also conducted. Again an initial Ames solution using GASP for the smooth OML instance of the RCC panel 9 series was first conducted. The CFD case calculated was point 1 as defined in table 4.3-4. The mesh had an identical number of points to the equivalent RCC panel 6 case – 1.86 million points. For a comprehensive discussion on the motivation for running this case, the reader is referred to the RCC panel 6 equivalent case above. Figure 5.2.4-79 and Figure 5.2.4-80 show the side and planform views of the heating for this case. The images are very similar to those shown earlier for the smooth OML RCC panel 6 results, and thus will not be discussed in any more detail.

RCC Panel 9, Lower Half Panel Out Solution with Solid Side Walls (ARC)

The next case in the series of RCC panel 9 related CFD solutions, calculated with GASP at NASA Ames, follows the same sequence as that followed for the RCC panel 6 series. Specifically, the current case models a lower half RCC panel 9 out. A pictorial representation of the geometry for this damage

configuration at Panel 9 is shown in Figure 5.2.4-78. The construction of the lower half RCC panel out cavity used cutting planes just as in the corresponding half RCC panel 6 out case. The number of mesh points and the topological details of the mesh were also the same as those used for the RCC half panel 6 out case. A GASP simulation with the lower half RCC panel 9 removed and solid wall boundary conditions inside the resulting cavity is depicted in Figure 5.2.4-81 and Figure 5.2.4-82. Again, virtually nothing happens on the lee side, either on the upper wing surface or on the side of the body. A detailed examination showed that the differences in surface heating on the side fuselage and OMS pod, between the present case and the smooth OML RCC panel 9 case, are of the same order as the solution noise present for any calculation with the convergence tolerance used for this study. Thus, it can be concluded that the lower half RCC panel 9 damage case, at CFD flight condition 1, shows no leeside heating effect, within the tolerance of the CFD simulation. Note that the equivalent lower RCC half panel 6 out case discussed above showed slight but not negligible heating differences. The observation is that the attachment line along the leading edge that separates flow traveling to the lee side and the wind side moves higher with increasing span position. It is therefore expected that lower panel damage to the higher panel numbers will show less and less leeside influence. By the time lower RCC panel 9 is reached, essentially no leeside effects can be observed. Wind tunnel tests discussed earlier confirm this trend and demonstrate that rather sizeable leeside effects can be seen if the lower panel damage is as far inboard as RCC panel 3. Although it is not presented pictorially in this report, the RCC lower half panel 9 out does cause significant changes to the windside heating on the wing lower surface. However, these effects are well within the limits that can be tolerated by the RCG coated tiles.

RCC Panel 9, Lower Half Panel Out Solution with Vented Side Walls into the RCC Channel (ARC)

Solid sidewalls within the RCC cavity were used in the flight simulations discussed above, and it was recognized that those solutions could produce misleading results. Thus, an alternate CFD simulation of the lower half RCC panel 9 out scenario was conducted. There is one primary difference between this simulation and the previous RCC lower half panel 9 out case. Instead of the lower half panel out cavity being confined to the lower portion of the wing leading edge section, the entire extent of the RCC cavity bounded by the local RCC panel definition is modeled. This cavity modeling leaves the upper RCC half panel 9 hanging in space; its exterior OML side is exposed to the external flow and its interior cavity side is exposed to the interior flow. The actual RCC panel in this calculation is modeled as a zero thickness surface for the remaining upper section of RCC panel 9. The zero thickness approximation may not be appropriate to capture details of the internal cavity flow, but should suffice to model the leeside effects. In the actual case of a removal of just a lower half panel, a detached bow shock would form on the lip of what remains of the panel and disturb the flow inside the cavity in a way that is different from an attached shock caused by the infinitely thin edge used for the present calculation. This case also differs from the previous solutions in that the location of the RCC channel is defined, or scribed, on the sidewall mesh faces. The sidewall boundary conditions within the RCC channel regions are switched from being modeled as solid to being modeled as exit flow, with a (very low) fixed back pressure. By changing the sidewall boundary condition, we attempted to model the venting relief that occurs down the RCC channel in both spanwise directions. The upper left hand corner inset in Figure 5.2.4-91 shows details of the channel definition across which the exit/venting boundary condition is applied. The back pressure specified for these RCC channel vents was set to 0.1 lbf per ft^2.

The exterior mesh used for this case was identical to that used in the immediately preceding case. Again, only CFD point 1 was computed due to time and resource constraints. The interior mesh was actually identical to the next two full panel 9 out cases, using the 7-block internal topology with 252 thousand grid points. The side walls outside the vented regions, the back wall and the interior surface of the RCC 9 upper half panel were all model as solid walls with RCG catalysis, radiative equilibrium and an emissivity of 0.89.

The side and planform views of heating shown in Figure 5.2.4-83 and Figure 5.2.4-84 are indistinguishable from those shown in Figure 5.2.4-81 and Figure 5.2.4-82. The conclusion is that for the lower half RCC panel out case presented thus far, the details of the cavity modeling seem to have little leeside flow field influence. In general, for RCC panel 9, removal of the lower half does not propagate effects into the leeside flow. As noted previously leeside effects resulting from having a lower half panel out seem to increase as the removed half panel location is moved forward along the wing leading edge.

This result is consistent with experimental leeside heating data presented in Section 4.3.1 and 5.2.3. Lower wing heating differences were again observed but not examined in detail.

RCC Panel 9, Full Panel Out Solution with Solid Side Walls (ARC)

A damage scenario with all of RCC panel 9 removed, and the sidewall boundary conditions within the cavity returned to solid walls with RCG catalysis and radiative equilibrium, is considered next. The case is analogous to the simulation computed for the RCC panel 6 study at Ames. The grid was identical to that used in the preceding case. Figure 5.2.4-85 and Figure 5.2.4-86 show the heating levels from a side view and a planform view. Immediately clear from these figures is the presence of significant side fuselage heating. To reveal the details of this heating pattern more clearly, the heat flux ratio between this solution and the smooth OML panel 9 solution is depicted in Figure 5.2.4-87. Significantly increased heating levels are seen across a wide range of the lower part of the side fuselage, extending substantially upstream of the damage location. The peak heating increase shows a ratio of heating relative to the smooth OML case of above 50. Ahead of this increased heating region is a prominent section of reduced heating extending up and onto the payload bay doors. Unlike the full RCC panel 6 out with solid side walls solution that showed a decreased heating on the OMS pod, this full RCC panel 9 out solution shows a significant heating increase on the OMS pod. The differences in heating effects for RCC panel 6 missing and a RCC panel 9 missing show that leeside heating effects depend upon the actual leading edge damage location. Further information regarding leading edge panel parametrics with a much larger series of RCC panels removed can be found in the wind tunnel discussion of Section 5.2.3.

Figure 5.2.4-88 through Figure 5.2.4-90 show temperature contours across cuts through the solutions for the half and full panel solid sidewall RCC panel 9 damage scenarios. As in the RCC panel 6 equivalent images, the half RCC panel out case is virtually identical to the smooth OML solution. The solution with the full RCC panel 9 out shows very complex flow structures on the lee side above the wing. These “hot” flow structures interact with the side fuselage, resulting in surface heating similar to that seen in the Panel 6 plots of Figure 5.2.4-72 - Figure 5.2.4-77. The reader is referred back to the detailed discussion for the Ames full panel 6 out calculation to gather an understanding of the off body flow phenomena.

RCC Panel 9, Full Panel Out Solution with Vented Side Walls into the RCC Channel (ARC)

The next in the ARC series of panel 9 damage scenarios was the vented side wall version of the above RCC full panel 9 out calculation. In this computation the solid inboard and outboard sidewalls have been changed to the vented sidewalls boundary conditions. This boundary condition was analogous to what was already discussed above for the half RCC panel out cases. The mesh used in the previous computation was recycled for this case to compute CFD point 1. The objective of this simulation was to better understand the differences that RCC channel venting might have on the leeside flow field and surface heating.

Figure 5.2.4-101 and Figure 5.2.4-102 display the side and top planform views of surface heating. The figures show that a geometry with RCC channel venting also has very large heating increases on the lower part of the side fuselage, similar to the unvented full RCC panel 9 out case. Figure 5.2.4-103, illustrates the ratio of heat fluxes between the current case and the smooth OML case. A comparison with Figure 5.2.4-87 (RCC Panel 9 out unvented) leads to the observation that approximately the same side fuselage region experiences increased heating with or without RCC channel venting. However, the level of heating augmentation and the forward extent of the heating footprint are both somewhat reduced for the vented case compared with the unvented case. In addition, the vented RCC channel case experiences very significant cooling on the OMS pod region compared with the slight heating that was present in same location for the solid wall case. The conclusion is that venting down the RCC channel reduces the strength of the high-pressure jet emanating from the full RCC panel out cavity region. As a result, the effects on the side fuselage are less extreme than without the venting.

RCC Panel 9, Full Panel Out Solution with Vented Side Walls into the RCC Channel (LaRC)

A computational analysis of the flow field effects due to RCC panel 9 loss on the Orbiter was performed using the LAURA code. For this analysis, gas entering the cavity formed by the missing RCC panel was

allowed to flow into the outboard RCC channel by imposing vacuum conditions on the sidewall. Note that the previous GASP-calculated full RCC panel 9 out case used 0.1 psf back pressure instead of a hard vacuum. The inboard side of the cavity was modeled as a solid wall. For the vented outboard cavity surface, the solution remains independent of RCC channel back pressure as long as the back pressure is low enough to produce supersonic flow. This stipulation is true for all the vented cavity sidewall solutions. This is the only boundary condition that can be applied for a well-posed computation of flow through a sidewall without interior RCC channel modeling. The full scale computation at flight conditions was performed on a grid with 2 million cells where over half a million cells were located in the cavity.

An approximation of the RCC channel geometry was made for hardware exposed to the external flow by a missing panel 9. These features are shown in Figure 5.2.4-91. As noted in the illustration, the geometry modeled in the cavity extended to the main wing spar. This approach allowed for an approximation of the spanner beam/earmuff blockage, as well as the windward and leeward carrier panels. An additional detail modeled by this simulation was to maintain the height of the RCC rib exposed on panel 9. A vent area of about 312 square inches resulted after this rib surface was included in the geometry.

Figure 5.2.4-92 shows a cross-section of the flow field density at a constant waterline through the wing for the region surrounding RCC panel 9. Results for both the smooth OML geometry and the case of missing RCC panel 9 are shown. The density contours approaching the cavity are identical between the two solutions as expected, and a complex shock structure is observed in the cavity of the missing panel. At the upstream edge of the cavity an expansion fan propagates into the shock layer, accelerating and turning the flow into the gap. A weak recompression wave, also emanating from the upstream edge of the cavity, processes the over-expanded flow. On the outboard RCC rib, an embedded bow shock forms with one-half of the wave ingested into the RCC channel and the other half forming a second interaction with the downstream wing shock. The effects of this interaction with the wing shock appear to be very minor since the intersection angles of this secondary interaction are small and the incident wing shock is already weakened by ingestion of flow into the RCC channel. The shock layer thickness is approximately 20% smaller over the wing downstream of the missing panel. This is due to flow ingestion into the missing panel region, which is then convected into the outboard RCC channel, or is spilled over to the leeside of the wing.

A view of the missing panel cavity presented in Figure 5.2.4-93 illustrates the major surface and flow field features in the cavity. Color contours in the figure represent surface pressures, while volume streamlines are plotted to indicate flow direction. The streamlines illustrate that a substantial part of the flow entering the missing panel cavity also continues directly into the RCC channel. An attachment line is formed on the outboard RCC rib that separates flow going into the RCC channel from flow continuing onto the wing upper surface. The interior cavity, formed by the presence of upper and lower carrier panels and the spanner bar, produced additional flow features of note. Streamlines that flow into this cavity region are deflected toward the wing spar by the spanner bar (away from the outboard RCC channel). A circulation is formed within the volume encompassed by the interior cavity and the inboard sidewall. This recirculating flow is “spun” out the top of the missing RCC cavity into the leeside flow field.

Predicted heating rates to surfaces in the interior of the missing RCC panel area are presented in Figure 5.2.4-94. The heating contours closely follow the pressure contours shown in the previous figure except on the exposed edge of the lower carrier panel. It appears that heating in this area is elevated due to a thin boundary layer and high shear stresses. These two effects, in combination, lead to the highest heating rate observed in this simulation.

A simple view of the streamlines emanating from the leeside of the missing RCC panel is shown in Figure 5.2.4-95. The streamline patterns illustrate that the flow leaving the gap corner nearest the inboard sidewall and spar is directed straight toward the fuselage. Flow leaving the gap from other locations along the spar and toward the outboard cavity area is increasingly turned downstream. The end result is a small area of flow diverted low along the upper wing and toward the side fuselage in this simulation.

Temperature contours normal to the vehicle axis are shown in Figure 5.2.4-96 to Figure 5.2.4-99 for both the smooth OML and the missing RCC panel 9 solutions. The first figure, Figure 5.2.4-96, shows the temperature contours at X = 1051 inches which is 40 inches upstream of the missing RCC cavity. The

contours are symmetrical, illustrating that the cavity has no effect on the flow at this upstream station. The location at X=1051 inches is within a region of the volume grid which was significantly modified from the original common baseline grid. The solution's similarity for the nominal OML and the Panel 9 cavity grid demonstrate that the cavity modifications did not result in noticeable flow field differences in the computations forward of the damage site. Figure 5.2.4-97 shows the temperature contours at X = 1091 inches, corresponding to the inboard corner of the cavity. The missing RCC panel 9 solution produces a jet of hot gas which exits the cavity and scrubs the leeside of the wing in the direction of the fuselage. At this station, however, the side of the fuselage appears unaffected by the jet. Figure 5.2.4-98 shows the temperature contours at X = 1204 inches, halfway between the cavity and the OMS pod. At this downstream station, the jet from the cavity has been turned downstream and is scrubbing the side of the fuselage with the highest temperature gas near the intersection of the fuselage and the wing. Figure 5.2.4-99 shows the temperature contours at X = 1316 inches at the beginning of the OMS pod. The increased temperatures along the side fuselage persist at this station, although they have decreased somewhat. A region of off-nominal low temperature is also evident on the leeside surface of the wing for this missing RCC panel 9 solution. The most predominant feature, however, is the high temperature gas near the OMS pod surface. While both the baseline smooth OML and the missing RCC panel 9 solutions show hot gases in this region, a higher temperature gas occurs for the baseline solution. This effect can be noted by the white levels in the contours for the smooth OML solution, as opposed to the magenta contours in the missing panel 9 solution.

The leeside flow field perturbation seen in Figure 5.2.4-95 to Figure 5.2.4-99 causes the surface heating effect illustrated in Figure 5.2.4-100. Here the amplification of heating rate relative to the nominal (undamaged geometry) is plotted to isolate missing RCC panel 9 effects. As would be expected from the streamline patterns, the fuselage heating is increased in the area where the flow diverted through the missing panel gap strikes the fuselage. In this damage scenario, the heating augmentation pattern assumes a horizontal orientation and is confined near the wing-fuselage juncture. Augmentation factors up to 2 over the nominal heating case are predicted on the side fuselage. The effect on the OMS Pod is lower heating (approximately 70%) for the missing panel solution relative to the baseline. The results of other CFD simulations presented in this section, as well as the wind tunnel results in Section 5.2.3 with missing RCC panels have shown similar trends, but quantitatively different heating patterns. In many of those cases, the side fuselage heating augmentation is higher up on the fuselage, occurs more upstream, and the pattern assumes an angled orientation. Also, heating to the OMS pod in those cases generally increased. Differences in leeside surface heating characteristics between this simulation and the other results are primarily believed to be due to the amount of flow venting into the RCC channel and to the presence of an embedded cavity behind the missing RCC panel. This simulation illustrates the sensitivity to venting effects down the RCC channel, as well as the geometry of hardware in the RCC cavity.

RCC Panel 9, Half Panel Out Solution with Vented Side Walls into the RCC Channel and the Upper Carrier Panel Out (ARC)

The damaged RCC panel configurations discussed up to this point all involved permutations on the location of damage on the RCC panel, and different extents of vertical damage (i.e.., half or full panel). Concurrent with the development of the grid systems and the understanding developed from those CFD simulations, as well as on-going wind tunnel studies and observations from the debris, our understanding of the parametrics involved in wing leading edge damage increased dramatically. Late in the investigation, it became apparent that the extent of the initial wing leading edge damage was not likely to include large leeside sections of the RCC panels missing. Wind tunnel testing was indicating that some windward damage, together with some leeward damage near the RCC, could produce signatures consistent with the surface instrumentation responses during the early part (i.e., < EI + 480 seconds) of the STS-107 trajectory. With these observations from the later stages of the investigation in hand, a final solution at flight conditions was pursued with the lower half of RCC panel 9 removed, and an approximation of upper carrier panel damage. This configuration was deemed to be more representative of potential early timeline damage to Columbia, and complements a similar geometry considered in the wind tunnel testing (see Section 4.3.1). Similar to the more complicated half panel 9 out case discussed previously (i.e., with vented side walls and the complete RCC cavity modeled), the current case modeled the full RCC cavity with a zero thickness RCC upper half panel 9 and venting down the RCC channel through the inboard and outboard sidewalls. However, to model the desired upper carrier panel removed configuration, the last 4 inches of upper RCC panel 9 along the wing spar was also removed. Flow-

through boundary conditions were applied across this gap at the top of the RCC panel, allowing communication of the flow from the RCC cavity to the wing lee side. A graphic depicting the geometry is shown in Figure 5.2.4-104.

CFD condition 1 was calculated using GASP with the mesh remaining consistent with the other panel 9 out ARC cases. Figure 5.2.4-105 and Figure 5.2.4-106 show side and top planform views of the leeside heating. While the visible effects in these images are mild compared with those seen for the full RCC panel 6 or 9 out cases, the surface heating effects are still substantial compared with those seen on the previous half RCC panel out cases. Figure 5.2.4-107 depicts the ratio of the heat fluxes between the present case and the smooth OML panel 9 case. The figure shows that the primary leeside fuselage influence is a cooling effect on the OMS pod region. There is also some local increased heating near the wing-body intersection aft of the damage location.

5.2.4.5.2 Concluding damage scenario comments.

Because the exact damage to the wing leading edge of Columbia will remain unknown, a limited matrix of damage configurations were examined using CFD and focusing on RCC panels 6 and 9. These solutions suggest that initial damage to only the windside leading edge coupled with significant venting to the interior of the WLE cavity (possibly also with some open vent paths from the RCC channel to the lee side via T-seal gaps and upper carrier panel gaps) would result in only minor temperature anomalies on the fuselage, and potentially, decreased heating on the OMS pod. Also, as the damage geometry changed during the re-entry of Columbia, the footprint on the side fuselage and OMS pod would also have changed. Furthermore, a breach from the windward side via lower RCC panel damage coupled with significant upper carrier panel damage would be associated with initial moderate heating anomalies on the side fuselage. To experience extensive heating anomalies on the fuselage would require additional damage including either more upper carrier panel damage (e.g., more than a single upper carrier panel removed), loss of an entire RCC panel, or an equivalently large wing breach allowing windside flow to feed directly to the lee side. Venting to the interior of the wing leading edge (through the RCC channel) delays the extent of leeside anomalies. This is due to reduced mass flow to the lee side associated with the jet from the wind side to the lee side, emanating from the leading edge damage cavity. The existence of this jet due to wing leading edge damage is shown conclusively in the CFD simulations presented in this section. The character of that jet is such that, with sufficient damage to the wing leading edge, high temperature gas is driven toward the side fuselage of the Orbiter which can propagate *upstream* of the damage site. The most dramatic heating increases and the largest extent of surface heating effects occur when the leading edge cavity jet is driven by wing leading edge stagnation pressure due to a significant breach in the wing leading edge on the wind side. As a final comment on the damaged leading edge CFD simulations, it must be pointed out again that the nature of these simulations, and the conclusions to be drawn from them, should be restricted to an engineering perspective. The CFD simulations conducted as part of the investigation were performed on representative geometries. The particular geometries that have been assessed were chosen in a very dynamic environment of wind tunnel, CFD, flight instrumentation, and recovered debris investigations. The fact that these geometries were chosen for investigation does not mean that the damaged geometry experienced by Columbia is exactly represented in this suite of simulations. In fact the dynamic/progressive nature of the actual Columbia data coupled with the time responses for the sensors will likely mean that a direct one-to-one match between CFD simulations and instrumentation flight data will never be achieved.

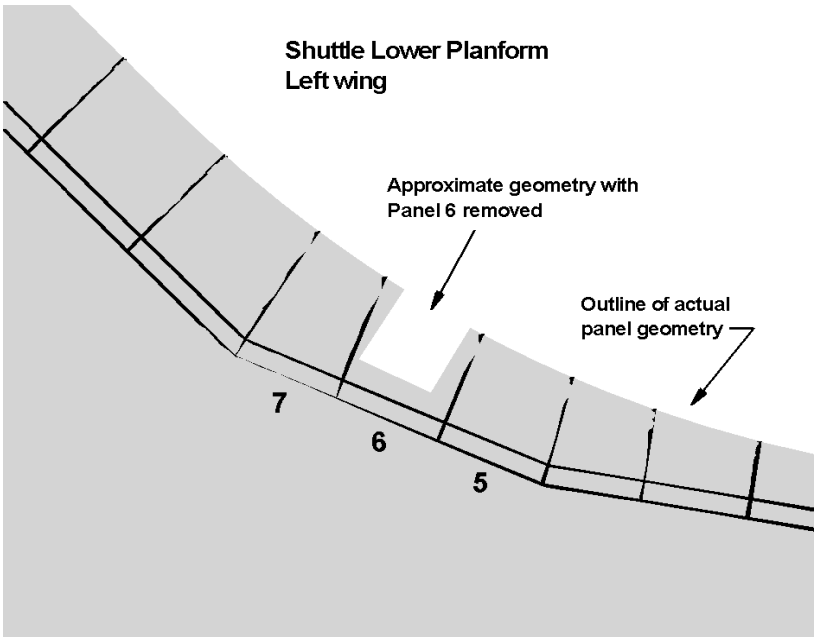

Figure 5.2.4-61 Planform view of missing panel 6 "notch"

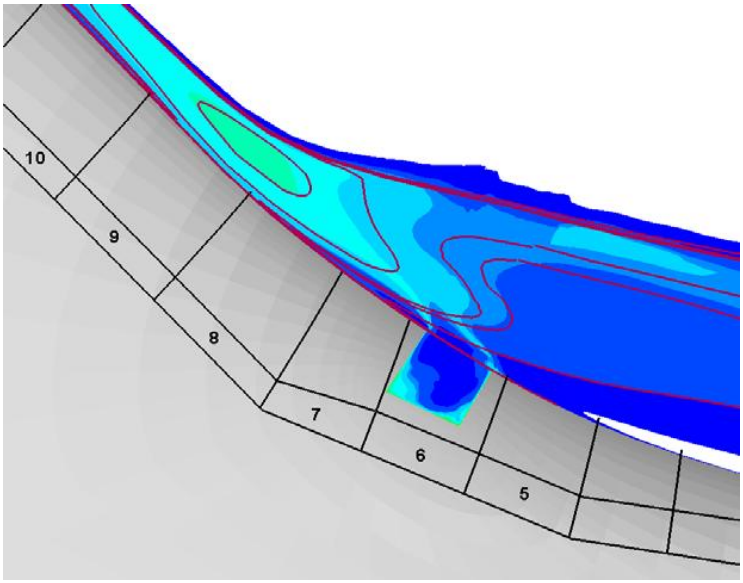

Figure 5.2.4-62 Planform view of flow field density contours for nominal geometry (contour lines) and for missing RCC panel 6 (flooded contours)

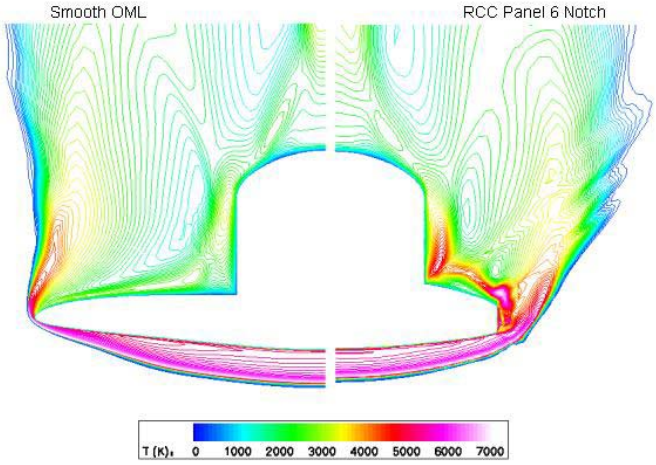

Figure 5.2.4-63 Temperature Contours at X = 1036 inches (through panel 6 notch)

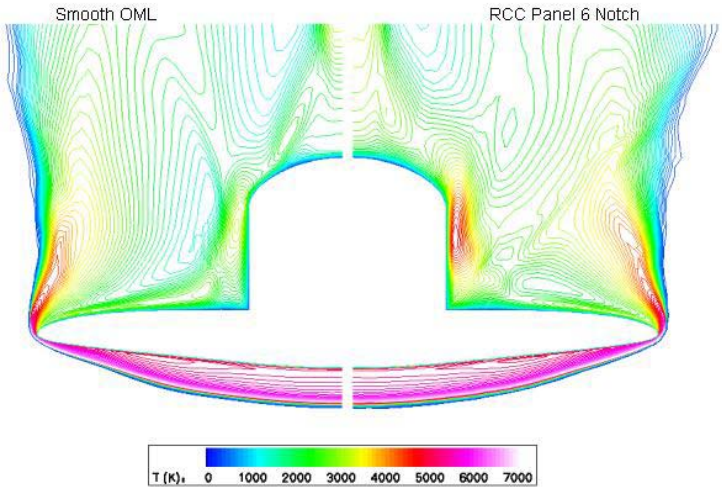

Figure 5.2.4-64 Temperature Contours at X = 1181 inches (halfway between notch and OMS pods)

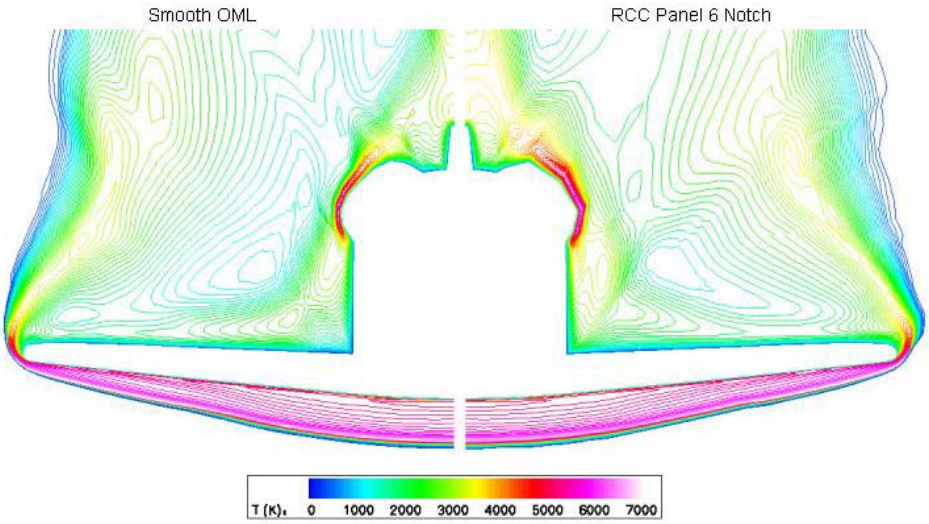

Figure 5.2.4-65 Temperature Contours at X = 1326 inches (forward face of OMS pod)

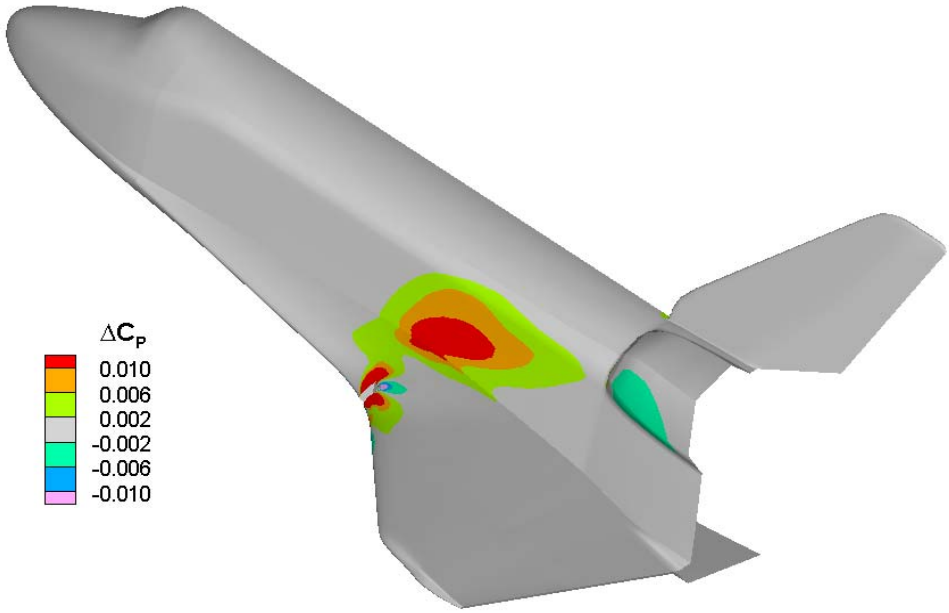

Figure 5.2.4-66 Difference in pressure coefficient due to missing RCC panel 6 "notch"

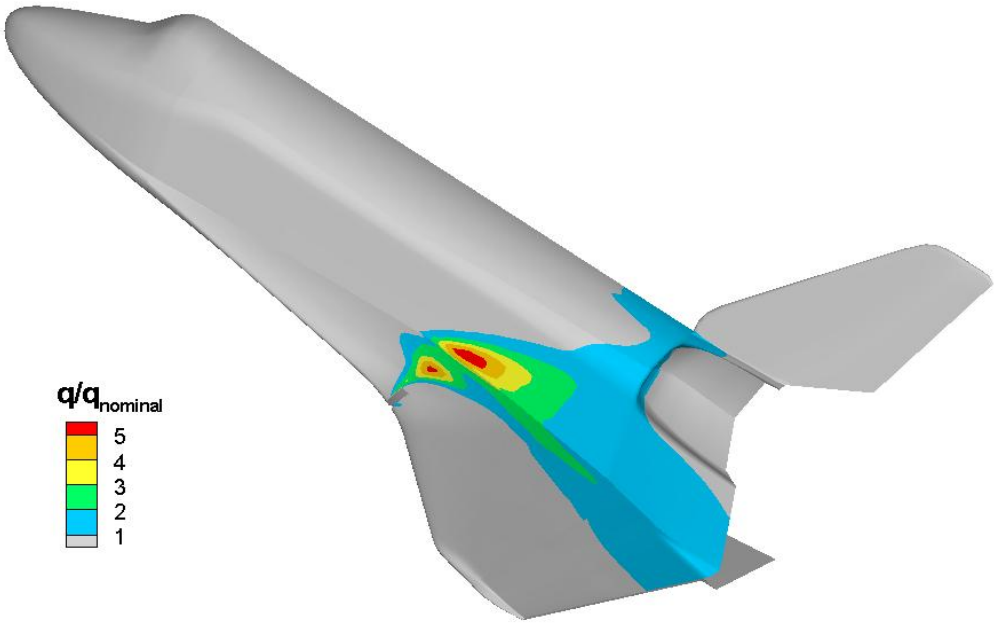

Figure 5.2.4-67 Heating augmentation due to missing RCC panel 6 "notch"

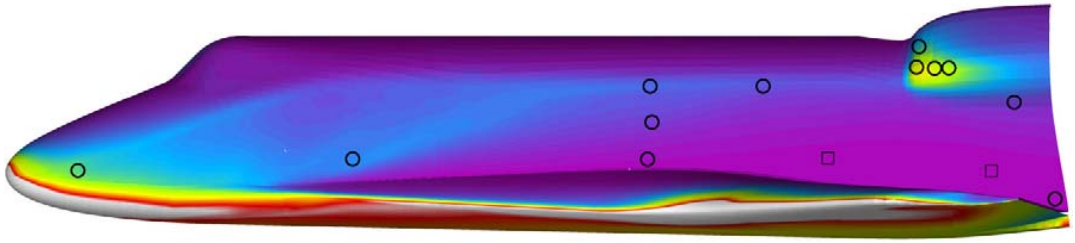

Figure 5.2.4-68 Smooth OML RCC Panel 6, Side View, Heating Rates

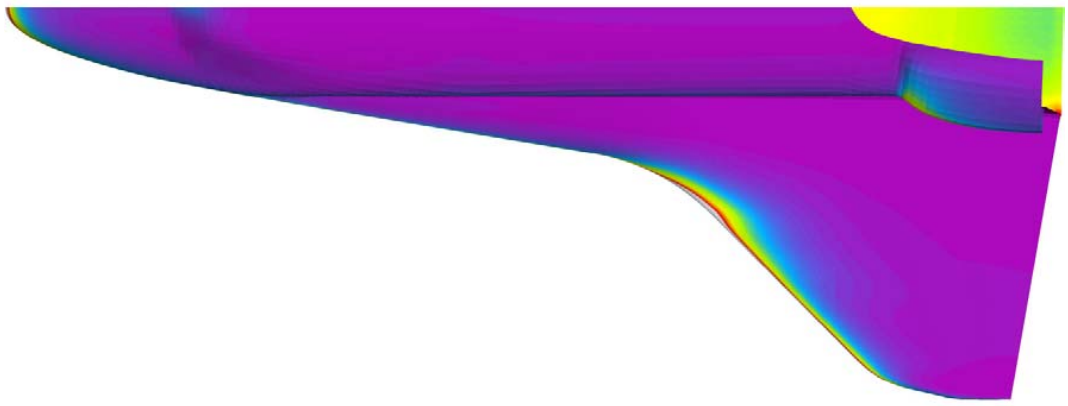

Figure 5.2.4-69 Smooth OML RCC Panel 6, Planform View, Heating Rates

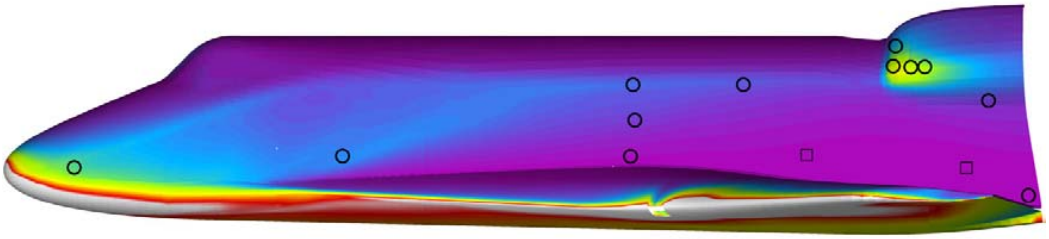

Figure 5.2.4-70 Lower Half RCC Panel 6 Out, Side View, Heating Rates

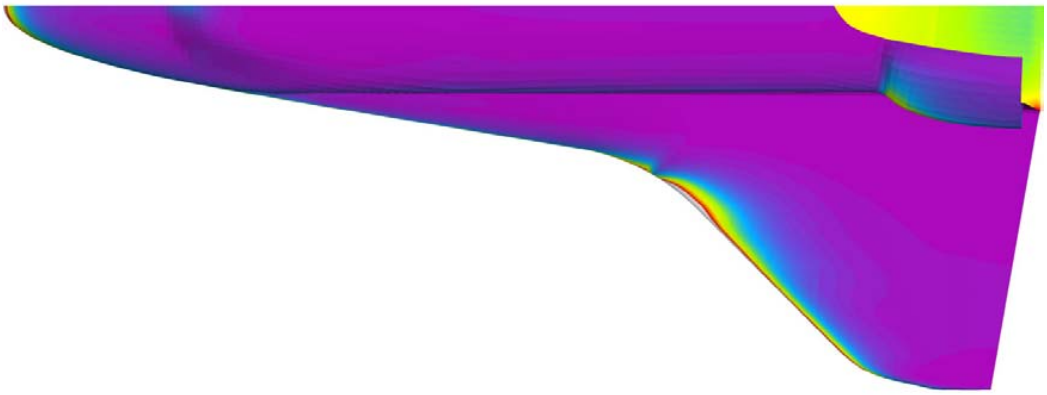

Figure 5.2.4-71 Lower Half RCC Panel 6 Out, Planform View, Heating Rates

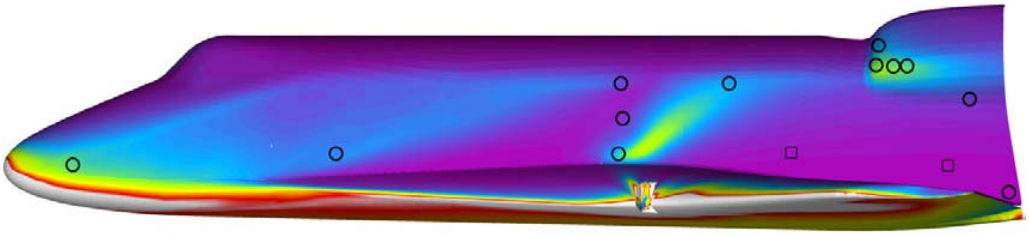

Figure 5.2.4-72 Full RCC Panel 6 Out, Side View, Heating Rates

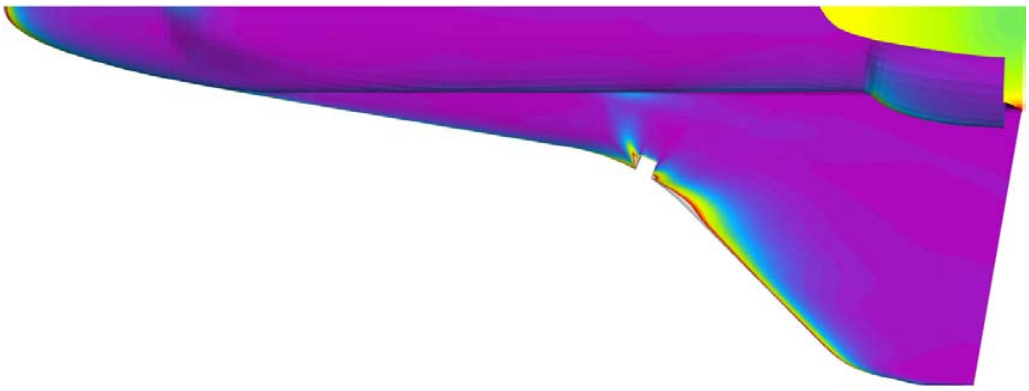

Figure 5.2.4-73 Full RCC Panel 6 Out, Planform View, Heating Rates

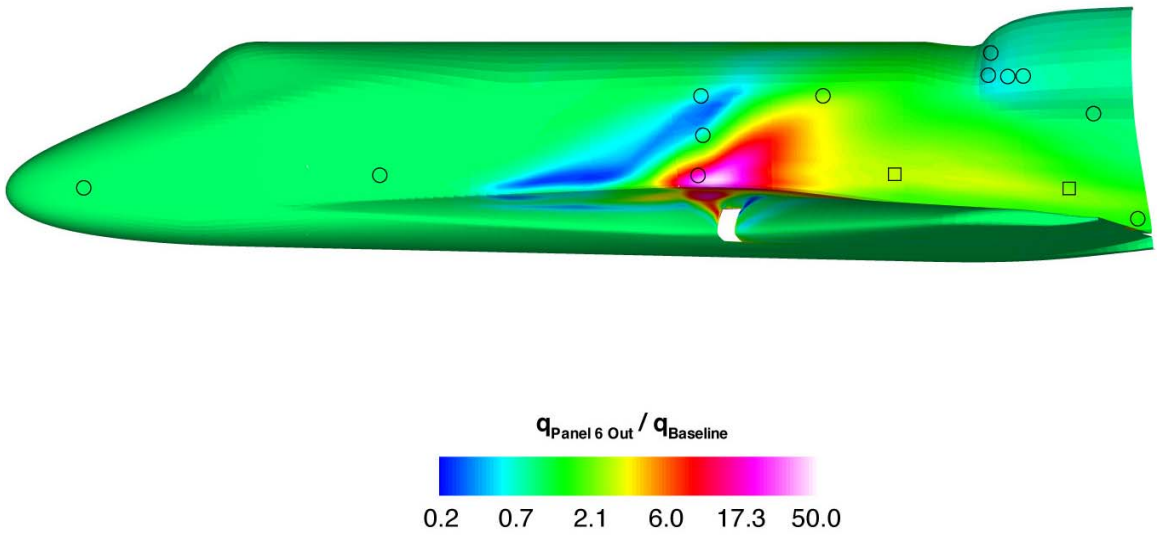

Figure 5.2.4-74 Full RCC Panel 6 Out, Side View, Ratio of Heat Fluxes

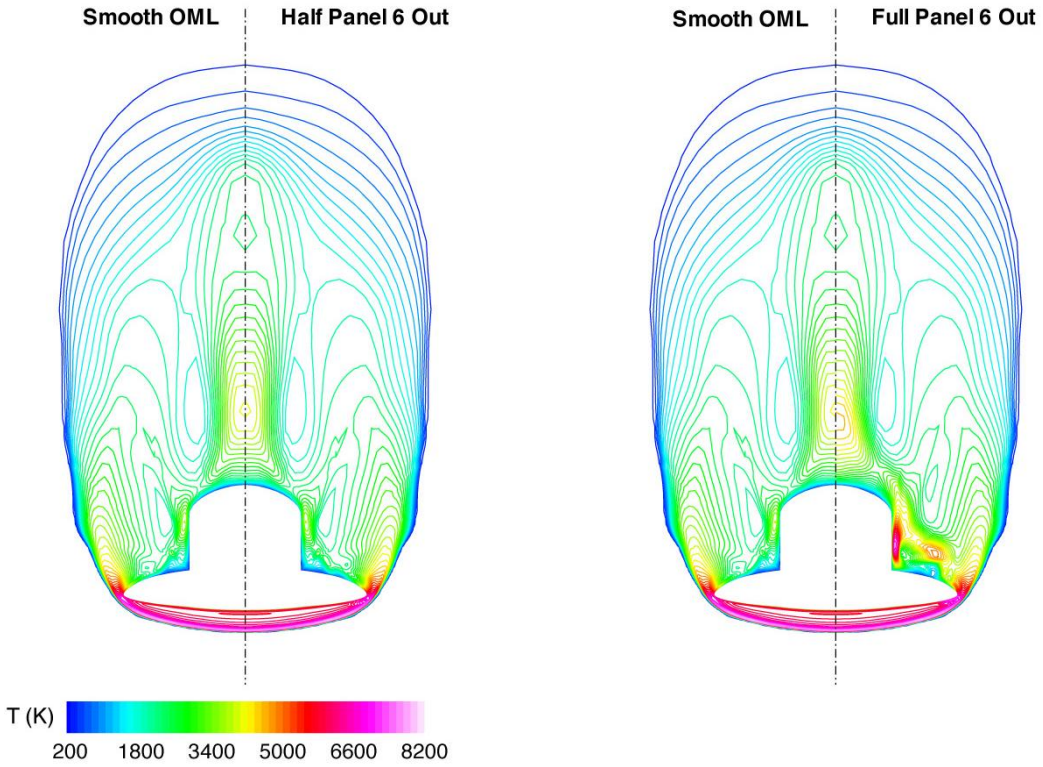

Figure 5.2.4-75 RCC Panel 6 Out, Y-Z Solution Cut at X = 27 m, Temperature Contours

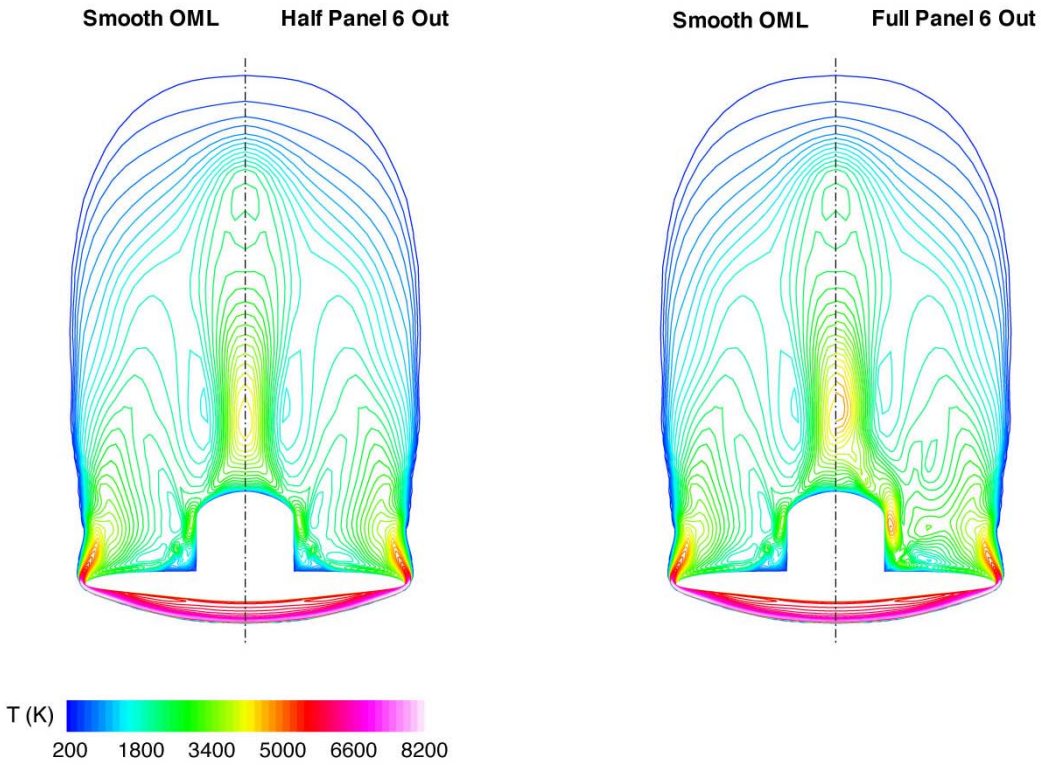

Figure 5.2.4-76 RCC Panel 6 Out, Y-Z Solution Cut at X = 30 m, Temperature Contours

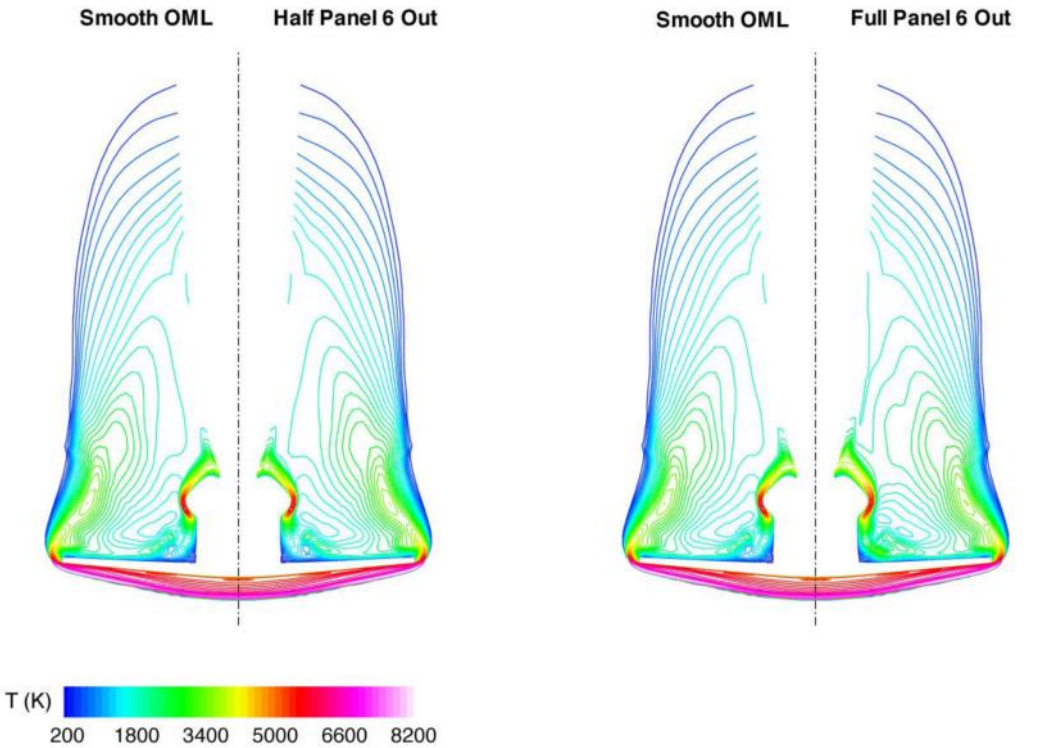

Figure 5.2.4-77 RCC Panel 6 Out, Y-Z Solution Cut at X = 35 m, Temperature Contours

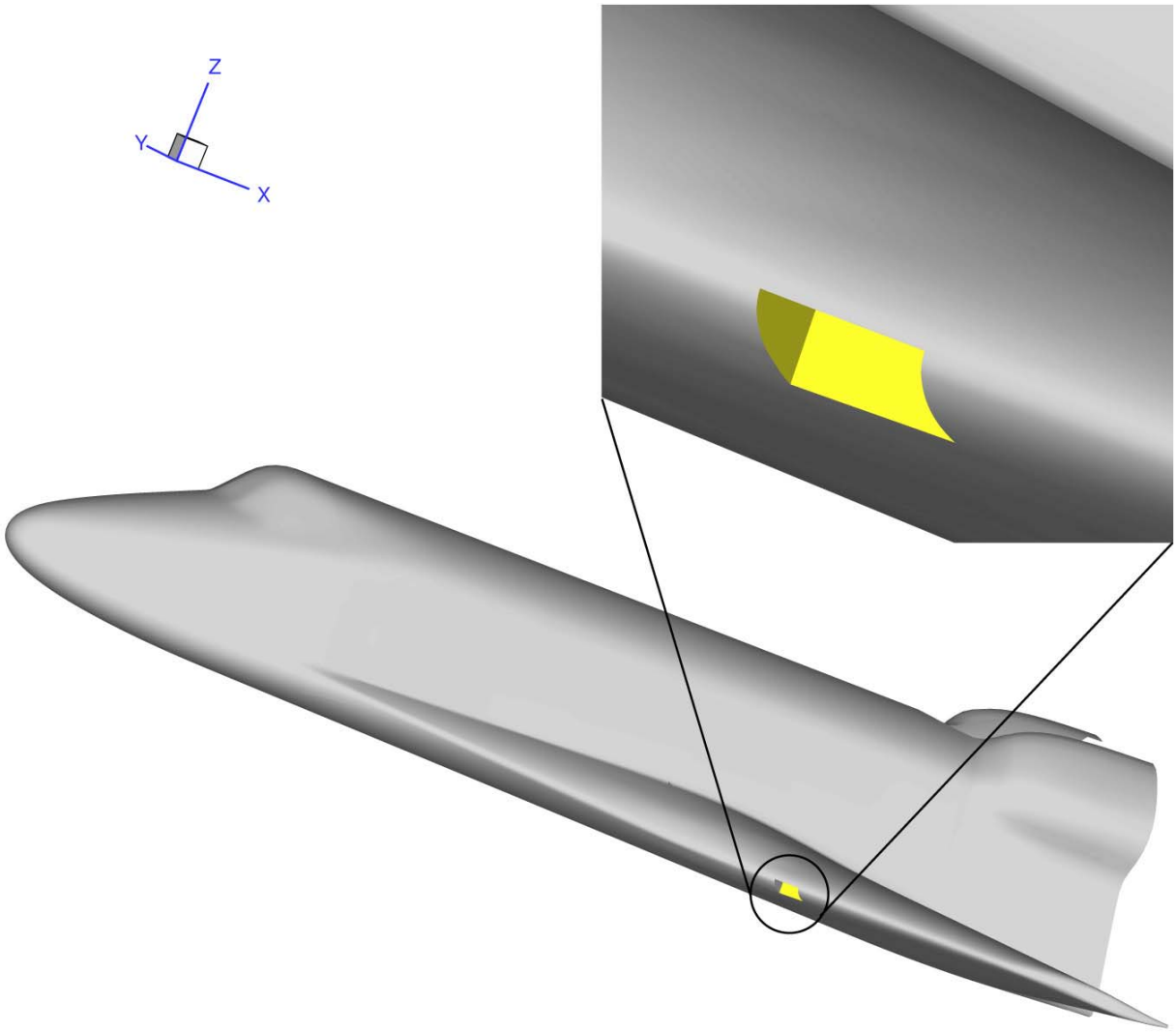

Figure 5.2.4-78 Lower Half RCC Panel 9 Out Geometry

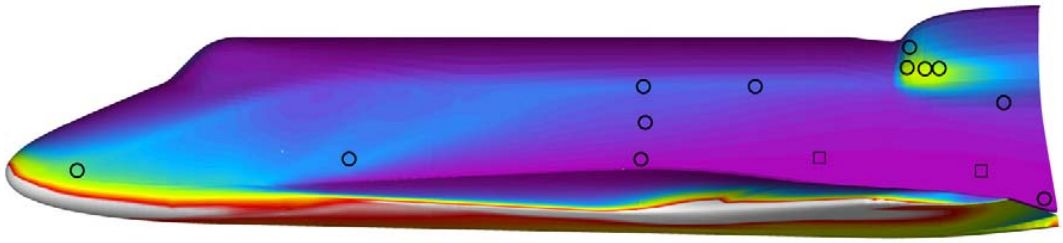

Figure 5.2.4-79 Smooth OML RCC Panel 9, Side View, Heating Rates

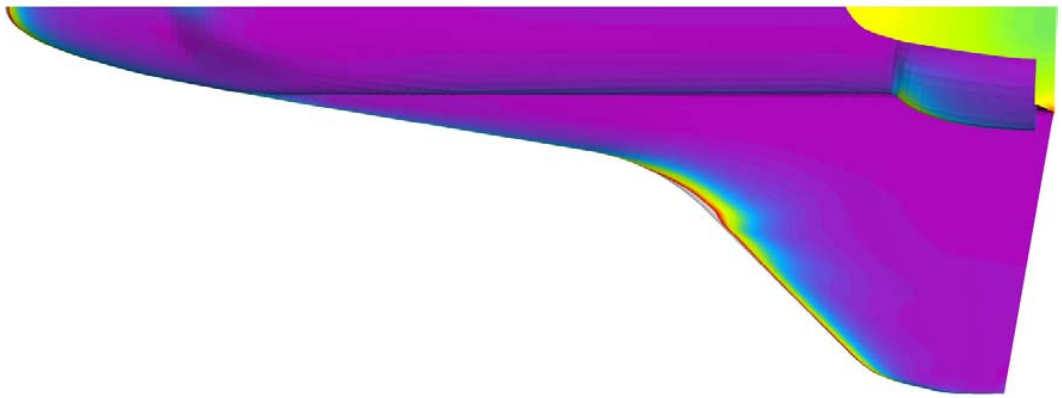

Figure 5.2.4-80 Smooth OML RCC Panel 9, Planform View, Heating Rates

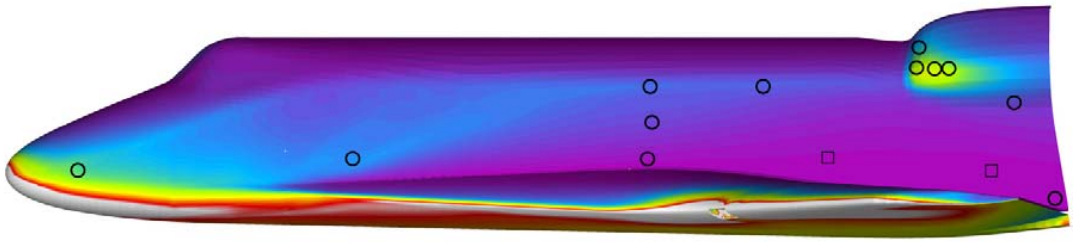

Figure 5.2.4-81 Lower Half RCC Panel 9 Out, with Solid Side Walls, Side View, Heating Rates

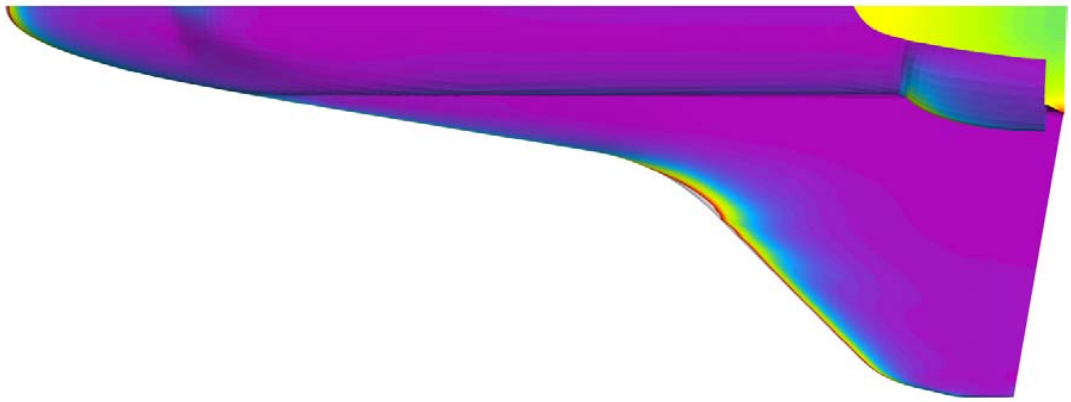

Figure 5.2.4-82 Lower Half RCC Panel 9 Out, with Solid Side Walls, Planform View, Heating Rates

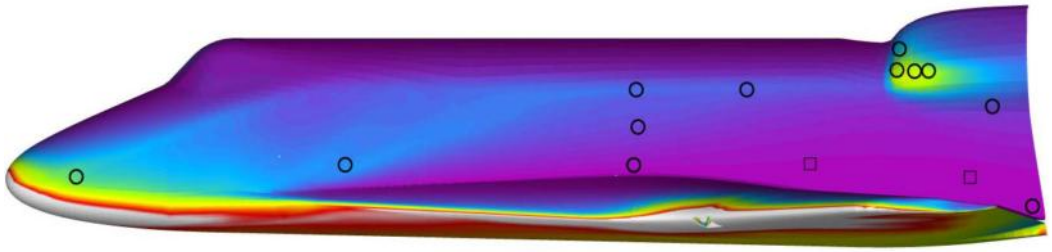

Figure 5.2.4-83 Lower Half RCC Panel 9 Out, with Vented Side Walls, Side View, Heating Rates

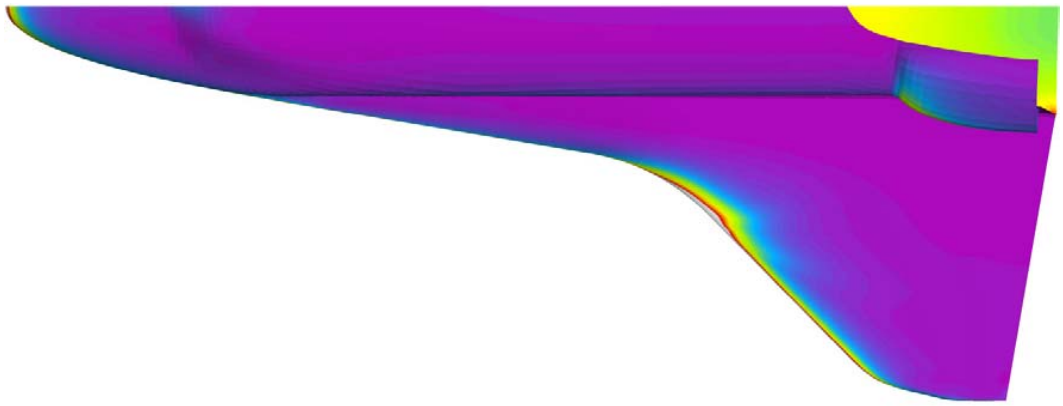

Figure 5.2.4-84 Lower Half RCC Panel 9 Out, with Vented Side Walls, Plan View, Heating Rates

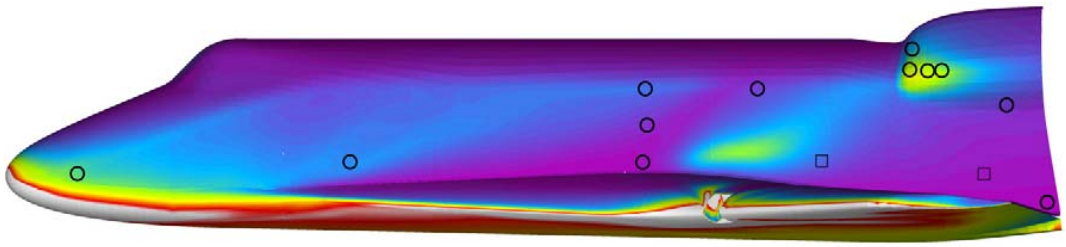

Figure 5.2.4-85 Full RCC Panel 9 Out, with Solid Side Walls, Side View, Heating Rate

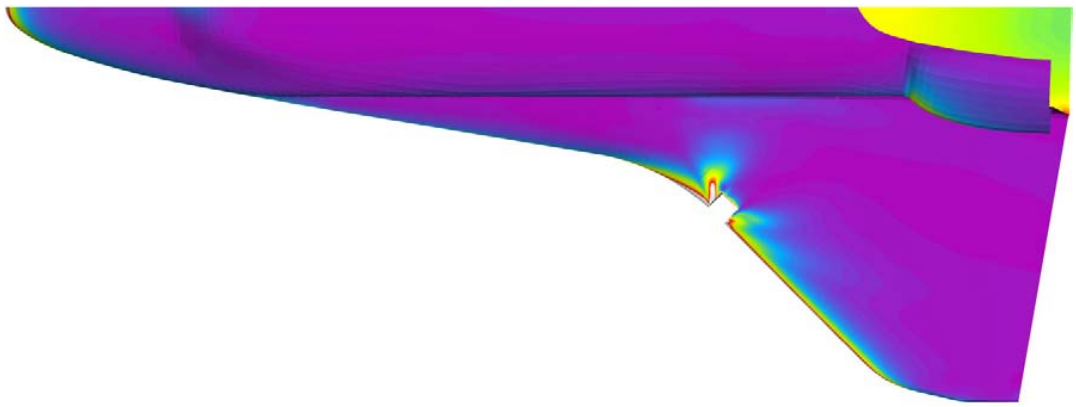

Figure 5.2.4-86 Full RCC Panel 9 Out, with Solid Side Walls, Planform View, Heating Rate

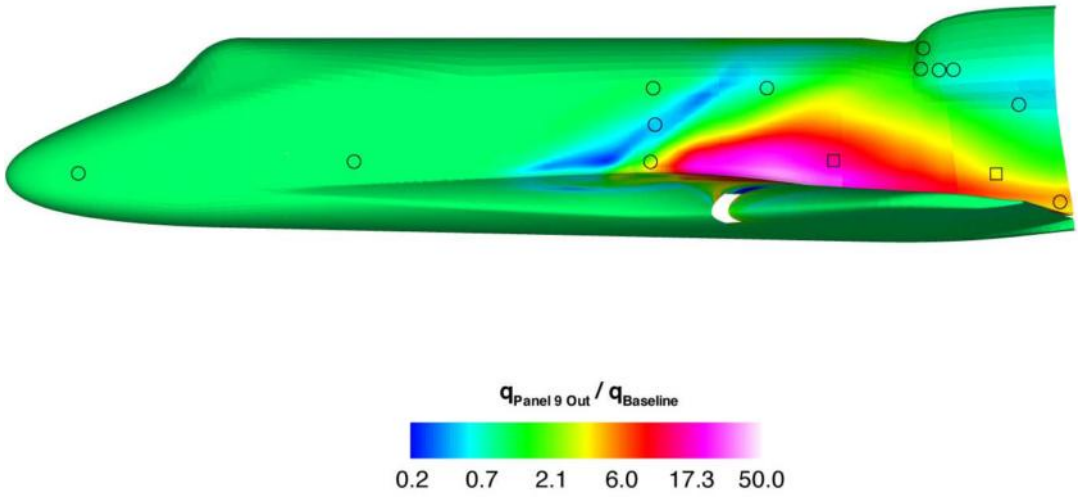

Figure 5.2.4-87 Full RCC Panel 9 Out, with Solid Side Walls, Side View, Ratio of Heat Fluxes

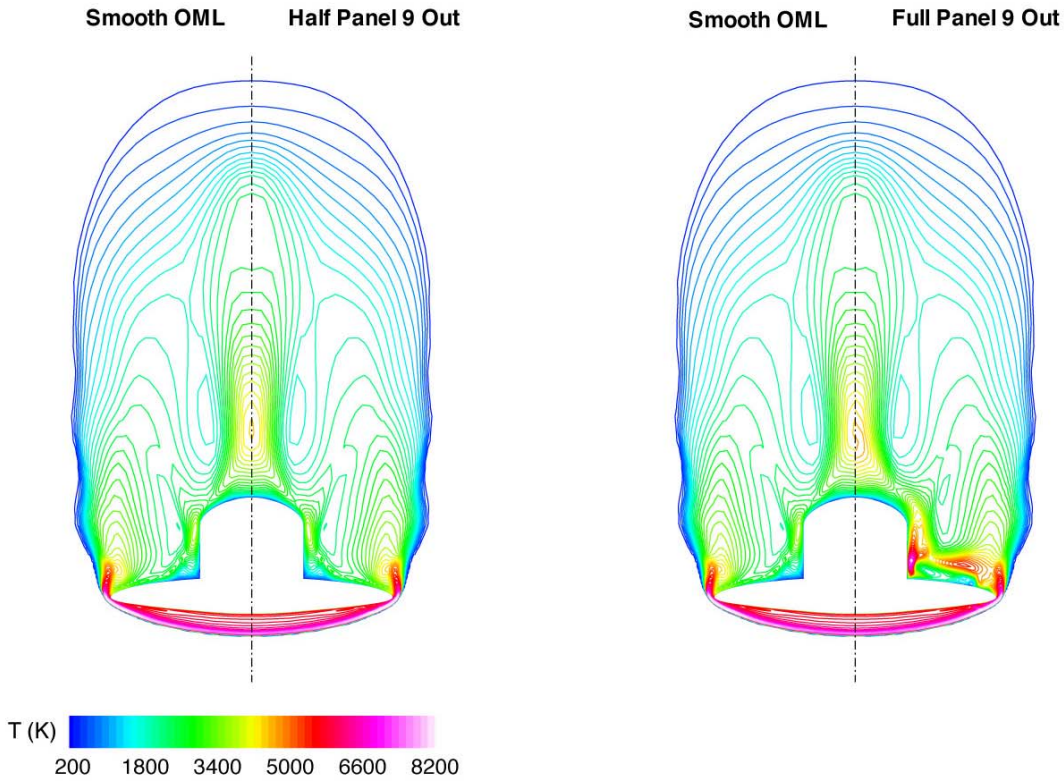

Figure 5.2.4-88 RCC Panel 9, Y-Z Solution Cut at X = 28.5 m, Temperature Contours

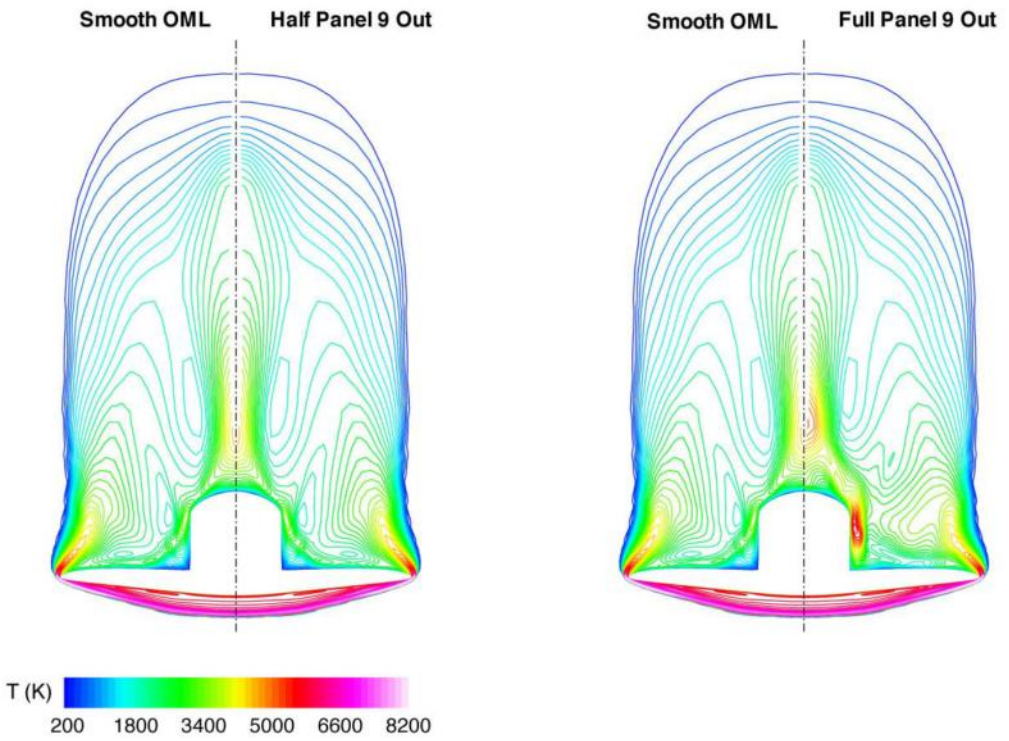

Figure 5.2.4-89 RCC Panel 9, Y-Z Solution Cut at X = 31.5 m, Temperature Contours

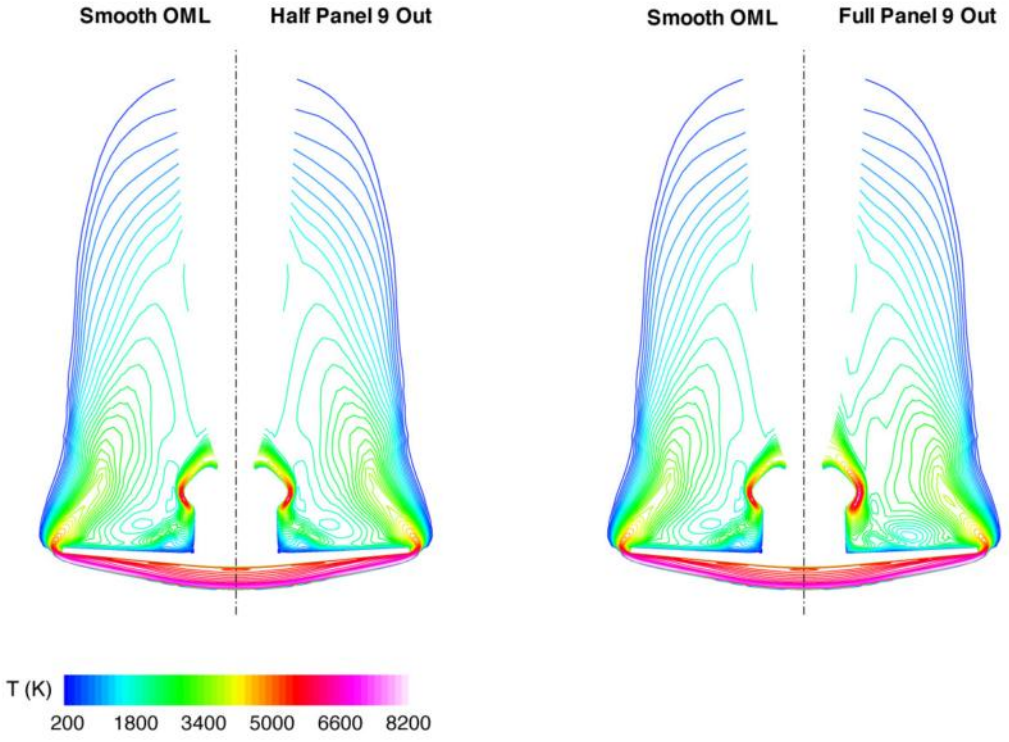

Figure 5.2.4-90 RCC Panel 9, Y-Z Solution Cut at X = 35.0 m, Temperature Contours

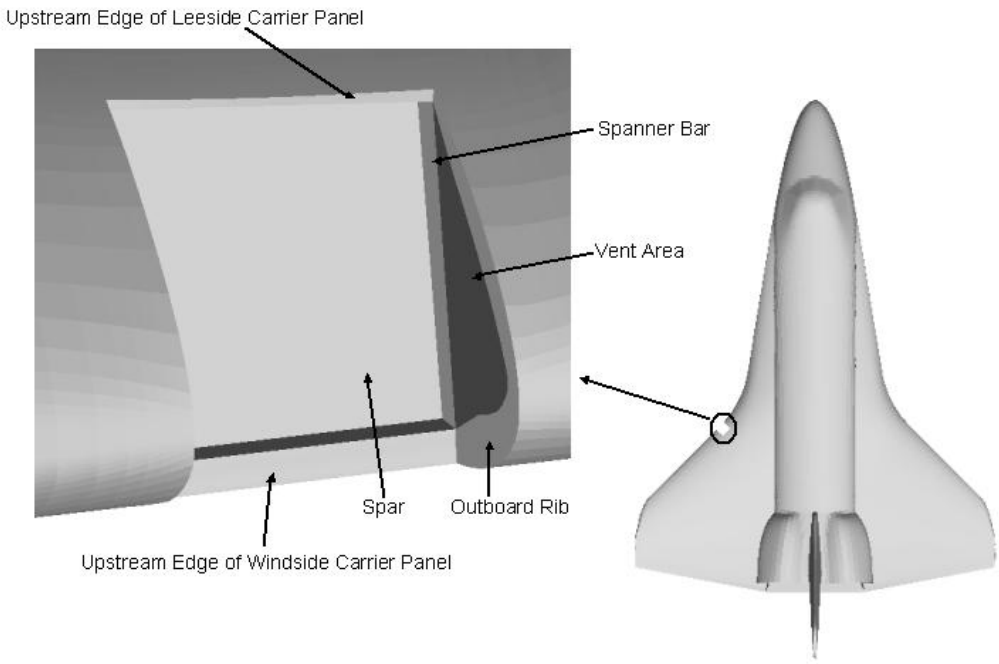

Figure 5.2.4-91 Geometry for Missing RCC Panel 9 with Venting in RCC Chamber

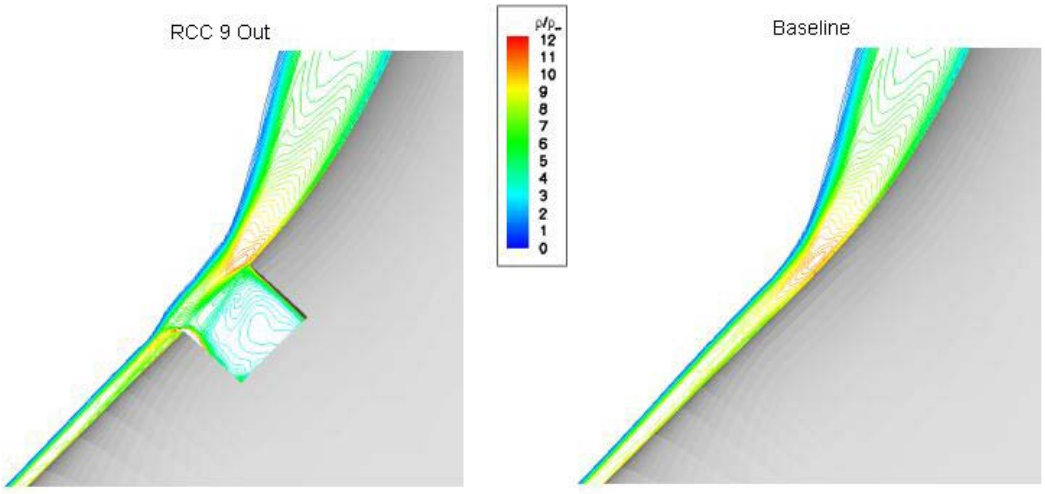

Figure 5.2.4-92 Comparison of Density Contours in Missing RCC Cavity and on Smooth OML Baseline Grid

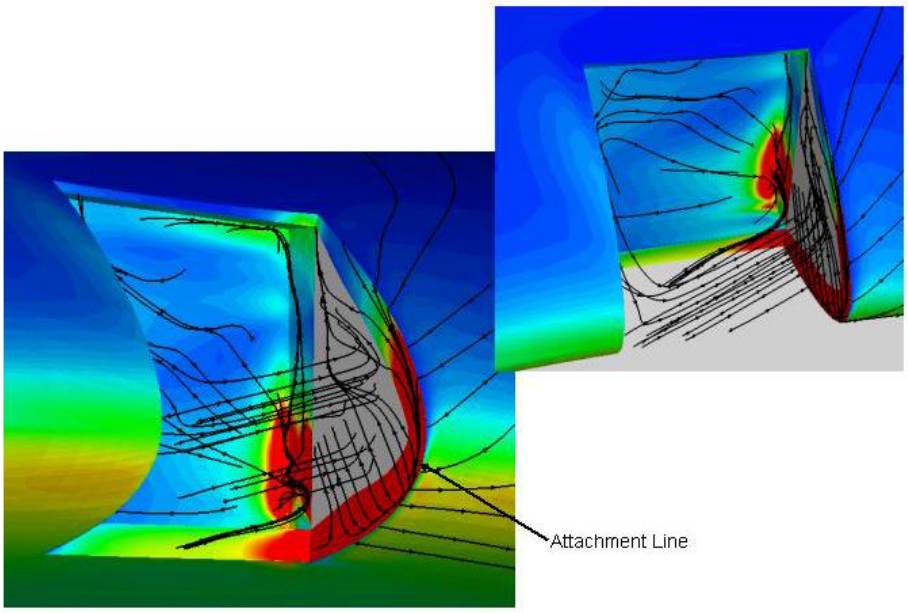

Figure 5.2.4-93 Pressure Contours, Volume Streamlines and Surface Streamlines in Vented RCC Panel 9 Cavity

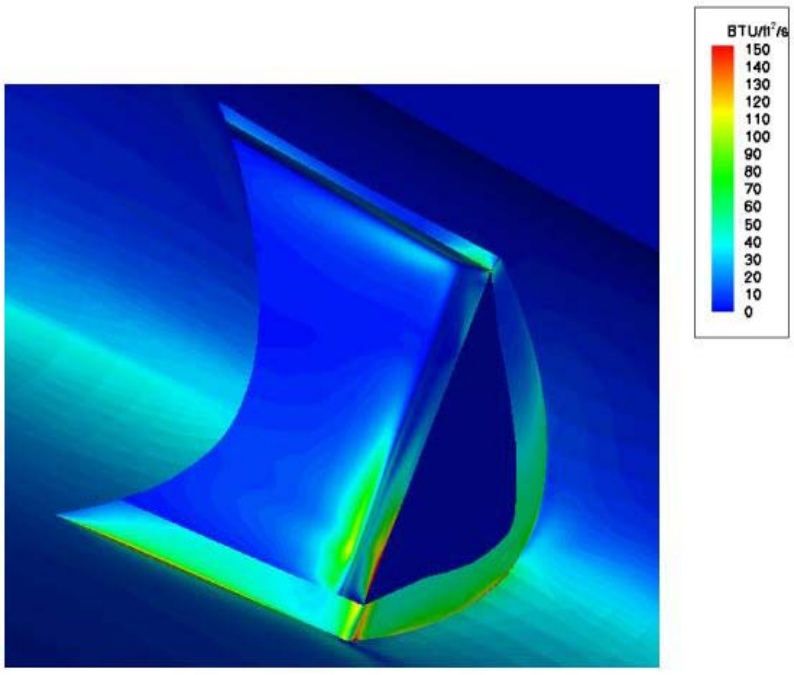

Figure 5.2.4-94 Heat Flux Contours in the Vented RCC Panel 9 Cavity

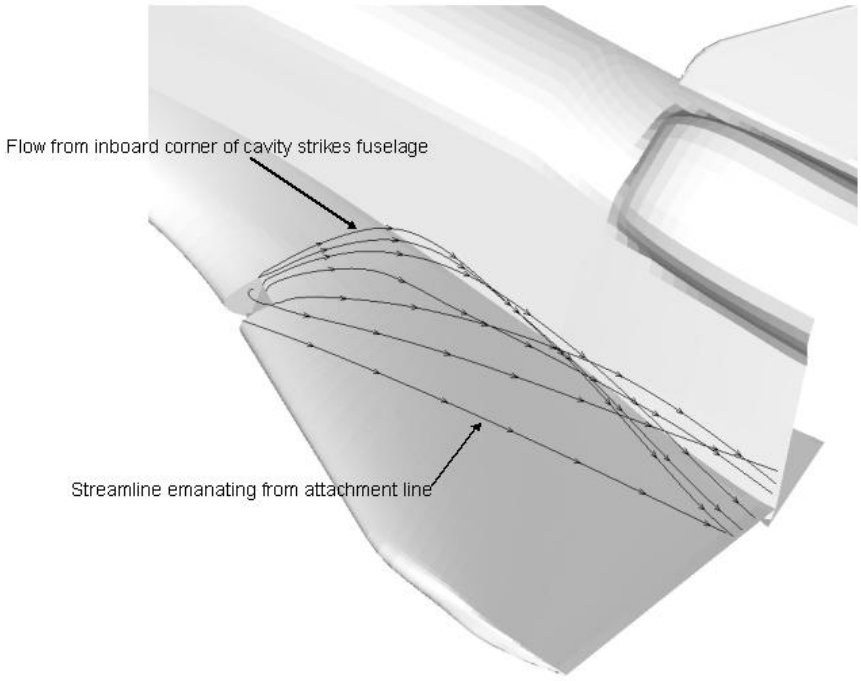

Figure 5.2.4-95 Streamlines on the Body Emanating from the RCC Panel 9 Cavity

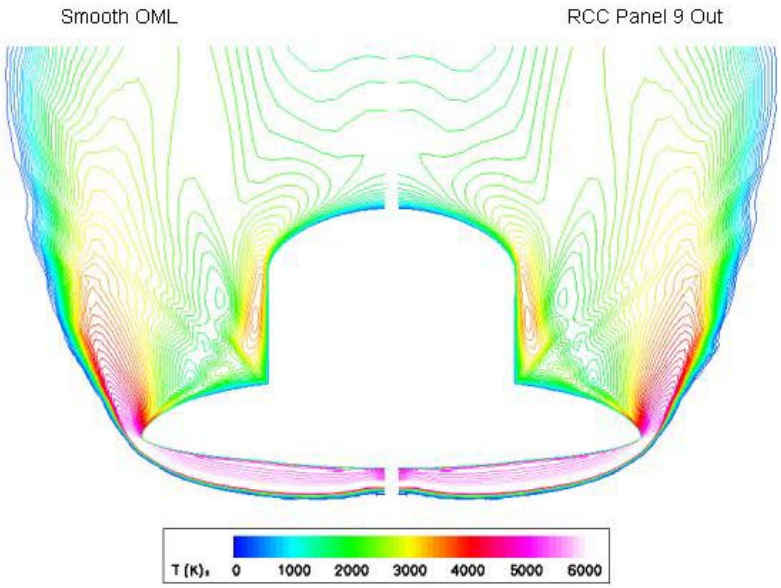

Figure 5.2.4-96 Temperature Contours at X = 1051 inches (40 inches upstream of RCC Panel 9 Cavity)

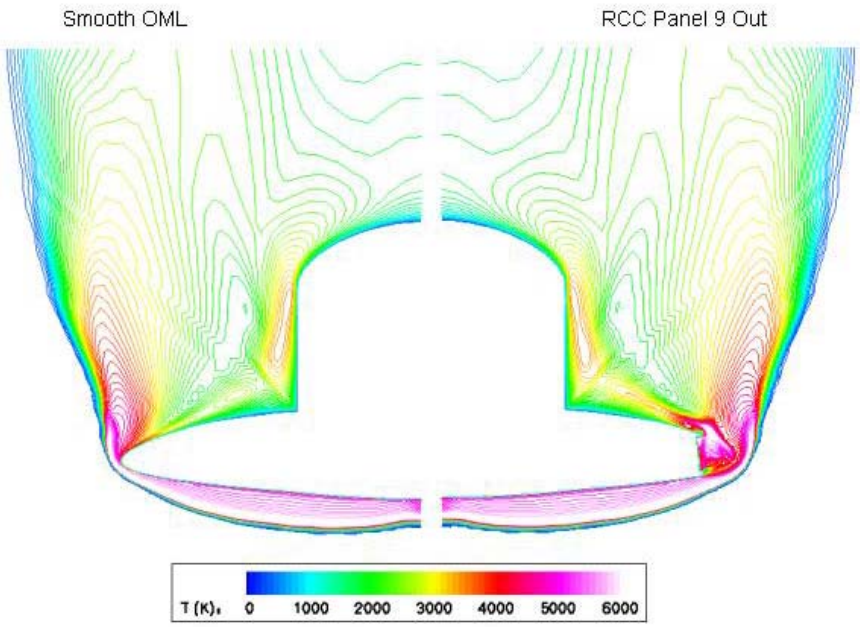

Figure 5.2.4-97 Temperature Contours at X = 1091 inches (at inboard corner of cavity)

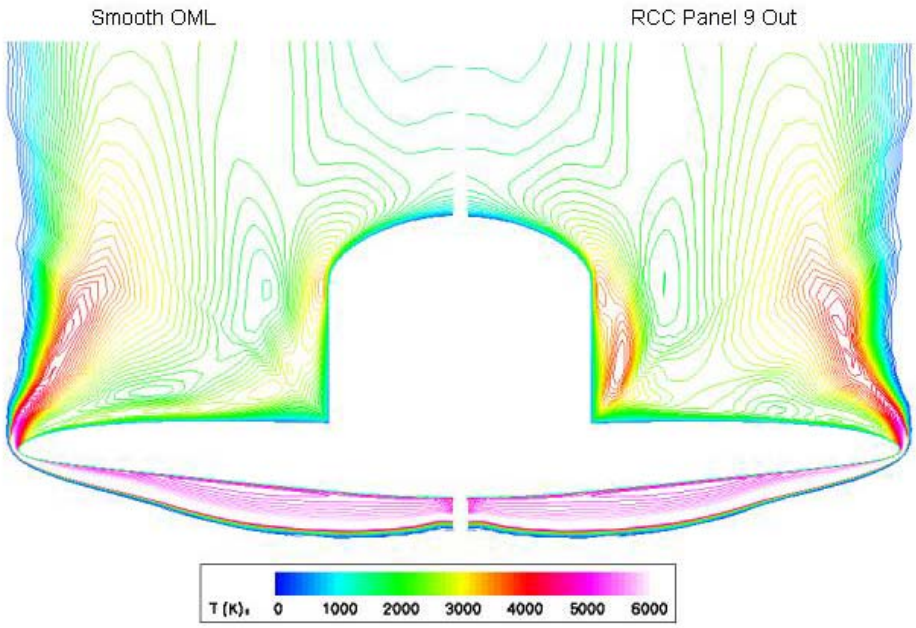

Figure 5.2.4-98 Temperature Contours at X = 1204 inches (halfway between cavity and OMS pods)

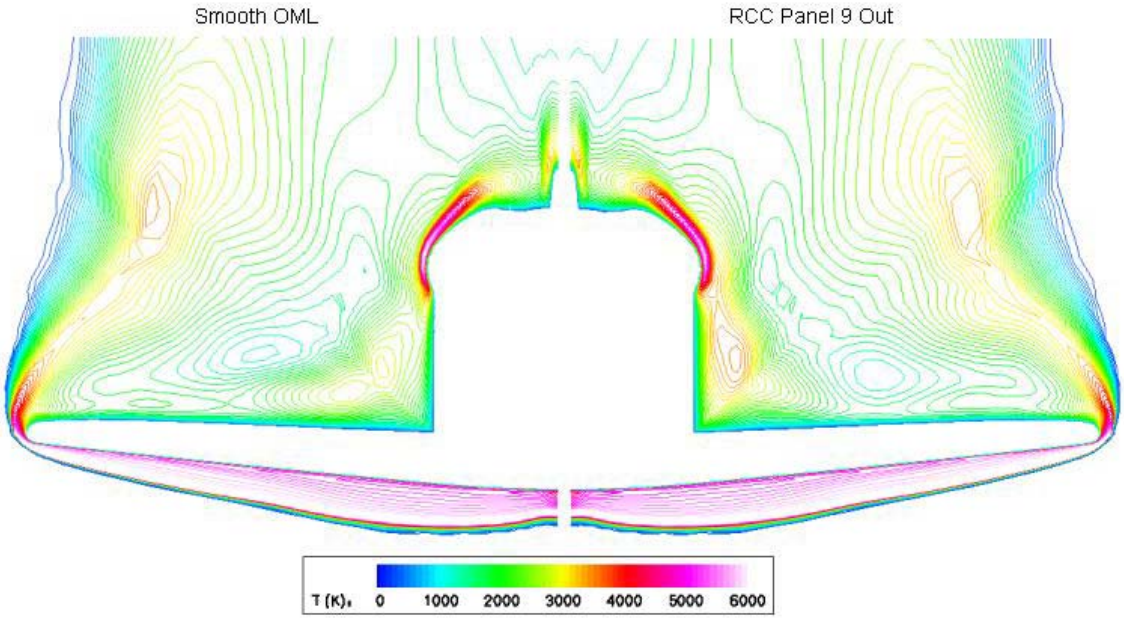

Figure 5.2.4-99 Temperature Contours at X = 1316 inches (at forward portions of OMS pods)

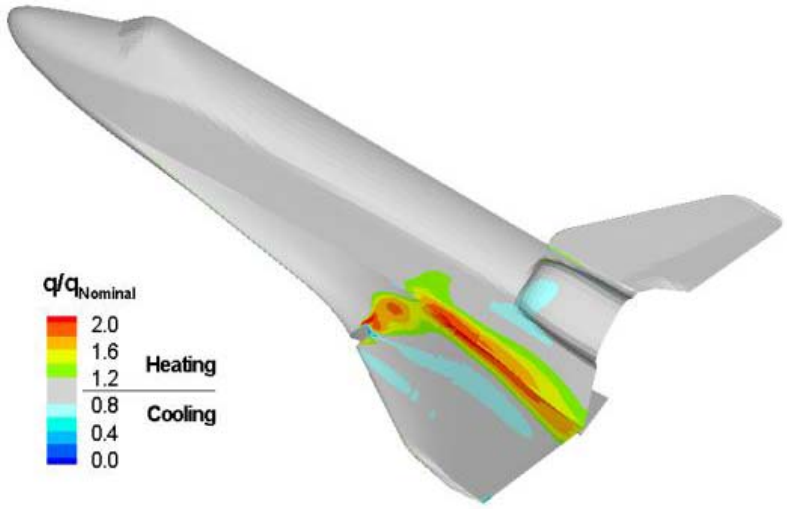

Figure 5.2.4-100 Magnification Factor for Missing RCC Panel 9 Heat Flux

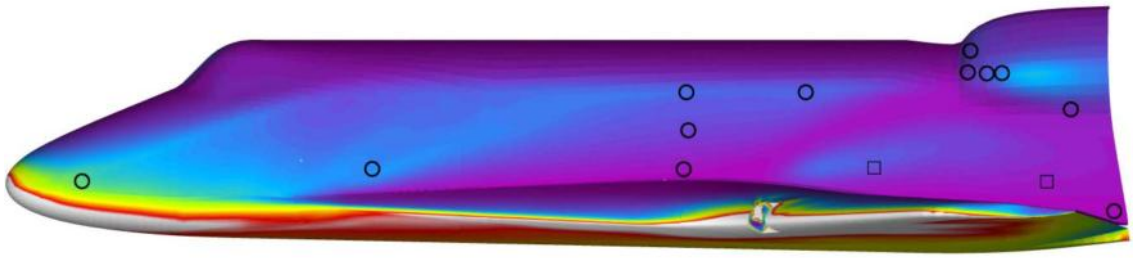

Figure 5.2.4-101 Full RCC Panel 9 Out, with Vented Side Walls, Side View, Heating Rate

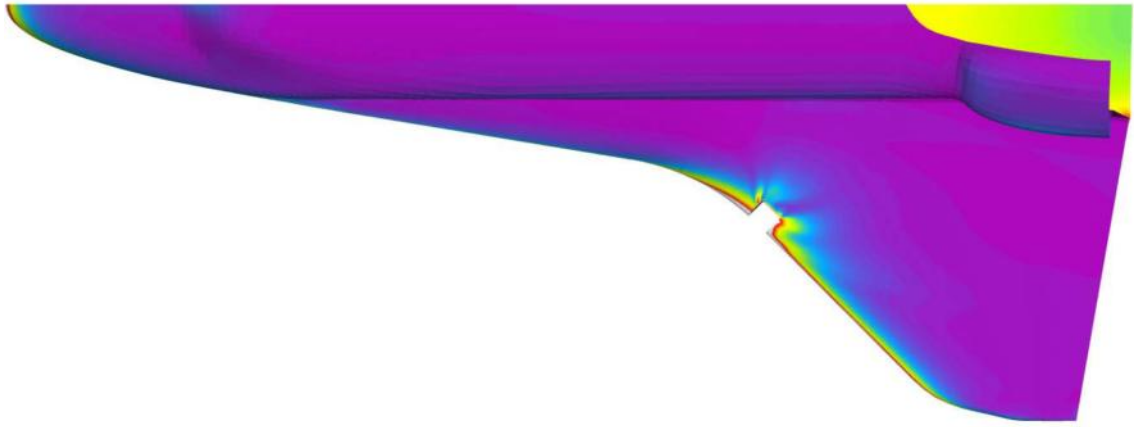

Figure 5.2.4-102 Full RCC Panel 9 Out, with Vented Side Walls, Planform View Heating Rate

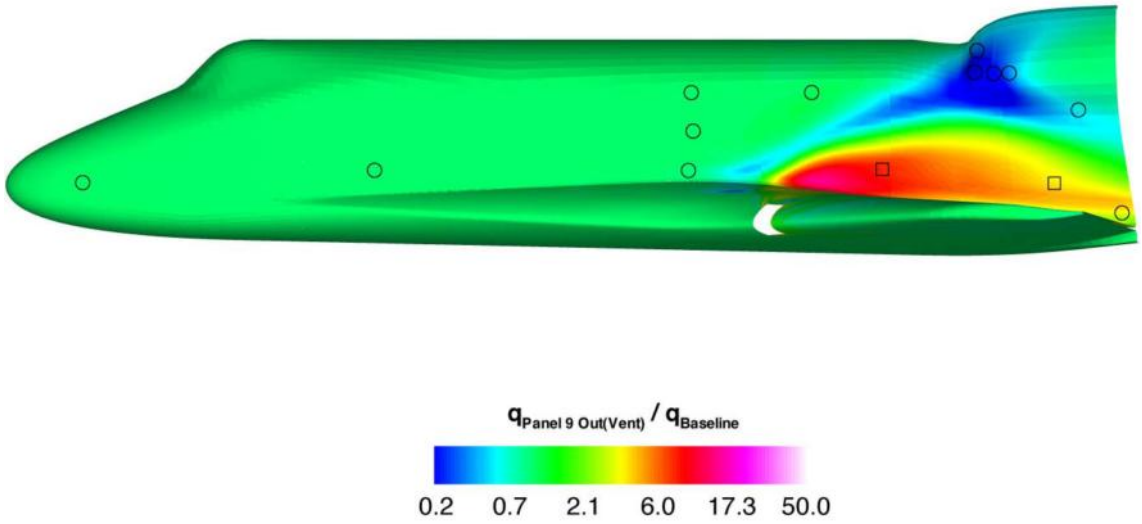

Figure 5.2.4-103 Full RCC Panel 9 Out, with Vented Side Walls, Side View, Ratio of Heat Fluxes

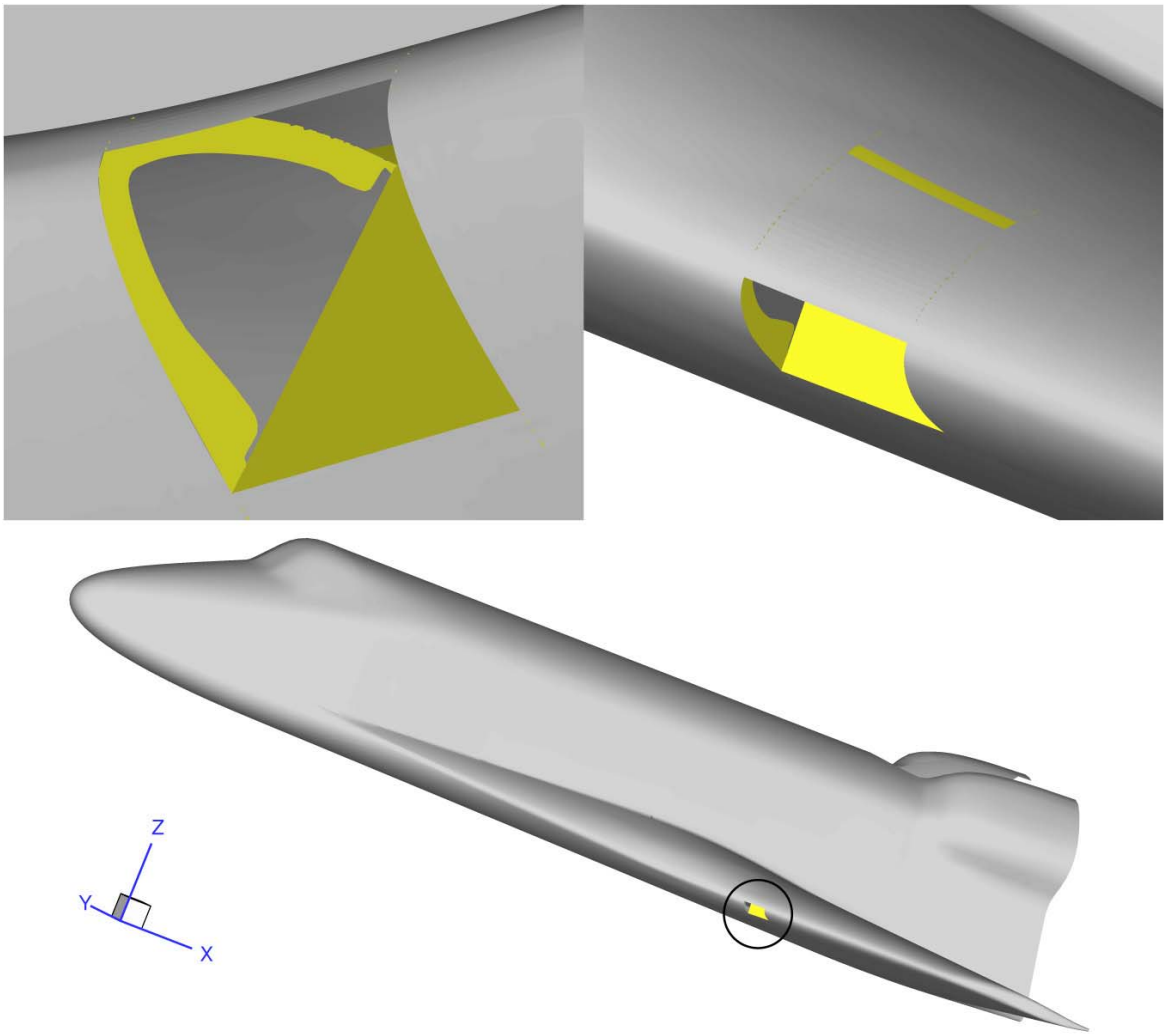

Figure 5.2.4-104 Lower Half RCC Panel 9 Out with Upper Carrier Panel Damage Geometry Used in GASP Simulations

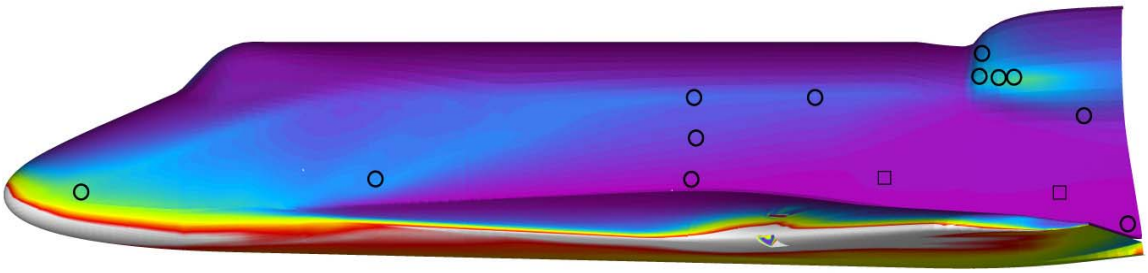

Figure 5.2.4-105 Lower Half RCC Panel 9 Out + Upper Carrier Panel 9 Out, with Vented Side Walls, Side View, Heating Rate

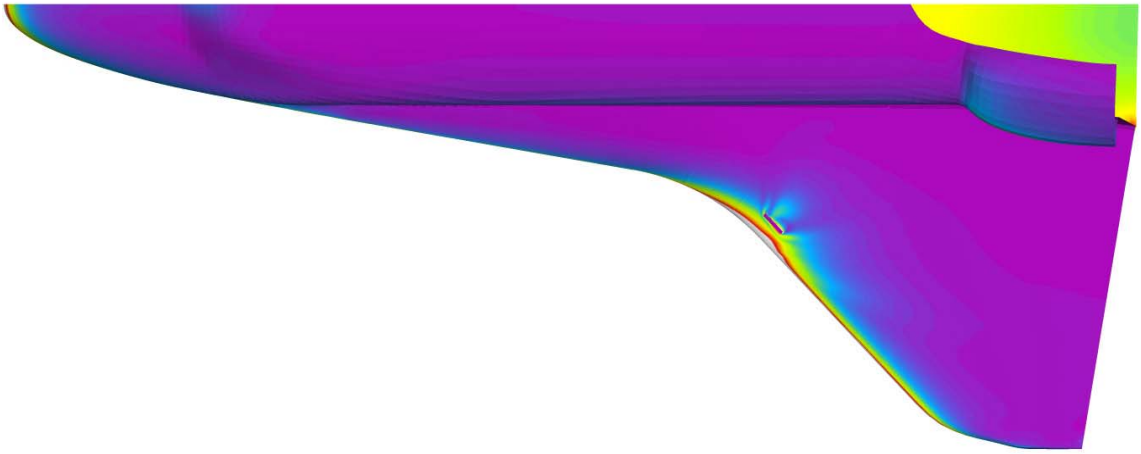

Figure 5.2.4-106 Lower Half RCC Panel 9 Out + Upper Carrier Panel 9 Out, with Vented Side Walls, Planform View, Heating Rate

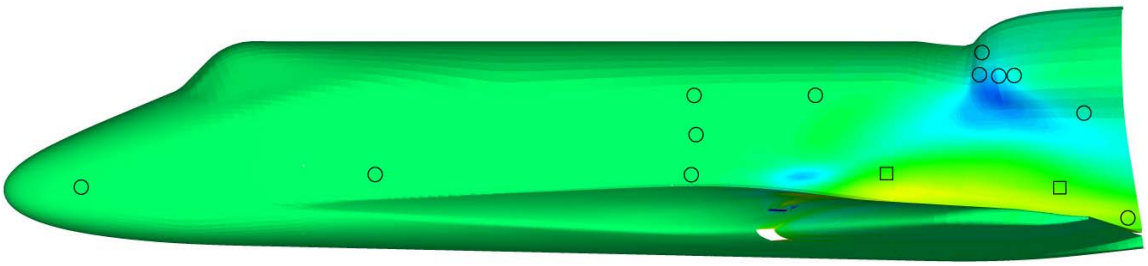

Figure 5.2.4-107 Lower Half RCC Panel 9 Out + Upper Carrier Panel 9 Out, with Vented Side Walls, Side View, Ratio of Heat Fluxes

5.2.5 Application of External Environments Data to the Working Scenario

The objective of this section is to provide a plausible explanation of the observed STS-107 flight data presented in Section 5.2.1 using the results from the various analyses and testing presented in sections 5.2.2 – 5.2.4 above or section 5.3 to follow.

5.2.5.1 Side Fuselage and OMS Pod

The decreased and increased temperature response on the side fuselage and OMS pod can be explained by the working scenario involving damage to the WLE, RCC panels 5 through 9. In Section 5.2.3, sufficient empirical evidence has been obtained to indicate that reduced heating exhibited early in flight (< EI + 480 sec) on the side fuselage and OMS pod sensors was due to changes in the leeside vortex field of the Orbiter, Figure 5.2.5-1, possibly coupled with the dynamics of flow emanating from the WLE damage which perturbs the WLE separation zone. For this reduced heating segment of the flight the most consistent result that matched the flight data was obtained by a case where there was flow through degraded RCC WLE cavity vents, Figure 5.2.3-22 through Figure 5.2.3-24. During this period of the flight, changes in the vortex field were likely caused by additional gas entering the leeside flow field through the vents designed into the upper RCC panel and T-seals, and in possible combination with small local upper carrier panel damage. The correlation of the vented flow to the lee side with flight data necessitates that there was a windside breach along the WLE in order to have the pressure necessary to drive the flow to the leeside with sufficient momentum. The momentum scaling, typically used for flows injected into a cross flow, was used to verify that a proper simulation of the flight environment was being performed and checked against various WLE breach CFD simulations, Figure 5.2.3-23. However, the slot in the wind tunnel model was an order of magnitude larger (1” width full scale, as opposed to 0.1” width full scale) than for the nominal Obiter WLE vent configuration. Therefore, local small damage to the vent area, which could easily occure where the RCC and upper carrier panels meet, has to be present to yield these leeside heating effects. The need for additional vent area was also confirmed using a coupled venting and thermal math model of the wing, Section 5.3.5, for a 10” diameter hole in the windward side of RCC panel 8. For this analysis, the hole existed at EI and the simulation was terminated at the estimated latest point of spar breach, Figure 5.2.5-2. Although mass flow rate is presented, the trend would be similar for momentum. The momentum scaling ratio is on the order of 0.6 from the coupled venting and thermal model. Venting of the RCC WLE cavity with a breach begins to increase significantly at the time the decreased temperature response is recorded on the Orbiter leeside instrumentation. However, the momentum ratio scaling parameter and the information from the wind tunnel tests and venting analyses allow the conclusion to be made, that the mass flow rates, and thus the momentum rates, out of the nominal 66 square inch leeside vent area would be too small to result in the initial side fuselage and OMS pod disturbance. Thus, before either the spar is breached or additional significant damage to the upper carrier panel occurs, the flow entering the WLE from the windward side was exiting through the leeside vents with locally damaged upper carrier panel(s), Figure 5.2.3-24.

The increase in side fuselage and OMS pod heating that occurred later in flight (> EI + 480 sec) can be explained by progressively worsening damage to the upper portion of the RCC panel, upper carrier, and eventually the upper wing skin. Although the increased side fuselage and OMS pod heating began as early as EI+510 seconds, significant changes in the off-nominal leeside temperature response can be attributed to the observed debris events. For instance, debris # 5 (considered to be more of a flash event than a debris event, as a result of ballistic coefficient and luminosity analyses) is closely tied to changes in the temperature response of gauges V07T9220, V07T9976, and V07T9978, Figure 5.2.1-6. Likewise, flash event 1/debris # 6 can be related to significant changes in slopes for gauges V07T9253 and V07T9925, Figure 5.2.1-5. It is important to note that debris # 5 is also closely correlated to the slope change in the delta rolling moment, discussed in Section 4. Therefore, significant changes in the increased heating signatures can be correlated to the observed debris events, which imply progressively worsening damage on the Orbiter.

During the increased heating period, the actual Orbiter configuration remains unknown; thus, multiple leading edge damage geometries, full and half panels, missing T-seal 8, and holes through the wing were evaluated in both the Mach 6 Air and CF_4 facilities. This information has been used to determine the

effect on side fuselage and OMS pod heating of different types of damage, Section 5.2.3. Since holes through the wing showed no evidence of sidewall and OMS pods heating augmentation, the focus turned towards some form of leading edge damage. Leading edge damage is required in order to provide the energy and pressure necessary to affect the leeside flow field. As can be seen in Figure 5.2.3-8 and Figure 5.2.3-16, the results from the Mach 6 air and CF_4 facilities show significant side fuselage and OMS pod disturbances for full RCC panel out cases 5 through 9 (Working Scenario). Overlaid on these figures are the MADS and OI measurement locations. As shown, the impingement footprint is dependent on the removed panel location and the facility. It was noted in the Mach 6 air results for panels 5 through 8 that although increased heating was indicated on the side fuselage, decreased heating was observed on the OMS pod. This combination is inconsistent with the flight data. However, when panel 9 was removed the results in the air facility were more consistent with the flight data. The results for the CF_4 facility showed that increased OMS pod heating was observed for all of the removed RCC panel cases. Setting aside the differences between the two facilities, there is substantial evidence that a damaged WLE will result in increased heating to the side fuselage and OMS pod. The testing results showed heating augmentation factors of from 2 to 10, whereas flight data indicated factors of 1.7 to 5.2 for the MADS data and up to 13 times for the OI V34T1106A gauge (Section 6).

However, the debris evidence indicates that most of the RCC panels were recovered with the exception of a majority of panel 9 and a large segment of panel 10. In addition, all the recovered RCC panel debris was found in Texas. It is believed that having substantial portions of the RCC missing as early as EI+510 seconds is not consistent with the vehicle flying all the way to Texas airspace. It is noted that the debris contains only a single interior tile for upper carrier panel 8 and that neither of upper carrier panels 9 and 10 was recovered. This lack of debris along with the above discussion on the reduced heating provides a consistent explanation for the initial cause of increased heating on the side fuselage and OMS pod. The explanation is that damage to the upper carrier panels became severe enough to allow substantial flow through the WLE vents, with at least a compromised vent path geometry. In order to demonstrate this, a half RCC panel 9 removed model configuration was modified to include the upper carrier panel missing. This geometry allows WLE damage to provide gas flow through the WLE and out the leeside venting location. The results of that wind tunnel test, shown in Section 4.3.1, indicated similar heating trends as the full panel out case.

As was stated above, a compromised upper surface geometry coupled with windward RCC damage was the most likely cause for the initial increased heating. Note that during this time the spar had already been breached and that significant damage was occurring to the wiring instrumentation along the spar and the wheel well. The analysis shown in the next section and the related results discussed in Section 6 will indicate that damage was also occurring to the intermediate wing structure. Since debris event 5 (flash 0) and flash event 1 / debris event 6 closely tie to changes in the side fuselage and OMS pod temperatures as well as the vehicle aerodynamics, it could be postulated that they are indications of upper wing skin breach in the intermediate wing area. The flash events are believed to be the release of small high temperature particles which rapidly decelerate in the Orbiter wake, as concluded from a ballistic coefficient. These particles, as will be shown, could have been combusting aluminum present in the intermediate wing interior, which was then vented to the exterior when the upper wing was breached.

A final question, that of determining which facility provides the more appropriate simulation of the Orbiter leeside flight environment for a damage configuration, may be addressed computationally Extensive aero/aerothermal calculations for the Orbiter with missing half and full RCC panels 6 and 9 were performed at CFD Case # 1 flight condition. Both the half panel out cases showed similar results to the wind tunnel in that no significant heating augmentation could be seen on the side fuselage and OMS Pod, although local disturbances do occur on the leeside of the WLE very near the damage location. The full RCC panel out cases with solid sidewall boundaries also showed side fuselage and OMS pod effects comparable to the wind tunnel results, and tend to favor the CF_4 measurements. However, because of uncertainties in grid resolution requirements and the physical modeling assumptions needed to simulate the leeside flow field accurately, it remains a judgment as to whether or not CFD solutions can be used to differentiate which facility best represents the Orbiter flight environment.

5.2.5.2 Wing Surface T/C V07T9666A

The response of V07T9666A is closely related to the events on the side fuselage and OMS Pod. As mentioned previously, the off-nominal trend for this T/C does not begin until after the indications of reduced side fuselage and OMS pod heating, off-nominal response of the spar temperature and strain gauge at RCC panel 9, and off-nominal clevis temperature response at the RCC panel 9/10 interface. There are two possible explanations for the V07T9666A measurement response. The first possibility is that an external flow disturbance caused by the damage site on the WLE propagated downstream to the measurement location via boundary layer transition. The second possibility is that disturbed flow came out of the WLE damage back onto the windward surface as a result of high temperature gas ingestion into the WLE cavity.

For the first possibility, a boundary layer transition analysis of the Orbiter near this point of the flight was performed. Figure 5.2.5-5 indicates that it would require a trip height of between 1.2" and 1.4" to result in an effective transition trip (see Appendix 5.6 for more information on effective trip calculation). At EI+370, the free stream Reynolds number for the Orbiter, presented in Figure 5.2.5-3, is approximately 5.0×10^5. Given a large enough damage site, a boundary layer disturbance could propagate downstream. No correlation is presented between the effectiveness of a protuberance versus that of a cavity, but a cavity would be more representative of a damaged WLE. However, protuberances are typically more effective at promoting boundary layer transition. For example, Figure 5.2.5-4 shows the limited downstream effect of a 6" diameter hole on the windward side of RCC panel 6. However, it will be shown that the damage necessary to cause the Columbia accident has been narrowed down to either a significant portion of a T-Seal, or RCC acreage damage on the order of 30 to 80 square inches. Moreover, this size of damage would be large enough to result in a locally disturbed flow extending from the damage site to this region of the wing given a high enough Reynolds number. Figure 5.2.5-6 presents a surface streamline plot of the Orbiter WLE region showing how the flow passes over the vehicle at EI+404 seconds. Since the working scenario addresses damage to the WLE in the area of RCC panels 5 through 9, this damage zone propagates streamwise effects which would pass over this gauge.

For the second possibility, the debris along with the above mentioned flight data provide a supporting rationale for the off-nominal temperature responses. As was noted, heating was already occurring in the WLE cavity at the time of leeside surface heating excursions. Therefore, flow was entering the cavity and exiting the WLE vent system (nominal configuration or damaged) prior to EI+370. Close inspection and reassembly of the debris in the RCC panel 8 and 9 area, Figure 5.2.5-7, indicated that flow out of the WLE cavity from a manufactured slot at the back corner of RCC panel 8 did occur. This flow is evidenced as well by the erosion on the RCC panel 9 lower carrier panel tiles. The answer for how flow can exit the WLE cavity to the lower surface of the wing is that the interior of the WLE cavity must be at a higher pressure than the local external pressure. At the high angle of attack during entry, the local pressure on the lower surface of the wing beyond the leading edge is approximately equal to the free stream dynamic pressure. In order to determine the relative pressure of the two regions given a damaged WLE condition, a coupled external / internal CFD of the Orbiter must be performed. This issue will be addressed in the section on internal aeroheating environments.

5.2.5.3 Chin Panel and Vacuum Vent / Water Supply Dump Nozzles

A possible explanation for the temperature responses of the chin panel and vacuum vent/water supply dump nozzles in flight is that a local disturbance to the flow, such as a protrusion, could have existed which then burned away over the period of time in question. For the chin panel gauge, the protrusion itself would have to be the gap between the nose cap and chin panel, exactly where the expansion seal resides. Preflight inspection of the gap, (see Boeing TM, ATA-TM-02-0009) indicated a small excursion of 0.002" beyond the equivalent roughness requirement of 0.120" just left of the vehicle centerline. Again referring to Figure 5.2.5-5, boundary layer transition analysis of the Orbiter at this point of the flight indicates that it would require a trip height of between 1" and 1.4" to result in an effective transition trip. Also, this trip had to be located at or outside the attachment line streamline such that the disturbance in the flow was swept overboard, because no disturbance was observed on any of the windward fuselage T/Cs downstream from the nose cap, see
Figure 5.2.5-8. Therefore, from an aerothermodynamic perspective, the response of the chin panel expansion seal gauge cannot be readily explained. Adding to that, as will be discussed in Section 6, is

the fact that the temperature response of the expansion seal gauge is non-physical with respect to how it recovers to the original slope of the curve.

For the vacuum vent and water supply dump nozzles, two possible explanations for the transient were proposed and investigated: (1) change in the vehicle orientation, and (2) a local flow disturbance just upstream from the two nozzles that flows along the same streamline. The nozzles are right above the beginning of the wing glove (forward wing extension). At this location the flow wraps around the chine of the wing glove, forming a vortex. This vortex is the source for the nominal heating in this region, Figure 5.2.5-9. Where the vortex scrubs the surface there is higher heating than where it does not; this can be seen in Figure 5.2.5-10. The location of this vortex is a function of the angle of attack and angle of sideslip, shown in Figure 5.2.5-11 and Figure 5.2.5-12, respectively. The variation in the angle of attack during this period is negligible with respect to the variation of the aeroheating environment. The variation of the angle of sideslip, although small, was investigated as a potential source for the off nominal events. As was seen in the aerodynamics section, this variation of sideslip was not outside previous flight experience of the Orbiter during this portion of the re-entry. CFD analysis of the Orbiter forebody showed insignificant changes in the heating due to variations in sideslip from 0 to –0.5 degrees.

From a local flow disturbance perspective, as can be seen in
Figure 5.2.5-9, the flow crossing both the vacuum vent nozzle and the water supply dump nozzle would also cross V07T9522, a surface T/C. Any disturbance strong enough to cause a change in the heating of the nozzle should have also disturbed the heating to this surface T/C. As was indicated previously, the only anomaly seen on this gauge is a sharp drop in temperature for one cycle during this time; otherwise, the response was determined to be nominal. Thus, again, from an aerothermodynamics perspective, the responses of the vent nozzle and water supply dump nozzle cannot be readily explained. Therefore, both the off-nominal events related to the chin panel and these nozzles should be listed as unexplained anomalies (UA).

5.2.5.4 Kirtland Photo

As was shown in Section 5.2.4, no dramatic changes to the windward and leading edge shock shapes could be discerned from the CFD solutions with RCC panel 6 or panel 9 removed. However, the source of the bulge in the light from the leading edge could have been either from embedded shocks in the damage zones or from additional particulates in the flow field as the damage progressed, or a combination thereof. No supporting evidence for the proposed particulate explanation exists. For the proposed imbedded shock explanation, Figure 5.2.5-13 is an example of the resultant embedded shocks due to WLE damage. The additional shocks would likely re-excite the N_2 first mode, which is the principle light source in the shock layer immediately around the vehicle. However, this explanation remains speculation, and thus there is no substantial evidence that can explain the Kirtland photo.

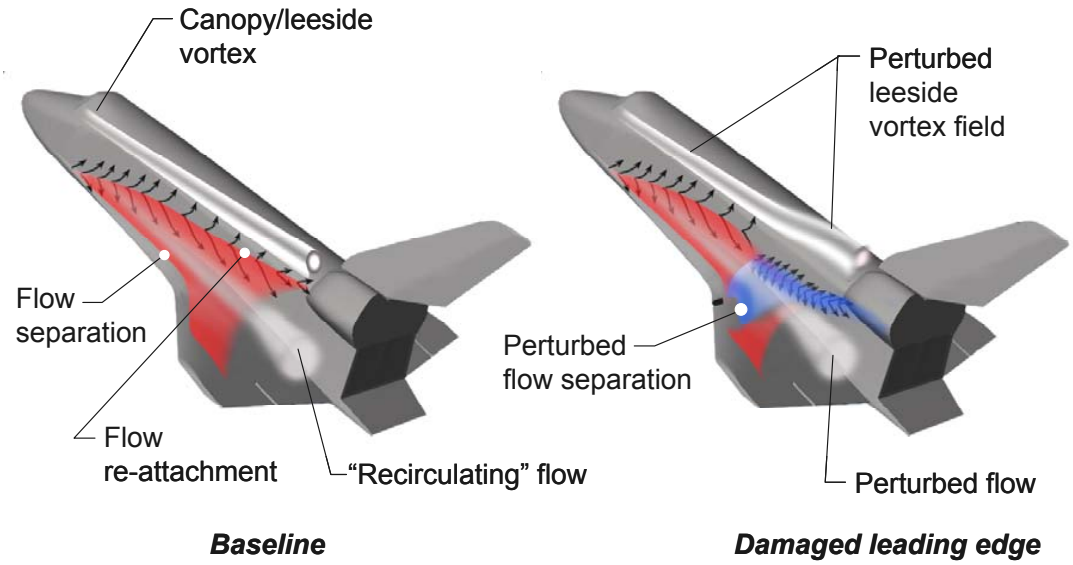

Figure 5.2.5-1 Postulated Orbiter Leeside Flowfield Associated With Wing Leading Edge Damage. Wing leading edge damage perturbs leeward flow separation and re-attachment locations as well as leeward embedded shocks (not shown).

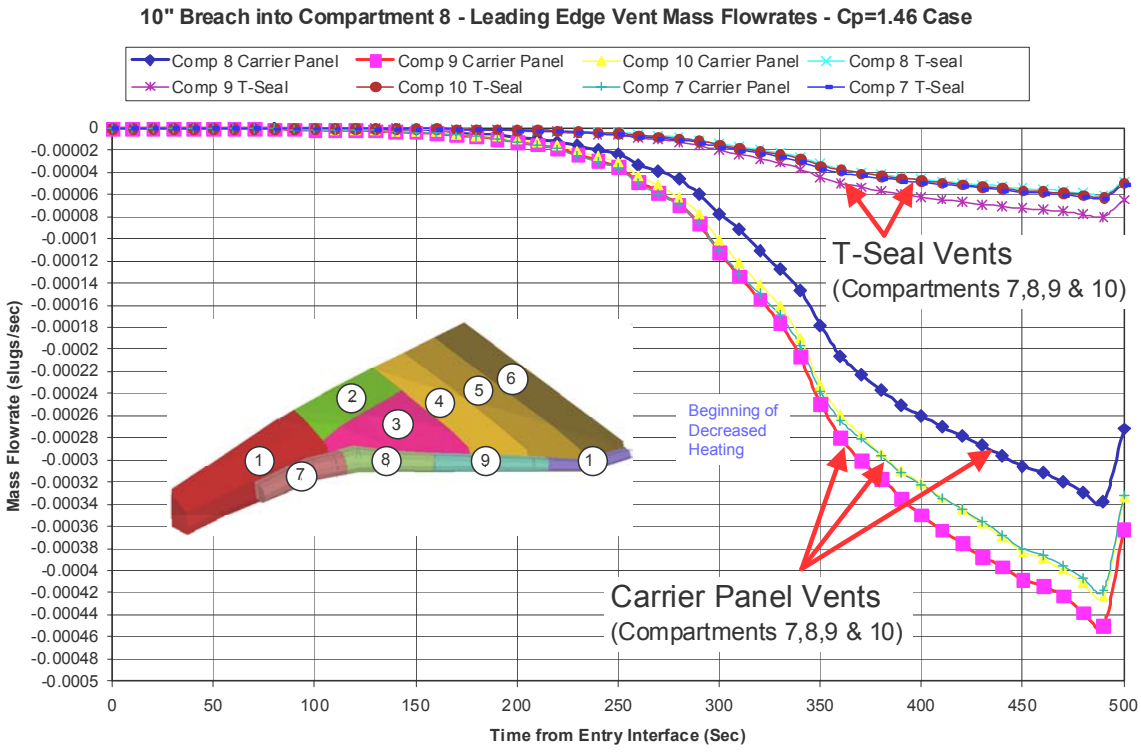

Figure 5.2.5-2 Leading Edge Vent Mass Flow-rate Summary - 10" Breach Cp=1.46. Results from MSFC-developed coupled venting and thermal wing model.

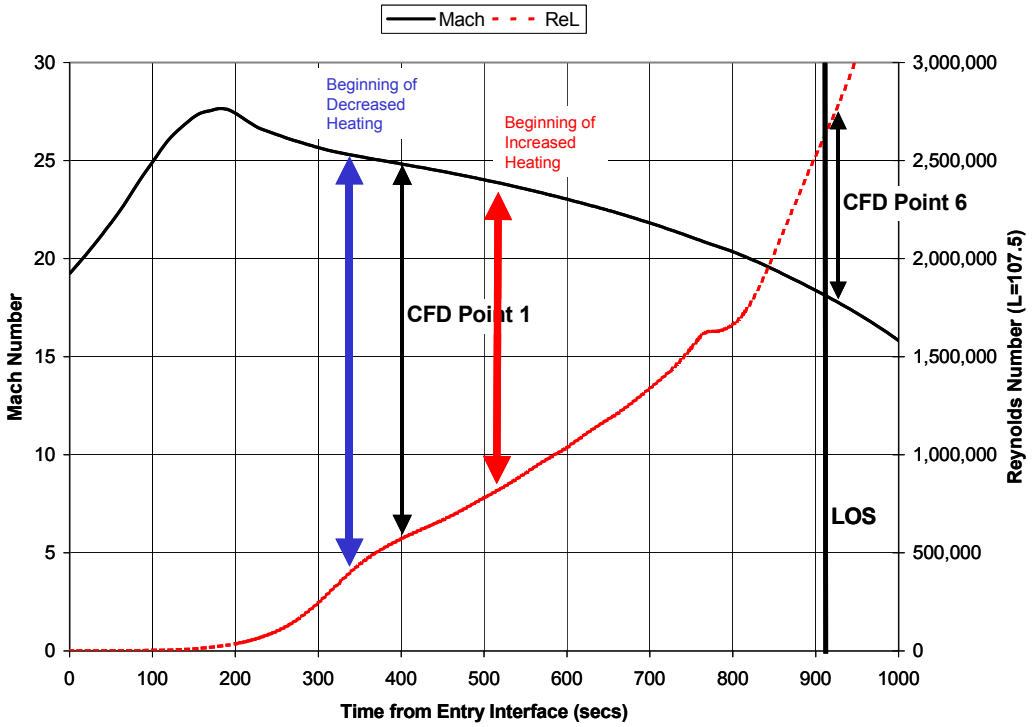

Figure 5.2.5-3 STS-107 entry trajectory, Mach No. and Reynolds No. from entry interface

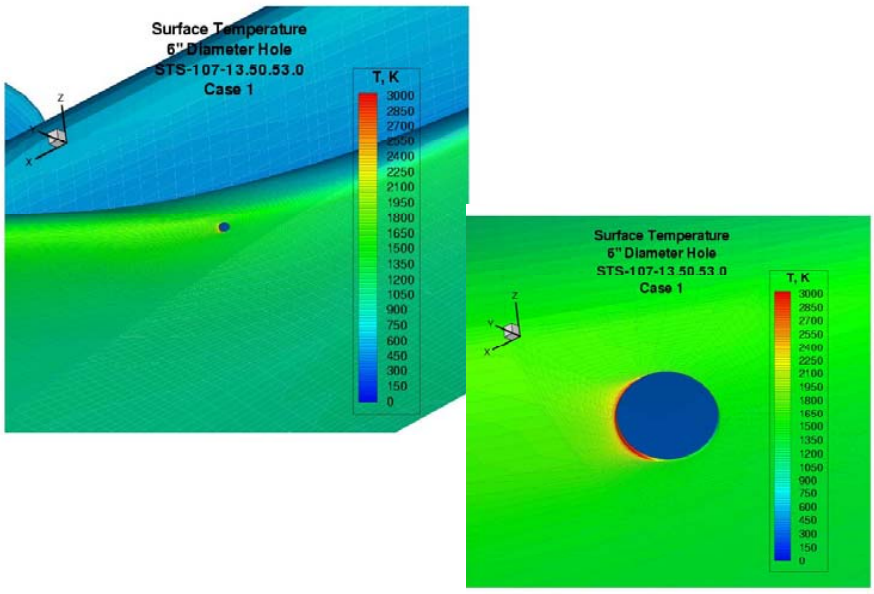

Figure 5.2.5-4 NASA LaRC LAURA CFD solution of a 6" hole on the windward side of Panel 6. Note the limited downstream disturbance of the flow.

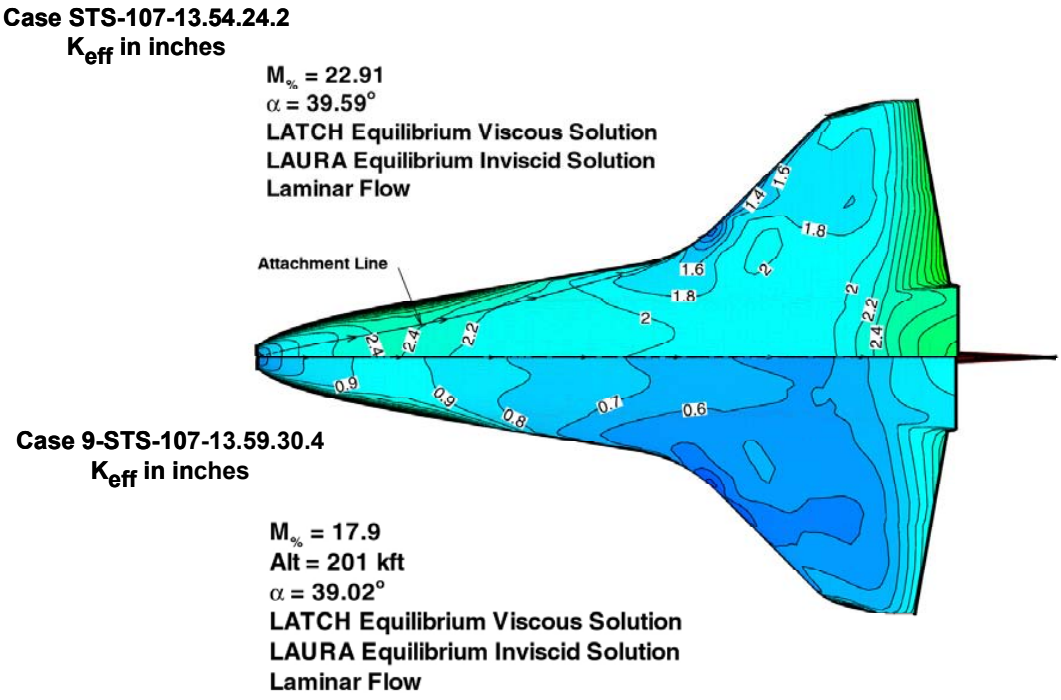

Figure 5.2.5-5 Effective Roughness Height for Transition

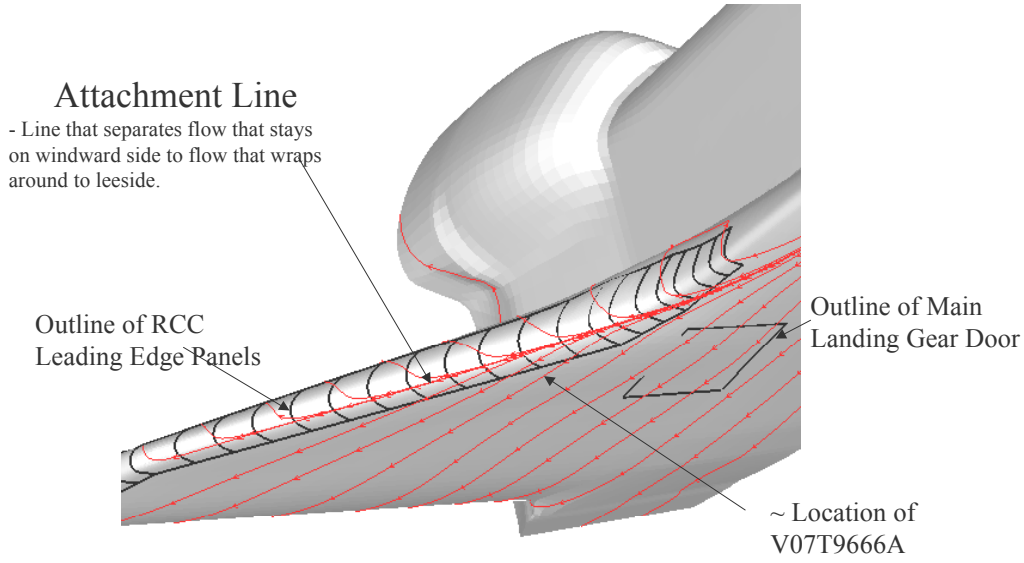

Figure 5.2.5-6 Orbiter surface streamlines. CFD Point 1, EI+404, Mach 24.9, 243 kft.

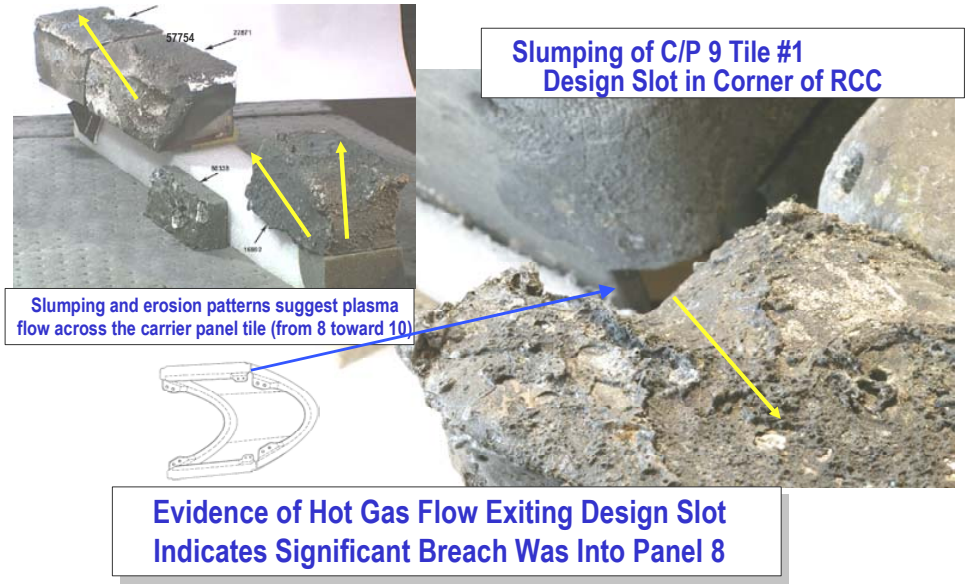

Figure 5.2.5-7 Hardware Forensics Team reassembly of RCC Panel 8 with RCC Panel 9 Lower Carrier Panel Tiles. April 28, 2003 presentation to the OVEWG.

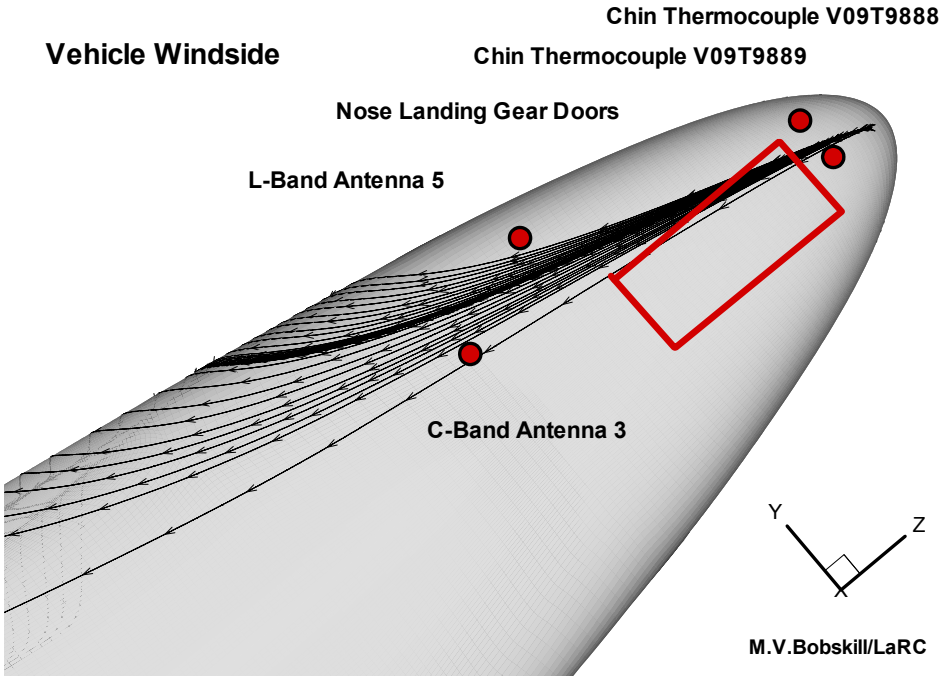

Figure 5.2.5-8 Orbiter surface streamlines crossing chin panel region.LaRC LAURA solution of CFD Case #1. CFD solution is of right side when angle of sideslip equals 0. Chin Panel gauges are in the correct relative position.

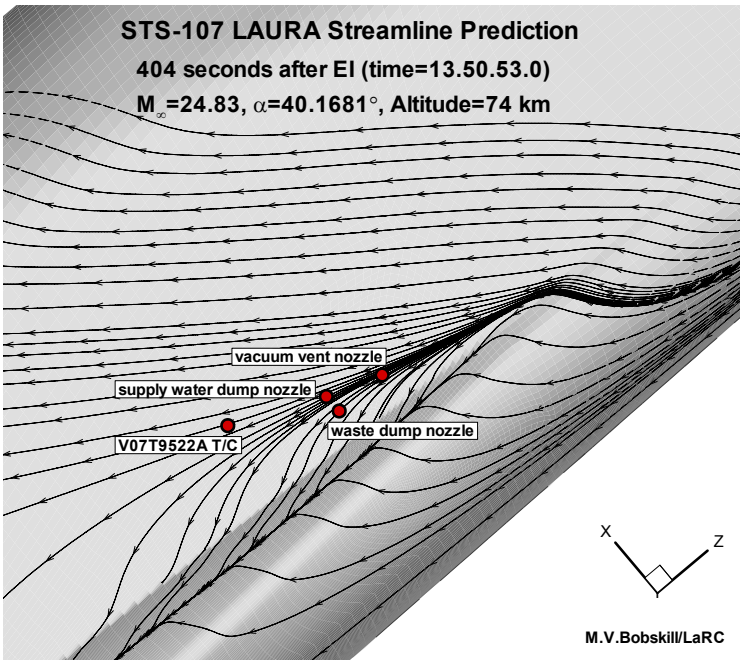

Figure 5.2.5-9 Orbiter surface streamlines in vent nozzle region. CFD solution is of right side when angle of sideslip equals 0. Nozzles are in the correct relative position.

.

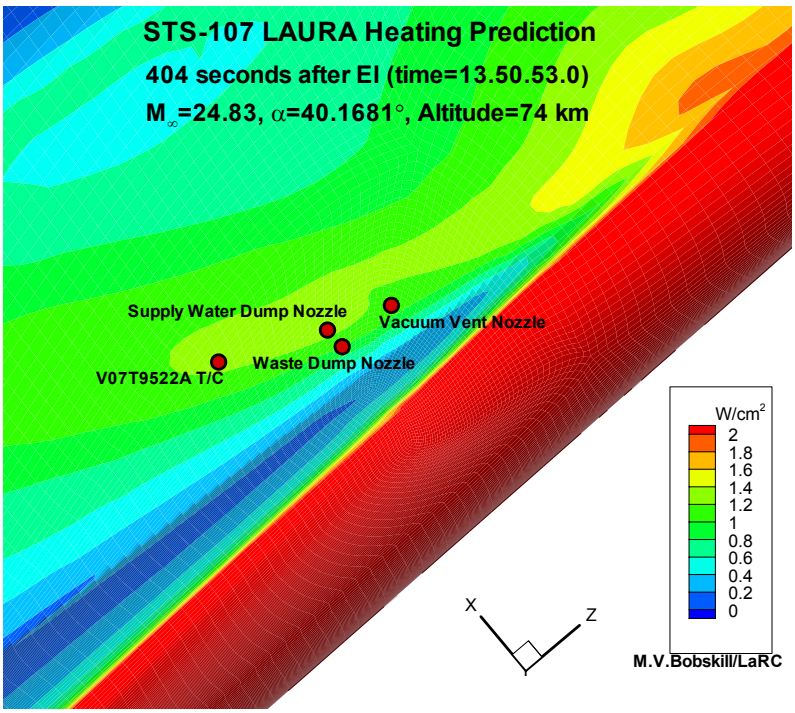

Figure 5.2.5-10 Orbiter surface heating in vent nozzle region. Note CFD solution is of right side when angle of sideslip = 0 deg. Nozzles are in the correct relative position.

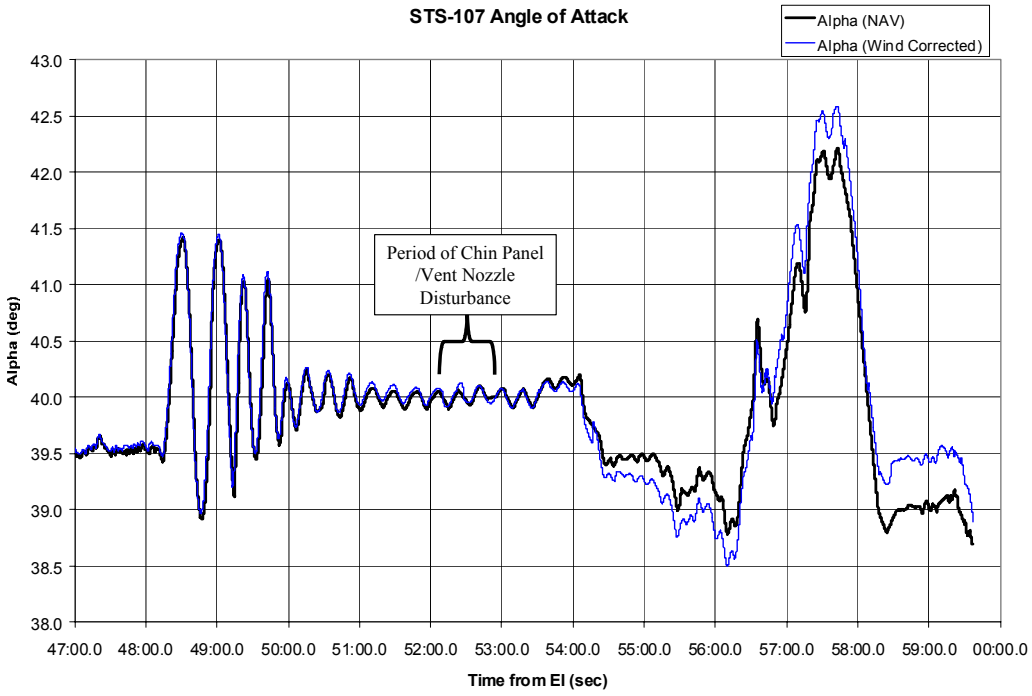

Figure 5.2.5-11 STS-107 Angle of Attack History with and without modeled winds. See Section 4.0 for further detail on model wind effects.

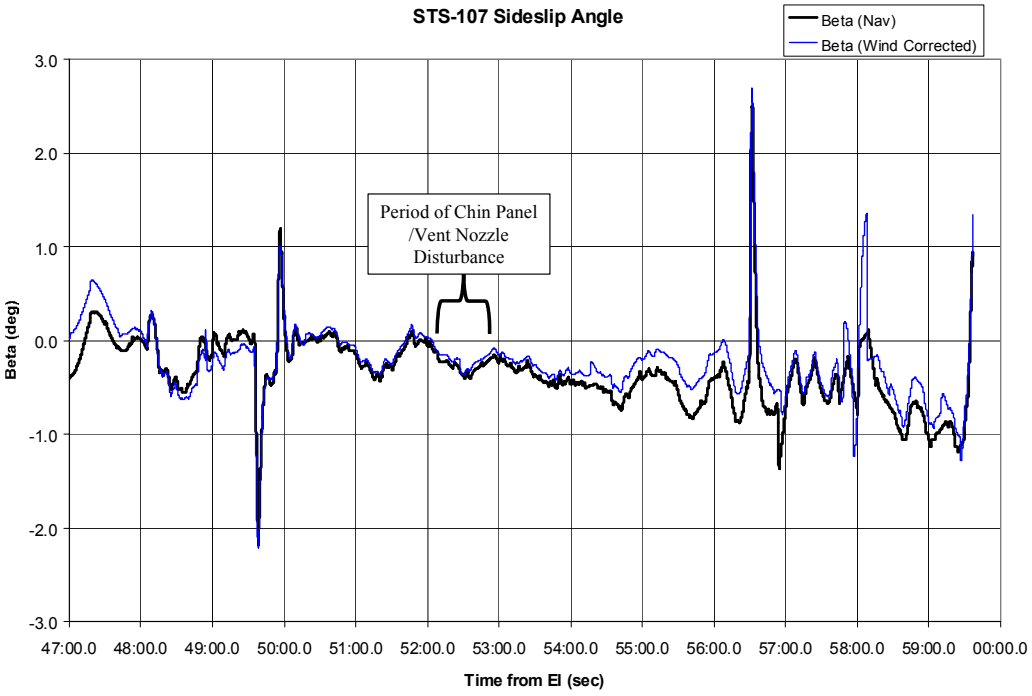

Figure 5.2.5-12 STS-107 Angle of Sideslip History with and without modeled winds. See Section 4.0 for further detail on model wind effects.

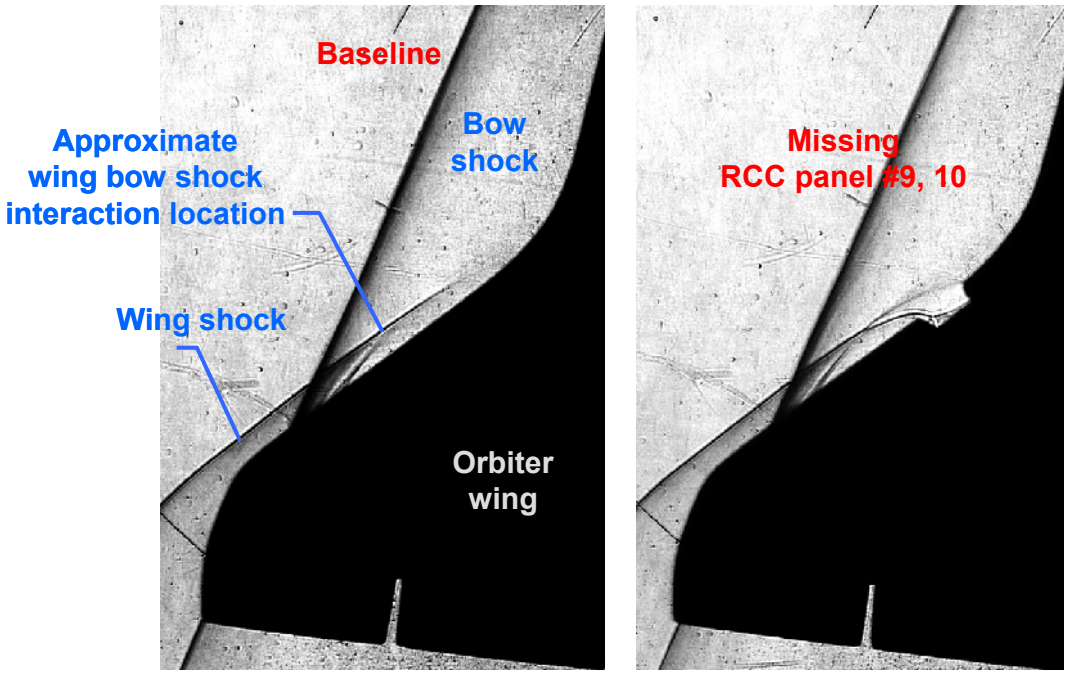

Figure 5.2.5-13 An example of imbedded shocks along the wing leading edge as a result of wing damage. Schlieren images taken in the LaRC Mach 6 Air facility. Note, shock locations are freestream Mach No. dependent.

5.3 Damaged Orbiter Internal Aerothermodynamic Environments

This section of the report details Internal Aerothermodynamic team activities contributing to the STS107-investigation working scenario. Internal environment team members focused on the analysis, investigation, prediction, and understanding of the complex, high temperature gas dynamics environment within the Orbiter wing following a breach of the external thermal protection system. From this point of view, the internal environment interfaced to the external environment activities, previously discussed, at the undisturbed outer mold line of the vehicle. Preliminary assessments, assuming independence of the two separate environments, proved to be inadequate, however, and required the complete integration and coupling of the exterior flow field with the internal breach environments. This direction led to the development and application of new aerothermal tools and techniques, which are discussed in the following sections below.

Section 5.3.1 will discuss the overall process of developing the internal environments used for thermal analysis as detailed in Section 6. Sections 5.3.2 through 5.3.6 detail the individual activities and tool development efforts required to produce integrated environments. Finally Section 5.3.7 will pull together the lessons learned and insight provided by the studies as an application to the present working scenario.

By the very nature of internal flow environments (that a hole has to exist before they come into play), the results of all analysis are highly scenario dependent. While insight and general understanding of the dominant fluid dynamics can guide engineering analysis, one must keep in mind that a small change in hole location or diameter may produce entirely different results. Given the degree of uncertainty regarding the actual damage, internal engineering predictions of heating were generally characterized with +/- 50% levels of uncertainty. These models were most useful for matching trends and understanding major phenomena. Refined CFD analyses, discussed in Section 5.3.6, emerged late in the investigation that locally produced peak heating rates several factors larger than engineering model results. The large heating rates predicted result from extreme flowfield gradients picked up in the finer grid solutions. Comparisons with the engineering distributions are presented in Section 5.3.7.

5.3.1 Process of Determining Internal Aerothermodynamic Environments

The use of Computational Fluid Dynamic tools for high temperature gas dynamic environments has progressed significantly over the last decade in the development of external aerothermal environments. With experienced CFD personnel and baselined tools, the external Aerothermodynamic teams were primed to get started within a relatively short time. Internal environments, however, were a different story. The following process was developed from scratch specifically for the STS107 investigation and drew on tremendous talent from across the country. (Note: the work covered in this report represents only a fraction of the total effort put forth by the Internal Flow team. Much of the unique and cutting edge analysis did not have direct bearing on the present working scenario, and thus, was not reported here. The remaining work will be reported in the future.)

5.3.1.1 Process Development

Immediately following the demise of Columbia, the aerothermal community came together and brainstormed activities required for understanding fluid dynamics of the entry event timeline leading to the loss of vehicle. In the process, a framework for constructing the necessary information and toolsets emerged with clear delineation between external and internal aerothermodynamics. The internal team was given the challenge of developing insight and tools to understand an environment involving multiple penetrations of supersonic, high temperature gases into complex geometries with coupled heat transfer to structures. The starting point for the process was identification of the types of analyses that would be required, identification of personnel and tools to perform the analysis, and establishment of a plan to meet all objectives in a short few months. Table 5.3.1.1-1 displays the five major fields of analysis identified and how they play together to provide a clear picture of three early scenarios. Given the unique nature of the investigation it was clear to the team that the required expertise to complete the analysis did not presently exist within the aerothermal community and would have to be developed.

At the outset the team developed a series of Unit Physics benchmarks, see Table 5.3.1.1-2, that separated the fully coupled, complicated problem into smaller pieces that could be individually simulated and compared to

calibration quality test data to assure the tools and capabilities could accurately simulate the necessary phenomena. These pieces would then be built upon through a series of increasingly complicated, more flight-like cases, leading to the fully coupled external/ internal failure simulation at true flight conditions. This process, as developed, is summarized in Figure 5.3.1-1.

Implementing the entire process shown in Figure 5.3.1-1 proved to be untenable within the time constraints of the investigation. Therefore, the majority of the internal team's CFD analysis relied on current best practices. However, for three specific failure scenario analyses the CFD did proceed through the key steps of this process. The CFD tools implemented for the two and three-dimensional T-Seal damage and the RCC Panel 8 10" breach (Sections 5.3.6.2.2, 5.3.6.2.4, 5.3.6.1.2, respectively) were benchmarked to the key Unit Physics and Unit Physics Extension relevant for those failure scenarios.

Thermal analysts require heating distributions and histories to assess structural temperatures and hardware failure times. Engineering methodologies for predicting internal environments were developed in parallel with the CFD techniques for the full-scale problem to meet thermal analysts data and schedule requirements. In order to provide greater consistency and accuracy, the interface for all internal tools was always the latest, most complete CFD analyses available from the external environments team. These additional tools include boundary layer extraction and mass/energy balance tools, venting and coupled thermal/venting tools, engineering plume impingement heating tools, and basic engineering support CFD for tool assessments. Figure 5.3.1-2 presents the internal environments process and some of the interactions between components.

	A. MLGD Penetration	**B. Wing Leading Edge Damage**	**C. Acreage Tile Loss**
1. Venting Analysis	1. Mass flow analysis 2. Energy balance 3. Penetration parametrics	1. Mass flow analysis 2. Energy balance 3. Penetration parametrics	1. Penetration location parametrics
2. Fluid Thermal Coupling	1. Flow past seal 2. Flow through crack	1. Flow past seal 2. Energy loss to wing structure	
3. Engineering Model CFD Support	1. 2D/Axi Jet modeling 2. Flow into cavities 3. Simplified 3D	1. Swept cylinder with hole 2. 2D into RCC cavity	1. Flow over cavity with penetration
4. Penetration flow engineering models	1. Modeling of Jet 2. Impingement modeling	1. Spar Impingement 2. Attach Hardware	1. Test data analysis 2. 3D heating factors
5. Large Scale CFD	1. Wheel Well Penetration 2. Door Ajar/Seal Breach 3. Vent ingestion	1. RCC Leading Edge penetration 2. Lower Seal breach 3. Missing panel	1. Wing Box Flow

Table 5.3.1.1-1 Internal Flow Team Analysis Matrix

Unit Physics	Benchmark Dataset	POC and Consolidator	Location or Date Available
High Enthalpy Flow (HEF)	Sphere Flows. LAURA Cases	P. Gnofo, 757 864 4380 p.a.gnoffo@larc.nasa.gov	simak.jsc.nasa.gov/pub/from_hermes/LargeInternalFlow/Continuum/Benchmarks/HEF/
Underexpanded Jet (UEJ)	Donaldson & Snedeker '71	Joe Ruf, 256 544 4942 Joseph.h.ruf.nasa.gov	simak.jsc.nasa.gov/pub/from_hermes/LargeInternalFlow/Continuum/Benchmarks/UEJ/
Shock – Shock Interaction (SSI)	Glass's Material	Kim Bey, 757 864 1351 k.s.bey@larc.nasa.gov	
Cavity Flow (CF)	1) Laminar, Hahn '68, & Wyborney,AGARD 2) Turbulent, 3) Pressure Gradient	Kim Bey, 757 864 1351 k.s.bey@larc.nasa.gov	simak.jsc.nasa.gov/pub/CavityFlow_Bey/
Wall Bounded Jet (WBJ)	In work -	Chris Glass, 757 864 1350 c.e.glass@larc.nasa.gov	Experimental Data being generated

Table 5.3.1.1-2 Unit Physics Benchmarks

Large Scale Wing Internal CFD Roadmap Overview

- **Multiple Failure Scenarios to be assessed**
  - Many similarities, some uniqueness
  - Basic fluid physics broken down to several Unit Physics
- **Unit Physics Problems**
  - Each addresses a unique set of physics
  - Codes are compared to available test data for each unit physics
- **Unit Physics Extensions**
  - Extend the Unit Physics problems to flight fluid properties
- **Bridging Problems**
  - Combine all relevant physics together in a geometrically representative problem
- **CFD of the Failure Scenario**
  - Lessons learned from the process applied to improve the result of the 'Large Scale Wing Internal CFD'

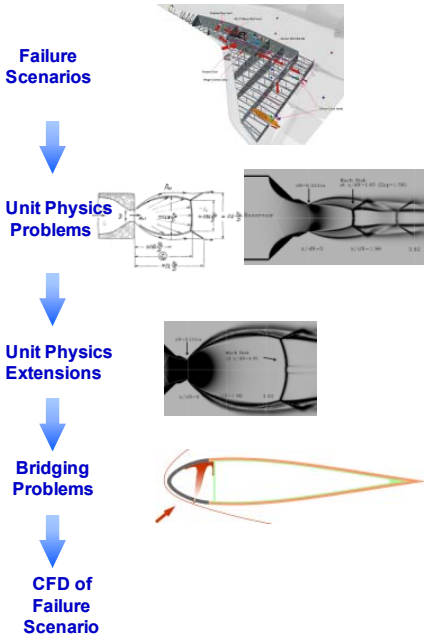

Figure 5.3.1-1 Large Scale Internal CFD Roadmap

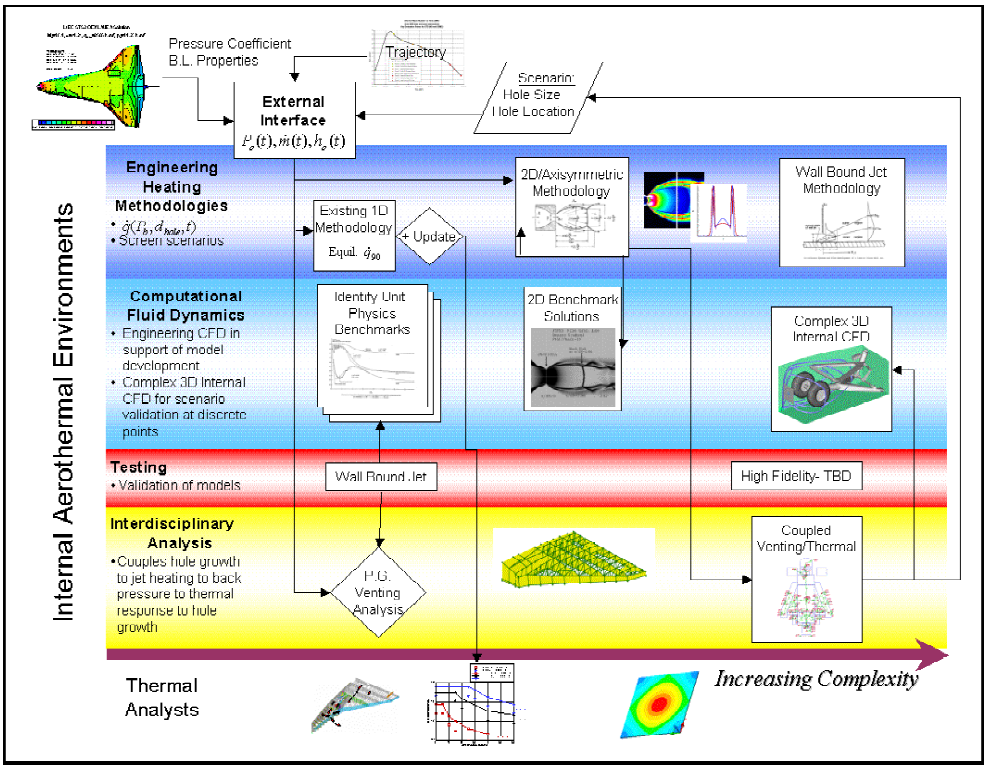

Figure 5.3.1-2 Internal Environments Flow

5.3.1.2 Tools

The unique application of aerothermodynamic analysis to the Orbiter internal environments required the development of a suite of unique capabilities and tools previously not available. A natural basis for much of the internal environment work involved the application of several CFD codes with diverse backgrounds. Each of the tools developed during this investigation for the assessment of the Orbiter, post breach, internal environment will be described in the following sections.

5.3.1.3 Integration

The original time-dependent, integrated analysis plan is given in Figure 5.3.1-3. In this original schematic, the intent was to fully assess a dynamic, multiple failure scenario leading to the STS-107 observed timeline. Within this schematic, the loop starts in the upper left with an assumed hole size, trajectory condition, and external properties from CFD solutions. This information is passed off to the external flow interface, which provides predictions of penetration mass and energy flux through the hole, as well as specifying fluid properties at the penetration. Fluid flow into the Orbiter through the penetration pressurizes the interior volume and transfers energy to the vehicle structure as modeled in the coupled venting thermal analysis loop. Once the quasi-steady internal properties are established, engineering predictions of jet impingement heating to internal structures are generated and fed to the detailed thermal models for local temperature predictions. Based on vehicle loads and material limits, breach and/or structural failure assessments are made and hole diameter/breach status is updated and the process starts the loop over again. The internal flow process, backed by the blue background, would be assessed at discrete time points by application of large-scale CFD solution methods and engineering validation for simplified jet impingement models.

This process was ultimately untenable within the time constraints of the investigation, given the distributed nature of the internal flow team. (Boeing Huntington Beach successfully implemented a similar process for their Progressive Failure Analysis as detailed in Section 6: provided a priori prediction for the hole diameter and internal heating distributions.) The present working scenarios are analyzed with fixed hole diameters up to

the point of structural failure, allowing specification of complete heating distribution histories to be computed and provided to thermal analysts for failure analysis.

Figure 5.3.1-4 presents the final integrated process for developing the internal heating environment for a breach into the wing leading edge RCC system. Starting in the upper left, the external team CFD solutions using LAURA are probed at the assumed hole location and values extracted as inputs to the external flow interface routines which generate bulk enthalpy values into the breach and into pressure inputs to the coupled thermal/venting methodology for the prediction of internal pressures and mass flow within the vehicle. Peter Gnoffo's LAURA calculations also serve as the basis for the fully coupled jet penetration calculations. *(Though larger holes were assessed later, the final environments produced utilized jet directions derived to match two-inch hole results.)* Potential penetration locations were screened along the predicted debris impact footprint to determine a worst-case penetration producing the peak impingement heating on the internal insulation surfaces. With the hole location specified, axisymmetric heating predictions are generated utilizing the previously calculated mass/energy flux and CFD predicted surface pressures. These results are then fed into the internal heating distribution methodology, which provides time histories of convective heating values over the internal volume of the RCC cavity. The final heating distributions and accompanying trajectory corrections are then provided to the thermal community. Use of large-scale CFD results is two-fold in this approach: 1) to independently assess the applicability of the final methodology, and 2) provide additional fluid insight in order to explain observed debris forensics.

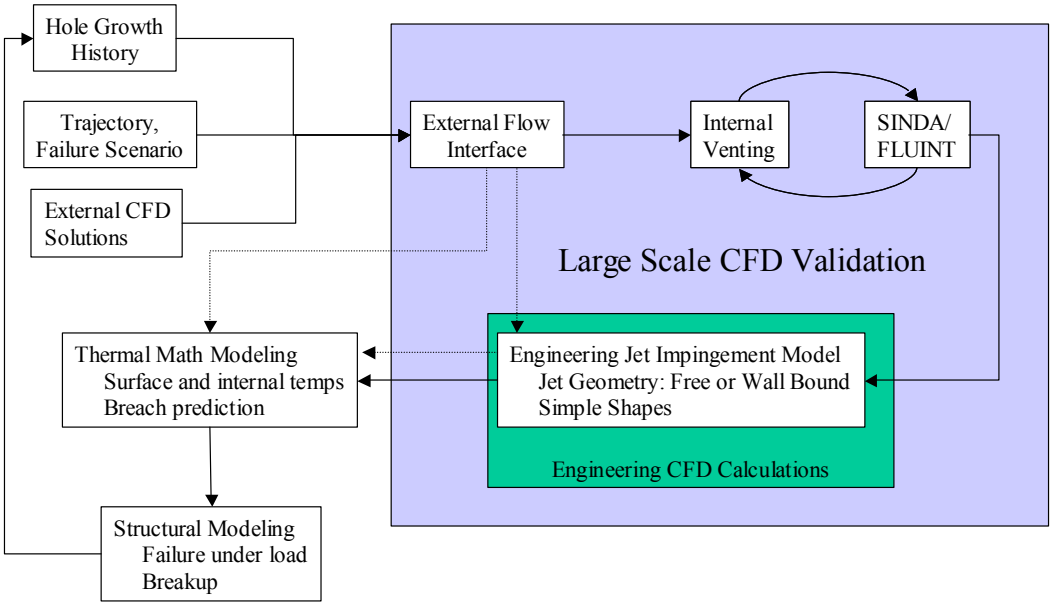

Figure 5.3.1-3 Closed Loop Integrated Analysis

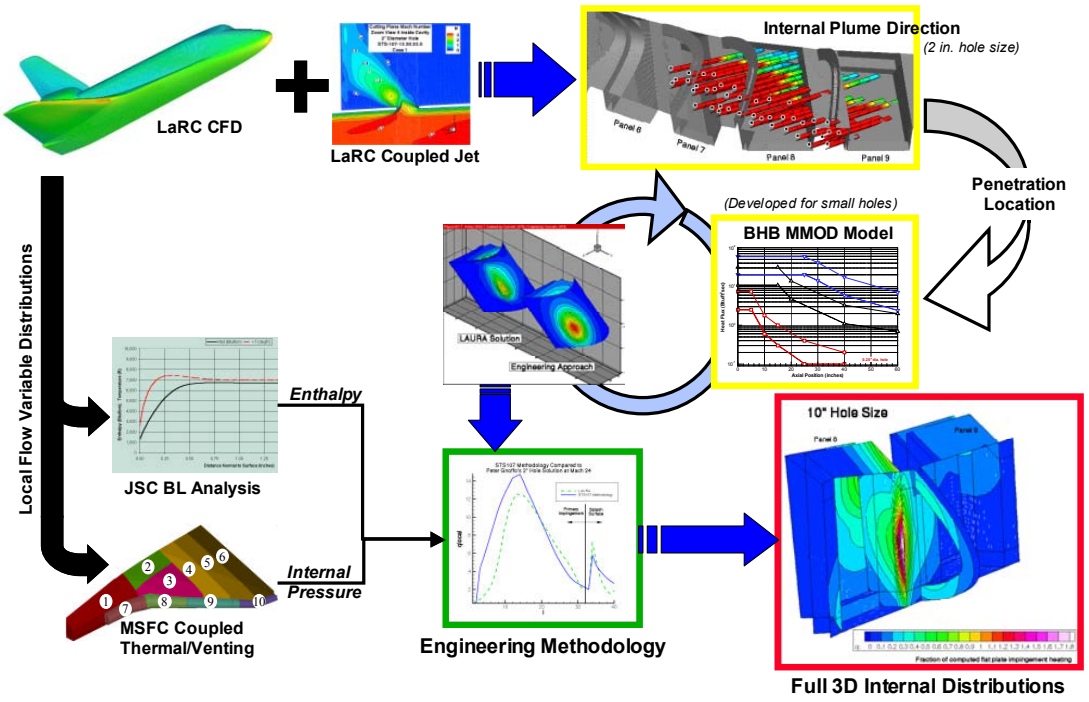

Figure 5.3.1-4 Integrated Internal Environments Schematic

5.3.2 External/Internal Environments – Engineering Analysis

In order to evaluate the effects of ingested reentry gases on the internal structure of the Orbiter wing, a method was needed that would provide the properties, e.g. mass flow rate and energy flux, of the ingested gas as a function of time through the trajectory. These values were needed as input to the 'plume' models that provided the local heating to internal hardware and as input to the coupled venting/thermal codes that modeled the flow and bulk heat transfer inside the wing. CFD solutions require significant resources to setup and then provide detailed data for only one or two free stream conditions. Therefore, selected CFD solutions were used to aid in the development of engineering tools that provided the histories of the ingested gas flow rate, bulk enthalpy and bulk temperature needed to evaluate the propagation of damage inside the vehicle.

5.3.2.1 Overview of Breach Hole Engineering Analysis Methodology

Figure 5.3.2-1 provides a sketch of the basic aspects of a breach flow field. Once a breach hole opens in the Orbiter aeroshell the pressure differential between the outside flow field and internal volume will cause reentry gases to enter the vehicle and generate a gas 'plume' that then impinges on internal structure. The flow rate and energy of the flow ingested depends on the size and shape of the hole and the properties of the gas just upstream of the hole. The gas properties in the external flow vary by location on the vehicle and by distance from the surface. For small breach holes, only a portion of the gas near the surface, as shown in Figure 5.3.2-1, is ingested. As the hole increases in size, more of the boundary-layer gas is ingested until the entire boundary layer is swallowed. Further increases in hole-size results in the boundary layer and a portion of the high enthalpy shock-layer gases to be ingested. The mass flow rate of gas through the breach hole is a function of the mass-averaged enthalpy of the boundary-layer gas that is ingested. Therefore, a mass balance between the gas flowing through the hole and that extracted from the external flow was used to obtain an engineering estimate of the mass flow rate and energy flux of the gas ingested.

The mass-flow rate through the hole was computed by the following isentropic relation from Shapiro:

$$\dot{m}_{hole} = Area\sqrt{\frac{\gamma}{R_{gas}}}\frac{P_o}{\sqrt{T_o}}\frac{M}{\left(1+\frac{\gamma-1}{2}M^2\right)^{\frac{\gamma+1}{2(\gamma-1)}}} \qquad (5.3.2\text{-}1)$$

where $\dot{m}_{hole}$ = mass flow rate through hole
Area = cross-sectional area of hole
γ = Ratio of specific heats
R_{gas} = Gas constant
P_o = External Pressure
T_o = Bulk temperature of ingested gas
M = Mach number at hole

The mass flow relation above has a maximum value when the Mach number is 1.0. The following isentropic relation was used to compute the Mach number as a function of the internal and external pressures, P_{int} and P_{ext}, respectively.

$$\frac{P_{ext}}{P_{\text{int}}} = \left(1+\frac{\gamma-1}{2}M^2\right)^{\frac{\gamma}{\gamma-1}} \qquad (5.3.2\text{-}2)$$

P_{ext} was used for the P_o value in Eqn. 5.3.2-1. The values γ, R_{gas}, *and* T_o are a function of the average gas properties of the flow extracted from the external flow field. To obtain these values it was assumed that chemical equilibrium air properties could be used given a pressure and an enthalpy. The average, or bulk, enthalpy of the ingested gas was obtained from the following relation:

$$H_{Bulk} = \frac{\int \rho u H dA}{\int \rho u dA} \qquad (5.3.2\text{-}3)$$

where H_{Bulk} = Bulk gas enthalpy
ρ = gas density in external flow field
u = gas velocity in external flow field
H = total gas enthalpy
dA = cross-sectional area of external flow ingested

The quantity ρudA is the mass flow rate through the cross-sectional area of the external flow streamtube that enters the hole. Therefore, to obtain the bulk enthalpy, the area of integration is enlarged until the quantity ρudA equals the mass flow rate through the hole, $\dot{m}_{hole}$. For this analysis, the local external flow properties were assumed to vary only in the y-direction normal to the surface. The area of integration was assumed to be

$$A_{st} = C\sqrt{A_{hole}}\int_0^y dy \qquad (5.3.2\text{-}4)$$

where A_{st} = cross-sectional area of external flow streamtube
C = constant derived from CFD solutions
A_{hole} = area of breach hole
y = normal distance from the surface

The value C was set to 0.4 to better match the ingested mass flow rate predicted by a CFD solution for a 2-inch diameter hole in Panel 6 (see Sec. 5.3.2.2). Therefore, the ingested streamtube had a rectangular cross-

sectional shape with a fraction of the square-root of the hole area defining the transverse dimension. The vertical distance was defined by integrating through the flow field until the value $C\sqrt{A_{hole}}\int_0^y \rho u dy$ equaled the hole mass flow rate, $\dot{m}_{hole}$.

Applying these assumptions for the ingested cross-sectional area, accounting for the enthalpy difference across the boundary layer, and non-dimensionalizing the values by the boundary-layer edge values, the bulk enthalpy relation used in the engineering analyses was obtained.

$$H_{Bulk} = \frac{\int_0^{y/y_e} \frac{\rho}{\rho_e}\frac{u}{u_e}\frac{(H - H_{wall})}{(H_e - H_{wall})} d\left(\frac{y}{y_e}\right)}{\int_0^{y/y_e} \frac{\rho}{\rho_e}\frac{u}{u_e} d\left(\frac{y}{y_e}\right)} + H_{wall} \qquad (5.3.2\text{-}5)$$

where the subscript *e* corresponds to the boundary-layer edge value and H_{wall} is the gas enthalpy at the wall temperature. As described in the next section, polynomial curve-fits for the quantities $\frac{\rho}{\rho_e}\frac{u}{u_e}$ and $\frac{\rho}{\rho_e}\frac{u}{u_e}\frac{(H - H_{wall})}{(H_e - H_{wall})}$ as a function of the non-dimensional distance, $\left(\frac{y}{y_e}\right)$, through the boundary layer were obtained from CFD solutions.

A FORTRAN computer code was used to solve for the breach hole gas mass flow rate, bulk enthalpy and bulk temperature using the relations above. The solution process included the following steps:

1) Compute the boundary-layer thickness and edge quantities as described in the next section.
2) Compute the bulk enthalpy and mass flux for the ingestion of the entire boundary layer and then compare the boundary-layer mass flux (denominator of Eqn. 5.3.2-5) to the hole flow rate (Eqn. 5.3.2-1). If the hole flow rate is greater than the boundary-layer mass flux, then it was assumed that more than the boundary layer was ingested into the hole. Outside of the boundary layer it was assumed that the gas properties are equal to the edge values. Increments of one-tenth of a boundary-layer thickness were used to find the vertical distance and therefore the external mass flux that best matched the flow rate through the hole.
3) If the hole-flow rate was less then the boundary-layer mass flux, then the vertical distance inside the boundary layer was varied by increments of one one-hundredth of a boundary-layer thickness to best match the flow rate through the hole.

5.3.2.2 Use of CFD Solutions

Two sets of CFD solutions were used to develop the engineering methods to estimate the ingested gas properties. The first set included two CFD solutions of the nominal undamaged Orbiter. These solutions were used to obtain curve-fits of flow field parameters just upstream of the assumed breach hole. The second set of CFD solutions were coupled external/internal flow field solutions for various size circular breach holes in the wing leading edge. These solutions were used to calibrate the engineering tool and to confirm its results.

5.3.2.3 External Flow Parameter Curve-fits

Two LAURA CFD solutions for the nominal Orbiter provided curve-fits for use in the breach hole gas ingestion engineering analysis. The CFD solutions for the following two flight conditions were chosen:

1) CFD Point 1: EI+404 secs.; Mach =24.9; Altitude = 243,000 ft; Angle-of-attack = 40 degs.; Dynamic pressure = 22.0 psf.
2) CFD Point 6: EI+921 secs.; Mach = 17.9; Altitude = 200,767 ft; Angle-of-attack = 40 degs.; Dynamic pressure = 83.5 psf.

For each of these 3-D flow field solutions, two points on the wing leading edge were selected – one on Panel 6 and one on Panel 8.

Panel	X (in)	Y (in)	Z (in)
6	1038	-193	284
8	1070	-211	294

At each of these points, predicted flow field properties were extracted from the CFD solutions as a function of the normal distance from the surface. Figure 5.3.2-2 presents the variation of gas temperature and enthalpy predicted by LAURA for the Panel 8 location at the CFD Point 1 flight condition. The boundary-layer thickness is 1.4 inches and was determined by selecting the first grid point from the wall where the total enthalpy value is approximately 99% of the free stream total enthalpy.

For use in the engineering analysis, curve fits of the quantities $\frac{\rho}{\rho_e}\frac{u}{u_e}$ and $\frac{\rho}{\rho_e}\frac{u}{u_e}\frac{(H-H_{wall})}{(H_e-H_{wall})}$ were defined using the extracted CFD values which were non-dimensionalized by the edge values. Figure 5.3.2-3 and Figure 5.3.2-4 present these curve-fits for the Panel 8 location. The extracted and curve-fit CFD values included both the CFD Point 1 and 6 data.

Since all of these values were non-dimensionalized by the boundary-layer edge values, relations also had to be developed to estimate the edge values as a function of nominal free stream parameters. Two values were needed – the boundary-layer thickness and the edge mass flux, $\rho_e u_e$. It was assumed that the boundary-layer thickness, δ, is a linear function of the square-root of the free stream Reynolds number, Re_L, based upon the length of the Orbiter (L=107.5 ft). Using the boundary-layer thickness values at the Panel 8 location from the two CFD solutions, the following relation was obtained.

$$\delta = \frac{1250}{\sqrt{\mathrm{Re}_L}} - 0.1617 \text{ (inches)} \qquad (5.3.2\text{-}6)$$

The edge mass flux , $\rho_e u_e$, was assumed to be a linear function of the free stream dynamic pressure, P_{dyn}, with the edge values for curve-fitting obtained from the two CFD solutions at the Panel 8 location.

$$\rho_e u_e = 1.0567E-03 P_{dyn} \text{ (slugs/ft}^2\text{-sec)} \qquad (5.3.2\text{-}7)$$

The relations and curve-fits presented are unique for the Panel 8 location. Additional relations of the same form were generated for the Panel 6 location.

5.3.2.4 Calibration of Engineering Tool

Several CFD solutions were generated for holes in the Orbiter wing leading edge. Four of these solutions described in Sec. 5.3.6.1.3 were used to calibrate and evaluate the engineering method for estimating the mass flow and energy flux of gas entering a leading edge breach hole. CFD solutions for 2, 4 and 6-inch diameter circular holes in Panel 6 and one for a 10-inch diameter hole in Panel 8 were reviewed and the predicted mass flow rate and energy flux flowing through the plane of the hole were computed. All of these values are for the same flight condition – CFD Point 1.

Case	Mass Flow Rate (lbm/sec)	Energy Flux (Btu/sec)
Panel 6: 2-in Dia. Hole	0.00152	9.4
Panel 6: 4-in Dia. Hole	0.00562	43.6
Panel 6: 6-in Dia. Hole	0.01247	110.9
Panel 8: 10-in Dia. Hole	0.04839	498.0

5.3.2.5 Properties of Flow into Breach Holes

The engineering method was exercised for four hole sizes in leading edge Panel 6 – 1, 2, 4, and 6 inches in diameter. Figure 5.3.2-5 presents the predicted fraction of the boundary layer that is ingested into the hole. Both the 4 and 6-inch diameter holes result in the ingestion of the entire boundary layer at later times in the trajectory. Figure 5.3.2-6 and Figure 5.3.2-7 present the predicted bulk gas temperature and enthalpy of the ingested gas. The gas temperatures are mostly between 9,000 and 10,000 R. Figure 5.3.2-8 and Figure 5.3.2-9 present the predicted mass flow rate and energy flux and compare the results to the values obtained from the CFD solutions for the holes in Panel 6. For the smaller holes – 2 and 4-inch diameter – the engineering method provides a very good estimate of the ingested flow rate and energy flux. However, as the hole is increased in size to the 6-inch diameter, the engineering methods tend to under predict the values.

Breach holes in Panel 8 were also analyzed with the engineering method. In this case, the external pressure used for the computation (C_p=1.46) was for a location slightly different from the location where the curve-fits were obtained. Figure 5.3.2-10 and Figure 5.3.2-11 present the predicted mass flux and energy flux into the holes. The values for the CFD solution with a 10-inch diameter hole are also plotted and indicate that the engineering method is under predicting the energy ingested into large breach holes.

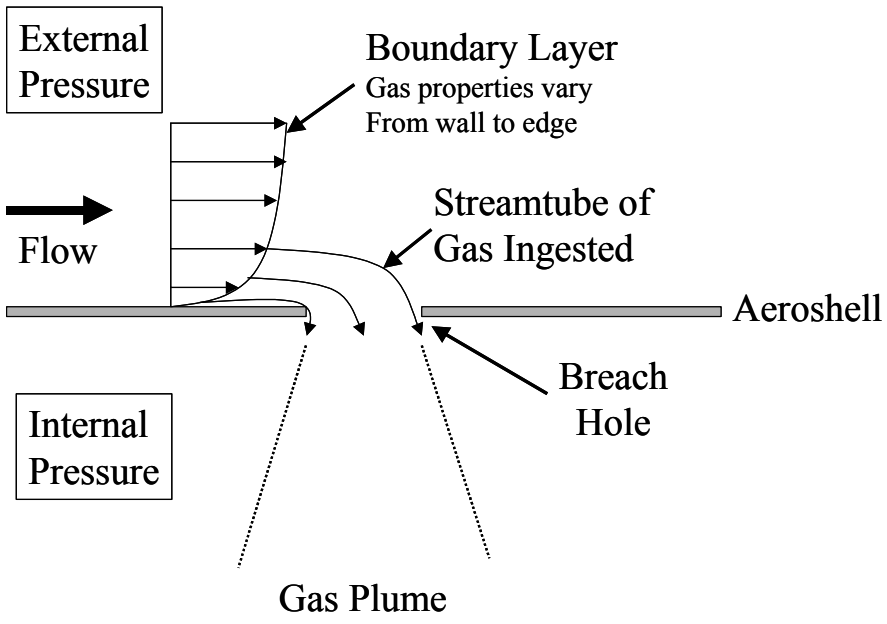

Figure 5.3.2-1 Sketch of Breach Flow Field

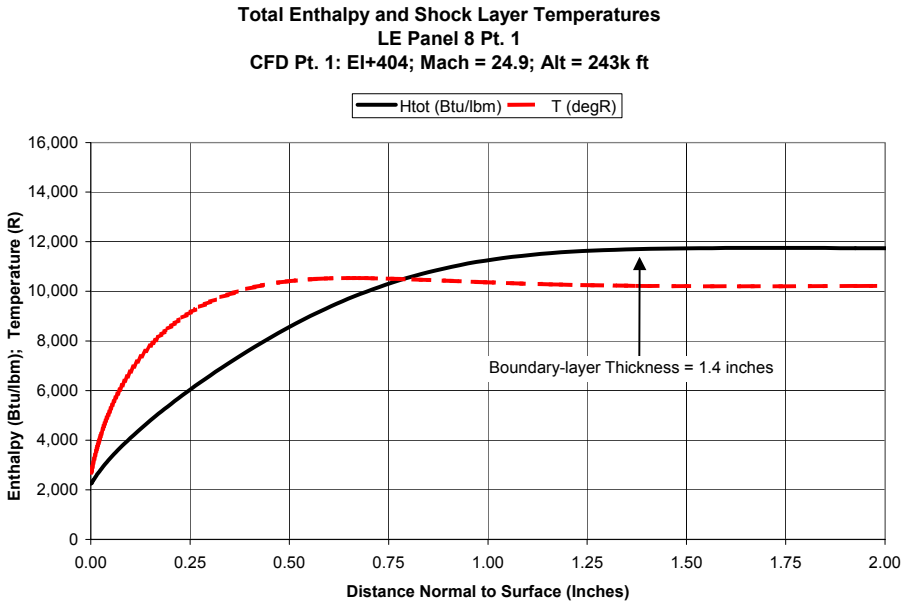

Figure 5.3.2-2 Total Enthalpy and Temperature Profiles at LE Panel 8 for Mach 24.9.

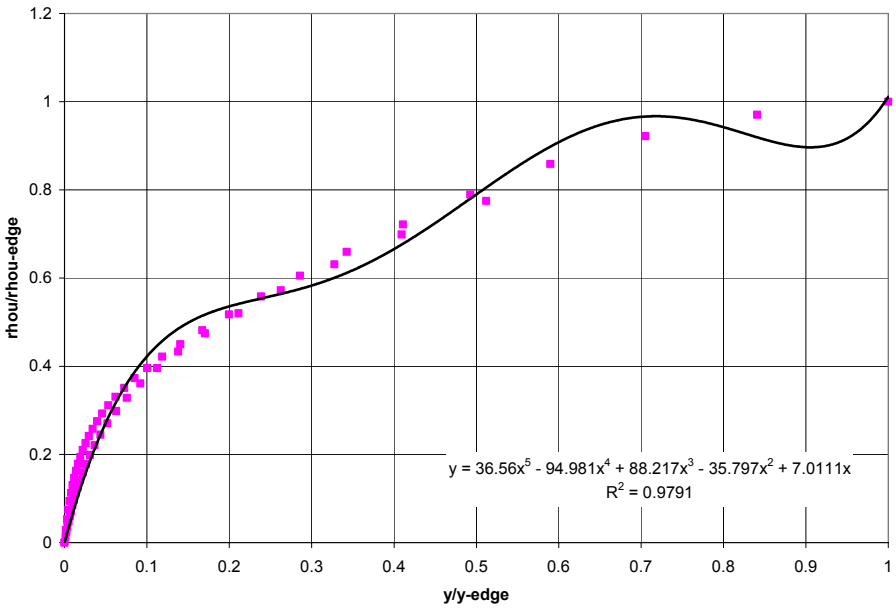

Figure 5.3.2-3 Boundary-layer Mass Flux, $\frac{\rho}{\rho_e}\frac{u}{u_e}$, Curve-fit for LE Panel 8.

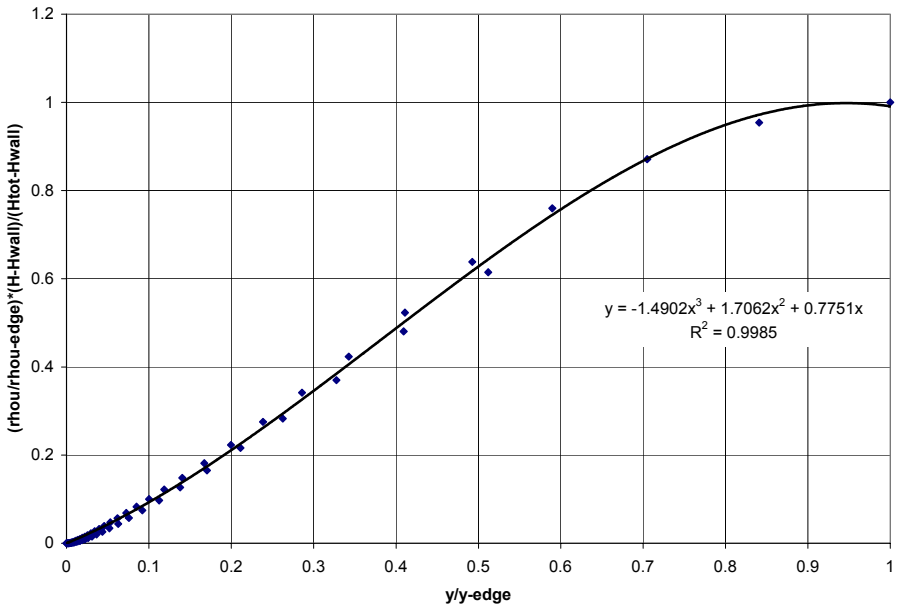

Figure 5.3.2-4 Boundary-layer Energy, $\frac{\rho}{\rho_e}\frac{u}{u_e}\frac{(H-H_{wall})}{(H_e-H_{wall})}$, Curve-fit for LE Panel 8

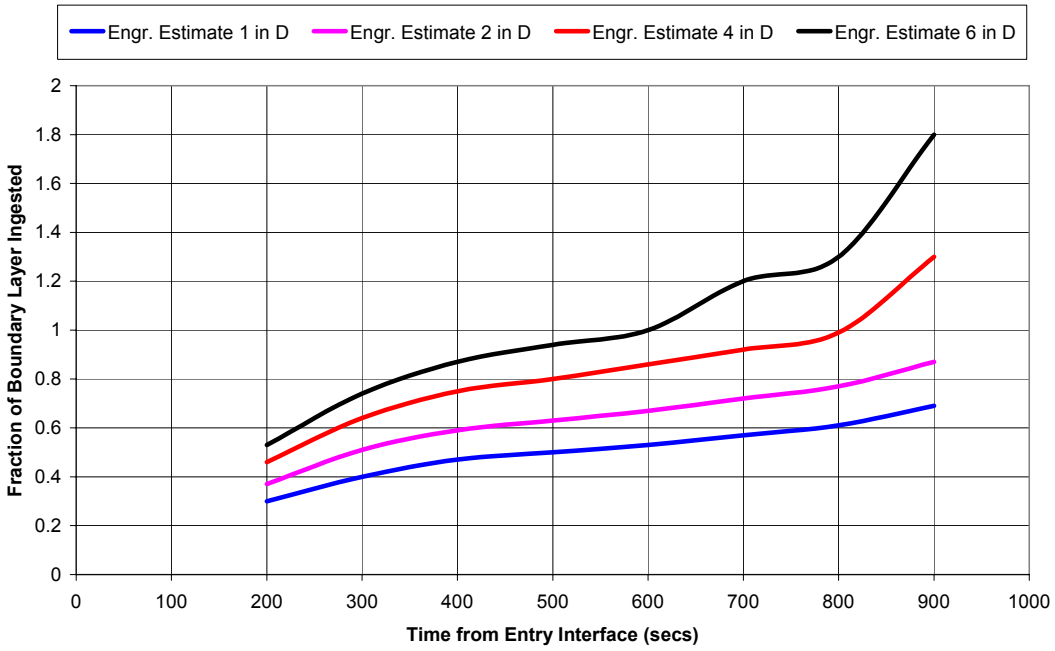

Figure 5.3.2-5 Predicted Fraction of Boundary-layer Thickness of Gas Ingested into Hole in LE Panel 6.

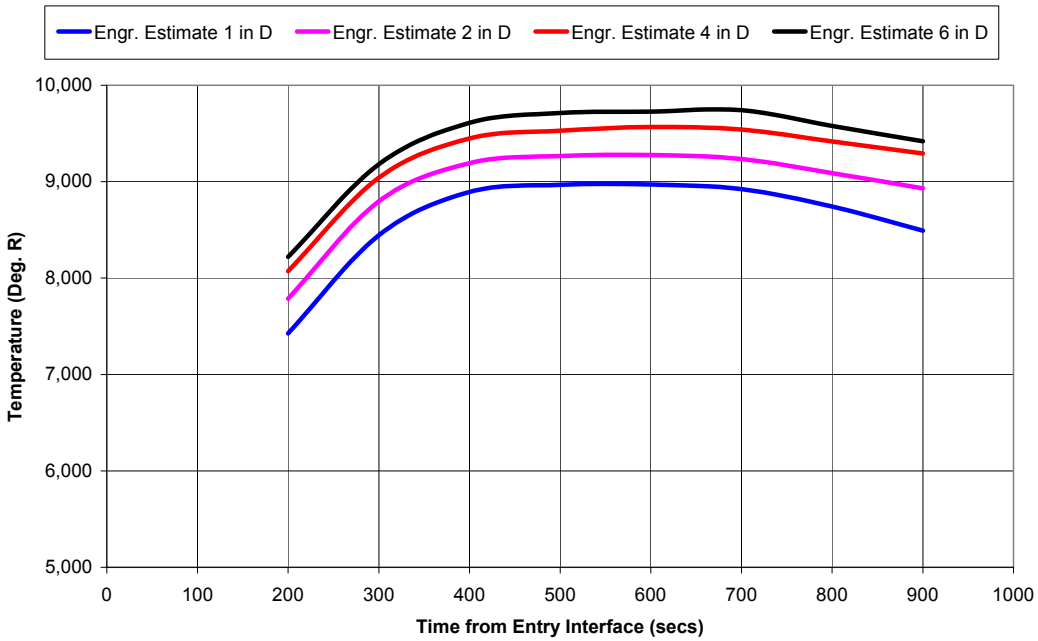

Figure 5.3.2-6 Predicted Bulk Temperature of Gas Ingested into Hole in LE Panel 6.

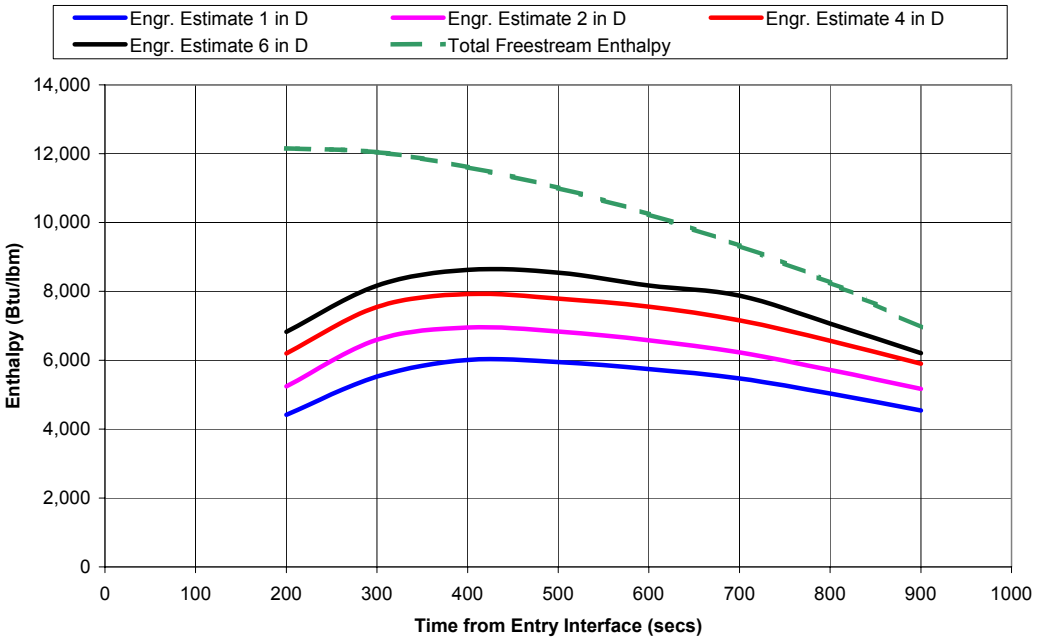

Figure 5.3.2-7 Predicted Bulk Enthalpy of Gas Ingested into Hole in LE Panel 6.

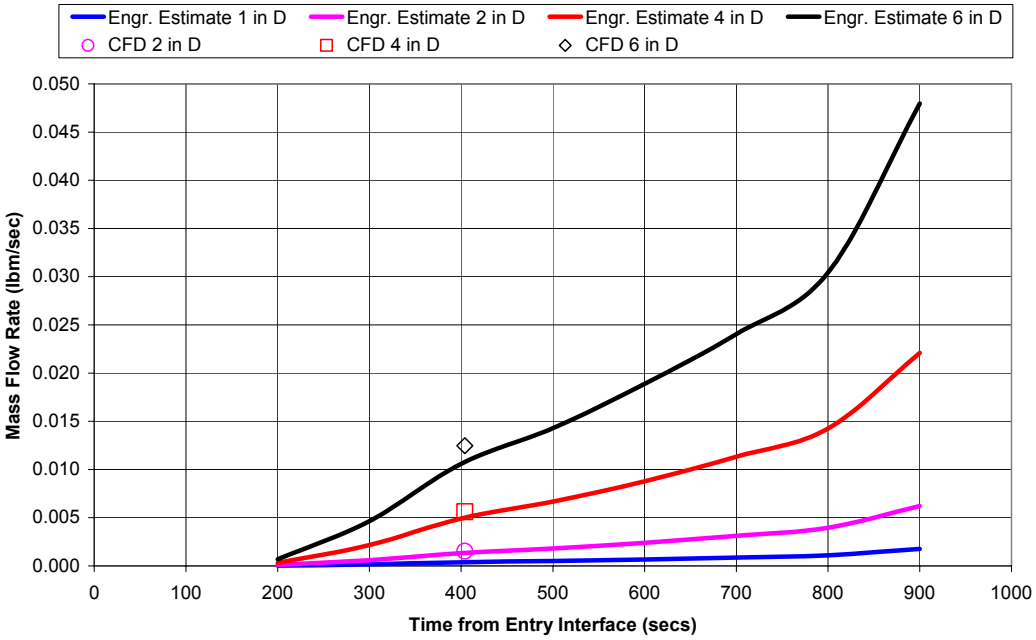

Figure 5.3.2-8 Predicted Mass Flow Rate of Gas into Hole in LE Panel 6.

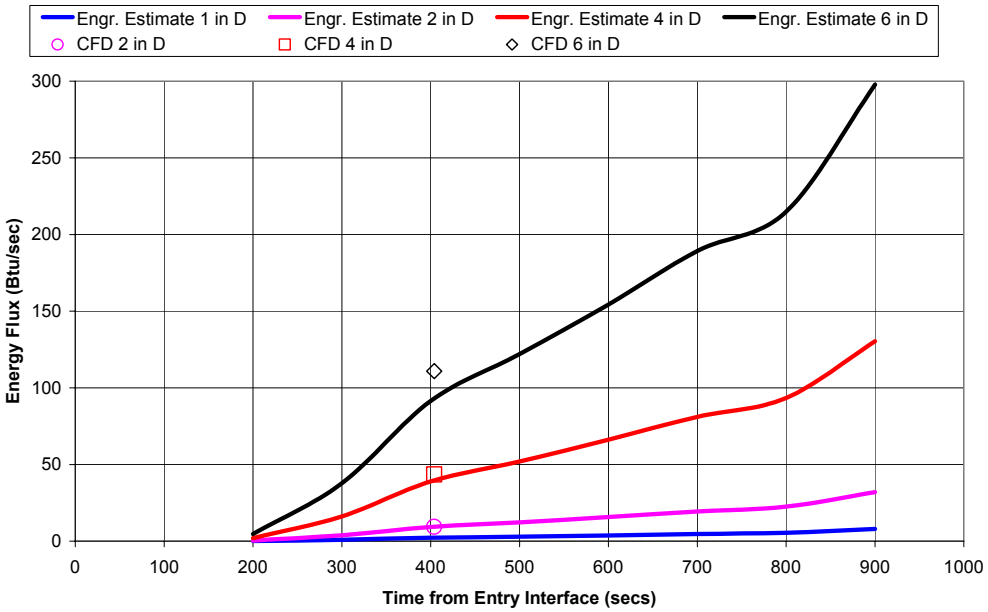

Figure 5.3.2-9 Predicted Mass Flow Rate of Gas into Hole in LE Panel 6.

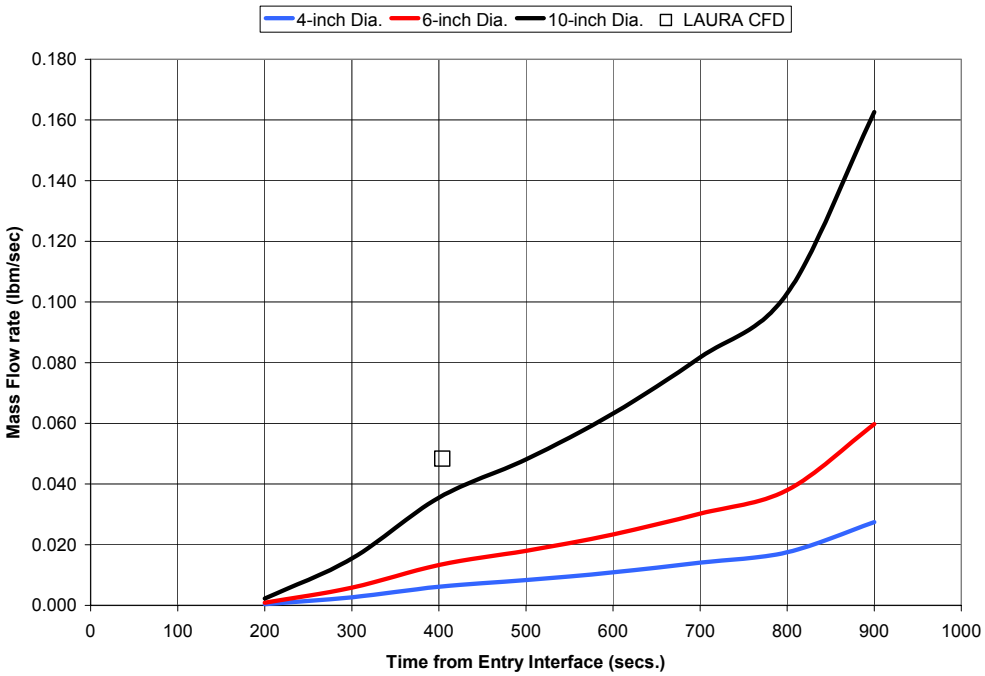

Figure 5.3.2-10 Predicted Mass Flow Rate of Gas into Holes in LE Panel 8.

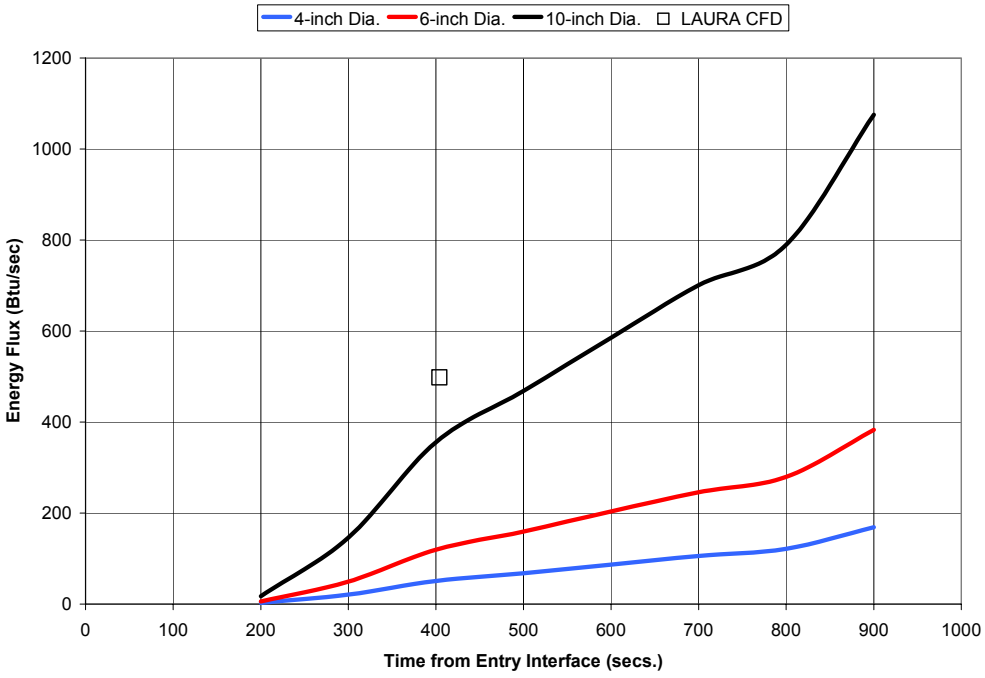

Figure 5.3.2-11 Predicted Energy Flux of Gas into Holes in LE Panel 8.

5.3.3 Plume Model Development

Engineering models of internal jet impingement heating are necessary to assess localized heating in the primary impingement zone for burn through and structural failure analysis. Heating distributions are produced based on:

1) Assumed hole diameter and shape
2) Assumed hole location
3) Freestream conditions
4) Internal pressure
5) Internal geometry
6) External boundary layer properties

The results must be in a form suitable for thermal analysis, typically closed form functions or tables that may be linearly interpolated. Computational results are very expensive to obtain and are only available at discreet points in the trajectory. Engineering models, though, if properly setup, allow for parametric studies in order to match flight data in terms of hole diameter, location, and jet direction. Such studies will be presented in the thermal analysis portion of the report. The following two sections describe the development of an engineering model to predict internal plume impingement values for circular holes, while the model developed to assess missing T-seal segments in described in Section 5.3.3.6.

5.3.3.1 Basic internal plume physics and impingement issues

The nature and structure of a free jet issuing into the Orbiter interior through a breach in the thermal protection system is dictated by the total pressure difference across the surface, the hole diameter, boundary layer properties, and local boundary layer edge Mach number. For small orifices, on the order of one inch, the jet may be assumed to enter normal to the internal surface with a sonic condition. For such a case the governing parameter that dictates shock structure and mixing of the jet is the ratio of external driving pressure to internal pressure. Bulk fluid properties are a function of the percentage of external boundary layer drawn off into the hole. For very small hole, the properties will be near wall conditions, whereas larger holes can produce internal flows with enthalpy levels approaching free stream total values. As the high-speed gas enters the cavity, it immediately starts mixing with the ambient fluid at the boundaries of the jet. This mixing zone gets larger as the jet progresses, until finally the core portion of the jet has been consumed and the jet has reached a fully developed condition. Depending on the conditions driving the jet, this may not occur until ten's of diameters downstream. In the highly under-expanded state, the jet shock structure is dominated by a normal shock downstream of the initial expansion called the Mach disk. Immediately downstream of the Mach disk the flow is subsonic, though it may re-expand to supersonic flow. Figure 5.3.3-1 displays variations in free-jet structure and with varying pressure ratios. Figure 5.3.3-2 shows the impact of pressure ratios in the range expected for Orbiter penetrations on computed flow structure.

Larger hole diameters display significant departure from this relatively simple structure as larger percentages of the highly energetic boundary layer are ingested and increased transverse momentum bends the jet over in the direction of the boundary layer edge flow. This effect was discovered with the first fully coupled, internal/exterior flow solution performed for a two-inch breach into RCC panel 6. Complete results are presented in Section 5.3.6.1.4. Larger diameter penetrations tend to carry highly supersonic, high temperature gases directly to the interior surfaces and produce highly complex shock/impingement structures that can significantly impact local heat transfer rates.

Two dimensional jet structure differs from that of the axisymmetric jet, primarily due to conservation constraints. The three-dimensional source flow falls off as $(1/r^2)$ versus $(1/r\ lnr)$. The effect of this can be seen in Figure 5.3.3-3 where the two-dimensional flow structure is quite different and maintains the first shock cell considerably further downstream.

Also, of note in predicting internal jet flow fields is the importance of modeling chemistry correctly. Jet structure and spreading are strongly a function of the ratio of specific heats of the gas. Additional considerations of chemistry are the energies absorbed in chemical reactions and the net energy transfer to the surface. This study will focus equilibrium chemistry options in internal flow computations in order to provide the most reasonable predictions of plume heating with sufficient conservatism.

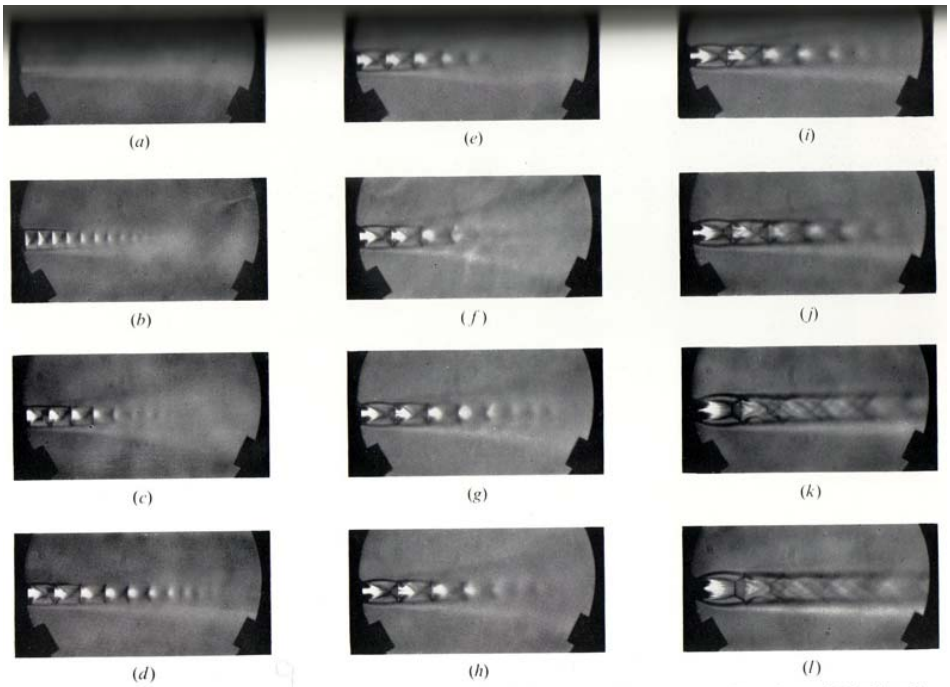

FIGURE 8. Free jet from convergent nozzle photographed with double-pass schlieren system. (a) $p_1/p_\infty = 1{\cdot}00$ (subsonic). (b) $p_1/p_\infty = 1{\cdot}15$. (c) $p_1/p_\infty = 1{\cdot}42$. (d) $p_1/p_\infty = 1{\cdot}59$. (e) $p_1/p_\infty = 1{\cdot}71$. (f) $p_1/p_\infty = 1{\cdot}84$. (g) $p_1/p_\infty = 2{\cdot}00$. (h) $p_1/p_\infty = 2{\cdot}13$. (i) $p_1/p_\infty = 2{\cdot}31$. (j) $p_1/p_\infty = 2{\cdot}59$. (k) $p_1/p_\infty = 3{\cdot}57$. (l) $p_1/p_\infty = 4{\cdot}09$.

Figure 5.3.3-1 Free jet mixing and structure with pressure ratio

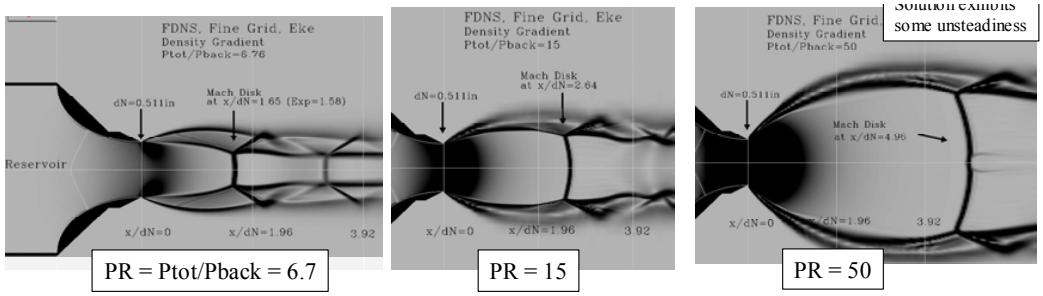

Figure 5.3.3-2 Computed pressure ratio effect on near orifice flow

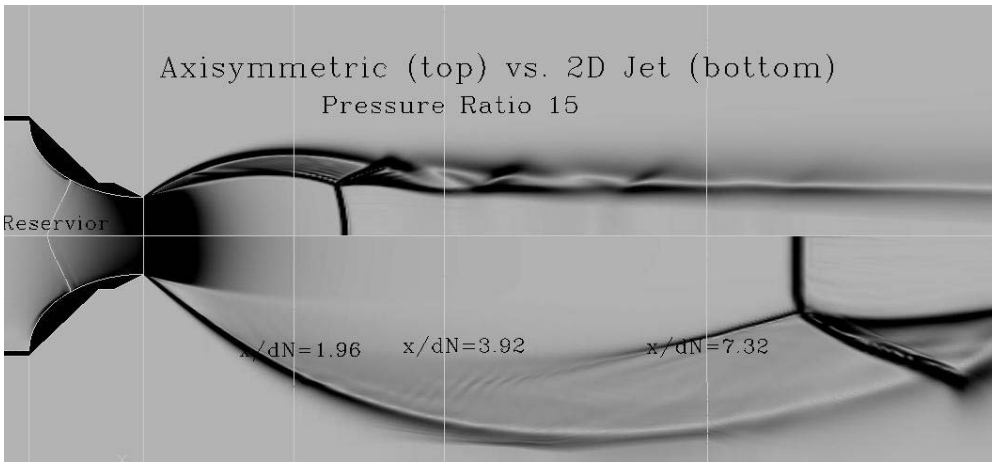

Figure 5.3.3-3 Axisymmetric vs. 2D Jet structure

5.3.3.2 1-D Axisymmetric Equilibrium Plume Heating Model

5.3.3.2.1 History

The plume model used to support the STS-107 accident investigation is a version of that originally developed to support Space Shuttle mission risk definition due to micrometeoroid and orbital debris hazards. The study objective, prompting the original model development, was to define levels of on-orbit impact damage that subsequently results in catastrophic loss of vehicle during entry. Under these conditions, on-orbit penetrations of the OML would result in ingestion of high enthalpy gas during reentry due to the pressure differential across the penetration. Heating environments due to this internal flow were required for thermal and structural analysis of the affected structure. As a result, a simplified internal jet flow model was developed to conservatively estimate time-dependent internal heating environments required for this study. During the course of this work, the analysis methodology and results were presented in 1997 to the National Research Council Review on Shuttle Meteoroid Risk Management.

For the STS-107 investigation, this model was employed for scenario feasibility and screening assessments.

5.3.3.2.2 Development

To provide the required time-dependent environments throughout an entry trajectory, it was desirable to develop a simplified method using closed form expressions to obtain characteristics of such internal flows, primarily impingement heating. The development of this method is described in this section.

5.3.3.2.3 Assumptions/limitations

- Due to the nature of the on-orbit impact hazard, the penetrations analyzed were limited to small holes of 1 inch diameter or less
- As a result, internal flow was modeled as an axisymmetric free jet issuing from a sonic orifice normal to the vehicle OML at the penetration location.
- Jet decay characteristics are based on empirical relations for properly expanded jets
- To maintain a conservative approach, internal heating levels were based on normal impingement angles for surfaces within the jet flow field

5.3.3.2.4 Theoretical Description of the Jet and Impingement Regions

To analyze the impinging jet, four distinct regions of flow are considered. First, a zone of flow establishment extends from the orifice to the apex of the potential core along the centerline of the jet. Within this core the velocity of the jet remains constant. It is surrounded by a region in which mixing occurs between the jet and ambient gas. In the second region, established flow in the direction of the jet beyond the apex of the potential core is characterized by a dissipation of the centerline jet velocity and temperature, and by a spreading of the

jet in the transverse direction. At this point, usually several nozzle diameters downstream from the orifice, the mixing region has spread inward enough to reach the centerline. Beyond this point the mixing region continues to spread as the velocity decays at a rate required to conserve axial momentum. These first two flow regions are shown in Figure 5.3.3-4. A third region is characterized by deflection of the jet from the axial direction at the impingement surface. At this point, local flow conditions on the jet centerline, including the effects of an impingement shock if present, are used to compute a stagnation heating level to a desired surface geometry, either a flat plate or cylinder in crossflow. In the final region of the jet the redirected flow increases in thickness as the boundary layer builds up along the solid impinged surface. Convective heating continues on these surfaces although at levels that progressively drop from the maximum achieved at the stagnation point at the jet centerline.

5.3.3.2.5 Analysis Methodology

Properties of the external flow ingested through the damaged OML are based on a bulk gas enthalpy defined by the method described in Section 5.3.2.1 and the local surface pressure at the hole. With the internal pressure within the RCC cavity controlled by the local pressure at the passive vent located on the upper surface of the wing, a small penetration in the RCC is expected to act as a choked sonic orifice. Flow at the exit of the orifice is based on the 1-D nozzle equation:

$$\begin{aligned} mdot &= \rho_j U_j A_{hole} C_D \\ &= p_s (1+((\gamma-1)/2)M_j^2)^{-(1+\gamma)/2(\gamma-1)} M_j (\gamma g/(zRT))^{0.5} A_{hole} C_D \end{aligned}$$

where $M_j = 1$ when $P_s/P_a \geq ((1+\gamma)/2)^{\gamma/(\gamma-1)}$, and P_a is the internal pressure within the RCC cavity.

Isentropically expanding this sonic flow to the required internal pressure produces an initial supersonic condition in the flow that is accompanied by a strong normal shock, or Mach disc, in highly underexpanded flows. A calculation procedure conserving mass, momentum and energy fluxes across a normal shock are used to account for the total pressure loss in the jet core due to this shock. High temperature equilibrium air properties are used in all flow property calculations.

A continued expansion to the established internal cavity pressure defines the conditions within the jet core downstream of the Mach disc. Although experimental values of potential core length reported in the literature vary from 4.7 to 7.7, a value of 6.5 orifice diameters was used in this analysis, close to the median reported in the literature. Beyond that point, decaying values of centerline velocity and temperature are given by:

$$U_{cl}/U_c = 6.5 / (X / D_{orifice})$$

$$T_{cl} = T_{ambient} + 0.722 (T_c - T_{ambient}) U_{cl}/U_c .$$

As illustrated in Figure 5.3.3-5, flow conditions approaching the impingement point represent the upstream properties for a normal shock solution, if required, to provide local and total flow properties downstream of the impingement shock. Based on the experimental work in the literature, post-shock properties are used in the calculation of laminar stagnation heat flux:

$$q_{fp} = 0.763\, g\, Pr^{-0.6} (\rho_s \mu_s U_{cl} / r_5)^{0.5} (\rho_w \mu_w / \rho_s \mu_s)^{0.1} (H_s - H_w)$$

$$q_{cyl} = 0.763\, g\, 2^{-0.5} (Pr)^{-0.6} (\rho_s \mu_s)^{0.4} (\rho_w \mu_w)^{0.1} (du/dx)^{0.5} (H_s - H_w)$$

$$\text{where } du/dx = R_{cyl}^{-1} [2 (p_s - p_j) / \rho_s]^{0.5}$$

The stagnation point velocity gradient for the flat plate is experimentally derived as reported in the literature, while that for the cylinder is based on modified Newtonian flow.

5.3.3.2.6 Results Summary

Early in the investigation, impingement heating levels were computed parametrically for various hole sizes on RCC panel 9, several impingement distances and two surface geometries, flat plate and cylinder. The results

of these calculations are shown in Figure 5.3.3-6. Stagnation heating values for ingested flow through large diameter holes in RCC panel 8 were also provided later in the investigation in support of the Working Scenario. Table 5.3.7.2-1 lists these heating values.

As described in Section 5.3.7, these values were used to create internal heating distributions within the RCC cavity.

5.3.3.2.7 Validation/Verfication

To gauge the usefulness of this simplified model, comparisons were made with available CFD solutions discussed in Section 5.3.3.4. Figure 5.3.3-7 shows the results of this comparison and indicates the simplified model off-axis heating profiles generally envelope CFD results and have much smaller rate of decay in radial direction.

Nomenclature

A	Hole area
C_D	Discharge coefficient
D	Hole diameter
H	Enthalpy
M	Mach no.
P	Pressure
Pr	Prandtl no.
q	Heat flux
r_5	Radial distance from jet centerline at $U=U_{cl}/2$
R	Gas constant, Geometric radius
T	Temperature
U	Jet axial velocity
z	Gas compressibility
γ	Ratio of specific heats
ρ	Gas density
μ	Gas viscosity

Subscripts

c	Core
cl	Center line
cyl	Cylinder
fp	Flat plate
j	jet
s	stagnation
w	wall

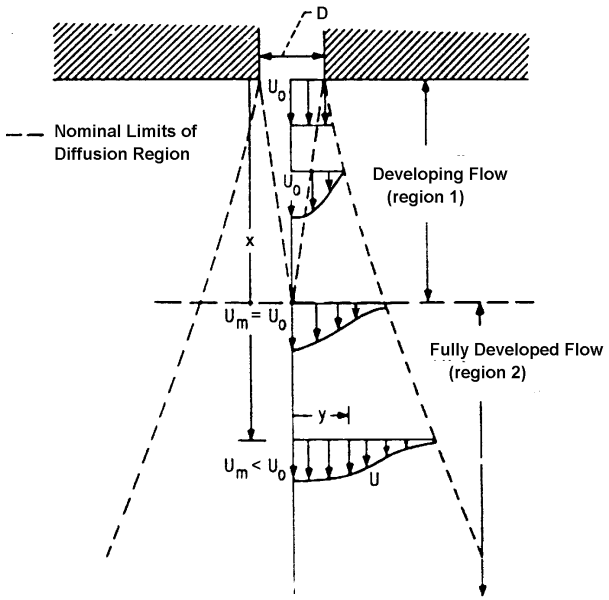

Figure 5.3.3-4 Flow Regions in Free Jet

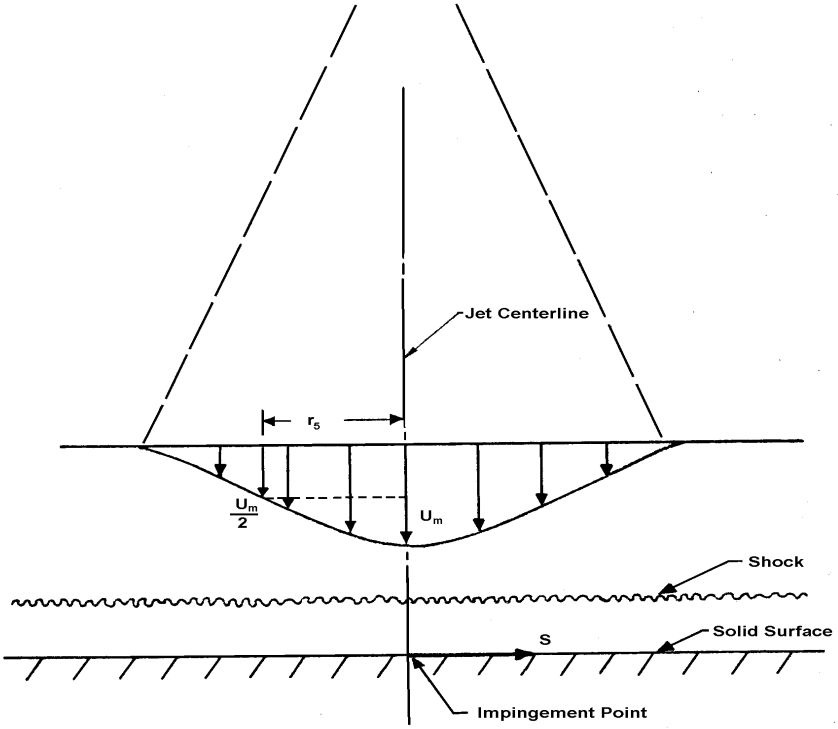

Figure 5.3.3-5 Jet Impingement Within Developed Flow Region

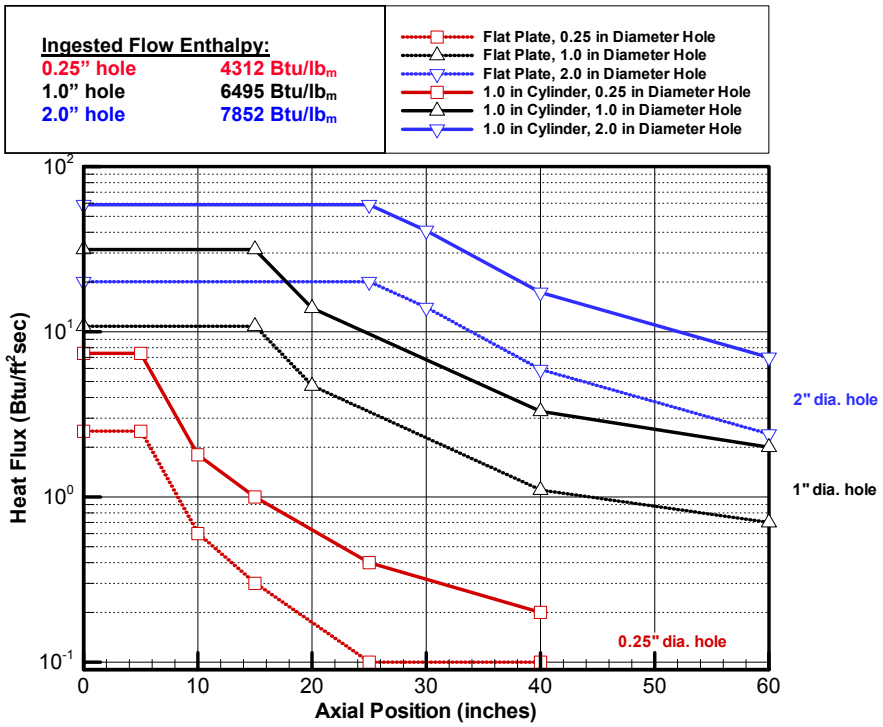

Figure 5.3.3-6 Simplified Plume Model Heating Results at 491 seconds After EI

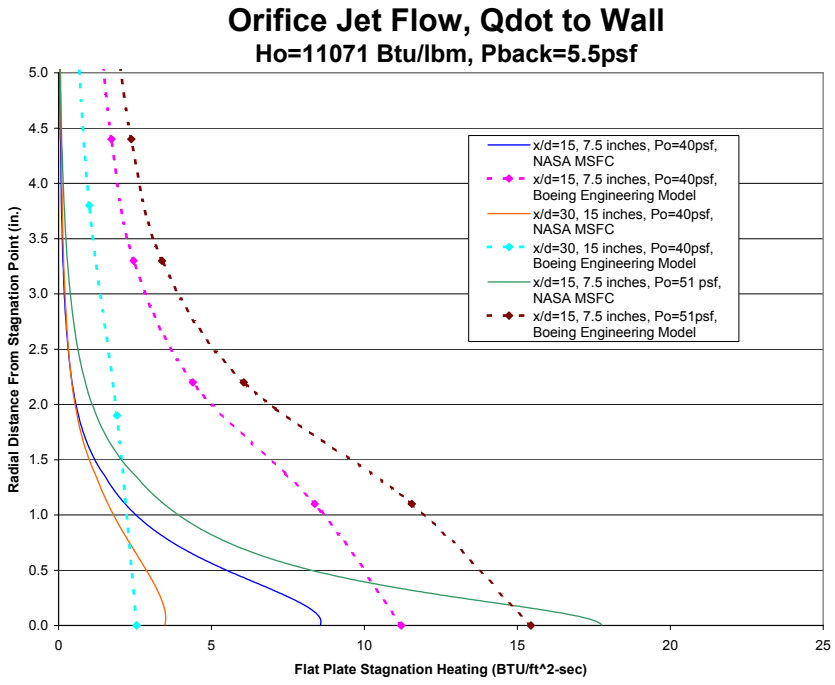

Figure 5.3.3-7 Comparison of Simplified Plume Model Results With NASA MSFC CFD Results

5.3.3.3 Engineering Corrections to Plume Model to Produce Heating Histories

The methodology of 5.3.3.2 allows the computation of stagnation heating to a flat plate, or cylinder, located along the axis of the jet, for fixed total conditions and a specified hole size. Early in the investigation process, the thermal community wanted a set of relations that would allow the assessment of heating distributions to flat plates and cylinders at arbitrary orientations to the jet orifice. The following analytical corrections allow the use of the data from Figure 5.3.3-6 for the assessment of burn-through times and hole sizes required to burn through in a specified time.

5.3.3.3.1 Radial coordinate correction

Axis values for stagnation heating are corrected for radial distance variation based on measured turbulent jet impingement heating characteristics with the distance to 50% of centerline velocity, r_5, as the similarity variable. r_5 is initially equal to the orifice exit radius, r_e, throughout the length of the undisturbed core and then slowly grows to reflect the entrainment and mixing with ambient air in the internal volume. Values from Table 5.3.3.3-1 are linearly interpolated to arrive at the ratio of local heating to centerline heating as a function of distance downstream, x.

r/r_5	$qdot/(qdot)_0$
0	1
1	0.748
2	0.392
3	0.219
4	0.154
5	0.119
6	0.1
7	0.0808
8	0.0615
9	0.0423

Table 5.3.3.3-1 Radial Jet Heating Correction

$$r_5 = r_e \qquad \text{for } x \le 7.0 r_e$$

$$r_5 = r_e + x \tan\left(\frac{\pi}{30}\right) \qquad \text{for } x > 7.0 r_e$$

5.3.3.3.2 Trajectory condition correction

Jet impingement heating values are directly dependent on the effective reservoir conditions driving the development of the plume. Figure 5.3.3-6 reflects the impingement heating values for 491 seconds from entry interface. In order to complete a thermal analysis, complete time histories of heating values must be computed. In order to do so, it is assumed that the internal heating scales with freestream dynamic pressure and the square of freestream velocity. This is equivalent to fixing the local Stanton number and scaling with mass flow through the hole (dynamic pressure) and enthalpy (velocity squared). The necessary equation is

$$\dot{q}(x,r,t,d_{hole}) = \dot{q}(x,0,491\text{sec},d_{hole}) \times \frac{\bar{q}(t)}{\bar{q}(491)} \times \frac{V_\infty{}^2(t)}{V^2{}_\infty(491)} \times \frac{\dot{q}(r)}{\dot{q}(r=0)}$$

5.3.3.3.3 Flat plate and cylinder attitude corrections

It is highly unlikely, given the geometry involved, that the jet will strike the impinged surface at a 90-degree angle. Therefore, corrections to the heating are required in order to reflect the known relationship between pressure and heating for more grazing angles. Using Newtonian theory for local pressures, the heating may be corrected by

$$q(x,r,t,d_{hole},\alpha) = q(x,r,t,d_{hole}) * \sin(\alpha)$$

For wire burn-through analysis, this equation takes the form of

$$q(x,r,t,d_{hole},\Lambda) = q(x,r,t,d_{hole}) * \cos(\Lambda)$$

where Λ is the sweep angle of the wire to the jet axis and is the complement to α, the local angle of attack.

5.3.3.3.4 Hole diameter effects

Holes greater than the two-inch diameter originally simulated can now be assessed for thermal effects through application of curve fit results for the 0.25, 1.0, and 2.0 inch holes. Notice that the exponent is not 2.0, which would be the case for area correction only. The larger exponent results from larger holes pulling off larger and larger portions of the boundary layer and much closer to the free stream total enthalpy.

$$q_{d_{hole}>2.0"} = q_{d_{hole}=2.0"} \times \left(\frac{d_{hole}}{2.0"}\right)^{2.6}$$

5.3.3.4 CFD Supporting the 1-D Axisymmetric Plume Model

CFD analysis was used to verify the Plume Model's (section 5.3.3.2.1) predicted heat transfer. The CFD tools were used to estimate axisymmetric plume impingement heating rates to a cold wall perpendicular to the plume axis. To facilitate the quick development of the Plume Model, the CFD analyses were set up based on past experience for what was required to produce accurate estimates of heat transfer. The CFD codes were not specifically benchmarked for conditions at which they were run. However, two CFD codes were run independently to develop confidence in the results.

5.3.3.4.1 General Boundary Conditions

The Plume Model support CFD analysis was done at conditions derived from the External CFD trajectory point #1, or EI +404 sec. These plume analyses assumed a reservoir condition which decoupled the plume flow from the external flow. Specifics of the boundary conditions for each case are given in the results section. Different chemistry models: frozen, finite rate and chemical equilibrium, were applied as needed. Two sets of plume CFD analyses were performed. The first was for a ½ inch orifice impinging on a flat plate 7.5 and 15 inches downstream from the orifice. The second set was for a six-inch orifice impinging on a plate 30 and 60 inches downstream. In all cases the downstream wall temperature was held at 540° R and was non-catalytic.

5.3.3.4.2 Laminar Flow

A key question about the plumes was whether the flow laminar or turbulent. This was important for two reasons. The first is that the heating rate of a turbulent plume would be higher than of a laminar plume. The second is that turbulent plumes are self-similar. That is, a solution for a plume from a small orifice, with the proper scaling, could be used to assess plume heating for other size orifices.

Mr. W. Dahm, NASA/MSFC, re-produced the Figure 5.3.3-8 from the literature. Although this chart maps plume characteristics for large pressure ratios (P_{total}/P_{back}) it was still useful for the relatively low pressure ratio plume calculations performed to support the Plume Model. The mapping of the plume character is done with Re_L, a Reynolds number based on the location of the plume Mach disk. It can be approximated by the orifice Reynolds number multiplied by the square root of the inverse of the total to static pressure ratio (equation shown in Figure 5.3.3-8).

The CFD plume heating calculations had orifice Reynolds numbers between 100 and 700 (Re_L between approximately 50 and 250) and pressure ratios of 5 to 15 and fell in the lower left had side of the graph. Reviewing Figure 5.3.3-9 the first observation is that for Re_L of 100 to 1000 the plume flow is laminar. The second observation is that the region of interest for the wing penetration was outside those regions in which the plumes would be self-similar. Two conclusions were made. One, the CFD analyses would be run laminar, and two, because the combinations of orifice Re and pressure ratio of interest were outside the regions of self similarity, the CFD results for one orifice size should not be scaled to other orifice sizes.

The three following calculations of a free jet (non-impinging) demonstrate the significant differences in plume structure due to different Re_L. The same total conditions were run for three different orifice sizes to assess the mixing characteristics of the resultant plumes. The orifices sizes were one-half, one and two inches

corresponding to Re_L of approximately 47, 86 and 178, respectively. As can be seen from the Mach number contours in Figure 5.3.3-9, the plume expanded to Mach 3.6 for the two-inch orifice, but only Mach 2.7 for the half-inch orifice. Additionally, the progression to fully developed flow took much longer (x=24") for the two-inch orifice than for the half-inch orifice (x=4").

5.3.3.4.3 Results

Two sets of plume heating rate calculations were performed. The first was done for a half-inch orifice with the freestream total conditions corresponding to a pressure coefficient of 1.5 at EI +404s. These conditions were, H_{total} =11071 Btu/lbm, P_{total} = 37 lbf/ft^2, T_{total}=10400 R. The back pressure was assumed to be 5.5 lbf/ft^2 resulting in a pressure ratio of 6.7.

Both NASA/MSFC and Sandia National Laboratory (SNL) personnel calculated heating rates for these conditions using the FDNS and the SACCARA codes, respectively.

This first set of heating calculations assumed frozen chemistry. The low density and rapid expansion of the gas from the orifice was the basis for this assumption. It was subsequently verified by a DSMC analysis at SNL, that few reactions occurred in these plumes. The gas was modeled as a single specie of average gas properties derived from the constituents of the disassociated gas at the total conditions. At these total conditions the equilibrium mole fractions of the constituents were N_2=0.2, N=0.55, O=0.25. The single specie molecular weight was 17.334 and the ratio of specific heats of was 1.59. Laminar flow was prescribed. Figure 5.3.3-10 shows a representative plume solution from FDNS.

Figure 5.3.3-11 shows the SACCARA and FDNS results for a subset of the cases run. For the half-inch orifice impinging on a plate 7.5 inches downstream the heating to the wall agreed within 20% between the two codes (comparing the solid blue line on the left with the solid red line on the right). Although the total conditions were slightly different, the conclusion drawn from this comparison was that the CFD codes were sufficiently accurate to provide verification for the Plume Model for a half-inch orifice.

The second set of CFD cases were run using the FDNS code. This set nominally modeled a six-inch hole in an RCC panel at EI +404s. The total conditions were based on average gas properties entering a six-inch hole in RCC panel 6 as calculated by a coupled external CFD solution (Section 5.3.6.1.3). Averaged properties of the flow entering the six-inch hole were used as total conditions. They were, H_{total} = 9004 Btu/lbm, P_{total} = 28 lbf/ft^2, T_{total} = 9796 R. At these conditions the equilibrium mole fractions were NO=0.0090, N=0.4151, O=0.2743, N_2=0.3097. The back pressure was set to 4.4 lbf/ft^2 based on the venting analysis (Section 5.3.5) for this size hole at this point in the trajectory. Frozen, finite rate and equilibrium chemistry models were run. The impinged plate was at 30 and 60 inches downstream from the orifice. Figure 5.3.3-12 shows a representative solution for these cases. Figure 5.3.3-13 shows the heating rates for the four calculations. Note that the equilibrium cases had significantly higher heating to the wall. This was a result of the full recombination of the species at the wall. Also note that the finite rate solution and frozen solution heating rates were essentially the same. The shape of the heating distribution indicates that the jet was not yet fully developed and possessed a large subsonic bubble on the axis at the impinged plate. Off axis peaks are the result of relatively high total pressure flow that has been processed through oblique shocks. Of particular interest is the comparison with engineering predictions under the same conditions. Here the model would predict that both the 30" and the 60" locations are still in the underdeveloped core region and hence have the same heating value - 30 Btu/ft^2sec. These results compare well with the peaks observed for both distances.

Nomenclature

x	axial station
d_N	Nozzle Diameter
H	Enthalpy
P	Pressure
Re	Reynolds Number
T	Temperature

Subscripts

L	Length to Mach Disk
total	total conditions

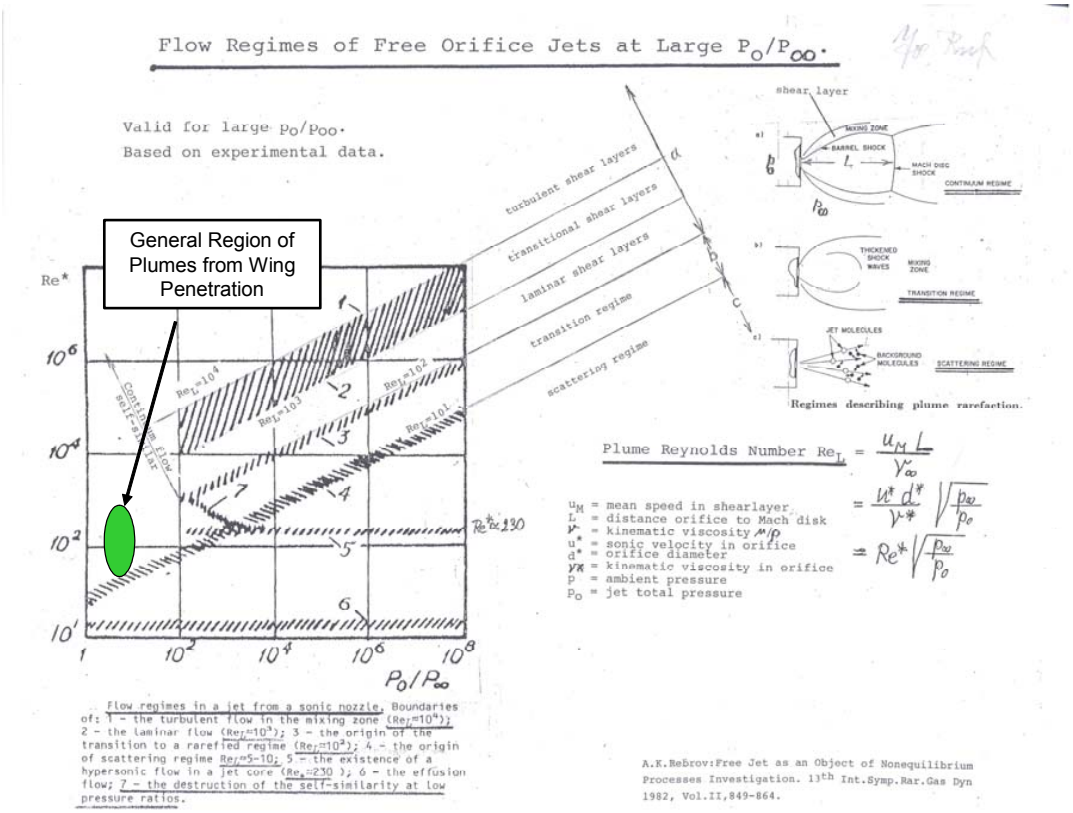

Figure 5.3.3-8 Flow Regimes of Free Jets from an Orifice.

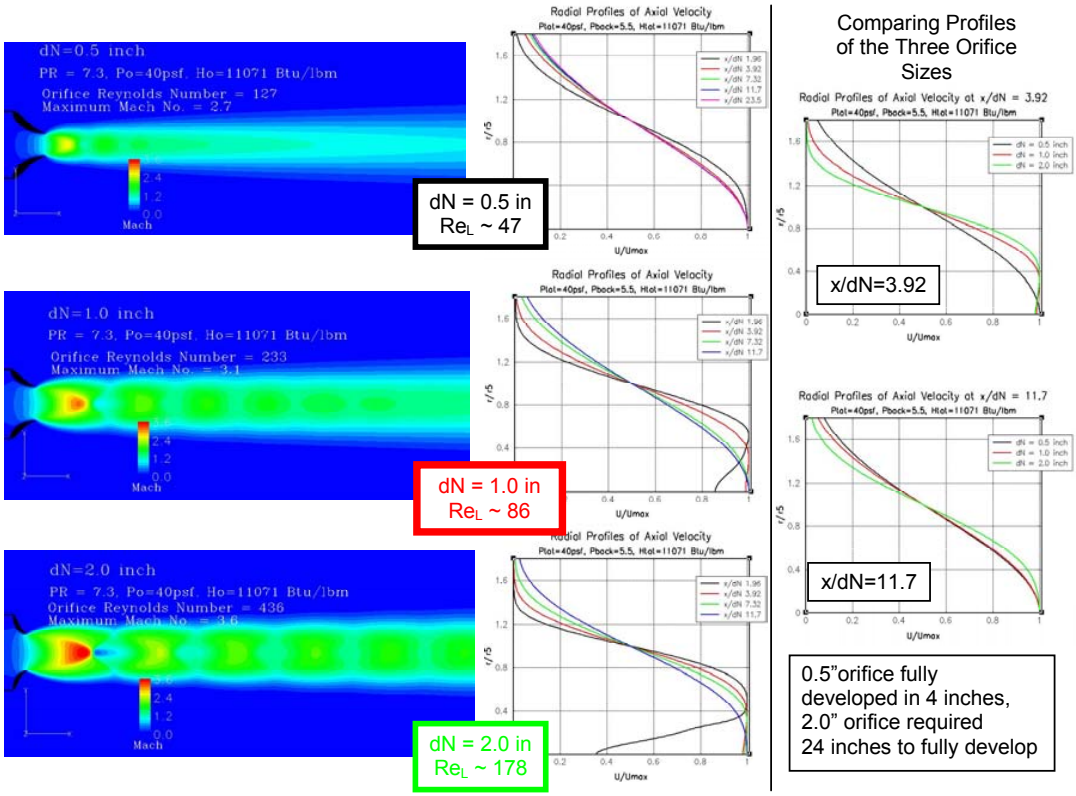

Figure 5.3.3-9 CFD Analysis of a Free Jet at Flight-like Total Conditions for Three Orifice Sizes.

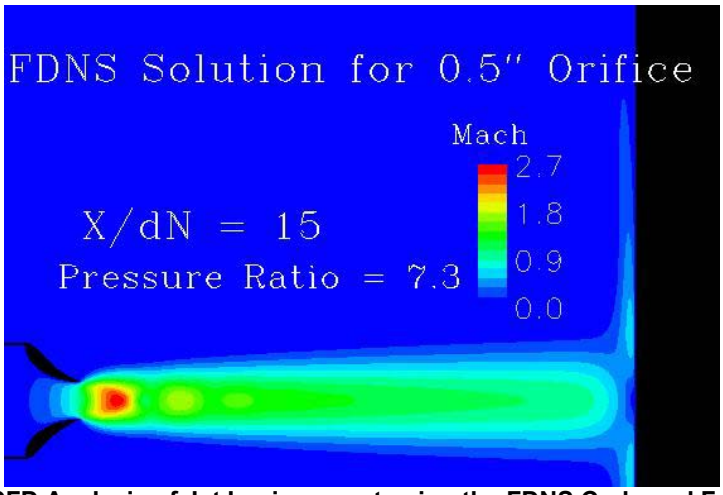

Figure 5.3.3-10 CFD Analysis of Jet Impingement using the FDNS Code and Frozen Chemistry.

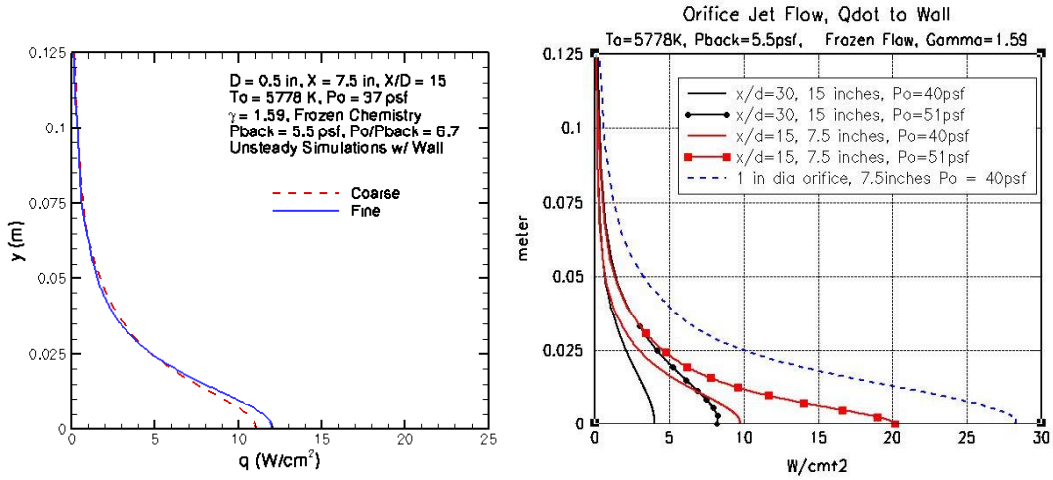

Figure 5.3.3-11 Heat Transfer for Half-Inch Orifice from SACCARA (left) and FDNS (right).

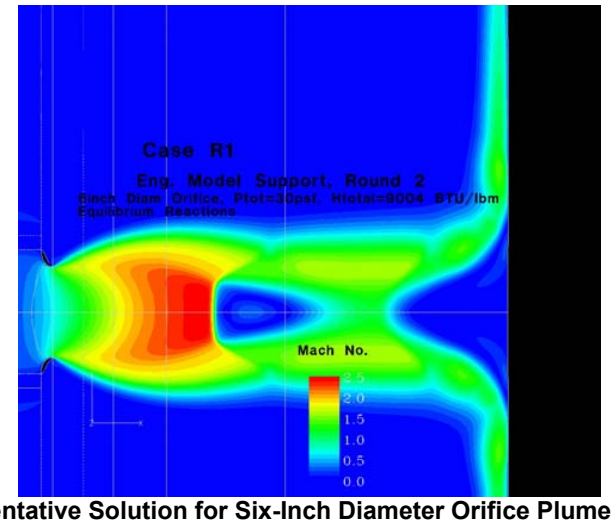

Figure 5.3.3-12 Representative Solution for Six-Inch Diameter Orifice Plume Impinging on a Plate 30 Inches Downstream.

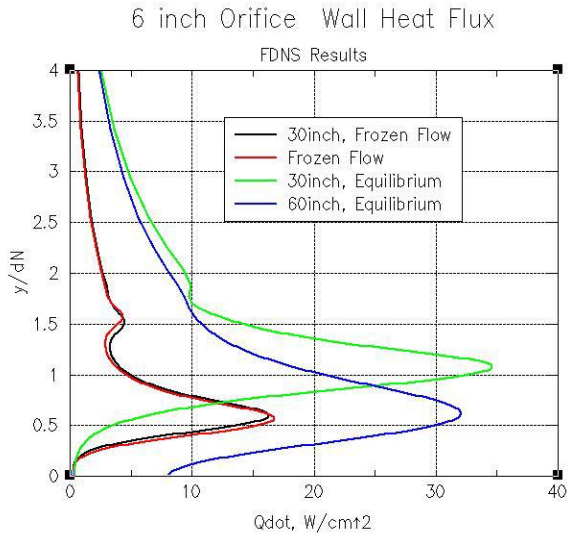

Figure 5.3.3-13 CFD Calculated Heating Rates for Six Inch Diameter Orifice Plume.

5.3.3.5 Arc-jet Test Data for Plume Heating Verification

5.3.3.5.1 Test Description

As described in Section 6.4, arc-jet tests were conducted in the NASA JSC facility to support the evaluation of effects of a breach hole in the Orbiter aeroshell. The test fixture, as sketched in Figure 5.3.3-14, was a rectangular cross-section box that was inserted into the flow exiting the arc-jet nozzle. Figure 5.3.3-15 shows the box with a hole in the front face and the location of test articles in the box downstream of the hole. Tests were conducted with a 1-inch and a 2-inch diameter hole in the front face. At the 15-inch test article location, pitot-probes, heat flux sensors and an instrumented cylinder were used to obtain data to verify the plume heating models.

Arc-jet test conditions were selected to be representative of those in flight by using total enthalpy and stagnation pressure as the simulation parameters. Figure 5.3.3-16 presents the STS-107 history of total enthalpy plotted as a function of the stagnation pressure. These values were derived from the STS-107 EOM3 trajectory simulation. A box is indicated on the plot that is labeled 'Zone of Interest' that corresponds to the range of total enthalpy and stagnation pressure for the time span of 300 to 600 seconds from entry interface. The two symbols on the plot indicate the total enthalpy and stagnation pressures that correspond to the two test conditions at which data were obtained. The arc-jet stagnation pressure was obtained from measurements of the pressure on the front face of the test fixture during runs. The arc-jet total enthalpy was derived from a combination of the stagnation pressure and the measured heat flux on a flat-face 1-inch diameter heat flux probe inserted into the arc-jet flow field at the same location at which the test fixture was located during runs. The following relation documented in Hiester and Clark was used with the measurements to obtain an estimate of the total enthalpy in the arc-jet flow field just upstream of the hole in the test fixture.

$$H_{total} = 24\dot{q}_{stag}\sqrt{\frac{R_{eff}}{P_{stag}}}$$

In this relation, R_{eff}, is the effective radius and is obtained by multiplying the flat-face cylindrical radius by a factor of 3.3, as recommended by Hiester and Clark.

The following table provides a summary of the two test conditions.

Test Configuration	Air Flow Rate (lb_m/sec)	Arc-jet Current (amps)	P_{stag} (psf)	q_{stag} (Btu/ft^2-sec)	H_{total} (Btu/lb_m)
1-inch Dia. Hole	0.3	1200	27	154	12,200
2-inch Dia. Hole	0.4	1200	35	139	9,700

5.3.3.5.2 Results

For the purpose of verifying plume-heating models, the most significant data obtained from this test series were pitot-pressure measurements and heat flux data on a 1.75-inch diameter cylinder at the 15-inch location downstream of the hole. The measured and predicted values are presented in the following table:

Test Configuration	P_{stag} (psf)	H_{total} (Btu/lb_m)	P_{box} (psf)	$P_{pitot-X=15"}$ (psf)	Measured q_{cyl} (Btu/ft^2-sec)	Predicted q_{cyl} (Btu/ft^2-sec)
1-inch Dia. Hole	27	12,200	0.88	2.02	4.7	21.1
2-inch Dia. Hole	35	9,700	0.68	3.18	12.1	39.3

The predicted values were obtained using the plume-impingement heating model described in Sec. 5.3.3.1. The test fixture stagnation pressures, P_{stag}, the box internal pressures, P_{box}, and a reduced total enthalpy were used as input to these predictions. It was assumed that the total enthalpy in the gas ingested through the test fixture hole was 84% of the arc-jet centerline total enthalpy, H_{total}, for the 1-inch hole case and 93% for the 2-inch hole case. These values were based upon mean temperature estimates for entry-length ducts, as described by Kays and Crawford. Clearly, the predicted values are significantly larger than those measured. It is believed that the test fixture box interfered with the free-jet flow field emanating from the hole and created shock waves inside the box. The simple plume impingement model was not created to predict heating in this type of flow field.

5.3.3.5.3 CFD Computation for Arc-jet Test Setup

At the time of report release, JSC was in the process of running CFD solutions for arc-jet conditions and the test hardware mockup. Preliminary results indicated that the test box walls constrained the plume expansion and created compression shocks that changed the plume flow field.

5.3.3.5.4 Conclusions

The breach hole arc-jet test provided valuable data about hole growth in aluminum plates and about the demise of flight-like instrumentation cable bundles. However, questions about the flow field inside the box prevent the impingement heating data to be used for verifying the plume impingement heating model.

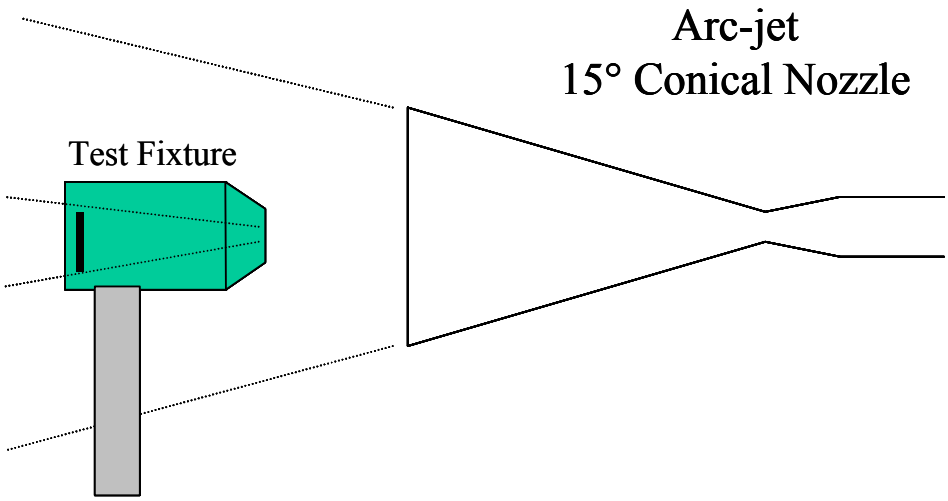

Figure 5.3.3-14 Sketch of Breach Hole Arc-jet Test Setup.

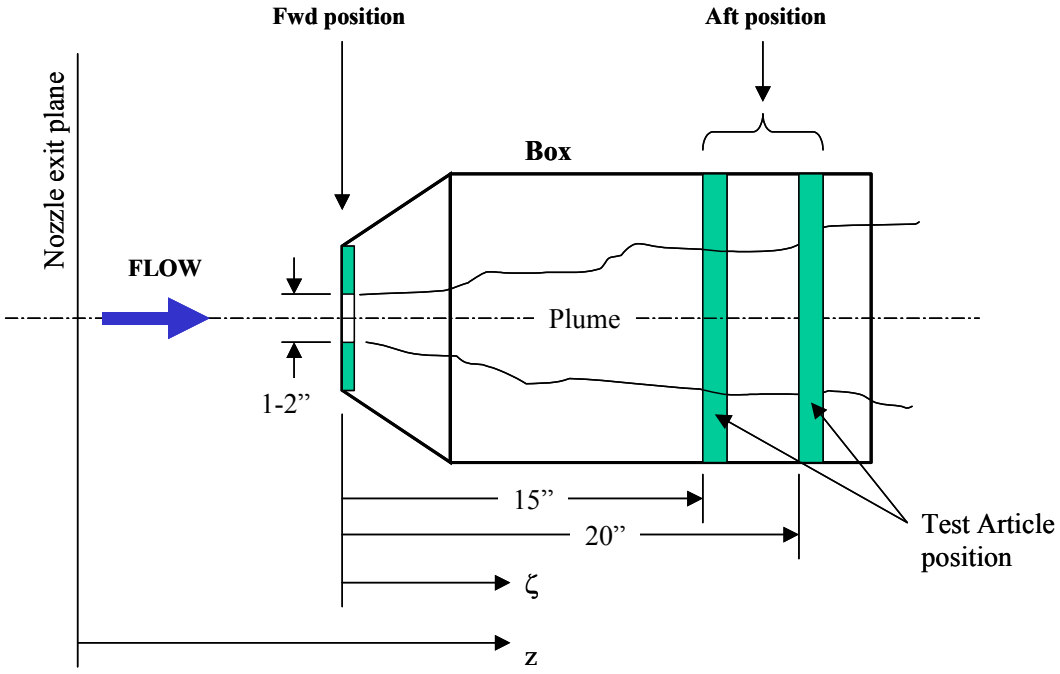

Figure 5.3.3-15 Sketch of Test Fixture and Locations of Test Articles

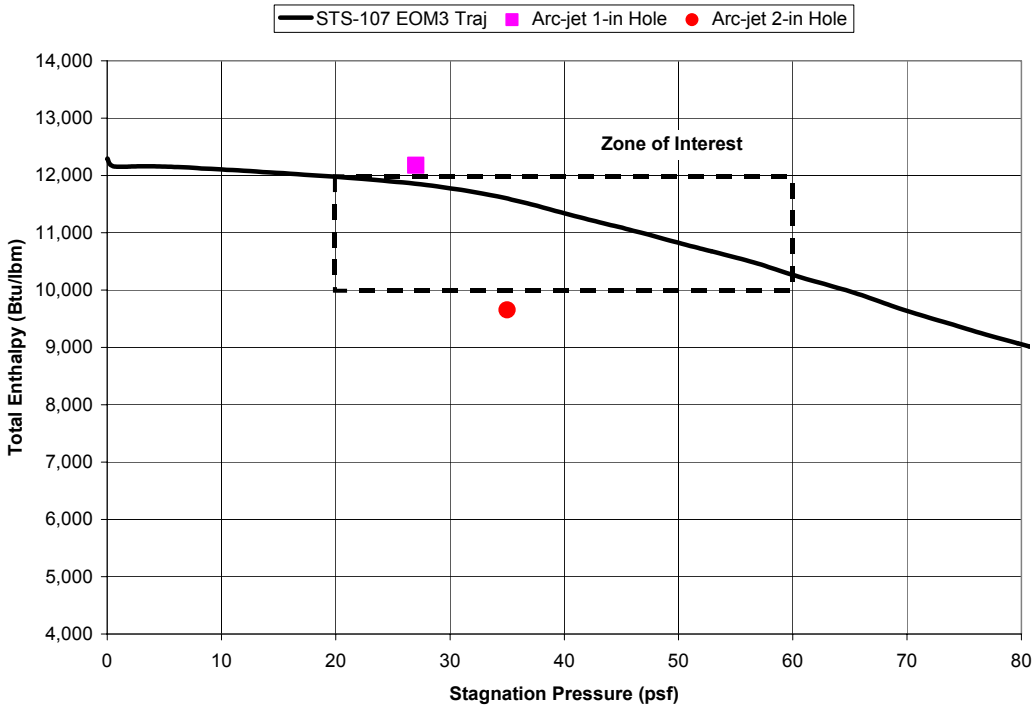

Figure 5.3.3-16 Comparison of STS-107 Flight Conditions and Arc-jet Test Conditions.

5.3.3.6 Slot Jet Heating Model (Missing Panel 8/9 T-seal)

5.3.3.6.1 Scenario Description

One of the damage scenarios evaluated was that the T-seal between leading edge panels 8 and 9 was damaged and missing at the beginning of the STS-107 reentry. In this instance it was postulated that only the lower portion of the T-seal between the apex and the beginning of the internal earmuff insulation was missing. Figure 5.3.3-17 provides a sketch of the geometry for this case. Panel 8 has been removed to permit a view of the internal structure.

5.3.3.6.2 CFD Predictions of Heating to Internal Hardware

Two sets of CFD solutions were used as the basis for developing the transient heating distribution to the earmuff insulation as a result of a missing T-seal between Panels 8 and 9. A 3-D Navier-Stokes CFD solution of the flow through the gap between panel 8 and 9 ribs for a missing 8-inch segment of T-seal has been provided by Boeing-Huntington Beach (see Sec. 5.3.6.2.3) for CFD Point 1:

> CFD Point 1: EI+404 secs.; Mach =24.9; Altitude = 243,000 ft; Angle-of-attack = 40 degs.; Dynamic pressure = 22.0 psf.

The heat flux distribution on the earmuff and spar insulation predicted by this solution is presented in Figure 5.3.3-18. The heat fluxes are for a wall temperature of 460° R. Note that the highest heating is concentrated at the edge of the earmuff closest to the rib channel outlet and quickly drops by a factor of ten on the rest of the earmuff front face. Heating to the earmuff sides and spar insulation is on the order of another factor of ten lower – less than 0.3 Btu/ft^2-sec.

Several 2-D Navier-Stokes CFD solutions were generated for the same flight conditions and for the perpendicular impingement of the flow emanating from the rib channel onto the earmuff insulation (see Sec. 5.3.6.2.1). Figure 5.3.3-19 shows the Mach number contours for the 2-D solution for a 5-inch distance between the rib outlet and the front face of the earmuff insulation. Cases were also run for 2-inch, 11-inch and 21-inch distances between the ribs and the earmuff. The resultant heat flux distributions predicted are presented in Figure 5.3.3-20 for a 1500° F wall temperature. The predicted heat fluxes on the edge of the earmuff are probably high due to a smaller than actual edge radius (0.25" modeled versus a 1.0" actual) used in these solutions. In order to apply the 2-D results to the actual hardware, lines perpendicular to the rib outer edge were projected to the earmuff front face centerline as shown in Figure 5.3.3-21. The radial distances between the rib and the earmuff were selected to approximate the perpendicular distances used in the 2-D CFD cases and the angles between the radial rays and the earmuff centerline were obtained. The 2-D CFD centerline heat flux values were then corrected by the cosine of the impingement angle. The resultant centerline heat fluxes are presented in the table below as a function of distance from the lower edge of the earmuff insulation.

Earmuff Location (inches)	Distance from Rib (inches)	Impingement Angle (degs)	CFD Prediction (Btu/ft^2-s)	Angle Corrected Heat Flux (Btu/ft^2-s)
2	2	70	46.7	15.9
6.5	5	70	17.5	6.0
12	11	65	7.1	3.0
20	18	55	3.1*	1.8

*Value derived by curve-fit since actual data were available for 2, 5, 11, and 21 inches.

5.3.3.6.3 Development of Engineering Model for Earmuff Insulation Heating

The CFD solutions provide heat flux predictions for a single flight condition – CFD Point 1. In order to conduct a thermal analysis and determine the response of the hardware, heat fluxes are needed as a function of time (varying flight conditions) and as a function of the surface temperature. Furthermore, the 3-D CFD solution was modeled with only an 8-inch length of the T-seal missing. Therefore, engineering judgment had to be used to estimate the effect of having a longer length of T-seal missing. The first step in the process of developing the engineering model was to assume that a majority of the heating was on the front face of the earmuff and then to establish the heating along the centerline of the earmuff in a local coordinate system. Figure 5.3.3-22 presents a sketch of the local coordinate system with an origin at the center lower edge of the earmuff and with the x-axis lying along the earmuff centerline from the lower to the upper edge. The z-axis is perpendicular to the earmuff front face.

The earmuff centerline heat fluxes in the local coordinate system are presented in Figure 5.3.3-23. Both the 3-D and corrected 2-D CFD values are shown. A best-estimate curve-fit is also provided that uses a reference maximum heating rate of 55 Btu/ft^2-sec at X_{local}= 0.25 inches.

$$q_{CL}(x) = \frac{0.412 q_{CL}(x = 0.25")}{x^{0.64}}$$

This curve-fit provided the basis for the earmuff centerline cold-wall heating distribution. In order to account for wall temperature effects and the energy available to heat the earmuff, the cold-wall heat fluxes were used to obtain enthalpy-based heat transfer coefficients. The final engineering model provides heat transfer coefficient and bulk enthalpy histories to use in calculating the transient heat flux to the earmuff.

$$q(x, y, t) = h(x, y, t)(H_{bulk}(t) - H_{wall}(T_{wall}))$$

In this relation, h, the heat transfer coefficient is a function of the location (x,y) and the time, t; H_{bulk} is the ingested bulk enthalpy of the flow through the rib channel as a function of time; and H_{wall} is the enthalpy of the gas at the wall temperature. Therefore, the centerline heat flux is defined by

$$q(x,0,t) = h(x,0,t)(H_{bulk}(t) - H_{wall}(T_{wall}))$$

with

$$h_{CL}(x,0,t) = \frac{0.412 h_{CL}(0.25",0,t)}{x^{0.64}}$$

The heat transfer coefficient at the reference point, h_{CL}(0.25",0,*t*) was obtained for *t*=EI+404 secs. from the peak cold-wall heat flux value of 55 Btu/ft^2-sec estimated from the CFD solutions and using a bulk enthalpy estimated from the 2-D CFD solutions.

$$h_{CL}(0.25",0,404\,\text{sec}.) = \frac{(5366 Btu/lbm) - H_{wall}(460R))}{55 Btu/ft^2 - \text{sec}} = 0.0105 lbm/ft^2 - \text{sec}$$

To obtain time dependent, and therefore flight condition dependent, values of the heat transfer coefficient at x=0.25" it was assumed that the heating varied as the square-root of the free-stream dynamic pressure. The rationale for this assumption is that impingement heating is proportional to the square root of the impingement pressure. In addition, the impingement pressure on the earmuff is driven by the wing leading edge external pressure which is a function of the dynamic pressure.

The variation of the bulk enthalpy with flight conditions was obtained by using the engineering analysis procedures discussed in Sec. 5.3.2. The effective gap width of the ingested flow was varied until the bulk enthalpy predicted by the engineering analysis matched that estimated from the 2-D CFD solution for t=404 seconds. The resultant bulk enthalpy history and the predicted maximum earmuff heating rate history are presented in Figure 5.3.3-24. The table below also presents the transient values.

EI Time (secs.)	Ingested Enthalpy (Btu/lbm)	Dynamic Pressure (psf)	$\sqrt{\frac{P_{dyn}}{P_{dyn,t=400s}}}$	q_{CL}(x=0.25") Tw=460 R (Btu/ft^2-s)	h_{CL}(x=0.25") (lbm/ft^2-s)
200	3781	1	0.23	8.81	0.0024
300	4861	8	0.65	32.26	0.0068
400	5366	19	1.00	55.00	0.0105
500	5387	25	1.15	63.34	0.0120
600	5273	33	1.32	71.20	0.0138
700	5095	41	1.47	76.63	0.0154
800	4741	48	1.59	77.02	0.0166
900	4334	69	1.91	84.23	0.0199

With the centerline heat transfer coefficients and bulk enthalpy values defined as a function of time, the lateral distribution of heat transfer on the earmuff was defined as a function of the centerline values using the results from the 3-D CFD solution. The non-dimensionalized values are presented in Figure 5.3.3-25 for five axial stations – x=0.25, 1, 2, 4, and 8 inches. Beyond 8 inches it was assumed that the distribution was the same as that for the 8-inch station.

Figure 5.3.3-26 presents a comparison of the cold-wall heat flux distribution on the earmuff front face from the 3-D CFD solution and that resulting from the engineering model. The acreage heating provided by the engineering model tends to be greater than that predicted by the CFD and that was done to provide an estimate of the effect of the increased length of the T-seal missing.

Heating to the sides of the earmuff and the spar insulation was assumed to be low and estimated to be below 0.5 But/ft2-sec at EI+404 seconds. Using this value a heat transfer coefficient of 0.0001 was estimated and the heat flux was then computed using the following relation:

$$q = 0.0001\sqrt{\frac{P_{dyn}}{P_{dyn,t=400s}}}(H_{ingested}(t) - H_{wall}(Tw))$$

5.3.3.6.4 Reduction of Heating with Distance from Rib Channel Outlet

In order to estimate the heating to hardware behind the earmuff after the earmuff is removed a relation was derived from the 2-D CFD solutions that provides an indication of the reduction in heating as a function of distance from the rib channel outlet. The relation is presented in Figure 5.3.3-27 and was obtained by curve-fitting the centerline heat flux predictions from the 2-D CFD solutions for a normal impingement.

This curve-fit was used to estimate the heating to a 1.75-inch diameter cylinder located 13 inches from the rib outlet. The cylinder represents an instrumentation cable bundle that would be located at the closest 13 inches from the rib channel outlet. Using the curve-fit from Figure 5.3.3-27, the heating to the front face of the earmuff would be approximately 4.7 Btu/ft^2-sec. However, the earmuff has a blunt front face with a width of 9 inches. To correct the heating for the difference in geometries between the earmuff and the cylinder the square root of the ratio of effective radii is used.

$$q_{cyl} = q_{earmuff-CL}\sqrt{\frac{R_{eff-earmuff}}{R_{eff-cyl}}}$$

The effective radius of the cylinder is half the diameter or 0.875 inches. With the blunt front face of the earmuff the effective radius is estimated to be 3 times the half-width or 13.5 inches. The estimated heat flux to the 1.75-inch cylinder would be 18 Btu/ft^2-sec. The factor of three is a typical ratio for scaling a flat-faced cylinder to an equivalent hemisphere as reported by Hiester and Clark.

This heating value was verified by extracting flow field properties from the 2-D CFD solution at a point 13 inches downstream of the rib channel outlet, and using a stagnation point relation also provided by Hiester and Clark to compute the heating.

$$q_{cyl} = \frac{H_{total}}{24}\sqrt{\frac{P_{stag}}{2R_{eff-cyl}}}$$

The factor of 2 in the relation is used for stagnation heating to cylinders. From the 2-D CFD solution the value of total enthalpy at 13 inches from the rib channel outlet was 5654 Btu/lb$_m$ and the stagnation pressure was determined to be 1.9 psf. Using these values, in the appropriate units, also results in a cold-wall heat flux on the cylinder of 18 Btu/ft^2-sec. This value contrasts with the results of section 6.0 in assessing the heating rate required to match the wire demise rate observed from flight of 89.6 Btu/ft^2-sec.

5.3.3.6.5 Heating to the Panel 8/9 Rib Channel with T-seal Removed

A 2-D CFD solution was also generated by Boeing-Rocketdyne for the detailed 2-D geometry of the channel between leading edge panels 8 and 9 for the CFD Point 1 flight conditions (see Sec. 5.3.6.2.2) with the T-seal removed. Figure 5.3.3-28 presents contours of the gas static temperature predicted by this solution. Three flow field regions were identified from these results – 1) separation region; 2) stagnation region; and 3) duct region. The flow along the Orbiter leading edge consists of a supersonic boundary layer that flows from inboard to outboard. When the flow encounters an open rib channel, the flow locally separates from the surface and then impinges on the downstream edge of the outboard rib. Some portion of the flow is turned inward and flows through the parallel ribs creating a flow similar to a two-dimensional duct. Using the characteristics of these flow regions and the heating distributions predicted by the 2-D CFD solution, an engineering model was developed to predict the local heat flux history in the rib channel for the STS-107 reentry trajectory.

The 2-D CFD solution provided heat flux distributions on the upstream and downstream rib surfaces in a local coordinate system shown in Figure 5.3.3-29. The CFD heat flux distributions for a wall temperature of 2900 R

were used to obtain enthalpy-based heat transfer coefficients, h, referenced to the heat transfer coefficient, h_{ref}, on the external surface of the leading edge.

$$\frac{h(s,t)}{h_{ref}(t)} = \frac{\dfrac{q(T_{wall} = 2900R)}{(H_{rec} - H_{wall}(T_{wall} = 2900R))}}{\dfrac{q_{ref}(T_{wall} = 2900R)}{(H_{fs-total} - H_{wall}(T_{wall} = 2900R))}}$$

To obtain the value h_{ref} the free stream total enthalpy, $H_{fs\text{-}total}$, was used. For the heat transfer coefficients inside the rib channel, the recovery enthalpy, H_{rec}, varied by the flow region. For the stagnation region, the recovery enthalpy was assumed to be equal to the free stream total enthalpy. For the separation and duct regions, the recovery enthalpy was assumed to be equal to the ingested bulk enthalpy found by the methods discussed in Sec. 5.3.2. The heat transfer coefficient distributions for the upstream and downstream surfaces were defined with linear segments based upon the local coordinate, s. A comparison of the heat fluxes derived from the engineering model with those provided by the CFD solution is presented in Figure 5.3.3-30. In order to obtain the transient variation of heat flux within the rib channel, values of the ingested enthalpy were provided as a function of time and it was recommended that the heat flux for BP 5505 on the leading edge of Panel 9 be used for the reference heat flux, q_{ref}. The resultant cold-wall heat flux histories for three locations in the rib channel are presented in Figure 5.3.3-31. These heat fluxes are very high since they use the high leading-edge heating associated with BP 5505 on Panel 9 (see Sec. 5.2.2).

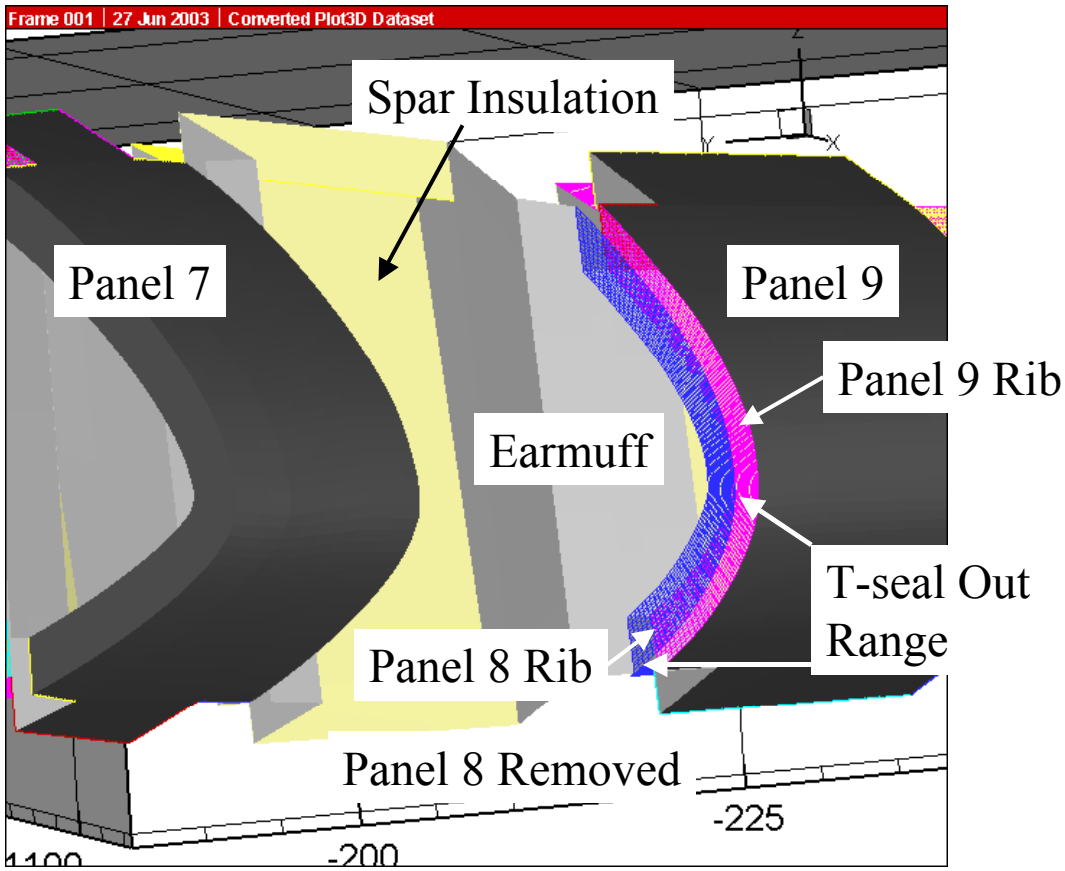

Figure 5.3.3-17 Sketch of Leading Edge Region for Panels 7, 8 and 9.

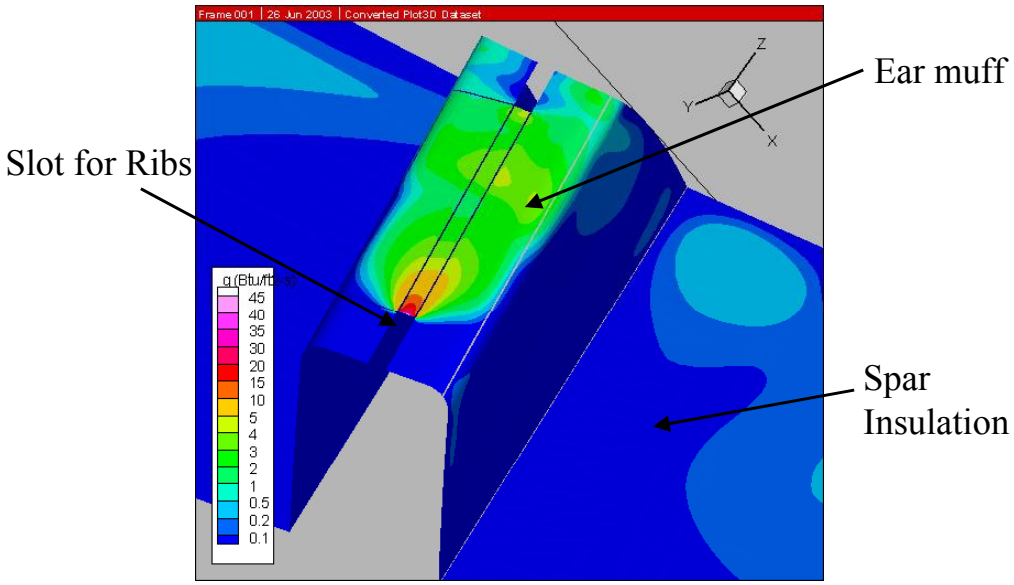

Figure 5.3.3-18 Earmuff and Spar Insulation Heating Predictions for CFD Point 1 from the Boeing-HB CFD Solution – Twall=460 R.

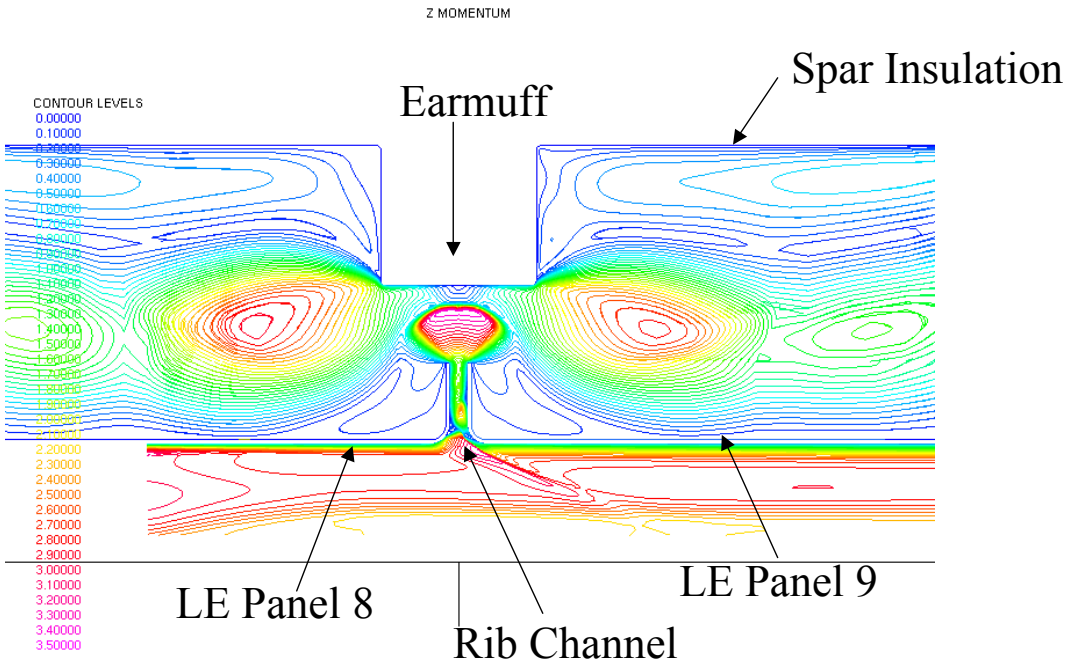

Figure 5.3.3-19 Mach Number Contours for 2-D flow impingement onto Earmuff and Spar Insulation – 5-inch Distance between Rib Channel Outlet and Earmuff.

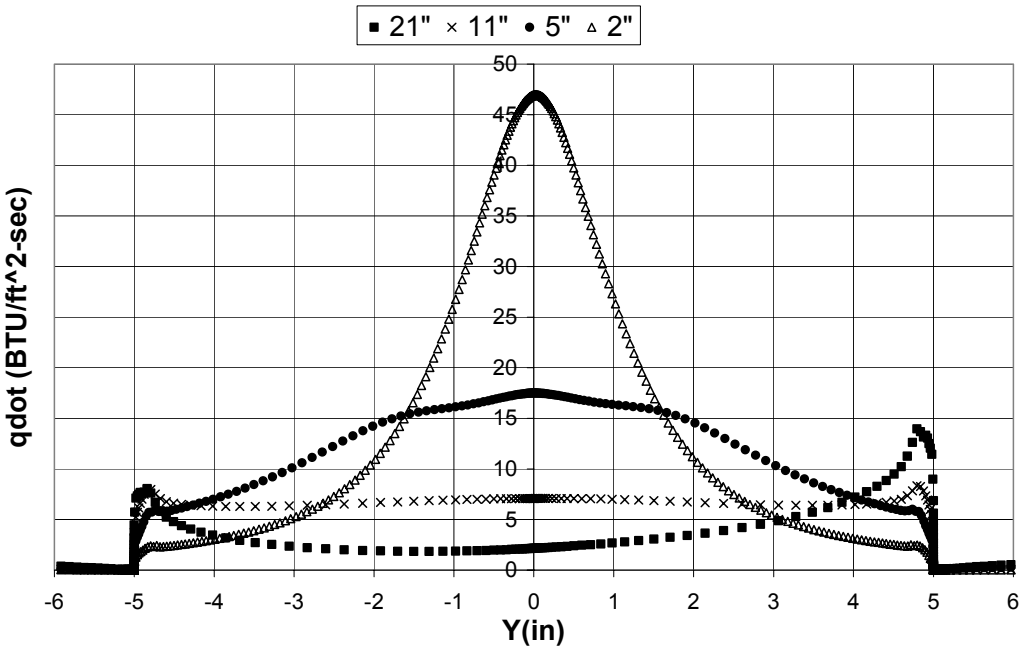

Figure 5.3.3-20 – Earmuff Heat Flux Distributions Predicted by the NASA JSC 2-D GASP CFD Solutions CFD Point 1.

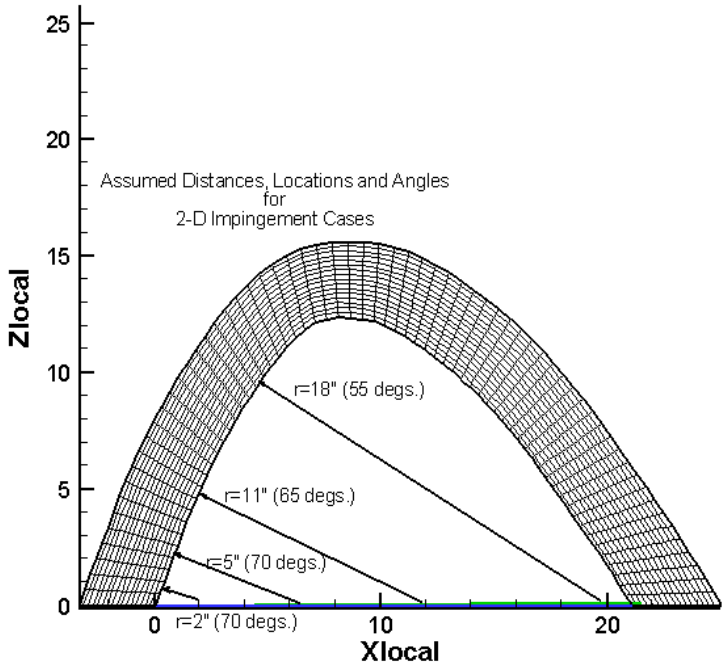

Figure 5.3.3-21 Application of 2-D CFD Solutions to the Actual Hardware

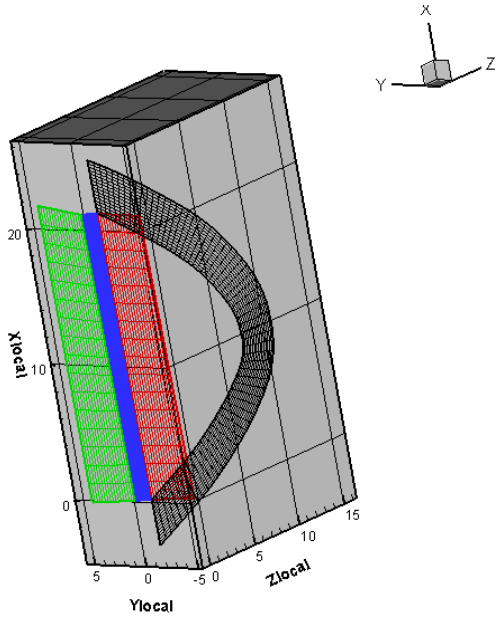

Figure 5.3.3-22 Local Earmuff Coordinate System
Figure 6 – Local Earmuff Coordinate System.

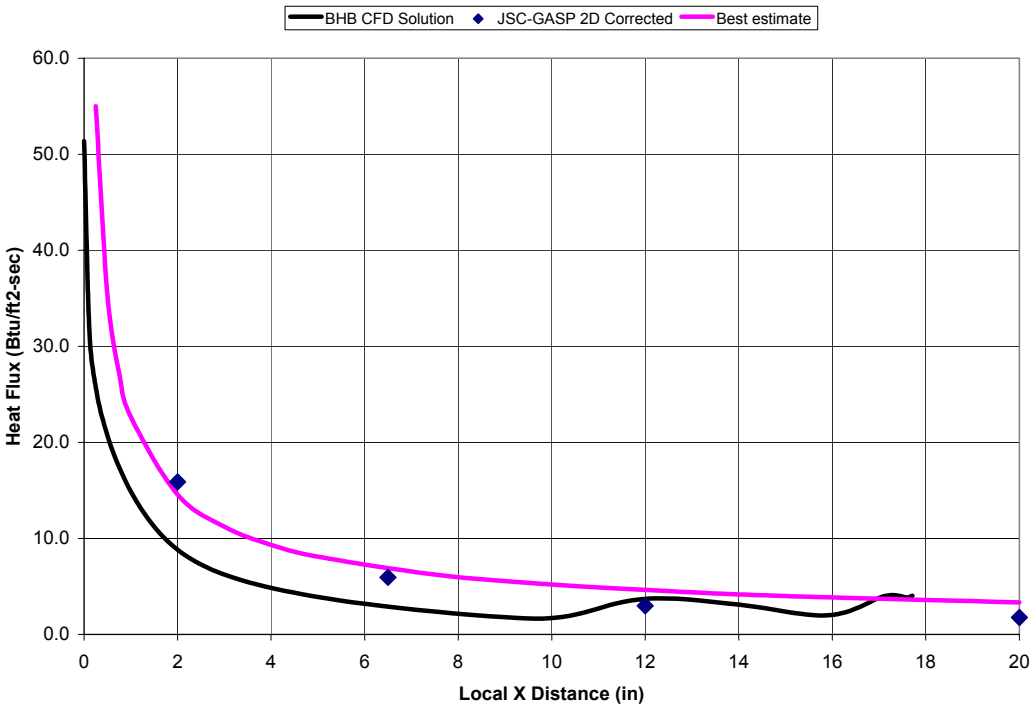

Figure 5.3.3-23 Comparison of Predicted Heat Fluxes on the Earmuff Centerline for CFD Point 1

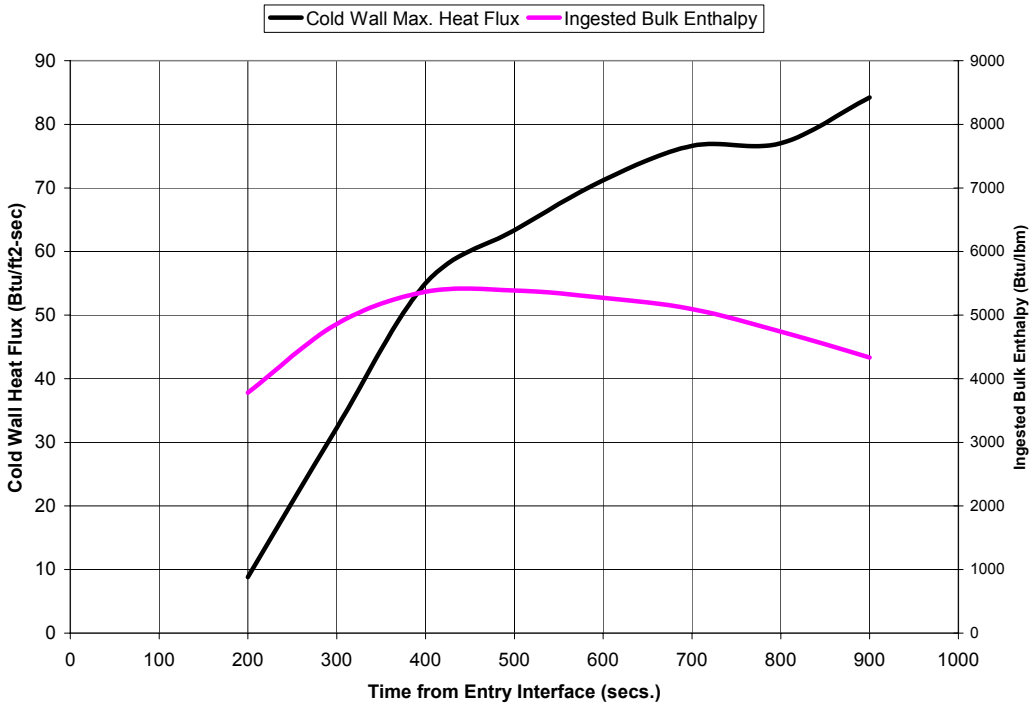

Figure 5.3.3-24 Predicted Maximum Cold-wall Heat Flux and Ingested Bulk Enthalpy Histories.

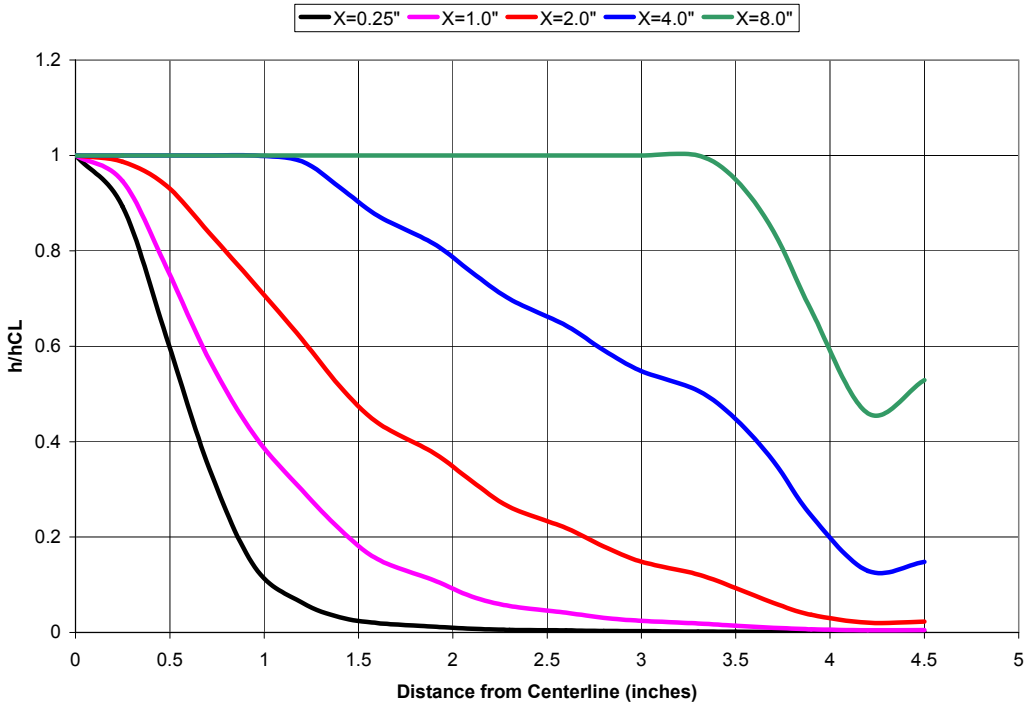

Figure 5.3.3-25 Predicted Maximum Cold-wall Heat Flux and Ingested Bulk Enthalpy Histories.

Twall=460 R

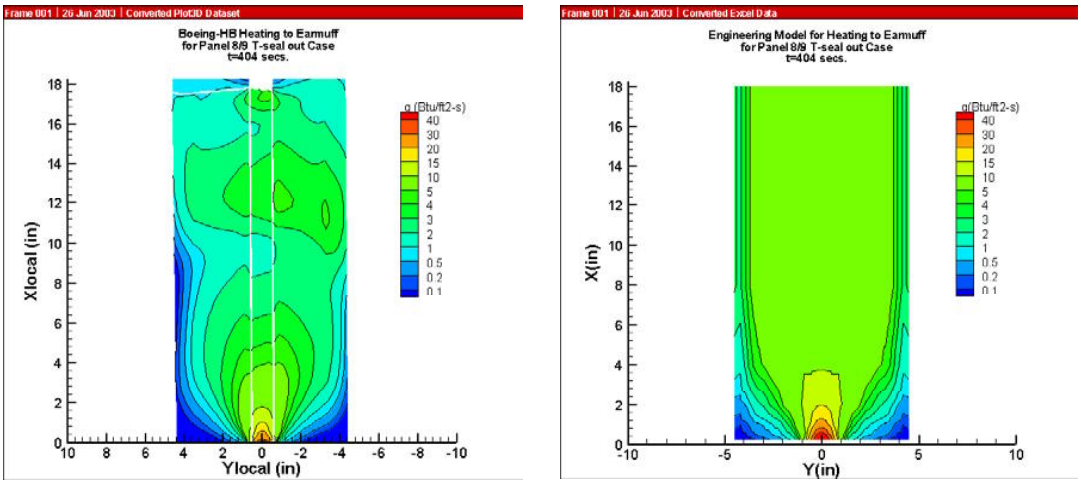

BHB 3-D CFD Results
8-inch T-seal out

Engr. Model Results

Figure 5.3.3-26 Earmuff Front-face Heating Comparison for EI+400 seconds. (Assumed results for 400 and 404 seconds are same.)

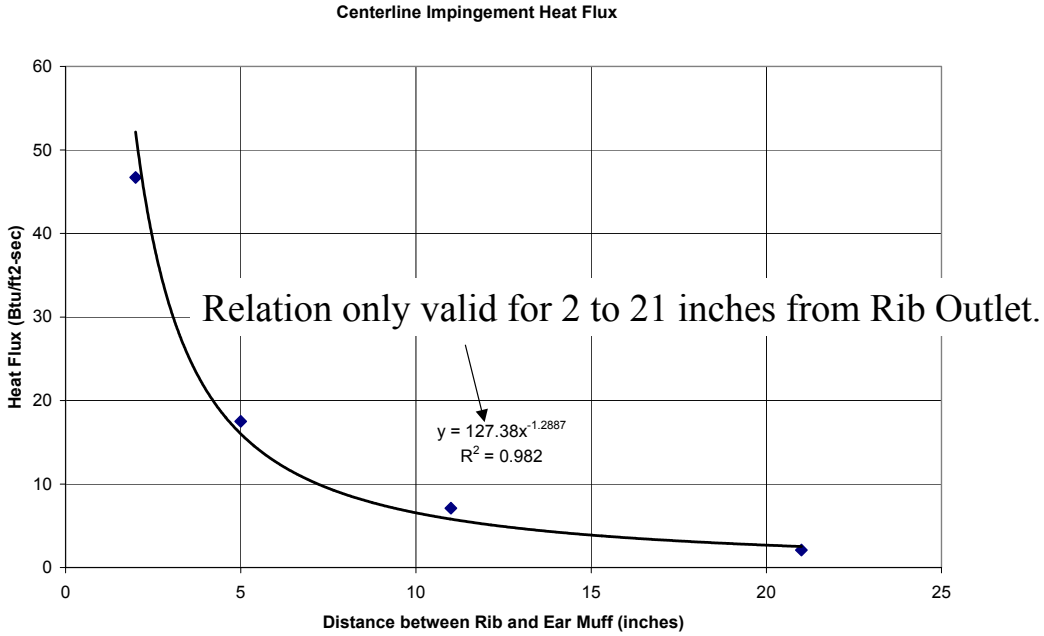

Figure 5.3.3-27 Relation for Estimating Reduction in Heating with Distance from Rib Channel Outlet.

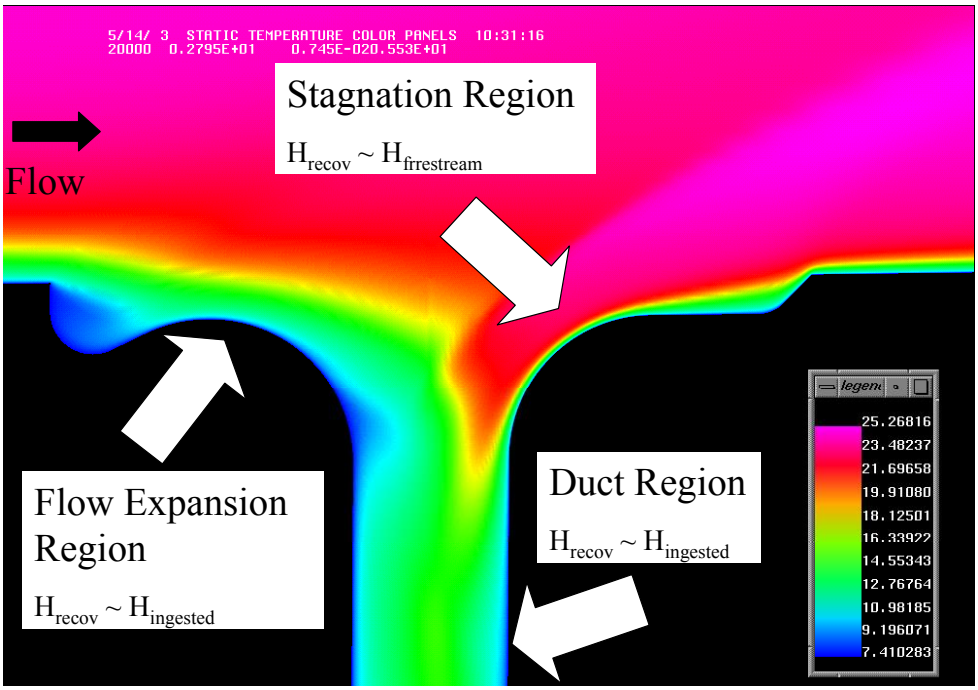

Figure 5.3.3-28 Regions of the Flow field in the T-seal Out Rib Channel.

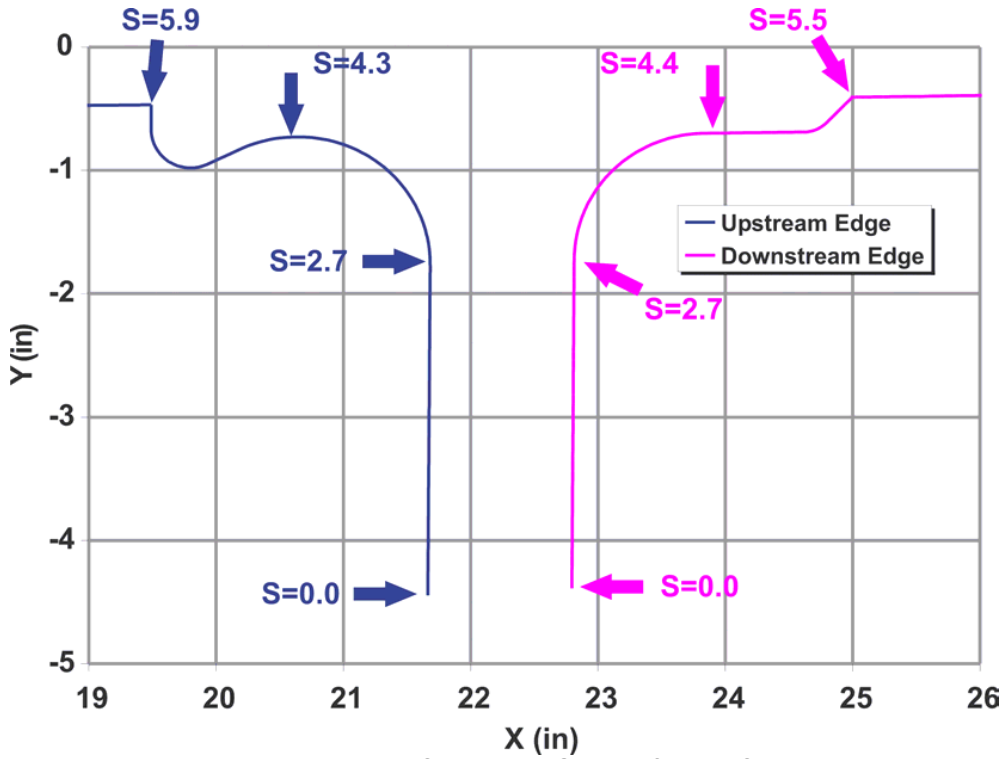

Figure 5.3.3-29 Local Coordinate System for Rib Channel.

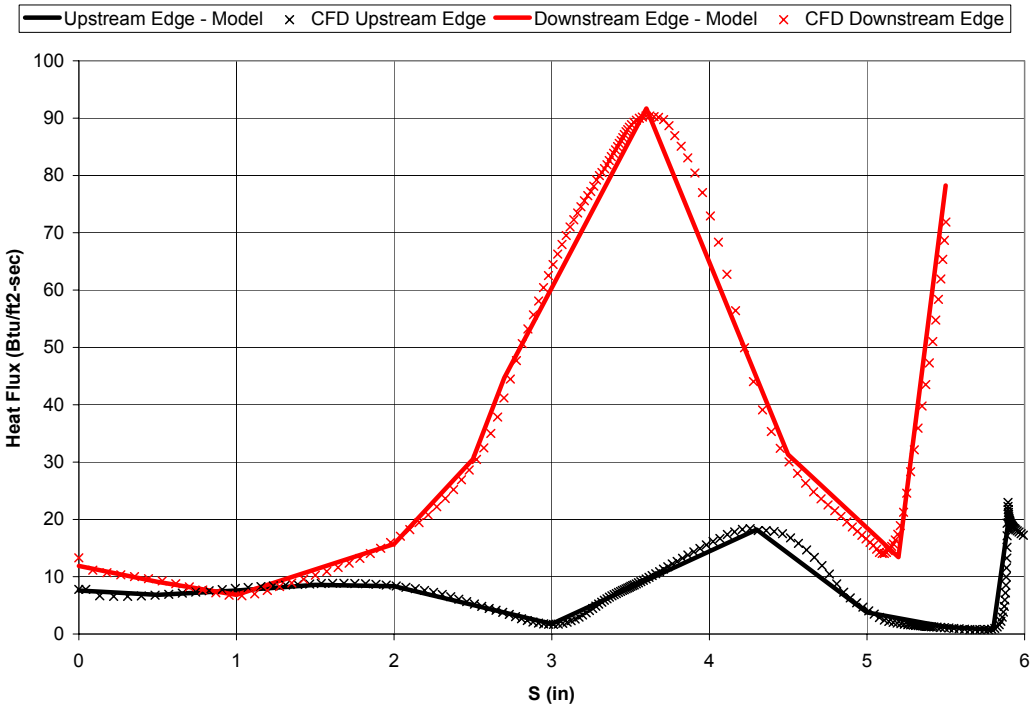

Figure 5.3.3-30 Comparison of Engineering Model Heat Fluxes with CFD Results.

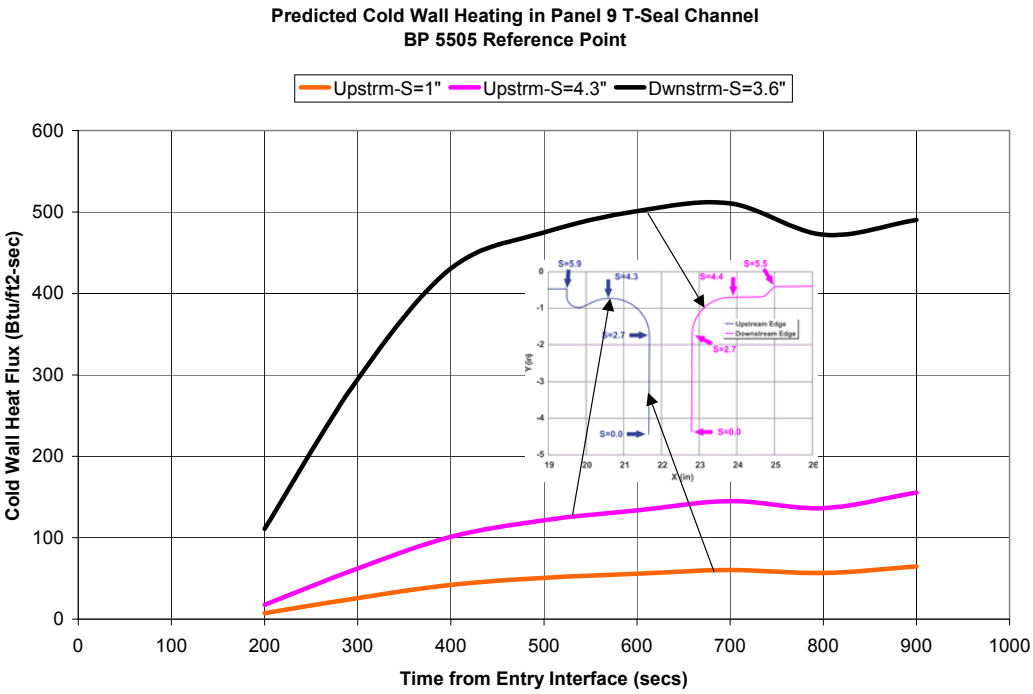

Figure 5.3.3-31 Predicted Cold-wall Heat Flux History for Locations in the Panel 8/9 Rib Channel

5.3.4 Effects of Burning Aluminum

In order to evaluate the effects of aluminum combustion on the STS-107 accident, a team was formed that included the following personnel:

NASA JSC Engineering Directorate Personnel (EG and ES Divisions)
NASA White Sands Test Facility Personnel
Boeing Huntington Beach Engineering Personnel
Lockheed Martin Space Operations Personnel
Sandia National Laboratories Personnel
Princeton – Dr. I. Glassman
Stanford – Dr. J. Jeffries
CalTech – Dr. P. Dimotakis

First, this team reviewed the aerothermodynamic environments associated with the STS-107 reentry. These environments are summarized in the following section. After reviewing these environments it was recognized that there was very limited experience with the exposure of aluminum to the high-temperature and low-pressure air resulting from a breach during reentry. Therefore, an air/aluminum chemical analysis that would determine the key reactions that would occur for the pressure and temperature range of the reentry gases was deemed necessary. Based upon the results of this analysis the heats of formations of the key reactions would be used to determine the additional energy available for propagating damage within the structure of the Columbia wing. A pictorial of the damage propagation process is provided in Figure 5.3.4-1.

5.3.4.1 Overview of STS-107 Aerothermal Environments

During the STS-107 reentry the total free stream energy of the gas surrounding the Columbia varies from about 12,000 Btu/lb_m-air in the early part of the reentry to about 7,000 Btu/lb_m-air at the time the vehicle was lost. Over this same time frame, pressures acting on the vehicle vary from near vacuum to less than 0.1 atmospheres. The resultant gas temperatures range from 6,000 R to over 10,000 R. A breach into the aeroshell exposes the aluminum structure to air at these pressures and temperatures. A more complete description of the STS-107 aerothermal environments is provided in Section 5.2.3.4.

5.3.4.2 Air/Aluminum Chemistry Analysis

5.3.4.2.1 Approach

The NASA Glenn Research Center's computer program for calculation of complex chemical equilibrium compositions and applications developed by S. Gordon and B. J. McBride was used to determine the chemical reactions that occur when aluminum is exposed to high-temperature air. This program was used to determine if the aluminum-oxygen reaction dominates the process or if aluminum-nitrogen reactions are prevalent enough to require consideration and was used to determine the appropriate heat of reaction to use in the plume energy calculations.

Several iterations of the Gordon-McBride program were run in which aluminum and air were present in stoichiometric proportions (phi=1), in fuel-lean proportions (phi=0.5), and in fuel-rich proportions (phi=2). For each fuel/oxidizer ratio a temperature-pressure problem was run in which the final temperature of the reactants were fixed at various temperatures ranging from 8000 to 520 R and the pressure was varied to represent the stagnation pressure at 8 points during re-entry (1.0, 5.1, 15.2, 35.5, 47.6, 76.0, 88.2, and 131.7 psf). More than 50 species were considered in this system including aluminum, oxygen, atomic oxygen, ozone, nitrogen, atomic nitrogen, aluminum oxide (various forms and states), and aluminum nitride (various forms and states).

Next, for each fuel/oxidizer ratio an enthalpy-pressure problem was run in which the initial temperature was input and the enthalpy was held constant for each of the 8 pressures. This calculation provided the adiabatic flame temperature of the reactants. This calculation was performed to provide a value to compare to the literature value of adiabatic flame temperature and thus provide a "sanity check" for the results.

5.3.4.2.2 Results and Conclusions

The results for the stoichiometric case (phi=1) indicate that the primary product of the reaction is Al_2O_3. Figure 5.3.4-2 presents the mole fractions for the 15.2 psf case. Figure 5.3.4-3 presents the enthalpy (energy) required to maintain the mixture at the specified temperatures. Note that for temperatures above ~5000 R energy is required to be input into the mixture to maintain the state and no aluminum oxide is formed. Below ~5000 R aluminum oxide is formed and energy is released.

These results were also confirmed in the fuel-lean case (phi=0.5). In the fuel-rich case (phi=2), aluminum nitride did appear, but it was observed that the presence of aluminum nitride did not significantly affect the calculated heat of reaction. Therefore, it was agreed by the team to use the heat of reaction of Al_2O_3 (1589 Btu/mole-Al_2O_3 (1676 kJ/mole-Al_2O_3) for subsequent calculations (see Glassman's text).

The calculated adiabatic flame temperatures in all cases compared favorably with the adiabatic flame temperatures provided by Glassman and were observed to be below the dissociation temperature of Al_2O_3 (6840 R (3800 K)). Figure 5.3.4-4 presents the flame temperatures for the stoichiometric case.

5.3.4.2.3 Additional notes

It was agreed by the team that aluminum burns if it is directly subjected to the ingested high-temperature 'plume' gases, but structural elements not directly impinged by the plume or not very near the plume will not necessarily sustain combustion. It is necessary to expose those aluminum structures to extreme heating conditions in order to get them to burn. Therefore, while the burning of aluminum contributes to the development of the breach hole and the propagation of damage inside the wing, it is not tangible for the entire wing structure to develop self-sustained burning simply as a result of that single, localized plume. It is important to realize that there are many conditions in which aluminum structural parts will not support self-sustained combustion. Factors that will hinder self-sustained burning of structural aluminum are as follows:

1) Thermal diffusivity: The thermal diffusivity of aluminum is very high enabling aluminum to rapidly conduct heat away from the burning region.
2) Radiative heat transfer: The energy radiated from a plume of hot air with burning aluminum is being distributed to a very large surface area at significant distances from the plume.
3) Fluid dynamics: The flow velocities of the plume are high. In such cases the molten and vaporized and burning aluminum will be rapidly blown downstream carrying much of the heat away from the high-temperature zone of the hole.
4) Protective oxide coating: In cases where the protective Al_2O_3 layer is not forcibly removed or penetrated, the ignition temperature of aluminum increases from the melting point of aluminum (1679 R (933 K)) to the point where the Al_2O_3 layer is breached. For systems with no mechanical disruption of the layer this is usually associated with the melting point of the oxide (4172 R (2318 K)) (see Werley et al).
5) Experience Base: WSTF has significant experience with the burning of structural aluminum and has many examples where aluminum did not support self-sustained combustion even in pure oxygen environments (see Newton and Stradling). The quenching of self-sustained combustion in these cases was clearly a function of heat transfer away from the burning region of the material.

5.3.4.3 Energy Comparison

Given the conclusion that the formation of aluminum oxide was the dominant reaction that would occur due to the exposure of aluminum structure to the reentry environments, an analysis was conducted to determine the maximum energy released by the reaction and compare that energy to the energy already in the reentry gases entering a breach into the aeroshell. As previously mentioned the heat of formation of aluminum oxide is (1589 Btu/mole-Al_2O_3 (1676 KJ/mole-Al_2O_3). Assuming that the reaction is limited by the available oxygen the energy released can be computed on a per mass of oxygen basis.

$$\left(\frac{1676 kJ / mole - Al_2O_3}{48 gm - O / mole - Al_2O_3} \right) = \frac{35 kJ}{gm - O} \text{ or } 14{,}982 \frac{Btu}{lb_m - O}$$

Using this value and the mass flow of air into a breach hole, the maximum energy flux due to aluminum combustion can be computed and compared to the energy flux associated with the high-temperature air. Of course this assumes that sufficient aluminum is available to react with all available oxygen. If the reaction is aluminum limited, then the energy released is

$$\left(\frac{1676kJ \,/\, mole - Al_2O_3}{54gm - Al \,/\, mole - Al_2O_3} \right) = \frac{31kJ}{gm - Al} \text{ or } 13{,}340 \frac{Btu}{lb_m - Al}$$

Assuming a 6-inch diameter hole into the leading edge spar, a quantitative comparison between the air energy flux and the aluminum combustion energy flux limited by the available oxygen is presented as a function time during the STS-107 trajectory in Figure 5.3.4-5. It is readily noted that the energy of the high-temperature air entering the breach hole is much greater than the energy released by the combustion of aluminum. At 600 seconds from entry interface, the reentry gas has a total enthalpy of 10,286 Btu/lb_m and flows into the 6-inch diameter hole at a rate of 0.038 lb_m/sec which results in an energy flux of 389 Btu/sec. Assuming that air is approximately 23% oxygen by mass, the energy flux associated with aluminum combustion is 133 Btu/sec or approximately one-third of the energy in the reentry gas. In order to compute the total energy available to heat wing internal structure due to a breach, the specific quantity of aluminum being heated must be considered since the energy required to raise the aluminum to the temperature at which it will begin to combust must be subtracted from the reentry gas energy.

5.3.4.4 Conclusions

Based upon this study several conclusions can be made. First, the ingestion of high-temperature reentry gases into the Columbia wing can result in the vaporization and subsequent combustion of aluminum with the primary reaction being the formation of aluminum oxide, Al_2O_3. Second, the energy released from this reaction is limited by the available amount of oxygen flowing into the wing. The aluminum combustion energy is approximately one-third of the energy already in the ingested reentry gas for the early portion of the reentry (less than 600 secs. from entry interface). Third, aluminum combustion occurs only for that portion of the wing structure being directly heated by the ingested reentry gases.

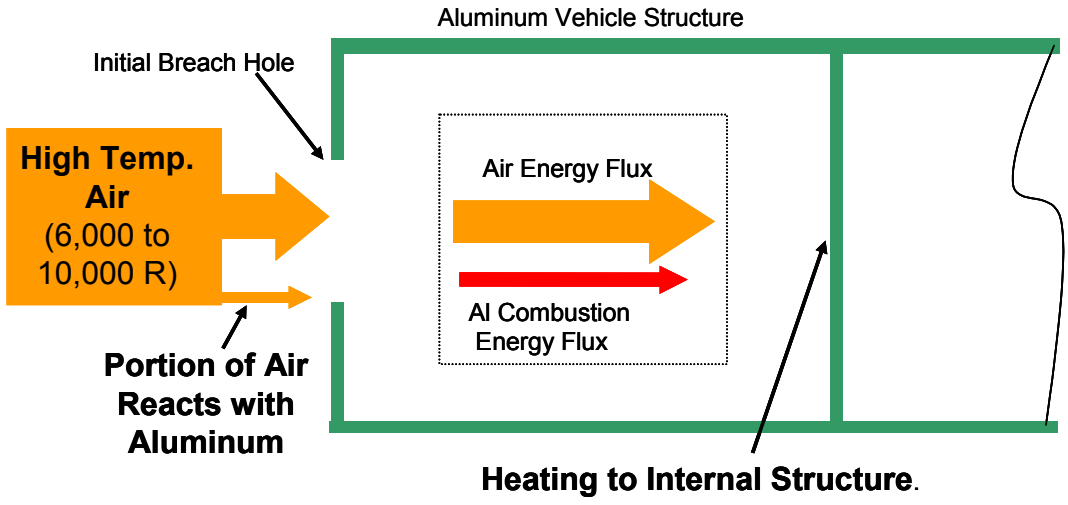

Figure 5.3.4-1 Breach Hole Scenario.

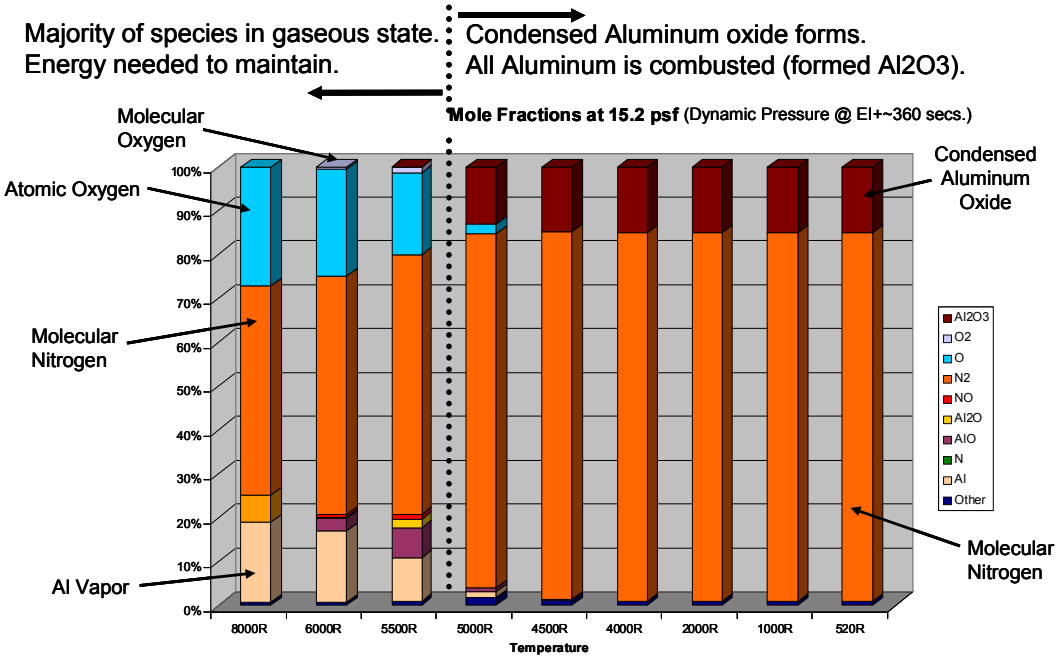

Figure 5.3.4-2 Aluminum/Air Mixture Mole fractions at 15.2 psf for Stoichiometric Conditions.

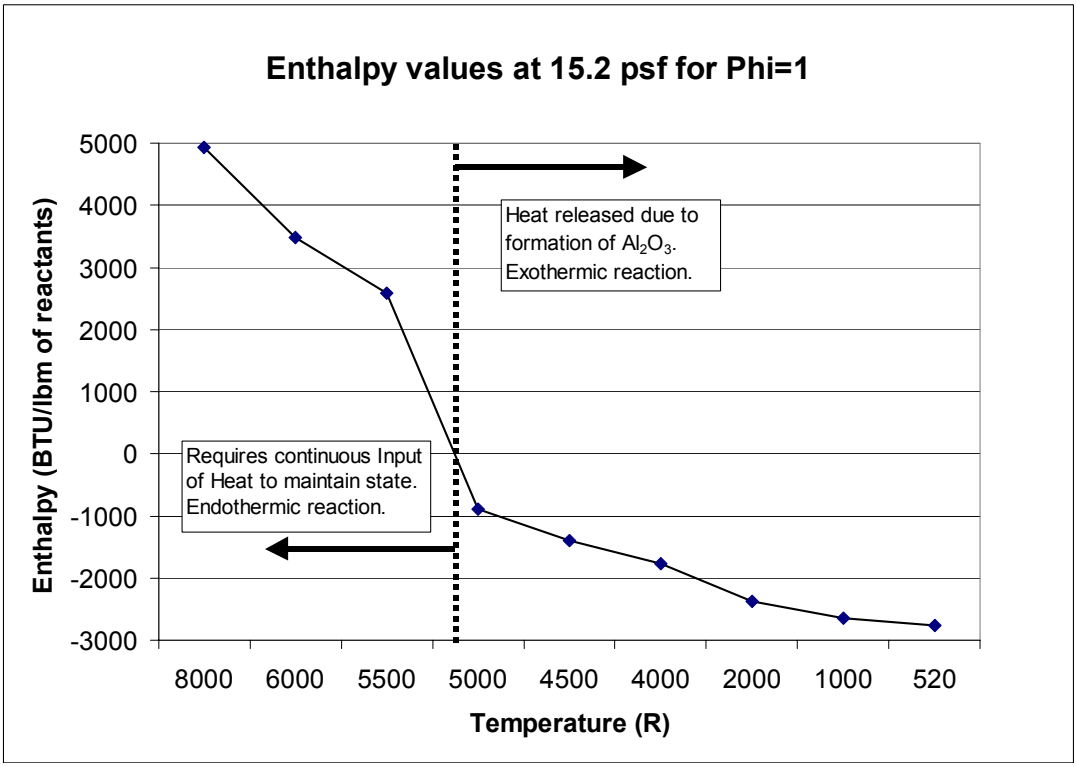

Figure 5.3.4-3 Energy Required to Maintain Air/Aluminum Mixture in Equilibrium State.

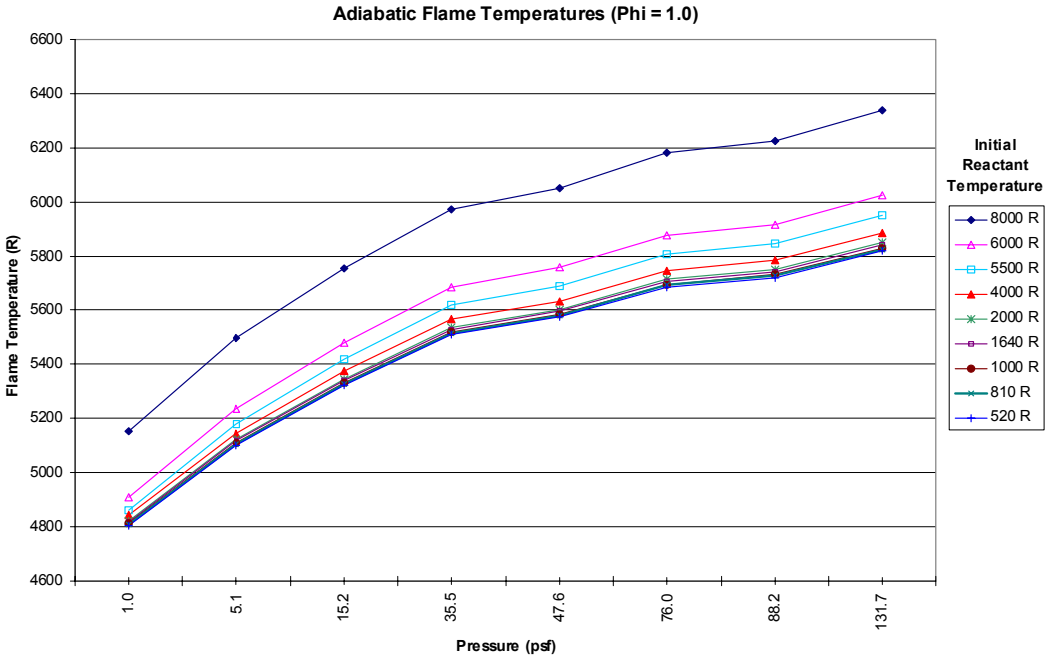

Figure 5.3.4-4 Adiabatic Flame Temperatures of Al Combustion.

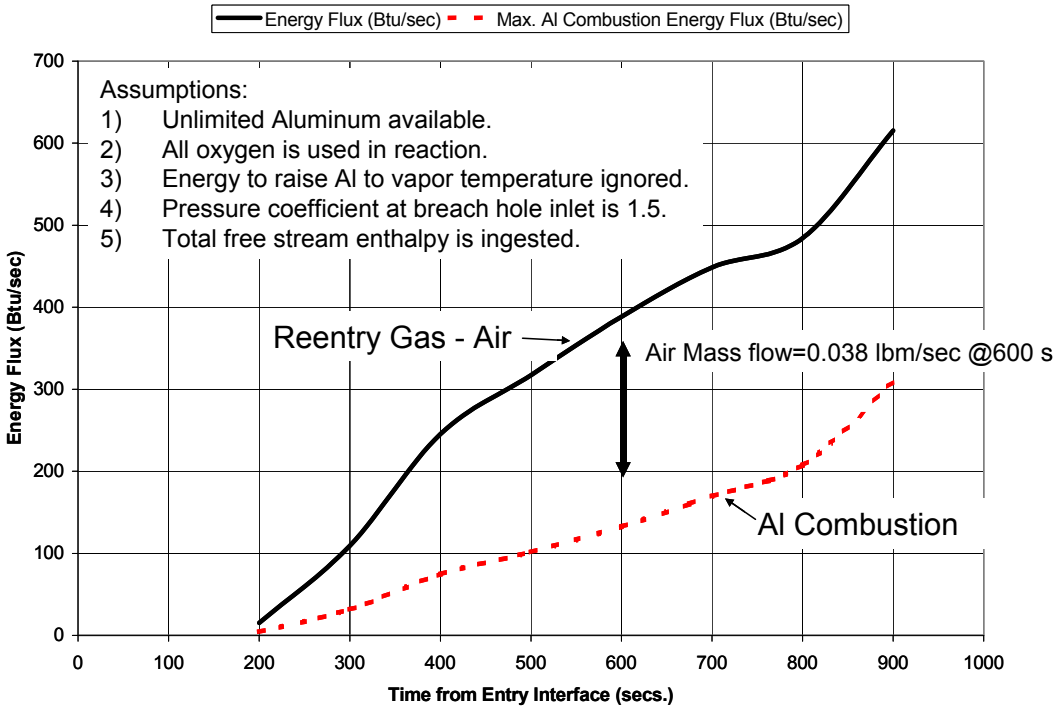

Figure 5.3.4-5 Comparison of Reentry Gas Energy Flux and Al Combustion Energy Flux for 6-inch Diameter Breach Hole in Leading Edge.

5.3.5 Coupled Venting and Thermal Model of Wing

5.3.5.1 Introduction

The objective of this analytical effort was to develop a tool capable of analyzing bulk flow in the STS-107 port wing for various breach scenarios. The intent was to utilize this transient modeling capability to provide pressure and flow rate boundary conditions to steady-state detailed CFD modeling and to screen the case matrix to isolate the more probable scenarios and decrease the number of cases for the more time intensive CFD work.

Originally, the scope was to utilize ideal gas venting codes (both CHCHVENT and FLUINT) and combine this venting model with a thermal representation (SINDA) of the wing for a coupled venting/thermal capability. Once preliminary results were achieved, the scope was increased to include the effect of dissociation and ionization of the ingested air, which was done assuming equilibrium air chemistry properties of the air as a function of air pressure and temperature instead of the ideal gas assumption.

5.3.5.2 Modeling Tools-Capabilities And Limitations

5.3.5.2.1 CHCHVent Program

Program CHCHVENT (see documentation by Fay) models the flow of a mixture of ideal gases with constant specific heats in the continuum flow regime between compartments arbitrarily connected by vents. It is primarily used to model launch vehicle compartment and payload venting environments. The program is based on the conservation equations of mass and energy with heat transfer in the chambers modeled as adiabatic, isothermal, or finite rate with a user-specified heat transfer coefficient.

Flow through the vents is assumed one-dimensional, isentropic, and is determined from the following equations (where subscripts U and D denote properties in the upstream and downstream compartments):

$$\dot{m} = C_d A P_U \sqrt{\frac{\gamma}{R T_U}} \frac{M}{\left[1 + \frac{\gamma - 1}{2} M^2\right]^{\frac{\gamma+1}{2(\gamma-1)}}}$$

where

$$M = \sqrt{\frac{2}{\gamma - 1}\left[\left(\frac{P_U}{P_D}\right)^{(\gamma-1)/\gamma} - 1\right]}$$

where:

$\dot{m} =$ Mass Flowrate

$C_d =$ Discharge Coefficient

$A =$ Flow Area

$P =$ Pressure; U=Upstream; D=Downstream

$M =$ Mach Number

$\gamma =$ Ratio of Specific Heats

$R =$ Gas Constant

T_U = Upstream Temperature

If the Mach number (*M*) is calculated to be greater than one, the program sets the Mach number to one (choked flow). A discharge coefficient (C_d) is used to correct the isentropic mass flow rate predicted from the

above equations. The C_d correction options included in CHCHVENT are: constant value, pressure-ratio dependent, and pressure-ratio-and-cross-flow dependent.

The program explicitly advances in time by numerical integration with the user having choices of 1st order Taylor series, 2nd order Modified Euler, 4th order Runge-Kutta and Runge-Kutta-Merson routines. Local pressure coefficients and local Mach numbers (which are specified as functions of free stream Mach number, vehicle angle of attack, and roll angle) and the trajectory parameters can be specified by the user.

The venting simulation is initialized by specifying pressures and temperatures for all chambers in the model. The total mass and internal energy derivatives with respect to time for a particular chamber are determined by summing the contributions from all vents connected to the chamber. These derivatives are used in the numerical routine to determine the chamber mass and internal energy at the next time, from which the remaining chamber properties are determined:

$$\rho = m / Vol \qquad T = U / mC_v \qquad P = \rho RT$$

where:

$\rho =$ Density
$m =$ Mass
$Vol =$ Compartment Volume
$T =$ Temperature
$U =$ Internal Energy
$C_V =$ Constant Volume Specific Heat
$P =$ Pressure
$R =$ Gas Constant

Using these chamber properties, the above procedure is repeated for the next time step.

5.3.5.2.2 SINDA/FLUINT Program

The Simplified Improved Numerical Differencing Analyzer (SINDA) with Fluid Integrator (FLUINT) is a software package, developed under contract to NASA, for solving lumped parameter network representations of heat transfer and fluid flow problems that are governed by conservation equations. For heat transfer problems, the physical system is partitioned into a Resistance-Capacitance (R-C) network that is analogous to an electrical circuit inasmuch as heat flows between nodes of unequal temperature, current flows between nodes of unequal potential (voltage) in an electrical circuit. Nodes within the thermal network represent discretized portions of the physical system and, in a transient simulation, may store or lose energy much like capacitors in an electrical circuit. Similarly, fluid systems are discretized into lumps and connectors where pressure differences between lumps and the resistance of the connectors determine both the magnitude and direction of the flow. The thermal and fluid networks may be seamlessly integrated through convective ties between fluid lumps and thermal nodes. The coupled thermal/fluid network is solved simultaneously by SINDA/FLUINT, thereby increasing stability and temporal accuracy.

Specifying the mass (or capacitance) of the thermal nodes and/or the volume of the fluid lumps permits transient as well as steady state simulations. A semi-implicit 2nd order forward-backward differencing scheme is used to advance the solution in time. The time-step is dynamically determined by the program to ensure stability with a user defined output interval available to provide results. The transient thermal network is solved such that the energy flows between nodes as well as the energy gained or lost by each node balance over the time-step. The transient flow network is solved such that conservation of mass and energy are maintained at each lump while momentum is conserved within each connector. FLUINT can handle compressible and incompressible flows up to the sonic limit (supersonic flows may be computed in special cases) and choked flows are automatically identified and computed by the program.

Connector-device models exist within FLUINT to allow the user to model a wide variety of flows. The orifice device is used almost exclusively in subsequent SINDA/FLUINT based analyses to describe the connectivity between flow compartments in the orbiter wing and associated volumes in the payload bay or fuselage. The orifice device is pictured below with the important input/output parameters noted. The subscripts U, D, and TH denote the upstream, downstream, and throat conditions, respectively. FLUINT automatically determines the direction of flow and the upstream and downstream conditions are derived from the fluid lumps between which the orifice device is connected. The throat conditions are only used in choking calculations and are determined by assuming an isentropic expansion from the upstream conditions. AORI is the actual physical area of the orifice and ATH is the effective area determined from AORI and a user specified discharge coefficient, CDIS. AF is the upstream area (generally intended for pipe flow) and is set to ten times the actual orifice area for the large freely vented volumes of the orbiter wing.

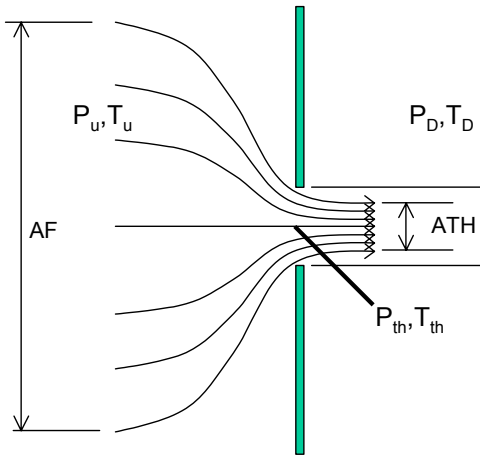

where:
AFTH = Throat Area (ATH)
CDIS = Discharge Coefficient
Cv = Velocity Coefficient
AORI = Orifice Area
P = Pressure (U=upstream; D=downstream; th=throat)

$$AFTH = \frac{CDIS}{C_V} AORI$$

$$C_V = .98$$

The internal algorithm for determining whether the flow-rate through the orifice device is choked is illustrated below. First, isentropic expansion from the upstream conditions and a velocity equal to the speed of sound at the throat are used to determine the critical (choked) flow-rate through the orifice. Next, the actual flow-rate through the orifice is determined from the pressure difference, average density, and a K-factor based upon the geometry of the orifice. Finally, comparing the actual flow-rate to the critical flow-rate yields the correct flow-rate.

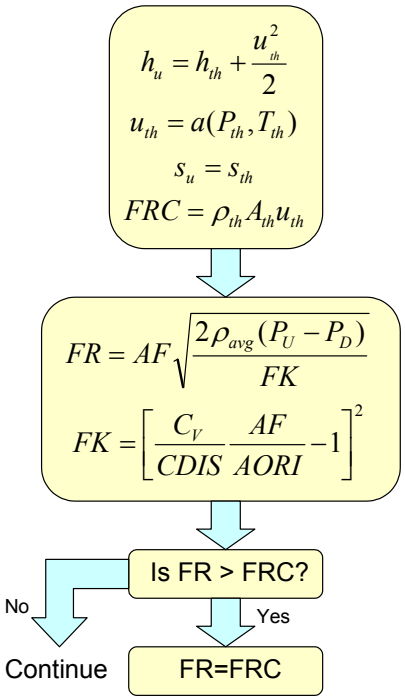

where:
h = enthalpy
u = internal energy
a = speed of sound
s = entropy
FRC = Critical Flowrate (for choking)
AF = Flow Area
FK = loss coefficient
FR = mass flowrate

5.3.5.3 Modeling Assumptions

5.3.5.3.1 Trajectory
The analysis is based on the STS-107 End of Mission 3 (EOM3) trajectory, where time zero corresponds to Orbiter Entry Interface (EI). The pertinent quantities used in the analysis are plotted in Figure 5.3.5-1 and Figure 5.3.5-2.

5.3.5.3.2 Discharge Coefficients
Two orifice discharge coefficient (C_d) corrections were used in the analysis. One is a pressure-ratio dependent C_d for a sharp-edged circular orifice from Shapiro, where C_d is a function only of the pressure ratio across the orifice. The second correction is a pressure-ratio-and-cross-flow dependent C_d for a circular orifice that is from CHCHVENT, which is based on experimental data documented by Haukohl and Forkois. The C_d in this correction is a function of both the pressure ratio across the orifice and the local external Mach number flowing past the orifice. Shapiro's correction is incorporated as a 5th order polynomial curve fit and is depicted in Figure 5.3.5-3. The pressure-ratio-and-cross-flow correction is incorporated as a bi-variant lookup and is depicted in Figure 5.3.5-4. For the high aspect ratio leading edge vents (carrier panel and T-seals), the Haukohl and Forkois data were consulted. Since the leading edge vents are choked for all the cases, the empirical data showed a less than 5% difference compared to the sharp-edged circular orifice correlations, so the circular orifice correlations were used in lieu of computing the family of curves needed to generically account for high aspect ratio vents.

5.3.5.3.3 Local Pressure Coefficients
The local pressure of the flow just outside a vent, leak, or possible penetration is crucial to the venting analysis because it is frequently very different from the freestream pressure. Local pressure coefficients (C_p) computed from LAURA CFD analyses were used as inputs to the venting programs for determining the local external surface pressures. These CFD solutions were completed by Langley Research Center for STS-2, and two solutions (Mach=18.1, angle of attack=41.2 degrees and Mach=24.3, angle of attack=39.4 degrees) were made available by Gnoffo.

In CHCHVENT, the C_p value at a particular location is determined by linearly interpolating between the C_p values for the two Mach numbers, 18.1 and 24.3. Since these C_p values were similar and in an effort to

expedite the process of adding this capability to FLUINT, the C_p values for the two Mach numbers were averaged in the FLUINT models. Also, since the vehicle angle of attack in the EOM3 trajectory is approximately 40 degrees from EI through EI+1000 seconds, the C_p values were considered virtually constant over this range. To validate this assumption, the CHCHVENT model was run with both linearly varying and constant averaged C_p values with negligible change in the results. Contour plots for the windward and leeward sides of the vehicle for the Mach=18.1 solution are depicted in Figure 5.3.5-5 and Figure 5.3.5-6, respectively.

5.3.5.3.4 Breach Boundary Conditions

The derivation for the local boundary conditions for a large breach is based upon the assumption that either all or a sizable fraction of the free stream total enthalpy is ingested at the breach or penetration. The flow through the large breach is modeled by the orifice device (within SINDA/FLUINT) and conditions at the upstream lump (or plenum) are updated each time-step based upon the assumed trajectory.

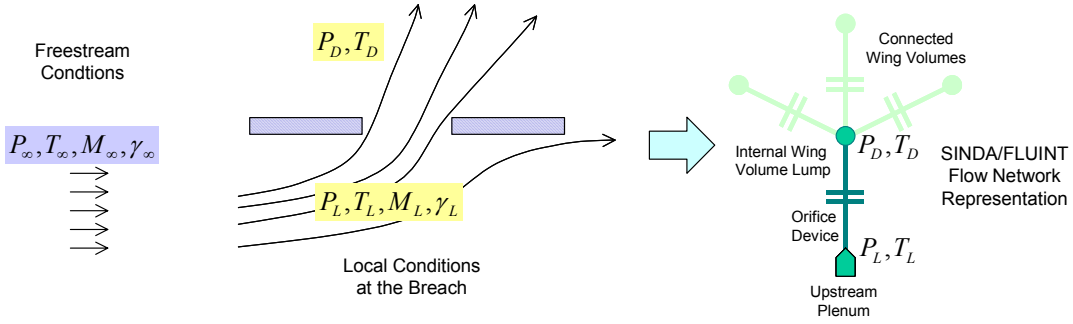

To determine the local conditions for the upstream boundary, the local enthalpy is scaled to the free-stream enthalpy (or taken from the engineering analysis described in Sec. 5.3.2.1) and the local pressure is derived from the free-stream pressure through an externally supplied pressure coefficient. Iteration within the equilibrium air property tables is required to determine the local conditions as a function of enthalpy and pressure for a real gas while a closed form solution exists for a perfect gas. An alternate model was created to more accurately model the period after the internal spar breach, where the local pressure from the jet impinging on the spar is assumed to equal the local external pressure. Also, the bulk enthalpy ingested through the leading edge hole was assumed to be ingested through the spar breach (consistent with jet flow through the breach).

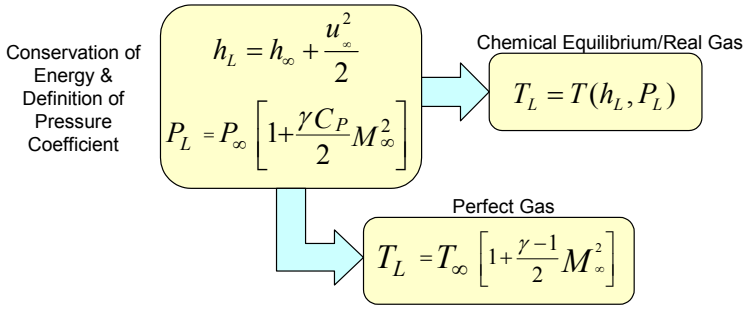

The derivation for the local boundary conditions for a small breach or vent is based upon the assumption that the flow into the small breach or vent is greatly influenced by the surrounding structure which necessitates the use of the local Mach number and the static conditions at the breach.

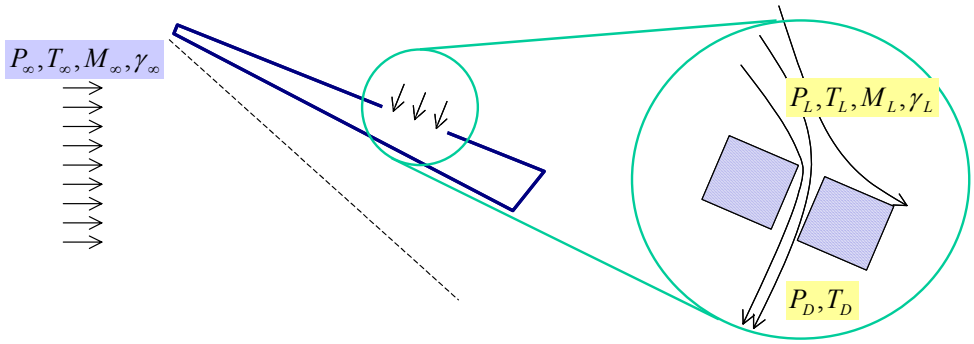

As in the case of the large breach, the local pressure is derived from the free-stream pressure via an externally provided pressure coefficient. The remaining state condition is determined by assuming constant entropy between the free-stream conditions and those locally at the breach or vent. This is not strictly correct if shock waves are present in the flow, but engineering judgement dictates that for wing locations away from the leading edge, the entropy increase through the shock will be largely offset by an entropy decrease due to the non-adiabatic nature of the flow over the wing. Determining the actual energy lost by the non-adiabatic flow to the wing structure is problematic for non-CFD based venting analyses and, for locations away from the leading edge of the wing (such as the windward elevon seals), it is anticipated that only a very small fraction of the free-stream enthalpy would be ingested. As before, a closed form solution exists for an ideal gas while a real gas demands use of the property tables.

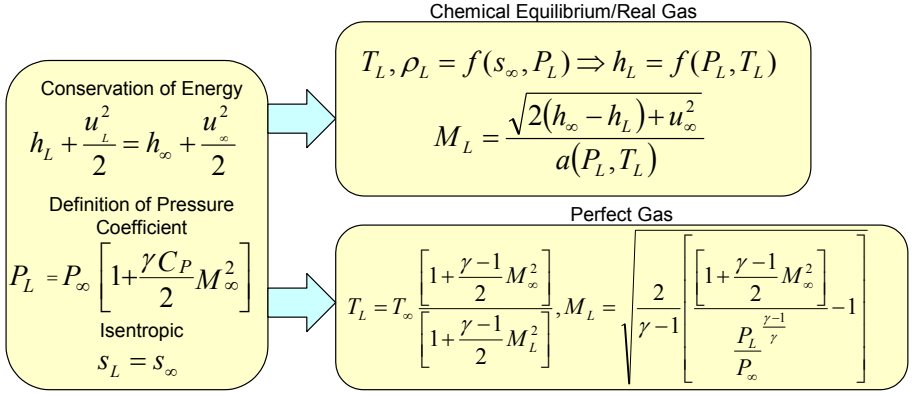

5.3.5.4 Vent-Only Model Development

5.3.5.4.1 Development/Description

The venting model was developed primarily from Rockwell International's 1994 "Orbiter Entry Venting Substantiation Report" by Wong, and a report documenting an integrated venting model for OV-102, Flight 27, STS-109 by Cline. The models used in the Substantiation Report were based on one-half of the Orbiter; whereas, the geometry was extended to include the complete vehicle to account for the non-symmetric nature of a possible breach in the left wing. The venting model was later modified based on results of a structural leakage test done for this investigation (Cline and Torres), suggested modifications from the JSC Aerothermal Internal Flow team, and estimated leading edge vent areas from Computer Aided Design (CAD) drawings. A graphical representation of the venting model is depicted in Figure 5.3.5-7.

Comparison Of CHCHVENT And FLUINT (Adiabatic/Ideal Gas)

FLUINT did not initially have the capability to calculate local external pressures from pressure coefficients or contain the discharge coefficient models included in CHCHVENT; therefore, these capabilities were added to FLUINT and comparisons between CHCHVENT and FLUINT were made for validation purposes. A typical plot from the comparisons is shown is Figure 5.3.5-8, where the predicted net rate of change of mass in the

left main gear wheel well assuming a 20 in^2 breach into the left wing front glove compartment (section between bulkheads 807 and 1040) is shown. This comparison was made assuming the air as an ideal gas with constant specific heats in both CHCHVENT and FLUINT. In addition, the boundary-condition temperatures used in the comparison cases only were calculated from isentropic equations. For the breach, the local ingested gas temperature was assumed to be the free-stream stagnation temperature and calculated from:

$$\frac{T_{local}}{T_{freestream}} = \left[1 + \frac{\gamma - 1}{2} M^2_{freestream}\right]$$ (Ideal Gas Case Only – Not used in Final Results)

For all other locations where gas could be ingested (i.e. lower elevon seals, wheel doors, etc.) the following equation was used for the ingested gas temperature:

$$\frac{T_{local}}{T_{freestream}} = \frac{\left[1 + \frac{\gamma - 1}{2} M^2_{freestream}\right]}{\left[1 + \frac{\gamma - 1}{2} M^2_{local}\right]}$$ (Ideal Gas Case Only – Not used in Final Results)

5.3.5.5 Chemical Equilibrium Air Properties

SINDA/FLUINT Property (FPROP) tables were generated using FORTRAN 90 property routines for chemical equilibrium air obtained from the NASA Langley Research Center (LaRC). Six property tables (all as a function of pressure and temperature) were generated from the property routines: specific volume, enthalpy, speed of sound, entropy, absolute viscosity, and thermal conductivity. Entropy was obtained by numerically integrating the enthalpy tables at constant pressure.

SINDA/FLUINT requires entropy as a function of pressure and temperature for choking calculations in real gas simulations. Entropy tables were generated from the LaRC routines by numerically integrating the relevant *Tds* equation along lines of constant pressure:

$$Tds = dh - vdP$$

$$\int_1^2 ds = \int_1^2 \frac{dh}{T} - \int_1^2 \frac{v}{T} dP$$

$$P = const$$

$$s_2 = \frac{T_1 + T_2}{2T_1T_2}\left[h_2 - h_1\right] + s_1$$

An arbitrary reference entropy of 10,000 J/kg-K (2.39 Btu/lb_m-R) was chosen for the pressure equal to 0.001 Pa (9.9e-09 atms) and temperature equal to 200 K (360 R). Initial conditions for the integration were based upon ideal gas estimates of the entropy at 200 K and for a pressure range of 0.002 Pa (1.97e-08 atms) through 101325 Pa (1 atm). The trapezoidal integration was performed row-by-row with each succeeding entropy numerically integrated from the previous row's entropy at the same pressure. The real gas properties of air are markedly different from those of a perfect gas as evidenced by the entropy versus temperature plot shown in Figure 5.3.5-9. The almost cyclical changes in entropy with increasing temperature indicate a pattern of dissociation/ionization as new species are continually formed.

Also to aid choking calculations, a frozen speed of sound was computed from the specific heat ratio and an effective gas constant ($R_{EFF}=P/\rho T$). SINDA/FLUINT utilizes internal routines to provide fluid properties either by direct interpolation or by iteration if not requested as a function of pressure and temperature (i.e. T=T[s,P]).

Several of the interpolation/integration routines were rewritten to remove any dependency on ideal gas assumptions and/or to remove the additional logic present for two-phase fluids.
The property tables were generated over a range of 200 K (360 R) to 9100 K (16,380 R) and from 0.001 Pa (9.9e-09 atms) to 101325 Pa (1 atm). At very low density (due to extreme temperature or low pressure), the LaRC property routines issued cautions. Some thermal conductivity and viscosity data were discarded and replaced with data obtained from the routines at a higher pressure (this is assumed reasonable given the range of pressure profiles expected in this analysis).

5.3.5.6 Thermal Model Development

Thermal representation of the main structure comprising the port wing was developed in order to determine the thermal coupling effects of the structure on the venting model. The model was developed in SINDA/FLUINT format with geometric modeling being performed in Thermal Desktop. The stand-alone thermal model was initially set up utilizing STS-5 re-entry environments (Hartung and Throckmorton) and compared to results from the Dryden Flight Research Center's STS-5 analyses (Gong et al). The model was then modified to STS-107 environments and convectively coupled to the vent models.

Configuration details for the SINDA/FLUINT thermal math model of STS-107 Columbia's left wing were obtained from several sources (Figure 5.3.5-10), Computer Aided Design (CAD) models developed by the STS-107 Accident Investigation Structures Team, Shuttle Drawing System (SDS) – Boeing North America (BNA), Shuttle Operational Data Book on the NASA Human Space Flight website, Space Shuttle Entry Heating Data Book, Volume III – STS-5 (Hartung and Throckmorton), and Dryden Flight Research Center's Space Shuttle SPAR wing model (Gong et al).

5.3.5.6.1 Thermal Model Description

The three-dimensional thermal model consists of six internal wing volumes (sections 1-6) and four wing leading edge volumes (sections 7-10) corresponding to the venting models. Details of the thermal model are shown in Figure 5.3.5-11 and outlined below.

- Wing internal geometry based on CAD model – model includes the wing spars but the struts are omitted.
- Landing gear/wheel assembly derived from CAD model and specifications.
- Spar, fuselage and wheel well closeout panels assumed to be 0.1 inch thick Al-2219.
- Skin Al and Al-honeycomb panel representations are included. Al-honeycomb core is thermally modeled based on X-33 leeward aeroshell skin.
- Leeward honeycomb is 1.15 inches thick including inboard and outboard face-sheets of 0.025 and 0.045 inches, respectively.
- Windward honeycomb is 0.75 inches thick. The face-sheets are the same thickness as the leeward side. Remaining wing skin was assumed to be 0.1 inch thick Al-2219.
- TPS is represented on both windward and leeward sides. Leeward TPS was assumed to be 0.16 inches of FRSI throughout. (LRSI tiles were not modeled). Windward TPS assumed to be HRSI. Thicknesses averaged for each wing section based on the Dryden model data (Gong et al).
- SIP and RTV layers are included.
- Internal radiation is included (Optical properties from Dryden model or estimated from material.)
- Leading edge geometry based on vent volumes in venting models and the spar geometry from the CAD model.
- STS-107 wing leading edge, windward and leeward heat rates for STS-107 End of Mission (EOM) 3 trajectory were supplied by Boeing-Houston.
- Material properties taken from (in order of preference) NASA RP-1193 or TPSX database (NASA ARC).
- Time dependent pressure arrays (required to interpolate pressure and temperature dependent property arrays) estimated from STS-107 EOM3 trajectory profiles, STS-2 LAURA windward and leeward C_p profiles.

5.3.5.6.2 Fluid/Structure Coupling

The lumps representing the air in each of the compartment volumes in the vent models were tied convectively to the internal wing structural nodes in the thermal model. Convection coefficients for each tie were derived from laminar flow, flat plate Nusselt Number correlations (Incropera & Dewitt) utilizing the total flow entering each compartment, the cross-sectional area at the centroid of each volume (roughly normal to the perceived main flow direction), the path length through the centroid (along the perceived main flow direction) and the fluid properties (evaluated at the average of the wall and lump temperatures). The thermal model was later modified to include convective coupling between the leakage into the wheel-well area through the MLG door seal and the door structure. Also, convective coefficients for compartment 3 were later derived from FLUENT CFD modeling of this flow (Sec. 5.3.6.3). A correction factor was derived between the flat-plate Nusselt relation and the CFD at time point 404-sec after entry interface and used for correcting the Nusselt relation for the remainder of the transient simulation.

5.3.5.7 Thermal/Venting Results

The results in this section were generated over several weeks as the modeling assumptions were evolving. The following matrix summarizes the cases for which results are presented in this report with the major assumptions at the time of that modeling effort. Many additional cases were generated, but are not included for brevity, but are available upon request.

Case #	Assumptions	Purpose
1	10”, 6” and 4” diameter RCC Breach hole with Cp=1.46 6” diameter internal Spar Breach hole at 490-sec after EI Ingested Enthalpy = 76% of freestream (based on Gnoffo CFD at 404-s) Local Pressure at Spar Breach calculated based on bulk compartment 8 pressure response. Flat Plate empirical Nusselt correlation for internal heat transfer	Assess leading edge pressure history for CFD boundary conditions and internal wing temperature response
2	10” diameter RCC Breach hole with Cp=1.46 10” diameter internal Spar Breach hole at 487-sec after EI Ingested Enthalpy based on Sec. 5.3.2 calculations. No heat transfer to leading edge structure – all ingested into spar breach. Local Pressure at Spar Breach assumed equal to external pressure (Cp=1.46). Flat plate empirical Nusselt correlation for internal heat transfer except for compartment 3, which uses FLUENT CFD heat transfer coefficient factor from Sec. 5.3.7.	Assess leading edge pressure history for CFD boundary conditions and internal wing temperature response
3	10” & 6” diameter RCC Breach Hole Cases with Cp=1.46 Ingested Enthalpy based on Sec. 5.3.2 calculations No internal Spar Breach	Provide pressure differential across leading edge spar for structural loads failure analyses.

5.3.5.7.1 Leading Edge Pressure Profiles

Case 1

The leading edge compartment pressures were of general use to providing CFD boundary conditions for various breach analyses. The Case 1 results are shown in Figure 5.3.5-12 for the three breach hole diameters. Prior to the EI+490-sec internal spar breach, the pressures represent the balance of flow coming in via the breach and the outflow from the T-seal and Carrier Panel vents of the leading edge. The pressure drop after the spar breach is due to flow into the low pressure compartment 3 volume.

Case 2

For Case 2, the leading edge was not modeled, but rather the spar breach local pressure was set equal to the external RCC pressure (assumed equal to jet impingement pressure). This approach results in a much higher local pressure to the spar breach as shown in Figure 5.3.5-13.

Case 3
The intent of Case 3 was to provide bulk pressure differentials across the leading edge spar, so the jet impingement local pressure to the spar was not appropriate. Therefore, this case models the leading edge bulk compartments (same as Case 1 except no internal spar breach). The pressure differentials for a 6" diameter and 10" diameter RCC hole are shown in Figure 5.3.5-14.

5.3.5.7.2 Internal Volume Pressure Profiles
The internal wing pressures are largely uninfluenced by the leading edge breach since there is only a very small nominal leak around the leading edge spar, but these pressures are dramatically increased by the subsequent internal spar breach at 487-seconds as shown in Figure 5.3.5-15 for both Case 1 and 2. The Case 2 post-spar breach pressures are much higher due to the larger local pressure and the 10" diameter spar breach instead of the 6" diameter breach in Case 1. The bulk of the wing is freely vented, but the forward wing-glove and wheel well compartments are slightly lower due to the large venting through the Payload Bay vent in the wing-glove as illustrated by the close-up of the Case 2 pressures in Figure 5.3.5-16.

5.3.5.7.3 Leading Edge Air Temperature Profiles

Case 1
The leading edge compartment temperatures are shown in Figure 5.3.5-17 for Case 1. Compartment 8 is the hottest due to the breach inflow and the other compartments are lower in temperature due primarily to the energy lost to structure (i.e., the RCC and leading edge spar insulation) and outflow from the leeside vents.

Case 2
As previously stated, Case 2 does not include the full representation of the leading edge, but rather just Compartment 8 treated as a plenum of local conditions for the spar breach. The air temperature for this plenum is illustrated in Figure 5.3.5-18. This is much higher than Case 1, which included the loss of energy to structure, where Case 2 assumes the jet energy carries through the internal spar breach. Therefore, the compartment 8 temperature represents the assumed bulk temperature of the flow entering the wing through the spar.

5.3.5.7.4 Internal Wing Air Temperature Profiles

Case 1
The internal wing compartment air temperatures are shown in Figure 5.3.5-19 for Case 1. The temperatures remain low until the leading edge spar breach at 490-seconds. Compartment 3 has the highest values since this is the compartment that the spar breach flows into directly. Temperatures in the other compartments are lower due to loss of energy to the wing structure. Compartment 1 has the next highest temperatures which is consistent with the mass flow and spar structural temperature results presented later.

Case 2
The internal wing compartment air temperatures for Case 2 are shown in Figure 5.3.5-20. These values are much higher than those for Case 1 due to the larger breach hole and much higher ingested enthalpy. The wheel well (Compartment 2) shows an elevation in temperature prior to the spar breach. This is due to an inflow from the payload bay, which is also at elevated temperature. This is an artificial effect since the standard leaks causing the elevated payload bay temperature would in reality lose energy to structure through those leaks, which the vent-only modeling does not capture. This effect is not a factor after the spar breach because the wheel well pressurizes with respect to the payload bay shortly thereafter.

5.3.5.7.5 Leading Edge Mass Flow Rate and Energy Rate In/Out
The leading edge RCC breach mass flow rate history is plotted in Figure 5.3.5-21 for Case 1. The Case 1 carrier panel and T-seal vent mass outflow is shown in Figure 5.3.5-22. The corresponding energy flux into the breach and out of the vents as well as heat transfer to the RCC and Cerachrome insulation is shown in

Figure 5.3.5-23. The mass flow through the spar breach for both Case 1 and 2 is compared in Figure 5.3.5-24 and the corresponding energy inflow is shown in Figure 5.3.5-25. The Case 2 mass and energy inflow are much higher due to the larger 10" hole instead of the 6" diameter and since energy is not transferred to structure before flowing through the spar breach in Case 1 as was shown in Figure 5.3.5-23.

5.3.5.7.6 Internal Wing Mass Flow Rate and Energy Rate In/Out

The forward and aft Compartment 3 vents (at Xo=1040 and Xo=1191) and wheel well forward Xo=1040 vent mass flow rates are plotted in Figure 5.3.5-26. The corresponding energy rates are shown in Figure 5.3.5-27.

The wheel well is of particular interest based on the flight data. The energy rates in/out from various vents/leaks for Case 1 is shown in Figure 5.3.5-28 and for Case 2 in Figure 5.3.5-29. Note the addition of energy into the wheel well prior to spar breach from the main landing gear door juncture leakage for Case 1. This energy is significant for Case 1 but not for Case 2 due to the much higher energy flux entering the wing for Case 2. Also, Case 2 reveals a brief inflow through the forward vent after the breach, but then the flow begins to outflow almost immediately. This transient is most likely due to the rapid pressurization of the wheel well from Compartment 1.

5.3.5.7.7 Leading Edge and Internal Wing Mach Number Histories

The RCC breach hole, the leading edge vents and the internal spar breach hole are almost immediately choked for all cases, so the plots of Mach Number are not presented. The Case 1 vent Mach Numbers for the Xo=1040, Xo=1191 and wheel well forward vents are plotted in Figure 5.3.5-30. The Case 2 results are shown in Figure 5.3.5-31.

5.3.5.7.8 Internal Wing Heat Transfer Coefficient Histories

Case 1 and 2

The heat transfer coefficients in Compartment 3 for Cases 1 and 2 are shown in Figure 5.3.5-32 and Figure 5.3.5-33, respectively. Case 2 includes the FLUENT CFD-based correction factors on these values. The wheel well (Compartment 2) Case 1 and 2 heat transfer coefficients are plotted in Figure 5.3.5-34 and Figure 5.3.5-35. The Case 2 values are higher primarily due to higher velocity flow rates.

Solid Wall Temperature Histories for the Leading Edge

The leading edge spar is insulated with Cerachrome that has a thin outer layer of Inconel. The Inconel temperature for Case 1 is plotted in Figure 5.3.5-36. Local heating effects caused by the leading-edge breach jet impinging on the insulation are not modeled and therefore the resultant temperatures for Compartment 8 are lower than what would be expected. However, for compartments away from the breach (7, 9, and 10) the predicted Inconel temperatures are considered realistic and indicate that the insulation would remain intact. The spar behind this insulation is plotted in Figure 5.3.5-37 and shows that the insulation performs very well.

Solid Wall Temperature Histories for Internal to the Wing

The Compartment 3 wall skin temperatures are shown in Figure 5.3.5-38 and Figure 5.3.5-39 for Cases 1 and 2, respectively. The wheel well wall temperatures are plotted in Figure 5.3.5-40 and Figure 5.3.5-41 for Cases 1 and 2, respectively. Case 2 temperatures are dramatically higher due to the larger hole in the spar, and the much higher ingested enthalpy. Note that the Case 2 temperatures exceed the aluminum melting point for many of the areas, which is known not to be the case from the telemetry data. This indicates that the Case 2 includes too much energy flowing into the wing (as compared to actual) due to either too large a size of the breach holes or the ingested enthalpy with local pressure assumptions being too high. The actual results are somewhere between the Case 1 and Case 2 predictions.

The spar temperatures for the remaining wing compartments are compared to Compartment 3 in Figure 5.3.5-42. The results indicate that heat is removed from the flow as it passes through the wing and that Compartment 1 structural temperatures are the next highest compared to Compartment 3. This trend is consistent with the higher flow rates through the 1140 vent into Compartment 1.

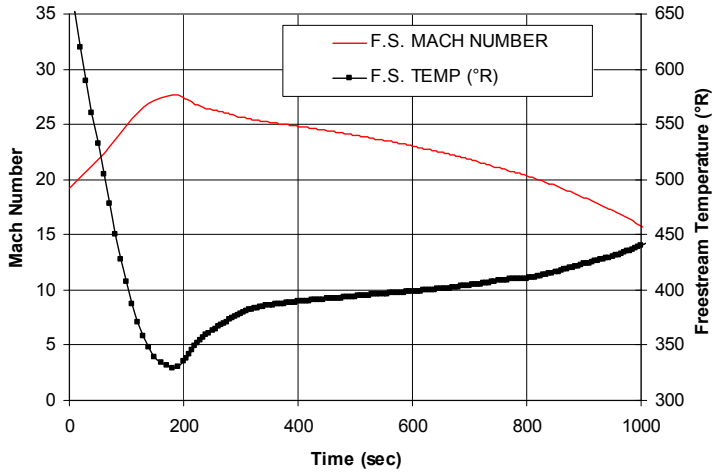

Figure 5.3.5-1 EOM3 Trajectory – Free-stream Mach Number and Temperature History.

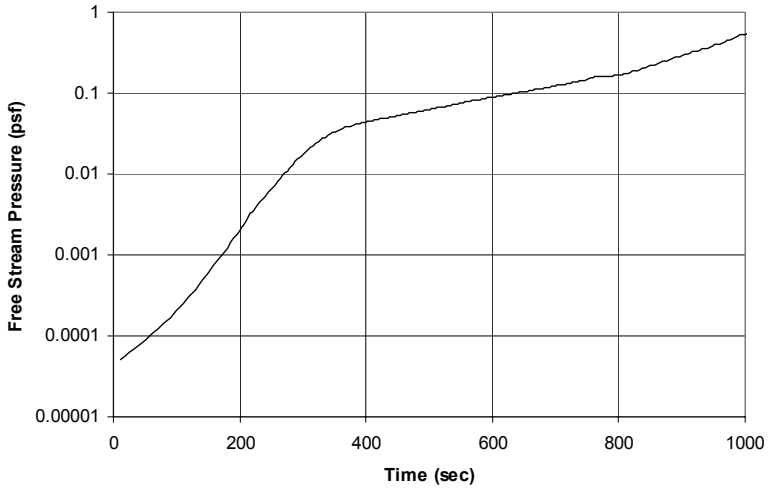

Figure 5.3.5-2 EOM3 Trajectory – Free-stream Pressure History.

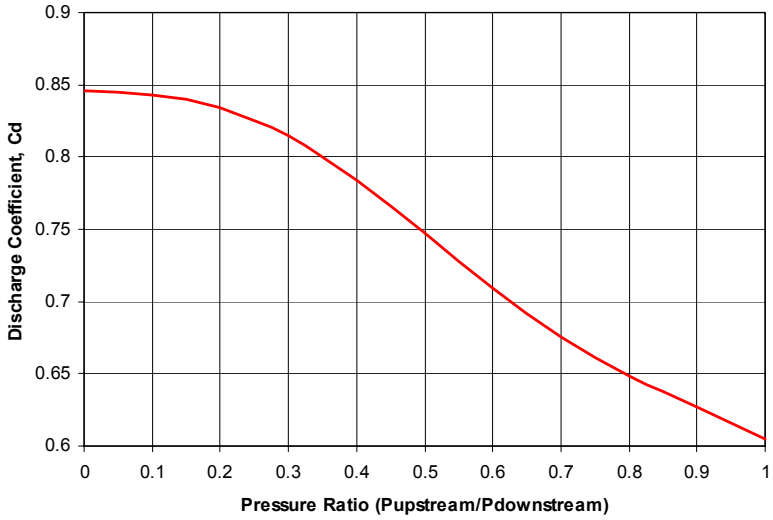

Figure 5.3.5-3 Pressure-Ratio Dependent Sharp Edge Orifice Discharge Coefficient .

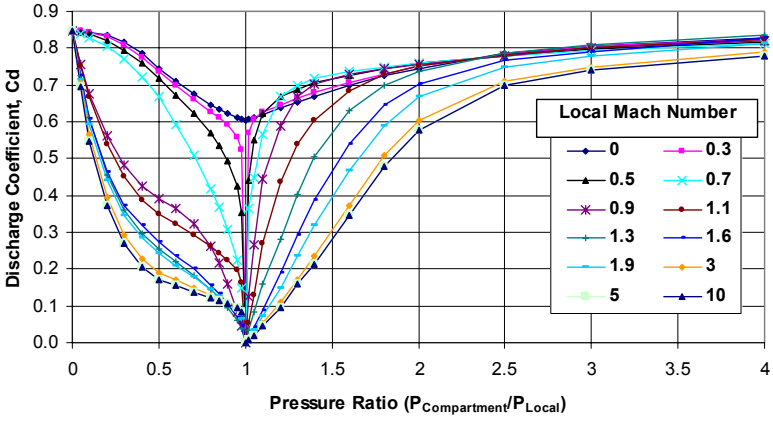

Figure 5.3.5-4 Pressure-Ratio-and-Cross-Flow Dependent Discharge Coefficient.

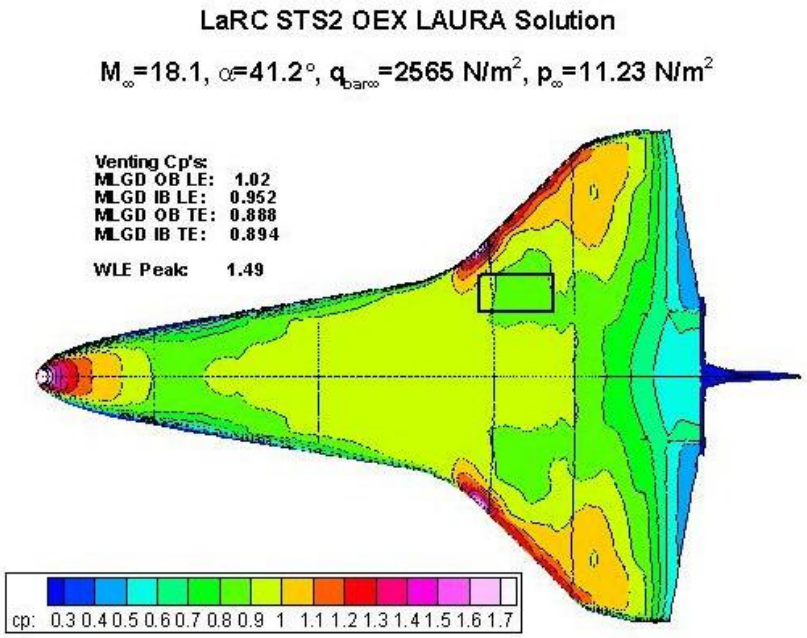

Figure 5.3.5-5 Windward LAURA Solution (STS-2, Mach 18) Surface Pressure Coefficient Contours.

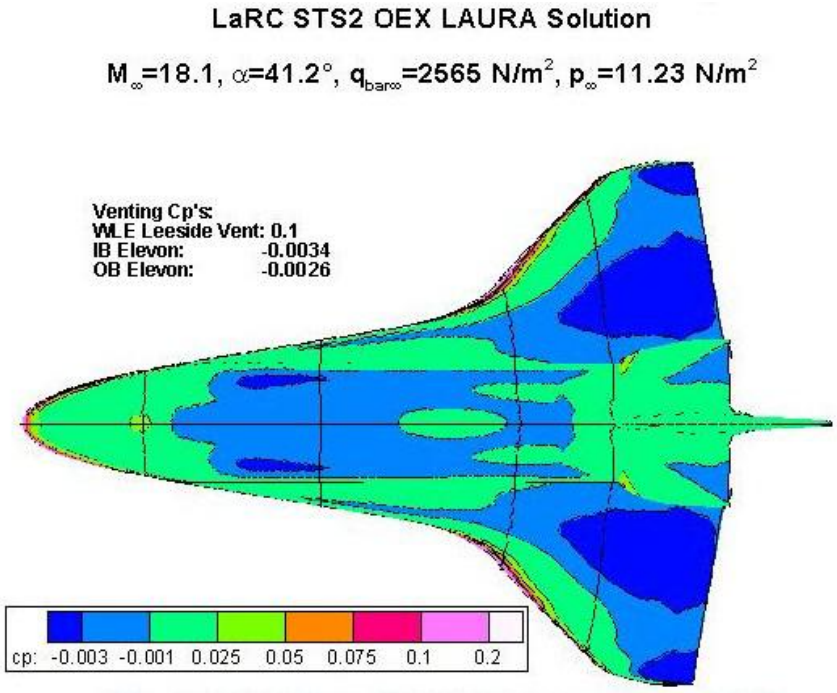

Figure 5.3.5-6Leeward LAURA Solution (STS-2, Mach 18) Surface Pressure Coefficient Contours.

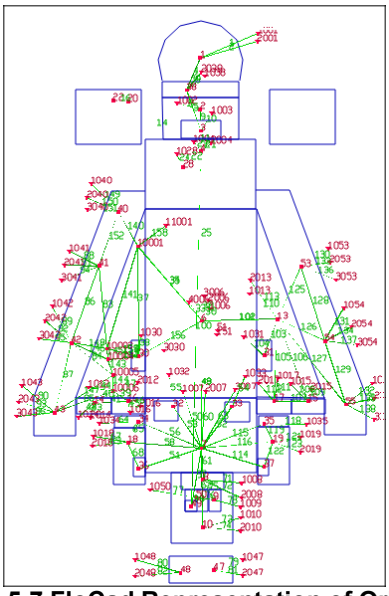

Figure 5.3.5-7 FloCad Representation of Orbiter Venting Model.

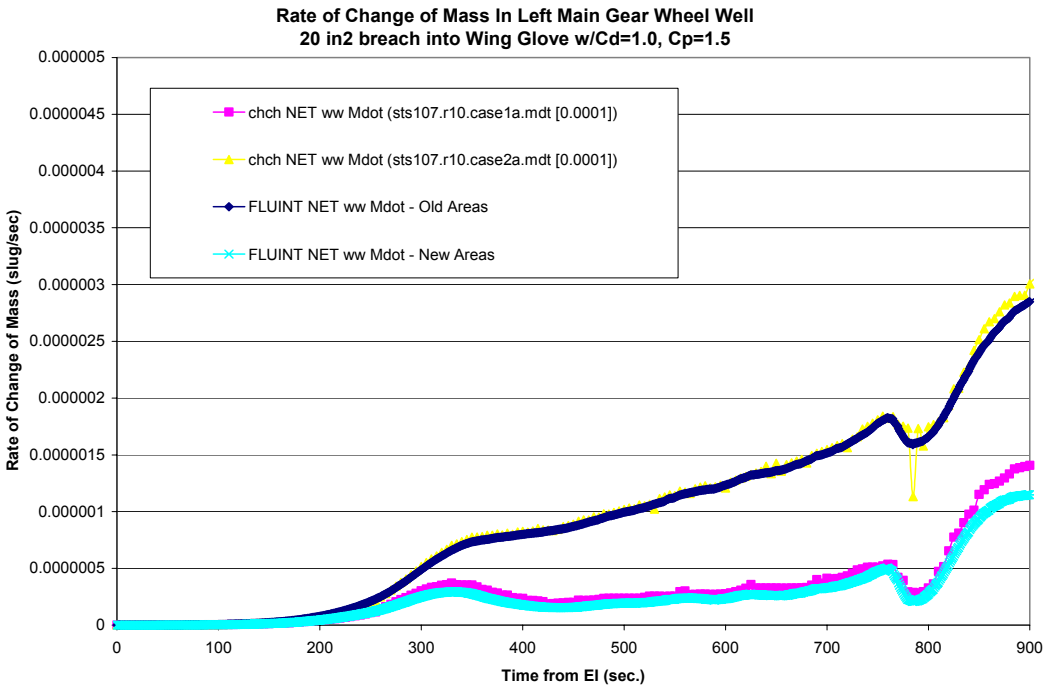

Figure 5.3.5-8 CHCHVENT and FLUINT Venting Comparison.

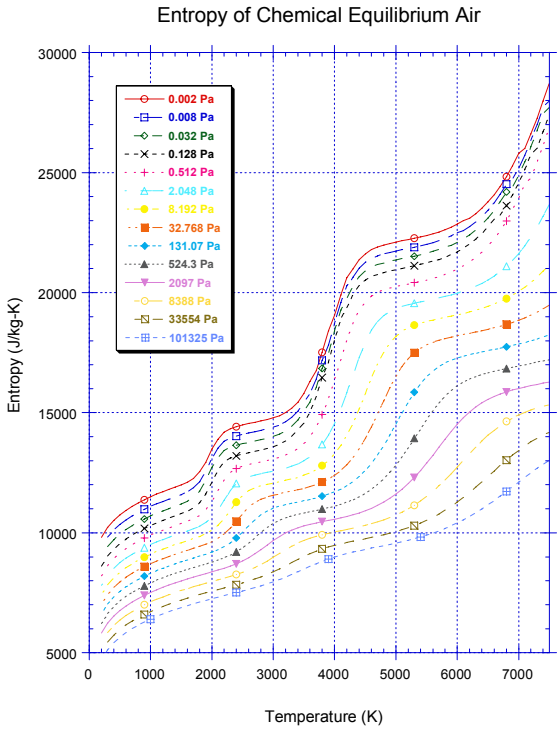

Figure 5.3.5-9 Equilibrium Air Entropy Variation with Temperature.

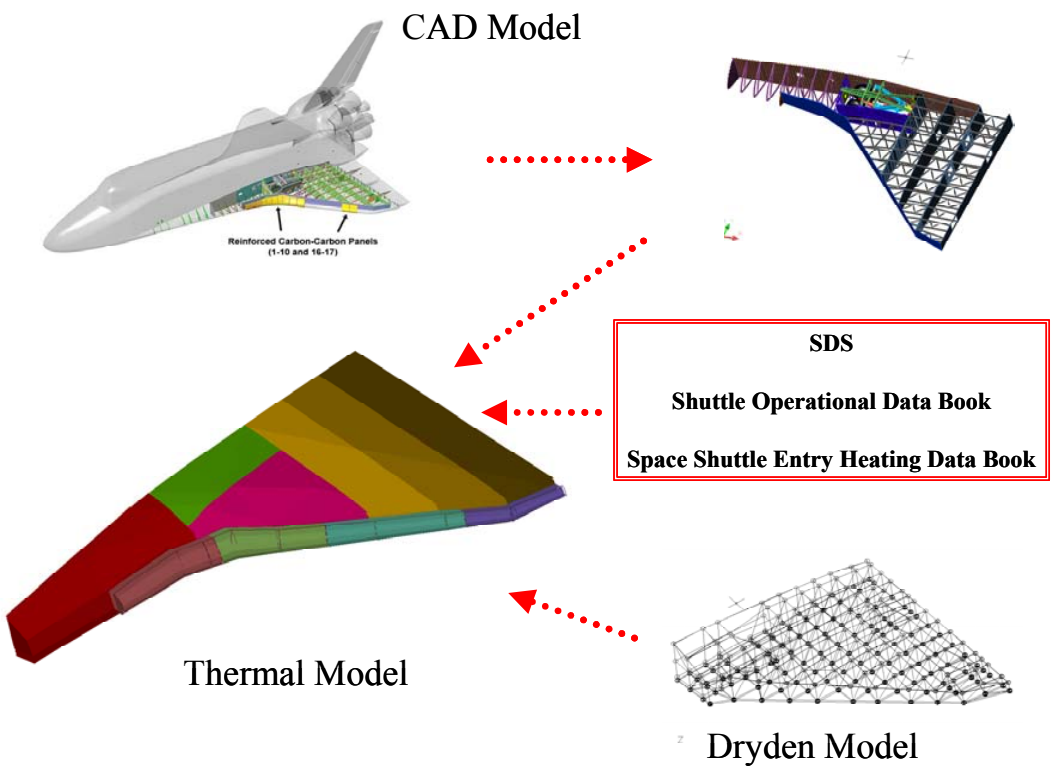

Figure 5.3.5-10 Orbiter Thermal Model Development Heritage.

RCC Leading Edge

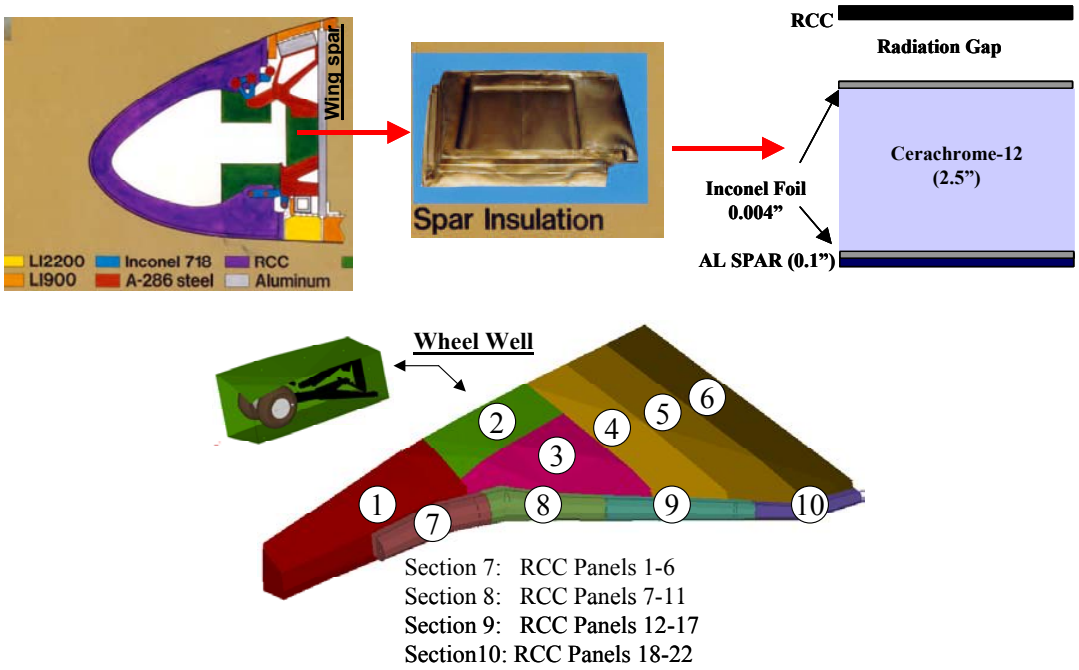

Figure 5.3.5-11 Thermal Model Configuration Details.

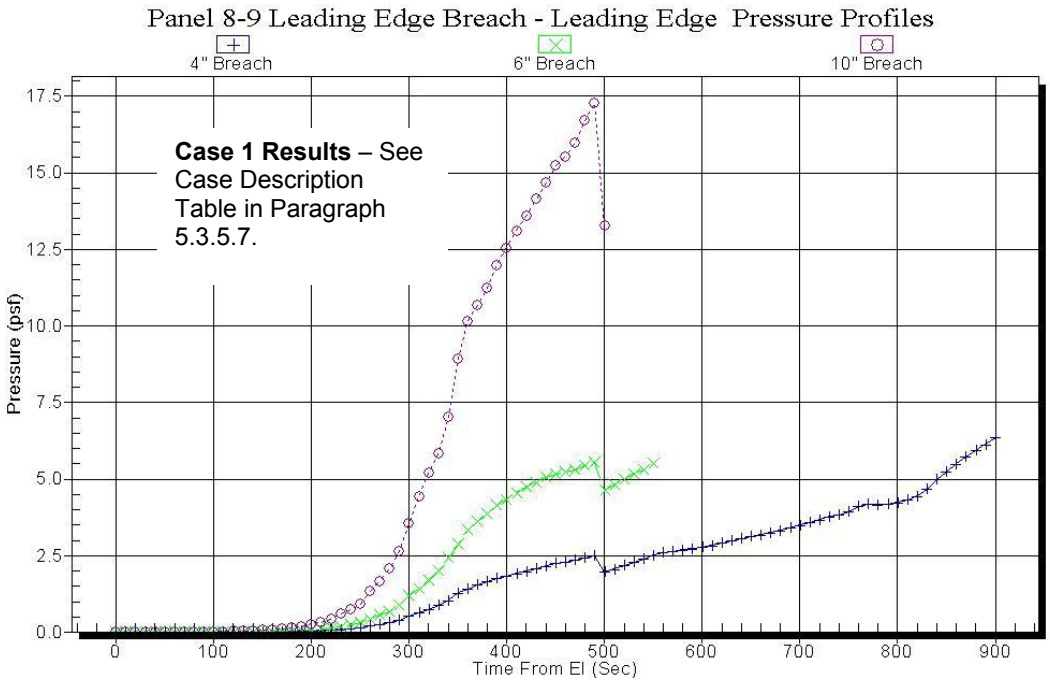

Figure 5.3.5-12 Case 1 Leading Edge Pressure History Plot for 4", 6" & 10" Diameter Breach

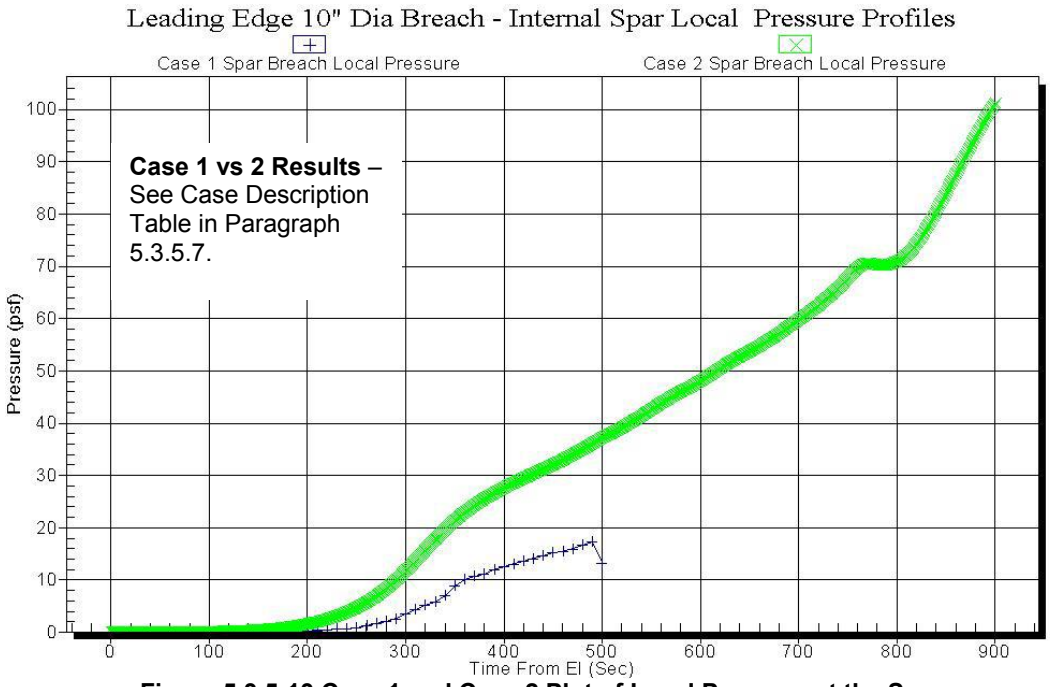

Figure 5.3.5-13 Case 1 and Case 2 Plot of Local Pressure at the Spar

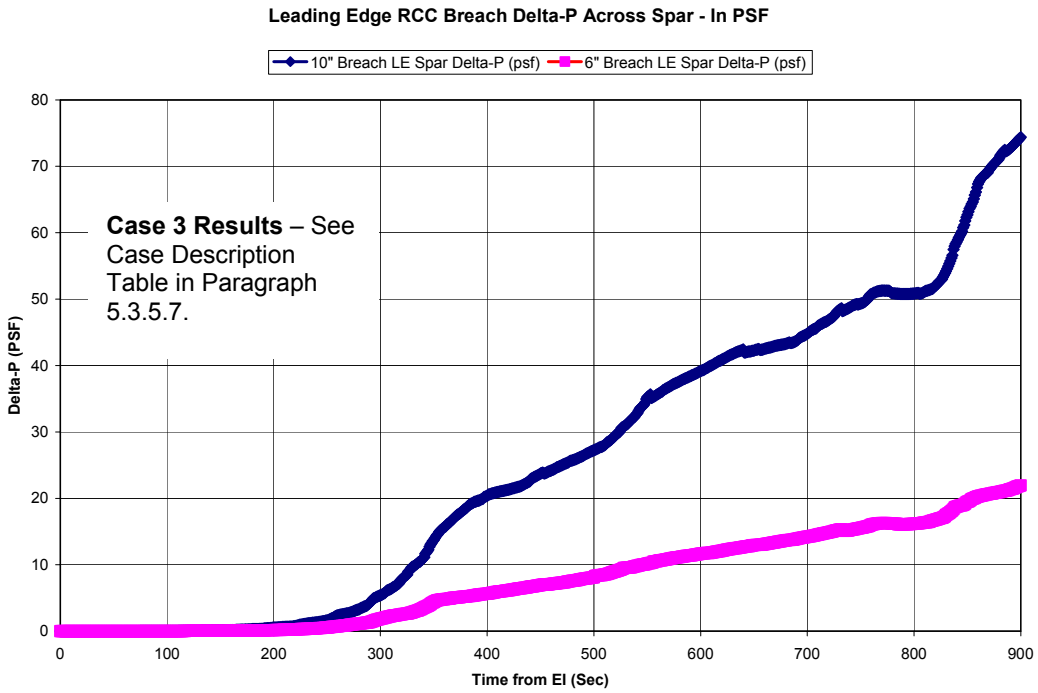

Figure 5.3.5-14 Case 3 Plot of Differential Pressure Across Leading Edge Spar for 6" and 10" Diameter Breach

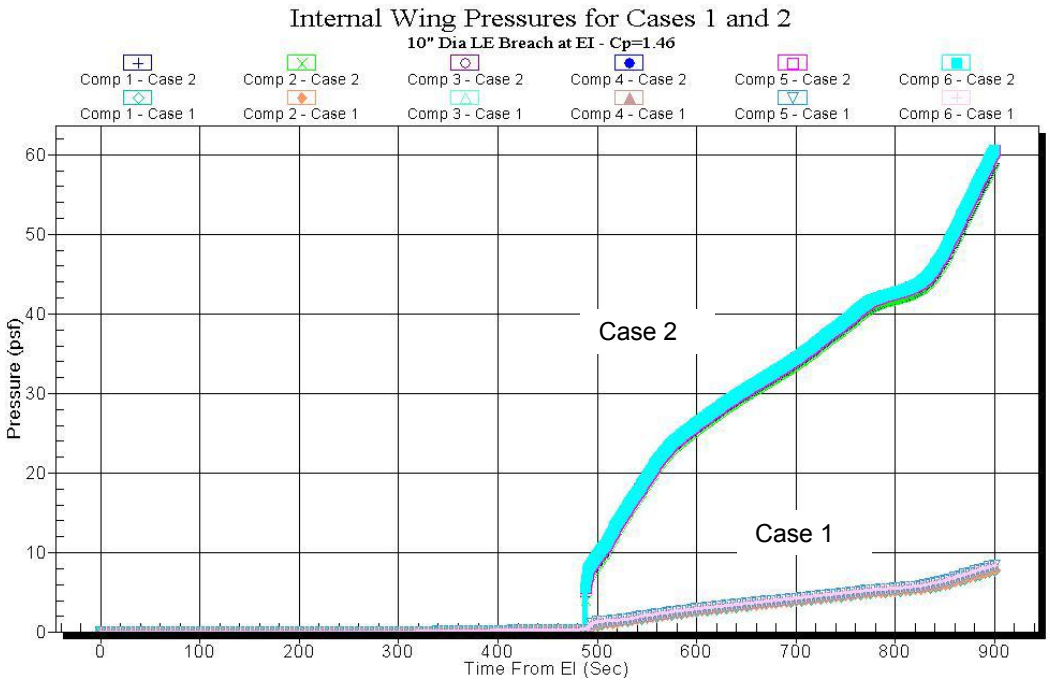

Figure 5.3.5-15 Internal Wing Pressure Histories for Cases 1 and 2

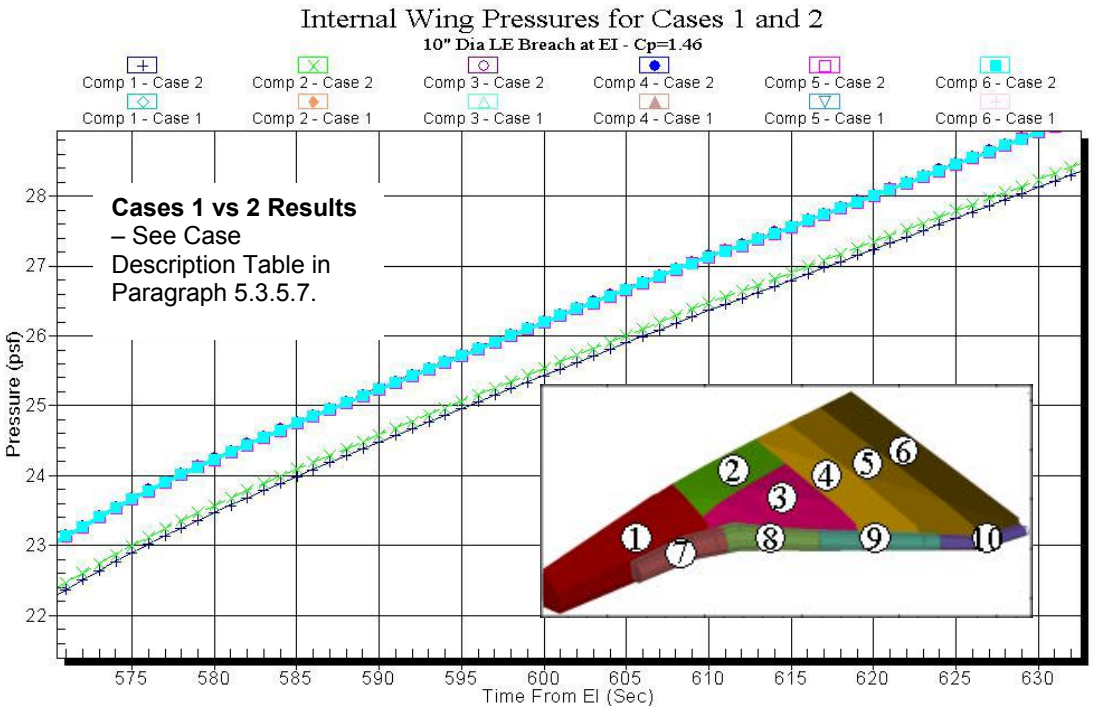

Figure 5.3.5-16 Detail Time-slice of Internal Wing Pressure Histories for Case 2

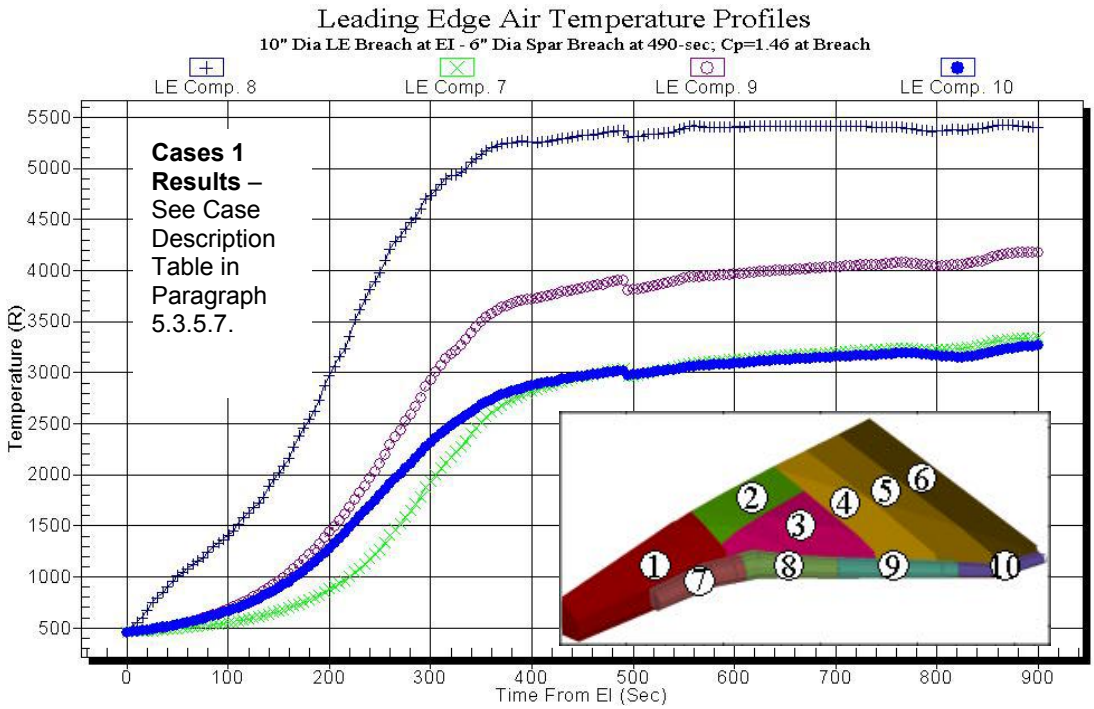

Figure 5.3.5-17 Leading Edge Air Temperature Histories for Case 1

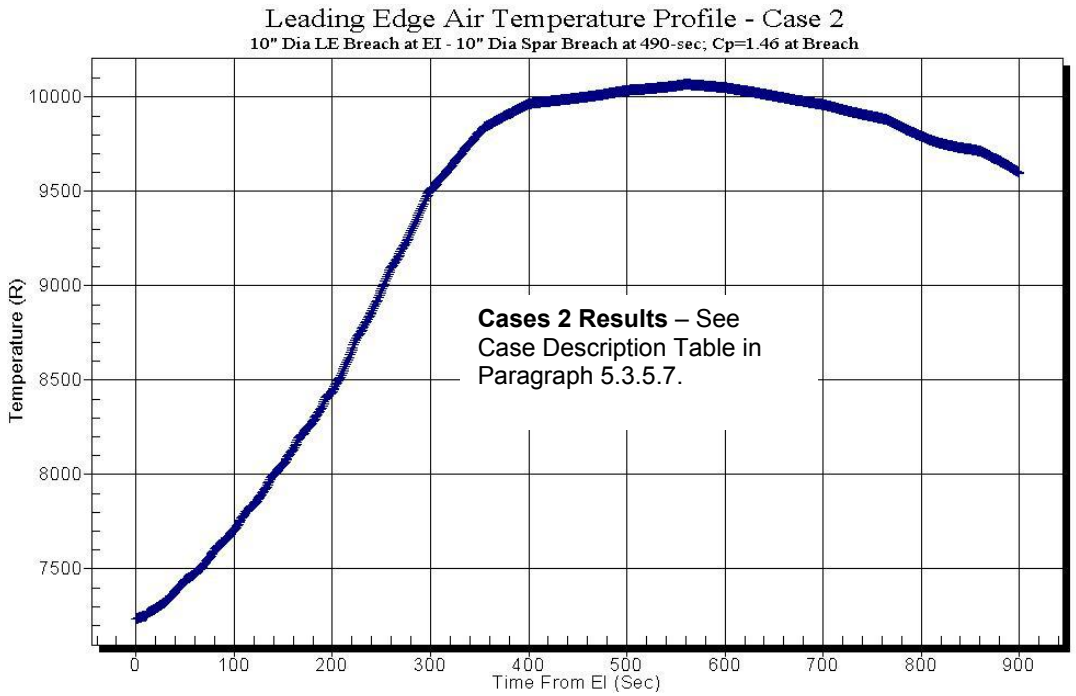

Figure 5.3.5-18 Leading Edge Air Temperature Histories for Case 2

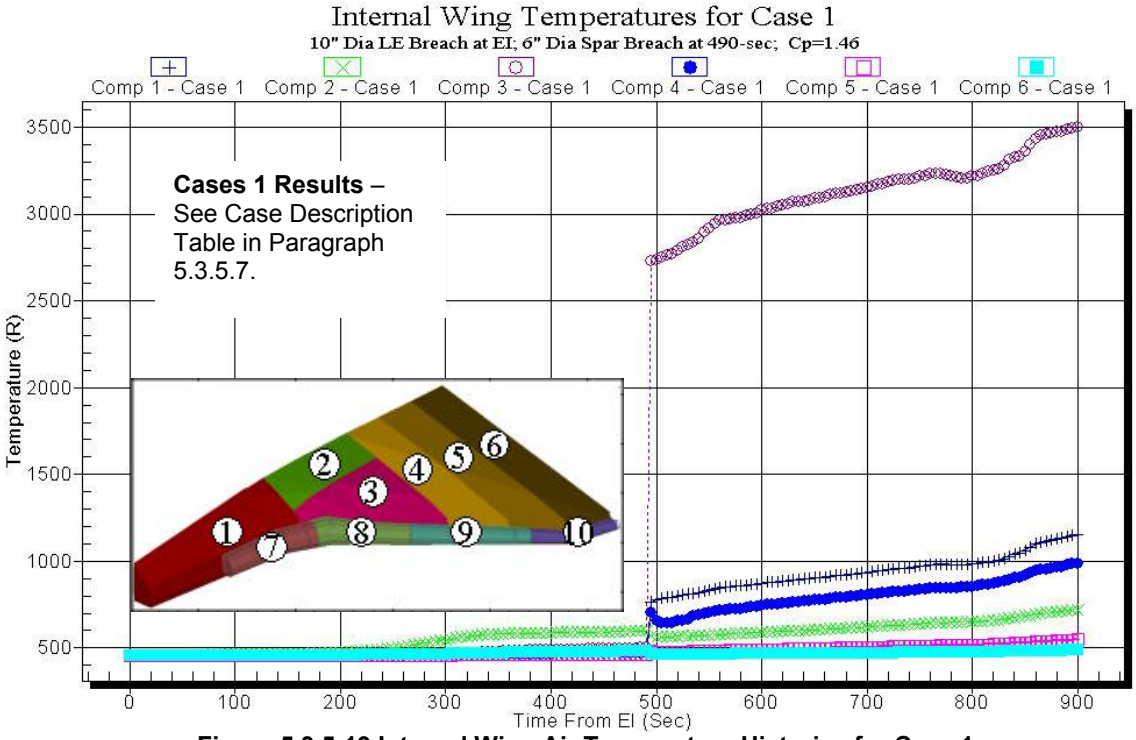

Figure 5.3.5-19 Internal Wing Air Temperature Histories for Case 1

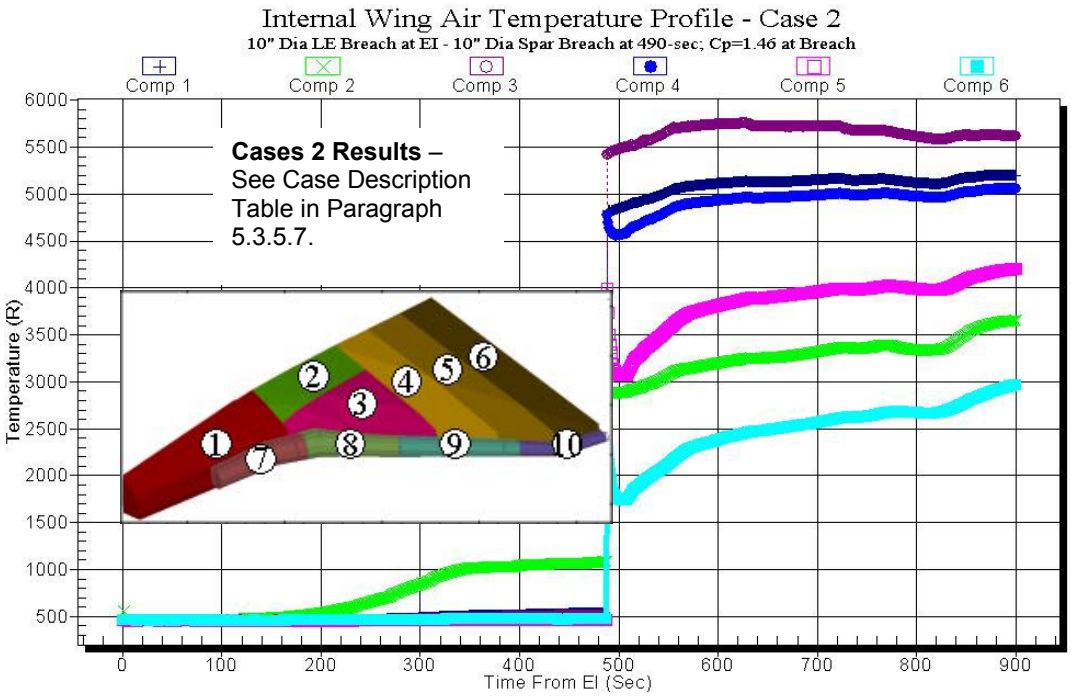

Figure 5.3.5-20 Internal Wing Air Temperature Histories for Case 2

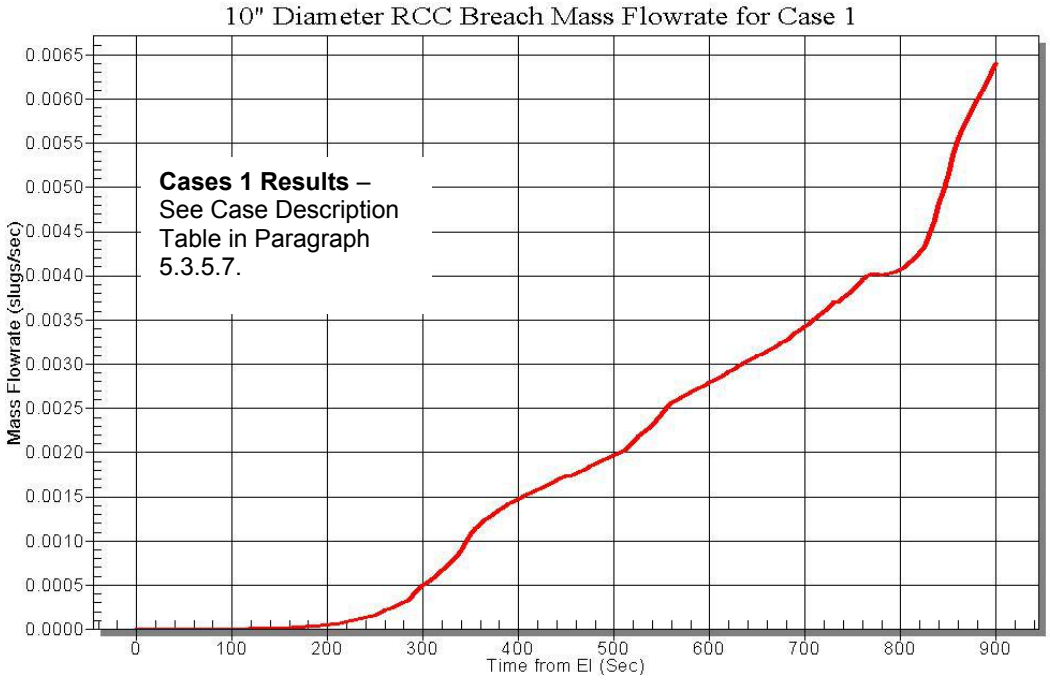

Figure 5.3.5-21 Leading Edge Breach Mass Flowrate for Case 1

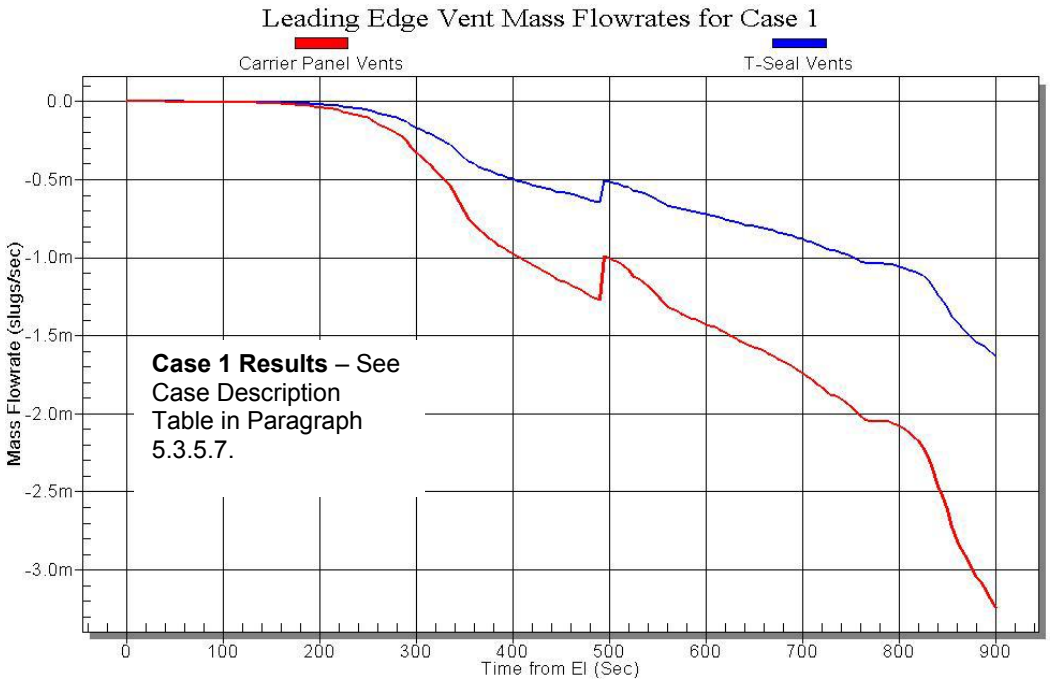

Figure 5.3.5-22 Leading Edge Vent Mass Flowrates for Case 1

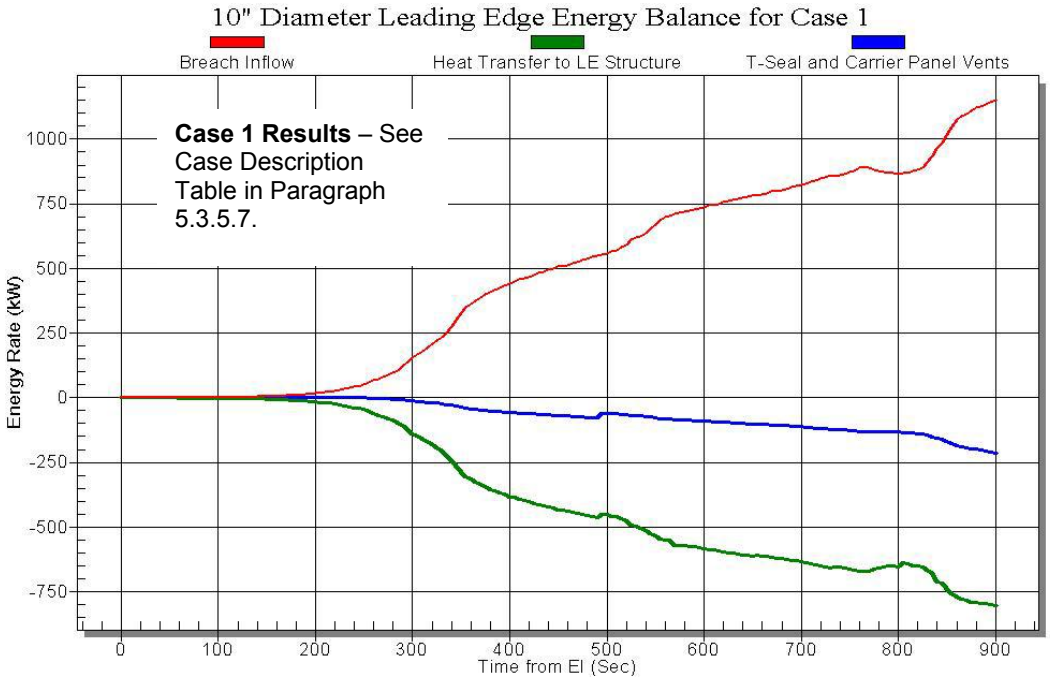

Figure 5.3.5-23 Leading Edge Breach Energy Inflow and Vent Outflow for Case 1

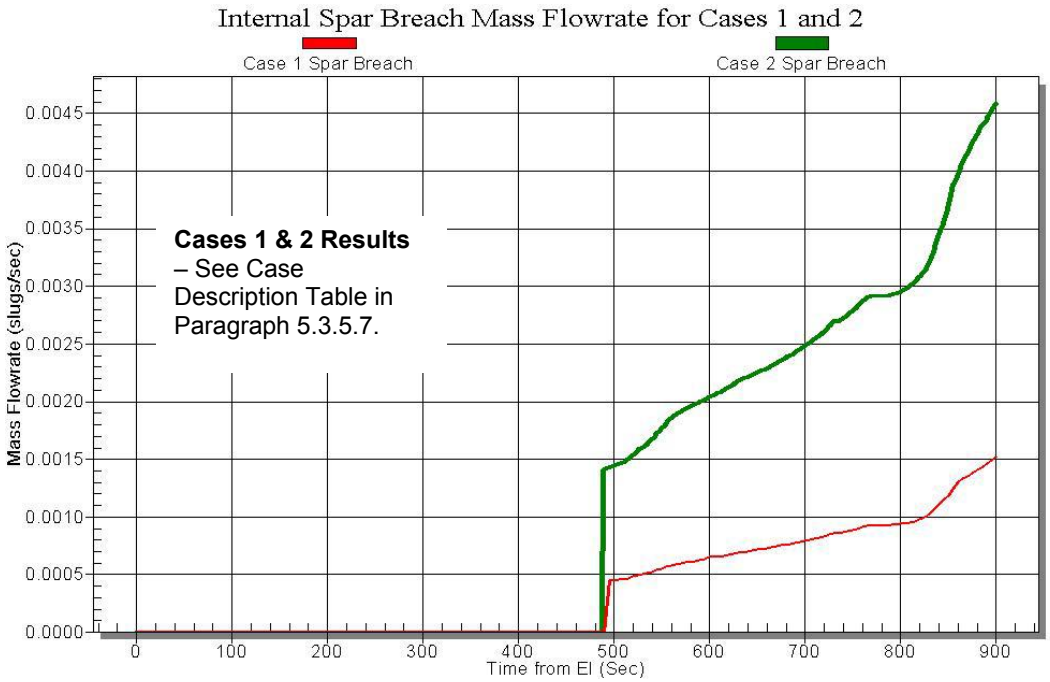

Figure 5.3.5-24 Spar Breach Mass Flowrate Comparison Between Case 1 and 2

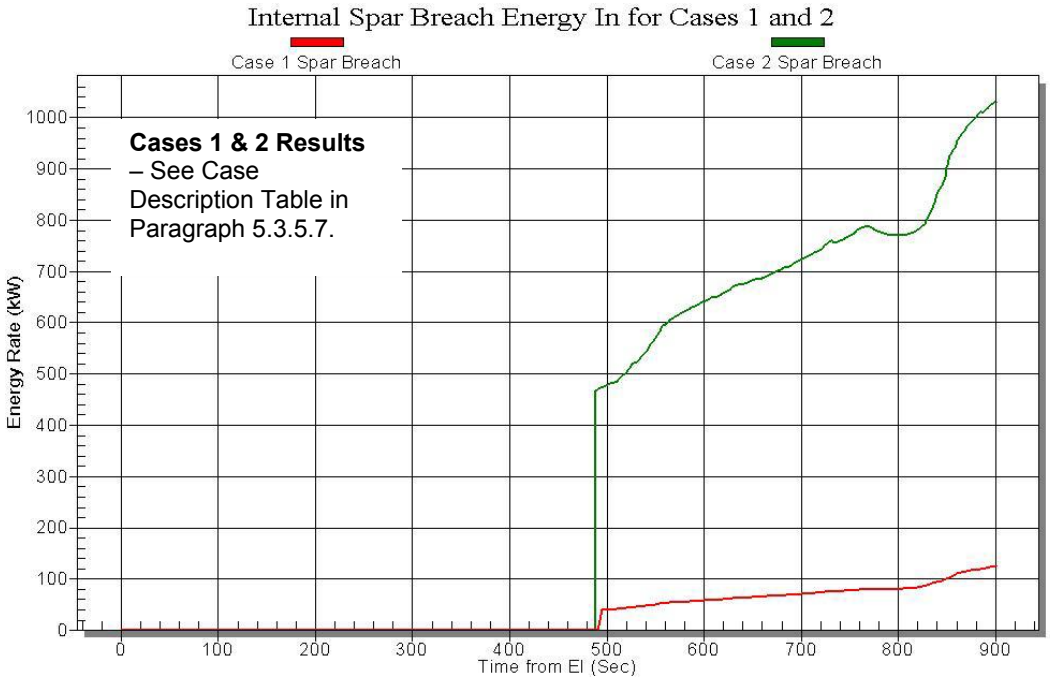

Figure 5.3.5-25 Spar Breach Energy Inflow Comparison Between Case 1 and 2

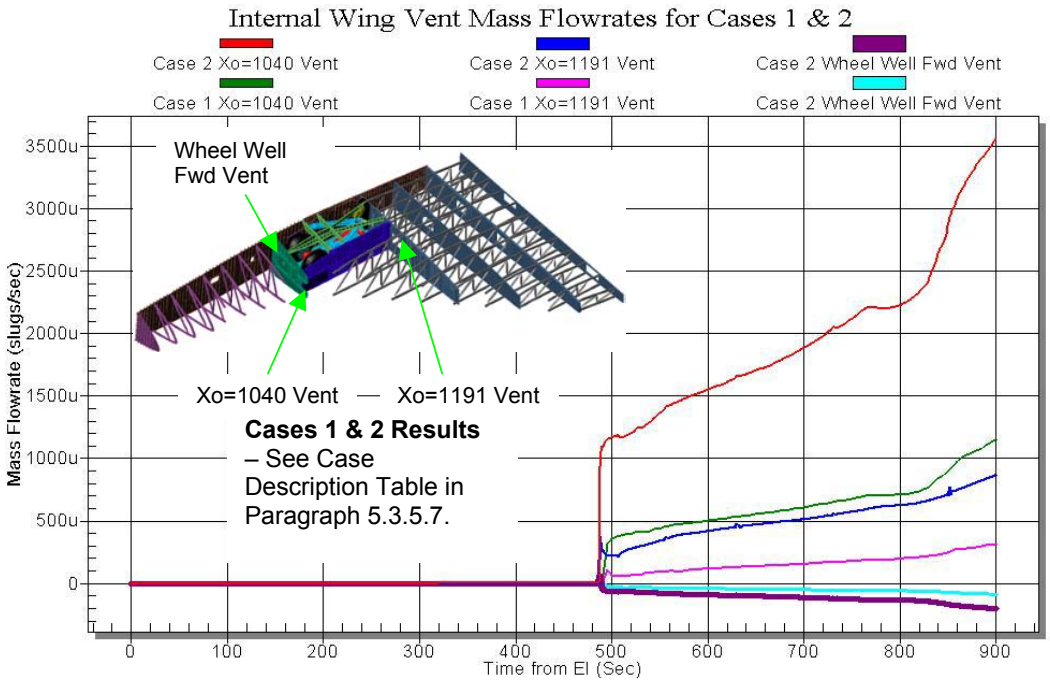

Figure 5.3.5-26 Internal Wing Vent Mass Flowrates for Cases 1 and 2

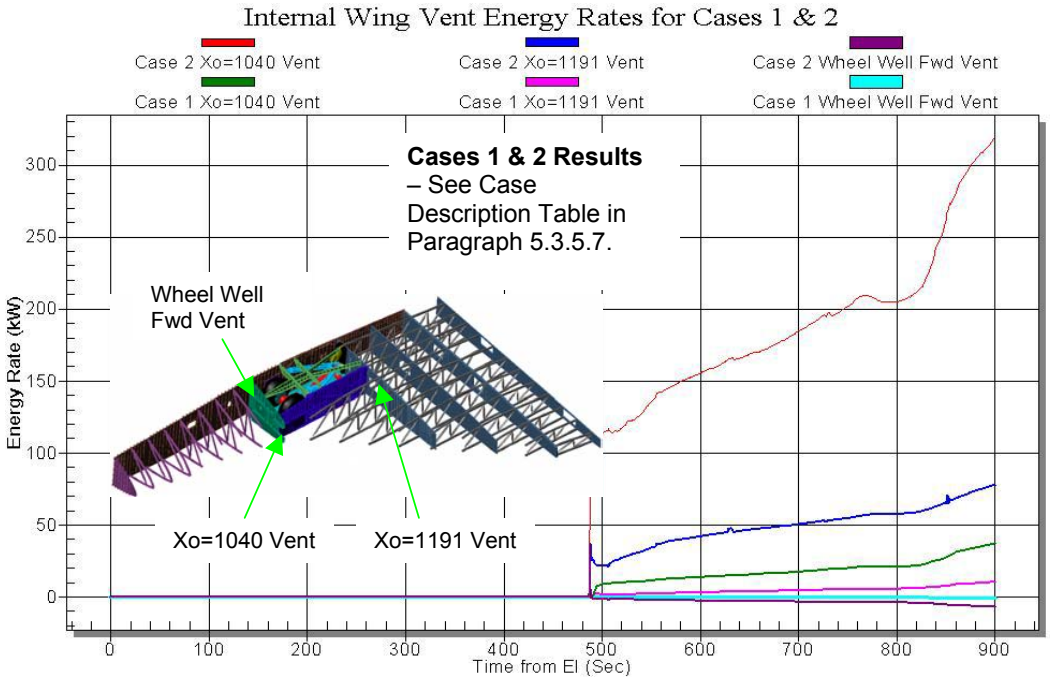

Figure 5.3.5-27 Internal Wing Vent Energy Inflows for Cases 1 and 2

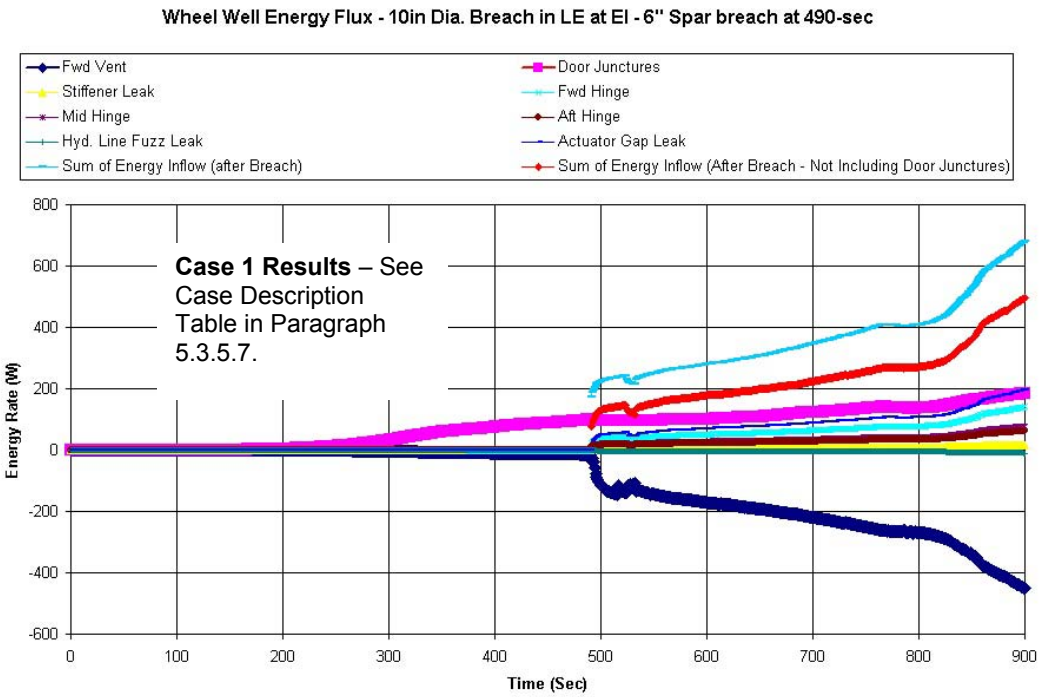

Figure 5.3.5-28 Wheel Well Energy Inflows for Case 1

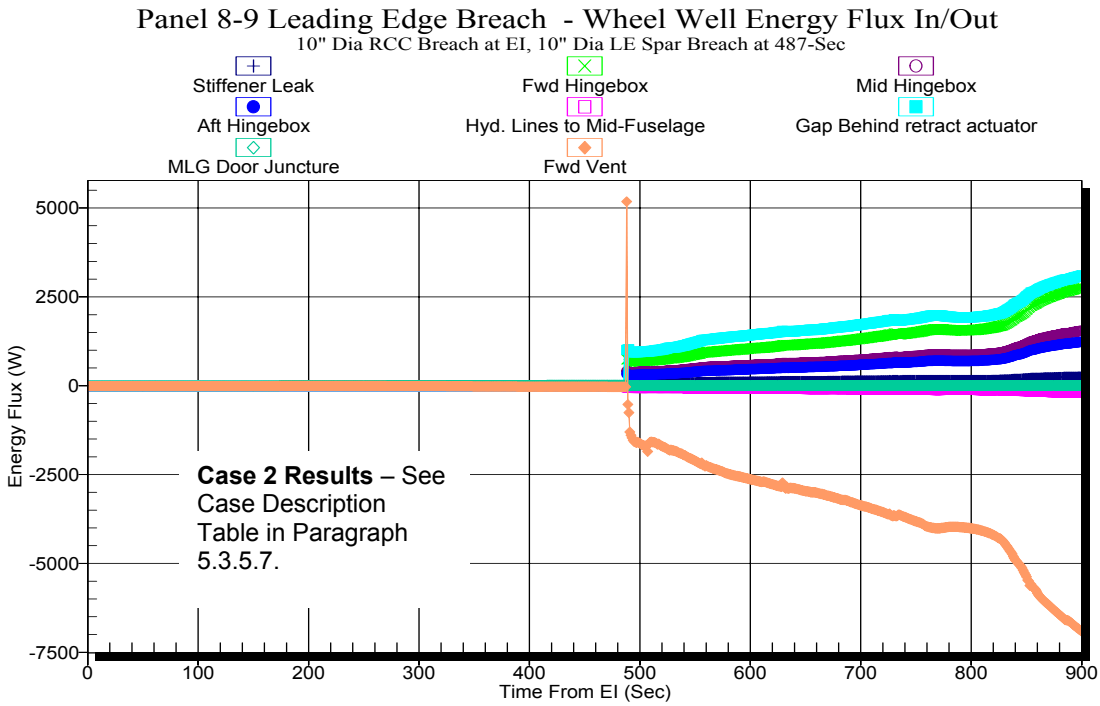

Figure 5.3.5-29 Wheel Well Energy Inflows for Case 2

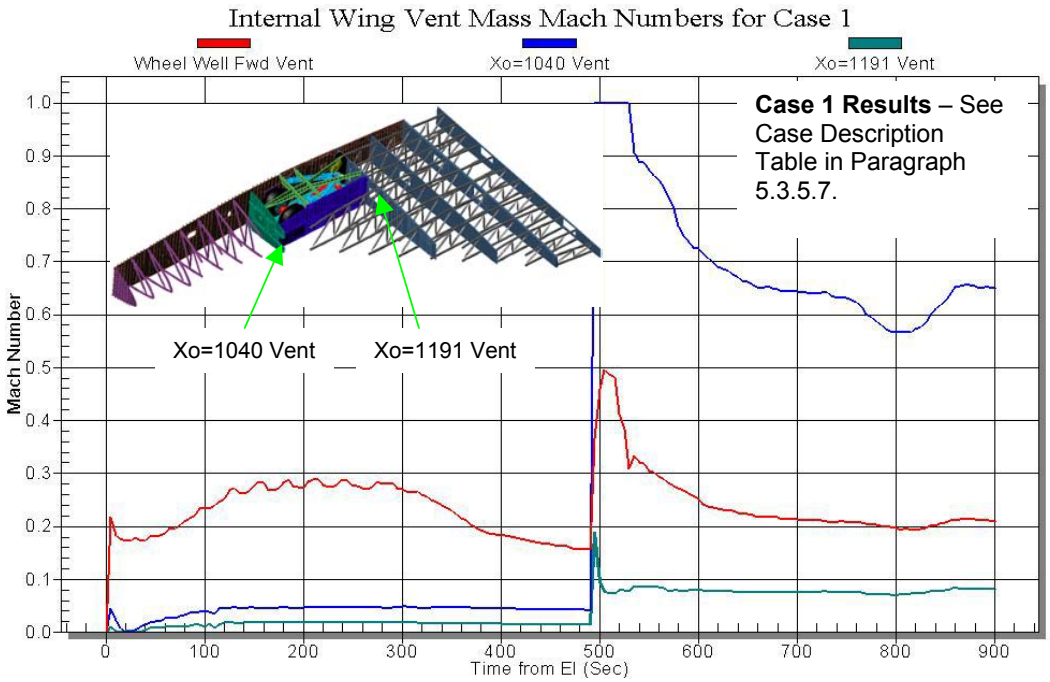

Figure 5.3.5-30 Internal Vent Mach Numbers for Case 1

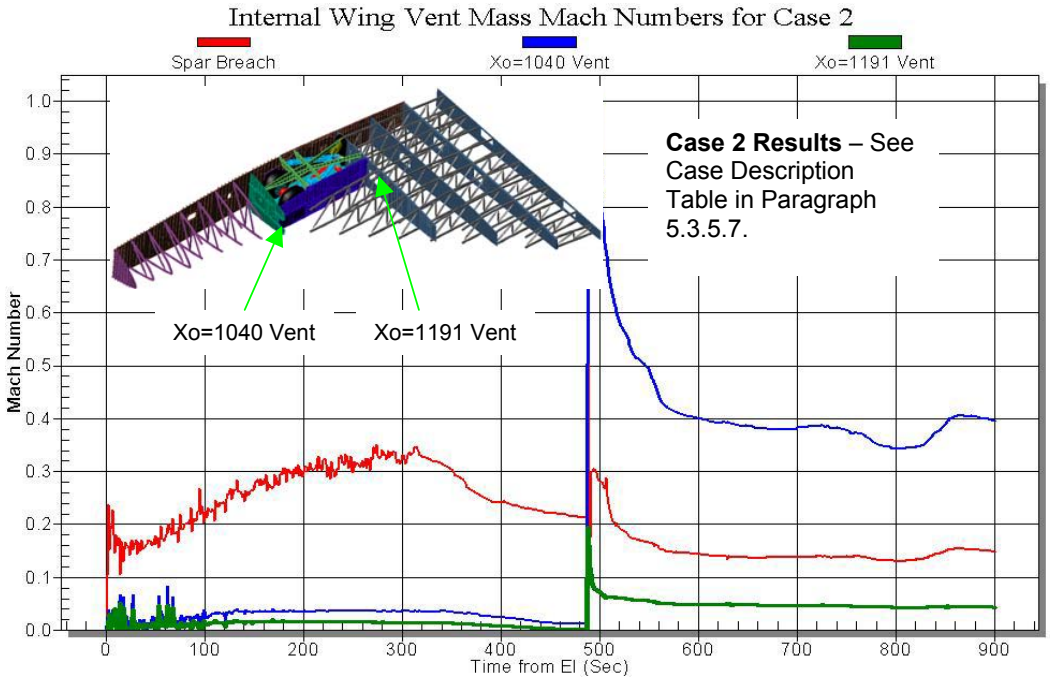

Figure 5.3.5-31 Internal Vent Mach Numbers for Case 2

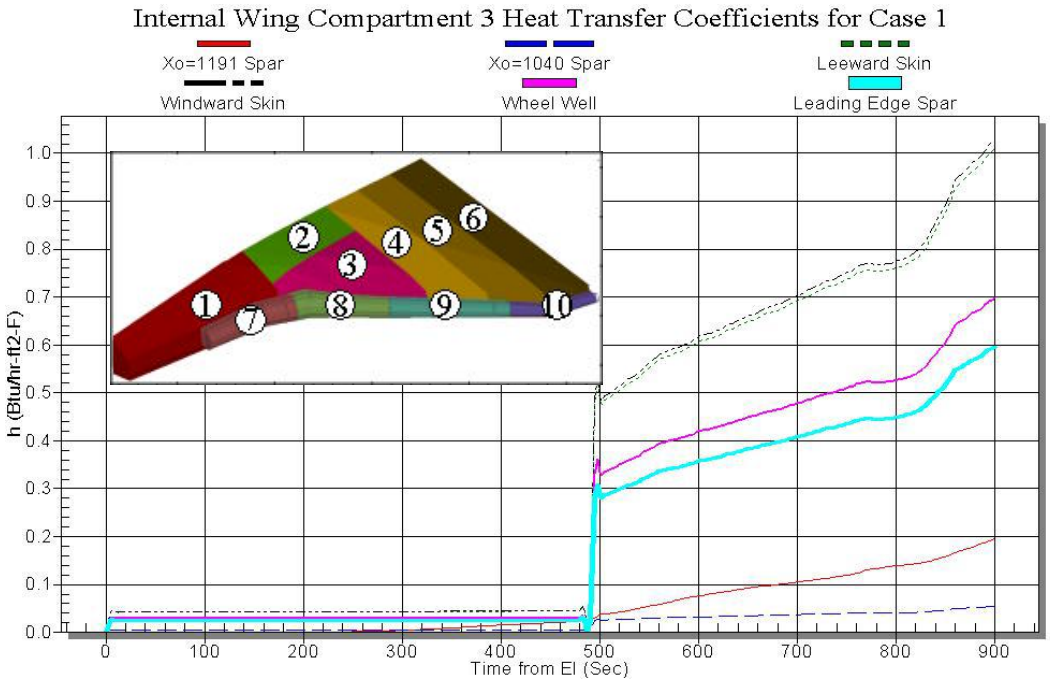

Figure 5.3.5-32 Compartment 3 Heat Transfer Coefficients for Case 1

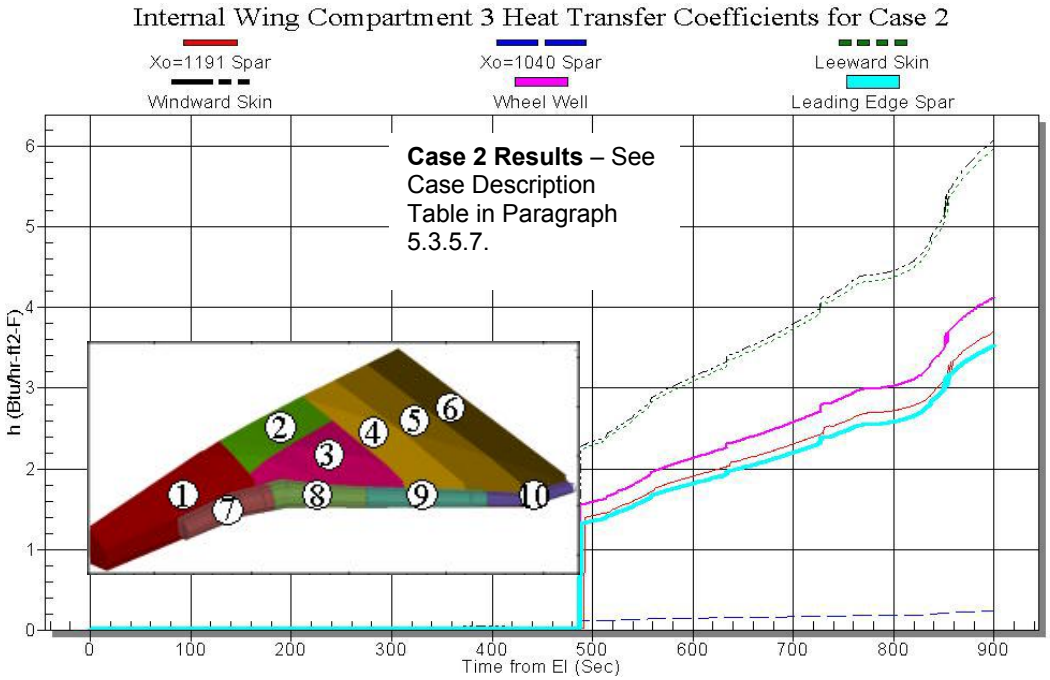

Figure 5.3.5-33 Compartment 3 Heat Transfer Coefficients for Case 2

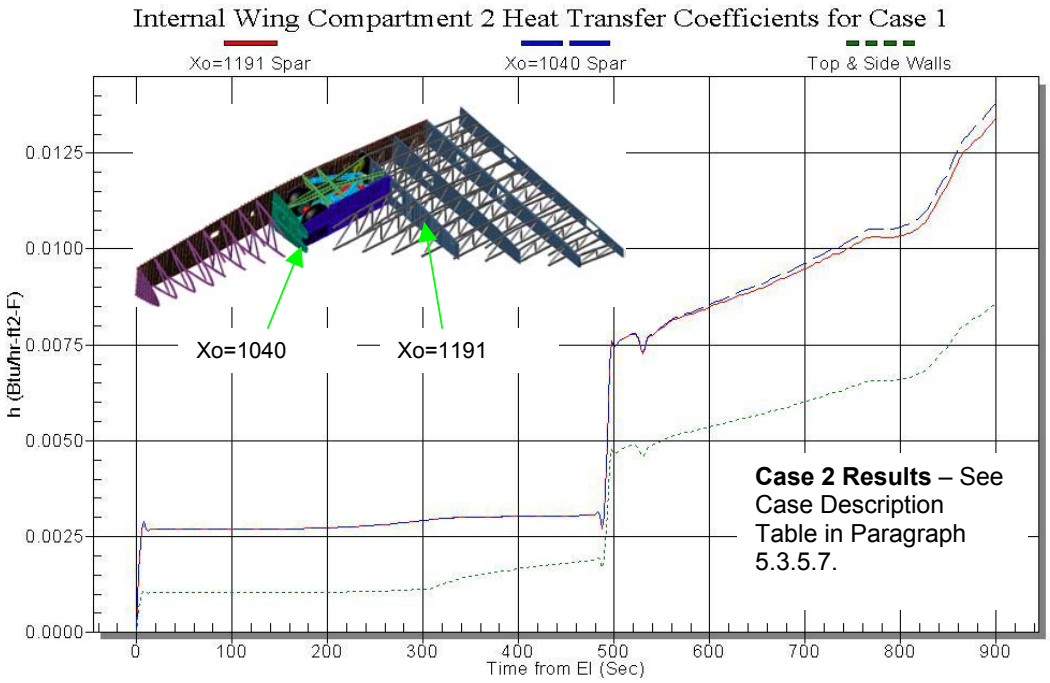

Figure 5.3.5-34 Wheel Well Heat Transfer Coefficients for Case 1

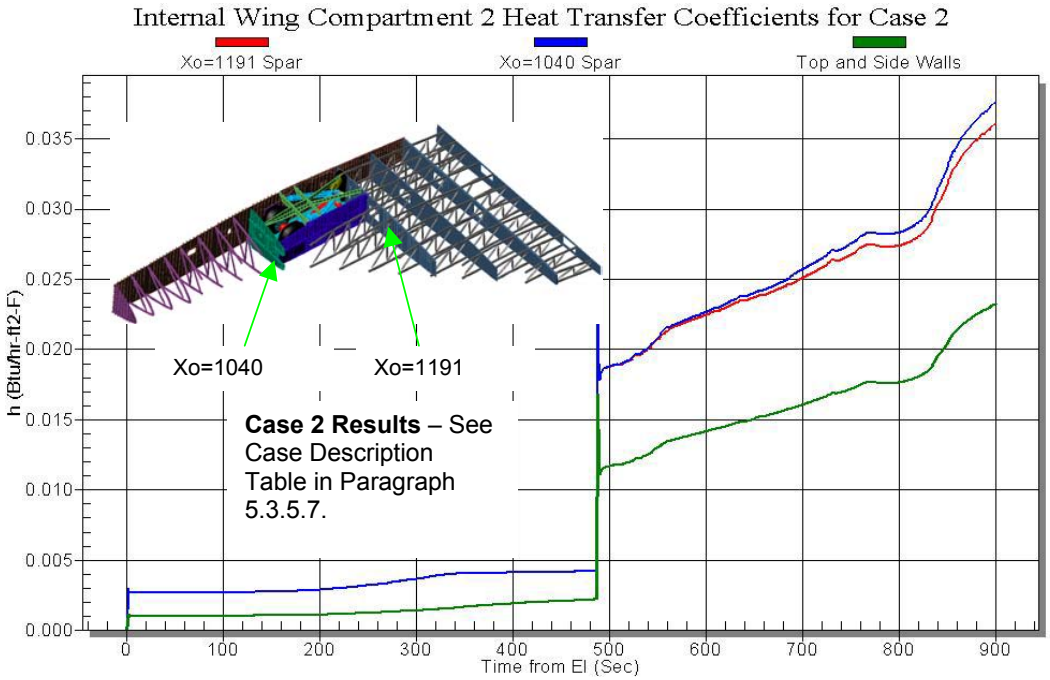

Figure 5.3.5-35 Wheel Well Heat Transfer Coefficients for Case 2

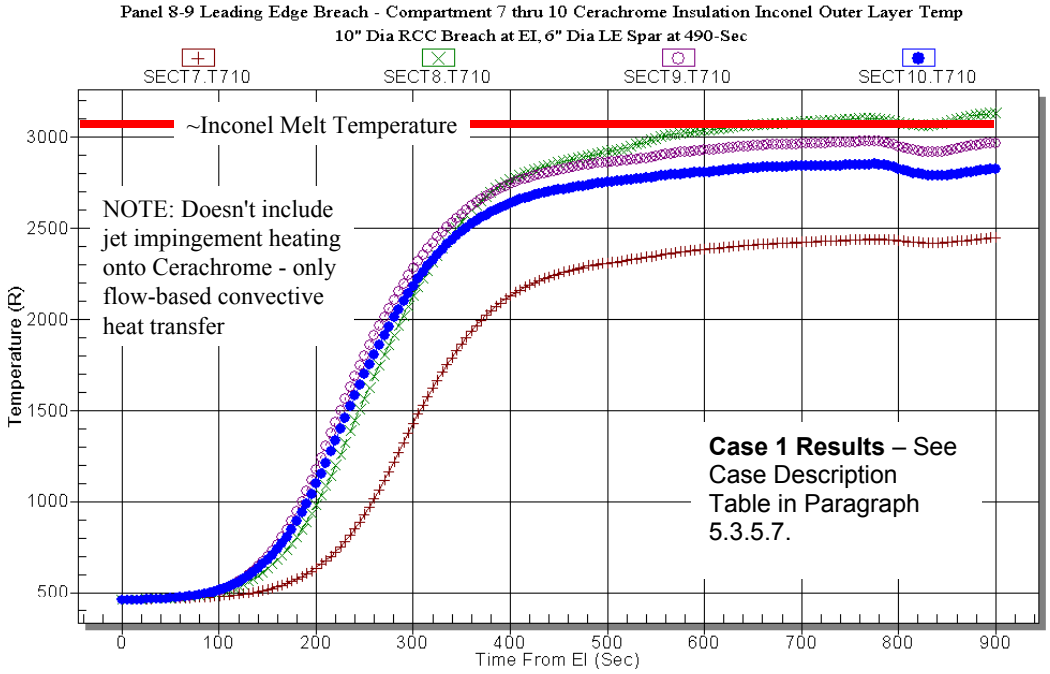

Figure 5.3.5-36 Leading Edge Cerachrome Insulation Inconel Outer Layer Temperature

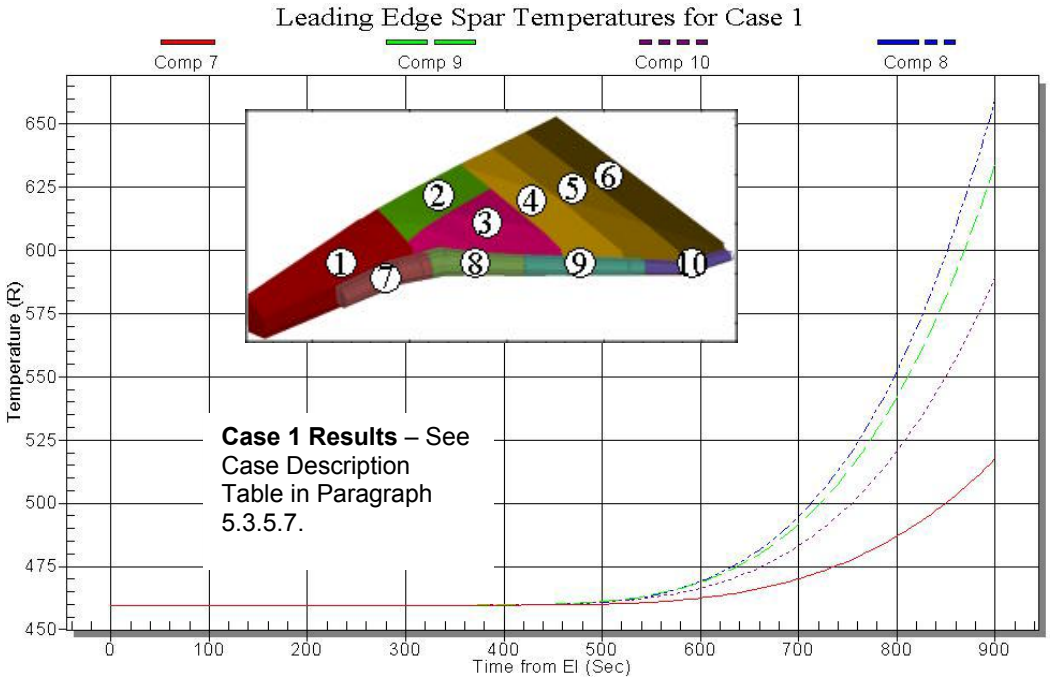

Figure 5.3.5-37 Leading Edge Structural Spar Temperature

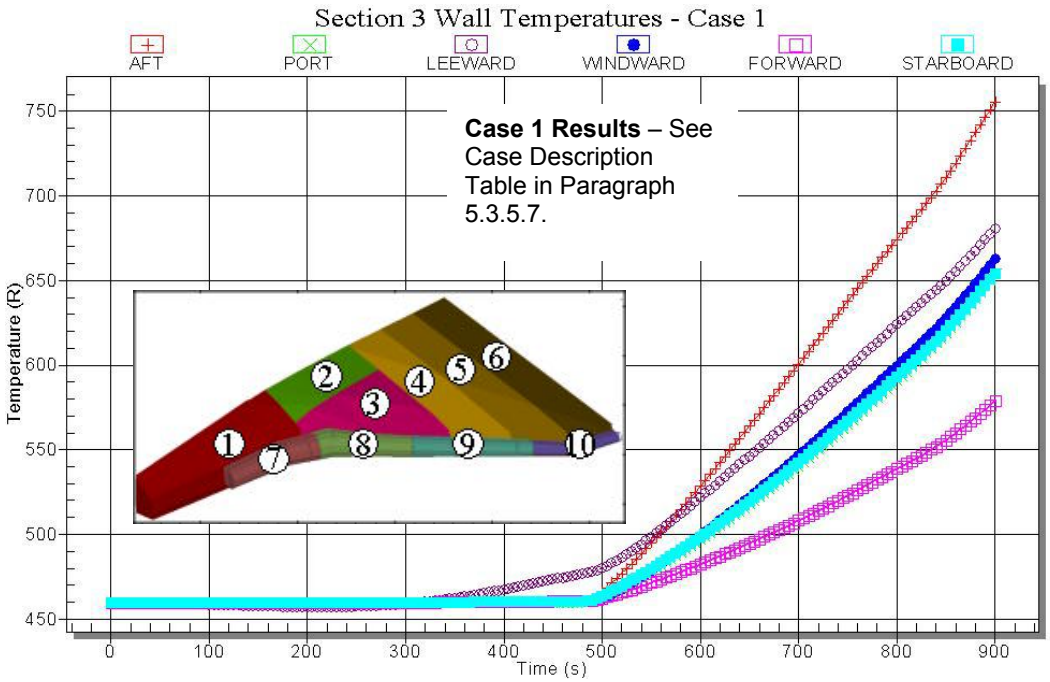

Figure 5.3.5-38 Compartment 3 Spar and Wall Skin Temperatures for Case 1

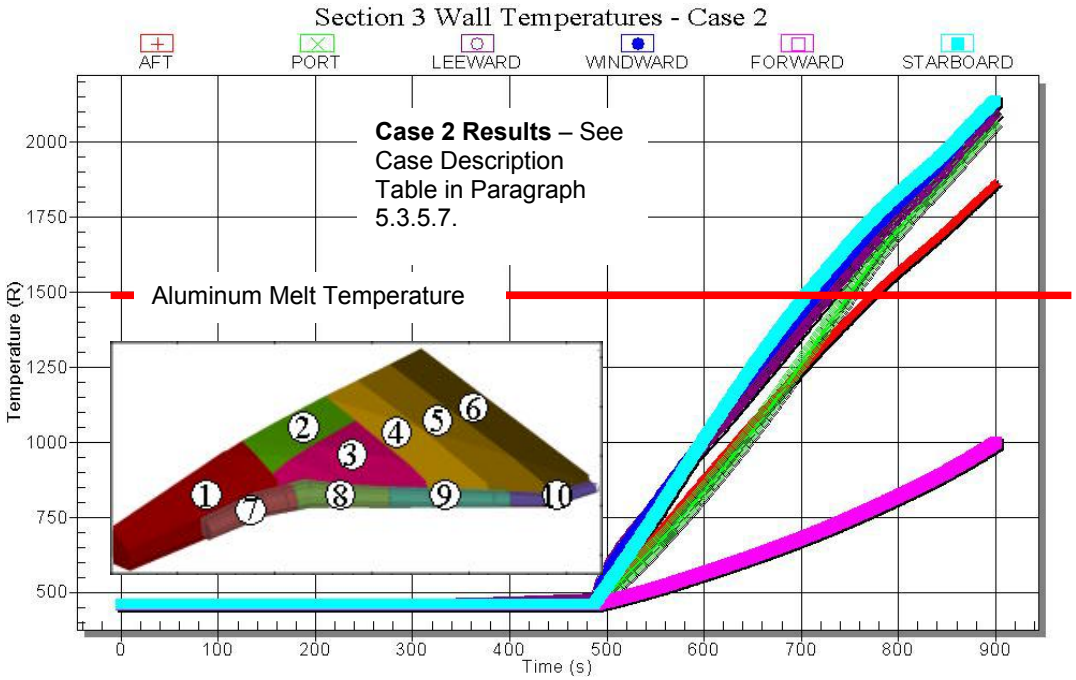

Figure 5.3.5-39 Compartment 3 Spar and Wall Skin Temperatures for Case 2

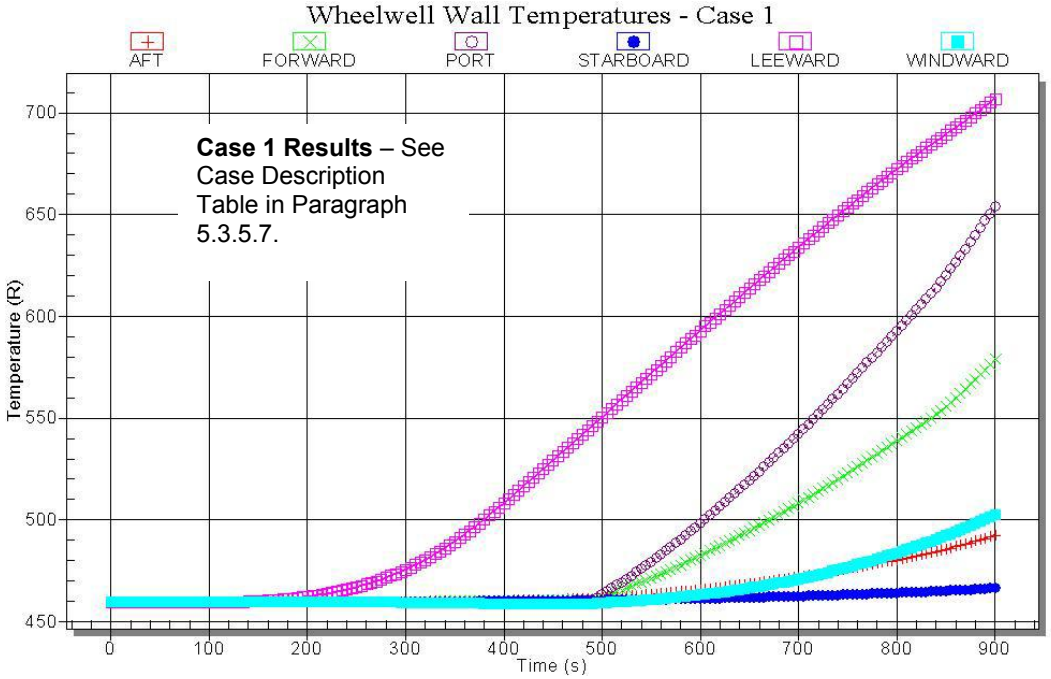

Figure 5.3.5-40 Compartment 2 Spar and Wall Skin Temperatures for Case 1

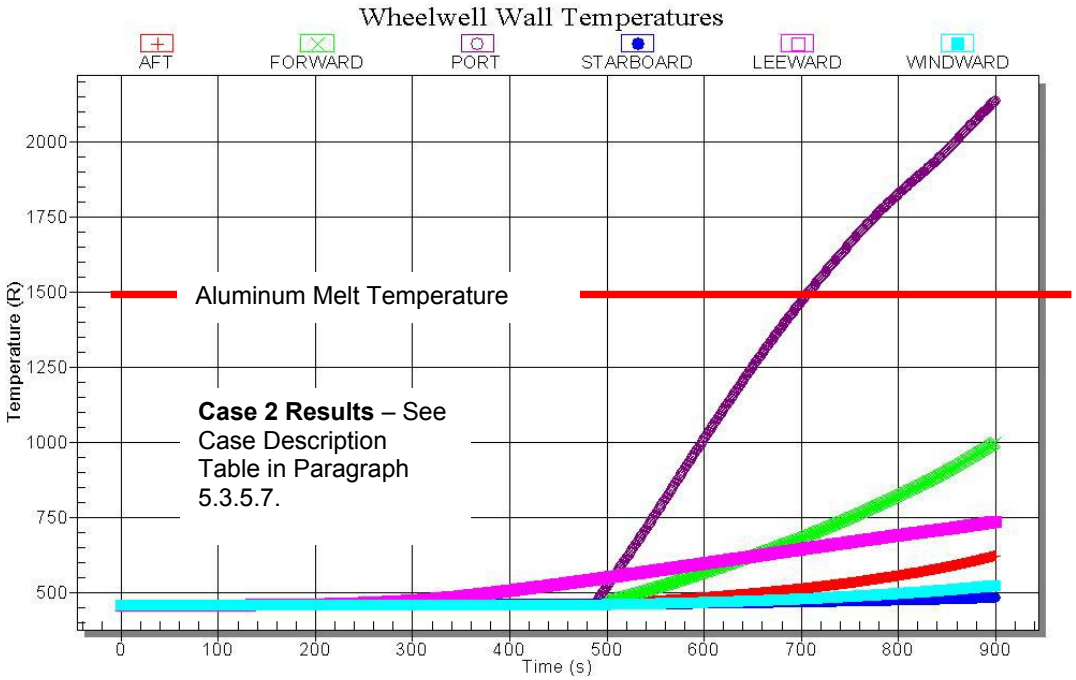

Figure 5.3.5-41 Compartment 2 Spar and Wall Skin Temperatures for Case 2

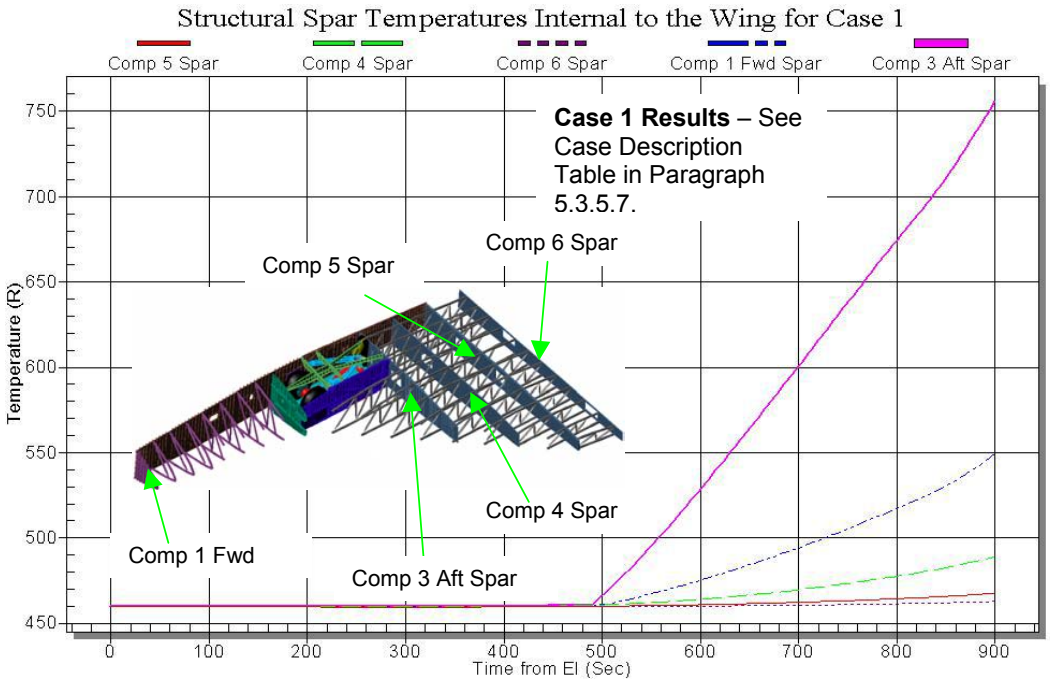

Figure 5.3.5-42 Internal Wing Spar Temperatures for Case 1

5.3.6 3D CFD & DSMC of Wing Leading Edge Cavity

5.3.6.1 CFD of RCC Panel Acreage Damage

5.3.6.1.1 Panel 7 6" Hole Decoupled Solution

5.3.6.1.1.1 Case description

This effort focused on a 6" diameter hole in RCC Panel 7 located on the attachment line at the panel midpoint (X = 1048 in, Y = -217 in, Z = 291.6 in). The attachment line location was determined from nominal geometry hypersonic Navier-Stokes solutions at approximately 40 degrees angle of attack. This study was conducted in two stages using the Unified Solution Algorithm (USA) flow solver with equilibrium air chemistry. The grid models were generated using ICEM/Hexa software. The first stage of the simulation involved a computational domain limited to the hole inlet and a section of the RCC channel from Panels 5-9, and is referred to as the decoupled internal flow case. Coupled external/internal flow simulations were performed next in the second stage. This decoupled internal flow simulation provided initial jet plume flow field information and convective heating environments to internal structure in the leading edge volume.

5.3.6.1.1.2 Geometry and Grid Definition

The CFD grid model used in this simulation included the ribs on both sides of Panel 7. Figure 5.3.6-1 show the surface grid. For the volume grid the wall spacing is 0.0005 inch to ensure a cell-Reynolds number of 1 or less. Rectangular openings to simulate the T-seal vent gaps were modeled on the leeside between Panels 5 and 6; Panels 6 and 7; Panels 7 and 8; and Panels 8 and 9. The respective areas of these vents are 0.5556, 0.642, 0.7704 and 0.642 square inches. These leeside rectangular vents of 0.2 inch width were modeled between the RCC panels in a chordwise orientation 2 inches ahead of upper carrier panels. To account for the vents in Panels 1-4, a circular vent of area 22.03 square inches was modeled at the inboard end of the Panels 5-9 channel. Similarly, another circular vent of area 55.29 square inches was modeled on the outboard end of the Panels 5-9 channel to account for the vents on Panels 10-22. The total vent area of about 80 square inches was purposely made to be about 20% larger than 66.4 square inches of all the documented spanwise vents in front of the upper carrier panels and the chordwise vents between RCC Panels just ahead of upper carrier panels.

5.3.6.1.1.3 Boundary Conditions

For the decoupled internal flow simulation the total conditions at the hole inlet were obtained from the Orbiter nominal geometry Navier-Stokes solutions for STS-107 CFD Point 2 flight condition (491.4 sec from Entry Interface). In this laminar simulation with equilibrium air chemistry, a pressure of 38.6 psf and temperature of 18,375° R were specified as the reservoir conditions at the hole inlet. This results in a total enthalpy of 27,500 Btu/lbm whereas the actual total enthalpy is 11,175 Btu/lbm for the flight condition at 491.4 sec after EI. The interior surfaces were kept at 0° F. A back-pressure of 0.5 psf was specified at the vents for the simulation.

5.3.6.1.1.4 Results

Figure 5.3.6-3 shows Mach contours of the jet plume with the corresponding jet pressure contours illustrated in Figure 5.3.6-4. The total enthalpy contours are shown in Figure 5.3.6-5. The pressure results on the RCC channel and the front spar are shown in Figure 5.3.6-6 and Figure 5.3.6-7, respectively. Similarly, Figure 5.3.6-8 and Figure 5.3.6-9 illustrate the heating on the RCC channel surfaces and on the front spar, respectively. The results discussed thus far in this section were obtained with a 2 million-cell grid model. Another simulation with a denser grid model of about 15 million cells was also conducted to evaluate grid convergence effects. Figure 5.3.6-10 and Figure 5.3.6-11 show the surface pressure and heating distributions, respectively, on the front spar and the RCC cavity from the 15 million-cell model simulation. The heating results are as high as twice the results from the 2 million-cell model simulation. The jet plume is probably better resolved as seen in the flow field Mach and pressure distributions illustrated in Figure 5.3.6-12 and Figure 5.3.6-13, respectively. The decoupled internal flow CFD heating results are higher than predictions from engineering models calculated at the same conditions. Nevertheless, the decoupled internal flow simulation provided a lead-in to the coupled external/internal flow simulations.

5.3.6.1.2 Panel 7 6" Hole Coupled External/Internal Flow Solution

5.3.6.1.2.1 Case description

Two coupled external/internal flow simulations were conducted during the second stage of this study for a 6-inch diameter hole in leading edge panel 7 using the freestream flow conditions from flight at 404 sec after EI. The first simulation used a finer grid but did not model the internal earmuff insulation between Panels 7 and 8. The second simulation used a coarser grid but the earmuff insulation between both panels 7/8 and panels 8/9 was modeled.

5.3.6.1.2.2 Geometry and Grid Definition

The grid models used for the coupled simulation included the RCC channel, vents and the 6” hole, as well as the Orbiter external flow grid in order to generate coupled external/internal flow solutions. In addition, the grid model used in the first coupled external/internal flow simulation included the ribs on both sides of RCC Panel 7 and Panel 8, along with the earmuff insulation between Panels 8 and 9. The far and close-up views of the surface grid of the external and internal flow regimes are shown in Figure 5.3.6-14 and Figure 5.3.6-15, respectively. Figure 5.3.6-16 and Figure 5.3.6-17 illustrate further the details of the geometry inside the RCC cavity, whereas a cross-section of the grid is shown in Figure 5.3.6-18. The wall spacing is 0.0005 inch to ensure the cell-Reynolds number of 1 or less on the surface.

5.3.6.1.2.3 Boundary Conditions

In this equilibrium air chemistry simulation, the RCC interior surfaces were kept at 0° F, whereas the Orbiter exterior surfaces were specified with radiative equilibrium temperature boundary condition. The vent areas and pressure boundary conditions used in the decoupled simulation were also applied to these simulations.

5.3.6.1.2.4 Results

Figure 5.3.6-19 and Figure 5.3.6-20 show the Mach and Pressure contours, respectively, in the jet plume for a planar cut through the leading edge cavity. Figure 5.3.6-21 illustrates the pressure contours in the flow field whereas the Mach contours in flow field are shown in Figure 5.3.6-22 and Figure 5.3.6-23 for a constant-z cut. The surface pressure distributions are shown in Figure 5.3.6-24 and Figure 5.3.6-25 on the RCC channel and the front spar, respectively. Similarly, the heating results are illustrated in Figure 5.3.6-26 and Figure 5.3.6-27 for the RCC channel and the front spar, respectively. These results are from a dense grid model with about 15 million cells. The heating environment inside the RCC cavity is converged, except on the front spar where there are some small variations. The secondary impingement of

the jet on the front spar is probably not a steady-state phenomenon, but the level of heating on the spar is not very high. The earmuff insulation between Panels 7 and 8 were not modeled in this simulation, because the jet was thought to be going straight toward the earmuff between RCC Panels 8 and 9. This simulation however showed that the jet hits primarily the outboard rib of RCC Panel 7 and the rib redirects the jet toward the region of the earmuff insulation between RCC Panels 7 and 8. The second coupled external/internal flow simulation in this study conducted included the earmuff insulation between RCC Panels 7 and 8.

Figure 5.3.6-28 and Figure 5.3.6-29 illustrate the external flow grid model for this simulation whereas the internal flow grid model is shown in Figure 5.3.6-30, Figure 5.3.6-31 and Figure 5.3.6-32. The results for this simulation using a grid model of about 2 million cells are discussed below. Figure 5.3.6-33, Figure 5.3.6-34 and Figure 5.3.6-35 show pressure distributions on the RCC channel, whereas similar heating distributions are illustrated in Figure 5.3.6-36, Figure 5.3.6-37 and Figure 5.3.6-38. Also, pressure contours in flow field are shown in Figure 5.3.6-39 and Figure 5.3.6-40, whereas Figure 5.3.6-41 and Figure 5.3.6-42 illustrate Mach contours in the flow field. The jet hits the outboard rib of Panel 7, then the outboard edge of the earmuff insulation between RCC Panels 7 and 8, and then the front spar behind RCC Panel 8.

• RCC Panels 5-9 with leeside vents modeled. (Side vents represent vents for other panels either side).

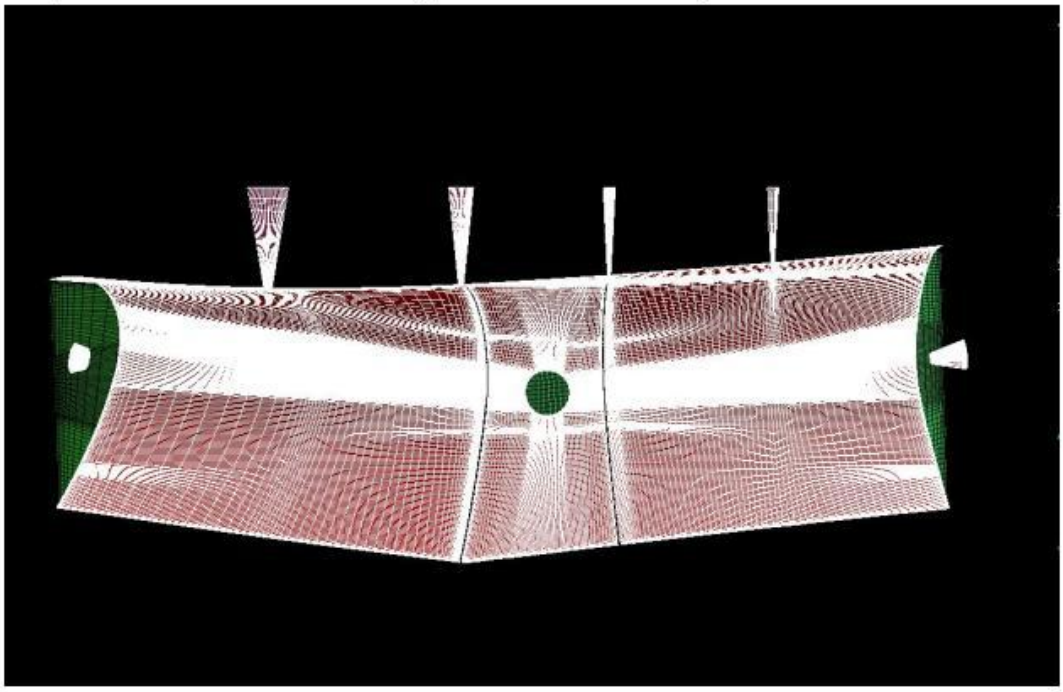

Figure 5.3.6-1 Grid Model for Panel 7 Hole Internal Flow Simulation

• Vents are connected to a fictitious dump chamber where back-pressure from leeside specified. (Brackets modeled either side of Panel 7)

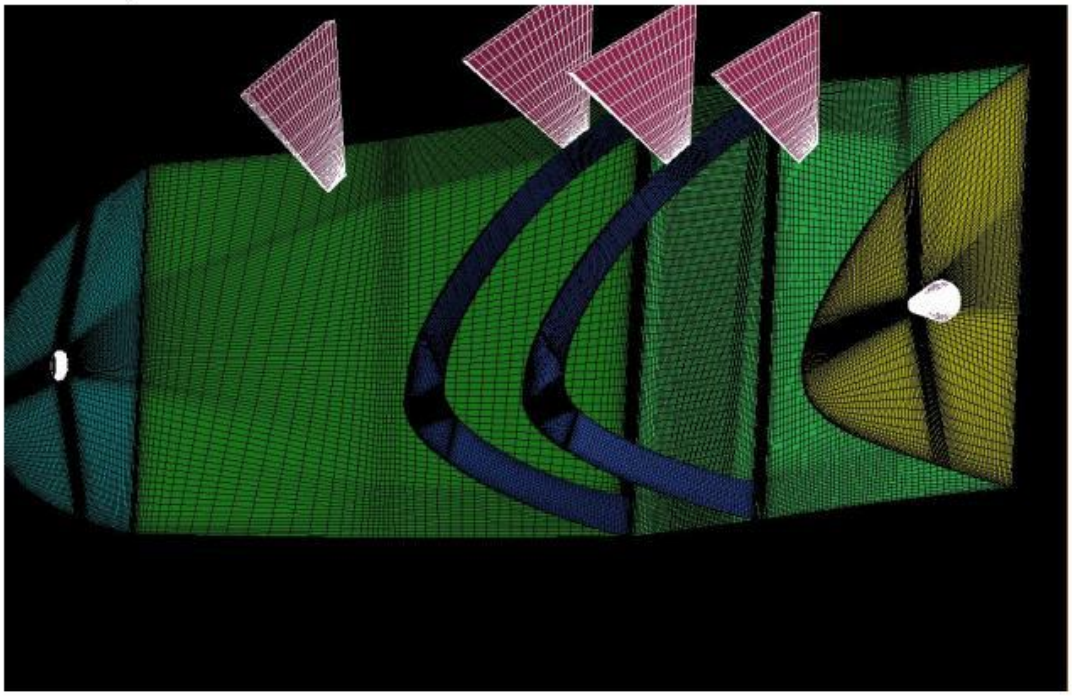

Figure 5.3.6-2 Grid Model for Panel 7 Hole Internal Flow Simulation

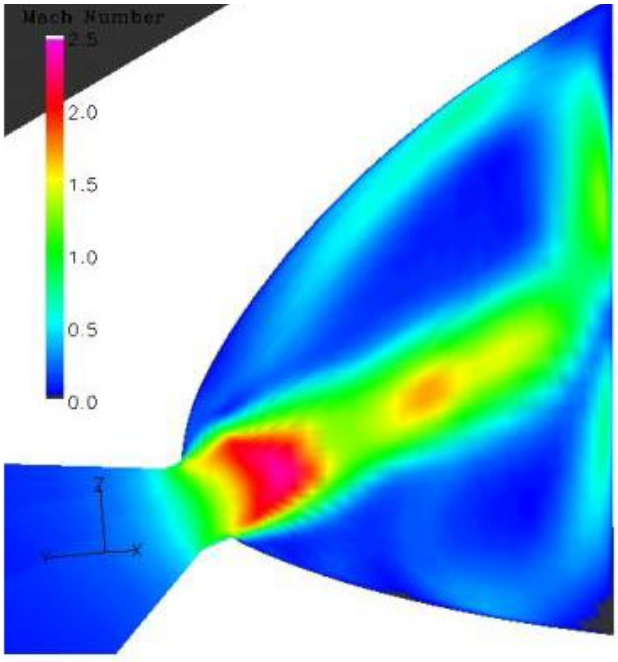

Figure 5.3.6-3 Mach Contours for Panel 7 Hole Internal Flow Simulation with 2 million-cell Model

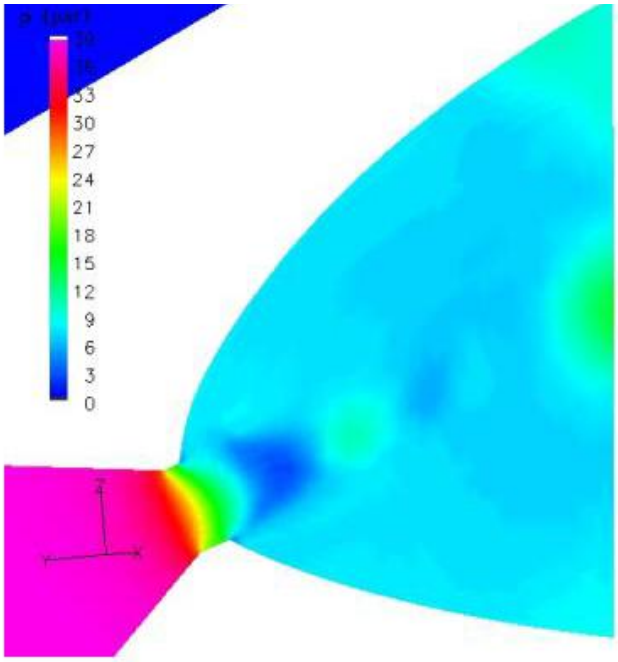

Figure 5.3.6-4 Pressure Contours for Panel 7 Hole Internal Flow Simulation with 2 million-cell Model

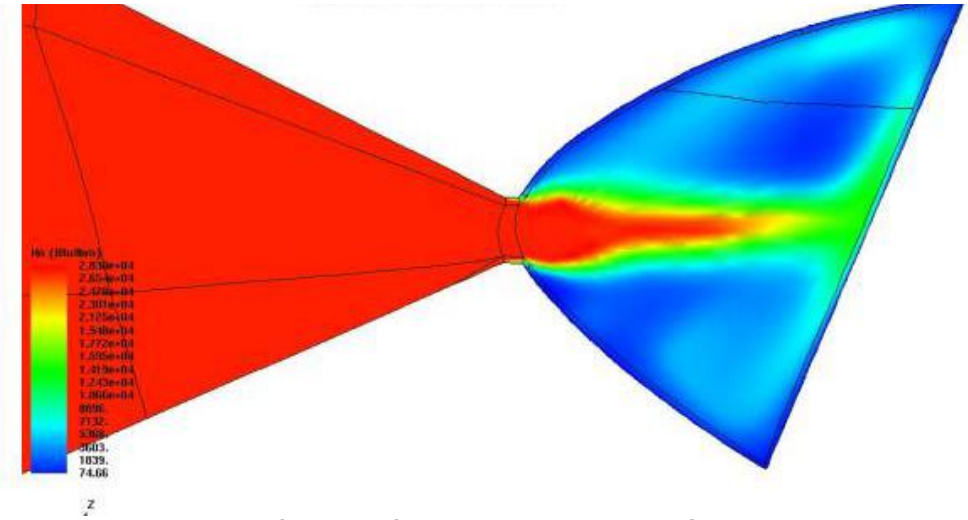

Figure 5.3.6-5 Total Enthalpy Contours for Panel 7 Internal Flow Simulation with 2 million-cell Model

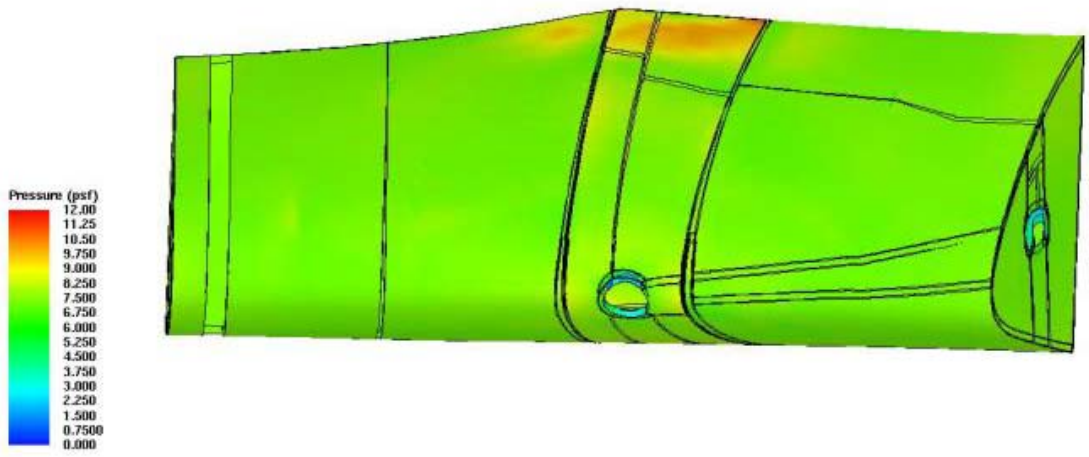

Figure 5.3.6-6 Pressure Contours on RCC Channel from Panel 7 Hole Internal Flow Simulation with 2 million-cell Model

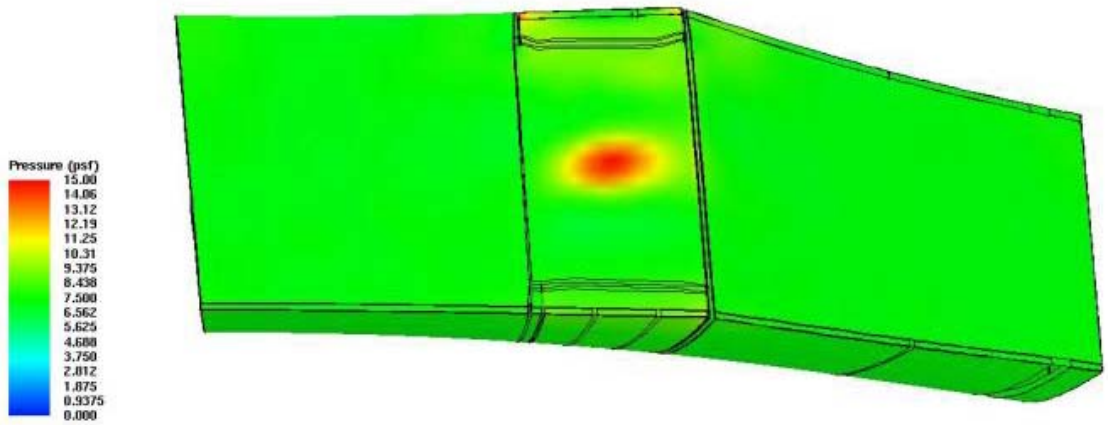

Figure 5.3.6-7 Pressure Contours on Front Spar from Panel 7 Hole Internal Flow Simulation with 2 million-cell Model

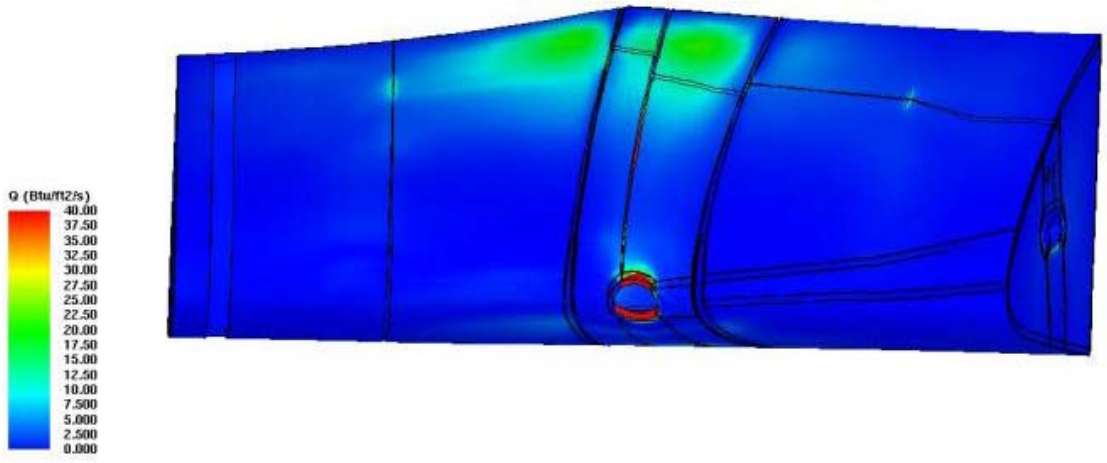

Figure 5.3.6-8 Heating Contours on RCC Channel from Panel 7 Hole Internal Flow Simulation with 2 million-cell Model

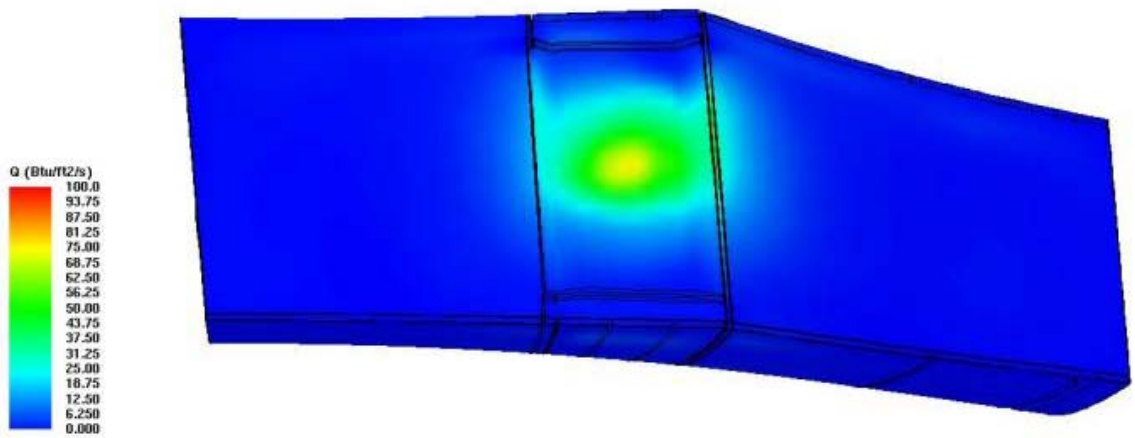

Figure 5.3.6-9 Heating Contours on Front Spar from Panel 7 Hole Internal Flow Simulation with 2 million-cell Model

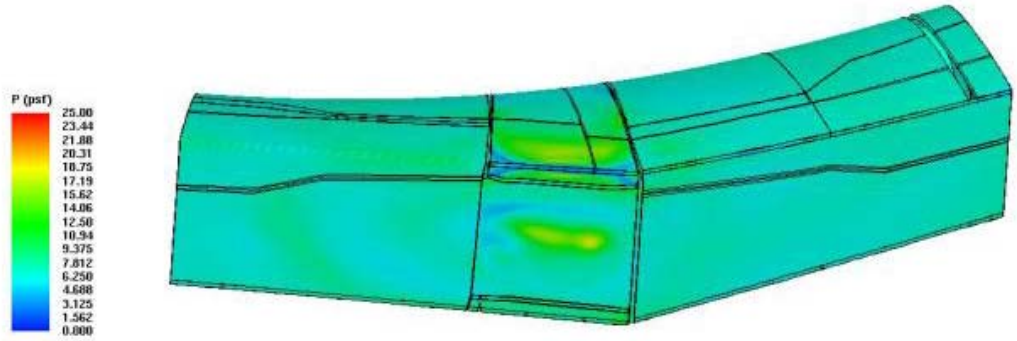

Figure 5.3.6-10 Pressure Contours on Front Spar and RCC Cavity from Panel 7 Hole Internal Flow Simulation with 15 million-cell Model

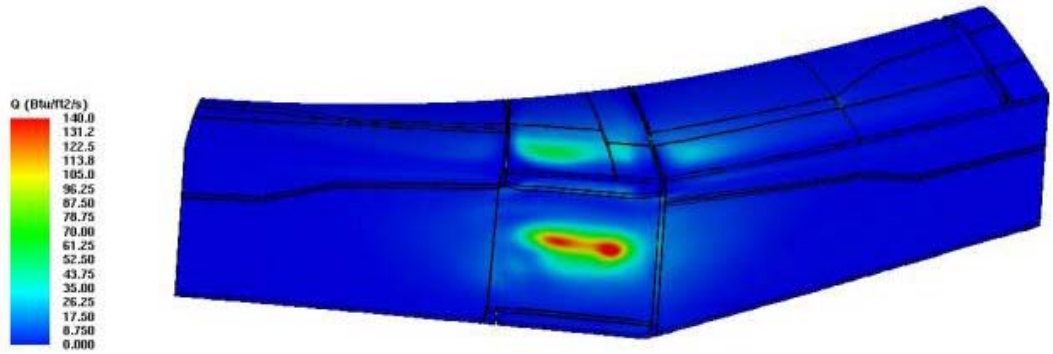

Figure 5.3.6-11 Heating Contours on Front Spar and RCC Cavity from Panel 7 Hole Internal Flow Simulation with 15 million-cell Model

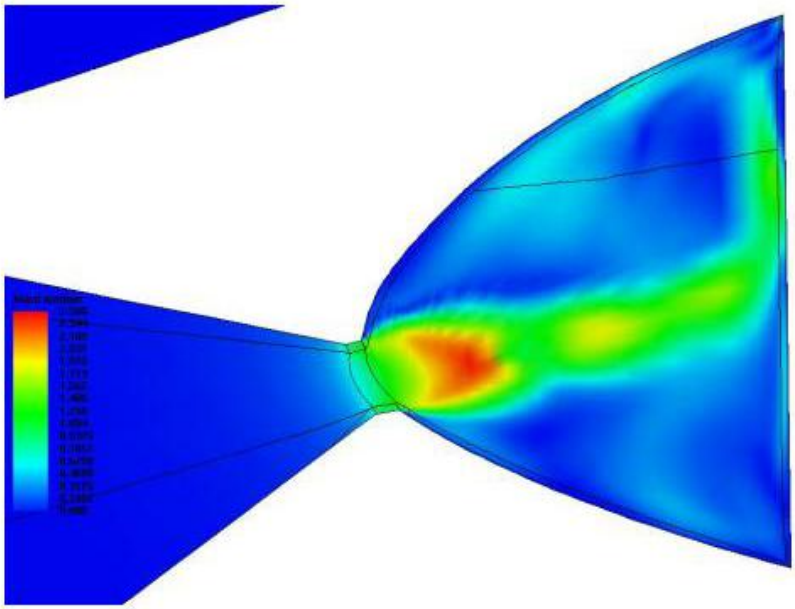

Figure 5.3.6-12 Mach Contours for Panel 7 Hole Internal Flow Simulation with 15 million-cell Model (Post-processed with every other points)

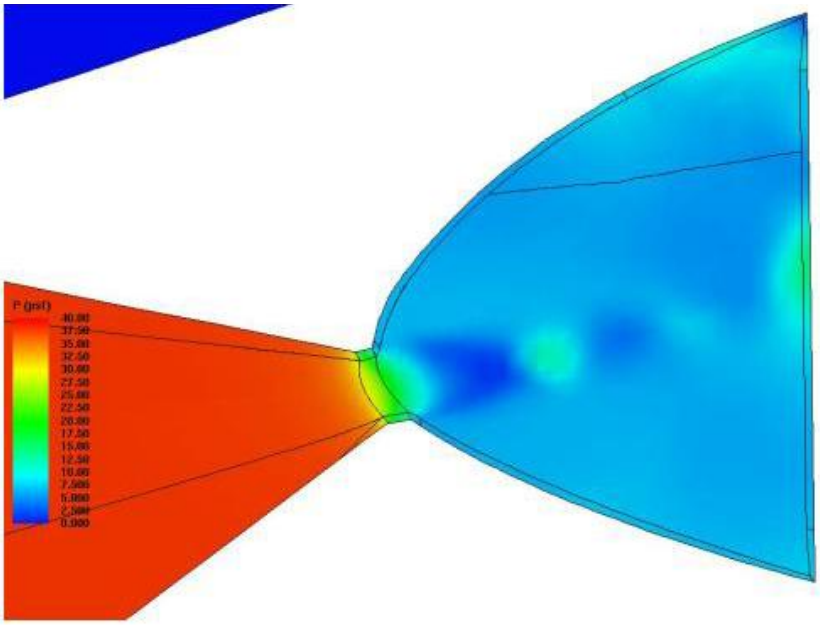

Figure 5.3.6-13 Pressure Contours for Panel 7 Hole Internal Flow Simulation with 15 million-cell Model (Post-processed with every other points)

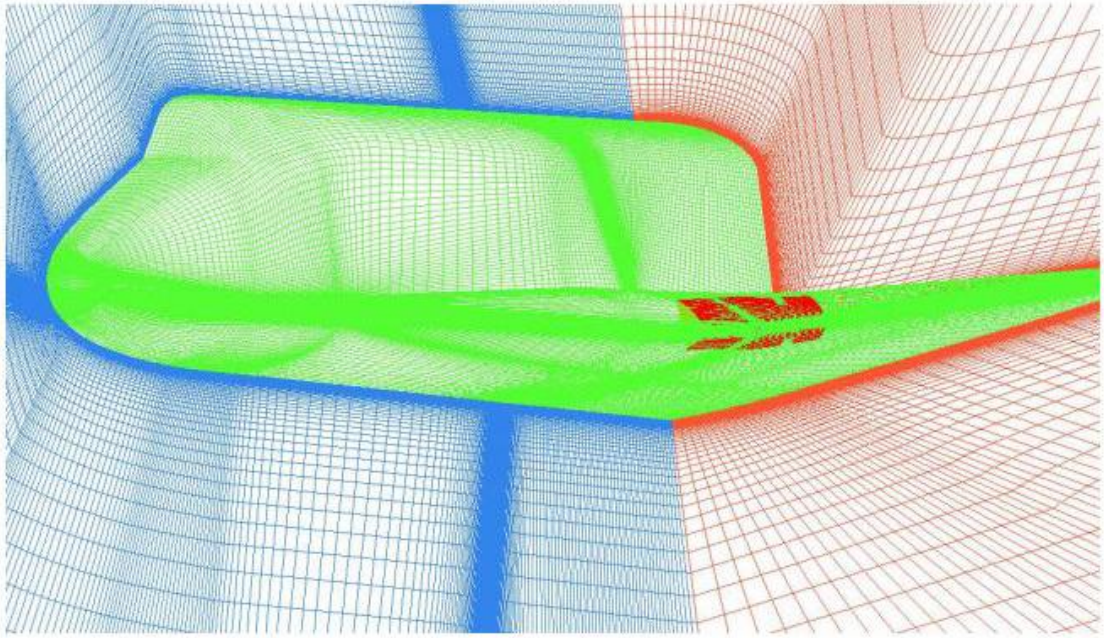

Figure 5.3.6-14 Grid Model for Panel 7 Hole Coupled External/Internal Flow Simulation I

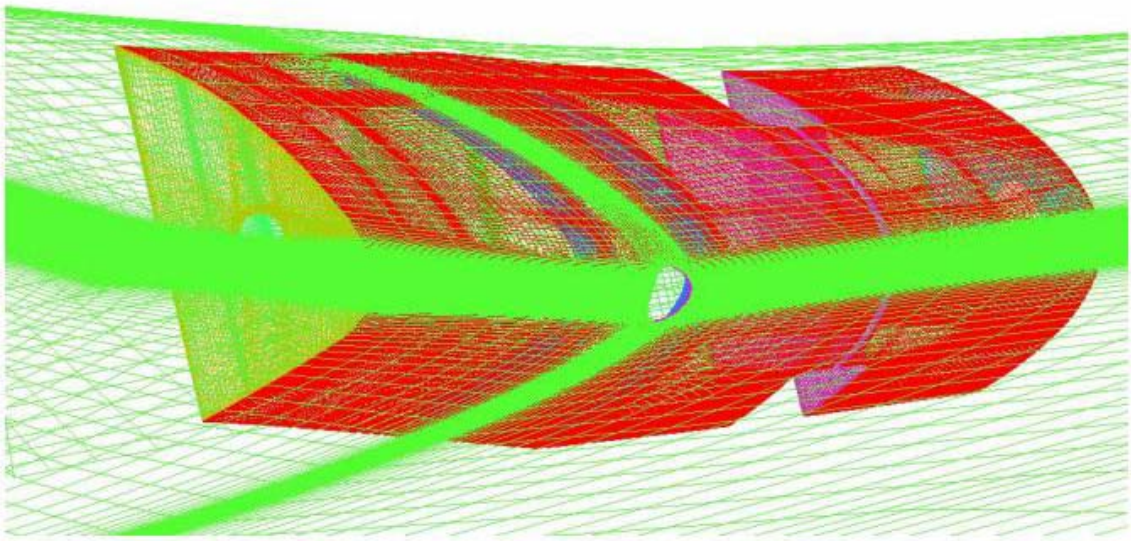

Figure 5.3.6-15 Grid Model for Panel 7 Hole Coupled External/Internal Flow Simulation I

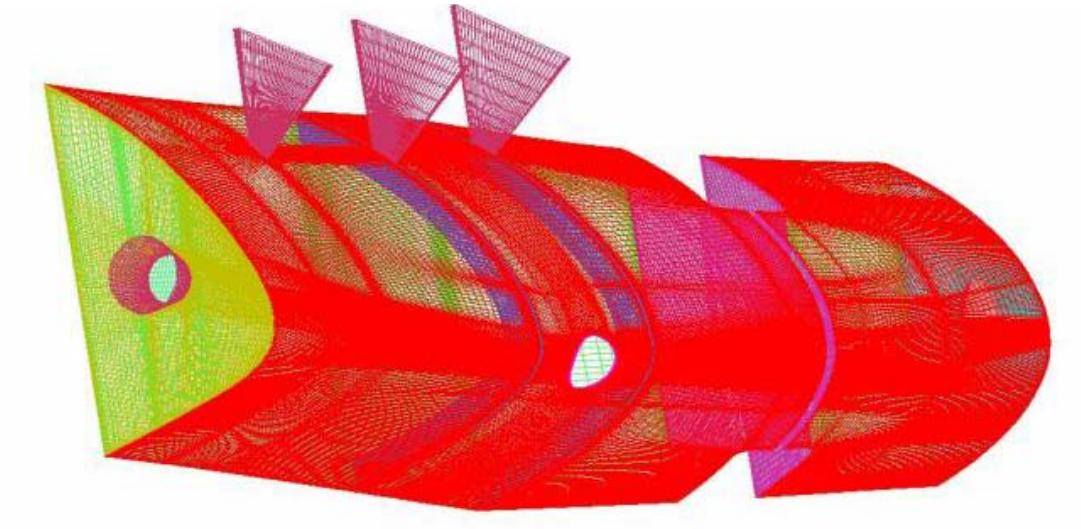

Figure 5.3.6-16 Grid Model for Panel 7 Hole Coupled External/Internal Flow Simulation I

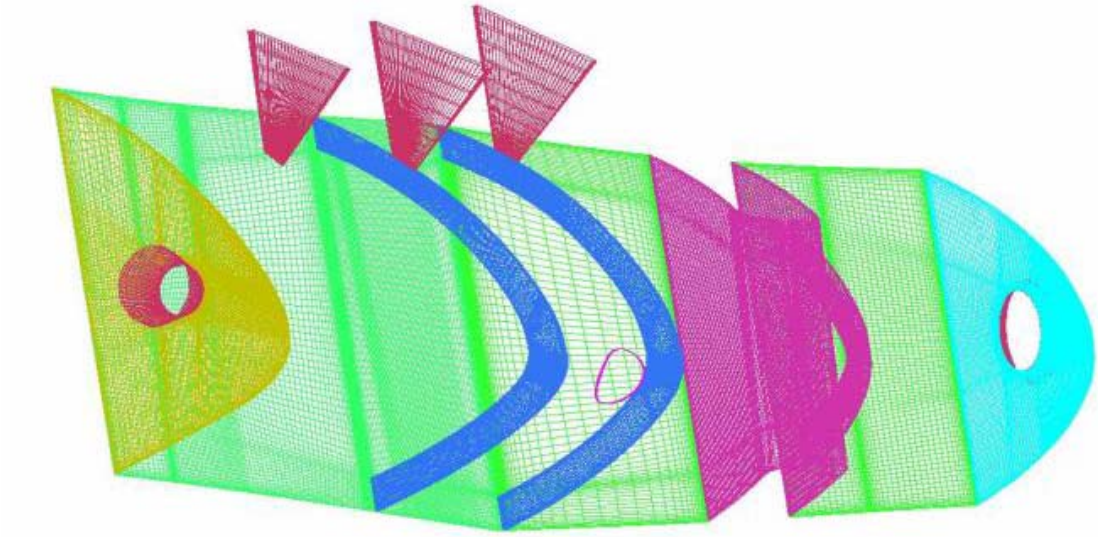

Figure 5.3.6-17 Grid Model for Panel 7 Hole Coupled External/Internal Flow Simulation I

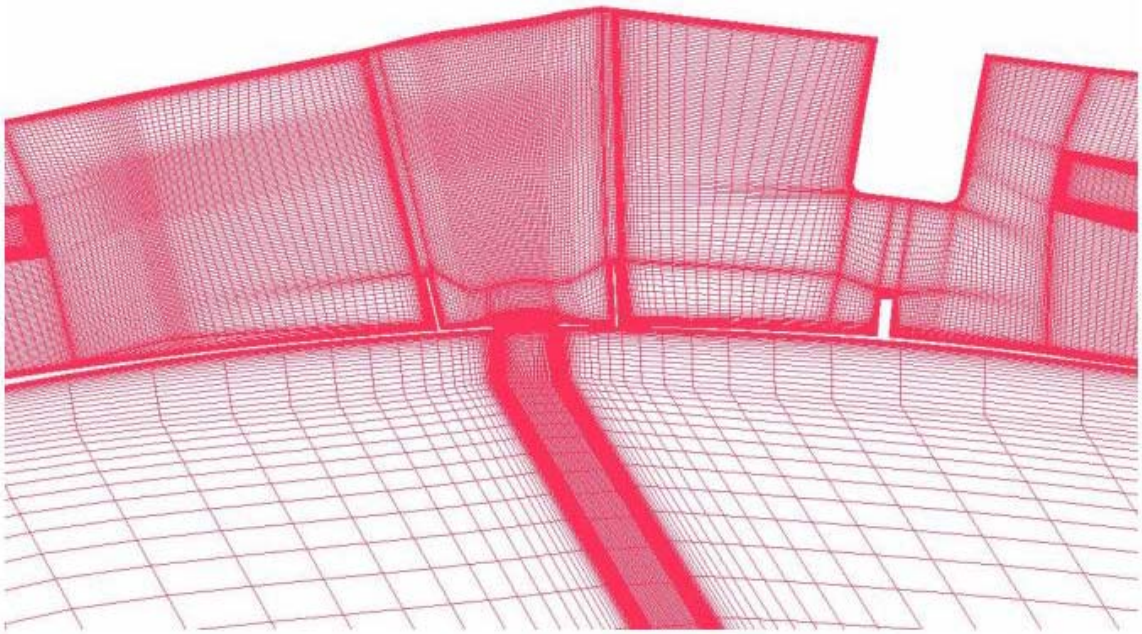

Figure 5.3.6-18 Grid Model for Panel 7 Hole Coupled External/Internal Flow Simulation I

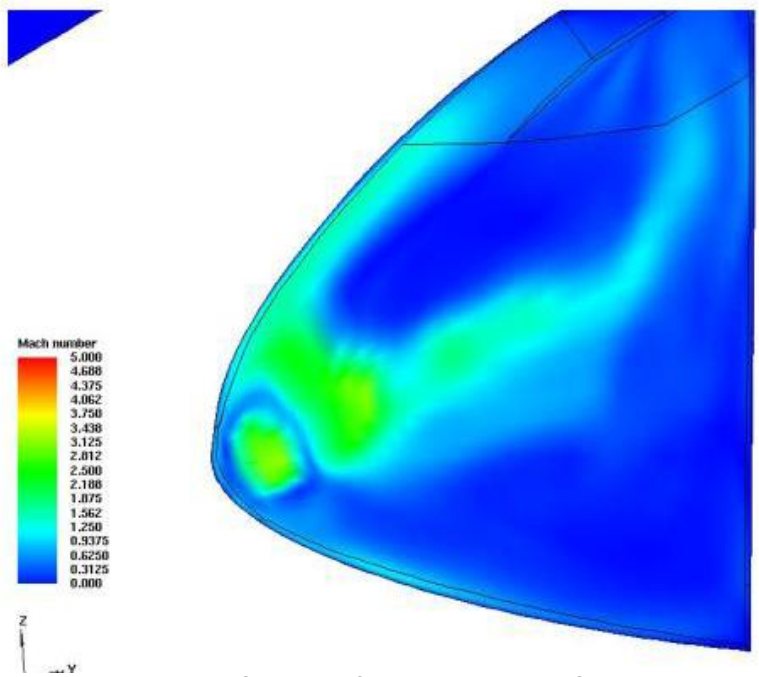

Figure 5.3.6-19 Mach Contours from Panel 7 Hole Coupled External/Internal Flow Simulation I (Postprocessed using every other points)

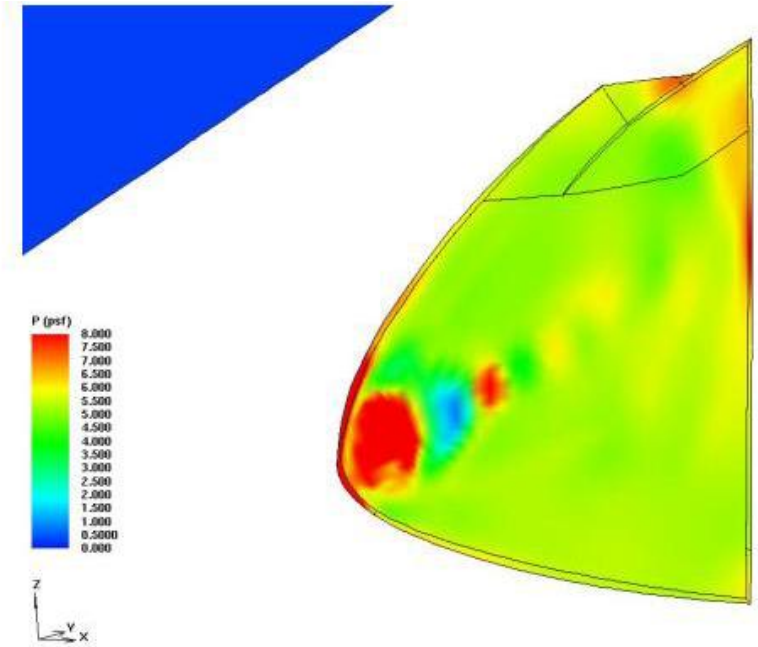

Figure 5.3.6-20 Pressure Contours from Panel 7 Hole Coupled External/Internal Flow Simulation I (Postprocessed using every other points)

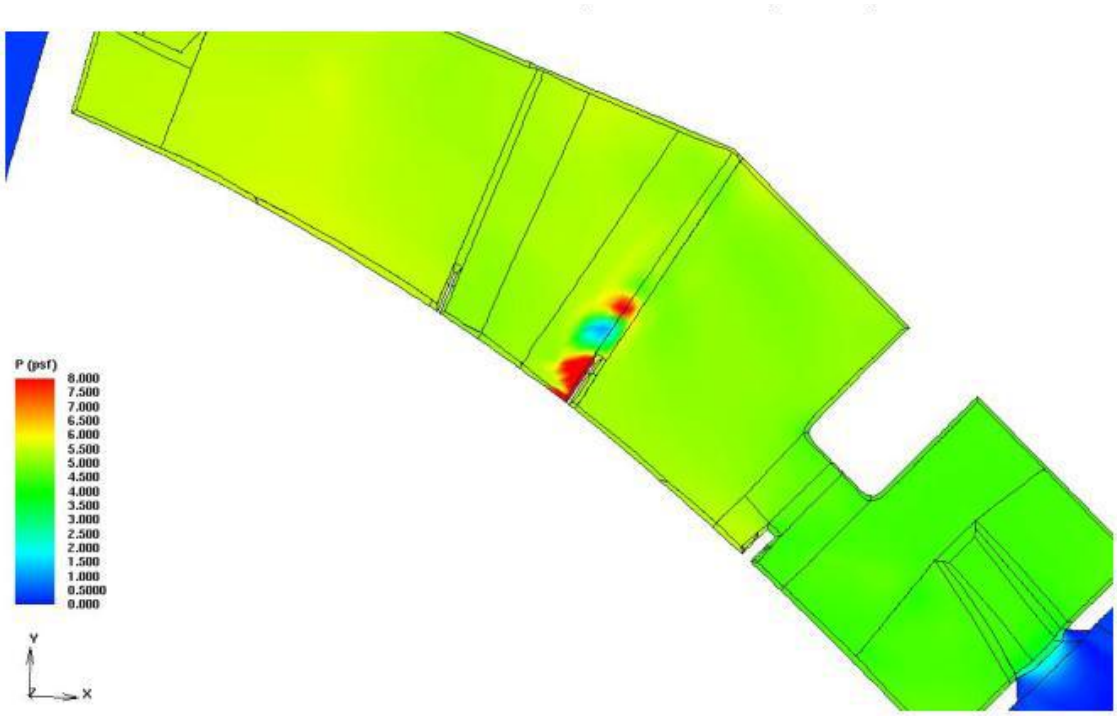

Figure 5.3.6-21 Pressure Contours from Panel 7 Hole Coupled External/Internal Flow Simulation I (Z=297.3; Postprocessed using every other points)

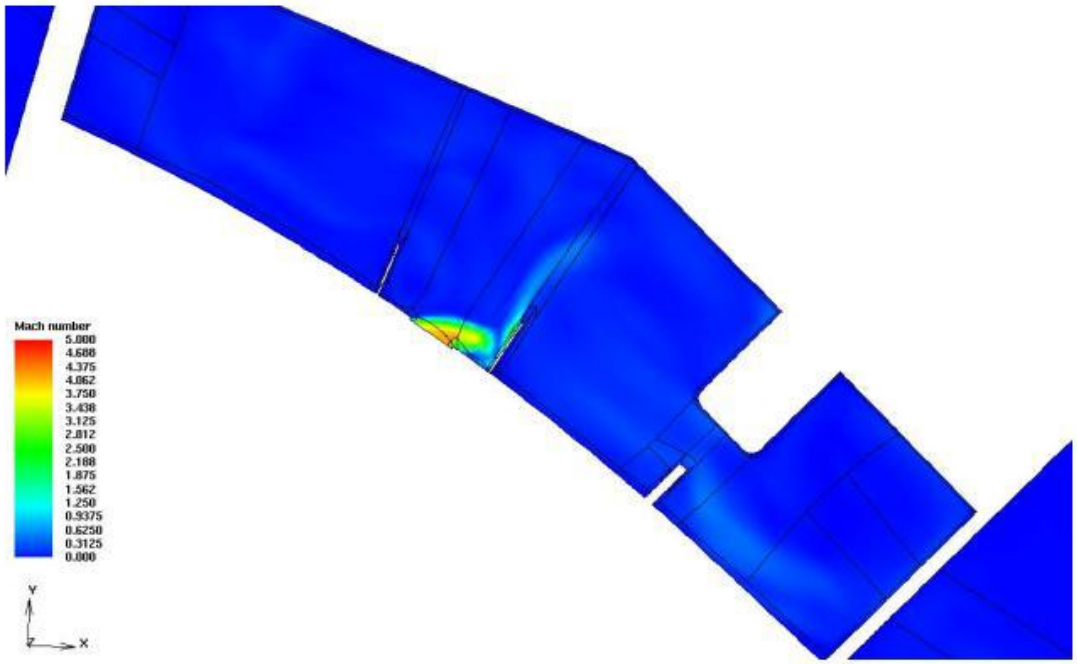

Figure 5.3.6-22 Mach Contours from Panel 7 Hole Coupled External/Internal Flow Simulation I (Z=291.6; Postprocessed using every other point)

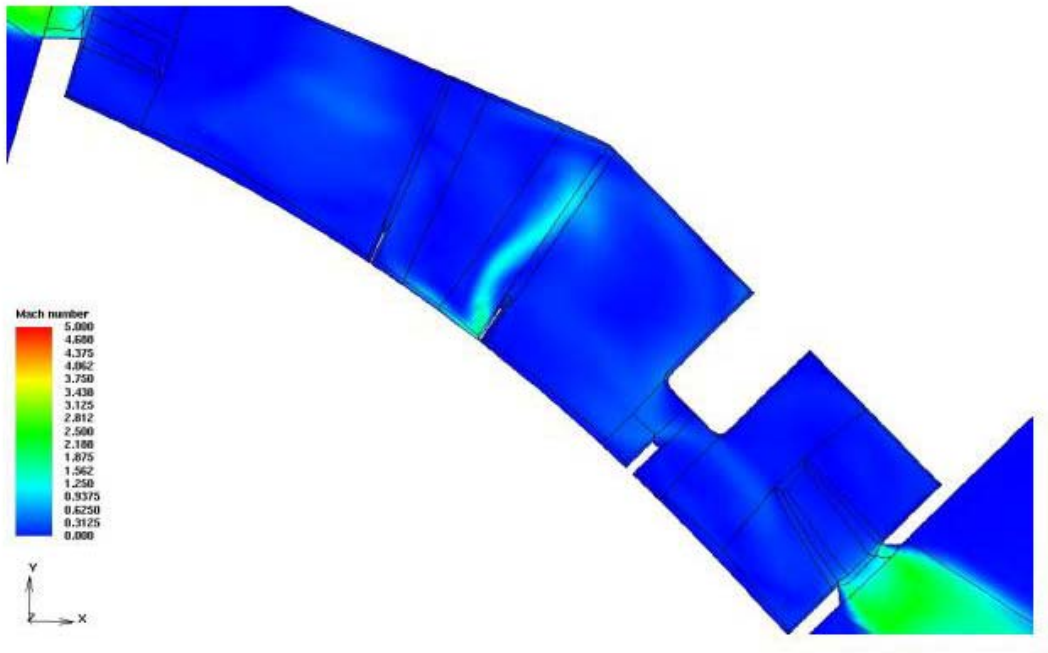

Figure 5.3.6-23 Mach Contours from Panel 7 Hole Coupled External/Internal Flow Simulation I (Z=301.6; Postprocessed using every other point)

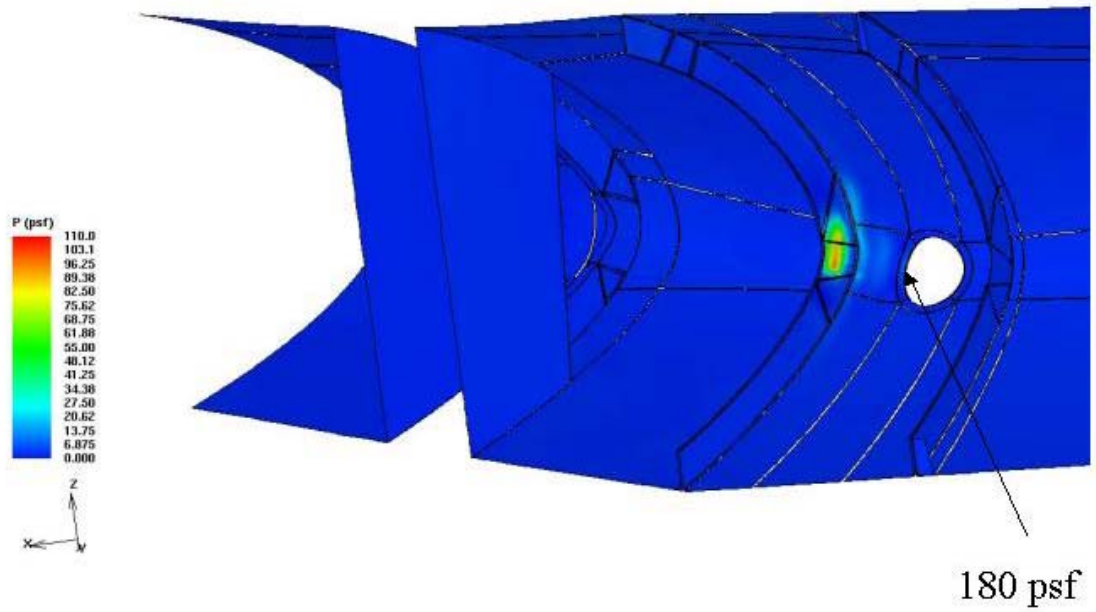

Figure 5.3.6-24 Pressure Contours on RCC Channel from Panel 7 Hole Coupled External/Internal Flow Simulation I

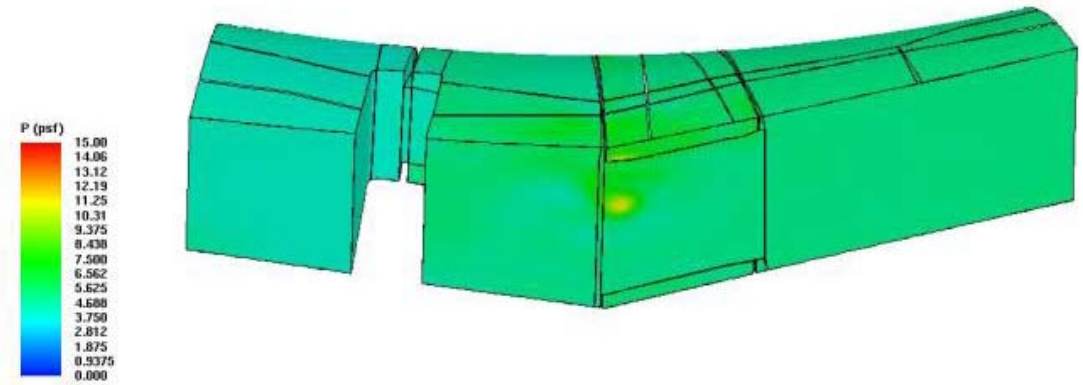

Figure 5.3.6-25 Pressure Contours on Front Spar from Panel 7 Hole Coupled External/Internal Flow Simulation I

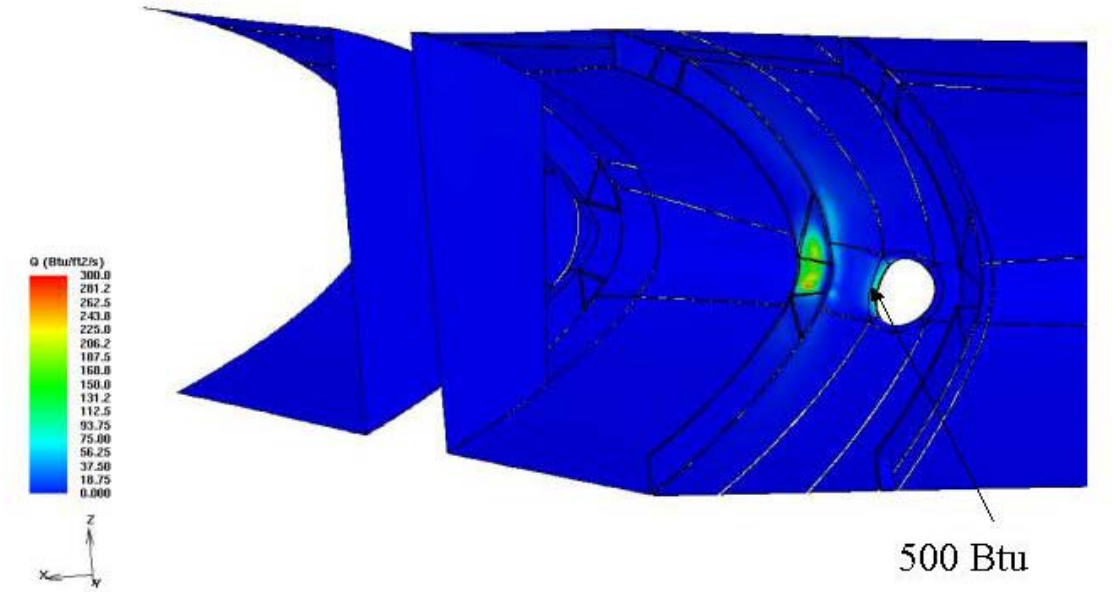

Figure 5.3.6-26 Heating Contours on RCC Channel from Panel 7 Hole Coupled External/Internal Flow Simulation I

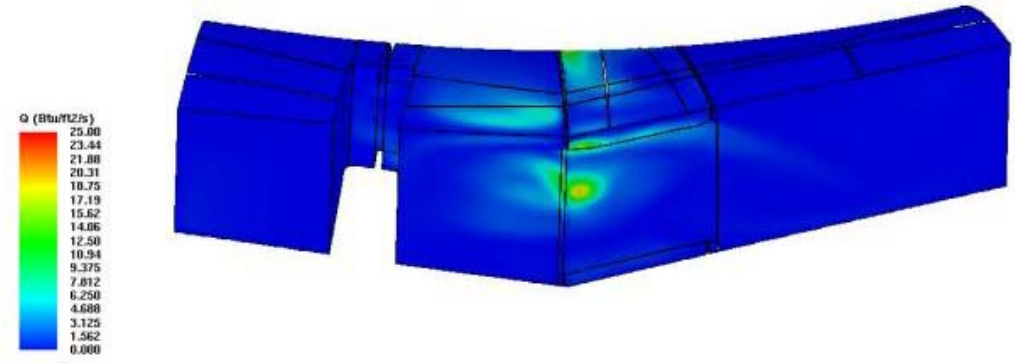

Figure 5.3.6-27 Heating Contours on Front Spar from Panel 7 Hole Coupled External/Internal Flow Simulation I

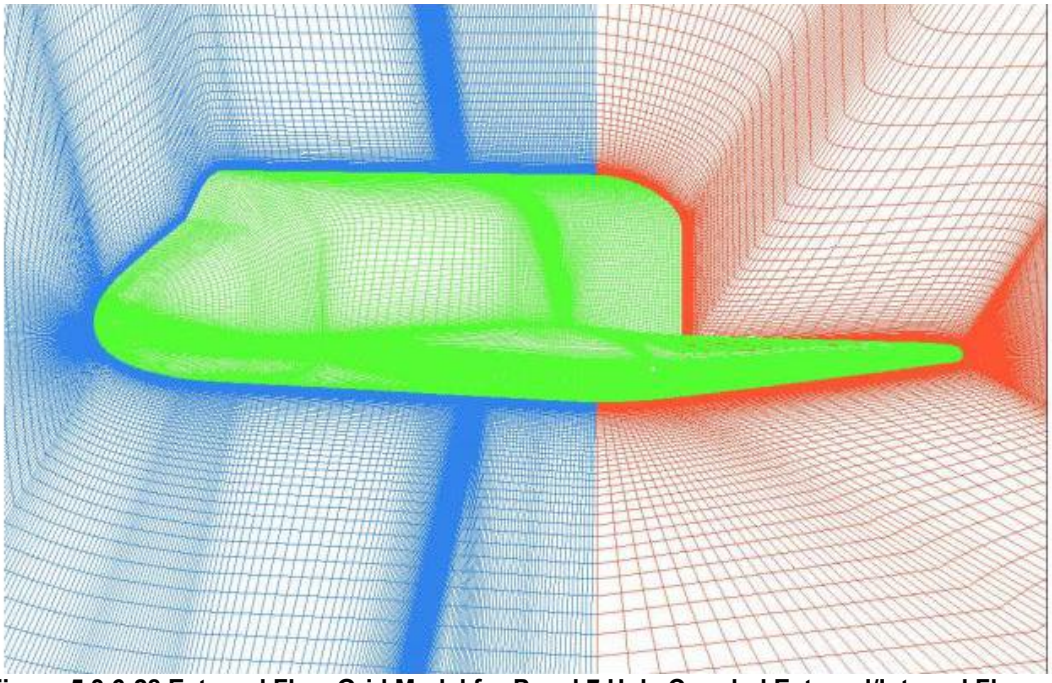

Figure 5.3.6-28 External Flow Grid Model for Panel 7 Hole Coupled External/Internal Flow Simulation II

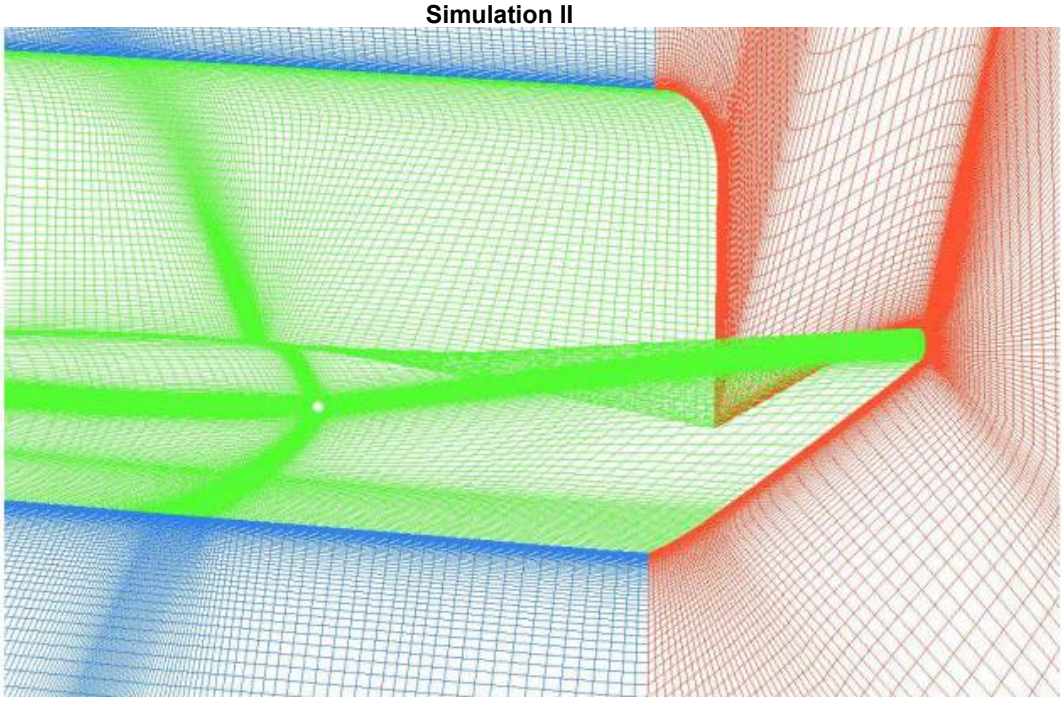

Figure 5.3.6-29 External Flow Grid Model for Panel 7 Hole Coupled External/Internal Flow Simulation II

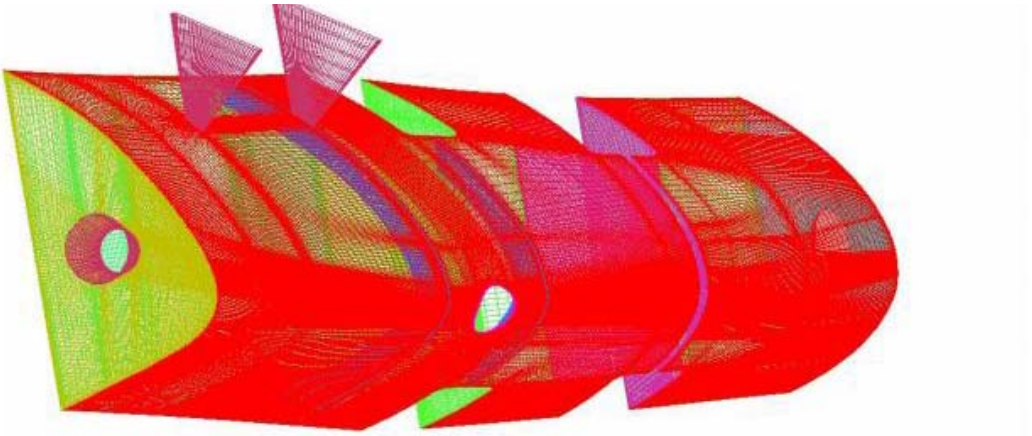

Figure 5.3.6-30 Internal Flow Grid Model for Panel 7 Hole Coupled External/Internal Flow Simulation II

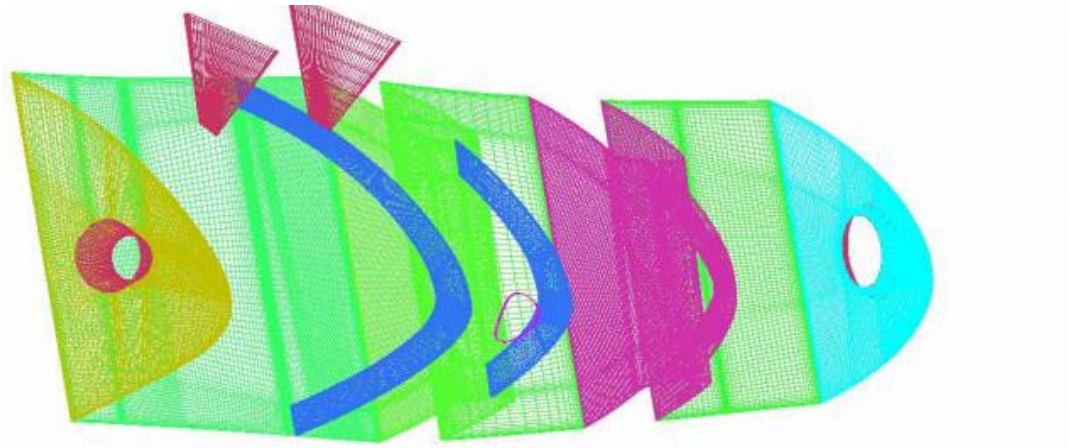

Figure 5.3.6-31 Internal Flow Grid Model for Panel 7 Hole Coupled External/Internal Flow Simulation II

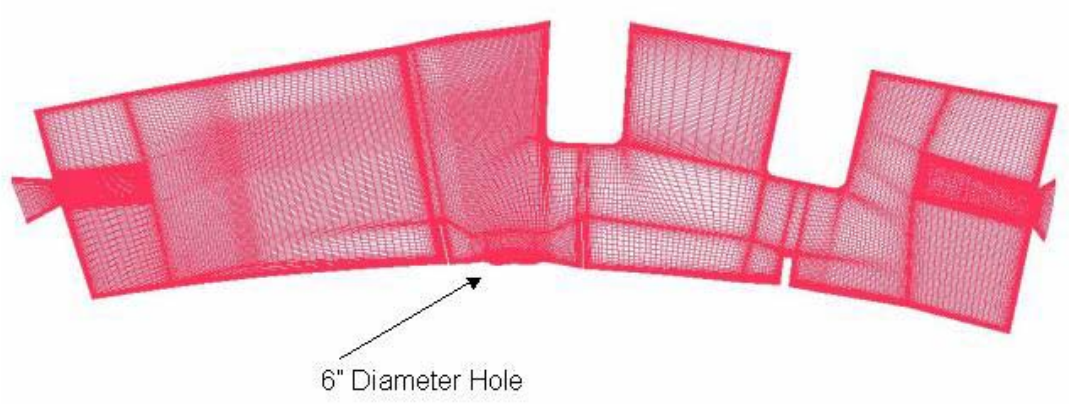

Figure 5.3.6-32 Internal Flow Grid Model for Panel 7 Hole Coupled External/Internal Flow Simulation II

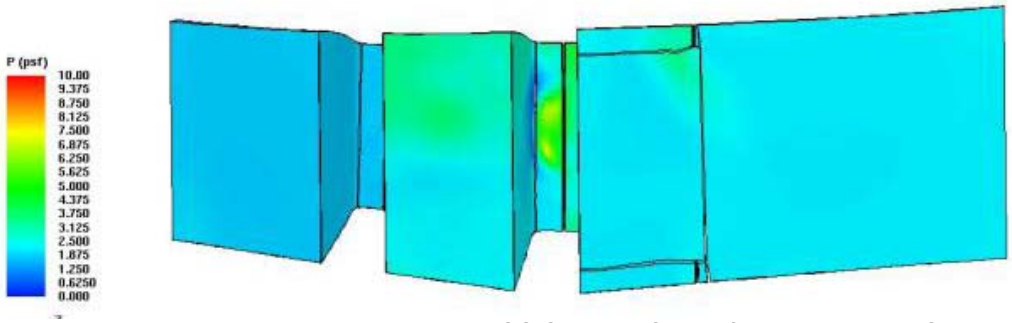

Figure 5.3.6-33 Pressure Distribution on RCC Channel Cavity for Panel 7 Hole Coupled External/Internal Flow Simulation II

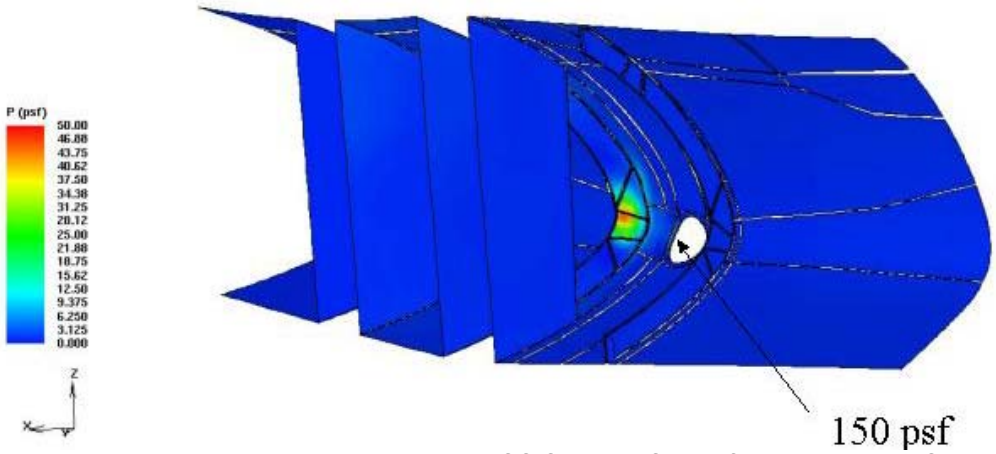

Figure 5.3.6-34 Pressure Distribution on RCC Channel Cavity for Panel 7 Hole Coupled External/Internal Flow Simulation II

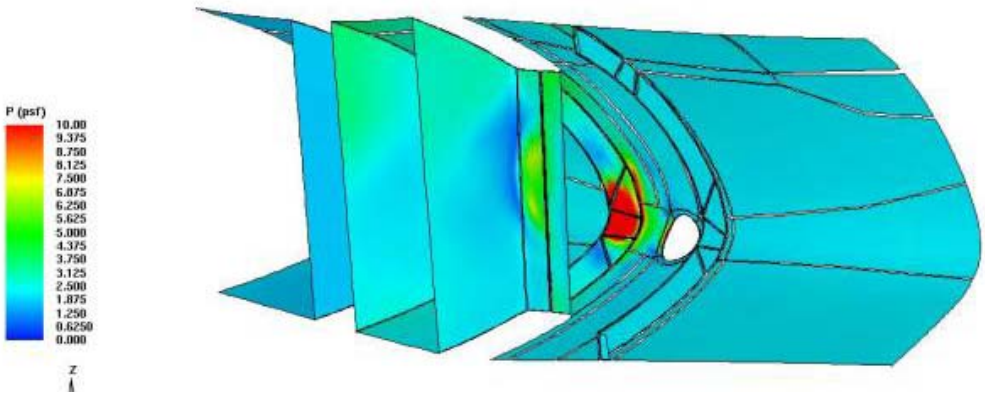

Figure 5.3.6-35 Pressure Distribution on RCC Channel Cavity for Panel 7 Hole Coupled External/Internal Flow Simulation II

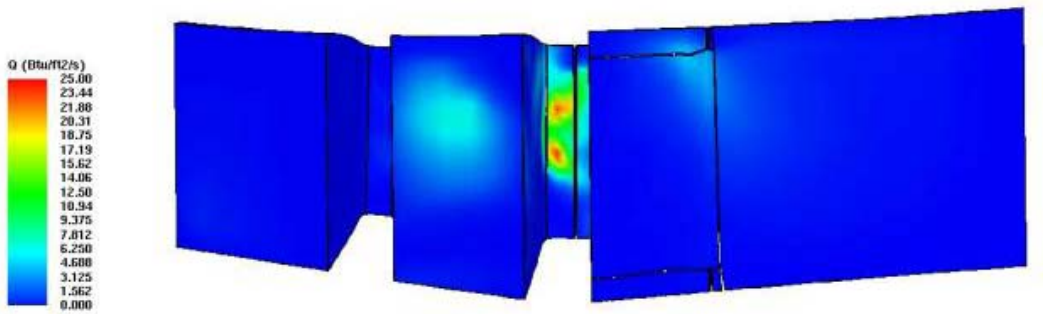

Figure 5.3.6-36 Heating Distribution on RCC Channel Cavity for Panel 7 Hole Coupled External/Internal Flow Simulation II

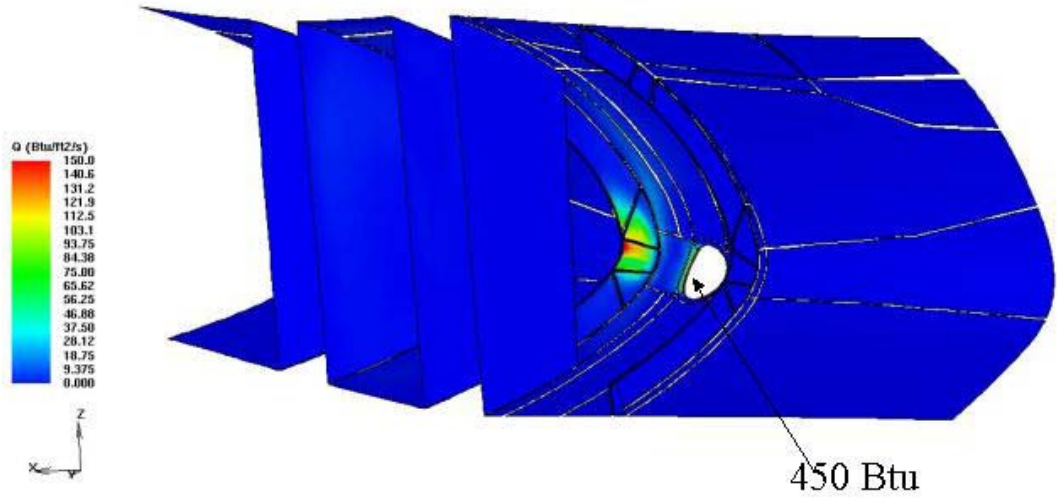

Figure 5.3.6-37 Heating Distribution on RCC Channel Cavity for Panel 7 Hole Coupled External/Internal Flow Simulation II

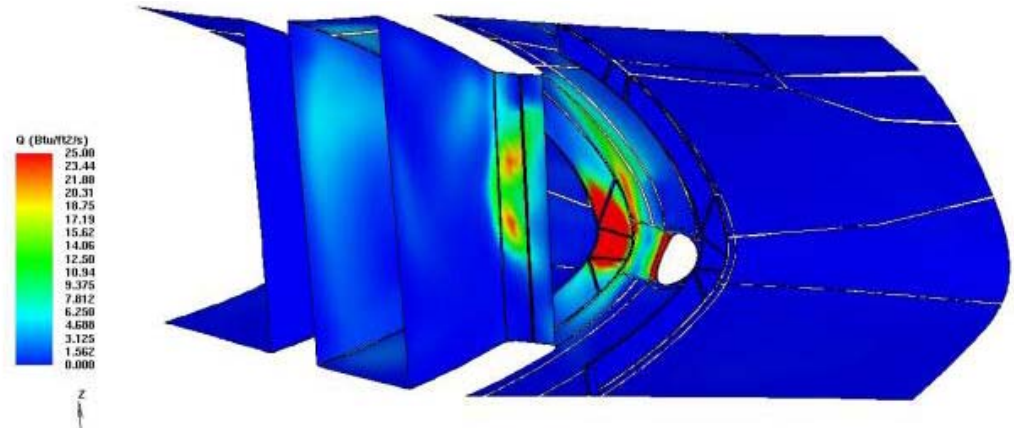

Figure 5.3.6-38 Heating Distribution on RCC Channel Cavity for Panel 7 Hole Coupled External/Internal Flow Simulation II

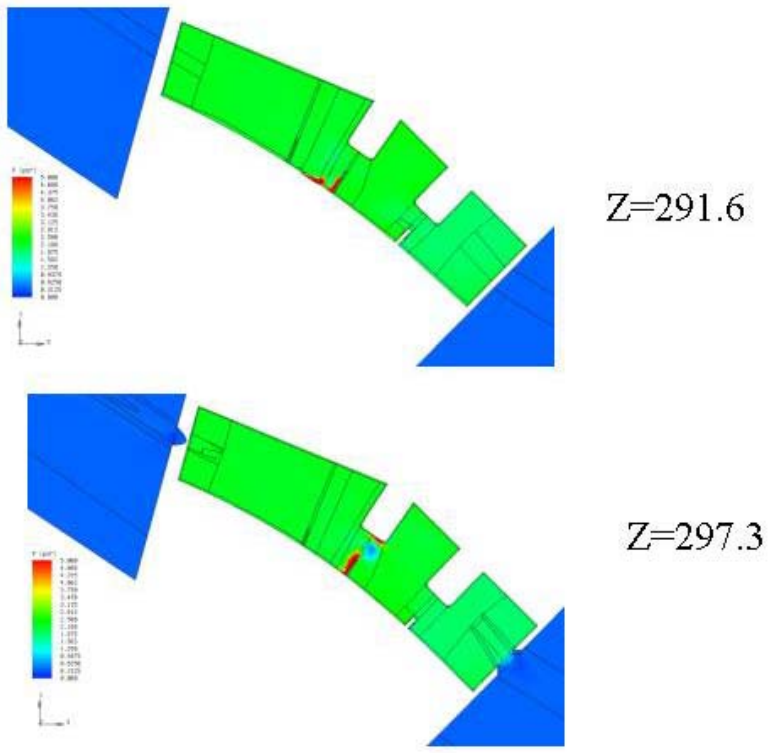

Figure 5.3.6-39 Pressure Contours in flow field for Panel 7 Hole Coupled External/Internal Flow Simulation II

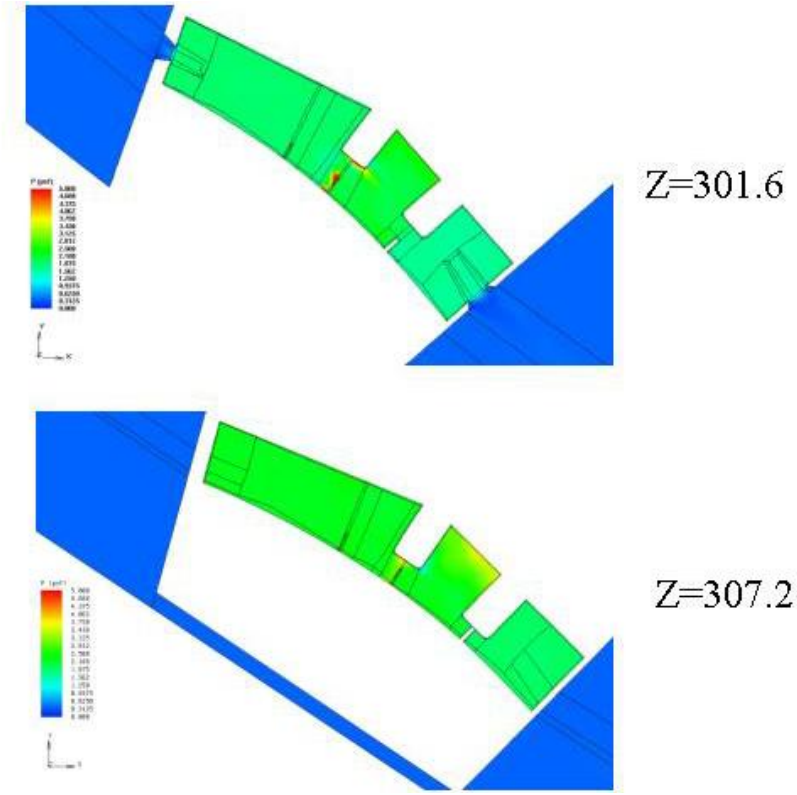

Figure 5.3.6-40 Pressure Contours in flow field for Panel 7 Hole Coupled External/Internal Flow Simulation II

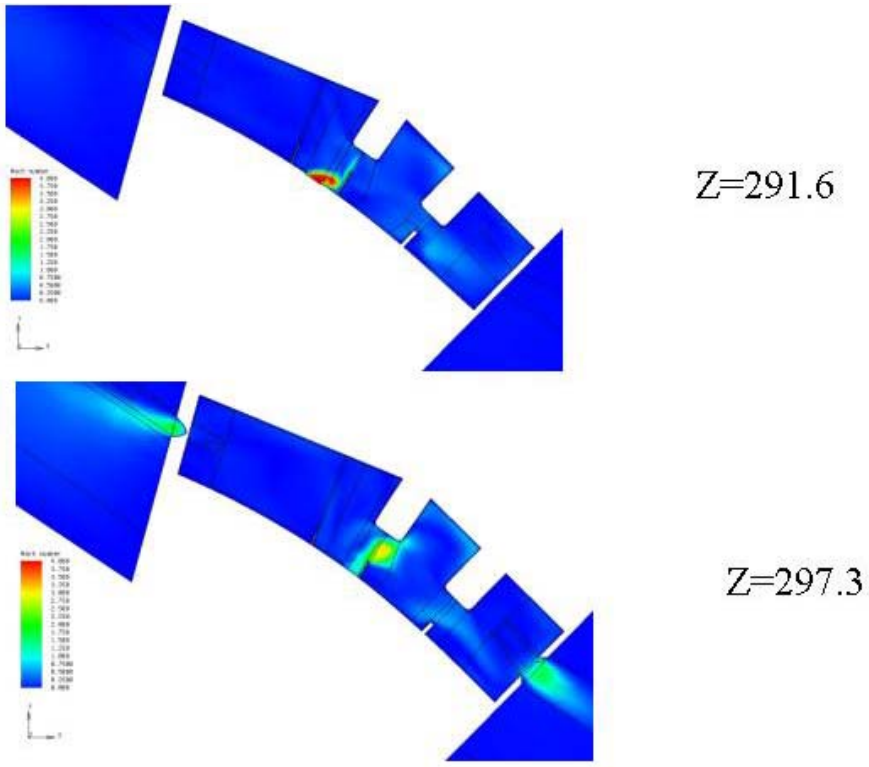

Figure 5.3.6-41 Mach Contours in flow field for Panel 7 Hole Coupled External/Internal Flow Simulation II

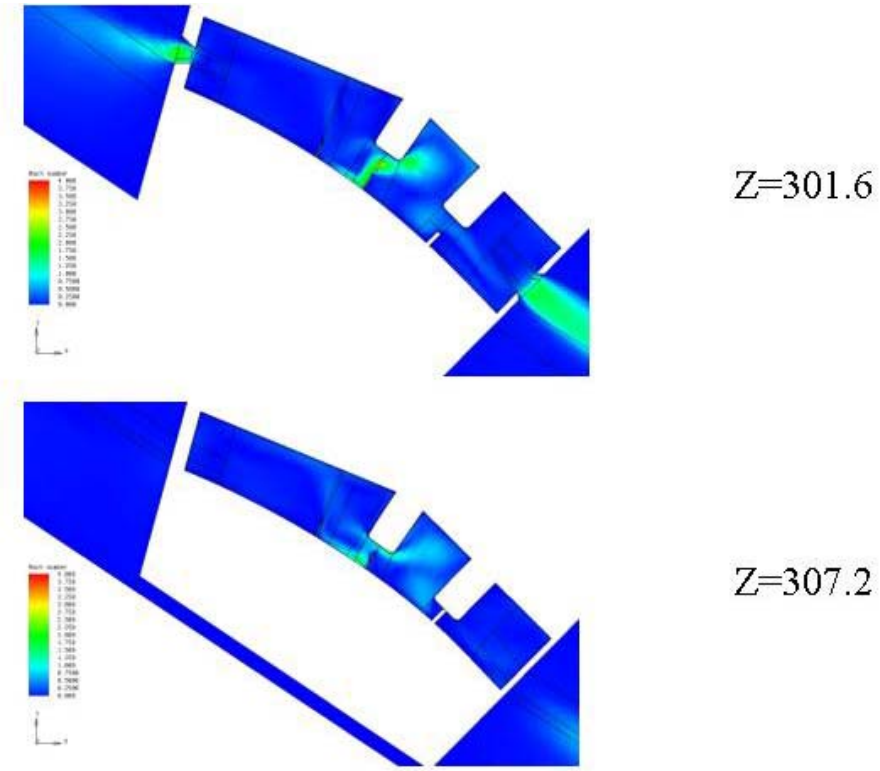

Figure 5.3.6-42 Mach Contours in flow field for Panel 7 Hole Coupled External/Internal Flow Simulation II

5.3.6.1.3 RCC Panel 8 10" - Boeing Rocketdyne

5.3.6.1.3.1 Case Description

The objective of this analysis was to compute convective heating rates on the Leading Edge Structural Subsystem (LESS) cavity internal surfaces. The intended application of the data was to enhance the engineering heat transfer models and to improve understanding of this flow field structure.

A 10 inch diameter hole was located at coordinates X=1066.00, Y=-214.75, Z=234.6 as shown in Figure 5.3.6-43. Also shown is a jet penetration analysis by NASA JSC based on a NASA LaRC LAURA external flow solution. This indicates that impingement will occur on the inboard side of the RCC 8/9 spanner beam insulators (earmuffs) given a hole at this location. These results were used as a guide for grid clustering in this analysis.

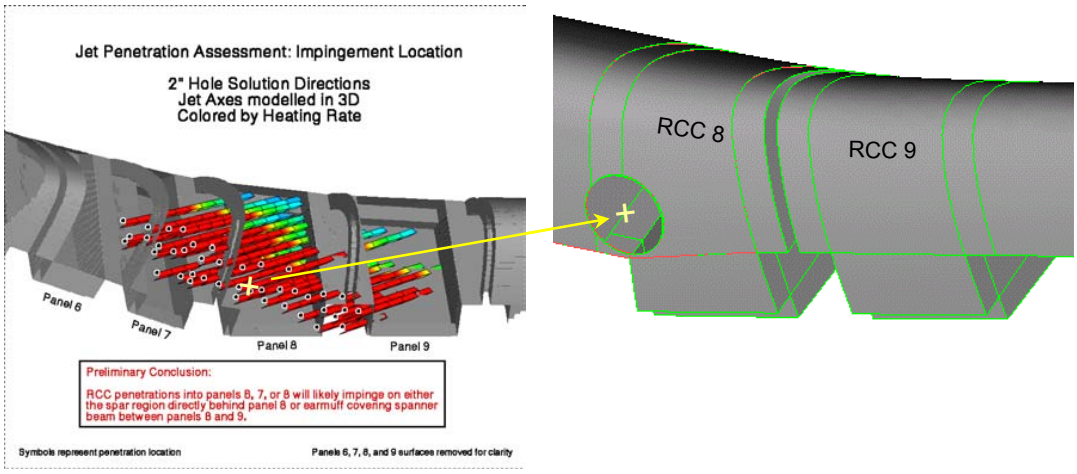

Figure 5.3.6-43 - 10 inch Hole Location Compared to Jet Penetration Analysis

5.3.6.1.3.2 *Grid/Solution Development*

The JSC model mentioned above was selected as the internal surface geometry for this analysis. This model had the benefits of possessing the RCC 7/8, 8/9, 9/10 earmuffs and the forward spar insulators (hot tubs) in between them. The hot tubs had been specifically requested for this analysis, while all three earmuffs were deemed desirable based on the anticipated flow field in this region. The negative aspects were that all of the edges are sharp, which conflicted with other models and photographs. Dimensions of key components, such as the earmuffs and hot tubs, were also somewhat uncertain since the JSC dimensions conflicted with a model used by Boeing Huntington Beach and some photographs. Due to time constraints however, the JSC model was employed while a more accurate model of the LESS was started using the Pro/Engineer CAD system. Extruded "dump" regions were added on either side of RCC 8 and 9 to enable the application of constant pressure outflow boundary conditions. The dimensions of these regions were based on the results of the 2-D T-Seal analysis (Section 5.3.6.2.2). Previous analyses had shown that a high degree of coupling existed between the internal and external flow fields. For a hole of this size, the external flow is capable of negotiating the opening while remaining supersonic. The LAURA external solution was used to provide the necessary coupling, but only a small two-zone (37 and 38) portion of it. This was carefully selected to reduce the size of the model while preserving the external solution in the region of interest (Figure 5.3.6-44).

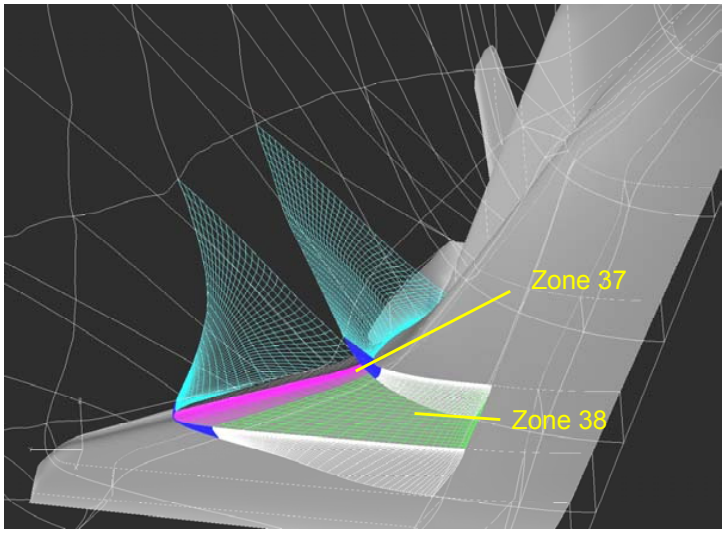

Figure 5.3.6-44 - LAURA Solution Zones Used as External Domain

The Boeing APPT system was used to generate the hybrid viscous unstructured computational grid. The unstructured approach greatly reduces the time required to generate the grid and eliminates wasted clustering cells in complex internal regions. After a number of revisions, final grids (Figure 5.3.6-45) were produced containing 4.1M elements with a wall spacing of $1.0e^{-4}$ inches (medium grid), and 4.9M elements with a wall spacing of $1.0e^{-5}$ inches (fine grid). The solutions were obtained using the Boeing ICAT code. Fully laminar flow was assumed based on the extremely low Reynolds numbers present. Liu-Vinokur equilibrium air thermochemistry and Tannehill transport properties were used. The convergence criteria were to drive net fluxes to an initial steady-state and also to drive integrated heat load in key areas to steady-state. Contours of heat flux in key areas were also plotted at different time steps.

The CFD Condition 1 trajectory point was used to define the freestream conditions. All wall temperatures were set to 3,000ºR. This corresponds to the melting temperature for the Inconel 601 outer layer of the Dynaflex surfaces such as the earmuffs and hot tubs. The pressures on the cavity outflow surfaces were established from the venting analysis (Section 5.3.5) and are presented in Table 5.3.6.1-1.

Cavity Outflow Pressure					
Cp	P/Pinf	*psf*	*psia*	*N/m^2 (Pa)*	
0.188	82.198	4.177	0.0290	200	Boeing Huntington Beach RCC7 6 inch hole
0.567	246.593	12.531	0.0870	600	This analysis

Table 5.3.6.1-1 – RCC Cavity Outflow Boundary Pressure

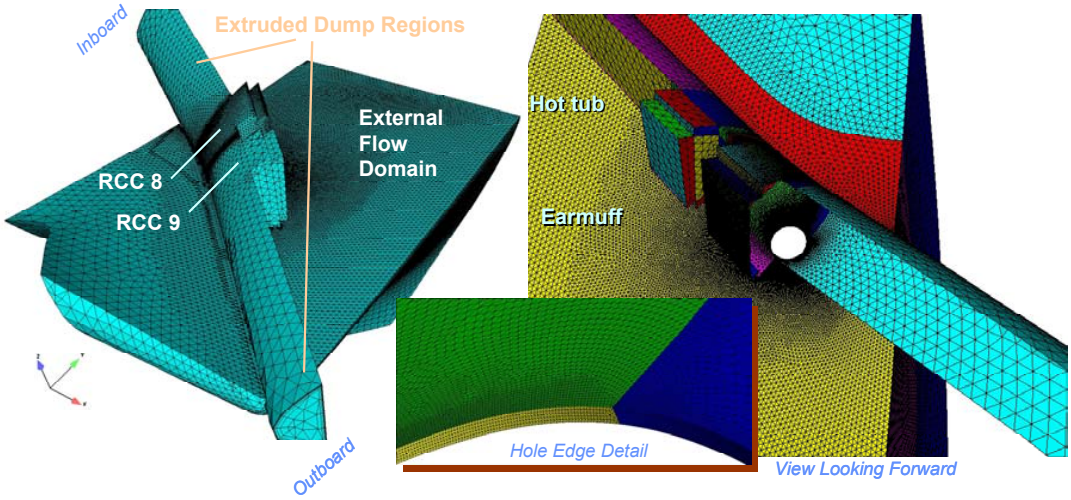

Figure 5.3.6-45 - Hybrid Viscous Unstructured Grid

5.3.6.1.3.3 Results

Major flow-structure comments

Figure 5.3.6-46 shows the flow inside the LESS cavity. The walls are colored by static pressure and the streamtubes are colored by Mach number. The primary jet issuing from the hole impinges on the inboard side of the RCC 8/9 earmuff. The jet makes a near constant-pressure turn (as observed by the small change in Mach number) and splits into two supersonic tails. This behavior was consistently observed in the T-Seal 2-D solutions (Section 5.3.6.2.2). The weaker tail (#2) impinges in upper corner of hot tub, while the stronger tail (#1) impinges in lower corner of hot tub. The latter impingement creates a transonic "re-tail" that impingements on RCC 7/8 earmuff outboard surface then shocks down to subsonic conditions. Entrainment of a subsonic vortex by the primary jet creates small supersonic impingement on RCC 8 rib. These features account for all of the supersonic flow inside the LESS cavity, and hence all of the high pressure and heat flux areas. Once subsonic, the flow twists into complex vortical patterns and makes its way to the outflow boundaries.

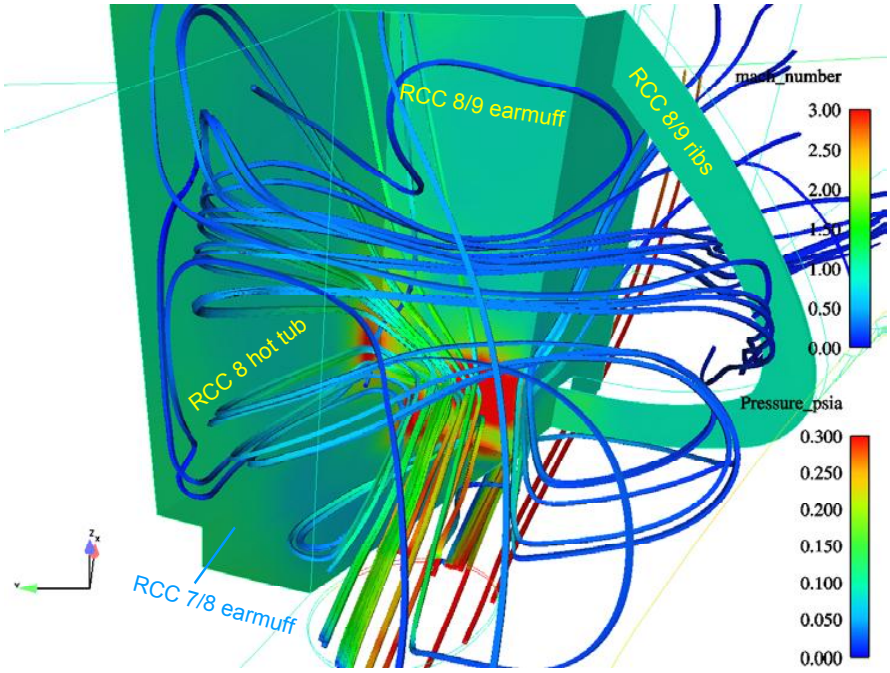

Figure 5.3.6-46 – Mach-colored Streamtubes and Wall Static Pressure Viewed from in Front of Leading Edge

Figure 5.3.6-47 shows static pressure on the walls and Mach number on a cutting plane. The cutting plane includes the internal and external flow fields. The external flow captured by the hole includes all of the wing boundary layer and some of the local freestream. Recall that the local freestream has been processed through the vehicle shock envelope that is oblique in this area. The captured flow expands through a 10° turn into the hole and forms the primary jet. The jet expansion is small internally since the pressure ratio due to the turn is only about 1.9. The primary jet then encounters a near-normal (80°) impingement onto the RCC 8/9 earmuff. The resulting stagnation pressure exceeds freestream-normal shock pressure due to recompression by oblique vehicle shock. Supersonic tail #2 is observed moving vertically along the earmuff.

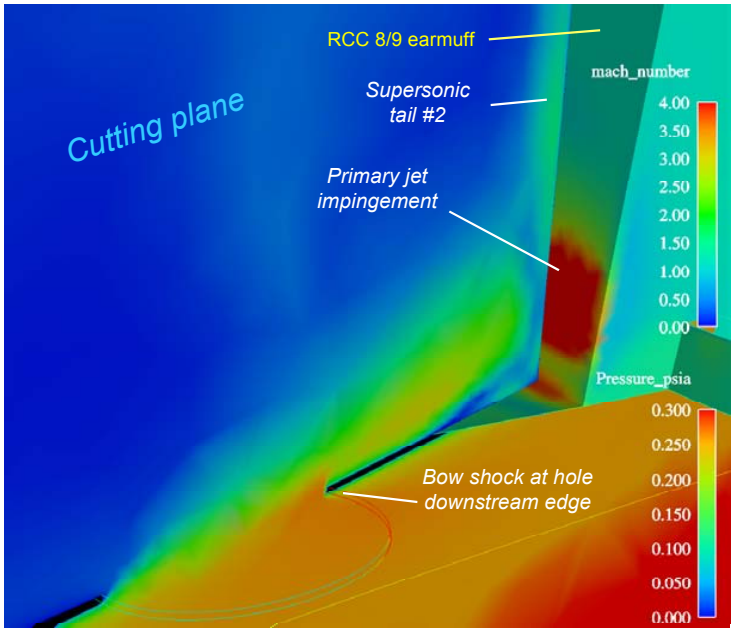

Figure 5.3.6-47 - Mach-colored Cutting Plane and Wall Static Pressure Detail View From in Front of Leading Edge

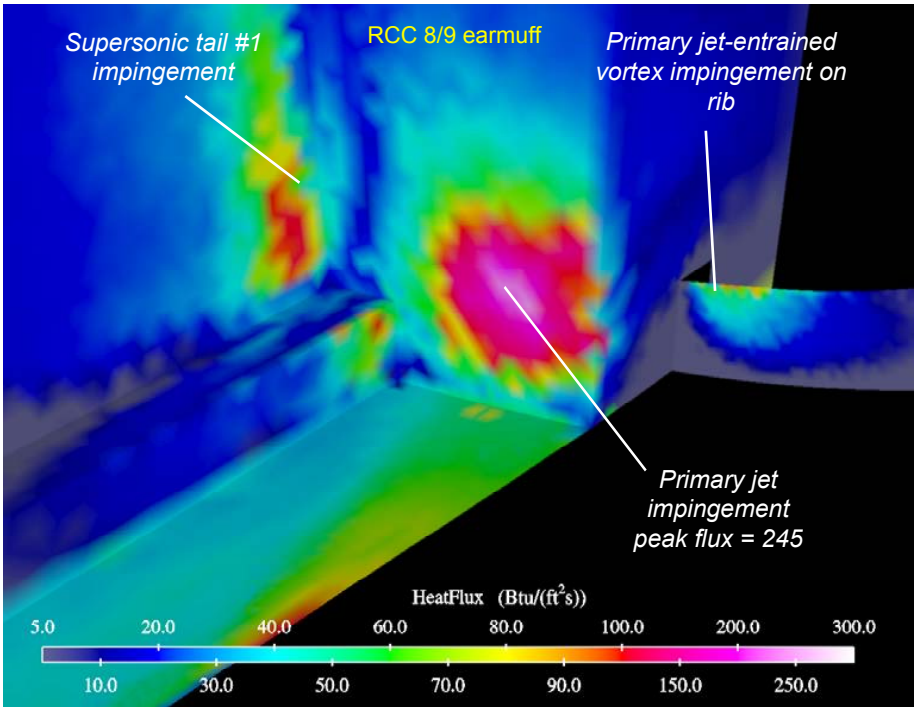

Figure 5.3.6-48 – Surface Heat Flux Detail View From in Front of Leading Edge – Medium Grid Solution

Surface heating and pressure comments

Figure 5.3.6-48 shows surface heat flux for the medium grid solution in the region where the RCC 8/9 earmuff and the RCC 8 hot tub intersect. This is the area of highest heating, as would be expected based on the pressure and Mach fields observed. The primary jet impingement produces the highest heating, while supersonic tail #1 produces the second highest. The tail flow has lost some total pressure due to shock waves encountered in the turning process that created it (Figure 5.3.6-48) so its stagnation pressure

and heat flux are lower. The RCC 8 rib encounters some heating do to the impingement of vortical flow that was reaccelerated to supersonic velocity via entrainment in the primary jet. Flow field animations were used to reveal this phenomenon as the source of that heating.

The fine grid solution is shown in Figure 5.3.6-49. The peak heat flux is 14% lower, however this occurs at a single surface cell. The integrated heat load in the regions of interest differs by only 2.3% with the fine grid solution having the lower value. Based on the proximity of these results, grid independence can be claimed. The medium grid solution was run a total of 30,000 time steps, while the fine grid solution was run a total of 32,000 time steps. Both were monitored periodically using flow visualization. No indication of unsteady flow was found, however there is still a possibility that this could occur. Many more time steps would be needed to be certain.

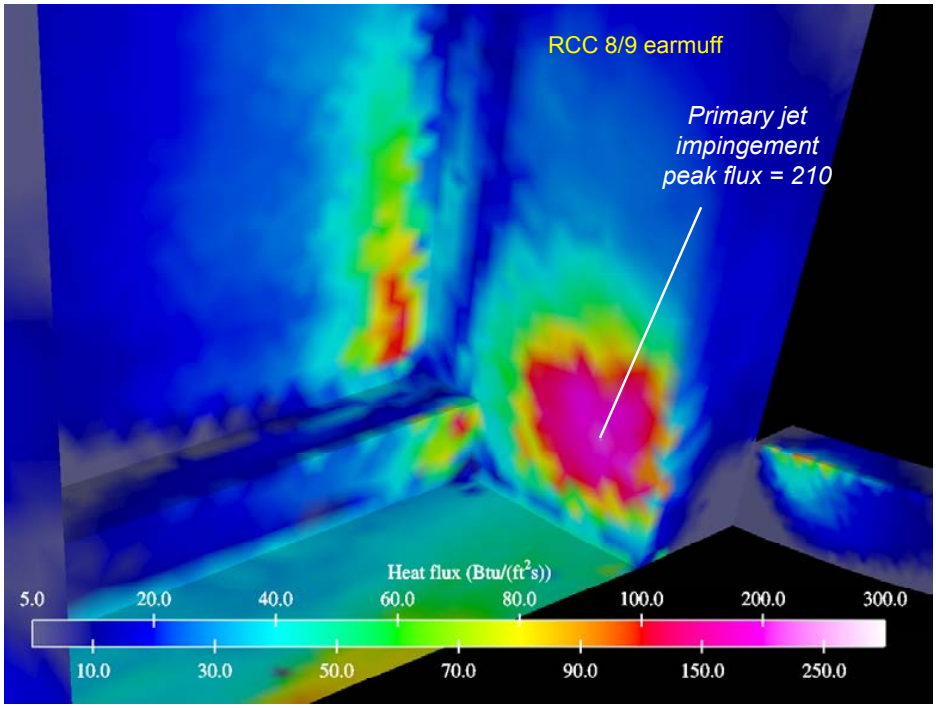

Figure 5.3.6-49 – Surface Heat Flux Detail View From in Front of Leading Edge – Fire Grid Solution

An equilibrium thermochemistry model was employed for computational efficiency based on the historical equivalence of surface heat flux from solutions using equilibrium air and those using finite-rate chemistry with a fully catalytic wall. The Dynaflex material covering the earmuff and hot tub surfaces has a 0.004" thick Inconel 601 foil. Figure 5.3.6-50 from Goulard shows that metals are highly catalytic under these conditions. The actual catalycity of the Inconel 601 and underlying materials under these conditions is not known at this time, however. Actual heat fluxes can range from 25%-80% less than the fully catalytic value if the materials have a lower catalycity.

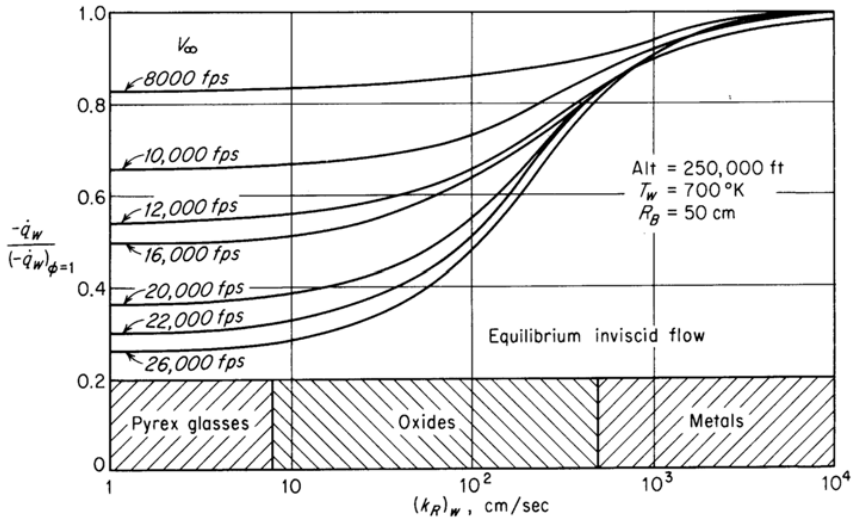

Figure 5.3.6-50 - Effect of Wall Material on Heat Flux (Goulard)

5.3.6.1.4 LaRC Solutions of Various Hole Size and Locations

The Langley Aerothermodynamic Upwind Relaxation Algorithm (LAURA) [NASA TM 4674, NASA TP 2867] was applied to external and internal flow simulations for the Columbia investigation. LAURA is a high fidelity analysis tool, specialized for hypersonic re-entry physics, utilizing state-of-art algorithms for computational fluid dynamic (CFD) simulations. Previous simulations of STS 1,2 and 5 with LAURA to resolve questions of a pitching moment anomaly (STS 1) and to validate heating predictions were published in the AIAA Journal of Spacecraft and Rockets in 1994 [JSR Vol. 31 No. 3]. All of the current simulations specify laminar flow of air in chemical nonequilibrium (N, O, N_2, O_2, NO) and thermal equilibrium. Only CFD point 1 is simulated with freestream conditions: V_∞ = 24,116 fps (7350.6 m/s), ρ_∞ = 7.5681 x 10^{-8} slugs/ft^3 (3.9005 x 10^{-5} kg/m^3), T_∞ = 391.2° R (217.3 K), α = 40.1681 deg., and time = 13.50.53.0 GMT. The external flow simulations are implemented on the shared, baseline grid developed for the External Environments Team. The baseline grid is modified to allow coupling of the external flow with flow through a breach in the wing entering a vented cavity.

The simulations described in this section were generated relatively quickly and early in the investigation on the NAS Cray SV1 because simplifications were made to the leading edge cavity geometry. These simplifications enabled (1) a very quick grid generation procedure; and (2) high fidelity corroboration of jet physics with internal surface impingements ensuing from a breach through the leading edge, fully coupled to the external shock layer flow at flight conditions.

5.3.6.1.4.1 Holes in Panel 6

The following material is the first application of LAURA to flow in a vented cavity. Consequently, geometric complexity was incrementally added to better understand ensuing flow physics and effects of boundary condition specification.

Initially, quarter inch deep holes with varying diameters were inserted into the baseline, external flow solution at Panel 6. (See Figure 5.3.6-51.) The boundary condition at the bottom of the hole used a zero-order extrapolation from interior points for density and velocity and a specified reservoir pressure equal to

2 p_∞ (approximately 0.1 psf). The flow through this boundary evolved to be substantially supersonic for hole-sizes greater than two inches. The vent backpressure is sufficiently low to maintain at least sonic conditions through the vent and is characteristic of leeside levels.

The two-inch-hole simulation was then expanded to include an internal cavity extruded from the backside of panel 6. The cavity was roughly 1ft x 1ft x 1ft but its shape evolved from an ad-hoc grid generation process. A two-inch vent hole was included at the far end of the cavity. Flow through the breach is fully coupled to the external flow and the vent boundary condition was transferred to its new location.

Methodology
An in-house utility to insert structured grids defining Reaction Control System (RCS) jets through the outer mold lines (OML) of hypersonic vehicles was modified to define a quarter-inch deep, circular hole through the leading edge of shuttle orbiter wing. The modified surface grid blends smoothly with the baseline external grid as shown in Figure 5.3.6-52. A detail of the surface grid defining the hole is shown in Figure 5.3.6-53.

Taking the inserted, rectangular domain surrounding the breach shown in Figure 5.3.6-52 and creating a quarter-inch offset orthogonal to the OML produced the near wall of the cavity. This surface was extruded into the interior in a direction defined by the axis of the hole. An initial cell size taken from the external flow domain was applied. A constant growth factor (1.20) grows the grid off the wall for 32 cells and then an inverse factor is applied for another 32 cells to resolve a boundary layer on the opposite wall. Sidewall boundary-layer resolution is achieved with a similar procedure in which additional points are added in directions defined by an extrapolated coordinate line. A view of this extruded cavity is shown in Figure 5.3.6-54.

Immediate vent (No internal cavity)
These simulations provided early evidence that the flow through a two-inch diameter (or larger) breach entered the cavity with significant retention of external flow directionality. A normal jet into the cavity was not an appropriate model for these conditions at CFD Point 1 (Mach 24). The breach diameters were of the same order or larger than the local, external boundary-layer thickness. High impingement heating and pressures on the downstream lip of the breach are computed. It is likely that hole shape would evolve as a slot cut in the direction of the external streamlines as shown in Figure 5.3.6-51. In the case of the six-inch diameter breach the boundary layer is fully ingested. Summary of results follow.

Two-inch hole
The contour plot of total enthalpy in Figure 5.3.6-55 shows the boundary edge as the transition from orange to red color. The total enthalpy above the boundary layer edge, outside of viscous dissipation effects, is a constant. The boundary layer thickness is roughly ¾ of the hole diameter. The pressure field and streamlines entering the breach (Figure 5.3.6-56) indicate significant retention of streamwise momentum after processing by a Prandtl-Meyer expansion emanating from the sonic line in the boundary layer. Surface heating rates exceed 264 Btu/ft^2-sec (300 W/cm^2) (Figure 5.3.6-57) and surface temperatures approach 5400° R (3000 K) (Figure 5.3.6-58) at the downstream lip of the breach where impingement is strongest. Ingested mass and energy rates are 0.00152 lb_m/s (0.000689 kg/s) and 9.4 Btu/s (9.92 kW), respectively. Boundary conditions (radiative equilibrium, finite catalytic wall) and examination of near surface grid quality (Re_{cell} of order 10 at impingement) suggest this heating rate is a lower bound. More data on grid convergence tests will be provided in the Panel 8 results to follow.

Four-inch hole
The contour plot of total enthalpy in Figure 5.3.6-59 is repeated for the four-inch diameter hole. The boundary layer edge impinges on the downstream lip. The pressure field and streamlines entering the breach (Figure 5.3.6-60) indicate even more retention of streamwise momentum as compared to the previous case for the smaller hole. Surface heating rates again exceed 264 Btu/ft^2-sec (300 W/cm^2) (Figure 5.3.6-61) and surface temperatures exceed 5400° R (3000 K) (Figure 5.3.6-62) at the downstream lip of the breach where impingement is strongest. Ingested mass and energy rates are 0.00562 lb_m/s (0.00255 kg/s) and 43.6 Btu/s (46 kW), respectively.

Six-inch hole
The contour plot of total enthalpy in Figure 5.3.6-63 is repeated for the six-inch diameter hole. The boundary layer edge and some inviscid flow at the maximum freestream total enthalpy above it are

completely ingested. The lip is impacted by streamlines carrying the total freestream enthalpy and a relatively large total pressure. The pressure field and streamlines entering the breach (Figure 5.3.6-64) show the same trends for retention of streamwise momentum as compared to the previous case for the four-inch hole. Surface heating rates again exceed 264 Btu/ft^2-sec (300 W/cm^2) (Figure 5.3.6-65) and surface temperatures exceed 5400° R (3000 K) (Figure 5.3.6-66) at the downstream lip of the breach where impingement is strongest. Of the three hole sizes, the present case should exhibit the largest heating because it is seeing undissipated flow from above the boundary layer edge. Ingested mass and energy rates are 0.0125 lb_m/s (0.00566 kg/s) and 111 Btu/s (117 kW), respectively.

Vented internal box

These simulations allowed the jet to develop naturally within the cavity and to view initial impingement and deflections of flow to other surfaces. Jet orientation is a strong function of hole depth to diameter ratio. Summary of results follow.

Two-inch hole to vented box

Figure 5.3.6-67 shows streamlines entering the breach and the ensuing reflected wave pattern producing compressions and expansions in the jet core. The jet is non-orthogonal to the back plane of the breach. It has a significant directional component defined by the external flow direction. An expansion off the upstream side of the hole overtakes a shock off the downstream side of the hole. The shock forms in response to supersonic flow from the upper portion of the boundary layer and the boundary layer edge impinging on the downstream lip. The Mach number distribution in Figure 5.3.6-68 provides additional detail of the jet entering the cavity. A sonic line sets up behind the inner edge of the breach lip shock indicating a choked condition. The interesting feature here is that the sonic line does not span the back plane of the hole but rather spans a smaller area defined by convergence of the streamlines entering from the circular border. Pressure coefficients in Figure 5.3.6-69 indicate the ambient pressure level in the cavity of approximately (1/8) $\rho_\infty V_\infty^2$. This level is attained at the back plane of the hole. The dependence of cavity ambient pressure on vent hole size has not been explored. It is interesting to note that a specification of the vent pressure immediately behind the back plane of the hole results in approximately the same ambient pressure level in the cell preceding the outflow boundary. Pressures exceeding the external pressure of approximately (1/2) $\rho_\infty V_\infty^2$ (C_p = 1) would effectively block ingestion of external flow.

The temperature in the shock over the downstream lip approaches 14,400° R (8000 K) in Figure 5.3.6-70. The corresponding total enthalpy profile is shown in Figure 5.3.6-71 that corresponds to the earlier result in Figure 5.3.6-55 except now the cavity beneath the hole is included. Conditions just below the boundary layer edge impact the lip to drive the large surface heating rates and surface temperatures (Figure 5.3.6-72). The impingement heating on the edge will tend to cut a slot along the surface in the external streamline direction.

The oxygen content of ingested flow is almost fully dissociated as indicated in Figure 5.3.6-73. A strong catalytic heating effect would be expected on metallic cavity walls but the finite catalytic boundary condition on the external surfaces was continued into the cavity. Also, the radiative equilibrium wall boundary condition assumes cavity walls can radiate to free space whereas the actual closed environment would restrict radiative cooling. Conductive cooling through metallic walls is not considered. Given these conditions (expected to produce lower heating rates) the surface temperatures on the cavity walls (Figure 5.3.6-74) exceed the melting point of pure aluminum at the impingement zone. Note that the breach hole through the lower surface is not visible in this figure. The vent hole on the top surface still sees temperatures that would melt aluminum.

Quarter-inch hole to vented box

A quarter-inch diameter hole was simulated to provide reference conditions in which the hole diameter was not larger than the hole depth and all hole dimensions were smaller than the local boundary layer thickness. In this case, the jet develops in an orthogonal direction to the wall as seen in the Mach number contour of Figure 5.3.6-75. Impingement heating and temperatures on the downstream lip are much more benign (Figure 5.3.6-76) because the energy content and total pressure of the impinging streamlines emerging from deep within the boundary layer is significantly dissipated. Temperatures entering the cavity (Figure 5.3.6-77) exceed 1800° R (1000 K).

5.3.6.1.4.2 Ten-inch Hole in Panel 8

These simulations were initiated in mid-May to complement ongoing simulation work on higher fidelity internal grids and to insure that sufficient corroborating data for engineering analyses could be made available as quickly as possible. However, greater fidelity to the internal geometry was requested (as compared to the ad-hoc cavity) so that jet development lengths and splash to adjoining internal surfaces may be better simulated.

A simulation plan was developed to maximize productivity in the limited, remaining time. First, the simulation of a ten-inch hole in Panel 8 into the ad-hoc cavity as described in the previous section was produced. (The grid in this case had to be post-processed by the VGM utility to compensate for problems associated with the larger ratio of local effective radius to hole diameter.) This simple simulation would next be used to initialize the cavity flow in a more realistic "chunnel" geometry generated concurrently. A grid sequencing process is used to complete the simulation and significant sharpening of the jet was observed in the transition from moderate to fine grid. When the jet boundaries sharpened, it was noted that the impingement location was under-resolved. An additional grid-processing step was required to bring a factor ten finer resolution on the wall at impingement.

The chunnel geometry was built off of the ad-hoc cavity and expanded to include the domain behind panels 7-9. The back plane was defined by the actual spar location. Two vent slots with combined area of 66 in^2 were included on the leeside, back surface. An internal core system of blocks was approximately bounded by the inner extent of ribs at the panel interfaces to accommodate possible future extensions of internal complexity. A combination of an O- and C- grid topology was used to accommodate the complex internal structure. The C-grid provides the ability to capture the rib and spar geometry while offering a decoupling of the grid requirements for stretching and clustering at the internal wall surfaces. As shown in Figure 5.3.6-78 and Figure 5.3.6-79, the C-grid easily captures the necessary chunnel features. Within the C-grid, in the bottom block, the hole in the RCC is accommodated by simply replacing the block of the C-grid with an "embedded" O-grid, which enables accurate modeling of the flow entering the chunnel. The O- and C-grid junction enables the accurate modeling of the existing geometry while offering the expandability to increasing geometric complexity without restructuring and regenerating the entire chunnel volume grid.

In the final simulation, the top vents were closed and the side core vents (combined area 79.3 in^2) were opened to enable the splash from an impinging jet to spill over a rib and through a vent. Summary of results follow.

Vented internal box

Mach number and streamlines entering the box through the ten-inch hole in panel 8 are shown in Figure 5.3.6-80. Streamlines exit a ten-inch diameter vent at the top of the box. The flow is strongly supersonic entering this cavity. The most interesting details of this simulation (that remain true for the subsequent chunnel simulations) are the high temperatures and pressures in the shock layer over the downstream lip of the hole. The high temperature (approaching 21,600° R (12000 K) in Figure 5.3.6-81) is easily explained because the lip is bathed in flow that carries the full freestream total enthalpy. The local pressure coefficient (C_p = 10) is higher than the stagnation point because the local streamlines here were processed by an oblique shock so that total pressure losses are less than those experienced in crossing a normal shock. Computed heating rates exceed 704 Btu/ft^2-sec (800 W/cm^2) in this case. When considering the factor of increase in pressure and factor decrease of local radius of curvature relative to the stagnation point one may expect this rate (ignoring ablative cooling) is a lower bound.

Chunnel with slotted leeside vents

Results in this section discuss the solution after adaptation of the finest grid to concentrate more mesh to the jet impingement point. Error norms had dropped to order 0.4 (a five to six order of magnitude decrease from the initial solution off the coarse grid). Some unsteadiness is evident when monitoring the solution but there was insufficient time to gather meaningful statistics on frequency. The jet impingement point has moved very little over about 10000 relaxation steps and it is believed that the basic flow physics presented here are correct.

Details of the jet in the cutting plane through the chunnel are presented in Figure 5.3.6-82 (total enthalpy), Figure 5.3.6-83 (Mach number), and Figure 5.3.6-84 (temperature). A tongue of high enthalpy flow persists up to the impingement point. A high temperature shock layer forms above this location. The jet initially scrapes the surface and then rises above it.

A "strip" of high pressure (Figure 5.3.6-85) and high heating rate (Figure 5.3.6-86) is evident at the relatively narrow impingement location. These figures show the sharpening of the profile associated with refinement from the medium grid to the fine grid (a factor of 2 in the i, j, and k directions). Review of solution metrics at the impingement showed high cell Reynolds number and large jump between imposed wall temperature (900° R (500 K)) and boundary cell center temperature (5184° R (2880 K)). Consequently, a grid adaptation was implemented to provide a target factor of 10 finer grid at the wall (i-direction) using a greater stretching factor for the same number of cells in the near wall blocks. Even with this refinement, the worst-case cell center temperature next to the wall was (2088° R (1160 K)). The convergence of peak impingement heating on these three sequential cases (not located at exactly the same surface mesh point) progressed from 102 Btu/ft^2-sec (116 W/cm^2) (medium grid) to 265 Btu/ft^2-sec (301 W/cm^2) (fine grid) to 635 Btu/ft^2-sec (721 W/cm^2) (adapted fine grid, Figure 5.3.6-87).

Chunnel with side vents

This side vent case (top vents now closed) was initialized from the previous top vent case with the finest grid and adaptation of grid on the impingement boundary.

The error norm for this case jumped about 4 orders of magnitude from the previous converged solution and returned to order 1 values at this "snapshot". An attempt to force the solution to advance more quickly with a constant, large time step eventually diverged. A smaller constant time step was again applied and the solution began to recover but insufficient time remained to drive it to convergence. The solution posted here is thought to have a jet impingement point that will continue to rise toward the side vent. The magnitude of jet oscillations cannot be estimated from the solution generated to date. A representative jet structure is presented in Figure 5.3.6-88 (total enthalpy) and Figure 5.3.6-89 (pressure). The basic structure is very similar to that observed in the previous case. The expansion process to sonic conditions at the side vent is displayed in Figure 5.3.6-90 (pressure) and Figure 5.3.6-91 (Mach number) in the impingement zone.

Top vent versus side vent internal surface pressures are compared in Figure 5.3.6-92. The equivalent heating comparison is presented in Figure 5.3.6-93 and Figure 5.3.6-94. Heating at impingement on the finest grid has remained between 440 and 616 Btu/ft^2-sec (500 and 700 W/cm^2).

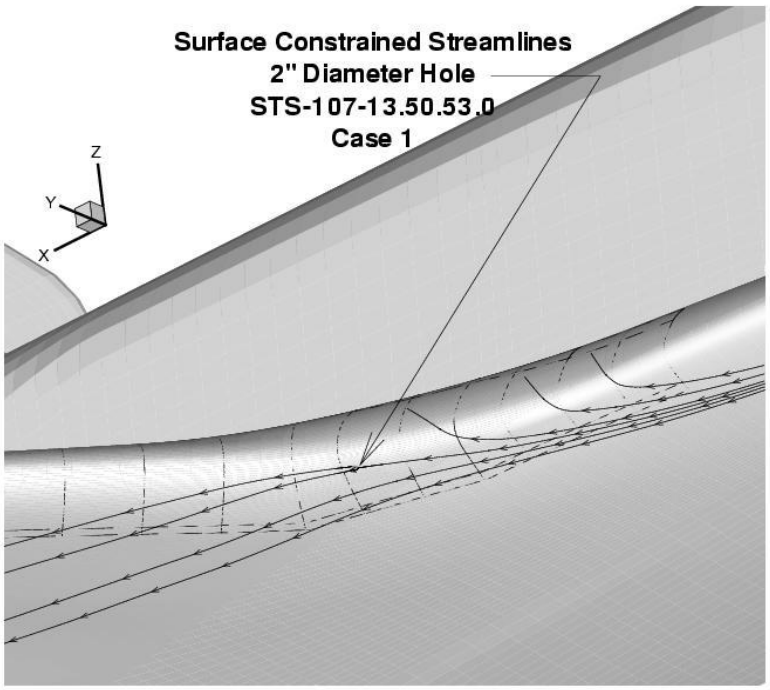

Figure 5.3.6-51 Streamlines over RCC panels on the leading edge and the location of the circular breach through the wing in panel 6.

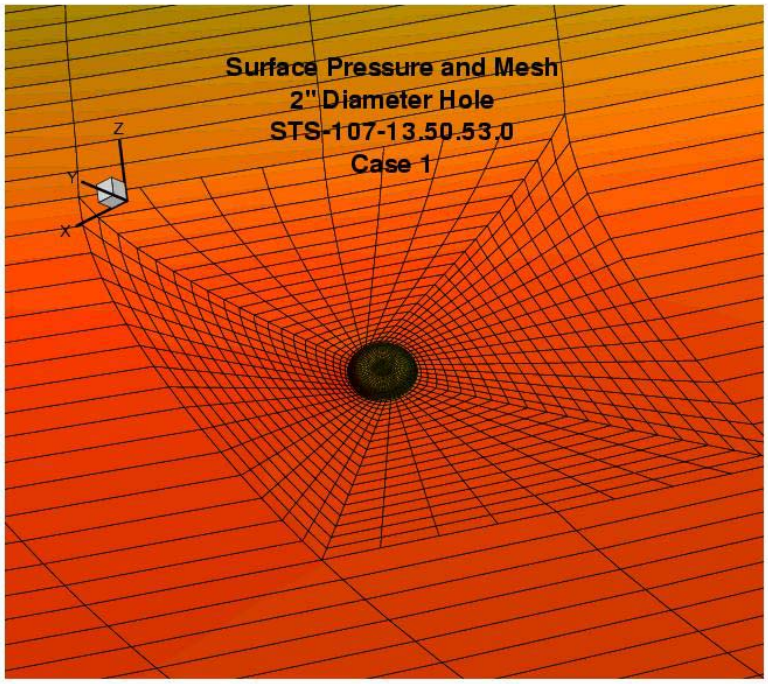

Figure 5.3.6-52: Modified surface grid in the vicinity of the hole.

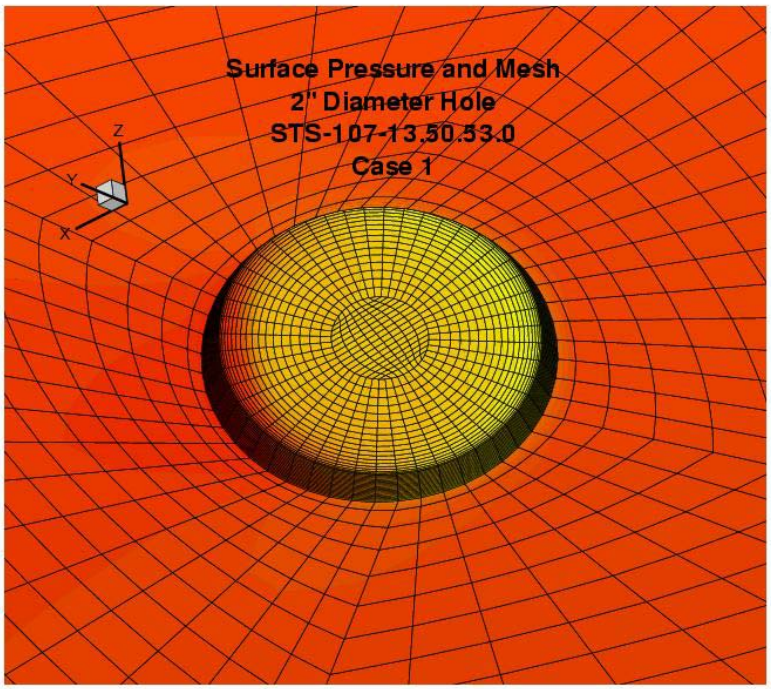

Figure 5.3.6-53: Structured grid within hole, approximately 20 cells deep and 60 cells across.

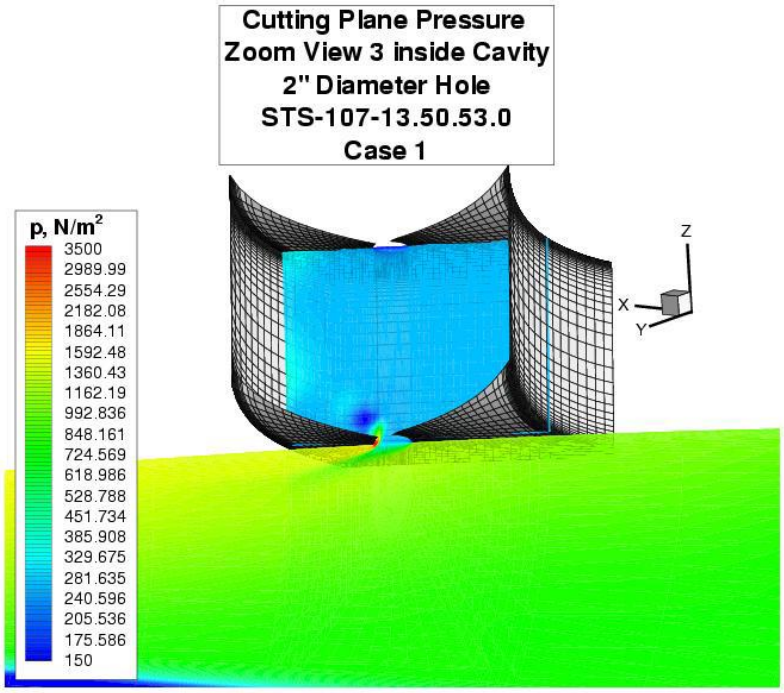

Figure 5.3.6-54: Pressure in cutting plane across breach and view of surface grid defining the vented cavity.

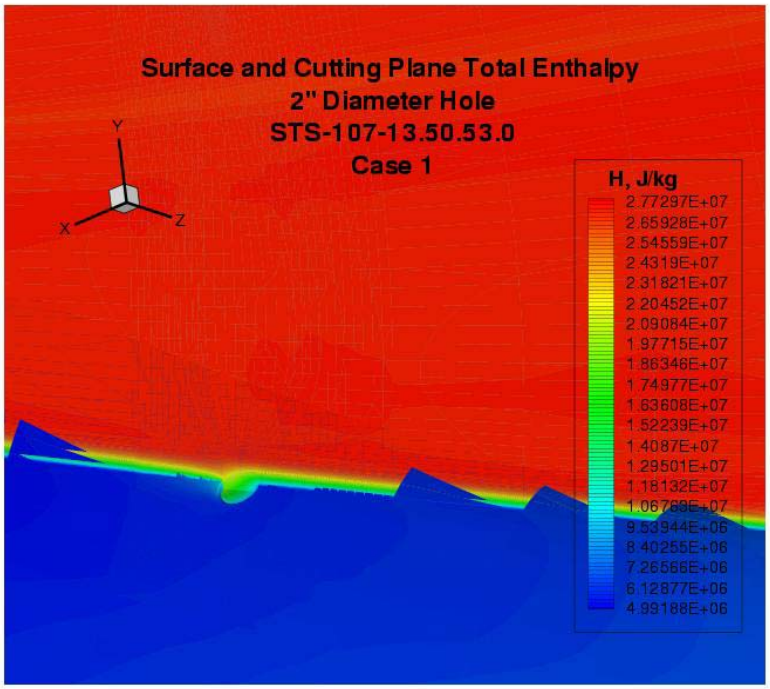

Figure 5.3.6-55: Total enthalpy in cut plane above hole showing partial ingestion of the boundary layer. (Blue jags are artifact of picture format conversion.)

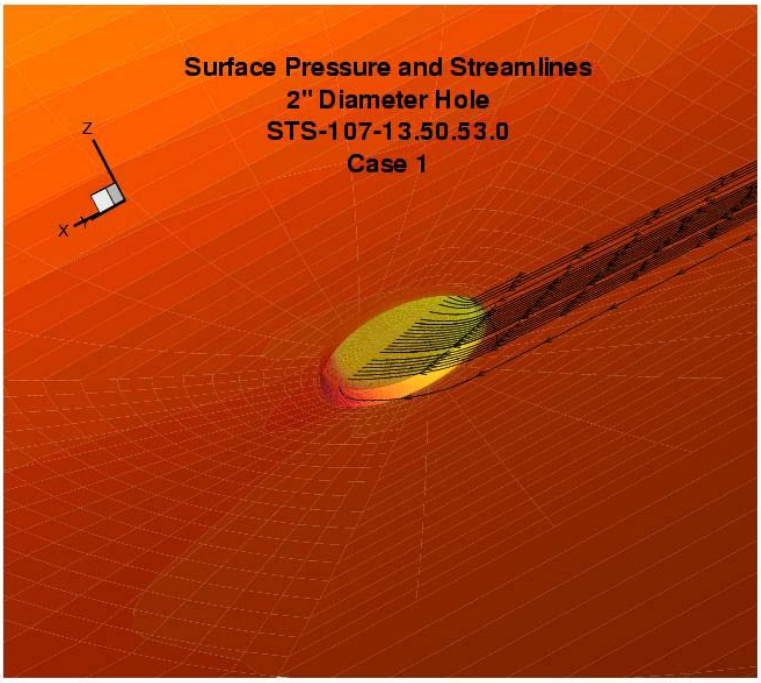

Figure 5.3.6-56: View of streamlines entering breach showing significant retention of external streamwise momentum.

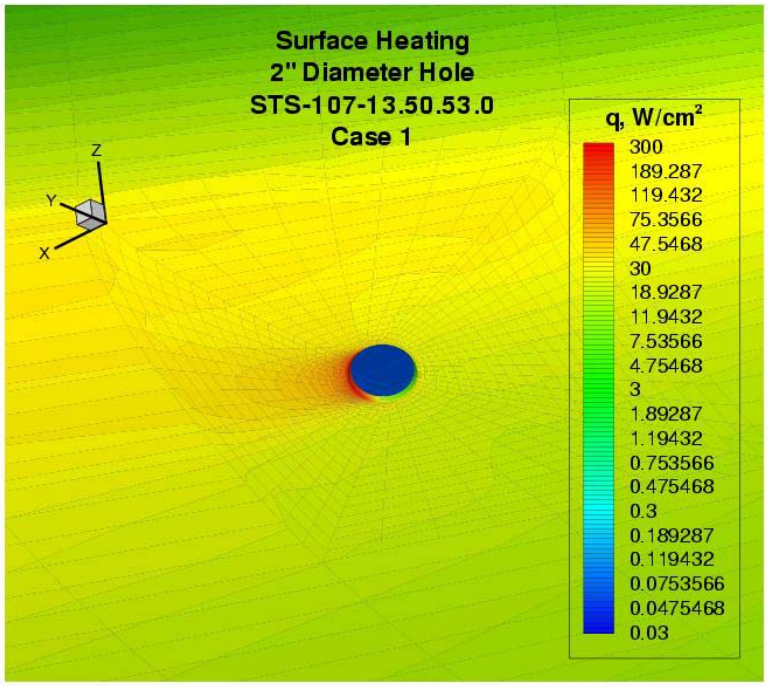

Figure 5.3.6-57: Surface-heating contours in the vicinity of the two-inch hole in Panel 6.

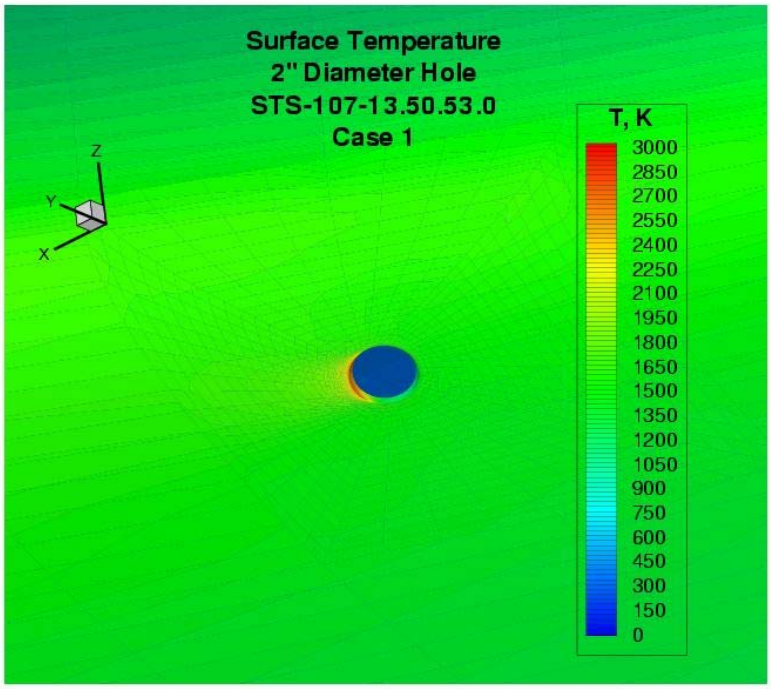

Figure 5.3.6-58: Surface temperature contours in vicinity of the two-inch hole in Panel 6.

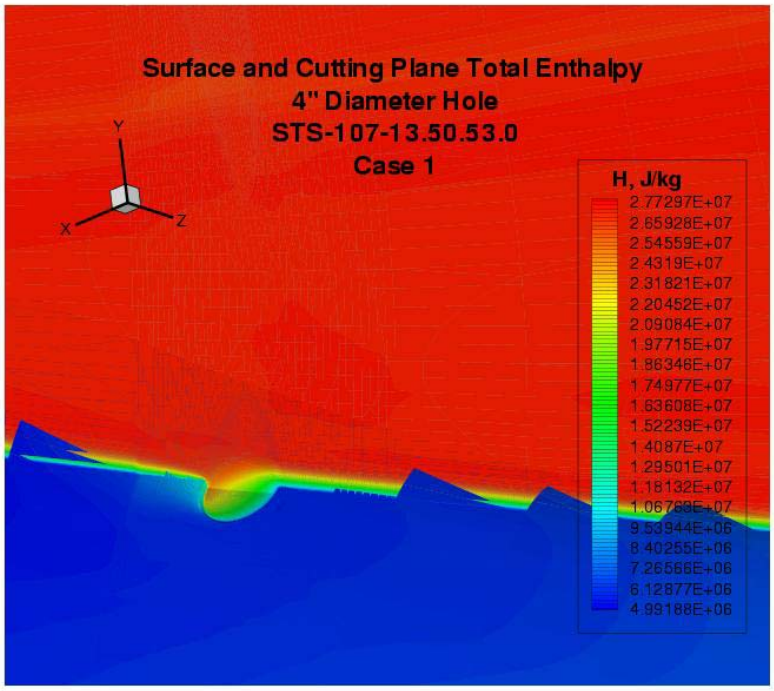

Figure 5.3.6-59: Total enthalpy in cut plane above four inch hole showing significant ingestion of the boundary layer. (Blue jags are artifact of picture format conversion.)

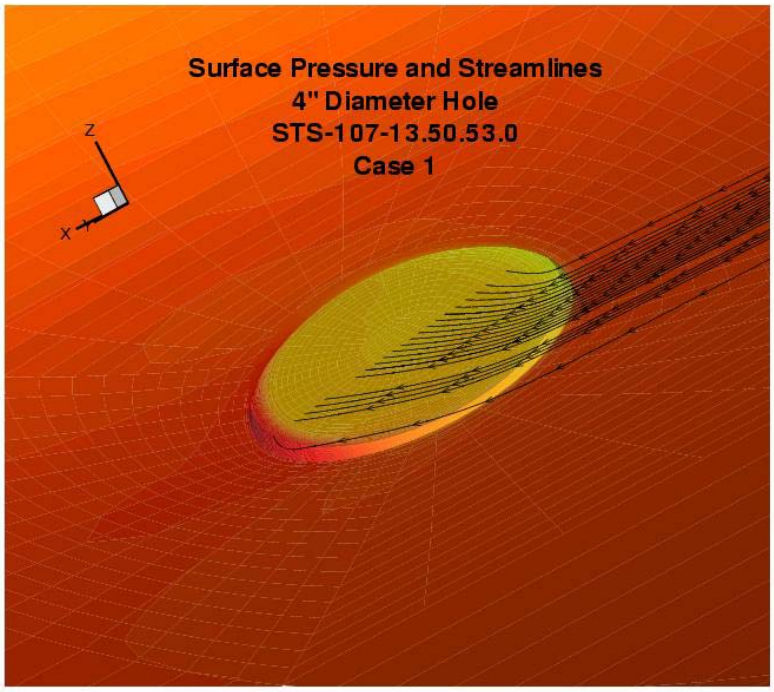

Figure 5.3.6-60: View of streamlines entering four-inch breach showing significant retention of external streamwise momentum.

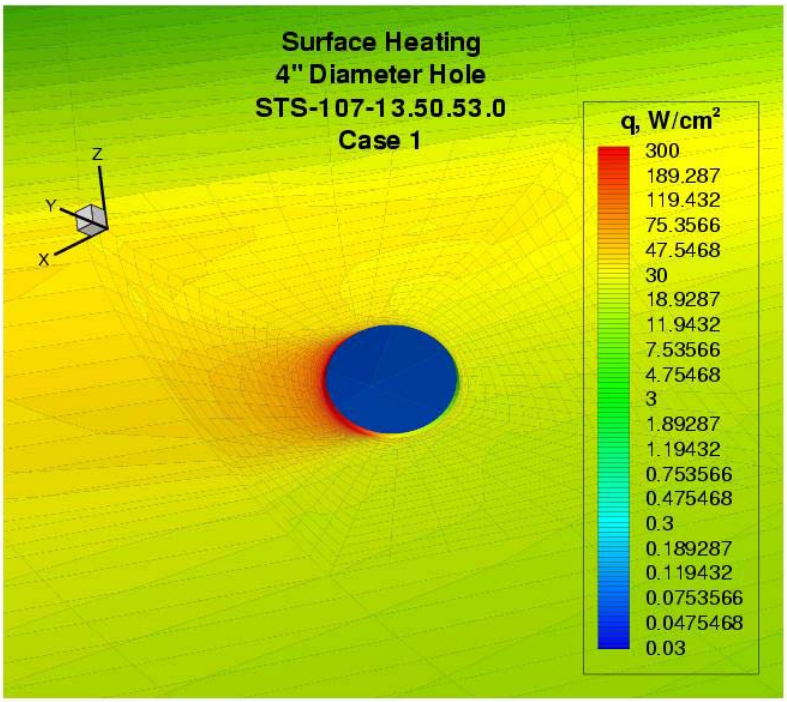

Figure 5.3.6-61: Surface-heating contours in the vicinity of the four-inch hole in Panel 6.

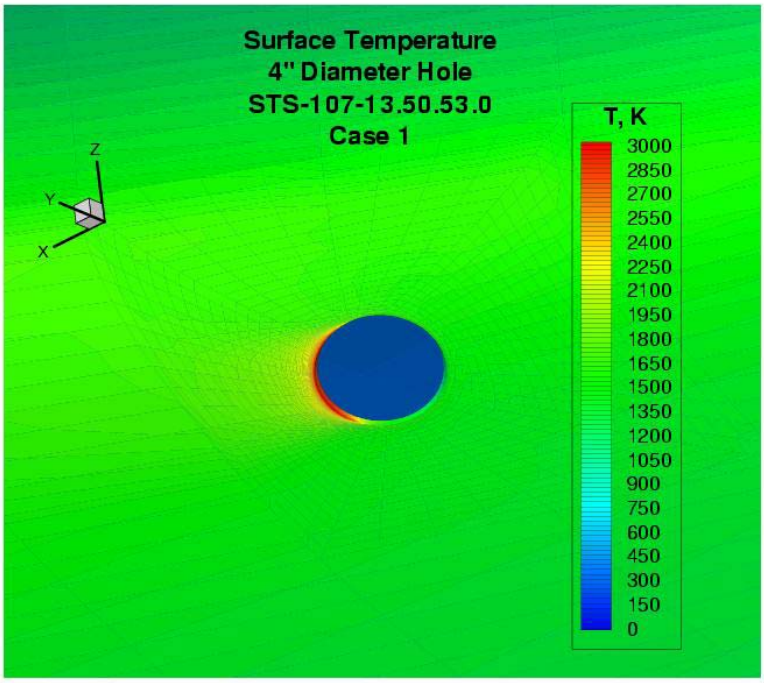

Figure 5.3.6-62: Surface temperature contours in vicinity of the four-inch hole in Panel 6.

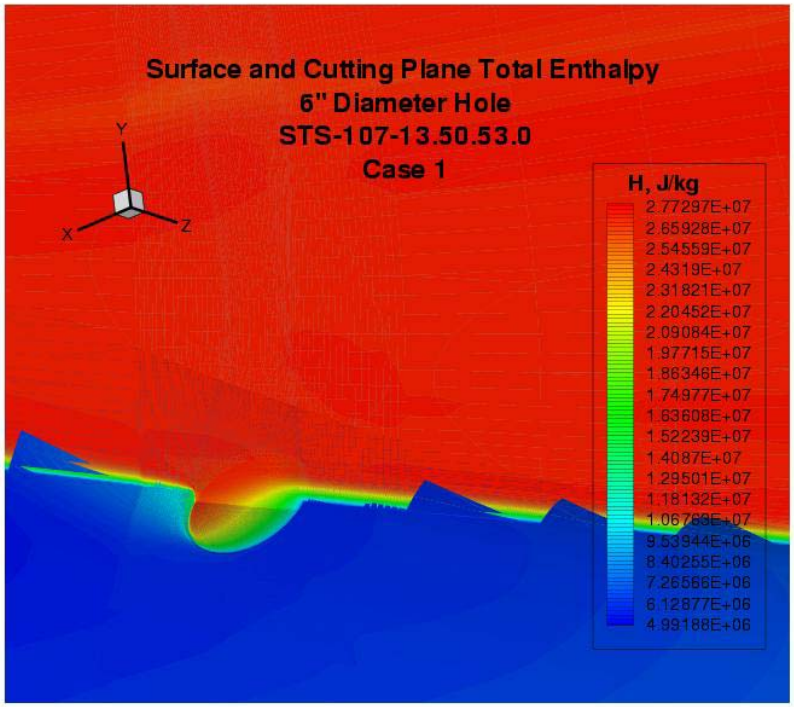

Figure 5.3.6-63: Total enthalpy in cut plane above six inch hole showing complete ingestion of the boundary layer. (Blue jags are artifact of picture format conversion.)

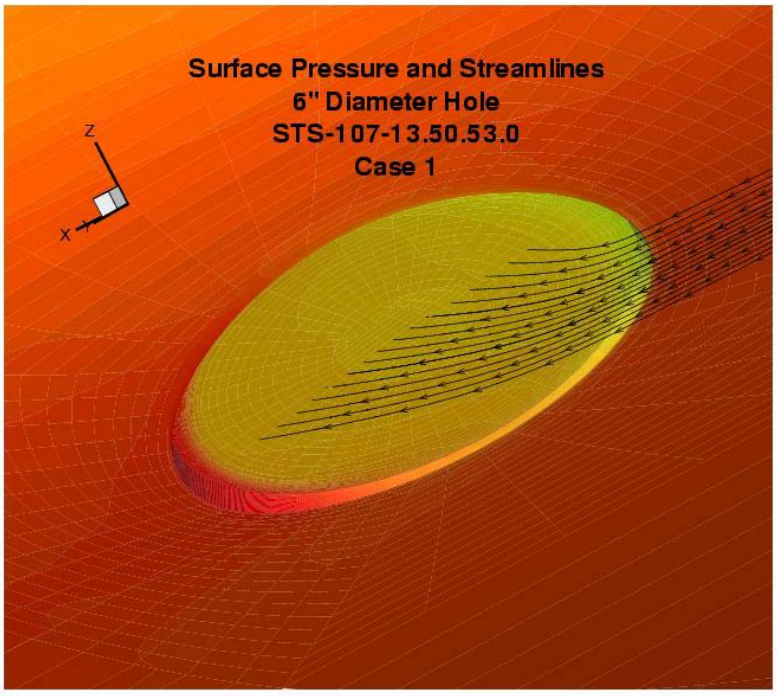

Figure 5.3.6-64: View of streamlines entering six-inch breach showing significant retention of external streamwise momentum.

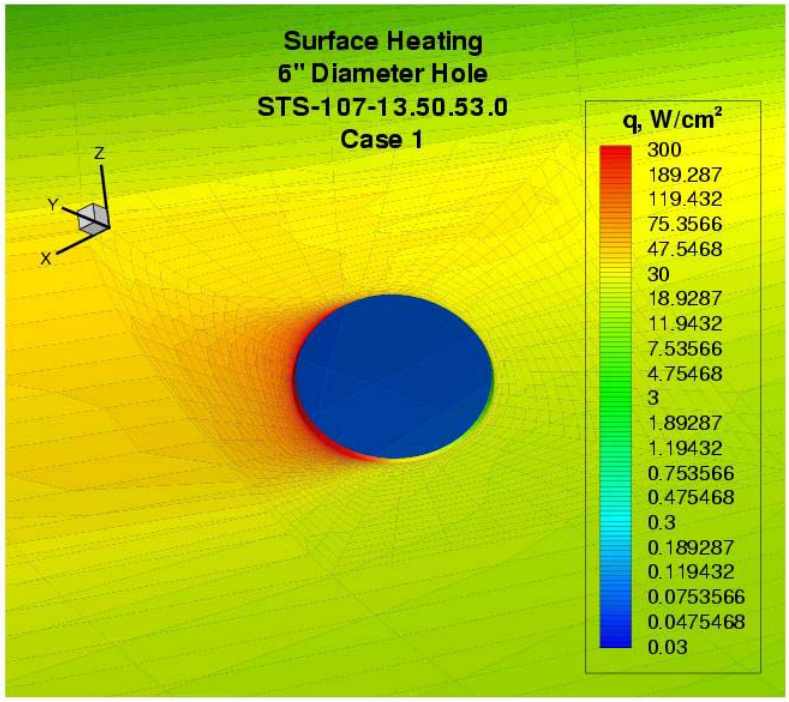

Figure 5.3.6-65: Surface-heating contours in the vicinity of the six-inch hole in Panel 6.

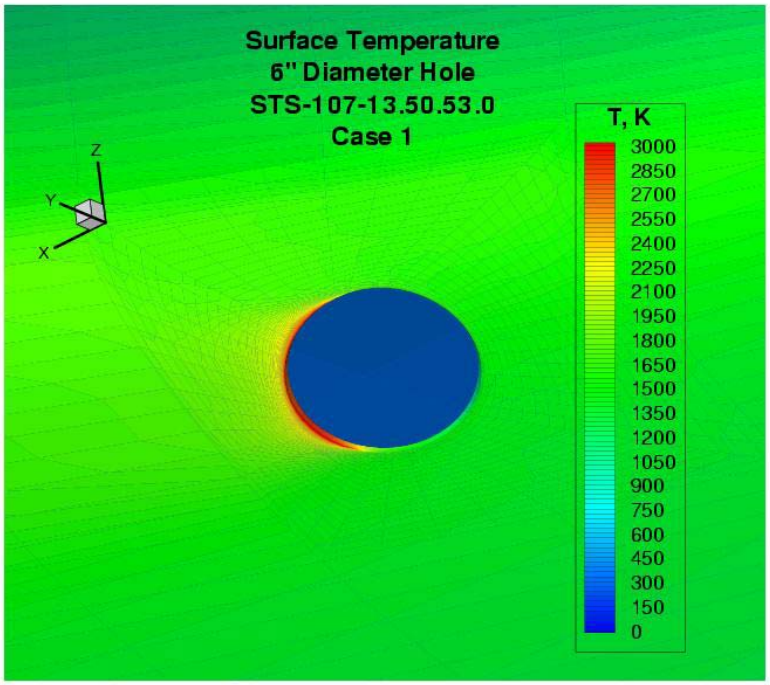

Figure 5.3.6-66: Surface temperature contours in vicinity of the six-inch hole in Panel 6.

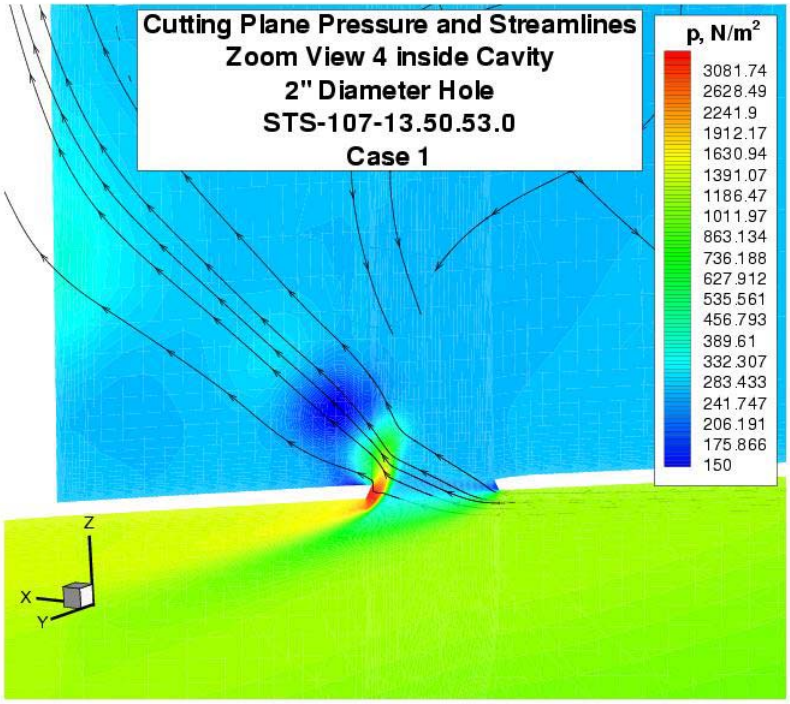

Figure 5.3.6-67: Streamlines entering the breach and pressure levels in the cutting plane. External flow direction is from the right to the left.

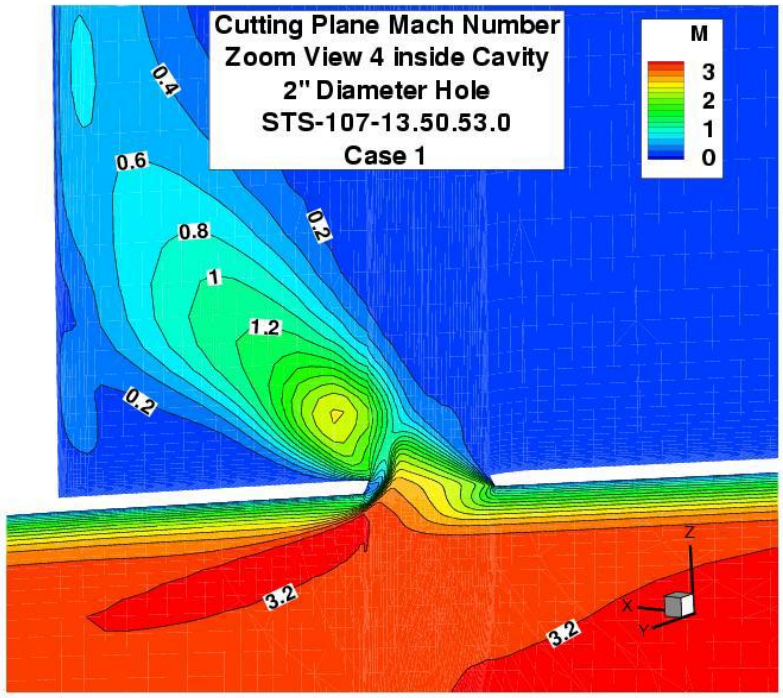

Figure 5.3.6-68: Mach number contours across the breach and in the jet entering the cavity. A sonic, choked condition sets up behind the lip shock over the downstream lip of the breach.

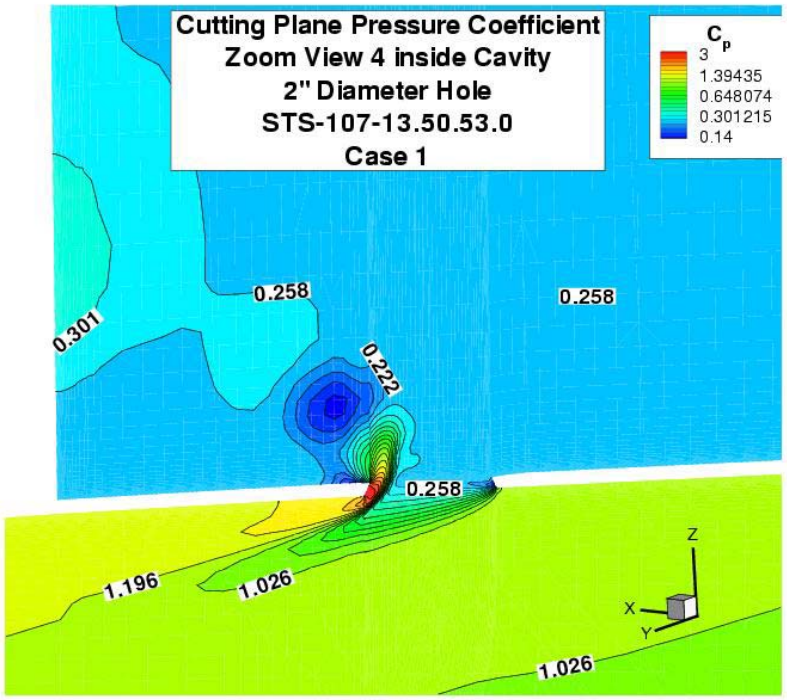

Figure 5.3.6-69: Pressure coefficient in vicinity of the breach.

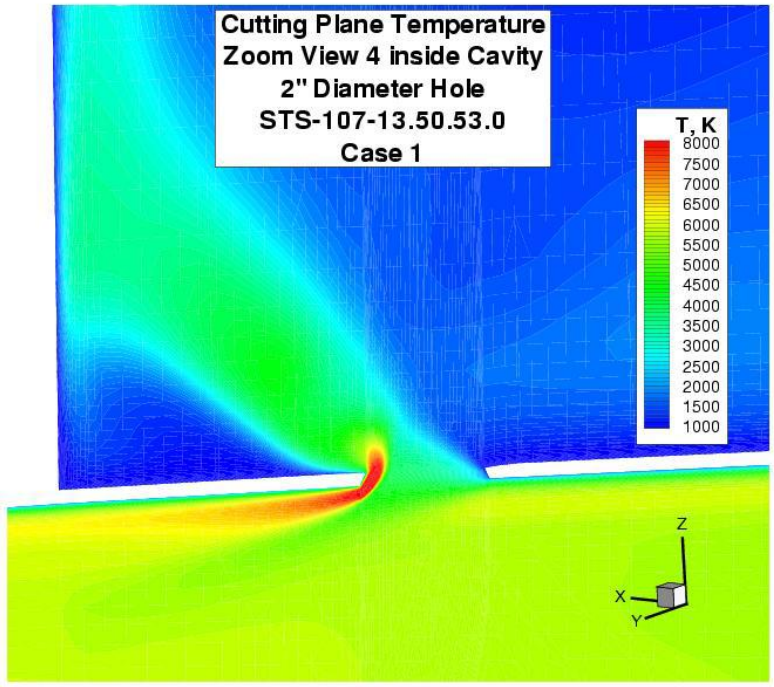

Figure 5.3.6-70: Temperature in vicinity of the breach.

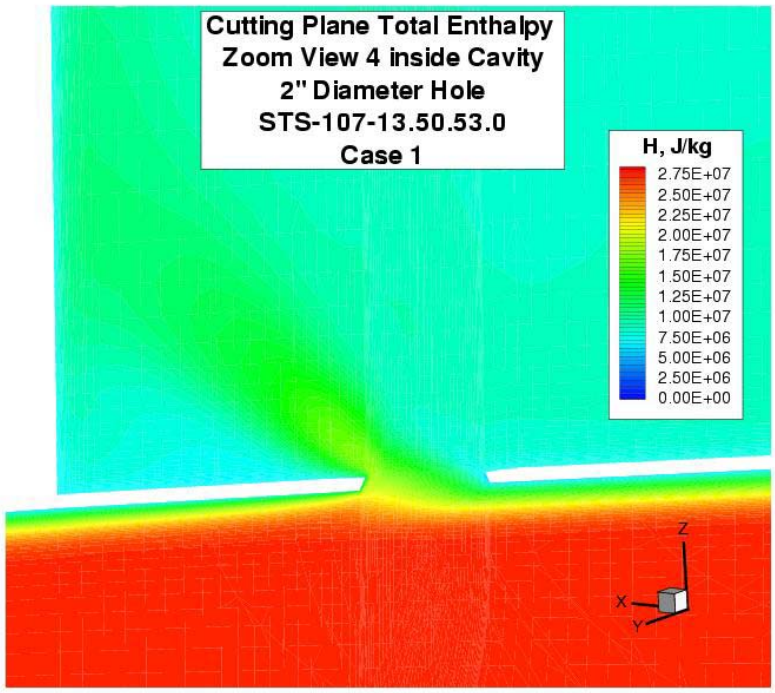

Figure 5.3.6-71: Total enthalpy in vicinity of breach indicating level of ingestion of the external boundary layer.

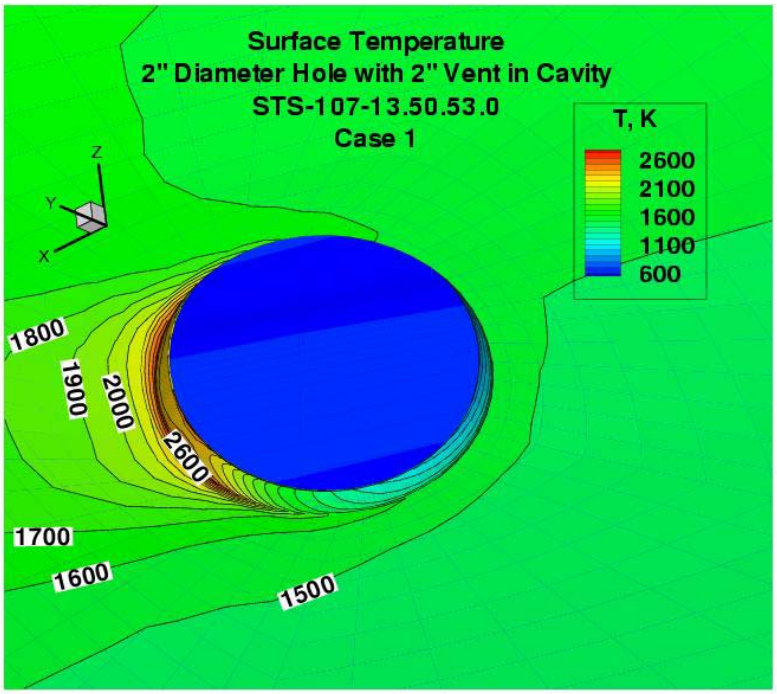

Figure 5.3.6-72: Surface temperatures in vicinity of downstream lip of two-inch hole over cavity.

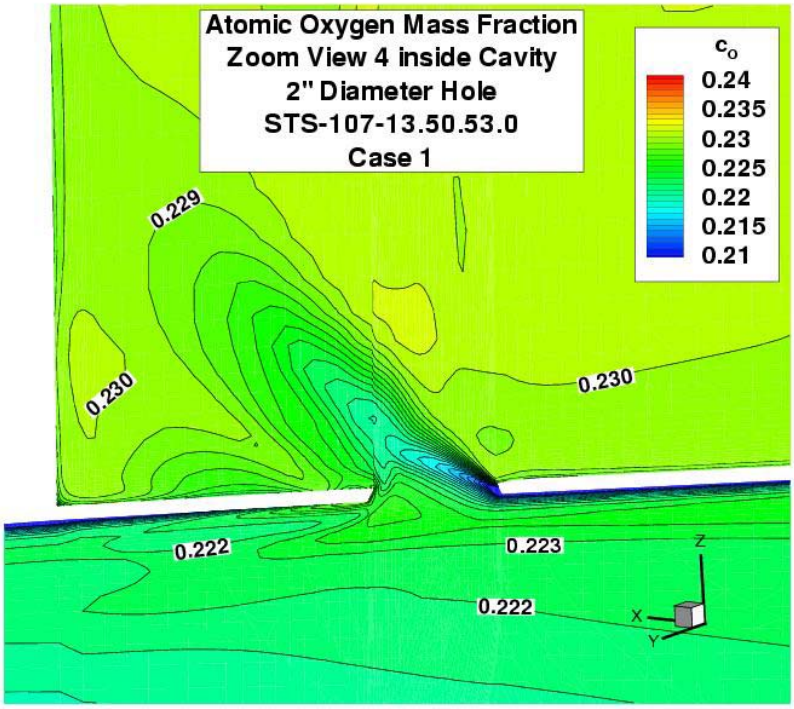

Figure 5.3.6-73: Atomic oxygen mass fraction ingested through breach.

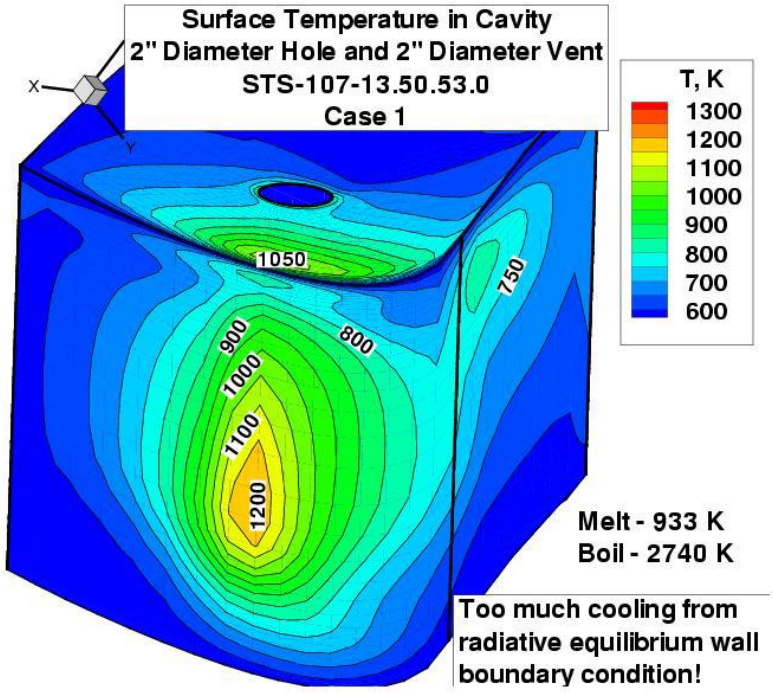

Figure 5.3.6-74: Surface temperature on cavity walls with identical cooling mechanisms as used for external flow.

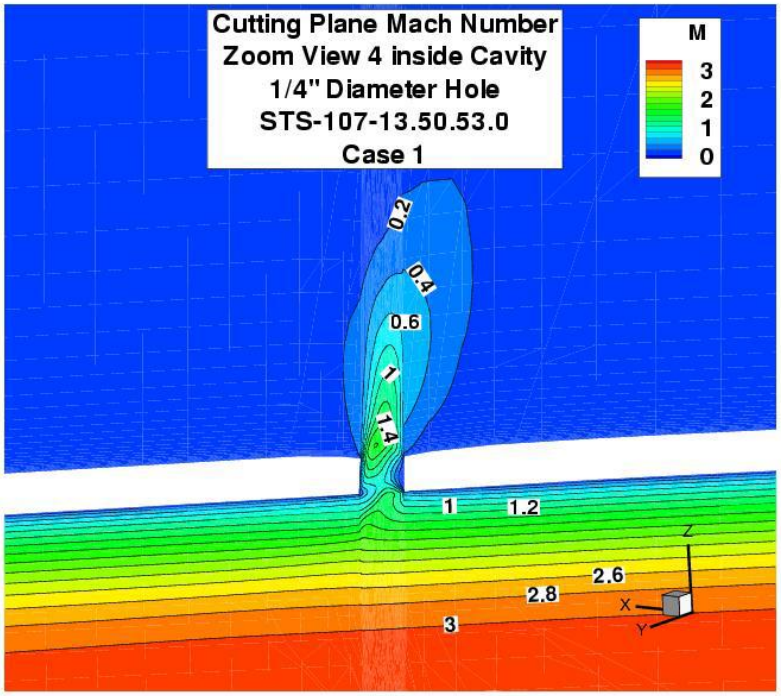

Figure 5.3.6-75: Mach number contours of jet entering cavity through quarter-inch diameter hole.

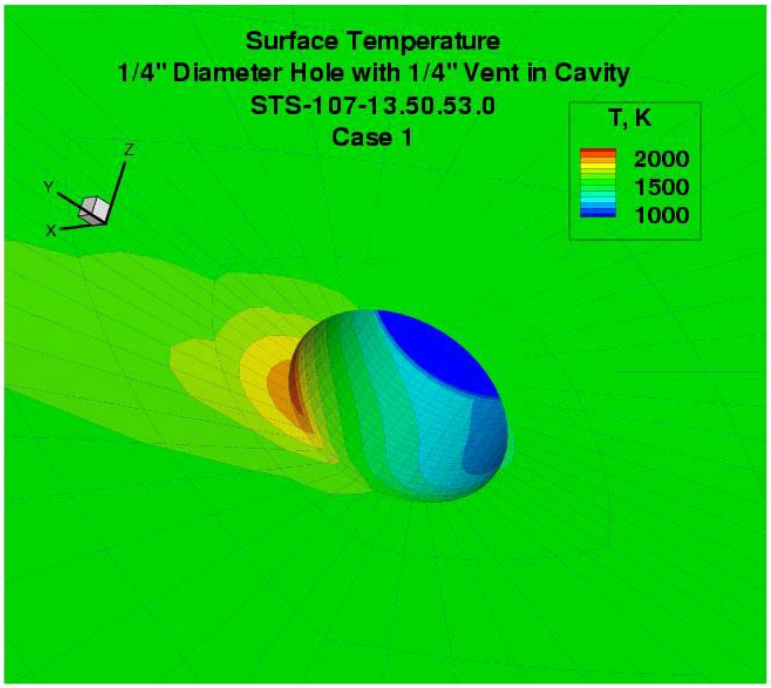

Figure 5.3.6-76: Surface temperatures in vicinity of quarter-inch hole.

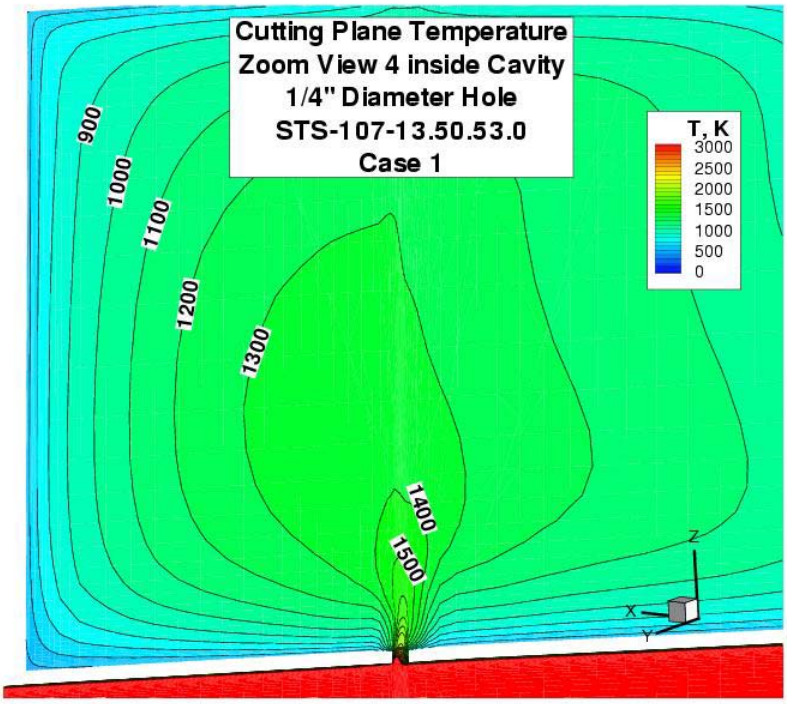

Figure 5.3.6-77: Jet temperatures in cavity bled from bottom of external boundary layer.

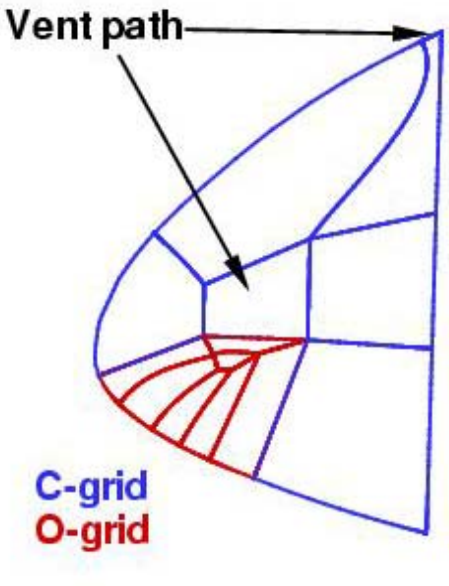

Figure 5.3.6-78: Internal block structure merging ad hoc cavity and chunnel showing relative vent positions.

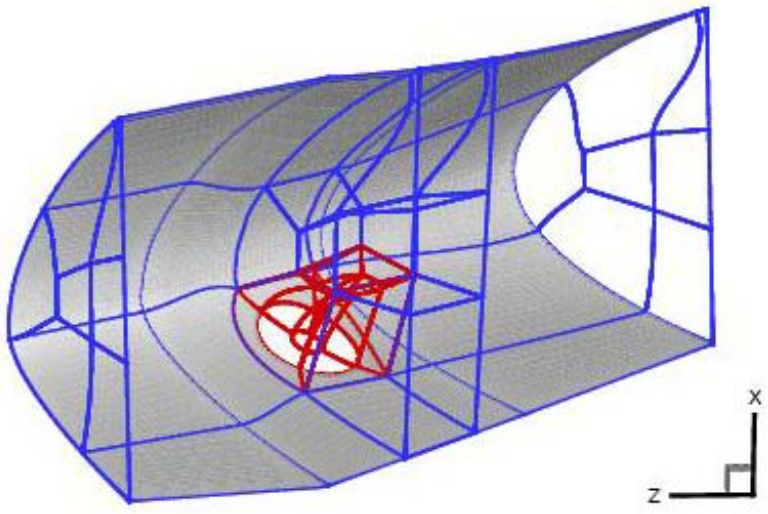

Figure 5.3.6-79: Global view of chunnel block structure.

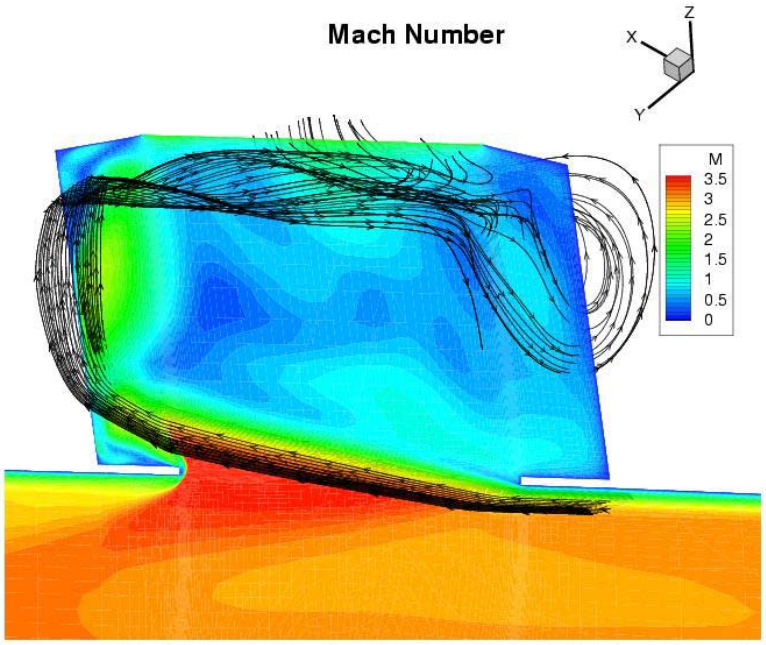

Figure 5.3.6-80: Mach number and streamlines in cavity behind panel 8 with ten-inch diameter hole and ten inch diameter vent.

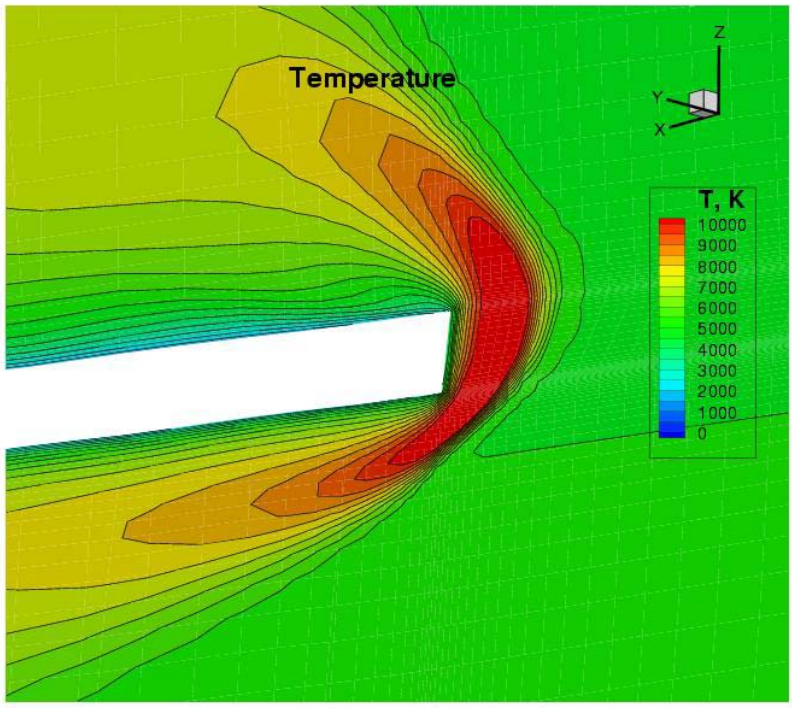

Figure 5.3.6-81: Details of temperature in shock layer over downstream lip with ten-inch breach through panel 8.

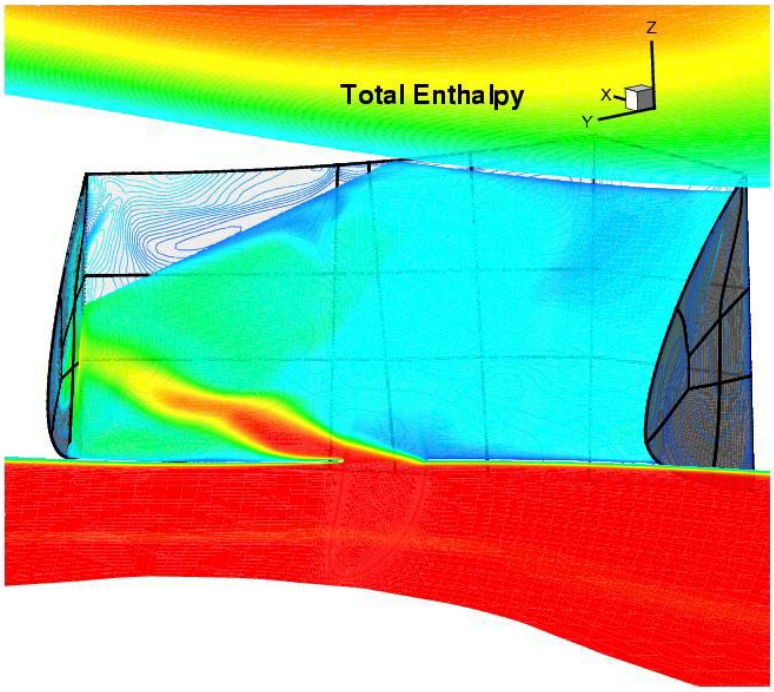

Figure 5.3.6-82: Total enthalpy entering chunnel through Panel 8. Venting is through slots on top of chunnel.

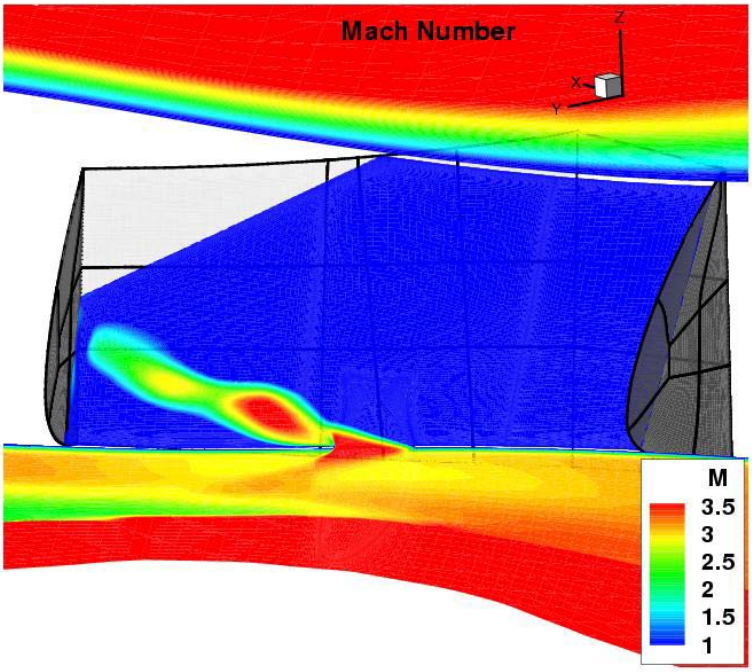

Figure 5.3.6-83: Mach number contours focused on supersonic domain.

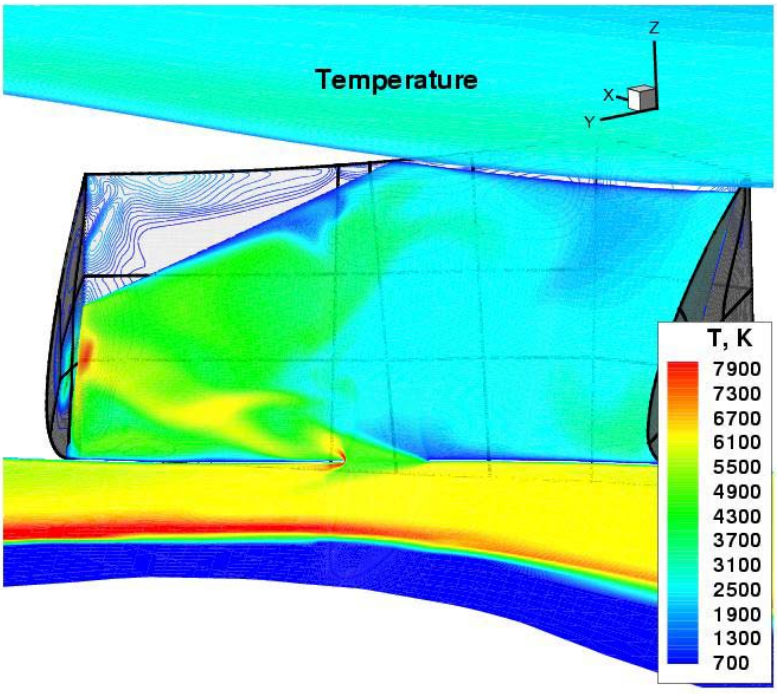

Figure 5.3.6-84: Temperatures in cutting plane through chunnel showing high temperatures at impingement of jet on the side wall.

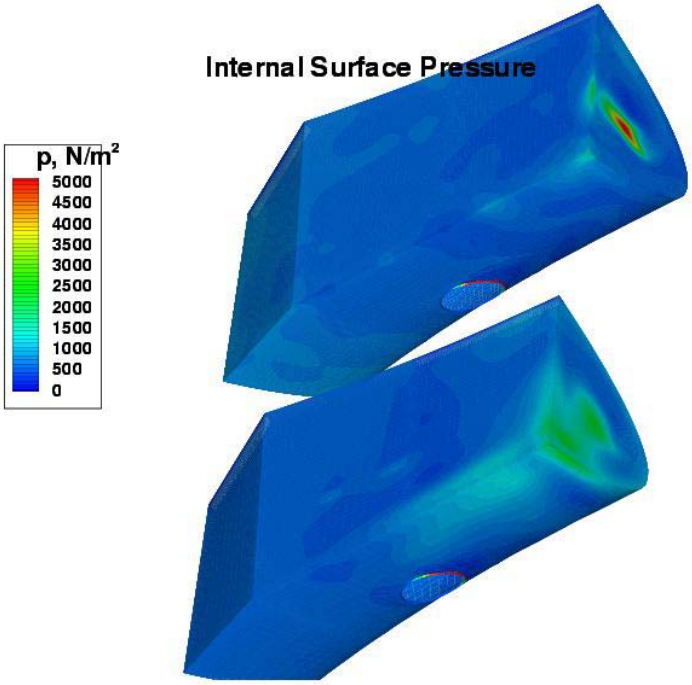

Figure 5.3.6-85: Comparison of chunnel surface pressures from medium grid and unadapted fine grid.

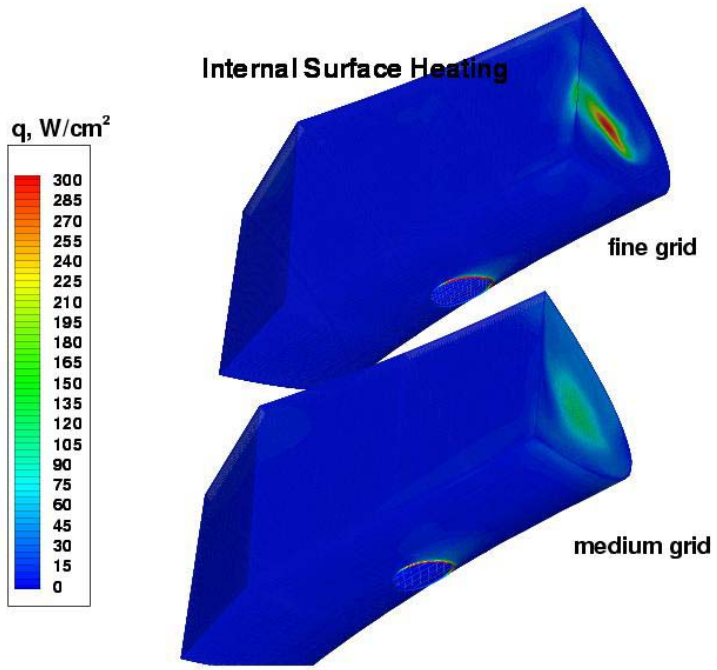

Figure 5.3.6-86: Comparison of chunnel surface heating from medium grid and unadapted fine grid.

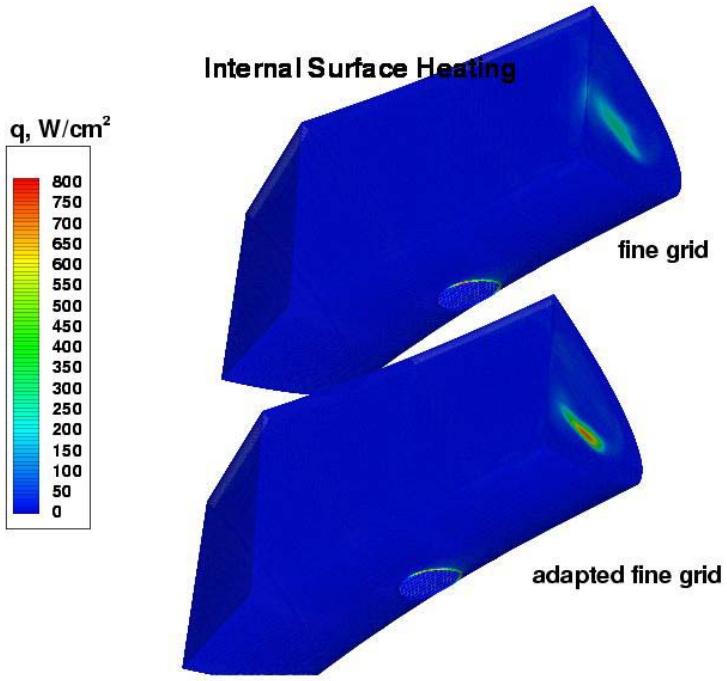

Figure 5.3.6-87: Comparison of chunnel surface heating from unadapted fine grid and adapted fine grid on impingement surface.

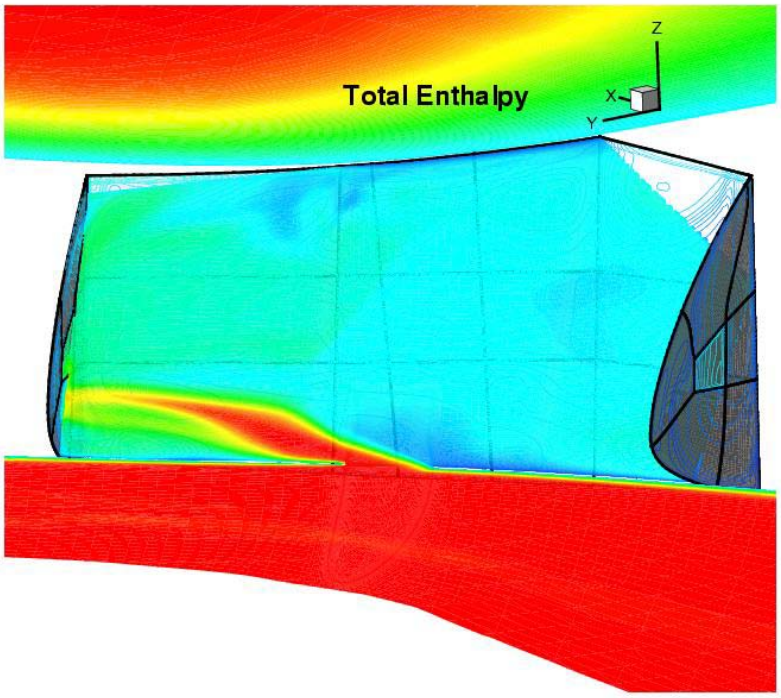

Figure 5.3.6-88: Total enthalpy in chunnel with side vents.

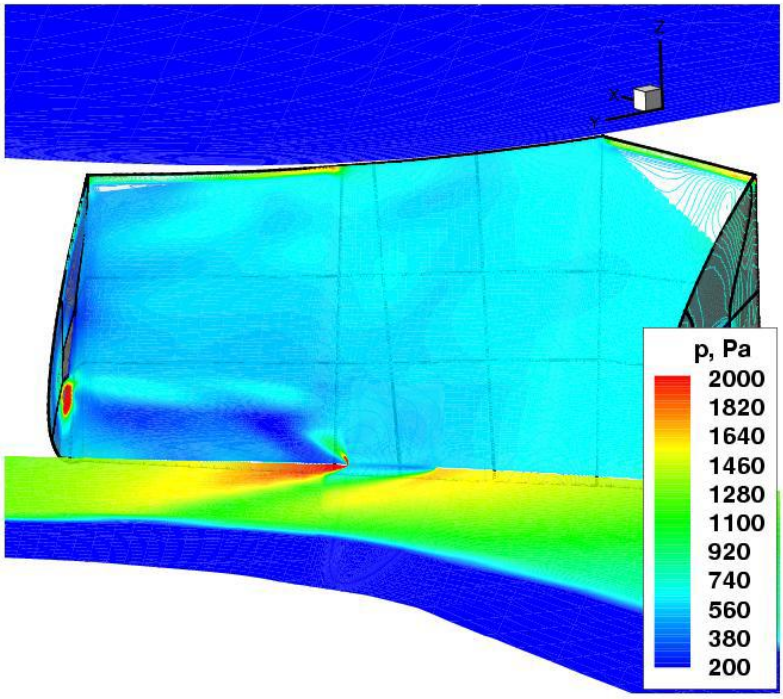

Figure 5.3.6-89: Pressures in chunnel with side vents.

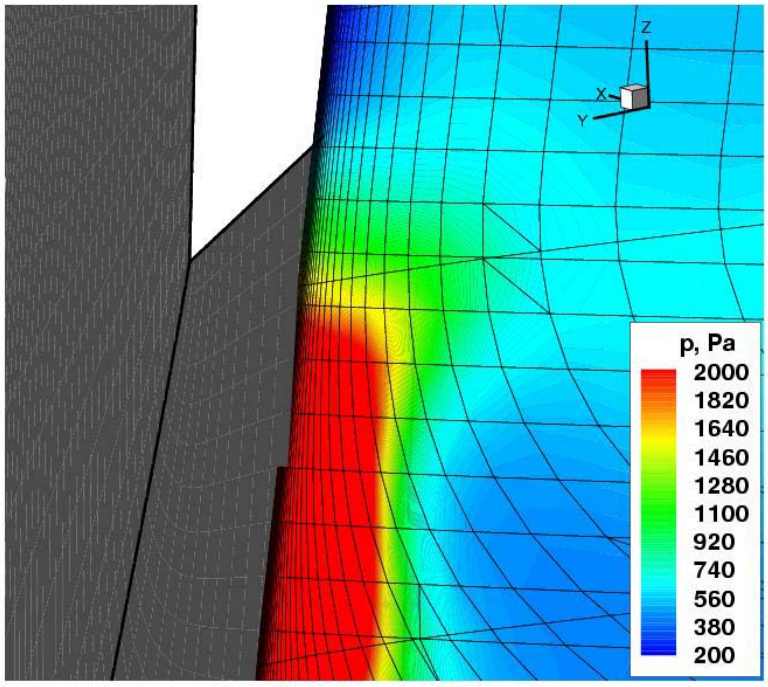

Figure 5.3.6-90: Detail of pressure at impingement location below side vent with supporting grid in the cut plane.

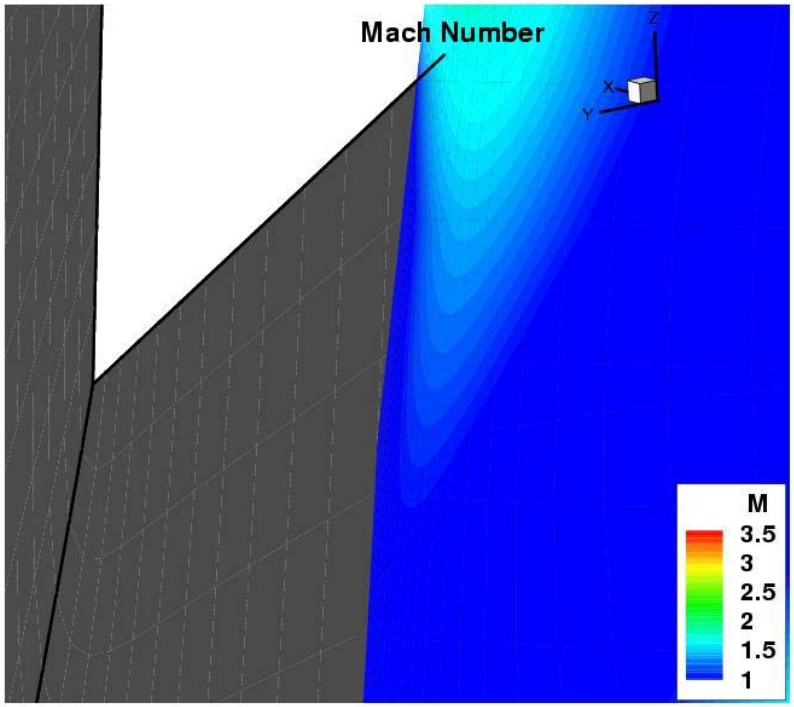

Figure 5.3.6-91: Magnified view of Mach number expanding to sonic condition at side vent.

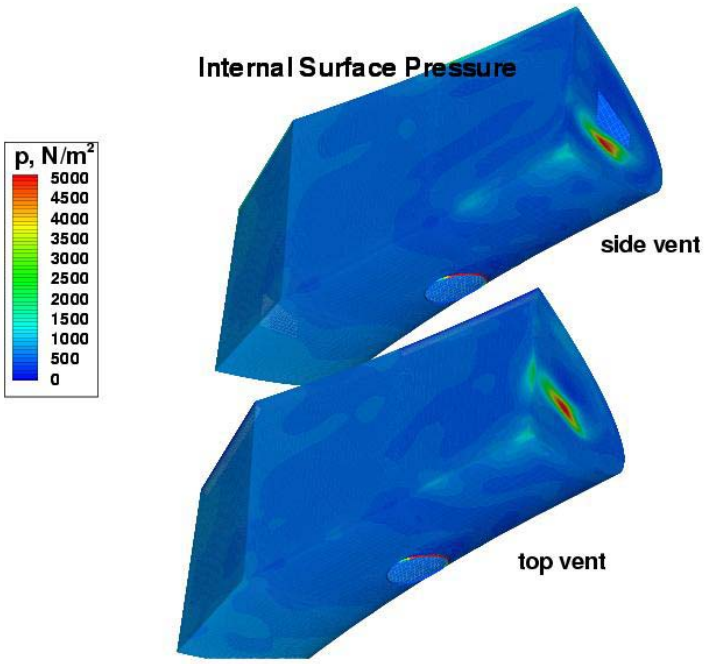

Figure 5.3.6-92: Comparison of chunnel surface pressures with top and side vents.

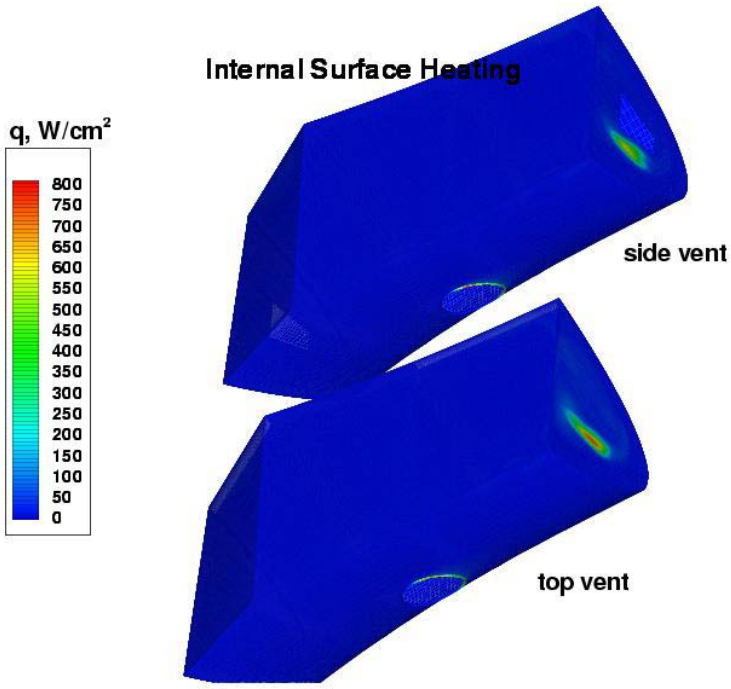

Figure 5.3.6-93: Comparison of chunnel surface heating with top and side vents.

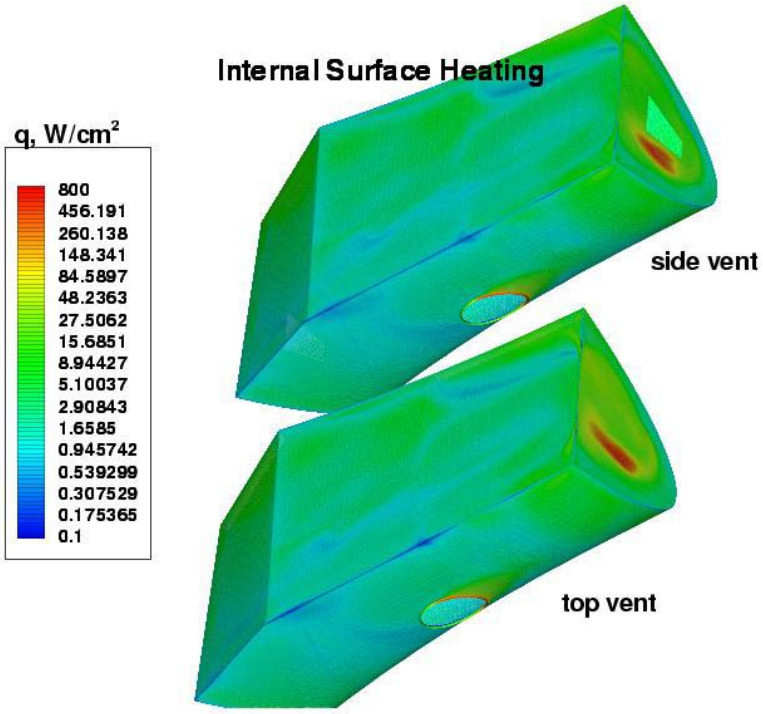

Figure 5.3.6-94: Logarithmic scaling of surface heating.

5.3.6.1.5 DSMC – Panel 8 10" Hole

5.3.6.1.5.1 Case Description

Using the DSMC Analysis Code, a DSMC case was run to simulate internal flow behind RCC panels 7, 8, and 9 due to a 10-inch hole in RCC panel 8. In this case, inflow boundary conditions were extracted from the previously run DSMC external flow solutions at an altitude of 350,274 and 300,000 feet. Vents were also applied to each side of the geometry with a total area equivalent to 66 inches squared.

5.3.6.1.5.2 Grid Development

Surface Grid
A heritage CAD definition for the RCC cavity was obtained from Jim Greathouse (NASA-JSC). This definition includes wing geometry from the leading edge back to the wing spar and includes a definition for the earmuffs between panels. The geometry used in this case was developed using the GridGen grid generation tool. After importing the CAD into GridGen, a 10-inch hole was generated in RCC panel 8 at a location of X = 1065 inches, Y = -219 inches, and Z = 286 inches in the orbiter coordinate system. Vent holes were included on each side of the geometry. It was assumed that the RCC thickness was uniform at ¼ inch, so the 10-inch hole in RCC panel 8 was given a thickness of approximately ¼ inch.

Since a DSMC solution had already been obtained for a nominal case at an altitude of 350,274 feet, it was felt that it was not necessary for a full-length shuttle case to be run for this failure scenario (1). Instead, an external flow field box-like "geometry" was created that connected to the hole from the external flow side. Great care was taken to create an external flow field geometry large enough so that the hole geometry would not significantly affect the flow at the upstream boundary, but small enough so that the case would run in a timely manner. The external flow field geometry was created to connect to a corresponding

portion of the outer RCC surface, which in turn, connected to the surface representing the thickness of the hole. Two different views of the surface geometry are displayed in Figure 5.3.6-95 and Figure 5.3.6-96.

In DAC, the surface geometry is represented as a collection of unstructured triangular elements and the entire surface geometry must be created to be "watertight" and possess continuous connectivity among triangles. In this case, the surface geometry contained approximately 53,000 surface triangles. Each individual surface triangle has specific boundary conditions associated with it. The triangles representing the surfaces of the wing were given the "solid wall" boundary condition, which means that no molecules are produced at the wall and none pass through. The triangles representing the vents were given the "outflow" boundary condition, which means that any molecules that hit the surface will disappear. Finally, the triangles representing the external flow field surface were given the "inflow" boundary condition. An inflow boundary creates molecules on the flow field side of the triangle, but any molecules that hit the surface will disappear.

Flow field Grid
The computational domain was specified to encompass the surface geometry created in this case and the boundary conditions of the computational domain were specified as vacuum. For the 350 kft case the internal flow field was discretized with Level-I Cartesian cells and each cell was specified to have a length of 1.18 inches (0.03 meters). The flow field grid was refined to the mean free path resolution though an adaptation process. After the adaptation process, the total number of cells in the computational domain was approximately 0.86 million cells. For the 300 kft case the Level I discretization employed cells of 0.059 inches (0.0015 meters). The total number of cells after the adaptation was approximately 40 million.

5.3.6.1.5.3 Input Parameters

The solution was run fully diffuse and the surface wall temperature was assumed to be 540° R (300 Kelvin). A chemistry model for high temperature reacting air was used that contained six molecular species – O_2, N_2, O, N, NO, and Argon. The mole fractions of these species were obtained from the 1976 Standard Atmosphere Model[1]. Number density, velocity, and freestream temperature were obtained from STS-107 flight data. To obtain the inflow boundary conditions from the full-length shuttle case already run at an altitude of 350,274 feet, the Surface Tools Plus (STP) DAC utility code was used to interpolate flow field properties onto the inflow geometry.

5.3.6.1.5.4 Results

Figure 5.3.6-98 and Figure 5.3.6-99 display a Y-slice of the flow field number density for the 350kft and 300 kft cases respectively. Due to the fact that the SLICE code (the DAC post-processing code that extracts the flow field properties of a certain plane) only has the capability to extract properties in a constant x, y, or z plane, Figure 5.3.6-97 was included to display a visual picture of the Y-direction cutting plane chosen. In Figure 5.3.6-98 and Figure 5.3.6-99, the streamlines shown depict the movement of the flow as it enters the hole in panel 8 and begins re-circulating inside the cavity. Figure 5.3.6-100 through Figure 5.3.6-103 (front and back view for the 350 and 300 kft cases, respectively) show the heating distribution in the RCC cavity while and Figure 5.3.6-104 through Figure 5.3.6-107show the corresponding pressure distribution. For the 350 kft case both the heating and pressure values shown in the legends on the right side of the figures have been normalized by reference heating and pressure values chosen from a point near the hole in panel 8 on the upstream RCC external surface. For the 300 kft case the heating and pressure were normalized by the free stream values at 300 kft. From these figures, it is evident that the area of highest pressure and heating due to the breach is near the earmuff between panels 8 and 9. In Figure 5.3.6-100 through Figure 5.3.6-103, a splash effect is shown on the panel 8 spar surface. As the flow hits the corner of the earmuff, a shock is formed and the flow is seen to splash onto the spar. Elevated heating levels are also seen near the earmuff between panels 7 and 8.

As was mentioned previously, mean free path resolution was obtained in the flow field grid for the 350 kft case. Historically, solutions that have reached mean free path resolution in their flow field grids have compared well with experimental data. The 300 kft case proved more challenging and although the available computational resources were exhausted mean free path resolution was not achieved throughout the domain. (That would have required a total number of cells in excess of 100 million). However, most cells were concentrated near the walls to capture the surface properties as accurately as possible.

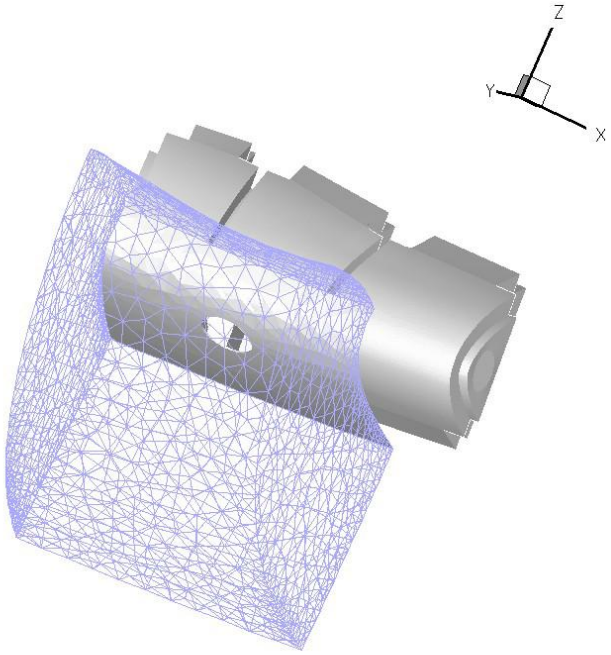

Figure 5.3.6-95 External (Triangulated) and Internal (Solid) Computational Domains – Front View

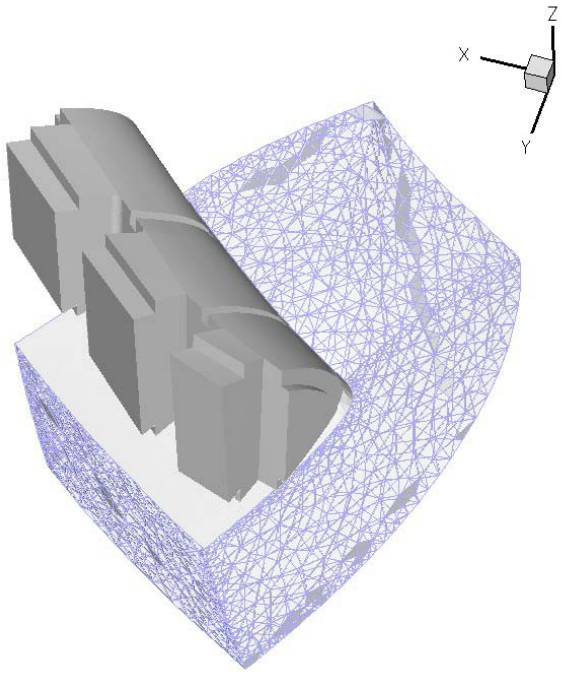

Figure 5.3.6-96 External (Triangulated) and Internal (Solid) Computational Domains – Back View

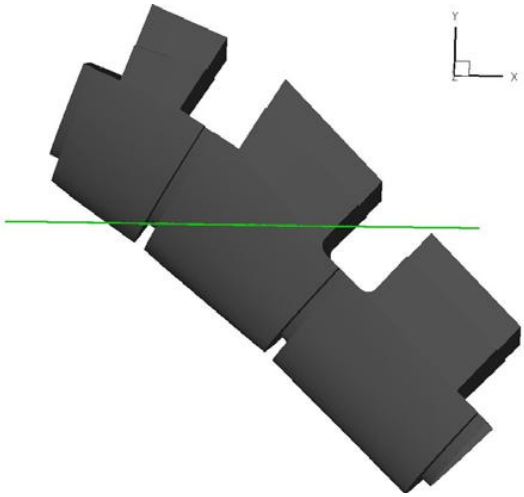

Figure 5.3.6-97 Visual of Cutting Place Chosen for Figure 5.3.6-98 and Figure 5.3.6-99

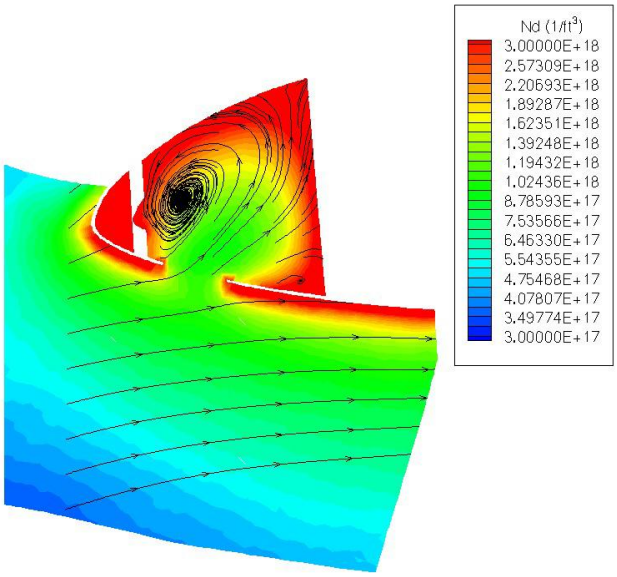

Figure 5.3.6-98 350kft Case-Number Density in Flowfield with Streamlines (Slice in Y-Direction)

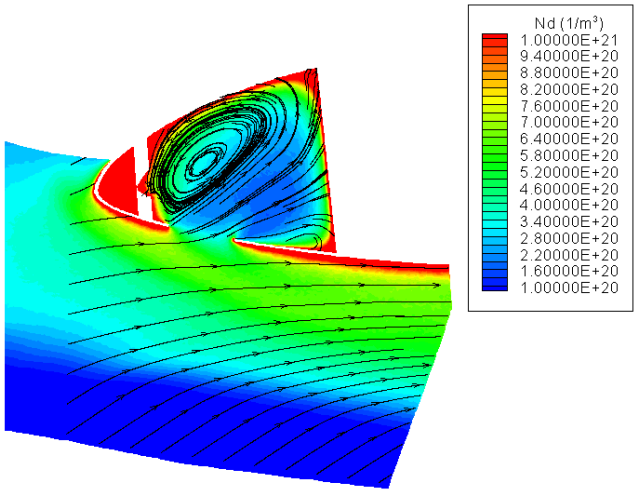

Figure 5.3.6-99 300kft Case-Number Density in Flowfield with Streamlines (Slice in Y-Direction)

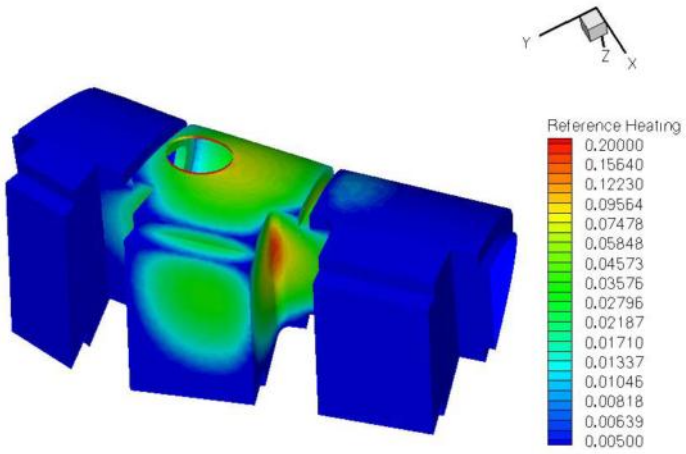

Figure 5.3.6-100 350kft Case-Reference Heating Distribution in RCC Cavity - Front View

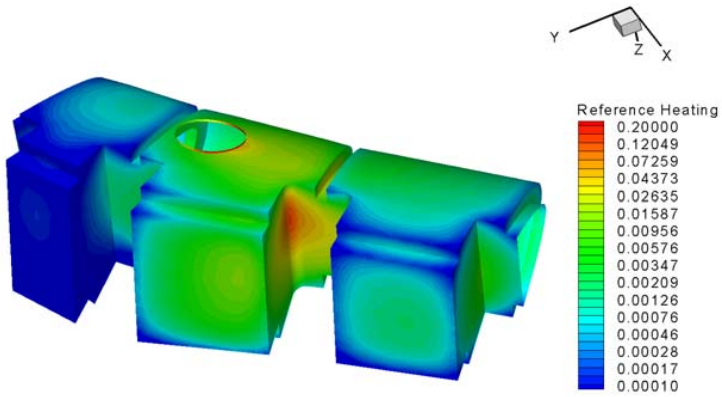

Figure 5.3.6-101 300kft Case-Reference Heating Distribution in RCC Cavity - Front View

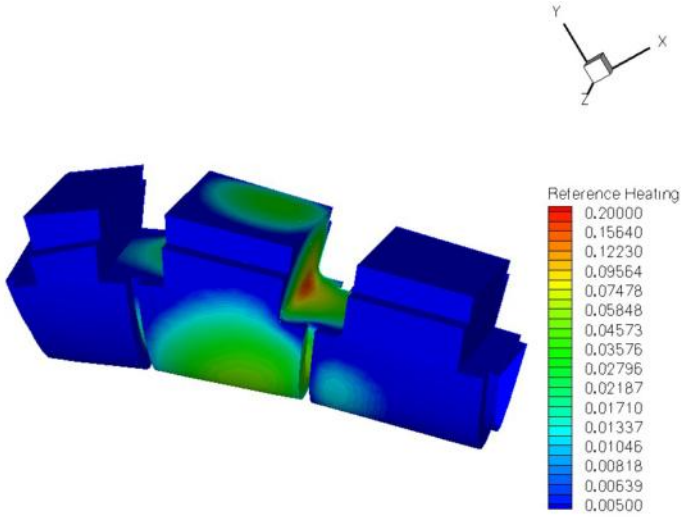

Figure 5.3.6-102 350kft Case-Reference Heating Distribution in RCC Cavity – Back View

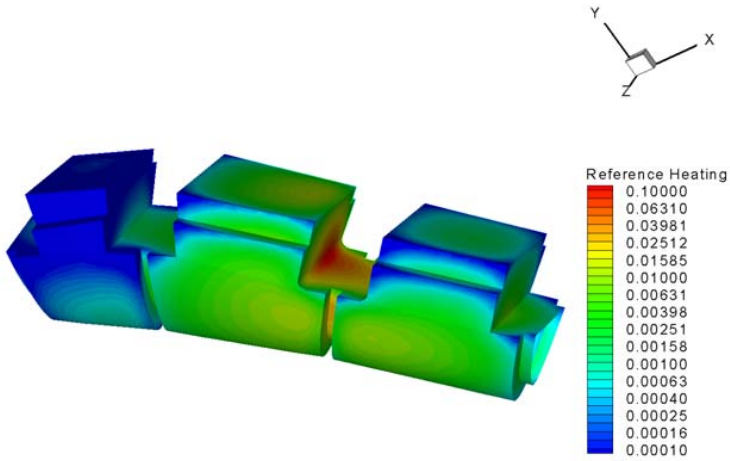

Figure 5.3.6-103 300kft Case-Reference Heating Distribution in RCC Cavity – Back View

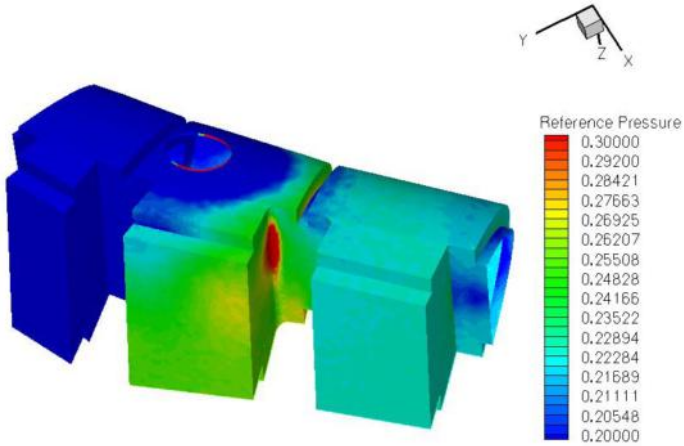

Figure 5.3.6-104 350kft Case-Reference Pressure Distribution in RCC Cavity – Front View

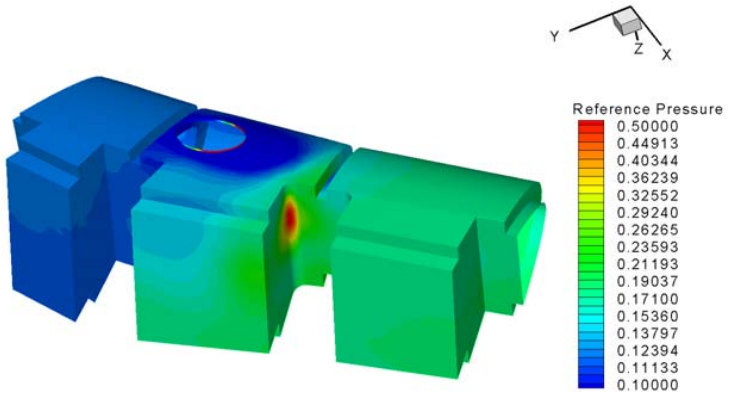

Figure 5.3.6-105 300kft Case-Reference Pressure Distribution in RCC Cavity – Front View

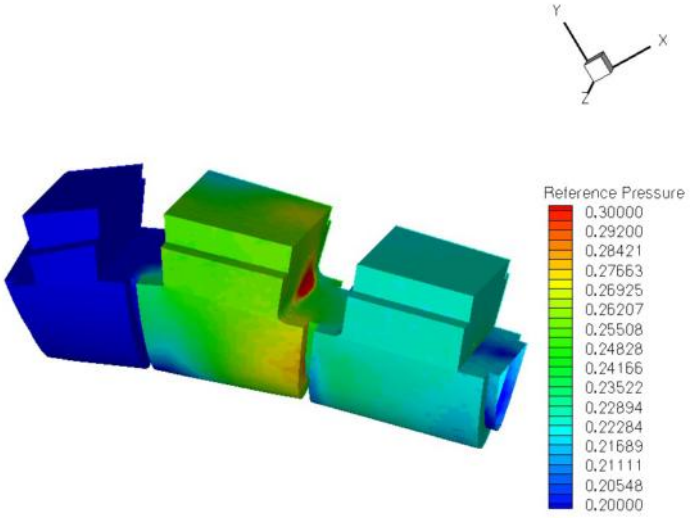

Figure 5.3.6-106 350kft Case-Reference Pressure Distribution in RCC Cavity – Back View

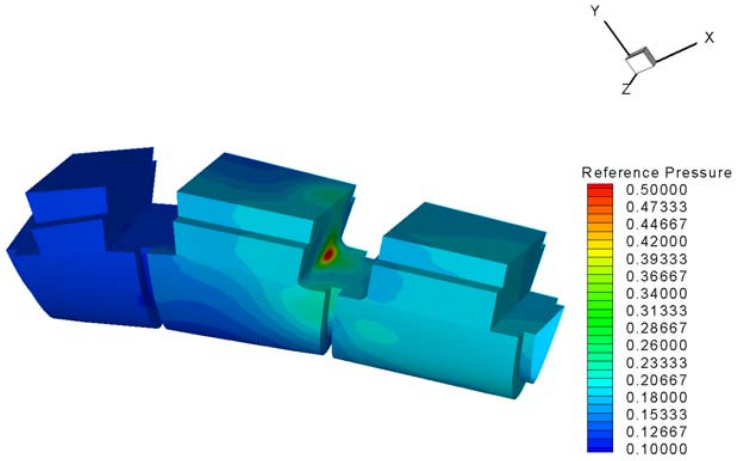

Figure 5.3.6-107 300kft Case-Reference Pressure Distribution in RCC Cavity – Back View

Footnotes

1. The value of the Knudsen number (a ratio of the molecular mean free path to a reference length) is often used as an indicator of rarefied flow. A Knudsen number of 0.01 or less is typically used to describe continuum flow, whereas higher Knudsen numbers indicate more rarefied flow. In this case, the Knudsen number is an order of magnitude larger when simulating only the portion of the flow field near the leading edge of the wing, than when simulating the entire flow field around the full-length vehicle. This corresponds to fewer computational resources needed due to fewer flow field molecules simulated.

5.3.6.2 CFD of RCC T-Seal Damage (Missing Portion of T-Seal)

5.3.6.2.1 JSC GASP 2D Solutions

5.3.6.2.1.1 Brief CFD Intro / Application Description

Two-dimensional simulations were done with GASP to model the internal wing flow field around the earmuff with a T-seal missing. Figure 5.3.6-108 is a representation of this simplified geometry. The true wall contour on the windward surface was not modeled in the GASP simulations. Instead, the windward surface was just a straight wall (black line instead of blue line in Figure 5.3.6-108).

GASP 4.1 with the overset grid option was used to expedite grid generation. Figure 5.3.6-109 shows the grid system. Sixteen grids were used with no overlap on the viscous surfaces. The upstream boundary was obtained by interpolating from a solution provided by the LAURA code from CFD point 1. The exact point to interpolate the boundary layer profile from was found by locating the attachment line on the wing leading edge and then locating the point between panels 8 and 9 that interested the attachment line. Figure 5.3.6-110 shows streamlines across the wing leading edge. The center of the red square is where the boundary layer profile was interpolated.

The interpolated boundary layer profile was in 3-D coordinate space, which was not the same coordinate system as the two-dimensional model problem. To transform the profile to the two-dimensional coordinate system the three-dimensional vector was dotted with the surface normal (along the attachment line) to get the x-component of the 2-D profile and dotted with the surface normal at the interpolation point to get the y-component of the 2-D profile. Figure 5.3.6-111 shows the boundary layer profile by components.

The out of page component is the velocity that would be out of the page in the 2-D simulation. It is small in comparison for the entire profile so it was ignored. The Mach number was used to limit the height of the profile that was used. The computational domain was limited to about 6.3 inches (0.16 meters) above the windward surface. Beyond that, the shock affected the Mach number profile.

5.3.6.2.1.2 Case Definition

The inlet to the simulation, as stated above, was a boundary layer profile from the LAURA code (CFD point 1). The internal back pressure was taken to be 0.835 psf (40 Pa). This was the leeside pressure above the leading edge from the same LAURA simulation (where the actual wing venting occurred). The internal wall temperature (on the earmuff) was held at 1500° F (fully catalytic surface). The external wall used the wall temperature from the LAURA solution (2794° F, partially catalytic surface).

5.3.6.2.1.3 Configurations Analyzed

The original geometry called for the internal surface to be 45” away from the windward surface of the wing. This made the distance from the earmuff to the T-seal exit to be 31” in the simulation. Four other cases were ran, with the distance from the earmuff to the T-seal exit being 21”, 11”, 5”, and 2”. The purpose for the fives cases was to create an earmuff heating model that varied as a function of distance from the T-seal exit to the earmuff. To speed up the running of the extra 4 cases, the original 31” solution was interpolated to each of the new grid systems (21”, 11”, 5”, and 2”) and the solution was ran from there. This saved the time of the flow setting up into the T-seal inlet. This was a legitimate way of running the cases because the flow out of the T-seal exit was supersonic thus the flow through the T-seal inlet never changed even when the earmuff was moved closer.

5.3.6.2.1.4 Heating Results

The heating distribution on the earmuff is shown in Figure 5.3.6-112. As the earmuff approaches the T-seal exit, the jet expands less, thus the heating on the earmuff is more localized and the peak heating is

much higher. The heating on the corners of the earmuff seems to increase slightly as the earmuff gets further from the T-seal exit.

5.3.6.2.1.5 Observations and Conclusions

The distance from the T-seal exit to the earmuff surface largely affects the plume structure. Figure 5.3.6-113 shows Mach contours for the 31" case. Figure 5.3.6-114 shows the mach contours for the 5" case. The maximum Mach number in the plume is at least 25% lower for the 5" case than the 31" case. Figure 5.3.6-115 shows the T-seal inlet flow structure. As the plume passes through the nozzle created by the missing T-seal, the flow directionality of the freestream is mostly washed away. This is evident by the symmetric flow at the exit of the T-seal.

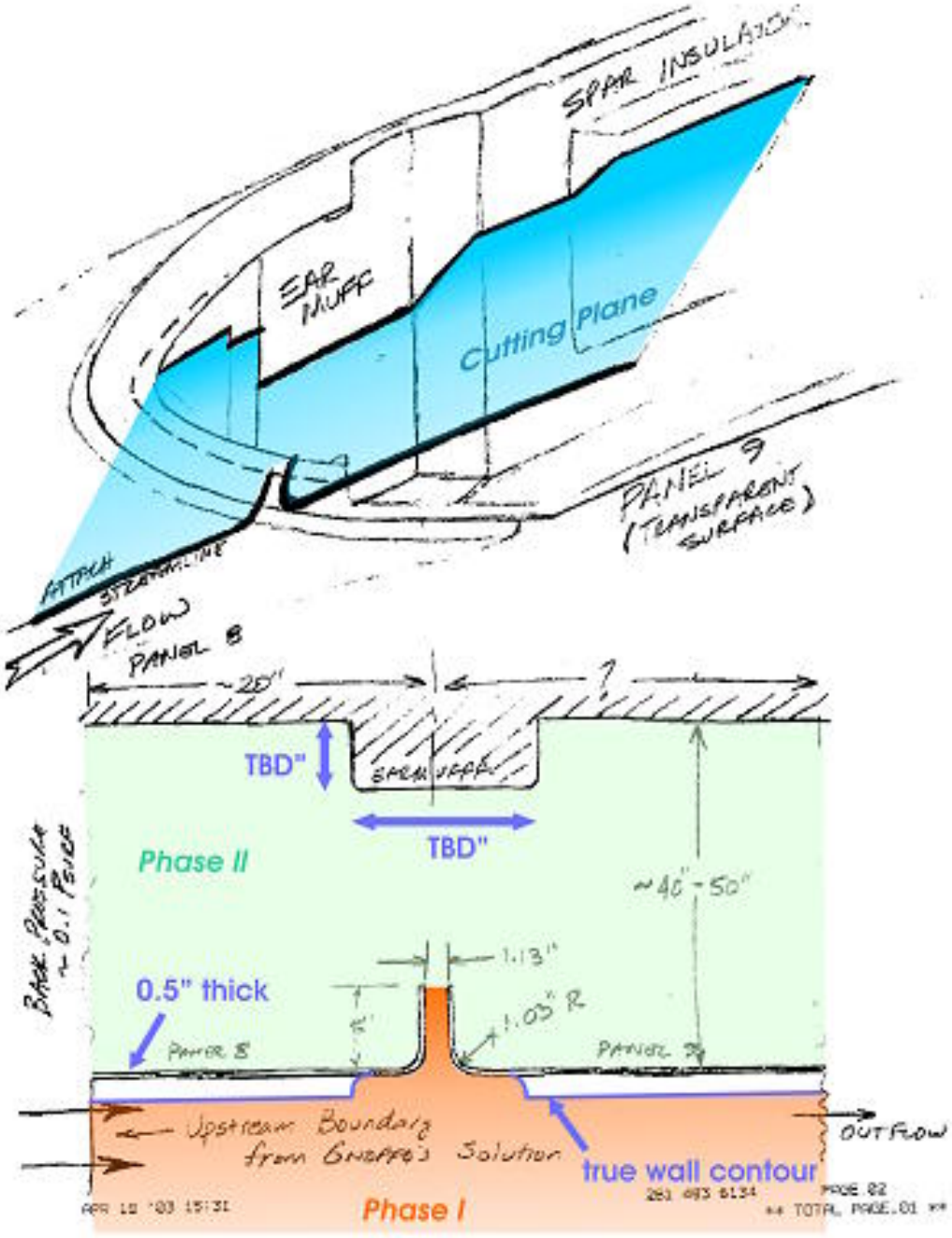

Figure 5.3.6-108 Representative T-seal geometry

a) Overview of Grid System

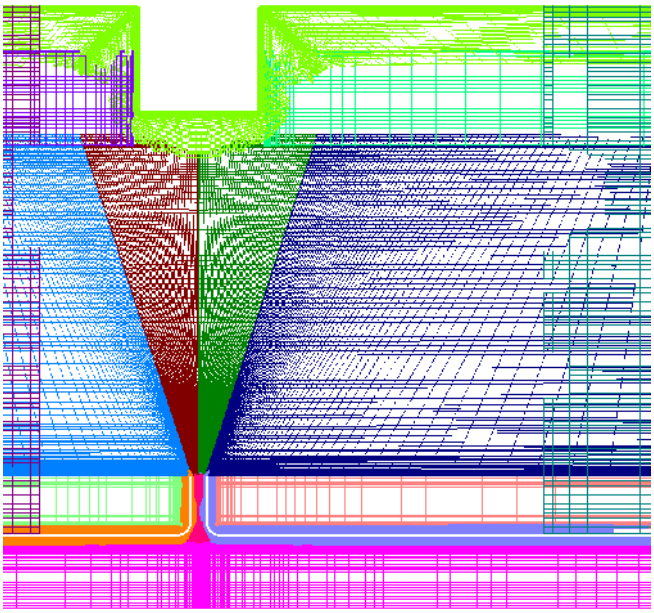

b) Close up of Earmuff Region

Figure 5.3.6-109 T-Seal Grid System

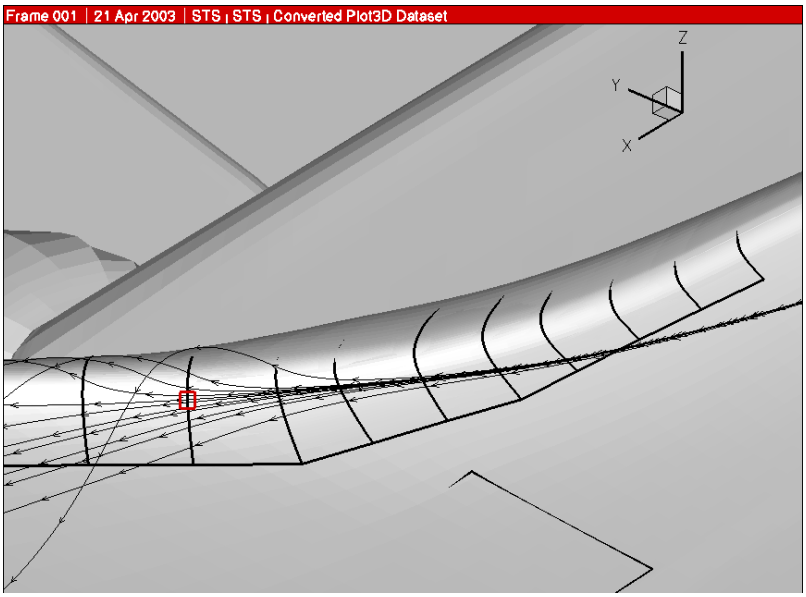

Figure 5.3.6-110 Panel 8 Attachment Line

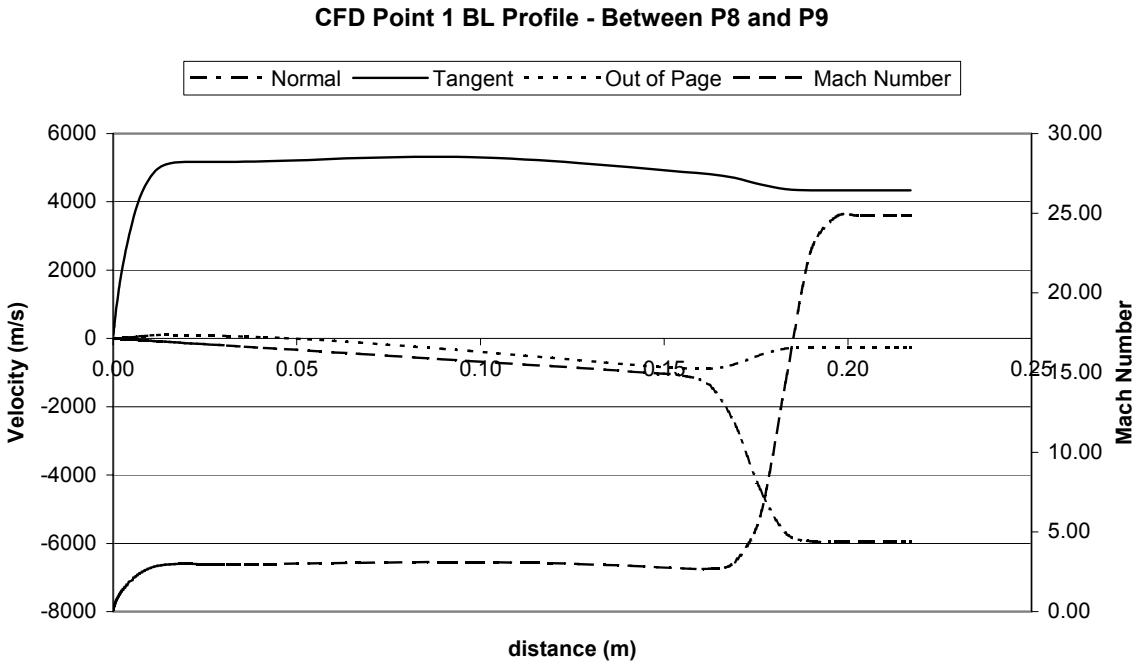

Figure 5.3.6-111 Transformed Boundary Layer Profile

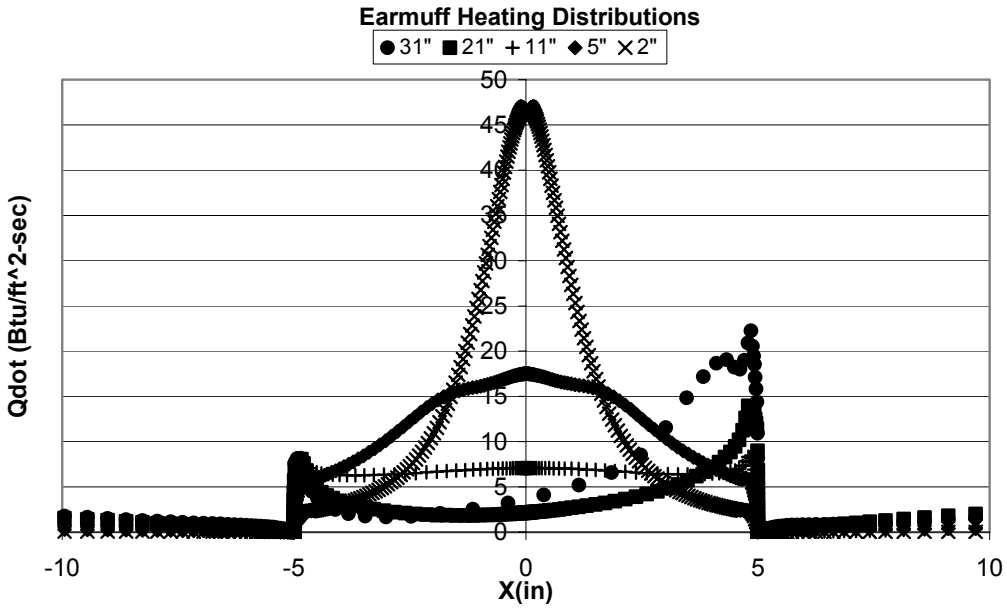

Figure 5.3.6-112 Earmuff Heating Distributions for Varying Distances

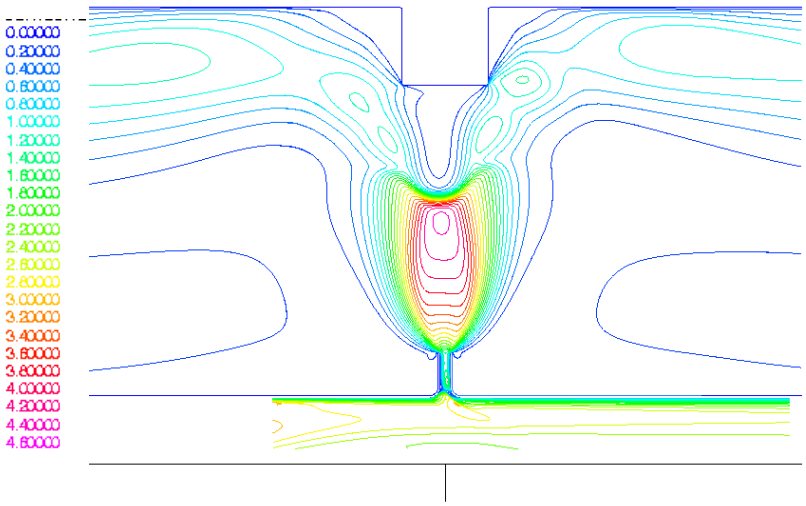

Figure 5.3.6-113 Mach contours for the 31" separation case

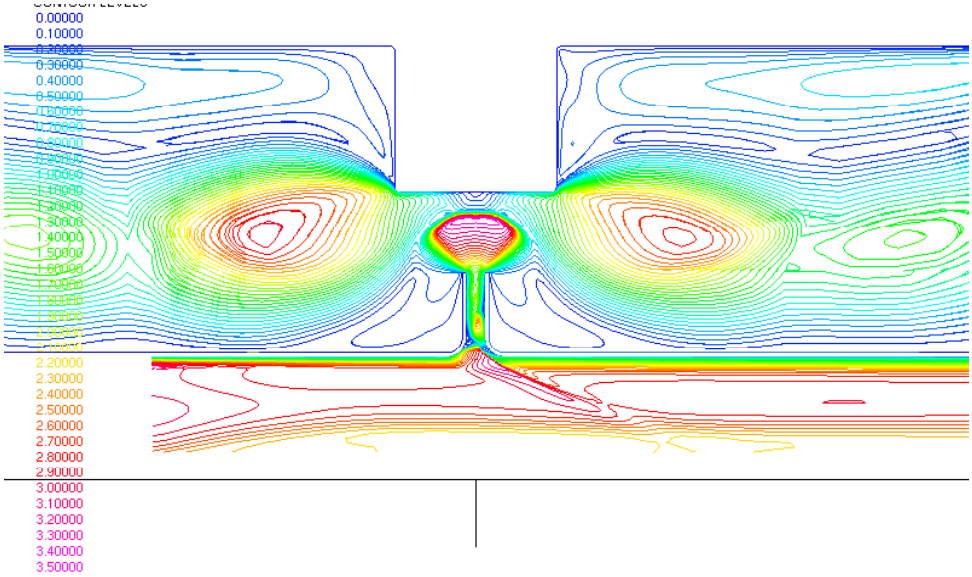

Figure 5.3.6-114 Mach contours for the 5" separation case

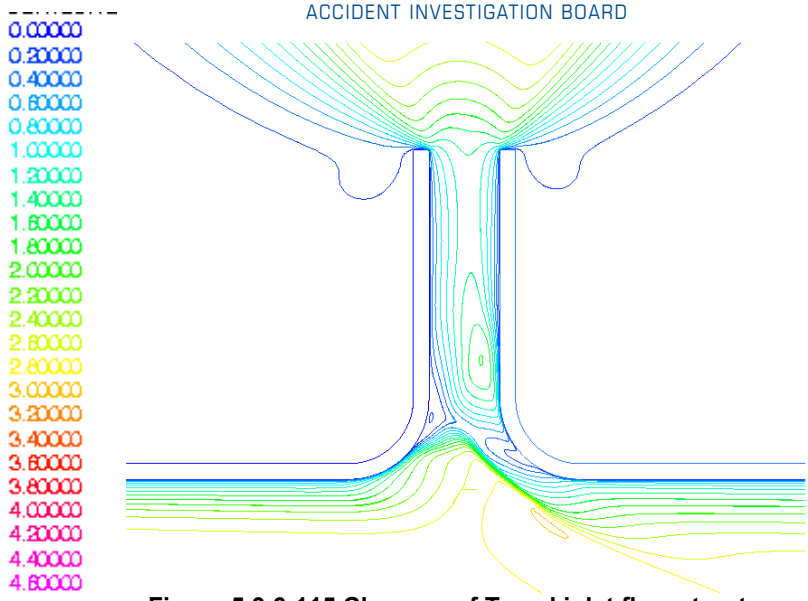

Figure 5.3.6-115 Close up of T-seal inlet flow structure

5.3.6.2.2 Rocketdyne 2-D T-Seal solution

5.3.6.2.2.1 Case description

The objective of the Rocketdyne 2-D CFD analyses was to compute convective heating rates on the RCC T-seal cavity and rib channel areas as well as on the spanner beam insulation directly behind the T-seal (RCC 8/9 "earmuff"). The motivation for these analyses was to create a "bridge" between the unit physics validation problems and the full 3-D failure scenario simulations. The experience obtained from these analyses was intended to improve the understanding of the flow field and heat transfer mechanisms applicable within the T-seal cavity and on the earmuff. The experience gained would be directly applied to constructing the models for 3-D failure scenarios. In order to obtain solutions in a timely manner and break down the complexity of the problem further, a two-phase approach was implemented for the 2-D analyses. The first phase examined only the external surface, T-seal cavity, and rib channel flow fields and heat fluxes. The second phase expanded upon the first phase to examine the flow field inside the RCC panel cavities and the heat fluxes the earmuff would be subjected to.

5.3.6.2.2.2 Grid/Solution development

A planar cut of the RCC T-seal cavity on the underside of the wing provided the geometry used to generate the grid. The cut was made through a Pro-E subassembly of RCC panels 8 and 9. A sketch of the flow domain and subassembly are shown below in Figure 5.3.6-116. External LAURA CFD solutions helped determine the appropriate placement of the planar cut to ensure that the flow was mostly perpendicular to the edge of the T-seal.

The grids for both phases were block structured and created using the Boeing APPT system. In the first phase, a dummy "dump" zone was added to the grid at the end of the T-seal rib channel to improve convergence time. The wall spacing used was 1.0e-4 in., and the grid was "wrapped" around the external surfaces and T-Seal cavity to maintain a consistent grid clustering normal to the walls. The phase I grid consisted of four zones, contained 38, 788 cells, and is shown in Figure 5.3.6-117.

The second phase grid was more or less identical to the first phase grid over the external region, T-Seal cavity, and rib channel, but several zones were created to replace the dump zone with a representation of the RCC panel internal geometry. Dimensions for the earmuff and some other geometrical information were extracted from the sketch in Figure 5.3.6-116 as well as the 2-D grid discussed in Sec. 5.3.6.2.1. Consequently, the representation of the wing leading edge internal geometry is not exact. Furthermore, the earmuff is modeled with sharp corners. This does not correspond to the actual geometry and does have an appreciable affect on the heat transfer as discussed in the results section below. The geometry, however, is good enough to provide a feel for the flow field and heat transfer. The outflow areas of the grid for phase II were expanded to include "dump" regions to allow the application of constant pressure boundary conditions. The wall spacing used was 1.0e-4 in. It should also be noted that the grid

coordinate system for phase II was different from that of phase I although this has no effect on the results. The phase II grid consisted of seven zones, contained 115,355 cells, and is shown in Figure 5.3.6-118.

For both phases of the 2-D analyses, solutions were obtained using the USA structured solver. Fully laminar flow was assumed based on the extremely low Reynolds numbers present. In phase I, Liu-Vinokur equilibrium air thermochemistry and Tannehill transport properties were used. In phase II, a finite rate thermochemistry model with five species and seventeen reactions was used and fully catalytic walls were assumed. The transport properties were determined using Sutherland's law. Additionally, a laminar Schmidt number of 0.52 was used. Also, for both phases of the 2-D analyses, the CFD Condition 1 trajectory point data provided the freestream conditions, and the external LAURA flow solution established the external flow boundary conditions. Three different wall temperature boundary conditions for the RCC external walls (2900° R – STS-5 nose temperature, 3523° R – approximate RCC coating loss temperature, and 5273° R – approximate RCC oxidation temperature) were run in both the first and second phases to obtain a "database" of wall heat fluxes versus temperature and wall location. In the second phase, a 3000°R boundary condition was applied to the earmuff wall. This specific temperature was chosen because it was assumed there was enough heating on the earmuff surface to melt the material and that insulation material has an external layer of Inconel, which has a melting point of 3000° R. The "databases" created by these analyses were intended to aid any subsequent radiation analyses. Furthermore, three different cavity backpressure values were set at the end of the extended outflow region (Cp = 0.02, Cp = 0.06, and Cp = 0.10) for phase II, while the phase I outflow condition was set to be supersonic outflow. In phase I, the convergence criterion was to drive the net fluxes to steady state. Phase II retained that same criterion, but also added another – steady state heat flux on the earmuff windward surface.

5.3.6.2.2.3 Results

5.3.6.2.2.3.1 Major flow structure comments

Figure 5.3.6-119 shows all the major flow structure features of interest from the phase I solutions. The image is for the 2900° R solution – all the other flow fields are similar in nature so only data from the 2900° R solution is presented. There are changes to the flow field with temperature, but the effects are negligible. There is a high degree of internal/external flow coupling and all of the captured flow is from the external boundary layer. Large recirculation regions exist in the T-Seal cavity corners, as is expected for laminar flow. There is also a "bow shock" on the downstream side of the T-Seal cavity as the flow in the boundary layer turns and hits the T-Seal rib cavity walls. Of particular interest is the aerodynamic throat in the T-Seal channel that is formed by this bow shock and the separation area on the upstream side of the rib channel. This aerodynamic throat chokes the incoming flow and leads to expanding supersonic flow leaving the rib channel. This, in turn, affects the heat transfer environment inside the RCC cavity.

In phase II of the 2-D analyses, the external flow field changes very little from that obtained in the phase I 2-D analyses. The internal RCC panel flow field structure, however, varies significantly depending upon the backpressure boundary condition chosen. The flow is not, however, particularly sensitive to external or internal wall temperatures. As a result, most of the following discussion focuses on the changes in flow structure arising from different backpressure boundary conditions.

In phase I, it was clearly established that the flow exiting the rib channel would be supersonic based upon an assumed low backpressure within the cavity. The pressure differential between the flow reaching the cavity exit and the RCC cavity backpressure would provide more than enough energy to accelerate the flow to supersonic speeds. Given such circumstances (a backpressure such that Cp <= 0.10), the rib channel flow becomes a supersonic jet fired into the RCC panel cavity, and some sort of plume expansion expected. The results of the phase II analyses showed that the amount of plume expansion in the cavity is closely tied to the cavity backpressure. Consequently, the higher the backpressure, the more mass flow that impinges on the "earmuff" and the larger the expected heat flux on the earmuff windward surface (given that the incoming jet flow does not unchoke). The following six figures (Figure 5.3.6-120 through Figure 5.3.6-125) clearly show the differences in the plume and shock structures of the RCC cavity jet flow as the backpressure varies. All three backpressures exhibit very large-scale separated regions resulting in large-scale constant pressure regions. Such separated regions are, again, expected because of the laminar nature of the flow. Similarly, all three backpressures have a canted stagnation streamline due to the asymmetric flow in the rib channel. In addition, supersonic "tails" develop in the interior of the RCC panel cavity. How those tails impinge upon the interior surfaces changes with the backpressure in a minor

way. Furthermore, those tails turn almost 90° while staying supersonic due to the constant pressure recirculation regions they see on either side of the earmuff.

Figure 5.3.6-120 and Figure 5.3.6-121 demonstrate that low backpressures (Cp = 0.02) result in a large plume expansion. Most of the incoming jet does not impinge on the earmuff, and the normal shock occurs at a considerable distance from the earmuff surface.

Similarly, Figure 5.3.6-122 and Figure 5.3.6-123 show that a slightly higher backpressure (Cp = 0.06) results in as much as a third of the incoming jet impinging on the surface. Furthermore, a complicated shock pattern develops and the normal shock is much closer to the earmuff surface. Unfortunately, the solution on the earmuff seems unsteady and goes through cycles. This adds uncertainty to the validity of any heat flux information that may be extracted. See the discussion in the section below for more detail.

Finally, in Figure 5.3.6-124 and Figure 5.3.6-125 when the highest backpressure is run (Cp = 0.10), all of the incoming jet impinges on the surface. Once again, there is a complicated shock pattern that develops and the standoff distance of the normal shock from the earmuff surface is at a minimum leading one to expect a higher temperature gradient and thus a larger heat flux.

5.3.6.2.2.3.2 Surface heating and pressure comments

The heart of these 2-D analyses is to help determine the heating environments on various internal structures of the orbiter wing and aid the heat transfer analysts by providing them insight into the flow field and heat transfer mechanisms. In the simplest terms, the largest heat fluxes occur where the largest temperature gradients reside. Most often, the largest temperature gradients occur at the geometrical features with the smallest radii (sharp corners, etc.) because more often than not such features thin or destroy the thermal and viscous boundary layers. This trend is observed in both the phase I and phase II results. As mentioned in Section 5.3.6.2, some parts of the geometry were modeled as having sharp corners even though pictures of the actual hardware indicated that the corners are actually rounded. One would expect to over-predict the heat flux at those corners, and indeed, large localized spikes in heat flux do occur in both the phase I and phase II solutions at any geometrical corner or feature with a small radius. Figure 5.3.6-126 shows the arc length coordinate system that is used to describe the positional heat flux along the walls of interest while Figure 5.3.6-127 shows the actual heat flux values along the T-Seal cavity from the Phase I solutions and Figure 5.3.6-128 shows a comparison of the phase I and phase II solutions on the external and T-Seal cavity surfaces. The heat flux predicted in phase II is quite a bit less almost over the entire length of the external, T-Seal cavity and rib channel walls, roughly 55% of the phase I solution. More importantly, except for at the sharp corners and other geometrical features with small radii, it is a consistent. The explanation for most of this difference lies in the different thermochemical and transport models used.

Figure 5.3.6-129 presents the heat flux predictions on the surface of the earmuff. Note the sharp spikes in heat flux at the sharp corners of either side of the top surface of the earmuff due to the thinning of the thermal boundary layer. There was a problem, however with the data obtained on the earmuff windward surface. For a backpressure of Cp = 0.06 (and probably Cp = 0.10), even though the solution seemed to have converged, there was a slow oscillation in the position and magnitude of the peak heat flux and pressures on the earmuff surface. In order to explain this discrepancy, the solver was allowed to run through twenty cycles (800 time steps each) of this oscillation. The data from the twentieth such cycle is shown in Figure 5.3.6-130. As is easily visible, the oscillation is not trivial and leads to a great deal of uncertainty in the results for $Cp \geq 0.06$. Even more unsettling is the fact that there is 13-fold change in the peak heat flux during the oscillations. This behavior points to unsteady behavior in the flow.

In summary, the Phase I and Phase II bridging problems provided a wealth of useful information and helped troubleshoot the CFD process for implementing full 3-D failure scenarios.

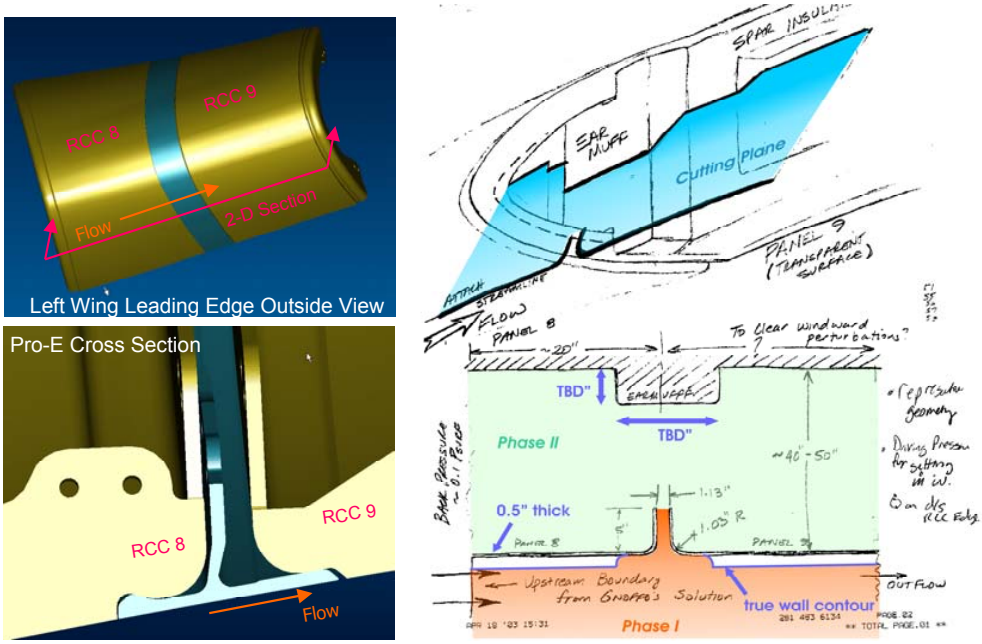

Figure 5.3.6-116 Assumed geometry and 3-D Pro/E subassembly

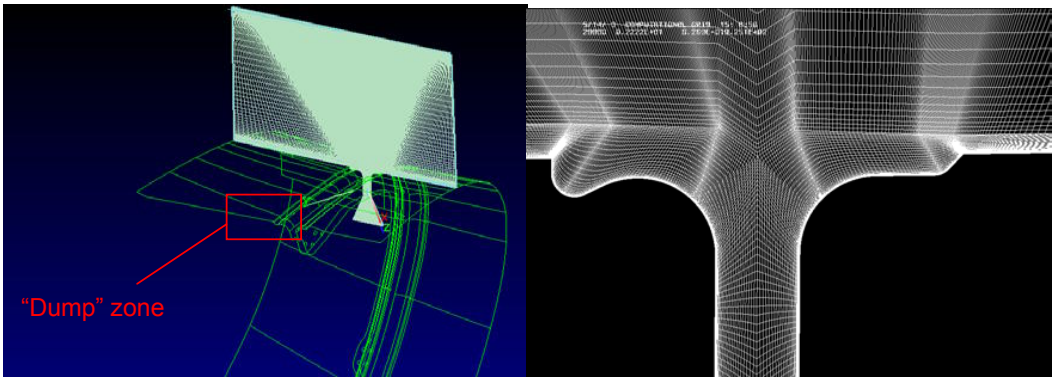

Figure 5.3.6-117 Phase I grid

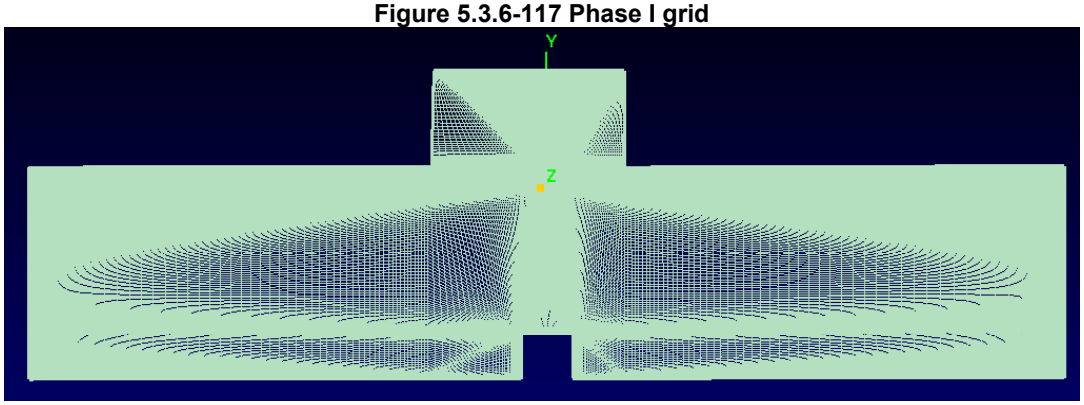

Figure 5.3.6-118 Phase II Grid

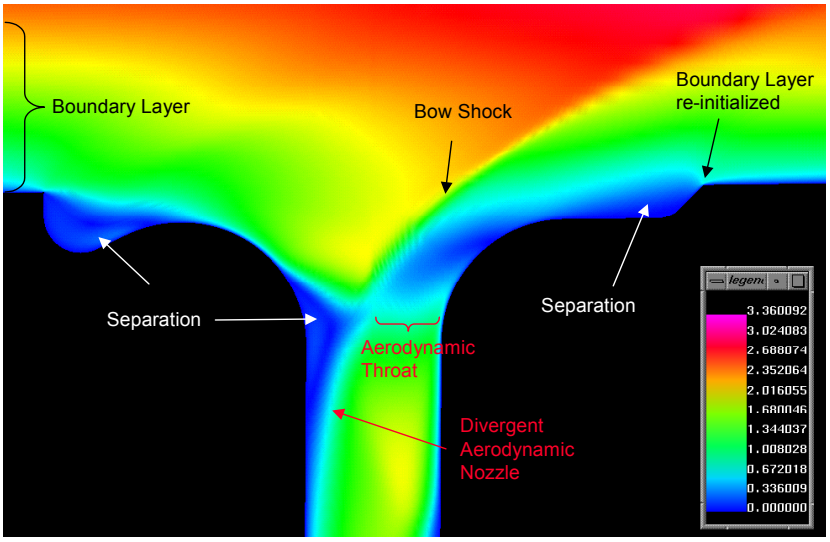

Figure 5.3.6-119 Mach Contours for T = 2900°R, phase I

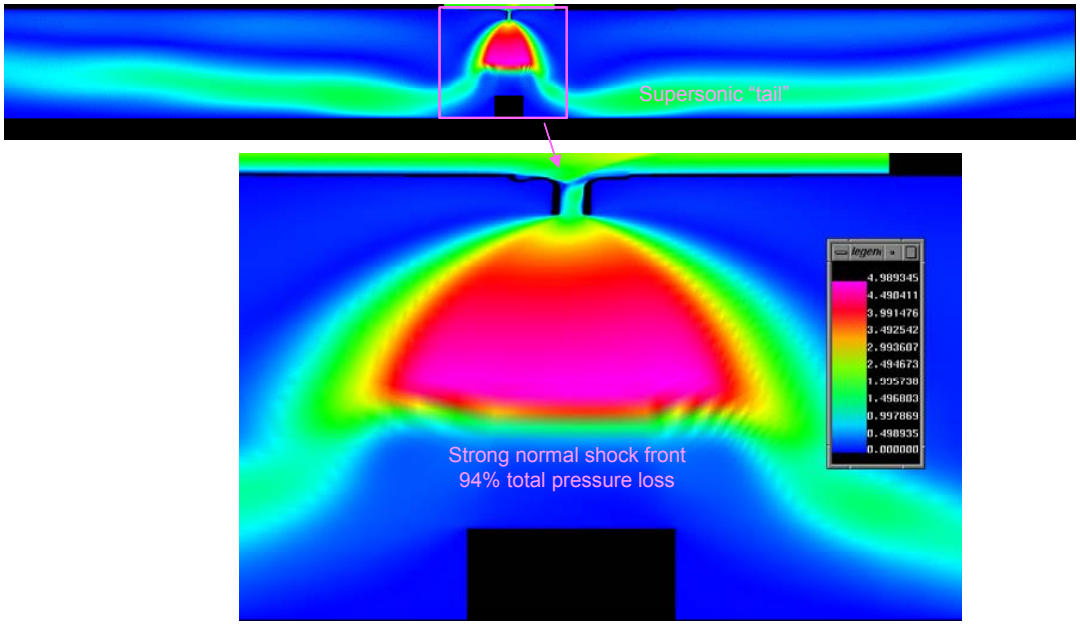

Figure 5.3.6-120 – Mach Contours for T = 2900°R and Cp = 0.02, phase II

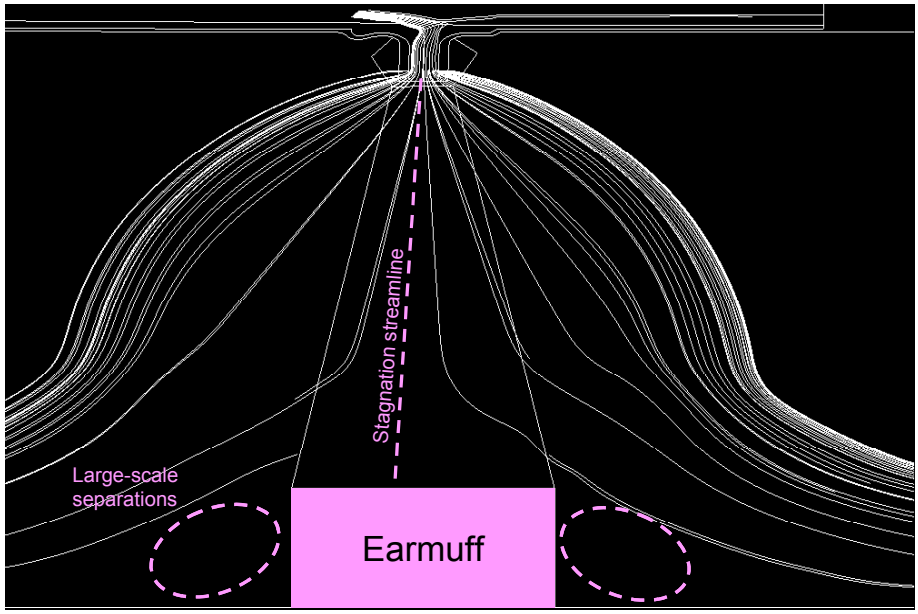

Figure 5.3.6-121 Streamlines for T = 2900°R and Cp = 0.02, phase II

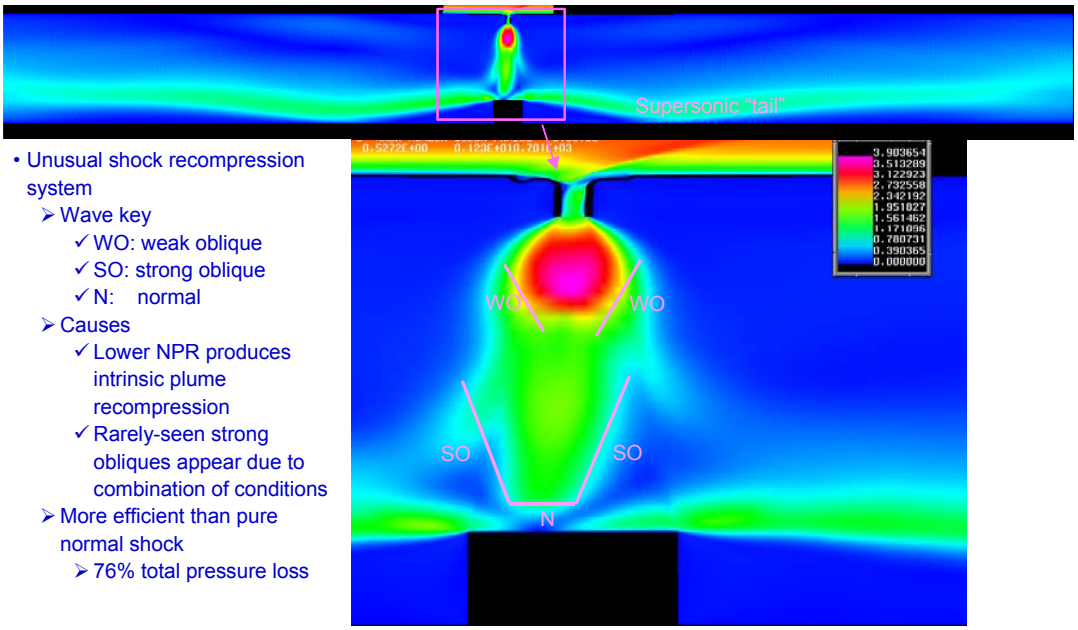

- Unusual shock recompression system
  - Wave key
    - ✓ WO: weak oblique
    - ✓ SO: strong oblique
    - ✓ N: normal
  - Causes
    - ✓ Lower NPR produces intrinsic plume recompression
    - ✓ Rarely-seen strong obliques appear due to combination of conditions
  - More efficient than pure normal shock
    - 76% total pressure loss

Figure 5.3.6-122 – Mach contours for T = 2900°R and Cp = 0.06, phase II

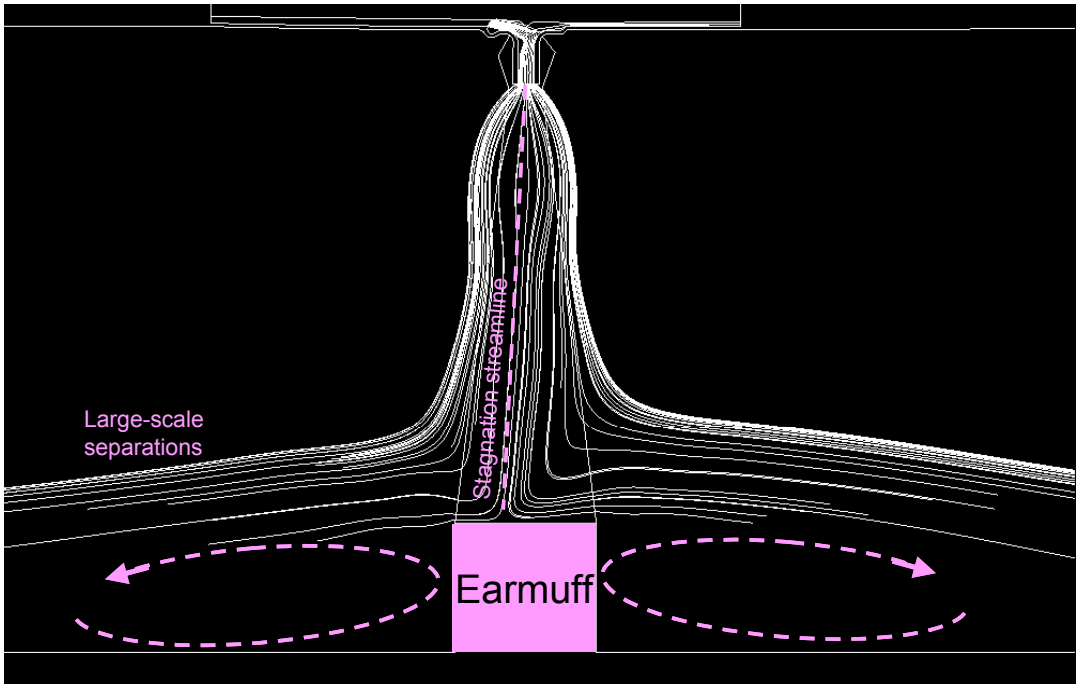

Figure 5.3.6-123 Streamlines for T = 2900°R and Cp = 0.06, phase II

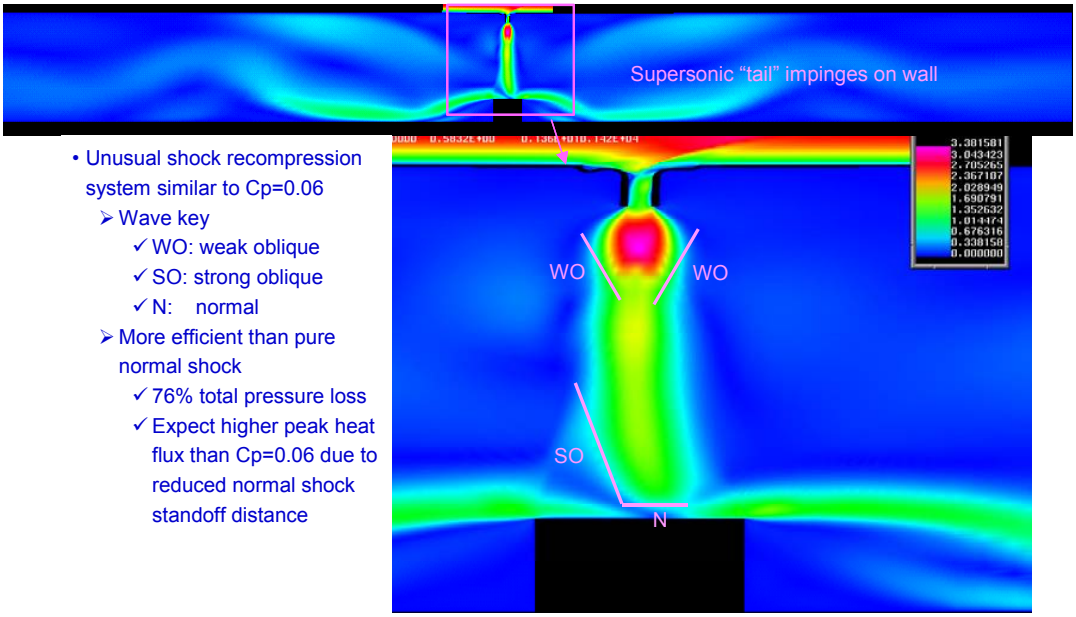

Figure 5.3.6-124 Mach contours for T = 2900°R and Cp = 0.10, phase II

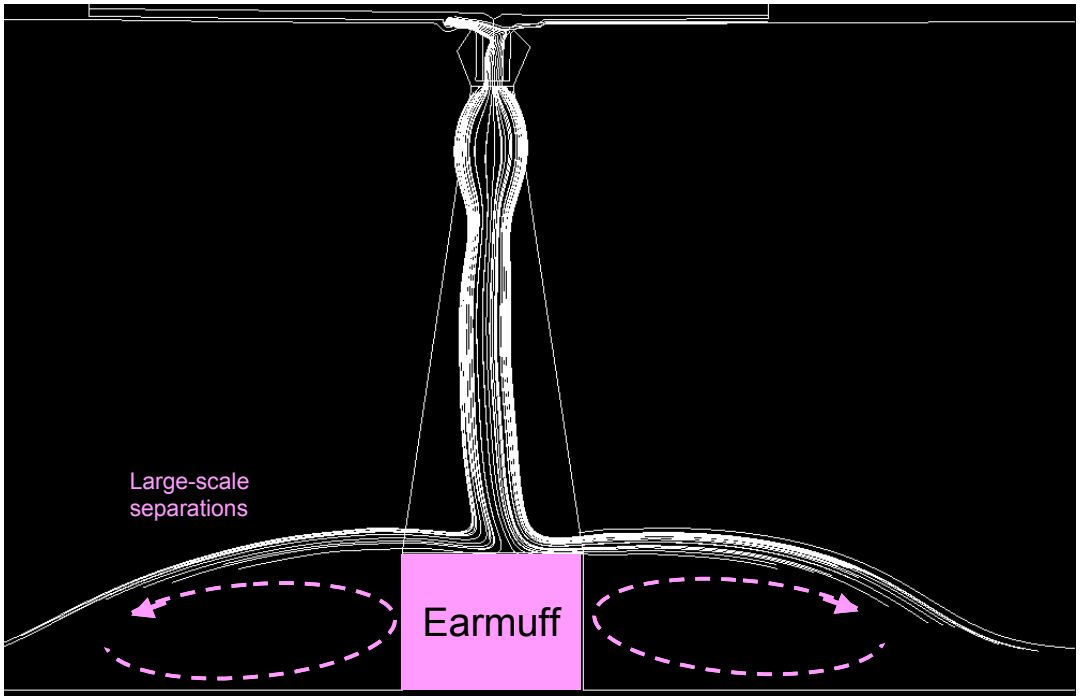

Figure 5.3.6-125 streamlines for T = 2900°R and Cp = 0.10, phase II

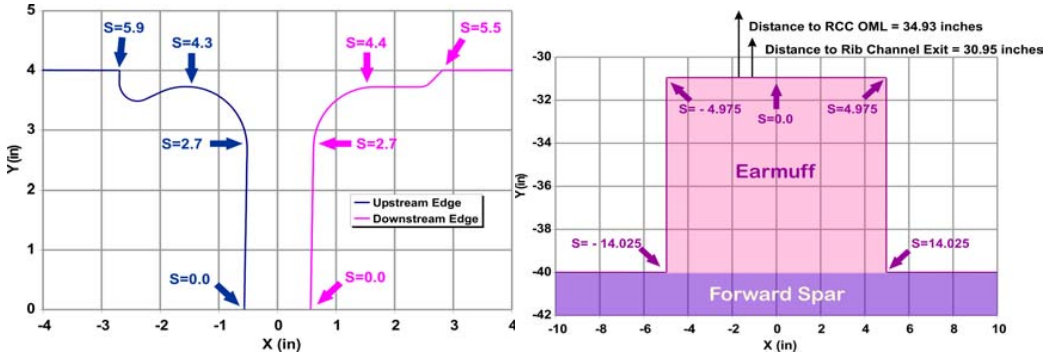

Figure 5.3.6-126 Arc length coordinate systems, phase I & II

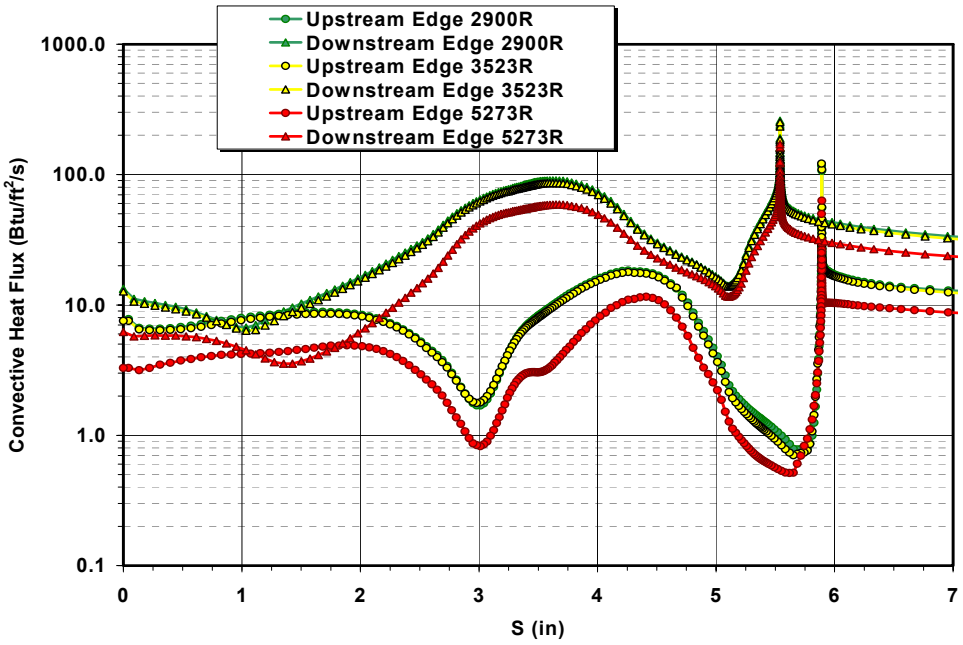

Figure 5.3.6-127 Convective heat flux on T-seal Cavity Surfaces, phase I & II

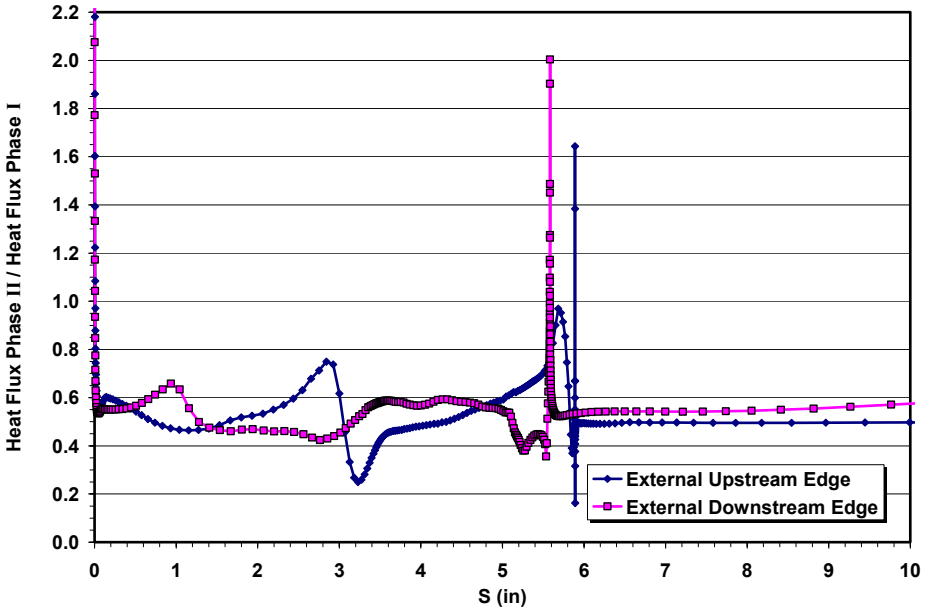

Figure 5.3.6-128 Phase I and phase II Comparison of T-seal Cavity Convective heat flux, T = 2900°R

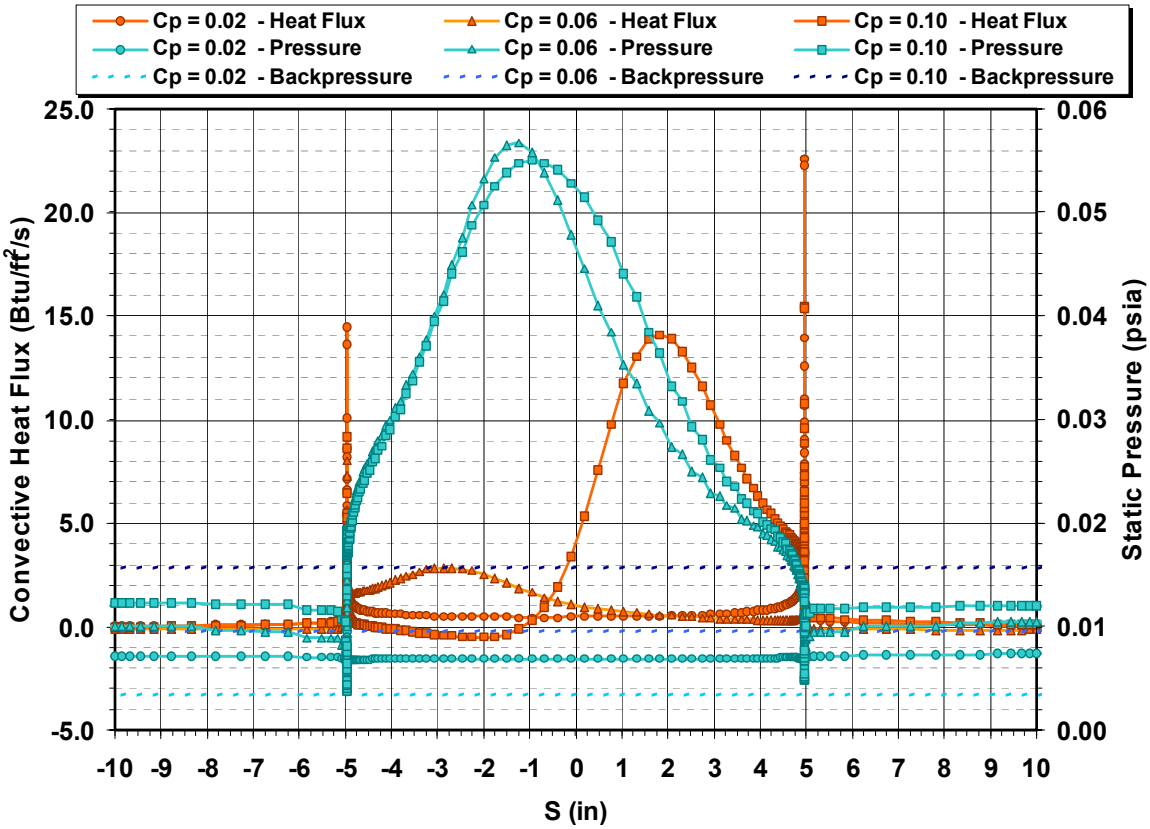

Figure 5.3.6-129 Earmuff Convective heat flux for T = 3000°R and Back-pressures, Phase II

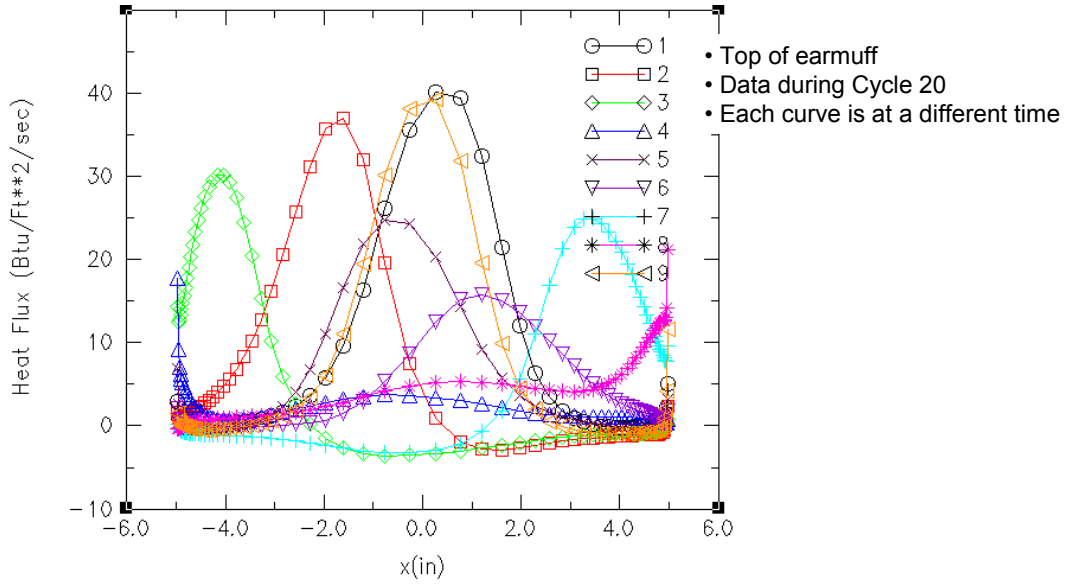

Figure 5.3.6-130 Earmuff Heat Flux Distribution Unsteadiness, phase II

5.3.6.2.3 BHB 3-D Panel 8/9 T-seal Damage

5.3.6.2.3.1 Case Description

T-seal damage between RCC Panels 8 and 9 was also one of the scenarios considered. This numerical study conducted with the USA flow solver at Boeing, Huntington Beach modeled a rectangular opening of 8" by 1.13" between the ribs of RCC Panels 8 and 9 on the windward side approximately 8" from the aft end of the lower carrier panel. This simulation included the ribs and the earmuff insulation between RCC Panels 8 and 9.

5.3.6.2.3.2 Geometry and Grid Definition

The external surface grid is illustrated in Figure 5.3.6-131, Figure 5.3.6-132 and Figure 5.3.6-133. Figure 5.3.6-134 and Figure 5.3.6-135 show the surface grid for the internal leading edge cavity. The volume grid was generated such that the wall spacing is 0.0005 inch to ensure the cell-Reynolds number of 1 or less near the surface. Solutions with both 2 and 15 million grid cells were generated.

5.3.6.2.3.3 Boundary Conditions

This equilibrium air chemistry simulation was conducted at the CFD Point 1 flight condition corresponding to 404 seconds after entry interface. The RCC interior surfaces were kept at 0° F, whereas for the Orbiter exterior surfaces a radiation equilibrium temperature boundary condition was applied.

5.3.6.2.3.4 Results

The flow field pressures are shown in Figure 5.3.6-136 and Figure 5.3.6-137 for chordwise and spanwise vertical cuts, respectively, through the T-seal damage. The corresponding Mach number distributions are illustrated in Figure 5.3.6-138 and Figure 5.3.6-139. The surface pressure and heating on the earmuff and the ribs in the vicinity of the T-seal damage are illustrated in Figure 5.3.6-140 and Figure 5.3.6-141 for the 2 million-cell model simulation. Similarly, Figure 5.3.6-142 and Figure 5.3.6-143 present the pressure and heating distributions for the 15 million-cell model simulation. The 15-million cell model results show as high as twice the heating levels, compared to the 2 million-cell model. The jet in this case acts like a wall-jet right next to the earmuffs.

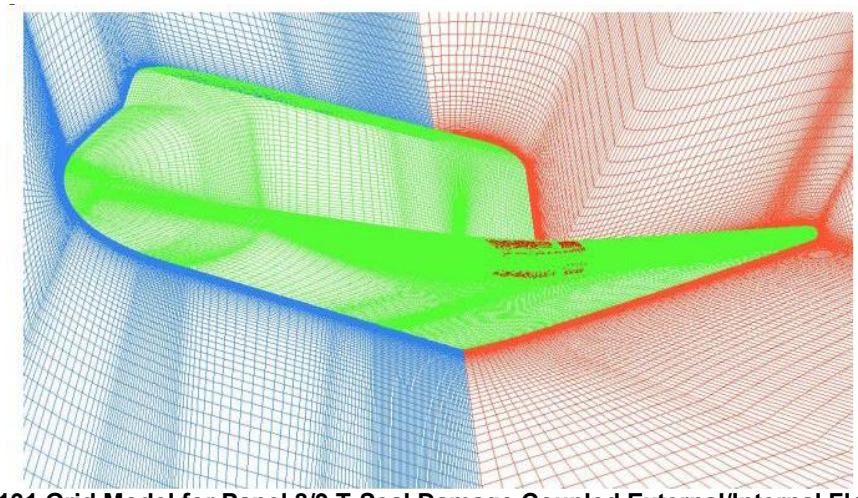

Figure 5.3.6-131 Grid Model for Panel 8/9 T-Seal Damage Coupled External/Internal Flow Simulation

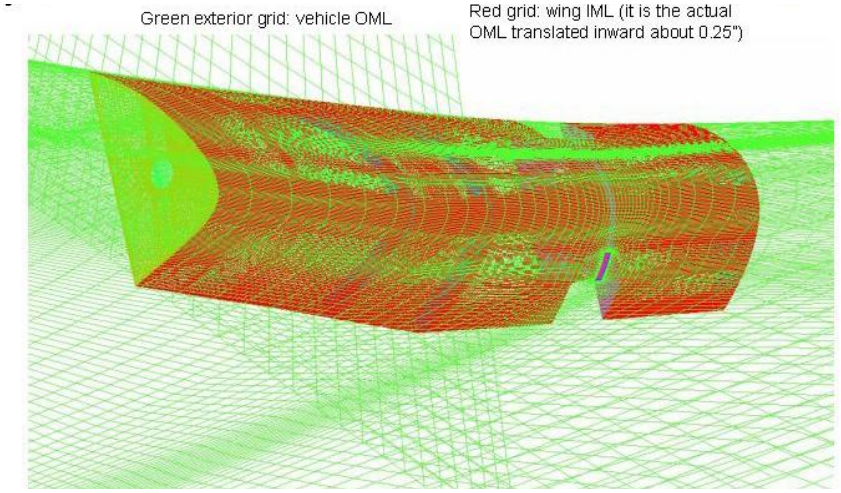

Figure 5.3.6-132 Grid Model for Panel 8/9 T-Seal Damage Coupled External/Internal Flow Simulation

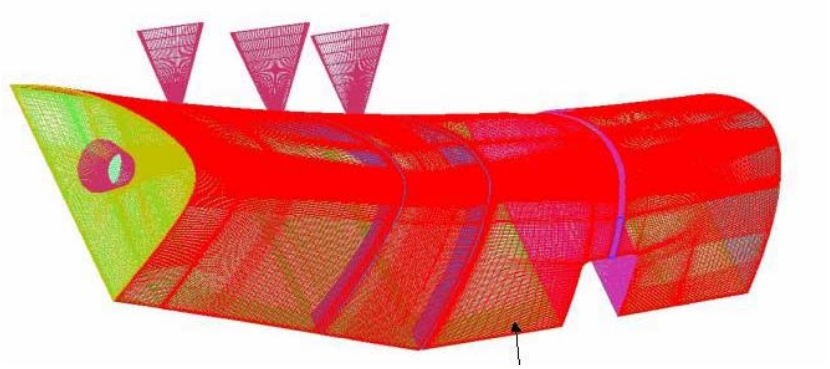

Figure 5.3.6-133 Grid Model for Panel 8/9 T-Seal Damage Coupled External/Internal Flow Simulation

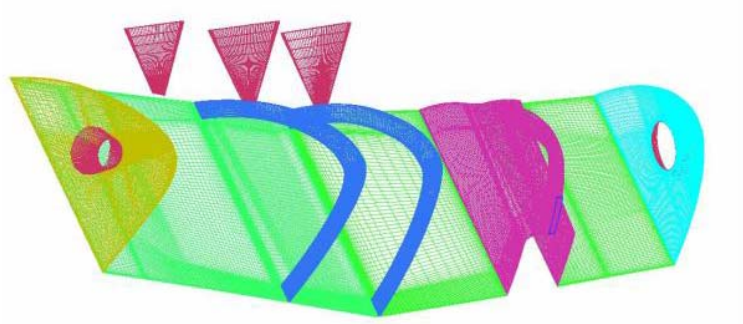

Figure 5.3.6-134 Grid Model for Panel 8/9 T-Seal Damage Coupled External/Internal Flow Simulation

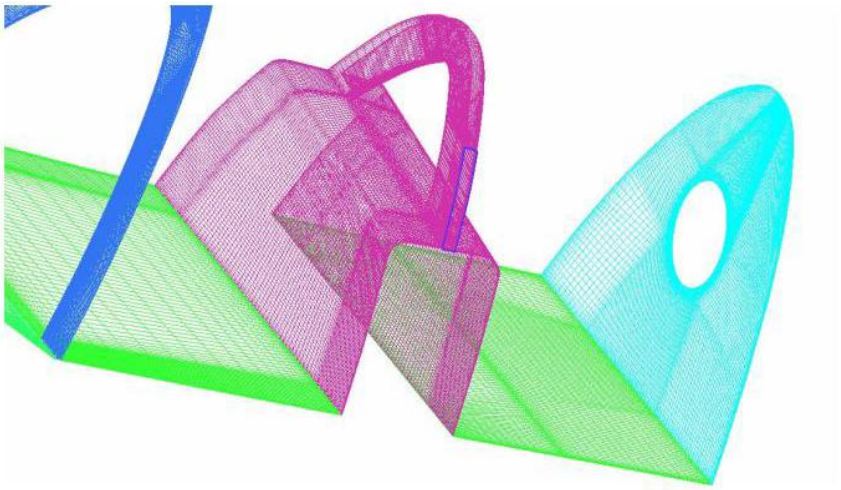

Figure 5.3.6-135 Grid Model for Panel 8/9 T-Seal Damage Coupled External/Internal Flow Simulation

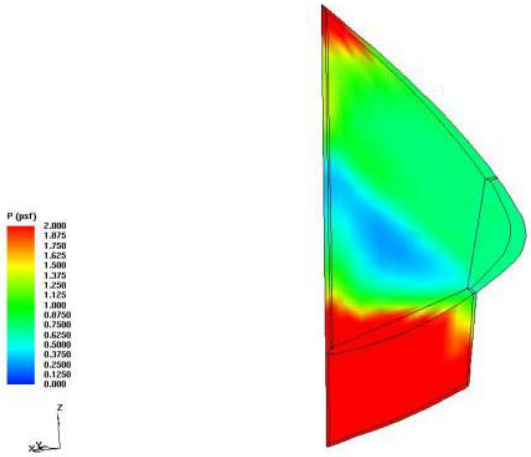

Figure 5.3.6-136 Pressure Contours from Panel 8/9 T-Seal Damage Coupled External/Internal Flow Simulation (15 million-cell Model; Postprocessed using every other points)

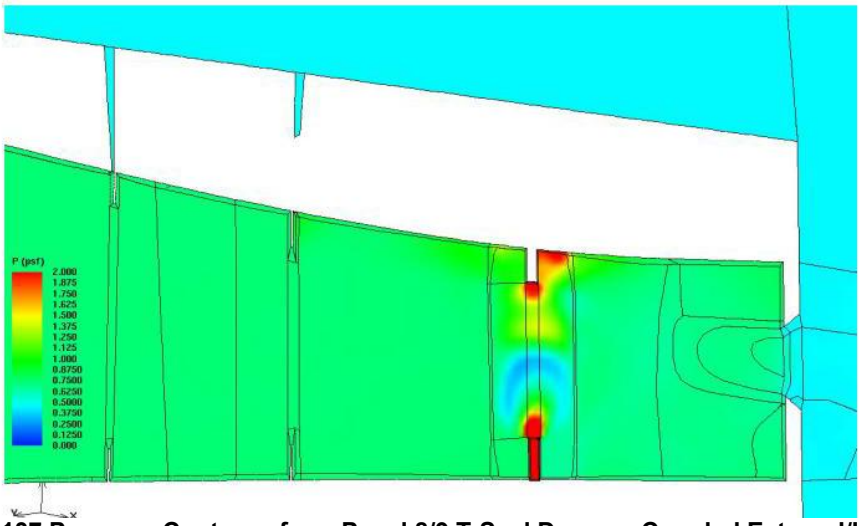

Figure 5.3.6-137 Pressure Contours from Panel 8/9 T-Seal Damage Coupled External/Internal Flow Simulation (15 million-cell Model; Postprocessed using every other points)

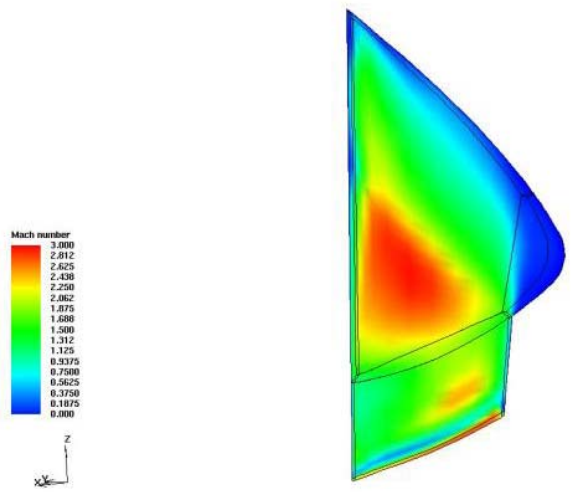

Figure 5.3.6-138 Mach Contours from Panel 8/9 T-Seal Damage Coupled External/Internal Flow Simulation (15 million-cell Model; Postprocessed using every other points)

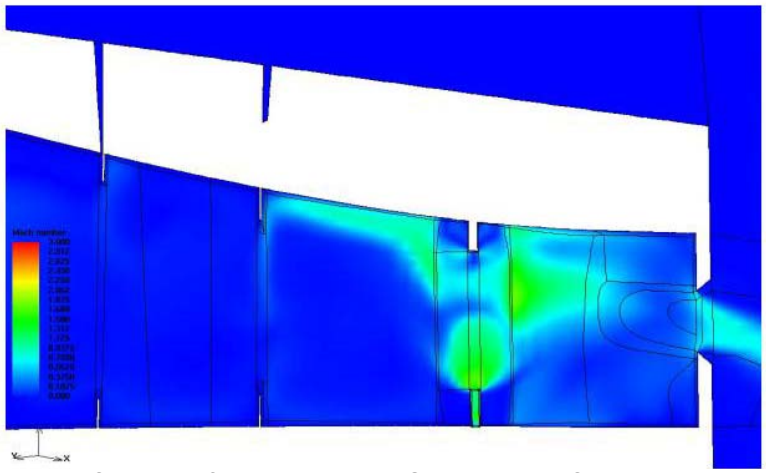

Figure 5.3.6-139 Mach Contours from Panel 8/9 T-Seal Damage Coupled External/Internal Flow Simulation (15 million-cell Model; Postprocessed using every other points)

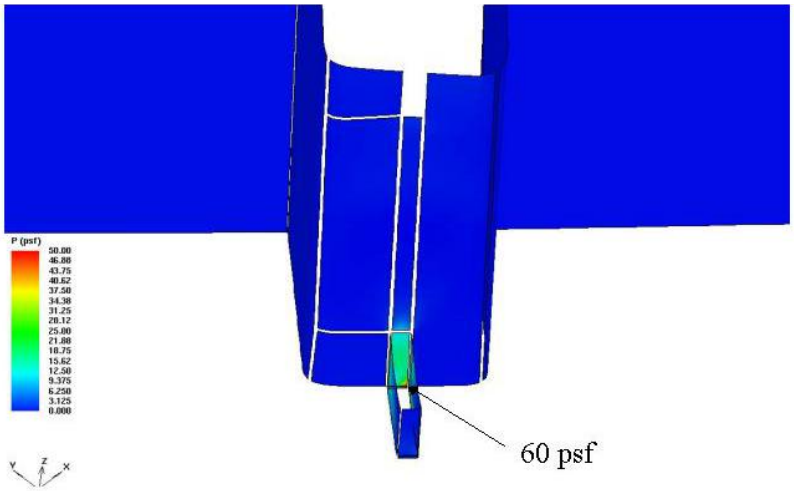

Figure 5.3.6-140 Pressure Contours on Earmuff Insulation and Rib Channel from Panel 8/9 T-Seal Damage Coupled External/Internal Flow Simulation (2 million-cell Model)

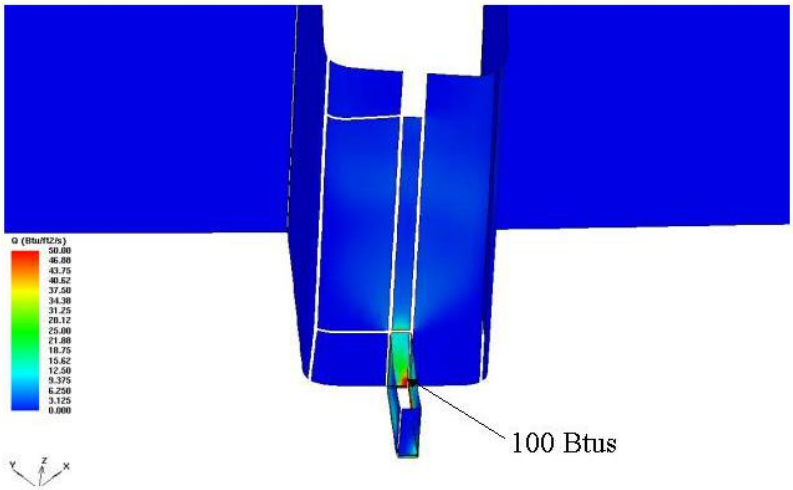

Figure 5.3.6-141 Heating Contours on Earmuff Insulation and Rib Channel from Panel 8/9 T-Seal Damage Coupled External/Internal Flow Simulation (2 million-cell Model)

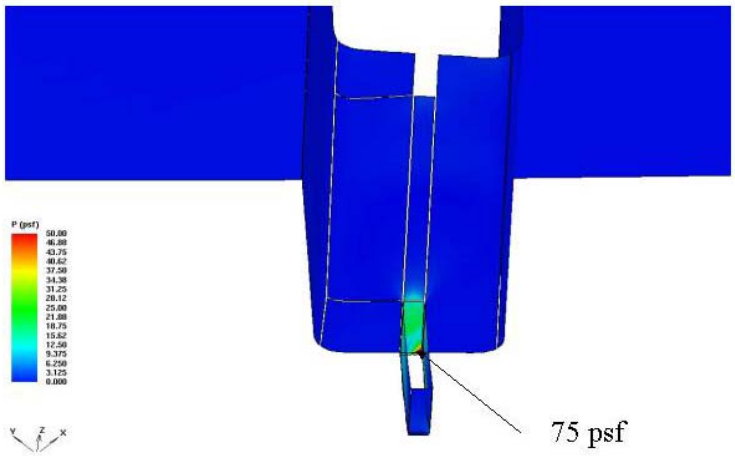

Figure 5.3.6-142 Pressure Contours on Earmuff Insulation and Rib Channel from Panel 8/9 T-Seal Damage Coupled External/Internal Flow Simulation (15 million-cell Model)

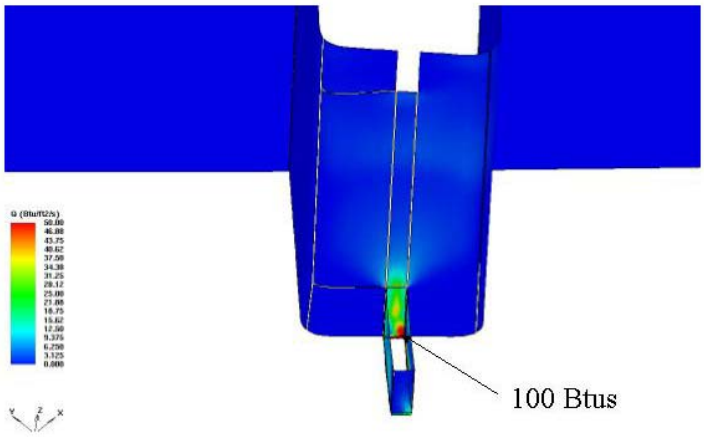

Figure 5.3.6-143 Heating Contours on Earmuff Insulation and Rib Channel from Panel 8/9 T-Seal Damage Coupled External/Internal Flow Simulation (15 million-cell Model)

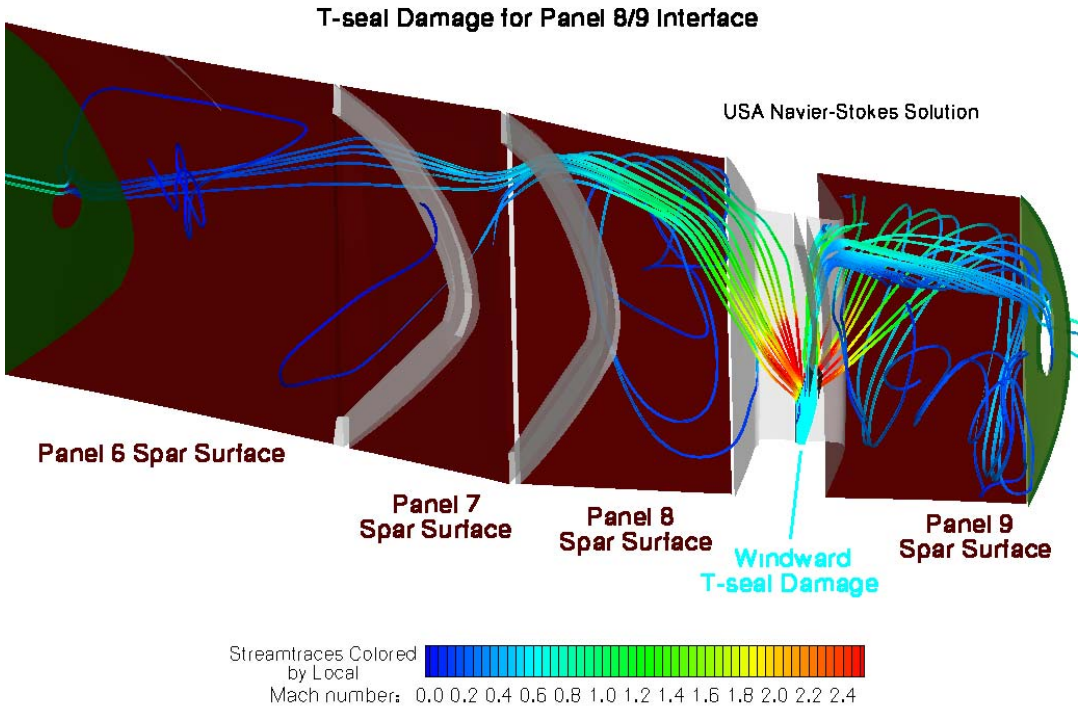

Figure 5.3.6-144 BHB Panel8/9 T-seal Damage Internal Streamtraces

5.3.6.2.4 BRPP 3-D Panel 8/9 Damaged T-Seal Solution

5.3.6.2.4.1 Case Description

The first objective of this effort was to compute convective heating rates on key surfaces of the Leading Edge Structural Subsystem (LESS) for the scenario of a damaged T-Seal in the RCC 8/9 location. These included:

- RCC T-Seal
  - Cavity
  - Rib channel
- Internal insulation units:
  - Forward spar insulator units (hot tubs)
  - Spanner Beam Insulator units (earmuffs)

The T-Seal damage was assumed to be a piece missing from the intersection of the T-Seal and the lower edge of the earmuff to the geometric leading edge as shown in Figure 5.3.6-145.

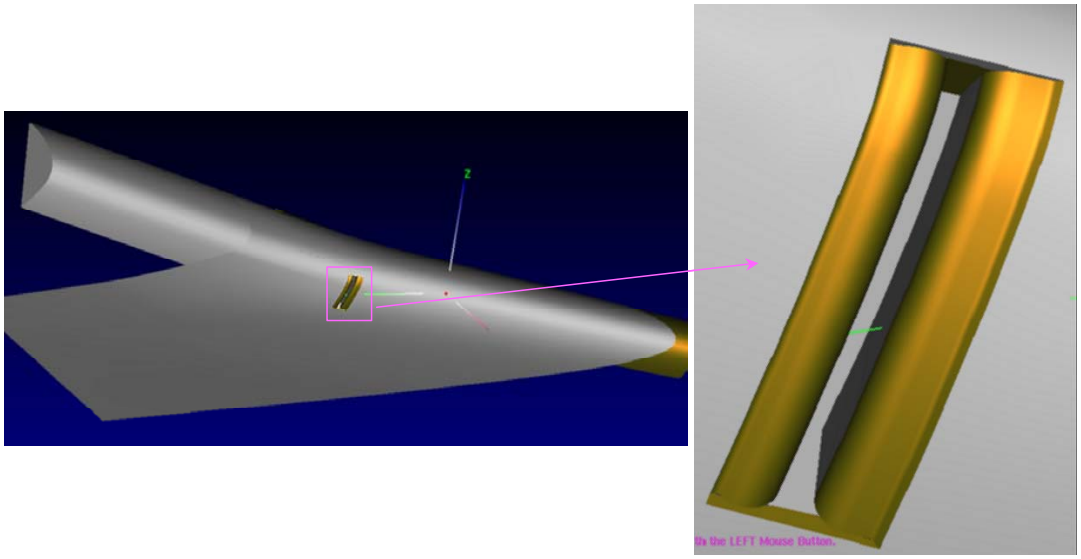

Figure 5.3.6-145 – Damaged T-Seal Geometry

The intended application of the data was to enhance the engineering heat transfer models and to improve understanding of this flow field structure. The second objective of this effort was to construct an accurate CAD model of the LESS components that would serve as a universal model usable for all types of multidimensional analysis via IGES export. This would possess clean, "watertight", trimmed surfaces for import to modeling software.

5.3.6.2.4.2 Grid/Solution Development

The universal CAD model was constructed with the Pro/Engineer parametric CAD system. Sources for geometry included imported CAD models for the RCC panels, forward wing spar, and RCC attachment brackets. Design specifications combined with photographs were used for the earmuffs, hot tubs, and wick insulators. No detailed drawings for the latter three components have been located to date. The model has been completed however issues precluded its use for CFD grid generation. The imported RCC parts were too complex for analysis use. They contained over 1,000 surfaces per RCC panel as well as duplicate surfaces. In addition, the model architecture requires a large amount of prep work prior to export for analysis grid generation due to the grouping of surfaces with solids. It was anticipated that an additional 1-2 weeks would be required to complete this task. A fallback plan was implemented in which development of the universal CAD model would continue, while the NASA JSC-based model for internal region used in for the 10" Leading Edge Breach would be modified for use in this analysis. The T-Seal channel geometry was extracted from the Pro/E CAD model and integrated into the JSC model (Figure 5.3.6-145). As discussed in Section 5.3.6.1.4, the JSC model included the RCC 7/8, 8/9, 9/10 earmuffs and the hot tubs in between them. The negative aspect of this model was that all of the edges were sharp, which conflicted with other models and photographs. Dimensions of key components, such as the earmuffs and hot tubs, were also somewhat uncertain since the JSC dimensions conflicted with a model used by Boeing Huntington Beach and some photographs.

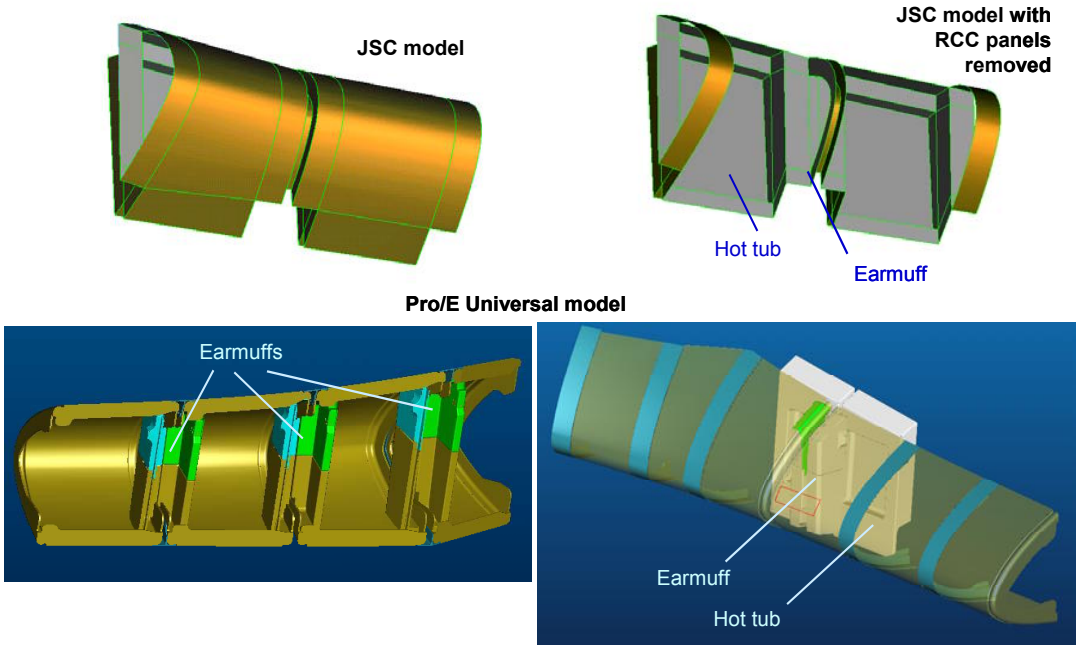

Figure 5.3.6-146 – Internal Region Geometry Models

The JSC and the Pro/E Universal model are compared in Figure 5.3.6-146. Extruded "dump" regions were added on either side of RCC 8 and 9 to enable the application of constant pressure outflow boundary conditions. The dimensions of these regions were based on the results of the 2-D T-Seal analysis of Sec.5.3.6.2.2.

Previous analyses had shown that a high degree of coupling existed between the internal and external flow fields. A NASA LaRC LAURA external flow solution was used to provide the necessary coupling, but only a small three-zone portion of it. This was carefully selected to reduce the size of the model while preserving the external solution in the region of interest (Figure 5.3.6-147). Not all of Zone 36 was required so it was sectioned with a cutting-plane interpolation.

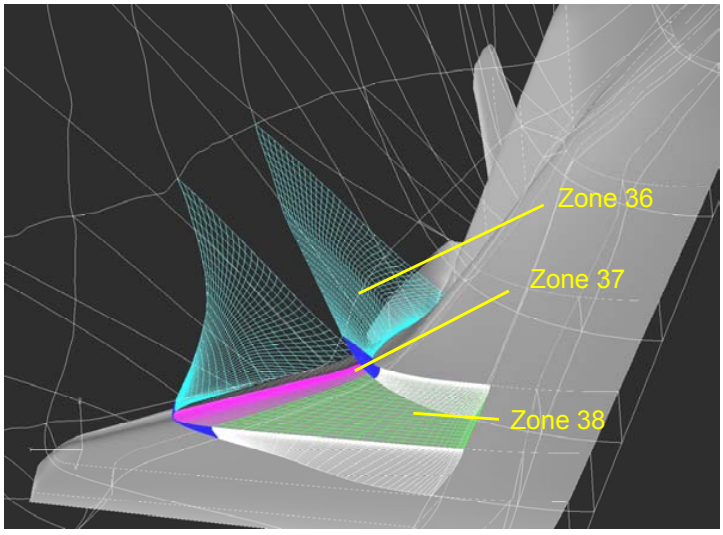

Figure 5.3.6-147 - LAURA Solution Zones Used as External Domain

The Boeing APPT system was used to generate the hybrid viscous unstructured computational grid. The unstructured approach greatly reduces the time required to generate the grid and eliminates wasted clustering cells in complex internal regions. After a number of revisions, final grids (Figure 5.3.6-148) were produced containing 4.1M elements with a wall spacing of $1.0e^{-4}$ inches, and 5.7M elements with a wall spacing of $1.0e^{-5}$ inches. Results from the 2-D T-Seal analysis (Sec. 5.3.6.2.2) along with a cardboard model and discussion among compressible flow experts were used to determine the clustering of elements in the internal region.

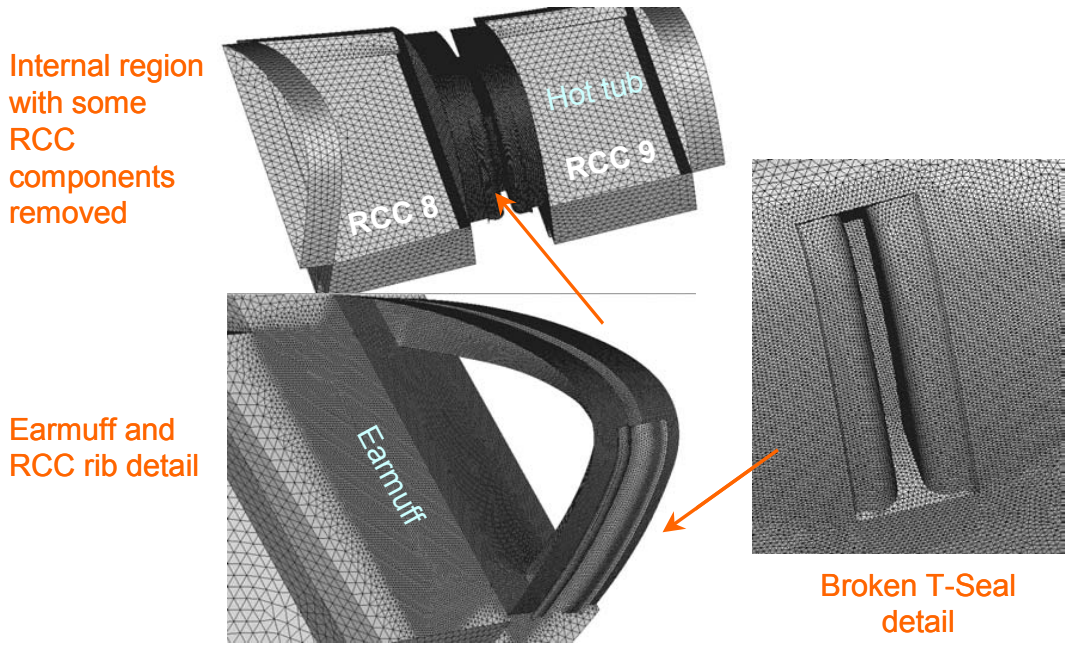

Figure 5.3.6-148 – Hybrid Viscous Unstructured Grid

The solutions were obtained using the Boeing ICAT code. Fully laminar flow was assumed based on the extremely low Reynolds numbers present. Liu-Vinokur equilibrium air thermochemistry and Tannehill transport properties were used. The convergence criteria were to drive net fluxes to an initial steady-state and also to drive integrated heat load in key areas to steady-state. Contours of heat flux in key areas were also plotted at different time steps.

The CFD Condition 1 trajectory point was used to define the freestream conditions. All wall temperatures were set to 3,000º R. This corresponds to the melting temperature for the Inconel 601 outer layer of the Dynaflex surfaces such as the earmuffs and hot tubs. The pressure on the cavity outflow surfaces was set according to Table 5.3.6.1-1. These values were established from venting analysis. Note that the values have evolved over time as has the venting analysis. The current level of 10.8 psf (517 Pa) is the result of the 2-D T-Seal computations being fed back into the venting analysis.

5.3.6.2.4.3 Results

5.3.6.2.4.4 Major flow structure comments

Figure 5.3.6-149 shows the flow inside the LESS cavity. The walls are colored by static pressure, and the streamlines are colored by Mach number and are launched from the center of rib channel. Subsonic flow is observed exiting the rib channel into the LESS cavity. This is due to the high cavity backpressure of .075 psia vs. ~.060 psia at the rib channel exit. The latter number comes from examination of the T-Seal 2-D solutions (Sec. 5.3.6.2.2) and represents the rib channel exit pressure without the influence of backpressure. Overexpanded laminar flow, such as this, easily separates, and normal shock structures reduce the flow to subsonic and also reduce total pressure. Both of these effects reduce the capability of the flow to generate heat flux on impingement surfaces. The majority of the LESS cavity flow is large-scale subsonic vortices.

Figure 5.3.6-150 shows the flow in the RCC rib channel. Again, the walls are colored by static pressure, and the streamlines are colored by Mach number, however this time they are launched from a boundary layer rake in the external flow. This flow field has features similar to the 2-D T-Seal solutions (Sec. 5.3.6.2.2). These include the aerodynamic throat, the upstream edge separation, and the downstream edge bow shock. Surface pressures are also close to the 2-D solutions.

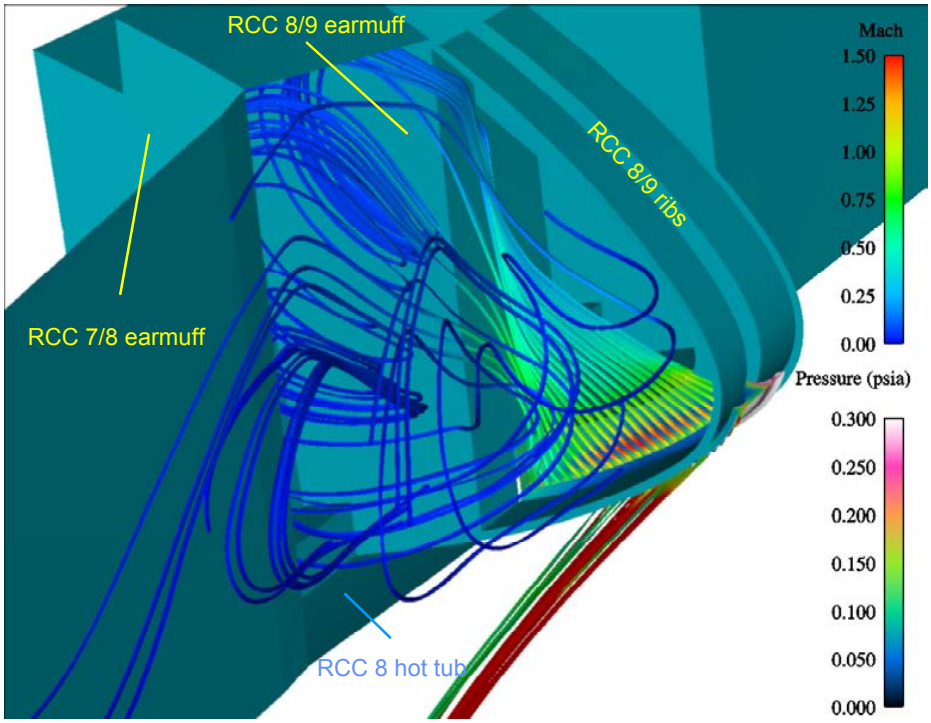

Figure 5.3.6-149 - Mach-colored Cutting Plane and Wall Static Pressure Detail View From in Front of Leading Edge

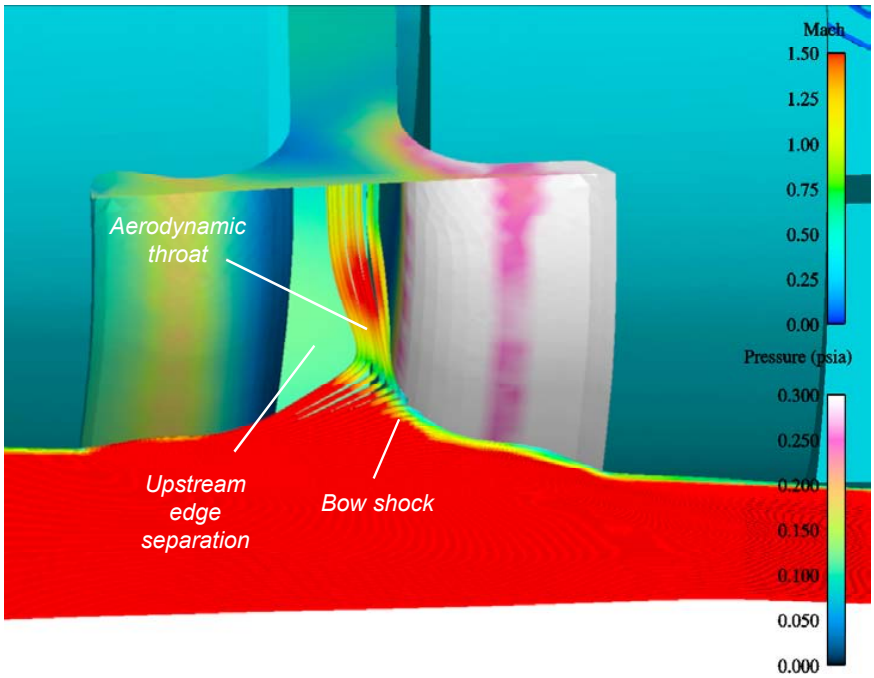

Figure 5.3.6-150 – View Into RCC Rib Channel

5.3.6.2.4.5 Surface heating and pressure comments

Figure 5.3.6-151 shows surface heat flux in the region where the RCC 8/9 earmuff and the RCC 8 hot tub intersect. This is the area of highest heating on the earmuff and hot tub surfaces, as would be expected based on the pressure and Mach fields observed. The levels are low compared to the peaks observed for the 2-D T-seal solution (Sec. 5.3.6.2.2) where supersonic flow is impinging on the earmuff. Heat fluxes in the rib channel closely match the USA 2-D T-Seal solutions (Sec. 5.3.6.2.2). The medium grid solution was run a total of 28,000 time steps. The solution was monitored periodically using flow visualization. No indication of unsteady flow was found, however there is still a possibility that this could occur. Many more time steps would be needed to be certain.

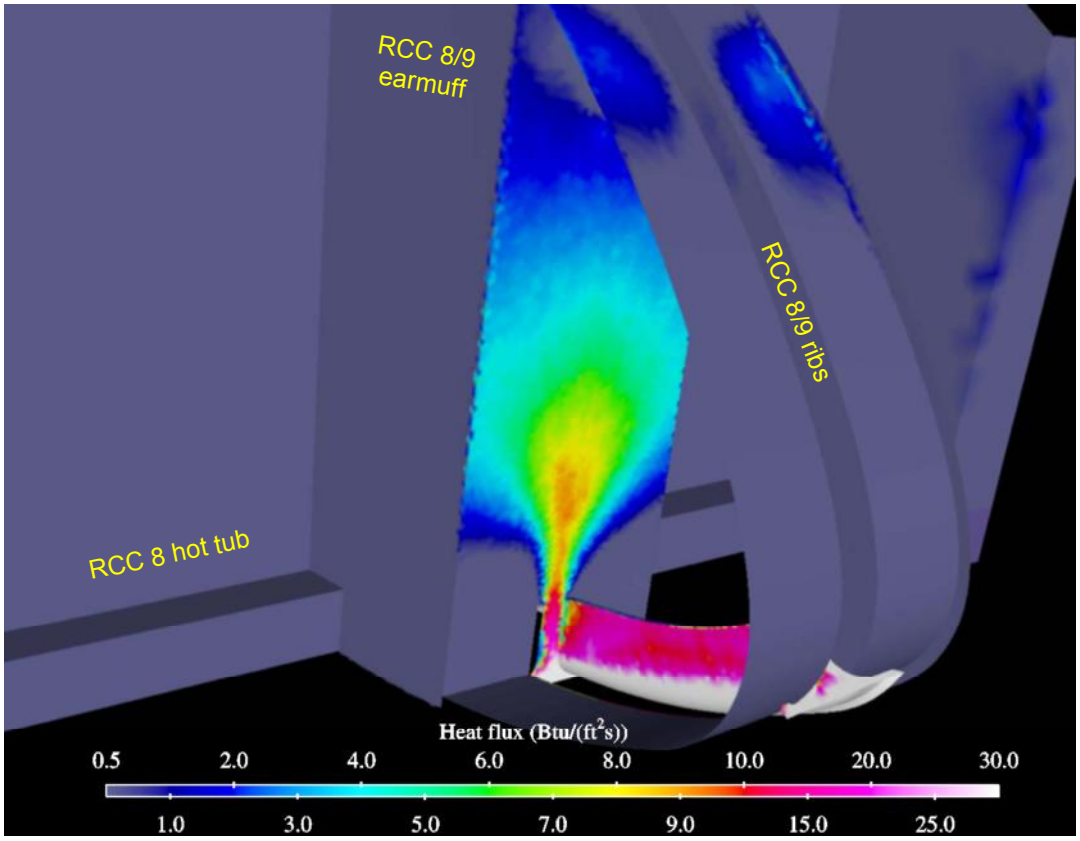

Figure 5.3.6-151 - Surface Heat Flux Detail View From in Front of Leading Edge

5.3.6.3 CFD of Simplified Internal Wing Geometry

5.3.6.3.1 Methodology and Philosophy of "Insight CFD"
CFD was used not only to help characterize fine details in the flow field with large, detailed CFD models, but also to help understand some of the larger scale flow phenomenon. For this purpose a few large scale, simplified models were created to understand the flow patterns once a breach of the internal wing cavity was initiated. These models were primarily used to visualize flow patterns within the wing cavity. They were not relied upon for detailed information such as wall heat fluxes, heat transfer coefficients, surface temperatures, or transient calculations.

Two simplified models were created. The first was a simplified model of the entire left wing aft of the 1040 wing spar and without the wheel well cavity. Wing spar designations are shown in Figure 5.3.6-153 for reference. This model did not include the RCC cavity along the wing leading edge. The purpose of this model was to visualize the flow field within the wing cavity immediately after the leading edge spar breach. This model assumed that the flow coming onto the wing cavity was normal to the spar. The second "insight" CFD model was a 2-D model of the left wing cavity and the RCC cavity. This model was used to visualize the flow through the RCC breach, through the wing spar breach, then into the wing cavity directly outboard of the wheel well. The purpose of this model was to verify whether or not it was possible for the flow to come into the wing cavity normal to the leading edge spar or not.

Models are "simplified" in the sense that only the necessary surfaces needed to characterize the flow field satisfactorily are included. The 3-D wing model has none of the internal circular struts connecting the upper and lower wing surfaces. Only the internal spars and spar vents and the wing upper and lower surfaces are included. The wing upper and lower surfaces were generated based solely on the spar outlines; therefore some of the finer details in the wing curvature were not captured in the models. All walls within the models are smooth walls, which in reality is not the case, particularly in the area of the wheel well walls.

FLUENT 6.1 was the CFD code used to model these simplified geometries. FLUENT 6.1 is a commercial Navier-Stokes solver for unstructured meshes. It is a cell-centered, finite-volume code. FLUENT's three solvers can be used to compute the flow and heat transfer for all flow regimes, from low subsonic via transonic and supersonic to hypersonic. The unstructured grid capability in FLUENT allows for modeling of complex geometries similar to the geometry found in the wing and wheel well areas of Columbia. A more detailed description of FLUENT can be found in the Appendix and in [1].

5.3.6.3.2 3-D Solution Cases

5.3.6.3.2.1 <u>3-D Wing Model, 6 inch and 10 inch Spar Breach</u>
The purpose of the analysis was to determine the flow path of the plume entering the wing through the wing leading edge spar. A steady state analysis was done using boundary conditions corresponding to the time immediately following the wing spar breach, approximately 490 seconds after entry interface.

A simplified model of the left wing of Columbia was created, Figure 5.3.6-152, and shows the outer wall boundaries of the model including the wing upper and lower surfaces and the leading edge spar. A circular breach hole was located in the wing spar leading edge at the intersection of RCC panels 8 and 9. Two different spar breach hole diameters were modeled - circular breach sizes of 6 inches and 10 inches diameter were chosen based upon other analyses performed as part of the investigation. An assumption was made that the flow coming into the wing area would be normal to the spar.

Figure 5.3.6-153 shows the internal spars and vents not visible in Figure 5.3.6-152. Three flow exit areas are included in the wing model and are shown in Figure 5.3.6-153. A rectangular vent area of 180 in^2 is located in the 1040 wing spar. The internal wing volume forward of the 1040 spar was not included in the model, instead pressures obtained from the MSFC analyses outlined in Section 5.3.5.7 were used to set the conditions at that interface. The other two flow exits are located at the rear of the model at the 1365 spar location. These vents are located at the approximate locations where the inboard and outboard elevons penetrate the 1365 spar. Vent areas were 2.55 in^2 and 5.5 in^2 for the inboard and outboard

elevons, respectively. Four internal vents allow for flow between the various internal wing compartments and are shown along with their areas in Figure 5.3.6-153.

The wing geometry was simplified in order to reduce the computational expense of the model. None of the tubular struts supporting the upper and lower wing surfaces were included in the model. As mentioned previously, the wing volume forward of the 1040 spar was not included. The wheel well volume was not included due to the complex geometry in the wheel well and because the primary focus of the analysis was flow paths within the wing, not the wheel well area. Another area of simplification was the wing surfaces. These were not imported directly from CAD geometry, but were created within the FLUENT geometry generation program. This means that there may be subtle differences between the FLUENT wing surfaces and the actual wing surface geometry, however due to the overall size of the model it is not anticipated that this difference would have a significant effect on the results. The size of the 3D wing model computational domain was approximately 340,000 cells.

Boundary conditions for the 3-D model are shown in Figure 5.3.6-154 for the 6-inch breach case and in Figure 5.3.6-155 for the 10-inch breach case. Pressure boundary conditions were applied at the breach hole and three flow exit boundaries. These pressure values were obtained from the MSFC venting model discussed in Section 5.3.5.7. The pressures correspond to the boundary pressures at 500 seconds after entry interface. This time is 10 seconds after the estimated spar breach time of 490 seconds.

The standard k-e turbulence model available in FLUENT was activated for all of the 3-D and 2-D analyses. The working fluid was air modeled as an ideal gas. No attempt was made to model the chemical reactions occurring within the gas at these elevated temperatures using FLUENT. A correlation for determining the specific heat of air as a function of temperature from 495 ^{o}R to 10400 ^{o}R was used in the all of the 2-D and 3-D FLUENT models due to the large variation of specific heat over this temperature range. This correlation was input into FLUENT as a piecewise-polynomial function, and a plot of this correlation versus the data used to generate it can be found in Figure 5.3.6-156. The models were run until convergence was met on the net mass flow in and out of the domain, and pressures reached a steady state value.

5.3.6.3.2.2 Results – 3D Model, 6 inch Breach hole

Results of the 3-D internal wing flow case with a 6-inch diameter spar leading edge breach are shown in Figure 5.3.6-157 through Figure 5.3.6-161. Figure 5.3.6-157 is a contour plot of velocity magnitude on a plane cut horizontally through the entire wing. The plot shows that the flow does not penetrate significantly beyond the 1191 spar, and that it tends to circulate within the cavity outboard of the wheel well and exit through the 1040 spar vent. Some flow does penetrate all the way to the rear elevon vents, and Figure 5.3.6-158 shows this with a velocity contour plot with a different scale.

Mass flow rates and Mach numbers for the flow inlet and three flow exits are shown in Table 5.3.6.3-1. The mass flow rates indicate that 78% of the incoming gas exits the wing cavity through the 1040 spar vent.

Table 5.3.6.3-1 6-inch Breach Hole Mass Flow Rates and Mach Numbers

Vent	Mass Flow Lb/min	Flow direction	Mach Number
6” Dia breach Hole	0.686	In	1.06
1040 Spar Vent	0.535	Out	0.105
Inboard elevon	0.0667	Out	0.83
Outboard elevon	0.0835	Out	0.39

Figure 5.3.6-159 shows pathlines (colored by velocity magnitude) to indicate the flow paths of hot gas entering the wing cavity. The pathlines begin at the breach hole location. The flow impinges directly on the outboard wheel well wall then turns 180 degrees and the majority of the flow exits through the 1040 vent hole. A small percentage of the flow does penetrate all the way to the rear of the wing but at a much slower velocity than seen in the cavity outboard of the wheel well.

Figure 5.3.6-160 shows a contour of static pressure within the wing. The figure indicates that the pressure at the 1040 spar vent drives the resulting static pressure. This is due to the large size of that vent in relation to the two smaller rear vents. Figure 5.3.6-161 shows a contour plot of static temperature within the wing.

5.3.6.3.2.3 3D Model, 10 inch Breach hole

Results of the 3-D internal wing flow case with a 10-inch diameter spar leading edge breach are shown in Figure 5.3.6-162 through Figure 5.3.6-166. Figure 5.3.6-162 and Figure 5.3.6-163 are contour plots of velocity magnitude on a plane cut horizontally through the entire wing using two different scales to help visualize both the higher speed flow outboard of the wheel well and the low speed flow rear of the 1191 spar. The plots shows that even with the higher energy flow coming in the breach, the flow still does not penetrate significantly beyond the 1191 spar. Table 5.3.6.3-2 lists the mass flow rates and Mach numbers that again indicate that the majority of the flow (87%) entering the wing exits forward through the 1040 spar vent.

Table 5.3.6.3-2 10-inch Breach Hole Mass Flow Rates & Mach Numbers

Vent	Mass Flow Lb/min	Flow direction	Mach Number
6” Dia breach Hole	7.13	In	1.06
1040 Spar Vent	6.19	Out	0.75
Inboard elevon	0.29	Out	0.95
Outboard elevon	0.65	Out	0.95

Figure 5.3.6-164 shows pathlines (colored by velocity magnitude) to indicate the flow paths of hot gas entering the wing cavity. The flow impinges directly on the outboard wheel well and exits primarily through the 1040 vent hole, similar to the 6-inch breach case. As in the 6-inch breach case some flow penetrates the cavity aft of the 1191spar. Figure 5.3.6-165 shows a contour of static pressure within the wing. Figure 5.3.6-166 shows a contour plot of static temperature within the wing. Comparing the temperature contour plots between the 6-inch breach (Figure 5.3.6-161) and the 10-inch breach case (Figure 5.3.6-166), the area behind the 1191 spar is much warmer in the 10-inch case. The larger breach hole size is able to push more flow beyond the 1191 spar vent into this region.

5.3.6.3.3 2-D Simplified Wing Model Solutions

The purpose of the analysis was to trace the flow path of the plume as it enters the RCC cavity and impinges on the RCC attach hardware, then passes through a breach hole in the wing spar. It was assumed that the plume would be deflected by the RCC attach hardware and burn a hole through the spar, entering the wing cavity in the direction approximately normal to the spar. The analysis is an attempt to support the 3-D model assumption that flow is entering the wing cavity normal to the spar. A steady state analysis was done using boundary conditions corresponding to the time immediately following the wing spar leading edge breach, approximately 490 seconds after entry interface.

A simplified 2-D model of the left wing of Columbia was created and is shown in Figure 5.3.6-167. The view is looking up from below the left wing. The model consists of the wing cavity bounded by the wheel well outer wall, the 1040 spar, the 1191 spar, and the leading edge spar. This wing geometry was derived from the 3-D model. A section representing the RCC cavity was added along the length of the wing leading edge spar. The 2-D RCC cavity geometry was approximated with a 29-inch deep channel. A 10-inch diameter hole was located on the leading edge of the RCC cavity in the approximate location of panel 8. The green lines shown in Figure 5.3.6-167 represent interior zones in the domain and are not hard walls.

Four flow exit areas are included in the wing model. A pressure outlet is located in the 1040 wing spar, and another pressure outlet represents the vent in the 1191 spar that allows flow to pass to the rear cavities of the wing. The RCC cavity has two pressure outlets located at either end of the RCC cavity. These openings were sized based upon leakage areas obtained from the MSFC venting model discussed in Section 5.3.5.7

Figure 5.3.6-167 also shows the simplified RCC attach hardware used in the model. The attach hardware (representing the spanner beam insulation) in the model represents the hardware associated with RCC panel #8, and the breach hole in the spar is located directly adjacent to this attach hardware.

Boundary conditions for the 6 inch and 10 inch breach hole 2-D models are shown in Table 5.3.6.3-3. Static pressure boundary conditions were applied at the four flow exit boundaries. These pressure values were obtained from the MSFC venting model discussed in section 5.3.5.7. The pressures correspond to the boundary pressures at 500 seconds after entry interface.

Table 5.3.6.3-3 2-D Model Boundary Conditions

RCC Leading Edge Breach	Breach Pressure Lb/ft^2	Breach Temperature ^oR	1040 Spar Vent Lb/ft^2	1191 Spar Vent Lb/ft^2	RCC Fwd Vent Lb/ft^2	RCC Rear Vent Lb/ft^2
6 inches	37	6000	0.92	1.04	13.2	13.2
10 inches	37	6000	8.6	9.65	13.2	13.2

The flow entering the RCC cavity was redirected to impinge directly at the corner of the RCC attach hardware. This assumption was supported by other coupled external/internal CFD analyses which show the RCC inlet plume impinging directly on the corner of the attach hardware. All walls of the domain were set at a constant temperature of 50 ^oF, and the same turbulence models and specific heat correlations were used as in the 3-D models.

5.3.6.3.3.1 2-D Results - 6 inch Spar Breach

Results of the 2-D internal wing flow case are shown in Figure 5.3.6-168 and Figure 5.3.6-169. The velocity contour plot of Figure 5.3.6-168 shows the flow does penetrate the spar approximately normal to the spar. This figure as well as the pathlines of Figure 5.3.6-169.shows how the spanner beam insulation hardware turns the flow. Both plots support the assumption made in the 3-D model that initially the flow coming into the wing cavity was normal to the spar. There are some differences in the flow patterns compared with the 3-D model results, and this is likely due to the restrictions on the flow imposed by the 2-D geometry. In the 3-D case the flow can circulate around the wing cavity by splitting and traveling over and under the incoming jet, while in the 2-D model the flow is blocked from doing this by the incoming jet. The flow direction into the wing cavity at a later time would depend upon the length of time that the RCC attach hardware remained in place.

5.3.6.3.3.2 2-D Results - 10 inch Spar Breach

Results of the 2-D internal wing flow case are shown in Figure 5.3.6-170 and Figure 5.3.6-171. As in the 6-inch wing spar breach case, the velocity contour plot of Figure 5.3.6-170 shows the spanner beam insulation hardware turns the flow so it enters the wing approximately normal to the spar. This is also indicated in the pathline plot of Figure 5.3.6-171. Both plots support the assumption made in the 3-D model that initially the flow coming into the wing cavity was normal to the spar.

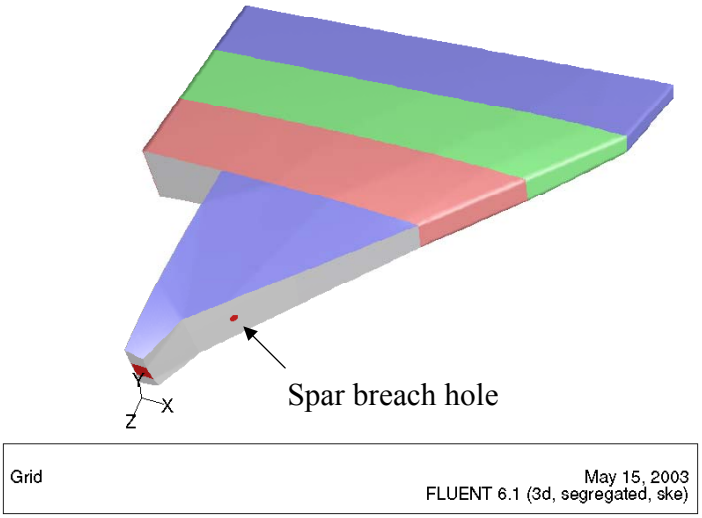

Figure 5.3.6-152 3-D Simplified Wing Geometry

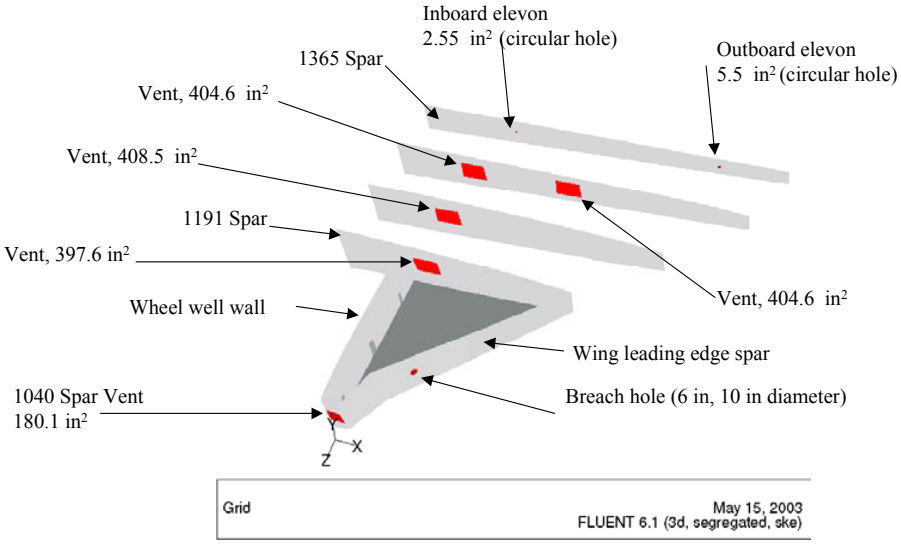

Figure 5.3.6-153 3-D Model Vent sizes

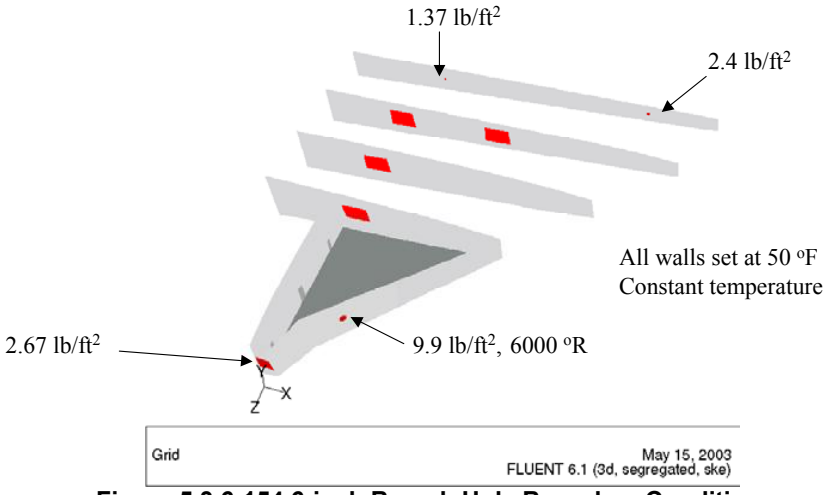

Figure 5.3.6-154 6-inch Breach Hole Boundary Conditions

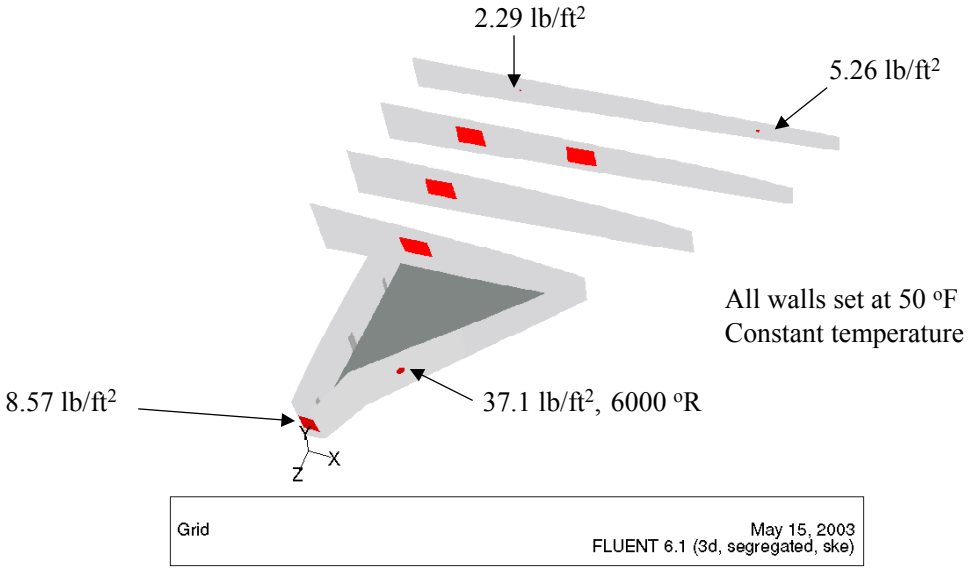

Figure 5.3.6-155 10-inch Breach Hole Boundary Conditions

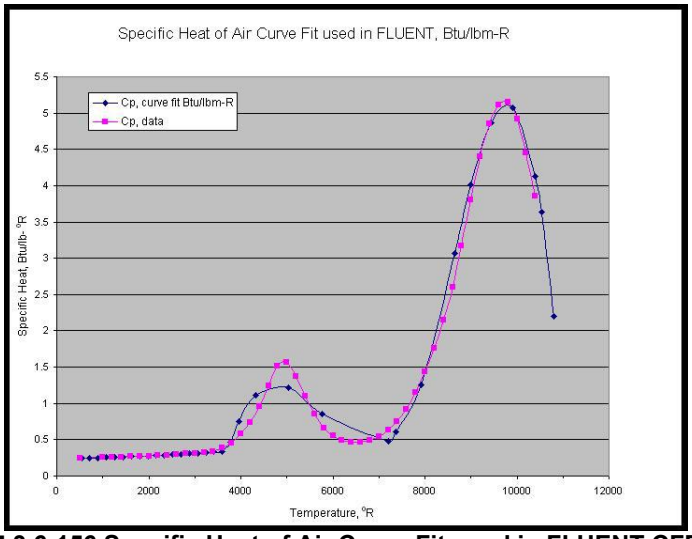

Figure 5.3.6-156 Specific Heat of Air Curve Fit used in FLUENT CFD Cases

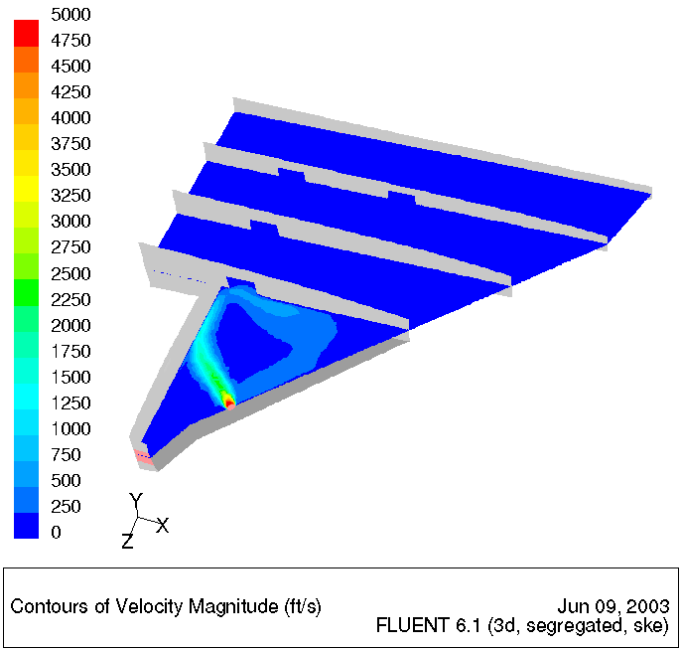

Figure 5.3.6-157 6-inch Breach hole, Velocity Contour Plot

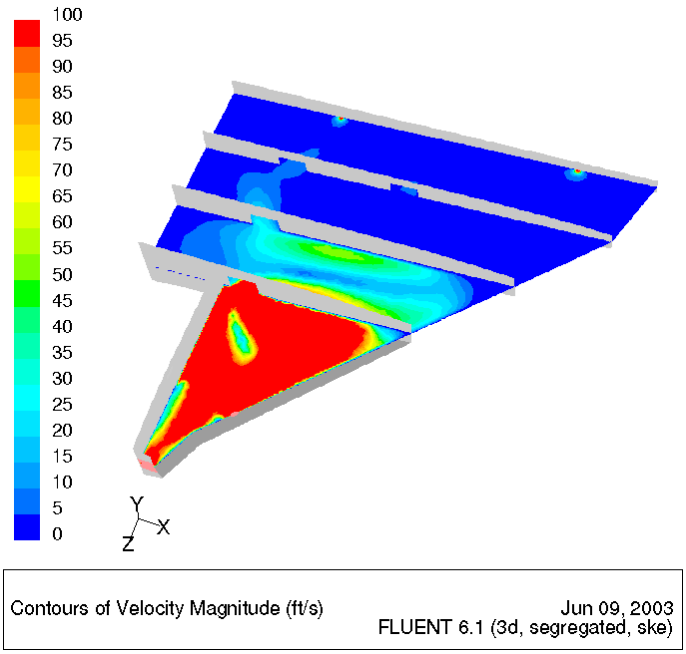

Figure 5.3.6-158 6-inch Breach Hole, Velocity Contour Plot

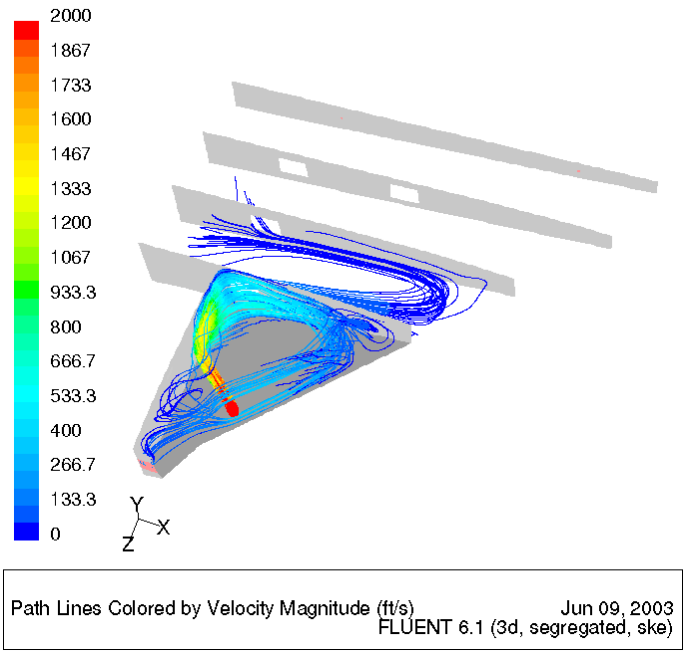

Figure 5.3.6-159 6-inch Breach Hole, Pathlines

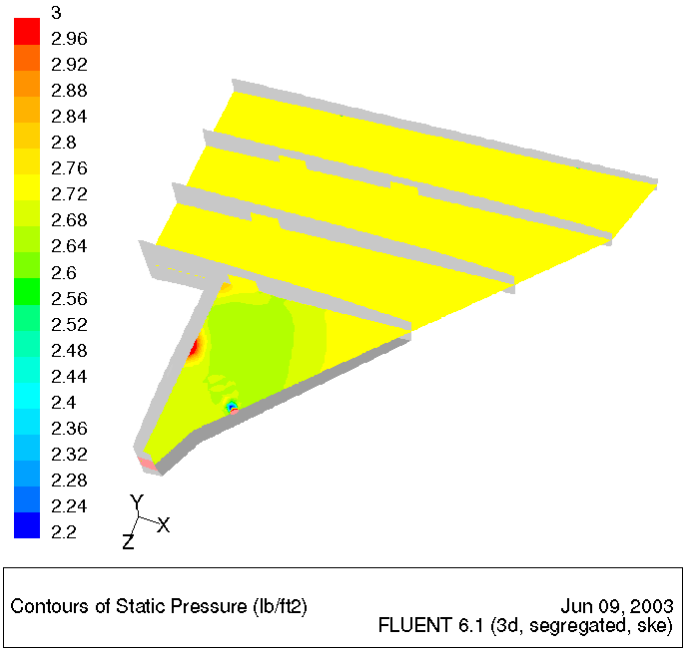

Figure 5.3.6-160 6-inch Breach Hole, Static Pressure

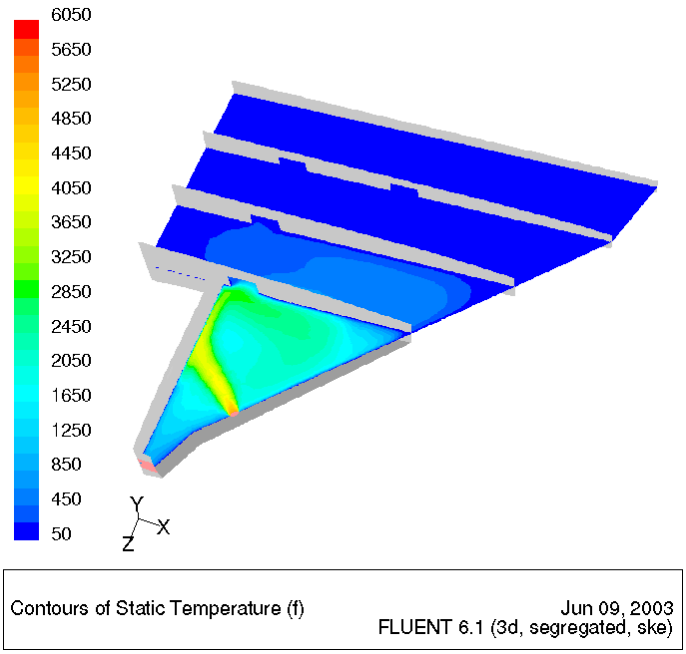

Figure 5.3.6-161 6-inch Breach Hole, Static Temperature

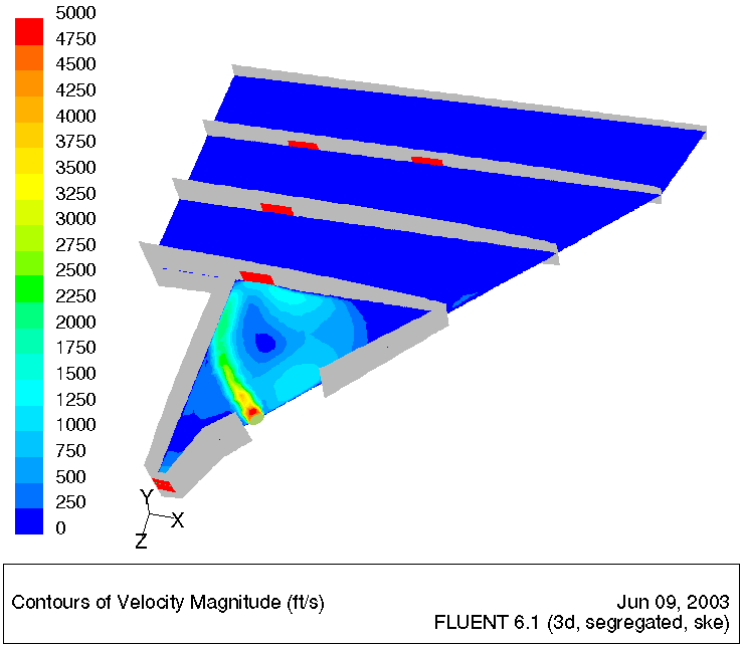

Figure 5.3.6-162 10-inch Breach Hole Velocity Contours

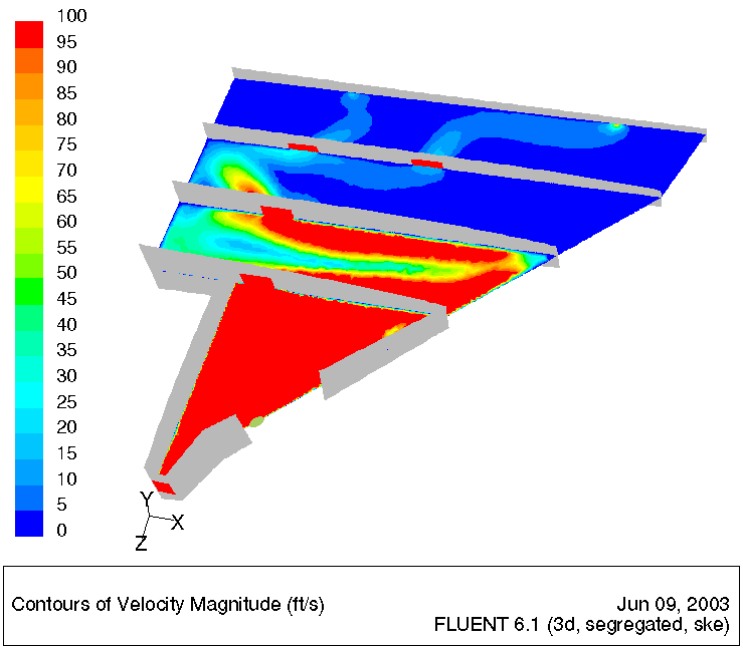

Figure 5.3.6-163 10-inch Breach Hole Velocity

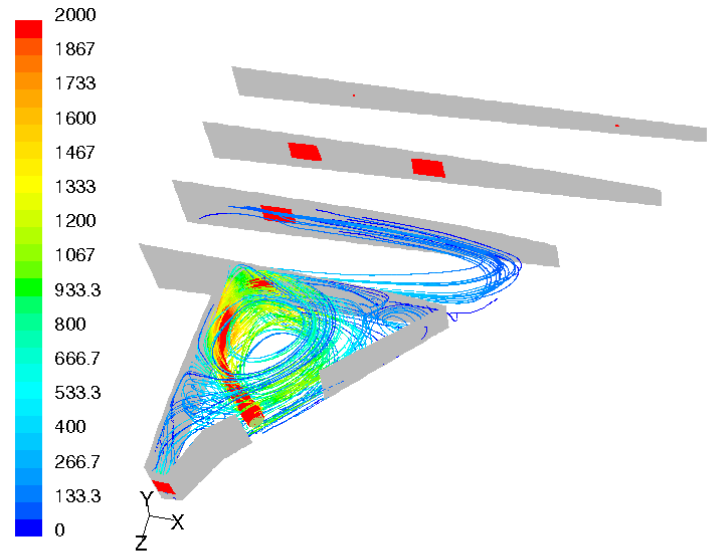

Figure 5.3.6-164 10-inch Breach Hole, Pathlines

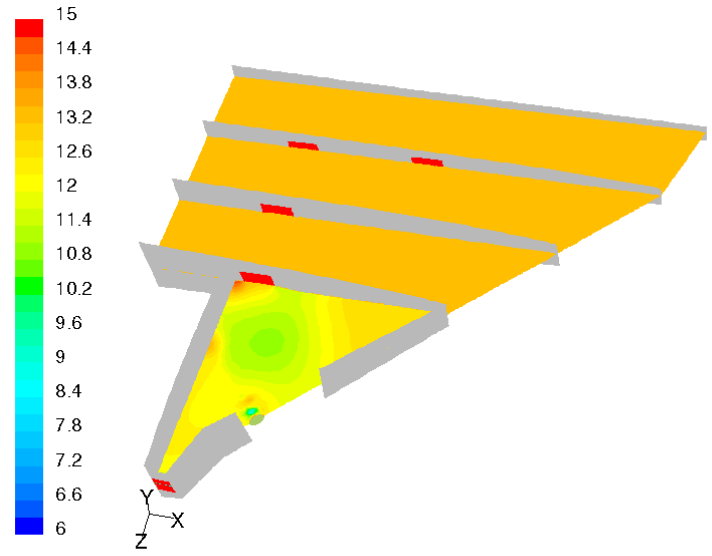

Figure 5.3.6-165 10-inch Breach Hole, Static pressure Contours

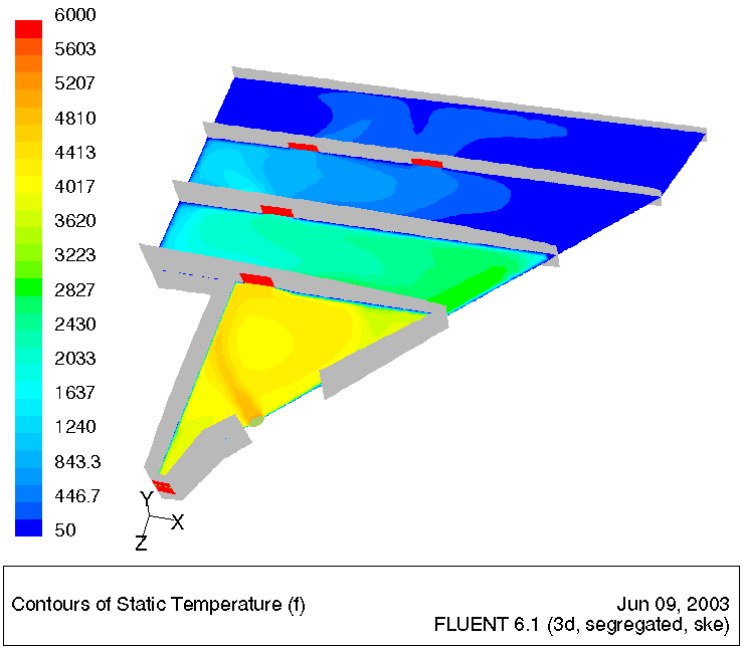

Figure 5.3.6-166 10-inch Breach Hole, Static Temperature Contours

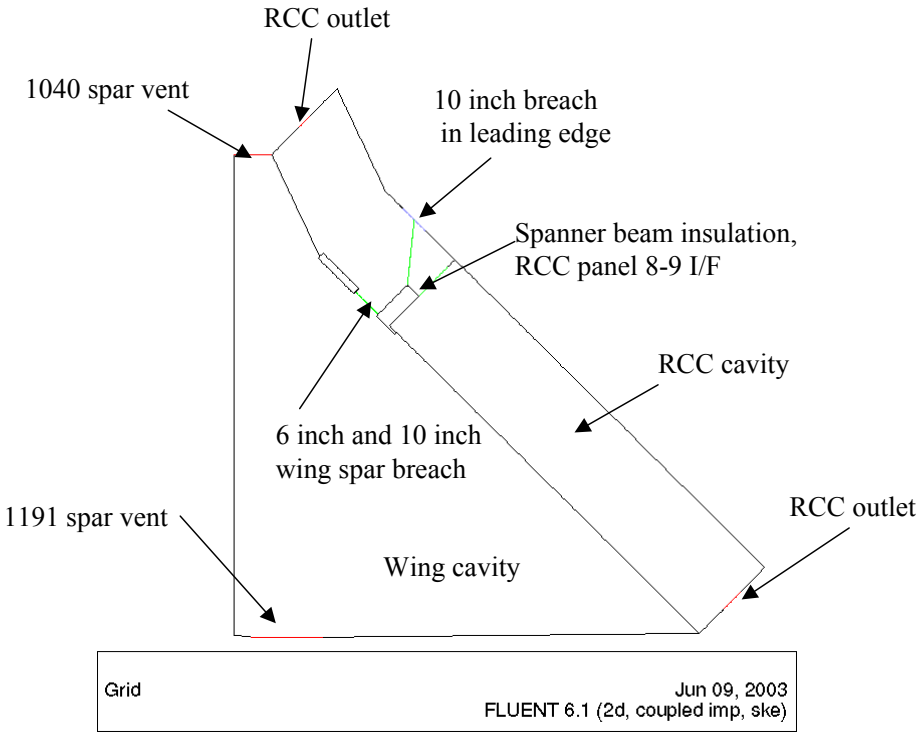

Figure 5.3.6-167 2-D Model Geometry – 10 inch Breach in RCC Leading Edge, 6 and 10-in Spar Breach

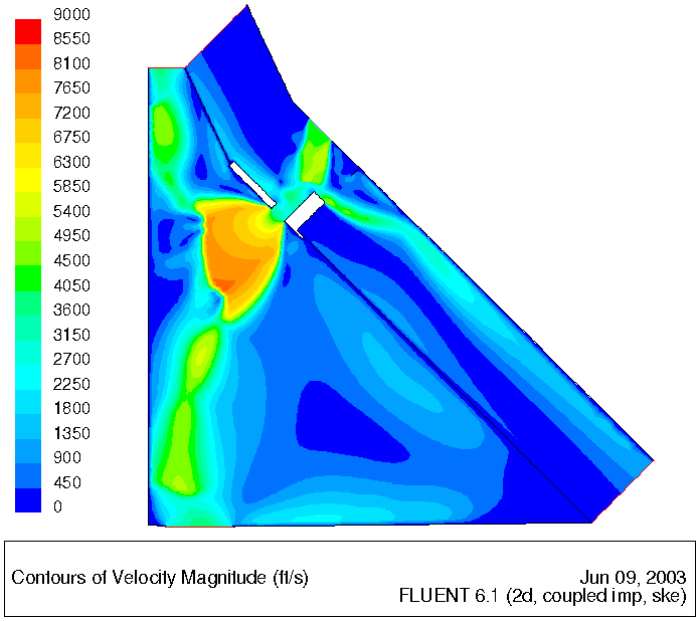

Figure 5.3.6-168 2-D Model, 6-inch Breach in Wing Spar, Velocity Contours

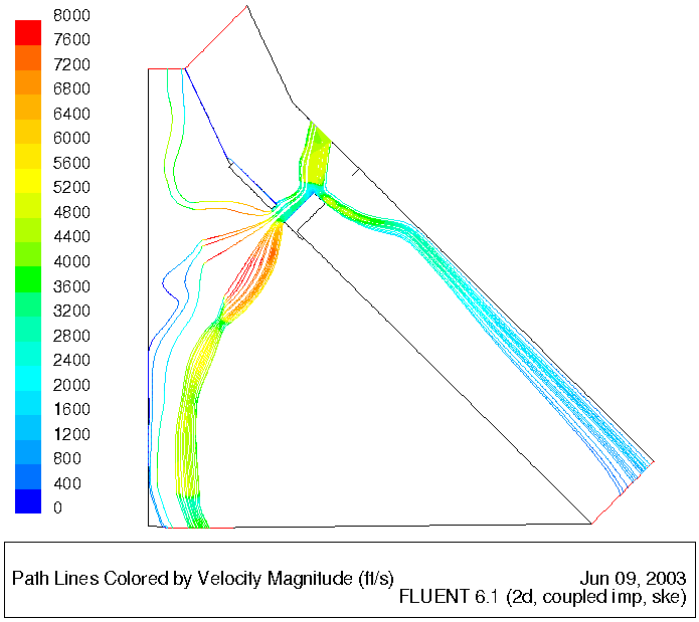

Figure 5.3.6-169 2-D Model, 6-inch Breach in Wing Spar, Pathlines

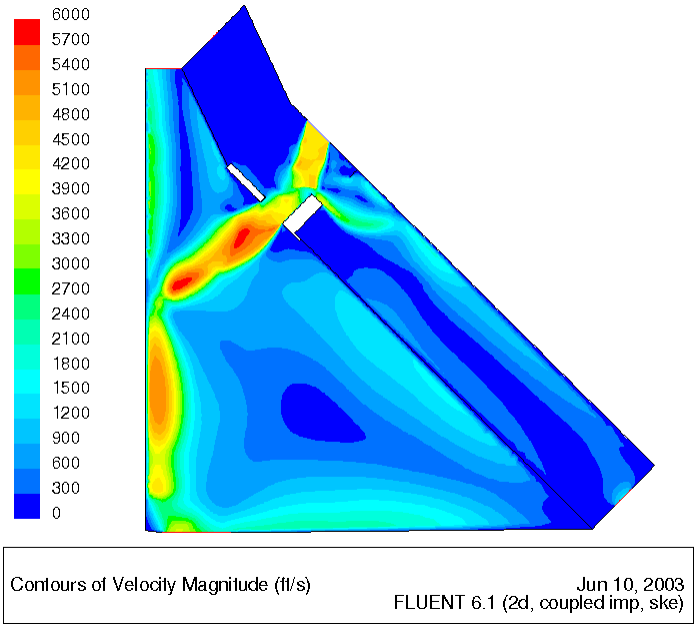

Figure 5.3.6-170 2-D Model, 10-inch Breach in Wing Spar, Velocity Contour

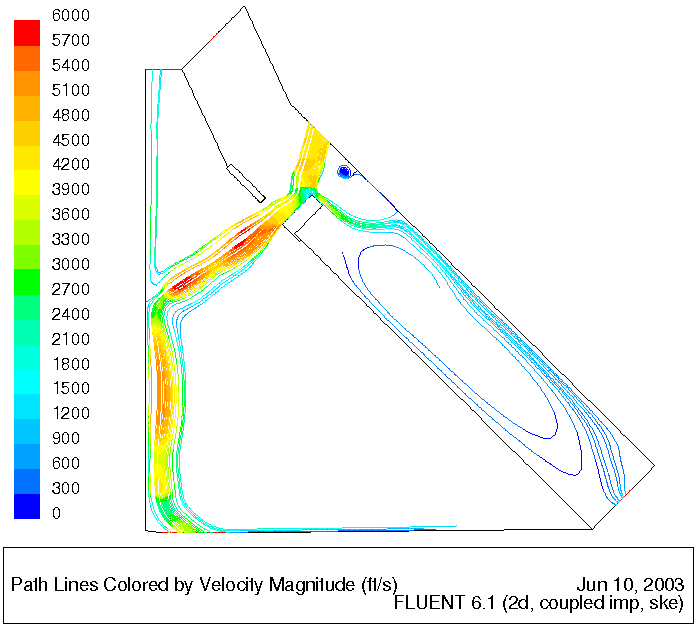

Figure 5.3.6-171 2-D Model, 10-inch Breach in Wing Spar Pathlines

5.3.7 Application of Data to the Working Scenario

5.3.7.1 Plume impingement angle in WLE

The insight provided by the CFD results for RCC penetrations with coupled flow fields allowed the adjustment of the assumed jet internal direction from normal to the interior surface to an angle reflective of the transverse momentum ingested into the RCC penetration. Figure 5.3.7-1 displays the two-inch penetration solution in RCC panel 6 by Peter Gnoffo. The streamlines turn into the hole initially at a 20-degree angle, that then interacts with the downstream lip shock resulting in a final flow turning angle of 41 degrees. It is desired to take advantage of this solution to generalize the internal jet direction to any penetration location. In doing so, the panel 6 results are assessed for a simple correlating parameter. A

local velocity based coordinate system is defined, as shown in Figure 5.3.7-1, with one component aligned with the velocity vector at the boundary layer edge and the other along the inward normal to the surface. Directional components were then assigned to the vectors. Many combinations of momentum components were tried, but with the uncertain impact of the lip shock, a simple correlation of boundary layer edge dynamic pressure (q_e) and surface static pressure (p_e) was chosen. The initial 20-degree flow turning angle was well reproduced with the ratio of static pressure over average ingested dynamic pressure. Boundary-layer edge properties are used to simplify the application to the entire wing. Figure 5.3.7-2 shows the process used to derive the correlation parameter, ***C***, to apply to the edge properties in establishing the flow turning into a penetration. Therefore, once the local coordinates are established, the predicted internal jet direction can be calculated as

$$\vec{J} = \left(0.176 \times \bar{q}_e\right)\vec{V} + p_e\vec{P}$$

With this definition established, a series of points along the projected debris path were chosen as illustrated in Figure 5.3.7-3 with the symbols. The ***J*** vectors are represented in three dimensions in the accompanying views of Figure 5.3.7-3, with the view from inboard on top and the view looking down on the RCC outlines on the bottom. Due to the double delta shape of the Orbiter wing, and the projected impact path at the juncture, the vectors primarily point to the spar region behind panel 8.In Figure 5.3.7-4 a representation of the RCC insulation system has been added in investigating the impact points of the selected jet penetrations. Due to the vector alignment and insulation configuration the conclusion is that the most likely primary impingement location for an RCC penetration along the predicted foam path is the spar region behind panel 8 or the earmuff region between panels 8 and 9. Table 5.3.7.1-1 provides the selected penetrations and the associated jet direction unit vectors.

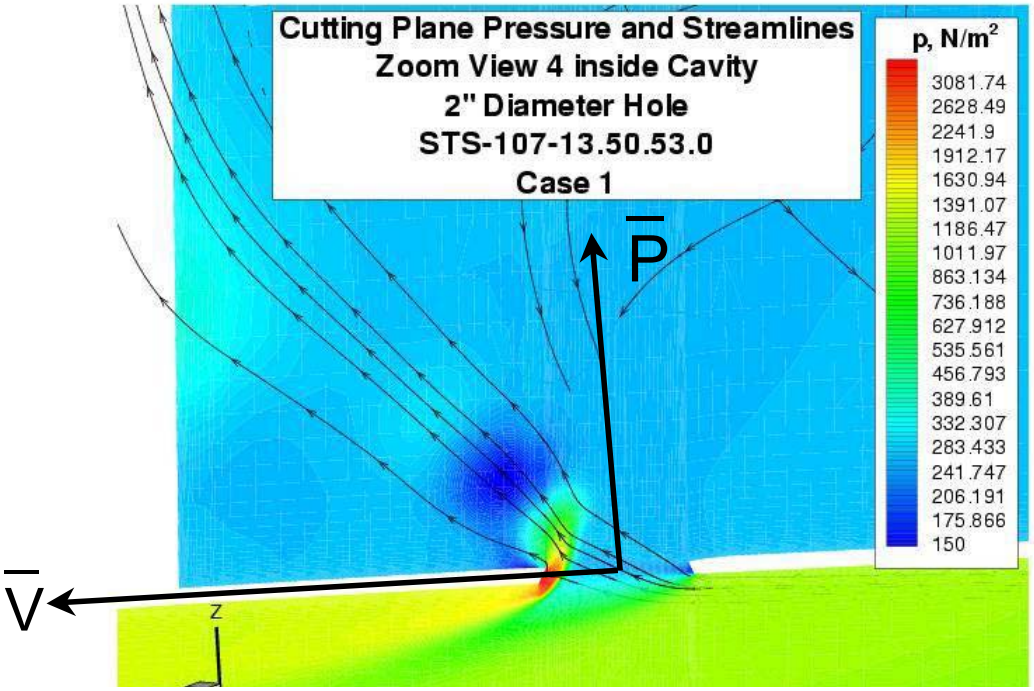

Figure 5.3.7-1 Panel 6 penetration and Jet direction coordinate system.

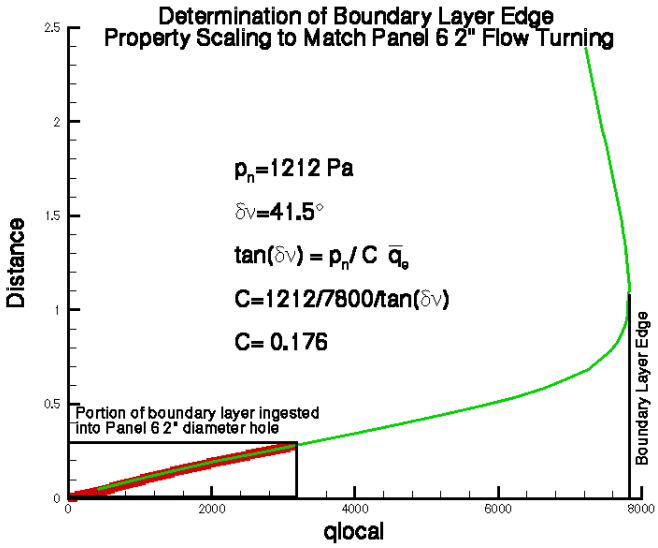

Figure 5.3.7-2 Jet direction correlation parameter derivation

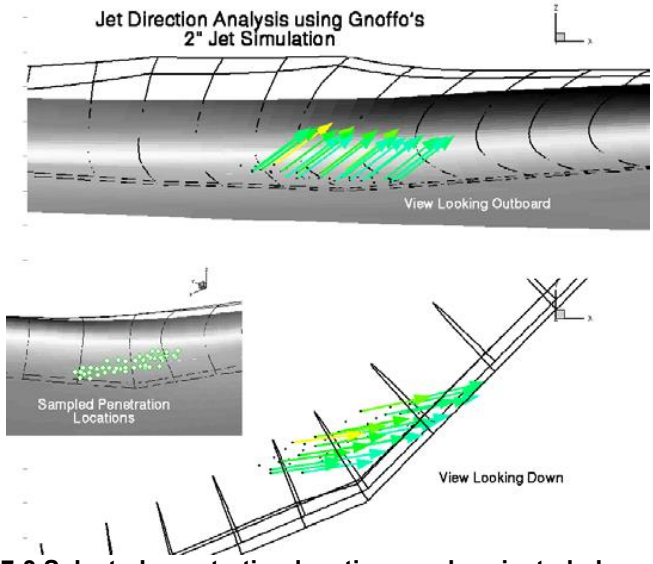

Figure 5.3.7-3 Selected penetration locations and projected plume directions

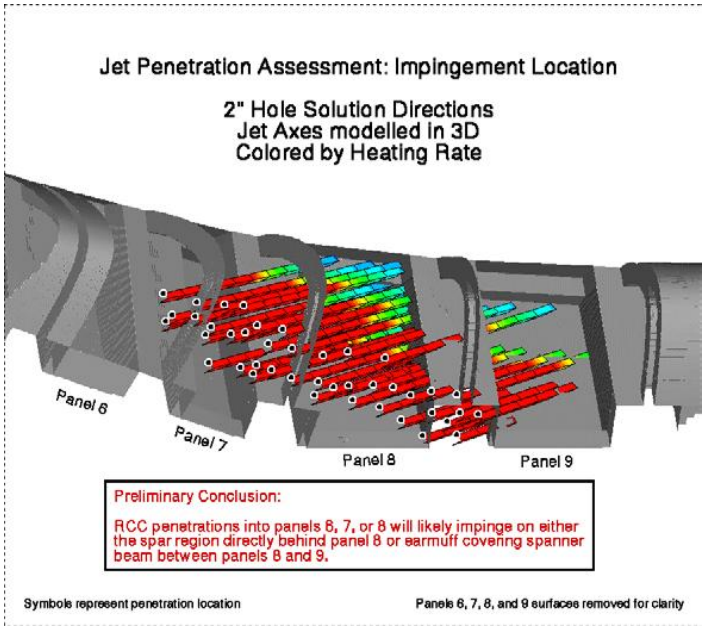

Figure 5.3.7-4 Jet penetration assessment

X	Y	Z	JetX	JetY	JetZ
1087.40	226.40	283.69	0.773	0.185	0.607
1088.09	221.74	282.61	0.775	0.173	0.608
1085.12	224.67	283.66	0.775	0.178	0.606
1082.34	226.31	284.54	0.776	0.179	0.605
1085.03	222.34	283.15	0.776	0.173	0.607
1084.47	218.03	282.33	0.777	0.165	0.607
1082.20	221.60	283.44	0.778	0.169	0.605
1079.10	223.87	284.55	0.779	0.169	0.603
1077.42	221.25	284.19	0.780	0.164	0.604
1079.82	217.54	282.90	0.780	0.159	0.605
1075.67	216.60	283.35	0.782	0.156	0.604
1074.39	220.23	284.52	0.783	0.157	0.602
1069.58	222.38	286.20	0.778	0.164	0.606
1071.82	218.29	284.50	0.784	0.151	0.602
1071.67	214.38	283.50	0.784	0.149	0.603
1067.86	213.76	284.04	0.786	0.145	0.601
1069.25	215.53	284.25	0.785	0.147	0.601
1064.78	218.99	286.31	0.785	0.149	0.601
1062.50	215.94	285.84	0.785	0.149	0.602
1065.37	212.72	284.25	0.788	0.141	0.600
1061.87	210.19	284.23	0.790	0.137	0.598
1058.09	213.32	286.04	0.792	0.135	0.596
1066.90	210.78	283.45	0.787	0.142	0.601
1058.65	208.86	284.49	0.792	0.134	0.596
1054.96	211.26	286.07	0.794	0.129	0.594
1051.40	211.92	287.24	0.797	0.121	0.592
1054.82	214.19	287.20	0.796	0.124	0.592
1050.94	209.88	286.56	0.797	0.122	0.591
1054.97	205.85	284.35	0.794	0.130	0.594
1057.20	206.49	284.10	0.793	0.132	0.595
1049.54	208.27	286.30	0.798	0.121	0.591
1045.30	210.44	288.34	0.801	0.104	0.590
1047.57	212.37	288.55	0.803	0.102	0.588
1046.34	206.93	286.58	0.798	0.119	0.590
1043.32	206.24	287.06	0.800	0.114	0.589
1041.77	207.76	288.11	0.806	0.104	0.583
1040.48	202.72	286.38	0.802	0.107	0.588
1036.79	205.16	288.31	0.810	0.087	0.581
1040.43	203.92	286.85	0.801	0.108	0.589
1046.73	205.56	285.99	0.797	0.119	0.591
1050.73	202.89	284.32	0.795	0.126	0.593
1056.37	207.78	284.63	0.793	0.132	0.595

Table 5.3.7.1-1Jet penetration directions

5.3.7.2 Plume heating distribution

As the investigation team narrowed in on a preferred working scenario, the internal flow team was asked to pull together internal heating distributions for assumed penetration locations that incorporate not only the primary impingement heating, like that described in 5.3.3.2, but also convective heating rates to the

surrounding internal TPS surfaces. Based on an assumed hole location and size, internal plume impingement environments were created that incorporate heating distributions for the panel 8/9 region based on assumed internal direction (5.3.7.1), degree of secondary splash heating, and geometric flow shadowing effects. Full 3-D CFD results for panel 7/8 penetrations were not yet complete, so the best fully coupled CFD solution with internal heating was used as a basis. Given the degree of engineering involved in producing the environments, uncertainty values of +/- 50% were applied to the final results and additional comparisons to higher fidelity CFD results were pursued to provide independent assessment of the expected internal heating.

5.3.7.2.1 Selection of assumed hole location

The present working scenario includes penetration of RCC from panels 6-9 with subsequent spar breach at 488 seconds from entry interface. The team chose a single penetration location for complete analysis in order to ballpark the hole size required to match the flight data for the panel 9 spar and clevis temperature measurements and the spar breach time of 488 seconds from E.I. Given similar heating analysis completed early in the investigation using the basic MMOD plume model, 5.3.3.2, hole sizes of 4, 6, and 10 inches in diameter were chosen and anticipated to bound the data. Hole location was chosen to maximize the predicted primary impingement heating rate, based on the internal flow direction analysis of 5.3.7.1. Using the simple 1-D plume heating model, the plume vectors of Table 5.3.7.1-1 were assessed and vector # 18 chosen and colored red in Figure 5.3.7-5. The anticipated heating rates at the primary impingement point are increased both by the short distance to the earmuff and the small radius of curvature on the TPS edge. The coordinates of the assumed penetration are X=1065 in, y=-219 in, and z= 286.3 in.

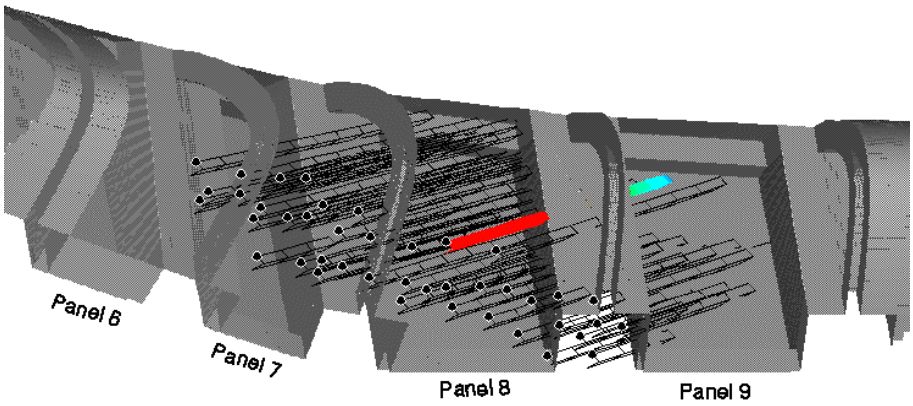

Figure 5.3.7-5 Panel 8 lower surface penetration location

5.3.7.2.2 Distribution methodology

Internal heating distributions are based on a modification of the baseline engineering methodology for holes as outlined Section 5.3.3.3 and take advantage of ingested flow enthalpy calculates using the methodology in Section 5.3.2 and a computed internal pressure using the methodology of Section 5.3.5. The local axis of the plume is assumed to align along the predicted direction of 5.3.7.1, independent of the hole diameter. This assumption was made due to the lack of available internal CFD at the time. (In truth, the larger holes will allow more transverse momentum to enter the hole and cause the jet to hug the interior RCC surface more than the present methodology based on 2" diameter hole results, but the heating distribution will only be shifted in space with little impact on peak heating values.) The radial position correction of the baseline methodology is replaced with computed three-dimensional factors as a function of hole size, which are presented in the results section below. Trajectory corrections remain the same, resulting in a final equation of

$$\dot{q}(x,y,z,t,d_{hole}) = \dot{q} \Big/ \dot{q}_{plate}(x,y,z,d_{hole}) \times \frac{\bar{q}_{\infty}(t)}{\bar{q}_{\infty}(488)} \times \frac{V_{\infty}^{2}(t)}{V^{2}{}_{\infty}(488)} \times \dot{q}_{plate}(d_{hole})$$

The baseline heating values, q_{plate}, are given for each hole size, computed for a trajectory time of 488 seconds from E.I., in Table 5.3.7.2-1.

10” Hole	55.9 Btu/ft^{2}sec for plate
6” Hole	30.1 Btu/ft^{2}sec for plate
4” Hole	27.1 Btu/ft^{2}sec for plate

Table 5.3.7.2-1 Panel 8 penetration heating values

5.3.7.2.3 Correlation and geometry correction factors

The methodology was adjusted based on the LAURA 2” diameter hole panel 6 penetration calculation of Section 5.3.6.1.4.1. Interior surface heating rates are extracted for the primary impingement region and the secondary splash surface. Corrections to the baseline model are made to bring the results into line with the CFD results. Comparison lead to a narrowing of the distribution by raising the values of Table 5.3.3.3-1 to the 1.6 power (also indicated by the comparisons in Figure 5.3.3-7) and the development of a splash heating approach to account for flow turning and secondary stagnation flows anticipated in the RCC cavity. Examination of the LAURA results indicated flow physics similar to a forward-facing step. Forward-facing step amplifications of 3.5 times the undisturbed value are appropriate for the observed internal Mach numbers and produced a good comparison on the splash surface of Figure 5.3.7-6. Secondary stagnation values are within 20% and the engineering methodology remains conservative as the flow moves down the surface.

In addition to secondary splash factors, other corrections to the baseline methodology are applied to account for “shadowing,” where the flow cannot directly impinge on the surface, local surface radius of curvature effects to earmuff edges and a general convective heating equal to three percent of peak values. The final geometry corrections are presented in Figure 5.3.7-7. Spar and carrier panel surfaces behind panel 8 are assumed to be secondary splash surfaces with a preference for the flow to splash on the upper surface and hence have amplification factors from 1 to 3.5. The edge of the panel 8/9 earmuff facing the assumed breach location shows high amplification factors to correct for local radius of curvature effects. The region behind panel 9 cannot be directly impinged upon from the assumed location and therefore has shadowing corrections that decrease the heating.

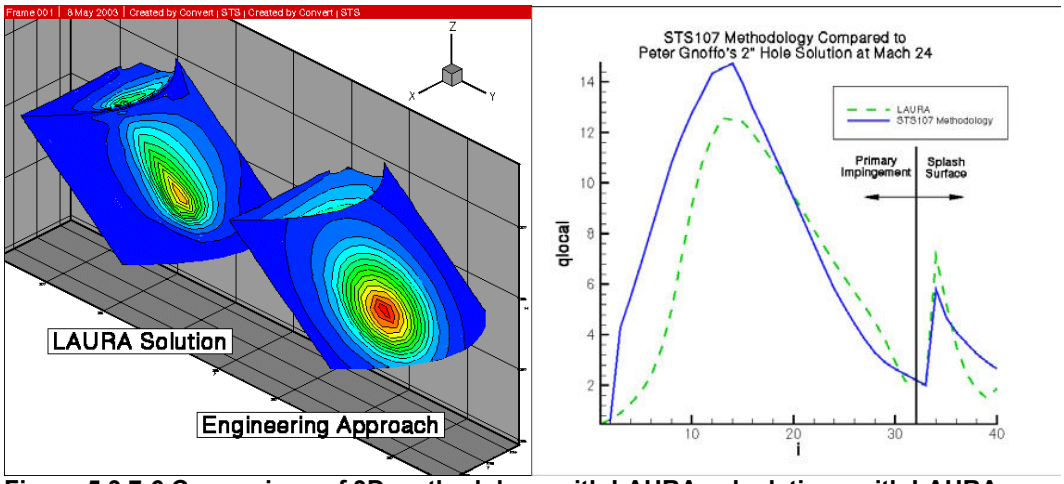

Figure 5.3.7-6 Comparison of 3D methodology with LAURA calculations with LAURA

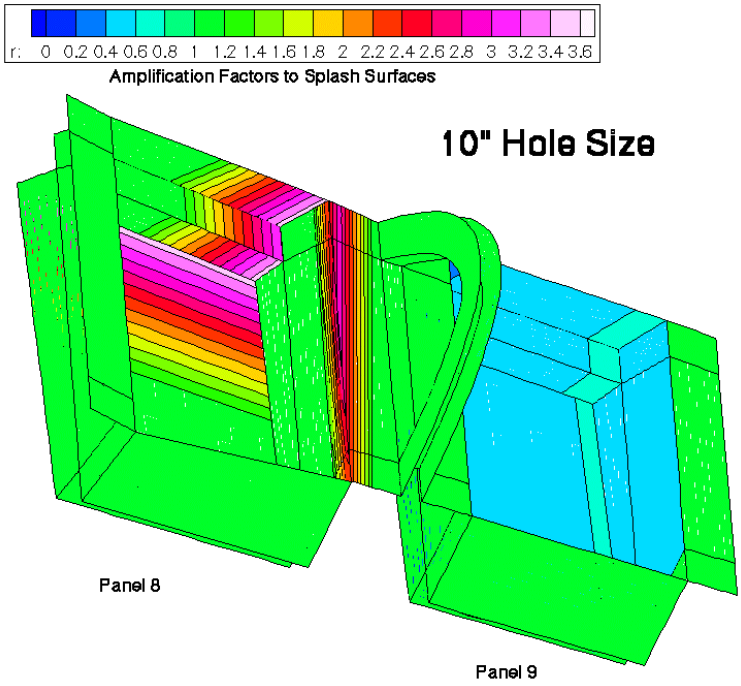

- Corrections given on a zone by zone basis to partially account for
  1. Secondary splash surface (based on forward facing step and panel 6 hole comparisons)
  2. Radius of curvature corrections to modeled geometry (Spanner beam insulation modeled with square corners, corrected to 1" radius heating)
  3. Line of sight shadowing and separation (panel 9 spar heating)
  4. Background heating values of 3% assumed on backward facing surfaces (on par with panel 6 and T-seal simulations)

Figure 5.3.7-7 Geometry correction for heating

5.3.7.2.4 Resulting Distributions

Engineering predicted heating distribution factors are presented in Figure 5.3.7-8 through Figure 5.3.7-10. All cases show a peak heating point on the earmuff between panels 8 and 9 at the edge of the TPS along the jet axis. By comparison, as the hole grows larger, so does the high heating region, with higher splash heating factors to secondary surfaces. Peak amplification factors do not change since the driving factor on the earmuff edge is local curvature, which is consistent between predictions. Keeping the previous equation and Table 5.3.7.2-1 in mind, however, shows that while the geometry amplification factors are the same, the 10" hole will experience significantly higher heating to the entire internal geometry.

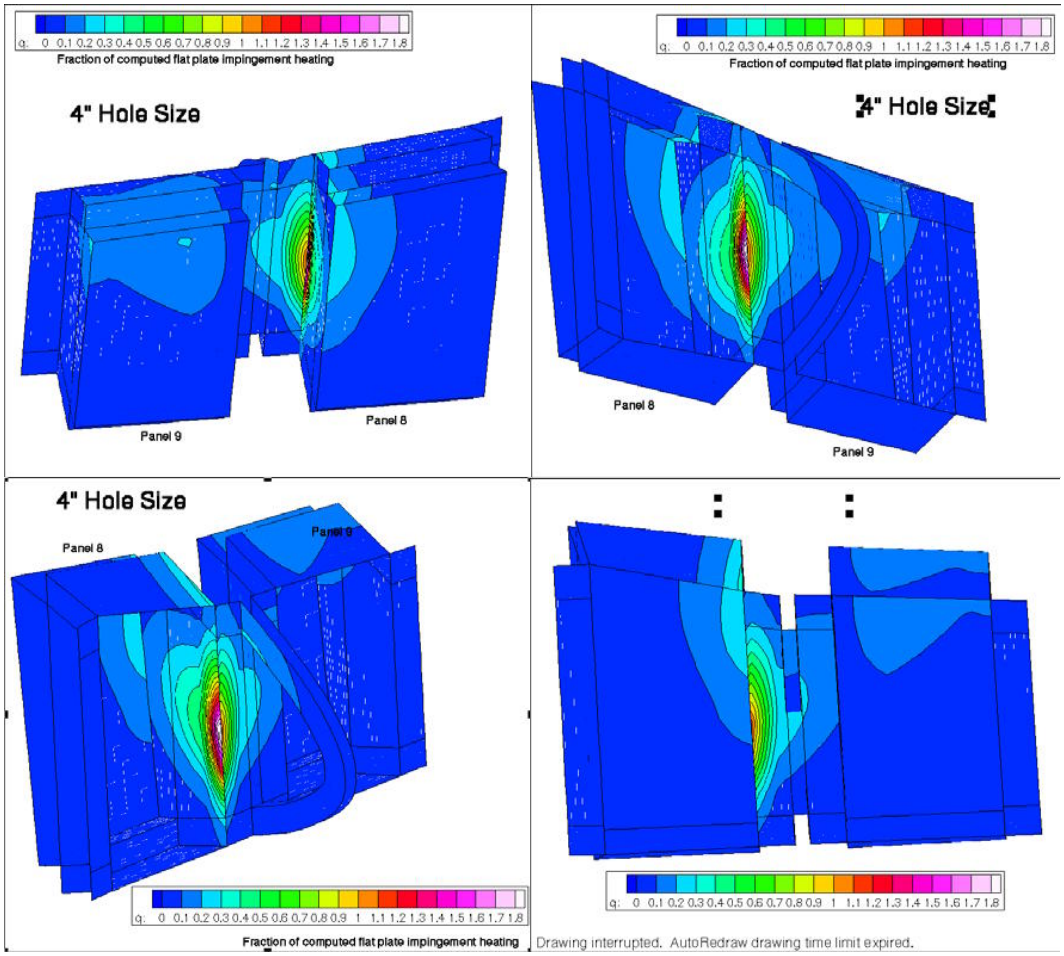

Figure 5.3.7-8 Heating factors for a 4" diameter hole in panel 8 lower surface

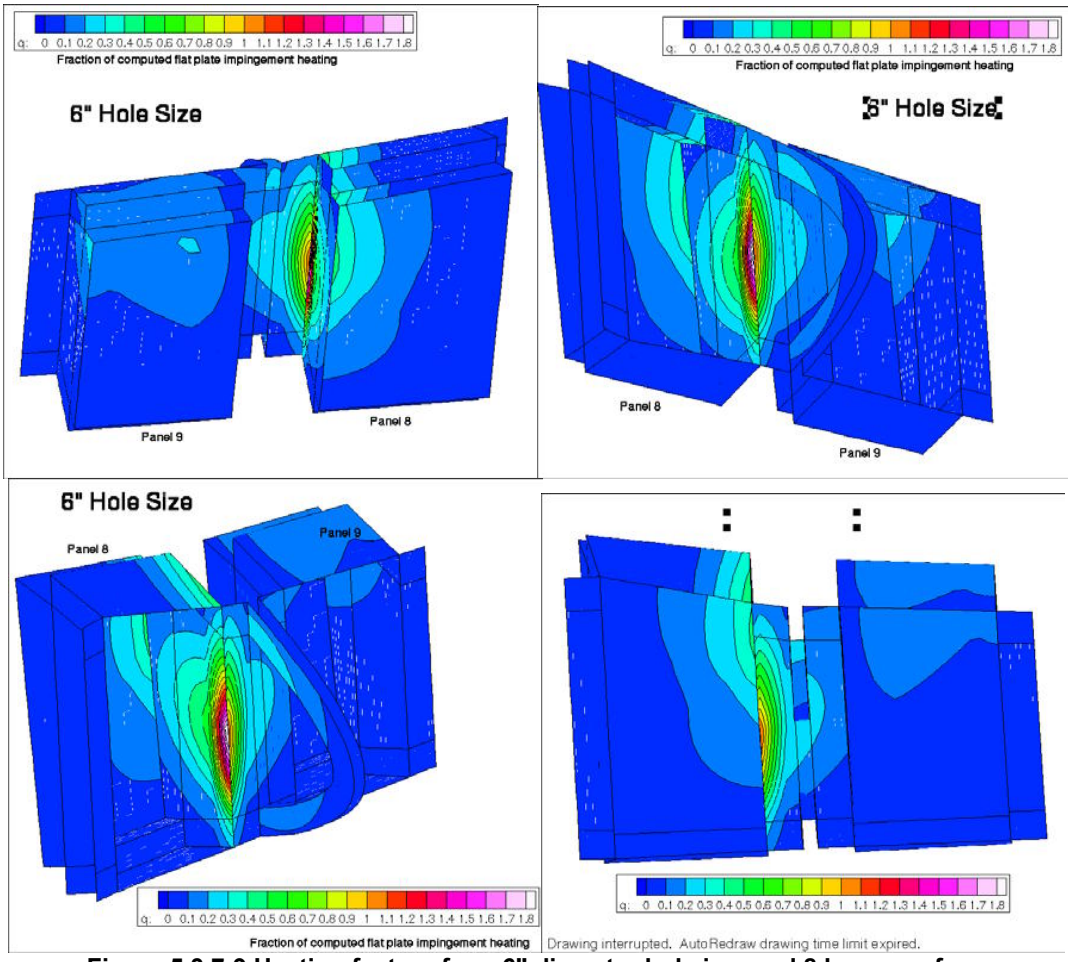

Figure 5.3.7-9 Heating factors for a 6" diameter hole in panel 8 lower surface

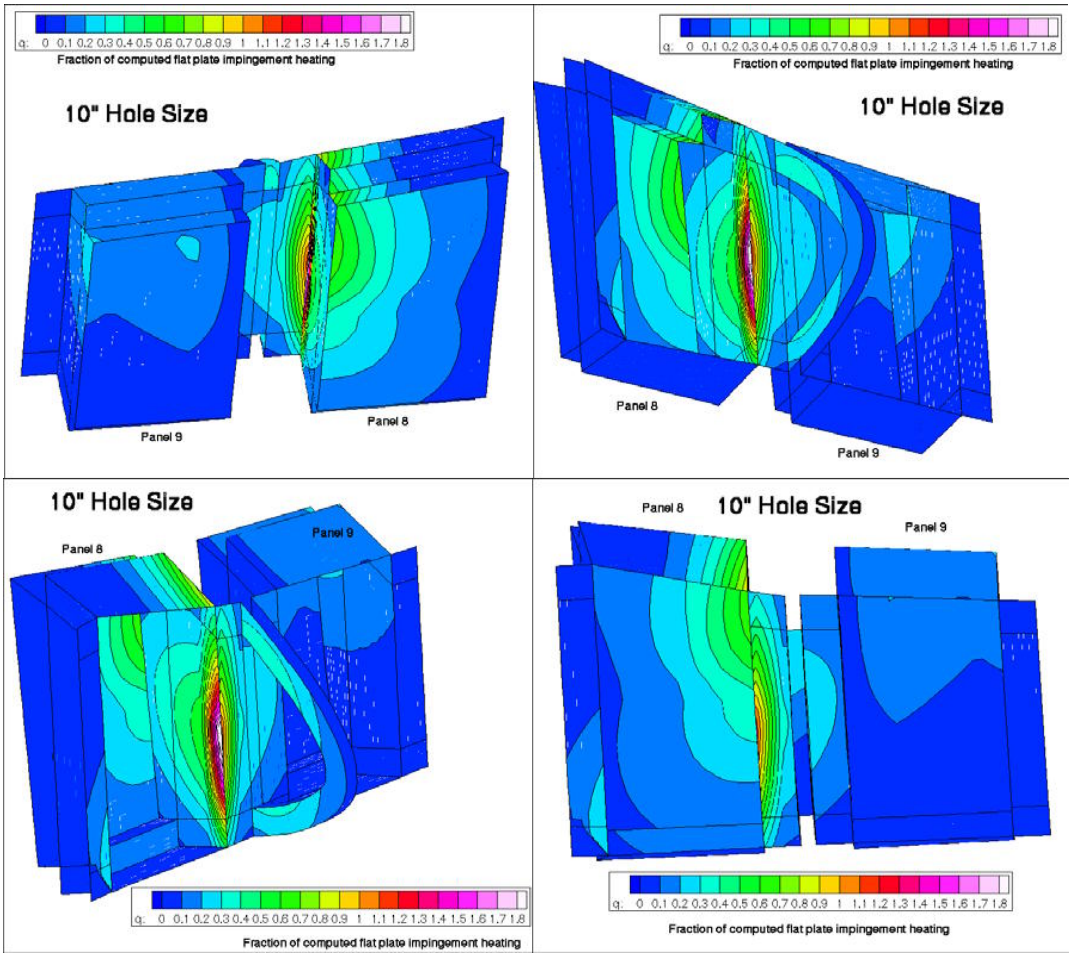

Figure 5.3.7-10 Heating factors for a 10" diameter hole in panel 8 lower surface

5.3.7.2.5 Comparison with 3D CFD/DSMC

The final STS-107 3-D plume heating methodology was developed based on very limited CFD results and represented a "highly engineered" environment for thermal analysis. It was desired to compare the engineering methodology to high fidelity CFD results for STS-107 type of geometries and assess the quality of the engineering predictions used for the subsequent thermal analysis. Given the complexity of the problem, the comparisons represent more of an independent assessment than a validation of the methodology, primarily since time did not allow a second loop through the process incorporating CFD lessons learned. Rather, the comparisons focused on gross fluid dynamic features and qualitative assessments. Comparisons with previously presented CFD results are given in Figure 5.3.7-11 through Figure 5.3.7-14.

Two types of comparisons with the DSMC results of 5.3.6.1.5 are displayed in Figure 5.3.7-11. On the left of the figure, both sets of data have been normalized by the peak impingement heating values on the panel 8/9 earmuff. The DSMC results fully couple the internal and external flow fields and provide additional support for the predicted internal jet direction since both methodologies predict peak heating values in the same location. DSMC results also provide an independent source for secondary splash heating to the spar region behind panel 8, again inline with the engineering methodology. Shadowing of the panel 9 spar region and some enhanced heating to the panel 9/10 earmuff are also predicted by the DSMC results inline with engineering assumptions. The right side of the figure provides a comparison of predicted heating magnitudes with the STS-107 engineering methodology. The engineering method predicts higher heating by roughly a factor of two. However, the engineering methodology is based on continuum assumptions and the calculations are made at rarefied condition so the conservatism is not surprising. Furthermore, the engineering method heat flux scaling appears to represent the physics well, given the two order of magnitude change in dynamic pressure.

Application of the engineering approach to the uncoupled panel 7 6" hole case, section 5.3.6.1.1, is displayed in Figure 5.3.7-12. Adjustments to the engineering methodology were made to account for the normal flow through the penetration, due to the uncoupled nature of the solution, and correction for total enthalpy variance. Comparison with two levels of grid refinement highlights a couple of conclusions. First, the STS-107 engineering methodology achieves qualitative agreement in terms of the size of the impinging jet, matching the spreading as the jet expands into the interior of the RCC. Peak heating values achieve excellent match with the medium grid results on the left. However, as more flow structure is captured with mesh refinement, the jet peak heating region changes shape and amplitude due to secondary flow patterns acting to self-focus the jet, enhancing peak heat transfer rates. While there remains a moderate level of unsteadiness in the results, as much as a factor of two increase over the engineering methodology is indicated. This phenomenon is independently predicted in the panel 8 results of section 5.3.6.1.4.2. The engineering methodology does not account for these flow interactions.

Figure 5.3.7-13 points out the dramatic change in internal heating distribution due to the external flow coupling. Here the same hole location produces a very concentrated, high enthalpy flow impingement on the interior rib surface of panel 7 just downstream of the hole. Examination of the engineering methodology indicates that the jet would, indeed, impact the rib, there is no automatic correction applied to account for it. The flow that strikes the rib has all of its downstream momentum arrested and winds up producing only moderate heating to the spar behind panel 7 while the STS-107 methodology shows a panel 8 spar impingement with elevated heating rates. Figure 5.3.7-14 shows the impact of local geometry changes to the distribution once more, as the earmuff between panels 7/8 is added and greatly changes the result. Fortunately, the additional interaction of the rib splash flow with the earmuff geometry produces heating distributions and magnitudes in line with the engineering methodology. While this is clearly a case of two wrongs make a right, it lends support to the use of the engineering approach for thermal analysis and does not negate the resulting outcome the thermal analysis to the panel 8 and 9 spar surfaces. RCC rib heating is handled by a separate modeling approach; section 5.3.3.6.5.

Overall, thermal analysis performed with the provided internal heat flux distributions will produce results consistent with CFD results, given the high levels of uncertainty applied to the approach. Final results may slightly change the hole size or hole location, but not invalidate the scenario.

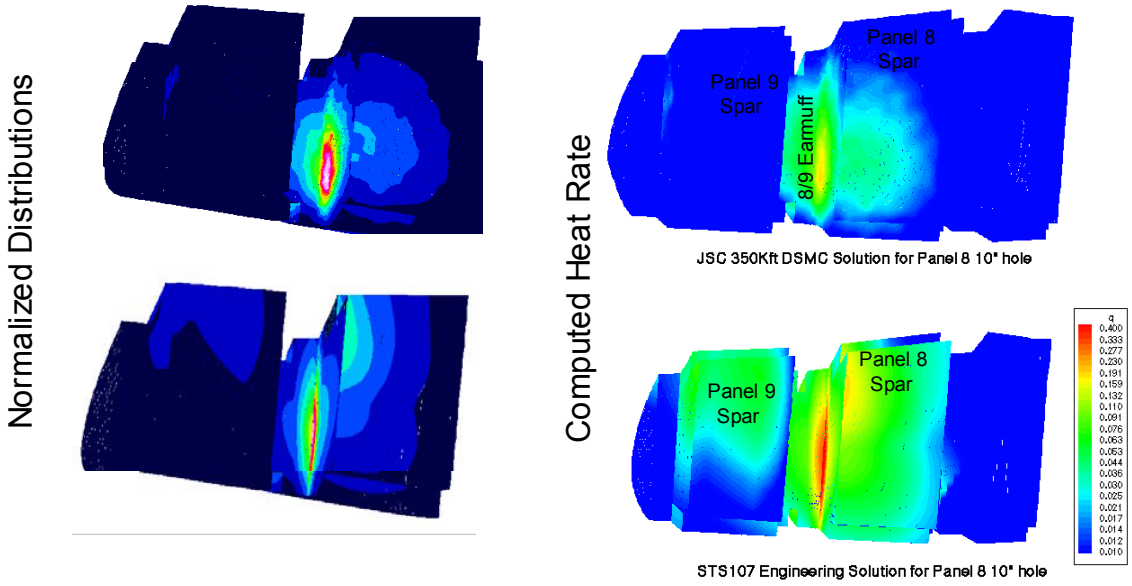

Figure 5.3.7-11 Comparison of engineering methodology with DSMC calculations at 350,000 feet

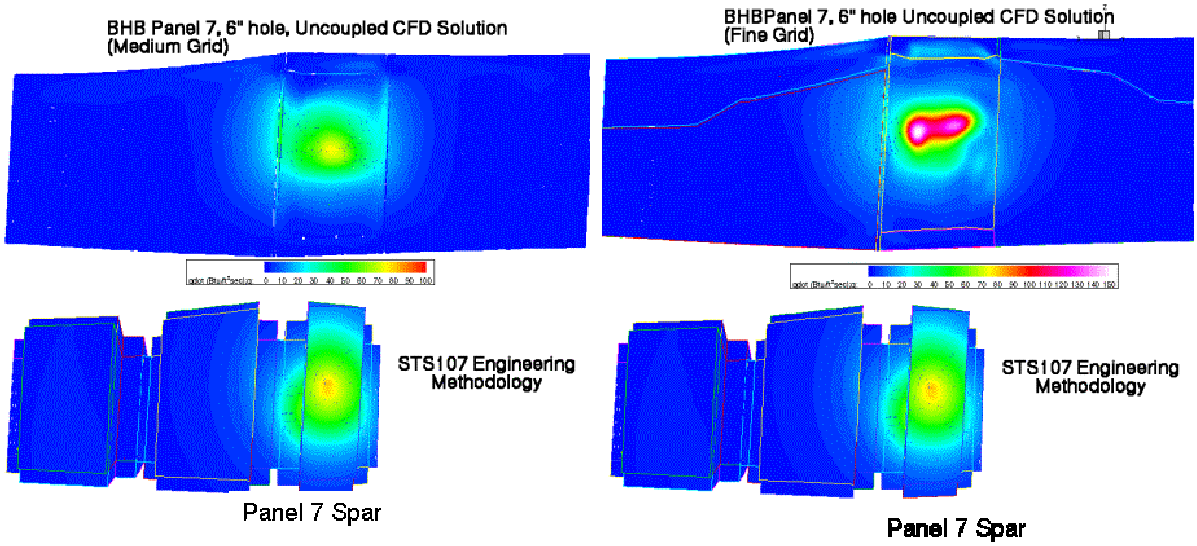

Figure 5.3.7-12 Comparison of STS107 methodology with panel 7 6" uncoupled CFD

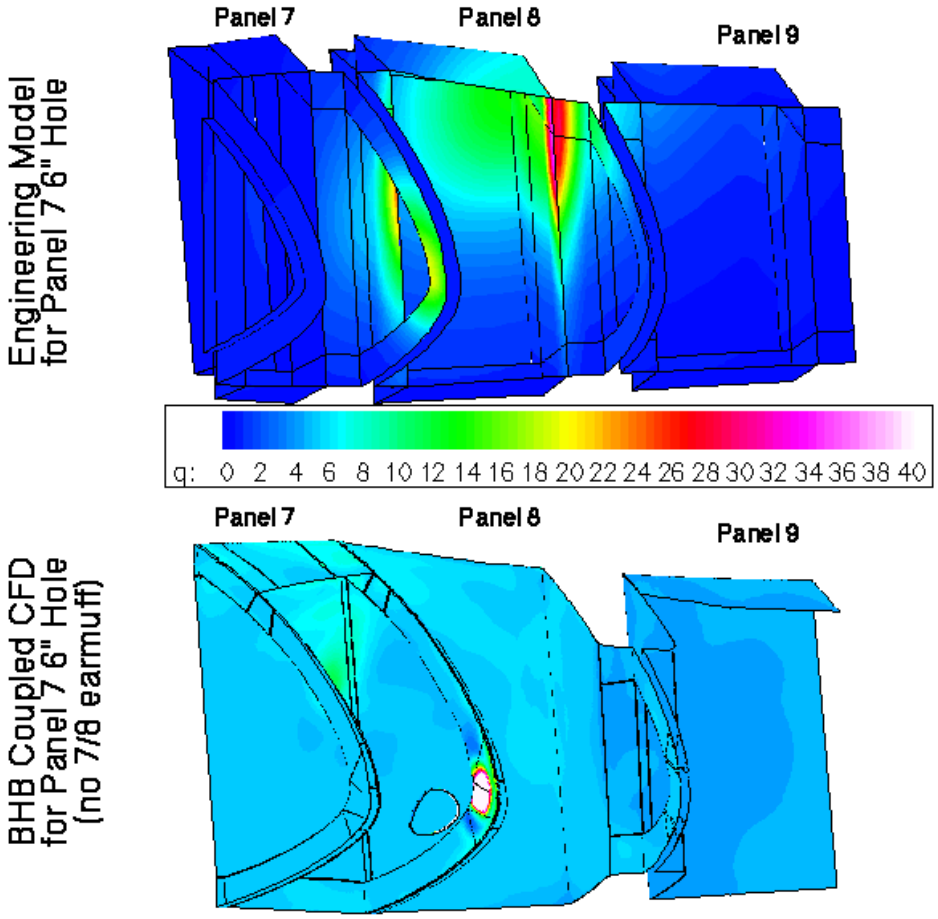

Figure 5.3.7-13 Comparison of STS107 methodology with panel 7 6" coupled CFD

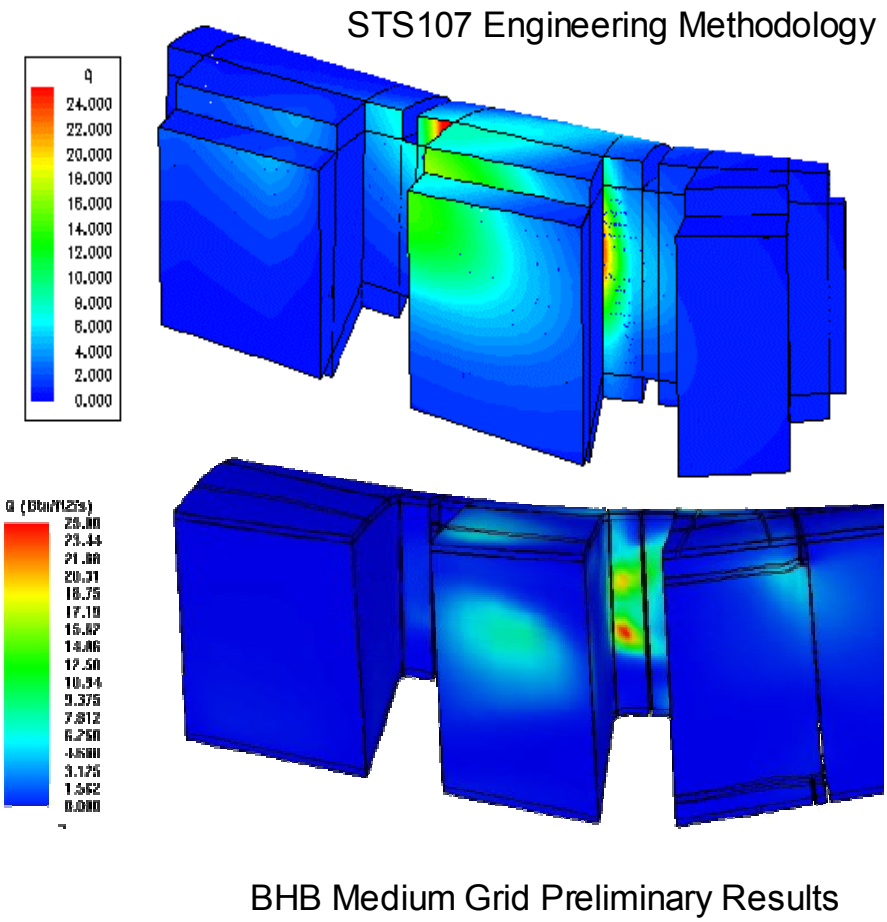

Figure 5.3.7-14 Comparison of STS107 methodology with panel 7 6" coupled CFD with earmuff

5.3.7.3 Assessment of Secondary Plume/Spar Breach

Thermal analysts keyed into wire burn-through times early in the investigation as a piece of known information that may be use to identify breach time, location, and size. The plume methodology of section 5.3.3.3 has been utilized in such assessment with one large, early assumption: that the plume enters through the spar normal to the surface. Early investigation activities, in fact, depended on the direction assumption with no conflicting information until the first coupled CFD results came out of Langley (5.3.6.1.4.1). With the additional knowledge that a significant fraction of transverse momentum is carried through the RCC breach, the question was raised about the secondary breach direction.

Secondary breach fluid dynamics are significantly different than RCC penetration for several reasons: 1) the internal RCC cavity geometry offers many surfaces to arrest momentum, 2) the highest heating point to the spar insulation is likely in a stagnant flow, high pressure region, 3) internal shock structures absorb significant portions of available flow energy, and 4) the flow must turn through several inches of structure and insulation rather than just 0.25 inches of RCC. With this information in hand, investigative activities continued assuming normal jet penetration. Final CFD calculations have continued to support the conclusion that the jet, at least initially, penetrated the spar normal to the surface.

Figure 5.3.7-15 represents the insight CFD results where the jet penetration direction was assumed normal to the spar. In the solution the jet structure remains coherent and impinges on the wheel well wall before being turned downstream and circulating through the mid wing volume. Figure 5.3.7-16 displays similar fluids dynamics from a two dimensional CFD solution where the flow initially carries streamwise momentum through the RCC breach and impacts internal geometry in the region where a hole is placed in the spar. This computed internal flow direction and mid wing fluid dynamic structure match the Figure 5.3.7-15 results quite well. While the two dimensional results modeled a large structural interference, the

BHB results of Figure 5.3.7-17 illustrate that even a relatively small geometric feature, in this case an RCC rib, can sufficiently absorb momentum to cause the jet to change direction completely. Any secondary burn-through of the spar in this case would clearly produce a normal jet through the breach.

In providing this assessment, however, the best that can be said is that **initially** the jet was certainly produced normal to the secondary breach surface. Given heating rates many times external values, eventually the primary impingement zone will be completely melted to the dimensions of the jet and there is then nothing to inhibit the free flow of the jet into the mid wing volume with full momentum. The time required to achieve such a state is entirely dependent on the initial damage and the TPS surface that is directly impinged.

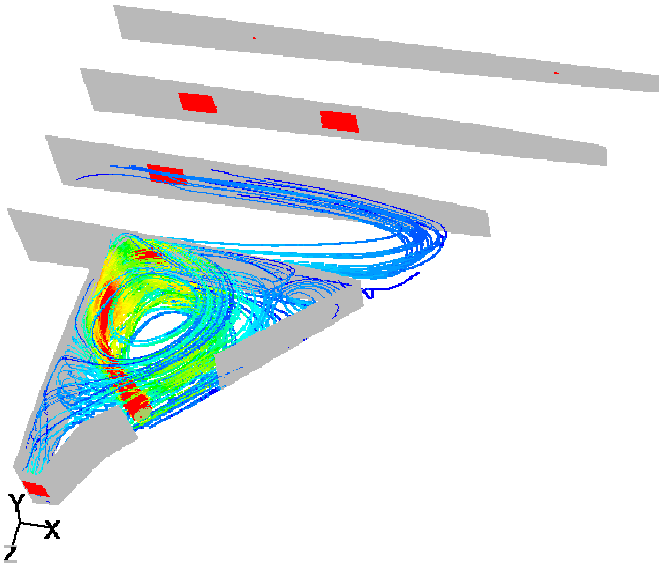

Figure 5.3.7-15 Assumed normal direction flow field

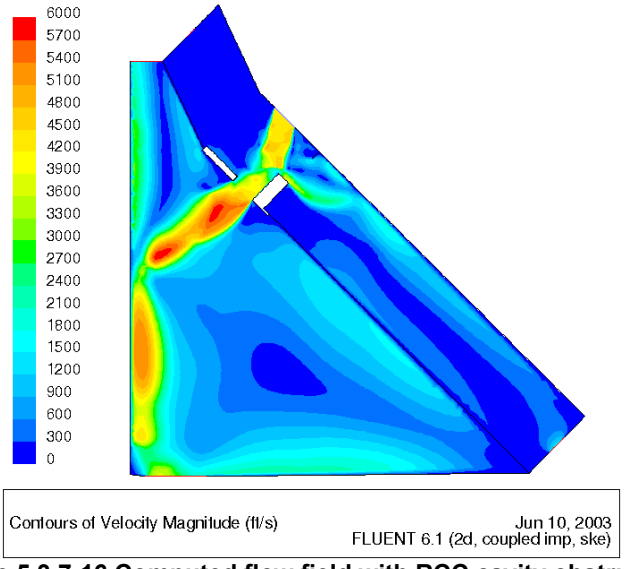

Figure 5.3.7-16 Computed flow field with RCC cavity obstruction

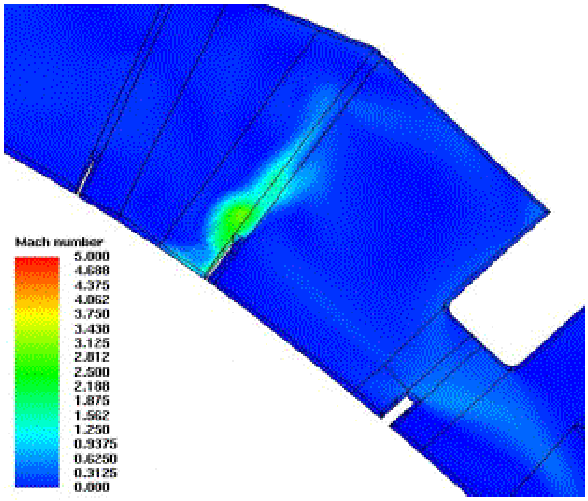

Figure 5.3.7-17 BHB Panel 7, 6" hole coupled internal flow field

5.3.7.4 Panel 8 penetration fluid dynamics and forensic evidence

Full three-dimensional CFD solutions for the panel 8 penetration provide invaluable insight into the flow inside the RCC that led to the eventual demise of the wing structure. Examination of the fluid dynamics and flowfield properties provides an explanation for, and independent verification of, hardware forensic evidence of a panel 8 breach. Figure 5.3.7-18 displays the internal streamline patterns for a 10" breach into the lower panel 8 surface. A supersonic stream of high-energy flow enters and directly impinges on the 8/9 earmuff, producing locally high pressures and heat rates. The flow re-expands and creates a supersonic "splash" flow that jets inward and upward into the panel 8 spar region before recirculating around to the panel 8 upper RCC inner surface and eventually exiting through the vents. This resultant flow field directly explains four key forensic features seen in the debris.

5.3.7.4.1 Inconel deposits on panel 8 inner surface

The initial deposits on the backside of the surviving panel 8 RCC have been analyzed and identified as Inconel nodules. The flow field predicted by BRPP provides the transport mechanism for the Inconel deposits. Initially high speed, high temperature flows impinge on the Dynaflex insulation, melting the outer Inconel surface. The melted/vaporized Inconel is deposited to the back of the panel as the supersonic tail jets scrub the panel 8 spar insulation and then the back side of panel 8.

5.3.7.4.2 Panel 8 and 9 rib erosion (knife-edging)

The BHB panel 7 CFD solution predicted heating rates over 200 Btu/ft^2-sec to the panel 7 interior rib surface in the primary jet impingement zone. BRPP results to the 8/9 earmuff are also over 200 Btu/ft^2-sec for the panel 8 penetration. Examination of Figure 5.3.7-18 shows how a slight adjustment of hole location would place the primary jet impingement heating region directly on the RCC rib. The directional aspect of the knife-edging observed in the debris can only be explained with a jet flowing internally from panel 8.

5.3.7.4.3 Erosion of panel 9 lower carrier panel tiles

Examination of panel carrier panel tiles shows clear indications of flow out from the corner of RCC panel 8, through the horse-collar seal and out and over the panel 9 lower carrier panel with significant erosion patterns. In order to produce such a flow, the internal pressure must be significantly higher than the lower surface pressure. In addition that erosion pattern indicates a coherent jet. Figure 5.3.7-19 shows the local pressure field for the panel 8 breach in the outboard lower panel 8 corner. Pressure values of 0.3 psia are greater than 2.5 times the external surface pressure at the same location on the lower surface of the Orbiter, more than sufficient to drive highly energetic flow out through the horse-collar. Of great significance is the localized aspect of the distribution: regions merely inches from the secondary stagnation point in the corner of the panel do not possess sufficient pressure to drive flow out onto the lower surface.

5.3.7.4.4 Panel 8 upper carrier panel "chimney" tile

Preferential jet splash patterns off of the earmuff surface and up and into the panel 8 spar region focus high temperature gases directly into the RCC leeside vents at the upper carrier panel. With the poor

radiation relief of tile to RCC, enhanced heating will quickly elevate the tile surface above the slump temperature and open the vent even more. Debris forensic evidence contains a panel 8 upper carrier panel tile with deposit buildup consistent with the internal insulation materials over 0.4" thick. Examination of Figure 5.3.7-20 shows the jet shape as it comes off the earmuff clearly heading directly into the region where the tile would be located, carrying with it any melted/vaporized material for deposit to the relatively cooler surface of the tile.

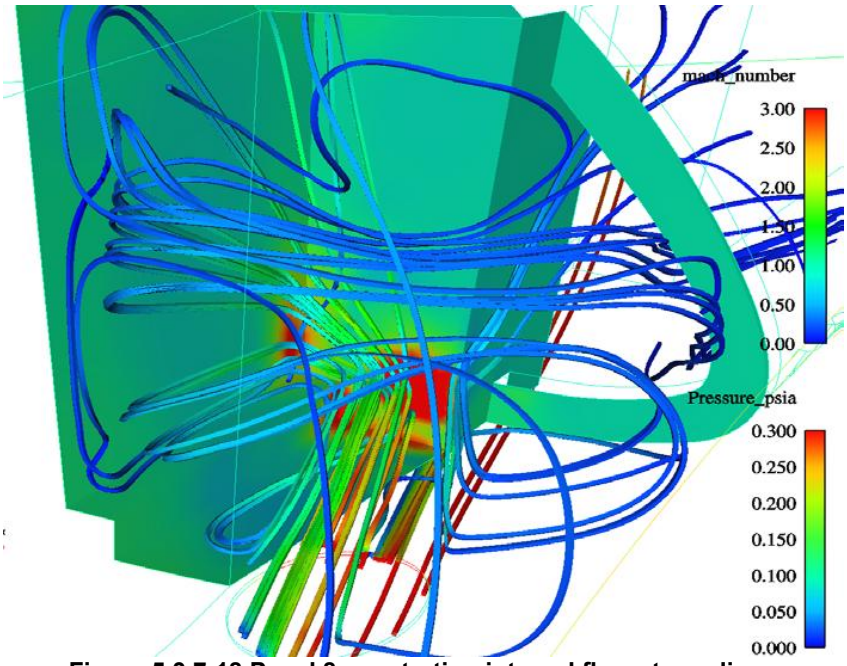

Figure 5.3.7-18 Panel 8 penetration internal flow streamlines

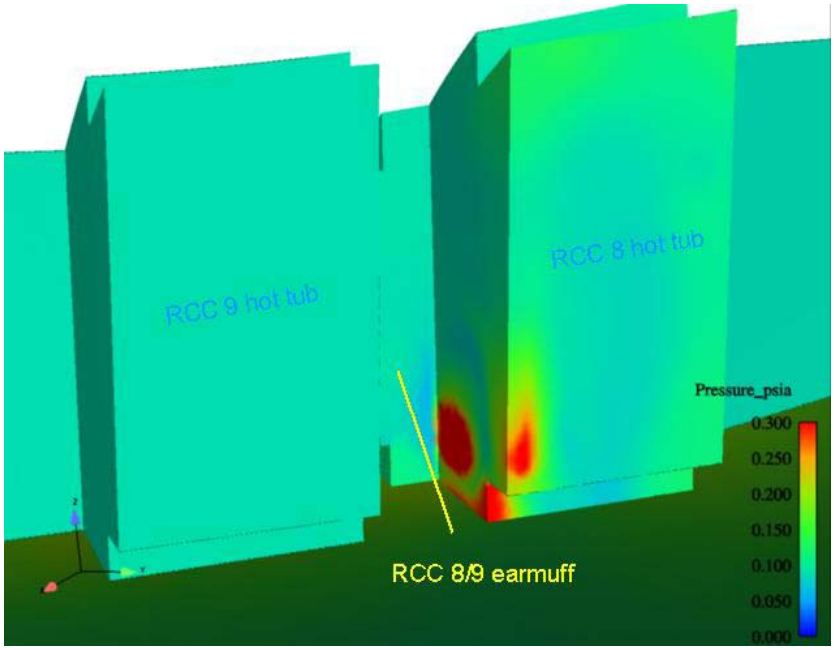

Figure 5.3.7-19 Panel 8 penetration internal stagnation pressures

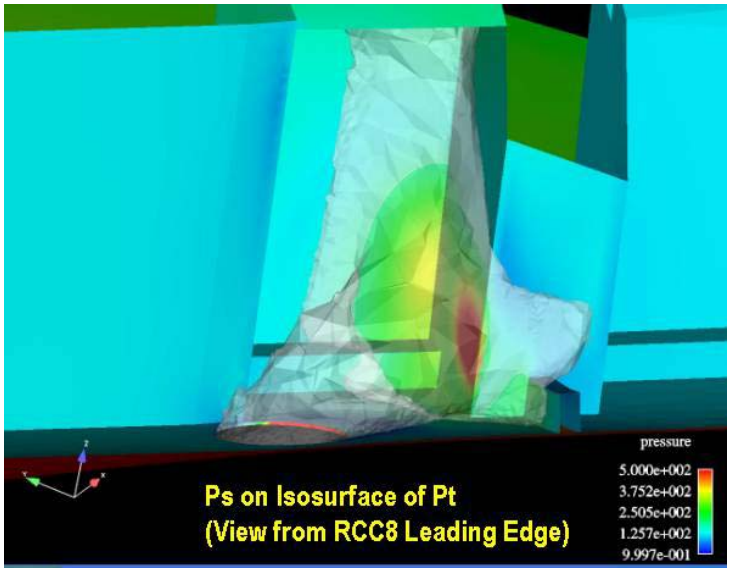

Figure 5.3.7-20 Panel 8 penetration internal jet shape

5.4 Aerothermodynamic Environments Summary

Aerothermodynamic analysis and testing has been conducted in support of the STS-107 Columbia accident investigation. The work presented above (in sections 5.1 – 5.3) explored various off-nominal external and internal aerothermodynamic events experienced by STS-107. The external aerothermodynamic analysis examined changes to the external Orbiter environment that result from a large matrix of possible damage types and locations. The internal aerothermodynamic analysis examined environments due to high temperature gas ingestion from the varying extent, location and type of damage. These analyses and test data were used to provide substantiating evidence in support of the Working Scenario: Damage to RCC Panels 5 through 9. In order to be considered as substantiating, the aerothermodynamic data had to be, (1) consistent with the results of data provided by the other technical disciplines and reported in this document, (2) consistent with evidence gathered through the recovered Columbia debris and data mapping, and (3) consistent with any other relevant evidence that became available during the investigation. Particularly important in this process of substantiating the aerothermodynamic data was correlating the aerothermodynamic team's analysis results with the data obtained from the STS-107flight instrumentation. Since the exact size, shape, and location of the damage was unknown, the process taken was to assume a damage configuration and evaluate the results on the aerothermodynamic environment. This was done by comparing the analysis or test results with the available flight data, as in the case of the surface thermocouples, or by providing the environments for thermal analysis to determine if the provided heating environment, coupled with the thermal model, was consistent with other data from the Orbiter.

Investigations of changes to the external environments through wind tunnel and numerical analyses have yielded much critical information. Although the chin panel and vent nozzle data could not be explained by these results, the side fuselage and OMS pod surface temperature and skin temperature responses were shown to be consistent with progressive wing leading edge damage. The extensive amount of wind tunnel test data obtained at Mach 6 Air and CF_4 facilities was mostly qualitative; however, the testing methods allowed for the rapid evaluation of multiple damage configurations and guided the focusing of the damage scenarios that were examined with computational analysis. High quality numerical simulations of the Orbiter with wing leading edge damage provided engineering information on leeside flow field features and surface heating. The combined efforts of numerical analyses and wind tunnel testing demonstrate that the reduced heating effect seen from the early part (< EI + 480 sec.) of the STS-107 flight instrumentation was caused by high pressure flow entering a hole on the windward side of the left wing leading edge and exiting to the lee side either through the leeside RCC channel vents or in combination with some localized leeside RCC/upper carrier panel breach. Analysis of the mass flow rates exiting the tested vent area

indicate that a hole size on the WLE windward side on the order of 80 square inches at flight scale was required to provide sufficient flow to affect leeside surface heating in a way that was consistent with flight data. The test and analyses data also showed that the increased leeside heating (side of fuselage and OMS pod) that occurred after EI + 480 seconds had to be associated with a significantly damaged leading edge; either severely damaged or missing upper carrier panels (more than one), the loss of significant portions of upper RCC panel(s), or even upper wing skin just aft of the WLE.

Supporting evidence for these damage geometries was generated with CFD tools, providing critical information at flight conditions. These CFD simulations represent a substantial effort, but they succeed in identifying the source of increased side fuselage heating as a jet emanating from a damaged RCC leading edge. This jet convects high-temperature/high-pressure gas onto the Orbiter leeside where, in sufficient strength, it both severely perturbs the leeside vortex flow field and impinges directly on the side fuselage. This side fuselage jet impingement was demonstrated to generate surface heating increases of more than a factor of ten. Damage configurations involving mass and energy convection to the Orbiter lee side, with less strength due to smaller leeside damage area, lack the strong coherent jet that impinges on the side fuselage. However, this weaker leeside flow disturbance still generates perturbations to the leeside vortex structure leading to movement of the wing strake vortices and the heating footprints associated with their flow structures. The identification of leeside surface heating differences was critical to interpreting these two classes of STS-107 flight data. The first being the early decrease in OMS pod and side fuselage heating, and the second being a substantially increased side fuselage heating together with moderate OMS pod heating increases.

The accuracy of leeside flow field computational simulations remains a concern for several reasons: (1) A comprehensive effort to validate leeside heating predictions has never been attempted. (2) The actual shape, location of the damage will never be known. (3) The progressive nature of the damage and the complicated mixed internal/external flows implies rapidly changing time dependent phenomena and hence unsteady solutions. (4) Details of modeling the proper internal cavity geometry and surface boundary conditions (both within the cavity and on the lee side) are beyond the scope of the currently available CFD methods. Nevertheless, the CFD simulations provided critical flow field information at flight conditions that allowed for an engineering perspective to draw the previously discussed conclusions. Similarly, questions remain about whether the Mach 6 air or Mach 6 CF_4 facility provide a more accurate representation of the high Mach number re-entry conditions of the Orbiter leeside flow field. However, these questions are less critical when considering the data in an engineering context and noting that the computational techniques are solving the equations for the conservation of mass, momentum, and energy and that both facilities reproduce the same basic physics of hypersonic flow.

In order to provide the internal heating environments in support of thermal analysis, new tools and techniques were developed. These included a process for the calibration and verification of the plume heating model, the development of a coupled equilibrium air venting and thermal model of the entire left wing, and the application of available CFD and DSMC computational tools on internal flows with complex geometry. As was discussed, the heating to an object is a function of its geometry. This problem is made even more difficult when the size, shape, and location of the original penetration is unknown, the internal configuration is complex and not designed for a convective environment, and the configuration is changing over the period in question. Thus, in order to provide internal heating environments, a static geometry strategy was pursued. For cases where a penetration in RCC panel acreage was assumed, a round hole was evaluated for simplicity. The area of the hole was the more critical factor because it determined the amount of energy ingested.

The engineering plume heating model used in the investigation had been previously applied for evaluation of micro-meteoroid penetrations of 0.25” to 1.0 “. For this work, holes as large as 10” in diameter were assessed. Experimental data for impinging plumes in a relevant environment were not readily available. This demanded that a process be developed to verify the applicability of the model to these larger diameter penetrations. The first step in the process was to analyze a series of relevant plume flows with two CFD codes. As there were no experimental data available, the CFD analysis relied on current best practices to estimate heat rates due to impinging plumes. Two CFD codes were run independently to develop confidence in the plume heating results. With confidence in the CFD established, the CFD results were compared to the engineering plume model at the same conditions. The engineering plume heating model was shown to compare to within +/- 30% of the CFD solutions. This plume model was used to evaluate plume heating on the wire bundles, wheel well wall, and the interior of the upper wing skin, as well as the

primary penetration in the WLE cavity. Arc jet tests were pursued to provide another source of verification of the plume model, the results of which are currently being evaluated.

An equilibrium air coupled venting and thermal model of the entire left wing of the Orbiter was developed principally to provide the best assessment possible of where the mass and energy of the high temperature gas was propagating within the wing outside of the direct plume impingement zone. This allowed for the evaluation of various penetration sizes and their effect on the interior surfaces and mass and energy distribution. This tool showed the internal compartment pressure and temperature effect that result from primary and secondary penetrations on the WLE, as discussed above, and a penetration of the wing spar. For the case of a 10" diameter hole in the wing spar behind RCC panel 8, it was shown that there was sufficient energy ingested to result in significant thermal damage to the interior of the intermediate wing prior to LOS. The case was used as substantiation for the configurations that were assessed for structural deformation. It also showed that the majority of the high temperature gas would flow towards the wing glove payload bay vent. These results provided the boundary conditions for CFD analysis of the interior wing volume.

CFD analysis was performed on the flow of the wing interior to provide insight into how the high temperature gases entering the wing from a breach of the spar behind RCC panel 8 would behave. The results of these analysis showed that a plume would remain coherent until impacting the wheel well wall and a majority of the flow would circulate back towards the 1040 spar vent as discussed above. The data from this analysis were used to update the heat transfer coefficients in the coupled vent / thermal analysis tool. Also, the analysis was used to assess whether or not an obstruction in the WLE cavity would be enough to redirect the flow such that it would enter into the wing interior normal to the spar. This assessment is important in that it would dictate the size of hole necessary to burn the wire bundle at the observed rate because of the distance involved in reaching the bundle from the WLE spar. The results indicated that any hardware impinged upon by the primary plume would be enough to arrest the momentum and redirect the flow. Since the interior geometry of the WLE cavity and the exact location, size, and shape of the WLE damage location remain unknown, it is likely that the plume entering the WLE did come in normal to the spar even if the flow entered the WLE cavity with some momentum.

Another concern of the internal heating group was the additional energy produced by the combustion of the aluminum that makes up the structure of the Orbiter. There was some concern that the combustion of aluminum could provide more than twice the energy available from only the ingested high temperature gas. Although more applicable to oxygen rich atmospheres, an analysis was performed to provide an estimate of the additional energy available at the high altitudes where the Orbiter was flying prior to breakup. The results showed that prior to EI+600 seconds only 30% additional energy could be released due to aluminum combustion and that variations in the breach hole size would result in larger changes in the total energy ingested. Given the uncertainty in the breach hole size, and therefore, the energy of the reentry-gas ingested, and the uncertainty in the predicted heating rates to the internal structures, the additional heating due to aluminum combustion was enveloped by these uncertainties.

In order to evaluate various size damage configurations of the WLE in support of the working scenario, an engineering heating distribution model of the internal WLE cavity was developed. This was needed not only to assess the direct plume impingement heating but also to provide secondary plume heating or "splash" effects. These "splash" environments were required in order to assess the thermal response of the RCC panel 9 clevis and spar temperature gauges, and again to establish consistency of the assumed damage size and location. But prior to this model's development, the question of, given a large enough hole, how does the external environment couple into the internal WLE cavity environment (i.e., does the plume come in normal to the penetration surface or does it flow in with momentum), had to be understood. The first ever coupled external / internal CFD analysis of the Orbiter was performed having only a simple one-foot vented cube as the interior volume. The results showed that for hole sizes 2" in diameter and greater, the majority of the upstream boundary layer was ingested into the interior volume. This result meant that the gases outside of the shock layer, at > 10,000° F, were being pulled into the WLE cavity. It also showed that the flow coming in carried with it its momentum and thus the plume no longer came in normal to the surface. This was critical for determining the location of plume impingement from a penetration in the acreage of an RCC panel. The initial engineering model was checked against these initial CFD solutions and provided to the thermal group for use in their analysis.

Additional CFD and DSMC analysis of the interior of the WLE was pursued to confirm the engineering model further and to include various degrees of complexity in the interior geometry of the WLE cavity. These involved holes in RCC panels 7 and 8 with and without the complex interior geometry and also partially missing T-Seal cases. All involved coupling the external flow field to the WLE interior. Each case provided further insight into the flow field of the interior WLE cavity. Several significant items resulted from these cases: (1) the heating rate on the edge of the RCC hole was an order of magnitude greater than the peak heating on the exterior of the Orbiter; (2) without a structural obstruction, the interior plume heating rate was an order of magnitude greater than the peak heating on the exterior of the Orbiter; (3) if obstructed, the momentum of the incoming gas would be arrested and redirected towards the spanner beam and spar insulation; (4) the heating distributions from the DSMC and CFD cases with obstructions agreed well with the engineering model; and (5) the heating from a partially missing T-Seal would be enough to burn through the spanner beam insulation but rapidly drops off as the flow reaches the spar. The latter indicated that although there was enough energy to get through the spar in the time required, there was not enough energy available to burn a wire bundle at the observed rate. Thus, the damage site was more likely either on the RCC panel acreage or a combination of panel acreage and T-Seal and less likely a partially missing T-Seal alone.

5.5 References

Bertin, John J. (1994), ”Hypersonic Aerothermodynamics,” American Institute of Aeronautics and Astronautics, Inc., Washington, DC.

Anderson Jr., John D. (1989), “Hypersonic and High Temperature Gas Dynamics,” McGraw-Hill, Inc., New York, NY.

NSTS-37384 Image Analysis Team Final Report projected completion date June 25, 2003

NSTS-37376 Data Review and Timeline Reconstruction Team Final Report in support of the Columbia Accident Investigation, June 3, 2003

NSTS-37379 Starfire Team Final Report in support of the Columbia Accident Investigation, June 3, 2003.

NSTS-37383 Vehicle Data Mapping Final Report in support of the Columbia Accident Investigation, June 18, 2003

NSTS-37385 Hardware Forensics Team Final Report in support of Columbia Accident Investigation projected completion, June 20, 2003

STS-107 Mishap Investigation – Combined Master Timeline, Revision 19.

NSTS-37397 Vehicle Reconstruction Team Final Report in support of the Columbia Accident Investigation, June 25, 2003

NSTS-60502 Columbia Working Scenario Final Report, projected completion date July 1, 2003

Chao, D. C. (2002), ”STS-107 Pre-Flight Aeroheating Report,” Boeing Technical Memorandum, Boeing NASA Systems – Houston, No. ATA-TM-02-0009.

Fay, J. A. (1958), and Riddell, F. R. “Theory of Stagnation Point Heat Transfer in Dissociated Air,” Journal of the Aeronautical Sciences, Vol. 25, No.2.

References for Section 5.2.2

“Orbiter Entry Heating Prediction Methods and Database,” Rockwell International Document STS 83-0948, Rev. 1, July 1988.

Fay, J.A. (1958) and Riddell, F.R., "Theory of Stagnation Point Heat Transfer in Dissociated Air," Journal of the Aeronautical Sciences, Vol. 25, No. 2, pp 73-85.

Beckwith, J.E. (1961), and Cohen, N.B., " Application of Similar Solutions to Calculation of Laminar Heat Transfer on Bodies with Yaw and Large Pressure Gradients in High Speed Flow," NASA TND-625.

Eckert, E.R.G. (1955), "Engineering Relations for Friction and Heat Transfer to Surfaces in High Velocity Flow," Journal of the Aeronautical Science, pp 585-587.

Spalding, D.G. (1964), and Chi, S.W., "The Drag of a Compressible Turbulent Boundary Layer on a Smooth Flat Plate with and without Heat Transfer," Journal of Fluid Mechanics, Vol. 18, pp 117-143.

Miller, B.A. (1984), "An Engineering Approach for Estimating Aeroheating to the Partially Catalytic STS Orbiter TPS Surface," Rockwell International Document STS 84-0015.

Holden, M.S. (????), "Boundary Layer Displacement and Leading Edge Bluntness Effects on Attached and Separated Laminar Boundary Layer in a Compressible Corner, Part I; Theoretical Study," AIAA Journal, Vol. 8, No. 12, pp 2179-2188, and "Part II: Experimental Study," AIAA Journal, Vol. 9, No. 1, pp 84-93.

Keys, J.W. (1973), and Hains, F.D., "Analytical and Experimental Studies of Shock Interference Heating in Hypersonic Flows," NASA TND-7139.

Bertin, J.J. (1975), Graumann, B.W. and Goodrich, W.D., "High Velocity and Real Gas Effects on Weak Two-Dimensional Shock Interaction Patterns," Journal of Spacecraft, Vol. 12, No. 3, pp 155-161.

Bertin, J.J. (1976), Mosso, S.J., Bacrette, D.W. and Goodrich, W.D., "Engineering Flowfields and Heating Rates for Highly Swept Wing Leading Edges," Journal of Spacecraft, Vol. 13, No. 9.

References for Section 5.2.3

Stone, David R. (1972), and Cary, Aubrey M. jr, "Discrete Sonic Jets Used as Boundary-Layer Trips at Mach Numbers of 6 and 8.5", NASA TN D-6802.

Zukoski, Edward E. (1964), and Spaid, Frank W., "Secondary Injection of Gases into a Supersonic Flow", AIAA J., vol. 2, no. 10, pp. 1689-1696.

References for Section 5.2.4

Steinbrenner, J. P. (1990), Chawner, J. R., and Fouts, C. L., "The GRIDGEN 3D Multiple Block Grid Generation System," WRDC-TR-90-3022, Wright Research and Development Center Report.

Alter, S.J. (1997), "The Volume Grid Manipulator (VGM): A Grid Reusability Tool," NASA CR-4772.

Sorenson, R.L. (1995), and Alter, S.J., "3DGRAPE/AL Users' Manual," NASA RP-1377, October 1995.

AMTEC Engineering Inc., (2002), "CFD Analyzer 3.0: User's Manual."

Olynick, D.D.R. (1996), "Importance of 3-D Grid Resolution and Structure for Calculating Reentry Heating Environments," AIAA Paper 96-1857.

Strang, W.Z. (1988), "QBERT: A Grid Evaluation Code," AFWAL Technical Memorandum 99-193, Wright Research and Development Center Report.

Thompson, J.F. (1985), Warsi, Z.U.A., and Mastin, C.W., *Numerical Grid Generation Foundations and Applications*, pp. 171-184, North-Holland, 1st ed.

Bird, G.A. (1976), Molecular Gas Dynamics, Clarendon Press, Oxford.

Boyles, K.A. (2003), LeBeau, G.J., Lumpkin, F.E., Wilmoth, R.G., "The Use of Virtual Sub-Cells in DSMC Analysis of Orbiter Aerodynamics at High Altitudes Upon Reentry", *41st AIAA Aerospace Sciences Meeting and Exhibit*, Reno, NV.

Stewart, D. (1997), "Surface Catalysis and Characterization of Proposed Candidate TPS for Access-to-Space Vehicles," NASA TM 112206.

DeVenezia, J. (1995), Wang, K.C., and Caram, J.M., "Space Shuttle Orbiter Wing Leading Edge Heating Predictions and Measurements," NASA CP 3248, Part 2, pp.741-809.

Baranowski, L. C. (1983), and Kipp, H. W., "A Study of Leeside Flow Field Heat Transfer On Shuttle Orbiter Configurations," NASA Contract NAS1-16839.

Berry, S.A. (2002), Hamilton, H.H., "Discrete Roughness Effects on Shuttle Orbiter at Mach 6," AIAA Paper 2002-2744.

Bouslog, S.A. (1995), An, M.Y., and Derry, S.M., "Orbiter Windward-Surface Boundary-Layer Transition Flight Data," Orbiter Experiments (OEX) Aerothermodynamics Symposium, NASA CP 3248, Part 2, pp. 703-740.

Brauckmann, G.J. (1995), Paulson, J.W., and Weilmuenster, J.K., "Experimental and Computational Analysis of Shuttle Orbiter Hypersonic Trim Anomaly," *Journal of Spacecraft and Rockets*, Vol. 32, No. 5, pp. 758-764.

Buck, G.M. (1989), "Automated Thermal Mapping Techniques Using Chromatic Image Analysis," NASA TM 101554.

Buck, G.M. (2000), "Rapid Model Fabrication and Testing for Aerospace Vehicles," AIAA Paper 2000-0826.

Buck, G.M. (1993), and Vasquez, P., "An Investment Ceramic Slip-Casting Technique for Net-Form, Precision, Detailed Casting of Ceramic Models," U. S. Patent 5,266,252.

Daryabeigi, K. (2003), Berry, S.A., Horvath, T. J., and Nowak, R. J., "Finite Volume Numerical Methods for Aeroheating Rate Calculations From Infrared Thermographic Data," AIAA Paper 2003-3634.

Fay, J.A. (1958), and Riddell, F.R., "Theory of Stagnation Point Heat Transfer in Dissociated Air," *Journal of Aeronautical Sciences*, Vol. 25, No. 2.

Haney, J.W. (1995), "Orbiter Pre STS-1 Aeroheating Design Data Base Development Methodology: Comparison of Wind Tunnel and Flight Test Data," Orbiter Experiments (OEX) Aerothermodynamics Symposium, NASA CP 3248, Part 2, pp. 607-676.

Joels, M.K. (1982), and Kennedy, G.P., "The Space Shuttle Operators Manual," Ballantine Books, New York.

Jones, R.A. (1969), and Hunt, J.L., "Use of Tetrafluoromethane to Simulate Real-Gas Effects on the Hypersonic Aerodynamics of Blunt Vehicles,", NASA TR 312.

Merski, N.R. (1998a), "Reduction and Analysis of Phosphor Thermography Data With the IHEAT Software Package," AIAA Paper 98-0712.

Merski, N.R. (1998b), "Global Aeroheating Wind-Tunnel Measurements Using Improved Two-Color Phosphor Thermography Method" *Journal of Spacecraft and Rockets*, Vol. 36, No. 2, pp. 160-170.

Miller, C.G. (1982), “Experimental Investigation of Gamma Effects on Heat Transfer to a 0.006 Scale Shuttle Orbiter at Mach 6,” AIAA Paper 82-0826.

Miller, C.G. (1999), “Development of X-33/X-34 Aerothermodynamic Data Bases: Lessons Learned and Future Enhancements,” NATO Research and Tech. Org., Applied Vehicle Technology Symposium Aerodynamic Design and Optimization of Flight Vehicles in a Concurrent Multi-Disciplinary Environment, paper no. 32.

Miller, C.G. (1990), “Langley Hypersonic Aerodynamic/Aerothermodynamic Testing Capabilities - Present and Future,” AIAA Paper 90-1376.

Throckmorton, D.A. (1995), “Orbiter Leeside Surface Aeroheating Environment Characterization,” Orbiter Experiments (OEX) Aerothermodynamics Symposium, NASA CP 3248, Part 2, pp. 811-822.

Hartung, L.C. (1988), and Throckmorton, D.A., “Space Shuttle Entry Heating Data Book: Volume I – STS-2,” NASA RP 1191.

Stewart, D., (1997), "Surface Catalysis and Characterization of Proposed Candidate TPS for Access-to-Space Vehicles", NASA TM 112206.

References for Section 5.3.2

Shapiro, A.H. (1953), “The Dynamics and Thermodynamics of Compressible Fluid Flow,” John Wiley & Sons, Inc.

References for Section 5.3.3

Hiester, N.K. (1966), and Clark, C.F., “Feasibility of Standard Evaluation Procedures for Ablating Materials,” NASA CR-379.

Kays, W.M. (1980), and Crawford, M.E., “Convective Heat and Mass Transfer”, McGraw-Hill Book Company, 2nd Edition.

Shapiro, A. (1958), "The Dynamics and Thermodynamics of Compressible Fluid FLow – Volume 1", 1953.
Moeckel, W. and Weston, K. "Composition and Thermodynamic Properties of Air in Chemical Equilibrium", NACA TN 4265.
Hrycak, P. (1970), et al., "Experimental Flow Characteristics of a Single Turbulent Jet Impinging on a Flat Plate", NASA TN D-5690.

Abramovich, (1963), "Theory of Turbulent Jets".

O'Connor, T. J. (1965), Comfort, E. H., and Cass, L. A. "Turbulent Mixing of Axisymmetric Jets of Partially Dissociated Nitrogen and Ambient Air", AVCO Corp Report RAD-TR-65-18.

Donaldson, C. DuP. (1971), and Snedeker, R. S. "A Study of Free Jet Impingements, Parts 1 & 2", J. Fluid Mechanics, Vol 45.

Rebrov, A.K. (1982), “Free Jet as an Object of Non-equilibrium Processes Investigation”, 13th International Symposium on Rarified Gas Dynamics, Vol II, pgs 849-864.

Chen, Y.-S. (1993), Liaw, P., Shang, H.-M. and Chen, C. P., “Numerical Analysis of Complex Internal and External Viscous Flows with a Second-Order Pressure-Based Method,” AIAA Paper 93-2966.

Roy, C. J. (2002), McWherter-Payne, M. A., and Oberkampf, W. L., “Verification and Validation for Laminar Hypersonic Flowfields Part 1: Verification,” manuscript submitted to the AIAA Journal.

References for Section 5.3.4

Gordon, S. (1994), and McBride, B.J., "Computer Program for Calculation of Complex Chemical Equilibrium Compositions and Applications," *NASA Reference Publication 1311*, National Aeronautics and Space Administration.
Glassman, I. (1977), "Combustion," Third Edition, Academic Press.

Werley, B. (1993), Barthelemy, H., Gates, R., Slusser, J.W., Wilson, K.B., and Zawierucha, R., "A Critical Review of Flammability Data for Aluminum," Flammability and Sensitivity of Materials in Oxygen-Enriched Environments, ASTM STP 1197, D.D. Janoff and J.M. Stoltzfus, Eds., American Society for Testing and Materials.

Newton, B. (2000), Hull, W., Stradling, J., "Failure Analysis of Aluminum-Bodied Medical Regulators," Flammability and Sensitivity of Materials in Oxygen-Enriched Environments, ASTM STP 1395, T.A. Steinberg, B.E. Newton, and H.D. Beeson, Eds., American Society for Testing and Materials.

References for Section 5.3.5

Fay, J.F. (1993), "Program CHCHVENT Version 5 User's Manual and Software Description." Sverdrup Technology/MSFC Group, Report 631-001-93-007.

Gnoffo, P.A. (1995), Weilmuenster, K.J., and Alter, S.J., "A Multiblock Analysis for Shuttle Orbiter Re-entry Heating from Mach 24 to Mach 12," NASA CP 3248.

Shapiro, A.H. (1953), The Dynamics and Thermodynamics of Compressible Fluid Flow, Volume 1, New York: John Wiley & Sons.

Haukohl, J. (1972), and Forkois, J.L. "Inflow Venting Orifice Efficiency Test Report." Lockheed Missiles & Space Company Report LMSC-HREC D225598, January.

Wong, LC. (1994), et al, "Orbiter Entry Venting Substantiation Report." Rockwell International Space Systems Division, SSD94D0275.

Cline, D.E. (2002), "As Built OV-102, Flight 27, STS-109 Integrated Vent Model," Boeing Company-Houston, DWC-2002-003.

Cline, D.E. (2003), and Torres, "Main Gear Wheel Well Leakage Mapping and Model," presentation to Aero-Thermal Mishap Investigation team, Boeing-PVD.

Hartung, L.C. (1988), Throckmorton, D.A., "Space Shuttle Entry Heating Data Book, Volume III – STS-5", NASA RP-1193.

Gong, L. (1984), Ko, W.L., Quinn, R.D., "Thermal Response of Space Shuttle Wing During Reentry Heating", NASA TM-85907, June 1984.
Thermal Protection Systems Expert and Material Property Database (TPSX), Web Edition Version 3, NASA Ames Research Center, 2003.

Incropera, F.P. (1985), Dewitt, D.P., "Fundamentals of Heat and Mass Transfer", Second Edition, John Wiley and Sons, Inc..

References for Section 5.3.6

Anon. (1976), U.S. Standard Atmosphere, 1976, National Oceanic and Atmospheric Administration, NASA, and U.S. Air Force.

"RCC 8-9 T-Seal Coupled Internal/External 2-D Bridging Phase II Results", Boeing Rocketdyne Propulsion and Power, CFDPUB00862.

"High Enthalpy Flow Benchmark Results", Boeing Rocketdyne Propulsion and Power, CFDPUB00822.

"High Enthalpy Flow Benchmark Extension Results", Boeing Rocketdyne Propulsion and Power, CFDPUB00865.

"Underexpanded Jet Benchmark Results", Boeing Rocketdyne Propulsion and Power, CFDPUB00866.

"RCC8 10in Leading Edge Breach Results", Boeing Rocketdyne Propulsion and Power, CFDPUB00867.

"Hybrid Viscous Unstructured CFD Mesh Technology", Boeing Rocketdyne Propulsion and Power, CFDPUB00756.

"Application of ICAT/BCFD in the Rocketdyne Design Environment", Boeing Rocketdyne Propulsion and Power, CFDPUB00752.

Goulard, R., "On Catalytic Recombination Rates in Hypersonic Stagnation Heat Transfer," Jet Propulsion, vol. 28, no. 11, 1958, pp. 737-745.

FLUENT 6.1 Users Guide, Volumes 1-24. Fluent Incorporated, 10 Cavendish Court, Centerra Resource Park, Lebanon, N.H. 03766.

References for Section 5.6.3

Gnoffo, P.A. (1989), Gupta, R.N., and Shinn, J., "Conservation Equations and Physical Models for Hypersonic Air Flows in Thermal and Chemical Nonequilibrium," NASA TP 2867.

Cheatwood, F.M. (1996), and Gnoffo, P.A. "Users Manual for the Langley Aerothermodynamic Upwind Relaxation Algorithm (LAURA)," NASA TM 4674.

Roe, P.L. (1981), "Approximate Riemann Solvers, Parameter Vectors, and Difference Schemes," Journal of Computational Physics, Vol.43, pp357-372.

Yee, H.C., (1986), "On Symmetric and Upwind TVD Schemes," NASA TM-88325.

Weilmuenster, K.J. (1994), Gnoffo, P.A., Greene, F.A., "Navier-Stokes Simulations of Orbiter Aerodynamic Characteristics Including Pitch Trim and Bodyflap," Journal of Spacecraft and Rockets, Vol. 31, No. 3, pp355-366.

Gnoffo, P.A. (1994), Weilmuenster, K.J., Alter, S.J., "Multiblock Analysis for Shuttle Orbiter Re-entry Heating from Mach 24 to Mach 12," Journal of Spacecraft and Rockets, Vol. 31, No. 3, pp367-377.

Kleb, W.L. (1994), Weilmuenster, K.J., "Characteristics of the Shuttle Orbiter Leeside Flow Dring a Re-Entry Condition," Journal of Spacecraft and Rockets, Vol. 31, No. 1, pp8-16.

Orbiter Experiments (OEX) Aerothermodynamics Symposium (1995), Edited by David Throckmorton, NASA Conference Publication 3248, Part I and II.

Wong, C.C. (1995), Soetrisno, M., Blottner, F.G., Imlay, S.T., and Payne, J.L., "PINCA:A ScalableParallel Program for Compressible Gas Dynamics with Nonequilibrium Chemistry," SAND 94-2436, Sandia National Laboratories, Albuquerque, NM.

Wong, C.C., Blottner (1995), F.G., Payne, J.L., and Soetrisno, M., "Implementation of a Parallel Algorithm for Thermo-Chemical Nonequilibrium Flow Solutions," AIAA Paper 95-0152.

Hassan, B. (1998), Kuntz, D.W., and Potter, D.L., "Coupled Fluid/Thermal Prediction of Ablating Hypersonic Vehicles," AIAA Paper 98-0168.

Kuntz, D.W. (1999), Hassan, B., and Potter, D.L., "An Iterative Approach for Coupling Fluid/Thermal Predictions of Ablating Hypersonic Vehicles," AIAA Paper 99-3460.

Yoon, S. (1988), and Jameson, A., "An LU-SSOR Scheme for the Euler and Navier Stokes Equa-tions," AIAA Paper 87-0600.

Peery, K.M. (1986), and Imlay, S.T., "An Efficient Implicit Method for Solving Viscous Multi-Stream Nozzle/Afterbody Flow Fields," AIAA Paper 86-1380, June 1986.

Steger, J.L. (1981), and Warming, R.F., "Flux Vector Splitting of the Inviscid Gasdynamic Equations with Applications to Finite Difference Methods," *Journal of Computational Physic*s, Vol. 40, pp. 263-293.

Van Leer, B. (1979), "Towards the Ultimate Conservative Difference Scheme. V. A Second Order Sequel to Godunov's Method," *Journal of Computational Physic*s, Vol. 32, No. 1, pp. 101-136.

Payne, J.L. (1999), and Hassan, B., "Massively Parallel Computational Fluid Dynamics Calculations for Aerodynamics and Aerothermodynamic Applications," Proceedings of the 1998 HPC-CP/CAS Workshop, NASA/CP 1999-208757, pp. 111-116.

Srinivasan, S. (1986), Tannehill, J.C., and Weilmuenster, K.J., "Simplified Curve Fits for the Thermodynamic Properties of Equilibrium Air," ISU-ERI-AMES-86041, Iowa State University.

Roy, C.J. (2000), McWherter-Payne, M.A., and Oberkampf, W.L., "Verification and Validation for Laminar Hypersonic Flowfields," AIAA Paper 2000-2550.

Roy, C.J. (2002), McWherter-Payne, M.A., and Oberkampf, W.L., "Verification and Validation for Laminar Hypersonic Flowfields Part 1: Verification," manuscript submitted to the *AIAA Journa*l.

Payne, J.L. (1995), and Walker, M.A., "Verification of Computational Aerodynamic Predictions for Complex Hypersonic Vehicles using the INCA TM Code," AIAA Paper 95-0762.

Roy, C.J. (2002), Gallis, M.A., Bartel, T.J., and Payne, J.L., "Navier-Stokes and DSMC Simulations for Hypersonic Laminar Shock-Shock Interaction Flows," AIAA Paper 2002-0737.

Roy, C.J. (2002), Gallis, M.A., Bartel, T.J., and Payne, J.L., "Navier-Stokes and DSMC Predictions for Laminar Hypersonic Shock-Induced Separation," manuscript to be submitted to the *AIAA Journa*l.

Alter, S.J. (1997), "The Volume Grid Manipulator (VGM): A Grid Reusability Tool," NASA CR-4772,.

Taubin, G. (1995), "A Signal Processing Approach to Fair Surface Design," SIGGRAPH.

Bartel, T.J. (2001), Plimpton, S.J., and Gallis, M.A., "Icarus: A 2-D Direct Simulation Monte Carlo (DSMC) Code for Multi-Processor Computers: User's Manual - v 10.0," Sandia Report SAND2001-2901, Sandia National Laboratories, Albuquerque, NM.

Bird, G.A. (1994), *Molecular Gas Dynamics and the Direct Simulation of Gas Flows*, Clarendon Press, Oxford.

Wagner, W. (1992), "A convergence proof for bird direct simulation Monte-Carlo method for the Boltzmann-equation," *J. Stat. Phys.*, **66**(3-4), pp.1011-1044.

Gallis, M.A. (2001), Torczynski, J.R., and Rader, D.J., "An approach for simulating the transport of spherical particles in a rarefied gas flow via the direct simulation Monte Carlo method," *Phys. Fluids*, **13**(11), pp.3482-3492.

Gallis, M.A. (2002), Torczynski, J.R., and Rader, D.J., "Calculations of the near-wall thermophoretic force in rarefied gas flow," *Phys. Fluids*, **14**(12), pp.4290-4301.

Torczynski, J.R. (2002), Gallis, M.A., and Piekos, E.S., “Comparison of methods for simulating gas forces on moving microbeams,” ASME Paper IMECE2002-33788.

Roy, C. J. (2002), Gallis, M. A., Bartel, T. J., and Payne, J. L., “Navier-Stokes and DSMC Simulations for Hypersonic Laminar Shock-Shock Interaction Flows,” AIAA Paper 2002-0737.

Roy, C. J. (2002), Gallis, M. A., Bartel, T. J., and Payne, J. L., “Navier-Stokes and DSMC Predictions for Laminar Hypersonic Shock-Induced Separation,” manuscript to be submitted to the *AIAA Journa*l.

Shufflebotham, P.K. (1995), Bartel, T.J., Berney, B., “Experimental validation of a direct simulation by Monte Carlo molecular gas flow model,” *J. Vac. Sci. Technol. B*, **13**(4), pp. 1862-1866.

Johannes, J.J. (1997), Bartel, T.J., Hebner, G.A., Woodworth, J., Economou, D.J., “Direct simulation Monte Carlo of inductively coupled plasma and comparison with experiments,” *J. Electrochem. Soc.*, **144**(7), pp. 2448-2455.

Gallis, M.A. (1999), and Bartel, T.J., “Direct simulation Monte Carlo modeling of viscous interactions,” AIAA Paper 99-3453.

Chakravarthy, S.R. (1985), and Osher, S., Computing With High-Resolution Upwind Schemes for Hyperbolic Equations, Proceedings of the 1983 AMS-SIAM Summer Seminar on Large-Scale Computations in Fluid Mechanics, published by American Mathematical Society in Lectures in Applied Mathematics, Vol. 22.

Rajagopal, K. (1997), Numerical Simulation of Flow Inside an Orbiter Wing Section during Entry through a Hole from a Possible On-Orbit Debris Impact Damage, AIAA Paper No. 97-2227.

Bird, G.A. (1976), *Molecular Gas Dynamics*, Clarendon Press, Oxford (1976).

Wilmoth, R.G. (1996), LeBeau, G.J. and Carlson, A.B., “DSMC Grid Methodologies for Computing Low-Density, Hypersonic Flows About Reusable Launch Vehicles”, AIAA Paper No. 96-1812.

LeBeau, G.J. (1999), "A Parallel Implementation of the Direct Simulation Monte Carlo Method", Computer Methods in Applied Mechanics and Engineering, Vol. 174, pp. 319-337.

LeBeau, G.J. (2001), and Lumpkin III, F.E., “Application highlights of the DSMC Analysis Code (DAC) software for simulating rarefied flows”, *Computer Methods in Applied Mechanics and Engineering*, Vol. 191, Issue 6-7, pp. 595-609.

References for Section 5.6.4

Steinbrenner, J.P. (1990), Chawner, J.R., and Fouts, C.L., “The GRIDGEN 3D Multiple Block Grid Generation System,” WRDC-TR-90-3022, Wright Research and Development Center Report.

Alter, S.J. (1997), “The Volume Grid Manipulator (VGM): A Grid Reusability Tool,” NASA CR-4772.

Sorenson, R.L. (1995), and Alter, S.J., “3DGRAPE/AL Users’ Manual,” NASA RP-1377

AMTEC Engineering Inc. (2002), “CFD Analyzer 3.0: User’s Manual.”

Olynick, D.D.R. (1996), “Importance of 3-D Grid Resolution and Structure for Calculating Reentry Heating Environments,” AIAA Paper 96-1857.

Strang, W.Z. (1988), “QBERT: A Grid Evaluation Code,” AFWAL Technical Memorandum 99-193, Wright Research and Development Center Report.

Thompson, J.F. (1985), Warsi, Z.U.A., and Mastin, C.W., *Numerical Grid Generation Foundations and Applications*, pp. 171-184, North-Holland, 1st ed.

Alter, S.J. (1997) "The Volume Grid Manipulator (VGM): A Grid Reusability Tool," NASA CR-4772.

Taubin, G. (1995), "A Signal Processing Approach to Fair Surface Design," SIGGRAPH.

5.6 Appendix for Aerothermodynamics

5.6.1 Engineering Tools

5.6.1.1 XF0002

XF0002/Exact Attitude Aerothermal Heating Computer Program is the main tool utilized for predicting re-entry heating of the Orbiter. The XF0002 Aeroheating Computer Program was formulated as a design tool for predicting ascent or re-entry heating to geometrically simple vehicle shapes. The program accurately predicts local properties and heat fluxes within the scope of the many user selected options. The options were obtained through the application of open literature publications on the subject and have been modified as required.

For re-entry, 2008 body points (aeroheating models) are used to cover the whole Orbiter body. The models are correlated with wind tunnel test data and the flight data from STS-1 through 5. The technical approaches and the body point heating methodology used in this program are described in Section 5.2.1.

XF0002 is under configuration control by Boeing Orbiter Vehicle Engineering Office.

5.6.2 Wind Tunnel Facilities & Measurement Techniques

The purpose of this section is to provide brief descriptions of the hypersonic aerothermodynamic wind-tunnel facilities and global heating measurement techniques at the NASA Langley Research Center utilized in support of the STS-107 accident investigation. Details regarding these facilities can be found in Miller (1990,1999).

5.6.2.1 Mach 6 Air

Heated, dried, and filtered air is used as the test gas. Typical operating conditions for the tunnel are: stagnation pressures ranging from 30 to 500 psia; stagnation temperatures from 760 deg to 1000 deg R; freestream unit Reynolds numbers from 0.5 to 8 million per ft., freestream and post normal shock gamma of 1.4, and a normal shock density ratio of 5.3. A two-dimensional, contoured nozzle is used to provide nominal freestream Mach numbers from 5.8 to 6.1. The test section is 20.5 by 20 in; the nozzle throat is 0.399 by 20.5 in. The test core varies from 12 to 14 inches depending on the operating condition. A floor-mounted model injection system can insert models from a sheltered position to the tunnel centerline in less than 0.5 s. For heat-transfer and flow visualization tests, the model residence time in the flow is only a few seconds; nominal run time for force & moment testing is approximately 60 to 120 s in this facility although longer run times are possible. Table 1 (sec 4.3.2) summarizes the nominal test conditions for the tests performed for this investigation.

5.6.2.2 Mach 6 CF4

Heated, dried, and filtered carbon tetrafluoride (CF_4 or Freon 14; molecular weight of 88 which is three times heavier than air) is used as the test gas. Typical operating conditions for the tunnel are: stagnation pressures ranging from 60 to 2000 psia, stagnation temperatures up to 1300 R, freestream unit Reynolds numbers from 0.01 to 0.55 million per ft., freestream gamma of 1.21 and a post normal shock gamma of 1.1, and a normal shock density ratio of 11.7. A contoured axisymmetric nozzle is used to provide a nominal freestream Mach numbers from 5.9 to 6.0. The nozzle exit diameter is 20 in with the flow exhausting into an open jet test section; the nozzle throat diameter is 0.466 in. The test core varies from 12 to 14 inches depending on the operating condition. A floor-mounted model injection system can inject models from a sheltered position to the tunnel centerline in less than 0.5 s. For heat-transfer and flow visualization tests, the model residence time in the flow is only a few seconds; nominal run time for force &

moment testing is approximately 20 s. Table 1 (sec 4.3.2) summarizes the nominal test conditions for the tests performed for this investigation.

5.6.2.3 IR Thermography

Model surface temperatures were measured using a FLIR SC2000 infrared imaging system having an un-cooled microbolometer-based focal plane array detector with 320 × 240 detector elements. The imager has a field of view of 24° × 18°, and is sensitive to infrared radiation in the 7–12 micrometer range of the electromagnetic spectrum. An eight-inch diameter zinc selenide window with a transmittance of 0.98 in the 7-14 micrometer spectral range was used for optical access to the test section. The measured infrared radiation was converted to actual surface temperatures using the emittance of a target, which for the phosphor-coated fused silica model was determined to be 0.906. The imager produces 30 frames of images per second, while the data acquisition hardware used with the infrared imaging system was only capable of real–time digital storage of approximately 6 frames per second. With temperature images acquired at different times during a wind-tunnel run, global heat-transfer images are computed assuming one-dimensional semi-infinite heat conduction formulation with convective boundary conditions. Details regarding the test methodology can be found in Daryabeigi, (2003).

5.6.2.4 Phosphor Thermography

With the two-color relative-intensity phosphor thermography technique (Buck, 1989; Merski, 1998a-b), ceramic wind-tunnel models are fabricated and coated with phosphors that fluoresce in two regions of the visible spectrum when illuminated with ultraviolet light. The fluorescence intensity is dependent upon the amount of incident ultraviolet light and the local surface temperature of the phosphors. By acquiring fluorescence intensity images with a color video camera of an illuminated phosphor model exposed to flow in a wind tunnel, surface temperature mappings can be calculated on the portions of the model that are in the field of view of the camera. A temperature calibration of the system conducted prior to the study provides tables used to convert the ratio of green and red intensity images to global temperature mappings. With temperature images acquired at different times during a wind-tunnel run, global heat-transfer images are computed assuming one-dimensional semi-infinite heat conduction. The primary advantage of the phosphor technique is the global resolution of the quantitative heat-transfer data. Such data can be used to identify the heating footprint of complex, three-dimensional flow phenomena (e.g., boundary layer transition locations, flow separation and reattachment locations, etc.) that are extremely difficult to resolve by discrete measurement techniques.

5.6.2.5 Flow Visualization

Flow visualization in the form of schlieren and oil-flow techniques was used to complement the surface heating and force & moment tests. The LaRC 20-Inch Mach 6 air and CF_4 Tunnels are equipped with a pulsed white-light, Z-pattern, single-pass schlieren system with a field of view encompassing the entire test core. Images were recorded on a high-resolution digital camera.

Surface streamline patterns were obtained using an oil-flow technique. Orbiter models were coated with a phosphorescent material dispersed in a thin layer of silicon oil. After the model surface was prepared, the model was injected into the airstream and the development of the surface streamlines was recorded with a conventional video camera. The model was retracted immediately following flow establishment and formation of streamline patterns, and post-run digital photographs were taken.

5.6.3 CFD/DSMC Tools

5.6.3.1 GASP (ARC)

The GASP Real-Gas Navier-Stokes code was the primary code for solutions accomplished at Ames Research Center. This code originated as a commercially available code developed at AeroSoft, Inc, but has been modified at ARC to enhance both capability and robustness specifically for hypersonic reentry applications.

The GASP Reynolds Averaged Navier-Stokes code is a three-dimensional (3D) finite-volume code. Upwind flux options exist for this code, but for the present solutions the Van Leer inviscid flux formulation was applied in all three directions. A formally 3rd order upwind-biased MUSCL scheme combined with min-mod limiter is selected to provide higher order accuracy. Experience at ARC with this code has indicated that wall normal spacing is sufficient to obtain accurate heat transfer with the Van Leer flux formulation and 3rd order accuracy provided the wall node Cell Reynolds number is kept below a value of 5. For most of the calculations provided in the present work the wall node Cell Reynolds number is approximately 1, which yields the best results in convergence and accuracy. Time advancement to steady state is accomplished with either a 2D Approximate Factorization, AF2, in the nominal cross-flow plane with planar relaxation in the streamwise direction, or, alternatively, with a point-Jacobi algorithm with inner iterations. Experience at ARC has shown that these two time-advancement schemes as implemented in GASP are nearly identical in convergence, robustness and speed.

The 5-species finite reaction rate model for dissociating air of Park was used in these calculations using GASP. In this chemistry model, air is composed primarily of molecular nitrogen, N2, and molecular oxygen, O2, with the possibility of dissociation at high temperature into atomic nitrogen, N, and atomic oxygen, O, followed by formation of NO. For the high Mach number, high altitude portion of a low Earth orbit reentry trajectory as considered herein, the molecular oxygen, O2, present in the atmosphere will almost entirely dissociate into atomic oxygen, O, upon encountering the bow shock. However, N2 will undergo but slight dissociation with lesser amounts of N and NO formed. The reaction rates are typically slow enough that little recombination occurs for hypersonic flows prior to the exit boundary except for that due to the catalytic effect of certain thermal protection surface materials.

The real-gas air chemistry has an important effect on the hypersonic flow about the orbiter by altering the shock location since energy is required to dissociate the molecular oxygen through the shock, the temperature and density rise through the shock are not as great as would otherwise occur for a perfect gas thereby reducing the effective gamma for the real gas in the shock relations. A further real-gas effect is that chemical energy is released at the shuttle surface due to recombination of O to O2 as a consequence of the catalytic behavior of the RCG shuttle tile material. This catalytic wall effect yields a higher heating rate to the wall than for non-catalytic materials. Species transport properties are calculated using Blottner relations with mixture properties calculated using Eucken relations.

Stewart characterized the surface catalytic recombination of air due to various thermal protection system insulation materials including RCG as used on the windward side of the shuttle orbiter. RCG and other catalytic materials act to enhance the rate of recombination of atomic oxygen into molecular oxygen and of atomic nitrogen into molecular nitrogen. Molecular NO is assumed to experience no catalytic effect. In the process, additional thermal energy is released to the wall due to the chemical reaction occurring at the surface.

The primary wall boundary condition used for these shuttle calculations is that of radiative equilibrium combined with the above RCG catalytic behavior. In this viscous wall boundary condition, there is an assumption that the radiative heat transfer from the wall exactly balances the thermal energy transfer to the wall due to convective heat transfer combined with energy release to the wall due to the surface catalytic chemical reaction. The radiative equilibrium boundary condition requires the simultaneous solution of 4 species equations (molecular NO is not considered catalytic) combined with an equation for the energy balance, all of which are written at the wall node. To then solve this wall boundary condition for each Navier-Stokes solver iteration, a Newton-Raphson method achieves quadratic convergence.

Additional boundary conditions used include conventional point-to-point zonal boundaries, adiabatic viscous wall, free-stream, and a specified back-pressure outflow boundary condition. Point-wise boundary conditions can be specified optionally for any of the 6 faces of each grid block and were used for the vented cavity panel 9 solutions.

Most of the solutions delivered were laminar throughout the solution domain. However, some eddy-viscosity turbulence models calculations were conducted to establish approximate turbulence heating enhancements and for validation purposes. Turbulence models implemented into this code include the Baldwin-Lomax algebraic model of Baldwin-Lomax and the 2-eq SST/K-Omega turbulence model of Menter. These models have compressibility corrections suitable for hypersonic flows and have been validated for heat transfer in hypersonic strong interactions as implemented in the ARC version of the GASP code. A means for specification of turbulence transition is implemented in the code, but is not used for the present work.

The GASP code was run initially on a serial processor computer (Intel 2 GHz XEON processor running RedHat Linux v 7.3). These early runs were for fully catalytic solid surface rather than RCG on grids of approximately 3/4 million grid points and took 96 hours. To improve throughput, subsequent work was moved to the NAS parallel-processing cluster, chapman, which is based on up to 1024 SGI Origin O3K cpus. For the parallel processor runs, the grids were decomposed into as many as 48 grid blocks each of which was then run on a separate SGI processor in the NAS chapman cluster. With grids of 1.9 million grid points, the chapman parallel processor runs took approximately 48 hours.

Convergence criterion was based on examination of residual history, temperature and pressure history for selected surface points during the entire iteration sequence, and when convergence was nearly complete examination of delta T and delta P surface plots separated by 50 to 200 iterations. Typically the L2 residual would drop by 5 orders of magnitude and the selected surface temperatures and pressures would become constant. The delta T and delta P surface plots were facilitated by the gasptools package written by D. Prabhu and M. Wright of Ames and which is based on perl scripts making use of the GASP print utility and the Tecplot plotting package. Typically the delta T surface plots were examined for constant temperature within 5 degrees over the entire shuttle surface. Some of the damage cases exhibited some oscillation of approximately a 10 degree K magnitude which was deemed acceptable inasmuch as there existed a physical basis.

5.6.3.2 LAURA (LaRC)

The Langley Aerothermodynamic Upwind Relaxation Algorithm (LAURA) was applied to external and internal flow simulations for the Columbia investigation. LAURA is a high fidelity analysis tool, specialized for hypersonic re-entry physics, utilizing state-of-art algorithms for computational fluid dynamic (CFD) simulations. Key elements of LAURA include Roe's averaging and Yee's Total Variation Diminishing (TVD) formulation of second-order, inviscid flux. Yee's TVD formulation has been found to be exceptionally robust and Courant-number-independent using point-implicit relaxation for hypersonic flow simulations. The TVD algorithm uses a non-linear, minmod function as a flux limiter that maintains second-order accuracy away from extrema but can admit limit cycles in the convergence process, particularly in the vicinity of captured shocks. This occurrence usually manifests itself as a stalling of convergence at a very low error norm, essentially a benign ringing in the solution at a level that has no impact on aerothermodynamic quantities. Viscous flux is computed using central differences.

Previous simulations of STS 1,2 and 5 with LAURA to resolve questions of a pitching moment anomaly (STS 1) and to validate heating predictions were published in the AIAA Journal of Spacecraft and Rockets in 1994. Some of this material was also presented in an ITAR restricted document with more detail and dimensions. All of the current simulations specify laminar flow of air in chemical nonequilibrium (N, O, N_2, O_2, NO) and thermal equilibrium. Only CFD point 1 is simulated for internal cavity flow simulations with freestream conditions: V_∞ = 7350.6 m/s, ρ_∞ = 3.9005 10^{-5} kg/m^3, T_∞ = 217.3 K, α = 40.1681 deg., and time = 13.50.53.0. The external flow simulations are implemented on the shared, baseline grid developed for the External Environments Team. The baseline grid has been modified to allow coupling of the external flow with flow through a breach in the wing entering a vented cavity.

5.6.3.3 SACCARA (SNL)

The Sandia Advanced Code for Compressible Aerothermodynamics Research and Analysis, SACCARA, was developed from a parallel distributed memory version of the INCA code, originally written by Amtec Engineering. SACCARA employs a massively parallel distributed memory architecture based on multi-block structured grids. The solver is a Lower-Upper Symmetric Gauss-Seidel scheme based on the works of Yoon et al., and also Peery and Imlay, which provides for excellent scalability up to thousands of processors.

For the current simulations, SACCARA was used to solve the Navier-Stokes equations for conservation of mass, momentum, and energy. The convective fluxes at the interface were calculated using the Steger and Warming flux vector splitting scheme. Second-order reconstructions of the interface fluxes were obtained via MUSCL extrapolation. A flux limiter was employed which reduces the spatial discretization to first order in regions of large second derivatives of pressure and temperature. This limiting process is used to prevent oscillations in the flow properties at shock waves. The use of flux limitiers results in a mixture of first- and second-order spatial accuracy. In this study three different equations of state were used depending on the physics that where being modeled.

The simulations for wind tunnel conditions assumed a perfect gas equation of state. The ratio of specific heat and the gas constant were specified and the remaining state variables were calculated. The viscosity was calculated using Keyes curve fit for air and conductivity was determined by assuming a constant Prandtl number. An iso-thermal, no-slip wall boundary condition was applied to the shuttle surface. This boundary condition enforces a zero velocity condition at the surface and keeps the wall temperature fixed at specified a value, while also assuming a zero pressure gradient at wall. The supersonic inflow boundary condition allows the user to specify inflow variables which remain fixed during the simulation. The outflow boundary condition assumes a zero order extrapolation.

A number of the simulations at flight conditions assumed equilibrium air. Tannehill's curve fits were used to determine the pressure and temperature from the known energy and density. The viscosity was calculated using Sutherland's law for air. The conductivity was calculated by assuming a constant Prandtl number. A radiative-equilibrium, no-slip wall boundary condition was applied to the shuttle surface. The wall temperature was calculated using an emissivity of 0.9. Remaining boundary conditions were as stated above.

The solutions were assumed to be converged when the residuals dropped by six or more orders of magnitude. The iteration histories of the quantities of interest were also carefully examined

A number of code verification studies provide confidence that the SACCARA code is free from coding errors. These studies included comparison to established numerical benchmark solutions as well as code-to-code comparisons with Navier-Stokes and Direct Simulation Monte Carlo approaches.

5.6.3.4 USA (BHB)

The unified solution algorithm (USA) code is a very versatile flow solver that can be used to compute numerical solutions to a large class of aerodynamic and aerothermodynamic problems by solving the Euler or Reynolds averaged Navier-Stokes (RANS) equations. The discretization is of TVD formulation using finite volume framework. Various Riemann solvers can be used with the preferred one being the modified Lax-Freidrichs scheme. A multizonal structural grid bookkeeping method facilitates the treatment of complex geometric topologies. A real gas approach based on a finite rate chemistry formulation can be coupled or uncoupled with the fluid dynamics to treat reacting and nonreacting gaseous species. Additional information on the USA code can be obtained in Chakravarthy (1985). In this work, the approximate factorization scheme using the implicit time marching option was used. The simulations discussed in Sections 5.3.6.1.1 and 5.3.6.2.2 modeled laminar flow conditions using equilibrium air chemistry model. The external flow surface had radiative equilibrium temperature boundary condition whereas the internal surfaces were kept at cold wall temperature of 0 degree F. The simulations were speeded up using grid-sequencing. The convergence of flow simulations were confirmed by monitoring the time history of surface heating results. An additional reference for the framework in which the USA code was applied can be found in Rajagopal (1997).

5.6.3.5 ICAT (B-RKDN)

ICAT is a general Navier-Stokes code that extends the well-validated numerical algorithms and physical models found in the structured USA code into an unstructured solver. ICAT can be used to compute a numerical solution to a large class of aerodynamic and aerothermodynamic problems by solving the Euler or Reynolds averaged Navier-Stokes (RANS) equations, and offers most of the chemistry, boundary condition and solver features of USA. However, the unstructured grid solver available in ICAT offers the advantage of being able to use hybrid viscous grids, which take an order of magnitude less time to create than structured grids, for complex geometries. The use of ICAT, along with Boeing grid generation tools, enabled the modeling and solution of complex orbiter wing and internal geometries in days, rather than in the weeks required for a comparable structured grid model and solution. The most important features of ICAT are currently being integrated into BCFD, Boeing's next generation structured/unstructured solver.

5.6.3.6 FLUENT (LMSC)

FLUENT 6.1 is a commercial Navier-Stokes solver for unstructured meshes. It is a cell-centered, finite-volume code. It is easy to use and the license entails full technical support, as well as two meshing programs called "Gambit" and "TGrid". Users can add their own functionality and models to FLUENT through the use of C-programs, with
Fluent providing a wide range of looping macros for accessing cell centers and face centers.

FLUENT's three solvers can be used to compute the flow and heat transfer for all flow regimes, from low subsonic via transonic and supersonic to hypersonic. The turbulence can be modeled by means of the Spalart-Allmaras model, the k-epsilon or k-omega families, the Reynolds Stress Model, the LES model, or the DES model. The software includes an integrated postprocessing suite.

FLUENT's broad range of physical models, designed to work on unstructured grids, is what differentiates it from other codes. The physical models include combustion models and associated multi-species capability, multiphase models, and radiation models. Finally, problems in which object boundaries move with respect to each other (e.g., stage
separation and store separation) are treated via FLUENT's moving-deforming mesh model.

Fluent Inc. also offers two finite-element solvers - FiDAP and PolyFlow
for engineers working with low-Reynolds number flows, i.e., materials
processing applications, viscoelastic flows, etc.

5.6.3.7 DAC (JSC)

DAC represents NASA's state-of-the-art implementation of the Direct Simulation Monte-Carlo (DSMC) method for simulating rarefied gas dynamic environments. Different than traditional CFD techniques, the DSMC method is a more direct physical simulation of a gas at the molecular level. Molecules are tracked as they move in space and time, colliding with surfaces and other molecules. The move and collision phases are decoupled, allowing molecules to move linearly a distance corresponding to the product of the molecule's velocity and the size of the time step, before collisions are considered. The microscopic quantities tracked during the simulation are converted to more familiar flowfield quantities of density, velocity and temperature by statistically sampling the ensemble of particles in the simulation. Although DSMC solutions are continuously unsteady, steady-state results are achieved by averaging an ensample of samples once a pseudo steady-state condition is achieved. Often, the cells of the grid used to group the molecules for collisions are also used as sampling zones for the flowfield quantities. This provides a distribution of the flowfield quantities throughout the computational domain. Likewise, the molecule-surface collisions simulated at the microscopic level are also converted macroscopic quantities by employing appropriate sampling techniques. For example, the pressure on a surface element is simply the time-rate-of-change of momentum for molecules impacting the surface element, divided by the area of the element. Similar techniques are used to obtain shear stress and heating on surface elements. Further details on the DSMC method can be found in the Reference section.

The DAC Series can simulate 2D, axi-symmetric and 3D problems using a handful of programs that perform specific tasks in the analysis process. The software employs a two level embedded Cartesian grid system that is used to both pair neighboring molecules, and for sampling of the macroscopic quantities. Embedded within the flowfield grid is the surface geometry. DAC represents the surface geometry as a collection of unstructured triangular elements, which also act as sampling zones for surface properties. Each triangle in the surface geometry may be assigned a specific boundary condition type. There are five types of boundary conditions: 1) a solid wall, 2) an outgassing wall, 3) an inflow boundary, 4) an outflow boundary, and 5) as a freestream. A solid wall means no molecules are produced at the wall and none pass through. An outgassing wall is the same as a solid wall, except molecules are created on the flowfield side of the triangle at a rate that matches the specified flux. An inflow boundary also creates molecules on the flowfield side of the triangle, but any molecules that hit that surface will disappear, as will those that hit an outflow boundary or a freestream boundary. Three types of boundary conditions can also be applied to edges of the computational domain: 1) vacuum, 2) freestream, and 3) a symmetry plane.

The rectangular bounding box for the computational domain is specified by the user, as is the discretization in each of the three Cartesian directions. The cells created by this uniform Cartesian grid are referred to as Level-I Cartesian cells – or simply Level-I cells. Each of these Level-I Cartesian cells can be further refined by its own embedded Cartesian grid. These embedded Cartesian grids allow varying degrees of refinement from one Level-I cell to the next as required by the local flowfield properties in that region of the computational domain. These embedded Cartesian grids form Level-II Cartesian cells – or simply Level-II cells. While the Level-II cells may be much smaller than their parent Level-I cell, they may be no larger than the parent Level-I cell, which would be the case if a Level-I cell was refined by a 1x1x1 Level-II grid.

The two-level embedded Cartesian grid system permits variable refinement throughout the computational domain, which is essential for meeting the local mean-free-path cell size requirement. The catch-22 here is that in order to create an appropriate grid, you need to know the local flowfield properties. But in order to accurately predict the flowfield properties, you have to have an appropriate grid. This issue is addressed in DAC through an adaptation process that allows the solution on one grid system to be used as the basis for the creation of a new more appropriate grid. This is an iterative process typically requiring one and sometimes two adaptations. Metrics provided by the post-processing software can be used to determine if additional adaptation in warranted. Figure 5.6.3-1 displays the ratio of the local mean-free-path to the flowfield cell size for the DSMC Point AA solution. As is shown in the figure, mean-free-path resolution was obtained near the body and greater-than-mean-free-path resolution was obtained everywhere else in the computational domain. Historically, solutions that have reached mean free path resolution in their flowfield grids have compared well with experimental data. It should be noted that for the DSMC Point A solution, the mean-free-path resolution requirement was approximated but not satisfied due to the excessive computational load that this would result in. Violation of this rule results in overestimation of the transport properties and the heat flux to the walls (the viscosity and heat conductivity of the flow is overestimated). Based on convergence analysis performed on these solutions the error should not exceed 10%, so the heat fluxes given Section 5.4 should be interpreted as maximum values.

In addition to controlling grid refinement, the adaptation process is also used to automatically specify other simulation parameters throughout the computational domain. The DSMC method also has very specific requirements for the size of the time step used in the simulation, and for having each cell be populated with an adequate number of simulated molecules. The DAC software efficiently addresses these requirements by allowing the time step and ratio of real-to-simulated molecules to be specified independently within each Level-I cell as needed.

In addition to the preprocessor (PREDAC) and the run code (DAC), the DAC Software also contains two post-processing codes, SLICE and SPROP, for viewing flowfield and surface properties, and a utility code, Surface Tools Plus (STP), which can be used for importing different file types, modifying boundary conditions, managing groups, manipulating geometry and performing diagnostic testing of the user created surface grids.

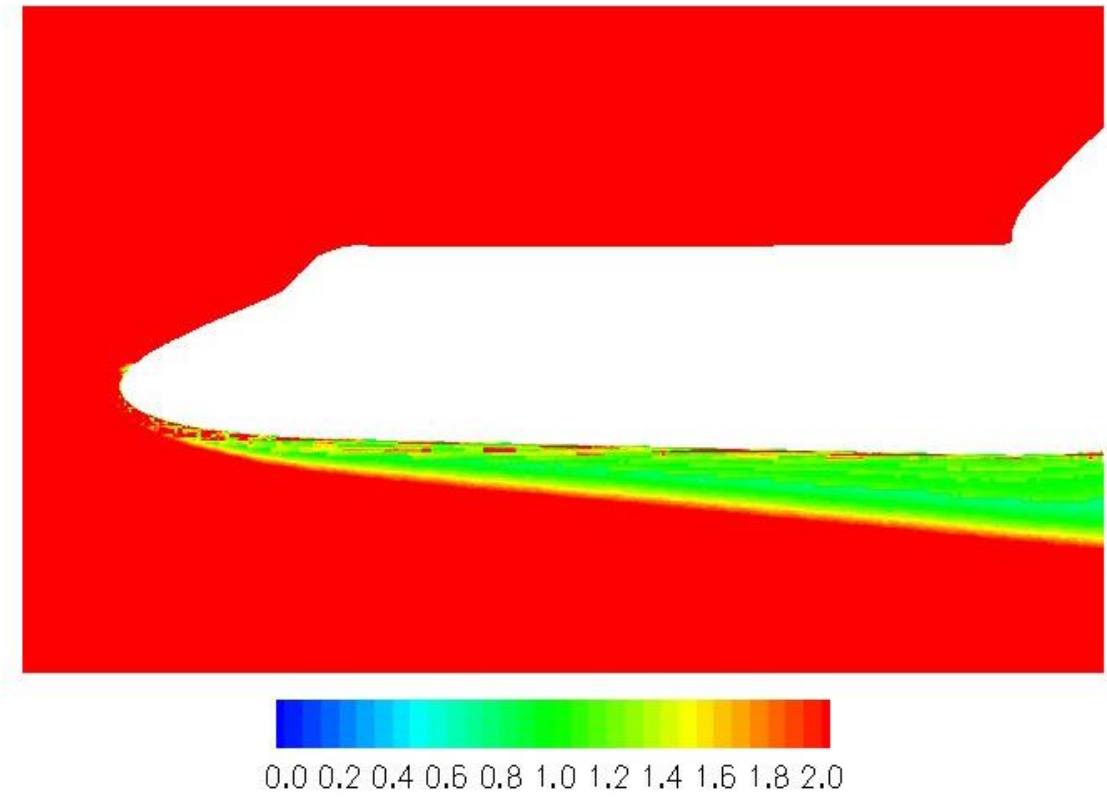

Figure 5.6.3-1 Ratio of Local Mean-Free-Path to Flowfield Cell Size for Nominal Orbiter Configuration DSMC Point AA.

5.6.3.8 ICARUS (SNL)

Icarus is a 2D gas dynamics code developed at Sandia by Bartel *et al.* based on the direct-simulation Monte Carlo (DSMC) method of Bird. It can model flowfields ranging from the continuum to the free molecular regime on Cartesian and axisymmetric grids. Icarus was optimized for a parallel computational environment with thousands of processors.

The DSMC method has been shown to approximate the Boltzmann equation. It employs computational particles that each represent a number of real molecules. During each time step, these particles undergo a deterministic move followed by a stochastic collision process. Collisions can involve multiple species, internal energy modes (rotation and vibration), and chemistry. Macroscale variables, such as temperature and velocity, are obtained by taking appropriate moments over the statistically-represented distribution functions.

The simulations of jet expansion were performed using both Cartesian and axisymmetric grids. The jet was modeled by introducing a constant flux of a given temperature, species mole fraction, and temperature. A vacuum condition was enforced at the outlet by deleting all particles that contact the boundary. The remaining boundaries were modeled as symmetry planes or solid surfaces, as the geometry required. Solid surfaces were treated as isothermal with full thermal accommodation.

The simulations of cavity flow were performed with Cartesian grids. A freestream boundary condition with a specified temperature, pressure, and velocity was enforced at the inflow edge. A vacuum was enforced at the outflow edge. Solid surfaces defining the wing and an open cavity were treated as isothermal with a specified thermal accommodation coefficient. In some calculations a vent was opened in the cavity with a specified outlet pressure.

The solutions were deemed steady-state when the total number of particles on the domain reached an asymptote. Statistical sampling then commenced and continued until the scatter was reduced to an acceptable level for all required quantities.

Extensive code verification studies have been performed on Icarus. These studies include comparison to data from analytic solutions, independent codes, and wind tunnel measurements.

5.6.3.9 VGM (LaRC)

The Volume Grid Manipulator (VGM) software was utilized on the Shuttle Orbiter Columbia Accident Investigation to modify, improve, refine, etc., structured surface and volume grids for viscous flow simulations. The software was developed in the late 1990's based on a set of existing grid manipulation tools. The suite of tools shared one specific drawback – they each required input and output which was the slowest part of operating on a grid. A grid manipulation language to couple the suite together was developed, and the VGM code was produced. Since its inception, the software has found application beyond its original intent, including the removal of negative celled volumes, feature based grid adaptation, and volume grid extrusion.

For the Columbia Accident Investigation, the VGM software was used to:

Correct negative celled volumes.

Transfer and adapt an existing solution to an entirely different topological grid.

Impose an orthogonal boundary condition on a block boundary attached to the wall of the shuttle orbiter.

Implement a C-II continuous matching block boundary condition in three dimensions.

Smooth surface and volume grids produced from adapting a grid to a specific solution.

Increase and decrease grid dimensionality to improve flow simulation accuracy without having to reconstruct the entire volume grid.

Expand existing volume grids to ensure outer bow-shock and entire flow field capture.

Reduce grid stretching and increase grid line intersection orthogonality to improve grid quality for flow simulations.

Smooth solution adapted grids through the implementation of method suggested by Taubin, but extended to fully three-dimensional problems.

The VGM language consists of 10 commands, where each command may have as many as 10 different options with up to 3 different settings for each option. Exercising each command with each option and setting produces a language with over 1000 individual operations. Coupling the individual operations enables the user to expand the capabilities of VGM to do extremely complex manipulations efficiently and with very few commands. Overall, the software provides a set of capabilities that do not exist in any other tool. As such, the user of this software can solve problems posed with structured grids that cannot be solved with any other grid generation software.

5.6.4 Hypersonic Boundary Layer Transition Effective Trip Height Calculation

The effective trip heights shown in Figure 5.2.5-15 were computed at Mach Numbers of 22.91 and 17.9 along the STS-107 flight path. The computations were based on a Euler/approximate boundary layer technique and on a Shuttle ground test boundary layer transition correlation (Berry,2002). Effective trip heights are defined in the study as the height required to move transition onset to the trip location. The transition correlation is presented by Berry as the momentum thickness Reynolds Number divided by the local Mach Number as a function of the roughness height divided by the boundary layer thickness (Figure 5.3.2.15). To establish the correlation, transition data were obtained on a Shuttle model over a range of

parameters including free stream Reynolds Number, angle of attack and roughness heights. The Euler/approximate boundary layer technique was used to compute the flow conditions to form the correlation parameters. Note that in Figure 5.3.2.15 the line defined as incipient transition relates to a trip height that promotes transition downstream of the disturbance(as opposed to occurrence at the trip). Data below the incipient line denote laminar flow, and data above the effective line represent turbulent conditions. Also, the data for the wing attachment line shown in the figure were obtained in the current study. The correlation results were extended to the two fight conditions shown in Figure 5.2.5-15 by first computing the momentum thickness Reynolds Number to Mach Number ratio over the Shuttle and mapping at the same locations the corresponding effective roughness height to boundary layer thickness ratio. For the computed values of boundary layer thickness, the appropriate effective trip heights were then computed and shown in the figure.

5.6.5 STS-107 End of Mission (EOM) 3 Pre-Entry Trajectory

STS-107 EOM3 1/22/03 KSC15 FEBRUARY WT/234200 XCG/1079.1 INC/39.0 D/L 8 XR								
Time (Seconds)	Altitude (Feet)	Velocity (Feet/Sec)	Alpha (Degrees)	Beta (Degrees)	Δ Elevon (Degrees)	Δ Body Flap (Degrees)	FS Density (Slugs/Ft^3)	FS Temp (°R)
0	399984.1	24639.3	39.53	0.46	1.98	-4.40	3.84E-11	682.9
10	395245.6	24651.6	39.71	0.43	1.98	-4.40	4.57E-11	650.9
20	390509.6	24661.4	40.09	0.38	1.98	-4.40	5.48E-11	619.8
30	385776.5	24668.6	40.20	0.31	1.98	-4.40	6.60E-11	589.7
40	381047.2	24672.2	40.00	0.23	1.98	-4.40	7.98E-11	560.5
50	376322.3	24671.4	39.46	0.13	1.98	-4.40	9.71E-11	532.1
60	371602.0	24668.9	39.40	0.01	1.98	-4.40	1.19E-10	504.6
70	366887.2	24663.7	39.54	-0.13	1.98	-4.40	1.47E-10	477.7
80	362178.4	24656.2	39.91	-0.30	1.98	-4.40	1.84E-10	450.7
90	357476.6	24646.7	40.10	-0.31	1.98	-4.40	2.30E-10	427.2
100	352782.9	24635.5	39.64	-0.03	1.98	-4.40	2.91E-10	406.8
110	348097.6	24623.6	39.44	0.28	1.98	-4.40	3.71E-10	387.3
120	343421.9	24612.9	39.82	-0.05	1.98	-4.40	4.76E-10	370.8
130	338757.1	24603.3	39.52	0.45	1.98	-4.40	6.12E-10	358.3
140	334104.5	24595.3	39.56	-0.12	1.98	-4.40	7.89E-10	348.4
150	329465.6	24589.4	39.63	0.20	1.98	-4.40	1.02E-09	339.5
160	324842.9	24585.3	39.61	-0.29	1.98	-4.40	1.32E-09	334.1
170	320238.7	24583.5	39.59	-0.30	1.98	-4.40	1.70E-09	331.5
180	315656.4	24583.6	39.59	-0.42	1.98	-4.40	2.18E-09	329.1
190	311100.3	24584.5	39.57	-0.39	1.98	-4.40	2.80E-09	330.0
200	306575.6	24585.9	39.55	0.21	1.98	-4.40	3.56E-09	334.9
205	304327.1	24586.9	39.59	0.25	1.98	-4.40	4.01E-09	338.2
210	302089.3	24587.8	39.59	0.04	1.98	-4.40	4.50E-09	341.7
215	299863.2	24588.6	39.56	-0.31	1.98	-4.40	5.05E-09	345.4
220	297649.9	24589.0	39.55	-0.30	1.98	-4.40	5.65E-09	348.9
225	295450.7	24589.2	39.58	-0.36	1.98	-4.40	6.31E-09	352.1
230	293267.3	24587.7	39.57	-0.03	-0.10	-4.40	7.03E-09	354.9
235	291100.9	24584.5	39.56	0.01	-2.15	-3.15	7.81E-09	357.0
240	288953.2	24580.9	39.58	-0.31	-4.24	-1.82	8.66E-09	358.9
245	286825.9	24576.9	39.62	-0.53	-6.32	-1.82	9.58E-09	360.7
250	284720.9	24572.3	39.82	-0.45	-7.28	-3.59	1.06E-08	362.7
255	282640.6	24567.1	40.46	-0.62	-5.80	-4.69	1.17E-08	364.6
260	280587.2	24561.0	41.26	-0.36	-2.87	-6.35	1.29E-08	366.5
265	278564.2	24551.6	41.32	-0.07	-1.52	-6.35	1.42E-08	368.2
270	276574.4	24541.8	40.55	-0.05	-2.32	-6.35	1.57E-08	369.8
275	274620.0	24531.8	39.45	-0.37	-4.80	-6.35	1.72E-08	371.3
280	272703.3	24520.6	39.16	-0.21	-5.63	-6.35	1.89E-08	372.8
285	270827.1	24508.2	40.17	-0.21	-3.08	-7.73	2.07E-08	374.2
290	268996.3	24494.3	41.21	-0.36	-0.63	-8.16	2.27E-08	375.6
295	267216.2	24479.3	41.08	-0.27	-0.48	-8.16	2.47E-08	377.1
300	265491.1	24463.8	40.01	-0.30	-2.70	-6.44	2.69E-08	378.3
305	263823.5	24448.1	39.37	-0.17	-3.70	-6.44	2.91E-08	379.6

310	262216.6	24431.6	39.99	-0.29	-2.10	-6.44	3.14E-08	380.7
315	260676.1	24413.5	40.77	-0.07	-0.60	-5.58	3.38E-08	381.7
320	259207.7	24394.4	40.44	-0.24	-2.02	-3.87	3.61E-08	382.5
325	257815.7	24375.1	39.80	-0.14	-4.02	-3.02	3.85E-08	383.2
330	256503.1	24355.2	40.10	-0.09	-2.47	-3.02	4.09E-08	383.8
335	255274.6	24333.9	40.51	-0.05	-2.00	-3.02	4.32E-08	384.3
340	254135.1	24311.9	40.22	0.04	-2.68	-3.02	4.55E-08	385.0
345	253087.5	24289.6	40.19	-1.99	-2.41	-3.02	4.77E-08	385.4
350	252135.7	24266.0	40.72	-0.41	-0.41	-2.40	4.97E-08	385.9
355	251278.6	24241.6	40.27	-0.29	-1.81	-1.03	5.17E-08	386.3
360	250503.9	24217.5	39.83	0.67	-2.30	0.39	5.35E-08	386.8
365	249792.7	24193.1	39.67	0.32	-3.60	0.39	5.52E-08	387.1
370	249134.9	24168.1	39.98	0.27	-3.27	0.39	5.69E-08	387.5
375	248524.0	24142.2	40.14	0.18	-3.34	0.39	5.85E-08	387.8
380	247953.5	24115.8	40.05	0.21	-3.52	0.39	6.00E-08	388.1
385	247417.5	24089.3	40.01	0.21	-3.36	0.39	6.15E-08	388.5
390	246911.2	24062.9	39.98	0.16	-3.45	0.39	6.29E-08	388.8
395	246430.6	24036.0	40.06	0.12	-3.38	0.39	6.42E-08	389.0
400	245973.2	24008.5	40.08	0.05	-3.49	0.39	6.56E-08	389.3
405	245536.9	23980.5	40.02	-0.06	-3.22	0.39	6.69E-08	389.5
410	245119.6	23952.3	39.96	0.01	-3.35	0.39	6.81E-08	389.8
415	244718.0	23923.6	40.03	-0.05	-3.32	0.39	6.94E-08	390.1
420	244329.6	23894.3	40.09	-0.02	-3.04	0.39	7.06E-08	390.3
425	243951.4	23864.7	40.00	-0.09	-3.17	0.39	7.18E-08	390.5
430	243581.0	23834.7	39.94	0.01	-3.36	0.39	7.30E-08	390.7
435	243215.1	23804.4	40.02	-0.07	-3.26	0.39	7.42E-08	391.0
440	242851.1	23773.4	40.04	-0.01	-3.04	0.39	7.54E-08	391.2
445	242485.7	23742.3	39.94	0.08	-3.20	0.39	7.67E-08	391.4
450	242116.3	23710.7	39.96	0.05	-2.85	0.39	7.80E-08	391.7
455	241741.2	23678.6	40.04	0.07	-3.11	0.39	7.93E-08	391.9
460	241359.5	23645.9	40.00	0.05	-3.43	0.39	8.07E-08	392.1
465	240971.8	23613.0	39.92	0.02	-3.24	0.39	8.21E-08	392.4
470	240579.1	23579.7	40.00	-0.01	-3.25	0.39	8.36E-08	392.6
475	240183.4	23545.8	40.03	-0.02	-2.90	0.39	8.51E-08	392.8
480	239787.2	23511.4	39.94	-0.11	-3.24	0.39	8.66E-08	393.1
485	239393.0	23476.7	39.96	-0.10	-3.23	0.39	8.82E-08	393.4
490	239002.9	23441.3	40.05	-0.15	-2.91	0.39	8.98E-08	393.6
495	238618.7	23405.3	39.98	-0.15	-3.29	0.39	9.13E-08	393.8
500	238241.2	23369.0	39.92	-0.18	-3.07	0.39	9.29E-08	394.0
505	237870.2	23332.3	39.98	-0.14	-2.87	0.39	9.45E-08	394.3
510	237504.4	23294.8	40.01	-0.11	-2.77	0.39	9.61E-08	394.5
515	237141.4	23256.9	39.94	-0.01	-2.95	0.39	9.77E-08	394.7
520	236777.7	23218.7	39.91	-0.06	-3.14	0.39	9.94E-08	394.9
525	236411.6	23179.8	40.00	0.01	-2.89	0.39	1.01E-07	395.1
530	236040.2	23140.4	39.95	0.05	-3.12	0.39	1.03E-07	395.4
535	235662.3	23100.6	39.90	0.06	-3.04	0.39	1.05E-07	395.6
540	235277.9	23060.2	40.00	0.07	-2.91	0.39	1.06E-07	395.8
545	234888.7	23019.0	39.98	0.03	-2.94	0.39	1.08E-07	396.0
550	234498.6	22977.4	39.92	-0.09	-2.90	0.39	1.10E-07	396.3
555	234112.4	22935.3	39.95	-0.12	-2.67	0.39	1.12E-07	396.5

560	233734.7	22892.3	39.98	-0.17	-3.18	0.39	1.14E-07	396.7
565	233369.4	22849.0	39.93	-0.19	-2.78	0.39	1.16E-07	397.0
570	233018.4	22805.0	39.91	-0.22	-2.87	0.39	1.18E-07	397.2
575	232681.6	22760.6	39.94	-0.20	-2.79	0.39	1.20E-07	397.4
580	232356.9	22715.7	39.92	-0.14	-2.84	0.39	1.22E-07	397.6
585	232039.2	22670.3	39.94	-0.04	-2.81	0.39	1.24E-07	397.8
590	231722.1	22624.3	39.92	0.04	-2.81	0.39	1.26E-07	398.0
595	231399.7	22578.0	39.93	0.08	-2.84	0.39	1.27E-07	398.2
600	231067.7	22531.0	39.95	0.12	-2.93	0.39	1.29E-07	398.4
605	230723.7	22483.6	39.91	0.09	-2.43	0.39	1.32E-07	398.6
610	230368.9	22435.8	39.74	0.04	-2.91	0.39	1.34E-07	398.9
615	230007.4	22387.5	39.82	-0.07	-2.56	0.39	1.36E-07	399.1
620	229646.0	22338.7	39.65	-0.10	-2.71	0.39	1.38E-07	399.3
625	229290.8	22289.6	39.71	-0.18	-2.27	0.39	1.41E-07	399.6
630	228946.8	22239.9	39.51	-0.22	-2.89	0.39	1.43E-07	399.9
635	228616.4	22189.9	39.58	-0.22	-2.21	0.39	1.45E-07	400.1
640	228299.4	22139.4	39.54	-0.18	-2.40	0.39	1.47E-07	400.4
645	227992.3	22088.4	39.54	-0.07	-2.44	0.39	1.49E-07	400.6
650	227689.0	22036.9	39.54	-0.03	-2.39	0.39	1.51E-07	400.9
655	227383.4	21985.1	39.55	0.02	-2.47	0.39	1.54E-07	401.1
660	227070.9	21932.6	39.55	0.00	-2.38	0.39	1.56E-07	401.4
665	226748.5	21879.6	39.56	0.04	-2.39	0.39	1.58E-07	401.7
670	226414.7	21826.1	39.55	0.00	-2.41	0.39	1.61E-07	402.0
675	226070.6	21772.1	39.59	-0.05	-2.25	0.39	1.63E-07	402.3
680	225719.2	21717.4	39.56	-0.10	-2.43	0.39	1.66E-07	402.6
685	225363.4	21662.0	39.57	-0.06	-2.74	0.39	1.69E-07	403.0
690	225005.7	21606.1	39.58	-0.14	-2.37	0.39	1.71E-07	403.3
695	224649.0	21549.6	39.56	-0.15	-2.45	0.39	1.74E-07	403.6
700	224294.1	21492.3	39.59	-0.11	-2.30	0.39	1.77E-07	404.0
705	223939.5	21434.5	39.58	-0.10	-2.44	0.39	1.80E-07	404.4
710	223582.2	21376.0	39.59	-0.06	-2.66	0.39	1.83E-07	404.7
715	223218.1	21316.9	39.59	-0.02	-2.38	0.39	1.86E-07	405.1
720	222843.4	21257.2	39.56	-0.03	-2.45	0.39	1.89E-07	405.5
725	222455.1	21196.6	39.60	0.00	-2.22	0.39	1.93E-07	405.9
730	222052.1	21135.4	39.59	0.00	-2.43	0.39	1.96E-07	406.3
735	221634.7	21073.3	39.51	-0.09	-2.50	0.39	2.00E-07	406.7
740	221205.8	21010.7	39.55	-0.07	-2.22	0.39	2.04E-07	407.1
745	220767.2	20947.2	39.54	-0.07	-2.15	0.39	2.08E-07	407.6
750	220320.4	20882.8	39.49	-0.07	-2.39	0.39	2.12E-07	408.1
755	219866.1	20818.0	39.47	1.91	-1.69	0.39	2.17E-07	408.5
760	219416.1	20750.2	39.74	0.39	-1.39	1.22	2.21E-07	408.9
765	219064.8	20683.0	39.21	-0.22	-1.59	2.88	2.25E-07	409.2
770	218859.4	20616.0	39.23	-0.30	-1.80	2.88	2.27E-07	409.5
775	218768.1	20549.0	39.22	-0.16	-2.22	2.88	2.28E-07	409.6
780	218696.7	20482.4	39.41	-1.77	-3.45	2.88	2.29E-07	409.6
785	218569.9	20414.7	39.91	-0.13	-3.75	2.88	2.30E-07	409.7
790	218392.9	20345.5	40.30	-0.07	-3.76	1.95	2.32E-07	409.9
795	218166.4	20274.7	40.60	-0.03	-3.31	1.02	2.34E-07	410.2
800	217889.0	20203.2	40.65	-0.04	-3.48	1.02	2.37E-07	410.4
805	217555.9	20130.6	40.84	-0.12	-3.62	1.02	2.41E-07	410.7

810	217162.0	20057.2	40.83	-0.20	-3.58	0.30	2.45E-07	411.1
815	216705.4	19982.2	41.03	-0.09	-3.44	0.09	2.51E-07	411.6
820	216190.2	19906.1	41.04	-0.14	-3.35	0.09	2.56E-07	412.1
825	215621.9	19828.7	41.04	-0.09	-3.67	0.09	2.63E-07	412.7
830	215009.4	19749.8	41.01	-0.09	-3.61	0.09	2.70E-07	413.2
835	214362.1	19669.6	40.86	-0.05	-3.29	0.09	2.78E-07	413.9
840	213690.7	19588.8	40.72	0.01	-3.23	0.09	2.87E-07	414.6
845	213005.6	19506.7	40.57	0.02	-3.18	0.09	2.95E-07	415.3
850	212313.4	19423.8	40.40	-0.10	-2.86	0.09	3.04E-07	416.0
855	211617.7	19339.5	40.27	-0.02	-2.91	0.09	3.14E-07	416.7
860	210923.6	19254.1	40.11	-0.02	-2.81	0.09	3.23E-07	417.5
865	210234.9	19167.5	39.99	-0.08	-2.75	0.09	3.33E-07	418.3
870	209553.6	19079.7	39.87	-0.08	-2.69	0.09	3.43E-07	419.0
875	208882.0	18990.7	39.75	-0.04	-2.77	0.09	3.53E-07	419.7
880	208222.7	18900.2	39.72	-0.08	-2.42	0.09	3.63E-07	420.4
885	207576.7	18808.7	39.64	-0.04	-2.59	0.09	3.73E-07	421.1
890	206944.3	18715.7	39.54	-0.06	-2.41	0.09	3.83E-07	421.8
895	206326.2	18621.5	39.55	-0.04	-2.39	0.09	3.93E-07	422.5
900	205722.0	18525.8	39.55	-0.10	-2.46	0.09	4.04E-07	423.2
905	205129.3	18428.6	39.54	-0.03	-2.47	0.09	4.14E-07	423.8
910	204545.9	18330.0	39.55	-0.08	-2.45	0.09	4.24E-07	424.4
915	203967.2	18230.1	39.55	-0.05	-2.46	0.09	4.35E-07	425.1
920	203388.7	18128.8	39.56	-0.04	-2.48	0.09	4.45E-07	425.8
925	202806.1	18026.1	39.55	-0.04	-2.51	0.09	4.56E-07	426.4
930	202213.9	17922.2	39.55	-0.10	-2.54	0.09	4.68E-07	427.1
935	201606.7	17816.8	39.65	-0.06	-2.59	0.09	4.80E-07	427.7
940	200980.4	17709.5	39.68	-0.06	-2.37	0.09	4.92E-07	428.5
945	200330.4	17600.9	39.75	-0.14	-2.52	0.09	5.06E-07	429.3
950	199653.1	17489.9	39.85	-0.07	-2.72	0.09	5.20E-07	430.0
955	198950.2	17377.0	39.92	-0.05	-2.90	0.09	5.35E-07	430.9
960	198224.3	17261.9	39.90	-0.10	-2.71	0.09	5.52E-07	431.8
965	197476.9	17144.9	39.98	-0.04	-2.77	0.09	5.69E-07	432.7
970	196710.1	17025.8	39.93	-0.08	-3.00	0.09	5.87E-07	433.7
975	195925.2	16904.5	40.01	-0.09	-2.91	0.09	6.06E-07	434.6
980	195124.4	16781.0	39.95	-0.03	-2.84	0.09	6.25E-07	435.8
985	194310.2	16656.0	39.99	-0.06	-3.13	0.09	6.46E-07	436.8
990	193484.9	16529.1	39.96	-0.08	-3.08	0.09	6.68E-07	438.0
995	192649.8	16400.4	39.94	-0.03	-3.07	0.09	6.90E-07	439.2
1000	191807.3	16269.1	39.94	-0.07	-3.00	0.09	7.14E-07	440.4
1005	190957.4	16135.7	39.98	-0.06	-3.12	0.09	7.38E-07	441.7
1010	190100.0	16000.1	39.95	-0.05	-3.02	0.09	7.63E-07	443.0
1015	189235.4	15862.3	39.95	-0.09	-3.26	0.09	7.89E-07	444.3
1020	188362.9	15722.2	39.93	-0.07	-3.49	0.09	8.16E-07	445.6
1025	187481.4	15579.5	40.00	-0.06	-3.56	0.09	8.45E-07	447.0
1030	186589.8	15434.7	39.97	-0.05	-3.53	0.09	8.74E-07	448.4
1035	185686.8	15287.5	40.03	-0.06	-3.61	0.09	9.05E-07	449.8
1040	184770.8	15137.9	40.06	-0.05	-3.89	0.09	9.37E-07	451.2
1045	183839.6	14985.8	40.10	-0.08	-4.09	0.09	9.71E-07	452.5
1050	182888.3	14831.0	40.17	-0.06	-4.19	0.09	1.01E-06	454.0
1055	181913.1	14673.7	40.19	-0.07	-4.57	0.09	1.04E-06	455.3

1060	180910.5	14513.1	40.36	-0.36	-4.71	0.09	1.09E-06	456.6
1065	179889.1	14350.3	40.21	-0.08	-4.64	0.09	1.13E-06	457.9
1070	178918.9	14186.9	39.91	0.21	-4.86	0.09	1.17E-06	459.1
1075	178067.7	14023.6	39.67	0.19	-4.56	0.09	1.21E-06	460.1
1080	177347.1	13860.6	39.52	0.03	-4.68	0.09	1.24E-06	460.9
1085	176724.9	13697.9	39.43	-0.13	-4.90	0.09	1.27E-06	461.6
1090	176152.3	13536.1	39.39	-0.16	-4.82	0.09	1.30E-06	462.2
1095	175593.1	13374.4	39.46	-0.10	-5.16	0.09	1.33E-06	462.8
1100	175031.4	13213.0	39.50	-0.08	-5.51	0.09	1.36E-06	463.5
1105	174461.4	13051.5	39.58	-0.05	-5.86	0.09	1.39E-06	464.1
1110	173878.9	12890.1	39.66	-0.07	-6.34	0.09	1.42E-06	464.8
1115	173276.2	12728.6	39.73	-0.05	-6.69	0.09	1.45E-06	465.5
1120	172645.7	12567.1	39.79	-0.05	-6.89	0.09	1.48E-06	466.1
1125	171982.4	12405.4	39.90	-0.03	-6.49	-0.86	1.52E-06	466.9
1130	171283.6	12244.0	39.84	-0.04	-6.75	-0.86	1.56E-06	467.7
1135	170547.6	12082.6	39.84	-0.08	-6.61	-0.86	1.60E-06	468.5
1140	169773.5	11921.5	39.83	-0.06	-6.99	-0.86	1.65E-06	469.3
1145	168966.5	11760.6	39.75	-0.06	-7.13	-0.86	1.70E-06	470.2
1150	168134.2	11599.5	39.69	-0.04	-7.35	-0.86	1.75E-06	471.1
1155	167281.4	11438.7	39.65	-0.03	-7.33	-0.86	1.81E-06	471.9
1160	166408.7	11278.1	39.59	-0.04	-7.40	-0.86	1.87E-06	472.8
1165	165514.7	11117.6	39.47	-0.05	-7.45	-0.86	1.93E-06	473.5
1170	164596.2	10957.6	39.34	-0.08	-7.39	-0.86	2.00E-06	474.2
1175	163649.5	10798.0	39.21	-0.06	-7.59	-0.86	2.07E-06	474.8
1180	162672.1	10638.6	39.10	-0.34	-7.24	-0.86	2.15E-06	475.5
1185	161677.1	10477.8	39.06	-0.24	-7.18	-0.86	2.23E-06	475.9
1190	160830.2	10316.7	38.82	-0.20	-6.97	-0.86	2.30E-06	476.1
1195	160265.4	10156.2	38.73	-0.10	-6.93	-0.86	2.35E-06	476.2
1200	159937.2	9996.5	38.68	-0.05	-7.19	-0.86	2.38E-06	476.2
1205	159630.2	9840.8	38.65	0.21	-8.15	-0.86	2.41E-06	476.3
1210	159171.9	9686.7	38.84	0.22	-7.97	-2.72	2.46E-06	476.3
1215	158523.9	9534.9	38.76	0.19	-7.55	-2.76	2.52E-06	476.3
1220	157702.7	9385.1	38.64	0.10	-7.61	-2.76	2.60E-06	476.3
1225	156769.7	9237.0	38.31	-0.20	-7.54	-2.76	2.69E-06	476.3
1230	155801.8	9091.0	37.98	-0.30	-7.25	-2.76	2.80E-06	476.3
1235	154846.5	8947.1	37.61	-0.26	-7.07	-2.76	2.90E-06	476.4
1240	153910.6	8805.3	37.26	-0.12	-6.93	-2.76	3.01E-06	476.6
1245	152971.8	8665.4	36.89	0.03	-6.59	-2.76	3.12E-06	476.8
1250	151997.5	8527.8	36.58	0.09	-6.64	-2.76	3.23E-06	477.1
1255	150968.2	8391.9	36.26	0.09	-6.35	-2.76	3.36E-06	477.3
1260	149885.0	8257.8	35.92	0.02	-6.47	-2.76	3.51E-06	477.3
1265	148768.0	8125.5	35.51	-0.09	-6.15	-2.76	3.66E-06	477.2
1270	147644.2	7994.6	35.13	-0.15	-5.97	-2.76	3.83E-06	476.8
1275	146532.0	7865.3	34.77	-0.17	-5.66	-2.76	4.00E-06	476.1
1280	145434.1	7737.4	34.33	-0.08	-5.61	-2.76	4.19E-06	475.1
1285	144338.0	7611.0	33.93	-0.02	-5.39	-2.76	4.38E-06	474.0
1290	143225.8	7486.2	33.58	0.01	-5.26	-2.76	4.58E-06	472.7
1295	142085.4	7362.9	33.18	-0.02	-5.15	-2.76	4.81E-06	471.4
1300	140912.7	7241.0	32.78	-0.06	-5.00	-2.76	5.05E-06	470.2
1305	139708.6	7120.4	32.39	-0.06	-4.60	-3.61	5.31E-06	468.8

1310	138474.9	7001.0	31.91	0.00	-4.52	-3.69	5.59E-06	467.6
1315	137213.0	6883.0	31.49	-0.02	-4.32	-3.69	5.89E-06	466.3
1320	135927.7	6766.3	31.05	-0.07	-4.05	-4.61	6.21E-06	464.9
1325	134625.6	6650.7	30.60	-0.05	-4.23	-4.61	6.56E-06	463.5
1330	133313.5	6534.3	30.44	-0.06	-3.76	-5.53	6.94E-06	462.1
1335	131989.1	6418.4	29.99	0.03	-3.55	-5.83	7.34E-06	460.6
1340	130641.9	6303.3	29.54	-0.02	-3.06	-7.37	7.78E-06	458.9
1345	129273.4	6189.6	29.02	-0.04	-3.27	-7.37	8.25E-06	457.1
1350	127888.4	6077.3	28.53	-0.04	-2.97	-7.50	8.76E-06	455.3
1355	126494.6	5965.6	28.07	-0.04	-2.65	-9.19	9.32E-06	453.3
1360	125095.7	5855.4	27.57	-0.03	-2.59	-9.19	9.91E-06	451.3
1365	123694.3	5746.2	27.08	-0.03	-2.59	-9.19	1.06E-05	449.2
1370	122292.7	5637.8	26.66	-0.02	-2.38	-10.10	1.12E-05	447.2
1375	120891.7	5530.4	26.15	-0.02	-2.25	-11.01	1.20E-05	445.2
1380	119488.9	5424.5	25.68	0.00	-2.31	-11.01	1.27E-05	443.2
1385	118083.1	5319.7	25.24	-0.04	-2.44	-11.01	1.36E-05	441.1
1390	116676.7	5215.7	24.84	-0.01	-2.59	-11.01	1.45E-05	439.1
1395	115269.8	5112.6	24.36	-0.04	-2.76	-11.01	1.54E-05	437.0
1400	113861.7	5010.4	23.89	-0.03	-2.78	-11.01	1.64E-05	434.9
1405	112454.1	4909.3	23.38	-0.01	-2.57	-11.01	1.76E-05	432.8
1410	111049.2	4809.3	22.88	0.00	-2.48	-11.01	1.87E-05	430.6
1415	109649.6	4710.2	22.40	0.00	-2.53	-11.01	2.00E-05	428.4
1420	108257.4	4612.0	21.98	0.59	-2.03	-11.01	2.14E-05	426.2
1425	106943.1	4512.5	21.62	0.15	-1.82	-11.01	2.27E-05	424.1
1430	105846.0	4412.5	21.20	0.12	-1.91	-11.01	2.39E-05	422.4
1435	104929.4	4313.0	20.92	-0.18	-2.00	-11.01	2.50E-05	420.9
1440	104021.4	4215.3	20.63	-0.01	-2.55	-11.01	2.61E-05	419.5
1445	103047.8	4119.0	20.47	0.03	-2.24	-11.01	2.73E-05	418.1
1450	102006.9	4024.6	20.19	-0.02	-2.48	-11.01	2.87E-05	416.5
1455	100890.1	3930.9	20.03	0.01	-2.38	-11.01	3.03E-05	414.8
1460	99695.7	3838.1	19.74	-0.03	-2.14	-11.01	3.21E-05	413.1
1465	98427.7	3746.1	19.43	0.01	-1.80	-11.01	3.42E-05	411.3
1470	97103.3	3655.7	18.97	0.00	-1.69	-11.01	3.64E-05	409.5
1475	95739.6	3566.6	18.56	0.00	-1.36	-11.01	3.89E-05	407.7
1480	94355.4	3477.7	18.15	0.01	-1.01	-11.01	4.16E-05	406.0
1485	92967.9	3389.3	17.72	0.04	-0.55	-11.01	4.46E-05	404.4
1490	91587.4	3301.5	17.29	0.04	-0.48	-11.01	4.77E-05	402.7
1495	90220.6	3214.1	16.78	0.01	-0.21	-11.01	5.10E-05	401.1
1500	88871.4	3127.4	16.35	0.03	-0.15	-11.01	5.45E-05	399.6
1525	82491.2	2702.0	14.77	0.03	-1.47	-11.01	7.49E-05	392.1
1550	76943.2	2283.9	13.52	0.20	-3.26	-11.01	9.92E-05	386.9
1575	72271.4	1882.0	11.73	0.10	-4.83	-11.01	1.26E-04	381.3
1600	66475.0	1568.7	10.26	0.10	-6.25	-11.01	1.72E-04	373.1
1625	59398.3	1276.8	9.30	0.17	-2.91	-11.01	2.52E-04	365.6
1650	52749.6	1010.9	8.98	0.27	2.18	-11.01	3.50E-04	368.7
1675	46737.0	848.5	10.47	0.28	7.04	-7.42	4.61E-04	378.1
1700	40406.4	777.7	11.07	-0.35	6.16	0.35	6.04E-04	392.0
1725	31130.9	801.1	10.03	-0.03	0.08	8.62	8.64E-04	420.0
1750	25762.5	735.9	8.30	-0.01	0.74	4.90	1.04E-03	441.3
1775	22151.3	675.3	8.16	-0.02	1.19	4.90	1.17E-03	455.9

1800	18315.8	636.5	7.52	-0.12	2.44	9.85	1.32E-03	470.8
1825	13676.3	604.1	7.19	-0.23	3.71	12.31	1.53E-03	485.9
1850	8865.0	593.3	5.14	-0.05	6.47	1.16	1.78E-03	500.7
1875	4352.1	544.0	5.17	-0.10	6.62	0.35	2.05E-03	511.1
1900	474.5	526.8	7.25	-0.07	2.96	0.35	2.31E-03	521.9
1923.48	-168.8	365.5	9.00	-0.02	2.14	0.35	2.35E-03	524.1

6 THERMAL

6.1 Panel 8/9 Spar & Clevis Thermal Analysis

A thermal analysis was conducted to compare the flight data instrumentation of the spar (V09T9895) and clevis (V09T9910) to the predicted thermal response in a plume heating environment of each of these panel 9 locations. The wing leading edge (WLE) cavity is shown in Figure 6-1. Two independent thermal math models, one from JSC and the other from Boeing Huntington Beach (B-HB), were utilized to perform this analysis.

The B-HB RCC panel 9 finite element model includes the entire RCC panel/T-Seal, internal insulation and metallic hardware including the spar aluminum honeycomb. Radiation between the RCC IML and internal insulation was simulated using the Thermal Radiation Analyzer System (TRASYS) software. Radiation was also simulated from the aluminum spar to the wing cavity using an existing structural model of the upper and lower wing without damage. The RCC inner mold line (IML), internal insulation, and metallic hardware, at the thermocouple locations, were compared to flight data to assure accuracy of the model. The flight certified model is used to support RCC mission life evaluation. This TMM was modified to simulate RCC damage with 6 and 10 inch holes at the center of the RCC panel. STS-107 nominal End-Of-Mission2 (EOM2) was utilized for the outer mold line (OML) heating. Internal plume heating, to be discussed later in detail, was taken from reference heating mapped on the internal RCC and insulation components with stagnation heating of 1.9 times the entering plume and significantly reduced over the spanner beam and spar insulation. As the internal components' material temperature limit exceeded its melting point the analysis was stopped in order to re-configure the TMM. A new geometry was developed to account for missing components and additional heating. The internal component material melting points used in the analysis are listed; Inconel (2500°F), Nextel Fabric (3000°F), Cerachrome (2600°F), and Aluminum (1000°F).

A simplified finite element TMM of the spar, spar insulation, and RCC fitting was developed by the JSC for this investigation. The spar is made entirely of Aluminum 2024-T6 with 0.03-inch thick facesheets that are adhesively bonded to a 1.0-inch thick honeycomb core. The Generic Honeycomb Modeling Tool was used to generate the effective heat transfer properties for the honeycomb spar. The honeycomb attributes for the spar in the region of panel 8 and 9 were gathered from stress report STS89-0537. These effective properties were then used to model the spar in the simplified finite element thermal model of the spar. The embedded aluminum fitting support bars are also included in the model. The spar insulation was modeled and an emittance of 0.85 was used for the outer Inconel foil material. The aluminum/cerachrome interface was assumed to be in intimate contact with no temperature difference at the gap. The four RCC attach fittings are made of steel A-286 and attached to the clevis hardware on the RCC. The RCC attach fittings were modeled each as a single diffusion node. The fitting temperatures are representative of the clevis temperatures and are reported as the clevis temperatures. Nominally, the clevis temperatures do not change until after 550 sec; well after STS-107 V09T9910 went off scale low. During this time, conduction from the RCC is insignificant and the only paths for heat to flow to the clevis are from the RCC fittings and through additional convective heating. The radiative boundary conditions for entry were based on the entry RCC inner mold line (IML) temperatures predicted for STS-107 by the Boeing Houston aero-thermal group. These boundary conditions were applied to the outer spar insulation surface. On the backside of the spar, where the inner wing structure is located, a constant boundary temperature of 22°F is used.

For the ascent thermal analysis using the JSC model, the boundary conditions are changed to the predicted ascent RCC IML temperatures. On the backside, the radiative boundary temperatures decreased from 55°F to 30°F. The backside spar ascent boundary conditions were determined by correlating the data to STS-109, since they had identical initial temperatures prior to the temperature increases at 300 seconds from launch.

The plume heating estimates for stagnation are and distributions within the cavity are discussed in section 5.3.3 and results summarized here for varying breach hole sizes in panel 8. Using equation (6-1), the time varying heat rate on panel 9 was generated.

$$\dot{q}(x,y,z,t,d_{hole}) = \dot{q}/\dot{q}_{plate}(x,y,z,d_{hole}) \times \frac{\bar{q}_{\infty}(t)}{\bar{q}_{\infty}(488)} \times \frac{V_{\infty}^{2}(t)}{V^{2}{}_{\infty}(488)} \times \dot{q}_{plate}(d_{hole}) \quad (6\text{-}1)$$

where;

$\dot{q}_{plate}(d_{hole})$ is 27.1, 30.1, 55.9 BTU/ft^2-sec for a 4 inch, 6 inch, and 10 inch hole respectively.

Figure 6-2 shows how $\dot{q}/\dot{q}_{plate}(x,y,z,d_{hole})$ varies for a 10 inch hole. The average distribution factor of the stagnation heating value over panel 9 for a 4 inch, 6 inch, and 10 inch hole are .02, .08, and .12, respectively. Additional heating behind the spar insulation, directly on the aluminum near bottom clevis locations, is also considered as a fraction of the panel 9 heating.

The ascent heating for internal flow impingement on the spar insulation was determined by normalizing the panel 8 stagnation heating with body point 5505 entry heating. The normalization factors are then applied to the STS-107 predicted ascent heating for body point 5505. The normalization factors used for the 4 inch, 6 inch, and 10 inch holes are 0.89, 1.0, and 1.8, respectively. The same distribution factors are then applied to the panel 9 spar insulation for ascent heating.

The thermal math models were solved using the Systems Improved Numerical Differencing Analyzer (SINDA). The B-HB model results are shown in Figure 6-3, through Figure 6-5. Figure 6-3 suggests that the heating through a 10 inch hole will produce a temperature rise on the back of the panel 9 spar that matches flight data V09T9895. The assumption of sneak flow directly onto the clevis, on the order of 1%, is necessary to match the flight data of V09T9910 as shown in the comparison of Figure 6-4 and Figure 6-5.

The JSC model predictions in Figure 6-6 and Figure 6-7 are shown for a 6 inch, and 10 inch hole. Figure 6-6 shows the instrumentation location on Panel 9 thermal response to varying hole sizes. A hole size between 6 inch and 10 inch will match the flight data V09T9895. The JSC model also requires a sneak flow assumption of 10% to match the clevis flight data, V09T9910 as shown in Figure 6-8. In Figure 6-9, sensitivity analysis of the thermal response was considered for a 50% variation in the heating data due to uncertainties.

The results from the ascent analysis are shown in Figure 6-10. Here it is shown that the predicted spar temperature rise during ascent is slightly higher with a pre-existing hole in the wing leading edge. STS-109 (undamaged condition) and STS-107 (presumably damaged condition) flight data are compared to these analytical results. It can be surmised that the thermal response of the STS-107 flight data is consistent with the analytical predictions for a damaged wing leading edge during ascent.

6.1.1 Damaged Tee-seal

An auxiliary analysis was performed to assess the feasibility for a damaged tee-seal between panel 8 and panel 9 to cause the observed flight data in the Panel 8/9 region. This analysis assumed that the tee-seal was damaged to the extent that it was completely missing for a 20 inch length on the lower portion of the seal. The same methodology as described in section 6.1 was used to compute the spar breach time and temperature response of the flight measurements using the heating rates described in section 5.3.3.

Analysis results using the Boeing-HB thermal math model is shown in Figure 6-11. This figure shows the computed temperature transients for the spar insulation immediately behind the tee-seal. This insulation does not have the Nextel fabric under the inconel foil and therefore has a lower failure temperature of about 2,600°F. Here the insulation fails within 400-500 seconds. The temperature response for the aluminum spar behind the insulation is predicted to fail at 360 seconds. This is earlier than the estimated actual spar breach time of 487 seconds.

Figure 6-12 shows the spar temperature transient prediction compared to the measured flight data. Here it is seen that the predicted temperature rise is much quicker than the flight data. Note that this analysis

is invalid after about 500 seconds because hot gases know to be within the wheel well at this time were not simulated. Figure 6-13 shows the analytical clevis temperature compared to the flight data. Here it is seen that the analytical prediction rises slightly earlier than the flight data but is not totally out of proportion.

This analysis and the analysis presented in section 6.5.1 suggests that a damaged tee-seal is not a likely scenario for initial damage to the wing leading edge.

6.2 Spar Burn Through Analysis

Several scenario-based and flight data-based data suggest that the wing leading spar experienced a breach during the mission. The most significant of these is the failure of the wire cables which run along the backside of the wing leading edge. Figure 6-14 shows a picture of this region and summarizes the failure times for each of these cables. Thermal analysis and torch testing has shown that the time for failure of one of these cables is less than three seconds. Therefore it is believed that the cable failure time gives a good indication of the when the spar is breached immediately in front of the cable. Since the cables do not provide full coverage of the spar and the original location of the breach is unknown, the exact time of the breach is uncertain but occurred no later than 487 seconds.

A geometric analysis was used to determine if the hole size as a function of time could be determined from the cable failure times. The result of this assessment is shown in Figure 6-15. Here it is predicted that the spar hole could reach a size of 580 in^2 by 520 seconds. It can be rationalized that the hole growth is eventually stunted and arrested as shown by the analysis due to the following factors:

- High mass of the spar embedded aluminum fitting support bars effectively “frames out” a rectangular limit for the hole
- Plume effect on the spar from the wing leading edge hole is arrested by the limited growth of the hole in the RCC.

A parametric analysis was also performed with this model to determine the initial breach time. Here the initial location was parametrically varied and the initial breach time computed. From these analyses, the spar could have been breached from 478 to 487 seconds from entry interface. Although the strain measurements and associated structural analysis suggest that the breach occurred between 420 and 470 seconds from entry interface, supporting data for a spar breach in this time frame comes from:

- Bundle 3 wire harness failure (before 498 sec)
- Bit flip in wheel well (488 sec)
- PNL 8/9 thermal analysis (490 sec)

6.3 Wheel Well Thermal Analysis

A thermal analysis was used to compare predicted heating to the flight data instrumentation summarized in Table 6-1 for the wheel well. Here a hot gas plume originating from the wing leading edge spar is assumed to impact the outboard wheel well wall. The hot outboard wall then conducts heat into the adjoining walls and radiates into the main landing gear (MLG) wheel well and the associated sensors within.

Table 6-1 - Wheel Well Sensor Summary

MEAS. NO.	DESCRIPTION
V58T0125A	SYS 1 LMG UPLK ACT UNLK LN
V58T0405A	L H MLG STRUT ACTUATOR
V58T0841A	SYS 2 L AFT BK SW VLV RTN
V58T0842A	SYS 3 L FWD BK SW VLV RTN
V58T1700A	L MLG BRK HTR LN 1 SYS 1&3
V58T1701A	L MLG BRK HTR LN 3 SYS 2&3
V58T1702A	L MLG BRK HTR LN 2 SYS 1&3
V58T1703A	L MLG BRK HTR LN 4 SYS 2&3

A thermal math model shown in Figure 6-16 was developed directly from computer aided design (CAD) models and used to predict the sensor responses in this presumed scenario. Shell elements were used where possible for simplicity with the remaining geometry represented by solid tetrahedral elements. Main Landing Gear (MLG) components were then thermally connected by combining nodes at joint locations. This allowed for faster analysis since arbitrarily low conductors (which is a common method to join components) can significantly reduce the time step in order to maintain a required accuracy. Internal radiation was also modeled using the Monte Carlo technique with 16000 rays per node. All of the nodes representing sensor locations had an initial temperature corresponding to the flight data. The rest of the components and the wheel well walls had an assumed initial temperature of 80°F.

The predicted plume heating distribution model is described in section 5.3.3. The heating was calculated for a 5 inch diameter hole in the wing leading edge spar assumed to appear instantaneously at EI+488sec (13:52:17 GMT). The plume impinged upon the outboard wheel well wall at location xo=1105, zo=309 and at a distance of 56 inch from the spar. Correction factors were applied for the 31.5 degree off normal impact angle as well as the internal wing pressure. The center of the plume had a heating rate of 22.1 BTU/ft^2-sec with the heating dropping off radially from the centerline. Melting of the outboard wall was not modeled, therefore, once a node reached melting temperature (935°F) it was then held at this temperature.

The thermal math model was solved using the Systems Improved Numerical Differencing Analyzer (SINDA). Predicted temperatures for the hydraulic lines and the strut actuator were obtained and are shown in Figure 6-17 through Figure 6-24. Initially, all the sensors begin to trend towards 80°F from radiation exchange with the 80°F surrounding structure. At 488 sec (GMT 13:52:17) the plume heating is applied to the outboard wall and the temperatures begin to trend upward at a rate dependant on their view factor to the outboard wall.

Table 6-2 - Sensor location and view factor summary

Sensor	Location	View Factor
V58T1700A	Bottom of strut	Good
V58T1701A	Bottom of strut	Good
V58T1702A	On inboard wall	Partial
V58T1703A	On inboard wall under debris shield	Poor
V58T0841A	On inboard wall under debris shield	Poor
V58T0842A	On inboard wall	Poor
V58T0125A	On upper wall behind structure	Poor
V58T0405A	Aft inboard corner of wheel well	Partial

At first glance sensors V58T1700A and V58T1701 correlate very well with the flight data. However, past EI+510 sec (GMT 13:52:39) the low mass honeycomb access panel has reached its melting temperature in the analysis as shown in Figure 6-25. This would allow hot gases to enter the wheel well and deposit energy through convection directly on the MLG components. However, one could argue that this convective energy then replaces radiative energy but CFD would have to confirm this. After EI+586 sec (GMT 13:53:55) the wall at the center of the plume reached its melting temperature as shown in . At this point the area available for hot gases to enter the wheel well increases rapidly as more of the outboard wall melts. The assumption of holding the wheel well wall at its melting temperature (935°F) is no longer valid for this analysis and CFD is required to determine the hot gas flow inside the wheel well in order to account for the convective heating.

From this analysis, it is possible to conclude that a portion of the hydraulic line temperature increase seen in the flight data can be attributed to radiation from the outboard wheel well wall being heating by a plume due to a spar breach.

6.4 Wire Bundle Burn-Through Tests

An Arc jet test program designed to simulate the flow of superheated air through a breach in the Space Shuttle Orbiter's Wing Leading Edge was performed at the Johnson Space Center's (JSC) Atmospheric Re-entry Materials and Structures Evaluation Facility (ARMSEF). Several of the test objectives listed in the test plan were met in this program. These objectives were:

- obtain test data to correlate and validate the axisymmetric plume heating methodology;
- obtain the failure mechanism characteristics, failure initiation time, failure rate, and burn-through time of a cable bundle when subjected to hot gas impingement with representative reentry plume environment;
- evaluate aluminum hole growth rates for aluminum flat plates;
- and evaluate aluminum burning phenomena and the effect of potential exothermic reactions on plume heating.

The test was accomplished through the use of a specially designed water-cooled "plume box" which was inserted in the arc jet flow field. The box was designed with interchangeable front plates with different hole sizes cut into them to represent the breach. The tests performed with this box show that a high enthalpy flow passing thorough a breach in Columbia's wing structure is not only capable of causing failures in flight-type wire bundles similar to what was seen flight, it is also capable of exacerbating the problem by rapidly increasing the size of the breach.

A total of three cable bundle tests were performed in this program. Each test was accomplished with a different plume box configuration. These configurations were, one-inch diameter hole in a cooled copper plate (the cooled plate resulted in a constant hole diameter), a two-inch diameter hole in a cooled copper plate, and a one-inch diameter hole in an uncooled aluminum plate. The arc heater power level for each test configuration were as follows: 3.27 MW for the one-inch hole test and 3.63 MW for both two inch hole tests. The one inch hole test resulted in a total of 6 wire failures in 837 seconds. That failure rate, a much lower rate than seen in the flight, necessitated an increase in heater power for the subsequent test runs. The increased power with a two-inch diameter fixed hole resulted in 33 wire failures (the total number of wires monitored) in 538 seconds. That rate approached what was experienced in the flight. The uncooled aluminum plate resulted in all 33 wires failing in 68 seconds as well as a complete disintegration of the bundle. The hole in the plate also grew from 1 inch in diameter to over 4 inches in diameter in approximately 13 seconds. This agreed well with pre-test analytical predictions.

Several calibration test runs were made to support the development of the analytical math models used to characterize the plume generated within the box. These test runs consisted of taking pressure and heat flux measurements along the centerline of the plume at different distances from the front hole. The heat flux and pressure of the arc jet free stream, the pressure on the front of the box, the static pressure within the box, and the static pressure of the test chamber were also measured. To estimate the heat flux that the cable bundle experienced, a tube calorimeter was built. The calorimeter consisted of a stainless steel thin walled tube with the same diameter as a cable bundle. To the inside of this tube were attached fine-gage thermocouples in a grid-like pattern. This tube was mounted inside the box in the same orientation as the cable bundles then exposed to the same environment. The response of the thermocouples was used to back out the absorbed flux.

Each cable bundle test article was approximately 1.75 inches in diameter and constructed to simulate the cable bundles that are routed along the Orbiter wheel well in the left wing. Each test bundle consists of 290 cables, of these, 33 cables were monitored with an auxiliary data system. Conductor-to-conductor resistance within each of the 33 cables was recorded during test operations. Each cable in the bundle was a Kapton insulated, 24 AWG, twisted, shielded, pair. Aluminum clamps from the vehicle installation were used to hold the bundle of cables together and for attachment to the box. A picture of the cable bundle test article is shown in Figure 6-27.

Previous test programs demonstrated the failure mode for Kapton insulated cables when subjected to extreme heating – a short circuit develops between the two conductors within a twisted shield pair cable. This occurs because the Kapton insulation breaks down and changes from an insulator to a resistor over a finite period of time. This means the resistance between the two conductors within a twisted pair cable changes from a very high value to a low value. An example of this from a previous test program is shown

in Figure 6-28. The cables of interest are connected to various sensors (temperature, pressure, strain). Measurements of conductor to conductor resistance are normalized by converting them to what the Orbiter signal conditioner would output for a –75 to 250°F hydraulic temperature sensor channel assuming initial actual temperature of 100°F and a short of this magnitude occurring in the cable. An example of the results from this conversion are shown in Figure 6-29. Note that this plot is similar to the actual sensor data observed from STS-107.

This test program was performed in Test Position #2 (TP2) of the ARMSEF. A video camera mounted on the test chamber was used to visually monitor the flow field and interior of the test chamber. This video was used to help determine if and when a particular test run should be terminated. A camera was also available to monitor the front of the box when a destructive test of that front plate was performed. A smaller camera was mounted inside the plume box and used to monitor the test specimens and determine if and when a particular test run should be terminated.

This test program was intended to simulate an internal convective plume resulting from penetration damage to the Orbiter wing. To facilitate a re-creation of this environment, a water-cooled copper box was fabricated and mounted to a specially designed insertion arm. The box was made of a stainless steel frame with 0.25-inch thick copper plates making up the walls and 0.25 inch diameter copper tubes were brazed to these walls to provide cooling. These walls also protect the test articles from the heating associated with reflected shocks within the test chamber. The front of the box had a 10”x10” square opening over which interchangeable faces could be attached. This position was designated the forward position. Four types of plates were manufactured to occupy this position. They were:

- Water-cooled copper plate with a 1-inch diameter hole
- Water-cooled copper plate with a 2-inch diameter hole
- Aluminum plate with a 1-inch diameter hole
- Aluminum honeycomb with a 1 inch diameter hole

Stainless steel brackets were mounted inside the box at 15 inches and 20 inches from this forward plate. The various test articles, cable bundles, calorimeters, etc., were attached to these brackets. These locations were designated the aft positions. Figure 6-30 gives a sketch of this set-up and Figure 6-31 shows the configuration and design of the box. Also within the box was mounted a video camera to record the response of the test article.

The test program consisted of two distinct phases: the calibration phase and the engineering test phase. Two different sized holes in the forward position provide two different plume geometries and two different ζ positions for the test article provide an array of test locations for this test program.

The test conditions attempted to match the arc jet flow free stream stagnation pressure and centerline enthalpy to the flight stagnation pressure and total enthalpy. The targeted conditions and results of arc jet calibration runs are shown graphically in Figure 6-32. The resultant heat rate at these conditions was measured. The calibration data for the flowfield free stream is compiled in Table 6-3

Table 6-3 – Test Conditions

Date	Run Number	Z-distance (in)	Current (amps)	Mass Flow (lbm/s)	Bulk Enthalpy (BTU/lbm)	Power (MW)	CL Pressure (psf)	CL Heat Rate 1" D (BTU/ft2-s)	CL Enthalpy (BTU/lbm)
05/01/2003	2-2509-3	10	530	0.2	3600	1.25	not measured	not measured	not calculated
05/01/2003	2-2509-3	10	1200	0.4	5400	3.62	not measured	not measured	not calculated
05/05/2003	2-2510-3	21.25	530	0.2	4100	1.25	15	52	5517
05/05/2003	2-2510-3	21.25	1400	0.4	6200	4.27	36	198	13560
05/05/2003	2-2510-3	21.25	1200	0.6	4700	4.44	46	149	9027
05/05/2003	2-2510-3	21.25	1300	0.67	4800	5.1	52	162	9231
05/05/2003	2-2510-3	21.25	1300	0.8	4500	5.43	60	not measured	not calculated
05/06/2003	2-2511-3	21.25	1000	0.3	5500	2.8	25	120	9862
05/06/2003	2-2511-3	21.25	1200	0.3	6400	3.26	27	154	12178
05/06/2003	2-2511-3	21.25	530	0.2	4080	1.26	15	60	6366
05/28/2003	2-2516-3	20.05	1200	0.4	5450	3.63	32	139	10097

Calibration runs were also performed to collect data on the plume generated within the box. The centerline pressure and heating rate of this plume was measured at specific test points established in the flow field calibration phase. In addition, a specially designed calorimeter was used to measure the heating distribution on a cylinder the same diameter as a cable bundle. This consisted of a 1.75-inch diameter thin-walled stainless steel tube to which several small gauge thermocouples were attached in a grid like pattern. The response of these t/c's to the plume environments was recorded and from this data the heat flux was determined. All of this data will be used to refine the thermal models used to analyze the cable bundle response to the breach environment. The results of these calibration runs are presented in Table 6-4.

Table 6-4 – Test Condition Summary

Arc-jet Parameters		Arc-jet Flow Conditions					Box Measurements							
Current	Flow Rate	Bulk Enthalpy	Chamber Pressure	q-4" FF	q-1" FF	P-4" FF	Hole Dia.	P-front	P-internal	Ppitot-10"	Ppitot-15"	q-probe-10"	q-probe-15"	q-cyl stag-15"
(amps)	(lbm/sec)	(Btu/lbm)	(psf) /w box in flow	(Btu/ft2-s)	(Btu/ft2-s)	(psf)	(inches)	(psf)	(psf)	(psf)	(psf)	(Btu/ft2-s)	(Btu/ft2-s)	(Btu/ft2-s)
1000	0.3	5800	0.902	62	122	26	1	28	0.78	2.06	No Data	No Data	No Data	4.3
1200	0.3	6600	0.966	74	154	27	1	29	0.88	No Data	No Data	No Data	No Data	4.7
1000	0.3	5800	0.902	62	122	26	2	28	0.47	1.45	2.06	No Data	11	7.9
1200	0.3	6600	0.966	74	154	27	2	29	0.42	1.49	2.02	No Data	13	9.4
1200	0.4	5500	1.153	71	139	35	2	35	0.68	2.18	3.18	No Data	16	12.1

Three runs with a cable bundle were performed at the test conditions shown in Table 6-5. After arc jet activation, the insertion arm with box and cable bundle inside were inserted into the flow field while cable resistance was monitored. When sufficient cable failures were observed or other arc jet constraints were reached, the arc jet was deactivated and the arm was moved to remove the box from the flow field.

Table 6-5 – Test Configuration Summary

Item	Run 1	Run 2	Run 3
Box Forward Plate Type	Cooled	Cooled	Uncooled
Forward Plate Orifice Diameter (in)	1 in	2 in	1 in (starting)
Bundle Distance Aft of Orifice (in)	15 in	15 in	15 in
Arc Jet Current (amps)	1200	1200	1200
Arc Jet Mass Flow (lb/sec)	0.3	0.4	0.3

Run 1: The test set-up incorporated a 1-inch diameter orifice in the forward position of the box with the cable bundle 15 inches aft. The relatively low heating rate of run 1 produced only a few cable failures, but all were on the cable side facing the plume.

Run 2: The test set-up incorporated a 2-inch diameter orifice in the forward position of the box with the cable bundle 15 inches aft. Higher heating rates of run 2 produced failures faster and the entire cable bundle failed. Photographs in Figure 6-37 shows the appearance of the bundle before and after the test.

Run 3: The test set-up incorporated an uncooled aluminum, 0.1 inch thick flat plate in the forward position box. This plate had a 1 inch diameter orifice on the centerline with the cable bundle 15 inches aft. The test demonstrated a rapid erosion of the uncooled aluminum orifice. The orifice grew to an estimated 4 inch dia in approximately 13 seconds. Orifice growth was somewhat arrested after 4-5 inch due to a heat sink designed around the perimeter. The cable bundle showed a very rapid and increasing failure rate as orifice diameter increased.

Figure 6-34 and Figure 6-35 shows a comparison of cable failure rates for this test series and that observed on the vehicle. Based on the various observed cable failure rates, heating rate for the vehicle cable bundle must have been between those of Run 2 and Run 3.

Table 6-6 – Test Results Summary

Item	Run 1	Run 2	Run 3
Cable Run Time (sec)	837	538	68
Heating Rate from Calibration (BTU/ft^2-sec)	4.69	12.13	Greater and increasing during run, but could not be measured
Time When First Cable Begins Failure (sec)	107	14	13
Time When Last Cable Begins Failure (sec)	635	351	66
Total Cables Failed (33 monitored)	6	33	33

Cable bundles were tested at three different test conditions. Test results showed the arcjet-induced heating produces the same cable failure mechanism as occurred during previous cable overtemperature tests - a short circuit between the two conductors within a twisted shield pair cable. Data obtained for cable failure rate as a function of heating rate can be used to validate thermal models of the vehicle cable bundles for the STS-107 Columbia investigation. These models can be utilized to determine the heating rate which the STS-107 bundle experienced. This in turn can be used to gain a better understanding of the vehicle failure scenario.

6.5 Wire Bundle Burn-Through Thermal Analysis

A thermal analysis was performed on the wire bundles, MLG wheel well wall, and wing upper skin shown in Figure 6-39. Separate Thermal Desktop TMM's were created for each hardware region. These math models were used to calculate the required breach sizes and breach locations along the wing leading edge spar that would cause failure of each item. Their best estimated failure times were determined from the flight data. The results of each analysis were mapped against each other at defined zones along the wheel well to determine if a common breach size and location could explain their collective failure. The zones and panel locations are defined in Figure 6-40.

The spar breach hole size is assumed to be constant with no growth for the purposes of this comparative analysis. In addition, any oxidation and combustion effects were not modeled. The plume is assumed to be perpendicular to the respective spar. In each analysis it is assumed to impinge directly upon the object (wire bundle, wheel well, upper wing). This is significant in that the wheel well wall should always have a direct impingement while the bundle will not necessarily have a direct plume impingent. The spar breach is assumed to be at EI+487 seconds.

The flat plate plume heating induced from a wing leading edge breach at EI+491 seconds as a function of hole size and distance was used in this analysis and is discussed in section 5.3.3. Figure 6-41 and Figure 6-42 show the heating rates for impingement on a flat plate and a 1-inch diameter cylinder, respectively. A heating factor time array was included to adjust the heating to represent a breach earlier in the re-entry profile. Also, adjustments were made for increased hole sizes and distances. The plume heating adjustment for breach hole sizes greater than 2-inch diameter are shown in equation 6-2 while plume heating adjustments for breach distances greater than 60 inches are shown in equation 6-3.

$$qdot(d_{hole}) = qdot_{2.0"hole} \cdot \left(\frac{d_{hole}}{2"} \right)^{2.6} \quad \textbf{(6-2)}$$

$$qdot(x) = qdot_{dist} \cdot \left(\frac{dist}{x} \right)^{2} \quad \textbf{(6-3)}$$

Corrections for local pressure coefficients, off-normal angle impingements, and radial distribution from the stagnation point are shown in Figure 6-43 though Figure 6-45. Plume impingement on the bundle was also adjusted for radius and circumferential distribution as shown in Figure 6-46 and Figure 6-47.

The wire bundles are comprised of several harnesses each comprised of cables. Each cable consists of 2, 3, or 4 wires as shown in Figure 6-48. The lost in-flight measurements experienced were due to cable failure.

Testing as described in section 6.4 was performed to correlate and gain confidence in the wire bundle TMM. Here, 1¾ inch diameter bundles were subjected to 8.08 BTU/ft^2-sec (large propane torch test), 4.69 BTU/ft^2-sec (arc jet test #1), and 12.13 BTU/ft^2-sec (arc jet test #2) heating rates (determined through calorimeter test runs). The TMM bundle failure rate test predictions were mapped against their respective test results in Figure 6-49 and Figure 6-50.

The wire bundle TMM represented the bundle as a lumped mass rather than a group of individual cables. A specific heat of 0.225 BTU/lb$_m$-F and thermal conductivity (along the length of the bundle) of 166 BTU/hr-ft-F were used. The density was calculated by dividing the bundle mass per unit length (0.197 lb$_m$/inch) by its cross sectional area. A factor of 2.14 was applied to account for the additional surface area present in the bundles but not in the TMM. A radiative boundary condition of 70°F (emittance = 0.88) was used. Bundle radial heat transfer and cable failure temperatures (800°F) were determined through large propane torch testing. How the cable failure temperature is determined is shown in Figure 6-51.

Heating was applied via film coefficients and a 1700°F flame recovery temperature during the large propane test correlation but was adjusted to the plume configuration for the arc jet test TMM simulations.

The test correlated TMM was adjusted to flight conditions by applying the corrected plume heating. It was also modified to represent flight bundle 3 as shown in Figure 6-52 by adjusting the mass per unit length to 0.303 lb$_m$/inch. A flight radiative boundary condition of 20°F was used (emittance = 0.88). Flight bundle 3 is assumed to have failed completely due to the likelihood that the measured failed cables are distributed throughout the bundle. The heating required to match flight bundle 3 failure rate was determined to be 89 BTU/ft^2-sec. This was used to determine the required spar breach sizes and locations.

The wheel well wall is constructed of ribbed aluminum 2024-T6 surfaces of varying thicknesses. Effective thicknesses were used along the wall to capture the appropriate thermal mass response as shown in Figure 6-53. Radiative boundary conditions were assumed to be 70°F based on wing structural temperatures. Koropon primer (emittance = 0.86) was assumed to be present during the duration of the analysis. A failure temperature of 935°F was assumed. Wall burn through was assumed at EI+599 due to the first indicated temperature rises of the wheel well. A failure time of 112 seconds (EI+599 – EI+487) was used to determine spar breach sizes and locations.

The upper wing is made up of Aluminum 2024-T6 honeycomb structure (melting temperature of 935°F). The thicknesses of the honeycomb facesheets and core are 0.025 and 0.9684 inches respectively. The Generic Honeycomb Modeling Tool was used to generate the effective conductivity through the honeycomb core. An adiabatic upper surface boundary condition and a lower surface radiative boundary condition (70°F) were assumed. A Koropon coating (emittance = 0.86) was applied and assumed to be present throughout the analysis. Upon burn through of the lower facesheet, heating is applied to the upper facesheet. The FRSI layer attached to the upper surface of the wing is assumed to fail when or slightly before the wing structure fails. A burn through time of EI+536 seconds is assumed due to a plateau in the wire bundle failure rate. Spar breach hole sizes and locations were determined using a failure time of 49 seconds (EI+536 – EI+487).

The TMM spar breach results for flight wire bundle 3, the wheel well wall, and the upper wing (for the partitioned zones of the wheel well) are compared in Figure 6-54 through Figure 6-57. Since the assumed failure times of the wheel well and the upper wing are not exact, error bars are included for the wall in zone 2 to indicate the sensitivity of the comparison to the chosen failure times. The locations of highest probability for the plume impingement are zone 1 (panel spar 6 and 7 coverage) and zone 2 (panel spar 8 coverage).

In this analysis, the most probable spar breach diameters ranges from 2 to 6 inches. This estimated hole size in the spar is not entirely consistent with the analysis described in section 6.1. It should be realized that this analysis had to make gross assumptions for the plume characteristics which biased the heating rates on the high side. Application of these heating rates resulted in demise rates for the cable which were higher than actually observed in flight. Therefore, from the cable demise rates which were correlated to the observed flight data, the estimated spar hole size should be considered as a lower bound.

6.5.1 Tee-seal scenario

In addition to the damaged tee-seal analysis comparison to the flight data in the panel area described in section 6.1.1, the damaged tee-seal scenario was evaluated for wire cable bundle burn rates. In the case of a damaged tee-seal where the flow entrance area aspect ratio is high in comparison to a round-shape hole, the plume heating drops off much quicker along the flow axis (refer to section 5.3.3). To bound this analysis in terms of feasibility, assumptions were biased to predict the most rapid burn rate for the cable bundle. The bundle was assumed to be directly behind the spar although the closet bundle is actually at least 12 additional inches away from the spar. Using the heating rate profile shown in figure 5.3.2-27, the predicted wire burn rate is shown in Figure 6-58. In comparison to the burn rate observed in flight, this analytically predicted burn rate is lower due to rapid drop in heating rate. This analysis coupled with the panel 8/9 thermal analysis provides evidence that a damaged tee-seal scenario is not consistent with the flight data and observations.

6.6 Orbiter Sidewall Bondline Thermal Analysis

A thermal analysis was performed on the area surrounding OV102's V34T1106 sidewall bondline temperature sensor. The sensor is located on the inboard surface of the port sidewall at XO: 1215.5, ZO: 355.5 as shown in Figure 6-59. A Thermal Desktop TMM was created to determine whether its temperature rise during the re-entry was produced by increased external heating, by the addition of internal heating, or by the loss of the FRSI layer. The assumptions used in the analysis, the TMM correlation with flight data, the analysis and its results are discussed below.

The sidewall is an aluminum honeycomb structure with a layer of FRSI on the outboard surface as shown in Figure 6-60. Conduction was assumed to be 1-D through the sidewall. Internal and external convection were negligible. Radiation heat loss was assumed from the FRSI (emittance = 0.8) to the external air temperature and from the inboard facesheet (emittance = 0.86) to the Orbiter internal structure. The internal structure temperatures are shown in Figure 6-61 and Figure 6-62 for STS-109 and STS-107 respectively. Conduction through the honeycomb core (density = 3.8 lb/ft^3) was assumed to be 0.095 BTU/hr-in-F. The honeycomb facesheet densities were adjusted to account for the honeycomb adhesive. The RTV density surrounding the sensor was modified to account for the sensor mass (1.5 g).

The inner facesheet, outer facesheet, and RTV densities became 223, 201.7, and 278.4 lb/ft^3, respectively.

Confidence in the TMM was obtained through correlation with STS-109 flight data as shown in Figure 6-63. Nominal STS-109 external heating can be seen in Figure 6-64 and corresponding pressure profiles were used in the analysis. To achieve correlation a factor of 1.986 was applied to the inboard RTV density to account for missing thermal mass.

Upon correlation, the TMM was used to investigate the possible STS-107 heating cases shown in Figure 6-65. Nominal STS-107 external heating and pressure profiles were applied except as otherwise noted.

The study showed that the temperature rise can be explained by an external heating 13x nominal applied after EI+600 seconds or the application of internal fuselage heating (0.16 Btu/ft2-sec) after EI+648 seconds. These heating profiles are shown in Figure 6-66 and Figure 6-67 respectively. The temperature rise, however, cannot be explained by the loss of the FRSI layer under nominal external heating. The results of the three cases studied are mapped against STS-107 re-entry flight data in Figure 6-68 (external heating case), Figure 6-69 (internal heating case), and Figure 6-70 (loss of FRSI case).

6.7 Damaged Wing Leading Edge Coupled Aero-Thermal-Structural Analysis

A multidisciplinary process was developed to simulate the initiation and propagation of thermal/structural failure in the left wing during reentry. The objective of the analysis was to evaluate the plausibility of RCC damage in the form of 6 or 10 inch diameter holes near the apex of panel 7 in leading to the observed pattern of thermal/structural failure established for STS-107. Critical conditions assessed during the simulation included front wing spar burn-through time, panel 8 spar rear facesheet temperature response, and eventual failure of the RCC panels and attachments.

The process, depicted in Figure 6-71, consisted of defining external and internal aerodynamic heating and airloads environments throughout the entry, generating high fidelity thermal response of the internal insulation blankets, wing and spar structure, and RCC panels, and performing a detailed structural failure analysis of the thermally and mechanically loaded system. Multiple failure mechanisms were examined including failure of wing spar insulation, aluminum melting, honeycomb face sheet/core debond and loss of structural integrity, and loss of RCC wing leading edge attachments. This section of the report describes the analysis methodology and solution results for a damage scenario consisting of vehicle reentry with a 6 or 10 inch diameter hole in the left wing leading edge. Predicted temperature distributions and structural analysis results showing material failure and damage propagation during entry are presented and compared with available flight data.

To provide a common basis for the multidisciplinary analysis, a detailed finite element model of the wing leading edge covering RCC panels 6 through 8 was developed and is shown in Figure 6-72. In addition to the RCC panels, the model encompassed the associated honeycomb wing spar, internal insulation blankets and earmuff, representative attachment fittings and spanner beam, surrounding wing acreage TPS and underlying honeycomb wing structure.

Utilizing a CFD solution derived from the Orbiter common grid system described in Section 5.2.4.2 and trajectory flight condition at 491.4 seconds after entry interface, external aerodynamic heating and pressure distributions were mapped onto the finite element model as analysis boundary conditions. These values were scaled with STS-107 trajectory-based reference stagnation heating and freestream dynamic pressure levels, respectively, to provide time-dependent external environments for analysis. On surfaces inside the RCC cavity, an internal convective heating distribution described in Section 5.3.7.2 – scaled with reference stagnation heating - and internal pressure level predicted by the coupled flow CFD solution described in Section 5.3.6.1.2 - scaled with freestream dynamic pressure - were applied to the model to serve as time-dependent internal environments.

Using the SINDA thermal analyzer code (Ref 6-3), transient temperature distributions were computed throughout the model due to the internal and external aerodynamic heating. Although absent from the finite element model due to their complexity, surrogate surfaces were added in the thermal model to represent T-seals, completing the internal radiation enclosure within the leading edge. Other features of the analysis included:

- Radiation from external surfaces to space at 0°F
- Surface-to-surface radiation within the RCC cavity, earmuff/spanner beam cavity, wing bay cavity, and spar honeycomb structure
- Temperature-dependent material properties

To simulate the melting failure of affected surfaces within the limited schedule available for the analysis, internal convective heating was applied to interior portions of the model as outer surfaces reached their melting temperature limits. This avoided the time-consuming process of node removal and, coupled with the imposition of temperature limits for failed nodes to prevent nonphysical levels during the analysis, served as a reasonable approximation to the actual structural heating during failure. The heat of fusion for the materials was not accounted for in this study. Resulting temperature histories throughout the insulation and spar are shown in Figure 6-73 for both the 6-inch and 10-inch damage cases.

Next, time-dependent temperature distributions were coupled with pressure-based mechanical loads during structural analysis to determine the sequence and timing of structural failure within the model. NASTRAN structural solutions were coupled with a with a progressive failure analysis and life prediction software code, Generalized Optimizer and Analyzer (GENOA, Ref. 6-5) to provide detailed information on temperature and stress distributions within the structure and consequent levels of physical damage such as fracturing, melting and displacement within the structure. Solutions were generated at ten-second time intervals throughout the entry. Upon achieving measurable levels of structural damage, subsequent solutions were processed using equilibrium analysis at each succeeding time step, allowing removal of melted/failed material and redistribution of mechanical loads to surviving structure.

To accommodate the challenging schedule associated with this effort, the present analysis contains a number of limitations and uncertainties. The use of panel 7 as the site of the initial RCC breach was based on the most current working scenario at the time of the analysis. More recent thinking during the investigation has placed the likely hole location at panel 8 with the bulk of internal thermal damage occurring at the junction of panels 8 and 9. This analysis is thought to be relevant even for this scenario by considering the damaged panel in the model as representative of panel 8 and viewing the results occurring between panels 8 and 9. Consistent with such an approach, the OEX flight data for the panel 9 spar rear facesheet thermocouple, V09T9895, has been compared with the thermal response of a comparable panel 8 location in the model as discussed in the Results section below. Other analysis limitations are reflected in the uncertainties surrounding the internal convective heating environment, the approximate nature of the RCC attachment fittings, the absence of inertial loads, and the absence of T-seals in the structural model.

Several events observed during the course of the solutions were considered particularly significant with respect to the overall structural failure of the wing leading edge. In order of occurrence they are listed below:

- Melting of the Inconel 601 foil overwrap on the internal insulation blankets indicated the onset of thermal failure of the insulation, eventually allowing convective heating to approach the spar.
- Initiation of wing spar damage and fracture.
- Melting of the rear facesheet indicated breach of the spar has occurred.
- RCC panel failure.

Analysis results at these conditions are shown in Figure 6-74 through Figure 6-77 for the 10 inch case and Figure 6-78 through Figure 6-81 for the 6 inch case. Predictions for both damage cases show eventual failure of RCC panels through fracturing and breakup.

A comparison of the times at which these critical events occur during the entry is shown in Table 6-7. As expected, failure times are accelerated for the 10 inch case compared with the 6 inch due to the higher levels of internal heating. Thermal response of instrumentation within the left wing of STS-107 have suggested the initial breach through the spar occurred at 491 seconds after entry interface. With a predicted spar breach time of 470 seconds, the 6 inch provides a better comparison to flight data than the 10 inch case. As shown in Figure 6-82, better agreement for the 6 inch damage case can also be seen by comparing the temperature response of V09T9895 (panel 9 spar rear facesheet thermocouple) from the OEX flight data with the model predictions at an analogous location on panel 8 (in this case panel 8 in the model is used as a surrogate for panel 9 as noted previously). The average predicted temperature of two nodes on the rear facesheet are used in the comparison for each damage case. Up to

the flight estimated time of spar breach at approximately 490 seconds the predicted thermal response for the 6 inch case is in reasonable agreement. After this point, the predicted temperature rise rates are much slower than flight data, indicating the effect of convective heating experienced during flight in this area from the hot gas jet expanding into the wing interior. Modeling of such heating was not included in this analysis.

Table 6-7 - Critical Failure Times For 6 Inch and 10 Inch Damage Cases

Critical Event	*10 inch hole*	*6 inch hole*	*Time difference*
Failure of Inconel 601 foil overwrap on thermal insulation.	***210 seconds***	***230 seconds***	***20 seconds***
Heating is applied to the aluminum spar surface. Initial structural failure of spar.	***320 seconds***	***380 seconds***	***60 seconds***
Initial spar breach. Inside now exposed with small gaps, growing into a large spar breach (28 inches x 4 inches; 38 inches is spar height).	***380 – 410 seconds***	***470 – 510 seconds***	***90 – 100 seconds***
Fracturing of RCC Panels Evident	***450 seconds***	***500 seconds***	***50 seconds***

6.8 Chin Panel Temperature Anomaly

Starting at 490 seconds from entry interface, a temperature measurement on the RCC chin panel recorded a sharp rise in temperature followed by a drop. Eventually, the temperature measurement recorded a trend that followed the expected nominal transient. The transient is shown in Figure 6-83. It has been concluded that this transient had to have been caused by a data system anomaly rather than an anomaly with the chin panel hardware of thermal environment.

- The anomalous transient picks up the thermal profile where it left off is unlikely for a real transient. This is very coincidental for a thermal transient since there is no reason for the temperature to return to the previous slope and absolute value (extrapolated).
- The recorded temperature actually cools down repeatedly during the transient. It is very difficult to cool this structure during entry because:
  - The surrounding hardware contributing to the radiation environment is getting hotter and the convection environment during this time period is heating (not cooling)
  - Thermocouple is on a heavy piece of hardware interior to the chin panel
- Anomalous behavior occurs after wing breach at 487 seconds. Postulate that the hot gases and associated heating and/or free electrons cause a data system malfunction.

6.9 Truss Tube Thermal Analysis

A thermal sensitivity study was performed on OV-102's left wing truss tubes. A Thermal Desktop TMM was created to gain an understanding if and when the tubes would fail if exposed to plume heating caused by a breach in the wing leading edge spar. Tubes at various distances from the spar were chosen as shown in Figure 6-84. The size of the breach was varied.

The tubes are aluminum 2024-T6. For analysis sake they are designated tubes 1 through 4. Table 6-8 shows their differences in outer diameter, wall thickness, length, and distance from spar panel 8.

Table 6-8 – Tube Summary

Tube	Outer Diameter (in)	Wall Thickness (in)	Length (in)	Distance (in)
1	3.75	0.048	48.41	15.94
2	3.75	0.031	39.04	96.44
3	2.00	0.018	38.37	37.80
4	2.25	0.020	38.02	94.49

Their diameters and wall thicknesses were assumed to be constant throughout their respective lengths. Their distances were measured in plane from their midpoints to the spar.

A radiative boundary condition of 20°F was assumed. The tubes were coated with Koropon (emittance = 0.86) throughout the duration of the analysis.

A spar breach is assumed at EI+488 seconds. It was assumed to be in spar panel 8 and to be constant in size. Oxidation and combustion effects were ignored. The plume was assumed to impact the middle portion of the tubes directly. Plume heating methodologies similar to section 6.5 were incorporated in this analysis. Correction for panel 8's local pressure coefficient, off-normal angle impingement, and radial distribution from the stagnation point were applied. The plume heating used is shown in Figure 6-85 and the heating correction for angular impingement is shown in Figure 6-86. Plume impingement on the tubes was also adjusted for radius and circumferential effects.

Failure was determined when the entire cross section of the tube at the point of plume impingement reached a temperature of 935°F. The failure times of the 4 tubes are shown in Figure 6-87 for varying breach hole sizes.

6.10 RCC Knife Edge Tests

STS-107 recovered debris for reinforced carbon-carbon (RCC) panels 8 and 9 showed "knife-edge" erosion. A test program was initiated in order to confirm uncoated RCC sharpening and determine if coated RCC will sharpen as seen in Columbia debris of RCC Panels 8/9 rib sections.

Two test fixtures were designed and developed for this test and are shown in Figure 6-88. The single plate fixture was used to simulate flow impinging onto a breach edge with an angle of 20°. The dual plate fixture was used to simulate flow impinging onto a near-normal (70°) surface representative of the RCC panel ribs.

RCC test specimens were prepared from an existing RCC panel rib section and RCC plate. The RCC test plates for the single plate fixture were 2.5"x3" in dimension and .25-inch thick. Closeout RCC pieces were used to prevent flow from entering into the copper holder and were of the same thickness of the single plate test specimen. Two uncoated specimens and one coated specimen were tested.

The RCC test plates for the dual RCC plate test fixture were 3"x3" in dimension and .375-inch thick. Smaller plates were used to model an offset RCC rib and were 1.6"x3" with an equivalent thickness. A coated and uncoated offset RCC plate was tested.

This test program was performed in test position #2 of the JSC Atmospheric Reentry and Structures Evaluation Facility (ARMSEF). Inside this facility, test gases (77% nitrogen and 23% oxygen) are head by a segmented constricted arc heater and injected into a vacuum chamber through a water-cooled 5-inch diameter nozzle that has a 15-degree half angle. While tests are in progress the facility vacuum chamber is maintained below 200 microns of mercury. Test models are mounted on a two water-cooled, remotely actuated sting arms that allow them to be inserted after test conditions are stabilized. The stagnation pressures experienced by test specimens were determined with a 0.5-inch diameter water-cooled pitot probe prior to specimen insertion.

Laser pyrometers monitored the center of the test specimens away from the edge to evaluate the gross temperature response of the RCC using an emissivity of 0.9. In addition, a stroboscopic camera was used to monitor the RCC test specimen edge for knife-edging. This camera provided real-time video data, which eliminated the effects of temperature on the image.

The test conditions were defined by enthalpy and pressure. The test points were derived from the predicted STS-107 RCC hole edge impact pressure and total enthalpy provided by JSC/EG. Three test conditions were established based on the profile shown in Figure 6-89.

A dual calibration model with a 1" flat face heat rate sensor and a pitot probe measurement was used to determine the heat rate and pressure. The actual test points that were calibrated for in the arc jet simulation are shown in Table 6-9.

Table 6-9 – Target Test Conditions

	Test Conditions	
	Pressure (psf)	Bulk Enthalpy (BTU/lb)
Condition #1	75	11200
Condition #2	129	10800
Condition #3	147	7400

The three test conditions were used to simulate a flight profile. For the first two tests, only condition #1 was used. Based on the results from these tests, conditions #2 and #3 were added and the flight profile developed. Figure 6-90 illustrates the simulated flight profile used during testing. It should be noted that the enthalpy specified is the centerline enthalpy and should be multiplied by a factor of two to correspond to the targeted total enthalpy.

In evaluating the results of the testing, the boundary conditions should be taken into account. The RCC test specimens were mounted in water-cooled copper holders, thus, slightly affecting the three mounted edges of RCC through conduction. There was an effort to minimize radiative losses from the back of the specimens using insulation and graphfoil (used to prevent any chemical reactions). However, both test fixtures could not prevent the large view factors from the front of the main RCC pieces to the chamber walls. The test run configurations are shown in Table 6-10.

Table 6-10 – Test Run Configuration

Run #	Angle	# of Plates	Offset	Coating
1	70	2	no	coated/coated
2	70	2	yes	coated/uncoated
3	20	1	n/a	uncoated
4	70	2	yes	coated/uncoated
5	20	1	n/a	coated

Test #1 produced no knife-edging since the conditions could not generate temperatures on the RCC specimen greater than 3250°F. Pre- and post-test photos are shown in Figure 6-91.

Test #2 used the same test conditions as Test #1, but the front specimen was exchanged with an offset RCC plate representing an offset RCC rib. Condition #1 could not produce temperatures greater than 3250°F on the SiC coating, but did oxidize the exposed carbon, leaving a white residue from the impregnated TEOS, as seen in Figure 6-92.

Test #3a utilized the simulated flight profile with conditions #1 though #3. Condition #1 did not create knife-edging, only localized oxidation on the exposed carbon. Condition #2 began after 200 seconds in

the stream, and created temperatures on the edge above 3250°F and initiated knife-edge like erosion. After 69 seconds at Condition #2, the environment was changed to condition #3. Condition #3 was a significant reduction in heating compared to condition #2, and the knife-edge features began to blunt. The decision was made to preserve the knife-edge features created in Condition #2 by removing the sting arm out of the flow. The pre- and post-test photos are shown in Figure 6-93.

Test #3b used another uncoated piece of RCC with the same simulated flight profile. The test, although, not required to run, reproduced the results in Test #3a with the same knife-edging.

Test #4 involved the same specimens tested in Test Run#2 in the dual plate fixture since there was minimal oxidation on the exposed edge and a limited amount of test specimens. The simulated flight profile was used, but the copper test fixture could not withstand the high heating rates at condition #2. Prior to the sting arm being removed from the flow, the SiC coating began eroding at the center of the front offset RCC piece. This suggests that the hottest portion of the RCC at this condition was not at the edge and that erosion would have propagated from the center outward. It must be noted that the front of the copper holder could have influenced the flow field and altered the heating distribution along the plate. Pre- and post-test photos are shown in Figure 6-94.

Test #5 used the single plate fixture with a coated RCC specimen. Knife-edging was produced on the main RCC specimen as shown in Figure 8. Test conditions did produce temperatures above 3250°F. The test condition profile was stopped at condition #2 in order to preserve the knife-edging features for posttest evaluation. A diagram showing the approximate dimensions of the knife-edging is shown in Figure 6-95.

In addition to the main RCC knife-edging on Test #5, the closeout RCC pieces also produced knife-edging as seen in Figure 6-96. The closeout pieces prevent flow from entering the copper test fixture. The erosion occurred from a secondary shock impinging on the closeout pieces. The knife-edging was sharper than what occurred on the main RCC piece.

The test facility was able to simulate predicted environments on RCC ribs and breach edge on six RCC test specimens. Knife-edging was apparent on specimens where the temperature on the SiC coating was above 3250°F. Knife-edging was also apparent on the closeout piece in test #5. This data along with the results from previous RCC testing suggests that under stagnation flow with temperatures above 3250°F, the RCC will erode in a knife-edge manner. If hot gases flowed into the wing leading edge through a breach with sufficient enthalpy and impact pressure, the RCC would have eroded in a similar manner as seen in the debris.

6.11 Leading Edge Reinforced Carbon-Carbon (RCC) Hole Growth Thermal Analysis

A prediction of RCC hole growth was performed using JSC arc jet test data obtained from hypervelocity impacted RCC test specimens when subject to a high temperature entry environment. The objective of the arc jet testing was to establish the oxidation characteristics of RCC with thru holes obtained from hypervelocity impacts. The specimens were exposed to constant heating conditions at temperatures of 2500 and 2800F and pressures of 50 to 180 psf. Correlations were developed from the data for use in trajectory simulations to predict hole growth and hot gas flow through an enlarging hole into the wing leading edge cavity.

A 0.75 inch diameter hole in the RCC was assumed for analysis purposes. Figure 6-97 shows the heat flux and pressure environment at the hole while Figure 6-98 shows the resulting RCC surface temperature as a function of time. The predicted RCC temperature of approximately 4800°F is assumed to be consistent with a diffusion-limited erosion regime for bare or uncoated RCC. With this assumption, the erosion or hole growth rate measured for the 2800°F arc jet tests can be used for erosion rate estimates here. The erosion rate in this flight environment and regime is .0032 in/sec. Figure 6-99 reveals the results of the analysis and shows the predicted growth to a final OML diameter of 4.0 inches. The predicted IML (back-face) diameter is slightly smaller at 3.0 inches. Extrapolation of this analysis to higher RCC temperatures (sublimation regime) or larger initial hole diameter is not recommended since the data base is very limited.

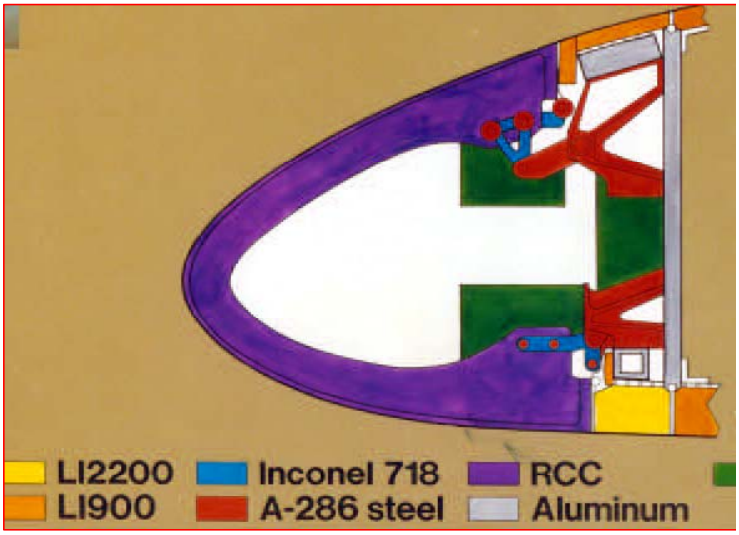

Figure 6-1 - Wing Leading Edge Cross-section

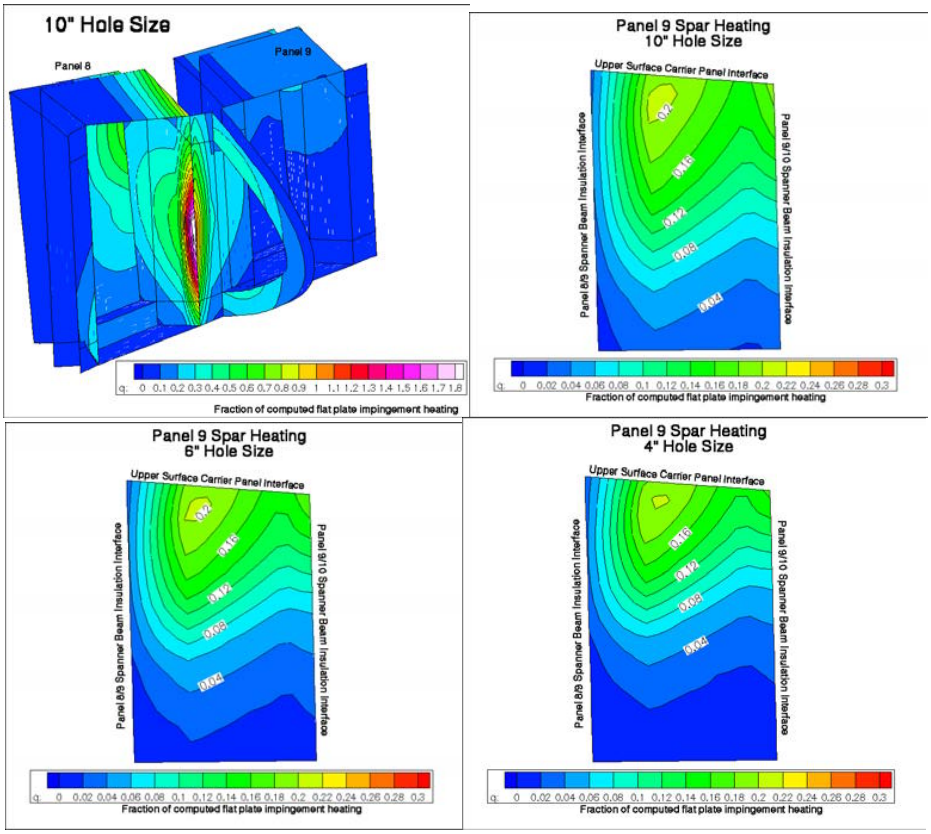

Figure 6-2 - Heating Distribution

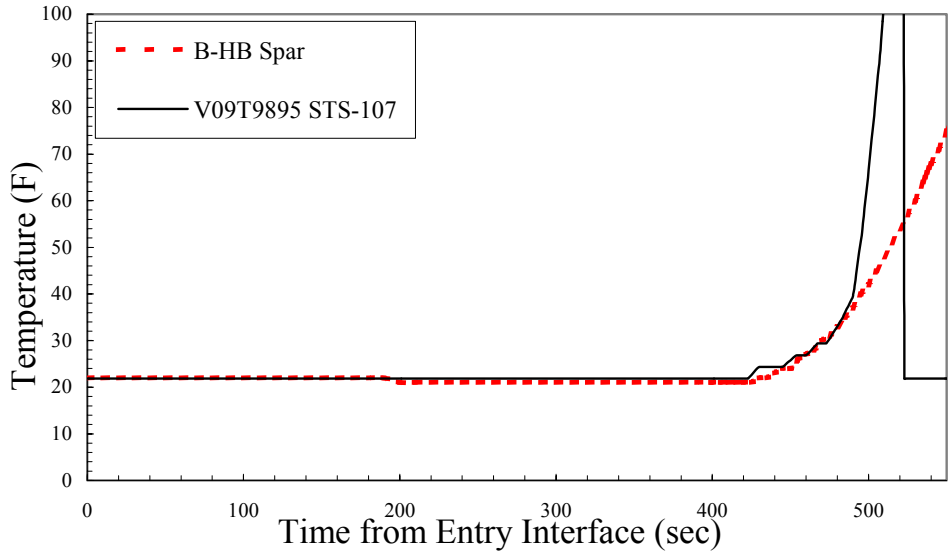

Figure 6-3 - Spar Temperature Prediction vs. Flight Data

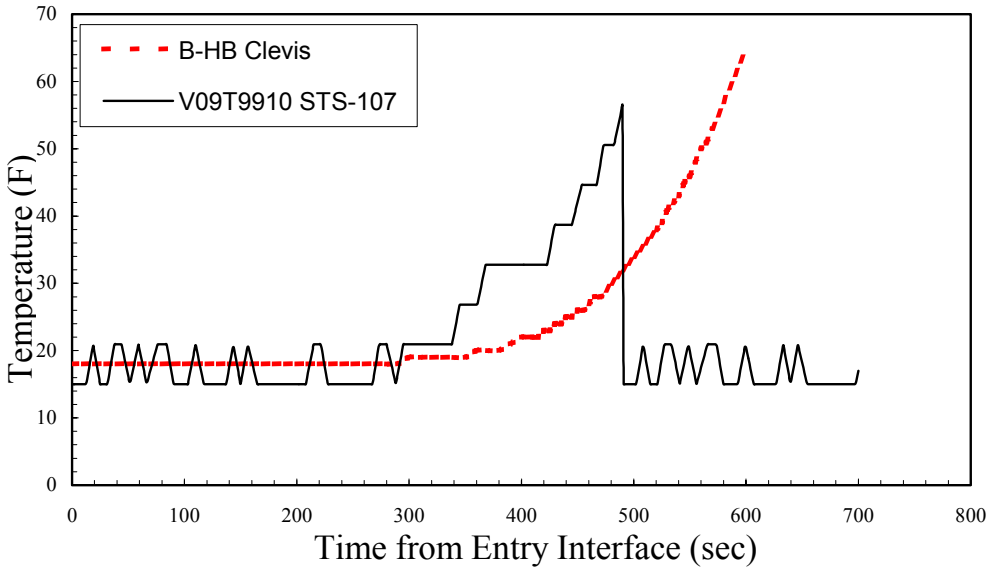

Figure 6-4 - Clevis Temperature Prediction vs. Flight Data

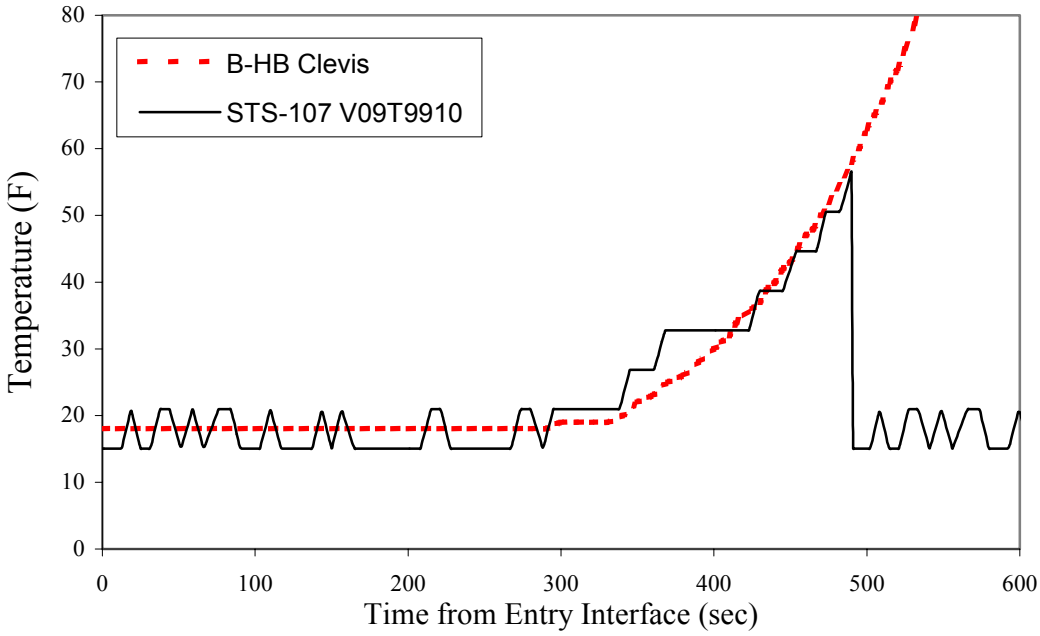

Figure 6-5 - Clevis Temperature Prediction vs. Flight Data

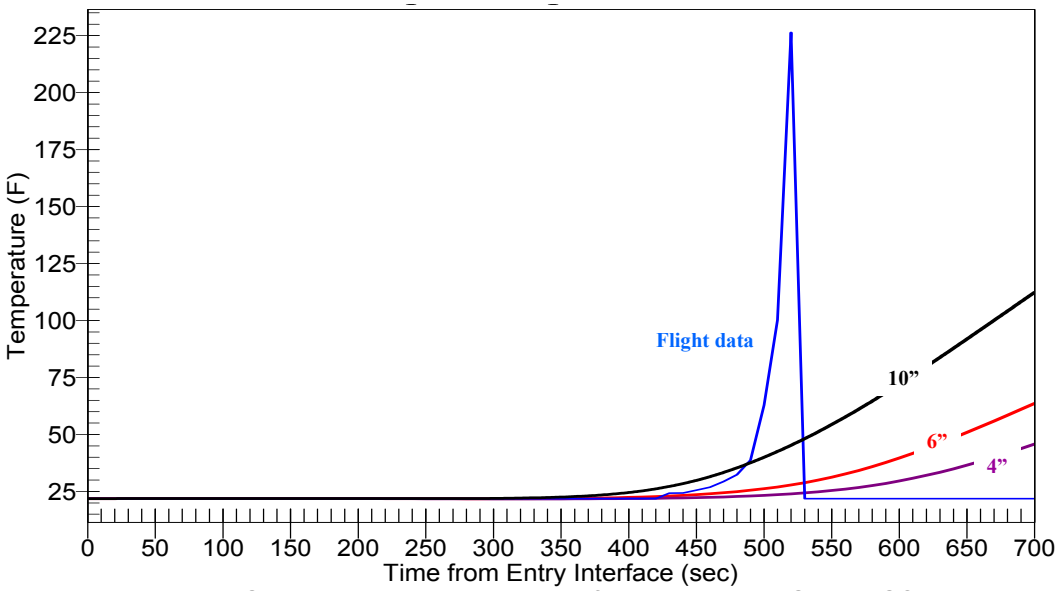

Figure 6-6 - Spar Temperature Prediction for Varying Hole Size – JSC TMM

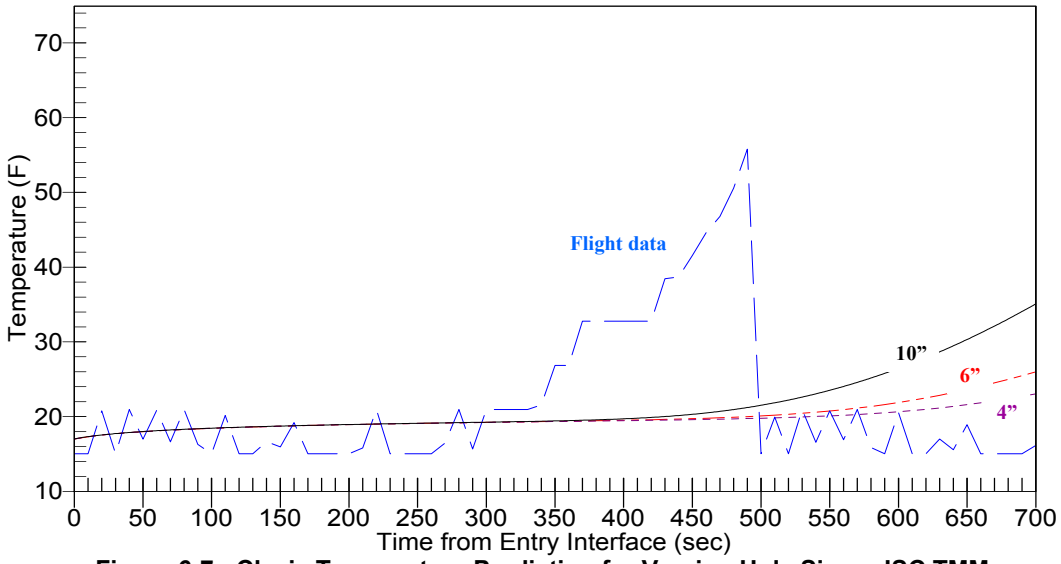

Figure 6-7 - Clevis Temperature Prediction for Varying Hole Size – JSC TMM

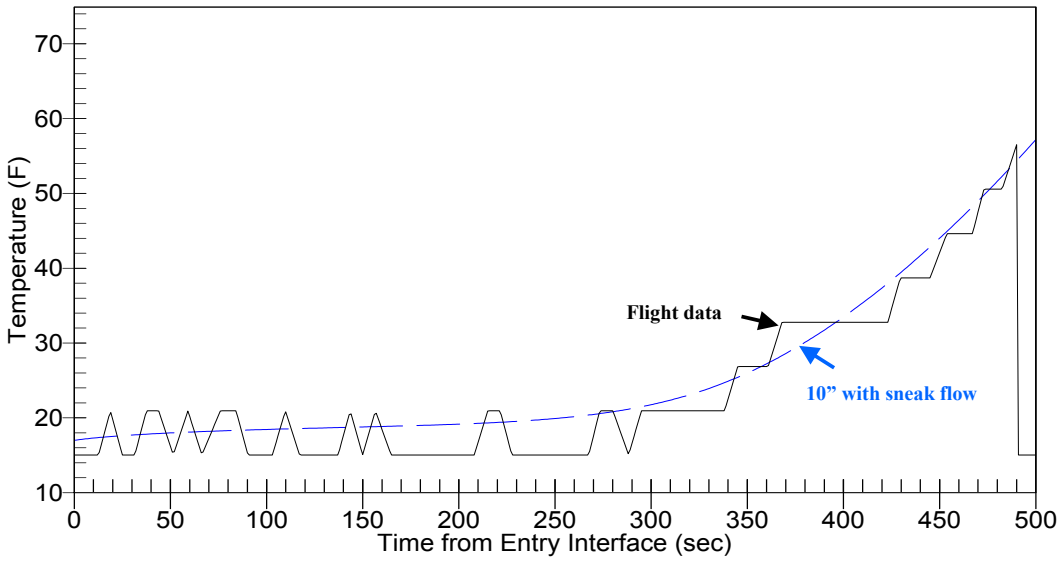

Figure 6-8 - Clevis Temperature Prediction (with 10% Sneak Flow) – JSC TMM

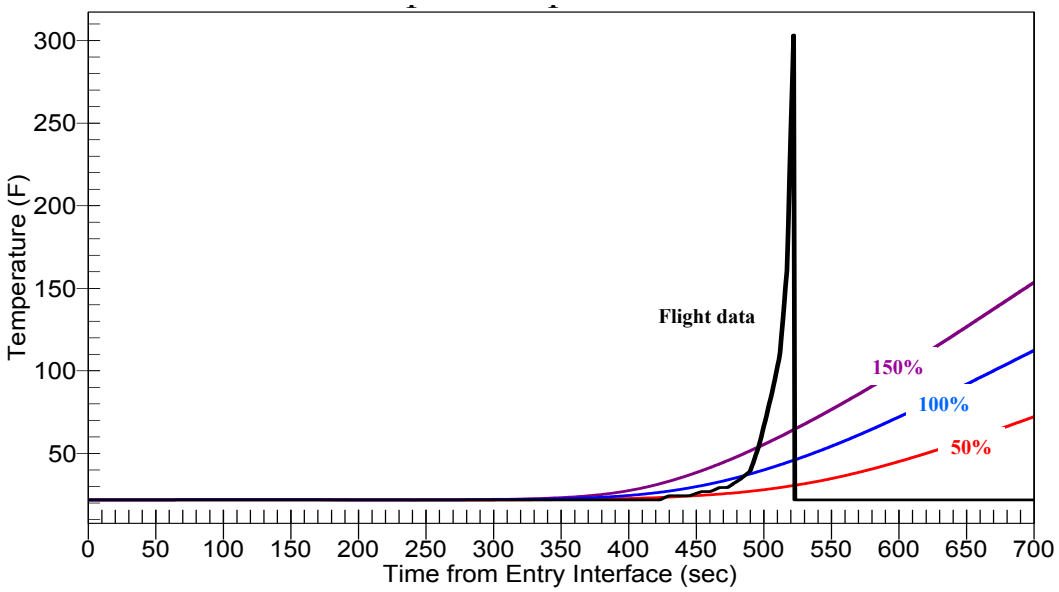

Figure 6-9 - Spar Temperature Predictions with Heating Uncertainties

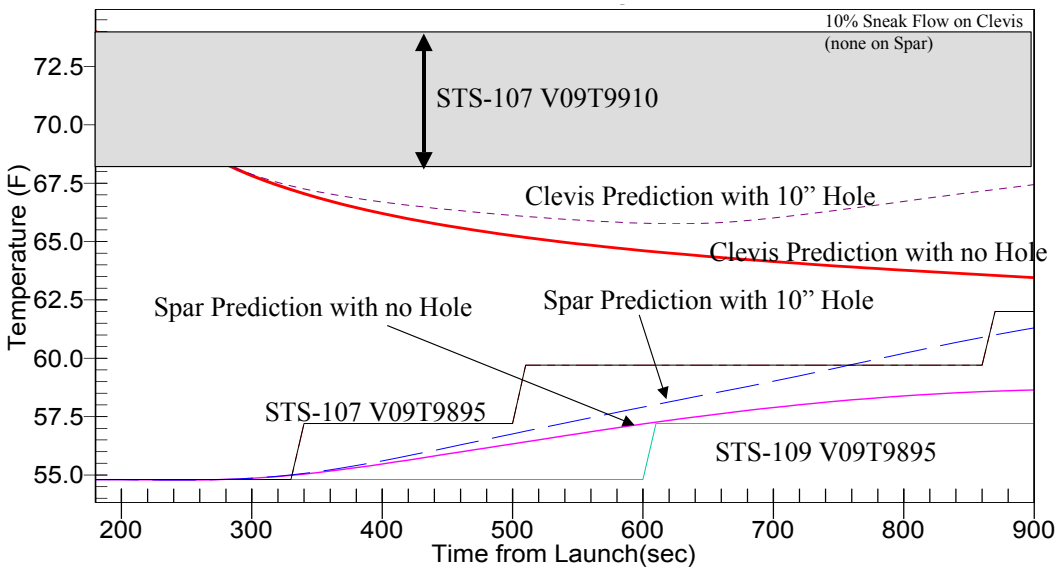

Figure 6-10 - Spar and Clevis Ascent Predictions Compared to Flight Data – JSC TMM

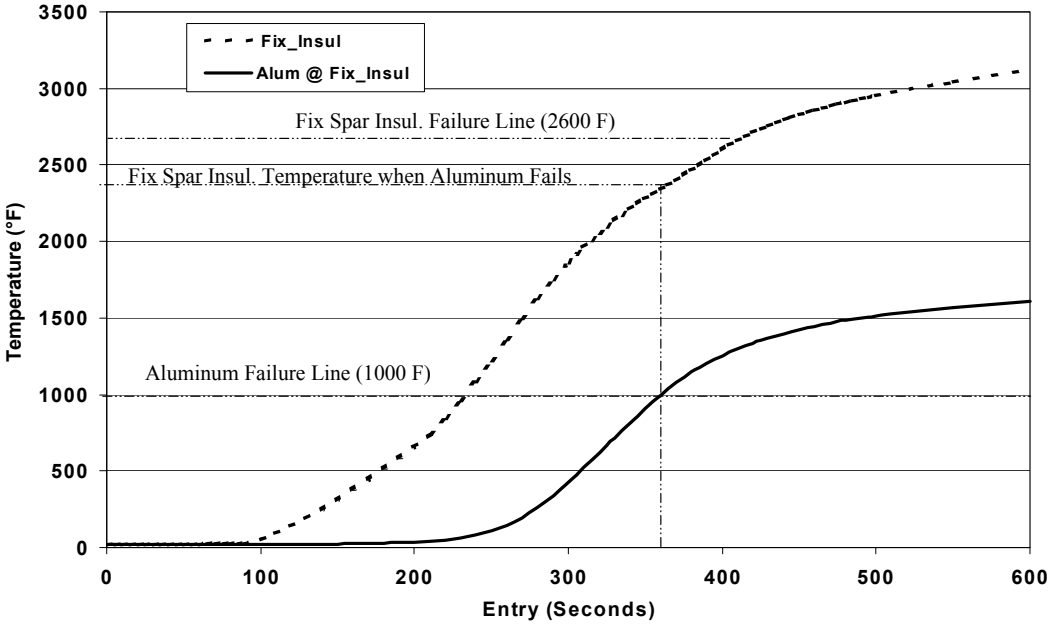

Figure 6-11 - Damaged Tee-Seal - Spar Insulation Transients

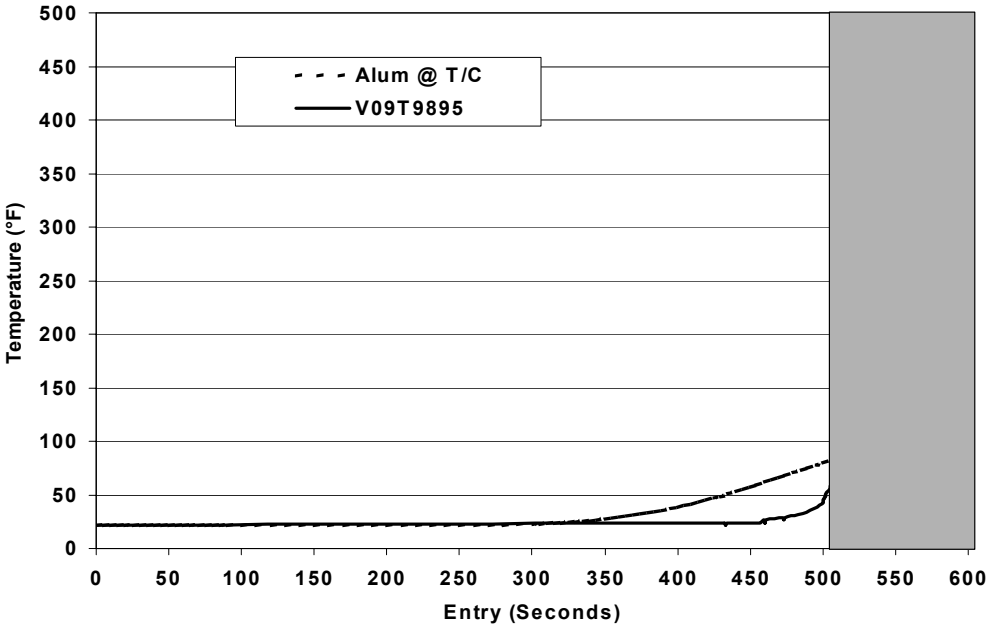

Figure 6-12 - Damaged Tee-seal - Spar Temperature Transients

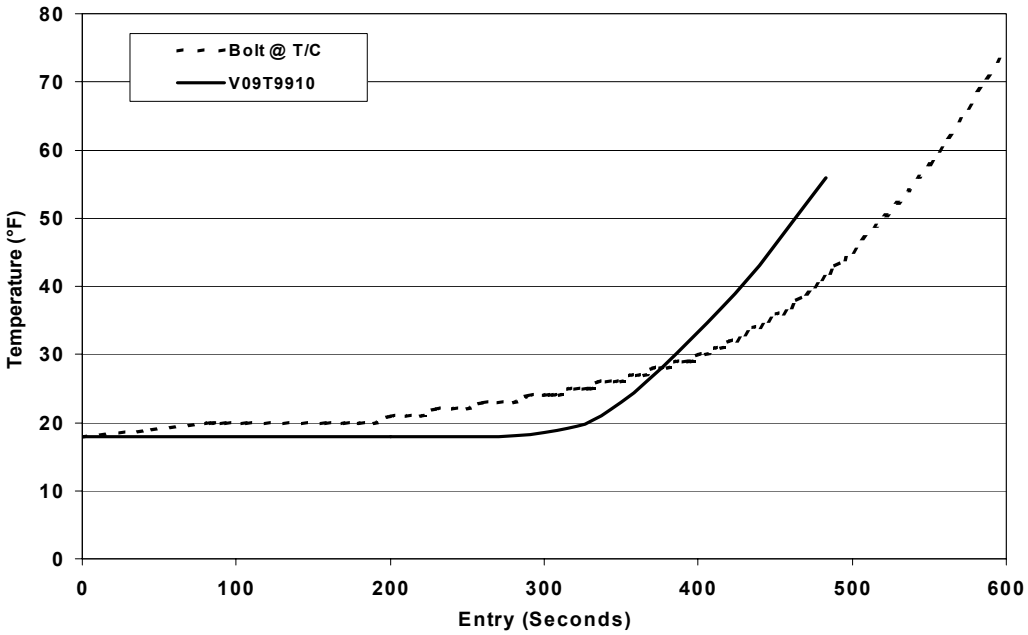

Figure 6-13 - Damaged Tee-seal - Clevis Transients

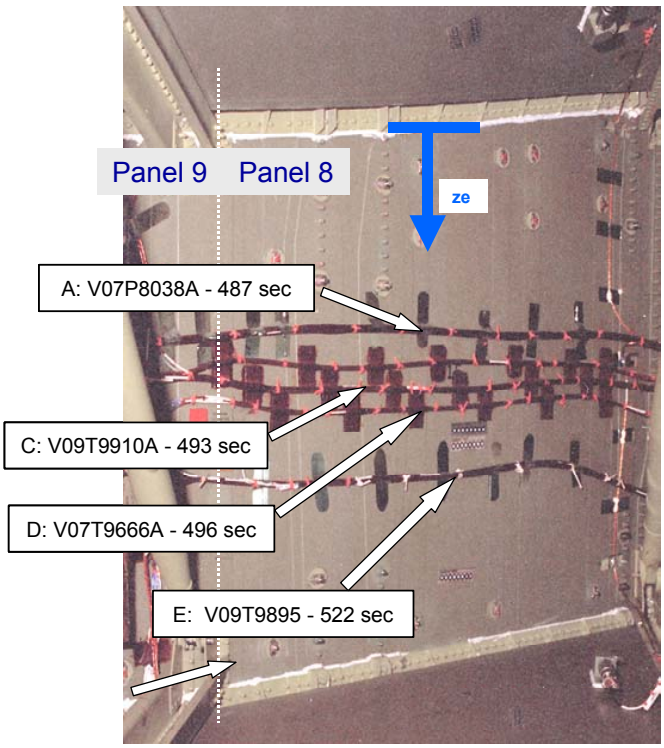

Flight data

	Time from e.i. (sec)	ze (in)
A	487.0	16.5
C	493.0	19.8
D	496.0	21.3
E	522.0	25.8
B		18.3

Figure 6-14 – Leading Edge Spar (view from within wing looking fwd)

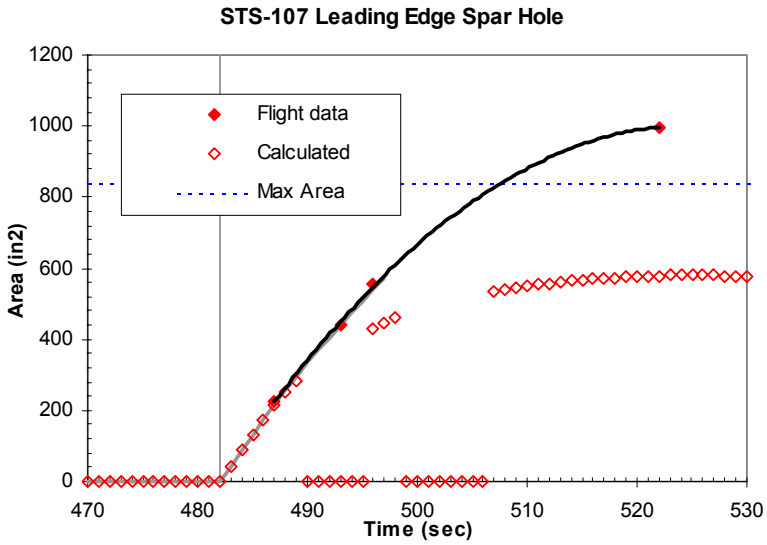

Figure 6-15 – Spar Hole Growth Analysis

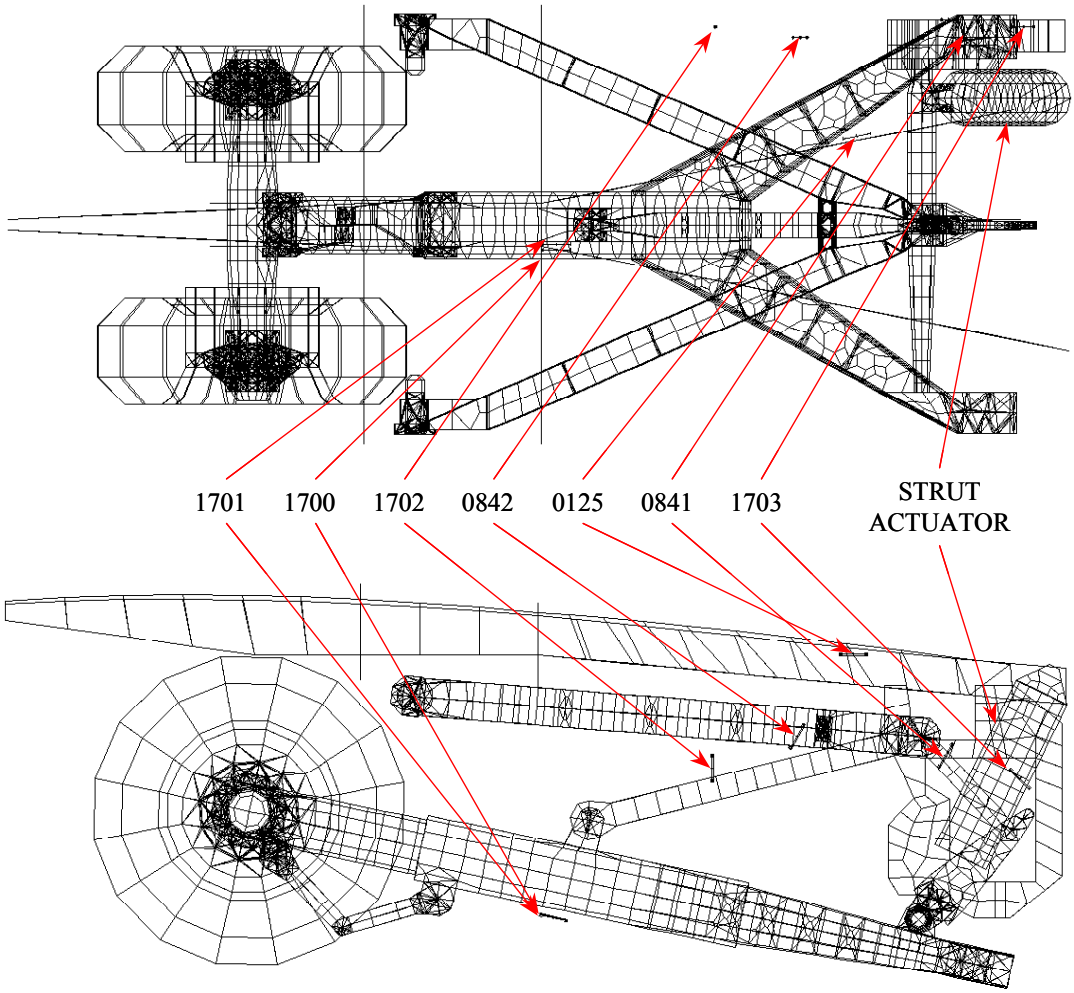

Figure 6-16 – Left Main Landing Gear Sensor Locations

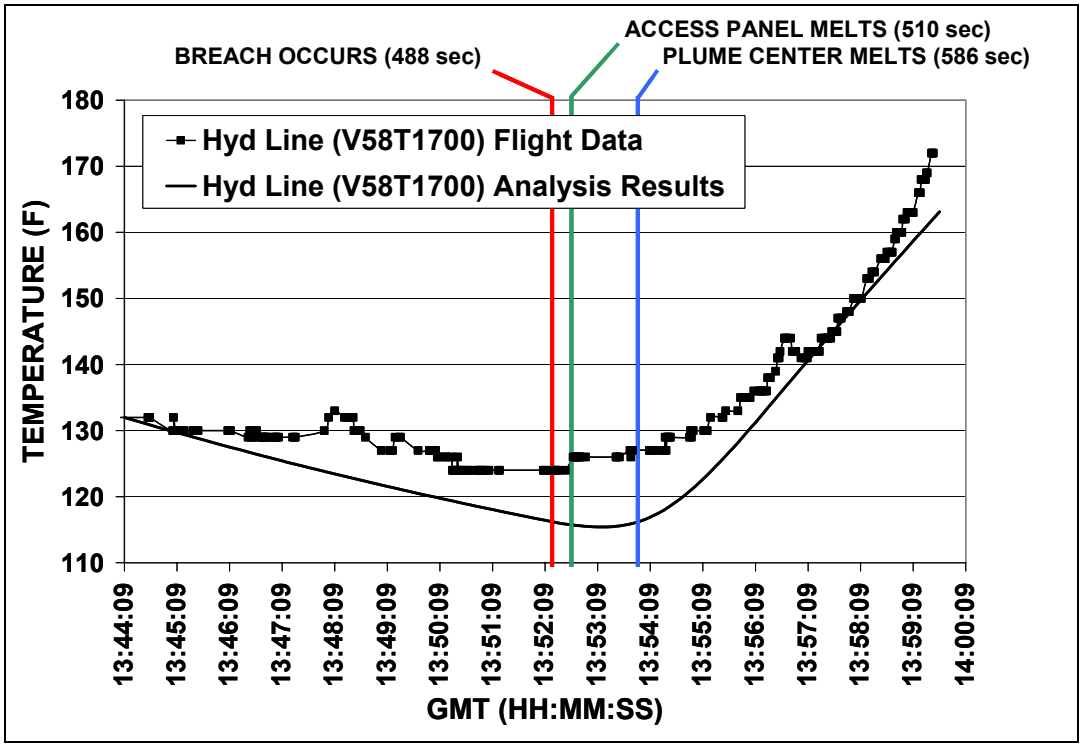

Figure 6-17 - V58T1700A analysis results

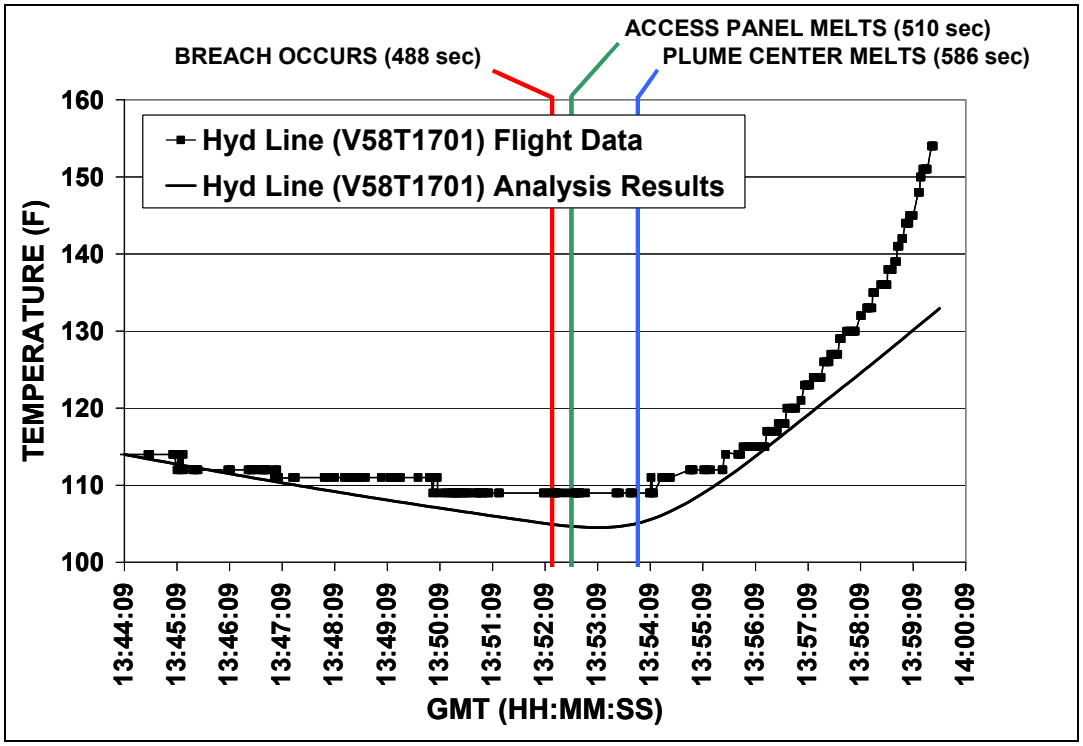

Figure 6-18 - V58T1701A analysis results

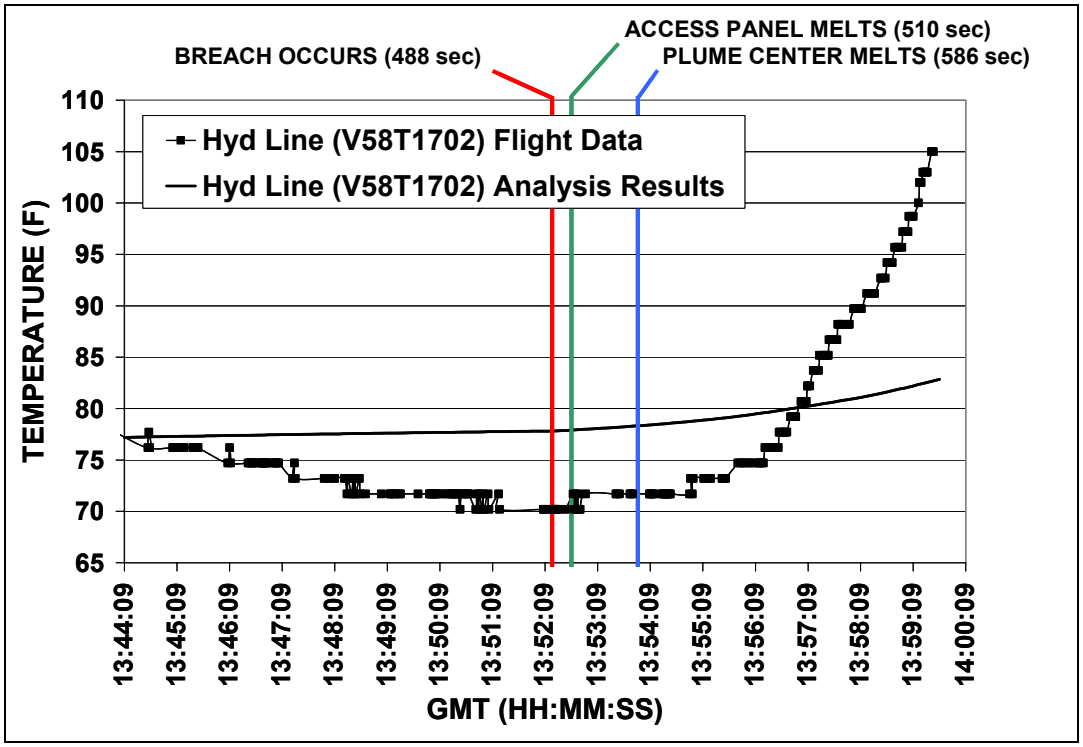

Figure 6-19 - V58T1702A analysis results

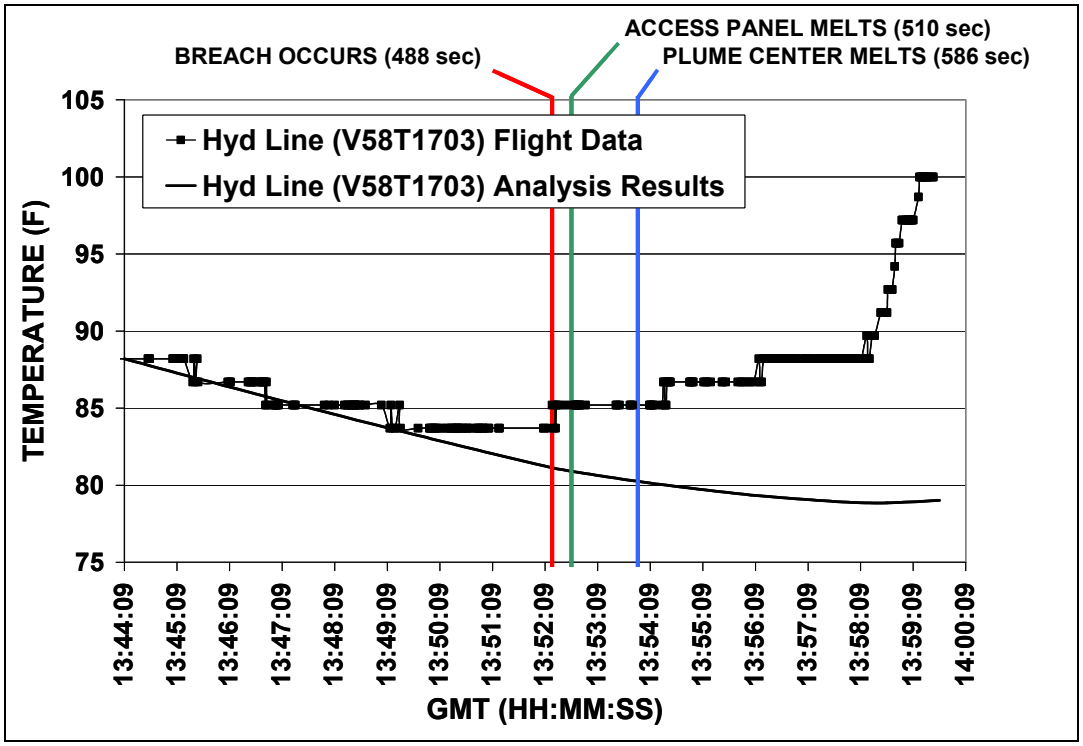

Figure 6-20 - V58T1703A analysis results

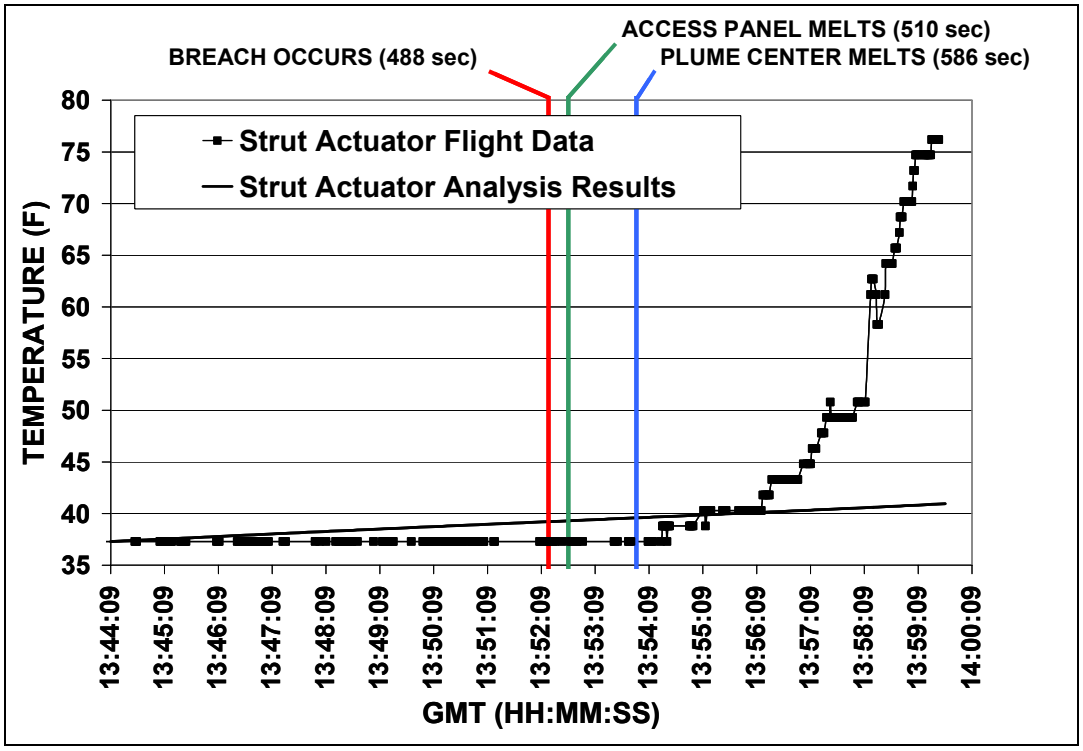

Figure 6-21 - V58T0405A (strut actuator) analysis results

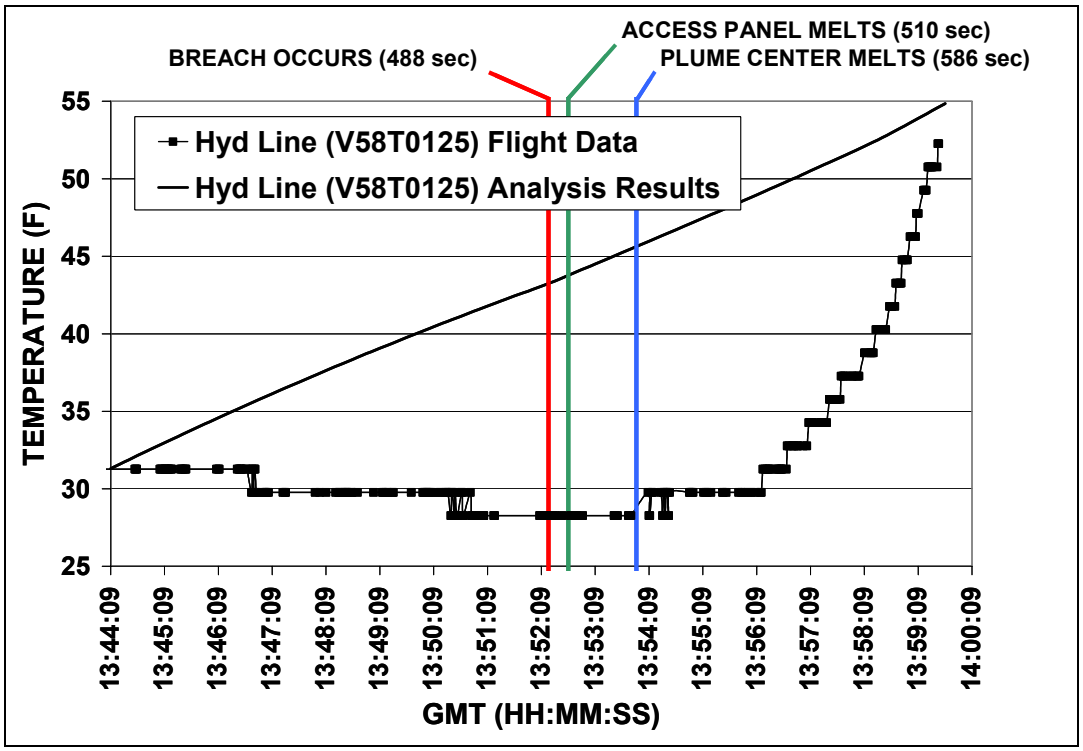

Figure 6-22 -V58T0125A analysis results

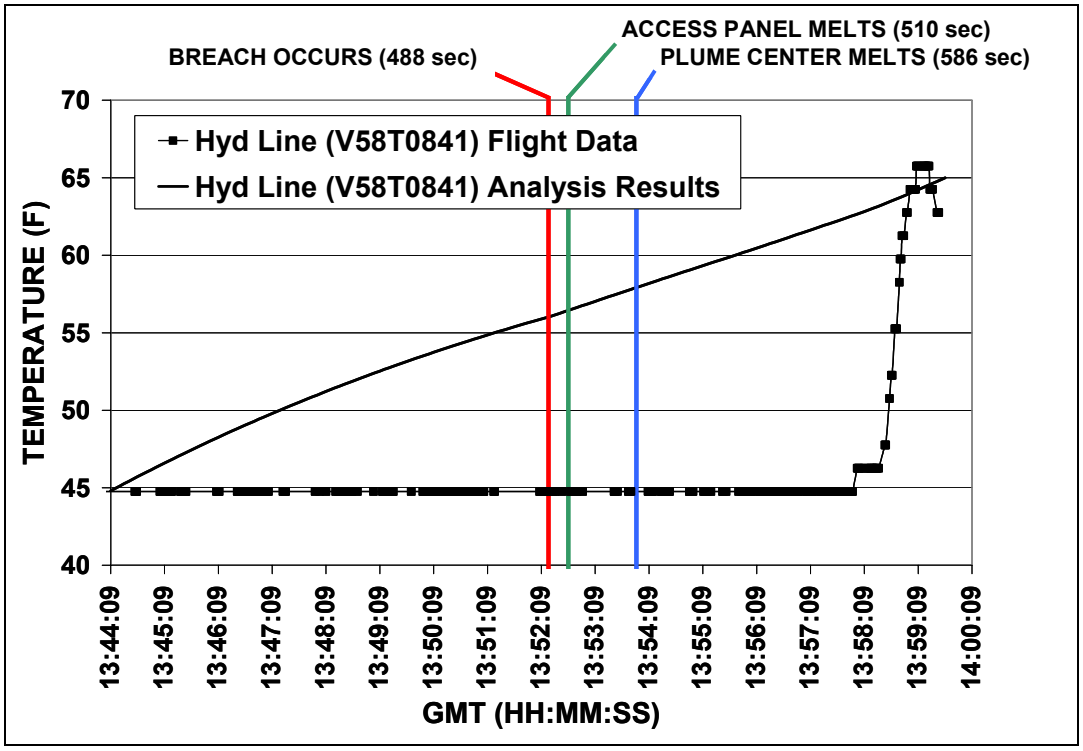

Figure 6-23 - V58T0841A analysis results

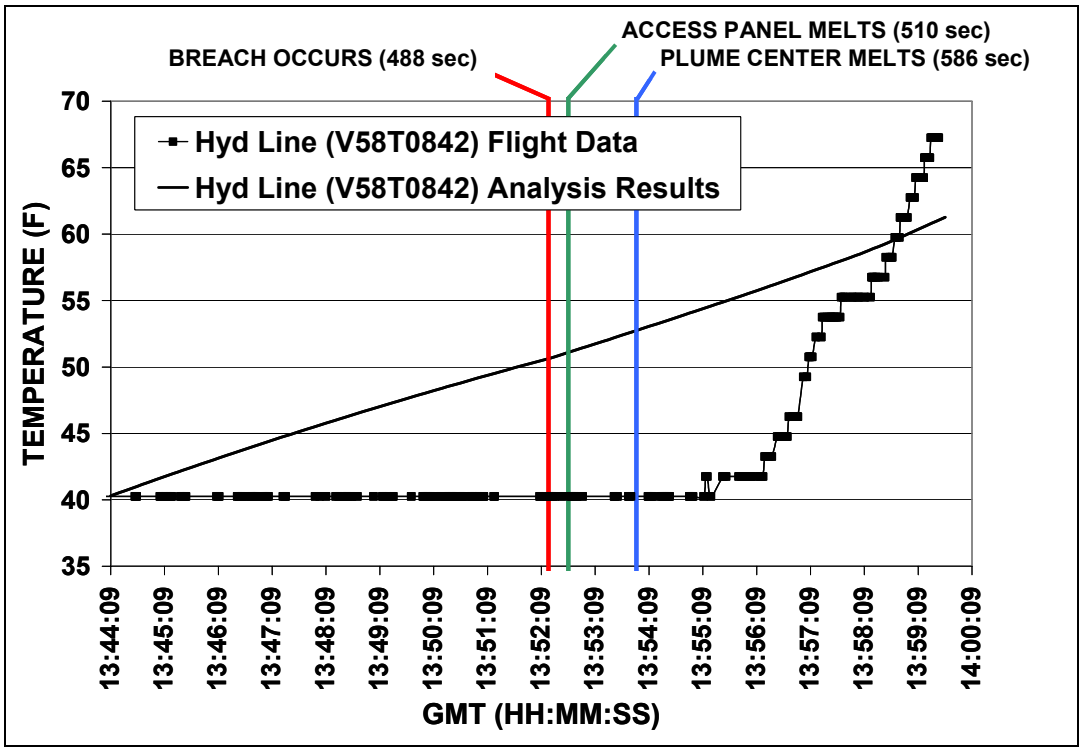

Figure 6-24 -V58T0842A analysis results

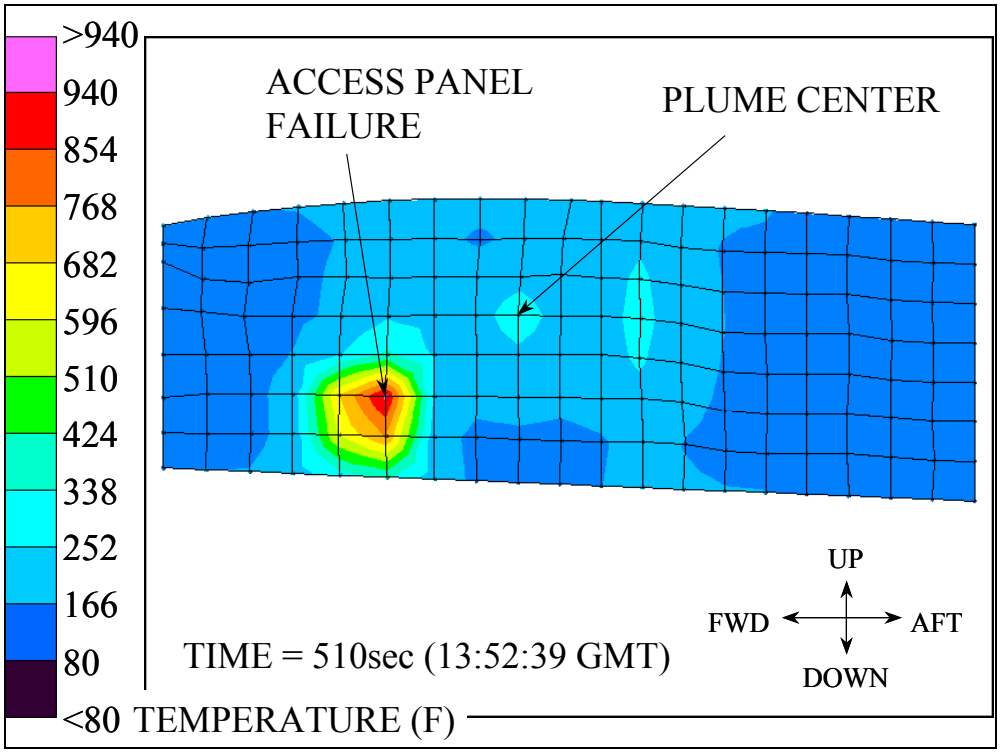

Figure 6-25 - Outboard wheel well wall temperature at 13:52:39 GMT

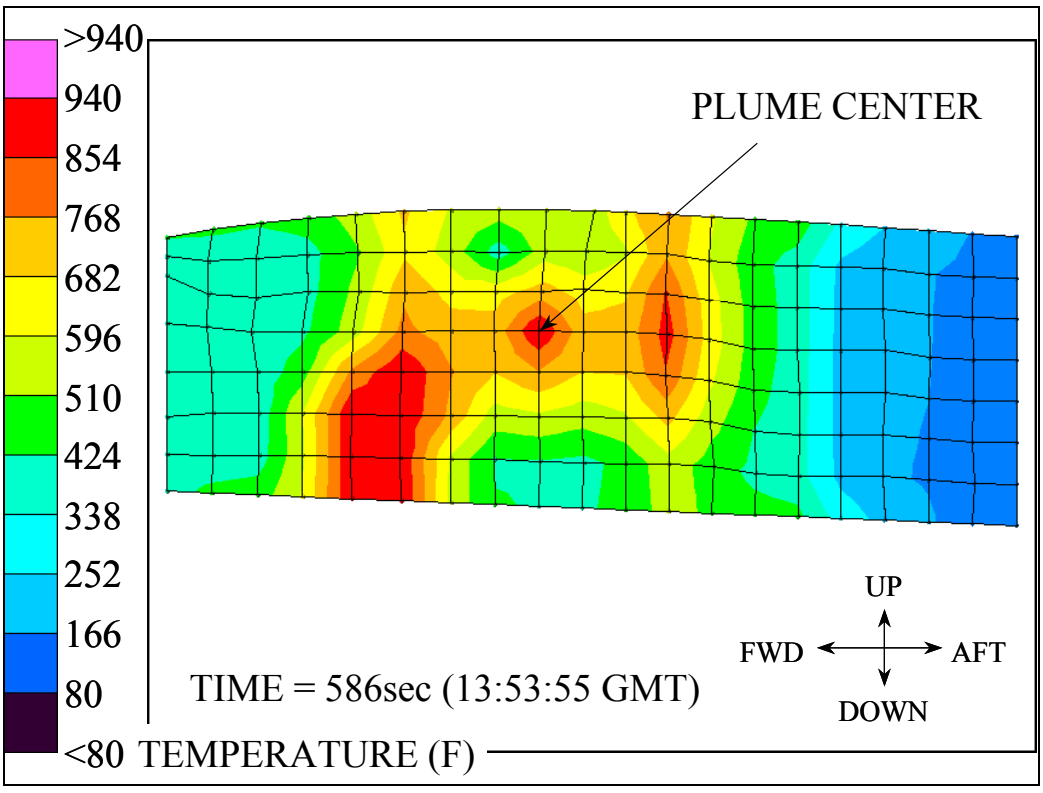

Figure 6-26 -Outboard wheel well wall temperature at 13:53:55 GMT

Figure 6-27 – Cable Bundle Test Article

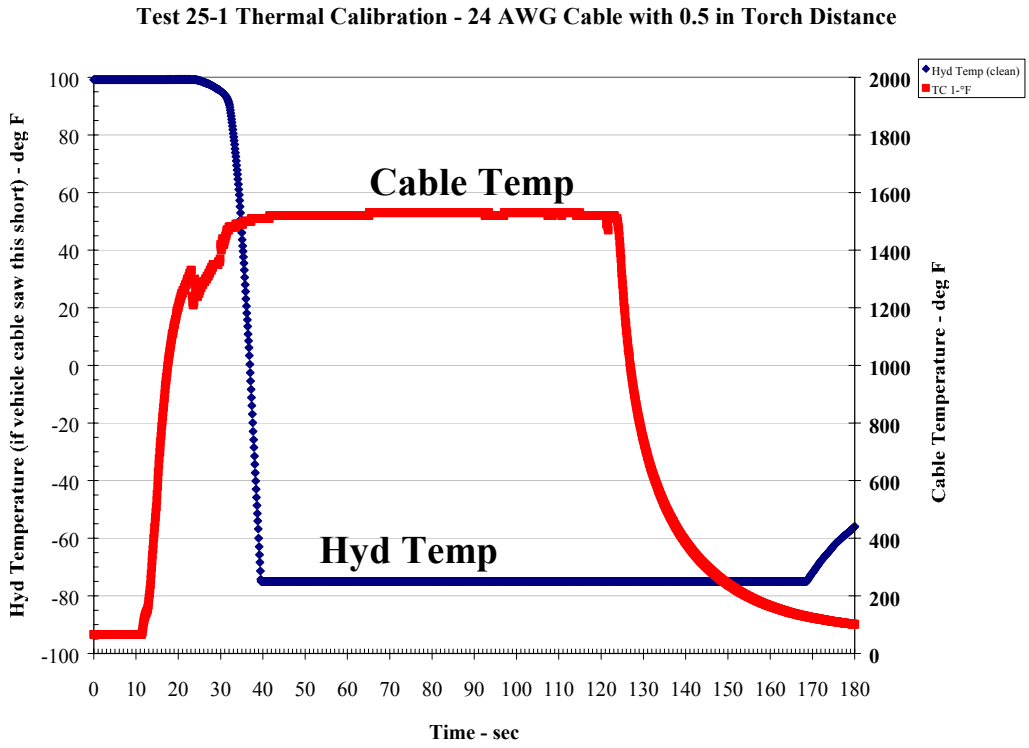

Figure 6-28 – Cable Failure Signature

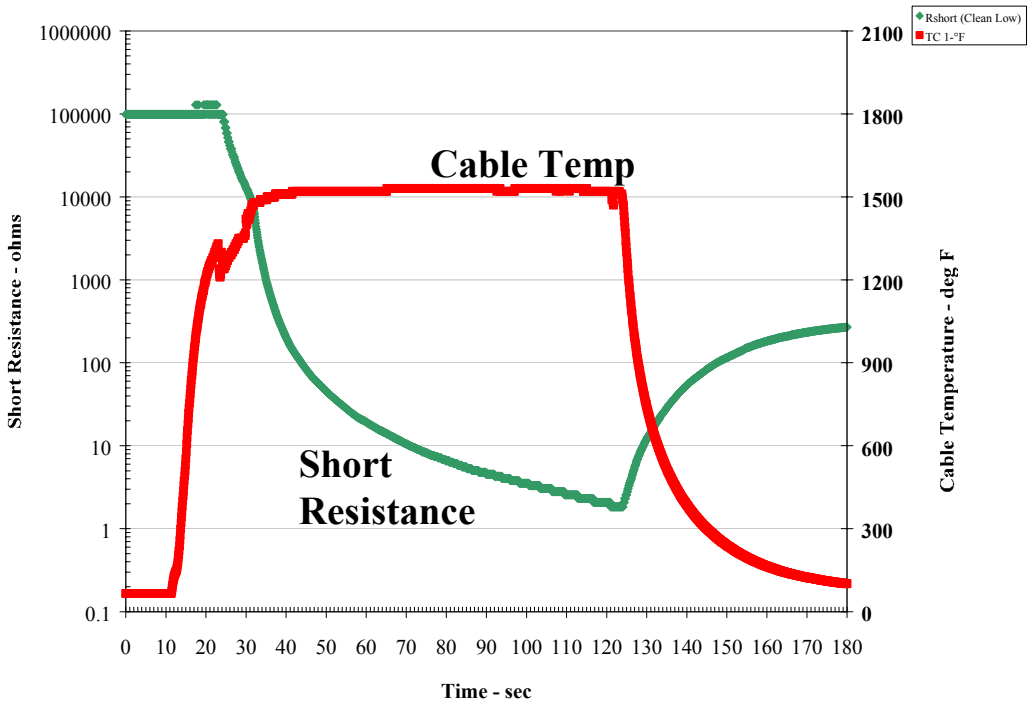

Figure 6-29 – Cable Failure Signature

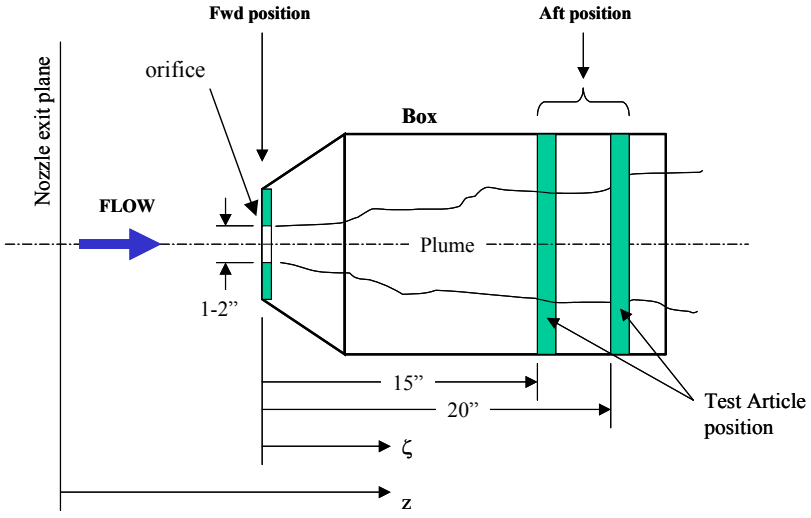

Figure 6-30 – Box Test Support Equipment

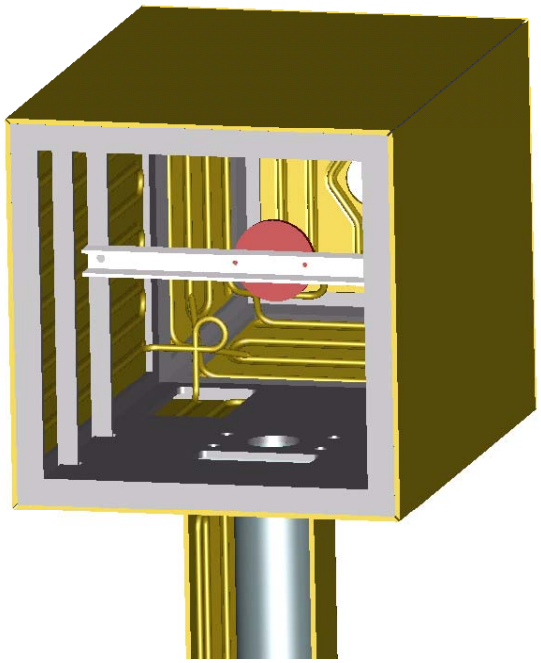

Figure 6-31 – Box Test Support Equipment

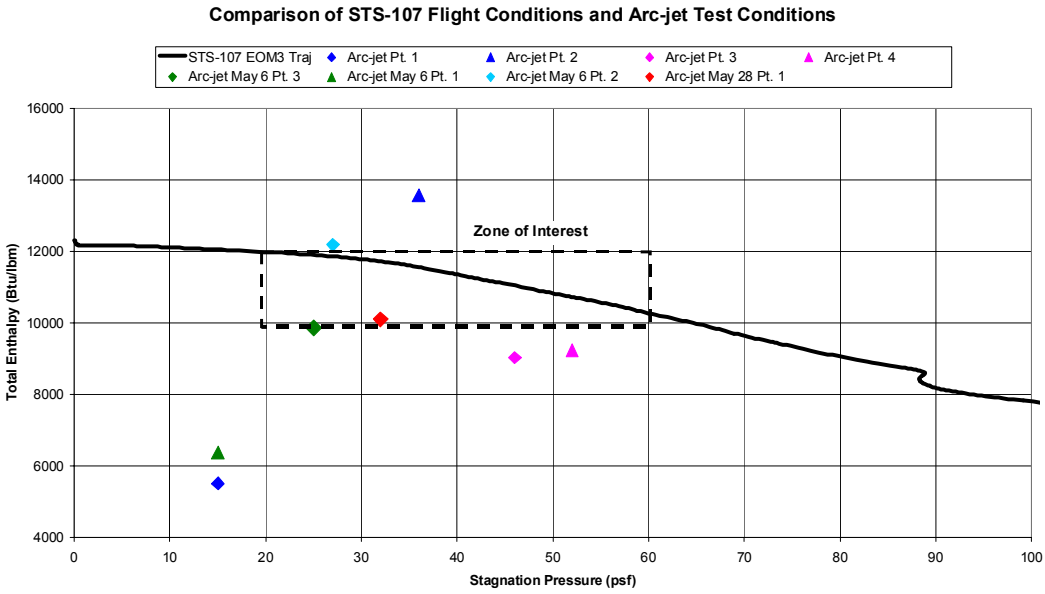

Figure 6-32 – Arc-Jet Test Conditions

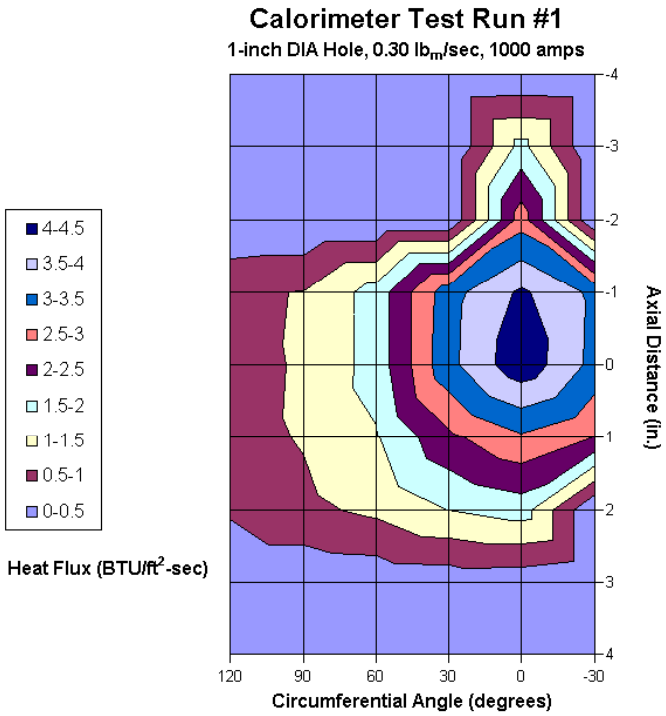

Figure 6-33 - Calorimeter

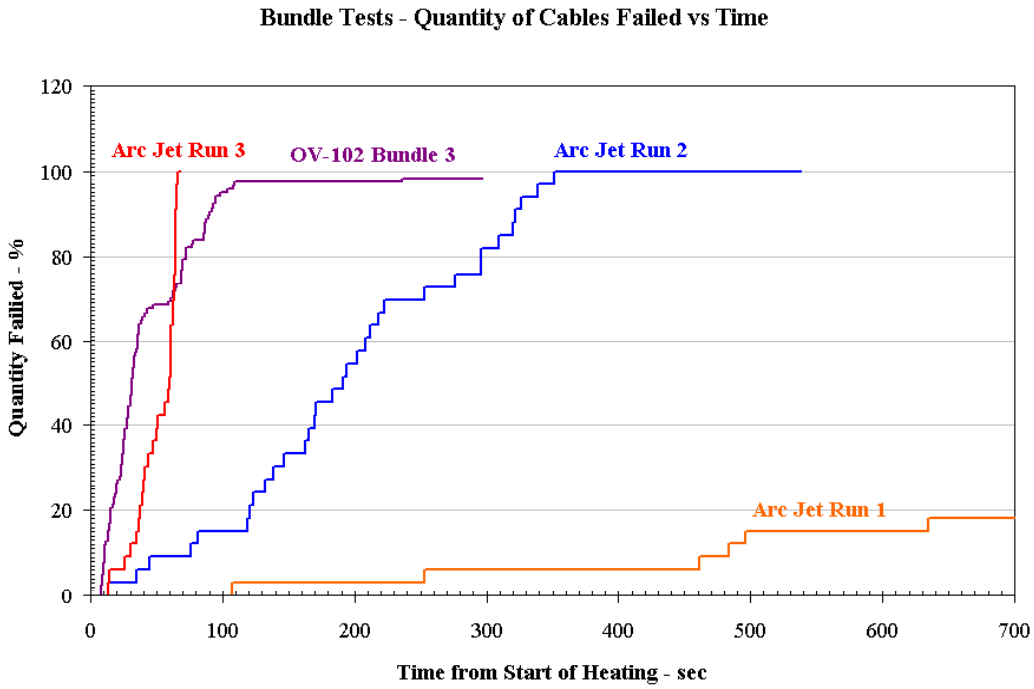

Figure 6-34 – Cable Failure Rates

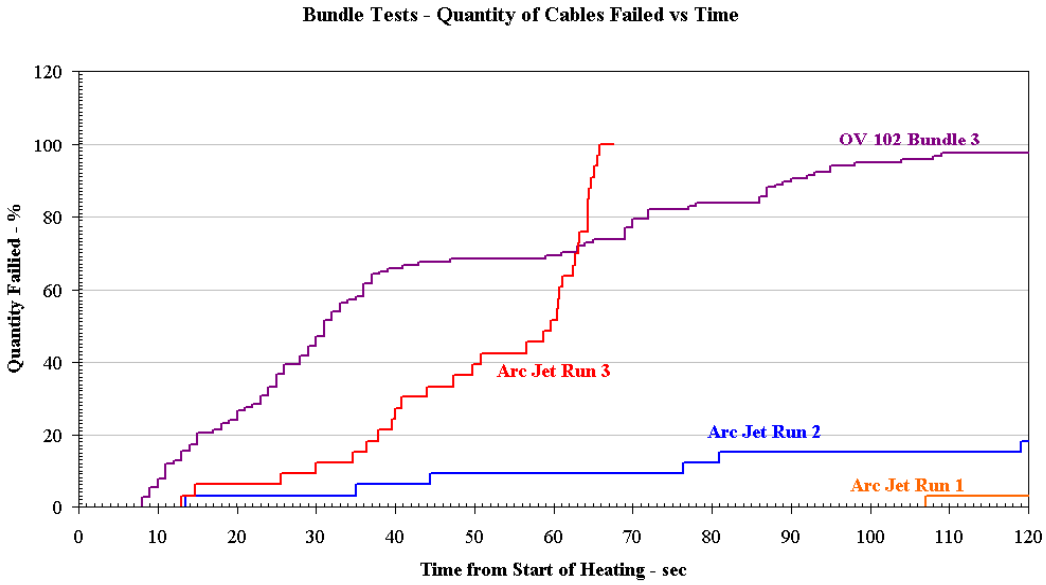

Figure 6-35 – Cable Failure Rates (expanded)

Figure 6-36: Wire bundle arc jet testing (before test)

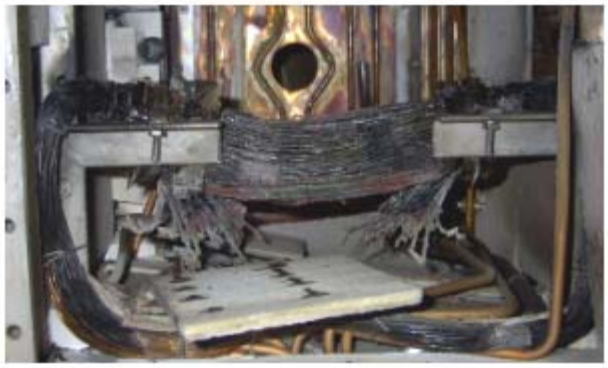

Figure 6-37 – Cable Bundle Post-Test Run #2

(1)
Test Article Inserted

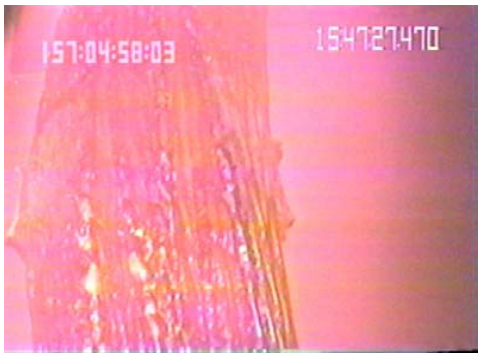

(2)

(3)

(4)

(5)

(6)

Figure 6-38 – Video Sequence of Cable Bundle Test (Run #3)

Figure 6-39 - MLG outboard sidewall (looking fwd)

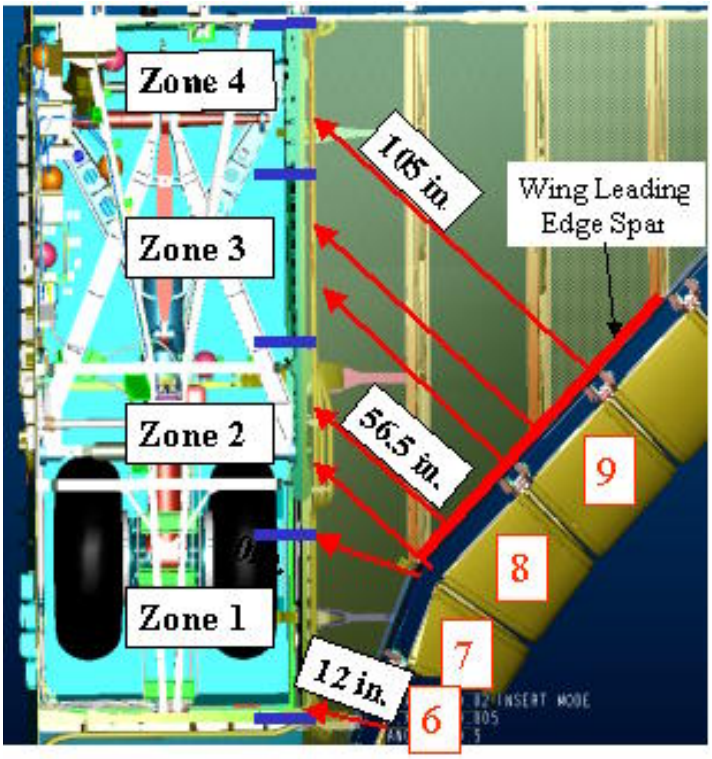

Figure 6-40 - MLG wheel well wall partitioning (view from top)

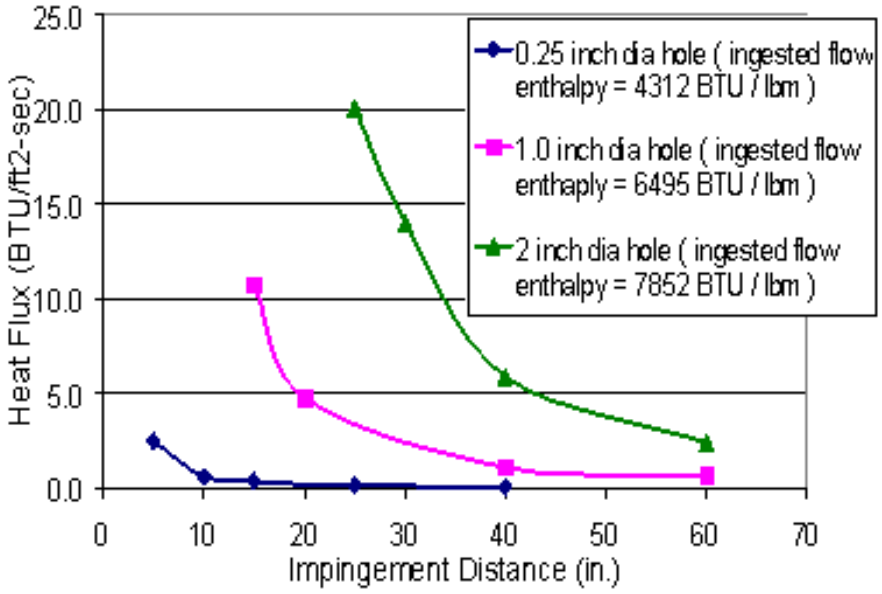

Figure 6-41 - Panel 9 internal plume flat plate impingement heating at EI+491 seconds

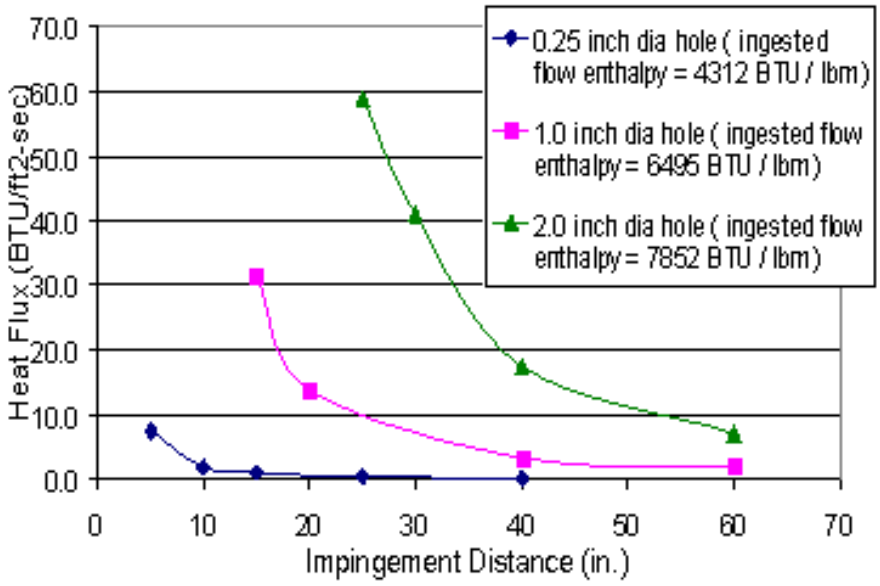

Figure 6-42 - Panel 9 internal plume impingement heating on 1" diameter cylinder at EI+491 seconds

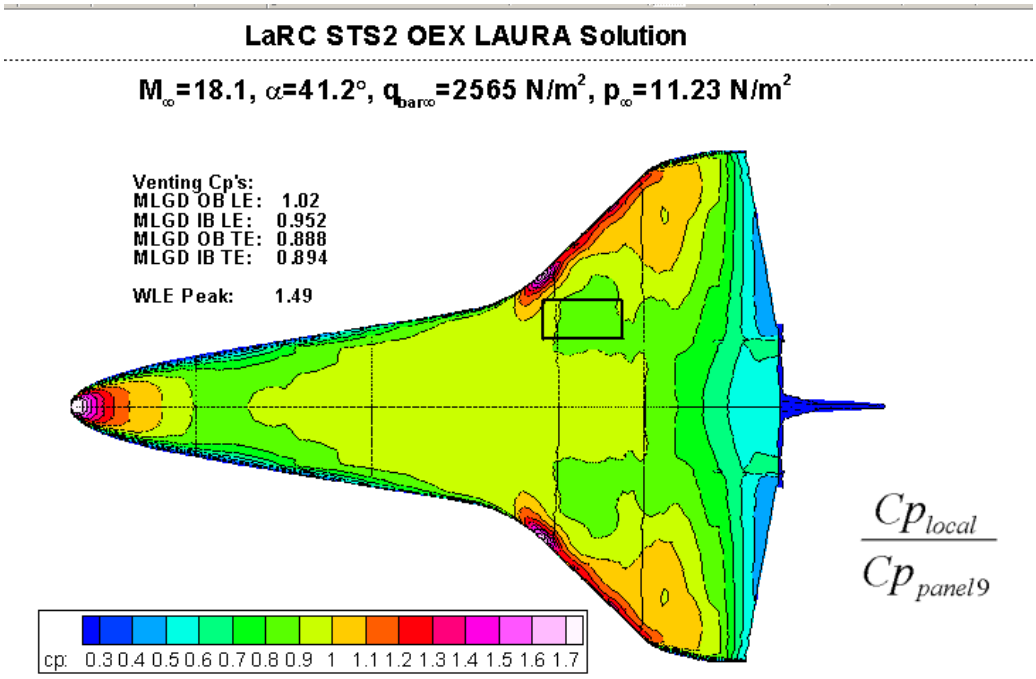

Figure 6-43 - Plume heating correction for local pressure coefficient

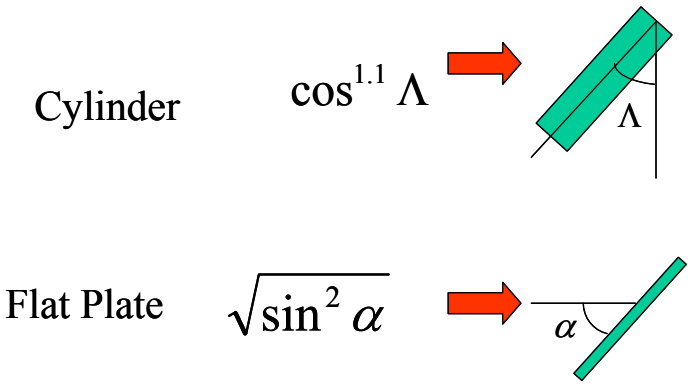

Zone	a	L
1	67.5	22.5
2	58.5	31.5
3	58.5	31.5
4	58.5	31.5

Figure 6-44 - Off-normal angle impingement plume heating correction for a cylinder and flat plate

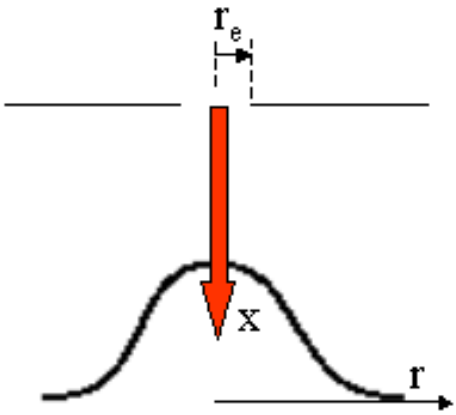

r/r_s	$qdot/(qdot)_0$
0	1.000
1	0.748
2	0.392
3	0.219
4	0.154
5	0.119
6	0.100
7	0.0808
8	0.0615
9	0.0423

$$r_s = r_e \quad \text{for } x \le 7.0 r_e$$

$$r_s = r_e + x \tan\left(\frac{\pi}{30}\right) \quad \text{for } x > 7.0 r_e$$

Figure 6-45 - Plume heating corrections for radial distribution from the stagnation point

$$\frac{\sqrt{r_{1"diametercylinder}}}{\sqrt{r_{bundle}}}$$

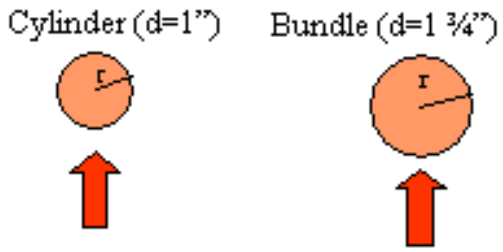

Figure 6-46 -Correction of plume heating due to radius effects

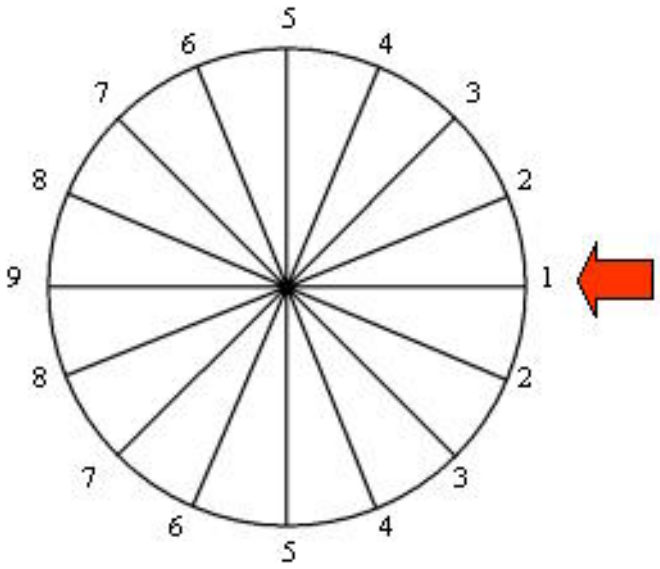

station	$qdot/(qdot)_0$
1	1.0000
2	0.9155
3	0.7080
4	0.4490
5	0.2230
6	0.0830
7	0.0320
8	0.0325
9	0.0370

Figure 6-47 - Circumferential plume heating corrections

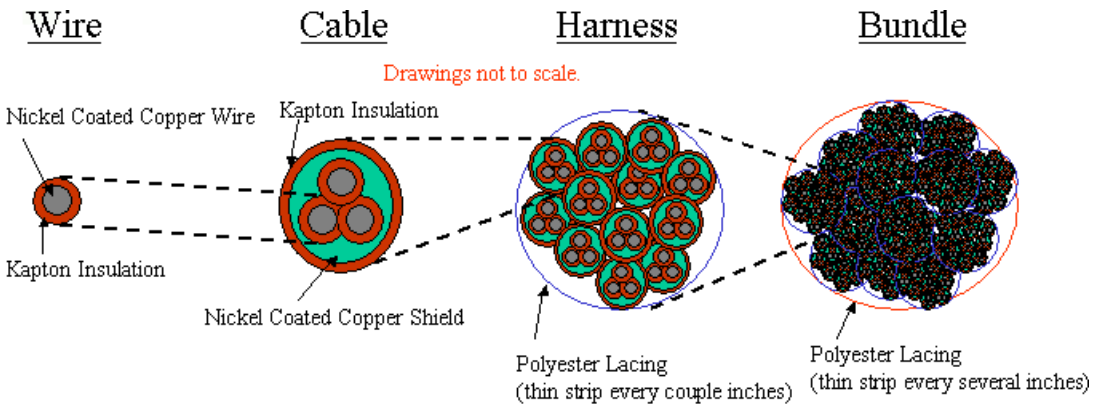

Figure 6-48 - Wire bundle configuration & terminology

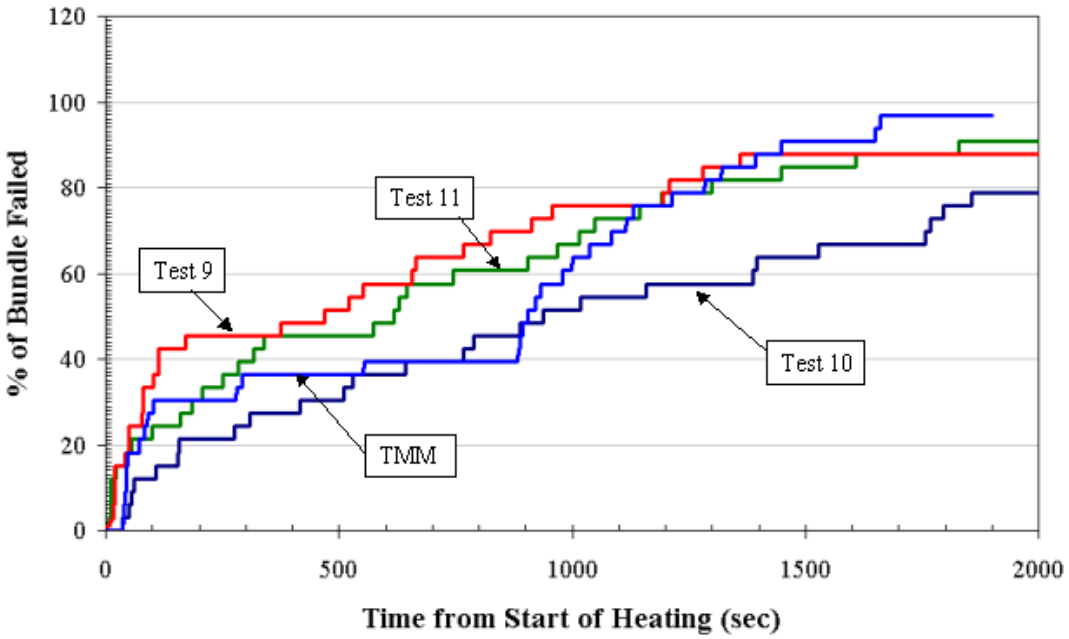

Figure 6-49 - Large propane torch test results vs. TMM test predictions

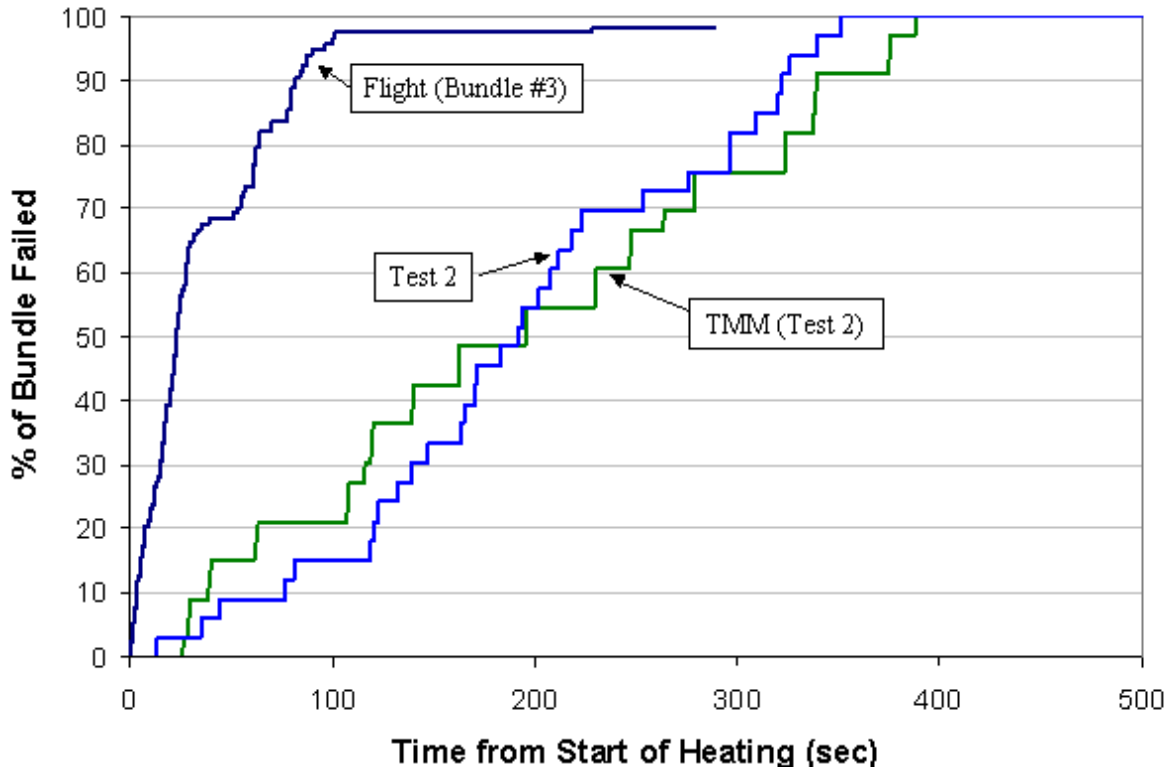

Figure 6-50 - Arc jet test 2 results vs. TMM test predictions

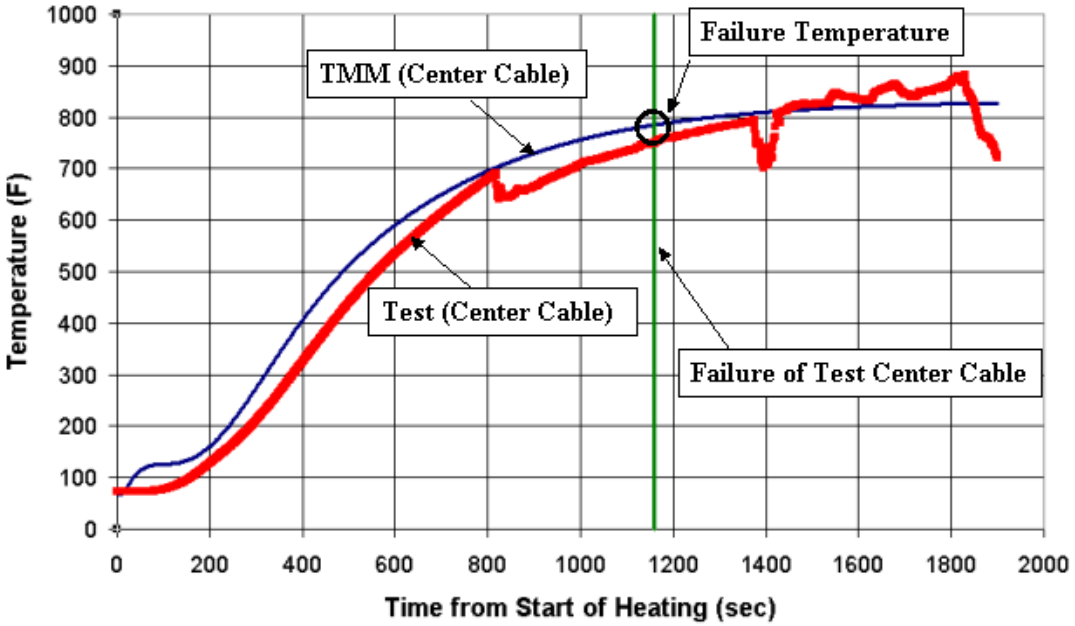

Figure 6-51 - TMM cable failure temperature determined through large propane torch testing

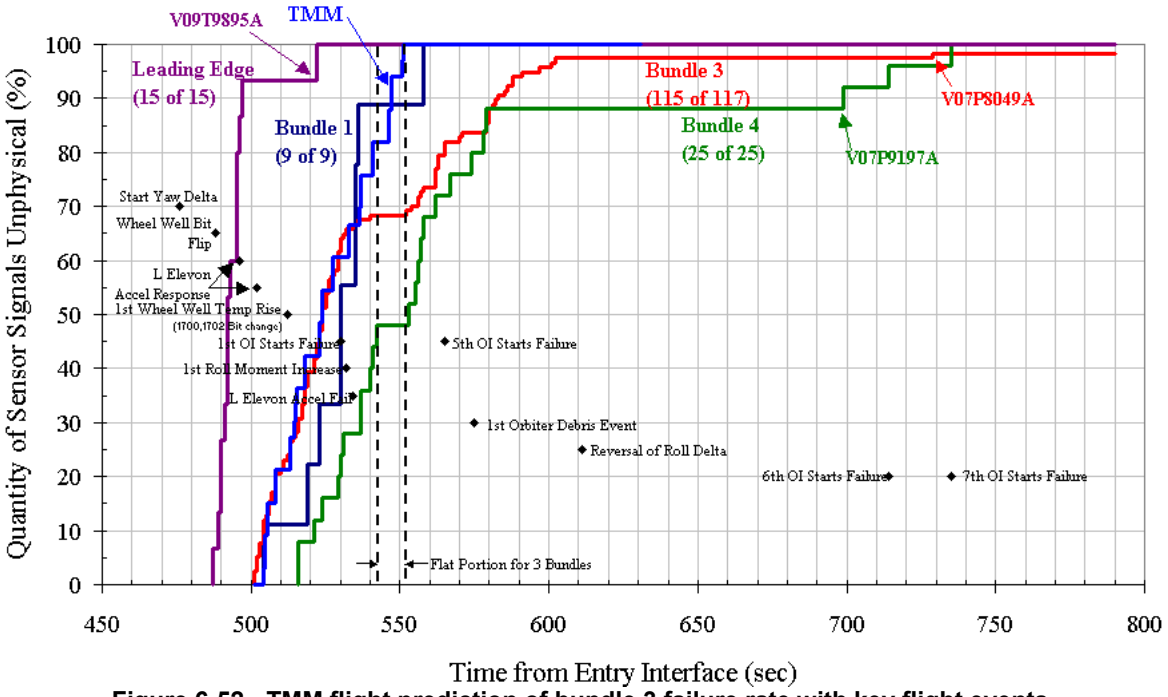

Figure 6-52 - TMM flight prediction of bundle 3 failure rate with key flight events

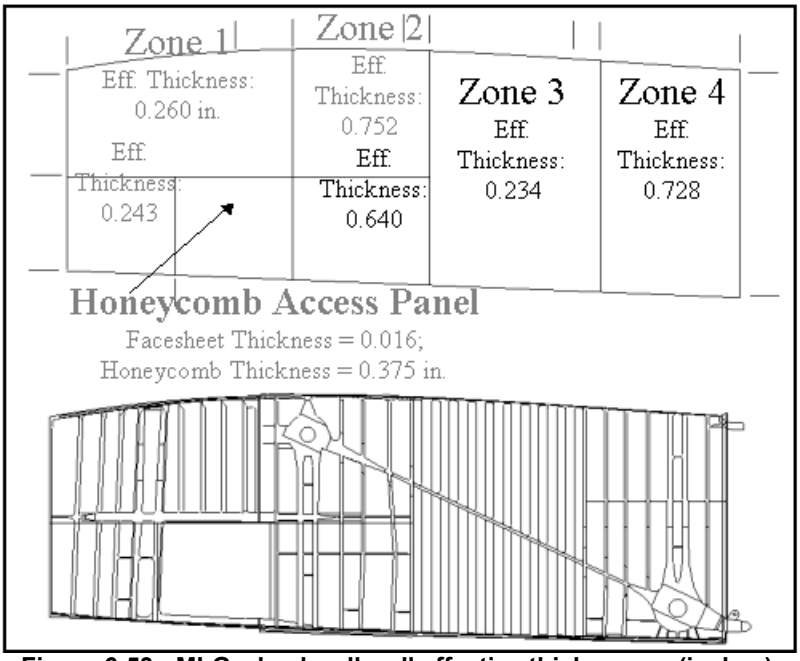

Figure 6-53 - MLG wheel well wall effective thicknesses (inches)

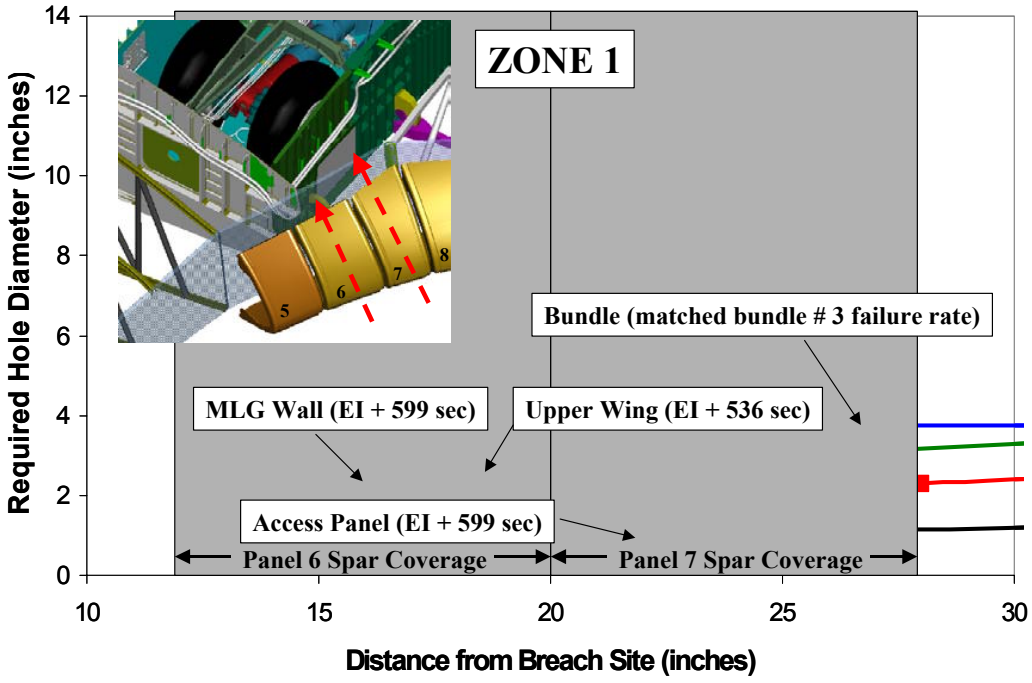

Figure 6-54 - Zone 1 plume heating result comparisons

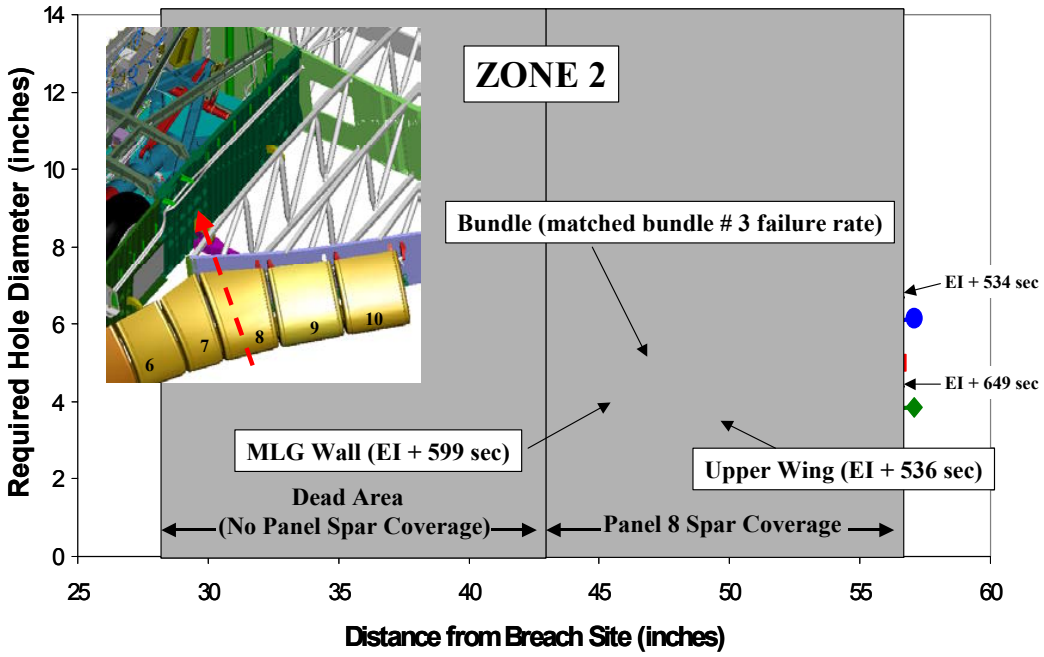

Figure 6-55 - Zone 2 plume heating result comparisons

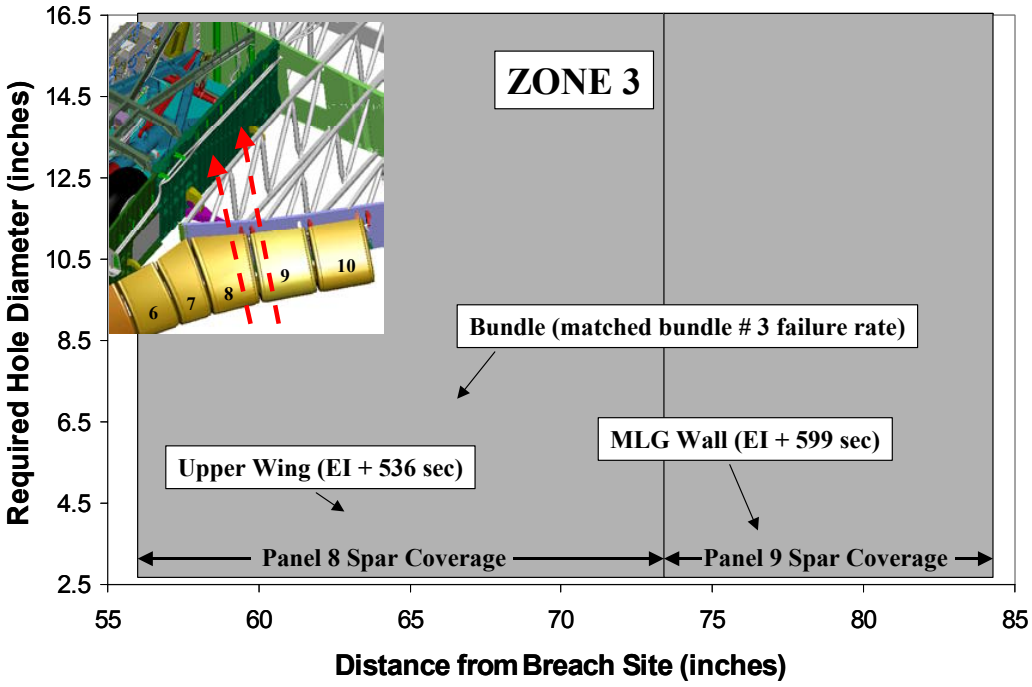

Figure 6-56 - Zone 3 plume heating result comparisons

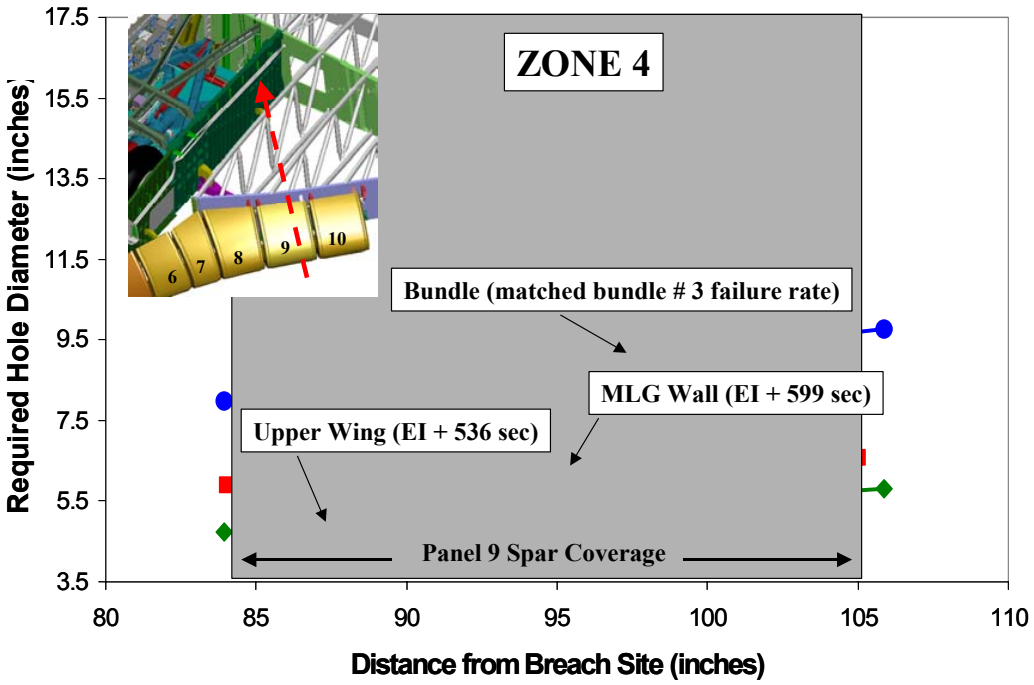

Figure 6-57 - Zone 4 plume heating result comparisons

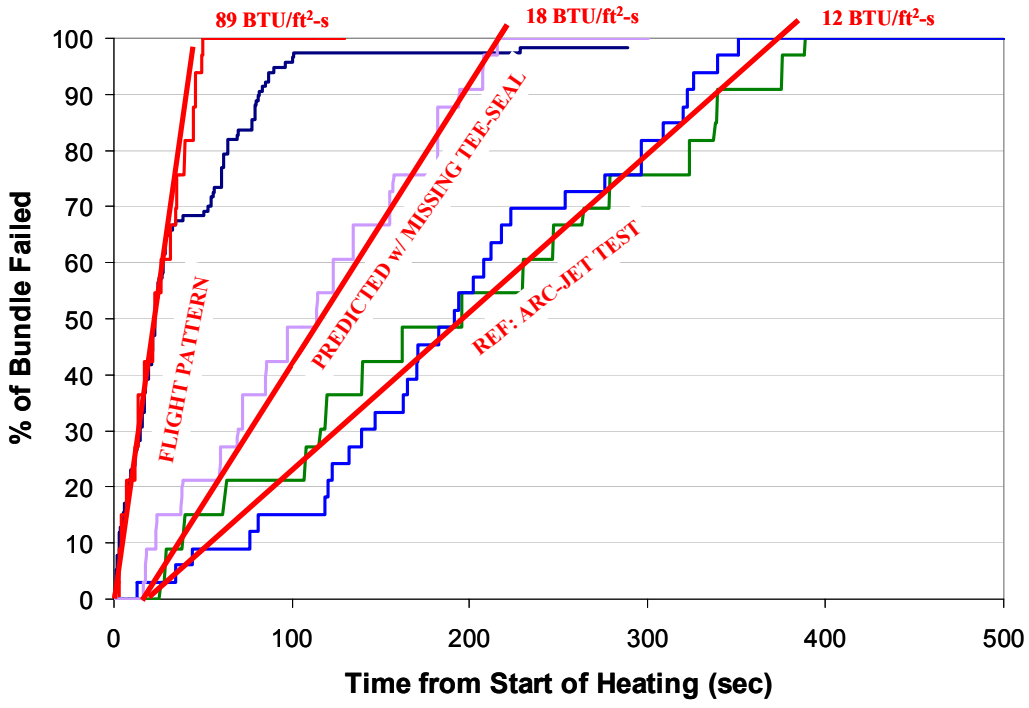

Figure 6-58 - Damaged Tee-Seal Bundle Failure

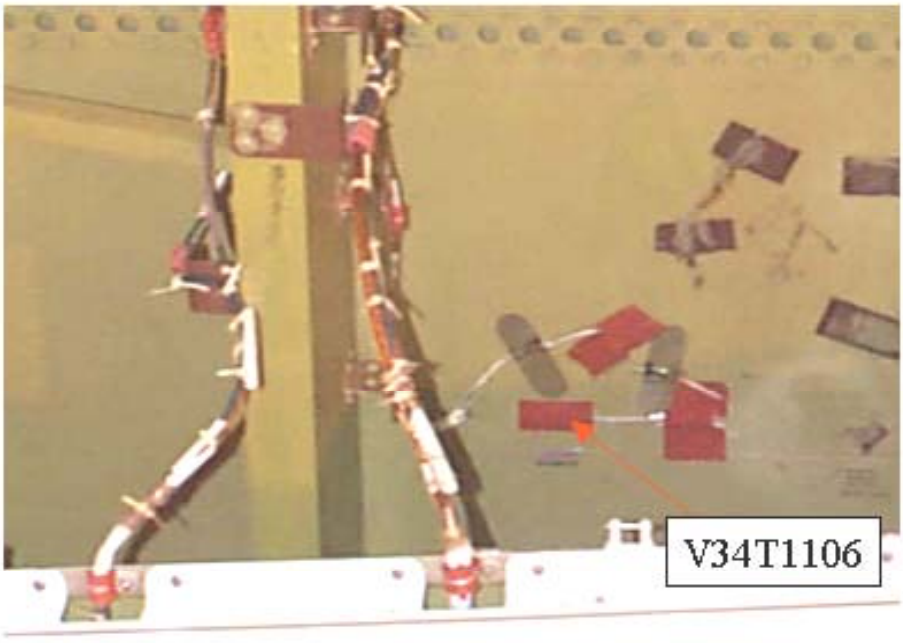

Figure 6-59 - OV-102 V34T1106 Temperature Sensor (looking outboard)

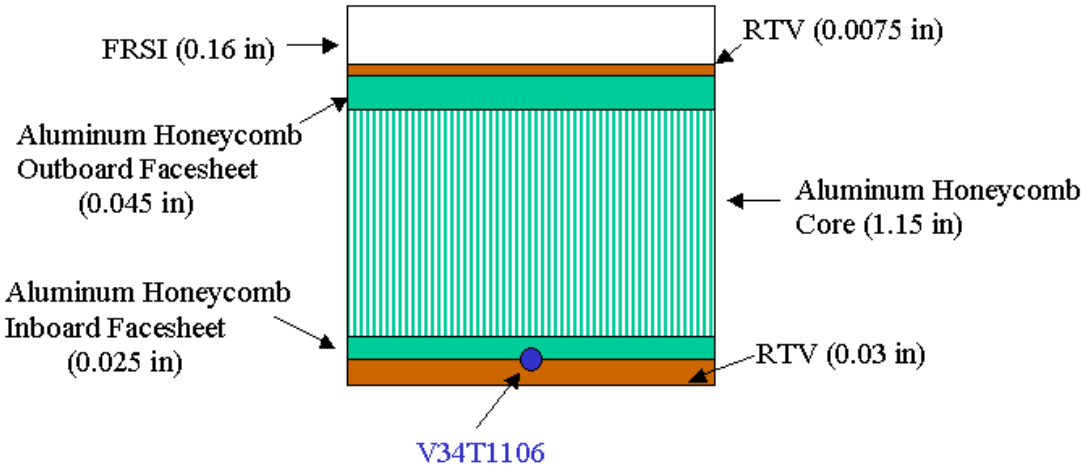

Figure 6-60 - OV-102 V34T1106 Port Sidewall Configuration for TMM

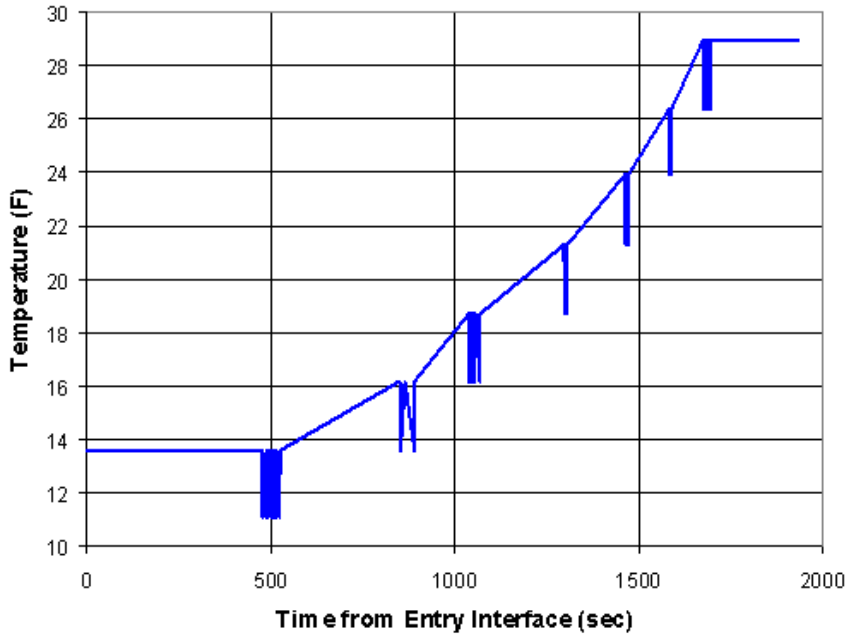

Figure 6-61 - STS-109 V34T1118 Structure Temperature Flight Data

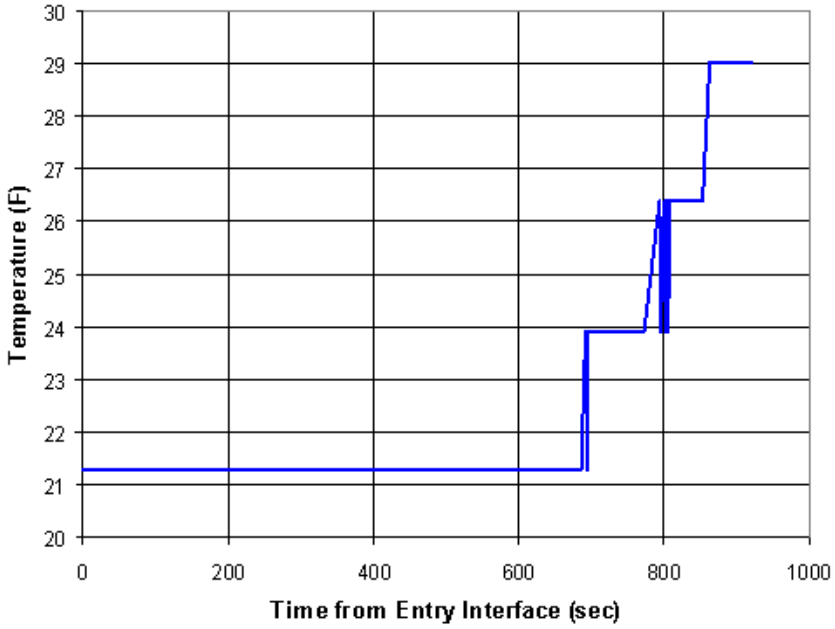

Figure 6-62 - STS-107 V34T1118 Structure Temperature

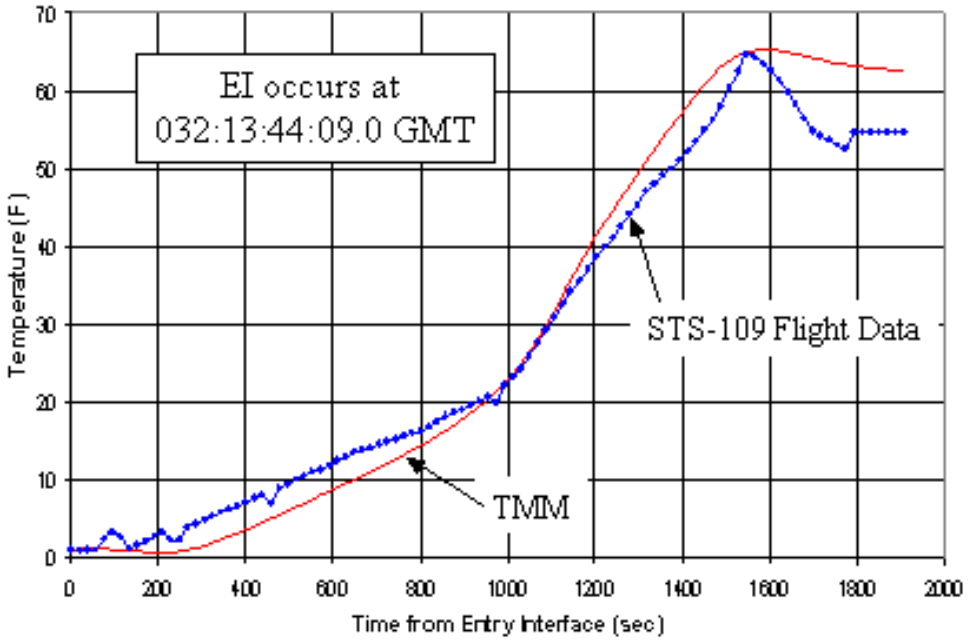

Figure 6-63 - STS-109 TMM Correlation to Flight Data

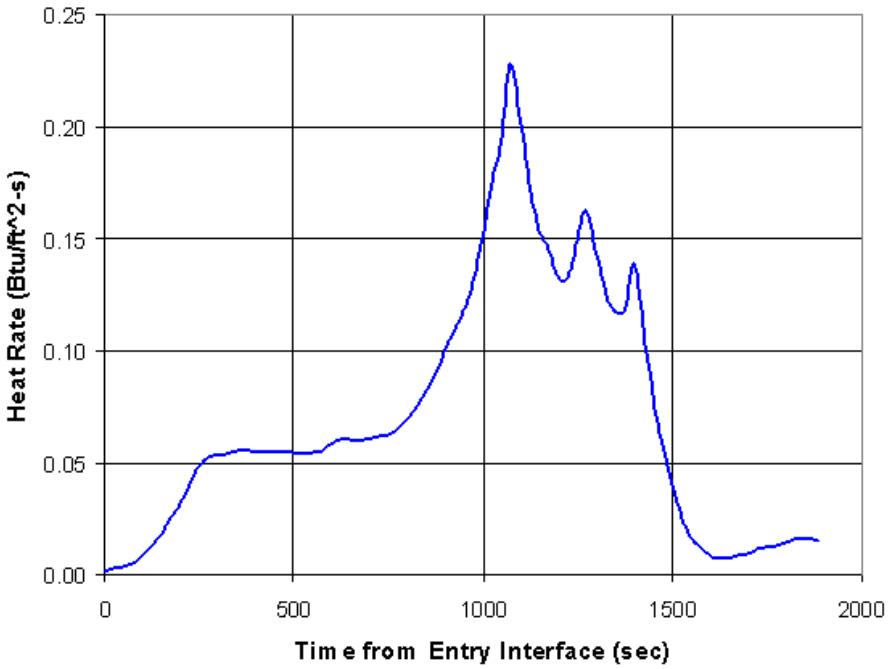

Figure 6-64 - STS-109 Nominal Aerothermodynamic Heating

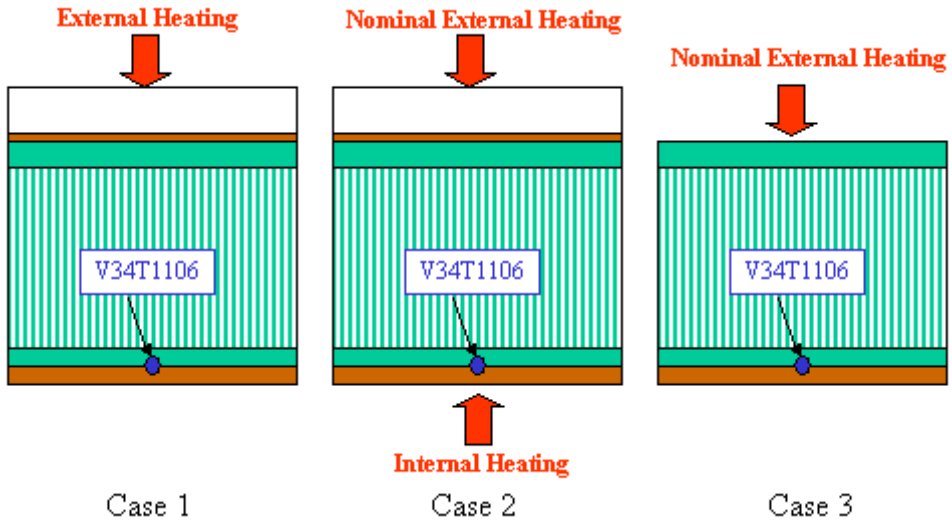

Figure 6-65 - Sidewall Heating Cases

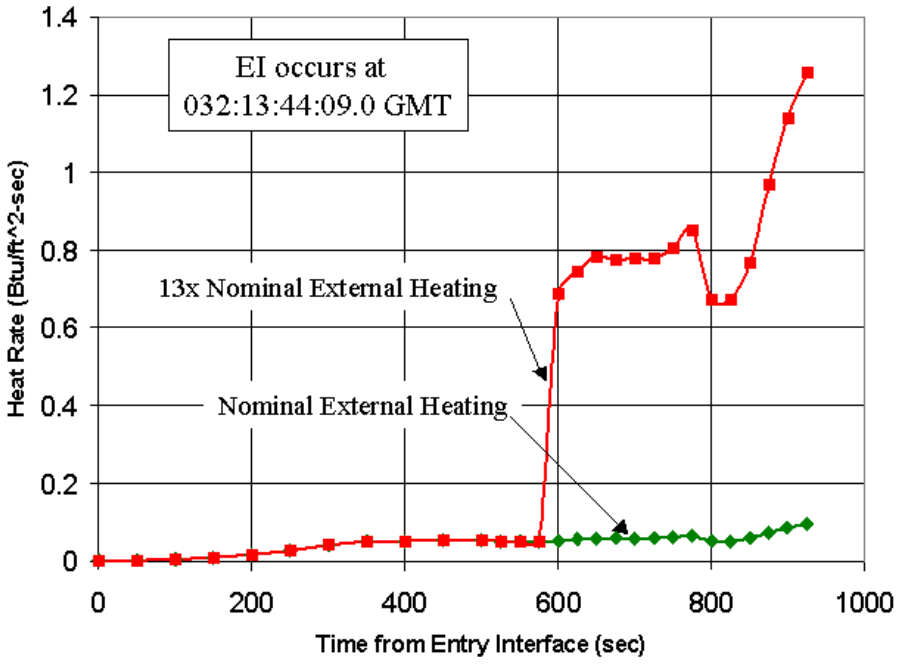

Figure 6-66 - STS-107 Aerothermodynamic Heating

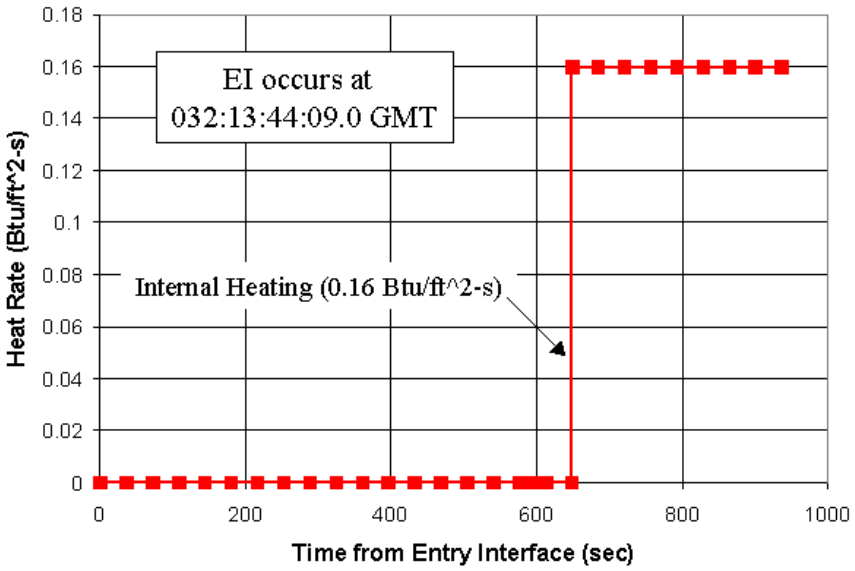

Figure 6-67 - STS-107 Internal Fuselage Heating

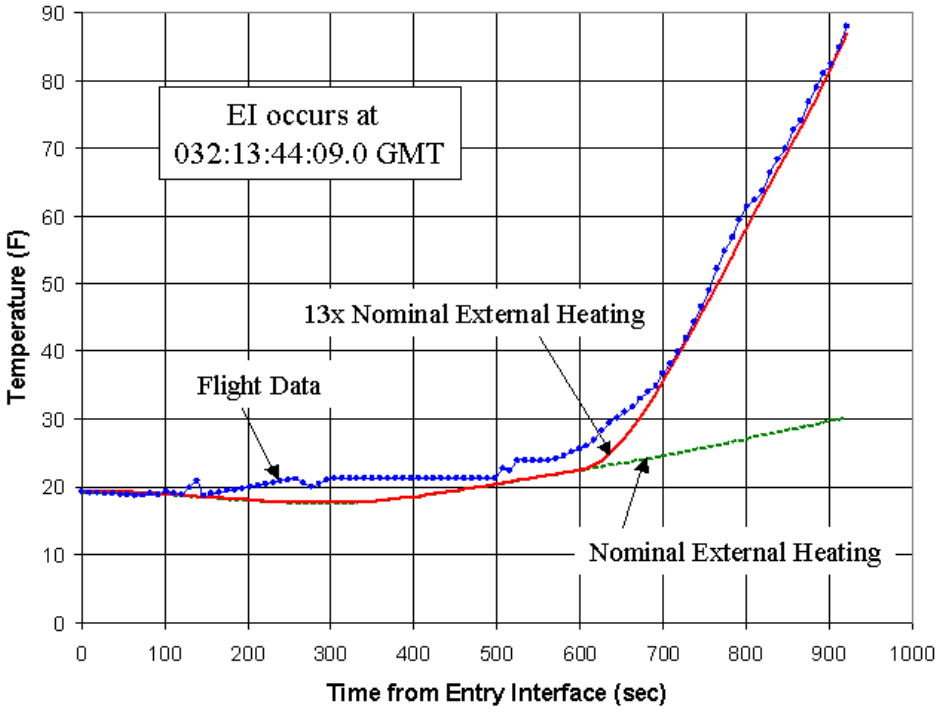

Figure 6-68 - Case 1: TMM Comparison to STS-107 Flight Data

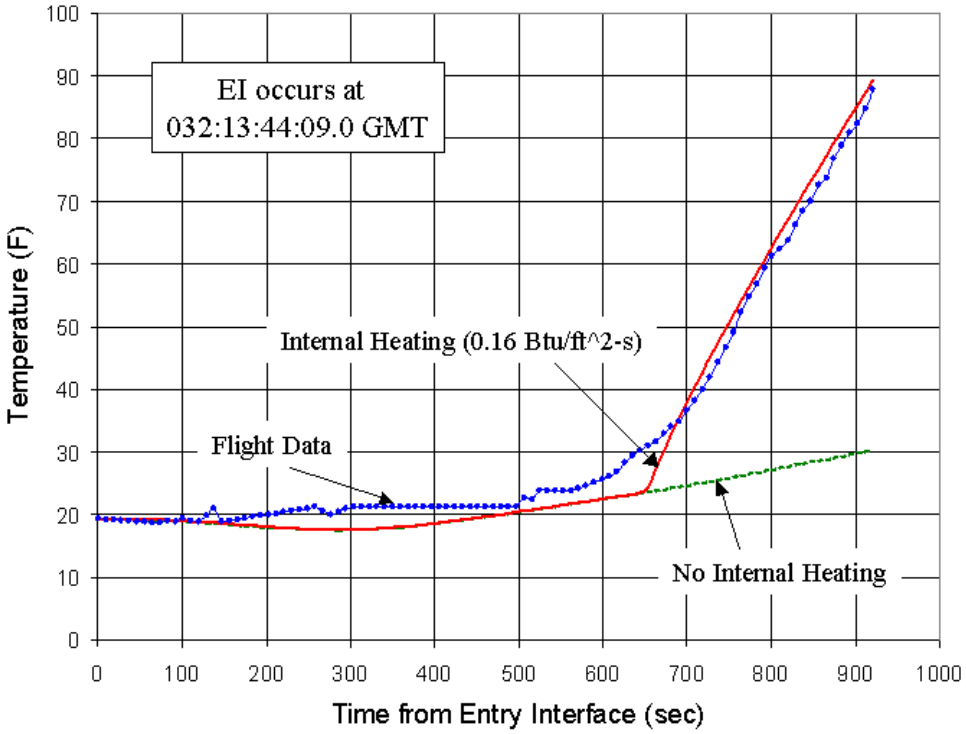

Figure 6-69 - Case 2: TMM Comparison to STS-107 Flight Data

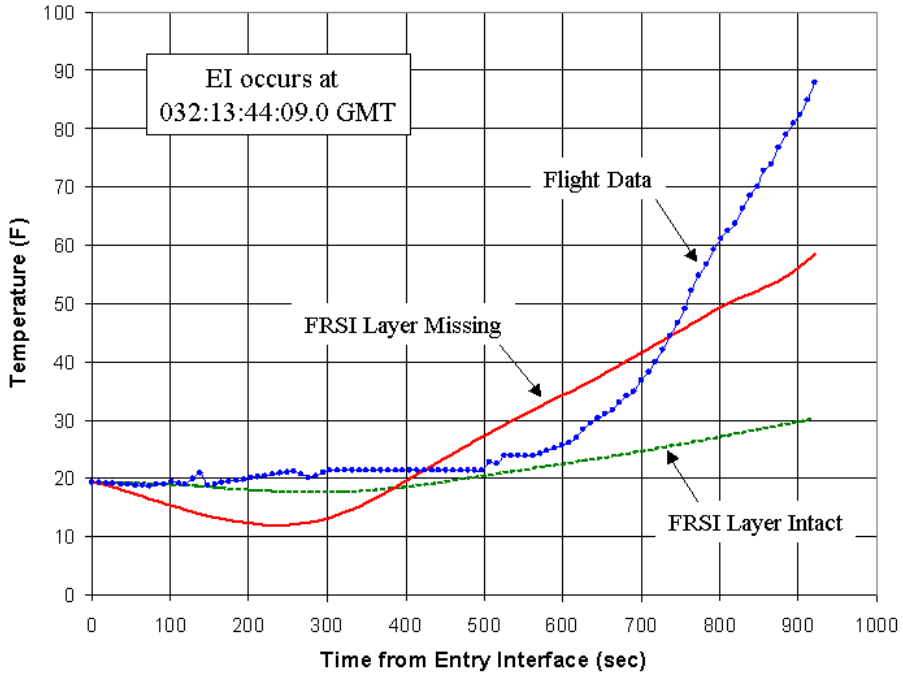

Figure 6-70 - Case 3: TMM Comparison to STS-107 Flight Data

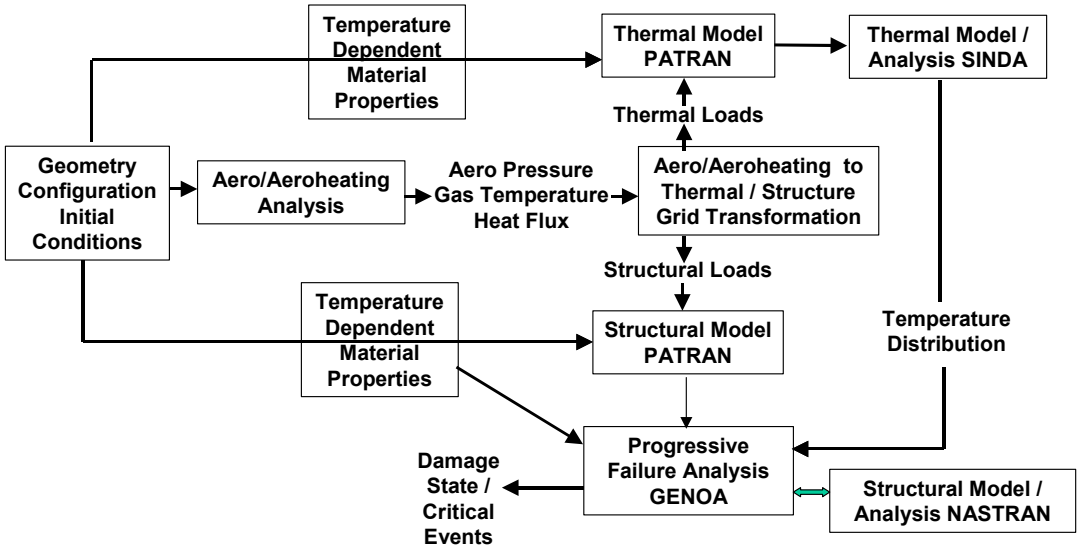

Figure 6-71 - Wing Leading Edge Failure Analysis Methodology

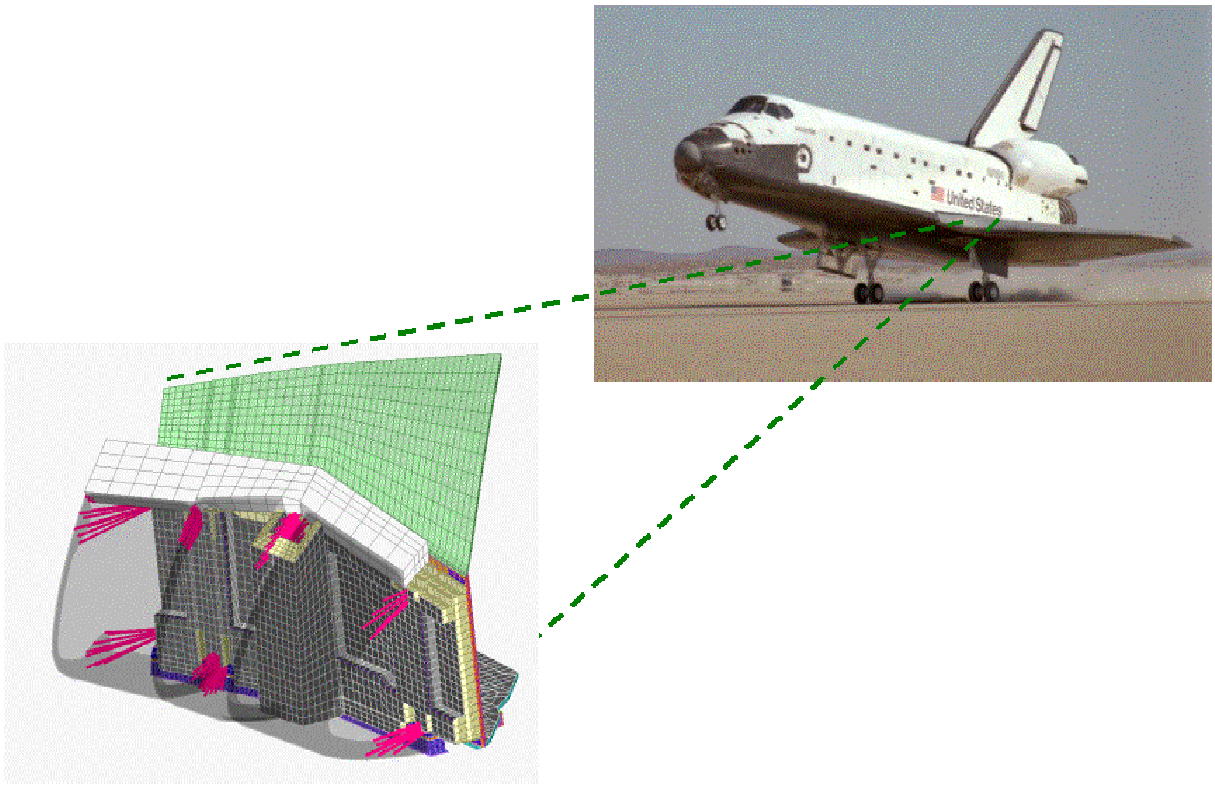

Figure 6-72 - Wing Leading Edge Finite Element Model

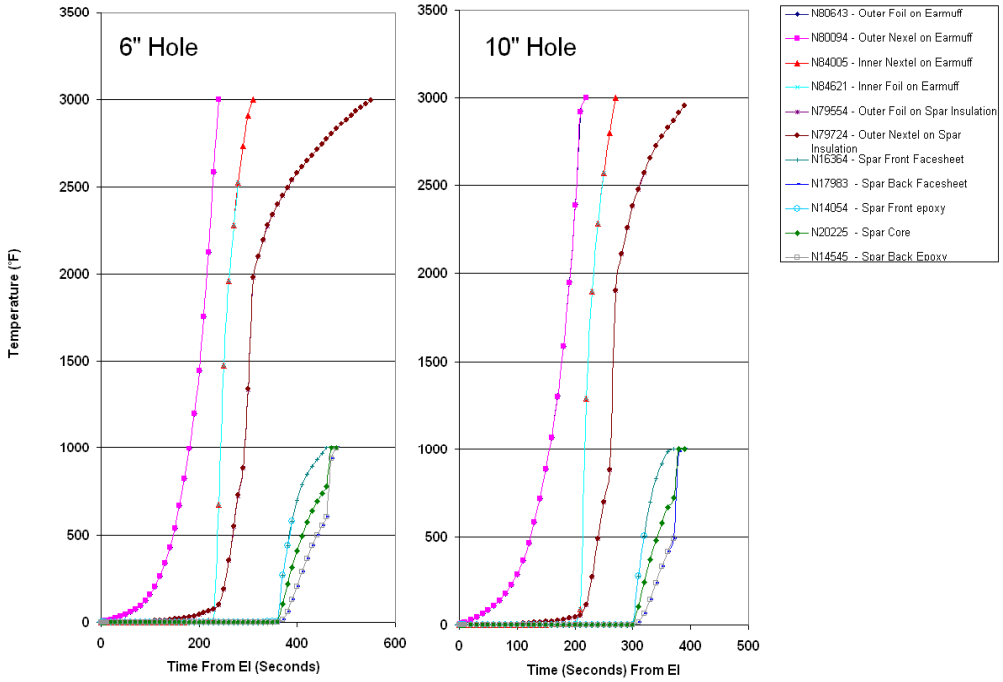

Figure 6-73 – Predicted Wing Spar Insulation and Structure Transients

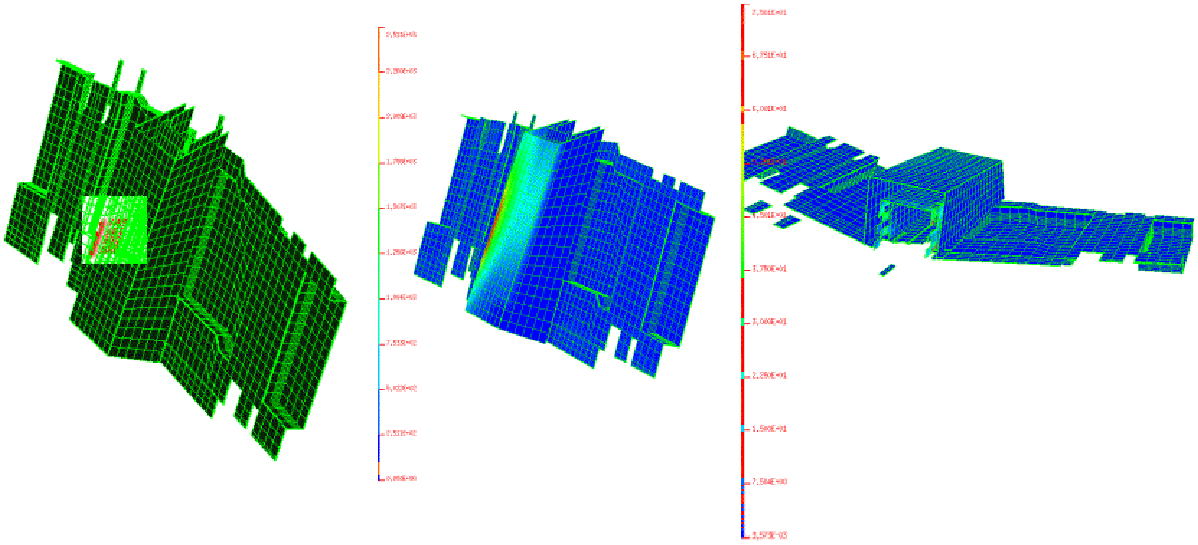

Figure 6-74 - Earmuff Insulation Analysis Results for 10 Inch Hole at t=210 Seconds

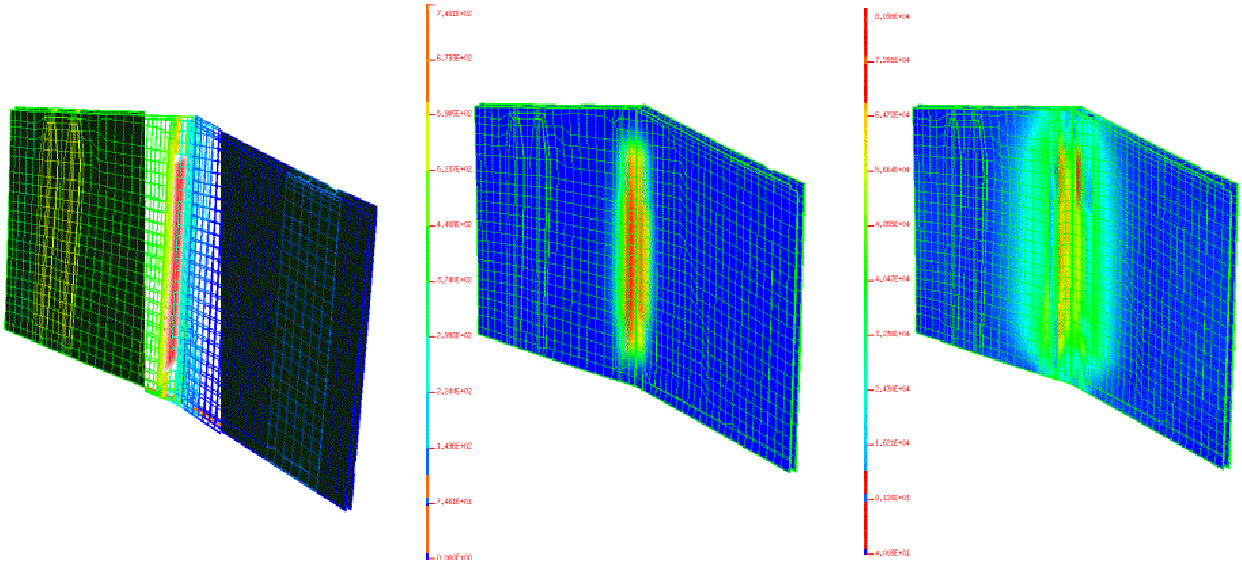

Figure 6-75 - Front Facesheet Analysis Results for 10 Inch Hole at t=320 Seconds

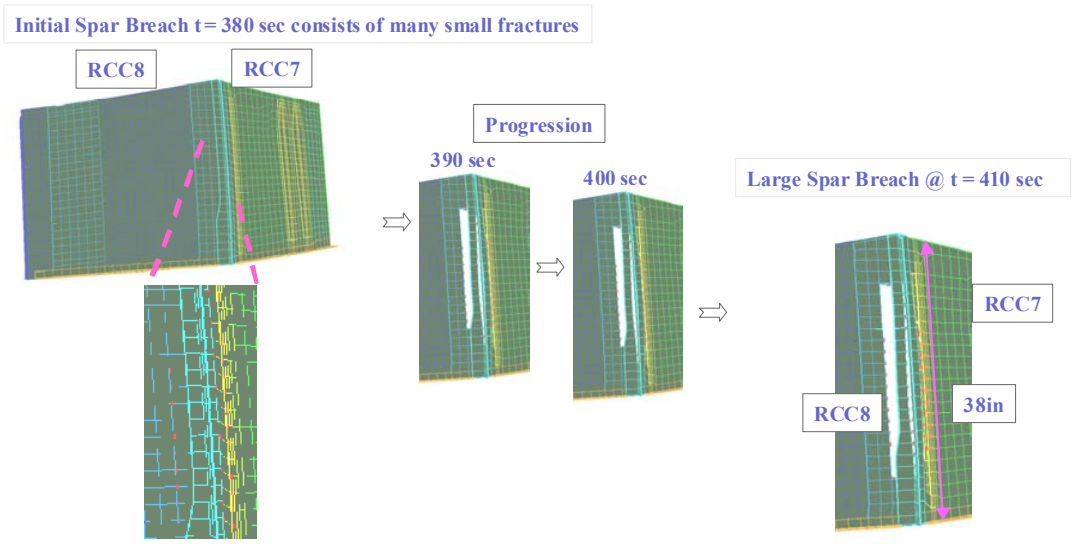

Figure 6-76 Rear Facesheet Analysis Results for 10 Inch Hole at t=380 Seconds (View of Spar From Inside Wing)

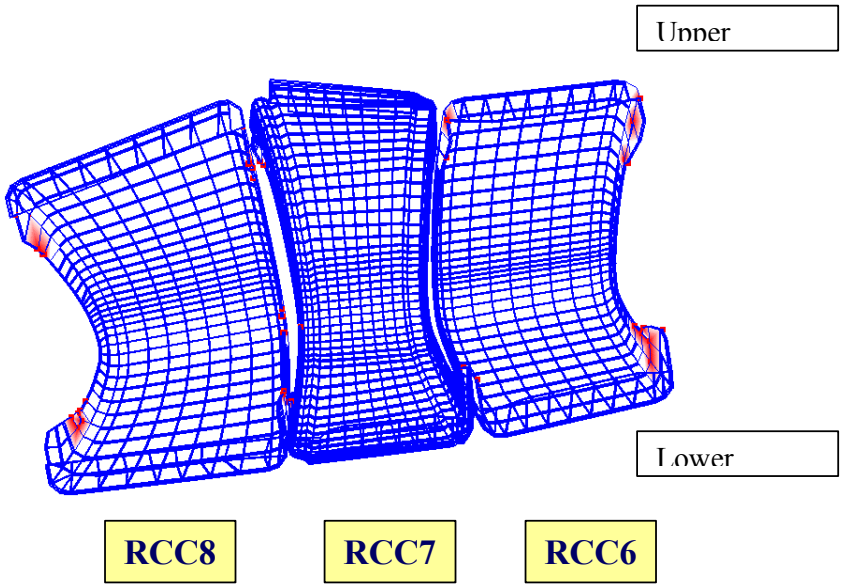

Figure 6-77 - RCC Panel Fracturing at 450 Seconds With 10 Inch Hole (View Looking From Inside RCC Cavity

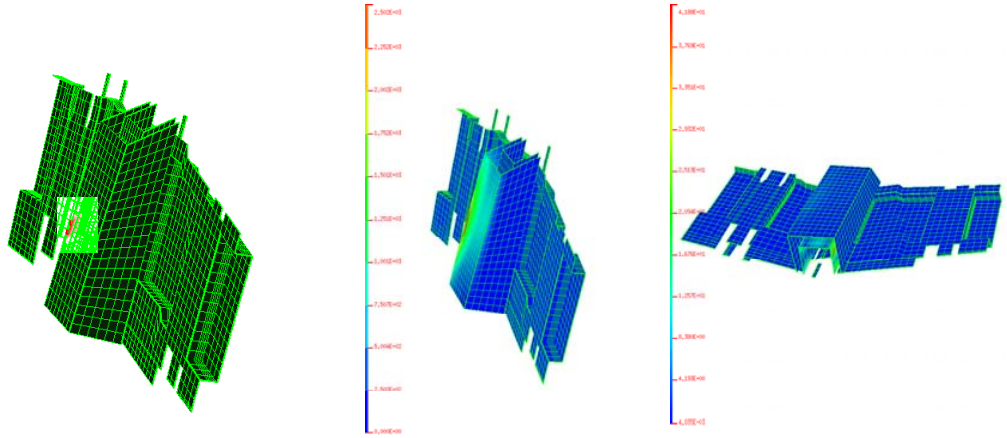

Figure 6-78 - Earmuff Insulation Analysis Results for 6 Inch Hole at t=230 Seconds

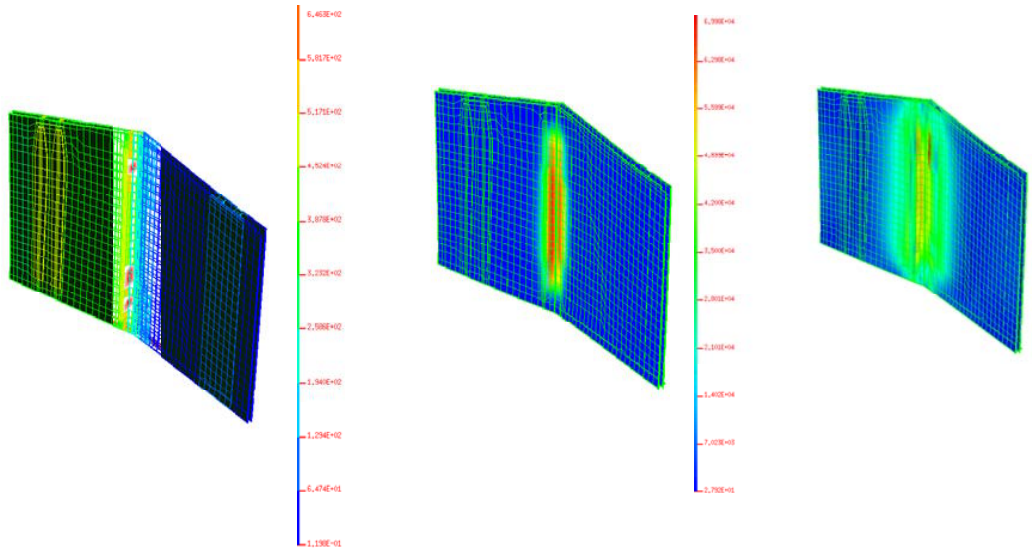

Figure 6-79 - Front Facesheet Analysis Results for 6 Inch Hole at t=380 Seconds

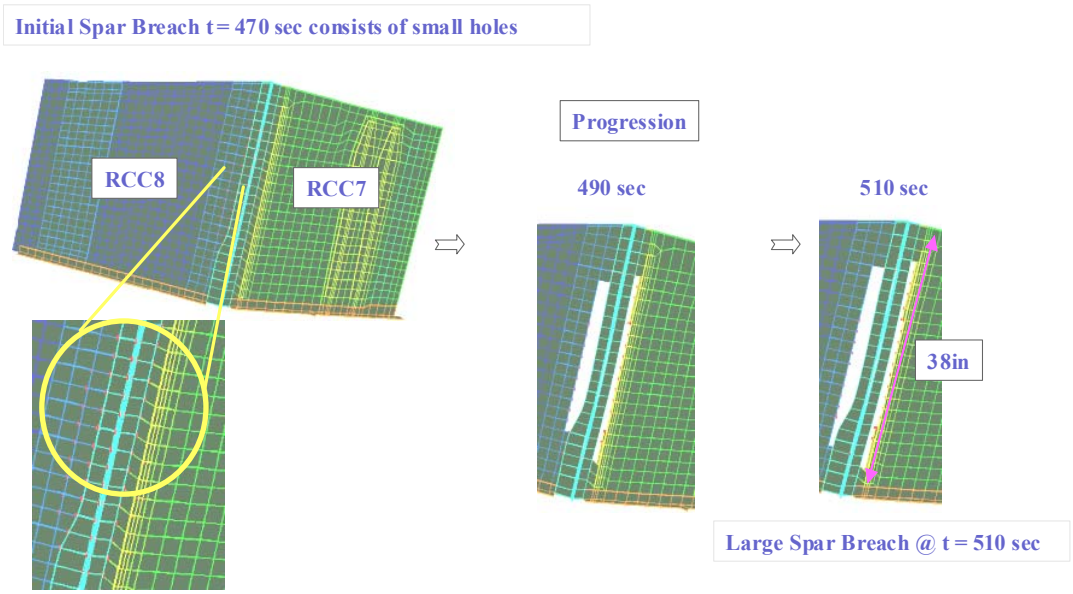

Figure 6-80 - Rear Facesheet Analysis Results for 6 Inch Hole at t=470 Seconds (View of Spar From Inside Wing)

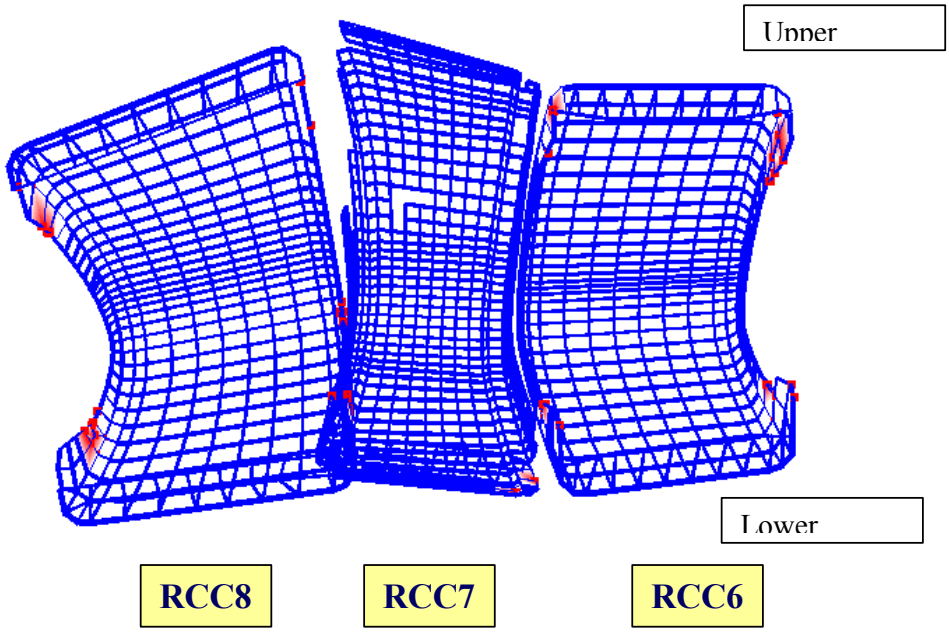

Figure 6-81 - RCC Panel Fracturing at 500 Seconds With 6 Inch Hole (View Looking From Inside RCC Cavity

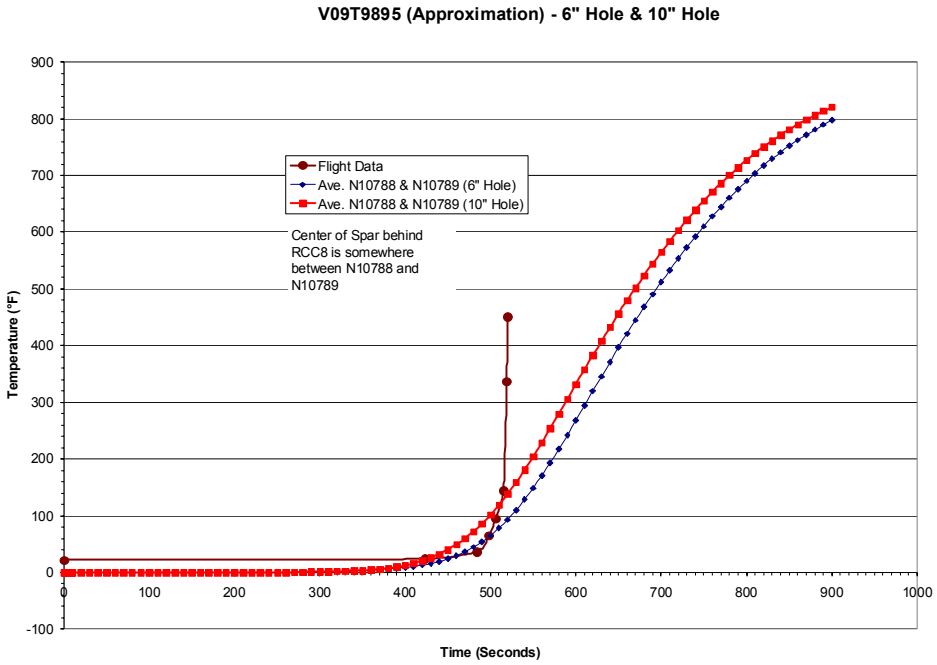

Figure 6-82 - Comparison of Panel 8 Rear Spar Temperature Prediction with Panel 9 Flight Data (V09T9895)

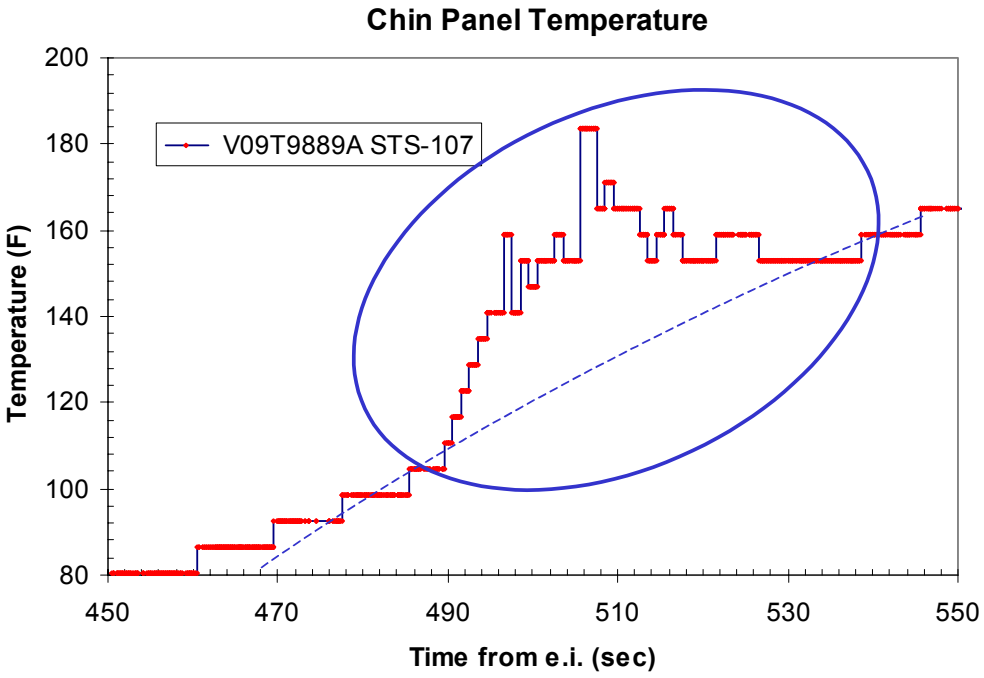

Figure 6-83 - Chin Panel Temperature Anomaly

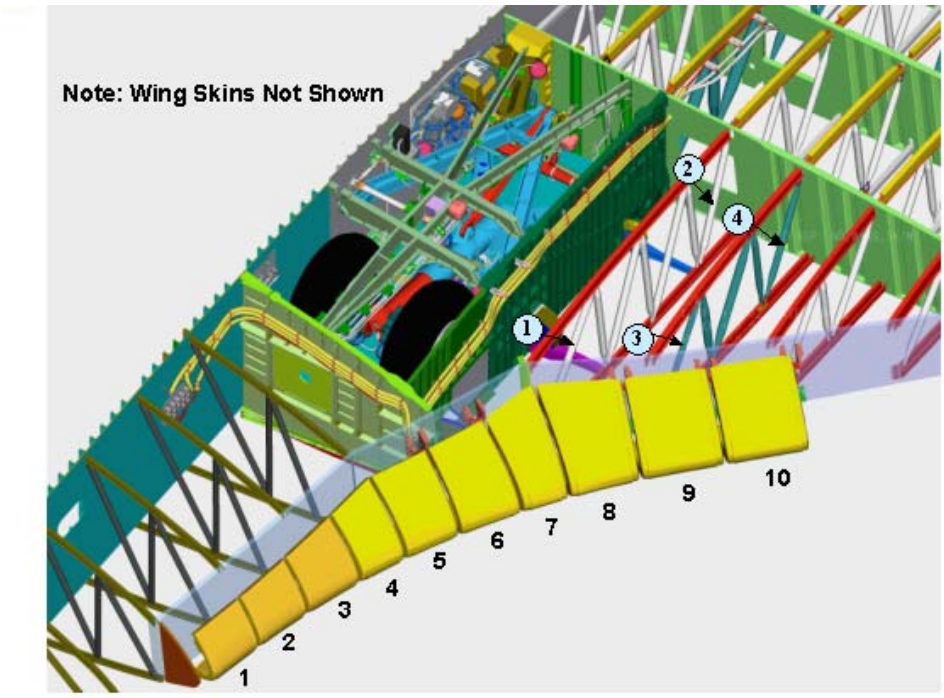

Figure 6-84 - Location of truss tubes (labeled 1-4) studied

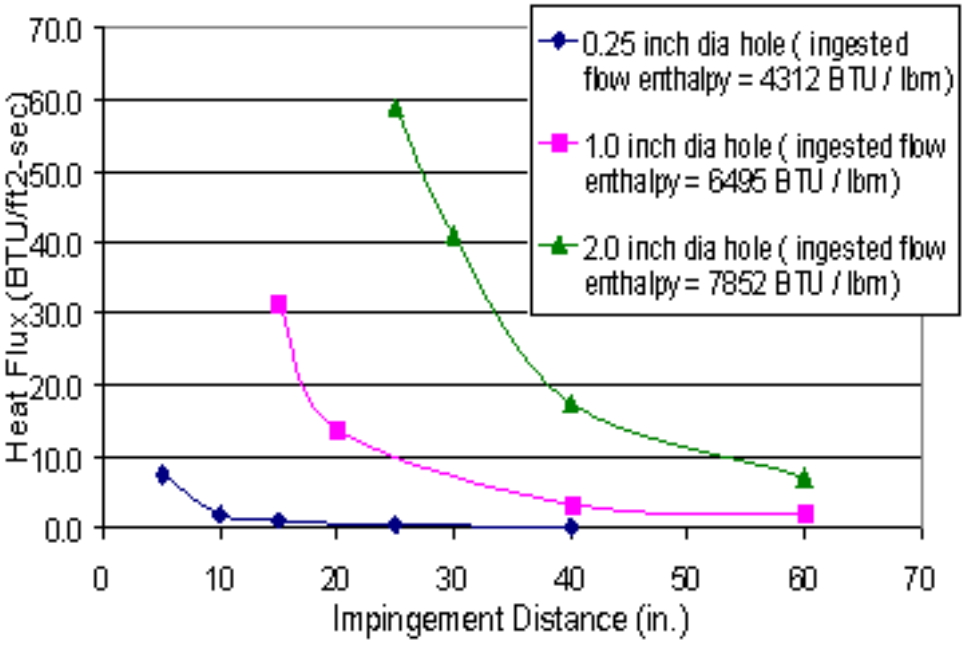

Figure 6-85 - Panel 9 internal plume impingement heating on 1" diameter cylinder at EI+491 seconds

$$\cos^{1.1}\Lambda_1 \cdot \cos^{1.1}\Lambda_2$$

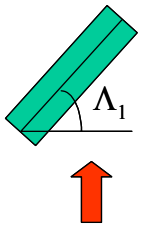

Tube	L_1	L_2
1	31.5	48
2	31.5	60
3	73.73	50
4	64.53	56

L_2 is out of the page

Figure 6-86 – Heating Correction for Angular Impingement

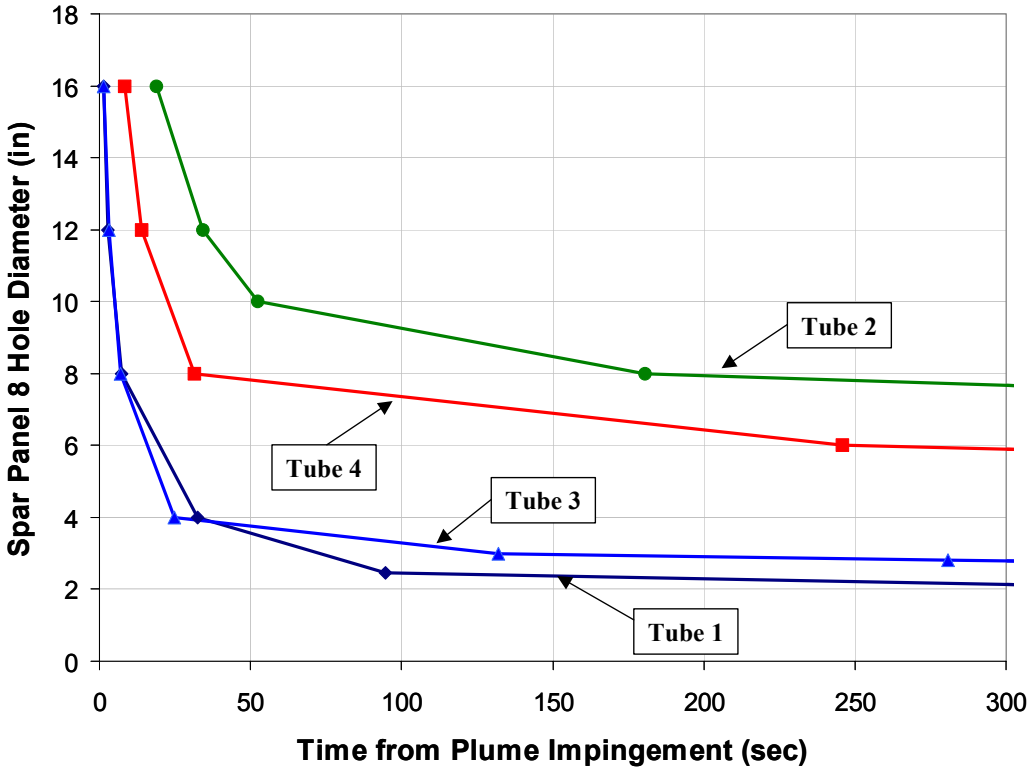

Figure 6-87 - Wing truss tube failure times with respect to breach sizes

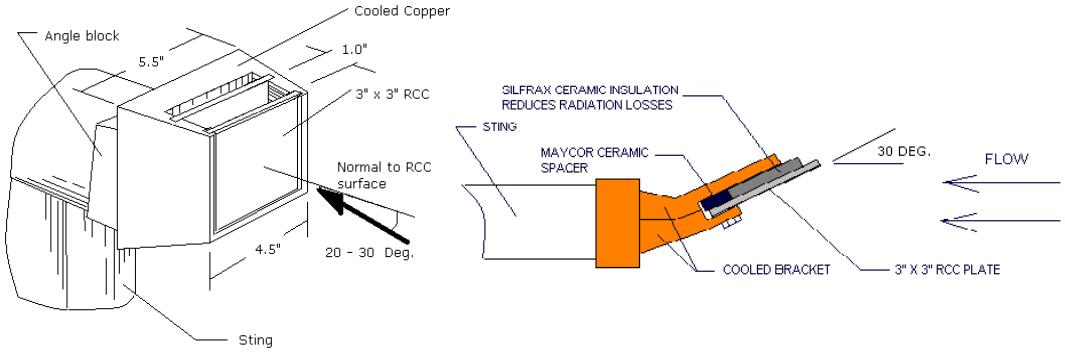

Figure 6-88 – Test Fixtures

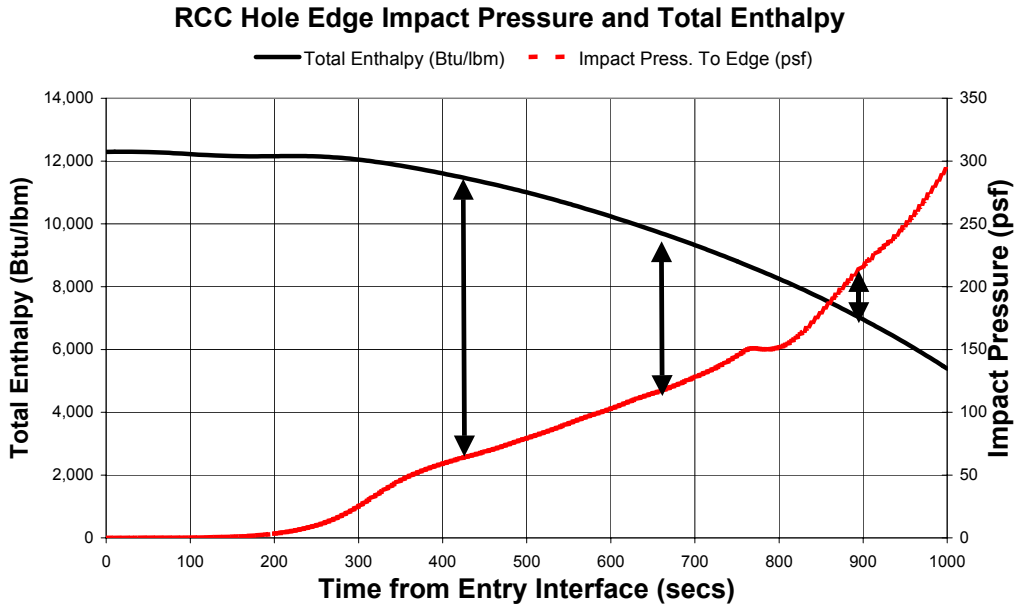

Figure 6-89 – Flight Environment

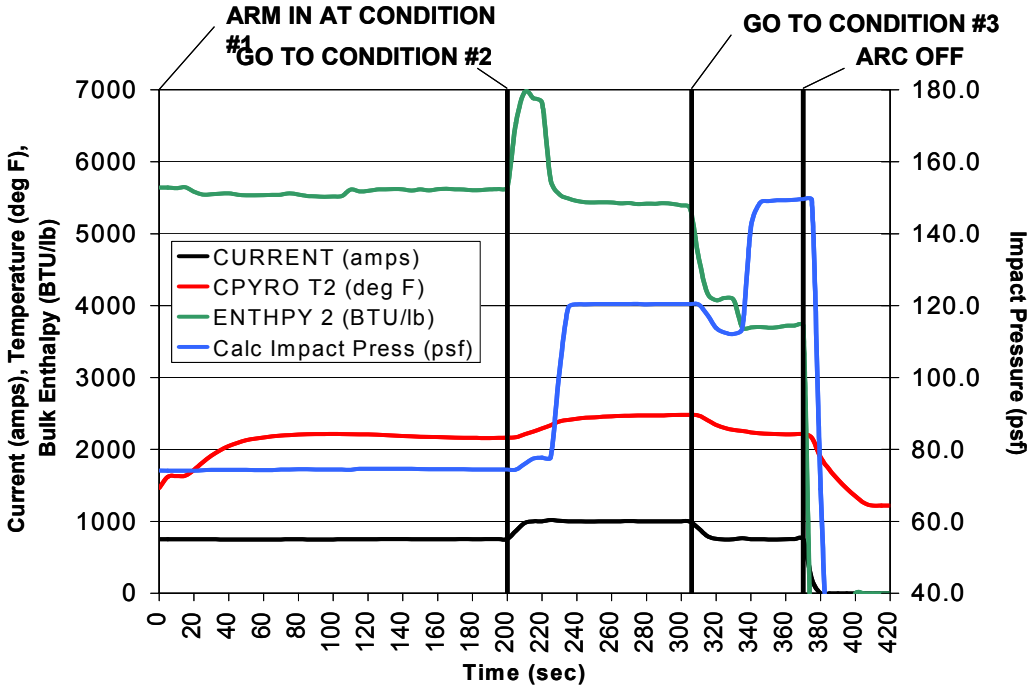

Figure 6-90 -Test Run #__ Actual Profile

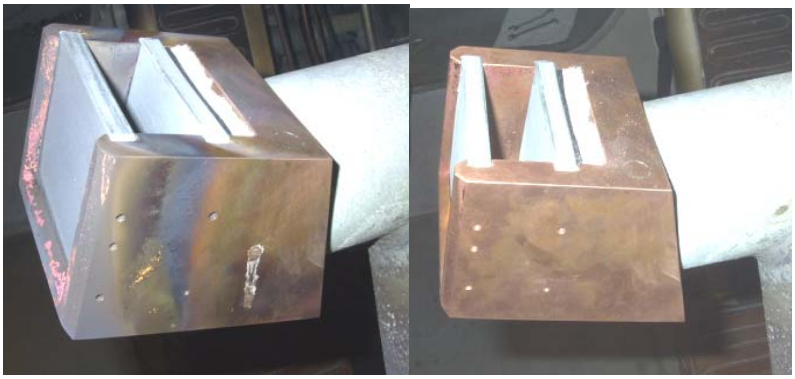

Figure 6-91 -Test #1 Pre and Post Test

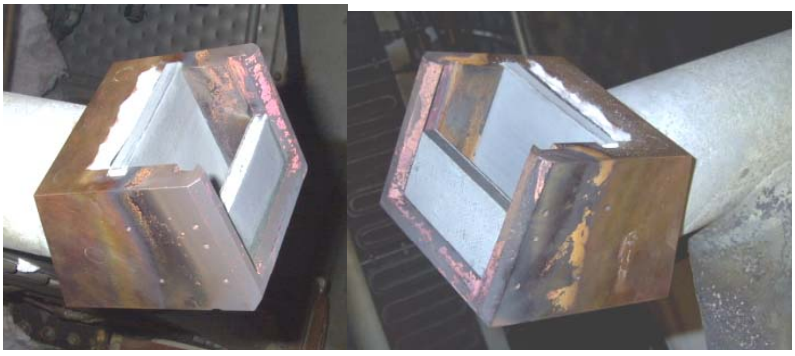

Figure 6-92 -Test #2 Pre and Post Test

Figure 6-93 -Test #3 Pre and Post Test - Knife-Edging Apparent

Figure 6-94 -Test #4 Pre and Post Test

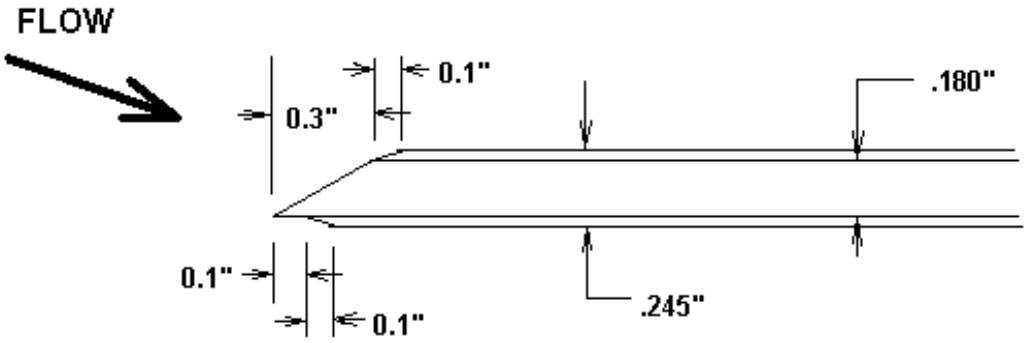

Figure 6-95 – Schematic of knife-edging dimensions

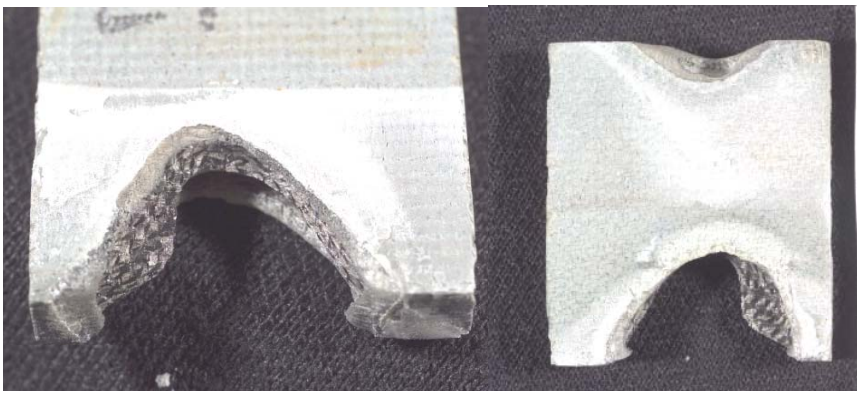

Figure 6-96 -Test #5 Closeout RCC Pieces with Knife-Edging

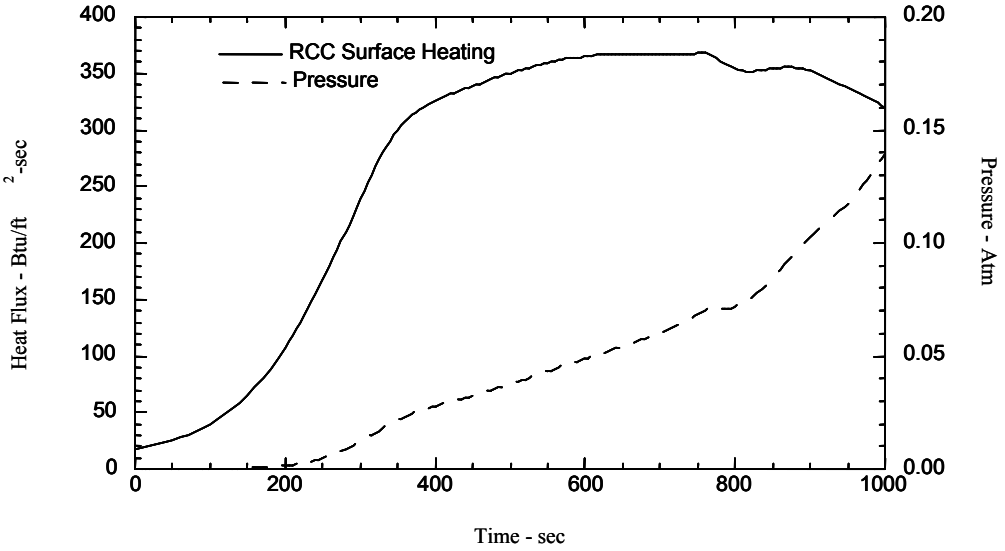

RCC Surface Heat Flux & Pressure History

Figure 6-97 – RCC Hole Environment

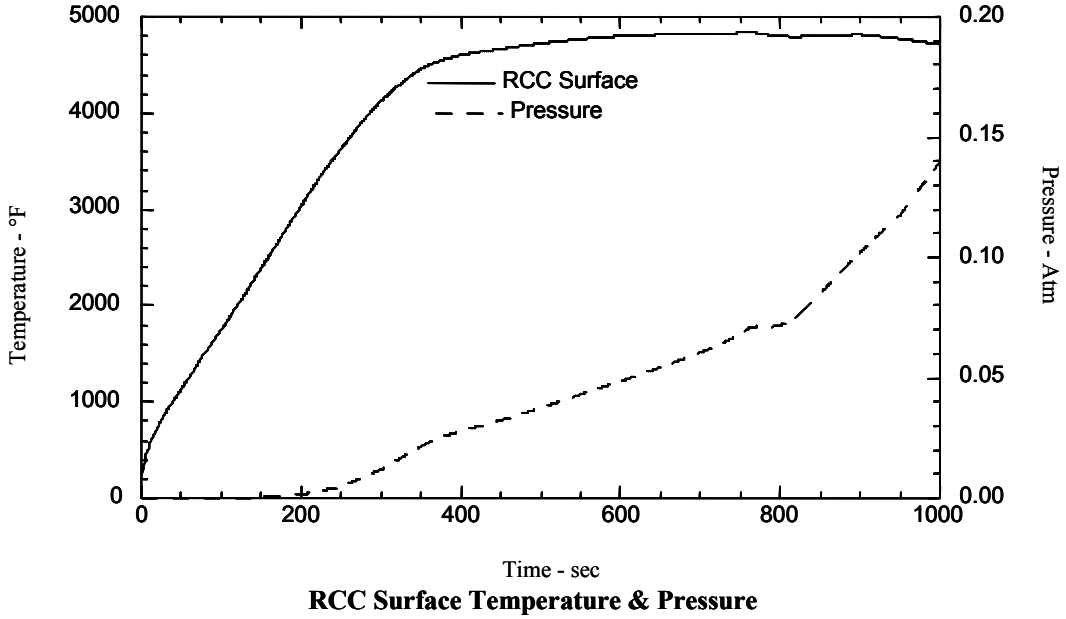

RCC Surface Temperature & Pressure

Figure 6-98 – RCC Temperature Response

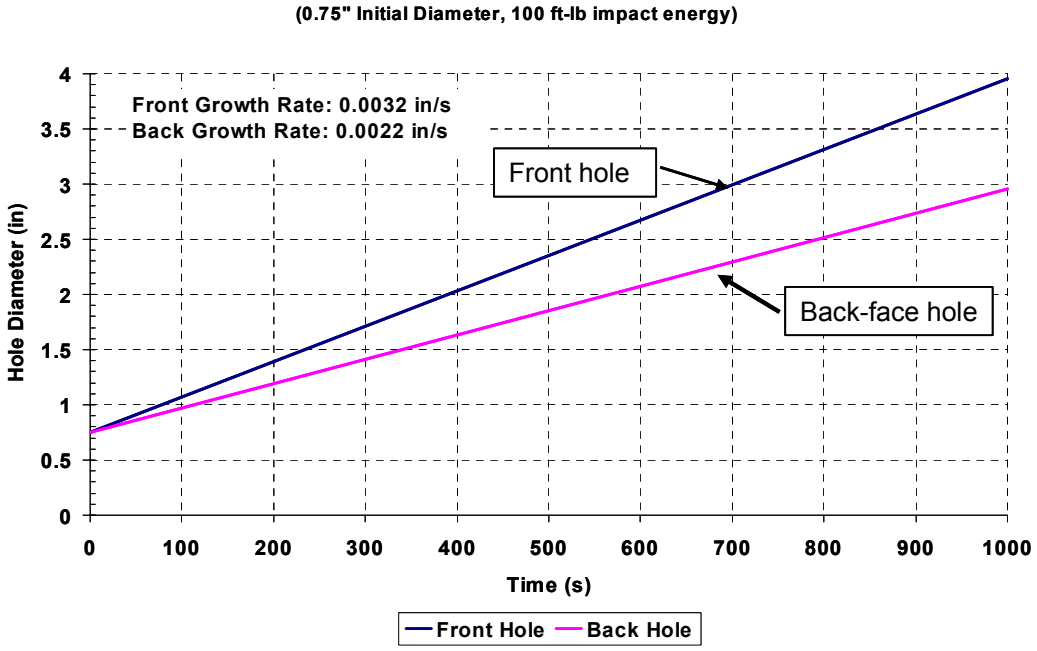

Figure 6-99 – RCC Hole Growth Calculation

References - Thermal

6-1. Generic Honeycomb Modeling Tool.
6-2. Stress report - STS89-0537
6-3. SINDA/FLUINT Version 4.4, C&R Technologies, Littleton CO.
6-4. Alpha Star Corporation, “Phase II Final Report, GENOA Progressive Failure Analysis of X-37 Reusable Launch Vehicle (RLV) Program”, June 24, 2000.
6-5. GENOA

7 STRESS

7.1 Panel 9 Spar Strain Gauge Evaluation

7.1.1 Analysis Objective

The objective of this analysis was to determine how a significant thermal event in the WLE spar would influence shear strain readings in the spar web shown in Figure 7.1-1. The location of the strain gage is shown in Figure 7.1-11. Primary focus was placed on thermal loading because mechanical loading would not produce the type of shear strain responses seen; maneuver type loads would have been seen on other strain gages and would have registered on the flight control systems. Mechanical load deviations would also be of relatively short duration. Pressure differentials across the WLE spar web would produce out of plane bending, but would not contribute to the shear strains in the web.

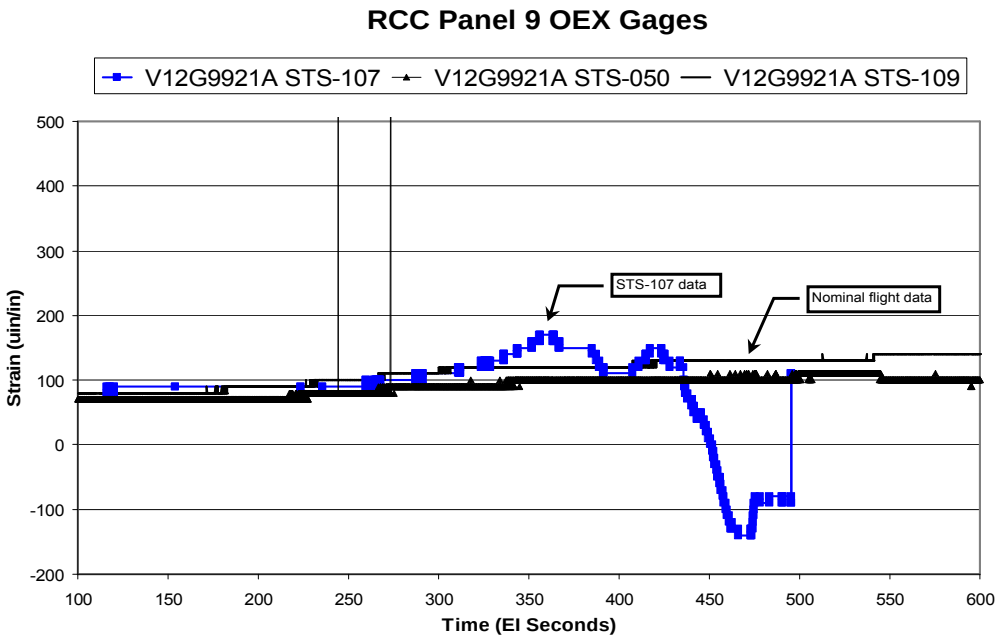

Figure 7.1-1 STS-107 V12G9921A strain gage data overlay with nominal strain gage flight data.

The two primary characteristics of the curve that need to be explained are the increase in shear strain with a sudden sign reversal. In addition to recreating the shear strain trends, interest was placed on how close to the thermal event would shear strain gage V12G9921A need to be to record the type of signal seen on STS-107. This gage is located roughly in the middle of the spar web near WLE panel 9. The thermal effects will register on the WLE spar strain gage even though it is some distance from the thermal event. Thermal sensors in the vicinity of panel 9 did not respond to a thermal event until much later. The quick response of the strain gage compared to the thermal sensors allows it to be used as a remote thermal sensor as shown in Figure 7.1-2. Near the boundary of a local thermal event, peak strains are expected because of the large thermal gradient. With increased distance from the thermal event the load will redistribute as illustrated and the influence of the thermally induced strain will eventually become negligible compared to the mechanical strain.

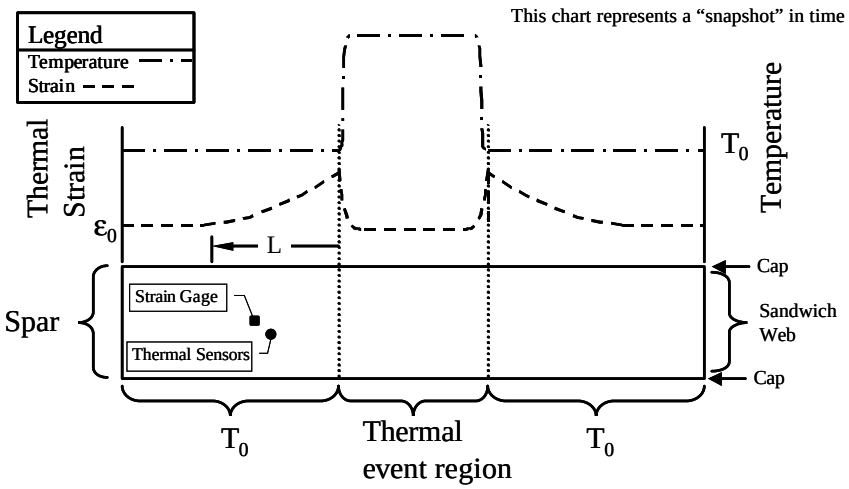

Figure 7.1-2 Temperature measurements lag strain measurements

7.1.2 Analytical Approach

A finite element model of the local wing area of interest was used because of the complex structural response to the thermal loading conditions. A total of 5 different assumed load cases were run. Initially a simple symmetric distribution was chosen. Because the strain gage is located near the middle of the WLE spar web, the shear strain response for a uniform thermal field is low. A number of unsymmetrical thermal fields were then analyzed, which created comparatively large shear strain responses similar to those seen during flight. The shear strain responses at the middle of the spar web were analyzed from the edge of the thermal event outward for each case. Based on the findings a possible scenario was then developed.

7.1.3 Model Description

The existing ASKA/NASTRAN loads finite element model of the wing was modified to perform a local analysis on the WLE spar. The coarse mesh on the original model in the WLE area near panel 9 was refined, as shown in Figure 7.1-3, to determine the local response of the structure to the thermal load cases being analyzed. In addition material properties were updated to include temperature dependent effects.

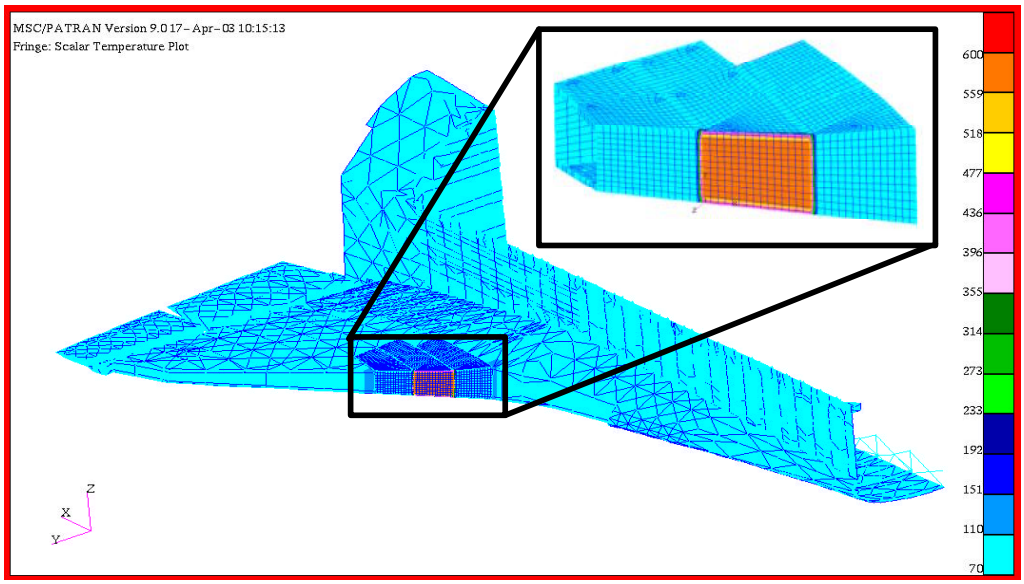

Figure 7.1-3 Refined region of wing used in thermally induced strain analysis

7.1.4 Thermal Profiles

Thermal profiles used in the analysis were assumed to be high heating events with large gradients between thermally protected and unprotected structure to induce large strain deviations from nominal flight data. A temperature of 600°F was chosen as the maximum temperature because reliable material properties were not available for higher temperatures. Also, since a uniform temperature region was used, this represented a reasonable average of temperatures ranging from melting of the aluminum (>900°F) to more moderate temperatures at the edge (400°F). Five different assumed thermal profiles were analyzed in developing the scenario.

Initially a temperature of 600°F was applied on WLE web while the spar caps were at 400°F. The rest of the structure was taken to be 70°F.

The second case assumed that the upper half WLE sees primary heating and it is initially heated to 300°F on upper half of WLE spar web and cap. Temperature from the middle of the WLE to the bottom of the WLE cap is linearly distributed from 300°F to 70°F and the rest of the structure is at 70°F. This case is an intermediate case between nominal heating and load case three.

For case three the upper half of the WLE sees continued primary heating up to 600°F on upper half of WLE spar web and cap with the temperature being linearly distributed from 600°F to 70°F at middle of WLE web to the bottom WLE cap. The rest of the structure is at 70°F.

For the fourth case a burn through is assumed on upper half WLE spar web. A temperature of 600°F is applied on upper WLE cap, wing skin, and wing ribs up to 16 inches from WLE. A linearly distributed temperature of 600°F to 70°F was applied from the edge of burn through (middle of WLE web) to bottom WLE cap. A temperature of 70°F was applied to the rest of structure.

The final case is a continuation of the fourth case. A burn through is now assumed on upper half WLE spar web and spar cap. A temperature of 600°F is applied on upper wing skin and wing ribs up to 16 inches from WLE. A linear temperature distribution of 600°F to 70°F from the edge of burn through (middle of WLE web) to bottom WLE cap is applied and the rest of the structure is sees 70°F. Contour plots of all five temperature profiles are shown in Figure 7.1-4 through Figure 7.1-7 below.

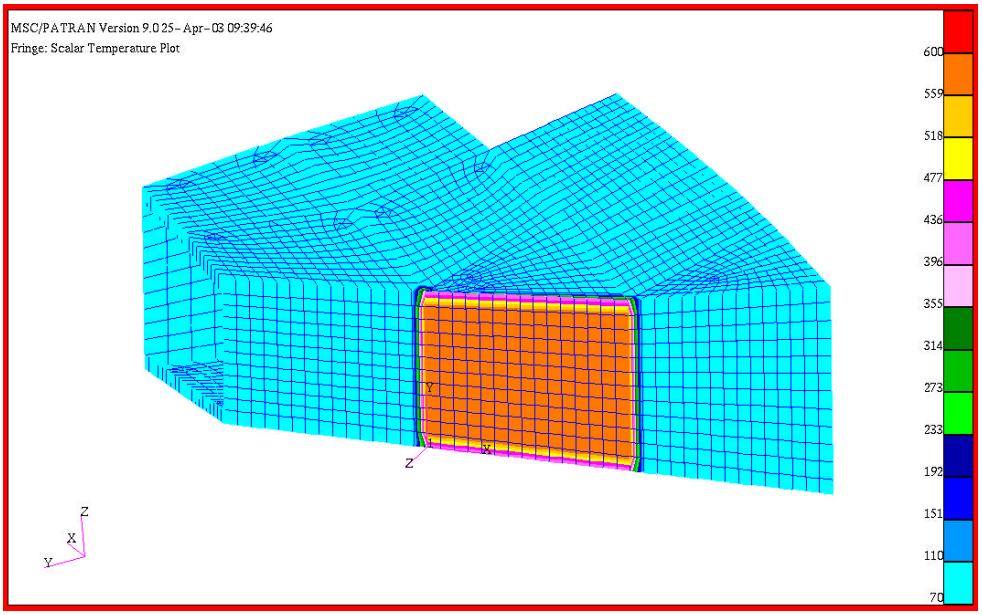

Figure 7.1-4 Contour plot of the initial symmetric temperature profile.

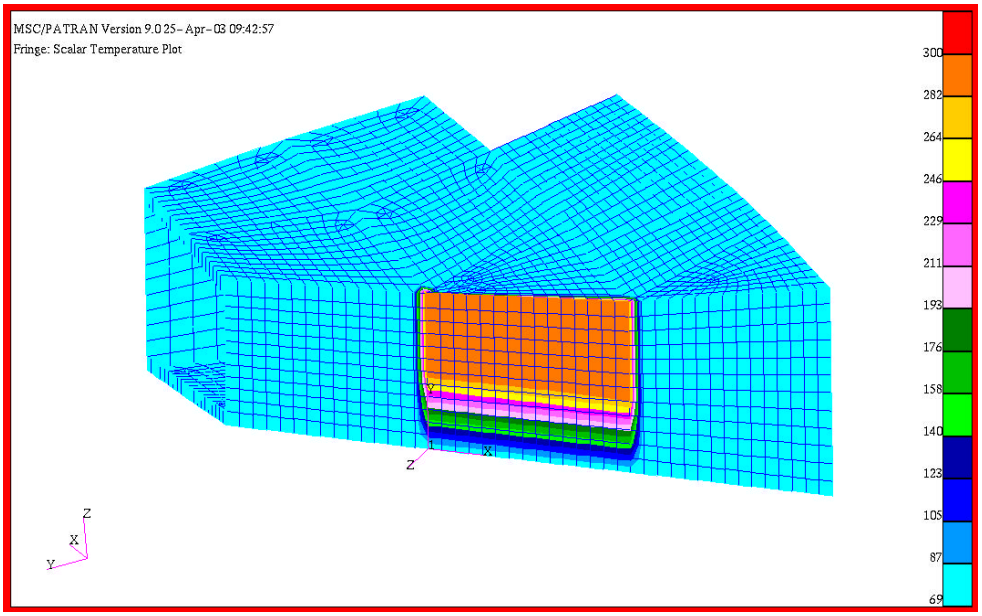

Figure 7.1-5 Temperature plot for the initial heating of WLE upper spar, second thermal profile.

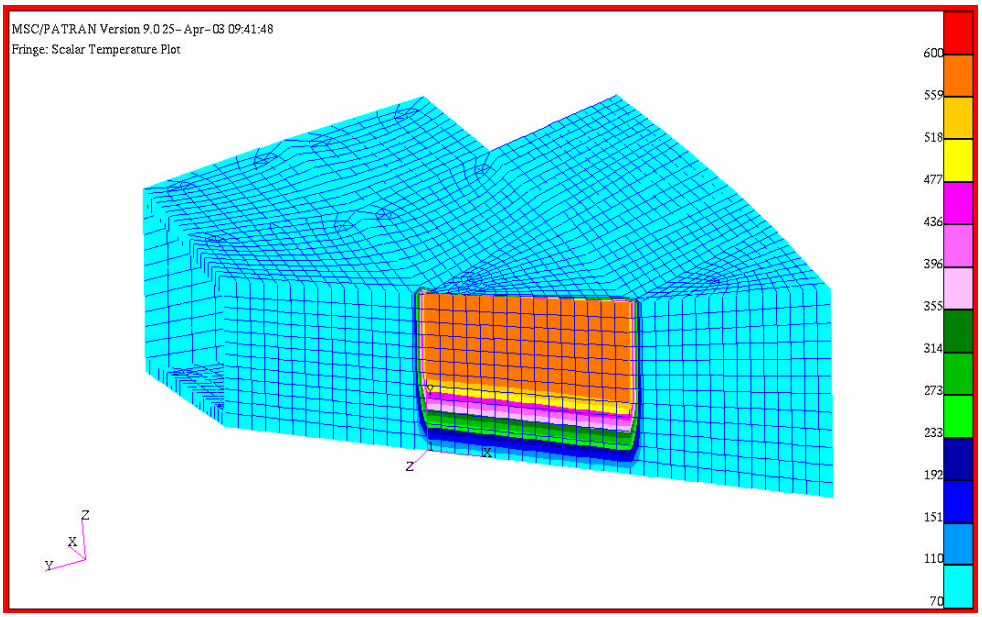

Figure 7.1-6 Contour plot for continued WLE upper spar heating, temperature profile three

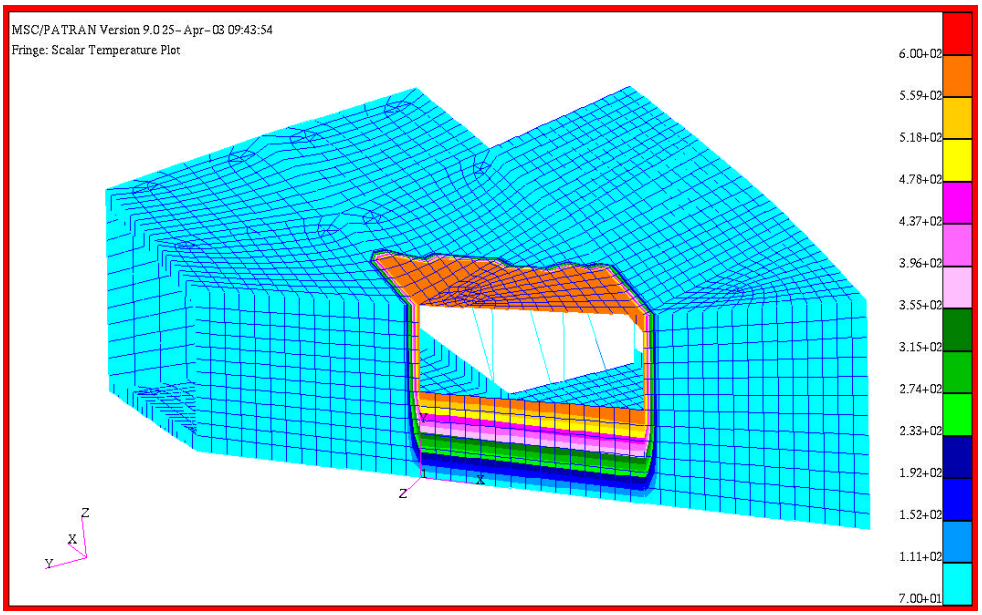

Figure 7.1-7 Temperature contour for WLE spar burn through, profiles four and five

7.1.5 Results

The shear strain results along the mid-span of the WLE spar outside of the thermal event for the five cases are shown in Figure 7.1-8 . The dashed lines on the chart show the amount of increase in shear strain that was seen during STS-107.

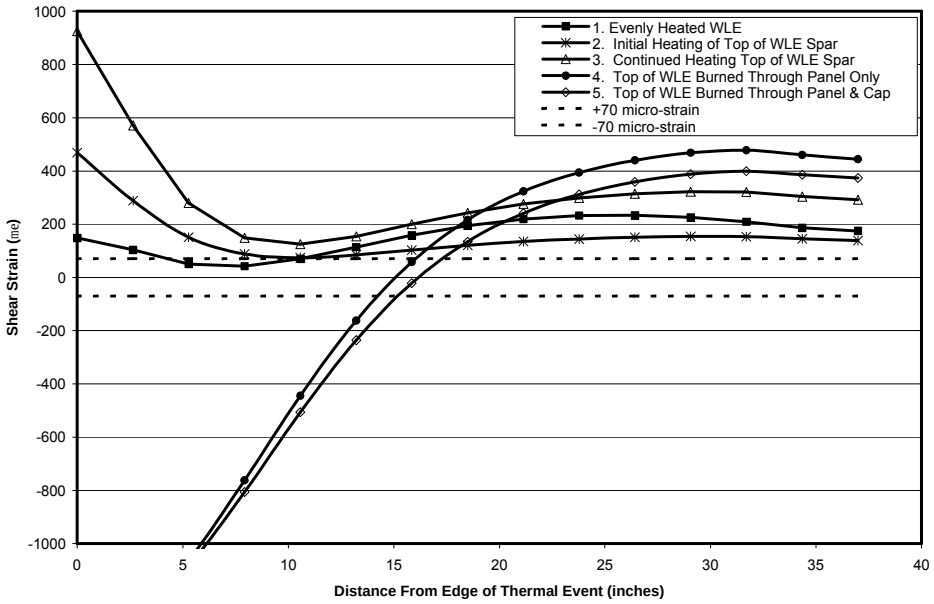

Figure 7.1-8 Shear strain results along midspan of WLE spar outside of the thermal event.

Thermal case one shows an increase in shear strain magnitude along the middle of WLE from the edge of thermal event outward but no significant magnitude. It is also noted that the sign remains the same for all locations plotted.

Thermal event two does show a significant rise in shear strain magnitude near the thermal event boundary that reduces with increased distance from the thermal event boundary. At distances greater than 18 inches from the thermal event boundary shear strain magnitude changes little. As with case one there is no change in sign of the shear strain at any distance from the thermal event.

Case three trends are very similar to case two trends but the magnitude of the shear strains has increased.

Case four produces the first reversal in shear strain sign. Even more than cases two and three there is a significant rise in shear strain magnitude near thermal event boundary. For distances less than 15 inches from thermal event boundary strain sign is negative. More importantly the shear strain from 15 to 19 inches reverses sign with magnitudes similar to the third case. There is a decrease in shear strain magnitude with increased distance from thermal event boundary as seen before. Shear strain magnitude changes little at distances greater than 26 inches from thermal event boundary.

Thermal event five is very similar to case four with increased magnitude. At distances less than 16 inches from the thermal event boundary the shear strain sign is negative and for the range of 16 to 23 inches from the boundary the shear strain is less than noted in the undamaged structure. With increased distance from the thermal event boundary the shear strain magnitude decreases and is relatively unchanging at distances greater than 26 inches from the thermal event boundary.

The results of cases four and five are significant findings. First it shows that a loss of the WLE spar structural capability is needed for a reversal of the shear strain sign seen on the gage. Additionally the results help bound the location of where the strain gage may be located. For both cases four and five sign reversals are see up to 15 or 16 inches away from the thermal event boundary, which establishes an outer limit location for this scenario.

7.1.6 Conclusions

Scenario Description

Based on the results of the five thermal cases coupled with previous OEX strain gage flight data, STS-107 strain gage and STS-107 thermal data, a possible scenario has been developed. It is hypothesized that a partial breech in a WLE RCC panel allowed hot gas impingement on WLE spar causing an unsymmetric temperature increase on WLE spar web and cap. The onset of this thermal event was slow to occur, probably due to the presence of WLE insulation, but caused shear strains to begin to deviate around 270 seconds as shown in a comparison to of STS-107 data with prior nominal flight data, Figure 7.1-9. The upper WLE spar web and cap were then subjected to heating and a temperature gradient occured on WLE spar from top to bottom. This increased shear strain gage readings until about 360 seconds from EI; during this time the structure remained intact. Shear strain data between approximately 360 to 400 seconds indicated the increasing temperatures were beginning to soften the structure but it was still carrying load in the heat affected region. Between 400 and 425 seconds there was a rise in shear strain that could be caused by heating at a second location closer to the strain gage; possibilities include a sudden loss of a large piece of insulation on the WLE spar or rapid temperature increase in the aft facesheet of the WLE sandwich panel. At 425 seconds, loss of structural capability was initiated causing the shear strain sign reversal. The loss could initially be attributed to debond on the facesheet of the WLE sandwich or significant loss of modulus (T>800°F) and, later, melting of the aluminum. Thermal stresses were relieved and the damage size continued to grow from this point on. The strain data is not considered reliable after about 470 seconds.

In summary, the main conclusion of this hypothetical scenario is that a loss of WLE spar structure is needed to reverse strain. Although this probably started as a facesheet debond or loss of modulus, it eventually proceeded to loss of the aluminum through melting. Secondly, the strain gage would need to be located in close proximity to the thermal event to record the type of signal seen for STS-107. For this scenario the strain gage would be located within 15” of edge of thermal as shown in Figure 7.1-8.

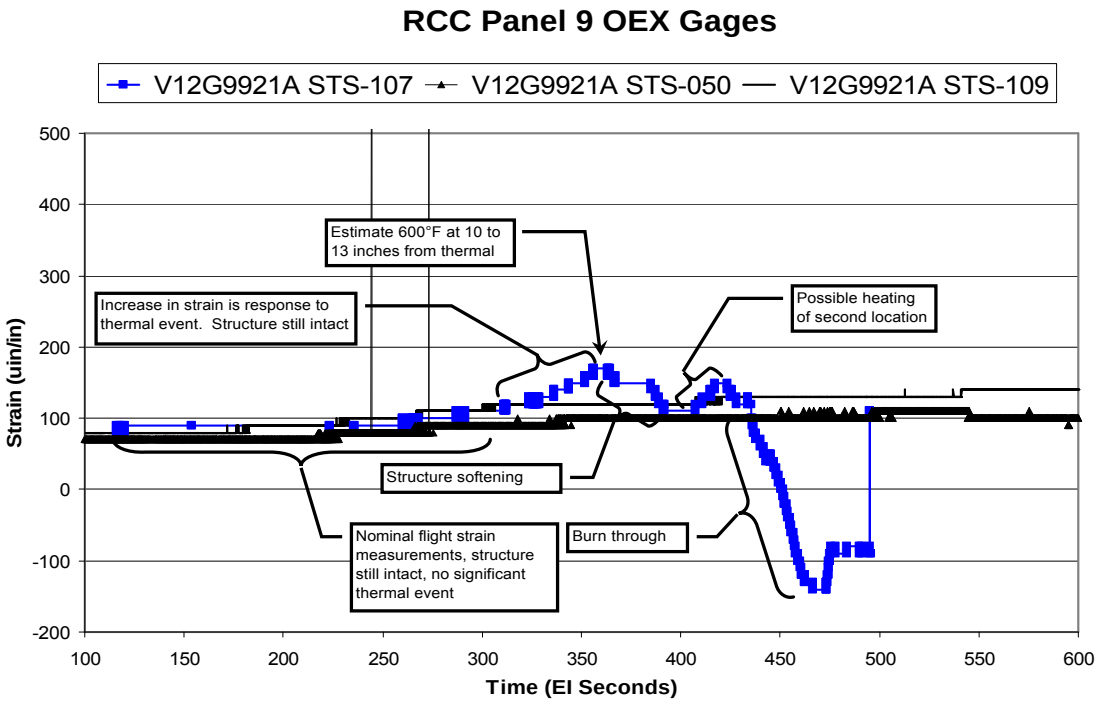

Figure 7.1-9 Scenario description overlay with nominal strain OEX strain gage data

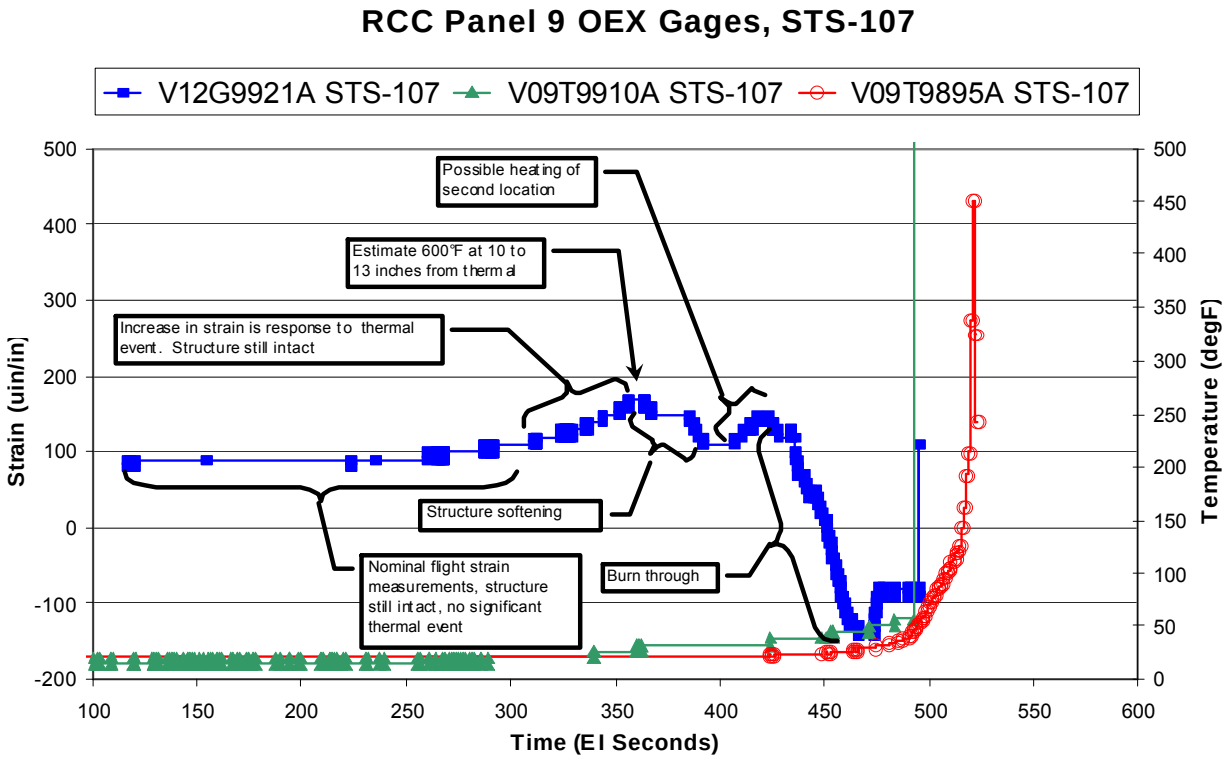

Figure 7.1-10 Scenario description overlay with STS-107 thermal flight data.

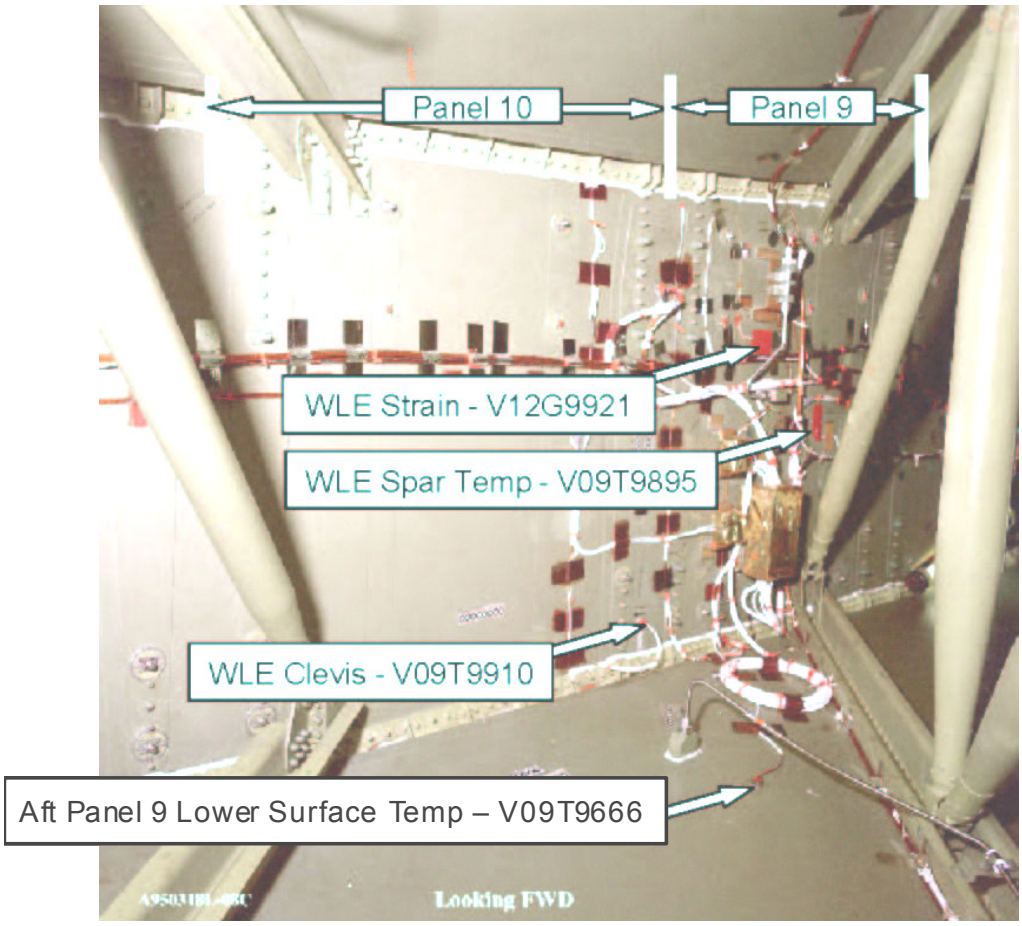

Figure 7.1-11 Location of WLE Strain Gage

7.2 1040 Spar Strain Gauge Evaluation

7.2.1 Analysis Objective

This analysis seeks to provide explanation for observed off-nominal strain signatures in gages V12G9048A and V12G9049A during STS-107 entry. Mechanical loading, pressure loading, load redistribution, thermally induced strain, and instrumentation malfunction were all considered as potential contributors. Strain due to local thermal effects in the region of the two gages is considered the most rational explanation, and is the primary focus of the analysis effort.

7.2.2 Analysis Inputs, Models, Assumptions, and Approach

7.2.2.1 Background

Axial strain gages V12G9048A and V12G9049A are located on the lower and upper caps of the left wing Xo1040 spar, respectively. The Xo1040 spar is the forwardmost of five major wing spars. Forward lies the wing glove area. Aft lie the main landing gear wheel well (behind the section of the spar inboard of the Yo167 rib), and the main wing cavity (behind the section of the spar outboard of the Yo167 rib). The outboard section of the spar includes a cutout that provides a path through to the main cavity of the left wing. There is also a cutout in the inboard section of the spar providing access to the MLG wheel well. Just forward of the Xo1040 spar on the Yo105 sidewall is a vent into the main fuselage. Figure 7.2-1 provides an illustration of the area.

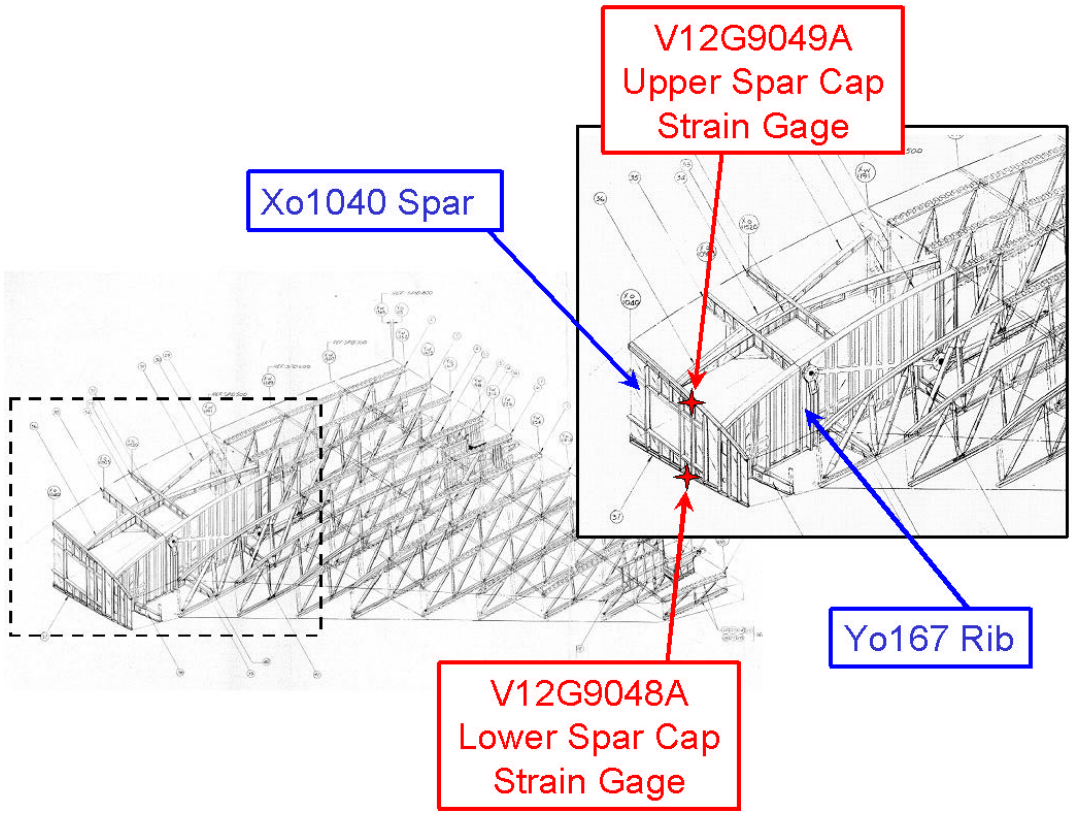

Figure 7.2-1 Xo1040 Spar Cap Strain Gage Locations

7.2.2.2 STS-107 Data Analysis & Reconstruction

As-recorded STS-107 data was refined in order to isolate suspected off-nominal behavior from nominal loading effects. To do so, a nominal profile, based on STS-109 (previous OV-102 flight) was compared with the recorded data. EI+488 seconds was chosen as an initial data point, up to which STS-107 data is considered nominal. The offset between STS-109 data and STS-107 data at this time was removed to generate a reconstructed nominal profile. Figure 7.2-2 illustrates the as-recorded STS-107 data versus the reconstructed nominal profile, based on STS-109.

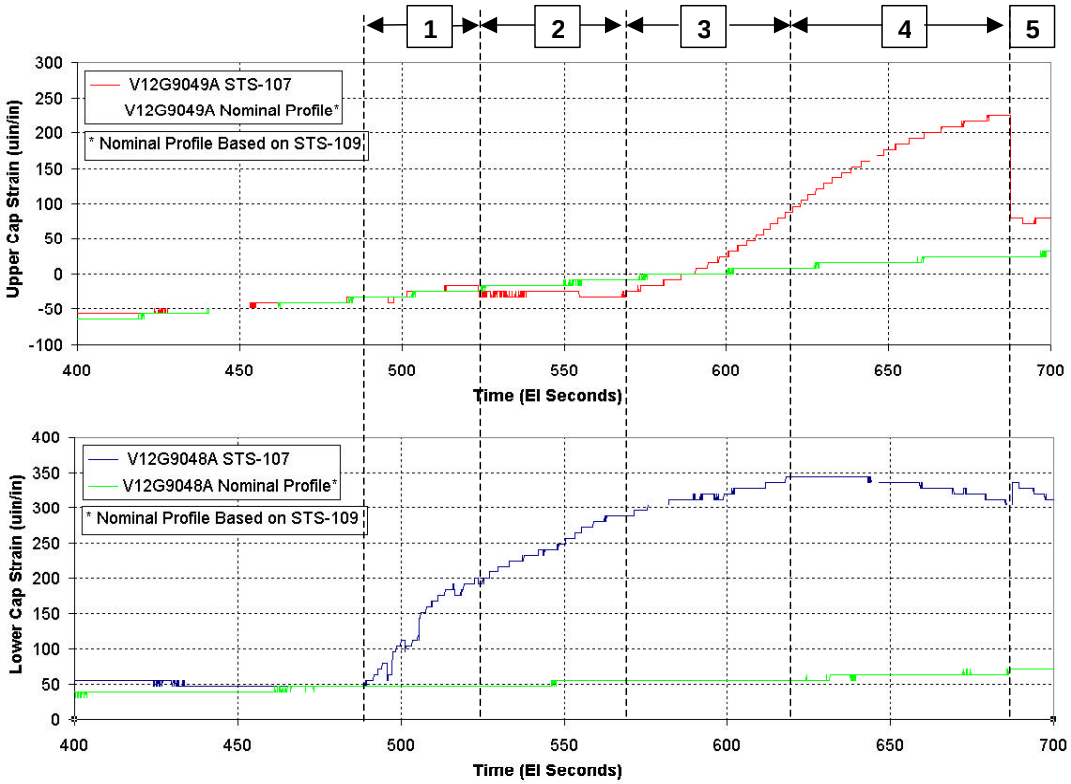

Figure 7.2-2 Observed STS-107 Strain Data versus Reconstructed Nominal Profile

Differentials between the nominal profile and the as-recorded profile represent strain values due to off-nominal loading during STS-107.

An illustration of the complete STS-107 Xo1040 spar cap strain data reconstruction is included for reference as Figure 7.6-2 of the Stress Appendix, Section 7.6.

The anomalous data profile has the following approximate timeline:

1. (EI+488 to EI+523 seconds)
   Minimal tension (8 µin/in) builds in the upper spar cap.
   Significant tension (152 µin/in) builds in lower spar cap.

2. (EI+523 to EI+569 seconds)
   Reversal causes minimal compression (-16 µin/in) in the upper spar cap.
   Tension continues to build to 232 µin/in in the lower spar cap.

3. (EI+569 to EI+618 seconds)
   Another reversal causes significant tension (72 µin/in) in the upper spar cap.
   Tension builds to a maximum (288 µin/in) in the lower spar cap.

4. (EI+618 to EI+687 seconds)
   Tension builds to a maximum (200 µin/in) in the upper spar cap.
   Tension reduces to 232 µin/in in the lower spar cap.

5. (EI+687 seconds)
   Instantaneous, high magnitude strain decrease (-144 µin/in) in the upper spar cap.
   Instantaneous, low magnitude strain increase (32 µin/in) in the lower spar cap.

Data following the instantaneous change at EI+687 seconds has not been conclusively verified as reliable strain data. There has been no instrumentation malfunction identified in these measurements at this time, or any time prior to EI+930 seconds. However, the instantaneous changes at EI+687 seconds are not considered rational from a real strain perspective. As such, there is no conclusive explanation for the instantaneous changes in strain values at that time. Without such an explanation, data beyond this point must be considered suspect, and therefore was not considered in the analysis that follows.

The observed off-nominal strain signatures during STS-107 are believed to be the result of instrumentation malfunction, thermally induced strain, or a combination of these two factors. Mechanical loading, pressure loading, and load redistribution were also evaluated as potential causes, but are believed to be unlikely explanations.

The primary evidence refuting mechanical loading, or more specifically, wing bending, is the agreement in sign between the off-nominal strains. That is, both the upper and lower caps show tensile loading. A nominal entry plot for these two gages from STS-109, included for reference as Figure 7.6-1 of the Stress Appendix, Section 7.6, illustrates that under significant wing bending loads in the TAEM portion of entry, the spar cap strains are of opposite sign; tension on the lower cap, compression on the upper cap. It should also be noted, however, that in the nominal profile, tensile loads exist in both spar caps during the period of entry in which off-nominal trends were recorded on STS-107. This phenomenon is attributed to the influence of upper skin heating, which generates a tensile effect in the upper cap that counteracts the mechanical compression load. The thermal effect on the lower cap is nominally much less pronounced.

An internal pressure load would not be consistent with the observed strain data, as the initiation times of off-nominal trends in the upper and lower spar caps, respectively, are not consistent with one another. Load redistribution also is largely unsupported by the data. The lower spar cap, for example, shows a reduction of tensile loading after EI+618 seconds, following the initial off-nominal rise. This would not be the expected behavior of a structure that had compensated for failure elsewhere by taking on additional load, namely as it would imply some sort of regaining of previously lost capability.

This evidence leaves localized thermal effects as the most reasonable explanation for the observed off-nominal strains. The analysis that follows considers thermal effects arising from intrusion of hot gas into the main wing cavity, which subsequently vents into the area in front of the Xo1040 spar. In combination with heating of the upper wing skin, due to breach into the main wing cavity and/or the MLG wheel well, localized heating in these regions could potentially give rise to temperature differentials that drive the observed spar cap strains.

7.2.2.3 Finite Element Model

The OV-102 Orbiter NASTRAN finite element model, based on the ASKA certification model, was used for assessment of localized heating. Selected FEM nodes were held at higher temperatures than others in order to produce thermally induced strain. FEM elements corresponding to the locations of the strain gages were then checked for strain response to the applied loads.

All elements in the model were assigned a default thermal expansion coefficient of a=0.000013/°F, and a default reference temperature of 70°F. Node temperatures by default were set to 70°F, with selected nodes raised to higher temperatures. It is important to note that the analysis does not attempt to model actual structural temperatures, but rather to gage structural response to local temperature differentials. The following structural areas were selected for application of local elevated temperature fields:

- Xo1040 Spar Web
- Xo1040 Upper Spar Cap
- Xo1040 Lower Spar Cap
- Wing Upper Skin, immediately forward of Xo1040
- Wing Lower Skin, immediately forward of Xo1040
- Wing Upper Skin between Xo1040 and Xo1090, Yo167 and Yo193
- Wing Lower Skin between Xo1040 and Xo1090, Yo167 and Yo193
- Wing Upper Skin between Xo1040 and Xo1090, Yo105 and Yo167
- Wing Leading Edge between Yw198 and Yw226 ribs
- Yo167 Rib Web between Xo1040 and Xo1098

Numerous combinations were run in order to assess the effects of different heating inputs on spar cap strains. These results were then compared to the observed strains to develop potential scenarios to explain the observed behavior.

Illustrations of the complete FEM, as well as specific areas of emphasis, are included for reference as Figure 7.6-3 to Figure 7.6-5 of the Stress Appendix, Section 7.6.

7.2.3 Results

The following table provides a qualitative summary of analyzed FEM cases and results:

Table 7.2-1 Qualitative FEM Results Summary

Case	Description	Upper Cap Reaction	Lower Cap Reaction
4A	Calibration (all nodes @ 70°F)	None	None
4B	Equal heating of spar web, forward upper and lower skins	Significant tension (20% higher than lower cap)	Significant tension
4C	Heating of outboard, aft, upper skin only	Significant tension	Very low tension
4D	Combined 4B and 4C	Significant tension (effects additive)	Significant tension (effects additive)
4F	Heating forward lower skin only	Very low compression	Significant tension
4G	Heating of WLE nodes	Very low compression	Low compression (2x upper cap)
4H	Heating of outboard, aft, lower skin only	Very low compression	Very low tension
4I	Heating of spar web nodes only	Very low tension	Low tension (2x upper cap)
4J	Heating of Yo167 rib sections	Very low tension	Very low tension
4L	Heating of upper spar cap only	Significant compression	Very low compression
4M	Heating of aft upper skin only	Significant tension	Very low compression

Numerical results from each of the load cases may be found in the Table 7.6-1 summary table of the Stress Appendix, Section 7.6.

The qualitative trends above were utilized to guide development of several temperature profiles that produce strains as observed in the STS-107 flight data. These profiles were screened versus scenario

evidence from the accident investigation team in order to define the most reasonable profile that could have produced the observed strains. The preferred profile, included in the scenario timeline that follows, corresponds to sequences 1-4 from the observed data timeline.

These results indicate that local temperature gradients on the order of 100-200°F could potentially explain the observed strains. These gradients may be consistent with scenarios involving hot gas intrusion from the wing cavity, passing in front of the Xo1040 spar enroute to the mid-fuselage, combined with heating of the wing upper skin just aft of the Xo1040 spar.

The major assumption of the selected temperature profile is that the lower spar cap has less heating than the structure around it; namely the upper spar cap, spar web, and wing skins immediately forward of Xo1040. The temperature rise in the lower spar cap thereby lags behind that of the adjacent structure and the upper spar cap. Note that sections A2 and A3 of the temperature profile indicate a transition from heating of the upper skin outboard of Yo167 to the upper skin atop the MLG wheel well, inboard of Yo167. This is one of a number of ways that a significant change in upper skin heating characteristics may be represented. The same effect could also be achieved, for example, by continued higher heating on the outboard section. It should be noted that the initiation of significant upper spar cap tension at this time is attributed to some substantial change in upper skin heating, but not necessarily by this particular means.

Scenario Timeline

1. (EI+488 to EI+523 seconds)
   Following WLE spar breach, hot gas vents into the region forward of the Xo1040 spar, providing heating to the spar web, nearby forward wing skins, and the upper spar cap. The lower spar cap temperatures lag behind the upper spar cap. Heating is also present in the upper wing skin just aft of the Xo1040 spar and outboard of the Yo167 rib.

2. (EI+523 to EI+569 seconds)
   Hot gas flow continues to drive temperature differentials in front of the Xo1040 spar, as the lower spar cap slowly begins to react. Heating to the upper wing skin outboard of Yo167 is effectively lost. Heating is now present only along skin at the top edge of the Yo167 rib.

3. (EI+569 to EI+618 seconds)
   Hot gas flow continues to drive temperature differentials in front of the Xo1040 spar. The lower cap is still slowly catching up. Breach into the MLG wheel well allows heating along the upper wing skin of the MLG well.

4. (EI+618 to EI+687 seconds)
   Xo1040 spar web, forward wing skins, and upper spar cap reach temperature equilibrium. Lower spar cap is slowly catching up, with continued heating of the upper wing skin above the MLG wheel well.

Table 7.2-2 Scenario Timeline FEM Results

Case	Description	Upper Cap Reaction	Lower Cap Reaction	Scenario
A1	+40°F applied to spar web, forward upper & lower skins, and upper spar cap +75°F applied to outboard, aft, upper skin	13 µin/in **(8 µin/in) (Recorded strain)**	146 µin/in **(152)**	Heating in front of spar and aft upper skin.
A2	+75°F applied to spar web, forward upper & lower skins, and upper spar cap +120°F applied to aft, upper skin along y167 rib +5°F applied to lower spar cap	-11 µin/in **(-16)**	225 µin/in **(232)**	Continued heating in front of spar and aft upper skin. Some heating in lower spar cap.
A3	+105°F applied to spar web, forward upper & lower skins, and upper spar cap +145°F applied to aft, upper skin above MLG wheel well +10°F applied to lower spar cap	73 µin/in **(72)**	291 µin/in **(288)**	Continued heating in front of spar and aft upper skin. Continued heating in lower spar cap.
A4	+105°F applied to spar web, forward upper & lower skins, and upper spar cap +190°F applied to aft, upper skin above MLG wheel well +20°F applied to lower spar cap	200 µin/in **(200)**	237 µin/in **(232)**	Thermal EQ in spar web, forward skins, and upper cap. Continued heating in lower cap. Continued heating of aft upper skin.

7.2.4 Conclusions

It is possible that the observed strains on V12G9048A and V12G9049A were a result of local thermal effects in the region of the Xo1040 spar. Given appropriate temperature gradients, the upper and lower spar caps are subjected to significant thermally induced strain, and could produce the observed strain gage signatures.

The STS-107 strain gage data offers some support for failure scenarios that involve intrusion of hot gas from the wing cavity into the glove area and/or the MLG wheel well. The timing of strain gage events shows some alignment with suspected breach times of the WLE and MLG well in these scenarios. Magnitudes of the observed strains, arising from local temperature gradients, could reasonably be generated by the suspected heat sources.

The strain gage data does not, however, conclusively indicate these scenarios. Numerous potential temperature profiles exist that would produce the observed strains. While a reasonable temperature profile has been suggested based upon corroborating evidence, this profile requires significant assumptions about the heat transfer properties of the local structure, the heat sources, and their combined ability to generate thermal gradients. A conclusive assessment would require conclusive identification of local structural temperatures, and significantly developed corroborating thermal analysis.

7.3 Overall Wing MADS Evaluation

7.3.1 Analysis Objective

This analysis compared recorded Modular Auxiliary Data System (MADS, a.k.a. OEX) wing strain gage measurements for STS-107 versus the same data for selected previous flights of the OV-102 vehicle. Both ascent and entry regimes were reviewed. Where appropriate, anomalous strain gage responses were identified, categorized, and in several cases, selected for additional in-depth analysis efforts.

7.3.2 Analysis Inputs, Models, Assumptions, and Approach

The OV-102 vehicle contained significantly greater MADS wing strain gage instrumentation than other vehicles in the STS fleet. There were 247 total strain gages available on the wings (Gage MSIDs begin with V12G); 121 of these gages were on the left wing, with the remaining 126 on the right. Additionally, 52 gages were located on the elevon structure, divided equally with 26 on each side of the vehicle (Gage MSIDs begin with V13G). In general, strain gage locations were symmetric between the two sides of the vehicle. Figure 7.6-23 and Figure 7.6-24 of the Stress Appendix, Section 7.6 illustrate strain gage locations on the vehicle. References in section 7.7 list relevant installation drawings.

OV-102 MADS strain gage data was recorded on three Pulse Code Modulation (PCM) data channels. Wing gages associated with channels PCM1 and PCM2 had continuous data recording at 10 samples per second for both ascent and entry flight regimes. There were 131 wing strain gages (45 left wing, 86 right wing) on channels PCM1 or PCM2. Gages associated with channel PCM3 had continuous 10 samples per second data recording during the ascent flight regime. During entry, PCM3 gage data was recorded in “snapshot mode” at periodic 1-minute-on, 4-minutes-off intervals (data rate during on-time was 10 samples per second). Elevon gages (PCM1 for right wing, PCM2 for left wing) had continuous data recording at 10 samples per second for the ascent regime. For entry, 20 of 52 gages (10 on each side) had continuous recording. The remaining 32 gages (16 on each side) were recorded in snapshot mode.

Seven previous OV-102 flights were selected for comparison with STS-107. These selections were made based upon similar mass properties and similar inclinations, starting with the most recent flights. Comparison flights were as follows:

STS-109, STS-093, STS-090, STS-087, STS-094, STS-073, and STS-050.

Comparison plots showing STS-107 data versus each of these previous flights were generated using in-house tools developed specifically for the STS-107 accident investigation. Comparison plots showed the entire duration of the ascent regime, and the first seventeen minutes of the entry regime, beginning at entry interface. This time frame includes all available data for STS-107, prior to loss of the vehicle and the end of data recording.

Comparison plots for each of the MADS strain gages were individually reviewed and assessed. Where appropriate, tabular point-by-point data was extracted, and additional analysis performed. Trends amongst gages were assessed, and gage response categories were defined.

7.3.3 Results

7.3.3.1 Ascent

All STS-107 MADS PCM strain data, without exception, was nominal during the ascent flight regime. No significant anomalies were noted. Comparison of ascent strain gage load indicators showed STS-107 ascent loads to be within the family of previous OV-102 flight experience. There was no discernable evidence of an impact load to the vehicle near MET +81.7 seconds. At the PCM sample rate of 10 samples per second, no such evidence is expected to be present. Both the extremely short duration of the impact load (0.003 to 0.005 seconds), and the range of wing modes (6 Hz and above) preclude such evidence. An interesting signature near this time was evident in some strain gages. The response was noted on left wing, right wing, and vertical tail gages. Further study and scrutiny showed that the signature was inconsistent with impact loading, and attributable to a nominal ascent load response. A review of accelerometer data did show signatures consistent with impact loading. This assessment is discussed in Section 7.4.

For reference, a typical PCM ascent strain gage comparison plot is shown in the Stress Appendix, Section 7.6, as Figure 7.6-6. Figure 7.6-7 illustrates the interesting signature noted near the suspect debris impact event, in comparison to data from STS-109, the previous flight of OV-102.

7.3.3.2 Entry - General

Comparison plots for the entry flight regime showed STS-107 data to be appreciably off-nominal versus previous flight experience after EI+490 seconds. Numerous anomalies were noted, most significantly on the left wing and elevon gages.

Due to the snapshot mode data recording on channel PCM3, data for these strain gages was largely not helpful in providing significant inputs to the analysis effort. Without continuous data, reliable conclusions regarding structural responses were not possible. Where possible, implications of off-nominal trends were identified, and data provided to the timeline team. This was the extent of the analysis effort for PCM3 strain gages.

Two sample PCM3 plots are included in the Stress Appendix, Section 7.6. Figure 7.6-8 shows a typical PCM3 comparison plot. Figure 7.6-9 illustrates a PCM3 gage with an apparent off-nominal trend.

The analysis effort focused on PCM1 and PCM2 gages that provided continuous data during the entry flight regime. This includes all PCM1 and PCM2 gages on the left and right wings, and 20 gages (10 on each side) on the elevon structure.

Loading levels during the initial stages of entry, prior to observation of significant off-nominal trends, were nominal as compared to previous flight experience. Maximum entry loading levels are nominally recorded during the TAEM region of flight, as shown by example in Figure 7.6-21.

7.3.3.3 Entry - Right Wing

In general, right wing strain gages showed nominal responses on STS-107 versus previous flights until immediately prior to loss of data (approximately 930 seconds after entry interface). Most, 49 of 85, right wing gages show this typical, nominal response, along with 8 of 10 right wing elevon gages. A sample plot is included for reference as Figure 7.6-10.

There were 19 right wing gages that show evidence of a brief, low magnitude off-nominal response initiating at EI+500 seconds. This signature is characterized by a 1 or 2 bit discrepancy versus previous flight experience, lasting as long as approximately 30 seconds. Following this time, strain values return to nominal tracking. This response was also noted on two right wing elevon gages. No instrumentation

malfunction has been identified in these gages at this time. The only reasonable hypothesis from a real strain perspective is internal pressurization following initial breach of the wing leading edge spar (both wings and the mid-fuselage share common venting). However, this hypothesis would not be consistent with the almost immediate return to nominal readings. The source of this phenomenon therefore is not conclusively understood at this time. A sample plot is included for reference as Figure 7.6-11.

There were 17 right wing gages that show an off-nominal response, initiating near EI+500 seconds, which creates a subsequent data offset versus previous flight experience. This signature is characterized by an off-nominal slope change of approximately 120 seconds duration, followed by a return to nominal tracking with a built-in offset, up to the loss of data. Again, this phenomenon may be explained by a transient internal pressurization effect, instigated by initial WLE spar breach, and relieved by a secondary external breach that subsequently reduces internal pressure. No instrumentation malfunction has been identified in these gages at this time. A sample plot is included for reference as Figure 7.6-12.

One right wing gage, V12G9653A (right wing upper skin at Xo1218, Yo245) showed a nominal response during ascent, but had no data recorded for entry. This gage is presumed to have failed at some point during the on-orbit period of STS-107. This type of on-orbit gage failure is not unusual in previous flight experience.

7.3.3.4 Entry - Left Wing

In contrast, the majority of left wing gages show indications of failure initiating between EI+486 seconds and EI+590 seconds. The vast majority, 42 of 45, of left wing gages, and all 10 left elevon gages show this typical response. The gage failure signature is characterized by sudden, rapid slope change driving strain to off-scale band edge values. In many instances, the gage signature oscillates between off-scale high and off-scale low values before settling at a “flatline”, steady-state response. This steady-state value is dictated by the instrumentation bias of a particular gage, and may or may not equal zero. Numerous gages show an off-nominal slope change that significantly precedes the dramatic off-scale event. The off-scale event, as well as the preceding off-nominal slope change, is attributed to burning of the strain gage wiring. These events are not consistent with literal strain responses to mechanical, thermal, or pressure loading. No significant correlation was found between strain gage location on the vehicle and initiation time of strain gage failure, as illustrated in Figure 7.6-22.

Significant unpredictability in the burning phenomenon dictates that individual gages show unique manifestations of the failure event. For example, not all gages “flatline” following the off-scale excursions. The period or number of oscillations between upper and lower band edge values also is variable from gage to gage.

Following the initial off-scale excursion, or off-nominal inflection toward such an excursion, strain gage data is considered invalid, due to the wire burning condition. Subsequent data therefore is an indication only of the wire-burning phenomenon, and not of structural strain gage responses.

Several representative samples of left wing and left wing elevon strain gage failure comparison plots are included for reference in the Stress Appendix, Section 7.6. Please refer to Figure 7.6-13 through Figure 7.6-17.

The remaining three left wing strain gages were the subjects of significant additional analysis effort. V12G9921A, located on the wing leading edge spar near RCC panel #9, showed the earliest off-nominal response of any strain gage, initiating near EI+270 seconds. Numerous slope changes and a change in sign of the strain value followed, prior to initiation of a gage failure signature after EI+470 seconds. Off-nominal strain values for this measurement are attributed to localized, thermally-induced strain and structural failure. This analysis is discussed separately in Section 7.1. The comparison plot for V12G9921A is included for reference as Figure 7.6-18.

Gages V12G9048A and V12G9049A, located on the lower and upper Xo1040 spar caps, respectively, in the center of the wheel well forward wall (Yo135) were the only two left wing gages that did not clearly indicate failure prior to EI+930 seconds. As these gages did not join wire bundles until just prior to

penetration of the mid-fuselage sidewall, this data would suggest an absence of direct plume impingement in the glove area forward of the wheel well. Both of these gages showed significant off-nominal trends, however, at earlier times. V12G9048A showed initiation of an off nominal trend at EI+489 seconds, which continued to the loss of data. Likewise, V12G9049A first showed initiation of an off-nominal trend at EI+568 seconds, again continuing until loss of data. These off-nominal trends are likely attributable to local thermal effects, possibly combined with instrumentation malfunction, as discussed separately in Section 7.2. Comparison plots for V12G9048A and V12G9049A are included for reference as Figure 7.6-19 and Figure 7.6-20, respectively.

7.3.4 Conclusions

Comparison of STS-107 MADS PCM strain gage data to previous flight data offers strong evidence and support for the STS-107 accident investigation. Specifically, the strain data offers support for failure scenarios with breach of the wing leading edge spar outboard of the Yo167 rib.

PCM strain gage data from the ascent regime shows no indications of off-nominal structural loads. Load levels for ascent are within the family of previous OV-102 flight experience.

During the entry regime, significant off-nominal behavior was identified. This off-nominal behavior is attributed primarily to combined influences of instrumentation failure and localized off-nominal thermal effects.

The typical left wing entry signature is indicative of instrumentation failure due to burning of wires inside the left wing. This failure pattern corroborates wire bundle burn-through scenarios developed in the previous analysis of telemetered OI data.

Significant early off-nominal strains in V12G9921A provide evidence of localized thermal effects in the area of RCC Panel #9.

Gages V12G9048A and V12G9049A, unlike all other left wing strain gages, do not show clear indications of instrumentation failure prior to loss of data. These two gages' wiring join bundles further forward than all other strain gages. Again, this data supports evidence of wire burning in the main left wing cavity. Off-nominal strains due to local thermal effects in these gages provide further clues regarding hot gas venting following initial intrusion into the left wing cavity.

7.4 Accelerometer Evaluation

Accelerometer and higher sample rate strain gage responses during STS-107 are studied during ascent and entry phases of the flight to identify any anomalous response. They were also compared to STS-109 and other OV-102 flight data to determine if the responses are within the family experience.

7.4.1 Ascent

The locations of the accelerometers are shown In Figure 7.4-1. They include 15 accelerometers on the wing/elevons, body flap and vertical tail/rudders, and 11 measurements on the longeron. In addition, there are 36 strain gages in the vertical tail and OMS deck area.

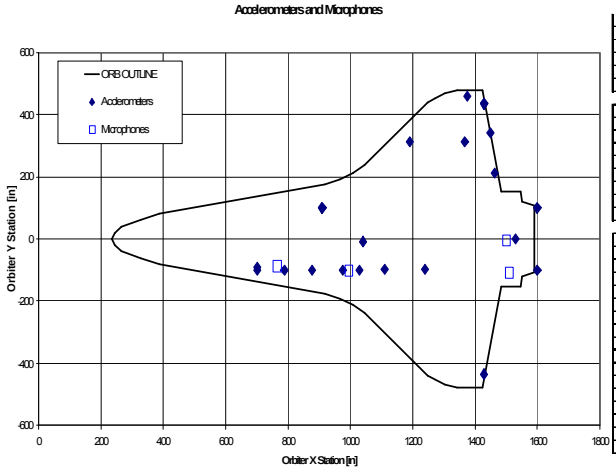

MISD	DFI	NOMENCLATURE	X	-Y	Z
		Microphones			
V08Y8006A	MADS	LH PAYLOAD BAY VENT #3 X765	765.3	-86.5	382.6
V08Y8039A	MADS	PAYLOAD BAY LH VENT NO 5 X994	994.0	-100.0	
V08Y9684A	MADS	AM ON HT SHLD Y-100 Z320 MAF004	1510.1	-107.3	316.4
V08Y9686A	MADS	AM AFT FUS HS CTR YO Z400 MAF006	1499.6	-2.4	384.9
		Accelerometers			
V34A9432A	MADS	LH LNGN ACCEL Z-AXIS X976	976.5	-101.5	407.5
V34A9460A	MADS	LH LNGN ACCEL Y-AXIS X701	701.2	-100.8	407.0
V34A9461A	MADS	LH LNGN ACCEL Z-AXIS X701	701.2	-91.3	407.5
V34A9464A	MADS	LH LNGN ACCEL Z-AXIS X877	877.2	-101.3	407.5
V34A9481A	MADS	KEEL ACCEL V-AXIS X1040,Y=0	1040.0	-8.5	LWR
V34A9482A	MADS	LH LNGN ACCEL Z-AXIS X790	788.3	-101.3	407.5
V34A9483A	MADS	LH LNGN ACCEL X-AXIS X1029	1029.0	-101.3	407.7
V34A9484A	MADS	LH LNGN ACCEL Z-AXIS X1110	1110.0	-96.8	407.3
V34A9485A	MADS	LH LNGN ACCEL Z-AXIS X1229	1238.7	-97.0	407.5
		Accelerometers			
V08D8037A	MADS	RH LONGERON Y-AXIS VIB	910.0	99.4	409.0
V08D8038A	MADS	RH LONGERON Z-AXIS VIB	910.0	99.4	409.0
V08D9062A	MADS	LFAF BF AFT-R Z-VIB AOB-16	1600.0	100.0	
V08D9063A	MADS	LFAF BF AFT-L Z-VIB AOB-17	1600.0	-100.0	
V08D9064A	MADS	LFAF BF HL CTR Z-VIB AOB-18	1530.0	0.0	
V08D9699A	MADS	LFAF L OTBD ELEV OTBD Y-VIB	1429.4	435.0	
V08D9729A	MADS	LFAF R OTBD ELEV OTBD Z-VIB	1428.6	-435.0	
V08D9737A	MADS	LFAF R OTBD ELEV OTBD Z-VIB	1428.6	435.0	
V08D9738A	MADS	LFAF R OTBD ELEV INBD Z-VIB	1449.1	342.5	
V08D9764A	MADS	LFAF R WING TIP AFT Z-VIB	1376.0	460.0	
V08D9765A	MADS	LFAF R WING OTBD-MID Z-VIB	1191.0	312.5	
V08D9766A	MADS	LFAF R WING X1365,Y312 Z-VIB	1367.0	312.0	
V08D9784A	MADS	LFAF R INBD ELEV-CTR Z-VIB	1462.6	212.0	
V08D9694A	MADS	LFAF V/S RSS262 A SPAR Y-VIB	1569.9	LH	710.0
V08D9789A	MADS	LFAF V/S RSS158 F SPAR Z-VIB	1459.9		671.5
V08D9795A	MADS	LFAF R SP BK UPR BOT Y-VIB	1620.9	RH	633.0
V08D9797A	MADS	LFAF R SP BK LWR TOP Y-VIB	1600.4	RH	593.2

Figure 7.4-1 Measurement Locations

In general, the responses from STS-107 and STS-109 are very similar for the most part. Shown in Figure 7.4-2 is a comparison of typical accelerometer responses. The magnitude is very comparable throughout the flight. The large amplitude responses at near M=1 are also very similar. (The peak response noted at ~82 seconds will be discussed later in detail) The RMS (Root Mean Square) values of all accelerometers for wing and tail accelerometers are shown in Table 7.4-1 and illustrate the overall amplitude is very similar. The PSD's of three measurements (Left outboard elevon, Right wing tip, Body flap) are shown in Figure 7.4-3. The results computed using 20-80 second data block demonstrate no significant change in the magnitude and frequency contents between the two flights.

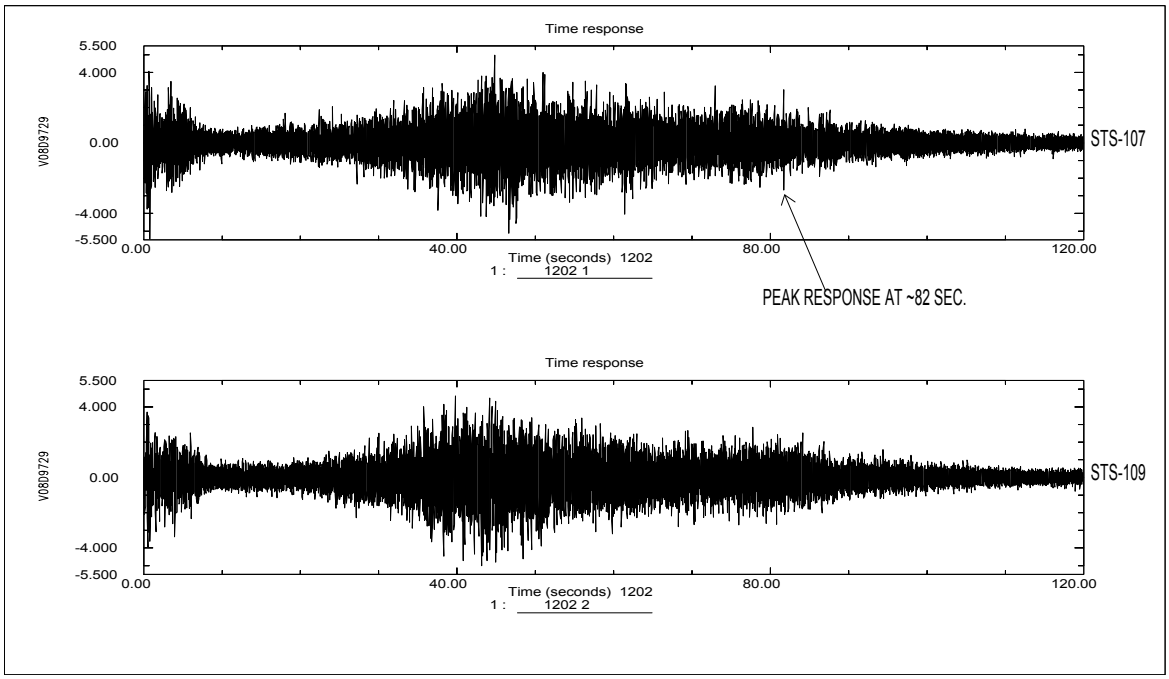

Figure 7.4-2 Comparison of Left Outboard Elevon Response (STS-107 VS. STS-109)

Table 7.4-1 Summary of RMS Acceleration

	T= 0-120 sec		T= 20-80sec.	
	STS107	STS109	STS107	STS109
VO8D9729A (L. OB Elevon)	.74	.78	.92	.98
VO8D9737A (R. OB Elevon)	.75	.75	.95	.95
VO8D9738A (R. OB Elevon)	.78	.75	.99	.95
VO8D9784A (R. IB Elevon)	.91	.90	1.23	1.22
VO8D9764A (R. Wing)	.73	.74	.92	.92
VO8D9766A (R. Wing)	.42	.41	.52	.51
VO8D9765A (R. Wing)	.35	.35	.40	.39
VO8D9064A (Body Flap)	.74	.85	.96	1.09
VO8D9062A (Body Flap)	3.51	3.79	4.85	5.09
VO8D9063A (Body Flap)	1.74	1.78	2.03	1.90
VO8D9699A (Vertical Tail)	.40	.36	.44	.37
VO8D9795A (Upper R. Rudder)	.52	.52	.68	.67
VO8D9694A (Vertical Tail)	.30	.28	.38	.33
VO8D9789A (Vertical Tail)	.43	.39	.52	.44
VO8D9797A (Lower R. Rudder)	---	---	---	---

Left Outboard Elevon Accelerometer

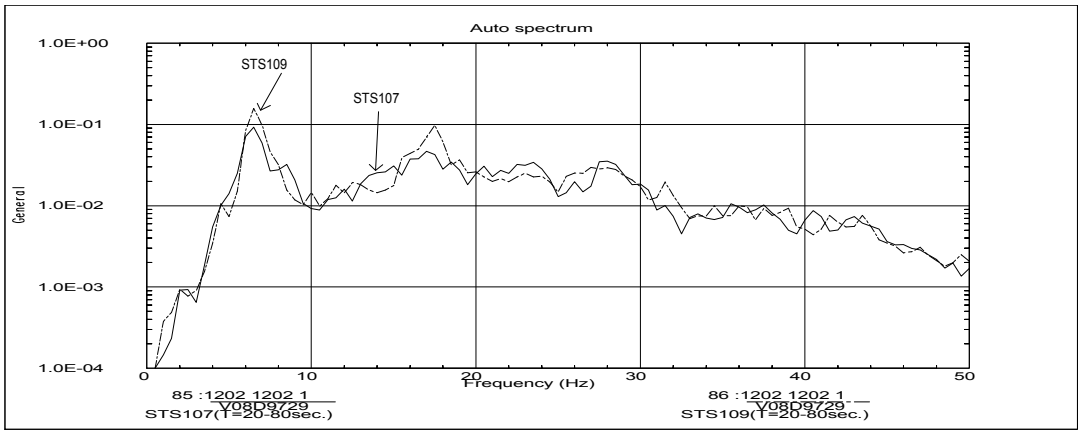

Right Wing Tip Accelerometer

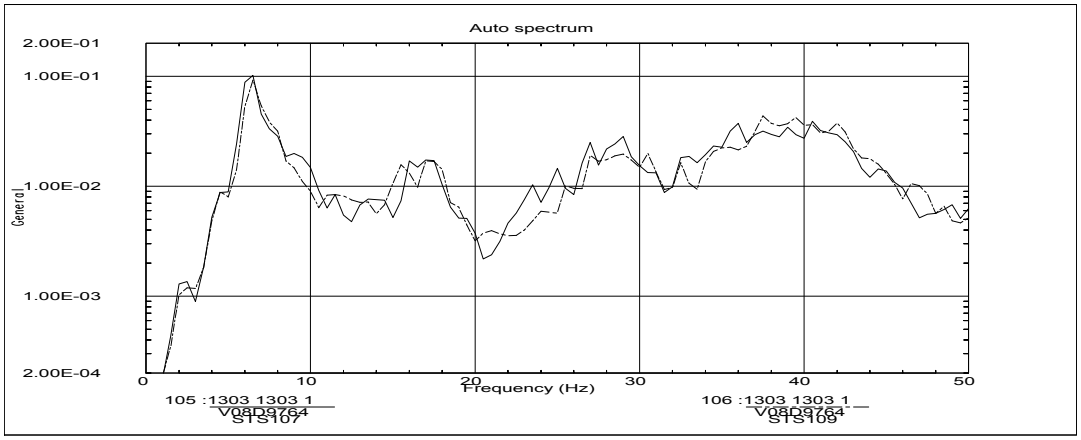

Body Flap Accelerometer

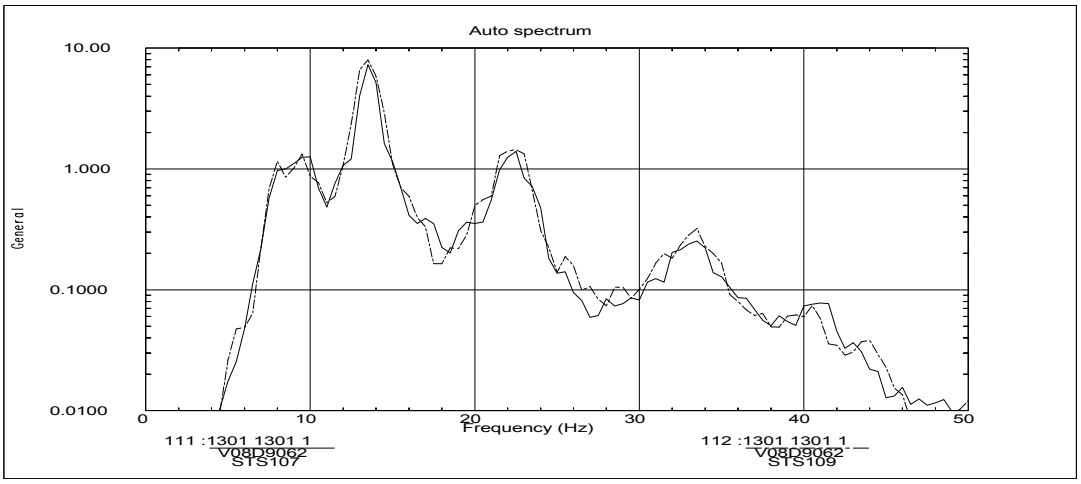

Figure 7.4-3 PSD's Comparison (STS-107 VS. STS109)

The only notable differences in the RMS acceleration are the three tail accelerometers, which are highlighted in the table. They show approximately 15-20% higher response during STS-107 compared to STS-109 results. The reason for the increase is the difference in the tail response near 40-42 second range, as noted in Figure 7.4-4. The PSD's during this time period shown in Figure 7.4-5 verify significantly higher response of the tail's 2nd and 3rd bending modes at the 20 to 40 Hz range.

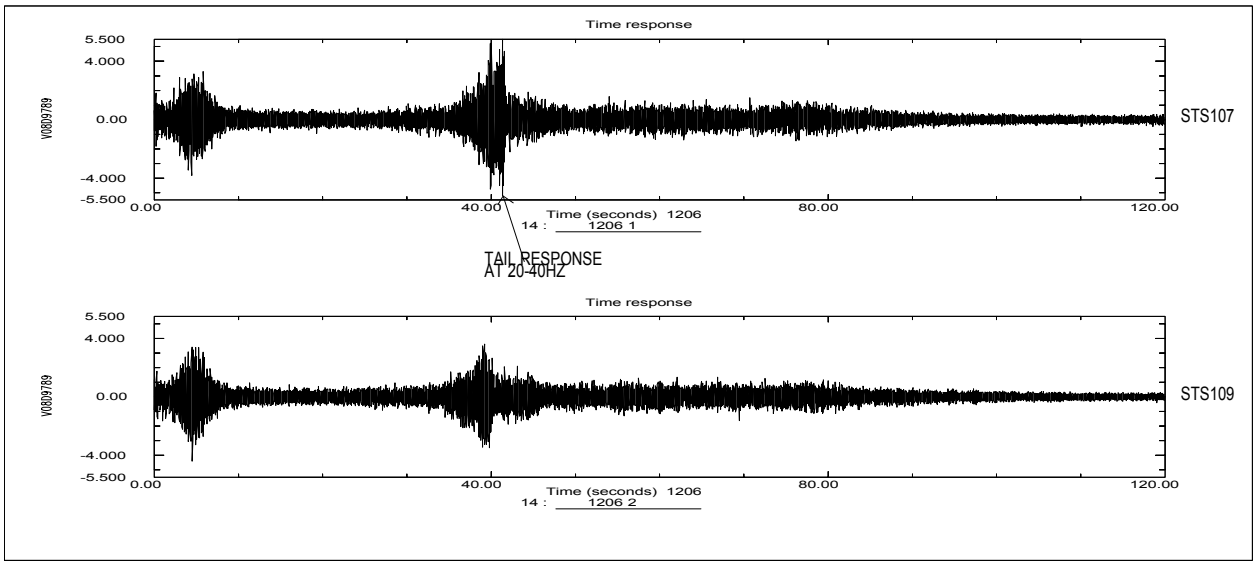

Figure 7.4-4 Vertical Tail Response during Ascent (STS-107 VS. STS-109)

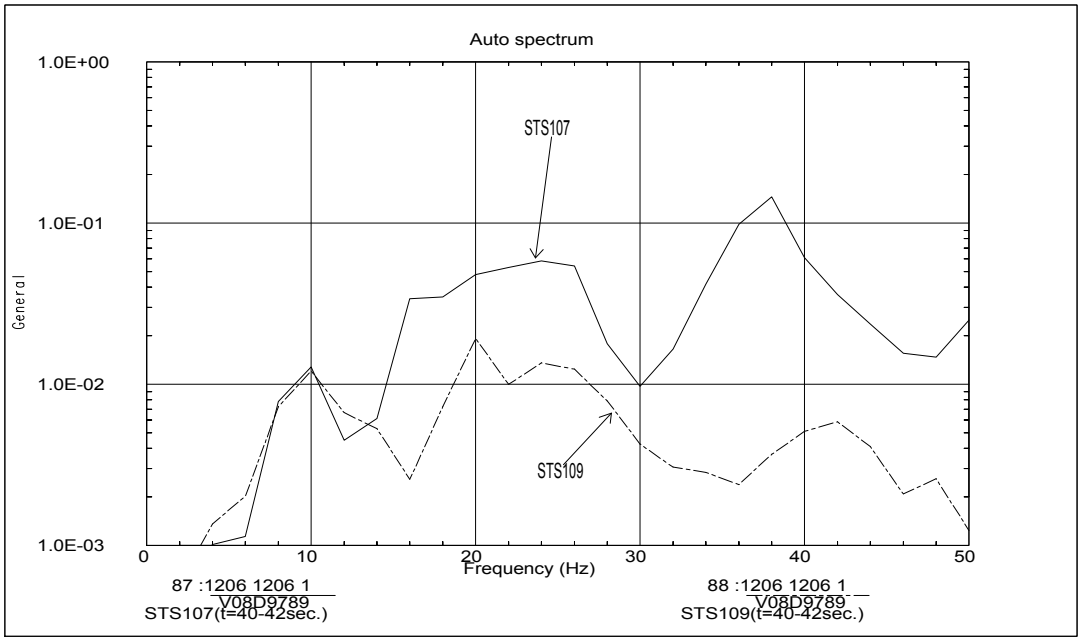

Figure 7.4-5 PSD Comparison of Vertical Tail Response at T=40-42 sec. (STS-107 VS. STS-109)

This type of variation in response is considered a normal behavior of tail reacting to buffeting environment near M=1, where the turbulent effect of the air is the greatest. The degree of turbulence level and the frequency content in air flow can vary flight to flight, which can result in different types of modes being excited. A similar characteristic was observed during STS-87 as presented in Figure 7.4-6. The PSD's from two flights are remarkably similar in magnitude and frequency contents. The results indicate the excitation of higher order tail mode during STS-107 is not unique and is considered within the family experience.

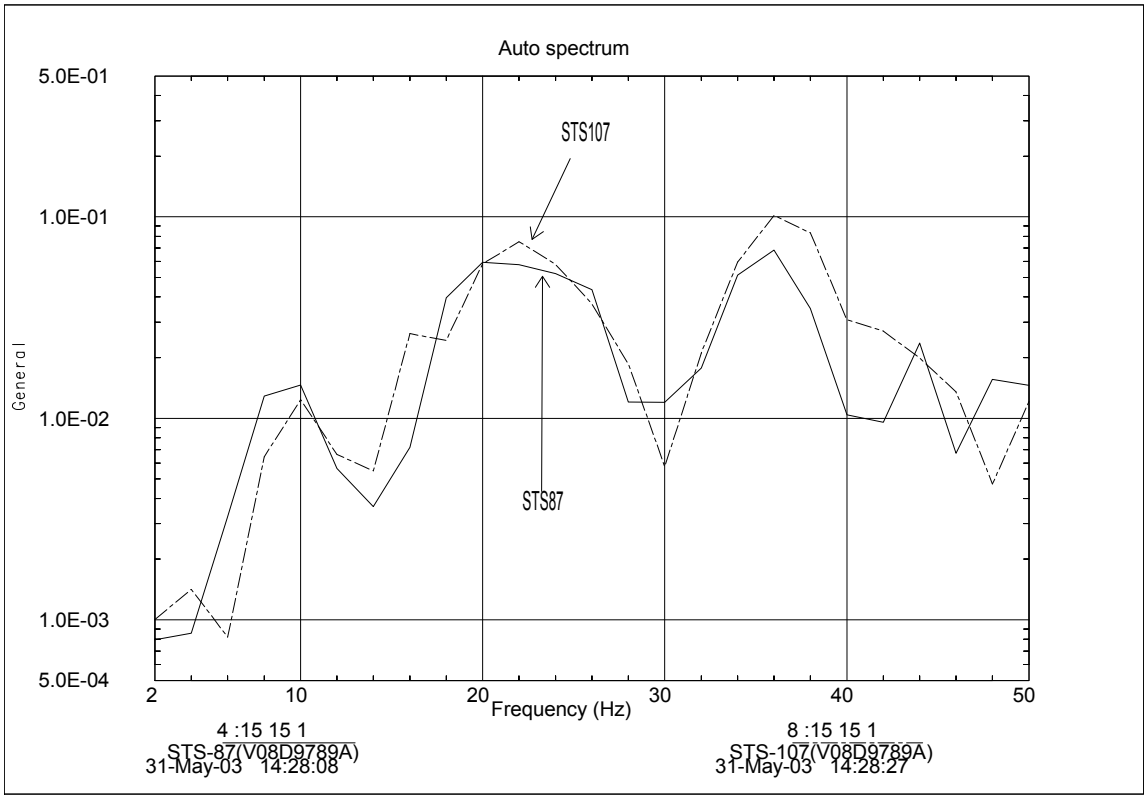

Figure 7.4-6 PSD Comparison of Tail Responses (STS-107 VS. STS-87) (T=40-42 sec.)

7.4.1.1 Evaluation of Peak Response at ~82 Seconds

An in-depth study was made to investigate if the peak responses observed at the left outboard elevon accelerometer at ~82 seconds is due to the debris impact. Normally, sharp spikes in acceleration are observed at times during the ascent phase of the flight due to buffeting event(s). The buffeting load is most significant during the transonic region. However, it still exists at higher Mach numbers, which results in structural excitation. Shown in Figure 7.4-7 is the left and right outboard elevon comparison for the 10 second period near 82 seconds. The peak response is noticeable only for the left outboard location. Filtered responses presented in Figure 7.4-8 verify several wing/elevons were excited at 82 seconds. The 2nd wing bending response constitutes the largest component of the peak amplitude. In addition, the responses of 3rd wing bending and elevon torsion modes contributed to the peak response.

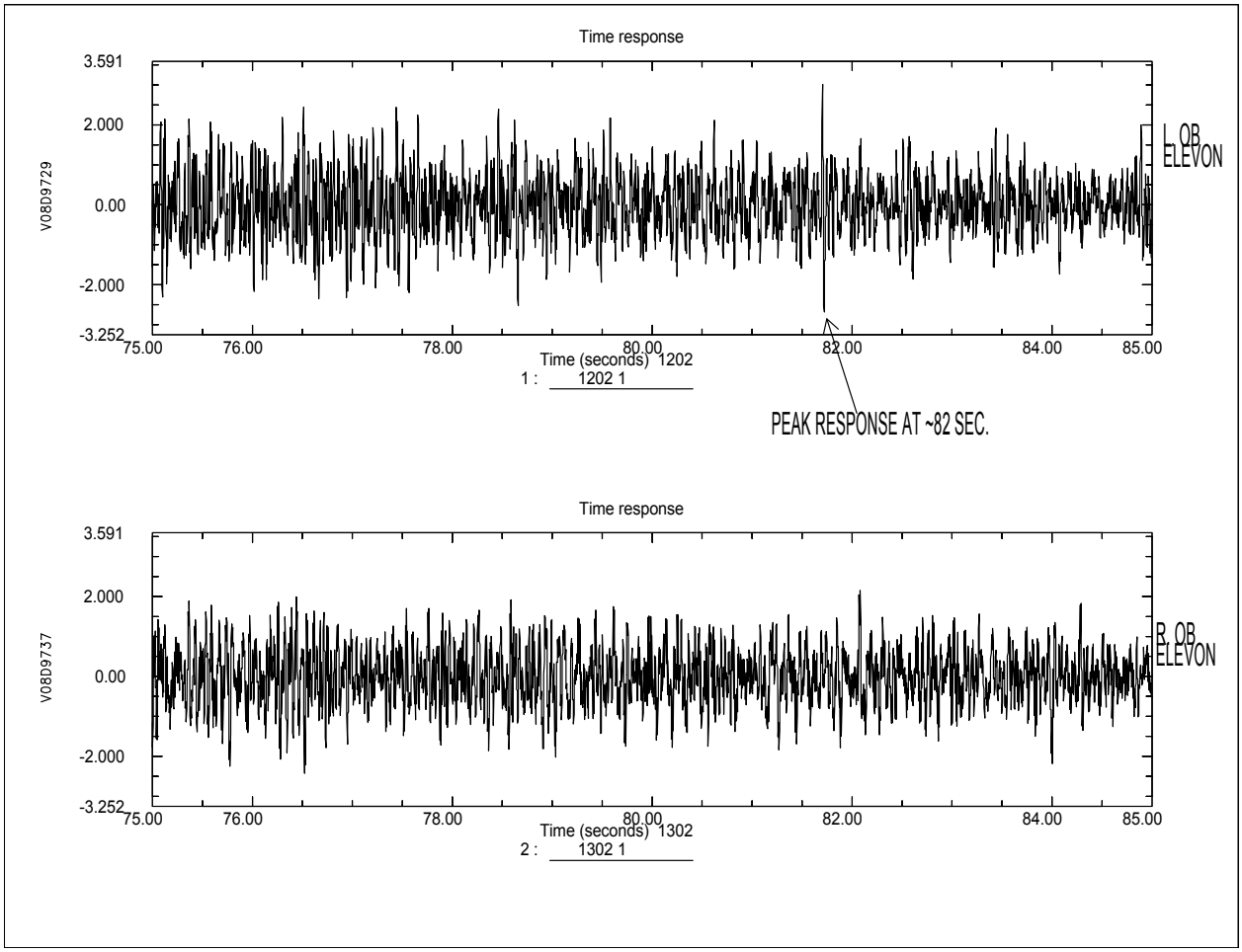

Figure 7.4-7 Right and Left Outboard Elevon Response at ~82 seconds

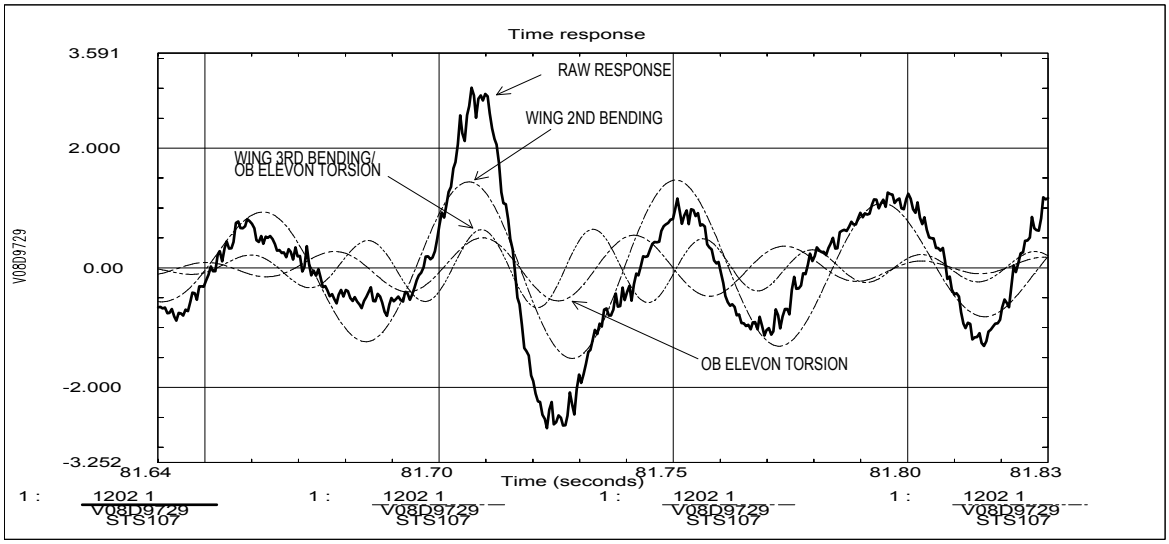

Figure 7.4-8 Excitation of Various Wing/Elevon Modes at ~82 sec. (Left Outboard Elevon)

To determine if the debris impact can cause the type of responses observed in the flight data, analyses were performed using the FEM model of the wing combined with the reduced model of the Orbiter, which provides the back-up structure's stiffness and mass (Figure 7.4-9). An impulse of 3,000 lbs force (with 0.005 second duration) in Z-direction was applied to the node closest to the RCC panel #8. The impulse of this magnitude is reasonable for a 1.5 lb object with a velocity of 530 MPH impacting the surface at 15 degrees inclination.

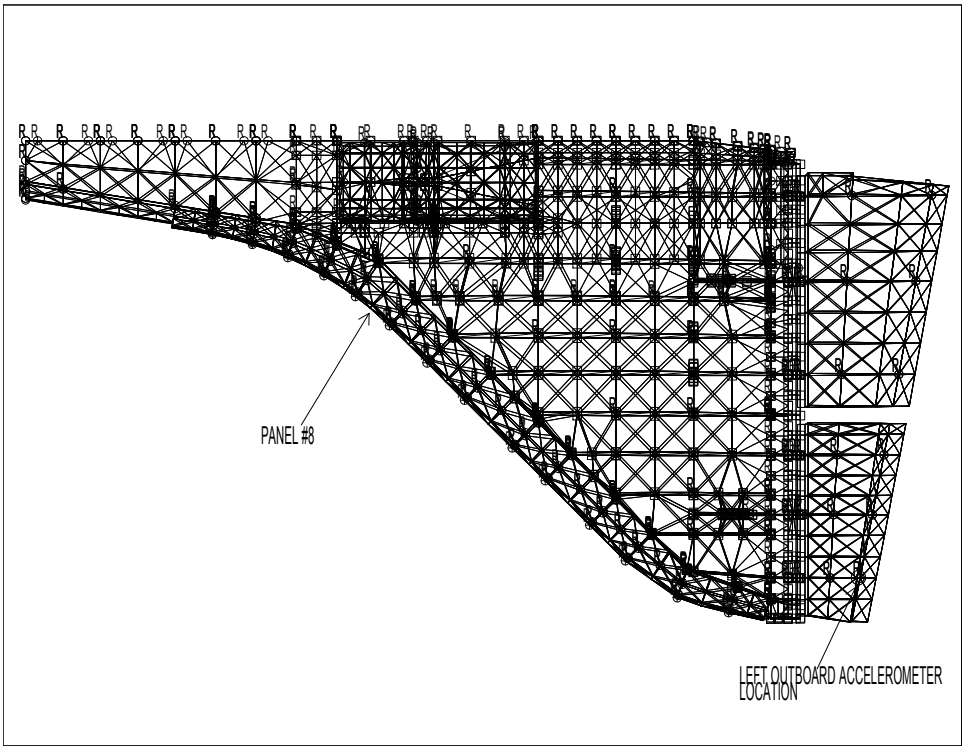

Figure 7.4-9 FEM Model of Wing Structure

Shown in Figure 7.4-10 is the recovered acceleration at the left outboard elevon location from the transient analysis. The FFT (Figure 7.4-11) of the response indicates excitation of several wing modes, including wing's 2nd and 3rd bending modes. The filtered responses shown in Figure 7.4-12 illustrate the 3rd wing bending mode constitutes the majority of the peak amplitude, while the 2nd wing bending and elevon torsion modes also contribute to the peak response. The acceleration computed using the FEM model is shown along with the flight measured data in Figure 7.4-13. The shapes of acceleration signatures are comparable at the onset of debris impact. The frequency from the analysis is higher, since the 3rd wing bending mode is excited the most compared with the 2nd wing bending mode experienced during STS-107. More pronounced 3rd wing bending response from analysis could be attributed to possible deviations from the assumed location and duration of impact event, and some uncertainty in the FEM models for higher order wing modes. Nevertheless, similar acceleration signature and the excitation of higher order wing modes from the analysis indicate that the debris impact quite possibly could have caused the peak acceleration on the left outboard elevon at ~82 seconds in addition to other aerodynamic disturbances, such as buffeting and shocks. An absence of additional sensors on the left wing make it difficult to make conclusive remarks.

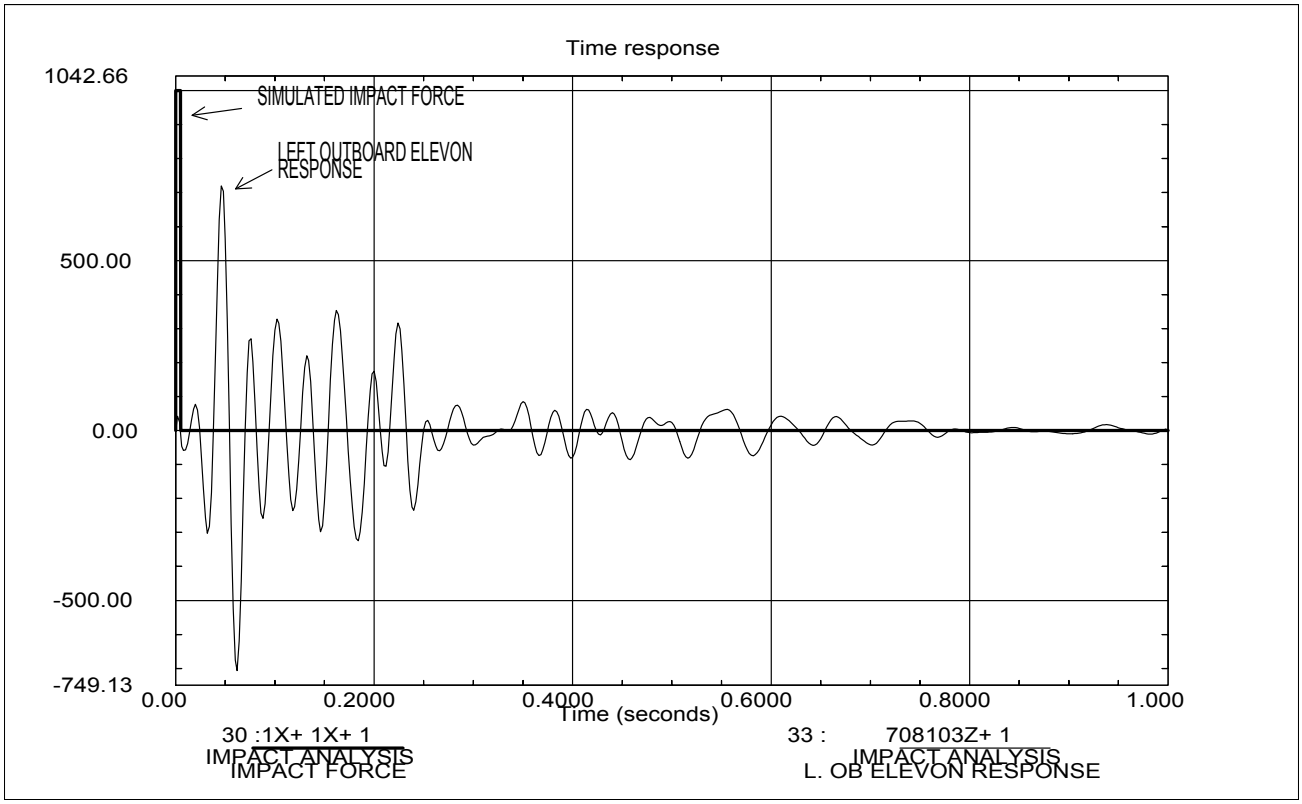

Figure 7.4-10 Outboard Elevon Response from Impact Analysis

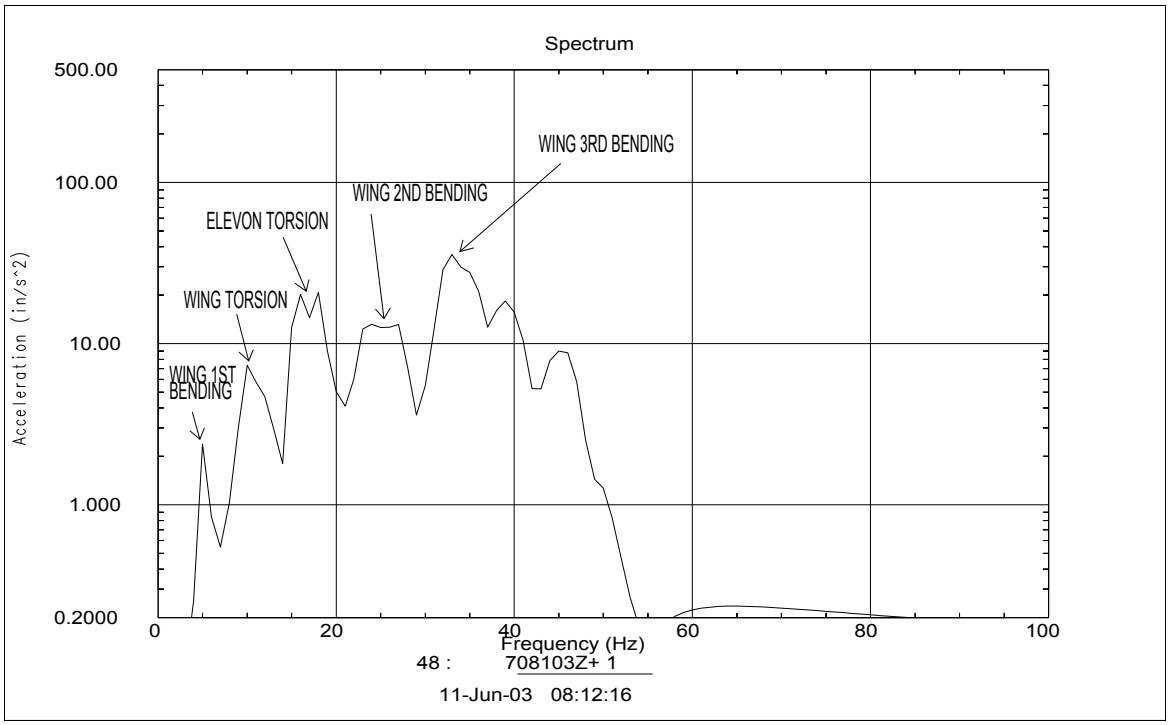

Figure 7.4-11 FFT at Outboard Elevon Location (Impact Analysis)

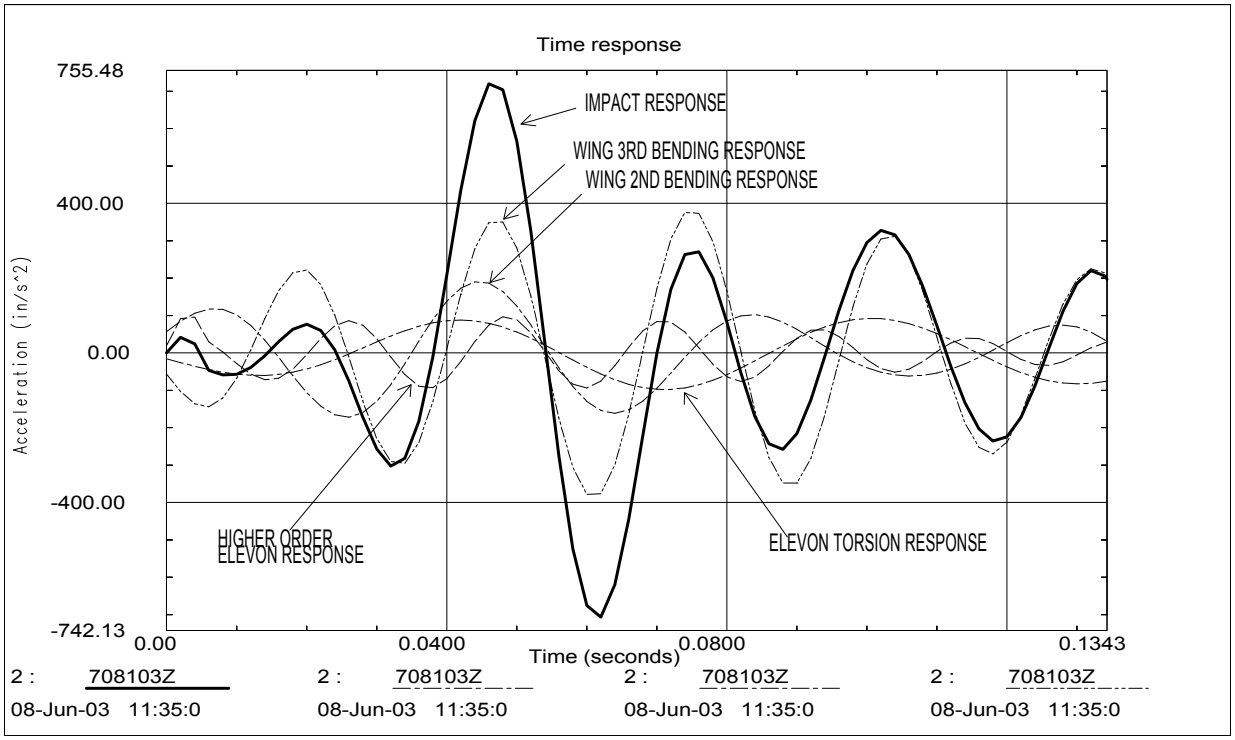

Figure 7.4-12 Excitation of Various Wing/Elevon Modes (Impact Analysis)

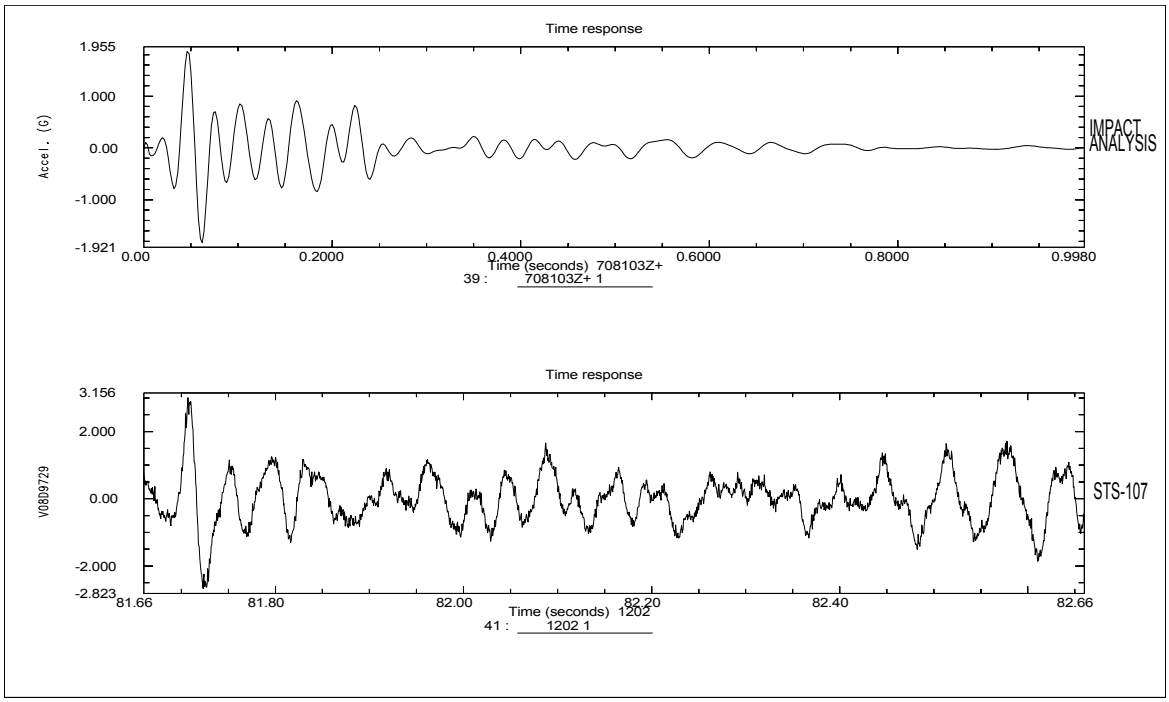

Figure 7.4-13 Comparison of Analysis and Flight Measurement

7.4.1.2 Flutter Assessment

A flutter assessment was made using wing and tail accelerometers. Previous flutter analysis had indicated the tail is the most critical component of the Orbiter for flutter instability. Flutter typically involves a coalescence of bending and torsion modes and is considered most critical near M=1. To determine if flutter had occurred during STS-107, PSD's from tail accelerometers were computed at various times during ascent. The results displayed in Figure 7.4-14 show distinct peaks for the 1st bending mode of tail at 3-4 Hz and the torsion mode at 10-11 Hz throughout the flight. This demonstrates that the mode coalescence did not occur and the tail was stable. Shown in Figure 7.4-15 are the filtered responses of the lower rudder. The raw accelerometer responses are filtered so that predominantly the bending and torsion responses are displayed. The figure illustrates that the response for critical modes always decayed after external disturbances. Also, the responses of the tail's bending and torsion mode are clearly visible, which verify that two modes did not coalesce and, consequently, the flutter instability did not occur.

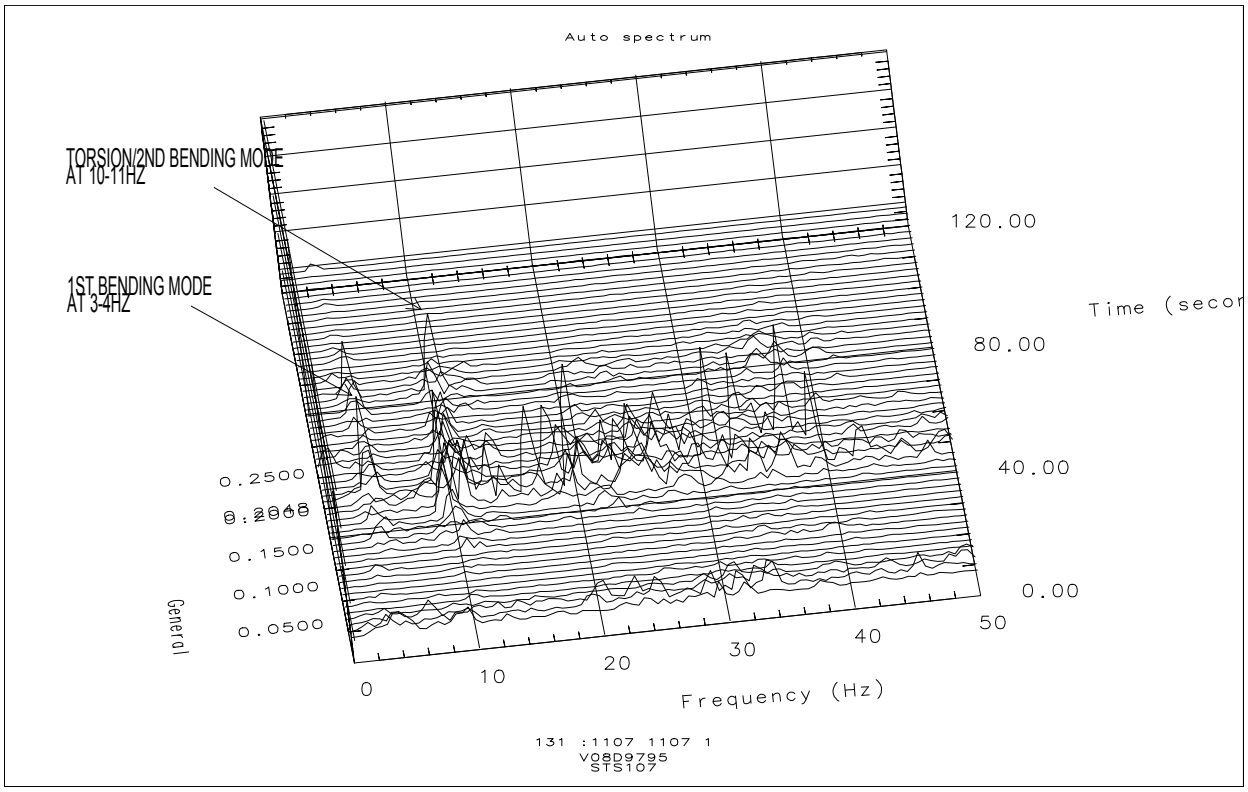

Figure 7.4-14 Vertical Tail Modes during STS-107

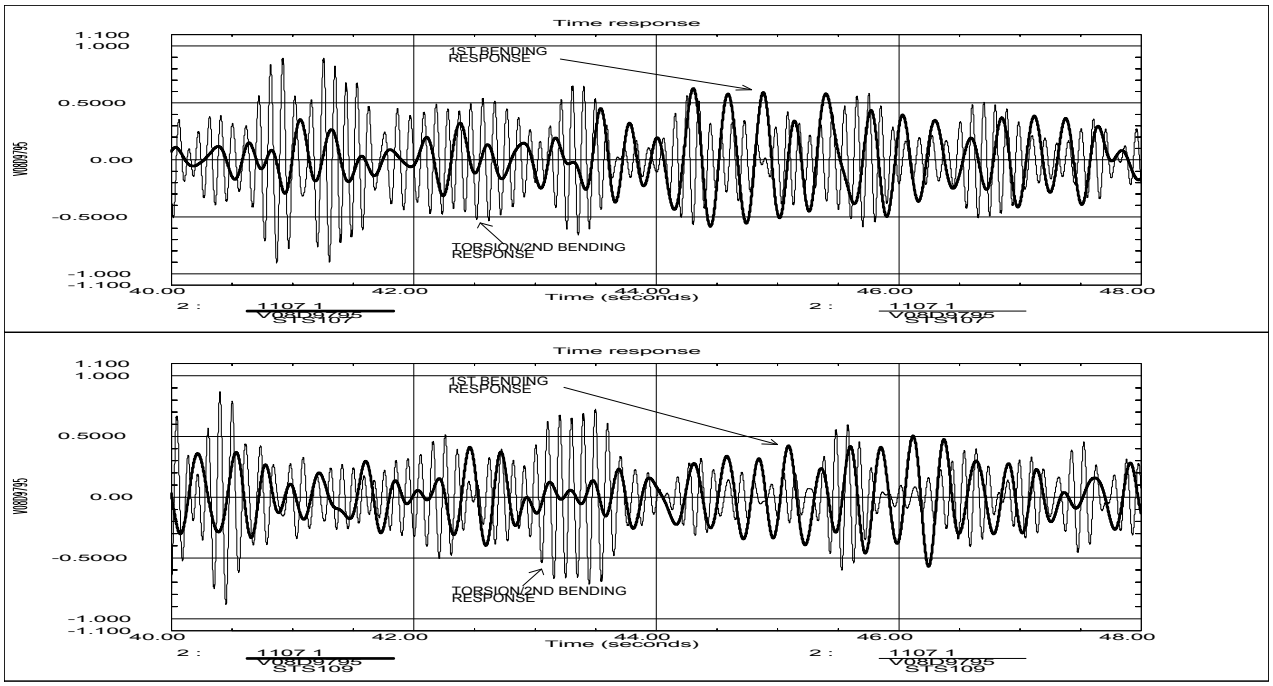

Figure 7.4-15 Filtered Response of Lower Rudder (STS-107 and STS-109)

For assessment of wing flutter instability, a similar process was employed. Presented in Figure 7.4-16 are the PSD's of the left outboard elevon accelerometer for STS-107 and STS-109. The distinct peaks for the 1st bending mode at ~6 Hz and torsion mode at ~8 Hz near M=1 are clearly visible. Thus, the mode coalescence did not occur for the wing during STS-107. The filtered responses shown in Figure 7.4-17 demonstrate the response of wing's bending and torsion modes did decay after aerodynamic disturbance, which confirms that the wing was far from flutter instability.

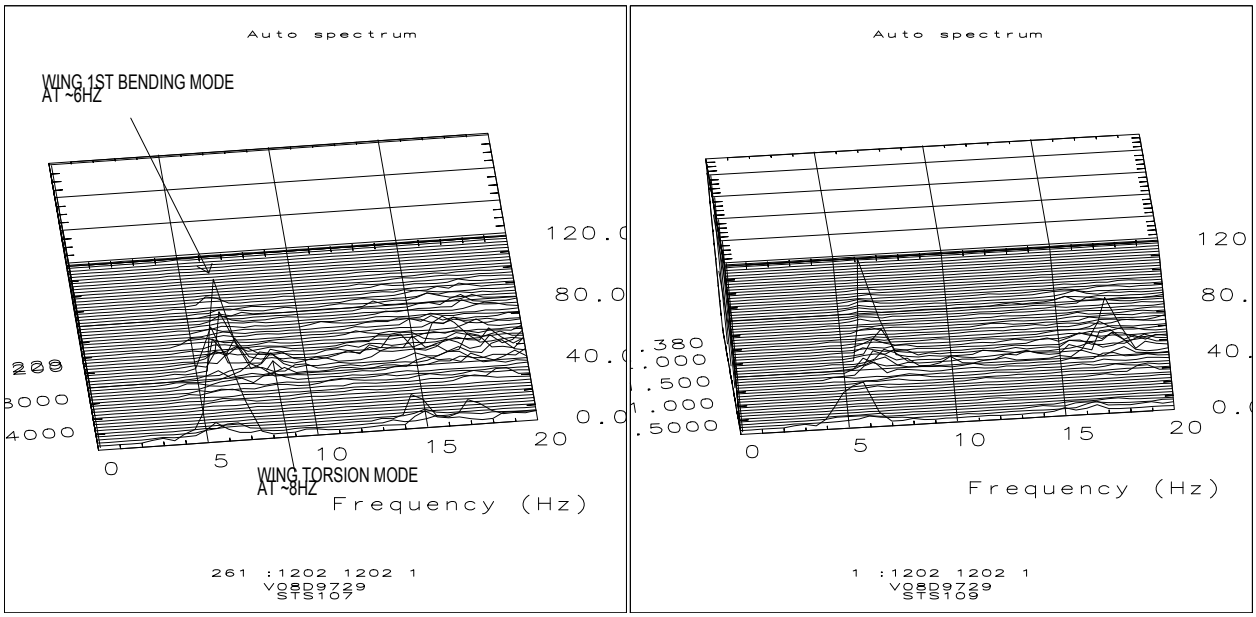

Figure 7.4-16 Wing Modes during STS-107 and STS-109

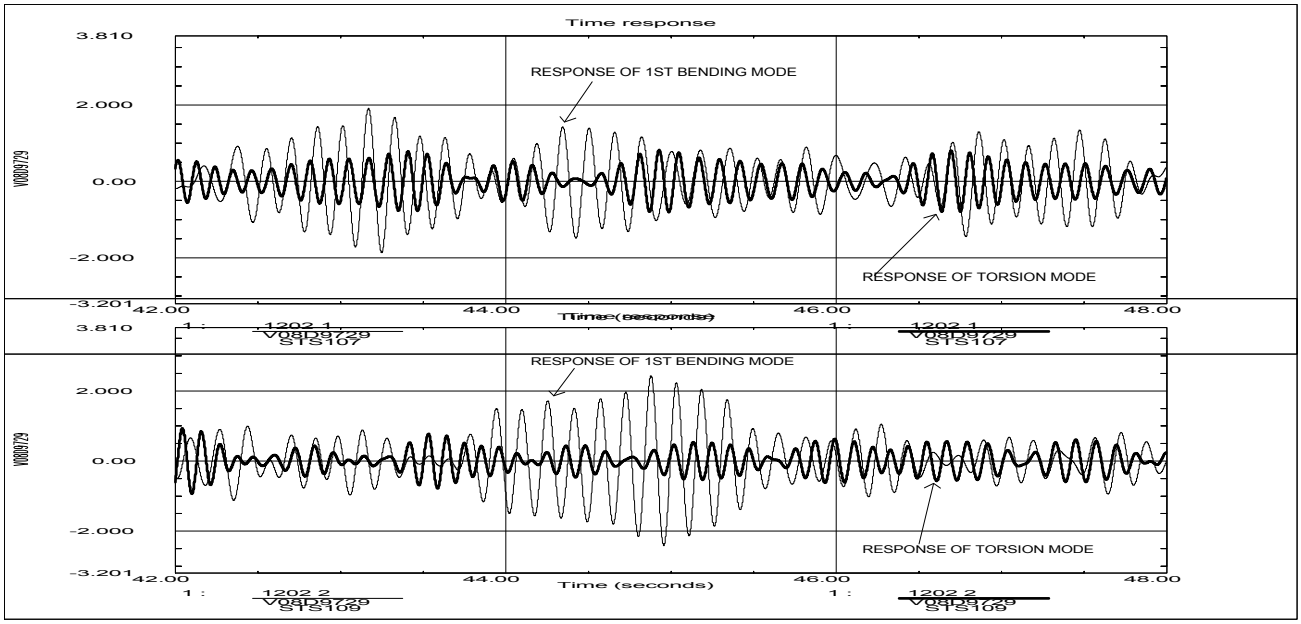

Figure 7.4-17 Filtered Response of Left Outboard Elevon (STS-107 and STS-109)

7.4.1.3 Strain Gage Response

The ascent strain gage data revealed the responses were very similar to STS-109. A comparison of typical gage response is shown in Figure 7.4-18. To compare the dynamic contents of the measurement, a 2-50 Hz band pass filter was applied to isolate the dynamic components. Plots shown in Figure 7.4-19 illustrate the response from two flights are very similar. The RMS values of strain shown in Table 7.4-2 also confirm that the overall level of dynamic strain is very comparable.

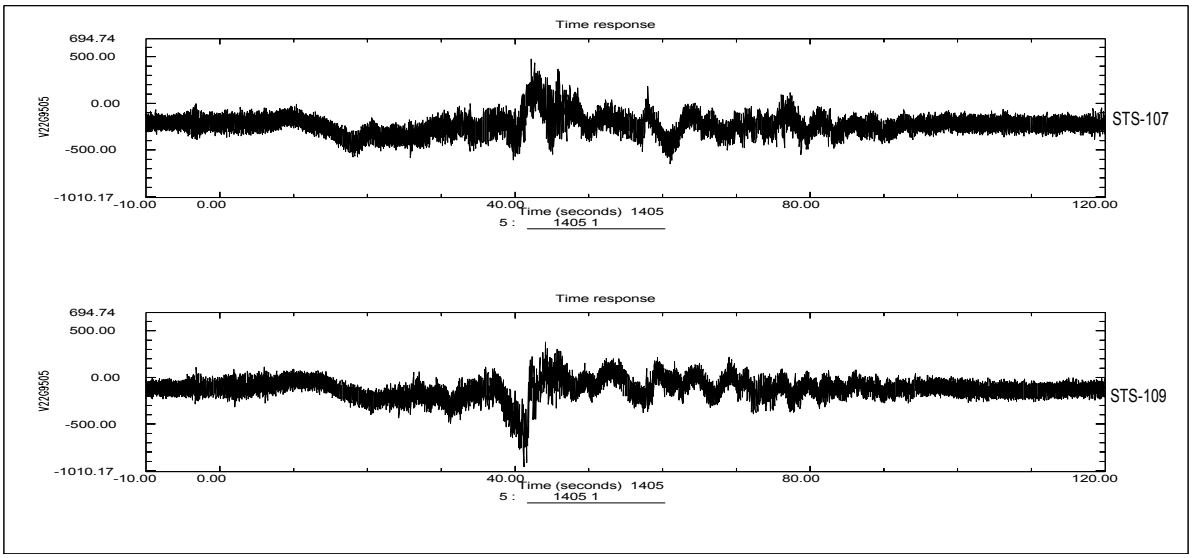

Figure 7.4-18 A Comparison of Strain Gage Response (Tail, Aft Spar Web)

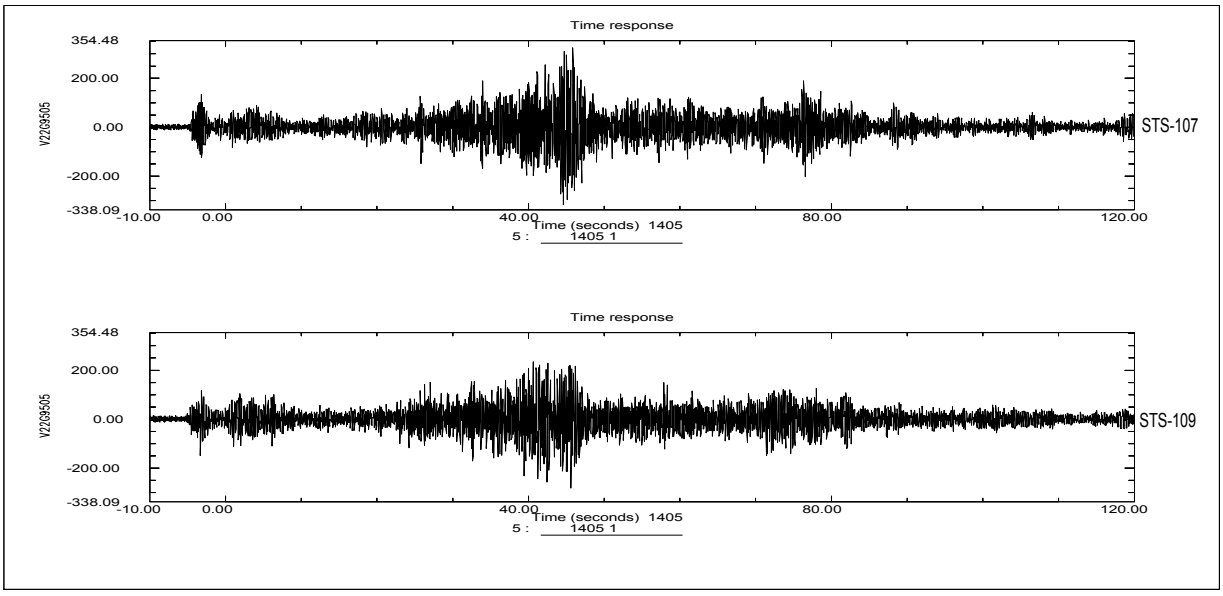

Figure 7.4-19 Dynamic Components of Strain Gage Response (Tail, Aft Spar Web)

Table 7.4-2 A Summary of RMS Values for Strain during Ascent

	T= 0-120 sec		T= 20-80sec.	
	STS107	STS109	STS107	STS109
V22G9501 A(V Fin, Aft Spar Web)	12.8	12.7	16.7	16.3
V22G9502 A(V Fin, Fwd Spar Web)	6.9	6.5	9.0	8.3
V22G9503A(V Fin, Aft Spar Web)	29.0	28.5	36.9	35.5
V22G9504A(V Fin, Fwd Spar Web)	8.9	8.3	11.7	10.9
V22G9505A(V Fin, Aft Spar Web)	45.1	41.5	59.6	53.6
V22G9506A(V Fin, Fwd Spar Web)	12.9	12.5	16.2	15.5
V35G9610A(Aft Fus, OMS Deck)	3.9	4.0	3.8	4.0
V35G9611A(Aft Fus, OMS Deck)	3.2	3.3	3.8	4.0
V35G9612A(Aft Fus, OMS Deck)	1.4	1.5	1.4	1.5
V35G9613A(Aft Fus, OMS Deck)	4.6	4.7	4.6	4.7
V35G9614A(Aft Fus, OMS Deck)	5.1	5.7	5.2	5.9
V35G9615A(Aft Fus, OMS Deck)	4.4	4.6	4.9	5.2
V35G9616A(Aft Fus, OMS Deck)	4.0	4.0	4.7	4.7
V35G9617A(Aft Fus, OMS Deck)	1.8	2.0	2.0	2.2
V35G9618A(Aft Fus, OMS Deck)	3.8	4.1	4.1	4.2
V35G9619A(Aft Fus, OMS Deck)	8.3	8.9	9.7	10.4
V35G9620A(Aft Fus, OMS Deck)	4.1	--	4.1	--
V35G9621A(Aft Fus, OMS Deck)	3.5	--	4.2	--
V35G9622A(Aft Fus, OMS Deck)	1.6	--	1.6	--
V35G9623A(Aft Fus, OMS Deck)	3.9	4.5	4.0	4.6
V35G9624A(Aft Fus, OMS Deck)	6.2	7.0	6.6	7.7
V35G9627A(Aft Fus, OMS Deck)	--	--	--	--
V23G9203A(L. Rud Hinge)	14.3	13.6	19.0	17.5
V23G9204A(L. Rud Hinge)	6.1	6.2	7.1	7.1
V23G9211A(L. Rud Hinge)	4.5	4.5	5.8	5.6
V23G9212A(L. Rud Hinge)	8.9	8.5	11.9	11.1
V23G9215A(L. Rud Hinge)	16.3	16.3	21.7	21.2
V23G9216A(L. Rud Hinge)	18.2	18.9	22.8	23.2
V23G9223A(R. Rud Hinge)	18.7	17.7	24.9	23.3
V23G9224A(R. Rud Hinge)	6.4	6.3	8.3	8.1
V23G9227A(R. Rud Hinge)	13.9	13.1	18.9	17.6
V23G9228A(R. Rud Hinge)	5.2	7.7	6.5	8.8
V23G9235A(R. Rud Hinge)	4.9	4.7	6.1	5.9
V23G9236A(R. Rud Hinge)	9.6	8.7	13.0	11.4
VO8G8041A(Heat Shield)	10.5	10.6	11.8	12.0
VO8G9091A(STN BHS Strut)	37.9	39.5	41.3	43.5

7.4.2 Descent

Although the overall level of acceleration during entry was small compared to ascent, accelerometer data were examined in detail to identify anomalous responses, which might correlate with events during entry. In particular, the left outboard elevon accelerometer (VO8D9729A) was thoroughly studied, since this was the only accelerometer on the left side of the wing. The responses of the accelerometer along with one on the right outboard elevon are shown in Figure 7.4-20. In the figure, responses following three particular events are of interest, thus, are studied in depth: Elevon activation at EI+223 sec., Transient responses at EI+496 and EI+502 sec., and Onset of signal saturation at EI+534 sec. (Note that frequent one-sided spikes are data anomalies and are not valid responses)

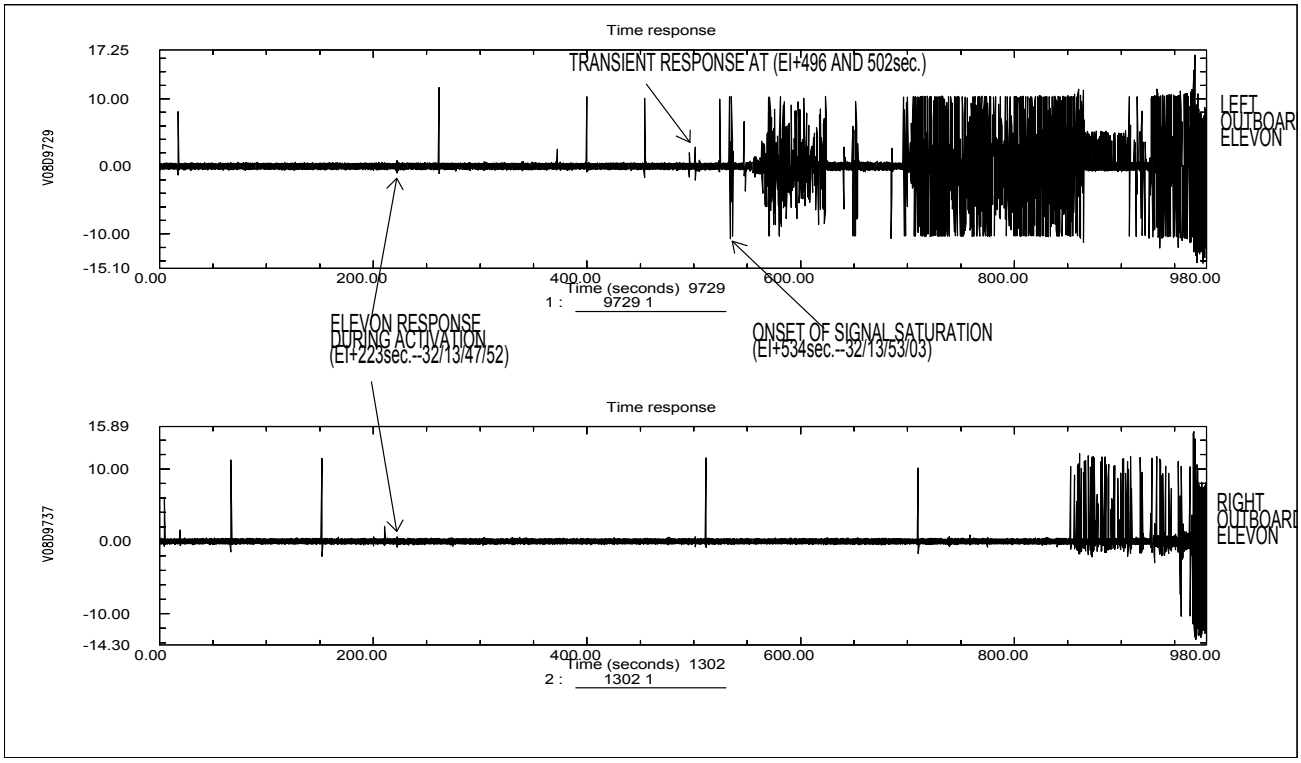

Figure 7.4-20 Left and Right Elevon Response During Entry (STS-107)

The detail plot of elevon response during activation is displayed in Figure 7.4-21. The 6 Hz response of the wing's 1st bending mode is clearly visible on both left and right outboard elevon channels. The presence of this mode verifies a proper operation of both accelerometers.

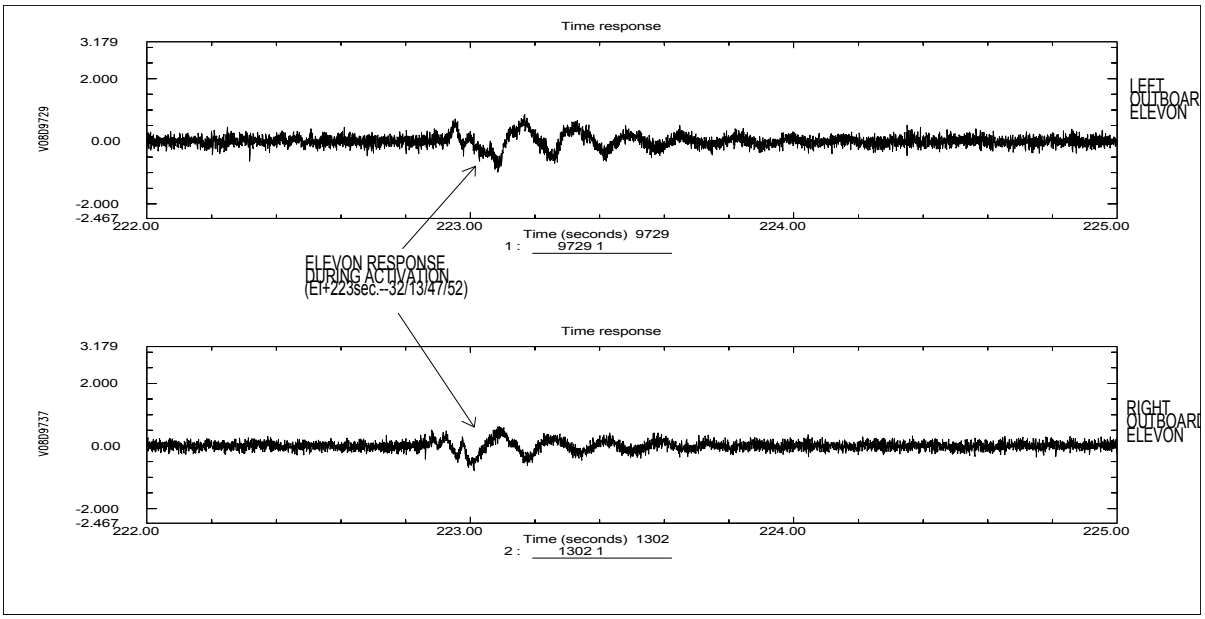

Figure 7.4-21 Elevon Responses during Elevon Activation at EI+223 sec

The second set of events occurred at EI + 496 and 502 seconds, which followed some type of external excitation. The transient response in Figure 7.4-22 was mainly noticeable for the left outboard channel. The PSD's (Figure 7.4-23) of the left outboard elevon channel following these disturbances confirm the existence of wing's 6 Hz bending and other wing/elevon modes. These times coincide with the RCS jet firings, however, similar type of transient response was not observed during other RCS jet firings.

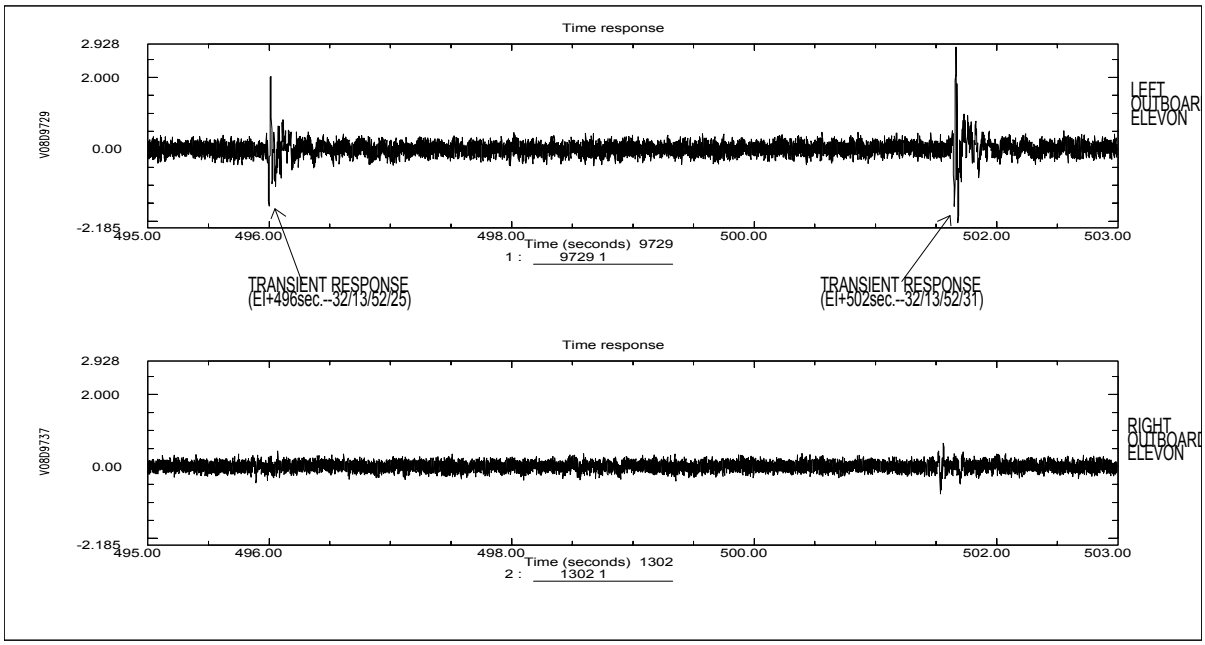

Figure 7.4-22 Transient Responses of Elevons at EI+496 and 502 sec.

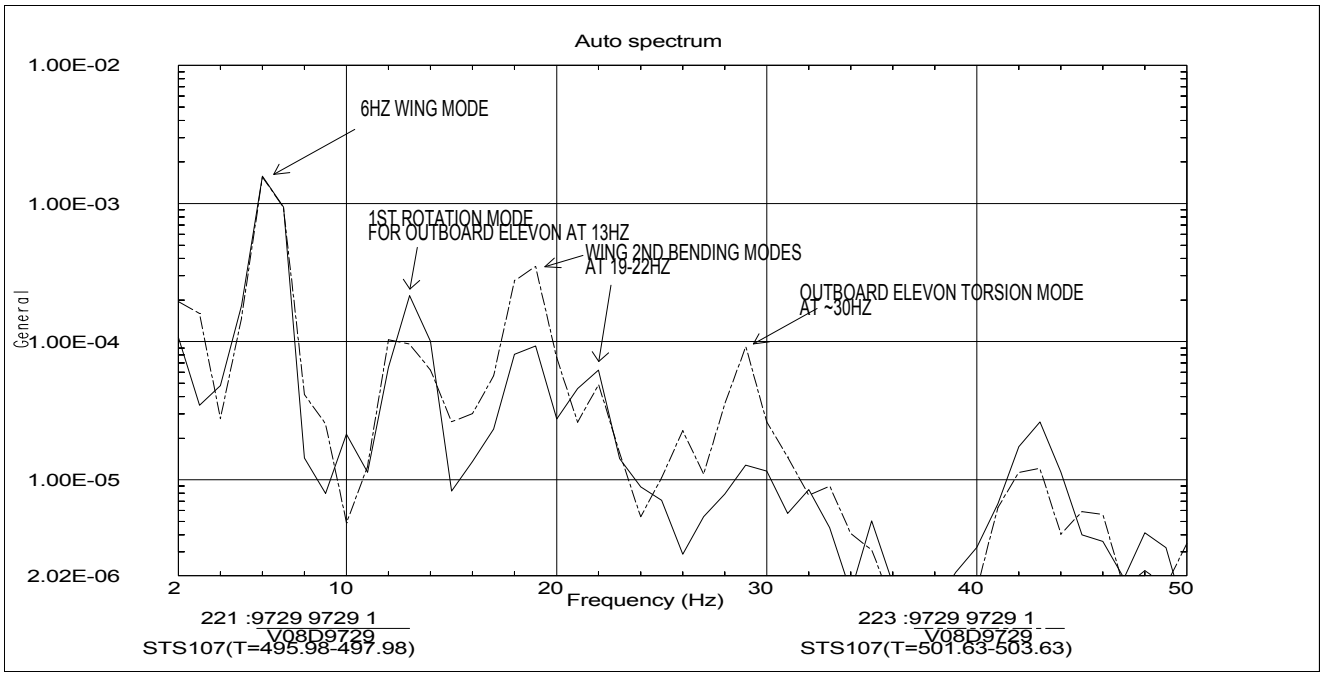

Figure 7.4-23 PSD's of Transient Response at EI+496 and EI+502 sec.

The third event observed at EI+534 indicates an onset of signal saturation for the left outboard channel. The accelerometer reading reached the maximum instrumentation range of 10G (Figure 7.4-24). The displacement computed (Figure 7.4-25) using the acceleration data results in an unrealistic number, which indicates a bad signal. The FFT's computed at various time segments during entry is shown in Figure 7.4-26. The figure illustrates a notable absence of 6 Hz response for the left outboard elevon channel after the onset of signal saturation, while the right outboard data exhibited 6 Hz response beyond EI+534 sec. This finding indicates malfunction of the left outboard channel past this time period.

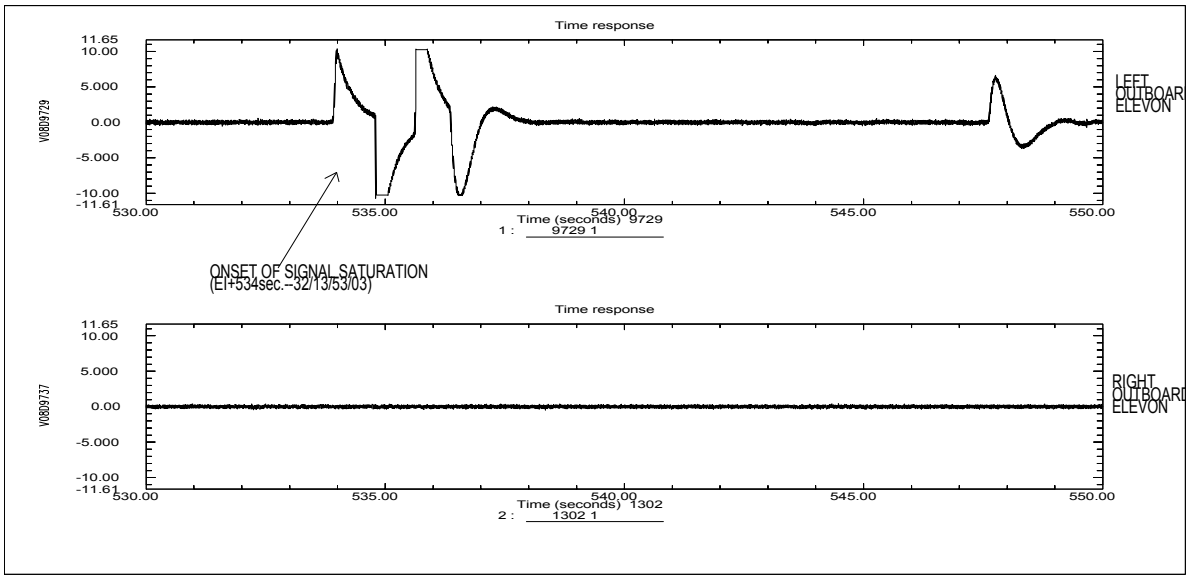

Figure 7.4-24 Onset of Signal Saturation for Left Outboard Elevon at EI+534 sec.

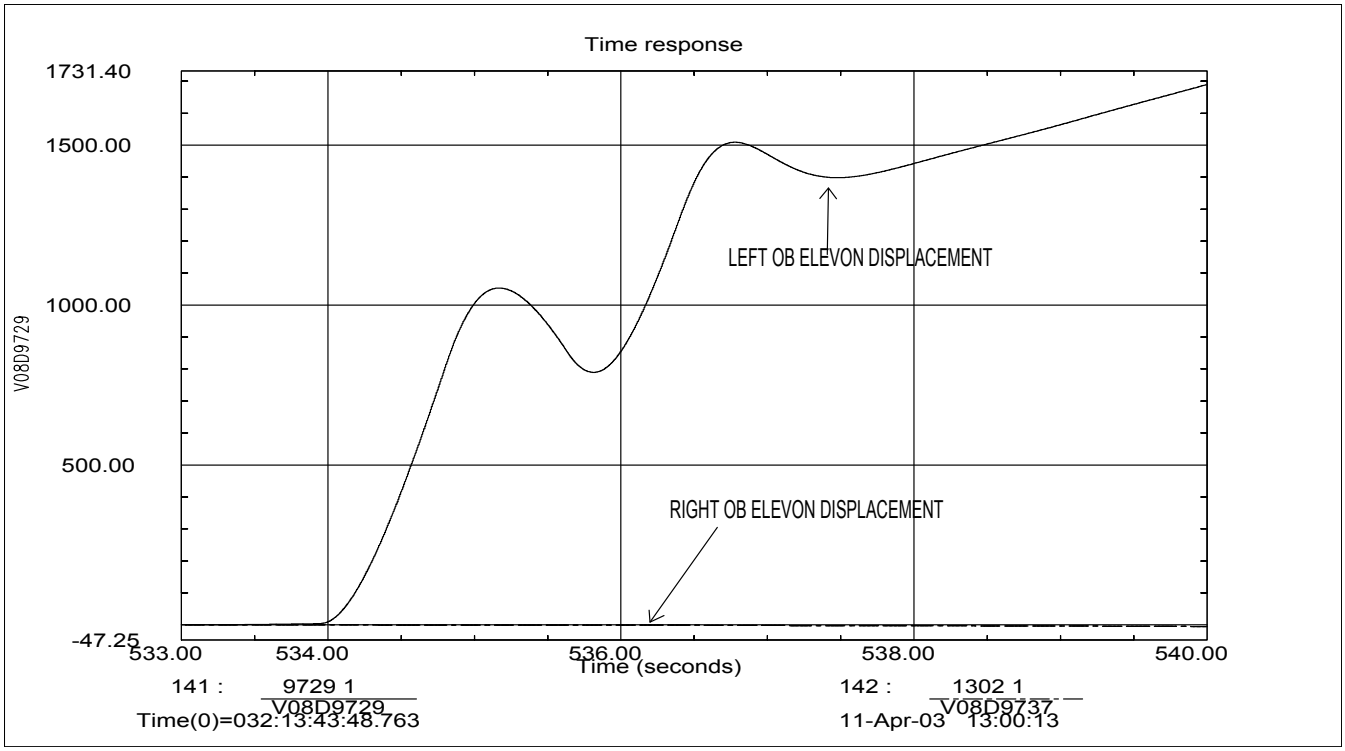

Figure 7.4-25 Displacement of Outboard Elevon Locations

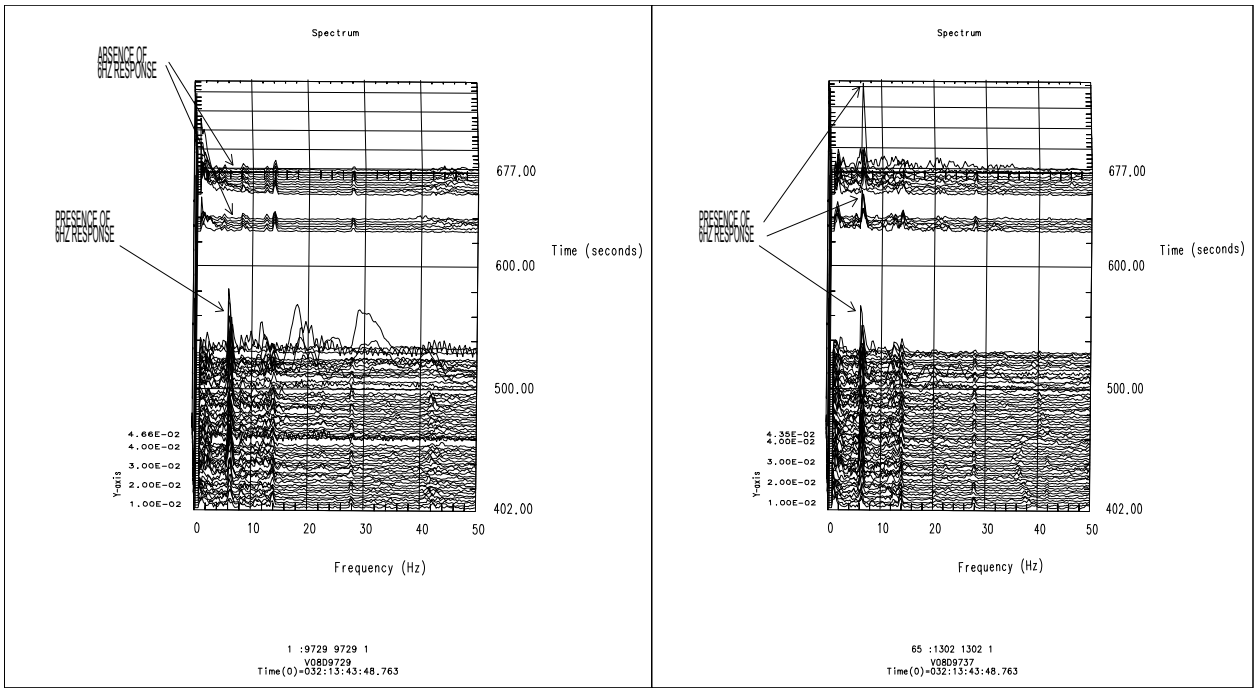

Left Outboard Elevon Right Outboard Elevon

Figure 7.4-26 FFT of Left and Right Outboard Elevon Responses

7.4.2.1 Strain Gage Data Evaluation

Typical strain gage responses are shown in Figure 7.4-27. For the most of entry phase, the strain gage channels are in "snap-shot" mode, where the readings are recorded for one minute and turned off for 4 minutes. Therefore, the only reading during the one minute period (where the strain level is near zero) is valid. In general, frequent one-sided spikes (which are not valid response and should be ignored) were observed during STS-107, which indicate the data quality was not quite as good. Also, extremely low strain level during "on" period makes the accurate assessment of the gage response very difficult. Only qualitative assessments are made. A PSD comparison for typical STS-107 and STS-109 strain data recorded at similar time period is shown in Figure 7.4-28. The figure illustrates the spectral contents are pretty similar. The large amplitude near 20 Hz and 40 Hz for STS-107 is due to the one-sided spikes, thus should be ignored.

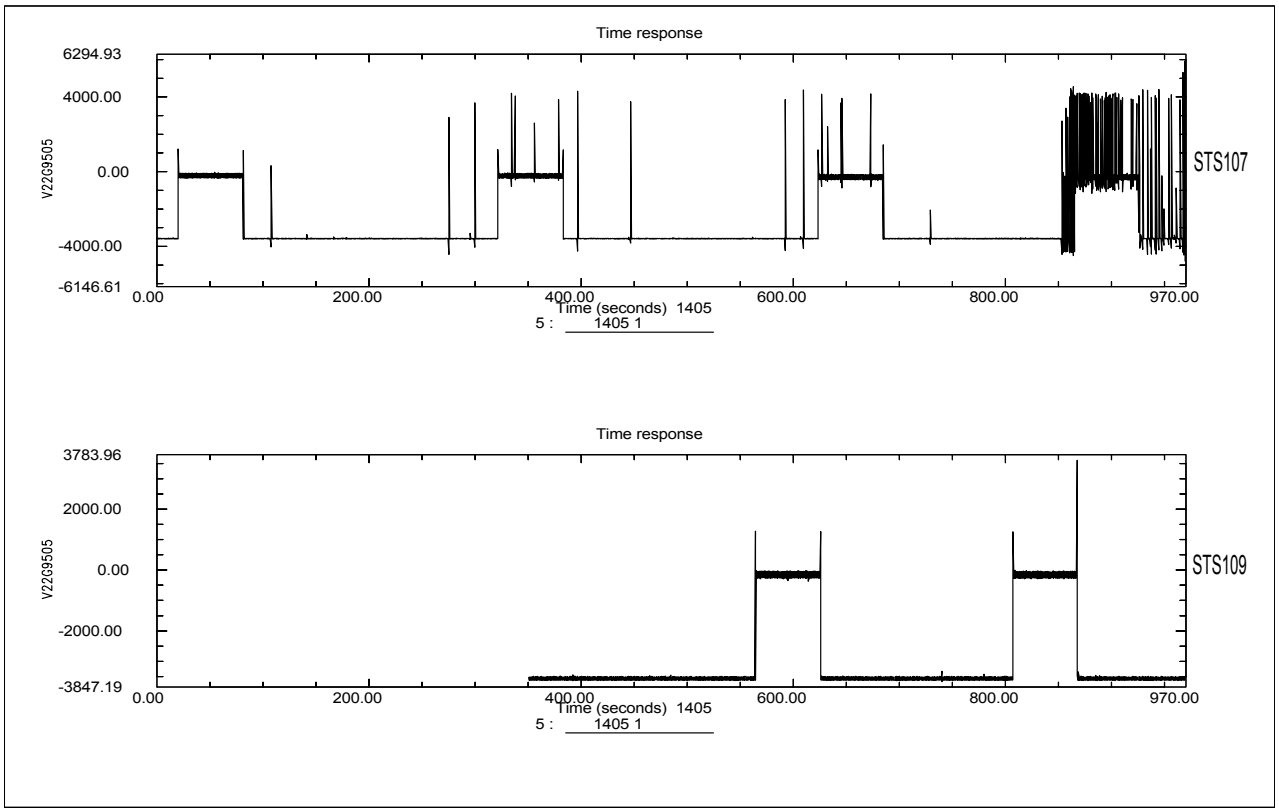

Figure 7.4-27 Strain Gage Response during Entry (Tail Aft Spar Web) STS-107 VS. STS-109

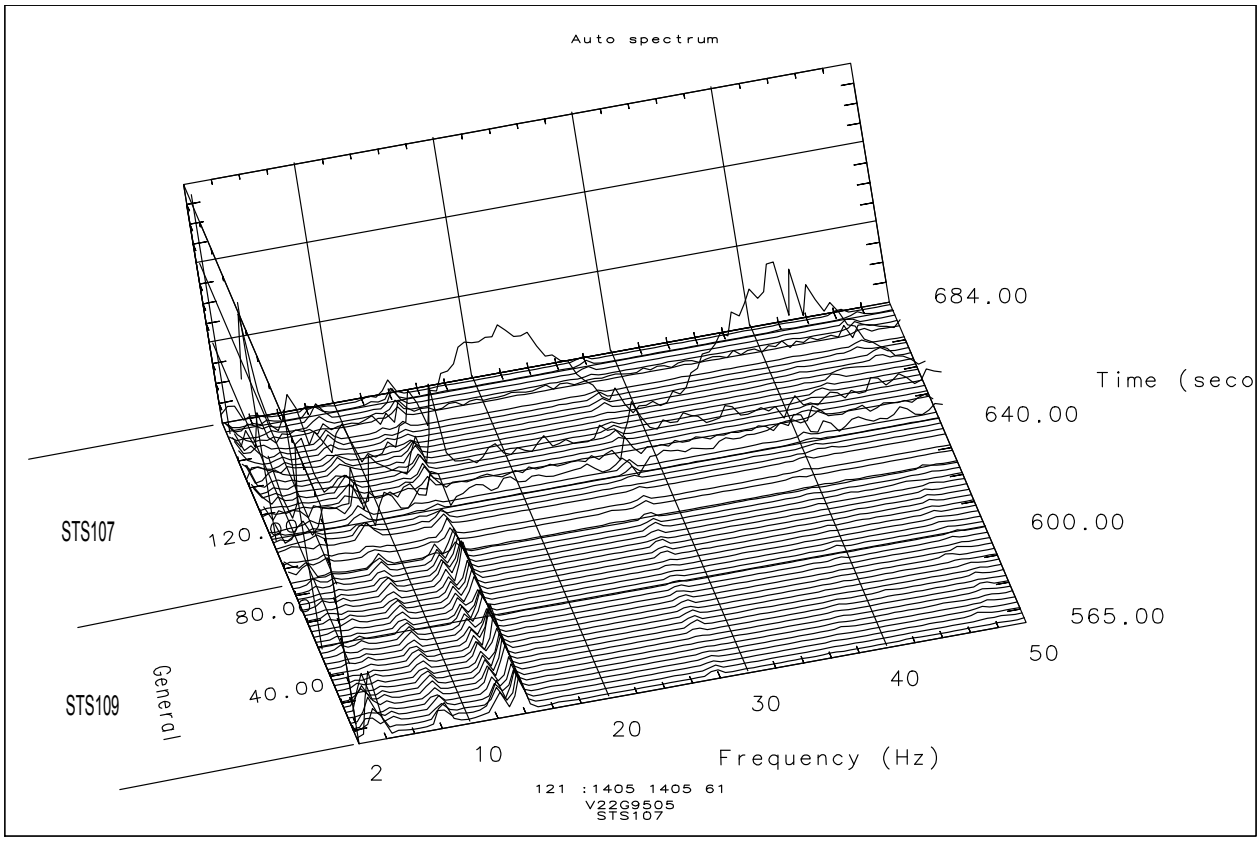

Figure 7.4-28 PSD Comparison of Strain Gage Response During Entry (STS-107 VS. STS-109)

7.4.3 Summary

Accelerometer and high sample rate strain gage responses were evaluated during ascent and entry phases of the STS-107 flight. The magnitude and the frequency contents of the measured acceleration and strain are considered within the family experience based on PSD's and computed RMS values. The excitation of the higher tail modes at 40-42 second period during ascent is similar to what's been experienced during STS-87, thus is considered normal. The distinct peaks observed for the bending and torsion modes of the wing and the tail demonstrate the flutter instability did not occur during ascent. The in-depth study of the left outboard elevon acceleration from flight and analysis using FEM models indicate the peak response observed at ~82 seconds could have come from the debris impact in addition to other aerodynamic disturbances. An absence of additional accelerometers on the left wing make it difficult to determine with certainty. During descent, the accelerometer data revealed the malfunction of the left outboard elevon accelerometer channel starting at EI+534 seconds

7.5 Feasible Wing Deformation Prior to Loss of Signature

7.5.1 Analysis Objective

The objective of the wing deflection analysis can be categorized into three distinct phases:

- Initial - the first analytical purpose was to assess OV-102 for gross left wing failure due to localized weakening of structural members. This analysis was performed during the early stages of the STS-107 accident investigation. Weakened structural members were assumed to occur from localized thermal heating due to damaged tile and RCC panels. This was considered the first approximation in determining the wing response due to various structural failure scenarios.
- Extended - the second analytical purpose was to expand the damage scenarios to include larger areas of the forward and intermediate wing sections. The analysis attempted to quantify the effects of losing major portions of the wing structure, instead of localized failure of structural elements. For this analysis, complete bottom to top cuts were made at critical structural locations around the main landing gear door wheel well, the wing leading edge spar and the honeycomb skin panels on the top and bottom wing surfaces. Structural member loss was assumed to occur from hot gas ingestion into the wing cavity; however, thermal degradation on the non-failed structures was assumed to be negligible.
- Refined - as the investigation continued, the analysis shifted from investigating various damage scenarios to cases that reflected the most probable events occurring during STS-107. The primary purpose of this analytical phase was to support an integrated analysis of the wing deformation with the aerodynamics group. The damage model was refined to represent a thermal breach at RCC panels 8 & 9, with subsequent hot gas flow into the intermediate wing cavity. Hot gas ingestion was assumed to lead to a loss of the intermediate wing tube struts and the upper wing skin panels. Also considered in this case was thermal weakening of the cavity walls, skins and rib caps.

7.5.2 OV-102 Wing Finite Element Model

A NASTRAN, OV-102 finite element model (FEM) was used to perform the analyses. An illustration of this model is shown in Figure 7.5-1. MSC-PATRAN was utilized for pre-processing of the model and post-processing of the results. The NASTRAN FEM was created from the original ASKA FEM and was previously used as part of the Performance Enhancement (PE) certification analyses, circa 1996. Due to the size and complexity of the FEM, only the wing and portions of the aft and mid fuselage were used. The mid-fuselage and the aft fuselage structure are present to allow for redistributing wing root reactions and deflections.

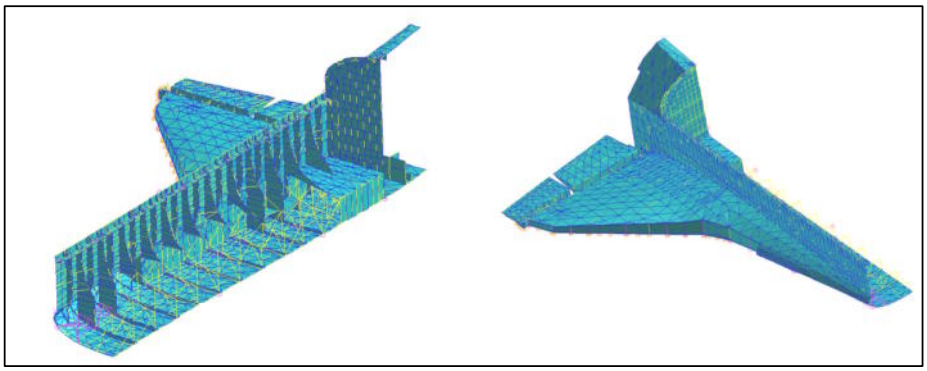

Figure 7.5-1 OV-102 Wing FEM

7.5.3 Load Cases

During the recent contingency abort project, a computational fluid dynamics (CFD) program was used to create a distributed aero pressure database for loads evaluation. This data provided Orbiter aerodynamic loads up to Mach 15. Subsequent to STS-107, and in support of the investigation, the database was expanded beyond Mach 18 in order to determine wing loads similar to those that occurred prior to the breakup. A portion of the Mach 18 expanded database is shown in Table 7.5-1. The dynamic pressure (Qbar) in the table is 70 psf and that angle of attack (Alpha) is 40 °. The load set that most closely resembles STS-107 is for an elevon angle of –2.98 degrees (De). This load set is highlighted in the table.

Table 7.5-1 Wing Loads, M=18

Wt	Xcg	Mach	Qbar	Altitude	Alpha	De	Dbf	Nx	Nz	Indicator		Wing Mx			Wing My			Wing Sz		
										Wing Mx	Wing Sz	Total	Aero	Inertial	Total	Aero	Inertial	Total	Aero	Inertial
234215	1078.3	18	70	207175	40	-11.37	11.30	0.05	0.92	0.267	0.181	4691114	6447031	-1755917	5296937	6648960	-1352023	39307	54275	-14968
234215	1078.3	18	70	207175	40	-10.40	10.60	0.05	0.92	0.253	0.181	4790338	6547683	-1757345	5229462	6582854	-1353391	39870	54851	-14980
234215	1078.3	18	70	207175	40	-9.64	9.90	0.05	0.92	0.243	0.181	4871794	6629995	-1758201	5174314	6528539	-1354225	40336	55324	-14988
234215	1078.3	18	70	207175	40	-9.02	9.20	0.05	0.92	0.233	0.181	4945690	6704639	-1758949	5124006	6478890	-1354883	40761	55755	-14994
234215	1078.3	18	70	207175	40	-8.40	8.50	0.05	0.92	0.223	0.182	5017525	6777221	-1759696	5075182	6430722	-1355540	41173	56174	-15001
234215	1078.3	18	70	207175	40	-7.78	7.80	0.04	0.92	0.214	0.182	5087389	6847831	-1760442	5027778	6383975	-1356196	41574	56581	-15007
234215	1078.3	18	70	207175	40	-7.16	7.10	0.04	0.92	0.205	0.182	5155312	6916500	-1761188	4981776	6338628	-1356853	41962	56976	-15013
234215	1078.3	18	70	207175	40	-6.54	6.40	0.04	0.92	0.196	0.182	5221298	6983232	-1761934	4937171	6294680	-1357509	42339	57359	-15020
234215	1078.3	18	70	207175	40	-5.92	5.70	0.04	0.92	0.187	0.182	5285425	7048106	-1762682	4893914	6252080	-1358166	42705	57731	-15026
234215	1078.3	18	70	207175	40	-5.48	5.00	0.04	0.92	0.181	0.182	5331767	7094767	-1763000	4862904	6221390	-1358486	42970	57999	-15029
234215	1078.3	18	70	207175	40	-5.10	4.30	0.04	0.92	0.176	0.183	5372428	7135619	-1763190	4835843	6194549	-1358706	43203	58233	-15030
234215	1078.3	18	70	207175	40	-4.74	3.60	0.04	0.92	0.171	0.183	5410271	7173639	-1763369	4810722	6169622	-1358900	43419	58451	-15032
234215	1078.3	18	70	207175	40	-4.44	2.90	0.04	0.92	0.166	0.183	5441861	7205389	-1763528	4789779	6148810	-1359031	43600	58633	-15033
234215	1078.3	18	70	207175	40	-4.14	2.20	0.04	0.92	0.162	0.183	5472515	7236202	-1763687	4769510	6128672	-1359163	43775	58810	-15035
234215	1078.3	18	70	207175	40	-3.84	1.50	0.04	0.92	0.158	0.183	5502245	7266091	-1763846	4749910	6109204	-1359294	43945	58981	-15036
234215	1078.3	18	70	207175	40	-3.54	0.80	0.04	0.92	0.157	0.183	5531060	7295065	-1764005	4730971	6090396	-1359426	44109	59146	-15037
234215	1078.3	18	70	207175	40	-3.25	0.10	0.04	0.92	0.157	0.183	5557818	7322008	-1764190	4713405	6072962	-1359557	44261	59300	-15039
234215	**1078.3**	**18**	**70**	**207175**	**40**	**-2.98**	**-0.60**	**0.04**	**0.92**	**0.157**	**0.183**	**5598759**	**7363171**	**-1764412**	**4685453**	**6045141**	**-1359688**	**44500**	**59540**	**-15041**
234215	1078.3	18	70	207175	40	-2.71	-1.30	0.04	0.92	0.157	0.183	5643147	7407781	-1764634	4655014	6014834	-1359820	44760	59802	-15043

A certification load case at Mach 18 does not exist for the Orbiter since structural significant loading does not occur during this portion of the descent phase. At the time of PE, descent load cases used for analyzing the Orbiter only extended to Mach 1.5. After STS-107, it was decided that creating a Mach 18 load case was not feasible due to the time constraint; therefore, it was decided that a currently existing load case would be used. Determining the applicable case was based upon two criteria: that the environment needed to be supersonic and that the wing shears and moments between the two load cases were of similar magnitude. A steady pitch terminal area energy management (TAEM) load case was selected. The aerodynamic loads for the selected case, TA2130, are shown in Table 7.5-2. Note that the wing moment values are approximately three times the aerodynamic values seen during STS-107. Root shear values are roughly 2 times the STS-107 conditions. Results, such as deflections and stresses, from this case need to be divided by 2 to approximate the STS-107 conditions just prior to vehicle break-up. It should be noted that the wing is designed to withstand root moments (Mx) up to a limit value of 32 million in-lbs, with a factor of safety of 1.4 above this load; the maximum loads for STS-107 entry were below 20% of the ultimate capability of an intact wing.

Table 7.5-2 Analytical Load Case

Report Condition	Mach	Description	Q (psf)	S/B (deg)	B/F (deg)	Elv (deg)	a (deg)	NZ (g's)	Mx	My	Sz
TA2130	**1.50**	**STEADY PITCH**	**375**	**55**	**16.57**	**-14.32**	**8.28**	**1.21**	**14,732,017**	**12,493,593**	**94,399**

7.5.4 Analytical Procedure

7.5.4.1 Damage Simulation

In order to simulate damage to the Orbiter wing, the modulus of elasticity for each damaged FEM element was reduced. This removed the stiffness of the elements, thus degrading the load carrying capability of the structural members. During the initial analysis phase, the modulus was reduced to 10% of nominal value for failed members. Reducing the stiffness by an order of magnitude was appropriate since the purpose was to gain an understanding of load distribution through the wing due to localized damage. The extended analytical phase; however, used a modulus of elasticity reduced to 1% of nominal value. This was done in order to help ensure that the damaged FEM elements were having no effect on the results. During the refined analytical phase, wing structures that were being heated, but not failed, were also reduced in stiffness. Wing honeycomb skin panels were reduced to 50% of nominal modulus value. This simulated de-bonded inner face-sheets. Other primary structural members, such as ribs, spars and skin panels away from the damage, but still exposed to thermal extremes were reduced to 30 % of modulus.

7.5.4.2 Screening Criteria

After running and obtaining results for the damage cases, a generalized screening process was used to find structures where load redistribution showed a significant increase. The screening was necessary to post-process large amounts of data in a reasonable amount of time and to provide a consistent methodology for the different analysts working on the project to employ.

The screening process consisted of comparing the stresses, loads and displacement for an undamaged element to a damaged element. A ratio of damaged to undamaged results was developed for each element and node within the wing. The definition of the load ratio is shown below:

$$R_{load} = \frac{\text{Damaged}}{\text{Undamaged}}$$

A large ratio does not necessarily equate to a significant change. A relatively small change could easily result in a large load ratio if the magnitudes of the data were small. As an example, a deflection changing from 0.001 inch to 0.002 inch would represent a 100% increase; however, due to the low magnitude, the increase would not represent a significant shift. Similarly, certain stress and load levels, depending on the magnitude, could be rationalized to be inconsequential. Table 7.5-3 shows the screening criteria that were established to reduce the amount of post-processed data.

Table 7.5-3 FEM Result Screening Criteria

FEM Entity	Data Type	Screening Criteria		Comment
		Load	Ratio	
Nodal	Displacement	--	> |15%|	--
Element	Stress	> 5000 psi	> |1.4|	Element types: CROD, CTRIA, CTRIA, CQUAD, CSHEAR
Element	Force	> 500 lbf	> |1.4|	Element types: CROD

7.5.4.3 Sub-Structuring

Wing elements and nodes were “sub-structured” into groups for comparative purposes. By organizing the structure into manageable groups, quicker conclusions could be drawn as to load re-distribution and deflections of the wing. Table 7.5-4 shows the sub-structure identification names associated with the associated portions of the model.

Table 7.5-4 Sub-Structured Identification

Location	Data Type	Sub-Structure ID
Leading Edge	Displacement	global_disp_LE
Leading Edge	Stress, Force	global_elem_LE
Fuselage to Wing Interface	Force	global_elem_IF
Global Wing Beams	Stress, Force	global_elem_Beams
Web Elements Inboard of Y_O198	Stress	global_webs_quad4 global_webs_tria3
Global Wing Nodes	Displacement	global_disp_WG

The first two sub-structured groups in Table 7.5-4 are for the wing leading edge (WLE) spar. Refer to Figure 7.5-2 and Figure 7.5-3 for the locations of these elements and nodes. The groups expand from panel 6, just forward of the Xo1040 spar, to the Xo1307 spar. The WLE was sub-structured separately from the rest of the wing due to the significance of the WLE in this investigation.

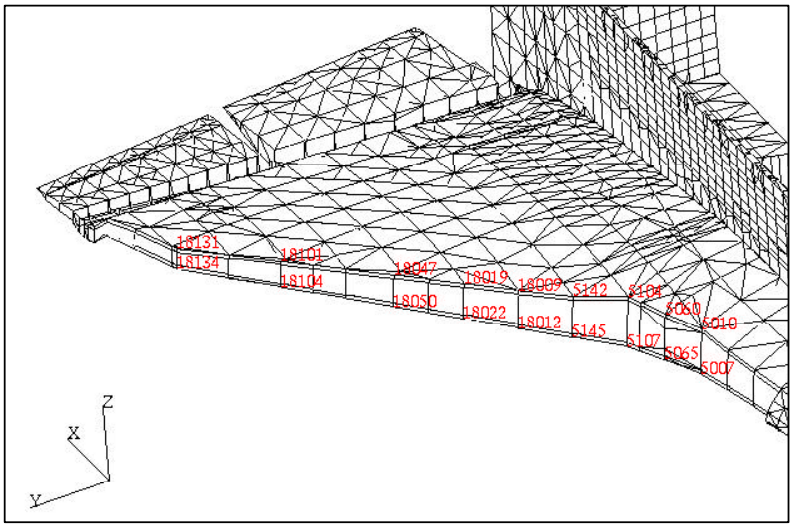

Figure 7.5-2 WLE Nodes

Only selected nodes along and the top and bottom of the WLE were sub-structured. Nodes were selected in order to provide an overall view of deflections along the WLE; therefore, a smaller sampling was appropriate. Similarly, only the WLE webs were selected for this sub-structured group. This was done in order to obtain an overall idea of the WLE load distribution as opposed to the rest of the wing.

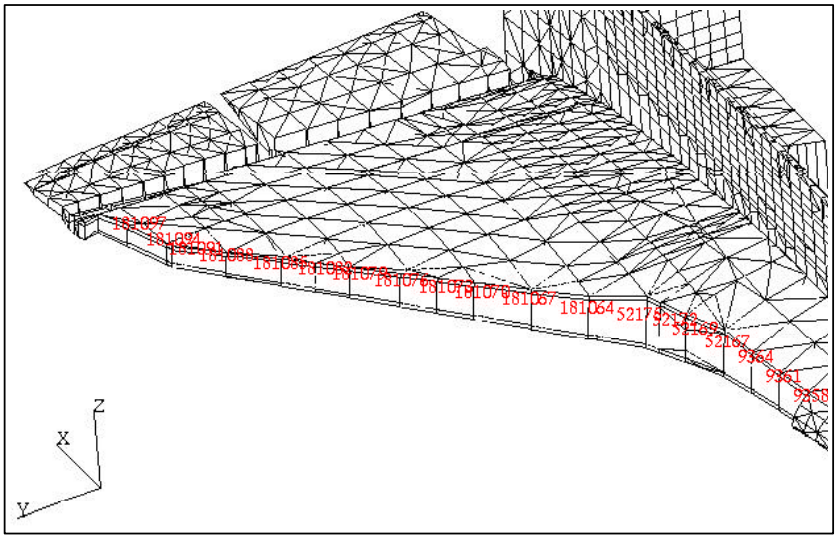

Figure 7.5-3 WLE Panel Elements

The wing torque box attaches to the wing carry thru (WCT) structure at locations Xo1191, Xo1249, Xo1307 and Xo1365. Additional bolts are located along the upper skin contour between the major spar attachments. The upper wing-to-WCT are loaded in tension and the lower wing-to-WCT is made through shear splices. Beam elements representing the wing interface bolt locations were sub-structured into a separate group. Figure 7.5-4 shows these elements and the location relative to the vehicle.

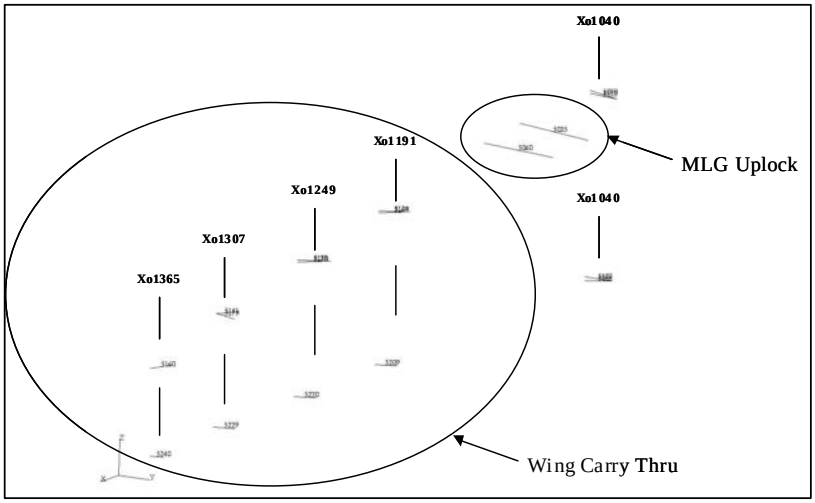

Figure 7.5-4 Wing-to-Fuselage Interface Elements

Due to criticality of the wing beam elements, most all were sub-structured for post-processing. These elements, shown if Figure 7.5-5, spanned the entire wing and included the glove area. Some areas, such as the main landing gear door hinges, were not included since damage would not produce a large effect to the wing.

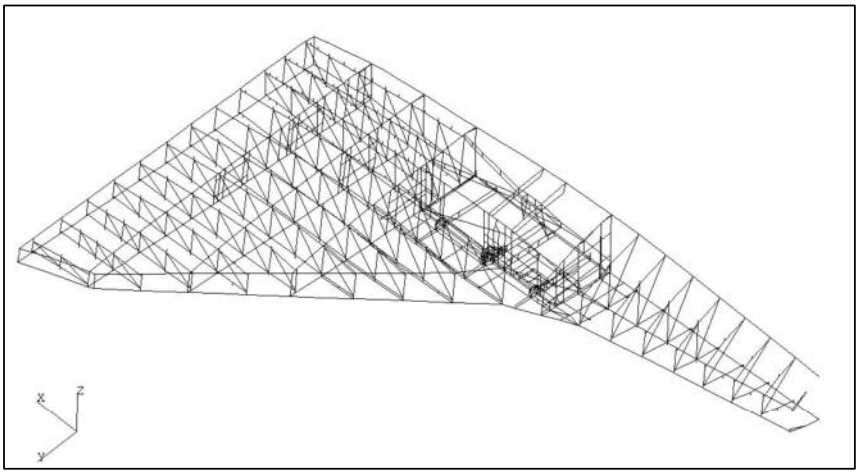

Figure 7.5-5 Wing Beam Elements

The wing model consists of a large amount of web elements. Early on in the analysis, it was decided that the beam elements provided good coverage for load distribution for the overall wing. This included load distribution through skin panels and spar webs. Therefore, to help limit the amount of elements data for post-processing, only the webs inboard of Yo198 would be sub-structured as being of particular interest relative to outboard rib webs. This group is shown in Figure 7.5-6. The X-station locations of the web elements spanned from Xo1010 to Xo1307.

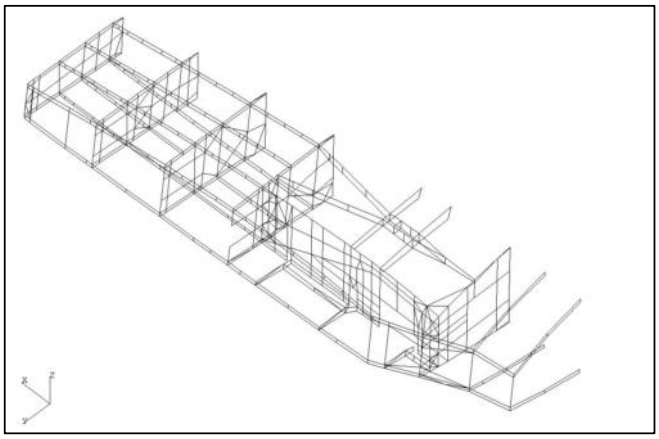

Figure 7.5-6 Inboard Wing Web Elements

As with the wing beam elements, all wing nodes were sub-structured. An illustration is provided in Figure 7.5-7. These groups of nodes were used to obtain an understanding of wing deflections based upon the various damage cases.

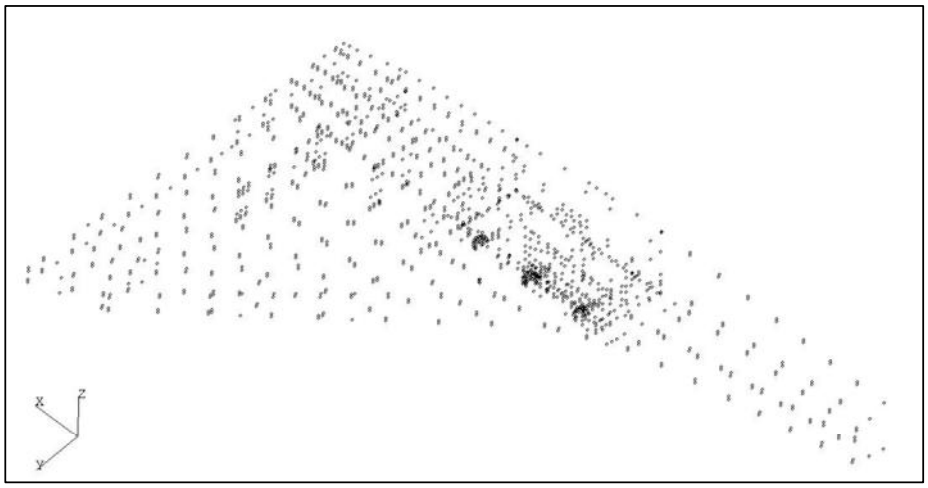

Figure 7.5-7 Wing Nodes

7.5.4.4 Post-Processing Tools

Two separate in-house Excel utilities were used for post-processing the analysis data. One utility reads the NASTRAN data output files for each damage case and creates separate files that categorizes results based upon the sub-structured elements. The second utility compares the results from each sub-structured data file to the undamaged results. Each utility was written in Visual Basic and provide a consistent and quick method for screening the sub-structured element by the criteria shown in Table 7.5-3.

7.5.5 Analysis Results

7.5.5.1 Initial (Small) Damage Analysis

The initial phase of the wing analysis attempted to assess the impact of localized skin, spar and rib damage to an overall effect on the wing. The analysis was performed for thermally weakened structure in locations deemed to be structurally significant. The screening criteria provided in Table 7.5-3 were used to determine wing areas where stresses, forces and displacements showed a significant increase in deflection and load.

The locations studied, along with the corresponding case files, are shown in Table 7.5-5. Most of the damaged areas are located in the intermediate wing with some WLE locations forward of the Xo1040 spar.

Table 7.5-5 Damage Locations, Initial Damage Failure Analysis

Case File	Location Studied
dam1191_1	Xo1191 lower spar cap and bottom skin aft of MLG well, aft, outboard corner
damle_1	MLG fwd hinge fitting, adjacent bottom skin and leading edge lower cap
damle_2	MLG fwd hinge fitting, adjacent bottom skin and leading edge lower cap and web to upper cap
damtube_1	Removed fwd diagonal truss tube from Yw198 rib (Elem 5812)
damtube_2	Removed fwd vertical truss tube from Yw198 rib (Elem 5561)
dis1191L	Disconnected Xo1191 spar cap and attached elements from mid-fuselage
dis1249L	Disconnected Xo1249 spar cap and attached elements from mid-fuselage
dis1307L	Disconnected Xo1307 spar cap and attached elements from mid-fuselage
dis1365L	Disconnected Xo1365 spar cap and attached elements from mid-fuselage
yo167_01	Yo167 rib lower spar cap at Xo1040 bulkhead
yo167_02	Yo167 rib lower spar cap at near door hinge point 1
yo167_03	Yo167 rib lower spar cap at near door hinge point 3
yo167_04	Yo167 rib lower spar cap at Xo1191bulkhead
yo167_05	Yo167 rib lower spar cap at near door hinge point 2
x1040y167-Damage1	Intersection Xo1040 spar and Yo167 rib at the lower wing surface

Table 7.5-6 lists the results for the initial damage failure analysis. As can be seen, the relative stress/load ratios show reasonable increases in element forces, stresses and displacements. The maximum load increases occurred for case damle_2. Wing beam elements showed a maximum increase 3.06 for case damle_2; however, the magnitude of the beam force was lower than the certified design load. The maximum wing-to-fuselage interface forces show a maximum increase of 8%. Based upon the capability of the interface bolts, an 8% increase is not considered significant. Maximum displacement was on the order of 39%. This was from a damaged element and was not considered realistic.

Table 7.5-6 Damage Locations, Initial Damage Failure Analysis

Case File	Maximum Load Ratio Results			
	Beam Force	Displ	LE Stress	IF Force
dam1191_1	1.54	1.03	1.02	1.08
damle_1	1.68	1.20	1.03	1.04
damle_2	3.06	1.39	1.16	1.08
damtube_1	2.29	1.08	1.07	1.02
damtube_2	1.72	1.03	1.02	1.02
dis1191L	2.00	1.17	1.05	1.06
dis1249L	2.00	1.17	1.01	1.02
dis1307L	2.90	1.23	1.00	1.03
dis1365L	1.06	1.06	1.00	1.01
yo167_01	1.58	1.01	1.00	1.00
yo167_02	2.18	1.01	1.00	1.01
yo167_03	1.41	1.01	1.00	1.01
yo167_04	--	1.01	1.00	1.01
yo167_05	1.92	1.01	1.00	1.00
x1040y167-Damage1	1.76	1.05	1.00	1.01

For the six separate locations along the Yo167 bottom rib cap, surrounding skins and web were checked for the effects of thermal degradation. Five of the damage locations were assessed along the Yo167 rib, lower cap and skins. For these cases, only the rib caps and skins were damaged. A sixth case with damaged Yo167 rib web elements was then considered. This case assumes impingement of hot gases onto the web and is indicative of burn through at Yo167 lower rib skins. Based upon the results, it was determined that localized failures of these locations are not sufficient to induced an overall wing structural failure. One element for all six damage locations violated screening criteria. As shown in Table 7.5-6, this element had a 2.18 load ratio. Element still maintains positive margin of safety based upon comparison to the certification database.

The conclusion from the analysis of small damage regions was that only the local areas were significantly affected. These would not produce a general wing failure, nor would they cause the local failure to propagate to a wider area.

7.5.5.2 Expanded Damage Analysis

The expanded damage analysis was performed to create more severe damage scenarios and to assess the wing response to a complete loss of load path due to damage in major structural areas. Seven damaged locations, shown in Figure 7.5-8, were examined during this phase of the analysis. The first two cases were centered about the WLE spar panels, just forward and aft of the Xo1040 spar. Cases 3 through 5 concentrated on the wheel well. In these areas, structure was assumed to be completely lost from the bottom wing surface to the top wing surface. Case 6 was created to see the effects of losing bottom surface honeycomb skin panels. Case 7 was the first attempt at specifically recreating the probable damage scenario experienced during STS-107. Case 7 was eventually modified to create the refined damage FEM.

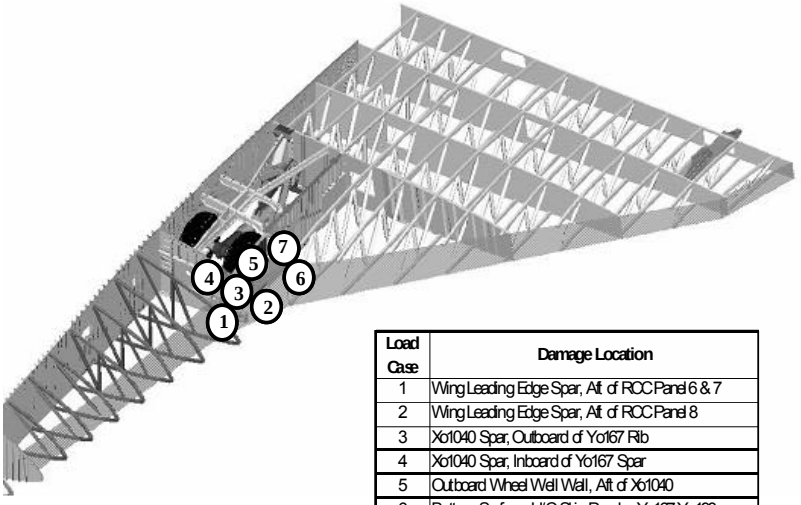

Load Case	Damage Location
1	Wing Leading Edge Spar, Aft of RCC Panel 6 & 7
2	Wing Leading Edge Spar, Aft of RCC Panel 8
3	Xo1040 Spar, Outboard of Yo167 Rib
4	Xo1040 Spar, Inboard of Yo167 Spar
5	Outboard Wheel Well Wall, Aft of Xo1040
6	Bottom Surface, H/C Skin Panels, Yo167-Yo198
7	- Upper Surface, H/C Skin Panel, Yo167-Yo198 - First Diagonal and Vertical Struts on Yo198 Frame

Figure 7.5-8 Damage Locations, Expanded Analysis

The total number of criteria violations for various data types, as described in Section 7.5.4.2, is shown in Table 7.5-7. From this table it can be noted that no significant fuselage interface violations occurred. This suggests that the amount of applied damage was not significant enough to cause the wing to detach from the main body. The total number of displacement criteria violations increases from the initial damage case, suggesting larger overall wing deflections. The stress violations also increase from the initial case. Some of these stress violations are significant, but a review of the certification analysis suggests that the parts still maintain a positive margin of safety. Overall, these results suggest a large amount of load redistribution does occur; however, wing failure from re-distribution is unlikely.

Table 7.5-7 Expanded Damage Analysis, Criteria Violations per Case

Damage Case	Stress	Displacement	Fuselage I/F Forces
1	135	26	0
2	94	11	0
3	94	0	0
4	61	0	0
5	20	0	0
6	131	21	0
7	142	0	0

7.5.5.2.1 Wing Displacements

Table 7.5-8 lists the total wing deflection criteria violations. Of the seven cases, cases 1, 2 and 6 showed displacement ratios greater than ±15%. The other cases displayed no criteria violations for deflections. (Note that for the expanded analysis, the deflection criterion was changed from a ±5% increase from damaged-to-undamaged condition, to a ±15% increase.) The maximum delta deflection was 0.24 inches, occurring for Case 2. A review of these violations suggests nothing significant from a structural strength standpoint.

Table 7.5-8 Wing Nodal Deflection Violations per Case

Damage Case	Criterial Violations		Wing Ratios		LE Ratios	
	Total Wing	LE Only	Max	Min	Max	Min
1	26	4	1.23	0.79	1.22	1.20
2	9	8	1.22	1.16	1.22	1.20
3	0	0	0	0	0	0
4	0	0	0	0	0	0
5	0	0	0	0	0	0
6	21	0	1.31	0.79	0	0
7	0	0	0	0	0	0

Note that these results contain ratios that are lower than the initial damage case results shown in Table 7.5-6. This is due to damaged elements being included in the initial analysis results. For the expanded case, localized damage effects were screened out.

Illustrations of the case 1, 2 and 6 displacement violation nodes are shown in Figure 7.5-9. For case 1, the violations are located in the glove area and near the WLE spar. This is consistent with a loss of load path between glove area and Xo1040 spar. The change in magnitude from undamaged to damaged are relatively small (0.11 inches), however. For Case 2, displacement violations are located at the WLE, which is consistent where the damage was located. As previously stated, the maximum delta deflection was 0.24 inches. The load path between the Xo1040 bulkhead and glove area has been restored, resulting in no violations in the glove area. For case 6, displacement violations are located at the wing glove area, suggesting that the lower panels help provide structural rigidity to elements of the Xo1040 spar.

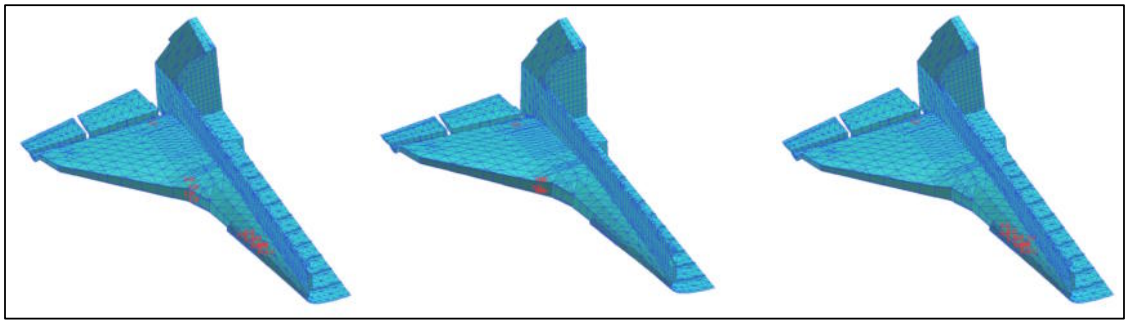

Figure 7.5-9 Node Displacement Violations

7.5.5.2.2 Wing-To-Fuselage Interface

As seen in Table 7.5-9, the results from the wing-to-fuselage comparison show no significant rise in loading from expanded damage conditions. The maximum load increase of 8% occurs for damage case 7. The location is at the X_O1040 upper wing-spar to fuselage interface. The maximum load increase along the lower wing interface is 7%, occurring at the X_O1191 wing-spar to fuselage interface. Note that the wing-carry-thru (WCT) interface reactions remain largely unchanged. This suggests that the main wing structure attaching the wing to the fuselage is not being compromised. The largest change for the lower wing interface is 7% at the X_O1191 lower spar interface.

Table 7.5-9 Wing-to-Fuselage Reaction Data

I/F Location	ELEM ID	Node ID	X_o	Y_o	Z_o	Case01	Case02	Case03	Case04	Case 05	Case06	Case 07	
Upper Wing	5070	5021	1040	105	342	1.04	1.00	1.01	1.02	1.00	0.97	1.00	
	5122	5023	1040	105	341	1.01	1.03	1.00	0.99	1.00	0.97	1.08	Max
	5035	5123	1090	105	339	0.97	0.97	0.95	0.95	0.99	1.00	0.97	
	5060	5194	1116	105	336	0.97	0.97	0.96	0.97	1.00	0.99	0.97	
	5124	5269	1191	105	325	0.99	0.99	0.99	1.00	1.00	0.97	1.00	Wing Carry Thru Locations
	5169	5054	1191	105	324	1.01	1.01	1.00	1.00	1.00	1.01	1.00	
	5133	5360	1249	105	317	1.02	1.01	1.01	1.01	1.00	1.03	1.00	
	5170	5059	1249	105	317	1.00	1.00	1.00	1.00	1.00	1.00	1.00	
	5141	5435	1307	105	308	0.99	0.99	0.99	1.00	1.00	0.97	1.00	
	5179	5435	1307	105	308	1.01	1.01	1.00	1.00	1.00	1.01	1.00	
	5160	5626	1365	112	300	1.02	1.02	1.01	1.01	1.00	1.04	1.00	
Lower Wing	5088	5018	1040	105	272	0.86	0.86	0.81	0.77	0.97	0.65	0.99	
	5123	5029	1040	105	273	0.85	0.85	0.80	0.77	0.97	0.60	0.99	
	5209	5265	1191	105	269	1.06	1.04	1.03	1.03	1.01	1.07	1.01	Wing Carry Thru Locations
	5220	5362	1249	105	267	1.01	1.01	1.00	1.01	1.00	1.01	1.00	
	5229	5437	1307	105	266	1.00	1.00	1.00	1.00	1.00	1.00	1.00	
	5240	5624	1365	112	267	0.98	0.98	1.00	0.99	1.00	0.99	1.00	

7.5.5.2.3 Stress & Force Results

Stress and force violations are summarized in Table 7.5-10. The most significant increases occur with cases 1, 6 and 7. Generally, the criteria violations are concentrated around the areas that have been damaged, with little impact to wing-to-fuselage interface, torque box or glove area.

Table 7.5-10 Stress and Force Violations

Damage Case	Element Type				Total Violations
	CTRIA3	CSHEAR	CROD	CQUAD4	
1	11	6	98	20	135
2	3	4	68	19	94
3	13	4	59	18	94
4	8	3	42	8	61
5	4	1	14	1	20
6	29	4	73	25	131
7	14	8	99	21	142

The stress violation dispersions illustrate load re-distributions within the wing. Dispersions for each of the cases are shown in Figure 7.5-10. Note that cases 2 & 7 show the widest area of dispersion. Case 2 load ratios are highly concentrated around the damaged WLE spar web, with some ratios scattered aft. Suggesting that there is not much load transfer moving toward the inboard wing structure. Case 7 also has high ratios around the damage area, but shows loads being distributed toward the wing-to-fuselage interface. Cases 4 & 5 show the least amount of dispersion, suggesting that the loads being routed around the wheel well is being more evenly distributed than with cases 2 & 7. Highly concentrated load

redistribution is observed for case 1, 3, & 6 around the area of damage. However, the dispersion does not move inward or outward.

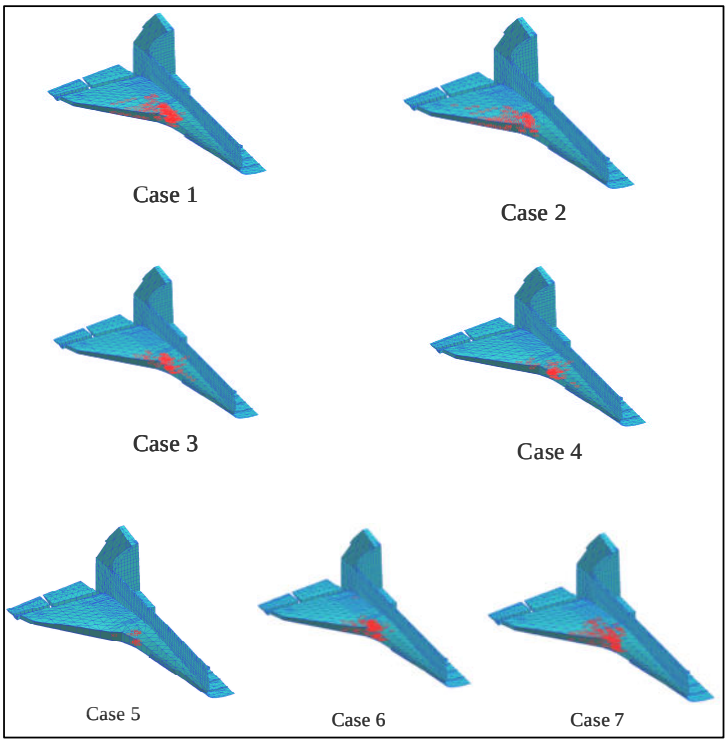

Figure 7.5-10 Stress/Force Violation Dispersions per Case

Table 7.5-11 shows the critical elements for each load case. The results show that, although load redistribution increases significantly with the expanded damage cases, the magnitudes were well within certification limits. The critical element for case 1, element 5515, was the closest to the certification load. This element is located in the Yo167 rib, near the main landing gear door forward hinge. The increase results from the damage WLE spar transferring the loads to the Xo1040 spar and Yo167 rib. The highest load shown in Table 7.5-11 is at element 5116, case 3. This element represents a beam in the Xo1040 spar. The load increase is to be expected since the element is close to the damaged area. Element 9053 represents a wing glove truss tube strut, located at the aft end of the glove at station Xo1010. Case 3 is the most critical for this element. This is due to the load path from the Xo1040 spar being lost and distributing an increased load forward.

Table 7.5-11 Critical Elements

Damage Case	Data	Type	Comp	ID	Damaged	Undamaged	Maximum Cert Load
1	Element Force	Crod	N (lb)	5515	820	51	967
2	Element Stress	Crod	Sx (psi)	5614	3542	204	10839
3	Element Stress	Crod	Sx (psi)	9053	-6774	-3853	-9886
4	Element Stress	Crod	Sx (psi)	5116	29731	11181	42877
5	Element Stress	Crod	Sx (psi)	5121	-3884	-1105	-10291
6	Element Stress	Ctria3	Sxy1 (psi)	51942	2699	1454	14111
7	Element Stress	Crod	Sx (psi)	5344	-4659	-1937	-14848

7.5.5.3 Refined Wing Stress Analysis

Structural analysis of a significantly damaged wing was requested to investigate potential sources of wing deformation. Correlation between the analytical results and the STS-107 measured aerodynamic data was the primary purpose of the analysis. Results were delivered to Aerodynamics group to study changes in aero coefficients seen during STS-107 descent.

The study was primarily focused on damage to the intermediate wing section. An attempt was made to model damage as closely as possible to the most probable failure scenario on STS-107, i.e., WLE spar breech at RCC panels 8 & 9. Three types of damage were applied to the FEM for this analysis. The first damage type was at areas where hot gas impingement was assumed to fail the structure. Susceptible structures were all the rib struts in the intermediate wing, the WLE spar behind RCC panels 8 & 9 and the top honeycomb panels just outboard of the wheel well wall. The modulus in these areas was set to 1% of their normal value. The second type of damage was concentrated on the upper and lower intermediate wing panels. The assumption was that the skin panels were affected by hot gas ingestion into the cavity, but not failed. The stiffness for these structures was reduced by a factor of two. The final type of damage was at the intermediate wing rib spars, Yo167 rib and the Xo1191 spar. Hot gas ingestion was assumed to lower the modulus of these locations by 30%. Refer to Figure 7.5-11 for the damage areas and modulus reduction values.

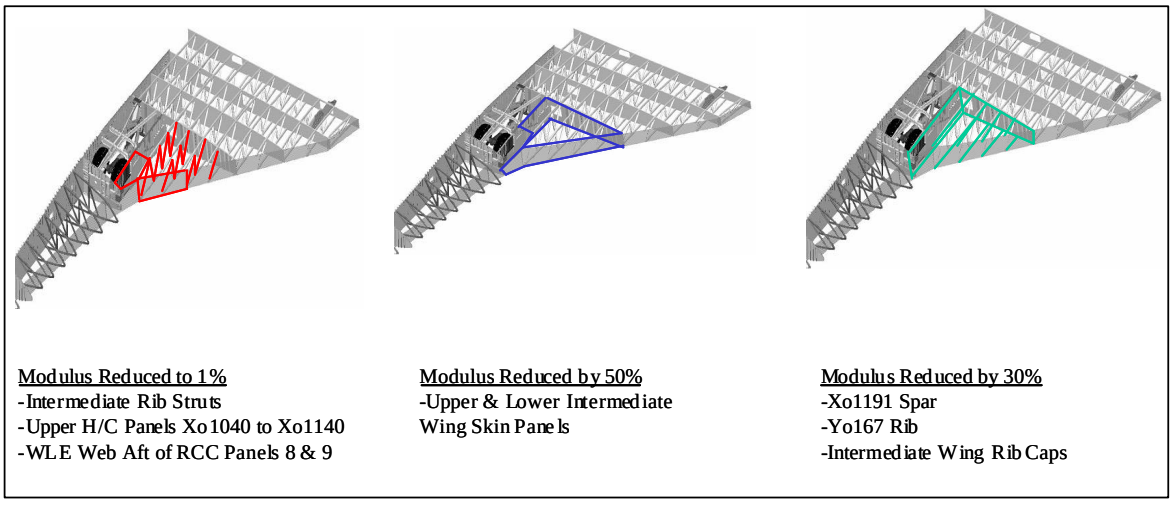

Figure 7.5-11 Refined Wing Damage Case

This linear FEM analysis was performed to show overall wing deformation, while hand calculations were done for local, non-linear effects on the lower wing skin. The FEM results show small deflections even with severe damage to the intermediate wing. The maximum delta deflection was 0.78 inch (Z), while the wing tip deflection increases to 0.25 inch. The wing tip deflection is nominally 1.1 inch. Maximum deflection results for the undamaged and damaged cases, as well as the difference between the two cases, are provided in Table 7.5-12.

Table 7.5-12 Refined Wing Damage, FEM Deflection Results

Condition	X (in)	Y (in)	Z (in)	RSS
Damaged Wing	0.1541 -0.1176	0.2298 -0.1334	1.3603 -0.0783	1.38817 0.19432
Undamaged Wing	0.0768 -0.1222	0.0681 -0.1236	1.0999 -0.0895	1.1047 0.19551
Delta Deflection	0.0774 -0.0195	0.2546 -0.1174	0.7822 -0.2561	-- --

Figure 7.5-12 shows the deflection of the wing with the refined damage. Significant distortion occurs around the intermediate wing just aft of RCC panels 8 & 9. Beyond this region, the wing deflections increase towards the wing tip. No significant deflections occur inboard of RCC panels 8 & 9. This is due to a denigrated load path from the outboard wing to the inboard wing.

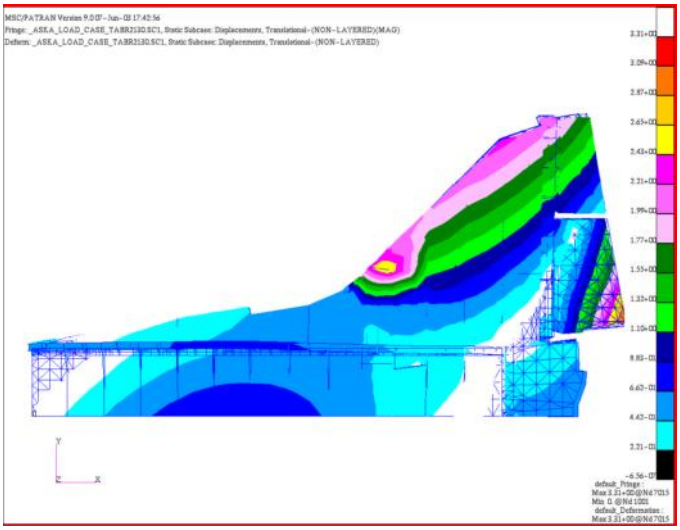

Figure 7.5-12 Refined Wing Damage, FEM Deformation Plot

Wind tunnel testing indicated that deflections of up to five inches are required to emulate the aerodynamic profile experienced during STS-107. These results show that the aerodynamic load at Mach 18 was not able to achieve overall wing deflections of this level, even with severe damage.

Hand analyses were performed to determine the maximum deflections that could occur on the lower wing skin panels. Three components were considered to cause the deflections. The first was a differential pressure across the panels. The difference in the free stream flow and the heated intermediate wing compartment was calculated to be 0.25 psi. This delta pressure was based on a pressure coefficient (Cp) of 1.0 and a dynamic pressure of 70 psf. The external pressure was approximately 0.5 psi with an

internal pressure of 0.25 psi, post breach. Potential loss of rib capability was considered as part of the analysis. As the loss of a rib can effectively double the width of the analysis panel, this can have a significant effect on the deflections calculated. For example, deflection increases as the fourth power of panel width based on this uniform pressure loading. To account for the partial effectivity of the rib cap, after the rib struts are lost, a factor (Leff Factor in Table 7.5-14) was assumed to produce an effectively shorter panel. The loss of the Yo198 rib is somewhat less effective based on the presence of the MLG door hinge backup structure found between panels 4,5, and 6. The effect of the loss of the rib between panel 8 and 9 is also less, because the rib is relatively short.

Two thermal scenarios were considered in addition to the pressure deflection: a thermal gradient across the honeycomb panel face sheets and a de-bonding of the inner face sheet. The deflection due to thermal gradient is a function of temperature differential from the inner to outer face sheet. This deflection increases as square of the panel width. The loss of the inner face sheet assumes a new stable configuration occurring when the tile gaps (.045 inch design; 0.050 inch assumed) are closed. Once the de-bonding occurs and the stable configuration has been reached, it was assumed that the outer face sheet acts as a membrane. This deflection is also a function of the square of panel width. The de-bond deflection is additive with delta pressure, but not thermal gradient deflection.

The hand analyses show that larger deflections are possible if a face sheet de-bond occurs. Note that this local, non-linear deflection scenario was not modeled in the FEM. The hand analysis results are shown in Table 7.5-13 and Table 7.5-14, with the wing panel layout shown in Figure 7.5-13. The results indicate that deflections are still relatively small without the loss of any ribs. Expanding the analysis to include damaged ribs, however, indicates that deflections of up to 5” are possible with the loss of three ribs and debond of the inner facesheet.

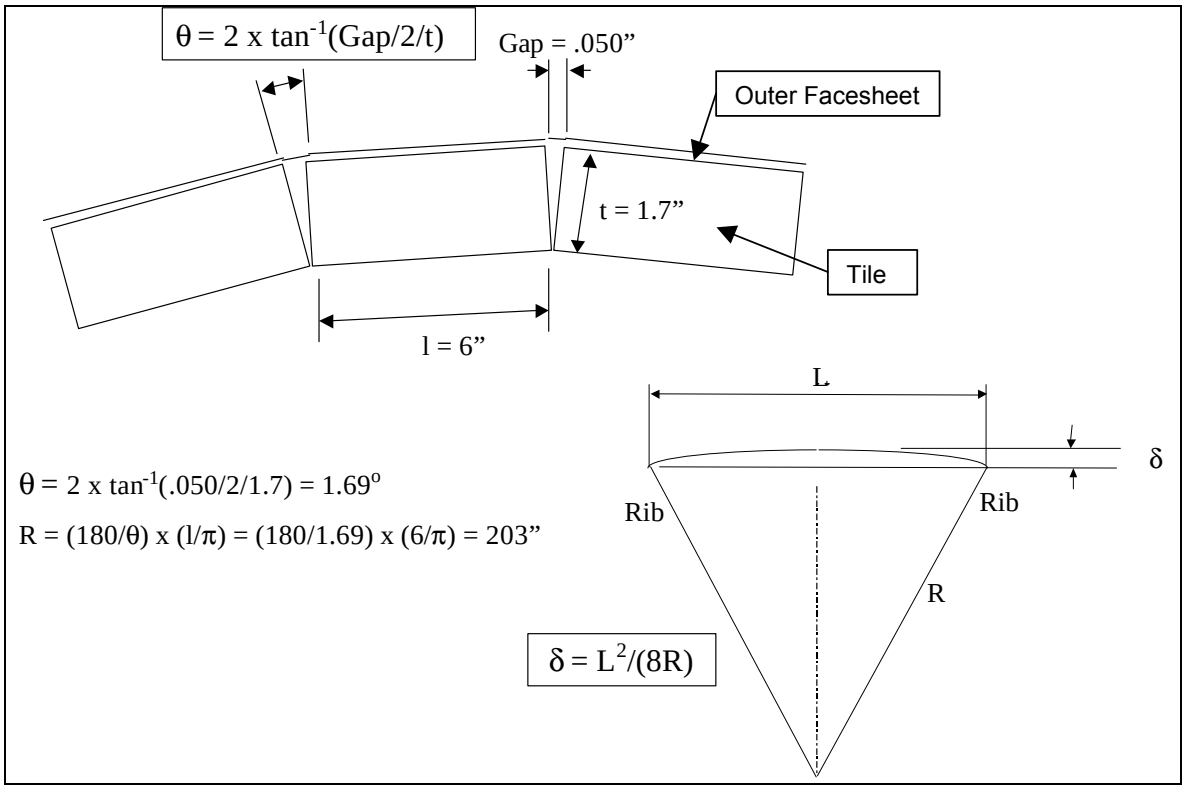

Figure 7.5-13 Calculations for Outer Facesheet and Tile Deflection

Table 7.5-13 Refined Wing Damage, Panel Deflection Results

Single Panel (Ribs Intact)									
Panel ID	Length	Leff Factor	Leff	Deflection for DP	Tile Gap	Deflection	Total Deflection	Yinbd	Youtbd
4	31	1	31	0.015	0.05	0.61	0.63	167	198
5	31	1	31	0.022	0.05	0.61	0.63	167	198
6	31	1	31	0.017	0.05	0.61	0.63	167	198
7	28	1	28	0.027	0.05	0.50	0.53	198	225
8	28	1	28	0.035	0.05	0.50	0.54	225	254
9	28	1	28	0.035	0.05	0.50	0.54	254	282

Table 7.5-14 Refined Wing Damage, Multi-Panel Deflection Results

Multiple Panel										
Panel ID	Length	Leff Factor	Leff	Deflection	Tile Gap	Deflection	Total Defl	Yinbd	Youtbd	Condition
4,5,6,7	59	0.8	47	0.13	0.05	1.42	1.56	167	225	1 rib lost
7,8	56	0.9	50	0.31	0.05	1.62	1.93	198	254	1 rib lost
4,5,6,7,8	87	0.7	61	0.67	0.05	2.37	3.04	167	254	2 ribs lost
4,5,6,7,8,9	115	0.65	75	1.52	0.05	3.56	5.09	167	254	3 ribs lost

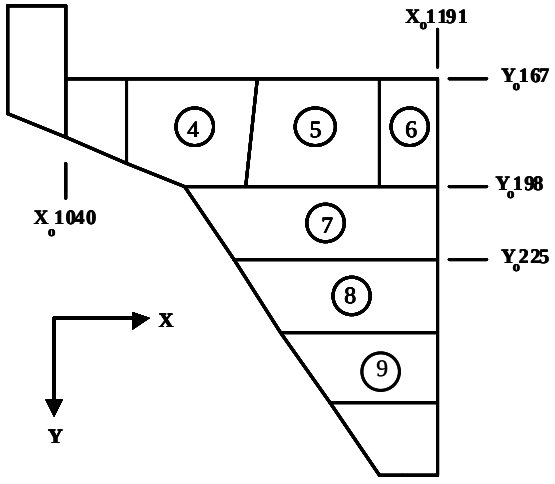

Figure 7.5-14 Lower Wing Panel Layout

7.5.6 Conclusions

Three distinct phases of analysis were performed on the OV-102 wing in order to help determine the most probable cause of the vehicle breakup. The “initial” analysis phase was performed to assess gross wing failure possibilities due to localized weakening of wing structural members. Results from this analysis showed that, although localized load increases do occur, the possibility of a gross wing failure or further damage propagation due to localized damage is highly remote. The “extended” analytical phase expanded the damage to larger areas of the forward and intermediate wing sections. These analyses attempted to quantify the effects of losing major portions of the intermediate wing structure. For this analysis, complete bottom to top “cuts” were made at critical structural locations around the main landing gear door wheel well, the wing leading edge spar and the honeycomb skin panels on the top and bottom wing surfaces. Results showed significant load redistribution throughout the wing; however, no structural members were shown to fail. The “refined” phase changed the investigative focus to a damage case that reflected the probable scenario occurring prior to the breakup. This analysis was initiated at the request of the Orbiter Aerodynamics groups in order to support an integrated analysis of the wing deformation. A combination of FEM analyses and hand analyses were used for this phase. The FEM results showed a change in overall wing panel deflections of approximately ¾”. However, hand analyses were able to show up to 5” inch deflections of the wing lower surface with de-bonded inner wing skin facesheets and loss of the intermediate wing ribs outboard of Yo167.

7.6 Stress Appendix

Appendix for Section 7.2

Table 7.6-1 FEM Summary Table of Results

		Temperatures									Results		
Case	Description	Default	Spar Web	Upper Skin	Lower Skin	Upper Spar Cap	Lower Spar Cap	Obd/Aft Upper Skin	Other (see notes)		Stress	Microstrain	Notes
4A	Calibration Case	70	70	70	70	70	70	70	-	Upper Cap (5073)	0	0	
										Lower Cap (5090)	0	0	
4B	Equal heating of spar web, upper and lower skins	70	180	180	180	70	70	70	-	Upper Cap (5073)	3749	354	
										Lower Cap (5090)	4445	419	
4C	Heating of only outboard, aft upper skin	70	70	70	70	70	70	400	-	Upper Cap (5073)	6668	629	
										Lower Cap (5090)	451	43	Nodes 73, 84, 95, 104, 103, 116, 141, 129
4D	Heat spar web, upper & lower skins, and outboard aft upper skin	70	180	180	180	70	70	400	-	Upper Cap (5073)	10416	983	
										Lower Cap (5090)	4896	462	
4E	Unequal heating of spar web, upper and lower skins	70	110	180	180	70	70	70	-	Upper Cap (5073)	3025	285	
										Lower Cap (5090)	2935	277	
4F	Heat lower skin near spar only	70	70	70	180	70	70	70	-	Upper Cap (5073)	-171	-16	
										Lower Cap (5090)	2210	208	
4G	Heat WLE nodes near panels 8/9	70	70	70	70	70	70	70	400	Upper Cap (5073)	-276	-26	
										Lower Cap (5090)	-602	-57	Nodes at y226 to 400°F
4H	Heating of only outboard, aft lower skin	70	70	70	70	70	70	70	400	Upper Cap (5073)	-377	-36	
										Lower Cap (5090)	119	11	Outboard, aft lower skin
4I	Heat spar web nodes only	70	110	70	70	70	70	70	-	Upper Cap (5073)	413	39	
										Lower Cap (5090)	863	81	Compare to 4E
4J	Heat sections of y167 Rib	70	70	70	70	70	70	70	200	Upper Cap (5073)	1	0	
										Lower Cap (5090)	5	0	167 Rib Web Nodes to 200°F
4K	Heating of only outboard, aft upper skin (see 4C)	70	70	70	70	70	70	200	-	Upper Cap (5073)	2627	248	
										Lower Cap (5090)	178	17	Compare to 4C
4L	Heating of only upper spar cap nodes	70	70	70	70	150	70	70	-	Upper Cap (5073)	-5474	-516	
										Lower Cap (5090)	-343	-32	
4M	Heating of only aft upper skin (wheel well)	70	70	70	70	70	70	70	200	Upper Cap (5073)	1273	120	Heating of aft upper skin in MLGD compartment
										Lower Cap (5090)	-108	-10	
4N	Heating of only aft upper skin (wheel well)	70	70	70	70	70	70	70	200	Upper Cap (5073)	3951	373	
										Lower Cap (5090)	-184	-17	4M plus nodes 73,95,103,116,129
M1	Mechanical load case TABR 2130 No Damage	-	-	-	-	-	-	-	-	Upper Cap (5073)	-1472	-139	
										Lower Cap (5090)	5868	554	
M2	Mechanical load case TABR 2130 Removed outboard aft upper skin	-	-	-	-	-	-	-	-	Upper Cap (5073)	-1432	-135	
										Lower Cap (5090)	5802	547	
A1	Combined heating	70	110	110	110	110	70	145	-	Upper Cap (5073)	141	13	
										Lower Cap (5090)	1549	146	
A2	Combined heating II	70	145	145	145	145	75	-	190	Upper Cap (5073)	-116	-11	Lose outboard aft upper skin (set to 70) Heat nodes 73,95,103,116,129 only
										Lower Cap (5090)	2388	225	
A3	Combined heating III	70	175	175	175	175	80	-	215	Upper Cap (5073)	777	73	
										Lower Cap (5090)	3082	291	Heat aft upper skin (wheel well) to 215
A4	Combined heating IV	70	175	175	175	175	90	-	260	Upper Cap (5073)	2122	200	
										Lower Cap (5090)	2513	237	Heat aft upper skin (wheel well) to 260

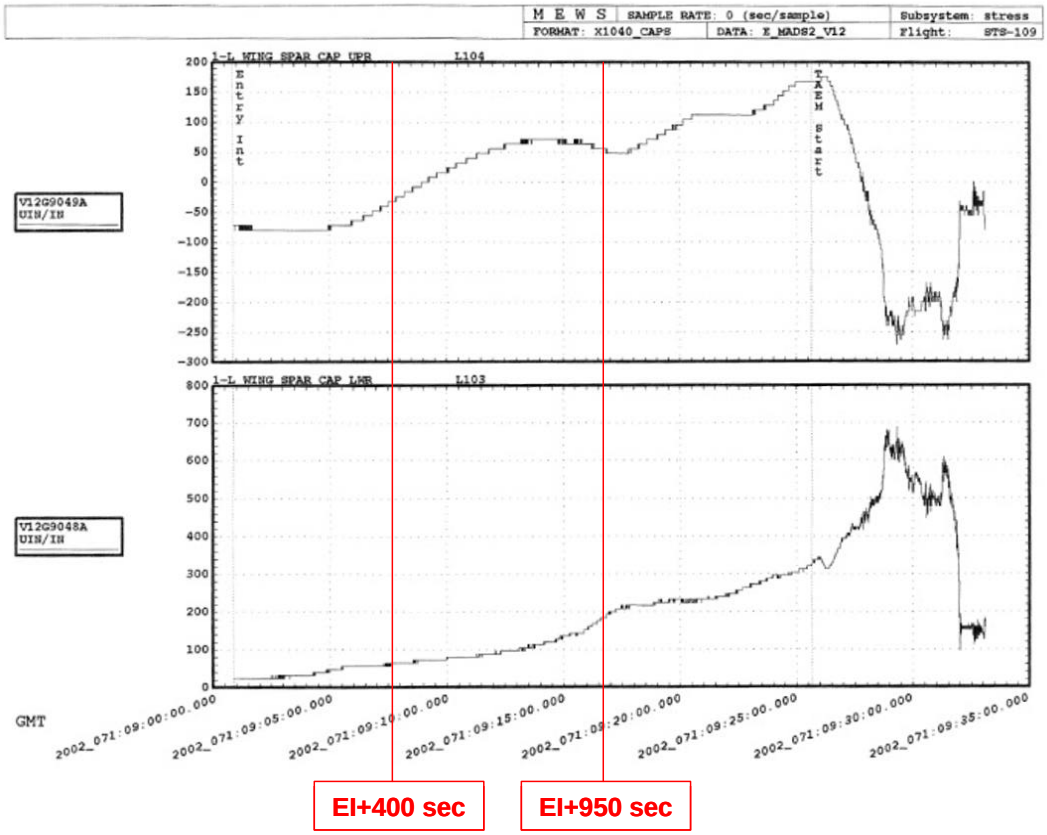

Figure 7.6-1 STS-109 Nominal Entry Strains

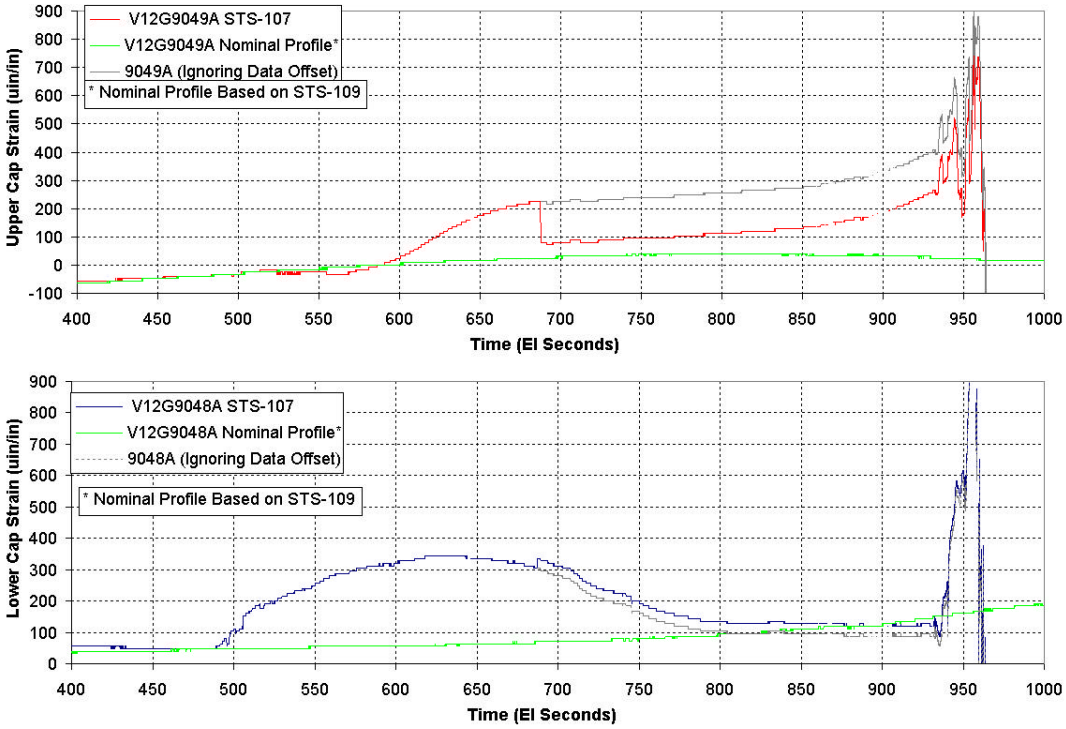

Figure 7.6-2 STS-107 Full Data Reconstruction

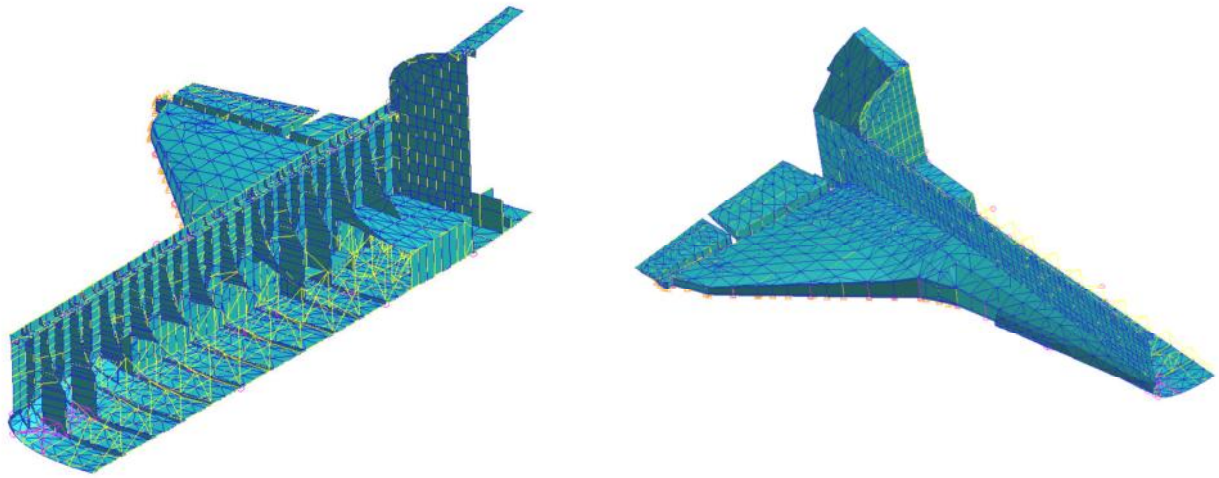

Figure 7.6-3 Complete FEM Model Illustration

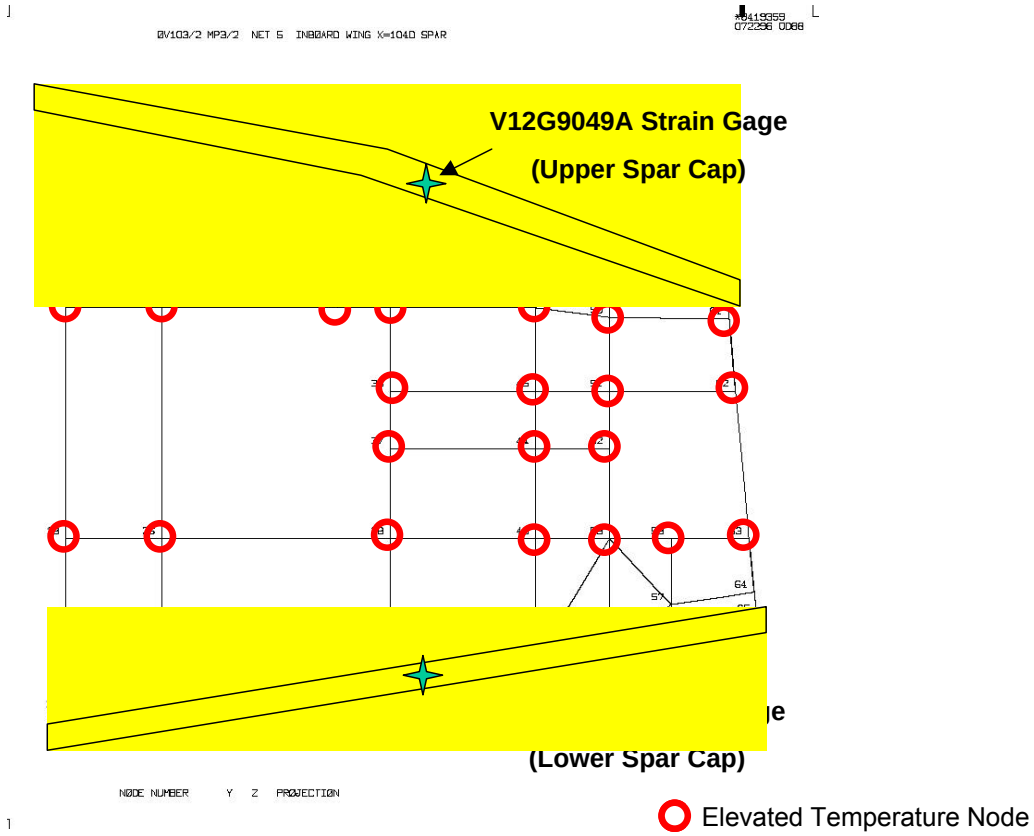

Figure 7.6-4 FEM Illustration, Xo1040 Spar Nodes

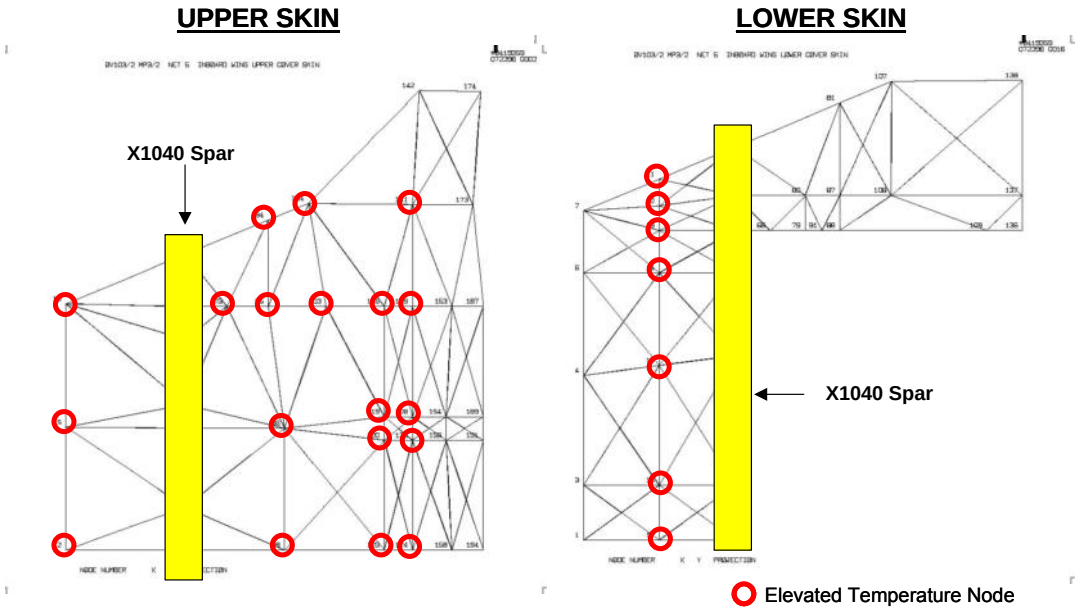

Figure 7.6-5 FEM Illustration, Nearby Skin Nodes

Appendix for Section 7.3

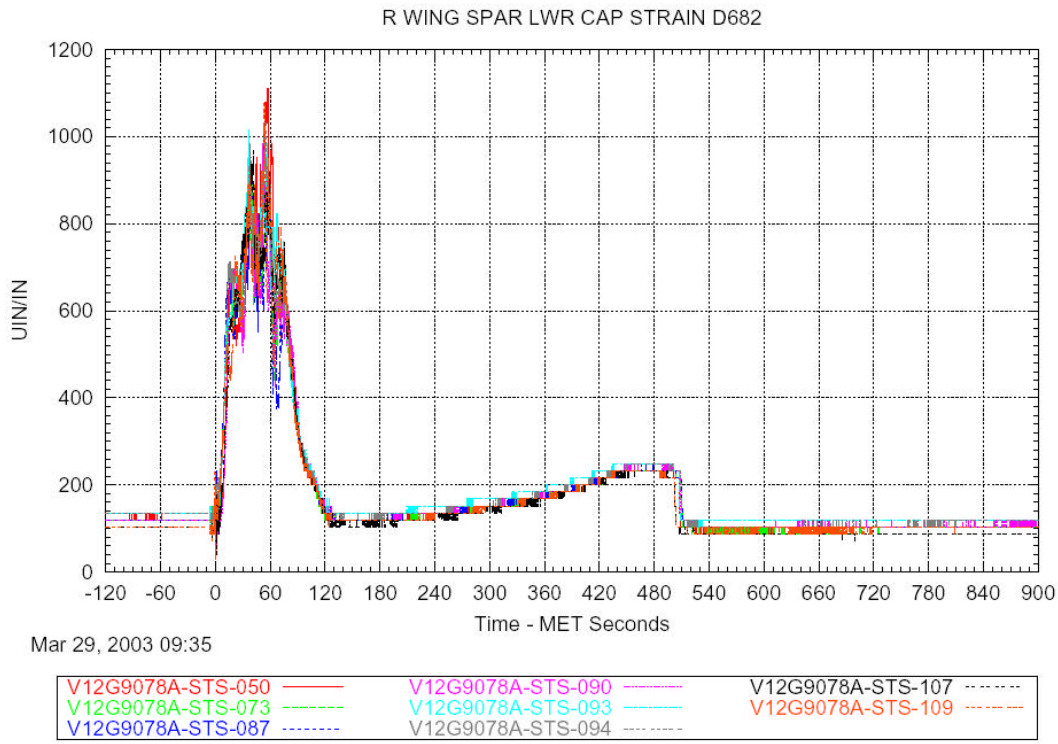

Figure 7.6-6 Typical Ascent Response

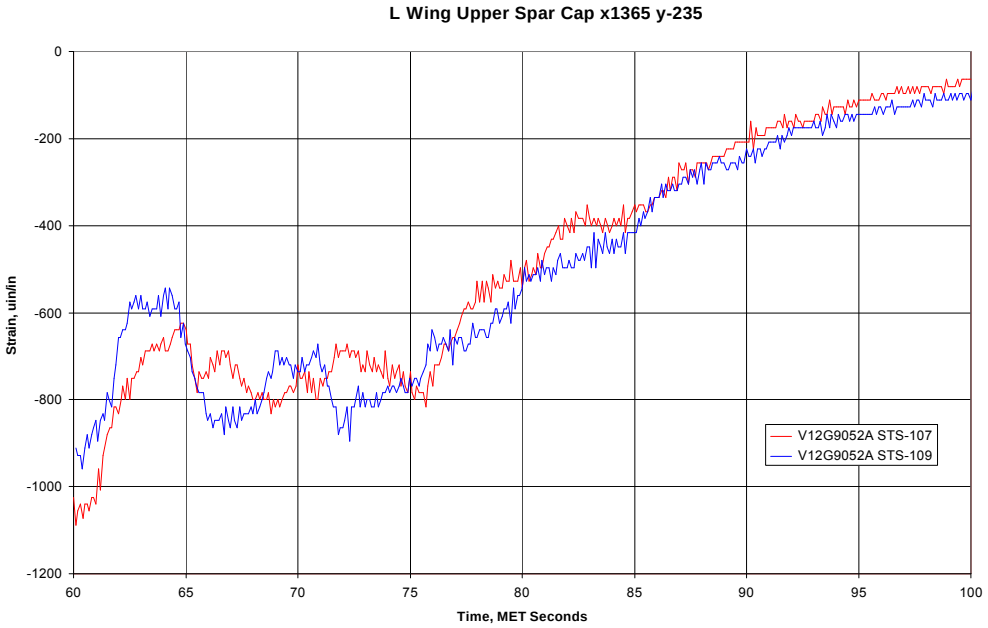

Figure 7.6-7 Interesting Signature Near Suspect Debris Impact Event

642

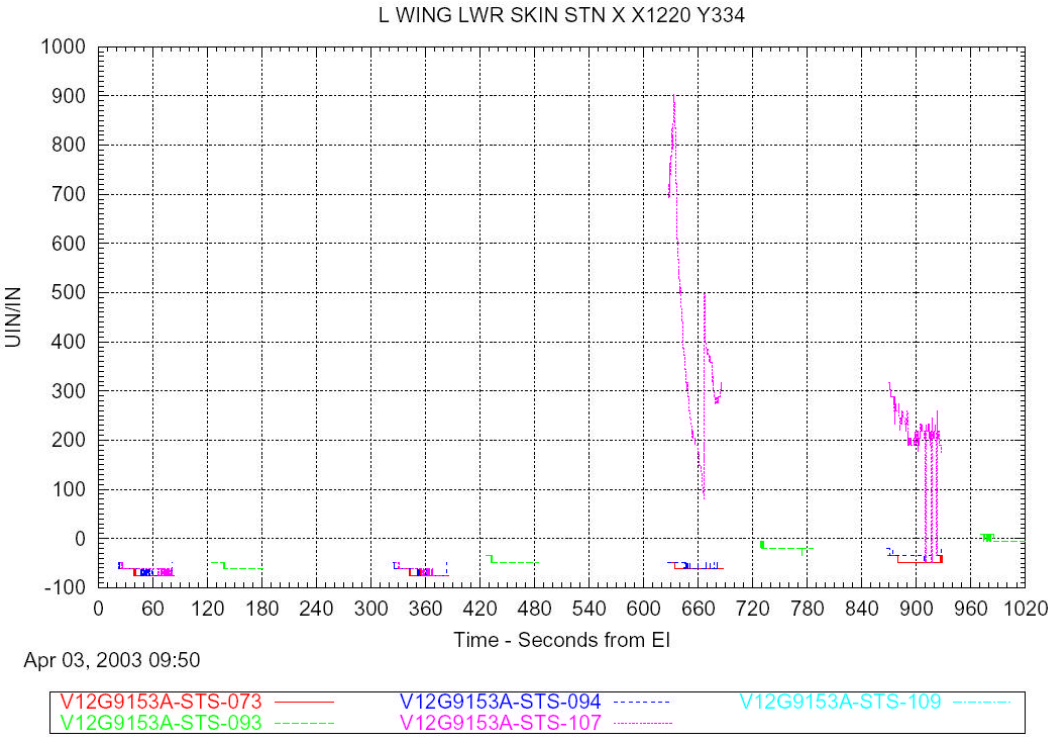

Figure 7.6-8 Typical PCM3 Entry Response

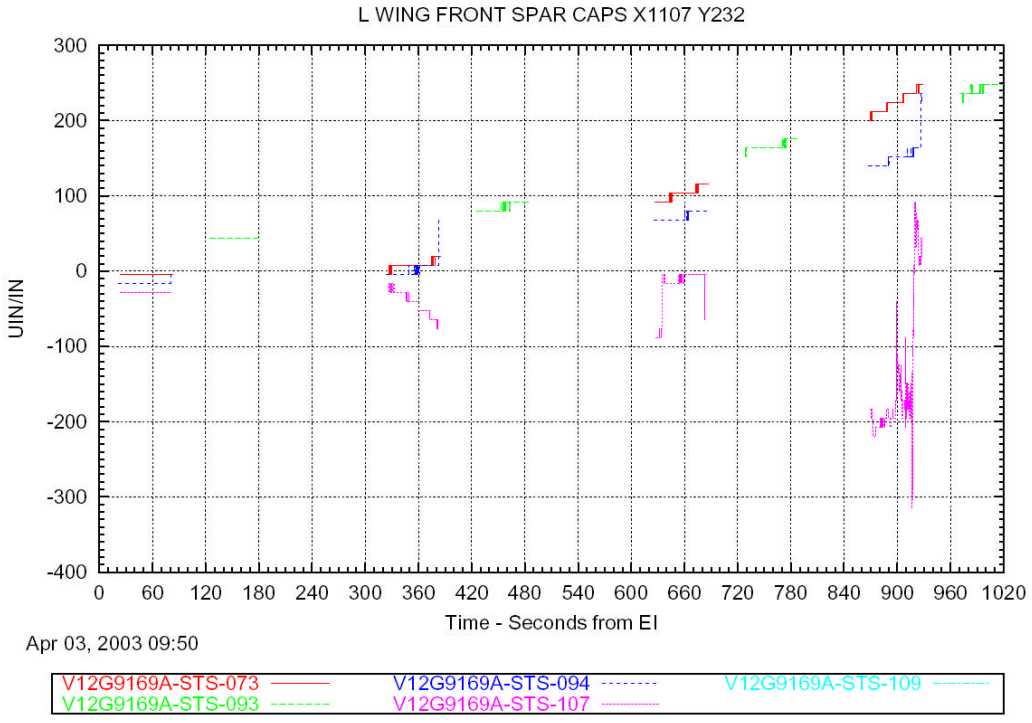

Figure 7.6-9 PCM3 Entry Response With Suspected Off-Nominal Trend

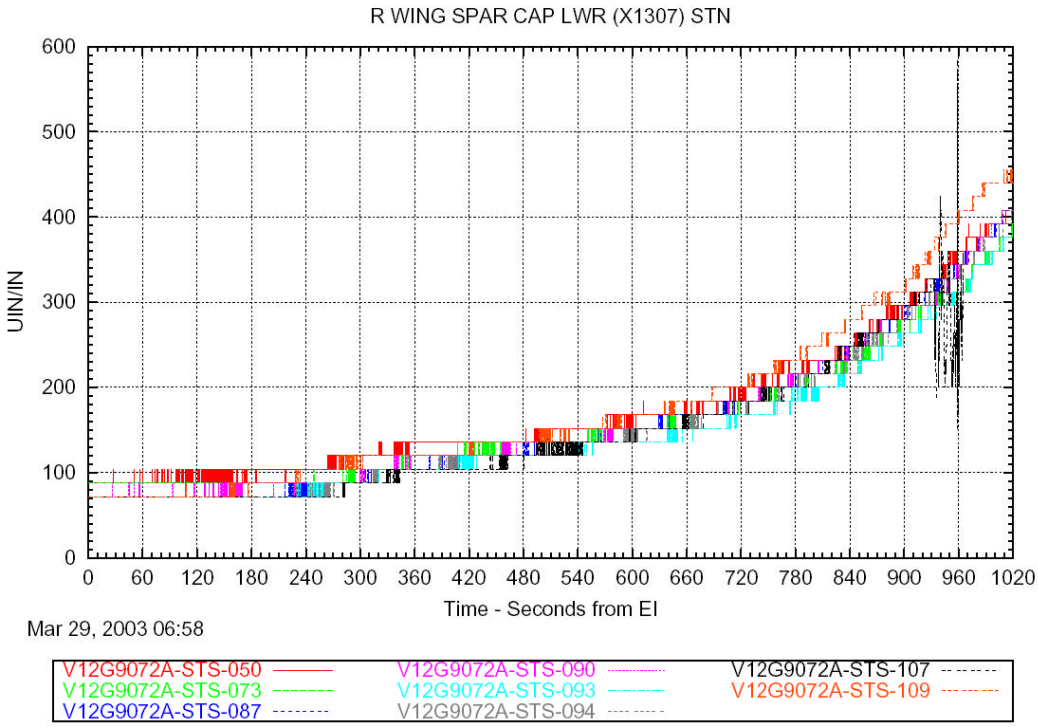

Figure 7.6-10 Typical, Nominal Right Wing Entry Response

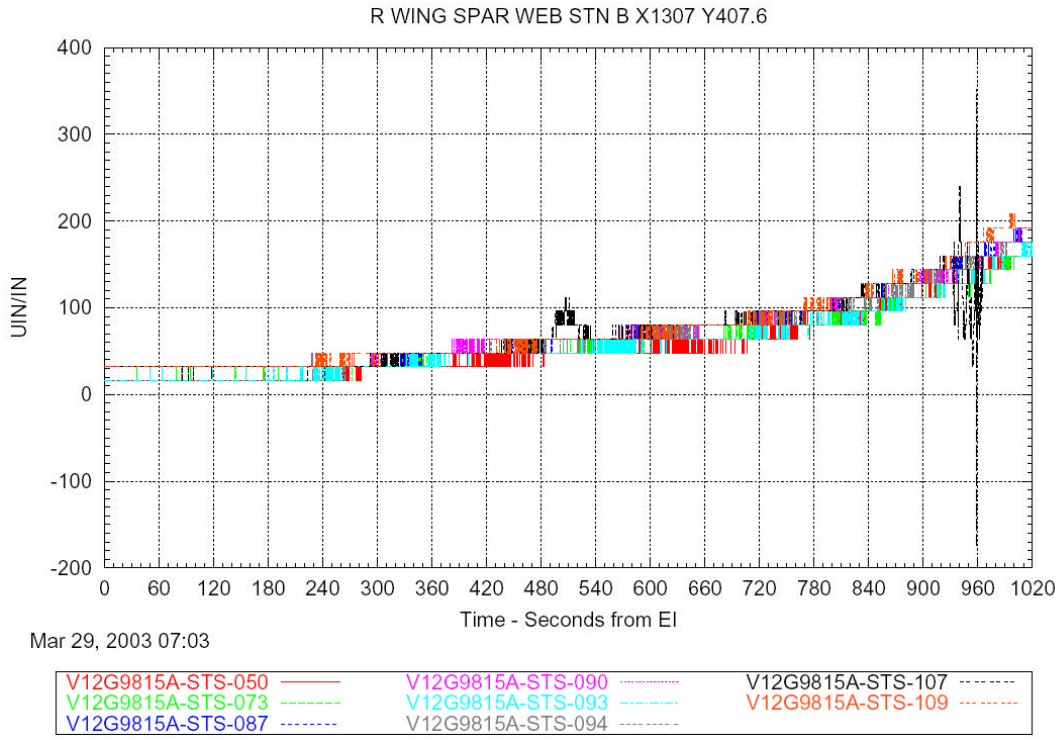

Figure 7.6-11 Right Wing Entry Brief Off-Nominal Response With Subsequent Return to Nominal

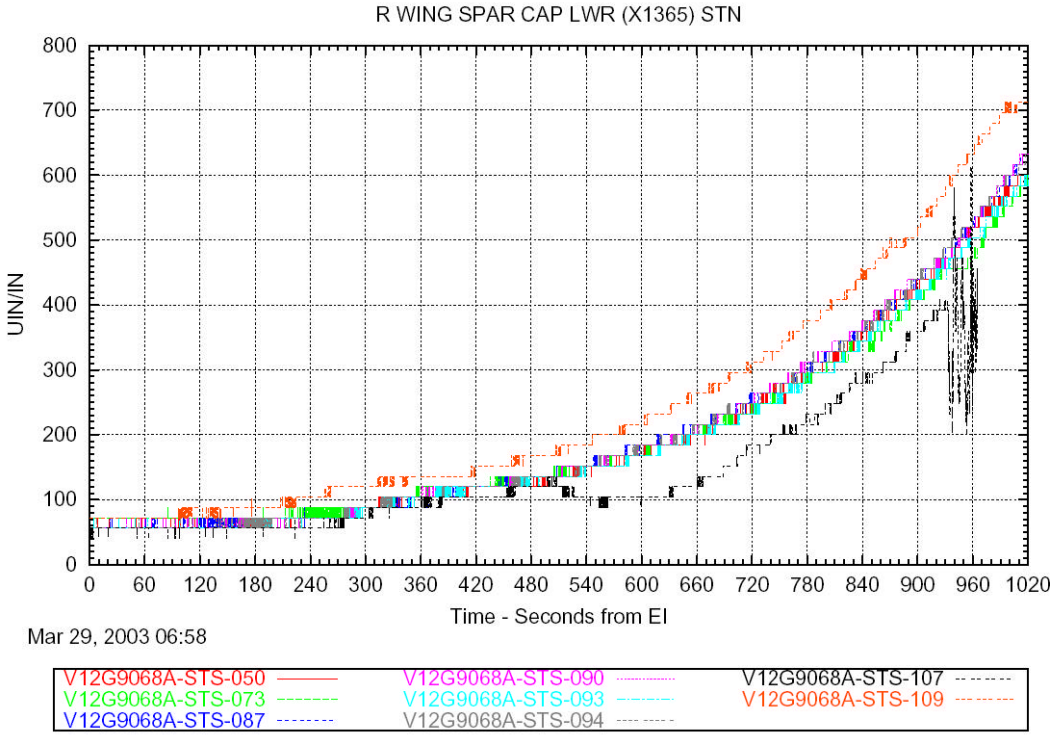

Figure 7.6-12 Right Wing Entry Off-Nominal Response With Subsequent Data Offset

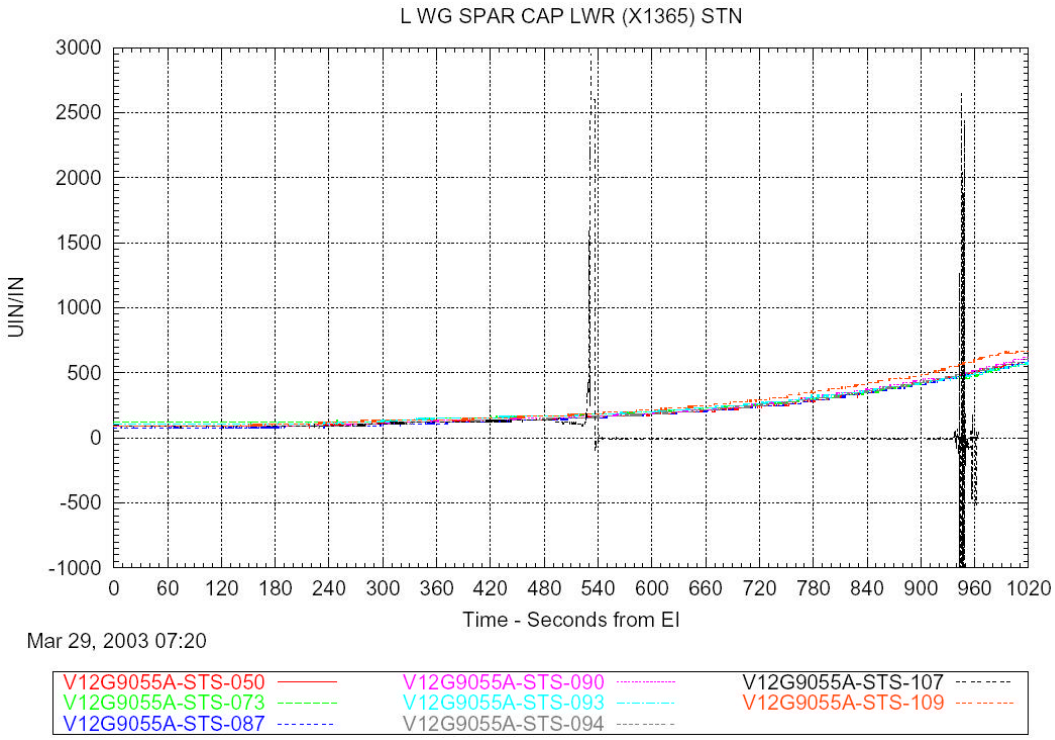

Figure 7.6-13 Typical Left Wing Entry Gage Failure

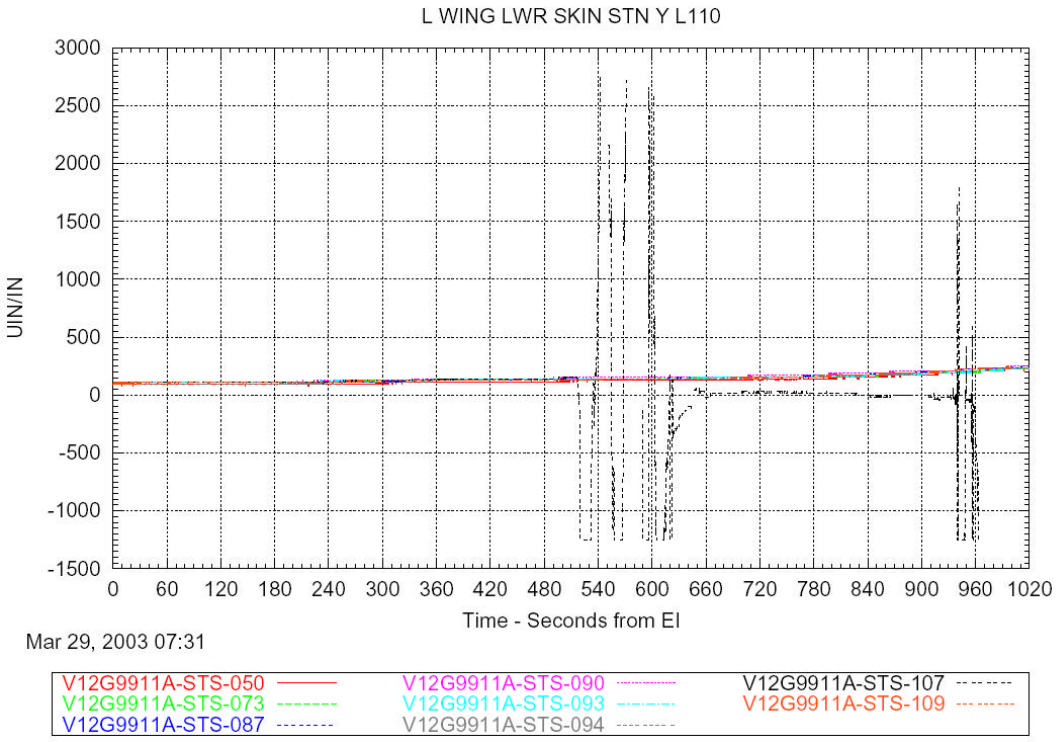

Figure 7.6-14 Left Wing Entry Gage Failure With Multiple Off-Scale Oscillations

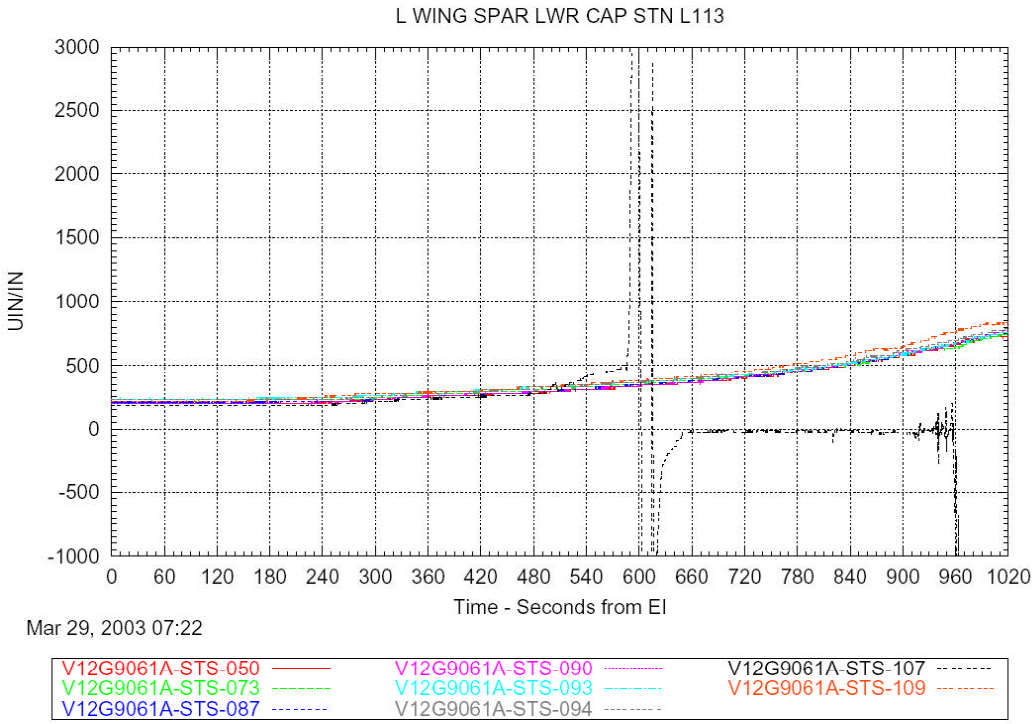

Figure 7.6-15 Left Wing Entry Gage Failure With Preceding Off-Nominal Inflection

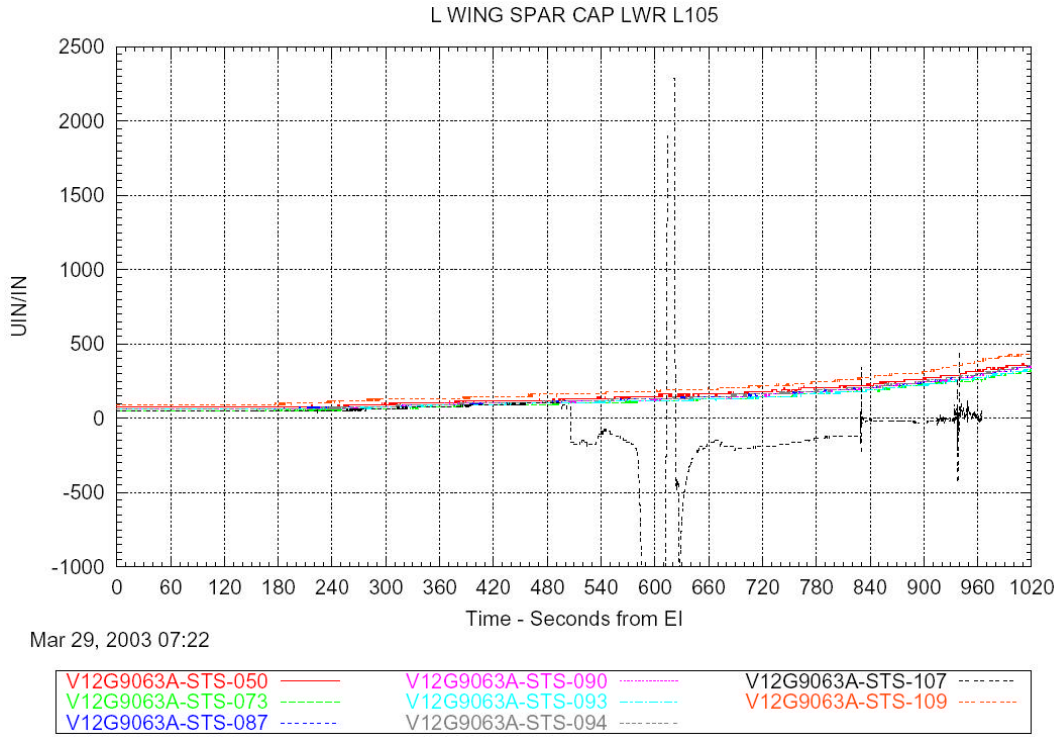

Figure 7.6-16 Left Wing Entry Gage Failure With Subsequent Nonzero Response

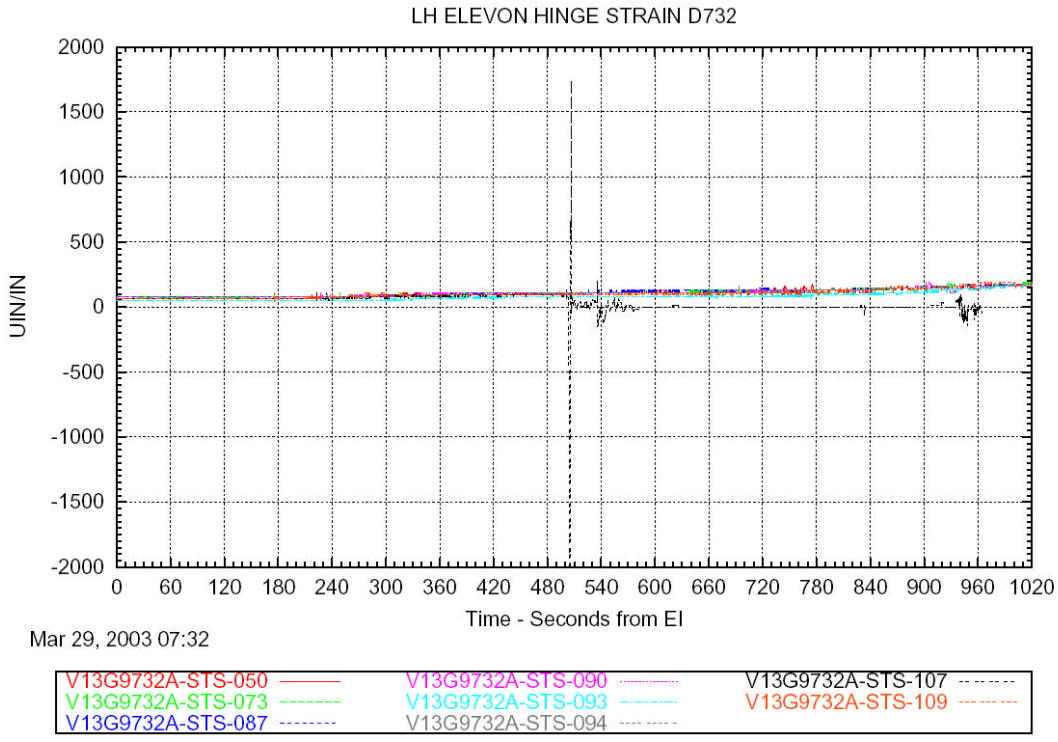

Figure 7.6-17 Typical Left Wing Elevon Entry Gage Failure

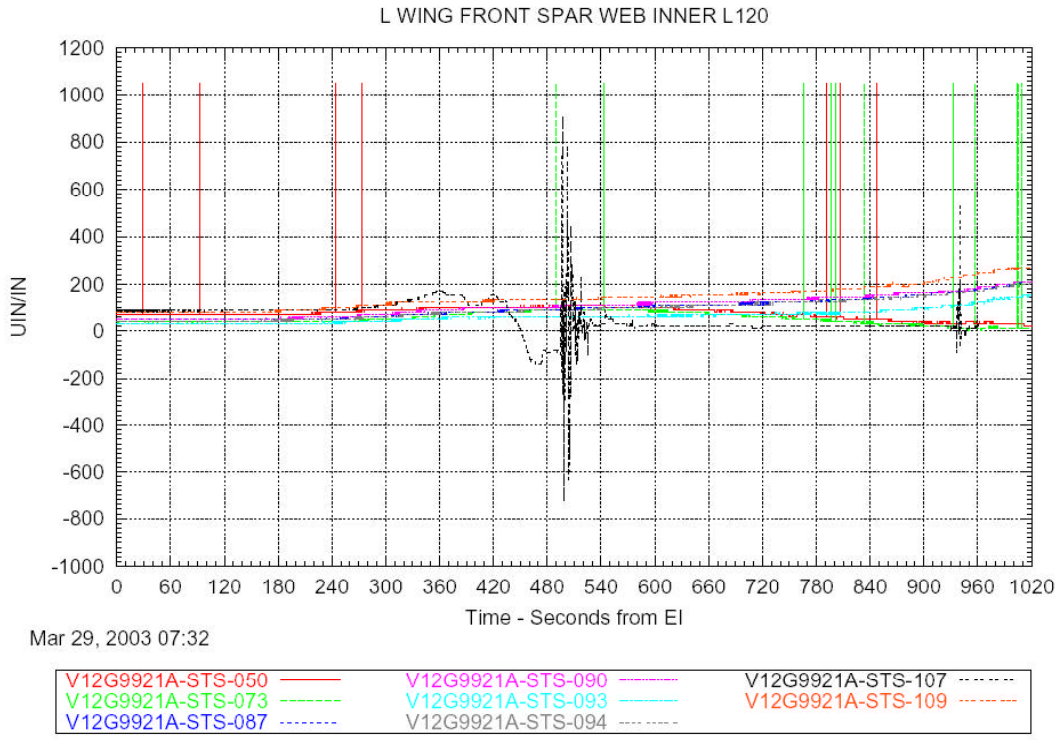

Figure 7.6-18 V12G9921A Entry Response

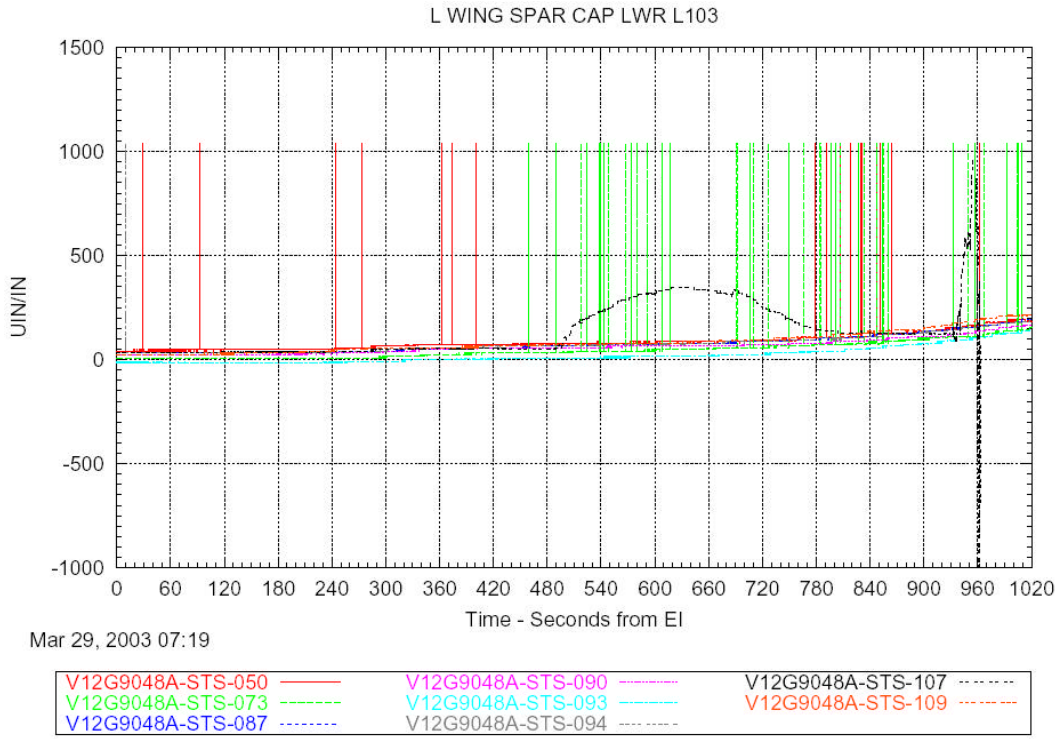

Figure 7.6-19 V12G9048A Entry Response

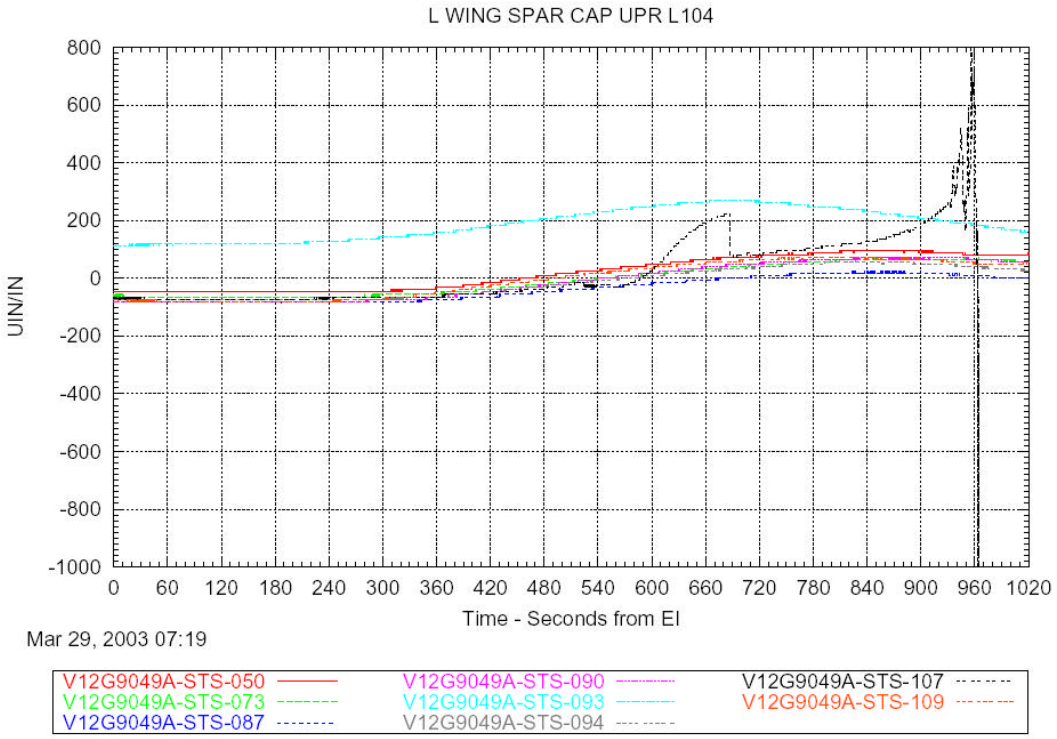

Figure 7.6-20 V12G9049A Entry Response

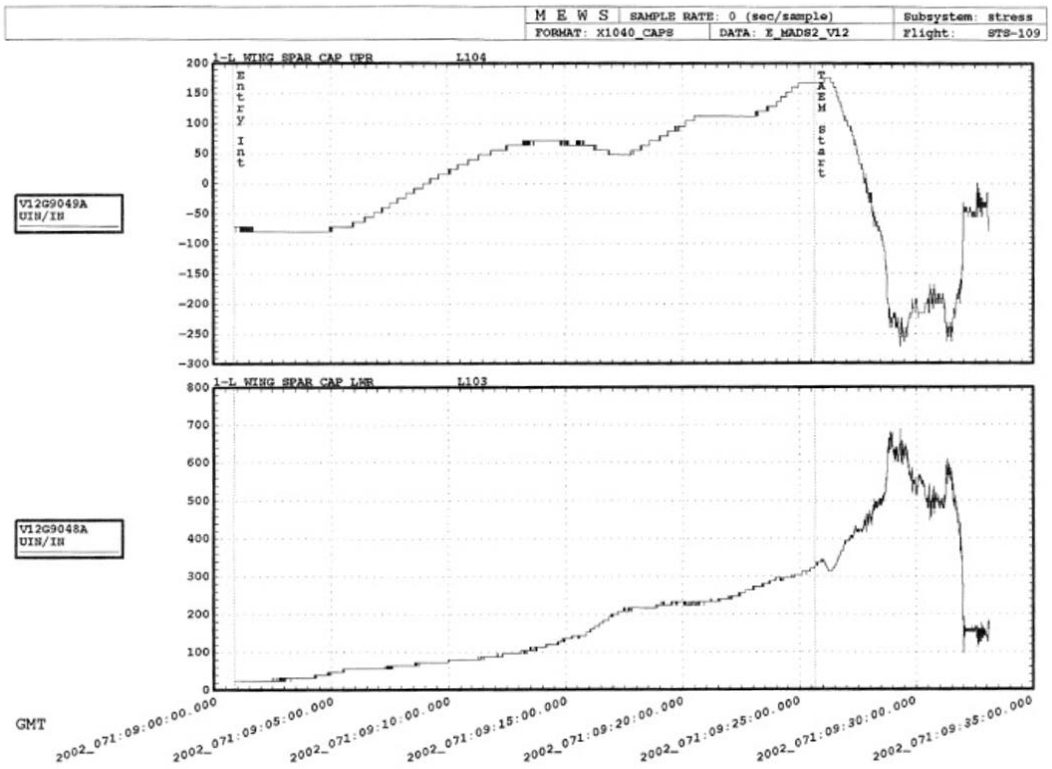

Figure 7.6-21 Xo1040 Spar Caps Nominal Entry (STS-109)

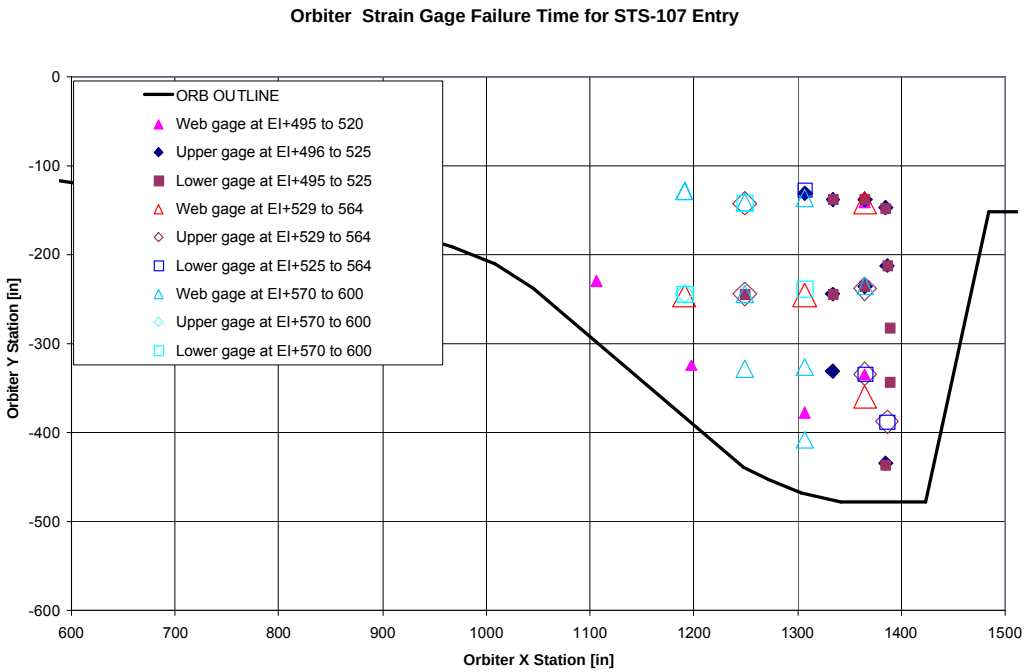

Figure 7.6-22 Left Wing Strain Gage Failure Times

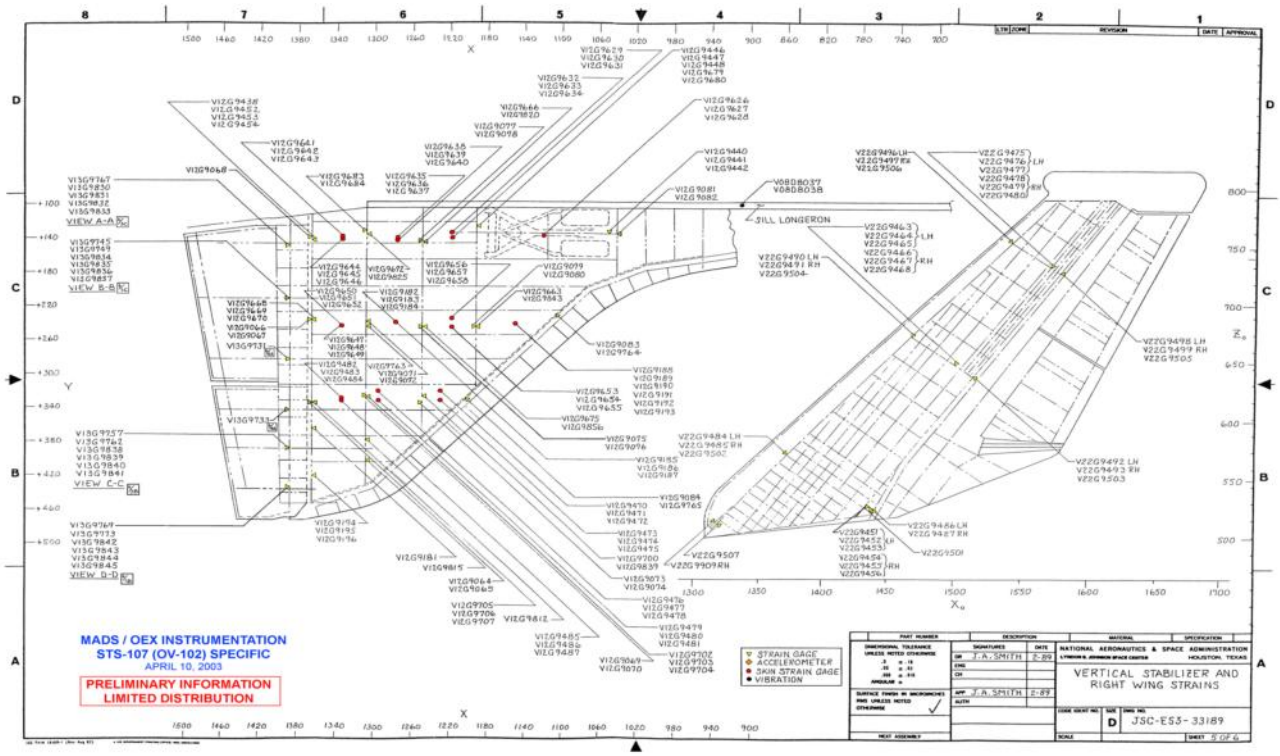

Figure 7.6-23 Right Wing Strain Gage Locations

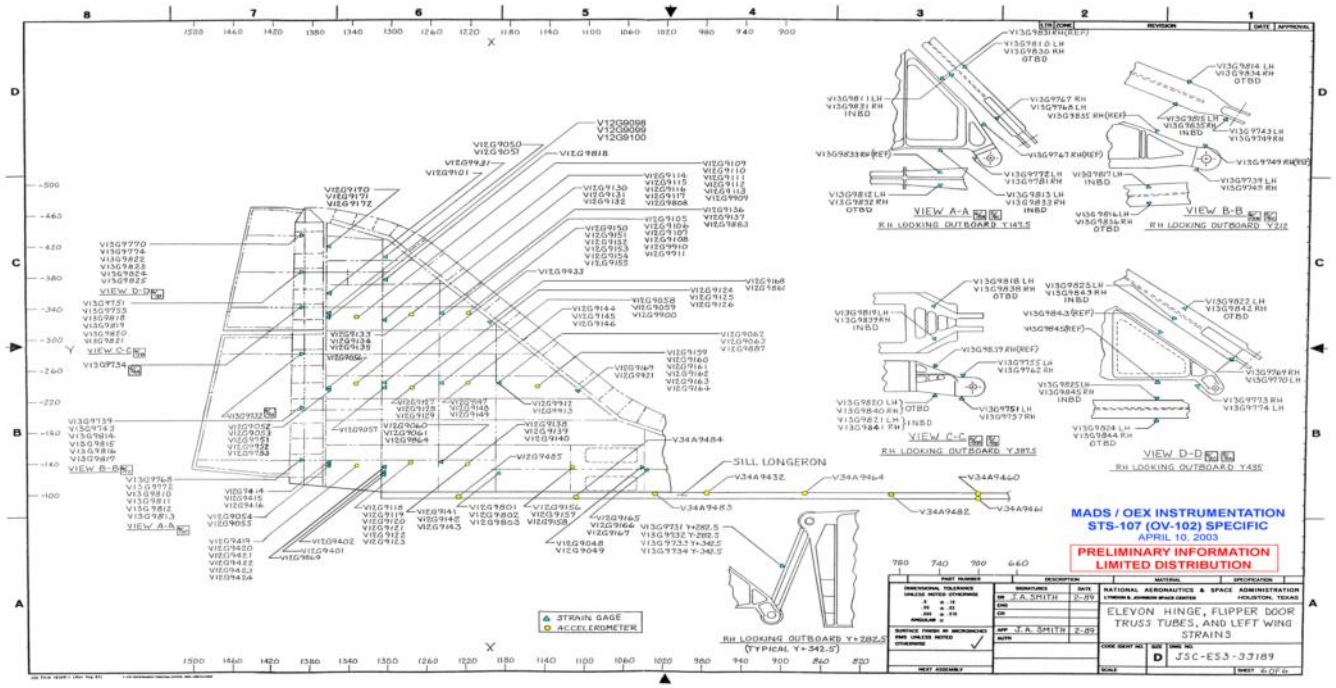

Figure 7.6-24 Left Wing Strain Gage Locations

7.7 Reference – MADS PCM Installation Drawings

Installation drawings for MADS PCM strain gages are as follows:

M072-754119
M072-754120
M072-755107
M072-756106
MC621-0004
V070-784102
V070-786117
VR70-754001

The appropriate drawing for a given strain gage installation may be determined from reference to document number JSC 23560, “OV-102 Modular Auxiliary Data System Measurement Locations”. All relevant installation drawings are included for reference in the data CD that accompanies this report.

8 CONCLUSIONS

The Aerodynamic/Aerothermodynamic/Thermal/Structures Team has completed analyses to support the Columbia Accident Investigation. The completion of this activity has resulted in the formulation of a most probable initial damage and damage progression scenario that can be used with results of other teams to identify the root cause of the Columbia accident.

The culmination of multiple analyses and tests suggest the following entry damage scenario:

Entry Interface to spar burn through:

Columbia began entry with damage to the wing leading edge reinforced-carbon-carbon (RCC) most likely in panels 7 or 8.

Hot gas was ingested into the cavity behind the RCC panels from the beginning of the entry profile. Internal aerothermodynamic and venting analyses show that the flow of hot gas into the RCC cavity was vectored outboard down the RCC cavity and up and aft toward the top of the wing leading edge spar. The hot gas impinged on the RCC panel rib and spanner beam insulation resulting in very high localized heating.

The panel 9 spar strain gage registered the first off-nominal indications at approximately 270 seconds from EI. Stress analysis shows that the panel 9 spar strain gage readings are consistent with shear strain associated with a temperature gradient that developed as the top of the spar is heated by the ingestion of hot gas.

Panel 9 clevis temperature began an off-nominal temperature increase at approximately 290 seconds from EI due to heating from conduction through the insulation and heating from convection due to sneak flow between the insulation and the clevis. Thermal analysis suggests that this response is consistent with flow entering an aperture with an area consistent with a ten inch diameter hole.

CFD analysis and wind tunnel test results modeling increased flow out of thermally degraded/expanded vents located at the top of the RCC cavity suggest that disturbed flow on the leeside of the vehicle can displace the strake and canopy vortices and temporarily reduce localized heating to the left sidewall and left OMS pod.

The damage magnitude is consistent with negligible aerodynamic increments experienced during this period.

Spar burn through to off-nominal increase in sidewall and OMS pod temperatures:

Spar burn through occurred by approximately 487 seconds from EI. This time is supported by:

Wing Spar Strain analysis	-> 420 - 470 sec
1040 Spar Strain analysis	-> 488 sec
Leading Edge Spar wire harness failure	-> 487 sec
Bit flip in wheel well measurement	-> 488 sec
Panel 8/9 thermal analysis	-> 490 sec

Analyses of spar burn through times suggest that the initial damage was consistent with a breach in the lower portion of RCC panel 8 with an area consistent with a six to ten inch diameter hole.

CFD analysis suggests that the transverse momentum of the flow of hot gas entering the RCC cavity is redirected as the flow impinges on RCC ribs and spanner beam hardware and insulation. As a result, the local pressure is increased and the plume entering the intermediate wing is directed normal from the spar toward the main landing gear compartment wall.

Thermal analysis of plume heating on wire bundles and the wheel well wall supports the location of the breach on the panel 8 spar.

Thermal analysis of measured temperature profiles for components in the wheel well show that convective heating is required to produce the measured results. This is consistent with the modeled burn through of the main landing gear compartment wall at approximately EI+601 seconds.

Increased heating of the left sidewall and OMS pod can be explained by redirection of the wing leading edge windward flow to the leeside through either a severely damaged and/or missing upper RCC carrier panel(s), severely damaged or missing full RCC panel (e.g. panel 9), or damaged upper wing just aft of the wing leading edge. Test and analyses of these damage conditions yields aerodynamic increments consistent with flight extracted aero between EI+500 to EI+600 seconds.

Evaluation of final aerodynamic increments:

Damage in the left wing cavity continued to progress until loss of signal. This damage resulted in a significant depression forming on the lower surface of the left wing due to burn though of intermediate wing truss tubes and compromised structural strength associated with heating internal to the wing. The depression in the lower wing resulted in external flow patterns that effectively increased the lift and drag on the left wing resulting in the large positive rolling moment and large negative yawing moment just prior to loss of signal.

As a final comment on the damaged configuration test and analysis results, it must be pointed out again that the nature of this analysis and the conclusions to be drawn from them should be limited to a proper engineering perspective. The test and analysis conducted for the investigation were performed on representative geometries. The representative geometries that have been assessed were chosen in a very dynamic investigation environment as engineers interpreted the latest results from wind tunnel testing, CFD analysis, flight measurement evaluation, recovered hardware forensics, etc. The fact that these geometries were chosen for investigation purposes should not be misconstrued as exactly reproducing the damaged configuration encountered in flight. These representative damaged configurations, however, do provide an insight into the nature and level of damage necessary to result in the loss of Columbia and her STS-107 crew.

9 CREDITS

The authors wish to recognize the outstanding efforts of the many personnel that directly or indirectly supported the AATS team. Numerous personnel from various organizations provided data, products or services in support of AATS team activities. Personnel supporting the accident investigation primarily through the AATS team are listed in Appendix B of this report. Many others, however, provided support through other teams and therefore are not individually credited here. The following teams are recognized for providing essential support to the AATS team:

Timeline Team
Vehicle Data Mapping Team
Integrated Entry Environments Team
Hardware Forensics Team
Scenario Team

In addition, many AATS team members did not author parts of this final report even though they were key contributors on the team, mostly due to reassignment to other activities later in the investigation. These individuals provide invaluable expertise, especially during the initial phase of the investigation. These team members are listed below:

Aerodynamics
Gary Bourland, NASA Johnson Space Center
James Brown, NASA Ames Research Center
Joe Gamble, NASA Johnson Space Center
Jim Greathouse, NASA Johnson Space Center
Gerald LeBeau, NASA Johnson Space Center
Chris Madsen, NASA Johnson Space Center
Charles Miller, NASA Langley Research Center
Phil Stuart, NASA Johnson Space Center

Aerothermodynamics
Ed Alexander, Boeing Houston
Maria Barnwell, Boeing Houston
Basil Hassan Ph. D., Sandia National Laboratories
Ron Merski, Ph. D., NASA Langley Research Center
Charles Miller, NASA Langley Research Center
Habib Sharifzadeh, Boeing Huntington Beach
Carl Peterson, Sandia National Laboratories
Richard Wheless, NASA Langley Research Center

Thermal
Stan Bouslog, Lockheed
Kevin Bowcutt, Boeing Huntington Beach
Doug Cline, Boeing Houston
Dianna Coronado, Boeing Houston
Don Curry, NASA Johnson Space Center
Fred Ghayasi, Boeing Huntington Beach
Andy Hong, NASA Johnson Space Center
John Kowal, NASA Johnson Space Center
Ronald K. Lewis, NASA Johnson Space Center
Jim Milhoan, Lockheed
Don Picetti, Boeing Huntington Beach
Steve Rickman, NASA Johnson Space Center
Dave Russell, Boeing Houston
Habib Sharifzadeh, Boeing Huntington Beach
John Sharp, NASA Marshall Space Flight Center
Lung-Chen Wong, Boeing Houston

Stress
Tony Chi, Boeing Huntington Beach
Scott Foust, Boeing Huntington Beach
Bill Novak, Boeing Huntington Beach
Dave Okino, Boeing Huntington Beach
Steve Scotti, NASA Langley Research Center

10 Acknowledgements

The work presented in this document is but a small demonstration of the total efforts of more than one hundred dedicated engineers and scientists across the country in support of the aerodynamic, aerothermodynamic, thermal, and structural analysis portion of this investigation. Those efforts are not only applicable to understanding Columbia's fate, but will also be used to improve future human space flight vehicle designs. Regardless of how outstanding our efforts, they merely shadow the tragic loss of Columbia and her crew. We dedicate these efforts and the immediate sacrifices of our families and loved ones since the morning of February 1, 2003, to Columbia, her crew, and the lifelong sacrifices of the crew's families and loved ones.

We would also like to recognize the devotion to space flight on the part of the Orbiter program engineers and flight controllers, as well as the dedication of the Space Shuttle and Orbiter program managers. The extreme energies put forth by the manned space flight community during this investigation must be acknowledged, for without their incredible insight, experience and focused drive, the understanding of Columbia's final flight would not have been possible within the allotted time frame. The passion exhibited by this team is the same unyielding dedication that keeps us moving forward, pursuing the vision of manned space flight.

Finally, we dedicate these results, the methods developed and the understanding acquired, to the future of manned space flight and all future crews. By pushing our limitations with each ensuing flight, we utilize the wisdom of the many sacrifices of the past in conjunction with our curiosity, to learn more and continue to follow the better path in mankind's quest for the stars.

References

1. NSTS-37376 Data Review and Timeline Reconstruction Team Final Report in support of the Columbia Accident Investigation

2. NSTS-37382 Integrated Entry Environment (IEE) Team Final Report in support of the Columbia Accident Investigation

3. NSTS-37383 Vehicle Data Mapping Final Report in support of the Columbia Accident Investigation

4. NSTS-37385 Hardware Forensics Team Final Report in support of Columbia Accident Investigation

5. NSTS-37386 Materials and Processes Failure Analysis Team Final Report in support of Columbia Accident Investigation

6. NSTS-37397 Vehicle Reconstruction Team Final Report in support of the Columbia Accident Investigation

7. NSTS-60502 Columbia Working Scenario Final Report

APPENDICES

Appendix A - Acronyms and Abbreviations

AATS	**Aerodynamic/Aerothermodynamic/Thermal/Structures**
ABLT	**Asymmetric Boundary Layer Transition**
ADTA	**Air Data Transducer Assembly**
aero	**Aerodynamic**
AFB	**Air Force Base**
Al	**Aluminum**
APU	**Auxiliary Power Unit**
ARC	**Ames Research Center**
ASA	**Reacting Flow Environments (Branch)**
BC	**Boundary Condition**
BFS	**Backup Flight System**
BHB	**Boeing Huntington Beach**
BL	**Boundary Layer**
BP	**Body Point**
B-RKDN	**Boeing Rocketdyne**
BTU	**British Thermal Unit**
CAD	**Computer-Aided Design**
CAIB	**Columbia Accident Investigation Board**
CART3D	**Cartesian Three Dimensional**
CF4	**Carbon Tetra-Flouride**
CFD	**Computational Fluid Dynamics**
CG	**Center of Gravity**
Comm	**Communication**
DAC	**DSCM Analysis Code**
DAO	**Data Assimilation Office**
DSMC	**Direct Simulation Monte Carlo**
EI	**Entry Interface**
ENV	**Environment**
EOM	**End of Mission**
FC	**Flight Control**
FCS	**Flight Control System**
FEM	**Finite Element Model**
FFT	**Fast Fourier Tranform**
FRSI	**Flexible Reusable Surface Insulation**
ft	**Feet**
FWD	**Forward**
GMT	**Greenwich Mean Time**
GN&C	**Guidance, Navigation and Control**
GNC	**Guidance, Navigation and Control**
GPS	**Global Positioning Satellite**
GRAM	**Global Reference Atmosphere Model**
GSFC	**Goddard Space Flight Center**
Hyd	**Hydraulic**
IEE	**Integrated Entry Environment**
IML	**Inner Mold Line**
IMU	**Inertial Measurement Unit**
INBD	**Inboard**
IR	**Infrared**
JSC	**Johnson Space Center**
Kn	**Knudsen Number**
KSC	**Kennedy Space Center**
LaRC	**Langley Research Center**
LE	**Leading Edge**
LESS	**Leading Edge Subsystem**

LG	**Landing Gear**
LH	**Left Hand**
LHIB	**Left hand Inboard**
LMG	**Left Main Gear**
LMSC	**Lockheed Management Sevices Company**
Ln	**Line**
LOS	**Loss of Signal**
LT	**Left**
M	**Mach**
MADS	**Measurement Acquisition Data System**
MEDS	**Multifunction Electronic Display Subsystem**
MET	**Mission Elapsed Time**
MLG	**Main Landing Gear**
MLGD	**Main Landing Gear Door**
MMOD	**Micro Meteoroid Orbital Debris**
MPH	**Miles per hour**
MPS	**Main Propulsion System**
MSFC	**Marshall Space Flight Center**
MSID	**Measurement Stimulus Identification**
NAIT	**NASA Accident Investigation Team**
NASA	**National Aeronautics and Space Administration**
NAV	**Navigation**
NLG	**Nose Landing Gear**
NSTS	**National Space Transportation System**
OADB	**Operational Aerodynamic Data Book**
OARE	**Orbital Acceleration Research Experiment**
OB	**Outboard**
ODRC	**Orbiter Data Reduction Complex**
OEX	**Orbiter Experimentation**
OFT	**Operational Flight Test**
OI	**Operational Instrumentation**
OML	**Outer Mold Line**
OMS	**Orbital Maneuvering System**
OSH	**Off Scale High**
OSL	**Off Scale Low**
OUTBD	**Outboard**
OVE	**Orbiter Vehicle Engineering**
OVEWG	**Orbiter Vehicle Engineering Working Group**
PCM	**Pulse Code Modulation**
PCM	**Pulse Code Modulation**
PDSS	**PRACA Data Support System**
PIC	**Pyro Initiator Controller**
PRACA	**Problem Resolution And Corrective Action**
Press	**Pressure**
PRSD	**Power Reactant Storage and Distribution**
PRT	**Prevention / Resolution Team**
PSD	**Power Spectral Density**
psf	**Pounds per square foot**
RCC	**Reinforced Carbon-Carbon**
RCG	**Reaction Cured Glass**
RCS	**Reaction Control System**
RMS	**Root mean square**
RTD	**Resistant Temperature Devise**
RTV	**Room Temperature Vulcanizing**
SABER	**Sounding of the Atmosphere using Broadband Emission Radiometry**
sec	**second**
SES	**Shuttle Engineering Simulator**
SGS	**Simple Geometric Shapes**
SiC	**Silicon Carbide**

SILTS	**Shuttle Infrared Leeside Temperature Sensing**
SLA	**Stereolithography**
SNL	**Sandia National Laboratories**
SOFI	**Spray On Foam Insulation**
SPR	**Suspect Problem Report**
SR&QA	**Safety, Reliability & Quality Assurance**
SSVEO	**Space Shuttle Vehicle Engineering Office**
STS	**Shuttle Transportation System**
Surf	**Surface**
Sw	**Switch**
Sys	**System**
TAEM	**Terminal Area Energy Management**
TAS	**True Air Speed**
TC	**Thermocouple**
Temp	**Temperature**
TEOS	**Tetraethyl Orthosilicate**
TIM	**Technical Interchange Meeting**
TIMED	**Thermosphere Ionosphere Mesosphere Energetics and Dynamics**
TMM	**Thermal Math Model**
TPS	**Thermal Protection System**
Unlk	**Unlock**
Uplk	**Uplock**
USA	**Unified Solution Algorithm**
USA	**United Space Alliance**
VGM	**Volume Grid Manipulator**
Vlv	**Valve**
VT	**Vertical Tail**
WBS	**Work Breakdown Structure**
WCT	**Wing Carry Through**
WLE	**Wing Leading Edge**
WSTF	**White Sands Test Facility**
WT	**Wind Tunnel**
WTT	**Wind Tunnel Test**

Appendix B - Team Member List & Biographies

Team Lead Biographies

Pam Madera
Ms. Madera has twenty years of experience in the Space Shuttle Program. Her current position is Subsystem Area Manager for Orbiter Vehicle and Systems Analysis for United Space Alliance in support of the NASA JSC Orbiter Vehicle Engineering Office. She provides oversight of analysis activities associated with the flight readiness, mission support as well as design changes.

Steven Labbe – Aerodynamics Team
Mr. Steven G. Labbe is a 1984 graduate of the University of Cincinnati with a Bachelor of Science Degree in Aerospace Engineering. He has been employed by NASA since 1981, beginning as a cooperative education student at the Lewis (now Glenn) Research Center. He transferred to the Johnson Space Center as a coop and accepted a full-time position in 1984. He currently serves as the Chief of the Applied Aeroscience and Computational Fluid Dynamics Branch. Previous positions at NASA include: Aeroscience Branch Engineer responsible for the development and analysis of Shuttle aerodynamic characteristics; Professional Development Program (PDP) participation via rotational assignment at NASA Ames Research Center in the Applied CFD Analysis Branch; Space Shuttle Ascent Aerodynamic Sub System Manager; Aeroscience Branch Aerodynamics Group Leader; X-38 Project, Aeroscience and Flight Mechanics, Division Chief Engineer/Flight Dynamics Team Lead; X-38 Aerodynamics Lead; and Deputy Chief, Applied Aeroscience & CFD Branch.

Joe Caram – Aerothermodynamics Team
Mr. Caram is an aerospace engineer employed at NASA Johnson Space Center since 1989 working in the Aeroscience and Flight Mechanics Division of the Engineering Directorate. He received his Bachelor of Science and Masters of Science degrees from Texas A&M University in 1986 and 1989, respectively. Until recently he was serving as chief engineer for the feasibility studies of the Orbital Space Plane on Expendable Launch Vehicles (08/02 – 01/03) and X-38 Project EG Division Chief Engineer / Flight Dynamics Lead (03/96 – 07/03). Previous positions at NASA include: Aeroscience Branch engineer responsible for development and analysis of aerothermodynamic environments of various configurations including the Space Shuttle Orbiter. In that position Mr. Caram was responsible for developing math models of the shock-shock interaction heating to the wing leading edge of the Orbiter (9/89 – 3/91) and lead a team investigating Orbiter early/asymmetric hypersonic boundary layer transition (6/92 – 12/95). Other activities during the 1991 to 1995 time frame included being aerothermodynamics team lead in support of advanced projects such as Assured Crew Return Vehicle, First Lunar Outpost, Single Launch Core Station, and Liquid FlyBack Booster. Mr. Caram is an Associate Fellow of AIAA and author or co-author of 20 publications including AIAA conference papers and journal articles, NASA TM's and Symposia.

Charles Campbell – External Aerothermodyanamic Environment Sub-team Lead
Chuck Campbell has been a member of the Applied Aeroscience and CFD Branch at NASA Johnson Space Center since 1990 and has had extensive experience in the application of CFD and wind tunnel testing to manned spacecraft design. Significant activities he has been involved with include the Orbiter Boundary Layer Transition Working Group in the mid-1990's, and hypersonic aerodynamic and aerothermodynamic design for the X-38 Crew Return Vehicle. He holds an Bachelor of Science from the University of Minnesota (1990) in Aerospace Engineering and Mechanics, and a Master of Science from the University of Houston (1998) in Mechanical Engineering.

Team Lead Biographies, Concluded

Steve Fitzgerald – Internal Aerothermodyanamic Environment Sub-team Lead
Steve Fitzgerald joined the Applied Aeroscience and CFD Branch of the Johnson Space Center as a cooperative education student in 1984. Since that time, he has worked a wide range of fluid dynamic fields ranging from numerical simulation of arcjet flows and re-entry flows to rarefied gas dynamics and on-orbit plume impingement flows. As the JSC plume lead, he was a principal author of the Orbiter plume impingement enviromnents and served as a principal investigator for two space flight experiments. In his role as X-38/Crew Return Vehicle aerothermal lead, he oversaw the development of the complete aerothermal database for the X-38, integrating CFD efforts from three separate agencies, and hypersonic wind tunnel testing results from both U.S. and European facilities. Steve holds Bachelors (1986) and Masters (1988) degrees from Texas A&M University in Aerospace Engineering. He presently serves as deputy chief for the GN&C Design and Analysis Branch.

Chris Madden – Thermal Team Lead
Mr. Christopher B. Madden is a 1987 graduate of the University of Texas at Austin with a Bachelor of Science Degree in Aerospace, Aeronautical and Astronautics. He completed his Master of Mechanical Engineering at the University of Houston in 1993. He has been employed by NASA/Johnson Space Center since 1984 where he began as a cooperative student in the Thermal Analysis Section. Mr. Madden is currently serving as the Deputy Chief of the Thermal Design Branch. His previous duties included performing thermal analysis of reentry spacecraft thermal protection systems including the Space Shuttle and other advanced spacecraft; investigation of Space Shuttle thermal anomalies; design and planning of arc-jet tests in support of thermal protection system design and analysis; conducting simulations of orbital debris reentry, and lead engineer for the X-38 structures team including the composite aeroshell and thermal protection system.

Mike Dunham – Stress Team Lead
Mike Dunham is currently is the Boeing Subsystem Manager for Orbiter Stress, Loads and Dynamics. He has worked on Shuttle Orbiter program for 21 years and has a Masters in Civil Engineering Structures from the University of Missouri-Columbia.

Aerodynamics Sub-Team

NASA Johnson Space Center

Rick Barton
Jerry Borrer
Gary Bourland
Kevin Dries
Joe Gamble
Reynaldo Gomez
Jim Greathouse
Mark Hammerschmidt
Steve Labbe
Gerald LeBeau
Randy Lillard
Forrest Lumpkin
Ricardo Machin
Chris Madsen
Fred Martin
Phil Robinson
Steven Robinson
Josh Schneider
Melanie Siloski
Phil Stuart
Tuan Truong
Darby Vicker

Ames Research Center

James Brown
Carol Carroll
David Kinney
James Reuther

Langley Research Center

Karen Bibb
Maria Bobskill
Greg Brauckmann
Pete Gnoffo
Bill Scallion
Charles Miller
Ramadas Prabhu
Bill Woods

Boeing - Houston

Olman Carvajal
Brandon Reddell
Georgi Ushev

Aerodynamics Sub-Team, Concluded

Boeing - Huntington Beach

Rick Burrows
Sergio Carrion
Ron Pelley
Karuna Rajagopal
Harry Sexton
Jeff Stone

Aerothermodynamics Sub-Team

NASA Johnson Space Center

Jerry Borrer
Katie Boyles
Chuck Campbell
Joe Caram
Steve Derry
Kevin Dries
Steve Fitzgerald
Gerald LeBeau
Chien Li, Ph. D.
Forrest Lumpkin, Ph. D.
Randy Lillard
Carl Scott, Ph. D.

NASA Johnson Space Center – White Sands Facility

Harold Beeson, Ph. D
Tim Gallus
Miguel Maes
Mike Shoffstall
Joel Stoltzfus
Bruce Wilson, Ph. D

Langley Research Center

Steve Alter
Kim Bey, Ph. D
Maria Bobskill, Ph. D
Kamran Daryabeigi
Joel Everhart, Ph. D
Chris Glass, Ph. D
Pete Gnoffo, Ph. D
Frank Greene
Harris Hamilton
Tom Horvath
William Kleb
Ron Merski, Ph. D
Charles Miller
Bob Nowak, Ph. D
Ricky Thompson
Bill Wood, Ph. D
William Wood??
Richard Wheless
Kay Wurster
Vince Zoby

Aerothermodynamics Sub-Team, Continued

Ames Research Center

James Brown, Ph. D
Dean Kontinos, Ph. D
Ryan McDaniel
Joe Olejniczak, Ph. D
James Reuther, Ph. D

Marshall Space Flight Center

Herb Bush
Mark Cousins
W. Dahm
Will Downs
Tim Karigan
Ken Kittredge
Al Mayers
David McDaniels
Stu Nelson
Richard Norman
Maurice Prendergast
Joe Ruf
Greg Schunk
John Sharp
Jim Sieja
Mickey White
Joe Wilson

Boeing - Houston

Ed Alexander
Maria Barnwell
Dennis Chao
Mark Fields
Ignacio Norman
K.C. Wang
Lung Wong

Boeing - Huntington Beach

Kevin Bowcutt, Ph. D
Michelle Chaffey
Dan Dominik
Fred Ghahyasi
Suk Kim, Ph. D.
Gerry Kinder
Todd Magee
Kurian K. Mani, Ph. D
Charles R. Olling , Ph. D
Don Picetti
Karuna Rajagopal, Ph. D
Leonel Serrano
Habbib Sharifzedah

Aerothermodynamics Sub-Team, Concluded

Boeing - Rocketdyne

Shashi Aithal
Edward Ascoli
Cliff Bampton
Steve Barson
Pai Chang
Willard Clever
Adon Delgado Jr.
John Fasheh
Scott Halloran
Yann-Fu Hsu
Zhining Liu
Michael Jacques
Dale Ota
S, V. Ramakrishnan
Touraj Sahely
Mark Stewart
Wallace Weider
Kaye Yun

Sandia National Laboratories

Tom Bickel, Ph. D
Michail Gallis, Ph. D
Basil Hassan, Ph. D
Roy Hogan, Ph. D
Dave Kuntz, Ph. D.
William Oberkamphf, Ph. D.
Jeff Payne
Carl Peterson, Ph. D
Ed Piekos, Ph. D.
Don Potter
Art Ratzel, Ph. D
Chris Roy, Ph. D.

AFRL

Susan Arnold
Peter Erbland
Roger Kimmel
James Miller
Richard Neumann

Lockheed Martin

Stan Bouslog
Jose Dobarco-Otero
Tom Paul
Bill Rochelle
Ries Smith

Thermal Sub-Team

NASA Johnson Space Center

Michael Baine
Stan Bouslog
Charlie Camarda
Chuck Campbell
Joe Caram
Joyce Carpenter
Harry Chang
Eric Christiansen
Don Curry
Horatio De La Fuente
Steven Del Papa
Steve Derry
Bonnie Dunbar
Steve Fitzgerald
Mike Fowler
Vadim Gandelsman
Andrew Hong
Eric Hurlbert
Justin Kerr
John Kowal
Gerald LeBeau
Ronald K. Lewis
Stan Love
Chris Madden
Robert Maraia
Tom Modlin
Dan Newswander
Tom Paul
Steve Rickman
Rodney Rocha
Alvaro Rodriguez
Stephanie Wilson

NASA Johnson Space Center – White Sands Facility

Joel Stoltzfus

Langley Research Center

Brian Hollis
Stephen Scotti

Ames Research Center

Scott Lawrence

Thermal Sub-Team, Continued

Marshall Space Flight Center
Joe Ruf
Greg Schunk
John Sharp

Boeing - Houston

Ed Alexander
Maria Barnwell
Shannon Belknap
John Blake
Scott Christensen
Doug Cline
Dennis Chao
Diana Coronado
Tim Davies
Stan Kennedy
Mohammed Nasrullah
Than Nguyen
David Norman
Ignacio Norman
Alfred Olaleye
Renee Rabke
Dave Russell
Steven Tidwell
John Tran
K.C. Wang
Lung-Chen Wong
Michael Zhang

Boeing - Huntington Beach

Kevin Bowcutt
Michelle Chaffey
Dan Dominik
Faustino Garcia
Fred Ghahyasi
Gerry Kinder
Kurian K. Mani
Charles R. Olling
Don Picetti
Karuna Rajagopal
Habbib Sharifzedah

Cimarron

James Smith

Thermal Sub-Team, Concluded

Boeing – Kennedy Space Center

Dan Bell

Boeing - Rocketdyne
Steve Barson
Scott Halloran

Sandia National Laboratories

Tom Bickel
Michail Gallis
Basil Hassan
Roy Hogan
David Kuntz
Jeff Payne
Carl Peterson
Ed Piekos
Don Potter
Art Ratzel

SAIC (Science Application International Corporation)
Omar Hatamleh
Mohamed Ishmael

AFRL
Peter Erbland
Roger Kimmel

Lockheed Martin
Stan Bouslog
Bill Rochelle
Jim Milhoan
Matthew Vogel

United Space Alliance
Pam Madera

Structures Sub-Team

NASA Johnson Space Center

Trevor Kott
Julie Kramer
Tom Modlin
Deneen Taylor

Langley Research Center

Max Blosser
Lynn Bowman
Roger Chen
Kamran Daryabeigi
Christapher Lang
Stephen Scotti

Boeing - Houston

Jason Adair
Bob Clark
Mike Dunham
Danny Le
Aaron Leinmiller
Gus (Constantine) Michalopolous
Darwin Moon
Paul Parker
Shawn Sorenson

Boeing - Huntington Beach

Tony Chi
Gary Collier
Ken Fiorelli
Scott Foust
Judy Goldish
George Hartnett
Mahesh Jain
Mike Koharchick
Jerry Lai
John McKinney
Bill Novak
Dave Okino
Charles Park
Al Richardson
Lou Swayne
Ed Tong
Jerry Warren